

Architectural and social potential of urban lighting

A field study of how brightness can affect the experience of waiting for public transportation

Hvass, Mette; Hansen, Ellen Kathrine

Published in:

Planning Post Carbon Cities: 35th PLEA Conference on Passive and Low Energy Architecture, A Coruña, 1st-3rd September 2020

DOI (link to publication from Publisher):

[10.17979/spudc.9788497497947](https://doi.org/10.17979/spudc.9788497497947)

Creative Commons License
CC BY-NC-SA 4.0

Publication date:
2020

Document Version
Publisher's PDF, also known as Version of record

[Link to publication from Aalborg University](#)

Citation for published version (APA):

Hvass, M., & Hansen, E. K. (2020). Architectural and social potential of urban lighting: A field study of how brightness can affect the experience of waiting for public transportation . In J. Rodríguez-Álvarez, & J. C. Gonçalves (Eds.), *Planning Post Carbon Cities: 35th PLEA Conference on Passive and Low Energy Architecture, A Coruña, 1st-3rd September 2020: Proceedings* (Vol. 1, pp. 683-688). University of A Coruña & Asoc.. <https://doi.org/10.17979/spudc.9788497497947>

General rights

Copyright and moral rights for the publications made accessible in the public portal are retained by the authors and/or other copyright owners and it is a condition of accessing publications that users recognise and abide by the legal requirements associated with these rights.

- Users may download and print one copy of any publication from the public portal for the purpose of private study or research.
- You may not further distribute the material or use it for any profit-making activity or commercial gain
- You may freely distribute the URL identifying the publication in the public portal -

Take down policy

If you believe that this document breaches copyright please contact us at vbn@aub.aau.dk providing details, and we will remove access to the work immediately and investigate your claim.



PLEA 2020 A CORUÑA



35th PLEA Conference on Passive and Low Energy Architecture

Planning Post Carbon Cities

Editors:

Jorge Rodríguez Álvarez

&

Joana Carla Soares Gonçalves



PLEA

Sustainable Architecture and Urban Design



UNIVERSIDADE DA CORUÑA



35th PLEA Conference on Passive and Low Energy Architecture

Planning Post Carbon Cities

A Coruña, 1st-3rd September 2020

PROCEEDINGS

Vol. 1

Editors:

Jorge Rodríguez Álvarez

&

Joana Carla Soares Gonçalves

Design and layout:

Daniel Zepeda Rivas



Sustainable Architecture and Urban Design



UNIVERSIDADE DA CORUÑA



Sustainable Architecture and Urban Design



Escola Técnica Superior de Arquitectura
Universidade da Coruña



UNIVERSIDADE DA CORUÑA

PLEA 2020 - Planning Post Carbon Cities

Proceedings of the 35th International Conference on
Passive and Low Energy Architecture
A Coruña, 1st - 3rd September 2020

Organized by the University of A Coruña
and Asoc. PLEA 2020 Planning Post Carbon Cities
www.plea2020.org
www.udc.es

Conference Proceedings edited by:

Jorge Rodríguez Álvarez and Joana Carla Soares Gonçalves
Design and layout: Daniel Zepeda Rivas

© Edition: University of A Coruña and Asoc. PLEA2020 Planning Post Carbon Cities
© Individual papers: the respective authors

Portions of this publication may be freely reproduced subject to the contents being reproduced accurately, for academic purposes, with due acknowledgement to the authors and the conference proceedings title and editors. For use in citations: Paper Author(s) (2020) Paper Title. In J. Rodríguez Álvarez & J.C. Soares Gonçalves (Eds.) *Planning Post Carbon Cities. Proceedings of the 35th PLEA Conference on Passive and Low Energy Architecture*. A Coruña: University of A Coruña. DOI: <https://doi.org/10.17979/spudc.9788497497947>
This book was prepared from the input files supplied by the authors. The editors and the publisher are not responsible for the content of the papers herein published.

Electronic version as:

ISBN: 978-84-9749-794-7

Depósito Legal: C 1551-2020

DOI: <https://doi.org/10.17979/spudc.9788497497947>



This book is released under a Creative Commons license
Attribution-NonCommercial-ShareAlike 4.0 International
(CC BY-NC-SA 4.0)



PLEA 2020 - Planning Post Carbon Cities

35th International Conference on Passive and Low Energy Architecture

www.plea2020.org A Coruña, 1st - 3rd September 2020

Organising Committee

Dr. Jorge Rodríguez Álvarez.

Conference Chair, School of Architecture University of A Coruña

Dr. Amparo Casares Gallego. School of Architecture, University of A Coruña

Dr. Cristina García Fontán. School of Architecture, University of A Coruña

Dr. Emma López Bahut. School of Architecture, University of A Coruña

Dr. David Peón Pose. School of Economics, University of A Coruña

Prof. Santiago Pintos Pena. School of Architecture, University of A Coruña

International Advisory Board

Prof. Edward Ng, PLEA President. Chinese University of Hong Kong

Dr. Heide Schuster, PLEA Vice-President. BLAUSTUDIO/Frankfurt University of Applied Sciences. Germany

Dr. Paula Cadima, PLEA Director, Architectural Association School of Architecture. UK

Prof. Rajat Gupta, PLEA Director. Oxford Brookes University. United Kingdom

Prof. Pablo LaRoche, Cal Poly Pomona. United States

Dr. Sanda Lenzholzer, PLEA Director. Wageningen University. Netherlands

Prof. Ulrike Passe, PLEA Director. Iowa State University. United States

Prof. Sue Roaf, Heriot-Watt University. United Kingdom

Dr. Joana Carla Soares Gonçalves, PLEA Director. AA School of Architecture, UK; School of Architecture and Cities, University of Westminster. UK; FAUU São Paulo. Brazil

Dr. Simos Yannas, Architectural Association School of Architecture. UK

PLEA Team

Erika Bea Soutullo. Student, School of Architecture, University of A Coruña

Ana Fernández Santamaría. Student, School of Architecture, University of A Coruña

Alba León Álvarez. Student School of Architecture, University of A Coruña

Alvaro Queiro Arias. Graduate, School of Architecture, University of A Coruña

Daniel Zepeda Rivas. PhD student, University of A Coruña

Scientific Committee

Dr. Shabbir Ahmed, Bangladesh University of Engineering & Technology. Bangladesh
 Rafael Alonso Candau, Atmos Lab. United Kingdom
 Prof. Sergio Altomonte, Université Catholique de Louvain. Belgium
 Balint Bakos, Urban Systems Design. United Kingdom
 Prof. Michael Bruse, University of Mainz. Germany
 Prof. Vincent Buhagiar, University of Malta, Malta
 Prof. Waldo Bustamante, Pontificia Universidad Católica de Chile. Chile
 Dr. Paula Cadima, Architectural Association School of Architecture. United Kingdom
 Dr. Amparo Casares Gallego, University of A Coruña. Spain
 Florencia Collo, Atmos Lab. United Kingdom
 Dr. Raphael Compagnon, Haute École d'Ingénierie et d'Architecture Fribourg. Switzerland
 Prof. Marwa Dabaieh, Aalborg University. Denmark
 Dr. Ruth Domínguez Sánchez, European Commission. Spain
 Dr. Samuel Domínguez-Amarillo, University of Seville. Spain
 Angela Dub, University of Buenos Aires. Argentina
 Prof. Evyatar Erell, Ben-Gurion University. Israel
 Dr. Carlos Javier Esparza López, Universidad de Colima. Mexico
 Dr. Jesica Fernández-Agüera, University of Seville. Spain
 Prof. Carmen Galán-Marín, University of Seville. Spain
 Dr. José Roberto García Chávez, Metropolitan Autonomous University. Mexico
 Dr. Cristina García Fontán, University of A Coruña. Spain
 Marjan Ghobad, PJCarew. Germany
 Pablo Gugel Quiroga, Atelier Ten. United Kingdom
 Prof. Rajat Gupta, Oxford Brookes University. United Kingdom
 Navid Hatefnia, Technical University of Munich. Germany
 Prof. Runa T. Hellwig, Aalborg University. Denmark
 Prof. Ester Higuera, Universidad Politécnica de Madrid. Spain
 Eric Blake Jackson, Stantec. United States
 Gloria Cecilia Jiménez Dianderas, Pontificia Universidad Católica del Perú. Peru
 Dr. Werner Xaver Lang, Technical University of Munich. Germany
 Benson Lau, University of Westminster. United Kingdom
 Dr. Sanda Lenzholzer, Wageningen University. Netherlands
 Prof. James Owen Lewis, University College Dublin. Ireland
 Prof. Pablo LaRoche, Cal Poly Pomona. United States
 Florian Lichtblau, Lichtblau Architekten BDA. Germany
 Dr. María López de Asiaín Alberich, University of Seville. Spain
 Dr. Emma López-Bahut, University of A Coruña. Spain
 Ranny Loureiro Xavier Nascimento Michalski, Faculty of Architecture and Urbanism of the University of São Paulo. Brazil

Scientific Committee (cont.)

Dr. Leonardo Marques Monteiro, University of São Paulo. Brazil
 Dr. Roberta Consentino Kronka Mülfarth, Faculty of Architecture and Urbanism of the University of São Paulo. Brazil
 Dr. Emanuele Naboni, The Royal Danish Academy of Fine Arts. Denmark
 Jonathan Natanian, Technical University of Munich. Germany
 Prof. Edward Ng, Chinese University of Hong Kong. Hong Kong
 Prof. Marialena Nikolopoulou, University of Kent. United Kingdom
 Prof. Ulrike Passe, Iowa State University. United States
 María Paz Sangiao, Instituto Tecnológico de Galicia. Spain
 Dr. David Peón, University of A Coruña. Spain
 Dr. Alessandra Prata Shimomura, FAUUSP. Brazil
 Dana Raydan, Raydan Watkins Architects. United Kingdom
 Dr. Lucelia Taranto Rodrigues, University of Nottingham. United Kingdom
 Dr. Jorge Rodríguez Álvarez, University of A Coruña. Spain
 Prof. Jean-Francois Roger France, Université catholique de Louvain. Belgium
 Prof. Marco Sala, ABITA Interuniversity Research Centre. Italy
 Dr. Rosa Schiano-Phan, University of Westminster. United Kingdom
 Prof. Mattheos Santamouris, University of New South Wales. Australia
 Prof. Marc Eugene Schiler, University of Southern California. United States
 Prof. Masanori Shukuya, Tokyo City University. Japan
 Dr. Heide G. Schuster, BLAUSTUDIO. Germany
 Shruti Shiva, Terra Viridis. India
 Gunveer Singh, Atmos Lab. United Kingdom
 Dr. Joana Carla Soares Gonçalves, Architectural Association School of Architecture. United Kingdom; School of Architecture and Cities, University of Westminster. United Kingdom; Faculty of Architecture and Urbanism of the University of São Paulo. Brazil
 Victoria Eugenia Soto Magán, École Polytechnique Fédérale de Lausanne. Switzerland
 Prof. Thanos N. Stasinopoulos, Izmir University of Economics. Turkey
 Prof. Koen Steemers, University of Cambridge. United Kingdom
 Dr. Abel Tablada, Technological University of Havana. Cuba
 Dr. Mohammad Taleghani, University of Salford. United Kingdom
 Dr. Juan Antonio Vallejo Vázquez, NaturalCooling Ltd. Spain
 Leonidas Tsichritzis, University of Kent. United Kingdom
 Prof. Barbara Widera, Wrocław University of Science and Technology. Poland
 Dr. Feng Yang, Tongji University. China
 Dr. Simos Yannas, Architectural Association School of Architecture, United Kingdom
 Aram Yeretzian, American University of Beirut. Lebanon
 Dr. Gabriela Zapata-Lancaster, Cardiff University. United Kingdom
 Daniel Zepeda-Rivas, University of A Coruña. Spain



PLEA 2020 - Planning Post Carbon Cities

35th International Conference on Passive and Low Energy Architecture

www.plea2020.org A Coruña, 1st - 3rd September 2020

Sponsors & Supporting Organisations



Foreword

The organization of the 35th PLEA Conference has been an enormous challenge. The unprecedented circumstances that preceded it required flexible and, at the same time, determined decision making. Once finished, we hope that PLEA 2020 becomes a landmark in the longstanding and unique trajectory of PLEA. It has been its first virtual Conference; arguably, the one with the lowest carbon footprint (which is being calculated by some participants). The organizational expenses were lower than those for a physical conference, which allowed for a substantial reduction in the participation fees. According to the participants' comments and feedback, the event was quite satisfactory. The environment was, overall, dynamic and engaging, the debate was fluid and there were numerous opportunities for interaction, considering the limitations. The high quality of the technical presentations was one of the most important factors, as they kept ongoing attention during the three days. The keynote speakers brought fresh and diverse ideas to the discussion. The roundtables were often enriched with the comments and remarks from the participants, enhancing direct interaction with the speakers as well as among themselves.

On the other hand, it was a little disappointing that we couldn't share the experience of A Coruña's city life or the beautiful Galician landscapes with the PLEA community. As much as we and the environment can benefit from virtual events there are certain opportunities (immersion in other culture, casual encounters during coffee breaks...) that require physical presence. It seems likely that a balance between virtual and face to face meetings is to be found in future events. We hope we can host such an event in A Coruña after the pandemic is over.

The central theme of PLEA 2020 was the Post Carbon City. When the potential subjects to be addressed in the conference were first discussed, most of the topics were related to energy efficiency, ventilation, comfort, daylight, mobility, microclimate or materials...However, in our opening statement we also proposed a paradigm shift to start designing "the cities we want in the future, to construct utopian visions in which urban progress is based on ecology, equality and wellness". A few months later we find ourselves studying how buildings and cities influence wellness and disease. Some widely established assumptions about sustainable urban models need to be reevaluated according to a new set of criteria, which in some cases may contravene the rules of efficiency. However, the need for high quality indoor and outdoor environments will be strongly reinforced after this episode. People staying at home during lockdowns, quarantines or due to remote working create new scenarios and demand greater flexibility and performance in domestic environments. The provision of comfortable outdoor spaces where social interaction is safer during the epidemic has led to a number of cities taken unprecedented measures. This could be a unique opportunity to set up the urban agenda for the forthcoming climatic challenges. Quoting the PLEA 2020 Award acceptance speech by prof. José Fariña "We are already in a period of urgency and it is necessary to act".

A number of articles presented in the Conference have showcased novel methodologies, from data mining to machine learning, while other papers relied on well-established methods, such as field observations and measurements, physical prototypes or computer simulations carried out

by a wide array of software tools. Overall, reviewers seemed to praise those proposals with a clear potential to be implemented, regardless of their methodology. By contrast, very specific case studies that offered little insights beyond the case at hand or established knowledge tended to be penalized. Half of the awarded and commended papers and posters addressed urban aspects (the microclimatic effect of vegetation, temporary urban interventions, the value of urban nature, urban canyons...). The climatic adaptation of buildings for future conditions was also a central topic both in the conference and in five awarded papers; the social approach to sustainability was not a minor subject as it was thoroughly addressed in at least three awarded articles and in a good number of papers presented at the Conference.

The selection of the papers to be presented followed a rigorous process. We received around 850 abstracts, from 1,500 authors affiliated to some 300 organizations from 60 countries. All the abstracts were reviewed by at least two reviewers in a double blind process. The first round required some 1,700 reviews to select 450 abstracts, which were to be converted into full technical papers. A second round of reviews was conducted to finally select 306 articles: 37 as posters and 269 as oral presentations.

All the material generated from this Conference is now freely accessible through the official repository of the University of A Coruña (ruc.udc.es), the PLEA 2020 website (plea2020.org) and PLEA (plea-arch.org). In addition, all the videos have been uploaded to PLEA 2020 YouTube Channel, including the keynote sessions and roundtables.

([PLEA 2020 youtube channel](#)).

Finally, I would like to express my gratitude to the global PLEA organization, for keeping up an invaluable network and stewarding high quality standards in all its Conferences. I would also like to thank the University of A Coruña, and, particularly, the School of Architecture for their constant support during these months, the regional government of Galicia: Xunta de Galicia, the local council of A Coruña, and all our sponsors and supporters. The presence of the President of the Galician Government, Alberto Nuñez Feijóo, the Mayor of A Coruña Inés Rey, the Chancellor of the University of A Coruña Julio Abalde and the Dean of the School of Architecture Plácido Lizancos, in the inaugural Ceremony was very special moment and their speeches reflected a commitment with values and ideas shared by the PLEA Community. The organization of PLEA 2020 wouldn't have been possible without the whole local organizing committee (Amparo, Cristina, David, Emma and Santiago) and the assistance of the PLEA 2020 team (Alba, Alvaro, Ana, Daniel and Erika). I wish you can find the PLEA 2020 Conference Proceedings at least as useful and enlightening as a compilation of timely and relevant research in Sustainable Architecture and Urban Design as the previous 34 PLEA editions.

Jorge Rodríguez Álvarez
PLEA 2020 Conference Chair



PLEA 2020 - Planning Post Carbon Cities

35th International Conference on Passive and Low Energy Architecture
www.plea2020.org A Coruña, 1st - 3rd September 2020

PLEA 2020 – Planning Post Carbon Cities, the first on-line PLEA conference

The 35th International Conference on Sustainable Architecture and Urban Design, entitled PLEA 2020 – Planning Post Carbon Cities, was the first on-line PLEA conference. Due to the pandemic that hit the world in the beginning of 2020, the organizers from the University of A Coruña were forced to convert what was meant to be a live event with people's physical presence in the Spanish city of A Coruña, in Galicia, into an on-line one.

Despite the natural constraints of the on-line modus operandi upon human dynamics, the commitment of the organizers in providing an easy and reliable digital platform, coupled with the engagement of the participants populating live chats of technical and keynote presentations made the conference a vibrant forum of environmental technical knowledge sharing. The PLEA 2020 event had 306 papers presented and brought together more than 700 participants from over 60 countries who are interested and active in the field of environmental design, teaching and research, located in different parts of the world, spanning from the Americas to the Far-East Asia. The quality of the papers is particularly high. Members of the PLEA Board unanimously agreed to hand out 4 best paper awards and 3 best poster award, together with a number of commendations. Thanks must be due to the hard work of the members of the scientific committee and the conference organizers. Furthermore, during the opening ceremony of the conference, the PLEA Lifetime Achievement Award 2020 was presented to Professor Edna Shaviv and the PLEA Award 2020 was given to Professor José Fariña Tojo. May we send our congratulations again to both of them.

On a rather positive note, the virtual status of the conference in 2020, in which challenges and opportunities for the post carbon cities and, therefore, post carbon societies were broadly discussed, opened a new avenue for the PLEA community itself, focused on the reduction of its environmental impact, associated with air travel across the world to attend periodic scientific meetings. Following on the steps of organizers of the 35th International Conference on Passive and Low Energy Architecture, we expect that the next PLEA conferences will explore on-line possibilities, specially to facilitate the participation of those in regions of the world away from the conference location, whilst creating adequate conditions for safe physical presence, when possible, in order to bring back the unmeasurable richness of human interaction and the consequent advantages to knowledge sharing.

Joana Carla Soares Gonçalves
On behalf of the PLEA Board

About the Keynote Lectures

The six keynote speakers addressed the theme of Planning Post Carbon Cities from a strategic design perspective and vision, qualified by research activities in real context as well as in the analytical realm. The role of people's behaviour and behavioural change, alongside the design focus of fulfilling people's needs and expectation in both buildings and urban design defined a common thread seen across all the six talks spread along the three-days conference.

Susan Carruth, from GXN, in Copenhagen, and **Klaus Bode** from Urban Systems Design (USD), in London, open the keynote talks. Susan gave the talk on Cities of the Future: Behaviourally driven, Materially Bound, in which she explored two themes: circular design and how to scale-up from materials to the design of cities, alongside the so-called behavioural design and their applicability in the planning of future cities. Following up, Klaus' presentation about Planning Post Carbon Cities: Our Challenges and Opportunities could not stress more the key role of occupants in reducing energy demand in buildings, calling for a design approach that he entitles human centric design, whilst revealing the potential for innovative and effective solutions at both building and masterplan scales, when based on passive environmental strategies and low-energy engineering.

In the second day of the event, **Cynthia Echave**, Urban Ecology expert based in Barcelona, talked about Liveability and Resilience from an Ecological Approach. In her talk, Cynthia explored innovative ecosystemic solutions liaising green economy, social inclusiveness and governance, focused on the Euro-Mediterranean Region and African cities. In the sequence, **Helle Sørholt**, CEO and cofounder of Gehl, gave the talk The Need for People and Public Spaces. The long legacy of the design practice exercised by Gehl Architects in designing quality-urban spaces geared for pedestrians and social activities is well known. In this talk, Helle brought some of the latest examples of projects developed by the firm that contribute to make cities around the world more liveable and sustainable.

In the closing day, **Michael Smith**, from Entre Nos Atelier, in San José, Costa Rica, and **Belinda Tato**, from Ecosistema Urbano, in Madrid focused on social aspects. Michael's talk on Regenerative Design and Spatial Justice brought a number of successful real-life projects in Latin America which exemplify his commitment with a social design agenda including community empowerment, environmental awareness and hands-on experiences based on inclusive design processes, mostly developed upon low-income environments. Belinda spoke about Ecosistema Urbano, showing projects based on knowledge from urbanism, architecture, engineering and sociology, resulting in what she calls urban social design, in which the design of environments, spaces and social dynamics come together in order to improve the self-organization of citizens, social interaction within communities and their relationship with the local physical and natural environment. Regarding the design process, both talks drew on the opportunities laying in participatory processes to create spaces for people.

Concluding, in addition to the emphasis put on the role of people in the design and planning of the Post Carbon City, by addressing issues of existing built environments, the keynote speakers collectively showcased a wide range of successful real and experimental projects, that highlight the advantages of a multidisciplinary approach, in reverting the current environmental and social conditions in cities around the world, in a creative and environmentally sound manner.

Table of Contents

Committees

Foreword

Technical Articles

Volume I

1. Sustainable Buildings

SB-1

ID	Title	Authors	Page
1122	Embodied Carbon: A Comparison of Two Passivhaus Homes in the UK	Stevenson, Fionn; Arslan, Dilek; Gomez Torres, Sergio; Brierley, Jenny; Foster, Sam; Halliday, Sandy	2
1360	Critical Analysis on Passive and Low Energy Architecture Study Research Trend through Text Data Mining Technique in the Period of 2006 to 2018	Wang, Lan; Lee, Eric Wai Ming	8
1486	Analysis and Countermeasures of Problems in Pure Soil Construction---Take the Research and Development Centre for Rural Vitalization in Yunnan China as an Example	Tian, Fang; Bai, Wenfeng; Zhou, Lai; Liu, Xiaoxue; Wan, Li; Chi, Xinan; Ng, Edward	14
1688	Using In-Situ Building Fabric Thermal Performance Testing to Calibrate As-Built Models of Low Energy Dwellings in the UK	Gupta, Rajat; Gregg, Matt	20
1117	Impact of Renovation Measures on the Indoor Climate and Energy Use in Single Family Dwellings in Belgium	Breesch, Hilde; Beyaert, Axel; Callens, Alexander; Claes, Koen; Versele, Alexis	26
1390	Adjustable Light Shelf Angles for Different Sky Conditions: Daylighting Reading Space at University Libraries in Dhaka	Ferdous, Zannatul; Joarder, Md Ashikur Rahman	32
1315	The Modern Vernacular: Adapting Vernacular Architecture for a Modern Production Facility in the context of Rishikesh, India	Anand, Isha; Juneja, Aarushi; Rastogi, Sonali	38
1836	Occupant and Environment Related Parameters in the Evaluation of Visual Environment: An Experimental Design	Kaçel, Seda	43
1857	Occupants' Perception versus Daylighting Simulations': A Field Study on Lecture Halls to Correlate the Occupant's Subjective Responses and Climate-Based Daylight Metrics	Verma, Tarun; Gopalakrishnan, Padmanaban	49

SB-2

ID	Title	Authors	Page
1201	Solar Cube: An Affordable Answer to Address Housing Shortage and Energy Deficit in Argentina	Rojo Pla, Gustavo Adolfo; Rojo Pla, Xavier Emmanuel; Rojo, Ricardo Daniel; Garza Gonzalez, Ana Cecilia	55
1521	The Influence of Building Form on Energy Use, Thermal Comfort and Social Interaction. A Post-occupancy Comparison of Two High-rise Residential Buildings in Singapore	Gamero-Salinas, Juan Carlos; Kishnani, Nirmal; Monge-Barrio, Aurora; Gandhi, Bhavya; Bilgi, Megha; Sánchez-Ostiz, Ana	61

1677	Recorded Energy Consumption of NZEB Dwellings – and Corresponding Interior Temperatures. Initial Results from the Irish NZEB101 Project.	Colclough, Shane; O’Hegarty, Richard; Griffiths, Philip; Kinnane, Oliver; Rieux, Etienne	67
1300	Characterization of Library Lighting Design	Espinoza Cateriano, Eduardo; Coch Roura, Helena; Crespo Cabillo, Isabel	73
1309	Holistic Assessment of Highly Insulated nZEB Walls	O Hegarty, Richard; Kinnane, Oliver; Lennon, Donal; Colclough, Shane	79
1467	Climate Change Adaptation and Retrofit of a Victorian Townhouse in Margate: the 5-year Living Lab	Nikolopoulou, Marialena; Watkins, Richard; Rueda-de-Watkins, Elena; Dominguez-De-Teresa, Leire; Renganathan, Giridharan; Kotopouleas, Alkis	85

SB-3

ID	Title	Authors	Page
1563	Structural System Based on Robot Assisted Carpentry for Medium-Height Building in Wood	Hormazabal, Nina; Ramirez, Michelle; Sills, Pablo; Quitral, Francisco; Valdes, Francisco	91
1787	Finding Patterns of Openings Operation and its Influence on the Thermal Performance of Houses: A Case Study in Southern Brazil	Schaefer, Aline; Ghisi, Enedir; Eccel, João Vítor	97
1405	The Impact of Static and Dynamic Solar Screens on the Indoor Thermal Environment and Predicted Thermal Comfort	Naik, Niyati Sudhir; Elzeyadi, Ihab	103
1302	Living Roofs for Cooling. Impact of Thermal Mass, Night Ventilation and Radiant Evaporative Cooling	Rodriguez, Laura; La Roche, Pablo	109
1221	Revealing the Thermal Quality of the Modernism Legacy’s Architecture: Marcos Acayaba’s Single-family Houses in São Paulo	Gasparelo Lima, Eduardo; Soares Gonçalves, Joana Carla; Loureiro Xavier Nascimento Michalski, Ranny	115
1412	Responsive Design in the Outdoor Space of the Sea Ranch Architecture	Shimoda, Masunami; Murata, Ryo	121

SB-4

ID	Title	Authors	Page
1209	Field Study on Indoor Thermal Environment in Air-conditioned Offices in the Tropics: A Case Study of Indonesia, Singapore, and Thailand	Sikram, Tanadej; Ichinose, Masayuki; Sasaki, Rumiko	127
1583	Exploring Potentiality of Lightpipe: Daylighting Deep Plan Office Buildings in Dhaka	Paul, Shajib; Joarder, Md. Ashikur Rahman; Chowdhury, Sajal	133
1133	Embodied Carbon: A Brettstapel Passivhaus in the UK	Arslan, Dilek; Stevenson, Fionn; Foster, Sam; Halliday, Sandy; Nimmo, Ian; Nimmo, Anne	139
1229	Energy-Efficient Retrofit Strategies at the Building Envelopes of Higher Educational Buildings in Mediterranean Climates to Achieve Thermal Comfort and Energy Efficiency	Hany, Nermine Aly	145
1402	Assessment of Natural Ventilation on Thermal Comfort and Energy Consumption: The Case of a Natural-ventilated Shopping Mall in the Tropics	Yuan, Ye; Liu, Gang; Dang, Rui; Yan, Fangli	151

1401	Energy Retrofit of the Existing Residential Building Stock in Jiangsu Province, China - Study on Danyuan Apartment of 1979-1999	Chen, Xi	157
1805	Comprehensive Evaluation of Daylighting, Air Quality and Thermal Comfort as Renovation Impact in a Madrid Classroom	Lopez de Rego Garcia Arquimbau, Almudena; Arranz, Beatriz	163
1435	User Centered Lighting Environment. Assessing The Variables for a Biodynamic Health Enhanced Control Logic	Lopez, Remedios Maria; Aguilar, María Teresa; Dominguez-Amarillo, Samuel; Acosta, Ignacio; Sendra, Juan José	169
1115	Circular Construction: Circularity Through Business Models for Longer Building Life	Hale, Lara Anne	175

SB-5

ID	Title	Authors	Page
1514	Monitoring of Indoor Radon in Passive House Buildings	Mc Carron, Barry; Meng, Xianhai; Colclough, Shane	181
1278	Occupant-centric Radiant Cooling Solutions	Mahdavi, Ardeshtir; Teufl, Helene	187
1551	Are Green Buildings Doing Enough? The Role of Green Certification and Gender on Sick Building Syndrome	Elnaklah, Rana; Fosas, Daniel; Natarajan, Sukumar	193
1496	Does Sharing Mean Sustainability? The Potential for Sustainability of Shared Spaces and Facilities in Collective Residential Buildings	Duan, Siyu; Tweed, Chris	199
1255	Vacuum Insulation Panels in Building Sector	Aparicio, Xabier; Erkoreka, Aitor; del Portillo, Luis Alfonso; Giraldo, Catalina; Uriarte, Amaia; Eguia, Pablo; Sánchez-ostiz, Ana María	205
1586	'Industria Loci': The Energy of Place Achieving Energy Optimisation within Mixed Use Developments utilising Passivhaus Design Strategies in Urban Design	Murray, Martin Anthony; Colclough, Shane; Griffiths, Philip	211

SB-6

ID	Title	Authors	Page
1561	Thermal Comfort Metamodel Tool compared to EnergyPlus simulations: A comparison Using an University Building	Medeiros, Helder Gattoni; Veloso, Ana Carolina de Oliveira; Souza, Roberta Vieira Gonçalves de	217
1577	Biophilic Design in Architecture: A Case Study of University of Brasília's Buildings	Blumenschein, Raquel; Muza, Pedro	223
1181	Lessons Learnt from the Brazilian Bioclimatic Modernism: The Environmental Potential of Passive Design for Office Buildings In The City of Sao Paulo	C Kronka Mulfarth, Roberta; Soares Goncalves, Joana Carla; Loureiro Xavier Nascimento Michalski, Ranny; Marques Monteiro, Leonardo; Rodrigues Prata Shimomura, Alessandra; Nascimento e Souza, Beatriz; Reis Muri Cunha, Guilherme; Monroy, Manuel	229
1497	Exploration of an Architectural Component with Environmental Functions from the Mechanical Recycling of PET	Lucares, María Ignacia; Carbonnel, Alexandre; Pérez, Hugo; Escobar, Daniel; Jimenez, María Paz	235

1120	Influence of Air Movement and Air Humidity on Thermal Comfort in Office Buildings in Florianópolis, Brazil	Citadini de Oliveira, Candi; Forgiarini Rupp, Ricardo; Ghisi, Eneir	240
1312	Experimental Building of Nîmes Institute of Technology	Abbas, Abbas; Cevaer, Franck; Dubé, Jean-François	246

SB-7

ID	Title	Authors	Page
1342	Thermal Perception in a Room with Radiant Cooling Panels Coupled to a Roof Pond	Fernandes, Leandro Carlos; Krüger, Eduardo Leite; Erell, Evyatar	252
1818	Analysis of Different Wall Typologies: The Thermal Performance of a Naturally Ventilated Social Interest Housing	Costa, Isabely Penina; Neves, Leticia de Oliveira; Labaki, Lucila Chebel	258
1592	Using Architectural Assessment to Evaluate User Experience in a Pre- and Post-Move Study of an Office Environment	Peters, Terri; Cepic, Mimi; McArthur, Jenn	264
1226	The Design Process of Commercial High-Performance Buildings: with reference to the context of São Paulo and London	Pellegrini L. Trigo, J.; Soares Gonçalves, J.C., Hernández Neto, A.	270
1612	Severiano Mario Porto's Projects in the North of Brazil: A Bioclimatic Research about the Amazon Architecture	Medeiros, Ayana Dantas de; Amorim, Cláudia Naves David	276

SB-8

ID	Title	Authors	Page
1705	Designing Sustainable Office Buildings with Higher Value in Use	Raynaud, Camille; Flachaire, Constance; Etienne-Denoy, Ella	282
1602	Evidence-Based Calibration of an Energy Simulation Model: Dealing with Practical Issues of Data Availability and Granularity in an UK Apartment Block	Scortegagna, Elisa; Martins, Nelson; Jain, Nishesh; Sousa, Luis; Tindale, Andrew	288
1116	Building Performance Evaluation of a 14th Century Pargetted House: Hygrothermal comfort and energy efficiency.	Whitman, Christopher J.	294
1645	How to Transform European Housing into Healthy and Sustainable Living Spaces?	te Braak, Petrus; Minnen, Joeri; Fedkenheuer, Moritz; Wegener, Bernd; Decock, Friedl; Descamps, Filip; Pauquay, Sabine; Feifer, Lone; Hale, Lara Anne; Asmussen, Thorbjørn Færing; Christoffersen, Jens	300
1159	Methodology Proposal for the Evaluation of Energy Efficiency and Indoor Environmental Quality of School Buildings	Arranz, Beatriz; Pérez, Mariana	305
1776	An Investigation of the Luminous Environment in Nottingham H.O.U.S.E	Kankipati, Lakshmi Soudamini; Rodrigues, Lucelia; Kiamba, Lorna	311
1253	Retrofitting of Buildings: What About GHG Emission Reductions? The Case Study of Switzerland	Cozza, Stefano; Chambers, Jonathan; Patel, Martin K.	317
1485	Optimization of Building Facade Solar Protection Design in an Urban Context	Santiago, Pedro; Blanca-Giménez, Vicente	323
1694	Natural Ventilation of Double Skin Façade: Evaluation of wind-induced airflow in tall buildings	Matour, Soha; Garcia Hansen, Veronica; Drogemuller, Robin; Omrani, Sara; Hassanli, Sina	328

SB-9

ID	Title	Authors	Page
1621	A Common Language for Environmental Performance - Implementing the EU Level(s) Framework for Sustainable Buildings	Páez Pérez, Camilo; Galán González, Aránzazu; Cristoforetti, Sebastiano; Erten, Duygu; Ben Rajeb, Samia	334
1765	Biophilic Atrium Design: An Analysis of Photosynthetically Active Radiation for Indoor Plant Systems	Du, Jiangtao; Sharples, Steve	340
1121	Thermal and Light Impact of the Use of Translucent Glass Railings on Terraces of Residential Buildings. Case in Sant Cugat del Vallès	Zamora Mestre, Joan Lluís; Sorto Díaz, Estela Lourdes; Uriarte Ortazua, Urtza; Armas Cabrera, Maria Eugenia	346
1124	Can Daylighting Instinctively Receive More Acceptance Than Artificial Lighting at Workspaces?	Chen, Xiaodong; Zhang, Xin; Du, Jiangtao	352
1593	Comfortable and Energy Efficient Educational Spaces. Strategies, Methods And Building Components For Energy Retrofit In Different Climate Zones	Rossi-Schwarzenbeck, Monica; Romano, Rosa; Capasso, Mario	358
1633	Using Machine Learning to Predict the Daylight Performance of Top-lighting Strategies	Taube, Benjamin; Green, Valerie; Santos, Luis; Caldas, Luisa	364

SB-10

ID	Title	Authors	Page
1480	Thermal Comfort in a Bioclimatic Dwelling. The "habitable device" 20 years later. ITER-Tenerife-Spain	Oteiza, Ignacio; Mustieles, Francisco; Delgado, Maria; La Roche, Pablo; González, Ricardo	370
1437	Evaluating environmental performance of Mashrabiya - Generating guidelines for contemporary implementation	Salem, Rofayda Ibrahim; Rajput, Kartikeya	376
1331	Evaluation of Thermal Comfort and Energy Performance of a Case Study in Vernacular Architecture of Cyprus	Heracleous, Chryso; Michael, Aimilios; Charalambous, Chrysanthos; Efthymiou, Venizelos	382
1631	A Generative System for the Design of High-Performing Shading Devices: Exploring the Daylight Potential of Weaving Patterns	Santos, Luis; Caetano, Inês; Pereira, Inês; Leitão, António	388
1241	Hygrothermal and Mold Modeling of Building Envelopes Under Future Climate Conditions	Tepfer, Sara Rose; Samuelson, Holly Wasilowski	394

SB-11

ID	Title	Authors	Page
1680	Unlocking the Potential - Low-Energy Dwelling with Heat Pump	Colclough, Shane; Hewitt, Neil; Griffiths, Philip	400
1473	Research on Design Strategy and Thermal Performance of Surface Space in hot Summer and Warm Winter Area	Yu, Haowei; Song, Yehao; Chu, Yingnan; Chen, Xiaojuan; Sun, Jingfen; Xie, Dan	406
1174	Influence of Thermal Emissivity on Thermal Properties of the Double Membrane Envelope of Air-Supported Structures	Zrim, Grega	412
1349	Improving Building Performance Simulation Boundary Conditions	Simon, Helge; Bruse, Michael; Cramer, Laura; Sinsel, Tim	418
1271	Application of Mixed-Methods in the Analysis of Building Monitoring Data	Guerra-Santin, Olivia; Grave, Anne; Mohammadi, Masi	424

1345	Anthropogenic Heat Dispersion Modelling for Better Urban Planning at High Density Cities	Yuan, Chao; Mei, Shuojun; Adelia, Ayu Sukma; Zhu, Ruixuan; He, Wenhui; Li, Xianxiang	430
1757	New Approaches to Risk Assessment of Climate Stability in Archive and Depot Buildings	Steinbach, Sven; Michalke, Simon; Feneis, Charlotte	436
1537	Towards Zero-Waste In Sustainable Construction of Buildings: Strategies for a More Efficient Implementation of Reusable Building Components on a Broad Scale In Germany	Kader, Alexander	440
1132	Research on Astronomical Alignments in Greek Temples using Solar Analysis Software: The Parthenon as a Case Study	Uson Guardiola, Ezequiel; Guillen Amigo, Carles; Vives Rego, Josep; Uson Maimo, Elisabet	446

SB-12

ID	Title	Authors	Page
1428	Hex Primary School - A Sustainable Self-built Community Project. Cost Effective Vernacular Architecture for the Tropical Climates	Osoy Escobar, Maria; Cadima, Paula	452
1439	Embodied Energy and Carbon Assess in Passivhaus - a UK Case Study	Gomez Torres, Sergio; Stevenson, Fionn; Brierley, Jenny; Bradshaw, Fran	457
1417	Evaluating Neutral, Preferred and Comfort Range Temperatures and Computing Adaptive Equation for Kano Region	Ali, Sani Muhammad; Martinson, Brett David; Al-Maiyah, Sura	463
1732	Performance of an Air Radiative Cooling System in a Residential Building in Chile	Galvez, Miguel A.; Conteras, Jorge; Barraza, Rodrigo; Díaz, Daniela	469
1185	Single-Skin and Multi-Skin Building Envelopes in Extreme Sub-Arctic Climates: Biophilic, Healthy Lighting and Thermal Performance Evaluations	Parsaee, Mojtaba; Demers, Claude MH.; Hébert, Marc; Lalonde, Jean-François; Potvin, André	475
1251	Conserving 20th Century Historic Places and Buildings of Jinja (Uganda) Through Environmentally Sustainable Adaptive Reuse	Wako, Anthony Kalimungabo	480

2. Sustainable Communities

SC-1

ID	Title	Authors	Page
1565	Natural Capital Impact Assessment for New Urban Developments	Puchol-Salort, Pepe; Van Reeuwijk, Maarten; Mijic, Ana	487
1764	Towards Developing Sustainable Maintenance Guidelines for Heritage Architecture of Northern Nigeria	Adekeye, Olutola Funmilayo; Rodrigues, Lucelia; Kiamba, Lorna; Adamu Bena, Aminu	493
1280	Urban Growth vs Density: The Case of a Low-density and Hot Desert Climate City	Lopez-Ordoñez, Carlos; Crespo Cabillo, Isabel; Roset Calzada, Jaume; Coch Roura, Helena	499
1462	The Contribution of Anthropogenic Heat on Urban Air Temperature Elevation: A Case Study of the Singapore Residential area	Mei, Shuo-Jun; Yuan, Chao; Zhu, Ruixuan; He, Wenhui; Li, Xian-xiang; Talwar, Tanya	505
1294	Stall Prototype For Gandhi Street Market	Suresh, Anjana; Cadima, Paula	511
1128	A Dynamic Analysis of Daylighting Availability in Dense Urban Residential Areas: A Cross-region Study in China	Hong, Lishu; Zhang, Xin; Du, Jiangtao	517

1193	An Urban Usability Study for Exploring Socio-Cultural Sustainability in Contemporary Public Spaces: The Case of the New Abdali Development Project in Amman-Jordan	Al Dissi, Neamat Hussein	523
1421	"Are Children Independently Mobile to School Anymore?": A Comparative Study of Two Neighbourhoods in Kolkata, India	Tyagi, Megha; Raheja, Gaurav	529
1740	Greenway on Street Canyon of Residential Areas in Dhaka: Missing Link and Plausible Impact in Taming the Thermal Comfort	Tasnim, Zarrin; Joarder, Md Ashikur Rahman	535

SC-2

ID	Title	Authors	Page
1516	Urban and Building Integrated Vegetation and its Impact on London's Urban Environment	Silva, Joao; Schiano-Phan, Rosa; Scofone, Amedeo	541
1585	The Logistics of Energy. Strategies for achieving Energy Optimisation within nZEB Mixed Use Urban Developments	Murray, Martin Anthony; Colclough, Shane; Griffiths, Philip	547
1704	Post Occupancy Evaluation of Educational Buildings in Warm-Humid Climate: Using BUS Methodology to Understand the Implications of Naturally Ventilated Building Design on Human Comfort	Selvaraj, Subhashini	553
1259	Participatory Processes Impelling Urban Socioecosystem Renewal. Social Sustainability from an Environmental Approach	LopezDeAsiain, Maria; Castro-Bonaño, Juan Marcos; Mora-Estéban, Rubén; Lumbreras-Arcos, María	558
1767	Urban Microclimatic Diversity and Thermal Comfort: Do Variations in Sun and Wind Conditions Correlate with PET Grades?	Peng, Zhikai; Steemers, Koen	564
1404	Cooling Effect of Urban Parks in Metropolitan Region of Barcelona	Arellano, Blanca; Roca, Josep; García-Haro, Alan	570

SC-3

ID	Title	Authors	Page
1183	The Environmental Performance of Temporary Urban Interventions: Technical Assessment Of Regeneration Initiatives in the City Centre of São Paulo, With Focus on Thermal and Acoustic Performance	Loureiro Xavier Nascimento Michalski, Ranny; Rodrigues, Lucelia; C Kronka Mulfrath, Roberta; Soares Goncalves, Joana Carla; Marques Monteiro, Leonardo; Tubelo, Renata; Rodrigues Prata Shimomura, Alessandra; Bley, Carolina; Silveira Vitti, Mariana; Ferrara Bilesky, Daniel; Guimaraes, Maysa Maria	576
1154	Urban Growth with Greenhouse Gas Emissions Reductions	Jackson, Blake	582
1141	Adaptive Thermal Comfort Model Suitable for Outdoors Considering the Urban Heat Island Effect	Oropeza-Perez, Ivan	588
1422	Integrating Landscape Tactics into Building Energy Performance Evaluation Based on Urban Morphometry	Passe, Ulrike; Engler, Mira; Entezari, Hossein; Goetz, Victoria	594
1809	Disruptive Technologies on Mobility Raising New Opportunities for Urban Design	Fortes, Melissa Belato; Duarte, Denise Helena Silva; Giacaglia, Marcelo Eduardo	600

SC-4

ID	Title	Authors	Page
1873	Characterising Living Wall Microclimate Modifications in Sheltered Urban Conditions: Findings from Two Monitored Case Studies	Gunawardena, Kanchane; Steemers, Koen	606
1163	Thermal Conditions in Urban Settlements in Hot Arid Regions: The Case of Ksar Tafilelt, Ghardaia, Algeria	Telli, Mohamed Yacine; Renganathan, Giridharan; Watkins, Richard	612
1196	Energy Transition Challenges in Under-Occupied Homes: Assessment of Two Peri-Urban Neighbourhoods of Single-Family Houses	Drouilles, Judith; Rey, Emmanuel	618
1748	Sustainable Communities Through an Innovative Renovation Process - Subsidy Retention to Improve Living Conditions of Captive Residents	Bielen, Leontien; Versele, Alexis	624
1815	Designing the Future to Predict the Future: An 'Urban-First' Approach to Co-Creating Zero-Carbon Neighbourhoods	Jenkins, Andrew; Keeffe, Greg; Martin, Craig Lee; van den Dobbelaars, Andy; Broersma, Siebe; Pulselli, Riccardo Maria	630
1457	Influence of High-Density Mixed-Use Residential Neighborhood Building Layout on Building Energy Consumption: Taking ChuangZhiFang in Shanghai, China as an Example	Tian, Nannan; Yang, Feng	636
1499	Optimizing Social Benefit of Vertical Greening System in Open Residential Neighborhood Using a Multiple Raster Data Based Viewshed Analysis: A Case Study in Southern China	Feng, YiPeng; Yang, Feng	642
1726	A Critical Discussion of Sustainability Assessment Methods as Applied to Communities with Dual Urban-Rural Characteristics: Case Studies of Two Villages in Southwest China	Gao, Yun; Pitts, Adrian; Zhou, Zou; Chen, Xin; Zhou, Ling	648
1472	Modelling and Testing Extendable Shading Devices to Mitigate Thermal Discomfort in a Hot Arid Climate	Alharthi, Mohammed; Sharples, Steve	654

SC-5

ID	Title	Authors	Page
1392	Using Textile Canopy Shadings to Decrease Street Solar Loads	Garcia-Nevado, Elena; Bugeat, Antoine; Fernandez, Eduardo; Beckers, Benoit	660
1520	Thermally-Activated Water-Based Lattices: Thermal Control of Exterior Urban Areas Through Evaporative Cooling, Shading and Ventilation	Marcos, Ana; Tenorio, Jose A; Guerrero, María del Carmen; Pavón, María del Carmen; Sánchez, José; Álvarez, Servando	666
1788	The Effect of Street Grid Form and Orientation on Urban Wind Flows and Pedestrian Thermal Comfort	Ayyad, Yara Nehrow; Sharples, Steve	671
1751	Impact Of Urban Albedo On Microclimate: Computational Investigation In London	Salvati, Agnese; Kolokotroni, Maria; Kotopouleas, Alkis; Watkins, Richard; Giridharan, Renganathan; Nikolopoulou, Marialena	677
1550	Architectural and Social Potential of Urban Lighting: A field study	Hvass, Mette; Hansen, Ellen Kathrine	683
1653	Decarbonising Our Transport System: Vehicle Use Behaviour Analysis to Assess the Potential of Transitioning to Electric Mobility	Waldron, Julie; Rodrigues, Lucelia; Gillott, Mark; Naylor, Sophie; Shipman, Rob	689

SC-6

ID	Title	Authors	Page
1639	Analysis of Shrubby-Arboreal Species as a Barrier to Wind for Comfort in Open Spaces	Padovani Zanlorenzi, Helena Cristina; Marques Monteiro, Leonardo	695
1281	Energy Sharing Between Sustainable Residential and Conventional Commercial Buildings Cluster	Singh, Kuljeet; Hachem-Vermette, Caroline	700
1572	Characterization and Mitigation Through Urban Climatic Map. Investigations on the Climate of Curitiba - Brazil	Schmitz, Lisana Katia; Rossi, Francine Aidie; Katschner, Lutz; Mel, Alessandra; Almeida, Gabriela	706
1426	Multidisciplinary Local Teams and Technologies for Participatory Processes in Sustainable Territorial Strategies: The Integral Regeneration of an Agrarian Valley in the Galician Diffuse City	Pereira-Martinez, David	712
1495	Energy Democracy In Practice: A Participatory Approach to the Community Governance of Renewables	Törnroth, Suzanna; Sotoca, Adolfo	718

SC-7

ID	Title	Authors	Page
1408	Can Planning Mitigate UHI?	Biere, Rolando; Arellano, Blanca; Roca, Josep;	724
1305	Outdoors Thermal Comfort Approach in Summer Season for the City of Madrid. Influence of urban typologies in microclimate and the outdoor thermal sensation	Lopez Moreno, Helena; Sánchez Egidio, María Nuria; Giancola, Emanuela; Ferrer Tevar, José Antonio; Neila González, Francisco Javier; Soutullo Castro, Silvia	730
1746	Effective Food: Design and Urban Agriculture in the Post Carbon City	Cullen, Sean; Keefe, Greg	736
1609	Simulation Based Support for the Urban Energy Transition - Predicting Heating Energy Needs for Residential Building Clusters Using a Non-Linear Data-Driven Approach	Koch, Andreas; Sevenet, Marie	742
1279	Promoting a Dispersed Urban Mobility Approach for Rehabilitation of Historic Cairo	Elsayed, Doaa Salaheldin Ismail; Ismaeel, Walaa S.E.	746
1272	Analysis Of Courtyards Heat Mitigation Potential In Warm And Dry Urban Locations	Diz-Mellado, Eduardo; Rivera-Gómez, Carlos; Galan-Marín, Carmen; Rojas Fernández, Juan Manuel; Nikolopoulou, Marialena	752
1679	Stakeholder Engagement in Nature-Based Public Space Design: Sustainable Regeneration Of Urban Environments	Osei, Gloria; Pascale, Federica; Pooley, Alison; Delle, Nezhapi	758
1337	The Mixed-use Matrix: Developing Design Guidelines for the Mixed-use Typology for Mumbai	Shiva, Shruti	764
1137	Building Performance Simulation Supporting Typical Design Activities: The Case Of 'Volume Massing'	Purup, Pil Brix; Petersen, Steffen; Dunn, Andrew Ferguson; Gkaintazi-Masouti, Myrta; Visa, Ondrej	770

SC-8

ID	Title	Authors	Page
1469	When Water Does Not Cool: A Different Use of Water in Urban Design	Cortesão, João; Lenzholzer, Sanda	776
1310	Energy Efficiency and Comfort on a Deprived Neighbourhood in Madrid, Spain. The Gap Between a Predictive Model and Measured Data on Energy Consumption, Addressing Indoor Environmental Quality Assessment	de Frutos, Fernando; Martín Consuegra, Fernando; Oteiza, Ignacio; Alonso, Carmen; Frutos, Borja; Galeano, Javier	782
1670	Reference Weather Data Selection in Urban Weather Generator Model	Alchapar, Noelia Liliana; Pezzuto, Cláudia Cotrim; Ballarini, Santiago Mario; Correa, Erica Norma	788
1739	Building Performance, Climatic Variables, and Indices: Identification of Correlations for Social Housing Across the Mexican Territory	Zepeda-Rivas, Daniel; Loonen, Roel; Rodríguez-Álvarez, Jorge	794
1648	CFD Analysis for Appropriate Positions of Wind Turbines on Tall Building in an Urban Environment	Takkanon, Pattaranan; Pimolvichayakit, Pharpoom	800
1438	Investigating the Impact of Urban Fabric on Urban Albedo: Case Study of London	Yeninarçilar, Muhammed; Nikolopoulou, Marialena; Watkins, Richard; Renganathan, Giridharan; Kotopouleas, Alkis	806

SC-9

ID	Title	Authors	Page
1372	Improving Hyperlocal Air Quality in Cities	Borna, Mehrdad; Schiano-Phan, Rosa	812
1785	Impact of Built Density and Surface Materials on Urban Microclimate for Sao Paulo, Brazil: Simulation of Different Scenarios Using ENVI-met Full Forcing Tool	Gusson, Carolina S.; Simon, Helge; Duarte, Denise H. S.	818
1303	Shading and Temperature of Urban Canyons: An Analysis in the Downtown Area of Passo Fundo-Brazil	Furlani, Sinara; Maroni, Daniela; Tebaldi, Vanusa; Tibério Cardoso, Grace	824
1695	No Retreat from Change: Landscape Information Modelling as a Design Tool for a Resilient Community: the Case of Poço da Draga in Fortaleza, Brazil	Moura, Newton Célio Becker de; Carvalho, Tainah Frota	830
1482	'Urban Lab City' Investigating the Role of Built Form on Air Quality and Urban Microclimates – City of London Case Study	Fletcher, Julie Ann; Mills, Gerald	835
1771	A Simplified Approach for Designing Sustainable near Zero Energy Settlements	Pignatta, Gloria	841



SUSTAINABLE BUILDINGS

Embodied Carbon: A Comparison of Two Passivhaus Homes in the UK

FIONN STEVENSON¹ DILEK ARSLAN¹ SERGIO GOMEZ-TORRES¹
JENNY BRIERLEY¹ SAM FOSTER² SANDY HALLIDAY³

¹The University of Sheffield, Sheffield, UK

²Sam Foster Architects, Dunfermline, UK

³Gaia Group, Edinburgh, UK

ABSTRACT: To reach net zero carbon by 2050, significant reductions must be achieved in embodied carbon emissions as well as operational energy demand in buildings. This paper uses a mixed methods case study approach to compare two individual Passivhaus homes built within a few years of each other in the UK. The aim is to understand the level of importance to attach to embodied carbon emissions in new build Passivhaus homes, the degree of difference that occurs when different structural and finishing materials are used, and whether Passivhaus metrics are fit for purpose. In both cases the embodied carbon is relatively high with a long payback.

KEYWORDS: Embodied Carbon, Embodied Energy, Passivhaus, Housing, UK

1. INTRODUCTION

In 2019 the UK Government committed itself to a legally binding target of net zero carbon emissions by 2050, to mitigate the current global climate emergency and aim to keep global warming to below 1.5C. The UK Climate Change Committee states that all new homes must be low carbon, and that the 29 million existing homes in the UK are retrofitted to low carbon standards [1]. One solution is adopting The Passivhaus Standard, first developed by Wolfgang Feist and colleagues in Germany [2]. This stipulates that a new Passivhaus home should not use more than 15kWh/sqm/pa for heating and hot water, and no more than 125 kWh/sqm/pa as primary energy use overall. There is also an Enerphit retrofit version. This standard has become increasingly popular in the last decade with numerous local authorities mandating it in different countries. Post-occupancy evaluation has shown that on average, UK Passivhaus homes consistently outperform other low carbon homes built at the same time [3].

Despite this progress, there remains a major research gap in relation to understanding embodied carbon (EC) emissions in Passivhaus homes, with no requirement in the main Passivhaus Standard to take account of this, and no regulatory requirements either. As homes become more energy efficient, the embodied energy (EE) and resultant EC emissions, becomes increasingly important, to the point where it can outweigh the significance of the carbon emissions in use, when this figure is net zero.

This paper uses a case study approach to compare two Passivhaus homes built in the UK, and evaluate their EC emissions in relation to other examples. The aim is to understand the level of importance to attach to EC emissions in new build Passivhaus homes, the

degree of difference that occurs when different structural and finishing materials are used, and whether Passivhaus metrics are fit for purpose.

2. EMBODIED ENERGY AND CARBON

Three methods used to calculate EE and EC emissions are:

1. Input-output (IO) analysis which uses national financial transactions to establish the energy intensity of economic sectors and attributes this to individual products.

2. Process-based analysis (PA), which collects all data, including direct and indirect energy inputs, related directly to the individual building product.

3. Hybrid analysis (HI-O) which combines both IO and PA processes, making it the most reliable and comprehensive method [4].

Due to limited data availability, the process analysis method was used in this study. EE figures are typically converted to EC emissions using nationally or regionally defined carbon conversion factors. EE and EC emissions assessments define the material life cycle boundary as either: *cradle to gate* (material extraction to factory gate); *cradle to site*, (additionally including transportation to the construction site); *cradle to grave*, (additionally including in-use, maintenance and demolition); and lastly *cradle to cradle* (additionally including reuse, recovery and recycling). Defining the boundary for EE varies considerably in literature. Dixit et al. [5] considers the additional demolition and waste disposal stages while Chau, Leung and Ng [6] only include extraction, production, transportation to the site and constructional energy stages. There are also concerns about varying heating factors applied and whether or not renewable energy is accounted for [7].

Appropriate materials choices can significantly decrease EE and EC emissions [8]. Careful material selection during the design process is thus vital as low impact materials or highly re-useable or recyclable materials significantly decrease emissions [9]. Due to limited data availability for EE calculations, and the importance of climate change mitigation, the focus in this study is on EC emissions.

3. METHODOLOGY

A mixed methods approach was used to gather data and inform the quantitative EC analysis with a deeper qualitative understanding of additional contextual factors that can affect EC calculations. Additional methods included a document review, detailed site visit to each of the homes, with an interview of the home owner/client as well as the architect responsible for the design of the home. A careful photographic survey was also made of each home inside and out and compared to construction drawings and specifications in order to establish any alterations in construction subsequent to completion, which would require adjustment of the EC calculations.

The study followed the Royal Institution of Chartered Surveyors (RICS) guidance. This calculates the EC emissions per kilogram of product, using the *cradle to gate* framework that covers processing to the final product stage only and not to site [10]. It is based on an adapted form of Life Cycle Assessment (LCA) as defined by the International Standard ISO 14044:2006 [11]. Material intensity data was based on a combination of the Inventory of Carbon & Energy (ICE Version 3.0, 2019) open source database for carbon emission of construction materials [12], and additional Energy Product Declaration (EPD) data to supplement this database where data was missing [13]. A UK beta version embodied carbon emissions tool, H\B:ERT, was used initially to take off quantitative measurements from the drawings using a REVIT model [14]. This uses an earlier version of ICE Version 2.0, requiring further adjustments. No attempt was made to calculate *cradle to cradle* carbon emissions, given the significant contingencies relating to lifecycle assumptions for the materials and products involved, as well as their final destinations and the potentially significant construction alterations that can occur over the life of a home [15]. It is recognised, however, that transportation to the construction site can typically add 10% to the result.

The Passivhaus energy in use standard was converted to a carbon emissions equivalent using the UK carbon emission factors for the national energy grid, which are updated annually [16]. Finally the embodied carbon emissions were compared with the Passivhaus standard carbon equivalent using Treated Floor Area.

4. CASE STUDIES

4.1 Timber house

The first case study, Plummerswood, is an award-winning three bedroom detached Passivhaus home near Edinburgh in Scotland, completed in 2011 and designed by Gaia Architects (Figs. 1 and 2). It has a Treated Floor Area of 300 m². Two people living together currently inhabit the home.

Unusually, it uses a 'brettstapel' construction system that consists of 80mm solid timber beams connected by timber dowels to form panel walling and flooring, without the need of any other fixing material such as glue or metal. The design principle exploits the different moisture content of the two structural elements; beams (15%) and dowels (8%) [17]. The exchange in moisture levels causes expansion in the dowels to snugly fit into the panel holes. This system allows low grade home grown timber to be used, with more carbon sequestered than for an average timber frame structure. It also increases air tightness, with low thermal conductivity, and provides good air quality. There is 340mm woodfibre insulation in between the Brettstapel and outer timber cladding (Fig. 3). In theory, this should make the home low impact in terms of carbon emissions. However, the timber system was sourced from Austria, as there is no brettstapel factory in the UK, adding to transport emissions arising from travel from the factory to site (which are not calculated here).

Figure 1: Plummerswood House First Floor Plan (Gaia Architects).



The house uses a wood stove in the living room to generate space heating and uses mechanical ventilation with heat recovery (MVHR). A 5.6 m² solar thermal panel system provides some hot water and electricity from the grid fulfils any other energy needs.

Figure 2: Plummerswood House First Floor Plan (Gaia Architects).



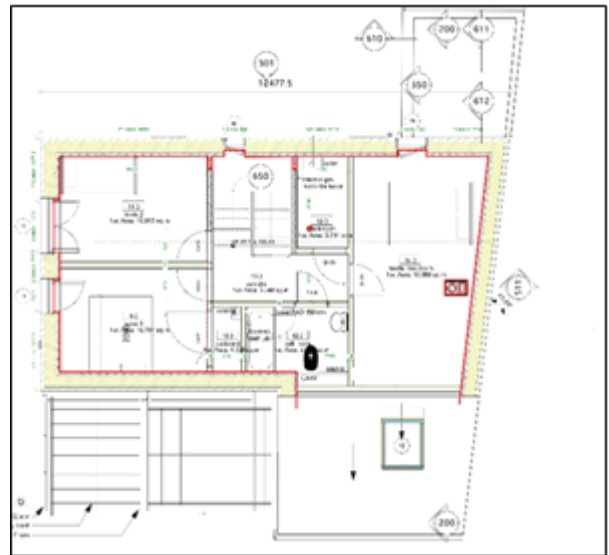
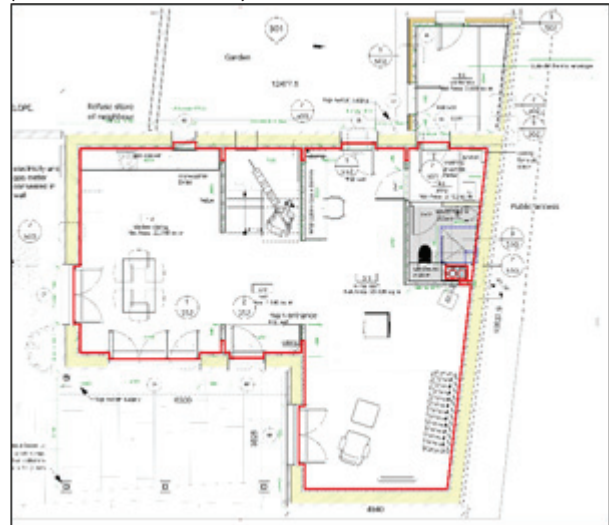
Figure 3: Plummerswood House (Exterior), Edinburgh (Gaia Architects)



sourced very locally (15 miles from site), minimising transportation.

This dwelling has 400 mm Polyisocyanurate (PIR) high performance insulation in the ground flooring. The tiled roof has high-density polyethylene between the battens and 300mm mineral wool insulation. The external Walls comprise 300 mm mineral wool insulation between 105mm handmade brick and 100mm aerated concrete block inner leaf resting on concrete foundations.

Figure 4: Ground floor Plan above: First Floor Plan below (Anne Thorne architects).



4.2 Brick/Concrete house

The second case study is a three bedroom detached Passivhaus home in York, England completed in 2015 and designed by Anne Thorne Architects (Figs 4 and 5). It has a Treated Floor Area of 127m². Originally planned for four people, the house is now mainly inhabited by one person. The house also has an MVHR system.

In contrast to the previous case study, it is built of handmade bricks that have much higher carbon emissions than the Brettstapel, but which were

Figure 5: External Views (Sergio Gomez Torres).



5. RESULTS AND DISCUSSION

5.1 Embodied carbon emissions timber house

The EC emissions of the timber case study house is calculated to be 452.47 kgCO₂e/m² which equates to 136,013 kgCO₂e in total as delivered to the factory gates. This virtually achieves the best practice figure of 450kgCO₂e/m² set for 2025 by the ground breaking RIBA 'Sustainability Outcome' targets set in 2019 [18]. The embodied carbon emissions from the superstructure (Brettstapel) materials, modelled with H\B:ERT is 273.8 kgCO₂e/m². The carbon sequestration capacity of the timber materials is ignored here because there is no guarantee of adequate tree replacement or that the building will lock up the sequestered carbon for a long enough time to the match regrowth period.

The total substructure EC was 178.67 kgCO₂e/m², which is lower than the superstructure figure and can be explained by the greater volume of material used for the superstructure. Steel and concrete materials were the main contributors to the substructure material emissions, with concrete embodying 52% of this. Substituting 70% blast furnace slag for virgin concrete aggregate could decrease the total EC of the substructure by 22%, which is significant.

The actual OE consumption of the timber house at 64.11 kWh/m²/pa (excluding estimated renewable energy contribution of 7.03 kWh/m²/pa), as monitored for one year, is under half the Passivhaus standard requirements for primary energy use (120 kWh/m²/pa) and equates to OC (operational carbon) emissions of 9.14 kgCO₂e/m²/pa or 2742 kgCO₂e/pa. This can be attributed to the exceptionally high insulation level as well only two people using the home, and the use of a woodstove for space heating, rather than electricity from the UK grid but grid electricity for hot water, when not heated by solar panels. This means that the EC emissions for the house as calculated to the factory gates is equal to 49 years of OC emissions, which is a significant proportion of a typical lifespan of 60 years for a home. This shows that when low carbon buildings are more realistically

analysed from a life cycle approach which includes the carbon emissions from material use, they can have a much heavier environmental impact than is indicated by simply examining the carbon emissions from the energy consumed in use.

5.2 Embodied carbon emission for brick/concrete house

The EC emissions for the brick/concrete house is 466.90 kgCO₂e/m² which equates to 59,295.95 kgCO₂e in total – less than half the total figure for the timber house, due to smaller size of the brick/concrete house.

The very low OE consumption for the home is 4,401.08 kWh/pa or just 34.65 kWh/m²/pa, as monitored over one year. This is even lower than the timber house and less than a third of the Passivhaus 120 kWh/m² primary energy target. This can be attributed to the exceptionally high insulation level as well as only one person using the home very frugally.

The OC emissions equates to 7.66 kgCO₂e/m²/pa or 973.34 kgCO₂e /pa. This rate per m² is lower than the timber house despite the different energy sources but the overall OC emissions total per year for the house is less than half that for the timber house. The EC emissions for this house as calculated to the factory gates is equal to 61 years of OC emissions, which is greater number of years than for the timber house. In other words the EC emissions just from cradle to gate is more than the OC emissions over a typical house lifespan of 60 years.

The above results and discussion of the two case studies is a summary only – more detail can be found in two accompanying papers [19]. The next sections discuss wider implications for Passivhaus metrics when assessing environmental impact.

5.3 Embodied Carbon 'sufficiency' in Passivhaus homes

While the above figures only show the overall impact of two homes, there are other similar Passivhaus detached homes that have also performed in a similar way. One 153m² detached home in the UK, completed in 2019, delivered a calculated figure of 338 kgCO₂e/m², which is slightly lower than the two case study homes shown here. Another 150m² detached home completed in 2015 did even better, reporting just 286 kgCO₂e/m² [20]. However, the EC tool used to calculate these figures, "PHRibbon", did not include the EC for services, which can be significant (e.g. the MVHR and hot water system) whereas the figures shown here include this. This shows the difficulty of comparing EC figures calculated using different tools, which use different boundary conditions.

It is important to consider two other factors that are not normally considered together in embodied carbon calculations: the size of the home and the

number of people living it. This generates the overall carbon emissions for a home which can then be expressed per person, which is a more useful figure in terms of the personal environmental impact that individuals have in relation to their chosen lifestyle in their home. This relates to an argument concerning the 'sufficiency' [21] of home size in relation to its carbon emissions, and whether the home is effectively utilised. Energy and resource 'sufficiency' moves beyond the rate at which energy or material resources are used in a home, to consider the overall impact of the energy in use and resources consumed in terms of overall carbon emissions per person.

When the two case studies are compared in terms of size and utilisation, the results are counter-intuitive in terms of overall carbon emissions. The seemingly more 'eco' material (brettstapel) house is much larger than the case study brick/concrete house, and at 300 m² is over three times larger than the average UK terraced family home and twice as large as the average detached house with an equivalent number of bedspaces according to government statistics. This significantly increases the impact of the timber components in terms of EC, given the extra wall and floor area needed, and means that the amount of substructure concrete could be easily halved for a home half the size, reducing embodied carbon emissions.

The comparison of resource use gets even more complicated however when the occupancy level is taken into account as a 'sufficiency' metric. The timber home is now doubly profligate in terms of 'sufficiency', given that only two people live in a relatively large house. The floor area provided per person is 150m² compared to just 25 m² per person for the average 4 person detached family home in the UK. The wide use of timber in the home offsets this space usage to a large degree, however, as does the low energy use, in terms of overall carbon emissions. This is particularly so, if the timber is not incinerated at the end of its life, and if it comes from guaranteed sustainable forestry sources. However, the 'profligate' Brettstapel house has twice as many occupants on average compared to the brick/concrete house. Thus, when resource use is considered per person as a comparison between these two cases, the overall EC figure for the Brettstapel house needs to be halved to provide the equivalent EC per person figure, giving it a *similar* EC impact *per person* to the brick/concrete house.

5.4 Brick versus Timber

Softwood timber clearly has less carbon emissions per volume than fired brick [19]. At the same time, timber also has better insulating qualities than brick, meaning that it needs less additional insulation material to bring the brettstapel construction up to Passivhaus standard. Nevertheless the timber

construction materials had to travel 1600 miles by truck and ferry to reach their destination, whereas the brick was manufactured very locally – just a few miles away from the home. The transportation factor has been excluded from this paper, but it is non-trivial, particularly given that many countries have to outsource their timber supplies, including the UK. At the same time, timber construction cannot be considered for carbon sequestration unless adequate re-forestation is certified and the building is not prematurely demolished before its predicted lifespan. the EE and EC for timber can also be surprisingly high, if it is a heavily manufactured product, such as Cross Laminated Timber, involving glues and multiple cutting, and if it is treated with chemical preservative.

5.5 Limitations

When comparing the percentage of EC emissions established by H\B:ERT against those calculated through the bill of quantities, this tool accounted for 16% less EC emissions, due to omission of services and other factors. Moreover, the accounting for EC emissions in the transport, construction and end of life is unclear in H:/BERT.

The H\B:ERT plug-in also has clear limitations during the modelling process. The materials are too generically defined in terms of density and embodied carbon. Missing materials need to be assigned by user from other sources, but this is time consuming. Worryingly, there are no defined products for the plumbing, sanitation, electricity services or other complex elements like bio disk units or boilers, which have to be estimated. The plug-in also needs to be updated as it uses the old version of the ICE database making it less reliable.

Another challenge during the research process was finding a reliable carbon database to calculate carbon footprint of the materials. ICE V3.0 is open source, but has less material profiles compared with ICE V2.0. The EPD reports were useful to compensate for this, but it was difficult to find exactly the same product. Similar products can vary from company to company as they use different material and energy sources and transportation. Finding the EPD reports for some fixing elements proved particularly challenging, so only the major materials were used for the embodied carbon calculations to generate approximate figures for these elements in this case. Further studies are needed to break down these individual elements and calculate them more accurately. All of this shows that EE and EC calculation processes in key tools have yet to mature.

6. CONCLUSION

The two case studies examined here easily meet the Passivhaus standard energy use requirements, yet the overall embodied carbon emissions in each case is significant for a variety of different reasons, including

house floor area and occupancy levels as well as materials specified. For a lifespan of 60 years, the embodied carbon emissions for both homes form a very significant proportion of the overall carbon emissions when compared with in-use emissions over this same period, despite using different materials. This demonstrates that a simple drive for energy efficiency in use through the mass deployment of Passivhaus standard new build homes will initially cause a major jump in carbon emissions during their construction (the carbon 'burp') unless appropriate measures are taken to mitigate this. It is essential therefore to compliment any Passivhaus energy efficiency drives with an equal emphasis on sufficiency as well as the type of material used to construct the homes in the first place. This demands that the Passivhaus Standard includes utilisation factors and overall size of homes, as well as embodied carbon emissions to generate a total carbon emissions result per person and per home. By taking all three of these factors into consideration a more accurate environmental impact of each Passivhaus home can be assessed.

REFERENCES

1. UK CCC (2019) *UK Housing: Fit for the Future?* UK Climate Change Committee, London, p.1-134
2. PassivHausInstitut.[Online].Available: <https://passiv.de/en/index.html> [Accessed 10 May 2020].
3. Johnston, D and Miles-Shenton, D and Farmer, D (2015) Quantifying the domestic building fabric 'performance gap'. *Building Services Engineering Research and Technology*, 36 (5): p.614-627.
4. Fenner, A., Kibert, C., Woo, J., Morque, S., Razkenari, M., Hakim, H. and Lu, X. (2018). The carbon footprint of buildings: A review of methodologies and applications. *Renewable and Sustainable Energy Reviews*, 94, p.1142-1152.
5. Dixit, M. (2017). Life cycle embodied energy analysis of residential buildings: A review of literature to investigate embodied energy parameters. *Renewable and Sustainable Energy Reviews*, 79, p.390-413.
6. Chau, C., Leung, T. and Ng, W. (2015). A review on Life Cycle Assessment, Life Cycle Energy Assessment and Life Cycle Carbon Emissions Assessment on buildings. *Applied Energy*, 143, p.395-413.
7. Rasmussen, F., Malmqvist, T., Moncaster, A., Wiberg, A. and Birgisdóttir, H. (2018). Analysing methodological choices in calculations of embodied energy and GHG emissions from buildings. *Energy and Buildings*, 158, p.1487-1498.
8. Pomponi, F. and Moncaster, A. (2016). Embodied carbon mitigation and reduction in the built environment – What does the evidence say? *Journal of Environmental Management*, 181, p.687-700.
9. WRAP (n.d.). Cutting Embodied Carbon in Construction Projects. [Online]. Waste and Resources Action Programme. Available at: <http://www.wrap.org.uk> [Accessed 10 May 2020].
10. RICS, (2017) *Whole life carbon assessment for the built environment*. Royal Chartered Institute of Surveyors, London, 2012.
11. Thormark, C. (2002) A low energy building in a life cycle – its embodied energy , energy need for operation and recycling potential, *Building and Environment* vol. 37 (4), p. 429–435.
12. ICE database V3.0 [Online]. Available <https://circularecology.com/embodied-energy-and-carbon-footprint-database.html> [Accessed 10 May 2020]
13. International Environmental Product Declarations. [Online]. Available at: <https://www.environdec.com/> [Accessed 10 May 2020].
14. H\B:ERT Tool. [Online] Available at: <https://www.hawkinsbrown.com/services/hbert> [Accessed 10 May 2020].
15. Gervasio, H. and Dimova, S. (2018). Model for Life Cycle Assessment of Buildings. [Online] JRC Science Hub.
16. UK Greenhouse gas conversion factors [Online]. UK Government. Available at: <https://www.gov.uk/government/publications/greenhouse-gas-reporting-conversion-factors-2019> [Accessed 10 May 2020]
17. Henderson, J., Foster, S. and Bridgestock, M. (2012). What is Brettstapel? [Online] Brettstapel Construction. Available at: http://www.Brettstapel.org/Brettstapel/What_is_it.html [Accessed 10 May 2020].
18. RIBA (2019), *Sustainability Outcomes Guide* [Online] Royal Institute of British Architects. Available at: <https://www.architecture.com/-/media/GatherContent/Test-resources-page/Additional-Documents/RIBASustainableOutcomesGuide2019pdf.pdf> [Accessed 10 May 2020].
19. Arslan, D. et al (2020) *Embodied Energy and Carbon in a Passivhaus: A Brettstapel House Case Study in the UK*, and Torres-Gomez, S. et al (2020) *Embodied energy and carbon assessment in Passivhaus: A UK case study*, PLEA 2020 A CORUÑA, Planning Post Carbon Cities, Conference proceedings.
20. Both homes are reported in *Passive House + Sustainable Building* , 53, p.24-39.
21. Shove, E.(2018) What is wrong with energy efficiency? *Building Research and Information*, 46(7): p.779-789.

Critical Analysis on Passive and Low Energy Architecture Study Research Trend through Text Data Mining Technique in the Period of 2006 to 2018

LAN WANG¹ ERIC WAI MING LEE¹

¹Department of Architecture and Civil Engineering, City University of Hong Kong, Hong Kong SAR.

ABSTRACT: As one of the leading conferences in the study area of passive and low energy architecture, the Passive and Low Energy Architecture (PLEA) Conference has presented continuously great efforts and innovative ideas from worldwide research communities and professional society in promoting the study of passive and low energy architecture. With the rapid urbanization and technological progress in the past decade, more and more research branches of PLEA emerged. Clarifying the research trend variation would benefit the research communities in identifying research gaps in this research area. This paper examines the PLEA proceedings from 2006 to 2018 with text data mining techniques in Python environment. More than three thousand lines of research paper titles have been analyzed to find out the research trend variations. The analysis reveals that main concerns of PLEA research have remained stable during the past decades. The main concerns are, indoor and outdoor thermal comfort in building level, and urban heat island effect in regional level. Natural ventilation is one of the most discussed technique in passive design strategies. Enlightening but rare mentioned keywords are 'visual comfort', 'life cycle', 'integrated design', 'urban morphology', 'urban micro-climate', 'climate change', 'parametric study', 'benefit reusing', 'neural network'. In 2018, more advanced computation methods have been involved in PLEA research. The social house, school, dwelling, office, and residential buildings are the building types that being focused most. Research gaps lie in rural buildings that are occupied by about half of the global population and the study on accessible daylight via reasonable architectural design. This study may serve as an informative reference for research communities, industry practitioners and non-profit organizations to appreciate passive and low energy architecture research trends and developments.

KEYWORDS: Text data mining; Passive; Low Energy; Architecture; Research trend.

1. INTRODUCTION

Passive and low energy architecture (PLEA) advocates the bioclimatic design and the application of natural and innovative techniques for sustainable architecture and urban design. Bioclimatic design, combining 'biology' and 'climate', is an approach to the design of buildings and landscape based on local climate [1]. The bioclimatic house uses the regular architectural elements to increase the energetic performance and get a natural comfort rather than expensive mechanical installations. Studies on PLEA make a lot of sense. Accessing to more daylight, natural ventilation rather than electrical lighting or heating ventilation and air conditioning (HVAC) system to achieve thermal and visual comfort would be healthier and more delightful for the occupants [2], and save significant building energy budget and reduce carbon dioxide emission [3].

The methodology of PLEA concerns the disposition of buildings, such as orientation related to the sun and wind, aspect ratio; site planning, air movement, openings and the building envelopes [4]. Specifically, a variety of strategies have been studied, including 'passive solar heating', 'active solar heating', 'cooling through a high thermal mass', 'cooling by high thermal mass with nocturnal renovation' and so on [5].

Clarifying the research trend variation would benefit the research communities in identifying the research gaps in this research area.

This paper examines the PLEA conference proceedings from 2006 to 2018 with text data mining techniques in Python environment. We analyzed 3336 lines of paper titles to find out the research trend variations through a three step work flow: pre-processing, processing and analysis. The PLEA conference proceedings are selected as the data pool since it is one of the most famous and long-lasting annual conference on this theme, and the proceedings are freely available on its website.

Previous literature has reviewed the studies on low energy architectural design. For instance, Agugliaro et al. [5] reviewed the bioclimatic architecture strategies for achieving thermal comfort. They examined the concept of bioclimatic architecture, the bioclimatic architecture construction strategies as a function of each climate zone with the objective of achieving the greatest climate comfort level within a specific building, and analyzed the principle scientific research trends in the relevant area. Chandel et al. [6] presented a comprehensive review of vernacular architecture research status to identify energy efficient vernacular architecture features affecting

indoor thermal comfort conditions for adaptation in modern architecture to suit present day lifestyle. Most of the review papers are based on a comprehensive collection of relevant literature to summarize the study trend with a subjectively categorization. This type of review papers has advantages in providing a holistic picture of the research area; but have limits in identifying the 'hot' topics which have been discussed too much and the 'less popular' topics which needs more attentions.

This paper is innovative in applying text data mining techniques to analyze research trends in PLEA area. With the data pool -- more than three thousand titles of relevant research papers, the fundamental concerns, 'hot' topics, 'less popular' topics, enlightening but rare discussed topics, new emerging topics can be identified objectively. Clarifying the research concerns and variation trends of passive and low energy architecture can provide informative references for research communities, industry practitioners and non-profit organizations in future study on passive and low energy architecture research.

Section 2 describes the basic information of the PLEA conference proceedings from 2006 to 2018, including the location, theme and amounts of research paper title lines; then specifies the flowchart of text data mining technique in Python environment. Section 3 presents the results and discussion; Section 4 draws conclusions.

2. METHODOLOGY

The text data mining technique is applied to the proceedings of PLEA from 2006 to 2018. This section describes the conference data pool in Section 2.1; introduces the diagram of the text data mining flowchart in Section 2.2.

2.1 Data Introduction

PLEA is an annual conference being held at different venues each year. The venue and theme of each year slightly affects the research concerns. Consequently, it is necessary to summarize the basic information, such as location, theme, and amounts of research paper titles, of the annual conference from 2006 to 2018. The conference has been held mainly in Europe, north America and Asia. The amounts of accepted research papers vary from 155 to 665, as shown in Figure 1 and Table 1.

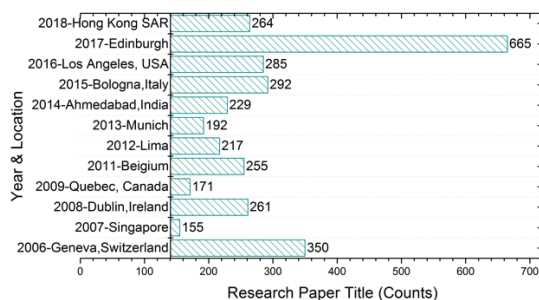


Figure 1: Year, location and counts of research paper titles of annual PLEA conference

Table 1: Theme of annual PLEA conference

Year	Theme
2006	Lessons From Traditional Architecture
2007	"Sun, Wind, and Architecture"
2008	Towards Zero Energy Building
2009	Architecture Energy and Occupant's Perspective
2011	Architecture and Sustainable Development
2012	Towards and Environmentally Responsible Architecture
2013	Architectural Quality in View of Future Based on Renewable Sources
2014	Sustainable Habitat for Developing Societies Choosing the Way Forward
2015	Architecture in (R)evolution
2016	Cities, Buildings, People: Towards Regenerative Environments
2017	Design to Thrive
2018	Smart and Healthy within the "2-degree Limit"

2.2 Diagram of text data mining approach

As shown in Figure 2, after extracting title text lines from PDF files, the text data mining mainly contains three steps--'pre-processing', 'processing' and 'analysis'. Pre-processing excludes the stopwords and punctuations and stems words of the raw corpus. The stopwords refer to the assistant words in a sentence such as 'the', 'is', 'are', 'they', 'of' and so on. The pre-processing is beneficial in reducing the work load to make the processing more efficient. Processing finds out the words' and strings' frequency ranking pattern of each year's proceeding to get the annual main research concerns. Single word, double-word string and triple-word string are studied to draw the entire pictures of the research concerns' variation. With the processing results, the variation trend of highly concerned research topics can be analyzed.

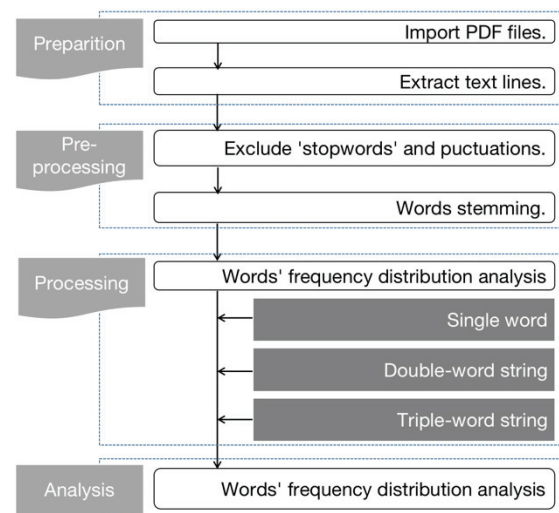
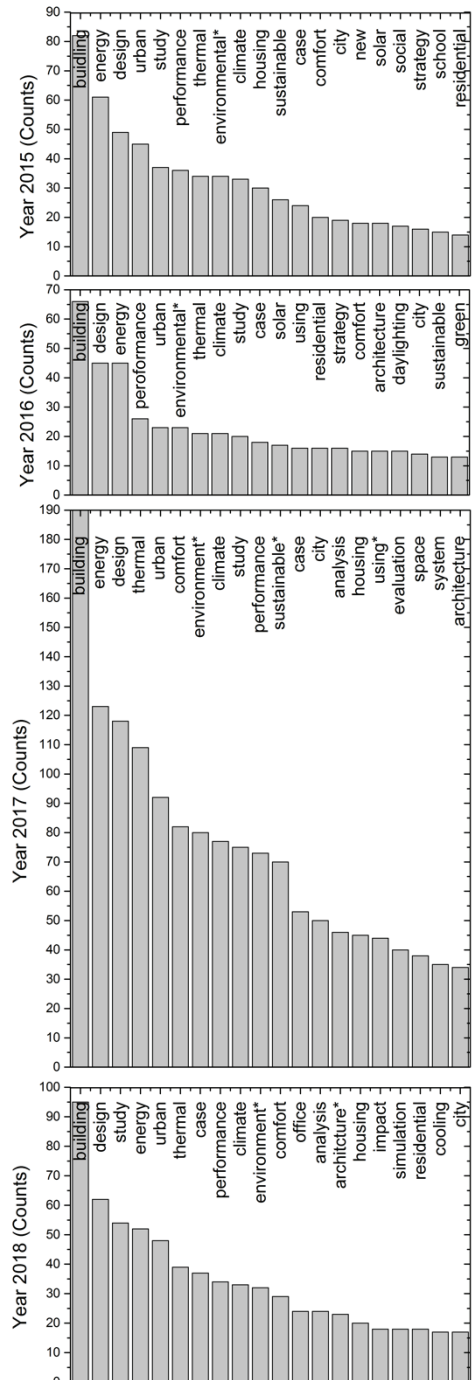


Figure 2: Diagram of text data mining approach

3. RESULTS and DISCUSSION

The frequency ranking of single word (first 20), double-word string (first 25) and triple-word string (first 20) provide very different information about the keywords of research concerns.

[illegible]

As shown in Figure 4, double-word string frequency ranking presents a different picture from that of single word. 'thermal comfort' has been the most mentioned string all through the past decade. Corresponding to the conference theme of 'Towards Zero Energy Building', the most mentioned string in 2008 is 'zero energy'. 'Sustainable building' or 'Sustainable architecture', which is a very general term to reflect PLEA theme, are mentioned a lot. Besides, 'post occupancy' (Year 2007, 2008, 2011, etc.), 'natural ventilation' (Year 2012, 2013, 2015, 2016, 2017, 2018) or 'natural ventilated' (Year 2006, 2009, 2014) are attractive topics. Interesting but rarely mentioned

concerns are ‘visual comfort’ in Year 2006 and 2014, ‘life cycle’ in Year 2009 and 2016, ‘integrated design’ in Year 2009 and 2013, ‘urban morphology’ in Year 2013, ‘urban micro-climate’ in Year 2014 and 2016, ‘climate change’ in Year 2017 and 2018. It is worthy mentioned that, in Year 2018, several new concepts emerged, such as ‘parametric study’, ‘benefit reusing’, ‘neural network’; it indicates more advanced computation methods are involved in PLEA research.

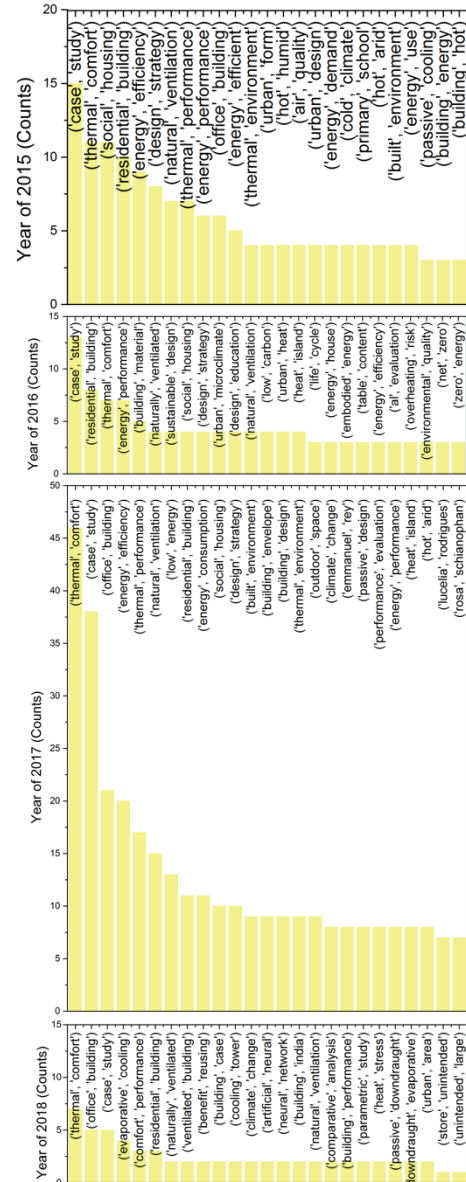


Figure 4: Double-word string frequency distribution

Triple-word string frequency ranking presents a different picture from those of single word and double-word string. The string ‘urban heat island’ turns out to be the most discussed topic in general. ‘Urban heat island’ is most popular topic in Year 2008, 2009, 2015, 2016 and 2017. Besides, the string ‘zero energy building’ has been mentioned most frequently in Year 2011 and 2013. In addition, strings that are repeated no less than 3 times are ‘thermal comfort zone’ in Year 2013; ‘hot arid climate’ in Year 2015 and 2017; ‘sustainable design education’ in Year 2016; ‘passive design strategy’, ‘indoor environmental quality’, ‘low energy building’, ‘hot humid climate’, ‘indoor thermal environment’ in Year 2017.

Concerns in Year 2006, 2007 and 2018 are diversely distributed as there is no extraordinary hot topics in these years. However, in Year 2018, we still can find out ‘artificial neural network’ repeating twice, which was proposed for the first time. Similar with the results of double-word string analysis, it indicates the

entrancement of advanced computation method in PLEA research.



Figure 5: Triple-word string frequency distribution

The frequency ranking of single word, double-word string and triple-word string outlines different pictures about the research concerns in the past

decades. They are complimentary by disclosing the research concerns through different perspectives.

From the single word to triple-word string, the counts of reappearance reduced generally. For example, in Year 2017, the top-ranking single word 'building' has been repeated more about 190 times within 665 research titles; the top-ranking double-word string 'thermal comfort' has been repeated about 48 times; the top-ranking triple-word string 'urban heat island' has been repeated 7 times. We can infer that, 'building' is the main research object other than 'urban' although 'urban heat island' is a popular topic that attracts lots of attentions. Indoor or outdoor 'thermal comfort' is the main concern in the building zone level. Similarly, in the year of 2009, 2015 and 2016.

To summary, the fundamental concerns of PLEA research have remained stable during the past decade. In the building level, indoor and outdoor thermal comfort has been discussed most; in regional level, the urban heat island effect attracts most attentions. Natural ventilation is one of most popular techniques in passive design strategies. The frequency ranking of double-word string indicates interesting but rare mentioned key words in the past decades, including 'visual comfort', 'life cycle', 'integrated design', 'urban morphology', 'urban micro-climate', 'climate change', 'parametric study', 'benefit reusing', 'neural network'. In 2018, more advanced computation methods have been involved in PLEA research. The social house, school, dwelling, office, and residential buildings are the building types that being focused most.

As to the research object, attentions are mainly paid on a variety of building type in cities and urban heat island effect. The research gap lies in rural buildings, which are occupied by 50% of the global population now [7]. As to the technique for passive design strategies, natural ventilation has been discussed a lot. The access to daylight via reasonable architectural design which improve visual comfort and benefit for thermal environment [8] needs more attention from the researchers.

4. CONCLUSIONS

The frequency rankings of single word, double-word string and triple-word string outline different pictures about the research concerns in the past decade, but are complimentary by disclosing the research concerns through different perspectives.

The analysis reveals that main concerns of passive and low energy architecture research have remained stable during the past decades. The main concerns are, indoor and outdoor thermal comfort in building level, and urban heat island effect in regional level. Natural ventilation is one of the most discussed techniques in passive design strategies. Enlightening but rare mentioned key words in the past decade are 'visual

comfort', 'life cycle', 'integrated design', 'urban morphology', 'urban micro-climate', 'climate change', 'parametric study', 'benefit reusing', 'neural network'. In 2018, more advanced computation methods have been involved in passive and low energy architecture research. The social house, school, dwelling, office, and residential buildings are the building types that being focused most. Research gaps lie in rural buildings and the study on accessible daylight via reasonable architectural design.

Clarifying the research concerns and variation trends of passive and low energy architecture can provide informative references for research communities, industry practitioners and non-profit organizations in the future study on passive and low energy architecture research.

ACKNOWLEDGEMENTS

This work described in this paper was fully supported by a grant from the Research Grant Council of the Hong Kong Special Administrative Region, China [Project No. CityU 11204117].

REFERENCES

1. Watson D. (2013) Bioclimatic Design. In: Loftness V., Haase D. (eds) Sustainable Built Environments. Springer, New York, NY. DOI: <https://doi.org/10.1007/978-1-4614-5828-9>
2. Bodach S., Lang W., Hamhaber J. (2014) 'Climate responsive building design strategies of vernacular architecture in Nepal', *Energy and Buildings*, 81, pp.227-242.
3. Chen X., Yang H., Lu L. (2015) 'A comprehensive review on passive design approaches in green building rating tools', *Renewable and Sustainable Energy Reviews*, 50, pp. 1425-1436.
4. Anna-Maria V. (2009) 'Evaluation of a sustainable Greek vernacular settlement and its landscape: architectural typology and building physics.' *Building Environment*, 44(6), pp. 1095-106. <http://dx.doi.org/10.1016/j.buildenv.2008.05.026>
5. Manzano-Agugliaro F., Montoya F., Sabio-Ortega A., and Garcia-Cruz A. (2015) 'Review of bioclimatic architecture strategies for achieving thermal comfort', *Renewable and Sustainable Energy Reviews*, 49, pp. 736-755. <http://dx.doi.org/10.1016/j.rser.2015.04.095>
6. Chandel S., Sharma V., Marvah B. (2016) 'Review of energy efficient features in vernacular architecture for improving indoor thermal comfort conditions', *Renewable and Sustainable Energy Reviews*, 65, pp.459-477.
7. United Nations, Department of Economic and Social Affairs, Population Division (2018). *World Urbanization Prospects: The 2018 Revision*, Online Edition.
8. Eltaweel A. and Su Y. (2017) 'Parametric design and daylighting: A literature review', *Renewable and Sustainable Energy Reviews*, 73, pp. 1086-1103.

ANALYSIS AND COUNTERMEASURES OF PROBLEMS IN PURE SOIL CONSTRUCTION

Take the research and development centre for rural vitalization in Yunnan China as an example

FANG TIAN, WENFENG BAI, LAI ZHOU, XIAOXUE LIU, LI WAN, XINAN CHI, EDWARD NG

¹The chinese university of HongKong, Hongkong, China

² Kunming university of science and technology, Kunming, China

ABSTRACT: Pure soil construction or raw material earthen construction (earthen construction technology without adding chemical stabilizers) is a sustainable construction method with the advantages of having no impact on the environment, low embodied energy and good indoor comfort. Both in China and western countries, this technology has a long history but it has some limitations as well: the construction process is not standardized, durability questioned, not waterproof and so on. Therefore, there are higher requirements for the design and building management in this kind of building, to avoid the occurrence of problems leading to the rework of the project which increases its cost and time limit. This research takes the pure soil construction technology as the research subject, combined with the research and development centre for rural vitalization in Yunnan China. Summarizes and analysis the problems in the process of building. And provides methods of preventing and solving those problems from three aspects, to achieve optimal management and accelerate construction.

KEYWORDS: rammed earth, sustainable development, raw material, Construction and management, contemporary earthen construction

1. INTRODUCTION

Pure soil construction or raw material earthen construction (earthen construction without the addition of chemical stabilisers) is a sustainable construction method with the advantages of low embodied energy, low construction cost and good indoor comfort.[1] Compared with that of modern buildings and even that of modern earth buildings with chemical stabilisers, the environmental performance of pure soil construction is the strongest. This technology has a long history in China and western countries. The most famous example is the Great Wall of China, which was built approximately 2,000 years ago using local materials: rammed earth (RE), stones, baked bricks and wood.[2] However, it has several limitations: the construction is neither standardised, durable nor waterproof. Therefore, the requirements for the design and building management in construction are high to avoid the occurrence of problems that lead to project reworking or safety problems, thus increasing costs and time limits. [3]

2. PROBLEMS IN CONSTRUCTION

2.1 Case background

The research and development centre for rural vitalization(The Terra center) is a research institution for

developing rural areas in China with sustainable methods. It also undertakes the training of craftsmen and holding academic conferences and activities. The RE walls of Terra center are built entirely of raw materials without any additives.



Figure 1 Terra center

2.2 Problems in construction

In most studies on earthen buildings, people only focus on investigating building materials and stabilisers, but often ignore the construction process. Moreover, construction problems are poorly analysed and summarised.

The extent of compaction affects the overall load-bearing performance and the texture of the finished surface. Therefore, the management of ramming is one of the most important parts of construction. The following is a summary of the problems in ramming.

2.2.1 Shrinkage

With the evaporation of moisture in the soil, the RE wall will shrink to a certain extent. Excessive shrinkage will cause extensive cracking. If cracking throughout the wall, then the first defect will affect the overall stability, whereas the second will affect indoor thermal comfort.



Figure 2 Shrinkage

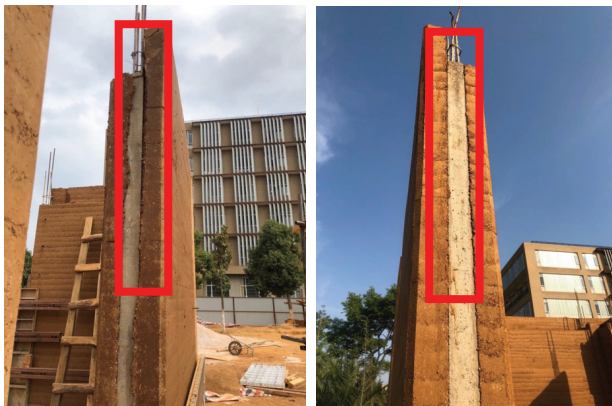


Figure 3 Deviation

2.2.2 Crack

The different physical properties of the soil and water content of the mixture will lead to different degrees of cracking. Cracks will affect the aesthetics of RE and its ability to adjust room temperature. Cracks will also affect the stability of the structure in severe cases.

Cracks are evaluated and regulated in different countries in accordance with earthen construction codes. Cracks that meet the requirements of those codes will be qualified because they will not cause safety problems. [4] However, given the absence of construction codes in China and that many parts of China are in earthquake zones, the formation of cracks in the earth construction of seismic areas should be strictly controlled in addition to referring to foreign codes.[5]

All cracking problems and locations during construction are summarised. Their causes are then analysed, and solutions to minimise the incidence of cracks are identified. (Table 1)

2.2.3 Deviation

If the mixing is too wet, then the RE wall will deviate from the contact site with the tie column. Deviation will also occur if the formwork is not calibrated in time.

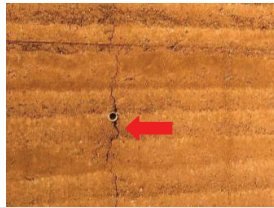

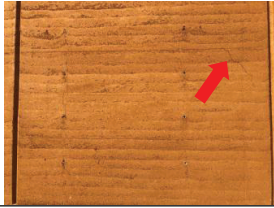

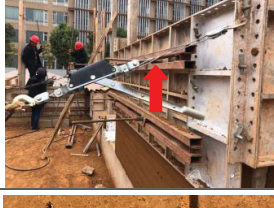

	Location: Around the tie rod of the formwork Cause: Given that the compaction force is uneven, soil around tie rod is not compacted tightly enough
	Location: Lower edge of the formwork Cause: Failure to remove the formwork in time results in uneven shrinkage along the top and bottom of the soil.
	Location: Wall surface Cause: Moisture content of the mixing is too high or too low
	Location: Above the opening Cause: The lintel above the door and window opening is too short or the material bearing capacity is insufficient.
	Location: Cracking due to incorrect operation Cause: Wrong way to use brace or knot on the top
	Location: Temperature difference on the two sides of the wall Cause: Different sunlight intensities on both sides of the wall lead to different degrees of drying and shrinkage

Table 1 Crack analysis

2.2.4 Wall damage

1) Damp

Raw soil buildings are limited in the aspect of waterproofing. Given the failure of waterproofing measures during the rainy season, sustained concentrated water flow will damage the RE wall, resulting in partial destruction, deformation and even collapse.[6] Some specific parts are easily dampened if

special treatments are not performed. Long-term dampness will also lead to damage. Therefore, detailing design is crucial and always needed for those parts.

All damping problems and locations during the construction process are summarised. Their causes are then analysed. (Table 2)

Location	Causes:
Junction with other materials	Water infiltration is present at the junction of the RE wall and concrete foundation.
Wall crown	The top of the rammed earth wall is the weakest location and will soften if constantly soaked in water.
Windowsill	Rainwater at the edge of rammed earth wall results in partial dampness and damage.

Table 2 Damp analysis

2) Leakage

Given that RE walls made of raw material are not waterproof, prolonged rain or concentrated leakage will lead to damage to RE walls.[7] Water leakage easily occurs where tarps are damaged or where they are connected. The second is the bottom of the RE wall that is easily damaged by the prolonged splashing of water on the ground.

When pouring the concrete floor, the cement slurry pollutes the RE wall along the crevices of the formwork because the concrete is too diluted or the formwork is poorly treated for leakage prevention.



Figure 4 Water leakage

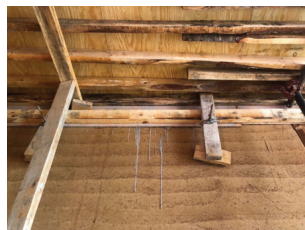


Figure 5 Cement slurry

3) Damage during formwork removal



Figure 6 Formwork removal damage

During formwork removal, wet clay is prone to adhering to the formwork and falls off together due to improper operation or the lack of oiling. [8]

3. COUNTERMEASURES

3.1 Design process

The design process involves the moisture-proofing of the bottom and top of the earth wall, the installation of doors and windows, the moisture-proofing of toilets and kitchens and the design of roofs and outer walls in accordance with the local climate.

3.1.1 stairs



Figure 7 Stairs



Figure 8 Footing

The wall compactness of pure soil is an important condition for ensuring its stability. Thus, drilling and processing after construction should be avoided. The staircase is designed in the form of a cantilevered central slab. The stair lintel is connected to other beams, and the ladder surface of the stairs is not in contact with the RE wall. (Figure 7)

3.1.2 footing and base details

The foundation of the building should have a waterproof layer above the ground to ensure that the RE wall at the bottom will not get wet. The height of the waterproof foundation can be determined in accordance with local weather conditions. (Figure 8)

3.1.3 openings and supports

The openings for door and window is usually reserved from top beam to floor beam, which can facilitate construction. And structural column should be embedded in both sides of the reserved openings to facilitate the installation of doors and Windows. Other forms of windowing shall be designed and constructed in strict accordance with the methods specified in the earth construction manual.[9]

3.1.4 protection given by roofs

Temporary roof protection is required during construction. During roof design, the expansion of the eave depends on the local weather and wind direction. Waterproof structures are required on the tops of RE walls after construction.

3.1.5 Services and fixings

Considering that embedded pipes are not conducive for repair, and leakage will damage the RE wall, all the pipes are not installed through embedding.

The water supply and drainage piping layout should be fixed using other parts instead of directly making holes in the RE wall. The wires should be installed through the floor slab, floor beam and roof beam.



Figure 9 Drainage



Figure 10 Wires

3.1.6 toilet

A double-layered wall in the toilet must be used to maintain the breathing performance, which is the ability to adjust temperature, of pure earth walls and to ensure that the room can meet reusable water supply and drainage demand and does not suffer from dampness.



Figure 11 Double layer wall



3.2 Construction management

3.2.1 Solution to shrinkage

To predict the degree of shrinkage of the RE wall, a test panel should be fabricated before construction. The test panel is 600 mm high by 1000 mm wide and 350 mm thick. The building method, material and moisture content of the test panel should be exactly the same as those of Terra Centre.(Figure12) The test panel must be checked after surface drying because a newly constructed RE wall is completely different from a wall that has dried out.



Figure 12 test panel



Figure 13'hit and miss'

We used the vertical ramming method to regulate shrinkage. During construction, the order and timing of ramming is monitored, and then the 'hit and miss' approach is adopted.(Figure13) That is, adjacent walls are not rammed at the same time. Every two walls are rammed. The tester then waits until the walls have completely dried and then rams the middle of the walls to minimise shrinkage.

3.2.2 Solution to cracks

Location	Solution
Around the tie rod of the formwork	Ramming should be reinforced around the tie rod and combined with a manual rammer
Lower edge of the formwork	Remove the formwork after ramming
Wall surface	Strictly supervise and control the moisture content of RE materials
Above openings	The sides of the lintel above the door and window openings must be extended by at least 30 cm
Cracks due to incorrect operation	Prohibit the practice of ropes on the top and strictly monitor the strength of the support
Temperature difference on two sides of the wall	Install a sun screen on the sunlit side to balance the drying of each side

Table 3 Solution to cracks

3.2.3 Solution to deviation

Mode	Merit and demerit
Overall frame mode	Merit Formwork calibration is convenient, and the probability of deviation is low.
	Demerit All formwork for building is needed, and failure to remove the formwork can lead to cracking.
Vertical frame mode	Merit Formwork calibration is convenient, and the probability of deviation is low.
	Demerit The amount of formwork is large, and the junction of two plates must buckle.
Rounds frame mode	Merit Formwork usage is small, and each plate is fixed firmly
	Demerit Layer-by-layer formwork calibration is time consuming, and the probability of deviation is increased.

Table 4 Formwork setting mode

The water content of the mixing should be checked regularly, whereas compactness and load-bearing capacity should be checked through on-site sampling. The installation, calibration and removal of formwork and the correctness of other construction operations should be strictly checked by on-site architects.

If the mixing is excessively wet, then the RE wall will deviate from the contact site with tie column. In this case, the RE wall must be slightly propped on both sides until drying is complete.

Three modes of formwork setting are introduced to avoid whole wall deviation, and the second method is adopted in this project. (Table4)

3.2.4 Solution to wall damage

Waterproofing and leakproofing measures should be taken in advance to prevent leakage. Covering the building with a plastic sheet or temporary roofing during construction is a good way to avoid rain erosion. However, a real roof is needed. In addition to providing sufficient eave extension, natural roof drainage should be avoided. The rain will flow back along the bottom of eaves, and in case of strong winds, the rain will erode the exterior walls. Thus, gutters and drains are essential.

When pouring the concrete floor, the cement slurry will pollute the RE wall along the crevices of the formwork because the concrete is too diluted or the formwork is not well treated for leakage prevention. Before pouring concrete, anti-leakage measures should be taken. If slurry leakage has occurred, then the leaked slurry should be cleaned in accordance with the texture of the RE wall after it has dried out.

The following treatments should be emphasised for components that are easily dampened.(Table5)




	Location: Junction with concrete Solution: Use a waterproof paintbrush on the foundation, floor and roof
	Location: Wall crown Solution: Use stone or cement to seal the top of the RE wall to ensure stability
	Location: Windowsill Solution: Install a windowsill to expedite rainwater

Table 5 Solution for wall damage

During mould removal, wet clay is prone to adhering to the formwork and falling off together due to improper operation or the lack of oiling. Therefore, the formwork should be cleaned and oiled before ramming to prevent this situation. In addition, the formwork should slide up instead of directly hinging away.

3.3 Training

In accordance with the design guidelines of earthen houses in various countries and regions, workers should be trained in the perception of soil and the construction method to improve their skills and accuracy before the project starts.



Figure 14 Mixing training



Figure 15 Ramming training

3.4 Repair

If wall damage occurs, but does not affect the overall structural safety of the building, then the damaged part can be repaired.

Generally speaking, repair is divided into the following steps: wetting, re-erecting formwork and ramming and removing formwork. During the repair of this project, we found that if the wall is thin (<300 mm), then the whole piece must be removed and re-rammed. The thickness of the damaged wall in this project is 600 mm, and the damaged part is half the thickness. We chose to remove the half part of the damaged wall and re-tamper it. Notably, however, the restoration work must be done with great care because the re-ramming part tends to detach from the original part.



Figure 16 Repair of damaged wall

4. CONCLUSION

Pure soil construction is a sustainable technology, and modern techniques help increase its strength and regulate its construction practices.

With the dissemination and popularity of sustainable technology and materials in recent years, a growing number of RE buildings are being built worldwide. However, this study finds that:

- 1) Designers and builders must increase awareness. Although modern techniques and equipment have been used in the construction of modern earth buildings, the design of modern earth buildings is different from that of modern buildings. Therefore, the plan should be discussed with earth experts before construction.
- 2) Even if the construction is performed by skilled workers, a certain period of construction training is necessary before the construction of raw soil buildings to familiarise workers with the characteristics of materials, construction tools and standard operations.
- 3) On-site instruction is crucial in the whole construction system. A soil specialist or on-site designer should frequently inspect the site.
- 4) In addition to optimizing the ratio of materials with different particle sizes in the mixture, we can minimise the disadvantages of earth construction and give full play to its advantages by doing a good job in construction management.

ACKNOWLEDGEMENTS

We especially thank Marc Auzet and Juliette Goudy of Atelier [tümù] Earth & Wood construction Design + Workshop, who are also soil experts of the project in this study. They helped us achieve a clear understanding of the construction technology and procedure of rammed earth buildings. This understanding is crucial for the analysis in this research. And thanks to Lucia Cheung of PLY Union Limited, the co-architect of this project, she helped to make the whole building more splendid and integrated with the raw material.

More importantly, we want to give thanks to Chan Cheung Mun Chung Charitable Fund Ltd and Mr. Chen, the construction sponsor of this project. Given his donation, we can also demonstrate rammed earth houses in many poor rural areas of western China and thus improve the living environment of farmers there.

REFERENCES

1. Back to earth: anti-seismic prototype in Guangming. Edward Ng, Li Wan, Xinan Chi, Austin Williams. *The Architecture Review*. 2017.
2. Various Types of Earth Buildings. Hamed Niroumand, M.F.M Zain, Maslina Jamil. *Procedia - Social and Behavioral Sciences* 89 (2013) 226 - 230 .
3. Recourse to earth for low-cost housing in Nigeria. A.O. Olotuah. *Building and Environment*, 37 (2002) .
4. A guideline for assessing of critical parameters on Earth architecture and Earth buildings as a sustainable architecture in various countries. Hamed Niroumand, M.F.M Zain, Maslina Jamil. *Renewable and Sustainable Energy Reviews*, 28 (2013) 130-165.
5. Experimental study on seismic performance of raw-soil structure walls in different construction technologies. A dissertation submitted for the degree of master, Chang'an university, Xi'an, China, 2011.6.
6. Rammed earth structure : a code of practice. Julian Keable and Rowland Keable. Practical action publishing ltd (2011) .
7. Earth Building Practice : Planning - Design – Building. Ulrich Röhlen, Christof Ziegert. Beuth Verlag (2011) .
8. Rammed earth : design and construction guidelines. Walker, Peter, 1957- & Great Britain. Department of Trade and Industry (2005).
9. The Australian earth building handbook. Standards Australia and Walker P. HB195: Sydney(Australia): Standards Australia, 2002.
10. Cob, a vernacular earth construction process in the context of modern sustainable building. Erwan Hamard, Bogdan Cazaciu, Andry Razakamanantsoa, Jean-Claude Morel. *Building and Environment* 106 (2016) 103-119.
11. A geotechnical perspective of raw earth building. Domenico Gallipoli, Agostino Walter Bruno, Céline Perlot, Joao Mendes. *Acta Geotechnica* (2017) 12:463-478.
12. International Advances in Raw Soil Materials. LIU Junxia, ZHANG Lei, YANG Jiujun. *Material guide A: overview*, December 2012 (I) volume 26 issue 12.
13. Building houses with local materials: means to drastically reduce the environmental impact of construction. Morel JC, Mesbah A, Oggero M, Walker P. *Building and Environment* 2001;36(10):1119-26.
14. UK National guidelines for rammed earth. Maniatidis V, Walker P. In: *Proceedings of the 9th International Conference on the Study and Conservation of Earthen Architecture*, Terra 2003. Yazd-Ira 29 November–2 December, 2003.
15. University-based rural sustainable development assistance strategies. Wan Li, Chi Xinnan, Ng Edward, et al. *Architecture and Resilience on the Human Scale* . 2015.

Using In-Situ Building Fabric Thermal Performance Testing to Calibrate As-Built Models of Low Energy Dwellings in the UK

RAJAT GUPTA AND MATT GREGG

Low Carbon Building Research Group, School of Architecture, Oxford Brookes University, Oxford, UK

ABSTRACT: *This paper presents the methodology and results of in-situ building fabric thermal testing to calibrate as-built energy models of three low energy dwellings in the UK, so as to examine the gap between the as-designed and as-built energy performance. The in-situ tests included air permeability testing, along with thermal imaging and heat flux measurement. Despite the dwellings being designed to high thermal standards, heat flux measurements showed poor thermal quality of the walls and roof section even for the 'good' quality sections that were measured. Thermal imaging surveys revealed air leakage pathways around door/window openings, penetrations and junctions between walls and ceilings indicating poor detailing and workmanship. Air permeability (AP) was found to have increased after the initial test due to post-completion alteration to the building fabric. Though the results were higher than expected they were within the UK Building Regulations limiting fabric parameters. Calibration of the model through temperature monitoring provided less extreme projected energy performance gap than simply replacing the designed AP values and U-values with test results. Insights from the study have reinforced the need for national Building Regulations to require as-built energy models with in-situ test data to measure the gap between intent and outcomes.*

KEYWORDS: *Building performance evaluation, performance gap, thermography, energy modelling*

1. INTRODUCTION

The UK Government is legally committed to a target of net zero for UK greenhouse gas (GHG) emissions by 2050 and to five-year carbon budgets in the interim set by the Committee on Climate Change [1]. Over the years various policies aimed at encouraging energy efficiency measures in domestic buildings such as Code for Sustainable Homes (CSH) and the Green Deal, have come and gone. According to the UK government's Department for Business, Energy and Industrial Strategy's (BEIS) Clean Growth Strategy [2], the UK has outperformed the target emissions reductions; however, the housing sector, will need to do more to meet its share of reductions.

These carbon budgets have driven the need for new dwellings to be built with high standards of insulation and airtightness with managed ventilation, high efficiency heating systems, and renewables. However, there is a growing concern that low/zero energy dwellings often underperform as compared to the design specifications, due to discrepancy in building fabric thermal performance, systems efficiency and occupant behaviour.

Building performance evaluation (BPE) studies offer a range of methods to evaluate the effectiveness of design and construction in meeting expected performance. Recent performance evaluation studies [3, 4] have demonstrated that in-use energy use can be up to three-five times more than design predictions. This energy performance gap (EPG) between the predicted energy performance of

a building (domestic or non-domestic) and its measured performance has been highlighted by several studies [5-14]. BPE studies of new dwellings [7, 14-16] have shown the reasons for performance gap to be related to discrepancies that arise across the building process, from the design and modelling tools used to design the building, through buildability, materials and build quality (as-designed and as-built), systems integration and commissioning but handover and operation, as well as the understanding, comfort and behaviour of the occupants. Clearly national policy targets for carbon reduction cannot be met without understanding, quantifying and minimising this performance gap between as-designed, as-built and in-use stages.

This paper uses in-situ building fabric thermal performance testing to examine the gap between as-designed and as-built energy performance to create and calibrate as-built energy models of three low energy dwellings in the UK. The study is part of a research project (2015 – 2020), funded by the European Union's Horizon 2020 Research and Innovation programme, called Zero Plus project which seeks to achieve net-regulated energy use of less than 20 kWh/m²/year. This paper presents the methods used and results of the pre-occupancy evaluation of three dwellings designed to meet the above target.

2. CASE STUDY DWELLINGS

The three case study dwellings in the study (Zero Plus project) are shown in Figure 1 on the following page. The dwellings are located in York (UK). The house numbering is from right to left in the images. ZP1 and ZP2 are both 2-bedroom semi-detached properties, consisting of two stories. These two properties are mirrored, and both share the party wall along the lounge wall. ZP3 is a 3-bedroom, plus study detached property, also with two stories.



Figure 1: Case study dwellings

All three dwellings were constructed to meet Code for Sustainable Homes (CSH) Level 4. Though CSH is no longer a standard used in the UK, it is the standard that was used when the development began design. Even to this day, though CSH has been abandoned, the standard fabric parameters used in the development to meet it still surpass the current UK Building Regulations (BRUKL) limiting fabric parameters (U-values and air permeability) as shown in table 1.

Table 1: Design and regulation fabric parameters

		ZP design	BRUKL
U-values	Wall W/(m ² ·K)	0.17	0.30
	Roof W/(m ² ·K)	0.16	0.20
	Floor W/(m ² ·K)	0.14	0.25
	Party wall W/(m ² ·K)	0.20	0.20
	Windows W/(m ² ·K)	1.33	2.00
	Air perm. (m ³ h ⁻¹ m ⁻²) @50pa	4.00	10.00

3. METHODOLOGY

The objective of pre-occupancy testing was to check the actual thermal performance of the building fabric and identify any areas of air leakage, thermal bridging or less than adequate insulation in the external fabric. The BPE methods included the use of a *blower door test to measure air permeability*, *heat flux measurement* to measure thermal transmittance (U-value) and *thermal imaging survey* to qualitatively document heat loss.

Air permeability tests were performed immediately following construction (January – February 2019) and again in April 2019. The test was conducted on each of the three dwellings in accordance with ATTMA TSL1 recommendations, using the Blower Door and depressurisation pressures up to 50Pa. All ventilation openings were closed and or sealed with an adhesive membrane. Measurements of air flow rate through the fan of a Blower Door fitted to the front door were recorded with fan speed varied to give pressures of approximately 10 to 60Pa. Calculations were then made to produce a figure for air permeability at a pressure difference of 50Pa.

Thermal imaging was carried out on the 3rd of April 2019 and performed twice for each property, before and during depressurisation. Depressurisation was used to highlight further areas of air leakage. A blower door was used and a pressure of around -50Pa was maintained for a period of 15 minutes before a second thermographic survey was undertaken. A 19°C difference was maintained between interior and exterior except for ZP2 where the heating was not working. In ZP2, temporary convection heaters were installed approximately four hours prior to the survey.

Heat flux plates were installed for 14 days to measure variations in thermal transmittance (U-value) between good and poor areas in close proximity. The detailed test method outlined in International Standard ISO 9869-1 was followed. Wall measurements on ZP1 and ZP3 were on North walls. The roof measurement was done on ZP2 in the first-floor bathroom. The locations for the Heat Flux plates were chosen as places where there were relatively good and poor areas of building fabric in close proximity (following the thermal imaging assessment). Air temperatures were measured in the

respective rooms and outside the fabric as near as possible to the same part of the fabric. The heat flux measurement for assessment of thermal transmittance was carried out from 3rd April to 24th April 2020. The process of quantifying the thermal transmittance involves data logging of the temperature on each side of the fabric element and the heat flow through the heat flux sensors. U-Value $W/(m^2 \cdot K)$ of a wall is heat flux (in W/m^2) divided by temperature difference (K). This is calculated from the average value of heat flux divided by the average temperature difference. Because temperatures and heat flow vary during the test, average values of each parameter need to be taken over an extended test period.

3.1 Energy model calibration

Throughout the design process, dynamic thermal simulation models were developed and maintained using the Integrated Environmental Solutions Virtual Environment (IES VE) suite of software, specifically ModelIT for modelling the external physical characteristics of the dwellings and Apache for setting thermal parameters and running simulations. IES VE thermal calculation and dynamic simulation software was selected since it is an approved industry standard, audited by the Chartered Institution of Building Services Engineers (CIBSE) and the United Kingdom Accreditation Service as well as being an accredited software for producing Energy Performance Certificates (EPCs) by the Building Research Establishment (BRE).

For modelling purposes ZP1 and ZP2 are a single model (semi-detached type), i.e. type 'B3' and ZP3 is a model of the detached type, 'C4'. The models were calibrated following the pre-occupancy evaluation results to observe potential performance gap issues, specifically where the building fabric may be performing differently from as-designed expectations. Two model calibration methods were explored as described below:

Method 1 (M1) - U-values through heat flux measurements: M1 used heat flux measurements and latest air permeability results to calibrate the model by using these values as parameters in the model. The mean of the air permeability results for ZP1 and ZP2, $5.42 \text{ m}^3 \cdot \text{h}^{-1} / \text{m}^2$ at 50 Pa, was used for model B3. External wall thermal transmittance of $0.56 \text{ W}/\text{m}^2 \cdot \text{K}$ was used for both B3 and C4. This is calculated by taking the 'good' and 'bad' heat flux measurements in ZP1 and using 'good' as 90% of wall and 'bad' as 10% of wall as the 'bad' measurements were at most representative of corners and trim conditions. A roof thermal transmittance of $0.3 \text{ W}/\text{m}^2 \cdot \text{K}$ was calculated in the same way.

$$\text{Thermal transmittance} = ('good' \times .9) + ('bad' \times .1)$$

Some limitations of M1 were as follows: ZP2 had inoperable heating, thereby limiting the temperature difference between the interior and the exterior. Also, the heat flux measurements were only taken on north walls in two instances and a ceiling in one instance. The worst areas were sought out for taking heat flux measurements; therefore, the thermal transmittance results from the assessment may be higher than the thermal transmittance in the dwellings overall.

Method 2 (M2) – U-values through temperature monitoring. An alternate method was explored for contrast. This method used temperature data measured during the summer in ZP2. Though the inoperable heating was problematic for pre-occupancy testing it provided an opportunity to study the dwelling unoccupied and free running for a longer period. As ZP2 remained unoccupied, this dwelling was used to calibrate the model using internal temperature data. Hourly external temperature data from Weather Underground¹ were used to align with external temperatures in the model. Similar temperature patterns were aligned from the same period for the day with the lowest temperature in the model. Observing the lowest temperature is helpful in observing the greatest strain on the external fabric albeit this evaluation was performed in the end of summer/shoulder season (September) and the lowest temperature was 6°C.

As the dwelling was unoccupied, all internal gains from occupant activity were removed from the model, that is, occupant body heat, appliance energy, domestic hot water energy, and lighting energy. In addition, occupant window opening patterns and heating patterns were removed from the model.

After the model was revised to mimic the pre-occupancy state of the unoccupied ZP2 dwelling, the thermal transmittance of the exterior walls and roof were adjusted to find the best match using simulated temperature data in the lounge. Two versions of the model were tested:

1. **Model A** – all parameters to match fabric details of the pre-occupancy evaluation (see details of method M1).
2. **Model D** – same air permeability as method M1, 'good' heat flux measurement for the roof of $0.19 \text{ W}/\text{m}^2 \cdot \text{K}$, and external wall thermal transmittance of $0.26 \text{ W}/\text{m}^2 \cdot \text{K}$ was used. This value was the change variable for finding the match between the monitored temperature data and model temperature data at the lowest point for the space simulated.

¹

www.wunderground.com/history/daily/gb/leeds/EGNM/date/2019-9-10

4. RESULTS

4.1 Air permeability testing

The results of the latest air permeability (AP) tests were compared with the test conducted at the completion stage, as shown in table 2.

Table 2: Case study form and air permeability details

	ZP1	ZP2	ZP3
Total floor area (TFA) (m ²)	84.4	84.4	129.6
Envelope area (m ²)	245.8	245.8	321.1
Design AP (m ³ h ⁻¹ m ⁻² @50pa)	4	4	4
Completion AP (m ³ h ⁻¹ m ⁻² @50pa)	3.94	3.97	2.77
Current AP (m ³ h ⁻¹ m ⁻² @50pa)	5.39	5.44	7.53

Interestingly all three dwellings were found to have better AP results than design targets when they were first tested. The current tests showed that none of the three dwellings met the design target of 4 m³ h⁻¹ m⁻² @50pa, although all dwellings remained within UK Building Regulations requirement of 10 m³ h⁻¹ m⁻² @50pa. ZP3 had deteriorated most significantly, and it was noted that there were holes in the kitchen wall where waste pipes had been fitted and the gaps around the pipes were not sealed properly. Other areas that had deteriorated included holes cut in the first floor, presumably to trace pipes or cables in the void and not properly filled, and cracks at the edges of the stairs and under the skirtings. These anomalies were re-confirmed in the thermal imaging survey under depressurisation. According to the developer some work had been done on the properties to fix defects between the first and second test.

4.2 Thermal imaging survey

Thermal imaging in all three dwellings showed air leakage pathways around openings and penetrations. Most surfaces were found to have a low thermal index which generally equals high U-values. The most common areas within ZP1 that these types of anomalies were seen were around skirting boards and at the junctions between the ceilings and walls (figure 2). ZP2 showed similar signs of air leakage throughout the property, as well as air leakage around the openable elements especially around doors and windows. ZP3 also showed similar signs of air leakage that was observed within the other two properties. This was mainly seen at the junctions between the ceiling and wall and around external doors.

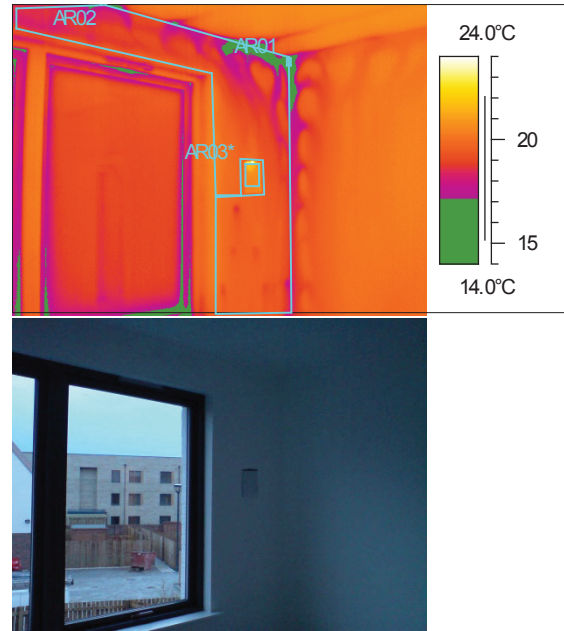


Figure 2: Air leakage in bedroom corner of ZP1

4.3 U-values through heat flux measurements

Overall heat flux measurements showed poor thermal quality of the walls and roof section that were measured. Whereas 'good' and 'poor' quality sections were measured, even the 'good' quality sections did not meet the design U-value. The measured values of thermal transmittance for the walls of the three dwellings were found to be significantly higher than design values as shown in Table 3. In fact, the wall U-values for ZP1 and ZP2 do not meet UK Building Regulations limiting fabric parameters. Similar differences were observed for the designed and measured U-values of the roofs. The U-values as calculated through the thermal imaging were a consistent 0.7 W/(m²·K); however, well-insulated fabric elements show greater uncertainties in measuring thermal transmittance through thermal imaging. Unfortunately, as the test were taken at a much later stage, the build quality, insulation thicknesses, and actual wall construction could not be reviewed.

Table 3: Heat flux measurements W/(m²·K)

	Wall ZP1	Wall ZP3	Roof ZP2
Design specification	0.17	0.17	0.16
Measured good area	0.47	0.56	0.19
Measured poor area	1.39	1.95	1.28

4.4 Calibrated energy models

Since in-situ measurements were mainly about building fabric thermal performance that affects space heating, as-designed energy models of the three dwellings were calibrated using the two methods (M1 and M2) to compare the difference

between as-designed and as-built (calibrated) space heating energy use.

Using method M1 that used measured U-values (through heat flux measurement) and measured air permeability (M1), as-built space heating was found to be about twice than the designed space heating energy for all three dwellings, as shown in Table 4.

Table 4: Calibration method 1 results

	ZP1/ZP2		ZP3	
	As-designed	As-built	As-designed	As-built
Space heating (kWh)	2,575	5,361	4,491	9,873

Using method M2, thermal transmittance of building fabric elements was manipulated to align the model's internal temperature with monitored data for the lounge. This resulted in an external wall U-value of 0.26 W/(m².K) in Model D. In Model A (external wall U-value of 0.56 W/(m².K) resulted in 1°C cooler internal temperatures in the model than what was monitored for the same period, which is why Model D was analysed further. In the case of method 2 (Model D), as-built annual space heating energy use was found to be 1.4 times more than designed space heating, as shown in Table 5.

Table 5: Calibration method 2 results (Model D)

	ZP1/ZP2		ZP3	
	As-designed	As-built	As-designed	As-built
Space heating (kWh)	2,575	3,596	4,491	6,002

5. DISCUSSION

The three in-situ tests revealed the magnitude of the gap between expected and actual thermal performance of the building fabric and the likely thermal defects that occurred in the three case study dwellings. Overall, most elements of the wall construction appeared to be well-insulated. However, depressurisation of the dwelling as part of the air permeability test highlighted the air leakage pathways and origins of some of these anomalies. Air movement was prevalent at the junction between walls and ceilings within all three properties, which could lead to thermal bypass. Air infiltration was seen around doors, particularly at the threshold of the doors to the garden area. The heat flux measurement showed areas of the building fabric that did not meet the limiting fabric parameters of Building regulations. It is recommended that the constructor addresses the

identified thermal defects before occupants move into the dwellings.

The second wave of air permeability tests showed higher AP values than those conducted post completion as part of compliance testing. This is a significant finding and implies that one-off tests are not adequate to identify thermal defects in dwellings since the building fabric thermal performance may deteriorate as works are undertaken, even after compliance testing. Moreover, there is very little research undertaken on longitudinal testing of building fabric performance; something that needs to be considered in future iterations of Building Regulations. The study has also exposed that communication of design intent amongst developers, constructors and designers is essential for achieving the intended thermal performance. If any works to the building fabric are undertaken (holes cut) following air-tightness testing, professionals responsible for ensuring a continuous air tightness layer must be involved.

Utilising in-situ testing data to calibrate as-built energy models is vital since it exposes the real difference between intended and actual energy performance without the influence of occupancy related factors since the dwellings are un-occupied. This is why calibration of the model through temperature monitoring provided less extreme projected energy performance gap than simply replacing the designed AP values and U-values with results from air permeability testing and heat flux measurements. It is evident that using more detailed data for calibration of energy models reduces the projected energy performance gap. To make this mainstream, future revisions of UK Building Regulations should require in-situ testing of building fabric thermal performance using a combination of tests (and not just air permeability tests), and submission of calibrated as-built energy models for compliance purposes.

6. CONCLUSION

The building fabric thermal performance of three low energy case study dwellings was systematically measured in-situ through concurrent tests involving air permeability, thermal imaging and heat flux measurements. The results were used to calibrate as-built energy models, so as to identify the real difference between as-designed and as-built energy performance.

Despite the dwellings being designed to high thermal standards, heat flux measurements showed poor thermal quality of the walls and roof section even for the 'good' quality sections that were measured. Thermal imaging surveys revealed where the fabric performance was being compromised. Air leakage pathways were found around door/window

openings, penetrations and junctions between walls and ceilings indicating poor detailing and workmanship.

Insights from the study have reinforced the need for national Building Regulations to require as-built energy models with in-situ test data to measure the gap between intent and outcomes.

ACKNOWLEDGEMENTS

The research study is part of the Zero Plus research project, which has received funding from the European Union's Horizon 2020 Research and Innovation programme under Grant Agreement No. 678407.

REFERENCES

1. HM Government, (2011). *The carbon plan: Delivering our low carbon future*. Department of Energy and Climate Change: London. p. 220.
2. BEIS, (2018). *Clean Growth Strategy: Leading the way to a low carbon future*, E.a.I.S. Department for Business, Editor. HM Government: London.
3. Monahan, S. and A. Gemmell, (2011). How occupants behave and interact with their homes. *The Impact on Energy Use, Comfort, Control and Satisfaction. HIS-BRE Press on behalf of the NHBC Foundation, Milton Keynes*.
4. Thompson, P. and J. Bootland, (2011). GHA monitoring programme 2009-11: technical report results from Phase 1: post-construction testing of a sample of highly sustainable new homes. *Report, Good Homes Alliance*.
5. Bordass, B. and A. Leaman, (2005). Making feedback and post-occupancy evaluation routine 1: A portfolio of feedback techniques. *Building Research & Information*, 33(4): p. 347-352.
6. Gaze, C., (2014). *How did the homes perform? The data.*, in *Proceedings of final AIMC4 conference*.
7. Gaze, C., (2014). *AIMC4 Information paper 5: lessons from AIMC4 for cost-effective fabric-first low-energy housing Part 5: As-Built performance and Post Occupancy Evaluation*. AIMC4 consortium.
8. Gill, Z.M., et al., (2010). Low-energy dwellings: the contribution of behaviours to actual performance. *Building Research & Information*, 38(5): p. 491-508.
9. Gupta, R. and M. Kapsali. *How effective are 'close to zero' carbon new dwellings in reducing actual energy demand: Insights from UK*. in *30th International PLEA Conference*. 2014.
10. Lowe, R., et al., (2007). Evidence for heat losses via party wall cavities in masonry construction. *Building Services Engineering Research and Technology*, 28(2): p. 161-181.
11. Stevenson, F. and A. Leaman, (2010). Evaluating housing performance in relation to human behaviour: new challenges. *Building Research & Information*, 38(5): p. 437-441.
12. Stevenson, F. and H.B. Rijal, (2010). Developing occupancy feedback from a prototype to improve housing production. *Building Research & Information*, 38(5): p. 549-563.
13. Williamson, T., V. Soebarto, and A. Radford, (2010). Comfort and energy use in five Australian award-winning houses: regulated, measured and perceived. *Building Research & Information*, 38(5): p. 509-529.
14. Wingfield, J., et al., (2011). *Elm Tree Mews Field Trial–Evaluation and Monitoring of Dwellings Performance (Final Technical Report)*, in *Leeds Metropolitan University: Leeds, UK*.
15. Wingfield, J., et al., (2008). *Evaluating the impact of an enhanced energy performance standard on load-bearing masonry domestic construction: Understanding the gap between designed and real performance: lessons from Stamford Brook*.
16. Gupta, R., M. Gregg, and R. Cherian. *Tackling the performance gap between design intent and actual outcomes of new low/zero carbon housing*. in *ECEEE Summer study proceedings*. 2013.

Impact of Renovation Measures on the Indoor Climate and Energy Use in Single Family Dwellings in Belgium

HILDE BREESCH¹, AXEL BEYAERT¹, ALEXANDER CALLENS¹, KOEN CLAES², ALEXIS VERSELE^{1,2}

¹Building Physics and Sustainable Design, Department of Civil Engineering, Ghent Technology Campus, KU Leuven, Ghent, Belgium

²Domus Mundi vzw, Ghent, Belgium

ABSTRACT: The “Dampoort KnapT OPI!” project in Ghent (Belgium) supported 9 families of captive residents in the necessary renovation of their dwellings. The aim of this study is to analyse the impact of these measures on the performance of the building envelope, energy use of and indoor climate in 3 single family dwellings. Measurements were carried out during the heating season in 2017-2018 (before) and 2018-2019 (after renovation). The monitoring campaign included pressurisation tests and infrared thermography. Temperature, relative humidity and CO₂-concentration were monitored during 2 to 4 consecutive weeks. Gas consumption (for heating) was measured on daily basis in a short period in dwelling A and B and annual values from 2016 to 2019 were acquired for all dwellings. The results show that it is difficult to draw general conclusions from comparable renovation actions in the studied dwellings. The air tightness increased in dwelling B while it decreased in dwelling C. Dwellings A and C have an increase of indoor temperature while the temperature is slightly decreased in dwelling B. The energy use for heating decreased in dwelling A and B but increased in C. The impact of the user on the indoor climate and energy use is also shown.

KEYWORDS: Renovation, Monitoring, Energy Use, Indoor Climate, Residential Buildings

1. INTRODUCTION

The city of Ghent (Belgium) is suffering from a lack of affordable, qualitative housing for people with low income. They are stuck in houses that are unsafe, of poor quality, not energy-efficient and not adapted to people's physical needs. 'Caught' in bad living conditions, these people are called 'captive residents'.

The “Dampoort KnapT OPI!” project of the public centre for social welfare of Ghent (Belgium) supports 9 families of captive residents in the Dampoort neighbourhood in Ghent in the necessary renovation of their dwellings. For each renovation, a starting capital of € 30.000 is provided with the focus on improvement of safety, quality of living and energy savings. This pilot project is up-scaled and applied to 100 dwellings in the new project “Gent knapt op” as described in [1].

The aim of this study is to analyse the impact of the renovation measures on the performance of the building envelope, the energy use of and the indoor climate in 3 different single family dwellings of the “Dampoort KnapT OPI!” project.

Other recent studies already determined the impact of an energy retrofit in residential buildings. Broderick et al. [2] measured the potential impact in fifteen semi-detached Irish homes on the indoor air quality (IAQ) and thermal comfort. They observed an increase of average

temperatures but no significant change in relative humidity. A significant change in concentrations of a number of pollutants was measured, attributed to reduced ventilation rates as a result of improved building air tightness. Földvary et al. [3] evaluated the impact of simple energy renovations on IAQ, air exchange rates and occupant satisfaction in Slovak residential buildings. Concentrations of total volatile organic components (TVOC) was elevated after renovation. It was concluded that energy renovation without considering its potential impact on the indoor environment could adversely affect the IAQ. La Fleur et al. [4] studied the measured and predicted energy use and indoor climate before and after a major renovation in a Swedish apartment building. An increase of indoor temperature was measured.

Major renovation projects in Northern Europe, including insulating building envelope and installation of a heat recovery system, cause reduction of normalized heating demand of 30 to 68% [4], [5], [6]. La Fleur et al. [4] also mentioned an Under-prediction of saving potential since indoor temperature has increased after renovation and the impact of the user behaviour on the energy-saving potential.

This paper is structured as follows. Paragraph 2 describes the characteristics of the buildings before and

after renovation and details of the monitoring campaign. The impact of the renovation on the building envelope, indoor climate and energy use is shown in the results part in paragraph 3, followed by conclusions.

2. METHOD

2.1 Description of the dwellings

2.1.2 Building characteristics and use

All buildings are originally built before 1945 and renovated in 2018. Figure 1 and 2 show the section respectively the ground floor plan of dwellings A and C while Figure 3 shows the ground floor plan of dwelling B. The heat loss area is indicated in red.

Table 1 summarizes the geometrical data of the 3 dwellings. Dwelling A and C are both terraced houses while dwelling B is a ground floor apartment with one common wall. Dwelling A and B have a similar net floor area and volume, while the volume and floor area of dwelling C is twice as large as this of the other buildings.

The use of the building, the heating set points and opening of the windows are shown in Table 2. Only living room, kitchen, bathroom and some sleeping rooms are heated. The occupants in dwelling C changed their habit of heating after renovation. The house is now constantly heated while before the retrofit the house was only heated when present. The other dwellings have a night setback for the heating. Windows are rarely opened.

Table 1: Geometrical data of the dwellings

	A	B	C
Building type	Terraced house	Apartment (ground floor)	Terraced house
Number of floors	2	1	3
Net floor area (m ²)	86.7	83.2	176.8
Heat loss area (m ²)	172.8	260.5	323.5
Volume (m ³)	263	291	611

Table 2: Usage data of the dwellings

	A	B	C
Occupants	1 to 2	3	2
Use weekdays	11h-15h30 18h-7h30	17h-8h30	17h30-10h
Use weekends	0-24h	0-24h	17h30-10h
Heating set point use (°C)	20	21.5**	21
Heating set point night (°C)	17	17	21/no heating*
Heated rooms	Living, kitchen, bathroom	Living, kitchen, bathroom, sleeping room 3	Living, kitchen, bathroom, sleeping room 1, 2
Opening windows	-	Only in sleeping room	-

* after/before renovation

** before renovation: thermostat was broken

2.1.2 Renovation measures

Table 3 gives an overview of the renovation measures in the three residential buildings.

Renovation in dwelling A includes the insulation of the sloped ($U = 0.19 \text{ W/m}^2\text{K}$) and flat roof ($U = 0.18 \text{ W/m}^2\text{K}$), replacement of the roof lights in the kitchen and bathroom ($U_w = 1.7 \text{ W/m}^2\text{K}$) and replacement of the roof window ($U_w = 1.0 \text{ W/m}^2\text{K}$) and the window in the sleeping room on the first floor ($U_w = 1.6 \text{ W/m}^2\text{K}$).

In dwelling B, both the building envelope and the heating system were refurbished. A new condensing boiler with a new thermostat and new radiators in the sleeping room, toilet and kitchen were installed. In addition, the windows in the kitchen, living room and toilet were replaced and also a new external door was foreseen ($U_g = 1.0 \text{ W/m}^2\text{K}$, $U_f = 1.6 \text{ W/m}^2\text{K}$).

The sloped ($U = 0.16 \text{ W/m}^2\text{K}$) and flat roof ($U = 0.14 \text{ W/m}^2\text{K}$) in dwelling C were insulated. In addition, a new door in the hall and new windows in the living room and sleeping room were installed ($U_g = 1.0 \text{ W/m}^2\text{K}$, $U_f = 1.1 \text{ W/m}^2\text{K}$).

The other walls and windows in all three dwellings are not insulated.

Table 3: Overview of renovation measures

	A	B	C
Sloped roof	x	-	x
Flat roof	x	-	x
Windows	x	x	x
Roof window	x	-	-
External door	-	x	x
Heating system	-	x	-

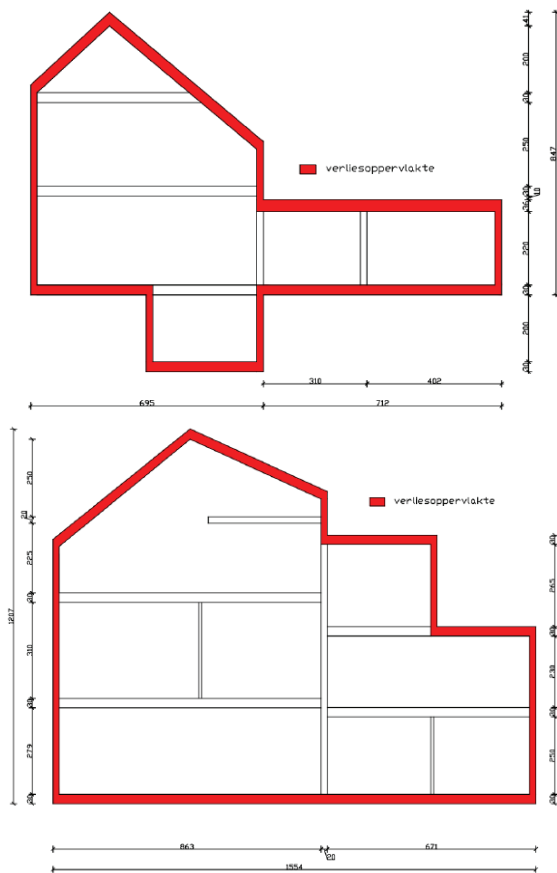


Figure 1: Section of dwelling A (above) and C (below)

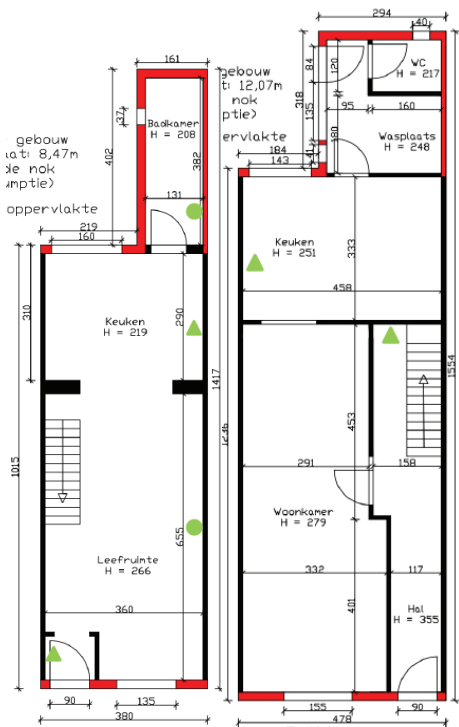


Figure 2: Grond floor plan of dwelling A (left) and C (right)

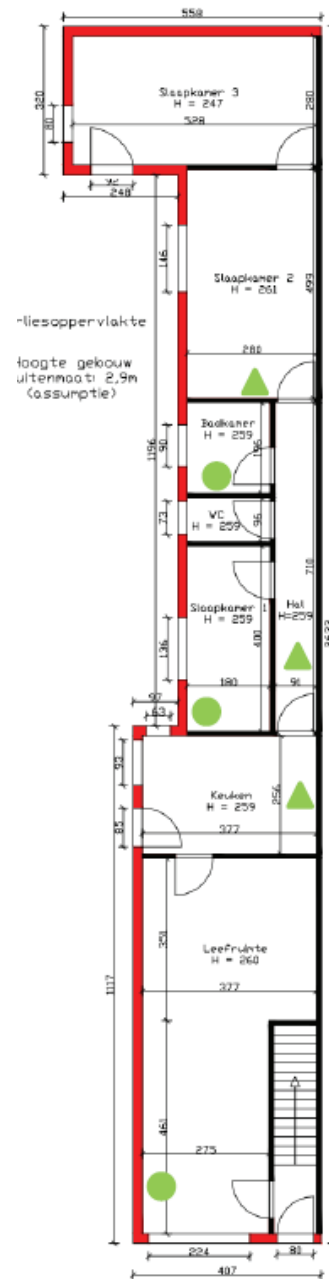


Figure 3: floor plan of dwelling B

2.2 Monitoring

The measurements were carried out during the heating season (winter) in 2017-2018 (before renovation) and 2018-2019 (after renovation). The monitoring campaign included pressurisation tests according to EN 13829 [7] to measure the air tightness of the whole building and infrared thermography to visualise the air leakage paths and thermal bridges in the building envelope. Infrared scans were executed in cloudy weather and with an indoor and outdoor temperature difference of 8 to 16°C.

The following parameters of the indoor climate were monitored every 5 to 10 minutes during 2 to 4 consecutive weeks in all the rooms in use: temperature, relative humidity and CO₂-concentration. The monitoring locations are indicated on the floor plans on Figure 2 and 3 with green dots (all parameters) and green triangles (only temperature and relative humidity). Table 4 shows the accuracy of the sensors.

Moreover, the gas consumption for heating was measured as follows. In dwelling A and B, daily values were monitored from March 18 to April 30 2019 via June Energy [8]. Annual values from 2016 to 2019 were acquired from the energy provider and subdivided per month based on the actual heating degree days.

Table 4: Accuracy of the sensors for indoor climate [9][10]

	HOBO U12	HOBO MX1102
Temperature (°C)	± 0.35	± 0.21
Relative humidity (%)	± 2.5	± 2.0
CO ₂ (ppm)	[10-90]	[20-80]
	-	± 50 ± 5% value

3. RESULTS

3.1 Building envelope and air tightness

Figure 4 shows the impact of the renovation on the measured global air tightness n_{50} of all dwellings, except for dwelling A, which had no reference value. The air tightness in dwelling B is improved due to new windows and external door with attention to airtight finishing. On the other hand, a small decrease is noticed in dwelling C. These results are in line with measurements in a comparable study in Belgium [11]. Some dwellings have an improvement of the air tightness of 5-30%, while other dwellings have a worse level of air tightness (19-40%) after renovation.

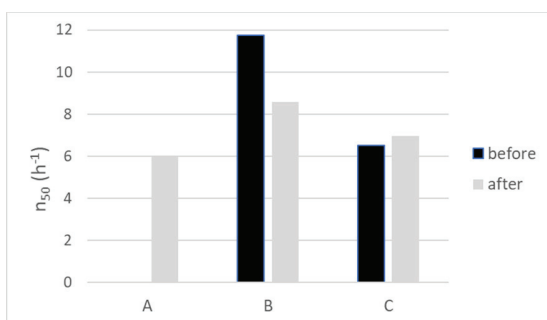


Figure 4: Measured air tightness (n_{50}) of the dwellings before and after renovation.

The results also indicate that the leakage rates after renovation remain relatively high due to significant air leaks as confirmed by infrared scans. Figure 5 shows e.g. the air leaks underneath the external door in dwelling A and B after renovation. Moreover, the infrared scans

prove that the overall insulation quality of the dwellings can be improved. Heat losses occur to a large extent along façades and non-renovated building envelope sections. However, the infrared scans did show that the renovated envelope elements were properly insulated.

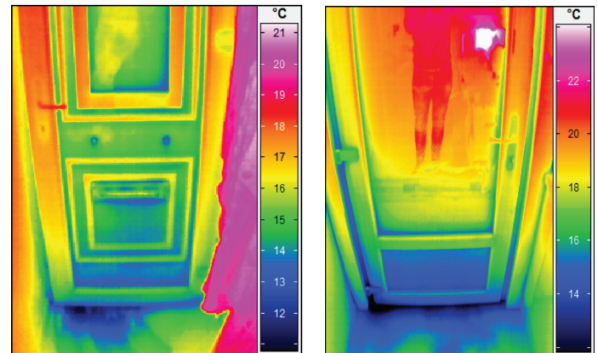


Figure 5: Infrared scan of the external door in dwelling A (left) and B (right).

3.2 Indoor climate

3.2.1 Temperature

The average indoor temperature before and after the renovation works is compared in all three dwellings in Figure 6. It is shown that the average temperature in dwelling A and C is increased as a result of insulating the roofs and the new windows. The temperature rise in dwelling C is more pronounced as a consequence of the changed heating habit from discontinuously to continuously. By contrast, the average temperature is slightly decreased in dwelling B due to better user control of the heating system to avoid high energy bills.

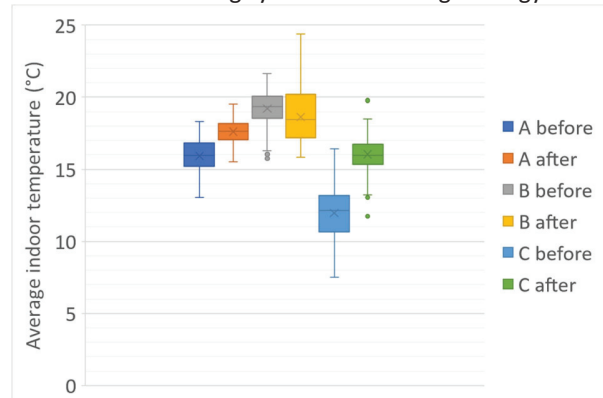


Figure 6: Comparison of measured average indoor temperature in all dwellings before and after renovation.

3.2.2 Relative humidity and CO₂-concentration

Figure 7 and 8 compare the average relative humidity respectively the CO₂-concentration before and after renovation in the living room of every dwelling.

In dwelling A and C, the average relative humidity in the living rooms is decreased due the increase in indoor temperature. In addition, the CO₂-concentration is only slightly influenced by the renovation.

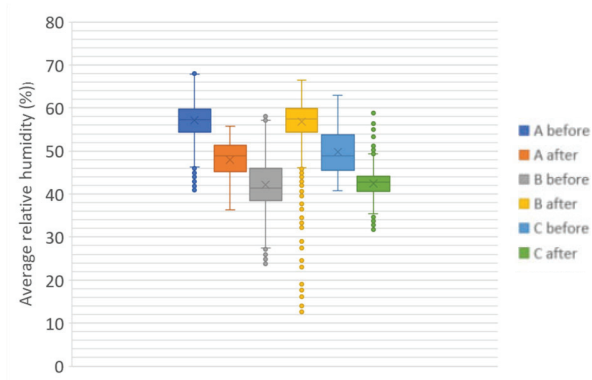


Figure 7: Comparison of measured average relative humidity in the living room in all dwellings before and after renovation.

In the meantime, renovation caused an increase of both the average relative and absolute humidity in the living room in dwelling B due to lower temperature and a higher air tightness level as shown on Figure 4. This is also noticed when comparing the average CO₂-concentration in the living room in dwelling B before and after renovation on Figure 8. The median of the CO₂-concentration is increased with 18%. All other rooms in dwelling B also have a significant rise of CO₂-concentration.

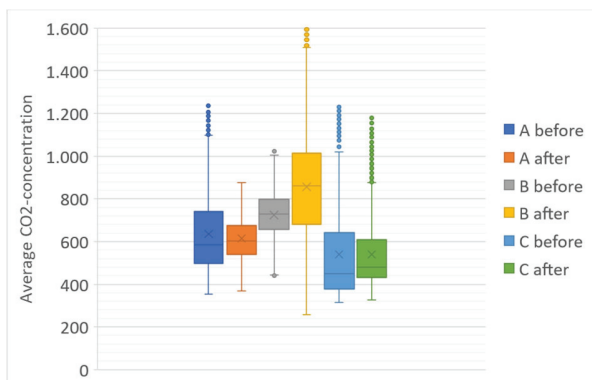


Figure 8: Comparison of measured average CO₂-concentration in the living room in all dwellings before and after renovation.

3.3 Energy use for heating

Figure 9 and 10 show the impact of the renovation on the energy use for heating in dwelling A and C, normalised for outdoor temperature respectively outdoor and indoor temperature.

The energy use in dwelling A is in both cases decreased caused by insulating the roofs. On the contrary, the energy use in dwelling C is increased. Only

when the energy use is corrected to the outdoor and the indoor temperature, a small decrease is noticed in this house. This means that the decrease caused by the insulation of the roofs is outweighed by the increase due to the changed heating regime, i.e. a rebound effect is noticed in dwelling C.

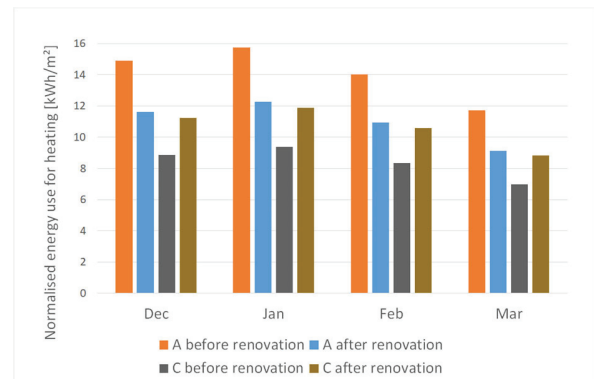


Figure 9: Measured average energy use for heating (normalised for the outdoor temperature) in dwelling A and C before and after renovation.

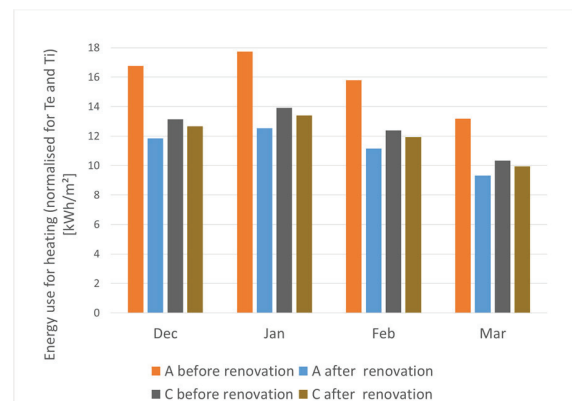


Figure 10: Measured average energy use for heating (normalised for the outdoor and indoor temperature) in dwelling A and C before and after renovation.

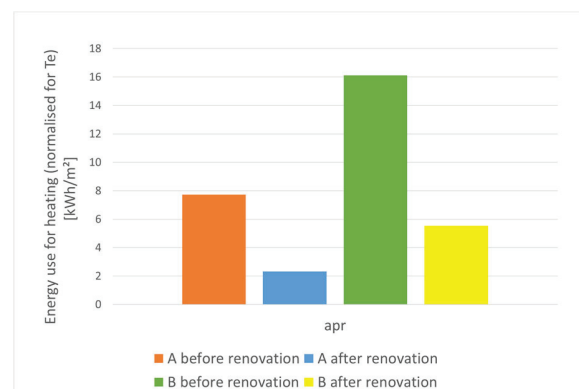


Figure 11: Measured average energy use for heating (normalised for the outdoor temperature) in dwelling A and B before and after renovation.

Figure 11 shows the impact of the renovation on the energy use for heating in dwelling A and B in April, normalised for outdoor temperature. This figures confirms the conclusions from Figure 9 in dwelling A. A significant decrease in energy use in dwelling B is also noticed as a result of the renewal of the control of the heating system in this house.

These results are in line with the findings of a comparable study in Belgium [11].

4. CONCLUSIONS

This paper analysed the impact of restricted renovation measures on the performance of the building envelope, the energy use of and the indoor climate in 3 different single family dwellings in a pilot project in Ghent (Belgium). The results of the monitoring have shown that it is difficult to draw general conclusions from comparable renovation actions in the three studied dwellings.

Regarding the building envelope, the air tightness is noticed to increase in dwelling B while it decreased in dwelling C. The overall insulation quality and air tightness of all dwellings can still be improved. Heat losses occur to a large extent along façades and non-renovated building envelope sections.

The renovation affects the indoor climate in all dwellings. Dwellings A and C have an increase of indoor temperature as a consequence of the renovation works (i.e. insulating the roofs). This is in line with recent studies about the impact of energy retrofit in residential buildings in moderate and cold climates [2], [4], [6], [12]. By contrast, the average temperature is slightly decreased in dwelling B due to better user control of the heating system. In addition, lack of ventilation combined with an increased air tightness causes an increase of absolute humidity and CO₂-concentration in dwelling B.

Although both dwelling A and C have an increase in indoor temperature, only dwelling A has a decrease of energy use for heating due to the insulation works. The impact of the user on the indoor climate and energy use is also shown. A rebound effect is noticed in dwelling C and the temperature decrease in dwelling B is caused by the change in heating regime after renovation. This conclusion is also supported by recent studies [13], [14] and is interesting for further research.

ACKNOWLEDGEMENTS

The authors would like to acknowledge the building residents for their support.

REFERENCES

- [1] L. Bielen and A. Versele, "Sustainable communities through an innovative renovation process: Subsidy

- retention to improve living conditions of captive residents," in *PLEA 2020: Planning Post Carbon Cities*, 2020.
- [2] Á. Broderick, M. Byrne, S. Armstrong, J. Sheahan, and A. M. Coggins, "A pre and post evaluation of indoor air quality, ventilation, and thermal comfort in retrofitted co-operative social housing," *Build. Environ.*, vol. 122, pp. 126–133, 2017.
- [3] V. Földváry, G. Bekő, S. Langer, K. Arrhenius, and D. Petráš, "Effect of energy renovation on indoor air quality in multifamily residential buildings in Slovakia," *Build. Environ.*, vol. 122, pp. 363–372, 2017.
- [4] L. La Fleur, B. Moshfegh, and P. Rohdin, "Measured and predicted energy use and indoor climate before and after a major renovation of an apartment building in Sweden," *Energy Build.*, vol. 146, pp. 98–110, 2017.
- [5] L. Liu, P. Rohdin, and B. Moshfegh, "Evaluating indoor environment of a retrofitted multi-family building with improved energy performance in Sweden," *Energy Build.*, vol. 102, pp. 32–44, 2015.
- [6] K. E. Thomsen *et al.*, "Energy consumption and indoor climate in a residential building before and after comprehensive energy retrofitting," *Energy Build.*, vol. 123, pp. 8–16, 2016.
- [7] EN 13829:2000, "Thermal Performance of Buildings - Determination of Air Permeability of Buildings - Fan Pressurization Method," 2000.
- [8] "June Energy." [Online]. Available: <https://www.june.energy/nl/>. [Accessed: 08-Jul-2019].
- [9] "HOBO MX1102." [Online]. Available: <https://www.mendelej.com/reference-management/web-importer> [Accessed: 06-Mar-2020].
- [10] "HOBO U12." [Online]. Available: <https://www.onsetcomp.com/products/data-loggers/u12-012>. [Accessed: 06-Mar-2020].
- [11] E. Lambie and D. Saelens, "Renoseec: Results monitoring (in Dutch)," 2018. [Online]. Available: <http://www.renoseec.com/>
- [12] A. Hambrug and T. Kalamees, "The Influence of Energy Renovation on the Change of Indoor Temperature and Energy Use," *Energies*, vol. 11, no. 11, p. 3179, 2018.
- [13] T. Hong, S. C. Taylor-Lange, S. D'Oca, D. Yan, and S. P. Corgnati, "Advances in research and applications of energy-related occupant behavior in buildings," *Energy Build.*, vol. 116, pp. 694–702, 2016.
- [14] Y. G. Yohanis, "Domestic energy use and householders' energy behaviour," *Energy Policy*, vol. 41, pp. 654–665, 2012.

Adjustable Light Shelf Angles for Different Sky Conditions: Daylighting Reading Space at University Libraries in Dhaka

ZANNATUL FERDOUS¹, DR. MD ASHIKUR RAHMAN JOARDER²

¹Department of Architecture, Ahsanullah University of Science and Technology (AUST), Dhaka, Bangladesh

²Department of Architecture, Bangladesh University of Engineering and Technology (BUET), Dhaka, Bangladesh

ABSTRACT: The challenge of daylighting is to assess light generated from sun and sky at a certain point, where sky luminance varies according to a series of meteorological, seasonal, and geometrical parameters that are difficult to codify. As daylight through windows, varies significantly by times and seasons, a common phenomenon in reading space of libraries are students more tend to draw the curtain when the weather is sunnier than usual, and turn on artificial lighting, resulting use of additional energy. Studies show in a tropical location the introduction of light shelf at any height produces an overall reduction of illumination on work plane and common light shelves cannot actively deal with external environmental factors. This paper studies on how to improve the daylight condition using angular light shelves in the reading space of a university library in context of Dhaka. Dynamic daylight simulation technique using DAYSIM, is applied in this research. Different angles of light shelves are found suitable for four dates which represents different seasons of the year, as 25° for 20 March, 20° for 21 June, 30° for 22 September and 35° for 21 December for a reading space in a university library in the context of Dhaka.

KEYWORDS: Daylighting, CBDM simulation, Library lighting, Adjustable Light Shelf, Angular Light Shelf

1. INTRODUCTION

Daylight is a feature of a space that can increase length and quality of stay [1]. As an important place for students to read and study, the quality of lighting in the reading space of university library has a great influence on the visual and learning efficiency of students [2]. A common phenomenon in the reading space of libraries is students more tend to draw the curtain when the weather is sunnier than usual, and turn on artificial lights, resulting in additional use of energy. The challenge of daylight design involves with the assessment of lighting generated from natural sources (sun and sky) at a certain reference point, where sky luminance varies according to a series of meteorological, seasonal, and geometrical parameters that are difficult to codify. The illuminance penetrations through the windows, vary significantly by times and seasons. Since the solar altitude is higher in summer, the penetration in summer is more tilted toward window adjacent areas than in spring and fall. Extreme illumination is produced that reached often the centre of the functional space in winter, probably because direct solar radiation comes from below the shades.

Light shelves have been discussed in numerous studies as suitable solutions for controlling daylight in side-lit spaces by offering shading and at the same time can redirect a significant part of the incoming light flux towards the ceiling to improve uniformity of daylight [3]. The light in a library need to be adequate for the users to see a particular task, usually reading a book or the text on a computer screen. Studies show,

in a tropical location, such as Bangladesh, the introduction of light shelf at any height produces an overall reduction of illumination on the work plane throughout the interior space; however, light shelf can be an effective element to enhance the quality of daylight in tropical buildings, if designed and located properly [4] and the common light shelves cannot actively deal with external environmental factors [5]. A slight tilt of a light shelf can increase the light flux entering the room especially during summer months. With increase of the latitude, angle of tilt decreases. The objective of this research is to identify the effectiveness of adjustable tilted angles of light shelf at south window façade of a university library reading space to ensure effective daylighting during different times and seasons considering the climate of Dhaka.

2. LIGHT SHELVES AND TILTINGS

Although a light shelf is supposed to produce an improvement of illumination conditions and energy savings, this is not always the case. Light shelves have maximum efficiency when the sun shines directly over the shelf. Study on light shelf performance on solar geometry and surface reflectance demonstrates the dependence of light shelf on solar angle, time of year and day, and model reflectance, yet illuminance level in the back of the room is not often improved [6].

To prevent unwanted solar heating, a window need to be shaded from the direct solar component and in some cases also from reflected components. It

is generally agreed that the principle of thermal solar control is to let the sun's energy into the building during the winter and to intercept it in the summer. The type, size and location of a shading device will therefore depend on solar angular relationships with the window in terms of solar altitude and azimuth. Shading the window perimeter by tilting the shelf downward will reduce the amount of light reflected to the ceiling. Upward tilting will improve penetration of reflected daylight and reduce shading effects (Fig. 1). Therefore, upward tilting angles are varied in this research to identify suitable angles for different times of days and seasons.

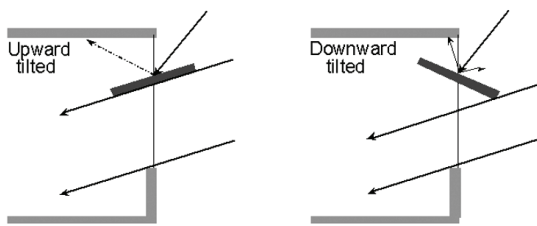


Figure 1: Upward and downward tilted light shelf influences shading and daylight reflection

3. METHODOLOGY

The seasonal positions of the sun are universally known in general terms. It is directly over the equator about 21 March, the vernal equinox; and thereafter it appears farther north each day until it reaches its zenith above the tropic of cancer about 21 June (the summer solstice in northern latitudes). Then the sun appears a little more southerly each day, rising above the equator about 21 September (the autumnal equinox) and reaching its most southerly point over the tropic of capricorn about 21 December (winter solstice).

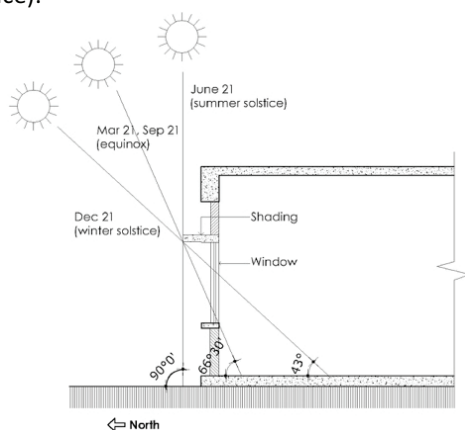


Figure 2: Solar solstice and equinox position for Dhaka.

Dynamic daylight simulation (DDS) technique using DAYSIM, is applied in this research. For finding the precise angles of light shelf on different seasons four dates have been selected to analyze according to different sky conditions and sunshine time. The dates are fixed on the 20 March, 21 June, 22 September

and 21 December; which are the equinox and solstice dates of Dhaka (Fig. 2) as mentioned. As the sun position also changes on different parts of a day, three times of a day are selected for analysis. The times are 8:30 at morning, 12:30 at noon and 4:30 at afternoon as the operation hour of the libraries are usually from 8:00 am to 5:00 pm.

As a case space, the designed central library of Bangladesh University of Engineering and Technology (BUET) is selected considering its size, width, orientation, and potential of daylight inclusion. The library building is north-south oriented (elongated to east-west) which is ideal for tropical climate of Dhaka considering the sun and wind (Fig. 3). The second floor of the building is taken as a case space with 72 reading tables with the capacity of 288 readers (Fig. 4).



Figure 3: South view of the BUET Central Library

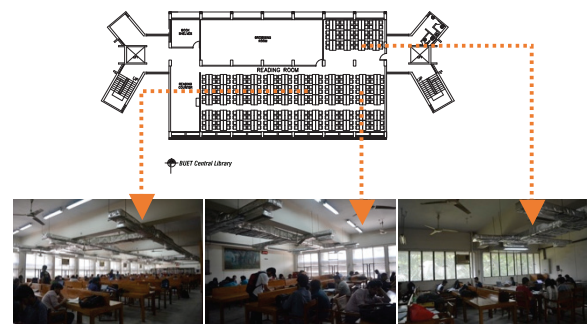


Figure 4: Interior views of the BUET Central Library

Daylight simulation allows to study the effect of one variable by keeping the others constant. To observe the variation of daylight penetration into the library the angles of light shelf is changed and the surrounding is considered as vacant [4]. The simulations are done considering the windows in north and south façades with constant sill level, lintel level, work plane height, materials and other surroundings as found during the field survey. There are horizontal louvers in the south façade which are eliminated during the simulation. The internal partitions are also not taken into consideration during simulation. Standard width of 1 m light shelves are installed at 2.4 m height in the south façade. A 3D model is built for the simulation as shown in Fig 5.

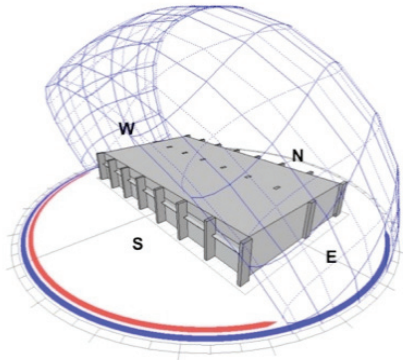


Figure 5: 3-dimensional exterior view of the case reading space with sun path diagram of Dhaka used for simulation.

A common approach for simulation is to define a grid of illuminance sensors that extends throughout a lighting zone [7]. 49 test sensor points are derived from seven lines in equal intervals on both horizontal and vertical axes in the reading area of the case library. These 49 sensor points are set into the height of 0.75m (Fig.7) from the finished floor level representing the work plane height for the reading spaces of Dhaka [8]. Intersection points in the plan are coded according to letter and number system as shown in Figure 6.

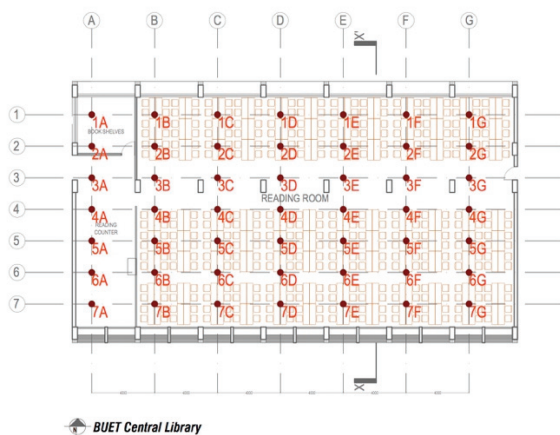


Figure 6: Location of the test sensor points in the case space



Figure 7: Schematic cross section of the case reading space towards XX' axis showing sensor points used for simulation.

4. SIMULATION

It is expected that among the illumination at 49 intersection points, the most crucial points are on the axis 7 and 1 (Fig. 6). Points on axis 7 is at the south façade of the case library with angular light shelf and points on axis 1 is at the north façade without light shelf. That is why there is high possibility of glare problem at the points on axis 7.

In this study, the initial 3D models for simulation are constructed in three phases with different angles (upward tilted) with the horizontal axis of light shelf. In the first phase, from 0° angled light shelf to 60° angled light shelf, models of five angles are constructed with a gap of 15° (i.e. 0°, 15°, 30°, 45° and 60°). In the second phase, the adjacent angles of the best found angle in the first phase (30°) with a gap of 5° are constructed in order to find out the more precise angles (i.e. 15°, 20°, 25°, 30°, 35°, 40° and 45°). In the third phase, the adjacent 15° angles of the best found angle in the second phase (30°) with a gap of 1° are constructed to specify the best light shelf angles with highest precisions for the year round (i.e. 15°, 16°, 17°, ... 45°). The detail results for the second phase, with an interval of 5° are presented in this paper, as in all cases these angles (i.e. 15°, 20°, 25°, 30°, 35°, 40° and 45°) (Fig. 8) perform better among all studied simulations and governed in decision support process.

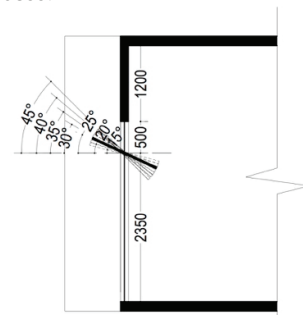


Figure 8: Studied angles (i.e. 15°, 20°, 25°, 30°, 35°, 40° and 45°) for the second phase, with an interval of 5°.

The design illumination on work plane height for the reading spaces of Dhaka was considered as 300 lux for 9 hours (8.00 to 17.00) [8]. Some variables are compared, such as average illumination, number of points below 300 lux (under light); number of points between 300-900 lux (effective light); and number of points above 900 lux (glare), for determining the best angles of the light shelves [4].

Performance metrics can be used for comparative studies to guide building design or to benchmark a building element against a pool of same elements with different configurations. Rating between different configurations is easier to interpret using specific variables. In the rating of the seven different studied angles of light shelf the highest value is considered as a rating of '6' points. When the values of the configuration types are decreased the rating point is also decreased respectively. The lowest value in any performance metric is counted as '0' rating points. When all the studied configurations have got the ratings for each of the performance parametric, the total rating is summed for each configuration individually. By comparing these individual performances of total ratings, a ranking is done to know which one secured the best position.

4.1 Rating points with ranks for different angles of light shelf on 20 March

On the 20 March, the illumination is high due to the position of the sun. To identify the best angles for three different times of the day rating points (RPs) with ranks for different angles of light shelf on the 20 March are considered and shown on Table 1.

Table 1: Rating points with ranks for different angles of light shelf on 20 March in different times

Time	Light Shelf Angles	Value and Rating point (RP)	Average Illumination	No of Point <300 lux	No of points between 300-900 lux	No of Glare Point >900 lux	Total Rating Points	Ranks
At 8.30 am	15°	Value	826	20	15	14	7	7th
		RP	0	4	2	1		
	20°	Value	849	19	17	13	20	2nd
		RP	4	5	5	6		
	25°	Value	856	18	18	13	23	1st
		RP	5	6	6	6		
	30°	Value	870	20	15	14	13	5th
		RP	6	4	2	1		
	35°	Value	832	20	16	13	15	4th
		RP	1	4	4	6		
	40°	Value	840	20	16	13	16	3rd
		RP	2	4	4	6		
	45°	Value	843	21	15	13	11	6th
		RP	3	0	2	6		
At 12.30 pm	15°	Value	2261	7	22	20	13	4th
		RP	3	6	4	0		
	20°	Value	2298	8	22	19	14	2nd
		RP	4	5	4	1		
	25°	Value	2307	9	24	16	20	1st
		RP	5	4	6	5		
	30°	Value	1470	10	21	18	7	7th
		RP	0	3	2	2		
	35°	Value	2696	12	21	16	14	2nd
		RP	6	1	2	5		
	40°	Value	1886	11	21	17	9	6th
		RP	2	2	2	3		
	45°	Value	1861	12	23	14	13	4th
		RP	1	1	5	6		
At 4.30 pm	15°	Value	414	30	12	7	16	4th
		RP	0	5	5	6		
	20°	Value	435	28	14	7	22	1st
		RP	4	6	6	6		
	25°	Value	437	31	11	7	19	3rd
		RP	5	4	4	6		
	30°	Value	438	31	11	7	20	2nd
		RP	6	4	4	6		
	35°	Value	422	34	8	7	13	5th
		RP	3	2	2	6		
	40°	Value	420	34	8	7	12	6th
		RP	2	2	2	6		
	45°	Value	419	35	7	7	9	7th
		RP	1	1	1	6		

4.2 Rating points with ranks for different angles of light shelf on 21 June

On the 21 June, the illumination is the highest due to the perpendicular position of the sun. To identify the best angles for three different times of the day RPs with ranks for different angles of light shelf on the 21 June are considered and shown on Table 2.

Table 2: Rating points with ranks for different angles of light shelf on 21 June in different times

Time	Light Shelf Angles	Value and Rating point (RP)	Average Illumination	No of Point <300 lux	No of points between 300-900 lux	No of Glare Point >900 lux	Total Rating Points	Ranks
At 8.30 am	15°	Value	828	18	17	14	10	6th
		RP	0	3	4	3		
	20°	Value	852	17	19	13	20	1st
		RP	4	5	6	5		
	25°	Value	858	17	16	16	12	5th
		RP	5	5	1	1		
	30°	Value	869	16	17	16	17	2nd
		RP	6	6	4	1		
	35°	Value	838	20	14	15	3	7th
		RP	1	0	0	2		
	40°	Value	848	19	17	13	14	4th
		RP	3	2	4	5		
	45°	Value	847	19	18	12	15	3rd
		RP	2	2	5	6		
At 12.30 pm	15°	Value	547	27	14	8	11	6th
		RP	0	6	5	0		
	20°	Value	564	27	15	7	20	1st
		RP	2	6	6	6		
	25°	Value	569	29	13	7	19	2nd
		RP	5	4	4	6		
	30°	Value	575	30	12	7	18	3rd
		RP	6	3	3	6		
	35°	Value	558	30	12	7	13	4th
		RP	1	3	3	6		
	40°	Value	569	31	11	7	13	4th
		RP	5	1	1	6		
	45°	Value	565	32	10	7	9	7th
		RP	3	0	0	6		
At 4.30 pm	15°	Value	477	27	14	8	12	5th
		RP	0	6	6	0		
	20°	Value	492	29	13	7	20	1st
		RP	4	5	5	6		
	25°	Value	501	31	11	7	18	3rd
		RP	6	3	3	6		
	30°	Value	499	30	12	7	19	2nd
		RP	5	4	4	6		
	35°	Value	485	33	9	7	9	7th
		RP	1	1	1	6		
	40°	Value	490	31	11	7	15	4th
		RP	3	3	3	6		
	45°	Value	487	33	9	7	10	6th
		RP	2	1	1	6		

4.3 Rating points with ranks for different angles of light shelf on 22 September

On the 22 September, the illumination is high due to the position of the sun. To identify the best angles for three different times of the day RPs with ranks for different angles of light shelf on the 22 September are considered and shown on Table 3.

Table 3: Rating points with ranks for different angles of light shelf on 22 September in different times

Time	Light Shelf Angles	Value and Rating point (RP)	Average Illumination	No of Point <300 lux	No of points between 300-900 lux	No of Glare Point >900 lux	Total Rating Points	Ranks
At 8.30 am	15°	Value	926	17	17	15	13	5th
		RP	0	6	4	3		
	20°	Value	953	18	17	14	17	2nd
		RP	4	4	4	5		
	25°	Value	960	17	18	14	22	1st
		RP	5	6	6	5		
	30°	Value	970	18	16	15	15	3rd
		RP	6	4	2	3		
	35°	Value	937	19	15	15	5	7th
		RP	1	1	0	3		
	40°	Value	951	18	16	15	12	6th
		RP	3	4	2	3		
	45°	Value	947	19	18	12	15	3rd
		RP	2	1	6	6		
At 12.30 pm	15°	Value	584	27	15	7	12	4th
		RP	0	3	3	6		
	20°	Value	603	26	16	7	22	3rd
		RP	4	6	6	6		
	25°	Value	607	26	16	7	23	2nd
		RP	5	6	6	6		
	30°	Value	608	26	16	7	24	1st
		RP	6	6	6	6		
	35°	Value	595	29	13	7	12	4th
		RP	2	2	2	6		
	40°	Value	599	30	12	7	9	7th
		RP	3	0	0	6		
	45°	Value	594	29	13	7	11	6th
		RP	1	2	2	6		
At 4.30 pm	15°	Value	224	41	7	1	17	3rd
		RP	0	5	6	6		
	20°	Value	232	42	0	7	8	6th
		RP	4	1	1	2		
	25°	Value	233	41	3	5	18	2nd
		RP	5	5	4	4		
	30°	Value	235	39	6	4	22	1st
		RP	6	6	5	5		
	35°	Value	228	41	3	5	14	4th
		RP	1	5	4	4		
	40°	Value	230	42	0	7	7	7th
		RP	3	1	1	2		
	45°	Value	229	41	1	7	11	5th
		RP	2	5	2	2		

4.4 Rating points with ranks for different angles of light shelf on 21 December

On the 21 December, the illumination is the lowest due to the position of the sun. To identify the best angles for three different times of the day RPs with ranks for different angles of light shelf on the 21 December are considered and shown on Table 4.

Table 4: Rating points with ranks for different angles of light shelf on 21 December in different times

Time	Light Shelf Angles	Value and Rating point (RP)	Average Illumination	No of Point <300 lux	No of points between 300-900 lux	No of Glare Point >900 lux	Total Rating Points	Ranks
At 8.30 am	15°	Value	433	29	13	7	18	2nd
		RP	0	6	6	6		
	20°	Value	440	30	12	7	17	3rd
		RP	1	5	5	6		
	25°	Value	513	34	8	7	17	3rd
		RP	6	2	3	6		
	30°	Value	499	31	11	7	19	1st
		RP	5	4	4	6		
	35°	Value	456	34	8	7	13	5th
		RP	2	2	3	6		
	40°	Value	460	33	8	8	9	7th
		RP	3	3	3	0		
	45°	Value	483	35	7	7	10	6th
		RP	4	0	0	6		
At 12.30 pm	15°	Value	1638	7	22	20	14	3rd
		RP	1	6	6	1		
	20°	Value	1824	9	18	22	11	6th
		RP	6	5	0	0		
	25°	Value	1687	11	19	19	14	3rd
		RP	4	4	3	3		
	30°	Value	1707	11	19	19	15	2nd
		RP	5	4	3	3		
	35°	Value	1641	11	21	17	17	1st
		RP	2	4	5	6		
	40°	Value	1642	12	20	17	14	3rd
		RP	3	1	4	6		
	45°	Value	1624	13	19	17	9	7th
		RP	0	0	3	6		
At 4.30 pm	15°	Value	188	40	9	0	10	7th
		RP	0	2	2	6		
	20°	Value	198	39	10	0	19	4th
		RP	5	4	4	6		
	25°	Value	199	39	10	0	20	2nd
		RP	6	4	4	6		
	30°	Value	197	36	13	0	20	2nd
		RP	4	5	5	6		
	35°	Value	192	35	14	0	21	1st
		RP	3	6	6	6		
	40°	Value	190	40	9	0	12	5th
		RP	2	2	2	6		
	45°	Value	189	40	9	0	11	6th
		RP	1	2	2	6		

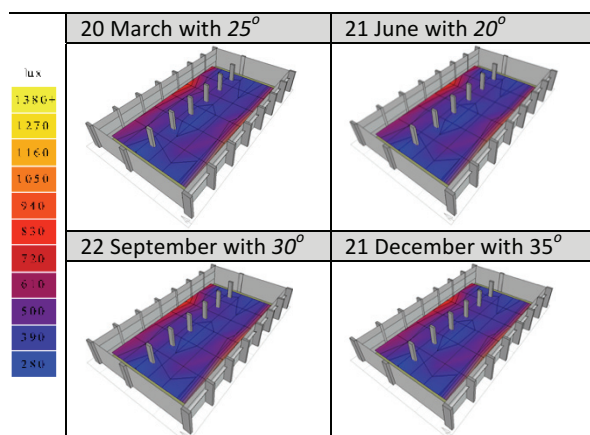
4. RESULTS

The simulation is done in order to find out the best angles for particular dates which might represent the seasons. From the comparison of the findings it is found that, 25° angular light shelf performs effectively on the 20 March whereas, on the 21 June 20° angular light shelf performs best. 30° angular light shelf performs well on the 22 September and 35° angular light shelf performs the best on 21 December comparing the results of different times of the day (Table 5). Though on the 20 March and on the 22 September the position of the sun is same (Fig. 2), but due to different sunshine hours and different cloud covers, the angles of the light shelves are different (Table 6).

Table 5: Summary result of the daylight simulation of equinox and solstice dates

Date	Time	Shelf Angles	Recommended Light Shelf Angle for the Date
20 March	8.30 am	25°	25°
	12.30 pm	25°	
	4.30 pm	20°	
21 June	8.30 am	20°	20°
	12.30 pm	20°	
	4.30 pm	20°	
22 September	8.30 am	25°	30°
	12.30 pm	30°	
	4.30 pm	30°	
21 December	8.30 am	30°	35°
	12.30 pm	35°	
	4.30 pm	35°	

Table 6: Daylight distribution of the reading space at work plane height on different dates with best angled light shelf.



Physical measurement of the actual daylight level in the existing case reading space of the library were compared with the illumination values generated by RADIANCE simulation tool at 12.30 pm on 8th October, 2018 according to climate data collected from Bangladesh Meteorological Department. The average illumination value of 49 sensor points found

in survey was 203 lux. On the other hand, average illumination value of 49 sensor points found in RADIANCE simulation tool was 193 lux. Therefore, there is an average deviation of 10 lux between actual condition and simulation results, which was approximately 4.93% (<5%) deviation of actual condition.

5. CONCLUSION

The natural lighting design of reading spaces in libraries not only affects the physical and mental health of readers, but also concerns the energy consumption of the buildings. The capital city Dhaka is one of the mega cities of the world. Most of the public and private university libraries in Dhaka lack the standard illumination and glare free uniform lighting in the reading spaces. Adjustable light shelves angles would be effective as the illumination varies with the changes of position of the sun and cloud cover in order to improve the uniform distribution of light at the reading spaces of a university library at different seasons of the year and times of the day.

ACKNOWLEDGEMENTS

This work has been carried out in the Department of Architecture, BUET. The authors gratefully acknowledge the support and facilities provided by BUET.

REFERENCES

- Wastawy, S.F., (2006). Libraries: The learning space within. Library of Alexandria. World Library & Information Congress, Egypt.
- Yang, Z., (2017). Research on natural lighting in reading spaces of university libraries in Jinan under the perspective of energy-efficiency. IOP Conference Series: Earth and Environmental Science, Volume 94, conference 1: 1-6.
- Kontadakis, A., Tsangrassoulis, A., Doulos, L., and Zerefos, S., (2017). A Review of Light Shelf Designs for Daylit Environments. Sustainability. 10: 1-24.
- Joarder, M.A.R., Ahmed, Z.N., Price, A.D.F., and Mourshed M.M., (2009). A Simulation Assessment of the Height of Light Shelves to Enhance Daylighting Quality in Tropical Office Buildings Under Overcast Sky Conditions in Dhaka, Bangladesh. 11 IBPSA Conference, 27-30 July, Glasgow, Scotland: 920-927.
- Heangwoo, L., Seonghyun, P., and Janghoo, S., (2018). Development and Performance Evaluation of Light Shelves using Width-Adjustable Reflectors. Advances in Civil Engineering, vol. 2018: 1-9.
- Claros, S.T., and Soler, A., (2002). Indoor Daylight Climate-Influence of Light Shelf and Model Reflectance on Light Shelf Performance in Madrid for Hours with Unit Sunshine Fraction. Building and Environment; 37:587-598.
- Reinhart, C.F., Mardaljevic, J. and Rogers, Z. (2006). Dynamic Daylight Performance Metrics for Sustainable Building Design. Leukos. 3(1). pp. 7-31.
- Bangladesh National Building Code (2006). House Building Research Institute. Ministry of Housing and Public Works. Government of People's Republic of Bangladesh.

The Modern Vernacular: Adapting Vernacular Architecture for a Modern Production Facility in the context of Rishikesh, India

ISHA ANAND, AARUSHI JUNEJA, SONALI RASTOGI

Morphogenesis, New Delhi, India

ABSTRACT: The paper describes the design process of a cosmetic and skin care production unit in the foothills of the Himalayas, that aims to be free-running and off grid. Through the combination of passive design and vernacular strategies, the building targets to achieve an energy efficient building envelope with an EPI (Energy Performance Index) of 38kWh/m2/year. The passive strategies integrated into the façade design give a strong architectural expression to the building that draws inspiration from its local context. Resource optimization has also enabled to economize investment in renewable sources of energy that helps in closing the loop, by offsetting the energy and water requirement of the facility.

KEYWORDS: Resource optimization, Passive Strategies, Vernacular architecture, Energy Positive

1. INTRODUCTION

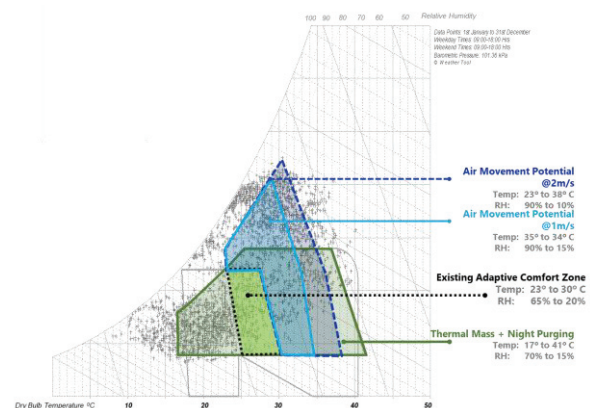
An Indian cosmetic, skincare brand that specializes in Ayurvedic preparations for its products commissioned the architectural practice to design their 1000sq.m production unit in Rishikesh, India. This was to imbibe the brand's philosophy of infusing ancient wisdom with modern aesthetics [1]. The remote location of the project and the limited availability of resources determined the budgetary and building constraints for the design.

The Architectural Practice set out to achieve a resource optimized and energy-efficient building through an integrated design approach. This approach is governed by the firm's copyright matrix of SOUL (i.e., S- Sustainability, O- optimization, U- unique, and L-Liveable) and illustrated through the design of this free-running and off-grid production unit.

2. CONTEXT

Nestled in the foothills of the Himalayas, along the banks of the river Ganga, Rishikesh is replete with natural beauty and resources. The site is located within a 600-acre village, about 50 kms away from the main town. The availability of basic infrastructure, vernacular houses constructed by using conventional building materials like mud, stone, and timber and agriculture being the main livelihood of the region, enforced the ideology of developing a self-sustaining building.

2.1 Climate



Analysing the local climate helps to understand
Figure 1: Potential of Passive Strategies

and identify the possible range of passive strategies applicable to the site. Rishikesh (30.08° N, 78.26° E) with an altitude of 372 m experiences hot summers (25-35°C), humid monsoons (25-30°C, RH 75-80%) and cool winters (15- 20 °C). Figure 1, illustrates the use of high thermal mass and night purging with a diurnal variation of 8-9 °C to tackle the hot summer period, whereas the humid period indicates the potential to employ physiological cooling by utilizing the prevalent Northeast and Southeast winds.

2.2 Learning's from Vernacular

The factors which guide the local architecture of the region are: a) easy access to building quality stone b) limited availability of good quality topsoil, c) varying availability of timber and water, d) moderate precipitation with no snow in winters [2].

The buildings are placed along the contours with an east-west orientation to benefit from the direct sunlight. The walls are typically made of stone, while the timber is used for structural purposes and slate for the sloping roof. In a typical traditional house i.e., the 'Kholi,' a central entry divides the house into two parts. Over time, both the parts evolved into two separate units on either side of the stairs. The ground floor is called 'Goth' and is meant for cattle, fodder, and storage. This helps to give warmth to the upper floors where the people reside in winters. [2].

3. DESIGN STRATEGY

The design brief clearly illustrated the sequential flow of the Ayurvedic preparation for the skincare products' manufacturing and packaging (i.e., Herbal soaps and Body scrubs). These products are made from local herbs and are manually processed and packaged.

Therefore, the building's functional division and space planning were not only to be sensitive to the production process but also to be user-centric (i.e., a secure, comfortable, and interactive environment) for the employees. The operative indoor environment was to be designed on the lines of human comfort standards and did not demand any conventional mechanical systems. Figure 2 highlights that thermal comfort can be achieved for almost 80% of the year by passive strategies.

The building design explores a healthy working environment through user-driven adaptive opportunities; the provision of manually operable window systems and basic active systems (i.e., ceiling fans) helps regulate the indoors during the warm and humid period. While thermal mass has an impact during the cold period.

3.1 Built Form Optimization

A rectangular volume of 30 X18m originated from the re-utilization of the existing footprint of the old building. The reformed building is oriented along the

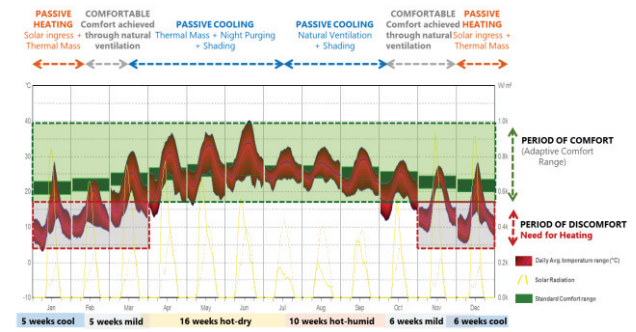


Figure 2: Human thermal comfort conditions for 80% of the year by passive strategies.

east-west axis with a central entry punctured by a light well. The arrangement of programs along the central court with a skylight above brings in daylight, eliminates the use of corridors, and provides the flexibility of spaces.

The spatial division was done based on the process-driven activities and was defined as follows: i) Manufacturing hall (Soap preparation and oil extraction process), ii) Herb Stores, iii) Herb Grinding, iii) Packaging hall. These spaces were arranged symbiotic to the traditional “Kholi” design highlighted in the previous section. The manufacturing hall and stores are planned on the ground floor (i.e., spaces with high internal heat gains), whereas the Packing hall and herb grinding spaces (i.e., spaces with higher occupancy) on the floor above—the well-lit central lobby functions as an interactive communal zone for the staff.

Further, the N-S orientated butterfly roof developed reminiscing the reverse form of the traditional roof provides not only a modern aesthetic but also allows larger operable windows which help in taking advantage of prevailing winds; Northeast and Southeast. In addition, allowing an 80%-day lit floor plate with unobstructed views of the valley. Also, the high volume of space created with facing the incline

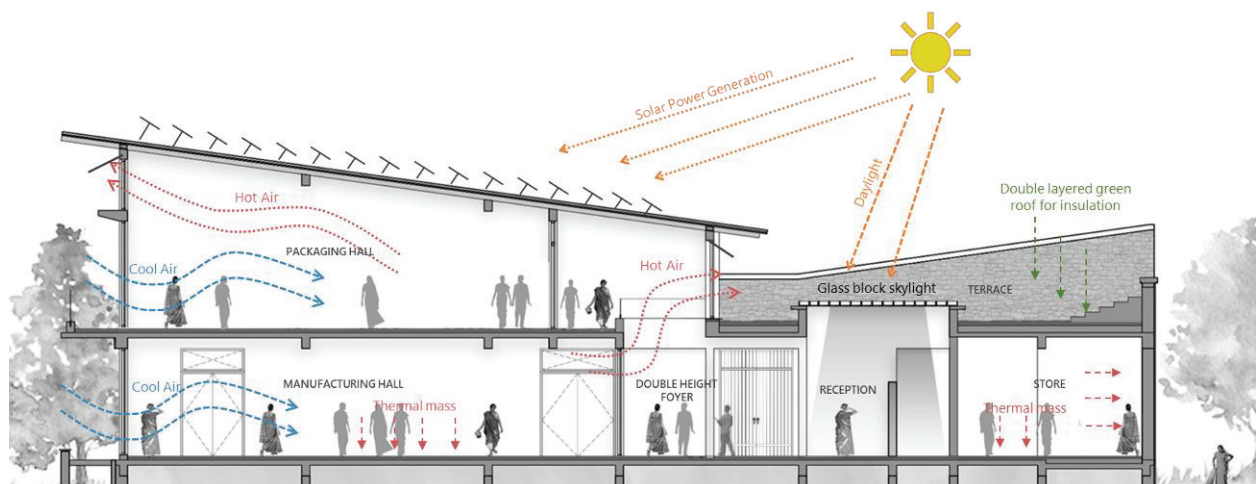


Figure 3: Section highlighting the application of passive design strategies

of the roof further explores power generation by the installation of PV panels (figure 3).

3.2 Building Envelope Optimization

Designing a building in hill settlements can be challenging due to the terrain, climatic conditions, vegetation, and limited access to resources. These factors force resource optimisation to become a vital component of the brief, thus leading to the adaptation of vernacular strategies and materials.

Building materials, glazing area (WWR-window to wall ratio), and façade shading determine the envelope's performance. Analysis of these three factors helps determine the sensitivity of each parameter to optimize the façade design for indoor thermal and visual comfort.

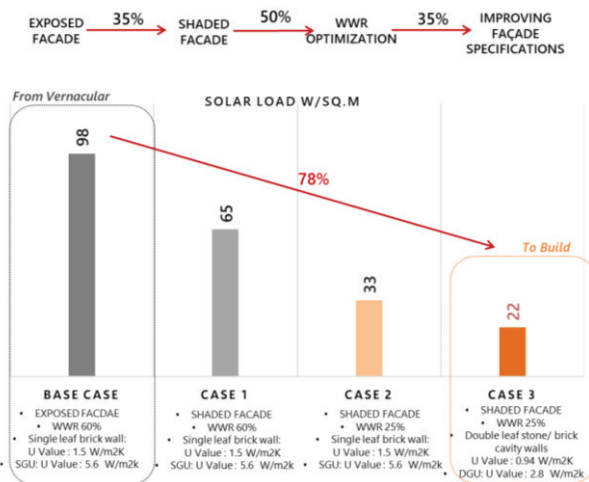


Figure 4: Facade Optimisation -Solar heat gain Analysis

Figure 4 illustrates the cumulative heat gain calculation for the building envelope on a peak summer day to assess its thermal efficiency. The base case is considered with envelope specifications, same as the vernacular (single leaf stone or mud wall with single pane glazing), WWR 60% with full exposure to the sun. Case 1 highlights the impact of façade shading, resulting in a reduction of solar heat gain by 35%. Further optimisation of WWR from 60% to 25% (case 2) allows another reduction of 50%. As discussed in section 2.1, the impact of thermal mass helps maintain constant indoor temperatures during both the winter and summer peaks; therefore, case 3 has been simulated by improving façade specifications. The high thermal mass façade was achieved using a double leaf stone/ brick cavity wall

instead of a single leaf brick wall and a basic double-glazed unit instead of single glazing. An overall improvement of 78% observed from the base case help set the façade design parameters.

4 BUILDING PERFORMANCE

4.1. Indoor thermal Comfort

The study of passive strategies highlighted that indoor comfort for users can be improved through enhancing air movement during the warm and humid period. A naturally ventilated building proves to perform better than an airtight building. Therefore, the window systems are designed with manually operable panels that encourage cross ventilation through the building. During the warm and humid period physiological cooling plays a significant role in increasing occupant comfort. Studying the impact of air movement through the CBE Thermal Comfort Tool resulted in cross ventilation coupled with ceiling fans to increase air movement up to 1m/s. This helps in enhancing the effect of physiological cooling and increases human adaptive comfort range by 2°C [3].

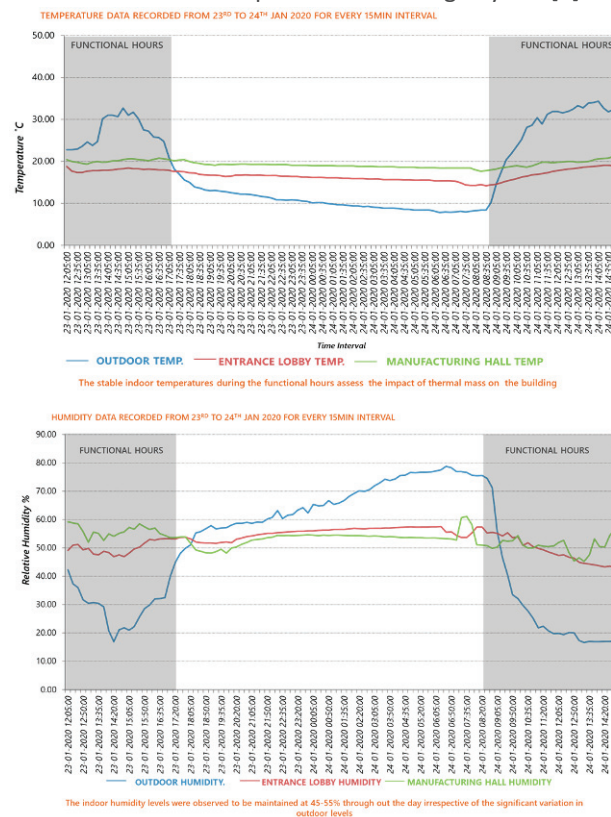


Figure 5: Temperature and humidity graphs highlighting the impact of thermal mass

The impact of thermal mass was observed through a post occupancy analysis done from 23rd to 24th Jan 2020 (winter day). Data loggers were placed in the manufacturing hall, entrance lobby, and outdoor. Data was logged every 15mins over 24 hours. Figure 5 highlights the stable temperature (17-20°C) and humidity range (55-60%) indoor irrespective of extreme outdoor fluctuations. Thus, clearly illustrating the impact of thermal mass. The maintenance of stable indoor temperatures by about overnight while the outdoor experiences an extreme drop of temperature. The heat absorbed during the day is restored within the building at night, keeping the indoor temps at about 17-20° C while outdoor drops to 8-10° C (i.e., building is in airtight mode). This helps to achieve occupant comfort during the early winter morning hours. The Manufacturing hall was observed to be 2° C higher than the Entrance hall due to the heat gain from the production process (figure 5).

The strategy of using natural ventilation through manually operable windows and ceiling fans help enhance air circulation to regulate the indoor environment in this area during the warm and humid period (figure 3).

4.2. Visual Comfort

Another critical aspect of a healthy working environment for users is visual comfort. The world health organisation suggests that lack of daylight and bad indoor air quality causes Sick Building syndrome [4], reducing attentiveness and energy levels of the users leading to low productivity. Therefore, the interior spaces have been designed to optimize daylight distribution and maintain the air quality of the space to make the workspace more desirable and increase productivity.

To maintain uniform and desired daylight levels in the facility, 25% WWR has been optimally distributed over all the four façades, maximized for the north façade (figure 6). The major work halls have been aligned along the same. Further, the depth of the



Figure 6: View of North façade of the facility

floor plate has been punctured with a glass block skylight allowing diffused light to enter the centre of the building, helping to maintain required Illuminance levels for all functional areas with internal glass partitions.

Figure 7, the spot measurements for indoor illuminance carried out on 23rd Jan 2020 (12.45 pm, Outdoor illuminance: 45000 lux) analyses the distribution of natural daylight over the floor plate. The daylight levels of the packaging hall on the first floor were observed to be uniform throughout ranging from 600 lux (near the window) to 275 lux (towards the corridor), the light levels on the ground floor's manufacturing hall were observed to range from 250 lux (near the windows) to 150 lux (towards the stores). The entrance lobby with a roof spills over diffused light throughout the facility with levels ranging from 2500 lux (centre of the lobby) to 500 lux around the corridors. Desirable light levels as per prescribed standards [5], are maintained across 80% of the entire floor plate (especially the working halls) during the operational hours, thus considerably reducing the dependence on artificial lighting.

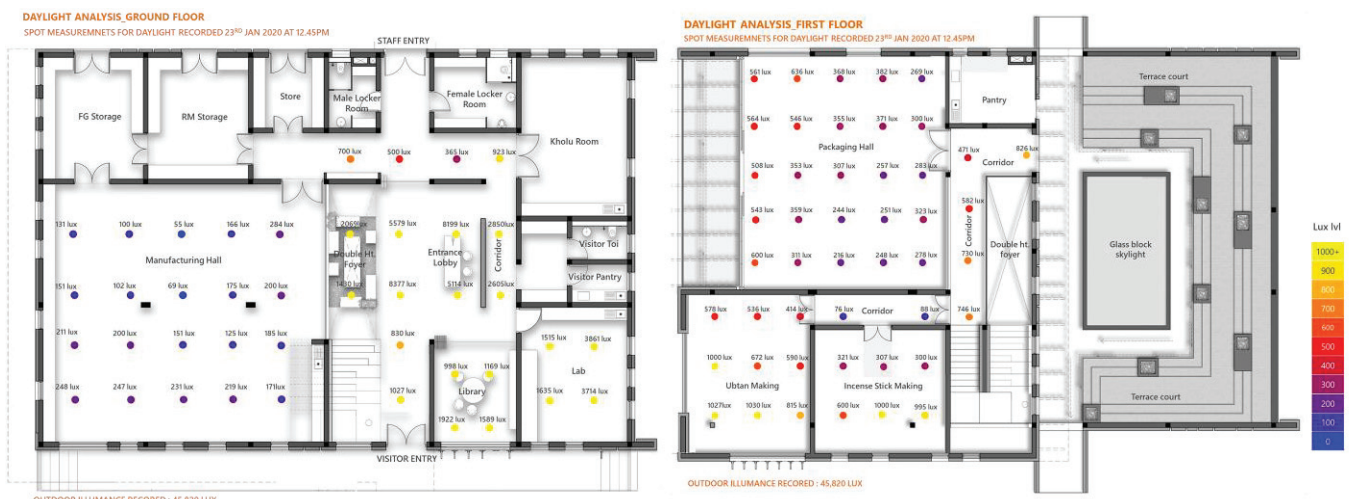


Figure 7: Spot measurements recorded for daylight levels across the factory

4.3 The NET “ZERO” Philosophy

The approach of ‘No is More,’ i.e., imagining one has no resources at one’s disposal, explores the potential for optimizing resources and targeting the Net Zero philosophy for energy water and waste.

Introducing renewable sources of energy helps close the loop by offsetting the facility's energy and water requirement. The microclimate generated through passive strategies proved to have an impact, which is demonstrated by the actual energy bill of 38kWh/m²/year of the facility. The 55kWp Solar plant, [7] installed on the roof does not only offset the facility’s own requirement but generates surplus to supply back to the grid proving it to be “Energy +”.

The carrying capacity calculation of the facility’s roof suggests a rainwater collection potential @740cu.m/year. However, due to site constraints, the rainwater tank has been optimized and planned to suffice for the two-day requirement of the facility, i.e., 60cu.m (as/ SVA GRIHA and NBC standards) [4][5].

Further to implementing the net-zero philosophy for water and energy, figure 8 highlights the innovative re-use of construction waste on site: the wooden and metal rafters were used to make light fixtures, Reinforcement bars as washbasin pedestal and a stone chisel as door handles. This enables the Net Zero philosophy for waste as well.

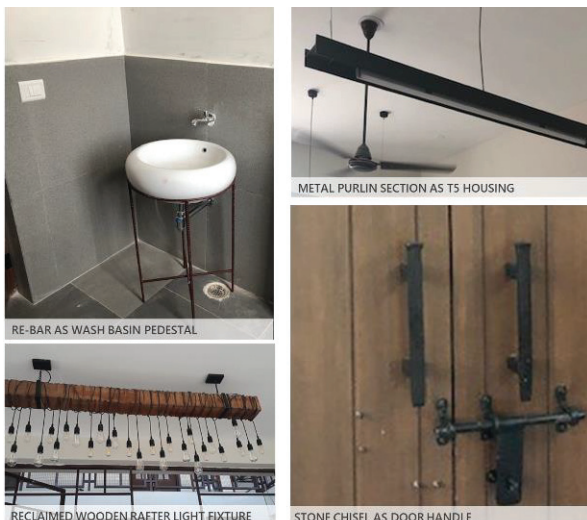


Figure 8: Optimisation of construction waste

5. CONCLUSION

The paper clearly illustrates the design process for off-grid architecture in the hills. The integrated design approach followed for the production unit through the implementation of passive strategies, and the study of vernacular helped develop an energy-efficient, resource optimized design that is unique and responds to the local context.

The building is symbolic of the fact that local materials and indigenous techniques used for centuries can still sustain a system and architecture that needs to function in this century (figure 9).



Figure 9: View of the Facility

ACKNOWLEDGEMENTS

This project is done with Morphogenesis under the guidance of the founding partners Manit and Sonali Rastogi. The project team to be thanked for the research work and design process. We would also like to thank our project clients Mira Kulkarni, Samrath Bedi and the entire team of Forest Essentials for their support and being receptive to the design vision. A special thanks to our consultants for their cooperation.

REFERENCES

1. Official website Forest Essentials available: <https://www.forestessentialsindia.com>
2. Negi S.K, Singh Vandana, Jain S.K, 2017, Architecture of Uttarakhand and Construction Techniques for Affordable Housing. *J. Environ. Nanotechnology. Volume 6, No.2, pp. 30-35.*
3. Hoyt Tyler, Schiavon Stefano, Piccioli Alberto, Cheung Toby, Moon Dustin, and Steinfeld Kyle, 2017, CBE Thermal Comfort Tool. *Center for the Built Environment, University of California Berkeley*, available: <http://comfort.cbe.berkeley.edu>
4. Indoor Air Quality Guide developed by American Society of Heating, Refrigerating and Air-conditioning Engineers”, *The American Institute of Architects, Building owners and Managers Association International, U.S. Environmental Pollution Agency, U.S. Green Building Council.*
5. National Building Code of India-2016, *Bureau of Indian Standards (BIS), 2016.*
6. Small Versatile Affordable Green Rating for Integrated Habitat Assessment (SVA GRIHA) Manual, the Energy and Resources Institute.
7. Solar Feasibility & Savings Report for Forest Essentials (2018), Sunfinity Solar Power LLP.

Occupant And Environment Related Parameters In The Evaluation Of Visual Environment: An Experimental Design

SEDA KAÇEL

Independent Researcher, Istanbul, Turkey

ABSTRACT: Post-occupancy evaluation (POE) is a procedure that assesses indoor environmental quality (IEQ), user satisfaction and building performance in a wide frame. This experimental study aimed to combine adaptive behaviour parameters with evaluation of lighting, spatial quality, user psychology and productivity. As the research methodology, the experiments contained between-groups and within-subjects tests. Occupant survey and field measurements of horizontal and vertical illuminance levels were carried out. As independent variables, different illuminance levels and correlated colour temperatures (CCTs) and different wall colours were tested in the between-groups tests. Different field of views were tested in the within-subjects tests. This research underlined how noteworthy occupant acceptance and preference were. It would be an asset to integrate adaptive behaviour, which contained modifications to improve comfort, into POE procedure of visual environment in order to achieve a holistic assessment. In other words, evaluation of occupant acceptance and preference would be merged with POE procedure.

KEYWORDS: Post-occupancy evaluation (POE), Visual environment, Adaptive behaviour

1. INTRODUCTION

Investigating parameters related to occupant and environment can provide valuable information in post-occupancy evaluation (POE) and indoor environmental quality (IEQ) studies. Occupant behaviour is affected by comfort and satisfaction. As a subtitle of occupant behaviour, adaptive behaviour is based on maintaining comfort and performing actions accordingly. Adaptive behaviour has been assessed widely in thermal comfort studies. Some studies underlined a wide range of adaptive behaviour measures as affecting visual comfort as well. This research evaluated adaptive behaviour parameters in relation to lighting, which were determined through a literature review. They were classified as occupant-related parameters and environment-related parameters. The environment-related parameters consisted of interior design-related parameters and lighting system-related parameters.

The research methodology is based on an experimental study in a full-scale test room with an office function. The experiments were organized as between-groups and within-subjects tests. The experiment investigated how occupant and environment affected mood, satisfaction, appearance and productivity.

This investigation is significant as it proposes to integrate the assessment of occupant-related and environment-related parameters into POE procedure for a holistic evaluation.

2. LITERATURE REVIEW

Illuminance level is one of the quantitative measures in lighting. Veitch and Newsham underlined the wide range of levels observed when performing visual tasks in various researches. The authors indicated that the adaptation capability provided users to perform in a good way under changing illuminance levels [1]. Fotios indicated a decrease in illuminance levels without having negative impact on spatial brightness in office spaces [2]. Referencing the research of Akashi and Boyce in offices [3], Fotios highlighted the 33% decrease in illuminance levels through the guidance of light sources with higher correlated colour temperature (CCT) and higher colour rendering index (CRI). This would provide a decrease in energy consumption without affecting visual performance and brightness of visual environment negatively. This is due to the fact that lighting would appear brighter when compared to the light sources with lower CCT and lower CRI [4]. Colour is another parameter that has been studied in lighting as affecting mood of occupants [5].

The experimental study of Veitch et al. investigated the links between user, perception of space, appraisal of light, task and satisfaction from workplace. In the study, it was found that lighting appraisal had impact on room appearance, which affected pleasure. Lighting appraisal and room appearance had impact on workplace satisfaction. Workplace satisfaction influenced environmental satisfaction and self assessed productivity [6].

Adaptive behaviour of occupants is performed to maintain personal comfort. The adaptive actions contain operating artificial lights, window blinds, thermostats, adjusting clothing level, using fan and door [7]. In their research Keyvanfar et al. interpreted pleasure through adaptive behaviour as a parameter not being included in the sustainable building assessment tools. The authors indicated the adaptive behaviour options such as covering the room surfaces (i.e. use of wallpaper), blind control, task lighting, changing the desktop or task surface, changing position or direction of furniture [8]. In the research of O'Brien and Gunay, interior design was indicated as a parameter affecting occupant behaviour for enhancing comfort. Flexibility of occupants related to changing their position or orientation was underlined for preventing glare. Besides, monitor orientation and furniture positioning were mentioned as being related to discomfort zones [9].

3. EXPERIMENTAL DESIGN

Experiments were conducted in the lighting laboratory at Istanbul Kültür University Ataköy Campus, Istanbul, Turkey. As the laboratory was located on the basement floor, there was no window and daylighting was excluded. There was a virtual window with metal venetian blind. The artificial lighting system had recessed TBS 631 luminaires (rectangular array: 9 luminaires x 2 rows, in total 18 luminaires). The luminaires had TL5 28W tubular fluorescent lamps (2 lamps in each luminaire, R_a : 85). They were controlled with Digital Addressable Lighting Interface (DALI) dimmable electronic ballasts.

The lighting laboratory contained a full-scale test office (length: 5.50m, width: 3.50m, height: 2.30m) (Fig. 1). The office had two office desks, two office chairs and a locker. The colour of the ceiling was white with the light reflectance of 0.80 and the colour of floor was grey with the light reflectance of 0.32 [10]. Through the sliding wall panels, there were two wall colours as blue and beige. The wall colour as beige (L90 C20 H55) had the light reflectance of 0.72. The wall colour as blue (L90 C10 H230) had the light reflectance of 0.74.

The experiments were carried out as between-groups (BG) and within-subjects (WS) designs as in the

researches of Veitch et al. [6] and Boyce et al. [11]. In the between-groups tests; different illuminance levels and CCTs (lighting system-related parameters) and different wall colours (interior design-related parameter) were tested as independent variables. In the within-subjects tests, different field of views (occupant-related parameter) were tested. The dependant variables were furniture position and orientation, field of view, colour of internal surfaces, lighting system, lighting appraisal, room appearance, pleasure, environmental satisfaction and self-assessed productivity: The variables lighting appraisal, room appearance, pleasure, environmental satisfaction and self-assessed productivity were taken from the model of Veitch et al [6]. The variables furniture position and orientation, field of view, colour of internal surfaces and lighting system were added as part of this research.

As the independent variables in the between-groups test, there were two lighting systems and two wall colours. The first lighting system Case 1 had the CCT of 3000 K and the illuminance level of 500lux on the workplane. The second lighting system Case 2 had the CCT of 6500 K and the illuminance level of 300 lux on the workplane. As the independent variables in the within-subjects tests, two occupant positions (Zone 1 and Zone 2) (Fig. 2) and three occupant orientations (0° , 45° and 90°) (Fig. 3) were tested.

Four null hypotheses were tested through analysis of variance (ANOVA):

- **Null hypothesis-1:** The evaluations of dependent variables under the lighting systems Case 1 (500 lux, 3000 K) and Case 2 (300 lux, 6500 K) do not vary for the beige wall colour.
- **Null hypothesis-2:** The dependent variables under the lighting systems Case 1 (500 lux, 3000 K) and Case 2 (300 lux, 6500 K) do not differ for the blue wall colour.
- **Null hypothesis-3:** The means of dependent variables for the beige and blue wall colours do not vary under the lighting system Case 1 (500 lux, 3000 K).
- **Null hypothesis-4:** The dependent variables for the beige and blue wall colours do not change under the lighting system Case 2 (300 lux, 6500 K).

As the research methodology, occupant survey and field measurement were carried out simultaneously. The between-groups and within-subjects experiments were conducted consecutively in the afternoon of the same day [6] [12]. Boyce et al. demonstrated different results in comfort and pleasure from morning to afternoon, in which comfort became worse and

pleasure decreased [13]. Thus the experiments of this research were carried out in afternoons.



Figure 1: The full scale test room with office function: The inner view towards the door with wall colour as blue.

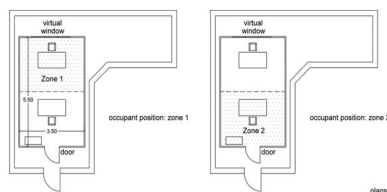


Figure 2: The occupant position as Zone 1 and Zone 2 shown on the plan of the test room.

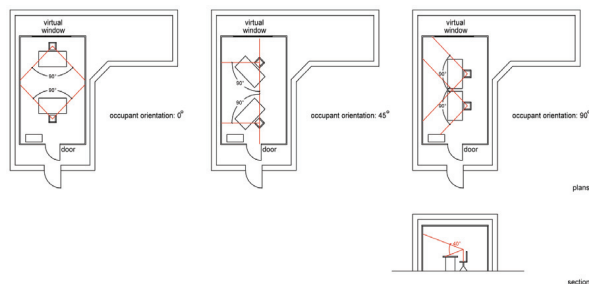


Figure 3: The occupant orientation as 0°, 45° and 90° with the field of views shown on plan and section of the test room.

In the occupant survey, the participants were given instructions on the between-groups design upon their arrival. While the experimenter gave the instructions, the participants walked around room for around one minute and then sat at the assigned desk for around four minutes. This approximate five minutes instruction time was for the participant to adapt to the workspace, lighting system and spatial conditions as applied by Saunders [14]. This was followed by the Ishihara colour blindness test [10] [13]. Later, the demographics survey was carried out [12] [13]. The participants performed a paper-based reading task as in the research of Saunders [14]. The reading text was taken from a coursebook on lighting [15]. The text was typed with Times New Roman 11pt (same as the questionnaire) with single spacing and printed on white matt A4 paper.

In the field measurement, the illuminance measurements were done horizontally on work plane as desk height (on desk and across room) and vertically

on the wall surfaces. The illuminance levels of each case was measured by Konica Minolta CL-200A Chroma Meter, which can measure both the illuminance level and CCT. The CCTs of the lighting systems were also checked by this chroma meter. The field of view was determined according to horizontal 40° band within a vertical 90° area in the view direction (Fig. 3) [16]. The illuminance levels were measured on the pre-determined grid points according to the EN 12464-1 Standard [17].

Sample was students at Istanbul Kültür University Atakoy Campus where the lighting laboratory was located. In the between-groups design, there were 36 participants. Each participant was assigned to one condition that contained the lighting systems Case 1 and Case 2 and the wall colours blue and beige. There were 13 students who preferred a different occupant position and/or orientation during the between-groups design. During the within-subjects design, each of 13 participants participated twice to the same condition as in the between-groups test with a different occupant position and/or orientation.

4. RESULTS

The data of the experimental design was analysed statistically. Descriptive statistics were analysed and ANOVA tests were carried out. The field measurements and within-subjects experiments were also analysed.

4.1 Descriptive statistics

IBM SPSS Statistics software was used. The sample size was 36. The average age of the participants was 21. 53% of the participants was female and 47% was male. No outliers (standardized scores >3 and <-3) were detected. Analyses of descriptive statistics included mean, standard deviation, skewness, kurtosis and Cronbach's α for the composite scales (Table 1). All variables were tested for normality with skewness values between -3 and +3 and kurtosis between -8 and +8 [18]. They met these criteria. Number of items and scales were stated for each variable.

Table 1: Descriptive statistics (N=36).

Variable	Mean	Standard deviation	Skewness	Kurtosis	Cronbach's α	Items	Scale
Furniture position and orientation	4.0139	0.21592	-0.554	-0.255	0.789	2	(1)-(6)
Field of view	4.0556	0.22073	-0.898	0.085	0.793	2	(1)-(6)
Colour of internal surfaces	4.3704	0.16628	-0.418	-0.177	0.705	3	(1)-(6)
Lighting system appraisal	4.20	0.262	-0.707	-0.367	-	1	(1)-(6)
Room appearance	3.4722	0.16630	-0.387	0.049	0.850	4	(1)-(5)
Pleasure	47.6698	3.95099	0.148	-0.395	0.913	9	(0)-(100)
Environmental satisfaction	4.2685	0.30249	-0.042	0.304	0.912	6	(0)-(8)
Self-assessed productivity	3.1806	0.15224	-0.051	-0.328	0.813	4	(1)-(5)
	6.31	0.301	-0.807	-0.163	-	1	(-4)-(4)

The bivariate correlations were calculated. It can be observed that one of the most significant correlations at the 0.01 level was between furniture position and orientation and field of view. As the others, colour of internal surfaces correlated with pleasure, environmental satisfaction and self-assessed productivity significantly. The correlation between lighting system and lighting appraisal, room appearance, environmental satisfaction and self-assessed productivity were significant. Correlations between lighting appraisal and room appearance, pleasure, environmental satisfaction and self-assessed productivity were significant. Room appearance correlated significantly with pleasure, environmental satisfaction and self-assessed productivity. Pleasure correlated significantly with environmental satisfaction and self-assessed productivity. Correlation between environmental satisfaction and self-assessed productivity was significant as well.

4.2 ANOVA tests

Analysis of variance (ANOVA) was used to test null hypotheses through comparing means of dependent variables. The null hypothesis defines that the populations that determine the samples would achieve the same means on the dependent variable [19]. The ANOVA tests evaluated the differences in the means of groups of the between-groups study that involved 36 participants.

ANOVA tests were carried out between the independent groups of the independent variable lighting systems (Case 1: 500 lux, 3000 K and Case 2: 300 lux, 6500 K) and the independent groups of the independent variable wall colours (Beige: L90 C20 H55 and Blue: L90 C10 H230) separately:

As the null hypothesis-1; for the beige wall colour and from Case 1 (500 lux, 3000 K) to Case 2 (300 lux, 6500 K), all $F_{obtained}$ values were smaller than $F_{critical}$ of 4.26 [19] for the degree of freedom associated with between estimate of variance of 1 and the degree of freedom associated with within estimate of variance of 24 at the alpha value 0.05. That is why, the null hypothesis could not be rejected.

As the null hypothesis-2; for the blue wall colour; the ratings of all dependant variables decreased from Case 1 (500 lux, 3000 K) to Case 2 (300 lux, 6500 K) (Table 2). There were statistically significant differences in between Case 1 and Case 2. $F_{obtained}$ values of 5.863, 5.878, 5.494, 13.003 and 9.333 for lighting system, lighting appraisal, room appearance, environmental satisfaction and self-assessed productivity respectively were larger than $F_{critical}$ of 5.32 [19] for the degree of freedom associated with between estimate of variance of 1 and the degree of freedom associated with within

estimate of variance of 8 at the alpha value 0.05. It is possible to reject null hypothesis for these five dependent variables and it can be said that the evaluation of lighting system, lighting appraisal, room appearance, environmental satisfaction and self-assessed productivity was different between Case 1 and Case 2 for the blue wall colour. The significances of 0.046, 0.042, 0.047, 0.007 and 0.018 were smaller than 0.05 ($p < 0.05$), which evidences that differences were statistically significant. No statistically significant difference was observed in other dependant variables.

Table 2: The ANOVA test between Case 1 and Case 2 for the blue wall colour.

Dependant variable	The lighting system	The wall colour		$F_{obtained}$	Significance
		Mean	Blue Standard deviation		
Furniture position and orientation	Case 1	4.4167	1.31972	0.503	0.498
	Case 2	3.7500	1.65831		
Field of view	Case 1	4.2500	1.50831	0.951	0.358
	Case 2	3.1250	2.17466		
Colour of internal surfaces	Case 1	4.8333	1.04881	0.138	0.720
	Case 2	4.5833	1.03190		
Lighting system	Case 1	5.40	0.894	5.863	0.046
	Case 2	4.00	0.816		
Lighting appraisal	Case 1	4.3333	0.66458	5.878	0.042
	Case 2	3.2500	0.73598		
Room appearance	Case 1	72.5926	19.45767	5.494	0.047
	Case 2	45.5556	14.85181		
Pleasure	Case 1	6.2778	1.56584	3.878	0.084
	Case 2	4.5000	1.06284		
Environmentalsatisf action	Case 1	4.3333	0.66458	13.003	0.007
	Case 2	2.5625	0.89849		
Self-assessed productivity	Case 1	8.00	0.632	9.333	0.018
	Case 2	6.67	0.577		

As the null hypothesis-3; for Case 1, the means of all dependant variables increased from beige to blue wall colour. There were statistically significant differences between beige and blue wall colours. $F_{obtained}$ values of 7.062, 8.027, 13.336 and 6.478 for room appearance, pleasure, environmental satisfaction and self-assessed productivity respectively were larger than $F_{critical}$ of 4.32 [19] for the degree of freedom associated with between estimate of variance of 1 and the degree of freedom associated with within estimate of variance of 21 at the alpha value 0.05. It is possible to reject null hypothesis for these four dependent variables and it can be said that the evaluation of room appearance, pleasure, environmental satisfaction and self-assessed productivity was different between beige and blue wall colours for Case 1. The significances of 0.015, 0.010, 0.001 and 0.019 were smaller than 0.05 ($p < 0.05$), which shows that the differences were statistically significant. No statistically significant difference was observed in other dependant variables.

As the null hypothesis-4; for Case 2 and from beige to blue wall colour, all $F_{obtained}$ values were smaller than $F_{critical}$ of 4.84 [19] for the degree of freedom associated with between estimate of variance of 1 and the degree

of freedom associated with within estimate of variance of 11 at the alpha value 0.05. That is why, the null hypothesis could not be rejected.

4.3 Analyses of the field measurements

The illuminance level measurements were carried out for two lighting systems (Case 1: 500 lux, 3000 K and Case 2: 300 lux, 6500 K) and two wall colours (Beige: L90 C20 H55 and Blue: L90 C10 H230). The horizontal illuminance levels on the workplane across the room (defined by the desk height) and the vertical illuminance levels on the four walls were measured. The average illuminance levels were calculated accordingly. The wall with the door was labeled as Wall 1, the left wall was labeled as Wall 2, the wall with the virtual window was labeled as Wall 3 and the right wall was labeled as Wall 4.

In the lighting system Case 1 (500 lux, 3000 K) and beige wall colour; the minimum illuminance level on the horizontal workplane across the room (E_{\min}) was 144 lux and the maximum illuminance level (E_{\max}) was 581 lux. The average illuminance level on the horizontal workplane, Wall 1, Wall 2, Wall 3 and Wall 4 were calculated as 362 lux, 111 lux, 126 lux, 169 lux and 186 lux (E_{ave}) respectively.

In the lighting system Case 2 (300 lux, 6500 K) and beige wall colour; the minimum illuminance level on the horizontal workplane across the room (E_{\min}) was 79 lux and the maximum illuminance level (E_{\max}) was 366 lux. The average illuminance level on the horizontal workplane, Wall 1, Wall 2, Wall 3 and Wall 4 were calculated as 232 lux, 71 lux, 101 lux, 99 lux and 87 lux (E_{ave}) respectively.

In the lighting system Case 1 (500 lux, 3000 K) and blue wall colour; the minimum illuminance level on the horizontal workplane across the room (E_{\min}) was 140 lux and the maximum illuminance level (E_{\max}) was 662 lux. The average illuminance level on the horizontal workplane, Wall 1, Wall 2, Wall 3 and Wall 4 were calculated as 398 lux, 120 lux, 196 lux, 272 lux and 220 lux (E_{ave}) respectively.

In the lighting system Case 2 (300 lux, 6500 K) and blue wall colour; the minimum illuminance level on the horizontal workplane across the room (E_{\min}) was 67 lux and the maximum illuminance level (E_{\max}) was 517 lux. The average illuminance level on the horizontal workplane, Wall 1, wall 2, Wall 3 and Wall 4 were calculated as 268 lux, 88 lux, 176 lux, 188 lux and 114 lux (E_{ave}) respectively.

4.4 Analyses of the within-subjects experiments

The within-subjects tests were carried out with 13 participants. Participant numbers were given from 1 to 13 in relation to the within-subjects test. The occupant

positions were Zone 1 or Zone 2 and orientations were 0°, 45° or 90°.

In the occupant questionnaire, the same questions were asked when the participant worked with the modified position and orientation. The means of the same questions during the between-groups test and the within-subjects tests were evaluated (Table 3).

Table 3: The means of the dependent variables for each participant that took the within-subjects test.

Dependent variables	Furniture position and orientation		Field of view		Colour of internal surfaces		Lighting system		Lighting appraisal		Room appearance		Pleasure		Environmental satisfaction		Self-assessed productivity	
									Mean									
	Participants of the within-subjects test								(BG: Between-groups, WS: Within-subjects)									
	BG	WS	BG	WS	BG	WS	BG	WS	BG	WS	BG	WS	BG	WS	BG	WS	BG	WS
Participant 1	3.00	4.00	3.00	3.00	4.00	3.67	5.00	4.00	3.50	4.25	41.11	25.56	2.33	2.33	4.25	3.50	7.00	4.00
Participant 2	4.00	4.00	3.00	4.00	4.33	3.67	2.00	1.00	3.00	2.00	20.00	24.44	3.50	3.50	3.00	3.25	7.00	7.00
Participant 3	3.00	3.00	5.00	1.00	2.00	3.00	4.00	4.00	3.75	3.25	58.89	54.44	1.67	2.67	3.50	2.75	5.00	5.00
Participant 4	1.50	2.00	4.50	1.00	5.33	6.00	3.00	2.00	3.25	3.25	56.67	55.56	5.17	3.17	3.00	2.25	8.00	6.00
Participant 5	3.00	3.50	2.50	3.50	5.33	5.67	5.00	5.00	4.50	4.50	71.11	71.11	6.33	7.00	3.50	4.75	7.00	8.00
Participant 6	4.00	6.00	3.50	6.00	4.33	6.00	6.00	5.00	4.75	5.00	78.89	96.67	5.83	7.00	3.25	5.00	5.00	9.00
Participant 7	3.00	2.50	4.00	4.00	5.00	5.00	4.00	4.00	3.00	3.00	38.89	38.89	3.67	3.67	2.50	2.50	4.00	4.00
Participant 8	6.00	6.00	5.00	6.00	4.33	5.00	6.00	6.00	4.00	4.00	65.56	70.00	5.50	6.83	3.25	3.25	8.00	8.00
Participant 9	4.50	2.00	4.00	2.00	4.67	4.67	4.00	5.00	2.50	2.75	38.89	55.56	4.00	6.50	2.25	2.25	7.00	8.00
Participant 10	4.50	5.00	4.00	5.00	4.67	4.67	4.00	4.00	3.50	3.50	42.22	46.67	3.67	3.67	3.00	4.00	6.00	5.00
Participant 11	2.00	2.00	2.00	2.00	3.67	3.67	3.00	3.00	2.25	2.25	14.44	14.44	2.33	2.33	2.25	2.25	6.00	6.00
Participant 12	4.00	4.00	3.50	3.50	4.33	4.33	4.00	4.00	3.25	3.25	64.44	64.44	5.50	5.50	4.00	4.00	7.00	7.00
Participant 13	3.50	3.50	2.00	2.00	4.33	4.33	6.00	6.00	4.25	4.25	58.89	58.89	4.33	4.33	4.25	4.25	8.00	8.00

Field of views changed when participants changed their positions and orientations in the within-subjects test. In other words; the walls, which the participants were facing, changed when they changed their positions and orientations. Thus, the average illuminance level in the field of view changed (Table 4).

Table 4: The average illuminance levels in the field of view in the between-groups test and within-subjects test.

Participants of the within-subjects test, lighting system and wall colour	Between-groups test			Within-subjects test			
	Position	Orientation	Average illuminance level (E_{ave})	Position	Orientation	Average illuminance level (E_{ave})	Difference in the average illuminance levels
Participant 1 Li • Wa +	Zone 2	0°	165 lux	Zone 1	45°	121 lux	44 lux ↓
Participant 2 Li • Wa +	Zone 2	0°	165 lux	Zone 1	45°	121 lux	44 lux ↓
Participant 3 Li • Wa +	Zone 1	0°	131 lux	Zone 2	0°	165 lux	34 lux ↑
Participant 4 Li • Wa +	Zone 2	0°	165 lux	Zone 1	90°	137 lux	28 lux ↓
Participant 5 Li • Wa +	Zone 2	0°	165 lux	Zone 1	45°	121 lux	44 lux ↓
Participant 6 Li • Wa +	Zone 2	0°	165 lux	Zone 1	45°	121 lux	44 lux ↓
Participant 7 Li • Wa +	Zone 1	0°	131 lux	Zone 2	45°	147 lux	16 lux ↑
Participant 8 Li • Wa +	Zone 1	0°	131 lux	Zone 1	45°	121 lux	10 lux ↓
Participant 9 Li • Wa +	Zone 1	0°	131 lux	Zone 2	90°	118 lux	13 lux ↓
Participant 10 Li • Wa +	Zone 1	0°	90 lux	Zone 2	45°	108 lux	18 lux ↑
Participant 11 Li • Wa +	Zone 2	0°	88 lux	Zone 1	45°	99 lux	11 lux ↑
Participant 12 Li • Wa ×	Zone 2	0°	259 lux	Zone 1	90°	235 lux	24 lux ↓
Participant 13 Li • Wa ×	Zone 2	0°	259 lux	Zone 1	90°	235 lux	24 lux ↓
Lighting system (Li)				Wall colour (Wa)		Difference	
• Case 1: 500 lux, 3000 K				+ Beige		↑ Increase	
• Case 2: 300 lux, 6500 K				× Blue		↓ Decrease	

4.5 Discussion

The ANOVA tests showed that the means of all dependant variables decreased from Case 1 to Case 2 for blue wall colour. The differences for lighting system, lighting appraisal, room appearance, environmental satisfaction and self-assessed productivity were statistically significant, for which the null hypothesis was rejected. For Case 1, the means of all dependant variables increased from beige to blue wall colour. The differences for room appearance, pleasure, environmental satisfaction and self-assessed productivity were statistically significant, for which the null hypothesis was rejected.

Considering the high illuminance level of Case 1, the highest differences were on the workplane, Wall 3 and Wall 4 for beige and blue walls. As for the vertical illuminance levels, there were higher illuminance levels on Wall 2 and Wall 3 for blue wall than beige wall.

In the within-subjects tests, differences between means of dependent variables evidenced the diversity in occupant acceptance. While the means of furniture position and orientation, field of view, room appearance and pleasure improved most, the means of lighting system both remained same and decreased most among the participants. The field of view changed based on changing the occupant position and orientation. The illuminance levels in the field of views either increased or decreased, the majority of which declined. The participants, who had a lower or higher average illuminance level in the field of view, evaluated the dependent variables with higher, same or lower ratings. The results demonstrated the importance of occupant acceptance.

5. CONCLUSION

This research worked on a holistic evaluation through integrating adaptive behaviour parameters into evaluation of visual environment. It highlighted the significance of assessing occupant and environment parameters.

ACKNOWLEDGEMENTS

The author would like to thank the participants in the experiments for their contribution in this research.

REFERENCES

1. Veitch, J. A. and Newsham, G. R. (1996). Determinants of Lighting Quality II: Research and Recommendations. In *the 104th Annual Convention of the American Psychological Association*, Toronto, Ontario, Canada, 9-13 August. ERIC Document Reproduction Service No. ED 408 543.
2. Fotios, S. (2011). Lighting in offices: lamp spectrum and brightness. *Coloration Technology*, 127, p. 114-120.
3. Akashi, Y. and Boyce, P. R. (2006). A field study of illuminance reduction. *Energy and Buildings*, 38, p. 588-599.
4. Fotios, S. A. (2001). Lamp colour properties and apparent brightness: A review. *Lighting Research and Technology*, 33, p. 163-181.
5. Küller, R., Ballal, S., Laike, T., Mikellides, B. and Tonello, G. (2006). The impact of light and colour on psychological mood: a cross-cultural study of indoor work environments. *Ergonomics*, 49:14, p. 1496-1507.
6. Veitch, J. A., Stokkermans, M. G. M. and Newsham, G. R. (2013). Linking Lighting Appraisals to Work Behaviors. *Environment and Behavior*, 45:2, p. 198-214.
7. Yan, D., O'Brien, W., Hong, T., Feng, X., Gunay, H. B., Tahmasebi, F. and Mahdavi, A. (2015). Occupant behavior modeling for building performance simulation: Current state and future challenges. *Energy and Buildings*, 107, p. 264-278.
8. Keyvanfar, A., Shafaghat, A., Majid, M. Z. A., Lamit, H. B., Hussin, M. W., Ali, K. N. B. and Saad, A. D. (2014). User satisfaction adaptive behaviors for assessing energy efficient building indoor cooling and lighting environment. *Renewable and Sustainable Energy Reviews*, 39, p. 277-295.
9. O'Brien, W. and Gunay, H. B. (2014). The contextual factors contributing to occupants' adaptive comfort behaviors in offices - A review and proposed modeling framework. *Building and Environment*, 77, p. 77-87.
10. Manav, B., Kutlu, R. G., Küçükdoğu, M. Ş. (2010). The Effects of Colour and Light on Space Perception. In *International Conference Colour and Light in Architecture 2010*, P. Zennaro (Ed.), *Proceedings of Colour and Light in Architecture*, Venice, Italy, 11-12 November, 173-178.
11. Boyce, P. R., Veitch, J. A., Newsham, G. R., Jones, C. C., Heerwagen, J., Myer, M. and Hunter, C. M. (2006). Lighting quality and office work: two field simulation experiments. *Lighting Research & Technology*, 38 (3), p. 191-223.
12. Newsham, G. R., Veitch, J. A., Arsenault, C. D. and Duval, C. L. (2003). *Lighting for VDT Workstations 1: Effect of Control on Energy Consumption and Occupant Mood, Satisfaction and Discomfort* (Report No. RR-165). National Research Council Canada Institute for Research Construction Report.
13. Boyce, P. R., Veitch, J. A., Newsham, G. R., Myer, M. and Hunter, C. (2003). *Lighting Quality and Office Work: A Field Simulation Study*. Report for the Right Light Consortium (Report No. PNNL-14506). Pacific Northwest National Laboratory (PNNL).
14. Saunders, J. E. (1969). The role of the level and diversity of horizontal illumination in an appraisal of a simple office task. *Lighting Research and Technology*, 1 (1), 37-46.
15. Berköz, E. and Küçükdoğu, M. Ş. (1983). *Çevre Kontrolünde Aydınlatma Ders Notları*. İstanbul: İTÜ Mimarlık Fakültesi, FÇK Birimi.
16. Loe, D., Mansfield, K. P. and Rowlands, E. (2000). A step in quantifying the appearance of a lit scene. *Lighting Research and Technology*, 32 (4), 213-222.
17. EN12464-1 (2011). *Light and lighting - Lighting of work places, Part 1: Indoor work places*.
18. Kline, R. B. (ed.) (1997). *Principles and practice of structural equation modeling*. New York: Guilford.
19. Healey, J. F. (2012). *Statistics: A tool for social research*. 9th ed. Wadsworth, Cengage Learning.

Occupants' Perception versus Daylighting Simulations': A field study on lecture halls to correlate the occupant's subjective responses and climate-based daylight metrics

TARUN VERMA, PADMANABAN GOPALAKRISHNAN

National Institute of Technology, Tiruchirappalli, India

ABSTRACT: Natural lighting plays an important role in the design of lecture halls in higher education institutes (HEIs). Many organizations and green building rating systems started to encourage daylight simulations to support better design incorporating natural lighting. The shift towards daylight simulations moves occupant perception away from the daylighting design theory and practice. It is, therefore, a need to correlate the daylight simulation results with the occupant's subjective responses. This study aims to correlate the occupant's subjective responses (n=207) with annual and point-in-time climate-based daylight simulations in the lecture halls (n=3) of HEI in India. This study also documents a novel comparison on correlating the daylight simulations with the subjective responses of architects (n=95) and non-architects (n=112). The findings reveal that point-in-time simulation results correlate better with the occupant's subjective responses than annual simulation results. The illumination range of 75-150 lux and 200-500 lux correlate best with subjective responses of architects for the annual and point-in-time daylight simulations, respectively. The results also suggest that architects can better predict the daylight simulation results than non-architects.

KEYWORDS: Subjective responses, daylight simulations, correlation, climate-based daylight metrics, lecture hall

1. INTRODUCTION

The higher education system of India is the largest in the world in terms of institutions (840 universities) and second largest in terms of enrolment (34.6 million students). The current gross enrolment ratio (GER) is 24.5% in the higher education system of India, and the government has set a target of 30% GER by the end of 2020. By 2030, every fourth graduate across the globe will be a product of the Indian Universities [1]. These stats substantiate the requirement of more number of higher education institutes (HEIs) in India. In HEIs, students spend a good amount of time in lecture halls. The design of lecture halls plays a crucial role in HEIs. There are many design parameters for designing a lecture hall, but natural lighting is the key to achieve performance goals. Natural lighting is utmost important for the students engaged in paper-based reading work. In windowless lecture halls, the students are less focused, unsociable and uncoordinated, so it is necessary to focus on daylighting while designing the lecture halls to enhance the health, performance and productivity of the students [2-5].

The occupants are more satisfied with the presence of natural lighting in indoors [6-7], resulting in, many green building rating systems and organizations have

started to encourage annual daylight simulation to support better design [8-10]. To support better design, the Illumination Engineering Society (IES) adopted spatial Daylight Autonomy (sDA; the percentage of analysis area exceeds 300 lux for 50% of analysis period) and Annual Sunlight Exposure (ASE; the percentage of analysis points in an analysis area exceeds 1000 lux of direct sunlight for 250 hours as calculated from 8 am to 6 pm) as a first human factors evidence-based annual dynamic daylight metrics in 2012.

The shift towards these dynamic daylighting simulations moves the occupant's perception away from the daylighting design theory and practice. It is, therefore, a need to correlate the daylight simulation results with the occupant's perception [9]. Previous studies suggest that the student's subjective responses correlate better with point-in-time simulation than annual daylighting simulation results [11-13].

The research on human subjective responses correlating with annual and point-in-time daylighting simulations appears to be in the amorphous stages in HEIs of India. The authors, therefore, saw a need to investigate the relationship between human subjective responses with daylighting (annual and point-in-time)

simulations in the HEIs of India. This study further attempts to answer the question raised by Van Den Wymelenberg [14]; "Is there an important difference between visual comfort research results obtained from naive versus expert participants?"

To the best of the authors' knowledge, this study is the first attempt in the context of HEIs of India to correlate human subjective responses with daylighting (annual and point-in-time) simulations. This study also documents a novel comparison on correlating the daylighting simulation results with the subjective responses of architects and non-architects. For this study, a lecture hall building is selected at the National Institute of Technology (NIT) Tiruchirappalli (10°45'36.6"N and 78°48'37.7"E), India. In total, 207 subjective responses (graduated architect's n=95 and engineering students n=112) collected from the three study spaces during five field trips in January and February. This study shapes upon a sequence of previous studies [13,15-18] and the methodology is adopted from the study done by Nezamdoost and Van Den Wymelenberg [17].

2. METHODOLOGY

2.1 Experiment setup

This study was conducted in a lecture hall building situated at NIT Tiruchirappalli. In total, 36 lecture halls are distributed on three floors in this building. The lecture halls are planned in various orientation with the window to wall ratio (WWR) of 40 per cent. Three lecture halls (G8, G10 and G12) (Fig. 1) have been selected on the ground floor for this study to perform the annual and point-in-time daylighting simulations. The study spaces were chosen with diverse orientation and exterior obstructions.

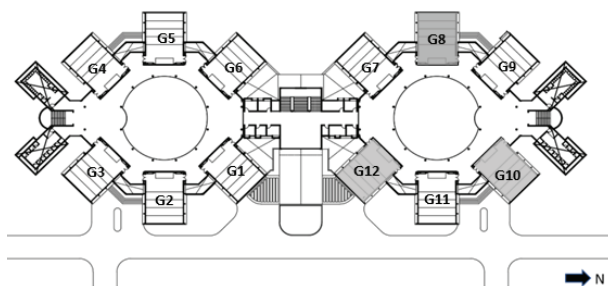


Figure 1: Ground Floor Plan - Lecture hall building at NIT Tiruchirappalli, India

Field trips (Fig. 2) were conducted during regular class timings between 10 am to 1 pm. In total, 207 responses were collected during five field trips, with an average of 41 responses per field trip for one study space. Each respondent was asked to complete a

questionnaire which consists of three sections concentrating on visual perception, visual comfort, daylight sufficiency, lighting conditions, brightness and glare. The questions were asked on a five-point Likert-scale. Clear instructions were given to the respondents to evaluate the space without consulting with other participants. According to the objectives of this study, the respondents were asked to evaluate the current (point-in-time) daylighting conditions as well as annual daylighting conditions based on their intuition. The authors decided to focus only on ten questions (5 questions per category), and each was assigned a code for analysis purpose. The questions are as followed:

- A2: I enjoy being in this room. (point-in-time)
- A3: I enjoy being in this room. (Annually)
- B2: I can work happily in this room with all the electric lights turned off. (point-in-time)
- B3: I can work happily in this room with all the electric lights turned off. (Annually)
- C2: The daylight in this room is sufficient. (point-in-time)
- C3: The daylight in this room is always sufficient. (Annually)
- D2: The daylight in this room is not too bright. (point-in-time)
- D3: The daylight in this room is never too bright. (Annually)
- E2: There is no glare from direct sun penetration. (point-in-time)
- E3: There is low probability of glare from direct sun penetration. (Annually)



Figure 2: Collecting subjective responses for one of the study space during a field trip

2.2 Simulations

The three-dimensional model for the lecture hall building was generated in SketchUp (version 2017) and exported into Rhinoceros (version 6). To perform the daylighting simulations, Grasshopper (rhino plugin), Ladybug and Honeybee (grasshopper plugins) were used with the RADIANCE daylight simulation engine. Table 1 shows the RADIANCE simulation parameters used for this study. An analysis grid of 0.5 x 0.5 meter was generated at a height of 0.75 meters from the

finished floor level. The analysis grid was generated based on the stepped floor profile of the lecture halls. The surface reflectance values were used, as mentioned in the simulation protocol LM-83 [10]. The glazing visual light transmittance (VLT) values were used as per data provided by the glass manufacturer. The modelling and simulation protocols were strictly followed, as mentioned in the simulation protocol LM-83.

Table 1: RADIANCE simulation parameters

-ab	-ad	-as	-aa	-ar	-dt
6	1000	1024	0.1	128	0

The illuminance values were calculated for the same date and time of when the participants assessed the study spaces during field trips. The annual daylighting simulations were conducted for the period (8 am to 6 pm) mentioned in LM-83. The simulation results were correlated with the participant's responses by using the following metrics [17].

Point-in-time:

- The percentage of the floor area, which meets the various threshold illuminance (50 to 5000 lux at distinct intervals) to examine the daylight sufficiency or excessiveness [17].

Annual:

- sDA n lux, 50% time: The percentage of the floor area at various threshold illuminance (50 to 5000 lux at distinct intervals) in 50% occupied hours around the year [17].

3. RESULTS & DISCUSSION

In total, 207 subjective evaluations correlated with the daylight performance metrics (annual and point-in-time) extracted from simulations. Pearson correlations were calculated to find the relationship between the participant's subjective responses and simulation

results. Probability values (p-value) were calculated to check the significance of correlation.

The statically significant ($p < 0.01$) correlation coefficients were marked with a double star (**) (Table 2 and Table 3), and statically insignificant correlation coefficients were colour coded with green colour (Table 2 and Table 3).

3.1 Descriptive statistics

Median, max, min and quartiles were plotted (Fig. 3) from the simulation results for the various illuminance thresholds (50 to 5000 lux at distinct intervals). The simulation results showed daylight deficiency in all three study spaces. The illumination thresholds were observed far below from the prescribed limit (300 lux; [19]) for lecture halls. The point-in-time simulation results showed that for all the study spaces, less than 30% of the room area meets the desired illuminance levels (Fig. 3). The annual simulation results also confirm the daylight deficiency in all the study spaces (Fig. 3). The sDA results confirm the lack of daylighting levels in all three study spaces (Fig. 4). In general, study spaces fall short of achieving the prescribed illumination criteria for lecture halls. The authors decided to focus only on significantly correlated ($p < 0.01$) illuminance thresholds for further analysis, i.e. 50 to 1000 lux for point-in-time simulations and 50 to 700 lux for annual simulations (Table 2 and Table 3). Other illumination thresholds were not correlated significantly with the participant's subjective responses.

Surprisingly, the questionnaire items D2, D3, E2 and E3 are not found any correlation with any of the illumination threshold range, so these items are not included in the further correlation analysis. However, in the previous study [17], these questionnaire items correlated significantly with very less correlation coefficients compare to other questionnaire items (A2, A3, B2, B3, C2 and C3). These findings show a gap on

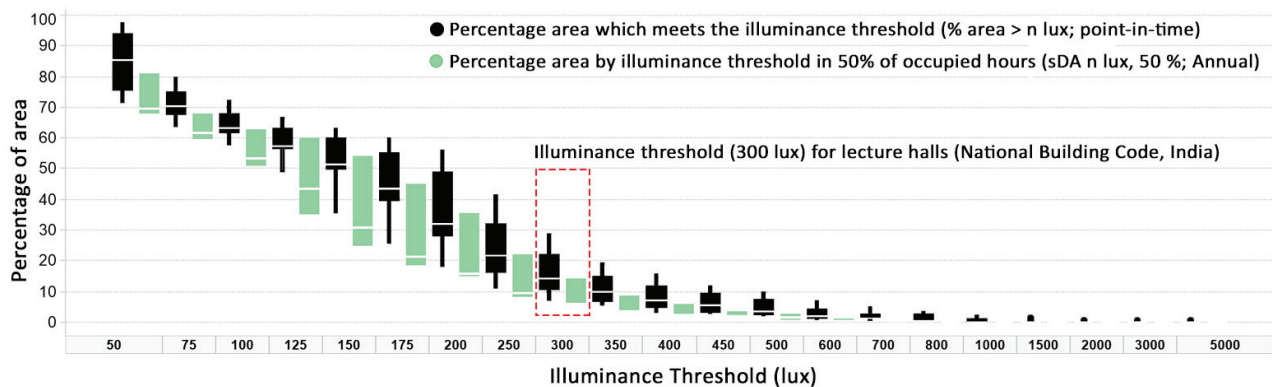


Figure 3: Point-in-time and annual simulation results showing the variability in percentage of area for different illuminance ranges

the predictive ability of questionnaire items D2, D3, E2 and E3. Future research should address this gap to find out the best-suited questionnaire items to predict the relationship between simulation results and subjective responses.

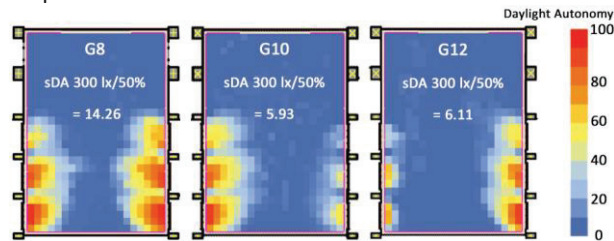


Figure 4: sDA 300 lx/50% annual simulation results

3.2 Point-in-time correlation results

The correlation results of point-in-time simulation and subjective responses are presented in Table 2. Three questionnaire items (A2, B2 and C2) were correlated with the point-in-time simulation results. The correlation results were divided into two groups: Architects (indicated by "AR") and Non-Architects (indicated by "N-AR").

Looking at the point-in-time correlation results for architects (AR), the highest correlation coefficient (r) observed at 800 lux with item B2. Even though the higher illumination thresholds (>500 lux) were also correlated significantly with the subjective responses, still, the authors decided not to include the higher illumination thresholds for further analysis because the percentage room area above 500 lux thresholds were observed very less (Fig. 3) in all the three study spaces. The items B2 and C2 were found as the most correlated indicators to predict the illumination threshold range, and this finding also confirms the previous study [17]. For each questionnaire item, the top 50 per cent correlation coefficients were represented in bold figures to find the most promising illumination threshold. By combining all the three questionnaire items (A2, B2, and C2), it was found that the illumination range 200-500 lux correlate best with the architects' subjective responses. However, the range observed in the current study was slightly different from the previous research (150-300 lux) [17].

Looking at the point-in-time correlation results for non-architects (N-AR), it was found that not even a single questionnaire item correlated significantly with any of the illumination thresholds. This finding reveals the answer to the question raised by Van Den Wymelenberg [14] that the expert participants (architects) can better predict the point-in-time simulation results than the naïve participants (non-architects).

Table 2 Correlations of point-in-time simulation illumination thresholds with the participant's subjective responses

% Area > n lux	A2		B2		C2	
	AR	N-AR	AR	N-AR	AR	N-AR
	Pearson Correlation (r)					
50 lux	0.373**	0.003	0.499**	0.009	0.311**	0.118
75 lux	0.373**	-0.033	0.492**	0.050	0.325**	0.076
100 lux	0.409**	-0.038	0.547**	0.055	0.394**	0.066
125 lux	0.405**	-0.043	0.530**	0.060	0.377**	0.049
150 lux	0.386**	-0.040	0.495**	0.057	0.340**	0.058
175 lux	0.386**	-0.037	0.499**	0.054	0.334**	0.068
200 lux	0.411**	-0.039	0.547**	0.056	0.382**	0.062
250 lux	0.421**	-0.042	0.568**	0.059	0.429**	0.051
300 lux	0.421**	-0.041	0.572**	0.058	0.430**	0.056
350 lux	0.438**	-0.044	0.599**	0.060	0.467**	0.046
400 lux	0.429**	-0.049	0.583**	0.064	0.445**	0.025
450 lux	0.453**	-0.050	0.624**	0.065	0.491**	0.017
500 lux	0.435**	-0.051	0.596**	0.065	0.461**	0.010
600 lux	0.399**	-0.053	0.554**	0.065	0.447**	-0.018
700 lux	0.409**	-0.053	0.565**	0.065	0.473**	-0.018
800 lux	0.458**	-0.053	0.638**	0.065	0.531**	-0.008
1000 lux	0.406**	-0.053	0.563**	0.065	0.466**	-0.008

** . Correlation is significant at the 0.01 level (2-tailed).

Correlation is insignificant.

Bold figures represent top 50% "r-values" for each item

3.3 Annual correlation results

The correlation results of annual simulation and the subjective responses are presented in Table 3. Looking at the annual correlation results for architects (AR), the highest correlation coefficient (r) observed at 700 lux with questionnaire item C3. Similar to point-in-time correlation results, the authors decided not to focus on those illumination thresholds (>=450 lux) which receive very less values for the percentage room area above specific thresholds (>=450 lux) (Fig. 3). Similar to the point-in-time correlation results, the items B3 and C3 were found as the most correlated indicators to predict the illumination threshold range. By combining all the three questionnaire items (A3, B3, and C3), it was found that the illumination range 75-150 lux correlate best with the architect's subjective responses. The illumination range observed in the current study does not match with the illumination range (100-300 lux) found in the previous study [17]. However, the authors acknowledge that the findings of the current study should be tested again in future researches because the present study did not include a variety of study spaces and daylighting strategies.

Looking at the annual correlation results for non-architects (N-AR), similar to the point-in-time correlation results, it was found that not even a single questionnaire item correlated significantly with any of

the illumination thresholds. This finding confirms that the expert participants (architects) can better predict both annual and point-in-time simulation results than the naïve (non-architects) participants.

Table 3 Correlations of annual simulation illumination thresholds with the participant's subjective responses

sDA n lux/50%	A3		B3		C3	
	AR	N-AR	AR	N-AR	AR	N-AR
	Pearson Correlation (r)					
50 lux	.374**	-.030	.399**	-.047	.373**	-.002
75 lux	.386**	-.041	.418**	-.033	.402**	.004
100 lux	.384**	-.040	.416**	-.034	.399**	.003
125 lux	.393**	-.053	.433**	-.016	.428**	.011
150 lux	.383**	-.038	.413**	-.037	.395**	.002
175 lux	.373**	-.029	.397**	-.049	.370**	-.003
200 lux	.363**	-.022	.383**	-.057	.351**	-.006
250 lux	.371**	-.028	.395**	-.050	.367**	-.003
300 lux	.355**	-.017	.371**	-.063	.335**	-.009
350 lux	.371**	-.028	.395**	-.050	.368**	-.003
400 lux	.365**	-.024	.386**	-.055	.355**	-.005
450 lux	.380**	-.035	.408**	-.041	.387**	.001
500 lux	.392**	-.052	.433**	-.017	.427**	.010
600 lux	.359**	-.019	.376**	-.060	.341**	-.008
700 lux	.324**	-.106	.396**	.086	.451**	.046

** . Correlation is significant at the 0.01 level (2-tailed).

Correlation is insignificant.

Bold figures represent top 50% "r-values" for each item

3.4 Point-in-time versus annual correlation results

In general, looking at the correlation results (Table 2 and Table 3), it is observed that point-in-time correlation results showed a stronger correlation than the annual simulation results. To check this, the authors decided to do further analysis using a statistical approach. By using independent sample t-test, t-score and p-value were calculated for the correlation coefficients of annual and point-in-time simulations. The 51 correlation coefficients for point-in-time simulation (Mean=0.4624, Standard Deviation=0.0820) compared to the 45 correlation coefficients in the annual simulation (Mean=0.3853, Standard Deviation=0.0269). The results showed a significant difference in mean correlation values between the point-in-time and annual simulations ($t_{61.918}=6.340$, $p<0.001$). The average correlation coefficient for point-in-time simulations was 0.077 (mean difference) more than the average correlation coefficient for annual simulations. This finding confirms the previous research results [11-13,17] that the point-in-time simulation results correlated better with participants subjective responses than the annual simulation results.

4. CONCLUSION

This study was conducted to find out the relationship between human subjective responses and daylighting simulations by using recently adopted climate-based daylight metrics. This study also aimed to compare the correlation results of daylighting simulations and participants subjective responses between architects and non-architects' group. Therefore, a daylighting simulation study was conducted, and participants were asked to evaluate three study spaces in a HEI at Tiruchirappalli, India.

The sDA simulation reveals that all three study spaces lack daylight. The findings of this study put up a question on the predictive ability of the questionnaire items D2, D3, E2 and E3 for the simulation results. This gap should be addressed in future researches to find out the best-suited questionnaire items to predict the relationship between simulation results and subjective responses. The questionnaire items B3, C3 and B2, C2 were found as the most correlated indicators to predict the annual and point-in-time daylighting simulations, respectively. The illumination range of 75-150 lux and 200-500 lux were correlated best with the subjective responses of architects for the annual and point-in-time daylighting simulations, respectively. The results of independent sample t-test revealed that the point-in-time simulation results correlated more with the participant's subjective responses than the annual simulation results. The findings of this study also gave an initial insight on the prediction ability of simulation results by architects and non-architects. The results suggested that the expert participants (architects) can better predict the daylight simulation results than the naïve participants (non-architects). In other words, architects were able to evaluate the daylighting performance of a space more precisely than non-architects.

However, the authors acknowledge that the results of this study should be tested again in future researches. Still, this study provides new findings regarding the predictive ability of simulation results by architects and non-architects. It also provides valuable inputs on the application of recently adopted climate-based daylight metrics and daylight simulations. This study was conducted in the context of the HEIs of India. Still, more studies are required to validate the findings of this study by including various building types, daylighting strategies across different climates.

REFERENCES

1. Federation of Indian Chambers of Commerce and Industry. (2020). *FICCI*. <http://www.ficci.in/sector-Details.asp?sectorid=11>

2. Jovanovic, A., Pejic, P., Djoric-Veljkovic, S., Karamarkovic, J., & Djelic, M. (2014). Importance of building orientation in determining daylighting quality in student dorm rooms: Physical and simulated daylighting parameters' values compared to subjective survey results. *Energy and Buildings*, 77, 158–170.
3. Korsavi, S. S., Zomorodian, Z. S., & Tahsildoost, M. (2016). Visual comfort assessment of daylit and sunlit areas: A longitudinal field survey in classrooms in Kashan, Iran. *Energy and Buildings*, 128, 305–318.
4. Zhang, A., Bokel, R., van den Dobbelsteen, A., Sun, Y., Huang, Q., & Zhang, Q. (2017). Optimization of thermal and daylight performance of school buildings based on a multi-objective genetic algorithm in the cold climate of China. *Energy and Buildings*, 139, 371–384.
5. Verma, T., & Valdaris, B. (2019). Evaluating the Daylighting Performance of Lecture Halls: A Simulation-Based Approach. *53rd International Conference of the Architectural Science Association*. 53rd International Conference of the Architectural Science Association, Roorkee.
6. Van Den Wymelenberg, K., Inanici, M., & Johnson, P. (2010). The Effect of Luminance Distribution Patterns on Occupant Preference in a Daylit Office Environment. *LEUKOS*, 7(2), 103–122.
7. Veitch, J. A., Charles, K. E., Farley, K. M. J., & Newsham, G. R. (2007). A model of satisfaction with open-plan office conditions: COPE field findings. *Journal of Environmental Psychology*, 27(3), 177–189.
8. U.S. Green Building Council. (2020). USGBC. <https://www.usgbc.org/>
9. Bureau of Energy Efficiency. (2017). *Energy Conservation Building Code*.
10. IESNA-Daylight Metrics Committee. (2012). *Lighting measurement LM-83, Spatial Daylight Autonomy (sDA) and Annual Sunlight Exposure (ASE)*. Illuminating Engineering Society of North America.
11. Nezamdoost, A. (2015). Daylit Area Revisited: A Comparative Sensitivity Study of Daylit Area Drawings with Daylight Results from Point-In-Time and Annual Simulations. *IES Conference*. IES Conference, Indianapolis.
12. Nezamdoost, A. (2016). Sensitivity Study of Annual and Point-In-Time Daylight Performance Metrics: A 24 Space Multi-Year Field Study. *ASHRAE and IBPSA-USA SimBuild 2016 Building Performance Modeling Conference*. ASHRAE and IBPSA-USA SimBuild 2016 Building Performance Modeling Conference, Salt Lake.
13. Nezamdoost, A., & Van Den Wymelenberg, K. G. (2017b). Revisiting the Daylit Area: Examining Daylighting Performance Using Subjective Human Evaluations and Simulated Compliance with the LEED Version 4 Daylight Credit. *LEUKOS*, 13(2), 107–123.
14. Van Den Wymelenberg, K. G. (2014). Visual Comfort, Discomfort Glare, and Occupant Fenestration Control: Developing a Research Agenda. *LEUKOS*, 10(4), 207–221.
15. Reinhart, C. F., & Weissman, D. A. (2012). The daylit area – Correlating architectural student assessments with current and emerging daylight availability metrics. *Building and Environment*, 50, 155–164.
16. Hesong, L. (2012). *Daylight Metrics: PIER Daylighting Plus Research Program* (p. 387). California Energy Commission.
17. Nezamdoost, A., & Van Den Wymelenberg, K. (2017a). A daylighting field study using human feedback and simulations to test and improve recently adopted annual daylight performance metrics. *Journal of Building Performance Simulation*, 10(5–6), 471–483.
18. Reinhart, C., Rakha, T., & Weissman, D. (2014). Predicting the Daylit Area—A Comparison of Students Assessments and Simulations at Eleven Schools of Architecture. *LEUKOS*, 10(4), 193–206.
19. *National Building Code*. (2016). Bureau of Indian Standards.

Solar Cube

An affordable answer to address housing shortage and energy deficit in Argentina

GUSTAVO ADOLFO ROJO PLA¹², XAVIER EMMANUEL ROJO PLA¹,
RICARDO DANIEL ROJO¹, ANA CECILIA GARZA GONZALEZ²

¹ Arquitectura Rojo Rojo, Córdoba, Argentina

² E.lab Eficiencia + Sustentabilidad, Monterrey, México

ABSTRACT: In the last decade, residential demand was responsible for 26% of Argentina's total energy consumption [2]. This research attempts to generate a reflection on the importance of energy efficiency applied to new social housing in Argentina to face two national problems simultaneously: the housing insufficiency and the energy deficit. For this purpose, a social housing model was developed for a family of up to four members, with the aim of being used as a basis for the development of future public housing programs. The starting point for this proposal is a precise climate analysis, which allowed us to choose the most effective strategies. During the design process, each strategy was analysed through an energy simulation software which showed the energy behaviour of the project. In addition, the universal accessibility regulations for public buildings were applied to the proposal. Finally, a comparison was made with conventional social housing, showing that a significant reduction in energy consumption can be achieved without increasing the cost of construction.

KEYWORDS: Nearly Zero Energy Building (NZEB), Passive House, Energy Simulation, Social Housing, Inclusive Design.

1. INTRODUCTION

In Argentina, according to the National Secretariat of Urban Development and Housing, the residential deficit is of approximately 3.5 million houses [1]. In addition, the National Energy Balance of Argentina [2] has been in deficit since 2011.

The demand for residential energy increased strongly in the last half century, from 18% to 25%. Furthermore, between 2005 and 2017, the demand for residential electricity grew by 86%, double the growth of the total electricity demand (43%) [3].

To tackle these issues it is necessary to build new social housing projects but it is of fundamental importance to reduce its energy demand through efficient construction.

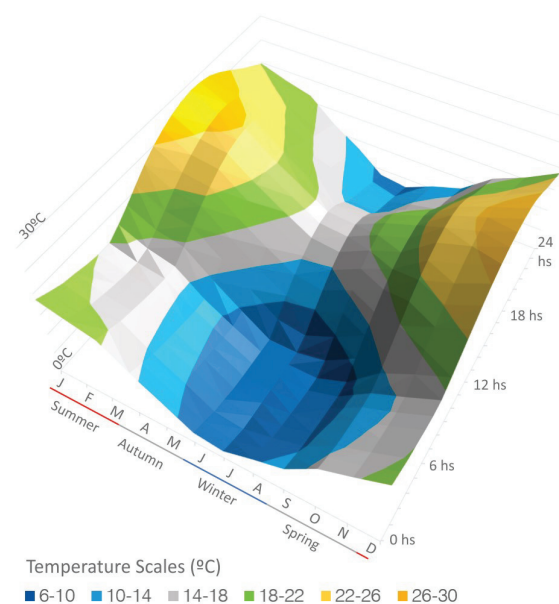
The objective of this project is to present an affordable residential typology with low impact in the site, energy efficient, and inclusive by taking into account the materials and labour available in the region.

The climatic zone selected is the Pampas region, which according to the latest National Population and Housing Census, accounts for 66.2% of the country's population [1].

2. CLIMATE ANALYSIS

The starting point of this project is a precise climate analysis, which is characterized by a clear differentiation of the four seasons of the year. Summer is known for its hot afternoons (average

30°C) and comfortable nights, while in winter, temperatures are constantly below 20°C, with average minimum temperatures of 0-5°C. The intermediate seasons have comfortable afternoons and cold nights. The average daily thermal amplitude is 12°C. The average hourly temperatures through the year are shown in Graph 1.



Graph 1: Average hourly temperatures per month

3. CONVENTIONAL ARCHITECTURE IN THE REGION

The lack of awareness of the population and professionals of the impact of construction and energy consumption, in addition to the low prices of energy resources [6-7], have led architecture to abandon old traditional construction techniques which passively protected buildings from exterior temperatures. Instead, now the buildings have poor envelopes and solve interior thermal comfort by installing inefficient active systems.

Nowadays, conventional architecture is characterized by the absence of thermal insulation in vertical facades and minimal in roofs. The windows consist of basic aluminium frames and single 4 mm glass.

4. DESIGN PROCESS

4.1 Form and Architecture

The project was developed for low density neighborhoods, in a site with the minimum width normally allowed: 10 meters.

The intention of this proposal was to find a compact form that could be built in any site maintaining each of its façades facing each “pure” orientation. After analysing several options, the final form chosen was a cube designed to fit in a 10 m diameter circle, so that it fits in every site of the project and could be rotated to maintain the ideal orientation for each facade (Figure 1).

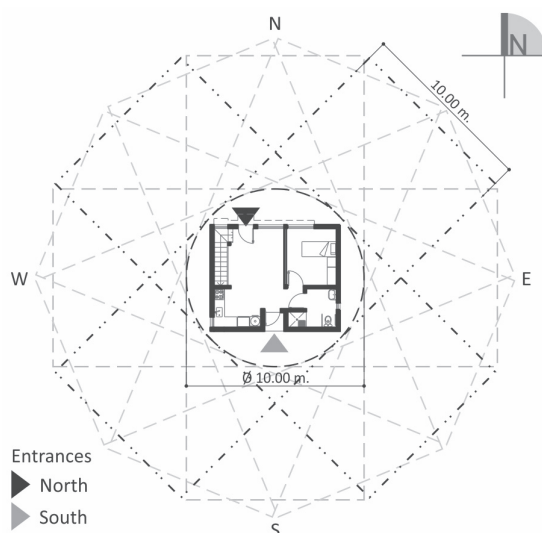


Figure 1: Site plan of a house showing the location in different land's orientations.

The idea of a compact form was to reduce the exposed surfaces to unwanted exchange of energy between interior and exterior, while the idea of maintaining “pure” orientations was to have defined strategies for each façade that could respond better to the climate through each day and season of the year. In Figure 2, it can be observed how the facades that receive higher radiation during summer, are

precisely the ones that receive less radiation in winter, and vice versa. This is due to the sun path, which responds to a geometric logic 100% predictable during time. The use of this information is essential to take advantage of the benefits of working with “pure” orientations.

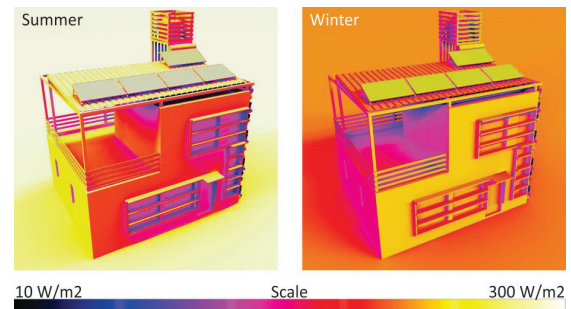


Figure 2: Solar radiation received per hour (W/m^2)

As shown in Figure 3, to prioritize the comfort in the living spaces, these were located to the north while service spaces were located to south. Also, in this way plumbing installations were reduced and more efficiently distributed. The stairs were designed in one line located in the west facade to optimize space and protect the living spaces from high solar radiation in summer.

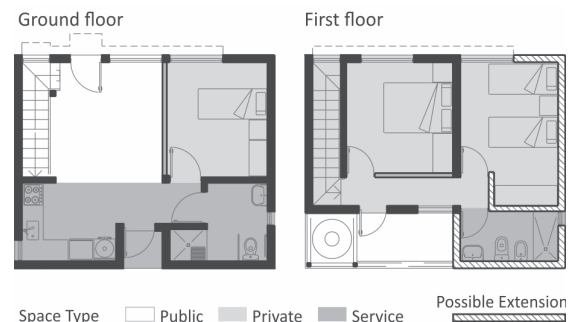
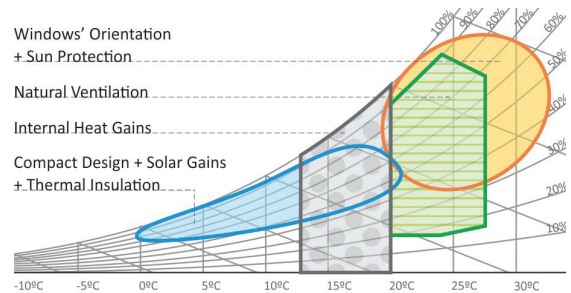


Figure 3: Location of different space types.

4.2 Passive Strategies

The design methodology used was based in two principles of NZEB (Nearly Zero Energy Building): First reduce the demands through passive strategies and then generate energy through renewable sources to satisfy the already reduced energy consumption.

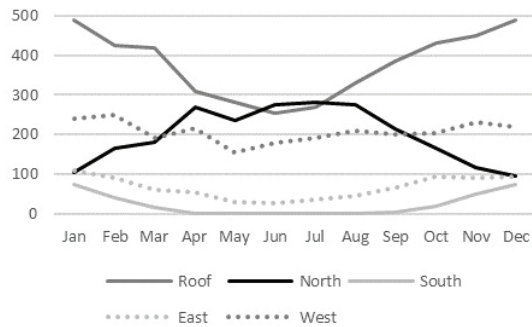


Graph 2: Psychometric graph with main design strategies

In order to reduce the energy demand of the house, a rigorous analysis of the climate allowed us to choose the most efficient passive strategies (Graph 2):

a) Solar Radiation

Graph 3 shows the amount of radiation that each facade receives through the year.



Graph 3: Average radiation per hour per facade (W/m2).

During summer, the facades that receive the highest radiation are west and horizontal (roof), so in order to protect them from heating which could increase the demand for cooling, a tensioned substructure with climbing plant was proposed in the west facade, and a vented over roof for the horizontal facade as shown in Figure 4.

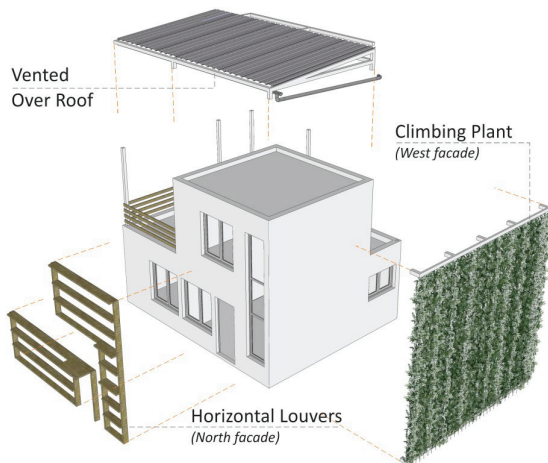
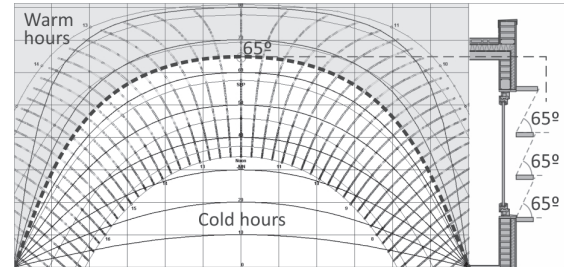


Figure 4: North, west and horizontal facades

The radiation received in the north facade is concentrated in winter, precisely when it is necessary to absorb heat. So, in order to take advantage of solar radiation for heating spaces, windows were designed to be mostly in this facade (Figure 4).

The windows have horizontal louvers which were calculated by analysing the sun path throughout the year (Graph 4), and defining the design angle that

could allow solar radiation during winter days but protect from it during summer days. In this case, the ideal angle to define the horizontal louvers is 65°.

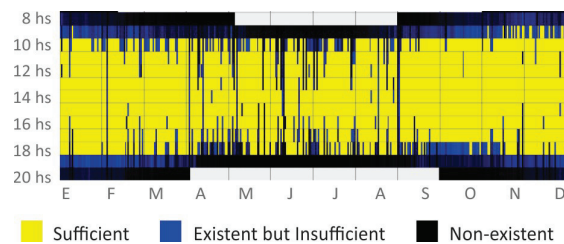


Graph 4: North windows' Shading overhangs calculation

The south and east facades are the ones that receive the least radiation throughout the year, even south facade receives no radiation at all the whole winter. Therefore, these envelopes are more opaque and insulated.

b) Daylight

Public and private living spaces have daylight autonomy during the day almost all year, as shown in Graph 5.



Graph 5: Daylight Autonomy (hours per month)

Even though daylight is more concentrated in living spaces, it can be observed in Figure 5 that it also reaches the service spaces with values around 300 lux which exceeds argentine standards and regulations [4].

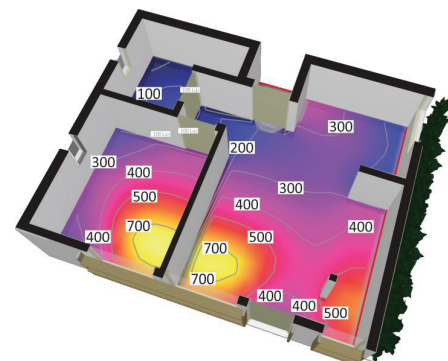
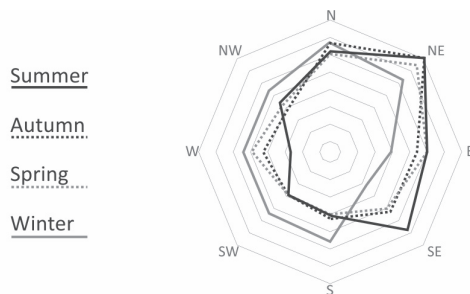


Figure 5: Distribution of daylight through the house (lux)

c) Natural Ventilation

As it was shown before in Graph 2 (Page 2), natural ventilation is possible as a passive cooling strategy taking advantage of winds and convection during certain periods of the year. This is possible when the ambient temperature is around 16-22 °C: during the summer nights and during the day in spring and autumn, in general. According to Graph 6, winds are predominant from the Northeast during the mentioned seasons [5].

The design allows these winds to pass through the house when convenient, which in addition to the thermal mass of the walls and slabs, allows us to reduce or eliminate the need of cooling during these times.



Graph 6: Wind direction per season

When wind speed is not enough for natural ventilation, an extractor is proposed to mechanically assist it with low energy consumption, as shown in Figure 6. It is located at the top of the western wall (staircase) to take out the hottest air and also, take advantage of convection.

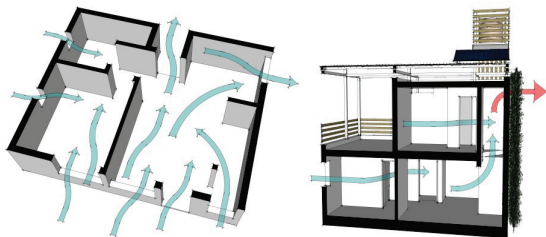
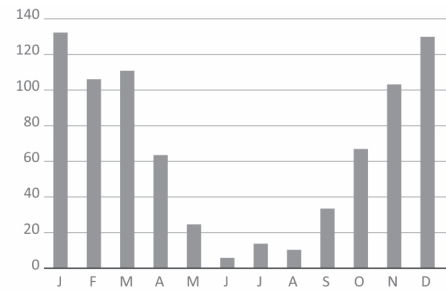


Figure 6: Natural ventilation and air extractor.

4.3 Water Efficiency

The efficient use of water was also a concern in this project. One of the proposed strategies to reduce potable water consumption was to collect rainwater from the roof into a 1,000 L tank and use it for the toilets.

In Graph 7 it is shown that the rains are seasonal, concentrated in spring-summer (120 mm per month) and almost no rains in winter [5]. This was considered to calculate the capacity of the rainwater storage tank.



Graph 7: Monthly Rainfall (mm.)

Besides rainwater, it is also proposed to use grey water among every five to ten houses for irrigation of green areas and cleaning of pavements. The necessary treatment to recover this water consists on regeneration stations of an underground tank with a bioreactor with membranes. The system works in 4 stages: roughing, biological oxidation, filtration and accumulation.

It is also important to install efficient sanitary equipment, for example faucets with aerators which reduce 50% of the water flow and hence consumption. Toilets should be double flush to also allow reduction of water use.

4.4 Community Garden

Thinking that sustainability consists of reducing the environmental impact of our actions in the planet, while preserving it for the future generations and at the same time improve the life quality of actual society, the proposal includes to generate community spaces in the project. Each site would share the courtyard forming a community garden in the “heart” of each block as shown in Figure 7. This will have recreational spaces and play yards for kids, in order to promote the good relationship between neighbours and productive activities. This space would also have a cultivating space for the following benefits:

- Provide organic food for the residents
- Avoid the CO2 footprint of food transportation
- Reuse greywater for irrigation
- Use the organic waste as compost

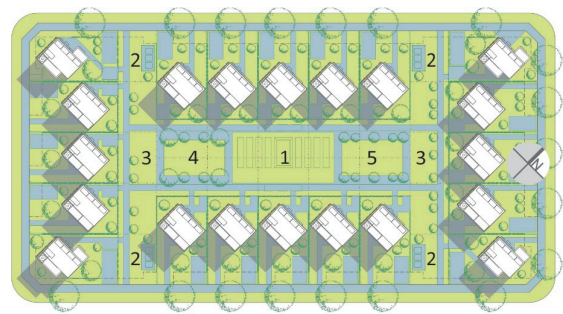


Figure 7: 1. Community Garden 2. Waste Separation 3. Gray Water Regeneration 4. Play Yards 5. Multiple Uses Space

4.5 Inclusive Design

Universal accessibility was resolved in the ground floor, where there are all the indispensable spaces easily accessible by wheelchair: handicapped bathroom, bedroom, kitchen, and dinner-living room.

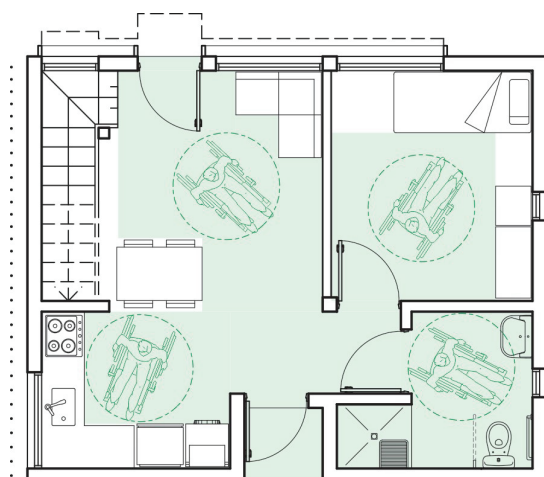


Figure 8: Ground floor. Scale 1:100

4.6 Construction System

The construction is simple and combines traditional techniques with new systems. The walls are made of bricks produced in the region, whose thermal inertia stabilizes the interior temperature. The thermal insulation is made of expanded polystyrene (20 kg./m³) and is located on the outer side of the shell. A metallic structure works as a roof cover, roof of the upper floor terrace, and support for railings and water tanks at the same time.

The construction of the walls has insulation and thermal mass by using thick bricks with exterior EWIS (External Wall Insulation System) system. The windows have PVC frames with double contact closing and double glazing.

4.7 Low Environmental Impact

One of the priorities was to maintain a low environmental impact, so different strategies were proposed according to the site and the selection of resources.

The project is developed in two floors, reducing the building footprint, and generating a larger green area. In the exterior an average of 6 trees of regional species per site were proposed.

The materials used for construction would be sourced regionally to reduce CO₂ from transportation. The wood would be from sustainable forests that are being constantly regenerated from the Cordoba mountains, oven dried and with immersion impregnation treatment. It is recommended that they have FSC (Forest Stewardship Council) certification or similar.

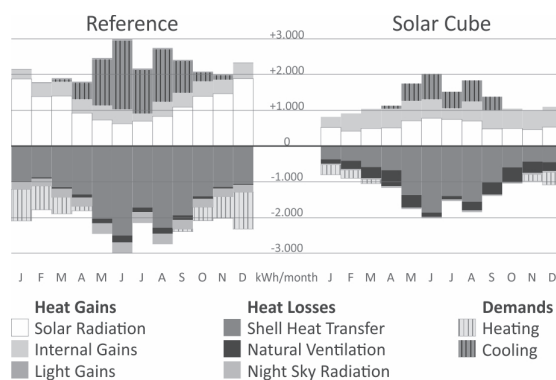
5. ENERGY CONSUMPTION

5.1 Comparison with Conventional Architecture

The energy balances in Graph 8 shows, as a mirror, how the gains and losses of thermal energy are compensated per month, first in a conventional social housing and then in the proposal.

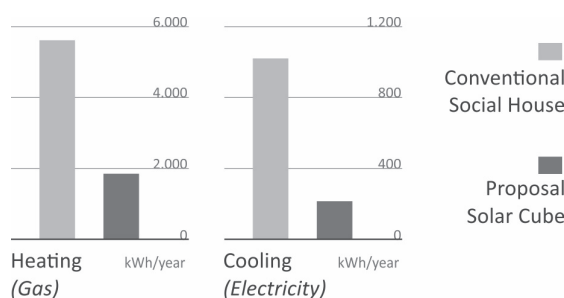
Is evident how the decrease of energy losses (through walls per transmission, as well as night radiation to the sky) reduces drastically the heating demands from 5.597 kWh/year to only 1.424 kWh/year (-75%). On the other hand, the considerable decrease of received solar radiation due to the orientation of the windows and the protection by overhangs, added to the use of natural ventilation for cooling, allows a cooling demand reduction of 80%, from 3.047633 kWh/year to only 633 kWh/year.

As a reference, the standard Passivhaus limits for cooling and heating demands are 15kwh/m² per year each one. In this case study, the heating demand was reduced from around 89 to 22 kWh/m² year, and the cooling demand from around 48 to 10 kWh/m² year.



Graph 8: Energy Balance

The set of strategies applied in this project decreases the demand for air conditioning and lighting by 75% compared to traditional social housing. This reduction directly impacts consumption, which can be further reduced using efficient equipment. For this analysis, a traditional social housing was taken as a reference, and the level of efficiency of the equipment was not modified to avoid distorting the comparison (Graph 9).

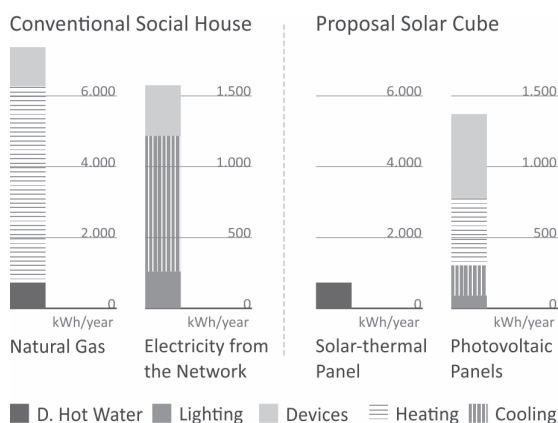


Graph 9: Energy Consumption

5.1 Renewable Energy (NZEB)

Considering that some states of this region, for example Córdoba, are moving forward towards distributed energy generation, which avoids the need of storing energy, it is proposed to install four photovoltaic polycrystalline panels of 270 W each with an inclination angle of 27°, to generate 344 kWh per year per panel. These are enough to cover the reduced demands of thermal conditioning, lighting and other electrical devices (Graph 10).

For the domestic hot water demand it is proposed a solar-thermal panel of 2m² area and a storage tank of 200 L. The inclination of the panel would be 45° in order to receive higher solar radiation during winter months, that is when the hot water demand is higher, as shown in Graph 10.



Graph 10: Energy Supply

As a result, using only 4 photovoltaic panels and 1 solar thermal panel, a Net Zero Energy Building is obtained.

6. HOME AFFORDABILITY

The total cost of this residential module, calculated in February 2019, is AR\$ 1,663,507 [8], equivalent to € 38,067 [9]. Thus, the cost per square meter is € 539 (AR\$ 23,650/m²), slightly less than the cost of standard construction in Córdoba (AR\$ 24,600/m² [10]).

Therefore, this project allows a typical family (3 to 4 members) to save approximately 1,000 kWh of electrical energy and 500 m³ of natural gas per year, without increasing construction costs.

Thus, the savings are \$ 7,425 [6] in electricity and \$ 7,331 [7] in gas, making a total of \$ 14,756 per year (equivalent to € 338 [9]). These annual energy savings represent about 1% of the total cost of building the home.

These savings do not include the energy generated by the installation of solar panels. In the case of installing one solar thermal panel (for DHW) and four photovoltaic panels, and in this way covering

the total energy consumption, the investment is amortized with the additional energy savings generated.

7. CONCLUSION

The low historical cost of energy and the lack of social awareness have led to the construction of precarious housing in terms of energy efficiency, so there is a big margin for improvement. This project demonstrates that it is possible to slash energy demands using simple application strategies without extra costs.

As a result, the Solar Cube makes it possible to reduce both, the housing and energy deficits, and shows us that sustainability is not necessarily complicated or expensive, but quite the opposite.

“Global warming, as well as growing inequality, are the main challenges that the planet is facing at the beginning of the 21st century” [11], and this proposal aims to help solve these two challenges partially.

There is a lot of work ahead.

ACKNOWLEDGEMENTS

This project was possible thanks to the encouragement and support of our families, our acknowledgements are especially to them.

REFERENCES

1. National Institute of Statistics and Censuses of the Argentine Republic (INDEC). www.indec.gob.ar
2. Ministry of Energy and Mining of the Nation. National Energy Balance of the Argentine Republic. www.argentina.gob.ar/produccion/energia/hidrocarburos/balances-energeticos
3. Lic. María Victoria Buccieri. “Energy deficit in Argentina: impact of alternative supply and demand policies”. Master Thesis, July 2018. Buenos Aires University (UBA), CEARE. www.ceare.org/tesis/2018/tes28.pdf
4. National electricity regulator (ENRE). IRAM-AADLJ20-06 Standard, Table 2, Minimum lighting intensity. www.argentina.gob.ar/enre
5. National Meteorological Service of Argentina. Pilar Meteorological Observatory. www.smn.gob.ar
6. End user rates table 02/2019 - Resolution ERSEP N° 01-2019 - EPEC - Provincial Electric Power Company of Córdoba (Argentina). www.ersep.cba.gov.ar
7. Residential user rates of natural gas in the Province of Córdoba (Argentina). Gas Distributor of the Center. www.enargas.gob.ar
8. Cost of Items in Architectural Works. Institute of Statistics and Census, Association of Architects of the Province of Córdoba, Argentina. Values February 2019. www.colegio-arquitectos.com.ar
9. Historical exchange rates of the Euro in Argentina, 02/14/2019, 43.70 \$/€. www.cotizacion-dolar.com.ar
10. Construction Cost Index (ICC-Cba). Base February 2019. www.datosestadistica.cba.gov.ar
11. PIKETTY, THOMAS. Capital and Ideology. France: Éditions du Seuil, 2019. 1.247 p.

The influence of building form on energy use, thermal comfort and social interaction

A post-occupancy comparison of two high-rise residential buildings in Singapore

JUAN CARLOS GAMERO-SALINAS ¹, NIRMAL KISHNANI ², AURORA MONGE-BARRIO ¹,
BHAVYA GANDHI ², MEGHA BILGI ², ANA SÁNCHEZ-OSTIZ ¹

¹ School of Architecture. Department of Construction, Building Services and Structure. University of Navarra (UNAV), Pamplona, Spain

² School of Design and Environment. Department of Architecture. National University of Singapore (NUS), Singapore

ABSTRACT: Two recently completed high-rise residential developments, located side-by-side in a neighbourhood in Singapore, are compared in a post-occupancy study. Both have near identical demographics, are exposed to the same microclimate, and constructed with a similar palette of materials. The primary difference is form. One has a high degree of porosity with inner voids that act as conduits for natural air flow and offer a sheltered space for social engagement. The other is more compact, less porous and has social spaces attached to the building's exterior. The study included surveys of residents, behavioural observations and environmental measurements. On three counts – self-reported energy use, thermal comfort and social interaction – the former appears to be more successful than the latter. Findings suggest that building form affects multiple outcomes at once. A form strategy that lowers energy use, for instance, can also improve social engagement. The implication of this socio-environmental approach to form-making is discussed in the context of high-density tropical typologies.

KEYWORDS: Building Form, Energy Use, Social Interaction, Thermal Comfort, Tropical Climate

1. INTRODUCTION

Building form is an important factor that shapes environmental performance. Form variables such as geometry, compactness and porosity play a key role in passive outcomes, such as shade, access to daylight and natural ventilation [1]. Passive design has long been a consideration at the drawing board, as this pertains to indoor comfort and energy demand [2], and more recently to overheating risk reduction [3,4,5]. In the tropical context, the emphasis on passive design and measured performance, as drivers of form-making, was first advocated by Malaysian architect, Ken Yeang, who applied it high-rise buildings in dense urban conditions [6]. His case for the *bioclimatic model* – which proposed form-features such as skyterraces and form-strategies like placement of service cores to reduce solar gains – was influential in the 80s and 90s in Southeast Asia, at a time when energy security was a concern [2]. With the advent of the Green movement in the 2000s, however, the question of performance was assigned to electro-mechanical solutions such as air conditioning. At this time, design firms like WOHA (Singapore) also began experimenting with new form typologies that could push the limits of passive design [7]. What is noteworthy about strategies by WOHA is that they merge the environmental and the social [8].

Gaps in buildings that facilitate airflow, for instance, are also the spaces for social gatherings.

2. BACKGROUND

In 2008, the Housing & Development Board (HDB) of Singapore commissioned two high-rise public housing developments (Figure 1) within the same neighbourhood. Both buildings, completed in 2015, have a near identical demographic breakdown, are exposed to a similar microclimate, and constructed with a similar palette of materials.



Figure 1: Building A (left) and Building B (right)

The primary difference is their approach to form. Building A (Figure 2), by architects WOHA

(Singapore), has a significant degree of porosity – gaps in the façade that let natural airflow pass through the towers. There are 12 vertically distributed skyterraces (four per tower) that, with the sky roof, act as social spaces. An inner void that runs vertically through each tower accelerates air flow, and acts as a semi-outdoor buffer space that mediates between outdoor conditions and apartment interiors. Each apartment opens onto this inner void, with which it interacts socially and environmentally.

Building B (Figure 3), by comparison, is compact and less porous. It has six skybridges for its residents, and one skygarden above a multi-storey carpark. None of these, however, are fully sheltered, nor are they directly connected to the apartments.

WOHA has stated that the design goals for Building A are occupant comfort, lower energy demand and social engagement [8]. The designer of Building B has spoken of creating a community building in the Modernist vocabulary [9,10].

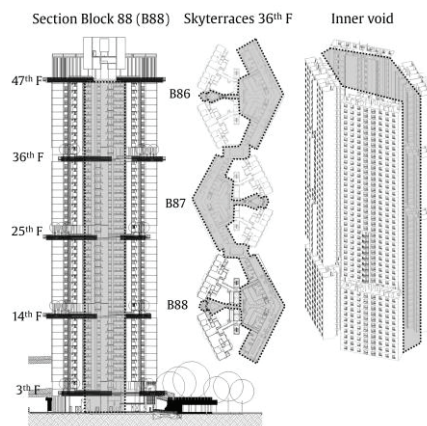


Figure 2: Building A showing section, floor plan with skyterraces and tower axonometric with inner void

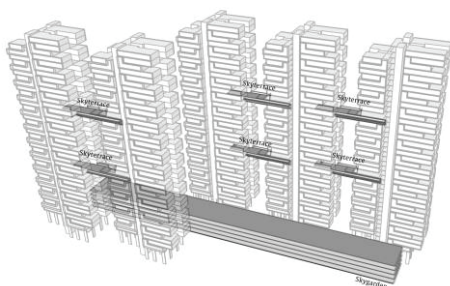


Figure 3: Building B axonometric showing skyterraces

This study set out to assess performance, as stipulated by the architects, and to gauge the extent to which performance can be linked to building form.

3. METHODOLOGY

The survey study began in August 2019 with residents of each building. Table 1 summarises the number of survey respondents in relation to the total number of apartments per building. This was augmented with behavioural observations,

estimation of building form variables and environmental measurements.

Table 1: Population and sample size for each building.

Building	Nº of apartments	Nº of surveys	%
Building A	960	49	5.10
Building B	758	46	6.07

3.1 Survey

Surveys were carried out in the common areas of each building. Surveyees were randomly selected

On energy use, surveyees were asked: ‘*what is your approximate monthly electricity bill?*’ (Q1). The options they were given were based on Singapore Power National Average Household Consumption for 2019 [11]. Surveyees were also asked ‘*do you have air-conditioning (AC) installed in your home?*’ (Q2), and ‘*at what time of the day is it usually turned on?*’ (Q3).

On use of social spaces, surveyees were asked ‘*do you visit the skyterraces in your estate?*’ (Q4). If they answered ‘yes’, they were then asked: ‘*how often?*’ (Q5), ‘*how much time do you spend in them?*’ (Q6), and ‘*why you visit them?*’ (Q7). Additionally, residents were asked (on a Likert scale) if ‘*skyterraces (including roof) are used by their neighbours?*’ (Q8).

To gauge social interaction between residents, surveyees were asked ‘*how many neighbours in your estate are you friends with?*’ (Q9). For this question, the answer options were ‘0-4’, ‘5-9’, ‘10-14’, ‘15-19’, ‘20-25’ and ‘25-30’.

On the question of comfort, surveyees were asked ‘*in terms of thermal comfort, how do you generally feel in the skyterraces and roof of your estate?*’ (Q10). They could answer from a 5-point thermal comfort scale, commonly used in comfort studies [12].

Each surveyee was asked his/her age, household size, floor level where s/he lives and how long s/he had been living in the development.

3.2 Building Form

The ratio of social space to total built-up area was calculated. The proportion of social areas in shade vs without shade was estimated. These calculations included both skyterraces and roofs above carpark. Another consideration was the percentage of building façade exposed to outdoor conditions. In Building A, the façade facing the inner void was deemed ‘not exposed’. For Building B, the façade adjacent to circulation corridors, voids and staircases was likewise categorised ‘not exposed’.

3.3 Behavioural Observations

Skyterraces in both buildings were visited every two hours from 14:00 until 18:00 (i.e. a total three times per afternoon) from August 6 to 9 and again, between August 12 to 14. During each visit, the number of visitors was counted. Counting was carried

out in the afternoons since occupants were observed to visit skyterraces mostly during the afternoon and evening, as observed during surveys.

3.4 Measurement of Environmental Conditions

The air temperature (T_a) of skyterraces and outdoor conditions was measured for 6 days (July 25 – July 30, 2019). Air velocity (V_a) was measured on day 1 and 2 of that same period, but only for Building A.

Only skyterraces linked to towers of buildings A and B were selected for temperature measurements (i.e. excluding social spaces on roofs of carparks). Three skyterraces on 14th, 25th and 36th storeys of Building A was selected, along with two on the 18th and 33rd storeys of Building B, which were at a similar height.

Readings were taken at 4pm, when the day was typically warmest. Reference ‘outdoor’ readings were taken on the roof of carparks of both buildings; the sensors here were sheltered from direct sun and placed less than 50 meters away from nearest skyterrace.

3.5 Statistical Analysis

Non-parametric statistical tests were carried out on data from the surveys. For Q1, Q8, Q9 and Q10 Mann-Whitney’s two sample test was performed; for Q2 and Q3 Fisher’s exact test; for Q4, Q5, Q6 and Q7 Pearson’s Chi-squared test. The analyses were done with Rstudio software. Rstudio functions *chisq.test*, *fisher.test*, *wilcox.test* and *shapiro.test* were used, respectively.

Mann-Whitney’s two sample test was used to compare measurements of buildings A and B.

4. RESULTS

Tables 2 and 3 summarise responses to survey questions. Table 4 summarises building form variables. Table 5 summarises mean values for each question and statistical significance (p-value) of the difference between the two buildings.

Table 2: Summary of responses to energy questions.

	Building A	Building B
Q1. What is your approximate monthly electricity bill?		
<\$100 (SGD)	2 (6.5%)	1 (2.7%)
\$50-\$99 (SGD)	13 (41.9%)	11 (29.7%)
\$100-\$149 (SGD)	12 (38.7%)	13 (35.1%)
\$150-\$199 (SGD)	2 (6.5%)	7 (18.9%)
\$200-\$249 (SGD)	2 (6.5%)	5 (13.5%)
Q2. Do you have installed AC in your home?		
Yes	48 (98.0%)	45 (100%)
No	1 (2%)	0 (0.0%)
Q3. At what time of the day are they usually turned on?		
Morning	0 (0.0%)	0 (0.0%)
Afternoon	1 (2.4%)	0 (0.0%)
Evening	2 (4.8%)	0 (0.0%)
Night	43 (93.5%)	43 (97.7%)

Table 3: Summary of responses to social questions.

	Building A	Building B
Q4. Do you visit the skyterraces of your own estate?		
Yes (1)	46 (93.9%)	36 (78.3%)
No (0)	3 (6.1%)	10 (21.7%)
Q5. How often do you visit the skyterraces?		
Every day or many times a week	18 (39.1%)	5 (13.9%)
Once a week	13 (28.3%)	12 (33.3%)
Once or twice a month	15 (32.6%)	19 (52.8%)
Q6. How much time do you spend on them?		
< 30 minutes	18 (41.9%)	16 (44.4%)
>= 30 minutes	25 (58.1%)	20 (55.6%)
Q7. Why do you visit the skyterraces and roof?		
a. Socialize with neighbours	13 (30.2%)	7 (19.4%)
b. Look at the views	27 (62.8%)	16 (44.4%)
c. To take kids to play	10 (23.3%)	15 (41.7%)
d. To exercise	5 (11.6%)	19 (52.8%)
Q8. Are the skyterraces used by your neighbours?		
1 Yes, a lot	7 (14.9%)	5 (10.9%)
2 Yes, somewhat	26 (55.3%)	15 (32.6%)
3 Yes, but not so much	12 (25.5%)	20 (43.5%)
4 Not at all	2 (4.3%)	6 (13.0%)
Q9. How many neighbours in your estate are you friend with?		
0-9 neighbours	16 (35.6%)	16 (44.4%)
10-19 neighbours	8 (17.8%)	3 (8.3%)
20-29 neighbours	3 (6.7%)	1 (2.8%)
Q10. In terms of your thermal comfort, how do you generally feel in the skyterraces of your estate?		
+2 (very comfortable)	8 (16.7%)	3 (7.3%)
+1 (Comfortable)	36 (75.0%)	21 (51.2%)
0 (Neutral)	4 (8.3%)	13 (31.7%)
-1 (Uncomfortable)	0 (0.0%)	4 (9.8%)
-2 (Very uncomfortable)	0 (0.0%)	0 (0.0%)

Table 4: Summary of building form variables

	Building A	Building B
Skyterrace area (social space)		
Shaded	13,404 m ² (63.2%)	582.6 m ² (11.8%)
Unshaded	7,800 m ² (36.8%)	4,352.2 m ² (88.2%)
Total	21,204 m ² (100%)	4,934.8 m ² (100%)
Gross floor area [13]	111,106 m ²	87,000 m ²
Skyterrace as % GFA	19.1%	5.7%
Percentage of façade directly exposed to outdoor conditions		
Directly exposed	43.3%	53.6%

Table 5: Mean responses and statistical significances of the difference between Building A and Building B.

	Building A	Building B	p-value
Energy-related aspects			
Average self-reported electricity bill (Q1)	\$107.3 (n=31)	\$130.4 (n=37)	0.038 (*)
Average number of dwellings with AC (Q2)	98.0% (n=49)	100% (n=45)	0.477
Average number of dwellings that turn on AC at night (Q3)	93.5% (n=46)	97.7% (n=44)	0.085 (.)
Social aspects			
Average number of neighbours that residents consider as friends (Q9)	10.2 (n=27)	7.5 (n=20)	0.0710 (.)
Average percentage of residents visiting skyterraces (Q4)	93.9% (n=49)	78.3% (n=46)	0.002 (**)
Average percentage of residents visiting skyterraces every day or many times a week (Q5)	39.1% (n=46)	13.9% (n=36)	0.000 (***)
Average percentage of residents that spend more	58.1% (n=43)	55.6% (n=36)	0.886

than 30 minutes on skyterraces (Q6)			
Average likelihood of neighbours visiting skyterraces, in Likert scale (Q8)	2.19 (n=47)	2.59 (n=46)	0.008 (**)
Average thermal comfort in skyterraces, in a 5-point thermal comfort scale (Q10)	+1.07 (n=48)	+0.53 (n=41)	0.000 (***)
Environmental conditions			
ΔT (Ta outdoor – Ta skyterrace)	1.39°C (n=6)	0.78°C (n=6)	0.003 (**)
Air temperature at skyterrace	29.65°C (n=6)	29.81°C (n=6)	0.189
Air temperature outdoors	31.04°C (n=6)	30.59°C (n=6)	0.115
Air velocity at skyterrace	1.39m/s	-	-
Significance codes: >0.1 (.) < 0.05 > (*) < 0.01 > (**) < 0.001 > (***)			

4.1 Survey

Analysis of data suggests that the two groups, Building A vs Building B, are not statistically different for any background variable. Normality is not found in their answers either.

On energy use, the reported electricity bill of surveyees in Building A is lower than Building B by almost \$23. Building A has a mean of \$107.3; Building B, \$130.4. This finding has statistical significance. *Note: data is filtered to surveyees between 19 and 59 years of age, who are more likely to be aware of the monthly bills.*

On use of AC, even though the two buildings are not significantly different in ownership of AC, approximately 93% of those from Building A say they use AC at night compared with almost 98% in Building B. This finding is marginally significant. *Note: the analysis is filtered for surveyees who say they use AC at night since this represents over 90% of responses in both buildings.*

On use of skyterraces, 94% of surveyees from Building A say they visit skyterraces, which is found to be significantly higher than 78% of surveyees from Building B. Additionally, skyterraces in A are visited more frequently than in B, with approximately 39% of surveyees in former saying 'every day or many times a week' compared with 14% in the latter. The perception of neighbours visiting terraces in Building A tends towards 'yes, somewhat'; in Building B it is closer to 'yes, but not so much'.

On why skyterraces are visited, 30.2% in Building A say 'socialise with neighbours' compared with 19.4% in Building B. The finding is not statistically significant.

Regarding social interaction, surveyees in Building A say that they consider, on average, 10.2 neighbours as friends in comparison to surveyees on Building B who consider 7.5 neighbours as friends. The difference is marginally significant. *Note: analysis is limited to those who say 'yes' to visiting skyterraces and say they spend more than 30 minutes per visit, so as to eliminate those who are just passing through.*

On perceived thermal comfort, 91.7% of surveyees in Building A say they feel 'very comfortable' or 'comfortable'; in Building B, the figure is 58.5%. The mean answer on the comfort scale is +1.07 for Building A (i.e. towards greater perceived comfort); the mean answer for Building B respondents is 0.53 (i.e. towards neutrality).

4.2 Building Form

Building A has four times more surface area for skyterraces than B: 21,204 m² and 4,935 m², respectively. As a proportion of total built up area, skyterraces in Building A account for 19.1%; Building B, 5.7%. In Building A, the surface area of skyterraces that is shaded is 63.2%; in Building B, 11.8%. The percentage of facade in A that is exposed to outdoors is 43%; in B it is 54%

4.3 Behavioural Observations

Skyterraces in Building A account for 257 visitors during the period of measurement; Building B, 60 (Table 6). Normalised against number of households, Building A has higher visitorship per household.

Table 6: Counting of people visiting skyterraces per building during period of observations (6-9, 12-14 August)

Building	Number of people on skyterraces	Number normalised against number of households
Building A	257	0.27 per household
Building B	60	0.08 per household

4.4 Environmental factors

The mean Ta of Building A is 0.16°C lower than that in B. This difference is not statistically significant. Measured outdoor temperatures at both buildings are not significantly different and are highly correlated (R = 0.92). However, the mean ΔT in A is almost 1.4°C (14thF: 0.99°C, 25thF: 1.41°C, 36thF: 1.79°C), while in B ΔT mean is almost 0.8°C (19thF: 0.67°C, 33thF: 0.89°C). The difference between the two is statistically significant. A mean air velocity of 1.85 m/s is measured in Building A (14thF: 2.26 m/s, 25thF: 1.82 m/s, 36thF: 1.48 m/s).

5. DISCUSSION

The architects for Building A, WOHA, have said they seek, through design, three outcomes: improved occupant comfort, lower energy use, and greater social interaction [8,14]. The findings from this study suggest that Building A does better on all three counts than Building B. *However, in what ways can the success of Building A be linked, directly or indirectly, to its built form?*

The distinguishing feature of Building A is its inner core – made up of voids and skyterraces – that acts as a conduit for natural air-flow and holds spaces for social interaction. As a result of this core, parts of the building envelope are inward facing. By contrast,

Building B is compact, without voids or inner facades. Its skyterraces are fewer and affixed to its façade, and therefore more exposed to outdoor conditions.

The first *form* hypothesis relates to comfort in skyterraces. The sheltered skyterraces of Building A should fare better in terms of thermal comfort than the exposed ones in Building B. The findings from this study support this. There is a measurable difference in the mean thermal comfort response of the two groups: +1.07 for A versus +0.53 for B, i.e. the former is more comfortable than the latter. This is corroborated by temperature and air velocity readings. In Building A, ΔT between skyterraces and outdoors is 1.39°K, almost twice the ΔT in Building B. The mean V_a in Building A voids is approximately 1.9 m/s. Lower temperatures and elevated air speeds should lead to high perceived comfort.

It is likely that comfort is a variable affecting visitor preferences. In Building A, where comfort levels are higher, 94% of those surveyed say they visit skyterraces; in Building B, only 78%. Thirty-nine percent in Building A also say they visit *'every day or many times a week'* compared with 14% in B. These findings appear to align with observed visitor numbers: skyterraces in A have 257 visitors versus 60 in B. Normalised against the number of households, skyterraces in Building A (0.27) appear to be more popular than in B (0.08), assuming all observed visitors are residents of the same building. It should be noted there are other reasons for visitorship. The survey suggests *'view'* is a factor. Skyterraces in Building A are also substantially bigger than the ones in Building B, with room for more people.

The second *form* hypothesis relates to social engagement: residents of Building A, who visit skyterraces more frequently, ought to know more neighbours. This is supported by the findings: surveyees from Building A say they know an average 10.2 neighbours, compared with 7.5 in Building B, i.e. 36% more. The difference is found to be marginally significant.

The third *form* hypothesis relates to energy use. Lower temperatures and higher air flows in the central void of Building A are likely to affect energy use. Apartments that open onto this cooler core can divert air flow through their living spaces, thereby reducing the need for mechanical cooling. Inner facades, opening onto a cool void, are likely to transmit lower solar heat gain into the apartments.

The findings show a difference in energy use. The monthly energy bill is 17% lower in Building A (\$107.3) than in Building B (\$130.4), notwithstanding identical ownership of air conditioners between the groups. Several variables that might affect energy consumption can be ruled out. Both buildings have near identical demographics; they rely on a similar palette of materials and comply with the same

regulatory limit for Residential Envelope Transfer Value (RETV) of 25 W/m² [15].

From this study, it is evident that Buildings A and B are two distinct form typologies. Findings suggest that form is a likely factor affecting performance in multiple ways. The significance of these findings become clearer when they are extrapolated to the urban scale. Singapore has 1 million HDB flats [16]. If the entire stock of housing were to perform at the same level as Building A, i.e. spending 17% less on energy, the impact at the city scale would be a saving of 729 GWh/year, based on a total of 4,287 GWh consumed in 2017 by public households [17,18]. This is equivalent to a reduction of 0.305 million metric tons of equivalent CO₂ emissions, based on Singapore's 2018 Grid Emission Factor of 0.4188 kg CO₂/kWh [17]. If every HDB household were to also interact with 36% more neighbours, is likely that social capital of the city would increase. Social capital is defined as the number of relationships between people in group that leads trust and cohesion [19].

6. CONCLUSIONS

Thermal comfort, energy use and social interaction are complex outcomes, affected by many variables. In this study, building form is found to be a factor that contributes to each outcome in direct and indirect ways. In Building A, the presence of sheltered and comfortable social spaces appears to lower barriers to neighbourly interactions. The inner void and skyterraces act as a nexus of social interaction. The core also affects the energy performance of the apartments. What is seen in Building A, therefore, can be described as the integration of social and environmental objectives through form-based solutions.

Architects and researchers in the tropical regions have in the past argued for the importance of form features and strategies, such as open-to-sky courtyards and sunshades, however, primarily for social or place-making purposes [20, 21]. The notion that a form-based design approach can simultaneously affect multiple outcomes in high-rise typologies is rare. Architect Ken Yeang made a case for this in the 80s and 90s, applying the bioclimatic model to office buildings in Malaysia which were said to deliver better energy performance and occupant comfort. Two noteworthy buildings of that era were evaluated in a study, with surveys and energy audits, that revealed them to be unsuccessful in both regards [2]. This was attributed to an inconsistent application of bioclimatic principles and to the underestimation of comfort expectations and preferences.

WOHA's approach to form, represented by Building A, differs from these earlier experiments in two ways. It sees environmental performance and social engagement as interdependent outcomes. The

building also creates an onsite microclimate with sheltered inner voids. These spaces are more comfortable; they also reduce thermal load and enhance the potential for cross ventilation. This form strategy is seen in other WOHA projects like the School of the Arts and Oasia Hotel Downtown [8,14] and in some of Yeang's more recent projects such as the National Library in Singapore [22].

Cities across the globe struggle to address environmental goals and social goals, which are sometimes at odds. Singapore offers lessons on integration in the high-density tropical context [23]. In this study, Building A demonstrates how this idea can be advanced further with form-based solutions at the building scale. Lessons learnt here are particularly relevant to developing countries where capital investment and access to technology are limited.

The limits of the current study should be countered in future research by increasing survey sample sizes and accessing actual energy bills. It should consider other factors that influence thermal comfort such as radiant temperature, relative humidity, activity level, and clothing. In the Singapore context, it would be necessary to compare Buildings A and B, both relatively new, with earlier generations of public housing typologies, which had different sizes and arrangements of social space.

ACKNOWLEDGEMENTS

We would like to deeply thank the Friends of the University of Navarra. Also, we would like to thank the University of Navarra, Obra Social 'la Caixa' and Caja Navarra Bank Foundation for the mobility grant that allowed the research stay at National University of Singapore (NUS). Special thanks to Mr. Wong Mun Summ, founding director of WOHA Architects, for supporting this research. We also acknowledge the kind permission from the Housing & Development Board (HDB) and Tanjong Pagar Town Council to access the public housing shown in this paper. Special thanks to Prof. Jesús Fidalgo of the University of Navarra for his guidance in the statistical analysis.

REFERENCES

1. Olgyay, V., (2015). Design with Climate: Bioclimatic Approach to Architectural Regionalism - New and Expanded Edition. *Princeton University Press*
2. Kishnani, N., (2002). Climate, Buildings and Occupant Expectations: a comfort-based model for the design and operation of office buildings in hot humid conditions (PhD Thesis)
3. Brotas, L., Nicol, F., (2016). Using Passive Strategies to prevent overheating and promote resilient buildings. In: *PLEA 2016 Los Angeles – 32nd International Conference on Passive and Low Energy Architecture. Cities, Buildings, People: Towards Regenerative Environments*
4. Hashemi, A., Khatami, N., (2017). Effects of Solar Shading on Thermal Comfort in Low-income Tropical Housing. *Energy Procedia*, 111, p.235-244

5. Gamero-Salinas, J.C., Monge-Barrio, A., Sánchez-Ostiz, A., (2020). Overheating risk assessment of different dwellings during the hottest season of a warm tropical climate. *Building and Environment*, 171, 106664. DOI: 10.1016/j.buildenv.2020.106664
6. Yeang, K., Balfour, A., Richards, I., (1994). Bioclimatic Skyscrapers. *Artemis, London*
7. Kishnani, N., (2019). Ecopuncture: Transforming Architecture and Urbanism in Asia. *BCI Media Group*
8. Bingham-Hall, P., WOHA, (2016). Garden City Mega City: Rethinking Cities for the Age of Global Warming. *Pesaro Publishing*
9. Powell, R., Chan, S., (2004). SCDA: The Architecture of Soo Chan. *Images Publishing*
10. SCDA. Skyterrace@Dawson. Available: <http://www.scdarchitects.com/> (accessed March 11, 2020).
11. Singapore Power Group (SGP), Billing, (2020). Available: <https://www.spgroup.com.sg/what-we-do/billing> (accessed February 12, 2020)
12. Becker, R., Paciuk, M., (2009). Thermal comfort in residential buildings – Failure to predict by Standard Model, *Building and Environment*, 44 (5): p. 948-960.
13. Council on Tall Buildings and Urban Habitat (CTBUH), The Skyscraper Center. <https://www.skyscrapercenter.com> (accessed May 5, 2020).
14. Wong, M.S., Hassell, R., Yeo, A., (2016). Garden City, Megacity: Rethinking Cities for the Age of Global Warming. *CTBUH Journal*, 2016 Issue IV, p. 46-51
15. Building and Construction Authority (BCA), (2008). Code on Envelope Thermal Performance for Buildings.
16. Housing and Development Board (HDB), (2020). Public Housing – A Singapore Icon. Available: <https://www.hdb.gov.sg/> (accessed February 13, 2020).
17. Energy Authority Market (EMA), (2019). Singapore Energy Statistics 2019. Available: <https://www.ema.gov.sg/Singapore-Energy-Statistics-2019/> (accessed March 11, 2020)
18. Energy Authority Market (EMA), (2018). Singapore Energy Statistics 2018. Available: https://www.ema.gov.sg/cmsmedia/Publications_and_Statistics/Publications/ses/2018/index.html (accessed March 12, 2020)
19. Ramboll Foundation, (2016). Strengthening Blue-Green Infrastructure in our cities. Enhancing blue –green Infrastructure & Social performance in high density urban environments. Available: <https://ramboll.com/megatrend/~media/B350ABC1D9D0489AA54955B43D853EE9.ashx> (accessed May 8, 2020)
20. Bay, J.H., (2004). Sustainable community and environment in tropical Singapore high-rise housing: the case of Bedok Court condominium. *Cambridge University Press*.
21. Powell, R., Tay, K.S., Lim, A.K.S., (1997). Line, edge & shade: the search for a design language in tropical Asia: Tay Kheng Soon & Akitek Tenggara. *Page One Publishing*
22. Hart, S., (2011). Ken Yeang's National Library of Singapore. *Architecture Week*. http://www.architectureweek.com/2011/1026/environment_2-2.html
23. Centre for Liveable Cities and Urban Land Institute, (2013). Lessons from Singapore 10 Principles for Liveable High-Density Cities. Available: <http://www.clc.gov.sg/> (accessed March 10, 2020).

Recorded energy consumption of nZEB dwellings – and corresponding interior temperatures.

Initial results from the Irish nZEB101 project.

SHANE COLCLOUGH^{1,2} RICHARD O HEGARTY¹ DONAL LENNON¹ PHILIP GRIFFITHS² ETIENNE RIEUX³
OLIVER KINNANE¹

¹University College Dublin, Dublin, Ireland

²Ulster University, Newtownabbey, BT370QB, UK

³School of Sustainable Civil Engineering, Transport and Planning, ENTPE, Lyon.

ABSTRACT: Ireland is mandating the unprecedented mass market deployment of low-energy dwellings via the near Zero Energy Buildings (nZEB) standard, from 1 January 2021 due to the EU wide Energy Performance of Buildings Directive (EPBD). This is among the first academic papers to provide recorded energy and temperature data for nZEB compliant dwellings in Ireland. It reports on initial results of the www.nZEB101.ie Post Occupancy Evaluation project, the objective of which is to uncover key nZEB design and operations lessons, to aid the next iteration of the country's building regulations. This paper reports on the analysis of winter temperatures and the energy consumption of 17 nZEB compliant dwellings, each of which have been monitored for at least a 12 month period. While analysis of further properties is needed to further validate the findings, key findings to date include significantly higher than expected interior temperatures and energy consumption, and a usage profile which is significantly different from the assumptions in the DEAP National energy rating software.

1. INTRODUCTION

The near Zero Energy Building Standard (nZEB) is required for all new dwellings which will be constructed in the European Union from 2020 [1]. However, with little track record in Ireland for building such low energy dwellings, objective information about how these dwellings will perform is required. This is the first academic paper to provide recorded energy and temperature data for nZEB compliant dwellings in Ireland.

Building on an established Post-Occupancy Evaluation (POE) monitoring project of low-energy dwellings which has been running for over three years, the nZEB101 project [2] is set to uncover the key nZEB design and operations lessons as the Republic of Ireland embarks on the construction of 550,000 of these low-energy buildings by 2040 [3].

Analysis of initial data indicates that

1. Interior temperatures are significantly higher in nZEB dwellings compared with those recorded in previous POE publications, e.g. [4].
2. Interior temperatures are higher than the assumed set temperatures in the national Building Energy Rating (BER) software during the winter period [5].
3. The temperature profile has changed with the living room and Rest of Dwelling (RoD)

temperatures more constant and similar than dwellings built to previous building regulations.

4. The regulated load energy consumption is higher than the BER predicted value the majority of the monitored dwellings – in some cases significantly so. Interior temperatures in the monitored nZEB dwellings are also higher than assumed in the BER software.

These findings are contrary to a recent evaluation of Irish dwellings which had undergone energy retrofit, which found that the DEAP software overestimated both the heating periods and interior temperatures of the pre-nZEB dwellings [6].

The findings are based on a sample of 1/6 of the dwellings which are planned to be monitored by the nZEB101 project.

However, the main finding to date based on the initial POE data is that the nZEB compliant dwellings demonstrate a disparity with the assumptions inherent in the National energy rating software.

2. METHOD

The nZEB101 project is undertaking an extensive Post Occupancy Analysis (POA) of over 100 dwellings which comply with the nZEB regulations. In order to comply with nZEB in Ireland, the buildings need to demonstrate an Energy Performance Coefficient of 0.3

and Carbon Performance Coefficient of 0.35, i.e. reductions of 70% and 65% in energy and carbon emissions respectively compared to a reference building built in 1985 [5].

Data is recorded on the overall energy consumption and the heating energy consumption for all dwellings (1 hour data) for a period of at least one year. In addition, there is five-minute data on the Indoor Environmental Quality (IEQ) parameters of air temperature, relative humidity and carbon dioxide. A subset of the dwellings (table 1) is considered here for the energy analysis and comprises.

- new and retrofit
- detached, semi-detached and terraced
- timber frame and block built and
- private and social housing

As can be seen, three of the new properties are of the same typology and are on the same site ("site I"), and four of the renovated properties are also co-located and of the same typology (site "K"). The majority of the new properties were constructed to the Passive House (PH) standard [7], and have Mechanical Heat Recovery and Ventilation (MVHR) systems for ventilation and all have triple glazed windows apart from nZEB6 which has double glazed fenestration.

Table 1: Selection of monitored nZEB101 dwellings

Dwelling id	New/Renovate	Site	Building type	Construction	Completed Year	Ventilation	Airtightness {n50/q50}
nZEB1	New	I	Semi-d, 2 stry	Timber Frame	2016	MVHR	0.4
nZEB2	New	J	Det, bungalow	Timber frame	2011	MVHR	0.54
nZEB3	New	L	Det, 2 Stry	Block	2005	MVHR	1
nZEB4	New	N	Det, 2 Stry	Block	2015	MVHR	0.50
nZEB5	New	P	Det, 2 Stry	Timber Frame	2011	MVHR	0.5
nZEB6	Renovate	O	Det, bungalow	Block	2016	Nat Vent	n/a
nZEB7	New	I	Semi-d, 2 storey	Timber Frame	2017	MVHR	0.3
nZEB8	New	I	Semi-d, 2 storey	Timber Frame	2017	MVHR	0.3
nZEB23	Renovate	K	Terraced 1 Storey	Block	2018	DCV	5
nZEB25	Renovate	K	Semi-d, 1 storey	Block	2018	DCV	4.12
nZEB26	Renovate	K	Semi-d, 1 storey	Block	2018	DCV	4.8
nZEB27	Renovate	K	Terraced 1 Storey	Block	2018	DCV	4.8

The majority of the dwellings which have undergone a Deep Energy Retrofit (DER) have Demand Controlled Ventilation (DCV). nZEB6 is a property which was constructed as a low-energy dwelling, with natural ventilation, and while it does not meet the current Irish definition of nZEB, it meets the indicative nZEB definition of regulated load primary energy consumption of less than 45 kWh/m²/a, and is included for comparative reasons [8].

Details of the recorded operational performance of the A-rated buildings, including indoor temperatures over the 2019/20 Winter period as defined by Met Éireann (December, January and February) and regulated load energy consumption which has been recorded over a period of at least one year per property have been provided (Table 2). The regulated load is that

as defined in the Dwelling Energy Assessment Procedure (DEAP) [5] and includes the energy to service the building i.e. Domestic Hot Water (DHW), space heating, fixed lighting and ventilation/pumps.

Given the significantly higher than expected interior temperatures identified in table 2, further, deeper analysis of interior temperatures across the homogeneous sample of nine of the DER properties has been carried out (Figs 2 and 3) and discussed below.

The DER scheme comprises 12 x 1 bed 30.77 m² social house dwellings (Fig 1), located in Wexford town, County Wexford, Ireland, which underwent the DER in 2018. The houses were originally built in the 1970s and house Wexford County Council local authority tenants, typically pensioners.

Prior to the upgrade, the dwellings had issues with inadequate ventilation and thermal bridging resulting in damp patches and mould on interior surfaces. The dwellings ranged from the second poorest Building Energy Rating (BER) rating of F (with a regulated load of 403 kWh/m²/a), to the worst BER (G), with the poorest performing dwelling consuming a regulated load of 1158 kWh/m²/a – as per the BER certificate.

Following the upgrade, the dwellings all are designed to operate in the BER category of A, with the majority having a BER of A2 (25 to 50 kWh/m²/a). The primary heating system is an electric Heat Pump (HP), and one of the dwellings (nZEB 27) also uses a Solid Fuel (SF) open fire with back boiler.

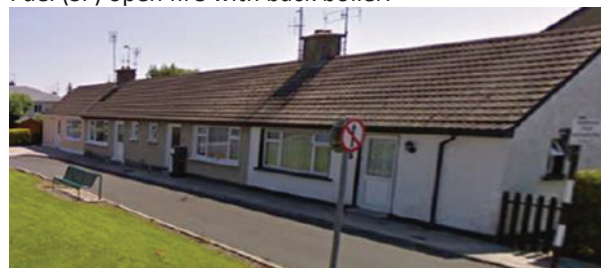


Fig 1 College View, Wexford town, County Wexford, Ireland – pre Retrofit

3. RESULTS

3.1 Overview

Table 2 gives the specific regulated load energy consumption, both in terms of the BER band rating and the specific primary energy consumption in kWh/m²/a. It also gives the recorded specific primary energy consumption, and the recorded average dwelling temperature during the winter (in degrees Celsius).

Table 2: Recorded Energy Consumption Vs Predicted

Dwelling Id	Heating System	Rating	BER Size (m2)	BER (kWh/m2/a)	Actual Reg Load Cons (kWh/m2/a)	Equiv BER Rating	Ave Dwelling Temp (Winter)
nZEB1	HP	A1	102	24.1	40.6	A2	20.1
nZEB2	HP	A3	182	61.6	52.6	A3	21.2
nZEB3	HP	A3	378	61.7	51.6	A3	21.8
nZEB4	HP	A1	285	23.7	26.3	A2	20.8
nZEB5	Gas	A3	271	56.7	72.8	A3	21.8
nZEB6	HP	A3	170	63.0	47.5	A2	18.9
nZEB7	HP	A1	102	24.4	52	A3	21.8
nZEB8	HP	A1	102	24.4	57	A3	22.3
nZEB23	HP	A2	31	47.4	165	C1	21.3
nZEB25	HP	A2	31	36.9	158	C1	21.5
nZEB26	HP	A2	31	36.2	267	D2	24.3
nZEB27	HP & SF	A3	31	65.7	181	C2	22.3

3.2 Energy Consumption

The buildings which exceed the expected energy consumption BER rating band are highlighted in orange in Table 2, and those which operated within or below the expected energy consumption band are highlighted in green.

For four of the dwellings (nZEB2, nZEB3, nZEB5 and nZEB6) the predicted regulated load matches or is below that expected by the Building Energy Rating software. In the case of nZEB4, while the BER A1 band was below the recorded regulated load energy consumption band (A2), the predicted regulated load was very close to the recorded regulated load (23.7 versus 26.3 kWh/m²/a). In the case of nZEB5, the recorded gas consumption (which is used for domestic hot water and space heating in addition to cooking) was being used to determine the regulated load. The dwelling significantly exceeded the expected consumption, and on further investigation it was found that a cookery school for children was being run as a home business, resulting in significantly higher than expected gas consumption.

The recorded performance does not match the predicted specific regulated load for the majority of the dwellings (eight of the 12). For nZEB 1, 7 and 8, the dwellings are on the same site, and were constructed to the Passive House (PH) standard with all having identical construction and heating systems. All three dwellings exceed the predicted Regulated load by approximately twice.

Similarly, in the case of the retrofit dwellings nZEB 23, 25, 26 and 27, all exceed the BER expected energy consumption, typically by a factor in excess of three, and in one case (nZEB 26) by a factor in excess of 7. These are the DER houses in Wexford – see Fig 1. The energy consumption was recorded using clamp on Loop energy meters, and were verified against data collected directly from the Daikin HPs.

Recognising that the regulated load (whilst also comprising fixed lighting and ventilation loads) is predominantly determined by the DHW and space heating loads, a focus was put on the interior temperatures, to determine if the dwelling temperatures matched the levels expected by the Dwelling Energy Assessment Procedure (DEAP)

software which is used to determine the BER and are reported on below.

3.3 Interior Temperatures

The Dwelling Energy Assessment Procedure (DEAP) software which produces the BER assumes that the heating system has a set temperature of 21°C in the living room, and 18°C in all other rooms for two hours in the morning and six hours in the evening. This equates to an average temperature of 18.9°C for eight hours of the day for a typical dwelling, and an unspecified (but assumed lower) temperature for the remaining period. Given that the heating is only expected to be on for one third of the 24 hour period, the overall average dwelling temperature during the winter is expected to be below the 18.9°C.

No nZEB dwelling presented in Table 2 records a temperature below 18.9°C, with nZEB6's *average* temperature at 18.9°, for the 24-hour period, indicating that the temperature during the 8 hour heating period would also be in excess of the DEAP assumptions. So, for all the DER nZEB dwellings analysed, temperatures are higher than expected.

The interior temperatures were compared with a sample of dwellings built to the pre-nZEB standard, it was found that the nZEB temperatures were higher [4]. Of particular note are nZEB 7 and nZEB 8, both of which exceed the energy consumption indicated by the BER rating by approximately 100% and which were also found to have higher than expected living room and bedroom temperatures [9]. As can be seen from table 2, the 24 hour interior temperatures are significantly higher than expected by the BER.

This indicates that there may be an element of “comfort taking”, i.e. the superior thermal performance of the nZEB dwellings is perhaps being used to increase thermal comfort rather than reduce energy consumption.

3.4 Temperature profiles – retrofit dwellings

Given the higher-than-expected overall temperatures, further investigation has been carried out across a sample of 9 of the homogeneous DER monitored dwellings which are located on the same site in County Wexford. This analysis was carried out to determine the interior temperatures:

1. For the eight-hour period heating period.
2. Outside of the heating period.

It was found that the temperatures were significantly different from those expected during the heating periods, and that the temperatures remained high outside of the heating period. See Fig 3 and Fig 4.

The red lines between 5 PM and 11 PM and between 7 AM and 9 AM indicate the expected

temperatures (i.e. 21°C in the living room, and 18°C in the bedroom). For the periods 9 AM to 5 PM and 11 PM to 7 AM, the heating is assumed not to be operational, with the interior temperatures expected to decline over those periods.

Box plots are used to represent the distribution of the dataset. In the box plots, numerical data is divided into quartiles, and a box is drawn between the first and third quartiles. The middle line of the box represents the median or middle value. The median divides the data set into a bottom half and a top half. The bottom line of the box represents the median of the bottom half or 1st quartile. The top line of the box represents the median of the top half or 3rd quartile. The whiskers (vertical lines) extend from the ends of the box to the minimum value and maximum value.

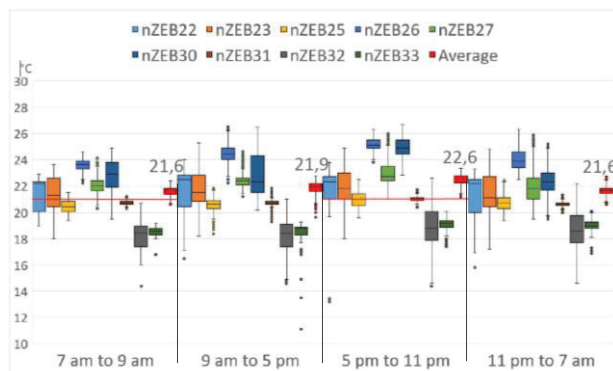


Fig 2 Winter Living room temperatures

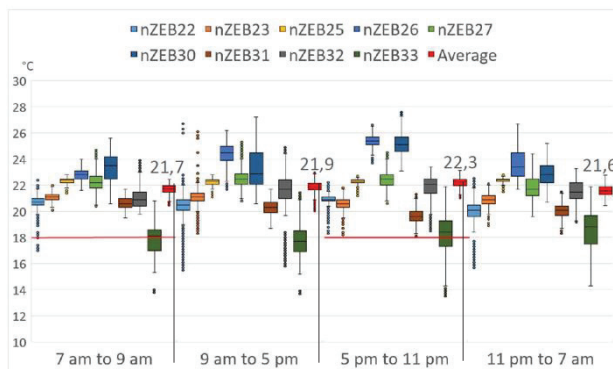


Fig 3 Winter Bedroom temperatures

The box plots give the range of temperatures for each dwelling for the living room (Fig 2) and bedroom (Fig 3). Each dwelling is represented by a box plot in a different colour and the box plots for the average values for the nine dwellings for each of the four time periods (two heating periods, and two non-heating periods) are presented in the red box plots seen on the right of each of the four time periods. The numbers above the average box plots give the overall mean

temperatures experienced for each of the four time periods.

3.5 Living room temperatures

Fig 2 indicates that median living room nZEB interior temperatures are higher than those expected by the energy rating software, for all of the properties apart from nZEB 32, and nZEB 33.

The average temperatures for the nine dwellings over the period 5 PM to 11 PM, continuously exceed the set temperature of 21°C and exceeds it for more than 75% of the time for the period 7 AM to 9 AM. In some cases the temperatures are significantly higher than those expected. For example nZEB 26 and nZEB 30 have median temperatures of 25°C with minimum temperatures in excess of 24°C and 23°C respectively and maximum temperatures of 26°C and 27°C between 5 PM and 11 PM.

Outside of the heating periods, again apart from nZEB 32 and nZEB 33 (which are seen to have the lowest temperatures), the majority of the dwellings continue to exceed 21°C outside of the heating periods. This is a significant finding and reflects high levels of occupancy during the day and a desire for continuous heating, even during the period 11 PM to 7 AM.

The mean temperature ranges between 21.6°C and 22.6°C over the 24 hour period, with relatively stable temperatures experienced by the majority of the properties.

3.6 Bedroom Temperatures

One of the most significant findings for the interior temperatures is that those in the bedrooms are much higher than assumed (Fig 3). The mean temperatures are significantly higher than the 18°C expected, ranging between 21.6°C and 22.3°C, irrespective of the heating/non-heating period.

While the living room temperature is expected to be 21°C during the heating period, the bedroom temperature is expected to be only 18°C during the heating period. Therefore the energy consumption required to maintain the temperatures circa 4°C higher than expected (at a median of c. 22°C) is significantly higher than that expected by the DEAP software.

3.7 Impact of Higher Than Expected Temperatures

The higher-than-expected temperatures will have a significant impact on the energy consumption for the buildings.

For example, in the case of nZEB 26, the average temperature over the winter period is 24.3°C, rather than the expected 19.14°C during the heating period for the individual dwelling, a difference of 5.16°C. The fabric heat loss for the dwelling is calculated at 73 W

per Kelvin by the DEAP software. Therefore to maintain the higher temperatures, $73 \times 5.16^\circ\text{C}$ (or 377 W) is required. Assuming an eight hour heating period (rather than the 24 hour period over which the average temperatures actually have been recorded), over 3 kWh extra energy is required per day, for the 8 hour heating period. Over the winter period alone, this would require an additional 275 kWh of heating, equivalent to 572 kWh of primary energy (conversion factor 2.08), for the eight-hour period. The DEAP software assumes no energy will be expended on heating for the other two thirds of the day. However, in order to increase the temperature from 19.14°C to the 24.3°C (rather than from the lower yet undefined temperatures outside the heating period, a conservative estimate of 1716 kWh would be required (i.e. multiplying the 572 kWh by three) in order to maintain the building at the recorded temperature for the winter period alone.

Dividing this by the 31 m^2 shows that a (very conservatively estimated) extra specific energy consumption of 55 kWh/m^2 is required to maintain the higher interior temperatures, for the three months of the winter. In order to heat the building for the year an estimate in excess of $100 \text{ kWh/m}^2/\text{a}$ would not seem unreasonable.

Table 2 shows that $245 \text{ kWh/m}^2/\text{a}$ was consumed compared with an expected $36.2 \text{ kWh/m}^2/\text{a}$. The calculations above show the considerable impact that the higher-than-expected interior temperatures had during the analysed winter period alone (c. 50% of the extra primary energy demand).

4. DISCUSSION

This paper has provided initial insights based on the recorded energy consumption of near Zero Energy Building (nZEB) dwellings, in advance of the standard being required for all buildings in the Republic of Ireland from January 2021. The analysis will be augmented as data from more dwellings become available via the nZEB101 project.

The main findings from the analysis:

1. The majority (75%) of the buildings are consuming more energy than predicted by the DEAP software.
2. For the A rated DER dwellings, the energy consumption ranged between 3 and 7 times higher than expected ($158 - 267 \text{ kWh/m}^2/\text{a}$).
3. Recorded interior temperatures are considerably higher than the 18.9°C (for an eight-hour periods) expected by the DEAP software, with 24 hr average temperatures ranging from 18.9°C to 24.3°C over the winter period (Table 2).

4. Analysis of nine dwellings which underwent a deep energy retrofit indicate that the higher interior temperatures are maintained throughout the 24-hour period
5. The bedroom temperatures were on average between 3.7°C and 4.3°C in excess of the 18°C assumed by DEAP.
6. The DEAP - assumed two-hour heating period in the morning and six heating period in the evening were not typical for the buildings monitored.

When the winter interior temperatures of nZEB compliant Passive Houses were compared with a sample of dwellings built to the pre-nZEB standard, it was found that the nZEB temperatures were higher than the dwellings constructed to the previous standards, and also higher than expected by the energy rating software [4], [9]. This indicated that there may be an element of “comfort taking”, i.e. the superior thermal performance of the dwellings is perhaps being used to increase thermal comfort rather than reduce energy consumption. It should also be remembered that a number of the nZEB dwellings monitored as part of the nZEB101 project were built to the Passive House standard, and this may also influence the interior temperatures, as the PH set temperature is assumed to be 20°C for 24 hours a day, which is nearer to the average temperatures measured. Also, higher-than-expected energy consumption and temperatures have been reported in the literature, especially in regard to the rebound effect associated with retrofit dwellings e.g. [10], [11].

On the other hand, the Hunter et al. study [6] of BER C & B Irish retrofit dwellings was conducted on data gathered over the 2011/12 and 2012/13 heating seasons found that DEAP over-estimated heating schedules and room temperatures by up to 37% and 1°C respectively. This is contrary to what was found for the new build and DER Wexford properties would be expected under the rebound effect. It may be explained by the fact that the earlier monitoring coincided with an economic recession during which oil prices were high potentially affecting homeowners’ heating practices. A recent paper [12] by Dennehy et al. found that the economic recession was principally responsible for the sharp fall in residential space-heating energy demand in Ireland between 2007 and 2012, rather than the energy retrofit measures.

Given that economic buoyancy was being experienced in Ireland over the 2019/2020 winter period, this may be a contributing factor to the higher than expected interior temperatures and energy consumption.

Equally, the reason for the higher than expected energy consumption and temperatures may be as a result of occupants reduced concern with heating costs given that they are significantly lower than normal in the PH & nZEB dwellings or for technical reasons e.g. if the Co-Efficient of Performance of the HP did not match that expected. Band C & B dwellings are harder to heat compared to band A, so underheating would be more prevalent for such dwellings as band A are easier to keep warm.

5. CONCLUSION

The potential reasons for the higher than expected energy consumption and temperatures presented is beyond the scope of this paper.

Further monitoring results are required to draw definitive conclusions e.g. with respect to the actual Vs assumed interior temperatures for the DEAP defined heating and non-heating periods, and the actual energy consumption versus predicted.

The contribution of the paper is to present the data on the initial sample of the dwellings complying with the Irish nZEB standard.

While the initial indications are that the heating periods and interior temperatures which were assumed 35 years ago based on the dwellings of the day may need to be revised, it is noted that the sample size of the dwellings is small, and that a significantly greater sample size will be reported on as part of the ongoing nZEB101 project.

6. ACKNOWLEDGEMENTS

This project is supported by the Sustainable Energy Authority of Ireland under Grant Agreement 18/RDD/358.

7. REFERENCES

- [1] Anon. Nearly zero-energy buildings. Energy - European Commission 2014.
<https://ec.europa.eu/energy/en/topics/energy-efficiency/energy-performance-of-buildings/nearly-zero-energy-buildings> (accessed September 30, 2019).
- [2] nZEB101 n.d. <http://www.nzeb101.ie/> (accessed September 26, 2019).
- [3] Anon. National Development Plan 2018 - 2027 2018.
- [4] COLCLOUGH S, GRIFFITHS P, HEWITT NJ. Winter performance of certified passive houses In a Temperate Maritime Climate – nZEB Compliant?, Jul 31 to Aug 3 2017a.
- [5] Anon. DEAP 4.2.0 Software. Sustainable Energy Authority Of Ireland n.d.
<https://www.seai.ie/home-energy/building-energy-rating-ber/support-for-ber-assessors/domestic-ber-resources/deap4-software/> (accessed May 12, 2020).
- [6] Hunter G, Hoyne S, Noonan L. Evaluation of the Space Heating Calculations within the Irish Dwelling Energy Assessment Procedure Using Sensor Measurements from Residential Homes. *Energy Procedia* 2017;111:181–94.
<https://doi.org/10.1016/j.egypro.2017.03.020>.
- [7] Anon. What is a Passive House? [] n.d.
https://passipedia.org/basics/what_is_a_passive_house (accessed March 11, 2019).
- [8] Anon. Department of Environment C and LG. Towards Nearly Zero Energy Buildings in Ireland, Planning for 2020 and Beyond. Dublin: Department of Environment, Community and Local Government; 2012.
- [9] Colclough S, Kinnane O, Hewitt N, Griffiths P. Investigation of nZEB social housing built to the Passive House standard. *Energy and Buildings* 2018;179:344–59.
<https://doi.org/10.1016/j.enbuild.2018.06.069>.
- [10] Gillingham K, Rapson D, Wagner G. The Rebound Effect and Energy Efficiency Policy. *Rev Environ Econ Policy* 2016;10:68–88.
<https://doi.org/10.1093/reep/rev017>.
- [11] Galvin R. Making the ‘rebound effect’ more useful for performance evaluation of thermal retrofits of existing homes: Defining the ‘energy savings deficit’ and the ‘energy performance gap.’ *Energy and Buildings* 2014;69:515–24.
<https://doi.org/10.1016/j.enbuild.2013.11.004>.
- [12] Dennehy ER, Dineen D, Rogan F, Ó Gallachóir BP. Recession or retrofit: An ex-post evaluation of Irish residential space heating trends. *Energy and Buildings* 2019;205:109474.
<https://doi.org/10.1016/j.enbuild.2019.109474>.

Characterization of library lighting design: A study of dynamic and static space

EDUARDO ESPINOZA CATERIANO¹ HELENA COCH ROURA¹ ISABEL CRESPO CABILLO¹

¹ Architecture, Energy & Environment. School of Architecture of Barcelona. UPC., Barcelona, Spain.

ABSTRACT: *The use of space is a fundamental variable in the creative process, so it is included in the lighting design. This paper presents a key to characterize the lighting space, to be used in the initial stages of architectural design. It aims to highlight the role of quantitative and qualitative lighting values of space. To carry on this study, two very different libraries have been analysed in Barcelona. The first case study corresponds to a university library whose function is reading and mainly individual study. The second case study, the community library, has a more participatory character with society, i.e. it includes reading spaces, meeting spaces, learning spaces for children and a conference hall. This research compares two library lighting design in terms of spatial configuration. Analysing false colour images reveals that there are different lighting intentions. The first case study shows that the difference between the luminance of the work area and the general environment is ten times greater. The second case study shows that the luminance in the work area is ten times less than the background. Therefore, it is suggested that the lighting design of those two libraries corresponds to the static and dynamic use of space.*

KEYWORDS: *Lighting design, library lighting, luminance value, false-colour image.*

1. INTRODUCTION

Today, libraries have transformed the use of studying space [1,2,3,4,5]. In the past, the architectural typology was configured to keep the knowledge acquired by civilizations. Subsequently, the function of the library included elite education, among which were religious groups. Monasteries, in particular, were characterized by introspection and self-learning. Throughout history, studies have been developed to analyse the impact of lighting in reading activities. Among them, the research of Arnau, Muñoz, and Gibson stand out due to the depth of their conclusions and the relevance to the subject of this study.

According to Arnau [6], colour and light play a primary role in the creation of space for worship. The binomial, subject-object, sustains its relationship in the inhabited space. Muñoz [7] shares Arnau's point of view, the sacredness of religious spaces is associated with libraries through light and silence. The user of libraries has multiple lighting needs. Lighting to focus on the main activity and environmental lighting to visualize the space limits [8]. Directional lighting tends to exclude distractions from reading. Meanwhile, diffuse lighting leans towards including another type of activities such as spatial orientation, social interaction and more. Artificial directional lighting enables concentration in user activity so long as there is light directed to work plane and there is less light reflected

in other surfaces. Natural diffuse lighting allows different activities at the same time in the libraries.

Thus, the primary activity in the old libraries was concentrated solely on reading; while, at present, the flexibility in the use of this type of space allows greater participation of society with culture. Finally, regarding visual perception, Gibson [9] clarifies the difference between the visual field (static use of space) and the visual world (dynamic use of space). Despite the differences in approach, the authors reach similar conclusions regarding the undeniable role of lighting in the construction of spaces dedicated to learning activities. Libraries spaces are therefore fundamentally concerned with the creation of an environment between the subject, the activity, and the light.

2. METHODOLOGY

The libraries chosen are typologically different, both stand out for their light qualities in terms of visual comfort [10]. It seeks to examine the relationship between the activities of the subject and the type of lighting of the objects. For this study, it has been chosen to analyse the libraries with digital pictures in High Dynamic Range (HDR). Each image corresponds to different scenes subjected to software that reveals luminance (L) value. To generate HDR images and false colour images, the website <https://www.jaloxa.eu> has been used in 2015, which is currently not in service. The

quantitative information of the scenes allows us to evaluate the luminance contrast in the visual field [11].

3. CASE STUDIES

The first case, owned by the Pompeu Fabra University since 1992, is the Dipòsit d'Aigües library. It is located opposite the Ciutadella park, in the Sant Martí district of Barcelona. Constructed in 1874 by Josep Fontserè as a water tank to feed the waterfall fountain inside the park, the old water tank was later refurbished as a library by Lluís Clotet and Ignacio Paricio [12]. The library is formed by eleven parallel arches of 14 meters high, which intersect by another eleven arches rows and extend along 65 meters. This generates that inside we find passages modified by a forest of high red brick columns on a grey carpeted floor, natural wood furniture and white metal luminaires.

Naturally lit from an overhead opening in the centre of the building and vertical windows in the perimeter. All photographs were taken on the same day, on June 16th, but at different hours. Three pictures were selected, as mentioned before, because is relevant to focus on reading activity and search book activity. At 14:00h the sky was partially clear. The library was illuminated by diffuse natural light through windows. Due to the distance of high-level windows from work plane, the artificial light plays a central role in the scenes studied. The lamp model used was fluorescents Philips Master TL5 HE 21W/830 SLV/40 on the furniture.

Because users are related to university studies, the lighting intention focuses on the reading activity. The floor plan (Fig. 1) shows three analysis scenes: collective reading, individual reading and corridors (Fig. 2-3-4).

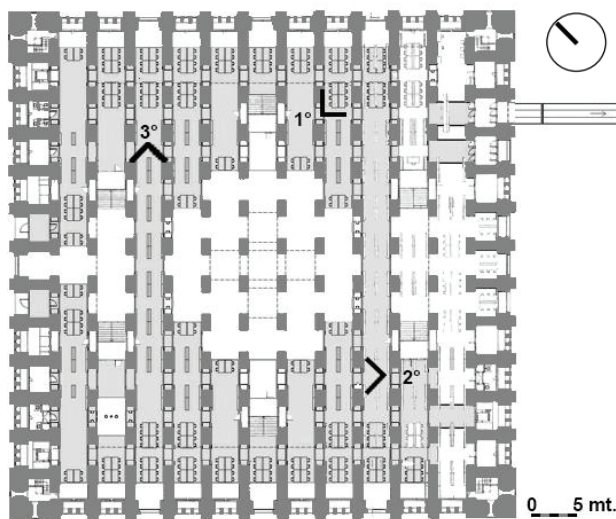


Figure 1: First floor plan Pompeu Fabra Library.



Figure 2: First HDR photo of group reading place.

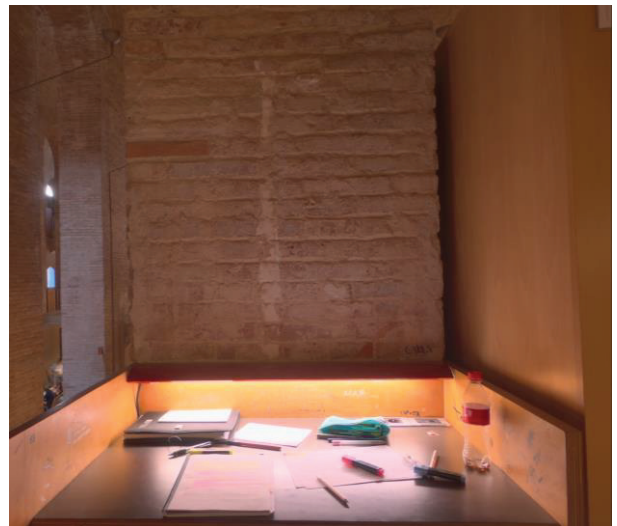


Figure 3: Second HDR photo of individual reading place.



Figure 4: Third HDR photo of corridors facing window.

The second case is the Agustí Centelles library, which opened in 2010. It is located in the Eixample district of Barcelona. The architects Rahola and Vidal had to group different uses and users in one building: a civic centre, an auditorium, a nursery school and a library [13].

The library starts from the third floor and occupies 4 levels, the double heights allow good views to the outside and diffuse light into the interiors (Fig. 5-6). The vertical surfaces are mostly white and are made up of the columns, the perimeter walls, the metal profiles that support the glazed facade and the shelves that delimit the reading areas of the circulation area. The horizontal surfaces are basically white for the ceiling of acoustic tiles and gray for the floor. As for the tables they are white except those of black color that are in front of the north-east glazed façade.

The interiors are illuminated by natural light through the north-east and south-west facing facade. These photographs were completed at 11:00h, on June 22nd, when the sky was partially clear. The artificial light comes from fluorescents Philips Master TL-D 58W/840 on the ceiling and Philips Tornado T2 8W WW E14 220-240V 1PF/6 on the table lamp.

The lighting design seeks to place the major activities next to the facades to allow the greatest entry of light from the outside. The choice of each HDR photo follows the same criteria as before: a place of shared reading, individual reading, and corridors (Fig. 7-8-9).

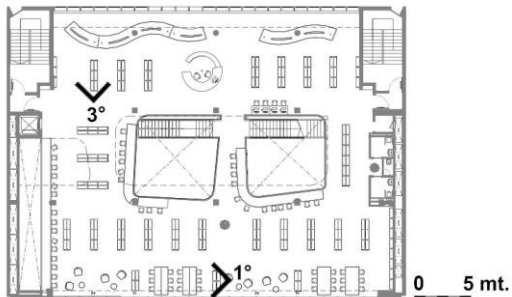


Figure 5: Fifth floor plan Agustí Centelles Library.

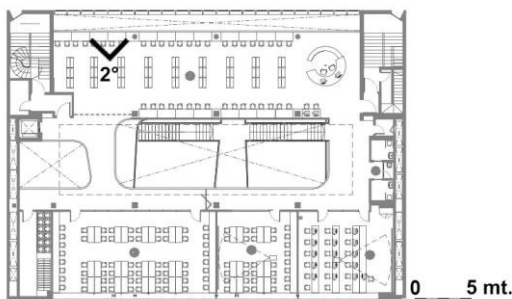


Figure 6: Sixth floor plan Agustí Centelles Library.



Figure 7: First HDR photo of group reading place.



Figure 8: Second HDR photo of individual reading place.



Figure 9: Third HDR photo of individual reading place.

4. RESULTS

The results in the university library (Figure 10-11), show that the luminance levels at the work plane are greater than the luminance levels in the environment. Also, in Figure 12, the luminance level on the bookshelves is higher than luminance level in other surfaces. The luminance values on the desk of group and individual reading place are between 10 cd/m² to 317 cd/m², but primarily near 100 cd/m², while the luminance values in the surrounding surfaces are mainly 10 cd/m². The luminance ratio of the environment and the work plane in this university library is near 1:10.

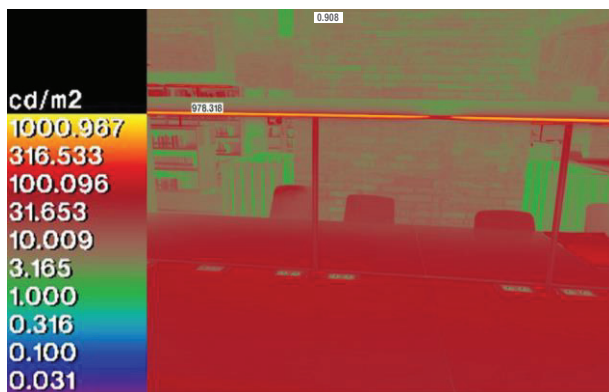


Figure 10: False colour photo of group reading place.

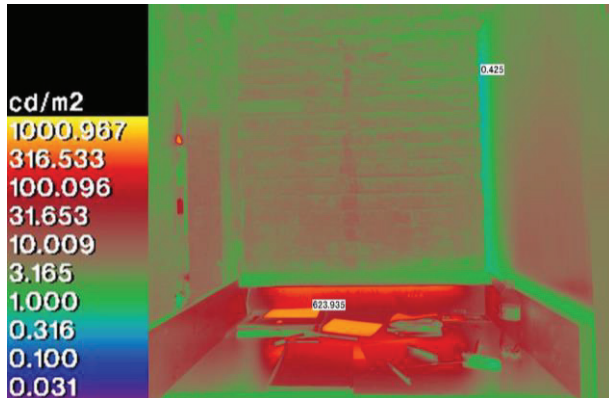


Figure 11: False colour photo of individual reading place.

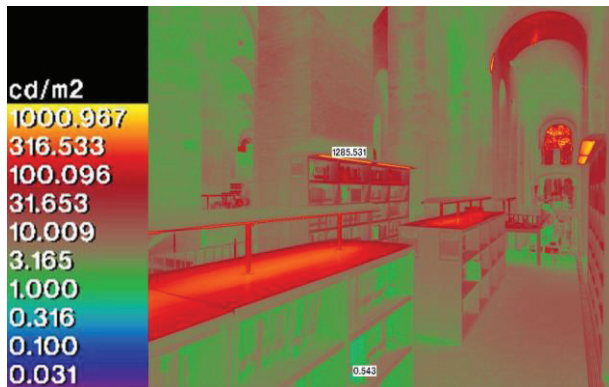


Figure 12: False colour photo of corridors facing window.

The false-colour photos in the community library (Figure 13-14), reveal that the luminance levels in the work plane of reading zone are lower than the luminance levels that surroundings. Figure 15 shows that luminance level in the interior is lower than the exterior, except from the artificial light source. The luminance values on the work plane are between 10 cd/m² and 317 cd/m², but mostly 100 cd/m². The luminance levels of surfaces from the exterior is between 317 cd/m² and 1000 cd/m², but primarily 1000 cd/m² when is facing window. The luminance ratio of the environment and the work plane in this community library is near 10:1.

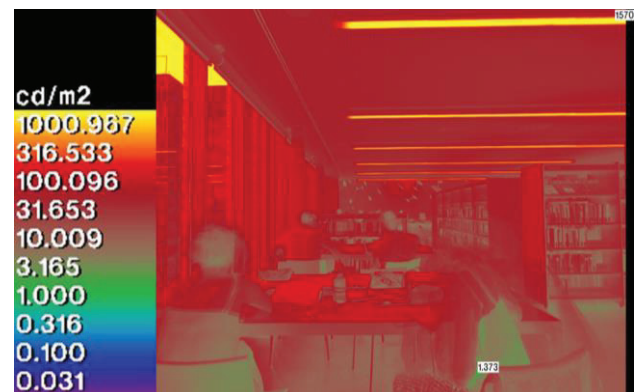


Figure 13: False colour photo of group reading place.

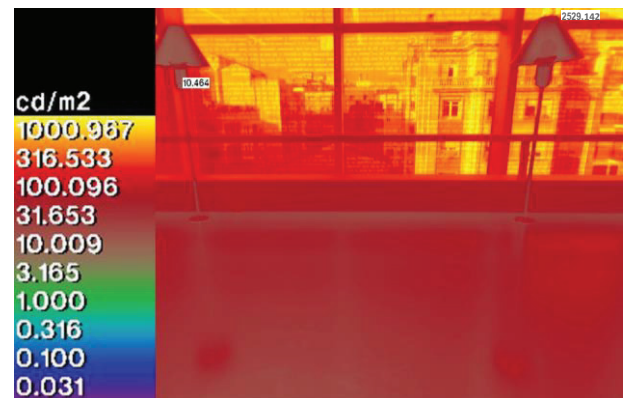


Figure 14: False colour photo of individual reading place.

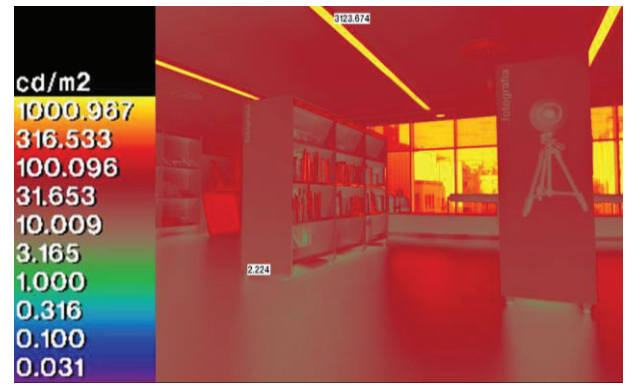


Figure 15: False colour photo of corridors facing window.

5. DISCUSSION

The analysis of false colour images mainly reveals that current library lighting regulations focus on the level of illumination on the work plane [14-15-16]. In both libraries, it was found that the work plane is sufficiently illuminated to carry out the reading activity, according to the UNE-EN 12464-1 standard [17]. The luminance value on the work plane is approximately 100 cd/m², which corresponds to an illuminance of approximately 500 lux depending on the reflection coefficient of the materials. Although it was not found a recommendation of specific luminance ratio for libraries, this work has adopted the proposed by the IRAM- AADL STANDARD J-20-06 [18], applicable to work areas or visual task, which are summarized in table 1.

Table 1: Maximum ratio between the Background Luminance (BL) and the Visual task (Vt).

Visual Field	Ratio BL:Vt
Central vision (30° cone opening)	3:1
Peripheral vision (90° cone opening)	10:1
Maximum L point of the visual field	40:1

It should be noted that all cases studied are under the ranges proposed in the table above. Considering any point of the work plane (100 cd/m²) and the maximum luminance point of the visual field, both cases studies are under the ratio of 40:1. In the first case, the university library, the maximum luminance point is 1285 cd/m², so the ratio is 13:1. In the second case, the community library, the maximum luminance point is 3123 cd/m², so the ratio is 31:1. The results obtained in this analysis show that these values are taken into account so as not to exceed the recommendations in the regulations.

However, we observed a great difference in the luminance contrast between the environment that surrounds the user of both libraries and the work plane. In the first case study, the ratio is shown to be 1:10, where the average luminance of the space limits is 10 cd/m² and the luminance on the reading activity is 100 cd/m². In the second case study, the ratio of the luminance contrast is reversed, with the ratio of 10:1, where the average luminance of the surfaces outside the building is 1000 cd/m² and the luminance of the work plane remains as 100 cd/m². The inversely proportional change between both libraries is the most noticeable light factor that the user experiences through the two buildings. The change of ratio corresponds to the change of the use of the space in each library. The first one is exclusively to reading activity while the second one has spaces for another activities besides reading books, such as children's area

to play and learn, meeting spaces to read newspapers, living rooms to play music with earphones and a conference hall. The luminance contrast in the university library is strongly ruled by the use of artificial source light, while the influence of natural light through windows in the community library is undeniable.

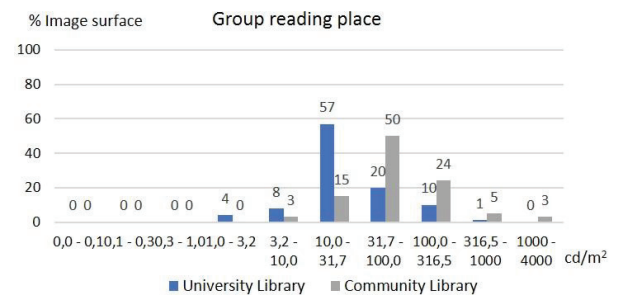


Figure 16: Luminance distribution of group reading

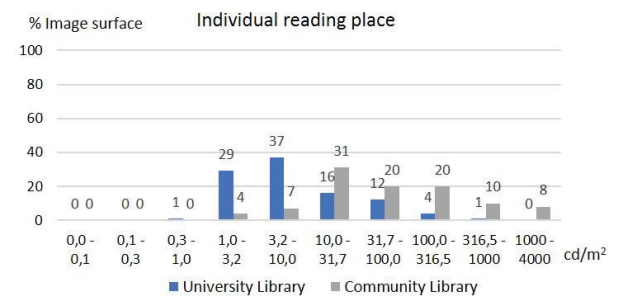


Figure 17: Luminance distribution of individual reading

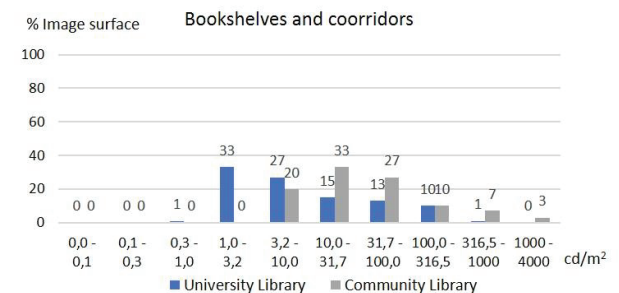


Figure 18: Luminance distribution of corridors and bookshelves

We can see (Fig 16-17-18) that the light distribution is more uniform in the community library than the university library. Also, the graphics show the percentage of light distribution is higher in the group reading place than the individual reading place. The luminance predominant in group reading place in the university library has 57% of luminance between 10 cd/m² and 32 cd/m², while the luminance predominant in individual reading place in the community library has 50% of luminance between 32 cd/m² and 100 cd/m². The comparison of each scene study between both libraries serves to conclude that the light distribution tends to be more uniform in a group reading place than an individual reading place.

6. CONCLUSION

The evaluation of the lighting design of these two libraries allows us to quantify the luminance in spaces with different lighting intentions. Group and individual reading spaces have been examined, as well as corridors with bookshelves. Due to the differences in the average illuminance in each library, an analysis of the luminance contrast between the work plane and the background has been carried out [19]. Both case studies present the same luminance in the task level, but the luminance of the surrounding surfaces is completely different. Current normative likely specify to lighting designer the illuminance in the work plane, however, the regulations are more flexible on how to illuminate other surfaces [20]. The chance is left to the lighting designer to choose how to light the rest of the surfaces taking into account the user's activities [21].

In the university library, the ratio between the luminance of the background and the work plane is 1:10, while in the community library the ratio is 10: 1. This inversely proportional change is perhaps due to the change in space usage of both libraries. In the first case study, it was found that all the spaces are conditioned solely for the study of university students. The university library, has directional lighting which helps to focus on reading activity, so it has mainly a static use of space. In the second case study, it was observed that there are a wide variety of activities in addition to reading, such as learning for children, meeting people for reading newspapers, searching for videos and music, among others. The community library, has diffuse lighting connecting the interior with the exterior visually, so it has mainly a dynamic use of space.

According to the results obtained, it seems that for spaces intended solely for reading, it is preferred to focus the highest luminosity on the work plane. In spaces that require multiple activities, there is a preference for putting more light intensity on the surfaces that define the space. Although it is evident that each activity requires a different lighting design, the present work reveals that the uniform light distribution allows the development of a greater number of activities simultaneously. The opportunity to carry out evaluations of different lighting environments could improve the specificity of the current regulation.

ACKNOWLEDGEMENTS

This research has been supported by the PRONABEC (RJ 4296-2018) and by the Spanish Ministry of Economy under the MOET project, code BIA2016-7765-R.

REFERENCES

1. Applegate, R., (2009). The library is for studying. *The Journal of Academic Librarianship*, 35(4): p.341-346.

2. Appel, J. and James J. M., (1975). How much light do we really need? *Building Systems Design* p. 27-31
3. CIBSE, (1991). Lighting Guide 5: The visual environment in lecture, teaching and conference rooms. London.
4. SLL, (2003). Addendum to CIBSE Lighting Guide 5 The visual environment in lecture, teaching and conference rooms. London, SLL.
5. Ramasoot, T. and Fotios, S. (2008). Acceptability of screen reflections: lighting strategies for improving quality of the visual environment in the Classrooms of the Future. In *25th Conference on Passive and Low Energy Architecture*. Dublin October 22-24
6. Arnau, J. (2014). El espacio, la luz y lo santo. Albacete: *UNO editorial*.
7. Muñoz, O. (2012). Luces y sombras: museos contemporáneos españoles. Sevilla: *University of Sevilla. Secretariado de Publicaciones*.
8. Kuliga, S. Dalton, R. and Holscher, C. (2013) Aesthetic and Emotional Appraisal of The Seattle Public Library and its Relation to Spatial Configuration. In *Proceedings of the 9th International Space Syntax Symposium*. Seoul: Sejong University.
9. Gibson, J. (1974). La percepción del mundo visual. Buenos Aires: *Infinito*
10. Espinoza, E. (2015). La iluminación para el culto: reflexiones del confort visual en la penumbra. [Online], Available: <https://upcommons.upc.edu/handle/2117/101100> [15 April 2020].
11. Jacobs, A. (2007). High Dynamic Range Imaging and its Application in Building Research. *Advances in Building Energy Research*, 1 (1): p 177-202.
12. Martí M. and Sarrà J., (1999). Una biblioteca bajo el agua. *El País semanal*, 1191 p: 49-54, [Online], Available: https://repositori.upf.edu/bitstream/handle/10230/20539/marti_biblioteca.pdf?sequence=1&isAllowed=y [15 April 2020].
13. Biblioteca Esquerra de l'Exemple Agustí Centelles [Online], Available: <https://bibliotecavirtual.diba.cat/documents/442130/0/BARCELONA+EIXAMPLE-biblioteca+Esquerra+de+L%C2%B4Eixample-Agust%C3%AD%20Centelles.pdf> [15 April 2020].
14. IESNA (2000). IES Lighting Handbook (9th edition). *Illumination Engineering Society*.
15. Standard Specifications, Layouts and Dimensions. (2007). Lighting System in Schools. *DCSF Publications*.
16. Martín, F. (2005) Manual Práctico de Iluminación. *AMV Ediciones*.
17. Iluminación. Iluminación de los lugares de trabajo. Parte 1: Lugares de trabajo en interiores. [Online], Available: <https://www.une.org/encuentra-tu-norma/busca-tu-norma/norma/?c=N0048898> [15 April 2020].
18. Iluminación artificial de interiores. [Online], Available: <http://www.aadl.com.ar/normas-iram-aadl/> [15 April 2020].
19. Bean, A. R., & Hopkins, A. G. (1980). Task and background lighting. *Lighting Research & Technology*, 12(3): p. 135–139.
20. Kwong, Q. (2020). Light level, visual comfort and lighting energy savings potential in a green-certified high-rise building. *Journal of Building Engineering*, 29: p. 101198.
21. Costanzo, V.; Evola, G.; Marletta, L. (2017). A Review of Daylighting Strategies in Schools: State of the Art and Expected Future Trends. *Buildings*, 7: p. 41.

Holistic Assessment of Highly Insulated nZEB Walls

In-situ measurement and embodied energy analysis

RICHARD O HEGARTY¹ OLIVER KINNANE¹ DONAL LENNON¹ SHANE COLCLOUGH¹

¹University College Dublin, Dublin, Ireland

ABSTRACT: Proponents of Passivhaus and nZEB often emphasise a ‘fabric first approach’ to ensure optimum envelope design, and by extension highest building energy performance. The energy performance of two similar walls, of two separate nZEB-compliant dwellings, are assessed in this paper. The walls have similar construction details, consisting of a layer of 200 mm of mineral wool on the exterior side and a block construction on the interior. The walls are investigated by comparing theoretical and in-situ conductance values while also estimating the embodied energy of both walls. The study found that, although the walls were of similar design and the test was conducted using the same methodology (in accordance with ISO 9869-1), that there was a significant difference between the in-situ performance of both walls. One wall performed only slightly worse than the design value while the other performed more than two times worse. This research extrapolates on the findings by comparing theoretical heat loss scenarios with both wall types and calculates A) the potential building energy performance for both walls and B) the carbon and energy payback for the insulation used to achieve such high performance. The results demonstrate the importance of good practice in construction of the building envelopes and in the manufacturing, robustness and quality control of the various building components.

KEYWORDS: U-value, in-situ measurement, embodied energy, nZEB, Walls

1. INTRODUCTION

The U-value and its reciprocal, the R-value, are used globally to quantify the heat loss through the fabric of buildings. They measure the heat transmittance (U-value), or heat resistance (R-value) of a building component; accounting for both the conductive and convective resistances. In near Zero Energy Buildings (nZEB), built to passive house specifications, when calculating the U-value of a component the conductive resistance accounts for more than 97% of the total thermal resistance – this is attributed to the thick insulation layers.

Building regulators are consistently specifying reduced U-values for building components in an effort to reduce the energy consumption of buildings [1]. This consequently means more insulation. But are these regulations sufficient – or indeed are they actually too stringent? And how accurately do these theoretical values describe the in-situ behaviour of building components?

This paper aims to try and address these questions by measuring the heat flow through the walls of two buildings built to nZEB specifications in Ireland and compare these with the theoretical U-values. The operational energy required to heat one of the homes for the design and measured U-values is estimated and compared. Further, the embodied energy required to achieve these low theoretical U-values is examined.

The construction details of the two walls compared in this study are from two completely separate buildings in two separate locations. The

construction details are very similar. This work forms part of a larger research project that focuses on the in-use energy monitoring of nZEBs in Ireland (nZEB101 - funded by the SEAI [2]).

2. LITERATURE REVIEW

Two review papers on the topic of in-situ U-value measurements have recently been published. Bienvenido-Huertas et al. [3] conducted a comprehensive literature review of the various methods used to determine building U-values. The authors categorise these into the 5 most common methods – one theoretical method (ISO 6946) and four experimental methods (including The Heat Flow Meter (HFM) method of ISO 9869-1). They outline the benefits and shortcomings of the different methods and conclude that the decision of which method to use is typically determined by the materials and equipment available. Teni et al. [4] also present a comprehensive review of the methods used – they categorise non-destructive in-situ measurements into two groups: those that use a HFM and those that don’t. They include the same methods as Bienvenido-Huertas et al. [3] in their study but also include the Natural convection and radiation method (NCaR) method, a method proposed by Jankovic et al [5] which requires inside and outside surface and ambient temperatures as well as the emissivity of the inner surface.

Gaspar et al. [6] identified the temperature difference, the test duration and the equipment accuracy as three critical parameters influencing the

accuracy of the in-situ U-value measurement. In their study of a test hut, which was specifically built for purpose, it was found that the average temperature difference between inside and outside has a major role in dictating the required test duration.

Throughout the literature, the deviation (ΔU) between theoretical (U_{th}) and experimental (U_{exp}) U-values is documented and is defined by Equation 1.

$$\Delta U (\%) = ((U_{exp} - U_{th}) / U_{th}) \times 100 \quad (1)$$

A deviation greater than zero indicates a building performing worse than what was calculated theoretically. Nardi et al. [7] found that the in-situ U-value could deviate from -6% to 83%. They showed an example historic building ($U = 1.17 \text{ W/m}^2\text{K}$) as performing slightly better than what was estimated theoretically and a heavily insulated wall of a private house performing 83% worse than the design U-value. A study conducted in Dublin (Ireland) found that the deviation in wall U-value ranged from 4% to 61% in a study of 6 walls, noting that all performed worse than designed [8]. Albatici et al. [9] also found that in none of the 5 walls they investigated did the experimentally measured U-value outperform the design, with deviations ranging from 0 to 43%.

The purpose of insulation is to reduce heat loss and thereby reduce the energy consumption (and associated carbon emissions) required to achieve and maintain a particular temperature for a desired thermal comfort setting. If, as outlined in the literature, some walls are not providing the amount of heat resistance as per design calculations, the question of the insulation's effectiveness is then raised. Can we justify the amount of energy that has been consumed in producing the thick insulation layers which remains embodied in the buildings fabric?

Whether the discrepancies between the real and design U-value are due either to misleading/inaccurate manufacturer specified values or due to poor installation during construction and the consequential effects (e.g. thermal looping [10]), the insulation itself remains the same. If the purpose of insulation is to save on energy and carbon then the energy and carbon that has gone into producing that insulation must also be considered.

An introduction to the embodied energy of insulation materials and their associated performance can be found on the GreenSpec® website [11] while individual Life Cycle Analysis (LCA) of specific products can be obtained on publicly available Environmental Product Declaration (EPD) databases – such as that of the Institut Bauen und Umwelt e.V. [12]. In a review and comparative study of insulation materials for the building sector, Schiavoni et al. [13] compared the embodied carbon and energy of

different insulation materials. They used a functional unit (f.u. = the amount of insulation required to achieve a thermal resistance of $1 \text{ m}^2\text{K/W}$ for a 1m^2 area) to compare the different materials. As an example, they observed that the embodied energy of a selection of stone wool based insulation products ranged from 5 to 18 kWh/f.u. while the embodied energy of expanded polystyrene base insulation products ranged from 32 to 36 kWh/f.u.; in terms of carbon these values were 1.45 to 3.62 $\text{KgCO}_2\text{eq /f.u.}$ and 5.05 to 8.25 $\text{KgCO}_2\text{eq /f.u.}$ respectively – these values are dependent on the fuel mix in the location where the materials were processed. The insulation material used in the buildings assessed in this paper is a commercially available stone wool.

3. METHODOLOGY

Prior to the embodied energy/carbon analysis, the thermal and operational performance of two walls of similar construction are investigated. First the theoretical U-values are calculated, and the heat loss is estimated over a one-year period. These results are compared with experimental results from in-situ monitoring of two nZEB dwelling walls in Dublin (Ireland) of typical construction. Finally, the embodied energy of the wall is calculated and compared with the operational energy savings/losses.

3.1 Theoretical values

The theoretical (or design) thermal conductance values, U_{con} ($\text{W/m}^2\text{K}$), are calculated using resistance networks as per ISO 6946 [14] for the two nZEB walls. The convective surface resistances add an additional and complex (if estimated accurately) variable to the problem which accounts for a small percentage of the thermal resistance of heavily insulated walls and so are omitted from this study. The thermal conductance is therefore calculated according to Equation 2.

$$U_{con} = 1 / (t_1/k_1 + t_2/k_2 + \dots t_n/k_n) \quad (2)$$

Where t_n and k_n are the thicknesses and conductivities of the n^{th} layers in a multi-layer wall build-up.

3.2 Whole building energy modelling

For contextual relevance, the annual heat requirements (kWh) are estimated for a hypothetical nZEB with different wall U-values. The hypothetical case study building considered for this part of the analysis is a detached two storey dwelling with a floor area of 113 m^2 (average dwelling size in Ireland in 2016 [15]) and constructed to nZEB standards (U-values for the walls, windows and roof are built to passive house specifications) with a glazing to opaque surface ratio of 20%. Real weather data from the year

2012 for Dublin, Ireland, is taken from the Met Eireann database and used for the analysis.

A number of assumptions and simplifications are made to obtain the building's heat demand. It is assumed that the only source of heat loss is through the fabric of the building and thermal bridging is neglected. A very simple heating schedule is also assumed whereby the daily heating schedule is from 06:00 to 09:00 and 18:00 to 23:00 and where the seasonal heating period starts on the 4th of October and ends on the 30th of April. The heating system considered is a 91% efficient gas boiler. The heat requirement, Q (Wh), is estimated at hourly average intervals which is calculated using Equation 3. The heat requirement is accumulated over a year for values within the assumed heating period and season.

$$Q = \sum U_x A_x (T_b - T_o) \quad (3)$$

U_x (W/m²K) and A_x (m²) are the thermal transmittances and areas of the different components of the building and T_b is the assumed base temperature of 16°C. T_o is the outdoor averaged ambient temperature.

The primary energy and carbon emission factors are taken from the Sustainable Energy Authority of Ireland (SEAI) [17], which are 1.1 (Primary Energy Factor) and 204.7 gCO₂/kWh (Emissions factor) for natural gas.

3.3 In-situ thermal monitoring

In-situ conductance values, U_{con} [W/ m²K] are used as inputs to the model. These are obtained using quasi-steady thermal analysis of the building's envelope as per ISO 9869-1 [16]. To obtain these in-situ values heat flux and temperature sensors are installed on interior and exterior surfaces of the building's fabric. A schematic of the test set-up is presented in Figure 1. It also outlines the conductance calculation where HF is the heat flow density (W/m²), T_{si} (°C) is the internal surface temperature and T_{se} (°C) is the external surface temperature. The test is conducted at two locations so as to get two sets of results for each test site. The equipment therefore contains four surface temperature sensors (± 0.2 K) and two heat flux sensors (± 3 %). Before every test is initiated a thermal image is taken to identify a suitable test location free from thermal bridging. An image of an example test setup is presented in Figure 2.

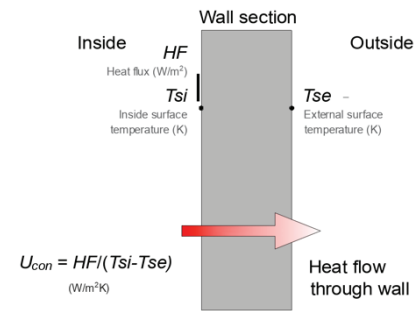


Figure 1. In-situ U-value measurement schematic.

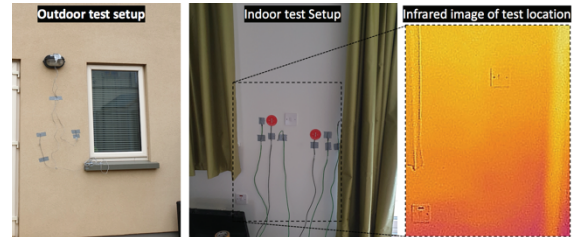


Figure 2. In-situ U-value measurement set-up for example wall.

3.4 Embodied energy & carbon analysis

The embodied energy and carbon of the insulation in the walls is quantified by simply cradle-to-gate boundary conditions. The data used to assess this is taken from the manufacturer's Environmental Product Declaration (EPD) for the high density stone wool; the results of which are presented in Table 1.

Table 1: Summary of environmental indicators for a commercially available stone wool

Parameter	value
Embodied carbon [kgCO ₂ eq/m ³]	197
Embodied primary energy [kWh/m ³]	589
Conductivity [W/mK]	0.032-0.05
Density [kg/m ³]	155

This data will be used to first compare the effectiveness of the insulation, by comparing the theoretical performance with the real in-situ performance. Secondly, the balance between the operational energy and embodied energy of the insulation will be compared. The carbon and energy payback as a result of the operational energy savings associated with incremental increases in the insulation thickness will be quantified assuming simple payback method as per Equation (4).

Payback = Embodied carbon and energy of the additional insulation / savings in operational energy by adding the extra insulation (4)

4. RESULTS AND DISCUSSION

4.1 Theoretical results

The theoretical thermal conductance values for the two nZEB walls presented in Figure 3 are 0.145

and 0.165 W/m²K for nZEB A and B respectively; calculated using Equation 2.

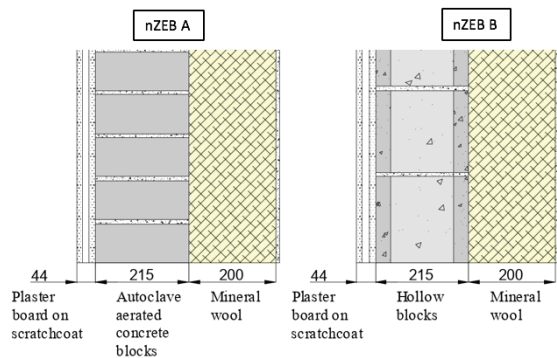


Figure 3. Wall sections for the two nZEB walls

The heat requirements for the theoretical case study described in Section 3.2. with these calculated U-values are presented in Table 2, along with the associated primary energy consumption and carbon emissions. The primary energy consumption associated to the heating per year per m² would be 12 kWh/m²/a for nZEB A and 13 kWh/m²/a for nZEB B.

Table 2: Summary of a case study nZEB performance with the theoretical wall conductance values of nZEB A and B. – based on the 113m² dwelling described in Section 3.2.

	nZEB A	nZEB B
Theoretical U_{con} [W/m ² K]	0.145	0.165
Heat requirement [kWh/a]	1145	1188
Primary Energy requirement [kWh/a]	1384	1436
Carbon emission [kgCO ₂ eq/a]	158	267

4.2 In-situ monitoring results

The actual thermal conductance of the two walls of nZEB A and B are measured following the procedure of ISO 9869-1, as outlined in Section 3.3. The tests were conducted at two different sites at different times of the year but with the same equipment and methodology. The results of both sets of sensors at both locations are presented in Figure 4. As the test for nZEB A was conducted in summer, the indoor temperature was boosted to 30 °C in order to obtain a sufficient temperature difference greater than 10 °C as per recommendations of Gaspar et al. [6] (Table 3).

It is evident that the two sets of monitoring sensors (HF , T_{se} and T_{si}) follow the same temperature and heat flux profiles for both tests, verifying the validity of the precise test locations at the two test sites.

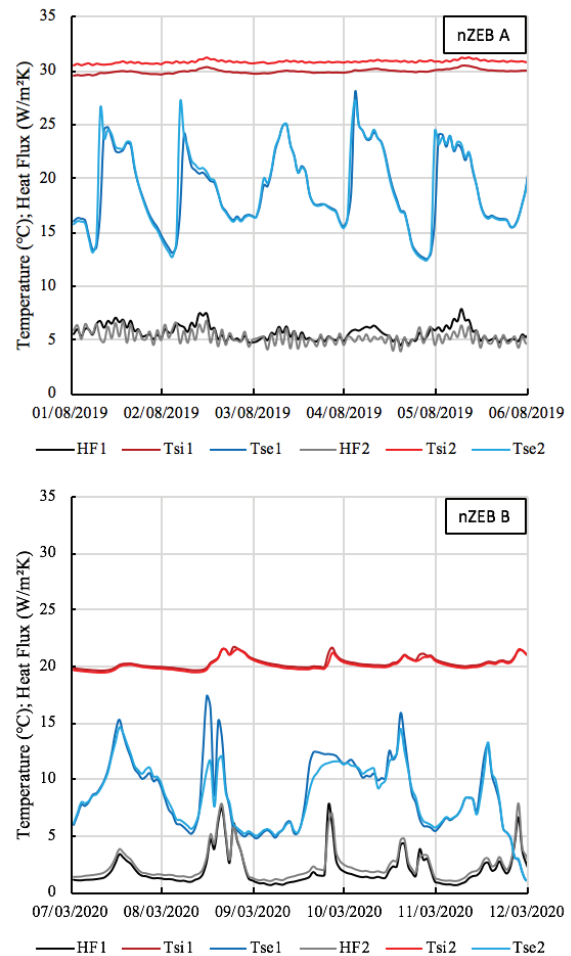


Figure 4. In-situ monitoring results for the two case study buildings - nZEB A (Top) and B (Bottom)

The thermal conductance, U_{con} (W/m²K), at a given time is calculated for both case study walls using results from the average of the sensor pairs. The actual thermal conductance of the walls is then calculated by cumulating these values over time as shown by the equation in Figure 5. The result is only valid once the three check criteria, outlined in Figure 5, are met. It is immediately evident from Figure 5 that the value of nZEB A is significantly greater than that of nZEB B as well as its theoretically calculated design value. A summary of these findings is presented in Table 3.

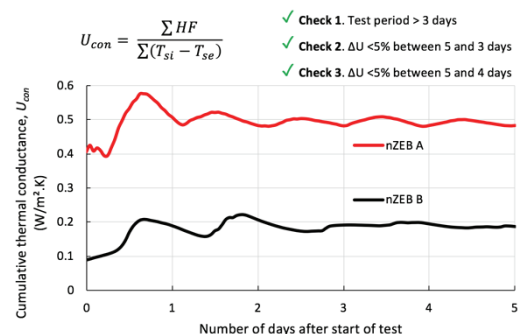


Figure 5. The cumulative thermal conductance over a 5 days test period for both wall tests.

Table 3: Summary of results from the two case study walls

	nZEB A	nZEB B
Average ($T_{si} - T_{se}$) [°C]	11.3	11.6
Theoretical U_{con} [W/m ² K]	0.145	0.165
In-situ U_{con} [W/m ² K]	0.482	0.187
Deviation (Equation 1) [%]	232%	13%

Considering the similarity of the two walls the difference in performance is stark. Possible explanations for the significant difference in the performance of the two walls could be due to any or a combination of wet/damaged insulation or inadequate/discontinuous wall construction.

Considering the first theory, that the insulation is either wet or damaged, it should be remembered that the high thermal resistance of most insulation materials is due to the small pockets of stagnant air within the material. Unlike most foam based insulation materials, stone wool is an open structure and so is susceptible to moisture ingress. If this moisture replaces the air, the insulation's performance can be significantly reduced [18].

The other potential cause for such a reduction in the thermal performance of the wall is a discontinuous layer of insulation. Such discontinuities formed from e.g. cyclic shrinkage and expansion or poor initial placement (not staggering the insulation layers or leaving gaps around the edges) could result in air gaps between the layers of insulation layer and the adjacent block layer which could result in thermal looping, which can significantly compromise the performance of the wall [10].

The precise reason for the variation in in-situ thermal conductance is subject to continued investigation in the nZEB101 project. But whether the higher-than-expected values arise from poor construction or inadequate insulation materials, the knock-on effect on the building energy performance is considerable. Table 4 presents a copy of Table 2 but with the experimentally measured values used to model the building in place of the theoretical ones – these results represent a 63% increase in the primary heat requirement for nZEB A and a 4% increase for nZEB B.

Table 4: Summary of a case study nZEB performance with the experimental wall conductance values of nZEB A and B.

	nZEB A	nZEB B
Experimental U_{con} [W/m ² K]	0.482	0.187
Primary Energy requirement [kWh/a]	2263	1494
Carbon emission [kgCO ₂ eq/a]	421	278

4.3 Embodied Energy and Carbon

The differences in U-values as a result of potentially poor construction, improper preparation of insulation materials on site and/or inadequate insulation has a significant and negative impact on

the operational performance. But unfortunately the material used to obtain the design criteria, remains embodied in the building. This results in insulation material that effectively has a reduced functionality – the same amount of insulation no longer provides the same level of thermal resistance. A comparison of the amount of energy used to produce the different amount of insulation for a given functionality is presented in Figure 6. It is evident from the logarithmic-scaled figure that the functionality of insulation has reduced substantially. Similar comparisons could be drawn for the embodied carbon where a different multiplier is used.

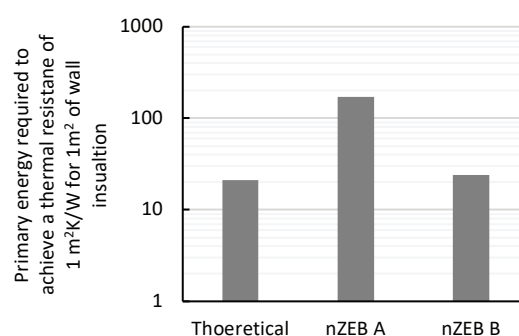


Figure 6. Comparing the effectiveness of the different case scenarios.

Based on the observed results it would be safe to assume that the theoretical case would likely provide the optimum results in most scenarios. And that, although it is likely the performance will be worse in reality (as shown by the results in this study and throughout the literature cited in this paper), it would be interesting to investigate the balance between operational energy and embodied energy for this best case scenario. To do this, the hypothetical case study described in Section 3.2 is used again and the theoretical wall build-up of nZEB A is assumed.

The amount of time, in years, required to pay back the primary energy and carbon associated with different incremental increases in insulation is presented in Figure 7. It is evident that there are diminishing returns as the thickness of the insulation is increased. This is because the heat loss is inversely proportional to the thickness of the insulation. This is a simple analysis and, as our grid electricity becomes greener, the carbon payback periods will increase; likely stretching beyond the life of the building. With other foam insulations which embody more energy and carbon per functional unit the payback periods would be longer.

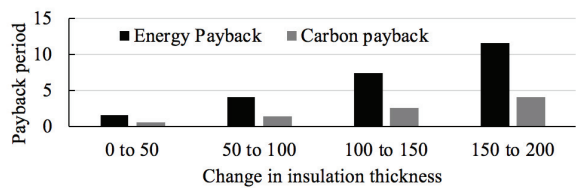


Figure 7. The number of years it would take to pay back incremental increases in thickness of the mineral wool insulation layer in terms of carbon and primary energy.

CONCLUSIONS

There exists a clear and unnerving discrepancy between the design and actual thermal performance of walls. The cause of which is subject to continued research, but the effect of which is significant.

In addition to potential concerns outside the scope of this paper (such as the consequential undersizing of mechanical system within a building) the deviations mean that the functionality of insulation material is significantly reduced. Not only does this add an unnecessary extra cost to the building, which in countries with housing shortages (such as Ireland) can lead to less homes being built for a given pot of money, it also means there is unnecessary extra energy and carbon embodied in the building. Even when the theoretical performances are met, the carbon and energy payback periods for heavily insulated walls are not particularly desirable in some cases e.g. the Irish case study building in this paper.

It is further interesting to remember that as our electricity becomes less carbon intensive – which European legislation is enforcing – the amount of carbon embodied in the walls will remain and the payback period on carbon will increase. We need to stand back from the “target” of low u-values, outlined in standards, and instead focus on the target of lower carbon. Implementation of such a broad target is of course challenging and more detailed targets are needed; but pushing the boundaries without addressing the current discrepancies between design and actual is not conducive to a low-carbon built environment. Our efforts might currently be better focused on building strategy rather than insulation quantity.

ACKNOWLEDGEMENTS

This work forms part of the nZEB101 project, which is supported by the Sustainable Energy Authority of Ireland under Grant Agreement 18/RDD/358.

REFERENCES

1. TGD Part L, Technical Guidance Document L - Buildings other than Dwellings - Conservation of Fuel and Energy. Dublin: Environment, Heritage and Local Government, 2017.
2. SEAI, 'nZEB101', 2020. <http://www.nzeb101.ie/> (accessed Apr. 08, 2020).

3. D. Bienvenido-Huertas, J. Moyano, D. Marín, and R. Fresco-Contreras, 'Review of in situ methods for assessing the thermal transmittance of walls', *Renewable and Sustainable Energy Reviews*, vol. 102, pp. 356–371, Mar. 2019.
4. M. Teni, H. Krstić, and P. Kosiński, 'Review and comparison of current experimental approaches for in-situ measurements of building walls thermal transmittance', *Energy and Buildings*, vol. 203, p. 109417, Nov. 2019.
5. A. Janković, B. Antunović, and L. Preradović, 'ALTERNATIVE METHOD FOR ON SITE EVALUATION OF THERMAL TRANSMITTANCE', *Facta Universitatis, Series: Mechanical Engineering*, vol. 15, no. 2, pp. 341–351, Aug. 2017, doi: 10.22190/FUME1704190171.
6. K. Gaspar, M. Casals, and M. Gangoells, 'In situ measurement of façades with a low U-value: Avoiding deviations', *Energy and Buildings*, vol. 170, pp. 61–73, Jul. 2018.
7. I. Nardi, D. Ambrosini, T. de Rubeis, S. Sfarra, S. Perilli, and G. Pasqualoni, 'A comparison between thermographic and flow-meter methods for the evaluation of thermal transmittance of different wall constructions', *J. Phys.: Conf. Ser.*, vol. 655, p. 012007, Nov. 2015.
8. C. Flood, 'In Situ Thermal Transmittance of Case Studies in Dublin.', *Sustainable Ecological Engineering Design for Society (SEEDS)*, Leeds Beckett University, 2016.
9. R. Albatici, A. M. Tonelli, and M. Chiogna, 'A comprehensive experimental approach for the validation of quantitative infrared thermography in the evaluation of building thermal transmittance', *Applied Energy*, vol. 141, pp. 218–228, Mar. 2015.
10. H. Hens, A. Janssens, W. Depraetere, J. Carmeliet, and J. Lecompte, 'Brick Cavity Walls: A Performance Analysis Based on Measurements and Simulations', *Journal of Building Physics*, vol. 31, no. 2, pp. 95–124, Oct. 2007.
11. Greenspec®, 'Environmental impacts of Building Mineral Insulation compared', 2020. <http://www.greenspec.co.uk> (accessed Apr. 08, 2020).
12. IBU, 'EPD-online. Institut Bauen und Umwelt e.V.', 2020. <https://epd-online.com> (accessed Apr. 08, 2020).
13. S. Schiavoni, F. D'Alessandro, F. Bianchi, and F. Asdrubali, 'Insulation materials for the building sector: A review and comparative analysis', *Renewable and Sustainable Energy Reviews*, vol. 62, pp. 988–1011, Sep. 2016.
14. ISO 6946, Building components and building elements - Thermal resistance and thermal transmittance - Calculation method. London: British standards institute, 2007.
15. M. Mahon, 'The true cost of building a house', *Surveyors Journal*, 2016. <http://www.surveyorsjournal.ie> (accessed Apr. 09, 2020).
16. ISO 9869-1, Thermal insulation. Building elements. In-situ measurement of thermal resistance and thermal transmittance. Heat flow meter method. British standards institute, 2014.
17. SEAI, 'Conversion Factors - Sustainable Energy Authority of Ireland', Sustainable Energy Authority Of Ireland, 2020. <https://www.seai.ie/> (accessed Apr. 09, 2020).
18. A. Karamanos, S. Hاديarakou, and A. M. Papadopoulos, 'The impact of temperature and moisture on the thermal performance of stone wool', *Energy and Buildings*, vol. 40, no. 8, pp. 1402–1411, Jan. 2008.

Climate change adaptation and retrofit of a Victorian townhouse in Margate: the five-year living lab

MARIALENA NIKOLOPOULOU, RICHARD WATKINS, ELENA RUEDA DE WATKINS, LEIRE DOMINGUEZ, GIRIDHARAN RENGANATHAN, ALKIS KOTOPOULEAS

Centre for Architecture and Sustainable Environment (CASE), Kent School of Architecture and Planning, University of Kent, Canterbury CT2 7NZ, United Kingdom

ABSTRACT: This paper focuses on the analysis of a longitudinal five-year study following the retrofitting and post-occupancy evaluation of a heritage townhouse designed for multi-generation living in Margate. The three-generation family of five adults and one child are renting the council-owned 420m². The POE confirmed 100% satisfaction and thermal comfort during both winter and summer. The results from the extensive monitoring confirmed the acceptable thermal environment during the free-running mode in the summer, when for a significant amount of time parts of the property were below the Cat II category. The thermal environment in winter was very stable varying from 19.9°C in the basement, to 23.2°C in the third floor living room, while in the non-refurbished property across the square, which was used for comparison, mean temperature was 15°C. The average 5K temperature difference between the two properties highlight the success of the refurbishment, which was sympathetic to the original character of the house, respecting the heritage features.

KEYWORDS: Refurbishment, Climate Change, Thermal Comfort, Energy, Heritage, Multi-generation living

1. INTRODUCTION

Margate, in Kent (51.39°N, 1.39°E) has a rich heritage with houses surviving in the Cliftonville area from the period 1850-1914, as well as conservation areas and numerous listed buildings. Margate's heritage has recently acted as a catalyst for regeneration, with major public sector investments. However, Thanet has the weakest economy of the Kent districts with Margate Central and Cliftonville West Wards having the highest levels of deprivation and unemployment, and life expectancy of men being 18 years below that of the healthiest wards in Kent.

The physical environment has exacerbated the above conditions, with poorly converted building stock, large provision of houses of multiple occupancy and overcrowding. However, the large size of such properties (many of them at around 400m² each), which are very energy intensive, and coupled with the socio-economic problems of the local population highlight an urgent need for a range of refurbishment strategies addressing energy, environmental and social concerns.

Margate has a warm and temperate climate, with a Cfb Köppen-Geiger classification (Table 1)

Table 1. Margate monthly air temperatures

Tair (°C)	Jan	Feb	Mar	Apr	May	June	July	Aug	Sep	Oct	Nov	Dec
Avg	4	4.1	6	8.3	11.5	14.6	16.8	17	15	11.6	7.4	5.2
Min	1.5	1.6	2.8	5	7.8	10.8	13	13.1	11.3	8.5	4.7	2.7
Max	6.5	6.7	9.3	11.6	15.3	18.5	20.7	20.9	18.7	14.8	10.2	7.7

2. REFURBISHMENT

To address the above challenges Thanet District Council and Kent County Council through the 'Thanet Heritage Initiative' have been working with external partners on the refurbishment strategies of an 'Exemplar Climate Change Project in Cliftonville' [1], while testing the concept of multi-generation living. The 420m² five-storey, mid-terrace, Victorian house in Dalby square was built in 1870. It was fully restored with low carbon measures for climate change.

The house was thermally upgraded (Fig. 1) using; external insulation in the 330 mm rear wall (120mm of Pavatex Diffutherm finished with a lime render), internal insulation on the front wall to maintain the heritage façade (40mm of Pavatex Pavadentro), loft insulation (400mm Rockwall mineral fibre quilt), and woodfibre insulation treatment within the floor zones. The UPVC windows to the front façade were replaced with purpose made 1870 design British Columbian pine sliding double glazed sash windows, accurate replicas of the original windows in design, are krypton filled and double glazing with krypton filled coating. The chimneys to the rooms were repurposed to provide natural ventilation with heat recovery (Fig. 2).

With increased evidence that overheating in the domestic sector is a real concern in the UK, particularly for new dwellings with increased insulation and airtightness [2], a key objective was to prevent overheating in the summer. For that, a key strategy was to maintain the central core of the stairs open to enhance stack effect ventilation for cooling with a rooflight at the head of the staircase to open

automatically in hot weather to increase airflow. Additional cooling strategies included openings for cross-ventilation, the repurposed chimneys to the rooms, exposed thermal mass where possible, i.e. the rear wall and the boundary walls, while the windows on the front façade have a high performance solar control clear outer pane and a float glass inner pane (laminated) with a slight grey tint and a g-value of 0.27.

The key innovation, however, has been the refurbishment of the property for multi-generation living, providing three living rooms (basement, ground and first floor), three kitchens (basement, ground and first floor), four/six bedrooms, and four bathrooms. The extensive three-generation family of five adults and one child, who were selected to live in the property (Fig. 3), include the upper generation, which consists of the Matriarch and Patriarch, as well as the Matriarch's brother, the mid-generation consisting of the Son and Daughter, while the lower generation consists of the daughter's young child.



Figure 1: The front and rear of the five-storey refurbished property in Dalby square, Margate (UK).



Figure 2: Chimneys to all the rooms repurposed to provide natural ventilation with heat recovery.

3. MONITORING

The house underwent extensive environmental monitoring to evaluate the thermal performance of the house supplemented by post-occupancy evaluation during the different seasons.

The monitoring included; pre-refurbishment, post-refurbishment without occupants and continuing with the residents, living in the property. Air temperature, surface temperature and relative humidity were measured in different rooms at different floors using



either HOBO loggers or Tinytag loggers, recording data every 15 minutes. They were positioned at 1.5m above Figure 3: Three-generation living and space allocation with logger positions (source: Lee Evans Partnership LLP)

the floor level, at all five storeys of the house, in different rooms to account for orientation (Table 2). CO₂ was measured using Tinytag loggers (0-2000ppm). Gas use was recorded using a Tinytag pulse counting logger attached to the existing gas meter, while gas and electricity meter readings were taken when visiting the house to collect data.

Table 2. Test House – Logger positions

Code	Parameter	Location
B	T / RH	Basement, front room (Living room)
A	T / RH	Ground floor (Hall, entrance)
J	T / RH	Ground floor, front room (Living room)
C	T / RH	First floor, front room (Family living room)
D	T / RH	First floor (Family kitchen)
H	T / RH	Second Floor, back room (dressing room)
G	T / RH	Third floor, back bedroom
E	T / RH	Third Floor, (top landing)
F	T / RH	Third Floor, front room (Living room)
K	Tsurface	Basement, front room (Living room)
L	Tsurface	Ground floor (Hall, entrance)

M T_{surface} Second floor, back room (dressing room)
 Text. External Temp. (back patio) in radiation shield
 AA CO₂ First Floor, front room (Family living room)
 BB CO₂ Second Floor, front room (Master bedroom)
 GR Gas Pulse Count data Basement

The data gathered was to be compared with additional data from periodic monitoring of an identical house across the square, which has not undergone any refurbishment, to evaluate the effect of the refurbishment. The monitoring in the Control House included three loggers, two T_{air}/RH in the basement front room (Living room) and the second on the first floor, front room (Family living room), while a CO₂ logger was placed in the first-floor room (Family living room). It is worth highlighting that the control house was also used as a multi-generation living, with an extended family living there for many years.

4. RESULTS

4.1 Post-occupancy evaluation

The occupants reported 100% satisfaction with the controls of the house, through operation of windows and doors for enhancing natural ventilation as well as blinds for shading. They also reported 100% satisfaction with the thermal environment. The comfort survey demonstrated that the house is perceived predominantly as warm in both winter and summer (Fig. 4a), and all found it comfortable/very comfortable (Fig. 4b) in both seasons.

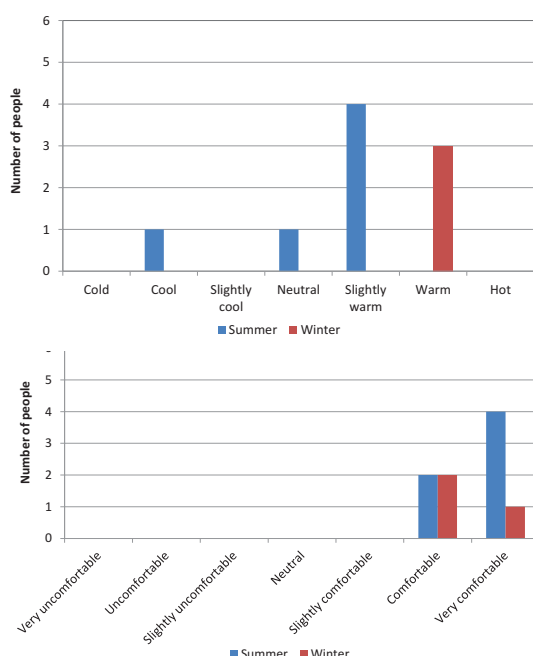


Figure 4: (a) Thermal Conditions (top); (b) Thermal Comfort (bottom) in the house in the Summer and Winter.

4.2 Thermal environment

Examining the conditions in the different rooms, the mean air temperature during the heating season

remains fairly stable for the different spaces (Fig. 5), the biggest difference found between spaces. The back bedroom on the third floor (pink line) is not used frequently which is reflected in the lower values, as also discussed below.

In January (the coolest month), the mean temperatures in the front four rooms is very similar, between 19.9°C and 20.3°C (Table 3). The temperature difference between maximum and minimum temperature was lowest in the basement, 2.4K, and highest in the ground floor living room, 9.4K, which is next to the entrance hall.

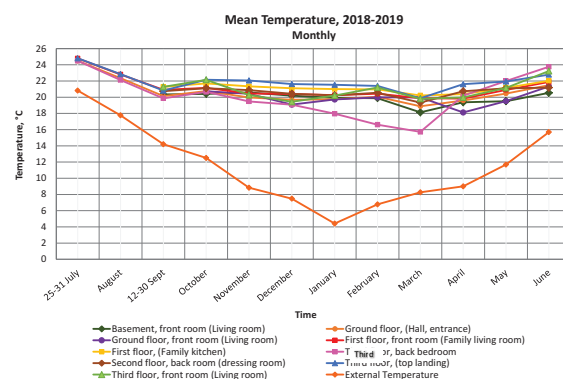


Figure 5: Monthly mean internal and external air temperature (°C)

In the summer, the house operates in a free-running mode without artificial cooling. In June, the mean temperatures in the front four rooms varied from 20.5°C in the basement, being the coolest space, to 23.2°C in the third floor living room. The maximum temperature was also found in the third floor living room, 27°C, 3K warmer than in the basement. The minima in June were closer, between 19.1°C in the basement and 20.2°C in the third floor living room.

Table 3. Internal temperatures (°C) in the front rooms

	Basement, Living room		GF, Living room		1st floor, Family living room		3rd floor, Living room	
	Jan.	June	Jan.	June	Jan.	June	Jan.	June
Mean	19.9	20.5	19.7	21.3	20.3	21.9	20.2	23.2
Min.	19.0	19.1	14.7	19.0	17.9	19.4	17.0	20.2
Max.	21.4	23.8	24.2	24.6	22.8	25.0	22.6	27.0

The rear third floor bedroom is used as a guest room and remains mostly unoccupied. This is why it experiences both high and low temperatures; a minimum of 10.5°C in January and maximum of 30.5°C in June (Table 4). The dressing room, on the same floor, does not experience these extremes, with the maximum temperature being 25.3°C in June and the minimum 17.2°C. The difference in temperatures between these two rooms is to be expected. The rear third floor bedroom projects from the main building and is therefore more exposed to the sun, while at the same time shades the dressing room. In addition, the

door of the dressing room is left open to the stairwell whilst the rear bedroom's door is kept closed.

Table 4. Internal temperatures (°C) in the rear rooms

	3rd floor, back bedroom		2nd floor, back room dressing room	
	Jan.	June	Jan.	June
Mean	18.0	23.8	20.2	21.2
Min.	10.5	20.1	17.2	17.2
Max.	24.7	30.5	25.0	25.3

Circulation spaces do not experience wide fluctuations (Table 5). The mean temperature in the entrance hall on the ground floor and on the third-floor landing are very similar to those in occupied spaces. As would be expected the third-floor top landing is warmer than the ground floor, on average by 2.5K at the different months.

Table 5. Internal temperatures (°C) in circulation spaces

	GF hallway		3rd floor, top landing	
	Jan.	June	Jan.	June
Mean	19.8	21.5	21.5	22.8
Min.	18.1	18.9	18.9	20.1
Max.	22.4	23.7	24.9	26.2

4.2.1 Thermal environment in the Control House

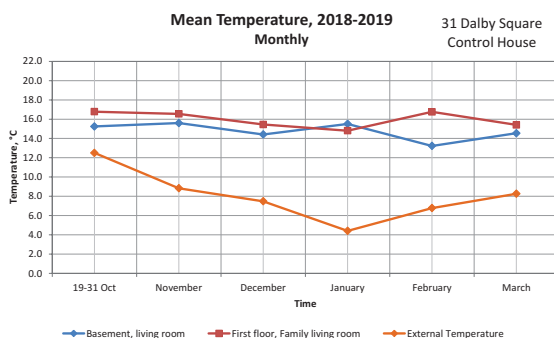


Figure 6: Monthly mean internal and external air temperature in the Control House.

When looking at the conditions from the six-months monitoring period in the control house across the square, which hasn't been refurbished, in wintertime, it is surprising how low the temperatures are. The mean monthly temperature on the first floor varies from a high of 16.8°C to 14.8°C, while in the basement the highest mean monthly average is 15.6°C in November and drops to 13.2°C in February (Fig. 6). Combined with fuel poverty and scarce operation of the heating system, it is clear that the resulting conditions are very low, with the minimum temperature reaching 10°C in the basement in January, well below the CIBSE recommendations for thermal comfort in dwellings [3]. Considering that these are the living conditions for an elderly family member, who cannot go up the stairs, the detrimental

effect on their health from the very low temperature and resulting damp conditions can be easily appreciated.

When the internal conditions are compared with those of the refurbished property, the average temperature differences are striking (Table 6), varying from 4.4K for the basement to reaching 5.5K for the first floor living room. The differences in the minimum temperature reached are even higher, with 5.8K in the first floor and 9K temperature difference in the basement, which highlights the higher fluctuations of the uninsulated property.

Table 6. Comparison of internal temperatures (°C) in the Control and the Refurbished House in January

	Basement, living room		1st floor, front, family living room	
	Control	Refurbished	Control	Refurbished
Mean	15.5	19.9	14.8	20.3
Min.	10.0	19.0	12.1	17.9
Max.	18.6	21.4	17.3	22.8

Another interesting point arises from comparing the mean temperatures in the two houses, and the different stages of the refurbishment of the main property. The data for pre-refurbishment (2015), when the house was monitored for a short period of time and post-refurbishment but pre-occupancy (2017), both periods representing free-running conditions without heating, are compared with the occupied conditions in the two houses in 2018. The data for the month of December is examined in the different years (Table 7).

Table 7. Comparison of internal temperatures (°C) in the Control and the Refurbished House in December

	Test House			Control House
	2015 Pre-refurbish	2017 Post-refurbish	2018 Post-Occupancy	2018
Mean	13.8	18.1	20.4	15.4
Min.	12.4	16.0	17.8	12.5
Max.	15.2	18.9	23.0	18.0

The mean and minimum temperature in the control house in December 2018 is remarkably similar to the pre-refurbish test house in December 2015 which was unoccupied and unheated. The similarity reflects the lack of insulation and low levels of heating in the control house.

4.3 Thermal comfort and overheating

A key factor in the refurbishment was to ensure it preparedness for climate change. To address such concerns analysis of thermal comfort in the summer was conducted, to identify whether overheating was prevalent. For the thermal comfort analysis, the CIBSE

recommendations are used, examining both the static and dynamic criteria [4].

The residents moved into the refurbished property in July 2018, hence the results are presented for the first summer of operation, the period August to October 2018.

The indoor temperatures for the different floors during the cooling period are presented in Figure 7. The thresholds for the static CIBSE criteria of 25°C and 28°C are also plotted. For the living areas, to avoid overheating the operative temperature should not exceed 28°C for more than 1% of the occupied hours. In fact, most of the temperatures are within the comfort range. In fact, only the third floor experiences overheating with 3.49% of the hours above the 28°C. This is within the first week of August, where outdoor temperature was very high, exceeding 28°C in various instances, with a maximum of 33.9°C recorded.

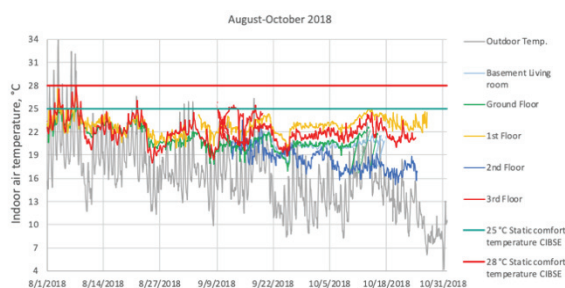


Figure 7: Indoor air temperature in relation to the outdoor temperature for the period 1/8/2018-31/10/2018 shown against the CIBSE static comfort criteria.

Comparing with the adaptive thermal comfort standards BSEN15251, for Category II, new buildings (Fig. 8) highlights that overheating does not appear to be an issue. The analysis of occupied hours within category II highlights that the only rooms with a small risk of overheating are the GF living room (1.32% above Cat. II) and the bedroom on the top floor at the rear of the property with a western orientation (0.14% above Cat. II). It should be noted that the analysis has been conducted with air rather than operative temperature, based on the assumption that the two values are similar under the monitored conditions.

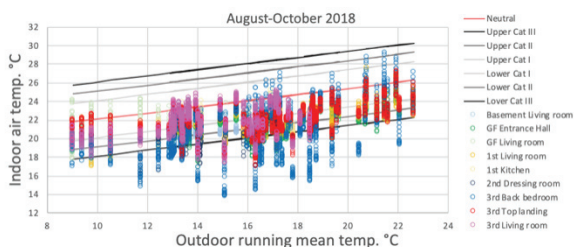


Figure 8: Indoor air temperature against the running mean temperature for the period 1/8/2018-31/10/2018, against the BSEN15251 adaptive comfort criteria

Focusing on August (Fig. 9), which was the hottest month, potential overheating is only observed on the

top floor at the rear bedroom, with the conditions exceeding Category II for 0.4% of the 745 hours monitored, is less than 3 hours for the whole month.

What is noticeable is the number of hours which could be classified as cold discomfort. Although the majority of the time spaces are within the required category II for comfort, large percentages depending on the room, from 23% for the top floor landing to 44% for the top floor rear bedroom, are below Category II, for comfort.

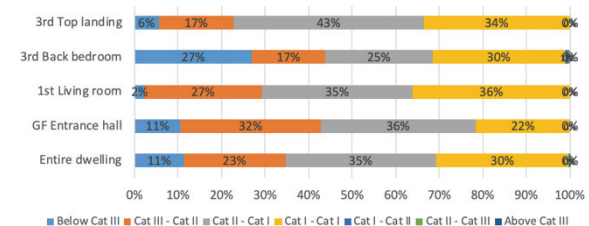


Figure 9: Distribution of percentage hours within the different categories of the BSEN15251 adaptive model, for August 2018.

Monitoring of the property continued until June 2019, so it was possible to analyse the following summer, specifically May and June 2019, for thermal comfort and potential overheating (Figs. 10-11).

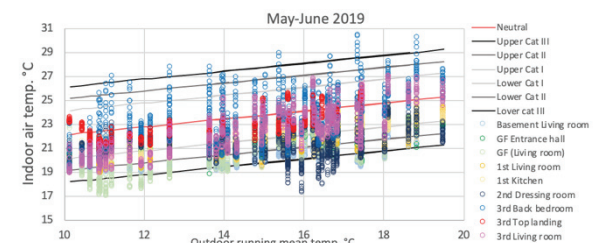


Figure 10: Indoor air temperature against the running mean temperature for May-June 2019, against the BSEN15251 adaptive comfort criteria

With the house running in free-running mode in May and June, the different spaces are within the comfort category for the majority of the time (Category II). Looking at the results in tabular form (Table 8), each floor behaves differently. Overheating is experienced for 4% of the time, on the top floor, the rear bedroom, which appears to be the main space with such risk. This is attributed to the fact that, as mentioned in Section 4.2, the rear third floor bedroom is therefore more exposed to the sun. while it shades the dressing room, which is reflected in the comfort hours between these two spaces.

Overall, cold discomfort is more noticeable, with the conditions at the basement being below Category II for 86% of the time. This percentage decreases moving up through the different floors, with stratification leading to cold discomfort being less noticeable. In fact, the landing at top of the stairs is 100% within the Category II range.

Table 8: Distribution of hours that different rooms are below, within, and above Category II, BSEN15251, May-June 2019.

	Hrs below Cat II	Hrs within Cat II	Hrs above Cat II	% hrs below Cat II	% hrs within Cat II	% hrs above Cat II
Entire dwelling	2904	8282	56	26%	74%	0.5%
Basement	1129	191	0	86%	15%	0
GF entrance	286	1034	0	22%	78%	0
GF L.R	654	666	0	50%	50%	0
1st floor L.R	196	1124	0	15%	85%	0
1st floor kitchen	98	1222	0	7%	93%	0
2nd floor dressing-room	427	893	0	32%	68%	0
3 rd floor bedroom	36	1228	56	3%	93%	4%
3rd floor landing	0	682	0	0	100%	0
3rd floor Liv.r.	78	1242	0	6%	94%	0

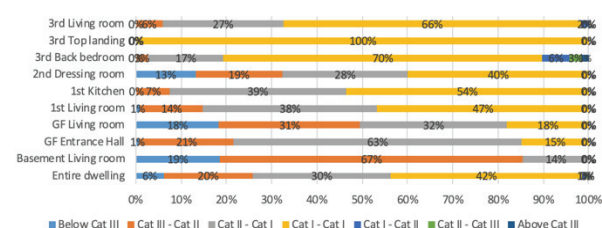


Figure 11: Distribution of percentage hours within the different categories of the BSEN15251 adaptive model, for May-June 2019.

4.4 Energy consumption

To determine the annual energy consumption (Table 9) the measured data were combined with estimated gas and electricity use. Measured gas data were available from 20 October 2018 to 28 June 2019, i.e. for 70% of the year. For the summer, consumption of gas was assumed to be for hot water and cooking only. Meter readings of electricity use taken on regular visits were used to estimate the annual use by extrapolating using the mean consumption.

Table 9: Annual Energy Use

Fuel	kWh/year	kWh/m ² .year
Gas	41,014	97.7
Electricity	5,883	14
Total	46,897	111.7

Although the overall energy consumption for gas in the domestic sector appears high, taking into account the large size of the property, the annual use weighted for floor area is lower than the average profile for new domestic buildings [5].

4. CONCLUSION

This paper focused on the analysis from a longitudinal five-year study of the retrofitting and post-occupancy evaluation of a heritage townhouse designed for multi-generation living in Margate. The three-generation family of five adults and one child, lived in the 420m² house for a year while the house was being monitored. The POE confirmed 100% satisfaction and thermal comfort during both winter and summer. The results from the monitoring confirmed the acceptable thermal environment during the free-running period in the summer, when for a significant amount of time parts of the property were below the Cat II category. The thermal environment in winter was very stable in the occupied rooms varying from 19.9°C in the basement, to 23.2°C in the third floor living room, while in the non-refurbished property across the square, mean temperature was 15°C. The average 5K temperature difference between the two properties highlight the success of the refurbishment, which was sympathetic to the original character of the house, respecting the heritage features.

The work supported the development of a Sustainable Heritage Toolkit for coastal towns [6] and guidelines for multi-generation living as a viable alternative to address social challenges in the era of climate change. In summary, the project, which the Academy of Urbanism highlighted as 'ground-breaking', provides a prototype for how to adapt historic buildings to accommodate projected changes in society and climate.

ACKNOWLEDGEMENTS

The project was funded by the Thanet Heritage Initiative from the UK National Lottery Heritage Fund. KSAP was working with Dr Hannah Swift from School of Psychology, along with Nick Dermott, Heritage Advisor- Thanet District Council, Kent County Council, Daedalus Environmental Ltd and Lee Evans Architects.

REFERENCES

1. Thanet District Council (2018). *Historic house in Margate part of pioneering multi-generational living project*. <https://www.thanet.gov.uk/historic-house-in-margate-now-part-of-pioneering-multi-generational-living-project/>
2. Lomas KJ & Porritt SM (2017). Overheating in buildings: lessons from research, *Building Research & Information*, 45: 1-2, pp 1-18.
3. CIBSE (2015). *Guide A: Environmental Design*. London.
4. CIBSE (2013). TM52 The Limits of Thermal Comfort: Avoiding Overheating in European Buildings.
5. NEED (2019). *Energy consumption in new domestic buildings 2015-2017*. <https://www.gov.uk/government/collections/national-energy-efficiency-data-need-framework>
6. The National Lottery Heritage Fund. (n.d.) *Climate change adaptation and Heritage buildings: a retrofitting toolkit*. http://heritageclimateadaptationtoolkit.org.uk/wp-content/uploads/2018/03/Retrofitting_Toolkit.pdf

Structural System Based on Robot Assisted Carpentry for Medium-Height Building in Wood: Metamorphosis Building – FENIX 2.0 Prototype

NINA HORMAZÁBAL¹, MICHELLE RAMÍREZ¹, PABLO SILLS¹,
FRANCISCO QUITRAL¹, FRANCISCO VALDÉS¹.

¹Architecture Department, Universidad Técnica Federico Santa María, Valparaíso, Chile

ABSTRACT: *This study addressed the issue of the reduced application of wood as a predominant structural material in medium-rise buildings in Chile, which for a wood producer nation seems like a contradiction. Besides, being Chile a highly seismic country, timber high-rise construction appears as not a viable solution, mainly due to the little knowledge of engineering wood and its technical potentials, besides, regulations in timber building construction are precarious. Thus, this applies research proposed to advance in this aspect through the development of posts and beams structural system for medium-rise building, based on engineering wood manufactured with robotic processes, which we have denominated Robot Assisted Carpentry (RAC corresponds to CAR, 'Carpintería de Armar Robotizada', in Spanish), is the process in itself the innovation. The final objective is to build, analyze and test a prototype of a fully equipped housing unit being developed by Team Chile of the Universidad Técnica Federico Santa María (UTFSM) to compete at Solar Decathlon U.S. 2020 Competition, to be held in Washington D.C. With the correct execution of this project, it is expected not only to demonstrate an innovative, efficient and sustainable way to conceive a structural system; but also to promote and disseminate in Chile, the use of timber as construction and structural building material robot-assisted and industrialized with innovative technologies.*

KEYWORDS: *Medium-rise timber building, Wood Engineering, Robot Assisted Carpentry*

1. INTRODUCTION

Despite, the great tradition of wood structures in houses in Chile, inherited and brought by European immigrants that came at the end of 19th century and the beginning of 20th centuries, British, Germans and Croatians, timber is not culturally appreciated in Chile as a building material, it is normally associated to poverty and “non-solid” or “not-resistant” construction. However, wood as a construction material possesses distinctive features, it is considered a durable, ecological and sustainable material. Its structural composition of cellulose fibers, lignin, and hemicellulose adds firmness and flexibility, extreme forces resistance and non-permanent deformations.

The timber industry of the world has largely developed with much diversity of products for the building construction sector. Currently, in countries of wood tradition such as Canada or Switzerland, the development of engineering wood and the growing awareness of the use of sustainable materials in urban constructions, has promoted a new architecture currently focused on wood as a predominant material in tall building systems, relying on computational parametric design, structural analysis, and developments in advanced manufacturing and robotics. All the above has come together in a reinvention of wood as a construction material, and forced the re-design of assemblage, joinery and structural models based on current and

innovative technologies; where our architecture department at UTFSM has not been absent.

Therefore, Team Chile from UTFSM applied for the Solar Decathlon U.S. 2020[1] being selected to compete with Casa FENIX 2.0 prototype built in wood as its main construction material. For which, the most important requirements within our architectural concept was that the wooden structural system had to allow modifications in its spatial configuration, in order to ensure architectural flexibility and the possibility of transformation over time, which is normally demanded by occupants of multifamily housing complexes as family life develops [2]. The carpentry of robotic assembly, apart from providing modularity and assembly characteristics in the construction process, is the articulator between the structure and the architectural design supporting a transformable system of customized joints that allow spatial modifications within the building. The demand of precision design, analysis and manufacture of joints lead us to the use of robotics or numerical control tools. Therefore, the correct transmission of loads is achieved through a larger contact for the joints robot-machined by the Robot Assisted Carpentry (CAR) [3], providing an excellent thermal and structural performance, compared to steel or reinforced concrete structures.

2. A WOOD PRODUCER COUNTRY

Chile has a consolidated timber industry that last year exported US\$ 6,836 millions comprised of 16,3

million tons of wood products [4]. Therefore, timber as a construction material has an enormous potential for wood based buildings in our country. In addition, the Chilean Ministry of Housing (MINVU) has recently committed to double by year 2025, the use of wood as the based construction material for social housing [5]. And, currently, the Ministry of Housing and Planning (MINVU) is promoting the first social housing low-rise building of 6-story height to be built in Rancagua city [6].

2.1 Sustainability of wood construction

There is a lot of evidence of market potential to promote wood as a building construction material; it is well recognized and demonstrated as the most sustainable material within the building construction industry, especially in developed countries. Despite of this and despite Chile is a timber producer country, the housing industry has been and it is based in reinforced concrete as the main structural building material, being characterized as a time consuming industry, high-energy consumption, high in CO₂ emissions, water dependent and high in costs, although, it is also a proven technology in terms of earthquakes resilience, completely comparable to the timber construction.

Taken into consideration the above described aspects, in order to avoid the negative features of concrete based structure, for the design of timber structural system to be prefabricated and modular, reducing the carbon footprint in the use of machinery, less pollution when prefabricating and less on-site contamination when building (assembling). If we add to this structural system, the use of robotic assembly carpentry for the joints, the CO₂ emissions decrease even more, since the manufacture of the steel parts produces more pollution than the design of the joints. On the other hand, the total cost of the structure increases to 40% of the final value when including metal joints.

In addition to sustainability and building life cycle, the use of nationally manufactured glued laminated wood and considering it comes from a sustainable forest management, these provide the project with low CO₂ emission values.

2.2 Innovating with wood construction

The low and medium rise wood base building is new in Chile, and we have the opportunity to prove that there is a market for them based in the fast construction, industrialized production, cost effective and sustainability commitment; besides adding opportunities to innovate on the Chilean housing industry sector. Chile has an almost lost tradition of wood structures and construction that were built in places around the world (South) and mine (North and South) industries in Chile, inherited and brought by European immigrants that came at the end of the 19th century and the beginning of the 20th, examples of wood residential buildings are the balloon frame and

derived typologies brought by British and Americans to Valparaíso and Iquique and the Nordic tradition brought to the Southern cities of Chile (Lake District, Chiloe Island and the Magellan Region).

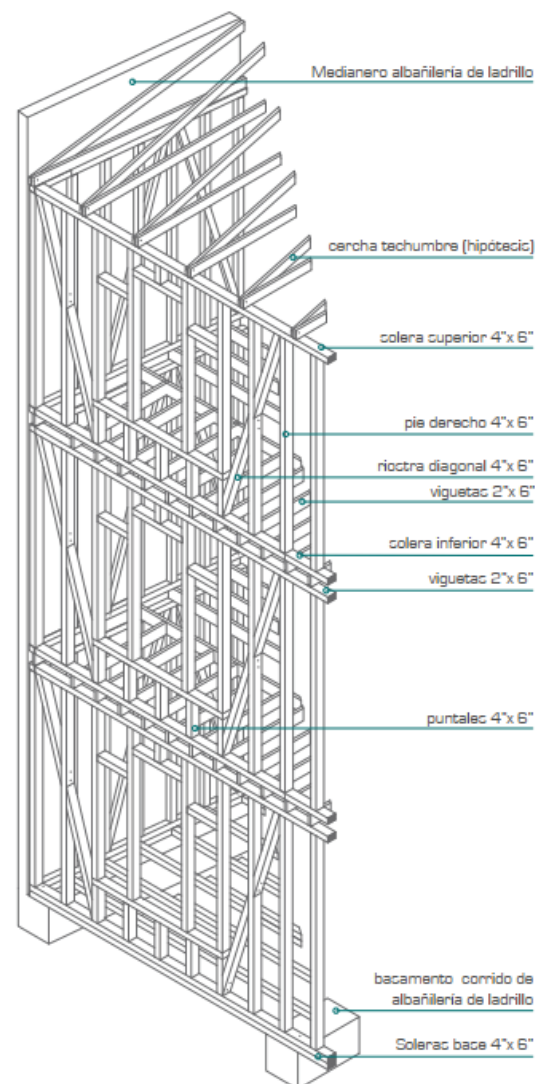


Figure 1: Valparaíso's typical housing of platform frame structure. Valparaíso. [7]

By analyzing this type of timber structures, it can be inferred that mainly the sections of their studs and the structural use for which they are designed divide the types of wooden frames. That is why, for this research, only the heavy frames or large studs will be considered as the primary structure, and light frames such as the platform frame as the design basis for the new structural system.

Besides the analysis made to these existing derivations from balloon frame timber structures brought from abroad and adopted by locals in different places in Chile, the review of two particular precedents of old and new mass timber construction systems enlighten this study to define the proposal of the Metamorphosis Building. On one side, the study of the Portland Observatory built in 1807 on Munjoy Hill, Maine, U.S. designed by a ship

captain for a lighthouse. The design therefore follows the logic of naval design for a medium-height building of 26 meter high, fully built in timber frame assembled by old technics of timber joints (Fig. 2 left), made of old growth wood post and beams system radially structured and anchored with 122 ton of granite blocks piled up on top of the lower crossbars and beams (Fig. 2 right).

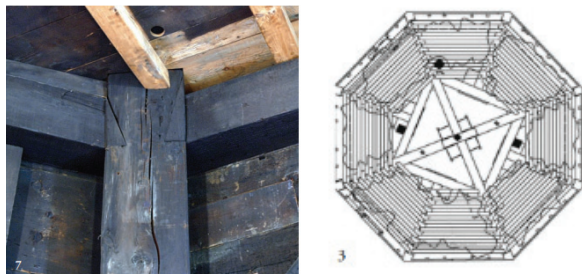


Figure 2: Timber joint and plan view of the Portland Observatory (1807) Munjoy Hill, U.S. [8]

On the other side, the analysis of the construction system of the mass timber and concrete tall building Mjøstårnet, built in Mjøsa Lake in Norway, finished in 2019, designed by Arthur Burchardt was revealing from the sustainability and mixed-use aspects. The building has an area of 11,300 sqm distributed within 18-story with 81 m height. Floor two to floor eleven are timber built with Trä8 Molven system, while from floor twelve up is built on concrete and Glulam beams, as shown in figure 3.



Figure 3: Mass timber and concrete structure of the Mjøstårnet building, Mjøsa Lake, Norway (2017-19). [9]

2.3 Structural system definition

The main characteristics to be used for the definition of the construction system to be developed are defined in relation to the revised precedents, both globally and nationally. These characteristics

meet the condition of responding to wooden buildings that are between 3 to 5-story height [10].

It can be determined that for a heavy framework system of post and beam construction type, large studs are required when it comes to medium-height buildings, and even more so when it comes to timber joinery or timber joints. This is due to the fact that when manufacturing a wood joint, a section of the wooden element is cut, so when using large stud it does not lose its structural capacity. In addition, it is established that the junction of the post and beam construction system is usually elastic structures in order to resist damage caused by earthquakes.

Secondly, it is established, mostly according to the precedents in Valparaíso, that the wooden framework systems, thanks to the flexibility of design, allow mainly orthogonal buildings to be adapted to any location. The flexibility of design is also established in the flexibility of internal diaphragm variations, determining for most cases of study that the trusses are the responsible for managing global forces (horizontal and vertical), in such a way to provide the necessary rigidity only with the primary structure. On the other hand, it is determined that the most efficient way to build the secondary structure is independent from the primary one, since, by supporting the secondary structure on the primary one, it produces an effect of diminishing the global structure capacity, adding extra weight and subsequently producing failures [10].

Then, the construction system is defined by establishing a mixed structural system. The Metamorphosis building is defined with an orthogonal structural system with a first level of reinforced concrete for greater moisture isolation from the wooden structure. The two systems are connected though seismic isolators that separate the movements of both structural systems, maintaining the common load transmissions lines. The post and beam construction system is robot-machined with timber joinery fixed with steel pins, modular every two stories and assembled by a platform system between the 3rd and 4th level. Finally, the primary structure is completed with CLT slabs, precast and dimensioned in medium sections for horizontal closing of the laminated timber framework.

3. ROBOT ASSISTED CARPENTRY (CAR), THE ARCHITECTURAL CONCEPT AND SD2020 TEAM-CHILE PROPOSAL

The proposal addresses innovation associated through flexibility and adaptability of its spaces proposing innovations on architectural solutions in social housing based on the lifecycle of families and their homes. Is the technical applications of the Robot Assisted Carpentry that made this proposal possible, ensuring the use of materials with low carbon emissions and overall, innovative for the

Chilean reality. However, it is important to mention that the robotic technology is still quite expensive in Chile, making this process not yet competitive.

3.1 Flexibility to adapt to changes in lifestyles

As part of the flexibility, it proposes a main timber structural system composed by post and beam framing that allows for continual metamorphosis of domestic spaces through the occurrences and changes of a family. The design contemplates a new system of interior walls that can move and set according to the needs of each family and beyond that in the lifetime of the house. These walls will be able to incorporate system of electrical installations depending on the case, taking the adaptability of the house to its maximum level.

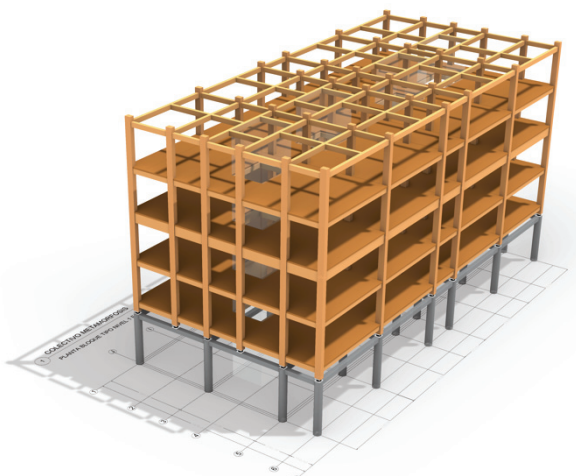
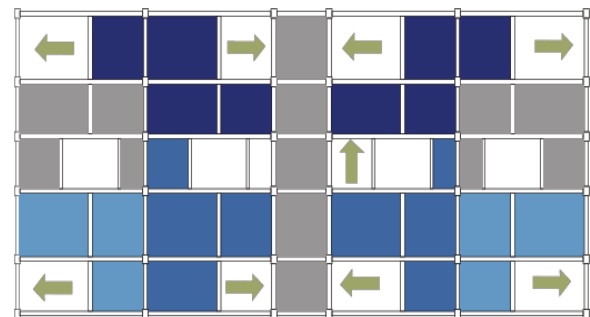


Figure 4: Proposal for medium-rise housing building of Team Chile on reinforced concrete and seismic isolators for SD 2020 competition. [10]

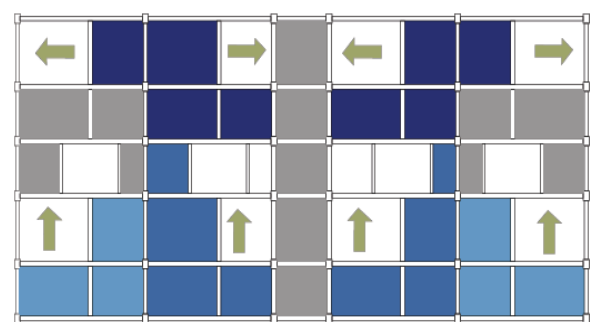
The wooden structure is projected by means of a system of glued laminated post and beams that constitute a reticule, inscribed within a mesh to modulate the operations of spatial variations. This 15x28 m wooden frame will be industrially manufactured through CAR a robotic parametric design composed of linear component of laminated wood assembled with the CAR process. The floors, supported by the structure described above, are built with 3-layer CLT panels (10 cm thick), on top of which a layer of mortar slab will be placed. For this, a lower reinforced concrete grid of 24 posts with a circular base of 50 cm in diameter and beams of 30x30 cm. For the laminated wood structure, an upper grid of 36 posts transversally crossed in relation to the general rectangle. This is done, to provide greater structural ordering and modular proportions for the housing units in both directions. The wooden framework configuration allows 6 rigid axes (grid), which balance the reticule and define the fixed non-transformable areas (gray color) or their limits (see Figure 5).

Household spaces are distributed according to operations with the greatest possible flexibility,

excluding humid zones, facilities and general circulation, which are kept fixed on the vertical volumetric bands. These 3D vertical components determine and limit the number of variations for the metamorphosis of the space; they are prefabricated on woodshop site and transported to the construction site. [10]



PLANTA NIVEL 4



PLANTA NIVEL 5

Figure 5: Proposal for transformation of houses. Team Chile for SD 2020 US competition. [10]

3.2 Chile Prototype – SD 2020

The built prototype to exhibit at SD 2020 U.S. is a chosen housing unit of the Metamorphosis building comprising of a 2-storey height and located at the edge of the building (see Fig. 6).



Figure 6: Rendered section Chile Prototype – Team Chile SD 2020. [10]

This prototype, Casa FENIX 2.0, will be monitored and the proposed structural system signed by a licensed structural engineer and the building permit has been approved for construction. It will house a family of Valparaíso, whom lost their home in the last fire of December 2019, it is being built with MINVU

reconstruction subsidy. This 2-story house has 78 m² and the structure was adjusted and redesigned to avoid oversizing the laminated wood elements and a better use of the interior spaces of the house. It is in this way that not only the structural design is adapted, but also new technical solutions for the development of joints and manufacturing details of the CAR system were established, testing the flexibility of the proposal and maintaining the sustainability principle Team Chile established.

The structure corresponds to laminated certified Oregon pine wood, provided by a local sawmill, from the Southern part of Chile. The post and beam structure new dimensions were 185x185 mm for the shorter beams and 185x360 mm for the longer posts and beams. The total amount of laminated wood used was 11.85 m³. The redesign of the wooden elements produced new technical details and structural calculations that modify the load lines and changed the directionality of the posts and beams inverting the load lines of the original reticle.

The development of the Chile prototype encompasses not only the structural design, but also validated the design of the CAR for the construction system, performing the robot-machined of the wooden elements. Fulfilling the objectives and requirements established for the structure of the Metamorphosis Building.

3.3 Robot Assisted Carpentry (CAR)

The CAR offers a proposition of value based on the prefabrication of timber frames assembly using complex geometry timber joints. This way, the industrialized production of wooden houses with timber joints made by robots, will allow us to take advantage of the Chilean timber industry, lower costs in metal joints and take advantage of development by reducing construction times in the future. In Chile there are currently approximately 500 industrial robots installed, which serve different areas of the industry, without considering a significant usage in the building construction sector, and only one in the laminated wood industry [8]. For this reason, it is intended to shorten this technological gap, by disseminating the CAR process through the demonstration home Casa FENIX 2.0.

Considering the above, the joinery design of CAR is proposed as a technical solution to the proposed double modular structural system with joint connection of the posts and beams platform, in which three critical design aspects are considered; 6.30 m long longitudinal posts and beams connection, 2.40 and 3 m long traversal posts and beams connection and the connection of both posts and beams modules.

In order to define the final design for assembly, the structural engineer was consulted prior to the robot-machined process, to corroborate the most

efficient design of the structural framework (2 posts and 3 beams 6.30 m long). The final design corresponds to a rectangular mortise and tenon joint with steel pins, as shown in figure 8.

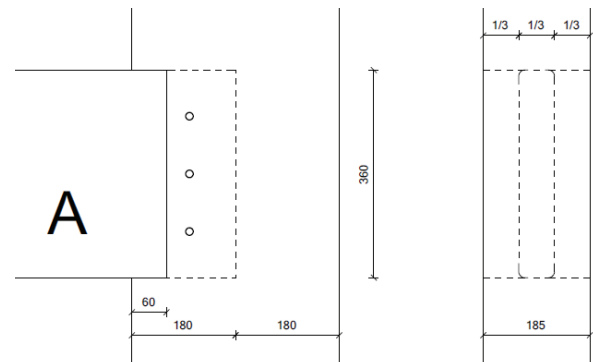


Figure 7: CAR's mortise and tenon joint for Casa FENIX 2.0 prototype – Team Chile SD 2020.

For the robot-machined process, a prefabrication of 24 tenon in 12 beams of 185x360 mm section and 6300 mm long were made. And 24 mortise in 8 pillars of 185x360 mm section and 6,600 mm long. These junctions build up four primary structure transversal frames made of Douglas Fir (Oregon pine) laminated wood.



Figure 8: CAR's Mortise and Tenon joint for Casa FENIX 2.0 prototype frame – Team Chile SD 2020, Villarrica. [10]

After the robot-machined process was done, a comparison analysis of the prefabrication and materials of the structure of casa FENIX 2.0 prototype with other construction materials was carrying out. Relevant aspects were established to compare and evaluate the life cycle and span of the prototype.

Table 1: Evaluation of Prefabrication. Comparison of 3 Types of Beams [8]

ASPECT	LAMINATED WOOD	STEEL	REINFORCED CONCRETE
Costs (CLP)	\$8.982.500	\$9.145.698	\$7.521.132

Fabrication time (days)	20 days		60 days
CO ₂ [Kg] Emissions	233,88	418,22	2025,7
Labor (# person)	3	6	10
Structure Weight [Kg]	5600	4825	40514,4
Ductility	✓	✓	Higher Seismic Risk
Pre-fabrication	✓	✓	Lower Design Complexity
Home Extension	✓	✓	Higher Complexity
Reutilization	✓	✓	NO

4. CONCLUSION

Based on this work it was possible to determine that the most favorable construction typology for the space transformation is the post and beam construction system. When considering symmetrical and orthogonal proportions the system does not require greater reinforcement of diagonals, leaving only the enveloped/partition diaphragms as secondary structure. On the other hand, as it is a structured system designed to be prefabricated and modular, production costs and construction times decreases in theory and provided the industry is technically and machinery prepared for it.

The Robot Assisted Carpentry (CAR) has several advantages, among them three can be technically defined: The first corresponds to the specific joint for used in the proposed construction system, which by being elastic or not completely rigid, contribute to the global structure of the building, providing greater resistance to damage caused by earthquakes. The second, proposing an orthogonal structural system allows greater flexibility to the design diaphragms, allowing a faster and more efficient development in terms of modular height increase and as elements for CAR's joints. The last, when using exclusively CAR's joints, it was found in the literature that it provides the proposed structure type with greater resistance to fire, increasing its collapse time, carbonizing the wooden elements before reaching the core for the subsequent collapse. This is a very important factor for families that had lost homes in an urban fire, which will be the case for the family that Casa FENIX 2.0 prototype is for.

It is important to take into consideration for timber joints design where they are going to be and the number of them in one spot, since more than one joint can cause some problems; depending on the section used, it is necessary to define which are the minimum requirements for the joint to be correctly

functional, in relation to the lengths of the mortise or the minimum dimensions of support or shoulder. In the case of the robot-machined of Casa FENIX 2.0 prototype, it was determined that it was not possible to have a timber joint in the extreme of the building, three beams on the same post, not only due to the dimensions of the elements and tenon, but also due to difficulties for the assembly process.

Wood structural systems by themselves are largely sustainable, since they absorb CO₂ throughout their life cycle. In addition, if we consider that it is a system designed to be prefabricated and modular, the decrease in the carbon footprint will be even greater through the buildings life cycle, reducing emissions with less use of machinery, less pollution when prefabricating and less pollution during construction. Wood emits 10.9% of the total CO₂ emissions of steel and 17.8% of the total CO₂ emissions of a concrete throughout its life cycle, considering the emission of the structure from its extraction to its construction.

Finally, in addition to everything previously described, the use of sustainable and nationally manufactured wood, with a good forest management from the beginning, besides from contributing to the benefits of CO₂ emissions from its raw material, enhance the sustainability of the project even more by extending longer its life cycle.

REFERENCES

1. U.S. Department of Energy, "Solar Decathlon," April 2020. [Online]. Available: <https://www.solardecathlon.gov/>.
2. ValSust UTFSM, "Design Development SD2020 Deliverable 2," Universidad Técnica Federico Santa María, Valparaíso, 2019
3. González L., Quiral F., Maino S. and Hurtado M. "Reconstrucción robotizada del patrimonio arquitectónico chileno en madera," in SIGRADI, Concepción, 2017.
4. Estadísticas Forestales, INFOR. Ministry of Agriculture [Online], Available: <https://wef.infor.cl/> [March 2019]
5. Une la Ciudad, Ministry of Housing [Online], Available: http://www.minvu.cl/opensite_det_20181116211656.aspx [March 2019]
6. Diario de la Construcción. Innovación [Online], Available: <https://www.diariodelaconstruccion.cl/edificios-de-madera-se-construiran-en-rancagua/> [27th September 2019]
7. Jiménez, M. 2015 "Los entramados tradicionales de madera en los Cerros Alegre y Concepción", UTFSM, Valparaíso.
8. Clark E. TIMBER FRAMING: Journal of the Timber Framers Guild, British Columbia, Canadá: profusely illustrated. Embossed hardcover, 2011.
9. Abrahamsen R. Mjøstårnet - Construction of an 81 m tall timber building,» de 23. Internationales Holzbau-Forum IHF 2017, Moelv, Norway, 2017.
10. Ramírez, M. 2020, "Sistema Estructural basado en carpintería de armar robotizada para edificación en madera de mediana altura," UTFSM, Valparaíso

Finding patterns of openings operation and their influence on the thermal performance of houses: A case study in Southern Brazil

ALINE SCHAEFER¹, ENEDIR GHISI¹, JOÃO VÍTOR ECCEL¹

¹Federal University of Santa Catarina, Florianópolis, Brazil

ABSTRACT: User behaviour regarding opening and closing windows is one of the factors that most impact the performance of houses. In addition, the variability of user behaviour is a factor that often leads to inconsistencies between reality and computer simulation, but this is not usually taken into account. For this reason, this study aimed to obtain different user profiles regarding openings operation based on actual data and analyse their influence on the energy performance of buildings. The method applied in this research consists of three steps: data collection, finding patterns of opening operation through cluster analysis and computer simulation for thermal performance analysis. Cluster analysis resulted in four distinct groups. For each group, one reference model was obtained, corresponding to those objects closest to the centroid, and described by a distinct hourly schedule, representing the time of the day doors and windows remained open. The thermal performance analysis has shown that different profiles may have a huge impact on the performance of houses due to heat losses and gains and air change rate through doors and windows. It was possible to conclude that the use of reference models based on actual data may lead to more reliable performance indicators.

KEYWORDS: User profile, Reference model, Opening pattern, Thermal performance of buildings, Low-income housing

1. INTRODUCTION

Users strongly influence the thermal performance of houses by the way they operate them. User behaviour regarding opening and closing windows is one of the factors that most impact the performance of houses [1-3]. In Brazil, which is a country with abundant winds, the operation of doors and windows can deeply contribute with energy efficiency in buildings, as this helps to provide thermally comfortable rooms naturally [4].

Several studies have applied computer simulations to infer about the effectiveness of energy efficiency measures, which allows to assess the impact of those measures before they are implemented. However, it is important to use reliable input data to avoid inconsistent results [5, 6]. Thus, by using real data in simulations one can achieve better and more coherent results, as the studies developed by Andersen et al. [7] and Haldi and Robinson [8] have shown.

In addition, another important factor is the variability of user behaviour. This is a factor that often leads to inconsistencies between reality and computer simulation, and this is not usually taken into account. Some studies [3, 7, 9], though, have proved the importance of applying more than one user profile in simulation to obtain more reliable results.

One way to find patterns in data is the use of some data mining technique, such as cluster analysis. Cluster analysis is an exploratory unsupervised method that aims to divide a sample into groups or clusters of similar individuals. Clusters must have high internal homogeneity and high heterogeneity between them [10, 11]. Cluster analyses have already been applied in other studies that aim to determine user behaviour patterns [6, 9, 12].

Regarding this context, this study aimed to obtain different user profiles regarding openings operation based on actual data and analyse their influence on the thermal performance of buildings.

2. METHOD

The method applied in this research consists of three steps: data collection, finding patterns of opening operation through cluster analysis and computer simulation for thermal performance analysis.

First, data regarding openings schedule were collected in single-family low-income housing, in southern Brazil. Data were collected for living-room and bedrooms (long-stay rooms only) of each house, and organized in binary hourly basis, resulting in 24 intervals. For each hour, it was recorded if windows and doors remained open or closed, adopting "0" (zero) when closed and "1" (one) when open. Data were

organized in a spreadsheet in order to obtain easy access to the information.

Then, data collected were organized and submitted to cluster analysis, which combined hierarchical and non-hierarchical procedures. Squared Euclidean distance and Ward algorithm were applied for the hierarchical procedure, while k-means algorithm was used for the non-hierarchical procedure. The hierarchical procedure was performed in order to determine the ideal number of clusters to be formed, according to the similarity level found for each step of cluster analysis. The number of clusters was determined according to the stop rule, which represents the moment when a joint between two clusters produces an increase of the similarity level relatively higher than the former step. The ideal number of clusters corresponded to those formed at the time the stop rule was applied. The non-hierarchical procedure was performed in order to define the final formation of clusters, taking into account the number of clusters determined with the hierarchical procedures.

Reference models of each group obtained from cluster analysis were used to represent different profiles in computer simulations. Each reference model was defined as the closest object to the centroid (multivariate mean) of its group and was described by an hourly schedule, representing the time of the day doors and windows remained open. The cluster analysis was based on the method proposed by Schaefer and Ghisi [13].

Finally, computer simulations were performed using the software EnergyPlus (version 8.9). Natural ventilation availability was configured according to each reference model's windows and doors operation schedule, since pre-established comfort conditions were considered [14]. All other parameters were kept constant. Florianópolis climatic reference year file was used to represent the weather conditions in simulations. Fig. 1 shows predominant wind speeds for each direction and season of year. The geometry and construction systems of the envelope were configured as the reference building found by Schaefer and Ghisi [13]. The building consists of a 36.00m² single-family low-income house, composed of a combined living-room and kitchen and two bedrooms. The construction system was composed of ceramic brick and mortar walls ($U = 2.39 \text{ W/m}^2\cdot\text{K}$, $C = 152.00 \text{ kJ/m}^2\cdot\text{K}$, $\alpha = 0.5$), roof composed of ceramic tile, concrete slab and wooden lining ($U = 2.05 \text{ W/m}^2\cdot\text{K}$, $C = 238.00 \text{ kJ/m}^2\cdot\text{K}$, $\alpha = 0.6$) and a concrete slab covered with ceramic tile floor ($U = 3.40 \text{ W/m}^2\cdot\text{K}$, $C = 293.80 \text{ kJ/m}^2\cdot\text{K}$). Internal gains were configured as suggested by CB3E [15]. Table 1 show the details of each opening.

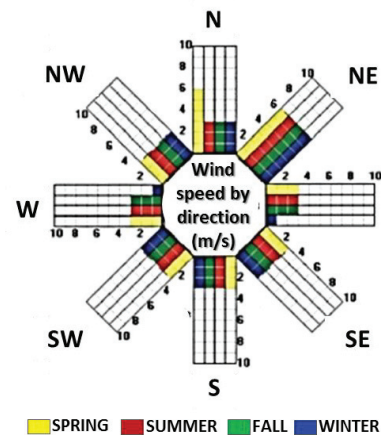


Figure 1: Predominant wind speeds for each direction and season of year in Florianópolis (m/s).

Table 1: Doors and windows description

Name	Type	Room	Dimension (m)	Solar Orientation
D1	Exterior door	Living-room	0.80x2.10	East
D2	Interior door	Main bedroom	0.80x2.,10	-
D3	Interior door	Secondary bedroom	0.80x2.10	-
W1	Window	Living-room	1.20x1.00	East
W2	Window	Kitchen	130.00x0.60	South
W3	Window	Main bedroom	1.20x1.00	North
W4	Window	Secondary bedroom	1.20x1.00	West

Two indicators, i.e. air change rate and sensible heat gains and losses, were obtained from the computer simulations. These indicators were used to verify the impact that different user profiles have on the building performance.

2. RESULTS AND DISCUSSION

3.1 Profiles obtained

Cluster analysis resulted in four distinct groups. For each group, one reference model was obtained. Each reference model represents the opening schedule of doors and windows of all houses from its cluster.

Fig. 2 shows the hourly opening schedule for all reference models. These schedules can be applied in computer simulations in order to provide more reliable results, since they represent the variability that can be found in field. Horizontal axis shows the 24 hours of a day. Vertical axis shows the openings, one of each

represented by a colour. The circles filled with colours represent the hour of the day in which each opening remained open (e.g., if the circle is coloured at 9:00, it means that the opening remained open from 9:00 until 10:00).

Reference model 1 has all windows and doors open from 10:00 to 18:00. Windows from Reference model 2 remain open from 9:00 to 20:00 while the doors remain closed part of the day (except for Main Bedroom, which remains open all day long). Windows of Reference model 3 remain open from 9:00 to 17:00, and so does

the external door. Internal doors remain open all day. Finally, Reference model 4 has shown the most irregular schedule. Living room windows remain open from 7:00 to 18:00. Windows of Main Bedroom and Secondary Bedroom remain open from 7:00 to 21:00 and from 12:00 to 18:00, respectively. Doors remain open part of the day, except for Secondary Bedroom, which remains closed all day long.

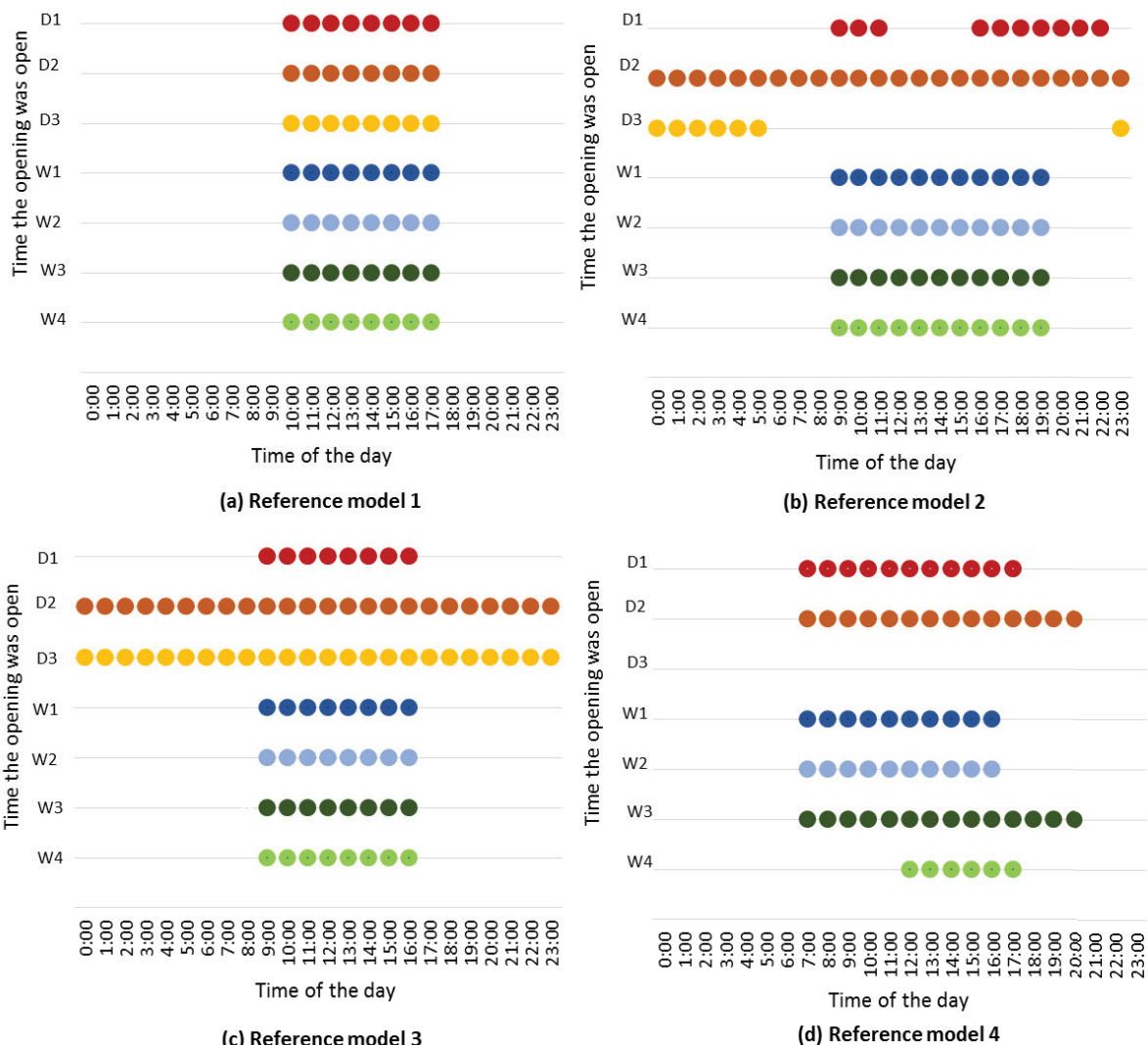


Figure 2: Windows and doors opening schedule of each reference model.

3.2 Thermal performance

Figs. 3 and 4 present the thermal performance indicators obtained through computer simulation for each of the reference models: the air change rate (ach) and sensible heat gains and losses (W), respectively.

The air change rate measures the amount (volume) of air that have been added to or removed from the room in relation to the volume of the room. It represents the air renewal of that room.

The air change rate was obtained for each reference model and it is shown in Fig. 3. In order to summarise,

only results obtained for the living room are shown. Data are presented in hourly basis for two typical weekdays, one in the hot season (February 21th) and the other in the cold season (July 19th), represented by a red line and blue line, respectively.

It is possible to observe that the air change rate differs for each reference model and occurs accordingly to their opening schedule. For all reference models, air change rates occur more often from 10 ach to 20 ach. The most expressive air changes were observed in the cold season for Reference models 1 and 3 (almost 40

ach) and in the hot season for Reference model 2 (almost 60 ach). Although Reference model 1 and Reference model 3 have similar schedules, a slight difference can be observed on the air change pattern of these two models. This indicates that even small differences in their schedule can influence the performance of a building, which highlights the need to consider user variability in thermal and energy simulations (i.e., to adopt more than one user reference model to represent user opening operation profile).

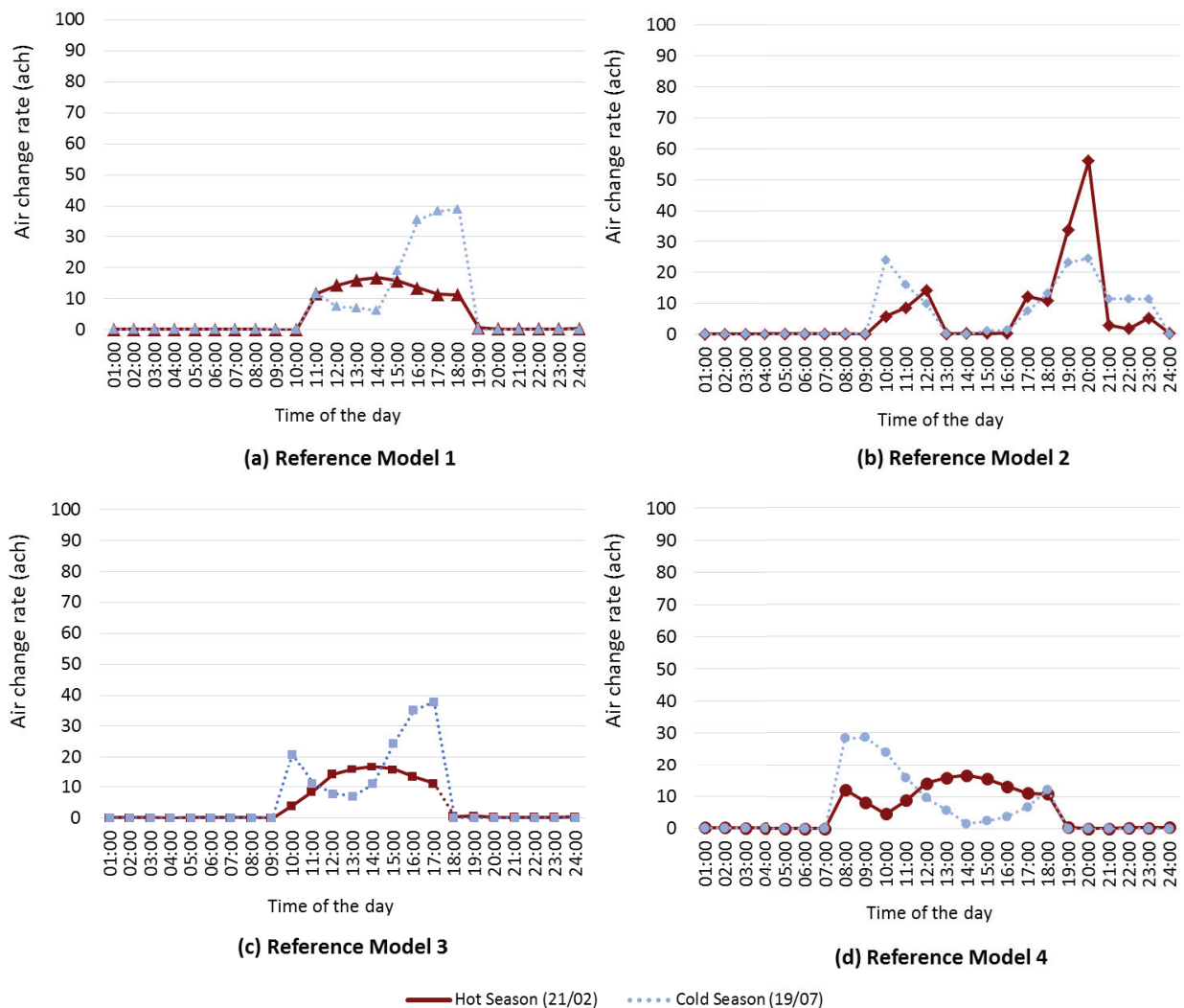


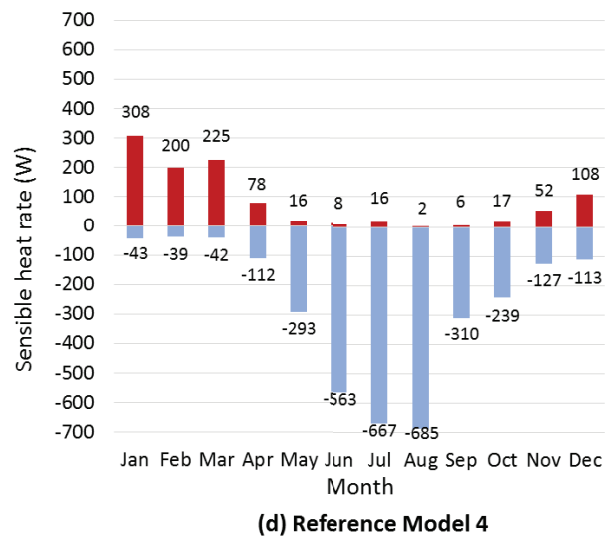
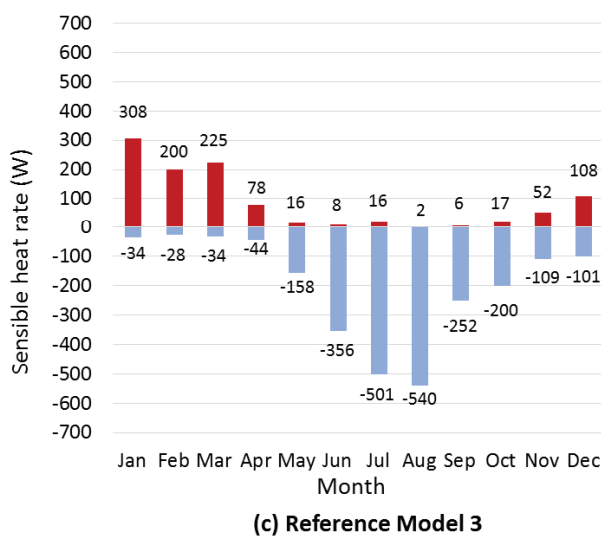
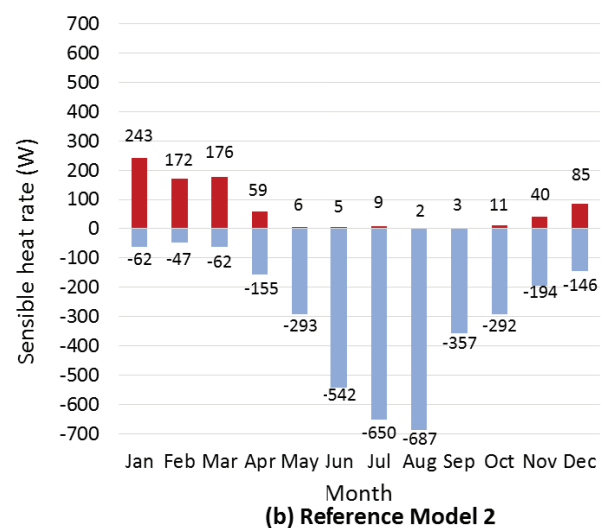
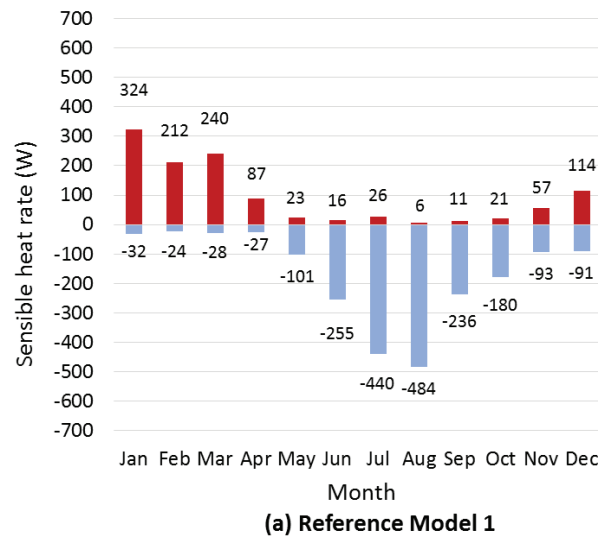
Figure 3: Air changes per hour due to different operation of doors and windows in the living room, in the hot (21/02) and cold (19/07) season.

The sensible heat gains and losses (W) obtained through the computer simulation represent the amount of energy that would be required to maintain the temperatures in each room within a predetermined limit range.

Fig. 4 shows a summary of monthly sensible heat gains and losses throughout the year, for all reference models. Horizontal axis displays all months of a year. Vertical axis shows the sensible heat gains (positive values) and sensible heat losses (negative values).

In general, sensible heat losses were greater than sensible heat gains for all models. Reference model 4 showed greater sensitivity to the effects of air infiltration, as it had the highest gains in the hot season and high losses in the cold season. This is also the reference model in which openings remain open for the longest period of time (from early in the morning until night). Reference model 2 was the one which suffered the greatest heat loss in both winter and summer. Although this reference model external openings remain open for a shorter period of time than Reference model 4, its internal doors remain open for a longer period. This influences the performance of models by allowing cross ventilation. Due to different pressure coefficients, internal air exchanges are

intensified, which impacts the thermal performance of rooms. Reference models 1 and 3 had similar results for both sensible heat gains and losses, but losses were slightly higher for Reference model 3. These two models had a similar operation of doors and windows, but internal doors from Reference model 3 remain open for the whole period. The opening schedules of internal doors are usually not taken into account in most studies, being configured as closed for the whole period. In this study, however, a difference related to the opening of the internal doors in the performance of the buildings was observed, from which the importance of taking them into account in computer simulations is verified.



■ Sensible heating gains ■ Sensible heating losses

Figure 4: Sensible heat losses and gains due to air infiltration in the living room throughout the year for each reference model.

4. CONCLUSION

This research aimed to obtain reference models regarding the opening of doors and windows in single-family low-income houses in Florianópolis, Brazil, for use in studies of thermal and energy performance. Four different reference models were found through the application of cluster analysis on an actual database. Each reference model represents a distinct doors and windows operation schedule. The schedules obtained can be applied in other thermal performance studies focused on single-family low-income housing in subtropical climate regions. From computer simulations, it was possible to verify the influence that different schedules have on the thermal performance of the house due to heat losses and gains and air change rate through doors and windows. The air change rates have shown that indoor air flows occur accordingly to the openings schedules. Additionally, sensible heat losses have found to be greater than sensible heat gains for all reference models. The study also highlighted the importance to determine operating schedules for internal doors, which is usually neglected in thermal performance studies. It was possible to conclude, at last, that the use of more than one reference model, obtained based on actual data, may lead to more reliable performance indicators.

ACKNOWLEDGMENTS

The authors acknowledge with thanks the financial support of Higher Education Personnel Improvement Coordination (CAPES) of Brazil.

REFERENCES

1. Wang, L. and Greenberg, S., (2015). Window operation and impacts on building energy consumption. *Energy and Buildings*, v. 92, p. 313–321.
2. Moghadam, S.T., Soncini, F., Fabi, V. and Corngati, S., (2015). Simulating window behaviour of passive and active users. *Energy Procedia*, v. 78, p. 621–626.
3. D’oca, S. and Hong, T., (2014). A data-mining approach to discover patterns of window opening and closing behaviour in offices. *Building and Environment*, v. 82, p. 726–739.
4. Sorgato, M.J., Melo, A. P. and Lamberts, R. (2016). The effect of window opening ventilation control on residential building energy consumption. *Energy and Buildings*, v.133, p. 1–13.
5. Silva, A.S. and Ghisi, E. (2014). Uncertainty analysis of user behaviour and physical parameters in residential building performance simulation. *Energy and Buildings*, v. 76, p. 381–391.
6. Aerts, D., Minnen, J., Glorieux, I., Wouters, I. and Descamps, F. (2014). A method for the identification and modelling of realistic domestic occupation sequences for building energy demand simulations and peer comparison. *Building and Environment*, v. 75, 67–78.

7. Andersen, R., Fabi, V., Toftum, J., Corngati, S. P. and Olesen, B. W., (2013). Window opening behaviour modelled from measurements in Danish dwellings. *Building and Environment*, v. 69, p. 101–113, 2013.
8. Haldi, F. and Robinson, D. (2009). Interactions with window openings by office occupants. *Building and Environment*, v. 44, n. 12, p. 2378–2395.
9. Balvedi, B. F., Schaefer, A., Bavaresco, M. V., Eccel, J. V. and Ghisi, E. (2018). Identificação dos perfis de comportamento do usuário para edificações residenciais multifamiliares e naturalmente ventiladas em Florianópolis. *Ambiente Construído*, v. 18, n. 3, p. 149–160.
10. Hair, J.F., Anderson, R.E., Tatham, R.L. and Black, W.C., (2009). *Análise Multivariada de dados [Multivariate data analysis]*. 6. ed. Porto Alegre: Bookman. (in Portuguese).
11. Bussab, W.O., Miazaki, E.S., and Andrade, D. F., (1990). *Introdução à análise de agrupamentos [Introduction to cluster analysis]*, IX Simpósio Nacional de Probabilidade e Estatística, São Paulo, SP. (in Portuguese).
12. Yu, Z., Fung, B. C. M., Haghighat, F., Yoshino, H. and Morofsky, E., (2011). A systematic procedure to study the influence of occupant behaviour on building energy consumption. *Energy and Buildings*, v. 43, n. 6, p. 1409–1417.
13. Schaefer, A. and Ghisi, E., (2016). Method for obtaining reference buildings. *Energy and Buildings*, v. 128, p 660–672.
14. American Society of Heating, Refrigerating and Air-Conditioning Engineers (2010). *Thermal Environmental Conditions for Human Occupation*. ANSI/ASHRAE Standard 55. American Society of Heating, Refrigerating and Air-Conditioning Engineers, Inc. Atlanta.

The Impact of Static and Dynamic Solar Screens on the Indoor Thermal Environment and Predicted Thermal Comfort

NIYATI NAIK¹ and IHAB ELZEYADI¹

¹School of Architecture and Environment, University of Oregon, Eugene, USA

ABSTRACT: Vernacular solar screens are popular design inspirations for contemporary facades which can be either static (i.e., fixed) or dynamic (i.e., operable). This study presents a comparative assessment of the impacts of static and dynamic screen prototypes on the indoor thermal conditions in an experimental, single occupancy office set-up, in ASHRAE Climate Zone 4C. Results demonstrate that static screen led to uniform indoor conditions within thermal neutrality limit established by ASHRAE-55 (2017). In comparison to the static screen prototype, the dynamic screen led to indoor environmental transience between thermal comfort and thermal neutrality zones. This non-uniformity in the indoor environment produced by the dynamic screen encourages exploration of their design potential in eliciting thermal pleasure and a state of alliesthesia for occupants. This work proposes an approach to design building envelopes with dynamic shading opportunities for occupant's comfort and pleasure.

KEYWORDS: Dynamic screens, thermal comfort, thermal pleasure, alliesthesia

1. EXTERNAL DYNAMIC SOLAR SCREENS: RESEARCH GAPS AND OPPORTUNITIES

Vernacular solar screens applied to exterior surfaces of building facades have aesthetic, environmental, and cultural significance. Due to these aspects, they are popular as design inspirations for contemporary façade design, both in their static or dynamic state. Static screens are non-movable/non-operable “bris de soleil” with optimized designs to respond to extreme solar conditions. On the contrary, dynamic screens are movable/operable that are typically designed to change their geometric parameters to respond to outdoor-indoor climatic conditions and/or occupants' needs.

The complex designs of dynamic screens have led to substantial research dealing with their movement and control technologies [1]. Few investigations on dynamic screens conducted using computational simulations have proven their high building energy efficiency and provision of occupant's visual comfort performance [2, 3, 4]. In addition, dynamic screens were able to reduce cooling loads on mechanical systems and provided thermal regulations to perimeter spaces within 15' (6 meters) of the building envelope, resulting in 12%-33% energy savings [2]. Despite promising results on building performance, their impact on thermal comfort remains unknown [5,6]. Quantifying their impacts on occupant's comfort is important to inform logical building envelope designs and their market adaptability.

1.1 Existing research on static solar screens: parameters investigated and findings

Unlike their dynamic counterparts, static screens have been extensively investigated for their building energy and occupant comfort performance [8, 9,10]. More than twenty-five studies have researched static screens in recent years. Most of them carried out optimization of screen geometric parameters such as perforation ratio (PR = % of open) and depth ratio (DR = perforation depth/perforation width) to determine the most suitable static design for building energy efficiency and occupant's comfort during a worst case climatic condition (i.e., extreme summers).

Static screens with 30 to 50% PR and 1:1 DR are recommended for maximum building cooling energy savings in hot climates [9]. For composite climates that have characteristics of hot-dry, warm-humid, and cold conditions, static screen designs optimized for hot-dry summers lead to over-shading and thermal discomfort during moderate winters [11]. As opposed to the optimized static screens, dynamic screens are climate responsive. Thus, if designed appropriately, dynamic screens have the potential to outperform the static types [12].

1.2 Occupant's thermal comfort in buildings

Building envelopes and mechanical systems are designed to maintain thermally uniform indoor conditions as required by the thermal comfort standards [13-15]. These standards prescribe narrow limits of thermal conditions as 'comfortable'. Predicted mean vote (PMV) is a widely used metric for thermal comfort assessment [13]. PMV values are

computed using a steady state mathematical model, which comprises of dry bulb temperature (DBT), relative humidity (RH), mean radiant temperature (MRT), air speed (m/s), occupant metabolic rate (met), and clothing insulation (clo), as its independent variables. PMV values in the range of (-0.5) to (+0.5) determines the thermal comfort zone. It is predicted that this limitation keeps a minimum of 80% of occupants satisfied [13,14].

1.3 Advances in thermal comfort research and opportunities for contribution

Over the past twenty years, there has been a paradigm shift in the conception of provision for thermal comfort [16]. The notion of a uniform thermal environment continues to be challenged. Investigations of different types of thermally non-uniform indoor conditions involving parameters such as air movement and body localized heating/cooling on occupant thermal perception and satisfaction is one of the currently sought out directions in thermal comfort studies [17-21].

Recent studies suggest that thermally non-uniform environments within a broader comfort range of +1 to -1 PMV can lead to occupant's well-being [17,22,23]. They can evoke perception of thermal pleasure among occupants [20]. Occurrence of thermal pleasure is explained by changes in physiological state of occupants within the boundaries of thermal comfort range, termed as alliesthesia. In addition to their potential to evoke thermal pleasure, the thermally non-uniform environments are also considered to be energizing for the occupants [17]. These environments can potentially affect occupants' resilience and adaptability to their surroundings, thereby positively influencing long-term well-being [22,23]. These studies provide a motivation for deeper investigations to uncover occupant's thermal perception and satisfaction in a wide variety of non-uniform environments.

Although there can be multiple techniques to create thermally non-uniform indoor environment, the operability of dynamic screens provides a unique opportunity to design them for creating non-uniform thermal environments within the broader comfort range that can potentially induce thermal pleasure among occupants. The present study aims to explore this opportunity.

2. CURRENT WORK, SOLAR SCREEN PROTOTYPES, AND STUDY DESIGN

This study attempts to address the following question: how can dynamic screens be designed to create thermally non-uniform indoors for occupant's thermal comfort and thermal pleasure within an accepted yet broader comfort range? It also provides

a comparative assessment of the impacts of dynamic and static screens on predicted thermal comfort and indoor thermal environment. Full-scale prototypes of static and dynamic screens were developed and installed on east facing, single-occupancy office set-up in the moderate climate of Eugene, Oregon (ASHRAE, Climate Zone 4C). The impact of five different conditions including non-screened, static, and dynamic screens (with three different movement frequencies) on the indoor thermal environment was recorded for sunny-sky, hot days during typical summer months in July and August.

2.1 Static and dynamic screen prototypes

The static screen prototype was intended to create a uniform thermal environment within the ASHRAE-55 comfort range, whereas the dynamic screen prototype was intended to create non-uniform indoor thermal conditions within the expanded boundaries of the ASHRAE-55 comfort range. To inform design of the prototypes, a sensitivity analysis delineating effects of screen geometric parameters such as PR and DR on predicted indoor thermal comfort was simulated in computational environment for summer months (June-September) for ASHRAE Climate Zone 4C using computational modelling and simulations in the IESVE software [24]. The results were used to decide the geometric parameters for static and dynamic prototypes. Details on the sensitivity investigation have been reported in a previous study [24].

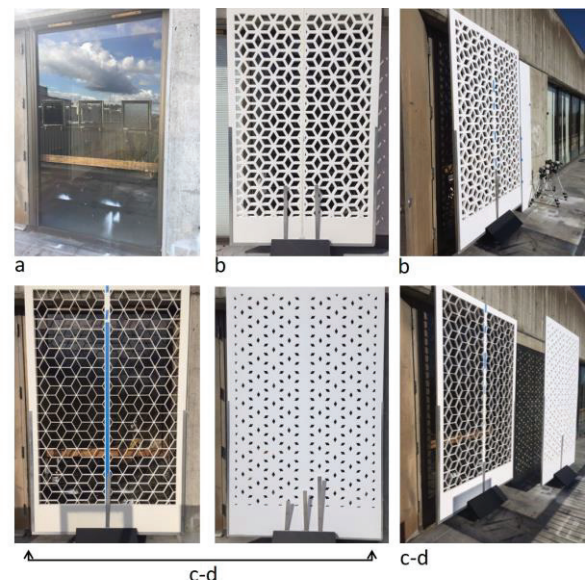


Figure 1: (a) non-screened window, (b) window with static screens having (PR, DR) = (50, 0.1), (c-d) dynamic screened window with overlapping panels having (PR, DR) = (90, 0.1) and (PR, DR) = (10, 0.1).

The screen prototypes were designed to be two-dimensional, thick planar surfaces, which were non-movable/fixed and moveable/operable in static and

dynamic conditions respectively (Fig. 1). Based on results of the simulations [24], the optimized static screen prototype was designed to have (PR, DR) = (50%, 0.1) (Fig. 1b) which were predicted to produce uniform thermal condition close to the neutral line (PMV = 0) within the thermal comfort zone [13]. The results of simulations also suggested that a dynamic screen with the geometric parameters altering between (PR, DR) = (10%, 0.1) and (PR, DR) = (90%, 0.1) can produce desired nonuniform thermal conditions that transition between the upper and the lower limits ($-0.5 < \text{PMV} < +0.5$) of the thermal comfort zone. Hence, a dynamic screen prototype was built comprising of two sliding panels (one with (PR, DR) = (10%, 0.1) and the other with (PR, DR) = (90%, 0.1) which could overlap sequentially (Fig. 1, c-d).

2.2 Experimental set-up

The current study was carried out in a 10' x 10' (3 x 3 m) experimental, single occupancy office set-up arranged in the perimeter space of an open-plan, east-facing studio in an educational building. The set-up was physically isolated by 7' high partitions and had a single-glazed 5' (wide) x 8' (high) fixed window ($T_{vis} = 0.80$, $SHGC = 0.80$) on its east facing wall. The dynamic and static screen prototypes shaded the outer surface of the window. Inside the set-up the work-desk arrangement faced south. Equipment required to measure thermal and visual environment was placed inside the set-up in the occupant's seating position plane. Figure 2 shows the details of the set-up.

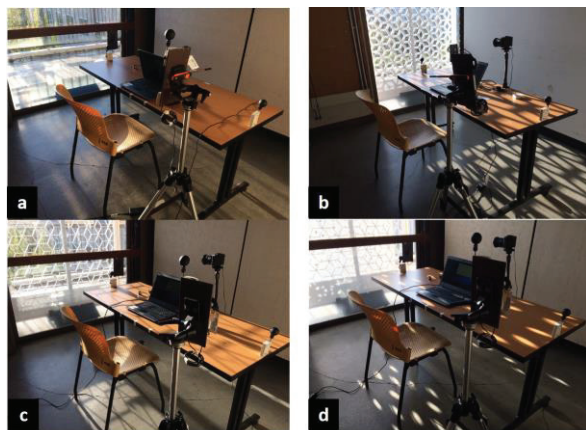


Figure 2: (a) non-screened condition, (b) static screened condition, (c-d) dynamic screened condition with screen in open position 'O' in (c) and closed position 'C' in (d).

Pre-programmed data-loggers (Onset HOBO U-12, accuracy: $\pm 0.35^\circ\text{C}$ ($\pm 0.63^\circ\text{F}$)) were placed at three locations horizontally and at three stratified levels vertically at 0.1 m (3.93"), 0.6 m (23.6"), and 1.1 m (43.3") to measure dry-bulb temperatures, relative humidity and globe temperatures. Globe temperature sensors fabricated and used for the study [25] were

connected to HOBO-U-12's extra-channel. Hot wire-anemometer (Testo 405i, accuracy: $\pm (0.1 \text{ m/s} + 5 \% \text{ of mv})$, measurement range: 0 to 2 m/s) was mounted at a seated-human's head-height on a tripod placed in the center of the set-up. The pre-programmed data logging unit to measure solar radiation (W/m^2) consisted of a calibrated pyranometer sensor (LI-COR LI-200R) connected to a calibrated transconductance amplifier (UTA for LI-COR™ sensors) and a data logger (Onset-HOBO U-12). Of the two solar radiation logging units, one was placed on the window surface behind the screen and the other in the outdoor environment.

2.3 Study Design

The non-screened, static, and dynamic screened conditions were tested during morning hours (8:30 AM - Noon) for the east-facing set-up. The dynamic condition transitioned between open 'O' position (screen panel with (PR, DR) = (90%, 0.1)) and closed 'C' positions (when screen panel with (PR, DR) = (10%, 0.1) overlaps the 'O' position). With the dynamic condition, it was intended to create variable thermal environment that could transition between the upper and lower fringes of the ASHARE-55 thermal comfort zone. Beginning with 'O' at 8:45 AM the position was changed to 'C' after 30 thirty minutes continuing the cycle until 12:15 PM. This movement, however, did not produce the desired indoor thermal variability. Hence, it was decided to test the dynamic condition with increased movement frequencies. As shown in Fig. 3, the following three dynamic movement frequencies were tested during a typical morning hour, beginning from 8:45 AM: (i) every 15 min (O-C-O-C), (ii) every 20 min (O-C-O), and (iii) every alternate 10 min (O) and 20 min (C) (O-C-O-C).

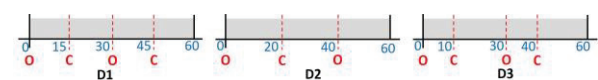


Figure 3: D1, D2, D3 are three different movement frequencies of dynamic screened condition tested during a typical morning hour. 'O' and 'C' denote open and closed positions of the dynamic condition.

3. DATA COLLECTION AND ANALYSIS

Outdoor and indoor environmental data consisting of solar radiation (W/m^2), dry-bulb temperature ($^\circ\text{F}$), globe temperatures ($^\circ\text{F}$), relative humidity (%), and airspeed (m/s) were recorded every minute during the study runs. The metabolic rate ($\text{met} = 1.2$) and clothing insulation ($\text{clo} = 0.5$) were kept constant during the experiment. The globe temperatures were used to calculate the mean radiant temperatures using Equation (2). Infrared images (IR) were captured at regular intervals using IR portable camera attachment to a mobile phone (FLIR

One Pro LT iOS camera, accuracy: $\pm 5\%$, resolution: $0.1^\circ\text{C}/0.1^\circ\text{F}$).

The measured indoor environmental thermal data comprising of DBT, RH, MRT, and airspeed was used to predict occupant thermal comfort by computing PMV values [13]. Occupant metabolic rate and clothing value were assumed as 1.2 met and 0.5 'clo' for PMV calculation. Metabolic rate of 1.2 was assumed for an occupant in the one-person office where he/she could be involved in light office work. Occupant clothing value of 0.5 'clo' was used for a person occupying the set-up during moderate summers in ASHRAE Climate Zone, 4C. The R package, "comf" with in-built functions for thermal comfort indices was used to compute the PMV values [27]. The computed PMV values were used to predict indoor thermal conditions inside the screened set-ups. PMV values between (i) (+ 0.5) and (-0.5) indicate the thermal comfort zone, (ii) (+1) and (-1) indicate the thermal neutrality limit, and (iii) (+1) and (+2) indicate a slightly warm thermal environment which could produce slight discomfort and heat stress.

Difference between outdoor and behind-the-shade solar radiation data was used to determine the reduction in solar radiation due to static and dynamic screen shading. The infrared images were analyzed in FLIR's computer-based program 'ResearchIR' to understand distribution of surface temperatures in the screened conditions.

4. FINDINGS

As hypothesized the reduction in solar gain due to the static screen panel with (PR, DR) = (50, 0.1) was 45-70%. In comparison, the dynamic screen in positions 'O' (i.e., (PR, DR) = (90, 0.1)) and 'C' (i.e., (PR, DR) = (10, 0.1)) reduced 80-90% of the solar gain. This suggests that dynamic screen with carefully designed movement frequency can achieve higher reduction in solar gain compared to the static screen. It is evident that the static and dynamic screens can effectively reduce surface temperatures compared to non-screened conditions (Fig. 4). In the case of dynamic screened condition, transition from 'O' to 'C' reduces indoor surface temperature further by an additional 6°F (Fig. 4 c-d).

Both static and dynamic screened conditions created an indoor environment consisting of patterned solar patches (Fig. 4) with higher surface temperatures on the floor and work plane. Moreover, they also created conditions wherein the radiant temperatures varied between the two boundaries of the space left and right to the occupant; a condition termed as 'radiant temperature asymmetry'. The surface temperatures in the static and dynamic set-ups remained within the range of 75°F - 80°F . However, the solar patches had temperatures

between 85°F and 90°F , which could potentially be the sources of local thermal discomfort. Difference between mean radiant temperatures (i.e., ΔMRT) at two points in the set-up showed that the approximate radiant asymmetry between the warm-window and the cool wall was less than 15°C (Fig. 5). This suggested that radiant asymmetry in the set-up did not exceed the limits of predicted local thermal comfort (i.e., predicted dissatisfaction, PD < 10) which requires $\Delta\text{MRT} < 30^\circ\text{C}$ [13].

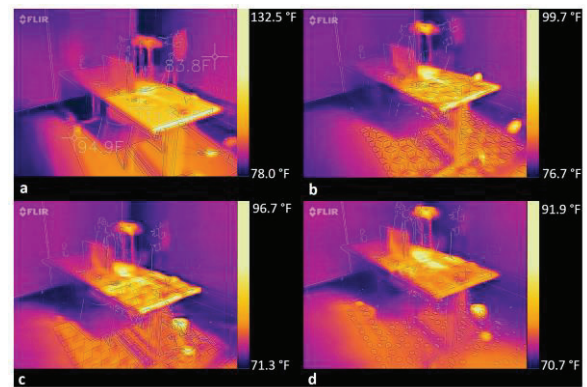


Figure 4: Infrared images of (a) Non-screened condition, (b) Static screened condition, (c-d) Dynamic screened condition with screen in open position 'O' in (c) and closed position 'C' in (d) at 9:30 AM.

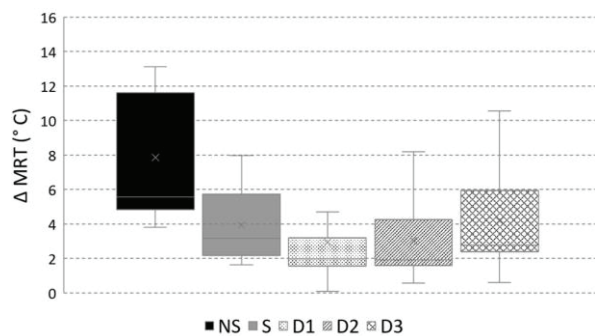


Figure 5: Difference in Mean Radiant Temperature (MRT) between warm and cool wall inside non-screened (NS), static screened (S) and dynamic screened conditions with movement frequencies (D1, D2, D3).

Analysis of the distribution of PMV values of the set-up under different conditions suggest that the non-screened condition was slightly warm as indicated by PMV values within 1.0 to 1.5. Results plotted in Fig. 6 indicate that the static screen and dynamic screens with movement type D3 were effective in keeping the indoor conditions within thermal neutrality limit (PMV < 1). The quartile range of PMV values in the set-ups with static screen and dynamic screens indicated that the later caused higher variability in the indoor thermal environment by creating transitions between 'neutral' and 'slightly warm' conditions. Dynamic screens with movement type D3 kept the indoor environment 'neutral' for most of the time besides creating instances of slightly

warm/ discomforting conditions when PMV values exceeded one (i.e. PMV=1).

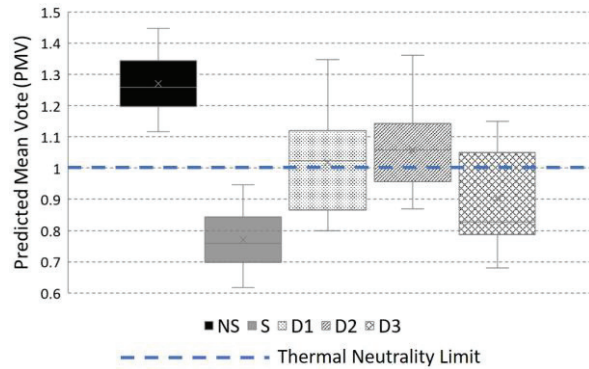


Figure 6: Distribution of Predicted Thermal Comfort inside non-screened (NS), static screened (S) and dynamic screened conditions with movement frequencies (D1, D2, D3).

As depicted in Fig. 7, a further analysis of indoor thermal environment for the dynamic screen set-up with movement type D3 revealed that the transition from 'O' to 'C' position and vice-versa decreases or increases the indoor air-temperature by 4-6° F. This can be attributed to the control of solar radiation with the screen's movement. The drop or rise in the temperature occurred during the early morning hours, with-in five minutes after the screen's position change.

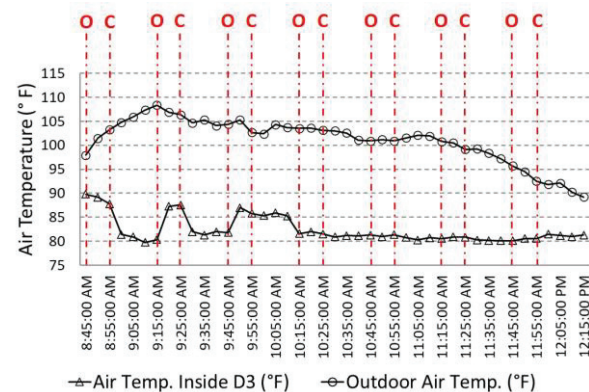


Figure 7: Air Temperature trend inside the set-up shaded by dynamic screens with movement type D3. 4-6° F drop/rise is observed after change in the screen position from 'O' to 'C' or vice-versa during early morning hours.

5. CONCLUSION

A comparative evaluation of effects of external static and dynamic screens on the indoor thermal conditions for a single occupancy office set-up in the moderate climate of Eugene, Oregon (USA) (ASHRAE, Climate Zone 4C) has been presented. As hypothesized, the static screen produces more comfortable indoor conditions with PMV < 1 as compared to the non-shaded set-up. The dynamic screened condition with an appropriate movement

design, introduce thermal variability in the indoor conditions that can potentially create instances of slight discomfort and comfort when the screen is, in the open 'O' (high PR) position and slides to closed 'C' (low PR) position, respectively.

These findings indicate the potential of dynamic screens to evoke sensation of 'temporal' and/or 'spatial alliesthesia' in occupants. 'Temporal alliesthesia' is the feeling of pleasure perceived because of a thermal stimulus, which brings human body from a slightly less comfortable state towards comfort. 'Spatial alliesthesia' is the perception of pleasure felt when there are differences in local skin temperatures across a person's body [17]. It should be noted that this study is specific to ASHRAE Climate Zone 4C and east facing single occupancy office settings. Future studies should investigate the applicability of these findings to different climate zones, orientations, and space types. The study suggests an approach to design and employ dynamic solar screens for occupant's thermal pleasure in work environments. This provides a novel perspective, which can be followed by architects and façade designers. This work proposes and emphasizes that designs for external dynamic façade shading systems need to be occupant centric and should expand our thermal comfort provisions to include thermal pleasure and alliesthesia.

6. EQUATIONS

The globe temperature, GT, is computed using Eq. (1) [26]:

$$GT = \frac{1.8}{A + A_1 + A_2} - 459.67 \text{ (°C)} \quad (1)$$

Where

$$A = 1.12886430756012 \times 10^{-3},$$

$$A_1 = B \times \text{LN}(10000(2.5/V - 1)),$$

$$A_2 = C [\text{LN}(10000(2.5/V - 1))]^3,$$

$$B = 2.34149078860173 \times 10^{-4},$$

$$C = 8.77065543744161 \times 10^{-8}, \text{ and}$$

V = voltage equivalent to the resistance measured through US sensor 10,000 Ω curve "J" thermistor. The symbol 'x' in the equation denotes the multiplication.

The mean radiant temperature, MRT, is computed using Eq. (2) [30]:

$$MRT = \left[(GT + 273)^4 + \frac{1.1 \times 10^8 v_a^{0.6}}{\epsilon D^{0.4}} (GT - T_a) \right]^{1/4} - 273 \quad (2)$$

Where

MRT is the mean radiant temperature (°C), GT the globe temperature (°C) computed using Eq. (1), v_a the air velocity at the level of the globe (m/s), $\epsilon = 0.95$ is the emissivity of the globe, $D = 0.15$ is the diameter of the globe, and T_a is the air Temperature (°C).

REFERENCES

1. Attia, Shady, Senem Bilir, Taha Safy, Christian Struck, Roel Loonen, and Francesco Goia. "Current trends and future challenges in the performance assessment of adaptive façade systems." *Energy and Buildings* 179 (2018): 165-182.
2. Elzeyadi, I. (2017). The impacts of dynamic façade shading typologies on building energy performance and occupant's multi-comfort. *Architectural Science Review*, 60(4), 316-324.
3. Karamata, Boris, and Marilyne Andersen. (2014). Concept, design and performance of a shape variable mashrabiya as a shading and daylighting system for arid climates. In 30th PLEA Conference on Sustainable Habitat for Developing Societies, 2, 344-351. CEPT University Ahmedabad.
4. Curcija DC, M Yazdanian, C Kohler, R Hart, R Mitchell, and S Vidanovic. 2013. Energy savings from window attachments. Prepared for U.S. Department of Energy under DOE EERE award #DE-FOA-0001000. October 2013. Lawrence Berkeley National Laboratory, Berkeley, California.
5. Attia, Shady, Fabio Favoino, Roel Loonen, Aleksandar Petrovski, and Aurora Monge-Barrio. "Adaptive façades system assessment: An initial review." *Advanced building skins* (2015): 1265-1273
6. Kunwar, Niraj, Kristen S. Cetin, and Ulrike Passe. (2018). Dynamic shading in buildings: A review of testing methods and recent research findings. *Current Sustainable/Renewable Energy Reports*, 5(1), 93-100
7. Alawadhi, E. M. (2018). Double solar screens for window to control sunlight in Kuwait. *Building and Environment*, 144, 392-401.
8. Chi, D. A., Moreno, D., Esquivias, P. M., & Navarro, J. (2017). Optimization method for perforated solar screen design to improve daylighting using orthogonal arrays and climate-based daylight modelling. *Journal of Building Performance Simulation*, 10(2), 144-160.
9. Elzeyadi, I., & Batool, A. (2017). Veiled facades: Impacts of patterned-mass shades on building energy savings, daylighting autonomy, and glare management in three different climate zones. In proceedings of International Building Performance Simulation Association conference (IBPSA, 2017), San Francisco, CA.
10. Gandhi, D., Garg, V., Rawal, R., Smith, M. The Stone Jaali, a critical inquiry into daylight performance. *Indian Architect and Builder*; December 2014
11. Mousa, W. A. Y., Lang, W., & Auer, T. (2017). Assessment of the impact of window screens on indoor thermal comfort and energy efficiency in a naturally ventilated courtyard house. *Architectural Science Review*, 60(5), 382-394.
12. Elzeyadi, I., Abboushi, B., Hadipour, H., & Riviera, I. (2016). High performance facades: Measuring the impacts of dynamic shading prototypes on indoor environmental quality using yearly simulations and field tests. *PLEA Cities, Buildings, People: Towards Regenerative Environments*, Proceedings, 1023-1032.
13. ASHRAE 55, Thermal Environmental Conditions for Human Occupancy. ASHRAE Standard 55-2017, American Society of Heating, Refrigerating and Air-Conditioning Engineers, Atlanta, Georgia (2017)
14. Indoor environmental input parameters for design and assessment of energy performance of buildings- addressing indoor air quality, Thermal. EN-15251
15. ISO 7730, Ergonomics of the thermal environment - analytical determination and interpretation of thermal comfort using calculation of the PMV and PPD indices and local thermal comfort criteria (2005)
16. De Dear, R. (2011). Revisiting an old hypothesis of human thermal perception: alliesthesia. *Building Research & Information*, 39(2), 108-117.
17. Brager, G., Zhang, H., & Arens, E. (2015). Evolving opportunities for providing thermal comfort. *Building Research & Information*, 43(3), 274-287
18. Parkinson, T. & de Dear, R. (2015). Thermal pleasure in built environments: physiology of alliesthesia. *Building Research & Information*, 43(3), 288-301.
19. Parkinson, T., de Dear, R., & Candido, C. (2012, April). Perception of transient thermal environments: pleasure and alliesthesia. In *Proceedings of 7th Windsor Conference*, Windsor, UK.
20. Parkinson, T., de Dear, R., & Candido, C. (2016). Thermal pleasure in built environments: alliesthesia in different thermoregulatory zones. *Building Research & Information*, 44(1), 20-33.
21. Naik, N. & Elzeyadi, I. (2020 a). Investigating the impacts of solar screens on occupant's thermal comfort: an observational field study. In *proceedings of American Society of Heating Refrigeration and Air Conditioning Engineers Winter Conference*, ASHRAE Transactions, 126, Part 1
22. van Marken Lichtenbelt, W., Hanssen, M., Pallubinsky, H., Kingma, B., & Schellen, L. (2017). Healthy excursions outside the thermal comfort zone. *Building Research & Information*, 45(7), 819-827.
23. Kingma, B. R. M., Schweiker, M., Wagner, A., & van Marken Lichtenbelt, W. D. (2017). Exploring internal body heat balance to understand thermal sensation. *Building Research & Information*, 45(7), 808-818
24. Naik, N. & Elzeyadi, I. (2020 b, March). External dynamic screens for thermal delight and alliesthesia. In the proceedings of Associate Collegiate Schools of Architecture (ACSA) 108th Annual Meeting, San Diego, CA, USA.
25. Abboushi, B., Elzeyadi, I., Taylor, R., & Sereno, M. (2019). Fractals in architecture: The visual interest, preference, and mood response to projected fractal light patterns in interior spaces. *Journal of Environmental Psychology*, 61, 57-70.
26. https://www.littelfuse.com/products/temperature-sensors/thermistor-probes-and-assemblies.aspx?utm_source=ussensor.com&utm_medium=redirect&utm_campaign=ussensor-lf
27. Schweiker, M. (2016). comf: An R Package for Thermal Comfort Studies. *The R Journal*, 8(2), 341.
28. Schweiker, M., Schakib-Ekbatan, K., Fuchs, X., & Becker, S. (2020). A seasonal approach to alliesthesia. Is there a conflict with thermal adaptation? *Energy and Buildings*, 212, 109745.
29. Son, Y. J., & Chun, C. (2018). Research on electroencephalogram to measure thermal pleasure in thermal alliesthesia in temperature step-change environment. *Indoor air*, 28(6), 916-923.
30. ISO, E. (1998). 7726. Ergonomics of the Thermal Environment-Instruments for Measuring Physical Quantities (ISO, 7726, 1998).

Living Roofs for Cooling.

Impact of Thermal Mass, Night Ventilation and Radiant Evaporative Cooling.

LAURA RODRIGUEZ¹, PABLO LA ROCHE²

¹ La Universidad del Zulia, Maracaibo, Venezuela

² Cal Poly Pomona / CallisonRTKL

ABSTRACT: Living roofs are surfaces that are substantially covered with vegetation. Among other things they reduce the energy requirements for cooling, the heat island effect in cities, and storm water runoff, while sequestering CO₂ from the atmosphere. This paper discusses the cooling potential of two types of living roofs: one of them insulated as typical living roofs and the second one with a radiant-evaporative cooling system. Both of these are compared to a control cell built with a regular insulated roof. Both living roofs were developed by the authors from previous prototypes and tested between July and August of 2018. Results indicate that the living roof with radiant evaporative always performs better than the other cells. With the full amount of thermal mass the living roof with the radiant- evaporative cooling system performs better than the cell with the insulated living roof and the control cell. And when all the thermal mass is removed from the floor of the cells, the radiant evaporative cooling system still performs better than the other living roof and the control cell.

KEYWORDS: Living roofs, cooling, night ventilation, thermal mass.

1. INTRODUCTION

Living roofs are substantially covered with vegetation. Among other things they reduce the energy requirements for cooling, the heat island effect in cities, and storm water runoff, while sequestering CO₂ from the atmosphere. [1]

In a typical non- vegetated roof with some thermal mass, accumulated daytime heat continues its transfer to the interior during the night, while on living roofs, vegetation reduces the solar gains so that less heat enters to the interior, reducing cooling loads and improving comfort. [2]

This paper discusses the cooling potential of two types of living roofs: one of them insulated as are typical living roofs and the second one with a radiant-evaporative cooling system designed by La Roche & Yeom [3]. Both are compared to a control cell built with an insulated non green roof. These living roofs were tested between July and August of 2018.

2. METHODOLOGY

2.1. Experimental set up

The test modules are located at the Lyle Center for Regenerative Studies at Cal Poly Pomona University, 30 km east of Los Angeles, in California. The climate is hot and dry with an average high temperature of 31.5°C in August and an average low of 5.3 °C in January.

All modules are 1.35 m. × 1.35 m. × 1.35 m. with south facing windows and similar characteristics in the walls, windows and floor. The only differences are in the roofs. These are compared and tested in several series with varying amounts of thermal mass. Each cell has cement bricks placed on the floor; weighting 2.5 kg each. A total of 16 bricks, or 40 kg was used in the first series with the full mass, equivalent to 28 Kg/m² of the thermal mass on the floor. In the second series, eight bricks were removed (20kg) or half of the thermal mass, equivalent to 14Kg/m². In the third series, the rest of the thermal mass is removed from the floor of the tested cells. All series still have thermal mass in the gypsum board in the walls. Night ventilation is provided with a fan and all the cells are equipped with a timer, set in these series from 9pm to 6am.



Figure 1: View of the all Test Cells with Shade

2.2 Monitoring System and Schedule

Data loggers by Onset computer were used for data collection (Models: U12-012, UX 120-006 M, TMC6-HD). These sensors were installed in different locations in the test cells to monitor dry bulb temperature and relative humidity and compare with exterior values also collected on site.

3. LIVING ROOF SYSTEMS

3.1. Radiant-Evaporative cooled living roof

The radiant-evaporative cooled living roof consisted of a radiant water pipe, water pump, and sprinkler (mist type) on the green roof. The water flow in the pipe and the sprinklers can operate on different schedules, based on their different functions. The sprinkler was typically scheduled to operate during the daytime and reduced the soil temperature with the evaporatively cooled water.

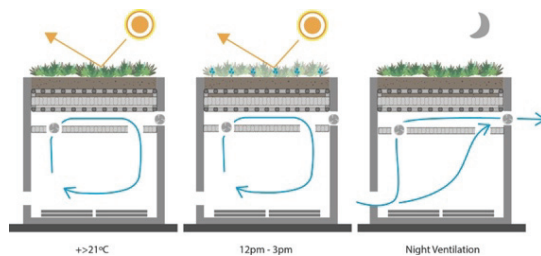


Figure 4: Radiant- Evaporative Living Roof

#	Material	mm	W/mK	U-Value (W/m ² K)
1	Soil	130	0.610	0.282
2	Gravel	20	2.000	
3	Water Proofing Liner	1	0.210	
4	Metal Pan	2	44.000	
5	OSB	11	0.130	
6	Glass Wool	21	0.044	
7	XPS	127	0.043	
8	Dry Wall	11	0.180	

Figure 5: Radiant- Evaporative Living Roof U-Value

The radiant system consists of a closed-loop pipe with a total length of 33 m. embedded in the soil of the green roof and which continued inside the test cell. A pump circulates the water inside the pipe and was operated by a digital timer, which turned on or off according to different schedules. The pipes are separated from the space by a plenum and an insulated ceiling (Fig 4), also with a sensor operated fan that provides cool air when needed below. The radiator absorbs heat from the interior of the cells which is dissipated through the green roof and the evaporation. The U value of the radiant- evaporative living roof was 0.282 W/m² K. (See Fig: 5). The

activation temperature of the fan is set at 21 °C, transferring air from the plenum, cooled by the radiant system, to the interior of the space, thus cooling it.

3.2. Insulated living roof

This living roof had insulation underneath the planting material (Fig. 2). The U value of the insulated green roof including the wood structure was also 0.282 W/m² K (See Fig: 3). The conditions inside the insulated green roof are affected by the thermal mass inside the space, the ventilation rates, and the amount of shade in the window.

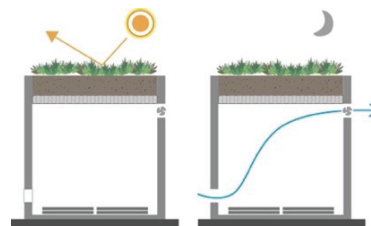


Figure 2: Insulated Living Roof

#	Material	mm	W/mK	U-Value (W/m ² K)
1	Soil	130	0.610	0.282
2	Gravel	20	2.000	
3	Water Proofing Liner	1	0.210	
4	Metal Pan	2	44.000	
5	OSB	11	0.130	
6	Glass Wool	21	0.044	
7	XPS	127	0.043	
8	Dry Wall	11	0.180	

Figure 3: Insulated Living Roof U- Value

4. RESULTS AND DISCUSSION

Results indicate that the living roof with a radiant evaporative cooling system always performs better than the insulated living roof and the control roof.

The comfort zone used for this analysis is generated by combining the winter and summer zones proposed by ASHRAE Standard 55, between 20°C and 27 °C DBT, Absolute Humidity below 12 g / Kg and a Relative Humidity above 10%. Also, an extended comfort zone was proposed, extending high values from 27°C to 31°C Dry Bulb Temperature [4]. This extended comfort zone accounts for an increased tolerance to higher temperatures with some air movement and reduced CLO levels.

For this analysis, the maximum and minimum temperatures outside were plotted on a chart to show the behavior of the temperature inside the cells during the months where the series were collected. The black vertical lines represent the maximum and minimum

temperature outside. The light green area represents the comfort zone and a dark green area represents the extended comfort zone. The outdoor average temperature is represented with a red dotted line and the thermal amplitude with a yellow dotted line. The vertical black line represents the outside temperature variation in a day and the color lines perpendicular to it, represents the maximum average temperature reached by each of the living roof tested and the control roof. Below, Fig. 6 and Fig. 8 show a comparison between the performance of the radiant evaporative living roof and the control roof, with the maximum and minimum exterior temperatures and the daily exterior swing and Fig. 7 and Fig. 9 show a comparison between the performance of the insulated living roof and the control roof, with the maximum and minimum exterior temperatures and the daily exterior swing.

Fig. 6 indicates that the maximum temperature inside the living roof with radiant- evaporative cooling system is lower than the control roof, with an average for the entire full mass series of 3°C DBT lower during the period, and almost always inside the extended comfort temperature zone.

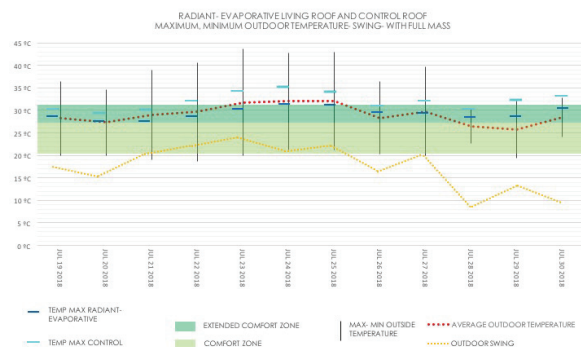


Figure 6: Radiant- Evaporative living roof and Control roof with full mass.

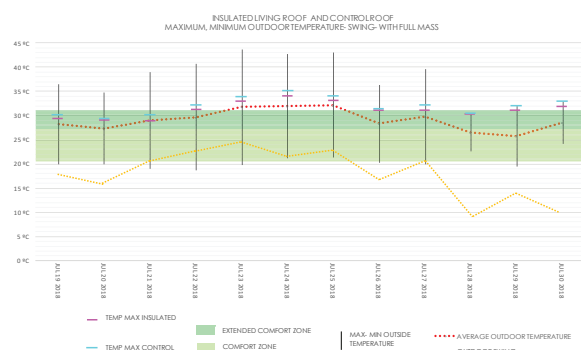


Figure 7: Insulated living roof and Control roof with full mass.

Fig. 7 indicates that the maximum temperature inside the insulated living roof is lower than the control roof, with an average difference for the entire full mass series of 0.7°C DBT.

Fig.8 indicates that the maximum temperature inside the living roof with radiant- evaporative cooling system is lower than the control roof, with an average difference for the entire without mass series of 1°C DBT below in most of the days of the entire series, and always inside or above the extended comfort temperature zone.

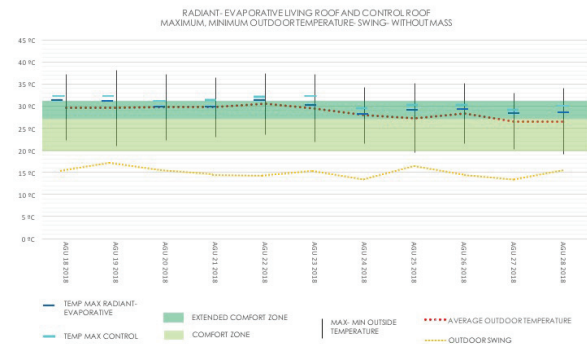


Figure 8: Radiant- Evaporative living roof and Control roof without mass.

Fig. 9 indicates that the maximum temperature inside the insulated living roof is lower than the control roof in almost every day of the series, with an average difference for the entire series without mass of 1°C DBT, and always inside or above the extended comfort temperature zone.

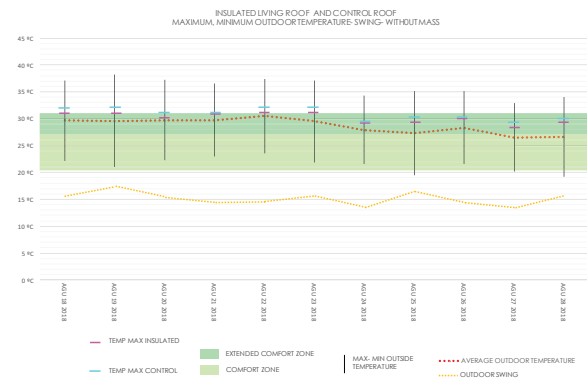


Figure 9: Insulated living roof and Control roof without mass.

Results indicate that with the full amount of thermal mass the test cell with the radiant- evaporative cooling system performs better than the cell with the insulated living roof and the control cell, with a difference with the control roof that varies from 2°C to 3.9°C, and with the insulated living roof from 1.7°C to 2.8°C.

With medium thermal mass in the floor, the indoor temperatures between the radiant evaporative living roof and the insulated living roof are almost the same and between the control roof, the radiant evaporative living roof performs better with a difference between 0.3°C and 0.9°C.

And when all the thermal mass is removed from the floor of the cells, the radiant evaporative cooling system performs better than the other living roof and the control cell, with a difference with the insulated living roof from 0.4°C to 0.7°C, and with the control roof from 1°C to 1.2°C.

5. APPLICABILITY OF LIVING ROOF SYSTEMS WITH DIFFERENT AMOUNTS OF THERMAL MASS

To understand the performance of the system, daily recorded indoor and outdoor maximum temperature and minimum relative humidity were plotted on the Building Bioclimatic Chart superimposed on the psychrometric diagram. Best performing series will have more values inside the comfort zone.

A lower indoor maximum temperature indicates a better cooling performance. The limits of outdoor optimum performance for each system are determined by the relationship between the indoor temperature and the comfort zone for a given exterior maximum temperature. If the indoor conditions are inside the comfort zone, the strategy is assumed as effective for those conditions of exterior temperature and relative humidity. [4]

Data for the maximum temperature and minimum relative humidity outside and compare with the inside data, then were plotted on the psychrometric chart. A total of 33 usable data points was plotted for 33 selected days tested under different conditions with full, medium and no thermal mass.

The goal of this analysis was to determine the applicability of the different living roof strategies under varying amount of thermal mass. Colors were used to represent each option (different shades of blue for the radiant- evaporative living roof and different shades of green for insulated living roof), if the indoor temperature was inside the comfort zone (up to 27 °C) when the outdoor temperature was above the comfort zone, the strategy was assumed to be effective to achieve thermal comfort. If the maximum temperature inside the cell was between 27°C and 31 °C this indicated that the strategy was somewhat effective to achieve thermal comfort. As you can see in the Fig. 6-7-8-9, all the maximum temperature data inside the cells was greater than 27°C, that is all the data and strategies are handled when the system is somewhat effective to achieve thermal comfort, for that reason the analysis was done only with the extended comfort zone.

5.1 Radiant- Evaporative Living roof

Fig. 10 shows the Building Bioclimatic Chart with the data for the cell with the radiant- evaporative

cooling living roof and full thermal mass. The deep blue dotted lines define the period during which this design strategy is somewhat effective, up to 44°C Dry Bulb Temperature; to 32 °C wet bulb temperature; and below the 60% Relative Humidity curved line.

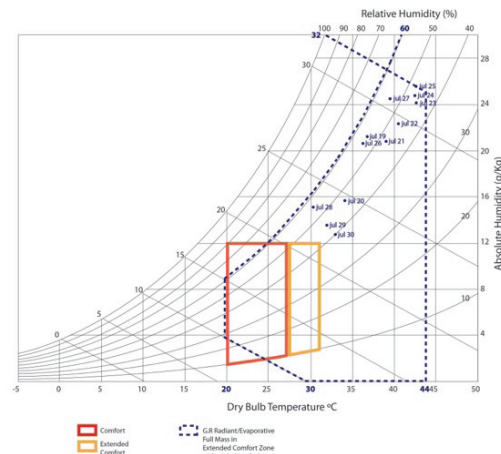


Figure 10: Psychrometric Chart for radiant- Evaporative living roof with full thermal mass

Fig. 11 shows the Building Bioclimatic Chart with the data for the cell with the radiant- evaporative cooling living roof and medium thermal mass. The blue dotted lines define the period during which this design strategy is most effective, up to 40°C Dry Bulb Temperature; to 29 °C wet bulb temperature; and below the 60% Relative Humidity curved line.

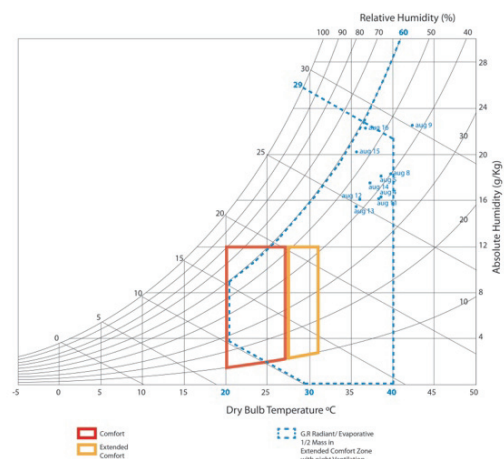


Figure 11: Psychrometric Chart for evaporative –radiant cooling green roof with medium thermal mass

Fig. 12 shows the Building Bioclimatic Chart with the data for the cell with the radiant- evaporative cooling living roof and no thermal mass. The light blue dotted lines define the period during which this design strategy is somewhat effective, up to 38°C dry bulb temperature; to 29°C wet bulb temperature; and below the 60% Relative Humidity curved line.

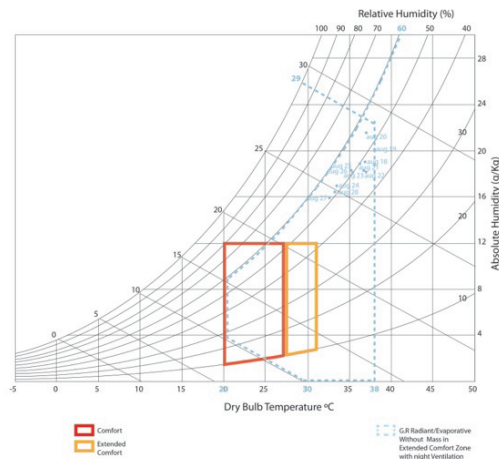


Figure 12: Psychrometric Chart for evaporative –radiant cooling green roof with no thermal mass

5.2 Insulated Living roof

Fig. 13 shows the Building Bioclimatic Chart with the data for the cell with the insulated living roof and full thermal mass. The deep green dotted lines define the period during which this design strategy is somewhat effective, from 32°C to 41°C Dry Bulb Temperature; to 30 °C Wet Bulb Temperature; and below the 60% Relative Humidity curved line.

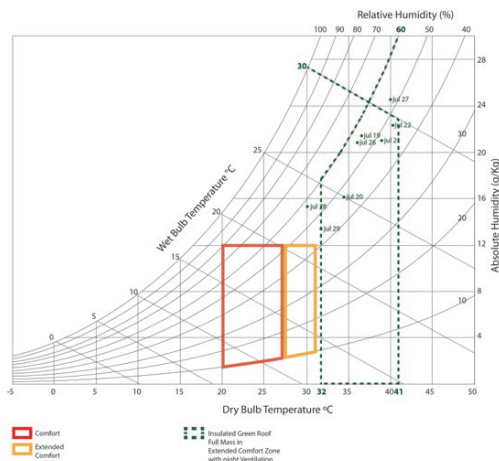


Figure 13: Psychrometric Chart for insulated green roof with full thermal mass

Fig. 14 shows the Building Bioclimatic Chart with the data for the cell with the insulated living roof and medium thermal mass. The green dotted lines define the period during which this design strategy is somewhat effective, from 32°C to 39°C Dry Bulb Temperature; to 29°C Wet Bulb Temperature; and below the 60% Relative Humidity curved line.

Fig. 15 shows the Building Bioclimatic Chart with the data for the cell with the insulated living roof and no thermal mass. The light green dotted lines define the period during which this design strategy is somewhat effective, from 32°C to 38°C Dry Bulb

Temperature; to 28°C Wet Bulb Temperature; and below the 60% Relative Humidity curved line.

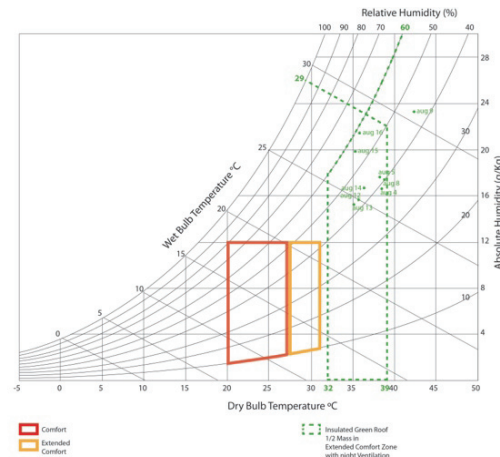


Figure 14: Psychrometric Chart for insulated green roof with medium thermal mass

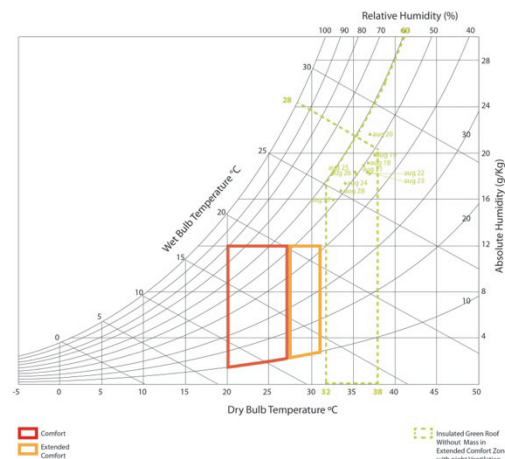


Figure 15: Psychrometric Chart for insulated living roof with no thermal mass

6. CONCLUSION

On hotter days, when the dry bulb temperature reaches 44 °C and the wet bulb temperature reaches 32 °C, the radiant- evaporative living roof with full thermal mass works better than the insulated living roof with full mass, with a difference between of 3°C dry bulb temperature and 2°C wet bulb temperature.

When the living roofs has medium thermal mass and when the dry bulb temperature reaches 40°C, the radiant- evaporative living roof works better than the insulated living roof, with a difference of 1°C dry bulb temperature between them.

With no thermal mass and when the dry bulb temperature reaches 38°C, both the radiant-evaporative living roof and the insulated living roof, perform similarly, with a difference between them of 1°C in wet bulb temperature.

There is not much difference in Dry Bulb Temperature with medium or less thermal mass is used. The full amount of thermal mass used for the study is 40Kg or more will perform better.

To understand the performance of the system developed in each living roof, the data collected was plotted and compared on the Building Bioclimatic Chart. The results of this analysis are shown in Fig. 17 and Fig 18, in which the psychrometric Chart shows the outdoor conditions under which each specific strategy will help achieve comfort.

The strategy “radiant- evaporative cooling with full thermal mass” is indicated with a deep blue dotted line from 20°C and 44°C Dry Bulb Temperature; 10 °C and 29 °C Wet Bulb Temperature; and below the 60% Relative Humidity curved line.

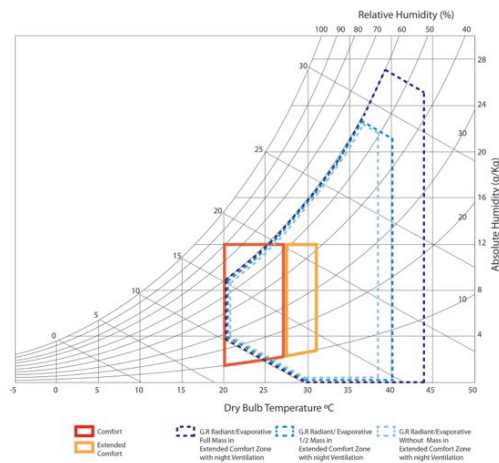


Figure 15: Psychrometric Chart for radiant- evaporative living roof

The strategy “radiant- evaporative cooling with medium thermal mass” is indicated with a dotted blue line from 30°C to 40°C Dry Bulb Temperature, to 23 g/Kg of absolute humidity and up to 60% relative humidity.

The strategy “radiant- evaporative cooling with no thermal mass” is indicated with a dotted light blue line from 30°C to 38°C Dry Bulb Temperature, to 29 °C wet bulb temperature up to 60% relative humidity.

The strategy “insulated living roof with full thermal mass” is indicated with a dotted deep green line from 32°C and 41°C Dry Bulb Temperature; to 30 °C Wet Bulb Temperature; and below the 60% Relative Humidity curved line.

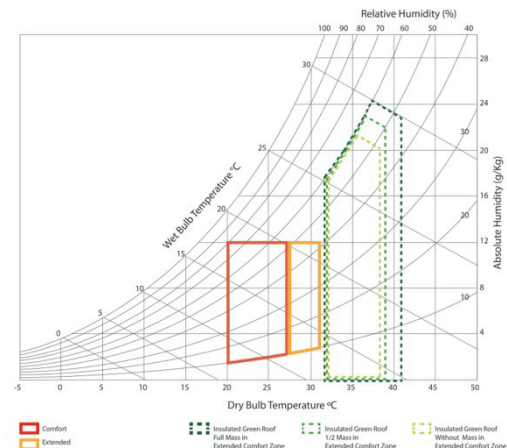


Figure 16: Psychrometric Chart for insulated living roof

The strategy “insulated living roof with medium thermal mass” is indicated with a dotted green line from 32°C to 39°C Dry Bulb Temperature, to 29 °C Wet Bulb Temperature; and up to 60% relative humidity.

The strategy “insulated living roof with no thermal mass” is indicated with a dotted light green line from 32°C to 38°C Dry Bulb Temperature, to 28 °C Wet Bulb Temperature and up to 52% relative humidity.

REFERENCES

1. U. Berardi, A. Ghaffarian Hoseini, (2014). A critical analysis of the environmental benefits of green roofs, *Applied Energy* 115 411–428.
2. Castleton, H.F. Stovin, V. Beck, S.B.M. Davison, J.B. (2010) *Green roofs; building energy saving and the potential for retrofit. Energy and Buildings*. Volume 42, Issue 10, October, Pages 1582-1591
3. D. Yeom, P. La Roche, (2017). Investigation on the cooling performance of a green roof with a radiant cooling system. *Energy and Buildings* 149 26–37
4. L. Rodriguez, P. La Roche, (2018). Green Roofs for Cooling. Test in a Hot and Dry Climate, *Passive Low Energy Architecture Conference PLEA* 79–84

Revealing the Thermal Quality of the Modernism Legacy's Architecture:

Marcos Acayaba's single-family houses in São Paulo

EDUARDO GASPARELO LIMA¹, JOANA CARLA SOARES GONÇALVES¹,
RANNY LOUREIRO XAVIER NASCIMENTO MICHALSKI¹

¹ Faculty of Architecture and Urbanism of the University of São Paulo (FAUUSP), São Paulo, Brazil

ABSTRACT: *This paper shows performance evaluations of the solutions and design strategies used in the period after Brazilian Bioclimatic Modernism that continues its environmental design legacy in the architecture of Marcos Acayaba. This research investigates the performance and quality of such buildings, never quantitatively evaluated before. For this purpose, three houses in São Paulo were selected as case studies for fieldwork: Marlene Milan House (1972), Hélio Olga House (1987), and Vila Butantã Residential Complex (1998). Whilst the research project involved thermal, daylight, and acoustic conditions, the work presented here focus on the results from fieldwork of thermal variables. Besides the data collected, interviews were done with the architect and with residents to complete the studies. The results were compared and confronted with performance criteria established by ASHRAE 55. The thermal quality of the case-studies in the warmer period is favourable to comfort, given the efficacy of the design strategies, including shading, thermal mass and controlled ventilation. However, the winter performance proved to be problematic, with temperatures below the comfort zone during day and night, but with room for improvement still within the realm of passive strategies.*

KEYWORDS: *Marcos Acayaba, Thermal response, Measurements, Design strategies*

1. INTRODUCTION

The Brazilian Modernist Architecture developed between 1930 and 1964 had special focus on questions related to comfort and environmental performance [1]. In this scenario, building design aimed to respond to local microclimatic conditions, as well as to the cultural habits, following bioclimatic precepts. As reported by Marta Romero [2], Bioclimatism takes into account the environmental aspects of building's local context, aiming to achieve passive natural environmental conditions through an integrated approach of thermal attributes, daylight, sound, and colour. Hence, the application of these principles must inevitably reflect in appropriated design to the place and to the local materials, demonstrating historical, cultural, environmental, and technological mastery.

The distinguishable and creative manner by which principles of environmental design were introduced in Brazilian Modernism made architecture from that period known as Brazilian Bioclimatic Modernism [1]. The performance of buildings from this time has been evaluated by a few researchers [1, 3]. In this context, this paper shows the results from the performance assessment of three case-studies designed based on the legacy of Brazilian Bioclimatic Modernism, continuing with the key strategies from the local environmental architecture. The value given by the architect Marcos Acayaba to design solutions related

to the comfort of occupants and quality of space (commonly reported in testimonials and interviews) makes him a key figure of his generation. Having said that, this research aims to investigate the environmental performance and quality in single family homes designed by him and never quantitatively evaluated before.

Acayaba was graduated in 1969 from Faculty of Architecture and Urbanism of the University of São Paulo (FAUUSP). Acayaba's architectural education was influenced by the need to contribute to technological development, coupled with the idea of integration between building, site and climate, learning from creative lessons from Brazilian Modernist Architecture.

When it comes to his buildings, the architect himself states that the concern with construction, production processes and maintenance is decisive to the definition of the architectural key design features, along with the specific geography of the building site [4]. Thus, free from any style type, the building form in Acayaba's architecture, almost always new, results from rigorous analysis of specific local conditions, looking for the highest efficiency of the building techniques, environmental comfort, quality of space, and, as a consequence, architectural beauty, where, in the words of the architect, "*nothing is left and nothing is missing*" [4].

Three houses in the city of São Paulo were selected as case studies. The reason for this specific selection can be explained by the different materials and construction techniques applied in their architectural design, showing an evolution in striving for an own design process. In addition, this also denotes a vast technological and constructive knowledge of the architect, which works the plasticity expression of his buildings based on the constructive techniques that best suit site demands, reinforcing the role of bioclimatic principles.

This study is part of a wider research project started in 2014, aiming to evaluate the environmental performance of iconic architecture in the city of São Paulo, birthplace of the *Escola Paulista* (São Paulo School) of Modern Architecture in Brazil. In respect to this research in particular, the overall scope includes the assessment of thermal, daylighting and acoustic conditions, counting on measurements *in situ* completed by analytical work. For the sake of this paper, the focus is on the thermal performance taken in measurements.

2. RESEARCH METHODS

The method is experimental inductive, with fieldwork regarding the measurement of thermal variables. Besides the *in situ* collected data, the architect and the residents were interviewed in order to complement the studies.

The measurements recorded values of dry bulb air temperature, globe temperature, air movement, and relative humidity, taken every 15 minutes with data loggers HOBO Onset (U12-013), installed in the living-room and in a bedroom of the three case studies, simultaneously, in summer and winter periods of 2019. For the warmer period, 15 days between March and April were selected, followed by 15 days in September to capture a cooler period. Measurements of external temperatures, humidity levels, and global radiation were registered at an open space on site, by means of a Campbell weather station.

For the purpose of this analysis, only the living-room data is presented, for a period of seven consecutive days, encompassing week and weekend, of stable conditions, close to the typical days of each period. The results from the three case-studies were analysed in a comparative way and confronted with the comfort zone of 80% acceptability range for occupant-controlled naturally conditioned spaces established by ASHRAE 55 [5].

3. SÃO PAULO CLIMATIC CONTEXT

With regards to the climate, the city of São Paulo (Latitude 23.85° S; Longitude 46.64° W; Altitude 792 meters above sea level) is located in a subtropical region, characterized by warm-humid summer days with predominantly partially cloudy sky, cool and drier

winter days with predominantly sunny sky, with prevailing wind directions being South, South-Southeast and Southeast during the year. Air temperatures are moderate for most of the year with an annual average temperature of 19.3°C, according to data from the climatological bank of the National Institute of Meteorology [6]. In typical warm days with clear sky, temperatures can reach figures above 30 °C in the beginning of the afternoon. On the other hand, under a cloudy sky, air temperatures in a warm day stay around 20 °C. In typical cooler days air temperatures can go as high as 24 °C, due to the solar radiation impact, whereas in a cooler cloudy day, air temperatures struggle to get above 15 °C [7].

4. CASE STUDIES: DESCRIPTION OF ARCHITECTURAL AND ENVIRONMENTAL ASPECTS

4.1 Marlene Milan House (1972)



Figure 1: Marlene Milan House, 1972. Photo: Jomar Bragança.

Figure 1 illustrates the first design project by Acayaba, still as a young architect. According to Pedreira [8], the architect made a synthesis of Oscar Niemeyer and Artigas influences. The design strategies, the aesthetics and the space layout are directly related to the modernist legacy. In Marlene Milan House, Acayaba proposed a cast-in-place concrete arch, under which the uses are allocated and organized on three semi-levels, a common solution to São Paulo's architecture at that time and appropriate to the specific site conditions.

The social areas were coupled with dining-room at the lower floor, whilst also being physically and visually integrated with the upper level where the bedrooms are located, increasing space volume. This spatial integration, associated with the variable heights of the multiple areas, creates one single volume that facilitates convective air movements, as well as cross ventilation. The fluidity between internal and external areas is guaranteed by the high glazed panels, shadowed by the over-arching concrete roof. Internally, separation between rooms consists of large movable wooden panels (Figs. 2 and 3).

Perforated concrete blocks with single glass coverage were also used in some external walls at lower levels, in order to maximize daylight and natural ventilation. Furthermore, these elements commonly named in Brazil as *cobogós* were characterized by

perforations to allow daylight and maintain internal natural ventilation (Fig. 4). In order to enhance ventilation, adjustable lower openings in the glass panels were introduced (Fig. 5), favouring the stack effect through higher openings placed near the concrete surface, positioned above the hydraulic columns in the social area.

Under the originally uninsulated concrete roof structure ($\lambda = 1.75 \text{ W/m}^\circ\text{C}$), the internal space is enclosed with operable single glass panels ($0.8 \text{ W/m}^\circ\text{C}$). Internal surfaces and partitions were made in *Cedro* wood ($\lambda = 0.12 \text{ W/m}^\circ\text{C}$). After residents reported high internal temperatures during the first occupied summer, a layer of thermal insulation made of polyurethane ($\lambda = 0.03 \text{ W/m}^\circ\text{C}$) was added to the external surface of the roof. In addition to that, the external surface was painted in white to increase reflectivity of global radiation (Fig. 6). Another strategy that helped to lower temperatures was the high vegetation density of the landscape design, providing shading to the glass panels and to the roof.

It is necessary to emphasize once again the architect concern to technical and constructive issues to establish design strategies. The construction technique and the aspirations for the form did not allow the installation of *brises* on the external face of the glass panels. Thus, the solution found was to extend the concrete roof in a way that it created a transition space between exterior and social area, resulting in a horizontal shading device, as illustrated in Figure 2. Regarding the design strategies for the cold period, the most notable one is the provision of a fireplace, in a prominent spot in the living-room, as shown in Figure 7.

All the rooms in the residence can be coupled with the outside, in thermal, daylight and visual terms. During the course of the day, it is possible to notice differences in the internal environment due to changes in the aspects of daylight and solar access.

Although measurements of acoustic conditions were not brought to this discussion, it is also worth mentioning that the residence has the lowest sound insulation performance of the three case-studies due to a high degree of sound leakage from the exterior in association with a large amount of reflexive surfaces (concrete, glass and ceramic tiles), that can cause high rates of room reverberation.

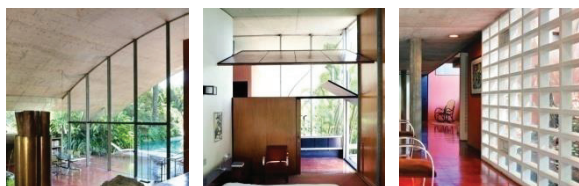


Figure 2 (left side): Extended roof and an integrated area with high room's height.

Figure 3 (in the middle): Movable wooden panels.

Figure 4 (right side): Perforated elements wall.



Figure 5 (left side): Natural ventilation devices.

Figure 6 (in the middle): Vegetation that provides shading and roof painted white with a thermal insulation layer.

Figure 7 (right side): Fireplace in a prominent spot.

Photos: Jomar Bragança (Fig. 2 and Fig. 5); Nelson Kon (Fig. 4 and Fig. 6); and Richard Powers (Fig. 3 and Fig. 7).

4.2 Hélio Olga House (1987)

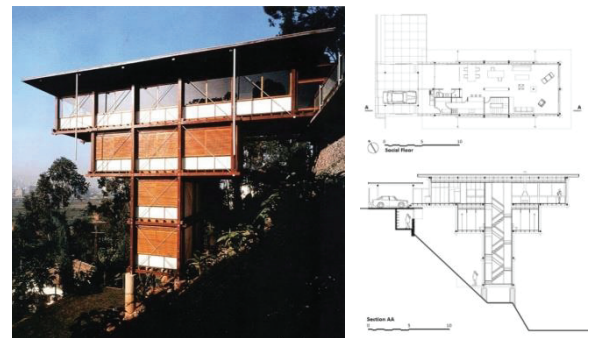


Figure 8: Hélio Olga House, 1987. Photo: Nelson Kon.

The concept of Hélio Olga House (Fig. 8) is the result of the structural concept defined to solve the challenging steep geographic site (100% of slope). Inspired by proportions, simplicity of form, lightness, transparency, and spatial continuity of Japanese Architecture [9], Acayaba sought solutions in the modular and standardized wooden structures, specialty of the engineer and owner of the residence. The Smith House (1955) and Weekend House (1964), both by the Miesian architect Craig Ellwood, were taken as reference to this design project.

An independent wooden structure was envisioned, supported by only six points, preserving the site natural geographic characteristics. A 3.30 meter modular cubic system was adopted, creating a residence of four floors. The living-room and bedrooms, facing Northeast, benefit from the best orientation in this climate, in terms of capturing solar gains during the winter period. The main facade is Northeast, receiving direct sunlight between 5 a.m. and 12 a.m. in the summer, and from 7:45 a.m. to 4 p.m. in the winter. For the subtropical climate of São Paulo, this is one of the best orientations for a long permanence place, maximizing solar access during winter and minimizing in the summer months.

Light-weight building components were specified for external and internal walls, as well as the roof, in *Angelim* wood ($\lambda = 0.23 \text{ W/m}^\circ\text{C}$), in order to minimize the total structure weight, resulting in a light thermal mass building, highly coupled with outdoor temperature fluctuations. In this design, maximum ventilation is the main strategy to control the rise of

internal temperatures. To assist in the comfort conditions, internal translucent blinds were added by the occupants to block solar radiation through the windows in summer. As a matter of fact, ventilation plays a central role in the thermal performance of this residence. As mentioned, the wooden structure is exposed on all sides, including the floor area, where adjustable trickle vents were inserted as part of the inlets to increment air flows, as shown in Figure 9. Besides, the uninsulated slabs of all floors are exposed to outside (Figs. 10 and 11).

The extended roof works as a shading device for the access floor (Fig. 12). On the other hand, the trees' canopies have the same effect on the lowest floors (bedrooms), as Figure 13 illustrates. In the lower floors, where the bedrooms are located, internal movable shutters provide adjustable shading. The light colour of the external opaque white panels reflects a great deal of the impinging solar radiation on all orientations, given to the very low absorption coefficient (between 0.2 and 0.3).

As seen in Marlene Milan House, the fireplace in Hélio Olga House also occupies a central area in the social floor (Fig. 14). In the winter, the great number of exposed surfaces may increase the indoor air temperature during sunny periods with clear sky. However, despite the provision of the fireplace in the living room, the level of exposure to the exterior environment due to the uninsulated envelope raises concerns about the night-time performance during the winter months.

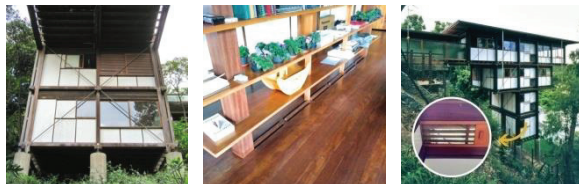


Figure 9 (left side): House detached from the ground.
Figure 10 (in the middle): Fins underneath bookshelves.
Figure 11 (right side): Vertical circulation and slabs with openings for ventilation.

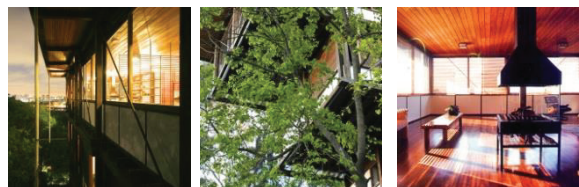


Figure 12 (left side): Roof used as shading device and large openings with internal shading devices.
Figure 13 (in the middle): Vegetation shading lower floors.
Figure 14 (right side): Fireplace in the social floor.
Photos: Marcos Acayaba's personal collection (Fig. 9 and Fig. 11); Sebastian Crespo (Fig. 12 and Fig. 13); Cristiano Mascaro (Fig. 14); and authors (Fig. 10 and detail in Fig. 11).

The way daylight reaches the interior spaces can change the occupants' space perceptions, in the same way as in Marlene Milan House, animated by a

dynamic change of internal colours throughout the day, as a function of the changing aspect of daylight. Acoustically, the residence takes advantage of its calm and isolated location, where eventual urban noise from a nearby busy road in rush hours is a rare problem to the overall comfort of occupants.

4.3 Vila Butantã Residential Complex (1998)

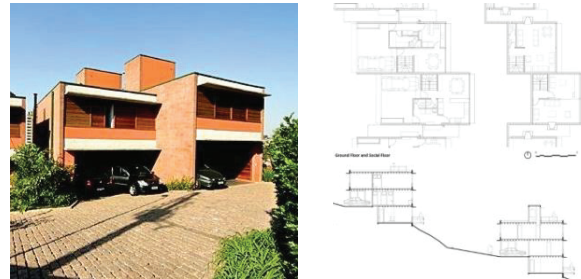


Figure 15: Vila Butantã Complex, 1998. Photo: Gal Oppido.

Vila Butantã Complex (Fig. 15) consists of a set of sixteen semi-detached single-family units. The houses were designed in order to favor the communal leisure and adapt to the terrain slope. In a semi-detached formation, two rows of houses were created following the boundaries of the site: one near street level, with four houses, and the other lower, with twelve houses (Fig. 16). Key local factors that drove the design project were topography (average slope of 45%), landscape and views. In addition, floor plans rationalization and building construction systems were a major drive to reduce building costs to design a flexible middle-class market-type housing typology.

The construction system is a structural masonry with pigmented concrete blocks ($\lambda = 0.91 \text{ W/m}^2\text{C}$), reinforced concrete slabs and wooden beams. This residential complex was designed with a considerable amount of opaque and heavy mass building components, guaranteeing considerable thermal inertia to its interior.

Aside from the *brise-soleils* designed to block the solar radiation (Fig. 17), in this specific case, the site planning arrangement of misaligned semi-detached residences facing East and West, resulted in shading benefits during the summer period (Figs. 17 and 18).

Following the same strategy as the other cases, the shading is associated with ventilation to achieve comfortable temperatures in the warm period. The air flow not only can enter by generous window openings that are not common in São Paulo real estate market (Figs. 19 and 20), but also can cross all the space when doors are maintained open. It is interesting to note that these openings have an adjustable panel to block sunlight into the bedrooms, shown in Figure 19.

One more time, a fireplace for the social floor as a strategy for the cooler periods of the year was provided (Fig. 21). On the other hand, daylight inside the residence does not have the same sensorial proposal as the other two cases. However, the

aesthetic created by the arrangement of the houses, their materials and their self-shadowing effect is something to be noticed. With regards to the acoustic performance, the calm vicinity and the predominant residential use of the area, provides good acoustic conditions in terms of external sound sources.



Figure 16 (left side): Misaligned residences.

Figure 17 (in the middle): Use of horizontal brise-soleils.

Figure 18 (right side): Volume shadows and shading devices.

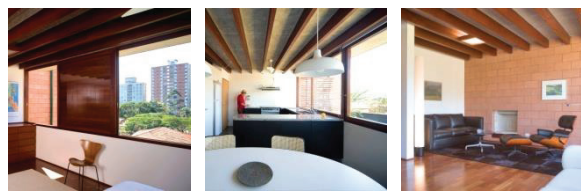


Figure 19 (left side): Windows with adjustable protection.

Figure 20 (in the middle): Large openings for ventilation.

Figure 21 (right side): Fireplace in a prominent spot.

Photos: Gal Oppido (Fig. 16, Fig. 18 until Fig. 21); and Nelson Kon (Fig. 17).

5. FIELDWORK: RESULTS AND DISCUSSION

Looking first at the measurements carried out during the warm period, as it can be seen in Figure 22, when external temperatures do not get above 30 °C, indoor air temperatures figure around 26 °C in Marlene Milan House and in Olga House, and 24 °C in Vila Butantã Complex. When the outdoor values are higher than 30 °C, the indoor air temperature can reach 28 °C in Marlene Milan House; between 30 °C and 32 °C in Olga House; and 26 °C in Vila Butantã Complex.

In the three cases, globe temperature is constantly below the air temperature, which is positive for thermal comfort of the occupants, during warm days. However, this difference decreases as the constructive materials are lighter and the solar radiation is available.

Overall, the three case-studies have a good response for warm periods. Almost all of the indoor air temperatures have complied with ASHRAE 55 comfort zone, with exception of a few hours in Hélio Olga House, when outdoor temperatures reached over 30 °C. It may be explained by the house low thermal mass, which also reflects on higher thermal amplitude, showing a similar pattern of temperature oscillation to the exterior one. Nevertheless, as internal conditions are quite coupled with the external ones (whilst shading is provided), internal temperatures are comfortable during mild periods.

Furthermore, looking at the measurements in Hélio Olga House, it is noticeable the effect of

ventilation rates to control internal temperatures. In this respect, on April 4th, when external temperatures exceed 30 °C, the reduced ventilation rates in the living-room maintained indoor temperatures below the external ones by keeping all windows minimally opened, despite the light-weight building fabric. In the next day, when ventilation was increased, a sensible increase of internal temperatures was observed.

Different from that, a considerable effect of thermal inertia can be seen in the measurements collected in Vila Butantã Complex with a significant thermal delay (3 to 4 hours), accompanied by the reduction of peak temperatures. The difference between peak internal temperatures comparing the two extreme cases, being Hélio Olga the light-weight house and Vila Butantã the one with more thermal inertia, was of approximately 5 °C on a summer day.

In this context, the Marlene Milan House is in the middle of the others, also in the middle of the comfort zone, with constant temperatures. Such a thermal response can be explained by the shading strategy together with the external insulation and reflectivity of the concrete roof. It is worth mentioning that the overwhelming shading strategy creates shaded outdoor spaces that characterize the microclimatic conditions in the immediate surroundings of the house.

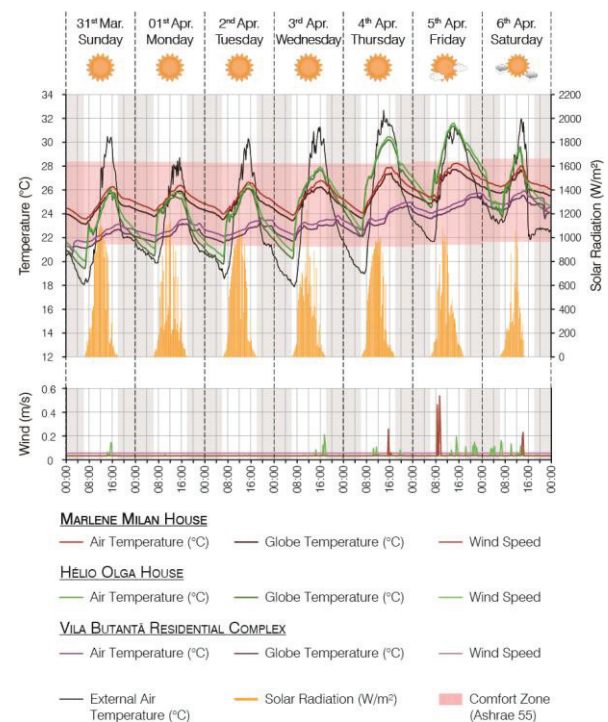


Figure 22: Measurements of dry bulb air temperature, globe temperature and wind speed during warm period (March/April 2019) in the living-rooms of the three case-studies with external air temperature and solar radiation.

For the cold period, Marlene Milan House had the best response of the three. As expected, Hélio Olga House has the closest thermal conditions to the exterior, having issues to comply with the thermal

comfort zone limits. As seen in Figure 23, in the coldest day with external temperatures around 14 °C during the day, indoor air temperatures figured around 19 °C in Marlene Milan House; 15.5 °C in Hélio Olga House and 17.5 °C in Vila Butantã Complex. The higher internal temperatures in the Milan House than in the Butantã Complex during the winter (despite the higher thermal inertia of the second) can be explained by the higher solar access in the first case due to the orientation and bigger glass panels. None of them reaches the 80% acceptability (with the windows closed).

It is important to highlight that these measurements were taken in places where temperatures could be increased by using the fireplaces provided in the design stage, although they were not used. One way of improving temperatures in cold days would be decreasing infiltration by increasing the windows airtightness. However, due to the São Paulo climate (subtropical) and the consequent predominance of warm periods, traditionally buildings have not been designed and built for airtightness, undermining the thermal performance in the colder periods.

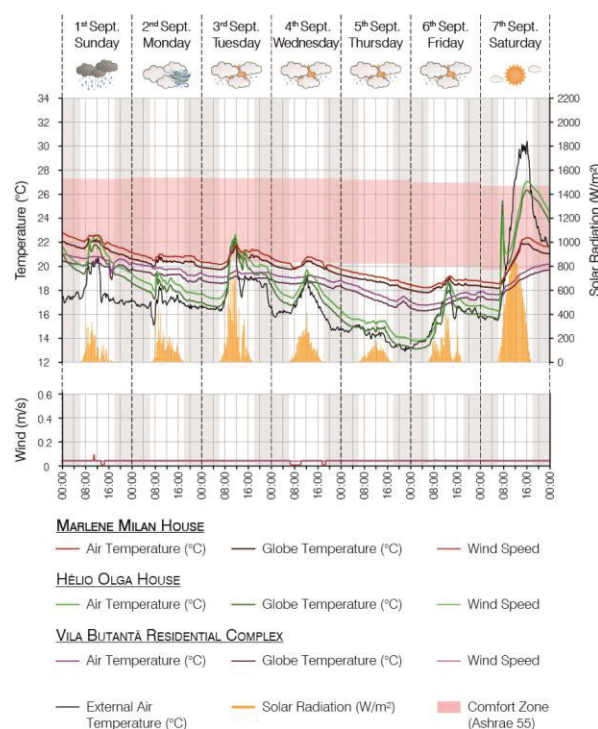


Figure 23: Measurements of dry bulb air temperature, globe temperature and wind speed during cold period (September 2019) in the living-rooms of the three case-studies with external air temperature and solar radiation.

6. FINAL CONSIDERATIONS

After analysing the three residences, it is clear that, in the Marlene Milan House, the strategies applied were related to the roof, including shading, as the concrete structure was made into a big and wide solar “umbrella”, reflectivity provided by the white external surface and thermal insulation. In addition, the

physical and environmental integration of the internal spaces facilitate air-flow. In Hélio Olga House, the strategies were mainly related to natural ventilation and light-weight components, as well as solar access and solar protection by dealing with orientation and large openings. In Vila Butantã Residential Complex, the main design drive was the adequacy of the semi-detached houses to the local topography, whilst for the building components, the material choice favoured thermal inertia, coupled with large openings to controlled ventilation and solar access, with movable external shading.

Despite the differences in the overall thermal response between the three case-studies, the thermal quality in all of them is unquestionable in the summer, with a few moments when the internal temperature reaches or exceeds the external one. On the other hand, whilst focus was put in dealing with the summer conditions, the winter performance was left with room for improvement. The adequate response to the summer conditions (predominant over the year) is directly related to the appropriate combination of multiple design strategies and, therefore, to the design synthesis, bringing together building techniques, site conditions and environmental strategies, on a case by case basis, moving away from the idea of the optimum or pre-determined solutions for the adequate environmental performance.

ACKNOWLEDGEMENTS

Thanks to FAPESP, the Research Funding Agency from the State of São Paulo (Process N° 2018/19902-8) for supporting this research project and to the residents that opened their homes. And special thanks to Marcos Acayaba for sharing his stories and knowledge and, in particular, for providing most of the images from his personal collection to compose this article.

REFERENCES

1. Corbella, O. and Yannas, S., (2009). Em busca de uma Arquitetura Sustentável para os Trópicos.
2. Romero, M., (2012). Estratégias Bioclimáticas de Reabilitação Ambiental Adaptadas ao Projeto. Brasília: p. 3.
3. Gonçalves, J. et al., (2018). Revealing the thermal environmental quality of the high-density residential tall building from the Brazilian bioclimatic modernism: the case-study of Copan building. *Energy and Buildings*, 175: p. 17-29.
4. Filosofia de trabalho, [Online], Available: <http://marcosacayaba.arq.br/> [30April 2020].
5. American Society of Heating, Refrigerating and Air Conditioning (2017). ASHRAE Standard 55-2017.
6. Climate data. [Online], Available: <http://climate.onebuilding.org> [16 February 2020].
7. Roriz, M., (2012). Arquivos climáticos em formato EPW. São Carlos, Brazil.
8. Pedreira, L., (1986). Prancheta. *Revista AU*, 7: p. 57-59.
9. Acayaba, M. A., (2004). Projeto, Pesquisa e Construção.

Responsive design in the outdoor space of the Sea Ranch Architecture

Relationships between spatial composition and environment

MASUNAMI SHIMODA ¹ RYO MURATA ²

¹Tsuruta architects, London, UK

² Tokyo Institute of Technology, Tokyo, Japan

ABSTRACT: Sea Ranch, California is the place where the coastal resort is designed by architects, landscape architects, and many kinds of researchers aiming for environmental and sustainable design since 1960's. It is important to reassess the Sea Ranch Architecture in the respect of environmental design as a significant practice of architecture responding to the environment. Thereby the goal of this research is to illustrate the characteristics of the relationship between the spatial design and the environmental situation calculated by simulation tool. Since wind, sunshine and view are important factors especially in coastal villas, these environmental factors are investigated regarding the spatial composition in the outdoor living spaces. Finally, various systems responding to the environment were found out in Sea Ranch Architecture.

KEYWORDS: Sea Ranch Architecture, Outdoor space, Passive design, Responsive design, Spatial composition

1. INTRODUCTION

A group of buildings at Sea Ranch, California, is known as villas that have been developed in harmony with the natural environment. The initial idea for the symbiosis of architecture and nature can be seen from the drawings of Lawrence Halprin, who designed the master landscape plan of Sea Ranch[1]. More than a half century has passed, this built environment can be regarded as an important masterpiece of architecture responsive to the environment in addition to the presence of a living heritage as modern architecture. Especially, it is assumed that various characteristics on design of outdoor spaces could be found as combinations of building's form and environmental phenomena, such as natural air flow, light and view to the surrounding, and they could be related to a passive design on the climatic and locational uniqueness in California. For instance, the sunny entrance terrace enclosed with walls has the modest wind or the poolside surrounded with a mound has the ocean view. However there is no research on these Sea Ranch Architecture using simulation yet. Thereby the purpose of this study is to illustrate the characteristics of the outdoor space design of Sea Ranch Architecture as seen from the spatial composition and the environment. This research is based on Climate data from the California Climate Data Archive offered by the Institution of Oceanography[2].

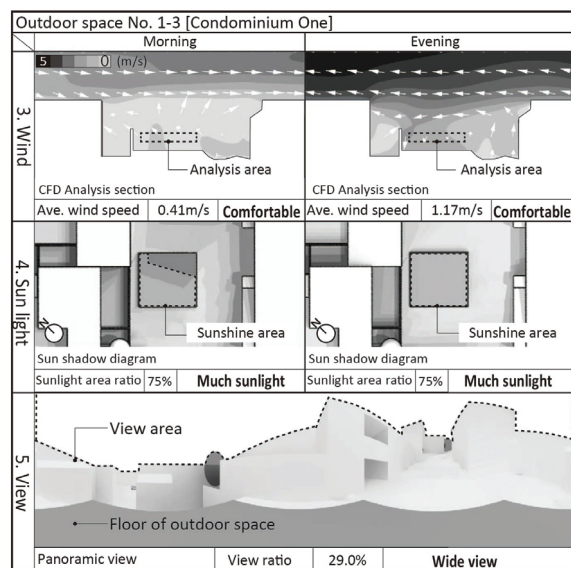


Figure 1: Analysis example

2. Spatial composition of outdoor space

2-1. Location and landscape

The spatial form of the outdoor space is analysed in this chapter. Firstly, it investigates the geographical characteristics of all 17 buildings in Sea Ranch. Mainly the location of buildings are on the coast or in forest. And more cases are located on the coast where wind blows stronger than in forest(13/17) [Table 1].

Table 1: Building location

Site	Forest	Coast
Cases	4/17	13/17

As suggested by Lawrence Harplin, landscapes such as the trees and mounds are distributed around the buildings as an enclosure. While many trees are enclosing around the building, a mound can be found in a few cases [Table 2,3].

Table 2: Trees distribution

Orientation	East	West	South	North
Number	11	9	12	11

Table 3: Mound distribution

Orientation	East	West	South	North
Number	3	1	2	2

2-2. The number of Outdoor space

47 outdoor living spaces were found within 17 buildings[Table 4]. Most of the buildings have multiple outdoor spaces(13/17). However there are only 4 outdoor spaces which have eaves over.

Table 4: Number of Outdoor space

The number of Outdoor space per building	Single	Multiple						
	1	2	3	4	5	6	7	8
Cases	4	5	4	2	1	0	0	1
Total number of Outdoor space								47
Thenumber of Outdoor space with roof								4

In addition, regarding the use, most of Outdoor spaces are common use such as Living room terrace or Dining terrace(36/47) [Table 5].

Private (4)	Lt- Loft terrace (2), Bd- Bedroom terrace (2)
Common (within a dwelling) (36)	En- Entrance terrace (8), Lv- Living terrace (9), Jc- Jacuzzi terrace(5),Pl- Play room terrace (1), Dn- Dining terrace (6), Kt- Kitchen terrace (3), Ln- Laundry terrace (2), St- Studo terrace (2)
Common (between dwellings) (7)	Co- Common terrace (1), Po- Pool side (2), Tn-Tennis court (3), Ba- Basketball court (1)

Table 5: Use of Outdoor space

2-3. Enclosure pattern of Outdoor space

Enclosure patterns are investigated by looking at the patterns of boundary types as listed in [Fig. 2].

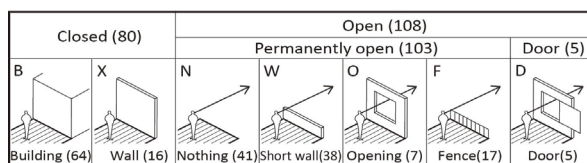


Figure 2: Boundary types

All cases are classified into three enclosure patterns; **OPEN** has open boundaries more than three, **EVEN** has two open boundaries, and **CLOSED** has an open boundary or less [Table 6]. **OPEN** is the majority among the cases(22/47) next majority is **EVEN** (16/47). **CLOSED** are only 9 cases. Consequently, the majority of wall patterns showed a tendency to open the space towards the southwest where the seaside is facing.

Table 6: Enclosure pattern of Outdoor space

Outdoor space No.	Roof	Wall				No. of Open wall	Use	Single Enclosure pattern
		E	S	W	N			
1-3	x	N	N	N	N	4	Co	
2-1	x	N	N	N	N	4	Jc	
3-2	x	F	F	F	F	4	Tn	
5-3	x	O	N	W	N	4	Kt	
2-3	x	N	N	N	B	3	Pl	
3-1	x	W	N	N	B	3	Po	
10-4	x	N	F	F	B	3	Tn	
12-3	o	W	W	W	B	3	Lo	
10-2	x	F	F	F	B	3	Tn	
9-1	x	W	W	B	W	3	En	
13-1	x	W	W	B	W	3	Ln	
14-5	x	W	W	B	W	3	St	
15-1	x	F	F	B	F	3	Ln	
5-1	x	W	B	N	N	3	Lv	
10-1	x	N	X	F	F	3	Ba	
10-3	x	N	B	F	F	3	Po	
2-2	x	B	N	N	N	3	Lv	
1-1	x	B	W	W	X	2	En	
1-7	x	B	D	D	B	2	Lv	
4-1	o	B	O	O	B	2	Bd	
4-2	x	B	W	N	B	2	Dn	
5-2	x	B	O	O	B	2	Kt	
7-1	x	B	W	W	B	2	Dn	
15-2	x	B	F	N	B	2	Lv	
17-1	x	B	N	N	B	2	Dn	
12-2	x	W	O	B	X	2	Jc	
13-4	x	B	B	W	N	2	En	
13-2	x	D	B	N	B	2	Dn	
8-1	o	N	B	B	B	1	En	
17-2	x	D	B	X	B	1	Jc	
1-6	x	X	W	X	B	1	Lo	
8-2	x	B	N	B	B	1	Lv	
1-2	x	X	X	B	B	0	En	
1-4	x	B	X	X	B	0	Lv	
1-5	x	X	X	B	B	0	En	

Legend: Closed Open

3. Wind environment of outdoor space

3-1. Outline of simulation

In this chapter the wind behaviour of the 47 outdoor spaces is analysed by the thermal fluid simulation based on the prominent natural wind condition of Sea Ranch[2][Figure 3]. The wind environment of each outdoor space is calculated under the setting of a constant prevailing wind condition from April to October[Figure 3]. Average wind speed 3.6m/s in morning and 3.2m/s in evening are set as Inflow wind speed in the simulation. Both of them are faster than 2.3m/s [4]. That is to say this area has **Strong** wind both in the morning and evening on average. Comfortable wind is defined as the wind speed slower than 1.5m/s[4].

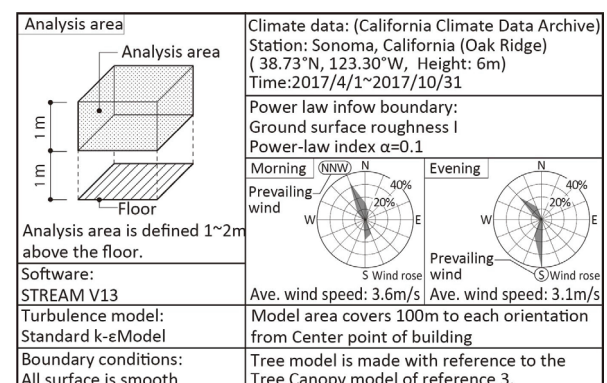


Figure 3: Outline of wind simulation

3-2. Average wind speed of Outdoor space

In order to analyse how much the wind is reduced in all cases, categorising the wind speed into three groups as below; **Comfortable** wind(1.5m/s) **Middle** wind(2.3m/s) and **Strong** wind[Figure 4]. Although the inflow wind is strong, most cases are mildened to comfortable wind in both morning and evening (morning:34/47) (evening:37/47) [Figure 4]. Also there are only a few cases has **Strong** wind (morning:2/47) (evening:3/47).

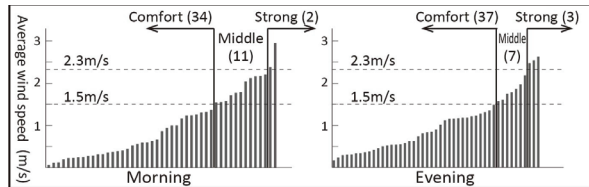


Figure 4: Average wind speed

In addition to this, most cases has always comfortable wind through a day(29/47)[Table 7]. This result shows how successful outdoor design can milden the wind.

Table 7: Transition of wind comfortability

Always comfort	Morning comfort	Evening comfort	Non comfort
29/47	5/47	8/47	5/47

4. Sunshine environment in outdoor living space

4-1. Outline of simulation

No matter how mild the wind, sunshine is also important and needs to be taken into Outdoor space. Therefore in this chapter the sunshine environment for these outdoor spaces are analysed by simulating. The simulating day is elected from July when the average amount of solar radiation is the highest in the year. The sunshine area for each hour is examined by the use of shadow maps exported from 3D modeling software. Then, the sunshine area ratio is investigated as a characteristic of the sunshine environment in each shadow map. It is the ratio of the sunshine area per the whole area of outdoor space [Fig. 5].

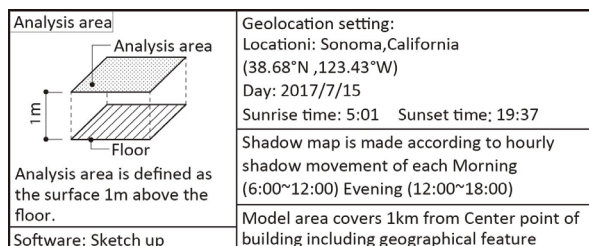


Figure 5: Outline of sunshine simulation

4-2. Sunshine area ratio of Outdoor space

In the case of morning hours, the patterns of the sunshine area ratio showed a consistent tendency among three groups, which are **Much**(16/47), **Middle**(15/47), and **Little**(16/47). In contrast, in the evening sunshine tends to be **Middle** or **Much**. That is to say sunshine area tends to become more over a wide range in evening.

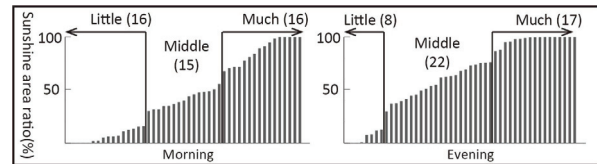


Figure 6: Sunshine area ratio

Besides, these outdoor living spaces get more sunshine at sunset time rather than sunrise [Table9, 10]. This result is related to the tendency of the outdoor space to open towards the sea.

Table 8: Transition of Sunshine area ratio

Always much sunlight	Morning much sunlight	Evening much sunlight	Always less sunlight
8/47	8/47	9/47	22/47

Table 9,10: Sun rise/Sun set visibility

Sun rising visible	Sun set visible
4/47	21/47

5. View of outdoor space

5-1. Outline of simulation

As in the sunshine environment, the view is also an important environmental factor in Sea Ranch. The view from each outdoor living space is analysed in this chapter, such as the sky and the sea by the use of panoramic view images exported from 3D modeling software. Each viewpoint is set at the centre of each outdoor space. Then, the view rate which is the ratio of the view to the outside per the whole area is investigated as a characteristic of visual environment in each panoramic view [Fig. 7].

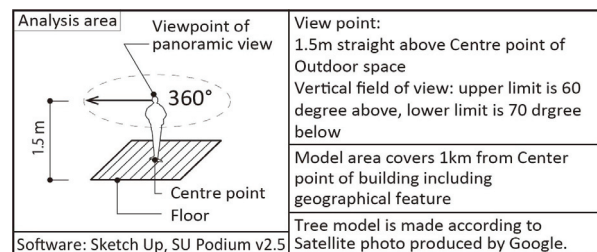


Figure 7: Outline of view simulation

5-2. View ratio of Outdoor space and view to the sea

Each view ratio is classified into three groups; **Wide** (29/47), **Middle** (12/47), and **Narrow** (6/47). As a result, more than half cases obtain **Wide** view [Fig. 8]. Maximum value of the view ratio is 50%. In addition, more than a half of these outdoor spaces has the view of the sea.

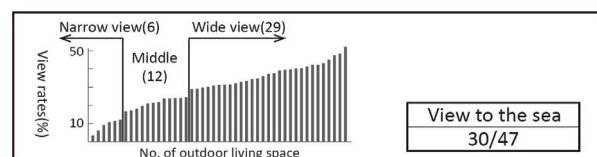


Figure 8: View analysis example

Table 10: Number of view to the sea

6. Environmental type and enclosure pattern

6-1. Environmental type

This chapter investigates the relationship among above three environmental factors and the spatial composition for 47 outdoor living spaces. Initially investigating the relationship between three environmental types, 6 types of unique environmental patterns were found out through the combination of the three environment aspects[Table 12]. ① **All-round** type (5 cases) has Much sunshine and Comfortable wind in both morning and evening. This pattern also has Wide view. That is to say this pattern takes all three environmental factors thoroughly in outdoor space. Open composition is more common than other patterns. More than half of the cases have a sunset view (3cases). ② **Wind,View** type (8 cases) also has comfortable wind in both morning and evening. And it has Wide view. More than half of the cases have Much sunlight in either morning(4 cases) or evening (2 cases). ③ **Wind** type (16 cases) also has comfortable wind in both morning and evening. This pattern is most common among all 6 patterns. ④ **Sun, View** type (4 cases) has Much sunshine and Wide view. ⑤ **View** type (12 cases) has only Wide view. Most of the cases have views of the sea. That is to say this pattern is specialized in view of the sea. ⑥ **Moderate** type (2 cases) does not have comfortable wind through a day, Much sunshine or Wide view. The result that there are only 2 cases of ⑥ **Moderate** out of 47 cases, means that most of the outdoor spaces have environmental characteristics such as environmental type ①~⑤. Although there are Wind type and View type, no Sun type is found among 47 cases. All Sun factors exist with the other environmental factors such as ① **All-round** type or ④ **Sun, View** type. Therefore it can be said that the Sunshine is the more additional factor than the other two factors.

6-2. Combination of Environmental pattern and enclosure pattern

This chapter investigates the relationships between enclosure types and environmental types acquired in the previous chapter. Three types which include Wide view has tendency of OPEN enclosure patterns such as ① **All-round** type ② **Wind-View** type ④ **Sun-View** type ⑤ **View** type. Especially ④ **Sun-View** type has only OPEN enclosure patterns. Therefore Openness is key to obtain view and sunlight in Outdoor space. On the other hand, ③ **Wind** type has most of CLOSED enclosure type (8 cases)and at same time it also has OPEN type (3 cases). ③ **Wind** type is the only type which has Open and Closed type in the same environmental type.

Table 12: Environmental types

Outdoor space No.	Ave. Wind speed		Sunshine area ratio		View ratio	Sun rise	Sun rise	View to the sea	Environmental Pattern
	Morning	Evening	Morning	Evening					
10-4	○	○	○	○	○	○	○	○	① All-round (5)
13-3	○	○	○	○	○	-	○	○	
15-2	○	○	○	○	○	-	○	○	
3-1	○	○	○	○	○	-	○	-	
1-3	○	○	○	○	○	-	○	-	
1-6	○	○	○	△	○	-	-	○	② Wind,View (8)
14-4	○	○	○	△	○	-	-	○	
14-5	○	○	○	△	○	○	-	○	
9-1	○	○	○	△	○	-	-	-	
15-3	○	○	×	○	○	-	○	○	
17-1	○	○	△	○	○	-	-	○	
5-1	○	○	×	△	○	-	-	○	
12-2	○	○	△	△	○	-	-	○	
12-3	○	○	△	○	△	-	○	○	③ Wind (16)
1-1	○	○	×	△	△	-	○	○	
12-1	○	○	△	△	×	-	○	○	
1-2	○	○	△	△	×	-	-	○	
1-7	○	○	△	△	△	-	-	○	
11-1	○	○	△	△	△	-	-	○	
4-1	○	○	×	×	△	-	○	-	
8-2	○	○	○	△	×	-	-	-	
1-4	○	○	△	△	×	-	-	-	
1-5	○	○	×	×	×	-	-	-	
1-8	○	○	×	×	×	-	-	-	
5-3	○	○	×	×	×	-	-	-	
8-1	○	○	×	×	△	-	-	-	
14-1	○	○	△	△	△	-	-	-	
17-2	○	○	△	△	△	-	-	-	
5-2	○	○	×	×	○	-	-	-	
10-2	△	○	○	○	○	○	○	○	④ Sun,View (4)
10-3	△	○	○	○	○	-	○	○	
3-2	△	○	○	○	○	-	○	-	
10-1	△	○	○	○	○	-	○	-	
6-1	○	×	×	△	○	-	○	○	⑤ View (12)
2-3	△	○	×	○	○	-	○	○	
2-1	△	○	×	×	○	-	○	○	
2-2	△	○	×	△	○	-	○	○	
13-4	△	×	×	○	○	-	○	○	
14-2	△	△	△	○	○	-	○	○	
13-2	○	△	○	△	○	-	-	○	
7-1	△	×	△	○	○	-	-	○	
15-1	△	△	×	△	○	-	-	○	
16-1	△	△	△	△	○	-	-	○	
4-2	○	△	△	△	○	-	-	○	
13-1	△	○	○	△	○	○	-	-	
16-2	○	△	×	×	△	-	-	○	⑥ Moderate (2)
14-3	○	△	○	△	△	-	-	○	

Legend: Average wind speed {○ Comfortable, △ Middle, × Strong} Sunshine area ratio {○ Much sunlight, △ Middle, × Little sunlight} View ratio {○ Wide view, △ Middle, × Narrow view}

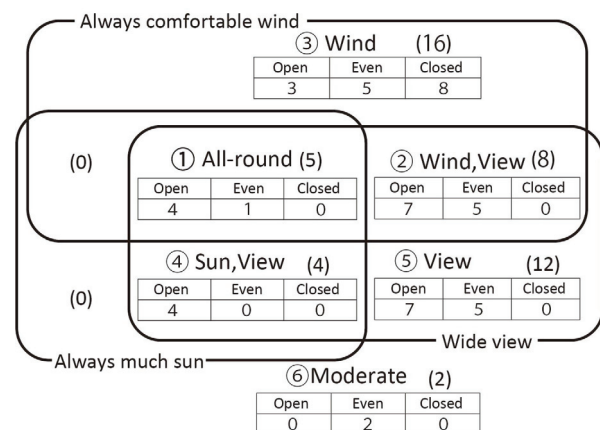


Figure 9: Venn diagram of Environmental types

7-2. Case study

As explained at the previous chapter, it is obvious that there are mainly two major groups of systems. First one is Close-dominated systems which have the outdoor spaces enclosed with walls and they milden the wind to a comfortable level. Second one is Open-dominated systems which have the outdoor spaces open to outside and have diverse environmental factors. This chapter focuses on the case studies of All-round type outdoor space belonging to each open-dominated system and Close-dominated system.

First case study is Outdoor space No.1-3 in Condominium one designed by MLTW and also Lawrence Harplin. Although this building belongs to **Close-Wind** system, No.1-3 is Open All-round type and used as common area for the entire building.

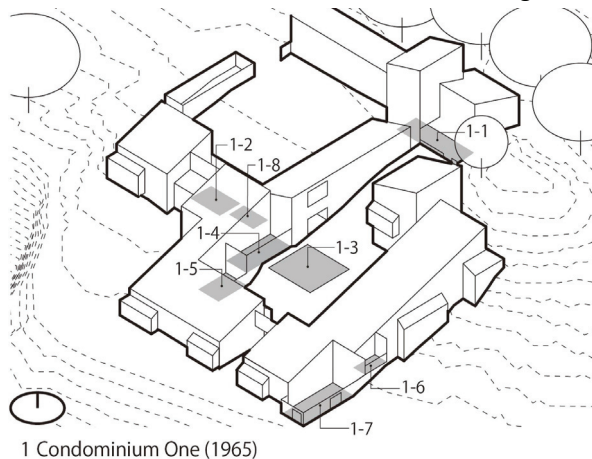


Figure 11: Case study 1 Condominium One

By assigning roles to the outdoor spaces, selective environment and spatial composition can be obtained into the life at this building. Also paying attention to the location of No.1-3 outdoor space the space itself is open but it is surrounded by the Volume of each dwelling unit. This makes it possible to obtain the comfortable wind and open space at same time. Thus It can be said that a courtyard is effectively utilized to milden the strong wind from a completely different direction in the morning and evening. And this is also what was proposed by Lawrence Harplin.

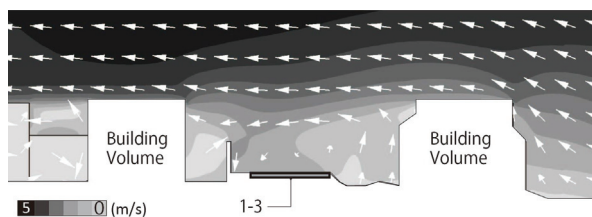


Figure 12: Case study 1 Wind direction map

Next, looking at Case No.3, this building is Open pattern and Sun-view type. Also most of the wind is mildened except for only the evening wind at

Outdoor space 3-2. Thus it can be said that this building succeeded in mildening the wind. Especially in No. 3-1 the wind is mildened to a comfortable wind speed both in the morning and afternoon. It can be seen that the mound is effectively utilized as a windbreak. On the other hand, No. 3-2, which is also surrounded by mounds, has an area larger than No. 3-1. So the wind cannot be weakened, and the average wind speed is Middle in the evening. Therefore the landscape is incorporated as an element for operating the environment in this case study.

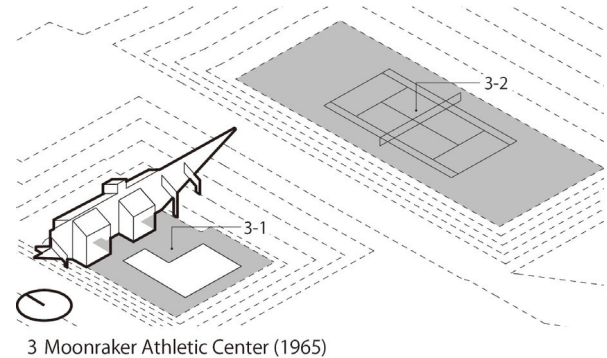


Figure 13: Case study 2 Moonraker Athletic Center

8.Conclusion

Although it is ideal that these three factors are obtained in each space, it is not easy as it is shown that the **All-round** type can be found in only 5 cases out of 47 cases. This is partly because wind type tends to be closed space composition meanwhile view type and sunshine type tends to be open in terms of wall composition. This is why case study shows that the idea of landscaping such as a mound or building position is an important factor of obtaining the three environmental factors at same time especially where the space is open. Therefore it can be said that the responsive design method of Sea Ranch Architecture is to make the outdoor space open and enclose it with a mound or locate it within the courtyard. This is exactly what Lawrence Heparin meant in his master plan guideline with his sketch. From the results mentioned above, various systems responding to the environment and the design method of outdoor space in Sea Ranch Architecture were found out.

REFERENCES

1. Donlyn Lyndon et al. : The Sea Ranch, Princeton Architectural Press, 2013.12
2. California Climate Data Archive (<https://calclim.dri.edu/>)
3. Tatsuaki IWATA, Atsuko KIMURA, Akashi MOCHIDA, and Hiroshi YOSHINO, (2005). Optimization of Tree Canopy Model For CFD Prediction Of Wind Environment At Pedestrian Level, National Symposium on Wind Engineering No. 18
4. Shuzo Murakami, and Yasushige Morikawa, (1985). Criteria For Assessing Wind-Induced Discomfort Considering Temperature Effect,, Transactions of AIJ. Journal of architecture and planning No.358, 1985.12

Field Study on Indoor Thermal Environment in Air-conditioned Offices in the Tropics: A Case Study of Indonesia, Singapore, and Thailand

Tanadej Sikram¹, Masayuki Ichinose¹, Rumiko Sasaki¹,

¹ Department of Architecture and Building Engineering, Graduate School of Urban Environmental Sciences, Tokyo Metropolitan University, Tokyo, Japan

ABSTRACT: A study of indoor thermal environment in office buildings is significant to satisfy people living in, especially in the tropics where temperature and humidity are high throughout the year. This study aims to clarify the actual thermal environment in office spaces in Southeast Asia countries; Indonesia, Singapore, and Thailand. The field measurement was in 2017–2019 by collecting thermal variables and a questionnaire survey. The results show that most of thermal variables were in the 1.0 clo zone due to the overcooled condition. The thermal sensation votes and the predicted mean votes (PMV) showed a similar trend as a negative scale which refers to the cold sensation. Based on Griffith's method, the average comfort temperatures are 26.8 °C (Indonesia), 24.8 °C (Singapore), and 24.0 °C (Thailand), respectively, lower than the actual operative temperatures. To reduce discomfort, the indoor temperature could be increased to be higher than the current actual values about 1–2 °C.

KEYWORDS: Thermal environment, Thermal comfort, Air-conditioned office, Tropics

1. INTRODUCTION

In a tropical region, office buildings consume high energy to provide a cool indoor environment for human comfort [1]. An air-conditioning system of the office in the operation and maintenance stage uses over half of the electricity distribution (56%) [2] reaching the highest demand compared with the use of other building types in the commercial sector [3]. Both international and local guidelines for indoor environments have been adopted in air-conditioned offices. However, climates and social context in this region are specific in many factors, such as long-term thermal experience, human behavior, human preference, etc. [4]. It is important to survey the thermal performance of the office in the after-built stage and compare it with both the design criteria and human comfort. Due to the limited number of air-conditioned cases in a tropical region [5], This study aims to give more details about thermal comfort based on the large number of on-site cases by clarifying thermal performance and determining the comfort temperature from data of thermal variables and human factors. It would be beneficial to compare the values among three Southeast Asia countries; Indonesia, Singapore, and Thailand to calibrate a suitable indoor environment to be implemented in the future.

2. METHODOLOGIES

The field surveys of an indoor thermal environment were conducted between 2017 and

2019 in one office in Indonesia (Jakarta), four offices in Singapore, and eight offices in Thailand (Bangkok and Nonthaburi), which were 13 cases in total. All offices are air-conditioned open-plan offices equipped with a cooling air-conditioning system. The offices belong to either private companies or government sectors. Table 1 describes the details of each office building.

Table 1: Information on surveyed offices

Case	D/M/Y	FL/All-FL	Area	AC	N
Indonesia					
I-1	28-29/9/17	17/21	1207	C	74
Singapore					
S-1	31-1/10-11/18	4/9	550	I	104
S-2	2-3/11/18	31/42	879	C	387
S-3	13-14/3/18	3,5/5	360	I	158
S-4	30-31/5/18	5/17	1761	C	465
Thailand					
T-1	24,27/4/18	4/7	862	I	97
T-2	2-3/5/18	14/40	437	C	151
T-3	12-15/6/18	14/19	737	I	315
T-4	19-22/6/18	7/20	372	C	470
T-5	24-26/9/18	11/25	674	C	492
T-6	4-6/3/19	17/29	290	C	305
T-7	12-13/3/19	32/43	492	C	142
T-8	9,12/9/19	7/20	576	C	225

Note: D/M/Y: Date/Month/Year of survey; Period: FL/All-FL: surveyed floor/total floor; Areas: Investigated area; AC: Air conditioning type; C: Central unit; I: Individual unit; N: Number of occupants.

Table 2 describes the automatic measuring devices used in this study. An anemometer was installed on a tripod that measured air velocity every 10 min per position. The air temperature and relative humidity were measured by the device named TR-74Uvi that recorded automatically in 1-min intervals. We used the RTR-52A 7" Globe attached to a partition nearby occupants' working desk at 1.1 m high from the floor. All devices were installed at every orientation in the office.

Table 2: Measuring devices and methods.

IEQ parameters	Measuring devices	Record interval	Number of measuring points
Air temperature and humidity	TR-74Uvi	10 min	4–13
Mean radiant temperature	RTR-52A 7" Globe	10 min	4–13
CO ₂	TR-76Ui	10 min	2–13
Air velocity	Anemometer	60 sec	5–6

The questionnaire sheet was given to occupants in the office to evaluate subjective perception towards thermal environments which was derived from the ASHRAE 55 [6] and the ISO 9920 [7] described in Table 3. There were three main questions, including a seven-point scale of thermal sensation vote (TSV), a five-point scale of thermal comfort vote (TCV), and a five-point scale of preference (TPV). We asked occupants twice a day at 11:00 and 15:00, together with collecting the thermal variables. We could collect data from 802 persons. We had 134 votes from Indonesia, 1,253 votes from Singapore, and 2,197 votes from Thailand.

Table 3: Questionnaire information.

Scale	Sensation (TSV)	Comfort (TCV)	Preference (TPV)
-3	Cold	-	-
-2	A bit cold	Uncomfortable	Colder
-1	Cool	A bit uncomfortable	A bit colder
0	Neutral	Neutral	No change
1	Warm	A bit comfortable	A bit warmer
2	A bit hot	Comfortable	Warmer
3	Hot	-	-

3. RESULTS AND DISCUSSION

3.1 Thermal environments

The results are arranged by following a name of countries; Indonesia, Singapore, Thailand, respectively. As the results, Figure 1 shows that the median of room temperature was 24.4 °C, 23.3–24.0 °C, and 22.2–23.6 °C respectively. The lowest value was in Thailand (Office TH-3), while the highest value was in Indonesia (Office I-1). The smallest temperature gap was in Singapore (Office S-2) reading as 22.7–24.0 °C ($\Delta T = 1.3$ k) but the largest

one was in Thailand (Office T-3) reading as 20.3–24.7 °C ($\Delta T = 4.4$ k). Two cases exhibited the median values ranging from 24 °C (Office I-1 and Office S-4). Especially in Thailand, the median room temperatures in five offices were lower than the recommendation from the ASHRAE standard (23.2 °C).

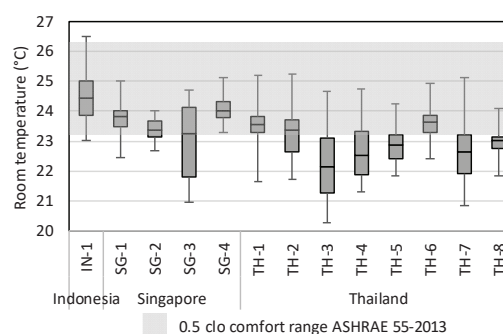


Figure 1: Distribution of air temperature.

The results of relative humidity (RH) were plotted in Figure 2. The median was 48% (Indonesia), 45–66% (Singapore), and 47–63% (Thailand). In Indonesia, Office I-1 performed the well-controlled rate being within 40–60%, whereas there were some cases in Singapore and Thailand exhibiting the relative humidity higher than 60%.

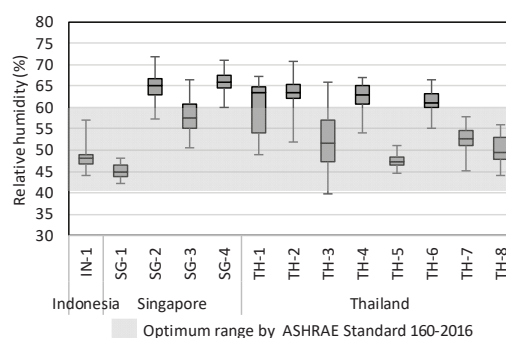


Figure 2: Distribution of relative humidity.

We compared the results of outdoor temperature derived from the online database [8-10]. The gap between outdoor and indoor conditions was severe in the offices that were overcooled inside but the outdoor temperature was excessively high. The average outdoor temperature was 26.7–31.7 °C with 64–85% (Indonesia), 28.3–31.1 °C with 64–84% (Singapore), and 31.1–35.6 °C with 33–67% (Thailand). Thai cases were expected to be most critical when temperature gaps between two sides were higher than Indonesian and Singaporean cases mainly because of low indoor temperatures.

The average air velocity was quite stable at 0.10–0.20 m/s which was normal in air-conditioned buildings. The operation of a fresh air ventilation

system in most cases was quite normal due to the control of CO₂ levels. The values of 12 cases were below 1000 ppm which fitted to the indoor environment [11]. There was only Office T-1 being slightly higher than the mentioned value at 1,050 ppm. It can be implied that the mechanical ventilation system of most case studies was in a normal situation providing sufficient fresh air volume.

We calculated the operative temperature and absolute humidity from the values from measuring devices to plot a psychrometric chart based on the ASHRAE standard [6]. The recommendation zone for people wearing loose clothes is the 0.5 clo comfort zone which fits weather conditions in the tropics. In Figure 3, it is noticeable that thermal environments in Indonesia were different from those in Singapore and Thailand. Most thermal points in Indonesia were in the 0.5 clo zone (95%), while those in Singapore and Thailand belonged to the 1.0 clo zone (72% and 85%). There are some values in Office S-2, S-4, T-1, T-2, and T-7 shifting out of the comfort zone due to the absolute humidity that was higher than 0.012 g/g. Based on a psychrometric chart, thermal environments were not appropriated to people in the tropics.

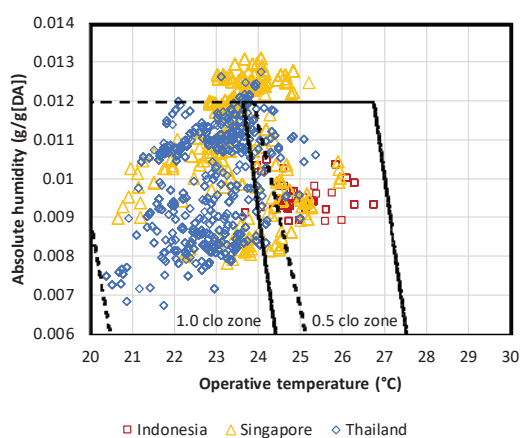


Figure 3: A psychrometric chart.

3.2 Clothing Insulation

Figure 4 presents the trend of clothing insulation based on the calculation from ISO 9920 [7]. The percentage of clothing insulation rate of occupants in all countries was the highest at 0.5 clo (33–37%), which fitted to the comfort zone for people in the tropics. The average clothing rates were 0.59 clo (Indonesia), 0.61 clo (Singapore), and 0.61 clo (Thailand), respectively. Even if the thermal environment in each country were different, the clothing rate was likely to be similar to each other. High outdoor temperature and relative humidity are the main factors for a clothing wearing decision. However, there were about 31–44% of occupants wearing clothing higher than 0.5 clo and more than

50 % of them reported that they felt slightly cold or cold during the day. However, people in this group voted comfortable due to clothing adaptation. They wore additional clothes, such as sweaters, cardigans, and scarves, etc., to make themselves warm. It could be implied that in open plan offices, people adapt themselves to the overcooled environment to become comfortable by adjusting their own garments without personal control of indoor environment.

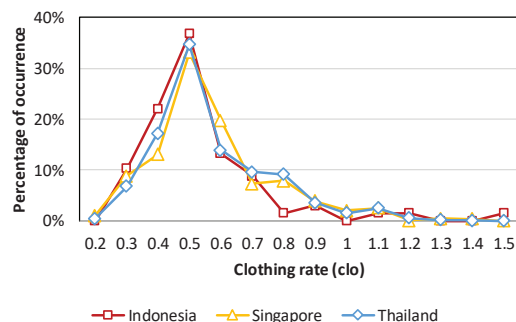


Figure 4: Clothing insulation rate.

3.3 The predicted mean votes

The predicted mean votes (PMV) is a well-known benchmark to evaluate thermal comfort in the office building. We use this model to estimate how much thermal environments and people's uncomfortable rates in this study could be fitted into that the tropical climate zone. It uses the data referring to 1) thermal variables that were measured during working hours; temperature, relative humidity, and wind velocity, 2) occupant's information; metabolic rate, and clothing insulation from the questionnaire. The value of metabolic rate was 1.1 met according to a typical rate for occupants' activities in the office written in ASHRAE 55 [6]. In Figure 5, the results are categorized into 3 groups; $PMV < -0.5$, $-0.5 \leq PMV \leq 0.5$ (a recommended zone), and $PMV > 0.5$. The results show that the recommended values belonged to Indonesia (80%), Singapore (62%), and Thailand (38%), respectively. Due to warm temperature and optimum relative humidity, the suitable PMV was the highest in the Indonesian case two times higher than Thai cases. When most values were lower than -0.5 , the suggested values in both countries could not reach over 80%.

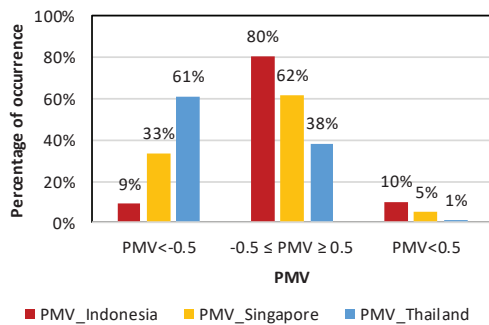


Figure 5: PMV estimation.

3.4 Subjective votes

Considering the thermal sensation votes (TSV) in Figure 6, the average was -0.9 (Indonesia), -0.8 (Singapore), and -0.6 (Thailand). Samples in all countries voted for the colder-than-neutral votes (TSV = -1, -2, and -3 or TSV-) rather than the warmer-than-neutral votes (TSV = 1, 2, and 3 or TSV+). The voting ratio between two sides was 62:16, 48:11, and 41:8, respectively. The percentage of TSV between Singapore and Thailand was a similar trend when TSV- was generally higher than the TSV+ which was counted as about 4 times higher in Singapore and 5 times higher in Thailand (48:11 and 41:8, respectively) and votes declared the highest values were feeling neutral (TSV = 0). The thermal acceptable range (TSV = -1 to +1) [6] was counted as 54%, 70%, and 76%, respectively. TSV was contradicted to a psychometric chart when the offices with cooler temperatures had higher acceptable TSV votes. The votes from Indonesia were the highest in feeling cold even indoor temperature was the warmest. The cold sensitivity and thermal neutrality of each country would be different and correlated to the comfort temperature that was discussed in Part 3.6.

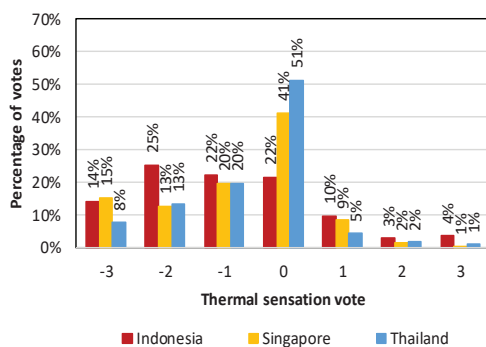


Figure 6: Distribution of thermal sensation votes.

Thermal comfort votes (TCV) are presented in Figure 7. The average was 0.5 (Indonesia), 0.4 (Singapore), and 0.4 (Thailand). The rate of all countries was the highest in a neutral scale (TCV = 0). The rate of uncomfortable votes (TCV = -1 to -2 or

TCV-) was 13%, 17%, and 20%, respectively. The total rate of each country was lower than 20% discomfort, however, the rate of uncomfortable votes reached over 20% in many cases; one office in Singapore (S-3) and five offices in Thailand (T-1, T-2, T-3, T-5, and T-7). Two highest uncomfortable rates were in Office S-2 (29%) and Office T-3 (28%) which the average room temperature was quite low and TSV was high on the cold side.

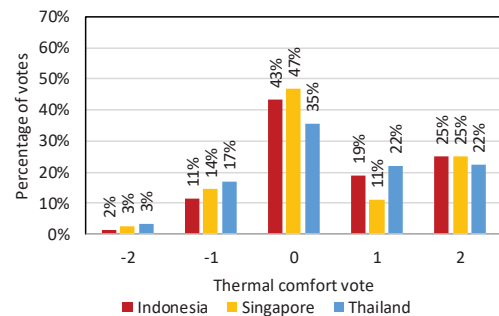


Figure 7: Distribution of thermal comfort votes.

To emphasize discomfort, the relation between TSV and TCV is plotted in Figure 8. The votes are categorized by the scale of TSV- and TSV+ without TSV0. The results show that TSV- of Indonesia was higher in TCV+ (84%), while TSV- of Singapore and Thailand was higher in TCV- (76% and 74%). In contrast, TSV+ of all countries became the highest rate in TCV- (Indonesia = 53%, Singapore = 21%, and Thailand = 17%). Even though most people voted more comfortable when they felt cold rather than hot, the number of uncomfortable votes remained higher in TSV- rather than TSV+. Especially in Singapore and Thailand, the percentage of TSV- in discomfort was 55% and 57% higher than that of TSV+ in discomfort. It could be implied that cold sensation may cause discomfort and people have to tolerate overcooling environments [12]. To decline discomfort, the indoor temperature should be slightly warmer so that people will satisfy more with the overall thermal environment.

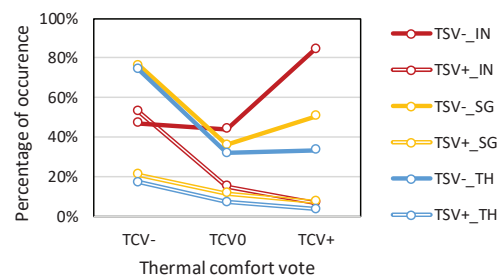


Figure 8: TSV and TCV.

Thermal preference votes (TPV) are shown in Figure 9. The average was -0.2 (Indonesia), 0.1

(Singapore), and 0.2 (Thailand). Considering the highest rate, samples voted “no change” as 69%, 65%, and 63%, respectively. In Indonesia, the percentage of “prefer a warmer temperature” (TPV+) was lower than that of “prefer a colder temperature”, while the other two countries gave the different results. The percentage of TPV- in Indonesia was 17–18% higher than that of Singapore and Thailand, respectively. On the other hand, the percentage of TPV+ in Indonesia was 16–17% lower than that of Singapore and Thailand, respectively. TPV is corresponding to TSV when 87% of people in Singapore and 83% of those in Thailand who answered TSV- would like to change into warmer temperature, whereas 64% of those in Singapore and 47% of those in Thailand voting TSV+ would like to change into a colder temperature (correlation coefficient = -0.8 and -0.7). People may normally feel neutral (TSV = 0) towards thermal environments, however, there is a possibility to adjust a slightly warmer temperature to a better rate of TPV with higher “no change” preference.

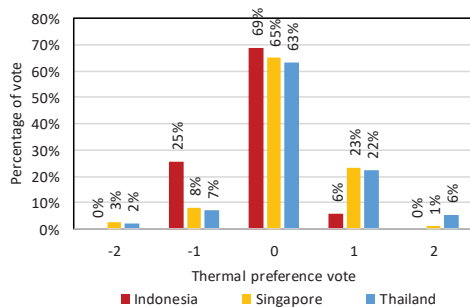


Figure 9: Thermal preference votes.

3.5 Comparison between PMV and TSV

Figure 10. Illustrates the mean PMV and the mean TSV plotted against the operative temperature of each 0.5 °C ranging from 21.5 °C to 26.5 °C. Most values fell in the negative zone lower than a 0 point scale. The trendline of the Indonesian case was a bit different from that of Singaporean and Thai cases by the small ranges of operative temperature that fitted to a 0 scale at a higher degree Celsius. By the PMV, an Indonesian case is obtained the highest rate mainly due to indoor warmer temperatures. The PMV prediction becomes 0 when the operative temperature is 25.5 °C, 24.6 °C (Singapore), 24.8 °C (Thailand), respectively. By the TSV, the average when lower becomes 0 when the operative temperature is 26.3 °C, 25.3 °C, and 24.9 °C, respectively. The values from the actual votes were higher than the PMV estimation.

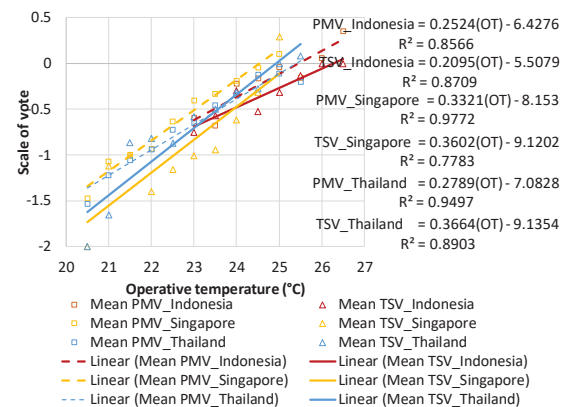


Figure 10: PMV and TSV against operative temperature.

3.6 Comfort temperature

To estimate the comfort temperature, we use an equation based on Griffiths' method which is suggested to apply to air-conditioned building types and climate zones including a hot-humid climate zone [13]. The equation is $T_c = T_r (0 - C)/a$, where T_c means the comfort temperature (°C), based on T_r which is temperature (°C); C is the thermal sensation vote on the scale, where 0 defines as a neutral condition; and a defines the constant rate of thermal sensation change with the room temperature which is 0.5, as had been used with a seven-point thermal sensation scale by the study of Humphreys [14]. By this method, the average of comfort temperatures are found to be 26.8 (Indonesia), 24.8 °C (Singapore), and 24.0 °C (Thailand). The average comfort operative temperatures are different from the actual measurement about +2.4 °C (Indonesia), +0.8–1.5°C (Singapore), and +0.4–+1.8 °C (Thailand). Comparing with the previous research of Damiani et al. [4] in South East Asian countries: Malaysia, Indonesia, and Singapore, it was found that the mean comfort temperatures of this study are lower than the actual mean temperatures. The main reason for a low comfort temperature in Thai offices was the low actual temperature with the high number of neutral votes and no change preference votes. The comparison between this study and the mentioned study is listed in Table 4.

Table 4. Comparison of the comfort temperature.

Country	N	T _{com} (°C)	S.D.	Source
Malaysia	1114	25.6	2.2	[4]
Indonesia	90	26.3	2.3	
Singapore	14	26.4	2.1	
Indonesia	134	26.8	2.9	This study
Singapore	1685	24.8	2.7	
Thailand	2197	24.0	2.3	

T_{com}: Comfort operative temperature, S.D.: Standard deviation.

4. CONCLUSION

This field study surveyed the thermal environment of air-conditioned offices in a tropical region, which were located in Indonesia, Singapore, and Thailand. To compare thermal variables and to estimate the comfort range, data loggers and the questionnaire were used in this study. The median room temperature ranged between 22.2 °C and 24.4 °C which was quite low in the offices in Singapore and Thailand. The median relative humidity was 40–66%, which some cases reached higher than the recommendation. Considering a psychometric chart of ASHRAE, most thermal environments fitted to the 1.0 clo comfort zone which was not a recommended zone for air-conditioned offices in the tropics. Offices in Thailand and Singapore were similar in terms of thermal performance, whereas a case in Indonesia had the highest values. Thermal environments affected the thermal sensation votes when a cold side was 3–5 times higher than a hot side. The thermal comfort votes also declared that the high number of feeling uncomfortable votes was from occupants who voted feel colder than neutral. The predicted mean vote (PMV) and the thermal sensation vote (TSV) were different in some cases that showed occupants still felt colder than the prediction. The median neutral temperature of the case studies was found at 24.0–26.3°C. In conclusion, these findings strongly support a better indoor environment in offices in a hot and humid region in terms of adjusting the temperature setpoint to be about 1–2 °C higher than the current situation. Air-conditioning loads could be decreased and occupants could be more relaxing with a warmer thermal condition.

ACKNOWLEDGMENTS

This research was granted by the Tokyo Metropolitan Government Platform Collaborative research project under the representative Asso. Prof. Masayuki Ichinose. We would like to thank all participants both building management teams who provided data on the case studies. Also, we would like to express the appreciation to all occupants who filled out the questionnaire.

REFERENCES

1. Sekhar, S.C., Thermal comfort in air-conditioned buildings in hot and humid climates – why are we not getting it right? *Indoor Air*, 2016. 26(1): p. 138-152.
2. Kofoworola, O.F. and S.H. Gheewala, Life cycle energy assessment of a typical office building in Thailand. *Energy and Buildings*, 2009. 41(10): p. 1076-1083.
3. Yamtraipat, N., J. Khedari, and J. Hirunlabh, Thermal comfort standards for air conditioned buildings in hot and humid Thailand considering additional factors of acclimatization and

education level. *Solar Energy*, 2005. 78(4): p. 504-517.

4. Damati, S.A., et al., Field study on adaptive thermal comfort in office buildings in Malaysia, Indonesia, Singapore, and Japan during hot and humid season. *Building and Environment*, 2016. 109: p. 208-223.
5. Rodriguez, C.M. and M. D'Alessandro, Indoor thermal comfort review: The tropics as the next frontier. *Urban Climate*, 2019. 29: p. 100488.
6. ASHRAE, Standard 55: Thermal environmental conditions for human occupancy. 2017: Ashrae Atlanta.
7. ISO, I.O.f.S., ISO 9920: Ergonomics of the thermal environment — Estimation of thermal insulation and water vapour resistance of a clothing ensemble. 2007.
8. Underground, W., Jakarta, Indonesia Weather History. 2019.
9. Underground, W., Singapore, Central Region, Singapore Weather History. 2019.
10. Underground, W., Bangkok, Bangkok Metropolitan Region, Thailand Weather History. 2019.
11. American Society of Heating, R.a.A.-C.E., ASHRAE Standard: Ventilation for Acceptable Indoor Air Quality. 1989: American Society of Heating, Refrigerating and Air-Conditioning Engineers.
12. Eco-Business. Freezing in the tropics - Asean's air-con conundrum 2018 [cited 2019 22 December 2019]; Available from: http://www.eco-business.com/media/uploads/freezing_in_the_tropics.pdf.
13. Griffiths, I.D. and C.o.t.E. Communities, Thermal Comfort in Buildings with Passive Solar Features: Field Studies. 1991: Commission of the European Communities.
14. Humphreys, M.A., H.B. Rijal, and J.F. Nicol, Updating the adaptive relation between climate and comfort indoors; new insights and an extended database. *Building and Environment*, 2013. 63: p. 40-55.

Exploring Potentiality of Lightpipe: Daylighting Deep Plan Office Buildings in Dhaka

SHAJIB PAUL¹, DR. MD ASHIKUR RAHMAN JOARDER², SAJAL CHOWDHURY¹

¹Department of Architecture, Chittagong University of Engineering and Technology (CUET), Chittagong, Bangladesh

²Department of Architecture, Bangladesh University of Engineering and Technology (BUET), Dhaka, Bangladesh

ABSTRACT: With rapid development, commercial and economic activities increase to accommodate a large number of office spaces and buildings in Dhaka. Deep plans are a common practice in middle and high-rise office building designs and large open plans are preferred office layout by modern businesses due to the flexibility of the space and economic benefits. Daylight produces positive effects, both physiological and psychological. The deep core areas of office buildings are often difficult to be naturally illuminated by side windows, and depend entirely on electricity for illumination. Lightpipes are innovative devices able to transport and distribute daylight in dark rooms. To explore the possibilities of installing lightpipes, experimental scale models and parametric computer simulation analysis by 'EnergyPlus™' with Openstudio plugin is used in this research to study different design parameters, e.g. length and width, number and position of lightpipes for effective use of daylighting. Results indicate combination of artificial light and lightpipe can ensure standard illumination at deep spaces of offices. It is expected that the design strategies and recommendations from this research will improve the luminous environment of deep plan office buildings in Dhaka.

KEYWORDS: Lightpipe, Daylighting, EnergyPlus™, Scale Model, Office Building.

1. INTRODUCTION

Many of the existing high rise office buildings in Dhaka are constructed too closely that the gap between two buildings is not enough to allow daylight from side windows, even though the building codes and setback rules set by the city authority (RAJUK) is followed. Contextual physical, environmental and socio-cultural effects on the overall condition of the city has been neglected [1, 2] in these cases. The buildings which are designed and constructed in such a way where little daylight may enter at the peripheral portion of the buildings; middle portion of the floor areas often deprived of daylighting. Skylight is only applicable to top floors, but not at the intermediate levels. The intermediate floor areas that are deprived of daylight, driving the occupants to rely on artificial lighting that increases energy consumption. From the year 2005 to 2011, electricity consumption of Dhaka city has been doubled [3]. Effective office space design is a challenging issue in case of building design to ensure effective inclusion of daylight as it embraces varieties of activities and users with different age groups.

Innovative daylighting strategies seek to break the conventional strategies barriers and 'guide' daylight beyond their limits to the remote zones and windowless spaces, whether in new or existing buildings [4]. Tubular daylight guidance systems (DGS) are linear structures that channel daylight utilizing optical interactions into the core of a building, with minimal impacts on the building design [4-6]. The installation of tubular lightpipe system

could be a brilliant solution that may ensure the quality working environment, energy saving, reduction of costs and effective space management [7]. The objective of the research is to evaluate the potentiality of lightpipe to initiate standard illumination levels in the deep office spaces in the context of Dhaka.

2. METHODOLOGY

Possibilities of installing lightpipe are explored, first by observing the daylight inclusion pattern of different lightpipes with experimental scale models. Then parametric computer simulation studies are conducted for a space (18m x12m) by EnergyPlus™ with Openstudio plugin. Several parametric simulations are done by changing different parameters such as length and width. Number and position of lightpipes on the same space to achieve effective use of daylighting.

The case office space is selected by a field survey. A total number of ten offices were surveyed from different locations of Dhaka [8]. The survey covered a broad area through a questionnaire about the physical characteristics of the offices of Dhaka such as area lighted with daylight and lighted with artificial light, heights of openings and types, and health symptoms of the employee of the offices. The case office building should represent the trend of typical office design in Dhaka and internal layout of the case office space should be such that, there should be provision for daylight inclusion near openings along

with deep areas where direct sunlight cannot reach by side openings.

According to the above criteria the nine storied Oposonin Building (Corporate office of Oposonin Chemical Industries Ltd, Dhaka) is selected for detailed examination and simulation study [8]. The 5th floor of the building is chosen as the case space for a detailed experiment (Figure 1). This floor is one of the typical levels, the plan of which is repeated on other floors. The building has a 7m wide road on the west, some single-storied semi-pucca establishments on the east, another nine-storied building 2.5 m from the northern edge and 2.5 m from the south is a three-storied building. There is a four-storied building and some greenery just opposite the road in front of the office building (Figure 2).

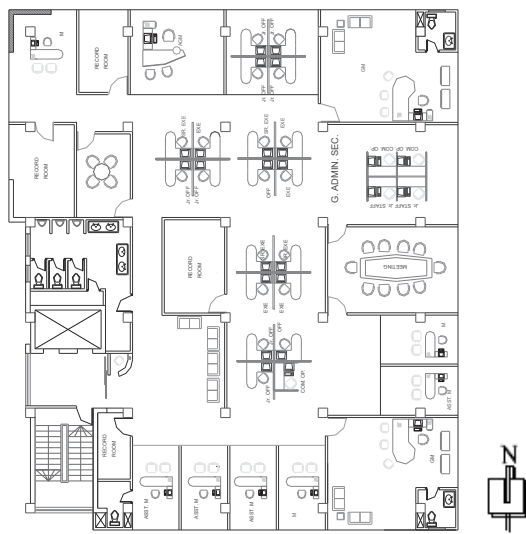


Figure 1: 5th floor plan of Oposonin building

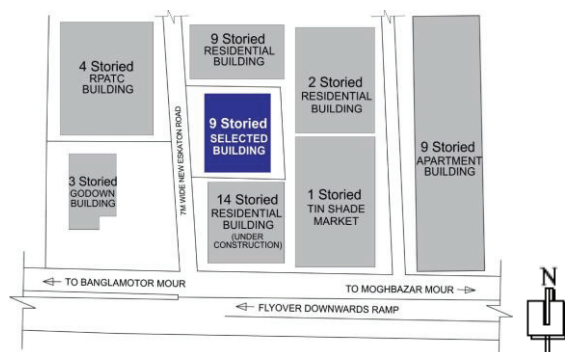


Figure 2: Location Map (With Site and Surroundings)

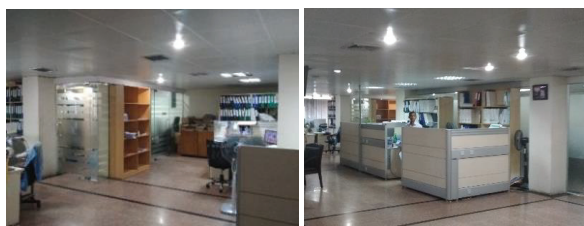


Figure 3: Interior view of the case space

Tubular daylighting devices (TDDs), also known as tubular skylights or lightpipes, are used to bring

daylight into the hard-to-reach, interior spaces of the case space. TDDs consists of three components: a dome, a pipe and a diffuser (Figure 4).

In EnergyPlus™ each of these components corresponds to an object in input file. The dome and diffuser are defined in the same way as windows using the fenestration surface detailed object. The surface type field specified as tubular daylight dome or tubular daylight diffuser accordingly.

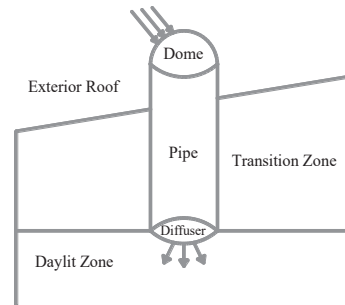


Figure 4: Tubular daylighting device diagram

The location and orientation of the dome surface affect the total amount of daylight collected. The base surface of the diffuser object determines to which zone the daylighting is delivered. The location and orientation of the diffuser surface affect the amount of daylight received at the daylighting: controls reference points.

Although the object definition is the same as for a window, there are several restrictions on tubular daylight dome and tubular daylight diffuser objects in EnergyPlus™ that is followed in this research as following [9].

- No outside face environment, objects, shading control devices, frames and dividers are installed.
- Multipliers are 1.0.
- Dome, diffuser, and pipe areas (as given by diameter) are approximately equal.
- Dome and diffuser constructions are in one layer
- The actual TDD projects some height above the roof surface is located to the tubular daylight dome coordinates.

3. EXPERIMENTAL STUDY

The experimental study is conducted in two phases. In the first phase a single-story building model in 1:60 scale is made with thick white paper. The model (2mx1m) height is 1m (Figure 5). The model is placed outdoor where the sunlight comes uniformly. Observation is done by modifying the model wall and roof. Daylight illumination is measured by a lux meter (Dr.meter-LX1330B).



Figure 5: Model for experiment 01

In the second phase, a multi-storeyed model in 1:100 scale is made with thick white paper to observe daylight inclusion pattern by lightpipe. The model is built with half of the previously selected open office area (18m x 12m) whose length is 9m and width is 6m. Each floor height of the model is 3.6m and the total height is 10.8m. The model is built considering the surveyed floor and it is a part of the real space, maintaining the scale of the model as comparable to the real scaled floors. A reflective paper is used as the inner side material of the lightpipes and the cross-sectional area of the tube is 6.25 cm² (2.5cm x 2.5cm). Observation is done by modifying the length and direction of lightpipes.

3.1 Inclusion of daylight by straight lightpipe

Firstly two lightpipes are built with paper whose inner side is with the reflected surface. The length of the pipes is different to observe different situations. One pipe connects the roof to the ground floor and other connects the roof to the 1st floor. This experiment is done in an indoor environment by artificial light. When artificial light is on, a significant amount of light travelled through the lightpipes and it reached to respective floors by both tubes (Figure 6).

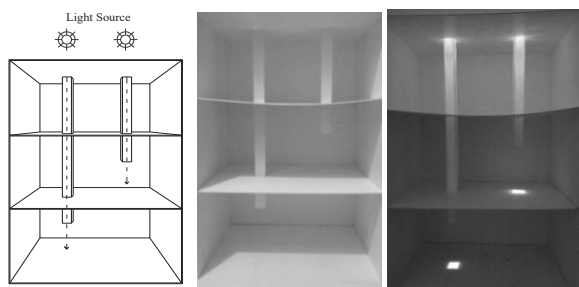


Figure 6. Model for experiment 02 (Straight Pipe)

3.2 Inclusion of daylight by bending lightpipe

At this stage, one lightpipe is started at the roof, bend 90 degrees at the 1st floor level and bend 90 degrees again before entering at ground floor (Figure 7).

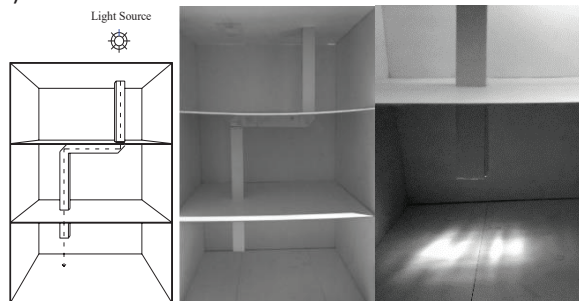


Figure 7. Model for experiment 02 (Bent Pipe)

This experiment is done in indoor environment by artificial light. When artificial light is on, light travelled through the lightpipe and it reached the ground floor by bending lightpipe.

3.3 Observation from the experiments

The target of the experimental setup as well as the scaled model study is to observe the daylight inclusion pattern in different spaces of the office by side openings and by lightpipes where daylight cannot reach by windows and roof. The findings of the experimental set are summarized as following.

- Light comes through the peripheral sides of office by side windows (if there are no obstructions) on any floor. If the window height is "h", direct daylight reach at the distance of "2h".
- The centre of office at intermediate floor can be illuminated by installing lightpipes, where there is no provision of entering daylight from side windows or roof.
- Straight lightpipe should be used where there is no obstruction on the upper floor of the target space.
- Light can be penetrated by bending of lightpipe where there are some obstructions at the upper floors of the target space.

4. SIMULATION STUDY

Simulation model is created only with the open office area of case office where direct sunlight cannot be entered and with vacant interior space without any partitions or furniture, to avoid the effects of such surfaces, which both block and reflect daylight (Figure 8).

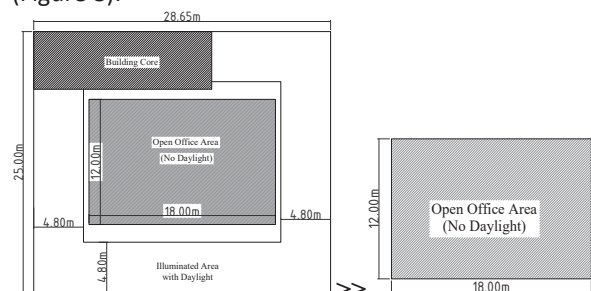


Figure 8: Model plan generation from selected office area

The other parameters of the model of case space are as following.

Selected Office Floor

5th floor dimensions	: 25m X 28.65m
Total floor area	: 692 sqm
Open office area	: 216 sqm (12m X 18m)
Clear height of space	: 3m (without false ceiling)
	: 2.4m (with false metal ceiling)
Work plane height:	: 0.75 m above floor level
Glass specification	: Thickness: 10mm.
	Conductivity: 0.9 W/m-K.
	Visible Transmittance: 0.55.
	Solar Transmittance: 0.775.
	Density: 160 lb/ft ³

Simulation Model

Simulation area	: 216 sqm (12m X 18m) [Open office area]
Simulation model height	: 3.5m
Transition floor height	: 3.5m
Work plane height	: 0.75 m above floor level

EnergyPlus™ Parameters

Version	: 8
Location	: Dhaka(time zone +6)
Month	: 6 [June]
Day type	: Summer design day
Simulation time	: 12 Hours(6 am to 6 pm)
Max. dry bulb temp.	: 36°C
Sky model	: Clear sky

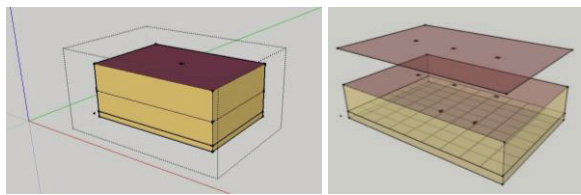


Figure 9: View of models used for the simulation.

In the simulation model there is an illuminance plane with 100 illuminance point to measure daylight at the work plane height (Figure 9). Commonly it is found that maximum light entered in the middle of the day-that is at 12.00 pm. For this reason, the illuminance analysis of every case was considered at 12.00pm. There is also two daylight reference points named “Daylighting Reference Point 1” and “Daylighting Reference Point 2” (Figure 10 and 11). Daylight is measured at both the points.

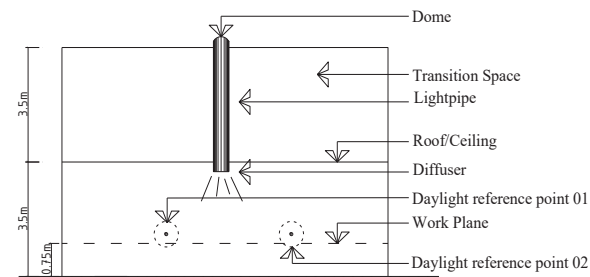


Figure 10: Typical section of one straight lightpipe

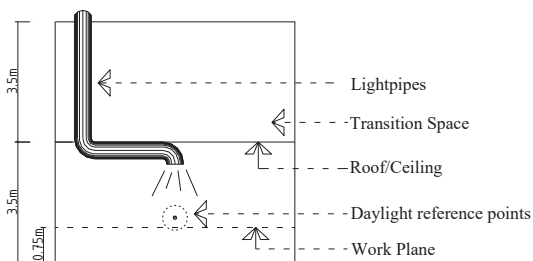


Figure 11: Typical section of one bending lightpipe

Simulation is done for both straight and bending lightpipes. Results for straight lightpipes are presented in three segments by changing three variables: lightpipe diameter, lightpipe length and lightpipe number.

Simulation results of the bending lightpipes are presented in two segments by changing two variables: lightpipe length and lightpipe number. The diameters of lightpipes start from 0.25m and end with 0.5m. The lengths of the lightpipes are varied according to floor heights such as one-floor height (3.5m), two-floor height (7.0m), three-floor height (10.5m) and four-floor height (14.0m). Variation of diameter and length are determined from the varieties of lightpipes available in market and used by previous researchers [10].

Lightpipe of 0.5m diameter is found with the highest illuminance and kept fixed during other parametric simulations of lightpipes at bending position (Figure 11). Bending angle is fixed at 90° for all cases.

Figure 12 shows the light levels at the 100 points of the illuminance plane of the simulation model at 12.00pm for the lightpipe of 0.25m diameter and shows that daylight can only illuminate at the center of space and constantly decreases at the periphery areas. The brightest level of light (165 lux) is found at the center of the space and the light located at the periphery area is lower (less than 50 lux). The average light is only 20 lux and the standard deviation is 31 lux. The median is 7 lux. The uniformity ratio below the light at work plane is 0.4. A total of 24 nos of the simulations are done with varying different perimeters following same methods [8].

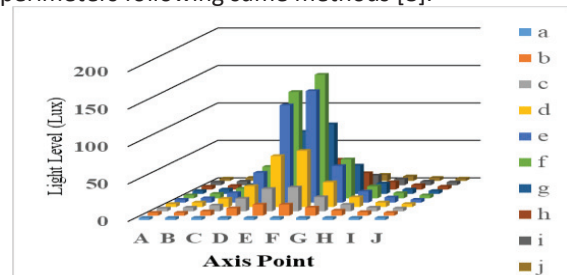


Figure 12: Daylighting distribution for 0.25m diameter

4.1 Simulation analysis: diameter (straight lightpipe)

Figure 13 shows the daylight levels at the central part of the illuminance plane for different diameters of lightpipes with the simulation model (deep part of the office floor). From these data, it is observed that penetration of light increases with the increasing diameters of lightpipes; however, the amount of increase is little. The maximum illuminance found with the lightpipe of 0.50m diameter and minimum illuminance found with the lightpipe of 0.25m diameter.

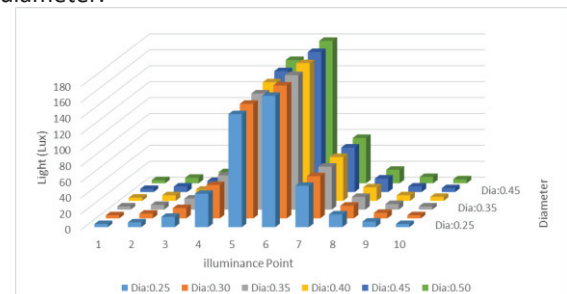


Figure 13: Daylight variation of different lightpipe diameters

The uniformity ratio below the lightpipes at work plane varied from 0.36 to 0.37. Daylight entered into the office space at the same ratio by the time (hour) and reached the maximum level at 12.00 pm. After 01.00 pm, it starts to decrease and arrive at the minimum level at the end of the office time (06.00 pm).

4.2 Simulation analysis: length (straight lightpipe)

Figure 14 shows the daylight levels at the central part of the illuminance plane for various lengths of light pipes with simulation model. From these data, it is observed that the difference in amount of daylight entered by lightpipe of different length is little. Maximum daylight entered by the lightpipe of 3.65m length; and minimum daylight found by the lightpipe of 14.60 m length. The uniformity ratio below the lightpipe at work plane was found 0.36. Daylight entered into the office space at the same proportion by the time (hour) and reached the maximum level at noon (12.00 PM). After 01.00 PM, it starts to decrease and reached the minimum level at 06.00 PM (end of the office time).

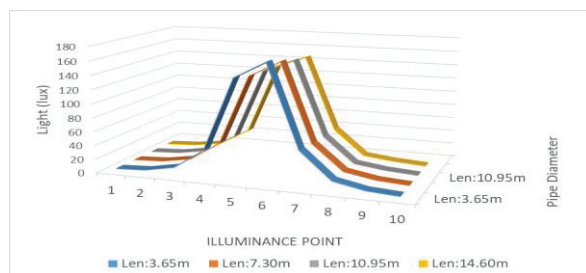


Figure 14: Daylight variation for different lightpipe lengths.

4.3 Simulation analysis: lightpipe numbers (straight lightpipe)

Daylight levels at simulation model at the central part of the illuminance plane shows that increasing number of lightpipes results increase in illumination (Figure 15).

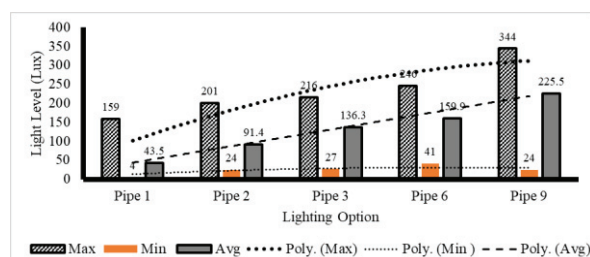


Figure 15: Daylighting distribution of straight lightpipes

Maximum daylight is found with nine lightpipes in the maximum illumination points of the illuminance plane. The standard light level (>300 lux) is found in two locations under the lightpipe and the average daylight level is 225 lux (below standard level). It can be stated that nine lightpipes are not enough to ensure standard luminous environment. It can be achieved by installing more lightpipes or adding artificial lights.

4.4 Uniformity ratio (straight lightpipe)

The uniformity ratios found for different numbers of lightpipes are shown in Table 1. The ratios increase with the increased numbers of lightpipes. The uniformity ratio of three pipes and six pipes have met the standards of the ratio most accurately which is $\geq 0.60\%$.

Table 1: Uniformity ratio for Straight lightpipe

Pipe No.	1	2	3	6	9
	Pipe	Pipes	Pipes	Pipes	Pipes
Uniformity Ratio	0.36	0.48	0.65	0.68	0.91

4.5 Simulation Analysis: Length (Bending Lightpipe)

Daylighting levels at the central part of the illuminance plane for different lengths of bending light pipes with simulation model shows that the highest illumination found under the diffuser and decreases with the distance from diffuser (Figure 16). Maximum daylight entered by lightpipe of 3.5m length and minimum light found by the lightpipe of 14.0 m length; however, the difference of the amount of daylight entered by lightpipe of different lengths are little. Daylight entered into the office space at the same ratio by the time (hour).

The uniformity ratio below the lightpipe at work plane found 0.37 for all cases.

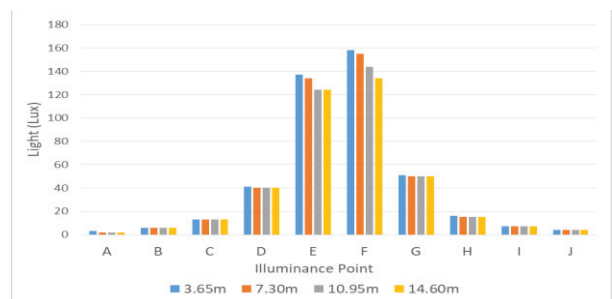


Figure 16: Daylight variation for different lightpipe lengths

4.6 Simulation analysis: lightpipe numbers (bending lightpipe)

Daylight levels at the central part of the illuminance plane for different light pipe numbers with simulation model shows that amount of daylight increases significantly with the increasing number of light pipes (Figure 17).

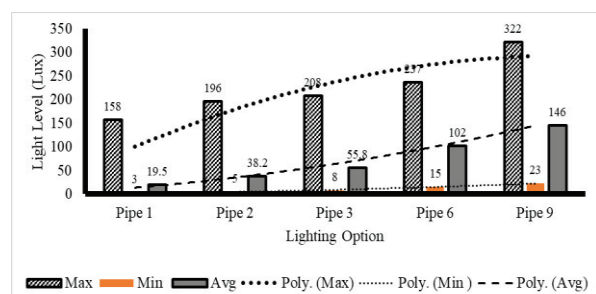


Figure 17: Daylighting distribution for bent lightpipes

Maximum daylight is found with nine bending lightpipes in maximum illumination points of the illuminance plane. As in maximum points' illumination are higher than 300 lux (standard light level) and the highest daylight level found is 708 lux, which may create over lighting and glare. The average light level is 344 lux. Simulation with six bending lightpipes are given more preferred daylight according to the illumination requirement with, few over illuminated points. Average daylight level with one pipe to three pipes do not meet the standard daylight levels.

4.7 Uniformity ratio (bending lightpipe)

The uniformity ratios found for different numbers of lightpipes are shown in Table 2. The ratios increased with the increasing numbers of lightpipes. The uniformity ratio of six pipes and nine pipes meet the standards of the ratio most accurately which is $\geq 0.60\%$.

Table 2: Uniformity ratio for bending lightpipe

Pipe No.	1 Pipe	2 Pipes	3 Pipes	6 Pipes	9 Pipes
Uniformity Ratio	0.37	0.45	0.58	0.65	0.77

4.8 Observation from the simulation models

The following observations are made after performance analysis of the experimental parametric simulation study.

- The illuminance is higher under the lightpipes and daylight decreases at the edge of the space.
- The maximum daylight enters at 12.00 pm (2015 lux) to 01.00 pm (1228 lux) through a single straight lightpipe.
- The penetrated daylight increases with the increasing diameters of lightpipes, maximum light found with the lightpipe of 0.50m diameter.
- As the penetrated daylight decreases with the expanding length of lightpipes, maximum light found with the minimum length of lightpipe which is found 3.5m.
- Uniformity ratio met the standard for simulation with three lightpipes for selected area.

5. CONCLUSION

Due to the limitation of energy resources, ever-increasing energy prices and global warming, the necessity to reduce the energy consumption in the buildings is an essential issue in developing countries such as Bangladesh. In such a context, it is needed to develop the use of daylight in deep spaces of office buildings and the efficient design of lightpipes can address these issue significantly. The amount of daylight increases considerably with the increased number of lightpipes. The combination of artificial lights and lightpipes can ensure a standard lighting environment at the deep spaces of office buildings. It is expected that the design strategies and recommendations from this research will improve the

luminous environment of deep areas of office buildings in Dhaka.

The present research work focuses mainly on the performance of lightpipe to improve the daylighting condition of the office building in the context of Dhaka.

In the tropics, with the daylight unwanted heat may enter and too much daylight may cause glare. This study concentrates on strategies for daylight inclusion into the office's task spaces. Besides improving the luminous environment, daylight inclusion is also associated to aesthetics, energy consumption (electric lighting, mechanical heating and cooling), heat loss and gain, sound transmission, economics, glare control, ventilation, safety, security and subjective concerns of privacy and view. Considering time and resource constraints for the research, the consequence of daylight inclusion on the previously mentioned concerns is however, beyond the scope of this paper.

ACKNOWLEDGMENTS

This work has been carried out at the Department of Architecture, BUET. The authors gratefully admit the support and facilities provided by BUET.

REFERENCES

1. Iqbal, A. and Khan, M. (2005). Tall buildings in the urban context of Dhaka city, in *CTBUH 7th World Congress*. Council on Tall Buildings and Urban Habitat, October 16-19. New York.
2. Hafiz, R. (2000). High-Rise Residential Buildings and the Urban Environment: A Study in Dhaka, *PLEA 2000*, UK.
3. Mondal, M. A. H. and Denich, M. (2010). Assessment of renewable energy resources potential for electricity generation in Bangladesh, *Renewable and Sustainable Energy Reviews*, 14(8), p. 2401–2413.
4. Carter, D.J. and Marwaee, M.A. (2008). User attitudes toward tubular daylight guidance systems. School of Architecture, University of Liverpool, Liverpool, UK, July.
5. Mayhoub, M.S. and Carter, D.J. (2012). How Hybrid Lighting Systems can be integrated into Building Design? 28th Conference, *Opportunities, Limits & Needs Towards an environmentally responsible architecture*, Lima, Perú, November 7-9.
6. Mayhoub, M.S. and Carter, D.J. (2011). The costs and benefits of using daylight guidance to light office buildings, *Building and Environment*, Vol. 46: p. 698-710.
7. Malet-Damour, B., Boyer, H., Fakra, A.H. and Bojic, M. (2013). Light Pipes Performance Prediction: inter model and experimental confrontation on vertical circular light-guides, 2013 ISES Solar World Congress.
8. Paul, S. (2019). An Investigation of Dual Ducting System for Daylighting Office Buildings in Dhaka, *Unpublished M.Arch Thesis. Department of Architecture, BUET, Dhaka*.
9. Input Output Reference — EnergyPlus 8.3 (<https://bigladdersoftware.com/epx/docs/8-3/input-outputreference/groupdaylighting.html#daylightingdevicetubula>).
10. Mayhoub, M.S. (2014). Dualducting: An innovation to increase the use of daylight in buildings, *Lighting Res. Technol.* Vol. 47: 2015; pp. 712–729.

Embodied Carbon: A Brettstapel Passivhaus in the UK

DİLEK ARSLAN¹, FIONN STEVENSON¹, SAM FOSTER², SANDY HALLIDAY³
IAN NIMMO⁴, ANNE NIMMO⁴

¹The University of Sheffield, Sheffield, UK

²Sam Foster Architects, Dunfermline, UK

³Gaia Group, Edinburgh, UK

⁴Home Owner, Scottish Borders, UK

ABSTRACT: In order to achieve net zero carbon by 2050, significant reductions must be achieved in embodied energy and carbon emissions from construction materials as well as operational energy demand in buildings. In this research, a unique timber Brettstapel Passivhaus case study demonstrates the effectiveness of glueless timber to improve building performance. The mixed methods used included a home tour, photo survey, interviews and Revit plug-in H\B:ERT for the calculations. Carbon intensities are taken from ICE V3.0 materials database and EPD reports. The results show that Brettstapel is an effective construction technique to help lower the embodied carbon in buildings, and the overall energy demand in the operational phase is lower than the Passivhaus standard.

KEYWORDS: Embodied Carbon, Embodied Energy, Passivhaus, Timber, Brettstapel

1. INTRODUCTION

The Climate emergency is a global challenge just now and for future generations. According to the IPCC, a temperature rise of +1.5 degree is likely, making the environment difficult to live in [1]. To avoid this, UK Greenhouse Gas (GHG) emissions are legislated to decrease by 50% by 2030 and to net zero by 2050 from a 1990 baseline. The building industry uses 45% of global energy production, producing a third of its carbon emissions [2] suggesting that a significant decrease in the embodied material energy and carbon emissions is required.

The latest RIBA policy is for new buildings to be net zero carbon and with a very low energy demand [3]. Standards are helpful to meet the above targets. The Passivhaus standard, increasingly used in the UK, has proven improved performance compared to other approaches [4].

Despite these efforts to mitigate climate change, there is little account taken of the impact of construction materials and their embodied carbon emissions, especially in Passivhaus projects where associated recurring embodied energy can be up to half of the life cycle energy of a building, and is vital to reduce in the sector [5].

In this research, a case study was used to evaluate, a unique timber Brettstapel Passivhaus in terms of using timber to improve building performance and decrease the embodied carbon. This case study was the subject of a previous POE study [6] which this paper builds on. Mixed methods are used in this paper to demonstrate a concrete understanding of findings based on real life applications.

2. LITERATURE REVIEW

2.1 Embodied Energy and Carbon

Embodied energy and carbon assessments define the material life cycle boundary as either: *cradle to gate* (material extraction from source to factory gate); *cradle to site*, (additionally including transportation to the construction site); *cradle to grave*, (additionally including in-use, maintenance and demolition); and lastly *cradle to cradle* (including reuse, recovery and recycling). Embodied carbon calculations are here based on the *Cradle to Gate* system boundary, which has the greatest data on intensities availability and because cradle to grave and cradle to cradle have many assumptions which affect reliability [7].

Defining the boundary for embodied energy varies considerably in literature. Dixit et al. [8] considers the demolition and waste disposal processes energy while Chau, Leung and Ng [9] just consider extraction, production, transportation to the site and constructional energy as initial energy. Another concern for embodied energy is that the energy sources used in material production often do not include renewable energy and it is not clear whether higher or lower heating figures are applied for the energy values [10].

Carbon emissions can be significantly decreased through the appropriate material choices [11]. Careful material selection during the design process is thus vital. Low impact materials like timber or highly recyclable materials like reclaimed brick significantly decrease the carbon emissions [12].

Due to limited data availability for embodied energy calculations, and the importance of climate

change mitigation, the focus here is on embodied carbon emissions.

2.2 Embodied Carbon Calculation Methods

There are three different assessment methods widely used in literature: Process, Input-Output and Hybrid Analysis.

Process analysis defines the specific carbon/energy of materials during the production stages but excluded steps (e.g. manufacturing machinery) might affect the data reliability [13]. Input-output analysis uses national cost data for products and their energy/carbon intensity. Its limitation is the variation in transactions and age of the data. Hybrid analysis is the combination of input-output and process analysis, which helps to overcome the limitations of the previous methods and provides more reliable data. However, subjectivity and time constraints can still be a limitation for this method.

Although the hybrid analysis method is superior to other methods, due to data availability, the process analysis method was used in this study.

2.3 Passivhaus and Principles

Rigorous standards can decrease energy demand in-use improving the energy performance of the buildings. Passivhaus requires a maximum of 15 kWh/m²/pa for heating and cooling and 120 kWh/m²/pa for the primary energy consumption. It is based on building fabric efficiency and exceptional air tightness.

The Passivhaus standard is proven to significantly reduce operational energy demand [14]. However, it does not usually include the embodied energy. This means a Passivhaus building can still have high overall energy consumption due to the material choices which can account for 20-50% of the total lifecycle energy of the building [5]. This is a weakness in the current standard, which this study addresses.

2.4 Timber Material and Brettstapel

Timber is widely used in building construction. It is easy to source as a low carbon highly recyclable and reusable, low impact material. It also has a relatively low thermal conductivity compared to other structural materials. Despite the upwards trend for use of the home-grown timber, 80% of UK timber supplies still come from other countries [15]. There are also concerns about deforestation and the flammability of timber. However, forest management strategies such as FSC certification and legislation for fire protection, such as Eurocodes, address these issues.

The Brettstapel technique uses timber as a combined structural and insulation element without any glue or adhesives. The design principle is based on the moisture content of the different structural

elements; posts have 15% and dowels have 8% [16]. The exchange in moisture levels cause expansion in the dowels to snugly fit into the panel holes. The benefits of this system are; (1) low grade home grown timber can be used; (2) more carbon is sequestered than for an average timber frame structure; (3) it provides high levels of air tightness with extra layer of moisture resistant sheathing boards, low level of thermal conductivity and good level of air quality; (4) it decreases the labour needed during the construction process.

The first Brettstapel Passivhaus home in the UK is investigated here as an 'exemplar' case study to address the research gap in relation to the embodied carbon emissions in timber Passivhaus homes.

2.5 Databases

Various embodied carbon and energy databases are available. WRAP's UK database includes only building level carbon data rather than individual material carbon information. The Athena Lifecycle Inventory is based on ISO standard procedures but focuses on North American carbon data, and is not relevant for the UK context. The ICE database V3.0, EU Environmental Product Declarations (EPD) and UK conversation factors from DEFRA databases were used to establish the materials' energy intensities in this study. ICE is based on process lifecycle assessment and cradle to gate (A1-A3) boundary conditions. Unfortunately, the embodied energy data for the materials are no longer available and some materials are missing in the latest version. EU EPD reports were thus used to compensate for this.

EPD is an eco-labelling system which is based on Product Category Rules and ISO 14025 standard. It provides life cycle impact data directly from the manufacturer. The reports for up to five years providing relatively current data for the calculations.

UK Government Conversation Factors for converting cumulative operational energy data to carbon are chosen here, rather than UK Standard Assessment Procedure (SAP) figures, since they are updated every year according to changes in fuel mixes.

2.6 Embodied Carbon Software

In this study a novel Revit software plug-in H\B:ERT was used to assess materials' carbon intensities. The advantages of this plug-in are that it provides material carbon emissions individually, and also shows the total emissions during the design modelling process.

3. METHODS

A case study method examines real-life situations and is a useful for understanding new phenomena in more detail [17].

A mixed method approach collected data as follows; a home tour by the researcher to identify any contradictions or changes between the construction and technical drawings, interviews with both occupants and the architect to understand their experiences of using the materials in the construction process and as lived with. Further documentary analysis and photo survey methods revealed how the building is constructed in reality. Lastly, embodied energy and carbon calculations were combined with energy in use calculations to show the overall house performance.

The superstructure of the house was modelled with H\B:ERT and the material specifications such as densities, volumes and weights extracted from the programme. To avoid the risk of double accounting, the materials were defined individually according to their functions. As the plug-in is based on the ICE V2.0 database, more updated and reliable data, material information was also taken from the new ICE V3.0 database. Additionally, Environmental Product Declaration (EPD) reports provided material data missing in the latest database. For the substructure, a bill of quantities provided from the architect was used with calculations combining ICE V3.0 and EPD for the embodied carbon emissions on an Excel spreadsheet.

Energy meter readings (electricity), amount of wood used (wood stove) for one year and solar thermal (hot water) energy generation data were collected from occupants for the energy in use calculations, and converted to carbon emissions. The Passivhaus standard was converted to carbon to compare and contrast the overall in use and embodied carbon data.

4. CASE STUDY: PLUMMERSWOOD

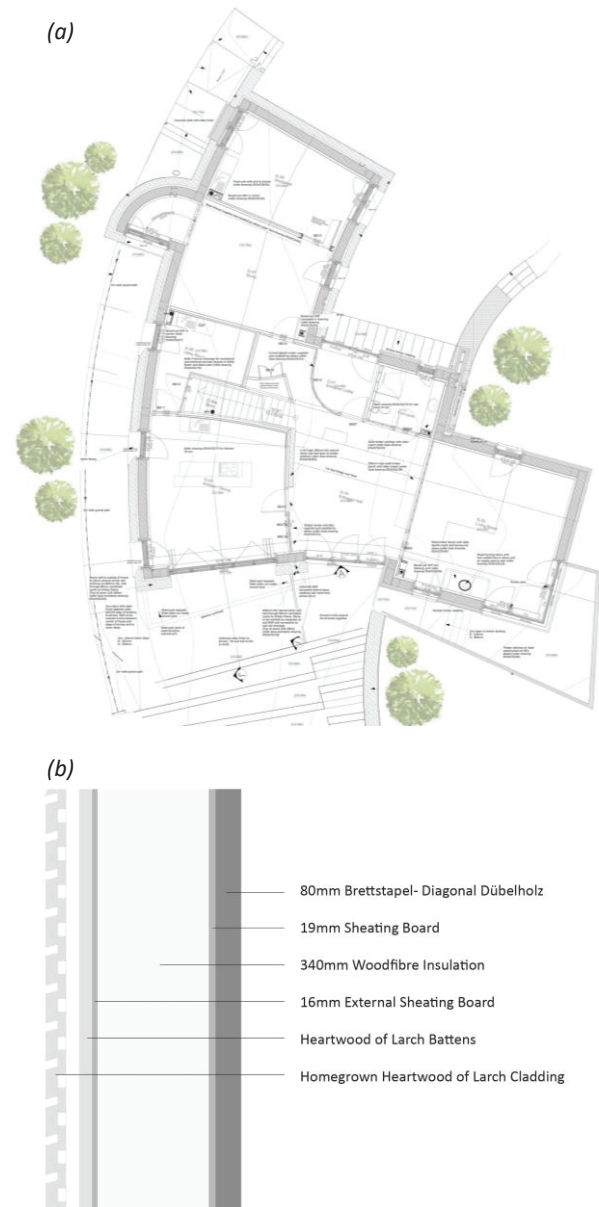
Plummerswood is a three bedroom detached Brettstapel house, located in the Scottish Borders. The house was designed by Gaia Architects and completed in 2011 (Figure 1 and 2). With no Brettstapel factory in the UK, these elements had to be transported from Austria.

Figure 1: Plummerswood House (Exterior), Scottish Borders (Dilek Arslan, 2019).



The house uses mechanical ventilation with heat recovery (MVHR- with post-heater) with no space heating other than a wood stove in the living room. There is a 5.6 m² solar thermal panel system to provide hot water for the 300 m² house. All other energy needed for the house relies on electricity.

Figure 2: Plummerswood House Ground Floor Plan (a) and Brettstapel exterior wall construction detail (b) (not to scale) (Gaia Architects, 2011).

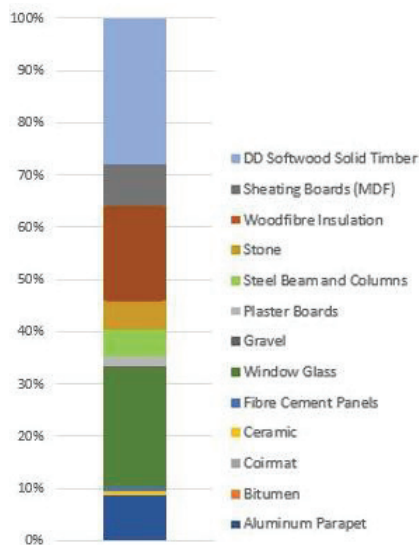


5. RESULTS AND DISCUSSION

5.1 Embodied Carbon from Materials

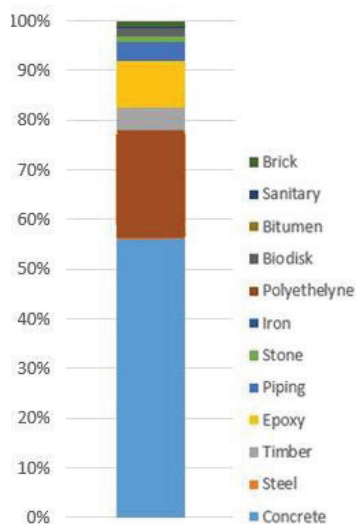
The total emission of the case study house is 452.47 kgCO_{2e}/m². The embodied carbon from the superstructure (Brettstapel) materials, modelled with H\B:ERT is 273.8 kgCO_{2e}/m². Due to the uncertainty of the end of life usage, such as landfill, reuse or recycle, the carbon sequestration capacity of the timber materials is ignored here.

Table 1: Embodied Carbon Emissions (kgCO_{2e}) of the Superstructure Materials.



As can be seen from the Table 1, the impact of the aluminium was almost same as the total for steel and stone, although the quantity was much less. Also, glass and solid timber are similar percentage because glass is a very high intensity while the volume was forty times lower than solid timber material.

Table 2: Embodied Carbon Emissions (kgCO_{2e}) of the Substructure Materials.



The substructure embodied carbon emission was $178.67 \text{ kgCO}_{2e}/\text{m}^2$, which is considerably lower than the superstructure. While steel and concrete materials were the main contributors, concrete materials formed 52% of the total carbon emissions, which is the highest percentage among the substructure materials (Table 2). However, although the resin anchors have the highest carbon intensity ($4.06 \text{ kgCO}_{2e}/\text{kg}$) their total carbon emission was low (13.74 kgCO_{2e}) as the quantity was relatively small.

The generic embodied carbon emission figures for the fixing elements such as bolts, steel plates or adhesives are noticeably higher in the ICE database, also.

Careful material replacement can significantly reduce the embodied carbon emissions from the substructure. Substituting 70% blast furnace slag for virgin concrete decreases the total carbon emission of substructure materials by 22%.

5.2 Energy In-Use

The primary energy consumption, including the energy transmission losses, from the electricity was $31.72 \text{ kWh}/\text{m}^2/\text{pa}$ for cooking and lighting, equipment, fans and pumps, hot water which is noticeably low compared to Passivhaus standard maximum of $50 \text{ kWh}/\text{m}^2/\text{pa}$ for these particular sections [18]. The renewable energy contribution for domestic hot water was $7.03 \text{ kWh}/\text{m}^2/\text{pa}$, also (Table 3). However, this value was taken from the annual energy simulation of T*SOL Pro 4.5 tool which gives an estimated figure to be careful.

Annual usage of the wood stove (10 kg per day x 175 days, pa) equates to $25.36 \text{ kWh}/\text{m}^2/\text{pa}$. This is higher than the Passivhaus requirements for the space heating. There is, however, an important misunderstanding concerning this figure. The Passivhaus standard considers either heat load ($10 \text{ W}/\text{m}^2$) or heat demand ($15 \text{ kWh}/\text{m}^2/\text{pa}$) for the space heating, which is commonly highlighted in the definition of the standard. This energy threshold can vary depending on the fuel and country context and have higher or lower values for the same heating load ($10 \text{ W}/\text{m}^2$). Therefore, the heating load from the wood stove is actually $2.9 \text{ W}/\text{m}^2$. Adding $6.6 \text{ W}/\text{m}^2$ from the post-heater and heat batteries on the MVHR, then total will be $9.5 \text{ W}/\text{m}^2$, meaning that Plummerswood meets the Passivhaus standard [19].

Table 3: Energy in Use Comparison between the Case Study House and Passivhaus Standard.

Building Energy Usage from Operational Energy Demand					
Case	Regulated Energy kWh/m^2 per year		Unregulated Energy kWh/m^2 per year		Total Energy Demand kWh/m^2 per year
Passivhaus Standard	Space Heating	Hot Water	Lighting, fans, pumps	Equipment	Cooking, catering
	15	55	10	25	15
					120
Plummerswood	Space Heating (actual)	Hot Water- Solar Contrib. (estimated)	Lighting, fans, pumps (actual)	Equipment (actual) - including hot water	Cooking, catering (actual)
	25.36	7.03		31.72	
					Total Energy Demand kWh/m^2 per year- including estimated solar
					64.11

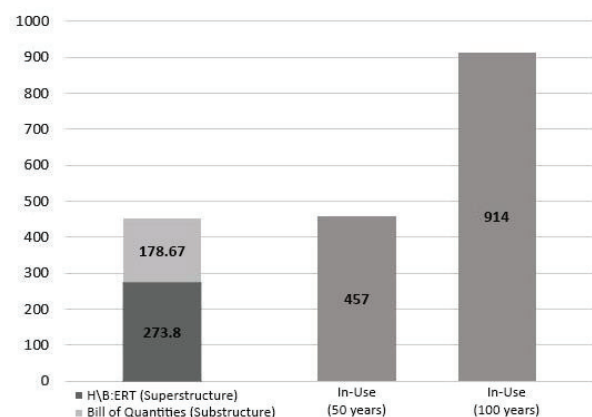
The total primary in-use energy of the house at $64.11 \text{ kWh}/\text{m}^2/\text{pa}$ is almost twice lower than the Passivhaus standard ($120 \text{ kWh}/\text{m}^2/\text{pa}$). This equates to $9.14 \text{ kgCO}_{2e}/\text{m}^2/\text{pa}$ (Table 4) and demonstrates that the cumulative carbon emissions for the house is almost equates its 50 years and half of its 100 years

operational carbon emissions (Table 5) which differs from other studies, in terms of embodied and operational carbon ratio [20]. This is because Plummerswood has remarkably good performance in operation. In the standard scenario which is 35-45 kgCO_{2e}/m² [18] for in-use emissions, the embodied carbon emissions for the house would be one fifth of its 50 years operational emissions which is relatively low compared to current studies.

Table 4: Energy in Use Carbon Emission Comparison between the Case Study House and Passivhaus Standard.

Building Carbon Footprint from Operational Energy Demand						
Case	Regulated carbon Emissions KgCO _{2e} /m ² per year			Unregulated Carbon Emissions KgCO _{2e} /m ² per year		Total Emissions KgCO _{2e} /m ² per year
	Space Heating	Hot Water	Lighting, fans, pumps	Equipment	Cooking, catering	
Passivhaus Standard	3-8	11	5	13	3-8	35-45
Plummerswood	Space Heating (actual)	Hot Water-Solar Contrib. (estimated)	Lighting, fans, pumps (actual)	Equipment (actual) - including hot water	Cooking, catering (actual)	Total Emissions KgCO _{2e} /m ² per year-actual
	0.40	0		8.74		9.14

Table 5: Comparison of embodied carbon emission (kgCO_{2e}) of the materials and carbon in-use.



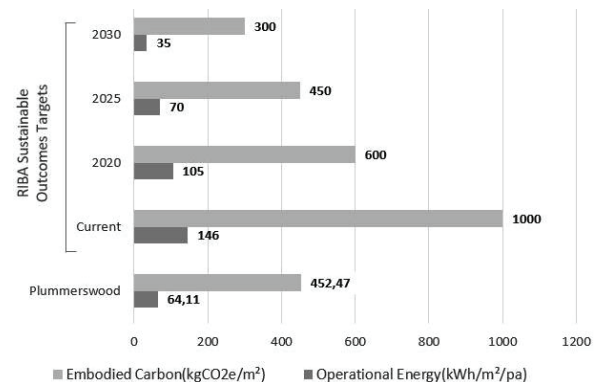
5.3 Carbon Challenges and Construction

Despite the Brettstapel building elements being imported, they still have a lower impact on the environment in terms of carbon emissions compared to other structural materials and provide fast construction, with less labour and no glue nor nailing for the joints. Significantly, the use of Brettstapel in this case study helped to lower the in-use energy to 75% less than the Passivhaus maximum. Given that the UK aims to decrease its carbon footprint to zero, choosing this system can help significantly to achieve this goal. It can be seen that, the building figures are little less than the RIBA 2025 target even though it was constructed over 10 years ago (Table 6).

Woodfibre has one of the lowest carbon emissions factor among all the construction materials in the case study. It has a good level of insulation. Insulation thickness is usually between 250-400 mm for the Passivhaus buildings to provide stable indoor

environment at 21°C. The wood fibre insulation thickness is 340 mm in the case study and achieves significantly lower energy in use figures than the standard requires. The findings from this study show that the more timber that can be used in Passivhaus building construction, the lower the embodied carbon emissions are likely to be.

Table 6: Comparison Embodied Energy (kWh/m²/pa) and Embodied Carbon (kgCO_{2e}/m²) of Plummerswood House and RIBA Sustainable Outcomes targets compared to current performance targets.



5.4 Limitations

The H\B:ERT plug-in had clear limitations during the modelling process. The materials are too generically defined in terms of density, embodied carbon. Missing materials need to be assigned by user from other sources which is time consuming. Worryingly, there are no defined products for the plumbing, sanitation, electricity services or other complex elements like bio disk units or boilers, which have to be estimated. The plug-in also needs to be updated as it uses the old version of the ICE database making it less reliable.

Another challenge during the research process was finding a reliable carbon database to calculate carbon footprint of the materials. ICE V3.0 is open source, but has less material profiles compared with ICE V2.0. The EPD reports were useful to compensate this, however it was difficult to find exactly the same product. Similar products can vary from company to company as they use different material and energy sources and transportation. Finding the EPD reports for some fixing elements proved challenging as there were no available data for them. Therefore, only the major materials were used for the embodied carbon calculations to generate approximate figures in this case. Further studies are needed to break down these individual elements and calculate them [21].

6. CONCLUSION

6.1 Summary

This paper shows that timber construction is highly effective for lowering overall carbon emissions.

In the case study, a half of the total carbon emissions of the house over a 100 year period comes from construction phase. If the house is demolished after only 50 years, this figure doubles. Using low impact materials is therefore essential for Passivhaus buildings in the UK, in order to achieve overall 2050 carbon targets. Using solid timber structure as insulation further decreases energy consumption, such that in use carbon emission of this house is remarkably lower than the Passivhaus standard.

6.2 Recommendations

More resilient data are needed for every single construction material. EPD reports are needed for every product in the sector as they provide more robust data, including both embodied energy and embodied carbon emissions of the product. There is also an urgent need for more reliable and broader databases for carbon calculations. Brettstapel should be manufactured locally using local timber where possible. Material substitution for concrete and steel substructure elements is urgently required. Further research is needed on optimal insulation thicknesses for Brettstapel elements, showing how these affect airtightness and thermal conductivity. Finally, the Passivhaus standard should include embodied energy and carbon emissions in its requirements, given the impact of these factors on overall energy consumption and carbon emissions.

ACKNOWLEDGEMENTS

This study was supported by Turkish Government. Also, we wish to thank the construction company (Sohm) for their generous help and all the information they provided during this research.

REFERENCES

- Intergovernmental Panel on Climate Change (2018). Global Warming of 1.5 °C. Switzerland: IPCC.
- Ibn-Mohammed, T., Greenough, R., Taylor, S., Ozawa-Meida, L. and Acquaye, A. (2013). Operational vs. embodied emissions in buildings—A review of current trends. *Energy and Buildings*, 66, pp.232-245.
- RIBA (2020). RIBA Sustainable Outcomes Guide. Royal Institution of British Architects, London.
- Johnston, D and Miles-Shenton, D and Farmer, D (2015) Quantifying the domestic building fabric 'performance gap'. *Building Services Engineering Research and Technology*, 36 (5): p.614-627.
- Sartori, I and Hestnes, A.G. (2007). Energy Use in the Life Cycle of Conventional and Low-Energy Buildings: A Review Article. *Energy and Buildings*, 39, pp: 249-257.
- Gaia and Arup (2014). *Plummerswood Performance Evaluation*. Gaia Publications.
- Gervasio, H. and Dimova, S. (2018). Model for Life Cycle Assessment of Buildings. [online] JRC Science Hub. Available at: http://publications.jrc.ec.europa.eu/repository/bitstream/JRC110082/report_d1_online_final.pdf [Accessed 18 Jul. 2019].
- Dixit, M. (2017). Life cycle embodied energy analysis of residential buildings: A review of literature to investigate embodied energy parameters. *Renewable and Sustainable Energy Reviews*, 79, pp.390-413.
- Chau, C., Leung, T. and Ng, W. (2015). A review on Life Cycle Assessment, Life Cycle Energy Assessment and Life Cycle Carbon Emissions Assessment on buildings. *Applied Energy*, 143, pp.395-413.
- Rasmussen, F., Malmqvist, T., Moncaster, A., Wiberg, A. and Birgisdóttir, H. (2018). Analysing methodological choices in calculations of embodied energy and GHG emissions from buildings. *Energy and Buildings*, 158, pp.1487-1498.
- Pomponi, F. and Moncaster, A. (2016). Embodied carbon mitigation and reduction in the built environment – What does the evidence say?. *Journal of Environmental Management*, 181, pp.687-700.
- WRAP (n.d.). Cutting Embodied Carbon in Construction Projects. [online] Waste and Resources Action Programme. Available at: <http://www.wrap.org.uk/sites/files/wrap/FINAL%20PRO095-009%20Embodied%20Carbon%20Annex.pdf> [Accessed 19 Jul. 2019].
- Fenner, A., Kibert, C., Woo, J., Morque, S., Razkenari, M., Hakim, H. and Lu, X. (2018). The carbon footprint of buildings: A review of methodologies and applications. *Renewable and Sustainable Energy Reviews*, 94, pp.1142-1152.
- Department for Business, Energy & Industrial Strategy (2010). 2050 Pathways Analysis. [online] HM Government, pp.101-102. Available at: https://assets.publishing.service.gov.uk/government/uploads/system/uploads/attachment_data/file/68816/216-2050-pathways-analysis-report.pdf [Accessed 9 Aug. 2019].
- Forestry Commission (2018). *Forestry Statistics 2018*. [online] Forestry Commission, pp.81-84. Available at: <https://www.forestryresearch.gov.uk/tools-and-resources/statistics/forestry-statistics/forestry-statistics-2018/> [Accessed 5 Aug. 2019].
- Henderson, J., Foster, S. and Bridgestock, M. (2012). What is Brettstapel? [online] Brettstapel Construction. Available at: http://www.Brettstapel.org/Brettstapel/What_is_it.html [Accessed 12 Feb. 2019].
- Souza, R. F. C. (2015). Case Studies as Method for Architectural Research. [online] Available at: https://www.researchgate.net/publication/314147521_Case_Studies_as_method_for_architectural_research [Accessed 23 Mar. 2019].
- Pelsmakers, S. (2016). *The Environmental Design Pocketbook*. 2nd, rev. ed. London: RIBA Publishing.
- Passipedia.org. 2020. Heating Load In Passive Houses. [online] Available at: https://passipedia.org/basics/building_physics_-_basics/heating_load [Accessed 6 August 2019].
- Iddon, C. and Firth, S. (2013). Embodied and operational energy for new-build housing: A case study of construction methods in the UK. *Energy and Buildings*, 67, pp.479-488.
- Din, A. and Brotas, L. (2016). Exploration of life cycle data calculation: Lessons from a Passivhaus case study. *Energy and Buildings*, 118, pp.82-92.

Energy-Efficient Retrofit Strategies at the Building Envelopes of Higher Educational Buildings in Mediterranean Climates

To achieve thermal comfort and energy efficiency

NERMINE ALY HANY

Arab Academy for Science, Technology and Maritime Transport, AAST, Alexandria, Egypt

ABSTRACT: Energy consumption has increased during the last decade, which contributes to high level of carbon dioxide emissions leading to climate change. The building sector has a significant role in this as their share of energy consumption is remarkably high, they are responsible for 33% of global energy. Therefore, strategies for improving buildings' energy performance become an urging demand for a sustainable future. The number of existing buildings compared to new buildings is very high. Moreover, their rate of replacement is very low. Therefore, retrofitting of existing buildings is crucial to reduce their high level of energy consumption.

This paper focuses on retrofitting of higher educational buildings' envelopes as they have unique patterns of use according to building activities, times of use and the number of users. The paper proposes energy-efficient retrofit strategies for higher educational buildings in Mediterranean climate in Egyptian cities to improve its energy performance and indoor comfort. The Department of Architectural Engineering building located at the AAST is selected as case study. Building envelope retrofit strategies were investigated and simulated to calculate energy savings achieved. Results show that the retrofit strategies applied have potential energy consumption reduction of 46.7% compared to the base case.

KEYWORDS: Building envelope retrofit, Energy-efficient retrofit strategies, Energy performance, Indoor thermal comfort, Higher educational buildings.

1. INTRODUCTION

Global climate change has been a rising issue in the last decade. Human activities have led to an alarming level of Greenhouse gases emissions (GHG) and consequently global warming. Specifically, in Egypt GHG emissions grew 133% from 1990-2012 [1]. Most of these emissions come from the combustion of fossil fuels to provide electrical energy in buildings for cooling, lighting, appliances and electrical equipment. Moreover, the International Energy Agency's (IEA) data show that Egypt's total primary energy supply more than doubled from 1990-2012. Egypt's dependence on fossil fuels is expected to continue increasing with the current social and economic development.

Energy consumption in Egyptian public buildings including administrative, commercial, educational and health buildings is (9%) of the total energy consumption in the building sector [2]. Enhancing energy performance in higher educational buildings will have a significant impact on the reduction of electrical energy consumption, resource efficiency, and the nation's energy footprint [2].

Moreover, according to the International Energy Agency (IEA) which defines energy efficiency as a method of managing and restraining the growth in energy consumption published a report by IEA'S EBCP

stating that educational buildings consume high energy and therefore their retrofit is a necessity [3]. Since, the number of existing buildings is much than the number of new ones. Also, the majority of energy used is by existing buildings and the rate of replacement of an existing building by a new one is very low around (1-3%) yearly [3]. Therefore, sustainable retrofitting of existing buildings is crucial to reduce energy consumption. Retrofit refers to any update in existing buildings that can be made either to repair any shortages in the building performance or to comply with new standards [4]. Energy-efficient retrofits would refer to improvements done to a building with the purpose of reducing its energy consumption and improving its energy performance [4].

Therefore, energy-efficient retrofits for existing buildings are a necessity. Accordingly, this paper will focus on the energy-efficient retrofitting of higher educational buildings' envelopes in Mediterranean climate in Egyptian cities as educational buildings are building types that consumes energy due to its building's activities, time of use, pattern of occupancy number of students and academic staff throughout the year. In most of the retrofit projects, there is a lack of application of energy-efficient retrofit strategies due to the lack of knowledge about the

quantity of investment required and the efficiency of the potential energy savings that could be achieved through energy-efficient retrofits.

Governments around the world have taken strong measures towards the energy-efficient retrofits of existing educational buildings in terms of improving their energy performance and improving the internal comfort conditions to improve thermal conditions and air quality inside educational spaces resulting in the improvement of educational activities [5]. The ODYSSEE database provides a comprehensive monitoring of energy efficiency trends in all sectors and priority areas to address EU policies [6]. For example in Greece, the energy consumption of educational buildings represent a significant amount of the country's total energy consumption consequently, the country is looking for alternatives to reduce energy consumption in educational buildings as an important approach for sustainability [6]. Unfortunately, this is not the case yet in Egypt and in the Egyptian universities.

Retrofitting in Egypt, especially for energy saving and energy efficiency, is a new concept which started to gain momentum in mid-2014 as a result of the electrical power shortage in the summer and frequent power cuts due to load sharing. The retrofitting actions taken at the time focused mainly on changing inefficient bulbs with CFLs or LEDs, and in some government buildings, photovoltaic (PV) arrays were installed to generate electrical energy during working hours. In general, this is not a holistic approach. Therefore, Egypt is in need of an approach or guide to be issued for retrofitting its higher educational buildings.

In educational buildings, students spend long hours in lecture halls and classrooms, labs and libraries. The relationship between indoor environmental conditions and student performance is well established [7]. Improving energy performance in educational buildings will have a significant impact on reducing electrical energy use and enhance resource efficiency and, above all, the nation's footprint.

The study presented here is intended to assess existing educational buildings to understand its energy performance with the intent of saving energy and transforming it to energy efficient using energy-efficient retrofitting strategies to address Egypt's energy challenges.

2. OBJECTIVES

The objective of this study is to investigate experimentally energy-efficient retrofit strategies for higher educational buildings envelopes to improve the indoor thermal comfort and reducing thermal energy demand during summertime through application of energy-efficient retrofit strategies. First

the study aims to present the potential energy savings in the existing building compared to the case after applying energy-efficient retrofit strategies using simulation tools.

Second, the case study is presented as an example to promote and provide guidelines for energy-efficient retrofit of higher educational buildings in Alexandria and other Mediterranean cities in Egypt. The proposed work is suitable for a considerable number of higher educational buildings in a view of global approach to the issues of retrofitting the existing educational building stock in Egypt which were built during the same time at 1990s and have the same building characteristics. Moreover, these concluded energy-efficient retrofit strategies can be set as a legislative measure for achieving energy-efficient educational spaces as it is essential to set energy-efficient and code enforced retrofit measures to be implemented on the national levels in Egypt.

3. METHODOLOGY

The study adopts an inductive methodology as it starts with defining the problem and presenting relevant practices about retrofitting of educational buildings globally. The study proceeds with an analytical part through analysis of three higher educational buildings in Mediterranean climate that have undergone through building envelope retrofit strategies in order to conclude the most commonly used energy-efficient retrofit strategies in the analysed examples that could be applied in the case study. As the study proceeds into the application part the multiplicity of challenges unfolds. Specific parameters and factors are cross-examined and checked to reveal a definite course of action and possible required interventions of energy-efficient retrofit strategies.

The paper consists of two parts; the first part presents a theoretical discourse that reviews retrofitting existing building envelopes with a special focus on approaches found in different Mediterranean cities designated to address energy efficiency and achieving thermal comfort in higher educational buildings. The second part is an experimental study applied locally on the Department of Architectural Engineering building located at the Arab Academy for Science, Technology and Maritime, Abu Qir, Alexandria Campus.

The experimental study aims to show the potential energy savings in the existing campus building compared to the case after applying energy-efficient retrofit strategies in order to test the theoretical views on pragmatic level to help in better addressing the general research problem in a local climatic context with its precise conditions and particular circumstances and this suggest adequate energy-efficient retrofit strategies to be applied on

buildings built in 1990s with same building characteristics in Mediterranean cities in Egypt.

4. LITERATURE REVIEW ABOUT EDUCATIONAL BUILDING ENVELOPES RETROFIT STRATEGIES

The literature review is divided into two parts; the first part shows different studies and researches done by previous researchers on the building envelope energy-efficient retrofit strategies for educational buildings, while the second part will explain special aspects concerning retrofitting educational buildings and the comfort requirements required for educational buildings.

4.1 Previous Research work on Retrofitting Educational buildings in Mediterranean Cities

As overheating is becoming a key problem in building design, the present study aims to investigate how educational buildings will perform in view of rising temperatures in the future and examine the implications on both energy performance and occupant's health and performance.

A study made by Ardente et al. indicated that the most significant benefits of energy consumption assessment were the improvement of envelope thermal insulations, lighting and glazing [8]. Further studies targeted the retrofitting of educational buildings in specific as in the study made by Basarir et al. on energy efficient retrofit methods at the building envelopes of the school buildings in Turkey. It was found that if retrofit is applied, annual fuel cost would be reduced approximately one-third of the current situation of the building [9]. In Tripoli, Lebanon, the energy performance of the Faculty of Architecture Engineering is studied for zero energy university buildings. Osama et al. found that retrofitting strategies in the envelope could reduce energy up to 28% [10]. In another study made by Aboulnaga et al. on sustainability of higher educational buildings in Egypt, it was found that with some retrofitting in glazing, insulation and green roof could reduce 15% electrical energy consumption from the baseline energy use [11].

Through all the previous research work done on energy-efficient retrofitting strategies, it may be concluded that there are most common retrofit strategies that were previously used which are applying thermal insulation layer, low emissivity coated window glazing and green roof applications.

However, little has been done in the context of higher educational buildings, where the typological features and use patterns are different. Thus, this paper will highlight the need to act on that particular typology, which merits an individual analysis and tailored approach.

4.2 Special Aspects of Retrofitting Higher Educational buildings

Good indoor comfort and air quality are essential for appropriate educational development considering

the long hours that students spend in buildings of this type. Moreover, the achievement of adequate comfort levels is essential in order to reduce energy consumption. A study conducted at the Polytechnic University of Timisoara (Romania), revealed that the classroom temperature affects the ability of students to grasp instruction [12]. Furthermore, a favourable learning environment correlates significantly to student involvement, teacher support, and classroom order and organization [13].

Educational buildings have many special aspects which should be considered in retrofitting plans. First, educational buildings have different age, size, and volume and can contain various space types with different optimum temperatures and activities. This diversity of floor use creates both challenges and opportunities for implementing energy-efficient retrofitting projects of varying size and scope. Second, the variety of different materials used in the educational building.

To conclude, existing educational buildings are not similar to newly built ones, as they already have geographical constraints as their selected site and orientation as well as the technical, economic, social, environmental and architectural history which gives a unique framework for the retrofitting application.

4.3 Comfort Requirements in Educational buildings

Studies have indicated a correlation between the way educational buildings are designed or retrofitted and their student's performance [14]. In fact, the educational process is strongly influenced by thermal, visual and acoustical comfort of the building which will be discussed below. Accordingly the indoor comfort of the educational buildings is a significant point to consider during energy-efficient retrofit strategies application.

First, thermal comfort is an important variable in the performance of the occupant's as teachers and students. Hot, stuffy rooms and cold, draughty ones reduce attention spans and limit productivity. In addition of wasting energy that adds unnecessary cost to the energy bills. Thermal comfort is highly affected by how classes are designed and how effectively the cooling and heating systems can meet the specific needs of that room [14].

Second, visual comfort means that the lighting quality in the spaces provides the visual tasks easier to users, such as reading and classroom presentations. Visual comfort results from a well-designed, well integrated combination of natural and artificial lighting. Retrofitting strategies aiming to improve visual comfort must target the size and configuration of both these systems [15].

Third, acoustic comfort means teachers and students can hear one another easily. If noise levels in the classroom are too high, students and teachers will lose the ability to intelligibly understand each other.

Typical sources are outdoor sounds; therefore, to achieve acoustic comfort energy-efficient retrofitting strategies must consider creating sound barriers between classrooms and exterior sources of noise [15].

The thermal, visual and acoustic comfort, and even indoor air quality are key players for comfort of educational spaces. The retrofitting process must consider and work to achieve those three variables simultaneously.

5. ANALYSIS OF HIGHER EDUCATIONAL BUILDINGS IN THE MEDITERRANEAN REGION

The study proceeds with an analytical part through analysis of three educational buildings in Mediterranean climate that have undergone through building envelope retrofit actions in order to conclude the most commonly used energy-efficient retrofit strategies in the analysed examples that could be applied in the case study.

This will help conclude the most commonly used retrofit strategies and methodology to apply in the case study to achieve energy efficiency and thermal comfort in the educational spaces.

Example 1:

-Name of project: Democritus University of Thrace,(D,U.TH.) School of Engineering [16]

-Location: Xanthi, Greece

-Project Description: It consists of four floors; the long axis of the rectangular building is oriented along the axis SE - NW, while the main façade is oriented southwest. The building includes classrooms, offices and public areas. It was constructed in 1990.

-Project Objectives: To investigate the best energy-efficient retrofit solutions to achieve minimal energy consumption for the building, while improving the desired internal occupant's conditions resulting in the improvement of educational activities.

-Energy-Efficient Building Envelope Retrofit Strategies Applied: -Application of thermal insulation at building's envelope walls, roof and floors consisting of graphite expanded polystyrene with thermal conductivity $\lambda=0,0320$ W/m K.

-Glazing upgrade from single glazing to low-e Argon filled double glazed windows taking into account the building's operating conditions.

-Results and Conclusions: The application of external thermal insulation and the glazing upgrade reduces its energy consumption by 49.69%.

Example 2:

-Name of project: University of Molise [17]

-Location: Termoli, Italy

-Project Description: It consists of four floors It is located in the north-south direction. The building shape is rectangular and consists of two rectangular blocks, connected by the stairwell. It was constructed in 1990.

-Project Objectives: The retrofit was aimed at reducing the increasing energy demands for the summer space cooling.

-Energy-Efficient Building Envelope Retrofit Strategies Applied: - Application of thermal insulation

at the external side the building envelope walls with expanded polyurethane = 0.026 W/m²K, the achieved U value is 0.22 W/m²K.

-Application of green roof, this proposed intervention involves the installation of an intensive type roof, characterized by stomata resistance equal to $120s/m$ It reduces the thermal resistances of the roof to reaching the value of 0.32 W/m²K.

-Results and Conclusions: The application of thermal insulation at the building's envelope external walls shows a yearly reduction of primary energy demand of 1.9% referred to the whole facility and all energy uses and the application of the green roof produces primary energy reduction of 1.6% in summer.

Example 3:

-Name of project: University of Basque, Architecture Faculty [18]

-Location: San Sebastian, Spain

-Project Description: It consists of 6 floors; the building is rectangular shape, where the main facade is oriented towards the southeast. The building was constructed in 1992 and the design style is based on "Tendenza", a post-modern architectural movement.

-Project Objectives: To propose energy-efficient retrofit strategies in order to become the first University in Spain to achieve the NZEB target, in order to present the best retrofit strategies where user preferences have been considered as an energy saving opportunity.

-Energy-Efficient Building Envelope Retrofit Strategies Applied:-Application of external walls insulation 10cm polystyrene.

-Application of roof insulation 10cm polystyrene

-Glazing upgrade by alternative found in the Spanish market to the north-facing windows.

-Results and Conclusions: The application of exterior insulation (10 cm polystyrene) to walls and roofs, the cooling demand for the entire building drops 4%. The application glazing upgrade reduces the energy consumption by 11%.

Table 1 shows the summary of the energy-efficient retrofit strategies used in the three analysed examples. The most commonly used strategies are external insulation of walls and the installation of double glazed window and application of green roof. These energy-efficient retrofit strategies will be applied and simulated in the case study.

Table 1: Shows the summary of the energy-efficient retrofit strategies used in the three analysed examples.

Building Envelope	Ex.1	Ex.2	Ex.3
Walls	Application of external thermal insulation	Application of external thermal insulation	Application of external thermal insulation

Roof	Application of roof thermal insulation	Application of green roof	Application of roof thermal insulation
Glazing	Low-e double glazed windows	N/A	Low-e double glazed windows

6. THE CASE STUDY: ARCHITECTURAL ENGINEERING BUILDING, AAST, ALEXANDRIA, EGYPT

-Name of project: Department of Architectural Engineering building, AAST

-Location: Abu Qir, Alexandria.

-Project Description:

The chosen case study is the Department of Architectural Engineering building located at the AAST Abu Qir campus in Alexandria constructed in 1996. The building is one of five buildings of the engineering campus complex. It is oriented along the North-East and South-West axis. It consists of four floors. Educational zones such as a library, classrooms and design studios all surrounding the building's central atrium used for natural lighting and visual connectivity. Also, the building includes other non-educational zones such as an exhibition, a multipurpose hall, administrative and lecturers' offices as shown in figure 1.

The building has a brutalism architectural style; the building facades are modularly designed. The building has three main facades and one secondary façade attached to the engineering building complex. The facade consists of a regular module of recessed glazing shaded by the extruded building elements. The building's four floors are shaded by the extruded roof slab.

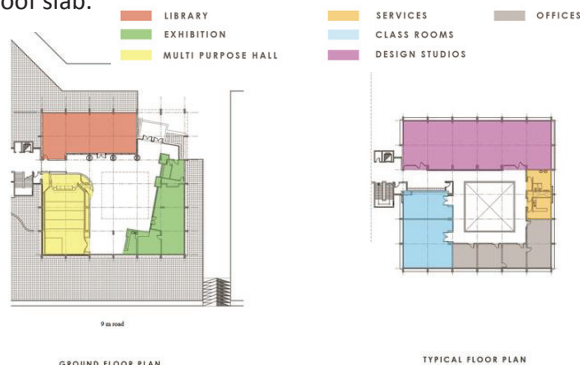


Figure 1: Showing the AAST Architectural Engineering building's ground, typical and roof floor plans. Source: by researcher

-Existing Building Envelope Conditions:

-Walls: 20 cm external brick wall without external insulation.

-Glazing/Windows: 6mm Single glazing and clear.

-Roof: Flat roof with reinforced concrete with bituminous water proofing, and screed.

-Project Objectives:

- Investigate experimentally energy-efficient retrofit strategies in attempt to improve energy efficiency in a sample of higher educational buildings in Egypt.

- Propose a suitable retrofitting strategy for higher educational buildings that could be applied in other Mediterranean cities in Egypt built during the same time and have the same building characteristics.

-Summary of Problems found through the Building's Energy Audit

- High indoor temperatures and overheating of the building's different zones in the summer time.

- Educational spaces do not provide thermal comfort for the student which has a negative impact on the educational process.

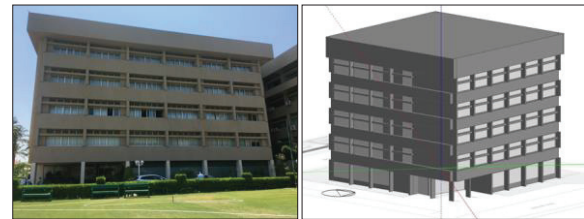


Figure 2: Showing a photo for the real building and the building model in the design builder. Source: by researcher

6.1 Case Study Methodological Steps

Step 1: A base case of the building is modelled and simulated using DesignBuilder incorporating the Energy Plus calculation engine as shown in figure 2. The location and associated weather data file is selected to simulate the building's energy performance and calculate the baseline energy consumption (kWh / m²)

Step 2: Energy-efficient retrofit strategies for the building envelope were investigated. Three energy-efficient retrofit strategies were proposed concluded from the three previously analysed examples.

Step 3: The proposed retrofit variables are simulated and the building's energy consumption is calculated.

Step 4: Comparative analysis between the energy consumption of the base case and the case after the application of retrofit strategies is conducted to find the achievable energy reduction.

6.2 Selected Retrofit Strategies

-Window glazing: Replaced from single glazed aluminium framed with a high solar heat gain coefficient (SHGC) of 0.81 and a high U-value of 4.8 W/m²K by a double glazed windows low-E Argon filled (Changing the glazing to a low-E double glazing (Solar Control-Saint Gobain Glass, Egypt, ST450—Reflecta-Sol glass) with a U-value of 1.50 W/m² K, SHGC of 0.33, light transmission of 0.38.

-Insulation: External insulation EPS external thermal insulation was chosen with thickness 0.05m.

-Green Roof Application: A green roof (GR) was applied on the accessible roof of the fourth floor to act as a heat insulator. An extensive GR type was used (U-value of 0.14 W/m² K), which requires low maintenance and which is supported by the current roof structure and characterized by a thin growing medium which is Coleus Blumei: is a reddish-green leafed plant that is commonly used in Egypt. These

plants require medium watering, it requires minimal maintenance, has low initial cost and low weight.

6.3 Simulation Results Discussion

The energy performance investigations and the impact analysis of the applied energy-efficient retrofit strategies were analysed through dynamic simulation studies by using the software Energy plus, by defining the model geometry through design builder.

For the base case the simulations show the building consumes 175.5 kWh/m². First, after the replacement of the windows to low-e Argon filled double glazed windows, the energy consumption decreased to 157kWh/m² which indicates an energy reduction of 10.28 %. Second, through the addition of external thermal insulation of 0.05m of EPS, the energy consumption simulated was 147kWh/m², results in a reduction of 16.2%. Third, the application of a green roof to the 4th floor showed the highest energy saving of 20.22% as plants can effectively reduce operative temperatures, heat gains and exterior roof temperature. The building's energy consumption recorded was 140 kWh / m².

The implementation cost of the green roof is calculated as the price of 1 m² of Coleus Blumei is LE 90. Therefore, the entire system costs 60,750 LE. This system needs to be watered every other day and requires 6 L of water/m² and therefore consumes a total of 1,080 L yearly.

By integrating of all the three previously mentioned retrofit strategies, energy reduction of 46.7% can be achieved. This is summarised in the following Table 2.

Table 2: Showing the comparison between the energy consumption kWh per m².

Retrofit Strategy	Base Case	Double glazing	External insulation	Green Roof
Energy consumption (kWh / m ²)	175.5	157	147	140
Percentage Reduction (%)	N/A	10.28	16.2	20.22

7. CONCLUSIONS

To conclude, the existing higher educational buildings building envelope's in Mediterranean cities may differ in their construction materials. However, the process and approach followed in this research can demonstrate the possibility of energy consumption reduction and achieving better indoor thermal comfort for the occupants.

This study is designed as a roadmap for energy efficient retrofit of educational building stock, through the analysis of case studies of major significance in term of building characteristics and period of construction in 1990s. The recognition of the consistency of the existing universities building stock and the subsequent selection of buildings that are representative of general conditions allowed comparing the results and drawing from them energy-efficient retrofit strategies that are applicable

to the higher educational stock in Mediterranean cities in Egypt.

REFERENCES

- [1] World Resources Institute Climate Analysis Indicators Tool (2015, November). Greenhouse Gas Emissions Factsheet: Egypt. Retrieved May 2019, from Climate Links: <https://www.climatelinks.org/resources/ghg-emissions-egypt-factsheet>
- [2] El-Darwish, I., & Gomaa, M. (2017). Retrofitting strategy for building envelopes to achieve energy efficiency. Alexandria Engineering Journal, 579-589
- [3] International Energy Agency (2016). Egypt Energy Balances data. Retrieved April 2019.
- [4] Dino, G., & Jahed, N. (2018). Performance-Based Façades: Retrofit Strategies for Energy Efficiency and Comfort in Existing Office Buildings. 13th International Conference on Advances in Civil Engineering. Turkey
- [5] Puteh M., Ibrahim M.H., Adnan M., Che Nidzam Che Ahmad C.N.C Noh N.M (2012), Thermal comfort in classroom: constraints and issues, Procedia –Social and Behavioural Sciences 46, 1834-1838.
- [6] oydyssee-mure.eu, Retrieved 3, 12, 2019 from <http://www.odysee-mure.eu/national-reports>, 2019.
- [7] Standards Australia, Australia(2000)/New Zealand standard: Energy audits: (AS/NZ 3598:2000), Standards Australia International Ltd., and Standards New Zealand.
- [8] F. Ardente et al, Energy and environmental benefits in public buildings as a result of retrofit actions, Renew. Sustain. Energy Rev. 15 (1) (2011) 460–470.
- [9] B. Basarir, et al., (2012). Energy Efficient Retrofit Methods at the Building Envelopes of the School Buildings retrieved 10.9.2019. www.academia.edu/Ellipsis/Energy_efficient_retrofit_methods_at_the_building_envelopes.
- [10] O. Osama et al, (2015) Zero energy university buildings energy performance evaluation of faculty of architectural engineering, Arch. Plan. J. 23 13–21.
- [11] Aboulnaga, M., & Moustafa, M. (2016). Sustainability of higher educational buildings: Retrofitting approach to improve energy performance and mitigate CO₂ emissions.
- [12] I. Sarbu, C. Pacurar, (2015) . Experimental and numerical research to assess indoor environment quality and schoolwork performance in university classrooms, Build. Environ. 93 (Part 2) 141–154.
- [13] B.J. Fraser, Research on classroom and school climate, in: G. Gabel (Ed.), Handbook of Research on Science Teaching and Learning, 1994, pp. 493–541, Washington, D.C
- [14] Cantin, R., Adra, N., & Guarracino, G. (2002). Sustainable Comfort for retrofitting educational buildings. Sustainable buildings International conference. Norway.
- [15] High Performance Schools, Best practices Manual, The Collaborative for High Performance Schools: CHPS, March 2001, Volume I, II and III: Design, Planning and Criteria
- [16] C.K. Mytafides et al, (2017). Transformation of a University Building into a Zero Energy Building in Mediterranean Climate. Energy and Buildings.
- [17] Ascione, F., Bianco, N., De Masi, (2019). Phase Change Materials for Reducing Cooling Energy Demand and Improving Indoor Comfort: A Step by Step Retrofit of a Mediterranean Educational Building. Energies, September issue.
- [18] O. Irulegi, A. Ruiz Pardo, A. Serra, J.M. Salmeron, R. Vega, (2017). Retrofit Strategies towards Net Zero Energy Educational Buildings: A case study at the University of the Basque Country. Energies and Building, March issue.

Assessment of Natural Ventilation on Thermal Comfort and Energy Consumption

The Case of a Natural-ventilated Shopping Mall in the Tropics

YE YUAN^{1, 3}, GANG LIU^{1, *}, RUI DANG¹, FANGLI YAN²

¹School of Architecture, Tianjin University, Tianjin, 300072, China

²Tianjin University Research Institute of Architectural Design, Tianjin, 300072, China

³Department of Architecture, National University of Singapore, 117566, Singapore

ABSTRACT: *The semi-outdoor space is a popular design method of architects in the tropics to introduce natural ventilation into buildings. This paper presented a simulation-based comparative analysis of an existing shopping mall in Singapore. Different ventilation schemes and techniques were applied to improve its thermal comfort and energy consumption. Two parts of simulations were carried out, including computational fluid dynamics (CFD) in PHOENICS for wind velocity and energy simulation in EnergyPlus for discomfort hours and energy consumption. Results show that adopting more semi-outdoor spaces being open to the prominent wind direction does not cause discomfort for the wind velocity, on the contrary, it is beneficial to the natural ventilation effect, which reduces discomfort hours and provides a better shopping experience for consumers. Moreover, results also find the open scheme with air curtains is the optimum solution for energy consumption, being conducive for shop tenants and mall managers to reduce both energy cost for cooling and mechanical ventilation.*

KEYWORDS: *Shopping mall, Natural ventilation, Thermal comfort, Energy consumption*

1. INTRODUCTION

Building energy consumption is one of the major components of social energy consumption in modern world, accounting for around 40% of the total [1]. This situation is even worse in large-scale public buildings like shopping malls. In order to maintain the thermal comfort, the full-time air-conditioning must be applied, resulting in its energy consumption four to eight times that of other ordinary buildings [2]. According to statistics, shopping malls have been built in large numbers all over the world [3]. Influenced by tourism and high-class lifestyles, this number grows much more rapidly in Singapore [4]. Therefore, it is necessary for architects to adopt appropriate design methods to achieve both low energy consumption and thermal comfort in shopping malls.

Natural ventilation is one of the key methods to provide optimum indoor air quality and maintaining an acceptable thermal comfort even without the employment of HVAC systems [5], and research have indicated that it could decrease 60% of the total building energy consumption [6-7]. In shopping malls, it is also a popular choice to incorporate semi-outdoor spaces that are naturally ventilated, especially in the tropics [8]. However, the applicability of this design method is unknown in shopping malls due to the building characteristics. In order to attract customers,

retail stores in shopping malls always adopt an open storefront to reduce the psychological barrier for customers to come in [9], resulting in high air exchanges there and the increased energy consumption [8]. Therefore, although the utilization of natural ventilation in shopping malls can reduce the energy consumption of public spaces, it will significantly increase the energy consumption in stores, both of which need to be considered comprehensively.

With the advent of the experience economy era, consumers are no longer limited to obtaining goods and services but focus more on seeking unique and memorable experiences [10]. Studies have shown that shopping environment directly determines the success of a shopping mall [11], and its impact on consumer-buying decisions is more significant than products themselves [12]. Thermal environment is a basic physiological demand of customers, and it has been proved to be able to enhance consumer experience and the attractiveness of shopping malls [13-14]. Different from other building types, the circulation space in shopping malls is continuously occupied by consumers to roam in the building through the entire shopping process, making its thermal comfort more important than other building types. Adopting semi-outdoor space designs for the circulation space can surely provide a rich space experience for consumers, but it is also

difficult to guarantee their thermal comfort by mainly relying on the natural ventilation. Several studies have been conducted on the semi-outdoor and outdoor thermal comfort in the context of Singapore [15-16]. However, specific design strategies of applying these obtained conclusions into natural-ventilated spaces is not provided, especially considering the characteristics of shopping malls.

Since there is no research on the natural ventilation design for shopping malls in the tropics, this study concentrates on it by exploring the design method of natural ventilation in the semi-outdoor space to achieve both goals of thermal comfort and energy saving based on the characteristics of shopping malls.

2. METHODS

This paper presents a case study of a partially natural-ventilated shopping mall that has been frequently complained by both retailers and customers since opened. In order to address the existing problems, different ventilation schemes were applied to find the optimal solution for it, and all of the alternatives were compared according to both criteria for thermal comfort and energy consumption. The simulation work was carried out into two stages including the CFD simulation and energy simulation.

2.1 The building

Westgate (Fig. 1) is a 7-level lifestyle and family shopping mall in Jurong East, Singapore. The whole building is divided into two parts – The Courtyard (naturally ventilated part) and the conventional closed indoor part. The Courtyard is a semi-outdoor space with large glazing walls and direct connections to the outside. Although it offers a holistic shopping experience there, shop tenants of that part always complained about their energy consumption being obviously higher than that in the indoor part, and customers there also want to stay indoors when it is hot outside.

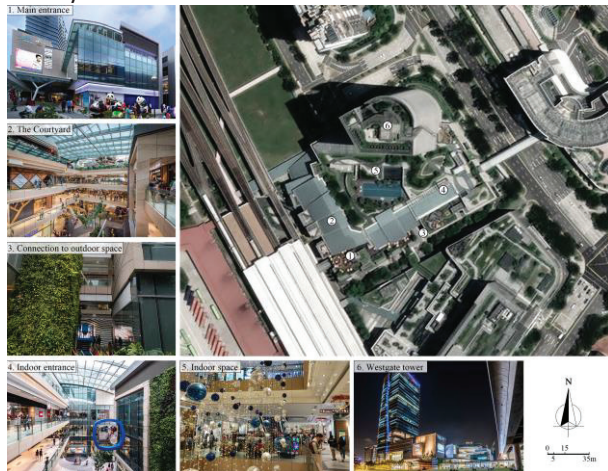


Figure 1: Building information of Westgate Mall in Jurong East, Singapore (source: Google Maps, used to present the location of the mall).

2.2 Ventilation schemes

To solve the existing problems, there are mainly two options: one is to eliminate The Courtyard and adopt the conventional closed mall solution for the entire building, and the other is to incorporate techniques and improve the building performance of the semi-outdoor part. Based on these two options, there are four ventilation schemes to be simulated (Fig. 2):

Alternative A - Original scheme: the naturally ventilated semi-outdoor space is in the southwest of the building and the indoor part is in the northeast direction. This alternative is utilized as the base model in this study.

Alternative B – Conventional closed scheme without natural ventilation: The Courtyard is closed by walls and roofs the same with the indoor part to eliminate natural ventilation and simultaneously reduce effects of cross ventilation between retail stores and the original semi-outdoor space. The window wall ratio (WWR) and skylight roof ratio (SRR) in that area are all controlled the same with the original building scenario. Afterwards, the entire building is air-conditioned.

Alternative C – Opened scheme with fully natural ventilation: to make full use of the natural ventilation, the indoor part in the northeast, direction of the prominent wind in Singapore, is also opened with connections to the outside and adopt fully naturally ventilation. In this context, only stores are air-conditioned.

Alternative D – Opened scheme with air curtains: on the basis of Alternative C, air curtains are adopted at the entrance of all stores to reduce air exchanges between stores and the semi-outdoor space.

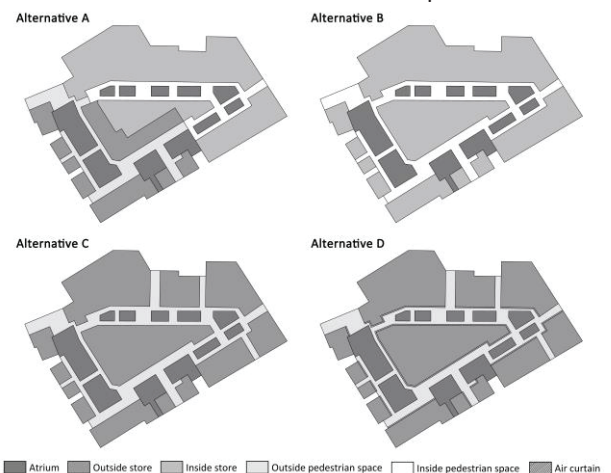


Figure 2: Four Ventilation Schemes of Westgate Mall.

2.3 CFD model and energy model

The simulation work was performed in two stages: all schemes were simulated for both thermal comfort in PHOENICS [17] and the energy consumption in EnergyPlus [18].

Fig. 3 presents the CFD model and simulation domain including cell numbers and surrounding buildings (i.e. Jem Mall, Ng Teng Fong General Hospital, Jurong East Station, etc.). The incoming wind was modelled using a power law profile [19] with a reference velocity of 3.0 m/s at a 10 m height above ground level. The speed is the maximum mean monthly wind speed from northeast in February of Singapore, and related data were obtained from the website of Meteorological Service Singapore (MSS) [20]. Moreover, the k-ε turbulence model, which has been proved to be accurate for global flow simulations [21-23], was used for the simulation in this study.



Figure 3: Top view of the CFD model.

Regarding the energy model, the simulation data for dimensional construction (Table 1) and indoor heat gains (Table 2) used in the thermal model are listed as follows according to Green Mark [24] and CIBSE [25], respectively. In order to calculate air exchange between retail stores and the outdoor air, the dynamic thermal modelling (DTM) of Airflow Network (AFN) for the natural ventilation was utilized to simulate multizone airflows driven by outdoor wind pressure [26]. The ventilation schedule of stores in the semi-outdoor part were opened the same with occupancy schedule.

Table 1: Properties of key building elements pertinent to energy simulation.

Parameter	U-value	Unit
Wall	1.6	Wm ⁻² K ⁻¹
Roof	0.8	Wm ⁻² K ⁻¹
Skylight	2.2	Wm ⁻² K ⁻¹
Window	2.8	Wm ⁻² K ⁻¹

Table 2: Internal conditions of the building.

Parameter	Value	Unit
Internal condition of retail stores		
Occupancy density	5	m ² /person
Lighting	25	Wm ⁻²
Electrical equipment	5	Wm ⁻²
Infiltration rate	0.5	ach
Internal condition of circulation spaces		
Occupancy density	5	m ² /person
Lighting	6	Wm ⁻²
Infiltration rate	0.5	ach
Ventilation rate	1.0	ach

The heating, ventilation, and air conditioning (HVAC) system was scheduled the same with the opening hours from 10:00 a.m. to 10:00 p.m. every day, and the cooling set point was 24 °C throughout the year. The cooling coefficient of performance (COP) for the system was calculated according to the following Equation (1) [27]. Moreover, there were mechanical ventilation systems operated during the opening hours for both indoor circulation spaces (fan power 8.4 kW/m²) and all shops (fan power 2.6 kW/m²), while the outdoor circulation spaces in Alternative A, C, and D were naturally ventilated. In addition, different from Alternative C, Alternative D adopted air curtains with the efficiency of 70%, reducing heat flux to 30% of the original flux.

$$\text{COP} = T_c / (T_H - T_c) \quad (1)$$

where T_c – Temperature of the cold reservoir (°C);

T_H – Temperature of the hot reservoir (°C).

2.4 Evaluation index

The evaluation for thermal comfort includes two indexes for both wind velocity and air temperature. As for the wind-generated discomfort of outdoor environments, NEN 8100 [28] was utilized to calculate the possibility of wind velocity exceeding the threshold of 5.0 m/s. In addition, the acceptable temperature ranged from 23.0 to 31.2 °C in semi-outdoor spaces of Singapore obtained by Song [16] was used as the criteria to evaluate the thermal comfort for temperature. The simulated operative temperature beyond this range was considered uncomfortable, thus the annual discomfort hours during the opening period can be used as the evaluation index for thermal comfort.

In addition to the thermal comfort of consumers, energy consumption concerned by tenants and mall managers was another important evaluation index. In order to assess different building scenarios, the energy use intensity (EUI), annual energy cost per square meter, was used as the benchmark for assessing building energy consumption. The final total energy

consumption includes both energy for cooling and the mechanical ventilation energy cost.

2.5 Weather data

Singapore (1°18'N, 103°51'E), situated near the equator, has a typically tropical climate with abundant rainfall, high and uniform temperatures, and high humidity all year round. The mean annual dry bulb temperature is 27.46 °C, and the most prominent winds are from the northeast and south, reflecting the dominance of the monsoons there.

3. RESULTS

3.1 Wind velocity

The comparative analysis of outdoor wind velocity is for Alternative A, C, and D, which contain the semi-outdoor spaces. Fig. 4 illustrates CFD simulation results of 1.5 m above the highest floor of the building (the most influenced area in it). It can be seen that even under the condition of the maximum monthly wind speed, there is no area exceeding the threshold of 5.0 m/s, meaning that the wind generated discomfort will not occur in the semi-outdoor space of all alternatives.

As natural ventilation can take away the excessive heat, the better ventilation effect, the more heat it will be removed. It can be seen that the ventilation effect in Alternative C and D is obviously improved by setting the whole circulation space as semi-outdoor spaces. Therefore, it is beneficial for building to make full use of natural ventilation by incorporating more open spaces, especially open towards prominent wind directions.

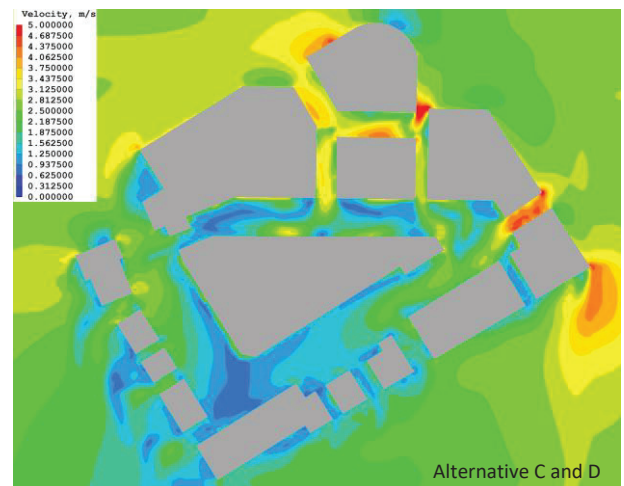
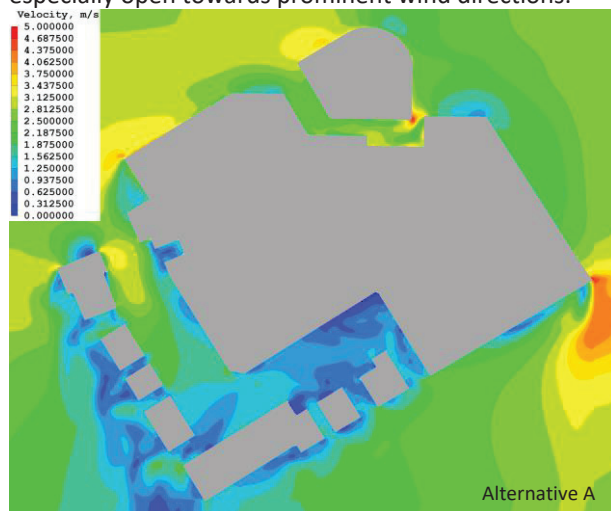


Figure 4: CFD simulation results of Alternative A, C, and D containing the semi-outdoor space for the highest floor.

3.2 Discomfort hours

Due to large glazing walls, there are lots of heat gains received during daytime, especially for the highest floor area. Fig. 5 presents simulation results of the circulation space in the highest floor area for all alternatives during the business hours.

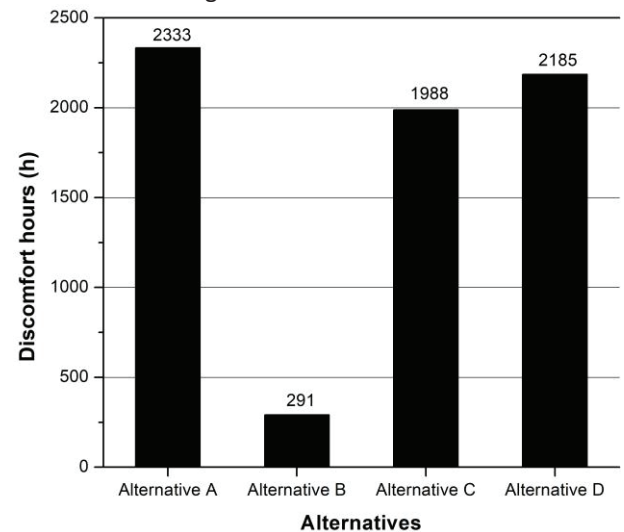


Figure 5: Simulation results of annual discomfort hours in the circulation space of the highest floor for four alternatives.

Alternative B, all spaces with HVAC systems, has the least discomfort hours compared with other three naturally ventilated alternatives. The 291 discomfort hours occur only when the solar radiation is strong under some extreme weather conditions, which result in the radiant temperature being too high. For the other three naturally ventilated ones, Alternative C and D, with more open spaces, have less discomfort hours than Alternative A because of the better natural ventilation effect. This again proves that good natural ventilation is conducive to the thermal comfort of semi-

outdoor spaces. In addition, as the air curtain can weaken air exchanges between semi-outdoor spaces and retail stores, the air temperature in the semi-outdoor space of Alternative D is higher than Alternative C, resulting in its discomfort hours also being slightly more than Alternative C.

3.3 Energy consumption

Fig. 6 illustrates energy simulation results of HVAC systems including both energy cost for mechanical ventilation and cooling. It can be seen that Alternative D, the open scheme with air curtains, is the most energy efficient solution, while Alternative C is the worst solution among all. Compared with Alternative C, air curtains adopted at the shop enhance can obviously reduce the cooling energy cost. In addition, although the indoor design scheme (Alternative B) can reduce the cooling energy consumption for the building, more indoor areas of the circulation space result in the significant increase of energy for mechanical ventilation. Thus, the total energy cost of Alternative B is even a little more than Alternative D.

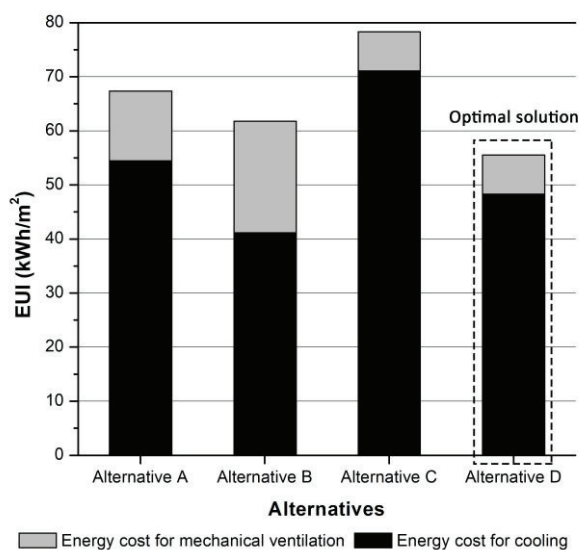


Figure 6: Energy simulation results of four alternatives including both energy consumption for mechanical ventilation and cooling.

Table 3 presents the energy simulation results of cooling energy cost in different thermal zones. It can be seen that there are obvious differences of cooling energy cost in different thermal zones: first, according to the simulation result of Alternative A, continuous air exchanges between outdoor shops and the semi-outdoor space result in the cooling energy cost in shops there is nearly 4 times that of indoor shops; second, due to the better ventilation effect, cooling energy cost of outdoor shops in Alternative C decreases by 47.19 kWh/m² compared with the outdoor shops in

Alternative A; third, through the comparison between Alternative C and Alternative D, air curtain is an effective method for shops to decrease the energy cost for cooling with a reduction of 35.85 kWh/m².

Table 3: Energy simulation results of cooling energy consumption in different thermal zones including indoor shops, outdoor shops, and circulation spaces.

Alternatives	Shop (kWh/m ²)		Circulation space (kWh/m ²)
	Indoor	outdoor	
Alternative A	40.66	159.10	34.80
Alternative B	41.68	-	40.20
Alternative C	-	111.91	-
Alternative D	-	76.06	-

4. CONCLUSIONS

This paper presented a case study of shopping mall in tropical climate conditions and shows the influence of natural ventilation on both thermal comfort and energy consumption. The research was carried out by comparative analysis of four different alternatives through CFD simulation and energy simulation. The original building was redesigned as both conventional closed scheme and open schemes, and in order to weaken the continuous air exchange, air curtains were applied to improve the building energy performance. Implications for natural ventilation design in shopping malls are outlined as follows:

(1) Thermal comfort

- The open scheme, especially when open to prominent wind directions, does not cause discomfort for wind velocity. On the contrary, it is beneficial to the natural ventilation effect.
- Better conditions of natural ventilation can improve thermal comfort by reducing discomfort hours of semi-outdoor spaces.

(2) Energy consumption

- The open scheme with air curtains by incorporating more semi-outdoor circulation spaces can reduce both energy cost for cooling and mechanical ventilation, making it the optimal solution for the building.
- Stores located in the semi-outdoor space consume nearly 4 times of energy that of the indoor ones.
- Better ventilation can reduce the cooling energy cost for outdoor shops by 47.19 kWh/m², and the potential energy savings of air curtains there is 35.85 kWh/m².

To conclude, natural ventilation can improve thermal comfort of semi-outdoor spaces in shopping malls, and it is also beneficial for building energy performance by reducing air exchanges. The results and findings can not only guide design practice of architects

in the tropics but also achieve a win-win situation for consumers, tenants, and mall managers.

ACKNOWLEDGEMENTS

This research is financially supported by the National Key R&D Program of China (Grant No. 2016YFC0700200), and the Program of Introducing Talents of Discipline to Universities (Grant No. B13011). We would like to thank China Scholarship Council for providing us with financial support to carry out the study at the School of Design and Environment in National University of Singapore.

REFERENCES

- Huang, J., Lv, H., Gao, T., Feng, W., Chen, Y. and Zhou, T., (2014). Thermal properties optimization of envelope in energy-saving renovation of existing public buildings. *Energy and Buildings*, 75: p. 504-510.
- Building energy conservation research centre, Tsinghua University, (2014). *Annual report on China building energy efficiency*. China Architecture & Building Press, Beijing, China. (in Chinese)
- CBRE Group, (2017). Global Shopping Centre Development, [Online], Available: <http://cbre.vo.llnwd.net/grgservices/secure/ViewPoint%20-%20Global%20Shopping%20Centre%20Development.pdf?e=1533469442&h=f65552e965fb94d3f0dfc884380ab401> [18 April 2017].
- Coclanis, P., (2009). A city of frenzied shoppers? Reinterpreting consumer behavior in contemporary Singapore. *Journal of The Historical Society*, 9(4): p. 449-465.
- Moosavi, L., Mahyuddin, N., Ab Ghafar, N. and Ismail, M. A., (2014). Thermal performance of atria: An overview of natural ventilation effective designs. *Renewable and Sustainable Energy Reviews*. 34: p. 654-670.
- Thirugnanasambandam, M., Iniyan, S. and Goic, R., (2010). A review of solar thermal technologies. *Renewable and sustainable energy reviews*. 14(1): p. 312-322.
- Chan, H. Y., Riffat, S. B. and Zhu, J., (2010). Review of passive solar heating and cooling technologies. *Renewable and Sustainable Energy Reviews*. 14(2): p. 781-789.
- da Graça, G. C., Martins, N. R. and Horta, C. S., (2012). Thermal and airflow simulation of a naturally ventilated shopping mall. *Energy and Buildings*. 50: p. 177-188.
- Ebster, C., (2011). *Store design and visual merchandising: Creating store space that encourages buying*. Business Expert Press, New York, NY.
- Pine, B.J. and Gilmore, J.H., (1999). The experience economy: Work is theatre and every business a stage. *SGB*. 18 (2): p. 129-130.
- Bitner, M.J., (1990). Evaluating service encounters: the effects of physical surroundings and employee responses. *Journal of Marketing*. 54 (2): p. 69-82.
- Kotler, P., (1973). Marketing during periods of shortage. *Journal of Marketing*. 38 (3): p. 20-29.
- d'Astous, A., (2000). Irritating aspects of the shopping environment. *Journal of Business Research*. 49 (2): p. 149-156.
- Kwok, T.F., Xu, Y. and Wong, P.T., (2017). Complying with voluntary energy conservation agreements (I): air conditioning in Hong Kong's shopping malls. *Resources, Conservation and Recycling*. 117: p. 213-224.
- Yang, W., Wong, N. H. and Jusuf, S. K., (2013). Thermal comfort in outdoor urban spaces in Singapore. *Building and Environment*, 59: p. 426-435.
- Song, J., (2006). Thermal comfort for semi-outdoor spaces in the tropics. *PHD thesis*, Department of Building, National University of Singapore.
- PHOENICS, Version 2019. Available: <http://www.cham.co.uk/phoenics.php>
- EnergyPlus, Version 8-9-0. Available: <https://energyplus.net/>
- ASHRAE, (2005). *Handbook—Fundamentals*, American Society of Heating, Refrigerating, and Air-Conditioning Engineers. Inc., Atlanta, Chapter 16.
- Meteorological Service Singapore. Climate of Singapore, [Online], Available: <http://www.weather.gov.sg/climate-climate-of-singapore> [8 May 2020].
- Zhang, Z., Zhang, W., Zhai, Z. J. and Chen, Q. Y., (2007). Evaluation of various turbulence models in predicting airflow and turbulence in enclosed environments by CFD: Part 2—Comparison with experimental data from literature. *HVAC&R Research*, 13(6): p. 871-886.
- Nishizawa, S., Sawachi, T., Ken-ichi, N., Seto, H. and Ishikawa, Y., (2004). A wind tunnel full-scale building model comparison between experimental and CFD results based on the standard k-ε turbulence representation. *International Journal of Ventilation*, 2(4): p.419-429.
- Cheung, J. O. and Liu, C. H., (2011). CFD simulations of natural ventilation behaviour in high-rise buildings in regular and staggered arrangements at various spacings. *Energy and Buildings*, 43(5): p.1149-1158.
- BCA, (2015). *Green mark for non-residential building NRB: 2015*. 5th ed.
- CIBSE, (2006). *Environment design CIBSE guide A*. 7th ed. Page Bros. (Norwick) Ltd.
- Chen, Q. Y., (2009). Ventilation performance prediction for buildings: A method overview and recent applications. *Building and environment*, 44(4): p. 848-858.
- Winterbone, D. and Turan, A., (2015). *Advanced thermodynamics for engineers*. Butterworth-Heinemann.
- Blocken, B. and Persoon, J. (2009). Pedestrian wind comfort around a large football stadium in an urban environment: CFD simulation, validation and application of the new Dutch wind nuisance standard. *Journal of wind engineering and industrial aerodynamics*, 97(5-6): p. 255-270.

Energy Retrofit of the Existing Residential Building Stock in Jiangsu Province, China

Study on Danyuan Apartment of 1979-1999

XI CHEN

¹Xi CHEN, the University of Liverpool, Liverpool, UK; Xi'an Jiaotong-Liverpool University, Suzhou, China

ABSTRACT: *The operational energy use in buildings in China represents over 1/5 of the total national energy consumption, from which urban residential buildings takes over 38% in the building sector. China has committed to established policies to promote clean and renewable energy and energy efficient buildings, to decrease carbon emission by 60% to 65% by 2030. This paper focuses on the multi-Danyuan residential apartment building typology constructed between 1979 to 1999 in Jiangsu Province, and expected to investigate the applicability and the potential of innovative measures and approaches to low energy retrofit for the residential building stock in Jiangsu Province that fit different future social and climate context scenarios through an innovative energy model that is able to perform different analysis with particular regard to sustainability, adaptation and resilience of the housing stock retrofit. The optimal solution for this study is to improve the thermal performance of the building envelopes and thereby reducing the energy demand on indoor space heating and cooling based on the UK Building Regulations 2010 L1B Existing dwellings.*

KEYWORDS: *Energy, retrofit, residential buildings, energy simulation, bottom-up model*

1. INTRODUCTION

This research aims to investigate the applicability and the potential of innovative measures and approaches to low energy retrofit for the residential building stock in Jiangsu Province that fit into future social and climate context. This paper addresses Multi-Danyuan apartment constructed in 1979 to 1999, which is one of the most representative housing types in the urban areas.

The operational energy use in building sector in China represents over 1/5 of the total national energy consumption, from which urban residential buildings takes over 38% in the building sector [1]. 76% of the energy use on building operation in China is produced by the burning of coal, which is a high polluting non-renewable fossil fuel [2]. Despite the fact that the energy intensity of urban residential buildings is lower than public buildings, the large total building area leads to high total energy consumption.

The growing construction of buildings and infrastructures lead to massive consumption of building materials and energy. The energy use on building construction was doubled than what it was a decade ago by 2014, which accounts for 27.5% of the total primary energy consumption and 1/3 of the total carbon emission [3]. As one of the biggest energy-consuming countries, China is committed to promoting clean and renewable energy and energy-efficient buildings, to decreasing carbon emissions by 60% to 65% from 2005 by 2030 [4].

Low energy retrofit of the existing housing stock can significantly reduce energy consumption and

carbon emissions. This research focuses on Multi-Danyuan apartments, one of the main existing residential building typologies constructed from 1979 to 1999 in Jiangsu Province. It intends to investigate innovative low energy retrofit approaches through energy modelling that is able to perform different analysis with particular regard to sustainability, adaptation and resilience performance of the housing stock retrofit. A bottom-up model was established to simulate the energy use condition of this building type. The simulation results suggest that retrofit strategies compliant with the Building Regulations 2010 L1B Existing dwellings (UK), can reduce the total energy use for the apartment buildings by 66% to 68%, by improving the thermal performance of the building envelopes and thereby reducing the energy demand on indoor space heating and cooling under the current and the future climate. On the other hand, adding a shading system, in spite of increasing the energy demand for heating, would moderate the solar radiation penetration and reduce the energy use on space cooling.

2. BACKGROUND

2.1 Urban housing development

In the era of planned economy 1949-1978, China's urban housing was distributed under a low-rent welfare-oriented system, which provided safeguards for residents' basic housing needs. However, this system increased the burden for the government and state-owned enterprises. Thus, by the end of 1977, there was a severe housing shortage [5]. As part of

the economic institution reform initiated in 1978, China has gradually sought to resolve these problems by reforming the urban housing system since 1980. By 1998, China's urban housing system reform had entered a crucial stage. The commercial housing developed rapidly, and housing conditions of urban residents also quickly improved [5]. From 2007, China entered the accelerating stage of the housing system.

Currently, the total urban residential building floor area in Jiangsu takes around 10% of the whole national urban housing area and the residential energy consumption per capita in Jiangsu was 34.2% higher than the average national level in 2017 [6].

2.2 Urban housing regulations

The early regulation for building design in 1950s (Code for Design of Civil Buildings) was neither targeting at the housing sector, nor on a specific climate region, which led to low-quality buildings unsuitable for specific regions. The first regulation specifically formulated for urban housing was published in 1987, which illustrated details on the indoor environment and building facilities. The building codes for urban housing have been amended and developed many times over the decades. The current regulation is the Design code for residential buildings GB50096—2011 (published in 2011), which may require updating for the development of building materials, construction methods and advanced technologies.

Along with the development of urban housing regulation, design codes aiming to improve building energy performance have also been developed during the past decades. The codes for building energy performance appeared in 1986 but not targeting specifically residential buildings. The first one for civil buildings in Jiangsu Province was issued in 2001, and the first one for urban residential buildings in Jiangsu was published in 2008. The current regulation on the energy efficiency of urban residential buildings in Jiangsu Province is the Design Standard of Thermal-Environment and Energy Conservation for Residential Buildings in Jiangsu Province (2008).

The research and practice on the sustainable renovation of housing arose very early in Europe and achieved satisfactory results. China's in-depth research on urban housing renovation started after the turn of the 21st century, but mainly focused on the clearance of slums and building reconstruction and aimed at space heating in northern China [7]. The first regulation on energy retrofit of urban houses is the Technical Specification for energy efficiency retrofitting of existing residential buildings JGJ/T129-2012, issued in 2012. In Jiangsu Province, there is still a lack of appropriate regulation on the energy efficiency for the retrofitting of urban residential buildings. The previous researches also indicated that

the exploration of same climate zone were either over-dependent on traditional approaches or lacking innovative and specific strategies [8, 9].

3. RESEARCH METHODS

3.1 bottom-up modelling and simulation

The bottom-up modelling approach works at a disaggregated level, providing flexibility and the powerful capability to investigate the impact of a specific action, measure or intervention at higher levels of aggregation that has been validated in several different countries and climatic contexts [10]. By modelling the representative building typologies which are assigned a statistical weight in the whole building stock, a reliable projection of the entire groups can be established [11].

However, this approach is highly dependent on the available, reliable and quality of the input data and the capability of the modelling and calculation [12]. The research scope for building type was selected based on reliable statistical data. The energy performance under different climate scenarios was simulated, and the energy conservation efficiency was tested to explore the optimal retrofit strategies.

3.2 Representative residential building type

The 6th National Population Census in 2010, indicates that around 50% of existing housing stock in the urban area of Jiangsu Province was built in the 1980s and 1990s, which is higher than the average proportion in the whole nation (Figure 1). It also shows that over 46% of existing residential buildings are multi-storey (4-6 storey) apartments, which makes up the most substantial proportion. On the other hand, the hybrid structure (brick and reinforced concrete structure) buildings take the highest proportion of over 52% of the total area of existing residential stock in urban area of Jiangsu Province.

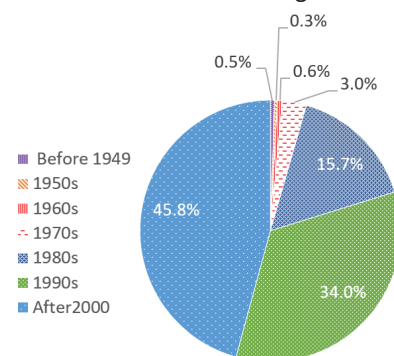


Figure 1 Proportion of housing stock by the age of completion of Jiangsu – city area

The promotion for building type diversity in the 1980s and 1990s results in a variety of urban housing typologies nationwide [13]. The construction records of each city of Jiangsu Province shows that around 70% to 80% of the existing buildings constructed

during the 1980s and 1990s are multi-Danyuan apartment, which makes this building type the most typical existing urban residential type constructed in that time period.

‘Danyuan’ apartment in Chinese stands for two or more household sharing one staircase, and two or more Danyuan can be combined in one building (see Figure 2). This type of building usually came in a leaner and simple shape. Figure 2 shows one typical plan of the multi-Danyuan apartment of the 1980s. The buildings were constructed in a very simple and rapid way to solve the housing shortage problem; thus there was no insulation. This resulted in very poor thermal performance and indoor comfort.

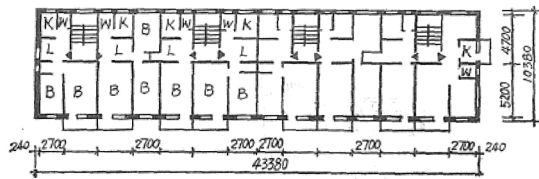


Figure 2 A four-Danyuan apartment building plan

Several reconstruction and update events have been implemented in the past decades. The open balconies on the south facade are often enclosed by residents to expand the indoor space and to improve the thermal performance at the same time. According to observation from 42 big-scale neighbourhoods constructed in the 1980s and 1990s of 6 main cities of Jiangsu Province, around 80% to 90% of the apartments had the balconies enclosed. Another update on the buildings is to mend and repaint the building façades sponsored by the government or the neighbourhood management; but no upgrades on the building envelopes.

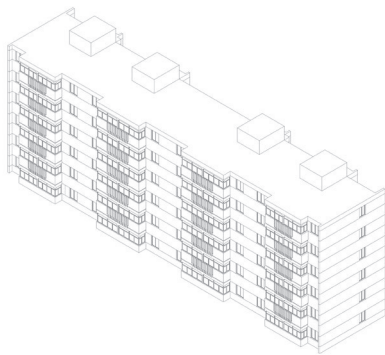


Figure 3 case study four-Danyuan apartment building

Table 1 descriptive statistics for case study building

Construction Year	1986
Floors	6 (5+1)
Staircase (Danyuan)	4
Dwelling Unit per Danyuan	2
Number of apartment	48
Area per storey (sqm)	470
Orientation	E-W
Compactness	0.42

In this paper, a representative case study building (Figure 3) is selected to model and simulate the energy performance of current and future scenarios, and to test the energy retrofit strategies. Table 1 provides a description of this building. It is assumed that all the balconies are enclosed by the residents and the building structure has been strengthened.

3.3 On-site investigation

The on-site data collection includes measurements of the building plan, building components, adjacent constructions, the electricity bills, etc. Several temperature sensors were placed in the living areas and bedrooms to collect the indoor temperature of a selected apartment. The climate data of the monitoring period time were collected from the local weather station. The whole temperature data collection took 48 days. The data collection had no impact on the daily life of the residents. The electricity bills were collected from the STATE GRID Corporation of China.

3.4 Climate data and future scenarios

The future climate data for 2020 to 2100 used for this paper were generated by Meteonorm 7.3, and the accuracy and feasibility have been well-studied and validated [14-17]. This study used A1B 2020, 2050 and 2080 scenario, the projections regarding future global carbon emissions, for the simulation of future climate context. Due to the level of completeness, accuracy and accessibility of climate data, hourly weather files for Shanghai was selected for the replacement of south Jiangsu, for Shanghai is adjacent with south Jiangsu Province and share the same climate, while the same time has a more integrated climate database.

3.5 Calibration and validation

The simulation results of a digital model were validated against the measured data from the real case. An apartment of the building was selected for the calibration and validation of the model. The hourly indoor temperatures were monitored and collected for 38 days, and the energy bills for the past two years have also been collected. Due to the complexity and uncertainty of the using pattern of residential buildings, the model was calibrated through multiple iterations to reduce the error value to below 15%. The possible reasons for the differences on the energy use situation is the wide variety of residents' behaviour patterns, schedules and the facilities types that will have a significant impact on the energy use, which is an inevitable factor, but not the research focus for this paper, which is the properties of building envelopes.

4. MODELLING AND SIMULATION

The modelling of the case study building was conducted with DesignBuilder, a graphical user interface software developed for EnergyPlus, and the accuracy and feasibility of simulation have been validated by many researchers and organisations [18].

The simulation process of the model has two parts, the first part focuses on the preliminary retrofit on building envelope based on three retrofit scenarios, from which the optimal scenario will be further tested for other energy improving approaches at the second part of the simulation process.

4.1 Preliminary retrofit on building envelope

The poor quality of the original building and outdated facilities result in an unsatisfactory indoor thermal condition. Due to the lack of management, monitoring and record, the thermal characteristics were not accessible from the on-site investigation and relevant authority. The construction details are therefore determined according to multiple building standards, design codes, thermal codes for residential buildings and construction records of the 1980s and 1990s, which can represent the construction conditions of most of the existing building stock in Jiangsu Province. The thermal characteristics were calculated based on the Thermal Design Code for Civil Building GB50176-93 and the built-in database (the EnergyPlus database) of DesignBuilder software (Table 2).

This stage focuses on the upgrade of the building envelope, including adding insulation on the walls and roofs, and changing the window components into higher-performance products. The efficiency of HVAC systems, or other factors that do not directly affect the building qualities are not taken into account.

Table 2 input thermal specifications of the original building without retrofit

components	Before retrofit
external wall u-value	1.789
Roof u-value	3.252
window u-value(glazing)	6.121
window frame u-value	5.881
Aluminium	
SHGC	0.810
Air tightness	2.000
shading	-

Three retrofit scenarios were designed to meet three different building thermal regulations, the Design standard of thermo-environment & energy conservation for residential building in Jiangsu Province DGJ32-J71-2014 (China), The Building Regulations 2010 L1B Existing dwellings (UK) and Criteria for the Passive House, EnerPHit and PHI Low Energy Building Standard (Germany). These three

standards have different criteria for the thermal performance of the retrofit building components, with the Chinese regulation having the lowest requirement and the German one the strictest.

Table 3 input thermal specifications of three scenarios

Components	Before retrofit	Sce 1	Sce 2	Sce 3
External wall u-value	1.789	0.739	0.499	0.299
Roof u-value	3.252	0.552	0.347	0.295
window u-value	6.121	2.549	1.322	0.786
window frame u-value	5.881	4.719	4.719	3.476
SHGC	0.810	0.698	0.478	0.470
Airtightness ACH	2.0	1.0	0.5	0.5

At this stage, based on the local building material market, retrofit scenario1 is set to meet the Chinese regulation requirement by applying 0.03m EPS expanded polystyrene as wall insulation, 0.03m foam-polyurethane as roof insulation, and double glazing window with argon gas and aluminium window frame with thermal break, with 1.0 airtightness (Air Changes per Hour). Scenario2 is set to meet the L1B by applying 0.06m EPS expanded polystyrene as wall insulation, 0.06m foam-polyurethane as roof insulation, and double glazing Low-E glass window with argon gas and aluminium window frame with thermal break, with 0.5 airtightness. Scenario3 is set to meet the EngyPhit by applying 0.09m XPS Extruded polystyrene as wall insulation, the same for roof insulation, and triple glazing Low-E glass window with argon gas and UPVC window frame, with 0.5 airtightness. The thermal parameters run in DB are shown as Table 3.

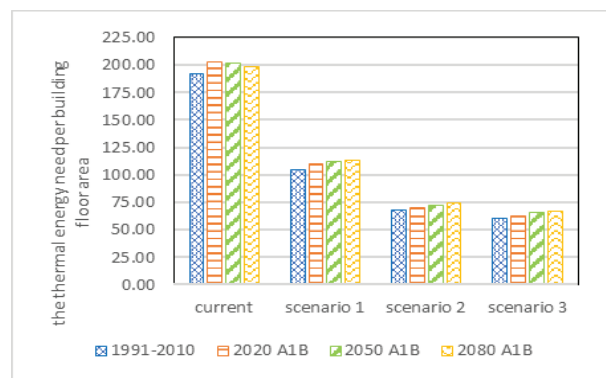


Figure 4 Energy per Total Building Area [kWh/m2]

Figure 4 shows the results of the simulation of the energy use per total building area [kWh/m2] of the current situation and the retrofit scenarios. Figure 5 illustrates the energy use of indoor space heating and cooling per building floor area. The following findings can be observed:

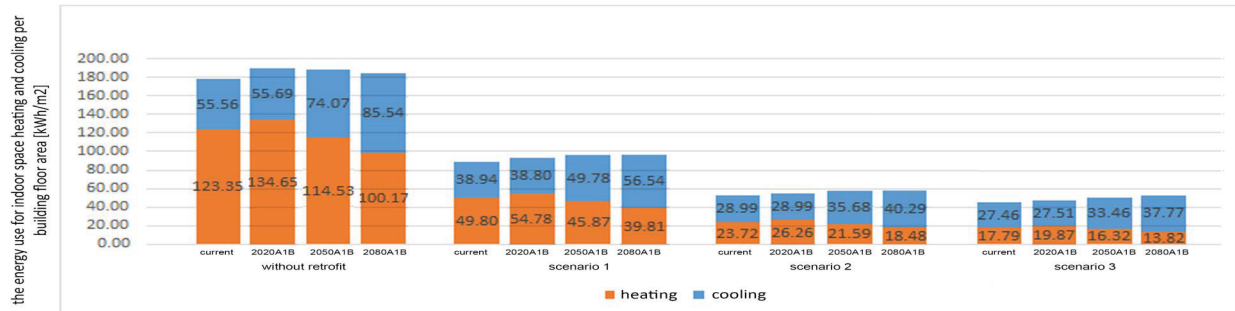


Figure 5 energy use of indoor space heating and cooling Per Total Building Area [kWh/m2]

- All three retrofit scenarios can reduce the total energy use significantly, while scenario 3 has the best effect of 68% reduction at the current time and 66% at 2080 A1B climate context.
- Compared with scenario 2, the reduction in energy use of scenario 3 is not very evident. Also the reduction trends for the heating and cooling sector are very similar.
- The reduction on the energy use for indoor space heating is much higher than the one for indoor space cooling. The energy use for space heating is higher than for cooling before retrofit on the building envelope, but the energy demand on space cooling will dominate the total energy use after retrofit along with the changing of climate change scenario context. In the 2080 A1B climate scenario context, with retrofit scenario 3, the energy use for cooling can reach triple to the one for heating.

The total energy need for the building would rise by 3 to 4% in 2080 without intervention. However, whilst heating energy is predicted to drop by up to 19%, cooling energy is expected to rise by up to 54%. Cooling demand is therefore expected to account for 46% of the total energy need in 2080. However the energy use for space heating still takes the largest proportion of all, which indicate that the heat preservation will be the primary issue to be solved. Thus, adding insulation on the building envelope and upgrade the thermal performance of the window components are the priority of the retrofit strategies.

The observations suggest that all the three retrofit scenarios can reduce the energy demand at the current time and in the future time, while the last two retrofit strategies are apparently more efficient than the first one. However, the energy reduction effects of the retrofit scenario 2 and 3 are very close, even though the cost for materials for scenario 3 can be much higher than scenario 2, and the requirement for the construction and the quality of the original

building would also be higher. Therefore, despite the Passivhuas standard is more popular at Chinese building market right now, scenario 2 (UK L1B regulation) is regarded as a better solution for the energy conservation retrofit for multi-Danyuan Apartment from long term consideration.

As a result, basic retrofit measures on the thermal envelope of the most poorly performing buildings can significantly reduce the energy consumption by 64% to 67% in the current and future climate context. The scenario2, which is designed to meet the requirement for UK L1B regulation would achieve the better effect on reducing energy use with the reasonable cost and feasible construction methods.

4.2 Further retrofit on the window shading system

The second part of the simulation process will be the tests of different shading systems based on retrofit scenario 2.

From the analysis of the above, it is clear that the energy demand for heating will reduce since the increasing global temperature, while the indoor overheating problem might occur over time. Many overheating mitigation approaches have potentials in energy retrofit on this building type, while this paper tested different external shading systems for the energy-saving effects, for shading system is the most effective and easily constructed of retrofitting approaches of the existing buildings. The options of the shading system that have been simulated are shown in table 4.

Table 4 shading options

Option	Description	Location
1	0.5m overhang	South façade, exterior
2	1m overhang	South façade, exterior
3	0.5m overhang and sidefin	South façade, exterior
4	1m overhang and sidefin	South façade, exterior
5	0.5m projection louvre	South façade, exterior
6	blinds with high reflectivity slats	South façade, exterior

The simulation results for current time indicate that the most effective alternative on reducing energy on space cooling is option 4, which can reduce energy use on cooling by 19% compared with no shading scenario; but at the same time increase the energy use on heating by 24%. Despite the big

increase on the percentage of energy use on heating, the total number do not increase much since the energy need for heating would be much lower in the future after retrofit on the building envelope. The final results unexpectedly suggest that Option 1 and 3 for shading system achieves the best solution for current and 2080 scenario, which respectively would reducing 1.1% and 3.1% of total energy use two climate scenarios. The effect is even less under other circumstances. Thus, consider the capital cost for the retrofit, this shading system might not be an effective solution for this case.

5. CONCLUSION

This paper illustrate the current situation of the poor thermal and energy performance of one of the most representative urban residential building types in Jiangsu Province.

A model for this building type has been built and simulated as a part of a wider bottom up stock model, to study the energy performance in current and future climate scenarios. The importance of establishing such models lies in the fact that a good understanding of the building situation of Jiangsu Province has the potential to avoid a significant unnecessary waste of energy and resources by developing an innovative and dynamic energy model.

The simulation results suggest that the retrofit strategies can refer to the regulation L1B for Existing dwellings, which can significantly reduce the total energy use by 66% to 68% by applying basic upgrading measures for the building envelopes, to improve the thermal performance and cut down the energy demand for indoor space heating and cooling in current time and the future climate context.

Further research would emphasise the following topics: (1) the potential of different HVAC system and the impacts on energy consumption; (2) the integration of renewable energy system, such as solar panel and ground source heat pump, for deep retrofit to pursue ultra-low power consumption; (3) the use of renewable and environmentally-friendly materials; (4) the performance in other cities in Jiangsu Province that may have different climate conditions and the respective optimal retrofit strategies; (5) different adjustable shadings, combination forms and control schedules in further study.

ACKNOWLEDGEMENTS

This research is funded by Xi'an Jiaotong-Liverpool University Research Development Fund (RDF-16-01-46) and Zhejiang Provincial Natural Science Foundation (LY19E080001). This research has been approved by XJTU University Research Ethics Committee.

REFERENCES

1. China Association of Building Energy Efficiency. (2019) China Building Energy Consumption Research Report 2019. November 2019, Shanghai
2. Center of Hubei Cooperative Innovation for Emissions Trading System. (2017) Annual Report of Carbon Emissions Trading Scheme 2017. Social Science Academic Press (China).
3. Tsinghua University Building energy conservation research centre. (2017). Annual Report on China Building Energy Efficiency 2017. China Architecture & Building Press.
4. Su, W. et al. (2015) Enhanced Actions on Climate Change: China's Intended Nationally Determined Contributions. Beijing.
5. Deng, Y. (2017) 'Urban housing system reform and real estate market development in China', Housing Finance International, pp. 15–18.
6. Jiangsu Statistical Bureau & Survey Office of National Bureau of Statistic in Jiangsu. (2017). Jiangsu Statistical Yearbook 2017.
7. Suo, J., Wu, D., & Tian, D. (2015). Study on Sustainable Renovation of Urban Existing Housing in China. China Architecture & Building Press.
8. Chinese Society of Urban Studies (Ed.). (2017). China Green Building 2017. China Architecture & Building Press.
9. China Academy of Building Research (Ed.). (2017). Review and prospect of China green building standard code. China Architecture & Building Press.
10. Loga, T., Stein, B., & Diefenbach, N. (n.d.). TABULA building typologies in 20 European countries—Making energy-related features of residential building stocks comparable. Energy and Buildings. JOUR.
11. Cimillo, M. et al. (2019), "Energy Modelling and Retrofit of the Residential Building Stock of Jiangsu Province" in 2019 XJTU International Conference: Architecture across Boundaries, KnE Social Sciences, pages 1–10. DOI 10.18502/45
12. Kavacic, M. et al. (2010) 'A review of bottom-up building stock models for energy consumption in the residential sector', Building and Environment. Elsevier Ltd, 45(7), pp. 1683–1697. doi: 10.1016/j.buildenv.2010.01.021.
13. Lv, J., Rowe, P. G., & Zhang, J. (2001). Modern Urban Housing in China 1840-2000. Prestel Pub.
14. Remund, J. (2016) Accuracy of Meteonorm. A detailed look at the model steps and uncertainties.[online] Available at: http://www.meteonorm.com/images/uploads/downloads/Accuracy_of_Meteonorm_7.pdf [Accessed 21 Apr. 2016], 2015.
15. Remund, J. (2008) Quality of meteonorm version 6.0. Europe, 2008. 6(1.1): p. 389.
16. Remund, J. (2008) Chain of algorithms to compute hourly radiation data on inclined planes used in Meteonorm, in Modeling Solar Radiation at the Earth's Surface. 2008, Springer. p. 393-410.
17. Remund, J., et al. (2010) the use of Meteonorm weather generator for climate change studies. In 10th EMS Annual Meeting, 10th European Conference on Applications of Meteorology (ECAM) Abstracts, held Sept. 13-17, 2010 in Zürich, Switzerland.
18. Foliente, G & Seo, S. (2012) Modelling building stock energy use and carbon emission scenarios. Smart and Sustainable Built Environment. Vol. 1 No. 2, 2012. pp. 118-138

Comprehensive evaluation of daylighting, air quality and thermal comfort as renovation impact in a Madrid classroom

ALMUDENA LÓPEZ DE REGO GARCÍA-ARQUIMBAÚ,¹ BEATRIZ ARRANZ ARRANZ²

¹VELUX Spain, Madrid, Spain

² UPM, Madrid, Spain

ABSTRACT: *This project evaluates the impact of a small envelope renovation on indoor comfort and energy efficiency in a classroom in Madrid. The project addresses the issues of indoor air quality, visual comfort with daylight and hydrothermal comfort, parameters linked to students' performance and wellbeing. The renovation, consisting on the addition of new automated windows and shutters in the roof, was designed to transform the classroom in a desirable and healthy space for education. The performance of both scenes has been evaluated through three outlooks: energy and daylight simulations, comfort parameters monitoring and users' perspective.*

KEYWORDS: *Schools, Healthy renovation, Renovation, Children, IEQ*

1. INTRODUCTION

The indoor environment should not hinder the learning of the children. The main aspects to be considered to ensure the Indoor Environment Quality (IEQ) must satisfy the conditions of hygrothermal comfort, acoustic comfort, luminous comfort, physical-chemical and microbiological contaminants in the air [1]. IEQ attracts scientific interest especially when it concerns the health of vulnerable populations such as children. Studies carried out in which students performance has been analysed, conclude that heat makes pupils lethargic, can affect concentration and lead to fainting [2]. Good lighting results in better job performance, the higher the daylight level the higher the achievement of the pupils, schools in the study [3,4] show a 7 to 18% higher performance in those classrooms with the most daylight compared to those classrooms with the lowest amount of daylight. Daylight has also a positive effect in health, in 2002 David Berson et al. [5], identified a new type of retinal photoreceptor cell which regulates biological effects. The light sends signals through the photoreceptor cells to our body clock, which regulates the circadian (daily) rhythms and the circannual (seasonal) rhythms in a variety of very different body processes. For good health it is important that these rates are not too altered. If the rhythm has been altered, the morning light helps to restore normal rhythm [6]. Natural light provides the only light with the entire radiation spectrum. In addition, daylight provides less heat in relation to performance than artificial light and is free.

Air quality influences learning. CO₂ concentrations seem to affect attendance. A 1000 ppm-rise in CO₂ concentration leads to increased absenteeism of 10-20% in one study [7], in another

study [8], every increase of 100 ppm leads to a decrease in annual attendance of about 0.2%.

Many schools do not provide an adequate indoor environment and need to make renovation in order to provide an appropriate learning environment for the children.

This paper analyses the effect of a renovated school classroom in Madrid. The renovation consists in increasing the glazing surface incorporating smart windows with automatic opening system, which operates depending on the indoor and outdoor conditions (CO₂, solar radiation and temperature). The objective of this work is to demonstrate whether the renovation impact is successful.

2. METHODOLOGY

The methodology consists of the integration of three approaches: theoretical studies, experimental studies, and participative research. This work started in February 2019, renovation was performed in August 2019 and after renovation research is ongoing.

The School "Waldorf Aravaca" is in a residential area very close to Madrid City. It educates children between 5 and 11 years old. Classrooms under the roof have very poor daylight levels and ineffective ventilation.

The project addresses the issues of indoor air quality, visual comfort with daylight and hydrothermal comfort. The intention is to prove that very good performance levels can be achieved in those fields without compromising the hydrothermal comfort during school hours.

The project of adding three windows in the roof is designed to transform the classroom in a desirable and healthy space for education. The performance of both scenes will be evaluated through three outlooks:

energy and daylight simulations, comfort parameters monitoring and users' perspective.

2.1 Previous simulations

In order to establish the optimal size, number and position of the windows, energy and daylight simulations were carried out. Real energy consumption was not considered in the project due to the difficulties to measure it under reliable methodology.

2.1.1 Energy simulations

Energy simulations were developed to find the best balance between indoor visual and thermal comfort. The objective was to find the right amount of glass that provides enough daylight without dramatically increasing the temperature during school hours in cooling season.

Simulations were run in Design Builder using local climate data from Energy Plus.

Simulations cover 2 different scenarios: original number of windows and final number of windows. For each of them, annual demand and consumption data have been compared as well as indoor temperatures in the warmest hour of the school hours in the summer.

With a total increase of hole area of 4.49 m², the results on energy demand and consumption show an increase of heating needs and a slight decrease of cooling needs (Table 1). The total impact on energy consumption is a raise of an 11.3%.

Table 1: Heating and cooling annual energy demands for before and after renovation scenes. Results of simulations calculated with Design Builder.

Annual analysis			
Scenes	Original	Final	Δ
Cooling energy demand [kWh/m ²]	-39.79	-32.96	-17.2%
Heating energy demand [kWh/m ²]	10.59	13.92	31.4%
Total H + C consumption [kWh/m ²]	21.30	23.70	11.3%

As seen on Table 2, simulations show that the addition of new windows does not result in significant temperature changes. Average annual temperatures remain practically the same, even though average solar gains increase by almost 29%. This could be due to the increase of thermal loss through the glass both during cooling and heating seasons. While there are four new windows losing heat, only the two facing south provide solar gains.

Table 2: Indoor temperature and solar gains for before and after the renovation scenes. Annual average. Calculated with Design Builder.

Annual analysis			
Scenes	Original	Final	Δ
Ganancias solares [kWh/m ²]	27.57	35.54	28.9%
Temperatura del aire [°C]	20.15	20.03	-0.6%
Temperatura operativa [°C]	20.24	20.11	-0.7%

When looking at the warmest time of the school hours through the year (June 12th at 15 p.m.), the results are very similar. Higher punctual solar gains do not drive to overheating (Table 3). Because outdoor temperature (29.5 °C) is much lower than the one indoor at this exact time, higher thermal transmittance of the roof due to the addition of the windows seems to compensate the new solar gains.

Table 3: Indoor temperature and solar gains for before and after the renovation scenes. Annual average. Calculated with Design Builder.

Warmest hour of school year (June 12th 15 p.m.)			
Scenes	Initial	Final	Δ
Solar gain [kWh/m ²]	0.81	1.07	33.1%
Air Temperature [°C]	36.35	35.18	-3.2%
Operative Temperature [°C]	35.82	34.72	-3.1%

The simulations do not include the use of solar control devices or the free cooling of the space during the night. Both strategies improved thermal comfort in the experimental part of this investigation. Energy simulations results need to be validated with the experimental data.

On the other hand, according to simulations performed with Design Builder, lighting consumption drops to a 10% of its original value, showing a great improvement (Table 4).

Table 4: Lighting consumption for before and after the renovation scenes. Annual consumption calculated with Design Builder.

Annual analysis			
Scenes	Original	Final	Δ
Lighting consumption [kW]	1.17	0.12	-90%

Economic and environmental savings in lighting are also interesting when considering improving daylight in school buildings.

2.1.2 Daylight simulations

Daylight simulations were done with Daylight Factor methodology. Different scenarios were simulated with a number of windows between 2 and 8, and with sizes between 0.47 to 0.91 m² of glass.

According to EN 17037 Daylight in buildings [9], recommended daylight values in buildings for Madrid swing between 0.6% and 4.4% DF to achieve interior illuminances between 100 and 700 lux (Table 5).

Table 5: Daylight Factor D equivalent to typical indoor illuminance requirements. UNE-EN 17037:2019 Daylight in buildings.

City	Geographical Latitude φ [°]	Median External Diffuse Illuminance $E_{v,d,med}$	D to exceed 100 lx	D to exceed 300 lx	D to exceed 500 lx	D to exceed 750 lx
Madrid	40.45	16900	0.6%	1.8%	3.0%	4.4%

With the final proposal of 4 windows with 0.91 m² of glass surface, the results are a median DF value of 4.1% and a 1.8% DF value across 91% of the surface of the room. In Madrid, a Daylight Factor of 1.8 % corresponds to 500 lux, which is the illuminance required in classrooms by Spanish legislation (Fig. 1).

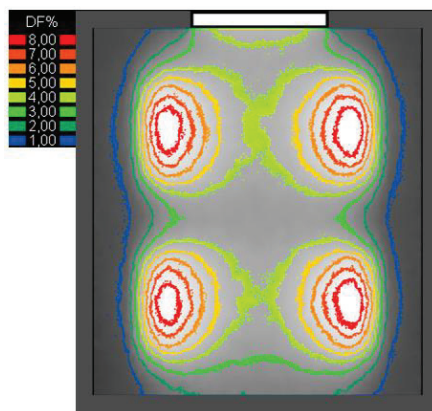


Figure 1: Daylight Factor representation of the final project.

Since the school closes during the summer, the objective was to achieve proper daylight levels through the school months at school hours. Daylight simulations show that with only two windows facing north, the DF is acceptable (Fig. 2), showing that in case of extreme overheating, the roller shutters of the windows facing south could be closed and still achieve a median DF of 1.8% (which is equivalent to 500 lux) and 0.6% DF across 99% of the surface of the room, which is equivalent to 300 lux.

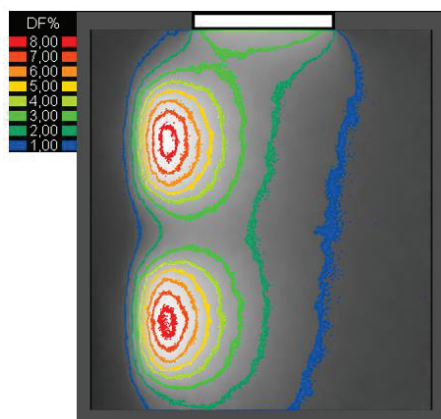


Figure 2: Daylight Factor representation when two windows are darkened by roller shutters to avoid overheating.

2.2 The renovation

The works in the envelope consist in the introduction of new automated windows in the learning space. The roof presented an acceptable level of insulation, so no further actions were implemented.

A total of 3.64 m² of glaze surface (3.17 m² more than original state) were installed distributed in four roof windows, equipped with interior and exterior dynamic sun control devices connected to an automatic system. Every product installed is a standardized market solution. The project does not aim to be a prototype, but a replicable experience.

The new glazed façade connects with the natural surroundings and reduces the dependence on artificial lighting.

The automation of the windows includes opening of windows for ventilation and activation of exterior roller shutters, to cover both thermal and IAQ driven ventilations and overheating prevention. The automatic system combines indoor measurements with weather forecast to make optimized decisions regarding efficient natural ventilation, minimisation of overheating and high comfort and health levels.

2.3 Monitoring

The evaluation of the performance has looked at relevant parameters such as thermal and visual comfort, as well as indoor air quality. Temperature, humidity and CO₂, sensors have been registering data and will stay in place until the end of the project. Daylight measurements have been taken 4 times in each period: outcast and sunny days in summer and winter for both, before and after the works scenes. The collection of data was taken from February to July 2019 as before the intervention performance, and between September 2019 and March 2020 as after the renovation data (COVID situation prevented from getting any later measurement).

2.4 Interviews

Healthier environments are often easily detected by users. Wellness and mood are linked to the spaces we live in and it is a connection we make very well when we choose our homes, but not so much when regarding working or learning spaces.

Short intentional interviews will be carried out during autumn of 2020. Students and teachers will be asked for 3 to 5 minutes about their experience in the classroom before and after the renovation. Questions will relate to daylight, indoor air, sick days, views, and thermal comfort.

The objective of this section is to identify which of the improvements are most valued and to get the interviewees to really connect with their sensations in the space.

2.5 Workshops at the school.

Workshops to increase awareness of children about the relevance of the IEQ and the use of energy of the buildings will be performed to promote their involvement in the use of the classroom. They need to take responsibility to ensure the common interests and become aware of the environmental significance of their actions. The active participation of users helps the changes implemented to be replicated in other cases.

3. RESULTS

Monitoring results were expected to show how air quality and visual comfort can be achieved with acceptable indoor temperatures throughout the year with a precise and optimal management of sun radiation and smart natural ventilation.

Results have been less complete than expected at this time due to the early finish of this school year because of the COVID-19 situation.

3.1 Indoor Air Quality

The concentration of CO₂ shows big changes, even in the months when the smart natural ventilation system wasn't working due to issues with the network.

CO₂ concentration before the renovation was over 4000 ppm for more than 75% of the school hours in February of 2019 (Fig. 3), reaching values up to 8400 ppm. With the new windows, in January of 2020, 85% of the measurements are under 1500 ppm and the curve is more stable (Fig. 4).

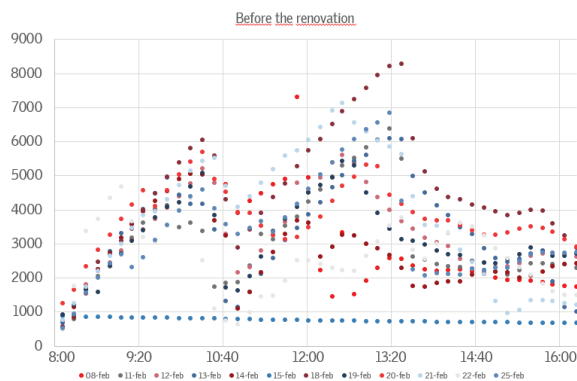


Figure 3: CO₂ concentration in school hours in February 2019. Before the renovation.

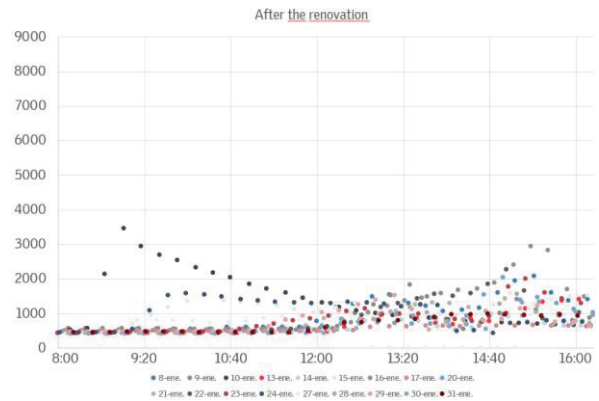


Figure 4: CO₂ concentration in school hours in January 2020. After the renovation.

When looking at the performance of the smart natural ventilation system, we see an improvement. It was working for the last two weeks of November (Fig. 6). When we compare them against the first two weeks (Fig. 5), we see lower CO₂ concentrations and more stable levels during school hours.

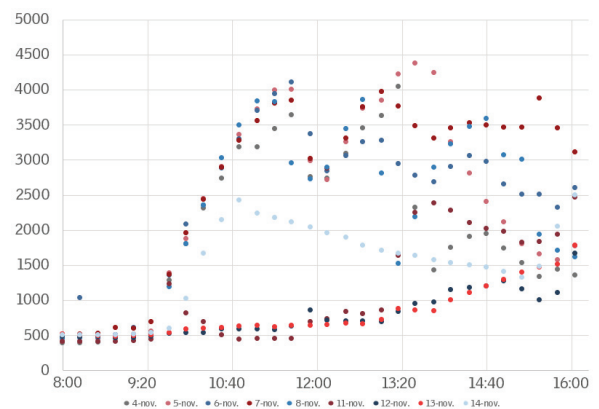


Figure 5: CO₂ concentration in school hours without smart natural ventilation system. November 2019.

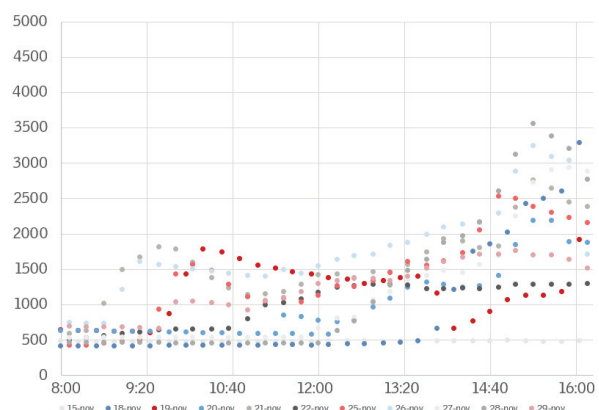


Figure 6: CO₂ concentration in school hours with smart natural ventilation system. November 2019.

3.2 Indoor thermal comfort

Summer and winter scenes have been compared to determine if the addition of daylight has had a negative impact on thermal comfort. Results show a

very similar thermal comfort level after the renovation, in both seasons.

In winter, when comparing February of 2019 and January of 2020, even with the necessary level of ventilation to ensure an adequate IAQ, indoor temperatures are a little closer to thermal comfort after the renovation. While before the renovation, students sat in a classroom between 18 and 20° C (Fig. 7), after the renovation the temperature along the day stays between 19.5 and 21.5° C (Fig.8).

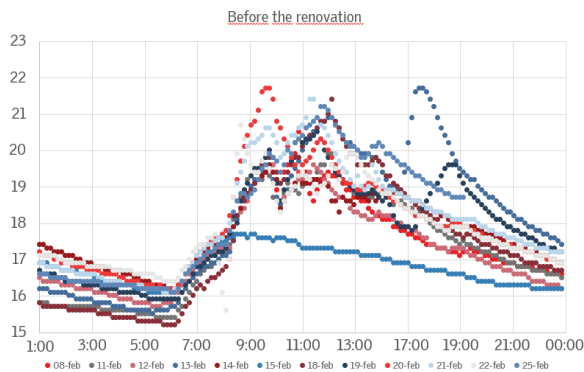


Figure 7: Indoor temperature along the day. Before the renovation in February 2019.

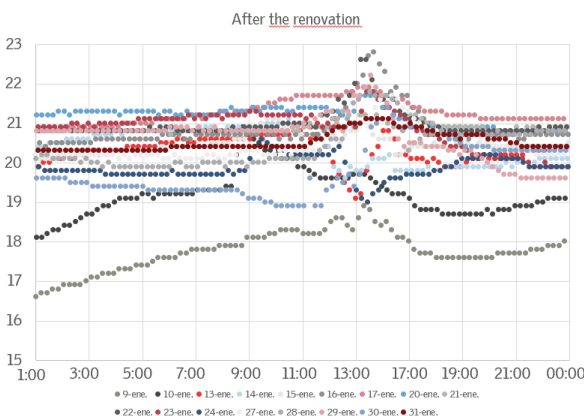


Figure 8: Indoor temperature along the day. After the renovation in January 2020.

The radiation enters the classroom through the new glazed surface increasing the solar gains , which heat the classroom during the day. This positive impact is bigger than the thermal loss at night due to the low thermal transmittance of the windows (1.3 W/m²K).

In order to extract conclusions on the performance during the cooling season, we will need further measurements, as planned. At this moment, we can compare the data of indoor temperatures on the school months before and after the renovation (Fig. 9). Outdoor temperatures were more similar in May and September 2019.

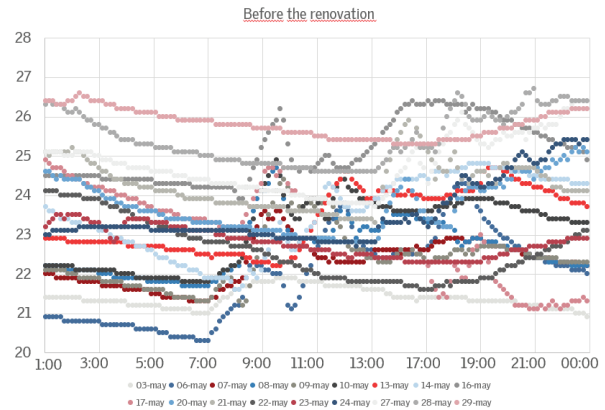


Figure 9: Indoor temperature along the day. Before the renovation in May 2019.

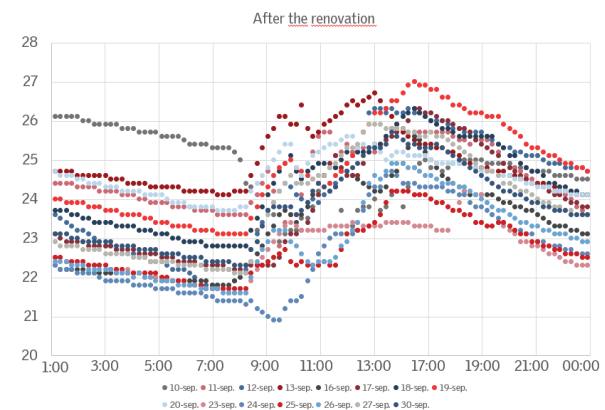


Figure 10: Indoor temperature along the day. After the renovation in September 2019.

Temperatures gathered after the renovation show almost no points over 26° C in September thanks to the possibility to ventilate properly, as well as to shade the windows when necessary.

The classroom can lower the temperature through the night better in September (Fig. 10), which helps reset the building into the comfort range. Indoor temperatures are very similar in both scenes, even though the envelope has increased the glazing area in 3.17 m². Considering the outstanding improvement in daylight and this data, we can say, for the end of the summer scene, the renovation was very successful.

Further data on the performance of the classroom in June, usually the warmest month of school year, needs to be gathered in order to evaluate the intervention at a full perspective.

3.3 Daylight improvement

The measurements of daylight have been taken in an average of 27 points on the students tables.

If we look at the measurements, the median amount of daylight inside is at least 10 times higher after the renovation on all weather and season scenarios (Table 6).

Table 6: Daylight measurements in different weather scenes, before and after renovation.

	BEFORE RENOVATION			
	WINTER		SPRING	
	High rad.	Low rad.	High rad.	Low rad.
Exterior (lux)	30.000	25.000	25-30.000	8.500-9.500
Median (lux)	62	65	58	80
	AFTER RENOVATION			
	WINTER		AUTUMN	
	High rad.	Low rad.	High rad.	Low rad.
Exterior (lux)	25-30.000	10.500	20.000	11.000
Median (lux)	843	1012	647	782
Improvement	1359.68%	1556.92%	1115.52%	977.50%

Only a maximum of 25% of the measurement spots are under the 500 lux, medium level of lighting according to EN 17037 Daylight in buildings [9]. This requirement is usually met with artificial lighting, but in this case, daylight autonomy is ensured through the most part of the school hours.

Daylight levels are even high on a third of the spots. This issue is addressed with the inside blinds and exterior shutters. On the months of more radiation, the two windows facing south can be completely blinded with the roller shutters and the classroom will still be daylit with the north windows, according to the simulations.

3.4 User's perspective

Interviews will take place later in 2020, as COVID 19 situation has impacted the calendar of this project. At this moment, we can only relay on how users have expressed their sensations during the informal team's visits to the school.

The experience of the users is extremely positive. Students as well as teachers have noticed a considerable improvement on energy and mood during lessons.

Interviews are expected to show the value of daylit spaces with views for users, as well as make the connection between this desirable room and better learning predisposition.

4. CONCLUSION

Small envelope renovations can highly improve comfort and health parameters in schools. Projects aiming to improve daylight and IAQ levels can take advantage of sun control devices and natural ventilation to get better environments without a significant impact on thermal comfort or energy consumption during school hours.

The improvement of daylight in the classroom is very high, reducing the dependency on artificial lighting by 90%.

The classroom had serious IAQ issues as concentration levels were extremely high. The improvement of this parameter is outstanding even when the smart ventilation was off and air renovation depended on users. The ability of the classroom to be ventilated with the new windows increased radically.

Thermal comfort has not been penalized by the new windows in any of the months during which data was collected. Thermal comfort in winter is very similar to the levels achieved before the renovation. Solar gains compensate increased thermal losses through the glass. Temperatures during the last month of summer show no overheating during school hours, due to the positive effect of free cooling and shading devices. However, monitoring results for June are necessary to ratify that cooling season is also safe from losing thermal comfort with a generous amount of glazing. This data will not be collected until June 2021 because schools will be closed in 2020 due to COVID 19.

Interviews and workshops with students and teachers will be rescheduled to, at least, Autumn 2020.

We expect, further data collection and analysis to show an adequate performance during the warmest month of the year. From the participative research, qualitative conclusions will be drawn. Both qualitative and quantitative conclusions will be analysed comprehensively to demonstrate that:

Healthier spaces can improve learning, education rates and energy efficiency.

Appropriate IEQ is vital to ensuring opportunities are being taken and children are being protected.

Small envelope renovations combined with automation improve comfort and health parameters.

Smart sun control allows better luminous comfort without compromising thermal comfort during school hours.

REFERENCES

1. Bluyssen, P.M. (2009). The Indoor Environment Handbook. How to make buildings healthy and comfortable". Ed. Earthscan.
2. Fergus Nicol. (2013) The Limits of Thermal Comfort: Avoiding Overheating in European Buildings. *TM52.CIBSE*.
3. Galasiu, A.D. et al. Occupant preferences and satisfaction with the luminous environment and control systems in daylit offices: a literature review.
4. Hescong, L. (2003). Daylighting in schools: an investigation into the relationship between day-lighting and human performance. Hescong Mahone Group.
5. Berson, D.M., Dunn, F.A., Motoharu Takao; (2002). Phototransduction by retinal ganglion cells that set the circadian clock, *Science*, (2002). 295(5557):1070-3
6. Brainard, G.C., (2002). Photoreception for regulation of melatonin and the circadian system in humans, Fifth International LRO lighting research symposium, Orlando.
7. Gunnar Grün, Susanne Urlaub. (2015). Impact of the indoor environment on learning in schools in Europe. *Study Report. Fraunhofer-Institut für Bauphysik IBP*.
8. Gaihe, S., Semple, S., Miller, J., Fielding, S., Turner, S. (2014). Classroom carbon dioxide concentration, school attendance and educational attainment. *Journal of School Health*.
9. Asociación Española de Normalización, (2019). UNE-EN 17037:2019 Daylight in buildings.

User centered lighting environment

Assessing the variables for a biodynamic health enhanced control logic

REMEDIOS M. LOPEZ-LOVILLO¹, MARIA TERESA AGUILAR¹, SAMUEL DOMINGUEZ-AMARILLO¹,
IGNACIO ACOSTA¹, JUAN JOSÉ SENDRA¹

¹Instituto Universitario de Arquitectura y Ciencias de la Construcción, Escuela Técnica Superior de Arquitectura,
Universidad de Sevilla, Seville, Spain

ABSTRACT: An approach is proposed to assess the different parameters used for the feeding of a biodynamic lighting-control system for both the integration of natural and electrical lighting, prioritizing health and the ergonomics of users. Accordingly, variables that directly affect the Circadian Stimulus (CS) such as illuminance levels or SPD will be analysed. The CS will be used as a primary indicator of the impact of the room lighting in the health and the performance of users. A case study is developed in an Intensive Care Unit (ICU) where the care-workers have uninterrupted shifts of 12 hours 24/365. The models integrate natural and electrical lighting through five scenarios involving standard, dimmable and tuneable-white luminaires, and the impact in the Circadian Stimulus (CS) is assessed. Two locations with different type of sky conditions (Seville and London) are tested during winter and summer typical days. The results determine that both the luminous flux and the SPD have a significative impact on CS, so the use of tuneable luminaires presents another worthy potential to optimize CS levels synchronization into shift-time environments as ICU's, since they allow both parameters to be regulated.

KEYWORDS: User-health, task-oriented, smart lighting control, biodynamic lighting, circadian stimulus.

1. INTRODUCTION

The conformation of the light environment is a key factor for the definition of architectural space. At present, within the configuration of the visual field, the integration of natural light is one of the main topics for reflection [1]. Its incorporation into interior spaces, does not only permit significant energy savings in lighting systems [2] and provide psychological and aesthetic aspects [3], but it also has a highly significant effect on the health and physiological-processes of the users [4]. Thus, multiple surveys demonstrate the capacity of natural lighting to regulate circadian rhythms and the alertness of occupants [5]. Natural light provides the appropriate characteristics to regulate the human circadian system [6]. However, nowadays we spend most of the day inside buildings, subjected in most cases to constant electric lighting and light spectrum in flux. The most extreme cases can be found in work centres where professionals work in shifts under artificial light following a 24/365 schedule. Several studies have shown that using illumination to reproduce the spectral distribution of natural light, it is possible to contribute to regulating the circadian rhythm [7], thus preventing health issues such as sleep disruption, depression, cardiovascular diseases or cancer among professionals [8].

There are two main parameters that affect circadian rhythm: Spectral Power Distribution (SPD) and the illuminance perceived by the eye [9]. These parameters must therefore be considered in the

lighting control system, proposing electrical sources that allow their emission to be regulated.

The latest research regarding lighting control views the user as a fundamental driving-factor, bearing in mind not only their presence and location but also considering their behaviour patterns while allowing a more autonomous control on their part [10].

To optimize lighting systems, it is important to evaluate and categorize the impact of different variables for managing (feeding) the systems of integral control of the lighting—natural and electric. This determines the importance in the lighting system response and especially, the impact of the different factors in the interaction with the indoor users and their performance. To do so an experiment is developed combining the simulation techniques of lighting models and control logic in a real space where a biodynamic luminaire control system is installed. In this case, the study of variables from building morphology, user-oriented, and dynamic biodynamic factors are assessed.

The aim is to propose a methodology to optimize a control system which allows the adjustment of the different variables affecting Circadian Stimulus (CS), evaluating the effects of each of these systems.

2. METHODOLOGY

Users are the most important components in a lighting system given their exposure to it. Therefore,

although it is necessary to propose a system that adapts to their needs to guarantee their comfort, it is also important to take their health into consideration.

This is decisive, especially in spaces that are in use 24/365, such as hospitals. In addition, this issue is even more important in Intensive Care Units where professionals work 24/365 in different shifts and sequences. In these settings the timing and optimization of alertness become key aspects to be added to the requirements of individual tasks.

In addition to variables such as illuminance levels or colour rendition, key to CS, other factors related to morphological or environmental aspects such as orientation, location, type of sky or time of year, are considered.

As well as the lighting values associated with the task and CS, it is important to establish the work plane on which these levels are to be achieved. This makes it essential to establish the analysis points of these values.

This analysis is carried out in an Intensive Care Unit where care personnel work two different shifts, one during the day from 8:00 am to 8:00 pm and another at night, from 8:00 pm to 8:00 am. This will be decisive in setting the parameters that regulate the CS.

All these determining factors then become the variables to be analysed with the DIVA for Rhino program, which operates in a similar way to Daysim or Radiance, and has been validated by several studies [11]. Although two locations are proposed, field measurements to calibrate the model will be carried out in Seville. The illuminance at each point will be analysed with this tool. Once these values are known, the CS calculator [12] will obtain the results for analysing the effect of the different control systems on CS. The CS calculator is based on a phototransduction model developed by Real et al. 2005 [12], which considers the melanopic response of the ipRGC cells of the eye, as well as the short-wavelength photoreceptors, such as rods and cones (S), in determining the melatonin suppression produced by the light perceived.

2.1 Description of the study space.

As indicated before, the experiments are carried out in an Intensive Care Unit. In this case (Fig. 1, Fig. 2), the room has a central space where care personnel and nurses perform their normal activity and a peripheral area where patients are located. The central space receives natural lighting from two sides of the unit, complemented by an electric lighting system. Previously, this space had an electrical installation based on the requirements and needs of the space. It has now been replaced by a system of modular LED luminaries arranged in the central area, coinciding with the nursing control area, so that the lighting affects hospitalized patients as little as

possible. Thus, patients are only exposed to lighting in cases when cures or treatments have to be performed.

2.2 Lighting definition

The new lighting system consists of LED luminaires which can be controlled through the electrical flow and SPD. This allows electrical light to emulate the spectrum of natural light and to contribute to the correct regulation of circadian rhythms.

Several design iterations are carried out previously and contrasted with DIALUX [11] software to optimize the arrangement of the luminaires to ensure uniform illuminance levels—a key design aspect—and a work-plane average level of around 500 lux, as required for the activity in compliance with standard EN 12464-1: 2012 [13].

2.3. Parameters

Due to the complexity of quantifying the priority of each variable when defining the lighting control system, it is crucial to specify which parameters are the determining variables to optimize CS. In this case, fewer variables were chosen to achieve reliable results in a simple way, saving on computational efforts. These variables will be the inputs of the system so that they can be classified according to different categories.

In terms of the morphology of the space, the location is decisive. In this sense, two locations were selected for a wider range of results: Seville and London. The former location corresponds to a predominantly clear sky type (CIE D55) and the latter represents a typically overcast sky (CIE D65), so that environmental variables such as the influence of sky type will also be considered here. As it is also worth noting the influence of the direct incidence of the sun, two different time periods will be analysed, winter (December 21) and summer (June 21).

This aspect is fundamental in the regulation of the CS since these factors are linked to the amount of natural light that the spaces receive [14]. These lighting levels will also be related to the type of task being performed, as well as users' schedules. These two variables are related and lighting levels of 500 lux

Table 1: Proposed parameters

BUILDING MORPHOLOGY	LOCATION	Seville
		London
DYNAMIC FACTORS	TYPE OF SKY	Overcast sky
		Clear sky
	TIME PERIOD	Winter (12/21)
		Summer (06/21)
TASK-ORIENTED	TASK	500 lx
		100 lx
	SCHEDULE	8:00 am – 8:00 pm
		8:00 pm – 8:00 am
Cs FACTORS	LIGHT INTENSITY	4100 lm
	CCT	5000 K
		3500 K

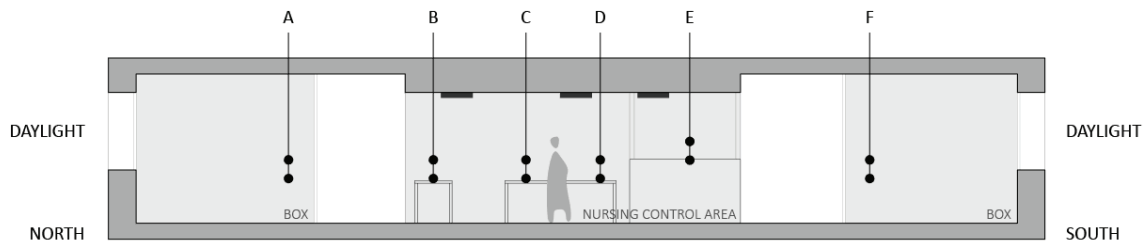


Figure 1: Setting analysed points

two variables are related and lighting levels of 500 lux are required for daytime hours, coinciding with the hours of most activity, while 100 lux are established for night time to ensure patient rest while allowing workers to continue their tasks, since it is an Intensive Care Unit where patients are cared for 24 hours. These thresholds have been established after carrying out several visual perception surveys of healthcare personnel, from which it has been obtained that during the day, values higher than 500 lux cause visual distress, and the same with values higher than 100 lux at night.

Regarding the CS components, it is essential to determine the colour temperature so that a predominantly blue light, at 5000 K, is needed during the daytime, while, in order to promote melatonin secretion among the workers at night, temperatures of 3500 K is used. Light sources have been selected from those with an emission spectrum (represented by their colour temperature) linked with the predominance of short-wavelength cone photoreceptors, in the most common lighting systems in public buildings such as hospitals, corresponding to a CCT value between 3500 and 5000 K [15]. This is because the circadian system is more sensitive to short wavelengths, so that a cold light result in greater suppression of melatonin while a warmer light produces lower suppression.

Table 1 shows the different variables proposed to analyse their influence on CS.

2.4. Study points

The results of 6 locations in the space will be analysed, corresponding to the workplaces.

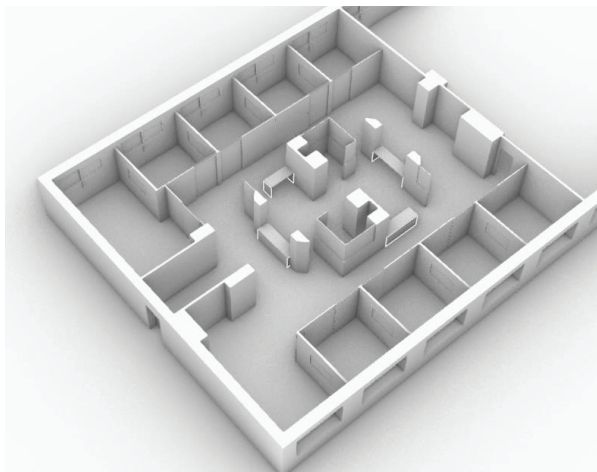


Figure 2: Space model

Two points are analysed in each of the locations: one corresponding to the work plane and the other to the line of vision of the workers. Thus, for cases A, B, C, D and F, a work plane located at + 0.80 m with respect to the ground and a line of vision of +1.22 m is analysed. For case E, whose activity is carried out standing, the work plane is located at +1.22 m and the vision plane at +1.55 m with respect to ground level. The 12 analysis points are shown in Fig. 1.

2.5. Model description

The modelling of this Intensive Care Unit (Fig. 2) is carried out using Rhino 6 and analysed by DIVA for Rhino 4.1.0.11.

Once the model was completed, it was validated to ensure that the results were produced in the most reliable way possible. To do so, a series of points were selected for various measurements in the Seville location, using a Konica Minolta CL-70 F spectrometer to measure the horizontal illuminance and spectrum in four vertical directions. Furthermore, to produce a more reliable model, the colour spectra of the different surfaces of this space were analysed using a PCE-CSM 8 spectrophotometer.

2.6. Metrics

It is necessary to analyse both the natural lighting and the levels of electric lighting at each of these 12 points. To do this, we use the Illuminance (lux) metric defined by the CIE (International Commission of Illumination) [16] to assess the impact of natural light. With all these conditions, the lighting levels will be analysed hourly in each case.

Moreover, to determine the illuminance levels offered by electric lighting in different configurations, the levels reached at each point (night situation) are analysed with the above metric and assuming only electric light.

Based on all the illuminance values established it is possible to derive the Circadian Stimulus (CS), a metric based on the calculation model developed by the LRC (Lighting Research Centre). This metric evaluates the regulation of melatonin considering the adjustment of the luminous flux of the lamps, seeking an accurate forecast of the lighting requirements necessary for the correct operation of the electric installation [17]. Several studies have quantified the influence of light on circadian rhythms by establishing optimal CS parameters. In the research carried out by

Table 2. Case study summary.

SC	LUMINAIRE	LUMIN. FLUX (lm)	CCT (K)	ILLUM. LEVEL (lx)	SCHEDULE
0	STANDARD FLUORESC.	1800	4000	500	8:00am–8:00am
A	STANDARD LED	4100	5000	500	8:00am–8:00am
B	STANDARD LED	4100	3500	500	8:00am–8:00am
C	DIMMABLE LED	4100	5000	500 100	8:00am–8:00pm 8:00pm–8:00am
D	DIMMABLE LED	4100	3500	500 100	8:00am–8:00pm 8:00pm–8:00am
E	TUNEABLE WHITE LED	4100	5000 3500	500 100	8:00am–8:00pm 8:00pm–8:00am

Figueiro [5] it is concluded that a CS value of 0.3 is sufficient for the synchronization of the circadian rhythm. However, overnight CS levels should be below 0.1 for proper regulation of the circadian system.

2.7. Study cases

This methodology is applied to 5 case studies analysed in comparison with case study 0, which is the one currently found in most hospital buildings. For this, a combination of systems with the parameters defined in the previous section is proposed. Thus, standard ON / OFF systems are considered as well as adjustable intensity systems which are tuneable in terms of intensity and CCT. Table 2 shows a summary of the cases.

- Case study 0: it starts from the initial situation where there are standard fluorescent luminaires emitting at 1800 lm and 4000 K.
- Case study A: analysis of a standard modular LED luminaire that emits at 4100 lm and 5000 K colour temperature. Since there is no regulation, natural lighting is not considered, and the electric light

will always be on to reach 500 lux.

- Case study B: this case is similar to the previous one although here the emission is at 3500 K.
- Case study C: an analysis of an adjustable modular LED luminaire, emitting at 4100 lm and 5000 K. In this case, illuminance levels are regulated, starting from natural lighting, complementing with electric lighting until the lighting levels required in each schedule are achieved.
- Case study D: analysis as in the previous case, modifying the colour temperature to 3500 K.
- Case study E: this case is presented as an evolution of the previous two. Starting from a tuneable white luminaire, with a flow of 4100 lm, the aim is to regulate the illuminance levels while changing the colour temperature since this type of luminaire can be graduated from warm white to cold.

3. RESULTS

Tables 3 and 4 show the illuminance and CS levels reached in each time zone in each calculation model, and in the periods from 8:00 am to 8:00 pm and 8:00 pm to 8:00 am.

Before comparing the results obtained, it should be noted that in none of the models is the natural light sufficient to guarantee an adequate level of illumination at all points of the space (500 lx in the morning and 100 lx in the late afternoon and at night) since in Seville only 500 lux are reached at one of the established points (F) and in London, the maximum value reached is 230 lux at point A, at 12 noon in summer. Therefore, the results shown have been obtained from electric lighting sources. Proposing control systems that act on all the luminaires at the same time does not allow them to act by zones, which would be the ideal way to take advantage of

Table 3: Illuminance and CS levels in each case study. Schedule from 8:00 am to 8:00 pm

8:00 am - 8:00 pm									
STUDY CASES	CONTROL	LUMINOUS FLUX	CCT	ILLUMINANCE			CIRCADIAN STIMULUS		
				Min	Max	Average	Min	Max	Average
0	ON/OFF	1800 lm	4000 K	163 lx	481 lx	254 lx	0.048	0.279	0.148
A	ON/OFF	4100 lm	5000 K	538 lx	969 lx	709 lx	0.466	0.58	0.495
B	ON/OFF	4100 lm	3500 K	538 lx	969 lx	709 lx	0.33	0.481	0.369
C	DIMMER	4100 lm	5000 K	500 lx	500 lx	500 lx	0.385	0.385	0.385
D	DIMMER	4100 lm	3500 K	500 lx	500 lx	500 lx	0.247	0.247	0.247
E	TUNEABLE	4100 lm	5000 - 3500 K	500 lx	500 lx	500 lx	0.385	0.385	0.385

Table 4: Illuminance and CS levels in each case study. Schedule from 8:00 pm to 8:00 am

8:00 pm - 8:00 am									
STUDY CASES	CONTROL	LUMINOUS FLUX	CCT	ILLUMINANCE			CIRCADIAN STIMULUS		
				Min	Max	Average	Min	Max	Average
0	ON/OFF	1800 lm	4000 K	163 lx	481 lx	254 lx	0.048	0.279	0.148
A	ON/OFF	4100 lm	5000 K	538 lx	969 lx	709 lx	0.466	0.58	0.495
B	ON/OFF	4100 lm	3500 K	538 lx	969 lx	709 lx	0.33	0.481	0.369
C	DIMMER	4100 lm	5000 K	100 lx	100 lx	100 lx	0.117	0.117	0.117
D	DIMMER	4100 lm	3500 K	100 lx	100 lx	100 lx	0.057	0.057	0.057
E	TUNEABLE	4100 lm	5000 - 3500 K	100 lx	100 lx	100 lx	0.057	0.057	0.057

natural light at the points closest to the windows where, as can be seen below, sufficient lighting levels are reached with natural lighting alone. Thus, in this case, the worst scenario was adopted using only electric light, although the individual control of luminaires would be advisable for future research.

Initially, the situations with standard luminaires and the current situation of this space were analysed (cases 0, A, B). Although the control system is the same with standard luminaires in both cases, we found a greater benefit in cases A and B than in case 0 due to the use of LEDs rather than fluorescent lamps. As seen in Table 3, this results in a 230% increase in average CS during the morning. The current luminaires provide an average CS of 0.148 during the morning, below the established minimum value of 0.3, and the value of 0.466 for static LED luminaires with a CCT of 5000 K and 0.33 with a CCT of 3500 K. These would already both be in compliance with minimum CS in the morning. At night, however, since the two luminaires are static, both are detrimental to circadian rhythms as they should have values lower than 0.1.

The transition to luminaires with adjustable intensity using a dimmer control system (cases C, D) allows us to improve these CS values at night, as seen in the table. During the morning optimum CS levels (>0.3) are reached in both standard and dimmable

lighting. However, adjustable lighting achieves a homogeneous CS throughout the space by being able to adjust illuminance to 500 lx on the work plane. Comparing cases C and D with cases 0, A, B, it is observed that the average CS achieved is approximately 30% higher with static lighting. This occurs because, with static lighting, some points are over-lit, reaching values 93.8% higher at the appropriate value of 500 lx and causing visual discomfort as we have been able to verify in on-site tests with the ICU health personnel. Therefore, with adjustable lighting, lower average CS levels are reached in the morning, although they are enough to promote adequate circadian stimulation with a more homogeneous field of vision and visual disturbances. At night, the adjustable system represents a considerable improvement and is able to provide an illuminance level of 100 lx in the field of work, therefore reducing CS levels by up to 320% with a CCT of 5000 K and by 540 % with a CCT of 3500 K. With a standard illumination at night, a CS value four times greater than the established limit of 0.1 is obtained, while with an adjustable system, values that are reached are close to the maximum of 0.1, and are 17 % higher than 0.1 with a CCT of 5000 K and 43 % lower than 0.1 with a CCT of 3500 K.

Another aspect to consider is the CCT of the luminaires. In the case of both standard and

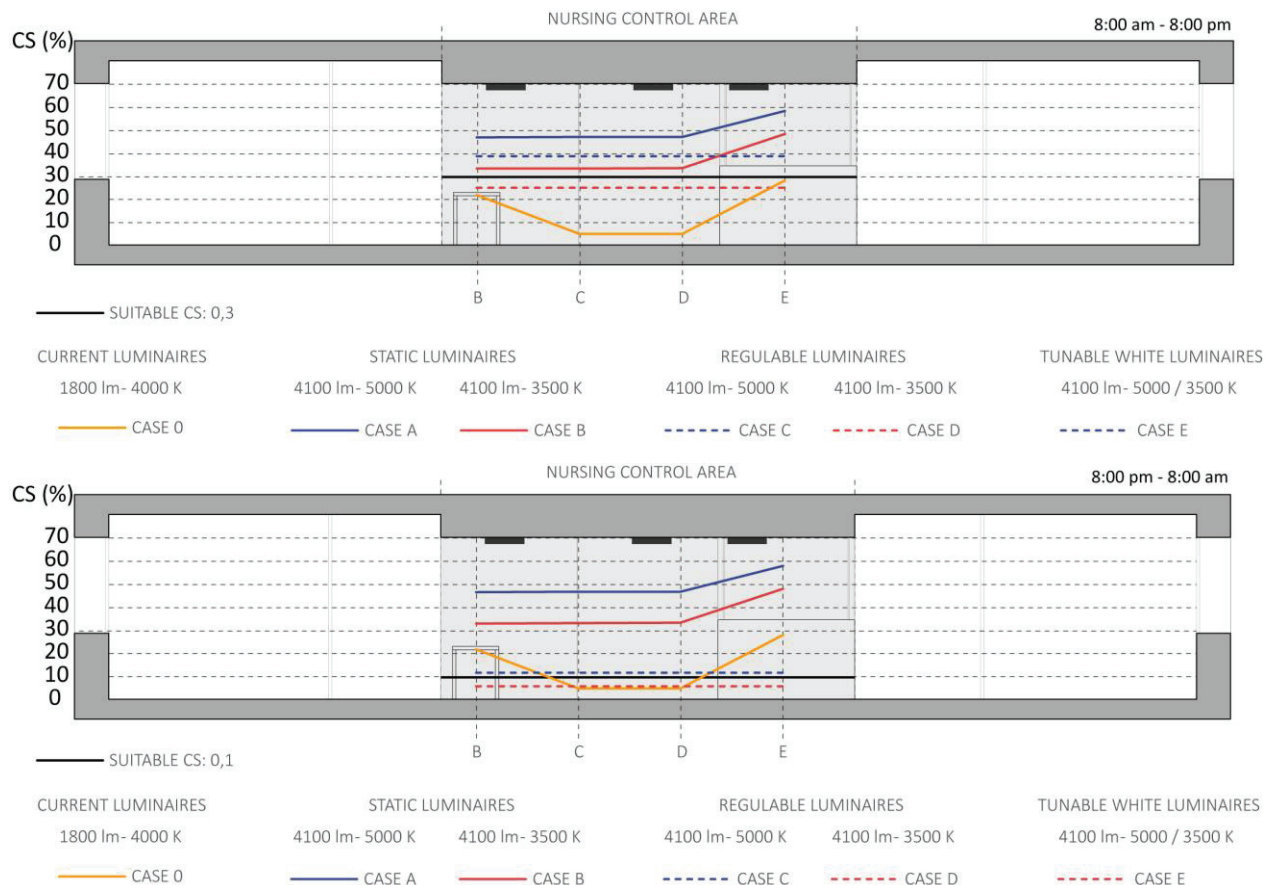


Figure 3: CS influence

dimnable luminaires, the CCT influences the CS, with a 5000 K CCT, which is better during the day since higher CS levels are achieved while lower values of 3500 K are obtained at night. This is followed by the next level of lighting control system, dimmable white tuneable luminaires (case E). These share the advantages of previous dimmable luminaires in terms of intensity and allow the spectrum to be modified both day and night. Compared to the adjustable 5000 K this system reduces night time CS by 51%, approaching the maximum level of 0.1. Compared to the adjustable 3500K daytime CS increases by 56%.

Fig. 3 shows how the CS influences each of the case studies at each point in the nursing control area.

4. CONCLUSIONS

The results obtained from the simulation show that, due to the non-influence of natural lighting, variables such as location, type of sky or time period are not relevant. This occurs in this case because the work area of the care personnel analysed is quite far from the natural light sources of space.

If considering the parameters directly affecting CS, it is possible to observe the effect of both SPD and the lighting level. This confirms the direct influence of the luminaires on the CS according to the type and the regulation capacity (illuminance and spectrum). In the case of a fluorescent luminaire which does not comply with CS values ($0.148 < 0.3$), the proposed LED luminaires provide a better adjustment to these values for cases with both 5000K (0.495) and 3500K (0.486) CCT, although this aspect can be modified by the characteristics of specific luminaires.

It is also confirmed that dimmable lighting offers better CS values compared to standard lighting since, in addition to achieving the optimum values for day and night, it avoids visual disturbances caused by excess lighting according to care personnel preferences.

As a significant advance, it should be noted that if both illuminance levels and SPD are varied, better CS values are obtained, concluding that tuneable white luminaires should be used in 24/365 work centres to optimize the CS of the workers.

From the results obtained, it is also concluded that the zoning of the luminaires is a fundamental strategy for lighting control systems which aim to regulate CS, since more optimized levels are reached at the points near the windows compared to centrals.

For future research, it is worth mentioning the use of this methodology including other variables such as orientation, window size, room depth... as well as more complex control systems. Depending on the results obtained, tuneable luminaires will be chosen. From the results obtained, it is also deduced that for the same SPD value, optimized results can be

obtained by varying the spectrum, making this topic a potential future line of research.

REFERENCES

1. L. Bellia and F. Fragiasso, (2017). New parameters to evaluate the capability of a daylight-linked control system in complementing daylight. *Building and Environment*, 123: p. 223–242.
2. I. Acosta, M. A. Campano, S. Dominguez-Amarillo, and C. Muñoz, (2018). Dynamic daylight metrics for electricity savings in offices: Window size and climate smart lighting management. *Energies*, 11 (11): p. 2-27.
3. O. Grigore, I. Gavat, and M. Cotescu, (2008). Stochastic algorithms for adaptive lighting control using psychophysiological features. *International Journal of Biology and Biomedical Engineering*, 1 (4): p. 68-77.
4. L. Bellia, F. Fragiasso, and E. Stefanizzi, (2016). Why are daylight-linked controls (DLCs) not so spread? A literature review. *Building and Environment*, 106: p. 301–312.
5. M. G. Figueiro et al., (2017). The impact of daytime light exposures on sleep and mood in office workers. *Sleep Health*, 3 (3): p. 204–215.
6. P. R. Boyce, (2010). Review: The impact of light in buildings on human health. *Indoor Built Environment*, 19 (1): p. 8–20.
7. K. M. Kim, Y. W. Kim, S. T. Oh, and J. H. Lim, (2019). Development of a natural light reproduction system for maintaining the circadian rhythm. *Indoor Built Environment*, 29 (1): p. 132–144.
8. R. G. Stevens, (2009). Light-at-night, circadian disruption and breast cancer: Assessment of existing evidence. *International Journal of Epidemiology*, 38 (4): p. 963–970.
9. L. Bellia, F. Bisegna, and G. Spada, (2011). Lighting in indoor environments: Visual and non-visual effects of light sources with different spectral power distributions. *Building and Environment*, 46 (10): p. 1984–1992.
10. H. Zou, Y. Zhou, H. Jiang, S. C. Chien, L. Xie, and C. J. Spanos, (2018). WinLight: A WiFi-based occupancy-driven lighting control system for smart building. *Energy and Buildings*, 158: p. 924–938.
11. I. Acosta, J. Navarro, and J. J. Sendra, (2011). Towards an analysis of daylighting simulation software. *Energies*, 4 (7): p. 1010–1024.
12. M. S. Rea, M. G. Figueiro, J. D. Bullough, and A. Bierman, (2005). A model of phototransduction by the human circadian system. *Brain Research Reviews*, 50 (2): p. 213–228.
13. AENOR, Norma UNE-EN 12464-1:2012. Iluminación. Iluminación de los lugares de trabajo. Parte 1: Lugares de trabajo en interiores. 2012.
14. L. Bellia, A. Pedace, G. Barbato, and F. Fragiasso, (2015). Complete evaluation of daylight characteristics in working environments. *6th VELUX Daylight Symposium*, 1: p. 2–3.
15. R. J. Lucas et al., (2014). Measuring and using light in the melanopsin age. *Trends in Neurosciences*, 37 (1): pp. 1–9.
16. F. Maamari, M. Fontoynt, and N. Adra, (2006). Application of the CIE test cases to assess the accuracy of lighting computer programs. *Energy and Buildings*, 38 (7): p. 869–877.
17. M. G. Figueiro, K. Gonzales, and D. Pedler (2016). Designing with Circadian Stimulus. *Ld+a*, 9 (3): p. 31–33.

Circular construction

Circularity through business models for longer building life

LARA ANNE HALE¹

¹Copenhagen Business School, Copenhagen, Denmark

ABSTRACT: *This paper investigates the problem of the undervalued 'use' phase in circular construction business models, and how smart building technologies, especially the Internet of Things (IoT), can enable elongated use of buildings. Despite the recent attention to circular economy in both research and practice, applications to the building industry are falling short. The aim of this research is to examine the opportunities and barriers to the circularity of resources in the building sector. Based on an ethnographic study and two workshops, the research finds that although the use phase is not currently valued in circular construction business models; that there are (a) multiple use phase values to be capitalized upon, (b) both economic and practical drivers for doing so, and (c) technological advancements that can facilitate this.*

KEYWORDS: *Circularity, Circular Construction, Business Model Innovation, Smart Building, Use Phase*

1. INTRODUCTION

This paper investigates the problem of developing circular construction business models and the challenges facing the building industry in practice. Despite the recent attention to circular economy in both research and practice, applications to the building industry are falling short [1, 2, 3]. The aim of this research is to examine the opportunities and barriers to the implementation of circular economy in the building sector, also referred to as *circular construction*. In particular, building organizations have recently demonstrated an interest in innovating circular business models in order to transition their cradle-to-grave business to circularity.

The building industry is particularly ripe for transition, given that it produces the largest total amount of waste in the world [4] and is a massive consumer of energy. In Europe, the industry is responsible for 40% of total energy use and 36% of greenhouse gas emissions [5]. In recognition of these issues, several companies, such as Arup, the Ellen McArthur Foundation, and 3XN Architects and GXN Innovation, have taken up the mantle to initiate the first steps towards building based on circular economy, or circular construction [6]. Yet, despite the recent attention to circular economy in both research and practice, implementation of circular construction is not advancing [1,2,3]. At the same time, innovation under the auspice of 'Industry 4.0' -- referring to business applications of the Internet of Things (IoT) and smart technologies -- opens up the possibility of smarter circular business models across industries.

Recognition of this challenge arose from ethnographic research in the building organization the VELUX Group, a company best known for its roof windows, but also deeply engaged in the research into

and development of sustainable buildings. The research was then furthered with two workshops -- one internal and one external -- and secondary data such as circular building materials and events concerning circular construction. The research finds that -- akin to other industries -- the building industry places an inordinate amount of attention on the reuse and recycling of material and little attention on extending the use of buildings (and thus their materials). This paper argues that one of the major shortfalls of current circular economy approaches in building is a lack of business models valuing the use phase of buildings and economically driving implementation of technologies for longer life.

2. THEORETICAL BACKGROUND

Theory development on sustainable business models including a circular economy approach is expanding [7,8,9]. Scholars utilize different definitions of circular economy that may consider the material dimensions, or economic aspects; but for the purposes of this paper, the Ellen McArthur Foundation (EMF) definition is used: 'A Circular Economy is an economic and industrial system where material loops are closed and slowed and value creation is aimed for at every chain in the system' [10], a system which 'aims to redefine growth, focusing on positive society-wide benefits' [11].

Thus far, the focus on circular economy business models has tended towards easily handle-able and transferable products, as opposed to durable goods [12]. Part of the problem could be the tension between economic and social or ecological valuation, because there is more economic activity involved in shorter-lived products that can be transformed into new products for consumption. Following these views,

Flynn and Hacking (2019) describe the ideological conflict arising from circular economy standards within a neoliberal governance system [13]. These material input and output focused valuations can reduce (or even eliminate) waste and improve efficiencies (and global trade), but they neglect a true life-cycle approach and potentially encourage design for planned obsolescence.

In theory we can see this reflected in the consideration of time as a factor for sustainable business models: As Lozano (2018) underlines in his review of sustainable business model literature: 'The time dimension is conspicuously missing in SBMs discourses' (p.4) [14]. Indeed, the tendency of research on circular economy for building tends to focus on two distinct time frames, pre-construction and re-use, while glossing over the use phase [12,3]. In their literature review of circular economy for buildings, Hossain and Ng (2018), find that most research that considers circular economy for building either consider cradle-to-grave (planning to demolition) or cradle-to-gate (planning to construction approval), and only 2% consider cradle-to-cradle (planning to next integration) (p.767) [15]. They also point to economic and social sustainability, fundamentally tied to the use phase of buildings: 'Sustainability assessment cannot be fully evaluated without considering the economic and social aspects, and most of the studies did not take those aspects into account' (p.776) [15].

Terms such as the *Internet of Things (IoT)*, *digital technologies*, and *smart technologies* are used interchangeably herein to refer to the combination of physical products and digital connectivity that yields benefits to a product or service. The potential game-changing effect on business of these technological advancements is collectively referred to as 'Industry 4.0' [16,17,18]. As Garcia-Muiña et al. (2018) venture: "Industry 4.0 and circular economy are candidates to be two sides of the same coin" (p. 256) [17]. But they also point out that this depends on industry's commitment to sustainability and argue that such responsibility "shifts the attention from a product-oriented production and consumption model to a solution-oriented model" (p. 279). Parida, Sjödin, and Reim (2019), in their literature review on digitalization, business model innovation, and sustainable industry, also claim that business model innovation is essential to harnessing the potential of IoT, given the growing demand for continuous improvement and long-term value for customers. They similarly underline the challenges of shifting business models from revolving around products or services to results [19].

Yet, despite multitudinous hurdles, a transformation is certainly underway; and digital technologies offer potential directions in which to develop circular construction business. For example,

Jensen & Remmen (2017) consider circular business models through IoT in practice and present how businesses are implementing IoT-based servitized business models in the automotive, shipping, and aircraft industries [18]. Another technology especially bridging data and design in the industry is Building Information Modeling (BIM), a tool for data-driven planning of construction based on the assembly of virtual BIM 'objects' containing detailed information about real-world products [20]. The uncertainty in design and material choice can be reduced by combining BIM and LCA [21]; and BIM can be more specifically used to design for circular economy [20]. Other opportunities include but are not limited to: building or material passports; sensor systems for modeling user behaviour; Big Data analytics; and building automation, including artificial intelligence mediation.

3. METHODOLOGY

This research uses qualitative methodology based on an ethnographic study at VELUX and two industry workshops. The ethnographic study involved office presence 1-3 times per week between January 2018 and June 2019, and it included observation of daily activities, informational meetings, and internal workshops and events, which were documented in note taking. The first workshop took place on the 25th of October 2018 in Zurich, Switzerland, and involved approximately 25 VELUX architects from VELUX sales offices, primarily from Europe. During this workshop, architects were asked to identify what the value during the use phase of the building is.

The second workshop took place on the 8th of November 2018 in Lecco, Italy, and involved about 20 architects and engineers from the Active House Symposium. They were asked to rank aspects of Building Information Management (BIM) by *sustainability importance*, *professional practicality*, and *economic viability*. Participants could rank levels 1-3 for each of these categories, with one being the top priority, and then scaling down to the third most prioritized aspects. The aim was to identify how a design tool that can be combined with life-cycle approaches (such as life-cycle assessment, LCA) to design for circular construction might imbed a variety of building aspect prioritizations in the industry. These rankings were then compiled into a spreadsheet, from which the BIM aspects were given an average rank and weighted average rank for each category.

3. FINDINGS

The VELUX case as derived from the ethnography is first shown, and then the outcomes from Workshops 1 and 2 are presented.

3.1 The VELUX Case

The VELUX Group ('VELUX') is a building company based in Hørsholm, Denmark with over 10,000 employees in sales offices and manufacturing facilities in 40 countries around the world. Villum K. Rasmussen founded the company following his original invention of a rooftop window in 1941, at a time when Europe was facing a shortage of healthy housing; and these roof windows allowed for the renovation of attic spaces into living quarters or improvement of upper levels in buildings. Although the company portfolio now includes such products as flat-roof windows, blinds, shutters, and even bespoke solutions, the development of the portfolio revolves around the central value of providing a healthy indoor climate through daylight and fresh air. In other words, despite its multitude of building *components*, the business model is based on a *whole building* approach. This is most emblemized in VELUX's co-founding of and participation in the Active House Alliance, where like-minded, cross-sector partners promote sustainable building based on a combination of energetic, environmental, and comfort specifications, while placing the utmost priority on the humans in buildings.

The idea of integrating technology into buildings is far from new. In fact, since 2005 VELUX has been a member of the consortium that developed io-homecontrol, a wireless communication protocol for home connectivity and automation (established by companies such as Somfy, Niko, and Renson, but now with a different set of partners). To this day, motorized VELUX windows and blinds can be controlled through io-homecontrol. Nonetheless, the advent of smart building sensor-, app- and voice- controlled devices, primarily provided by the 'tech giants' Apple (Apple HomeKit), Google (Google Home), and Amazon (Alexa), has turned smart building on its head, especially since the advent of Project Connected Home Over IP, an alliance including Zigbee, Apple, Google, and Amazon to standardize smart technology protocols. These developments have formed a new interface with building users and opened the building business ecosystems [22,23] to include technology companies. VELUX is also committed to engagement in a number of industry events and conferences for knowledge-sharing and partnership formation (e.g. participation in the Urban Tech program for urban innovations). This kind of technological- and collaborative foresight lends to business model development within circular construction. Examples of notes related to circular construction and building use from the ethnography can be seen below in Table 1.

Table 1: Ethnographic note samples.

"Much of company does not appreciate the need to understand the users better." 1 April 2018, internal meeting, anonymous
"At the end of the day, what's really important is how it's operating, how it's being used." (referring to the building), 24 Sept. 2018, external event, Nadia Yen, First Gulf
"The most sustainable thing you can do is to build a building that will last 500 years or more." 26 Sept. 2018, internal event, John Sommer, MT Højgaard
"The renovation rate is too slow, the renovation depth is too shallow, and it's not clear which buildings most need renovation." 26 Sept. 2018, internal event, Andreas Hermelink, Ecofys
"It's very much the agenda now to talk about the value of circularity." 20 Nov. 2018, external event, Torben Klitgaard, BLOXHUB
"Buildings that are loved are used for 100s of years. Now they completely skip the whole use phase." 25 Jan. 2019, internal meeting, anonymous
"When we brought circular economy to the World Economic Forum, it was a niche topic. And now it's broadly recognized, also from our clients." (Moderator: Isn't there a discourse around capitalism still being the driving force?) "Indeed we see those opportunities that have a real business case...if you can show the business case, you can get them to change." 18 Feb. 2019, external event, Stephanie Hubold, QVARTZ
Efforts at changing company mindset from being just about product to being about "green" and "healthy" outcomes, including circularity. 26 Feb. 2019, internal meeting, anonymous
Three phases: business model, product, process. Process as most interesting because you can look at it more systematically, and this goes back to the business model. Don't start with good product now, but ask what is there demand for in the market? And then figure out how to make it economical. 4 April 2019, external event, Ditte Lysgaard Vind, Lendager Group

In addition to potential support of circular construction, there are a number of advantages of smart building systems for VELUX, for example: improving the direct relationship with customers, protecting the indoor climate from conditions that could be detrimental to people's health, increasing awareness about healthy indoor climate, automating and personalizing energy consumption, and creating optimal conditions for the building. Following from this, in July 2018, VELUX launched a smart device, VELUX ACTIVE with NetAtmo, which automates natural ventilation via motorized roof windows and blinds based on sensor readings of CO2 levels, humidity, and temperature and which can be controlled through its own app, the Apple HomeKit app, or a wall-mounted remote. Further, 2018 saw the official adoption of BIM as the standard interface system for architecture and product integration across the VELUX Group. Nonetheless, the question arises: if there is the motivation for the whole building

approach, as well as advancing technologies that could support it, what is interfering with circular construction business models? The main observation crosscutting the ethnography is the rising popularity of circular construction that appears to come at odds with the status quo of construction sector business models.

3.2 The Workshops

Simultaneous to attempts to generate new business from trade activity based on reusing and recycling building materials, there is an increasing concern for (and helplessness about) the use (or *operations*) of buildings. The initial findings from Workshop 1 (Table 1) demonstrate the use phase value that could potentially be captured in circular construction. Further, the initial findings from Workshop 2 (Table 2) show that building professionals do not rank operation and maintenance, the factor most linked to the use phase, as the most important for sustainability (landing instead at fourth place out of the factors). However, they do rank it as the number one most practical factor, as well as the second most economical factor.

Table 2: Workshop 1 – Building use phase value.

Inputs (e.g. materials, energy, finance)	Process (e.g. visioning, drawing, collaboration, certificates)	Outputs (Use Phase)
		knowledge
		good sleep quality
		motivation
		understanding / awareness
		comfort
		pride / privilege
		innovation
		uniqueness
		health
		privacy / security
		happiness
		productivity
		well being
		recharging

Table 3: Workshop 2 - Summary of BIM rankings.

Ranking	Sustainable	Practical	Economical
1	Integrated design	Energy Analysis	Construction management
2	From concept to as-built detail	Operation & maintenance (tied for 1 st)	Integrated design
3	Construction management	Integrated design	Operations & maintenance (tied for 2 nd)

4. DISCUSSION

These findings underscore a disparity between the value placed on buildings in use and the reflection of this value in current business models for building, wherein economic value capture is heavily focused on

the production phase, despite resource intensity. But they also indicate that there is a practical and economic opportunity to develop business models around the durable use of buildings. In particular for the building industry, wherein the durable life of the product can extend to hundreds of years, it makes sense that building companies would need to utilize service-oriented business models to support the circularity and sustainability of buildings over their full life span. Arguably, this was not possible due to a fragmented industry with multitudinous shortages of information -- until the advent of smart technologies. Though, as much of the literature on IoT cautions, just because digital technologies can facilitate circularity, does not necessarily mean they will.

There are a number of ways to strategically approach circular construction business models and best capture the value of business use. For example, the findings from Workshop 2 suggest that focusing on economic and practical advantages of using BIM for extending the life of buildings would more likely result in using this technology for circularity business models than if sustainability was emphasized. Putting together the research and the literature, what is highlighted here is that technological added value can best be captured if businesses focus on (at least) three priorities: ensuring data analysis connects back to design; networking across multiple stakeholders; and starting from customer needs.

With VELUX ACTIVE, data on the usage of the system and interactions with customers is needed to design not only a better version of ACTIVE, but also to design better buildings and customer relationships. Linking the data analysis back to design leads to “improve[d] both assessment and continuous improvement process in the product design stage” that facilitates product stewardship (p. 381) [18], be that through customer or producer ownership. Bakker et al. (2014) similarly emphasize the role of design for ‘products that go round’, or circularly designed products, in order to combat the trend of decreasing lifespans [24]. For the building industry, data on materials and quality can affect construction design [25], and the data analysis is especially useful for planned and predictive maintenance and renovation.

As Teece (2010) stresses: “History shows that, unless they can offer compelling value propositions to consumers/users and set up (profitable) business systems to satisfy them with the requisite quality at acceptable price points, the innovator will fail, even if the innovation itself is remarkable, and goes on to be widely adopted by society” (p. 186) [23]. Bakker et al. (2004) also point to economic viability of CBMs as an aspect that cannot be compromised [24]. When it comes to the VELUX case, it was the building users who drove the rise of app- and voice-controlled smart building technologies; and it is the users who will

determine the attractiveness of circular construction. For one, users are more interested in circularity for psychological or economic reasons than environmental or sustainability ones [26], which is supported by the results from Workshop 2. And the IoT offers opportunities to better understand and, in a sense, collaborate with users to create the economic systems of tomorrow. By going beyond daily life based on readily available information, the IoT can bring value to customers through more interconnected, informed decision-making.

There are certainly both barriers and opportunities for servitized, circular business models in the building sector that would capture value from the extended life of buildings. On the one hand, there are stakeholders in the building industry who benefit from the status quo and who profit from new construction, even if it means demolishing buildings before their justified end of life [26]. Or, as EMF points out, the industry could swing the opposite direction towards modularity-driven short-lived buildings. Further, there is a fair amount of uncertainty and risk involved in switching to service-based business models [27], and Leising, Qvist, and Bocken (2018) point out the building industry's difficulty in reimagining value due to the multifarious partners, materials, and life spans involved [12].

On the other hand, the IoT is a game changer, metamorphosing and connecting several areas of the business, while gaining in strategic importance. Bressanelli et al. (2018) highlight that the combination of smart technologies, circular economy value drivers, and a lifecycle perspective "allows managers to align their company strategy to the desired path" (p. 656) [16]. And despite interest in modular construction (which can also lend flexibility to durable buildings), the greatest value for the building industry is in the longevity of these resource-intensive products. From the pure newness of being able to leverage digital technologies, IoT for circular construction business models can bring building companies into a 'blue ocean', where there is "fertile ground for innovation and value creation" (p. 128) [28]. Though in order to do so, businesses need to capitalize on the design-improving capacity of digital technologies, establish new business models, and approach customers with flexible design strategies a sensitivity to their needs.

5. CONCLUSION

This research sheds light on the neglected use phase in circular construction. Although circular economy aims to approach sustainability from a life cycle perspective, not all phases are considered equally in construction. Yet, this blind spot to the use phase overlooks promising value, as elucidated in the results in Table 1. And these aspects could be practically and economically addressed, as highlighted

in Table 2, by incorporating use phase value – for example with the use as smart technologies such as building automation systems and life cycle tools such as BIM combined with LCA. This is not disconnected from the transition from product to service economy. Thus, the challenge is not just the circular flow of materials through the life of buildings, but the care and renewal of materials throughout the long life of buildings.

Ultimately this is a problem of time and business models. For durable goods, be they buildings, refrigerators, or automobiles, it is easy to imagine that the financial value capture will be more tangible for companies attempting circular economy if their business focuses on rapid production, even if that means shortening the products' life span. Yet in terms of sustainability, there is some irony here: the business models that could make building companies more sustainable in the long run are dropped to the wayside when companies consider they might not last long enough for the total value to be relevant to them down the line. Thus, the challenge is not just the circular, slowed flow of materials through multiple cycles, but rather the innovation of circular business models that enable companies to profit from utilizing a lifecycle perspective, even if their products are extraordinarily long-lived. In this light, servitized business models hold much promise, so long as building companies can form technology platforms and consumers can steer well enough to shift both supply and demand in a timely enough manner to satisfy business. Governments and policy making can also play a significant role in facilitating and accelerating this transformation.

This research builds upon the excellent work of many talented scholars, and naturally, can be furthered with additional research. Future research areas could, for example, include: How can different business models be set up to capitalize on the use phase data from IoT technologies? How can networked platforms organize business models that ensure the benefits of building use are distributed fairly among partners? What is the role of consumers in shaping circular construction business models? As with most sector-focused works, it would be interesting to examine the relevance of the presented model for other sectors, especially regarding long-lived products. But perhaps even more intriguing would be research into the industry-spanning mechanisms of IoT, and how that works in practice with servitized business models.

ACKNOWLEDGEMENTS

This research is part of the Danish 'Smart Buildings and Cities' research cluster and is made possible by funding from The Danish Innovation Fund and Realdania. I would also like to thank the VELUX Group and BLOXHUB for their collaboration, welcoming, and forward-thinking.

REFERENCES

1. Geldermans, R.J. (2016). Design for Change and Circularity – Accommodating Circular Material & Product Flows in Construction. *Energy Procedia*, September 2016 (96), 301–311.
2. Ghisellini, P., Ripa, M., and Ulgiati, S. (2018). Exploring environmental and economic costs and benefits of a circular economy approach to the construction and demolition sector. A literature review. *Journal of Cleaner Production*, March 2018 (178), 618–643.
3. Nußholz, J. L. K., Nygaard Rasmussen, F., & Milios, L. (2019). Circular building materials: Carbon saving potential and the role of business model innovation and public policy. *Resources, Conservation and Recycling*, 141(October 2018), 308–316.
4. Clark, C., Jambeck, J., & Townsend, T. (2006). A review of construction and demolition debris regulations in the United States, critical reviews in. *Environmental Science & Technology*, 36(2), 141–186.
5. IEA. (2019). Tracking Energy Transitions. Retrieved from: <https://www.iea.org/tracking/>
6. Acharya, D., Boyd, R., & Finch, O. (2018). From Principles to Practices: First steps towards a circular built environment. Report by Arup, the Ellen McArthur Foundation, and 3XN Architects and GXN Innovation.
7. Lacy, P., & Rutqvist, J. (2015). Waste to wealth: The circular economy advantage. Basingstoke, UK: Palgrave Macmillan.
8. Bocken, N. M. P., De Pauw, I., Bakker, C., & van der Grinten, B. (2016). Product design and business model strategies for a circular economy. *Journal of Industrial and Production Engineering*, 33(5), 308–320.
9. Simons, M. (2017). Comparing Industrial Cluster Cases to Define Upgrade Business Models for a Circular Economy. In S. N. Grösser, A. Reyes-Lecuona, & G. Granholm (Eds.), *Dynamics of Long-Life Assets: From Technology Adaptation to Upgrading the Business Model* (pp. 327–356). New York, NY: Springer International Publishing.
10. EMF. (2013). Towards the Circular Economy - Opportunities for the Consumer Goods Sector. Ellen MacArthur Foundation.
11. EMF. (2019). Concept: What is a circular economy? A framework for economy that is restorative and regenerative by design.
12. Leising, E., Quist, J., & Bocken, N. (2018). Circular Economy in the building sector: Three cases and a collaboration tool. *Journal of Cleaner Production*, 176, 976–989.
13. Flynn, A., & Hacking, N. (2019). Setting standards for a circular economy: A challenge too far for neoliberal environmental governance? *Journal of Cleaner Production*, 212, 1256–1267.
14. Lozano, R. (2018). Sustainable business models: Providing a more holistic perspective. *Business Strategy and the Environment*, 27(8), 1159–1166.
15. Hossain, M. U., & Ng, S. T. (2018). Critical consideration of buildings' environmental impact assessment towards adoption of circular economy: An analytical review. *Journal of Cleaner Production*, 205, 763–780.
16. Bressanelli, G., Adrodegari, F., Perona, M., & Sacconi, N. (2018). Exploring how usage- focused business models enable circular economy through digital technologies. *Sustainability (Switzerland)*, 10(3).
17. Garcia-Muiña, F., González-Sánchez, R., Ferrari, A., & Settembre-Blundo, D. (2018). The Paradigms of Industry 4.0 and Circular Economy as Enabling Drivers for the Competitiveness of Businesses and Territories: The Case of an Italian Ceramic Tiles Manufacturing Company. *Social Sciences*, 7(12), 255.
18. Jensen, J. P., & Remmen, A. (2017). Enabling Circular Economy Through Product Stewardship. *Procedia Manufacturing*, 8(October 2016), 377–384.
19. Parida, V., Sjödin, D., & Reim, W. (2019). Reviewing literature on digitalization, business model innovation, and sustainable industry: Past achievements and future promises. *Sustainability (Switzerland)*, 11(2).
20. Akanbi, L. A., Oyedele, L. O., Akinade, O. O., Ajayi, A. O., Davila Delgado, M., Bilal, M., & Bello, S. A. (2018). Salvaging building materials in a circular economy: A BIM-based whole-life performance estimator. *Resources, Conservation and Recycling*, 129(May 2017), 175–186.
21. Röck, M., Hollberg, A., Habert, G., & Passer, A. (2018). LCA and BIM: Visualization of environmental potentials in building construction at early design stages. *Building and Environment*, 140(December 2017), 153–161.
22. Zott, C., & Amit, R. (2010). Business model design: An activity system perspective. *Long Range Planning*, 43(2–3), 216–226.
23. Teece, D. J. (2010). Business Models, Business Strategy and Innovation. *Long Range Planning*, 43(2), 172–194.
24. Bakker, C., Wang, F., Huisman, J., & Hollander, M. Den. (2014). Products that go round: exploring product life extension through design. *Journal of Cleaner Production*, 69, 10–16.
25. Højbye, L., & Sand, H. (2018). Circular Economy in the Nordic Construction Sector: Identification and assessment of potential policy instruments that can accelerate a transition toward a circular economy. TemaNord, Report 517.
26. Wuyts, W., Miatto, A., Sedlitzky, R., & Tanikawa, H. (2019). Extending or ending the life of residential buildings in Japan: A social circular economy approach to the problem of short-lived constructions. *Journal of Cleaner Production*, 231, 660–670.
27. Linder, M., & Williander, M. (2017). Circular Business Model Innovation: Inherent Uncertainties. *Business Strategy and the Environment*, 26(2), 182–196.
28. Hatzivasilis, G., Fysarakis, K., Soutatos, O., Askoxylakis, I., Papaefstathiou, I., & Demetriou, G. (2018). The Industrial Internet of Things as an enabler for a Circular Economy Hy-LP: A novel IIoT protocol, evaluated on a wind park's SDN/NFV-enabled 5G industrial network. *Computer Communications*, 119(January 2018), 127–137.

Monitoring of Indoor Radon in Passive House Buildings

A post occupancy study of indoor radon concentrations in certified Passive House buildings

Barry Mc Carron^{1 2}, Xianhai Meng², Shane Colclough³

¹ South West College Belfast, Ireland

² Queens University Belfast

³ University College Dublin

ABSTRACT: The acceleration of the climate emergency is having a profound effect on European Union (EU) policy influencing energy efficiency standards and targets. The Intergovernmental Panel on Climate Change (IPCC) Fourth Assessment Report (AR4) and the Emissions Gap Report from the UN have outlined and advocated the use of the passive house standard. This study is both important and original given it is the first research attempt to examine radon distribution in Passive House buildings in Ireland and the UK. The World Health Organization (WHO) has identified radon as a known human carcinogen. Radon is a colourless, odourless and tasteless radioactive gas. It is formed by the radioactive decay of the small amounts of uranium that occur naturally in all rocks and soils. The Passive House standard has two inherent principles which should mitigate against high radon levels. These are Airtightness and Mechanical Ventilation Heat Recovery (MVHR). This research is of significance because it provides evidence of how effective the transferred air principle is with a correctly installed and commissioned MVHR unit in the domestic setting. A striking observation to emerge from the data shows a difference in radon distribution between upstairs and downstairs when compared against regular housing.

Keywords: Certified Passive House, EnerPHit, Radon, Indoor Air Quality, Energy Efficiency

1. INTRODUCTION

The UK Parliament became the first in the world to declare a climate emergency on 1st May 2019. The Irish government declared a climate emergency a week later and the Northern Ireland Assembly followed suit in February 2020 [1].

The Paris Agreement, signed in 2016, is an agreement within the United Nations Framework Convention on Climate Change (UNFCCC), dealing with greenhouse-gas-emissions mitigation, adaptation, and finance. [2]. The most recent report issued by the IPCC is called the Special Report on Global Warming of 1.5 °C (SR15). The report assesses projected impacts at a global average warming of 1.5°C and higher levels of warming. Its crux finding is that meeting a 1.5 °C target is possible but will require deep emissions reductions and rapid, far-reaching and unprecedented changes in all aspects of society [3].

The influential Emissions Gap Report, advocates for the passive house standard in its 2016 edition. This consolidated a recommendation for the standard as a climate mitigation solution in the IPCC 4th assessment report released in 2007 [4]. It is in this context that buildings are central to meeting the sustainability challenge as currently European buildings account for approximately 40% of total energy consumption within the European Union (EU) [5].

The Energy Performance in Buildings Directive (EPBD) mandates that all EU member states build Near Zero Energy Buildings (NZEB) by 2021. The EPBD defines near zero energy buildings, in broad terms, as those with high levels of energy efficiency. The directive further states that the very low amount of energy required should be provided to a very significant degree by energy from renewable sources, preferably produced on or near site [6].

The UK's Climate Change Committee (CCC) is an independent, statutory body established under the Climate Change Act 2008 [7], in 2019 they published a report titled "UK housing: Fit for the future?" [8] states that 'Greenhouse gas emission reductions from UK housing have stalled, and homes across the UK must be improved now to address the challenges of climate change.

The costs of building to a specification that achieves the aims set out in this report are not prohibitive and getting design right from the outset is vastly cheaper than forcing retrofit later'. The CCC is calling for a UK "ultra-energy efficient standard" with a space heating demand of 15-20 kWh/m²/yr ideally heated with an electric Heat Pump[8].

The International Passive House Standard offers a proven methodology to achieve this standard. The combination of Passive House with heat pump and renewable energy production presents a suitable solution to move to the proposed low/zero carbon objective given the context. Passive Houses focus on energy saving and are designed to have an energy demand that is as low as practically achievable. With such a small amount of energy to be supplied, it is easier to meet the subsequent demand with renewable sources [9]. To meet the Passive House Standard, the airtightness of a building must achieve an air change per hour rate of less than 0.6 air changes at 50 Pascals of pressure (n50), and have ventilation provided by a balanced mechanical ventilation heat recovery system. Existing research in the UK and Ireland has predominantly focussed on Indoor Air Quality (IAQ) and overheating [10]. To date, no research in the UK or Ireland has investigated the relationship between the unique characteristics of certified Passive House buildings and indoor radon concentrations.

This study aims to assess if certified Passive House buildings, with the associated high levels of air tightness coupled with mechanical ventilation, will result in a reduction in indoor radon gas concentrations compared to conventional buildings. It includes the following detailed objectives:

- Evaluating the findings against the target level (TL), Action Level (AL) and the national average;
- Comparing radon distribution levels between upstairs and downstairs;
- Identifying the influence of main construction materials on corresponding radon concentrations;
- Determining the indoor radon concentrations of the Passive House Retrofit standard (EnerPhit) sample; and
- Carrying out case studies on a direct comparison of indoor radon concentrations in a high-risk radon area.

2. PASSIVE HOUSE CRITERIA

Passive House (or Passivhaus) refers specifically to the International Passive House Standard as developed, defined and administered by the Passive House Institute (PHI) in Darmstadt, Germany. Passive House has a very clear set of requirements, so it is possible to check if a building meets the definition of the Passive House Standard. Rigorous modelling and verification are required in the design and construction stages to meet Passive House certification standards. This research will monitor only Passive House buildings certified by the PHI [11].

The Passive House Standard employs a mixed mode ventilation strategy combining a Mechanical Ventilation System and Heat Recovery (MVHR) with summer ventilation/cooling using windows. Mixed mode ventilation allows for Passive House airtightness/air leakage criteria: 0.6 air changes/hour under a blower door test. This minimizes energy loss to the outside, improves insulation performance and reduces moisture ingress into the building fabric. This standard contrasts sharply with natural ventilation methods where sufficient ventilation for occupants is achieved, in part, due to a leaky building fabric. The resultant draughts in naturally ventilated buildings are often exacerbated using open fires which further draw in air for combustion. As concerns about IAQ and health grow, ensuring good IAQ is critical. Available research already indicates that a correctly installed and operating MVHR system has a positive effect on IAQ and humidity levels [12]. The Passive House Standard uses the European air quality category IDA 3 (Moderate IAQ CO₂ level 600–1000ppm) to define MVHR operating parameters along with output that is based on the number of people (30 m³/h per person) according to DIN 1946, the German standard for ventilation [13]. The Passive House certification criteria set out key metrics for compliance in respect to MVHR including early design consideration, successful installation and commissioned units. This is confirmed by academic research into the performance of the Passive House Standard [12]. The standard is based on compliance of the International Standard for Thermal Comfort ISO 7730 [14].

3. RADON IN BUILDINGS

Radon is a naturally occurring, radioactive gas that results from the decay of uranium in rocks and soils. It is the major source of ionizing radiation exposure to the population. Radon decays to form tiny radioactive particles, some of which stay suspended in the air as colourless, odourless, tasteless gas that can only be measured using special equipment. Normally, when radon is emitted into the open air, it is quickly diluted to harmless concentrations. However, when radon enters an enclosed space, (such as a house) through cracks in floors or gaps around pipes and cables, it can build up to a dangerously high concentration. Inhaled radon particles give a radiation dose that may damage cells in the lung [15].

The WHO has identified radon as a known human carcinogen and has reported a wealth of biological and epidemiological evidence connecting radon exposure and lung cancer [16]. Radon is estimated to cause 1,100 deaths per year in the UK and is the second largest identified cause of lung cancer after smoking [17]. In addition to the UK, approximately

300 cases of lung cancer in Ireland every year can be linked to radon [18]. Considering that the typical person in industrial countries (such as the UK and Ireland) spends approximately 90% of their time indoors,[19] there are surprisingly few academic studies on radon in the home. Monitoring indoor radon is of fundamental importance and this research represents an opportunity to advance an understanding of the effect of increasing energy performance standards and the role of increased airtightness and mechanical ventilation. The Health Protection Agency (HPA) in the UK estimates that with an increase in radon concentration of 100 Becquerels per cubic metre (Bq/m³), the risk of a smoker developing lung cancer increases by up to 31% with a central estimate of 16% [20]. The HPA advises that homes with smokers or ex-smokers should seriously consider reducing radon levels, where concentrations are measured above the target level (TL) of 100Bq/m³ because of the substantial risks associated with a combination of smoking and radon exposure [20].

Radon prevention and mitigation

Radon measurements are typically made with two radon detectors, one in the main living area and the other in a regularly used bedroom, reflecting the parts of the home that are most often occupied. Detectors are left in place for three months. Radon is measured in Becquerels per cubic metre of air (Bq/m³). The governments in both Ireland and the UK recommended an 'action level' for radon in homes as 200 Bq/m³. Above this level, it is recommended that householders act to reduce their radon levels [16].

Prior to construction, it is not possible to predict the radon concentration in a dwelling. However, probability or risk maps are available, which show the probability of radon concentrations in areas across Ireland and the UK (see Figure 1). These maps are colour coded by concentration level. Indoor radon concentration may be mitigated by two preventative measures: basic radon protection and full radon protection. Basic radon protection is provided by a damp-proof membrane modified and extended to form a radon-proof barrier across the ground floor of the building. Full radon protection comprises a radon-proof barrier across the ground floor and provision for subfloor depressurization (a radon sump) or ventilation (a ventilated subfloor void). The radon sump is not initially activated, rather it is capped and available for use as a secondary measure in case the radon-proof barrier is insufficient for reducing radon levels below the AL of 200Bq/m³. These requirements for preventative measures are largely similar in both Ireland and the UK, depending on location on the radon risk maps.

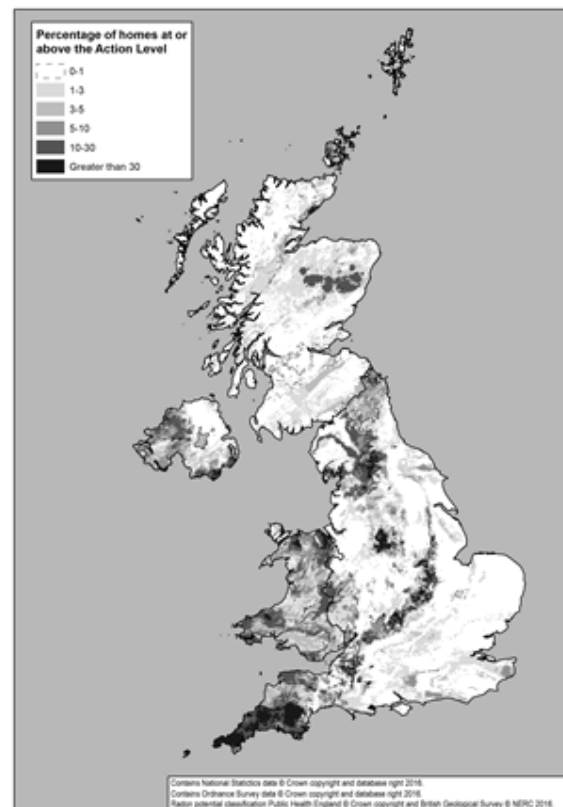


Figure 1: Radon Risk Map of the United Kingdom.

4. SAMPLE SELECTION AND CHARACTERIZATION

The sample in this study comprises 97 certified Passive House buildings in Ireland and the UK and consists of two-house classifications, 92 are passive house certified and five meet the passive house EnerPHit standard (namely passive house retrofit). In addition to these, 25 comparison homes were also selected simply because of their proximity to corresponding certified homes. The oldest of these passive house homes was built in 2005 with the most recent being constructed in 2019. The entire sample is also all two-story domestic dwellings. The largest of these is 455m² while the smallest is 122m². Of the 97 homes, 54 are of masonry construction and the remaining 43 are of timber frame construction. All the homes are passive house certified and all have a balanced mechanical ventilation heat recovery unit and have an airtightness level (n50) of <0.6 of new homes and the EnerPHit <1.0. The building characteristics and materials are significant, as the most common sources of radon are gas from the soil/ground and off-gassing from building materials containing radon [21]. Building material radon emissions are much lower than radon gas being emitted from soil/ground gas and only apply to such building materials as ground rock and those which originate from ground rock (e.g. sand, soil and cement). Concentrations of radon present in these building materials will vary, depending upon

geological origin [22]. The small number of homes retrofitted to the EnerPHit standard are significant as other studies show that energy retrofitting of homes may reduce the potential for ventilation flushing of radon gas from the house, increasing radon levels [23]. Retrofit houses may also have an existing floor that does not include radon protection and sealing the full footprint of the building may prove difficult. Therefore, it is difficult to predict the effect of applying Passive House techniques to existing buildings on indoor radon concentrations: a properly installed and operating MVHR system could reduce the radon level but failing to completely seal the building envelope could increase the radon level.

Radon monitoring

In 2010, the HPA updated its advice on the limitation of human exposure to radon, maintaining the national AL at 200Bq/m³ and introducing the concept of a TL at 100Bq/m³ [24] The TL refers to an annual average concentration of 100Bq/m³ or below as the ideal level acceptable in a building. The HPA, WHO and most international governments recognize that homes which exceed the radon AL (200Bq/m³) should reduce their radon levels with immediate effect. In this study, indoor radon levels were measured by CR-393 alpha track diffusion radon gas detectors placed in the main living area (Room 1) and the main bedroom (Room 2) for just over three months in three different stages from October 2017 to June 2019. Radon results are presented as an annual average using the seasonal adjusted average (SSA) method. The test results are compared with the existing national averages data on radon both in Ireland and the UK.

5. RADON TESTING RESULTS

Radon measurements were completed in a total of 123 homes; 97 certified (including 5 EnerPHit) passive house buildings and 25 comparison homes. None of the 97 certified passive homes surveyed had radon concentrations exceeding the 200 Bq/m³ (see Figure 3) national Reference Level. Only 6.79% of the sample breached the target level of 100 Bq/m³. The maximum concentration measured was 149 Bq/m³ in a home in Northern Ireland located in a defined higher risk area.

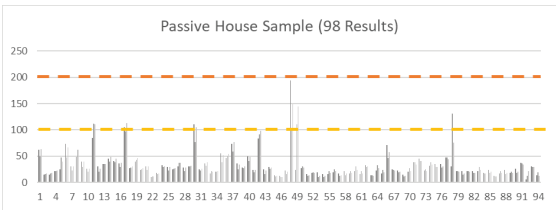


Figure 2: Passive House Sample (97 homes) with AL and TL shown with dashed lines.

The Environmental Protection Agency (EPA) carried out the National Radon Survey (NRS) of Ireland between 1992 and 1999 [18]. The survey characterized areas of Ireland in terms of their radon risk and one of the key findings was that the geographic weighted national average indoor radon concentration at that time was 89 Bq/m³. Since then, several developments have taken place in Ireland that are likely to have impacted on the national average radon concentration. These include the introduction of amended Building Regulations in 1998, requiring radon preventive measures in new buildings in High Radon Areas (HRAs), between 1999 and 2014 the number of dwellings in Ireland increased dramatically by an estimated 47%. To re-assess the national average indoor radon concentration, a survey protocol was carried out in 2015, which would measure radon in a sample of homes as the representative of radon risk and geographical location. This new national average was published in 2017 and could then be used to assess the effectiveness of the measures that have impacted on this metric since it was first established in the 2002 NRS [18]. The results showed that the national average indoor radon concentration for homes in Ireland was 77 Bq/m³, a decrease from the 89 Bq/m³ reported in the 2002 NRS. This figure of 77 Bq/m³ is now a baseline metric for the National Radon Control Strategy (NRCS) [18].

Radon levels against national average

The average indoor radon level based on the 98 certified passive homes monitored in this study is 36 Bq/m³ as shown in Table 1. It can be directly compared with the national average of 77 Bq/m³. The radon level of certified passive homes is directly compared with the non-passive houses (namely comparison homes), which were also monitored in this study. The average of comparison homes was found to be 88 Bq/m³ which is broadly in line with NRS.

Table 1: Radon results showing the EPA 2015 NRS, the comparison sample and finally the Passive House sample.

Metric	EPA 2015 NRS	Comparison Sample	PH Sample
Number of homes measured	649	25	97
No. of homes >200 Bq/m3	8%	8%	0%
No. of homes >100 Bq/m3	25%	16%	7%
Minimum concentration measured (Bq/m3)	14	21	10
Maximum concentration measured (Bq/m3)	1393	598	149
Seasonally adjusted annual average for Sample	77	88	36

Radon distribution

The single most striking observation to emerge from the data shows a difference in radon distribution between upstairs and downstairs when compared against regular housing. In previous UK research,

radon levels were found to be typically 35% lower on first floor bedrooms compared to ground floor living rooms [25]. In this research, the radon concentrations between both floors tested interestingly found that levels were only 6% lower on the first-floor bedrooms compared to ground floor living rooms. This sample included the analysis of 344 standard two-story homes from the EPA 2015 NRS and the Passive House sample of 97 two-story homes, which presented this different radon distribution. Distribution ratios shown in Table 2 of the bedroom/living room radon levels in the standard two-story homes presented as gaussian distribution (mean 0.79, median 0.74 with a standard deviation of 0.37). The results of the certified passive house sample are significantly anomalous (mean 1.03, median 0.92 with a standard deviation of 0.56).

Table 2: Radon distribution results comparing the passive house sample tested in this study against the EPA NRS 2015.

Study	No of Samples	Average Ratio	Mean Ratio	Standard Deviation
National Radon Study (2 Storey)	344	0.79	0.74	0.37
PH Study	97	1.03	0.92	0.56

A possible reason for the difference may lie in the fact that the Passive house standard has a defined specification for airtightness and MVHR systems, unlike much of the standard dwellings. In addition to this, there is a consistent framework on design, installation and commissioning of these systems. This quality assurance coupled with typical layout of a two-storey dwelling combine to produce the lower indoor concentrations and closer distribution levels between upstairs and downstairs.

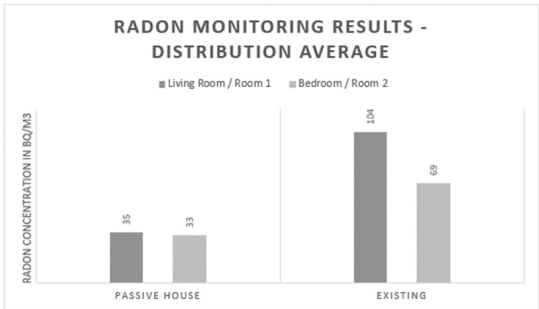


Figure 3: Radon monitoring results Distribution Average.

Radon from building materials

While the influence of building materials on indoor radon concentrations is recognized, there is a paucity of quantitative data representing the structural contribution to domestic radon. A figure on 20 Bq/m³ has recently been suggested for the contribution from building materials to indoor radon concentrations [21]. In this study, 54 are constructed from masonry and the remaining 43 are of timber frame construction. The analysis results shown in

Figure 5 reveal that the timber frame group has a slightly lower radon level than the masonry group. This corresponds with previous research [25]. However, as the number of houses investigated in this research was relatively small and it was not the key focus of the research, the results should be treated with caution.

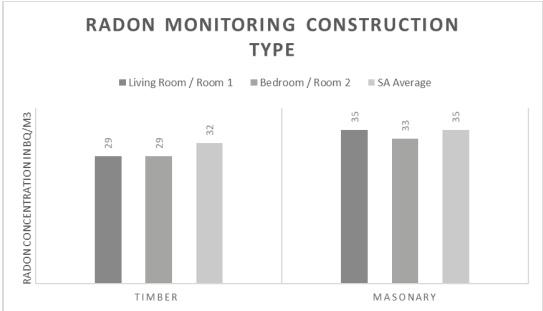


Figure 4: Radon Monitoring Construction Materials.

A total of 10 comparative case studies were also carried out, which were in known high risk areas. For each case study, the comparison is between a certified passive house and the home directly next door. The findings here are significant as conventional homes demonstrate elevated levels in all 10 case studies. As shown below in Figure 6, a clear differentiation is also found in levels among 50% of the case studies between the two groups.

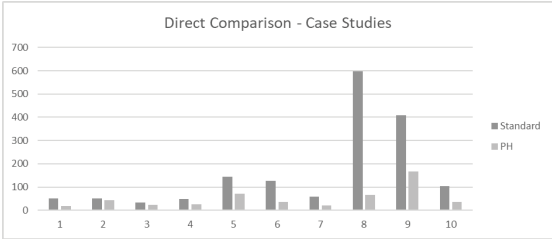


Figure 5: Direct comparative case studies.

The figure above illustrates that in the five case studies with the clear differentiation, (5, 6, 8, 9 and 10), the conventional home sample all have levels on or above the Action Level of 100 Bq/m³. From the figure above, it is also seen that Homes 8 and 9 have significantly elevated levels 598 Bq/m³ and 400 Bq/m³. By comparison, the corresponding passive houses next door in both case studies have levels of 67 Bq/m³ and 166 Bq/m³, respectively.

6. CONCLUSION

Radon is perhaps the most dangerous contaminant within the IAQ spectrum. The accumulation in houses can increase the risk of lung cancer, especially in individuals who smoke. This study presents the key findings of a larger PhD research project into the indoor radon levels in Passive House buildings compared national averages in conventional

buildings. The results support the hypothesis that certified Passive House buildings perform better in respect to indoor radon concentrations compared to conventional homes given less airtightness and no MVHR systems. The research also consolidates this with individual findings. The clearest illustration of this was in the presentation of the ten case studies, which highlighted elevated levels in the comparison homes against all ten Passive House buildings coupled with five distinctive contrasting results showing clear differentiation from the corresponding comparison home. The radon distribution results indicate that the passive house framework for quality assurance of the design, installation, and commissioning promote a properly functioning MVHR system. This will result in more extract on the ground floor thus reducing the ground floor radon level and lowering the distribution gap. On the other hand, the findings on the relationship with construction materials and radon concentrations are not statistically significant to make claims about background radon emissions.

This project is the first comprehensive investigation of indoor radon in certified passive house buildings in the UK and Ireland. The analysis of the radon levels undertaken here has extended our knowledge of the effect of airtightness and mechanical ventilation heat recovery systems combined in a clear methodology such as the passive house standard. The findings of this study have important implications for future practice. It illustrates the value of having a clear methodology of quality assurance (integral to the passive house process). Passive House exhibits better radon performance which is ascribed to the combination of reduced air infiltration combined with mechanical ventilation. Other possible implications include:

1. There is the need for quality assurance in design and construction.
2. The potential offered by ensuring the MVHR system is balanced such that the house is at a slight positive pressure.

ACKNOWLEDGEMENTS

Barry McCarron would like to acknowledge the contribution from Xianhai Meng and Shane Colclough with the development of this paper. He would also like to thank Dr. Stephanie Long and Rachel Flynn of the Environmental Protection agency (EPA).

REFERENCES

1. BBC News, "UK Parliament declares climate change emergency," *BBC News*, 2019.
2. UN, "The Paris Agreement - main page," *The Paris Agreement*, 2016. .
3. IPCC, *Global warming of 1.5°C*. 2018.
4. IPCC, "Fourth Assessment Report (AR4): Mitigation of Climate Change," *Work. Gr. III*, 2007.

5. UNEP, *The Emissions Gap Report 2017 - A UN Environment Synthesis Report*. 2017.
6. D. 2010/31/CE, *Directive 2010/31/EU of the European Parliament and of the Council of 19 May 2010 on the energy performance of buildings*. 2010.
7. CCC, "Net Zero: The UK's contribution to stopping global warming," *Committee Clim. Chang.*, 2019.
8. Committee on Climate Change, "UK housing: Fit for the future?," no. February, p. 135, 2019.
9. S. Colclough, J. Mernagh, D. Sinnott, N. J. Hewitt, and P. Griffiths, "The Cost of Building to the nearly-Zero Energy Building Standard: A Financial Case Study," 2019.
10. J. Foster, T. Sharpe, A. Poston, C. Morgan, and F. Musau, "Scottish Passive House: Insights into environmental conditions in monitored Passive Houses," *Sustain.*, vol. 8, no. 5, 2016.
11. Passive House Institute, "Certified Passive House - Certification Criteria for Residential Passive House Buildings," *Passiv. House Inst.*, 2013.
12. J. Schnieders and A. Hermelink, "CEPHEUS results: Measurements and occupants' satisfaction provide evidence for Passive Houses being an option for sustainable building," *Energy Policy*, 2006.
13. Passive House Institute, "Criteria for the Passive House, EnerPHit and PHI Low Energy Building Standard," *Passiv. House Inst.*, 2016.
14. ISO, "ISO 7730: Ergonomics of the thermal environment Analytical determination and interpretation of thermal comfort using calculation of the PMV and PPD indices and local thermal comfort criteria," *Management*, 2005.
15. S. Dempsey, S. Lyons, and A. Nolan, "High Radon Areas and lung cancer prevalence: Evidence from Ireland," *J. Environ. Radioact.*, 2018.
16. WHO, *Indoor Radon a Public Health Perspective. A public health perspective*. 2009.
17. J. Milner *et al.*, "Home energy efficiency and radon related risk of lung cancer: Modelling study," *BMJ*, vol. 348, no. January, pp. 1–12, 2014.
18. A. Dowdall, P. Murphy, D. Pollard, and D. Fenton, "Update of Ireland's national average indoor radon concentration – Application of a new survey protocol," *J. Environ. Radioact.*, 2017.
19. N. E. Klepeis *et al.*, "The National Human Activity Pattern Survey (NHAPS): A resource for assessing exposure to environmental pollutants," *J. Expo. Anal. Environ. Epidemiol.*, 2001.
20. Health Protection Agency, "Radon and Public Health RCE 11," *Radiation, Chem. Environ. Hazard*, p. 258, 2009.
21. A. R. Denman, C. J. Groves-Kirkby, N. P. Groves-Kirkby, R. G. M. Crockett, P. S. Phillips, and A. C. Woolridge, "Factors Influencing Upstairs and Downstairs Radon Levels in Two-Storey Dwellings," *2006 IRPA Paris*, 2006.
22. T. Woolley, *New Homes and Wellbeing : Building Materials , Health and Indoor Air Quality New Book raises issue about hazardous materials in buildings. .*
23. M. Collins and S. Dempsey, "Working Paper No. 554 March 2017," 2017.
24. P. H. England, "UK National Radon Action Plan About Public Health England."
25. W. Ringer *et al.*, "The Effect of New Building Concepts on Indoor Radon Austrian Agency for Health and Food Safety (AGES), Wieneringerstrasse 8 , 4020 Linz , Austria," no. May, pp. 13–18, 2012.

Occupant-centric radiant cooling solutions Requirements, designs, assessment

ARDESHIR MAHDAVI, HELENE TEUFL

Department of Building Physics and Building Ecology, TU Wien, Vienna, Austria

ABSTRACT: *The effects of global warming and urban heat islands have led to an increased cooling demand for buildings. Due to the considerable energy consumption of conventional air-conditioning systems, alternative solutions are needed to cool indoor spaces. Radiant cooling systems can represent a possible solution for this challenge. They have been promoted for their potential for enhanced thermal comfort provision and energy efficient operation. Nonetheless, the implementation of radiant cooling elements must address multiple considerations (e.g., condensation risk, climatic region of the building, position of the radiant panel). The present contribution discusses radiant cooling solutions relevant to the aforementioned considerations. Thereby, the main approach aims at positioning the radiant cooling panel close to occupants. The potential of such occupant-centric solutions is explored via preliminary computational studies pertaining to an office environment setting in the city of Vienna, Austria. The results point to the thermal comfort improvement potential due to radiant panels positioned in the proximity of occupants.*

KEYWORDS: *Climate Change, Cooling Demand, Radiant Cooling, Thermal Comfort, Condensation Risk*

1. INTRODUCTION

Adequate thermal design of buildings can ideally eliminate – or at least reduce – the need for energy intensive environmental control systems for heating, cooling, and ventilation. However, under predominantly cold or hot climatic conditions, even optimal designs (in view of building fabric, geometry, and materials) cannot ensure that passive building operation alone would offer adequate indoor environmental conditions. Specifically, the combined consequences of climate change and urban heat islands have led to an ever-expanding need for space cooling.

Conventional air-conditioning technologies do not necessarily represent a scalable solution for this challenge, given their considerable energy demand. Radiant cooling techniques have been promoted in view of their potential with regard to both enhanced thermal comfort provision and energy efficient operation [1-3]. However, radiant cooling solutions require specific considerations. One challenge concerns the coordination of radiant cooling systems with buildings' ventilation systems [4-5]. Another challenge concerns the water vapor condensation risk [6]. In this context, the present contribution explores the potential of innovative occupant-centric radiant cooling solutions. Thereby, a key strategy involves the positioning the radiant cooling panels close to occupants. Two related computational case studies are presented in this contribution. Furthermore, a number of technical radiant cooling strategies are alluded to that could address, in principle, the aforementioned challenges.

2. BACKGROUND

Radiant cooling systems use temperature-controlled surfaces to remove sensible thermal loads from an indoor space. The controlled surfaces commonly maintain their temperature by chilled water, which is circulated through integrated pipes. Thereby, heat from an indoor space is absorbed by the actively cooled surface [7]. Note that the cooling capacity of radiant panels may have to be limited due to condensation risk. Condensation occurs when the surface temperature of the cooling panel is lower than the dew point temperature of the adjacent air layer. Especially in a hot and humid climate, radiant cooling can be challenging, due to the high-moisture ambient air [4-5]. This results in an increased risk of condensation due to ventilation or infiltration.

In comparison to conventional air cooling systems, radiant cooling does not address the air change requirement. Given an additional controlled ventilation system, incoming air may have to be dehumidified to reduce the condensation risk. Likewise, building envelopes shall be highly tight to avoid unwanted infiltration. As such, provision of fresh air through a secondary ventilation system is more cost and energy-intensive.

Typically, radiant cooling systems are integrated with ceilings, floors, or walls of a building. In recent years, some efforts have been made to incorporate radiant cooling functionality in personal comfort systems. These systems can improve occupants' thermal comfort but also reduce buildings' cooling energy demand [8]. An instant of such efforts pertains to the integration of radiant cooling panels in

an office desk (tabletop and panels mounted to the back and sides of the table). Thereby, surface condensation had to be avoided. For this purpose, the surface temperature of the panels was set to be approximately 3 K higher than the dew point temperature [8]. The study pointed to a certain thermal comfort improvement potential. However, the cooling effect influences mainly the upper body parts of the participants.

A project in India explored the energy efficiency and thermal comfort potential of radiant cooling systems [9]. The study was conducted in an office building, which was divided into two similar zones (i.e., similar floor plan and orientation). One zone of the building included a radiant cooling and dedicated ventilation system. The other zone incorporated a variable air volume system for cooling. A two-year comparison showed that the radiant cooling system used 34% less energy. Furthermore, a thermal comfort survey revealed that 63% of the occupants from the buildings' radiant cooling zone felt "satisfied" or "very satisfied". Only 45% of the other zone's occupants selected one of these categories [9].

3. A PRELIMINARY POTENTIAL ASSESSMENT

We conducted a preliminary computational study to analyze occupants' thermal comfort within a building that is equipped with radiant cooling elements. Instead of a chilled ceiling, which is a common application form of radiant systems, vertical panels are used. These are positioned close to the occupants. As a result, they provide more personal control opportunities and increase the energy efficiency. For the purpose of this study, the Predicted Mean Vote (PMV), which is a common indicator of thermal comfort, was considered [10]. It represents a seven-point thermal sensation scale ranging from the subjective evaluation of "cold" (-3) to "hot" (+3). According to ISO 7730, the recommended limits for the PMV are -0.5 and +0.5 [9]. Another common indicator which is related to the PMV is the PPD (Predicted Percentage of dissatisfied) [10]. It denotes the predicted percentage of thermally dissatisfied people and was also considered in the present assessment. The aim of this computational study was to show at which ambient air temperature the PMV is still within the recommended range. In case the radiant panel is not enough to keep the PMV lower than +0.5 (e.g., at significantly high temperatures), the air speed can be increased using a fan. The calculations can point to the needed air velocity at any given temperature in order to keep the PMV below +0.5.

In the course of this study, the PMV is calculated for two different procedures: *i)* the classical PMV method according to ISO 7730 [10]; *ii)* the PMV with elevated air speed method provided by the ASHRAE

55 document [11,12]. The latter method calculates PMV differently, if the air speed is above $0.2 \text{ m}\cdot\text{s}^{-1}$. This is due to assumed cooling effect of higher air flow velocities [11].

The study was conducted with specific assumptions. The relative humidity was assumed to be 70%. Furthermore, a clothing value of 0.5 and a metabolic rate of 1.1 were used. The estimation of the mean radiant temperature required the calculation of the shape factor from the occupant to the radiant element. The surface temperature of the radiant cooling panel was set at 15°C . The surface temperature of the other surrounding surfaces was assumed to be equal to the ambient air temperature. The size of the radiant cooling panel is 2.25 m^2 and it is located 0.75 m from the occupant. The detailed dimensions of the panel are illustrated in Figure 2.

Figure 1 and Table 1 show which air flow speed is needed at specific temperatures to keep PMV within the recommended range ($-0.5 < \text{PMV} < +0.5$) [10]. This is illustrated for the two aforementioned PMV calculation methods. It is noticeable that the radiant cooling panel does not need to be activated below an air temperature of 27°C . After that, the PMV does not exceed the recommended limit of +0.5, if the radiant cooling panel is used. At higher temperatures, the radiant element can be supported by an additional fan. The results differ depending on the PMV calculation method. In case of the classical method according to ISO 7730, the PMV is still within the recommended range at an air temperature of 29°C . However, in this case an air speed of $1 \text{ m}\cdot\text{s}^{-1}$ is needed. In case of the ASHRAE 55 calculation method, the PMV can be kept below +0.5 at an air temperature of 30°C if an air flow speed of $0.7 \text{ m}\cdot\text{s}^{-1}$ is provided. Note that, given the assumed relative humidity level (70%), condensation occurs for all calculated scenarios with an activated radiant panel. As a result, the panel must accommodate surface condensation. Toward this end, special designs (e.g., those with integrated drainage elements would be necessary).

Table 1: Necessary air flow speed at various ambient air temperatures to keep PMV below +0.5 (Assumptions for the calculation: RH=70%, clo=0.5, met=1.1, panel surface temperature= 15°C).

Ambient air temperature[$^\circ\text{C}$]	≤ 26	≤ 27	≤ 28		≤ 29		≤ 30
Air speed [$\text{m}\cdot\text{s}^{-1}$] ASHRAE 55	0.1	0.2	0.4	0.25	0.6	0.4	0.7
Air speed [$\text{m}\cdot\text{s}^{-1}$] ISO 7730	0.1	0.2	0.6	0.25	-	1.0	-
Radiant cooling panel	-	-	-	✓	-	✓	✓
Surface condensation	no	no	no	yes	no	yes	yes

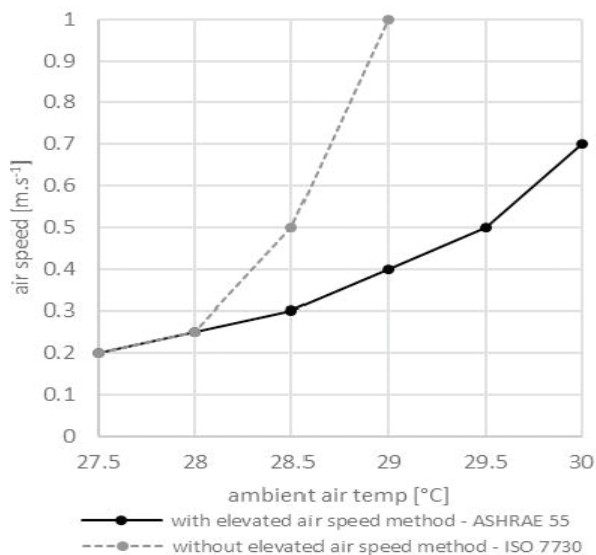


Figure 1: Necessary air speed at specific temperatures to keep PMV below +0.5 with an activated radiant panel (Assumptions for the calculation: RH=70%, clo=0.5, met=1.1, panel surface temperature= 15°C).

4. A CASE STUDY

Given the promising results of the preliminary assessment above (see section 3), we conducted a computational case study to evaluate occupants' thermal comfort at an office area with vertically positioned radiant cooling elements. The selected office area is located in Vienna, Austria. Within this case study, the PMV was used as the pertinent performance indicator. It was calculated on an hourly basis for the warmest period (June – August) of three selected years (2017 – 2019). The PMV calculations were conducted for multiple scenarios: *i)* without radiant cooling panels, *ii)* for one radiant panel, and *iii)* for two radiant cooling panels close to the occupant's workstation. The arrangements for the scenarios with radiant elements are illustrated in Figure 2.

Measured values from the office area, more specifically the indoor temperature as well as the relative humidity, were used for the PMV calculation. Moreover, a clothing value of 0.5, a metabolic rate of 1.1, as well as an air velocity of 0.2 m.s⁻¹ were assumed. The influence of an additional fan on the occupants' thermal comfort was explored as well for all scenarios. In these cases, the generated air flow speed was assumed to be 0.5 m.s⁻¹. It was assumed that the radiant cooling panel is activated, every time the PMV exceeds +0.5. Consequently, the surface temperature of the cooling panel is reduced. This is done until the PMV is within the recommended range, or in case one of the two following conditions occurs. The first condition concerns the water vapor condensation risk. With this case study, surface condensation is to be avoided. For this reason, the surface temperature of the radiant panel was not allowed to be lower than the dew-point temperature.

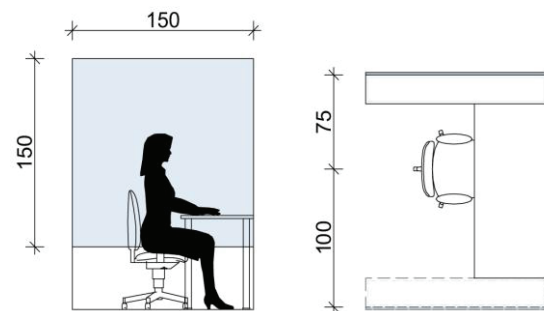


Figure 2: Arrangement for one or two (dashed line) radiant panels (dimensions in cm).

To avoid discomfort due to radiant asymmetry, it has been recommended that the difference between the air temperature and the panel's surface temperature shall not exceed 15 K [9]. The present case study involved, whenever necessary, the modulation of the panel's surface temperature so as to meet this condition. Figure 3 shows the outcome for one of the scenarios, more specifically for an arrangement with one radiant cooling panel, no additional fan, and within the warmest months of 2017. It illustrates the calculated hourly values of PMV and PPD, as well as the dynamically adjusted surface temperature of the radiant panel. It is noticeable that even with one radiant cooling panel in the close proximity of the occupant, the PMV mostly remains below +0.5, and is rarely exceeds a value on 1, which corresponds to the subjective evaluation of "slightly warm". Likewise, PPD rarely exceeds 25%. A higher percentage of dissatisfied occurs only on a few occasions. Note that, in this scenario, specific minimum panel surface temperatures were maintained to avoid surface condensation. As such, PMV could have been further improved if the panel's technical design would allow for – and accommodate – surface condensation. Table 2 presents a summary of the results for all three scenarios and all three years. The table shows the percentage of time, in which the PMV is higher than +0.5 within the assumed office working hours (8 am to 6 pm). The percentage of time in which the PMV exceeds 1 is presented as well. These results suggest that the percentage of time with higher thermal discomfort probability (PMV > 0.5) is much smaller when a radiant cooling panel is placed close to an occupant. For the calculated scenarios with a second radiant cooling panel or an additional fan, the percentage of time in which the PMV exceeds the specified limits is further reduced. The PMV is rarely larger than 1 in all scenarios with radiant cooling panels. Specifically, depending on the year, the number of panels, and the air velocity, percentage of time with PMV outside the recommended range lies somewhere between 1.7% (2 panels, 0.5 m.s⁻¹, 2017) and 12.7% (1 panel, 0.2 m.s⁻¹, 2018). Figure 4 presents the outcome of all scenarios from 2017 in more detail.

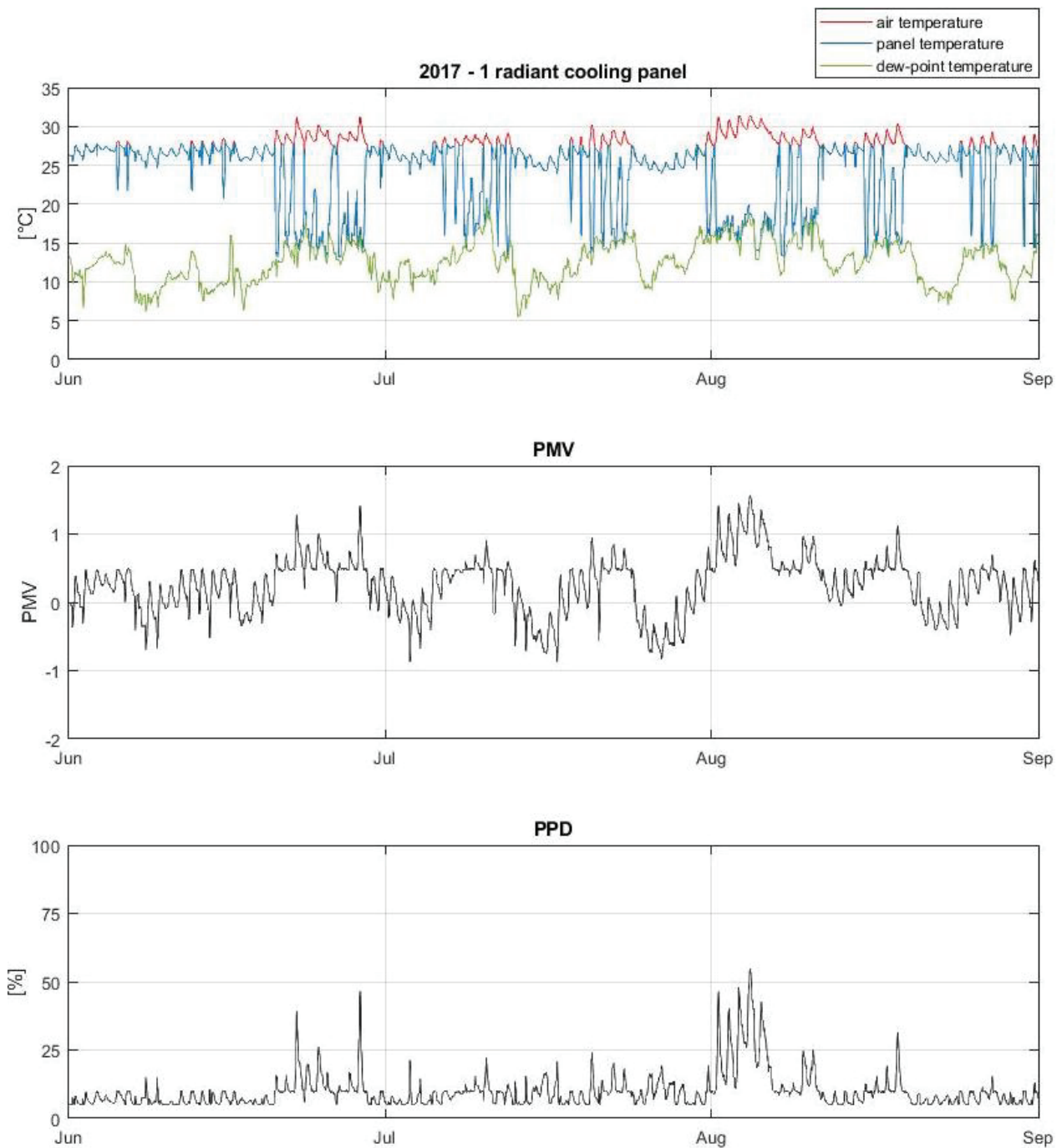


Figure 3: Calculated PMV, PPD, and surface panel temperature with one radiant cooling panel, no additional fan (June, July, and August of 2017).

Table 2: Percentage in which the PMV exceeds 0.5 or 1 within the working hours (8:00 AM – 6:00 PM).

	No radiant cooling panel				1 radiant cooling panel				2 radiant cooling panels			
	PMV > 0.5		PMV > 1.0		PMV > 0.5		PMV > 1.0		PMV > 0.5		PMV > 1.0	
	Air velocity [m.s ⁻¹]											
2019	0.2	0.5	0.2	0.5	0.2	0.5	0.2	0.5	0.2	0.5	0.2	0.5
	49.9	36.6	20.9	7.0	34.2	19.5	4.3	2.5	18.4	6.8	2.4	2.1
2018	0.2	0.5	0.2	0.5	0.2	0.5	0.2	0.5	0.2	0.5	0.2	0.5
	42.4	28.9	21.3	14.2	27.4	19.9	12.7	9.4	19.1	14.9	7.6	5.0
2017	0.2	0.5	0.2	0.5	0.2	0.5	0.2	0.5	0.2	0.5	0.2	0.5
	41.2	25.2	14.1	7.2	22.9	13.1	5.1	3.5	12.5	7.3	2.6	1.7

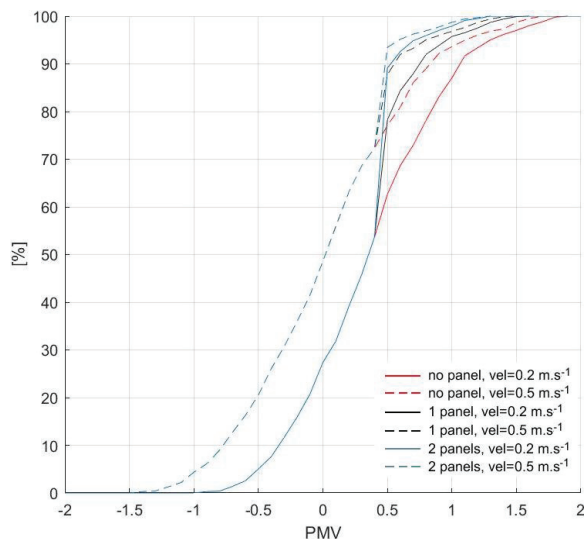


Figure 4: Cumulative distribution of the percentage of time when PMV exceeds a specific value (all scenarios of 2017).

It shows the percentage of time in which the PMV exceeds a specific value. As such, this Figure illustrates the relative thermal comfort improvement potential of radiant and convective cooling options, both individually and in combination.

5. CONCLUSION AND FUTURE RESEARCH

This contribution explored the thermal comfort provision potential of occupant-centric radiant cooling solutions via computationally-based studies. Bringing radiant cooling elements closer to occupants, reducing thus the view factor and increasing the efficiency and personal control opportunity. A preliminary study shed light on the performance of radiant panels under specific climatic assumptions (e.g., a relative humidity of 70%). The study showed that by using a radiant cooling element, the PMV does not exceed the recommended limit of +0.5, if the air temperature is within a specific range. With the addition of a fan functionality, even higher ambient air temperatures could be dealt with. Depending on the PMV calculation method, the room air temperature can reach 29 or 30 °C for the PMV to be still within the recommended range. However, surface condensation cannot be avoided, given the boundary condition assumption pertaining to the assumption of a rather high water vapor concentration in the air.

A further computational case study examined occupants' thermal comfort for a deployment scenario of user-centric radiant panels in an office area in Vienna, Austria. The results suggest that thermal comfort can be noticeably improved via such a solution. The computed percentage of time in which PMV exceeds +0.5 was significantly lower when radiant panels were used. Further improvement was predicted when a second radiant panel and/or fan-triggered convective cooling was assumed. These results obviously are specific to the relevant climatic

context. Similar investigations are being thus carried out for a larger number of climatically distinct locations around the world [13].

Future research must address the problem that, despite their advantages, classical solutions for radiant cooling may not be applicable in all situations. For instance, the technical requirements for the installation and maintenance of full-fledge chilled beam and chilled ceiling technologies may not be feasible for low-cost and low-tech applications. As mentioned before, especially in hot and humid climatic regions, humidity control represents a major challenge [4-5]. Water vapor condensation risk on large-area radiant ceilings is often cited as an argument against such systems. Moreover, the provision of fresh air through a secondary air-conditioning system may not be cost-effective. Likewise, to eliminate condensation risk due to unwanted air infiltration, building envelope construction must be highly tight. As a result, installation of radiant cooling systems in existing buildings (with frequently leaky facades) does not offer itself as a feasible solution. These challenges underline the need for alternative radiant cooling solutions, especially in case of low-tech buildings in hot and humid climatic regions.

To address these challenges, we are currently developing occupant-centric radiant panel designs that can accommodate surface condensation and are thus compatible with natural ventilation options even if outdoor air is highly humid (see Table 3).

Table 3: Schematic illustration of a number of conceived solutions for the design of radiant cooling elements

Base-element	Base-element + vegetation
Base-element + drainage element	Base-element + vegetation + drainage element
Two-sided base-element + drainage element	Base-element + flower box
Two-sided base-element + PCM + drainage element	Base-element + PCM + drainage element

Whereas technical details of the developed solutions cannot be included in the present contribution, the schematic illustrations entailed in Table 3 provide a broad overview of a number of the developed design concepts.

To implement these solutions, water-resistant radiant panels are vertically positioned and equipped with condensed water drainage details. Furthermore, we are exploring the potential for incorporating vegetation in the radiant panel designs. Hence, instead of strictly avoiding surface condensation, the solutions are conceived so as to be compatible with deployment scenarios under hot and humid conditions. These designs will be further refined in future. Moreover, we are in the process of physically implementing instances of such solutions in a laboratory setting. This will facilitate the empirical assessment of the proposed systems' potential by human participants in a realistic office setting.

REFERENCES

1. Khan, Y., Khare, V.R., Mathur, J. and Bhandari, M., (2015). Performance evaluation of radiant cooling system integrated with air system under different operational strategies. *Energy and Buildings*, 97: p. 118-128.
2. Feustel, H.E. and Stetiu, C., (1995). Hydronic radiant cooling – preliminary assessment. *Energy and Buildings*, 22: p. 193-205
3. Rhee, K.N. and Kim, K.W., (2015). A 50 year review of basic and applied research in radiant heating and cooling systems for the built environment. *Building and Environment*, 91: p.166-190.
4. Bayoumi, M., (2018). Method to Integrate Radiant Cooling with Hybrid Ventilation to Improve Energy Efficiency and Avoid Condensation in Hot, Humid Environments. *Buildings*, 8 (5): 69.
5. Nutprasert, N. and Chaiwiwatworakul, P., (2014). Radiant Cooling with Dehumidified Air Ventilation for Thermal Comfort in Buildings in Tropical Climate. *Energy Procedia*, 52: p. 250-259.
6. Rhee, K.N., Olesen, B.W. and Kim, K.W., (2017). Ten questions about radiant heating and cooling systems. *Building and Environment*, 112: p. 367-381
7. ASHRAE, (2012). Handbook – Heating, Ventilating, and Air-Conditioning Systems and Equipment. Atlanta, GA.
8. He, Y., Li, N., He, M. and He, D., (2017). Using radiant cooling desk for maintaining comfort in hot environment. *Energy and Buildings*, 145: p. 144–154.
9. Sastry, G. and Rumsey, P., (2014). VAV vs. Radiant. Side-by-Side Comparison. *ASHRAE Journal*, May 2014: pp. 16–24.
10. EN ISO 7730, (2006). Ergonomics of the thermal environment - Analytical determination and interpretation of thermal comfort using calculation of the PMV and PPD indices and local thermal comfort criteria.
11. ASHREA 55, (2017). Thermal Environmental Conditions for Human Occupancy.
12. CBE Thermal Comfort Tool, [Online], Available: <https://comfort.cbe.berkeley.edu/> [4 March 2020].
13. Teufl, H. and Mahdavi, A., (2020). Toward user-centric radiant cooling solutions. In *AIRAH Outlook 2020 – International HVAC&R Conference*. Sydney, Australia, November 08-10. to be published.

Are Green Buildings Doing Enough?

The role of green certification and gender on sick building syndrome

RANA ELNAKLAH^{1,2*}, DANIEL FOSAS¹, SUKUMAR NATARAJAN¹

¹ Department of Architecture and Civil Engineering, University of Bath, BA2 7AU, Bath, UK;

² Faculty of Architecture and design, Al-Ahliyya Amman University, Amman, Jordan;

* Corresponding author: rade20@bath.ac.uk

ABSTRACT: One of the promised benefits of green buildings is providing healthier indoor environments for their occupants, however, this notion is still debated. To test this, a sample of 502 office-based workers from 13 air-conditioned office buildings (44.4% female and 55.6% male) in Jordan completed a questionnaire on Sick Building Syndrome (SBS) symptoms. The role played by gender in symptom-reporting was also investigated. Findings showed that building type made no significant difference to the prevalence of all SBS symptoms except the tiredness symptom which was slightly higher in the occupants of conventional buildings. Surprisingly, green buildings and conventional buildings had a higher occurrence of SBS symptoms than what industry standards allow for (up to 20%), suggesting that both building types would be classified as sick buildings. Results have also shown that the only significant difference between male and female workers was in the cough and sore throat symptom, which was reported more often by female workers. These findings reinforce the need for further attention to the occupants' perceived health in the green buildings, which may use as an indict of the building performance.

KEYWORDS: Green building, Sick Building Syndrome, Workplaces, Gender differences, Jordan

1. INTRODUCTION

There is an increasing interest in how the Indoor Environment Quality (IEQ) of the green building promotes occupants' health, productivity, and satisfaction [1], particularly in office buildings, where employees spend about a third of their time at the workplace. This is could be an important issue considering that prolonged exposure to environments with poor IEQ parameters (e.g. air quality, lighting, thermal comfort, and acoustic) could lead to the well-known Sick Building Syndrome (SBS). According to a definition provided by the World Health Organization (WHO), the SBS is a group of medical symptoms that affect buildings' occupants and linked to the time spent in the building, and usually disappear when the person is away from the building [2].

The benefits of the green building design are not limited to reduction in the energy consumption and the subsequent harmful impact on the environment, they can also include potential benefits of creating a healthier indoor environment for occupants [3]. There is an increasing concern of whether green buildings deliver a healthier indoor environment they promised or rather, they increase the prevalence of SBS compared to conventional buildings [4].

To date, the research evidence on the effect of green buildings on the frequency of SBS symptoms is

limited and equivocal. Although the study by Tham et al. in Singapore showed that the occupant perception of IEQ was slightly higher in the green building compared to the non-green building, no statistical differences in the proportion of SBS symptoms were found between the two occupants groups, also, the number of sick leave days was similar in both building types [5]. In contrast, a pre- and post-evaluation study in the United States showed an improvement in the employees' perceived health and reduction in the self-reported absenteeism after moving to the green buildings [6].

However, building physical features such as ventilation, lighting, temperature, etc. are not the only reasons behind the prevalence of SBS. Other psychological and physiological factors like job satisfaction, work-related stress, and gender differences might be as important in predicting SBS symptoms [7]. Of these, the effect of gender differences on the prevalence of SBS is still debated. Several attempts had been made to clarify the role gender differences might play in explaining changes to the frequency of SBS symptoms reported by occupants. Findings suggested that female workers usually reported higher levels of SBS symptoms (e.g. fatigue, headache, irritated eyes or nose, cough, and dry skin) compared to male workers [8–10]. This might be due to

three factors are namely biological (e.g. genes, hormones, and metabolism), behavioural (e.g. smoking, diet), and social (e.g. stress, social network) [7]. Unfortunately, other researchers did not consider gender as a predictor for the frequency of SBS symptoms, missing the opportunity to clarify whether this is indeed the case or not [11,12].

Given the uncertain evidence concerning the role of green certification and gender differences on SBS, this paper aims to answer two questions, which are studied from a holistic perspective that accounts for both factors the physical (i.e. building type) and physiological (i.e. gender differences) that underpin SBS prevalence, the two questions are:

- Do occupants in the green office buildings have a lower prevalence of SBS symptoms compared to their counterparts in the conventional buildings?
- Do gender differences affect the prevalence of SBS symptoms in the workplace?

2. METHODS

To answer the two questions, the data collection campaigns were designed to gather the responses of occupants in green and non-green office buildings, each of which has a random proportion of self-identified male and female employees. The dataset sample in this study reflects 502 responses from full-time office-based employees. The participants were selected randomly from five green buildings (n=261 respondents) and eight conventional buildings (n=241 respondents). Surveyed buildings are in Amman, the capital city of Jordan. All buildings are offices occupied by the private sector and did not report any known indoor air quality issues previously. The data were collected between summer 2017 – winter 2019.

2.1 Survey

The questionnaire was adapted from the Health and Work Performance Questionnaire produced by World Health Organization (WHO HPQ) [13]. It consists of two sections, the socio-demographic to collect information from employees on potential covariates (e.g. age, gender, work experience, job role, weight, and height). The second section includes ten questions to assess the prevalence of SBS, these questions were classified into three groups based on the WHO classification of SBS symptoms (Figure 1).

Respondents were asked to rate the frequency of SBS symptoms during the 28 days preceding the survey date. A 5-point Likert scale was used per question [14]. The scale ranged between 'not at all', 'a little of the time', 'some of the time', 'most of the time', 'all the time'. Further, the frequency of each symptom was

compared to the ASHRAE standard 62.1 threshold [15]. According to this standard, a building can be labelled as sick when 20% or more of its occupants reported discomfort symptoms linked to the time spent in the building for a period exceeding two weeks.

The paper-based survey was used. The questionnaire was designed and wrote originally in English, then translated to Arabic, the first language of most participants. Both versions of the questionnaire were combined with the consent form and distributed in the selected buildings during working hours between 0900 – 1700. Of the 502 participants, 55.6 % were Male and 44.4 % were female.

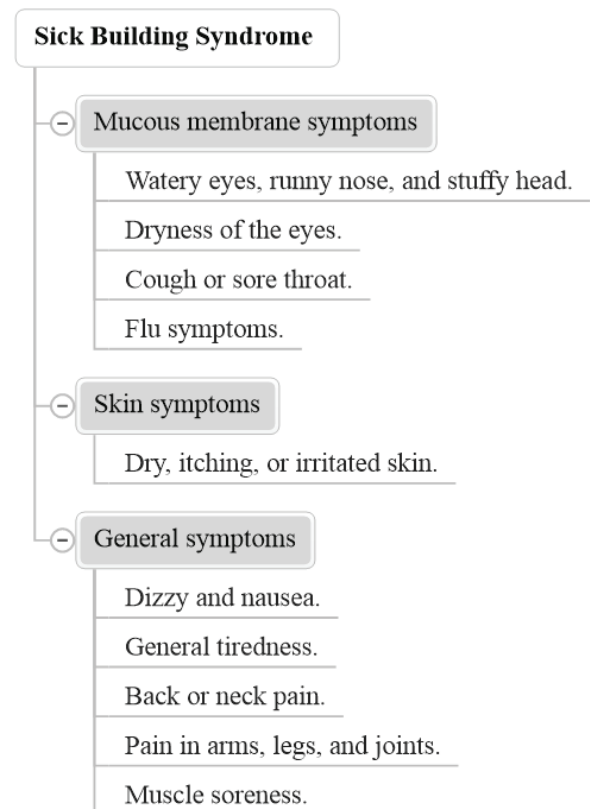


Figure 1: The categories of sick building syndrome symptoms.

2.2 Data Analysis

Each of the two research questions can be translated into the following questions: are the overall median prevalence of SBS symptoms the same between the two groups under consideration? Where the median is taken as an indicator of the overall change in self-reported SBS symptoms and the two groups under consideration refer to the conventional and green building types or male and female workers when addressing potential differences due to employees' self-

reported gender. Each question is studied through the following analysis methods:

- I. Graphical inspection: A normalised stacked bar-chart of the response counts for each category and question, split by the variable of interest, should reveal any differences through the relative offset of the stacked bar of a group over that of the other.
- II. Statistical hypothesis testing: We have conservatively chosen to appraise medians since responses to the questions in the survey are Likert items. To this end, the non-parametric Mann-Whitney U test (Wilcoxon's rank-sum test) is used to test the null hypothesis of no differences between groups at the 0.05 significance level.
- III. Analysis of effect size: Coherently with the numerical analysis based on medians, the Rank Biserial Correlation (RBC) [16] was chosen as the measure of effect size, i.e. quantification of the magnitude of the difference between any two groups, regardless of their statistical significance. Similarly, to other correlation coefficients, the value of RBC is within $[-1, +1]$, where 0 indicates no correlation, +1 a (perfect) positive correlation, and -1 a (perfect) negative correlation.

These were possible thanks to the following open source software: R [17], including the Tidyverse family [18] and HH libraries [19], and Python [20], including Numpy [21], Pandas [22] and Pingouin [23] libraries.

3. RESULTS and DISCUSSION

This section presents the results of the analysis of the impact of the green certification and gender

differences on the SBS prevalence in workplaces, and it discusses the findings.

3.1 Building type and SBS

Figure 2 shows the breakdown of the scores for each SBS symptom in both building types. The occupants in the conventional buildings had a higher prevalence in most of SBS symptoms compared to the occupants in the green buildings. Moreover, from Figure 2 we can see that more than 20% of the participants in both building types experienced six SBS symptoms for '*some of the time*', these symptoms are namely watery eyes, neck pain, arms, legs and joints pain, muscle soreness, eye dryness and stuffy head, and tiredness (see Appendix A). Compare this finding to the ASHRAE standard 62.1 threshold, both building types in this study would be classified as sick.

Table 1 shows the results of the Mann-Whitney U test, which fails to reject the null hypothesis of no difference between the median scores according to the building type for nine SBS symptoms (In cases $p\text{-value} > 0.05$). While the U test suggests rejecting the null hypothesis of no difference between the median response according to the building type for tiredness symptom ($U=27490.5$, $p\text{-value} < 0.01$, $RBC = 0.12$), which was higher between the occupants in the conventional buildings.

This outcome is contrary to that of Tham et al. (2015) who reported no significant difference in the frequency of SBS symptoms between the occupants of the green and non-green buildings in Singapore, while both building types were below the recommended threshold [5]. This discrepancy could be attributed to the cultural and personal variances [24,25] or due to the differences in the buildings' characteristics [26].

Table 1: Statistical analysis of individual SBS questions according to the Mann-Whitney U test ($n_{\text{Green}}=261$, $n_{\text{Conventional}}=241$); GB indicates green buildings and CB indicates conventional buildings.

SBS symptom	μ_{GB}	μ_{CB}	$\Delta\mu_{\text{GB-CB}}$	U	Tail	p-value	RBC
Dizzy	1	1	0	31475.0	Greater	0.49	≈ 0.00
Tired	1	2	-1	27490.5	Less	< 0.01	0.12
Back or neck pain	1	2	-1	31957.5	Less	0.62	-0.02
Pain in arms, legs, or joints	1	2	-1	30264.0	Less	0.22	0.03
Muscle soreness	1	1	0	30851.0	Greater	0.64	0.01
Watery eyes, runny nose, or stuffy head	1	1	0	31227.5	Greater	0.55	≈ 0.00
Dryness of the eyes	1	1	0	29869.5	Greater	0.84	0.05
Cough or sore throat	0	0	0	29605.5	Greater	0.89	0.05
Flu symptoms	0	0	0	31753.0	Greater	0.41	-0.01
Dry, itching or irritated skin	0	0	0	29040.5	Greater	0.95	0.07

Table 2: Statistical analysis of individual SBS questions according to the Mann-Whitney U test ($n_{\text{Female}}=223$, $n_{\text{Male}}=279$); F indicates female subjects and M indicates male subjects.

SBS Symptom	μ_M	μ_F	$\Delta\mu_{M-F}$	U	Tail	p-value	RBC
Dizzy	1	1	0	31238.5	Greater	0.47	≈ 0.00
Tired	1	1	0	28498.0	Greater	0.96	0.08
Back or neck pain	1	2	-1	30740.5	Less	0.41	0.01
Pain in arms, legs, or joints	1	2	-1	28826.0	Less	0.07	0.07
Muscle soreness	1	1	0	29961.0	Greater	0.77	0.04
Watery eyes, runny nose, or stuffy head	1	1	0	30631.0	Greater	0.62	0.02
Dryness of the eyes	1	1	0	27601.5	Greater	0.99	0.11
Cough or sore throat	0	1	-1	26960.5	Less	<0.01	0.13
Flu symptoms	0	0	0	27612.5	Greater	0.99	0.11
Dry, itching or irritated skin	0	0	0	28835.0	Greater	0.94	0.07

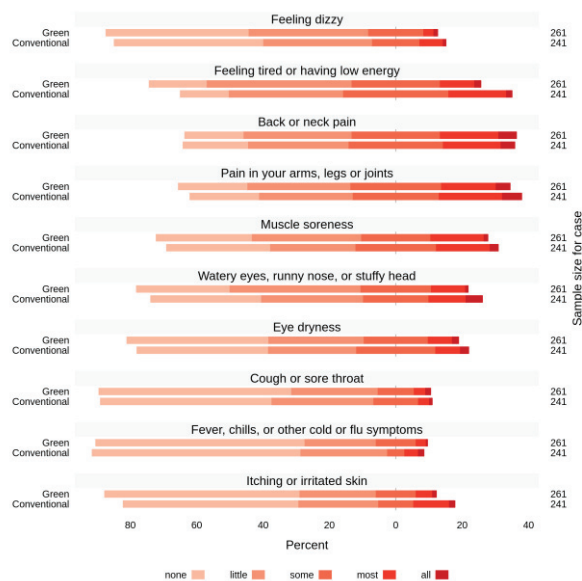


Figure 2: Breakdown of responses to SBS symptoms questions according to the building type (statistical analysis in Table 1).

3.2 Gender differences and SBS

Figure 3 shows the results of the breakdown for the scores of SBS symptoms according to the occupants' gender. The female workers tend to have a higher frequency of SBS symptoms compared to the male workers for all symptoms except two symptoms are namely dizzy and watery eyes, runny nose and stuffy head, that were reported more often between male workers.

Table 2 shows the results of the Mann-Whitney U test which fails to reject the null hypothesis of no difference between the median responses according to the occupants' gender for all SBS symptoms (In cases p-value > 0.05) except the cough and sore throat symptom ($U=26960.5$, p-value < 0.01, RBC = 0.13), which has a negligible effect size.

This finding is consistent with other studies in this area that found the gender differences is small and inconsistent in the self-reported symptoms [12]. Also, the differences between male and female workers in SBS were observed to be reported frequently in particular symptoms included cough, sore throat, fatigue, and eye irritation [9], this variance can be attributed to the biological and behavioural differences.

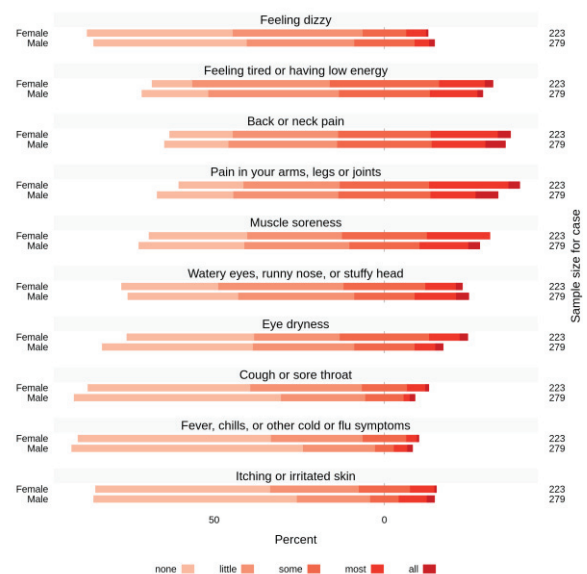


Figure 3: Breakdown of responses to SBS symptoms questions according to gender differences (statistical analysis in Table 2).

4. CONCLUSION

This study investigated if the occupants of green office buildings in Jordan have a lower prevalence of SBS symptoms compared to those in the conventional buildings. It investigated as well if gender differences play a role in the frequency of SBS symptoms.

The findings of our analysis based on 502 office occupants show that building type made no significant difference to the frequency of all SBS symptoms except the tiredness symptom, which was found to occur more

often between the occupants of conventional buildings. However, according to the ASHRAE standard 62.1 threshold, both building types can be classified as sick buildings, as more than 20% of their occupants had experienced six SBS symptoms '*some of the time*' during 28 days preceding the survey.

Also, the present analysis indicates that female and male office workers reported the same frequencies for most of SBS symptoms, with a statistically significant higher prevalence of cough and sore throat symptom between the female workers albeit of negligible effect size. However, this study had a cross-sectional research design, and an absolute conclusion of causation cannot be made, thus longitudinal with repeated measures could assist in capturing any differences between the two samples.

Overall, our findings highlight a clear problem in the office buildings in Jordan and suggest that architects, designers, and building owners need to pay further attention in the future to the unintended consequences of green office buildings, that could potentially impose on employee health and affect the work performance and the financial return of the business.

ACKNOWLEDGMENTS

This research is funded by Al-Ahliyya Amman University in Jordan "International Grants Program". The authors would like to thank Mr Mualla for helping with the data collection, Dr Ian Walker for helping in the design of the questionnaire, and the management of the surveyed buildings for allowing the authors to conduct the study.

DISCLOSURE STATEMENT

The authors reported no potential conflict of interest.

REFERENCES

1. WGBBC. Health, Wellbeing & Productivity in Offices The next chapter for green building [Internet]. London; 2017 [cited 2020 Jun 14]. Available from: <https://www.ukgbc.org/ukgbc-work/health-wellbeing-productivity-offices-next-chapter-green-building/>
2. Hedge A, Erickson WA, Rubin G. Predicting sick building syndrome at the individual and aggregate levels. *Environment International*. 1996;22(1):3–19.
3. WGBBC. BUILDING THE BUSINESS CASE: Health, Wellbeing and Productivity in Green Offices [Internet]. 2016 [cited 2020 Jun 4]. Available from: <https://www.worldgbc.org>
4. Yudelson J, Meyer U. The World's Greenest Buildings: Promise Versus Performance in Sustainable Design. New York: Routledge; 2013.
5. Tham KW, Wargocki P, Tan YF. Indoor environmental quality, occupant perception, prevalence of sick building syndrome symptoms, and sick leave in a Green Mark Platinum-rated versus a non-Green Mark-rated building: A case study. *Science and Technology for the Built Environment*. 2015;21(1):35–44.
6. Singh A, Syal M, Grady SC, Korkmaz S. Effects of Green Buildings on Employee Health and Productivity. *American Journal of Public Health*. 2010;100(9):1665–8.
7. Rostron J. Sick building syndrome: A review of causes, consequences and remedies Received. *Journal of Retail and Leisure Property*. 2008;7(4):291 – 303.
8. Aries MBC, Veitch JA, Newsham GR. Windows , view , and office characteristics predict physical and psychological discomfort. *Journal of Environmental Psychology*. 2010;30(4):533–41.
9. Bakke JV, Moen BE, Wieslander G, Norback D. Gender and the Physical and Psychosocial Work Environments are Related to Indoor Air Symptoms. *JOEM*. 2007;49(6):641–50.
10. Brasche S, Bullinger M, Morfeld M, Gebhardt H, Bischof W. Why do women suffer from sick building syndrome more often than men?--subjective higher sensitivity versus objective causes. *Indoor Air*. 2001;11:217–22.
11. Norback D, Edling C. Environmental , occupational , and personal factors related to the prevalence of sick building syndrome in the general population. *British Journal of Industrial Medicine*. 1991;48:451–62.
12. Kinman G, Griffi M. Psychosocial factors and gender as predictors of symptoms associated with sick building syndrome. *Stress and Health Stress*. 2008;171(24):165–71.
13. Kessler R, Petukhova M, McInnes K. Short WHO HPQ Absenteeism and Presenteeism Questionnaire [Internet]. world health organization/ HWP. 2007 [cited 2020 Jun 15]. p. 156–74. Available from: <https://www.hcp.med.harvard.edu>
14. Garland R. The mid-point on a rating scale: Is it desirable? *Marketing Bulletin*. 1991;2:66–70.
15. ANSI and ASHRAE 62.1. Standard 62.1 - Ventilation for Acceptable Indoor Air Quality. Atlanta: American Society of Heating, Refrigerating and Air-Conditioning Engineers, Inc.; 2019.
16. Guttman L. "Best possible" systematic estimates of communalities. *Psychometrika*. 1956;21(3):273–85.
17. R Core Team. R: A Language and Environment for Statistical Computing [Internet]. R Foundation for Statistical Computing. Vienna, Austria, Austria: R Foundation for Statistical Computing; 2019 [cited 2020 Jun 2]. Available from: <https://www.r-project.org/>
18. Wickham H, Averick M, Bryan J, Chang W. Welcome to the tidyverse. *Journal of Open Source Software*. 2019;4(43):16–86.
19. Heiberger RM, Robbins NB. Design of Diverging Stacked Bar Charts for Likert Scales and Other Applications. *Journal of Statistical Software*.

- 2014;57(5):1–32.
20. Python Software Foundation. The Python Language Reference [Internet]. 2020. Available from: <https://docs.python.org/3/reference/> Accessed: 2020-06-10
 21. Oliphant T. A guide to NumPy [Internet]. 2006 [cited 2020 Jun 10]. Available from: <https://numpy.org/>
 22. McKinney W. Data Structures for Statistical Computing in Python. In: Proceedings of the 9th Python in Science Conference. 2010. p. 51–6.
 23. Vallat R. Pingouin: statistics in Python. Journal of Open Source Software. 2018 Nov 19;3(31):1026.
 24. Norback D, Torgen M, Edling C. Volatile organic compounds, respirable dust, and personal factors related to prevalence and incidence of sick building syndrome in primary schools. British Journal of Industrial Medicine. 1990;47(11):733–41.
 25. Runeson R, Norbäck D, Klinteberg B, Edling C. The influence of personality, measured by the Karolinska Scales of Personality (KSP), on symptoms among subjects in suspected sick buildings. Indoor Air. 2004;14(6):394–404.
 26. Skyberg K, Skulberg KR, Eduard W, Skaret E, Levy F, Kjuus H. Symptoms prevalence among office employees and associations to building characteristics. Indoor Air. 2003;13(3):246–52.

APPENDIX A: The percentage of occupant response for each SBS symptom in both buildings types during 28-day preceding the survey

SBS Symptom	None of the time		Little of the time		Some of the time		Most of the time		All of the time	
	GB	CB	GB	CB	GB	CB	GB	CB	GB	CB
Dizzy	43%	45%	36%	33%	17%	15%	3%	7%	15%	1%
Tired	17%	15%	44%	34%	27%	32%	10%	17%	2%	2%
Back or neck pain	18%	20%	33%	30%	27%	29%	18%	17%	5%	4%
Pain in arms, legs, or joints	21%	21%	31%	28%	28%	26%	16%	19%	4%	6%
Muscle soreness	29%	31%	33%	26%	21%	24%	16%	16%	1%	2%
Watery eyes, runny nose, or stuffy head	28%	33%	39%	31%	21%	20%	10%	11%	1%	5%
Dryness of the eyes	43%	39%	29%	27%	20%	24%	7%	7%	2%	2%
Cough or sore throat	58%	51%	26%	31%	11%	14%	3%	3%	2%	1%
Flu symptoms	63%	63%	21%	26%	12%	5%	3%	4%	0	2%
Dry, itching or irritated skin	59%	53%	23%	24%	12%	11%	5%	11%	1%	2%

Does Sharing Mean Sustainability The Potential for Sustainability of Shared Spaces and Facilities in Collective Residential Buildings

SIYU DUAN^{1*} CHRIS TWEED¹

¹Welsh School of Architecture, Cardiff University, Cardiff, United Kingdom,

ABSTRACT: *The building sector contributes to over 40% of total energy use in the UK, among which the space heating in winter accounts for over 60% of domestic energy end-use. Additionally, occupants' energy-related behaviour accounts for a significant part of domestic building energy consumption. This paper studies the building energy performance and occupant behaviour pattern of a co-living building in London, which contains over half of the usable floor space sharing in the community. This research aims to explore the impact that shared spaces and facilities in co-living building typology have on occupants' energy-related behaviour and unwrap the reasons and concerns behind it. The results show that occupants' patterns in shared spaces and facilities buildings are different from a typical residential building, as well as their energy consumption in the building. The reasons are various and are related to the residents' age, occupation and attitude towards the shared living.*

KEYWORDS: *Sharing in housing, Common spaces, Energy use, Human-related energy behaviour*

1. INTRODUCTION

1.1 Research context and background

Living is the highest form of privacy, and living together is trying to expand the sense of community and sharing. There have been constant exploration on where to draw the line between private and public in residential living under different economic and social contexts. From the 1960s co-housing, a popular form of community living, began supporting women back to workplace [1] and helping take care of children with help from the community. From this it developed and expanded to respond to wider community needs. Co-housing has formed as a community for a particular resident group, developed to solve urban housing problems, and been designed to practice sustainability and help achieve low energy goal. In recent years, the environmental advantage of co-housing has been discussed by researchers. Building physics, low carbon technologies, household size, occupants' behaviours, openness to sustainable technologies and adopting pro-environmental behaviour are some of the aspects studied by researchers. Williams [2] agrees with Marcus and Dovey's view (1991) that the cohousing model is a sustainable alternative to other housing models, and summarises the sustainability objectives of cohousing model in two perspectives – 'well-being and affordability' and 'networks, cohesion and inclusion'. However, the sustainable aspect of cohousing model has not been fully discussed.

Community with shared spaces and facilities are influenced and has developed rapidly by the sharing economy. Inspired by the concept of co-housing, a co-

living apartment is a modern form of shared living emerging in many urban cities. Co-living apartments usually have a higher common space ratio than co-housing developments because they have smaller room sizes. This character has the potential to reduce energy use from space heating, while in the meantime, residents have more choice to spend time in the building with all the common functional rooms. Numbers of corporation co-living model are emerging worldwide, including The Collective (London and New York), Roam (Miami, Bali, Tokyo, San Francisco and London), Zoku (Amsterdam) [3], and You + (multiple cities in China). However, the main focus was on co-living, providing an alternative for modern living and providing social benefits. As the common space layout and occupants' activities are different from either co-housing or standard residential buildings, the energy efficiency of this building typology is still lack of discovering.

1.2 Sharing in housing

Humans have a long history of living together and living as a community. The Co-housing concept (began in Denmark in the 1960s) became popular and known by the public since the 1980s; it is an intentional community where residents have their self-contained spaces as well as shared spaces, and they come together to manage their community, share activities and regularly eat together [4]. Moreover, the growing contemporary collaborative housing schemes are embedding co-housing building concepts into modern society.

Sharing has different scopes, purposes, types of occupants and correspondingly different challenges. Vestbro and Horelli [5] clarified several concepts used to study housing with shared spaces and shared facilities - these concepts include co-housing which is defined as housing with common spaces and shared facilities, where residents organize regular community events; collaborative housing is used for housing that is oriented towards collaboration among its residents; collective housing is focusing on the collective organization of services. Other sharing in housing may be designed to a specific type of people, like shared accommodation aiming to provide living spaces for homeless young people. The challenges include restricted choice, health and well-being problems due to the living environment, parenting and family relationship issues, vulnerability, on-site management difficulties, and insecurity [6]. In the meantime, sharing in housing has a number of benefits both for residents and societies, especially in the current sharing economy.

There is a good deal of ambiguity in the terminology when defining collaborative housing, and several concepts have been used to identify similar phenomena in the study of housing with shared spaces and facilities [1]. Elements like participation in different stages, living styles, organization types, and residential management are all considered in the sharing practice.

The mainstream discussions about these collaborative community that contains shared spaces and facilities focus on their social perspective. Their sustainability discussions are limited and lack in-depth study.

1.3 Human-related energy use

Energy use in residential buildings includes space heating (68%), hot water (13%), electrical appliances (12%), cooking (5%), and lighting (2%) at the EU level [7] (European Commission 2020). Each of the above elements can be primarily influenced by occupants' behaviour, and researchers point out the importance of occupant behaviour studies [8-9].

Occupant behaviour research in buildings can be traced back to the 50s and 60s, which were focused on occupants' interaction with the ventilation system and window opening [10]. From the 1980s, there are grown interests in occupants' behaviour studies regarding energy use in buildings. The main topics include adaptive occupant behaviour, thermal comfort and model research. Since the 1990s social science researchers got involved in this field and also contributed to the body of knowledge [11].

Primary factors of occupants' behaviours, which influence building energy use in domestic building include climate, occupants' control of building settings,

the characteristics of the dwelling, and the profile of the occupants [12].

Shove explains in a presentation [13] that attitudes of individuals drive their behaviour. Steemers and Yun [12] also point out that energy use is directly impacted by climate, building physics and equipment, but these in turn affect behaviour. Moreover, they suggest to better understand, evaluate and predict building energy use researchers need to pay attention to the occupant and behavioural aspects in the building performance.

Occupants related factors are different from a typical residential building in the co-living building model. This building typology minimises the influence of individuals by designing small private spaces and large common spaces.

1.4 Sustainability related discussion and gaps in existing research

Researchers pay attention to occupants' behaviour when investigating building energy. In recent years, the research of occupant aspect has shown the trend of gaining more attention. Gram-Hanssen [14] points out in the research that in regards to environmental sustainability, occupants' household routines are as essential as the physical and technical aspect of buildings. A number of studies have been designed to test out how much occupants' behaviour has an impact on commercial buildings, and in turn, what ways building features are influencing occupants. Fewer studies have researched the occupant behaviour and energy using pattern of residential buildings due to ethic limitation. The studies exploring residential buildings with shared spaces and facilities needs in-depth research as well. Williams [15] suggested it is more efficient for more people to live together with regard to energy, resources and time. However, the sharing system relays highly on individual resident's sense of responsibility and desire to form a community.

There are some discussions in the field about the sustainability aspect of co-housing typology. Discussions mainly focused on its social and economic benefits, and fewer studies explored the sustainability capacity in the co-housing model. However, there is not much in-depth research on the sustainability capabilities of co-living developments, nor the role that common space plays. This paper, therefore, hopes to provide insights and discussions about the sustainability and energy-saving potential of common spaces in co-living development in urban cities. The data was collected during a field study to a co-living project through observation, conversations and interviews.

2. RESEARCH METHOD AND METHODOLOGY

The research methodology was developed to explore how residents in the co-living community use different common spaces as well as their private units and how much impact does the co-living building typology have on occupants' energy-related behaviour. The chosen co-living case is the largest of its kind in London; occupied since 2016, with over 500 residents, it provides a significant amount of data for understanding different types of residents. The data analysis is conducted to reveal the link between occupants' activities and energy consumption in various common spaces in the co-living building and interpret the reasons why occupants behave in a certain way.

This research is produced in two steps, including a desk-based search and a field study. The desk-based resource search includes the following: 1) existing literature of the co-living project, from online publications; 2) onsite services and organization of the management team and the existing sustainability strategies; 3) the building information of the co-living project. The field study, which includes observation and interviews, was carried out in winter. The observation was taken from 13th Feb to 20th Feb – a week-long, on-site observation at a co-living project in London. It aimed to gain primary data about occupants' usage and behaviour in a co-living building. More specifically, to observe what people do in each functional space, and how they interact with their neighbours and common facilities. Yan et al. [9] pointed out that occupants' behaviour includes occupant presence, pattern of movement, and an individual's interaction with building appliances and services system. Therefore, the observation in this field study focused on collecting occupant behaviour data from the above aspects. During the observation period, data relating to occupants' activities, how long they stayed in the spaces, their movement in the building and the occupant density in spaces, was collected. The semi-structured interviews were conducted with residents of the co-living building from 13th February – 17th March 2020, the interviewees were selected with a sampling method, and each interview lasted for about 60 mins. The sampling method considered the following features of the residents: their length of tenancy, whether they lived alone or with a partner, their employment, and their gender. The researcher went to various common spaces in the building and approached residents with the following rules: interviewing both male and female residents and trying to approach residents of all ages. In order to get views from residents who did not use common spaces very often, some interviewees were also recruited with the help from the building manager team.

3. DATA INTERPRETATION AND RESULTS

3.1 Benchmarking the case study project

The case study project is a co-living apartment with a capacity to accommodate 550 people, located in west London, with a very diverse resident population. 70% of the residents are under 30 with the age range from 18 to 61. 90% of the residents are from the UK and EU. The most popular occupations living there are doing consultant, operation and finance jobs. The building information is listed as follow (Table 1):

Table 1: Project building information.

Term		Area	%	M ² /pers.
Outdoor spaces (m ²)		830	/	1.5
Total floor area (m ²)	Total	11880	100	21.6
	Public access	1915	16	3.5
	Common use	4720	40	8.6
	Private use	5245	44	9.5

3.2 Usage patterns of the common spaces

The common spaces are located on the ground floor and the middle part of each floor that is close to the lifts. The designed space functions and activities in each space are listed as follow (Table 2):

Table 2: Activities in different common spaces in the co-living building.

Floor	Space	Activities in the spaces	
		Energy-related activities	Non-energy-related activities
10 th , 9 th and 8 th	Themed kitchen	Cooking meals Working	Relaxing Gathering
2 nd to 7 th	Common kitchen in each floor	Cooking meals	Working Communicating
7 th	Library	PC	Reading/Studying
6 th	Game room	Watching TV Video games/Music	Board game Ping-Pong, Pool
5 th	Cinema	Watch film Watching TV	Relaxing Chat Eating
4 th	Secret Garden	PC	Reading Relaxing Eating Gathering
3 rd	Spa	/	Relaxing
2 nd	Laundry room	Washing/Drying Watching TV Ironing	Chatting
1 st	Office	/	/

GF	Gym, Lobby, Co- working space, Bar & Kitchen	PC	Chatting Gathering
----	--	----	-----------------------

The usage pattern in each common space various as well as in different times of the week. For example, in general, people spend more time at the bar, cinema, laundrette and library at weekends, whilst the co-working space is more prevalent during the weekdays. Because the co-working space is also open to the public if they pay a sign-up fee, people who do not live in the building could also use this space to work. The following chart is generated from the data collected on-site. The data was collected during the field study period by visiting each space every three hours (Fig.1).

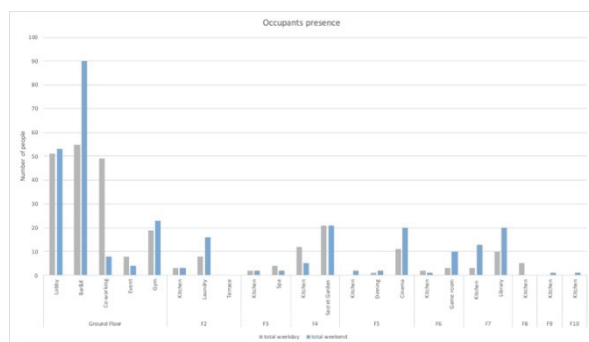


Figure 1: Occupants' presence.

Activities related to cooking

The cooking-related energy consumption in domestic accounts for 5% of total end-use energy in the EU (3% in the UK). While parts of the electricity consumption are related to cooking activities. For example, the use of lighting in the kitchen and dining room. The location and accessibility of cooking spaces are varied depending on the purpose of designed target users. Furthermore, the freedom to use the communal kitchen spaces provide more flexibility for residents to meet their cooking and gathering purpose, depending on whether they are preparing individual meal or shared meals. There are four types of kitchens in the building, including the private kitchen either shared by two residents or within the studio unit, a common kitchen in each floor, themed kitchen on the top floors, and the kitchen in the event rooms on the ground floor.

The equipment in private and common kitchens are slightly different. The private kitchens are equipped with a microwave, a two-zone electric hob, and a mini-fridge. In communal kitchens there is an additional oven, dishwasher, two refrigerators and a four-zone electric hob. Since residents have the choice of using different kitchens, how do they decide where to cook? Moreover, what influences their decisions

and preferences? These questions were posed when interviewing the residents about their usage preferences for cooking activities. People's choices were varied: some residents cooked most of their meals in the common kitchen and rarely used their private kitchens because of the kitchen layout - 'my kitchen is so small, and the smell after cooking is hard to go away' [16]. Others enjoyed the social environment of the common kitchen, and reported: 'I like to come to the common kitchen where I normally could meet people and talk during dinner' and 'sometimes when I run out of something I could check all the free stuff in the common kitchen' [17]. Conversely, others rarely used the common kitchen because 'it is far from my room and I have to bring all my cooking stuff with me and pass two doors, while my kitchen has all I need for cooking' [18]. Though all the common kitchens and themed kitchens are open to all residents, residents might feel the boundary between private and public (or semi-public). As the themed kitchens are on the 8 – 10th floor which also has residential living spaces, some residents said that they rarely or never go there even though it has a better view and beautiful decoration, because they feel they are 'step[ping] into other people's space' as they do not live in that floor [16].

Therefore, residents' usage pattern of cooking is not only related to the designed cooking spaces but also closely associated with an individual's preference. There is a bottom-up solution to reduce individual cooking by organizing group meal among residents [19]. They have a group where people meet up once a week for a group meal, which is generally cooked by one or two people in the group. However, this form of a shared meal is not stable as the residents may come and go year by year.

Where to work?

When talking about the location of where people work, the residents have several options within the building. The building was designed to let everyone have their spots, even though there are lots of spaces for events and gathering, people who prefer quiet can still find places to go [20]. Furthermore, due to the modern working flow, a great number of people can work anywhere as long as they can access power and have an internet connection. This also means that people have different preferences with the way they work.

The main concerns for people when choosing a working place include noise level, privacy, and comfort. People do not necessarily prefer to work in designed workspaces. Their reasons for liking or disliking a working spaces are summarized from interviews with residents (Table 3), which shows a high level of disagreement about the same features [21]. For example, 'quiet' could simultaneously be an

advantage or a disadvantage for different people. This was also found in relation to the 'privacy in common spaces', the 'background noise', and 'access to people'.

Table 3: Reasons collected from residents about liking or disliking working spaces in the co-living building.

	Reasons for like this working space	Reasons for dislike this working space
Library	'It is <u>quiet</u> , I would go to the library when I really need to get something done.'	'It is just <u>too quiet</u> . I worried about bothering other people if I make any noise.'
The Exchange (co-working space)	The atmosphere of working - surrounded by people busy at work.	'There always have someone talking on their phones.' Uncomfortable table and seats. No view to the outside.
The Galley	Big window. Fewer people	Unable to fit many people.
Lobby	Big window beautiful view. <u>Good background noise</u> . Able to make social contact with people.	Privacy (apply to all common spaces) <u>Too loud</u> .
Common kitchen	Quiet when not during mealtime. Convenient to get some food. 'I <u>could socialise when I want to</u> .'	The smell of food. <u>Interrupt by people</u> .
Private room	'It is a habit to study on my bed.' 'I have all my settings in my room, and these are comfortable for me.'	Small space, especially for couples. 'There are too many disruptions – my bed, snacks, TV.'

People's preference for the working environment is different, as some choose to use a quiet space while others may prefer to have some degree of noise and random conversations. There are also a number of interviewees who said that they prefer to work in their own room, either because of the excellent level of privacy or because it is more convenient. They did mention that they spend more time working outside of their room than in their previous accommodation. Some residents commented that they might spend less time in their room and on their computer because they found themselves more involved in community activities and meet more neighbours in a day.

3.3 Gradation between private and public

The boundaries between private and public influence the coexistence of the residents living in shared spaces and facilities spaces on a day to day

basis [22]. Architects could create a different level of accessibility and publicness by space design.

Not only is energy-related behaviour found to be different in private spaces and common spaces, but the energy adaptive behaviours are also varied in these areas. The observational studies and the interviews with residents highlighted a number of factors that might result in different occupants' behaviour in private and common spaces in co-living buildings. Interviewees were asked to number their reactions to discomfort in both their private rooms and in common spaces. The result is summarized in the following Table 4 (numbered by the frequency of mention).

Table 4: Energy adaptive behaviours in different areas.

Energy adaptive Behaviours in different areas	Private	Common
Open/close the window	1	3
Open/close the door	4	/
Adjust clothes	3	1
Go to another place	5	2
Do some exercise to warm-up	/	/
Adjust the radiator	2	4
Use an extra electric heater	/	/
Ask the manager to adjust room temperature	/	5

Residents tended to adapt to the room environment in their private spaces by opening or closing the window, adjusting the radiator and changing their own clothes. In common spaces most frequent behaviour included adjusting clothes, moving to another place and opening or closing the window. As the private rooms are small, opening or closing the window and adjusting the radiator could quickly change the room temperature, whereas in common spaces the room temperature is pre-set at 21 degree and occupants are unable to alter it.

4. DISCUSSION AND CONCLUSION

The paper argues that the residential building with common spaces and facilities have different occupant behaviour pattern from normal residential buildings, which has the potential to influence building energy consumption by occupants' behaviour in different ways. One co-living residential building was picked as case study to conduct the observation and interviews in order to find out which occupant behaviours related to energy use in both private and common spaces in a co-living building model and the reasons behind them.

Through the analyses of cooking and working practices, the result shows that the residents' patterns of using each space are highly individual. This does match with the design intention of providing multiple spaces for people with different preferences and needs. However, the complex user patterns are

difficult for architects to predict and simulate in the design stage. Therefore, more detailed research of how occupants' multiple patterns differ from the 'occupant simulation' in models should be designed. The energy adaptive behaviour of the residents in private rooms and common spaces shows different preferences. Adjusting the windows and radiators are mostly chosen by interviewees in private rooms, whilst for common spaces, the top choices are adjusting clothes and moving to other places. The reason for residents' behaviour in private rooms include the fact the room temperature could be adjusted quickly by change the temperature of the radiator or adjusting the windows. Because the room space is small, some interviewees accordingly think it would not cost too much energy to heat up the room due to its size. Meanwhile, for the common spaces, residents have little control of the temperature setting and they need to consider others when adjusting windows.

More detailed analyses and research should be conducted on the comparison of the designed energy consumption and the measure of energy consumption. The analyses of occupants' behaviour can play a part in explaining where the gaps emerge and how to reduce the mismatch between as-design and in-use energy consumption in the co-living building model.

ACKNOWLEDGEMENTS

The authors would like to thank staff from the case study project to facilitate access and support during the field study. My thanks also go to the project architect for kindly explaining the design process of this co-living project. Also, a huge thanks to all the interviewees who participated in this study.

REFERENCES

1. Vestbro, D. U., and Liisa H., (2012). Design for Gender Equality: The History of Co-Housing Ideas and Realities. *Built Environment*, 38(3):315–35.
2. Williams, J., (2005). Sun, Surf and Sustainable Housing - Cohousing, the Californian Experience. *International Planning Studies*, 10(2):145–77.
3. Reinventing Density: Co-Living, the Second Domestic Revolution, [Online], Available: <https://theconversation.com/reinventing-density-co-living-the-second-domestic-revolution-66410> [27th April 2020].
4. About Cohousing, [Online], Available: <https://cohousing.org.uk/about/about-cohousing/> [30th April 2020].
5. Vestbro, D. U., (2010). Living Together – Cohousing Ideas and Realities Around the World. In *International Collaborative Housing Conference*. Stockholm, Sweden. 5th – 9th May 2010.
6. Green, S., and McCarthy, L., (2015). Is Sharing the Solution? Exploring the Opportunities and Challenges of Privately Rented Shared Accommodation for Single People in Housing Need. *People, Place and Policy Online* 9(3):p. 159–76.
7. Energy Use in Buildings, [Online], Available: <https://ec.europa.eu/energy/en/eu-buildings-factsheets-topics-tree/energy-use-buildings> [27th April 2020].
8. Stazi, F., Federica N., and Marco D'Orazio., (2017). A Literature Review on Driving Factors and Contextual Events Influencing Occupants' Behaviours in Buildings. *Building and Environment*, 118:40–66.
9. Yan, D., Tianzhen, H., Bing D., Ardeshir, M., Simona, D'Oca., Isabella, G., and Xiaohang, F., (2017). IEA EBC Annex 66: Definition and Simulation of Occupant Behavior in Buildings. *Energy and Buildings*, 156:258–70.
10. Tam, Vivian W. Y., Laura A., and Khoa Le., (2018). Energy-Related Occupant Behaviour and Its Implications in Energy Use: A Chronological Review. *Sustainability (Switzerland)*, 10(8):1–20.
11. Guy, Simon., and Shove, E., (2000). Theories of Knowledge and Practice. *A Sociology of Energy, Buildings and the Environment*. p. 56. London: Routledge
12. Steemers, K., and Geun Young Yun., (2009). Household Energy Consumption: A Study of the Role of Occupants. *Building Research and Information*, 37(5–6):625–37.
13. Shove, E., (2011). How the social sciences can help climate change policy. Script of lecture, London. 17th January 2011. Available: <https://www.lancaster.ac.uk/staff/shove/exhibits/transcript.pdf>
14. Gram-Hanssen, K., (2013). Efficient technologies or user behaviour, which is the more important when reducing households' energy consumption? *Energy Efficiency*, 6(3):447–457.
15. Williams, J., (2007). Innovative solutions for averting a potential resource crisis - The case of one-person households in England and Wales. *Environment, Development and Sustainability*, 9(3):325–354.
16. Duan, S., (2020a). Interview by Siyu Duan, Structured interview, London, 20th February.
17. Duan, S., (2020b). Interview by Siyu Duan, Structured interview, London, 18th February.
18. Duan, S., (2020c). Interview by Siyu Duan, Structured interview, London, 12th March.
19. Duan, S., (2020d). Interview by Siyu Duan, Structured interview, London, 12th March.
20. Duan, S., (2020d). Interview by Siyu Duan, Structured interview, London, 14th January.
21. Duan, S., (2020e). Multiple interviews by Siyu Duan, Structured interview, London, 18th February – 12th March.
22. Schmid, S., and CU-Lucerne., (2019). A History of Collective Living, edited by S. Schmid, D. Eberle, and M. Hugenobler. Basel: Birkhauser. p. 16.

Vacuum Insulation Panels in Building Sector: Case study in Spain of Vacuum insulation panels in construction for energy efficient retrofitting of buildings.

XABIER APARICIO,¹ AITOR ERKOREKA,¹ LUIS ALFONSO DEL PORTILLO,¹ CATALINA GIRALDO,¹
AMAIA URIARTE,² PABLO EGUIA,³ ANA MARÍA SÁNCHEZ-OSTIZ,⁴

¹ University of the Basque Country (UPV/EHU), Bilbao, Spain

² Fundación Tecnalia Research and Innovation, Zamudio, Spain

³ University of Vigo, Vigo, Spain

⁴ University of Navarra, Pamplona, Spain

ABSTRACT: *With the installation of 1800 m² of Vacuum Insulation Panels in the entire opaque façade of an existing building, it has been demonstrated that the use of Vacuum Insulation Panels is possible in energy efficient building retrofitting, even in complex façades with low modularity. It has also shown the possibility of using Vacuum Insulation Panels in larger construction works. After the works, the state of the façade has been monitored. Damaged panels have been quantified during the construction phase and one year after the completion of the works.*

This work presents the lessons learnt during the design and installation process of the vacuum insulation panel integrating solutions, including the key improvements that are necessary to be implemented in the VIPs production process to guarantee their technical and economical viability for their use in edification.

KEYWORDS: *Energy efficiency, Vacuum Insulation Panels, Building Retrofitting.*

1. INTRODUCTION

One of the important challenges in the framework of energy saving is to improve energy performance in the construction sector. To enable truly effective measures, actions must be carried out both in new construction and in the rehabilitation of buildings, taking into account that a large part of the building park is built before the first regulations regarding energy measures.

Framed in this context, this summary presents the application of a new material for the rehabilitation of a building with the aim of improving its thermal insulation: Vacuum Insulation Panels (VIP). Said material has been applied to the building envelope, integrated into an industrialized system.

The VIPs give thermal transmittance values of 0.28 W / m²K within a 10 cm retrofit construction solution. This feature of the vacuum panels represents a great opportunity for energy saving in the construction world, both for new buildings and for their rehabilitation. However, they present problems for manipulation and installation that have made the application of the material on the façades of buildings impossible until now. Furthermore, the uncertainty of property loss during their lifetime has also hindered their use as an energy efficient solution in building sector [1, 2].

In this document, we analyze the specific action to rehabilitate a public building of the University of the Basque Country (UPV/EHU), the Rectorate

Building. The project has been developed within the FP7 A2PBEER research project funded by the European Commission as detailed in [3].

We provide details of the project that has tried to systematize the placement of the panels in the building and the data obtained from the execution of the work in order to convert the VIPs into a real alternative for their application in building rehabilitation works.

Finally, the physical inspection carried out later to determine the state of the vacuum panels time after their placement is included in this document to showcase the reliability of the solution under real conditions.

2. CASE STUDY BUILDING

With the aim of verifying the applicability of vacuum panels as insulation, the Rectorate building has been rehabilitated at the University of the Basque Country. The demonstration building is located on the Leioa University campus. The Leioa University campus is located on top of a hill, about 11 km from Bilbao.

The building was built in 1970. It has a rectangular floor plan of dimensions 110 x 22 m. It is made up of three blocks with a maximum height of 18 meters and heights from two to four floors. The retrofitting has been carried out only in the west block.

The original envelope was executed without any energy efficiency measures. Most of the façade is built with 10 cm precast concrete panels with vertical

and horizontal ribs of reinforcement and an interior layering with a discontinuous air chamber. The composition of the façade is carried out with large windows in contrast to the precast concrete ones. Towards the south it has concrete parasols on the windows that have been kept in the restoration.

In this project, a total of 1,800 m² of ventilated façade has been installed, taking the original precast concrete façade as support. The insulation is VIP, completing borders and unique points with traditional high-performance insulation.

Another series of energy saving measures were also carried out in the rehabilitation of the building; recovery systems in ventilation systems, windows, improvement in lighting systems, etc. However, these actions are not analyzed in this document.

The building's energy use has been monitored before and after the performance. Following the completion of the works, follow-up visits have been made to the action, highlighting the visual inspection of the situation of the VIPs.



Figure 1: University of the Basque Country, rectorate building. South façade.

Figure 2: Silica core of vacuum insulation panels.

Figure 3: Vacuum insulation panel pallet.

3. VACUUM INSULATION PANEL

The insulation used in the rehabilitation of the building was developed by the company Isoleika S.Coop. This company dedicates its products mainly to industrial uses and household appliances but did not have experience in the production of VIPs for building envelope.

The insulating panel is composed of a core of smoked silica (pyrogenic) and reinforced with fibers, wrapped in an aluminum bag. Silica is compressed into sheets of desired thickness. Later it is cut in the established measures and it is introduced in the aluminum bag. Finally, the interior air is removed from the bag and sealed to guarantee vacuum. The excess flaps of the envelope fold and glue on the panel itself.

The maximum dimension of the panel is 1100 mm² × 700 mm², and with a thickness of 30 mm. It is a light panel, easily manipulated on site.

The declared thermal conductivity of the panels is 0.005 W / mK that applied to a thickness of 30 mm, can lead to a surface-surface thermal transmittance (U) of 0.17 W / m²K. In case of loss of vacuum, the core conductivity increases to 0.021 W/mK, and the surface-surface thermal transmittance increases up to 0.7 W/mK.

The interior composition of the insulation panel and the way it is built generate certain conditions that must be considered when putting the material into use:

1. The edges of the panels do not offer a completely flat surface, nor well-defined angles. The first panels presented a dimensional variation of 10 cm for every 10 meters. As an example, ceramics offered a variation of 1 cm for every 10 meters.
2. The panel behaves well in compression against well distributed loads. However, sharp edges or sharp elements can damage the aluminum bag, eliminating at that time the conditions of interior vacuum and losing much of the insulating properties. That is why the company supplied the material with an adhered asphalt sheet to offer greater resistance to punching.
3. The panel cannot be modified on site. In order to guarantee vacuum conditions, it cannot be cut or drilled for placement. Thermal bridges must be properly resolved in conjunction with other materials and fasteners, but without cuts or holes.

The panel has a flat but irregular surface, due to the pressure of the vacuum in the aluminum bag. Considering the said aluminum surface, it is easy to check if a panel is punctured since the bag has a smooth surface, without vacuum pressure. However, depending on the perforation hole, the air filling of the panel does not take place immediately, so it is advisable to check the panels sometime after their placement to confirm that the panel is not really damaged.



Figure 4: Punctured vacuum insulation panel (left) next to a vacuum insulation panel in good condition (right).

4. PROCESS OF THE WORKS

Given the particularities of VIPs, a series of investigations and checks were carried out on the material and the way it was placed within the final retrofitting solution. Several samples were carried out both in the Rectorate itself and in a test building located at the Tecnalia facilities.

Finally, the way to fix the panel was defined and the complete execution project was written. The project contemplated the execution of the entire façade of the building but divided into two phases. The first phase is the one that is the object of this document and corresponds to the west block of the Rectorate Building with a total of 1,800 m² of façade. The second phase has not yet been developed.

Table 1: Dates of works and revision.

Architectural project	May 2017
Start of construction works	Jun 2017
End of construction works	Nov 2017
VIPs review	May 2019

4.1 Special features of the building

As we have mentioned, the rector's building original façades were built with 10 cm precast concrete panels with vertical and horizontal ribs of reinforcement and an internal brick layering with discontinuous air chamber. It does not have insulation. The parasols on the south façade are also made of concrete, proving to be very effective in their function.

In general, the façade presents numerous outgoing volumes, with structural floor in flight and pillars that are part of the envelope.

The solution to improve the thermal behavior of the façade had to take this situation into account, covering not only vertical walls, but also horizontal and cantilevered ones, giving continuity to the thermal insulation layer in those areas.

4.2 Construction system

Works were carried out with a ventilated façade system anchored to the existing precast concrete panels in the building.

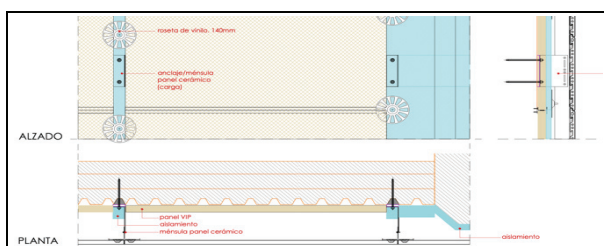


Figure 5: Execution project. Constructive detail of the façade.

The new façade is made up of the following elements and materials:

1. Wall mounted PVC profile and grooved rail clip system for pressure fixing VIPs. Horizontal fixing by pressure on top and bottom of the VIPs.
2. 30 mm thick VIP insulation layer of 10 different measures (maximum 1100 × 700 mm²), arranged horizontally and vertically, with an asphalt protection layer.
3. Metal anchoring supports on thermal break pads, for fixing the aluminum substructure that supports the external ceramic cladding of the ventilated façade.
4. Vertical rockwool insulation strips with a 40 mm and 60 mm vapor-permeable black veil between each VIP column and on an aluminum substructure, and in general for

special points. Insulation fixed with rosette type circular pieces of large diameter that also allow to fix by pressure the VIP faces not caught with the PVC profile (see Fig. 5).

5. Ceramic finish substructure consisting of vertical aluminum T-profiles lacquered in black that support the external cladding 5 cm away from the insulation; leaving a ventilated cavity.
6. 2 cm thick extruded ceramic cladding superimposed in various colors.

4.3 Installation methodology

Firstly, a complete scan of the building was carried out in order to have the exact geometry and to be able to generate all the VIPs and ceramics with maximum precision in view of the impossibility of cutting on site. In relation to the VIPs, it was tried to cover the maximum surface of the building playing with a maximum of 10 different measures of panels. All of them were marked with a sticker to facilitate on-site installation.

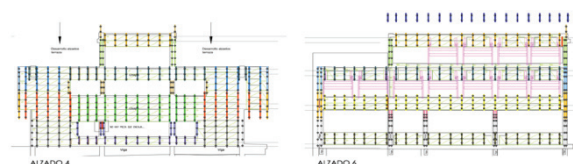


Figure 6: Execution project. Façade detail with the position of vacuum insulation panels.

Prior to the placement of the ventilated façade and thermal insulation, the situation of the façade original panels and concrete structure was analyzed, cleaning and repairing, where appropriate, the deteriorated points. The surface was revised to avoid points and edges that could damage the VIPs.

The concrete parasols were removed to clean them up and paint them on the ground and replace them with new brackets that allowed the insulation to pass, eliminating thermal bridges.

For the placement of the VIPs, a special profile composed of two pieces with a grooved rail clip system was designed (see Fig. 7). One piece was screwed to the existing façade with countersunk screws to avoid damaging the VIP, later the VIP was placed and finally the second piece of the PVC profile was clipped by pressing the VIP.

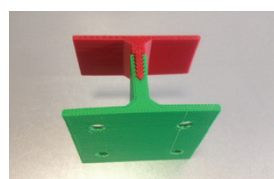


Figure 7: Profile of slotted rail clip system for fixing the vacuum insulation panel. Prototype section.



Figure 8: Profile of slotted rail clip system for fixing the vacuum insulation panel. Test sample on the building.

First of all, the position of the panels is projected onto the façade and marked precisely. The second step is to fix the first piece of the PVC profile, the metal anchor support for fixing the ceramic cladding substructure and the anchors for the circular pieces of support for the rock wool (see Fig. 9 and 10).



Figure 9 and figure 10: Wall fixing of the first piece of the PVC profile to support the VIPs, metal anchoring supports on thermal break pads for fixing the aluminum substructure that supports the external ceramic cladding of the ventilated façade and anchoring for circular support pieces of rockwool insulation.

Once all the holes have been drilled and the anchors are fixed, the VIP is placed and the second piece of the PVC profile is clipped by pressing the panel at the top and bottom (see Fig. 11). Subsequently, the rockwool is put in its position and is fixed with double fixation on the same anchor, one with a larger diameter to also fix the sides of the VIP in a timely manner and another with a smaller size that exerts pressure on the assembly.

In relation to the VIPs, a material collection procedure was established on site to prevent them from being damaged once received. Similarly, the status of the placed VIPs was monitored. A review of the panels was established after 48 hours of placement to detect punctured VIPs and proceed to replace them. Therefore, the ceramic coating could not be installed until the end of this quarantine period.

In accordance with normative criteria on the spread of fire in ventilated façade chambers, it was necessary to remove the asphalt coating from part of the VIPs, mainly those located in the accessible part of the façade.



Figure 11: VIPs placed in position using a horizontal PVC profile and rockwool fixed with circular pieces.

Figure 12: Isolation at singular points. Rockwool insulated abutment in continuity with VIP insulation.

Figure 13: Detail of the metallic anchor support for the ceramic cladding substructure with the green thermal bridge break pad.

The black lacquered aluminum vertical T-substructure that supports the external cladding was fixed on the metal anchoring supports.

Finally, the ceramic pieces were placed in the anchorages of the vertical aluminum substructure and the finishes of the singular points of the façade were made (see Fig. 14 and 15).



Figure 14: Façade of the rectored building with VIP insulation placed and awaiting ceramic laying.

Figure 15: Façade detail. Cladding ceramic piece, black lacquered aluminum substructure for fixing ceramic, circular pieces pressing rock wool and VIPs fixed with PVC profile.



Figure 16: University of the Basque Country, rectorate building. North façade after retrofitting.

Figure 17: University of the Basque Country, rectorate building. South façade after retrofitting.

4.4 Results of intervention

The following aspects and data after the complete execution of the façade are quite remarkable:

1. Accuracy in setting out was fundamental to be able to bring the work to a successful conclusion. In the case of the metal anchor support, the thickness added by the placement of the thermal bridge break pad was not considered in origin. Since the VIP was placed just in contact with the base of said support, it was decided to introduce a pad that would protect not only the base, but also the metallic side of the support edge. This change modified the staking of the entire façade. Similarly, the control of the panel tolerance by the manufacturer has been essential to carry out the work. In this way, the affection of the possible thermal bridge in the joints between panels is mitigated (see Fig. 13).
2. The PVC profile for fixing the VIPs was effective, not giving any closure stability problems during the construction process. However, once clipped, if it was reopened under pressure, the grooving teeth were deformed and subsequently offered a

weakened seal with undesired opening in some cases.

3. The company's proposal to cover the VIPs panels with a cheap and resistant material such as asphalt sheets provides protection to the panel against punctures, but generates other added problems regarding fire behavior, so other materials should be considered.
4. The 48-hour quarantine times to verify the existence of punctured panels generates problems in the execution rates of the work, delaying the execution and generating more indirect costs for the works.
5. During the construction phase, the following punctured VIP panels were counted.

Table 2: Panels punctured until end of works.

Total VIPs installed on site	1.515	
After storing 1 year in factory	13	1%
Handling on site	15	1%
On the façade (48h quarantine)	221	15%
TOTAL PUNCTURED VIPs	249	17%

6. Data on the cost of executing the work:

Table 3: Works costs before taxes.

VIPs	209.658,80€
Clips for VIPs	24.096,32€
Traditional insulation	4.656,00€
Ventilated façade	328.013,26€
Façade installation	230.640,42€
TOTAL COST	797.064,80€
Façade surface	1.800 m ²
COST / SURFACE	442,81€/m²

7. The placement of the VIPs, with the limitation of 10 types of different measures, was carried out to the maximum possible surface area of the façade. A total of 1,112 m² of VIPs and 688 m² of traditional insulation were placed, that is, 62% of VIPs compared to 38% of traditional insulation.
8. In relation to the building, there was a substantial improvement in energy savings. The measured space heating energy use reductions were of 23% as depicted in the table below. Nevertheless, up to 51% energy reductions would have been expected if no other energy efficient measures that considerably reduced the internal heat gains of the building were implemented (see details in [4]). Furthermore, as shown in [4], the indoor temperature set point increases after rehabilitation has also hindered the energy savings of the retrofiting.

9. Finally, the reduction on the building Heat Loss Coefficient has been estimated based on the pre- and post-retrofitting monitoring data, and even after the introduction of the mechanical ventilation system, it has been reduced in a 28% as detailed in [5,6].

5. REVIEW OF THE STATE OF VACUUM INTEGRITY OF THE VIPs

As we have indicated, several panels installed on the façade had an appearance of correct vacuum conditions, but after a 48-hour quarantine, it was found that they were punctured. These panels suffered in the handling or installation some type of smaller perforation that generated a very slow air intake and therefore gave the false feeling of not being punctured.

That is why, after the completion of the works in late 2017, it was decided to review the status of the VIP panels in May 2019.



Figure 18: North façade during insulation review.

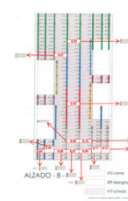


Figure 19: VIPs review sheet.



Figure 20: Ceramic pieces removed. Punctured insulation at the top and good condition insulation at the bottom.

5.1 Review methodology

The inspection of VIPs was by visual. VIPs that have lost their vacuum show an aerated envelope. Using auxiliary means such as scaffolding and telescopic lifts, it was decided to carry out a sampling on the façade of the building. The industrialized system used to fix the ceramic to the aluminum substructure allows releasing these ceramic pieces and replacing them individually without damaging them.

All the rehabilitated façades were analyzed, making a representative sampling of the different positions of the VIPs and the ceramic pieces (height, position, dimensions, etc.).

As a complement, an attempt was made to review the VIPs puncturing using thermographs. However, the air chamber and the ceramic of the ventilated façade did not allow perceiving information on the state of the insulation layer below them.

5.2 Results of revision

The following data has been obtained analyzing all the information collected during the review:

Table 4: Result of the inspection of punctured panels divided into upper floors (UF) and ground floor (GF).

Elevation sections	Total VIPs	Revised VIPs	Revised/ Total	Punctured VIPs	Punctured/ Revised
UF 1	107	38	36%	4	11%
UF 2	147	19	13%	1	5%
UF 3	51	14	27%	1	7%
UF 4	215	28	13%	1	4%
UF 5	52	15	29%	2	13%
UF 6	191	53	28%	21	40%
UF 7	71	6	8%	1	17%
UF 8	87	22	25%	14	64%
UF 9	48	14	29%	4	29%
SUBTOTAL	969	209	22%	49	23%
GF 1+2	104	40	38%	3	8%
GF 3+4	119	54	45%	2	4%
GF 5	117	58	50%	7	12%
GF 6+7	29	4	14%	1	25%
GF 8	9	3	33%	1	33%
GF 9	146	32	22%	3	9%
GF 10+11	22	16	73%	1	6%
SUBTOTAL	546	207	38%	18	9%
TOTAL	1.515	416	27%	67	16%

According to the random check and subsequent statistical analysis carried out, a total of 16% of VIPs punctured are counted on a review of 27% of the installed VIPs. A higher number is detected in higher plants (23%) than in the ground floor (9%). Analyzing by façade sections we have a dispersion from 4% to 64%. However, we found only three cases with values above 30% (64%, 40% and 33%). Among others, the great importance of labor can be interpreted to understand this dispersion.

Furthermore, it might be that the review times of 48 hours to verify the existence of punctured panels is insufficient.

6. CONCLUSION

The installation of an industrialized façade with the incorporation of VIPs has been shown to be technically feasible, being a great opportunity to improve the thermal performance of façades.

The necessary construction details have been developed to solve the challenge of VIPs in relation to the impossibility of cuts and drills.

However, improvements must still be made to the performance of the panel to offer greater resistance to punctures and to avoid having values of vacuum losses in panels of around 15% on commissioning and 16% after more than a year from end of the work. Similarly, VIPs must be improved to guarantee flat sides and reduce dimensional tolerances in order to avoid thermal bridges in joints.

The incorporation of VIPs in the construction also requires an execution project drawn up with total precision and a qualified workforce that respects and knows the peculiarities of the material.

The VIP panel therefore has real options to enter the ventilated façade market, providing very interesting features. However, it is still necessary to make improvements to the panel, it will require drafting of projects in great detail and training for the installation must be taken care of. But above all, it will have to lower the cost at more competitive prices to be able to enter to compete in actual market.

ACKNOWLEDGEMENTS

The authors acknowledge the Affordable and Adaptable Public Buildings through Energy Efficient Retrofitting (A2PBEER) project, grant agreement no. 609060, funded by the European Commission for providing resources for the monitoring system and, at the same time, to the University of the Basque Country (UPV/EHU) for providing the studied in-use office building to the A2PBEER project.

This work was supported by the Spanish Ministry of Science, Innovation and Universities and the European Regional Development Fund (grant number RTI2018-096296-B-C22) through the MONITHERM project 'Investigation of monitoring techniques of occupied buildings for their thermal characterization and methodology to identify their key performance indicators', project reference: RTI2018-096296-B-C22 (MCIU/AEI/FEDER, UE).

REFERENCES

- 1.-B.P. Jelle , S.E. Kalnæs , Chapter 7: nanotech based vacuum insulation panels for building applications, in: Nano Biotech Based Mater. Energy Build. Effic., 2016, pp. 167–214.
- 2.-S. Brunner, T. Stahl, K. Ghazi Wakili, An example of deteriorated vacuum in- sulation panels in a building façade, Energy Build. 54 (2012) 278–282, doi: 10.1016/j.enbuild.2012.07.027.
3. A2PBEER, 2013. Affordable and Adaptable Public Buildings through Energy Efficiency Retrofitting. Project under the European 7th Framework Program for Research. Available at: www.a2pbeer.eu.
- 4.- A. Uriarte, I. Garai, A. Ferdinando, A. Erkoreka, and O. Nicolas, "Energy & Buildings Vacuum insulation panels in construction solutions for energy efficient retrofitting of buildings . Two case studies in Spain and Sweden," Energy Build., vol. 197, pp. 131–139, 2019.
- 5.- I. Uriarte, A. Erkoreka, C. Giraldo-Soto, K. Martin, A. Uriarte, P. Eguia, Mathematical development of an average method for estimating the reduction of the Heat Loss Coefficient of an energetically retrofitted occupied office building, Energy Build. 192 (2019) 101–122. doi:10.1016/j.enbuild.2019.03.006.
6. L.A. del P. J. Terés-Zubiaga, K. Martin , A. Erkoreka, X. Aparicio, Chapter 18 Cost effective energy retrofitting of buildings in Spain: An office-building of the University of the Basque Country, in: Cost-Effective Energy Effic. Build. Retrofit., 2017: pp. 515–551.

‘Industria Loci’, The Energy of Place: Achieving Energy Optimisation within Mixed Use Developments utilising Passivhaus Design Strategies in Urban Design

MARTIN MURRAY¹, SHANE COLCLOUGH¹, PHILIP GRIFFITHS¹

¹ Belfast School of Architecture and the Built Environment,
Ulster University, Shore Road, Jordanstown, Belfast, Co Antrim, BT37 0QB

ABSTRACT: *The human population of cities in 2020 consume 75% of the world’s resources in the form of energy, water and materials. 55% of the world’s population live in urban environments and by 2050 this figure is expected to rise to 65%. These facts combined with the reality that residential energy use alone, accounts for almost 40% of global carbon emissions indicates that the challenge of reducing our profligate use of residential energy, and thus reducing our greenhouse gas emissions, is first and foremost an urban challenge and opportunity. The theme of this paper is prioritisation. By prioritising the development of low rise, integrated mixed-use developments we are facilitating energy use in the most efficient and beneficial way, toward achieving these reductions. The authors argue that such developments are also societally enriching, through the creation of another layer of understanding of the urban environment, achieved through reflecting key energy engagements between buildings, uses and sites. The energy logic of such developments is further justified and enabled, if combined with the reuse of serviced ‘brownfield’ urban sites, a variety of user profiles, long life facilitation of habitation use, and resource efficiencies; all achieved whilst facilitating low carbon living at an urban microscale.*

KEYWORDS: *Urban design, Resource optimisation, Mixed-use.*

1. INTRODUCTION

This paper reflects on best practice in urban design from an energy and resource perspective, using case studies of both existing developments and a proposed low energy mixed use development located near Dublin City, in the Republic of Ireland. Such case studies are of value, not for being representative of a ‘status quo’ but rather as a reflection of methodology insights, demonstrating the optimisation potential of mixed-use urban development, using integrated Passivhaus (PH) design strategies, within 21st century, post carbon cities.

There is a growing and recognised challenge and opportunity within contemporary urban and city design to create sustainable mixed-use developments which allow people the opportunity to live, work, dine, shop and socialise, without excessive travel or commuting, – *the village within the city concept*. There is also a growing desire for these spaces to be community-friendly with an emphasis on well-being, scale and environmental credibility. Initiatives such as the Walkable City and the Economic City are direct reflections of these aspirations.

Central to such credibility is the need to make such developments (i) energy efficient in use and (ii) low carbon in construction and operation. The complexity of these needs brings with it a number of challenges. across the key early design phases, within which the

initial concepts and strategies are formulated. On brown field sites these early strategies require an urban design sensitivity. Urban Design itself has always had a difficulty in establishing its own authenticity, being lost somewhere between ‘architecture’ and ‘framework planning’. The emerging legislative requirement in Europe for the design of nearly Zero Energy Buildings (nZEB), across all building typologies, is an opportunity and catalyst to investigate how the requirements of nZEB metrics might challenge and merge with urban design to best create sustainable developments in the context of our future urban and city planning.

2. CONTEMPORARY URBAN DESIGN

What constitutes ‘Urban Design’ throughout history has been determined usually by societal preference. In a hierarchical sense there is, at the bottom, the prosaic creation of public policy and its implementation, in the hope that continuity, rigour and the market place will allow a coherent urban fabric to emerge. The typical development plan of contemporary Irish Local Authorities aspires to this rather low level of aspiration.

Further up the aesthetic scale there is the deliberately beautiful city of Piranesi’s Rome or Hausmann’s Paris. In recent years the free wheel ‘Ballet of Urban Life’ promoted by theorists such as Jane Jacobs [1], have been identified as worthy of consideration and implementation. In all cases an

endeavour of understanding into how vibrant and exciting urban (and suburban) environments come into being has been central to the task in hand.

In the post carbon city however, active engagement must begin with our concept of an 'Energy of Uses' and an eye to resources. Heretofore common metrics of urban planning would have been reflected in zoning use, site coverage, site ratios and contextual heights. The challenge in a post carbon reality however, is to ask how such metrics facilitate a low carbon future, respectful of resource availability. This question requires us to give voice to metrics promoting energy and carbon optimisation; in buildings this presupposes optimal orientation for solar gain, fabric design to reflect this, shading optimisation, energy storage and sharing, distribution of energy, and site biodiversity. In such ways the urban quarters of the post carbon city are energy quarters, with optimised district area energy controls and distribution; in effect an optimisation of energy related to mixed use development profiles.

Unlike current urban design practice, this new urban design strategy of the 21st century, must address itself to the paradigm of optimal supply, to meet an efficiency of use; this is 'microsurgery'; just-in-time localised delivery, particular to a specific location, use and time. It is in contrast to, and opposed to, the current paradigm of concentrating grid infrastructure and traditional delivery with large inefficient centralised generation, a type of 'open-heart surgery' whereby the efficiency of 'supply' is uppermost in prioritisation, without questioning the overall efficiency of 'end-use'.

The current 'near Zero Energy Building Directive', (nZEB) lies within the context of the latter paradigm, with a fabric specification, derived from EU energy policies going as far back as 2002. In contrast the theme of this paper is that we can - if we promote a more demanding wholistic design approach, utilising fabric-first principles of energy reduction, combined with process efficiency and on site generation - optimise supply and carbon emissions control. What then are the determinants of such an approach?

2.1 The Determinants of 'Genius Loci'

The Urban Design theorist Norberg-Schulz, in his analysis of 'Genius Loci', (Spirit of Place), identified three prevailing determinants of cities which render them identifiable and visually cohesive; in effect pleasant places to be in:- (a) a Comprehensible City Pattern, (b) a Consistent Set of Building Typologies and (c) a Consistent Collection of Building Morphologies, reflecting the way things are made, materials used and facades created; all traditional key determinants [2].

The expansive internationalism of the 1950's, through to recent years, wiped away these coherent

architectural expressions. Materials and building typologies transcended beyond their location and region. Architectural design spoke to formal design theories, methodologies, and post-modern facadism. In response the architectural critic Kenneth Frampton wrote of the imperative of an architecture of 'Regionalism', all this in an era before climate change itself became an impelling reason for such a call. Now Frampton's 'Critical Regionalism' is a compelling metaphor for responsible design and zero carbon priorities, creating the urban design determinants of the new post carbon city [3].

If our understanding of 'Genius Loci' leads us to appreciate it as a physiological determinant in enjoying the visual cohesiveness of the environment around us, then our understanding of '*Industria Loci*' would allow us to appreciate and enjoy energy resilience as the measured use of limited resources within the post carbon city.

'Urban mixed-use developments', designed as energy positive developments, where activity and urban life is energised through localised use patterns and engagement, offer themselves as potential anchors for such zero carbon cities. They in effect express a reality that such cities must consist of smart interlocking parts, epitomised by such energy positive developments. So if the key determinates of Genius Loci are as defined above what might those of '*Industria Loci*', the 'Energy of Place' be?

2.2 The Determinants of '*Industria Loci*'

People are attracted to and attune to urban environments they have a tangible understanding and comprehension of [4]. 'Energy-collated' mixed-use developments therefore offer an opportunity for communities of energy users to coalesce, and social engagement to emerge, from an acknowledged and shared understanding of careful resource utilisation, and energy efficiency; attracting understanding, enjoyment and creating an '*Industria loci*'. Since cities account for 30% of total CO₂ emissions within the construction sector, cities are the single largest contributor to climate change. Thus it is important that we progress within them the development of low-carbon infrastructures such as these

In the mixed-use domain reducing carbon emissions has been intensively explored with solutions ranging from energy efficiency constructions, combined with building informatics, user behaviour modelling and building information modelling. The determinants of success lie in the ability of our buildings to give vision to a virtue; an architecture to provide a 'protected space' in which low-carbon systems and leadership can develop. Without the vision, the virtue can become

eroded by the real challenges of low energy design:- avoiding summer overheating, end-user satisfactions, performance gaps, coordination of mechanical installations and planned commissioning.

None of these issues are significant, if the design and performance indicators are shared by all, are clearly understood and sufficiently robust. Local electrical generation is key. The first determinant therefore must be a cohesive pattern of energy use and distribution, with an understandable energy hierarchy, the more localised the better [5]. Secondly in mixed use terms the energy needs of spacial adjacencies ought to be complimentary in regard to balancing and utilising energy demand. Thirdly these needs will give rise to increasingly flexible building typologies that are capable of meeting different end uses without significant remodelling. All buildings will need natural (minimal) ventilation, optimal orientation and specific façade design, the trade mark ‘curtain wall’ is perhaps a thing of the past, both in regard to customisation of facades, energy and airtightness; each site and project is unique.

To progress understanding we provide two contributions to this endeavour dating back to 1998, when we had an opportunity to address our carbon emissions and global temperature variation was 50% (.3°C) less than the 2018 figure of 0. 6°C (Figure 1) [6]. Across the intervening years we have failed to meet our energy reduction commitments. believing that the market place will give rise to natural adaptation when in fact time and resources are running out [7].

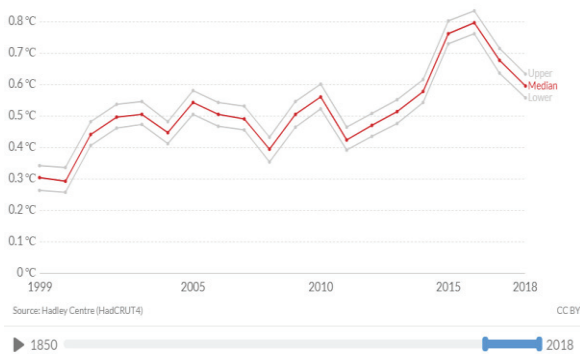


Figure 1: Temperature increase globally since 1999.
(Our world in Data) [6]

The central theme of this paper therefore is to press the energy advantages of ‘energy plus, mixed use developments’; which grant measurable return on scarce resources and can provide fossil-fuel-free energy to older poorer performing adjacent buildings if required. This would reduce their immediate fossil energy needs, and thus buys us all time to create closed loop supply chains to progress the time and labour

consuming effort of retrofitting with controlled embodied carbon, using bio-based materials.

Since such developments must be energy positive, nZEB cannot therefore, in its current configuration be an energy standard ‘fit for purpose’, as the energy reach is too low, and the expectation of ongoing variable building types for non-domestic buildings is naïve in the face of the growing resources timebomb. Building typologies will need to converge to ensure their greatest possible level of flexibility, as to their future use.

The nZEB energy demand criteria in Ireland lack these specific performance indicators and incentives to reduce future energy use. However, despite these shortcomings nZEB is now the common legislative energy language for buildings across all use-sectors in Europe. In this given context, the authors seek to demonstrate how nZEB optimisation may be developed by improving its metrics to reflect PH design strategies (Premium) across - in particular - mixed use developments, and utilising resources to optimise benefits to all. What is proposed is not new however the import of its success has now a focused relevance.

Below are recorded current, previous and proposed efforts at such developments and lessons learned. We reflect also on a contemporary project which is in design development and the design variables and criteria at play. What is effectively at play, is the need to generate and pay a ‘ransom energy’, an energy of atonement by ensuring that all new developments are robustly energy positive. This will buy us time to allow the long and arduous journey of energy retrofitting of existing buildings to progress, the embedded carbon of which impels us to retain and reuse them. Demolition may no longer be always, an unchallenged option.

3 THREE CASE STUDIES: ‘NOW, THEN, & TOMORROW’

Energy simulations and built prototypes of different types of buildings indicate that detached and attached houses can achieve an energy positive status, under most climatic conditions. Passivhaus has become a recognised methodology for achieving such low energy buildings, across a range of performance criteria from its ‘Classic’ model of design, through to Passivhaus ‘Plus’ and Passivhaus ‘Premium’ [8].

Difficulties can arise in regard to the on-site generation of the energy consumption needs of apartment blocks, and offices, due to the limited availability of roof surfaces relative to the occupied volume and energy demand within. In Urban design terms, six storeys appears to be the modest equilibrium, whereby achieving carbon neutral and energy positive use within a building/ development becomes compromised by its height [9]. Emerging

examples however do exist of low rise buildings, which generate a large peak electrical output with associated battery storage [10].

3.1 Ransom energy

The operational benefits to the grid are significant; in effect we are paying through these net zero energy buildings a 'ransom energy of atonement' back to the grid to compensate for the sins of our poorer performing existing buildings elsewhere. However this reality can buy us time to meet the challenge of retrofitting these existing buildings. This is not possible if our new buildings are not energy positive and are not ambitious in regards to fabric controls and indoor environment quality, (IEQ); in these circumstances, it is an opportunity lost and scarce resources not used to their optimal societal benefit. We are creating no inherent societal value and creating a lock-in of poor standards that will stay with us for at least 50 years [7].

However if grid peak energy demand is reduced through energy plus developments, the need for new power stations and centralised windfarms can also be reduced, avoiding significant energy loss in transit and millions of euro spent on building, operating, fuelling and, eventually, decommissioning these facilities. Instead we build, create, convert more buildings, reduce power station expenditure, and create more low carbon jobs; a really healthy feedback loop [10].

3.2 Ransom Energy: then

In Dublin in 1998, the city embarked on two adjacent but disparate development projects; the conservation, protection and development of an area of the inner city known as Temple Bar, full of characterful but poorly performing buildings in energy terms, and the construction of a large new office building; in effect a new City Hall.



Fig 2. Aerial view of Temple Bar Development looking South

The project of linking these two construction projects to achieve an overall energy and carbon reduction was commissioned in 1996 and after five years of operational monitoring received the Bremen Partnership Award in 2001 [11], beating 140 other international projects for innovative energy management. The project achieved a 40% reduction in Carbon Dioxide emissions compared to conventional heating systems of the time. This was achieved through the use of a gas fired combined heat and power (CHP)

plant which generated heat and electricity for the offices and heat for the neighbouring buildings, (Fig. 2 & 3) [11].

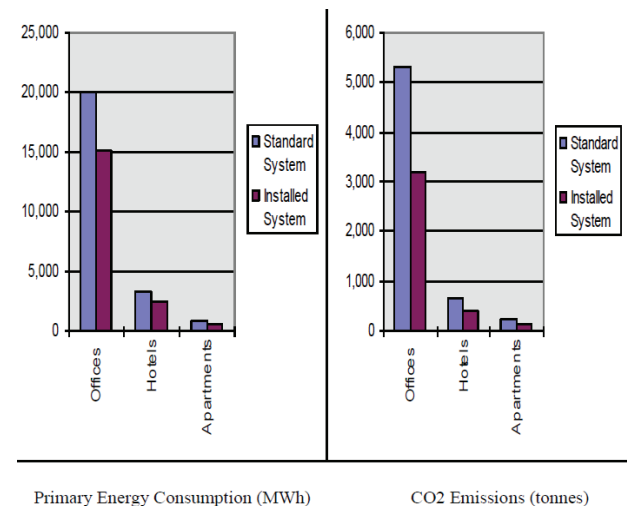


Fig. 3. Comparative energy and carbon performance across Temple Bar Development, (standard vs installed) (Vertical metric units as indicated.) [11].

This match between energy need and energy generation is the key challenge and opportunity in the optimisation of energy usage within mixed use developments. Energy storage and management become significant issues in addressing the seasonal variations, equating peak generation with use requirements, minimising the energy gap across the whole development and contributing to its overall energy efficiency performance.

In the case of the Temple Bar project any differences in return water temperatures from the serviced adjacent buildings, (four hotels, one hostel and one new apartment building), was compensated for by three shallow wells utilising ground water which controlled the temperature of the water returning to the CHP unit. All of this achieved with Building Energy standards as set by the 1991 Irish Building Regulations.

Had improved design strategies been operational at the time of the Temple Bar Project the carbon savings would have been dramatically better; (using the current nZEB standard probably in the order of an 60% improvement), and so the opportunity to sustain and reduce the poor energy carbon emissions of even a greater number of buildings was lost.

This potential energy contribution of developments to buildings beyond themselves, is directly reflective of 'the whole being greater than the sum of the parts', in itself a working definition of Urban Design.

3.3 Ransom energy: now

A more recent example of a ground breaking customised low energy mixed use neighbourhood initiative was the Beddington Zero Energy Development (BedZED) in South London (Fig. 4, 5 & Table 1), developed by the Peabody Trust and constructed 2000 through to 2002, to be an exemplary zero carbon neighbourhood with 82 homes, 17 apartments and 1,405m² of live - work units .

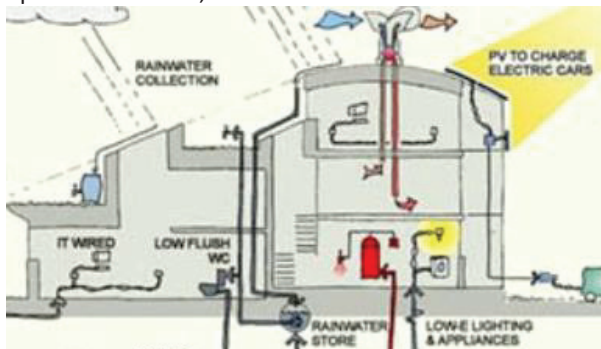


Fig. 4. Section thru' BedZED. (B. Dunster ZED Factory) & Bioregional (2003)

Table 1. Comparative energy performance between BedZED and UK national standards reflecting fabric first approach. (Source: Energy Saving Trust, 2002).

Element	1995 Regs Wim ² /K	BedZED Wim ² /K	BedZED material
Roof	0.25	0.10	300mm styrofoam
Exposed Walls	0.45	0.11	300mm Rockwool
Floors	0.45	0.10	300mm expanded polystyrene
External Windows, doors and roof lights	3.3	1.2	Argon filled triple glazing on all elevations except south facing. double glazing on south facing

Source: Energy Saving Trust (2002) Table 1

The principle of the overall 'zero heating specification' was to minimise space heating so that the overall resulting thermal demand is for hot water only. This remains largely consistent all year round which facilitated - with oversized local hot water storage tanks - meeting peak demands - space-heat and water - whilst still allowing trickle recharging throughout the day. This allowed the power plant to more or less match average electrical demand, exporting to grid when surplus power was generated on site - and importing to meet peak demand. The advantage of the biomass CHP system was reflected in the intention to generate electricity from flue gases, energy which would have been otherwise lost. The woodchip fuelled centralised CHP plant however never performed to its intended specification and subsequently was replaced by condensing gas boilers. Nevertheless BedZED would still be considered a successful endeavour for its time [12].

An evaluation by Bioregional in 2009 showed that the homes used 45 percent less electricity than an average home in the locality. BedZED homes also used

81% less gas to heat and less than half the water used by locals in housing of a similar nature and size [12].

BedZED switched back to a biomass pellet boiler in 2017 however electricity is now sourced from the grid on a green tariff and the biomass pellets are sourced from Spain, not locally. What BedZED did show was the benefit of building to a fabric first principle, which ensured overall internal comfort levels despite summer overheating issues. It also displayed an attempt to create flexibility in use; of the units constructed, all blocks of accommodations have similar technologies and physical properties and so, conversions have occurred with little difficulty.

Fig. 5. BedZED accommodations; note high embedded carbon materials. (B. Dunster ZED Factory)



3.3 Ransom Energy: tomorrow

Neither of the developments referenced above stand as direct role models for similar future developments. At Temple Bar, the buildings being serviced were poorly insulated by contemporary standards, whilst the low discounted energy provided led to a rebound effect of increased (or rather unnecessary) energy use in the served buildings [11]. The CHP plant in Temple Bar utilised fossil based energy, (gas). At BedZED, the energy demands of the various building types were significantly reduced, notwithstanding that the ambitious Biomass CHP plant carried significant operational failings and defects [12].

The mixed-use developments of the future may well be smaller in scale than BedZED, will have an energy use profile so low that the overall energy need will be negative, allowing energy to be dissipated back into the grid or used locally to promote energy protection for adjoining sites, uses and buildings, all of which determines and supports an urban design aesthetic and discipline.



Fig. 5. Proposed mixed use development, (Murray Mews) (Martin Murray Architects)

This is a particularly attractive option where urban environments contain buildings of architectural or historic significance where retrofitting to a low energy need may not be possible due to fabric constraints. The Murray Mews project - in design development - builds on the lessons of these previous case study

developments. The 0.1 hectare site is located in the centre of an Irish provincial town, close to Dublin, and contains all of the typical design opportunities and challenges of such a typical urban site. An energy positive development in this part of the old town will greatly facilitate energy supply to adjacent older buildings and will be able to sell energy back to the national grid within the next two years. This latter benefit is due to Renewable Energy Directive II (RED II) adopted by the EU in December 2018 which sets a binding target, that 32% of the EU's energy demand is to be met by renewable technologies by 2030.

What is notable is that the RED II Directive sets unequivocally an '*energy efficiency first*' principle by acknowledging that the '*cheapest and cleanest source of energy is the energy that does not need to be produced*'. The design of Murray Mews therefore is focused on optimising flexible plan configurations with a fabric first design principle of high embodied carbon materials and a low carbon threshold for manufactured non-bio construction materials. Bio-based materials will be sourced to reflect a closed loop supply chain. The operational use of the buildings will encompass a balance of retail, office and residential use and design development is investigating scenarios of optimum proportionality of façade, roof and orientation to ensure maximum Primary Energy Renewables.

Preliminary Design and merging case studies would suggest that a peak electrical output of c. 32kW on a sunny day from 160m² of solar photovoltaic panels (PVs) is possible, (modelled). Excess power will go to the local electrical grid. However at present Ireland has a 6kW electrical export limit requiring a 32 kWh battery installation. Current data suggests that as a general rule, 1kWh of battery storage per 1kWp of PV.

The software model is currently based on the Passive House 'Plus' standard however design exploration is intended to progress toward the passivhaus premium standard and the Living Building Challenge, due in particular, to the latter's identification of 'step change' benefits across different sites.

4 CONCLUSION

The premise of this paper is that mixed use urban developments, utilising proven and focused low energy methodologies such as Passivhaus 'Plus' and 'Premium' offer the greatest hope of reducing our urban carbon emissions to zero within the suggested time limit of 30 years. The 'Passive House Premium' energy standard-the economic and ecological challenge of which is justified by the societal benefits - is the ideal standard for such a fabric first approach.

The authors argue that by minimising the initial energy demand, we can begin to tackle time and

seasonal disparities across uses, thus allowing optimal local energy distribution. In particular such developments feeding into the national grid have the capacity to buy time in regards to allowing us the operational space to ramp up our national retrofit programmes, particularly in regard to closed loop supply chains. Such developments will only achieve energy optimality if the building fabric standards are sufficiently robust so as to minimise the energy needs of the overall site and create a 'flat line' energy profile. The 'mixed use' profile facilitates some addressing of troughs and peaks of use and need.

The significantly reduced energy demand, combined with optimal energy use and supply will contribute greatly to successful urban planning and thus contribute to addressing the emerging climate emergency. Mixed-use development in this way allows for a clear urban design strategy with well-defined methodologies and reflecting significant benefits within urban environments, thus fulfilling the urban design criteria of the 'whole being greater than the sum of the parts'. This is urban design for the 21st century.

ACKNOWLEDGEMENTS

This paper is intended as foundation research in support of Ph D Study at Ulster University, Jordanstown. I wish to thank the University for their sponsorship of these studies and their support in the development of this paper.

REFERENCES

1. J. Jacobs, (1961). The Death and Life of Great American Cities. (*Vintage books reprint (1992)*).
2. C. Norberg-Schulz, (1980). Genius Loci: Towards a Phenomenology of Architecture. (*Rizzoli International Publications; (1 Dec. 1980)*)
3. K. Frampton, (1983). Towards a Critical Regionalism: Six Points for an Architecture of Resistance, (1983).
4. K. Lynch, The Image of the City, (MIT press (1960))
5. Implementation of the Energy Efficiency Directive (2012/27/EU), *EPRS Review* 579.327, April 2016
6. H. Richie, M. Roser (2020) - "CO₂ and Greenhouse Gas Emissions". *OurWorldInData.org*. Retrieved from: '<https://ourworldindata.org/co2-and-other-greenhouse-gas-emissions>' (*Online Resource*).
7. R. Rovers, People vs Resources. (Eburon, Utrecht 2019).
8. International Passive House Association. <https://passivehouse-international.org/>
9. The new Irish Building Regulations, *Arup*, (2017).
10. J. Bere, An introduction to Passive House. (*RIBA Publications, London., 2016*).
11. T. Cooper, Optimized Energy System for City Centre Urban Renewal Project. *Conservation Engineering Limited*, (2004).
12. J. Young. Towards Zero Energy Buildings: Lessons learned from the BedZED development. *PhD thesis Bartlett School of Graduate Studies, UCL*, (2015).

Thermal Comfort Metamodel Tool compared to EnergyPlus simulations:

A comparison using an University building

HELDER GATTONI MEDEIROS¹, ANA CAROLINA DE OLIVEIRA VELOSO¹, ROBERTA VIEIRA GONÇALVES DE SOUZA¹

¹Universidade Federal de Minas Gerais, Belo Horizonte, Brazil

ABSTRACT: This paper aims to compare the percentage of occupied hours in thermal comfort (PHOCT) in an under construction naturally ventilated building in the Campus of the Federal University of Minas Gerais (UFMG) obtained by an EnergyPlus simulation and by a metamodel tool developed by Rackes et al. The building has 5 floors with a total area of 2678 m². PHOCT was obtained considering the adaptive comfort model for naturally conditioned environments proposed by ASHRAE 55-2013 in both cases. To use the metamodel it was necessary to adequate the following input parameters: 1) building maximum depth, 2) maximum floor to floor height and 3) maximum room power density of the occupied spaces to fit them within the range of the metamodel. Although such adjustments had to be made so the metamodel could be used to evaluate the thermal comfort it is considered that the proposed tool presented close PHOCT estimations both for INMET and TRY weather files when compared to simulations. Results found in metamodel were of 89% and 71% of occupied hours in comfort while the results obtained by EnergyPlus were of 92% and 77% for each weather file, the tool presenting a huge time saving when compared to simulation.

KEYWORDS: Simulation, Thermal Comfort, EnergyPlus, Natural Ventilation.

1. INTRODUCTION

The important role of buildings in energy consumption opened the eyes of the world for building energy efficiency. This is no different in Brazil which launched in 2009 the Technical Quality Regulation for the Energy Efficiency Levels of Commercial, Service and Public Buildings (RTQ-C) published by Inmetro (National Institute of Metrology, Quality and Technology), the agency responsible for the Brazilian Labelling Program, PBE. This Regulation aims to create conditions to rate the energy efficiency level of buildings [1,2]. This regulation aims to label the level of energy efficiency of office buildings, hospitals, schools, museums and other non-residential buildings.

In this Regulation the air conditioning system has a final weight of approximately 70% in the definition of the rank (approximately 40% directly for the air conditioning system (AC) efficiency classification and 30% indirectly for the building envelope (ENV) classification [1]. The criteria adopted to evaluate the ENV efficiency level focused on the development of a regression equation which provides an electricity consumption indicator [3]. The envelope prescriptions in this Regulation are based on electricity consumption equations developed with 5000 simulations to provide a method to evaluate the envelope efficiency level when two HVAC efficiencies

were used (3.19 W/W and 1.82 W/W for cooling and 2.39 W/W and 1.36 W/W for heating) [3].

AC and ENV evaluation present both 1) a simplified calculation system based on tabulated values and on equations developed by linear regressions and 2) an energy simulation method.

The full implementation of the RTQ-C regulation in Brazil may potentially reduce the buildings energy consumption significantly in the long term [4], and simplified methods should help in this way. Even though computational simulation does not represent the reality in its totality, it is considered to be the most flexible and complete way to evaluate issues related to the energy efficiency of buildings [5]. But to get reliable simulations results, there must be a great investment both in financial and in time consuming terms demanding highly skilled and experienced workforce [5]. In Brazil, less than 18% of the buildings labelled by RTQ-C from July 2009 to February 2020 used the simulation method [6].

As previously seen, RTQ-C is strongly oriented to air-conditioned buildings even though there are many buildings in Brazil that tend to be naturally ventilated in the commercial, service and public sectors. Schools, public universities, public health centres, small street stores are examples of buildings that use natural ventilation as their main means of air conditioning in the country. In this sense the problem regarding naturally ventilated buildings is that in RTQ-

C [1] the efficiency of naturally ventilated buildings must be calculated via a thermal simulation, with no simplified method. The analysis of naturally ventilated spaces is made through the calculation of the Percentage of Occupied hours in Thermal Comfort, PHO_{Ct}. A PHO_{Ct} of 80% would give an A level to the analysed spaces that would substitute the evaluation of the air conditioning system in these spaces [1].

PHO_{Ct} estimation has great importance in the labelling of passive buildings but simulations to obtain internal temperatures values are complex due to the need of controlling the opening and closing of windows according to the external and internal conditions taking a long time to be done and needing specialized consultants to carry out reliable simulations. This fact may discourage the construction industry to test the performance of natural ventilated buildings.

In fact, this tendency could be inferred when the building energy efficiency labels emitted in Brazil are analysed. In the Brazilian system when all systems are evaluated a Global label is emitted but a Partial label can also be emitted provided the building envelope is analysed. Of the buildings simulated until March 2020, 24% did not evaluate the efficiency of the air conditioning system - only the envelope performance was evaluated, probably using an auto-sized air conditioning system, indicating that those buildings may be naturally ventilated. 26% of the buildings evaluated by the prescriptive method did not evaluate this system either indicating that those buildings may be naturally ventilated too. [6].

In order to overcome this and other barriers as appointed by Wong & Kruger [4] the Brazilian Government opened a public consultation by Ordinance No. 248 of July 10, 2018, with the objective of improving the RTQ-C. The proposal renames the regulation to INI-C - Inmetro Normative Instruction - Commercial, Service and Public Buildings [7]. INI-C proposes a new method which uses the building's energy consumption as an evaluation parameter, comparing it with reference conditions. For each of the evaluated items, it is possible to use a simplified method or a simulation method. In the case of naturally ventilated buildings the novelty is the proposal of a simplified method capable of estimating the percentage of occupied hours in thermal comfort (PHO_{Ct}) with the input of simplified climate-related parameters and building characteristics [8].

The simplified method uses a tool proposed by Rackes et al. [8] supposed to promote the validation of natural ventilation strategies. The importance of such a tool relies on the fact that it was verified that in mild temperate climates present in many regions of Brazil, naturally ventilated buildings can

significantly diminish energy use intensity [9,10] and have a better chance to adapt to climate change [11]. In this sense buildings with natural conditioning must be proven to meet the conditions of thermal comfort when not using artificial conditioning systems. It is not enough that they present a lower energy consumption. That is, a building is considered more energy efficient than another when it provides the same environmental comfort conditions to its user, with lower energy consumption [12].

Although the simplified method is considered easier to use than the thermal simulation, studies testing it against real buildings could not be found in the literature. It also presents ranges to some input parameters values which might not correspond to an actual building design. This paper then aims to estimate the PHO_{Ct} of an academic building in the Campus of the Federal University of Minas Gerais (UFMG) using the metamodel proposed by Rackes et al. [8] and to compare the results obtained by the computational simulation method using EnergyPlus software.

2. STUDY CASE

The study case is the under construction building of the School of Fine Arts of UFMG, located in the Campus Pampulha in Belo Horizonte, MG, Brazil.

The building will have 5 floors with a total area of 2678 m². It has 24 professor offices, 4 dancing rooms, a library, 13 administrative rooms, as well as living areas and toilets (see figure 1).

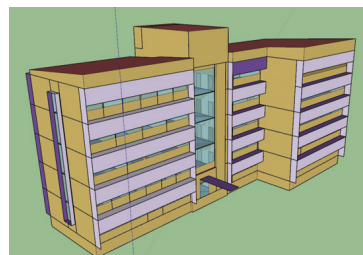


Figure 1: Analysed building

The construction is in reinforced concrete coated structure and presents an internal vertical circulation box with reinforced concrete stairs and 2 elevators. The building has internal divisions and external walls in masonry, wooden doors and lining only in the sanitary areas. The windows are sliding sheets with aluminum frames.

The external walls are to be built in 14x19x29cm ceramic brick and the internal walls in 09x19x29cm ceramic brick. The external painting will be white and yellow, with 89% of the area in white and 11% in yellow with absorptances of 0.2 and 0.3, respectively. The building will have a white sandwich panel roof above a concrete slab. Simple 6mm glass will be used in the openings, and solar shading devices will be

used on all windows. It is intended that the building will operate using natural ventilation and therefore no air conditioning system was envisaged. Figure 2 show a picture of the building.



Figure 2: Analysed building under construction

Brazilian territory is divided into 8 climatic zones [13]. Belo Horizonte is in Bioclimatic Zone 3 that represents the temperate mild climate with hot rainy summers and mild dry winters. This climate is classified as temperate (Cwa), according to Köppen's climatic classification. Average winter temperatures are of 18°C and average summer temperatures are of 27°C. The annual relative normal humidity is 67%, the annual average of total precipitation is 1,602.6 mm. The climate presents, according to the adaptative model of ASHRAE 55-2017 [14], from 61% (TRY weather data) to 66% (INMET weather data) when natural ventilation is used according to the software Climate Consultant 6.0 and considering the operating hours of 8 a.m. to 10 p.m. corresponding to the academic buildings operating hours.

3. METHODOLOGY

The building's PHOCT was evaluated both by computer simulation in EnergyPlus and by the metamodel. For both evaluations, the adaptive comfort model for 80% acceptability proposed by ASHRAE 55-2017 [14] was used to define the acceptable thermal conditions for naturally conditioned environments. This is an empirical model based on users' continuous adaptation to outdoor temperatures which uses equations 1 and 2 to determine the upper and lower limit for the operative temperature to grant 80% acceptability.

$$T_U = 0.31T_{pmao} + 21.3 \quad (1)$$

$$T_L = 0.31T_{pmao} + 14.3 \quad (2)$$

Where T_U – Upper 80% acceptability limit (°C)

T_L – Lower 80% acceptability limit (°C)

T_{pmao} – Prevailing mean outdoor air temperature.

The temperature limits and T_{pmao} both vary with time. The window for T_{pmao} can be from 7 to 30 days. In the simulation and metamodel the window used is of 7 days.

2.1 Simulation Methodology

To evaluate PHOCT through simulation, the building was modeled in SketchUp Make, version 2017, using the Euclide plug-in version 0.9.3 and each room was considered a thermal zone. The simulation was performed in EnergyPlus Software version 8.7.0.

The operating schedules of occupancy, lighting, and equipment use were obtained with the building administrators. The *Ventilation Control Mode* for window and doors opening chosen was the “TEMPERATURE” rule, thus they were set to open only when the rooms are occupied AND the temperature is above 20°C AND the zone internal temperature is higher than the outside temperature.

Two climatic files were used in this study for the city Belo Horizonte: TRY and INMET [15]. Both files were used to the simulation and in the metamodel tool to estimate de PHOCT.

As the output of the simulation software we obtained the operative temperature (T_o) of each zone and the dry bulb external temperature (T_e) were obtained. With these data and considering Equation 1 and 2 (ASHRAE 55-2017) the PHOCT, and the number of exceedance hours (EH), or hours in which the comfort limit was exceeded, divided by the total number of occupied hours were obtained. According to Rackes et al the EH is the standard metric indicated by ASHRAE 55-2017 for evaluating thermal acceptability over time and two indexes were defined by the authors: the “exceedance hour fraction – hot” ($E_{HF_{hot}}$) and the “exceedance hour fraction – cold” ($E_{HF_{cold}}$), were calculated, representing the hour fractions that exceeded the upper and lower limits respectively. [8]

2.1 Metamodel Methodology

The creation of the metamodel is expected to facilitate the validation of passive ventilation systems, encouraging the use of this solution. The climates found in Brazil have great potential to use passive solutions which also avoid problems of concentration of pollutants (such as CO_2) in the interior and offer significant savings in energy costs of the building. This tool was designed to be used in warm and hot climates in which comfort performance was quantified by the average annual fraction of occupied hours that exceeded the upper limit of an adaptive comfort zone [8].

According to INI-C, PHOCT may be estimated by simulation or using the metamodel. When using the metamodel the PHOCT is 100% minus the best value for $E_{HF_{hot}}$ estimated by the metamodel. The metamodel consists in a routine developed in Python version 2.7. The user must enter 38 parameters to determine the occupant comfort in naturally ventilated buildings in hot and mild climates [8]. The first nine parameters refer to climate, derived from

weather files. The program provides data for 428 cities in Brazil although if users want to analyze a building in a different place or with a newer climate data the program presents a routine to translate a weather file into those nine parameters. The other 29 parameters are related to building characteristics. Table 1 presents the 9 parameters related to climate data with their units and the values entered for the two weather files TRY and INMET, available for the city of Belo Horizonte.

Table 1: Metamodel input climate data

Parameter	Unit	Climate data	
		TRY	INMET
Tout	°C	22.6	21.8
ToutDailyVar	°C	10.4	9.4
ToutAnnualVar	°C	13.8	13.6
CDD18	°C *days	1764	1483
CDD25	°C *days	304	164
radDirNorm	W/m ²	175	95
radDiffHoriz	W/m ²	108	91
windSpeedMet	m/s	2.1	2.2
elevation	m	785	869

Where:

- Tout – Mean annual outdoor air temperature (To,a)
- ToutDailyVar – Annual mean of To,a daily amplitude
- ToutAnnualVar – Annual mean of To,a daily amplitude
- CDD18 – Cooling degree days base 18 °C
- CDD25 – Cooling degree days base 25°C
- radDirNorm – Mean direct normal solar radiation
- radDiffHoriz – Mean diffuse horizontal solar radiation
- windSpeedMet – Mean wind speed at meteorological station
- elevation – Elevation above sea level

The others 29 parameters entered in the metamodel are shown in Table 2, which also shows the minimum and maximum limits for each parameter allowed by the metamodel.

Table 2: Metamodel input building data

Parameter	Unit	Min	Max	Adopt.
bldgLength	m	13	200	45.56
bldgDepth	m	8	50	12.73
floorHeight	m	2.75	4.25	3.20
Nfloors	-	1	5	5
roomSize	m ²	9	400	33.81
stairFracFPA	-	0	0.28	0.052
WWR	-	0.05	0.70	0.264
shadingAngle	°	0	45	37.41

extWallAbs	-	0.2	0.8	0.211
extWallU	W/m ² *K	0.1	5.0	1.85
extWallCT	kJ/m ² *K	40	500	105
roofAbs	-	0.2	0.8	0.259
roofU	W/m ² *K	0.1	5.0	0.558
roofCT	kJ/m ² *K	10	400	247
SHGC	-	0.2	0.8	0.635
windowU	W/m ² *K	1.0	6.0	5.792
roomELPD	W/m ²	1	25	25
publicELPD	W/m ²	1	15	2.933
occDensity	occ/m ²	0.01	1.00	0.274
dayStart	h	6	10	8
dayEnd	h	14	22	22
windAlpha	-	0.10	0.40	0.22
averageShelter	-	0.3	1	0.9
windowMaxOpenFrac	-	0.2	1.0	0.442
NVW_WWR	-	0	0.17	0.0125
PW_width2height	-	0.1	50	4.513
PW_Cd	-	0.4	0.8	0.6
interiorELAperLen	-	0.0001	.4	0.21
ceilFanAirSpeedDelta	m/s	0	0.9	0

Where

- bldgLength – Building Length (higher dimension)
- bldgDepth – Building depth (shorter dimension)
- floorHeight – Floor-to-floor height
- Nfloors – Number of floors
- roomSize – Average room size
- stairFracFPA – Fraction of the building footprint area occupied by stairwells
- WWR – Window-to-wall ratio
- shadingAngle – Shading angle from building façade
- extWallAbs – Exterior walls solar absorptance
- extWallU – Exterior walls overall thermal transmittance
- extWallCT – Exterior walls thermal capacity
- roofAbs – Roof Solar Absorptance
- roofU – Roof overall thermal transmittance
- roofCT – Roof thermal capacity
- SHGC – Windows solar heat gain coefficient
- windowU – Windows thermal transmittance
- roomELPD – Occupied room power density
- publicELPD – Public spaces power density
- occDensity – Occupants density
- dayStart – Day starting hour
- dayEnd – Day ending hour
- windAlpha – wind speed correction factor
- averageShelter – Sheltering obstacles correction factor
- windowMaxOpenFrac – Maximum windows fraction opening
- NVW_WWR – night ventilation window-to-wall ratio
- PW_width2height – Typical windows width divided by its height
- PW_Cd – Typical windows discharge coefficient

- interiorELaperLen – Effective leakage area between occupied rooms and public spaces per length of shared wall
- ceilFanAirSpeedDelta – Air speed enhancement provided by fans

As a result, the metamodel estimates the building's EHF_{hot} generating 5 values, the best estimated value by the metamodel, minimum and maximum for a precision of 95% and minimum and maximum for a standard deviation.

Since the metamodel method is simplified, it has limitations. Thus, it was necessary to modify some parameters of the real building to make them fit within the range of the metamodel. Among them we can mention adequacy in the width of the building (bldgDepth) due to its shape. As it can be seen in figure 03, the building is not a rectangular one, so it was necessary to calculate a mean building depth.

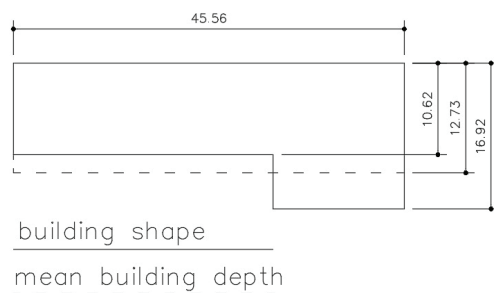


Figure 3: Building shape with an indication of the mean building depth (m).

It was also necessary to adequate the floor-to-floor height (floorHeight) due to the metamodel limit of the building height of 16m. The actual floor-to-floor height is of 3.75 and the total building height is of 18.75. The adjustment implied in a 15% decrease in the floor-to-floor height.

A more extreme limitation was verified in the installed power density in occupied rooms (roomELPD) where the limit imposed by the metamodel tool is of 25 W/m² and the value found for the building is of 39.9 W/m². It is important to reinforce that ELPD is calculated for the occupied rooms associating both lighting and equipment. This high value found in the building is due to a high power density in illumination (50 W/m²) for the dance rooms due to the use of special lights for their practice and also because in teacher offices the equipment power density is high (51.5 W/m²) because the layout estimates that there'll be 3 computers in an area of 10.3 m.

3. RESULTS

Table 3 shows the metamodel estimated exceedance hour fraction EHF_{hot} estimated using TRY and INMET weather files.

Table 3: EHF_{hot} estimated by the two precisions given in the metamodel (%)

	Best Value	95% precision		One Standard deviation (68.2% precision)	
		Min.	Max.	Min.	Max.
TRY	28.5	12.9	51.4	20.8	37.7
INMET	11.3	4.1	25.7	7.6	16.4

Using INMET weather file the PHOCT obtained was 91.7% for EnergyPlus simulation and 88.7% for the metamodel (3.0% difference). While using TRY weather file the results was a PHOCT of 76.6% for simulation and 71.5% for the metamodel (5.1% difference). Both results, using TRY or INMET, were considered to be very close for PHOCT. The metamodel is only capable of evaluating the hot discomfort while with EnergyPlus it is possible to evaluate hot and cold discomfort. Figure 3 compares each result.

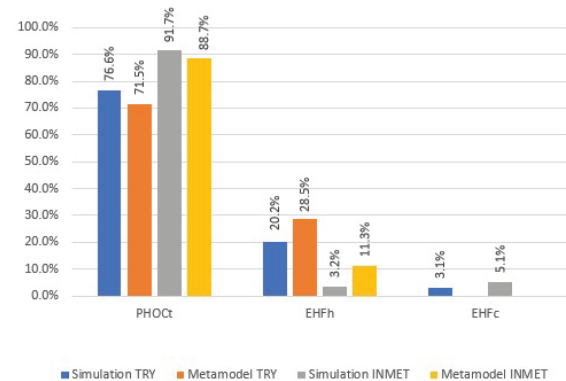


Figure 3: PHOCT, EHFh e EHFc for each method.

As we can see, although PHOCT values given by the simulation and by the metamodel present values that could be considered similar (a maximum difference of 5,1%), when EHF_{hot} is analyzed higher differences are found. This may be because the exceedance hour fraction for cold is not considered in the metamodel but appears in the simulation process.

4. CONCLUSION

The tool presented close PHOCT results to those obtained through simulation with a huge time saving.

Some parameters limitations restrict the application of the simplified method. In this study it was necessary to adjust the parameters "bldgDepth", "floorHeight" and "roomELPD". These adjustments may have influenced in the divergence in the values obtained.

The adequacy in the parameters were the reduction of the installed power density of the occupied rooms (roomELPD) from 39.9W/m² to

25.0W/m² to input a value for this parameter inside the metamodel range. A “virtual” width has been inputted to maintain the building area because it does not present a rectangular shape such as required by the metamodel. And the floor-to-floor height (floorHeight) had to be changed from 3.75m to 3.19m because the metamodel only accept buildings with total height under 16m.

In tropical countries like Brazil the increment in floor-to-floor height is a recommended strategy to improve the comfort, especially in high density occupation rooms like classrooms. The edification code of Belo Horizonte city [16] for instance considers 4.00m as the minimum floor-to-floor height for classrooms with 48m² or more, which is almost the upper limit of the tool (4.25 m). Thus, the limit of 16 meters for the building height would allow the evaluation of schools up to 4 floors only. This may not be a problem for schools evaluation, but it should be a problem when naturally ventilated office building towers are evaluated once they present a higher number of floors.

This analysis is of special importance once the metamodel was specially targeted to verify comfort based on office and school buildings such as the one analysed in the present study. INI-C could provide guidelines for acceptable parameter adequacy to fit then in the range to extend the application of the simplified method and to promote natural ventilated buildings.

If a compliance range is sought for the PHOCT, it is important to verify the influence of the weather file selection as results between files varied in approximately 20%.

Studies with more buildings should be performed to ensure that adjustments do not make the results unusable.

ACKNOWLEDGEMENTS

The authors would like to thank CNPq - National Council of Technological and FAPEMIG - Minas Gerais State Research Support Foundation for the financial resources invested in this research.

REFERENCES

1. Brasil. Instituto Nacional de Metrologia, Normalização e Qualidade Industrial, (2013). Portaria n° 299, 19 de junho de 2013. Regulamento Técnico da Qualidade para o Nível de Eficiência Energética de Edificações Comerciais, de Serviços e Públicos (RTQ-C). Rio de Janeiro. Available: <http://www.inmetro.gov.br/legislacao/> [30 August 2019].
2. Brasil. Instituto Nacional de Metrologia, Normalização e Qualidade Industrial, (2012). Portaria INMETRO n°18, 16 de janeiro de 2012. Regulamento Técnico da Qualidade para o Nível de Eficiência Energética de Edificações Residenciais (RTQ-R). Rio de Janeiro, Available: https://www.normasbrasil.com.br/norma/portaria-18-2012_236244.html [10 January 2019].

3. Carlo, J. C. and Lamberts, R., (2008). Development of envelope efficiency labels for commercial buildings: Effect of different variables on electricity consumption. *Energy and Buildings*. Volume 40, Issue 11, Pages 2002-2008. <https://doi.org/10.1016/j.enbuild.2008.05.002>
4. Wong, I. L. and Krüger, E., (2017). Comparing energy efficiency labelling systems in the EU and Brazil: implications, challenges, barriers and opportunities, *Energy Policy*, vol. 109: p. 310-323.
5. Carlo, J. C. and Lamberts, R. (2010). Parâmetros e métodos adotados no regulamento de etiquetagem da eficiência energética de edifícios – parte 2: método de simulação. *Ambiente Construído*, 10: p. 27-40.
6. Instituto Nacional de Metrologia, Qualidade e Tecnologia. Tabelas de consumo/eficiência energética - Edificações Comerciais. [Online], Available: <http://www.inmetro.gov.br/consumidor/pbe/edificacoes.asp> [15 March 2020]
7. Inmetro, (2018). Portaria n.º 248, de 10 de julho de 2018. Consulta pública - Aperfeiçoamento do Regulamento Técnico da Qualidade para a Classe de Eficiência Energética de Edifícios Comerciais, de Serviços e Públicos. Brasil, Available: <http://cb3e.ufsc.br/etiquetagem/desenvolvimento/atividades-2012-2016/trabalho-1/pesquisas/> [09 May 2019].
8. Rackes, A., Melo, A. P. and Lamberts, R. (2016). Naturally comfortable and sustainable: informed design guidance and performance labeling for passive commercial buildings in hot climates. *Applied Energy*, 174: p. 256-274.
9. Alves, T.; Machado, L.; Souza, R. V. G. and Wilde, P., (2017) A methodology for estimating office building energy use baselines by means of land use legislation and reference buildings. *Energy and Buildings*, 143: P. 100-113.
10. Veloso, A. C. O.; Souza, R. V. G.; Koury, R. N. N., (2017) Research of design features that influence energy consumption in office buildings in Belo Horizonte, Brazil. *Energy Procedia*, 111: p. 101-110.
11. Kwok, A. G. and Rajkovich, N. B. (2010). Addressing climate change in comfort standards. *Building and Environment*, 45: p. 18-22.
12. Lamberts, R., Pereira, F. O. R. and Dutra, L., (2014). Eficiência Energética na Arquitetura. 3a edition ed. Rio de Janeiro: ELETROBRAS.
13. ABNT, (2005). NBR15220: Desempenho térmico de edificações – parte 3: Zoneamento bioclimático brasileiro e diretrizes construtivas para habitações unifamiliares de interesse social. Associação Brasileira de Normas Técnicas. Rio de Janeiro, RJ.
14. ASHRAE, (2017). 55- Thermal Environmental Conditions for Human Occupancy. American Society of Heating, Refrigerating and Air-Conditioning Engineers. Atlanta, GA: ASHRAE.
15. Climate One Building. Repository of free climate data for building performance simulation, [Online], Available: http://climate.onebuilding.org/WMO_Region_3_South_America/BRA_Brazil/index.html [24 September 2019].
16. Belo Horizonte, (2009). Lei N° 9.725, de 15 de julho de 2009, Código de Edificações do Município de Belo Horizonte. Belo Horizonte, MG.

Biophilic design in architecture

A case study of University of Brasília's buildings

RAQUEL NAVES BLUMENSCHNEIN, PEDRO HENRIQUE FERREIRA MUZA

University of Brasília – FAU - Faculty of Architecture and Urbanism - LACIS (Built Environment, Inclusion and Sustainability Laboratory) -, Brasília, Brazil

ABSTRACT: More recently, Sustainable architecture has been reinventing the way in which we solve paradigms and dilemmas faced in urban centers. In this process, it is possible to observe that new dimensions have been incorporated in addition to the environmental impacts caused by construction. Assuming the plurality of the word sustainability and the need for a holistic approach, it is possible to argue that economic, cultural and well-being aspects must also be taken into consideration in order to achieve more efficient architectural features. As follows, Biophilic design proposes architectural solutions for spaces based on nature. Thus, it promotes an integrative design with sustainable features and provides a restorative experience to users. It aims to provide well-being and balance artificial spaces with nature, establishing connection between nature and humans as the theory of biophilia states. This paper aims to identify biophilic design patterns at the University of Brasília, as proposed by a literature review. The Users perspective was gathered through a questionnaire so as to investigate users' affinities with biophilic patterns. in order to point out which architectural features can offer better restorative and welfare conditions to people.

KEYWORDS: Biophilic Design, Sustainable Buildings, Architecture, Well-being, Survey

1. INTRODUCTION

Biophilic Design has as its main characteristic the use of elements of nature in favor of constructed spaces. Thus, its application is wide, varied, and can have restorative and well-being effects on space users. Human resilience is a term that can be understood as the result of various stimuli that an individual receives by interacting with society and spaces. Therefore, in a sense of conflicting urban times, buildings can be considered hostile places as they tend to gain more artificial features over natural ones.

[1] With this panorama, it can be argued that the current innovations proposed by construction and architecture create the illusion that people are beings dissociated from nature and their biological functions. Thus, having a posture of superiority and distance from the natural environment, results in the belief that basic needs arising from evolution and genetic heritage can be left aside. This belief leads to methods of construction and design that exhaustively exploits natural resources, dissociating natural environments from society.

In architectural projects, Biophilic Design assumes that the health of a human being has a biological basis that depends on direct contact with nature. Thus, it is established that the user of the space tends to feel emotionally and physically better. According to a research conducted by the group Terrapin Bright Green [2], biophilic design can reduce stress, improve

cognitive function, creativity and well-being, as well as accelerate the healing process.

This study aims to identify in a practical way biophilic design practices in existing buildings in the University of Brasilia that have a restorative effect on its users and that strengthens human resilience through direct contact with elements of nature, based on user perspective and opinion.

2. HUMAN RESILIENCE AND BIOPHILIA

The lack of contact with nature, as well as the massive consumption and neglect of the environment, may lead cities to become hostile places to human life. In this way, they can increase the frequency of diseases, stress, and decrease the quality of life of the population. Steg argues [3] that physiological responses to environmental stressors can be attenuated through design, allowing the restoration of bodily resources before system damage occurs.

Research points out to the human preference for the natural environment over the artificial environment. Edward O Wilson [4], in 1984, popularized the concept of biophilia. This concept highlights the need for a connection between nature and the human being, enabling restorative responses in the individual's health. Having a biological and evolutionary vision, Wilson and Kellert [5] argue that contact with nature is something that humans have evolved and need for their well-being. Their work also

points out that individuals are genetically predisposed and programmed to respond to natural stimuli, both physiologically and psychologically. Meanwhile, the term biophilia had already been used and defined by the psychoanalyst Erich Fromm [6] in his productions on the essence of the human being. In general terms, he explained it as "the human being's love for life".

More recently, the healing power of a connection with nature was established by the study of Roger Ulrich [7], which compares the recovery rates of patients with and without nature. Browning and Romm [8] suggest that with the emergence of the ecological construction movement in the early 1990s, links were established between improved environmental quality and worker productivity. Hence, it may be possible to relate the importance of architecture to users respond and react when surrounded by built environments, emphasizing the impacts of architecture in one's well-being.

In general, studies on the impacts of environments and natural elements on people can be observed both in physical and psychological aspects of health. For example, McCaffrey's studies [9] Grafetstatter et al. [10] demonstrate decreased levels of stress, depression and anxiety in patients. Research by Latkowska [11] and Berger [12] points to reduced pain and recovery time.

Biophilic Design can be understood as any and all attempts, conscious or unconscious, to reinforce these ties with the natural. Whether by subtle interventions such as allusions to nature forms in buildings, or nature itself shaped by man and translated into urban parks and gardens. The identification of biophilic design patterns shows how subtle the reference to nature can be and yet contribute significantly to the positive user experience. The more of those elements a space contains, the greater the chance of providing a restorative experience for the community.

3. BIOPHILIC DESIGN

The biophilic design idea increases the growing recognition that the human mind and body evolve in a sensorially rich world, which remains critical to people's emotional and psychological health, and spiritual well-being. During a modern era of large-scale agriculture, industry, artificial manufacturing, engineering, electronics and the city represent only a small fraction of the evolutionary history of our species. Humanity has evolved in adaptive responses to natural conditions and stimuli, such as sunlight, climate, water, plants, animals, landscapes and habitats, which remain essential for human maturation, functional development and, finally, survival.

Kellert and Finnegan [13] argue that one of the biggest challenges in biophilic design is to address the

gaps in contemporary architecture. In this sense, it aims to propose a new structure to benefit the experience of contact with nature in the built environment. [14] This design presents a new dimension to architectural projects, called "restorative environmental design". In addition to encouraging and improving contact between people and nature in the urban context, biophilic design also aims to minimize environmental impacts, preserving natural resources, and assuming low-environmental-impact strategies.

Nature can be used in the design of buildings in several ways: shapes, materials, symbols and spaces that make references to nature. Throughout the history of architecture, biophilic design has expressed itself in different ways. Not always identified or conscious, it transmitted certain subjectivity using several devices that attest the bond between nature and the human being. [15]

[16] Fourteen biophilic design attributes that can be applied to the design of the built environment and landscape architecture have been developed by Browning, Ryan, and Clancy (2014); Hildebrand (2008); and Kellert (2008). Heerwagen and Gregory (2008) outline seven attributes, whereas Kellert (2008) suggests there are six elements and 70 design attributes to biophilia. Ryan et al. (2014) outline 14 patterns of biophilia.

In his research, Kellert [17] divides the biophilic attributes of design in two main dimensions called "organic or naturalistic" and "place-based or vernacular". From these two classifications, 70 biophilic attributes emerge. The author argues that the classification of these parameters can aid designers to apply the concepts of biophilic design in project development in a practical way.

The first dimension of biophilic design, organic or naturalistic, classifies elements that allude, directly or indirectly, to nature's forms. It is characterized by contact with elements of self-sustainable characteristics, such as the predominance of natural light, plants, ecosystems and animals. The elements called indirect include representations of the natural world through images, metaphors and symbols. The indirect form can also be achieved by experiencing with natural elements manipulated by humans, such as plant pots, water sources or aquariums.

The second dimension attributed by Kellert, called "place-based or vernacular", refers to landscapes and buildings imbued with the historical and cultural context of a social organization, linked to a specific locality or geographical area. It can be understood as actions that modify the natural environment starting from principles that form the collective identity of a community.

As explained, biophilic design comprises a wide field of symbologies and patterns in architecture. It can be understood with gestures that allude directly or

indirectly to natural elements that provide contact with nature for the user of the buildings. Thus, establishing a greater connection between constructive elements, the natural and the human being, having the potential to positively impact people. Holistically, it embraces several dimensions of sustainability.

3.1. Healing effects

The restorative power of direct contact with nature proposed by biophilic design can be attested in the scientific literature. In addition to the consolidated facts about improving air quality, nature can contribute to other aspects of human health. In a survey conducted in 2011 by Professor Qing Li of Nippon Medical School [18], volunteers were invited to spend a certain period of time emerging in direct contact with nature. Further analysis indicates that the number of immune cells increased by 40%. This fact may indicate that person's immune system is identifying and eliminating viruses and cancer cells more efficiently. In addition, [19] other research results indicate that people tend to suffer less than cancer compared to people who live in regions without contact with nature.

In experiments with people diagnosed with diabetes, [20] Yoshinori Ohtsuka, Hokkaido University, assessed the blood sugar levels of 116 patients after a walk through the woods. The results showed that blood glucose levels of patients after exposure to natural environments decreased significantly. Ulrich [21] has shown in research that a simple view of nature can accelerate effects of patient recovery after surgery. The group of patients looking out the garden window also needed lower doses of painkillers in the recovery process.

In another aspect of studies, researchers at the University of Illinois [22] found that children also benefit positively from contact with nature. Studies show that observed children improved their power of concentration and communication when playing in gardens.

4. METHODS

The research process was divided in two phases. The first refers to the theoretical compilation of biophilic design and its applications in architecture. In this part, a systematic literature review was carried out using the databases Spocus, SciELO and Web of Science. This procedure aimed to elect the productions about biophilic design and to identify the biophilic patterns to be considered in the second phase of the research. In the subsequent phase, an online based survey was applied to building users, asking them to evaluate and give their opinion on how they

experience these biophilic patterns and their effects on their well-being. The intent of this analysis was not only statistical, but mainly to corroborate pre-existing raised hypotheses about biophilic design.

4.1. Identifying Biophilic patterns

The databases chosen for the research were: SciELO, Scopus and Web of Science. The search strings were: "Biophilia", "architecture" and "well-being". The search was not restricted to a specific period of publications. In order to discard articles that were not relevant to the research objective, two screenings were performed. The first excluded very specific subjects linked exclusively to medicine, psychology and biology. The second took into account the keywords of the publications. With this, one can find about 23 publications relevant to the context of biophilic design. This may indicate how the subject is still little explored in general. This procedure was important to define the subsequent biophilic patterns used in this paper.

The method of analysis was inspired by the results of a study carried out by Terrapin Bright Green [2]. It consists on the identification of patterns that favor and reinforce the bonds between the built environment and the natural one. The Buildings chosen for this stage were The Memorial Darcy Ribeiro (Figure 1) and the Instituto de Ciência Central - ICC - Oscar Niemeyer (Figure 2).

The choice of buildings was based on the diversity and intensity of the flow of people during a normal day of university activities. The criterion was also to choose two buildings with different construction dates and constructive methods. The Memorial Darcy Ribeiro was constructed in 2010 and its constructive method uses modulated metallic structure, having an area of approximately 2 thousand m². The memorial includes spaces for cultural activities, classrooms and a library open to the entire community. The Instituto Central de Ciência (ICC) dates from 1971 and its composition is made of reinforced concrete. ICC is one of the main buildings of the University of Brasília, having 120 thousand m², featuring several teaching and research activities in its various laboratories, classrooms and academic centers.

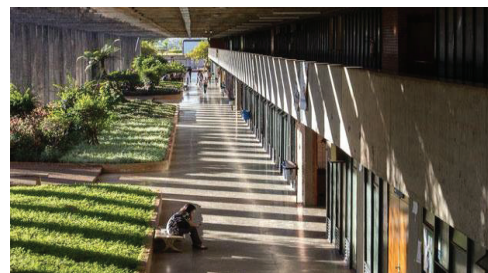


Figure 1: Instituto Central de Ciência, Internal perspective. Fount: University of Brasília (UnB)



Figure 2: Memorial Darcy Ribeiro, Internal perspective. Fount: UnB

The most common aspects about the biophilic patterns identified in the research were taken into account in the subsequent phase. It concluded with visits to the places, in order to experience the environment from the users view. The analysis first took into consideration the visual stimulation in space. Secondly, the sensation caused by the natural elements in counterpoint to the built environment. And in a third moment, the aim was to analyse more objectively the materials and volumes that made up each space. Based on the Analyses of these two buildings, it was possible to identify 10 Biophilic Design Patterns:

1. Possibility of non-visual experiences with natural elements;
2. Visual effects by natural elements;
3. Landscape framing;
4. Use of natural elements by contrast;
5. Elements that enable natural lighting and ventilation;
6. Patina – The time dimension of the building;
7. Path and places that triggers exploration;
8. Microclimate - Creation of small ecosystems;
9. Use of material in its natural state;
10. Forms analogous to natural elements in building composition

4.2 Questionnaire

Using the platform available online, google forms, the questionnaire was sent via email to users of both buildings. In the questionnaire, one could judge anonymously, using the Likert scale, statements corresponding to each of the 10 biophilic standards. The questionnaire was made available to professors, students and university staff. After a first period of testing and calibration, its final version was made available online during the month of April 2019. In this period, the research collected 510 responses.

The questionnaire was divided into two sections, intended to collect data from the user's profile, such as: age range, function they perform, frequency of use of spaces and average length of stay. In this step, the user also identified one of the buildings to respond. The subsequent stage of the questionnaire consisted

of ten statements, each corresponding to each of the biophilic patterns, which could be assessed on a scale of 1 to 5 (1 being "totally disagree" and 5 "totally agree").

In summary, the questionnaire method using Likert scale generates quantitative data about a subject. However, as it is an instrument that can be used to measure the degree of satisfaction of an user on certain aspects, it can be said that a qualitative analysis can also be extracted from the results generated by the research.

Biophilic Design Patterns
1. Natural lighting inside the building is sufficient for activities most of the day.
2. The building's external shape is inviting and encourages you to discover its internal space.
3. The internal space of the building allows positive experiences that instigate other senses such as hearing, olfactory and touch experiences
4. The conditions of the indoor spaces make you feel comfortable enough to spend long periods of time.
5. The building's internal temperature is pleasant and there are sufficient openings for natural ventilation
6. Once inside the building, having eye contact with the landscape around the building is pleasant feature
7. The internal layout of spaces in the building is inviting and easy to understand.
8. The building's maintenance conditions (condition of materials, garden conditions) make the building experience more pleasant
9. The gardens and natural elements (plants, water mirrors) are a positive point in the building.
10. The use of materials in their natural state (exposed concrete, steel, glass) and the apparent structure enrich the sensory experience in the building.

Table 1: Affirmations corresponding to each pattern used in the questionnaire. Fount: Author.

5. RESULTS

Data analysis was performed in two stages. The first prioritized the compilation of data from demographic users and their relationship with spaces. The second part of the results focused on analysing users' preferences according to their responses to the Likert scale. For research purposes, positive responses to biophilic patterns were considered responses that marked `` Agree`` and `` Strongly agree`` (table 1).

Demographic data showed that the majority of respondents were students from the university, adding up to 74%. Age data show that most respondents were over 30 years of age. The frequency of use of the spaces was defined mainly by two types of users: Sporadic (37%) and Frequent (45%).

Regarding the time spent using the spaces, the group with the highest percentage was made up of respondents who claimed to spend 1 to 4 hours a day, followed by respondents who reported spending 4 to 8 hours a day at the university.

The analysis of the collected data indicates a relationship between the daily time spent in the spaces and some patterns. The longer users spend in the space, the more they tend to value visual stimuli such as "Use of natural elements by contrast" and "Forms analogous to natural elements in building composition". The use of materials in their natural state also presented expressive preference in the judgment of welfare in buildings. Dias e Santos [23] Argue that the different textures employed in a building can serve as a guide for visually impaired users, improving the user's experience.

As shown in the graphic 1, the most scored, and accepted by the users, are: *Possibility of non-visual experiences with natural elements (54%); Landscape framing (77%); Use of natural elements by contrast (72%); Use of material in its natural state (72%); Forms analogous to natural elements in building composition (61%).*

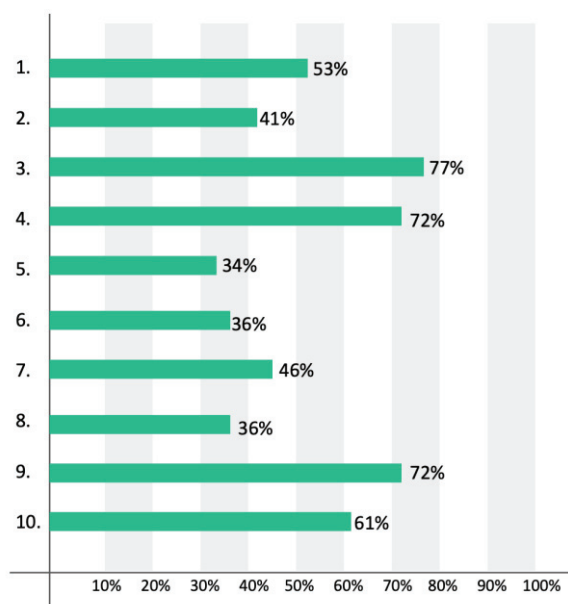


Figure 3 : Overview results. People's acceptance of Biophilic Patterns in percentage. Fount: Author.

The best standards accepted by users in general come from visual stimuli linked directly or indirectly to contact with natural elements in spaces or the allusion of forms of nature. This fact can show that users are more likely to feel good when they are stimulated mainly by the sense of sight. To understand the importance of visual stimulation in architecture, Santaella [24] points out that 75% of human perception comes from visual stimuli. This characteristic is due to the human evolutionary importance of vision for survival. Hearing would be

responsible for 20% of the stimuli perceived in space and touch, taste and smell would add the remaining 5%.

Another interesting point raised by the user's opinion is that 53% of respondents stated that the pattern "Possibility of non-visual experiences with natural elements" also positively influences their experience with space. The engagement of other senses such as hearing and tactile can also enrich the feeling of well-being in buildings. [25] The transformation of a space into a place can only occur through the recognition and creation of a bond of affection between the user and the place. This occurs concomitantly between the sensory stimuli given by the space and the memorization of it by the apprehension of the whole. (Yi-Tuan 1997).

6. CONCLUSION

It can be said that in order to create truly sustainable and efficient environments, human physical and psychological health must be taken into account. The built environment directly impacts people's experience and, consequently, their health and well-being. In this sense, biophilia is directly linked to the restoring power of the human organism. In some respects, biophilic design can be considered as a recent attribute or as a future trend in the design of built environments. However, its theoretical bases rest on concepts established throughout history.

One may argue that the bond between nature and humans may have healing effects. [26] Kellert and Calabrese identified fundamental conditions for the effective practice of biophilic design, including parameters such as: stimulating greater sensitivity to natural spaces, promoting positive interactions between people and nature, increasing the sense of well-being and restorative effects. As this article points out, people can relate their comfort and well-being in built environments taking into account their senses, especially visual stimuli, and elements linked to natural landscapes or similar forms.

The bibliographic review identified the recent effort to converge evidence to prove the bonds between health and nature in a building's design. As can be inferred, some aspects of biophilia may be difficult to quantify. Furthermore, as it is a new approach, it is possible to conclude that the field of study is vast and still little explored, opening up for future work. Ryan et al. [27] argues that in the field of sustainability, biophilic design shows great aggregating potential. In order to achieve a truly sustainable architecture, low environmental impact projects can incorporate the aspects proposed by biophilic design as a complementary dimension.

7. REFERENCES

- 1.P.B. Roös, Regenerative-Adaptive Design for Coastal Settlements: A Pattern Language Approach to Future. Resilience. (unpublished PhD Thesis), School of Architecture & Built Environment, Geelong: Deakin University, (2016).
2. Bronwing, Ryan, Clancy. (2016) 14 Patterns of Biophilic Design – Improving Health and well-being in the built environment [Online], Available: <http://www.terrapinbrightgreen.com/wp-content/uploads/2014/09/14-Patterns-of-Biophilic-Design-Terrapin-2014p.pdf> 20/11/2016. [20 June 2017].
3. Steg L., (2007) Environmental Psychology: History, Scope & Methods. In L. Steg, A.E. van den Berg, & J.I.M. de Groot (Eds.), *Environmental Psychology: An Introduction* (1-11), First Edition. Chichester: Wiley-Blackwell.
4. Wilson, E. O. (1984). *Biophilia*. Cambridge, MA: Harvard University Press.
5. Wilson, E. O. (2008). The nature of human nature. In S. R. Kellert, J. Heerwagen & M. L. Mador (Eds.), *Biophilic design : The theory, science and practice of bringing buildings to life* (pp. 21-25). Hoboken, NJ: John Wiley.
- 6.Fromm, E. (1964). *The heart of man*. New York, NY: Harper & Row.
- 7.. Ulrich, R.S. (1993) Biophilia and Natural Landscapes. In: S.R. Kellert & R.S. Wilson. *The Biophilia Hypothesis* (73-137). Washington: Island Press.
8. J Room, Browning W. (1994) *Greening the Building and Bottom Line. Increasing Productivity Through Energy-Efficient Design*. Rocky Mountain Institute.
9. McCaffrey, R., and P. Liehr. (2016). The Effect of Reflective Garden Walking on Adults With Increased Levels of Psychological Stress. *Journal of Holistic Nursing* 34 (2): 177–184.
10. Grafetstatter, C., M. Gaisberger, J. Prosegger, M. Ritter, P. Kolarz, C. Pichler, J. Thalhamer, and A. Hartl. (2017). “Does Waterfall Aerosol Influence Mucosal Immunity and Chronic Stress? A Randomized Controlled Clinical Trial.” *Journal of Physiological Anthropology* 36 (1).
11. Latkowska, M. J. (2015). “‘Green Care’ in Poland – Application of Horticulture for Improvement of Human Life Quality and Environment Protection.” In *Acta Horticulturae*, edited by C. Shoemaker, and S. A. Park, 125–131. Leuven: International Society for Horticultural Science.
12. Berger, R. (2017). “Nature Therapy – Highlighting Steps for Professional Development.” In *Environmental Expressive Therapies: Nature-Assisted Theory and Practice*, edited by Alexander Kopytin, and Madeline Rugh, 48–60. New York: Routledge.
- 13.Kellert, S., & Finnegan, B. (2011). *Biophilic Design: The Architecture of Life*. A 60-minute video.
14. Heerwagen, J., & Gregory, B. (2008). Biophilia and sensory aesthetics. In S. R. Kellert, J. Heerwagen & M. L. Mador (Eds.), *Biophilic design: The theory, science, and practice of bringing buildings to life* (pp. 227-241). Hoboken, NJ: John Wiley.
- 15.. Söderlund, J. Newman P. (2017). Improving Mental Health in Prisons Through Biophilic Design. *The Prison Journal* 2017, Vol. 97(6) 750–772. 2017 SAGE Publications.
16. C.O. Ryan, W.D. Browning, J.O. Clancy, S.L. Andrews, N.B. Kallianpurkar. (2014). *BIOPHILIC DESIGN PATTERNS: Emerging Nature-Based Parameters for Health and Well-Being in the Built Environment*. *International Journal of Architectural Research. Archnet-IJAR*, Volume 8 - Issue 2 – July 2014 - (62-76) – Regular Section
17. Kellert S. Heerwagen J. Mador. (2008) *Biophilic Design. The Theory, Science and Practice of Bringing Buildings to Life*. Chapter I, Dimensions, Elements, and Attributes of Biophilic Design. John Wiley and Sons, Inc.
18. Li Q. Kawanda (2013) *The Effect of the Phytoncides From Trees on Immune Function in Forest Medicine*,ed. Qing Li (New York; NOVA Biomedical), 71.
19. Li Q. Kobayashi M. Kawada T.(2008) *The Relationships Between Percentage of Forest Coverage and Standardized Mortality ratios (SMR) of Cancer in All Prefectures in Japan*. *The Open Public Health Journal*.: 1-7.
20. Ohtsuka Y. (2013). *Effect of the Forest Environment on Blood Glucose*. *Forest medicine*. (New York: NOVA Biomedical,2013),111.
21. Ulrich R.(1984). *View Through a Window May Influence Recovery From Surgery*. *Science* 224. No 2 (April 27):420.
22. Taylor A, Kuo F, Sullivan W .(2001)*Coping with ADD: The Surprising Connection to Green Play Setting*. *Environment and Behaviour* 33, no 1.
23. Dias A. Anjos M. (2017) *Simpósio de sustentabilidade e contemporaneidades ciências sociais*.
24. Santaella L. (1998) *A percepção: uma teoria semiótica*. São Paulo: Experimento.
25. Tuan Y.(1997). *Space and Place: The Perspective of Experience*. Minneapolis: University of Minnesota Press.
26. S. Kellert, and E. Calabrese (2015) *The Practice of Biophilic Design*. www.biophilic-design.com .[23 abril 2019].
- 27.Ryan O. Browning W. Clancy J. Andrews S. Kallianpurkar N.(2014) *Biophilic Design Patterns. Emerging Nature-Based Parameters for Health and Well-Being in the Built Environment*. *Archnet-IJAR*, Volume 8 - Issue 2 – July 2014 - (62-76) – Regular Section.

Lessons Learnt from The Brazilian Bioclimatic Modernism: The Potential of Passive Design for Offices in the City of Sao Paulo, fieldwork in the building of *Complexo Conjunto Nacional* (1963)

ROBERTA C. K. MULFARTH¹, JOANA C. S. GONÇALVES², RANNY L. X. N. MICHALSKI³, LEONARDO M. MONTEIRO⁴, ALESSANDRA R. P. SHIMOMURA⁵, BEATRIZ N. E. SOUZA⁶, GUILHERME REIS MURI CUNHA⁷, MANUEL MONROY⁸

^{1,2,3,4,5,6,7,8} Faculty of Architecture and Urbanism of the University of Sao Paulo, Department of Technology (FAUUSP, AUT, LABAUT), Sao Paulo, Brazil.

ABSTRACT: In commercial buildings from the Brazilian modernism, built between 1930 and 1964, narrow plans allowed for good daylight and natural ventilation. However, little is known about the actual environmental performance of those buildings. In this context, the objective of this technical study is to draw lessons from the performance of the iconic office building of *Complexo Conjunto Nacional*, the CCN, (1963), in São Paulo (24° S), alongside Paulista Avenue, with focus on its thermal response. Since the case-study building has no external shading, the counter effect of the thermal mass of the construction coupled with the potential of natural ventilation was initially examined during fieldwork. The relation between solar exposure and daylight as well as the impact of operable windows in the internal acoustic environment were also addressed by in situ measurements. Despite the lack of external shading, thermal conditions during a typical summer week were proved to be below external temperatures and within the comfort zone by means of a selective control of the natural ventilation. Daylight measurements showed that illuminance levels remain within visual comfort range, when direct solar radiation is not impinging on windows. Noise levels above the recommended by the national standard were registered. Nevertheless, fieldwork confirmed that occupants open windows for natural ventilation.

KEYWORDS: Office building, Environmental performance, Subtropical climate, Fieldwork.

1. INTRODUCTION

In commercial buildings from the Brazilian modernist architecture built between 1930 and 1964, narrow plans of approximately 12 to 15 metres deep allowed for good daylight and natural ventilation [1]. However, little is known about the actual environmental performance of those buildings [2]. In the following decades, economic pressures led to taller buildings of sealed facades and larger floor plates, with major impact on the thermal response of buildings. As a result, one decade ago, space cooling in office buildings in Brazil accounted for approximately 47% of the total country's electricity consumption, followed by artificial lighting, that were in 22% [3].

In this context, the objective of this technical study is the assessment of the environmental conditions of the iconic building of *Complexo Conjunto Nacional* - CCN (1963), located in the city of São Paulo (latitude 24°S) (Fig. 1). Since the case-study building has no external shading, the counter effect of the exposed thermal mass of the construction, coupled with the potential of natural ventilation, was one of the main objectives of this technical study. In addition, the relation between solar exposure and daylight as well as the impact of operable windows in the internal acoustic environment were addressed by in situ measurements. With special regards to issues

of thermal performance, the research project about the CCN building encompassed by primarily fieldwork and complementary analytical studies. However, since the focus of the research is on the overall environmental performance of the case-study building, this paper brings together aspects of thermal, daylight and acoustics, and the discussion presented here refers to the results of the fieldwork.



Figure 1: *Complexo Conjunto Nacional* (1963), view from Paulista Avenue.

2. CASE-STUDY BUILDING

One notable building in São Paulo which exemplifies the best of Brazilian bioclimatic

architecture of office buildings is the mixed use *Complexo Conjunto Nacional*, located at Paulista Avenue [2]. Built to be an icon of the Brazilian economic prosperity and urban growth, the case-study is composed by 3 adjacent 27 story tall buildings (approximately 80 meters high), being 2 buildings dedicated to office spaces, located in the centre and on the southeast edge of the slab, and one residential building on the northwest edge (Fig. 1). The dual aspect slab-like building is 19 meters wide and 120 meters long stretching from one edge to the other of the site, and is oriented parallel to the busy Paulista Avenue, facing northeast, and to Alameda Santos (a much quieter road), facing southwest. The long tall building is placed on the 14 meters high terrace of the three-storey base-building that covers the entire rectangular urban site of 110 by 130 meters (Fig. 2).

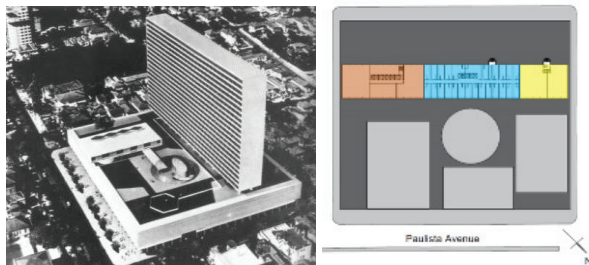


Figure 2: *Complexo Conjunto Nacional*. On the left, physical model of the project. On the right, diagrammatic plan of the several blocks of the CCN placed on the podium building.

Designed prior to the massive culture of air conditioned spaces, therefore, to be completely naturally ventilated, the main architectural and environmental features of the original design of the CCN office buildings are: thermal mass of the exposed concrete structure (in particular the slabs) and operable windows (with 50% efficiency of its area for natural ventilation). Different from the other iconic Brazilian office buildings of its time, the office blocks of the CCN have no external shading. Nevertheless, the window to wall ratio (WWR) of 60%, as opposed to the 90% WWR typical of the contemporary glass tower in the city [4], is a means of controlling the impinging solar radiation, whereas the thermal mass from the exposed concrete structure works as a heat-sink for the internal heat gains. Glare control has been managed in the office spaces with the use of internal blinds.

Since the 70s, changes in the internal spaces have been done to accommodate demands from occupants, including: subdivisions of the open plan and the reduction of the floor to ceiling height from 2.7 to 2.55 meters with the introduction of suspended ceilings for acoustic purposes. At the same time, the growing prestige of artificially controlled environments, coupled with the increasing air and

noise pollution from the busy surrounding urban environment, resulted in a wide adoption of air-conditioning window-machines in several office spaces of the CCN. Nevertheless, its actual use is primarily a choice of the occupants and not every working room is artificially air conditioned, as identified in the fieldwork described later in this article.

3. CLIMATE AND ACOUSTIC ENVIRONMENT

The city of São Paulo (Latitude 23.85° S; Longitude 46.64° W; Altitude 792 m) is located in a region of subtropical-humid climate (Cfa) [5], characterized by warm-humid summer days with predominantly partially cloudy sky, followed by mild and drier winter days with predominantly sunny sky. Predominant wind directions are southeast and south during the summer and northeast during the winter. Air temperatures are moderate for most of the year with an annual average of approximately 19 °C (Fig. 3). Due to the subtropical conditions, the annual frequency of overcast sky is of approximately 60%. Diffuse radiation in São Paulo accounts for approximately 50% of total annual global radiation on the horizontal plan, therefore, having a significant impact on buildings solar gains. Maximum global radiation on the horizontal plan in January, the warmest month in the year, is 1.068 W/m² being 578 W/m² diffuse radiation. July is the coolest, with absolute minimum of 8 °C and absolute maximum of 27 °C. Daily ΔT (temperature variation) varies between 6 °C and 12 °C.

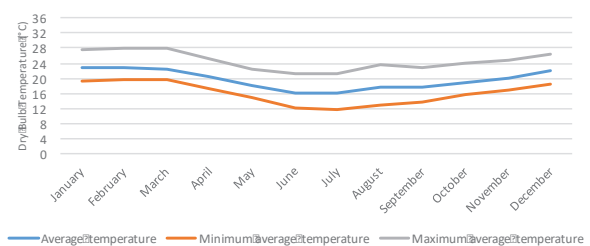


Figure 3: Annual distribution of dry bulb temperatures (DBT) for the climate of São Paulo [4].

In warm days shading is fundamental for the thermal comfort in buildings as well as natural ventilation, which can also be beneficial during night-time given the daily temperature differences. In cooler days, the benefits of passive solar gains are balanced with the contribution of internal gains. In other words, in office buildings, solar gains might be undesirable. It is worth mentioning that the climatic data presented here does not consider the influence of heat island effect, identified in the city centre of São Paulo [6].

The noise map of the area is presented in Figure 4 and indicates the A-weighted equivalent sound pressure levels (L_{Aeq}) at a height of 1.7 m. The colors

vary from green (for the lower noise levels) to black (levels higher than 80 dB). On the northeast front of the CCN building, facing Paulista Avenue, a level of 72 dB reaches the building, while in the southwest side, Santos Str., this level falls to 66 dB [7]. These values are likely to be higher at the upper floors, which are not protected by the barrier created by the base block and where, consequently, sounds from the streets can directly hit the facades.

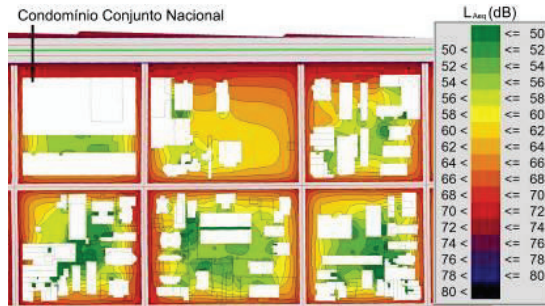


Figure 4: Partial noise map of the area, for a height of 1.7 m from ground level, including CCN (on the top left) [7].

4. METHOD

This research was developed based on fieldwork comprising environmental variables measurements in working spaces in the CCN building, including air temperature, globe temperature, relative humidity, illuminance levels, air movement and sound level. Measurements of thermal and daylight were registered for the entire months of March (summer) and August (winter) (using the data logger Hobo Onset U12). External measurements were registered by a portable weather station at the roof top of the building. Case study rooms for thermal and daylight studies included two office spaces located at the 24th floor of the edge block, both facing Santos Str., at the southwest orientation, being one naturally ventilated, room 1, and the other one air-conditioned, room 2, both shown in Figure 5. For this part of the fieldwork, the case-study rooms were selected by the building administration and no rooms facing the busy Paulista Av. were available at this time.

The adaptive comfort model proposed by ASHRAE [8] was adopted as the assessment criterion for the thermal conditions. As the studies of daylight searched for the probability of excessive illuminance levels due to the unshaded facades, measurements of illuminance levels shown here refer to the warm period only, when global radiation is at its yearly peak. During week days, the artificial lighting was operated in each room according to the occupants' usual routine, therefore, the measurements accounted for natural and artificial light, where and when both sources were present. The assessment was based on the range of useful daylight illuminances (UDI), between 300 and 3000 lux [9, 10]. Given the particularities of the local climate, the

analysis of thermal and daylighting measurements focused on the summer period, with results from one week in March.

In addition to the continuous monitoring of thermal and lighting variables, spot measurements of internal and external sound pressure levels were carried following the relative Brazilian technical standards (using the Larson Davis sound level meter SLM 831) [11]. Values of A-weighted equivalent continuous sound pressure levels (L_{AeqT}) were also compared against the standards recommendations. The fieldwork of acoustic conditions was done eight months after the thermal and daylight ones, because at the time the thermal and daylight conditions were performed, the appropriate acoustic measurement equipment was not available. At this time, it was possible to access two rooms facing Paulista Avenue, where higher noise levels were mapped in the surroundings of the building (rooms 3 and 4, Fig. 5). These rooms are located at the 12th floor.

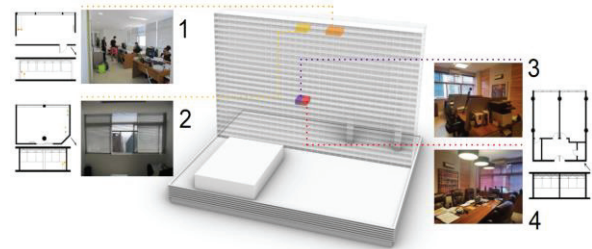


Figure 5: Localization of the case-study rooms in the slab building of the CCN.

5. FIELDWORK: IN SITU MEASUREMENTS

5.1 Thermal conditions

The measurements of the thermal conditions in the naturally ventilated case-study room (room 1), during the summer period, indicate that during the occupied hours the internal dry bulb temperatures are just below the external ones and within the comfort zone, with the exception of the weekends, when windows are closed for the whole day (Fig. 6). The only exception of this trend is observed on Friday, March 25th, when internal temperatures supersede external ones by approximately 1 °C.

During night-time, internal temperatures can reach up to 5 °C higher than outside, due to a decrease in the ventilation, as windows' apertures are reduced to a minimum opening. In this case, internal daily temperatures start at around 25 °C when outside temperatures are around 20 °C, but the opening of windows when occupants arrive causes a quick drop to approximately 23 °C. The highest internal temperature variation was found on Monday March 21st, being approximately 5.5 °C when internal temperatures varied between 22.5 °C during early morning (due to the effect of opening windows by the occupants) and 28 °C, touching the top limit of the comfort zone. In addition, as a consequence of

the opened windows, air speeds at the work-station (where measurements were taken) oscillated between 0.5 m/s and 1.5 m/s for most of the time during the week days, which are values perceived by occupants and sensible to improve thermal comfort conditions in warm days. Peak measurements reached figures higher than 3.0 m/s in a few moments. At night-time, when windows' aperture is reduced, air speeds are lower, staying below 1.0 m/s.

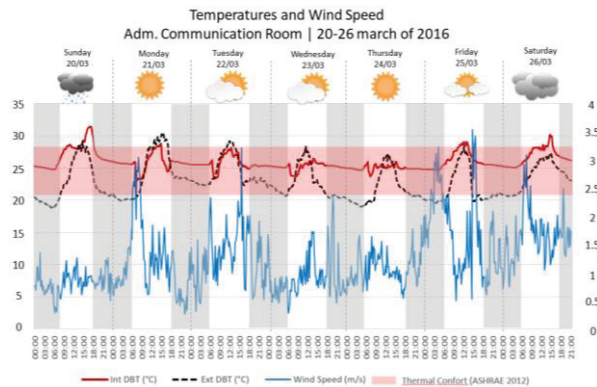


Figure 6: Measurements of air temperature and air movement in the naturally ventilated room at the 24th floor of the CCN, facing southwest, during the warm period.

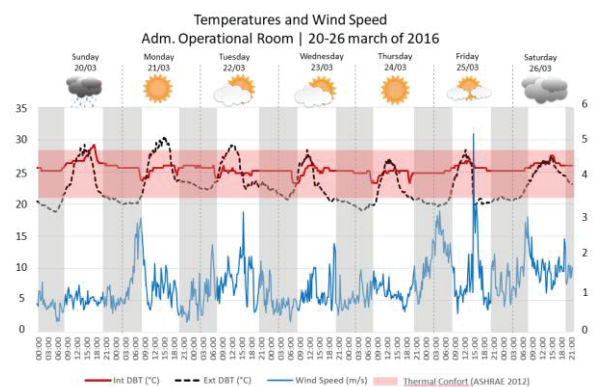


Figure 7: Measurements of air temperature and air movement in the air-conditioned room at the 24th floor of the CCN, facing southwest, during the warm period.

Steadier temperature conditions, well into the comfort zone, were found in the air-conditioned room (room 2) facing southwest (Fig. 7). During occupied hours of weekdays, when the air-conditioning system is switched on, internal air temperatures stay around 25°C, dropping to 24 °C and 23°C a few times during mornings, when occupants open the windows for a couple of hours, but going up again to 26°C in the afternoon, when windows are closed and the air-conditioning system is kept on. Air-movement in this room was determined by the cooler air pushed into by the air-conditioning system. At the work-station where the measurements were taken, most of the recordings during the week registered fairly high air speeds values, between 1 m/s and 2 m/s and reaching the mark of 3 m/s at

peak moments. During night-time, the air-conditioning system is switched off and the window is minimally opened, creating air movement in the room, but the resulting ventilation is not enough to lower temperatures down. As a matter of fact, night-time temperatures are very similar to daytime ones. The measurements depicted in Figures 6 and 7 make evident a missed opportunity for night-time cooling via natural ventilation, when the difference between internal and external temperatures can get up to 6 °C. Even in the naturally ventilated room, the window's aperture at night is not sufficient to bring internal temperatures close to the external conditions.

5.2 Daylight

Regarding the lighting conditions, Figure 8 brings recordings of illuminance levels from both rooms where air temperatures were recorded at the same time/week, characterized by days of clear and partially cloudy sky conditions. A significant difference in the daylight performance of both rooms was registered in the measurements (Fig. 8).

In room 1 (called *operational room*), the naturally ventilated one, artificial lights are switched-off for most of the time and internal blinds are used to control the penetration of daylight during clear sky days avoiding glare. In this case, illuminance values overtake the 300 lux threshold already at the first hours of a clear sky day, as it happens on Monday March 21st, achieving 1,100 lux at 9 am, raising to 1,390 lux at 12 pm and coming back to 1,130 lux at around 5 pm. Daily peaks occur in the afternoons due to the impact of direct solar radiation on the facade, reaching illuminance levels as high as 2,150 lux at 3 pm. During the partially clear sky days, such as Tuesday March 22nd, the measurements show lower but still high values, varying between 900 lux at 9 am and 750 lux at 5 pm, reaching the daily peak at 12 am with approximately 1,000 lux. In essence, the results for the 1st room indicate that the internal blinds are an efficient strategy to keep daylighting levels within the recommendable range for visual comfort, set between 300 lux and 3,000 lux [4], even at the moments of peak daylighting levels.

In the room 2 (called *communication room*), the air-conditioned one, higher values than in the previous case were found, on both clear and partially cloudy sky days, which can be explained by the intermittent use of artificial light (Fig. 8). In this room, because of the use of artificial light, blinds are likely to be put in a position to block more daylight than in the previous one and, therefore, illuminance levels are more constant, but still high, varying between 870 lux at 9 am and 975 lux at 5 pm, reaching high values of approximately 1,050 lux at 12 am, on Monday March 21st of, a clear sky day. On Thursday the 24th, the highest values are just about to touch

the threshold of 800 lux. During the partially cloudy days, Tuesday the 22nd and Wednesday the 23rd of March, maximum levels of illuminance surpass 800 lux, whilst on Friday the 25th levels stay below 400 lux for most of the day.

It is very likely that such differences reflect the operation of internal blinds, which could have been closed by the occupants during the days when lower illuminances were measured, in order to avoid direct solar radiation on the work-plan, but without compromising minimum illuminance levels to perform the office tasks. What cannot be identified in the measurements is how much of the illuminance levels in room 2, is still coming from the windows when the blinds were probably lowered and how much of the total lighting levels is coming from the artificial light.

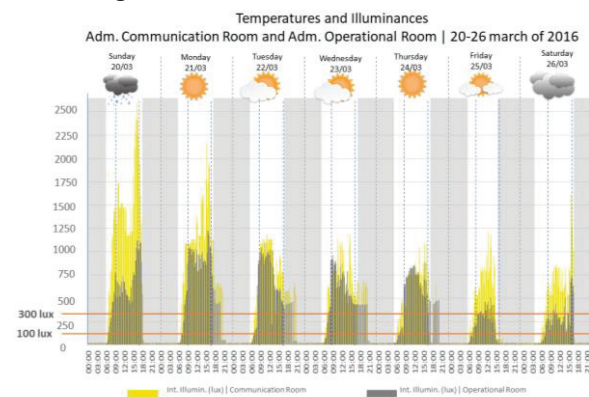


Figure 8: Measurements of illuminance levels in the 2 case-study rooms, at the 24th floor of the CCN, facing southwest, during the warm period. Operational room (grey) – room 1 (naturally ventilated), Communication room (yellow) – room 2 (air conditioned).

The measurements of lighting levels indicate that both rooms are within the recommended range of illuminance levels for comfort conditions. Nevertheless, in the naturally ventilated room, where the artificial light is less used, daylight has a more significant contribution to the visual comfort of the occupants than in the air-conditioned room, where artificial light is used more intensively.

5.3 Acoustic conditions

As mentioned earlier, acoustic measurements were taken in two office rooms facing northeast, towards the busy and noisy Paulista Avenue, with windows closed and opened. Outdoors measurements were taken in the same floor with the equipment held outside the windows. Outside measured A-weighted equivalent continuous sound pressure levels were basically the same in both cases, 67 dB for room 3 and being 68 dB for room 4, whereas indoors measured levels with the windows closed were 51 dB in room 3 and 52 dB in room 4 (Figs. 9 and 10). Both rooms proved to have similar sound pressure levels, with a difference from outside to inside of approximately 16 dB.

With the windows opened, this difference between inside and outside decreases to approximately 10 dB. Comparing with the national technical standards, recommended sound pressure levels for office environments are equal to or less than 40 dB, with a tolerance of up to 5 dB, whilst in open plan offices recommended values are equal to or less than 45 dB, with the same tolerance of up to 5 dB [12]. Although not shown here, sound pressure levels were also measured in octave band frequencies from 63 Hz to 8 kHz. It was found that the main contribution to sound energy is at low frequencies, typical of traffic noise.

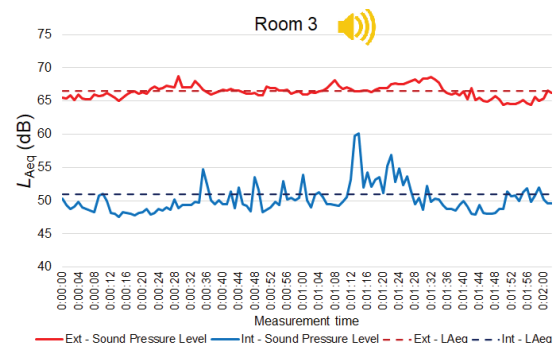


Figure 9: Measurements of sound pressure levels in dB in room 3, at the 12th floor, facing northeast (Paulista Av.).

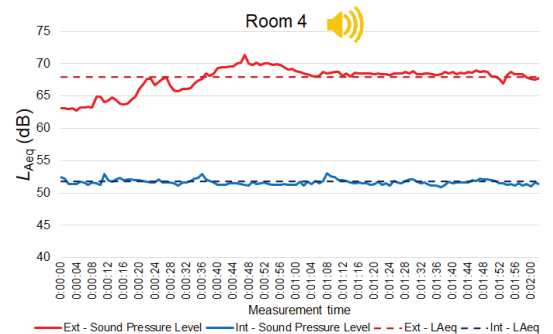


Figure 10: Measurements of sound pressure levels in dB in room 4, at the 12th floor, facing northeast (Paulista Av.).

Although the case-study rooms presented levels above the Brazilian standard reference values (51 dB in one and 52 dB in the other), these can be reduced by treating internal surfaces with sound absorption materials and improving facade sound-insulation. As it can be seen in Figure 11, the installation of the air conditioning machine left large openings at the pipe outlet locations, which allow noise to enter the rooms even when windows are closed.

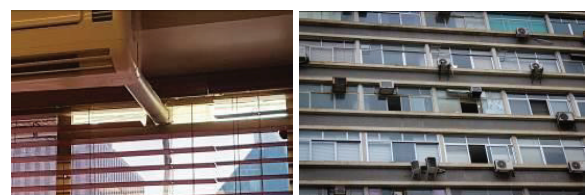


Figure 11: On the left, room 3, details of windows showing gaps in the glass. On the right, view of the facade of the CCN facing Paulista Av. showing air conditioning machines as well as windows opened for natural ventilation.

6. FINAL CONSIDERATIONS AND DESIGN RECOMMENDATIONS

Fieldwork showed that, despite the popular culture of artificially controlled workspace in São Paulo, some of the office rooms in the CCN buildings, facing both Paulista Av. and Santos Str., kept using natural ventilation, whilst others prefer a selective use of the artificial cooling in warm days of the year. The thermal response of the naturally ventilated case-study room in the warm period of the year leads to the hypothesis that there is no need in the CCN building to use air conditioning system for most of the occupational time.

It is also worth noticing how internal air temperatures quickly drop to values inside the comfort zone when natural ventilation is increased by means of opening more the windows. The good performance of the case-study rooms with the use of natural ventilation can be attributed to the thermal inertia of the internal spaces, coupled with the size of windows that allowed sufficient air-changes to remove the heat gains. At night, the difference between internal and external temperatures in both rooms indicates a missing opportunity of night-time cooling via natural ventilation with wider openings.

With regards to daylight, the measurements showed that when the direct solar radiation is not impinging directly on the windows, illuminance levels remain within the comfort range at the working plan height. Moreover, the internal blinds proved to be essential in the control of the amount of global radiation that falls on the desk and, therefore, keeping daylighting levels within the recommended comfort band, particularly in the absence of external shading devices. However, such devices block the view to the outside.

The impact of reduced views towards the outside on people's health, satisfaction and productivity is a sensitive issue but it was not assessed, as it was not part of the scope. It was interesting to notice that the room in which the occupants preferred natural ventilation to the air-conditioned alternative was also the room where the occupants make good use of daylight and have minimum the dependency on artificial light.

Although the study of acoustics registered levels above the Brazilian standards in the office rooms, with the windows opened and closed, it was verified during the fieldwork that occupants do open the windows for natural ventilation during the day in offices facing both orientations of the building, revealing their tolerance to noise levels above the national standards when natural ventilation is desirable and preferable to the air-conditioning alternative (Fig. 10). In other words, a number of occupants still open the windows to passively cool the internal spaces, proving that natural ventilation is

a potentially effective strategy to cool internal office spaces in São Paulo, in architectural and occupational scenarios such as the case of *Complexo Conjunto Nacional*, despite the absence of external shading.

Nevertheless, to avoid acoustic discomfort (and productivity reductions), night-time ventilation is a thermally beneficial strategy in the climate of São Paulo, where daily ΔT in January (the hottest month of the year) stays around 8 °C.

ACKNOWLEDGEMENTS

To the São Paulo Research Funding Agency, FAPESP (2014/15961-9, 2015/04646-8) and the Brazilian Research Funding Agency, CNPq, for supporting the research projects that based the work presented in this paper. Thanks also to the administration of CCN and the occupants of the offices that granted access to their premises for this research.

REFERENCES

1. Yannas, S. and Corbella, O., (2003). Em busca de uma Arquitetura Sustentável para os Trópicos (2nd Ed.). Rio de Janeiro: Editora Revan.
2. Gonçalves, Joana Carla Soares, (2016). A Clarion Call for a New Approach: Sustainability In: Brazil: Restructuring the Urban. Architectural Design (AD). 1 ed. London: John Wiley & Sons, v. 86, p. 126-135.
3. Romero, M. A., (2001). Dynamic Evaluation by Computer Simulation using ESP-r in Office Buildings in São Paulo. In: *Proceedings of PLEA 2001*. Florianópolis.
4. LABEEE – Laboratório de Eficiência Energética de Edificações, UFSC, UFSC, (2005). Arquivos climáticos em formato TRY, SWERA, CSV e BIN. Available at: <http://labeee.ufsc.br/downloads/arquivos-climaticos/formato-try-swera-csv-bin/>
5. Peel, M. C.; Finlayson, B. L.; McMahon, T. A., (2007). Updated world map of the Köppen–Geiger climate classification. In: *Hydrol. Earth Syst. Sci.* 11, p 1633-1644.
6. Tarifa, J. R. and Armani, G., (2000). As Unidades Climáticas Urbanas da Cidade de São Paulo. In: *Atlas Ambiental do Município de São Paulo*. São Paulo.
7. Sales, E. M.; Brito, A. C.; Aquilino, M. M.; Akutsu, M., (2018). Desenvolvimento de método para mapeamento sonoro da cidade de São Paulo. In: *Proceedings of XVII ENTAC*, Foz do Iguaçu.
8. American Society of Heating, Refrigerating and Air Conditioning, (2017). ASHRAE Standard 55-2013. Thermal Environmental Conditions for Human Occupancy. Atlanta.
9. Mardaljevic, I., Andersen, M., Roy, N., Christoffersen, J., (2012). Daylighting Metrics: Is there a relation between useful daylight illuminance and daylight glare probability? In: *First Building Simulation and Optimization Conference*. Loughborough, UK.
10. Nabil, A. and Mardaljevic, J., (2005). Useful daylight illuminance: a new paradigm for assessing daylight in buildings. *Lighting Res. Technol.* v. 37, n. 1, p. 41-59.
11. Associação Brasileira de Normas Técnicas, (2019). ABNT NBR 10151, Acústica – Medição e avaliação de níveis de pressão sonora em áreas habitadas, Aplicação de uso geral. Rio de Janeiro.
12. Associação Brasileira de Normas Técnicas, (2017). ABNT NBR 10152, Acústica – Níveis de pressão sonora em ambientes internos a edificações. Rio de Janeiro.

Exploration of an Architectural Component with Environmental Functions from The Mechanical Recycling of PET

MARÍA IGNACIA LUCARES¹ ALEXANDRE CARBONNEL¹ HUGO PÉREZ¹ DANIEL ESCOBAR¹
MARIA PAZ JIMENEZ¹ DAYANA GAVILANES²

¹Laboratory of Environmental Architectural Materials Exploration, University of Santiago de Chile, Santiago, Chile

²Laboratory of Polymers, University of Santiago de Chile, Santiago, Chile

ABSTRACT: This interdisciplinary research uses a process of mechanical extrusion and pressing to incorporate titanium dioxide nanoparticles (TiO₂) into a recycled PET plastic film in order to explore the potential for a new building envelope material with the capacity to degrade atmospheric contaminant gases. The behaviour of a new architectural material with 8% of photocatalytic nanoparticles incorporated in this mixture, microscopy observations confirm the presence of TiO₂ nanoparticles at the surface of the new material, reaffirming the photocatalytic potential. Assessment of the fragility properties showed tendency to break, with a loss of viscosity and elasticity, this combination and coordination of materials to achieve a new polymer with enhanced properties and characteristics constitutes an important opportunity in architectural design that could lead to the incorporation of new, environmentally beneficial functional properties and trigger a new phase of prototype development.

KEYWORDS: Recycled plastics, Architectural materials, Nanotechnology, Secondary raw material, Building envelope

1. INTRODUCTION

The present research concerns the creation of a new material and is oriented and motivated by the key materials design notions of origin, technological sense, and objectives. As such, it addresses the problems of plastic waste accumulation and urban atmospheric contamination by exploring the possibility of converting this waste into a new material with added photocatalytic properties which could contribute to atmospheric decontamination in cities. The proposal involves the manufacture of a new building envelope material from mechanically recycled polyethylene terephthalate (PET) imbued with photocatalytic potential by the incorporation of a semiconductor catalyst in the form of titanium dioxide nanoparticles.

1.1 Photocatalytic envelopes

In the context of the environmental challenges facing architects today, the issue of the envelope as a building component has opened up new, very specific fields within the development of new technologies and building systems. One of these fields concerns the problem of urban atmospheric contamination and addresses the possibilities of mitigating the impact of this environmental phenomenon by means of the building envelope itself.

The construction industry has embraced the notion of incorporating photocatalyst nanoparticles

into architectural materials based on their capacity, through a process of oxidation, to degrade contaminants such as carbon monoxide (CO), nitrogen oxide (NO_x), volatile organic compounds (VOCs), formaldehyde (CH₂O), and other industrial emissions.

According to data from the Iberian Association of Photocatalysis (AIF), in 2019, the principal applications for photocatalytic materials were paved surfaces (51%), façades (40%), interior surfaces (7%), and roofing (2%) [2]. The most commonly used photocatalytic façade surfaces include ceramic coatings and panels, cement mortars, waterproofing barriers, and photocatalytic vitrified steel panels. Our focus on the building envelope as the subject of exploratory research into plastic reuse is to expand this emerging field of application with the design of a new photocatalytic PET material.

1.2 Atmospheric contamination and its implications in Chile

Atmospheric contamination in urban areas remains one of the most severe environmental problems facing the fields of architecture and urban sustainability. On the global level, OECD estimates for 2050 suggest that, unless addressed immediately, poor air quality in cities may become the principal environmental cause of illness and death [6]. In this context, PM₁₀ and PM_{2.5} particulate matter are

among the main atmospheric contaminants, with the latter having the most serious effect on short- and long-term personal health.

The 2018 World Air Quality Report [1], which assesses the world's most polluted countries and cities, identified Chile as the country with the highest levels of PM_{2.5} contamination in the Latin American and Caribbean region. Of the ten most contaminated cities in the region, seven are in Chile, and the capital, Santiago, is the seventh most contaminated in the region. Of the remainder, the cities of Padre de las Casas and Osorno are categorised as "unhealthy for sensitive groups".

Although the problem of pollution has led to implementation of plans and programmes by the Chilean government, the focus has been on management of critical episodes in certain cities by means of palliative measures such as vehicle restrictions, transport management measures, clampdowns on fixed sources, agricultural burning bans, and bans on the use of solid fuel heating [7].

In light of this, one of the objectives of architectural and materials design should be to develop solutions to mitigate atmospheric contamination in urban centres. As such, the present research seeks to explore the possibility of creating a material which responds to its surroundings through its photocatalytic capacity to degrade atmospheric contaminants.

1.3 Plastic waste as a raw material

Initiatives aimed at the reintroduction of materials into production cycles have identified waste as a potential secondary raw material. The European Parliament Directive on waste (2008/98/EC) is one such initiative, and establishes that, by 2020, at least 70% of non-hazardous construction and demolition waste should be prepared for re-use, recycling and other material recovery [4].

Within this new cyclical notion of raw materials, particular attention has been paid to plastic waste. Plastic waste has been identified and documented as both a political and an environmental issue [3,5] and, given its potential toxicity and slow rate of degradation, has been identified as a risk to human health and ecosystem welfare. The present research therefore seeks to address the cycle of this material.

2. MICROARCHITECTURE OF A NEW PHOTOCATALYTIC ENVELOPE MATERIAL

Given the possibilities for reintroduction of plastic waste into the production cycle and the urgent need for atmospheric decontamination in cities, the present study focuses on the design of a new photocatalytic building envelope material. The first step in this process is the mechanical recycling of PET waste and its material stabilisation through incorporation of photocatalytic titanium dioxide (TiO₂) nanoparticles.

This was achieved by means of an interdisciplinary process that we have termed *microarchitecture*, and which involved various exploratory phases.

2.1 Stabilisation of the new material

An iterative, exploratory process of trial and error was used to achieve a stabilised mixture. The procedure involved qualitative analysis of certain mechanical properties of the new material, namely fragility, presence of bubbles, and calcination. This permitted us to determine the behavioural viability of the material in accordance with construction industry standards, as well as to establish the optimum procedure and raw material proportions.

Furthermore, in terms of its potential to degrade atmospheric contaminants, we needed to demonstrate the presence of nanoparticles on the surface of the material, thus ensuring a photocatalytic reaction upon exposure to ultraviolet rays. This was achieved by means of an electron microscopy of the semi-finished product, which revealed the presence of nanoparticles both within and on the surface of the material.

2.2 Exploratory questions

Exploration of the stability of the new material was conducted in response to two critical questions:

How does the new material behave in terms of fragility (tendency to break) and calcination (as a result of overheating)?

Does the process result in a presence of TiO₂ nanoparticles at the surface of the new material?

3. EXPLORATORY METHOD

Exploration of this new building envelope material was conducted at the Environmental Architectural Materials Exploration Laboratory (LEMAA, School of Architecture), the Polymers Laboratory (POLILAB, Faculty of Chemistry and Biology), and the Centre for Nanoscience and Nanotechnology (CEDENNA), all of which are part of the University of Santiago, Chile.

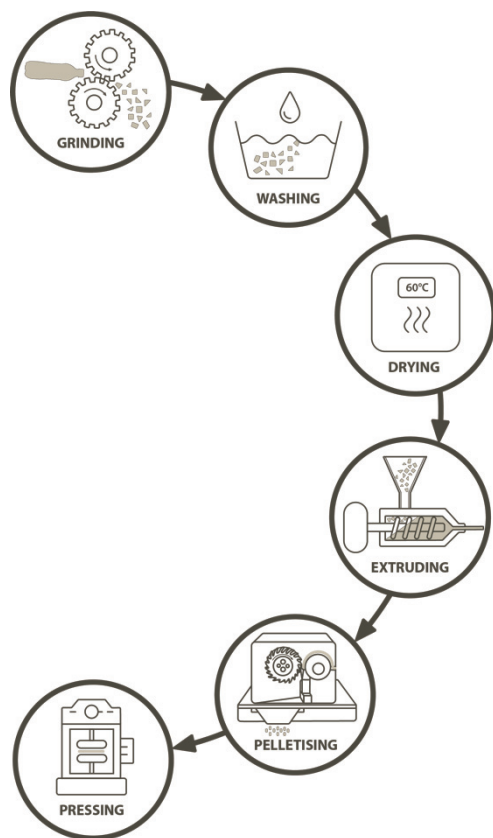


Figure 1: Mechanical exploration process.

As can be seen in Fig.1, PET waste is prepared by means of a mechanical process of grinding and washing in readiness to be mixed with the catalyst nanoparticles in an extruder, where temperature, pressure, and rotation speed variables are iteratively adjusted to achieve an optimal mixture. The newly extruded material, known as Masterbatch, is then pelletised.

Finally, the pellets are pressed according to different configurations of temperature, pre-contact time, contact time, and cooling time.

4. MICROARCHITECTURE RESULTS

Component proportions and a number of variables relating to the mixing process itself were found to be crucial to ensuring the stability of the new material.

We succeeded in establishing the optimum temperature and mixing duration for thermofusion and extrusion of the components.

Plastic materials are subject to two main transition temperatures: glass transition temperature (T_g) and melting temperature (T_m). As a material reaches each of these transition temperatures, changes occur to its properties and it transitions from rigid to rubbery, and eventually to liquid.

A differential scanning calorimetry (DSC) suggested that the material would become flexible at between 73°C and 80°C (T_g) and combine at between 240°C and 260°C (T_m).

A larger proportion of nanoparticles resulted in a more fragile Masterbatch with reduced elasticity and increased viscosity, while the incorporation of too few nanoparticles would diminish the photocatalytic properties of the material's surface.

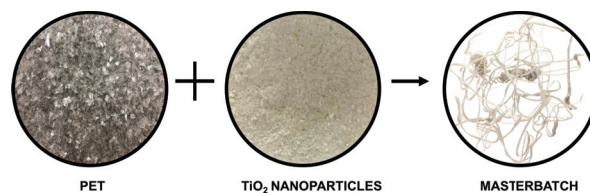


Figure 2: Exploratory microarchitecture: Masterbatch experimentation.

As can be seen in the right hand image of Fig.2, combination of PET waste and nanoparticles according to the temperature ranges established above resulted in a stable Masterbatch. The extruded mixture was irregular in thickness, cloudy white in colour, homogeneous in terms of component distribution, and had greater fluidity.

5. MECHANICAL QUALITATIVE ASSESSMENT

Having mechanically combined the two components, the resulting Masterbatch is then pressed according to certain temperature, pressure, cooling time and pressing time variables to produce films of 150 mm x 150 mm x 3 mm in accordance with Chilean testing standard NCh 873.

Changes to the pressing variables resulted in different film behaviours. Thermal treatment of the Masterbatch prior to pressing resulted in improved visual, mechanical and chemical behaviour.

Furthermore, addition of Teflon sheets over the stainless-steel plates to protect the material as it is pressed improved homogeneity and expansion within the pressing frame and reduced fragility caused by sharp changes in temperature.

5.1 Fragility

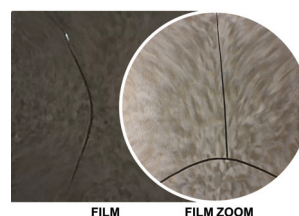


Figure 3: Qualitative assessment of brittle film.

As shown in Fig.3, analysis of pressed samples reveals clear differences between the films. The amount of moisture absorbed by the Masterbatch must be less than 4%, as greater humidity results in increased fragility and makes mechanical testing impossible. This was a novel finding that confirmed the value of the experimental procedure adopted by the present microarchitecture study.

5.2 Bubbles

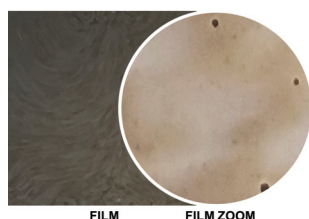


Figure 4: Qualitative assessment of film with bubbles.

The distribution of the pelletised Masterbatch on the pressing plates, i.e., whether all of the material is placed in the centre of the plate or spaced out evenly to the edges, is another variable that affects the behaviour of the film.

A study of the microarchitecture of the pressed film revealed the presence of surface bubbles as a result of uneven distribution of pellets on the pressing plates (Fig.4).

5.3 Calcination

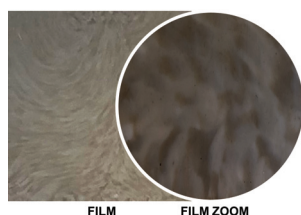


Figure 5: Qualitative assessment of calcinated film.

As shown in Fig.5, differences in film colouration are observed according to thermal treatment of the material during pressing. Temperatures higher than 260°C resulted in calcination at the edges of the film and directly affected the mechanical properties of the material.

6. CHEMICAL BEHAVIOUR

Following incorporation of the TiO_2 nanoparticles, the chemical behaviour of the mixture was analysed, and the films were studied to determine the presence of nanoparticles at the surface and thus establish the photocatalytic potential of the material.

Two electron microscopy analyses were conducted in order to test the behaviour of the nanoparticles within the film.

6.1 Transmission Electron Microscopy

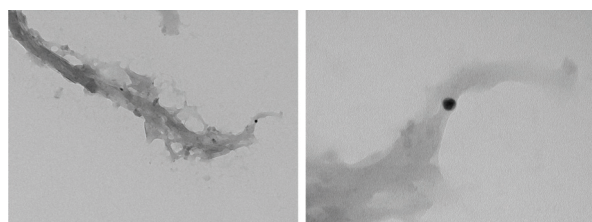


Figure 6: Presence of nanoparticles on film surface.

As can be seen in Fig.6, transmission Electron Microscopy (TEM) analysis of the samples revealed a distribution of the nanoparticles throughout the film, thus validating the proposed combination of recycled PET with TiO_2 to achieve a photocatalytic building envelope material.

6.2 Scanning Electron Microscopy

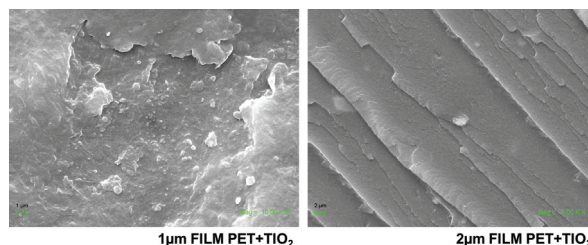


Figure 7: Surface analysis of new material.

Greater surface roughness would increase the area of contact between the film and the air, thus increasing its capacity for gas exchange. Scanning Electron Microscopy (SEM) analysis of the composition and surface of the material revealed an irregular but uniform microarchitecture that would not only improve its photocatalytic performance but would also make it tactile and easy to clean, making it more attractive as a potential building envelope material (Fig.7).

7. CONCLUSION

Analysis of the test samples suggests that effective combination of the two components is indeed possible.

Incorporation of 8% titanium dioxide (TiO_2) nanoparticles resulted in a loss of the original viscosity and elasticity of the recycled PET and the production of more aqueous and viscous extruded samples that showed greater crystallinity following pressing – in other words, greater fragility of the film. These observations constitute a basis for future studies into nanoparticle weights and proportions in order to improve compatibility of the two elements.

Using electron microscopy, we were able to identify varying distributions of TiO_2 nanoparticles throughout the recycled PET film according to different configurations of the production process, thus confirming the potential for the creation of a recycled polymer for photocatalytic applications.

According to data from the Iberian Association of Photocatalysis (AIF), the most commonly used photocatalytic façade surfaces include ceramic coatings and panels. Our focus on the building envelope as the subject of exploratory research into plastic reuse is to expand this emerging field of application with a new photocatalytic PET material, like an architectural component.

In the current state of this research, this film development is understood as a semi finished product, according to ISO 15270 [8]. Therefore, to validate a proof of concept it's necessary the elaboration of exploratory films in accordance with Chilean testing standard NCh 873 [9], could be scaled as a highlight to the possibility of design a prototype tile for exterior walls of buildings.

As demonstrated by the present study, the combination and coordination of materials to achieve a new architectural component with enhanced properties and characteristics constitutes an important opportunity in architectural design that could lead to the incorporation of new, environmentally beneficial functional properties and trigger a new phase of prototype development.

ACKNOWLEDGEMENTS

Environmental Architectural Materials Exploration Laboratory (LEMAA), School of Architecture, University of Santiago, Chile.

Polymers Laboratory (POLILAB), Faculty of Chemistry and Biology, University of Santiago, Chile.

Centre for Nanoscience and Nanotechnology (CEDENNA).

Acknowledgements to the POSTDOC_DICYT Project code 092090CT_AYUDANTE.

The study received funding from the National Commission for Scientific and Technological Research (CONICYT/FONDECYT), project no. 11180461.

REFERENCES

1. IQAir AirVisual, 2018. 2018 World Air Quality Report. Region & City PM2.5 Ranking. [Online], Available: <https://www.iqair.com/world-most-polluted-cities/> [10 May 2020]
2. Asociación Ibérica de la Fotocatálisis, (n.d.). Libro Blanco de la Fotocatálisis. *Tecnologías, Aplicaciones, Medición y FAQ*. Coordinator: David Almazán Cruzado.
3. European Commission, 2013. LIBRO VERDE. GREEN PAPER On a European Strategy on Plastic Waste in the Environment. Brussels, COM/2013/0123 final.
4. European Council, 2015. Directive 2008/98/EC of the European Parliament and of the Council of 19 November 2008 on Waste and Repealing Certain Directives.
5. Ministerio del Medio Ambiente, 2018. Informe Gestión de Episodios Críticos de Contaminación GEC 2018. Gobierno de Chile.
6. George, C., A. Beeldens, F. Barmpas, J.F. Doussin, G. Manganelli, H. Herrmann, J. Kleffmann and A. Mellouki, 2016. Impact of photocatalytic remediation of pollutants on urban air quality. *Environmental Science and Engineering*, 10(5): p. 2.
7. SEREMI, 2018. Plan Operacional para la Gestión de Episodios Críticos de Contaminación Atmosférica por Material Particulado Respirable (MP10 y MP2,5) en la Región Metropolitana. Gobierno de Chile.

8. ISO 15270, 2008. Plastics- Guidelines for the recovery and recycling of plastics waste. ISO (the International Organization for Standardization).

9. Norma Chilena Oficial NCh 873.Of1999, 1999. *Construction-Plastic Tiles-Test methods*. Instituto Nacional de Normalización.

Influence of Air Movement and Air Humidity on Thermal Comfort in Office Buildings in Florianópolis, Brazil

CANDI CITADINI DE OLIVEIRA¹, RICARDO FORGIARINI RUPP^{1,2}, ENEDIR GHISI¹

¹Federal University of Santa Catarina, Department of Civil Engineering, Laboratory of Energy Efficiency in Buildings, Florianópolis/SC, Brazil

²Technical University of Denmark, Department of Civil Engineering, International Centre for Indoor Environment and Energy, Kgs. Lyngby, Denmark

ABSTRACT: Thermal comfort presents high importance for user satisfaction and performance, as well as high potential for energy savings. Two relevant factors to be considered in thermal comfort analyses are air movement and air humidity, as they may enable expansion of the acceptable limits of air temperature. Based on this, this study was carried out to investigate the influence of air velocity and air humidity on users' thermal comfort in office buildings located in the humid subtropical climate of Florianópolis, southern Brazil. Using field data collected in one building with a central air-conditioning system and two mixed-mode buildings, statistical analyses were performed considering environmental variables and users subjective responses obtained by means of an electronic questionnaire. The results did not show a direct influence of air velocity and air humidity on users' thermal comfort, but a significant relationship between thermal comfort and both the perception of air movement and air humidity was verified. Therefore, it was found that air velocity and air humidity have an indirect influence on thermal comfort.

KEYWORDS: Thermal comfort, Hybrid ventilation, Air movement, Air humidity.

1. INTRODUCTION

According to data from the Brazilian Energy Balance [1], residential, public and commercial sectors represent 42.8% of Brazil's total electricity consumption. The commercial sector accounts for 14.4% of the national electricity consumption, showing great importance in the internal demand for energy. Therefore, it is necessary to explore energy-efficient alternatives that enable natural resources savings. One possible strategy is the use of natural ventilation or fans in hot or subtropical climates, which has lower power consumption than air conditioners and a high potential to improve thermal comfort [2,3].

Appropriate air velocity and air humidity values have the potential for energy savings due to the increase of acceptable internal air temperature limits [2-6]. In addition, they keep occupants comfortable as convection and evaporation processes in the body are intensified, thereby increasing heat loss to the environment in hot climates [5-8].

Many authors have identified the preference for high air velocity at high temperatures [2,6,9], which shows the importance of air movement for thermal comfort in hot climates. In some works, users' thermal sensation votes decreased as air velocity increased for air temperatures up to 30°C [10] or 32°C [11]. It was found that high air movement is effective in increasing heat loss and reducing skin temperature [10]. However, the use of fans is not enough to maintain thermal comfort at high-temperature conditions [12].

The air humidity was already studied in different places, such as climatic chambers [6,7,9,13,14], classrooms [11,15], houses [5], and offices [4], generally in hot and humid climates. Although most studies consider the relative humidity in their analyses, some authors suggest the use of absolute humidity [15,16], which can be expressed by the partial pressure of water vapour or the humidity ratio.

Research showed a tendency to improve thermal sensation and thermal comfort, as well as increase occupant thermal acceptability, by reducing air humidity and skin humidity [7,11,14]. In contrast, other works did not find a relationship between these variables [9,13,15]. Also, relative humidity and absolute humidity, as they are related to skin humidity, have an indirect influence on users' thermal comfort [4]. In this case, lower humidity values enable higher comfort temperatures and, therefore, reduce air-conditioning demand.

In this way, it can be seen that in mixed-mode and naturally ventilated buildings, air movement plays a fundamental role in occupants' thermal perception, generally providing a higher thermal comfort. However, the comparison of studies investigating the effects of air humidity on thermal comfort reveals the disparity of results regarding the importance of this variable. Thus, this work aims to investigate the influence of air velocity and air humidity on users' thermal comfort in office buildings located in the humid subtropical climate of Florianópolis, Brazil.

2. METHOD

This study is based on analyses of data collected during two years in three office buildings located in the humid subtropical climate of Florianópolis (latitude: -27°36', longitude: -48°33' and altitude: 7m), southern Brazil. One building with a central air-conditioning system (CC) and two mixed-mode buildings (H1 and H2), in which there was alternation between natural ventilation mode (NV) and air-conditioning mode (AC) according to user preference, were analysed.

It is noteworthy that mixed-mode buildings had split air conditioners and windows accessible and operable by the occupants, with direct entrance of external air. Also, there were individual portable fans on some workstations, operated by their respective users in all buildings.

2.1 Data contextualisation

Simultaneously, environmental variables were measured inside the buildings and subjective variables were obtained by means of an electronic questionnaire. Microclimate stations were used to measure air temperature, globe temperature, air velocity and relative humidity. A portable thermo-anemometer was also used to map air temperature and air velocity near the users.

For the collection of occupants' subjective data in the three buildings, an electronic questionnaire, which users accessed through their personal computers, was applied. The questionnaire contained background questions and questions related to users' thermal, air movement and air humidity perception. Table 1 presents the scales of each parameter regarding the answer options for each question in the questionnaire. Further information on field data collection can be found at [17].

2.2 Statistical analyses

In order to evaluate the relationship between environmental and subjective data, statistical analyses involving these variables were performed. For this purpose, absolute humidity was calculated based on measurements of air temperature and relative humidity. Since relative humidity is associated with temperature, it was considered more appropriate to use absolute humidity in the analyses, as suggested by some authors [15,16].

According to ISO 7726 [18], absolute humidity can be expressed by the partial pressure of water vapour, Equations (1) and (2), or the humidity ratio, Equation (3). Since partial pressure of water vapour and humidity ratio can be used interchangeably and the second is more often used in psychrometric charts, the analyses in this work were based only on humidity ratio.

Table 1: Scales of each parameter considered in the questionnaire.

Parameters	Scales	
Thermal sensation	Hot	+3
	Warm	+2
	Slightly warm	+1
	Neutral	0
	Slightly cool	-1
	Cool	-2
Thermal preference	Cooler	+1
	No change	0
	Warmer	-1
Thermal acceptability	Unacceptable	+1
	Acceptable	0
Thermal comfort	Uncomfortable	+1
	Comfortable	0
Air movement sensation	Very low air movement	+2
	Low air movement	+1
	Enough air movement	0
	High air movement	-1
	Very high air movement	-2
Air movement preference	More air movement	+1
	No change	0
	Less air movement	-1
Air movement acceptability	Unacceptable	+1
	Acceptable	0
Humidity sensation*	Very wet	+3
	Wet	+2
	Slightly wet	+1
	Neutral	0
	Slightly dry	-1
	Dry	-2
Humidity preference*	Very dry	-3
	Less humidity	+1
	No change	0
Humidity acceptability*	More humidity	-1
	Unacceptable	+1
	Acceptable	0

* The questions regarding humidity perception had the extra option "I do not know how to answer".

$$P_{as} = 0.611 \cdot \exp[17.27 \cdot T_a / (T_a + 273)] \quad (1)$$

where P_{as} – saturated vapour pressure (kPa);

T_a – air temperature (°C).

$$P_a = P_{as} \cdot RH / 100 \quad (2)$$

where P_a – partial pressure of water vapour (kPa);

P_{as} – saturated vapour pressure (kPa);

RH – relative humidity (%).

$$W_a = 622.0 \cdot P_a / (P - P_a) \quad (3)$$

where W_a – humidity ratio (g/kg);

P_a – partial pressure of water vapour (kPa);

P – total atmospheric pressure (kPa), equal to 101.325 kPa.

In order to identify the use of each operation mode throughout the year, data were distributed according to season and operation mode for each building. Also, analyses were performed between the environmental variables air velocity and humidity ratio and the subjective variables thermal acceptability and thermal comfort.

The relationship between air movement acceptability and thermal acceptability was verified. In addition, the thermal sensation was related to humidity sensation and humidity preference. The frequency of votes related to air movement and air humidity perception for each type of building and operation mode, for users in thermal comfort and thermal discomfort, was also analysed.

All data concerning air movement sensation and humidity sensation were grouped – for instance, "low air movement" corresponds to votes +1 and +2 on the air movement sensation scale and "wet" corresponds to votes +1, +2 and +3 on the humidity sensation scale.

3. RESULTS AND DISCUSSION

Collected data consist of 2644 measurements regarding environmental variables linked to subjective data (268 in building H1, 1767 in building H2, and 609 in building CC). Table 2 shows the mean and standard deviation of the environmental variables for each building and operation mode: air temperature (Ta), external air temperature (Text), air velocity (Va), relative humidity (RH), partial pressure of water vapour (Pa), and humidity ratio (Wa). In general, the mean air temperature and air velocity were similar for all the buildings and operation modes, with a high concentration of air velocity data around 0.1 m/s. Otherwise, the mean external air temperature was lower for mixed-mode buildings in natural ventilation mode, indicating that natural ventilation was mainly used during the intermediate seasons and winter. Regarding the relative humidity, partial pressure of water vapour and humidity ratio, higher values were observed for natural ventilation mode in comparison to air-conditioning mode. This may be related to air humidity reduction due to the use of air conditioners.

Figs. 1 and 2 show data distribution according to season and operation mode, for mixed-mode

buildings. In building H1, there was a predominant use of natural ventilation in all seasons, but air-conditioning was mostly used in summer. In building H2, there was a similar use of both operation modes during autumn and spring, with a slight predominance of air-conditioning. In summer, there was the exclusive use of air-conditioning and, in contrast, the use of natural ventilation predominated in winter. In the building with central air-conditioning system, 82.1% of the data were collected in the summer and 19.7% in the spring.

The subsequent analyses were performed considering the data of all the buildings and operation modes together.

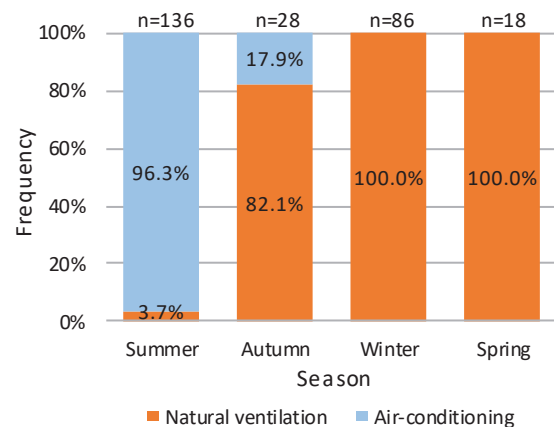


Figure 1: Frequency of votes collected according to season and operation mode for building H1.

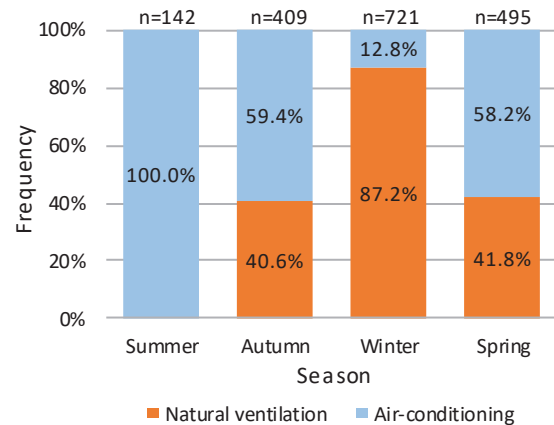


Figure 2: Frequency of votes collected according to season and operation mode for building H2.

Table 2: Statistical summary of the environmental variables for each building and operation mode.

Variables (mean ± standard deviation)	H1		H2		CC
	NV n=132	AC n=136	NV n=1002	AC n=765	AC n=609
Ta (°C)	23.0 ± 1.4	24.4 ± 1.2	23.5 ± 1.3	23.9 ± 1.2	24.0 ± 0.9
Text (°C)	18.6 ± 2.4	26.8 ± 1.1	18.8 ± 1.7	22.4 ± 2.8	23.6 ± 1.8
Va (m/s)	0.10 ± 0.01	0.19 ± 0.15	0.11 ± 0.08	0.11 ± 0.03	0.12 ± 0.08
RH (%)	69 ± 4	55 ± 8	66 ± 8	60 ± 5	63 ± 4
Pa (kPa)	1.614 ± 0.091	1.394 ± 0.232	1.590 ± 0.202	1.478 ± 0.147	1.558 ± 0.118
Wa (g/kg)	10.07 ± 0.58	8.68 ± 1.46	9.92 ± 1.28	9.21 ± 0.93	9.72 ± 0.75

In general, for all buildings and operation modes, the majority of votes showed neutral thermal sensation, thermal preference for “no change”, and acceptable and comfortable thermal environment. Regarding the air movement and humidity perception, most votes indicated enough air movement sensation, air movement preference for “no change”, neutral humidity sensation, and humidity preference for “no change”. Also, air movement acceptability and humidity acceptability remained above 80% for all cases. Since air humidity in Florianópolis is high all year round due to the proximity to the sea, users can be adapted to local humidity conditions. In addition, at high air temperatures occupants chose to use the air-conditioning system, which reduces the humidity of the environment. Thus, some thermal discomfort problems found in other studies [7,8,13] associated with high humidity at high temperatures were not observed in this work.

By relating air velocity and humidity ratio to thermal acceptability and thermal comfort, it was found that there is no correlation between the environmental variables and the subjective variables ($R^2 < 0.001$ for all cases). Thus, there is no direct influence of air movement and air humidity on users' thermal comfort.

The results show that by increasing air velocity, there was a slight tendency of preference for less air movement and less acceptability of air movement for mixed-mode buildings. The opposite was observed for the building with central air-conditioning system. Moreover, the thermal acceptability was high and low when air movement was considered acceptable and unacceptable, respectively (Fig. 3). It is important to note that thermal acceptability was lower when air velocity was considered very high. Thus, it was found that environment thermal acceptability is related to air movement acceptability.

Thermal sensation was related to humidity sensation and humidity preference, according to Figs. 4 and 5. The option “I do not know how to answer” was not considered in the analyses. The frequency of votes indicating neutral humidity sensation and humidity preference for “no change” was higher for thermal neutrality condition. As thermal sensation increased or decreased, there was a higher preference for dry or wet ambient and more humidity or less humidity. Thus, thermal sensation is related to humidity sensation and humidity preference.

It was found that comparing users in thermal comfort and discomfort they were exposed to similar environmental conditions, as air temperature, air movement and air humidity. The results show a high concentration of votes for users in thermal comfort, indicating neutral or slightly warm/cool thermal sensation. For occupants in thermal discomfort, the

thermal sensation was slightly warm/cool, contrarily to what was expected, which would be votes for extreme thermal sensation (hot or cold). In addition, it was found that most people in thermal comfort preferred to maintain the environment as it was at the time the questionnaire was answered. On the other hand, most users in thermal discomfort wanted the environment to be cooler or warmer.

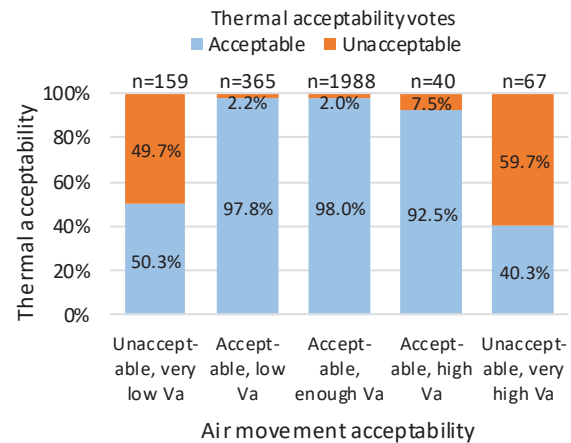


Figure 3: Relationship between air movement acceptability and thermal acceptability.

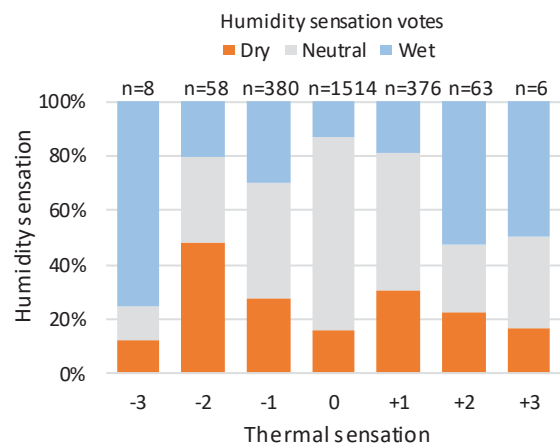


Figure 4: Relationship between thermal sensation and humidity sensation.

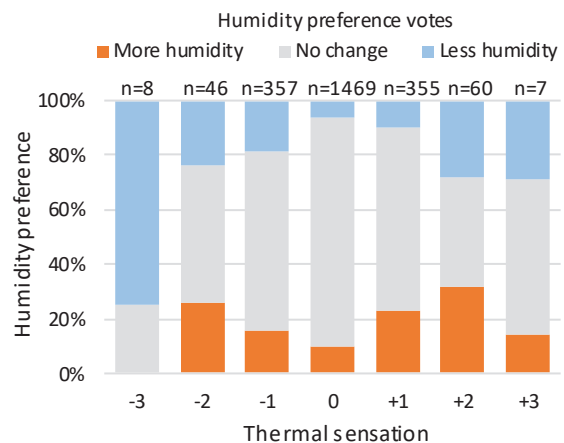


Figure 5: Relationship between thermal sensation and humidity preference.

It was also observed that most users felt thermal discomfort due to heat in all the seasons (Table 3). However, the percentage of discomfort due to cold was high, exceeding 30% in all seasons. Thus, even in summer and winter, there was a high number of users feeling discomfort due to cold and heat, respectively. So, discomfort may be related to other environmental conditions besides air temperature.

Table 3: Thermal discomfort according to season.

Thermal discomfort	Summer n=140	Autumn n=74	Winter n=113	Spring n=70
Heat	55.7%	63.5%	56.6%	64.3%
Cold	44.3%	36.5%	43.4%	35.7%

Figs. 6 to 9 show the frequency of votes related to air movement sensation, air movement preference, humidity sensation, and humidity preference for each type of building and operation mode, for users in thermal comfort and thermal discomfort. It can be observed that the frequency of votes showing enough air movement sensation and air movement preference for “no change” was higher for occupants in thermal comfort. Otherwise, the percentage of votes indicating low or high air movement and preference for more or less air movement was higher for users in thermal discomfort. It is notable that, for all cases, the frequency of votes regarding low air movement sensation and preference for more air movement was higher in comparison to high air movement sensation and preference for less air movement, respectively.

Similarly, it can be seen that the percentage of votes showing neutral humidity sensation and humidity preference for “no change” was higher for occupants in thermal comfort. Contrarily, the frequency of votes indicating dry or wet ambient sensation and preference for more or less humidity was higher for users in thermal discomfort. For thermal comfort and discomfort conditions in mixed-mode buildings in natural ventilation mode, the percentage of votes regarding wet ambient sensation and preference for less humidity was higher in comparison to dry ambient sensation and preference for more humidity, respectively. The opposite is observed for mixed-mode buildings in air-conditioning mode and the building with central air-conditioning system. It is noteworthy that the frequency of responses “I do not know how to answer” was higher for users in thermal discomfort.

Thus, the subjective variables related to air movement and air humidity influence users' thermal comfort.

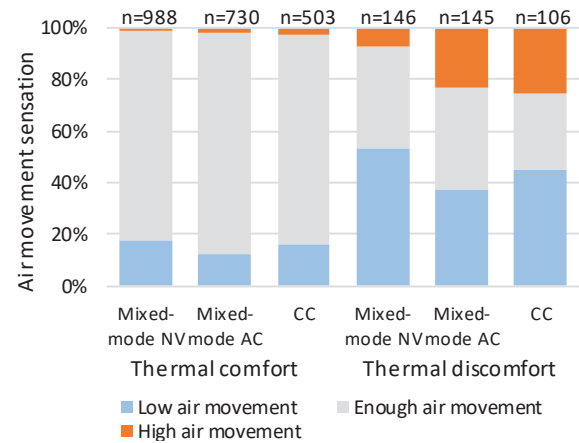


Figure 6: Frequency of air movement sensation votes for each type of building and operation mode for users in thermal comfort and thermal discomfort.

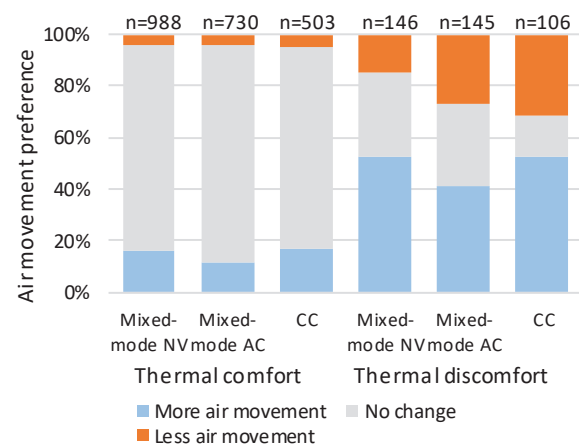


Figure 7: Frequency of air movement preference votes for each type of building and operation mode for users in thermal comfort and thermal discomfort.

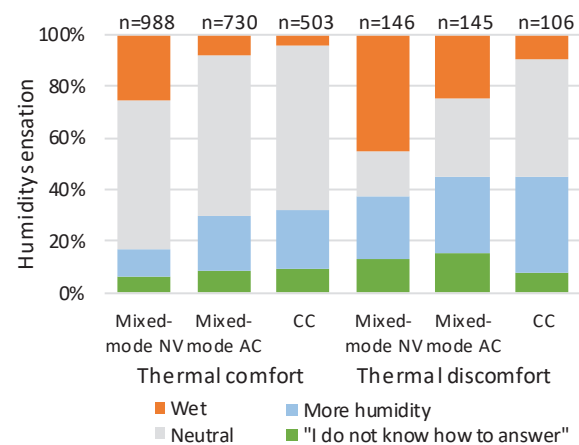


Figure 8: Frequency of humidity sensation votes for each type of building and operation mode for users in thermal comfort and thermal discomfort.

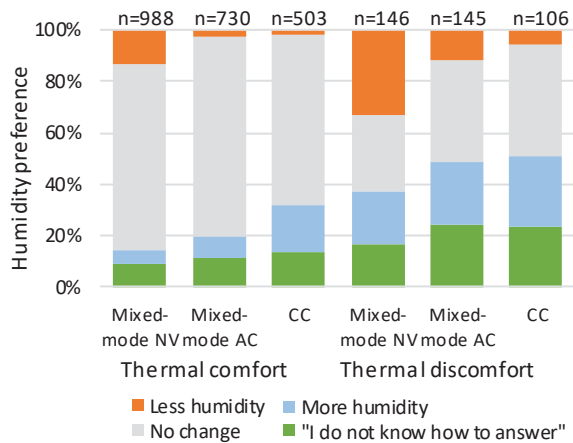


Figure 9: Frequency of humidity preference votes for each type of building and operation mode for users in thermal comfort and thermal discomfort.

4. CONCLUSIONS

This study evaluated the influence of air movement and air humidity on users' thermal comfort in the humid subtropical climate of Florianópolis, southern Brazil. In the analyses, field data were considered and, therefore, there was an unequal distribution of some environmental data. Although it was difficult to perform some analyses due to the small number of observations in some cases, data collection in existing buildings enables a more accurate representation of reality.

From the results, it was not identified a direct influence of air velocity and air humidity on users' thermal comfort, but a significant relationship between thermal comfort and both the perception of air movement and air humidity was found. Therefore, it was found that air velocity and air humidity have an indirect influence on thermal comfort. From these results, it is important to consider the variables air movement and air humidity in building design in order to improve users' comfort and satisfaction, as well as reduce energy consumption by means of decreasing the use of air-conditioning.

ACKNOWLEDGEMENTS

This work was funded in part by the *Coordenação de Aperfeiçoamento de Pessoal de Nível Superior* (CAPES) – Finance Code 001, Brazil. The authors would like to thank the Brazilian National Council for Scientific and Technological Development (CNPq), for financial support.

REFERENCES

[1] Brazil, Ministry of Mines and Energy, Brazilian Energy Balance 2018 – year 2017: Final Report, Rio de Janeiro, Brazil, 2018 (in Portuguese).
 [2] L. Huang, Q. Ouyang, Y. Zhu, L. Jiang, A study about the demand for air movement in warm environment, *Building and Environment*. 61 (2013) 27-33.
 [3] A. Lipczynska, S. Schiavon, L.T. Graham, Thermal comfort and self-reported productivity in an office with ceiling fans

in the tropics, *Building and Environment*. 135 (2018) 202-212

[4] S.A. Damiati, S.A. Zaki, H.B. Rijal, S. Wonorahardjo, Field study on adaptive thermal comfort in office buildings in Malaysia, Indonesia, Singapore, and Japan during hot and humid season, *Building and Environment*. 109 (2016) 208-223.

[5] H.B. Rijal, M. Humphreys, F. Nicol, Adaptive thermal comfort in Japanese houses during the summer season: behavioral adaptation and the effect of humidity, *Buildings*. 5(3) (2015) 1037-1054.

[6] Y. Zhai, H. Zhang, Y. Zhang, W. Pasut, E. Arens, Q. Meng, Comfort under personally controlled air movement in warm and humid environments, *Building and Environment*. 65 (2013) 109-117.

[7] S. Jing, B. Li, M. Tan, H. Liu, Impact of Relative Humidity on Thermal Comfort in a Warm Environment. *Indoor and Built Environment*. 22(4) (2013) 598-607.

[8] H. Tsutsumi, S. Tanabe, J. Harigaya, Y. Iguchi, G. Nakamura, Effect of humidity on human comfort and productivity after step changes from warm and humid environment. *Building and Environment*, 42(12) (2007) 4034-4042.

[9] Y. Zhai, E. Arens, K. Elsworth, H. Zhang. Selecting air speeds for cooling at sedentary and non-sedentary office activity levels, *Building and Environment*. 122 (2017) 247-257.

[10] C. Du, B. Li, H. Liu, Y. Wei, M. Tan, Quantifying the cooling efficiency of air velocity by heat loss from skin surface in warm and hot environments, *Building and Environment*. 136 (2018) 146-155.

[11] C. Buonocore, R. de Vecchi, V. Scalco, R. Lamberts, Influence of relative air humidity and movement on human thermal perception in classrooms in a hot and humid climate, *Building and Environment*. 146 (2018) 98-106.

[12] M. Indraganti, K.D. Rao, Effect of age, gender, economic group and tenure on thermal comfort: A field study in residential buildings in hot and dry climate with seasonal variations, *Energy and Buildings*. 42(3) (2010) 273-281.

[13] T.T. Chow, K.F. Fong, B. Givoni, Z. Lin, A.L.S. Chan, Thermal sensation of Hong Kong people with increased air speed, temperature and humidity in air-conditioned environment, *Building and Environment*. 45(10) (2010) 2177-2183.

[14] J. Toftum, A.S. Jorgensen, P.O. Fanger, Upper limits for indoor air humidity to avoid uncomfortably humid skin, *Energy and Buildings*. 28(1) (1998) 1-13.

[15] B. Givoni, J. Khedari, N.H. Wong, H. Feriadi, M. Noguchi, Thermal sensation responses in hot, humid climates: effects of humidity, *Building Research and Information*. 34(5) (2006) 496-506.

[16] F. Nicol, M. Humphreys, S. Roaf, Adaptive Thermal Comfort Principles and Practice, 2012, Routledge, London, England.

[17] R.F. Rupp, J. Kim, R. de Dear, E. Ghisi, Associations of occupant demographics, thermal history and obesity variables with their thermal comfort in air-conditioned and mixed-mode ventilation office buildings, *Building and Environment*. 135 (2018) 1-9.

[18] International Organization for Standardization. ISO 7726: Ergonomics of the thermal environment – Instruments for measuring physical quantities, 2. ed., 1998, Geneva, Switzerland.

Experimental Building of Nîmes Institute of Technology: The Occupant Behavior's Impact in Summer 2019

Abbas Abbas, Franck Cevaer, Jean-François Dubé

Mechanical and civil engineering laboratory of Montpellier, France

ABSTRACT: The building field represents the largest energy consumer in France and the second largest producer of greenhouse gases after the transport sector. In this context, within the IUT of Nîmes, a largely instrumented experimental building was designed for educational and research purposes. Several techniques and protocols are used to control the equipment and to acquire data. The analysis of the data collected should make it possible to understand the factors that contribute to the building's energy efficiency and to identify the equipment energy performance and the occupants discomfort.

This study focuses on two main topics: shutter control and domestic hot water (DHW) consumption; in which four occupant scenarios are simulated to identify their impact on the building's energy behavior. As for heating and cooling, they are carried out by a reversible air-to-water heat pump, the production of DHW is ensured by an electro-solar system. Also, six photovoltaic panels feed the building and the ventilation is done by a double flow controlled mechanical ventilation system coupled with an air-ground heat exchanger. The building is located in the Mediterranean region and the analysis will covers 2019 summer heat wave.

Keywords: Behavior, Building energy efficiency, Heat pump, DHW, energy consumption

1. INTRODUCTION

In 2017, the building sector's contribution in France was 44% from the total energy consumption, which is far more than that consumed by the transport sector (31.3%). It emitted into the atmosphere more than 123 million tons of CO₂, nearly 16.5% of greenhouse gases (Ministry of Ecological and Solidarity Transition).

The Energy Transition for Green Growth Act, an important law for an efficient energy building, published in August 2015, extends previous commitments (including the two Grenelle laws) and confirms that the measure will be sustainable by 2050.

The LTECV has many objectives: i) Reduce greenhouse effect by 40% in 2030 compared to 1990, ii) Increase the contribution of renewable energy to one third of the final energy consumption, iii) Reduce the fossil energy consumption by 30% in 2030 compared to 2012, iv) Diversify electricity production by reducing the nuclear power contribution to 50% by 2025 and to decrease the energy consumption by 50% at the end of 2050.

The law assigned specific objectives to the construction sector: BBC level for the entire housing stock by 2050, an annual renovation of 500,000 dwellings from 2017, 15% reduction in fuel poverty by 2020 and an energy renovation of dwellings with a primary energy consumption of more than 330 kWh/m².year before 2025. At the same time, the

global improvement of the sector is driven by higher energy and environmental requirements for new buildings, including the construction of positive energy and low carbon buildings, propelled by the Thermic Regulation RT 2012 and Energy Regulation RE 2020 regulations.

In 2018, the law on the housing evolution, known as the ELAN law, was published in the Official Gazette on 24 November 2018. It contains provisions on the evolution of social housing, which facilitate the transformation of offices into housing, and simplifies the building rules.

On November 28, 2016, the Occitanie region launched a project to become Europe's first positive energy region in 2050. The project aims to reduce energy consumption to a maximum level by sobriety and energy efficiency by covering 100% of the consumption by producing local renewable energy. For buildings sector, objectives have been set: to reduce energy consumption by 26% and renovate 52,000 dwellings per year until 2030, then 75,000 dwellings per year.

In 2019, the Occitanie region launched and financed a research project entitled Energy Optimization of the Mediterranean Habitat (OEHM). The aim of the project was to move towards minimizing the energy costs of Mediterranean housing. It is based on four stages: experimental aspects of materials, physical and numerical modelling, tests on instrumented structures and

habitats, the typology and morphology adapted to the Mediterranean climate.

This article, covers the third stages of the OEHM project, deals with the energy study of an experimental building at the University Institute of Technology of Nîmes, it presents the impact of the occupant's shutters management on the building's energy consumption during the summer period. This impact is studied by measuring the input and consumption of the several appliances installed in the experimental building.

2. Literature review

Nowadays, scientific community admits that occupants have significant impact on thermal comfort and energy consumption [3-6]. In Mediterranean area, the energy consumption for air-conditioning in summer can be equal to heating in winter, and it's expected to get worse due to global warming.

The heating and cooling systems have been developed to offer a better life conditions for occupants by compensating the external climate. Today occupants are cut off from their external environment, and simple actions like opening window or close shutter in summer are not used, which impacts the energy consumption. To compensate these counterproductive actions two studies should be considered:

- Changing occupant's behavior.
- Architectural solutions to adapt occupant's behavior.

To change the occupant's behavior, it is necessary to develop solutions by volunteer politicians and social scientists, initiated immediately [7-9]. Understand the possibilities that would limit the unfavorable behavior of the occupants by architects and thermal Engineers (in terms of comfort or energy consumption). Occupants can act on two main architectural elements: the windows and the shutters that can be modified by architects.

Opening of windows and shutters affects ventilation rate and excessive solar heat gain.

Nowadays, dynamic thermal simulations are made by thermal engineers and architects to predict energy consumption and internal temperature of a building, which helps in choosing architectural designs and systems to create energy efficient buildings.

The modeling, metrological data and uses of the building should be known by architects, as the first two elements are now known by architects and engineers the third one is established by hourly step scenarios. Numerous studies have highlighted the relationship between the use of windows [9-19] or shutters [13,15,19-30] and different parameters like external/internal temperature.

In most cases, these studies cover office buildings, while in house building, uses are different and occupants can bear a discomfort situation before modifying their environment. Therefore, a study of the use of housing building is of great importance to simulate real conditions and have good predictions of energy consumption and thermal comfort.

3. Experimental building

This experimental building is a project designed in 2009 and carried out by Civil Engineering students during their end of studies projects. It is designed with the idea of being a reference for the research team in the field of energy efficiency. It is an educational tool to enable students to gain an applied understanding of the building's energy issues.



Figure 1: The experimental building of Nîmes Institute of Technology.

3.1. Building characteristics

This experimental building (Fig. 1) is wood-framed, accessible to people with reduced mobility and has a total surface area of 20 m² divided into two rooms: a living room and a technical room host equipment such as the double flow ventilation system, the Solar Domestic Hot Water system (SDHW)...

The walls and ceiling are insulated with Métisse®, a bio-sourced type of insulation made from recycled cotton wool. The building is built on a soil composed of sand and lime containing a ground-air heat exchanger allowing the recovery of low emissions from the building floor. Heating and cooling are carried out exclusively by the floor.

3.2. Building systems

Heating and cooling of the experimental building are provided by a reversible air-to-water heat pump monobloc system GENIA AIR 6 - SAUNIER DUVAL. Energy from the air is absorbed into a fluid. This fluid transfers its temperature to the water in a 50L storage tank that supplies the dual-zone underfloor heating and cooling system controlled by a hydraulic module.

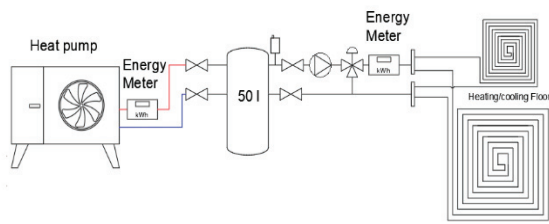


Figure 2: Technical installation of the heating/cooling system of the experimental building.

The production of DHW is ensured by a 250 L electro-solar DHW system installed in the technical room.

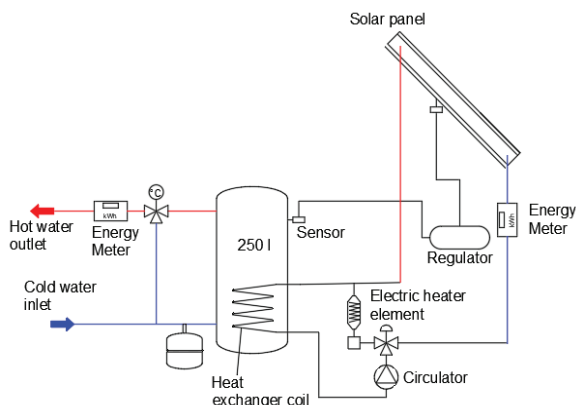


Figure 3: Domestic Hot Water technical installation

YL250P-29b solar panels with 1.5 kWp peak power are installed on the roof and on a supporting structure near the experimental building. The energy produced is brought by a SUNNY-BOY inverter, that's is self-consumed or reinserted into the Nîmes Institute of Technology's electricity grid. The outside air treatment is carried out by an earth-to-air heat exchanger under the building coupled to a Double Flow Controlled Mechanical Ventilation (DF CMV) DOME0 DF model. Two PVC windows with a 0.8 m² surface area are installed on the building's south facade, protected by controlled roller shutters.

For data acquisition and control we used several techniques and protocols to provide students with complete information about these systems. We used KNX, MBus systems and direct connection to a central acquisition system. The KNX system controls the various components such as lighting, shutters and electrical outlets using sensors (electrical energy, humidity, CO₂ levels, outdoor and indoor temperatures and luminosity). A digital interface (Node-Red - Influxdb - Grafana) connected to the KNX system allows data to be displayed and stored for analysis to students with an educational or experimental research purpose.

4. Scenarios summer model

The heat pump is controlled by a thermostat in the room. The outlet temperature of the heat pump is set at 10°C and the indoor temperature is set at 23°C to ensure thermal comfort for the occupant during the day and night. Roller shutter management scenarios are implemented in order to simulate 4 major occupant's behavior highlighted in a previous study of 13 instrumented dwellings of the same property complex in the Mediterranean area (Vauvert City, Gard) [1].

Active behavior V1 (2019/7/16 to 2019/7/23):

Total opening from 7pm to 10am, half-opening between 10am and 12pm then 4pm to 7pm then complete closure between 12pm and 4pm.

Intermediate behavior V2 (2019/7/23 to 2019/7/30): half opening of the flaps all day and night.

Counter-productive behavior V3 (2019/7/30 to 2019/8/6): Total opening during the day from 8am to 11pm and complete closure during the night.

Expert behavior V4 (2019/8/6 to 2019/8/13): Complete closure of the shutters during the daily period from 8am to 10pm.

The comparative energy analysis of the building is described according to the occupant's behavior impacting the solar gains to be combated by the heat pump, which are added to the internal gains (lighting, DHW system, etc.).

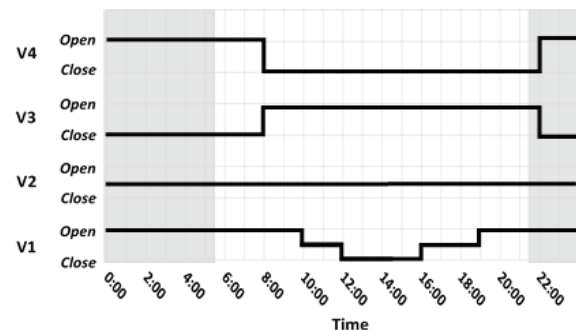


Figure 4: 4 roller shutter management modes

The individual use of domestic hot water is simulated by a solenoid valve controlled by the KNX system in three daily draws: morning, noon and evening.

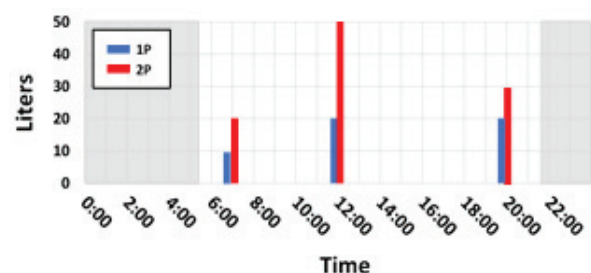


Figure 5: DHW consumption levels

Two different behaviors are set in relation to the daily needs per person. One person: about 50 liters at

50°C (10 - 20 - 20 liters). Two persons: about 100 liters at 50°C (20 - 50 - 30 liters).

4 user behaviors are defined with regard to their shutter management (V1 - V4) and their DHW consumption.

Scenario	Week	Set point T°C	Roller	DHW
Scenario 1	2019/16/7 to 2019/7/23	23°C	V1	100 l
Scenario 2	2019/7/23 to 2019/7/30	23°C	V2	100 l
Scenario 3	2019/7/30 to 2019/8/6	23°C	V3	100 l
Scenario 4	2019/8/6 to 2019/8/13	23°C	V4	0 l

Table 1: Description of scenarios studies

Many factors involved the comfort and energy efficiency of a building:

- The building itself (orientation, insulation, architecture, materials, inertia, ventilation...)
- Internal supplies (people, DHW tank, inverter and lighting...)
- External contributions by radiation (solar gain through glass surfaces).

These contributions, quantified in kWh for the experimental building for the day of July 3, 2019 are shown in Fig. 6 with a mean outdoor temperature at 35°C and daily solar radiation about 7.5 kWh.

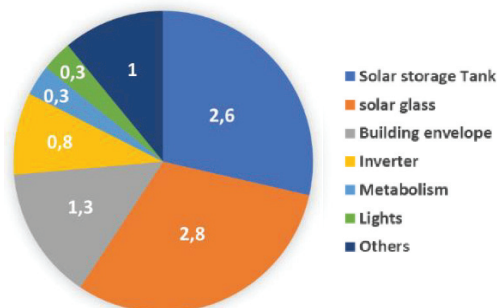


Figure 6: Internal and external contributions (kWh)

Figure 6 shows the internal and external inputs to be overcome by the heat pump. The contribution of the DHW storage tank is very high due to the experimental building 's small surface area. The solar energy gained through the scenario 4 is due to the cumulative glazed surfaces exposed to the south i.e. 1.6 m², which corresponds to one twelfth of the habitable surface, that constitutes half of the minimum regulatory surface. The solar energy gain through these south-facing glazed surfaces reflects a more realistic value compared to the other gains.

For a classic residential building, managing the solar energy gain through glazing is very important, since it helps in promoting the personal comfort and managing the consumption of the cooling system.

3. Results

The energy consumption/produced balance for each scenario is described in Figure 7.

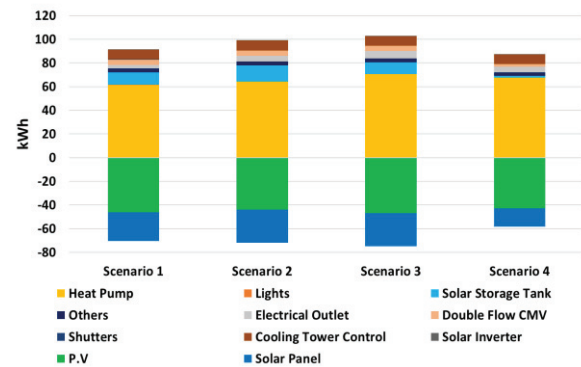


Figure 7: Energy consumption of building equipment

It shows that the building electrical energy consumed is a function of the occupant's scenarios and/or the weather for the corresponding week. Moreover, it also shows that the heat pump consumes more energy than all other elements.

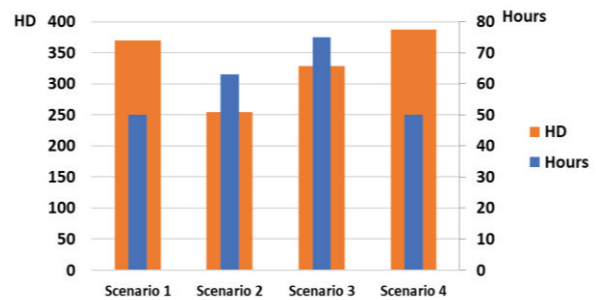


Figure 8: Comparison of cumulative degree hours and durations for which the indoor temperature exceeds 25°C

Figure 8 highlights the degree-hours in each period (accumulation over the week in question of the positive differences between indoor and outdoor temperatures) that reflect the climatic load for the building to be overcome by the heat pump.

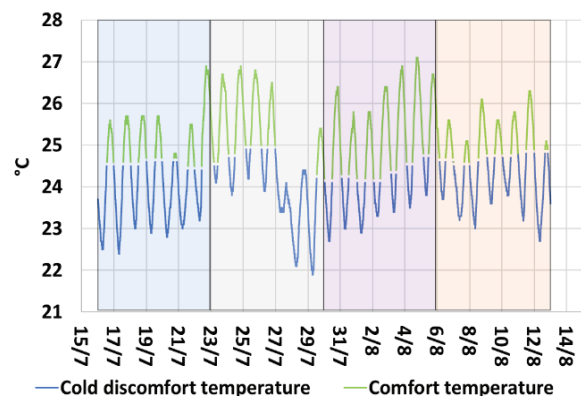


Figure 9: Change in building indoor temperature and indoor comfort in July and August 2019

To refine this analysis, we use the indoor comfort temperature (TRM7) which varies little over these 4 weeks and defines the comfort range $[T_c-3; T_c+3]$ with a lower limit close to 25°C. TRM7 is based on the evolution of the outside temperature of the previous 7 days. Therefore, we calculate the number of hours this temperature is exceeded by 25°C for each of the scenarios. We then obtain 50h, 63h, 75h and 50h respectively for scenarios 1 to 4, Fig.8.

The inside temperature of the experimental building, also the comfort and discomfort period during the 4 weeks are described in Fig. 9.

The indoor temperature does not respect the set point of 23°C maximum, this is probably due to the exchange weak surface of the cooling floor and the setting of the heat pump with a water inlet at 10°C. The measurements give identical power supplied by the heat pump over the 4 weeks with the same day and night evolution.

However, by correlating this temperature evolution with the degree hours of each week, we can see the effect of the openings. As an example, the evolution of the indoor temperature for scenario 1 (active) is lower than the one in scenario 3 (shutters open), while the cumulative degree-hours decrease from 458 K.h in scenario 1 to 446 K.h in scenario 3.

Figure 8 shows that scenarios 1 and 4 give an identical number of hours with a fairly similar cumulative degree hourly temperature (458 K.h and 441 K.h). Scenarios 2 and 3 with a lower cumulative degree-hours than the previous ones (390 K.h and 446 K.h) have a number of hours of 63 h and 75 h respectively for which the indoor temperature exceeds 25°C. The solar irradiation measured by the weather station installed on the IUT site for each week being more or less identical (about 49 kWh), it can be observed that opening of the shutters between 12:00 h and 16:00 h, even if limited, causes an increase in the indoor temperature and degrades summer comfort.

After analyzing the overheat due to the shutters management, it is interesting to study the gain through the solar panels installed.

The solar thermal panel covered the weekly DHW demand from 68% (Scenario 2) to 91% (Scenario 4) depending on the scenario.

Photovoltaic solar panels produced from 44% (Scenario 2) to 51% (Scenario 1) of the weekly electricity requirement.

4. DISCUSSION

This work is a continuation of a work initiated in the winter of 2019 [2].

It will be interesting to carry it out in the mid-season when the building will be on positive energy. It would be interesting to control the heat pump by

adjusting its set temperature to the comfort temperature deduced from the previous 7 days, which would drastically reduce the heat pump's electricity consumption.

The air conditioning temperature set point could not be controlled by the comfort temperature, it had been decided to set it at 23°C for the entire period studied. The summer studied had outside temperatures so high that on the one hand contained of the method of calculation of the TRM7, the temperature of comfort it was found to be of the order of 25° C and the pump functioned all the time for that one finds oneself with fresh periods.

The occupant of scenario 4 (expert) consumes less energy than for the other scenarios with an almost identical photovoltaic production and a production of domestic hot water by the water heater which is correlated with the consumption of hot water. This occupant has a better energy balance than the other occupants with a smaller variation in indoor temperature than the other scenarios, which puts him/her in the best comfort situation.

5. CONCLUSION

This article presents the impact of the occupant's shutters management on the building's energy consumption during the summer period.

The building envelope and systems are largely instrumented and equipped with a monitoring system to simulate the occupant's behavior. This tool allows the data acquisition for systems energy analysis and buildings according to the desired period (weekly, monthly, yearly). These data are accessible both to researchers in the laboratory to confront them with the theoretical models they develop, and to students in the teaching department to refine their understanding in the field of building energy.

These experimental means will allow the evaluation of the consumption in building with the conventional scenarios of the Thermal Regulations and the dynamic thermal simulation tools.

ACKNOWLEDGEMENTS

This study was carried out as a part of a regional collaboration within the OEHM project. The authors express their thanks to the team of IUT Nîmes, especially to technicians of the civil engineering department and the professors of the electrical department.

REFERENCES

1. C. BATIER, Confort thermique et énergie dans l'habitat social en milieu méditerranéen : d'un modèle comportemental de l'occupant vers des stratégies architecturales, p. 291.
2. A. ABBAS, F. CEVAER, J.F. DUBE, Bâtiment expérimental de l'IUT de Nîmes - Étude énergétique de la pompe à chaleur,

37èmes Rencontres Universitaires de Génie Civil de l'AUGC, Sophia Antipolis, FR, 2019-06-19.

3. R. HAAS, H. AUER, P. BIERMAYR, The impact of consumer behavior on residential energy demand for space heating, *Energy and Buildings*. 27 (1998) 195–205. doi:10.1016/S0378-7788(97)00034-0.

4. J.-M. CAYLA, B. ALLIBE, M.-H. LAURENT, From Practices to Behaviors: Estimating the Impact of Household Behavior on Space Heating Energy Consumption, in: *Summer Study on Energy Efficiency in Buildings*, 2010. <http://www.aceee.org/files/proceedings/2010/data/papers/2141.pdf> (accessed April 15, 2013).

5. Z. YU, B.C.M. FUNG, F. HAGHIGHAT, H. YOSHINO, E. MOROFSKY, A systematic procedure to study the influence of occupant behavior on building energy consumption, *Energy and Buildings*. 43 (2011) 1409–1417. doi:10.1016/j.enbuild.2011.02.002.

6. T. DE MEESTER, A.-F. MARIQUE, A. DE HERDE, S. REITER, Impacts of occupant behaviours on residential heating consumption for detached houses in a temperate climate in the northern part of Europe, *Energy and Buildings*. 57 (2013) 313–323. doi:10.1016/j.enbuild.2012.11.005.

7. C. FISHER, Feedback on household electricity consumption: a tool for saving energy?, *Energy Efficiency*. 1 (2008) 79–104. doi:10.1007/s12053-008-9009-7.

8. A. FARUQUI, S. SERGICI, A. SHARIF, The impact of informational feedback on energy consumption—A survey of the experimental evidence, *Energy*. 35 (2010) 1598–1608. doi:10.1016/j.energy.2009.07.042.

9. O. OULLIER, S. SAUNERON, “Nudges verts” : de nouvelles incitations pour des comportements écologiques, Centre d’analyse stratégique, Paris, 2011. www.strategie.gouv.fr (accessed February 18, 2013).

10. T. HARGREAVES, M. NYE, J. BURGESS, Keeping energy visible? Exploring how householders interact with feedback from smart energy monitors in the longer term, *Energy Policy*. 52 (2013) 126–134. doi:10.1016/j.enpol.2012.03.027.

11. G.W. BRUNDRETT, Ventilation: A behavioural approach, *Int. J. Energy Res.* 1 (1977) 289–298. doi:10.1002/er.4440010403.

12. P.R. WARREN, L.M. PARKINS, Window-opening behavior in office buildings, in: *ASHRAE Transactions*, Atlanta, GA, USA, 1984: pp. 1056–1076.

13. I.A. RAJA, J.F. NICOL, K.J. McCARTNEY, M.A. HUMPHREYS, Thermal comfort: use of controls in naturally ventilated buildings, *Energy and Buildings*. 33 (2001) 235–244. doi:10.1016/S0378-7788(00)00087-6.

14. F. HALDI, D. ROBINSON, On the behaviour and adaptation of office occupants, *Building and Environment*. 43 (2008) 2163–2177. doi:10.1016/j.buildenv.2008.01.003.

15. S. HERKEL, U. KNAPP, J. PFAFFEROTT, Towards a model of user behaviour regarding the manual control of windows in office buildings, *Building and Environment*. 43 (2008) 588–600. doi:10.1016/j.buildenv.2006.06.031.

16. F. HALDI, D. ROBINSON, Interactions with window openings by office occupants, *Building and Environment*. 44 (2009) 2378–2395. doi:10.1016/j.buildenv.2009.03.025.

17. V. FABI, R.V. ANDERSEN, S. CORGNATI, B.W. OLESEN, Occupants’ window opening behaviour: A literature review of factors influencing occupant behaviour and models, *Building and Environment*. 58 (2012) 188–198. doi:10.1016/j.buildenv.2012.07.009.

18. R. ANDERSEN, V. FABI, J. TOFTUM, S.P. CORGNATI, B.W. OLESEN, Window opening behaviour modelled from

measurements in Danish dwellings, *Building and Environment*. 69 (2013) 101–113. doi:10.1016/j.buildenv.2013.07.005.

17M. BONTE, F. THELLIER, B. LARTIGUE, Impact of occupant’s actions on energy building performance and thermal sensation, *Energy and Buildings*. 76 (2014) 219–227. doi:10.1016/j.enbuild.2014.02.068.

19. A.I. RUBIN, B.L. COLLINS, R.L. TIBBOTT, Window blinds as a potential energy saver - a case study, *NBS Building Sciences Series*. (1978). <https://www.ncjrs.gov/App/Publications/abstract.aspx?ID=64368> (accessed August 10, 2015).

20. M.S. REA, Window blind occlusion: a pilot study, *Building and Environment*. 19 (1984) 133–137. doi:10.1016/0360-1323(84)90038-6.

21. T. INOUE, T. KAWASE, T. IBAMOTO, S. TAKAKUSA, Y. MATSUO, The development of an optimal control system for window shading devices based on investigations in office buildings, in: *ASHRAE Transactions*, ASHRAE, Ottawa, Canada, 1988: pp. 1034–1049.

22. S. PIGG, M. EILERS, J. REED, Behavioral aspects of lighting and occupancy sensors in private offices : a case study of a „Energy Efficiency in Buildings, 1996: p. 8.161–8.171. http://aceee.org/files/proceedings/1996/data/paper/s/SS96_Panel8_Paper18.pdf (accessed August 10, 2015).

23. C.F. REINHART, K. VOSS, Monitoring manual control of electric lighting and blinds, *Lighting Research and Technology*. 35 (2003) 243–258. doi:10.1191/1365782803li0640a.

24. V. INKAROJIT, Balancing comfort: occupants’ control of window blinds in private offices, Thèse en Architecture, University of California, Berkeley, 2005. <http://escholarship.org/uc/item/3rd2f2bg> (accessed August 7, 2015).

25. F. NICOL, M. WILSON, C. CHIANCARELLA, Using field measurements of desktop illuminance in European offices to investigate its dependence on outdoor conditions and its effect on occupant satisfaction, and the use of lights and blinds, *Energy and Buildings*. 38 (2006) 802–813. doi:10.1016/j.enbuild.2006.03.014.

26. A. MAHDAVI, Patterns and Implications of User Control Actions in Buildings, *Indoor and Built Environment*. 18 (2009) 440–446. doi:10.1177/1420326X09344277.

27. J. DAY, J. THEODORSON, K. VAN DEN WYMELENBERG, Understanding Controls, Behaviors and Satisfaction in the Daylit Perimeter Office: A Daylight Design Case Study, *Journal of Interior Design*. 37 (2012) 17–34. doi:10.1111/j.1939-1668.2011.01068.x.

28. K. VAN DEN WYMELENBERG, Patterns of occupant interaction with window blinds: A literature review, *Energy and Buildings*. 51 (2012) 165–176. doi:10.1016/j.enbuild.2012.05.008.

29. P. CORREIA DA SILVA, V. LEAL, M. ANDERSEN, Occupants interaction with electric lighting and shading systems in real single-occupied offices: Results from a monitoring campaign, *Building and Environment*. 64 (2013) 152–168. doi:10.1016/j.buildenv.2013.03.015.

30. M. FRONTCAK, P. WARGOCKI, Literature survey on how different factors influence human comfort in indoor environments, *Building and Environment*. 46 (2011) 922–937. doi:10.1016/j.buildenv.2010.10.021.

Thermal perception in a room with radiant cooling panels coupled to a roof pond

LEANDRO FERNANDES¹, EDUARDO KRÜGER², EVYATAR ERELL³

¹ Postgraduate Program in Civil Construction, Federal University of Paraná, Curitiba, Brazil

² Postgraduate Program in Civil Engineering, Federal University of Technology - Paraná, Curitiba, Brazil

³ Dept. of Geography and Environmental Development, Ben-Gurion University of the Negev, Beersheba, Israel

ABSTRACT: Roof ponds (RP) can promote comfortable thermal conditions, particularly in single-storey buildings. They allow structural cooling or heating and stabilization of surface and air temperatures. When coupled to radiant panels cooled by the exposed pond, they can further improve their thermal performance. However, there is a lack of research on RPs focusing on the thermal perception of users indoors. The main objective of this study was to evaluate empirically under hot dry summer conditions the thermal perceptions of volunteer participants in an indoor environment conditioned by a system composed of radiant panels coupled to a RP. We also sought to assess the applicability of the PMV model and the passive building models of ASHRAE Standard 55 and EN-15251 under these conditions, through comparison with subjective thermal votes reported by the study participants. In a test building at Ben-Gurion University of Negev, Israel, a sample of 46 participants found a room cooled only by a RP. Thermal votes showed more agreement with the PMV and EN-15251 models than with the ASHRAE model.

KEYWORDS: Roof pond; Radiant cooling; Passive cooling; Thermal comfort models.

1. INTRODUCTION

Roof ponds (RP) can promote comfortable thermal conditions in some locations, particularly in single-storey buildings. They allow structural cooling or heating and stabilization of surface and air temperatures. Radiant cooling using ponds on metallic ceilings instead of concrete ones may be more effective, because the temperature difference between the reservoir water and indoor air below due to their higher thermal conductivity [1]. To compensate for this, the performance of concrete ponds may be improved by coupling them with water-based radiant cooling systems suspended below the ceiling. There is evidence that radiant cooling systems can provide equal or better comfort conditions compared to conventional air conditioning systems [2]. Tests in an experimental building equipped with radiant cooling panels showed that two thirds of the summer cooling occurred by radiation and only one third by convection [3]. Studies on radiant cooling and evaporative cooling still focus mainly on the optimization and performance of systems [4], and there have relatively few field studies involving occupants reporting feedback [5].

The main objectives of this study were: First, to verify empirically in warm summer conditions whether volunteers would evaluate as comfortable a thermal environment conditioned by radiant panels coupled to a RP. Secondly, to identify which thermal comfort model best agrees with the votes registered by the study participants.

2. METHODOLOGY

The experiment was performed in a room cooled with radiant panels suspended from the ceiling coupled with a roof pond. Volunteers were requested to assess the thermal conditions in the room by means of questionnaires, and their responses were compared with comfort indices calculated from environmental data recorded in the test room. The performance of the roof pond was assessed through comparison with conditions measured before installing the evaporative cooling system coupled to the radiant panels.

2.1 Test facility

The rooms are part of a test facility located at the Sde-Boqer Campus of Ben-Gurion University of the Negev, in Israel. The climate (Köppen Climate Classification subtype "Bsh") is characterized by large diurnal and seasonal thermal fluctuations, dry air and clear sky with intense solar radiation. Summer weather is extremely stable: temperature differences from day to day are minimal, with a typical maximum of 32-33°C and minimum of 18-19°C. The average wet bulb temperature in July is 16.8°C [6].

The facility incorporates three similar test rooms (9.45 m²) with a white-painted interior. The room on the right in Figure 1 had a roof pond installed on it, while the center room served as a control.

The setup in the RP room (Fig. 2) comprised 1) a 2 mm-thick white PVC roof, installed 1.5 m above the slab; 2) a spray system; 3) a water pump; 4) a floating layer of EPS; 5) 755 l of water; 6) two radiant aluminum panels with coils, placed inside the test environment; 7) a dummy conditioner unit working only as a fan.

The control configuration (CC) consisted of a 10 cm thick concrete slab roof with 10cm thick polystyrene thermal insulation covered with a light-coloured gravel ballast. The room was equipped with a split AC unit.



Figure 1: South façade of test building.

External environmental data were obtained from the campus weather station. Internal conditions monitored included air temperature (T_a), air velocity (V_a), relative humidity (RH), water temperature (T_w) and the temperature of all surfaces (T_s). The mean radiant temperature (T_{mrt}) was calculated from T_s , using the procedure in ISO 7726 [7], which then allowed the calculation of operative temperature (T_o).

Useful monitoring started on July 31 and ended on September 21 2017, covering 22 days.

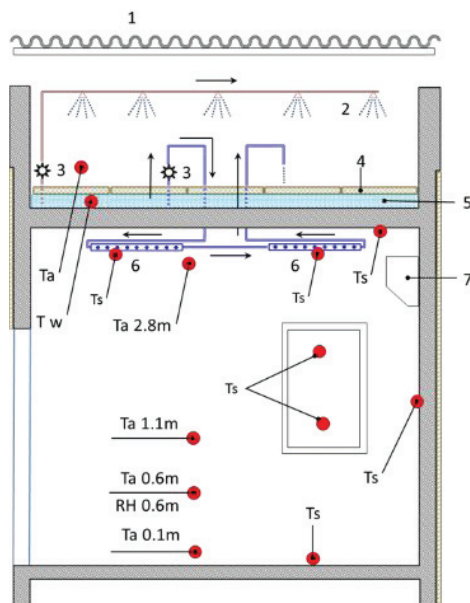


Figure 2 – RP section showing sensor locations.

2.2 Questionnaire and participants

Volunteers were recruited from members of the university community (students, staff and family members). The questionnaire was designed according to the guidelines of ISO 10551 [8], and included in addition questions about personal data and clothing.

Thermal perception was recorded by three metrics: thermal sensation (TS), thermal comfort (TC) and thermal preference (TP), as indicated below:

1 What is your general thermal sensation right now?

()	()	()	()	()	()	()
-3	-2	-1	0	+1	+2	+3
Cold	Cool	Slightly cool	Neutral	Slightly warm	Warm	Hot

2 How do you feel about the thermal environment?

()	()	()	()	()
0	1	2	3	4
Very uncomfortable	Uncomfortable	Neutral	Comfortable	Very comfortable

3 At this moment, would you prefer to be?

()	()	()	()	()	()	()
-3	-2	-1	0	+1	+2	+3
Much cooler	Cooler	Slightly cooler	Without change	Slightly warmer	Warmer	Much Warmer

2.3 Determination of thermal conditions in the experimental environment

The thermal conditions in the RP room were assessed 30 minutes before volunteers arrived to establish a reference condition, and again 5, 30 and 35 minutes after their arrival, using the Predicted Mean Vote (PMV). The PMV was calculated according to ISO 7730 [9] using WinComf [10] and the CBE calculation tool (<http://comfort.cbe.berkeley.edu>), assuming a 'standard' male person, aged 35, 1.75 m tall, weighing 75 kg [11], wearing light clothing (0.3 clo) and in sedentary activity (70 W). The data shown in the following analysis refer to conditions recorded between 30 and 35 minutes after the arrival of volunteers in the test room.

According to ISO 7726 [7], T_{mrt} , which is required to calculate PMV, can be estimated from the temperatures of the internal surfaces and their respective angle factors (F) using Equation 1:

$$T_{mrt} = \sum(F_i T_s) \quad (1)$$

Where T_s is the temperature of a surface and F_i is its angle factor from a given point of interest, so that the temperature of the surfaces is weighted according to their solid angles (Ω) in relation to the chosen point [12]. The angle factor (F) (Equation 2) corresponds to the relative solid angle around a point.

$$F_i = \frac{\Omega_i}{4\pi} \quad (2)$$

The angle factor can be approximated by the projection of the surface or object on a sphere whose center is the point of interest. It measures the apparent size of the object seen from that point, such that the sum of the solid angles of the surfaces that delimit it will be equal to the area of a sphere given in steradians (4π or 12.566). Taking the point of interest as the vertex and a surface (wall, for example) as the base of a pyramid, one can estimate the solid angle given by that surface with Equation 3 [13].

$$\Omega = 4 \tan^{-1} \left(\frac{ab}{2d(4d^2 + a^2 + b^2)^{0.5}} \right) \quad (3)$$

Where:

Ω is the solid angle given by the surface in relation to the point of interest.

a is the length of the base of the pyramid (length of the wall).

b is the width of the base of the pyramid (height of the wall).

d is the distance between the center of the base and the top of the pyramid.

2.4 Evaluating thermal perception

The thermal perceptions reported by the volunteers were assessed using the following models: a) the predicted mean vote (PMV), and the predicted percentage of dissatisfied (PPD) derived from it, calculated according to ISO 7730 [9]; b) the comfort range for passive buildings defined by ASHRAE Standard 55 [14]; c) and the comfort range for passive buildings defined by standard EN-15251 [15].

Thermally dissatisfied persons were classified as those who voted 'very hot', 'hot', 'cold' or 'very cold' (-2, -1, +1 and +2) on the seven-point thermal sensitivity scale suggested by ISO 7730 [9].

Thermal comfort models for passive buildings given by ANSI/ASHRAE Standard 55 [14] and EN-15251 [15] provide for the use of operative temperature (T_o) to derive neutral temperatures and comfort ranges in rooms with no air conditioning. T_o can be taken as the average between T_{mrt} and T_a [8, 16], if air speed in the environment (v_a) is less than 0.2 m/s (as was the case even when the dummy AC fan was turned on).

Standard EN15251 [15] establishes a comfort band for buildings with no mechanical cooling that is derived from the average daily outdoor temperature. The comfort band is defined around a neutral operative temperature ($T_{o\,comf}$) according to equation 5:

$$T_{o\,comf} = 0,33T_{ex\,ewa} + 18,8 \quad (5)$$

Where, $T_{o\,comf}$ is the neutral operative temperature and $T_{ex\,ewa}$ is the exponentially weighted running mean of the daily external air temperature.

$T_{ex\,ewa}$ can be calculated using Equation 6:

$$T_{ex\,ewa} = (1 - \beta) \times T_{ex\,m-1} + \beta \times T_{ex\,ewa-1} \quad (6)$$

In which:

β is a constant, equal to 0.8 [15];

$T_{ex\,m-1}$ is the mean air temperature of the previous day (°C);

$T_{ex\,ewa-1}$ is the exponentially weighted average external air temperature, calculated for the previous day.

The comfort range for "new construction and renovations with normal expectation" has a width of 6°C [15, 17].

ANSI/ASHRAE Standard 55 [14] also establishes a comfort band that is variable and is based on the average of external temperatures. The procedure is

applicable only when the average monthly temperatures are greater than or equal to 10 °C and less than or equal to 33.5 °C [14]. The neutral operative temperature according to this standard may be derived using Equation 7 [14]:

$$T_{o\,comf} = 0,31T_{ex\,ma} + 17,8 \quad (7)$$

Where $T_{ex\,ma}$ is the moving average of external temperatures (°C).

It is observed that $T_{ex\,ma}$ is a moving arithmetic mean, differing from the variable used by EN-15251 [15], which uses a weighted average. It must be based on no less than 7 and no more than 30 consecutive days before the day in question [14]. Around the neutral temperature, the range of thermal acceptability with 7 °C in width was adopted, to serve 80 % of the population [14].

2.5 Test sample

The test sample comprised 46 participants: 19 men (average age 33.9 years) and 27 women (average age 31.7 years). 91.3 % of subjects were aged from 16 to 40 years old, making the majority of the sample composed of young adults. Participants were from 13 different countries: Israel (25 participants), USA (5), India (3), Brazil (2), Germany (2), Russia (2), other countries (7). The Body Mass Index (BMI, calculated as the body weight divided by the square of the body height, expressed in kg/m²) varied between 18.4 ('underweight') and 35.5 kg/m² ('grade II obesity'), according to the categories of the World Health Organization [18]. Table 1 summarizes the physical characteristics of the test subjects.

Table 1 – physical characteristics of test subjects.

	average	std dev
Age (years)	32.6	8.8
BMI (kg/m ²)	23.4	3.6
Weight (kg)	67.1	12.9
Height (m)	1.69	0.08

Most of the subjects had just come from thermal environments without air conditioning (63.0 %), some from air-conditioned spaces (30.4 %) and some from public transportation/cars, typically with air conditioning (6.5 %). 32 of the volunteers arrived at the experiment site walking (69.6 %), 10 arrived by bicycle (21.7 %) and 4 by car/bus (8.7 %). 45 of the participants (97.8 %) took less than 10 minutes to arrive at the experiment site.

Most volunteers wore short-sleeved T-shirt, shorts, underwear and sandals, with a mean thermal insulation value of 0.32 clo and median of 0.24 clo.

3. RESULTS

3.1 Roof pond performance

The effect of the roof pond (experimental configuration - EC) was assessed by comparison with

conditions measured before (control configuration - CC) installing the evaporative cooling system coupled to the radiant panels. Results of measurements made of air temperature and the temperature of room surfaces including walls, ceiling and cooling panels (RP room only) are summarized in Table 2. During the monitoring period (6/16 – 6/24/2017), the average internal air temperature in the reference room was 2.2 °C higher than the average external temperatures, while in the experimental configuration (7/29 – 8/07/2017) the average was 0.3 lower than the average external temperatures. In the case of the surface temperatures of the ceiling, in the CC, the average value was 2.6 °C higher than the average of the external air temperatures, while in the EC it was 1.7 °C lower (the average of the surface temperatures of the radiant panels was even lower, 2.7 °C lower than the average outdoor temperature).

Table 2 - Averages of surface temperatures and internal and external air temperatures.

	Ta	Ta ex	Ts ceiling	Ts panels
Control Configuration	26,5	24,3	26,9	26,9
Experimental Configuration	26,8	27,1	25,4	24,4

3.2 External and internal environmental conditions

The weather during the experiment was generally warm and dry. During the sessions, the average outdoor temperature was 29.6°C, with a maximum of 34.6°C and a minimum of 24.3°C (Fig. 3). Internal conditions during the sessions were stable and almost uniform: The temperature ranged from 25.8°C (the coolest session) to 28.8°C during the warmest session, with an average of 27.2°C. Air movement (V_a) was less than 0.2m/s. Relative humidity averaged 62% , with a minimum of 50%, and a maximum of 70%. Thus, although the room lacked a mechanical AC system, the volunteers were exposed to mild internal environmental conditions. However, during some of the sessions there were substantial differences between external and internal air temperatures. In most cases, the external air temperature was higher than the internal one (Fig. 3), with a maximum difference between $T_{a\text{ ex}}$ and $T_{a\text{ in}}$ of 6.8°C.

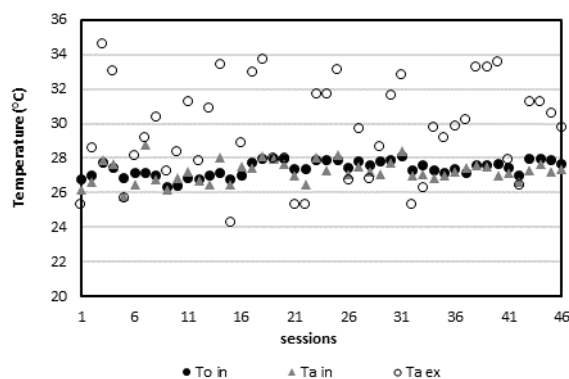


Figure 3 - Indoor and outdoor air temperatures during thermal comfort sessions

3.2 PMV and PPD during the sessions

In general, the values for the PMV (Fig. 4) were close to thermal neutrality (between -0.57 and 0.20, average -0.08). The values for the PPD were close to or below 10% (between 4.9% and 13.2%, average of 6.2%). That is, according to the PMV model, the volunteers were exposed to mostly comfortable environmental conditions during the sessions, or very close to them.

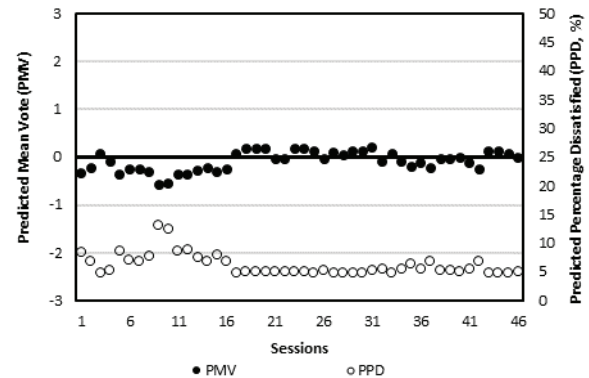


Figure 4 - PMV and PPD during thermal comfort sessions.

3.3 Thermal comfort ranges according to adaptive models during sessions

The operative temperatures during the sessions were plotted on the comfort ranges given by the standards ANSI/ASHRAE Standard 55 [14] (Fig. 5) and EN-15251 [15] (Fig. 6). The average values over the duration of the experiment are shown in Table 3 for the two comfort standards. In the case of the ASHRAE comfort range, the operative temperatures were between the upper limit of the comfort range and the neutral condition. In the case of the comfort range of EN-15251, operative temperatures were, in general, closer to neutral temperatures. Although the operative temperatures were closer to the recommended values for the EN 15251 model than for the ASHRAE model, there was a high probability that the volunteers' votes would indicate satisfaction with the thermal environment provided by the cooling system according to both.

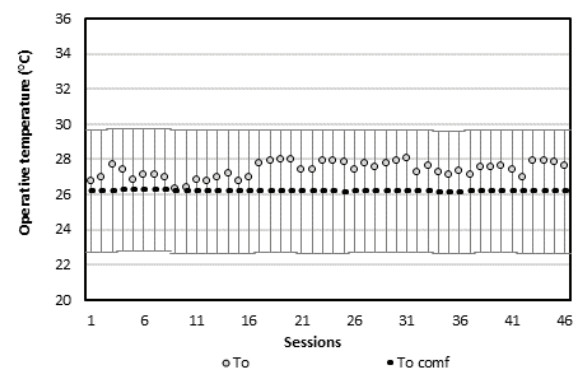


Figure 5 - Operative temperatures in the RP room and comfort range according to ANSI/ASHRAE Standard 55.

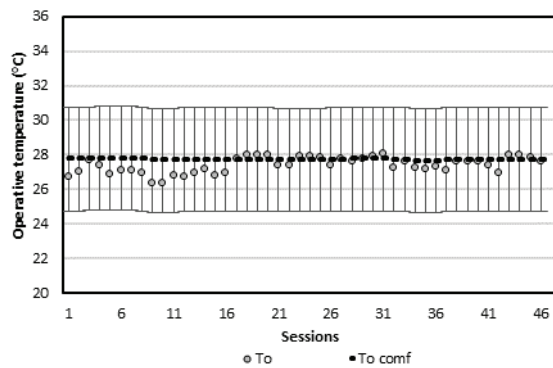


Figure 6 - Operative temperature in the RP room and comfort range according to EN 15251.

Table 3 – Comfort range averages to ANSI/ASHRAE Standard 55 and EN-15251.

	ANSI/ASHRAE 55 [14]	EN-15251 [15]
Upper limit (°C)	29.7	30.7
Neutral operative temperature (°C)	26.2	27.7
Lower limit (°C)	22.7	24.7

3.4 Subject Assessment of the Thermal Environments

THERMAL SENSATION (TS)

In response to Question 1, most of the volunteers considered thermal conditions in the test room to be either neutral (50%) or slightly cool (30.4%) (Fig. 7). The average operative temperature in the room when test participants reported a 'neutral' thermal sensation was 27.3 °C, or 1.1 °C above the ANSI/ASHRAE Standard 55 neutral temperature but 0.4 °C below the value indicated by the EN-15251 standard (Table 4). EN-15251 thus appears to give a better prediction of subjective TS under these conditions, with a trend to slightly cool sensation.

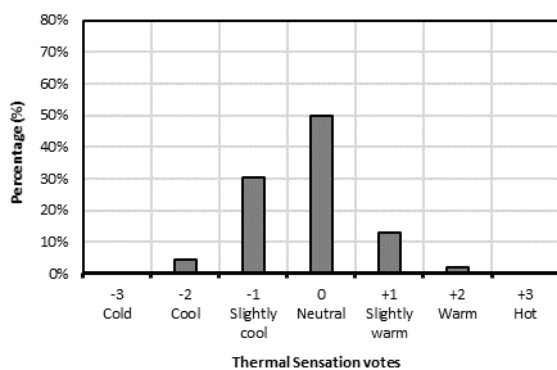


Figure 7 – Thermal sensation votes (TS).

The environment was considered satisfactory by 93.5% of the volunteers (Table 4), indicating a high degree of agreement with the PMV model adopted by ISO 7730 [9], from which it was estimated that 93.8% of the participants would report satisfaction with the thermal environment.

Table 4 - PMV and PPD versus reported data.

	Average PMV	Average reported TS	PPD (%)	Dissatisfied people according to the votes (%)
RP room	-0,08	-0,22	6,2	6,5 (2 due to cold and 1 due to heat)

THERMAL COMFORT (TC)

The average thermal comfort (TC) vote (Question 2), was 2.72 (between neutral and comfortable). Most of the subjects rated conditions as either 'comfortable' (43.5%), or 'neutral'. Only 1 participant found conditions 'uncomfortable', while 4 considered them 'very comfortable' (Fig. 8). The average operative temperature calculated when respondents rated conditions as 'neutral' was 27.5°C, 27.4°C for 'comfortable' conditions and 27.1°C for 'very comfortable' conditions (Fig. 9).

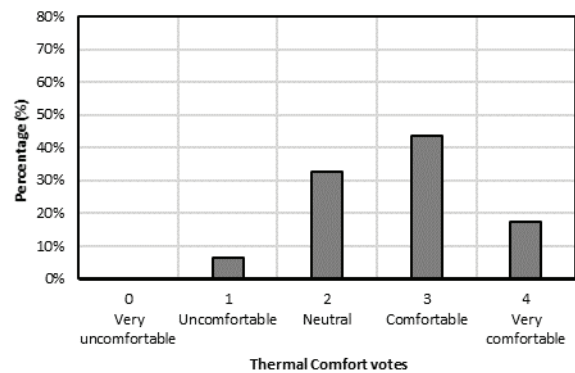


Figure 8 - Thermal comfort (TC) votes

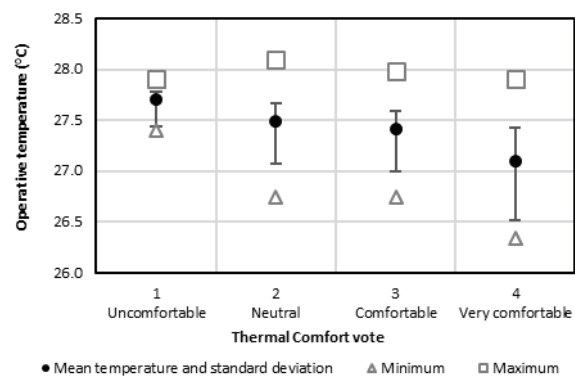


Figure 9 - Operative temperature for each thermal comfort (TC) class

THERMAL PREFERENCE (TP)

In response to Question 3, a majority of the participants voted for conditions to remain 'without change' (65.2%), and a sizable minority (30.4% of the participants) would have preferred 'slightly cooler' conditions (Fig. 10). The average operative temperature of the sessions whose participants opted for the first option (no change) was 27.4°C and that of the sessions whose participants opted for the second option (slightly cooler) was 27.3°C.

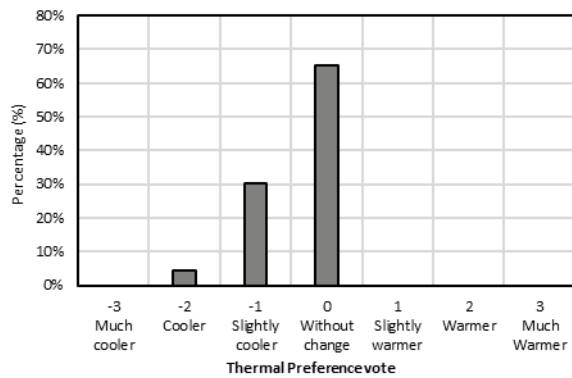


Figure 10 - Thermal preference (TP) votes

There is a small but important discrepancy between the reported thermal sensation (TS), which tended to be to the cool side (Figure 7 and Table 4), and the expressed preference for even cooler conditions (Figure 10). We hypothesize that this may be a reaction to consistently high temperatures people are exposed to outdoors, so that compensation through short-term exposure to conditions that might otherwise be considered too cool elicits a feeling of alliesthesia [19].

4. FINAL CONSIDERATIONS

The cooling system, characterized as 'radiant cooling panels coupled to a roof pond', was able to provide comfortable conditions for volunteers, despite the adverse conditions observed outdoors (summer in a desert climate). Most volunteers reported a sensation of 'thermal neutrality'.

Among the adaptive thermal comfort models assessed, EN-15251 [15] was closest to the stated comfort votes of the participants, but the PMV model was also satisfactory.

The thermal gradient observed in the room due to the colder ceiling did not appear to cause discomfort.

REFERENCES

- Garcia C, Givoni B. (2007). Cooling by roof pond with floating insulation in the hot humid climate of Veracruz, Mexico. *PLEA2007*.
- Karmann, C., Schiavon, S., & Bauman, F. (2017). Thermal comfort in buildings using radiant vs. all-air systems: A critical literature review. *Building and Environment*, 111, 123-131.
- Mirieli, J.; Serres, L.; Trombe, A. (2002) Radiant ceiling panel heating-cooling systems: Experimental and simulated study of the performances, thermal comfort and energy consumptions. *Applied Thermal Engineering*, v. 22, n. 16, p. 1861-1873.
- Sharifi, A.; Yamagata, Y. (2015) Roof ponds as passive heating and cooling systems: A systematic review. *Applied Energy*, v. 160, p. 336-357.
- Mustakallio, P., Bolashikov, Z., Rezgals, L., Lipczynska, A., Melikov, A., & Kosonen, R. (2017). Thermal environment in a simulated double office room with convective and radiant cooling systems. *Building and Environment*, 123, 88-100.

- Bitan, A., & Rubin, S. (1991). Climatic atlas of Israel for physical planning and design. *Israel Meteorological Service and Ministry of Energy and Infrastructure*.
- ISO (1998). 7726. *Ergonomics of the thermal environment-Instruments for measuring physical quantities*.
- ISO (1995). 10551. *Ergonomics of the thermal environment. Assessment of the influence of the thermal environment using subjective judgement scales*.
- ISO (2005). 7730. *Ergonomics of the thermal environment - Analytical determination and interpretation of thermal comfort using calculation of the PMV and PPD indices and local thermal comfort criteria*.
- Fountain, M. E.; Huizenga, C. (1996). WinComf: A Windows 3.1 Thermal Sensation Model - User's Manual. Berkeley: Environmental Analytics.
- Daneshvar, M. R. M.; Bagherzadeh, A.; Tavousi, T. (2013). Assessment of bioclimatic comfort conditions based on Physiologically Equivalent Temperature (PET) using the RayMan Model in Iran. *Central European Journal of Geosciences*, v. 5, n. 1, p. 53-60.
- Romana, F.; Dell, M.; Igor, B.; Riccio, G.; Russi, A. (2013). On the measurement of the mean radiant temperature and its influence on the indoor thermal environment assessment. *Building and Environment*, v. 63, p. 79-88.
- Fernández-González, A.; Costache, F. I. (2012). Cooling Performance of a Wet Roofpond System in Las Vegas, Nevada. In: *Proceedings of World Renewable Energy Forum (WREF)*, Denver: C. Fellows.
- ANSI/ASHRAE S. (2013). 55-2013. *Thermal Environmental Conditions for Human Occupancy*.
- CEN (2007). EN 15251. *Indoor environmental input parameters for design and assessment of energy performance of buildings addressing indoor air quality, thermal environment, lighting and acoustics*.
- INMETRO. (2010). *Portaria 449 - Regulamento Técnico da Qualidade para o Nível de Eficiência Energética das Edificações Residenciais*.
- Nicol, F.; Wilson, M. (2010). An overview of the European Standard EN 15251. In: *Proceedings of Windsor Conference: Adapting to Change*. Windsor, London: Network for Comfort and Energy Use in Buildings.
- Status, W. P. (1995). The use and interpretation of anthropometry. *WHO technical report series*.
- De Dear, R. (2011). Revisiting an old hypothesis of human thermal perception: alliesthesia. *Building Research and Information*, 39: 108-117.

Analysis of Different Wall Typologies: The thermal performance of a naturally ventilated social interest housing

ISABELY PENINA COSTA ^{1, 2}, LETICIA DE OLIVEIRA NEVES ¹, LUCILA CHEBEL LABAKI ¹

¹State University of Campinas, Campinas, Brazil

² Federal Institute of Alagoas, Batalha, Brazil

ABSTRACT: *Natural ventilation an essential passive strategy for thermal comfort in hot-humid regions. The existence of external elements near the building, for example, the wall, frequently impaired this resource. The objective of this study is to evaluate the influence of the different types of walls on the thermal performance of residential buildings in Brazil. The method is based on parametric analyses performed by computer simulations with EnergyPlus software. Three models of walls were defined: one without openings and two with laminated porous components. Also, variable parameters were analysed: the porosity of the wall and the incidence of wind at the frontal façade. The cases were compared considering the number of air changes per hour, the air temperature and cooling degree-hours. The results indicate that the configuration with downward laminas and porosity of 75% showed slightly better values (air change rate 36% higher and cooling degree-hours 6% lower below the reference model). However, in general, the porous walls did not show significant advantages over walls without openings. Therefore, more studies should be carried out, considering other porous components and wind direction.*

KEYWORDS: *Natural Ventilation, Wind Action, Porous Wall, Thermal Performance.*

1. INTRODUCTION

Natural ventilation is one of the leading passive design strategies for thermal comfort in hot-humid regions. It can have the potential for reducing electricity consumption. Higher values of wind velocity, up to acceptable levels, can provide physiological cooling of users and cooling of buildings [1, 2].

However, the use of natural ventilation frequently is impaired by the existence of nearby external elements, for example, wall that delimits the lots [3]. These walls are a recurrent element in Brazilian houses, necessary for security and privacy.

Previous studies realized that walls without openings increase thermal discomfort in housings due to the reduction of wind velocity and air change rate [4, 5]. Other studies have shown that different wall settings and forms can change natural ventilation conditions in buildings [6, 7]. These research studies suggest the need of further investigation about porous walls and their relationship with the building's thermal performance.

This paper analyses the thermal performance of a naturally ventilated ground floor social interest housing in Brazil, surrounded by different types of walls.

2. METHOD

Parametric analyses were performed through computer simulations focused on thermal

performance. This research was organized in three stages: (1) the choice of the wall models; (2) the computer simulations with EnergyPlus software [8]; and (3) the analysis of the following variables: air changes per hour, air temperature and cooling degree-hours.

2.1 Wall models

Three models of walls were defined: one without openings (RM) and two with laminate components (LCW 1 and LCW 2) (Fig. 1). These components were selected due to their potential to generate settings that favours the privacy of the occupants. A real single-family social interest residence was considered. The users of the residence performed several modifications to the original project, such as the inclusion of high and enclosed walls around the house.

This study analyses two variable parameters:

(1) The porosity of the wall (0%, 50% and 75%), which was one of the most relevant parameters identified in the literature [6]. The porosity calculation considered the value of the open volume in relation to the total volume of the laminate component. The percentages were determined with variations in lamina dimensions (Fig. 1).

(2) The wind incidence angle at the frontal façade (45°, 90° and 135°): the focus was to evaluate the wall performance considering the windward direction to the frontal façade, perpendicularly and obliquely (Fig. 1). This parameter was linked to the use of pressure

coefficients (C_p) obtained through Computational Fluid Dynamics (CFD) simulations [9].

These definitions generated fifteen different cases (Fig. 1).

we did not model the geometry of wall models, because the differences between them were determined by specific C_p values for each one (see the next subsection).

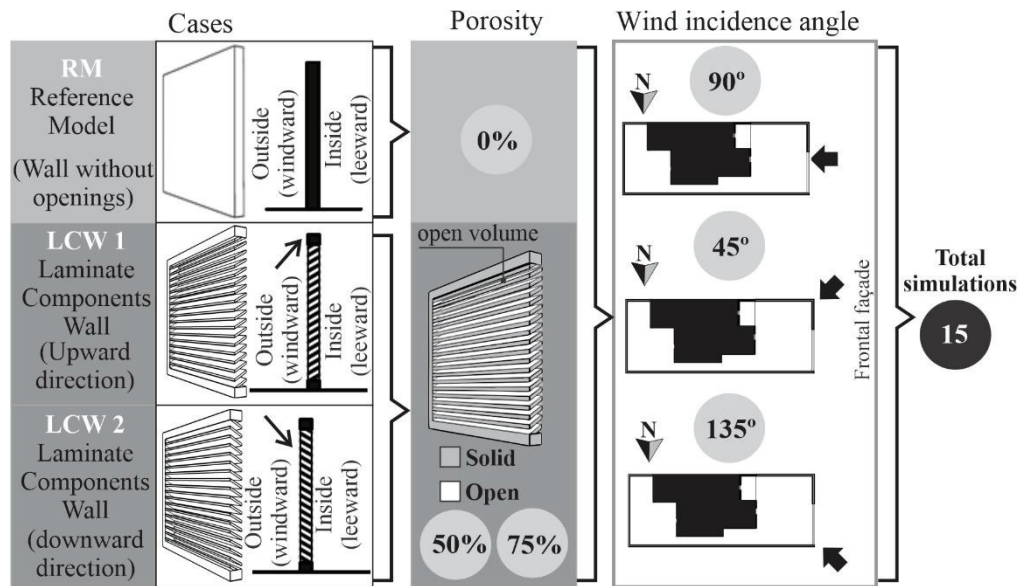


Figure 1: Cases and variable parameters of the study.

2.2 Computer simulations

The simulation settings are divided in: (1) Weather data, (2) Building modelling, and (3) Natural ventilation modelling.

2.2.1 Weather data

The weather data for the city of Maceió, Alagoas State, Brazil, was considered for this case study. The city is located at 9°40' South latitude and 35°42' West longitude with a hot-humid climate, being defined for two seasons: high summer temperatures and moderate winter temperatures [10]. The Brazilian Association for Technical Standards considers that the city of Maceió is located at bioclimatic zone 8 [11]. One of the most important passive strategies for thermal comfort recommended by the Standard for this zone is permanent cross-ventilation [11].

The monthly average wind velocity in Maceió is 3.1 m/s, varying between 2.40 m/s (May, June, and July) and 3.8 m/s (November). The predominant wind direction is Southeast (March until November) and East (December until February) [10].

The EnergyPlus weather file (epw) of Maceió in [12] was used to perform the simulations, with modifications to adapt to the analysed wind incidences (Fig. 1).

2.2.2 Building modelling

The building geometry was modelled in the plug-in Euclid for SketchUp software. The model contains seven thermal zones and the roof eaves and the walls were modelled as shading devices (Fig. 2). Therefore,

The thermal properties of the construction components and materials of the building envelope were determined based the NBR 15 220 Standard [11] (Table 1).

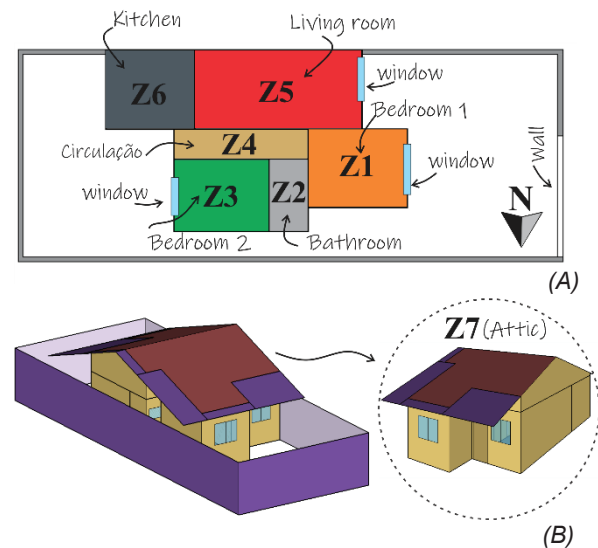


Figure 2: (A) floor plan with thermal zones; (B) building model.

The internal loads (occupation, lighting system and equipment) and schedules were based on the Brazilian Energy Efficiency Regulation for Residential Buildings [13] (Table 1).

Table 1: Characteristics considered for the construction components, internal load and schedules.

Opaque components	U (W/m².K)	Thermal capacity (KJ/m²K)	α
White wall (plaster + bricks + plaster)	3.29	247.20	0.20
Brown wall (plaster + bricks + plaster)	3.29	247.20	0.74
Floor (gravel + concrete + plaster+ ceramic)	3.27	269.36	-----
Roof (ceramic roofing tiles + plaster board)	6.80	43.60	0.75
Door (wood)	2.00	3.62	-----
Transparent components	U (W/m².K)	g (-)	
Window (colorless glass)		5.69	0.85
Internal load and schedules			
Type	Living room	Bedrooms	
Lighting	5 W/m² - 4:00 pm to 9:00 pm	5 W/m² - 6:00 am to 7:00 am and 10:00 pm to 11:00 pm	
Occupation	2:00 pm to 6:00 pm (50%) and 7:00 pm to 9:00 pm (100%)	1:00 am to 7:00 am and 10:00 pm to 12:00 pm	
Equipment	2:00 pm to 10:00 pm	not applicable	

2.2.3 Natural ventilation modelling

The natural ventilation modelling was performed through AirFlowNetwork (AFN) [8]. This module is based on the hypothesis of a uniform distribution of the surface temperature and the air within the same thermal zone.

The input data to calculate the airflow between thermal zones and the outside, such as the schedules for windows and doors openings and the natural ventilation parameters, are presented in Table 2. The schedules for opening windows were configured according to a data survey in Brazilian residences [14]. The dimensions and opening factor of the windows were based on the Brazilian Regulation [13].

The wind pressure coefficients (Cp) were inserted manually based on data obtained in Computational Fluid Dynamics (CFD) simulations [9]. Only the permanently occupied rooms (bedrooms and living room) were considered in the results analysis.

Table 2: Input data for the natural ventilation modeling.

Data	Conditions
Zones (rooms)	Z1, Z2 (bedrooms) and Z5 (living room)
Window type	Single sliding-window
Opening factor	0,5
Schedules: Windows	07:00 am to 10:00 pm
Schedules: doors	always closed
Wind Pressure coefficient	CFD simulation [9]
Discharge coefficient	0,6

2.3 Results analysis

Models with different wall settings were compared considering three variables: air changes per hour (ACH), indoor air temperatures and degree-hours based on the ASHRAE 55 adaptive comfort model, applicable for naturally ventilated buildings (Equations 1 and 2) [15].

$$\text{Upper 80\% acceptability limit (}^{\circ}\text{C)} = 0.31 \times T_{pma}(\text{out}) + 21.3 \quad (1)$$

$$\text{Lower 80\% acceptability limit (}^{\circ}\text{C)} = 0.31 \times T_{pma}(\text{out}) + 14.3 \quad (2)$$

Where $T_{pma}(\text{out})$ = mean outdoor air temperature.

The results analysis considered two periods: the most critical period of the year (a typical day in summer for Maceió-AL, February 16) and a yearly analysis.

3. RESULTS

3.1 Air changes per hour (ACH)

The model with downward direction laminate components (LCW 2) and 75% porosity displayed the highest values for ACH, especially in bedroom 1 with wind incidence angle of 45° (Fig. 3). During daytime (8:00 am to 1:00 pm), the living room had a subtle increase of ACH values for the model with upward direction laminate components (LCW 1) with 75% porosity, and wind incidence angle of 90° (Fig. 4). Lower ACH values were obtained in bedroom 2 (Fig. 5) due to the layout of the building: the bedroom 1 and the living room have windward openings (the living room being retreated in the façade) while the bedroom 2 has a leeward opening (Fig. 2).

During daytime, the air change rates increased subtly following the wind velocity, especially for the case with downward direction laminate components (LCW 2) in the bedroom 1. In general, higher ACH were obtained during the evening (6:00 pm to 10:00 pm).

We can observe a peak at 7:00 am in the bedrooms, when the windows are opened. This behaviour differs from the outdoor wind velocity profile and it can be related to the difference between the outdoor temperature (lower) and the indoor temperature (higher).

The annual analysis shows similar results. The ACH variations followed the wind velocity profile, being the highest observed values in the period from October to March (Fig. 6).

The wall with downward direction laminate components (LCW 2) shows a better behaviour than the other cases for the annual period, especially in the bedroom 1 and the living room with wind incidence angle 45° (Fig. 6). Bedroom 2 does not show significant differences between the three cases.

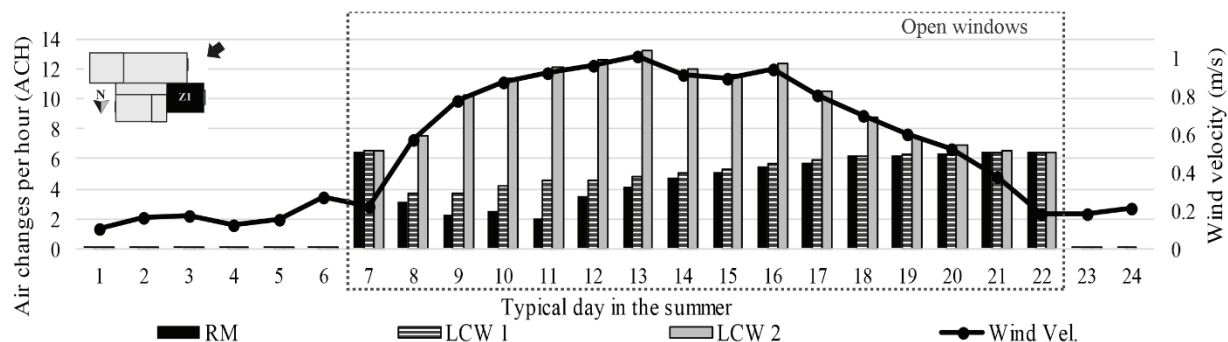


Figure 3: Air changes per hour x wind velocity on February 16. Bedroom 1 (Z1) – wind incidence angle: 45°.

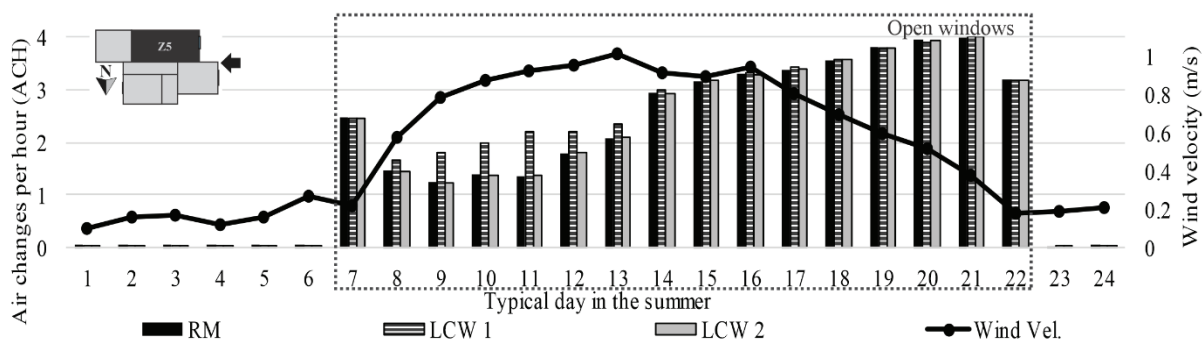


Figure 4: Air changes per hour x wind velocity on February 16. Living room (Z5) – wind incidence angle: 90°.

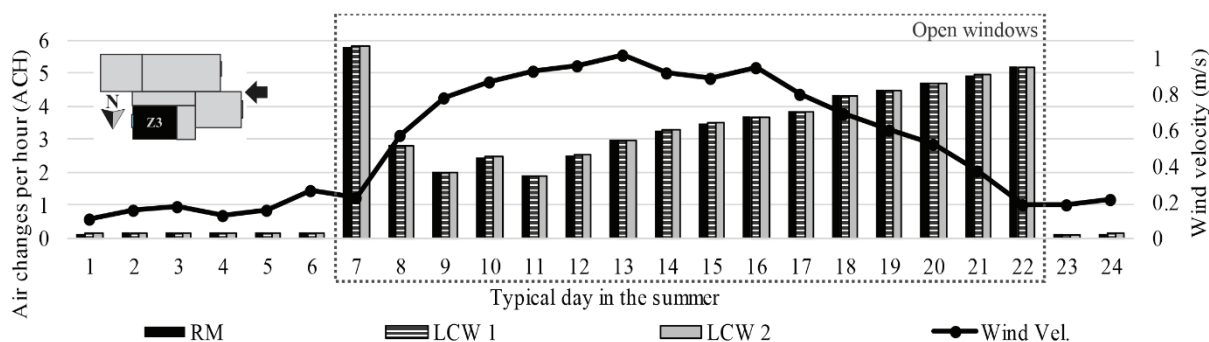


Figure 5: Air changes per hour x wind velocity on February 16. Bedroom 2 (Z3) – wind incidence angle: 90°.

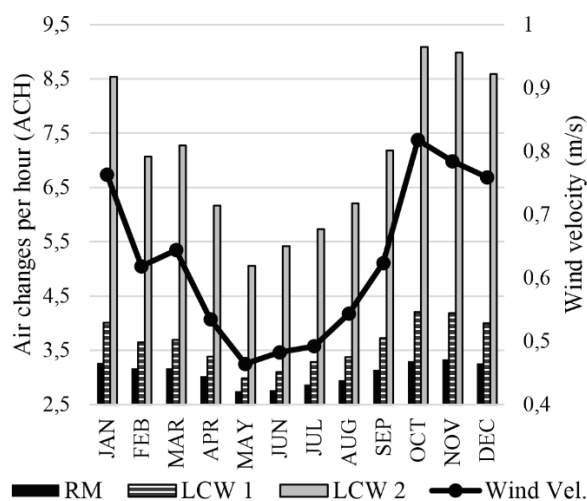


Figure 6: Annual air changes per hour x wind velocity.
Bedroom 1 (Z1) – wind incidence angle: 45°.

3.2 Air temperature

Indoor air temperature is higher than outdoor temperature, except for a short period in the morning (9:00 am to 10:00 am). The variation during the day was similar, except from 11:00 pm to 12:00 pm and at 7:00 am.

Indoor air temperature was similar for all scenarios and rooms. Bedroom 1 shows lower temperatures in the afternoon (12:00 pm to 6:00 pm) for the case with downward direction laminate components (LCW 2), with 75% porosity (Fig. 7), which matches with the highest values of the air changes per hour (Fig. 3).

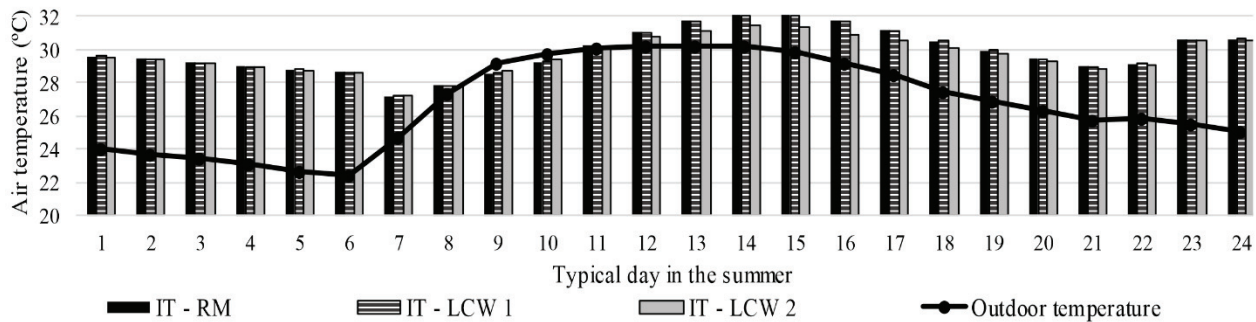


Figure 7: Indoor Temperature (IT)x Outdoor temperature on February 16. Bedroom 1 (Z1) – wind incidence angle: 45°.

3.3 Cooling degree-hours

Results show no thermal discomfort due to cold (heating degree-hours) and a high number of cooling degree-hours in the analysed rooms. However, there were no significant differences in the performance among the different wall models.

The cooling degree-hours in the living room ranged from 3400 to 3520 °Ch. The typology with downward direction laminate components and 75% porosity (LCW 2 - 75) shows better results for the wind incidence angle of 45° and 135° (Fig. 8).

The wind with 90° incidence angle shows better results for the typology with upward direction laminate components and with 75% porosity (LCW 1 - 75) (Fig. 8).

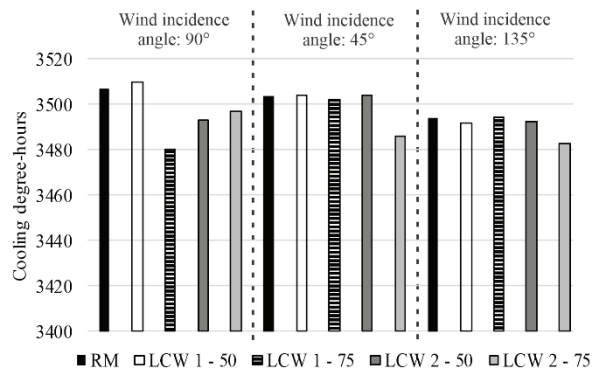


Figure 8: Annual Cooling degree-hours for the living room.

Results for bedroom 1 range from 3100 to 4000 °Ch. The LCW 2 and 75% porosity case (LCW 2 - 75) presents the lowest number of cooling degree-hours (Fig. 9). Bedroom 2 shows the same behaviour between the typologies, except for the LCW 1 with 50% porosity (LCW 1 - 50) (Fig. 10). This room presents the lowest result because of its East solar orientation, (Fig. 2).

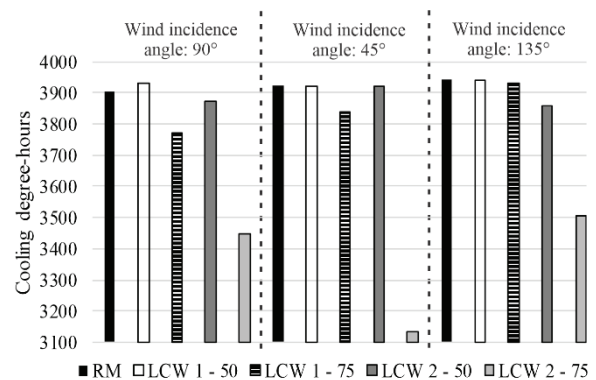


Figure 9: Annual cooling degree-hours for Bedroom 1.

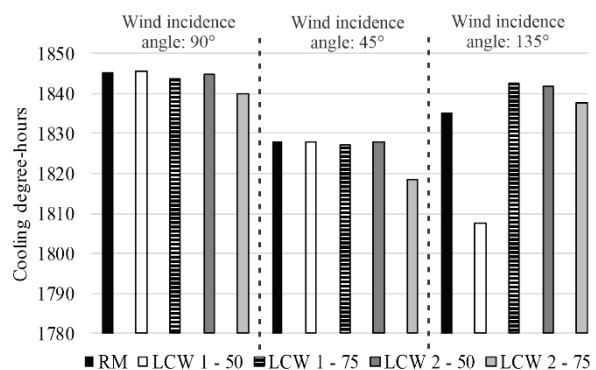


Figure 10: Annual cooling degree-hours for Bedroom 2.

In general, no significant differences in performance are observed between the wall models. However, it is observed that the typologies with 50% porosity present higher thermal discomfort due to heat. The solar orientation of the rooms influences the results. As expected, the West facing rooms show higher discomfort due to heat.

4. CONCLUSION

In this paper three models of a building's enclosing walls are compared, in order to investigate if the use of permeable walls could enhance the thermal performance of a ground floor social interest house. The following conclusions can be drawn:

- The configuration with lamina directed downwards (LCW 2) and 75% porosity showed

better results. This model had the highest air change rate (36% above the reference model) and the lowest value for cooling degree-hours (6% below the reference model).

- The 75% porosity showed better results than the 50% porosity: air change rate 16% higher and cooling degree-hours 3% lower.
- The wind incidence angle had no significant effect. The main variations in results were due to the wall typology and between the analysed rooms.

The porous walls do not have significant advantages over walls without openings, regarding thermal comfort inside the residence. However, more studies should be carried out, by considering a comparison with a building without the enclosing walls.

REFERENCES

1. GIVONI, B., (1994). Passive and low energy cooling of buildings. John Wiley & Sons, New York NY.
2. CÂNDIDO, C.; DEAR, R. J.; LAMBERTS, R. and BITTENCOURT, L., (2010). Air movement acceptability limits and thermal comfort in Brazil's hot humid climate zone. In: Building and environment, v. 45, p. 222-229.
3. TOLEDO, E (1999). Ventilação natural das habitações. Edufal, Maceió.
4. OLIVEIRA, M. C. A., (2009). Simulação Computacional para Avaliação dos Efeitos das Modificações em Casas Autoconstruídas sobre a Ventilação. Tese (Doutorado) – Universidade Federal de Campinas, Faculdade de Engenharia Civil, Arquitetura e Urbanismo. Campinas.
5. MARIN, H. F.C., (2017). Impacto de dispositivos de sombreamento externos e muro na ventilação natural e no desempenho térmico de uma habitação de interesse social térrea. Universidade de São Paulo, São Carlos.
6. CHANG, W. R., (2006) Effect of porous hedge on cross ventilation of a residential building. In: Building and Environment, v. 41, n. 5, p. 549-556. Elsevier Ltd.
7. CHANG, W. R. and CHENG, C. L., (2009) Modulation of Cross Ventilation in a Residential Building Using a Porous Hedge. In: Journal of the Chinese Society of Mechanical Engineers, Vol.30, No.5, pp.409-417. J. CSME.
8. ENERGYPLUS, (2018). EnergyPlus Version 9.0.1. Berkeley: U.S. Department of Energy.
9. COSTA, I. P. C., (2018). Influência de muros vazados laminados no desempenho da ventilação natural em habitações de interesse social. Universidade Federal de Alagoas. Maceió.
10. BRASIL (2018). Ministério da Agricultura, Pecuária e Abastecimento – Instituto Nacional de Meteorologia. Normais Climatológicas do Brasil 1981-2010, Brasil, [Online], Available: <http://www.inmet.gov.br/portal/index.php?r=clima/normaisclimatologicas> [20 April 2019].
11. ABNT - ASSOCIAÇÃO BRASILEIRA DE NORMAS TÉCNICAS (2015). NBR 15220: Desempenho térmico de edificações. Rio de Janeiro.
12. LABEEE - Laboratório de Eficiência Energética em Edificações (2018). Arquivos climáticos INMET 2018, Florianópolis, [Online], Available: <http://labeee.ufsc.br/downloads/arquivos-climaticos/inmet2018> [10 April 2019].
13. INMETRO - INSTITUTO NACIONAL DE METROLOGIA, QUALIDADE E TECNOLOGIA, (2018). Proposta de Instrução Normativa Inmetro para a Classe de Eficiência Energética de Edificações Residenciais. Florianópolis, [Online], Available: <http://cb3e.ufsc.br/sites/default/files/2018-09-25-INIR%20-%20Vers%C3%A3o02.pdf>. [10 May 2019].
14. CASATEJADA, M. P. and CHVATAL, K. M. S., (2017). Comparação entre os horários habituais e recomendados de abertura tanto de janelas quanto de portas internas em habitações brasileiras. In: XIV Encontro Nacional de Conforto no Ambiente Construído – ENCAC. Balneário Camboriú.
15. ASHRAE - AMERICAN SOCIETY OF HEATING, REFRIGERATING AND AIRCONDITIONING ENGINEERS, (2017). ASHRAE Standard 55 – 2017. Thermal Environmental Conditions for Human Occupancy. American Society of Heating, Refrigerating and Air-Conditioning Engineers, Inc. Atlanta.

Using Architectural Assessment to Evaluate User Experience in a Pre- and Post-Move Study of an Office Environment

TERRI PETERS¹ MIMI CEPIC¹ JENNIFER MCARTHUR¹

¹Department of Architectural Science, Ryerson University, Toronto, Canada

ABSTRACT: *This paper presents preliminary findings of the use of an Architectural Assessment to understand user experience in an office Case Study pre and post move. The paper reports on challenges encountered using this method, and the authors share experiences collecting and interpreting Architectural Assessment data, with the goal of informing future studies. The analysis was intended to lead to a greater understanding of the influence of environmental design on worker productivity and building performance. This paper concludes that Architectural Assessments can be a valuable tool in the context of analyzing work environments but that there are limitations inherent to this method, and caution should be taken in drawing specific conclusions. Architectural Assessments have potential to be of benefit to researchers planning future work and to offices as a way of gaining insights into how spaces are used but are not reliable as singular sources of data for comparing spaces as researchers plan a pre- and post- assessment.*

KEYWORDS: *Architectural Assessment, Post-Occupancy Evaluations (POE), Environmental Design, Performance Gaps, Observational Methods*

1. INTRODUCTION

In sustainable design, there is a need to better understand how people experience their environments, and the potential synergies and trade-offs between occupant comfort and building performance. Post Occupancy Evaluations (POE) are established methods that evaluate the discrepancies between predicted and actual performance [1]. Hadjri and Crozier (2008) traced a history of POE and report that researchers use a range of definitions, interpretations, and approaches to POE [2]. POE can address what researchers have identified the various “performance gaps” between a design’s intentions and the actual experience people have in buildings, and/or the building’s performance in use [3]. The data collected in a POE depends on who is carrying out the evaluation, the program type, and the desired outcomes. Accepted POE methods include user surveys, visual and participatory tools, focus groups and interviews, building walk throughs, and more [4]. POE are considered important tools to understand various aspects of how a building performs including how it meets the functional requirements, social and psychological performance and visual quality and satisfaction [5]. A POE can be defined as more than “an appraisal of the degree to which a designed setting satisfies and supports explicit and implicitly human needs and values of those for whom a building is designed” [6]. Details of challenges encountered when using POE are not typically published. This paper shares challenges and notes the benefits of collecting data using this method, to inform future studies.

2. METHODOLOGY

Collecting and interpreting various kinds of data rather than relying on a sole metric is more effective to understand people’s range of behaviours and experiences in spaces. An Architectural Assessment was carried out to gather data about occupant comfort and use of workspaces in two locations occupied by an office, before and after they moved. In this case, the Architectural Assessment provided insights into certain aspects of user behaviour in spaces that were not evident in the other data collection methods used. The Architectural Assessment was an observation of aspects of the work environment that studies have shown relates to employee satisfaction, including personalization, use and availability of personal storage and clutter, dishes and food providing evidence of eating at the desk, and a variety of adaptive thermal behaviours including heaters and sweaters.

The Architectural Assessment is one aspect of a larger study carried out over the course of a year to better understand the impacts of environmental design on worker productivity and building performance. This larger study collected, analysed and compared numerous sources of data including: environmental data using desk sensors; online qualitative surveys of user comfort relative to location in the office; employer provided productivity data and sick days; and, the focus of this paper, an architectural assessment of the spaces in the office.

2.1 Architectural Assessment

The Architectural Assessment is based on a walk-through observational method and was designed specifically to understand occupant comfort and uses of the office shared and desk spaces. The walk-through observational method has been identified as useful in POE and many benefits and challenges were found. The Architectural Assessments were carried out in two office spaces: the pre-move environment and the post-move environment. These were structured 3-hour walk-throughs of the building where environmental aspects were observed and documented in notes and photographs. Key data collected includes: evidence of adaptive comfort behaviors such as sweaters on chairs, personal fans, plants, desk personalization, clutter, headphones, blinds use, and use of standing or sitting desks.

2.1 The Role of this Architectural Assessment:

User behaviors in office environments are important to consider for multiple reasons including worker productivity, employee wellbeing, and impacts on a building's environmental performance. The role of the Architectural Assessment was to collect data that was not being collected in the other ways and to use focused observation, photography, notetaking and walking through a space to gain insights and give context to the other data.

There is a clear business case for providing optimal indoor environmental quality and comfort. Reports estimate that typically 1% of a business operating cost going to energy, 9% to rental costs, and 90% to staff costs, salaries and benefits [7]. The quality of the office environment and its impact on employee satisfaction and productivity can thus significantly affect the commercial performance of an organization, as demonstrated through significant research [8,9]. Quantifying the negative impact of poor thermal comfort on productivity.

Despite the use of thermal comfort standards such as ASHRAE 55 to inform building system design, the ability to measure thermal comfort as perceived by occupants is a complex challenge. There has been significant research investigating thermal comfort models and their relationship with occupant-perceived comfort [10,11,12]. The research undertaken addresses this latter impact; if workers are relying on personal fans for comfort, it is reasonable to assume the environmental conditions need improving, perhaps even if the sensor data shows otherwise.

Critical management studies have shown that from a management perspective, space serves three functions: *emplacement* – activity-specific spatial design, *enchantment* – design to ‘win the hearts and minds’ of employees, and *enactment* – the use of symbols, routes, and routines to create social meaning [13]. Within this context, it is important to consider the use of the space by employees, the impact of the design

quality and its perception by occupants, and the use of symbols and cues directing movement within the office as elements impacting occupant behaviour [13]. Desk personalization – where employees bring in their own symbolic elements to their workspace – and broader architectural design considerations have significant value from a management perspective. Traditional methods of POE engage minimally with these aspects of workspaces, and this is another way in which the value of the Architectural Assessment is evident.

3. RESULTS

The results of the Architectural Assessment are presented in terms of the pre-move observations, the post move observations of the new office, the comparison between certain environmental design elements and some findings relating to the difficulty of comparing spaces directly.

3.1 Pre-move Observations

The old office is in an urban setting, occupying one floor of a multi-story office building. Most employees sit together with colleagues in one of eight departments. Each department had a long, shared desk for collaborative work. There were two kitchenettes and a small lobby space with communal seating near the entry. The office colour scheme used mainly neutral colours with white desks, grey carpet and light grey walls. Collaborative desks were limited within the departments and were often used as storage. The private areas were restricted to 4 meeting rooms and a couple smaller spaces for discussions between 2-3 people. This office had a total of 157 desks and a total area of 1660m².

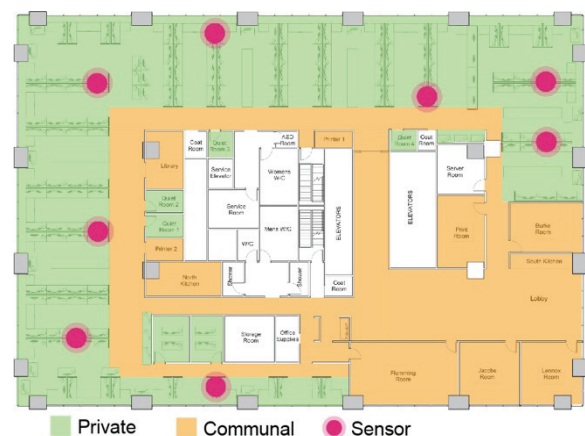


Figure 1: The first office space (pre-move). The red dots are the location of sensors used to evaluate environmental conditions. The green shows the work spaces and the orange colour shows the shared work areas.

The open plan office had large windows around the perimeter with manually operable blinds. There was non-adjustable fluorescent ceiling mounted lighting and during the walk-through it felt uncomfortably

bright. We observed only one task lights on a desk. During the walk-through we observed that the office feels cold. We observed many sweaters and scarfs left by employees on chairs suggesting dissatisfaction with thermal comfort. The windows do not open.

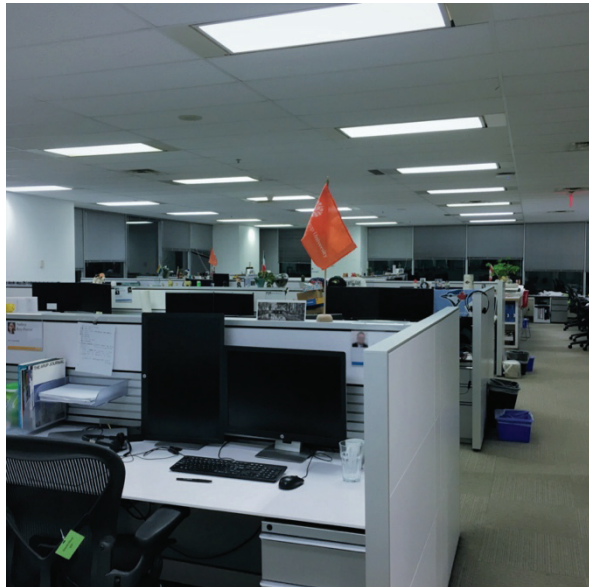


Figure 2: The interior of the first office space (pre-move) was well used and seemed that employees needed more space. Some areas were very cluttered.

The desks were arranged largely along the perimeter, perpendicular to the windows, and each employee desk area appears equal in size. All desks have daylight and a view, although view quality varies greatly. There were four semi-private meeting rooms. Almost all desks had personal items such as shoes, and boxes, stored underneath, and most also had work items such as binders, and boxes, suggesting that there is insufficient nearby storage provided per employee. We observed that most desks had a box of tissues on the desk. Many desks had coffee cups and also open food items such as chips, candy and other snacks. Solid grey partitions are used behind the desks, they are 128cm high.

3.2 Post-move Observations

The new office is also in urban setting, near to the first office, occupying three floors of a multi-story office building. As with the first office, the new office is open plan and has large windows around the perimeter with manually operable blinds. An LED circadian lighting system has been installed in the desk areas. This new lighting system varies the spectrum of color temperature and intensity to follow a specific light curve, adapting the quality of light based on the time of day, as well as the local conditions. This means the colour temperature changes through the course of the day, bluer in the morning and warmer in the afternoon. When we visited there were issues with the lighting and we were told it was not working as

planned yet. The office still seemed cold and as with the first office, the windows do not open. There were many sweaters and scarfs left by employees on chairs. The area of each floor was consistently 1520m², the number of individual workstations varied between each floor to accommodate for more communal space. The new office consisted of a total of 314 desks, double the amount of the previous office.



Private Communal Sensor

Figure 3: The new office space (post-move). The red dots are the location of sensors used to evaluate environmental conditions. The green shows the work spaces and the orange colour shows the shared work areas.

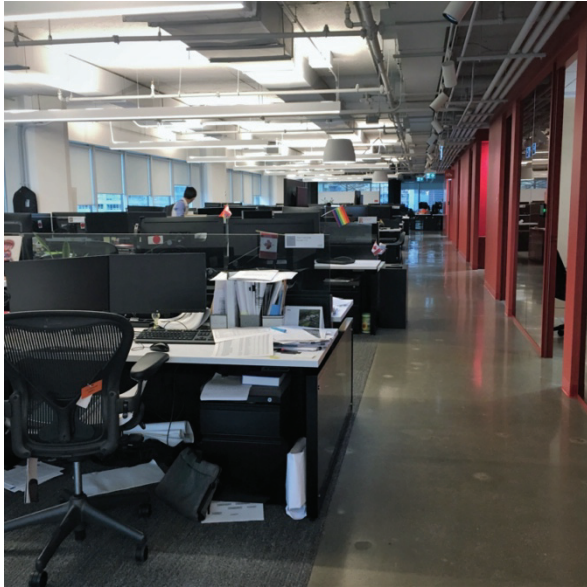


Figure 4: The interior of the new office space (post-move) has new lighting, new desks, a new colour scheme and is much larger than the old office.

The desks are arranged along the perimeter, with several semi-private, corner meeting rooms. In total there are 24 meeting areas in the new office. The chairs have remained the same in the new office but new dark tinted, transparent panels are used to cover the bottom of the desks, and are also dividers between individual workstations. The 3-drawer lockable under desk storage units have been replaced with the same size but black in colour. The new ones have cushions on top and wheels on the bottom, allowing for desk discussions and collaborative work. Rather than Individual garbage cans under desks as in the old office, there are now small, black bins at the end of every few aisles. We observed a number of food and drinks are left at desks, this may be because it is more effort to get up and walk to the shared garbage bins.

3.3 Observed Findings Relating to Both Office Layouts and Furnishings.

In each of the old and new offices, there were a high degree of uniformity in the office furniture. In the old office employees had the same standard issue chair, desk, headphones, wheeled storage, monitors and laptops. In the new office when new furniture was introduced it too was for everyone, such as the new desks. There is clearly a desire to make all of the work stations seem equal, despite the variety in the views.

In the old office, the shared tables were mainly used for storage and seemed like much needed surfaces. They were the same size in all departments, and always located behind people's chairs and offered no visual or acoustic privacy. In the new office, the shared tables are more public, facing the walkway around the core of the office. These also seemed well

used but rather dark, as the partition that offers visual privacy is a dark colour.

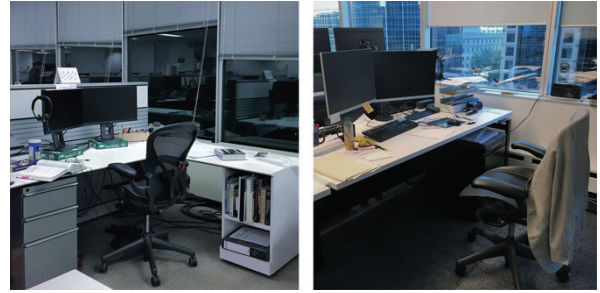


Figure 5 Comparisons of personal desks. The old office (left) and the new office (right).

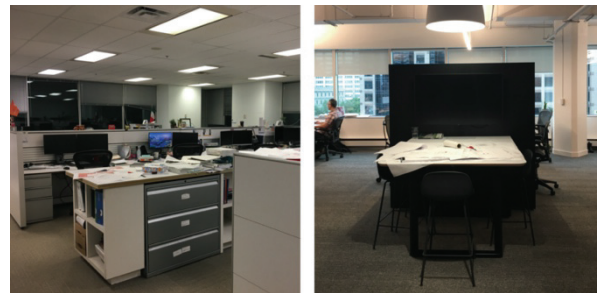


Figure 6 Comparison shared tables in the departments. The old office (left) has a long middle table within each department behind people's chairs. The new office (right) has the shared table in a dark colour, facing the corridor.

The new office saw the introduction of all desks being adjustable as sit-stand. In addition, the common area layout is different with new furniture. Now for each department, there is a dedicated common desk facing onto the corridor providing a visual buffer to the desks and also a shared desk area for layout and informal meetings. It was observed in the Architectural Assessment that people were using these desks and that they seem needed. Also, many people are using the sit-stand desks and this leads to a different work experience.

Post-move, the new office provided an increase in private work areas of various size and although the collaborative desks for the departments became smaller, more were provided, making it easier to work collaboratively. Each floor had collaborative zones from a cafeteria, to work booths to informal meeting spaces with lounge seating.

3.4 Difficulty in Comparing Spaces:

The Architectural Assessment did not yield clear and comparable results relating to occupant experience in these office spaces for various reasons. There were significant challenges to collecting, comparing and analyzing this data via an architectural analysis related the fact that the new office is so much larger than the old one, and also the new office is better equipped with new lighting and wayfinding.

The employees moved from a single level in an office building to a nearby building but this time having three floors. Numerous changes in the office layout and structure saw departments move relative to one another and – in some cases – split up and integrate with other department. This makes the data hard to decipher and impossible to clearly compare a person's experience in a department in the pre- and post- move study.

Environmental Design Improvements in the new office

In the new office, due to the larger space, there are many improved opportunities for people to sit together and collaborate.

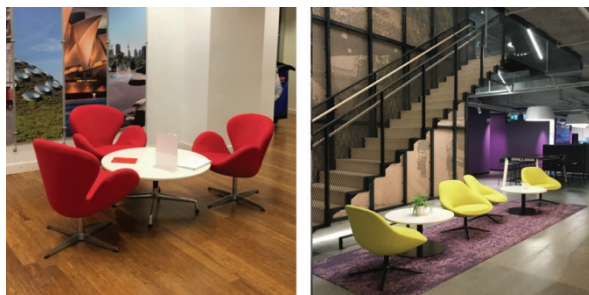


Figure 7 Comparison of spaces for collaboration are arranged differently and in different locations. The old office (left) and the new space (right).

The old space had only a few spaces for employees to sit together informally while working. The red chairs shown in Figure 7 were located in the old office near to the entry and to the dining area. The new office has several new collaborative areas near to the desks. As well, there are also other seating amenities in the new office such as booth seating away from the department, that offer visual and acoustic privacy.

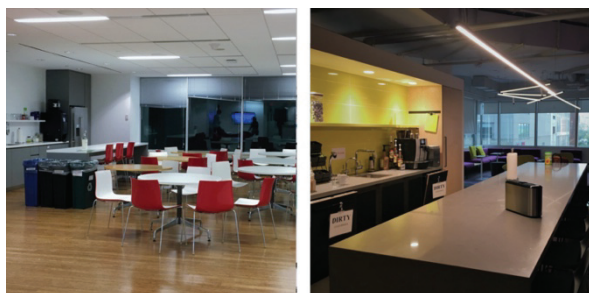


Figure 8 Comparison of spaces for coffee and eating. The old office (left) had two kitchenettes and a lunch room with plenty chairs and tables. The new office (right) has 3 kitchenettes each with bar seating areas.

The old office had a large meeting room/lunch room with a shared kitchen for employees. It was near to the lobby and away from the desks. The new office has open coffee areas on each level and the bar encourages people to eat and drink there, rather than bring food and drink back to their desks.

We observed 65 personalized desks in the old office and 188 personalized desks in the new office. We observed 19 small plants in the old office and 65 plants in the new office.

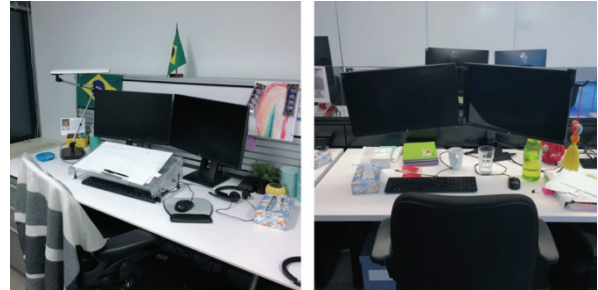


Figure 9 Comparison of personalization observed at desks. The desks in the old office (left) had fewer personalized items than the desks in the new office (right).

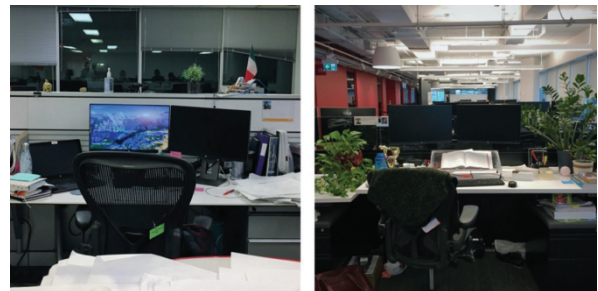


Figure 10 Comparison number of plants observed in the office. The old office (left) had fewer plants than the new office (right)

4. DISCUSSION

The Architectural Assessment provided valuable insights into how people used the spaces. In both offices many desks had signs of personalization, which is positively linked to a sense of feelings of productivity and health [14] and also related to creating a sense of privacy and avoiding emotional exhaustion at work [15]. Studies show that employee personalization of desk spaces can reduce negative impacts of low privacy at work [15], and this is relevant as both the old and new office have no full height partitions. Some personalization looks like clutter. The Architectural Assessment showed how different employees used their personal storage, as each workspace had the same locked cabinet under the desk yet some desks were extremely cluttered (mostly with papers not personalization) and others were nearly empty. Studies have shown that there are differing views of personalization and clutter in office cultures, and Wells (2000) found variations in personalization and desk clutter linked to gender and office policy [16]. There were some coffee mugs and dishes and a few food wrappers visible on desks, more in the old office,

than the new one which had visible coffee stations from more workspaces.

There were significant challenges in comparing the impact of indoor environmental quality in the two office environments: size differences, location and view differences, and interior design characteristics. First, the new office is substantially larger, arranged over three floors, with a significantly increased staffing complement, reorganized into more than twice as many departments. This size difference alone poses challenges for comparison because rather than all employees on a single floor, people's interactions change as they are spread out and work on different floors. This increases the mobility of workers within the office, and while this may have positive impacts, they are different and hard to compare. Second, the new office is in a different building, and therefore there are different views and fundamentally different interior organization, which would provide different experiences for employees. Third, the new office interior design is significantly different, with bright colours and varied furnishings used to effectively distinguish spaces from one another, and provide wayfinding as opposed to the monochromatic design of the previous office. This is evident in the themes of the meeting rooms, to the new kitchens, and new social areas. In addition, employees all have standing desks and there is more space to move around.

5. CONCLUSIONS: ARCHITECTURAL ASSESSMENTS THE VALUE OF OBSERVATION

This study found that this structured observation of the architectural and sensory qualities of the space provided an effective way to collect data not normally considered. The study collected data about adaptive thermal comfort and other aspects that have been linked to worker wellbeing. The study also found that while this data is important to collect and relatively straightforward to interpret, it is difficult to compare.

ACKNOWLEDGEMENTS

This research was partly supported by a grant from the Dean's Research Fund Undergraduate Research Experience Program at Ryerson University.

REFERENCES

1. Mallory-Hill, S., Preiser, W. F. E., & Watson, C. (2012). Enhancing building performance. Wiley-Blackwell.
2. Hadjri, K. and Crozier, C. (2009), "Post-occupancy evaluation: purpose, benefits and barriers", *Facilities*, Vol. 27 No. 1/2, pp. 21-33.
3. Coleman, S., Touchie, M., Robinson, J., & Peters, T. (2018). Rethinking performance gaps: A regenerative sustainability approach to built environment performance assessment. *Sustainability*, 10(12), 4829.
4. Hay, R., Samuel, F., Watson, K. J., & Bradbury, S. Post-occupancy evaluation in architecture: Experiences and perspectives from UK practice E & FN Spon.

5. Preiser W.F.E and Schramm, U. (1997) "Building Performance Evaluation" in Watson D et al (Eds) *Time Saver Standards*, 7th ed. McGraw-Will, New York, NY.
6. Friedman, A., Zimring, C. and Zube, C. (1978), *Environmental Design Evaluation*, Plenum, New York, NY.
7. United Kingdom Green Building Council, 2014 "Health, Wellbeing & Productivity in Offices: The Next Chapter For Green Building". Available <https://www.worldgbc.org/news-media/health-wellbeing-and-productivity-offices-next-chapter-green-building>
8. Tanabe, S.-i., Haneda, M., & Nishihara, N. (2015). Workplace productivity and individual thermal satisfaction. *Building and Environment*, 91, 42-50
9. Veselý, M., & Zeiler, W. (2014). Personalized conditioning and its impact on thermal comfort and energy performance –A review. *Renewable and Sustainable Energy Reviews*, 34(2014), 401-408.
10. Antoniadou, P., & Papadopoulos, A. (2017). Occupants' thermal comfort: State of the art and the prospects of personalized assessment in office buildings. *Energy and Buildings*, 105, 369-389.
11. Enescu, D. (2017). A review of thermal comfort models and indicators for indoor environments. *Renewable and Sustainable Energy Reviews*, 79, 1353-1379.
12. Mishra, A., Loomans, M., & Hensen, J. (2016). Thermal comfort of heterogeneous and dynamic indoor conditions An overview. *Building and Environment*, 109(2016), 82-100.
13. Burrell, G., & Dale, K. (2014). Space and organization studies. In P. d. Adler, G. Morgan, & M. Reed, *The Oxford Handbook of Sociology, Social Theory, and Organization Studies: Contemporary Currents*.
14. Kim, J., Candido, C., Thomas, L., & de Dear, R. (2016). Desk ownership in the workplace: The effect of non-territorial working on employee workplace satisfaction, perceived productivity and health. *Building and Environment*, 103, 203-214.
15. Laurence, G. A., Fried, Y., & Slowik, L. H. (2013). "My space": A moderated mediation model of the effect of architectural and experienced privacy and workspace personalization on emotional exhaustion at work. *Journal of Environmental Psychology*, 36, 144-152.
16. Wells, M. M., Thelen, L., & Ruark, J. (2007). Workspace personalization and organizational culture: Does your workspace reflect you or your company? *Environment and Behavior*, 39(5), 616-634.

The Design Process of Commercial High-Performance Buildings: with reference to the context of São Paulo and London

JULIANA PELLEGRINI L. TRIGO¹, JOANA C. S. GONÇALVES¹, ALBERTO HERNANDEZ NETO²

¹University of São Paulo, Faculty of Architecture and Urbanism, Department of Technology, São Paulo, Brazil

²University of São Paulo, Department of Mechanical Engineering, São Paulo, Brazil.

ABSTRACT: *The context of architectural design has changed in recent decades with increasing complexity of digital technologies and all the challenges related to sustainability and climate change. The demands for building performance have also changed with considerations to environmental internal quality, energy efficiency, water and material's consumption and cost, in the course of design, construction, operation and maintenance during building's life cycle and afterwards. The research based on interviews with the main architectural practices and stakeholders in the development of high performance buildings (HPB), included AKTII, ARCHITYPE, Foster and Partners, Rogers Stirk Harbor, SOM and Urban Systems Design in the city of London and Aflalo e Gasperini, Perkins + Will and Königsberger Vannucchi in the city of São Paulo, who are notable examples of design actors in their local context that brought significant transitions in the design process (DP) during the last decade. The professional experience of such references is presented in a comparative way, encompassing some key points of a holistic view of the DP of the commercial building. Finally, through the exemplification of the practice of HPB, this work highlights the current value of the design project as a whole, that contribute to the achievement of some of the sustainability and net zero carbon goals of the building sector for 2030 and 2050.*

KEYWORDS: *design process; performance design; architectural practice; high performance building; environmental performance;*

1. INTRODUCTION

The context of architectural design has changed in recent decades, becoming interdisciplinary or transdisciplinary among stakeholders, with the rapid development of digital technologies; in addition to the increase complexity of the projects and challenges related to the built environment, not least concerning issues of sustainability in all of its aspects [1]. The demands for building performance have also changed in these decades, in addition to its design and construction to the expected results of its performance on the period of operation and maintenance during its life cycle, concerns with the Environmental Internal Quality (EIQ), such as health and well-being for the occupants [2], efficient consumption of water and energy, as well as materials and their environmental impacts and all the associated costs.

The Royal Institute of British Architects (RIBA) [3] recognizes the close relationship between research and innovation in design, the role of research in design is in creating insights and knowledge in the statement [4]: *"Design practice can be understood as a form of scientific research when both are seen as projective activities."* In this way, research in design is essential in the formulation of pertinent inquiries and strategies, so as in the preparation for necessary rethinking and reskilling [1]. Although the benefits to the practice of architecture in the involvement with academic research are discussed in contemporary narrative and practice as something new for

architecture [3], what could be seen as new is the growing awareness, both in the architecture profession and established research, is that design practice is also a way of generating new knowledge and a means of research [4].

High-performance buildings (HPB) as defined by the National Institute of Building Sciences and the High-Performance Building Council (HPBC) deal with human, environmental and economic factors, having an enormous impact on society. They are also a product of the application of environmental design principles for construction, operation and maintenance, a paradigm shifts for the built environment.

In order to achieve these expected HPB objectives, a change in Design Process (DP) models it is on course. At the same token, the architecture model of most commercial office buildings, designed and built to date on a global scale, is still based on the values of an international commercial standard (International Style) fully air-conditioned sealed glass box [5]. In this sense, the same concept of commercial building project (in this work *project* refers to all phases of production of the building, from Strategic Definition to the Handover Stage [6]) has been in place since the 60's in particular in North American cities maximising usable area whilst minimising façade area and disseminating the well-known sealed glass box artificially controlled environments, with space cooling and artificial light due of deep plan buildings [7,8]. This model has been replicated since the 1980s in

parts of Asia and South America, which have places of warm climatic zones.

However, as well known, since the energy crisis in 1970, environmental issues began to be addressed, requiring civil and governmental solutions more sensitive to climate and energy-efficient buildings. In the 1980s, building performance rating systems or environmental certifications, began to be created, such as the Building Research Establishment Environmental Assessment Method (BREEAM), from 1988 in England, Leadership in Energy and Environmental Design (LEED), created in 1993 in the United States, which do not represent a design methodology for the best environmental performance but a tool to minimize the impact of buildings on the global environmental scenario. Today, there are several systems for evaluating and certifying buildings, systems that have introduced a notion of market value for environmental aspects of the building project, including certifications that focus on passive strategies and the internal environment quality and its occupants.

According to the World Green Building Council, given the fact that buildings accounts for 36% of all emissions, 40% of energy and 50% of raw material extraction in the EU, delivering a sustainable vision requires the establishment of strong policies that support transformative action within our sector [8]. Different declarations and manifests have been presented by entities and bodies of the construction sector clearly recognising the role that the building sector can play in delivering a climate neutral, addressing issues such water, health, circular economy, carbon emissions, resilience, biodiversity and cost. In June 2019 the UK Government committed to be net zero carbon by 2050, the RIBA and a large proportion of the construction industry, believe that to meet this target, practitioner must design and construct new buildings that do not need to be adapted before 2050. The achievement of such a goal requires urgent action involving immediate changes in the ways building are being designed [6].

In this context, the work presented in this paper seeks to understand how some of the main architectural practices and stakeholders in the cities of London and São Paulo conduct their design processes, taking the practice performed in London as a leading reference. History has shown that London design practices are internationally recognized for their avant-garde [10] approach with regards to HPB, with experience not only in the UK but in different cities around the world, with major influence in Asia and the Middle East. There is a movement in the building sector with a constant drive to remain in this leadership, among designers, RIBA, in addition to a growing increase in the regulatory restrictions that accompany this movement, not only to the building,

but in comfort and well-being for the user. São Paulo is the biggest city in South America with the main buildings in terms of design investment and technology from the commercial buildings sector in the continent, also where the largest concentration of buildings with environmental certification is also found.

From the main HPB designers, in the cities presented, the objective of this work is to highlight some considerations, methods and objectives in which the design teams are working, and thus contribute to the dissemination of these approaches to qualify the DP and a faster achievement for 2030 and 2050 goals.

2. THE MULTIDISCIPLINARY DESIGN PROCESS

The Whole Building Design Guide (WBDG) describes high-performance buildings from eight attributes: cost-benefit, safety, sustainability, accessibility, functionality, productivity, historical preservation and aesthetic [11]. In this definition, a project, is successful when the design's goals are identified from the beginning and maintained in proper balance during the DP; thus their interrelationships and interdependencies with all inputs in design, such passive and active strategies, building systems, building materials, security, cost, regulations and aesthetic are properly applied and coordinated simultaneously from the early stages in the DP. In this sense, with the specialization of disciplines and the increase in the number of stakeholders in the process, HPB cannot be achieved unless the integrated design approach is employed.

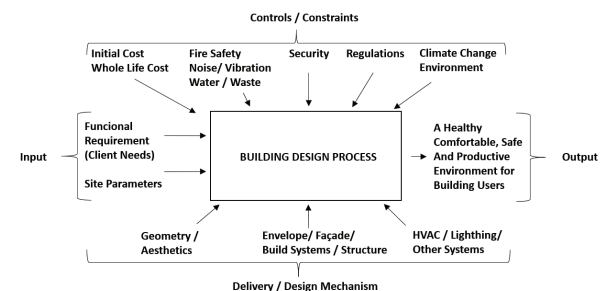


Figure 1: Holistic Approach to Design, CIBSE [14]

To achieve the new current demands, HPB requires a series of parallel and combine actions, such as the creation of more restrictive building codes and standards (ASHRAE Design of High-Performance Green Building 189.1- 2017 [12]; and Energy Performance of Buildings Directive (2010/31/EU) [13], as well as the qualification of everyone involved in the development of the project and consequently the DP as a whole, integrating agents in a more collaborative way since the early design. In this respect, three key references that address Integrated and Collaborative Design Process, bringing together the new culture of the stakeholders during the project development are: i) Environmental Design Guide A, from CIBSE [14], in

which the newest version of 2019 includes a Chapter about the quality of the environmental design, adopting a holistic approach to the design and integrated DP (Figure 1); ii) RIBA Plan of Work is a dynamic tool that helps the professional incorporated new concepts into the different design phases, its latest version, 2020; “Innovation can only be fostered if the construction industry shares experiences” [6]; iii) Integrated Project Delivery: A Guide from AIA, 2007 [15]. According to the AIA through the IPD it is possible to optimize results, increase project value, reduce waste and maximize efficiency in all stages of the design, manufacturing and construction. In this respect, an integrated multidisciplinary team, with the use of information management of construction, technology and modelling, can be a very powerful “tool” for the project delivery. Figure 2 shows the difference between conducting a typical design effort compared to IPD, where stakeholders are involved much earlier in the DP stages and, therefore, the exchange of expertise takes place from the planning stage and where the possibilities for changes and impact in costs due to more feasible changes.

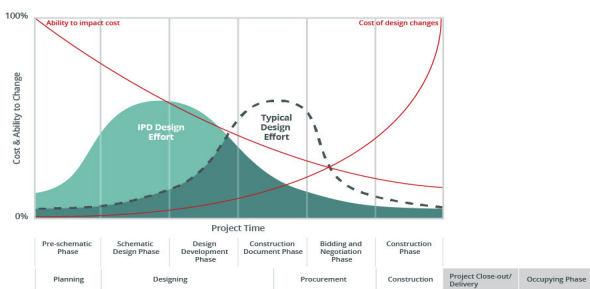


Figure 2: Integrated Project Delivery [16].

The architects had traditionally performed the Lead Design or Client Adviser [17,18], together with his DP scope. Nowadays they can combine that position or a specific professional can assume that role, which involves facilitating regular design reviews and managing a different wide range of tasks of the design progresses. They direct the work of the design team, coordinating efforts and liaising with the project team, including the client, stakeholders and the contractor, to determine the project's constraints and refine the Owner Project Requirement (OPR) as the project progresses develops [18]. Another significant change on DP was new tooling technologies such Building Information Modelling (BIM) and the environmental simulation tools, that do not only have a significant impact on the way buildings are designed, but also change the internal structures of architectural offices, the design methods these offices use and the way design is through [19].

3. DESIGN PROCESS (DP)

3.1 Methodology

This investigation uncovers the DP from the

conception at real estate until the end of the design phase, but understanding that the design covers the entire life cycle of a building. Through critical literature review, looking of specialise titles, in conjunction with Semi-structured interviews, in the cities of London and São Paulo during 2019, the questions were predetermined but the interviewer was free to modify them. The dialogue with different practices working in the disciplines inserted in the process. Some of the topics covered in the interviews were:

- 1) What is it HPB for this market? Which are the particularities of its design process?
- 2) Design projects have become highly complex nowadays, in your view, what is the role established for the architect and for the engineers in the project process? How is the integration between all designers involved in the DP?
- 3) How does the market read and understand strategies like Sustainability, Energy Efficiency, NZEB (Net Zero Energy Building), Well-Being and Carbon Emission?
- 4) What design software used in all stages of the project? How do simulations influence the design result and in what period of the project?
- 5) Is the building's operating data regarding consumption and requirements are collected and analysed? Does this data provide feedback to the project or optimize the building's operation??

All respondents are professionals who have notorious knowledge in their respective areas of expertise in the DP of HPB in the cities of London and São Paulo, they are presented in Table 1.

AREAS	NAME	POSITION / COMPANY / COUNTRY
ARCHITECTURE	Catherine Harrington	Senior Architect ARCHITYPE UK
	Daniel Toletto	CEO Konisberger Vannucchi Architecture BR
	Douglas Tolaine	Principal Design Perkins + Will São Paulo BR
	Flavia Marcondes	Project Manager Afalo Gasperini Architecture BR
	Gianfranco Vannucchi	Founding Architect of Konisberger Vannucchi Architecture BR
	Jack Newton	Senior Associate Architect Rogers Stirk Harbour + Partners - UK
	José Luis C. Lemos	Partner Afalo Gasperini Architects BR
	Marieli Sicoli	Senior Partner Foster + Partners - UK
REAL STATE	Miguel Afalo	ITECH Master / Project Manager Afalo Gasperini Architecture BR
	Diego Pastor	Former Managing Director at GTIS BR
	Daniella Equi	CBRE Project Management Director for Google USA
	Katia Goldberg	Psychologist and Director Lohn & Goldberg BR
CONSULTANTS	Luiz Henrique Ceotto	Former Managing Director at Tishman Speyer BR
	Walter Lenzi	Partner W&R Lenzi Comissioning BR
ENGINEERS	Bruno Martinez	Partner Petinelli Sustainability Consulting / NZEB BR
	Carolina Leme	Director Studio Symbios BR
	Eduardo Yamada	Building Systems Manager at CTE Sustainability Consulting BR
	Kartikanya Rajput	Head Sustainability Chapman BDSP - UK
	Klaus Bode	Director Urban Systems Design - UK
	Mina Hasman	Head Sustainability SOM - UK
	Marcelo Nudel	Partner of CA2 BR
INSTITUTIONS	Marcos Casado	Technical and Commercial Director Sustentech BR
	Marcos Maran	Director of the Board of ABRAFAC - Brazilian Ass. of Facilities BR
	José Roberto Muratori	Automation Designer / Director of AURESIDE Association BR
	Luiz Dornela	Proj Management and Business Management at Concremat BR
SIA	Ricardo Baptista	Director AKT II - UK
	Yopanan Rebello	Ycon Engineering Structure Project
	Maira Macedo	Inst. and Governmental Relations Manager of GBC Brazil BR
	Tim Dwyer	UCL Institute for Environmental Design and Engineering UK
SIA	Tercio Ambrizzi	IAG Professor at USP - Climate Change Committee BR
	Alberto Hernandez Neto	Researcher at USP Polytechnic School BR
SIA	Fabiano Ferreira	LEED Reviewer II Canada Green Building Council - CaGBC CA

Table 1: List of architectural practices and stakeholders who collaborated for the research [20].

4. DISCUSSION

Through the interviews with stakeholders, it was possible to highlight some considerations to the DP in both referential cities.

4.1 HPB and Environmental Certification

In the last three years with the greatest understanding of the issues addressed to climate change, the London market realized how advantageous it is an HPB, including long-term benefits, with the understanding that HPB can bring the quality of the environment for the occupants [10]. When the design is conducted from the beginning in an integrated and collaborative way, analysing various alternative scenarios and strategies, certification is a natural consequence [10]. According to a specialist in São Paulo, a narrower definition of the HPB was identified, restricted to that of the *green certification* alone [20], not looking at the broader context. The BREEAM certification system has proved to be a successful reference for environmental goals for projects in the UK as a whole, regardless of the level pursued. However, other metrics such whole life carbon assessment (WLCA) has recently become a major design driven tool, although the strategies for insertion in the regulations are still being discussed in new London Plan. Architect declares that the clients in the building sector, are increasingly realizing that what matters most are the sustainability strategies included in the project and not necessarily the need for certification [10]. In a nutshell, if there is no market demand for stem performative requirement no value is given to associated design decisions [10], all these strategies are still linked to capital cost, how much can be saved or how much can be added to the sale value of the building [10].

In São Paulo, the environmental certification is defining a new design culture over the past 10 years and LEED certification is the most representative in office buildings [21]. As the criteria for obtaining certification, they are linked to the quality and performance standards and requirements of their countries of origin, consequently the São Paulo DP had to adapt and qualify for its achievement, since local regulations do not include the same requirements. Furthermore, currently, a growing interest has been seen for certifications related to health and environment quality [21], begin considered as the new differential in the São Paulo market [21]. On the other hand, issues like carbon emissions are not yet on the agenda for discussion, but according to architect, it will naturally become a key topic as the market mature regarding environmental issues [21].

4.2 Design Process – The Role of Architect and Client

In both cities, agents in the process used the analogy with the architect being the conductor of the DP, orchestrating all the agents involved [10,21]. Experts point out that architect due to his greater proximity to the client, is responsible for introducing issues such as sustainability, climate change [10], considering a balance between aesthetic and

functional issues, in addition to demonstrating the importance of inserting IPD into the DP [21]. Architect in UK, considered that the architectural design is the one with the major scope, he gives the creative direction, keep everyone in tune for fluid design [10]. The responsibility of the architect has been gradually increasing in recent years [21] : i) the number of agents involved among architects, engineers and consultants has also grown due to multidisciplinary, we are living in an environment of specialization, becoming more and more granular [10]; ii) the expected high-performance result during the building's operating phase; iii) and increasing restrictions on local codes and standards.

As consequence the need for an interrelationship between the architect and the multiple design disciplines and the client it is necessary. Influential engineer, in London, said it was noticed that the traditional way of conducting the design is a very beginner format [10], and that ends up requiring a rework, explicit an architect from São Paulo [21]. The objective of the collaborative DP is that there is an exchange of knowledge between the professionals involved in the design and consequently qualify the DP. In London, what is perceive, when the collaborative integration of the project team is already incorporated into the office culture, the approach will always be the same, regardless of the size or typology of the building [10].

What can be seen in the architectural offices in São Paulo is that the conduct of the project is changing. IPD is recognized as a project qualification strategy by architects, who have sought to insert it into the process [10,21], however flow of agents in the project needs to change [10], which leads to a change in the flow of investment from the beginning of the process. From a perspective of an engineer in London, another significant change is the participation of the client who needs to decide parameters such as performance very early [10]. Stakeholders in São Paulo are being inserted in the initial design phase, but the interrelationship between them still needs to occur in a more collaborative and integrated way.

According to experts in both cities, key point for obtaining the best results for the ownership is the role of the client. A change in the mindset that establishes premises at the beginning of the project will impact the occupant's behaviour and occupation patterns in the building [10]. The client has a fundamental role in defining the dynamics and structure expertise and decision-making responsibilities, in addition to encourage the right level of exploration at early design stages to find the best design for the set- performative aims [21]. The opposite is also valid, when the client does not have the necessary knowledge to lead and all team members do not share common objectives, it is very

Likely that the project will achieve the best possible high-performance goals [10].

The project management is extremely important and is related to topics such as scope / schedule / cost and etc. In the last few years, it was inserted into the DP, however, increasing the level of bureaucracy and affecting the DP negatively, as his background is not related to design, there is a lack of understanding of how environmental issues are contemplated in the DP [10]. In this sense, the PMBOK is focused on deliverable and not benefit, so it is not suitable for the DP [21]. Within the already complex network of specialists, new professionals were added to the design team, into the London context, a Project Management that accompanies all meetings and guides the architects and the scope limits established in the contract [10]; and the Lead Design who was also inserted in the process to collaborate with this communication, it aims to organize all stakeholders with a holistic view of the DP, which gives him autonomy and knowledge to carry out the necessary changes to the achievement of the project goals and cost. With a distinct role from Project Management, Lead Design ensure communication and negotiation among all stakeholders in the DP, adding collaboration to the process. The composition of both agents, project management and client adviser, with the technical vision inserted in the management decision making is fundamental. As highlighted, each professional will limit their advice to topics within their areas of expertise [18].

The project starts from the design briefing defined together with the client. The construction of an OPR as a technical requirement, as declared by influential engineer, it needs to be detailed in the Concept Design Stage, needs to be a life document, which will be updated and have flexibility to accommodate changes during the process [10]. OPR will contain the objectives to be achieved by the design team; support the decision-making during DP; and it will be the metric for the success of the project, it is not a usual practice in São Paulo. "OPR is rarely seen in the project, usually what is used is the basis for approval by certification. The design briefing ends up being the certification" [21].

4.3 Design and Simulations Softwares

BIM (Building Information Modelling) has been used since 2017 in the development of HPB design, in São Paulo in the vast majority of architecture studios, which is perceived as an irrevocable trend, as in London. Another gain added to the process by the green certifications was the inclusion Environmental Simulations Tools (ESTs). The most commonly used tools simulations are the ones related to shadows and radiation analysis and energy modelling, mainly for systems, but also used to simulate future scenarios related to climate change. The ESTs help architects to

optimize the early design stages and quantify in more detail the performance figures, in order to ensure compliance with the project goals and certification levels, in the most advanced design phase. Simulation are normally used during the whole DP development in London [10]. In counterpoint, in São Paulo the simulations end up being used in specific phases in the design, recently linked to the NBR 15575 Performance Standard [21], mainly when they are necessary for the validation of the certification [21], often missing its role in influencing fundamental design decisions. Through parametric studies, used by architects, engineers and different consultants in the initial design phase [10], the volume of tested scenarios and design produced is much larger in London compared to São Paulo. However, the investment and specialists necessary for this design task, is not identifies in the context of São Paulo [10].

4.4 Feedback - Operation and Maintenance

Strategies for operation and maintenance (O&M) of buildings are being increasingly inserted into the development of the DP. In this respect, a new strategy that is beginning to spread in London is the use of the Data collected in buildings, such as through the Building Management System (BMS). Through the analysis of these Data, it is possible to draw comparisons between design outcomes and local benchmarks, with benefits in the optimization of building's operation, but also to provide feedback to stakeholders to requalify the DP for future enterprises [10]. This analysis of the BMS data for monitoring energy efficiency and comparative analysis with benchmarks is a recent practice in São Paulo, but the actual improvement of the DP has not yet been put in place. [20]

5. FINAL CONSIDERATIONS

This study aimed to describe how some of the main architectural designers and different stakeholders develop HPB in the cities of London and São Paulo, and how their design processes were carried out and lead. Having London as a reference, in a comparative way, with a holistic approach, trends and changes elapsed in the last 10 years in the DP of commercial buildings.

Through the interviews, it was possible to notice trends that will influence the future in the building sector, pointing to continuous improvement, that has had its limitations within the local context and the culture of the DP in each city. Improvements in the process and in the information deliverables that has brought about a change in the way buildings are being designed, constructed and operated. Performance design with the ultimate goal of a holistic and cyclical view of the entire process, with benefits to building's environmental performance in a rather broader sense.

Another major conclusion from the interviews is that the need for new knowledge about the practice of architecture and the performance of buildings in terms

of climate change, efficiency in consumption and the internal environment quality is an important impetus for research. This awareness puts pressure on all stakeholders involved in the design, construction, operation and maintenance processes to develop new knowledge and approaches to the current issues already presented. It is in the DP stage that the requirements and strategies foreseen for the construction phase and for the operation and maintenance phase need to be raised and contemplated, in order to achieve the expected results for the building during its life cycle and afterwards, within a circular economy concept. If these are not inserted during the DP, their insertions will be much more difficult to achieve and the cost of obtaining them will often make them financially unfeasible. In the Design Conception Stage, is where you have the lowest proportional cost and the greatest margin for change, through studies of analytical scenarios; different architectural designers and stakeholders, with the help of digital tools and new types of collaboration in new and integrating ways of design, managed to deal with the complexity and multidisciplinary of current DP to achieve a HPB.

Within the DP culture of each city and its possibilities for expansion and qualification, a fundamental action is the insertion of restrictions and incentives by local authorities. In Sao Paulo, in terms of DP, the requirements rule went up, in view of the certification metrics, the entire market chain was qualified, however, some points need to be developed and improved while others still need to be implemented. The same can be said about increasing restrictions and regulations as well as tax incentives, which need to be implemented by local governments.

The role of the architect and engineer is also one of education with the market, transmitting his expertise to members of the value chain of the building sector. The cost is still one of the biggest limitations in the process, and normally when you have never done specific work, your risk and cost margin inserted into the process is higher. In this sense, the transmission of this expertise, in order to leave the status quo, is important to be able to insert innovation into the process. Concluding a key point perceived in both cities was that in order to reach the level required for the HPB, the flow of conduction during the project design is extremely important. Management with the technical vision inserted in decision making is fundamental. The management decision matrix together with technical, in a conciliatory and viable way for each project, will directly influence the expected results for that project throughout the entire life cycle of a building. In addition to that, the change in the culture of the DP, in order to achieve net zero carbon buildings in 2050 is in progress but there is still a long journey, the time

needed to reach this goal is shorter, in a market where changes tend to be very slow.

ACKNOWLEDGEMENTS

The authors are grateful to all architectural practices and stakeholders who have contributed to this research.

REFERENCES

1. Hensel, M., Nilsson, F., (2016). The changing shape of practice. Routledge.p. xiv.
2. Olesen, O. (2005). Indoor Environment- Health-Comfort and Productivity. International Center for Indoor Environment and Energy, Technical University of Denmark. Proceedings of Clima.
3. RIBA - Royal Institute of British Architects, (2014). Architects and research-based knowledge.
4. Leatherbarrow, D., (2012). The project of design research. In: Hensel, M., ed., Design Innovation for the Built Environment. Routledge, 11.
5. Gonçalves, J. C. S.; Umakoshi, E. M. (2010). The Environmental Performance of Tall buildings. Earthscan.
6. RIBA - Royal Institute of British Architects (2020). Plan of Work 2020 Overview. Foreword.p.118
7. Gonçalves, J.C.S. (2016). The Value of Environmental Design in the Context of the Green Economy In: PLEA 2016, 32nd International Conference on Passive and Low Energy Architecture, Los Angeles: PLEA, v.3. p.1757 – 1766.
8. Gonçalves, J.C.S., Bode, K. (2011). The Environmental Value of Buildings. In: Innovation: The European Journal of Social Science Research. V.24, p.31 – 55.
9. WGBC- World Green Building Council, (2019). Europe publishes advocacy manifesto, A Sustainable Built Environment at the Heart of Europe's Future.
10. Industry Professional Statement in an interview with Juliana Pellegrini in physical meeting, London, UK, (2019).
11. WBDG- Whole Building Design Guide, (2003). Access: May 2020 <https://www.builup.eu/en>.
12. ASHRAE-American Society of Heating, Refrigerating and Air Conditioning Engineers. Design of High-Performance Green Building 189.1-2017. May 2020 <https://www.ashrae.org/technicalresources/standard-189-1>
13. Performance of Buildings Directive (2010/31/EU). Access: May 2020 <https://www.wbdg.org/>
14. CIBSE- Chartered Institution of Building Services Engineers. Guide A: Environmental Design 2019.
15. AIA - The American Institute of Architects. Integrated Project Delivery: A Guide. Version 1, (2007).
16. Castellanos, S., (2010). Integrated Project Delivery: A History of Leadership, Advocacy, and Commitment. Parametric and IPD. California Council arcCA issue 10.1
17. RIBA- Royal Institute of British Architects, (2019). Independent, Expert Advice that Puts you in Control of your Construction Project. Client Advisers. RIBA Architecture.
18. Sinclair, Dale., (2019). The Lead Designer's Handbook. RIBA Publishing.
19. Naboni, E., (2013). Environmental Simulation Tools in Architectural Practice. The impact on processes, methods and design, Conference: PLEA 2013.
20. List of architectural practices and stakeholders who collaborated for the research. Produced by the authors.
21. Industry Professional Statement in an interview with Juliana Pellegrini in physical meeting, São Paulo, BR, (2019).

Severiano Mario Porto's Projects in the North of Brazil: a Bioclimatic Research About the Amazon Architecture

AYANA DANTAS DE MEDEIROS, CLÁUDIA NAVES DAVID AMORIM

University of Brasilia, Brasilia, Brazil

The architect Severiano Mário Porto is a Brazilian icon. In Amazon region, his projects outstanding characteristics show the local climate potential, bioclimatic strategies, flexible design, cost optimization, renewable materials and regional labour techniques. This paper aims to present the results of an investigation to catalogue the bioclimatic strategies used Severiano Mario Porto design in Boa Vista buildings, focusing on daylighting, shading and ventilation strategies, also evaluated with user's perspective. The method includes documentary survey and case studies selection, the use of morphological diagrams, on-site monitoring, user feedback and computational analysis. The results identify 14 buildings and 4 from these were selected as case studies. Morphological diagrams demonstrate mixed solutions for design, resulting in an expressiveness work for treatment of local impasses. On site monitoring reveals problems related with low illuminance levels and some minimum view quality, due to solar protection elements. The users' opinion demonstrate satisfaction with the luminous environment, although it is always necessary to have artificial lights on. The results of lighting computer simulations, however, shows that the original project have good daylighting levels, before interventions like solar controls glazing with low transmittance. The main strategies used by the architect were... Crossing data, it is possible to conclude that the original projects of Severiano Mário Porto in Boa Vista present good quality in terms of daylighting and shading but, in practice, wasted by inadequate interventions

KEYWORDS: Bioclimatic architecture; Severiano Mario Porto; daylight; shading; natural ventilation.

1. INTRODUCTION

In architecture, the relation between building and users is a challenge to design with local conditions. Bioclimatism can be a way to match the challenge to build in a respectful and interactive relationship between man and climate. In this context, questions like daylight, ventilation and user are important aspects to be evaluated.

Regarding the use of daylight, this is an essential resource, with great capacity to transform the users experience in internal spaces into something pleasant [1]. Lighting a room is among the main reasons why architects try to apply daylight to their projects and, in addition, researches demonstrate the human health expectation to better responds for stimulus for natural exposure, mean a strong preference for the use of daylight. However, satisfactory levels of light are variable and individual [2].

About natural ventilation system, it is something defined in the initial design, privileging, or not, the orientation for prevailing winds and using devices that will favour heating or cooling in the environment [3]. In these sense, the passive cooling techniques in buildings are effective and can contribute significantly to reducing the thermal internal gains and can result in good conditions of thermal comfort and indoor air quality, as well as reduced energy consumption [4].

In these sense, the assertive application of resources such as daylight and natural ventilation in

architecture needs to be planned, where it is necessary to understand the comfort and climate criteria, realizing the influence of these elements in the built environment, since applying them can cause variations and unwanted behaviour in the building internal microclimate [5].

Thus, buildings in tropical climate are submitted to a dilemma: allowing daylight and natural ventilation to penetrate without solar gains. In this context, shading is one of the most effective resources to combat the discomfort; extensive roofs shadowing openings can be a good strategy [6]. Specifically, in hot and humid climates, like Amazon region, all openings and windows need a system that avoids direct sunlight, through the use of techniques of shading [7].

The shading deals with permanent or temporal, reduction of solar radiation transmitted through the building components. Dominated by need for cooling, solar control devices should reduce solar gains as much as possible, allowing enough daylight and visual contact with the view out. This can be done using external and internal devices, or even using variable transmittance glazing. Besides, researchers indicate that high luminosity of the sky, who causes glare, need control and the vision of the celestial dome must be limited by blockers as architectural frames or, even, through vegetation [6-7].

So, tropical buildings are typically composed for a light construction, with large openings and shading devices. However, the architecture always had as first paradigm meeting the expectations of users, from the basic aspects of habitability into the aesthetic enjoyment that this shelter can provide to humans. This is a professional challenge, who sometimes prioritize aesthetic-formal values over the performance of the built environment and its functional quality [8].

In these prerogatives, it is proposed the research about projects by Brazilian architect Severiano Mário Porto in the extreme North of Brazil. Icon of Brazilian architecture in second half of XX century, Porto studied in Rio de Janeiro, but his projects detach in Amazon cities, with outstanding characteristics in projects that enjoy the local potential and apply contemporary techniques, using resources like integration and harnessing the local bioclimatic potential, flexible design, cost optimization, renewable materials and regional labour techniques. Throughout almost 50-year career, his professional objective was to find simple solutions, conducted correctly, integrated into the site and well according to the scale of the problems [9].

The focus of this research is about buildings in Boa Vista city, capital of Roraima stated, in the extreme North of Brazil. With a hot and humid typical climate, the city is too close of Equator Line and has two defined seasons: summer (dry) and winter (rainy). According local data, the average temperature rates is around 27°C and relative humidity around 75.9%, being constantly in all the year. Sky condition is dominance for partly cloudy and, about sun exposure, the average is 4,500 Wh/m³ [10].

So, this paper aims to present the results of a master's research, in order to catalogue the bioclimatic strategies used Severiano Mario Porto work in Boa Vista buildings. It is analyse regarding about daylight, shading and ventilation strategies, allied with user's perspective. In this article, the results report about documentary survey and case study selections, morphological evaluation of buildings, apply a monitoring protocol and computer simulation for daylight.

This investigation integrates the work for International Energy Agency (IEA) for Solar Heating and Cooling Programme (SHC), in Task 61, Annex 77 - *Integrated Solutions for Daylighting and Electric Lighting*, Subtask D, who treats about lighting and general aspects, like energy, circadian elements, photometry and users. The aim of Subtask D is develop a monitoring protocol to evaluate the case studies, in different contexts, under a common framework [15].

2. METHOD

To achieve the proposed objectives, were necessary to work in different approaches, since access and treatment of primary data, until the exercise to validate qualitative an architecture. In this sense, applied some steps, aimed at achieving result, and for conclusions, analysed of data with cross studies, with attention to the bioclimatic elements present in the select projects, especially about daylight, shading and natural ventilation.

2.1 Documentary survey and case study selection

The first step is based in search for information in documents without scientific treatment, using materials that lack analytical procedures, consultation primary sources. Accordingly, the documentation of Severiano Mário Porto's projects was consulted. This material is part of Research and Documentation Centre, of the Faculty of Architecture and Urbanism of the Federal University of Rio de Janeiro.

After, began the selection of case studies. For a representative analysis, the focus was to identify the buildings with best conservation status in relation to the original project. So, applied the Brazilian standard about Valuation of Goods of Historical and Artistic Heritage [11] as an instrument. This standard parameter analyses the original project and classifies buildings according the state of conservation and integrity, in order to appoint it like preserved, restored or uncharacterized.

2.2 Morphological diagrams

To identify bioclimatic strategies in case studies, the methodology proposed are morphological diagrams. The instrument is a document for qualitatively evaluates architectural projects. It is apply with objective to composition a repertoire of architectural typologies and can be used in early stages of project and in exist building, in order to verify possible aspects that can still be optimized [12]. The selected diagrams study issues related to daylighting [12] and natural ventilation [13].

The morphological diagrams are compose into three moments: local place, building and environment. Through technical pieces, such as location, floor plans and cuts, it is possible to develop results in a report that presents the architectural solutions found.

2.3 Monitoring Protocol

The on-site verification of the lighting condition was determined using the guidelines of the Monitoring Protocols of the International Energy Agency [14-15]. According to IEA [15], protocols are instruments with credit and support, where a big amount of information is collected and made

available, in order to summarize this in an objective and easy to understand.

These protocols are integral part of research by the IEA-SHC Task 50 [14] and Task 61 [15], both about lighting with energy aspects. The *"Monitoring protocol for lighting and daylighting retrofits"* - Task 50 [14] and the *"A monitoring protocol to evaluate user-centered integrated solution"* - Task 61 [15] discuss procedures to verify the lighting condition in an environment. The mentioned documents establish measurement mechanisms on-site that have a common structure. In the developed dissertation, the dimensions of study used were photometry and users, with photometry and view out analyses and questionnaire survey.

2.3.1 Photometry and View Out

The photometric dimension includes environmental and spatial aspects of lighting. According to consolidated surveys, some of the quality indicators are illuminance and view out [15]. The protocol suggests the separate measurements with only daylight, only artificial light and both combine, in order to approximate the measured results to the real condition. In this research, data were collected for the analyses about: reflectance of surfaces, illuminance average, illuminance on the task, uniformity, and quality of the view out.

For the average illuminance verification, the protocol proposes a grid in place, which divides the room in small measurement areas. The method consists of a measurement points that must be drawn from the central axis of the window, towards the back of the room. A first measurement is made at 0.5m from the window, and then from 1.0m to 1.0m [14]. The capture of illuminance must be determined at 0.80m above the ground, with a luxmeter. These grid measurements assist in analyses of distribution of illuminance, illuminance on the task and uniformity of light. Simultaneously, the measurement of the global diffuse external illuminance is performed, for every 5 minutes. This measurement takes place outdoors, without obstruction of direct solar radiation, shading the external luxmeter cell with a small disc and recording the sky condition on time.

To verify the quality of view out, the monitoring protocol indicates the method proposed by European Standard for Daylight in Buildings [16]. This document present that the aesthetic value of a user's scene is related to complexity, maintenance, temporal aspect, among others. The composition can be examined with a photograph of the view out, taken from the landmarks within the environment (for this study, the photos was taken in centre of the rooms). For a good composition, the elements generally appreciated should not be fragmented, and a balance between the left and right sides of the image must be

guaranteed. In addition, information for location, weather, climate, surroundings and the flow of people outside is also important.

2.3.1 Questionnaire survey

The questionnaire applied is based on the proposal of International Energy Agency (IEA) [15], from April 26, 2018 version. This document was translated and adapted to investigate user's opinion regarding daylight and well-being conditions in the study case. Thus, the resulting document consisted of 50 questions, divided into 4 sections, namely: section 1 - general data; section 2 - social and physical climate; section 3 - user's experience with lighting; and section 4 - user's interest in building. It consisted of 4 pages, with predominance of objective answers.

2.4 Computer simulation for daylight

The computer simulation of daylight was modelling by DesignBuilder, version 6.0, and Radiance program. The idea was to cross these step results with data from morphological diagrams and measurement on site, simulating the original condition on Severiano Mario Porto design, without some recent changes in space, like addition of films on glass and internal layout.

3. RESULTS

3.1 Documentary survey and case study selection

According to the documentary survey, Severiano Mario Porto developed 14 projects in Boa Vista city. The original records are outdated and without any characterization of the current state of buildings. This information was updated and organized.

The state of conservation of Severiano Mário Porto's buildings in Boa Vista was the main criterion for choosing case studies. The cases that interests this research are those in which the project intention was preserved or partially preserved. From the 4 case studies selected, 03 are schools, partially preserved, and 01 is an institutional building for public use (Figure 01), with a good state of preservation.



Figure 01 – preserved case study

These 04 case studies were analysed with morphological diagrams; the on-site monitoring was

performed in the institutional building, in better stage of preservation (Figure 1), together with questionnaire survey and daylight computer simulations.

2.2 Morphological diagram

The morphological diagrams from 4 selected case studies appoint the common elements used in project for Severiano Mário Porto in Boa Vista: buildings with façades of low reflectance and specularity, high opening rates on the façades (between 25% and 50%); façades not uniform in relation to solar orientation; internal spaces with adjacent cross ventilation and use of pivoting windows (rotating on the vertical axis); and brises-soleil, cobogos, eaves and marquees, pergolas, and vegetation as elements of sun protection.

On the roof, all buildings have a robust eaves, with more than 2 meters, where this advance function as a horizontal element of shading. In schools, the corridors are used as structure and addition to sun protection (Figure 2).



Figure 02 - corridor on a Severiano Mario Porto school, east facade

With brises-soleil (Figure 1), it is possible analyse that the solutions, horizontally and vertically, provide protection at times when the solar path is most critical, close to midday (Figure 2). Although the often excessive sun exposure in Boa Vista, studying with solar map, it is possible verify how the structures show good shading angles, allowing the penetration of heat daylight until 9 am in the Northeast façade and after 3 pm on the southwest façade (a critical orientation).

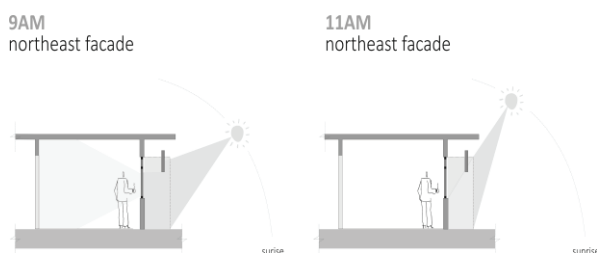


Figure 03 - solar path in case study room

The organization of the building's volumes also enables self-shading. In the case study in better conservation condition, the building is envelope with fixed brises that also collaborate as a solar protection element (Figures 1 and 3), without, meantime, compromising the view out.

Regarding window frames, there is a notable design intention in the use daylight and ventilation in the architect choices, with windows and structures designed in order to optimize the entry of daylight and circulation of the winds with the use of pivoting windows, lamellar openings and translucent surfaces. In classrooms, the distribution of frames in bilateral way, on opposite faces and with different heights, helps in cross-ventilation, indicated for the local climatic context.

3.3 Monitoring Protocol

3.3.1 Photometry and View Out

For the systematization of data from the application of the IEA Monitoring Protocol [15-16], it is worth commenting on some information observed. The first one is about windows in the building, received adhesive film blocking around 50% of direct solar radiation, which strictly interferes with the level of luminosity obtained through on-site measurements. Another comment is about rooms internal organization, flexible. In the investigated case study, the furniture itself blocks the openings and view out sometimes is a factor that compromises access to daylight and better lighting conditions in the workstations. However, they provide privacy and are not subject of complaints among users.

Regarding the lighting on task, the rooms with Northeast orientation facade show more desirable conditions as the rooms in the Southwest. In general, the results of the measurements in grid demonstrated there is not a satisfactory level of average illumination, below for the Brazilian lighting standard levels. When combined, daylight and artificial light, offer a good average of illuminance and even achieve good levels of uniformity. In all aspects analysed, the rooms on a higher floor offered better lighting conditions.

When analysing the quality of the view out, it is important explain that the entire building is envelop for fixed brises, in concrete sheets, for shading. However, internally, these elements do not compromise the contact with outside. Theirs modulation are strategically fitted in order to converge with the structure of the frames, which allows a continuity in the view out perceived, by the users.

All studied rooms have a high degree of view range (with an angle greater than 50°), a quality factor, in addition to a good indicator of external distance. Nevertheless, the number of layers varies from minimum to high, determining the general

quality of the view out analyses. The only room with low quality of the view out (due to the minimum number of layers) is located on the ground floor and oriented to an internal atrium of the building, limiting the visual layers.

3.3.1 Questionnaire survey

The application of the questionnaire resulted in 37 valid answers, that represents 20% of total population of the building. In general, the satisfaction with the built, 27% are satisfied, while 29.7% are neutral and 32.4% very satisfied

The levels about daylight satisfaction on your work plan, 27% are very satisfied, while 16,2% are very dissatisfied, and 21,6% in a neutral stage. About how apply daylight in your workstation, 86.5% answered never work using only natural light (highest percentage among all surveyed items). This is an interesting response when cross with the answers about lighting preferences, and the satisfaction rate with the natural light achieved on task.

About view out, the information are: 32.4% very satisfied, while 29.7% very dissatisfied and 37.9% not satisfied and not dissatisfied. In rooms with daylight access restriction, this discontent is higher.

3.4 Daylight Computer simulation

Regarding Severiano Mario Porto original design, the calculation of the Spacial Daylight Autonomy – sDA, verified that all the studied rooms show an expressive potential of daylight illuminance values, superior to 500 lux, in a good part of the year. These appoint that the original project has a better daylighting condition that your actual stage. The studied rooms have big part of evaluation plan with more than 500 lux, in more than 60% of the hours of the year. Only one simulated room, due to its internal location, has an unfavourable condition, with less than 40% of the hours of the year meeting this requirement.

About the glare probability, the levels of Annual Sun Exposure - ASE, greater than 2000 lux, was around 25% of the hours of the year. Without any apply of internal blocking device, such as the existing blinds, the occurrence of values above 2000 lux only appear in the areas close to the windows, in all rooms, representing a small area.

As for the Useful Daylight Illuminance - UDI, in an interval between 100 and 2000 lux, it is clear that, originally, there is a great vocation to use daylight in all verified rooms. The only place that needs attention are those close to the windows, with potential for glare, but with reduced area. In general, the potential for using daylight in all rooms is very satisfactory.

4. CONCLUSION

Proposing and performing a multimethod analysis on Severiano Mário Porto projects in Boa Vista city, the research conclusions converge to crossing data. Firstly, rescuing the understand that bioclimatic architecture brings man and environment closer together, it is possible to analyse that the strategies employed by Severiano Mário Porto, in Boa Vista projects, guarantee a bioclimatic bias in his design practice. This study admits that there is, in fact, a preponderant concern of the referred architect with the issue of shading in projects for the Amazon context.

Morphological diagrams demonstrate that the found answers are mixed solutions that, combined, such as form, coverage, hollow elements, orientation and set of frames - result in an expressiveness work for treatment of local impasses. The investigated projects have significant potential, in search of passive solutions for daylight, shading and natural ventilation, with the replicability of some elements employed in all case studies, like brises-soleil, cobogos, large eaves and vegetation as elements of sun protection.

For verification with a representative case study, in better state of preservation, through on-site visits, application of a monitoring protocol and consultation with users, some aspects were obtained about the real condition of use of the building and the changes imposed on the original project (such as applying window films). It was noticed that, in practice, in terms of daylight, the case study analysed does not present satisfactory conditions of illuminance, whether in average illuminance or on task plan. This observation also happens when checking the combined systems, natural and artificial light, which an unsatisfactory lighting performance. According Brazilian standards, none of the measured rooms offered a good lighting condition, in all the verified variables (illuminance average, on task and uniformity).

About view out of the windows, the results showed medium and high quality, with the number of layers being decisive. Of the 4 studied rooms, 1 presents with high quality of the view out, 1 with minimum quality, but, in general, all have high reach and high external distance as positive aspects of contact with the external environment.

About users' perspective as an element of investigation, in the representative case study, responses corroborated with some these results: the majority mention a little availability of daylight in their workstation and the respondents show there is no use only daylight as a source of light for your work. However, levels of satisfaction with general space are polarized but point to a positive majority. Satisfaction

with the view out and other qualities of the space may justify this fact.

For the same rooms where the real conditions of use were verified, with monitoring protocol, data regarding computer simulation of daylight are given. They indicate the potential for daylight use in original design. The results showed good levels of illuminance for daylighting, without presenting a high probability for internal glare. This concludes all the concern with shading and sun protection in Severiano Mário Porto's projects, in their original condition. Even though developed without the technology around software and computer simulation, they were designed to achieve a satisfactory performance for lighting with natural light, without propose too high thermal internal gains for direct solar radiation.

However, whether through the results of the measurement or the responses of users, it is concluded that the good levels of daylighting it is not, in fact, the reality of the studies rooms today, with a discrepancy between the original design intention and the existing building. This fact can be attributed to the modifications made to the original design, like the addition of films and the reduced of light transmission of the glasses. An unanswered question in this work is the motivation for adding these films to the original project.

Conducting the research and visiting on site Severiano Mario Porto buildings in Boa Vista city, the contempt for many of the design intentions was noticed. An example, closing the lamellar frames in schools, clearly indicates this fact.

Its assertive understand some demands for cooling, today, the rooms with artificial equipment. The extreme conditions of Amazon climate admit this option. But the wrong way to interfere in the space, reaches not just in thermal condition, they have implication in daylighting conditions too, clearly an original design presuppose.

Although designed to optimize the use natural ventilation and daylight, as well as promoting shading and sun protection for internal structures, these builds received interventions that sacrificed some of their original intentions. This is the case of the total closure of the shutters in the classrooms of the investigated schools, the arbitrary replacement of the original frames and the application of films on the windows. Here, the interventions carried out and necessary are not condemned, without the zeal to maintain the potential of the projects.

ACKNOWLEDGEMENTS

This research is grateful to the Laboratory of Environmental Control and Energy Efficiency at the University of Brasília (LACAM FAU UnB), University of Roraima (UFRR) and the Court of Justice of the State of Roraima (TJ/RR).

REFERENCES

1. Johnsen, K. and Watkins, R., (2010). Daylight in Buildings: ECBCS Annex 29/SHC Task 21 - *Project Summary Report*. EACOM IEA SHC
2. Galasiu, A.D. and Veitch, J.A., (2006) Occupant preference and satisfaction with the luminous environment and control systems in daylight offices: a literature review. *Energy and Building*, 38: p. 728-742.
3. Gratia, E., Bruyère, I., and De Herde, A., (2004) How to use natural ventilation to cool narrow office buildings. *Building and Environment*, 39: p. 1157-1170.
4. Santamouris, M., (2005). Passive Cooling of Buildings. In: *Advances in Solar Energy - An annual review of research and development in renewable energy technologies*. James and James Publishers, London.
5. Ghiaus, C. and Allard, F., (2006). Potential for free-cooling by ventilation. *Solar Energy*, 80(4): p. 402-413.
6. Koenigsberger, O.H., (1973) *Manual of tropical housing and building - part 1, climate design*. Longman press. London.
7. Hertz, J.B., (1988) *Ecotécnicas em arquitetura: como projetar nos trópicos úmidos do Brasil*. Pioneira: São Paulo.
8. Voordt, T.J.M. and Wegen, H.B.R., (2005). *Architecture in use: an introduction to the programming, design and evaluation of buildings*. Thoth Publishers: Bussum.
9. Porto, S.M.M., (1986). Criatividade, correção e beleza em quaisquer arquiteturas. *Projeto*, 83, p. 48-49.
10. Instituto Nacional de Meteorologia. *Arquivo Climático* (2019). [Online] Available: <http://www.inmet.gov.br/portal/index.php?r=bdmep/bdmep> [16 Jun 2019]
11. Associação Brasileira de Normas Técnicas, (2009). NBR 14.653 - Historical and artistic heritage assets. *Brazilian standart*.
12. Amorim, C.N.D., (2007). Diagrama morfológico parte II – projetos exemplares para a luz natural: treinando o olhar e criando repertório. In: *Paranoá: cadernos de arquitetura e urbanismo*, 3(1), p.78-98.
13. Sales, G.L. (2016). *Diagrama de ventilação natural: Ferramenta de análise do potencial da ventilação natural no estudo preliminar de projeto*. [Online] Available: <https://repositorio.unb.br/handle/10482/227> [19 Jun 2019]
14. International Energy Agency - Solar Heating and Cooling Programme (2019). Task 50: *Monitoring protocol for lighting and daylighting retrofits*, [Online], Available: https://task50.iea-shc.org/Data/Sites/1/publications/Technical_Report_T50_D3_final.pdf [08 May 2020]
15. International Energy Agency - Solar Heating and Cooling Programme (2019). Task 61/EBC Annex 77: *Integrated Solutions for Daylighting and Electric Lighting*.
16. EN 17037: Daylight in buildings, (2018). *European Standart*.

Designing Sustainable Office Buildings with Higher *Value-in-use*

The relevance of cocreation workshops to generate innovative ideas

CAMILLE RAYNAUD¹, CONSTANCE FLACHAIRE¹, ELLA ETIENNE-DENOY¹

¹Green Soluce, Paris, France

ABSTRACT: *This paper shares a co-creation approach to help real estate actors (developers and asset managers) identify specific stakes regarding the value-in-use in tertiary assets (i.e. the intangible value of an asset, that exceeds the simple material value, its location or price per square meter). In this approach, two workshops were designed with a real estate company and its internal (sustainability and commercial team) and external stakeholders (clients, service providers, partners...) to leverage on collective intelligence to identify different value propositions based on value-in-use. The global objective of the two workshops was to develop a methodological approach to define and create value-in-use scenarios, and to use the results to implement further actions for the change of use of existing buildings. The paper presents the conceptual problem, the methodological approach for ideation of such value-in-use scenarios and general outcomes for tertiary buildings. The conclusions are both on the methodological aspects of the process and the first actions and evaluation indicators identified.*

KEYWORDS: *sustainable buildings, value-in-use, collaborative design, workshop innovation, resilient design*

1. INTRODUCTION

Existing buildings are key assets towards a cleaner and low carbon city. Their correct management allows to optimize and reduce resource consumption. In addition to cost and resource management, existing buildings have the opportunity to further support an environmental transition by the intangible use of the building.

The term *use*, in this context, addresses the services that are provided to occupants (e.g. indoor comfort, basic services, digital connectivity, leisure spaces, neighbourhood opportunities, proximity to work, etc). Although these points are considered during the design stage of a new construction, they are less considered on transformations of tertiary buildings [1].

This transformation, based on the concept of *value-in-use*, is essential to create resilient cities that optimize the existing building stock for future societal needs while optimizing the need for resources demand (i.e. energy, material, water).

This paper shows the workshop experience with real estate stakeholders to identify innovative value-in-use scenarios for existing buildings and its impact on future cities.

2. BACKGROUND

To date, literature about *value-in-use* in office buildings focuses on the benefits for building tenants and building occupants [2,3], viewed from a client perspective and internal stakeholders.

The purpose of the workshop is to involve external stakeholders to better understand the direct and indirect opportunities for real estate companies (developers and asset managers) regarding the *value-in-use* in tertiary assets.

2.1 Concepts and definitions

Throughout this paper, the concept of *value-in-use* is meant to address the intangible value of an asset. Although the use of the space is intrinsic to the value of a building, it also exceeds the simple material value of the asset, its location or price per square meter.

The *value-in-use* offered by an existing building does not only improve the user experience, but furthermore it increases the perceived economic value on the market. As cities grow (in size, citizens, services), and integrate a more sustainable architecture and urban design, the concept of usage also evolves and adapts, with a special focus on the tertiary real estate field [4].

2.2 Need for case studies on *value-in-use* (or change of use)

Tertiary real estate developer and asset managers face a need for a different use of their existing building portfolio, where these portfolios are exposed to a high risk of inadequate buildings that will exist for decades. Due to changing urbanization trends and related sustainability requirements, these buildings might not adapt to the new building owner's objective or the final users' future needs.

This functional obsolescence of buildings favours their vacancy (office vacancy rate in 2019 Q3 was 11% in Milan and 8.6% in Berlin [5]), and in the long-term is conducive to the building destruction to build a new one more suitable to people habits. For developers and asset managers, it generates extra cost for deep further refurbishments or fits out. Moreover, the demolition to rebuild has a strong carbon impact, as 60% of buildings life-cycle CO₂ footprint come from the construction phase [6].

To contribute and support the case for low carbon cities, by avoiding buildings demolition and re-construction, the approach of *value-in-use* provides a new outlook. In France, over the last years, real estate players slowly integrate the concept of *value-in-use* within their corporate objectives. Thus, providing a space to build new methodologies and practices that can serve as example to other projects.

This paper is based on the workshop experience with a French financial actor who manages building assets. The workshop was designed to help the organisation define, identify and promote a different *value-in-use* for the transition of their existing building stock. This experience could be replicated by other real estate actors in order to build an urban resilience through the notion of *value-in-use*.

3. CONTEXT OF THE WORKSHOP

The workshop experience with the real estate actor was set up as: a) workshop context definition, b) workshop objective and sequences, and c) the workshops methodological approach.

3.1 Context definition

Today, co-working and co-living are new concepts of value proposition observed in the real estate market. These trends have forced actors to question their business proposition, where the concept of value-in-use has gained interest. Specially, when considering that sustainability topics have become more relevant to communicate the intangible value of a building.

In defining the workshop context with the real estate actor, it became evident the need to tackle three aspects: 1) the concept of value-in-use for their business, 2) the challenges and opportunities with its stakeholders, and 3) the need to break down these opportunities and challenges for tertiary buildings.

3.2. Objectives and sequences of workshop

To address the three aspects, two workshops were designed to engage the real estate actor and its stakeholders, and address expectations about *value-in-use*. The global objective of the two workshops was to gather the internal (sustainability and commercial

teams) and external stakeholders (customers, partners and service providers) and develop a methodological approach to define and create *value-in-use* scenarios, and to use the results to implement actions for the change of use of existing buildings.

The first workshop, divided in two sprints, identified prospective and strategic interests of a building's value-in-use.

- Sprint 1: Identify tertiary buildings major trends in tomorrow's city.
- Sprint 2: Identify levers of action that increase the *value-in-use* which respond to the major trends identified in sprint 1, and classify these actions under the corporate materiality matrix.

The second workshop, also divided into two sprints, deepened the initial reflection and results to shift from strategy to business operation. This part, identified some solutions (business and impact evaluation) towards a building's *value-in-use*.

- Sprint 1: Identify economic models using the Lean Canvas as a basis for reflection. The Lean Canvas was adapted for a commercial real estate player to analyse the different aspects of a project.
- Sprint 2: Identify indicators to evaluate the *value-in-use* of the building.

3.3. Workshop methodological approach

The workshops methodology is based on three main pillars: 1) a multi-stakeholder collaborative approach, 2) a prospective tool based on a project transition framework, 3) an agile method for collaborative co-creation.

3.1.1. A multi-stakeholder collaborative approach

The first pillar focused on a multi-stakeholder co-creation process. A process inspired by the theory of strategic management of stakeholders [7]. This theory takes into account the range of needs of a companies' stakeholders and by a confrontation of complementary expertise, and a combination of mutually enriching experiences it proposes more suitable products.

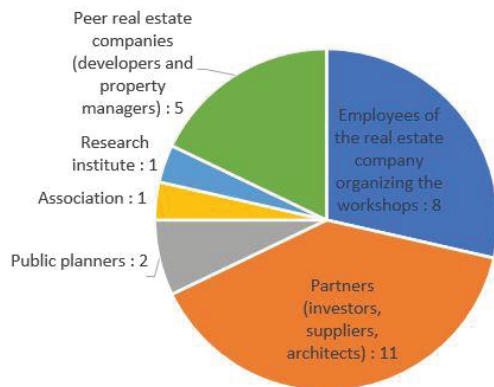


Figure 1: Number of participants and type of stakeholders participating in the workshop

The collaborative workshops were composed of 30 internal and external stakeholder representatives in total. Participants were mainly the same for the two workshops. They were classified into five groups: partners, employees, peer-real estate companies, public partners, associations and research institutes. The most represented stakeholders were partners which included investors, suppliers and architects (figure 1).

3.1.2. A prospective tool based on a project transitions framework

The second pillar addressed the prospective approach of the *value-in-use* as described in the context definition. A prospective analysis is not about predicting a certain future, but to project into long-term scenarios, making hypothesis on long-term socio-spatial variables [8]. It allows to define a desirable future vision for the territories and to anticipate actions to take to make this desirable future come true.

A prospective approach is particularly relevant with regard to the *value-in-use* of real estate projects. As real estate projects are planned, in general, five years before being occupied and used, they intrinsically should anticipate future needs and social evolutions when they are designed. This helps to avoid them being obsolete just when they open for service. Moreover, a prospective approach is essential when thinking about sustainable development, where issues are long-term and the nature, intensity and knowledge of the risks are likely to change significantly and rapidly over the next few decades.

The tool used during the workshop was based on a prospective reference framework, developed by the ESSEC Business School, which takes the form of a multi-level and multi-criteria mind-map (figure 2). The framework addresses a context under five large trends: work, habitat, new models, consume and develop, and a future city. From these trends several elements of evolution or potential impact branch out, e.g. the initial

category Habitat branches out into specific issues as informal dwellings, temporary buildings, increase migration, patrimonial values, accessibility and connectivity.

Based on this prospective approach, the objective of the first workshop was to project several *value-in-use* concepts over the long term and to evaluate them against the company's strategic framework. The mind framework tool helped identified the major trends likely to influence the future of cities and urban services over a time horizon of 20 years or more, which then were broken-down into specific issues. The workshop participants had to build their own reference frame, representing their vision of the evolutions that could impact strategic scenarios related to *value-in-use*.

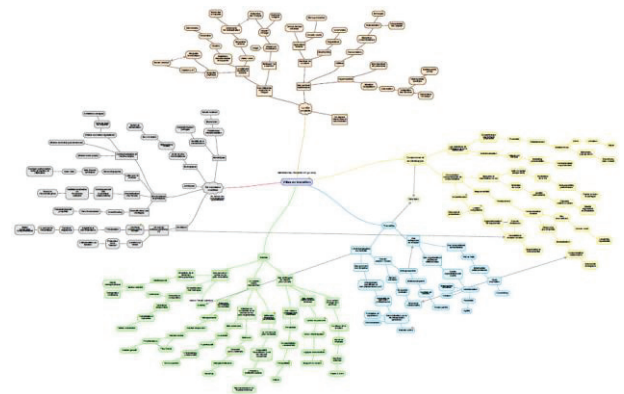


Figure 2: General image of the multi-level and multi-criteria mind map for the prospective reference framework

3.1.3. Agile and collaborative co-creation method

The third pillar integrates an agile collective intelligence process for ideation. Based on the literature, an agile project management [9] is founded on key principles of iteration and collaboration. More particularly, the agile methodology, was inspired by the computer coding sector to accelerate the generation of groundbreaking ideas with short but intense "sprints" of thinking and co-creation.

The workshop was sequenced into two sprints of co-construction and reflection, each of them lasting 75 minutes. Each sprint alternated an individual reflection, a collective reflection, a time for formalization within groups, and finally a global pooling with all the groups. The ideas arising from these sprints were placed on posters (figure 3).

The workshops' sprints were focused on the *value-in-use* of office buildings, which can result in innovative, relevant and long-lasting value propositions.



Figure 3: Example of posters gathering ideas co-created by participants written on post-its

4. OUTCOME

This methodology approach based on a prospective framework allowed to generated four key general outcomes about *value-in-use* for tertiary buildings (figure 4a and figure 4b).

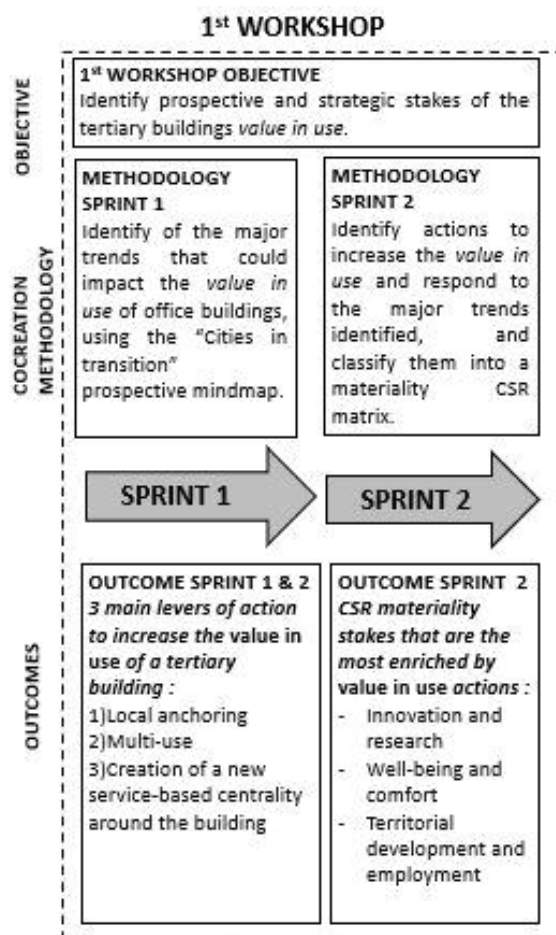


Figure 4a: Synthesis of the objectives, methodology and outcomes of the 1st workshop

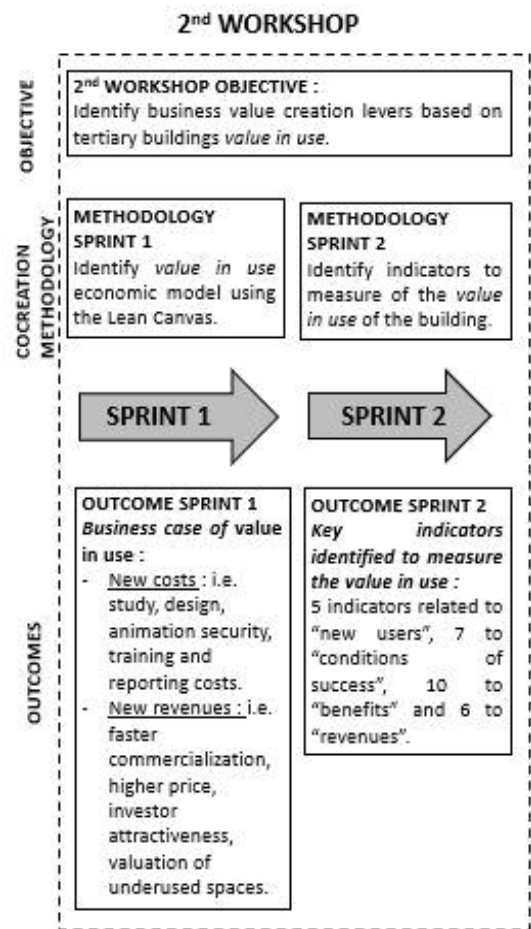


Figure 4b: Synthesis of the objectives, methodology and outcomes of the 2nd workshop

4.1. First outcome: Main levers of actions to reinforce the *value-in-use* of a tertiary building

During the first workshop, 100 ideas of levers of action to increase the *value-in-use* of a tertiary building, were generated by the participants. A post-workshop analysis of these ideas showed that most of the actions identified could be reunited in three categories of levers (figure 5):

- 22% of the proposed levers of actions concerned the **local anchoring**. Actions focused on the local ecosystem, e.g. opening of places as company restaurants, mutualization of services for the neighborhood centralized in the building.
- 15% of the ideas of levers of actions concerned the **multi-use of the building**, with actions linked to the modularity and adaptability of the spaces over time.
- Finally, 10% of the levers of actions concerned the creation **a new service-based centrality around the building**, through services offered to building users, such as concierge services.

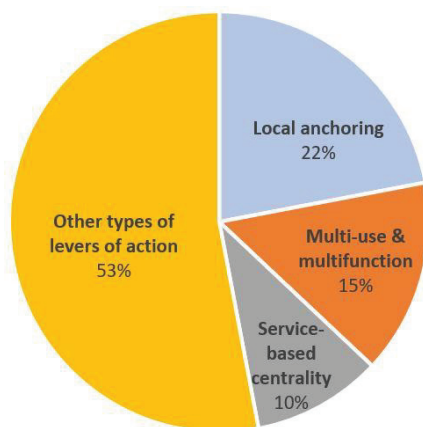


Figure 5 Repartition of actions to reinforce value-in-use by type of lever of actions (in %)

4.2. Second outcome: The link between sustainability issues and value-in-use

Also, the first workshop allowed to visualize the potential sustainable value of the solutions. Amid the 100 actions identified, the best of them were selected by the participants. The participants had to analyze the contribution of each action towards the *value-in-use* identified in contrast to several sustainability issues or priorities.

To contextualized this outcome, the sustainability issues identified during workshop were compared with the sustainability issues synthesized by the OID (The Observatory of the Sustainable Real Estate), a French real estate association around sustainability research [10].

The comparison showed that the ideated actions to reinforce *value-in-use* contributed mainly to the three large sustainability issues (in order of frequency): innovation and research (contribution of 35 actions), well-being and comfort (contribution of 32 actions) and territorial development and employment (contribution of 23 actions) (figure 6). The outcome confirmed that the *value-in-use* concept, under this approach, is a vector of opportunities in innovation for the company, the end-users and the local economy.

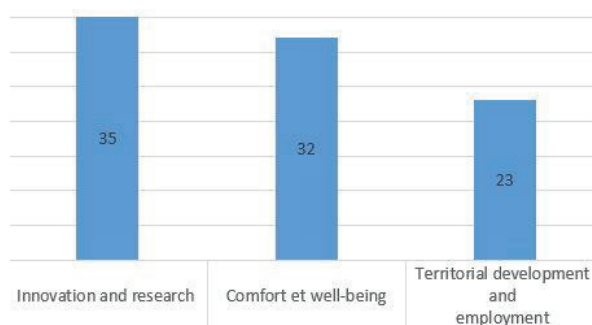


Figure 6: Main CSR stakes and number of actions of real estate players reinforced by value-in-use

4.3. Third outcome: Business case of the value-in-use for the real estate company

During the second workshop, participants worked on a specific Business Model Canvas adapted to tertiary real estate issues, inspired by the Lean Canvas by Ash Maurya (figure 7). This exercise clarified the business case of *value-in-use* for the developer and asset manager, with a deeper understanding of the costs and revenues a new model could generate for tertiary buildings.



Figure 7: The Lean Canvas by Ash Maurya

On the cost analysis of the canvas, some of the actions that had a higher impact on its augmentation were the followings: project design, animation, security, training, and reporting costs. Similarly, on the revenue analysis new streams were identified which could compensate the previously identified costs. In this regard, the main financial benefits identified were: faster commercialization, increased price, investor attractiveness, and a higher valuation of under-used spaces.

4.4. Fourth outcome: Impact indicators as a condition of success of the value-in-use

Lastly, at the end of the workshop, the participants identified several indicators to measure the *value-in-use* of a tertiary building, in relation to four categories of the Canvas analyzed during the first "sprint". Amid the indicators proposed: five indicators were related to new users (e.g. "number of typology of users per building"); seven were related to conditions of success, ten were related to the measurement of benefits (e.g. "carbon footprint of the building") and six were related to revenues.

6. CONCLUSION

This paper presents the results of a workshop experience with real estate stakeholders to identify levers of action of value-in-use scenarios for existing buildings and its impact on future cities. The workshop methodology and results address the importance of

designing a sustainable value proposition (tangible and intangible benefits) adapted to the challenges of a real estate actors.

The experience also serves as a base of discussion for similar approaches on how to re-design the existing building stock in cities in order to address environmental and societal challenges, and to define new viable and impacting propositions.

The four general outcomes identified: 1) actions to reinforce the value-in-use of a building, 2) link between sustainability issues and value-in-use, 3) the business case of value-in-use, and 4) impact indicators as condition for success, are relevant results which come out of a workshop approach to co-create and bring about innovation for existing office buildings. Thus, supporting the transition towards new business models that serve global sustainability objectives.

7. ACKNOWLEDGMENT

The authors would like to thank C. Papillon, Global Head of Sustainable Development & CSR at BNP Paribas Real Estate for her support and participation to reinforce the value in use of buildings.

REFERENCES

1. Remøy, H., *Out of Office; a Study on the Cause of Office Vacancy and Transformation as a Means to Cope and Prevent*. Delft, IOS Press, 2010
2. VIBEO, *Value-in-use in a building office*: p. 4-10, 2018
3. SHRM Research, *How Have Sustainable Workplace Practices Changed Over Time?* [ONLINE], 2013. Available on: <https://www.shrm.org>
4. Wilkinson, Sara J., Remøy, Hilde (Editors), *Building Urban Resilience through Change of Use*. Wiley Blackwell, 2018
5. Savills, *European Office Outlook 2020*, 2019, Available on : <https://bit.ly/2Wz9eZ5>
6. Bâtiment Bas Carbone, 2019 [ONLINE]. Available on <https://www.batimentbas carbone.org/carbone-batiment/>
7. F Ackermann, C Eden, *Strategic management of stakeholders theory and practice*, Long range planning, 2011. Available on : <https://www.sciencedirect.com/science/article/abs/pii/S0024630110000452>
8. De Jouvenel, Bertrand, *The Art of Conjecture*, Routledge, 2012
9. Schwaber, Ken, *Agile Project Management with Scrum*, Microsoft Press, 2004. Available on: <https://bit.ly/2JaIEgl>
10. OID, *Etude de marché – matrices de matérialité*, 2018

Evidence-Based Calibration of an Energy Simulation Model: Dealing with Practical Issues of Data Availability and Granularity in an UK Apartment Block

ELISA SCORTEGAGNA¹, NELSON MARTINS¹, NISHESH JAIN², LUIS SOUSA³, ANDREW TINDALE³

¹Universidade de Aveiro, Aveiro, Portugal

² University College London, London, United Kingdom

³DesignBuilder Software Limited, Stroud, United Kingdom

ABSTRACT: Several recent studies have emphasized considerable discrepancies between the measured and the simulated building energy performance. As buildings usually underperform during their operation when compared to the design prediction, a broad interest in building monitoring and operational diagnostic has developed. The gap between the measured and simulated energy consumption has thus become an important concern in the building simulation domain. For this reason, the calibration of building simulation models, which creates a virtual representation of an existing building, is of a growing interest. This work uses the data from the actual energy use and Indoor Environmental Quality (IEQ) measurements of a newly built residential apartment block in West London, UK, to develop a calibrated model. A systematic, evidence-based process is used for calibrating a typical apartment in the complex. Within the current data available, a calibrated model is created, however, it is found that there are multiple solutions that can meet the calibration criteria as per ASHARE Guideline 14/IPMVP. Therefore, conclusions drawn from 'a' calibrated model might not reflect the true reality. KEYWORDS: Evidence-based Calibration, Building Energy Performance Model, Indoor Environmental Quality, Uncertainty Analysis, Sensitivity Analysis.

1. INTRODUCTION

Dynamic simulation of buildings is an increasingly common practice in architecture and engineering. By constructing simulation models that mimic complex real-world physical processes, it is virtually impossible to evaluate all possible variations because of the large number of interdependent input variables. Although in recent years several Building Energy Performance Models (BEPM) have been developed, the amount and type of input data required creates difficulties in modelling and obtaining accurate results from simulations [1].

The Uncertainty Analysis (UA) and the Sensitivity Analysis (SA) of the results seek to evaluate the impact of the variations on the input parameters in the outputs, in order to create simplified models by identifying the most sensitive inputs which propagate the uncertainty in the results [2].

For high-quality, low-energy buildings to be designed, feedback from operational performance of real buildings is required. One way of obtaining this information is through post occupancy evaluations and energy audits. Analysis of these can be done by using calibration simulation of BEPM [3].

Several studies performed recently have emphasized considerable discrepancies between the measured and the simulated building energy performance. As buildings usually do not present the same performance during their operation as the one

predicted in the design phase [4], a broad interest in building real-monitoring and operation diagnostic has emerged and the gap between measured and simulated energy consumption data has thus become an elementary concern in the building simulation domain. For this reason, the calibration of building simulation models is of growing interest.

2. OBJECTIVE AND METHODOLOGY

The purpose of this paper is to explore the use of the energy use data and the Indoor Environmental Quality (IEQ) measurements, for calibrating a simulation model. This has been shown through a case study example of a newly built residential apartment in London, UK.

2.1. Detailed Methodology

This work focus is calibrating a BEPM to estimate its operational energy performance and assess the gap between the simulated results and the actual energy consumption, commonly referred as the 'performance gap' [5,6]. A systematic, evidence-based manual fine-tuning is done to calibrate performance of a typical flat in an apartment complex. The method has been adapted from a typical calibration workflow used in Jain et. al. [7]. The methodology applied to perform the UA is based on literature and previous case studies [8,9]. This

method is diagrammatically shown in Figure 1 and explained in detail below.

1. The building's design intents and actual data, for energy use and IEQ were collected from the design documentation and during the site visits.

2. A baseline model was then created based on the design data. The baseline results were compared to the actual measured and monitored data and the operational trends and deviations from design intents were analysed.

3. The model was procedurally fine-tuned based on identified deviations and the results were validated using monthly calibration criteria as per ASHRAE Guideline 14 [10] and IPMVP [11], CV(RMSE) and NMBE values should be $<15\%$ and $<\pm 5\%$ respectively.

4. Going beyond the ASHRAE Guideline 14 and IPMVP, the uncertainty in calibrated model results was also quantified. The range of variability in model input parameters was based on observed evidence in the building and as per existing literature [12,13].

5. Discrepancies between operation and design data and their potential causes were listed.

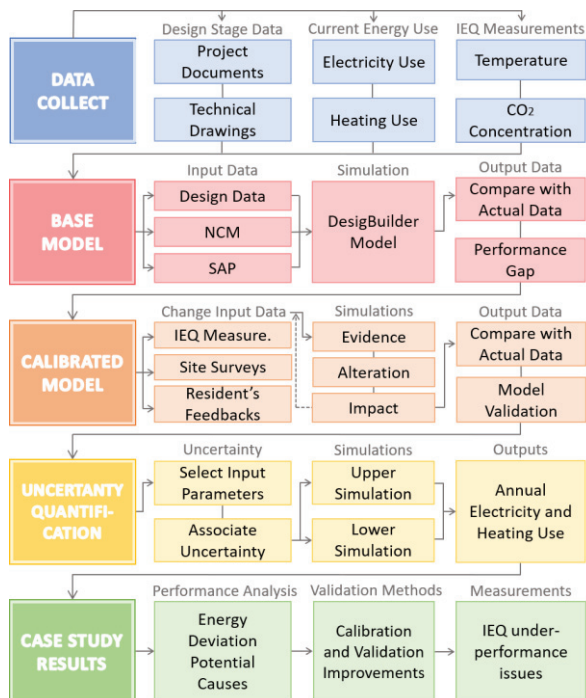


Figure 1: Calibration Methodology Diagram

3. CASE STUDY BUILDING

The case study is an apartment block located in East London, England. The buildings were completed in 2015, they attain high sustainability standards. The mixed-use development provides 98 flats, as well as community infrastructure and offices on the ground and first floors.

The apartment block has a district heating system, that provides heat for space heating and hot water. The electricity supplied is by the grid. All the flats have radiators installed for space heating and there is

no provision for mechanical cooling. A mixed-mode ventilation strategy uses both natural ventilation and Mechanical Ventilation with Heat Recovery (MVHR).

Only residents of five flats allowed the monitoring of indoor air quality and comfort conditions in their homes. Therefore, one of these flats was selected as typical for detailed performance analysis. The Figure 2 shows the spread of energy use in all the flats, the typical flat selected for calibration and detailed analysis, highlighted by the red line, has energy use near to the average value across the apartment block.

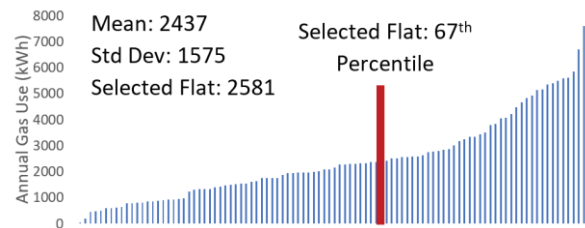


Figure 2: Spread of actual energy use in the apartment block

The flat analysed is occupied by a family of five people, three adults and two children, it's located on the eighth floor, facing southwest and southeast orientations, with total floor area of 98.3 m² and a height of 3 m. It has eight zones, which include three bedrooms, a living room, a kitchen, a bathroom, a toilet and a circulation area.

3.1. Building Data Access

Data for consumption of electricity and natural gas for heating was obtained during site visits from the respective meters. The data for IEQ parameters (air temperature and CO₂ concentration), was collected by data loggers installed on the walls of the regularly occupied spaces. Based on the availability and granularity, the data for the year 2017 was selected for use in model calibration. Design data were obtained from project documents, design plan and technical drawings.

3.2. Base Model



Figure 3: DesignBuilder Building Model

The model was created in DesignBuilder Software version 6.1 [14] based on the drawings and design projects of the selected apartment and the building. Figure 3 shows the flat model from the simulation software and its zones.

The parameters, profiles and schedules in the base model were as per the National Calculation Method (NCM) [15] database and Standard Assessment Procedure (SAP) [16] worksheets. NCM contains standard sets of data for different activity areas and call on common databases of construction and service elements. SAP is the standard methodology used in the UK to assess and compare the energy and environmental performance of dwellings. SAP calculations were done at the design stage by the project team as a part of performance projections.

Data on the dimensions, size and quantity of the openings and U-value of the exterior walls, floors and openings were obtained from project information and drawings. Infiltration rate, air exchange rate, the efficiency of system and construction were extracted from the SAP calculation table. Other data, such as DHW consumption, room heating setpoints temperatures, occupancy by day of week and space usage, were obtained from the NCM database, already incorporated into the software.

The outcomes from the simulation were compared with the actual energy consumption and elaborate the causes of discrepancies in the building predictions. The CV(RMSE) and NMBE values were calculated for the base model. For heat demand the values were respectively 56.21% and 45.31% and for electricity consumption were 9.97% and 3.42%. These are shown in Figure 4 and Figure 5.

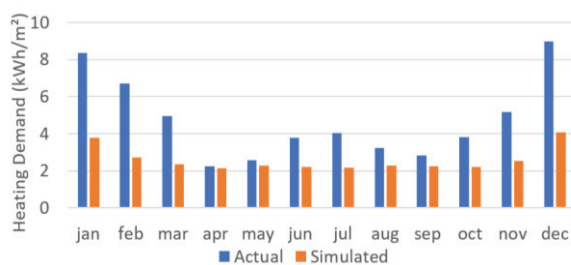


Figure 4: Actual versus Simulated Energy Consumption - Heating Demand (Gas)

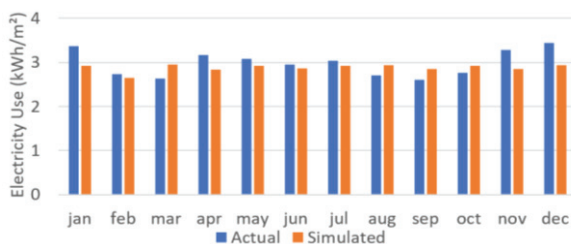


Figure 5: Actual versus Simulated Energy Consumption - Electricity Use

3.3. Calibration Process

After analysing the base model simulation results and comparing it with the data of the current IEQ measurements and energy consumption, some variables to be changed in the calibration process were established. These variables essentially include assumptions related to operational factors such as changing the heating setback and setpoint temperatures and the occupancy patterns and use.

The calibrated model was obtained by modifying the base model according to findings obtained from residents' feedbacks, actual IEQ and energy measured conditions. The parameters and values changed at each stage of the calibration process are described next and summarised in Table 1.

Table 1: Parameters and Values Changed in the Calibration

CM Stage	Parameter	Changed Values
Change 1	Heating Setback Temperature	12 °C to 18 °C: as per minimum internal temperature
Change 2	Number of Residents	4 (2 adults, 2 children) to 5 (3 adults, 2 children): as per resident's feedbacks
Change 3	Occupancy Schedules	Increased occupancy hours: based on CO ₂ concentrations data
Change 4	Holidays	Spring / Summer: based on CO ₂ concentrations and energy use patterns
Change 5	Heating Setpoint Temperature	18°C and 21°C to 21°C to 24°C: to meet average indoor temperature

By analysing indoor temperature data in the apartment rooms, was possible to conclude that the temperature did not fell below 18°C, which testifies the alteration made.

Based on feedback from residents' interviews, the actual number of inhabitants became known and was updated accordingly.

In the apartment rooms whose IEQ data were being measured, CO₂ concentration evidence occupation patterns for the living room, the kitchen and the bedrooms. The occupancy schedules assigned to each apartment space per day of the week have been changed as needed.

IEQ measurements analysis also show that the CO₂ concentration levels were closer to the external average concentration level in that region. This evidence, associated with the fact that the heating daily use for those days also presents a significant drop, and this period coinciding with the School Easter Holidays according with the school term dates by local Council, made believe that the family was in vacations during those days.

In order to access more accurate results, the hourly indoor temperature average values were compared with the occupation hours of the rooms.

Based on those evidences, the average temperature per room for each month have been changed as needed.

Incorporating all the changes based on evidence based method and empirical data, the actual heating and electricity consumption were compared with the simulation values of the calibrated model, as shown in Figure 6 and Figure 7. The CV(RMSE) and the NMBE are respectively 46.92% and 37.09% for heating (gas) and 11.36% and 0.46% for electricity. The energy consumption values simulated in the calibrated model do not accurately represent the actual consumption data.

As all empirical data has been used in previous changes, no further changes can be with high degree of certainty. More monitored data is required to complete the calibration process based on only evidence-based modification. However, the quantification of uncertainty based on observed and short-term data can help and facilitate obtaining 'a' calibrated energy performance model.

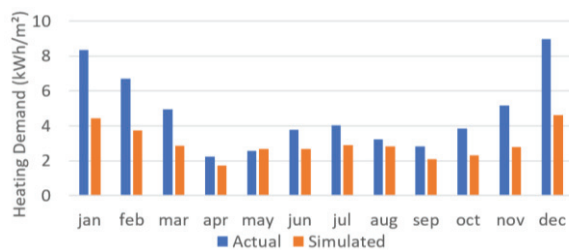


Figure 6: Actual versus Simulated Heating Demand - Calibrated Model

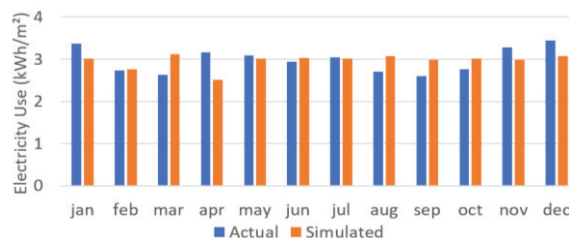


Figure 7: Actual versus Simulated Electricity Use - Calibrated Model

3.4. Uncertainty Quantification

Since all empirical data has been exhausted, and no other statement can be made with certainty based on the available data, the quantification of uncertainty helped and facilitated obtaining a calibrated energy performance model.

Inferences can be drawn from short term data, spot measurements and on-site observation, which may represent actual operations of the building over the longer term as well. These factors affecting trends of the electricity and heating energy consumption were selected for the uncertainty quantification. For each of those variables, associated uncertainty values according and designated distribution were based on the observed trends. Additional uncertain factors commonly seen in existing literature and case studies

researches[12,13] were also added to the uncertainty quantification. These have been listed in Table 2.

To quantify the overall uncertainty, two simulations were performed (Figure 8 and Figure 9). The lower bound simulation was performed to evaluate the scenario that presents the lower energy consumption, the best scenario. The upper bound simulation was performed to evaluate the scenario that presents the higher energy consumption, the worst scenario. In the Figure 8 and Figure 9 the values for actual energy consumption is in between the upper and lower values.

Regarding the heating consumption (gas), Figure 8, most of the monthly consumption values were close to the maximum estimates. For electricity consumption, Figure 9, the months of Mar and Apr are the only ones that still present lower and higher current consumption values than the minimum and maximum values of each month respectively. These could be attributed to Mar energy use being billed in Apr.

Table 2: Uncertainty variables and their range

Variable	Unit	Range
External Wall U-value	W/m².K	Lower 0.16 and Upper 0.55
Infiltration (Template)	-	Good and Medium
Natural Ventilation	°C	Values between 20 and 17
Heating Set point	°C	Values between 21 and 24
Occupancy	Num.	±10%
Equipment Power Density	W/m²	±10%
Lighting Power Density	W/m²	±10%
DHW Consumption	l/m² day	±20%

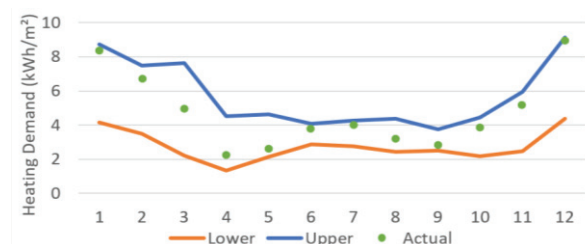


Figure 8: Sensitivity Analysis Heating Demand versus Actual Consumption

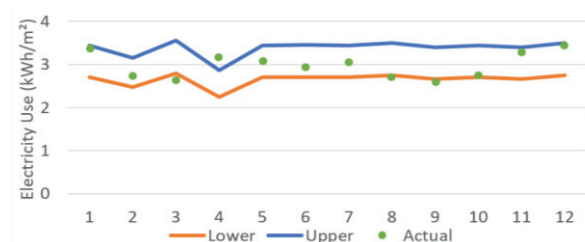


Figure 9: Sensitivity Analysis Electricity Use versus Actual Consumption

4. RESULTS AND DISCUSSION

Figure 10 and Figure 11 summarize the annual energy consumption for the actual energy use, the design projections in the base model, the partially calibrated model and the minimum and maximum values for uncertainty propagation.

It is possible to see that the simulated values in the calibrated model are still lower than the actual values, especially for heating consumption. After the evidence-based adjustments made during the calibration process, while there was a reduction in the existing gap between the actual demand and the design predictions simulated in the base model, the discrepancies were still very high.

The months with colder temperatures showed differences in the values greater than 40%, while for the months from Apr to Sep the simulated operational performance values were around 20% lower than actual values. On the other hand, the gap in the electricity consumption is considerably smaller when compared to the gaps in heating demand and is within acceptable error range.

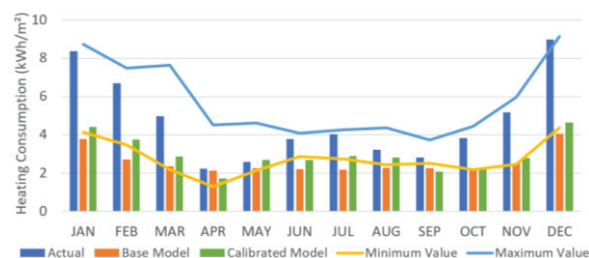


Figure 10: Annual Heating Consumption Summarized

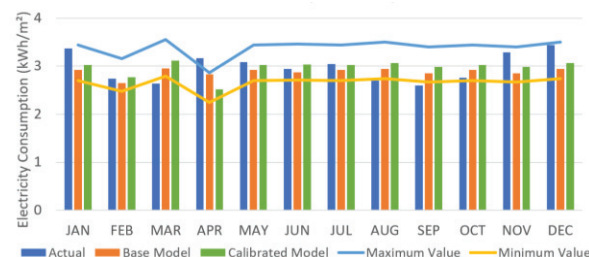


Figure 11: Annual Electricity Consumption Summarized

The discrepancies between the actual measured data and the design predictions in the base model and the partially calibrated model are shown in Table 3 and Table 4 respectively, as well as the CV(RMSE) and NMBE values for model validation.

Analysing the discrepancies in the different steps of the calibration process, the result is not ideal. The simulated values of annual heating consumption, Table 3, show that initially, the base model, which represent the design stage projection, had under predicted heating demand consumption by 45%. After the changes made in the partially calibrated model, this percentage decrease to 37%. Evaluating the gap in the simulated electricity consumption between the calibrated model and the actual annual

demand, Table 4, it was noted that the consumption reaches acceptable values of CV (RMSE) and NMBE.

Table 3: Annual Heating Consumption Discrepancies

Against Actual Data	Design projection (Base Model)	Partially Calibrated Model
Consumption (kWh/m²)	31.00	35.66
Absolute Error (kWh/m²)	25.68	21.02
Relative Error (%)	45.31	37.09
CV(RMSE)	56.20	46.92
NMBE	45.31	37.09

Table 4: Annual Electricity Consumption Discrepancies

Against Actual Data	Design projection (Base Model)	Partially Calibrated Model
Consumption (kWh/m²)	34.55	35.61
Absolute Error (kWh/m²)	1.22	0.16
Relative Error (%)	3.42	0.46
CV(RMSE)	11.35	11.35
NMBE	3.42	0.46

The uncertainties in the inputs specifications have significant impacts on the modelled energy results, as shown in the analysis process, so the energy performance gaps can be either smaller or larger than the final gaps of the calibrated model. While it was not possible to meet the validation criteria based on evidence-based calibration, actual results lie within your reasonably defined uncertainty range. It suggests that there might be multiple solutions that may meet the criteria.

Since there are huge discrepancies in the heating energy predictions of the base model, it is noticeable that the SAP table forecasts are not representative of the actual operating conditions. Bearing in mind that the real operating conditions of a building are dynamic, forecasts based on standardized conditions in the SAP tables, which use a quasi-steady state calculation method, are not suitable to be treated as expected energy performance.

Likewise, the NCM database used in the construction of the base model presents parameters that do not fully represent the real values. In this sense, the predictions of the base model, do not accurately reflect the real building performance.

Considering that the base model is the foundation for the calibration process, the parameters that would not be calibrated or modified in later stages should reflect the actual in-use conditions. For those building parameters and operational profiles which lack actual metered or better references, their values are maintained using dwelling templates in NCM,

what generates considerable uncertainties, non-negligible in the final energy performance gap.

The level of measurements need to improve, the scarcity of IEQ data, such as data losses, need to be overcome, more detailed sub-meters is necessary, the indirect calibration based on occupancy patterns need to be avoid, as it cause lack accuracy, and the impact of occupants-related activities has to be paid more attention.

Considering all the above, the calibration process of energy performance models does not reveal absolute truth, but one of many alternatives whose simulated output values are close to the actual energy consumption values of the analysed building. The final objective of the calibration simulation is to create 'a' calibrated model, which is within the limits of validation of existing models.

5. CONCLUSION

Through this case study, calibration based only on evidence-based findings shows that there can still remain a significant amount of discrepancy between measured and simulated heating consumption values.

Although the results are below expected due to some limitations in the data availability and granularity, the evaluation process applied in this case study is reasonable and necessary to modify the incorrect initial forecasts and reflect on the flexible and diverse real conditions of use in design stage model predictions for this flat. This work recommends some improvements in the calibration process to be better used in other projects for assessing the energy performance of residential buildings.

Better validation protocols of calibrated models and improvements in existing methods for calibration are required. A reduction in the acceptable MBE and CV(RMSE) values is suggested given the number of solutions yielded by the current acceptance criteria.

With currently available tools and the lack of access to more accurate measurements and data regarding building information, it is difficult to calibrate a BEPS model. A reduction of uncertainty in the model's input parameters is necessary, by facilitating access to operational performance data in buildings and improving data availability and granularity obtained by measurements.

Through model calibration process and the quantification of the buildings inputs uncertainties, IEQ parameters should be used to highlight the interrelationship of energy and IEQ and to assist in overall building energy performance assessment.

ACKNOWLEDGEMENTS

The authors wish to express their gratitude to DesignBuilder Software Ltd. and the 'Total Performance' of Low Carbon Buildings in China and the UK ('TOP') project funded by EPSRC

(EP/N009703/1), for the access the building details and monitoring data.

REFERENCES

1. Soto AM, Jentsch MF. Sensitivity and Uncertainty Analysis of Models for Determining Energy Consumption in the Residential Sector. 14th Conference of International Building Performance Simulation Association. 2015.
2. Tian W. A review of sensitivity analysis methods in building energy analysis. *Renewable and Sustainable Energy Reviews* [Internet]. 2013;20:411–9. Available from: <http://dx.doi.org/10.1016/j.rser.2012.12.014>
3. Raftery P, Keane M, Costa A. Calibration of a detailed simulation model to energy monitoring system data: A methodology and case study. In: *Proceedings of the 11th IBPSA Conference*. Glasgow; 2009. p. 1199–206.
4. Fabrizio E, Monetti V. Methodologies and Advancements in the Calibration of Building Energy Models. 2015;2548–74.
5. De Wilde P. The gap between predicted and measured energy performance of buildings: A framework for investigation. *Automation in Construction*. 2014;41:40–9.
6. Burman E, Mumovic D, Kimpian J. Towards measurement and verification of energy performance under the framework of the European directive for energy performance of buildings. *Energy*. 2014 Dec 1;77:153–63.
7. Jain N, Burman E, Mumovic D, Davies M, Tindale A. Improving the Energy Performance Contracting Process using Building Performance Simulation: Lessons Learnt from a Post Occupancy Investigation of a Case Study in the UK. *Proceedings of the 15th IBPSA Conference San Francisco, CA, USA, Aug 7-9, 2017*. 2017;1394–403.
8. Jain N, Burman E, Mumovic D, Davies M, Tindale A. Comparative Analysis of Protocols Used in Measurement and Verification of Energy Performance: Dealing with Practical Issues of Data Availability and Granularity in a UK School Building. *BSO2018 papers*. 2018;(September):11–2.
9. BSI, CEN. BS EN 15603:2008 Energy performance of buildings. Overall energy use and definition of energy ratings. *European Standard*. 2008. p. 1–45.
10. ASHRAE. Measurement of Energy, Demand, and Water Savings. *ASHRAE Guideline 14-2014* [Internet]. 2014;2014. Available from: www.ashrae.org/technology.
11. Efficiency Valuation Organization. IPMVP - International Performance Measurement and Verification Protocol - Concepts and Options for Determining Energy and Water Savings. 2012;1(January).
12. Rivalin L, Stabat P, Marchio D, Caciolo M, Hopquin F. A comparison of methods for uncertainty and sensitivity analysis applied to the energy performance of new commercial buildings. *Energy and Buildings* [Internet]. 2018;166:489–504. Available from: <https://doi.org/10.1016/j.enbuild.2018.02.021>
13. Ruiz GR, Bandera CF. Analysis of uncertainty indices used for building envelope calibration. *Applied Energy*. 2017;185.
14. DesignBuilder Software Ltd. DesignBuilder Software Ltd [Internet]. 2019 [cited 2020 May 13]. Available from: <https://designbuilder.co.uk/>
15. NCM. NCM - National Calculation Methodology modelling guide for buildings other than dwellings in England. 2017;2013 Editi(November).
16. BRE Group. SAP - The Government 's Standard Assessment Procedure for Energy Rating of Dwellings. 2014;(October 2013).

Building Performance Evaluation of a 14th Century Pargetted House:

Hygrothermal comfort and energy efficiency

CHRISTOPHER J. WHITMAN¹

¹Welsh School of Architecture, Cardiff University, Cardiff, Wales, UK

ABSTRACT: Building performance evaluation (BPE) provides the tools to begin to understand the operational efficiency and resultant occupant satisfaction of the built environment. This is particularly important with historic and traditionally constructed buildings, where perceptions of their performance are often based on preconceptions and generalisations. It is therefore important to undertake BPE of these buildings in order to establish their actual performance and inform the often difficult decisions regarding their ongoing use. This paper presents the BPE of a 14th century timber-framed house, with 17th century decorative pargetting in Saffron Walden, Essex. In situ monitoring and digital simulation were used to assess its current performance and inform the ongoing conservative repair work. The results show that although the thermal conductivity of the pargetting is not particularly low, the increased thickness, and more importantly the sealing of the commonly poor junction between the timber-frame and infill materials, do result in an external envelope with a higher thermal performance than many historic timber-framed buildings. The simulations show that whilst applying internal wall insulation would further improve this performance, it would also increase the risk of frost damage. This highlights the challenges of sustainable building conservation and the role of BPE.

KEYWORDS: Building Performance Evaluation, Hygrothermal monitoring, Energy Simulation; Energy Use In Historic Buildings, Conservation

1. INTRODUCTION

In order to understand the operational efficiency of our built environment and the levels of environmental comfort provided to its occupants, it is necessary to undertake Building performance evaluation (BPE). Through the combination of monitoring and simulation it is possible both assess the current conditions and make recommendations for improvements. When considering traditionally constructed and historic buildings, this becomes all the more important due to the preconceptions that exist as to their performance. It is generally accepted that the older the building, the less energy efficient it is. However, the results of some studies challenge this assumption [1-3]. Nevertheless, it is important that these studies do not themselves become the basis for further generalisations. It is therefore necessary to undertake BPE on all historic and traditional buildings, as part of their sustainable conservation, in order to inform decisions regarding their ongoing use, aiming to satisfy the needs of the buildings' users, whilst maintaining their heritage value.

This paper presents the BPE of a 14th century timber-framed mediaeval hall house (Figure 1) in Saffron Walden, Essex, in the East of England. The most significant feature of this property is its 17th century decorative pargetting, a layer of sculpted lime plaster externally covering the timber-frame.

In situ monitoring and digital simulation have been used to assess the buildings current performance and inform the ongoing conservative repair work currently being undertaken.



Figure 1. Laser Scan of North elevation. Eastern cross wing to the left and western to the left. Source: (Author's Own, 2017)

1.1 History

Described by Pevsner as "amongst the most precious of Saffron Walden" [4], the Grade I listed building was originally built in the late 14th century [5] as a single "hall house". In the 17th century it became part of the Sun Inn, later being divided into two dwellings, both remaining related to the inn until its closure in the 1870s. The cottages were then extended to the rear, with Tudor styled doors and

windows being fitted at this time [6]. In 1930 the ownership of both buildings was transferred to the Society for the Protection of Ancient Buildings (SPAB), who in turn vested the freehold in the National Trust, who own it to this day [6]. The leasehold of the cottages was acquired by the present owner in 2009, who embarked on the current ongoing conservative repair which aims to reunite the two cottages into one home fit for 21st century residential occupation.

1.2 Built Fabric

The structure of the main building is timber-framed, with closely spaced vertical timber members, forming tall vertical infill panels, a technique known as “close studding”. The ground floor has been underbuilt with brick, with the Victorian outshut also of brick construction. The infill panels to the upper stories are mainly wattle and daub, consisting of a clay plaster (daub) over a framework of woven thin timber elements (wattle work) wedged into the main structural timber-frame. It has been identified that some infill panels have been replaced at a later date with brick nogging [6]. The main roof is covered with clay peg tiles and the roof of the outshut is slated. As previously noted, the most distinctive feature is the main façade to the street which is covered in 17th century pargetting. The decorative elements include fruit, foliage, avian forms, a stocking and most notably two human figures. Since the acquisition of the property by the current owner, the pargetting has undergone extensive conservation repairs.

2. BPE METHODOLOGY

In order to understand the current and potential operative performance of this property, BPE was undertaken. The methodologies employed were internal hygrothermal comfort monitoring (dry-bulb air temperature and relative humidity), airtightness, thermography, in situ U-value measurements and digital energy demand simulation. As the property is currently uninhabited, occupant thermal perception surveys were not conducted.

The internal hygrothermal comfort was measured using TinyTag Ultra 2 TGU-4500 sensors, in addition to the owner’s Lascar® EasyLog® EL-USB-2 sensors, which were already in place. The sensors were located in seven internal locations and one external (Fig.2) and measured at half hour intervals from 11/03/17-16/08/17.

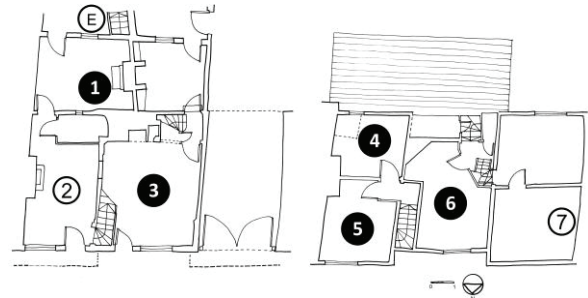


Figure 2. Ground (left) and first floor (right) plans showing hygrothermal monitoring locations. Open circles Lascar® sensors, solid circles TinyTag®.

Pressure testing to measure airtightness was undertaken on 12/03/17 according to BS EN ISO 9972:2015 [7] using a Minneapolis® blower door with analogue Magnehelic pressure gauges. The measurement procedure was conducted twice, once for the whole property and again for only the eastern portion, formerly number 25, in order to allow the comparison of the results with those undertaken previously in 2012 [8], prior to the reconnection of the two properties and removal of 20th century internal finishes. For this second measurement, the interconnecting door between the two halves was sealed with plastic sheeting and builder’s tape.

Thermography took place at 6:30am the same day following best practice guidance [9, 10], using a FLIR® B250 thermal imaging camera. During the measurements the building was unpressurised but electric heaters were used to augment the internal air temperature, achieving a temperature difference between inside and out of 11.5°C for the eastern cross wing and 5.5°C for the western.

The in situ U-value measurements were undertaken on two separate occasions (12/03/17-02/04/17 and 15/12/19-22/01/20) with two monitoring positions each time. The monitoring positions were chosen to measure two different thicknesses of pargetting. These are described in more detail in paragraph 3.4). The methodology followed BS ISO 9869-1:2014 [11] using Huxeflux HFP01 heat flux plates, held by pressure against the wall surface with a flexible plastic clip braced against adjustable building props. The surface of the plates was covered with paste to ensure complete physical contact, with the use of thin PVC film to avoid damage to the internal wall finish. Internal and external air temperatures directly adjacent to the wall surface were measured using type T thermocouples. On the first occasion the sensors were wired back to an Eltek® Squirrel® datalogger, whilst the second time a Campbell Scientific® CR1000 data logger was used. Both times the data was recorded with a five minute interval.

Digital simulations of the building’s current energy demand and potential future energy retrofit actions were undertaken using the software DesignBuilder®

Version 4.2.0.54, with measured U-values and airtightness imputed to improve accuracy. A climate file was created using the software Meteonorm® version 6.1 using the time period 1996-2005. Simulations were also conducted with the two-dimensional conduction heat transfer software THERM® version 7.5.

3. RESULTS

3.1 Internal Hygrothermal Comfort

Measurements were taken at half hour intervals from 11/03/17-16/08/17. During this time the property was unoccupied due to the ongoing conservation work. As such the results show that only the front bedrooms (locations 5 & 7 Fig.2) achieved any hygrothermal comfort during March. This was due to the electric heating used in both rooms to reduce the risk of frost damage to the 17th century pargetting. The heating was maintained for longer in front bedroom 5 to enable the in situ U-value monitoring. Being uninhabited, no space heating is provided in the rest of the house and hygrothermal comfort is only achieved in mid-May once external ambient conditions had also reached comfort conditions.

The reasons for hygrothermal comfort not being achieved are a combination of low temperatures and high relative humidity (Fig.3), with high relative humidity being a common problem on the ground floor. In two monitoring positions (2&3) relative humidity was recorded in excess of that measured externally. This may be partly due to the current uncontrolled connection of these spaces to a subterranean cellar.

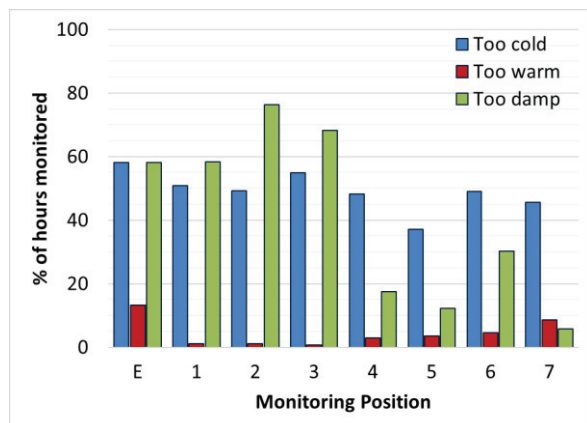


Figure 3. Graph showing percentage of time conditions do not achieve hygrothermal comfort conditions. 11/03/17-16/08/17 Refer to Fig.2 for location of monitoring positions.

3.2 Airtightness

The results (Table 1) showed that the work undertaken since 2012, removing inappropriate, 20th century, vapour impermeable internal finishes has

decreased the airtightness of property 1 by almost 50%.

Table 1: Airtightness results. (API) Air Permeability Index, (ACR) Air Change Rate @ 50 Pa

Property	API (m ³ /h.m ²)	ACR (/hr)
1*	7.3	10
1	14.2	18.8
1&2	58.6	56.6

* Previous measurement undertaken in 2012 [8]

The replacement internal finishes had not been installed at time of testing. It is assumed that these will result in increased airtightness. The reconnection of the two cottages has resulted in a particularly high air change rate, due to uncontrolled connections to roof voids and the cellar in property 2. Both the reinstatement of internal finishes and the closing off of the connection to the cellar are issues that will be addressed prior to the completion of the conservative repair process. Further testing is recommended following this work.

3.3 Thermography

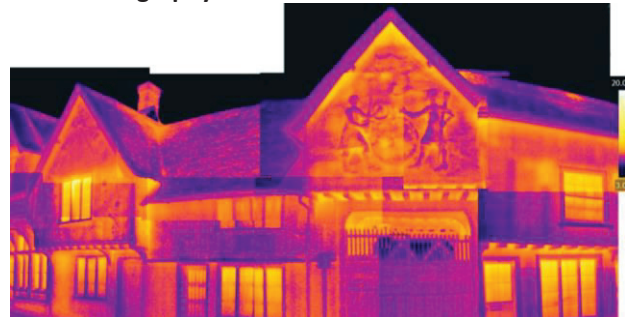


Figure 4. Thermography of north façade 12/03/17 6:30am. External temperature 10.5°C. Source: (Author's Own, 2017)

The thermography was undertaken unpressurised with an external air temperature of 10.5°C and internal temperatures between 13-22°C. A complete view of the whole north façade (Fig.4) appears to show that the pargetted upper façade is allowing less thermal transmittance than the lower brick underbuilding of the ground floor. Given the unequal heating of the corresponding internal spaces there may be some degree of error in this conclusion, however, the internal temperature of the ground floor was substantially lower at 13°C compared to the 16°C of the upper west cross wing bedroom (left) and 22°C of the upper east cross wing bedroom (right). Therefore, it could perhaps be presumed that if all spaces were at an equal temperature the difference in the thermal performance between the pargetting and the brick underbuilding would be even more apparent. Figure 4 also shows the differing thermal performance within the pargetted façade, with the thinner, plainer sections recording a higher surface temperature and therefor greater heat loss as compared to the thicker sculpted features. The

greatest thermal weaknesses of the envelope are however undoubtedly the single glazed windows, the protruding floor of the jettying and the exposed floor over the carriageway .

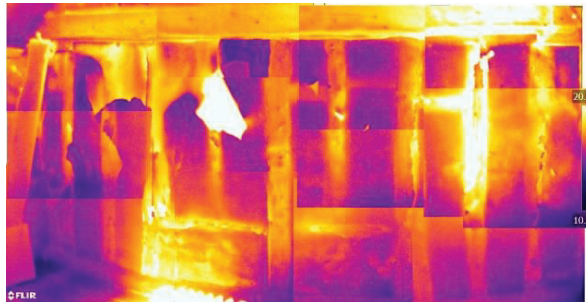


Figure 5. Internal thermography of west cross wing at 1st floor. 12/03/2017 6:30am. Internal temperature 16°C. Source: (Author's own, 2017)

Internal thermography of the north façade of the western cross wing upper bedroom (Fig.5) shows the higher thermal transmittance of the infill panels in comparison to the timber frame. Interestingly, by highlighting the timber-frame, otherwise hidden by the internal wallpaper, it also suggests the previous presence of a central window that may have predated the external pargetting. This demonstrates the advantages of BPE in understanding buildings, above and beyond reviewing their energy efficiency.

3.4 In situ U-Value

On the first occasion (12/03/17-02/04/17) the U-value was measured in two locations (M1 and M2 in Fig.6) on the first-floor elevation of the east cross wing (left in Fig.1).

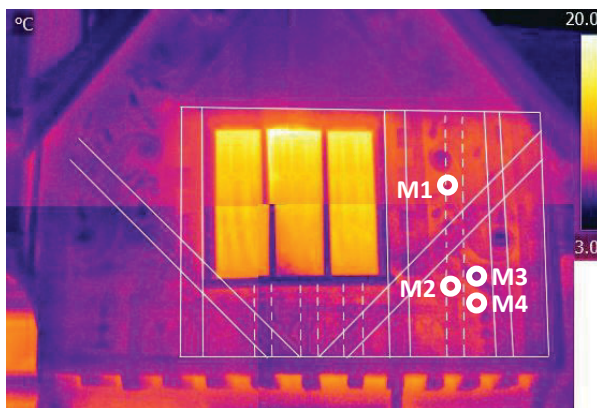


Figure 6. Thermography of eastern cross wing showing location of monitoring positions. M1 & M2 monitored 12/03/17-02/04/17 and M3 & M4 monitored 15/12/19-22/01/20. Source (Author's own, 2020)

The locations were chosen to measure two different thicknesses of pargetting, one plain section (M2) and a sculpted gourd or pear standing 40mm proud of the plain surface (M1). On first reading of the thermography it was believed both locations to be in the middle of an infill panel. Unfortunately,

closer inspection following completion of the measurements revealed faint signs of further timber-framing (dotted lines Fig.4), which was subsequently confirmed with the use of an electronic stud detector. This error was exacerbated by the heat flux plate in position M1 being accidentally dislodged after only five days. A second period of monitoring was therefore undertaken (15/12/19-22/01/20), again through two thicknesses of pargetting but this time avoiding the now identified timber-frame members. Position M3 was located to measure the body of an avian form, also 40mm proud of the surrounding plain surface, where M4 was located. The results of all four measurements are presented in Table 2.

Table 2: Measured U-Values

Monitoring location	Wall thickness (m)	U-value (W/m ² K)
M1*	0.170	0.85
M2	0.130	0.64
M3	0.170	1.29
M4	0.130	1.33

* Only measured over 5 days and so high error factor

The measured U-value at position M2, over a timber-frame member was 0.64 W/m²K, and as such below the UK Building Regulations threshold value (0.70 W/m²K) for retained thermal elements [12]. In the centre of a panel (M3 & M4) the values are higher, however, these are considerably lower than measurements of other historic timber-framed properties, with typical U-values 1.69-2.88 W/m²K [13, 14] for un-pargetted walls, suggesting that pargetting may be considered an early form of external wall insulation (EWI).

That said, the improvement in U-value provided with the increased thickness of pargetting is marginal in monitoring position M4. Assuming that this improvement is purely down to the additional pargetting, this would suggest the pargetting has a thermal conductivity of 1.72W/mK, similar to a hard limestone [15] and therefore not a particularly effective EWI. In the case of monitoring position M1, for the short period that monitoring did occur, the measured U-value was consistently higher than the thinner M2. Some speculation has been made over the influence of increased external surface area of the mouldings, however, further research is required to confirm this.

4.0 DIGITAL SIMULATION

4.1 DesignBuilder®

The simulation with DesignBuilder®, using the measured U-values and air-change-rates, showed a current heating energy demand of 179kWh/m². If the airtightness could be returned to that measured in 2012 this could be reduced to 96.6kWh/m², with a further 17% reduction possible by insulating roofs

and exposed floors. Insulating external walls internally with internal wall insulation (IWI) would result in an additional 12-20% reduction, however, there is concern over the potential increased risk of frost damage to the decorative 17th century pargetting.

4.2 THERM®

In order to assess this increased risk, simulations with THERM® were undertaken. Modelling was conducted, both in its current state uninsulated and with differing thicknesses of IWI, of a cross section of pargetted wall, including decorative sculpted elements, the profile of which was determined by data acquired through laser scanning.

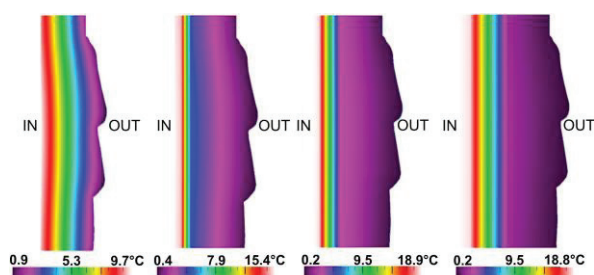


Figure 7. Simulations with THERM® version 7.5 of wall section through decorative pargetting showing temperatures with (left to right) no insulation, 25mm, 50mm and 100mm of wood fibre IWI. Exterior temperature 0°C and interior 21°C. Source: (Author's own, 2017)

The simulation demonstrated (Fig.7) that currently with no insulation, with an internal air temperature of 21°C and an external air temperature of 0°C, the external surface of the most protruding features of the pargetting would be almost 1°C higher than the surrounding air at 0.9°C. Any introduction of insulation will reduce this external surface temperature, thereby raising the risk of frost damage. In the case of the 25mm IWI, the external surface temperature is halved to 0.4°C when the external air temperature is 0°C. With the application of 50mm and then 100mm IWI this drops to 0.2°C, with much of the historic wall being below 1°C. Given the heritage value of this historic pargetting it is unlikely that this potential increase in risk of frost damage can be outweighed by the reductions in energy demand that would be achieved. As no decorative pargetting is present on the ground level, potentially this could be internally insulated with 25mm of IWI resulting in a 7% reduction in energy demand.

5. DISCUSSION

The monitoring at this un-retrofitted property has highlighted areas for improvement but has also shown that at times the historic fabric can perform better than expected. The measured u-values indicate that the pargetted wall is performing better than other infill panels of historic timber-framed

buildings, including some which have been replaced with modern insulation materials as part of energy retrofits [14]. The thermal conductivity of the pargetting is most likely only partially responsible for this performance, with the sealing of the joints between panel and timber-frame, thereby reducing infiltration and air movement also being influential.

The pressure testing showed that currently the property is not very airtight and that the work so far undertaken by the owner to remove 20th century finishes has made it even less so. If the property is to be an inhabitable dwelling, this is an area that will require careful consideration. The owner's intention is not to leave the property without internal finishes but rather to replace the impermeable 20th century finishes with traditional vapour permeable finishes that will be more sympathetic, both technically and aesthetically, to the historic building fabric. It is assumed that the reinstatement of complete internal finishes will lead to an improvement in airtightness. Whether these achieve a higher or lower airtightness is an area that a future BPE should investigate. At the same time the uncontrolled connection between the basement and attic spaces will be addressed, thereby further improving hermeticity. As shown by the DesignBuilder® simulation, even just returning the property to the airtightness levels measured in 2012 would see a 17% reduction in energy demand.

The thermography showed the single glazed windows and exposed floors, both over the carriageway and the jetttying, to be the areas of greatest thermal weakness. These areas would be relatively easy to address, with little adverse impact on the heritage value of the property. The current windows date from 1870 [5] and as such not one of the most significant features of the building, however it is unlikely that they would be replaced. Although, it would however be possible to repair the windows to increase airtightness, install secondary glazing, insulated internal shutters or thick curtains, all of which would improve the thermal performance of these elements [16]. The insulation of the exposed floors may be more difficult as this would most likely require the lifting of the existing floorboards, with the potential risk of damage that this entails. However, insulating the exposed floors and the roof do not pose the same risks of increased frost damage to the 17th century pargetting that would be involved in the use of IWI, as shown by the THERM® modelling. Given the high significance of the pargetted façades, a trade off could be made in allowing beneficial heat loss through the associated walls, whilst insulating elsewhere, even if this involved some limited loss or damage to historic fabric.

The hygrothermal monitoring shows that in its current unoccupied state, few rooms in the house achieve comfort levels. This is to be expected and the

measurements in the front bedroom of no.27 show that with heating, comfort can be achieved. Equally the controlling of the connection to the cellar should assist in resolving the high levels of relative humidity measured on the ground floor. However, further monitoring is recommended as the conservation of this building progresses

4. CONCLUSION

The use of BPE has enabled a greater understanding of this historic property which can now inform the continuing decisions in its conservative repair. Keys findings are:

- That the pargetting appears to improve the U-value of the timber-frame wall, acting as an early form of EWI.
- Conservative repair work removing inappropriate internal finishes has reduced the airtightness. The new finishes will hopefully rectify this.
- Improving airtightness and insulating roofs and floors could see a reduction in energy demand of 55%. However, the use of IWI on the pargetted walls would increase the risk of frost damage to this historically significant element and as such is not advisable.

The research presented in this paper has highlighted the role that BPE can play in understanding the complex performance of our historic built environment and the challenges that face us in balancing the conservation of heat and power and the sustainable conservation of our heritage.

ACKNOWLEDGEMENTS

Thanks to the building owner for allowing this monitoring to take place and for sharing their own monitoring data.

REFERENCES

1. Macalister, T., (2006). The green house of the future - built c.1550, *The Guardian*. [Online], Available <https://www.theguardian.com/uk/2006/nov/08/topstories3.ethicaliving> [28 July 2020].
2. Wallsgrove, J., (2008). The Justice Estate's Energy Use. *Context: IHBC*, 103(March): p. 19-20.
3. Oresrcryn, T., T. Mullany, and C. Ni Riain, (1994). A Survey of Energy Use in Museums and Galleries. In *Museums: Environment, Energy*, M. Cassar, Editor, Museums & Galleries Commission.
4. Pevsner, N., et al., (2007). Essex., New Haven (Conn.); London: Yale University Press.
5. Kent, D.D., (2015). 25-27 Church Street, Saffron Walden: A Brief Guide. p. 2.
6. Historic England, (2014). The National Heritage List for England, Historic England. [Online] Available: <https://historicengland.org.uk/listing/the-list/list-entry/1196155> [28 July 2020]

7. British Standards Institution, (2015). BS EN ISO 9972:2015 Thermal performance of buildings - determination of air permeability of buildings - fan pressurization method. British Standards Institution.
8. Hubbard, D., (2012). Air permeability testing and thermographic survey: 27 Church Street, Saffron Walden. ArchiMetrics.
9. Hart, J.M., (1991). Practical guide to infra-red thermography for building surveys, BRE: Bracknell, UK.
10. Young, M., (2015). Thermal Imaging in the Historic Environment, in Short Guide, Historic Environment Scotland. [Online]. Available: <https://www.historicenvironment.scot/archives-and-research/publications/publication/?publicationId=088dab34-1194-43e6-af5e-a62801090992> [28 July 2020]
11. British Standards Institution, (2014). BS ISO 9869-1:2014 Thermal insulation- Building elements- in situ measurement of thermal resistance and thermal transmittance Part 1: Heat flow meter method.
12. HM Government, (2018). Approved Document L1B; Conservation of fuel and power in existing dwellings. NBS.
13. Rye, C., C. Scott, and D. Hubbard, (2012). THE SPAB RESEARCH REPORT 1. U-Value Report. Society for the Protection of Ancient Buildings. [Online]. Available: <https://www.spab.org.uk/sites/default/files/documents/MainSociety/Advice/SPABU-valueReport.Nov2012.v2.pdf> [28 July 2020]
14. Whitman, C.J. and O. Prizeman, (2016). U-value Monitoring of Infill Panels of a Fifteenth-century Dwelling in Herefordshire, UK. APT Bulletin: *The Journal of Preservation Technology*. 47(4): p. 6-13.
15. British Standards Institution, (2000). BS EN 12524:2000 Building materials and products - Hygrothermal properties - Tabulated design values.
16. Wood, C., B. Bordass, and P. Baker, (2009). Researching into the thermal performance of traditional windows: timber sash windows. Historic England. [Online]. Available: <https://research.historicengland.org.uk/redirect.aspx?id=7273%7CResearch%20into%20the%20Thermal%20Performance%20of%20Traditional%20Windows:Timber%20sash%20windows%27> [28 July 2020]

How to Transform European Housing into Healthy and Sustainable Living Spaces?

– the RenovActive principles tackle climate and renovation challenges

PETRUS TE BRAAK², JOERI MINNEN², MORITZ FEDKENHEUER³, BERND WEGENER³, FRIEDL DECOCK⁴, FILIP DESCAMPS⁴, SABINE PAUQUAY⁵, LONE FEIFER¹, LARA ANNE HALE¹, THORBJØRN FÆRING ASMUSSEN¹, JENS CHRISTOFFERSEN¹

¹VELUX A/S, Hørsholm, Denmark

²Vrije Universiteit Brussel, Brussel, Belgium

³Humboldt University of Berlin, Berlin, Germany

⁴Daidalos Peutz, Leuven, Belgium

⁵VELUX Belgium, Brussel, Belgium

ABSTRACT: This renovation concept seeks to offer healthy, affordable, easy to reproduce, scalable solutions for the existing building stock of European housing. The concept was developed and tested in a prototype phase, where 7 principles have been applied to a semidetached house built in 1920s, situated in a garden city in Brussels. The prototype was now occupied by a family and monitored for two years. The monitoring was performed both through data, sensors and extensive interviews and questionnaires with the family. In general, living in the house is positively perceived by the family, who state they are very satisfied with the indoor environment, such as temperature, air quality and daylight. Sensor data results show a general indoor CO₂-concentration below 900 ppm. Indoor temperature measurements vary between 21°C and 26°C. The occupants are very satisfied with the house, however the technical and sociological monitoring show there is further potential to optimise and improve indoor comfort levels and perception. There are discrepancies between setpoints and programming, based on predicted behaviours, and user actions and preferences in real life, as well as situational perceptions and culture. This goes to prove that technical systems operating the indoor environment must be both flexible and robust to accommodate for multiple and varying preferences of building inhabitants.

KEYWORDS: Renovation, POE, Building Monitoring, Active House, Healthy Buildings

1. THE RENOVACTIVE CONCEPT

Through 2008-2012, several Model Home 2020 demonstration buildings were designed and constructed. The objective of the Model Home 2020 project was to combine excellent indoor environment with high energy efficiency. Thereby, the houses were designed, built and constructed as state-of-the-art homes with the newest technological developments and high-quality materials, and designed to strike the best balance between the three Active House principles [1] (Figure 1):

- Comfort: the building should provide indoor living conditions that support the health and comfort of its inhabitants
- Energy: the building achieves high levels of energy efficiency and makes use of renewable energy
- Environment: the building has a minimal impact on the environment.

In the Model Home 2020 projects, all buildings were monitored in use to measure and understand both the buildings' performance and the perception of the occupants. From the monitoring part, one of the conclusions was that it is possible with available

products and technology to meet the 2020 energy requirements without compromising sustainable living.

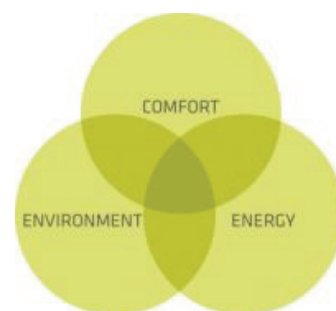


Figure 1 - The Active House principles

The need for meeting legislative requirements is especially poignant with pre-existing structures. The RenovActive project builds on these learnings, while focusing on renovation. Indeed, all the current dwellings in Europe have been built between 1945 and 1980, and the average age of our total building stock continues to grow increasingly older. Eurostat has registered a 30% decline in construction output in the EU's 28 member states since 2008. If the trend continues, 90% of our current residential properties

will still be in use by the year 2050. The RenovActive project in Anderlecht seeks to offer healthy, affordable, scalable solutions [2] by testing the Active House principles in social housing and in the single-family housing segment.

2. SEVEN PRINCIPLES FOR A HEALTHY AND AFFORDABLE CLIMATE RENOVATION

A key aspect of the RenovActive (Figure 2) project is to prove the financial viability of a renovation according to the Active House principles in social housing across Europe, where challenges are:

- Ill-maintained homes are more common in rental properties due to tenants' lack of ownership
- Energy poverty means that nearly 11% cannot afford to heat their home sufficiently
- Unsuitable behaviors, e.g. lack of regular airing and the drying of clothes indoors, lead to a bad indoor climate



Figure 2 RenovActive prototype before and after renovation

Dividing the concept into seven individual building elements makes it possible to create a better match between the financial plan of the project and the different needs of the housing company, and the very wide span of existing housing conditions. To be able to meet the different points of departure, and enable a standardized approach, the affordability concept bases on the proven quality of each principle, as well as the ability to be reproduced, allowing economies of

scale to take effect; as such it is an approach of systemic enablement with a combination of elements.

Table 1: Seven principles applicable and cost-effective solutions for renovation.

1: Attic conversion: The attic is converted into living space (area 12,5m ²) and connected to the home via an open stairwell.	
2: Increased glazed area: Distribution of windows (both new and existing) in every room and on every floor to improve daylight conditions	
3: Staircase shaft for daylight & ventilation: An open stairwell topped with roof windows allows ventilative cooling through open roof windows as well as downward daylight distribution.	
4: Dynamic sunscreening: External sun screening reduces overheating.	
5: Hybrid ventilation system: During summer, windows and stairwell are used to provide natural cooling in the building. During winter, mechanical ventilation maintains indoor air quality and while limiting risk of draughts.	
6: Improved thermal envelope: New facade insulation, a new roof construction and new windows all around ensure reduced energy consumption. New ground floor heating and modern radiators on the 1 st and 2 nd floors.	
7: Building extension: The extension (area 15m ²) creates additional living space on the ground floor and space for one more family member in total.	

The RenovActive Concept is based on seven principles, seen to be the most applicable and cost-effective solutions for renovation (Table 1). Each element is created to give existing buildings the ability to perform on the same level, or close to, as newly built houses. Depending on the existing building design and renovation budget, the different elements

can be implemented to increase the level of daylight, improve ventilation, strengthen the envelope or expand the living space through densification or extension. The concept's modularity adapts to each house typology.

To investigate the concept, the house has been tested by the first family to move in and monitored post occupancy to evaluate how the elements function in practice. The post occupancy evaluation is conducted by a research team of social scientists and engineers. The sociologists took a close look at the occupants' perspective, experiences and their interaction with the building. The engineers checked physical data and performances of the house. The post occupancy monitoring of the first RenovActive project wanted to explore the performance of this healthy and affordable renovation, targeting both energy savings and user comfort.

The following targets were laid down to make the RenovActive House in Belgium a success and validate the concept - all of them were met by the completion of the project:

- Indoor climate: The house offers high daylight levels, protection against overheating and a good indoor air quality
- Affordability: The renovation (incl. all technical equipment) is executed within the budget lines of social housing in Brussels
- Reproducibility: The concept should be based on existing technologies and materials
- Energy performance: The primary energy use complies with the strict Brussels EPB (Energy Performance of Buildings) legislation

2.1 From an occupant perspective

The sociological monitoring included three different instruments of data collection and several data collection points. There were face-to-face-interviews, online questionnaires and a time-diary-tool. These three instruments were linked together, and each is referring to the other. After filling in questionnaires, the adults were interviewed face-to-face by a scientist, directly after the interview, both adults were asked to fill in a time diary for a one-week period. The online questionnaire quantified the opinions, level of satisfaction and comfort behaviour of the dwellers, an input that was then extended during the face-to-face-interview.

2.2 From a monitoring perspective

The post occupancy building monitoring included measurements of indoor air quality and thermal comfort, as well as energy consumption. The monitoring aimed at establishing knowledge and documentation on the house's performance, the inhabitants' perceptions and on the contribution of the different renovation principles to both.

2.3 Methodological challenges

In this project, there proved to be several methodological challenges to be dealt with when monitoring and evaluating the results, the most prominent one being the dependency on a single case exploration, which makes generalising difficult. Some findings can thus be to some extent, related to the observed family and the special conditions of their former home.

3. RESULTS

The complete monitoring program took place from July 2017 until September 2019. Data from the social monitoring [3] show that the family is very satisfied with the level of indoor comfort. In the questionnaires, the time diary as well as during the interviews, the family stated that they were very happy with the indoor temperature, the indoor air quality and daylight levels. However, the family pointed towards too high temperatures during the summer months of the first year. Based on this feedback, adjustments were made to the ventilation system to improve the stack effect of the staircase by automatic window openings. Moreover, a better solar shading device in the attic significantly improved the indoor comfort. The occupants perceived the house to be well-lit by daylight thanks to the different windows, even if they were using the ground-floor solar protection almost all the time for privacy reasons.

There is generally enough space for the family and the layout ensures that the house can be used optimally.

To further improve the level of comfort, the family had various options to adjust appliances manually, such as opening windows, lowering blinds, adjusting heating and ventilation systems, etc. Besides daily adjustment of the heating in the bedrooms during winter, and the opening of windows during cooking and cleaning in order to let the 'smelly' air out, few adjustments were made to improve the indoor climate. Nevertheless, occupants reported a sense of being able to adjust the different indoor parameters according to their needs, and when doing so, to experience an improvement of the indoor environment. Interestingly, the ventilation system as well as the home automation system were left unadjusted, along with sporadic manual window opening to cool down the house.

The mother reports a positive development on her state of health. She reported irritated airways in the former home because of high humidity during winter. This has disappeared. The quality of sleep has also been greatly improved since the family moved in. Although the general perception of the house is very positive and associated with increase of happiness, health level and overall wellbeing, there are a few elements that occupants identify as challenging: the

presence of mosquitos during night, lack of outdoor storage facilities, and a technical mistake of the slope of the bathroom floor.

the lowest possible airflow (an airflow has to be maintained as the Healthbox unit contains the indoor climate sensors) and the windows are used to control

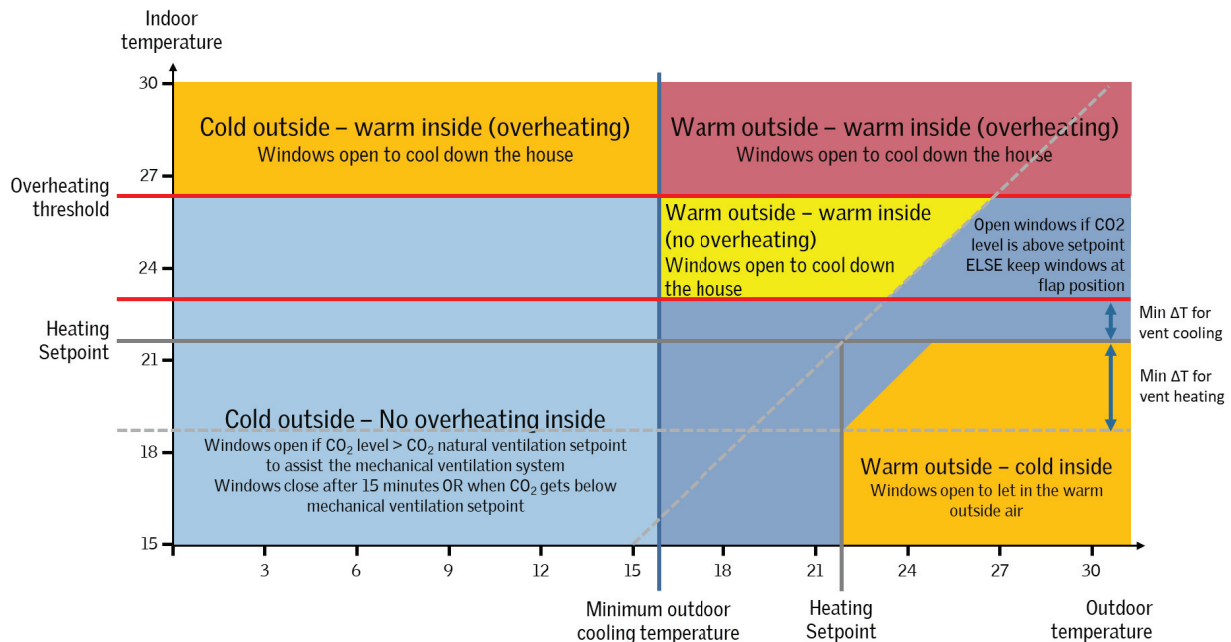


Figure 3: Schematic diagram explaining the hybrid ventilation system of the Healthbox.

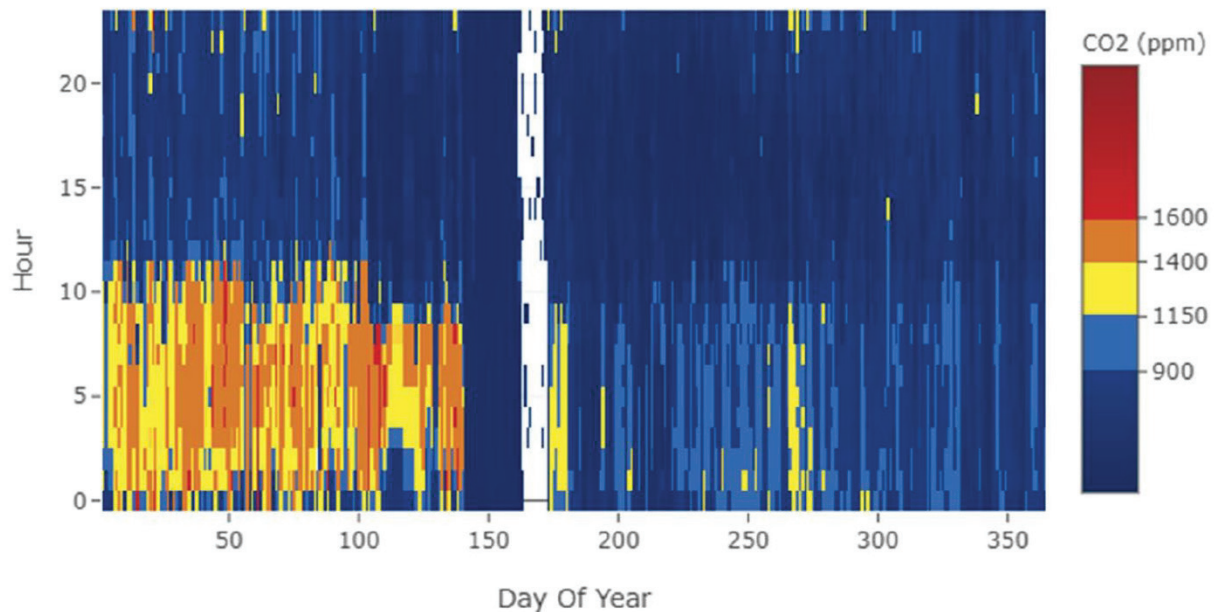


Figure 4: Temporal map of the CO₂ concentration in the parent's bedroom, 2018. Each column represents one day of the year and each of the rows the hours. The colour scale indicates the CO₂ level. The white area around May is due to a period of missing data.

From a monitoring perspective [4], the results show that the indoor air quality is very good. The hygienic ventilation system, Healthbox, in the house is a demand-controlled ventilation system with natural supply vents and mechanical extraction, designed according to Belgian standards. Figure 3 show the schematic diagram, where the control is based on the indoor and outdoor temperature. When the outdoor temperature is above "minimum outdoor cooling temperature, the mechanical ventilation is reduced to

the indoor climate. Below the setpoint the mechanical ventilation runs in demand control mode with the windows as a backup system (for birthdays and other occasions where the mechanical ventilation is not sufficient to cope with the pollution load).

The mechanical extract ventilation was roughly 9 L/s for the bedrooms and 22 L/s for the kitchen. Additionally, a peak ventilation through automatically controlled window openings is available. The control of the switch between hygienic and peak ventilation is

based on indoor air quality parameters (CO₂, RH) and indoor air temperature. The setpoint for the mechanical extract ventilation is 850 ppm. During warm periods, windows open at 1100 ppm and during winter at 1500 ppm (natural peak ventilation is thus used as a backup for the mechanical system providing hygienic ventilation). The design goal was to maintain at least category II of EN 16978-1 (5), Table B.12, corresponding to 1200 ppm (outdoor level 400 ppm). For more than 95% of the time, the CO₂-concentration in the house, in general, is below 900 ppm. Slightly higher values were measured in the parents sleeping rooms (e.g. 1100 ppm, Figure 4). On the other hand, the mechanical ventilation system did not perform according to the intended strategy from the beginning, due to some of the supply vents unintentionally closed, as well as the fact that the fan system was set, by the family, to eco-mode instead of demand control mode due to noise, resulting in low ventilation rates. Automatic operation of the staircase windows, and attic window was turned off at night (as a mosquito protection). In this timeframe, the 95th percentile CO₂ concentration where slightly above 1300 ppm. Indoor temperature measurements show that the thermal comfort is good, but in case of extremely hot temperatures, indoor temperatures increase quickly if the solar shading devices are not used as intended.

The temperatures stay for more than 95% of the time between 21°C and 26°C (e.g. similar to category II of EN 16978-1 Table B.4), while the attic has slightly higher values, but stays under 28°C, after improved staircase- and attic-window openings, especially by encouraging the family to use cross ventilation in the attic to reduce peak temperatures. During the 2018 hot spell, the indoor temperatures were too high, and the automatic system did not resolve this, but could have been improved by ensuring cross-ventilation operation.

Energy consumption for heating is higher than the predicted value, mainly due to higher indoor temperature (about 21°C) than the setpoint used in the calculation (19°C). The average yearly energy consumption for heating (gas consumption) and domestic hot water is around 70 kWh/m²/year. The electricity consumption is slightly above a moderate household use (+400 kWh). There is most likely a rebound effect as explanation on year 1, and the energy consumption was reduced during year 2.

4. CONCLUSION

In general, home satisfaction is very high. The family indicated that they are very happy with the indoor climate, such as the indoor temperature, air quality and the automatic system. The health and sleep quality of the family have improved considerably since they moved into the RenovActive house. They also report that their family life as well as social

contacts outside the family have greatly improved. During their daily life, few adjustments of the automatic system are operated by the family. One reason could be that the family indicates that they feel unqualified to make adjustments; they consider that the system is smarter than they are, not daring to overrule it. Another reasoning is that as long as the system does not interfere with their primary needs (privacy, mosquito bites etc.) they tolerate it.

Finally, an important learning is that the family operates the technical systems, as well as its adjustment possibilities, slightly differently than the intended strategy. Consequently, the flexibility and robustness of the technical systems operating the indoor environment is essential to accommodate for the occupants' preferences. For example, a system detecting significant deviations from planned parameters could return to a default setting or provide feedback to occupants to allow them to make informed decisions.

REFERENCES

1. Active House <https://www.activehouse.info/>
2. VELUX (2016). A healthy and affordable renovation concept Available: https://velcdn.azureedge.net/~media/com/case%20studdy/renoactive/renovactive_brochure.pdf [30 September 2019].
3. Vrije Universiteit Brussel (2019). User experience and post-occupancy evaluation - Final Report on the Sociological Monitoring June 2017 – June 2019 (Not published).
4. daidalos peutz (2019). RenovActive.monitoring - the results of the comfort and energy monitoring campaign from July 2017 - September 2019 (Not published).
5. EN 16798-1:2019 Energy performance of buildings – Ventilation for buildings – Part 1

Methodology proposal for the evaluation of energy efficiency and indoor environmental quality of school buildings: Case study in Aranjuez (Madrid)

Beatriz Arranz ¹, Mariana Perez Grassi ²

¹ Universidad Politecnica de Madrid, Madrid, Spain

² Habitar Sostenible, Madrid, Spain

ABSTRACT: Schools in Spain suffer significant deficiencies, which are related to three aspects: architecture, education, and energy consumption. The growing interest in school buildings is mainly due to high energy consumption in this sector and inadequate IEQ. Climate change is a challenge society is facing. In Spain, the final energy consumption in buildings for education amounted to 599 ktoe. In innovative pedagogies, the child has gone from being a passive subject to an active subject. The pedagogical importance of the environment takes centre stage when considering the autonomy of the child in the construction of knowledge. In this paper a technical-participatory methodology is proposed, incorporating the user into the process, as a subject that provides useful information and participates in the optimal functioning of the building. The first phase of this methodology is applied in a case study. According with the analysis the school indoor environment does not comply with the minimal requirements to promote optimal learning and there is not an efficient use of energy. The school community input has been of high value. Information has been shared with the City Council and the school along with improvement proposals. Awareness activities are recommended.

KEYWORDS: Schools, IEQ, energy efficiency, user behaviour, participation.

1. INTRODUCTION

Schools in Spain suffer significant deficiencies, which are related to three aspects connected to each other but that are usually dealt with independently: architecture, education, and energy consumption.

Spain has approximately 25,000 schools (65% public and 35% private) [1]; much of them built in the 70s. The main investments since then have been devoted to extensions to meet the needs derived from successive population growth. Sustainability levels in general and comfort and energy efficiency are in the most cases poor or very poor.

Today, climate change is a challenge society is facing. The EU has proposed an integrated package of measures on climate change and energy which establish stronger long-term renovation strategies, aiming to decarbonise national building stocks by 2050. The Energy Performance of Buildings Directive (EPBD) is the main European standard aimed at ensuring the achievement of the EU's objectives in relation to building construction. In view of the exemplary role that public institutions should have, the European Directive 2012/27 / EU required from January 1st, 2014 that 3% of public buildings must be renewed every year. In Spain, the final energy consumption in buildings for education amounted to 599 ktoe, 6.77% of the total energy consumption in the service sector, a percentage very similar to the 6.87% corresponding to the energy consumption in hospitals [2].

A similar thrilling challenge is concerning education nowadays. Schools must fulfil the important role of educating today's children. In innovative pedagogies, the child has gone from being a passive subject to an active subject, listening to the child, working collaboratively, being empowered by the child to experiment, and valuing the imagination. The pedagogical importance of the environment takes centre stage in this approach that considers the capacity and autonomy of the child in the construction of knowledge [3]. In 1998, neuroscientists Fred H. Gage and Peter Ericksson announced the discovery that the human brain can produce new nerve cells (neurons) favouring richly stimulating environments [4]. This was the birth of neuroarchitecture, according to Eve Edelstein, "Neuroarchitecture tries to consider how each aspect of an architectural environment could influence certain brain processes, such as those related to stress, emotion and memory." [5]

Architecture is decisive in relation to the Indoor Environment Quality (IEQ), the main aspects to be considered to ensure the internal environmental quality must satisfy the conditions of hygrothermal comfort, acoustic comfort, luminous comfort and air quality [6]. IEQ attracts scientific interest especially when it concerns the health of vulnerable populations such as children. The indoor environment should not hinder the learning of children, e.g. with high noise level, overheated rooms or inadequate lighting conditions or stuffy and unhealthy air.

Unfortunately, many schools do not provide an adequate indoor environment. Many schools fail to provide a sufficient outdoor air supply rate and are too warm in the summer months [7]. The growing interest in school buildings is mainly due to high energy consumption in this sector and inadequate IEQ [8].

In relation to **hygrothermal comfort** the regions of Southern Europe are already experiencing a marked increase in maximum temperatures and a consequent and marked decrease in rainfall. More frequent heat waves and changes in the distribution of infectious diseases sensitive to climate change are expected to increase, which will result in risks to human health and well-being. The month of June 2017 was marked by high temperatures across Western Europe with heat waves triggering national heat-health plans and wildfires requiring evacuations in Portugal and Spain, sending monthly mean temperatures about 3°C above normal levels (1981-2010). During these heat waves, temperatures above 32°C inside public education centers were reached. This problem has generated an important social alarm in the warmer regions of Spain, extreme circumstances occur in the warmest regions, and in large cities where the problem is accentuated by the thermal island effect. Studies carried out in which students performance has been analysed, conclude that there is an effect on students' performance because of anomalous temperatures inside their classrooms [9]. Heat makes pupils lethargic, can affect concentration and lead to fainting.

In relation to **lighting comfort**, high solar radiation climates, the effect of the large amount of light and the usual lack of daylighting control devices cause exterior sunscreen abuse, paradoxically generating artificially illuminated interior spaces. The consequences of living in areas with not enough daylight go beyond the impact on electricity consumption. The higher the daylight level the higher the achievement of the pupils, schools in the study [10,11] show a 7 to 18% higher performance in those classrooms with the most day-light compared to those classrooms with the lowest amount of daylight. In addition, daylight provides less heat in relation to performance than artificial light and is free.

Regarding **air quality**, in the early years specifically, poor air quality has a negative impact. CO₂ concentrations seem to affect attendance. A 1000 ppm-rise in CO₂ concentration leads to increased absenteeism of 10-20% [12]; every increase of 100 ppm leads to a decrease in annual attendance of about 0.2% [13]. Thus, there seems to be an influence of CO₂ concentration on attendance, however the dimension is unclear yet (factor of 10 between the studies) and may be related very strongly to specific school conditions. If ventilation rates were increased

over the recommended values, the illness caused absence rate would seem to be reduced by about 11-17% [14].

In relation to **acoustic comfort**, according to the World Health Organization, there are several problems that can be caused by noise, such as decrease in work or school performance: changes in blood pressure, cardiovascular effects, interference with communication and social behaviour. Other problems are effects on metabolism, decrease or loss of hearing; behavioural changes in children and sensitive people, hormonal changes, sleep disturbances causing difficulties in daytime and low immunity function [15]. The negative interference in learning caused by inadequate acoustics of classrooms has been established in several studies (e.g. [16-18]) and the main effect of noise in classrooms is to reduce speech intelligibility. In Spain, 40% of schools in Madrid suffer from disturbing levels of outdoor noise [19]; in addition, there are certain interior areas such as canteens or gyms where noise levels are too high. There is also some social alarm, the NGO Ecologistas en Acción calls for an urgent action plan by the Madrid City Council.

User behavior is one of the factors that most influence the energy consumption of the building and contributes to uncertainty in the prediction and simulation of energy use in the models [20-23], causing the greatest discrepancies between those stipulated by design and the energy consumed in the stage of use. The understanding of user behavior is insufficient at all stages of a building (design, use and rehabilitation), leading to erroneous simplifications in computer models and analysis [21]

The involvement of the user is relevant, first as a source of information on the building performance, secondly because when the user perceives they are needed for the optimal management of the building, they take responsibility to ensure the common interests, and become aware of the environmental significance of their actions. The active participation of users helps the changes implemented to become permanent.

In this paper an innovative methodology, aimed at the successful renovation of schools, is described, and the first phase of this methodology is applied in a case study.

2. METHODOLOGY.

The proposed methodology is designed with the conviction that by making users part of the process, the final solution will respond better to their needs and the user will take responsibility for the building management, making more efficient use of it.

The particularity of the proposed methodology consists of incorporating the user into the process, as

a subject that provides useful information and as a subject that participates in the optimal functioning of the building.

The **technical-participatory methodology** proposal is called “Escuelas que Cuidan Passport”, it is structured in four phases: analysis, design, construction, and monitoring.

Each one of them considers the involvement of the building user. This paper deals with the first phase of the “Escuelas que Cuidan Passport”, which has been applied in a school in the Community of Madrid.

Comprehensive technical-participative analysis.

The technical measures consist of Indoor Environmental Quality (IEQ) measurements, and an energy efficiency analysis. The technical process is accompanied by a parallel participative work consisting of interviews, meetings, workshops, and questionnaires with three objectives:

- Raising awareness on the importance of interior environmental quality and energy efficiency.
- Obtaining first-hand information on how users of the building feel in it.
- Involving the user in the search for solutions and in future efficient use of the building.

The Indoor Environmental Quality (IEQ), consists of measurements of temperature, humidity, lighting, acoustics, and CO₂ taken in different areas of the school (classrooms, hallways, dining room, gym, auditorium). Spot measures are carried out during specific visits to the school and several sensors are left recording data for three weeks in the 3 classrooms and the gym.



Figure 1. measuring devices.

The measuring device placed in the classrooms and used to record Temperature, Relative humidity and CO₂ is the WOEHLE CLD 210 (figure 1. left). The device used to do spot measurements during the visits to the school is the sensor MC350 with its mobile application (figure 1. right) to visualize the data, providing measurements of temperature, noise, lighting levels and humidity.

The energy analysis consists of carrying out an energy audit, thermographic images (Flir ONE Pro thermal camera), and the energy certificate.

Acoustic tests of insulation to external noise, airborne noise isolation between indoor rooms, impact noise and reverberation time are performed.

The participative activities consist of:

- Interviews with teachers and center staff aiming at generating awareness and detect the main deficiencies perceived by them.

- Questionnaires: The questions proposed are quite open, aiming at having objective input from the pupils, to obtain undirected responses.

- Workshops: The objective is to generate awareness. The devices used for the technical analysis, previously described, are also used as a teaching tool in workshops with children and in meetings with teachers.

Once the information is evaluated **the overall diagnostic is shared** along with improvements.

An indicators system is designed to communicate the results. A traffic light exercise represents the conditions of comfort and energy efficiency evaluated in the school. The results are classified according to the following colors and meanings: **GOOD**, **TOLERABLE (with observations)** and **CRITICAL**.

The values obtained from the analysis are compared to National Spanish Building Code (CTE) minimal requirements, if the results comply they are **GOOD**, if they are 5% under the requirements they are considered **TOLERABLE (with observations)** and if they do not comply they are **CRITICAL**. The indicators systems allow not only to quickly visualize the results of the diagnosis, but to prioritize them and plan the improvement actions.

2. CASE STUDY. “CEIP San Isidro”, Aranjuez (Madrid).

The school “CEIP San Isidro” has 6 buildings and 14,000 square meters of land where 1000 students, 50 teachers and 12 non-teaching professionals work every day.

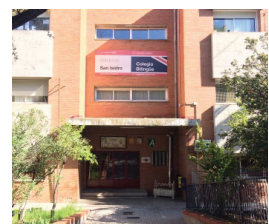


Figure 2. School main entrance.

The work was carried out during the second semester of the 2017-2018 school year, from January to June.

The energy analysis considers all school buildings and facilities. For the IEQ analysis, specific spaces were chosen with variable characteristics and representative of different circumstances that occur in the whole building. The spaces studied are:

- Classrooms: 3ºB (Building 2), 4ºD (Building 1), infant classroom 4años (Building1).
- Canteen, hallways, theatre, gym and outer space.

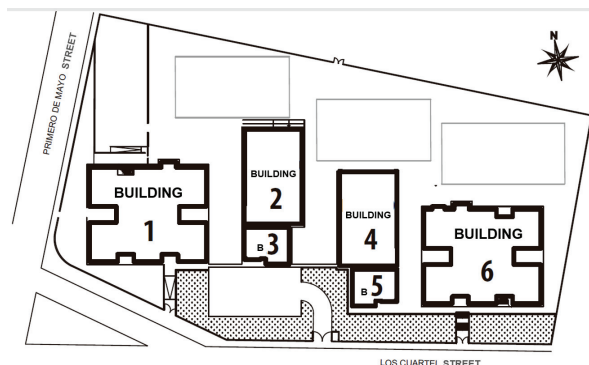


Figure 3. School layout

The comprehensive technical-participatory diagnostic consists of the integration of energy audit and certification, thermography, acoustic studies, lighting and indoor air quality, interviews with teachers, workshops and “idea boxes” in elementary classes and in common spaces.

Technical measurements:

Measurements of temperature, humidity and CO2 concentration were recorded every 10 s. for 3 weeks in 3 classrooms and for a week in the gym.

On 11 visits to the school, specific measurements of humidity, noise, temperature, and lighting were carried out in most rooms.

Measurements of lighting levels with artificial lighting switched on and off on days of high solar radiation were taken in the whole school. Special emphasis has been placed on measuring acoustics at particularly critical times and places, such as noise in the hallway during class changes and exits to recess and dining time.

Thermographic images were taken of all the building façades. (figure 4)

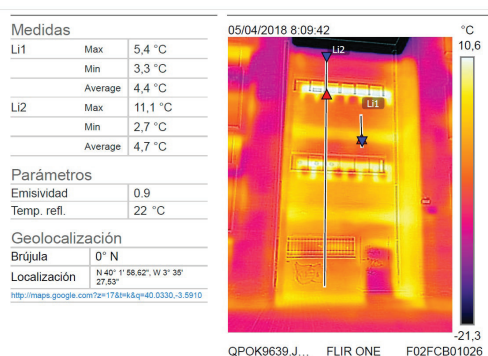


Figure 4. Façade thermographic image.

Acoustic tests were performed by GREENback R&D acoustics and noise control.

The participative activities consisted of:

- One-day interview with teachers and school staff.
- Mailbox placement with questions in building access 1, Building access 2, 2^oC, 1^oA, common area 2nd Floor building 1, 4^oD, 3^oD, 4^oB, 5^oA, 6^oA, dining room, 2nd Floor common area building 2.



Figure 5. Mailbox and mailbox answers.

- Workshops: "Experts in well-being" The objective is to generate some awareness and focus on comfort conditions.



Figure 6. "Experts in being well" workshop.

2. RESULTS

Temperature and humidity

There are classrooms in all orientations, so there are a variety of problems. Complaints are given both for episodes of heat and cold. As a general situation, the northern classrooms are cold in winter and the southern ones are hot in summer. In the gyms, in the afternoon, in winter the temperature falls below 18°C and in summer it rises above 30°C. The relative humidity in the classrooms and other analyzed areas remains within the comfort range (40% -60%) and does not present great variability, therefore that has acceptable levels. The thermographic study shows the lack of insulation on the facades. During visits to the center, we have verified that the heating system does not serve all rooms efficiently, in many classrooms there are phenomena of thermal asymmetry, due to cold walls and floors in winter and overheating in summer. From the interviews, we confirmed that the lack of thermal comfort occurs both in summer and winter, they also alerted us that simultaneously in temperate seasons, it can be hot and cold, due to the impossibility of regulating the radiators.

In the gyms the opening of the windows has been canceled, so that at times of overheating, when the

solution would be ventilation (day and night), it is impossible to dissipate this accumulated heat. For a complete analysis of thermal comfort it is convenient to carry out an annual monitoring.

Visual Comfort

The school has great availability of natural light, all classrooms are exterior and have a large area of windows. As a consequence of the effects of overheating, excess light or glare on the backboard, shutters are often used to prevent the entry of radiation or light and once they are down, they are left in that position all day. It is one of the most relevant facts regarding comfort conditions, since the beneficial effect that natural light has on people's health has been demonstrated, as well as its positive influence on performance.

Artificial lighting in classrooms generally reaches the minimum recommended levels in the work plane of 300 lux. In some classrooms, however the distribution is not the most suitable and most luminaires have ill-oriented screens that cause glare. Additionally, the possibilities of reducing electricity consumption for lighting are relevant. The school has not replaced the luminaires to introduce more modern and efficient models based on LEDs.

Regarding interior views, an excess of information is seen in most spaces, all the walls are covered with didactic material, which sometimes duplicates, which overexcites and leaves no empty space that invites relaxation. We have observed that in some classrooms didactic material is placed on the windows, shielding the access for natural light. Both students and teachers consider the school as very bright. It is noted, however, that many teachers are unaware of the time they spend with the blinds down. Artificial lighting provides adequate light levels for vision; however, natural light provides information to the body for the organic regulation of multiple processes.

Acoustic comfort

The noise reduction index obtained is 32 dB, which meets the level required in the area. Noise between classrooms has been measured obtaining 33 dB, less than the 50 dB required by the CTE-HR.

Impact noise has been measured in 5 primary classrooms, levels between 41 dB and 61 dB have been obtained, in all cases below the 65 dB required by the CTE-HR.

Classrooms have a reverberation time of 1.34 s., compared to 0.7s. maximum required for new buildings. This excessive reverberation makes listening difficult and can also generate stress for both teachers and students. Reverberation time of 1.92 s. have been obtained in the dining room. This

affects the students, teachers and especially the canteen workers. In the gym (1.46s), hallways (1.99s) and auditorium (1.74s), high reverberation times have also been measured.

Measures of sound pressure go up to 90dB, which undoubtedly generate an important situation of stress and tiredness.

In general, the educational community has transmitted their perception that lack of acoustic comfort is a priority problem. The students perceive the noise as one of the annoyances to highlight.

CO₂

CO₂ measurements have been made in two classrooms. In both cases they generally exceed 1000 ppm (figure 7). Above 1000 ppm, attention decreases and drowsiness appears in general and in specific cases discomfort and migraines occur. The CO₂ levels exceed the recommended limits, there is a decrease in both the temperature and the level of CO₂ concentration coinciding with recess. We interpret that during the rest of the day the classroom has not been ventilated. The ventilation mechanisms in all rooms are manual through the windows, even during periods of active heating.

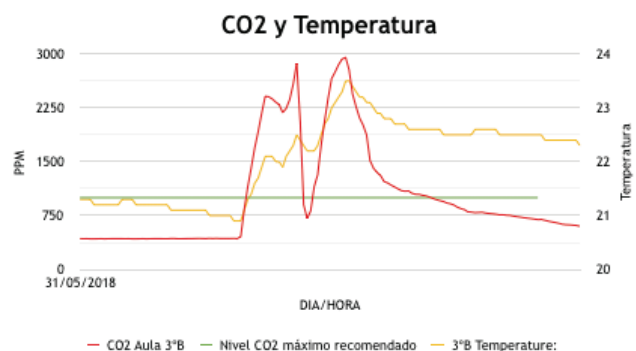


Figure 7. Measurements in 3ºB.

Considering the subjective evaluations of the teachers, the feeling of a stuffy atmosphere is usual.

Energy Audit

The consumption in relation to the installed power has been analyzed, determining that simply adjusting the contracted power to the actual consumption of the building, economic savings will be obtained without the need to reduce consumption. In addition, measures to reduce consumption have been detected:

- Replacement of luminaires, incorporation of presence detection sensors and greater use of natural lighting in common areas.
- Thermostatic valves in radiators and use of the boiler, adapting it to the needs of each moment.
- Replacement of gym heaters.

The overall results can be observed in the indicator (figure 8), which allows to quickly visualize the results of the diagnosis, to prioritize the solutions and plan the improvement actions.



Figure 8. Overall results in the school.

4. CONCLUSIONS.

According to the analysis, the school indoor environment does not comply with the minimal requirements to promote optimal learning.

The school has great potential for improvement in all the analysed items.

The school community have participated in the diagnosis; their input has been of high value. After the participation they are more aware of the school needs, of the importance of the indoor environment and they are committed as agents of change. Information of the comprehensive diagnosis is shared with the City Council and the school along with improvement proposals.

Challenges are proposed; building improvement has been submitted to the City Council and building use improvement communicated to the School (students, teachers, and non-teachers).

Different sensitivities are observed in relation to comfort, there are teachers who ventilate and are aware of the use of natural light, although this is not the general rule.

Some of the items analysed need a substantial investment to be corrected (thermal insulation, solar-daylight devices) but there are some which can be improved with modification of user habits (use of daylighting, ventilation, noise) and others require minimal investment (presence sensors, regulation of radiators, possibility to open windows).

Awareness activities are recommended regarding the use of blinds and the use of natural light, the ventilation and student behaviour regarding acoustics.

REFERENCES

1. Datos y cifras Curso escolar 2016/2017. (2017) Ministerio de Educación, Cultura y Deporte. Estudios Secretaría

General Técnica Subdirección General de Documentación y Publicaciones.

2. IDAE. Instituto para la Diversificación y Ahorro de la Energía (2016) Informe anual de consumos energéticos. <http://www.idae.es/index.php/idpag.802/recategoria.1368/reلمenu.363/mod.pags/mem.detalle>. Accessed 19 Apr 2016

3. Clara Eslava (2017). Environment and Education: An Invisible Tissue. A Journey from the City to the Classroom. Revista Internacional de Educación para la Justicia Social.

4. Ana Camarero (2017). Así influye el entorno físico de la escuela en el aprendizaje. El País.

5. Interview with Eve Edelstein. (2016) University of Minnesota. www.takingcharge.csh.umn.edu/interview-eve-edelstein.

6. Bluyssen, P.M. (2009). The Indoor Environment Handbook. How to make buildings healthy and comfortable. Ed. Earthscan.

7. Europe Gunnar Grün, Susanne Urlaub. (2015) Study Report. Impact of the indoor environment on learning in schools. Study Report. Fraunhofer

8. Arambula L et al (2015) Energy audit of schools by means of cluster analysis. Energy and Buildings 95: 160-171

9. Fergus Nicol. (2013) The Limits of Thermal Comfort: Avoiding Overheating in European Buildings." TM52.CIBSE.

10. Galasiu, A.D. et al. (2006). Occupant preferences and satisfaction with the luminous environment and control systems in daylight offices: a literature review. Energy and Buildings 38(7):728-742

11. Hescong, L. (2003). Daylighting in schools: an investigation into the relationship between day-lighting and human performance. Research Report, Hescong Mahone Group.

12. Gunnar Grün, Susanne Urlaub. (2015) Impact of the indoor environment on learning in schools in Europe. Study Report. Fraunhofer-Institut für Bauphysik IBP

13. Gaihre, S., Semple, S., Miller, J., Fielding, S., Turner, S. (2014) Classroom carbon dioxide concentration, school attendance and educational attainment. Journal of School Health 84. p. 569-574.

14. Mendell, M.J., Eliseeva, E.A., Davies, M.M., Spears, M., Lobscheid, A., Fisk, W.J., Apte, M.G. (2013): As-sociation of classroom ventilation with reduced illness absence: a prospective study in California elementary schools. Indoor Air, 23, p. 515-528.

15. Correa, S.; Osorio, M. y Patiño, V. (2011), "Economic valuation of noise: an analytical review of studies", in Semestre Económico, 4 (29), pp. 53-76 <https://doi.org/10.22395/seec.v18n37a2>

16. Hetu R, Truchon-Gagnon C, Bilodeau SA. (1990) Problems of noise in school settings: a review of literature and the results of an exploratory study. J Speech-LanguagePathol Audiol;14(3):31-8.

17. Berglund B, Lindvall T, Schwela DH. Guidelines for community noise. (1999) World Health Organization.

19. Shield BN, Dockrell JE. (2003) Invited review paper; the effects of noise on children at school: a review. J Build Acoust;10(2):97-116.

19. NGO: Ecologistas en acción. (2016). Análisis de la exposición a la contaminación acústica y atmosférica en los centros educativos de Madrid.

<http://www.ecologistasenaccion.org/article32018.html>

An Investigation of the Luminous Environment in the Nottingham H.O.U.S.E

The effect of shading devices on a building with change of use

LAKSHMI SOUDAMINI KANKIPATI¹, LUCELIA RODRIGUES², LORNA KIAMBA³

^{1, 2, 3} Architecture and Built Environment, University of Nottingham, Nottingham, UK

ABSTRACT: Daylight makes an important contribution to indoor quality and building occupants' wellbeing and productivity. Although it is well known that different spaces need different lighting quality for tasks to be performed effectively, the issue of change of use is rarely explored. This is particularly relevant now, not only because in many major cities where land is scarce and expensive building change of use is common, but also since the world is dealing with a major pandemic that has forced most people to start working from home for a significant period of time. Can homes provide good quality working environment? The Nottingham H.O.U.S.E (Home with Optimised Use of Solar Energy) was designed for the Solar Decathlon Competition in Madrid in 2010 as a starter home. It has found its lasting place on the University of Nottingham campus where it provides office space. In this work, the authors investigated the luminous environment of the office spaces within the house and compare the findings to its designed targets. Onsite measurements, computer simulations and interviews with the users were undertaken and the findings suggest that the building has adequate daylight levels for task performance according to benchmarks. However, the aluminium shading device, essential from a thermal performance perspective, causes impairing glare that can affect the users' performance. The reflective properties of the device were studied, and solutions were proposed.

KEYWORDS: Daylight, Nottingham H.O.U.S.E, Visual comfort, Glare, Shading devices

1. CONTEXT/BACKGROUND

There is a significant and growing body of research on the benefits that effective daylighting in buildings can provide. Daylight contributes to the overall indoor quality in terms of user productivity, comfort and wellbeing, and energy savings; it is preferred over artificial lighting in working spaces [1]. Different spaces have various lighting requirements for functional task performance [1, 6]. Effective lighting is particularly important for offices where more detailed tasks are conducted and, therefore, minimal lighting standards are specified. However, there could be potential drawbacks of daylighting like glare or overheating due to the type of glazing used in windows, shading devices, surface area of window discharging light and heat radiating through it.

In this paper, the authors investigated the luminous performance of the Nottingham H.O.U.S.E (Home Optimising the Use of Solar Energy) (Figure 1). The house was designed, built and entered into the US Department of Energy Solar Decathlon competition in 2010, an international competition aiming to advance the knowledge of sustainable homes. Designed as a starter home for two adults and one child, the design of the house was focussed on offering a sustainable solution for the UK housing market. It was designed to

meet the Passivhaus standards and the UK Code for Sustainable Homes Level 6 (zero carbon) [3].



Figure 1: The South Façade of Nottingham H.O.U.S.E, University of Nottingham.

Interestingly, as the competition was set to be held in Madrid, the designers had the task of making it perform to the climate requirements of both Madrid and Nottingham. In Nottingham (latitude 53 and longitude -1.2), the sky conditions are cloudy and overcast for about 50-70% of the year whereas in Madrid (latitude 40.4 longitude -3.7) it is mostly clear for around 30-70% of the year [2]. Currently, the Nottingham H.O.U.S.E is used as an office for research and teaching staff. It is situated at the Creative Energy Homes hub, which is a project led by the University of Nottingham to explore the various technological

developments in sustainable housing and energy efficiency [7]. The fact that the house is an environmentally efficient building, the transformed usage of the house from a home to an office building spurred the purpose of exploring the luminous environment.

The house consists of two floors, with a built-up area of 75 m². The ground floor consists of a lobby, kitchen, a living room (now an open office area), dining space (now a meeting space) and a toilet (Figure 2). The upper floor consists of a bathroom and two bedrooms which have been converted into two single-occupant offices (Figure 2). The windows and roof light were designed for passive natural ventilation. The building also uses external aluminium blinds as a shading device on its southern façade (Figure 1). For this study, all the office spaces within the house were reviewed and the issues that impact on adequate daylight identified and potential solutions proposed. Although the study was focused on an individual building, it presented an invaluable opportunity to highlight the issues faced when there is a change in use of space. Given that many are now working from home for an indefinite period of time in response to the Covid-19 pandemic, there is a need to examine the potential impacts on such shifts on user comfort and corresponding task lighting requirements.

2. RESEARCH METHODOLOGY

The objectives of this research were to examine the luminous environment of the house and to propose solutions for any daylight problems that were observed. To analyse the visual comfort from a user's perspective, all the research staff working in the house were interviewed. The aim was to acquire feedback of the design of the house in terms of comfort, the materials of construction and technology. Also, onsite daylight measurements were recorded to analyse the daylight received on the work planes. However, to support the data collected from the onsite measurements and the interviews, a set of computer simulations were analysed and correlated. From the daylight visual comfort findings, it was inferred that there was a potential daylight problem occurring because of the external shading device, such as glare. Further computer simulations were run to analyse the glare occurred and plausible solutions were provided with supporting analysis.

The research methodology was divided into two parts, the first part was the assessment of the daylight performance of the house and the identification of any problems. The second part was the analysis of glare and proposal of solutions to minimize the effect of it without compromising the other elements of daylight performance.

2.1 Daylight analysis and visual comfort

The Nottingham HOUSE was divided into three zones and daylight performance was analysed at the task plane level (Figure 2). Zone 1 consisted of the open office on the ground floor with four workstations, an open to the sky dining area and a kitchen. This space consists of windows on the north, south and the east facades. The first floor was divided into Zone 2 (the room on the southern end) and Zone 3 (the room on the northern end) because they are two single-occupant offices.



Figure 2: The Nottingham H.O.U.S.E. zones

The main intent was to check if the daylight on the workstation planes satisfies the requirements for the task performance. Following an assessment done using rule of thumb calculations, the daylight factor (DF), uniformity ratio (UR) and the useful daylight illumination (UDI) for all the zones were investigated using the software, Integrated Environmental Solutions Virtual Environment (IESVE). The simulations were carried out using the following assumptions:

1. Sky conditions: overcast
2. Occupancy hours: 9:00 am – 5:00 pm
3. Threshold lux levels: 300 lux (task lighting)[6]
4. Simulated for the weekdays throughout the year (occupancy days)

The reason to run the digital model under the assumption of an overcast sky condition was to understand the luminous environment inside the built structure when there is minimal daylight availability. Also, the sky conditions in Nottingham are cloudy for 50-70% of the year.

To understand the daylight performance during the days with various sky conditions such as sunny and overcast day, on-site spot lux level measurements were recorded. A series of lux level measurements were determined on the work plane at 3 different times of the day, 9:00am, 12:00pm and 3:00pm on the following days with the respective conditions:

1. An overcast day- artificial lights switched off and internal blinds 30% closed.
2. A clear sky day- artificial lights switched off with the internal blinds 100% open.

CIBSE (Chartered Institution of Building Services Engineers) comfort guidelines were used as a baseline for luminous standards and threshold criteria for office spaces. Various daylight parameters which measure the sufficient daylight levels on work planes were analysed. The following are the base guidelines:

1. DF- Minimum of 2% and an average of 5% [6]
2. UDI- 300-500 lux [6]
3. UR- More than 0.1 indicates borderline satisfied and more than 0.2 indicates good daylighting in the rear end of the room [10]
4. Glare- a) There would be an occurrence of glare if the DF is more than 5%
b) The contrast ratio, measured in cd/m^2 of the task luminance: immediate surroundings: non - adjacent surrounding should be 1: 3: 10 [5, 6]

2.2 Analysis of glare and shading device strategies

The results from the simulations and onsite measurements led to conclusions regarding the daylight performance of different zones. While correlating the data from the interviews, onsite measurements and the digital simulations, it was inferred that there was an occurrence of glare in Zone 1 and Zone 2. Furthermore, frequent visits and a set of interviews were conducted to understand the visual comfort from an occupant perspective. The authors visited the site every fortnight to record various data like onsite measurements, interview, to gain a first-hand experience of the space. The users were asked questions relating to their perception of the space, the daylight quality on various days, usage of the inner shading blinds and the frequency of using them. This led to the identification of experiential related issues like glare caused by the aluminium blinds used as an external shading device (Figure 1). Also, it was noticed that the inner blinds were used mostly to avoid the glare caused. As inferred from the interview and the daylight analysis, a set of digital analysis was carried out to understand the intensity of glare throughout the year by radiance mapping. The radiance mapping produces images which contain the glare components. The scope of the work presented in this paper was limited to only one component of glare, the daylight glare probability (DGP) because it is the most credible component which identifies the intensity of discomfort [11]. The Evalglare software was chosen to evaluate the DGP because it integrates radiance mapping to analyze it.

The probability of the occurrence of glare due to the shading device used in the southern facade in Zone 1 and 2 were identified in the occupant feedbacks and it was supported by the computer simulations. However, further analysis was required to measure the intensity of it. Zone 2 was simulated to arrive at various radiance mapping images to analyze the effect of glare. According to the CIBSE guidelines, if the DGP is higher than 0.35, it states that the glare occurred may cause discomfort, but it is tolerable. However, with the aim of establishing solutions for a glare-free working environment, few shading device strategies were worked out to compare their DGP.

3. RESULTS AND DISCUSSION

The results are presented in this section and divided to reflect the steps taken in the work.

3.1 Daylight analysis and visual comfort

The DF of the three zones as identified were analysed using Flucs DL, IES-VE. As observed in Table 1, the average daylight factor received in Zone 1 is 6.9%, Zone 2 is 5.8% and Zone 3 is 5.1%. This shows that all the zones satisfy the minimum required DF conditions. However, there could be a probability of glare near the windows because DF near the windows, especially in Zones 1 and 2, is nearly 20% [6].

Even though the DF is satisfied in all the zones, the uniformity ratios from Table 1 infer that Zone 2 and 3 are uniformly lit whereas the Zone 1 is not because of its longer plan depth (Figure 2).

Table 1: Average DF and UR of Zone 1, 2, 3

Zone	Avg. Daylight Factor (%)	Uniformity Ratio (UR)
1	6.9	0.02
2	5.8	0.13
3	5.1	0.14

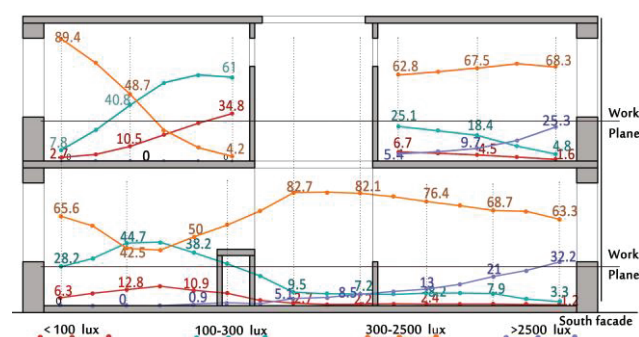


Figure 3: Section showing average UDI distribution on workplane throughout the year in all the zones

In-depth climate-based daylight illumination renders were analysed to identify the UDI distribution in all the zones throughout the year as shown in the

graph, Figure 3. The UDI range of 300-2500 lux, which is the sufficient natural daylight illumination for office task work, is satisfied in all the zones in the workstation areas for about 62%-89% throughout the year. It is clear that the house receives a part of direct daylight through the skylight window located at the centre of the building (Figure 2), providing ample daylight to the Zone 1. The central space (dining/meeting area) gets acceptable daylight of 300-2500lux for around 70-84%, annually. However, the kitchen receives daylight only for around 45-65% of the year because the window is orientated towards the north thereby receiving diffused daylight. The workstation area in Zone 1 receives around 63-80% of acceptable daylight levels throughout the year. Although the work-plane in Zone 2 achieves required lux level requirement for around 63-69% of the year Zone 3 receives 4.2-89% of acceptable daylight because of the window facing on the north facade. However, as indicated in Figure 4 it is noticed that the high daylight illumination on the work plane in Zone 2 is reduced because of the external shading device used. The present scenario proves that the existing shading device reduces the solar radiation yet maintains the useful daylight illuminance. To further investigate the luminous performance a set of onsite multi-meter measurements were recorded.

The occupants' feedback through interviews suggested there have been experiential problems like the occurrence of glare on their workstations during clear sky days and they tend to use the internal blinds to avoid it. The external aluminium blinds used for shading increases the effect of glare due to their reflective properties. Also, the windows on the southern facade are exposed to more solar radiation compared to other facades. This indicates more hours of daylight entering the workstation spaces. As shown in Figure 2, the majority of workstations are on the southern end of the building, 4 on the ground and 1 on first floor.

The daylight illuminance was reviewed during the occupant hours: 9:00 am – 5:00 pm on weekdays in the early summer season. During which, it was observed that there was a high UDI ranging from 2600 lux- 4861 lux on the workstations in Zone 1 and 2 during noon on clear sky days (Figure 5). When the UDI is more than 2500lux and has exceeded the useful range of illumination it means that there could be a phenomenon of glare and overheating thus causing discomfort in the indoor visual factors [8].

It is clear from occupants' feedback that there is an occurrence of glare, however, there is an increased chance of occurrence of glare near the windows affecting the work-plane areas from the onsite

measurements especially on sunny clear sky days. However, it is important to understand the intensity of glare caused. If this building was used strictly as a house instead of an office the occurrence of glare might not have negatively affected occupants due to the flexible nature of residential living spaces. The next discussion section gives more insight into the study on the intensity of glare.

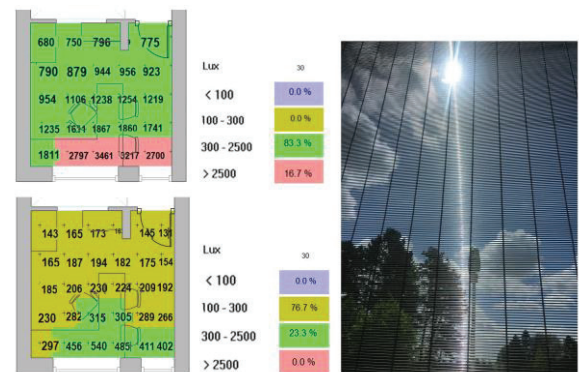


Figure 4: Average UDI of Zone 2, Base Case and Base Case + external shading measured in lux

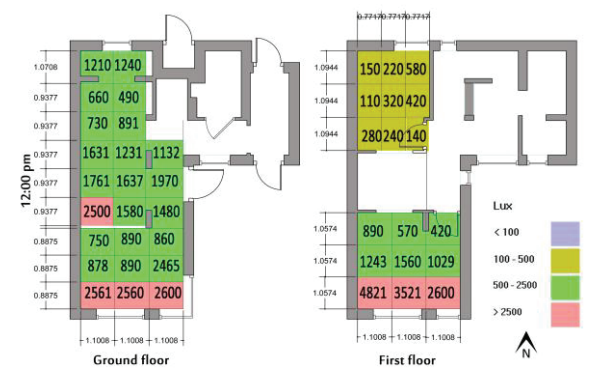


Figure 5: Onsite daylight illumination spot measurements of all the zones on a clear sky day (10th April 2018 12:00pm)

3.2 Glare analysis

It was inferred from the occupant interview feedback that two types of glare that persist, disability glare and veiling glare. The disability glare, which was observed only in Zone 1 and 2 was caused by the aluminium shading device which is constructed of several cylindrical wire-like blinds. Additionally, this glare was also due to the field of vision that the occupant has been exposed to while working on their computers. Due to the reflective properties of the polished surface, the shading device reflects the daylight (Figure 4). The veiling glare was caused due to the shadows of the blinds cast on computer screens resulting in reduced screen contrast. Generally, the occupants use internal blinds to avoid this glare, an action that decreased the daylight entering the space and curtailed views.

From Figure 4, it is inferred that Zone 1 and Zone 2 received the maximum illuminance of 2600-4821 lux near the windows thus indicating the occurrence of glare. To analyse the effect of glare due to the external shading device, Zone 2 was chosen for further findings. The digital model on IES-VE was simulated to generate radiance luminance map images. A hemispherical image with the view position angle as shown in Figure 6 was processed to analyze the effect of glare. There is no measure of a threshold for glare to state if it is high or low because it is personal perseverance which changes according to the individual [2,4]. To evaluate the glare caused by the daylight, Wienold and Christoffersen developed a glare index, DGP and the formula for which is following:

$$DGP = 5,87 \times 10^{-5} \times E_v + 9,18 \times 10^{-2} \times \log \left(1 + \sum_i \frac{L_{s,i}^2 \times \omega_{s,i}}{E_v^{1.87} \times P_i^2} \right) + 0,16$$

Equation 1: Daylight Glare Probability [9]

Where, L_s is Luminance of source, ω_s is the solid angle of the source, L_b is the background luminance i.e. adaptation luminance and P_i is the position index [9]. The following were the assumptions for simulations:

1. Sky condition: Overcast day /Sunny day
2. Task luminance: 180 cd/m²
3. Simulation day: 21st June (Summer solstice)

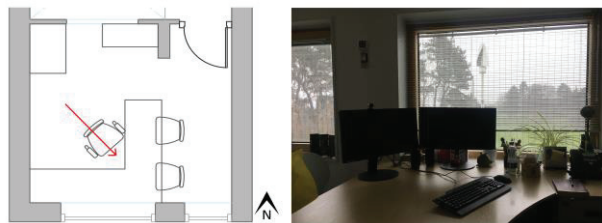


Figure 6: Zone 2 with the view position to analyse glare

The model was simulated under overcast day conditions without the shading device (Case 1) to analyze if there was an occurrence glare in this scenario. However, to analyze the current scenario the model was simulated on an overcast day and a sunny day to analyze the occurrence of glare (Cases 2 and 3). Further, the rule of thumb calculations and the DGP found from the processed images were analysed.

According to CIBSE, the contrast ratios, measured in cd/m², of the task luminance: immediate surroundings: non-adjacent surrounding should be within the ratio of 1:3:10 (180° Hemispherical view) [5]. The 3 cases were calculated using the rule of thumb from the digital image mapping from the IES-VE radiance luminance image. The results for the respective cases were 1:3.6:13.6, 1:4.7:10, 1:2.8:27.3. The high contrast ratio between the visual task and the

adjacent surface in Case 2 proved that the task was impaired by the glare. However, as inferred from the interviews and the high contrast ratios 1:27.3, Case 3 (sunny day) proves that the discomfort glare caused was due to the shading device.

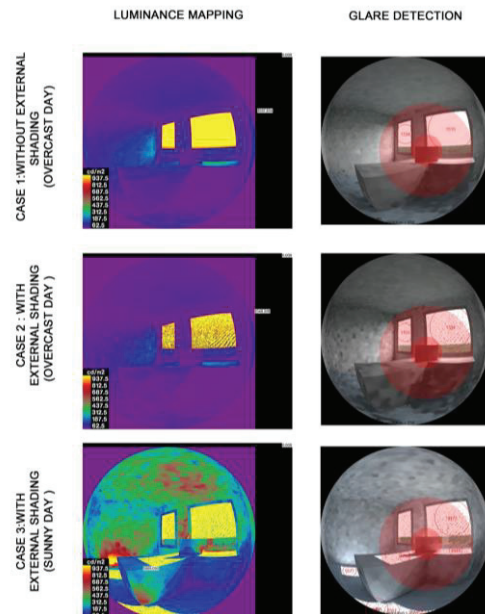


Figure 7: Luminance mapping and glare detection

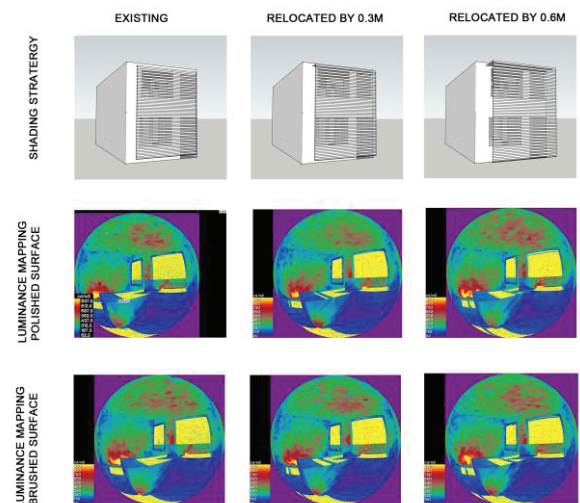


Figure 8: Shading device and Luminance mapping

While simulating the luminance maps, a parallel High Dynamic Range (HDR) image was produced. Wxfalse colour application in DIVA was used to produce the luminance mapping from the HDR image. The luminance mapping as shown in Figure 7 helped in analyzing the DGP. The Evalglare software was used to determine the DGP once we code the Radiance image or the HDR image into it. The DGP for the Case 3 image was 0.37. This indicates discomfort but at tolerable levels. However, the study intended to achieve a glare-free work environment, and, therefore, various shading device strategies were tested.

Table 2: Aluminium finishes vs. their DGP and contrast ratios (SD Shading Device, PF Polished Finish, MF Matte Finish)

	Finish	DGP	Uniformity ratio
Existing	PF	0.37	1: 2.8: 27.3
SD	MF	0.356	1: 3.0: 20.48
SD 2	PF	0.32	1: 2.4 : 21.47
	MF	0.311	1: 2.5: 20.43
SD3	PF	0.325	1: 2.4: 19.2
	MF	0.314	1: 2.2: 17.5

It is important to understand the material properties and the finishes of a shading device during their application because we know that the reflective properties of the polished surface resulted in discomfort glare. The next set of analysis focused on altering the shading device's material properties and the distance at which it could be placed from the building. There are various grades of aluminium finishes available currently in the market. The more polished the surface is the more reflective they are. Figure 8 shows the shading strategy used and Table 2 is the comparison between the aluminium finishes and their contrast ratios and DGP (SD- Shading Device, PF- Polished finish, MF- Matte/ Brushed finish). Zone 2 was simulated with following shading strategies and the different shading shown in Table 2:

1. Existing shading device
2. Existing shading device relocated 0.3 m away from the built structure
3. Existing shading device relocated 0.6 m away from the built structure

The reason for relocating the shading device was to explore whether that could help improve the results. Table 2 and Figure 8 show that the existing shading device portray the highest DGP and contrast ratios compared to the iterations. Also, it is evident that the surface finish of the blinds has an impact on the glare caused. The matte finished shading device simulations reveal a lower DGP and contrast ratios comparatively. However, it is also observed that the farther the shading device from the built structure, the lesser was the DGP. In the case of shading device strategy 3 (matte finish), where the existing shading device was being relocated by 0.6 m from the building, it showed the lowest contrast ratio of 1: 2.2: 17.5, but it exceeded the ratio of 1: 10. However, in the case of shading device strategy 2 (matte finish), where the shading device was moved by 0.3m, it resulted in the lowest DGP of 0.311. Finally, it is inferred that the matte finish shading device yield better performance than the existing polished surface. It is important to note that the glare can be reduced by moving the shading device further away from the building in such a way that the principal shading strategy of reducing solar radiation was not affected.

4. CONCLUSIONS

It is important to evaluate the indoor comfort

condition post-occupancy, especially when there is a change in building use as in the case with the Nottingham H.O.U.S.E. This can help in identifying any issues and the implementation of remedial measures. It is evident from the analyses conducted as part of this work that the Nottingham H.O.U.S.E satisfies the indoor daylighting requirements for the workstation task plane for 40-89% of the year. However, in the summer, especially during clear sky days the task is impaired due to visual discomfort caused by the glare due to the external shading device indoors. Given that the façade in question is orientated to the south, there would still be a need for a shading device to control daylight in the summer months. The reflective properties of the shading blinds are causing discomfort glare. It has been analysed that the glare can be avoided by changing the material finish of the shading device to a brushed or matte instead of polished finish. Also, by relocating the shading device further by 0.6m towards the south resulted in lower contrast ratios and a DGP of 0.311, which means the glare caused would be imperceptible. It can be observed that every building component that goes into the construction should be evaluated to understand the future impact of it. Especially the facade elements like the window, shading devices and the materials of their construction should be evaluated post-occupancy to decrease potential problems that might be caused by them.

REFERENCES

1. Osterhaus, W. (2009). Design Guidelines for Glare-free Daylit Work Environments. *Research gate*: p. 1-2.
2. Weatherspark, Available: <https://weatherspark.com/y/41783/Average-Weather-in-Nottingham-United-Kingdom-Year-Round> [March 2018]
3. Guzman, G. (2014). *An Exemplar of Low-Energy Offsite Manufactured Housing: Nottingham H.O.U.S.E*: p. 2.
4. Julieta Yamin Garreton, R. R. (2016). Effects of perceived indoor temperature on daylight glare perception. *Building research & information*, 44 (8), pp. 907-919: p. 2.
5. CIBSE. (2009). *SLL Lighting Handbook*. Society of Light and Lighting.
6. CIBSE. (2006). *Guide an Environmental Design*. CIBSE Publications: p. 1-20, 21
7. Creative Energy Homes. (n.d.). *University of Nottingham*. Available: www.nottingham.ac.uk/creativeenergyhomes/index.aspx [March2018]
8. Gherri, B. (2015). *Assessment of Daylight Performance in Buildings Methods and strategies*.
9. Daniel overbey, Available: <http://danieloverbey.blogspot.co.uk/2012/12/methodologie-s-for-glare-analysis.html>
10. David Rennie, F. P. (1998). Environmental design guide for naturally ventilated and daylit offices. Construction Research Communications Ltd, BRE Ltd.
11. Christoph Reinhart, Shelby Doyle, J Alstan Jakubiec and Rashida Mogri (n.d). Glare Analysis of Daylit Spaces: Recommendations for Practice. Available: http://web.mit.edu/tito/_www/Projects/Glare/GlareRecommendationsForPractice.html [March 2018]

Retrofitting of buildings: what about GHG emission reductions?

The case study of Switzerland

STEFANO COZZA¹, JONATHAN CHAMBERS¹, MARTIN K. PATEL¹

¹Energy Efficiency Group, Institute for Environmental Sciences and Department F.-A. Forel for Environmental and Aquatic Sciences – University of Geneva, Switzerland

ABSTRACT: The decarbonization of buildings is highlighted as a priority to achieve the EU's long-term energy and climate goals. In this work, the Swiss energy performance certificate database is used to assess the current state of the residential building stock in Switzerland and its characteristics in terms of greenhouse gas (GHG) emissions. The GHG emissions in kg CO₂-eq related to space heating and domestic hot water is calculated from the final energy used of each building type. Then, a sub-sample of buildings that have been retrofitted in recent years is established to analyse the type of renovation performed, its depth, and the GHG reduction achieved. The results suggest that energy retrofitting has mainly focussed on energy savings (leading to an overall GHG savings by 50%) without sufficiently integrating the GHG abatement of heat supply. The installation of heat pumps, which is essential for decarbonization of the heat used in buildings, proceeds very slowly. The current energy retrofit rate is found insufficient to achieve the objectives of the Swiss Energy Strategy 2050. It is therefore very important not only to increase the rate of energy retrofitting but also to ensure that the systems installed are more efficient in terms of GHG emissions.

KEYWORDS: Energy Performance Certificate, LCA, GHG emissions, Building retrofit

1. INTRODUCTION

Existing buildings account for approximately 40% of the energy consumption in the European Union (EU) placing them among the most significant CO₂ emission sources in Europe [1]. The decarbonization of the built environment is highlighted as a priority to achieve the EU's long-term energy and climate goals [2]. In Switzerland, the Federal Council has been developing the Swiss Energy Strategy 2050 (ES-2050) since 2011 [3]. The ES-2050 is based on three strategic objectives: increasing energy efficiency, increasing the use of renewable energy, and withdrawal from nuclear energy. For residential buildings, this translates into a target of 29 TWh/y consumed and 2.7 Mt CO₂/y emitted by 2050, with the final energy consumption to be reduced by 46% and CO₂ emissions by 77% compared to today levels [4].

More than 80% of the Swiss building stock was built before 1990 and the renovation rate is very low (about 1% per year) [5]. This makes it difficult to reach the objectives of the ES-2050, which would call for an energy retrofit rate of the building stock of 1.9% per year [4].

Given the importance of energy retrofitting for the abatement of greenhouse gases (GHG) [6], the objective of this paper is to assess how much GHG can be saved through energy retrofitting of Swiss residential buildings. In particular, the research

question of this work is whether the current rate and type of retrofit are adequate to meet the 2050 emissions targets for the residential sector.

2. METHOD

2.1 Data analysis

In this work, a large-scale dataset based on the Cantonal Energy Certificate for Buildings (CECB) has been used for the analysis [7]. The CECB was used to assess the current state of the residential building stock in Switzerland and its characteristics in terms of GHG emissions. The total GHG emissions and the median values per square meters for different building types were calculated.

The GHG emissions were calculated using the Life Cycle Assessment Data per fuel type based on the Ecoinvent methodology [8]. This database assesses the greenhouse effect as the cumulative effects of the different greenhouse gases which is expressed as kg CO₂-eq. Using this dataset, the application of the life cycle approach is limited to the fuel supply chain while we did not apply it to the building envelope.

We established a sub-sample of residential buildings that have been retrofitted in recent years and for which a CECB certificate was available both before and after retrofit. This sub-sample was used to analyse the type of renovation performed (e.g. the type of heating system installed), its depth (expressed by the number of energy classes gained) and the GHG

reduction achieved. The effectiveness of the retrofit was also evaluated through the carbon content of the heat supply per energy label before and after retrofit.

2.2 Potential scenarios

Based on a review of the cantons' energy strategies [9], three simplified potential scenarios for the year 2050 were compared to determine which one comes closest to the described scenario of the ES-2050. For the scenario analysis, the median GHG emissions of each label per m² of floor area (obtained from the CECB) were scaled to the entire Swiss residential sector as estimate of the GHG emissions related to heating. The scenarios were developed using the median GHG emissions of the energy label categories and the number of buildings in the stock undergoing energy retrofit. Therefore, these simplified scenarios disregard climate change, population growth, and a potential reduction of the carbon content of the electricity grid. The outputs are the GHG emissions and the retrofit rate that is required to reach the objectives by 2050.

3. DATA

The Swiss energy performance certificate CECB was created in 2009 based on the European standards SN EN 15217 and SN EN 15603 [10]. To date, the CECB dataset contains more than 50 000 buildings and it has been shown to be representative of the residential stock [11]. However, after having removed outliers and other implausible values, the sample size decreased to 34 816 residential buildings.

The thermal performance of buildings, expressed in kWh per m² and year is grouped in categories represented by energy labels between A and G (very efficient to very inefficient) [10]. The CECB dataset includes information on the following parameters which define the performance of the building:

- The energy label.
- The construction period.
- The energy reference area (ERA).
- The heating system installed.
- The actual energy consumption.

The actual consumption is obtained from energy bills for the energy carriers used in the building, after climate correction following the methodology described in SIA-2031 [10]. Actual energy consumption is determined as the average of measured energy use over at least three consecutive years. We then converted this value to GHG emissions using the emission factors from the KBOB database [8].

The CECB dataset did not specify information on retrofit occurrences, however many buildings had multiple certificates. In order to generate a sub-sample containing only retrofitted buildings, it was assumed that buildings with multiple certificates

representing different energy labels, with the newer energy label being better than the old one, had been retrofitted. This resulted in a sub-sample of 1172 residential buildings with a CECB certificate both before and after retrofit, allowing to analyse the GHG emissions before and after retrofit.

4. RESULTS

4.1 Building stock

We first focus on the characterization of the CECB database and therefore of the Swiss residential building stock. A wide range of GHG emission intensities was found across the different construction periods and energy labels, ranging from 4.1 kg CO₂-eq/(m²y) for newer buildings to 37 kg CO₂-eq/(m²y) for older buildings (see Table 1). For the median building in the residential stock, a GHG emission value equal to 28 kg CO₂-eq/(m²y) was found.

Table 1: GHG emissions in the CECB sample - median values by construction period.

Construction period	No. of buildings	GHG emission intensity [kg CO ₂ -eq / (m ² y)]
Before 1919	5352	27.9
1919 - 1945	3138	34.1
1945 - 1960	4613	36.1
1960 - 1970	4726	37.2
1970 - 1980	5843	32.4
1980 - 1990	5512	19.8
1990 - 2000	2705	21.9
2000 - 2010	2312	14.6
2010 - 2017	615	4.15
All	34816	27.9

The change in GHG emissions per square metre of ERA are determined by both energy consumption per m² as a function of construction period and the change in energy mix (increasing shares of renewable and heat pumps over time at the expense of oil and gas boilers).

The relatively narrow bandwidth of emission intensities suggests that the heating systems used in very old buildings (before 1960) are not substantially different from those used in the more recent ones (between 1960 and 2000). Indeed, a much larger contribution to GHG emissions would have been expected from older buildings due to their arguably inefficient and polluting heating systems. This is partially explained by the analyses shown in

Figure 1, where the heating systems are presented as a function of the construction period of the buildings.

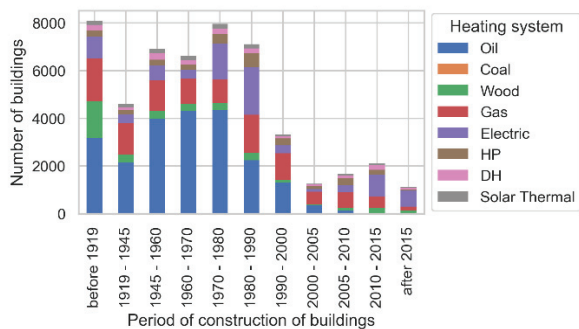


Figure 1: Heating system distribution in function of the buildings' construction period.

As shown in Figure 1, the mix of technologies and fuels used in buildings from 1919 to 2000 is quite similar and the presence of oil and gas boiler is predominant in these categories, leading to rather comparable GHG emissions. In contrast, the absence of oil boilers in buildings after 2000 reduces their carbon emissions by almost half (Table 1).

However, this effect is attenuated by the installation of new heating systems in old building. A supplementary analysis on the installation periods of the heating systems (Figure 2) shows that most old buildings are equipped with new boilers which are still powered by fossil fuels (74% of all the heating systems installed after 1990 in buildings constructed before that year are gas- and oil-fuelled).

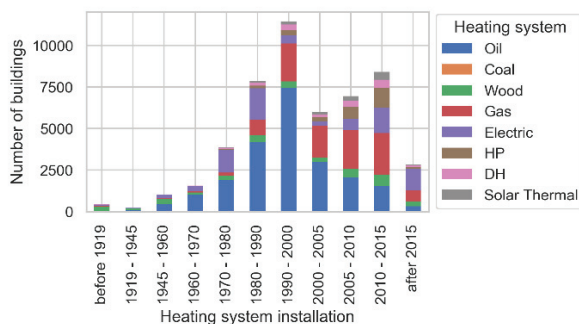


Figure 2: Heating system distribution as a function of the installation period.

This highlights an important challenge as newly installed fossil fuels systems have a lifespan of 20-30 years during which they contribute significantly to the GHG emissions released by the building stock.

4.2 Retrofitted buildings

Having evaluated the building stock, we focused on the most recent energy retrofit period (after 2012) to better understand the adopted measures. To do so, we used the CECB sub-sample of the 1172 recently retrofitted buildings.

The main energy and emissions figures of this sub-sample are reported in Table 2. While the ERA increased by 7%, energy retrofitting allowed to reduce both total final energy used (from 79.4 to 41.7

GWh/y) and GHG emissions (from 20.1 to 9.25 kt CO₂-eq/y), i.e. in both cases by approximately a factor of two. This indicates that practically the entire reduction in GHG emissions is due to the reduction in final energy consumption and not decarbonisation of the supply.

Table 2: Main figures of the CECB sub-sample.

	Before	After
Total consumption [GWh/y]	79.4	41.7
Total GHG emissions [kt CO ₂ -eq/y]	20.1	9.25
Consumption per m ² [kWh/(m ² y)]	147	59.3
GHG emissions per m ² [kg CO ₂ -eq/(m ² y)]	37.3	9.21
Total ERA [km ²]	0.54	0.58

We then analysed how this reduction was distributed among the different energy labels. Figure 3 shows a very similar pattern for GHG emissions (a) and final energy (b) before and after retrofit. This again reflects the fact that the carbon content of the heat supply remains practically unchanged across the different energy labels.

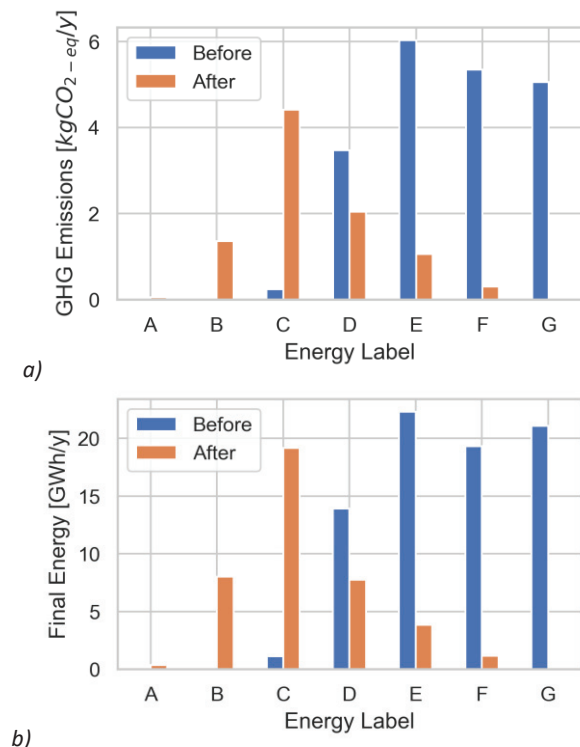


Figure 3: GHG emissions (a) and final energy (b) by energy label before (in blue) and after (in orange) retrofit (A = 0.05 ktCO₂/y and 0.4 GWh/y).

This result is largely explained by the analysis of the heating systems used in the buildings before and after retrofit (Figure 4). It revealed that in most cases the type of heating system used before and after retrofit is identical, with a notable difference only for the oil boilers. Figure 4 shows that 60% of buildings in the sample were equipped with oil boilers before

retrofit and 35% after retrofit, and that the remainder mostly switched to heat pumps (HP, +20% after retrofit). This, however, did not result in a large reduction in GHG emissions.

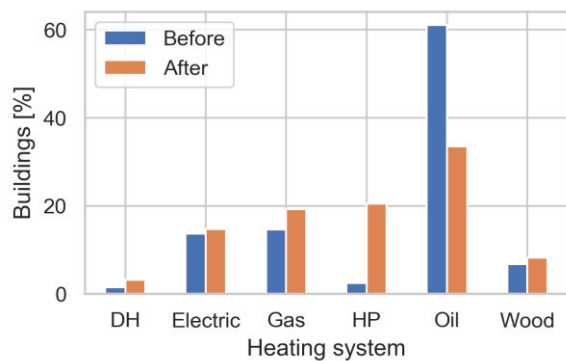


Figure 4: Heating system used in the building sample before and after retrofit (DH = district heating).

This explains why there is no significant difference in carbon content of the heat supply per energy label (Table 3). This means that buildings with a certain energy label generally use the same heating system, regardless of whether they are retrofitted or not. It also implies that the increase of heat pumps according to Figure 4 is primarily related to buildings which are renovated to A and B labels (according to Table 3, GHG emissions below 0.2 kg CO₂-eq/kWh are only found for energy labels A and B).

Table 3: GHG content of the heat supply before and after retrofit, and for the entire building stock by energy label.

Energy label	Heat carbon content [kg CO ₂ -eq/kWh]		
	Before retrofit	Building stock	After retrofit
A	-	0.108	0.109
B	0.102	0.129	0.122
C	0.205	0.202	0.199
D	0.243	0.250	0.246
E	0.251	0.251	0.254
F	0.263	0.238	0.222
G	0.222	0.215	-
All	0.239	0.224	0.182

Finally, it should be noted that the sub-sample before retrofit and the total CECB dataset (describing the building stock) are very similar in terms of GHG emissions (i.e. first and second column of Table 3), which seems to suggest a prevalence of unrenovated buildings in the building stock.

4.3 Retrofit actions

This paper does not examine the details of the different retrofit actions that were applied to the buildings in the sample. However, we analyzed the most common retrofit actions (i.e. additional

insulation, heating and ventilation system) for each building in the current stock to reach the minimum energy requirements. The “system solutions” proposed in [12] were used as they provide a pre-defined package for energy retrofit that can be applied to a wide range of buildings. The same ensure compliance with the legal minimum performance requirements for retrofitted buildings in Switzerland. Five system solutions with varying degrees of insulation by building element and boiler retrofit are proposed [12]. Usually, the retrofit starts with an additional insulation of the envelope and the installation of the ventilation system. Both retrofit actions reduce significantly the thermal losses and subsequently the useful energy demand, which means that the power of the new heating system can be reduced compared to the old system. Other retrofit actions are: insulation of the interior ground, exterior roof and walls; windows replacement to double or triple glazing; installation of a ventilation system, including a heat recovery unit for buildings with low heating efficiency; replacement of the heating system either with a new air source heat pump or with the original type of heating system.

4.4 Scenarios

The poor decarbonization of heating systems was analysed in terms of its implications for goal achievement under the ES-2050, through the creation of simplified technical scenarios for 2050. Scaling the CECB sample (with an ERA of 24 million m²) to the entire Swiss residential ERA (470 million m² [5]), resulted in total GHG emissions of 12.6 Mt CO₂-eq/y. This value is somewhat above the value published by Prognos [13], currently reported as 11.4 Mt CO₂-eq/y for the residential sector. The declared target of the ES-2050 for GHG emissions for heating of residential buildings by the year 2050 is 2.66 Mt CO₂-eq [4].

Based on a review of the cantons’ energy strategies [14], it was found that all their approaches to subsidising CECB energy label improvements fall into three main groups, which were used to create the three scenarios reported in Table 4.

Table 4: Technical potential scenario for the Swiss residential sector by 2050 (thermal performance only).

Year	Scenario	GHG emissions [Mt CO ₂ -eq/y]	Renovation rate [%]
2017	Our CECB Model	12.6	0
	Prognos	11.4	0
2050	1	10.7	0.82
	2	5.45	2.22
	3	2.73	3.11
	ES-2050	2.66	1.9

A business-as-usual case (Scenario 1) with no incentives was calculated for the year 2050, assuming an energy retrofit rate of 0.82% per year in line with the current level [15]. The resulting level of GHG emissions is very far from the objective (10.7 vs. 2.66 Mt CO₂-eq/y). This highlights the inadequacy of the business-as-usual scenario.

A second scenario (Scenario 2) assumes that energy retrofit improves the buildings' energy performance by three-label steps. Therefore, all buildings except for A, B, and C labels are renovated. This results in a retrofit rate which is slightly higher than the one proposed in the ES-2050 (2.2% vs. 1.9%). The result for this scenario indicates that the 2050 objective for GHG emissions will not be achieved unless the quality of the energy retrofit will be significantly improved.

The only scenario that approaches the objectives of the ES-2050 for GHG emissions is the one in which all the buildings are retrofitted to at least at B-label (Scenario 3). In this scenario, the GHG emissions slightly exceed the target set (2.73 vs. 2.66 Mt CO₂-eq/y). However, this requires a very high energy retrofit rate of 3.1% (compared to the proposed 1.9% and the current 0.82%), which does not seem to be realistic.

It is finally worthwhile to mention that these scenarios were calculated based on a conservative approach by basing the scenario analysis on median values, and therefore do not consider uncertainty in the results.

5. CONCLUSIONS

The analysis of the GHG emissions caused by heating of the Swiss residential building stock suggests that most old buildings have been equipped with new heating systems but that most of these are operated with fossil fuels. This explains why the emissions in terms of kg CO₂-eq/kWh are very similar from label C to label G, suggesting that the heating systems used in medium rated buildings are not substantially different from those used in the lower rating, and showing a large drop only for the labels A and B. This highlights the contribution of the high efficiency and low emissions of the heating systems installed in these new or deeply renovated buildings, and it further indicates a need for energy policy to incentivise carbon emission reduction in addition to requiring a minimum level of energy efficiency.

The results on the GHG savings for retrofitted buildings suggest that the energy retrofitting has mainly focussed on energy savings (leading to an overall GHG savings by 50%) without sufficiently mitigating GHG emissions from heat supply. Based on today's emission levels (11.4 Mt CO₂-eq/y for heating and hot water in residential buildings [5]), a much greater effort is required to achieve the 2050

objective, since it will be necessary to reduce emissions by at least 75% (objective ES-2050: 2.7 Mt CO₂-eq/y). The installation of heat pumps, which is essential for decarbonizing heat supply in buildings, is proceeding very slowly. The existing heating systems were replaced with heat pumps in only 20% of the energy retrofits performed.

This study also provides a first analysis of the feasibility of achieving the GHG emissions target of the national Energy Strategy 2050 (ES2050) for the residential sector. Scenarios allowing to establish the technical GHG emission reduction target for the year 2050 were defined based on three groups of energy policies linking incentives to energy label improvement.

The results show that with the business-as-usual approach (Scenario 1), maintaining the current retrofit rate, it is impossible to achieve the objective set. An intermediate approach, involving the improvement by three label steps and achievement of label D as minimum requirement (Scenario 2) would require a retrofit rate similar to the one proposed by the ES-2050 strategy. However, the resulting GHG emission level would still be twice as high as the target (5.45 vs. 2.22 Mt CO₂-eq/y). On the other hand, a more aggressive policy aiming at renovating all buildings to the highest standards (Scenario 3), would allow to nearly achieve the target but it would require a retrofit rate that seems unrealistically high (3.1% per year).

To conclude, the current energy retrofit rate and the retrofit depth were found to be insufficient to achieve the objectives of the ES-2050. It is therefore very important not only to increase the rate of energy retrofitting but also to ensure that the systems installed are more efficient in terms of GHG emissions. This must be pushed forward while maintaining the low carbon content of the Swiss electricity grid, otherwise the GHG target will be attainable only with an extremely high retrofit rate. However, our findings are based on the CECB database and further research would be required to understand how the buildings included in this sample perform compared to the Swiss average. Furthermore, the impacts for the electric grid and the total costs associated to the alternative strategies should be analysed.

ACKNOWLEDGEMENTS

This research is financially supported by the Swiss Innovation Agency Innosuisse and is part of the Swiss Competence Center for Energy Research on Future Energy Efficient Buildings & Districts (SCCER FEEB&D).

REFERENCES

- [1] Odyssee Project, Enerdata - Odysee: European Energy Efficiency Database, 2018.
- [2] EU Parliament, Directive 2018/844/EU Energy performance of buildings, in: Off. J. Eur. Communities, 2018: pp. 75–91.
- [3] Swiss Federal Office of Energy, Energy Strategy 2050 Once the New Energy Act Is in Force, Bundesamt für Energie (BFE), 2018.
- [4] Prognos, Die Energieperspektiven für die Schweiz bis 2050, Bundesamt für Energie (BFE), 2012.
- [5] FSO, Construction and housing - key figures, Federal Population Census, Buildings and dwellings statistics, 2017.
- [6] F. Filippidou, N. Nieboer, H. Visscher, Effectiveness of energy renovations: a reassessment based on actual consumption savings, *Energy Effic.* 12 (2018) 19–35. doi:10.1007/s12053-018-9634-8.
- [7] Conferenza Cantonale dei Direttori dell'Energia, CECB - Web Page, (2020). <http://cecb.ch/> (accessed January 7, 2020).
- [8] KBOB, Données des écobilans dans la construction 2009/1:2016, Koordinationskonferenz der Bau- und Liegenschaftsorgane der öffentlichen Bauherren, 2016.
- [9] R.W. Amstalden, M. Kost, C. Nathani, D.M. Imboden, Economic potential of energy-efficient retrofitting in the Swiss residential building sector: The effects of policy instruments and energy price expectations, *Energy Policy*. 35 (2007) 1819–1829. doi:10.1016/j.enpol.2006.05.018.
- [10] SIA, SIA 2031 - Energy certificate for buildings, Swiss Society of Engineers and Architects (SIA), 2016.
- [11] S. Cozza, J. Chambers, A. Geissler, K. Wesselmann, C. Gambato, G. Branca, G. Cadonau, L. Arnold, M.K. Patel, GAPxPLORE: Energy Performance Gap in existing, new, and renovated buildings, Swiss Federal Office of Energy (SFOE), 2019.
- [12] K.N. Streicher, S. Mennel, J. Chambers, D. Parra, M.K. Patel, Cost-effectiveness of large-scale deep energy retrofit packages for residential buildings under different economic assessment approaches, *Energy Build.* 215 (2020) 109870. doi:10.1016/j.enbuild.2020.109870.
- [13] Prognos, Der Energieverbrauch der Privaten Haushalte 2000 - 2016, Bundesamt für Energie (BFE), 2017. doi:31 - 27264.
- [14] S. Cozza, J. Chambers, M.K. Patel, Measuring the thermal Energy Performance Gap of labelled residential buildings in Switzerland, *Energy Policy*. (2020) 111085. doi:10.1016/j.enpol.2019.111085.
- [15] Conferenza Cantonale dei Direttori dell'Energia CDE, Il Programma Edifici nel 2016 - Rapporto annuale, (2016).

Optimization of building facade solar protection design in an urban context

Energy and interior comfort through BIM and evolutionary algorithmic modelling – a case study in two cities Porto, Portugal and Valencia, Spain.

PEDRO SANTIAGO, VICENTE BLANCA-GIMENEZ

Universitat Politècnica de Valencia, Valencia, Spain

ABSTRACT: To effectively design an efficient building, the evaluation of energy performance in the early stages of the project through simulation is an indispensable and inescapable, yet demanding and complex procedure. Over several decades, several tools and methods have been developed to address design issues related and articulated with performance, mostly using Multi-Objective Optimization Algorithms. Technological advances have revolutionized the way architects design and think, automating complex tasks and enabling the evaluation of multiple variants simultaneously. BIM methodologies and visual programming languages have opened up a wide range of design and analysis tools allowing architects to make informed decisions based on data extracted from models. In this article, a methodology and design workflow is proposed, integrating BIM in articulation with evolutionary algorithms and energy simulation systems, exploring its capabilities, advantages and limitations from the design of the building's façade, namely its openings and respective optimization. Part of two case studies present in two cities Porto and Valencia through the design of solar control façade membranes integrating local cultural values in their design. The method has shown that it is possible to optimize the façades of historic buildings for solar control.

KEYWORDS: Energy, Comfort, Optimization, BIM, parametric design

1. INTRODUCTION

Since half of the world's population lives in cities that collectively consume three quarters of global resources, with predictions of their increase to three quarters by 2050 [1], it is imperative to understand and create strategies to minimize energy consumption in this particular environment. Current energy efficiency directives in EU buildings (Directives 2002/91 / EC, 2010/31 / EU, Nearly Zero Energy Building) impose new requirements on the construction and renovation of buildings with the aim of creating a NZEB built-up landscape. Solar protection design in Mediterranean countries represents a both functional and cultural architectural element used for centuries to ensure the comfort of its occupants and nowadays to minimize energy consumption.

Solar gains can contribute positively to the thermal energy performance of the building, in the form of passive gains, or negatively, in case of need due to lack of exposure or formal and material lack of control. The urban landscape, with the surrounding built environment presents a great challenge to achieve this goal. The approach of maximizing the use of solar energy - whether for the active conversion using solar thermal and / or photovoltaic collectors, or by bioclimatic passive strategies, allows

the reduction of heating and lighting energy. The design team is presented with a challenging task that can be overwhelming. To work towards this goal, computational modeling directed to the availability of solar radiation can be a tool to support design decisions for architecture and urbanism. However, the probability of finding an ideal solution by manual trial and error method is extremely time consuming and does not guarantee the optimal result. Manual calculations can be made for determining the best solar envelope using the solar azimuth and elevation data alongside the projected shadows of neighboring constructions or context. However, manual calculations are a long and inaccurate process for urban environments.

Nonetheless, today with the aid of digital calculation designers can create workflows that may overcome these obstacles. Some computer-aided and parametric design programs integrate environmental simulation tools that include the ability to evaluate solar envelope performance. A procedure that requires some external information, such as location, surrounding volumes, plans that define the area to be evaluated and periods of analysis. However, this system only allows to evaluate the potential of the solar envelope, being the process of manual optimization, often based on the experience and

knowledge acquired from the designer, limiting the range of solutions to these factors and the time available for the design. Given the geometric and volumetric complexity of the urban environment along with the objectives of the study, an alternative and more efficient method is proposed.

2. METHODOLOGY

This paper proposes a method to generate solar envelopes that consider multi-directional requirements for access to direct solar gain in complex urban environments. This method was developed for the evaluation of the potential of construction in existing areas in the cities of Porto and Valencia, integrating calculations of solar direct access from environmental computational simulations, generation of solar envelopes using parametric design and optimization plugins. The theme of an outside protective skin intends to maintain the building tradition of both cities, even with different climates and locations. The result is a reinterpretation of this element maintaining its function based on data whilst still creating a cultural element.

In the city of Porto tiles have geometric designs inherited from ancient cultures. These patterns will be the basis for the skin design, parametrically built and fine-tuned (Fig. 1).



Figure 1: Example of tiles in Porto.

The same principle will be applied in Valencia. The traditional tiling in this city is the “trencadis” (Fig. 2).



Figure 2: Example of the traditional “trencadis” in Valencia.

The definitions are therefore different for each city. The one for Porto creates a tile pattern that can

be controlled parametrically through attractor points that result in a more open or closed sub pattern allowing the control of incident sunlight (Fig. 3).

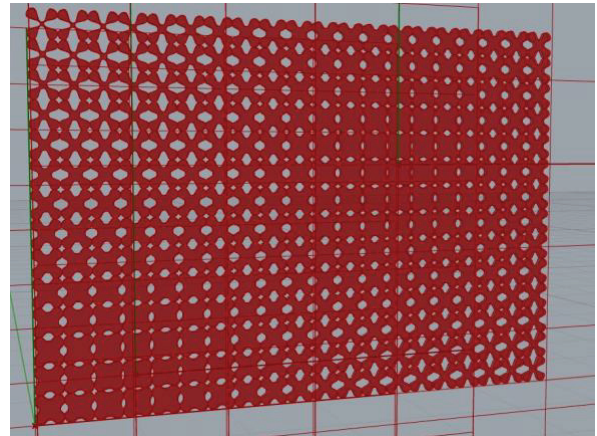


Figure 3: Porto parametric tile pattern.

For the city of Valencia, the “trencadis” effect was obtained by a Delaunay triangulation. The pattern can be tighter or looser depending on the amount of points that work as the parametric variation for achieving the desired sunlight control (Fig.4).

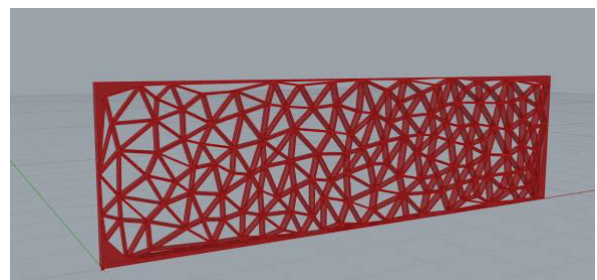


Figure 4: Valencia parametric tile pattern.

The urban models to integrate the proposal were imported from GIS and integrated in the BIM software, allowing real-time connection with the visual programming tool where the algorithm was developed (Fig. 5).

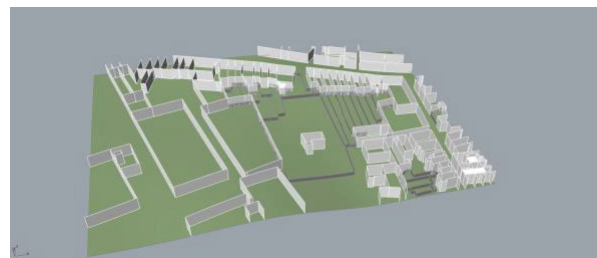


Figure 5: Urban model of case study from Porto.

The proposed method pretends to solve and to generate solar control envelopes that consider multidirectional access requirements for direct solar gains in complex urban environments considering local cultural factors. This method was developed to evaluate the solar control potential in consolidated areas existing in the cities of Porto and Valencia,

integrating calculations of direct solar access from environmental computational simulations, generation of solar control envelopes using parametric design and optimization plug-ins. The urban model to integrate the proposal was exported and rebuilt automatically a BIM program, Archicad that allows the connection in real time with the visual programming tool Grasshopper where the algorithm was developed. The environmental simulation tool used to calculate the hours of direct sun exposure in the Grasshopper is Ladybug [2], based on its sun-path Radiance component, a validated tool for simulation of solar radiation [2]. The optimization plugin used is the Galapagos [3] that allows applying the principles of evolutionary optimization in the Grasshopper.

The environmental simulation tools are both from the parametric tool [2] as well as from the BIM tool. The mutli – optimization tool runs in the parametric environment showing the results in real time in the BIM software. [3] [4] [5]

The method described is applied to two building sites located in a consolidated urban context of the cities of Porto and Valencia. In the first phase a study of the solar potential of the site is carried out in a period of one year (Fig. 6).

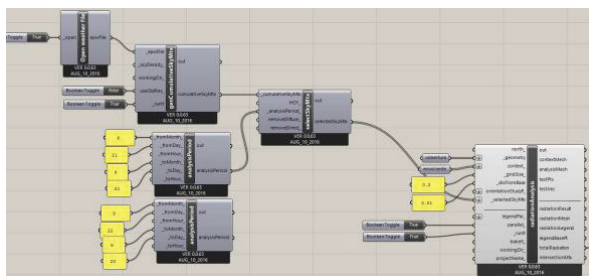


Figure 6: Analysis period.

The obvious or traditional design of concordances of alignments and geometry generated a volume that was also submitted to analysis for reference, base and comparison of results.

The surfaces and volumes generated in the BIM environment are integrated in the parametric software where the analysis are performed from the construction of an algorithm. Any change can be reintroduced into the BIM tool, which allows the addition of information, not loss, throughout the process.

The algorithm allows the control and manipulation of the size and openings of the patterns of the protective skin within a limit and direction. Since the system is not static it allows a great degree of freedom and combinations within the alignments and energy needs (Fig. 7). [6] [11] [12]

In the end these same surfaces are connected with the native construction elements of the BIM model still as elements of the algorithm allowing the symbiosis of the working systems. The algorithm is

run with the optimization plugin and the analysis focuses on the results of annual radiation values and time consumed to finish the optimization.

The results are then compared. The cross of parametric and BIM tools represents the key for the methodology and workflow creating several advantages. Working with real time data informed design decisions and extending the advantages of each method between each other allows the project team to work with the best of both worlds.

In both case studies the position of the solar control skin was placed on the south facing façade of the building. Since it is the façade with most solar exposure, the solar control is the most demanding as well.

3. RESULTS

The base of both case studies (without the solar control skin) was analysed for both the hot months of the year, which considered the period from 21st June to 21st of September, being the remaining months considered colder period. Even though the climates are quite different, as Valencia is much hotter than Porto, for comparison reasons, the analysis periods were the same.

Table 1 refers to the results from Porto. The improvement registered was of a total of 65% of less radiation. The distribution of this improvement was of 61% on the hot period and of 63% on the colder months.

Table 1: results for Porto

Month	HM	CM	Total
Base	161183	318016	479199
Proposal	63456	150159	213615
Dif.	-97727	-167857	-265584

Table 2: results for Valencia

Month	HM	CM	Total
Base	201586	526063	727649
Proposal	145141	331419	476560
Dif.	-56445	-194644	-251089

Table 2 refers to the results from Valencia. The improvement registered was of a total of 35% of less radiation. The distribution of this improvement was of 29% on the hot period and of 38% on the colder months.

The table represents the total radiation in kWh per period of analysis. This is computed through a mass addition of results at each of the test points in kWh/m2 multiplied by the area of the face that the test point is representing.

4. CONCLUSIONS

The type of pattern represented the main difference between the two case studies. It's pattern design and variables resulted in different approaches and results. The method worked but can still be improved.

The advantage of the proposed method is the real-time workflow, a very important factor in the development of the work process in the initial phase of the project, to constitute a work system that goes through the concept implementation process, its analysis and optimization processes, in this case using evolutionary processes. [7] The existing examples presented always refer to digital environments external to the base design program, which tend to compromise the agility of design thinking and analysis processes, along with errors in importing and exporting information and models and sometimes data loss. This proposal is integrated, dynamic and manages to harness the advantages of both systems. The result is a more advantageous base, allowing also the work with more adapted forms without compromising other factors and conditions. [8] [9] [10]

The tools and methodology presented, offer the architect an improved and clearer access to multiobjective optimization results along with the ability to classify, filter, understand the formal aspect of the solution, considering the overall performance of the project. Archicad provided a common platform for additional functionalities in the development of the building design by combining multiple different domains through the connection to Grasshopper3d and its sub products like Octopus, according to the architect's preferences and cognitive skills.

The potential of the workflow described is significant at the beginning of the project development which can be even more efficient, smart and flexible. The intention is to allow the architect to deal with an increasingly demanding field of complexity in a clear and visual way, always based on data and design.

One of the main objectives of the research described in this article was to reduce the distance and error inherent in the migration of information between various platforms in the project cycle through the integration of real-time parametric design cycles, multiobjective optimization, simulation and feedback. By holistically integrating the programs and automating the workflow using a common platform, some of the frequently encountered interpretation and data exchange problems were avoided.

As demonstrated in this case study, the suggested models not only offer good solutions, but also contribute to a better understanding of the design problems. The possibility of examining the same data set with different evaluation schemes allows us to

face and rethink the systems and methodologies inherent to architectural design problems. In other words, optimization models are a promising starting point for the development of generative design tools or tools that allow the exploration of informed solutions and establish new relationships between the architect and the computer and help to generate and visualize design knowledge in the form of models informed by concrete data.

This research focuses on the use of solar control devices acting as booth solar filter and cultural design element of the building. Further research on the same case studies could be carried out focusing on the interior consequence of this stage and design solution as far as occupant's comfort is concerned. Glare, view and interior temperature are directly linked to wellbeing and depend on the façade solutions. The same tools used for this research could be used to broaden the study and give the designer more information to work with.

The pursuit for better buildings based on data driven design is a way of achieving more sustainable solutions within an holistic approach.

REFERENCES

- [1] United Nations, World Urbanization Prospects: The 2014 Revision, 2004.
- [2] Sadeghipour, M. and Smith, A., Ladybug: a parametric environmental plugin for Grasshopper to help designers create an environmentally-conscious design, Proceedings of BS2013: 13th Conference of International Building Performance Simulation Association, 2013, p. 3128-3135.
- [3] Yi, Y. K. and Hyoungsub, K., Agent-based geometry optimization with Genetic Algorithm (GA) for tall apartment's solar right, Solar Energy, vol.113, 2015, p. 236-250.
- [4] G. Zemella, A. Faraguna,, Evolutionary optimization of façade design, a new approach for the design of building envelopes. Springer, 2014.
- [5] Kampf J.H, Robinson D., Optimisation of building form for solar energy utilisation using constrained evolutionary algorithms, Energy and Buildings vol. 42, 2010, p. 807–814
- [6] Huang Y., Niu J., Optimal building envelope design based on simulated performance: History, current status and new potentials, Energy and Buildings vol. 117, 2016, p. 387–398
- [7] D.A. Coley, S. Schukat, Low-energy design: combining computer-based optimisation and human judgement, Build. Environ. Vol. 37, 2002, p. 1241–1247.
- [8] W. Wang, H. Rivard, R.G. Zmeureanu, Optimizing building design with respect to life-cycle environmental impacts, in: Proceedings of the building simulation, Eindhoven, Netherlands, 2003.
- [9] W. Wang, R. Zmeureanu, H. Rivard, Applying multi-objective genetic algorithms in green building design optimization, Build. Environ. vol. 40, 2005, p.1512–1525.
- [10] W. Wang, H. Rivard, R. Zmeureanu, An object-oriented framework for simulation-based green building design optimization with genetic algorithms, Adv. Eng. Inform. Vol. 19, 2005, p. 5–23.

- [11] J. Wright, M. Mourshed, Geometric optimization of fenestration, in: Proceedings of the building simulation, Glasgow, Scotland, 2009.
- [12] D. Tuhus-Dubrow, M. Krarti, Genetic-algorithm based approach to optimize building envelope design for residential buildings, Build. Environ. vol. 45, 2010, p.1574–1581.

Natural Ventilation of Double Skin Façade: Evaluation of wind-induced airflow in tall buildings

SOHA MATOUR¹, VERONICA GARCIA-HANSEN¹, ROBIN DROGEMULLER¹, SARA OMRANI¹,
SINA HASSANLI²

¹Queensland University of Technology, Brisbane, Australia

²ARUP, Sydney, Australia

ABSTRACT: To improve the thermal performance of Double Skin Facades (DSF) in warm climates, the risk of overheating in the system's cavity must be addressed. The use of wind-driven airflow as the dominant force for the heat dispersion from the cavity has not been studied from a passive ventilation performance point of view. For this purpose, a series of CFD simulations were conducted on two basic wind-induced DSF configurations considering four wind incident angles (0°, 30°, 60°, and 90°). Cavity air velocity, airflow pattern, and distribution, and the function of openings were assessed as essential measures of natural ventilation. The results demonstrate that the cavity air velocity and airflow rate of the openings in the DSF configuration with lateral openings (M0) are highly affected by wind direction while the application of a central front opening on external skin (M1) can moderate the dependency of the DSF on wind direction. The central opening, therefore, would encourage faster flow/higher flow rate inside the cavity when considering all directions which would increase the heat dissipation from the cavity. However, uneven air distribution in M1 facing 30° wind direction needs openings design improvement to meet the ventilation criteria.

KEYWORDS: Double-Skin Facade, Cavity's openings, Natural ventilation, Wind, CFD simulation.

1. INTRODUCTION

The significance of the building envelope for reducing building energy consumption has been assessed up to 55% through the use of daylighting, solar heat gain control strategies, and natural ventilation strategies in a warm climate [1, 2]. For this purpose, Double Skin Façades (DSF) provide an opportunity to use the combination of external glazed skin and protected external shading devices for tall buildings. The literature review shows the efficiency of this system for solar heat gain reduction in a warm climate [3]. However, longwave radiation caused by absorbed and reflected solar radiation in the cavity increases the overheating risk in the hot months [4].

On the other hand, It has been proven that increasing the airflow rate in the cavity can result in reduced long-wave radiation exchange and convective heat flux [5] and finally dissipation of heat from the air gap [6, 7]. Therefore, to take advantage of external glazed skin and shading devices for facade solar heat gain reduction and increasing the overall thermal performance of DSF, natural ventilation of the cavity is a key alternative and needs more consideration in improving the cooling effect of DSF.

In the conventional type of DSF with limited opening size, buoyancy-driven airflow is the main driving force for cavity ventilation. However, for cavity ventilation in a warm climate, it can be claimed that DSF installations should not just rely on the stack

effect as airflow driven force [8]. For this purpose and to avoid the use of mechanical systems for cavity ventilation, the strategy described in this paper is the enhancement of wind-driven airflow [9] as a method for reducing the overheating risk of DSF in tall buildings.

In contrast with conventional DSF, two other kinds of DSF configurations have been introduced in the literature in which wind-driven airflow is the dominant flow regime: 1- DSF with lateral openings and 2- DSF with lateral and a front opening. An experimental study on the thermal performance of DSF with lateral openings [10] proved that horizontal ventilation mode (wind-driven airflow) outperforms vertical ventilation (buoyancy-driven airflow) which is a governing flow regime in conventional types of DSF. However, almost all of the studies in the literature focused on conventional DSF configuration for thermal performance assessment of DSF in a warm climate [11]. In these studies, despite the reduction in building cooling load, cavity overheating has been reported as an issue for this type of DSF.

According to the significance of DSF cavity ventilation and the lack of research on cavity wind-induced airflow assessment, a gap has been identified for improving DSF thermal performance in warm climates.

The objective of this research is to evaluate two introduced types of DSF configuration in the literature [12-14] from their thermal performance

and cooling capacity. For this purpose, the effects of influential factors on airflow behaviour across the cavity of DSF are investigated. The three main parameters studied are external skin openings, wind speed, and wind direction. The previous study conducted by the authors showed the effectiveness of external skin front openings in the perpendicular wind direction in terms of cavity airflow enhancement [11]. The current study focuses on the performance of openings and the contribution to natural ventilation improvement of the DSF cavity for different wind directions and velocities.

2. RESEARCH METHOD

Computational Fluid Dynamics (CFD) as a numerical approach was employed which is vastly used in industry and academia as a technique for assessing airflow in and around tall buildings [15] as well as building-integrated DSFs [2, 13]. This technique can provide a detailed description of the airflow by solving the Navier–Stokes equations [15, 16]. Steady-state Reynolds-Averaged Navier–Stokes (RANS) equations with $k-\omega$ -SST as the turbulence model was selected for this study.

A series of parametric simulations of the model considering the DSF types, wind direction, and wind speed (Table 1 & Fig.1) have been conducted and evaluated based on three main ventilation performance indicators: airflow distribution, cavity air velocity, and volumetric airflow rate through the openings. To ensure adequate fresh airflow across the cavity, an even distribution of induced air into the cavity is desirable and discussed as uniformity of air distribution in this paper. The ventilation rate of a space (volumetric flow rate), Q , is defined as the rate at which external air (fresh air) flows into the space [17]. The volumetric flow rate can be calculated as the product of the cross-sectional area (A) and the average flow speed (U) perpendicular to the area [18]:

$$Q=AU \text{ (m}^3\text{/s)} \quad (1)$$

Regarding the overheating reduction in a space, the rate at which heat is removed from the cavity (Heat loss) is influenced by the ventilation rate, Q , and the higher the value of Q , the higher is the cavity heat dispersion[17]. Both values of air velocity in the cavity and volumetric airflow rate of openings, hence, should be assessed to estimate the cooling capacity of each DSF configuration for different wind directions.

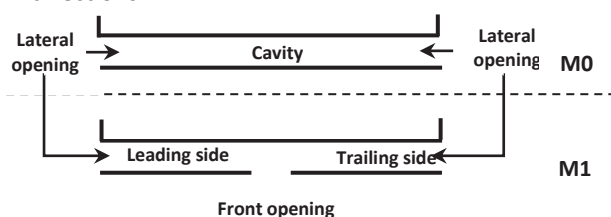


Figure 1: The studies DSF configurations and openings location.

Table 1: The studied parameters

Parameters	Parametric variations
External skin configuration	M0/M1
Wind direction (θ)	0°/30°/60°/90°
Wind speed at three building levels	Top (5/6 H) Middle (3/6 H) Bottom (1/6 H)

2.1 CFD SIMULATION

2.1.1 Numerical method and Model geometry

The CFD simulations have been carried out on a small scale (1/150) CAARC (Commonwealth Advisory Aeronautical Research Council) standard tall building with lateral and front openings. The dimension of the building model and configuration of openings are given in Table 2. Two different configurations for external skin openings were considered. In the first case (M0) cavity can be ventilated just through lateral and top openings while in M1, one opening was considered on the external skin of DSF in the middle of the external skin.

The commercial code ANSYS FLUENT 19.0 was used for the CFD analysis. The SIMPLE scheme was considered for pressure-velocity coupling with second-order discretization for pressure and momentum.

Table 2: The building dimensions.

	Scaled building	Prototype
Height	1200 (mm)	180 (m)
Width	200 (mm)	30 (m)
Length	300 (mm)	45 (m)
Cavity	6.6 (mm)	1 (m)
Openings width	6.6 (mm)	1 (m)

2.2. Computational domain and grid resolution

The CFD model was previously developed and validated against the wind tunnel test model [13]. The vertical cross-section of the computational domain was considered the same as wind tunnel condition (2 m × 3 m). For inlet and outlet distance, 3H and 11H were considered respectively, where H refers to the building height.

A fully structured mesh was constructed. A mesh sensitivity study was conducted for three levels of grid refinements to minimize the effect of grid size on the solution. Cavity depth as a region of interest was divided into 5, 10, and 20 cells and the results of air velocity were compared in the middle of the cavity along the building height (Figure 2, left). Less than 1% change occurred by increasing cell numbers from 10 to 20 while it was about 4% in the case of 5 cells. Therefore, the whole domain was divided by 10 million cells for more accuracy using the ICEM ANSYS meshing package. The minimum cell size of $6.5e^{-4}$ m and the growth rate of 1.1 were applied to the areas

of interest (i.e. walls and openings). This meshing property resulted in a y^+ value under 30 on all walls. Figure 3 shows the mesh resolution of CFD simulation in this study.

2.1.2 Boundary conditions

At the inlet boundary, the atmospheric wind profile corresponding to the wind tunnel testing profile for Terrain Category 2 of Australian Standard 1170.2 was imposed. The mean wind speed, turbulence kinetic energy, and turbulence frequency at the inlet section were calculated by:

$$U(z) = 0.564 \times \ln\left(\frac{z}{z_0}\right) \quad (3)$$

$$k(z) = \frac{3}{2} (U \times I)^2 \quad (4)$$

$$\omega(z) = k^{0.5}/L \quad (5)$$

where $U(z)$ refers to wind speed at height z , z_0 is the roughness length, and I and L are the turbulence intensity and the turbulence length scale determined in the wind tunnel test. For all simulations, the outlet boundary condition was set to outflow and top and lateral boundaries to symmetry while the ground and building's surfaces were set to no-slip wall. The convergence criterion was set to 10^{-6} for all equations.

To validate the accuracy of the wind profile, the profile at a location far from the building in the CFD simulation was compared to the wind tunnel data conducted in Hassanli's [13] experimental research. The normalized wind speed for the wind tunnel test and the CFD simulation at the target location is given in Figure 2 (Right) which shows a good agreement with R-squared of 0.95. Reference wind speed (U_{ref}) at the building height was reported as 12.56 m/s measured in the wind tunnel test.

3. RESULTS AND DISCUSSION

The flow characteristics (air velocity and distribution) inside the integrated DSF and volumetric airflow rate (Q) through the openings (lateral and front openings) were investigated for different wind directions.

To assess the airflow behaviour in the cavity, the mean velocity at the middle of each cavity section (between two openings) were calculated and normalized using the reference wind speed at the top of the building. Flow characteristics were evaluated at three building levels: middle of each one-third of the building height (Table 1). The airflow rate at openings for the entire building height was estimated as a performance indicator for introducing fresh air into the cavity.

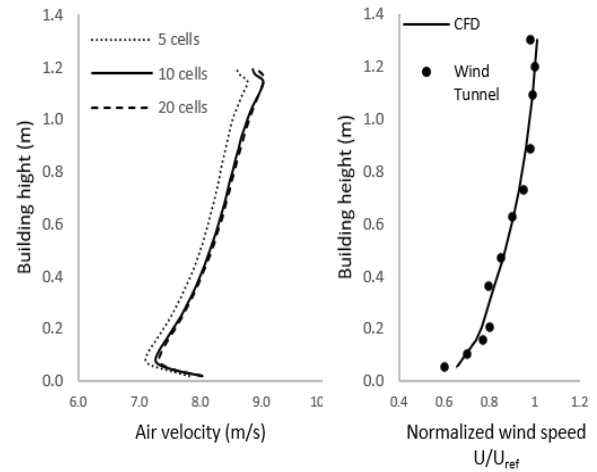


Figure 2: Results of grid Sensitivity analysis (Left) and normalized mean velocity at the empty domain (Right).

3.1 Effect of wind direction on cavity natural ventilation

3.1.1 Cavity air velocity and distribution

Figures 4 and 5 illustrate the distribution of the normalized air velocity (U/U_{ref}) and mean velocity in the cavity of all 8 studied cases at the Top level of the building ($5/6 H$) respectively. M0 with just lateral openings presents the lowest airflow speed of 1.5 m/s ($U/U_{ref}=0.12$) in the cavity for the winds perpendicular to the façade.

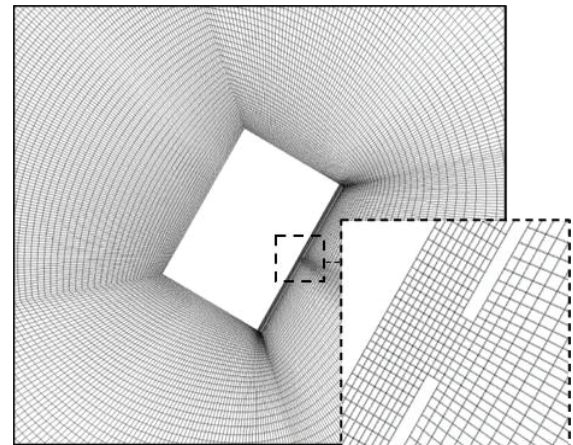


Figure 3: Mesh resolution around building and front opening

For wind direction of 30° , the speed is doubled to about 3 m/s ($U/U_{ref}=0.24$). However, the pressure distribution around the building and openings does not trigger the air movement towards the channel efficiently and creates a recirculation area at the inlet of the cavity. A greater change occurs for M0 under wind direction of 60° . Due to the higher differential pressure between two sides of the cavity, a larger mass flow enters from the leading side opening and discharges from the lateral opening at the trailing side of the cavity. This would result in the highest air

velocity in the cavity among all cases reaching an average of 10.2 m/s ($U/U_{ref}=0.82$).

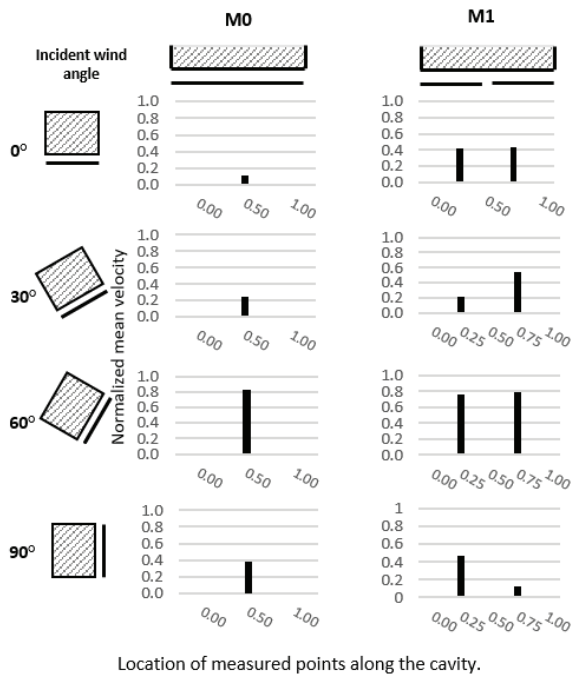


Figure 4: Normalized mean velocity (U/U_{ref}) in the middle of the cavity sections.

Increasing the incident wind angle to 90°, the cavity air velocity decreases to about 4.7 m/s ($U/U_{ref}=0.38$). For this wind direction, the mean velocity is still greater than 0° and 30° but it is not as high as when the wind direction is 60°. This is because the flow separation at the sharp edge of the lateral opening creates a bigger recirculation region which would reduce the effective opening area, thereby reducing the flow rate.

By introducing a central front opening to the external skin of DSF, the trend for air distribution along the cavity changes. In M1-0° air velocity in the middle of each section is about 5.3 m/s ($U/U_{ref} = 0.42$). This normal velocity is about 29% bigger than the same value measured in the experimental study on a full-scale DSF building with the lateral opening (10) showing the effectiveness of the central front opening for introducing wind to the cavity.

By increasing the wind incident angle to 30°, the flow uniformity and air distribution between two sections of the cavity change. On the leading side, air velocity is considerably lower than the trailing side as a result of pressure equalization between the leading side opening and the front opening. In another word, the front opening is only effective to drive the air to the trailing side.

The uniformity of airflow pattern can be seen in the 60° wind direction with a higher level of air velocity reaches 9.6 m/s and 9.9 m/s ($U/U_{ref}=0.76$ and 0.78) in leading and trailing sides. This is about 1.8 times higher than the airflow speed in M1-0°.

When the wind direction is 90°, the air distribution is approximately similar to 30° only mean airflow speed in the leading and trailing sides is swapped. Therefore, DSF with the lateral opening (M0) performs better for wind direction of 60° to 90° than the two other direction ranges, while M1 with a central front opening outperforms in wind directions of 60° and 0° compared to other directions.

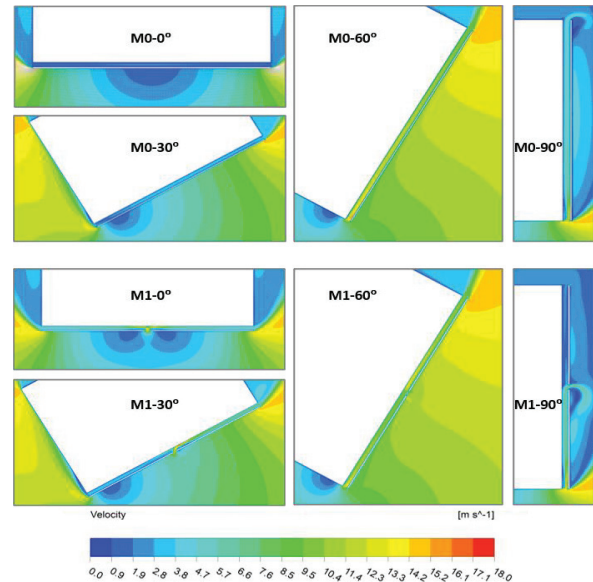


Figure 5: Mean velocity contours in the cavity in the plan view at the top level (5/6H).

3.1.2 Opening air flow rate

Figure 6 presents the total volume airflow rate through the openings in M0 and M1. The following observations can be made: The lowest air flowrates are for M0 openings for the wind directions of 0° and 30°. There is a considerable increase in the flowrate for openings at 60° wind direction in terms of inducing fresh air into the cavity (0.08 m³/s). Increasing the wind incident angle to 90°, the volume airflow rate through openings is decreased to about half that value and reaches less than 0.04 m³/s. In comparison with M0-0°, the airflow rate changes at 30°, 60°, and 90° are 75%, 2600%, and 1200% respectively.

In contrary to M0, M1 with a central opening produces the highest level of airflow rate through the openings when it faces the perpendicular wind direction. Changing the wind direction can decrease the cavity ventilation gradually. Compared with M1-0°, the ventilation rate through openings in M1-30°, M1-60°, and M1-90° declines by 20.3%, 14.1%, and 48.1% respectively. Therefore, it can be concluded that in the DSF configuration with one front opening, the effect of the wind incident angle from 0° to 60° on cavity ventilation rate is less notable compared with M0 with lateral openings.

Figure 7 indicates the performance of the central front opening utilising volume airflow rate vector for different wind directions. When wind approaches the building at 0°, the central front opening has the highest contribution for cavity ventilation. After a slight decrease at 30°, the decline at 60° is far more notable. Looking at figure 6 and Table 3 it can be concluded that the central front opening at 60° is not as effective as 0° and 30° and almost all the induced fresh air is provided by the lateral opening. This decreasing trend continues when the wind direction is at 90°. The opening in this condition works as an outlet instead of an inlet and exhausts the entered air to the outside of the cavity, which shown by a negative sign as an outflow. This airflow behavior can cause insufficient ventilation for the cavity trailing side.

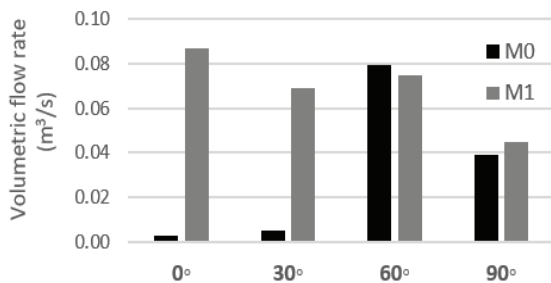


Figure 6: Total volumetric flow rate through the openings.

3.2 Effects of the configuration of openings on cavity natural ventilation

3.2.1 Cavity air velocity and distribution

Comparing both configurations in figure 4, it is noteworthy that the application of the central front opening can result in acceleration of air velocity across the cavity only in the case of 0° wind direction. For 30° and 90°, M1 outperforms M0 in just one side of the cavity (leading or trailing side) and another side remains even lower than the result for M0. Changes of air velocity in the cavity of M0-60° and M1-60° are less notable while a slight decrease in cavity air velocity results from using a central front opening on the DSF external skin.

3.2.2 Openings' air flow rate

Table 3 presents the volume flow rate of each opening and its contribution to cavity ventilation in all cases of the study. In all analysed wind directions, M1 outperforms M0 except at 60° which a slight decrease of about 6% can be observed. The airflow rate increase in M1 is about 186%, 172%, and 14.8% at 0°, 30°, and 90° respectively.

3.2 Effects of wind speed on openings function

DSF configurations have different behavior for wind speed increases along the building height.

Figure 8 presents the effect of wind speed on normalized mean velocity in the cavity for the studied cases. When M0 and M1 are at 60° of wind direction, the cavity air velocity increases more rapidly with wind speed along the building height than the other cases. On the other hand, in M1-0° increasing the wind speed has a slight effect on the cavity air velocity. It could be as a result of the high-pressure area around lateral openings when wind approaches the building with higher speed. The higher pressure does not allow the air to enter the cavity through the central opening as was expected. Therefore, in low wind conditions or lower levels of the building M1-0° is more capable of driving the wind into the cavity. The same trend happens in M0-0° while the increase of wind speed does not contribute to higher cavity air velocity. In other cases, the cavity air velocity is proportional to the incident wind speed.

Table 3: Details of volume flow rate m³/s (Q) through the openings showed as CFO (Central Front Opening), LO-L, and LO-T (Lateral Opening at Leading and Trailing side).

DSF Configuration	LO-L	CFO	LO-T
M0-0°	0.001	----	0.001
M0-30°	0.003	----	0.001
M0-60°	0.079	----	----
M0-90°	0.038	----	----
M1-0°	----	0.087	----
M1-30°	----	0.069	----
M1-60°	0.062	0.012	----
M1-90°	0.045	----	----

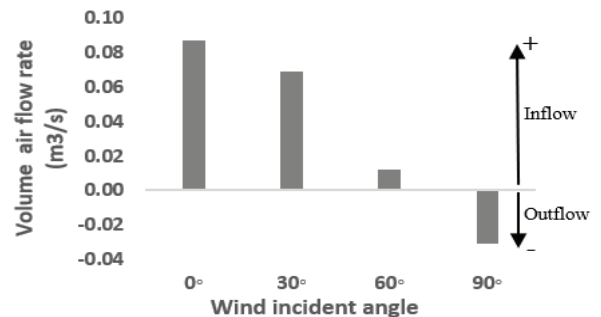


Figure 7: Volume airflow rate vector through the central front opening in M1.

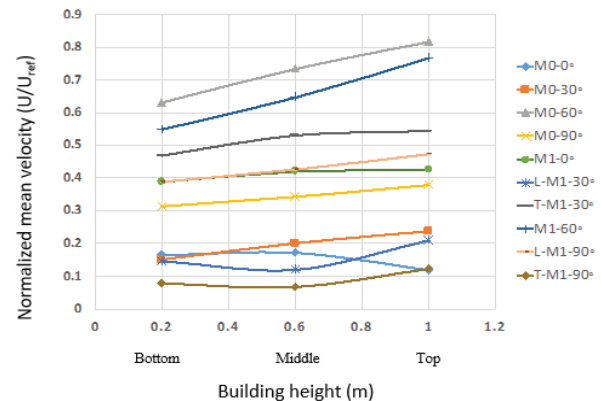


Figure 8: Effects of wind speed on cavity air velocity.

4. CONCLUSION

This study aims to improve natural ventilation in DSF cavity to reduce the common overheating risk of the system in a warm climate. A series of CFD simulations on two types of wind-induced DSF configurations were carried out by considering different wind incident angles and speeds. The findings of the study are outlined below:

- The airflow pattern in a DSF with the lateral openings is highly sensitive to the wind direction. To encourage airflow into the cavity for a wider range of wind directions, creating a front opening can be a potential strategy.
- Employing a front opening on the external skin is an effective strategy in perpendicular wind direction which drives the wind into the cavity while keeping the flow uniformity across the cavity. The volume air flow rate through openings in M1-0° is about 29 times higher than M0-0°.
- In M1-30° and M1-90°, despite the volume airflow rate increase through the openings the inflow cannot be distributed evenly across the cavity. Hence, while the heat at one section of the cavity could be adequately dissipated, there is a chance for overheating for the other section of the cavity.
- To assess the wind-driven natural ventilation in the cavity of DSFs' with front opening, it is necessary to evaluate the air velocity, distribution, and opening functions simultaneously.

This research is a preliminary step of a greater attempt to explore potential wind-driven mechanisms to overcome DSF overheating by passive design and suggests a future work for evaluating the effects of quantity and arrangement of front openings as well as cavity size for optimizing the cavity natural ventilation of DSFs.

REFERENCES

1. Haase M, Marques da Silva F, Amato A, (2009). Simulation of ventilated facades in hot and humid climates. *Energy and Buildings*, 41(4):361-73.
2. Nasrollahi N, Salehi M, (2015). Performance enhancement of double skin facades in hot and dry climates using wind parameters. *Renewable Energy: An International Journal*, 83:1-12.
3. Kim D, Cox SJ, Cho H, Yoon J, (2018). Comparative investigation on building energy performance of double skin façade (DSF) with interior or exterior slat blinds. *Journal of Building Engineering*, 20:411-23.
4. Olena Kalyanova L, (2008). Double-Skin Facade – Modelling and Experimental Investigations of Thermal Performance: Department of Civil Engineering, Aalborg University.
5. Hazem A, Ameghchouche M, Bougriou C, (2015). A numerical analysis of the air ventilation management and assessment of the behavior of double skin facades. *Energy and Buildings*, 102:225-36.
6. Luo Y, Zhang L, Liu Z, Su X, Lian J, Luo Y, (2018). Coupled thermal-electrical-optical analysis of a photovoltaic-blind integrated glazing façade. *Applied Energy*, 228:1870-86.
7. Kuznik F, Catalina T, Gauzere L, Woloszyn M, Roux J-J, (2011). Numerical modelling of combined heat transfers in a double skin façade – Full-scale laboratory experiment validation. *Applied Thermal Engineering*, 31(14):3043-54.
8. Poirazis H, (2004). Double skin facades for office buildings-Literature review report. Sweden: Lund University, Lund Institute of Technology, Lund.
9. Pomponi F, Barbosa S, Piroozfar PAE, (2017). On The Intrinsic Flexibility of the Double Skin Façade: A Comparative Thermal Comfort Investigation in Tropical and Temperate Climates. *Energy Procedia*, 111:530-9.
10. Flores Larsen S, Rengifo L, Filippín C, (2015). Double skin glazed façades in sunny Mediterranean climates. *Energy and Buildings*, 102:18-31.
11. Matour S, Garcia-Hansen V, Drogemuller, R, Omrani S, (2019). Adaptation of Double Skin Facade for warm climate from a wind harvesting perspective in tall buildings. in *53rd International Conference of the Architectural Science Association*.
12. Lou W, Huang M, Zhang M, Lin N, (2012). Experimental and zonal modeling for wind pressures on double-skin facades of a tall building. *Energy and Buildings*, 54:179-91.
13. Hassanli S, Hu G, Kwok KCS, Fletcher DF, (2017). Utilizing cavity flow within double skin façade for wind energy harvesting in buildings. *Journal of Wind Engineering and Industrial Aerodynamics*, 167:114-27.
14. Hu G, Hassanli S, Kwok KCS, Tse KT, (2017). Wind-induced responses of a tall building with a double-skin façade system. *Journal of Wind Engineering & Industrial Aerodynamics*, 168:91-100.
15. Omrani S, Garcia-Hansen V, Capra B, Drogemuller R, (2017). Natural ventilation in multi-storey buildings: Design process and review of evaluation tools. *Building and Environment*, 116:182-94.
16. Tian W, Han X, Zuo W, Sohn MD, (2018). Building energy simulation coupled with CFD for indoor environment: A critical review. *Energy and Buildings*, 165:184-99.
17. Hall M, (2010). *Materials for Energy Efficiency and Thermal Comfort in Buildings*. 1st edition ed. Hall MR, editor: Woodhead Publishing.
18. Tecle A, Bitsuamlak GT, Jiru TE, (2013). Wind-driven natural ventilation in a low-rise building: A Boundary Layer Wind Tunnel study. *Building and Environment*, 59:275-89

A Common Language for Environmental Performance Implementing the EU Level(s) Framework for Sustainable Buildings

CAMILO PÁEZ PÉREZ¹, ARÁNZAZU GALÁN GONZÁLEZ¹, SEBASTIANO CRISTOFORETTI²,
DUYGU ERTEN³, SAMIA BEN RAJEB¹

¹ULB Université Libre de Bruxelles - Ecole Polytechnique, Belgium; ²CRISCON Società di Ingegneria, Trento, Italia;

³Istanbul Medipol University - Civil Engineering Department, Turkey

ABSTRACT: *This paper develops an analysis of the potential and challenges of the European Commission Level(s) framework for assessing and reporting on the sustainability of buildings. Building upon the feedback from the beta version launched in 2018 – and tested in a wide variety of projects across several countries – a market-ready version is announced for mid-2020. This initiative aims to provide transparency and a harmonised reference to the market where multiple certification and rating approaches are available but of limited and complex application. The framework is intended to facilitate the mainstream implementation of sustainable practices in the building sector, making emphasis in the full life cycle of buildings and embracing health and wellness aspects, costs, resilience and adaptability to future conditions. How certification schemes can align with this framework is considered in detail. The implications of its use in the overall building process are evaluated as well. Finally, this study seeks to highlight points of attention for the evolution of Level(s). This latter task is done taking into account its potential for supporting the value-appraisal of green buildings, allowing to ease and secure investment, e.g. green-mortgage type financing, and hence market uptake.*

KEYWORDS: *Level(s), Sustainable Building, Assessment Methodology, Green-mortgage, Certification.*

1. INTRODUCTION

How does the use of sustainable-building guidelines affect the processes of planning, constructing and operating a building? How the Level(s) framework [1] would condition such processes? Can a common language be established, and effectively improve the sustainability of the built environment integrating a full life cycle thinking?

The present study addresses these questions in the task of evaluating the challenges and potentials of the Level(s) reporting system. The overall goal of this European Commission's initiative is to improve the sustainability of the building sector by means of a consistent and comparable voluntary assessment and reporting framework that focuses the attention on the "most important aspects of a building's performance" [1]. The use of a common language of Core Indicators and metrics is expected to foster harmonisation, understanding and the uptake by the market of holistic sustainable building practices.

The emergence of this institutional approach happens at a time when contemporary methodologies and technical solutions to achieve minimal environmental impact and maximal benefits from buildings have been developing and evolving for several decades [2]. However, if best practices emerging from these solutions and assessments methods become abundant, the required upscaling to the mainstream practice remains a pressing challenge [3]. It is also a complex challenge taking into

consideration that there are currently numerous and diverse assessment methods, ratings and certification schemes [4] and that misconceptions or inconsistencies can be found when applying such tools [5].

The implementation of the Level(s) reporting scheme underwent a one-year pilot testing phase that ended in 2019 that allowed gathering feedback from participants and key stakeholders across Europe such as Green Building Councils and professional associations that were actively involved in the process. Recent research projects reviewing or assessing the use of Green Building Rating System (GBRS), have evaluated the compatibility and alignment potential of those systems to the Level(s) structure. This is the case of the SMARTER Finance for Families (Green-Homes / Green-Mortgages) project [6].

This paper presents the results of the study built upon the institutional presentation of the beta-version of the Level(s) framework and late feedback. In particular, the outcomes of the integration of the Level(s) scheme into the SMARTER project are presented.

2. BACKGROUND AND CONTEXT

It needs to be acknowledged that accuracy may lack to some extent when using the terms 'sustainable building' and 'green building' [7] with 'sustainability' being a broader and evolving concept

[8]. The given title evokes the assessment of the environmental qualities which would be those that can appraise the sustainability of a building – evaluating its contribution to the consensual UN sustainable development goals. This approach corresponds to Level(s) initiative's scope addressed in this study. However, when considering certification and rating schemes of buildings' environmental performance, these are designated in this paper as Green-Building-Rating-Systems (GBRS) [8].

As an underlying context in which the Level(s) framework is being introduced, the codes and regulations of the construction and building sector are considered. The concerns of these regulations to ensure structural stability, safety and health have evolved in time to embrace increasingly environmental and energy-saving parameters.

In the domains of energy performance and efficiency, standards and calculation methodologies started to be developed forty years ago. In the last decade, the regulation in these fields has experienced a rapid evolution. In Europe, this evolution has mainly been driven by the EPBD Directive [3]. While the effectiveness in reducing the energy use in the building sector has so far been limited [9], a step change is expected in the coming years as ambitious energy efficiency goals are formally set for 2030 [10] and the vision for a climate-neutral economy in 2050 [11]. Currently, the growing trend of a broader-than-energy environmental scope in regulation is noticeable in, e.g. the European Circular Economy Action Plan [12].

Considering the holistic approach to the environmental performance of buildings, multiple sets of guidelines or certification schemes have emerged, starting from the early 90s'. Those have been used on a voluntary basis rather than integrated into regulation. The examples range from the pioneering labels of BREEAM (UK 1990), LEED (USA 1993) and HQE (France 1995) to several other national, or even local, initiatives around the world. Recent innovative and dynamic ones have emerged such as Living Building Challenge (LBC) (USA 2006) largely embracing the social dimension of sustainability [13] and DGNB (Germany 2007) which already integrates, in its 2019 update, sections for interacting with Level(s) [8]. These initiatives have been useful guidelines for green-building motivated stakeholders [4]. Exemplary and coherent projects conceived and built following such schemes, estimated to a 5% of the market [14], are today far ahead from the mainstream construction production. The Level(s) initiative aims at filling this gap between exemplary and mainstream practices allowing the scale-up of the building sector's sustainability [14].

The intention of Level(s) is not to set benchmarks or minimum requirements for performance indicators

but to acknowledge which indicators and metrics to use. With this framework, interested parties such as clients, service providers, certifiers, or policymakers, can set their reference values and required thresholds according to specific needs and goals.

The reporting scheme provided by Level(s) refers to 'calculations' for design and construction phases, and to 'measurements' for operation phase, allowing to consider the assessment of real performance.

Additionally, to complete this overview of Level(s), it needs to be highlighted how, besides assessing primarily the full life cycle environmental impact of buildings, there are indicators and tools addressing the complementary key sustainable performance aspects of health, comfort, life cycle cost, and future risks and adaptation [1].

3. APPROACH AND METHODOLOGY

3.1 Topics and Performance Indicators

Level(s)' macro-objectives structure and principles have been examined as well as the choice of its core-indicators. For this, recent research approaches in the field of Building Performance Modelling and Assessment that have analysed the indicators of building performance were referred to [15].

3.2 Approach to Rating and Certification Schemes

This previous characterisation contributed to establishing, in a second step, a general comparison of Level(s)' framework to the structure and principles of several GBRS present in the European market.

In this sense, three GBRS foreseen as certification schemes to support the implementation of the SMARTER Green Homes/ Green Mortgages (GH/GM) programme were analysed in detail. The SMARTER project is currently launching the implementation of such programme in 11 European countries, aiming to create a citizen-driven demand for green finance, and bringing around the table developers, financial institutions, and independent certifying bodies. These analysed certification schemes are the Romanian GBC Green Homes [16], the Irish GBC Home Performance Index (HPI) [17] and the Italian GBC HOME [18]. A recent review on the influence of Level(s) in the four main GBRS (BREEAM, DGNB, HQE and LEED) is additionally used as a reference [8].

3.3 Project Implementation Process Evaluation

A critical review of the implication of using Level(s) framework in the distinct phases of the development of building projects constitutes a third part of the study. In this stage, the study refers to the feedback from the testing pilot projects' stakeholders and takes into account *"the architect's role and point of view"* as expressed in the Level(s) scheme implementation report emitted by the Architects Council of Europe (ACE) [14].

The outcomes the review of this paper are meant to support the recommendations on how to potentially adjust and implement the Level(s) system in a way that strengthens its capacity to improve the overall environmental quality of buildings. For this review it was evaluated the potential of Level(s) for:

- Favouring and incorporating bioclimatic and passive-energy measures into projects.
- Supporting the project planning, management and implementation process.
- Incrementing of value and financial appraisal of real estate assets.

4. DISCUSSION AND RESULTS

4.1 Level(s) Structure and Indicators

As advanced in the Beta version of the framework, it embraces three thematic areas: Life cycle (LC) environmental performance; Health and comfort; Cost, value and risk.

Six macro-objectives address each of these areas: The LC environmental performance area will include the first three objectives: 1. Greenhouse gas emissions along the building's LC; 2. Resource-efficient and circular material LC; 3. Efficient use of water resources. The Health and comfort area is addressed by the 4th objective: Healthy and comfortable spaces. Objectives 5. Adaptation and resilience to climate change, and 6. Optimised Lifecycle cost and value address the area dedicated to Cost, value and risk.

Furthermore, the resulting precise objectives inscribed in this scheme are measured through a set of 9 indicators and 4 LC tools proposed by Level(s) that are synthetically compiled in Table 1.

Table 1: Level(s) structure and core indicators overview

Indicator or life cycle tool	Unit of measurement
1.1 Use stage energy performance	kWh/m ² /yr
1.2 LC Global Warming Potential	kg CO ₂ eq./m ² /yr
2.1 LC tool: Bill of materials	Reporting Building / Materials
2.2 LC tool: scenarios lifespan, adaptability, deconstruction	Reporting according to level of assessment
2.3 Construction and demolition waste and mat.	kg waste and materials/m ²
2.4 Cradle to grave LCA	7 impact category indicators
3.1 Total water consumption	m ³ of water/occupant/yr
4.1 Indoor air quality	Ventilation, CO ₂ and humidity +List of pollutants
4.2 Time outside thermal comfort range	% of time out of defined max. & min. temperatures/ season
5.1 LC tool: scenarios for future climatic conditions	Protection health and thermal comfort +2030 2050 scenarios
6.1 Life cycle costs	€/m ² /yr
6.2 Value creation + risk factors	Reliability ratings/ indicator.

Besides these set of indicators and tools, four other objectives are foreseen as potential indicators to be included at a later stage: 4.3 Lighting and visual comfort, 4.4 Acoustic comfort, 5.2 Risk of extreme weather events and 5.3 Risk of flooding events.

Lastly, three possible levels of detail and depth in the reporting are proposed to address different

degrees of expertise of users, different engagement possibilities of clients and different reporting purposes. These are a basic 'Common' assessment level, a 'Comparative' one and an 'Optimisation' assessment level nurtured with more precise and reliable data (Fig. 1).

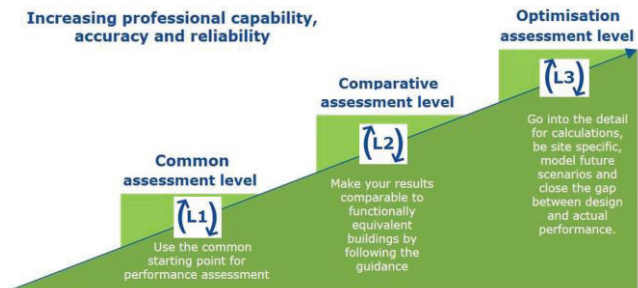


Figure 1. The three levels of performance assessment from Level(s) v1 - Part 1

The overall proposed scheme represents an appropriate strategy aiming to, on the one hand, to synthesise and simplify into a limited number of indicators and categories the vast possibilities of assessing sustainable performance. This synthesis is noticeable in reference, e.g. to the 130 KPIs of building performance compiled by the Eurac KPIs Database [15] or the 27 indicators retained for the ExCEED project [19].

On the other hand, the scope of Level(s) enlarges to allow the upfront integration of long-term perspective with a full-LC approach and the consideration of future scenarios for measuring building performance.

As in the piloting phase, the indicators to tackle and report were in some cases optional, and the system itself is of voluntary applicability; the indicators left in the beta version as a future possibility (§4.3, §4.4, §5.2, §5.3) could already be integrated into the core system. Doing so would allow strengthening of the assessment in the Health and Comfort thematic area that can underpin the overall sustainability of the projects. Actions in this area would interact and inform other areas. In particular, the Lighting and Visual comfort intertwine with passive-energy performance features (solar gains, solar protection) and merits to be integrated into the early design process with substantial benefits.

4.2 Alignment of GBRS to the Level(s) reporting

Level(s) does not set minimum requirements, nor a rating points scheme which implies a fundamental approach difference to the market GBRS considered in the paper.

GBRS systems may differ from each other in the weighting of criteria, the areas of focus, or even in the metrics used. They have, nonetheless, a common intention to offer a holistic assessment of a building's quality and tend to share most of their sustainability

objectives [20]. These schemes tend to focus on environmental aspects of the building with lesser attention to the other two canonical pillars of sustainability: the social and the economic. These aspects have only gained interest in recent GBRS version updates and developments as in DGNB [13].

Level(s) shares with the GBRS considered here, the main areas of environmental impact assessment as a base, applying, however, its full-LC approach in a systematic way (Fig. 2). Lifecycle analysis (LCA) is only partially -- or indirectly -- considered in most of the GBRS, being the RoGBC GH systems one of the exceptions where LCA is an upfront requirement. In this comparison exercise, it is worth recalling that Level(s) scope provides economic sustainability assessment within the dedicated thematic area of Cost, Value and Risk. The social dimension is considered in terms of health (indoor air quality) and comfort (thermal range and potentially visual and acoustics parameters).

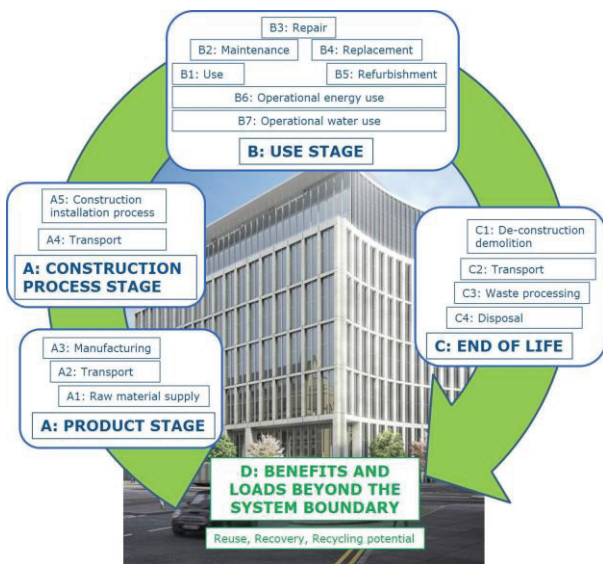


Figure 2. Modular schematic of building life cycle stages
Source: CEN (2011) from Level(s) v1 - Part 3

Additionally, it shall be noted that Level(s), despite aiming at mainstreaming sustainable practices, does include and offer designers refined tools – not usually applied in residential projects – such as the 5.1 Lifecycle tools: Scenarios for projected future (2030-2050) climatic conditions (linked to 4.2 Time outside of thermal comfort range). Likewise, 6.1 Lifecycle costs, under the three 2.2 scenarios for life span, adaptability and deconstruction, aren't quite commonly adopted, nor included within rating systems, with the scope Level(s) does.

On the contrary, many GBRS criteria are not included in Level(s) Beta-version objectives. This is the case, for instance, of the parameters regarding site-location, surroundings and accessibility to services. This area is not currently included in the

scope of Level(s) [20]. The fact that location, in particular, has an indirect influence in the environmental impact from material choices, from water use or use-stage energy consumption of the building itself, may have led to leaving them out from the synthesised core-indicators. The LC perspective would incorporate the impact of transportation in Production, Construction and End-of-Life stages. Nevertheless, location can influence the needs of transportation or other services during the use-stage of the building, with significant consequences on the overall sustainability. If it is not via Level(s), these aspects should be taken otherwise into account by the concerned stakeholders in the preliminary planning process of projects.

Similarly, criteria concerning the so-called "sustainable construction site" and related, e.g. to noise, dust and pollution minimisation are not explicitly included in Level(s) at this stage. These aspects remain under locally applicable regulations.

Considering the detailed compatibility potential evaluation and the alignment requirements for the GBRS considered for the SMARTER project, it appears that RoGBC GH scheme is the closest in covering the Objectives and Indicators of Level(s). Some of the Lifecycle Scenarios (2.2) from Level(s) are not covered: Refurbishment, Adaptability and End of life. Lifecycle Cost Level(s) criteria are partially addressed by RoGBC scheme, same as it is by the Irish HPI rating but missing in the Italian GBC HOME. What all three systems are missing are the future extreme weather risk assessments (5.1, 5.2) and the Risk and Value criteria (6.2).

Iris HPI Index stands out in the Level(s) alignment readiness as being the only one of the three to address, even if it is partially, the Time Out of Thermal Comfort criteria (4.2 in table 1) and the Lifecycle scenarios for Adaptability and Refurbishment (2.2 in table 1). The latter criteria is, on the contrary, not at all considered within the Italia GBC HOME system, and would thus require adaptation to include the appropriate criteria.

Given the fact that the structure of Level(s) and the GBRS – corresponding to different purposes and maturity stages – don't allow their overlapping to carry out a granular matching, two complementary evaluation angles have been considered. First, examining the GBRS from the Level(s) implementation perspective. Then, from the embedding point of view of each of the three rating systems considered, which led to more practical entailments. The first analysis allowed, the previous description, in short here, of the extent at which the ratings already include Level(s)' indicators. In the second, a detailed review was conducted for each GBRS, aimed at assessing the adaptation to Level(s). A concise "translation rating" (TR) 0 to 4 was used to

represent the grade of usability of the Level(s) indicators for the actual ratings' goals. The scores spanned from 0 – for the cases where an indicator was not considered in the Level(s) framework – to 4 – for the opposite cases where Level(s) is going beyond, offering metrics in a broader extent than the ratings. Intermediate values account for aspects from the GBRS criteria that are implicit, partially or fully included in level(s) [20].

From the compatibility evaluations behind the summary above, different sets of recommendations, indicator by indicator, were formulated for each of the three GBRS. These recommendations, classified in three levels of importance (Key, Normal, Further), are to be implemented progressively. With the final goal being to ensure an operative alignment of these systems with the Level(s) framework and the purpose of certification of SMARTER GH/GM projects. Attention was paid to a timeline of adaptation, considering as well the upcoming release of the formal market version of Level(s) framework.

In Huelva University's review, the structure of Macro-objectives, Core-Indicators and Indicators of Level(s) is systematically compared to the hierarchical structure of the studied GBRS. This comparison confirms the global correspondence, for instance, to the Category, Criteria, Issue, Indicator scheme of BREEAM. Yet, it underlines at the same time, the heterogeneity of methodologies that makes necessary translation and ad-hoc alignment procedures. As well, lack of detailed information for some of the indicator-systems (IDS) may undermine the accuracy of comparisons and underlines the importance of 'IDS analysis' for this task [8].

Among the four GBRS analysed in Huelva University's review, DGNB and HQE, which embrace an LCA approach, are much closer to the structure of Level(s) hence, easier to align than BREEAM or LEED. DGNB system even includes all six macro-objectives of Level(s) in its categories. This trend of convergence to European policy and UN SDG is expected to appear in future versions of GBRS.

4.3 Potential and Implication of using Level(s) in the Project Implementation Process

Although Level(s) intends to foster and up-scale sustainability in the building sector through essential indicators and a common language, to succeed it should embrace the potential to be more than a reporting framework and offer some basic benchmarking references and requirements upfront. Market appropriation of such a scheme would as well be eased by ensuring user-friendliness and by providing practical solutions to the needs of the different stakeholders to whom it is addressed.

The potential to represent all of the building's environmental performances in a concise graphical

form, including LCA's outputs such as, for example, the global warming potential (GWP100), in kg CO₂ eq / m², for the reference scenarios and stages, is a remarkable feature.

The role as a key decision-making tool, as support for design process optimisation and to ensuring the value creation and conservation in the built environment; are essential aspects that were underlined by the testing partners [14].

One point of conflict is the concerns about the progressive complexity and degree of detail foreseen in the three Levels of performance assessment. This scheme may correspond to different ambitions or capacity of the stakeholders – beginners and experimented users – but it does not reflect the planning and conception process of a project where these types of assessment could provide useful insight for value creation. Levels L2 and L3, 'Comparative' and 'Optimisation' assessment, are foreseen to be complemented with more detailed information. In contrast, optimisation and the comparison of design options may be made at the early stages of the conception process with a low resolution of details [14]. Highly detailed calculations and reporting at late stages would mainly ensure detailed compliance and the reliability of the data. Still, they would have, at this point, limited potential for optimising the configuration of the building or its technical systems. However, detailed and reliable data can be meaningful for stakeholders concerned by the operation phase of the building.

Another studied aspect, from the macro-objective of reducing the greenhouse gas (GHG) emissions along the building's life cycle, is the Use Stage energy performance (1.1). The metrics of this indicator are the – calculated or measured – energy consumption of the building in kWh/m² per year, in terms of Primary energy demand (Indicator 1.1.1) and of Delivered energy demand (Indicator 1.1.2). The provisions for these indicators refer to the national energy performance of buildings (EPB) regulations resulting from the European EPBD Directive, usually referring to the CEN standards of application and foreseen the use of EN ISO 52000 series [21].

The basic common assessment (L1) data for these indicators can directly be provided by the results of the national calculation methods required for building permits or for issuing Energy Performance Certificates (EPCs). For comparative assessment (L2), complementary simulations and calculation conditions need to be verified and reported, while for optimisation assessment (L3) detailed dynamic simulations are required, considering the representativeness and precision of the calculated performance.

From the L1 assessment, efficiency-first and envelope performance may be taken into account as

long as it is included in the national calculation methods, e.g. if they have been developed according to EN ISO 13790 and EN ISO 52016, where this the starting point (considering orientation, control of solar gains and daylighting, thermal inertia and zoning) [21].

Nevertheless, it would be coherent that provisions to favour incorporating bioclimatic and passive-energy measures into the conception of the project are embedded in the framework guidelines or as explicit requirements of these indicators.

5. CONCLUSIONS AND CHALLENGES AHEAD

Level(s) initiative responds to an aching demand of the building sector, considering its potential and responsibility to contribute to UN Sustainable Goals and environmental restoration.

Level(s) reporting is meant to be used, at this stage, in a voluntary basis and can be applied either directly via the forms provided, or indirectly with the alignment of a third-party certification system. The alignment of GBRS to this reporting framework has a significant galvanising potential for the building sector.

The framework, as such, does not determine indicators' benchmarks nor minimum levels to comply. While this offers flexibility, it can also cause disengagement or confusion. In the midterm, compulsory minimum markers are likely to appear based on this framework.

The reporting structure implies a coherent Green Building approach promoting Life Cycle and Life Cycle Cost analysis. The latter, and the 'property valuation influence and reliability rating' provisions within the framework, linking environmental quality and the value of buildings, can foster investments, financing, and the upscaling of sustainable building practices.

While the three assessment levels of using the framework can facilitate reaching different levels of experience or engagement of stakeholders, this approach may fail to correspond to projects' workflows.

Adequate management and transparency of building's information in all phases is crucial to produce successful projects and for the improvement of environmental quality in particular. Linked data and digitalisation concerning construction are gaining mainstream market and have the potential to integrate Green Building practices, assessment and procedures efficiently.

Level(s) framework has essential challenges to embrace and overcome. Still, it has as well the potential to become an essential communication and multipurpose reporting tool. One that favours a radical improvement of the building sector and contributes to underpin clear and ambitious policies related to green public procurement, aligned to the

European Green Deal through the Circular Economy Action Plan [12].

ACKNOWLEDGEMENTS

This study is developed in the framework of the SMARTER project that has received funding from the European Union's Horizon 2020 programme under Grant Agreement No. 847141

REFERENCES

1. Dodd N, Cordella M, Traverso M, Donatello S. (2017). Level(s) A common EU framework of core sustainability indicators for buildings Parts 1 and 2 (Draft Beta v1.0).
2. Mulhall DG, Braungart M, Hansen K. (2019). Creating Buildings with Positive Impacts. p. 9.
3. Tsemekidi Tzeiranaki S, Bertoldi P, Diluiso F, Castellazzi L, Economidou M, Labanca N, et al. (2019). Analysis of the EU Residential Energy Consumption. p. 23.
4. Erten D. (2018). A Roadmap for Localising and Harmonising Existing Green Building Rating Tools. *Journal of Current Researches on Engineering*. pp. 182-183.
5. Shaviv E. (2011). Applications of simulation and CAD tools in the Israeli "Green Building" Standard for achieving low energy architecture. *12th BPSA Conference, Sydney*. P.1259.
6. SMARTER H2020 Project (2019). SMARTER, A Toolkit for Residential Investors and Developers.
7. Berardi U. (2013). Clarifying the new interpretations of the concept of sustainable building. *Sustainable Cities and Society*.
8. Sánchez Cordero A, Gómez Melgar S, et al. (2020). Green Building Rating Systems and the New Framework Level(s): A Critical Review of Sustainability Certification within Europe. *Energies* www.mdpi.com.
9. Watts, M (C40), Knupfer S. (McKinsey Center). (2017). Focused acceleration: A strategic approach to climate action in cities to 2030. P. 28.
10. DIRECTIVE (EU) 2018/ 2002 of the European Parliament and of the Council - 11.12.2018 on energy efficiency (recast).
11. European Commission. (2018). A Clean Planet for all A European, Strategic long-term vision for a prosperous, modern, competitive and climate neutral economy.
12. European Commission. (2020). A new Circular Economy Action Plan.
13. Danish Building Research Institut SBI, GXN - 3XN Architects. (2018). Guide to Sustainable Building Certifications. p. 88.
14. Sattrup PA, Braune A, Kimpian J, Federal Chamber of German Architects (BAK). (2019). ACE study on the Role of Architecture in Building Performance as Defined by the EU Level(s) Scheme. 5: p. 21
15. Antonucci D, Pasut W, Babich F, Avesani S. (2018). Eurac KPI database.
16. RoGBC. (2019) Green Homes and Green Mortgage Toolkit for Residential Investors.
18. GBC Italia. (2018). GBC HOME short V2-mag 18.
19. Exceed project.eu. (2019). D3.1 KPIs and needed data.
20. Cristoforetti S., SMARTER Project. (2019). WP2 D2_05 Recommended Adjustment to Incorporate the Level(s) Framework.
21. Dodd N, Cordella M, Traverso M, Donatello S. (2017). Level(s) – A common EU framework of core sustainability indicators for office and residential buildings (Part 3).

Biophilic Atrium Design: An Analysis of Photosynthetically Active Radiation for Indoor Plant Systems

Comparison between Two Climates

Jiangtao Du, Steve Sharples

Liverpool School of Architecture, University of Liverpool, Liverpool, UK
Jiangtao.du@liverpool.ac.uk

ABSTRACT: *Biophilic design aims to bring natural elements into the built environment. In urban buildings, an atrium can be adopted not only as an important passive solution to achieve natural light and ventilation, but also to provide significant biophilic opportunities by nurturing plant growth on floors and façades. Access to Photosynthetically Active Radiation (PAR) is critical for sustaining plant growth in and around the atrium well. Therefore, it is important to investigate the availability of PAR at the early stage of an atrium building design. Using advanced ray-tracing simulations, this study presents the analysis of PAR availability at various positions in atrium buildings, considering shapes, geometries, and climates (Beijing and London). Key findings from the study are: 1) Different from daylight metrics for human vision, the PAR metric Photosynthetic Photon Flux Density (PPFD) could be more useful in terms of planning planting systems in atria. 2) The impact of atrium shape and geometry on PAR availability is significantly linked to position in the atrium, while the effect of atrium geometry will also depend on the shape. 3) It seems that climate conditions might not substantially influence PAR frequency variations based on this metric for plants.*

KEYWORDS: *Photosynthetically Active Radiation, Indoor plants, Biophilic design, Atrium building, Simulation*

1. INTRODUCTION

Biophilic design [1], an emerging design concept in the built environment, is increasingly applied to improve occupants' connectivity to the natural environment through direct nature, indirect nature, space and place conditions, and climate. The atrium has been generally adopted in traditional and contemporary architecture as an efficient passive solution to achieve daylighting and natural ventilation, and thus human visual and thermal comfort [2, 3, 4]. An atrium can also produce creative interplays of sky and sun, spaciousness, plants, and water in a deep plan, and to simulate the qualities of natural settings in an indoor space [5, 6]. Thus, in urban buildings, the atrium has been well recognized as one important and practical biophilic design solution.

Studies of atrium daylighting generally target three aspects - occupants, plants, and energy [2, 7]. The atrium floor and façades can be used as possible positions to establish plants of various types and sizes [6, 8]. Plants have been shown to be an effective biophilic solution to achieve a direct contact with nature for building occupants [4]. To maintain plant growth within the atrium is one of key objectives for sufficient daylight level needs in atria [2]. Plants require plentiful amounts of natural light to support fundamental photosynthesis processes, and maintain normal growth [9, 10]. It is recommended that typical

needs of common plants lie in the range of 700 to ~1000 lx for twelve hours a day and that top lighting is more desirable as a direction-giver [2]. Therefore, daylighting in an atrium has been regarded as one of the most difficult environmental factors to predict and control on the basis of plant maintenance for the interior [2]. In many atrium buildings, supplementary electric lighting will have to be used to sustain the planting [9, 10]. However, the use of electric lighting would not just increase energy consumption, but also bring in undesirable negative effects on a biophilic space, where man-made environmental factors and relevant control measures should be minimized or even avoided [5].

For the planting in a controllable facility (e.g. chamber, greenhouse), the light levels required by plants can be measured by illuminance (unit: lux) or Photosynthetically Active Radiation (PAR, unit: W/m² or μmoles/m²/s) [10, 11]. The concept of illuminance was developed based on the human visual system [9], and it was also applied by horticultural scientists to indirectly indicate how much light is required by the plants [9]. Photosynthetically Active Radiation (PAR), the spectral range (wavelength) of solar radiation (400 to 700 nm) that photosynthetic organisms use in the process of photosynthesis, is a direct metric of energy critically required for sustaining plant and vegetable growth [10]. PAR varies seasonally and changes based on time of day and site latitude [10].

Investigating the availability of PAR is necessary when planning an indoor planting scheme and the relevant facilities for growing the plants.

Using advanced ray-tracing simulation and various weather data, this study presents the first analysis of PAR availability and distributions in atrium buildings, taking into consideration shape, geometries, and locations. The results could be developed into design guidelines for the establishment of a biophilic atrium with a high potential to bring indoor a 'green nature' for building occupants.

2. METHODOLOGY

2.1 Locations and climates

Two atrium locations with different climates were selected in this study - Beijing in China (39.9° N, 116.4° E) and London in UK (51.5° N, 0.128° W). Beijing has a continental climate with a cold winter and a hot and humidity summer, whilst a typical temperate oceanic climate is found in London. Total annual sunshine hours of Beijing and London are 2478 and 1481, respectively. Beijing has 67% more sun shining hours than London, indicating a much higher level of daylight availability.

2.2 Atrium models

At each location, two typical atrium models were digitally modelled with square and round floor plans (Figure 1). These models had a flat double-glazed roof with a visual transmittance 0.64, and their wall and floor have reflectance of 0.4 and 0.2, respectively.

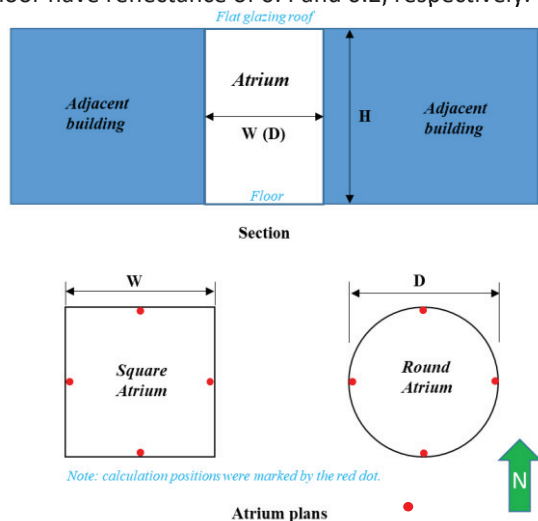


Figure 1: Section and plans of two atrium models.

Based on the configurations in Figure 1, six atrium models were studied in terms of shape and dimensions (Table 1). For a square atrium, the Well Index (WI) can be expressed by the equation:

$$WI = H/W \quad (1)$$

where H and W are the height and width of the atrium well respectively. Three types of square atrium were studied: shallow atrium (WI = 1), normal atrium (WI = 1.5), and tall/narrow atrium (WI = 2).

Similarly, the round atrium was categorized by the same three heights as the square atrium. For each height, the volume of the round atrium equalled that of the square one.

Table 1: Atrium types and geometries.

Shape	Name	W (m)	D (m)	H (m)	Well Index
Square	S-WI1	18		18	1.0
	S-WI1.5	18		27	1.5
	S-WI2	18		36	2.0
Round	R-WI1		20.32	18	
	R-WI1.5		20.32	27	
	R-WI2		20.32	36	

2.3 PAR simulation and metrics

Generally, PAR is quantified in terms of Photosynthetic Photon Flux Density (PPFD, $\mu\text{moles}/\text{m}^2/\text{s}$) [10, 11]. One indoor gardening guide book [11] provides PPFD ranges for sustaining the growth of indoor plants, such as (i) lower level (9.5-47.5 $\mu\text{moles}/\text{m}^2/\text{s}$); for example, Ficus Lyrate, Schefflera, Asparagus Fern; (ii) higher level (47.5-190 $\mu\text{moles}/\text{m}^2/\text{s}$); for example, Bromeliad, European fan palm, Mock Orange Bush. A very low PPFD (<9.5 $\mu\text{moles}/\text{m}^2/\text{s}$) and a very high PPFD (>190 $\mu\text{moles}/\text{m}^2/\text{s}$) will not be able to sustain a healthy growth of indoor plants. Thus, a PAR metric was applied based in this study on these four PPFD ranges.

The PAR calculations in the atrium models were achieved using the following steps: 1) The daylight illuminance (lux) at specific positions was simulated using the lighting software DAYSIM/RADIANCE and the weather data of the two locations; 2) The illuminance (visual part of solar irradiance spectrum) was converted to PPFD ($\mu\text{moles}/\text{m}^2/\text{s}$) using the algorithm given in [10]: $\text{PPFD} = 0.0185 \times \text{Illuminance}$. The daily analysis of PPFD was only considered within a daytime period of 9:00 - 16:00 [11]. The ambient settings for the RADIANCE simulations [12] were: Ambient Divisions 2048; Ambient Bounce 9; Ambient Super-Samples 1024; Ambient Resolution 128 and Ambient Accuracy 0.1. These atrium settings had been validated in a previous study by the authors [3].

Given the aim to place indoor plants in an atrium, this study investigated PAR availability at the centre atrium floor and three different façade heights, including low position (1/4H), middle position (1/2H), and high position (3/4H). Those calculation positions at atrium facades can be found in Figure 1 (red dots).

In this study, the PAR availability was assessed using the annual frequency in terms of the four PPFD ranges mentioned above. PAR levels at the façade were expressed by the averaged value of four positions at the same vertical position. The centre of the atrium floor PAR levels represented this area.

3. RESULTS

3.1 PAR performances on the atrium floor

Figures 2 and 3 show annual PPFD frequencies (four ranges) at the centre of the atrium floor for the six atrium models in Beijing and London, respectively.

In Beijing (Figure 2), square and round atrium models have similar varying trends of PPFD frequencies. Increasing WI or height will significantly increase the frequency of PPFD (<9.5) at the centre floor, while the frequency of PPFD (47.5-190) decreases. The tall atrium models (WI = 2.0) had no PPFD values falling in the range (47.5-190). Interestingly, the varying WI just slightly impacts on frequencies of PPFD (9.5-47.5). In general, all models can achieve the combined 'green' PPFD frequencies (9.5-190) > 50%, while high PPFD (>190) frequencies can be found in WI = 1.0 & 1.5 (< 5%). Thus, it seems that the PAR available at the atrium floor could be possible to sustain the normal growth of plants over half the working year.

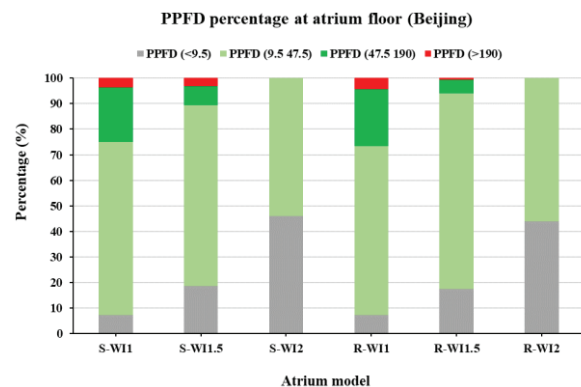


Figure 2: Frequencies of PPFD range at centre floor in various atria (Beijing).

For London (Figure 3), similarly, there are no big differences of PPFD frequencies found in square and round atrium models. The frequencies of PPFD (<9.5) tend to be larger with the increasing WI or height. As shown in Figure 3, There are no PPFD values falling in the range of (>190) in London, while only shallow atrium models (WI = 1.0) see the frequency of PPFD (47.5-190) of around 20%.

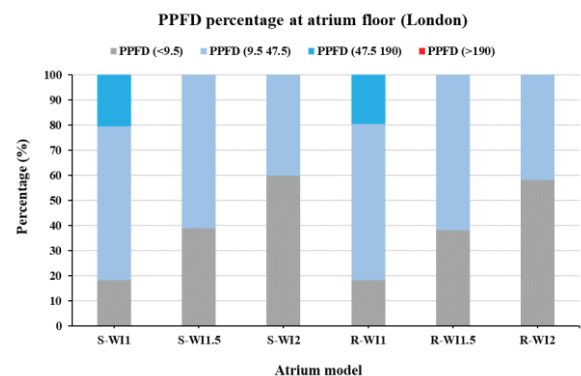


Figure 3: Frequencies of PPFD ranges at centre floor in various atria (London).

The shallow atrium models have very similar frequencies of PPFD (9.5-47.5) for normal atrium models (WI = 1.5). However, tall atrium models (WI = 2.0) achieve relatively lower PPFD (9.5-47.5) frequencies. Compared with Beijing (Fig. 2), London sees lower frequencies of PPFD (9.5-190), especially for tall atrium. However, all models achieve the frequency > 40%, and it possible to grow plants at the atrium floor in London for ~40% of the working year.

3.2 PAR performances at low levels of atrium façade

Figs. 4 and 5 present annual PPFD frequencies (four ranges) at the low levels of the atrium façade in six atrium models for Beijing and London, respectively. In Beijing (Fig. 4) there are big differences of PPFD variations between square and round models. For the square model, an increasing WI reduces frequencies of PPFD (9.5-47.5) and PPFD (47.5-190), while increasing the frequency of PPFD (<9.5). The tall atrium model (WI = 2) has the frequency of PPFD (9.5-190) < 35%, indicating a low possibility to place plants at this position. However, for the round model, frequencies of PPFD (<9.5) are less than 2%, while relatively higher frequencies of PPFD (>190) can be found at all heights (all values > 20%). Frequencies of PPFD (9.5-47.5) are generally higher than 65%. For each model, frequencies of PPFD (47.5-190) are much higher than frequencies of PPFD (9.5-47.5). This suggests that there is a high possibility to place plants at low façade levels in round models.

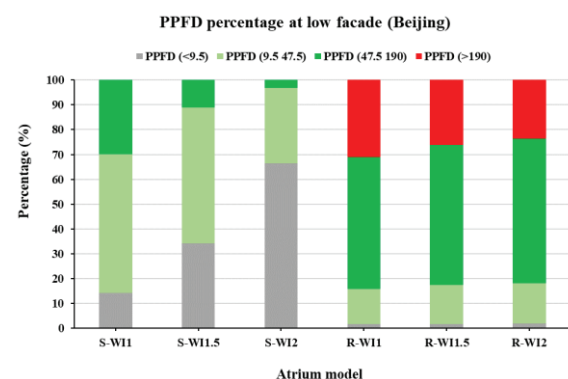


Figure 4: Frequencies of PPFD ranges at low levels of the atrium facade in various atria (Beijing).

For London (Fig. 5) similar variations of PPFD frequency in two types of atrium are seen. In general, the varying PPFD frequencies of square models are significantly different from round models. Compared with round models, square models see lower PPFD (9.5-190) frequencies and much higher PPFD (<9.5) frequencies. Round models have relatively higher PPFD (>190) frequencies (all values > 10%), while these values cannot be found in any square model. Increasing the WI increased the PPFD (<9.5) frequency in square models, while significantly decreasing frequencies of PPFD (9.5-47.5) and PPFD (47.5-190). In addition, heights of round models do

not have a significant impact on frequencies of PPFD (< 9.5), PPFD (9.5-47.5), and PPFD (47.5-190). Frequencies of PPFD (47.5-190) are higher than those of PPFD (9.5-47.5) in round models. Moreover, frequencies of PPFD (9.5-190) were over 70% in all round models. However, square models can see these values > 50% only when WI = 1. It could be found that for a location dominated by overcast skies the round atrium can still provide higher opportunities for plants applied at low atrium façade levels.

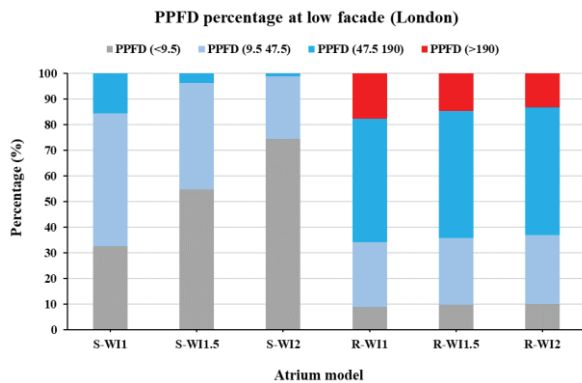


Figure 5: Frequencies of PPFD ranges at low levels of the atrium façade in various atria (London).

3.3 PAR performances at middle level atrium façade

The distributions of annual PPFD frequencies (four ranges) at the middle atrium façade level in the six atrium models are presented in Figs. 6 & 7 for Beijing and London respectively. In Beijing (Figure 6), the middle façades levels generally have high frequencies of PPFD (9.5-190) in both square and round models. The frequencies achieved in square and round models are >70% and > 65%, respectively. For square models, interestingly, increasing WI could increase frequencies of PPFD (9.5-47.5), while decreasing frequencies of PPFD (47.5-190). Frequencies of PPFD (9.5-47.5) are generally higher than those of PPFD (47.5-190). No PPFD (>190) values can be found at middle façade level of the square model.

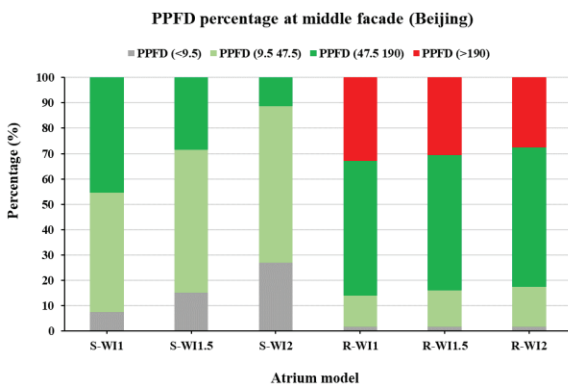


Figure 6: Frequencies of PPFD ranges at middle atrium façade in various atria (Beijing).

For round models, the varying height cannot significantly change frequencies of PPFD (9.5-47.5)

and PPFD (47.5-190). Frequencies of PPFD (>190) were above 27% at all heights, while frequencies of PPFD (< 9.5) were less than 2%. Different from square models, round models can see higher frequencies of PPFD (47.5-190) than those of PPFD (9.5-47.5). It seems that the choice of suitable types of plants would be linked with the type of atrium plan.

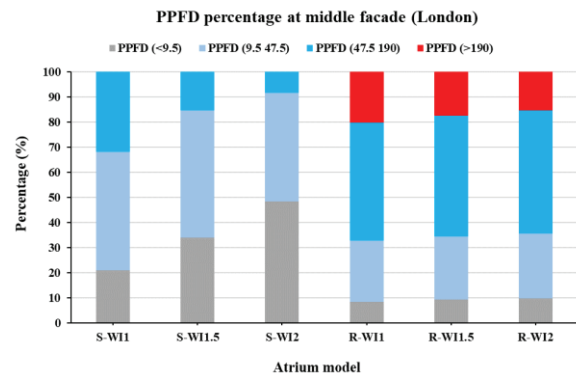


Figure 7: Frequencies of PPFD ranges at middle atrium façade in various atria (London).

Similar trends of PPFD frequency variations can be found for London (Fig. 7). At the middle level, both square and round models have high frequencies of PPFD (9.5-190). All square models have the values above 50%, while these values for round models are over 70%. An increasing WI increased frequency of PPFD (< 9.5), while decreasing frequencies of PPFD (47.5-190). However, no clear impact of WI can be found for the frequency of PPFD (9.5-47.5). Square models see higher frequencies of PPFD (9.5-47.5) than PPFD (47.5-190). In round models, similarly, no big impact of atrium height can be found on frequencies of the four PPFD ranges. Frequencies of PPFD (> 190) in all models were larger than 15%, while PPFD (< 9.5) frequencies were lower than 10%. Compared with the frequency of PPFD (9.5-47.5), a higher frequency of PPFD (47.5-190) was achieved in each round model. Thus, the atrium plan type can affect the plant types placed at middle façade levels.

3.4 PAR performances at high atrium façade levels

Figs. 8 and 9 show distributions of annual PPFD frequencies (four ranges) at the high atrium façade level for the six atrium models in Beijing and London, respectively. For Beijing (Fig. 8), it can be seen for square models that frequencies of PPFD (9.5-190) are over 90%. Compared with square models, round models see lower frequencies of PPFD (9.5-190). However, this value for each round model is still higher than 60%. In square models, shallow and normal atria (WI = 1.0 and 1.5) have higher PPFD (47.5-190) frequencies than PPFD (9.5-47.5) frequencies, while a tall atrium (WI = 2.0) sees similar frequencies between the two PPFD ranges (around 45%). For round models, there are higher frequencies of PPFD (>190) for three heights, such as 36% (R-

WI1), 35% (R-WI1.5), and 33% (R-WI2.0). Similar to results in Sections 3.2 & 3.3, no big impact of atrium height can be found on frequencies of PPFD (9.5-47.5) and PPFD (47.5-190) in round models. The PPFD (47.5-190) achieved much higher frequencies than the PPFD (9.5-47.5). It seems that plants requiring a higher PPFD (> 47.5) would be suitable for this façade position. In addition, the square plan for an atrium could be a proper solution to grow plants at this position.

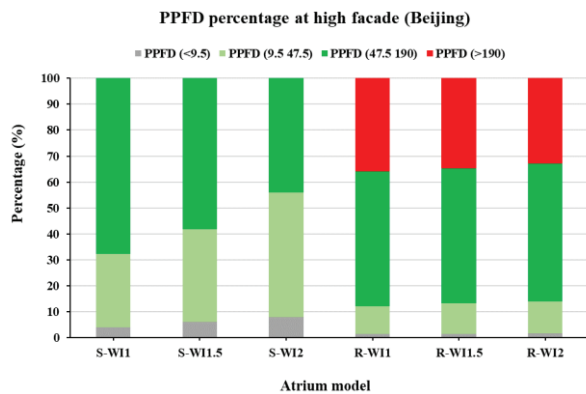


Figure 8: Frequencies of PPFD ranges at high atrium facade levels in various atria (Beijing).

In London (Fig. 9), similar varying trends of PPFD frequencies can be found. Both square and round models have high PPFD (9.5-190) frequencies (over 65%). Without any PPFD (>190) values, square models receive higher PPFD (9.5-190) frequencies than round models, while PPFD (> 190) frequencies in round models fall in a higher range of 20% ~ 24%. For square models, compared with PPFD (47.5-190), normal and tall models have higher frequencies of PPFD (9.5-47.5). The shallow atrium (WI = 1.0), however, sees an opposite trend. In round models, frequencies of PPFD (47.5-190) are significantly higher than those of PPFD (9.5-47.5). The frequency ranges for PPFD (47.5-190) and PPFD (9.5-47.5) are 45% - 24% and 22% - 25%, respectively. In addition, the big impact of WI or height on PPFD frequency can only be found in square models.

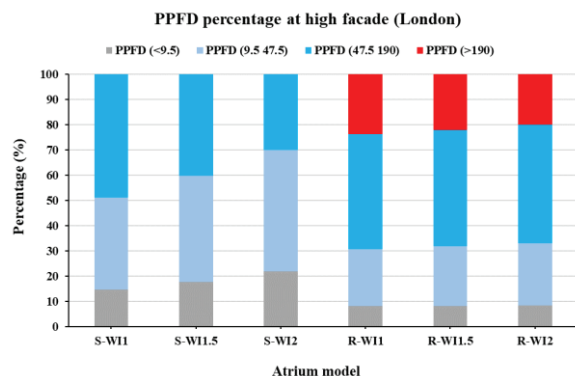


Figure 9: Frequencies of PPFD ranges at high atrium facade levels in various atria (London).

3.5 Comparisons between different atrium positions

Comparisons of frequencies of two PPFD ranges suitable for plants between different atrium positions are discussed in this section, including floor and three facade levels. Taking the high façade level as a reference, relative differences of frequencies of PPFD (9.5-47.5) or PPFD (47.5-190) [$R_{PPFD(9.5-47.5)}$ or $R_{PPFD(47.5-190)}$] can be expressed as follows:

$$R_{PPFD(9.5-47.5)} = \frac{[F_{PPFD(9.5-47.5), n} - F_{PPFD(9.5-47.5), \text{high facade}}]}{F_{PPFD(9.5-47.5), \text{high facade}}} \times 100\% \quad (2)$$

$$R_{PPFD(47.5-190)} = \frac{[F_{PPFD(47.5-190), n} - F_{PPFD(47.5-190), \text{high facade}}]}{F_{PPFD(47.5-190), \text{high facade}}} \times 100\% \quad (3)$$

where $F_{PPFD(9.5-47.5), n}$ or $F_{PPFD(47.5-190), n}$ is the frequency of PPFD (9.5-47.5) or PPFD (47.5-190) at floor, low or middle façade positions; $F_{PPFD(9.5-47.5), \text{high facade}}$ or $F_{PPFD(47.5-190), \text{high facade}}$ is the frequency of PPFD (9.5-47.5) or PPFD (47.5-190) at the high façade level; n means various atrium positions, including the centre floor, low and middle façades.

Table 2: Relative differences of frequencies of PPFD (9.5-47.5) between high façade and other three positions (S1–3 mean models of S-WI1, S-WI1.5, S-WI2; R1-3 means models of R-WI1, R-WI1.5, R-WI2.).

		$R_{PPFD(9.5-47.5)} (\%)$					
		S1	S2	S3	R1	R2	R3
Beijing	Floor	139	98	12	520	555	352
	Low facade	98	54	-37	32	35	32
	Middle facade	66	58	28	16	22	26
London	Floor	68	45	-16	175	160	71
	Low facade	42	-1	-49	12	10	10
	Middle facade	30	21	-10	8	6	6

Table 3: Relative differences of frequencies of PPFD (47.5-190) between high façade and other three positions (S1–3 mean models of S-WI1, S-WI1.5, S-WI2; R1-3 means models of R-WI1, R-WI1.5, R-WI2.).

		$R_{PPFD(47.5-190)} (\%)$					
		S1	S2	S3	R1	R2	R3
Beijing	Floor	-69	-87	-100	-57	-90	-100
	Low facade	-56	-81	-92	3	8	10
	Middle facade	-33	-51	-74	3	3	4
London	Floor	-58	-100	-100	-57	-100	-100
	Low facade	-68	-91	-96	6	8	6
	Middle facade	-35	-62	-72	3	5	4

Tables 2 and 3 give the calculated values of $R_{PPFD(9.5-47.5)}$ and $R_{PPFD(47.5-190)}$, respectively. According to Table 1, compared with the high façade, the floor can receive much higher frequencies of PPFD (9.5-47.5) in most models at two locations, except for tall

square atrium, while for the low façade significantly higher PPFD (9.5-47.5) frequencies can be just found in normal and shallow square atrium in Beijing and shallow square models in London. In addition, the middle façade level only sees higher PPFD (9.5-47.5) frequencies in Beijing's shallow square atrium. For the data of PPFD (47.5-190) in Table 3, the high façade in square models has higher frequencies than the other three positions at the two locations, whilst round models can only see this trend on the atrium floor. The middle and low facades levels in round models achieve very similar PPFD (47.5-190) frequencies as the high façade.

4. DISCUSSIONS AND CONCLUSION

Based on the simulation analysis of PAR availability and distributions in various atrium models at two locations, several key findings are discussed as follows.

Different from the daylighting metric applied for human visual function [9], the PAR metric (PPFD, $\mu\text{moles}/\text{m}^2/\text{s}$) recommended in this study could be more useful in terms of planning greenery systems to enhance biophilic aspects of atrium. This metric adopted three PAR thresholds [10] instead of illuminance levels to evaluate if plants can have a normal growth in an atrium space. This could be used to provide quick solutions for supporting landscape design (interior) in a straightforward way.

The impact of atrium shape on PAR availability is significantly linked to the position in an atrium. At the atrium façade, it can be found that there are big differences of PAR availability between square and round atrium models. Generally, round atrium model could achieve higher PAR levels than square models, thus leading to a higher possibility to set vertical greenery systems at low or middle façade levels. On the other hand, at high façade levels, round models would be less suitable for vertical planting due to the excessively higher PAR levels. However, on the atrium centre floor, the impact of shape on PAR variation could be negligible, since a very similar level of PAR can be found for both square and round atrium models. This could be explained by the same volume and height applied for both atrium types.

In addition, geometric atrium properties (Well Index or height) could affect the PAR availability in an atrium. Similarly, the effect can be associated with the atrium shape and positions. At the atrium centre floor, increasing the WI or height would significantly lower the possibility to apply planting systems due to the decreasing frequency of proper PAR ranges. However, at the atrium façade, some different trends can be found. In square atrium models, an increasing WI or height could reduce frequencies of PAR falling in a proper range for sustaining plants growing, while the change of WI or height in round atrium models

would not deliver big impact on such frequencies. Thus, round atrium models could provide designers with more opportunities for both spatial design and greenery system installations.

The frequency analysis indicates that climate conditions might not substantially influence the varying trends of PAR frequency according to the six atrium models studied here. Even though there is a big difference in climate between Beijing and London, the application of four frequency ranges (see section 2.3) might have reduced the divergence brought by the absolute PAR levels.

These results could contribute to design guidelines for the establishment of greenery systems in an atrium, and thus to increase opportunities to create a biophilic atrium with the 'green nature'.

Limitations and future work: this study only adopted two types of atrium. The atrium configurations were relatively simple. More work will be continuously conducted on parameters including interior properties, shapes, roofs, etc.

REFERENCES

1. Kellert, S. R., Heerwagen, J., Mador, M. (2008). *Biophilic Design: The Theory, Science and Practice of Bringing Buildings to Life*. John Wiley & Sons, New Jersey, USA.
2. Sharples, S., Lash, D., (2007). Daylight in atrium buildings: A critical review. *Architectural Science Review*, 50: p. 301-312.
3. Du, J., Sharples, S., (2010). Analysing the impact of reflectance distributions and well geometries on vertical surface daylight levels in atria for overcast skies. *Building and Environment*, 45: p. 1733-1745.
4. Du, J., Sharples, S., (2010). The variation of daylight levels across atrium walls: Reflectance distribution and well geometry effects under overcast sky conditions. *Solar Energy*, 85: p. 2085-2100.
5. Browning, W., Ryan, C., Clancy, J. (2014). *14 patterns of biophilic design: improving health and well-being in the built environment*. New York, USA: Terrapin Bright Green LLC.
6. Gauzin-Muller, D. (2002). *Sustainable Architecture and Urbanism: Design, Construction, Examples*. Switzerland: Birkhauser Verlag AG.
7. Littlefair, P. (2003). Daylight prediction in atrium buildings. *Solar Energy*, 73: p. 105-109.
8. Iguchi, M., Shen, Y., Saito, Y., Yamamoto, S. (2009). A study on landscape image evaluation of an atrium with plants. *Landscape Research Japan*, 72: p. 611-616.
9. Baker N., Fanchiotti A. and Steemers K. (1993). *Daylighting in Architecture, A European Reference Book*. London, UK: James and James.
10. Langhans, R.W., Tibbitts, T.W. (1997). *Plant Growth Chamber Handbook*. Iowa Agricultural and Home Economics Experiment Station, USA.
11. Van Patten, G. F. (1995). *Gardening Indoors: The Indoor Gardener's Bible*. Van Patten Pub., USA.
12. Ward, G.L. and Shakespeare, R. (1998) *Rendering with Radiance: The Art and Science of Lighting Visualization*. Morgan Kaufmann Publishers Inc, San Francisco, California.

Thermal and Light Impact of the Use of Translucent Glass Railings on Terraces of Residential Buildings

Case study in Sant Cugat del Vallès (Barcelona)

JOAN LLUIS ZAMORA MESTRE¹, ESTELA LOURDES SORTO DIAZ¹, URTZA URIARTE ORTAZUA²,
MARIA EUGENIA ARMAS CABRERA³

¹ UPC, Catalunya, Spain

² UPV EHU, Spain

³ Universidad Europea de Canarias, Spain

ABSTRACT: One strong current trend in architecture is to employ glass on façades. After its widespread application in administrative buildings, the use of glass is expanding rapidly on the terrace and balcony railings of many residential buildings. Glass is highly appreciated for its great transparency, adequate security and easy maintenance, especially in the hotel sector that wants to offer beautiful views to its customers. Railings are an element that has low surface dimensions compared to the entire surface of the façade. Hence, it is not generally considered that the use of glass railings has an appreciable impact on user comfort, either on the terrace itself or inside the adjacent room. This study evaluated the impact of glass railings and related phenomena, to promote a more responsible, efficient use of this architectural element from the environmental perspective in the future. It was considered a priority to conduct a field study. The selected case was a dwelling in a multi-storey apartment building in Sant Cugat del Vallès (Barcelona), which had a south-facing and a north-facing terrace. Thermal and light measurements in situ were made in the spring-summer period of 2017. The results show that there is not much greenhouse effect due to the large terrace and air ventilation. However, the ground does not have much shade and receives a lot of direct solar radiation, causing visual disturbance.

KEYWORDS: Glass railings, thermal comfort, light comfort, terraces, balconies

1. INTRODUCTION

From the second half of the twentieth century, when tempered or laminated glass became available, some avant-garde architects began to use glass on railings. Parallel fixing systems and metal profiles were developed that were suitable for this function.

A range of models and types can be found within the commercial offer of this type of railings. They vary in the arrangement of the metal elements that transmit the mechanical forces generated on the handrail to the general structure of the building (Figure 1).

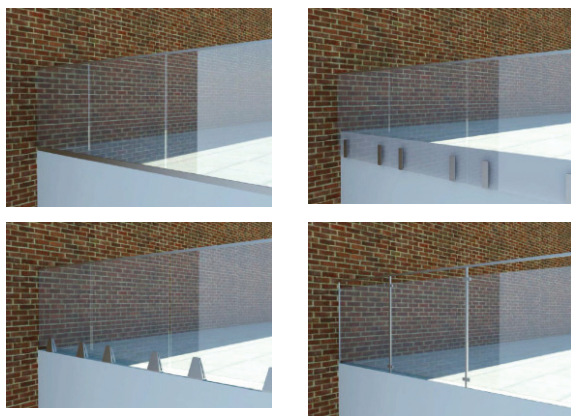


Figure 1. Different commercial types of glass railings.
Source: authors

2. STATE OF THE ART

Recently, some authors [1,2,3] have focused on the impact of greater use of glass on the traditional balconies and cantilevered terraces of apartment buildings in intensely sunny climates. These spaces were traditionally in semi-shade and exerted a visor effect that moderated in adjacent rooms the visual and thermal impact of the incidence of intense solar radiation on façades. In new apartment buildings, with an isolated urban arrangement and greater height, architects usually propose large sun-bathed terraces with beautiful views. An inexperienced use of glass railings in these cases could cause an increase in the temperature on the terrace itself due to the reduction of shadows and ventilation, as well as glare [4,5] caused by the increase in luminance in the visual field in the adjacent interior room that enjoys the views (Figures 2 and 3).

3. METHOD

To identify the thermal and light impact of the use of glass railings, a preliminary set of light and temperature measurements was carried out in a dwelling in a multi-storey apartment building in Sant Cugat del Vallès (Latitude 41°28'23.29"N, Longitude 2° 4'1.81"E), which had a terrace facing south and another north, and glass railings facing north, south, east and west.



Figure 2. General view of the apartment building. Case study terraces are identified (authors)

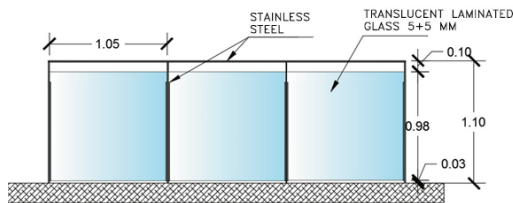


Figure 3. Terrace railings are made of stainless steel profiles and translucent laminated glass. Source: authors



Figure 4. View towards the south terrace taken from the interior of the dwelling. Source: authors



Figure 5. View towards the north terrace taken from the interior of the dwelling. Source: authors

The south terrace has an area of 34 m². It has only one access door and is not completely covered by the terrace roof (see the dashed lines). The north terrace has an area of 19.60 m² and is narrower than the south terrace. It is almost completely covered with a roof. This terrace has two entrances to the interior of the apartment, one with a north orientation and the other with an east orientation. Both terraces have some sections of railings facing east and west.

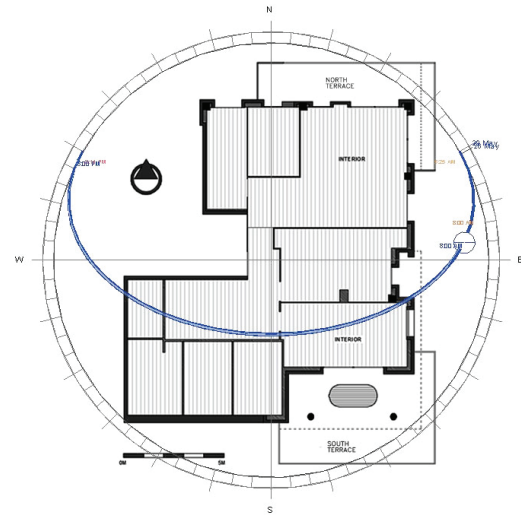


Figure 6a. Architectural plan superimposed on the solar route on the date of the measurements (authors)



Fig.6b. Main surface materials

Maximum temperature: 27.3°C
Average temperature: 20.5°C
Minimum temperature: 15.4°C
Global irradiation: 8,027.84 Wh/m²
Prevailing wind: southeast
Average wind speed: 22.7 km/h
Average relative humidity: 69%

Figure 6c. Meteorological data at the location of measurement

Measurements were taken on 26 May every hour from 08:00 to 19:00 (+2 GMT) (CEST) at predetermined points, using portable equipment, on the sunny terrace (south) and on the non-sunny terrace (north) (Figures 4 and 5).

A *Hagner Screen Master* portable luxmeter was used for the light measurements that can determine luminance and illuminance from 0.1 to 200,000 cd/m² and lux, respectively. Vertical and horizontal surfaces were considered work surfaces in illuminance; and the front, floor and sky or roof were considered as surfaces in luminance.

For the thermal measurements, an environment meter, PCE-EM882, was used to measure the air temperature and relative humidity. The surface temperatures of the floor and the glass of the railings were determined using a thermometer with the option of infrared laser.

4. RESULTS

4.1 Light results

Various points were selected for the light measurements: I1S, I2S and I3S (Figures 7 and 10) on the south terrace and I1N and I2N on the north terrace (Figures 8 and 11). To make the comparisons between the values clearer, time evolution graphs of illuminance and luminance were superimposed with the radiation evolution bars of meteorological data.

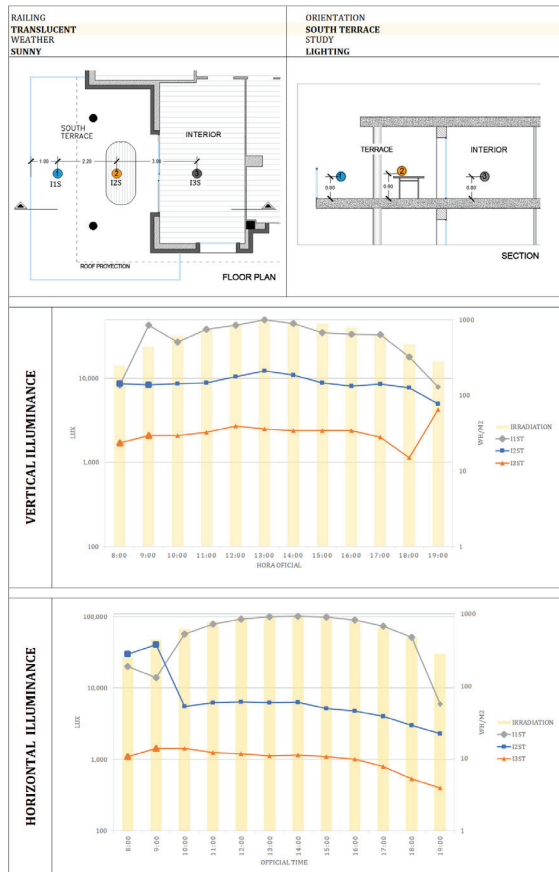


Figure 7. Illuminance (vertical/horizontal), south terrace

In general, the vertical illuminance is higher on the south terrace due to its direct sun exposure, and gradually decreases as it gets closer to the interior. The values at I3S and I2N are very similar. This is probably due to the presence of lateral openings to the east.

From 8:00 to 10:00 at I1S the vertical illuminance is very changeable. In the first two hours of the day, direct solar radiation hits the glass railing. Subsequently, a shadow is cast by the railing itself. The reflection of light on the floor is reduced and then gradually increases, depending on the intensity of the day's radiation.

Horizontal illuminance is also much higher on the south terrace. At I2N, the horizontal illuminance is also higher from 8:00 to 10:00, due to the direct entry

of the sun through the eastern opening. At I2S, from 8:00 to 10:00 there is intense direct radiation in the horizontal plane.

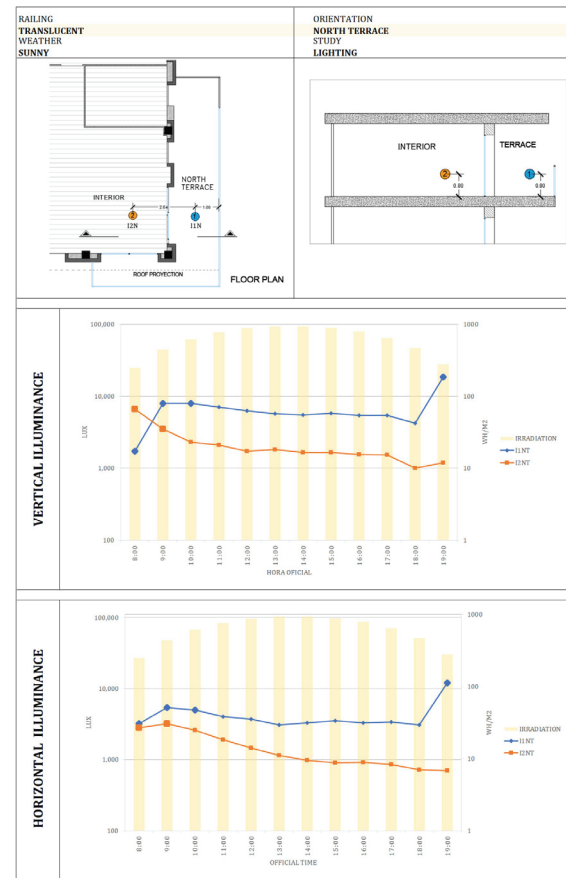


Figure 8. Illuminance (vertical/horizontal), north terrace

On the south terrace, in general, the floor luminance values follow the trend of irradiation throughout the day. Luminance is much higher at I1S, due to the incident direct solar radiation. At I2S and I3S, the same phenomenon occurs, but with less intensity. From 8:00 to 10:00, the sun from the east alters this situation. The frontal luminance at I1S and I2S does not vary greatly. However, at I3S it decreases earlier through the day because there are more visual obstructions to the outside.



Figure 9. Translucent glass railing on the south-east corner

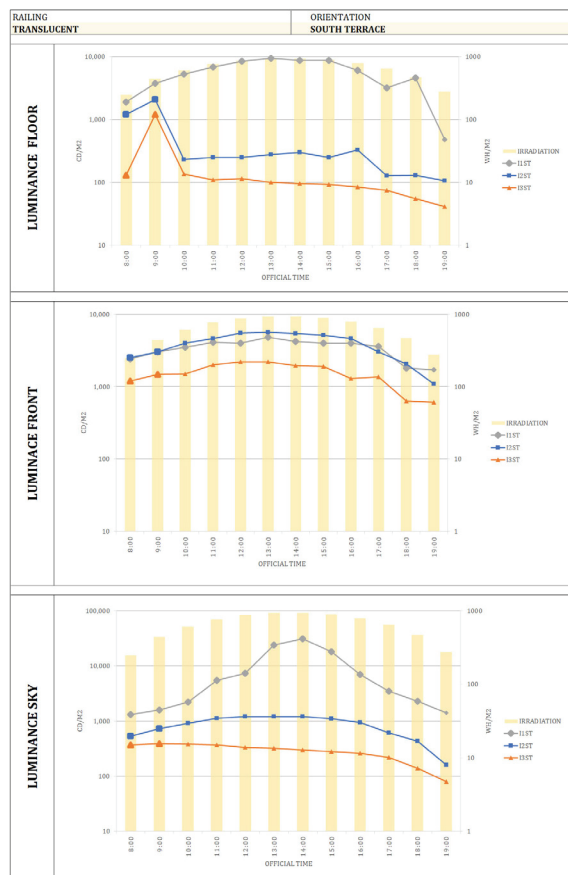


Figure 10. Luminance (floor, front & sky), south terrace

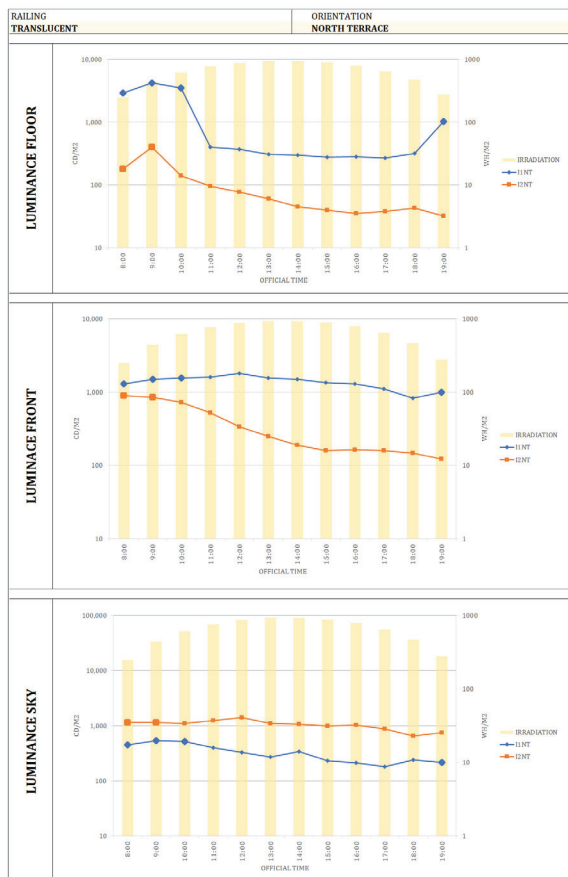


Figure 11. Luminance (floor, front & sky), north terrace

The sky luminance is quite constant on points with a roof. I1S is the only point without a roof, so the values of sky luminance are higher when taken directly from the sky. As there is more distance to the interior, and it is under cover, the luminance of the sky decreases on the south and the north terrace.

On the north terrace, the front luminance remains stable at I1N. At I2N, the values decrease progressively due to the radiation in the first few hours of the day from the east.

On both terraces, the values measured in the interior points were quite similar.

4.2 Thermal results

Various points were selected for air and surface temperature measurements: E1S, E2S, E3S, E4S and E5S on the south terrace (Fig. 12); E1N, E2N, E3N and E4N on the north terrace (Fig. 13). Some other measurement points were added: E4S and E3N (a closed 3 cm gap between the glass railing and the floor), E5S and E4N (an open 3 cm gap between the glass railing and the floor).

To make the comparisons between the values clearer, the time evolution graphs of the air and ground temperatures have been superimposed with the temperature evolution bars of the glass railing.

On the south terrace, the temperature of the air near to the railing at every point is a few degrees higher than the outside air temperature during sunny hours. The only exception is ES2 because it is most affected by wind. The temperature of the railing is quite similar to the nearby air temperature except on positions where, hour by hour, the sun radiation direction is perpendicular to the glass. In general, the temperature of the floor is similar to the outside air because of the beneficial effect of the shadow cast by the railing. The exception is at ES2, where the floor temperature is as high as 45°C, because of its position outside of the railing-cast shadow area. E4S and E5S reach a maximum temperature at noon that is close to the temperature of ES2 because of the confined area. E4S is a few degrees higher than E5S because of the closed 3 cm gap between glass rail and floor. At 14.00, two close points, E2S and E3S, can be in temperature ratio of 1:2.

On the north terrace, the railing temperature is quite strongly affected by a sunny morning at positions that are oriented to east. The rest of the day, the railing temperature descends to equilibrate with air temperature. The temperature of the air close to the railing is between 25°C and 30°C, as on the south terrace, where it is always some degrees above the railing temperature. The temperature of the floor is quite similar to the railing temperature, except at E3N (37°C) and E4N (47°C) because of the confined area.

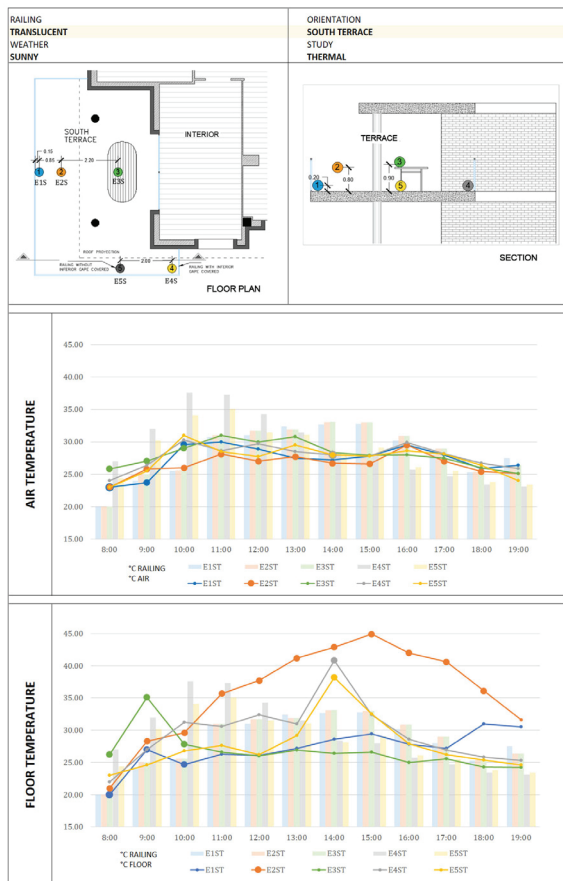


Figure 12. Temperature (air, floor), south terrace

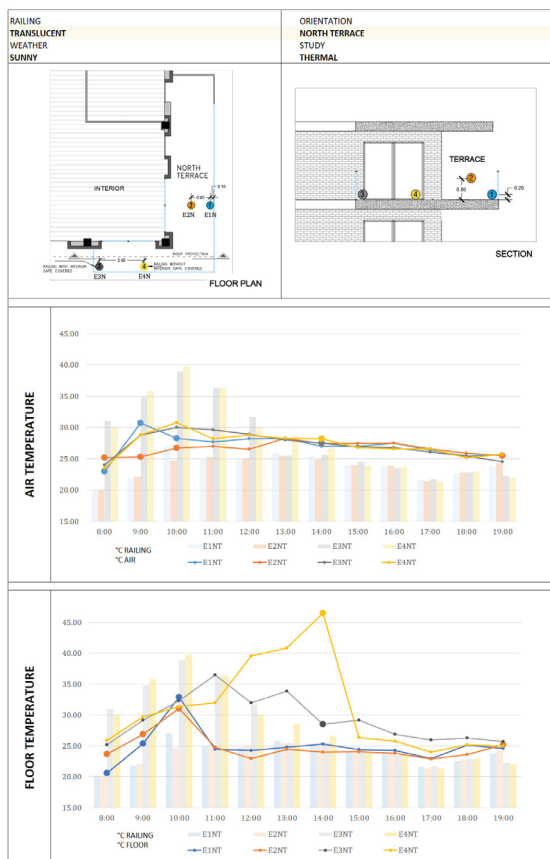


Figure 13. Temperature, north terrace

5. ANALYSIS

Direct sunlight is very intense in Mediterranean areas on the date of the study and usually causes glare and temperature increases on the surfaces where it falls most perpendicularly.

If we also consider that translucent glass is semipermeable to most of the solar radiation, this could enhance these effects and affect comfort on the terrace and/or in the adjacent interior area. From the above data, we analyse how and why lighting and thermal phenomena derived from the use of glass railings happen.

5.1 Light analysis

In this case, as the railing was translucent rather than perfectly transparent, some cast shadows appear and both the luminance (front, sky and ground) and illuminance (vertical and horizontal plane) values were modified, especially in southern orientations where there are more hours of incidence of direct solar radiation.

In this case, the depth dimension of the south terrace has a 1:4 ratio. Hence, the effect of the translucent railing in the interior spaces of the south terrace (IS3) does not have a high impact since they are relatively far away and the area that separates them is not sufficiently protected by the upper ceiling.

In contrast, the light effect of the translucent railing on the exterior spaces of the south terrace (IS2) near the railing is perceived as greater contrast and glare, which would be even more marked if the glass was transparent. Only in the early morning, due to the rising sun, can changes be noted from 08:00 to 10:00 in the measurement points oriented to the east.

It does not seem that the light results are affected by surface material color and brightness, as they are quite balanced in this case.

On the north terrace, there are no shadows cast, and the depth dimension of the terrace is at a 1:2 ratio. The situation is neutral and only altered in the early morning hours by the sunrise from the east.

5.2 Thermal analysis

On the south terrace, the air inside the railings remains slightly higher in temperature than the surrounding air due to the effect of protection from the wind, a phenomenon that does not occur in bar railings.

At the point closest to the glass railing (E1S), the impact of the translucent glass on heat gain seems evident. This gain is high, due to the absorption and subsequent thermal reemission of the glass itself.

However, this greater heat, in this case of the open terrace, is directly affected by the daytime wind typical of terraces in high-rise buildings, so as we move away from the railing (E2S) this effect decreases.

The south terrace pavement is the most affected by heat gain due to the use of the translucent railing, as it undergoes more changes in area and time of incidence of direct solar radiation.

These dynamic changes create a high thermal gradient on nearby surfaces, an aspect that can affect user comfort, material fatigue and the generation of new local air movements.

None of the above seems to apply to the north terrace. However, solar radiation does affect the glass of the railing to the east, which has a great thermal impact in a short period of time. Perhaps it would be advisable in these orientations to change the arrangement of the glass panels or to place plant shade elements in front of them or even resort to transparent glass exceptionally.

6. CONCLUSIONS

When glass railings are used on the terraces of any building, the impact of this decision on the thermal and lighting conditions of this privileged, protected space for domestic relaxation should be considered.

If a translucent glass railing is used on a terrace directly oriented towards the predominant solar radiation, the solar factor of the glass, the cast shadows over the glass and the ratio between the height of the railing and the depth of the terrace must be considered in detail. Translucent glass railings seem to increment luminance and cast shadow on the pavement, which increases glare.

It is very important to avoid confined spaces near the railing protected from wind because the temperature increases if there is not enough ventilation.

Even more specific are the railings oriented towards sunrise or sunsets because the sun radiation is more perpendicular to glass rails and the light and thermal effects are augmented in a short time.

In order to extend these preliminary conclusions, it is worth in the future continuing the tests in laboratory conditions:

- Modifying the degree of opacity and translucency of the glass railing.
- Taking the measurements at other periods of the year, especially in the boreal winter when the incident solar radiation has a greater horizontal component.

- Exploring other geometries of terraces with limited lateral radiation contributions from other orientations.
- Changing the surface of terrace with smaller one, mainly affecting depth.
- The influence of shadow on perception and inertia.
- Performing simulations of lighting conditions using software without depending on the variable sky cloud conditions.

ACKNOWLEDGEMENTS

This contribution is part of the final research carried out as part of the MBArch master, ITA option, at the Barcelona School of Architecture (ETSAB) of the Universitat Politècnica de Catalunya (UPC).

REFERENCES

1. Agüero, R. (2009). *El balcón y la celosía: elementos de confort lumínico y térmico en el clima de la ciudad de Lima*. Master thesis. [on line], Available [10 July 2019] at: https://wwwaie.webs.upc.edu/maema/wp-content/uploads/2016/06/07_Rafael-Aguero-Leon_Balcon-y-celosia_COMPLETO.pdf
2. Pagel, É. (2016). *The influence of glazed balconies in the thermal comfort in an urban tropical region*. SBE Series. Sustainable Urban Communities toward a Nearly Zero. Impact Built Environment. ISBN 978-85-92631-00-0.
3. Philip, H. S. (2015). *Thermal performance of glazed balconies within heavy weight/thermal mass buildings in Beirut, Lebanon's hot climate*. Energy and Buildings, Volume 108, pp 291-303.
4. Uriarte, U. (2016). *Light and taste, third plane side-view combined with complex Fenestration System atmospheres under midday clear sky at restaurants*. Doctoral thesis UPC, Barcelona. Retrieved 10 July 2019 from: <https://upcommons.upc.edu/handle/2117/105817>
5. Coelho, E., Alvarez Cristina, E. de, & Reis Neyval, C. (2016). *The influence of glazed balconies in the thermal comfort in an urban tropical region*. SBE Series Brazil & Portugal #16.2.

Can Daylighting Instinctively Receive More Acceptance Than Artificial Lighting at Workspaces?

New Evidence from a Field Experiment in Beijing

Xiaodong Chen¹, Xin Zhang¹, Jiangtao Du²

¹School of Architecture, Tsinghua University, Beijing, China

²Liverpool School of Architecture, University of Liverpool, Liverpool, UK

ABSTRACT: *This study presents an experiment on how the combination of daylighting and artificial lighting can affect participants' alertness, mood, and visual comfort in a full-scale office in Beijing, China. This experiment was conducted during a spring period (19th April ~ 17th May 2019). Research methods included lighting (Inc. spectrum) measurements, KSS (Karolinska Sleepiness Scale) alertness evaluation, PANAS (Positive and Negative Affect Schedule) mood survey, and self-reported satisfaction survey. Key findings are as follows: 1. When a proper lighting condition was achieved based on visual and circadian performances, increasing daylighting levels would significantly reduce negative mood while decreasing the level of alertness. 2. The artificial lighting could be still required to achieve visual comfort and a proper level of alertness, even when a high level of daylighting is available. 3. There might be an upper bound of illuminance for human non-visual performances at workspaces, including alertness and mood.*

KEYWORDS: *Integrated lighting solution, Alertness and mood, Self-reported satisfaction, Workplace, Beijing*

1. INTRODUCTION

Several experiments have exposed that there are significant effects of daylight on occupants' performances in an indoor environment, including visual and colour comfort, alertness, mood, and work productivity [1, 2, 3]. Recently studies of the impact of daylight on office workers' performances have received increasing attention in Europe and North America. A field study in ten Dutch office buildings [4] found out a significant link between occupants' visual comfort and wellbeing and the configurations and installations of the external windows, which could deliver daylighting and view. An on-site experiment conducted in Switzerland also showed that daylighting can improve office occupants' visual performance, mood, and alertness [5]. Another American investigation found that occupants' sleep quality and overall health can be improved with more exposure to daylight at workspaces [6]. In addition, a series of surveys in American office buildings in both summer and winter periods enhanced that daylight can apparently improve mood and sleep quality of office workers [1, 7]. Based on on-site lighting measurements and subjective assessments, Figueiro & Rea [1] recommended that more investigations would be continuously required in order to clarify how daylight regulates sleep and mood among office workers. All the findings above indicated

that a workspace with more daylight expose can receive higher occupants' preference in terms of both visual and non-visual response.

However, in a real space with both daylighting and artificial lighting available, effects of the integrated lighting on visual comfort and non-visual aspects including mood, alertness, and sleep quality tend to be more complicated. Using questionnaire a French study first investigated the response among office workers to different amount of daylighting or artificial lighting [8]. It was found that occupants tended to choose lower artificial lighting levels when daylight was bright, with an aim to use more daylight for supporting work. By using computer simulations in a small office with photosensors under various daylighting conditions, Kim and Mistrick proposed a method to integrate daylight with artificial light and developed an algorithm of lighting control to achieve visual comfort and reduce energy consumption [9]. Furthermore, from the perspective of the integration between daylight and artificial lighting, a Japanese study examined the visual harmony between daylight from the window and artificial light from the ceiling using a scaled room model [10]. Achieved results showed that daylight and artificial lighting could be harmonized through properly designed illuminance distributions. Recently a series of studies conducted by environmental psychologist

explored the natural preference with the occurrence of daylight and artificial light using online questionnaire [11]. It was suggested that beliefs regarding effects of light on health and concentration may mediate the naturalness-attitude relationship, confirming the instrumental motives behind the natural preference for daylight. Thus, due to the development of artificial lighting controls and increasing studies on non-visual effect of lighting, the integrated application of daylight and artificial light has again attracted attention. According to an opinion on daylighting standard and design [12], two key questions were raised as '(1) What makes a room appear daylit? (2) If a room is lit by a combination of daylight and electric lighting, what is the optimum balance of illuminance between the two sources?'. Several studies above [8-11] have just adopted simple methods, such as questionnaire, computer simulation or scale model, whereas few human experiments in a real space were conducted to explore the interaction effect between daylight and artificial light. Apparently, the lighting design at a workspace is still challenging researchers and practitioners in terms of visual perception, human psychological and physiological performances, especially when using both daylight and artificial light.

This article presents an on-site human experiment in an office lit by the combination of daylight and artificial lighting, aiming to answer if daylight can always be accepted as the first solution based on occupants' alertness, mood, and self-reported satisfaction.

2. MATERIALS AND METHODS

2.1 Workspace and participants

From 19th April to 17th May 2019, this experiment was conducted in an office building (Figure 1) in Beijing (Lat: 39.90° N, Long: 116.41° E). Figure 2 gives room plan and internal layout, dimensions, and window position. This room has a dimension of 7.6 × 4.3 × 3.0 m and the surface reflectance of 0.29 (floor), 0.90 (wall), and 0.90 (ceiling). Only one east-facing side window is available for daylighting and view. This east-facing window has the double glazing with a total visual transmittance of 0.78. Its thermal properties include 840 J/(Kg.K) for specific heat Capacity, 0.16 W/(m.K) for thermal conductivity, and 2.211 W/(m².K) for U-value. As displayed in Figure 3, the window is composed of two large components (3 × 1.2 m) and three small openable components (0.8 × 1.2 m). Several sitting positions were used for participants in the experiment, such as B1-6 (two workstations marked by the blue dash line).

Twenty-six participants were recruited from university students [age: 20.94 (±1.61) years; gender: male (13), female (13)].



Figure 1: Views of the workspace used for the experiment.

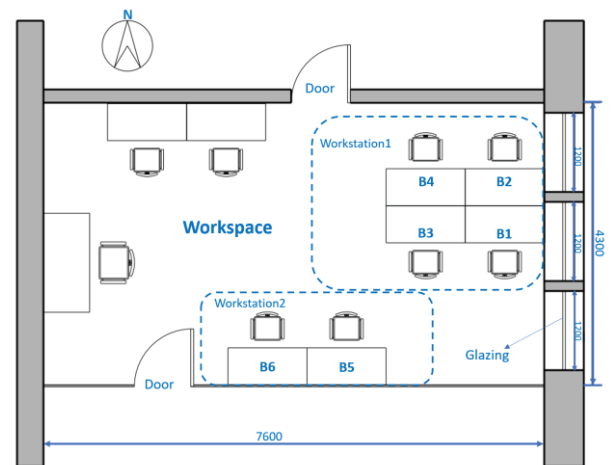


Figure 2: Layout of the workspace used for the experiment.

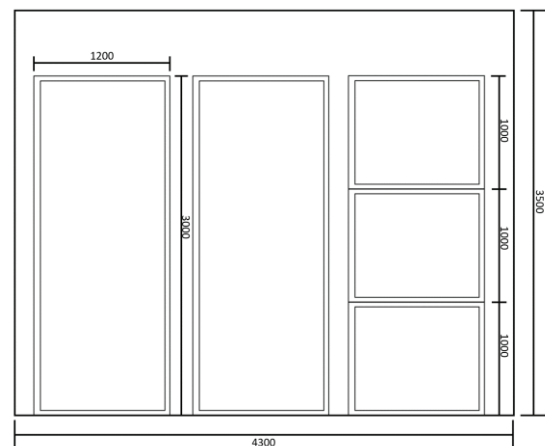


Figure 3: Dimensions and configurations of the window.

Both artificial lighting and daylighting were used during the experiment. The artificial lighting can be adjusted in terms of illuminance and CCT through a local control system called TE-LIG0001. During the experiment, the illuminance produced by the artificial system at the workplane has a range of 15.6 lx to 153.7 lx, while CCT produced by artificial lighting was kept on a constant value of 5200K. Thus, the variation of light

colour was only produced by the daylight from the side window.

2.2 Lighting measurement and Circadian Stimulus (CS)

Lighting was measured by a Spectral meter and several wireless lighting sensors to achieve values of illuminances at the table and near participant's eyes (lx), the light spectrum, and CCT (K). The lighting measurement was conducted every 5 minutes automatically. The measurement positions were at participants' working area on the table, and at the vertical plane near participant's eyes with a height of 35±5 cm above the table. The height could be changed according to the actual occupant's eyes position by using an adjustable stand. Thus, based on the measured data, Circadian Stimulus (CS) of ambient light can be calculated using the method in the reference [13]. The key algorithm is as follows (1):

$$CS = 0.7 - \frac{0.7}{1 + \left(\frac{CLA}{355.7}\right)^{1.1026}} \quad (1)$$

Where CL_A is circadian light, which means irradiance weighted by the spectral sensitivity of the retinal phototransduction mechanisms stimulating the response of the biological clock.

CS ranges from 0 to 0.7. The '0' value means the threshold for circadian system activation whilst the response saturation will be achieved at the value of '0.7'. CS is directly proportional to nocturnal melatonin suppression after one-hour exposure (0% to 70%). According to a field study in offices [14], $CS = 0.3$ has been recognized as the minimum requirement to reduce sleepiness and increase vitality and alertness of workers.

2.3 Measures: alertness, mood, and self-reported satisfaction

During the experiment, participants were asked to complete an assessment of alertness using the Karolinska Sleepiness Scale (KSS); while the Positive and Negative Affect Schedule (PANAS) was adopted as the mood measure including positive and negative affect [i.e. PANAS (p) and PANAS (n)]. In addition, a self-reported VAS (visual analogue scale) questionnaire was applied at the same time to assess satisfaction and visual performances of participants. Nine questions (Q1-9) were used, including comfort, attractiveness, colour appearance, brightness, glare, appearance of objects, acuity, brightness fluctuation, and light colour fluctuation.

2.4 Procedure

Four sessions in each testing day were used as follows: 08:30-10:00, 10:00-11:30, 13:30-15:00, and

15:00-16:30. Tasks at the start and the end of each session were displayed in Figure 4.

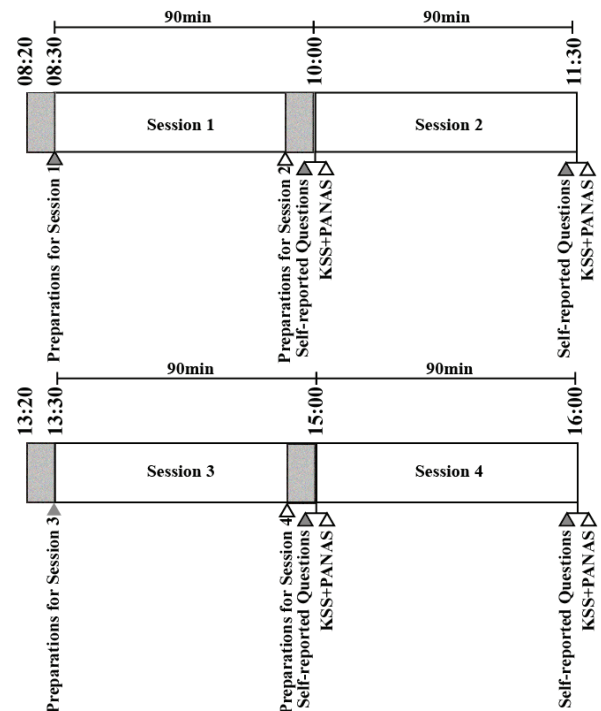


Figure 4: Experimental procedures in this study

The mode of artificial lighting was set before 08:10 in each testing day according to the experiment schedule. As presented in Figure 4, participants will arrive at the room 10 minutes before attending the sessional experiment. During each session, participants were asked to complete the self-reported VAS questionnaire, KSS questionnaire and the PANAS survey at the end of the session.

3. RESULTS

To quantify the amount of daylight and artificial light used during the experiment, two indicators are defined as follows: E_{D+A} is total vertical illuminance measured at eyes with both daylighting and artificial lighting, while R_D is the ratio of vertical daylight illuminance (E_D) at eyes over E_{D+A} . A Spearman correlation analysis was performed between R_D and the feedback of KSS, PANAS and self-reported questionnaire. All significant main effects were achieved when $p \leq 0.05$ or $p \leq 0.01$. IBM_SPSS (v24) was the statistical package used for all analysis in this study.

3.1 Frequencies of illuminance, CCT and CS values

Figure 5 displays frequencies of illuminance near participants' eyes across the whole experimental period. The mean illuminance is 653.84 lx, while 75% of the measured illuminance is above 300 lx and 48% of

the values is larger than 500 lx. In general, this office during the experiment has received a relatively high lighting level, which was supposed to be adequate according to the need of visual functions.

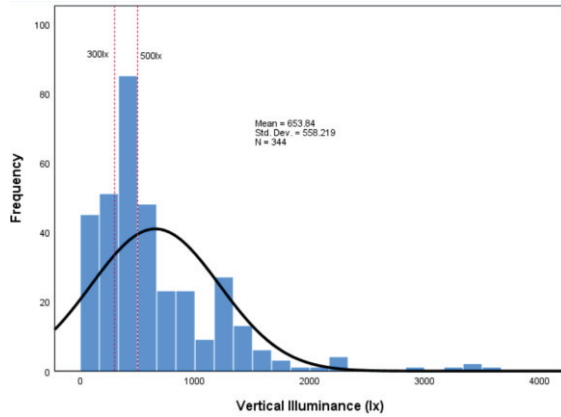


Figure5: Frequencies of measured illuminance near the eyes.

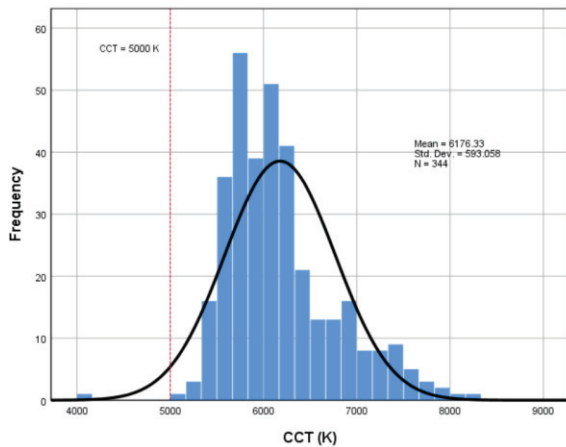


Figure6: Frequencies of measured CCT of light in this space.

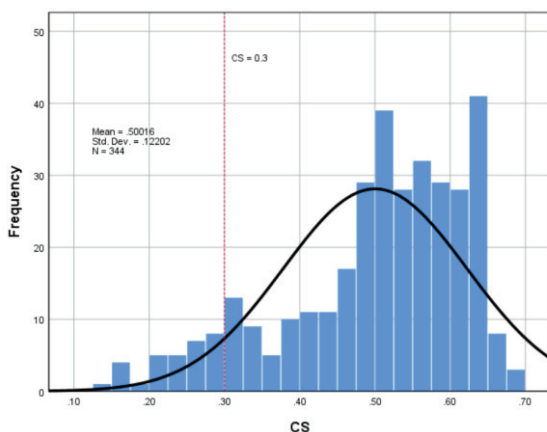


Figure 7: Frequencies of measured CS of light in this space.

Figure 6 and 7 show frequencies of CCT and CS values measured near participants' eyes during the experiment. 97% of the CCT values are above 5000 K, whilst the mean CCT is 6176 K. Since the CCT produced

by the artificial light was fixed at 5200K, it can be concluded that the overall CCT was mainly determined by the daylight. Moreover, the mean CS is 0.5. Thus, 91% of the measured CS values are above the threshold of 0.3 [1], which indicated a higher level of circadian stimulus can be achieved at most of testing period. The lighting condition in this office can significantly take positive effects on participants' circadian systems.

3.2 Effects of illuminance (day/artificial lighting) on KSS and PANAS

The Spearman correlation analysis was conducted between E_{D+A} , R_D and scores of KSS and PANAS. As given in Table 1, there is significant correlation between R_D and KSS / PANAS(n) scores, indicating that increasing the ratio of daylight illuminance (R_D) can significantly reduce alertness level (KSS) and negative mood [PANAS (n)]. However, no significant correlation can be found between E_{D+A} and KSS / PANAS scores.

Table 1: Spearman correlation analysis between E_{D+A} , R_D and scores of KSS, PANAS (p & n).

	Correlation coefficient (Spearman's rho)		
	KSS	PANAS (p)	PANAS (n)
E_{D+A}	0.016	0.020	-0.103
R_D	-.111*	-.053	-.165**

*. Correlation is significant at the 0.05 level (2-tailed).

**. Correlation is significant at the 0.01 level (2-tailed).

Given that the illuminance level could affect occupants' response, the overall experimental data were divided into four ranges according to the illuminance near participants' eyes, such as below 300 lx, 300 - 500 lx, 500 - 1000 lx, and above 1000 lx. Then, the spearman correlation analysis was separately tested in four sub-datasets.

Table 2: Spearman correlation analysis between E_{D+A} , R_D and scores of KSS for different illuminance ranges.

	Correlation coefficient (Spearman's rho) -KSS			
	<300 lx	300-500lx	500-1000 lx	>1000lx
E_{D+A}	-.005	-0.011	0.084	-0.347**
R_D	-0.26*	-0.204**	-0.113	-0.266*

*. Correlation is significant at the 0.05 level (2-tailed).

**. Correlation is significant at the 0.01 level (2-tailed).

For KSS, Table 2 shows that significant negative correlation could be found between R_D and KSS score among three illuminance groups except for the range of 500 - 1000 lx. For the illuminance < 500 lx, the correlation well corresponds to the results in Table 1 in that occupants tend to feel relaxed when the daylight proportion increased. Interestingly, when illuminance

was above 1000 lx, there was significant correlation between E_{D+A} and KSS score, indicating that occupants would become more relaxed and even feel sleepy when exposed to excessive daylight.

As regards PANAS, significant correlation could only be found when illuminance is between 300 lx and 500 lx (as shown in Table 3). With the increase of illuminance from 300 lx to 500 lx, occupants would achieve higher positive mood. Similarly, negative mood would be reduced if R_D increases. These results could be explained by the facts: vertical illuminance below 300 lx could not meet the basic requirement to active non-visual system, while occupants' non-visual system tend to be insensitive to the high illuminance (above 500 lx). Thus, with the vertical illuminance ranging from 300 lx to 500 lx, occupants preferred a relatively higher illuminance to help improve mood.

Table 3: Spearman correlation analysis between E_{D+A} , R_D and scores of PANAS (p & n) for different illuminance ranges.

Correlation coefficient (Spearman's rho) -PANAS					
		<300 lx	300-500lx	500-1000 lx	>1000lx
PANAS(p)	E_{D+A}	0.211	0.193*	-.042	-.082
	R_D	0.043	-.026	-.081	-.017
PANAS(n)	E_{D+A}	-.035	-.129	0.027	-.171
	R_D	-.214	.278**	-.065	-.053

*. Correlation is significant at the 0.05 level (2-tailed).

**. Correlation is significant at the 0.01 level (2-tailed).

3.3 Effects of illuminance (day/artificial lighting) on self-reported satisfaction

The spearman correlation analysis was also performed for nine self-reported questions. Table 4 shows that only the feedback of two questions is significantly linked with E_{D+A} (Q4 & 9) or R_D (Q1 & 2). Increasing E_{D+A} can lead to a brighter space, while lowering the perception of light colour. On the other hand, increasing the ratio of daylight illuminance could reduce comfort level and light attractiveness.

Table 4: Spearman correlation analysis between E_{D+A} , R_D and feedback of self-reported questionnaires.

Correlation coefficient (Spearman's rho)					
	Q1	Q2	Q3	Q4	Q5
E_{D+A}	-0.032	-0.021	-0.012	.182**	0.035
R_D	-.133*	-.109*	-0.105	0.050	0.020
	Q6	Q7	Q8	Q9	
E_{D+A}	0.025	0.100	-0.077	-.124*	
R_D	-0.046	-0.024	-0.049	-0.039	

*. Correlation is significant at the 0.05 level (2-tailed).

**. Correlation is significant at the 0.01 level (2-tailed).

Similar to Section 3.2, spearman correlation analysis was also conducted here in terms of four illuminance ranges. In Table 5, significant results were just found for two illuminance ranges, including < 300 lx, and 300-500 lx. To be specific, R_D was negatively correlated to Q1-comfort, Q2-attractiveness, Q3-color appearance, Q4-brightness, Q6-appearance of objects, and Q7-acuity. It seems that with vertical illuminance < 500 lx, the larger R_D values tend to make the room feel more uncomfortable, unattractive, and unnatural, whilst occupants would feel less bright and the object looks to be stiffer and dimmer. This result might conflict with the common knowledge that we prefer to have more daylight at a normal workspace. Given that at most time the experiment was conducted with a sufficient lighting level (contributed by daylight and artificial light), participants' feedback might support that a higher proportion of artificial lighting will be beneficial to the visual performance in the integrated lighting environment. On the other hand, high proportions of daylight may negatively affect occupants' visual functions. Most importantly, there is an apparent difference between light incident paths (daylight from side window and artificial light from ceiling). This could be used to explain the human response to the two light sources when a higher lighting level was achieved.

Table 5: Spearman correlation analysis between R_D and feedback of self-reported questionnaires.

Correlation coefficient (Spearman's rho) -Self-reported questionnaire				
	<300 lx	300-500lx	500-1000 lx	>1000lx
Q1	-.430**	-.260**	-.039	-.098
Q2	-.293**	-.268**	-.003	-.062
Q3	-.253*	-.172*	-.170	.041
Q4	-.253*	-.160*	-.123	.115
Q5	.014	-.093	-.056	-.125
Q6	-.267*	-.228**	.057	-.080
Q7	-.213*	-.163*	-.118	-.116
Q8	-.023	-.080	-.002	-.006
Q9	-.106	-.128	.128	.047

*. Correlation is significant at the 0.05 level (2-tailed).

**. Correlation is significant at the 0.01 level (2-tailed).

4. DISCUSSION AND CONCLUSION

First, when a proper lighting condition was achieved based on visual and circadian performances, increasing daylighting levels would reduce negative mood, while the alertness level could be decreased at the same time. Thus, even though the daylight may help improve office workers' mood and reduce stress, the increased body relaxation level might lead to lower alertness. A field study [8] found that the low-level artificial lighting was preferred by occupants when daylight was too bright. Visual comfort could be the direct reason for

explaining this choice. However, our study could expose another proof that office workers would keep a proper level of alertness to achieve normal work productivity by using controllable artificial lighting. Therefore, it is worthy of reconsidering and further exploring the visual and non-visual effects of daylight on occupants' performance under a high lighting level.

Second, at a workspace with a higher level of daylight availability through the side window, the artificial lighting could be still required, especially based on an aim to achieve visual comfort. Even though a psychological study [11] pointed out that the human tendency to prefer natural substances over their synthetic counterparts is also operative in the domain of light, some results would still support that the ability to easily control illuminance levels gives electrical lighting a benefit over natural daylight in an office environment [11]. Another study [10] found that artificial lighting from room ceiling could be required to adjust illuminance distributions caused by the daylight from side windows according to the visual harmony of occupants. Thus, it seems that the key aim to apply daylight would be targeted at the benefit of non-visual effects including mood and alertness, while the advantage of artificial lighting is to deliver proper visual functions.

Third, this study has supported that there might be an upper bound of illuminance for human non-visual performances. In this experiment, when the vertical illuminance near participants' eyes was above 500 lx, no correlations were found between the lighting levels and KSS scores, PANAS (p or n), and self-reported questions. Previous studies have found that if a higher CS level (≥ 0.3) can be achieved, the colour of daylight transmitted through the glazing would not significantly affect human's alertness, mood, and visual comfort [2, 3]. Exploring the upper bound may be useful for strategy development of both health lighting and energy efficiency.

Several limitations can be found. 1. The experiment was conducted in a specific office, and within a relatively short period (30 days). 2. All tests were achieved based on higher lighting levels according to visual and non-visual performances. Results did not include data achieved under low-level lighting conditions. 3. A higher proportion of daylight amount was prevalent across the experiment. The data might not be able to reflect the situation of a higher amount proportion of artificial light. More studies will be continuously carried out.

ACKNOWLEDGEMENTS

This work was funded by the National Natural Science Foundation of China through a project of

'Fundamental studies of non-visual and biological effects of daylight on the sleeping and alertness in young and middle-aged adults' (No. 51778322). The authors would thank Beijing Tongheng Energy & Environment Technology Institute for their invaluable support.

REFERENCES

1. Figueiro, M. G., Rea, M. S., (2016). Office lighting and personal light exposures in two seasons: Impact on sleep and mood. *Lighting Res & Tech*, 48(3): p. 352-364.
2. Chen, X., Zhang, X., Du, J., (2019). Glazing type (colour and transmittance), daylighting, and human performances at a workspace: A full-scale experiment in Beijing. *Building & Environment*, 153: p. 168-185.
3. Chen, X., Zhang, X., Du, J., (2019). Exploring the effects of daylight and glazing types on self-reported satisfactions and performances: a pilot investigation in an office. *Architectural Science Review*, 1: p. 1-16.
4. Aries, M. B. C., Veitch, J. A., & Newsham, G. R. (2010). Windows, view, and office characteristics predict physical and psychological discomfort. *Journal of Environmental Psychology*, 30(4), 533-541.
5. Borisuit, A., Linhart, F., Scartezzini, & J.-L., et al. (2015). Effects of realistic office daylighting and electric lighting conditions on visual comfort, alertness and mood. *Lighting Research & Technology*, 47, 1-18.
6. Boubekri, M., Cheung, I. N., Reid, K. J., Wang, C., & Zee, P. C. (2014). Impact of windows and daylight exposure on overall health and sleep quality of office workers: a case-control pilot study. *Journal of Clinical Sleep Medicine*, 10(6), 603-611.
7. Figueiro, M. G., Steverson, B., Heerwagen, J., Kampschroer, K., Hunter, C. M., & Gonzales, K. (2017). The impact of daytime light exposures on sleep and mood in office workers. *Sleep Health*, 3(3), 204-125.
8. Escuyer, S., & Fontoynt, M. (2001). Lighting controls: a field study of office workers' reactions. *Lighting Research & Technology*, 33(2), 77-94.
9. Kim, S. Y., & Mistrick, R. (2013). Recommended Daylight Conditions for Photosensor System Calibration in a Small Office. *Journal of the Illuminating Engineering Society*. 30. 176-188.
10. Han, S., & Ishida, T. (2004). A practical method of harmonizing daylight and artificial light in interior space. *Journal of Light & Visual Environment*, 28(3), 132-138.
11. Antal, H., (2014). The natural preference in people's appraisal of light. *Journal of Environmental Psychology*, 39: p. 51-61.
12. Tregenza, P., Mardaljevic, J. (2018). Daylighting buildings: Standards and the needs of the designer. *Lighting Research and Technology*, 50: p. 63-79.
13. Rea, M. S., Figueiro, M.G., Bierman, A., Hamner, R. (2012). Modelling the spectral sensitivity of the human circadian system. *Lighting Research and Technology*, 44: 386-396.
14. Figueiro, M. G., Kalsheer, M., Steverson, B.C., Heerwagen, J., Kampschroer, K., Rea, M.S. (2018). Circadian-effective light and its impact on alertness in office workers. *Lighting Research & Technology*, 0, 1-13.

Comfortable and energy efficient educational spaces Strategies, methods and building components for energy retrofit in different climate zones

MONICA ROSSI-SCHWARZENBECK¹ ROSA ROMANO² MARIO CAPASSO²

¹ HTWK Leipzig, Germany

² University of Florence, Italy

ABSTRACT: Europe is characterised by old and energy inefficient school buildings that show several technical problems. Furthermore, in the last years, many scientific studies have highlighted how the innovative technological solutions used for reducing energy consumptions are not able to increase the internal thermo-hydrometrical quality, in particular in the intermediate and summer seasons. In addition, issues relating to the environmental comfort of outdoor spaces are very often ignored. Accordingly, this research aims to propose an innovative methodology of renovation to increase indoor and outdoor comfort of school buildings located in different climate zones. The innovative features of the proposed approach are: 1) Taking into account not only indoor but also outdoor spaces; 2) developing a repeatable and effective retrofit strategy and constructive solution for the schoolyards and building envelopes able to guarantee an excellent environmental comfort level in the schoolyards as well as in classrooms also in the warm months.

The proposed retrofit methodology has been tested in two school buildings built in the 60s and 70s, located in Italy (Lucca) and in Germany (Leipzig), both characterised by high energy consumptions and discomfort problems during the whole year. This paper presents and evaluates the results of this experimentation.

KEYWORDS: school buildings, indoor comfort, outdoor comfort, energy retrofit, building envelope.

1. INTRODUCTION

Ensuring energy efficient school buildings, characterized by a high level of indoor and outdoor comfort, have a priority for EU as well as U.S. governments. An investigation carried out a few years ago by the U.S. Green Building Council estimated that in the U.S. more than 55 million schoolchildren and more than 5 million teachers and staff spend hours every day in buildings with poor ventilation, inadequate lighting, inferior acoustics and antiquated heating systems [1, 2]. Also in Europe, school buildings are frequently old and in poor condition [3].

The European "Directive 2010/31/EU on the energy performance of buildings" requires that "the public sector in each member state should lead the way in the field of energy performance of buildings" and that "buildings frequently visited by the public should set an example" [4]. Among the most promising public building types to act as lighthouse projects are school buildings.

Therefore, the European Commission has co-funded several projects like "School of the Future" (2011-2016), VERYSchool (2012-2014), "ZEMedS" (2013-2016) and "RENEW SCHOOL" (2014-2017) in recent years [5]. The international work is supported also by national programmes such as the EnEff:Schule research focus of the German Federal Ministry for

Economic Affairs and Energy that includes very interesting pilot projects dealing with energy efficient new schools and energy retrofit of existing school buildings [6]. Retrofit of schools in Europe is currently characterised by individual projects with a very heterogeneous architectural and energy quality. The application of repeatable strategies and practices would lead to an economy of scale and optimization of interventions, with an improving of the indoor comfort. Schoolyard renovations as undertaken in recent years focused only on functional improvement or addition of sports equipment, without focusing on the environmental comfort level. This topic on the other hand has been subject to many recent research projects and the simulation methods and results could be successfully applied to mitigate environmental conditions of schoolyards. [7]

2. ENERGY RETROFIT OF SCHOOL BUILDINGS: AN INNOVATIVE APPROACH

This research aims to devise an innovative methodology as well as to develop high quality design and technological solutions that can be applied in various energy retrofits of school buildings in different climate zones. The main innovation fields of this approach, compared to the above mentioned European and national projects, are:

- Improvement of indoor and outdoor comfort. The proposed renovation strategy intends to achieve a high level of environmental (thermo-hygrometric, visual, acoustic and olfactory) comfort not only in the classrooms, but also in the schoolyards where pupils spend their recreational breaks and part of the afternoon.
- Repeatable approach. Since energy inefficiency is a widespread problem common to thousands of European school buildings, the strategies and working methods, as applied in this research were developed with the idea to use them repeatedly in different climatic contexts.
- Architectural and construction solutions. Europe is characterized by different climates. Hence it is not possible to use the same materials and components everywhere although school buildings are often built with similar technologies. This work also aims at highlighting similarities and differences that occur when operating in different climate zones in order to identify buildings materials and components, which are efficient in a wide climatic range.

2.1 Instruments and methods

To achieve this goal, findings of European programs and pilot projects, as mentioned in the introduction of this paper, were evaluated, systematized and revised carefully in order to develop a new methodology for the energy retrofit of school buildings located in different European climate zones. The methodology is organized in the following phases and uses methods and tools as outlined below:

- 1) Climate analysis of the building location and evaluation of the microclimatic conditions of the site. Climate data of the last thirty years and the evaluation of future trends were verified with the software Meteonorm, defining a “typical year” and an “extreme day” for winter and summer (with the higher and lower values of temperature and solar irradiation) for Leipzig and Lucca. Furthermore, shading at the school buildings and courtyards were analyzed through the elaboration of solar diagrams.
- 2) Simulation of the schoolyards with the software ENVI-met and evaluation of the level of outdoor environmental comfort by analyzing several parameters such as PMV, PPD, temperature, wind speed and direction and relative humidity. ENVI-met is a three-dimensional non-hydrostatic computational fluid dynamics software, which in this research has been used for analyzing small-scale interactions between buildings, surfaces, plants and air inside the schoolyard environments.
- 3) Development of design strategies and technological solutions for the improvement of outdoor comfort and verification of these solutions through ENVI-met simulations.

- 4) Assessment of the energy efficiency of the existing buildings and the quality of the external spaces adjacent to it by means of energy audits, thermography, on-site measurement of environmental parameters (air, operative and surface temperatures, humidity), thermal bridges analysis, measurement of U-values and assessment of the level of conservation and efficiency of HVAC.
- 5) Simulation of indoor comfort level and energy demand of two classrooms for each of the two school buildings in the current status with the software EnergyPlus.
- 6) Testing with EnergyPlus of three different technological solutions for the restoration of building envelope to improve the indoor comfort level in the classrooms. Evaluation of results and choice of the most efficient façade system.
- 7) Development and testing of a retrofit kit for the renovation of the school envelope with additional technological devices (solar shading systems, and ventilation grids) to reduce the overheating phenomena inside the classrooms.

2.2 Case studies

In order to apply and verify the research methodology, two case studies, located in different European climates, were chosen (Fig. 1):

- 1) 66th Elementary school in Leipzig, Germany, 1977.
- 2) ITC School “F. Carrara” in Lucca, Italy, 1960.

Both school buildings present the construction features of the European educational buildings built quickly and at low cost, from the 60s to the 80s. A reinforced concrete structure, external walls in prefabricated concrete panels or brick infill without thermal insulation (Lucca) or with a very low one (Leipzig), large windows, realized with single, low quality glazing, without adequate solar shading characterized the chosen school buildings. These features determine a high-energy demand for heating and cooling and led to overheating and discomfort in the summer months.

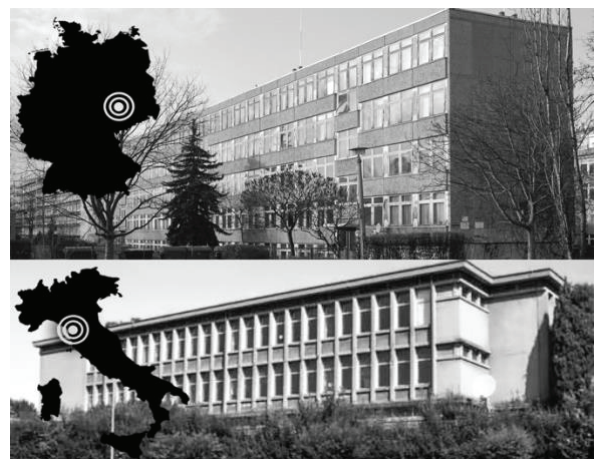


Figure 1: Top - 66th Elementary school in Leipzig, Germany. Bottom - ITC-School “Francesco Carrara” in Lucca.

3. RESULTS OF THE EXPERIMENTATION

3.1 Climate analysis and solar diagrams

Climate analyses of Leipzig showed relatively cold winters, particularly humid autumn months, significant rainfall throughout the year and moderately hot summers with, especially in recent years, high-temperature peaks. The solar diagrams (Fig.2) highlighted how the 5-storey building creates a large shadow in the northern part of the schoolyard during winter months.

Climate analyses of Lucca showed mesothermal warm temperate climate with mild winters, hot/dry summers and concentrated rain in winter. The solar diagrams (Fig.2) highlighted that the schoolyard between building blocks was partially shaded in summer months and almost totally shaded for most of the winter months.

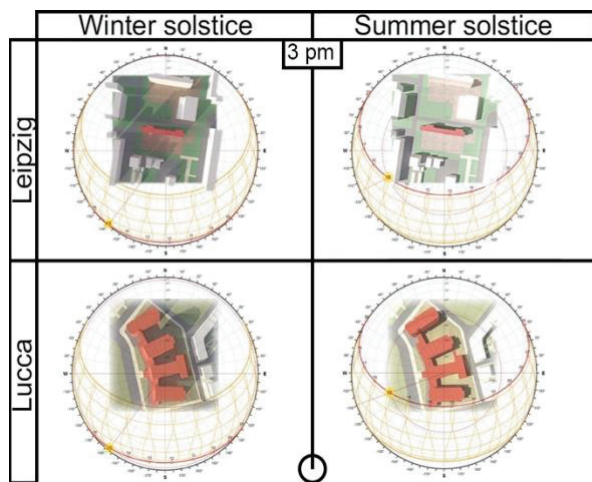


Figure 2: Solar diagrams and shadow analysis.

Leipzig and Lucca, despite being at different latitudes, have similar temperatures in summer. The main differences are the quantity and concentration of rainfall (in Leipzig more abundant and spread over several months), temperatures in the winter months (in Leipzig lower) and the wind velocity (higher in Leipzig than in Lucca) and sun angle.

3.2 Outdoor comfort simulations

The simulations with ENVI-met reproduced in a three-dimensional model the outdoor environmental conditions of the schoolyard during the two typical days (summer day and winter day) in order to evaluate the level of comfort condition. The simulations started at 6:00 a.m. (before sunrise) and were run during the daytime until 6:00 p.m.

The analyzed microclimate parameters were air temperature [K], relative humidity [%], wind velocity [m/s], wind direction [deg], surface temperature [K] at the building surfaces and the ground flooring. The analyzed comfort parameters were: Predicted Mean Vote Index, PMV [-] and Predicted Percentage of Dissatisfied Index, PPD [%].

The results of the simulations confirmed the assessments made in the climate data analysis and highlighted discomfort situations in the schoolyards in winter as well as in summer (Fig. 3).

3.3 Improvement of external space and results of new outdoor comfort simulations

Since pupils use the schoolyard mainly in summer and in intermediate seasons, it was decided to select microclimate mitigation devices to minimize discomfort during these periods of the year and to reduce the heat island effect.

The technological and bio-based solutions chosen to achieve these objectives were: reconversion of clay paving in the meadow, planting of deciduous trees and construction of solar shading systems such as sun sails or roofs with adjustable slats. Also, in this case, the ENVI-met simulations shown how microclimatic mitigation devices were able to increase the level of comfort even under extreme climatic situations such as on an extreme summer day at 3 pm in both schoolyards (Fig. 3 and Tab. 1). In fact, in selected areas of schoolyards, where schoolchildren can spend their breaks, PMV and PPD values improved from extreme discomfort condition (without mitigation devices) to comfort condition (with mitigation devices).

Table 1: PMV and PPD-values without and with microclimatic mitigation devices in a significant point of the two schoolyards

Leipzig	without	with
PMV	3.41	1.51
PPD	99.91%	51%
Lucca	without	with
PMV	2.83	0.92
PPD	98%	23%

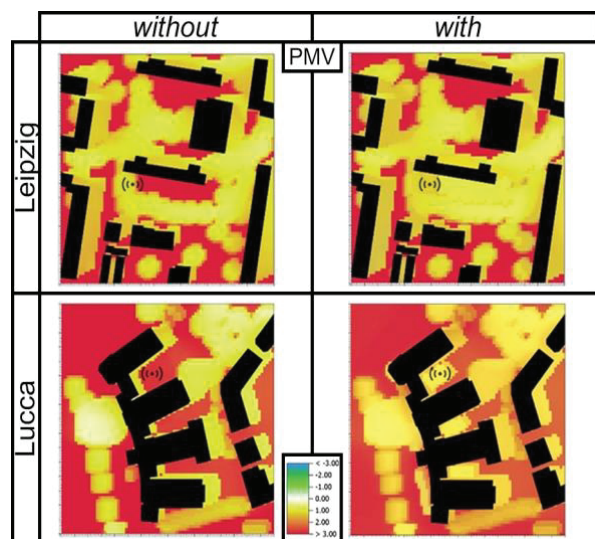


Figure 3: PMV-Values without and with microclimatic mitigation devices, with identification of the significant points whose values are shown in Table 1.

3.4 Buildings Energy Audit

Buildings energy audit, thermography, on-site measurement of environmental parameters and thermal bridges analysis shown an obsolete and poorly maintained building envelope in both school buildings. The highlighted problems were high thermal transmittance of the external walls, low windows performance, lack of solar shading and presence of thermal bridges (Tab. 2).

Table 2: Characteristics of the building envelope of the two school buildings.

	Leipzig	Lucca
U external walls [W/m ² K]	1.14	2.85
U windows [W/m ² K]	5.80	5.40
Solar shading	Internal blinds	Unavailable

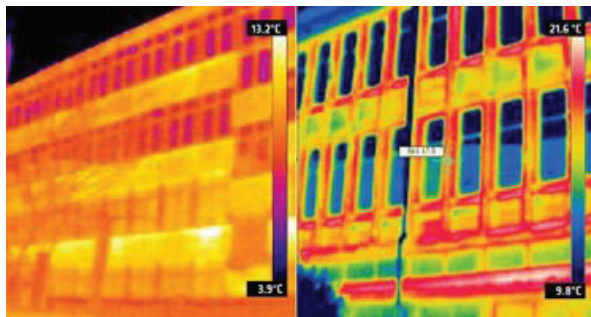


Figure 4: Thermography of the south facades of school buildings. Left: Leipzig, Right: Lucca.

The poor thermo-hygrometric performances (Fig. 4) of the building envelope lead to high heat losses in winter months (with consequent high energy consumption for heating) and overheating in summer (with a consequent discomfort condition), particularly in rooms with south-oriented large windows. Besides, both schools are not equipped with air conditioning, so high temperatures can only be reduced by natural ventilation. Furthermore, visual and acoustic comfort is not adequately guaranteed in all classrooms. The lack of adequate solar shading in some cases leads to glare phenomena on the students' desks. Finally, the need to open the windows in summer not only does not ensure sufficient air exchange, but also to avoid excessive overheating, leads to a considerable level of noise disturbance from the traffic on the nearby streets.

3.5 Simulation of comfort level of two classroom types

In order to analyze indoor thermo-hygrometric comfort level, two characteristic classrooms were selected for each of the two schools.

For the Leipzig school, the selected classrooms were: i) a ground-floor room with south-facing windows, ii) a first-floor room with double north and south-facing windows.

In the Lucca school, the selected classrooms were: i) a ground-floor room with north-facing windows; ii) a first-floor room with double south and west-facing windows.

These classrooms were modelled and simulated with the software EnergyPlus over a period of one year, with particular attention on the hottest summer week and the coldest winter week in order to assess the extreme conditions. Physical parameters concerning the classroom (e.g. air temperature [K], relative humidity [%], operative temperature [K]), as well as the thermal properties of external walls (e.g. inside and outside superficial temperature [K], heat storage energy [J]) and of windows (e.g. superficial temperature, heat gain/lost energy [J]), were analyzed in thermodynamic simulations. The level of indoor comfort was evaluated with PMV and PPD values.

3.6 Application of different facade solutions and results of new simulations

The three following technological solutions for the redevelopment of the building envelope on the outside were tested: 1) External thermal insulation: 2 x 12 cm EPS and external plaster; 2) Lightweight ventilated wall: 2 x 10 cm of polyurethane foam, ventilated air chamber, aluminum sheet cladding; 3) Heavy ventilated wall: like the light ventilated wall but with external covering in brick tiles.

In all three proposed solutions, the external walls of the Leipzig school reach a U-value of 0.13 W/m²K and those of the Lucca school 0.14 W/m²K.

The objective was choosing, after energy simulations (developed with Energy-plus), the best one that with the integration of a window realized with PVC frames and low-emission double-glazing (U-value 0.18) was capable of improving the energy performance and the comfort indoor of both schools during the whole year.

Accordingly, the classrooms chosen as case studies were simulated again for the typical winter and summer weeks with the new windows and for each of the three external walls solutions.

The results showed that:

- in winter, in both school buildings, the upgrading of the walls greatly decreased the level of indoor discomfort (Fig. 5);
- in summer in the school in Leipzig, there were no relevant improvements about the level of comfort, while in the school in Lucca there was a reduction of the PPD-values, particularly with the heavy ventilated wall. These improvements were sufficient to achieve an acceptable level of comfort in the north-oriented classrooms, but not in the south-west oriented one (Fig. 6);
- heavy ventilated walls guaranteed good performances in terms of thermal inertia in summer months in both climatic conditions.

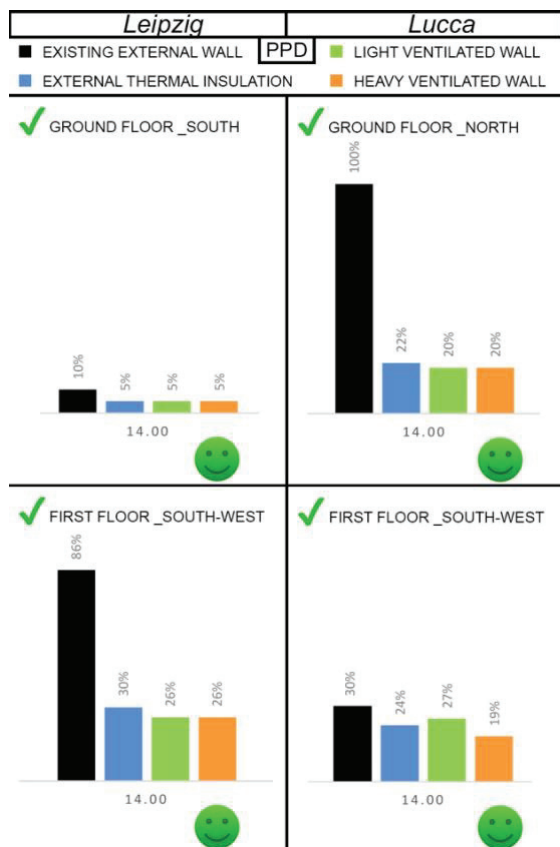


Figure 5: PPD values on the “extreme winter day” at 2 p.m. with different solutions. All the retrofit solutions include low-emission double glazing pvc window.

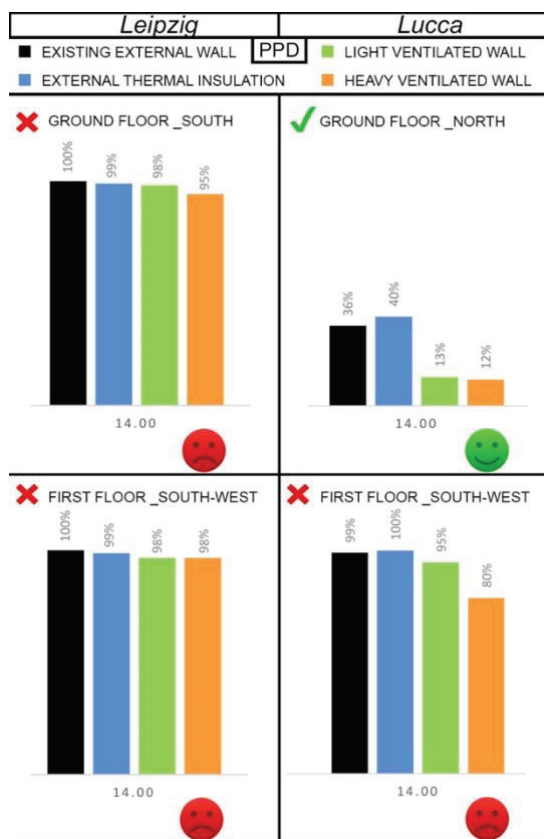


Figure 6: PPD values on the “extreme summer day” at 2 p.m. with different solutions. All the retrofit solutions include low-emission double glazing pvc window.

3.7 Additional energy retrofit devices to improve the indoor comfort in summer

The simulations have shown that improving the U-value of windows and walls was not sufficient in order to guarantee an adequate level of comfort and limit overheating in the hottest day of the year, particularly for the first-floor south-west oriented classrooms.

Consequently, also if the heavy ventilated wall ensured good thermo-hygrometric performances, it was necessary to develop and test additional mitigation technological devices such as shading systems (to control the solar gain through the glass surfaces) and windows ventilation grid to regulate the natural ventilation and to improve the air quality in the educational spaces of both school buildings.

The impact of these added envelope technologies was analyzed developing new simulations for a critical summer day in the typical year for the two classrooms that in Lucca and Leipzig had the worse comfort condition.

The results of this new phase of simulations showed that:

- the integration in the windows only of outside adjustable aluminum slats proved to be an efficient system in the Lucca school. However, in the Leipzig school, aluminum slats improved the PMV values, but these were still far from a comfort condition (Fig.7).

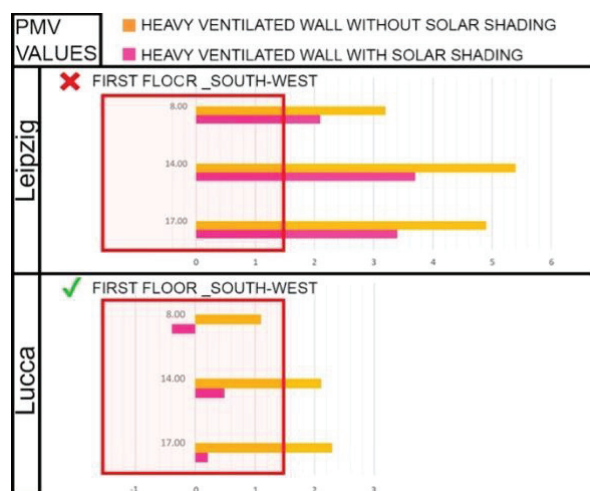


Figure 7: PMV values at different times of a typical summer day with and without solar shading.

- the ventilation grids allowed to achieve good comfort condition (PMV values between -1.5 and +1.5) in the Lucca school throughout the day. Otherwise, in the Leipzig school the comfort was guaranteed only in the morning with a worsening of the situation in the early afternoon hours (Fig.8).

The PMV simulation shows if that the retrofitting kit was useful to improve the level of thermo-hygrometric comfort indoor in the Lucca school throughout the year, also reducing the overheating phenomena in the warmer day, in the Leipzig school did not allow to achieve the same good result.

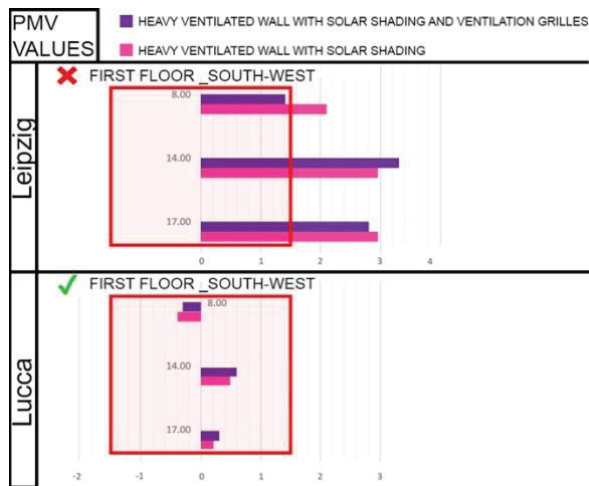


Figure 8: PMV values at different times of a typical summer day with and without ventilation grille.

However, the detailed analysis of the summer comfort in the Leipzig school for the summer season (Tab. 3) highlights how the complete renovation of the envelope with the proposed technologies guarantees to reduce from 62 to 28 the discomfort days (about four weeks: the same time of the summer holidays for the Leipzig schools). Consequently, though the result for the Germany case study is not excellent in terms of comfort in summer months, it can be considered acceptable to validate the developed renovation kit.

Table 3: Days with PMV-values over + 1.5 for the first floor South-West Leipzig classroom with the following retrofit solutions: a) heavy ventilated wall; b) heavy ventilated wall and solar shading; c) heavy ventilated wall, solar shading and ventilation grille. All the retrofit solutions include low-emission double glazing pvc window.

Retrofit solution	Day with PMV over +1.5			
	June	July	August	TOT
a)	14	23	25	62
b)	13	18	20	51
c)	9	11	8	28

4. COMPARISON OF RESULTS OF THE TWO CASE STUDIES AND CONCLUSION

The experimentation shows that it is possible to find similarities in school buildings built in the 60s and 70s in different climate zones and European countries and that it is desirable to envisage intervention strategies as well as constructive solutions repeatable in different retrofitting projects.

The highlighted analogies, at urban and at building scale are:

- Schoolyards have not been designed to ensure a good level of comfort. The main problem is the heat island in the summer months. It is difficult to guarantee the same level of comfort in the whole courtyard, especially if it is large. It is necessary to identify areas of aggregation and focus on achieving a

good level of comfort, at least in these areas. The application of simple mitigation devices has proven to be very efficient again, also in different climate zones. In particular, the replacement of pavements or rammed earth with lawns, the planting of trees and the use of adjustable or removable roofs or solar shading systems (roofs with adjustable slats or sun-blinds) have given excellent results.

- The indoor comfort level is mainly due to the building envelope, whose thermo-hygrometric performances are poor in hot as well as cold months. In both case studies, which represent two different European climate zones, to decrease the discomfort phenomena in the cold months, it is sufficient to replace the windows and apply outside insulation. In summer, without air conditioning systems, it is possible to combine new envelope solutions with shading device and ventilation grid, preferably connected to a home automation system that opens them when high temperature or a high level of CO₂ is reached inside the classroom.

In the future the work will deepen the following three topics:

- Link between the improvement of indoor and outdoor hydro-thermal comfort conditions, in order to evaluate how the internal and external environment can influence each other.
- Energy consumptions, to analyze if the retrofit kit allows achieving the nZEB target;
- Environmental assessment - in terms of LCA and LCC - of the proposed retrofit measures.

REFERENCES

1. Ford, A. (2007), *Designing the Sustainable School*, Images Publishing Group, USA.
2. Kluttig, H., Erhorn, H. and Mørck, O. (2003), "Retrofitting in Educational Buildings – REDUCE 25 Case Study Reports from 10 different Countries", in Ove Mørck, IEA ECBCS Annex 36: Case Study Reports.
3. Gaitani, N., Lehmann, C., Santamouris, M., Mihalakakou, G., Patargias, P. (2009), Using principal component and cluster analysis in the heating evaluation of the school building sector, in *Applied Energy* 87, Elsevier, p. 2079-2086.
4. Directive 2010/31/EU of the European Parliament and of the Council of 19 May 2010 on the energy performance of buildings.
5. Gallo, P., Romano, R. (2015), Studying in a "classy" school. Energy efficiency to save schools construction industry, in *Techne* 9, p. 274-287.
6. BUILD UP: The European portal for Energy Efficiency in Buildings [Online], Available: <https://www.buildup.eu/en/news/overview-school-buildings-leading-examples-energy-efficient-renovation-0> [14 March 2020].
7. Rossi, M. (2017), Efficient and Nice – Urban Metabolism and Urban Comfort, in *Quality of Life in Sargolini, M., Grifoni, C., D'Onofrio, R., Springer*, p. 125-130.

Using Machine Learning to Predict the Daylight Performance of Top-lighting Strategies

BENJAMIN TAUBE ¹, VALERIE GREEN ¹, LUIS SANTOS ², LUISA CALDAS ^{3,4}

¹ UC Berkeley, Center for the Built Environment, Berkeley, CA, USA

² Kent State University, College of Architecture and Environmental Design, Kent, OH, USA

³ UC Berkeley, College of Environmental Design, Berkeley, CA, USA

⁴ Lawrence Berkeley National Laboratory, Berkeley, CA, USA

ABSTRACT: Top-lighting is an effective design strategy both in introducing and controlling daylighting in buildings. Since it can assume many forms, architects and daylighting analysts use simulation tools to predict their behavior in capturing, transporting, and distributing light. However, the expertise required in setting up daylighting simulations and their excessive run times hampers their use in early-design phases when immediate feedback is desirable. The paper discusses the potential of using Machine Learning (ML) techniques as valid approaches to build good surrogate models for top-lighting that support instantaneous queries. The work compares different ML techniques in estimating different sensor grid-based daylight metrics. The goal is to identify suitable ML approaches and provide guidelines on how we should use them in the context of daylighting studies that use horizontal sensor grids. Finally, it discusses the application of ML in the design of simple top-lighting systems highlighting its advantages and limitations.

KEYWORDS: Daylight prediction, Machine Learning, Statistical Learning, Regression and Clustering Models

1. INTRODUCTION

Top-lighting is an effective strategy both in introducing daylighting in buildings and promoting uniform light distribution. Thus, this design strategy has the potential to substantially reduce lighting energy in buildings. Top-lighting includes countless variations of skylights, clerestories, roof monitors, and light wells. Since each strategy captures and distributes light differently, architects use simulation tools to predict their behavior. However, such simulations usually require specialized expertise to conduct, and are time consuming and incompatible with design times, particularly at stages when quick feedback is desirable.

Machine Learning (ML) techniques are useful to model different building physics related phenomena. ML enables the generation of black-box predictive models based on data either simulated with white-box approaches or collected in-situ. The use of ML in building science focuses either in building specific predictive models or in generating surrogate models typically used in building performance optimization to avoid the evaluation of computational costly unknown objective functions. Albeit their use is common in whole-building energy calculation [1]–[3], the application of such techniques in daylighting studies is more recent. Most approaches focus on side-lighting based designs either to optimize their daylight performance [4], or predict advanced daylighting metrics based on luminance images [5][6][7], usually used in later stages.

Considering the lack of ML-based approaches for the daylight analysis of top-lighting strategies, particularly at early-design phases, this work will discuss the potential of using ML techniques in the daylight analysis of top-lighting based designs.

2. BACKGROUND AND RELATED WORK

ML is a non-symbolic branch of Artificial Intelligence (AI) based on computational statistics. Contrary to symbolic AI approaches, it excuses the need to be explicitly programmed to perform a task. ML builds mathematical models from sampled data (training data) and uses self-improving techniques in problem solving or prediction tasks [8].

In recent years, ML is impacting different areas of human activity such as medicine [9], physics [10], and financing [11]. The design and simulation of high-performance-based buildings is not an exception. Although ML techniques have been widely used in whole-building energy modeling, their use in daylight prediction in buildings is more recent. Despite some early works that date back to 2006 [12], the literature only reports a consistent use of ML in the current decade (2010-2020). Based on the most recent literature review on ML for daylighting prediction in buildings [13], the most common application is predicting illuminance (E) – 53% of studies. Such works include [6][14][15][16] that used an Artificial Neural Network (ANN) to determine illuminance values on a horizontal grid. Only a few studies on illuminance prediction complemented the ANN

regression with other techniques such as Auto Regression (AR) [17] or Multiple Linear Regression (MLR) [18].

The application of ML to predict Daylight Factor (DF), such as in [19], only represents 4% of the body of work [13]. After illuminance, the literature shows that researchers use more ML to determine Daylight Autonomy (DA) (13%) and spatial DA (sDA) (11%). The computational cost of calculating annual illuminances for DA and sDA explain the use of ML techniques in the generation of surrogate predictors for such metrics.

Compared with *E* and DF research regarding ML and climate-based metrics is more recent and formulates the prediction problem either as a regression [20] or a classification [21]. The work presented in [22] is an exception since it formulates the prediction of DA as a clustering problem. Albeit, the recent efforts on applying ML in the prediction of climate-based metrics, the literature shows that the work mostly focuses on DA and sDA; thus, excluding other important annual metrics such as Useful Daylight Illuminance (UDI) or Annual Sun Exposure (ASE).

Additionally, most ML applications for daylighting analysis of buildings only address side lighting. In fact, no work mentioned in [13] investigates top-lighting. The work presented in [23] is one of the few ML applications to top-lighting. However, the research does not involve the prediction of daylighting metrics but the control of agricultural facilities. Finally, most studies only either use one or two ML techniques tailored to the specific problem at hands.

In sum, there is a need to (i) expand the application of ML to the daylighting design of top-lighting strategies, (ii) include in the same study relevant daylight metrics less addressed in the literature such as DF, DA, ASE, and UDI, (iii) study and compare the effectiveness of different ML techniques to discuss a possible general application.

3. RESEARCH GOALS

This paper investigates and compares the application of different ML techniques in the daylight analysis of different top-lighting strategies. The work compares in detail the application of some regression and clustering techniques such as Ridge regression, Lasso regression, K-nearest neighbors' regression (k-NN), and multilayer perceptron (MLP), a type of ANN. This comparative study encompasses three main goals:

1. Find suitable ML-based approaches to predict illuminance-based daylight metrics such as DF and climate-based metrics, particularly DA, UDI (all bins), and ASE.

2. Discuss best practices, guidelines, and limitations on the use of ML approaches in daylight prediction.
3. Propose a prototype of a computational tool that helps architects to quickly analyze the impact of different top-lighting designs on daylighting.

4. METHODS

The following details the methods used in generating the data set, training different ML algorithms, and selecting the most suitable approach.

4.1 Collection of daylighting data sets

The authors produced daylighting data sets by running multiple parameterized Radiance analyses through the DIVA plug-in for Grasshopper. Preliminary analyses used the same standardized 8 m by 10 m room with a single overhead skylight and room height varied in each run.

Each simulation had three variable parameters defining the room geometry and seven variable parameters defining the skylight geometry. A pseudo-random number generator in Python produced randomized geometry parameters to ensure coverage of the solution space. The probability of any set of specific parameters being repeated during a set of 5,000 simulations is approximately $1E-10$.

The three room geometry parameters are ceiling height, and two skylight location parameters. Ceiling height varies from 2.5 m to 5 m with a step size of 5 cm. Two variables, X and Y, define the skylight location in terms of cartesian coordinates. We constrained X and Y to ensure that the skylight does not overhang the exterior walls of the room. The skylights are pyramid lightwells (Figure 1) with geometry defined by seven variable parameters: depth, base length and width, top length and width, glazing tilt angle, and glazing tilt direction.

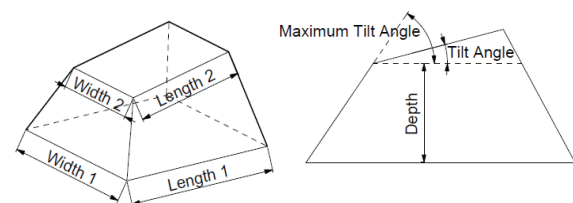


Figure 1. Geometry parameters for pyramid skylight.

Depth defines the lightwell height and varies from 0.25 m to 2.5 m. Base width (Width 1) and base length (Length 1) are varied from 0.25 m to 4 m. Only cases where the lightwell base is larger than or equal to the glazing area are considered. Glazing width (Width 2) and glazing length (Length 2) have a lower limit of 0.25 m and upper limits of Width 1 and Length 1 respectively. These five parameters are varied with a step size of 5 cm. The Tilt Angle rotates

the skylight's glazing. It varies from 0 degrees (horizontal) to coplanar with the lightwell wall as shown in Figure 2. For cases where lightwell walls are vertical, the glazing can be vertical as well. The glazing Tilt Direction is a discrete randomized variable that orients the glazing towards the main cardinal directions - North, South, East, or West.

Half of the simulations run using constraints on Width 2, Length 2, and Tilt Angle to produce only box lightwells with horizontal glazing (Figure 2).

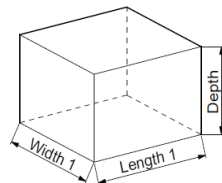


Figure 2. Geometry parameters for box skylight.

The authors used DIVA to run Radiance analyses for 20,000 randomized configurations (Table 1). For the first 10,000 runs, DF, was recorded at each of the 220 sensors in the model. For the remaining 10,000 runs, we recorded the values of the climate-based metrics listed in Table 2 at each sensor point. Sensors were evenly spaced 0.60 meters apart at a height of 0.75 meters, intended to approximate the work plane height in an office environment. The optical properties of the different room's surfaces are as follows: 80% of reflectance for ceiling surfaces, 70% for walls, 40% for floor, and a 64% of Visual Light Transmittance for the skylights glazing assembly.

Table 1. Breakdown of 20,000 randomized daylighting simulations.

Simulation #	Skylight	Simulation Type
1 - 5,000	Box	Daylight Factor
5,001 - 10,000	Pyramid	Daylight Factor
10,001 - 15,000	Box	Climate Based
15,001 - 20,000	Pyramid	Climate Based

Table 2. Climate based metrics recorded in simulations.

Climate Based Metrics
Annual Sunlight Exposure (ASE)
Daylight Autonomy (DA)
Useful Daylight Illuminance - Autonomous (300-3000 lux)
Useful Daylight Illuminance - Overlit (>3000 lux)
Useful Daylight Illuminance - Underlit (< 100 lux)
Useful Daylight Illuminance - Supplemental (100-300 lux)

3.2 Training the predictive models

We used the four resulting data sets — daylight factor and annual metrics for both the box skylights and the pyramid skylights — to train four separate machine learning models. The resulting data sets for the daylight factor and annual metrics simulations

included daylight sensors, each with X and Y coordinates, as well as the parameters described above and either a Daylight Factor (DF) value or the six annual climate-based metrics described in Table 2. We split the four data sets into a training set of 90% of the data and a test set of 10% of the data to be used for the models. We normalized all parameters from -1 to 1 so the models were not affected by the different scales of the parameters. We also one-hot encoded the Tilt Direction variable to use in the model as numeric substitutes for categorical data.

3.3 Predictive model selection

The predictive models we used were Ridge with 5-fold cross-validation, Lasso with 5-fold cross-validation, k-NN), and MLP. For the k-NN models, k values of 1-20 were tested and the k value that produced the minimum root mean square error (RMSE) was chosen. The resulting k value was 3 for daylight factor and 4 for annual metrics. The k-NN models used distance weighting (1/d) to give more weight to nearer neighbors. The MLP models had one hidden layer with 300 nodes, an adaptive learning rate, and 5000 maximum iterations.

5. RESULTS

5.1 Initial models

The Ridge ($R^2 = 0.228$), Lasso ($R^2 = 0.228$), and k-NN ($R^2 = -4.852$) models performed poorly. The negative R^2 indicates that the k-NN performs even worse than a fit of a horizontal line through the mean of the data. Given that Ridge and Lasso are both linear models, the results suggest that a linear model would not be suitable for this task. The performance of the two linear models—Ridge and Lasso—was practically identical. The difference can only be seen by moving out several more decimal places. Although the loss function for Lasso allows for regularization coefficients to go to zero, that was not a significant factor, suggesting that all of the factors are important in the model. The k-NN model performed well at predicting missing values withheld from a single case, but it was not able to extrapolate to new cases for which it had only the information about the parameters.

5.2 Final models and resulting tool

The MLP models proved to be much more accurate at predicting both DF and annual climate-based metrics than any of the previous models. However, these models have some limitations and required some post-processing of output data. The model predicted some values slightly below 0 and above 100. We changed the negative values to 0 and the ones above 100 to 100 since both DF and climate-base metrics range from 0 to 100. A more robust

model with a larger training set may be able to better understand the domains of the target variables and predict only values within the real domain. Table 3 presents the R^2 values after we made those adjustments to the predicted values.

Table 3. R^2 values for daylight metrics for box and pyramid skylights

Daylight Metric	Box Skylights	Pyramid Skylights
DF	0.996	0.980
ASE	0.929	0.679
DA	0.982	0.949
UDI-Autonomous	0.971	0.942
UDI-Overlit	0.910	0.726
UDI-Underlit	0.976	0.958
UDI-Supplemental	0.849	0.820

Figures 3 and 4 compares the simulated results of the test data that was withheld from training the model to the values predicted by the MLP models. For the box skylights, there is a strong correlation between simulated and predicted data, especially for DF, DA, and UDI-Autonomous. The correlation is not as strong for the other annual metrics.

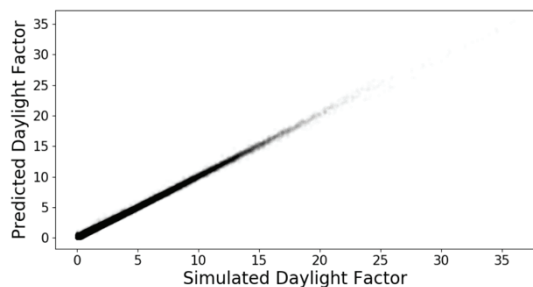


Figure 3. DF from the test data set vs predicted by the ANN for box skylights.

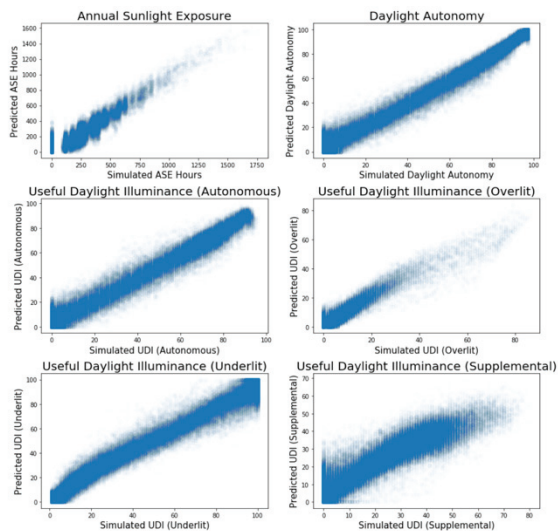


Figure 4. Climate-based metrics from the test data set vs predicted by the ANN for box skylights.

Figures 5 and 6 show that the correlations are not as strong for the pyramid skylights as they were for the box skylights, suggesting that the adding features to the model makes the prediction more challenging for the ANN.

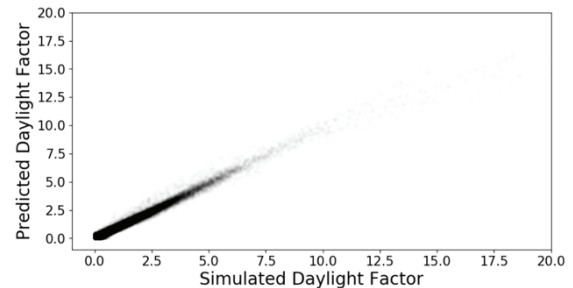


Figure 5. DF from the test data set vs predicted by the ANN for pyramid skylights.

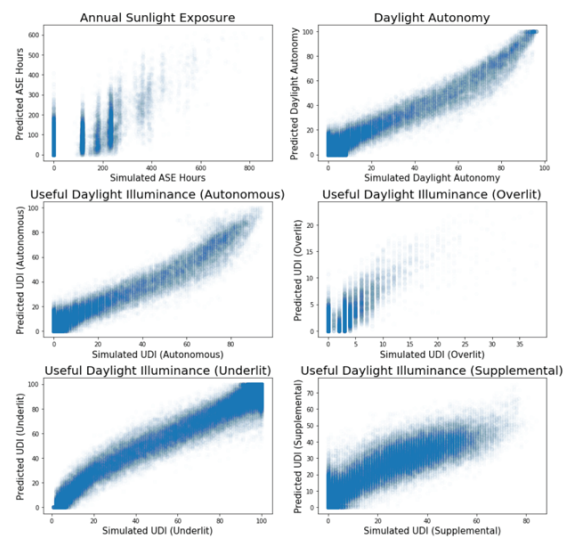


Figure 6. Climate-based metrics from the test data set vs predicted by the ANN for pyramid skylights.

5. APPLICATION AND VALIDATION

In addition to the correlation factors as an evaluation method of the models' performance, we apply the approach in a design simulacrum to assess how well it would predict DF and DA. Figure 7 shows the position of skylights of these additional cases. Test case 1 and 2 are pyramidal skylights while Test case 3 is a linear box skylight aligned with the East wall.

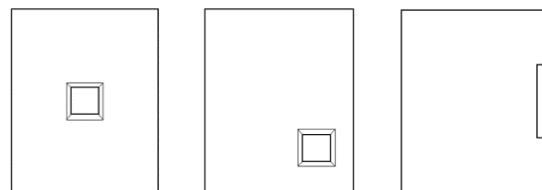


Figure 7. Design test cases 1-3 (from left to right) in plan view.

Figures 8 and 9 compare the models' predictions against simulated data for DF and DA respectively.

They show that the ML approach was able to identify the location of the hotspots, and that is better in predicting DF than climate-based metrics. The calculation process of DF and DA might be behind this performance difference. DF is a purely continuous variable. In contrast, although the DA domain is continuous, its calculation involves an *a priori* filtering, i.e., a classification process. Nevertheless, the DA predictions yield acceptable error values for most cases. The exception is Test case 3, indicating that probably the training data did not include enough of such cases.

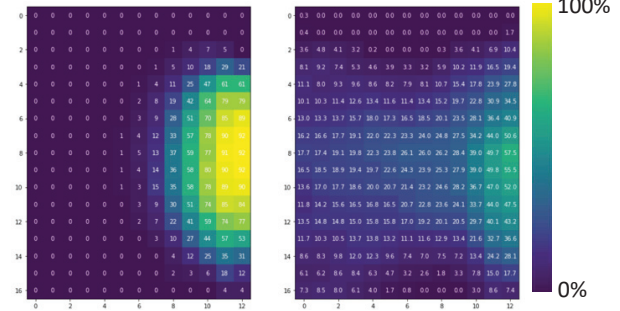
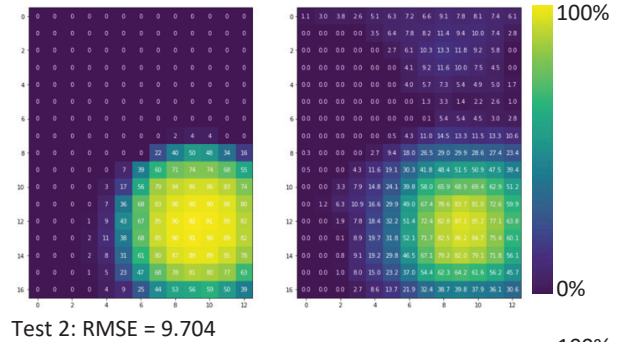
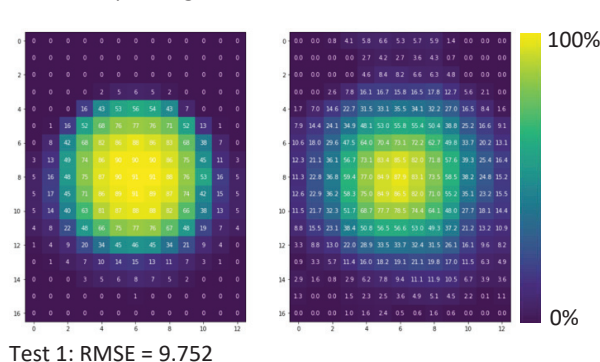
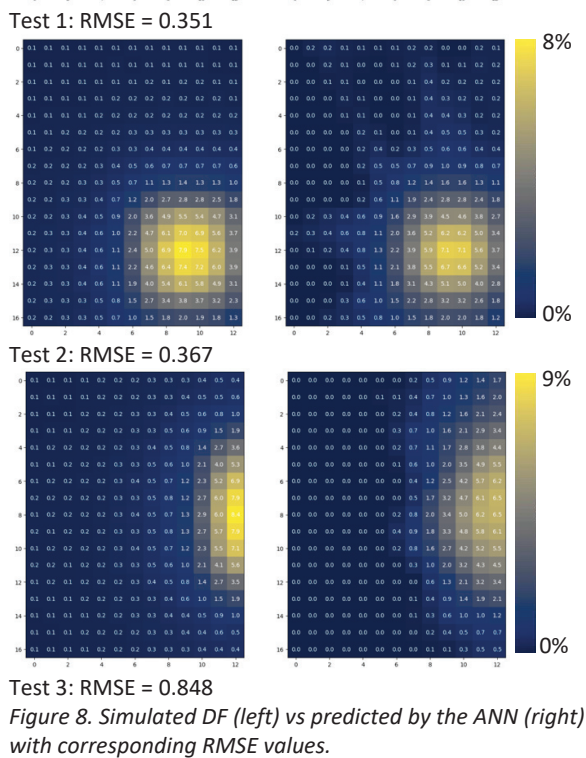
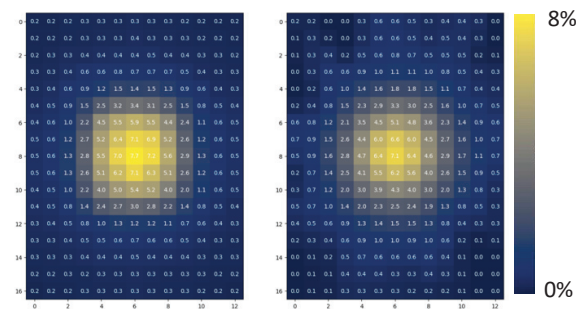


Figure 9. Simulated DA (left) vs predicted by the ANN (right) with corresponding RMSE values.

6. CONCLUSION

From all the tested approaches, a multilayer perceptron (MLP) neural network was the most effective learning algorithm for predicting daylight factor and selected annual climate-based metrics at any location on an analysis grid. This approach has potential application to predict DF and climate-based metrics grid in spaces for which we have not run simulations. It also yields the potential of generating useful predictive models that users can interactively query to obtain instantaneous performance feedback in top-lighting design tasks.

We also plan to apply these findings to an intelligent painting tool for defining daylight goals for goal-oriented design, such as the Painting-With-Light (PWL) [24]. We envision using the same method so that PWL can optimize skylight configurations towards a desired spatial pattern for any given daylight metric.

Although the results are promising, the proposed approach entails some limitations. Some of those seem to relate with the technique of sampling used. In our validation experiment, Test case 3 shows a bigger error both in DF and DA. This indicates that the parameter space was not properly sampled. Future work will assess the effectiveness of more robust sampling techniques such as orthogonal sampling or Latin Hypercube Sampling. Acquiring more data by simulating more cases would increase the model's performance but it would also entail a significant amount of time. Future work will deploy the use of already available simulation parallelization techniques [25] to speed up the generation of data.

Additionally, the training of the model using directly climate-based metrics is simplified since the data per sensor results from the reduction of an 8760 illuminance array to a single value. While this simplification reduces computational time in training the ANN, we lose some of the data's granularity and nuance. Moreover, although all climate-based output variables are continuous, the means by which they come about is through categorization. Consequently, and observing the No-Free-Lunch theorems [26], our regression-based ANN was more successful in predicting some metrics than others. Running a classification on the 8760-illuminance data might increase the models' accuracy. Finally, the annual climate-based metrics were simulated using the climate data of a single location: Phoenix, Arizona. In the future we will add additional climates to improve its usability across different climate-based annual sky types.

REFERENCES

1. Amasyali, K. and N. M. El-Gohary (2018). A review of data-driven building energy consumption prediction studies. *Renewable and Sustainable Energy Reviews*, 81: p. 1192–1205.
2. Robinson, C., Dilkina, B., Hubbs, J., Zhang, W., Guhathakurta, S., Brown, M. A. and R. M. Pendyala (2017). Machine learning approaches for estimating commercial building energy consumption. *Applied Energy*, 208: p. 889–904.
3. Mocanu, E., Nguyen, P. H., Gibescu, M. and W. L. Kling (2016). Deep learning for estimating building energy consumption. *Sustainable Energy, Grids and Networks*, 6: p. 91–99.
4. Wortmann, T., Costa, A., Nannicini, G. and T. Schroepfer (2015). Advantages of surrogate models for architectural design optimization. *Artificial Intelligence for Engineering Design, Analysis and Manufacturing*, 4(29): p. 471.
5. Liu, Y., Colburn, A. and M. Inanici (2019). Predicting Annual Equirectangular Panoramic Luminance Maps Using Deep Neural Networks. In *Proceedings of the Building Simulation 2019 Conference*, Rome, Italy, p. 996–1003.
6. Liu, Y., Colburn, A. and M. Inanici (2018). Computing Long-term Daylighting Simulations from High Dynamic Range Imagery Using Deep Neural Networks. In *The Building Performance Analysis Conference and SimBuild of ASHRAE and IBPSA-USA*, Chicago, IL, U.S., p. 8.
7. Chatzikonstantinou, I. and S. Sariyildiz (2016). Approximation of simulation-derived visual comfort indicators in office spaces: a comparative study in machine learning. *Architectural Science Review*, 4(59): p. 307–322.
8. Belém, C., Santos, L. and A. Leitão (2019). On the Impact of Machine Learning. Architecture without Architects? In *Proceedings of the 18th CAAD Futures Conference*, Daejeon, Korea, p. 148–167.
9. Magoulas, G. D. and A. Prentza. (2001). Machine Learning in Medical Applications. *ACAI 1999 - Lecture Notes in Computer Science*, 2049: p. 300–307.
10. Ferreira, D. R. (2018). Applications of Deep Learning to Nuclear Fusion Research. Available: <https://arxiv.org/abs/1811.00333> [29 May 2020].
11. Bolton, R. J. and D. J. Hand (2015). Statistical Fraud Detection: A review. *Statistical Science*, 17(3): p. 235–255.
12. Kurian, C.P., George, V.I., Bhat, J. and R.S. Aitha (2006). ANFIS model for the time series prediction of interior daylight illuminance. *ICGST International Journal of Artificial Intelligence and Machine Learning*, 6: p.35–40.
13. Ayoub, M. (2020). A review on machine learning algorithms to predict daylighting inside buildings. *Solar Energy*, 202: p. 249–275.
14. Hu, J. and S. Olbina (2011). Illuminance-based slat angle selection model for automated control of split blinds. *Building and Environment* 46: p. 786–796.
15. Logar, V., Kristl, Ž. and I. Škrjanc (2014). Using a fuzzy black-box model to estimate the indoor illuminance in buildings. *Energy and Buildings*, 70: p. 343–351.
16. Navada, S.G., Adiga, C.S., and S.G. Kini (2016). Prediction of daylight availability for visual comfort. *International Journal of Applied Engineering Research*, 11: p. 4711–4717.
17. Colaco, S.G., Colaco, A.M., Kurian, C.P. and V.I. George (2014). An Adaptive predictive framework to online prediction of interior daylight illuminance. In *International Conference on Advances in Energy Conversion Technologies (ICAECT)*, p. 174–180.
18. da Fonseca, R.W., Didoné, E.L. and F.O.R. Pereira (2013). Using artificial neural networks to predict the impact of daylighting on building final electric energy requirements. *Energy and Buildings* 61: p. 31–38.
19. Conraud-Bianchi, J. (2008). A Methodology for the Optimization of Building Energy, Thermal, and Visual Performance. In *Masters Abstracts International*, Montreal, Quebec, Canada, 47(4).
20. Ayoub, M. (2019). A multivariate regression to predict daylighting and energy consumption of residential buildings within hybrid settlements in hot-desert climates. *Indoor Built Environment*, 28: p. 848–866.
21. Zhou, S., and D. Liu (2015). Prediction of daylighting and energy performance using artificial neural network and support vector machine. *American Journal of Civil Engineering and Architecture*, 3: p. 1–8.
22. Liu, Y., Huang, Y. and R. Stouffs (2015). Using a data-driven approach to support the design of energy-efficient buildings. *Journal of Information Technology in Construction*, 20: p. 80–96.
23. Yu Y., Deng L., Wang L. and H. Pang H. (2017). A Skylight Opening Prediction Method Based on Parallel Dirichlet Process Mixture Model Clustering. In *Intelligent Computing, Networked Control, and Their Engineering Applications. ICSEE 2017, LSMS 2017. Communications in Computer and Information Science* 762: p. 240–251.
24. Caldas, L., and L. Santos (2016). Painting with light: An interactive evolutionary system for daylighting design. *Building and Environment*, 109: p. 154–174.
25. Jones, N. L., and C.F. Reinhart (2017). Experimental validation of ray tracing as a means of image-based visual discomfort prediction. *Building and Environment*, 113: p. 131–150.
26. Wolpert, D. H. (2002). The supervised learning no-free-lunch theorems. *Soft computing and industry*, p. 25–42.

Thermal Comfort in a Bioclimatic Dwelling The "habitable device" 20 years later. ITER-Tenerife-Spain

IGNACIO OTEIZA¹, FRANCISCO MUSTIELES², MARÍA DELGADO³,
PABLO LA ROCHE⁴, RICARDO GONZÁLEZ³

¹Instituto Ciencias de la Construcción Eduardo Torroja CSIC, Madrid, Spain

²University Iberoamericana, Puebla, Mexico

³Instituto Tecnológico de Energías Renovables-ITER, Tenerife, Spain

⁴Lyle Center for Regenerative Studies. Cal Poly Pomona. CA. USA

ABSTRACT: In 1995 the Official College of Architects of the Canary Islands, together with the International Union of Architects, launched an international competition for the construction of 25 bioclimatic houses, to be built in the area of the Technological Institute of Renewable Energies -ITER- in Granadilla, Tenerife, Spain. 24 of the 397 international proposals were built, completing the construction in 2010; currently these homes, use for tourism (lodging), making up the "Living-Lab, bioclimatic homes-ITER".

This work analyzes temperature, relative humidity, energy consumption and production data of the house known as "El Dispositivo". Data helped us understand that the bioclimatic concepts that guided the initial design were correct and the hypotheses raised in the design were fulfilled. Likewise, and after the different European requirements are included in the Energy Saving Standards of the Spanish Technical Building Code in its most current version (DB HE0.CTE 2020), it can be affirmed, based on the results of the measurements, that this house meets requirements for buildings with almost zero energy (EECN).

KEYWORDS: *Bioclimatic house, Energy, Comfort, Tenerife.*

1.-INTRODUCTION

The single-family house known at the ITER as "El Dispositivo" received one of the 25 prizes in the international contest "25 Bioclimatic Houses for Tenerife" organized by the College of Architects of the Canary Islands and sponsored by the International Union of Architects in 1995 <http://casas.iter.es/casas/el-Dispositivo/>. The construction of 24 houses -one was not built- was completed in 2010, and together with a visitor center, are part of a complex within the Technological Institute of Renewable Energies (ITER) of Tenerife Spain, dedicated to energy research and which allows the evaluation of sustainable design concepts of 24 different bioclimatic housing designs, whose habitability conditions (Temperature, Relative Humidity, Wind, Energy) have been monitored, for more than 7 years, in order to understand their hygrothermal behavior and comfort conditions (1).

Today, this house and the other 23, are all part of ITER's Living Lab, because in addition to being monitored, they are offered for rent, under the slogan of "vacations outside the tourist circuits" <http://casas.iter.es/>

In 1995, when this project was designed, we did not have any comprehensive set of sustainable design guidelines; these appeared years later, so we

proposed our own set of guidelines to achieve bioclimatic and sustainable housing. One of our main concerns at that time, during the design process, was the integration of sustainable and architectural concepts into a "habitable device", integrating technology and architecture. Our strategies to achieve a sustainable architecture, was to group them in different aspects: thermal comfort, energy efficiency, available materials and construction processes, and water and environment.

2.-CONCEPTION

Developing a housing project in a context devoid of urbanity, nestled in a warm semi-arid territory, with no known "neighbors" in 360º, and within what could be considered a new generation energy generating park, may give rise, among others approaches, extravagance, iconicity - sometimes associated with the previous one - to hide in or work with the territory.

We decided on the latter, to produce a building located in the territory, that is, cardinally referring to its major natural elements, but at the same time, "dressed" in it, that is, using the material qualities of those elements, to wrap it; a building that recognizes its "territorial parents": El Teide volcano and the Atlantic ocean.

At the same time, a building that is sensitive to the climatic conditions of the place, especially to the management of solar radiation and lighting, to the capture and generation of energy, and to the flow of the prevailing winds, to be in a comfortably sustainable situation, while using energy saving electrical, electronic and sanitary devices and equipment, and using mostly local materials.

That is why we have conceived this house from the beginning, as a habitable device, that is, as a comfortable and sustainable building that acts as an interface between the climatic conditions and the geographical characteristics of the place, not oblivious to the incorporation of technology to support the sustainability.

Architectural design concepts and bioclimatic design concepts have often been treated separately, contrary to how they were addressed in vernacular architecture; this disagreement ends up generating a building composed of a sum of devices that awkwardly accompany the architecture. This disagreement was very palpable at the time of the launch of this competition in 1994 (2).

Our proposal rethinks the dialogue between architecture and environmental conditioning by proposing a housing model that aims to be "integral" by combining early notions of sustainability and bioclimatic conditioning technologies with architecture. (Fig. 1)

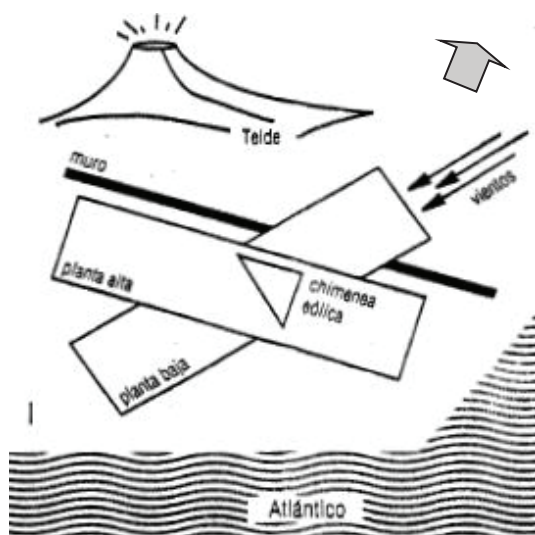


Fig. 1 Geo-references that determined the form.

2.1. Bioclimatic strategies. Energy and comfort.

The building was designed to reduce energy consumption and use renewable sources in the Technological Institute of Renewable Energy (ITER), a center specialized in renewable energy. We relied on the Givoni bioclimatic psychrometric chart, where outdoor conditions for the warmest and coolest months of the

year, January and July, were used to determine potential passive cooling and heating strategies. These two cases represent "winter" and "summer" with two conditions for each case: day and night (3).

Orientation

The building was designed so that it could be flexible in handling the sun and wind, to achieve comfort during daily and seasonal variations. The winds are generally from the northeast, sometimes with desert sand (haze).

The proposal is a two-story house, with an orientation determined by the winds, the views of the sea and the sun. The upper floor is oriented on its main axis in the east-west direction, responding to the sun and views of the sea (south); the ground floor is oriented at 45° to the upper floor, responding to the prevailing winds from the northeast and at the intersection of the two volumes a wind scoop was proposed, which crosses the two floors, to receive and direct the wind in a controlled manner throughout the house. The architectural proposal thus responds to both the architectural intent and the climate.

Passive strategies

Three passive strategies are present in the proposal and are named as systems (3):

a.) The Solar Regulatory System (SRS), regulates solar radiation in the home; on the south façade, with the rooms on the upper floor, a complete floor-to-ceiling glazing is proposed, which is protected by a operable slat closure, depending on the time of day and the season of the year, avoiding the overheating in summer, but allowing the passage of air in a controlled manner (Fig. 2).

On the ground floor, also to the south-east, it is protected with interior blinds and the upper volume acts as sun protection throughout much of the façade throughout the year. The other element of the SRS is the 60cm thick volcanic stone wall that protects the house mainly from the north winds and late summer sun.



Fig. 2 South facade, envelopes and exteriors.

b.) The Wind Regulatory System (SRE) modifies the conditions of the environment through heat transfer by the air and is made up of different

devices: the windows and the wind chimney or scoop (Fig. 3); this is located in the center of the house and crosses the two volumes, so the inhabited triangular chimney emerges, that faces northeast, collects the winds in a controlled way, in summer and circulates them inside the house through a vertical inhabited space that can be used with the placement of a triangular metal framework in the center of the floor (galvanized metal grid) on the first level (3.10mx 3.10m) (Fig. 4).

The upper part facing the outside of the wind scoop is protected by adjustable glass elements that are controlled to regulate the air flow that enters the home. The ventilation is one of most important tools to get better the climatic conditions. We studied incorporation in this homes cross ventilation systems, and this things was measuring with the help of the anemometers of hot wire.



Fig. 3 North facade. The MURO with the upper wind fireplace.

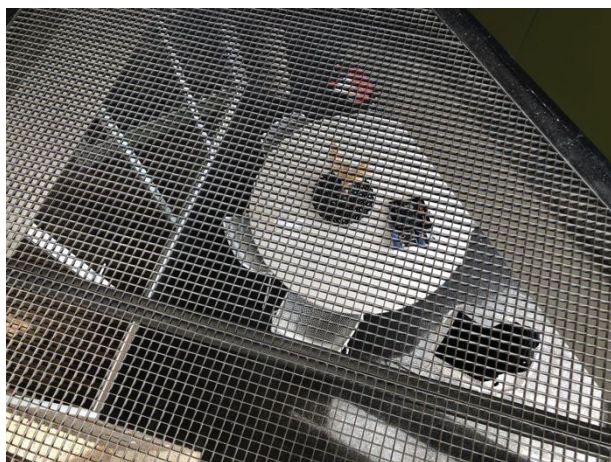


Fig. 4 Triangular metal framework-wind chimney.

As part of this passive wind strategy, in the lower part there is a small body of water (2.30m x 2.30m x 0.30m) that provides some air humidification and evaporative cooling.

c.) The Mass Regulating System (SRM) consists of strategically located thermal mass and

thermal insulation. The opaque envelope (vertical cladding and roof) is insulated to avoid conduction heat gains in summer and losses in winter. The windows are double-glazed aluminum without thermal bridge.

The so-called MURO, to the south, built with porous volcanic stone from the island, known as coarse block (Fig. 4), is made up of a central part of concrete block, covered by pieces of coarse block, whose constructive appearance is of a wall with a simple rigging; Inside, it has a reinforced concrete structure with its corresponding foundation, which allows the autonomous stability of the wall, separated from the building that appears on the south façade.

The MURO has a dimension of 19m in length, a height of almost 7m and a thickness of 0.60m; It is a screen that serves as a thermal regulator of external conditions and protects from cold winds in winter and especially strong ones, but with openings that can allow cross ventilation in summer; It is a solid wall with small perforations through which light, wind (Fig. 3) passes in a controlled way and it is also possible to look at El Teide, always present on the island

At the top of the wall there are solar collectors for domestic hot water, accessible via a sea ladder.

2.2. Construction materials.

The structure is made up of 3 modules of 4m x 4m reinforced concrete grid, with circular columns of 30cm in diameter free of the walls and the enclosures.

The roof is a ribbed slab of reinforced concrete, with polystyrene sheet insulation, and the floor and the north terrace, of precast reinforced concrete ribs with concrete block vaults and stone (volcanic) stone.

The exterior walls are two-leaf walls of vibrated concrete blocks (e-20cm) with an air chamber (10cm). The non-opaque envelope is made up of laminated glass (4+4) from floor to ceiling (south façade) with aluminum carpentry, protected with sliding slat frames on rails.

The water supply for the entire ITER complex (bioclimatic houses and offices) comes from sea water that is transformed into drinking water through a desalination plant owned by the ITER.

2.3. Renewable energy equipment.

-Photovoltaic energy (Fig. 5)

The photovoltaic system consists of 17 panels facing south and with a 10° inclination on a fixed structure on the highest roof of the house. The panels are of the multicrystalline type with a peak power of 170Wp and 2.89kWp of total generation power. This installation has an inverter to allow connection to the electrical grid.

Components:

Photovoltaic panel model ITER ST 170 P-1 multicrystalline with dimensions 1,036x991x40mm³, a weight of 16kg and a collection area of 1.29m², made up of 48 cells in series.

The main electrical properties are:

- Maximum power 170 +/- 3%.
- Voltage at maximum power: 23V
- Intensity at maximum power 7A
- Open circuit voltage 28V
- Short circuit current: 8,3A
- Efficiency of the module 13%

Single-phase photovoltaic inverter for grid injection. Conceived for a typical string of panels with a maximum voltage of 600VDC, 3kW of maximum power and 230VAC for connection to the network. Peak efficiency is around 97%. It is monitored through an RS-485 line with MODBUS RTU protocol through the photovoltaic inverter.



Fig. 5 Photovoltaic panels on the roof.

-Solar Thermal Installations. (Fig. 6)

The installation for the production of hot water is made up of six custom-made collectors, with an inclination of 20°, supported on the wall and facing south. The 200 lt capacity inter-accumulator tank is necessary for the expected consumption of the home and a pumping group necessary for the correct operation of the system.

Components:

Custom-made solar collectors of the Constant Solar brand, with a total area of 3.35m². Each collector is made up of tempered solar glass, a grill with 2 absorber tubes per copper panel, with a selective coating of Cr+Si+Ni with high absorbance.

The main parameters are:

Profit factor: $n_0 = 0,790$

Loss factor: $a_1 = 3,641$ $a_2 = 0,016$

Inter-accumulator tank model 209 SPTE of the SICC brand with a fixed coil of 200 lt capacity and with

internal anticorrosive treatment. For vertical or horizontal arrangement, with an unladen weight of 79kg and dimensions 1,465m long and 0.6m in diameter.

These equipments are accessible through a marine ladder supported on the MURO.



Fig. 6 ACS solar collectors on the MURO.

3.-METHODOLOGY AND ANALYSIS

The goal is to analyze the building's bioclimatic behavior, its connection with thermal comfort, its adaption to the climate and its real energy efficiency, after more than 25 years of making the proposal to determine if the building is performing as intended. To achieve this data from a monitoring system that has been in place for more than 7 years is used. This system has collected data that includes comfort variables (in different spaces of the home) and energy consumption (since 2012) (4).

The monitoring system of the houses that conform the "Bioclimatic Laboratory" project is made up of different components of interconnected elements. During the construction, different sensors were installed in each of the ITER homes; in this house –*El Dispositivo*–, the sensors installed were Temperature (T) and Relative Humidity (RH) (SHT11 Sensirion)-5, Surface Temperature (TS) -3 (TC77 de Microchip), and Air flow meter- Anemometer (A) -1 (Hot wire anemometer for measuring velocity.). On the floors of the house (Fig. 7), the location of the different sensors is indicated.

An anemometer was included as it had a wind scoop that runs through the entire house. T and RH data collection is performed every minute. In some periods, the data is not complete, so data from 2016 is shown as an example, allowing to compare the conditions of the interior of the house with those of the exterior.

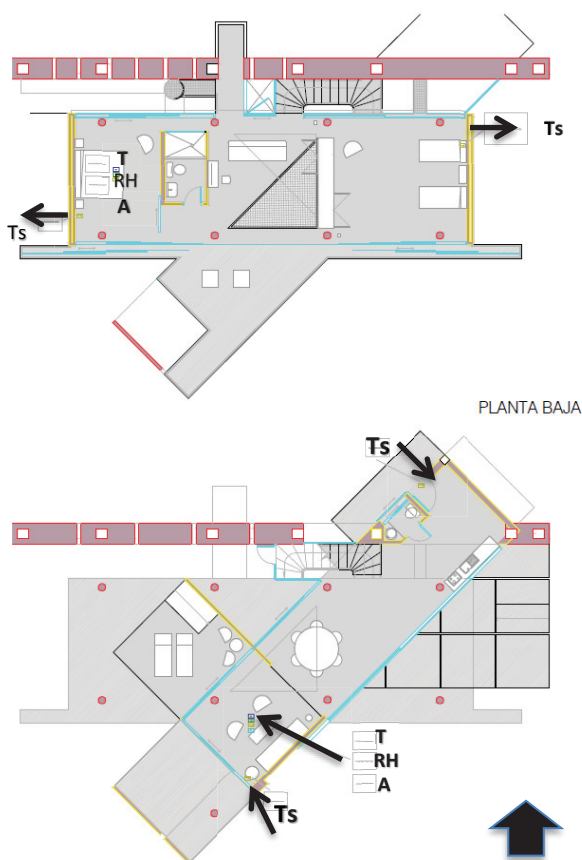


Fig. 7 Location of the different sensors T, Ts and RH, Anemometer-A.

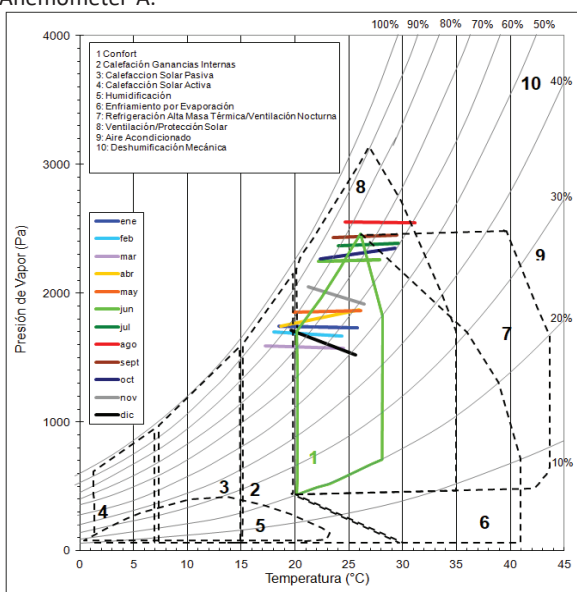


Fig. 8 Outside temperatures / humidities (ITER Urbanization weather station), mean Max and Min, mean Year 2016 (5).

When comparing the graphs of Figs. 8 and 9, it can be seen that the relative temperatures and humidity of the year analyzed (2016), inside the house, are mostly within the comfort zone in Givoni's psychrometric chart (5), with the exception of the months

of August and September, that conditions enter area 8, whose bioclimatic strategies seek better ventilation and solar protection, easily achievable with the design. The Canary Islands, and specifically the area near the coast, where the project is located, is in Spain's climate zone ($\alpha 3$) the most benign in winter and the one that requires the least heating energy.

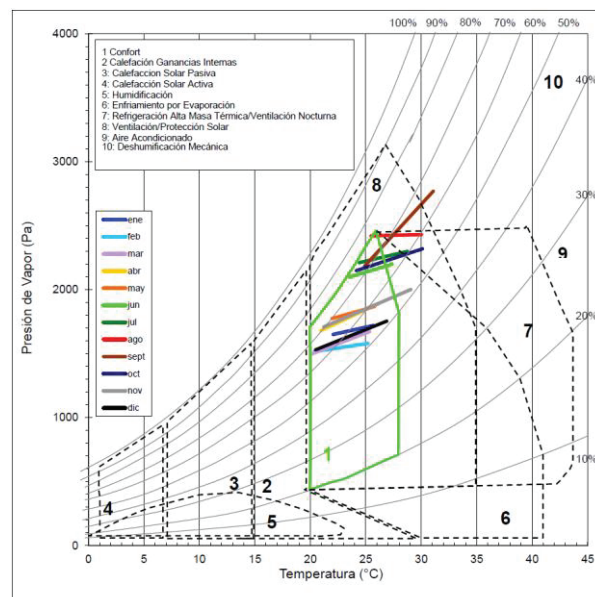


Fig. 9 Givoni psychrometric chart. Temperatures / humidities inside the house each month of the Year 2016 (5).

The monitoring of the dwellings also provides energy balance information (energy generated-consumed). In addition updated information on the energy consumption allows to propose better energy saving and efficiency strategies, through the feedback offered to the inhabitants about the consequences that the connection of household appliances has on consumption; the electrical panel of the house gives us this information.

Two months of 2019 are presented, January with the least production or renewable energy and July, which is the month with the highest production and occupation.

Fig. 10 shows the production of energy by renewable sources (photovoltaic and solar collectors) in two different months of the year 2019, January, where consumption is greater than production during every day of the month and in July, where the generation is always higher than the consumption.

The total balance between what was generated and what was consumed in 2019 was 1.378.866 kWh in favor (Fig. 11). It is important to note that these experimental houses are currently being used as lodging, with an average occupancy rate in the last 2 years of 90.32%. In the CTE Standard DB-HE0 (6), there are two requirements for residential use (which must be

complied with): the first, for climate zone $\alpha 3$, is that the consumption of non-renewable primary energy (Cep, nren) , must be less than 25kWh/m² year, and the total primary energy consumption (Cep, nren) of 46kWh/m² year, in terms of limiting energy use. In the case of this house, the total consumption is 26.76 kWh/m² year of primary energy

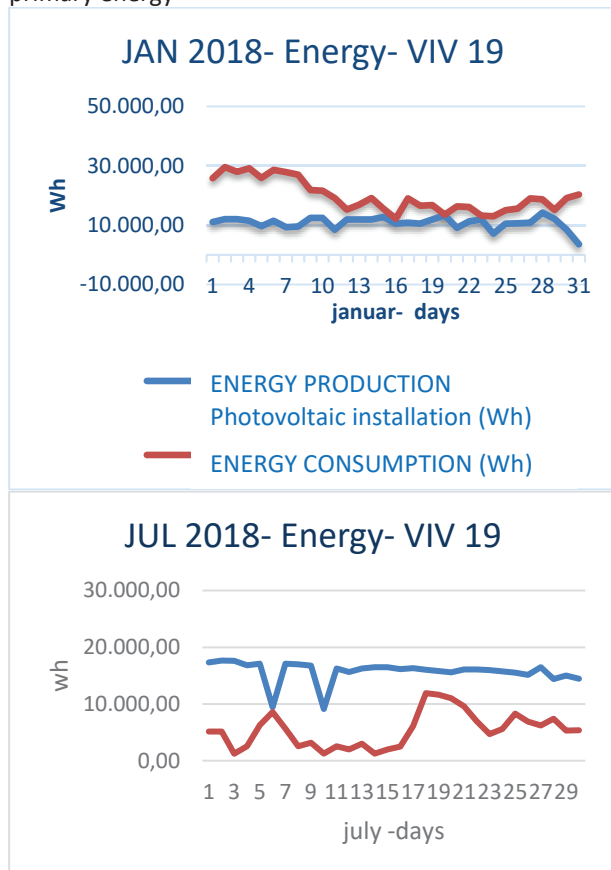


Fig. 10. Production and consumption of energy (Wh) in the months of January (upper) and July (lower) of 2019.

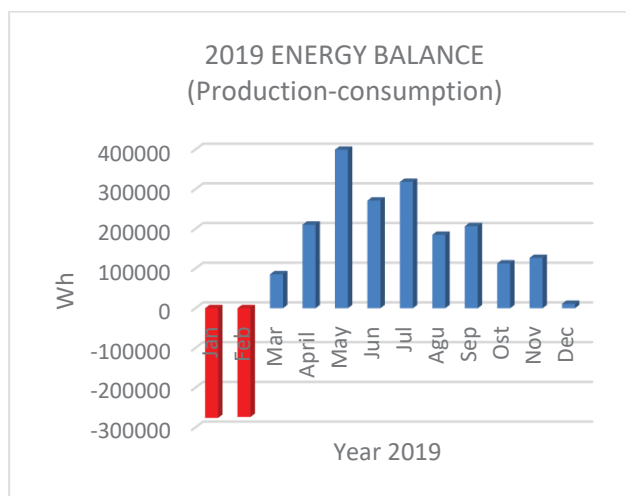


Fig. 11. Energy balance (Wh) between that generated by renewable energies and that consumed in 2019.

4.- CONCLUSIONS

Thanks to monitoring, it has been possible to analyze the real data on the hygrothermal and energy behavior of the home; the bioclimatic design strategies proposed 25 years ago could be determined as valid, showing very few deviations from what was originally planned.

Over 90% of the hours of the year, this building is within the comfort zone, without the use of any mechanical heating and cooling systems, demonstrating that it is possible to achieve thermal comfort inside the building with passive bioclimatic measures, such as better ventilation and sun protection in the months of August and September.

This building, designed more than 25 years ago and built 15 years ago, with the bioclimatic criteria indicated in point 2.1, would be complying with the current requirements of the European energy efficiency directives and specifically with the regulations of the Technical Building Code –DB -HE0 2019 (Limitation of energy consumption), below 58.1%, which is required for nearly zero consumption energy buildings (nZEB).

ACKNOWLEDGEMENTS

The team of the Technological Institute of Renewable Energies (ITER), Tenerife-Spain; to the University of Zulia, Maracaibo-Venezuela, to the engineer S. Delgado and the architects N. Soles and H. Sánchez, and the students in 1995 who collaborated on the project, especially M. Machado, L. Rodríguez and C. Urdaneta. Spain Ministry of Science and Innovation for support the project HABITA-RES, BIA 2017- 83231-C2-1-R. And the INTERREG-MAC 2014-2020 Project, funded by the European Union SOSTURMAC (MAC/4.6c/115).

REFERENCES

- (1) Mustieles, F; La Roche, P.; Oteiza, I. (1996) «Vivienda bioclimática, como Dispositivo habitable». *Revista Tecnología y Construcción*. Volumen 12 (I). págs. 21-31. Caracas, Venezuela.
- (2) La Roche, P., Machado, M., Mustieles, F., Oteiza, I. (1999). «El Dispositivo habitable». *Revista Informes de la Construcción*, 50 (460): 39-52. Madrid, España.
- (3) Mustieles, F, La Roche, P., Machado, M., Oteiza, I., Soles, N., (1998). "To inhabit the Devices: Bioclimatic house for Tenerife. Bioclimatic Proposal towards a sustainable future" Proc. of PLEA 1998, The 15th International Conference on Passive and Low Energy Architecture ISBN-13:978—1-873-93681-8, Lisbon, Portugal.
- (4) ITER (2020) Data on the monitoring of the habitability of the Device House. - Living Lab- ITER- Tenerife 2012-2020 Spain.
- (5) Allaker, K. (2000) The Climate and Givoni tools were developed by *Architecture, En & .Env. Program*. Belgium.
- (6) Ministerio de Fomento. España. (2019) Código Técnico de la Edificación- DB-HE0. Madrid, Spain.

Evaluating Environmental Performance of Mashrabiya Generating Guidelines for Contemporary Implementation

¹ROFAYDA SALEM, Cairo, Egypt

² KARTIKEYA RAJPUT, London, United Kingdom

ABSTRACT: Extreme climatic conditions have given birth to different passive solutions. One of them: façade perforated screens, varying from one place to another according to cultural and climatic factors. Mashrabiya is an element that gathers both passive environmental solutions, traditional art and cultural aspects. It is also a façade component with various geometrical forms that can combine different screens typologies. Implementation of the perforated screens in vernacular architecture has been conducted by designing a façade component that balances the need for shading and convenient natural ventilation. Reintroducing Mashrabiya in contemporary design can be the starting point towards achieving passive buildings in hot climates. Nowadays, there is a vast reduction in the use of this powerful traditional shading tool in contemporary buildings, endangering Mashrabiya as an art. So, this thesis aims to illustrate the environmental performance of the existing traditional perforated screens and re-evaluate them in a practical way. Reintroducing Mashrabiya can be Through systematic analyzation of these façade components with the help of analytical tools. This study can portray the implementation of Mashrabiya in a more appropriate way, through providing design recommendations that emphasize the most applicable use for various patterns according to the location, orientation and type of the space.

KEYWORDS: Passive design, Mashrabiya, perforated screens, facades.

1. INTRODUCTION

The word “Mashrabiya” is defined in the Oxford dictionary as a latticework of Islamic architecture. Its meaning in the Arabic language is driven from the primary function required from Mashrabiya. Where the word “Mashrabiya” in the Arabic language is driven from the word “sharab” which means drink, this is rooted in the primary function of Mashrabiya where its perforated screens allow air to flow and cool down the ceramic pots placed near the screens. From that, the users used to place a ceramic pot in front of inlet pattern, in order to achieve a multi proposal process. where the air passing gets colder and moisturized while interring the space, and the water inside the pot is cold for drinking as if it is a “natural refrigerator.”

Mashrabiya as a concept is a component developed by time to balance the environmental and cultural requirements. It was based in Islamic architecture to achieve the balance between making comfort and preserving the privacy of the indoor spaces. Based on that, the typology of the Mashrabiya itself started to evolve through time, to achieve the required and desired functions it was created for.

In the past hot climatic regions used to respond to extreme climatic factors through implementing thick

walls with small openings, to maintain the number of solar gains resulted from the light entering the space. Also, the urban fabric used to provide more adaptability towards these extreme climatic conditions. In hot climates, especially the middle eastern countries, the urban fabric used to be close with the narrow streets. That brought the buildings close to each other to provide mutual shading. But this typology forced the buildings to have small and narrow openings respecting the privacy of the houses.

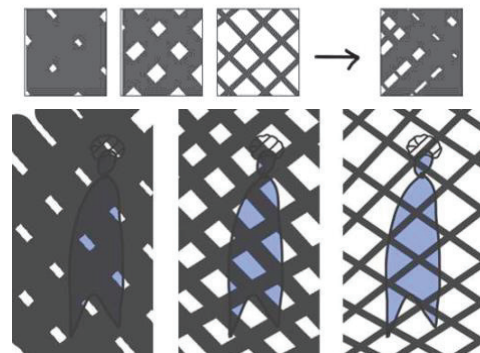


Figure 1: analytical sketch explaining the concept of screens

2. Context and precedent of Mashrabiya

The idea of Mashrabiya expanded with the expansion of the Islamic culture, and the patterns

implemented in it started to vary according to the culture and the heritage of each place. And based on that many typologies of Mashrabiya were formed.

The typologies of Mashrabiya used to vary according to geometry, function and the patterns used in the component. Also, the name and the material used to vary from a region to another according to its climatic factors and cultural aspects.

As the typology of the Mashrabiya changes the environmental performance changes as well, based on that, the scope of this paper was oriented towards two main types of Mashrabiya, which are:

Andalusian Mashrabiya- based in Spain and Morocco
Ottoman Mashrabiya based in Egypt
These two types were selected because they represent the majority of the existing Mashrabiya in the middle east, and there are huge variations between the two models. This will expand the documentation of the analysis of different patterns and forms.

2.1 Scope of the study

The study aims to evaluate the environmental performance of the different typologies of Mashrabiya. As follows, it was important to fix certain environmental parameters for all the patterns in order to provide a technical quantification.

2.2 Observing Mashrabiya

To understand how different typologies perform, it was important to observe the characteristics and test their environmental performance in terms of shading and ventilation. For that, fieldwork was held to provide sufficient data and satisfying background of these different forms and patterns. Objectives of fieldwork were not limited to monitoring the environmental performance and understand the variations in the performance from a case to another. It was also for documenting the dimensions of each pattern and the details of the different components. Afterwards, a systematic dimensional sketch was made in order to guarantee the accuracy in the modelling of the patterns and components in different softwares. During the fieldwork, a survey was held among the craftsmen and carpenters to understand how they used to model the Mashrabiya and state what patterns should be applied. This step was essential to know how the majority of contemporary Mashrabiya examples were modelled.

In this study, to make a good understanding of the performance of facade perforated screens, it was necessary to do the study on a wide parameter of sites in different climatic regions to understand different uses of Mashrabiya. To have a full understanding of the environmental performance of Mashrabiya and be able to quantify its performance, it was necessary to run fieldwork studies to understand how the living examples perform. The fieldwork was necessary to illustrate the reason behind the drop in the implementation of traditional Mashrabiya

2.3 Field work and site analysis:

To understand how the performance of Mashrabiya might vary from a case to another according to the variation in both geometry and patterns it was important to study different typologies of Mashrabiya. Based on the previous facts Spain and Egypt were selected as they represented the cradle of the most famous two Islamic architecture schools:

- Andalusian architecture
- Ottoman architecture

The field work held in Spain was centred in Andalusia part that mainly started in Granada and expanded by time towards Cordoba. While the Ottoman Mashrabiya was mainly found in Cairo where it was commonly implemented during the Ottoman Rule on Egypt.

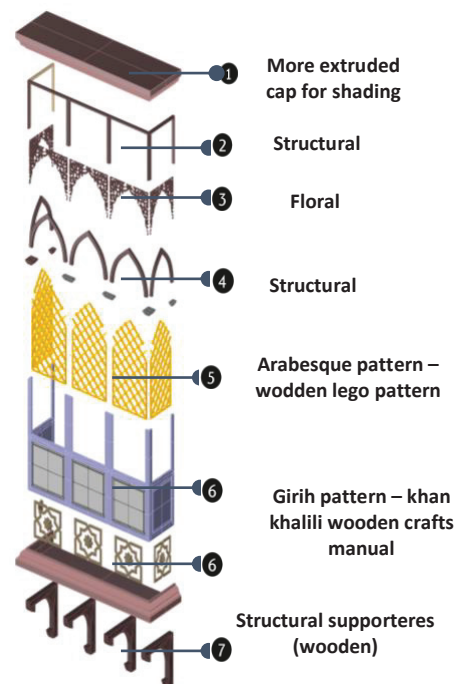


Figure 2: Analytical disassembled model to show the elements of Ottoman Mashrabiya

The difference between the ottoman and Andalusian Mashrabiya represented in different geometries and different types of patterns, which enhanced the difference in the performance according to different environmental parameters.

The extruded style of Mashrabiya mainly found in ottoman architecture providing a self-shading technique as well as additional space that encouraged the implementation of more than one pattern on the same component. This complexity helped in the evolving of Mashrabiya from just a faced perforated screen to complex component with an adaptable performance that can change according to the users' needs.

To have a full understanding of the environmental preform according to its climatic context, Spain was visited in order to see the different typologies and shapes of patterns. The objective of the fieldwork wasn't only to understand the environmental performance of Andalusian or ottoman Mashrabiya but also to understand the difference between them in terms of details and patterns.

- Spot Measurements were taken
 - Photos were taken to provide a full understanding of the details
 - Measurements were made to know the dimensions of the components that formed the patterns Sketches were drawn to keep the details of the measures for the modelling stage to be used in the analytical work.
- In Spain the following sites were selected:

- 1.Alhambra palace
- 2.Placiodedar al hora
- 3.The great mosque de Cordoba

These sites were selected according to the typologies of the perforated screens inside them. These buildings managed to maintain the screens implemented in it, which was considered to be the pure definition of Andalusian Mashrabiya.

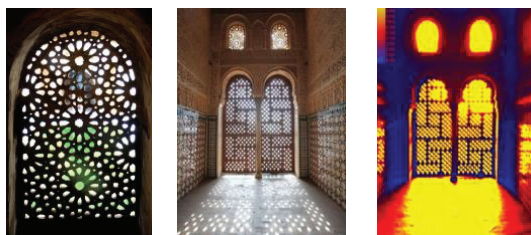


Figure 3: Aftab analytical photo of Alhambra palace Ambassador hall window

For security issues, the long-time continuous monitoring devices couldn't be applied. So, spot

measurements were taken on a three days interval in each site. Measurements were taken more than once through the day in order to estimate the average performance of the patterns.

Estimating the average performance of the patterns was through comparing the outdoor conditions and indoor conditions at different depths of the spaces. Some of the patterns in Alhambra palace were cover with glass in order to maintain the ornaments curved in the wall by protecting it from different climatic factors. But the performance was measured during the maintenance period where the glass was removed to be cleaned.

The journey to Spain started on 2nd of May 2019 and continued to 15 days after. Each site took an average of 5 to 3 day of monitoring and observing, except for the great mosque de Cordoba the fieldwork and observing occurred in one day as the patterns were totally covered with fixed glass that can't be removed during the maintenance.

The great mosque de Cordoba was an observing case to understand how the pattern was created in terms of geometry and dimensions if it is applied in large scale windows or arches. Also, to understand its performance in terms of shading in such a scale.

To understand the variation in performance and typologies of Mashrabiya it was important to see living examples of ottoman Mashrabiya. For that Egypt – Cairo- old Cairo was selected to see and understand different typologies of Mashrabiya, based on these 2 sites were monitored for two consecutive days. The sites were:

- 1.Wikala Al Ghouri
- 2.Bayt Al-Suhaymi

After that, there was a survey represented in friendly chatting with the carpenters and craftsmen who are still working in crafting Mashrabiya until nowadays in Al Moez street.

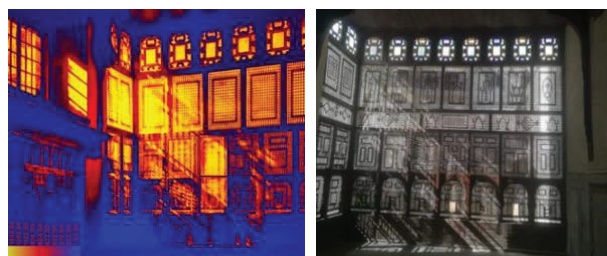


Figure 4: Aftab image of Bayt al suhaymi, Cairo

3. Analytical quantification of the environmental performance of Mashrabiya

3.1 Methodology:

This study depends on empirical evidence and fieldwork documentation besides the literature review of previous paper works and books that contributed a lot to understanding Mashrabiya. Based on literature review, fieldwork and systematic quantification of the environmental performance of Mashrabiya.

After observing and concluding a lot of facts about Mashrabiya, the analysing process was shaped according to the outcomes of the fieldwork. It was found that Mashrabiya performance varies significantly by changing the smallest details of it, as well as the change in the integral component. This shaped the process of quantification of Mashrabiya performance to be divided into two main parts:

A. Micro-level: where the main focus will be on the patterns and how they differ in shape and performance. To quantify these shapes, seven patterns were selected based on its variation, where each pattern represent a representative example of a category of patterns similar to it in form, dimensions and perforation percentage. Then the seven patterns were correlated with each other in order to understand the variation in the performances in terms of shading and ventilating.

B. Macro-level (component level): where the main focus was to understand how the Mashrabiya preforms as a component with different typologies. In consequence, different geometries were tested with various forms and patterns. In this part, the study aimed to understand the outcomes of combining different patterns in the same component and set the baseline of understanding the different combinations.

According to the fieldwork and literature review, a lot of factors were found, and from that, it was concluded that the performance of Mashrabiya in terms of shading and ventilation varies according to:

- The perforation percentage of the pattern
- The type of the pattern, whether it could be floral or geometrical
- The thickness of the pattern, as it was found in the great

mosque de Cordoba, where the patterns that were applied to a bigger scale

maintained the same ratio between the depth and the length of gapes.

- The activity preformed in the transitional space created by Mashrabiya affects its performance significantly. Whether an evaporative cooling element is added or not

indeterminably, the performance of the Mashrabiya varied in terms of shading and ventilation according to the patterns, the component style and whether it had more than one pattern combined on it as it was found in the ottoman Mashrabiya examples found in Egypt. All these factors managed to shape the process of analysis and quantification of the environmental performance of Mashrabiya. According to that, the analytical method was formed and divided into two main steps:

- 1st step was to understand the performance of Mashrabiya on the micro level and start understand and quantify the performance of different patterns on micro level
- 2nd step was to study the performance as a component and understand the variation of performance in different environmental parameters

A. Micro level:

Where the main focus was on the patterns and zooming on the smallest details of Mashrabiya. after that, start testing them under studied and fixed conditions to understand the difference of each pattern in terms of performance if they are exposed to the same climatic and physical surrounding conditions.

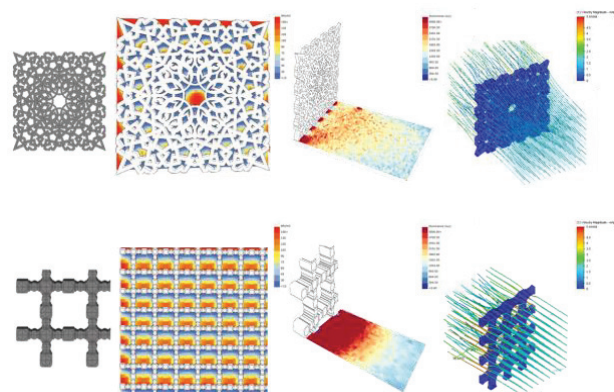


Figure 5: different patterns micro analysis for solar radiation, illuminance and discharge coefficient

B. Macro (component) level:

After realizing how each pattern preforms in terms of light, solar radian and airflow, the next step scope is adjusted to zoom out and focus on the change in the performance according to the whole component. And understand how the geometry and combination of patterns can significantly change the performance. Also, in the macro level, the effect of adding an evaporative cooling element in the transitional space created by the component will be roughly estimated.

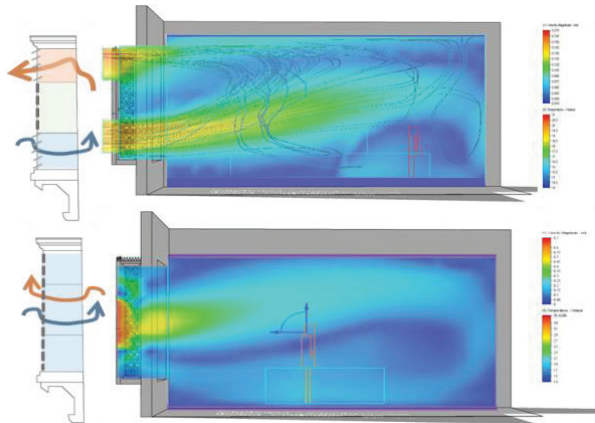


Figure 6: CFD analysis for Mashrabiya with same perforated screen and with different screens together.

3.2. Analytical quantification outcomes:

Based on the analytical quantification of Mashrabiya in terms of screens and component. It was found that Mashrabiya, as a façade component, can have an impressive impact in improving the indoor conditions of the space. But it also can have a negative effect by not preforming efficiently if the wrong pattern is applied to the façade.

From all the parts of the analytical work, it was found that Mashrabiya within its simplicity as a solution there is a lot of complexity in its performance. To understand and quantify its performance a lot of analytical tool were used, and despite software limitations, a total figure was formed about the performance of Mashrabiya. This analytical work managed to show us how Mashrabiya varies significantly in its environmental performance from the smallest change in any of its details.

That's why it was important to make a full understanding towards the details of the Mashrabiya. Despite the complications in analysing the details of the components that form each pattern, this step was essential to understand and compare the main details of Mashrabiya.

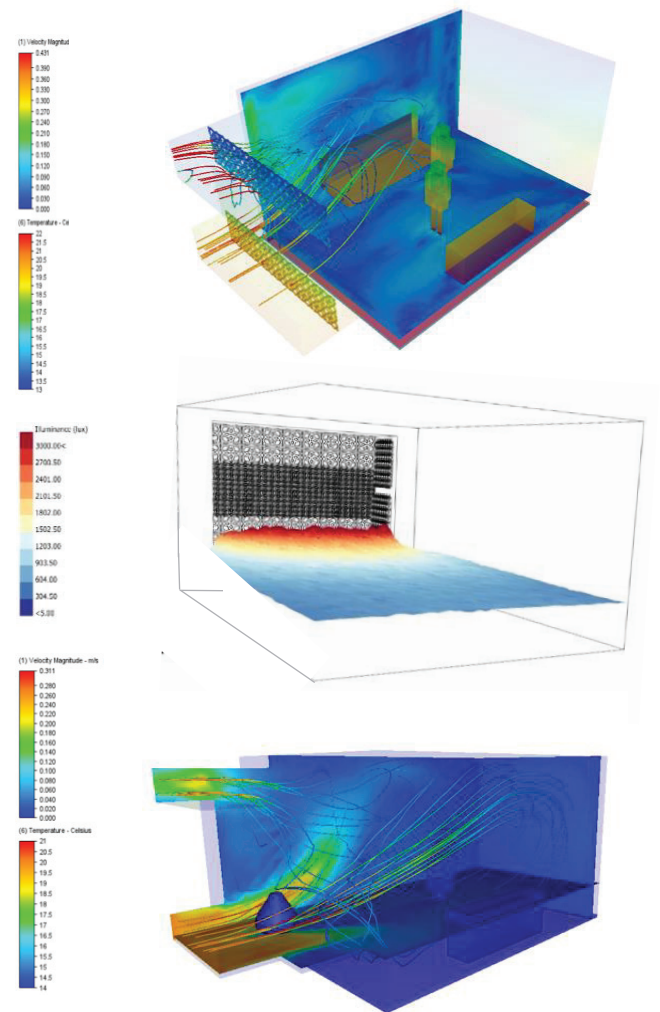


Figure 7: different macro level analytical quantification through CFD and grasshopper.

Regarding, the macro level analysis it was found that combining patterns is significantly influencing the total performance of Mashrabiya in both: ventilation and shading. This can be considered as a double-edged tool, that can improve and strengthen the performance of Mashrabiya, or drain and demolish the strength points that exist in Mashrabiya as a passive solution. For that, design guidelines and recommendations must be provided to encourage the implementation of Mashrabiya in contemporary designs with the most accurate and precise methods.

4. Design guidelines:

Designing a shading element that preforms efficiently on different sun angles is quite challenging and that's why perforated screens can be reintroduced in a systematic study in order to achieve such approaches. So, a formula was made in order to link the depth of the required horizontal shading element to shade a window and the perforated screens that will replace it. This replacement will manage to provide a better shading performance for

most of the sun angles for different parts of the year on different orientations.

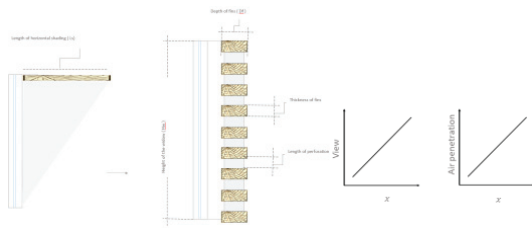


Table 1: Equation sectional explanation and relativity fun.

Equation (1):

Depth or length of the horizontal shading element

$$(Ls) = \text{depth of fins } (Df) * \text{No. of fins} \quad (1)$$

Where Ls – depth of horizontal shading element (m);

Df – depth of fins (m);

Equation (2):

Perforation percentage of a screen =

$$\left[\frac{\text{Total Length of the gaps}}{\text{total length (height of window)}} \right] * 100 \quad (2)$$

Where total length of gaps = $(Hw) - (\text{thickness of fins} * \text{No. of fins})$

Where Hw – height of the window (m)

Thickness of fins can be determined through this formula:

$$\left[\kappa^{-1} * \text{height of the window} \right] \div \text{No. of fins}$$

Where κ - a variable No. that depends on how much allowance of other environmental and architectural parameters:

And based on that a matrix was formed to suggest the studied patterns for different orientations and different space usage.

5. Conclusion:

Mashrabiya can be a very effective tool towards achieving indoor comfort and balancing the user's requirements in different environmental parameters. From observing the environmental performance of some Mashrabiya typologies it was found Mashrabiya can block up to 72% of the daylight that can enter to the space, this is accompanied by more efficiency in protecting from solar gains resulted from the radiations which contribute a lot in reducing the indoor temperature up to 10 degrees less.

Mashrabiya's role in reducing the indoor comfort is not limited on preventing excessive solar radiation from entering the space, it is also through orienting the air passing through it flow at different depths of the room. In the field work it was found Mashrabiya can reduce the indoor temperature up to 10 °c compared to the same neighbouring rooms that didn't implement any shading element.

the complexity found in the details Mashrabiya could gather, shaped the analytical work to focus on the quantification of Mashrabiya on different levels and scales. For that the patterns were analysed on a small scale, and it was found that the performance of the patterns in terms of shading and ventilation in not always related to the perforation percentage of the patterns, it is more related to the shape and forms of the pattern's component. It was also found that Floral patterns tends to allow more uniform distribution of light inside the space.

Analysing Mashrabiya as a component showed how can the total performance of the Mashrabiya can vary significantly if patterns were combined in a way that can create stack ventilation. The performance of Mashrabiya can be improved through applying the accurate pattern in the suitable place for the right orientation. Within the experimental steps of the analytical study it was found Mashrabiya can have inoperative impact by having impractical performance, this can happen through applying un recommended patterns to the wrong façade. For that it was important to supply the users and decision makers with recommendation and guidelines that orient the total performance of Mashrabiya towards the maximum efficiency.

In the end Mashrabiya is a component that merged art and passive environmental solutions, for that it was widely implemented in the past. Now the contemporary implementation of Mashrabiya is lamented on façade perforated screens in modern building and some few crafts for low cost buildings and common houses. Going through these examples showed the fact of how Mashrabiya got so disconnected from its original functional forms. After testing Mashrabiya with its different forms with analytical tools it was found that Mashrabiya can be a double-edged weapon, and its impact can be useless if it is applied in a wrong way. Accordingly, this paper aims to revitalize Mashrabiya and reintroduce this solution. This paper can be the starting step towards so many future studies that can document all the other typologies that this paper didn't mention and using environmental design as a tool to preserve heritage and traditional architecture.

REFERENCES

1. Igawa, N. and H. Nakamura, (2001). All Sky Model as a standard sky for the simulation of daylight environment. *Building and Environment*, 36: p. 763-770.
2. Kittler, R., (1985). Luminance distribution characteristics of homogeneous skies: a measurement and prediction strategy. *Lighting Research and Technology*, 17(4): p. 183-8.
3. Perraudau, M., (1988). Luminance models. In *National Lighting Conference*. Cambridge, UK, March 27-30.
4. International Daylight Monitoring Programme, [Online], Available: <http://idmp.entpe.fr/> [16 June 2008].

Evaluation of thermal comfort and energy performance of a case study in vernacular architecture of Cyprus

CHRYSO HERACLEOUS¹ AIMILIOS MICHAEL¹, CHRYSANTHOS CHARALAMBOUS¹, VENIZELOS EFTHYMIU¹

¹ FOSS Research Centre for Sustainable Energy, University of Cyprus, Nicosia, Cyprus

ABSTRACT: *The conservation and rehabilitation of buildings of vernacular architecture is a sustainable approach, not only because it leaves a small ecological footprint, compared to the erection of new buildings, but also due to the passive bioclimatic design features integrated in vernacular buildings. This paper will investigate the thermal performance of vernacular architecture in lowland area in diverse climatic contexts. The findings of the current research are based on an on-site investigation carried out in a representative vernacular building that is going to be upgraded to a hands-on technology exhibition area of renewable energy systems complemented with visual means to enhance the experience of visitors under a Research European Programme (Horizon 2020). The current study provides a basis for the formulation of a site-specific design strategy to improve thermal conditions and achieve energy conservation within lowland constructions in diverse climatic conditions. Understanding and analysing the thermal behaviour of these spaces is the first step towards this strategy. The quantitative analysis reveals the various challenges faced and opportunities provided by lowland structures and contributes to informing current design policies. Moreover, the analysis will inform the sizing of the technical systems throughout the year.*

KEYWORDS: *Thermal comfort, Vernacular architecture, Mediterranean climate, Lowland region*

1. INTRODUCTION

The conservation and rehabilitation of buildings of vernacular architecture is a sustainable approach, not only because it leaves a small ecological footprint, compared to the erection of new buildings, but also due to the passive bioclimatic design features integrated in vernacular buildings [1-3]. The vernacular architecture of Cyprus, as well as of other eastern Mediterranean areas with similar climatic conditions and building typologies, can be characterized as an excellent example of bioclimatic architecture, since it incorporates a series of environmental features, appropriate for both the heating and cooling period [4-8]. In addition, a series of recent studies performed on vernacular architecture of Cyprus indicate the environmental adaptability of traditional settlements located in different climatic regions of the island [9, 10]. A traditional building was selected to be an example where a hybrid electrical-thermal storage system will be installed in the Mediterranean region as part of an ongoing research programme i.e. HYBUILD, which is funded by the European Union through HORIZON 2020. The selection aims at the rehabilitation of vernacular buildings and the promotion of both bioclimatic features incorporated in vernacular architecture and new technologies that can be adapted in such buildings. This study focuses on the environmental assessment of these spaces, through the monitoring of air temperature and relative humidity. These structures are quite common in the vernacular architecture of the island; therefore, their scientific examination produces useful knowledge in terms of energy savings.

2. METHODOLOGY

2.1. Case study building and area

For the purpose of the present study, a representative vernacular dwelling was selected for an in-depth investigation. The study of a representative case study, in terms of typology and building materials, allows the wider exploitation of the research results. The building under study is located in the core of the traditional settlement of Aglantzia (lowland region - climatic zone 2). Like the rest of the island, Aglantzia has a Mediterranean climate with hot-dry summers and relatively cold-wet winters. With regard to typology, the building plan is "I"-shaped as a more compact and simple form of linear placement of the individual spaces. The interior arrangement of the central part of the building volume is divided to double bay (dichoro). The traditional buildings are characterized by main spaces with high ceiling of approximately 3.5-4.5m. The high ceilings help in the isolation of heat gains on upper levels maintaining indoor spaces cooler during the summer period while enhancing the potential for natural ventilation. The traditional buildings were mostly made of materials available in the region. Thick masonry walls made of adobe and stones are the most common materials. The building under study has a 50-55cm thick stone masonry wall with rubble infill providing high thermal inertia. The thermal conductivity of the stone is estimated at 0.538W/m²K based on laboratory measurements and calculations. The roof is slightly inclined and originally was comprised of a thick layer of beaten earth which was laid on matting. The roof layers were supported by timber beams. At the retrofitting stage the beaten

earth was replaced with OSB and thermal insulation of 12cm extruded polystyrene giving a thermal conductivity of U value = $0.28 \text{ W/m}^2\text{K}$. The windows consists of single glazing with 30% of surface to be wooden frame of total U value $4.7 \text{ W/m}^2\text{K}$.



Figure 1. External view of the building under investigation, located at the traditional core of Aglantzia.

2.2. Field measurements

For the investigation of the thermal performance of the vernacular building, a field study has been carried out from January 2019 and is still in progress, covering all seasons. During the period under investigation, specific environmental parameters were recorded in the outdoor and indoor environment. Specifically, air temperature, and relative humidity, were measured using the UX100-003 HOBO data logger (DL) and mean radiant temperature, globe temperature and air velocity using the LSI-Lastem Heat Shield base module (ELR610M). As per the European standard EN ISO7726:2001 [11], all parameters were logged at 1.1m height from the floor. The equipment was placed in selected locations, as shown in Fig. 2.

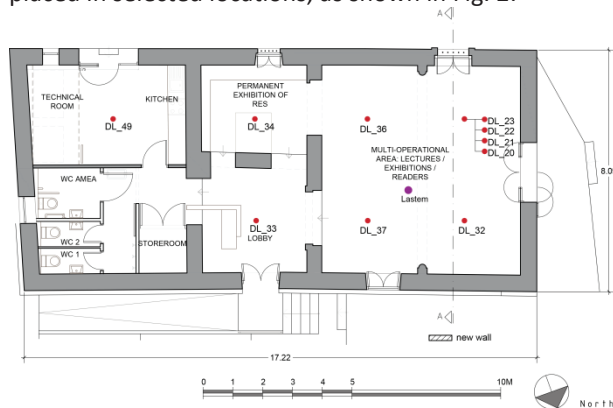


Figure 2. Plan of the building with positions of measurement equipment.

In addition, data loggers were placed in one selected position along different heights of the room, i.e. 1.1 m, 1.7 m, 2.3 m, 2.9 m in order to examine the contribution of temperature along the height. An outdoor weather station is installed in Aglantzia at the University of Cyprus at a height of 3-4 m above street level, at a small distance from the demo-site of Aglantzia (less than 1.8km).

2.3. Data analysis methodology

The objective was to evaluate the thermal comfort conditions of traditional buildings. Thermal comfort is assessed using the Adaptive Comfort Standard (ACS) which is incorporated in ASHRAE 55 [12]. The acceptable indoor operative temperatures are determined within the 80% and 90% acceptability limits, calculated as a moving average of the mean daily outdoor air temperatures (T_{rm}), using a seven-day moving average. Particularly, the 80% acceptability limits are calculated as indicated in Eqs. (1) and (2), while the corresponding 90% acceptability limits result after subtracting 1°C from the upper 80% acceptability limit and adding 1°C to the lower 80% acceptability limit:

$$\text{Upper: } T_c (^\circ\text{C}) = 0.31T_{rm} + 21.3 \quad (1)$$

$$\text{Lower: } T_c (^\circ\text{C}) = 0.31T_{rm} + 14.3 \quad (2)$$

where, T_c is the predicted comfort temperature when the running mean of the outdoor temperature is T_{rm} .

With regards to the thermal environment, the degree-hours which fall outside both the higher and lower limit margins can be employed as a performance indicator when building either for warm or cold seasons.

3. RESULTS

The analysis of the onsite recordings includes maximum, minimum and mean temperatures of different spaces of the building, the percentage of spaces within the comfort zone and the heating and cooling degree hours throughout the year. It is worth noting that the building was free of users while the shutters, where available, were closed during the monitoring period. Figure 3 shows the indoor temperatures evolution in the different rooms of the building and outdoor temperature throughout the year.

The outdoor temperature during the winter period i.e. December to February varies from -0.59°C to a peak of 23.06°C with a mean diurnal fluctuation of 11.43°C (Fig. 4). The outdoor mean average temperature during the winter period was 11.6°C . Based on the onsite recordings, mean average temperatures in all spaces are found to be low but stable and all rooms show similar behaviour in terms of temperature. Nevertheless, it is interesting to mention that, during the winter period, the building shows much higher temperatures compared to the outside conditions. Specifically, the mean average indoor temperatures in the building during winter period range from 12.1 to 16.3°C . The results indicate that the south-oriented spaces (kitchen/technical room (DL_47) and the permanent exhibition space (DL_34) exhibits generally slightly higher temperatures and diurnal temperature fluctuations compared to the north-oriented one. Specifically, the mean maximum temperature during the winter period in the multi-purpose area (DL_20, DL_32,

DL_36, DL_37) ranges from 12.3 to 16°C with a mean diurnal fluctuation varying from 0.3°C to 0.5°C; while in the south-oriented space of the kitchen/technical room and permanent exhibition (DL_47 and DL_34) the mean maximum temperature range from 12.9°C to 16.3°C with mean diurnal fluctuation varying from 1 to 1.7°C. This variation in temperatures of spaces with different orientation is mainly attributed to the impact of direct solar radiation. It is worth noting that these spaces are also not shaded by external shutters. The mean maximum temperature in the spaces under study remains lower compared to the outdoor environment however, indoor temperature fluctuations indicate that temperatures in spaces remain fairly constant. Due to their high thermal stability, all spaces present a beneficial thermal effect during night-time hours when temperatures are minimal. Specifically, mean minimum temperatures in the building range from 11.8°C to 16.0°C while the mean minimum temperature in the outdoor environment is between 4.5°C-6.7°C (Table 1).

The outdoor temperature during the intermediate spring period, i.e. March to May, varies from 2.8°C to a peak of 42.2°C with a mean diurnal fluctuation of 14.6°C. The outdoor mean average temperature during the mid-season period was 19.2°C. Regarding indoor temperatures, the highest temperatures are recorded again in south-oriented spaces i.e. kitchen/technical room (DL_47). The mean average indoor temperatures in the building ranges from 14.9°C to 15.5°C during March, from 17.4°C to 17.7°C during April and from 23.1°C to 23.7°C during May, i.e. a mean difference of 0.3-0.6°C between the spaces. It is worth mentioning that only during May the mean average temperature is within comfort levels. The building keeps thermal stability, having slightly higher mean diurnal fluctuation in each individual space, compared to the winter period ranging from 0.5 to 1.7°C. Again, the indoor mean minimum temperatures that appear during night-time are above the minimum outdoor temperatures. Specifically, the indoor mean minimum temperatures range from 14.6°C to 14.9°C during March, from 16.9°C to 17.2°C during April and from 22.7 to 23°C during May while the mean minimum temperature of the outdoor environment is 8.7°C, 11.8°C and 16.1°C respectively (Table 1).

The outdoor temperature during the summer period, i.e. June to August varies from 15.4°C to a peak of 41.1°C with a mean diurnal fluctuation of 15.1°C (Fig. 5). The outdoor mean average temperature during the summer period was of 28.8°C. Only during June and July, the average temperature of all spaces falls within the comfort zone. Regarding indoor temperatures, throughout the examined seasons, indoor maximum temperatures are, to a great extent, below maximum outdoor

temperatures i.e. of 9-10°C lower and with small diurnal fluctuation i.e. from 0.7 to 1.8°C in different spaces. However, due to this low fluctuation, the indoor average temperature is always higher than the corresponding outdoor one during the whole summer period ranging from 27.7-31.7°C. The highest temperatures are again recorded in south-oriented spaces, i.e. kitchen/technical room (DL_47). Specifically, the mean maximum temperature in the kitchen ranges from 29°C to 32.8°C compared to the multi-purpose area (DL_20) that ranges from 28.6°C to 31.8°C. The indoor mean minimum temperatures that appear during night-time are, to a great extent, above the mean minimum outdoor temperatures i.e. 7.4-7.6°C during June, 7.7-8.1°C during July and 8.6-8.9°C during August, above the minimum outdoor temperature. Specifically, the indoor mean minimum temperatures range from 27.4°C to 27.6°C during June, from 29.8°C to 30.2°C during July and from 30.7 to 31°C during August while the mean minimum temperature in the outdoor environment is 20°C, 22.1°C and 22.1°C respectively.

The outdoor temperature during the intermediate autumn period i.e. September to November varies from 6°C to a peak of 15°C with a mean diurnal fluctuation of 14.3°C. The outdoor mean average temperature during the autumn period was of 21.8°C. The highest indoor temperatures are also recorded in south-oriented spaces i.e. kitchen/technical room (DL_47). The mean average indoor temperatures in the building range from 20.2°C to 30.1°C during autumn in all spaces. The average temperature indicates that the building is within the comfort levels most of the time. The mean diurnal fluctuation in each individual space ranges from 0.5 to 2.2°C. Again, the high thermal mass masonry construction leads to indoor mean minimum temperatures during night-time above the minimum outdoor temperatures, keeping the building warmer during night. Specifically, the indoor mean minimum temperatures range from 20.1°C to 29.4°C from September to November while the mean minimum temperature in the outdoor environment ranges from 10.4°C to 19.6°C (Table 1).

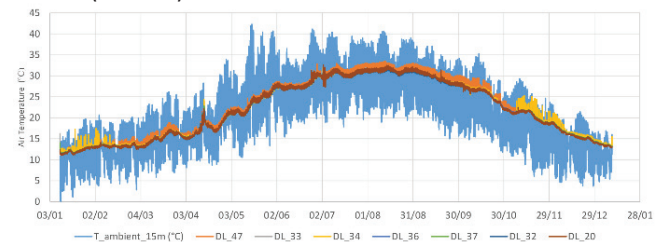


Figure 3. Indoor temperatures evolution in the different rooms of the building and outdoor temperature throughout the year.

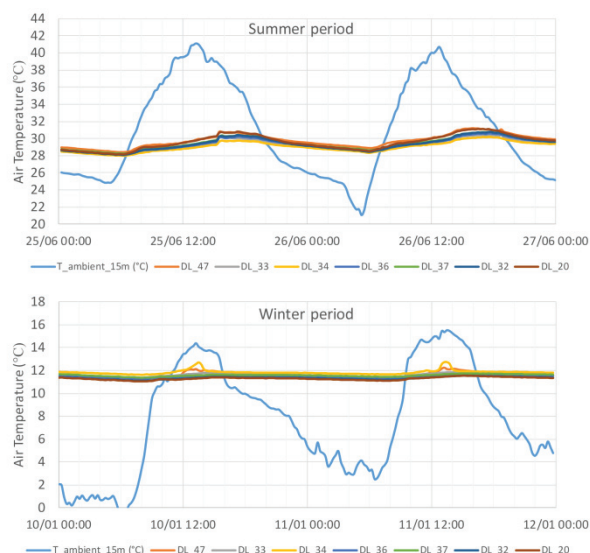


Figure 4. Indoor temperatures evolution during the warmest and coldest week of the year.

The results indicate that spaces with southern orientation could provide a warmer space during a cold, sunny winter day while spaces with northern aspect could offer greater thermal stability and a cooler space during a hot, summer day.

The results of different data loggers along different heights of the room show that during the winter period the difference is negligible (0.1°C) while during the summer period, the mean difference between the lower data logger at 1.1m and the higher data logger at 2.9m is about 0.5°C . Taking into account that the building has a mean height of 4.30m, the difference is expected to be much higher at the top. This shows the positive contribution of high ceilings, keeping indoor spaces cooler during the summer (Fig.5).

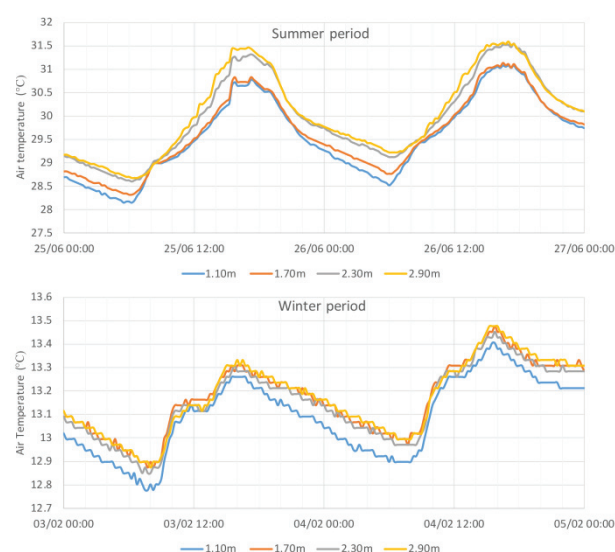


Figure 5. Indoor temperatures evolution along different heights of the room, i.e. 1.1 m, 1.7 m, 2.3 m, 2.9 m.

Table 1. Synthesis table of all the recorded temperature values ($^{\circ}\text{C}$) carried out for the investigation of thermal comfort from January to December 2019.

Months	Mean temp.	Outdoor	DL_47	DL_33	DL_34	DL_36	DL_37	DL_32	DL_20
Jan	Min	4.5	12.0	12.0	12.2	12.0	12.1	11.9	11.8
	Max	16.3	12.9	12.6	13.9	12.4	12.5	12.3	12.3
	Average	10.0	12.3	12.2	12.4	12.2	12.3	12.1	12.1
	St. Dev.	4.2	0.6	0.5	0.6	0.5	0.5	0.6	0.6
	Diurnal fluctuation	11.8	1.0	0.6	1.7	0.3	0.4	0.4	0.4
Feb	Min	6.7	13.1	13.1	13.4	13.2	13.2	13.0	13.0
	Max	17.8	14.4	13.5	14.4	13.5	13.5	13.5	13.5
	Average	12.0	13.5	13.3	13.5	13.3	13.4	13.2	13.2
	St. Dev.	3.8	0.5	0.2	0.3	0.2	0.2	0.2	0.3
	Diurnal fluctuation	11.1	1.3	0.5	1.1	0.3	0.3	0.5	0.5
Mar	Min	8.7	14.9	14.6	14.9	14.8	14.8	14.6	14.6
	Max	21.5	16.6	15.3	15.5	15.3	15.3	15.3	15.3
	Average	14.7	15.5	14.9	15.2	15.0	15.0	14.9	14.9
	St. Dev.	4.5	1.4	1.3	1.3	1.3	1.3	1.3	1.3
	Diurnal fluctuation	12.8	1.8	0.7	0.5	0.5	0.5	0.7	0.7
Apr	Min	11.8	17.1	16.9	17.2	17.1	17.1	16.9	17.0
	Max	24.9	18.7	17.9	18.1	18.0	18.1	18.0	18.0
	Average	18.1	17.7	17.4	17.5	17.4	17.5	17.4	17.4
	St. Dev.	5.2	1.7	1.6	1.7	1.7	1.7	1.7	1.7
	Diurnal fluctuation	13.1	1.7	1.0	1.0	1.0	1.0	1.0	1.1
May	Min	16.1	23.0	22.7	22.8	22.8	22.9	22.8	22.9
	Max	33.9	24.6	23.7	23.5	23.7	23.8	23.8	24.0
	Average	24.9	23.7	23.1	23.1	23.2	23.3	23.2	23.4
	St. Dev.	6.7	2.1	2.0	2.0	2.0	2.1	2.1	2.1
	Diurnal fluctuation	17.8	1.6	1.0	0.8	0.9	1.0	1.0	1.2
Jun	Min	20.0	27.6	27.4	27.4	27.4	27.5	27.4	27.5
	Max	34.8	29.0	28.3	28.1	28.3	28.4	28.4	28.6
	Average	27.1	28.2	27.8	27.7	27.8	27.9	27.8	27.9
	St. Dev.	5.0	1.1	1.1	1.0	1.2	1.1	1.1	1.1
	Diurnal fluctuation	14.8	1.4	0.9	0.7	0.9	0.9	1.0	1.1
Jul	Min	22.1	30.2	30.0	30.0	29.9	30.0	29.8	29.9
	Max	37.1	32.0	30.9	30.8	30.9	31.0	31.1	31.2
	Average	29.4	31.0	30.4	30.3	30.4	30.4	30.4	30.5
	St. Dev.	5.1	0.8	0.5	0.6	0.6	0.6	0.7	0.7
	Diurnal fluctuation	15.0	1.8	1.0	0.8	1.0	1.1	1.3	1.3
Aug	Min	22.1	31.0	30.8	30.9	30.8	30.8	30.7	30.9
	Max	37.5	32.8	31.4	31.4	31.5	31.5	31.6	31.8
	Average	29.5	31.7	31.1	31.1	31.1	31.2	31.1	31.2
	St. Dev.	5.0	0.7	0.3	0.3	0.4	0.2	0.4	0.4
	Diurnal fluctuation	15.4	1.8	0.7	0.6	0.7	0.7	0.9	0.9
Sept	Min	19.6	29.4	29.2	29.3	29.1	29.1	29.0	29.2
	Max	34.0	31.3	29.7	29.9	29.7	29.7	29.7	30.0
	Average	26.5	30.1	29.5	29.5	29.4	29.4	29.3	29.5
	St. Dev.	4.7	1.2	1.0	1.0	1.1	1.1	1.1	1.1
	Diurnal fluctuation	14.4	1.9	0.5	0.6	0.6	0.6	0.7	0.8
Oct	Min	15.9	25.5	26.2	25.4	26.7	26.7	26.4	25.3
	Max	29.8	27.7	26.8	25.9	27.4	27.4	27.1	25.9
	Average	22.2	26.2	-	26.6	25.7	27.1	26.8	25.6
	St. Dev.	11.8	2.0	-	1.1	1.7	0.5	0.5	1.8
	Diurnal fluctuation	13.8	2.2	0.7	0.5	0.7	0.7	0.7	0.7
Nov	Min	10.4	20.4	20.2	23.0	20.4	20.2	20.1	20.2
	Max	25.1	21.5	20.7	20.5	20.8	20.6	20.5	20.7
	Average	16.8	20.8	20.3	20.7	20.6	20.4	20.2	20.4
	St. Dev.	5.6	1.3	1.2	1.3	1.2	1.2	1.2	1.2
	Diurnal fluctuation	14.8	1.1	0.4	2.0	0.3	0.3	0.3	0.5
Dec	Min	6.4	15.6	15.7	16.0	15.8	15.8	15.6	15.5
	Max	18.3	16.3	16.1	16.9	16.0	16.0	15.9	15.9
	Average	11.9	16.0	16.0	16.3	16.0	16.0	15.8	15.8
	St. Dev.	4.2	1.3	1.3	1.3	1.3	1.3	1.3	1.3
	Diurnal fluctuation	11.9	0.7	0.4	0.9	0.3	0.3	0.3	0.3

*Bold indicates the peak values

Depending on the external conditions, the thermal comfort zone ranges from 17.4°C - 23.5°C to 24.4°C - 30.5°C for 80% acceptability and from 18.4°C - 24.5°C to 23.4°C - 29.5°C for 90% acceptability.

During January, February and March, the building fails to maintain indoor thermal comfort as no recorded time falls within 90% or 80% acceptability limits described by ASHRAE (Table 2). The maximum average temperature in the building during these three months is 15.47°C . However, it is interesting to mention that the mean minimum temperature indoor

is about 7-7.5°C above the outdoor temperature. During April, the percentage within the 80% and 90% acceptability limit is only 10.3% and 3.1% of the time respectively. During May, the building is within the 80% and 90% acceptability limit for 61.7% and 52.9% of the time respectively, while during June the building achieved one of the highest percentages within the comfort zone compared to other months. Specifically, the operative temperature was within the 80% and 90% acceptability limit for 88.1% and 81.1% of the time. During July, the percentage within 80% acceptability limit drops to 46.8%. The percentage within the 90% acceptability limit drops to 4.6%. It is worth noting that the whole building fails to maintain indoor thermal comfort during August as none of the spaces exhibits temperatures within the comfort zone. However, it should be noted that although the outside temperature reaches up to about 40°C, the indoor temperature shows small temperature deviation from the acceptable limits in a range of 1 - 2.3°C difference from the 80% acceptability limit (Fig. 6). The building remained closed; therefore, the heat absorbed by the building could not be released to the outside environment leading to higher indoor temperatures. During September, the building is within the 80% and 90% acceptability limit for 50.4% and 28.6% of the time, while during October, the building is nearly all the time within the comfort zone with a percentage of 99.4% for the 80% acceptability limit. During November, the percentage is reduced to 69.8% and 60.7% for the 80% and 90% acceptability limit, while during December, the temperature falls out the comfort zone most of the time, being only 5.5% of the time within the 80% acceptability limit.

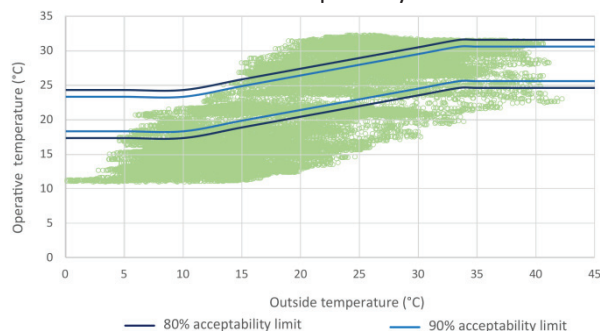


Figure 6. Brager Index of operative temperature in multi-operation area of the building from Jan. to Dec. 2019.

The onsite monitoring results during the winter period, and early intermediate period, show that the thermal comfort conditions of spaces are unsatisfactory and require a large amount of energy to keep indoor thermal comfort (Table 2). During the late intermediate period, and early summer period, the building provides acceptable indoor temperatures without the aid of an artificial system. However, the building requires much less energy for cooling.

Specifically, the building needs 13 times less energy for cooling than for heating.

Table 2. Percentage of data within thermal comfort zone for the 80% and 90% acceptability limit and degree hours

	% of data within thermal comfort zone		Degree hours	
	80% acceptability	90% acceptability	heating	cooling
Jan.	0.0%	0.0%	2942.6	0.0
Feb.	0.0%	0.0%	3330.6	0.0
Mar.	0.0%	0.0%	3045.9	0.0
Apr.	10.3%	3.1%	1774.0	0.0
May	61.7%	52.9%	313.1	0.0
Jun.	88.1%	81.1%	0.0	25.0
Jul.	46.8%	4.6%	0.0	139.9
Aug.	0.0%	0.0%	0.0	515.9
Sept.	50.4%	28.6%	0.0	314.7
Oct.	99.4%	79.0%	0.0	0.2
Nov.	69.8%	60.7%	157.1	0.0
Dec.	5.5%	0.0%	1687.8	0.0
Total			13251.0	995.7

The recorded data for relative humidity show that for most of the time (from May to December) the building totally meets the norms with values between 40-70%. During February and March, the building exhibits higher relative humidity due to lower indoor temperatures having only 20-30% of the data between acceptable limits (Table 3).

Table 3. Summary of registered RH values throughout the year

	Absolute values RH (%)			% of data in which RH=40-70%
	max	min	mean	
Jan.	72.1	55.8	67.9	79
Feb.	76.8	64.3	71.6	21
Mar.	77.8	54.1	71.1	26
Apr.	79.2	53.6	69.3	54
May	79.2	53.6	69.3	100
Jun.	71.3	43	59.6	100
Jul.	61.8	44.1	54.1	100
Aug.	64.5	43.8	56.6	100
Sep.	63.5	39.8	56.8	100
Oct.	65	47.7	58.8	100
Nov.	66.8	52.4	61.1	100
Dec.	70.0	50.5	64.6	100

For the improvement of thermal comfort and energy performance, passive measures should be considered during the normal operation of the building. Based on the bioclimatic chart (Fig. 7), during the heating period, i.e. from November to April, passive solar systems and internal gains are required. During the intermediate period, i.e. October and May, the temperatures are mild and overlap the comfort zone for the largest part of the day. During the cooling period, i.e. from June to September, a number of cooling strategies are proposed. The appropriate passive cooling design strategies include

ventilation, night ventilation and evaporative cooling. Daytime ventilation should be carefully applied and restricted to the periods of the day when the exterior temperature is lower compared to the interior temperature. The high thermal mass of the building also works beneficially to the cooling of the building when combined with natural ventilation.

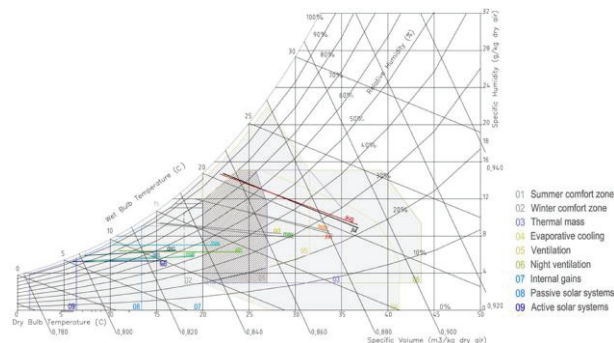


Figure 7. Plotting the Aglantzia's Weather Data at Givoni's chart.

4. CONCLUSION

This paper investigates the thermal performance of vernacular architecture in lowland area Nicosia, Cyprus in diverse climatic contexts. The findings of the current research are based on an on-site investigation carried out in a representative vernacular building that is going to be upgraded to a hands-on technology exhibition area of renewable energy systems complimented with visual means to enhance the experience of visitors under a Research European Programme (Horizon 2020). The results of the current research show that vernacular buildings perform very well during the intermediate and summer period keeping within the comfort zone most of the time, while during the winter period, the building requires additional heat gains to maintain indoor thermal comfort and acceptable relative humidity levels. This study provides a basis for the formulation of a site-specific design strategy to improve thermal conditions and achieve energy conservation within lowland constructions in diverse climatic conditions. Understanding and analysing the thermal behaviour of these spaces is the first step towards this strategy. The quantitative analysis reveals the various challenges faced and opportunities provided by lowland structures and contributes to informing current design policies. Moreover, the analysis will inform the sizing of the technical systems throughout the year.

ACKNOWLEDGEMENTS

The research described in this paper is based on the HYBUILD project funded by the European Union through HORIZON 2020 under grant agreement N° 768824.

REFERENCES

- [1] S. Saljoughinejad, S.R. Sharifabad, Classification of climatic strategies, used in Iranian vernacular residences based on spatial constituent elements, *Build. Environ.* (2015) 475–493.
- [2] A.-M. Vissilia, Evaluation of Greek vernacular settlement and its landscape: architectural typology and building physics, *Build. Environ.* (2009) 1095–1106.
- [3] M.S. Sozen, G. Z. Gedik, Evaluation of traditional architecture in terms of building physics: old Diyarbakir houses, *Build. Environ.* (2007) 1810–1816.
- [4] M. Philokyprou, A. Michael, Evaluation of the environmental features of vernacular architecture. A case study in Cyprus, *Int. J. Heritage Digital Era* 1,(2012) 349–354.
- [5] M. Philokyprou, A. Michael, The contribution of the courtyard to the environmental perception of residential architecture in Cyprus, in: I. Michaelides, A. Papadopoulos, A. Poullikkas (Eds.), 4th International Conference Renewable Energy Sources & Energy Efficiency, New Challenges, Nicosia, Cyprus, Proceedings, 2013, pp. 166–178.
- [6] M. Philokyprou, A. Savvides, A. Michael, E. Malaktou, Examination and assessment of the environmental characteristics of vernacular rural settlements. Three case studies in Cyprus, in: M. Correia, G. Carlos, S. Sousa (Eds.), *Vernacular Heritage and Earthen Architecture: Contribution to Sustainable Development*, Taylor & Francis Group, London, 2014, pp. 613–618.
- [7] A. Savvides, A. Michael, E. Malaktou, M. Philokyprou, Examination and assessment of insolation conditions of streetscapes of traditional settlements in the Eastern Mediterranean area, *Habitat Int.* 53 (2016) 442–452.
- [8] A.M. Papadopoulos, D. Aravantinos, G. Ekonomides, Analysis of the energy significance of openings in modern residential buildings with traditional design in Northern Greece, in: *Proceedings of the 11th International Conference Passive and Low Energy Architecture*, Negev Israel, 1994, pp.455–462.
- [9] E. Malaktou, M. Philokyprou, A. Michael, A. Savvides, Thermal assessment of traditional: partially subterranean dwellings in coastal and mountainous regions in the Mediterranean climate. The case of Cyprus, *J. Sustain. Archit. Civil Eng.* 3 (16) (2016) 82–96.
- [10] M. Philokyprou, A. Michael, E. Malaktou, A. Savvides, Environmentally responsive design in Eastern Mediterranean. The case of vernacular architecture in the coastal, lowland and in the coastal, lowland and mountainous regions of Cyprus, *Build. Environ.* 111 (2017) 91–109.
- [11] EN ISO7726 (2001) Ergonomics of the thermal environment instruments for measuring physical quantities. Brussels: International Standardisation Organisation.
- [13] American Society of Heating, Refrigerating and air-conditioning engineers, in: *ASHRAE Standard 55- Thermal Environmental Conditions for Human Occupancy*, Atlanta, Georgia, 2013.

A Generative System for the Design of High-Performing Shading Devices:

Exploring the Daylight Potential of Weaving Patterns

LUIS SANTOS¹, INÊS CAETANO², INÊS PEREIRA², ANTÓNIO LEITÃO²

¹ Kent State University, College of Architecture and Environmental Design, Kent, USA

² INESC-ID/Instituto Superior Técnico, University of Lisbon, Lisbon, Portugal

ABSTRACT: Designing and optimizing a Façade Shading Device (FSD) involves conflicting goals related to view access, visual comfort, energy, daylighting, and thermal performance. The optimization becomes particularly challenging when the FSD entails a complex geometry facing different orientations and solar exposure levels. Current literature focuses on the optimization of simple discrete FSDs based on horizontal or vertical shades, favoring one or the other depending on orientation. The optimization of complex FSDs that suit different orientations and solar angles is generally limited to the control of glass fritting or screen perforation density. Considering this, we present a novel Generative Design System to study the potential of weaving horizontal and vertical shades in the design of high-performing, three-dimensional, complex FSDs.

1. INTRODUCTION

Designing and optimizing a Façade Shading Device (FSD) is a difficult task that involves conflicting goals regarding view access, visual comfort, energy, daylighting, and building thermal performance. This task becomes particularly challenging when creating geometrically complex FSD that simultaneously face different orientations and solar exposure levels.

Current literature on discrete FSDs optimization focuses on horizontal and vertical shades, favoring one system over another, depending on orientation [1-2]. Regarding continuous FSDs, the research generally focuses on the use of fritting or perforation density to control sunlight [3]. Considering this, we present a novel Generative Design System (GDS) addressing weaving patterns for the design and optimization of three-dimensional complex FSDs that can balance conflicting daylighting design goals.

2. BACKGROUND

The standard IES LM-83 [4] focuses on Climate-based Daylight Modeling by proposing two metrics for the assessment of daylighting in buildings. The first one is the Spatial Daylight Autonomy (sDA), which measures the amount of area that reports an illuminance (E) ≥ 300 lux for at least 50% of the occupied annual schedule, i.e., that registers a Daylight Autonomy (DA) 300 lux (DA_{300lux}) $\geq 50\%$ – $sDA_{300/50\%}$. The second one is the Annual Sun Exposure (ASE), which measures the percentage of area that, under direct visible light conditions, reports at least 250 hours above 1000 lux - $ASE_{1000,250h}$. Henceforth, the acronyms $sDA_{300/50\%}$, DA_{300lux} , and

$ASE_{1000,250h}$ will be simplified to sDA, DA, and ASE, respectively.

Higher values of sDA improve daylight availability and subsequently decrease artificial lighting energy consumption. A lower ASE reduces the risk of visual discomfort. Thus, it is desirable to maximize sDA and minimize ASE. Based on the recommendations presented in [4] and assuming that $ASE_{1000,250h}$ is below 10%, or between 10% and 20% with additional strategies to mitigate glare, LEED V4.1 Daylight Credit Option 1 [5] awards the points described in Table 1.

Table 1: Use of sDA in the calculation of LEED V4.1 BD+C Daylight Credit Option 1 (values in %).

sDA _{300/50%} Credit	
≥ 40	1
≥ 55	2
≥ 75	3

However, simultaneously maximizing sDA and minimizing ASE poses an ill-defined problem since lower ASE values typically entail lower sDA scores and vice-versa. The multi-objective optimization of FSD is a useful approach in solving this problem. However, the literature presents a limited amount of studies that directly address it. Most of the related work in daylight optimization either is single-objective [3] or combines one of the metrics with energy-related metrics [6] or uses a single or limited range of solvers [6]. Additionally, the optimization of FSD geometry is generally limited to simple shading elements, such as louvers, fins, or perforated screens [3,7]. The few studies of complex FSD, such as [8], typically focus on

sizing and positioning an existing FSD, not addressing the optimization of the geometry of such systems.

Considering the current limitations, there is a need to study different approaches in the design and optimization of high-performing complex FSDs.

3. RESEARCH GOALS

We propose a cross-platform GDS that combines algorithmic design, daylight simulation, and performance optimization to design high-performing FSDs. The GDS interfaces with different design tools, namely AutoCAD and Rhino, and different analysis tools, including Radiance and Daysim for daylighting simulation. Moreover, it supports several black-box optimization algorithms.

This paper explores the potential of weaving patterns as valid daylighting design strategies. The aim is to produce complex architectural screens that adapt to different design requirements, such as building form, orientation, and daylight performance. We describe how the GDS manipulates weaving patterns to control daylight in buildings, particularly to balance sDA and ASE.

4. METHODS

The research comprises two phases with the following methods: (1) Implementation, which includes the development of the proposed GDS; (2) Evaluation, which consists of using the GDS in the refinement of weaving FSDs, and testing the GDS' optimization abilities to find designs that both maximize sDA and minimize ASE. The next sections describe in detail each phase.

4.1 GDS implementation

The proposed GDS has four modules: (1) one providing the algorithmic modeling of interweaved elements; (2) another delivering daylight simulation abilities; (3) a third one providing optimization capabilities that enable the automatic search for high-performing solutions; (4) a final one enabling designers to explore, query, and visualize the optimization results interactively.

Module 1: weaving patterns

Weaving is a technique based on bending and interweaving stripe-shaped elements that yields the potential to generate diverse, intricate patterns and structures. This module delivers the ability to create complex FSD based weaving patterns.

To implement it, we extended a previously developed framework specialized in weaving façade designs [9]. The framework is formalized in terms of higher-order functions, geometric transformation rules, and matrix algebra. The framework is entirely algorithmic and generates weaving patterns composed by multiple horizontal and vertical stripe-

based elements, strategically bent to avoid intersections. The framework allows the user to select: (1) the surface shape on which the weaving pattern will be created, (2) the numbers of horizontal and vertical stripes composing the pattern, and (3) the weaving strategy to apply. The proposed extension to this framework adds functionalities to control both the stripes' rotation and width along the façade surface in order to satisfy different shading requirements. Fig. 1 shows two examples of weaving patterns produced by the GDS.



Figure 1: Two examples of weaving patterns.

Module 2: daylight simulation

Module 2 is responsible for analyzing and comparing the performance of different solutions produced by module 1 using (1) visual analysis based on High-Dynamic Range (HDR) renders and false-color images, and (2) quantitative assessments of illuminance-based metrics in horizontal sensor grids placed at work plane height (≈ 0.75 m). To conduct both analysis types, the GDS uses Radiance and DAYSIM either directly or through DIVA 4.0 due to its ability to parallelize Radiance and DAYSIM simulations and therefore reduce calculation time.

Module 3: optimization packages

Our GDS takes full advantage of optimization and machine learning libraries available for the programming languages Python and Julia, namely, the black-box optimization algorithms available in Scikit-learn, Platypus, and JuliaOpt.

In this paper, we use black-box population-based metaheuristics and model-based optimization algorithms to explore the conflicting multi-criteria problem caused by sDA and ASE. We selected three optimization approaches: two metaheuristics – the Non-dominated Sorting Genetic Algorithm II (NSGA-II) and the Optimized Multi-Objective Particle Swarm Optimizer (OMOPSO) –, and a model-based technique that uses a Gaussian Process Regression (GPR) combining the Radial Basis Function (RBF) kernel with the Strength Pareto Evolutionary Algorithm 2 (SPEA-2) solver (GPR_SPEA2).

We selected NSGA-II due to its successful use in building design and optimization [10], and OMOPSO

because it was shown as the most performant of Particle Swarm Optimizers [11], which are particularly effective in building performance optimization [12]. For the model-based optimization approach, we selected the RBF kernel because it provides good results when combined with the SPEA2 optimizer [3], a popular optimization algorithm in performance-based design.

Module 4: optimization visualizer

Our GDS supports the interactive visualization of the optimization results. The goals are to (1) explore and assess the different solutions found in the search, particularly the Pareto-front ones, (2) identify the relevant decision variables and their domain, and (3) query the results. The visualizer includes an interactive scatter plot of dominated and non-dominated solutions and automatically traces the Pareto-front. The user can select any solution in the scatter plot, and the system interactively generates the corresponding 3D model and displays relevant information regarding design variables and daylight metrics. This on-demand 3D visualization also supports the analysis of other design factors not included in the search process, particularly the solutions' visual composition/aesthetic quality. Additionally, the visualizer creates parallel-coordinates graphs that allows the user to filter solutions by interactively selecting different ranges of values for decision variables and objectives/daylight metrics. This visualization facilitates iterative explorations and more refined optimizations.

4.2 Evaluation

The GDS evaluation entailed two experiments: (1) generation, iteration, and refinement, and (2) performance optimization. Both experiments consisted in the design of a weaving FSD for a 12 x 9 x 2.7 m test cell representing a typical office space located in a hypothetical commercial tower with an east and south curtain wall. We modeled these two openings to examine how the proposed system simultaneously handles two orientations with different types of solar exposure and penetration. Fig. 2 presents an exploded axonometric of the test cell fully annotated with the optical surface properties used in both experiments. Note that the interruption of the weaving pattern in the south screen aims at creating less obstructed views to the outside.

The optimization considered two metrics: sDA and ASE. Since the goals were to maximize sDA and minimize ASE, we used the guidelines of LEED V4.1 Building Design and Construction (BD+C) Daylight Credit – Option 1 (Table 1). Our test cell, with its fully glazed south and east façades, increased the difficulty of achieving the objective since it is challenging to

diffuse the Eastern low angle sunlight in clear sky conditions through a static FSD.

In both experiments, the calculation of sDA and ASE is based on a sensor grid located at work plane height (≈ 0.75 m) with sensors evenly spaced ≈ 0.6 m in both directions. The climate data used in the annual sky matrix generation is from Phoenix, AZ – a location dominated by clear skies [13].

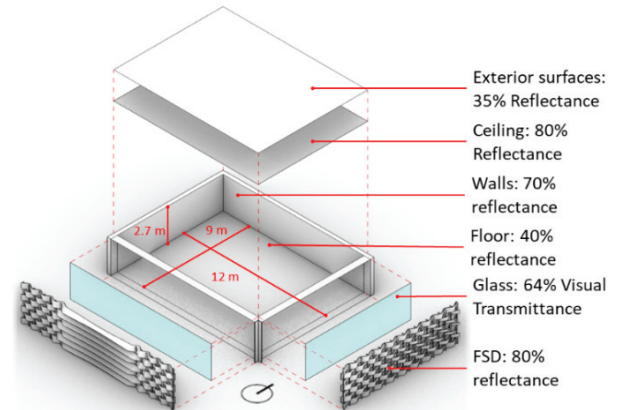


Figure 2: Exploded axonometric illustration of the test cell used in the evaluation of the GDS.

Finally, the weaving FSD generative algorithm has three main discrete variables: the number of horizontal stripes $X1 \in \{6, 7, \dots, 20\}$, the rotation of the south horizontal stripes $X2 \in \{-\pi, -\pi + 0.02, \dots, \pi\}$, and the reduction factor of the east horizontal stripes $X3 \in \{0, 0.02, \dots, 1.6\}$. Regarding $X2$, 0 or π values generate parallel horizontal stripes in the center of the south façade, while $\pi/2$ or $3\pi/2$ create perpendicular ones. Regarding $X3$, the range results from a sinusoidal behavior wherein 0 means no reduction, and 1.6 means maximum reduction. The following describes the two experiments.

Experiment 1: generation, iteration and refinement

This experiment focused on assessing the GDS' generative and daylight abilities in a user-driven iterative process. It illustrates how a user can incrementally refine the design of an FSD based on the feedback provided by the proposed digital tool. In this experiment, point-in-time HDR renders and false-color images complemented the assessment of sDA, DA, and ASE. The production and visualization of those point-in-time images helped the designer evaluate the spatial and lighting quality of the solutions under specific circumstances. Due to space constraints, we present two user-driven explorations to illustrate the iterative use of the tool.

Experiment 2: performance optimization

In this experiment, we tested the GDS' capability to automatically search for solutions that yield a good balance between sDA and ASE, in two phases. In the first one, we used the GDS to test the performance of

the selected optimization algorithms in advancing plausible trade-offs to the optimization problem. The analysis of the first optimization results allowed us to detect, isolate, and redefine the most sensible decision variables for a more refined optimization in the second phase. The refinement consisted of first selecting the two best performing search algorithms and, then, constraining the range of the most sensible decision variables. The restraining focused the search in areas of the solution space that yield more potential to contain high-performance candidates. In both phases, the unconstrained optimization used the following objective functions:

$$\min f(x_1, x_2, x_3) = ASE_{1000,250h}(x_1, x_2, x_3) \quad (1)$$

$$\max g(x_1, x_2, x_3) = sDA_{300/50\%}(x_1, x_2, x_3) \quad (2)$$

where x_1 , x_2 , and x_3 are the variables of the algorithm that produces the weaving FSD (see section 4.2). All optimization runs analyzed 400 solutions grouped in populations or swarms of 20.

5. RESULTS

The following presents the results per experiment.

5.1 Experiment 1 results

A designer used our GDS to explore different solutions to the problem. Based on the analysis of both ASE and sDA results, the user selected a point-of-view (POV) and a time event of interest to conduct a visualization of the proposed design with HDR renders and false-color images that mapped illuminance and luminance on the room surfaces. Fig. 3 shows the results of the initial design solution proposed by the user, which has 8 horizontal stripes (x_1), a rotation of -1.5 radians (x_2), and a reduction factor of 0.75 (x_3). The goal was to allow some view in the east façade and to channel light in the south façade by tilting the stripes towards the sky. To assess east low sun angles, the user decided to conduct a point-in-time visual analysis of a POV that overlooked the southeast corner at 9 am in Winter solstice. This initial solution reported an sDA of 74.3% and an ASE of 34.7%. The good sDA score came at the expense of admitting too much direct light.

Based on the results, the user changed the rotation of the south façade horizontal stripes (x_2) to 1.1 radians to block direct light (Fig. 4). This solution reduced ASE to the acceptable value of 15.3%, but sDA dropped to a low score of 32.3%, demonstrating the limitations of using iteration in balancing both metrics.

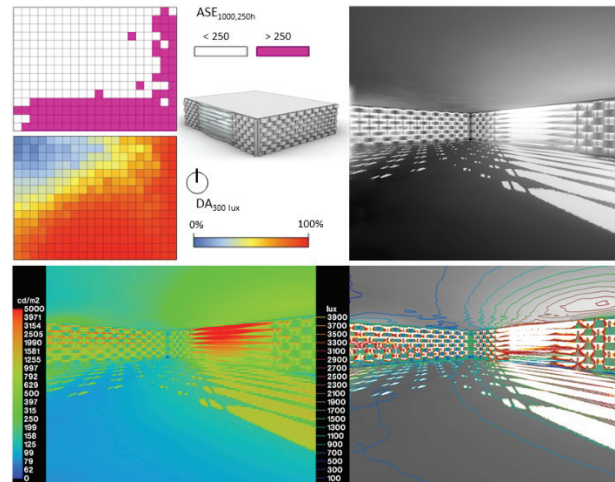


Figure 3: Initial solution. Top: DA and ASE distribution in grid of sensors. Bottom: Illuminance contour mapped on HDR render (left) and luminance false color image (right) of the select POV at winter solstice 9 am.

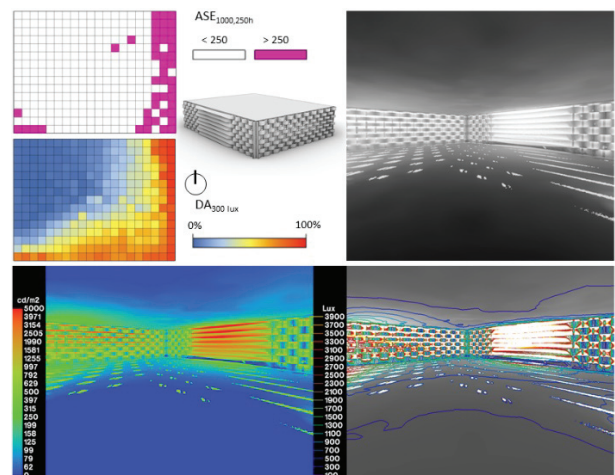


Figure 4: Alternative solution. Top: DA and ASE distribution in grid of sensors. Bottom: Illuminance contour mapped on HDR render (left) and luminance false color image (right) of the select POV at winter solstice 9 am.

5.2 Experiment 2 results

Fig. 5 compares the different search mechanisms used in the first phase of this experiment. It shows that NSGA-II outperformed OMOPSO and GPR_SPEA2, which was the least performant. Both NSGA-II and OMOPSO found solutions scoring 2 points in the LEED V4.1 Daylight Credit Option 1. NSGA-II found solutions with a better sDA score than OMOPSO.

Fig. 6 Parallel-coordinates graph maps all the solutions analyzed in terms of their decision variables, sDA, and ASE score. The figure also presents the result of an interactive filter of the solutions by acceptable ranges of sDA ($\geq 40\%$) and ASE ($\leq 20\%$).

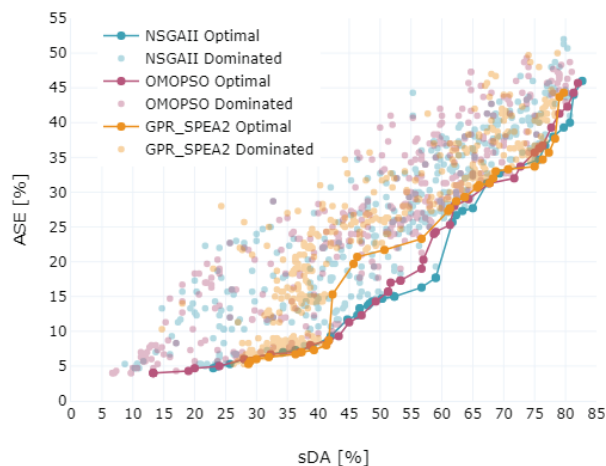


Figure 5: NSGAII, OMOPSO, and GPR_SPEA2 optimization results and their respective Pareto-fronts.

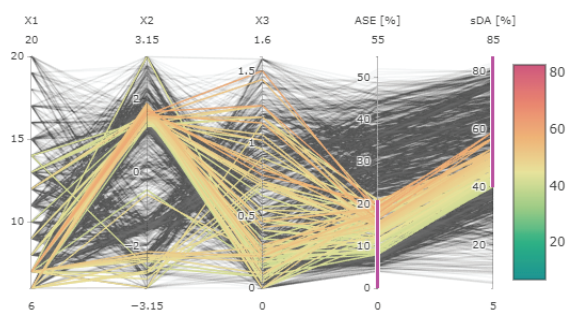


Figure 6: Parallel-coordinates analysis of the results of the first optimization phase. The filtered solutions are color-coded by sDA and are the ones that yield acceptable values of sDA and ASE.

The Parallel-coordinate visualization showed that the variable X3 (reduction factor of the east stripes) is the least influential. Therefore, the GDS can balance higher porosity levels in the east façade by controlling the size, proportion, and rotation of the south horizontal elements. The key variables are X1 (number of horizontal stripes) and X2 (rotation of the south stripes). The most successful designs in balancing ASE and sDA limit X1 to the range [6, 9] and X2 to $[33\pi/10, 64\pi/10]$.

Based on these results, the second phase of this experiment refined the optimization process by only using NSGA-II and OMOPSO and constraining X1 and X2 to the intervals mentioned above. We still selected OMOPSO since it had just a slightly worse behavior than NSGA-II in the first phase. Fig. 7 shows that both algorithms have very similar results. OMOPSO conducted broader searches, identifying solutions that yield the highest sDA scores. NSGA-II found solutions with the best balance between the two metrics, despite the small difference to analogous solutions found by OMOPSO.

The constraining of the optimization problem resulted in a higher number of solutions that yield a good tradeoff between ASE and sDA. In the first phase, OMOPSO and NSGA-II identified a total of 20 solutions eligible to score a LEED V4.1 Daylight Credit.

In the second phase, the same algorithms found 32, with 2 solutions yielding higher sDA than the best LEED V4.1 Daylight Credit qualified solution found in the first phase.

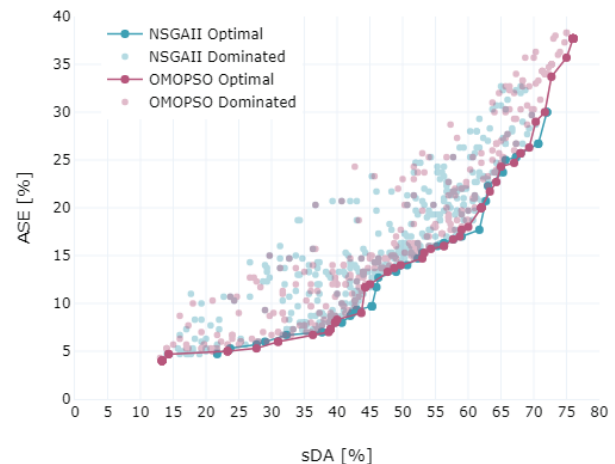


Figure 7: Results of the second optimization experiment.

6. DISCUSSION

The first experiment showed the generative and simulation capabilities of our tool by allowing users to develop design solutions based on feedback from simulation. It also revealed that an iterative use of the GDS benefits from combining quantitative data with spatial visualizations. Fig. 3 and 4 illustrate how on-demand HDR-based visualizations properly depict spatial light distribution patterns. Designers can explore this feature to complement quantitative simulation data. The experiment also showed the limitations of a user-driven iterative approach. Although the designer used the analysis feedback to propose a design alternative, the new solution was insufficient, indicating that iterative design and analysis tasks can be time-consuming and biased to the finding of few satisfactory solutions.

The second experiment showed the tool's ability to use several optimization algorithms to explore the solution space effectively. It demonstrated the benefits of conducting a two-stage optimization workflow that first compares the effectiveness of several search algorithms and isolates key decision variables to then conduct a more refined search in the second stage. The results of the first phase showed that the metaheuristic approaches (OMOPSO and NSGA-II) were better than the model-based one (GPR_SPEA2). Nevertheless, this finding does not exclude the usefulness of model-based approaches; they rather stress that design optimization is problem-dependent and that there is no universal approach. The results of the first stage also showed the benefits of using multi-objective optimization in the design of complex FSDs over user-driven approaches. Only in the first optimization, the GDS was able to find 24 eligible solutions to score at least

1 point in the LEED V4.1 Daylight Credit (Option 1) and 3 solutions qualified to 2 points. NSGA-II found the best solution with an ASE of 17.7% and an sDA of 59%. Using the GDS, we analyzed the optimization results and redefined the optimization problem by constraining the key decision variables range. As a result, the following optimization increased the pool of qualified solutions to score a LEED V4.1 Daylight credit by 60%. Moreover, all the solutions found either below ASE 10% or between 10-20% had a higher sDA score.

7. CONCLUSION

This paper presents a modular GDS that combines 3D modeling, daylight simulation, and optimization algorithms to design high-performance FSD based on complex weaving patterns. Its modular nature allows us to use the system iteratively or as a goal-oriented design tool. Our first experiment showed how a designer could use the tool to generate and evaluate the daylight performance of weaving FSD. The visualization of the different solutions showed that by manipulating the weaved elements, it is possible to shape the lighting environment in different ways, such as redirecting and diffusing daylight or even making parts of the weaving FSD glow, acting as passive luminaires (Fig. 3 and 4). Additionally, the ability of the GSD to use a wide range of black-box optimization algorithms demonstrates its versatility in deploying goal-oriented design approaches to the multi-objective problem based on sDA and ASE. The proposed GDS can compare different search algorithms and perform a sensitivity analysis of the design variables to further refine the optimization-driven process. The second experiment demonstrated that the use of such capabilities improves the effectiveness of goal-oriented design approaches.

Nevertheless, our GDS entails two main limitations. The first is the lack of embedded expert knowledge to assist the user in iterative design-analysis tasks. When used iteratively, the tool-user interaction relies exclusively on the user's expertise. The second relates to the time cost of evaluating the objective functions, which might hamper the application of the tool in real design situations. To overcome such limitations, future work contemplates the development of heuristics that effectively helps users find critical time events and POVs, such as those proposed in [14], and the use of faster daylight simulation techniques as the ones suggested in [15]. Future developments will also include the study of different complex FSD.

ACKNOWLEDGEMENTS

This work was supported by national funds through *Fundação para a Ciência e a Tecnologia* (FCT) with references UIDB/50021/2020 and PTDC/ARTDAQ/31061/2017, and by the PhD grant

under contract with FCT with reference SFRH/BD/128628/2017.

REFERENCES

1. Khoroshiltseva, M., D. Slanzi and I. Poli, (2016). A Pareto-based multi-objective optimization algorithm to design energy-efficient shading devices. *Applied Energy*, 184: p. 1400–1410.
2. Gagne, J., and M. Andersen, (2012). A generative facade design method based on daylighting performance goals. *Journal of Building Performance Simulation*, 5(3): p. 141–154.
3. Wortmann, T., A. Costa, G. Nannicini and T. Schroeffer, (2015). Advantages of surrogate models for architectural design optimization. *Artificial Intelligence for Engineering Design, Analysis and Manufacturing*, 29(4): p. 471–481.
4. IESNA, I, (2012). LM-83-12 IES Spatial Daylight Autonomy (sDA) and Annual Sunlight Exposure (ASE).
5. Council, UGB, (2020). LEED v4.1 for building design and construction.
6. L Liu, S., X. Meng and C. Tam, (2015). Building information modeling based building design optimization for sustainability. *Energy and Buildings*, 105: p. 139–153.
7. Manzan, M., (2014). Genetic optimization of external fixed shading devices. *Energy and Buildings*, 72: p. 431–440.
8. Kazanasmaz, T., LO. Grobe, C. Bauer, M. Krehel and S. Wittkopf, (2016). Three approaches to optimize optical properties and size of a South-facing window for spatial Daylight Autonomy. *Building and Environment*, 102: p. 243–256.
9. Caetano, I. and A. Leitão, (2019). Weaving Architectural Façades: Exploring algorithmic stripe-based design patterns. In *Proceeding of the 18th CAAD Futures Conference*. Daejeon, South Korea, 1023–1043.
10. Carlucci, S., Cattarin, G., Causone, F. and L. Pagliano (2015). Multi-objective optimization of a nearly zero-energy building based on thermal and visual discomfort minimization using a non-dominated sorting genetic algorithm (NSGA-II). *Energy and Buildings*, 104: p. 378–394.
11. Durillo, JJ., J. García-Nieto, AJ. Nebro, CA. Coello, F. Luna and E. Alba, (2009). Multi-objective particle swarm optimizers: An experimental comparison. *Lecture Notes in Computer Science*, 5467 LNCS: p. 495–509.
12. Wetter, M. and J. Wright, (2004). A comparison of deterministic and probabilistic optimization algorithms for nonsmooth simulation-based optimization. *Building and Environment*, 39(8): p. 989–999.
13. Santos, L., A. Leitão and L. Caldas, (2018). A comparison of two light-redirecting fenestration systems using a modified modeling technique for Radiance 3-phase method simulations. *Solar Energy*, 161: p. 47–63.
14. Santos, L. and L. Caldas, (2018). Assessing the Glare Potential of Complex Fenestration Systems: A Heuristic Approach Based on Spatial and Time Sampling. In *Proceedings of PLEA 2018*. Hong Kong, 445–451.
15. Jones, NL. And CF. Reinhart, (2015). Validation of GPU Lighting Simulation in Naturally and Artificially Lit Spaces. In *Proceedings of Building Simulation 2015*. Hyderabad, India, 1229–1236.

Hygrothermal and Mold Modeling of Building Envelopes Under Future Climate Conditions

SARA TEPFER¹, HOLLY SAMUELSON¹

¹Harvard University Graduate School of Design, Cambridge, MA, USA

ABSTRACT: *Climate-responsive design now includes design for future climate, which involves design for gradually changing climate conditions. Here we examine the importance of an overlooked aspect of climate-adaptive design: the susceptibility of residential lightweight timber construction to mold growth in future climate conditions. This paper seeks to understand the hygrothermal performance of newly built, code-compliant residential building envelopes under future climate conditions across U.S. climate zones. Combined hygrothermal and mold modeling is performed on a typical, code-compliant exterior residential wall assembly, using morphed future climate data in representative cities in three climate zones. The results suggest widespread mold issues under future climate conditions. Mold risk was identified in each of the three climate zones tested (ASHRAE climate zones 4A, 5A, and 6A). Mold issues emerge as early as the mid-21st century for climate zones 4A and 5A. These findings suggest the need for the consideration of climate adaptation and resilience in the development of building codes.*

KEYWORDS: *Hygrothermal simulation, mold growth modeling, health, climate adaptation, resilience*

1. INTRODUCTION

Our climate is warming, historically defined climate zones are shifting, extreme weather events are increasingly frequent and severe, and these changes affect the thermal and hygrothermal performance of our buildings. The scope of climate-responsive design now includes design for future climate, which means design for gradually changing and increasingly severe climatic conditions [1]. Urban areas across the United States (U.S.) are expected to become warmer due to climate change [2], with North American populations living in temperate climates expected to suffer from an increase in the frequency and severity of extreme heat events [3]. While our codes and regulations remain largely based on historical data [1], our approach to the design of buildings, including envelope design, will need to evolve as the climate warms [4,5].

Wall cavity surfaces vulnerable to condensation can facilitate the conditions necessary for mold growth [5,6]. The geographical locations and types of cavity constructions that are most vulnerable will change as our climate warms [5]. Molds grow everywhere there are nutrients and biologically available moisture. Building materials are included among the many potential substrates for mold growth. Wall cavities in moisture-damaged homes can become a virtually unlimited feedstock upon which fungal growth can be established. To avoid mold growth, building design must meet the needs of the regional climatic conditions. “Imported” design strategies do not perform well in new climates [6]. Though limited,

studies show that buildings will face greater risk of rot-decay damage if located in one of the many climates that will experience warmer, wetter weather [5].

Mold growth in wall cavities causes moisture-induced decay, which, under certain conditions, can negatively affect structural integrity over time. Such decay problems in buildings are most often the result of moisture damage, which can result from water leakage, convection of damp air and moisture condensation, and structural moisture accumulation. High wood moisture content and persistent high humidity exposure pose high risks for bio-deterioration of unprotected timber [7]. Damage due to biological action is the main mechanism that affects wood durability in building structures [8]. It is estimated that approximately 90% of damage in residential wood buildings is the result of temperature and moisture effects [9].

Furthermore, mold growth has adverse effects on indoor air quality. Occupants may be exposed to mold growth in wall cavities, and such exposures can have health implications. Numerous studies have shown that water-damaged homes are associated with adverse respiratory effects [10-12]. Though mechanisms and processes for fungal spores to move through building envelopes are complex [13], one source of microbial exposure may be attributed to the migration of spores through penetrations in wall constructions [14]. Additionally, asthma severity can be affected by microbial exposures: exposure to allergenic fungi in homes has been associated with a

36-48% exacerbation of current asthma symptoms [15].

Given this context, this paper seeks to understand the hygrothermal performance of newly built, code-compliant residential building envelopes under future climate conditions across U.S. climate zones. The results of this study may help practitioners understand retrofit needs and approaches as our climate changes, as well as effects of climate change on anticipated building service lives. This study poses the following hypotheses: (1) Certain climate zones are at higher risk than others for mold growth in wall constructions; (2) Wall constructions that perform well under historic conditions will show mold growth under future conditions.

2. METHODOLOGY

This methodology, which expands on past work [20], involves a three-step process. First, a morphing process is used to convert typical meteorological year (TMY) weather files to future weather files. Second, a hygrothermal simulation is performed on an exterior wall assembly in WUFI Pro 6. Third, simulated temperature and moisture data from the hygrothermal model are used to simulate mold growth potential using the VTT model [16-18]. The resulting 10-year mold index time series is used to evaluate how climate affects mold growth.

2.1 Future Weather Files and Climate Selection

As outlined above, the first step in this study is to morph a TMY weather file to future conditions. The

Weather File Module of the WeatherShift™ tool [19] is used to perform the morphing procedure. TMY files are composed of twelve “typical” months that comprise a “typical” year. These are derived from historical weather data using statistics. The WeatherShift™ tool takes the TMY data as an input and “morphs” each variable, using several relatively simple transformations. Because they are based on historical data, the morphed data are meteorologically realistic. However, because most of the transformations preserve historical variability, the morphed data may understate changes in future extremes [19].

The morphing technique transforms historical time series data based on projected changes in the monthly averages of several climatic variables. Future values of these variables are uncertain, particularly at local scales; thus, the offset values are calculated for a group of climate predictions that are generated from the Coupled Model Intercomparison Project Phase 5 (CMIP5). The CMIP5 models are run for the Intergovernmental Panel on Climate Change (IPCC) Fifth Assessment Report (AR5) Representative Concentration Pathways (RCPs). Offsets are calculated for several future time periods (2026-2045, 2056-2075, and 2080-2099) for both the 4.5 and 8.5 RCPs. A cumulative frequency distribution (CFD) of the offset in mean monthly temperature is constructed for each combination of time period and RCP. It is based on the percentile rankings of the projections within the initial group of climate predictions [19]. This study uses the RCP 8.5 scenario and several different percentiles.

Table 1: Case study cities

City [Code reference]	ASHRAE Climate Zone	Predominant Exterior façade for new construction [27]	Code-required R-Value (m ² ·K)/W [h·ft ² ·F /BTU]	Vapor retarder	Continuous air barrier
Baltimore [2015 IECC]	4A	Vinyl	3.5 or 2.3 + 0.9 continuous [20 or 13 + 5 continuous]	Code- required	Code- required
Raleigh [2015 IECC*]	4A	Vinyl	2.6 or 2.3 + 0.4 continuous [15 or 13 + 2.5 continuous]	Code- required	Code- required
Boston [2015 IECC]	5A	Vinyl	3.5 or 2.3 + 0.9 continuous [20 or 13 + 5 continuous]	Code- required	Code- required
Chicago [2019 Chicago Bldg. Code]	5A	Vinyl	3.5 or 2.3 + 0.9 continuous [20 or 13 + 5 continuous]	Code- required	Code- required
Columbus [2019 Res. Code]	5A	Vinyl	3.5 or 2.3 + 0.9 continuous [20 or 13 + 5 continuous]	Code- required	Code- required
Omaha [IBC 2018*]	5A	Vinyl	3.5 or 2.3 + 0.9 continuous [20 or 13 + 5 continuous]	Code- required	Code- required
Milwaukee [WI Uniform Dwelling Code]	6A	Vinyl	3.5 or 2.3 + 0.9 continuous [20 or 13 + 5 continuous]	Code- required	Code- required
Minneapolis [IECC 2012*]	6A	Vinyl	3.5 or 2.3 + 0.9 continuous [20 or 13 + 5 continuous]	Code- required	Code- required

* Plus amendments

While the WeatherShift™ tool is able to morph most TMY variables, rainfall data are not projected.

These data are crucial for hygrothermal simulation [20]. Therefore, rainfall data were manually extracted from the historical dataset and added, unchanged, to

the projected dataset via Excel. This is a conservative approach.

Cities from ASHRAE climate zones 4A, 5A, and 6A [21] were selected for this study, as they are mixed-humid climates that will see increased temperature and absolute humidity [22-25]. Average monthly temperatures for cities in each of the three selected climate zones are shown in Figure 1. Selected cities and their corresponding 2020 code requirements are shown in Table 1. These code requirements were used to develop a standard test wall assembly for each city.

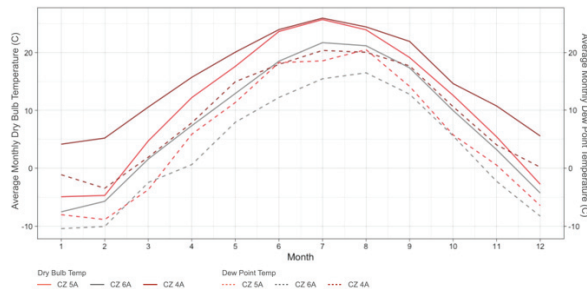


Figure 1: Average monthly temperatures for representative cities in each of the three climate zones (4A, 5A, and 6A).

2.2 Hygrothermal Model

The second step uses hygrothermal simulation to understand heat and moisture transport through each assembly. The dynamic hygrothermal simulation software package WUFI Pro 6 is used to perform this simulation. This model is well validated [27-28].

The program considers three groups of parameters: the component, including the envelope assembly, orientation, surface transfer coefficient, and initial conditions; the control, including the calculation period and related parameters; and the boundary conditions, including hourly indoor and outdoor temperature and relative humidity.

Hygrothermal outputs from WUFI were used to assess temperature and moisture changes at various points within the wall section.

As shown in Figure 2, the wall section includes fiberglass insulation between standard Douglas Fir studs. The total thickness of the wall is 17.4 cm, with a U-value of 0.22 W/m²K (R-Value of 24 ft²°F h/Btu). Table 2 provides properties for each material. A north orientation was used for the wall, and the initial condition of the assembly is 80% relative humidity and an initial temperature of 20°C. These initial conditions are consistent with previous studies [20].

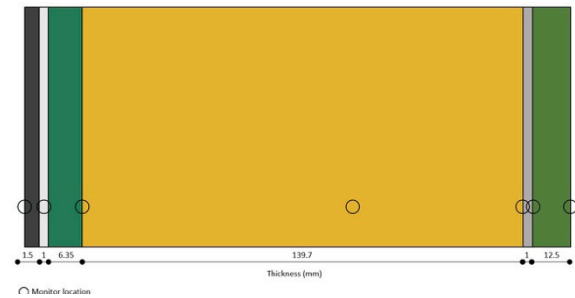


Figure 2: Wall section, including the following materials from left (exterior) to right (interior): vinyl siding (1.5mm), air barrier (1mm), oriented strand board (6.35mm), fiberglass batt insulation (139.7mm), 1-perm vapor retarder (1mm), gypsum board (12.5mm).

Table 2: Materials Data

Material	Thermal Conductivity [W/mK]	Density [kg/m ³]	Specific Heat [J/kgK]
Vinyl siding	0.1696	829.0	2300
Air barrier	0.047	1.298	999.8
Polyolefin membrane	2.3	65	1500
Oriented Strand Board	0.084	575.1	1879.9
Fiberglass batt	0.035	19.22	841.5
Vapor retarder	2.3	130	2300
Gypsum board	0.163	850.6	870.9

Ten-year hygrothermal simulations were run in WUFI Pro, to confirm the equilibrium mold growth condition. The indoor climate follows ASHRAE 160 standards [29], such that indoor conditions were maintained between 21.1°C and 23.9°C via mechanical heating and cooling. Indoor moisture gains were specified at 0.000105 kg/s, and the maximum indoor relative humidity is capped at 50%.

2.3 Mold Model

The third step is to simulate mold growth. The VTT model [16] was used to simulate mold growth based on hygrothermal data from WUFI Pro. This model is derived from experimental studies on pine sapwood and spruce, and it was later expanded to include other building materials [30]. The simulation accounts for mold growth and decay based on dry-bulb temperature, relative humidity, and the material's sensitivity to mold growth. Model validation and details have been published widely [30-32]. The model calculates mold index (MI) hourly. The MI ranges from zero, which represents no growth, to six, which represents 100% surface coverage. The MI levels are shown in Table 3.

Table 3: The VTT Mold Index [17]

MI	Description
0	No growth.
1	Some growth detected only with microscopy.
2	Moderate growth detected with microscopy
3	Some growth detected visually.
4	Visually detected coverage >10%.
5	Visually detected coverage >50%.
6	Visually detected coverage 100%.

Mold growth calculations are performed in WUFI Mold Index VTT 2.0, which uses temperature and relative humidity outputs from WUFI Pro. Conditions are assessed at various points within the wall, with the interior face of the insulation cavity showing the highest potential for growth. Based on this, mold growth modeling is performed for the interior face of the insulation cavity, at the timber framing.

Lightweight timber residential walls in the US are typically framed with Douglas Fir, which is included in the VTT classification of “pine sapwood”. The default sensitivity and specifications of pine are therefore used for subsequent mold index simulations.

3. RESULTS

Figures 3 and 4 show the results of the mold simulations. Figure 3 shows a 10-year time series for each city under different warming percentiles from the Weathershift™ cumulative frequency distributions; TMY3, 50th percentile 2080-2099, and 95th percentile 2080-2099 scenarios are shown.

In contrast, Figure 4 shows the equilibrium mold indices, which are extracted from the end of the ten-year simulations in Figure 3, at different periods of time and under different warming percentiles.

3.1 Impacted Climate Zones

As shown in Figure 3, the performance of the interior of the insulation cavity is as expected, i.e. no sustained mold growth, when using present-day weather data. A low MI (corresponding to minor mold growth detectable only with microscopy [16]) occurs only seasonally, which is considered acceptable [32].

The results change when modeling with morphed weather data. Under the highest warming scenario (95th percentile), an MI above 3, which corresponds to visible mold, is observed in every climate zone and in every city except Minneapolis. This result occurs because moisture from the warm, humid outdoor air builds up within the envelope. The higher temperature difference between the outdoor air and the cool interior air leads to moisture accumulation.

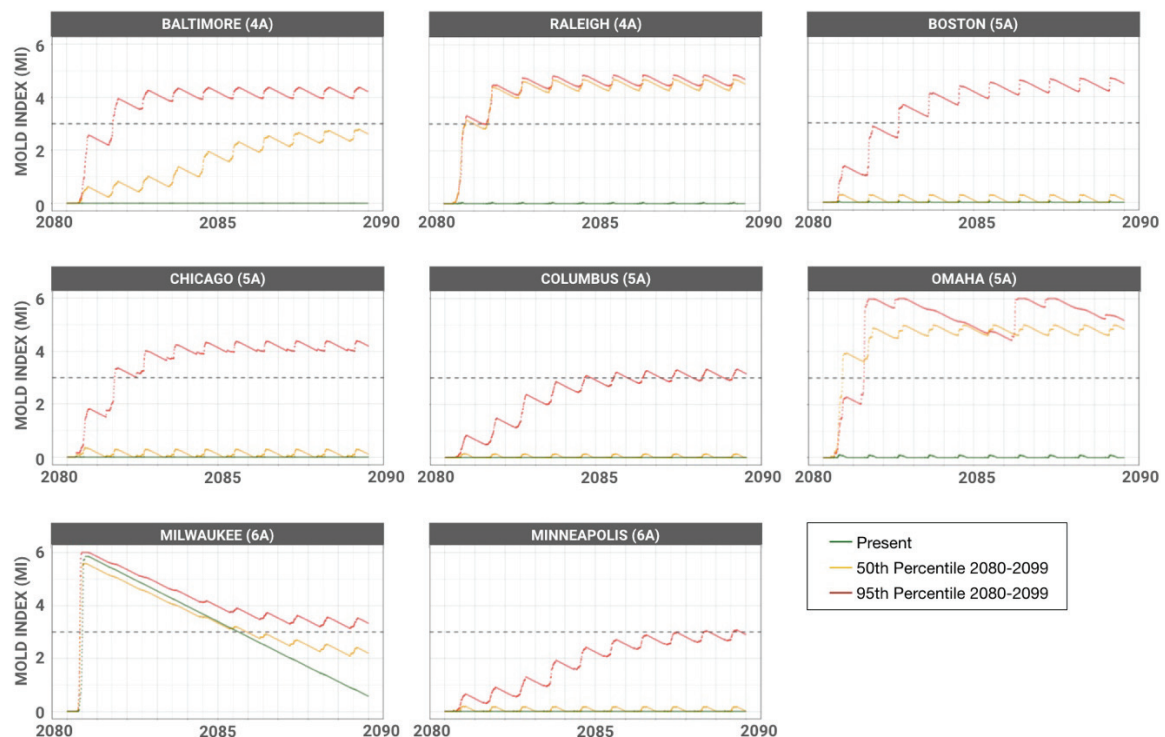


Figure 3: 10-year time series Mold Index for each case study city under different warming percentiles drawn from the Weathershift™ cumulative frequency distributions.

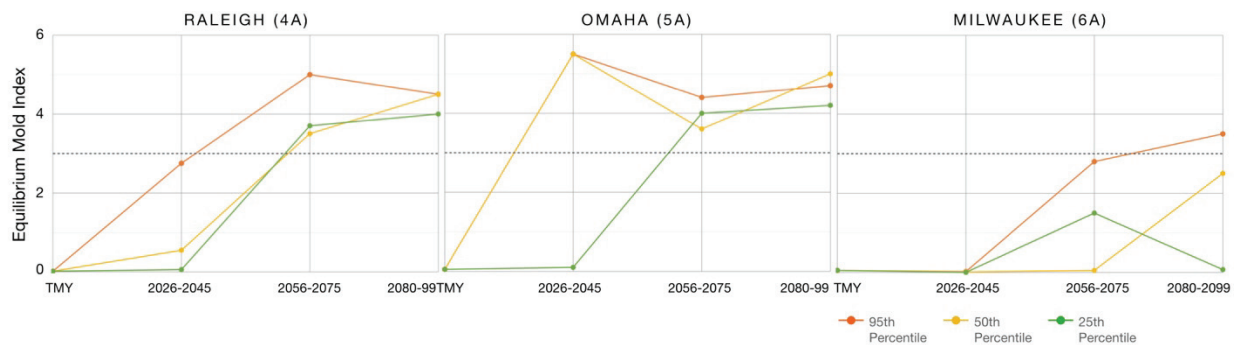


Figure 4: Equilibrium mold indices during different periods of time and under different warming percentiles.

The variability within climate zones is likely observed for two reasons. First, the nature of the rain data strongly affects the hygrothermal and mold modeling outputs [20]. This may explain the observed differences within climate zones, such as the difference between Boston and Columbus, which are both in climate zone 5A. Second, the assumed initial conditions strongly affect the early MI calculations. The initial conditions were assumed to have an 80% relative humidity and 20°C temperature; however, these assumptions may be incorrect, and the conditions need to self-correct over time. This is why Milwaukee appears to have significant mold growth in the first few months/years of simulation, while arriving at a different equilibrium MI after ten years. This is an artifact of the initial assumptions.

2.4 Predicted Onset

Figure 4 shows the predicted onset of mold growth for three representative cities. Equilibrium MI represents the average MI at the end of the ten-year simulation. As Figure 4 shows, visible mold issues begin in the mid-21st century for both climate zones 4A and 5A, regardless which warming percentile is used. Climate zone 6A does not become sufficiently warm until 2080-2099, and even then, the projected MI is less than those predicted for climate zones 4A and 5A.

The results of this analysis also suggest the significant variability among the different warming percentile scenarios generated by Weathershift™. This is shown in both Figure 3 and Figure 4.

4. DISCUSSION

This study confirms the first hypothesis, which stated that certain climate zones are at higher risk than others for mold growth in wall constructions in changing climates. The study indicates that climate zones 4A and 5A are particularly vulnerable to significant mold growth in the building envelope type tested, while 6A is less vulnerable. We predict that dry (climate type B) and marine (climate type C) climates will not have mold risks, even in future climate conditions, as walls in these climate types will have the opportunity to dry, unlike climate type A (humid). Further work is needed to confirm these predictions.

This study also confirms the second hypothesis, which predicted that wall constructions that perform well under historic conditions will show mold growth under future conditions.

The future hygrothermal and mold problems observed in this study are sustained and extreme versions of what already occurs during the summer in mixed-humid climates. In these mixed climates, vapor barriers are placed on the interior (warm side) of the exterior wall construction to prevent warm, humid air from reaching the insulation layer during the winter. This approach is ill-suited for summer, when hot, humid air is instead on the exterior of the envelope, and migrates inward, into the cool wall assembly (assuming air conditioning). Sometimes this results in condensation in the wall, but these events are sufficiently brief and infrequent that sustained mold growth is not an issue, as observed in the analysis of present-day data in this study. However, when summer conditions become more frequent, sustained, and extreme, as they will in the future, the suboptimal envelope design provides adequate conditions for sustained mold growth, as we have observed here.

4.1 Future Work

This and previous studies [20] show the sensitivity of the analysis to climate data. Further work is needed to identify the sensitivity of the results to specific climate inputs and to develop more accurate ways of morphing currently missing parameters (i.e., rain).

Further research is also needed to understand the sensitivity of the hygrothermal and mold analysis to other parameters in the model, such as indoor climate conditions (i.e., building operations), construction parameters (e.g., choice of materials and insulation levels), and other numerical parameters of the simulations.

Additionally, while this research has identified future susceptibility to sustained mold growth, the scale of the problem has not been quantified, nor have mitigation techniques been identified and assessed. Each of these questions remain for future work.

5. CONCLUSION

This study demonstrates that lightweight timber building envelopes constructed to today's code requirements are not well-adapted for future conditions across several climate zones. This finding implicates a large number of single-family residential dwellings in the U.S and suggests the need for the consideration of climate adaptation and resilience in the development of building codes.

ACKNOWLEDGEMENTS

This work was supported in part by a Harvard University Research Enabling Grant and by the Harvard Graduate School of Design. The authors would like to thank Pamela Cabrera for her insight.

REFERENCES

1. de Wilde, P., Coley, D., (2012). The Implications of a Changing Climate for Buildings. *Building and Environment*, 55: p.1-7.
2. Bartos, M., Chester, M., (2014). *Assessing Future Extreme Heat Events at Intra-Urban Scales: a Comparative Study of Phoenix and Los Angeles*. Center for Earth Systems Engineering and Management, Arizona State University.
3. Meehl, G., Tebaldi, C., (2004). More Intense, More Frequent, and Longer Lasting Heat Waves in the 21st Century. *Science*, 305(5686): 944.
4. Phillipson, M., Emmanuel, R., Baker, P., (2016). The Durability of Building Materials under a Changing Climate. *Wiley Interdisciplinary Reviews: Climate Change*, 7(4).
5. Almas, A., Lisø, K., Hygen, H., Øyen, C., Thu, J., (2011). An Approach to Impact Assessments of Buildings in a Changing Climate. *Building Research and Information*, 39(3): p. 227-38.
6. Small, B., (2003). Creating Mold-Free Buildings: A Key to Avoiding Health Effects of Indoor Molds. *Archives of Environmental Health: An International Journal*, 58(8): p.523-27.
7. Viitanen, H., Vinha, J., Salminen, T., Ojanen, R., et al. (2010). Moisture and Bio-deterioration Risk of Building Materials and Structures. *Journal of Building Physics*, 33(3): p. 201-24.
8. Nofal, M. Kumaran, K., (2011). Biological Damage Function Models for Durability Assessments of Wood and Wood-Based Products in Building Envelopes. *European Journal of Wood and Wood Products*, 69(4): p. 619-31.
9. Zabel, R., Morrell, J., (1992). *Wood Microbiology: Decay and its Prevention*. San Diego: Academic Press.
10. Prussin, A., Marr, L., (2015). Sources of Airborne Microorganisms in the Built Environment. *Microbiome* 3(1): 78.
11. Heseltine, E., Rosen, J., (2009). *WHO Guidelines for Indoor Air Quality: Dampness and Mould*. Copenhagen: World Health Organization.
12. Dales, R., Zwanenburg, H., Burnett, R., Franklin, C., (1991). Respiratory Health Effects of Home Dampness and Molds Among Canadian Children. *American Journal of Epidemiology*, 134: p. 196-203.
13. Rao, J., Fazio, P., Bartlett, K., Yang, D., (2009). Experimental Evaluation of Potential Transport of Mold Spores from Moldy Studs in Full-Size Wall Assemblies. *Building and Environment*, 44(8): p. 1568-77.
14. Muise, B., Seo, D., Blair, E., Applegate, T., (2010). Mold Spore Penetration Through Wall Service Outlets: a Pilot Study. *Environmental Monitoring and Assessment*, 163(1-4): p. 95-104.
15. Sharpe, R. Bearman, N., Thornton, C., Husk, K., Osborne, N., (2015). Indoor Fungal Diversity and Asthma: a Meta-Analysis and Systematic Review of Risk Factors. *Journal of Allergy Clinical Immunology*, 135: p. 110-22.
16. Hukka, A., Viitanen, H.A. (1999). A mathematical model of mould growth on a wooden material. *Wood Science and Technology*, 33(6): p. 475-485.
17. Viitanen, H., A. Hanhijärvi, A. Hukka, K. Koskela. (2000). Modeling mould growth and decay damages. *Healthy Buildings, Espoo, August 6-10*, 3:341-346.
18. Viitanen, H., Ojanen, T. (2007). Improved model to predict mold growth in building materials. *Thermal Performance of the Exterior Envelopes of Whole Buildings X – Proceedings CD*, 2-7.
19. Dickinson, R., Brannon, B. (2016). Generating Weather Files for Resilience. *Proceedings of the Passive Low Energy Architecture Conference*. Los Angeles.
20. Cabrera, P., Samuelson, H., Kurth, M. (2019) Simulating Mold Risks under Future Climate Conditions. *Proceedings of Building Simulation*. Rome, Italy.
21. ASHRAE. (2019). ASHRAE 90.1-2019: Energy Standard for Buildings Except Low-Rise Residential Buildings.
22. Brown, P.J., DeGaetano, A.T. (2013). Trends in US surface humidity, 1930-2010. *Journal of Applied Meteorology and Climatology*, 52(1), 147-163.
23. Dai, A. (2006). Recent climatology, variability, and trends in global surface humidity. *Journal of Climate*, 19(15), 3589-3606.
24. Trenberth, K.E., Jones, P.D., Ambenje, P., Bojariu, R., Easterling, D., Klein Tank, A., et al. (2007). Observations: surface and atmospheric climate change. Chapter 3. *Climate change*, 235-336.
25. Willett, K.M. (2007). *Creation and analysis of HadCRUH: a new global surface humidity dataset*. (Doctoral dissertation, University of East Anglia).
26. U.S. Census Bureau. (2018). Survey of Construction Microdata Files. Accessed 12 February 2020.
27. Alev, Ü., & Kalamees, T. (2016). Avoiding mould growth in an interiorly insulated log wall. *Building and Environment*, 105, 104-115.
28. Mundt Petersen, S., & Harderup, L-E. (2014). A method for blind validation of hygrothermal calculation tools. In M. Quattrone, & J. Vanderley (Eds.), *Proceedings XIII DBMC - XIII International Conference on Durability of Building Materials and Components* (pp. 624-631).
29. ASHRAE. (2016). *ASHRAE 160-2016: Criteria for Moisture-Control Design Analysis in Buildings*.
30. Ojanen, T., Viitanen, H., Peuhkuri, R., et al. (2010). Mold-growth modeling of building structures using sensitivity classes of materials. *Proceedings Buildings XI, Florida*.
31. Vereecken, E., Roels, S. (2012). Review of mould prediction models and their influence on mould risk evaluation. *Building and Environment*, 51, 296-310.
32. Gradedi, K., Labonnote, N., Time, B., & Köhler, J. (2018). A probabilistic-based methodology for predicting mould growth in façade constructions. *Building and Environment*, 128, 33-45.

Unlocking the potential - Low-Energy Dwelling with Heat Pump. Investigating their multiple benefits, and how to increase adoption rates

SHANE COLCLOUGH¹, NEIL HEWITT¹, PHILIP GRIFFITHS¹

¹Ulster University, Newtownabbey, Co. Antrim, UK

ABSTRACT: *This paper is novel in that it is a first attempt to analyse the direct and indirect costs and benefits of constructing a 3-bed social house dwelling to low-energy standards in Northern Ireland. It uses data on direct construction and energy costs and augments this with estimates for some of the indirect benefits for three potential low energy upgrade for the real scheme of new dwellings. While estimation of Indirect Benefits is by its nature imprecise, the analysis provides fresh insights and indicates that a financial argument exists for constructing to low-energy standards at both societal and individual levels. However the analysis also demonstrates that the decision-maker is dis-incentivised, leading to poor adoption rates for the low energy, carbon efficient dwellings. This has potential policy implications for UK social housing given the conflict with the UK's stated decarbonising objectives.*

KEYWORDS: *Passive House, Low Energy Dwelling, Social House, Financial Analysis, Multiple Benefits*

1. INTRODUCTION

The benefits of energy efficient housing are multiple and varied, and appear to be an obvious solution for the provision of current and future sustainable buildings. However, despite possessing a multitude of benefits, low-energy, for example houses built to the Passive House (PH) standard, have not been universally deployed. This paper inquires as to why this is so, by carrying out a holistic cost and benefit analysis by including estimated economic value for a range of indirect benefits. By looking beyond energy cost savings, it aims to inform discussion and identify the means of unlocking the potential of low-energy home provision.

The paper quantifies the energetic and financial benefits of low-energy and PH in combination with low temperature Heat Pumps (HP), by optimising the design for a real case study building in the UK. Three potential energy upgrade options for the new-build three bedroomed 94m² social house are presented. A detailed energy, cost and direct benefits analysis is carried out based on the UK's SAP energy rating software and the Passive House Planning Package (PHPP), for the three options including that of a PH with HP. The paper applies the 'Multiple Benefits' (MB) framework [1] to enable comparison of the indirect financial benefits for current and future building regulations. It then uses the Multi-Beneficiary Analysis (MBA) to determine the costs and benefits for the involved stakeholders, based on a number of seminal studies identified in the literature. It should be noted however that there is a paucity of published analysis of certain benefits.

The analysis indicates that in order to realise the considerable potential of low energy social housing,

tailored government support is required (and justified) to address the "split incentives" dilemma which the analysis has unveiled and quantified.

2. METHOD

2.1 Overview

The analysis was carried out on a scheme of 12 x 95 m² properties as described in [2] which are planned to be constructed to the optional social housing low-energy Energy Efficiency Multiplier (EEM) standard in Northern Ireland (NI). This is a voluntary standard for which Housing Associations (HA) receive a multiplier of 1.03 on the agreed costs of delivering the standard dwelling (equivalent to approximately 50% of the cost differential of achieving the higher energy efficiency standard).

The EEM Standard is equivalent to the current English building regulations [3] while the PH [4] standard is similar to the Change Committee's (CCC) recommended standard for the UK. For the PH dwelling, two different heating systems (Gas and electric HP) are considered.

The four energy efficiency standards were analysed and compared, with all but the base case qualifying for the EEM incentives for the Housing Association (HA):

1. Base Case of current NI minimum building regulations – assessed with SAP 2009 – "Base SAP 2009".
2. The English Building Regulations standard equivalent to the base EEM standard (assessed with SAP2012 and referred to as "EEM" below).
3. The PH standard using gas fired central heating- "PH (Gas)".
4. The PH standard heated with a HP integrated into the Heat Recovery and Ventilation system

“PH (Heat Pump)” is a design which is novel in NI but has proven successful elsewhere [5].

2.2 Energy Consumption

All four variants are presented in Table 1 with the predicted space heating demand calculated using both the SAP rating system and the PHPP software. Table 1 shows that in the case of the EEM and PH dwellings, the building fabric is considerably more energy efficient than the dwelling complying with the minimum building regulations (see PHPP output in the bottom line). While the standard house requires 77.6 kWh/m²/a for space heating and the EEM requires 44.6 kWh/m²/a while the 2 PH variants only require 18.2 and 18.9 kWh/m²/a.

Item	Base SAP 2009	EEM	PH (Gas)	PH (Heat Pump)
Floor (W/m ² ·K)	0.2	0.12	0.1	0.1
Walls (W/m ² ·K)	0.21	0.17	0.18	0.18
Roof (W/m ² ·K)	0.14	0.09	0.08	0.08
Windows (W/m ² ·K)	1.4	1	0.75	0.75
Doors (W/m ² ·K)	1.6	1	0.75	0.75
Average U Value	0.71	0.476	0.372	0.372
Ventilation	Trickle Vents, Mech extract	Vertaxia MVHR	Nilan MVHR	Nilan MVHR
Air Permeability	5 m ³ /m ² ·hr ⁻¹	3.5 m ³ /m ² ·hr ⁻¹	0.35 ach ⁻¹	0.35 ach ⁻¹
Air Permeability	5	3.5	0.35	0.35
Heating	Condensing Gas Boiler	Condensing Gas Boiler	Condensing Gas Boiler	MVHR & integrated HP
Renewables	none	2kW PV Panels	1.5 kW PV Panels	900W PV panels
SAP Space Htg (kWh/m ² /a)	36	26	10.6	12.85
EPC	B83	A92	A92	A93
PHPP (kWh/m ² /a)	77.6	44.6	18.2	18.9

Table 1 Energy Specific Parameters for Social House dwelling

2.3 Costs

The costs for each of the upgrade options considered comprise the year one costs (the cost of upgrading to the EEM standard & PH standard in year one).

2.4 Quantification of Benefits

The MB and Multiple Beneficiary Analysis (MBA) captures the overall benefits and assigns them to the three beneficiaries – tenant, HA and government/common purse. This enables an analysis of not only the financial benefits for the four variants of the case study dwelling, but also to whom they accrue.

Direct benefits (reduced energy costs and associated carbon taxes) and indirect benefits accrue [1] (increased capital and rental value, benefits to the local economy and the financial benefits associated with improved health). While the quantification of the indirect benefits (increased capital & rental value and benefits to the local economy) is difficult and imprecise, their exclusion from analysis would lead to an underreporting of the full economic benefit for policy makers.

3. RESULTS

3.1 Extra construction costs

Table 2 gives the breakdown of the base costs and additional costs for each of the higher energy performance variants [2]. All benefit from the EEM financial incentive of 3% of the construction costs and so

the HA will benefit from a 3% contribution based on the assumed construction cost of £110,000 (i.e. £3,300).

Item	Base SAP 2009	EEM (Gas)	PH (Gas)	PH (Heat Pump)
Floor	5,030	368	892	892
Walls	20,019	441	263	263
Roof	7,000	112	260	260
Windows & Doors	4,155	435	3,149	3,149
Mech & Electrical (excl renewables)	11,900	-	-	1,800
Renewables	-	3,020	2,020	1,270
Ventilation	-	2,980	2,980	2,980
Airtightness	940	-	784	534
Construction cost differential	-	7,356	10,348	11,148
Preliminaries	-	-	-	2,523
PH - Optional extras - Certification	-	-	1,100	1,100
Total Extra Cost incl Certification	-	7,356	11,898	10,175
Total Extra Cost excl certification	-	7,356	10,798	9,075

Table 2 Cost differential for energy influencing elements per three bed social house variants

The extra cost of upgrading to the EEM standard (in year one) is calculated at £7.4k.

The government contributes £3.3k via the EEM incentive, and the HA contributes the remaining £4.1k. It is assumed that the HA will have to meet the full cost of upgrading in year 20 in order to meet the net carbon commitments. The extra costs of constructing the dwelling to the PH standard are:

1. Integrated HP/HRV system (£9.1k).
2. Traditional gas central heating (£10.8k)

3.2. Benefits – EEM / English Building Regulations

Heating Energy savings. Due to the upgrade in the building standard from the Base Case (BC) to the EEM specification, the space heating energy consumption reduces by 28% from 36 to 26 kWh/m²/a (based on the SAP rating), or from 77.6 to 44.6 kWh/m²/a (47%) based on the Passive House Planning Package (PHPP) predictions - Table 3. The two software packages (PHPP and SAP) provide different predictions due to their different assumptions. The savings associated with the improved EEM standard range from £1,463 to £4,829, (depending on the space heating energy consumption prediction software employed) accrue to the tenant (Table 5).

Calculation Methodology	Spec energy consn (kWh/m2/a)	EEM	Extra Consumption (BC Vs EEM)		SpC Htg Cost (Gas) (£/a)	Min/Max Cost Savings (£)
SAP	36	26	10	950	73.18	1463.51
PHPP	77.6	44.6	33	3135	241.48	4829.58

Table 3 EEM Minimum and Maximum Energy Consumption Cost Savings

Given that the cost differential for upgrading to the EEM standard is £7,356, the simple payback period is approximately 100 years (based on the SAP annual space heating cost reduction of £73.18), or 30 years (based on the PHPP annual space heating cost reduction of £241

.48). However, this payback does not recognise the extra indirect multiple benefits which accrue:

Carbon emissions savings

Table 4 shows that carbon emissions for the base case total 17.26 tonnes for the gas heating system, and 4.79 tonnes in the case of the same dwelling built to the EEM standard, representing a saving of 12.47 tonnes (equivalent to £947 at a potential cost of £76 per tonne[6]) over the 20-year period). Based on the PHPP predictions for the energy consumption, the savings amount to £1,625 over the same period. Table 5 shows that the benefits accrue to both the tenant (through reduced carbon taxes) and the Government (through reduced emissions penalties).

Calc Method	Min Bldg Regs (kWh)	Min Bldg CO2 (tons)	EEM (kWh)	EEM CO2 (Tons)	CO2 Saved (Tons)	£ Saved
SAP	83786.19	17.26	23273.94	4.79	12.47	947.38
PHPP	180605.79	37.20	76804.01	15.82	21.38	1625.12

Table 4 carbon emissions savings

Value of building

Many studies have estimated the effect of improved energy efficiency on property values. While a review of the associated literature is beyond the scope of this paper, based on the analysis by Fuerst et al [7] an assumption of a 2% increase in the value of the property is viewed as reasonable. This would lead to an increase in value by £2,656 due to the increase in energy efficiency.

In another study Cajias et al [8] propose that the value of the property will increase by 0.45% per 1% decrease in energy costs, leading to an increase in the value of the property by as much as £5,738. This is calculated as follows: based on the SAP predictions the total primary energy consumption of the dwelling is 7,927 kWh/a, of which 2,740 kWh/a is used for space heating. The space heating element will be reduced from 36 to 26 kWh/m²/a (72%) leading to a reduction in space heating from 2,740 to 1,979 kWh/a. This is equivalent to a reduction of 761 kWh/a, representing a 9.6% reduction in the overall energy consumption of the dwelling, leading to a 4.3% increase in the value of the property for the HA.

It is noted that the lower values for the property increase are less than the cost required to upgrade the property to the higher energy efficiency standard, and the upper value approximates the upgrade cost.

Increase in rent

In NI, social housing tenancies that commenced prior to September 1992 have a controlled rent, while all other properties have a decontrolled rent, with rents set by individual HAs [9], who can charge a premium for newer units. HA's can assess each scheme individually, with rent set to reflect the cost of building (including finance) and maintenance.

Assuming that 50% of the estimated energy savings costs are paid by the tenant, the extra rental payment will range between £0.7k and £2.4k over the 20-year period. This equates to between £0.67 and £2.30 per week. Given that the average HA weekly rent for a 3 bed *general needs* accommodation is £93.97 [9], this equates to an increase of no more than 2.4% for the HA, paid by the tenant (Table 5).

Benefits to the local economy

The GDP of NI [10] is estimated at €53.3bn (£47.97bn), equating to £68,207 per household per annum, if the total is simply divided by the number of households (703,300 households). In a study from Scotland [11] it was proposed that a 5% decrease in energy consumption would lead to a 0.1% improvement in GDP, equivalent to a contribution to the economy of NI of £1,364 per household over the 20-year period. Based on this increase in GDP for every 5% decrease in expenditure on energy costs [11], the increased benefit to the common purse per household is between £2,620 (SAP) and £4,010 (PHPP).

Health benefits

Parameter	Benefit (£ '000)		Beneficiary (£ '000)		
	Range	{£k/dwelling}	HA	Tenant	State
Extra Cost for EEM Vs Base (Yr 1)	n/a	-7.4	-4.1	0.0	-3.3
Heating energy saving	Lower	1.5	0.0	1.5	0.0
	Upper	4.8	0.0	4.8	0.0
CO2 Saving	Lower	0.4	0.0	0.4	0.4
	Upper	1.2	0.0	1.2	1.2
Value of building increase	Lower	2.7	2.7	0.0	0.0
	Upper	8.8	8.8	0.0	0.0
Increase in rent	Lower	0.7	0.7	-0.7	0.0
	Upper	2.4	2.4	-2.4	0.0
Economy Benefits	Lower	2.6	0.0	0.0	2.6
	Upper	4.0	0.0	0.0	4.0
Health benefits	Lower	1.5	0.0	0.0	1.5
	Upper	2.0	0.0	0.0	2.0
Total Benefit	Lower	9.1	3.4	1.1	5.0
	Upper	20.3	11.2	3.6	6.7

Table 5 MBA for social house built to the EEM standard (Gas Heating)

Estimation of the economic value of energy efficiency on home occupant health is based on the Kirklee project benefits analysis [12]. The estimated for the health benefits associated with the energy upgrade is 20% of the upgrade cost, equivalent to £1,471, while the Chief Medical Officers [13] estimate of 42% of expenditure saving on health costs is equivalent to up to £2,028, based on a heating cost saving of £4,830 over the period.

Who Benefits and who pays?

The 'Extra Cost ...' row in Table 5 indicates a total cost of £7.4k (from Table 2), split between government (£3.3k (the EEM incentive)) and the HA (£4.1k (=£7.4-3.1k)). Total benefits are calculated to range from £9.1k to £20.3k over the 20-year period, split between HA (£3.4k to £11.2k), tenant (£1.1k to £3.6k) and government (£5k to £6.7k).

The (year 1) extra cost for upgrading to the EEM standard (rather than the prevailing minimum building regulations) is £7.4k, comprises mainly of additional

costs associated with the building. It is seen that for a cost of £7.4k, benefits of between £9.1k and £20.3k represent paybacks of between 124% and 276%.

In terms of the Multi-Beneficiary Analysis, the figures show that the tenant benefits significantly, and the government accrues a significant portion of the benefits, based on the year one investment of £3.3k and the £4.1k by the HA. The stakeholder charged with providing the higher standard accommodation may not recover the investment (if only the lower estimated £3.4k benefit is realised), although the HA may realise a substantial benefit of £11.2k, the largest potential benefit. This benefit is achieved primarily as a result of the increased capital value of the property (a metric on which the HA is not assessed).

3.3 Passive House Standard

3.3.1 Overview

The MB and MBA analysis was also carried out using the same methodology for the dwelling constructed to the PH standard for the two heating systems.

Extra cost is incurred in upgrading the building fabric to the PH standard (to achieve the 15kWh/m²/a which the CCC proposes). However, the benefit is that air can be used as the heat transport mechanism, eliminating the need for a Gas Fired Central Heating (GFCH) system. While it is recognised that HAs may have a preference for GFCH as it is well established (and maintenance is standardised and understood), significant extra cost would be incurred in installing a gas central heating system and replacing it in 20-year's time to meet the CCC recommendations.

The PHs have been designed to comply with the EEM standard and therefore also avail of the 1.03 multiplier, equivalent to a £3,300 contribution from the government towards the upgrade costs in year one.

3.3.2 PH with integrated HP/HRV system

Table 6 shows that the additional year one cost of constructing the electrically heated PH compared with the base case is £9.1k. These costs are split between the HA (£5.8k) and the government (£3.3).

The cost of £9.1k yields benefits of between £15.2k and £29.1k over the 20-year period, representing a payback of between 167% and 321% (see table 8).

The largest beneficiary is the Government, with between £8.5k and £13k accrued over the 20 years (for the investment of £3.3k), and the HA is the next largest beneficiary at between £4.7k and £11.4k (due primarily to increased property value). The tenant is seen to benefit by between £2.6 and £6.6k.

Table 7 shows that the extra cost of constructing the dwelling to the PH standard with GFCH is £10.8k. The

benefits which accrue due to the year one cost of £10.8k range from £16.1k to £28.4k over the 20-year period.

Parameter	Benefit (£ '000)		Beneficiary (£ '000)		
	Range	(£ k/dwelling)	HA	Tenant	State
Extra Cost for EEM Vs Base	n/a	-9.1	-5.8	0.0	-3.3
Heating energy saving	Lower	4.0	0.0	4.0	0.0
	Upper	9.5	0.0	9.5	0.0
CO2 Saving	Lower	0.6	0.0	0.6	0.6
	Upper	1.8	0.0	1.8	1.8
Value of building increase	Lower	2.7	2.7	0.0	0.0
	Upper	6.6	6.6	0.0	0.0
Increase in rent	Lower	2.0	2.0	-2.0	0.0
	Upper	4.8	4.8	-4.8	0.0
Economy Benefits	Lower	6.1	0.0	0.0	6.1
	Upper	7.1	0.0	0.0	7.1
Health benefits	Lower	1.8	0.0	0.0	1.8
	Upper	4.0	0.0	0.0	4.0
Total Benefit	Lower	15.2	4.7	2.6	8.5
	Upper	29.1	11.4	6.6	13.0

Table 6 MBA for social house: PH with Heat Pump

3.3.3 PH with traditional gas central heating

Parameter	Benefit (£ '000)		Beneficiary (£ '000)		
	Range	(£ k/dwelling)	HA	Tenant	State
Extra Cost for EEM Vs Base (Year 1)	n/a	-10.8	-7.5	0.0	-3.3
Heating energy saving	Lower	3.7	0.0	3.7	0.0
	Upper	8.7	0.0	8.7	0.0
CO2 Saving	Lower	0.9	0.0	0.9	0.9
	Upper	2.2	0.0	2.2	2.2
Value of building increase	Lower	2.7	2.7	0.0	0.0
	Upper	6.6	6.6	0.0	0.0
Increase in rent	Lower	1.9	1.9	-1.9	0.0
	Upper	4.3	4.3	-4.3	0.0
Economy Benefits	Lower	6.7	0.0	0.0	6.7
	Upper	7.2	0.0	0.0	7.2
Health benefits	Lower	2.2	0.0	0.0	2.2
	Upper	3.7	0.0	0.0	3.7
Total Benefit	Lower	16.1	4.5	2.8	9.7
	Upper	28.4	11.0	6.5	13.0

Table 7 MBA for social house: PH with gas heating

Given that the PH complies with the EEM standard, the HA will benefit from the government payment of £3.3k in relation to the additional construction costs in year one. Therefore the HA would have to pay the remaining £7.5k in the case of gas-fired central heating.

The largest beneficiary is the Government with between £9.7k and £13k benefits accrued over the 20 years, for an outlay of £3.3k. The tenant also benefits significantly (by £2.8k to £6.5k), and does not have to make any investment. The HA benefits by between £4.5k and £11k, again primarily as a result of the increase in the capital value of the dwelling due to the investment of £7.6k.

4 DISCUSSION

4.1. Overall Returns

Table 8 gives an overview of the benefits which accrue over a 20 year period, (without considering the extra 20 year upgrade costs to meet the CCC recommended energy efficiency standard). The payback for the PH (HP) is 19 years, with the worst-case (EEM) resulting in 30.5 years to recoup the extra initial cost.

Overall returns for the respective investments were estimated at between 124% to 276% (EEM), 148% to 263% (PH with GFCH) and 167% to 321% (PH with HP). Therefore, it is seen that the overall business case for energy upgrades is positive.

Item	EEM	PH (Heat Pump)	PH (Gas)
Extra initial cost (£)	7356	9075	10798
Heating Energy Saving (PHPP) (£ pa)	241	477	435
Payback (Operational Energy) (Yrs)	30.5	19.0	24.8
Overall Benefits (MBA) - Worst case (£)	9132	15197	16112
Overall Benefits (MBA) - Best case (£)	20298	29145	28367
Return (MBA) Worst case (%)	124%	167%	149%
Return (MBA) Best Case (%)	276%	321%	263%

Table 8 Summary of 20-year Benefits for the three Social House Variants

There is however an additional significant benefit which accrues to the HA - that of avoided future energy upgrade costs required to meet UK net zero carbon commitments. Based on the CCC's recommendation that new dwellings are built to meet 15 kWh/m²/a (equivalent to that the PH standard) [14], dwellings constructed to lesser standards will need to be upgraded in the future. It costs significantly more to build dwellings to current minimum building regulations and subsequently upgrade (£26,300) compared with incorporating the extra insulation and airtightness etc at the initial design and build stage (£4,800) [14].

4.2 Future Upgrade Costs

When the future upgrade costs are added to the initial costs estimated as part of this study, a more holistic perspective is obtained. See Fig 1. On the left (in orange) are the costs associated with carrying out the energy-efficient upgrade at the build stage and (in red) the additional costs associated with the future upgrade costs to meet a space heating requirement of 15 kWh/m²/a, and the installation of a HP (all assumed take place in year 20).

For the EEM, it is seen that at the end of the 20-year period, a significant extra cost of £26.3k will be incurred to upgrade the building fabric to the required standard, and install a heating system based on a low-temperature HP. This is a significant future liability.

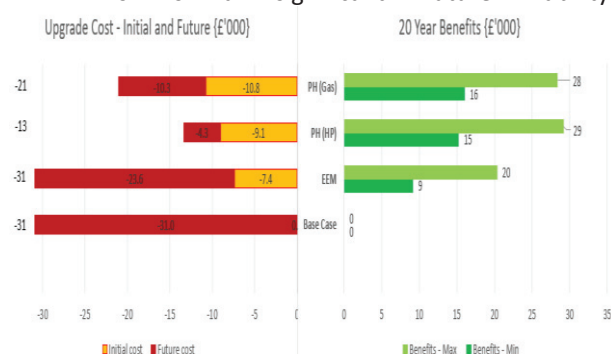


Fig 1 Costs and 20-year Multiple Benefits of 3 Bed Low-Energy social house Dwelling

For the PH, the building fabric would meet the CCC proposed standard, and in the case of the PH heated with HP, replacing the installed HP in year 20 costs £4.3k. For the PH with GFCH, the cost of upgrading from a gas

fired heating system in Year 20 to an electric HP is estimated at £11,250 [5].

4.3 Returns per beneficiary

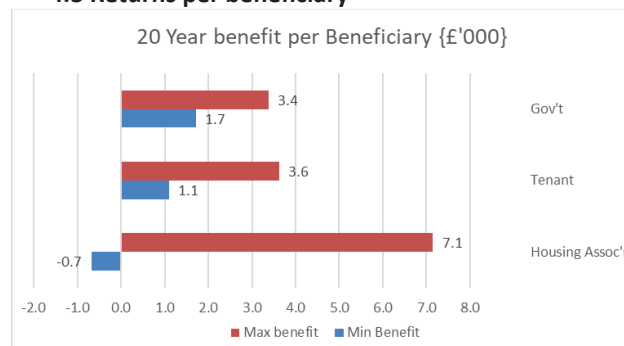


Figure 2 Summary of Benefits per beneficiary (EEM)

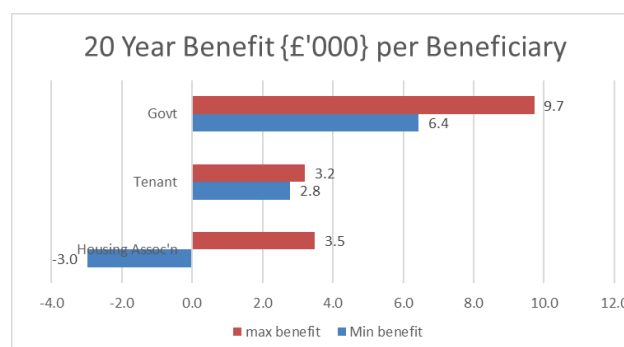


Figure 3 Summary of Benefits per beneficiary (PH, Gas)

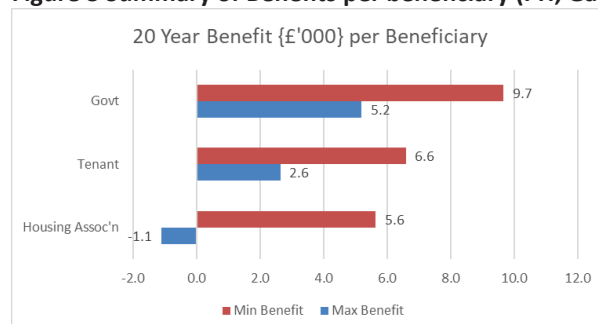


Figure 4 Summary of Benefits per beneficiary (PH Dwelling with HP)

Figures 2, 3 and 4 show the 20 year benefit per beneficiary for each of the upgrade scenarios considered.

In each case the summary of the 20-year benefits per beneficiary shows that the public purse (government) is a net beneficiary, and in two cases enjoys higher benefits than any other stakeholder. The tenant also accrues significant benefits.

The government benefits, not only through the avoidance of health costs and carbon emissions penalties, but also from the substantial economic benefits which accrue as a direct result of reduced social housing energy consumption.

The tenant accrues significant benefits through avoided heating costs and associated carbon dioxide levies (which will likely be levied on fuel in the future).

However, while the tenant and government benefit significantly, the stakeholder charged with deciding on the extra investment, the Housing Association is seen to have to bear significant increased capital costs of between £4.1k (Table 5) and £7.6k (Table 7). The benefits which accrue to the HA are in all cases potentially insufficient to cover the costs and any potential net benefits are based on property values, a metric which is not of interest to the HA.

5. CONCLUSION

This analysis has the limitations of being based on predicted energy consumption rather than recorded data. Further, assumptions have had to be made to provide estimates for a number of the often intangible indirect benefits. It also doesn't consider possible rebound, or comfort taking phenomena that has been reported in the socio-technical literature.

However, a number of insights are emerging from the Multiple Benefits and stakeholder analysis.

1. Overall, upgrading to improved energy efficiency standards is seen to be financially beneficial, with the PH standard heated with an electric HP being most advantageous (Table 8).
2. When the future upgrade cost to the CCC recommended standard is included in the analysis, lowest overall cost (£13.4k) and the highest overall benefits (£29k) are achieved with the PH heated with HP (Fig 1).
3. The future liabilities (should the HA defer the decision to meet the CCC standard) are seen to be significant (£26.3k), compared with building to the standard now (£13.4k).
4. Substantial individual & societal benefits accrue over the 20 year period by adopting improved energy efficiency standards now (fig 1).
5. The HA must fund an extra £4.1k (Table 5) to £7.6k (Table 7) and, irrespective of the energy-efficient upgrade path chosen, the HA is disincentivised from making the upgrade decision now (figures 2, 3 and 4).
6. It is noted that the Government ultimately is responsible for providing social housing at least cost and greatest value, and enjoys significant benefits over the 20 year period (in two cases being the principal beneficiary).

Given the significant benefits which accrue, and the often life changing impact on typically disadvantaged social housing tenants, the paper indicates that potential exists for strategic investment by government (via HA's) to unlock the significant multiple benefits of low energy

dwellings. Further, investment would make a significant contribution to achieving much needed carbon savings.

ACKNOWLEDGEMENTS

This project was supported by InvestNI under its Collaborative Growth Programme.

REFERENCES

- [1] IEA. Capturing the Multiple Benefits of Energy Efficiency: A Guide to Quantifying the Value Added. Paris: 2014.
- [2] Colclough S, McWilliams M. Cost Optimal UK Deployment of the Passive House Standard, ISBN 978-1-912532-05-6; 2019.
- [3] Approved Documents. GOVUK n.d. <https://www.gov.uk/government/collections/approved-documents> (accessed May 15, 2020).
- [4] PHI. What is a Passive House? 2011. https://passivehouse.com/02_informations/01_what_is_a_passive_house/01_what_is_a_passive_house.htm.
- [5] UK housing: Fit for the future? 2019.
- [6] Carbon pricing is crucial to save planet. Financial Times 2018. <https://www.ft.com/content/adaafba6-bdbc-11e8-8274-55b72926558f> (accessed March 11, 2019).
- [7] Fuerst F, McAllister P, Nanda A, Wyatt P. Does energy efficiency matter to home-buyers? An investigation of EPC ratings and transaction prices in England. *Energy Economics* 2015;48:145–56. <https://doi.org/10.1016/j.eneco.2014.12.012>.
- [8] Cajias M, Piazzolo D. Green Performs Better: Energy Efficiency & Financial Return on Buildings. Rochester, NY: Social Science Research Network; 2013.
- [9] Northern Ireland Federation of Housing Associations. HOUSING ASSOCIATION RENTS: GENERAL NEEDS & SHELTERED, 2016/17. n.d.
- [10] Anonymous. Northern Ireland 2010. <https://ec.europa.eu/growth/tools-databases/regional-innovation-monitor/base-profile/northern-ireland> (accessed April 17, 2019).
- [11] Turner K, Riddoch F, Figus G. How improving household efficiency could boost the Scottish economy. <https://strathprints.strath.ac.uk/id/eprint/57955>. 2016.
- [12] International Energy Agency. Capturing the Multiple Benefits of Energy Efficiency. 2014.
- [13] Anon. 2009 ANNUAL REPORT of the Chief Medical Officer. http://www.sthc.co.uk/Documents/CMO_Report_2009.pdf. 2009.

Research on design strategy and thermal performance of surface space in hot summer and warm winter area

HAOWEI YU¹, YEHAO SONG², YINGNAN CHU², XIAOJUAN CHEN³, JINGFEN SUN³, DAN XIE³

¹China Architecture Design and Research Group, Beijing, China

² Tsinghua University, Beijing, China

³ Beijing Tsinghua Tongheng Urban Planning and Design Institute, Beijing, China

ABSTRACT: In the past several decades, architects and engineers have been seeking sustainable design strategies which integrate the technologies to architectural design, and testing them in practices. In terms of hot summer and warm winter area, from traditional residential buildings to modern sustainable buildings, the proper utility of the semi-outdoor space is always an important approach in climate adaptability design. Based on such design experience, this article advances the concept of "Surface Space", within the frame of the buffer layer of biological climate, which stands for the semi-outdoor space extended from the building envelope, with effects of improving the microclimate around the building and decreasing the energy consumption during the use. Meanwhile, based on a real experimental project in Hainan, China, the article provides a research method of using ENVI-met to simulate the thermal performance of the surface spaces and verifies the effects of the surface spaces in the project in Hainan by using such simulating method. Further, this article focuses on one courtyard in the project and studies the influences of different spatial designs on the thermal performance of such surface spaces.

KEYWORDS: Surface space, Courtyard, ENVI-met, Buffer layer of biological climate

1. INTRODUCTION

As the development in the abilities of building design and construction, an obvious promotion has been spotted in terms of the complexity of building functions and requirements for the comfort of built-up space. Meanwhile, faced with global environmental problems and energy crisis, buildings need to be designed, built and used more sustainably. As a result, in hot summer and warm winter area, mere traditional approaches of climate adaptation design, which mostly emphasize the use of passive strategies such as shading and natural ventilation, can hardly match such demands. However, nowadays the typical procedure of "design- optimization" (architects focus on the spatial design while engineers optimize the material and HVAC system to lower the energy consumption) in green building designing has gradually shown its negative effects in the design of sustainable buildings, that architects and designers are losing voice in the field of sustainable building.

In the history of contemporary architecture, Charles Correa and Kenneth King Mun YEANG are regarded as two of the pioneers in sustainable building design in India and Malaysia. In their works, comprehensive design from the location, orientation and shape of the buildings, the arrangement of courtyards, atriums and verandas, to the details of shadings, greenings, etc., forms a system to improve the thermal performance of the building and meanwhile create comfortable and

unique spaces which make the building outstanding in the field of architecture design. The success of such works emphasizes the importance of the spatial system of comprehensive sustainable strategies.

Adjustment of the microclimate around the building, thermal protection of the building envelopes, and use of mechanical heating or cooling are regarded as 3 phases of adjusting the interior temperature. The spatial system mentioned above mainly works in the first stage. Further, the concept of a buffer layer of biological climate was advanced to identify such kind of spaces and building components and build a theoretical frame of related sustainable strategies [2]. The concept of surface space is advanced within such frame and especially refer to the semi-outdoor spaces extended from the building envelope, including courtyards, atriums, verandas, etc.

For the buildings in hot summer and warm winter area, the increasing requirements for comfort resulting in the extensive use of AC in closed interior space during summer, and huge energy consumption. Surface space acts as a buffer layer, which aimed to partly decrease the air temperature of the outdoor space close to the building envelopes, generally using passive solutions such as shadings, greenings, water landscape for cooling the air, and natural ventilation in courtyards and atriums, etc., by which means interior cooling load in summer could be partly decreased (Fig. 1). Meanwhile, for architects, those surface spaces can be designed as

spaces that connected the internal space and the external environment, where various activities and events take place. The design of surface space integrates architectural design and sustainable technologies.

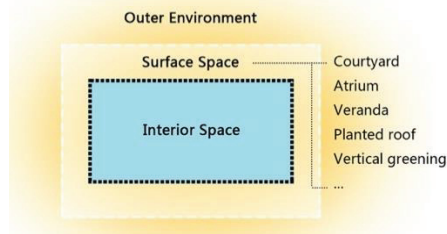


Figure 1: Diagram of the concept of surface space.

The following parts of the article will further discuss the simulating method of surface space and apply it in the evaluation of surface spaces of different spatial design based on a real project in Hainan, China.

2. RESEARCH METHOD

Researches of the quantitative relationship between spatial design and its thermal performance are increasingly important for both researchers and architects.

2.1 Simulating method of surface space

The effect of surface space, as a buffer layer, can be directly evaluated by the difference of air temperature between the outer environment and the interior space surrounded by the surface space. However, in such calculation, the thermal conductivity of the building envelop is also considered, which has no relevance with the spatial design of the surface space. Consequently, the effect of surface space can be shown by the temperature distribution inside the space itself. The difference in temperature between the area near the outer environment and the area near the boundary of internal space reflected the effect of surface space (Fig. 2 to 3).

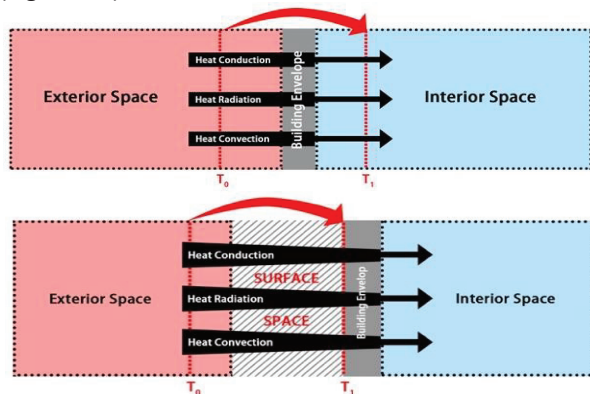


Figure 2 & 3: The comparison between typical simulating method and the simulating method of the surface space. The value of T_0-T_1 reflects the effect of surface space.

Accordingly, in this article, ENVI-met (ver.4.4) is used for the simulation and evaluation of surface space. The minimum module of modelling and simulating is 0.5m, which provides results precise enough for architects in the early stage of design.

Though the software was originally developed for simulating the thermal performance of the space between building groups. in recent years it was gradually proved credible for space of building- scale. S. Berkovic with his colleagues applied ENVI-met in the simulation of a courtyard of 20m x 40m x 9m [3], while A. Ghaffarianhoseini and his colleagues applied it in the research of a courtyard of 24m x 24m, and discussed how the orientation, spatial proportion and crown density of the landscape influenced the distribution of temperature and thermal comfort in the courtyard [4]. S. H. Xue applied the software in the simulation of the outdoor thermal environment of the south of the five ridges gardens in China, which showed the capacity of ENVI-met for simulating open system consisting of buildings, water, landscape and open space [5].

As the simulation of ENVI-met only focuses on the outdoor environment (and semi-outdoor environment) and ignores the use of the space, the results are not the real value of the thermal environment of the surface space. However, such results can be used in the quantitative comparisons of different design, as well as the study of a long-term pattern.

2.2 Case project

The case project is a 4-floor office building located in Chengmai County, Hainan Province, China (109.99°E, 19.69°N), which is designed to be a sustainable building according to the concept of surface space.

The building was designed to be multi-functioned, with the building area of 11,000m². An exhibition hall and a multi-functioned lecture hall is arranged on the 1st floor, together with the lobby, café shop and a series of courtyards. The 1st floor is earth-covered in the south and west, where the solar radiation is relatively high during the day, and such layer of soil and plants also acts as a buffer layer, as well as a park for users and visitors (Fig. 4). All the courtyards on the 1st floor is integrated with the landscape and become part of the park, connecting the internal space and the natural environment outside (Fig. 5). The office space on the 2nd to 4th floor is arranged around the main semi-outdoor atrium facing southeast (Fig. 6), and surrounded by terraces, roof gardens and side courtyards. Each courtyard, atrium and terrace of different floor levels in the building connect and form the system of public space, which is also the system of surface space in the building.



Figure 4: Aerial view of the project under construction.

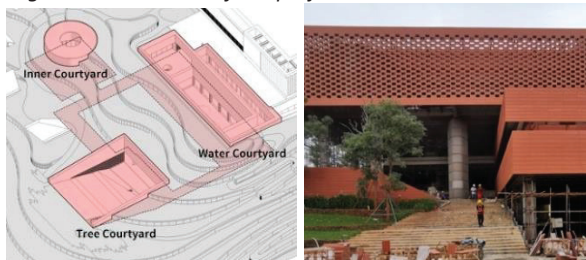


Figure 5&6: The courtyard and atrium in the project.

2.3 Simulation task arrangement

The simulating and research of the surface space in the project have 2 phases. First, in terms of the whole building space, the validity of the surface space improving the microclimate should be tested, meanwhile, the connection and difference between various surface spaces will be analysed. After that, in the second phase, typical space with apparent effect in the design will be isolated and simulated, to show the relationship between spatial design and its effect as surface space. Such two phases as well show the process of design optimization using ENVI-met in a real project.

Considering the accuracy of the simulation and the module in architecture design, the cell size of modelling and simulating is set to 0.6m x 0.6m x 1m. Meanwhile considering the stability and duration of computing, the project is divided to 2 parts to be simulated separately, namely the part of the courtyard and the part of the atrium (the 2 parts of surface space are of different orientation and separated by interior office space, which can be regarded as 2 isolated parts). The weather data applied in the simulation is that of the typical summer day of Haikou provided in Energy Plus database (Fig. 7). The main façade of the project is a ceramic plate curtain wall and glass curtain wall.

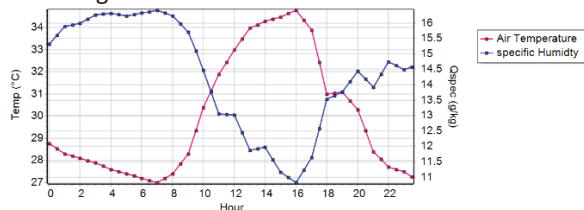


Figure 7: Weather data input for the simulation.

3. RESULT

3.1 Results of courtyards

This part contains 3 different courtyards on the 1st floor, including a water courtyard of 9m x 24m, a tree courtyard of 17m x 21m, and a courtyard inside the exhibition hall of 12m x 12m. All 3 courtyards are connected together with an outdoor corridor, and most of the part except for the courtyards is covered by earth.

First, the simulation result shows a general decrease in air temperature inside each courtyard and the corridor, and basically, the locations near the edge of the courtyards perform better than that in the centre. Meanwhile, the average temperature (T_a) inside the surface space shares the same variation trend with the outside dry-bulb temperature (T_{DB}), and the two parameters reach the peak synchronously at 16:00. Such phenomena show the validity of courtyards surface space as a buffer layer. The difference between T_a and T_{DB} can be regarded as the equivalent thermal resistance of the surface space, while such kind of surface space has little equivalent thermal inertia compared with ordinary building materials, as the surface space is directly connected with the outer environment.

The temperature difference between T_a and T_{DB} in the whole system reaches the maximum of 6.3°C at 13:00 at the inner corner of the corridor, and the temperature near the edge of the courtyards is also declined by more than 5°C in the small courtyard inside the exhibition hall (Fig. 8).

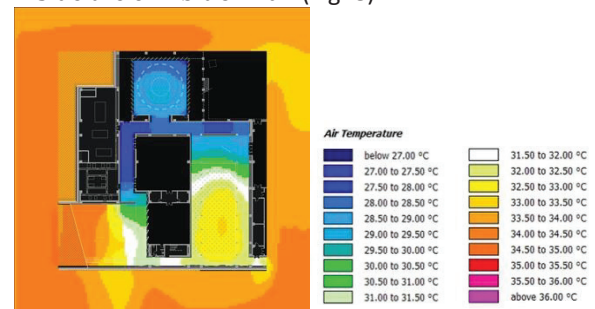


Figure 8: Temperature distribution ($h=1.5m$) in the part of the courtyard at 13:00 and the legend of the temperature.

Through the comparison of the temperature distribution in the 3 courtyards, it is apparent to see the square courtyard inside the exhibition hall performs better than the other two- the temperature in that courtyard is at least 2°C lower than that in other courtyards. One of the most important reason is over 80% of the space is covered by a concrete roof. Meanwhile, the height of the courtyard is more than 9m, and its proportion between height and width on the section is close to 1:1. Both two conditions reduce the radiation that reaches the bottom of the courtyard. It can also be proved by the temperature distribution of the section, that the air temperature increases slightly from the

ground to the level of 3m (no more than 0.5°C), but apparently above the level of 4m (Fig. 9). However, the chimney effect in the courtyard is not apparent, and it is unlikely to improve natural ventilation through such surface space.

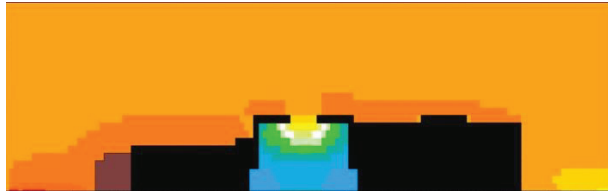


Figure 9: Temperature distribution in the section of the courtyard inside the exhibition hall at 13:00.

In terms of average air temperature, the thermal performances of water courtyard and tree courtyard are relatively similar, as both of them use high walls on the edges and hanging terraces for shading, with most of the space uncovered. However, the different spatial design creates different microclimate and different temperature distribution in the two courtyards.

The water courtyard has a closed boundary of walls of 9m high, meanwhile, the space of the courtyard is longer in a north-south direction, and the proportion of width and height of the space in the section of the short axis is smaller than 1:1. Such design improves the effect of self-shading, especially during the morning and afternoon. The boundary on the 1st floor is an inward colonnade, which helps to provide extra shading. The simulation shows that such design can effectively lower the air temperature on the edge of the courtyard. The temperature difference between the east and west edge(beneath the colonnade) and the centre variable from 1.5°C (before 11:00 and after 16:00) to 3°C(at 13:00). Such a difference is much more remarkable on the north edge, beneath the large terrace, which can be up to 5.6°C at 13:00 (Fig. 10).

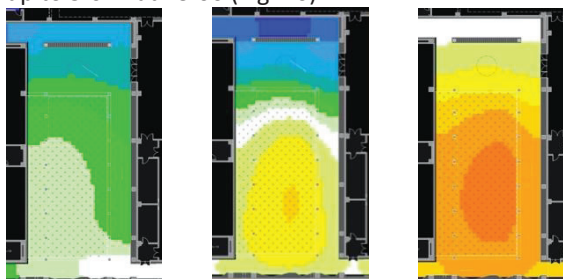


Figure 10: Temperature distribution ($h=1.5m$) in the water courtyard at 11:00, 13:00 and 16:00.

While the tree courtyard is open on the west, which to some degree weakens the effect of self-shading. It is clear in the figure that during the afternoon the air temperature in the tree courtyard rises much faster than that in the water courtyard. However, the opening let in

the wind to the courtyard and the surrounding corridors, which lowers the value of PMV in the courtyard.

3.2 Results of the atrium

This part focuses on the atrium in the east of the building. The atrium is 4 floors high, as the main entrance of the building. The atrium works as a large surface space, with its south and east sides open and its top covered by several skylights equipped with fans for ventilation. The atrium is surrounded by interior office space on the north and west, and on 3rd and 4th floor several terraces and outdoor corridors extend from the office space and form a ventilating shaft in the centre. There is a set of stairs and landscape at the bottom of it as well, which helps to lead and precool the wind.

As the volume of 4th floor and the terraces hanging out and providing shading for space beneath, the air temperature in the atrium is lower than outside, the difference ranges from 4.4°C to 0.4°C, and space deep inside the atrium is cooler, which shows the effectiveness of the atrium as surface space for the surrounding office space. Such difference is variable according to the height as well, which on one hand due to the shading condition, and on the other to the chimney effect in the atrium (Fig. 11 to 12).

The simulation shows the existence of the chimney effect in the atrium, though it is relatively an open system. In the case of southeast wind, the wind accelerates in the centre of the atrium. The wind speed inside can reach up to 2.2m/s. (Fig. 13) And a temperature gradient can also be read in the section.

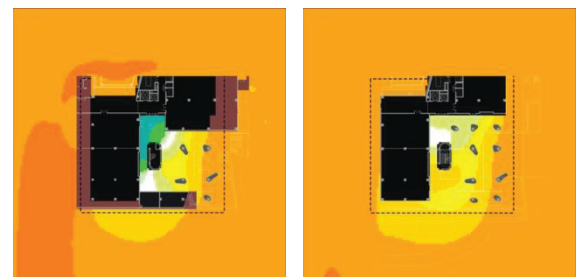


Figure 11 & 12: Temperature distribution ($h=6.5m, 10m$) inside the atrium at 13:00

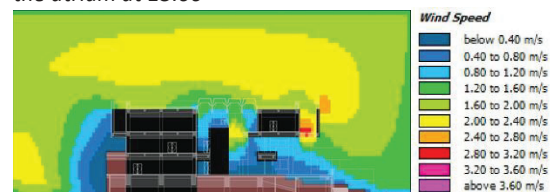


Figure 13: Wind speed distribution in the section of the atrium and the legend of wind speed.

However, it should be noted that high wind speed for ventilation is not always the correct design for the atrium as a surface space. In the project, the columns in

the atrium are wrapped by GRC plates, to make the ventilating shaft narrower and to some extends decline the wind speed in the atrium. Through a comparison simulation of 2 conditions of with and without such thick columns, it is revealed that as the wind speed decrease by around 50% in the atrium, T_a of each floor decline by 0.3 to 0.4°C (Fig. 14 to 15). The columns cannot provide extra shadings, but reduce heat transfer by convection. Such phenomenon indicates that for surface spaces, in some situation, natural ventilation increases the cooling load in turn during summer in hot summer and warm winter area.

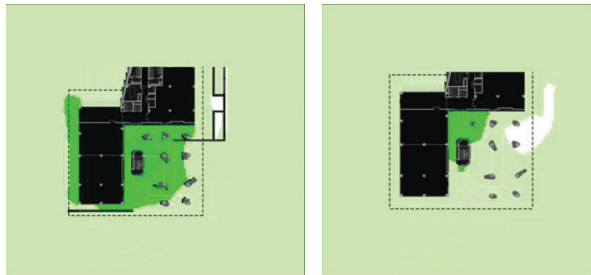


Figure 14 & 15: The comparison of the temperature distribution ($h=10m$) in the atrium with (L) and without (R) the GRC columns at 11:00.

4. DISCUSSION

The simulations and researches above basically focused on a comprehensive effect of multiple surface spaces, or one surface space with multiple design strategies. It is proved that surface spaces of proper design are indeed capable of adjusting the microclimate inside and help to decrease the cooling load of surrounding rooms to some extends. Besides, in terms of single surface space, its basic thermal performance and to what end proper spatial design could improve it, still need to be discussed. Meanwhile, such discussion also shows the approaches of design optimization of surface space with the help of simulation tools.

The prototype model for simulation is furtherly simplified. The cell size is set to 2m x 2m x 1m, and the area of the courtyard is around 40 blocks in the modelling, which is close to the water courtyard. The courtyard is surrounded by rooms with the depth of 10m, and with a corridor of 2m wide connecting with the outer environment. Beyond the rooms, space of 10m long is spared, for more convincible wind simulation, and more importantly, such space works as a contrast. The effect of the courtyard in different orientation can be measured by the temperature difference between the inner surface of the courtyard, and the outer surface of the building (which exposed without the surface space) in the same orientation.

First, the variable of the simulation is the proportion of the courtyard, including its shape and height. Through cross-comparison, it can be concluded that in hot

summer and warm winter area, during the summer days in terms of the shape, a courtyard which is long in north-south direction can be more beneficial, especially during the afternoon, and in terms of the height, a higher courtyard can enjoy better self-shading condition, which eventually leads to a lower temperature at the edge. However, it should be noted that higher courtyard may be weak in natural ventilation, and visually the experience in a high courtyard could be depressive. The simulation of various conditions shows that the courtyard of 8m x 20m (long in the north-south direction) with 3 floors height has the best thermal performance, and the mere courtyard can help to lower the air temperature by up to 3°C at the northern and western surface, during the hottest period of 3-4 pm (Fig. 17).

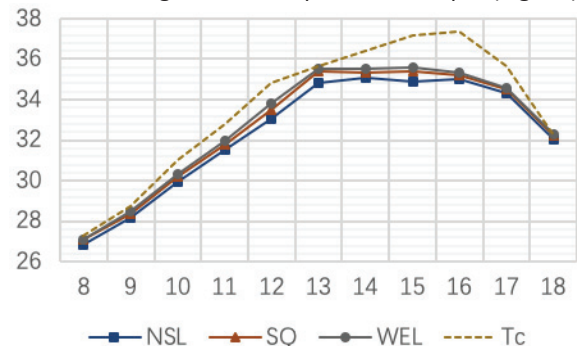


Figure 17: T_a of the northern surface in the courtyards (3 floors high) of different shapes.

(NSL: long in north-south direction, SQ: square, WEL long in west-east direction, T_c: contrast temperature outside the courtyard)

Then, different conditions of shading in the courtyard need to be discussed. In the research contains 4 types of shading, including roof shading, inward colonnade, a terrace as shading and walls for shading. The effect of the courtyard is improved as the shading increases. Meanwhile, different kind of shadings works well at different periods. The roof shading can lower the air temperature at the edge of the courtyard before 14:00, but its effect is not outstanding in the afternoon. Inward colonnade and terraces have a similar effect, that the air temperature at the edge can be controlled in the morning and the afternoon, while from 12:00 to 15:00 the temperature rises rapidly, and the peak temperature is close to the blank contrast condition. Shading walls only have a slight effect before 12:00, however, it helps to decline the peak of the temperature at 13:00. From 13:00 to 14:00, shading walls and roof shading can furtherly lower the peak temperature by more than 1°C comparing with the blank contrast condition. It should be considered in the design to apply more than one type of shadings to get the better effect (Fig. 18).

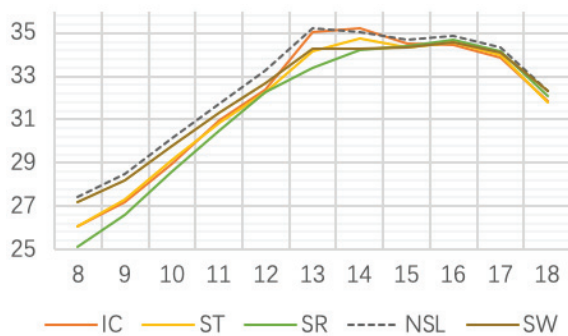


Figure 18: T_a of the western surface in the courtyards (3 floors high) of different types of shading.

(IC: inward colonnade, ST: shading terraces, SR: shading roof, SW: shading walls, NSL: contrast without extra shading)

Different conditions of ventilation are also studied in the research. In the condition of south wind as the dominant wind direction during summer, the simulation result shows that a ventilating shaft in north-south direction is much more effective than one in west-east direction. The previous one of the same widths can increase the wind speed in the surface space to more than 2m/s. Meanwhile, increasing the widths of the corridor or add an extra corridor can both furtherly enhance the natural ventilation. The ventilating shaft of north-south direction can effectively lower the air temperature comparing with the contrast condition, especially from 12:00 to 14:00. The ventilating shaft can be integrated with the inward colonnade, which can furtherly improve its effect. The condition of the courtyard with 2 shafts of 4m wide can decline the air temperature inside by up to 2.2°C at 13:00. However, natural ventilation brings in the warm air outside the courtyard, and that explains the reason that ventilating shafts like a narrow corridor or shaded colonnade perform better than a large opening (Fig. 19).

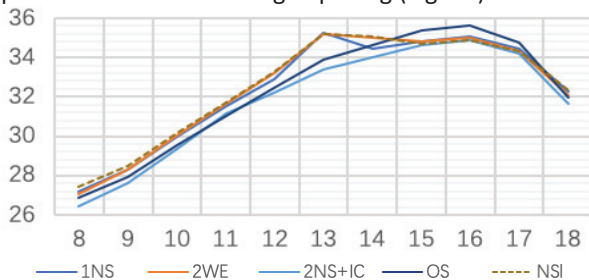


Figure 19: T_a of the western surface in the courtyards (3 floors high) of different ventilation conditions.

(1NS: single shaft of north-south direction, 2WE: double shafts of west-east direction, 2NS+IC: double shafts of north-south direction integrated with inward colonnade, OS: opening at the southern edge, NSL: contrast without ventilation shaft)

Eventually, one solution (Fig. 20) was provided based on the analysis above which has a comprehensive design strategy of integrating inward colonnade, ventilating

shaft and shading walls. Its simulation result showed that such design provided a decline in air temperature at each inner surface of up to 2.8°C and 1.3°C in average on the ground floor during the daytime (Fig. 21). Meanwhile, such solution performs more equally at different surface.

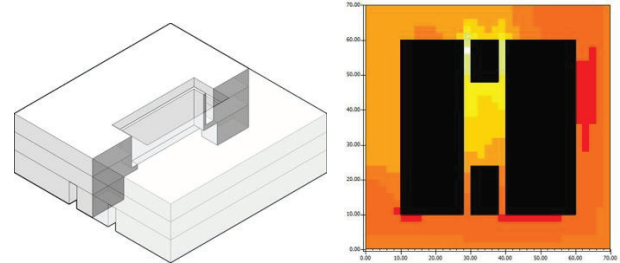


Figure 20 & 21: Optimized design solution for the courtyard prototype and simulation result of temperature distribution ($h=1.5m$) at 14:00.

5. CONCLUSION

This paper advances the concept of surface space as a sustainable design strategy in the hot summer and warm winter area and provides a simulating method for evaluating in research and design optimization. With the simulation and analysis of the project, surface space is proved to be effective in improving the microclimate and decreasing energy consumption.

Besides, based on the simulation and analysis of the project, this paper provides the theoretical basis and key points for the design of surface space in hot summer and warm winter area in China, such information may be helpful for architects, meanwhile, such research can also become an example of design optimization of the surface space by using ENVI-met.

ACKNOWLEDGEMENTS

This work was funded by National Natural Science Foundation of China (Project No. 51678324) and National Key R&D Program of China Technical System and Key Technology Development of Nearly Zero Energy Building (No.2017YFC0702601).

REFERENCES

1. Song, Y. H. & Li, D. X., (1999). A General Sense of Ecological Architecture, a Structural Framework of Ecological System and a Buffer Layer of Biological Climate. *Architectural Journal*, 03: p.4-10.
2. Berkovic, S., Yezioro A. & Bitan, A., (2012). Study of thermal comfort in courtyards in a hot arid climate. *Solar Energy*, 86(5): p. 1173-1186.
3. Ghaffarianhoseini, A., Berardi, U. & Ghaffarianhoseini, A., (2015). Thermal performance characteristics of unshaded courtyards in hot and humid climates. *Building and Environment*, 87: p. 154-168.
4. Xue, S. H., (2016). Study on the Space Elements Layout Pattern of the Lingnan Garden Based on Climate Adaptation, Ph.D. Dissertation. Guangzhou, China: South China University of Technology.

Influence of Thermal Emissivity on Thermal Properties of the Double Membrane Envelope of Air-Supported Structures

GREGA ZRIM

Aerogel EEC, Ljubljana, Slovenia

ABSTRACT: *The intention of this paper is to present how thermal emissivity of external surface of double membrane envelope inner membrane influences the thermal resistance of the whole constructional complex. Three envelope assemblies were considered: one made of two PVC and PVDF coated polyester fabrics; one made of two ethylene tetrafluoroethylene foils and the later insulated by aerogel insulation composite. In the given parametric study, the envelope's cross-section geometry and velocity of air in the channel between the membranes were also considered. Lastly, heating and cooling demand calculations were run with EnergyPlus, in order to assess the influence of optical and thermal properties alteration. The air-supported structure at Brezovica pri Ljubljani and its double membrane envelope were considered as the study case.*

KEYWORDS: *Air-supported structures, Double membrane envelope, Thermal emissivity, Thermal resistance, Aerogel*

1. INTRODUCTION

The main goal of this paper is to explore how thermal emissivity of external surface of double membrane envelope inner membrane influences its thermal resistance. For this purpose, properties of three constructional complexes were studied: one made of two PVC and PVDF coated polyester fabrics (DME_I), one made of two ethylene tetrafluoroethylene foils (DME_II) and the later insulated by aerogel insulation composite (DME_III). DME_I is a translucent complex with low solar transmittance and low thermal resistance. DME_II, having practically the same thermal resistance is, in contrast to DME_I, transparent and has high solar transmittance. Finally, DME_III [1] is translucent with low solar transmittance but high thermal resistance comparable to contemporary highly thermally insulative glazing [2].

In general, thermal resistance of building envelope (opaque, transparent or translucent) is one of its key properties on basis of which assessment and comparison of properties among different constructional complexes is made [3]. In temperate and heating predominant climate, such as Ljubljana's, increase in thermal resistance of any conventional building envelope component is inexpertly considered as an improvement in thermal properties. In order to check if this is true for the increase in thermal resistance due to described reduction of inner membrane thermal emissivity of DME_I, DME_II and DME_III a set of heating and cooling demand calculations of study case air-supported structure was made in addition. As in case of the studied building at Brezovica, envelope of such structures is often whole translucent and solar control, apart from membrane

optical properties, is demanding. Thus, keeping solar gain and possibilities of heat dissipation in balance is of high importance. In other words, optical and thermal properties need to be expertly selected [4, 5] to provide comfortable indoor conditions at high energy efficiency. In the presented paper, the comparison between two technologies of heat retention is facilitated.

Not so long ago, use of low emissivity coating in air-supported structures was investigated by Suo, Angelotti and Zanelli [6]. Envelope of their study case building was made of two polyester fabric coated with PVC. By using transient energy modelling program ESP-r, they showed that, in climate of Milan, the application of low-e coating on inner side of single membrane envelope would provide about the same reduction of heating demand as the two other double membrane options. More recently, an option of ethylene tetra-fluoroethylene foil with reduced transmittance and increased absorptance including longwave infrared radiation for reducing overheating potential was introduced for cushion membrane constructions made of ethylene tetrafluoroethylene foils [7]. TRNSYS simulations have shown a reduction of cooling demand by up to 35% in climate of Stuttgart [7].

After the thermal emissivities were obtained from total reflectance spectra, the thermal transmittances of envelope with parallel sides were calculated. Thermal transmittance calculations of actual envelope cross section were established using the method of heat radiosity in an enclosure and the crossed-string method of view factor determination. Finally, the results of energy demand calculations in local climate were obtained.

2. METHODOLOGY

2.1 Study case envelope and building

The geometry of double membrane envelope studied in this paper, was taken from the study case air-supported structure at Brezovica (Fig. 1). The translucent dome covers the multipurpose court used mainly by the Brezovica primary school and local sport clubs. The double membrane envelope originally consists of two polyester fabrics coated with PVC and PVDF (PES), which form curved tubular segments (Fig. 1) with characteristic cross section shown in Fig. 2. The segments are welded together along their edges, where the outer and the inner membrane join. An overpressure relative to external and internal environment is maintained in order to keep the two membranes apart. A small air current was recorded in the gap [1].

2.2 Thermal emissivity

Thermal emissivities e_T of polyester fabric coated with PVC and PVDF and ethylene tetrafluoroethylene foil (ETFE) were experimentally determined from total spectral hemispherical reflectance $TR_{IR}(\lambda)$ recorded in the spectral range between 2.5 and 16 μm . The reflectance spectra were recorded with spectrometer Bruker IFS 66/S (measurement resolution 4 cm^{-1}) equipped with integration sphere (OPTOSOL). A gold plate was used as the reference surface for diffuse reflectance. The spectral thermal emissivity $e(\lambda)$ was determined according to Equation (1). The process of spectra integration to obtain e_T at different temperatures is described in various sources [8]. By use of e_T grey radiation characteristics are implied.

$$e(\lambda) = 1 - TR_{IR}(\lambda) \quad (1)$$

where $e(\lambda)$ - spectral thermal emissivity (-);

$TR_{IR}(\lambda)$ - spectral reflectance (-);

λ - wavelength (nm).

Even though the $TR_{IR}(\lambda)$ spectra were not recorded on full radiation heat transfer spectrum (from 2.5 to 100 μm) [5], e_T were determined in wavelength band region where the heat exchange between surfaces is the strongest. Partially due to the spectral distribution of black body radiation at surface temperatures between -10 to 50 $^{\circ}\text{C}$ and its peaks overlapping the atmospheric window (from 8 to 14 μm) wavelength band (clear sky, low humidity). In the given measurement spectral range, a black body radiates from 52 to 66 % of energy considering surface temperatures from -10 to 50 $^{\circ}\text{C}$.

2.3 Thermal resistance calculations

Thermal resistance of the double membrane envelope segment R_{DME} (welds (Fig. 2) not included)

was calculated according to international standard ISO 15099:2003 [10] using Equation (2).

Thermal resistance of its air channel R_{ch} , as well as the resistances of external and internal surfaces, R_o and R_i , were calculated as reciprocal value of corresponding convective (h_c) and radiative (h_r) heat transfer coefficients' sum following Equation (3) [11].



Figure 1: Indoors of study case air-supported structure at Brezovica.

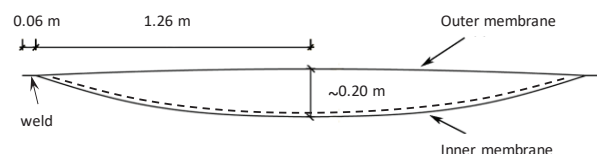


Figure 2: Cross section of the tubular double membrane envelope segment of the air-supported dome at Brezovica with potential low-e coating on external side of inner membrane (dashed line). After [9].

$$R_{DME} = R_o + R_z + R_{ch} + R_n + R_i \quad (2)$$

where R_{DME} - thermal resistance of double membrane envelope ($m^2.K/W$);

R_o - external surface resistance ($m^2.K/W$);

R_z - thermal resistance of external membrane ($m^2.K/W$);

R_{ch} - thermal resistance of air channel between membranes ($m^2.K/W$);

R_n - thermal resistance of internal membrane ($m^2.K/W$);

R_i - internal surface resistance ($m^2.K/W$).

$$R = 1 / (h_c + h_r) \quad (3)$$

where R - thermal resistance ($m^2.K/W$);

h_c - convective heat transfer coefficient ($m^2.K/W$);

h_r - radiative heat transfer coefficient ($m^2.K/W$).

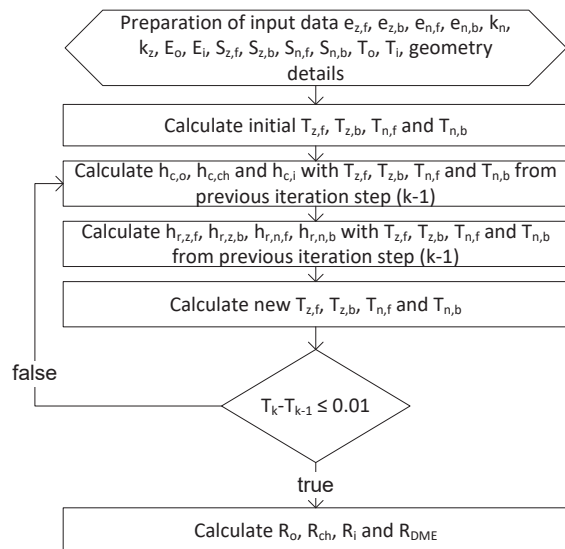


Figure 3: Calculation procedure of the double membrane envelope thermal resistance (R_{DME}).

Due to the fact that the convective and radiative coefficients are temperature dependent, the surface temperatures ($T_{z,f}$, $T_{z,b}$, $T_{n,f}$, $T_{n,b}$) were determined according to the numerical methodology also used in EnergyPlus software [12, 13]. The system of linearized heat balance equations (Equations (4) to (7)) was prepared and iteratively solved on basis of [12] as shown in Fig. 3. This procedure was repeated for each parametric case of the thermal emissivity $e_{T,n,f}$ and air velocity in the air channel v_{ch} (m/s).

$$E_o e_{T,z,f} - h_{r,z,f} T_{z,f} + k_z (T_{z,b} - T_{z,f}) + h_{c,o} (T_o - T_{z,f}) + S_{z,f} = 0 \quad (4)$$

$$k_z (T_{z,f} - T_{z,b}) + h_{c,ch} (T_{n,f} - T_{z,f}) + h_{r,n,f} T_{n,f} - h_{r,z,b} T_{z,b} + S_{z,b} = 0 \quad (5)$$

$$h_{c,ch} (T_{z,b} - T_{n,f}) + k_n (T_{n,b} - T_{n,f}) + h_{r,z,b} T_{z,b} - h_{r,n,f} T_{n,f} + S_{n,f} = 0 \quad (6)$$

$$E_i e_{T,n,b} - h_{r,n,b} T_{n,b} + k_n (T_{n,f} - T_{n,b}) + h_{c,i} (T_i - T_{n,b}) + S_{n,b} = 0 \quad (7)$$

where E_o , E_i - incident exterior and interior longwave radiation (W/m^2);

$e_{T,z,f}$, $e_{T,n,b}$ - thermal emissivity of external face of outer membrane and internal face of inner membrane (-);

k_z , k_n - thermal conductance of outer and inner membrane ($W/m^2.K$);

$h_{c,o}$, $h_{c,i}$, $h_{c,ch}$ - convective conductance of outer and inner air boundary layer and air channel ($W/m^2.K$);

$h_{r,z,f}$, $h_{r,z,b}$, $h_{r,n,f}$, $h_{r,n,b}$ - radiative conductance of external and internal face of outer membrane and external and internal face of inner membrane in case of parallel channel sides ($W/m^2.K$);

$T_{z,f}$, $T_{z,b}$, $T_{n,f}$, $T_{n,b}$ - temperature of external and internal face of outer membrane and external and internal face of inner membrane (K);

$S_{z,f}$, $S_{z,b}$, $S_{n,f}$, $S_{n,b}$ - incident short wave radiation (solar and from lights) and longwave radiation from lights (W/m^2).

The original heat balance equations [12], valid for case of air channel with parallel faces, were linearized [12] with Equations from (8) to (11):

$$h_{r,z,f} = e_{T,z,f} \sigma T_{z,f}^3 \quad (8)$$

$$h_{r,z,b} = 1 / (1 / e_{T,z,b} + 1 / e_{T,n,f} - 1) \sigma T_{z,b}^3 \quad (9)$$

$$h_{r,n,f} = 1 / (1 / e_{T,z,b} + 1 / e_{T,n,f} - 1) \sigma T_{n,f}^3 \quad (10)$$

$$h_{r,n,b} = e_{T,n,b} \sigma T_{n,b}^3 \quad (11)$$

where $e_{T,z,b}$, $e_{T,n,f}$ - thermal emissivity of internal face of outer membrane and external face of inner membrane (-);

σ - Stefan-Boltzmann constant ($W/m^2.K^4$).

In order to take into account, the influence of actual air channel geometry (Fig. 2) on radiative heat transfer coefficient, the radiative conductances $h_{r,z,b,(l)}$ and $h_{r,n,f,(l)}$ were calculated according to the Equations (12), (13) and (14):

$$q_{net} = \sum q_{net,j} A_j / \sum A_j \quad (12)$$

$$h_{r,z,b,(l)} = q_{net} / (T_{n,f}^4 - T_{z,b}^4) T_{z,b}^3 \quad (13)$$

$$h_{r,n,f,(l)} = q_{net} / (T_{n,f}^4 - T_{z,b}^4) T_{n,f}^3 \quad (14)$$

where j - index of linear segment running from 1 to 12;

$h_{r,z,b,(l)}$, $h_{r,n,f,(l)}$ - radiative conductance of internal face of outer membrane and external face of inner membrane in case of curved channel sides ($W/m^2.K$);

q_{net} , $q_{net,j}$ - average net density of heat transfer and for its segments ($W/m^2.K$);

A_j - area of segments 1 to 12 (m^2).

The net density of heat transfer ($q_{\text{net},j}$) between surfaces within the air channel containing a non-absorbing medium was determined on basis of the radiosity method as described in [8]. This method predicts radiative heat exchange between flat grey surfaces, which form the sides of an enclosure. Therefore, the air channel cross sections geometry was approximated by 12 elements as shown in Fig. 4. Further on, the view factors (F_{pq}) between these 12 surfaces were calculated according to crossed-string method [8].

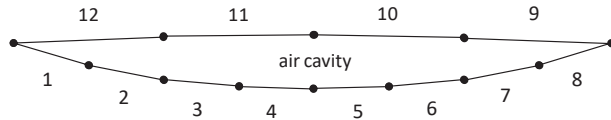


Figure 4: Cross section segmentation of the study case double membrane envelope.

Finally, the radiative heat transfer coefficient of the air channel $h_{r,\text{ch}}$ was calculated using Equations (15) and (16), second being reverse of Equation (6) in [10]:

$$h_{r,\text{ch}} = \sum h_{r,j} A_j / \sum A_j \quad (15)$$

$$h_{r,j} = q_{\text{net},j} / (T_{n,f} - T_{z,b}) \quad (16)$$

where $h_{r,\text{ch}}$, $h_{r,j}$ - average radiative heat transfer coefficient of the air channel between membranes and of air channel segments ($\text{W}/\text{m}^2\cdot\text{K}$).

The air channel convective heat transfer coefficients ($h_{c,\text{ch}}$) were calculated according to international standard ISO 15099:2003 [10]. Methodology given in this standard is experimentally developed and confirmed for air gaps of various inclinations and aspect ratios between flat plates [14]. For the purpose of this article, the input data, apart from surface temperatures and mean air temperature in the channel, from precedent research were used [1].

External (R_o) and internal (R_i) surface resistances and thermal resistances of outer (R_z) and inner (R_n) membrane were calculated according to international standard ISO 6946:2007 [15].

2.4 Energy use calculations.

The influence of thermal emissivity e_T on heating (Oct.-Apr.) and cooling (May-Sep.) energy demand of the study case building was assessed for temperate climate of Ljubljana [16]. The energy loads were obtained with EnergyPlus software [13], utilizing the same computer model as in preceding research [1]

3. RESULTS

3.1 Determination of thermal emissivity

From comparison of the recorded TR_{IR} spectrum of ETFE (Fig. 5) with the spectra for ETFE given in [7] it is possible to assume that the higher TR_{IR} peaks in the wavelength region between 2.5 and 7.0 μm are a consequence of the materials transmittance. Even so, the influence of the assumed transmittance amounts to below 3.1 % of its e_T values at different surface temperatures (Table 1). Finally, the e_T values were evaluated in waveband between 8 and 14 μm , where the given thermal resistance calculations are valid in terms of measured material optical properties. The whole recorded spectrum of PES (Fig. 5) is quite uniform and constant e_T is a good estimate. Also, for PES, the influence of surface temperature is negligible (Table 1).

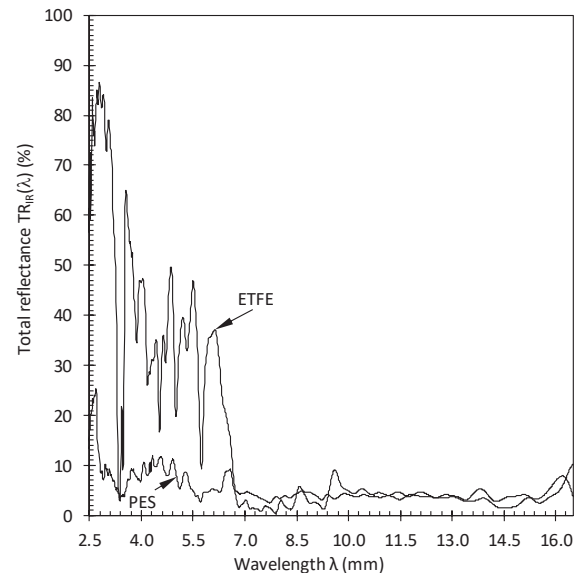


Figure 5: Total spectral reflectance of longwave infrared radiation ($\text{TR}_{\text{IR}}(\lambda)$) on spectral range from 2,5 to 16 μm of polyester fabric coated with PVC/PVDF and ethylene tetrafluoroethylene foil (ETFE).

Table 1: Thermal emissivity (e_T) of polyester fabric coated with PVC/PVDF (PES) and ethylene tetrafluoroethylene foil (ETFE) at different temperatures. Its values were determined from the measured total spectral reflectance of infrared radiation on gold background, in spectral range from 8 to 14 μm .

Temperature	$e_T (-)$		
	-10 °C	20 °C	50 °C
PES	0,96	0,96	0,96
ETFE	0,96	0,96	0,96

3.2 Thermal resistance calculations

Initial surface temperature ($T_{z,f}$; $T_{z,b}$; $T_{n,f}$; $T_{n,b}$) values were calculated using standard surface resistance values (external and internal) of a vertical wall and air gap thermal resistance, all proposed in international standard ISO 6946:2007 [15]. The

outdoor air temperature was -10 °C and the indoor 17 °C. There was no solar radiation taken into account ($S_{z,f}$, $S_{z,b}$, $S_{n,f}$, $S_{n,b}$ equal to zero) and the incident infrared radiation was evaluated on basis of T_o (overcast sky) and $T_{n,b}$. The thermal conductivities of materials were assumed to be 0,450 W/m.K for PES, 0,240 W/m.K for ETFE and 0,016 W/m.K for aerogel blanket composite. R_i and R_o were determined for each case separately.

From results of $R_{ch,||}$ and $R_{ch,()}$ calculation (Table 2) it can be observed that the relative contribution of e_T to thermal resistance of air channel is highly dependent on the v_{ch} value. In example, the reduction of v_{ch} of 0.5 m/s increases the R_{ch} almost equally as the reduction of e_T from 0.60 to 0.10, regardless of the studied air channel geometry case or inclusion of additional thermal insulation layer. As expected, the contribution to R_{ch} is higher at lower v_{ch} values (Fig. 6). In case of $R_{ch,||}$, the contribution of e_T to the thermal transmittance ranges from 6.8 to 91.0 % of initial value ($e_T = 0.96$) for DME_II and from 6.7 to 97.9 % for the DME_III. In case of $R_{ch,()}$, the contributions of e_T to the thermal transmittances are slightly smaller and range from 6.7 to 89.5 % of initial value ($e_T = 0.96$) for DME_II and from 6.5 to 96.1 % for the DME_III. Consequently, it is clear that geometry of air channel cross section, calculated according to presented procedure for the given temperature conditions, is almost insignificant (see also Fig. 6). The relative difference between $R_{ch,||}$ and $R_{ch,()}$ is in average equal to 0.24 % and is smaller than 1 % of $R_{||}$ for each individual pair of e_T and v_{ch} . These relative differences between $R_{DME,||}$ and $R_{DME,()}$ are even smaller and absolute ones lower than 0,001 m².K/W (unobservable in Fig. 6) for both analysed constructional complex cases.

The results for DME_I differ from results for DME_III for less than 1.6 % in case of $e_{T,n,f}$ is equal to 0.1 and less than 0.0 % for other $e_{T,n,f}$ cases. So, they are not given here in detail.

Table 2: Thermal resistance of air channel (R_{ch}) for the studied cases of double membrane envelope constructional complexes DME_II and DME_III, with parallel ($R_{ch,||}$) and curved ($R_{ch,()}$) sides.

$R_{ch, }$ (m ² .K/W)					
DME_II					
e_T/v_{ch}	0.0 m/s	0.5 m/s	1.0 m/s	2.0 m/s	4.0 m/s
0.96	0.146	0.115	0.094	0.069	0.045
0.60	0.181	0.136	0.108	0.077	0.048
0.40	0.210	0.152	0.119	0.082	0.050
0.10	0.278	0.185	0.138	0.091	0.053
DME_III					
e_T/v_{ch}	0.0 m/s	0.5 m/s	1.0 m/s	2.0 m/s	4.0 m/s
0.96	0.165	0.127	0.102	0.073	0.047
0.60	0.208	0.151	0.118	0.081	0.050
0.40	0.243	0.169	0.129	0.087	0.052
0.10	0.327	0.208	0.151	0.096	0.055

$R_{ch,()}$ (m ² .K/W)					
DME_II					
e_T/v_{ch}	0.0 m/s	0.5 m/s	1.0 m/s	2.0 m/s	4.0 m/s
0.96	0.147	0.115	0.095	0.070	0.045
0.60	0.182	0.136	0.109	0.077	0.048
0.40	0.211	0.152	0.119	0.082	0.050
0.10	0.278	0.185	0.138	0.091	0.053
DME_III					
e_T/v_{ch}	0.0 m/s	0.5 m/s	1.0 m/s	2.0 m/s	4.0 m/s
0.96	0.167	0.127	0.103	0.074	0.047
0.60	0.209	0.151	0.118	0.081	0.050
0.40	0.244	0.170	0.129	0.087	0.052
0.10	0.327	0.208	0.151	0.096	0.055

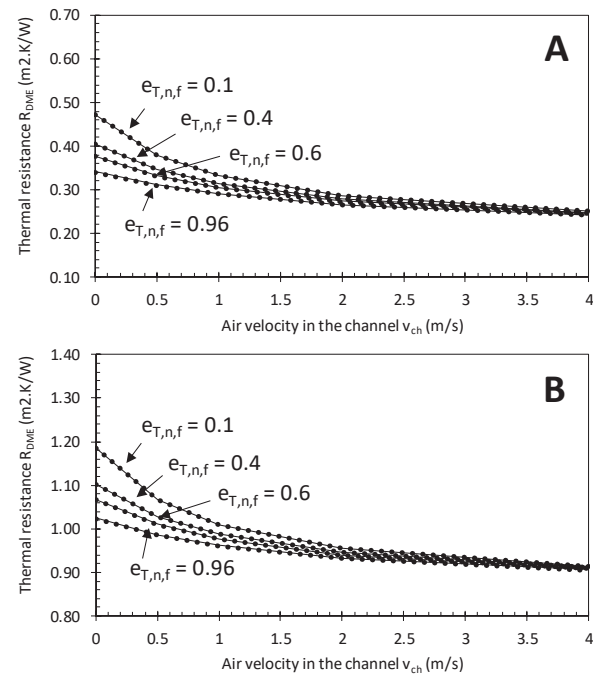


Figure 6: Thermal resistance of air-supported dome double membrane envelope (R_{DME}) constructional complexes DME_II (A) and DME_III (B) for cross section with parallel sides (dotted line) and the original envelope segment cross section (Fig. 2) (solid line).

3.3 Energy demand

The absolute and relative Q_{heat} savings, due to the reduction of e_T , were the highest for DME_III, except for $e_T = 0.1$ (Table 3). One can also observe, that the efficiency of $e_{T,n,f}$ in reducing Q_{heat} slightly increased when its value was decreased. Similar is true for DME_II in comparison with DME_I. The effect of adding aerogel insulation blanket had the inverse effect. In regards to Q_{cool} , it is interesting to point out that in case of DME_I, though not expected, the decreasing $e_{T,n,f}$ resulted in lowering Q_{cool} . This is just the opposite to what is true for other two envelope cases (Table 3). The presented calculations clearly show how the relationship between optical and thermal properties influences Q_{heat} and Q_{cool} .

Table 3: Yearly energy demand for heating Q_{heat} (Oct.-Apr.) and cooling Q_{cool} (May-Sep.) of study case building at Brezovica expressed as a percentage of base case demand.

	Q_{heat} (kWh/m ² .a)			
e_T	0.96	0.60	0.40	0.10
DME_I	100 %	97 %	95 %	91 %
DME_II	86 %	81 %	78 %	72 %
DME_III	78 %	77 %	76 %	74 %
	Q_{cool} (kWh/m ² .a)			
e_T	0.96	0.60	0.40	0.10
DME_I	100 %	91 %	84 %	66 %
DME_II	2518 %	3117 %	3462 %	4294 %
DME_III	531 %	578 %	622 %	749 %

4. DISCUSSION

The R_{DME} calculations are valid also for other structure typologies with double membrane envelope akin to the studied one (geometrical, optical and thermal properties).

The reduction of e_T by 0.03 (2.5 to 16 μm) results in 2.6 % higher value of $R_{\text{DME,II}}$ for DME_II. The effect is small, but even so, higher than the effect of curved geometry consideration. The optical properties, if not in full, at least in waveband up to 25 μm , should be determined and in case of noticeable total transmittance values, in region above 16 μm , also heat balance Equations (4) to (7) should be refined. But then again, the influence of atmospheric window should be investigated first.

The energy demand calculations were made for the case of double membrane envelope with a closed air gap, in which only natural convection occurs. Therefore, the influence of e_T value on Q_{heat} and Q_{cool} at higher values of v_{ch} remains unexplored.

5. CONCLUSION

To conclude, the use of low-e coating is not as efficient as inclusion of translucent, 10 mm thick, aerogel blanket in terms of increasing thermal resistance of double membrane envelope.

ACKNOWLEDGEMENTS

This work was supported by A-EEC d.o.o. and DUOL d.o.o.. The author would like to thank prof. dr. Boris Orel for his contributions to the presented research.

REFERENCES

1. ZRIM, G. (2019). *Implementation of aerogel insulation blanket Spaceloft into envelope of air-supported structures* [Doctoral dissertation, University of Ljubljana]. RUL. <https://repozitorij.uni-lj.si/IzpisGradiva.php?id=106593>.
2. Okalux. (2019). Comparison of the U_g -values depending on the position of installation. 5th April 2020, https://www.okalux.com/fileadmin/user_upload/aktuell/D_uploads/Infotexte/Infotext_OKALUXplus_en.pdf
3. Hutchins, M. G., & Platzer, W. J. (1996). The thermal performance of advanced glazing materials. *Renewable Energy*, 8(1), 540-545. doi:[https://doi.org/10.1016/0960-1481\(96\)88914-2](https://doi.org/10.1016/0960-1481(96)88914-2)

4. Wong, I. L., Eames, P. C., & Perera, R. S. (2007). A review of transparent insulation systems and the evaluation of payback period for building applications. *Solar Energy*, 81(9), 1058-1071. doi:<https://doi.org/10.1016/j.solener.2007.04.004>
5. Poirazis, H., Kragh, M., & Hogg, C. (2009). *Energy modelling of ETFE membranes in building applications*. Paper presented at the 11th International IBPSA Conference, Glasgow, Scotland.
6. Suo, H., Angelotti, A., & Zanelli, A. (2015). Thermal-physical behaviour and energy performance of air-supported membranes for sports halls: A comparison among traditional and advanced building envelopes. *Energy and Buildings*, 109, 35-46. doi:<https://doi.org/10.1016/j.enbuild.2015.10.011>
7. Cremers, J., Marx, H. (2016). Comparative Study of a New IR-Absorbing Film to Improve Solar Shading and Thermal Comfort for ETFE Structures. *Procedia Engineering*, 155, 113-120.
8. Gray, W. A., & Müller, R. (1992). *Engineering calculations in radiative heat transfer*. Oxford: Pergamon Press.
9. Duol (2012). *Slica membrane*. Duol. Brezovica pri Ljubljani.
10. ISO (2003a). ISO 15099:2003 Thermal performance of Windows, Doors and Shading Devices – Detailed Calculations. Geneva: International Organization for Standardization.
11. Duffie, J. A., & Beckman, W. A. (1991). *Solar engineering of thermal processes*. New York: John Wiley & Sons.
12. Winkelmann, F. C. (2001). *Modeling windows in EnergyPlus*. Paper presented at the 7th International IBPSA Conference, Rio de Janeiro, Brazil.
13. LBNL (2011). *EnergyPlus Engineering Reference. The Reference to EnergyPlus Calculations*. Berkeley, California: Lawrence Berkeley National Laboratory.
14. Hollands, K.G.T., Unny, T.E., Raithby, G.D., & Konicek, L. (1976). Free convective heat transfer across inclined air layers. *Journal of Heat Transfer*, 98(2), 189-193. doi:10.1115/1.3450517
15. ISO (2007). ISO 6946:2007 Building components and building elements - Thermal resistance and thermal transmittance - Calculation method. Geneva: International Organization for Standardization.
16. Meteotest (2009). *Meteonorm* (6.1). Meteotest.

Improving Building Performance Simulation boundary conditions

Urbanization of Building Performance Simulation input files using the microclimate model ENVI-met

HELGE SIMON¹, MICHAEL BRUSE¹, LAURA CRAMER¹, TIM SINSEL¹

¹Department of Geography, Johannes Gutenberg University Mainz, Mainz, Germany

ABSTRACT: Building Performance Simulations (BPS) are important tools to optimize the energy usage of a building and the thermal comfort for its occupants. In order to estimate the heating and cooling demands, boundary conditions for the outdoor meteorology are needed. Typical sources are local year-based weather files derived from outer-city measurement stations. These, however, do not include the imminent effects of the actual surrounding microclimate. Since the effects of the local climate can be quite substantial, failing to include them greatly reduces the accuracy of BPS. This contribution shows a way to overcome this shortcoming. By running microclimate simulations based on local weather files, local microclimate effects at building envelope are captured. This microclimatic information can then be used as input data to drive the BPS. A comparison of generic BPS input data with microclimate simulation outputs shows significant differences regarding important BPS parameters. While coupling of Building Performance Simulations with microclimate models presents a valuable approach to provide BPS models with more accurate meteorological data, the prolonged simulation times of microclimate simulations hinder coupling microclimate simulations with BPS models as a standard approach.

KEYWORDS: Energy Performance, Microclimate, downscaling, coupling models, TRNSYS

1. INTRODUCTION

Urban areas as well as their local microclimates are predominantly characterized by their buildings' structures. Buildings shape the microclimate in various ways: They modify the wind flow, cast shade, and alter the radiation and energy budget due to processes like heat storage, reflection, or reduction of sky view [1-3]. However, not only the microclimate is influenced by buildings, the indoor climate and the need to regulate the same (heating and cooling demands) strongly depend on the outside microclimate [5].

This interaction has been well-known for many years, yet little application has been found in the implementation of this knowledge. Building Performance (Energy) Simulations (BPS), which intend to optimize the energy usage of a building and the thermal comfort for its occupants, still use boundary conditions commonly derived from airport measurements as meteorological input data for building simulations [5-7]. Because the atmospheric conditions at the building envelope depend on the immediate local microclimate, their negligence leads to massive inaccuracies in building performance simulations and, ultimately, in an over/underestimation of the buildings' performance. To overcome these shortcomings of BPS, usual input data

provided by common weather files like EPW or TRY should be replaced by microclimate model outputs, which incorporate the local climate conditions at the building envelope [6-8]. This coupling of a microclimate simulation model, such as the state-of-the-art model ENVI-met, with Building Performance Simulation tools is thus a valuable approach to improve and urbanize the input data of BPS.

2. METHODS

As part of a case study, newest developments of the microclimate model ENVI-met aiming to urbanize BPS input files are implemented, applied, and analyzed. The developments include optimizations to enable year-long simulations and other improvements needed for the coupling with BPS, such as the implementation of precipitation, an enabling of the usage of TRY files as ENVI-met input data, and an export of the façade-based data in BPS input file format.

With ENVI-met being a dry model, as with most other microclimate simulations, i.e. neglecting water in liquid, running year-long simulations as needed for BPS has been hardly possible. When running a year-long simulation in order to get urbanized input data but without any added water to the water cycle, the soils

will eventually go extremely dry, thus leading to an overheating and eventual death of the vegetation. This, in turn, will lead to overall higher temperatures as transpiration and evaporation potential through plants can no longer be accounted for and instead of having a cooling effect, the dried-out plants may have the opposite effect [9-11].

This restraining limitation could be lifted by including a simplified abstraction of precipitation into the simulation process using full forcing. Full forcing is an operation mode, in which the user can provide hourly boundary conditions for various meteorological parameters such as air temperature and humidity, wind speed and direction and radiation (shortwave direct, diffuse and longwave). By adding precipitation in to the full forcing the accumulated precipitation is equally divided among the time steps between the current and prior forcing time step (see Equation 1).

$$P(t) = P_{cum} / dt \quad (1)$$

with $P(t)$ being the precipitation value at the time t in mm/s, P_{cum} the accumulated precipitation between the last and the current data point in mm and dt the time between the last and the current data point.

The resulting precipitation per second is then distributed using a simplified approach, where rain is falling exactly vertically and only onto plants and natural surfaces. Rain onto buildings or sealed surfaces, is – as of yet – not taken into account. When hitting a plant or soil cell, the water is partially intercepted by leaves and soil and can be further distributed downwards (see Figure 1).

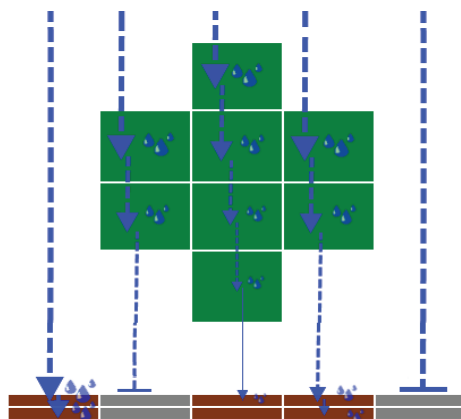


Figure 1: Schematic of the vertical distribution of precipitation.

To estimate the interception capacity of leaves, the local leaf area density as well as evaporation is taken into account. In case the rain water overcomes the interception capacity, the remaining water is transferred into the neighboring cell underneath. When rain

reaches unsealed soil, the water is taken up by the topmost layer as a first step. It is then distributed vertically using ENVI-met's prognostic water exchange equation (see Equation 2)

$$\partial \eta / \partial t = D_{\eta} * \partial^2 \eta / \partial z^2 + \partial K_{\eta} / \partial z - S_{\eta}(z) \quad (2)$$

with t as the time, z as the depth, η as the volumetric water content, D_{η} as the hydraulic diffusivity of the soil, K_{η} as the hydraulic conductivity of the soil and S_{η} as the water extraction from the soil by plants.

Precipitation data for the specific location can be obtained from measurements or common weather files. To improve the range of datasets that can be used as full forcing input data in ENVI-met, the possibility to create a full forcing file from TRY weather data was added to the already existing options of measurement and EPW data.

In order to improve BPS by integrating the urban influences caused by buildings, surfaces, and vegetation into their input files (Fig. 2), different measures for the ENVI-met simulation process were applied. The users can now define the building numbers of the buildings, which they want to further analyze with BPS and the urbanized meteorological data at building envelope is saved in a building specific CSV throughout the course of the simulation. The hourly microclimate output data that can then be used as building simulation input data can either be saved as averages for the cardinal directions of the façades or the individual values of each façade element. It currently includes the air temperature and air pressure in front of the façade and the wall shading flag, Sky View Factor, incoming longwave radiation, and the incoming direct, diffuse, and reflected shortwave radiation of the façade itself.

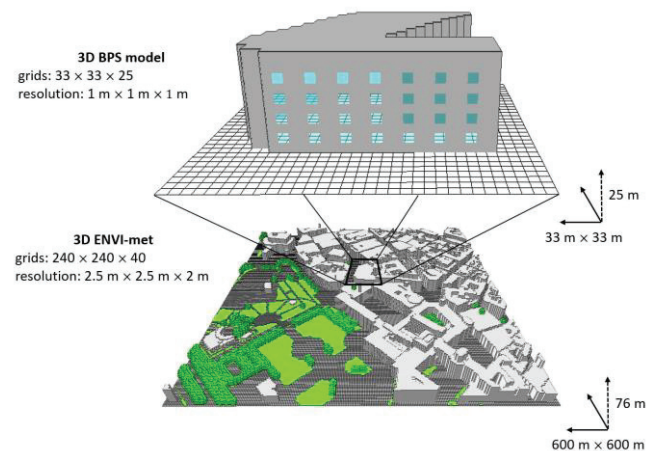


Figure 2: Exemplary building with no urban surroundings as simulated in BPS (top) and the same building in an urban context as simulated in a microclimate simulation (bottom).

In order to test the above-mentioned advancements of the ENVI-met model, year-long simulations for buildings in a medium dense urban area in Cologne, Germany were run (see Figure 3). The meteorological boundary conditions were taken from TRY-Datasets 2003 for Cologne.

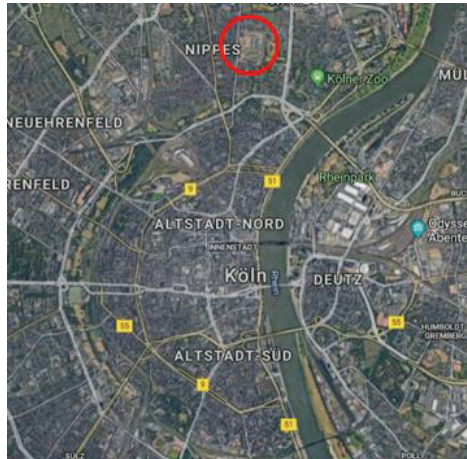


Figure 3: Location of the model area in the northern part of Cologne, Germany.

To save computational time, the simulation period was split into 12 month-long simulations. To account for processes that might build up during a simulation e.g. heat storage, the simulation periods overlapped for 10 days. Furthermore, the model area was digitized in a rather coarse resolution of 5 meters horizontally and 3 meters vertically and consists out of 100 x 120 x 22 cells (see Figure 4).

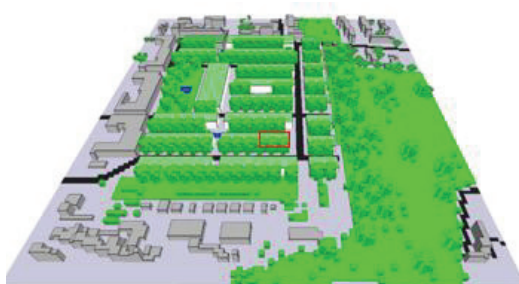


Figure 4: Model area for year-long simulation. Hourly BPS data was extracted for the highlighted building.

To evaluate the urbanization effect due to the microscale simulations the results of parameters in front of ENVI-met façades are compared against the generic BPS data input data – in this case the TRY-file for Cologne. Since year-long simulations generate large amounts of data, the comparison of the urbanized BPS inputs with the data provided by the TRY-file focuses on two months, July and January. This way, differences

caused by the incorporation of the local microclimate in summer and in winter can be evaluated. As ENVI-met's BPS outputs provide cell-based data of various meteorological information in front of individual façades, first three-dimensional model outputs at different times are shown to visualize the in-homogenous distribution at the observed building. In a second step, meteorological data of the individual façades is aggregated to the whole building envelope by calculating the mean over the whole façade area to directly compare the output data with the generic TRY-data.

3. RESULTS

Looking at the spatial pattern of various meteorological parameters in front of the façades of the observed building, the high spatial variation becomes clearly visible (see Figures 5 - 8). While BPS models also incorporate façade orientation, effects of the surrounding microclimate are not considered when using only a BPS model. However, variations caused by the local microclimate can be of substantial size, as for example demonstrated by the varying incoming shortwave radiation values between around 190 W/m² and 440 W/m² for the south facing wall at noon in Figure 5. Other parameters like the nocturnal longwave energy balance show distinct vertical patterns on the façade (see Figure 6 and 7).

The high spatial variation of important BPS input parameters such as the wind speed, which is used to calculate air pressure in front of façades for estimating natural ventilation, can be observed in figure 8.

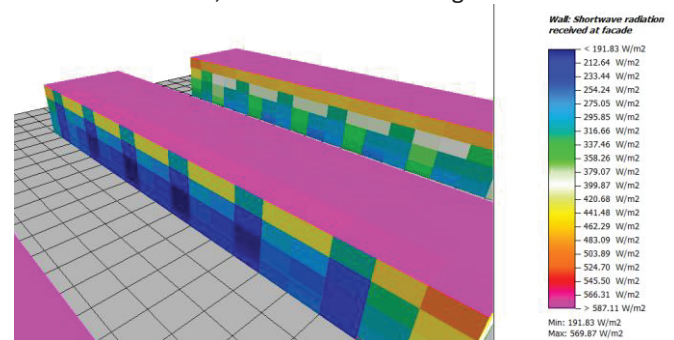


Figure 5: Distribution of shortwave radiation received at façade at noon on 21st July.

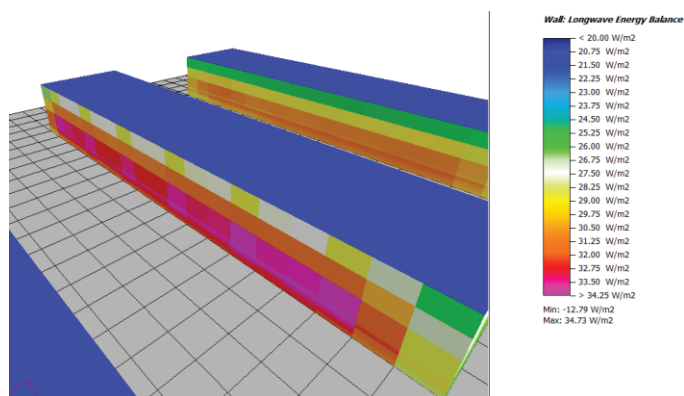


Figure 6: Longwave energy balance of façade at 4 am on 22nd July.

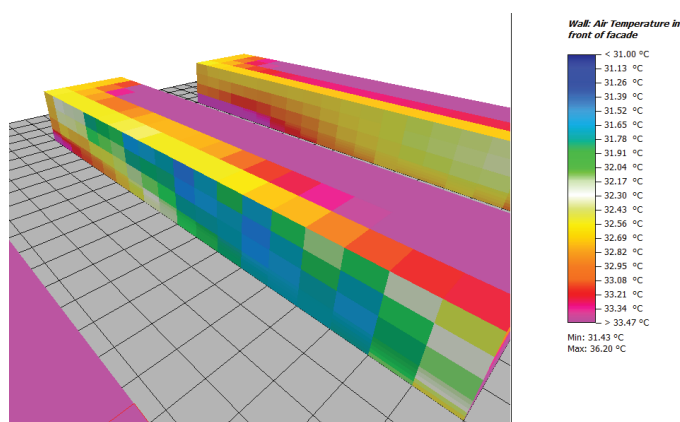


Figure 7: Air temperature in front of façade at noon on 21st July.

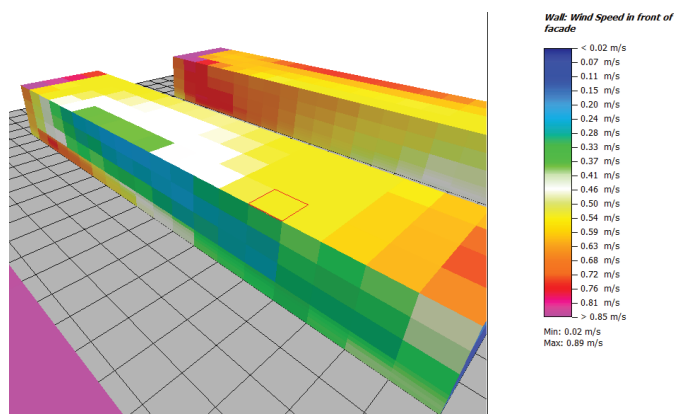


Figure 8: Wind speed in front of façade at noon on 21st July.

Aside from the high spatial variations in front of the façade, the comparison of façade mean outputs with TRY-file input data over time shows significant differences as well. As the statistical parameters in Table 1 and the comparison plots in Figure 9 – 14 show, large differences between the TRY-File data and the mean façade data can be attested.

Table 1: Minimum, maximum differences and Root Mean Square Error between TRY-file and simulated mean façade data for January and July.

	Wind Speed [m/s]	Air Temperature [K]	Relative Humidity [%]
<i>January</i>			
Minimum Difference	-0.34	-1.08	-51.95
Maximum Difference	12.38	4.07	12.06
RMSE	2.93	0.85	23.07
<i>June</i>			
Minimum Difference	-1.39	-2.88	-34.86
Maximum Difference	12.60	4.01	13.50
RMSE	2.35	1.13	12.53

Comparing the diurnal cycle of air temperature differences between the TRY-file data and the mean façade simulation outputs, it becomes apparent that the mean façade data generally shows lower values during daytime and higher air temperatures at nighttime. This might be caused by the effects of the nocturnal urban heat island, where due to the vertical structures in urban environments the increase of shade at daytime lowers the air temperatures and the higher heat storage of the thermal masses leads to increased air temperatures at nighttime. Since TRY-file data is generally obtained from open areas such as airports, a nocturnal heat island effect is not present.

The comparison of wind speed shows the effects of obtaining data in open areas even more drastically. Wind speed values are considerably higher in the TRY-file compared to the simulated façade means. With the surrounding buildings and vegetation in the microclimate simulation, the local wind speed is massively decreased and temporary gales of wind speeds greater than 10 m/s cannot be found in the microclimate simulation data.

Looking at the relative humidity differences, which is a good indicator of potential mold in BPS models, large differences can again be attested. Especially in January, the overall low air temperatures can lead to condensation of water at the façade surfaces. In June, ENVI-met seems to predict higher relative humidity values than the input TRY-data as well. This might be caused by the local vegetation, which, due to the transpiration processes, leads to an increase of water vapor.

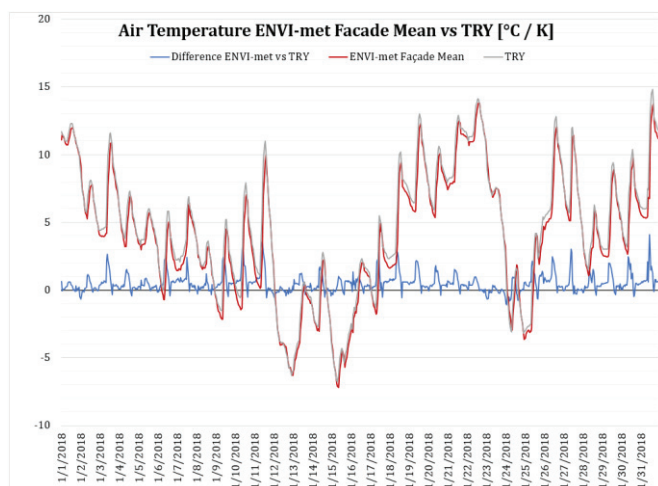


Figure 11: Comparison of air temperature in front of ENVI-met facades (mean over all facades) and input TRY air temperature for January.

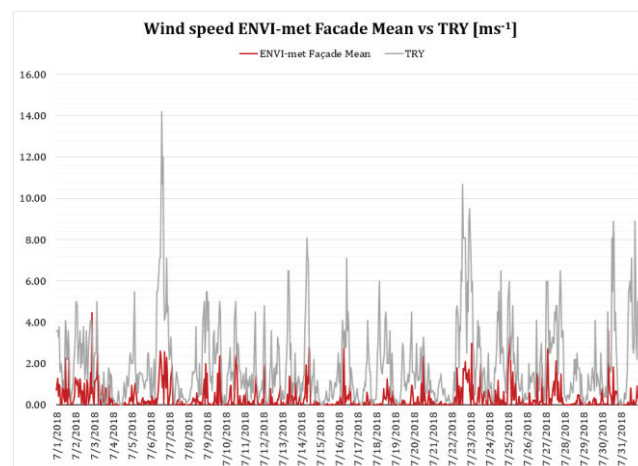


Figure 10: Wind speed values [ms^{-1}] in front of ENVI-met facades (mean over all facades) and input TRY wind speed values for July.

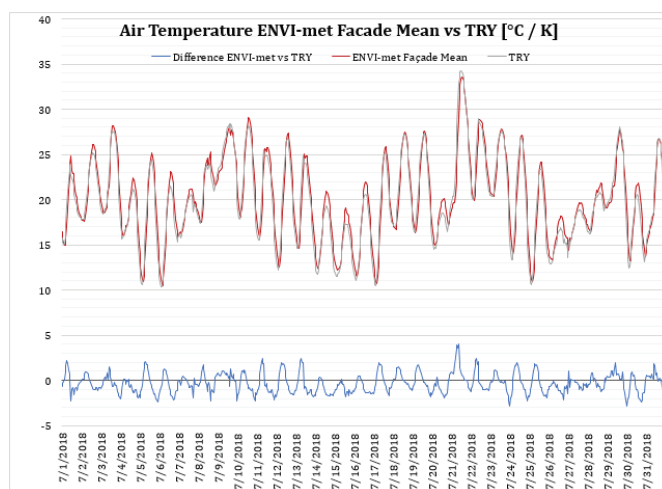


Figure 12: Comparison of air temperature in front of ENVI-met facades (mean over all facades) and input TRY air temperature for July.

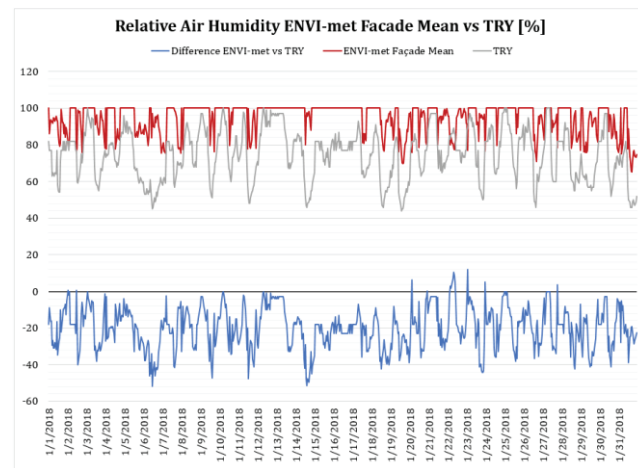


Figure 13: Comparison of relative air humidity in front of ENVI-met facades (mean over all facades) and input TRY relative air humidity for January.

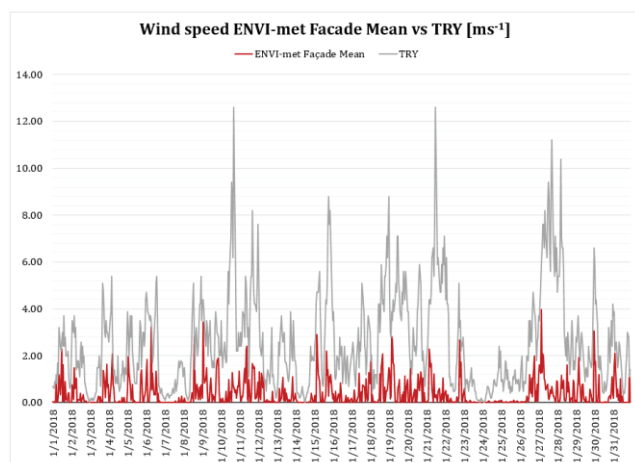


Figure 9: Wind speed values [ms^{-1}] in front of ENVI-met facades (mean over all facades) and input TRY wind speed values for January.

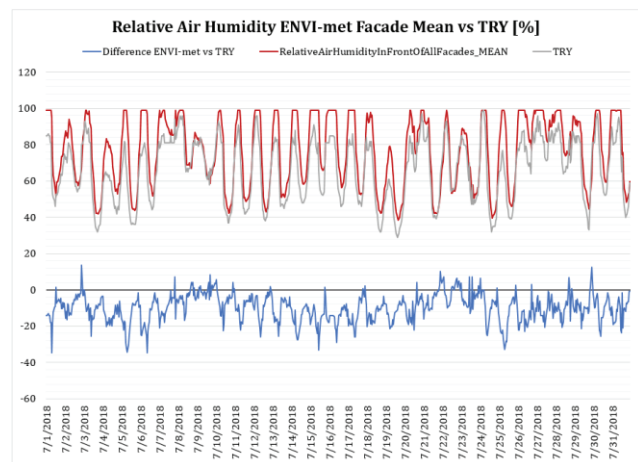


Figure 14: Comparison of relative air humidity in front of ENVI-met facades (mean over all facades) and input TRY relative air humidity for July.

4. CONCLUSION

The comparison of generic BPS input data with microclimate simulation outputs shows significant differences regarding important BPS parameters. By considering microclimate interactions between buildings, vegetation, and surfaces, effects like heat storage, radiative transfer, and wind flow can be accurately extracted from microclimate models and incorporated into BPS simulations. Using coupled simulation runs, ENVI-met can be used to generate boundary conditions accounting for the local microclimate around the building structure as input for BPS modelling. This allows much more precise representation of the actual microclimate at the building envelope which further increases BPS modelling.

The implemented adaptations to the microclimate model ENVI-met present a valuable approach to provide BPS models with more accurate meteorological data at the building envelope. The long simulation times of a year-long microclimate simulation (~13 days on three AMD Threadripper 1950x) are however still an obstacle that might hinder coupling microclimate simulations with BPS models. In order to overcome this, simulating only a handful of days featuring significant weather patterns might be an option. By extracting characteristic meteorological conditions from TRY-files, simulation only those in the microclimate model, and then using the data to extrapolate back to yearly information, effects of local microclimate might be captured without having to simulate a whole year. Further research has to be conducted in order to decide whether this is a viable option.

REFERENCES

1. Arnfield, A.J., (1990): Street Design and Urban Canyon Solar Access. *Energy and Buildings*, 14 (2): p. 117-131.
2. Blocken, B. and Carmeliet, J., (2004): Pedestrian wind environment around buildings: Literature review and practical examples. *Journal of Thermal Envelope and Building Science*, 28(2): 107-159.
3. Chudnovsky, A., Ben-Dor, E., and Saaroni, H., (2004): Diurnal thermal behavior of selected urban objects using remote sensing measurements. *Energy and Buildings*, 36(11): 1063-1074.
4. van Hooff, T., Blocken, B., Timmermans, H. J. P., and M., Hensen J. L., (2016): Analysis of the predicted effect of passive climate adaptation measures on energy demand for cooling and heating in a residential building. *Energy* 94: 811-820.
5. Sun, Y., Heo, Y., Tan, M., Xie, H., Wu, C.F.J. & Augenbroe, G., (2014): Uncertainty Quantification of Microclimate Variables in Building Energy Models. *Journal of Building Performance Simulation* 7 (1): 17-32.
6. Merlier, L., Frayssinet, L., Johannes, K. & Kuznik, F., (2019): On the Impact of Local Microclimate on Building Performance Simulation. Part I: Prediction of Building External Conditions. *Building Simulation* (12,5): 735-746.
7. Vuckovic, M., Hammerberg, K. & Mahdavi, A., (2019): Urban Weather Modeling Applications: A Vienna Case Study. *Building Simulation*: 1-13.
8. Merlier, L., Frayssinet, L., Johannes, K. & Kuznik, F., (2019): On the Impact of Local Microclimate on Building Performance Simulation. Part II: Effect of External Conditions on the Dynamic Thermal Behavior of Buildings. *Building Simulation* (12,5): 747-757.
9. Kim, H.H., (1992): Urban Heat Island. *International Journal of Remote Sensing* (13): 2319-2336.
10. Perini, K. & Magliocco, A., (2014): Effects of Vegetation, Urban Density, Building Height, and Atmospheric Conditions on Local Temperatures and Thermal Comfort. *Urban Forestry & Urban Greening* (13): 495-506.
11. Heusinger, J. & Weber, S. (2017): Surface Energy Balance of an Extensive Green Roof as Quantified by Full Year Eddy-Covariance Measurements. *Science of The Total Environment* (577): 220-230.

Application of mixed-methods in the analysis of building monitoring data

Lessons learned for user-centred design

OLIVIA GUERRA-SANTIN¹ ANNE GRAVE¹ MASI MOHAMMADI¹

¹Chair of Smart Architectural Technologies, Department of the Built Environment, Eindhoven University of Technology, Eindhoven, The Netherlands

ABSTRACT: *This paper presents the application of mixed-methods analysis of building monitoring data to draw conclusions for a user-centred design approach. The analysis is applied to a case study consisting of a Passivhaus care home in the UK, specialised on dementia care. User-centred design is especially important in older peoples' living environments due to specific needs and preferences associated to their pattern of daily activities and health condition. The analysis showed that the building tends to be uncomfortable for the staff, but it is kept within comfortable ranges for the residents. However, the energy use is higher than expected, because the building is managed in a way to preserve residents' health. The building design is able to meet the residents comfort because their needs, and the practices followed in a care home were taking into account during the design of the building.*

KEYWORDS: *Energy performance, Comfort, Care home, Dementia, User-centred*

1. INTRODUCTION

To battle climate change and reduce the Green House Gas emissions from the domestic sector different housing typologies are being developed and built, like Passivhaus [1]. However, that these buildings help with reducing energy consumption does not necessarily mean that the building provides a good living environment to its users. While further developing the Passivhaus concepts to reduce more energy it is also necessary to integrate a user-centred design approach, in this way the wishes and needs of the users can be integrated into the design.

Applying the user-centred approach is especially important when designing living environments for older adults with dementia due to specific needs and preferences associated to their pattern of daily activities and health condition. Due to demographic changes, the group of older adults with dementia is increasing with 850.000 people with dementia living in the UK in 2019 and it is expected that these numbers will rise to 1.6 million people by 2040 [2]. A significant group of people who will partly be placed in the energy-neutral newly built or renovated care homes. When this happens these living environments should meet the needs and wishes of its users.

Due to symptoms of dementia such as judgment, cognition, and perceptual deficits, the older adults with dementia have an altered sensitivity to environmental conditions [3,4]. Older adults may for example not realize that their living room is too cold, only that he or she is uncomfortable. A person with dementia will not associate this uncomfortableness with the room's temperature or is able to

communicate this to others [5,6]. This often leads to behavioural issues like agitation, frustration, and anger [3,5,7] or illnesses like colds or worse pneumonia which lead to a decrease in quality of life. Garre-Olmo and colleagues [8] showed that quality of life of nursing home residents with dementia was related to environmental factors such as temperature [8,9] not only because it reduced health risks and improved living comfort also because a good indoor climate also reduces behavioural issues like agitation and decreases pressure on the care professionals [7,8]. It is therefore important that indoor climate is properly regulated in Passivhaus care homes.

In this paper, a mixed methods approach is used to analyse building monitoring data, from a case study Passivhaus care home in the UK, to draw conclusions for a user-centred design approach when designing a Passivhaus care home.

2. MIXED METHODS APPROACH

A mixed methods approach was used in the data collection and analysis. In this approach, qualitative and quantitative data on building use and building performance in terms of energy and indoor environment are collected and analysed to determine the occupancy practices followed by the building users, and the reasons behind the practices. The practices analysed can be related to space heating, cooling, natural ventilation, use of appliances, domestic hot water, etc. The objective of the mix methods approach is to obtain a comprehensive understanding of the users' interaction with the building.

3. MONITORING CAMPAIGN – CASE STUDY

The case study consists of a 60-bedroom care home in England, specialised in providing care for older people with dementia. The building was designed according to Passivhaus requirements. The building is provided with radiators in bedrooms and an air conditioning system providing heating and cooling in common areas and a heat recovery ventilation system.

The monitoring campaign was carried out between June 2012 and June 2013. The designers of the building, who specialised in care homes, were interested in the suitability of Passivhaus technology in care homes and were mostly concerned about the air quality and the effect of airing rooms patterns usually needed in care homes, on the energy performance of the building.

3.1 Data collection and methods

Information on indoor and outdoor environmental conditions, energy consumption, and building operation were collected for the first year of occupancy. In the following sections, the details of the campaign are presented.

Indoor and outdoor conditions

Indoor temperature, relative humidity, and CO₂ measurements were taken in selected spaces. The care home was not fully occupied and so the selection of the spaces depended on the occupancy. Bedrooms facing north and south were selected to compare the effect of solar gains. External weather conditions were also measured with a weather station installed at the open area behind the building. Air temperature, solar radiation, humidity, wind speed, and wind direction were recorded at 30 minutes intervals.

Thermal comfort

The care home has different types of occupants, with very different activities and health conditions. Thus, the level of comfort of each group needs to be evaluated. The groups also differ in the areas of the building that they occupy. The building's occupants are: 1) residents are the most sensitive group since they are fulltime in the building and usually have poor health; they are very passive and have less control on the building systems; 2) nurses and carers have 12-hour shifts (day or night) and a moderate activity level; 3) housekeeping staff have an activity level higher than nurses and carers but only work the day shift; and 4) administrative staff have a lower activity level and work eight-hour day shifts.

Two methods were used to evaluate the comfort in the building: the first based on structured interviews and surveys with the occupants, and the

second based on the Predicted Mean Vote (PMV) method developed by Fanger [10]. The PMV method was used because of the impossibility to involve all the residents of the building in the monitoring campaign, especially those with dementia, and due to the effect of the large differences on activity types and clothing between the occupants in the building.

During the interviews, and on the questionnaire survey, carried out seasonally, staff members were asked to rate the temperature and air quality of the building and their thermal comfort based on the seven-point thermal sensation scale (-3 to +3). Four residents were interviewed in the winter because only residents without dementia and in good health could be considered. As an extra indicator of the thermal comfort of residents, the staff was asked about their opinion about the thermal comfort of the residents.

Energy and building operation

Energy sub-meters were used to measure electricity, gas, and heat for hot water. Building operation (occupant behaviour) was investigated to determine its effect on comfort and energy efficiency, but also to determine the actual heating and ventilating practices in the care home with the vision to inform future design. Data about the operation of the building were collected in three ways: installation of energy meters and sensors, analysis of indoor parameters and interviews with staff. The following data were used to determine building operation: 1) heat meters were installed in the radiators of 12 bedrooms; 2) sensors were installed in the windows in four bedrooms; 3) measurements of indoor parameters and outdoor conditions were used as indicators of natural ventilation; and 4) staff members were asked about their interaction with the building in terms of opening and closing windows, and use of the radiators.

3.2 Mixed methods approach to data analysis

A mixed methods approach to data gathering and analysis was followed to determine the building performance and occupancy practices. These performances and practices were analysed in relation to the initial project expectations to determine how users are considered during the design process. The results can be used to inform future design processes in relation to the type of information needed to carry out evidence-based (inform) design decisions, and the methods for data collection and analysis that can be employed during user-centred design approaches.

Qualitative data (such as user's interviews), quantitative subjective data (comfort votes) and quantitative objective data (opening windows, meters, and indoor parameters) were collected during a year. The different types of data were

analysed using triangulation methods 1) to determine occupancy practices regarding natural ventilation and use of heating and cooling, 2) differences between groups and individual preferences for temperature and fresh air, and 3) energy consumption. The relationship between occupancy practices, user preferences, comfort, and energy use were analysed to determine the effect of design intentions on building performance.

4. RESULTS

4.1 Indoor conditions

Temperature in monitored areas was analysed with statistics and with visualizations of plotted external in internal temperatures. Analysis of the temperatures shows similarity across the occupied spaces most of the time, usually within 22 to 24 degrees. The temperatures in occupied bedrooms are more or less steady, usually with less than 1°C Standard Deviation within one month.

The results show that there was an increase in temperature in common areas and unoccupied bedrooms in July, which was followed by starting using the air conditioning on a regular basis. The nurse station tended to be warmer than other common areas because there are no windows in the nurse stations and the air conditioning control is not easily accessible. The dining room tends to overheat at dinner time because food is kept warm in the place. However, the mean temperature does not show the overheating because of the use of air conditioning, especially in July. The coffee shop is the coolest common area because both air conditioning and crossed ventilation are used.

No large differences in temperature were seen between the seasons, but temperatures in the bedrooms vary more in warm days in the summer than in the winter. Common areas tend to overheat in the spring and summer, especially the dining room at dinner time, while bedrooms are less likely to overheat in the summer.

The difference in the summer between unoccupied bedrooms and occupied bedrooms is large, highlighting the use of natural ventilation for cooling. Bedrooms facing the North and South were monitored but no significant differences were found between the temperatures in bedrooms in the South in comparison to those in the North.

4.2 Users' comfort

Interviews

Three rounds of interviews were conducted in summer, autumn, and spring. In addition, a survey was carried out in the winter, because of the busy schedule of the care staff during this period.

Summer interviews showed that all the staff members consider the building to be too warm and

reported to be (thermally) uncomfortable most of the time. The only space considered comfortable was the coffee shop, where air conditioning and natural ventilation are most often used. The staff seem to be more forgiving of high temperatures in the bedrooms and lounge, places where the residents spent most of the time. These spaces are rated as neutrally comfortable while the temperatures were rated mostly as warm and hot (Figures 1 and 2). A large variation in comfort rating was found in the nurse station while the temperature was rated as warm and very warm. The dining room was rated as hot and uncomfortable.

During the winter, most spaces were rated as warm and hot, but as seen in the summer, the bedrooms were rated as neutral. The temperature in the dining room was rated as uncomfortable and hot and the reception area as neutral in comfort but varied in temperature rating. The largest difference in comparison to the summer was seen in the lounge, which was rated as very hot and uncomfortable.

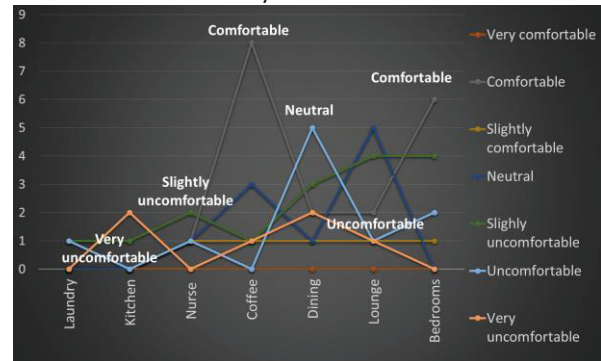


Figure 1: Staff thermal comfort votes in the Summer

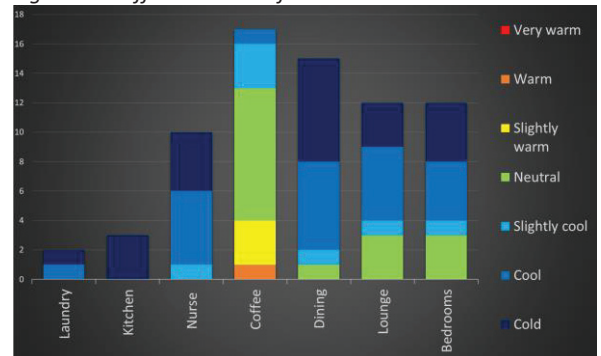


Figure 2: Staff temperature votes in the Summer

As other studies have shown [11], staff reported feeling “comfortable” working at the care home due to other factors such as the working conditions provided by the organisation. Some staff members, mostly care staff, stated that the building was too warm for them, but “just right” for the residents. However, there are spaces not intended for residents that were also rated too warm. Staff members reported the kitchen and laundry to be too hot and to have no control to change it, since on warm days opening windows does not cool down these rooms and no other ways to cool down the rooms are provided. Although the staff acknowledges their

discomfort ensures residents' comfort, some felt that their own comfort could be improved through more breathable uniforms and they expressed preferences for a polo shirt type of uniform.

PMV calculation

The residents were asked to rate different areas in the building based on the same thermal comfort scale (-3 to 3) given to the staff. In all areas, residents seem to feel warm and comfortable. Only one resident of those interviewed thought that the lounge was too warm for her but in her opinion, all other residents, especially those with dementia, felt comfortable and were usually wearing jumpers.

Since residents with a poor health condition or dementia could not be interviewed, we have assessed the thermal comfort of users of the building by calculating the Predicted Mean Vote (PMV) based on the ASHRAE standard 55:2004-04 [10] for thermal comfort. The comfort survey allows us to compare the results from the calculation with actual perceived thermal comfort.

The Predicted Mean Vote (PMV) was calculated for every monitored space and each measured interval (30 minutes). To calculate the PMV, we estimated the metabolic rate (MET) and clothing level (CLO) of the two main types of occupants in the building: housekeeping and care staff, and residents, due to their differences in activity level, clothing, and health condition. Two PMV calculations were made for each space, one per occupancy group. Clothing insulation values were calculated from observations. A value of 0.95 was used for residents. For staff, a value was derived for each of two uniforms: 0.472 (winter uniform) and 0.392 (summer uniform). The PMV of staff was calculated for both uniforms. Activity level was assumed to be 1.0 met for residents (sedentary activity level), mostly sitting and resting; and 2.0 met for the staff (moderate activity). These were also based on observations.

The ASHRAE standard 55:2004-04 introduces three categories of performance. These categories depend on the stringency of the building evaluation. The building can be evaluated based on the percentage of time that a given parameter (PMV, relative humidity, temperature, and CO₂) falls within the requirements of each category. The categories are: 1) higher than typical comfort standards; 2) new buildings and; 3) existing buildings (Table 1). The percentage of time that the building is within each category was calculated next. We consider that the building should be within Category 1 for the residents, and within Category 2 for the staff (Figures 3 and 4).

Results showed large variations on the comfort level in each monitored room in the different seasons. In general, most areas are too warm for the

staff. While for the residents, the causes for discomfort are caused by both low and high temperatures. In the winter, the bedrooms are between 10-50% of the time within Category 1 for the residents, and 40-60% the rest of the year. A larger variation is seen in common areas, going from 20-30% in the summer, to 30-50% in autumn and winter, to 40-70% in the spring.

For the staff, less comfort is seen in the summer, especially in the bedrooms (10-40% of the time within Category 2), and in the autumn, winter, and spring in the common areas (less than 10% of the time within Category 2 in the spring).

The very small percentage of time within Category 1 in all seasons is caused by the very narrow range of comfort within this category. Considering Category 2 (new buildings) significantly improves the thermal comfort performance of the building, especially for the residents. In some bedrooms, the percentage of time within comfort limits would raise to 95%.

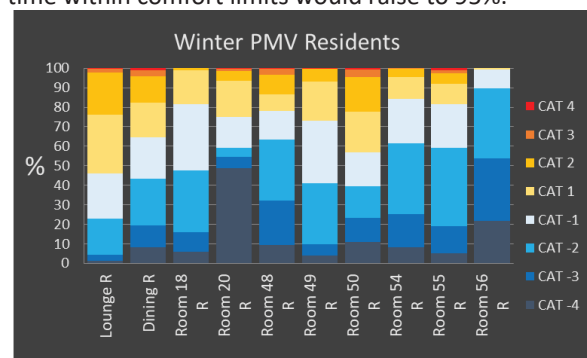


Figure 2: Residents' PMV in the winter period

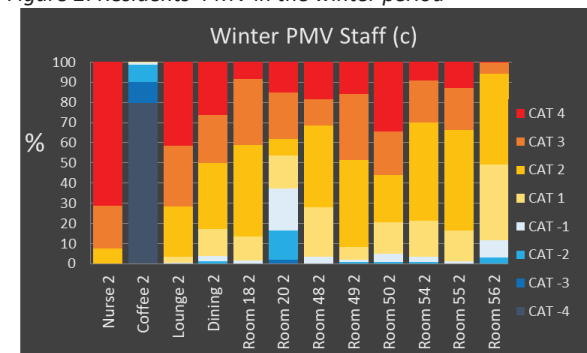


Figure 3: Staff PMV in the winter period

CO₂

Figure 5 shows the results of the categories for CO₂ concentration levels for winter. CO₂ is used as an indicator of indoor air quality. The percentage of time within Category 3 is considerable, especially in rooms 48, 49, 50 and 55. In common areas, the CO₂ concentration is within Category 3 for more than 50% of the time. In spring, indoor air quality is better in comparison to the winter. Similar conditions were found in the autumn. During the summer, better indoor quality is observed.

Higher mean CO₂ levels occur in colder months (January and February) and in specific bedroom (B49). Therefore, differences in CO₂ concentrations are

related to natural ventilation, raising concerns about the efficiency of the mechanical ventilation system. The outlet of the mechanical ventilation system is located in the bathrooms, which doors are usually closed due to the layout of the rooms.

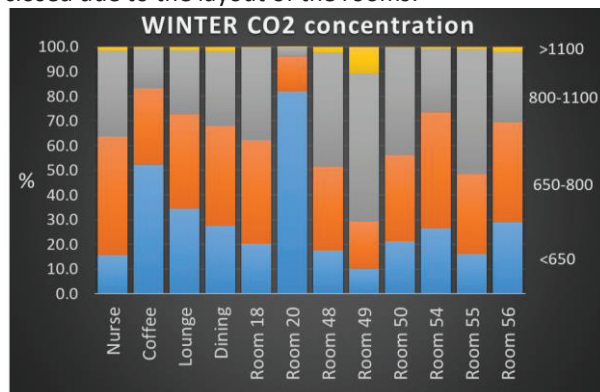


Figure 5: CO2 concentration per room in the winter period.

Table 1 Categories according to ASHRAE standard 55:2013.

	PMV	CO2 (ppm)	Building type
Cat -3	-0.7<PMV		Existing
Cat -2	-.05<PMV		New
Cat -1	-0.2<PMV		Higher comfort
Cat 1	PMV< 0.2	<650	than standard
Cat 2	PMV< 0.5	650-800	New
Cat 3	PMV< 0.7	800-1100	Existing

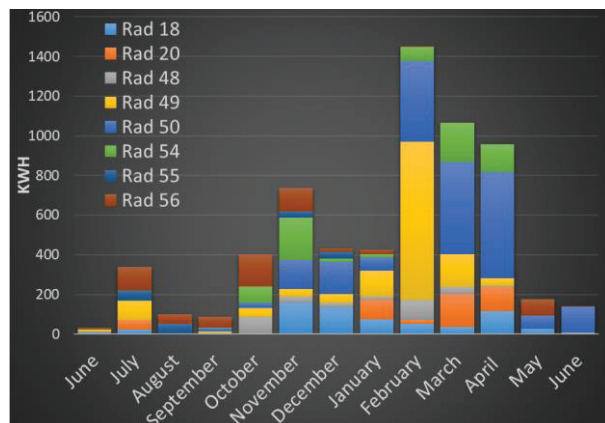


Figure 6: Heat to radiators per monitored room

4.3 Occupancy practices

The heat provided to radiators in a selection of bedrooms was monitored to determine the use of the radiators throughout the year. Figure 6 shows that radiators were on in some bedrooms during the summer and in the spring. It is also visible that some rooms are heated more than others. Room 49 and 50 utilising most of the heat in the monitored bedrooms. However, the temperature in the monitored rooms was not higher than the temperature in the other occupied monitored rooms because of the use of natural ventilation. This shows the large differences in energy requirements between bedrooms based on residents' preferences for temperature and natural ventilation.

In regard to heating practices, most of the staff reported to only open or close the radiator valve when asked by the resident.

Natural ventilation

During the summer, staff reported opening windows in the bedrooms in the morning mainly to get rid of stale air and odours, but if the resident was in the bedroom, they would ask them first about opening the window before doing so. Most of the cleaning staff reported opening windows as part of the normal routine. Staff also reported opening some windows in common areas to cool the spaces. However, few staff members reported having been instructed "not to open windows" during the winter, as it is usually recommended in Passivhaus buildings. During the autumn, staff reported to open windows less frequently than in the summer in common areas, but about with the same frequency as in the summer in the bedrooms. During all seasons the same natural ventilation operation routine was used in the bedrooms: windows being open to cool down spaces and to get rid of odour and stale air. In the winter, windows are open with less frequency in common areas, but bedrooms are still ventilated in the mornings.

To further investigate window opening behaviour, analysis of the data from window sensors in 4 bedrooms were used as indicators of natural ventilation in the building. We wanted to know whether windows were opened at all during the winter (opposed to the requirements of a Passivhaus building). Figure 7 shows the hours during the monitoring. Although according to the design of the building, windows should not be open during the cold weather period, the figure shows that in the monitored rooms, windows are opened. Long hours of ventilation in rooms 49 and 50 correspond to the higher heating requirement seen in Figure 6.

The staff reported to open the windows in two instances: cleaning staff reported to open windows shortly when cleaning the rooms in the morning and to get rid of stale air, and the caring staff reported to open windows to cool down the spaces or to refresh the air, but only when the resident asked for it, first asking the resident if it was ok to do it. This was also noticed in the analysis of CO2 levels in the bedrooms since no clear common ventilation pattern was found in the rooms.

The results show that the residents prefer warmer temperatures throughout the whole year, in the range of 23-25°C. This explains the use of the heating system during the warmer months. The results also showed large differences between residents, some preferring cooler rooms than others, as well as a preference for more fresh air both during day and night. These preferences for fresh air during the night had a visible impact on the indoor air quality of the

residents' bedrooms. Large differences were found in the air quality of the different bedrooms. The results showed that the occupancy practices related to heating, cooling and airing rooms, followed by the staff (carers and cleaning staff), were always focused on the needs of the residents.

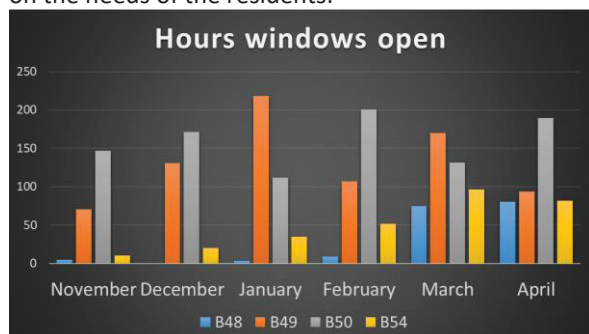


Figure 7: Hours windows open in selected bedrooms

4.3 Energy consumption

The energy consumption was much higher than expected, especially in comparison with the PHPP calculation software (Tables 2 and 3). The main reasons for these differences were that the actual needs of the users were not fully considered during the calculation of the expected energy use. It is important to remark that we refer to calculations and not to the design of the building and installations since the daily activities required in this type of building were actually well considered during the design of the building (e.g. provision of radiators in bedrooms, openable windows, etc.).

Table 2: Measured and calculated electricity consumption.

	Measured (kWh)	Calculated (kWh)
Electricity total	159,961	72,051
Lighting	51,407	1,914
Air conditioning	44,997	9,732
Ventilation	13,337	5,350

Table 3: Measured and calculated gas consumption.

	Measured (kWh)	Calculated (kWh)
Gas (excl. Laundry and kitchen)	267,446	98,804
Domestic hot water	124,858	70,544
Space heating	143,188	28,260

5. LESSONS LEARNED

The results of this study showed the importance of considering the final user during the design of a building. In this case, the managers of the care home were able to provide the required comfort level (in terms of thermal comfort and to a lesser extent on air quality) to the residents of the building due to the provision of radiators in bedrooms, air condition system in common areas and all-year round openable windows even though the building was defined as Passivhaus. However, and partially as a consequence of providing the residents with a good indoor

environment, the actual energy consumption of the building was much higher than the expectations, both in comparison with the Passivhaus calculations and with more realistic expectations defined by the design team. This shows the importance of considering the actual needs and preferences, and understanding the daily activity patterns of the users during the design of the building, and the effect on the energy gap of considering unrealistic occupants' behaviour.

REFERENCES

- McLeod, R. S., Hopfe, C. J., & Rezgui, Y. (2012). An investigation into recent proposals for a revised definition of zero carbon homes in the UK. *Energy Policy*, 46, 25–35. <https://doi.org/10.1016/j.enpol.2012.02.066>
- Alzheimer's society. (2020). Facts for the media. Retrieved January 17, 2020, from <https://www.alzheimers.org.uk/about-us/news-and-media/facts-media>
- van Hoof, J., Kort, H. S. M., Hensen, J. L. M., Duijnste, M. S. H., & Rutten, P. G. S. (2010). Thermal comfort and the integrated design of homes for older people with dementia. *Building and Environment*, 45(2), 358–370. <https://doi.org/10.1016/j.buildenv.2009.06.013>
- Weaverdyck, S. E. (1991). Assessment as a basis for intervention. In D. H. Coons (Ed.), *Specialized dementia care units* (pp. 205–523). Baltimore: The John Hopkins University Press.
- van Hoof, J., Kort, H. S. M., Duijnste, M. S. H., Schoutens, A. M. C., Hensen, J. L. M., & Begemann, S. H. A. (2008). The indoor environment in relation to people with dementia. In P. Strom-Tejsen (Ed.), *Conference on indoor air quality and climate*. Copenhagen: Indoor Air. Retrieved from www.tue.nl/taverne
- Warner, M. L. (2000). *The complete guide to Alzheimer's proofing your home*. West Lafayette: Purdue University Press
- van Hoof, J., Kort, H. S. M., van Waarde, H., & Blom, M. M. (2010). Environmental interventions and the design of homes for older adults with dementia: an overview. *American Journal of Alzheimer's Disease & Other Dementias*, 25(3), 202–232.
- Garre-Olmo, J., López-Pousa, S., Turon-Estrada, A., Juvinyà, D., Ballester, D., & Vilalta-Franch, J. (2012). Environmental Determinants of Quality of Life in Nursing Home Residents with Severe Dementia. *Journal of the American Geriatrics Society*, 60(7), 1230–1236. <https://doi.org/10.1111/j.1532-5415.2012.04040>
- Tartarini, F., Cooper, P., Fleming, R., & Batterham, M. (2017). Indoor Air Temperature and Agitation of Nursing Home Residents With Dementia. *American Journal of Alzheimer's Disease & Other Dementias*, 32(5), 272–281.
- American Society of Heating, Refrigerating and Air-Conditioning Engineers (ASHRAE), (2013). *ASHRAE 55:2013: Thermal Environmental Conditions for Human Occupancy*, Washington, DC.
- van Hoof J, HSM. Kort, H. van Waarde (2009). Housing and care for older adults with dementia. A European perspective. *Journal of Housing and the Built Environment* 24:3 p. 369-390.

Anthropogenic Heat Dispersion Modelling for Better Urban Planning at High Density Cities

CHAO YUAN¹, SHUO-JUN MEI¹, ADELIA, AYU SUKMA¹, RUIXUAN ZHU¹, WENHUI HE², XIAN-
XIANG LI²

¹National University of Singapore, Singapore

²Singapore-MIT Alliance for Research and Technology Centre

ABSTRACT: Anthropogenic heat is one of the key factors that causes intensive UHI due to its direct impact on ambient temperature in urban areas. Stagnated airflow due to closely packed tall buildings causes weak dilution and removal of anthropogenic heat. Consequently, research is critically needed to investigate the effect of urban morphology on anthropogenic heat dispersion and provide effective planning strategies to reduce UHI intensity, especially at the extreme scenario, such as with very low wind speed and high heat emission. This study provides scientific understanding and develops a GIS-based modelling tool to support decision-making in urban planning practice. We start from a computational parametric study at the neighbourhood scale to investigate the impact of urban morphology on heat dispersion. Site coverage ratio (λ_p), and frontal area density (λ_f) are two urban morphological parameters. Ten parametric cases with two heat emission scenarios are designed to study representative urban areas. Furthermore, based on the energy conservation within the urban canopy layer, we develop a semi-empirical model to estimate spatially-averaged in-canopy air temperature increment, in which the exchange velocity between the street canyon and overlying atmosphere is estimated by the Bentham and Britter model. The performance of the new model is validated by cross-comparing with CFD results from the parametric study. By applying this new model, the impact of anthropogenic heat on air temperature are mapped in residential areas of Singapore for both long-term annually averaged and short-term extreme low wind speed to improve urban climate sustainability and resilience.

KEYWORDS: Anthropogenic heat dispersion, Semi-empirical model, CFD simulation, Urban planning, GIS mapping

1. INTRODUCTION

With rapid urbanization, the urban heat island (UHI) effect has caused serious environmental challenges to both urban climate sustainability and resilience. Anthropogenic heat emission is one of the key factors that cause intensive UHI due to its direct impact on ambient temperature in urban areas. A Weather Research and Forecasting (WRF) modelling study conducted by Singapore-MIT Alliance for Research and Technology (SMART) indicates that the impact of anthropogenic heat on ambient air temperature is significant in the Central Business District, Singapore [1]. Chow and Roth [2] studied the temporal UHI of Singapore and concluded that UHI in Singapore is influenced by a combination of site-specific factors, such as low wind speed and intense anthropogenic heat emission. Weak anthropogenic heat removal and dilution is caused by stagnated airflow around closely packed and tall buildings. Therefore, effective strategies for anthropogenic heat removal and dilution are crucial to reduce the magnitude of the UHI. Many studies indicated that urban morphology has a significant impact on urban outdoor environment through modification on momentum, mass, and heat transfer around urban structures. Hence, research is critically needed to investigate the effects of urban morphology on anthropogenic heat dispersion at urban areas.

Computational Fluid Dynamics (CFD) simulation can provide accurate and high resolution modelling results of heat transfer and dispersion in the street canyon, and thus evaluate the effect of anthropogenic heat on air temperature. The numerical study conducted by [3] showed that differential heating can shift the in-street flow structure from one-vortex flow to several counter-rotating vortices, and Mei, et al. [4] indicates that buoyancy force induced by heated urban surfaces significantly alters temperature distribution inside street canyon. Kim and Baik [5] carried out extensive CFD simulations with various street canyon aspect ratios and street-level heating to characterize the flow regime. Oliveira Panão, et al. [6] applied a two-dimensional simulation to study the influence of a windward-heated wall on the airflow circulation in a street canyon with building height-to-street width ratio (H/W aspect ratio) from 0.7 to 1.5. The modelling results identified three airflow regimes. Regime (I) includes a single circulatory flow within street canyons. Regime (I) occurs for high wind intensities when the circulatory flow dominates over the thermal flow. By decreasing the Froude number ($Fr = \frac{Re^2}{Gr}$, where Gr is the Grashof number and Re is the Reynolds number), the flow within street canyons shifts to regime (II), with two counter-rotating vortices co-existing inside the canyon. When further

decreasing Fr number, the lower vortex dominates the air circulation inside street canyons, and it is defined as regime (III). Airflow regime III can efficiently remove the warm air inside the cavity due to a strong upward air current close to the surface opposite to the main flow direction. Rather than the above mentioned simulation work, Adelia, et al. [7] extended the anthropogenic heat study to the implementation of architectural design, by conducting a computational parametric study. Effects of building typologies on anthropogenic heat dispersion were investigated, and the understandings from this parametric study directly benefit the architectural design practice.

Apart from CFD simulation, wind tunnel and water channel experiments are also important approaches to model the flow and heat dispersion at urban areas. Ruck [8] measured the flow field around isolated buildings with heated surfaces with a 2D Laser Doppler Anemometer (LDA), and experimental results showed a significant change in the recirculation zone when the heat release increased above $Gr/Re^2 = 0.2$. Uehara, et al. [9] conducted a wind tunnel experiment, and investigated the effects of bottom heating and cooling on flow in urban street canyons. Allegrini, et al. [10] used Particle Image Velocimetry (PIV) to measure street canyon flow with heated surfaces in a wind tunnel. They reproduced a secondary counter-rotating vortex under a heated windward wall condition, as Sini, Anquetin and Mestayer [3] found in CFD simulation. The wind tunnel experiment conducted by Cui, et al. [11] covered a range of Richardson numbers ($Ri = Gr/Re^2$) between 0 to 4.77, and investigated thermal effects on both airflow and pollutant dispersion. The above wind tunnel experiments are significant because they provided not only the experimental results to validate numerical simulations, but also new understandings on effects of buoyance force on air flow.

2. RESEARCH METHOD

By conducting CFD simulation, we started from the computational parametric study at the neighbourhood scale to investigate the impact of urban morphology on heat dispersion. Total 10 parametric cases with two heat emission scenarios were conducted to make the parametric study representative to the real urban areas. More importantly, based on the understandings from parametric study and heat conservation, we developed a GIS-based modelling-mapping tool for planning practice.

A power law equation was applied for the incoming wind speed profile, i.e. time-averaged horizontal velocity, as:

$$U_h = U_{met} \left(\frac{h}{d_{met}} \right)^\alpha \quad (1)$$

where U_h is the wind speed at the height (h), U_{met} is the reference wind speed, 7.4 m/s, at reference height d_{met} , 300m, and α is the surface

roughness, 0.3 [7]. The turbulence originates only from friction and shear as [12]:

$$k(z) = \frac{u_{ABL}^*}{\sqrt{C_\mu}} \quad (2)$$

$$\varepsilon(z) = \frac{u_{ABL}^*}{\kappa(z+z_0)} \quad (3)$$

where u_{ABL}^* is the atmospheric boundary layer friction velocity, z the height above the ground, z_0 the aerodynamic roughness length, k the turbulence kinetic energy, ε the turbulence dissipation rate and $C_\mu = 0.09$ a constant of the turbulence model.

This study applied RANS $SST k - \omega$ model as turbulence model, which combines the advantages of standard $k - \omega$ model in the near wall region and $k - \varepsilon$ model in the far field [13]. $SST k - \omega$ model has been validated and employed in our previous studies related to urban flows, air pollutant and heat dispersions [7, 14, 15]. Specifically, we have validated the performance of $SST k - \omega$ to model the anthropogenic heat dispersion by cross-comparing with wind tunnel data provided by [10]. The validation result indicates a good agreement between the simulation result and wind tunnel data, as shown in Figure 1 [7].

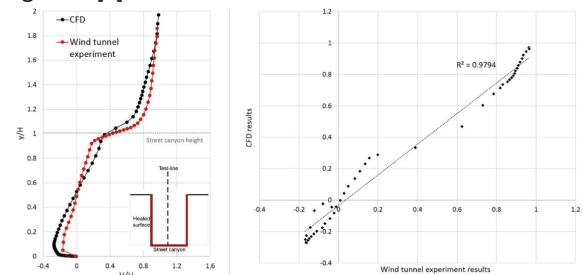


Figure 1: Validation of CFD simulations by cross-comparing with wind tunnel data. Left: modelling settings in the validation study; Right: cross-comparison result on air temperature increment.

3 COMPUTATIONAL PARAMETRIC STUDY

A neighbourhood scale parametric study was conducted, and 10 cases of urban morphology were designed based on permutations of urban planning indices, i.e. site coverage ratio (λ_p), and frontal area density (λ_f), as shown in Table 1. They are the ratio between element type (A_x), e.g. building footprint area (A_p) and frontal area approached by incoming wind (A_f), and total ground surface area (A_T) as [16]:

$$\lambda_x = \frac{A_x}{A_T} \quad (4)$$

In the parametric study, we kept urban density constant for the valid cross-comparison, and changed values of λ_p and λ_f by modifying building width (W) and building height (H), as shown in Table 1.

Table 1: Urban morphological parameters at 10 cases with the same plot ratio, 6.0.

Cases	H (m)	W (m)	λ_p	λ_f
01	30	48	0.60	0.38
02	32	45	0.56	0.40

03	36	40	0.50	0.45
04	40	36	0.45	0.50
05	45	32	0.40	0.56
06	50	28.8	0.36	0.63
07	60	24	0.30	0.75
08	72	20	0.25	0.90
09	90	16	0.20	1.13
10	120	12	0.15	1.50

Note: site area is 384000 m² and plot ratio is 6.

The modelling temperature field (Case 1 as an example) are shown in Figure 2.

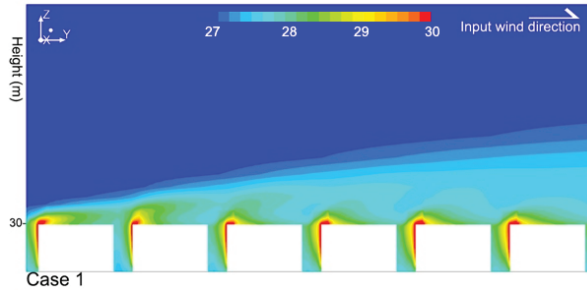


Figure 2: CFD simulation results (Case 1): Contour of air temperature.

4 DEVELOPMENT OF MODELLING-MAPPING TOOL

The semi-empirical model was derived from a box model, based on energy conservation within the urban canopy layer. The anthropogenic heat is ejected into the canopy air volume and heats the air within it. The heat emission within the canopy layer and heat exchange between the canopy layer and the air above are shown in Figure 3. The shear stress layer at the roof level induces air exchange, which exhausts warm air and inhales cool air. There is an energy balance in the canopy layer at the steady state condition, where the anthropogenic heat emission rate Q is equal to the heat flux at roof level Q_{roof} .

$$Q = Q_{roof}, \text{ where } Q_{roof} = \rho A_{opening} c_p U_E (T_c - T_0) \quad (5)$$

where, ρ is the air density, $A_{opening}$ is the opening area of urban canopy, c_p is the specific heat capacity of air, U_E is exchange velocity, T_c is the in-canopy air temperature, and T_0 is the ambient air temperature. Therefore, ΔT_c can be calculated as:

$$\Delta T_c = T_c - T_0 = \frac{Q}{\rho A_{opening} c_p U_E} \quad (6)$$

where $Q = Q_{A_site} A_T$ and Q_{A_site} is the heat emission intensity normalized by site areas (A_T).

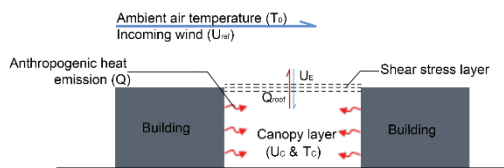


Figure 3: Schematic of the single-layer urban canopy model, derived from a box model, in which Q is equal to Q_{roof} .

The exchange velocity (U_E) needs to be solved to close equation 6. In a moderately densely packed

canopy, Bentham and Britter [17] suggested that the air exchange rate could be estimated as following:

$$\frac{U_E}{u_*} = \left(\frac{U_{ref} - U_c}{u_*} \right)^{-1} \quad (7)$$

where u_* is friction velocity, and U_c is spatially-averaged in-canopy velocity. Yuan, et al. [18] indicates that the above equation is also suitable in high density urban areas. Bentham and Britter [17] showed that the U_c in high-density urban areas can be calculated as:

$$\frac{U_c}{u_*} = \left(\frac{2}{\lambda_f} \right)^{0.5} \quad (8)$$

The friction velocity u_* depends on the urban morphology. Yuan, Norford, Britter and Ng [18] suggested that, when λ_f is larger than 0.4, u_* is almost constant and can be evaluated as:

$$u_* = 0.12 U_{ref}, \text{ where } \lambda_f > 0.4 \quad (9)$$

Based on equations (8), (9), (10), the exchange velocity could be calculated by:

$$U_E = \frac{u_*^2}{U_{ref} - U_c} = \frac{0.0144 U_{ref}}{1 - 0.12 \left(\frac{2}{\lambda_f} \right)^{0.5}} \quad (10)$$

Combining Equation (6) and (10), the in-canopy air temperature increment (ΔT_c) can be calculated by urban morphology parameters λ_f and λ_p .

$$\Delta T_c = \frac{Q_{A_site} A_T}{0.0144 U_{ref} \rho A_{opening} c_p} \left(1 - 0.12 \left(\frac{2}{\lambda_f} \right)^{0.5} \right) = \frac{1}{D_c} \frac{Q_{A_site}}{U_{ref} (1 - \lambda_p)} \left(1 - 0.12 \left(\frac{2}{\lambda_f} \right)^{0.5} \right) \quad (11)$$

where $D_c = 0.0144 \rho c_p$ is a heat capacity constant, 17.183 ($J K^{-1} m^{-3}$) related to the thermal characteristics of the air.

This model was then validated by cross-comparison with the previous CFD simulation results in Section 3, as shown in the Figure 4. Linear regression analysis shows a good agreement between the CFD model and semi-empirical model ($R^2 = 0.69$), which indicates that this semi-empirical model can be used to estimate the increment of in-canyon air temperature caused by anthropogenic heat emission in residential areas. It should be noted that we also calculated exchange velocity (U_E) using the Soulhac, et al (2013) model, and modelling results (ΔT_c) were included in Figure 4. It is clear that the semi-empirical model using Soulhac, et al (2013) could underestimate the ΔT_c because of overestimated U_E .

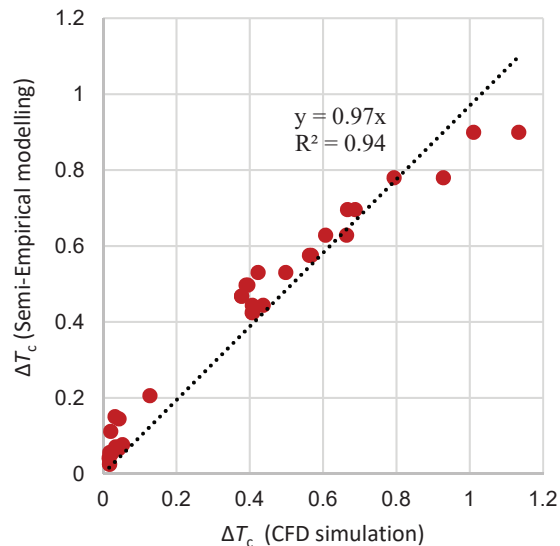


Figure 4: Cross-comparison of the in-canopy air temperature increments (ΔT_c) between the CFD and the semi-empirical model, adopting U_E estimated by both Bentham and Britter [17]

5. IMPLEMENTATION

In this section, we mapped anthropogenic heat emission and dispersion in residential areas of Singapore. As shown in Figure 5, the heat emission data, as the input data, is collected from an existing database of anthropogenic heat for Singapore (conducted by the Center for Environmental Sensing and Modelling team (CENSAM), Singapore-MIT Alliance for Research and Technology (SMART)). For HDB and condominiums, the heat emission of individual buildings was calculated based on dedicated energy consumption profiles within a postal code, which were provided by Singapore Energy Market Authority. For the landed properties, a top-down approach was adopted to calculate the heat emission from individual buildings, i.e. normalizing total energy consumption by gross floor area (GFA) as allocating factor.

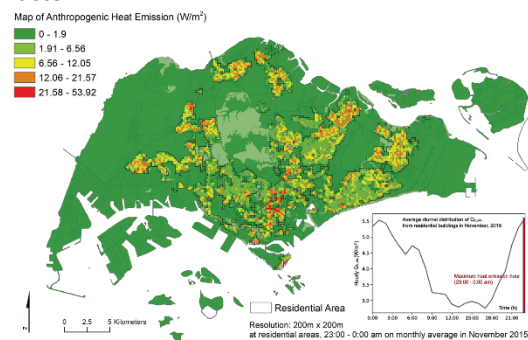


Figure 5: Map of anthropogenic heat emission from residential buildings at 23:00 – 0:00 am in November 2015. The monthly average diurnal distribution of Q_{A_site} is also presented.

Because only monthly electricity consumption data was available, the hourly electricity consumption was

estimated with the help of a representative daily electricity load profile from previous study [19], as shown in Figure 6. For this mapping study, we chose the hour with highest emission intensity, i.e., 23:00 – 0:00 am, in the monthly average in November 2015. Morphological indices λ_p and λ_f for residential areas of Singapore, shown in Figures 6 and 7, respectively, were calculated at each cell (200 m \times 200 m), using the building footprint data provided by Singapore Land Authority (SLA) [20] and the building height data extracted from the digital surface model (DSM) [21]. In the calculation of λ_f , prevailing wind directions in November 2015 for each cell were obtained from the nearest meteorological station [22].

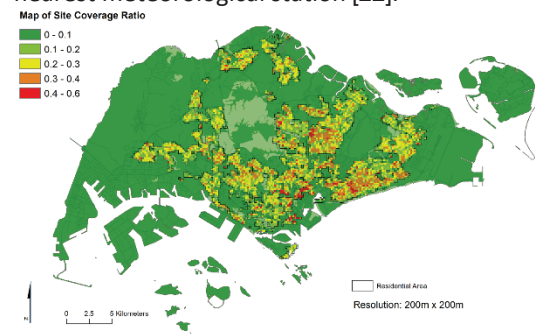


Figure 6: Map of site coverage ratio λ_p in Singapore.

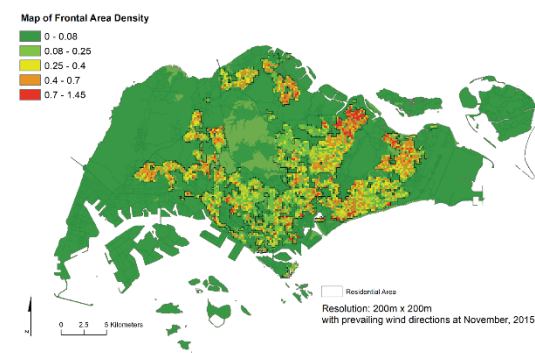


Figure 7: Map of frontal area density λ_f in Singapore. Prevailing wind directions in November 2015 from the nearest meteorological stations for each cell were applied in the λ_f calculation.

Using the new semi-empirical model developed in Section 4.2, the impact of anthropogenic heat on air temperature (ΔT_c) at residential areas was calculated in ArcGIS for scenarios with 1) annually averaged incoming wind; 2) minimum incoming wind (from 2009 to 2020). The reference wind speeds at 300m above the ground are 7.4 m/s and 1.1 m/s at scenarios I and II respectively. As shown in Figure 8a, the maximum value of ΔT_c is 0.34 $^{\circ}\text{C}$ at the downtown area, and ΔT_c is less than 0.2 $^{\circ}\text{C}$ at the most of residential areas. It indicates that anthropogenic heat has little impact on the spatially averaged air temperature in the normal, i.e. annually averaged, situation.

However, in the scenario II with high anthropogenic heat emission and very weak incoming

wind, which was measured in November, 9th, 2018, the air temperature increment is much more significant than in scenario I. As shown in Figure 8b, the maximum value of ΔT_c is about 2.3°C, which is significant for outdoor thermal comfort. This grid is located near the

Chinatown district, with total 1729.5kW heat emission and low dispersion potential (λ_f and λ_p are 1.02 and 0.5 respectively).

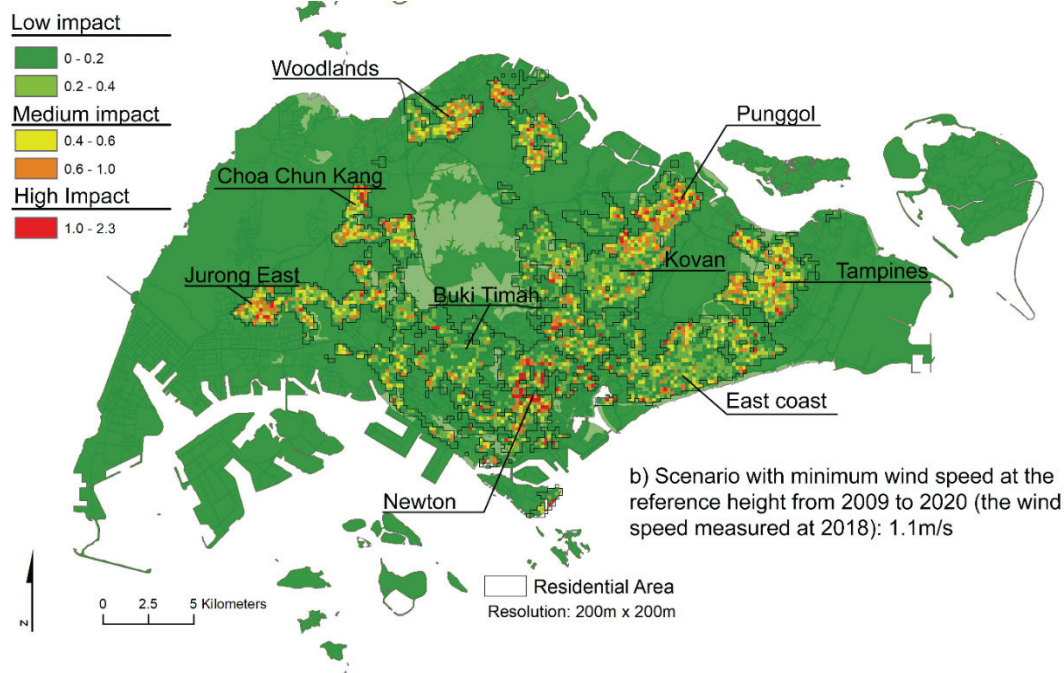


Figure 8: Map of air temperature increment (ΔT_c) at residential areas of Singapore with the heat emission at 23:00 – 0:00 with minimum incoming wind (from 2009 to 2020).

We categorized residential areas as: high, medium, and low impact zones as shown in Figure 8b. First, the areas with ΔT_c higher than 1.0°C, which is two times higher than the maximum value in the normal scenario (scenario I), are categorized as a high impact zone, about 3% of total residential areas, and mainly concentrated at the downtown area (Newton), Tampines, Punggol, Woodlands, Choa Chun Kang, and Jurong East. Both λ_p and Q_{A_site} at Punggol are much lower than at downtown areas, but because of higher values of λ_f , the values of ΔT_c at Punggol and downtown area are comparable. Secondly, 26 percent of residential areas with values of ΔT_c between 0.4°C to 1.0°C are categorized as a medium impact zone. Q_{A_site} at the most of these cells are higher than the mean value of residential areas, and normally λ_f is high. At last, the low impact zone with ΔT_c less than 0.4°C is occupied by low-rise buildings, such as the terrace buildings at the west region (Bukit Timah), middle area (Kovan) and the east coast region. Even though λ_p could be high at this zone, the heat emission is quite low compared with other areas.

The above analysis indicates that, if the incoming wind speed is extremely low, it is difficult for the anthropogenic heat to be dispersed. It is highly possible that heat stress risk could come from the temperature increment under an extreme situation with very low wind speed. The temperature increment

in the extreme scenario (scenario II) could be 6 times higher than the scenario I.

6. Conclusions

We conducted this study to support urban planning practice to mitigate the negative effect of anthropogenic heat on the microclimate in residential areas. The study is important to both urban climate sustainability and future resilience. We provided not only scientific understandings of anthropogenic heat dispersion in urban areas, but also the practical GIS-based modelling-mapping tool. This study was started by parameterizing urban morphology and conducting CFD simulations. The CFD simulation was validated by cross-comparing with existing wind tunnel experiment results. The heat transfer and dispersion at residential areas with different morphologies, i.e. λ_p and λ_f , were simulated by the SST k- ω model in ANSYS Fluent. To associate the urban morphologies with air temperature increment, we conducted the regression analysis using CFD simulation result, and developed the GIS modelling-mapping tool. The impact of anthropogenic heat in both annually averaged and short term extreme micro climate conditions was modelled and evaluated in Singapore.

The heterogeneous urban morphologies and emission scenarios certainly bring uncertainty to the performance of new semi-empirical model. Therefore,

more validation and modification of the new model is necessary in the future. Secondly, the heat storage in the building mass and urban ground surface is significant to the air temperature increment. The study on transient urban street air warming is needed. And last but not at least, more components need to be included in the model to cover the commercial, industrial, and traffic heat emissions, which were not included in the current study but have significant impact on ambient temperature.

7. Acknowledgment

This research is supported by Singapore National Research Foundation under its two Campus for Research Excellence and Technological Enterprise (CREATE) programmes: 1) Intra-CREATE seed research grant (Grant no. NRF2018-ITS003-022) and Singapore ETH Centre, Future Resilience System II grant (Grant no. R-295-000-169-592). The computational work for this article was partially performed on resources of the National Supercomputing Centre, Singapore (<https://www.nscg.sg>).

REFERENCES

- [1] X.-X. Li, L.K. Norford, Evaluation of cool roof and vegetations in mitigating urban heat island in a tropical city, Singapore, *Urban Climate*, 16 (2016) 59-74.
- [2] W.T.L. Chow, M. Roth, Temporal dynamics of the urban heat island of Singapore, *International Journal of Climatology*, 26 (15) (2006) 2243-2260.
- [3] J.-F. Sini, S. Anquetin, P.G. Mestayer, Pollutant dispersion and thermal effects in urban street canyons, *Atmospheric Environment*, 30 (15) (1996) 2659-2677.
- [4] S.-J. Mei, C.-W. Liu, D. Liu, F.-Y. Zhao, H.-Q. Wang, X.-H. Li, Fluid mechanical dispersion of airborne pollutants inside urban street canyons subjecting to multi-component ventilation and unstable thermal stratifications, *Science of The Total Environment*, 565 (2016) 1102-1115.
- [5] J.-J. Kim, J.-J. Baik, Urban street-canyon flows with bottom heating, *Atmospheric Environment*, 35 (20) (2001) 3395-3404.
- [6] M.J.N. Oliveira Panão, H.J.P. Gonçalves, P.M.C. Ferrão, Numerical analysis of the street canyon thermal conductance to improve urban design and climate, *Building and Environment*, 44 (1) (2009) 177-187.
- [7] A.S. Adelia, C. Yuan, L. Liu, R.Q. Shan, Effects of urban morphology on anthropogenic heat dispersion in tropical high-density residential areas, *Energy and Buildings*, 186 (2019) 368-383.
- [8] B. Ruck, Wind-tunnel measurements of flow field characteristics around a heated model building, *Journal of Wind Engineering and Industrial Aerodynamics*, 50 (1993) 139-151.
- [9] K. Uehara, S. Murakami, S. Oikawa, S. Wakamatsu, Wind tunnel experiments on how thermal stratification affects flow in and above urban street canyons, *Atmospheric Environment*, 34 (10) (2000) 1553-1562.
- [10] J. Allegrini, V. Dorer, J. Carmeliet, Wind tunnel measurements of buoyant flows in street canyons, *Building and Environment*, 59 (2013) 315-326.
- [11] P.-Y. Cui, Z. Li, W.-Q. Tao, Wind-tunnel measurements for thermal effects on the air flow and pollutant dispersion through different scale urban areas, *Building and Environment*, 97 (2016) 137-151.
- [12] P.J. Richards, R.P. Hoxey, Appropriate boundary conditions for computational wind engineering models using the k- ϵ turbulence model, *Journal of Wind Engineering and Industrial Aerodynamics*, 46-47 (1993) 145-153.
- [13] F.R. Menter, Two-equation eddy-viscosity turbulence models for engineering applications, *AIAA journal*, 32 (8) (1994) 1598-1605.
- [14] C. Yuan, E. Ng, L.K. Norford, Improving air quality in high-density cities by understanding the relationship between air pollutant dispersion and urban morphologies, *Building and Environment*, 71 (2014) 245-258.
- [15] C. Yuan, E. Ng, Building porosity for better urban ventilation in high-density cities – A computational parametric study, *Building and Environment*, 50 (2012) 176-189.
- [16] T.R. Oke, G. Mills, J. Voogt, *Urban climates*, Cambridge University Press, 2017.
- [17] T. Bentham, R. Britter, Spatially averaged flow within obstacle arrays, *Atmospheric Environment*, 37 (15) (2003) 2037-2043.
- [18] C. Yuan, L. Norford, R. Britter, E. Ng, A modelling-mapping approach for fine-scale assessment of pedestrian-level wind in high-density cities, *Building and Environment*, 97 (2016) 152-165.
- [19] A.K.L. Quah, M. Roth, Diurnal and weekly variation of anthropogenic heat emissions in a tropical city, Singapore, *Atmospheric Environment*, 46 (2012) 92-103.
- [20] Singapore Land Authority, Digitised Land Information. Retrieved October 25, 2019, in, 2012.
- [21] M.A. Dissegna, T. Yin, S. Wei, D. Richards, A. Grêt-Regamey, 3-D Reconstruction of an Urban Landscape to Assess the Influence of Vegetation in the Radiative Budget, *Forests*, 10 (8) (2019) 700.
- [22] Meteorological Service Singapore, Annual Climatological Report. 1–2. , in, 2015.

New Approaches to Risk Assessment of Climate Stability in Archive and Depot Buildings

Determination of storage safety of various stored goods based on prevailing climatic conditions

Prof. Dr.-Ing. Sven Steinbach¹, Simon Michalke¹, Charlotte Feneis¹

¹University of Applied Sciences Erfurt, Erfurt, Germany

ABSTRACT: The purpose of archive and depot buildings is to permanently store goods, to make them accessible, and to ensure protection against unauthorized use or destruction. As a result of this need for unlimited preservation, and due to the diversity of formats and materials, special requirements are claimed on storage and use. The prevailing temperature and humidity values are of crucial importance here. Applying the method for risk assessment elaborated in this text, allows the evaluation of recorded climate data with regard to their damaging effect, thus allowing significant statements on storage safety. The knowledge gained should help to create safer, more economical, and energy-efficient depot and archive buildings for future projects. It hence aims at achieving a positive ecological and economic influence on the storage of different goods.

KEYWORDS: Risk Assessment, Archive, Preservation, Climate, Storage

1. INTRODUCTION

The purpose archive and depot buildings is to permanently store goods, making them usable, and ensuring protection against unauthorized use or destruction. As a result of this need for unlimited preservation and due to the diversity of formats and materials, special requirements are claimed on storage and use [1].

The prevailing temperature and humidity values are of crucial importance here. A room climate which is not adapted to the stored goods can damage the archival material and thus shortens the service life considerably.

High temperatures and humidity accelerate the chemical degradation processes. Furthermore, a relative humidity of over 60% RH increases the risk of microbiological activity, which in turn allows harmful substances, from the materials themselves or from the environment, to penetrate deeply into the pieces. With highly hygroscopic materials, such as paper or parchment, this might result in swelling or deformation [2].

Therefore, the creation of a suitable and constant climate is one of the central tasks of archives [3].

evaluated with regard to their damaging effect on archive holdings.

The damage causing an effect, is best described based on the following three damage functions [4]:

- dose-response relationships
- thresholds
- chemical degradation processes

The purpose of risk assessment is to map all damage functions as comprehensively as possible. Based on this, quality statements can be formulated and summarized in a uniform risk assessment for storage security.

To achieve this, a selection of three different evaluation methods is applied. These methods are suitable for a long-term preservation of museum and archive collections. After the individual evaluation procedures have been carried out, the results are merged to form a new preservation risk index and are assigned to a preservation class (Fig. 1).

Selected were the 'ASHRAE' evaluation, the specific climate risk assessment by 'Martens', and the 'preservation index by Image Permanence Institute', which, in their entirety, cover all damage functions.

2. RISK ASSESSMENT OF CLIMATE STABILITY

To be able to assess the prevailing climatic conditions, climate data needs to be recorded and

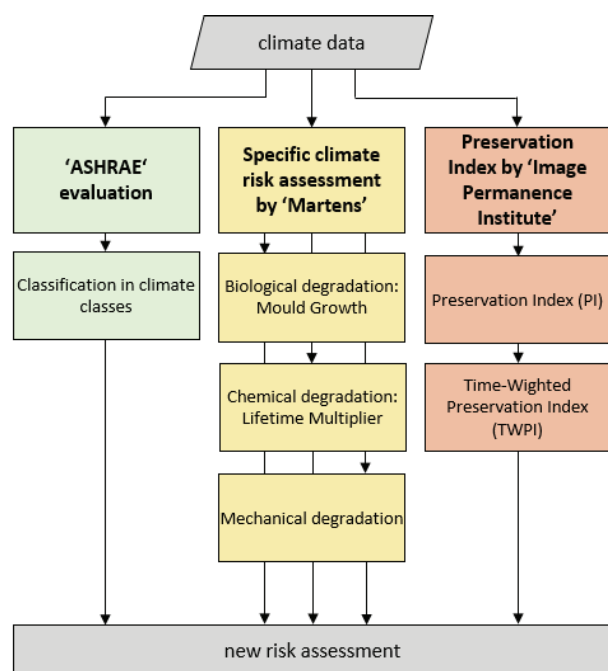


Figure 1: Schematic representation for the formation of a risk assessment.

As a result, the various damage functions can be regarded holistically in only one evaluation. This makes it easier to view the results of the individual evaluation procedures in their entirety and thus facilitates the interpretation of the total risk.

2.1 'ASHRAE' evaluation

For the evaluation of the indoor climate conditions according to the 'ASHRAE' classes, it is necessary to compare the collected climate data with the generally accepted design criteria of the individual classes. The degree of fulfillment of each class is shown as a percentage (Fig. 2).

This statistical evaluation of the measurement data allows a quick and easy comparison of different areas.

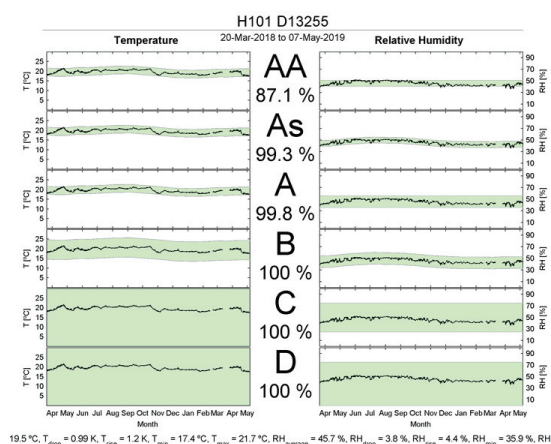


Figure 2: Exemplary ASHRAE classification of the temperature and the relative humidity.

When interpreting the results, one has to take into consideration, that they only represent the proportion of measurement points that lie within the climate corridor.

Statements on damage forecasts are only possible if they are completely fulfilled. Therefore, for example, irreparable damage can already occur in a small period of non-fulfillment of a class with a low risk of damage.

According to the fulfillment of the individual AASHRAE classes, the classification into a corresponding risk class takes place.

2.2 Specific climate risk assessment by 'Martens'

The Martens model for the assessment of climate risk for museum objects, provides for the determination of the risk of damage to typical collection objects. It does so, by examining the indoor climate and determining, whether or not conditions are favorable for damage.

The focus lies on the actual reactions of the objects. This allows an evaluation of the main risk factors and the preservation qualities of the indoor climate, independent of any specifications. The typically stored materials are classified according to their characteristics and their susceptibility to damage.

This risk assessment examines the various damage functions consisting of biological, chemical, and mechanical degradation [5].

Biological degradation meaning the promotion of mold growth. The prevailing conditions are considered safe if germination does not take place. If the conditions for germination are fulfilled, the mold growth is calculated [6].

The chemical degradation process of many objects depends mainly on their water content. As the water content of the air increases, so does the amount of water inside each object, which in turn increases the speed of the reaction [7].

In this approach, the objects' reactivity is expressed by the lifetime multiplier. It refers to a comparative state and shows, whether the climate acting on the object has had a positive or negative effect.

Further examination focuses on the moisture reaction behavior of the objects with a corresponding moisture change. If the breakage limit is exceeded, this will lead to breakage. Permanent deformations, on the other hand, occur when stresses exceed the yield point but not the breaking point. On condition that the individual changes stay within the elastic range, this will not lead to deformation and can thus be classified as safe. Changes within the plastic deformation range, can lead to damage if repeated (Fig. 3).

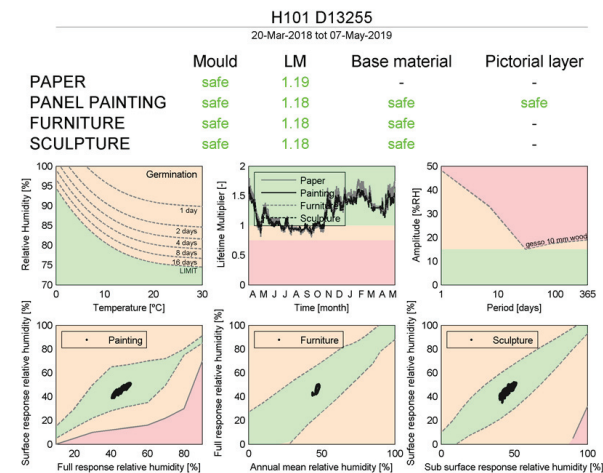


Figure 3: Exemplary valuation according Specific climate risk assessment by 'Martens'.

Risk indices are formed based on the individual results, according to defined evaluation tables.

2.3 Preservation index by 'Image Permanence Institute'

The 'Image Permanence Institute' has introduced a time-weighted preservation index (TWPI). This index intends to provide information on the conservation quality of the environment, and thus to simplify the interpretation of temperature and humidity data.

It is based on the preservation index (PI). The preservation index describes the effect of certain combinations of temperature and humidity conditions, at the time of each measurement. Similar to the Martens lifetime multiplier. The PI values represent the approximate period of time, an organic material will last at a given combination of temperature and humidity (Fig. 4) [8].

		Temperature (°F)															
		32	37	42	47	52	57	62	67	72	77	82	87	92			
% RH	5	2634	1731	1147	767	516	350	240	165	114	80	56	40	28	PI Values, in Years		
	10	2254	1473	979	656	443	302	207	143	99	70	49	35	25			
	15	1897	1255	837	562	381	260	179	124	86	61	43	30	22			
	20	1613	1070	716	482	328	224	155	107	75	53	37	27	19			
	25	1373	914	613	414	282	194	134	93	65	46	33	23	17			
	30	1170	781	525	356	243	168	116	81	57	40	29	21	15			
	35	998	668	451	307	210	145	101	71	50	35	25	18	13			
	40	852	572	387	264	182	126	88	62	43	31	22	16	12			
	45	729	491	333	228	157	109	76	54	38	27	19	14	10			
	50	624	421	287	197	136	95	66	47	33	24	17	12	9			
	55	535	362	247	170	118	82	58	41	29	21	15	11	8			
	60	459	312	213	147	102	72	51	36	26	18	13	10	7			
	65	394	269	184	128	89	62	44	31	22	16	12	9	6			
	70	339	232	160	111	77	54	39	28	20	14	10	8	6			
	75	292	200	138	96	67	48	34	24	17	13	9	7	5			
	80	251	173	120	84	59	42	30	21	15	11	8	6	4			
	85	217	150	104	73	51	36	26	19	14	10	7	5	4			
	90	187	130	90	63	45	32	23	16	12	9	6	5	3			
	95	162	112	79	55	39	28	20	15	11	8	6	4	3			

Figure 4: Determination of PI values depending on temperature and relative humidity.

By means of an evaluation table, a risk index is formed and classified in the appropriate risk class (Fig. 5).

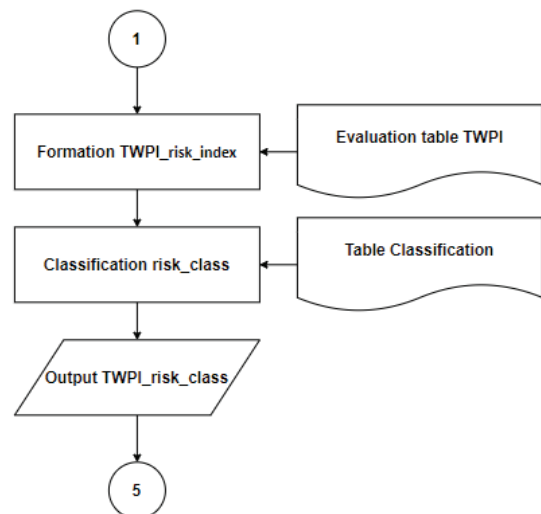


Figure 5: Procedure of classification 'TWPI' risk class.

2.4 New Preservation Risk Index

The different results of all risk assessment methods considered in the previous sections of this elaboration, must be combined into a uniform assessment to be able to make a uniform statement on the safety of storage. The results will then be evaluated with an 'Excel' tool, specifically developed for this purpose.

The tool's purpose, on the one hand, is the formation of a comprehensive preservation risk index in dependency of all input data. On the other hand, it aims at the subsequent classification of the data in a preservation risk class.

Weighting factors help to calculate the overall risk index. These factors are used to regulate the influence of the various components.

The calculation of the risk index depends on the nature of the stored materials. Photographic materials are not considered. They make special demands on the climatic environment.

Based on the risk index formed, it is possible to make a corresponding classification into a preservation risk class from each procedure, (Fig. 6). The final preservation risk class is the lowest class value from the previously determined classes. This procedure prevents a possible compensation of low risk class values.

Preservation Risk Index

General input:

Room designation:

Type:
Stored material:

ASHRAE input:

Class coverage: AA: % A: % B: % C: %

IPI input:

TWPI:

Specific risk assessment by Martens input:

Mould risk:

Lifetime multiplier:

Paper:
Panel Painting:

Furniture:
Sculpture:

Mechanical load:

Base material:

Panel Painting:
Furniture:

Sculpture:

Pictorial layer:

Panel Painting:

Preservation risk class:

High safety level
Good conditions for long-term storage!

1

2

3

4

5

1

2

3

4

5

REFERENCES

1. DIN 67700:2017-05, (2017). Bau von Bibliotheken und Archiven - Anforderungen und Empfehlungen für die Planung: p. 16.
2. Petra Hauke, (2009). Klaus Ulrich Werner. Bibliotheken bauen und ausstatten. s.l. : BOCK + HERCHEN Verlag: p. 159.
3. Glauert, Mario and Ruhnau, Sabine, (2015). Verahren, Sichern, Erhalten. Handreichungen zur Bestandserhaltung in Archiven. Potsdam: Landesverbandes Brandenburg des Verbandes deutscher Archivarinnen und Archivare e.V.: p. 55.
4. Kilian, Ralf, (2013). Klimastabilität historischer Gebäude. Stuttgart: Fraunhofer Verlag: p. 94.
5. Martens, Marco, (2012). Climate risk assessment in museums. s.l.: Technische Universität Eindhoven: p. 96.
6. Martens, Marco, (2012). Climate risk assessment in museums. s.l.: Technische Universität Eindhoven: p. 109.
7. Martens, Marco, (2012). Climate risk assessment in museums. s.l.: Technische Universität Eindhoven: p. 61.
8. James M Reilly, Edward Zinn, Douglas W Nishimura, (1995) New Tools for Preservation: p. 13.

Figure 6: Input mask of the developed evaluation tool.

In addition to the preservation risk class, the procedure also provides information about class name and class description. Moreover, a scale is used for graphical classification. This allows the user to gain a better understanding of the prevailing conditions for long-term storage.

3. CONCLUSION

Applying the developed method for risk assessment helps to evaluate recorded climate data in regard to their damaging effect. This allows to make significant statements on storage safety. These quality statements can indicate a possible need for action in the individual areas.

The knowledge gained should help to create safer, more economical, and energy-efficient depot and archive buildings for future projects. This approach hence aims at achieving a positive ecological and economic influence on the storage of different goods.

Towards Zero-Waste In Sustainable Construction Of Buildings

Strategies For A More Efficient Implementation of Reusable Building Components On A Broad Scale In Germany

ALEXANDER KADER¹

¹ German University of Technology in Oman (affiliated with RWTH Aachen), Muscat, Oman

ABSTRACT: *The construction methods used today, do not sufficiently integrate the future requirements which will be necessary in regard to resource efficiency. Many building parts are neither reusable nor recyclable and the amount of waste created from the demolition of buildings is unnecessarily high. A paradigm shift is required to achieve an implementation of more efficient construction methods on a broad scale. The introduction of integral construction principles is overdue. By comparing today's common building practice with zero-waste construction techniques of innovative exemplary projects, this study asks: how can reusable building components be more efficiently integrated into the common building practice? Within this paper, at first the principles of zero-waste construction are illustrated and its key terms explained. Thereafter, three examples of innovative zero-waste architecture have been analyzed. The following part consists of a comparison between the analysed zero-waste building methods and the common building practice. Within an evaluation, these differences are used for the elaboration of improvement options which form the basis for the final part of this study. The conclusion provides a series of proposals of how the identified zero-waste construction principles could be effectively established into the common building practice on a broad scale in the future.*

KEYWORDS: Zero-Waste, Cradle to Cradle, Resource Efficiency, Circular Economy, Reuse

1. INTRODUCTION

In contrast to a number of other sectors such as the car industry which has a material recycling rate of more than 90%, the construction and demolition sector remains underdeveloped in regard to effective concepts to reuse building parts. Today's common construction methods are in large parts based on outdated techniques and use of unsustainable elements like reinforced concrete and composite components with synthetic materials which are available at low costs [1]. Utilizing new methods of construction can significantly reduce the carbon footprint of a building.

It is essential to recognize the need for a more ecological approach – one that addresses energy efficiency, material efficiency and the concept of zero waste, prioritizing the use of natural and local materials with less embodied energy; thus resulting in a more responsible consumption, incorporation and usage of materials [2]. This study illustrates approaches how zero-waste and cradle to cradle concepts can be integrated into today's construction industry to pave the road towards a circular and closed loop system to better protect our built environments.

2. DEFICITS OF CURRENT METHODS

A building's overall energy demand consists of the

energy required for its production, maintenance and operation, demolition and disposal of its waste at the end of its life span. In regard to current construction methods, all factors mentioned contain an immense potential for optimisation.

Since many building parts are neither reusable nor even recyclable, as of today, the amount of raw materials consumed and waste created by the construction sector worldwide is unnecessarily high [3]. Many of these raw materials are part of a linear process where they end up in landfills after the lifespan of the building ("cradle to grave" approach) [4]. Switching to recyclable materials would be a first step towards a zero-waste future for the industry. However, the recycling process of many composite materials, such as reinforced concrete, still requires an enormous amount of additional energy and labor force for their demolition and separation to its constituent elements, making the procedure complex [5].

Building regulations and governmental incentives today do not sufficiently enforce the implementation of reusable building components.

3. IMPROVEMENT GOAL

Due to the pressing need for emission reduction in current circumstances, the integration of zero-waste and cradle to cradle principles with reusable building components is expected to play a major role

in the future of the building industry. Prefabricated building parts could be designed, produced and assembled in a way that most, if not all, building parts could be easily dismantled and reused. In this manner, the life-cycle of more and more resources in the building industry could change from linear “cradle to grave” to circular “cradle to cradle”; a concept of mimicking the regenerative cycle of nature in which waste is reused [6].

4. PRINCIPLES AND KEY TERMS OF ZERO-WASTE AND CRADLE TO CRADLE CONSTRUCTION

The fundamental idea of zero-waste and cradle to cradle construction is to ensure that no waste is created. The cradle to cradle approach formulates the idea that, when a building’s life span ends and it must be demolished, all building parts become a new resource or “nutrient”, either technical for new building processes, or biological, thus contributing to the cycle of nature [7]. Nonetheless several steps need to be taken to realize this idea.

At the beginning of a planning process, the building must be designed not conventionally, but according to zero-waste principles. Thereafter, all construction techniques and materials have to be selected according to their suitability for easy disassembly and reuse after the building’s life span. An early prototypical building in which most components are reusable is House R128 in Stuttgart, built by Werner Sobek in 2000 [8]. Biodegradable materials (such as untreated wood) can be used as building parts to avoid any waste creation, such as demonstrated by the Woodcube building in Hamburg [9].

5. EVALUATION OF CASE STUDY BUILDINGS

Some projects in Germany are showcasing these zero-waste and cradle to cradle construction principles already today. Within this study, the following buildings are analysed as case studies:

“Aktivhaus Development” in Winnenden by Werner Sobek; “Woodcube Building” in Hamburg by IfuH architecture office and Architekturagentur; “ICON Rheinlanddamm Building” in Dortmund by William McDonough + Partners and IAA Architects.

5.1 “Aktivhaus Development” in Winnenden

Designed by the engineer and architect Werner Sobek from Stuttgart in 2016, the housing project for refugees in Winnenden, Germany is making use of the Aktivhaus modules which are flexible to be applied for many different functions and locations. A total of 38 modules from the Aktivhaus 700 Series were deployed at the project in Winnenden. This number included examples of the 701 model (45 m²) and the 702 model (60 m²). Built using a timber frame construction method, the Aktivhaus modules were

stacked to a height of two storeys. Besides the residential units, there is a technology module, two community rooms and a multifunctional space [10].

5.2 “Woodcube Building” in Hamburg

The “Woodcube” building in Hamburg, Germany, by IfuH architecture office from Berlin and Architekturagentur from Stuttgart, was completed in 2013 as part of the International Building Exhibition in Hamburg-Wilhelmsburg. The five-storey building has the structure of a cube with dimensions 15.1 m x 15.1 m x 15.6 m (length x width x height), on a footprint of approximately 228 m². Most building parts are prefabricated consisting of untreated wood, with the exception of the basement and staircase core of reinforced concrete [11]. The Woodcube nearly reaches the passive-house certification energy standard while also achieving a CO₂-neutral life cycle assessment, while consistently abandoning any contaminating construction chemicals. All essential materials are recyclable as well as biodegradable, leaving behind no waste which might harm future generations. The prefabricated wooden construction is part of a modular building kit developed, produced and marketed by the company Holz Thoma from Austria [12].

5.3 “ICON Rheinlanddamm” in Dortmund

The “ICON Rheinlanddamm” building in Dortmund, Germany, has been designed by William McDonough + Partners from Charlottesville, USA and is being realised in cooperation with IAA architects from Enschede, Netherlands. Scheduled to be completed in 2022, the six storey office building has dimensions of approximately 80 m x 50 m (length x width). Among other characteristics, the building features terraces on the upper floors, green façade elements on its front side and green interior walls in the atrium. The multilayered roof acts as a rainwater collector to irrigate the green elements of the building, while also shading the atrium with its sun-oriented glass surfaces equipped with photovoltaic elements. Surpluses from electric energy generation can be utilized not only for the building’s operation, but also to charge electric cars in the parking area. A mass of concrete slabs is used for cooling and heating the building, making use of a combination of passive strategies. Biological and technical materials ensured to be demountable and reusable in the future are used in this building along with many cradle to cradle certified components designed for reuse [13].

5.4 Evaluation of essential characteristics

The following table 1 describes the characteristics of the three case study’s building elements in regard to zero-waste and cradle to cradle. Through careful assessment of these building elements used in the

three case study houses, this paper attempts to derive conclusions about which design solutions work

best in order to achieve a zero-waste building within the cradle to cradle paradigm.

Table 1: Comparison of the components of the three case study buildings in regard to reusability

Elements	Aktivhaus Winnenden	Woodcube Hamburg	ICON Dortmund
Constructive system, building structure	Prefabricated wooden frame construction; modular, flexible and reusable	Prefabricated wood, reusable. Staircase core and basement reinforced concrete, not reusable	Reinforced concrete skeleton, not reusable
Exterior walls and opaque façade elements, insulation material	Modular and reusable prefabricated wooden modules with a total thickness of 31 cm, insulation mineral fibreboard 28 cm, exterior and interior larch wood surfaces	Solid wood building kit of untreated prefab wooden elements, 32.4 cm thickness, reusable. Two integrated layers of wood fibreboard insulation, each 2.2 cm; exterior surface of larch wood [14]	Aluminium frame construction, thermally separated; sandwich panels filled with 16 cm mineral wool insulation, reusable, exterior panel surface of colored glass
Windows, glazed façade elements	Wooden frame, with double glazing, modular, reusable	Untreated wood frame, reusable and biodegradable; triple glazing	Curtain wall, alu frame construction, reusable; triple glazing
Interior walls	Wooden panels with three layers; visible surfaces made of spruce plywood, reusable	Solid wood building kit wall system with wooden frame partitions, reusable	Cradle to cradle certified drywall partitions, suitable for biological or technical reuse cycle
Roofs	Modular and reusable prefabricated wooden modules, insulation mineral fibreboard, no photovoltaics, no green roof	Solid modular wood construction with unglued cross laminated timber, sloping insulation layer of mineral fibreboard, photovoltaics, no green roof [15]	Multifunctional, with photovoltaics, partial green roof, rainwater collection, greenhouse to clean and preheat incoming air (winter) or precool (summer). Reinforced concrete slab [16]
Floor slabs	Wood, reusable. Floor slabs are part of the prefabricated module [10]	Untreated solid wood and ceiling integrated beams made of wood and steel, prefabricated, modular, reusable	Reinforced concrete, not reusable; massive slabs contain tubes for cooling (summer) or heating (winter)
Foundations and ground floor slabs	Reinforced concrete strip foundations, removable, reusable	Reinforced concrete ground floor and basement slabs, not reusable, basement on pile foundation	In-situ reinforced concrete foundations and ground floor slab, not reusable
Interior fittings; floor, wall and ceiling surfaces, furniture	Linoleum floors, spruce plywood wall and ceiling surfaces, all components are reusable and/or biodegradable	Untreated wooden boards on floors, walls and ceilings, most components are reusable and/or biodegradable	Most interior materials according to cradle to cradle principle (floors, ceilings, appliances), reusable and/or biodegradable [16]
Connections techniques building components	All building components can be assembled and disassembled with use of reversible connections, e.g. screws, brackets, dowels, clamp connections and magnets	All building components can be assembled and disassembled with the use of reversible connections, mainly wooden. e.g. dowels, form fitting joints, clamp connections and steel brackets [11]	Reinforced concrete structure not easily disassembled and reused. Connections of façade and interior components designed in reversible way for future reuse
Use of pollutants, chemicals	Wood surface of façades are impregnated, interior wooden surfaces untreated, some building materials contain color coatings (e.g. window frames)	All wooden components are untreated, no use of glue, adhesives, protective chemicals or solvents	Use of cradle to cradle products which are free of pollutants, some building parts (e.g. façade components) contain color coatings, glue and adhesives
Technical installations	All technical installations can be disassembled and reused; software controlled energy optimisation, underfloor	Heating provided by external renewable sources. Decentral controlled ventilation system with heat recovery. Photovoltaic	Cradle to cradle certified installation material. Heat pump, photovoltaics, software control. Cavity floor installations, mas-sive

	heating	roof. Electric cabling PVC free, pipework made of steel and copper instead of plastic. All parts reusable; software controlled	floor slabs for cooling and heating. Rainwater catchment, stored in tanks to irrigate green, atrium plants and toilet flushing
--	---------	--	--

6. COMPARISON COMMON PRACTICE AND ZERO-WASTE

While energy efficiency has been a hot topic for over a decade in the world of construction and architecture, today there are urgent challenges around the supply of resources, materials, energy, food and water. It is vital for the focus to now shift to include further resources and material efficiency [17]. Despite the commonly debated topics of energy efficiency and recyclability being an important factor

to be addressed, it is now increasingly important to rethink the practices of the construction industry as a whole. With the following table 2, the differences and similarities of the three case study buildings are assessed. The table sets a comparison of building components in the case studies analyzed above against those used in common practices. It then proposes certain guidelines and exemplary solutions to be practiced in order to set towards 100% zero waste construction and operation of buildings.

Table 2: The different building parts in comparison with today's common building practice and cradle to cradle / zero-waste approach

	Common practice in today's construction sector	Disadvantages of common practice	Improvements towards zero-waste and cradle to cradle buildings as represented by case study buildings	Requirements for buildings which are entirely built according to zero-waste and cradle to cradle principles
Constructive system, building structure	Most common are reinforced concrete skeleton, load bearing walls, steel skeleton, wooden systems (rarely applied)	Very limited reusability, effortful recyclability, high amount of embodied energy is wasted after building's life cycle	Reusability of constructive parts only partially fulfilled; often buildings are marketed as much more sustainable as they are in reality	Zero-waste standard can be achieved e.g. with constructions of untreated wood, prefab steel modules; reinforced concrete to be avoided
Exterior walls and opaque façade elements, insulation material	Masonry, two layered walls, thermal insulation composite system (fossil fuel based), plaster, insulating bricks, aerated concrete	Most materials designed for single-use. Creation of large amounts of waste which partially is toxic	Prefab and modular panels or façade systems which contain insulation and are demountable for reuse	Prefab modular panels, reusable, possibly untreated, made of natural materials, low amount of embodied energy, high insulation quality
Windows, glazed façade elements	Frames of PVC, wood, aluminium, double glazing (sometimes triple glazing)	Components mostly recyclable: Insulation and air tightness to be optimised. External shading devices often lacking. Unsustainable materials (e.g. PVC)	Reusable components, increased use of natural materials for frames, triple glazing, external sun protection	Standardised window and glazing components, designed for multiple use. Production local and with renewable energy sources, embodied energy possibly low
Interior walls	Drywalls with aluminium stud frame and gypsum boards, masonry and plaster	Not reusable, effortful recyclability, embodied energy gets lost in large parts	Reusable, modular elements, natural materials	Lowtech, reusable components screwed together which can be easily disassembled
Roofs	Flat roofs with wood or steel joists, concrete slabs, sloping insulation layer, often hard exterior surfaces or roofing felts (often with bitumen coating); inclined roofs with wooden or steel construction, roofing tiles	Most components are not reusable; fossil based materials are used for insulation and other roof materials. Roofing tile construction method from past times, not up to date. Hard, often dark surfaces contribute to urban overheating	Reusable, modular elements. Only some case study buildings have multifunctional roofs with green, rainwater collection, renewable energy generation	Multifunctional roofs. Renewable energy generation with photovoltaic, warm water collectors, wind turbines; rainwater collection, green roofs, urban agriculture
Floor slabs	Reinforced concrete, floating screed, firmly connected building	Many components not separable from each other and not reusable	Prefabricated modular components, reusable	Prefabricated, modular, reusable parts, untreated materials, no poured

	components			layers, dry screed flooring
Foundations and ground floor slabs	Main components made of reinforced concrete	Demolition and recycling require high effort and energy, no reusability	Only few case study buildings have improved solutions with screw foundations or prefabricated reinforced concrete foundation parts which are separable and can be reused	Prefabricated reusable modular pieces of reinforced concrete strip foundations; screw foundations; foundations of natural materials such as natural stone or brickwork
Interior fittings; floor, wall and ceiling surfaces, furniture	Single use, many elements are composite materials and contain chemicals	Waste, partly hazardous, embodied energy is lost	Recyclable and reusable products, possibly untreated, cradle to cradle certified products	Reusable products, materials possibly untreated, cradle to cradle certified products
Connection techniques between building components	Many building parts are composites consisting of different materials which can not be separated easily, use of glue, single use	Many building parts not separable, not easily recyclable nor reusable. Immense losses after end of products' lifespan	Use of reversible connections, different construction materials can be separated and reused	Clamping, click, screw, magnet connections, all materials or products can be reused. All building components are designed for reuse
Use of pollutants, chemicals	Many components contain chemicals and fossil fuel based materials, some are even toxic. Gluing techniques widely used	Many products are only designed for single use. Toxic materials can be harmful for health. High amount of pollution and greenhouse gas emissions during production and disposal	Some case study buildings are refusing the use of products which contain harmful chemicals and pollutants	Use of untreated natural materials. No toxic materials. Possibly only carbon free products, no products which contain chemicals. All embodied primary energy of products to be offset
Technical installations	Mainly fossil fuel based heating, cooling and warm water heating. PVC pipe installations. Low proportion of renewable energy generation	Buildings are generating emissions. Not all technical installations can be reused. Potential of renewable energy production not sufficiently used. Often energy wasted by improper user behaviour	Emissions minimised, reusable installations, intelligent energy saving software	Entire energy demand can be generated by the building from renewable sources with photovoltaics, wind turbines and solar water heating collectors. Installation of efficient water use. Rainwater, grey water use, treatment for irrigation of green, toilet flushing etc.

7. CONCLUSION – PROPOSALS FOR THE FUTURE

Summarizing the above, several proposals have been deduced as an approach towards a zero-waste future in the building industry.

Proposal 1 – Reusable building structures. Constructions shall be made of prefabricated standardised elements of wood, steel or reinforced concrete. The use of untreated wood has the advantage that it can either be reused or wastelessly disposed. Steel profiles as modular construction systems in standard dimensions also would provide a way for effective constructions in the future (example: R128 building [8]). Both wood and steel can be fire-protected with standardised demountable protection coverings. Reinforced concrete shall only be used if standardized prefabricated and demountable elements would be developed, preferably made of recycled materials [18].

Proposal 2 – Modular exterior walls. They can consist either of reusable prefabricated panels, i.e. wood

with natural insulation material (example: Woodcube [19]), or of components with layers of different materials assembled on site. Green components may be integrated for a better microclimate inside and outside the building. There may be façade integrated photovoltaics and solar warm water collectors.

Proposal 3 – Improved insulation material. Insulation shall either be degradable, reusable or both (e.g. wood fibreboard). Building practices could adhere to natural insulation materials, while standardized insulation materials with reusable properties might be developed.

Proposal 4 – Standardised windows and glazed façade elements. Cradle to cradle certified glass shall be used. Reusable or degradable materials such as wood, aluminium or steel shall be used for frames. Façade system producers and specialists such as could focus on developing building kits with reusable standardized elements.

Proposal 5 – Prefabricated interior wall components. Standardised prefabricated interior wall components, easily demountable and reusable could be an effective alternative to current practice. Construction

companies shall be encouraged to develop such systems.

Proposal 6 – Multifunctional roofs. Roofs shall become multifunctional. In addition to weather protection they can serve as energy generators, water collectors, green space, food production. They shall improve the location's microclimate. The paradigm of a roof would shift from being a passive to an active building component.

Proposal 7 – Demountable floor slabs. Floor slabs would comprise a system of prefabricated beams along with other elements and plates. Dry materials such as dry screed flooring would prove to be an effective solution.

Proposal 8 – Demountable foundations. Prefab modules in separable pieces would make up the foundations of a building. Such reusable parts could either be made of reinforced concrete, stone or bricks. Ground floor slabs could either follow this principle, or could be of wooden or steel construction, ventilated from below. Screw foundations are another viable solution.

Proposal 9 – Reusable technical installations. Standardised reversible components shall be used, such as provided by the cradle to cradle certified products or as practiced in the car industry.

Proposal 10 – Leasable interior fittings, furniture and other items. Products shall be reusable, possibly being "leased" from the producers for their lifecycle.

Proposal 11 – Pollutant and glue free connection techniques of building components. Reversibility is to be enabled with clamping, clicking, screwing, drilling or by magnets.

Proposal 12 – Efficient water (re)use. Water could be treated locally on or within the building to be reused for irrigation of green, passive temperature control, toilet flushing etc. Rainwater is also to be collected and used.

Proposal 13 – Circular household waste treatment. Waste shall be separated into organic and non organic. Organic waste could be composted and used locally, non-organic waste could be sold for reuse or recycling.

To ensure that the above mentioned practices are implemented on a broad scale, government incentives would have to come into play. As a start, in Germany building regulations and standards such as EnEV, DGNB criteria and Bauordnung would have to integrate the cradle to cradle and zero-waste concepts. For a holistic ecological and energy efficient future of our built environments, factors such as sufficient insulation, embodied energy, and energy performance of building operation must be combined with the concepts demonstrated in this paper. Furthermore, the use of vernacular architecture and passive design principles must also be regulated and standardized, maximizing resource

and energy efficiency. With the integration of all of the aforementioned factors, a comprehensive building industry could be established, which celebrates a range of cultural and natural pleasures while rejoicing in the technological advances of mankind.

REFERENCES

1. Lehmann, S. and Crocker, R., (2012). Designing for Zero Waste, Earthscan: p. 210 – 222.
2. Berge, B., (2009). The Ecology of Building Materials: p. 5
3. Elgizawy S. M., El-Haggar S. M., and Nassar K. (2016). Approaching Sustainability of Construction and Demolition Waste Using Zero Waste Concept. *Low Carbon Economy*, 7, 1-11. [Online], Available: 10.4236/lce.2016.71001.
4. McDonough, W. and Braungart, M., (2002). Cradle to Cradle: Remaking the Way We Make Things, p. 93-97.
5. Schilperoort H., (2016), Reusing concrete elements, Eindhoven University of Technology, Netherlands, [Online], Available: <https://www.researchgate.net/publication/314206868> [June 2016].
6. Beney J. F., Attia S. and Andersen M., (2013), Application of the Cradle to Cradle paradigm to a housing unit in Switzerland: Findings from a prototype design, *Sustainable Architecture for a Renewable Future, PLEA 2013*, Munich.
7. Kloeppfer, W., (2008). Life cycle sustainability assessment of products. *Life Cycle Assessment* 13: p. 89-94.
8. Blaser W., Heinlein F., (2002), R 128 by Werner Sobek: Architecture in the 21st century.
9. Smart Material House Woodcube, (2014). IBA Hamburg, [Online], Available: <https://www.internationalebauausstellung-hamburg.de>.
10. Aktivhaus Project, [Online], Available: <https://ah-aktivhaus.com/> [26 April, 2020].
11. Lennartz, M. W. and Jacob-Freitag S., (2015). New Architecture in Wood: Forms and Structures: p. 128 - 134.
12. Holz-Thoma Bauteilkatalog (2017) [Online], Available: <https://www.thoma.at>.
13. ICON Dortmund, [Online], Available: icon-dortmund.de/gebaeude.html [22 April 2020].
14. Green, M. and Taggart, J. (2017), Tall Wood Buildings: Design, Construction and Performance: p. 84 - 95.
15. Deutsche Bauzeitung, [Online], Available: <https://www.db-bauzeitung.de> [24 April 2020].
16. Dortmund ICON [2020]. Building Description document by IAA Architekten.
17. Lehman, S., (2011), Optimizing Urban Material Flows, *Sustainability* [Online], Available: doi:10.3390/su3010155 [2 May 2020].
18. Godelet, A. and Schuster, H. G., (2018), A Material World, *Smart and Healthy within the 2-degree Limit, PLEA 2018*, Hong Kong.
19. Mayo, J., (2015), Solid Wood: Case Studies in Mass Timber Architecture, Technology and Design: p. 153

Research on astronomical orientation in the Greek Temples using solar analysis software

The Parthenon as a case study

EZEQUIEL USON GUARDIOLA¹, CARLES GUILLEN AMIGO¹, JOSEP VIVES REGO²,
ELISABET USON MAIMO³

¹School of Professional & Executive Development, UPC, Barcelona, Spain

²Universidad de Barcelona UB, Barcelona, Spain

³Polytechnic University of Catalonia, UPC, Barcelona, Spain

ABSTRACT: *The aim of this research was to analyse the astronomical orientation of Greek temples and the relationship between that and the religious rituals carried out in them, using solar analysis software tools. For our case study, we chose the temple of the Parthenon. Highly practical solar analysis software tools enabled us to determine the astronomical azimuth of the building's main longitudinal axis with a high degree of accuracy and to simulate the manner in which solar radiation was allowed to penetrate the innermost areas of the sanctuary. We also calculated the intensity of natural lighting entering the building and the time of year when this would have happened. The methodology applied in this research could be extrapolated to undertake similar analyses of other Greek temples.*

KEY WORDS: *Astronomical Orientation, Solar Analysis Software Tools, The Parthenon, Panathenaea festival.*

1. INTRODUCTION

One of the most potent tools that the Ancient Greeks developed and exploited was solar geometry. As already widely reported by other authors, the Ancient Greeks achieved a high level of astronomical precision that allowed them to lead the development of solar architecture. Their knowledge of the path of the sun, in the different seasons of the year, allowed them to choose the most appropriate orientation when laying out new settlements and designing significant buildings [1]. In addition, their sophisticated geometric knowledge helped the Ancient Greeks to accurately determine the astronomical orientation of their sanctuaries and temples. Such astronomical observations were also fundamental to the celebration of religious rituals in honour of the deities to which sanctuaries, and the main temples within them, were dedicated. These celebrations would usually take place on a set day of the year. It was important to ensure that such festivals were held on the correct day and that the calendar did not move out of season. However, it is not unreasonable to expect that Greek architects working more than two thousand years ago, and who would have had only basic topographic tools and trigonometric calculations at their disposal, could have made errors of several degrees in their astronomical alignments. This has, in fact, been demonstrated by recent examinations using modern instrumentation.

2. THE ASTRONOMICAL ORIENTATION OF THE GREEK TEMPLES

Greek temples were generally built facing eastwards. In an analysis of 113 temples previously studied by Heinrich Nissen (1910), William Bell Dinsmoor (1939) discovered that approximately 73% were oriented within 60° of due east, 8% within 60° of due west, and 19% in other directions [2]. Dinsmoor's general conclusion about the orientation of Greek temples was that their positioning was determined by the need to face either the rising or the setting sun. Their eastern orientation could also be explained by Egyptian influences. [3]. More recent studies using archaeoastronomy techniques have concluded that their eastward orientations were dictated by ritual, which required them to be brightly lit only at a specific time and on a specific day (Belmonte y Hoskin, 2002) [4]. George Pantazis and Evangelia Lambrou (2004), who have studied both the Parthenon and Hephaestion temples in Athens, concluded that "...both were aligned with dawn on the day on which the feasts of their respective deities were celebrated. Each temple was orientated so that the statue of the deity to which the temple was dedicated would be illuminated by the rays of the rising sun, at dawn, on the day of its official festival.....the Parthenon is oriented towards the point where the sun rises on the day of the celebration of the goddess Athena..." [5].

To achieve this, it was very important to establish the astronomical azimuth of the building's main

longitudinal axis, and the location of the statue inside it, with a high degree of accuracy.

2.1 Natural light and worship

By the classical period, Greek temples varied considerably in detail, although almost all of them consisted of simple rectangular buildings that were constructed to hold statues of gods. The side walls of these structures usually extended forwards to form a porch, which was embellished with columns. The statue of the God stood in the cella or naos which was supposed to be half-shrouded in darkness. Natural light was only allowed to enter the temple through the main doorway when the great doors were opened. As already mentioned, this use of natural light was primarily achieved through the alignment of the temple with the position of the sun in order to restrict sunlight entering the cella to a certain time on a specific day. This implied that at other times of the day or year temple interiors remained dark and visually unimportant and that they had to be lit by other means, such as with lamps or torches. This dim lighting created a gloomy interior but also an otherworldly, sacred atmosphere inside the temple.

3. THE PARTHENON

The temple of the Parthenon (447-432 BC) was built on the south side of the Acropolis at the initiative of Pericles. It was designed by the great architect Ictinus, in the Doric style, using the highest quality Pentelic marble. It was the brightest construction of the classical era of Athens and was dedicated to Athena, the city's goddess and protector (Fig. 1). The sides of the building follow a 4:9 ratio, with the monument being 30.8m wide and having a 69.5m long stylobate. It is 8 columns wide, 17 columns long, and 20 metres high, and its main entrance is in its eastern façade [7].

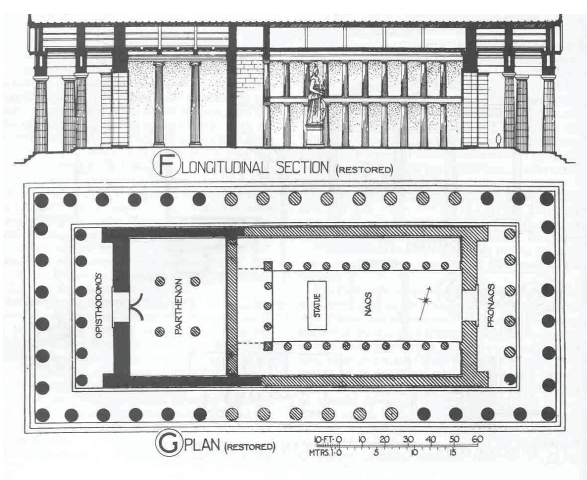


Figure1: Temple of the Parthenon (source Banister Fletcher).

One innovation in the interior space of its cella was the creation of a superimposed double

colonnade with an architrave in between. This was designed to enlarge and magnify the interior space surrounding the statue of the goddess Athena Parthenos: a colossal, 11-metre-high chryselephantine statue made by Phidias. This image was first built on a wooden frame lined with bronze plates and then completely covered with pieces of gold and ivory and with precious stones.

On the pediment of the east façade, above the entrance to the cella and following the axis of the rising sun, there is a sculptural group that was also created by Phidias and which represents the triumph of day over night. At the western end of the building, the god Helios appears on the horizon, at sunrise, with his chariot, while at the eastern end, the goddess Selene disappears behind the horizon at dusk. In front of the chryselephantine statue of Athena Parthenos, there was a small, shallow, rectangular pond, measuring approximately 9.0 m x 9.5 m, creating a reflective sheet of water. [8].The building was possibly designed in this way with the aim of improving the lighting cast on the statue by reflecting the light that would have entered through the open door.

3.1. Orientation

The astronomical orientation of the Parthenon has been studied by many researchers over the last 200 years with them reporting different results (table 1). This was first done using simple instruments like compasses and poles (Penrose1846). More recently, research has been carried out using modern instrumentation and applying geodetic methodology (Pantazis 2014) [9].

Table 1: Measurements of the astronomical orientation of the Parthenon; comparing earlier readings with the findings of our research.

Source	Azimuth (°)
Penrose (1846)	76° ±1°
JN Lockyer (1964)	72°
Sault	76°±1°
NASA	72°±2°
Boutsikas (2007)	77°±1°
Pantazis (2014)	77°07'±1°
Research of this paper	77° 11'±1°

4. DETERMINATION OF THE ASTRONOMIC ORIENTATION OF THE PARTHENON USING SOLAR ANALYSIS SOFTWARE

The methodology applied in our research consisted of the following steps:

We established the position (coordinates) of the monument's site on the Earth's surface using the positioning software on Google Earth.

A 3D plan of the monument was made using SketchUp software [10]. Its geometry was determined and also the position and dimensions of the statue of Athena located inside it.

Once the exact location of the Parthenon had been determined, an EPW (Energy Plus Weather) file was created using Meteonorm software [11]. This software contains a digital terrain model that automatically recognises any solar obstructions caused by the local terrain. Based on the orthographic horizon, the astronomical azimuth of the monument's main longitudinal axis was determined to be $77^{\circ}.11' \pm 1$. To avoid any potential obstructions generated by the horizon, the solar height had to be $2^{\circ}72'$. (Fig 2)

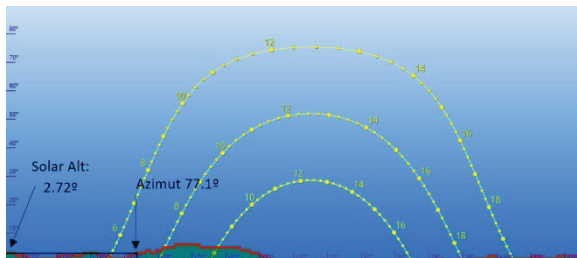


Figure 2: Diagram showing the plane of the horizon of the Parthenon, generated using the EPW file (Solar Azimuth $77^{\circ}.11' \pm 1$, Solar altitude $2^{\circ}.72'$).

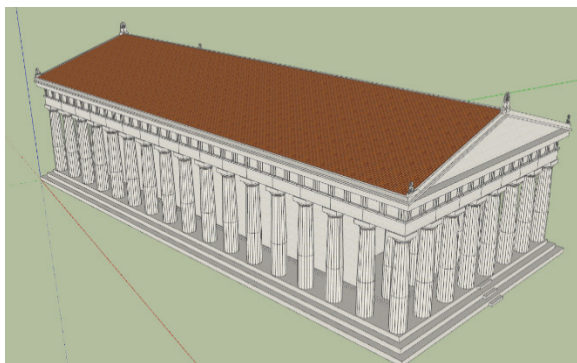


Figure 3: 3D plan of the Parthenon created using SketchUp software and highlighting the main orientation of the building, (azimuth $77^{\circ}.11'$). The green axis indicates cardinal north and the red axis indicates cardinal east.

Once the 3D model of the temple had been drawn from the building plans, it was imported into Graitec ArchiWizard software, together with the EPW file [12]. Its position was then defined, using the EPW file, and its solar orientation was determined using the imported geometry. This made it possible to generate diagram of the sun's path and to superimpose this onto the 3D model of the temple. (Fig. 4).

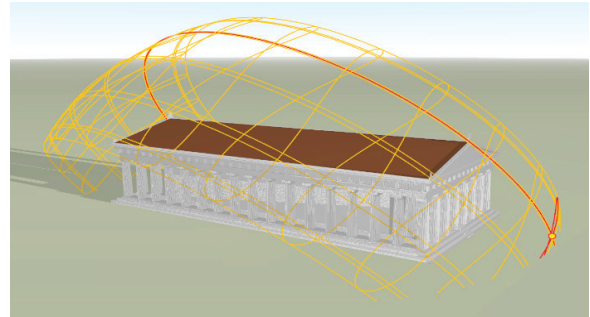
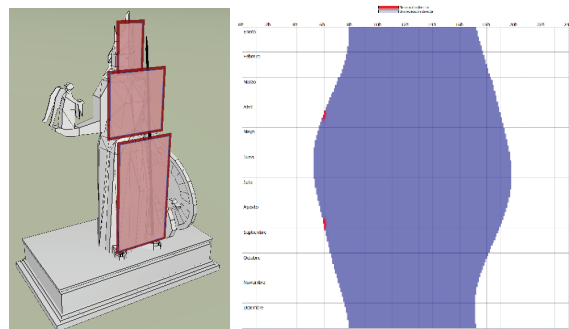


Figure 4: Incorporating the sun's path over the model with Archiwizard software.

Three surfaces of analysis (solar receiver) were then assigned to the statue of the goddess Athena to determine the day and time when it would have been fully illuminated. To do this, the statue was divided into three parts: the head, the torso, and the lower extremities. Direct solar radiation would have fully illuminated the statue when the solar receiver corresponding to its head received direct solar radiation. With a solar Azimuth of $77^{\circ}.11' \pm 1$ and a solar height of $2^{\circ}.72'$, this would have occurred at dawn (6:07 am) on August 22, according to solar time based on the current (Gregorian) calendar. (Figs. 5, 6 and 7).



Figures 5 and 6: On the left, the three analysis surfaces (solar receiver) assigned to the statue: head, torso and lower extremities. On the right, the verification that the statue's head would have received direct solar radiation (in red) in mid-April and in the second half of August.

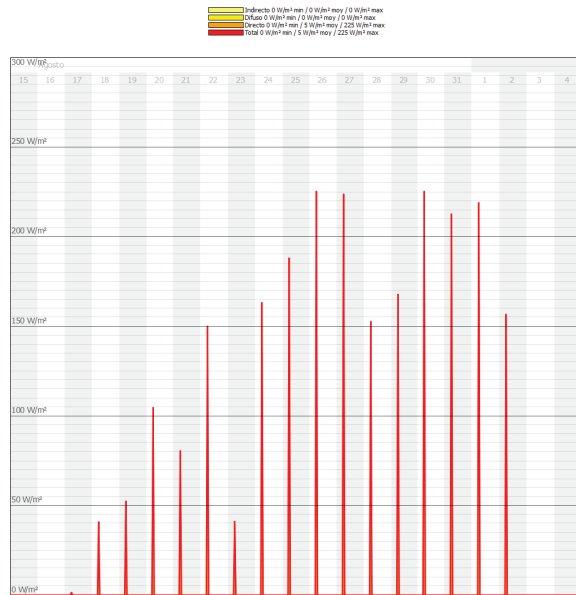


Figure 7: Direct solar radiation received by the statue in W/m² from August 18 to September 2 (of the current Gregorian calendar).

To check this more graphically, we generated a stereographic diagram which was projected onto the current remains of the Parthenon. This verified that, at 6:07 am (solar time) on August 22 of the current (Gregorian) calendar, the sun shines perpendicularly to the statue of Athena (Figures 8 and 9). The intensity of solar radiation shining on the statue between 6am and 7am (the maximum precision of the programme is 1 hour) was also quantified (Figures 10 and 11).



Figure 8: Stereographic diagram of the existing remains of the Parthenon (solar azimuth 77° 11' and solar altitude 2° 72').

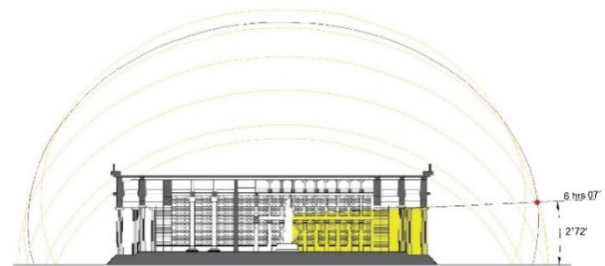
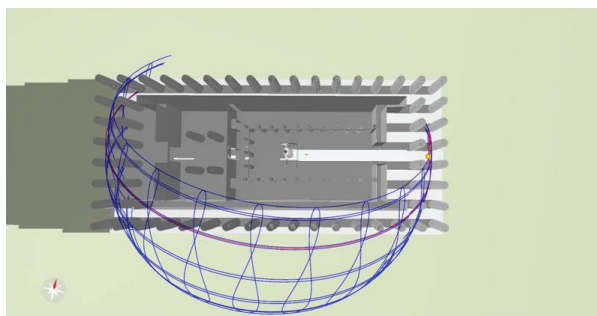
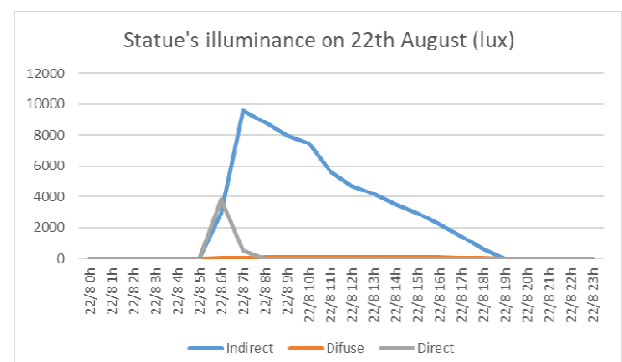
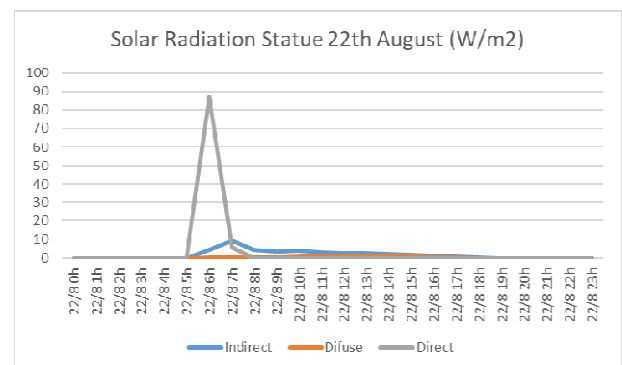


Figure 9: Direct incidence of solar radiation striking the statue at 6:07 am on August 22, according to the current (Gregorian) calendar.

We ran a simulation using the ArchiWizard software to calculate the intensity of the internal illumination of the temple on August 22, at this precise time. Properties were assigned to the different materials, which made it possible to take into account the reflection of the solar radiation inside the temple (Figures 10 and 11). As the whole temple had been built with Pentelic marble, white marble was assigned as the material (diffuse reflection: 75%; specular reflection: 30%).



Figures 10 and 11 - Global radiation levels (W/m²) and illuminance (lux) on the statue at 6.07am on August 22.

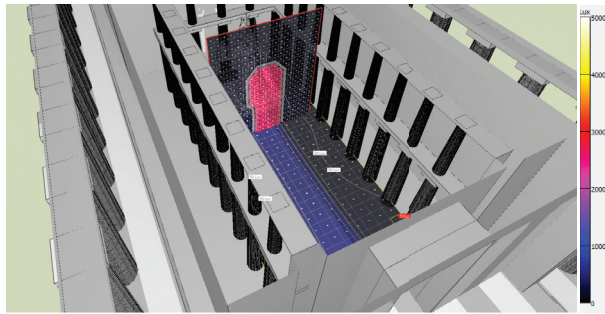


Figure12: Graphic Simulation of the illuminance levels (lux) inside the cella at 6.07am on August 22, according to the current (Gregorian) calendar.

5. RELIGIOUS RITUAL AND TEMPLE LIGHTING

Once every year, Athenians used to pay tribute to their protecting divinity, Athena, at the Panathenaia festival; and every fourth year, they would do the same at the Great Panathenaia.

This religious celebration centred around a procession that started on the outskirts of the city, climbed up to the Acropolis, and ended, at dawn, at the eastern facade of the temple, where the faithful delivered their offerings to the goddess Athena. According to historians, this important moment in the Athenian calendar coincided with the rising of the sun on the 28th day of the Greek month of Hekatombaion [13].



Figure 14: Life-size replica of Phidias's statue of Athena Parthenos (as presented in Nashville's Parthenon), fully illuminated and with its reflecting pool.

As a result, on that day and at the time, the temple doors were opened to the people of Athens so that they could adore the statue and present offerings to Athena, in what was the main festival in her honour. On that day, the people's attention was monopolised when a priestess presented a peplos to the goddess, in the cella of the Parthenon, inside the sumptuous niche in which the colossal image was housed. It is not difficult to imagine the impression that this must have made on the citizens of Athens. At precisely 6:07 am, the chryselephantine statue of the goddess Athena would have received the perpendicular impact of solar radiation and would have been fully illuminated, shining in all its glory and in various shades of gold and ivory. (Figure 14)

5.1 Correspondence of dates: Attic calendar vs. Gregorian calendar.

There is no direct correspondence between the dates of the Athenian calendar and our current (Gregorian) calendar. The Athenians used star calendars to set the dates for their religious celebrations. The Panathenaia festivities took place throughout the month of Hekatombaion, which was the first month in the Attic calendar. As this was the feast of the city's goddess and protector, it was important to make sure that the festivities took place on the correct day and that the calendar was not out of synchronisation on that day. Using a lunar calendar, it was difficult to meet this requirement. The Greeks were fully aware of the fact that their 12-month, approximately 29.5-day, lunar cycle did not fit the 365-day year. They used to make up for the difference by inserting an additional month approximately once every three years. With each reform, a new calendar was generated, with different month names and times of insertion. Furthermore, although a new month always began with the sighting of the new moon, the exact determination of the best day on which to celebrate the peplos ritual was always subject to the interpretation of local observers and to the constellations in the night sky. For this reason, the Attic calendar was not fixed, and the correspondence of dates between the Attic calendar and our Gregorian calendar changed from year to year. [14].

6. DISCUSSION AND CONCLUSIONS

The basic findings of this research were:

We checked the validity of the solar analysis software to determine astronomical orientation. In the case of the Parthenon (solar azimuth $77^{\circ}11'$), our result significantly coincided with those obtained by other contemporary authors who had used geodetic measurement. The determination of the astronomical azimuth of the monument's main longitudinal axis also confirmed the influence of its use as a place of

worship. When designing this building, the goal had been to allow the rising sun to cast light on the statue of the goddess. The statue therefore occupied a specific position within the temple. It was particularly important that the first morning sunlight fell on the statue on the day dedicated to the goddess Athena during the Panathenaea festival. Our research led us to hypothesize that the Greek architects who built the Parthenon temple must have had advanced knowledge of solar geometry to achieve this. There was a non-causal correlation between the dimensions of the cella, the astronomical orientation of the Parthenon, and the position of the chryselephantine image of the goddess Athena Parthenos.

Based on the results obtained using the solar analysis software, we concluded that the statue of Athena would have been fully illuminated at 6:07 am on a date corresponding to August 22 of the current (Gregorian) calendar. Due to the illumination reflected by the pool, and to the marble cladding inside the cella, the statue would have received illumination at dawn for a period of almost two weeks. Research conducted by historians suggests that the offering that was made to the goddess Athena during the Panathenaea festival coincided with the rising of the sun on the 28th day of the month of Hekatombaion in the Attic calendar. Although we cannot make an exact conversion between the Attic and Gregorian calendars, we do know that this would have corresponded to the same season of the year.

With this work, we have increased awareness of the potential use of direct sunlight in temple interiors in classical times. Morning sunlight was shown to have fallen directly between the central columns of the Athenian Parthenon on a specific day related to the festival dedicated to Athena Parthenos. (Figure 7).

Another important question relates to the methodology for verification used in this investigation. This could be extrapolated to undertake similar analyses of other temples built by the Ancient Greeks.

ACKNOWLEDGEMENTS

This applied research benefitted from input from some of the students on the UPC's MSc course in "Architecture and Sustainability: Design Tools and environmental control techniques": Lucia Igoa and Julieta Norali Pardo. Under our leadership, they developed a graphical approach that greatly helped us in the development of this research.

REFERENCES

1. Butti, K. and Perlin, J. (1981). *A Golden Thread, 2500 years of solar Architecture and Technology*, Marion Boyars Publishers Ltd. London.
2. Dinsmoor W.B. (1939). *The Architecture of Ancient Greece: an account of its historic development*. Biblo and Tannen: p. 149-50.
3. Nissen H. (1906). *Orientation, Studien zur Geschichte der Religion*, 3 v. in 1, Berlin: Weidmann.
4. Belmonte J.A., Hoskin. M. (2002). *Reflejo del Cosmos, Atlas de Arqueoastronomia del mediterraneo antiguo*. Madrid, Equipo Sirius.
5. Lambrou, E. Pantazis, G. (2008). *Astronomical azimuth determination by the hour angle of Polaris using ordinary total stations*. Survey Review, vol.40. Nº308: p. 64-172.
6. Williamson C. (1993) *Light in dark places. Changes in the application of natural light in sacred Greek architecture*. PHAROS Journal of the Netherlands Institute at Athens, vol, I: p. 23, JC. Gieben publisher. Amsterdam.
7. Fletcher, B. (1987). *Sir Banister Fletcher's a History of architecture*, BUTTERWORTHS, London: p. 112-116.
8. Miles, M (2016). *A companion to Greek Architecture*. John Wiley& Sons, Inc.: p. 216-220.
9. Pantazis, G. (2014). *The symmetric placing and the dating of the Parthenon and Hephaisteion in Athens (Greece)*. Mediterranean Archaeology and Archaeometry, vol.4, nº2: p. 273-279.
10. SketchUp Software Available: <https://www.sketchup.com/>
11. Meteonorm Software: Available <https://meteonorm.com/en/> EPW Energy Plus Weather File: Available <https://energyplus.net/weather>
12. Graitec Archiwizard Software. Available <https://fr.graitec.com/archiwizard/>
13. De la Nuez Pérez. M.E. (2008). *Las Panateneas: un ejemplo de relaciones sociales a través de la fiesta*. Gerion nº.26 (1): p. 255-265.
14. Ancient Attic calendar. Available: <https://www.epistemeacademy.org/calendars>

Hex Primary School - A Sustainable Self-built Community Project

Cost Effective Vernacular Architecture for the Tropical Climates

MARIA ANDREE OSOY ESCOBAR¹, PAULA CADIMA¹

¹Sustainable and Environmental Design, Architectural Association School of Architecture, London, UK

The standard of education in Guatemala is ranked one of the lowest in Latin America. This is due to the low economic growth, failure from governments to invest funds in education and the lack of a linear and incremental growth of the educational system. This lack of funds to the educational sector has affected the access, coverage and quality of educational centers in rural communities; where literacy levels, school attendance and student retention are pressing problems. This paper focuses on the design development of a low-cost self-built prototype unit for primary schools that can adapt to any urban or suburban site in the hot tropical climate while achieving environmental qualities and a free running, net zero passive design. The design project was inspired by vernacular architecture in similar climates and promotes the use of traditional construction methods and local materials

KEY WORDS: Comfort, energy, ventilation, thermal performance.

1. INTRODUCTION: Hex Primary School : A Sustainable self-built community project

The standard of education in Guatemala is ranked one of the lowest in Latin America. Due to Guatemala's low economic growth the evolution of the educational system has not been linear or has had an incremental growth. [1] Dictatorship regiments and the government's failure to properly invest funds in the education system has had a negative impact in literacy and academic levels. Guatemala suffers of low levels of literacy, attendance and retention. The lack of funding into the educational sector has not permitted rural communities in the country to have access to good quality education or educational centers. Due to budget restrictions family members see themselves taking charge of the educational centers available which compromises the proper management and maintenance of school centers. Research has demonstrated that educational buildings in the country do not follow design guidelines to provide safe and comfortable environments for students in rural areas.[2] Such is the case of Colonia Nueva Esperanza School located in Izabal, Guatemala, where 200 students are forced to seek shelter under the neighborhoods trees and shaded areas to be able to perform their daily school activities. Mean temperatures in Izabal are in general quite mild throughout the year. The highest temperatures occur during the wet season between the months of May to October with average maximum temperature about 31°C and average minimum around 24°C, Fig 1.1. Tropical cyclones are common in the wet season when

days are usually overcast causing flooding in schools and neighborhoods. *Canicular*, the dry period, is common in July and August and typically lasts between 4 to 7 weeks, during which the highest temperatures of the year occur. A rainy season follows this *canicular* period with intense rainfall until October. The wind direction is usually from the north. Fig 2.1

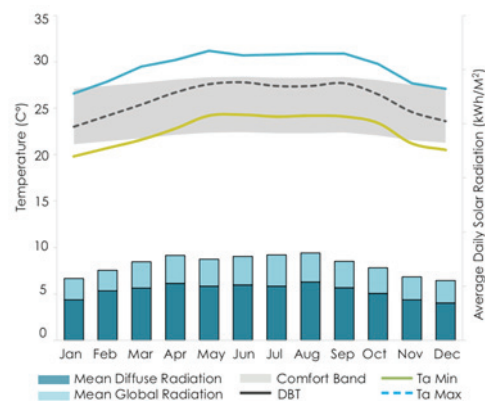


Fig. 1.1 Izabal Climate Analysis

As part of a research for a design project aimed at generating a learning environment able to promote sustainable living and a sense of community in Puerto Barrios, a village in Guatemala.[3] Colonia Nueva Esperanza educational center was studied and used as an example to set a base case study to determine the main problematics that schools in the hot tropical climate of Guatemala face.

2. Establishing the Base Case Model

A typical school complex in the area of Izabal was studied to help defining a base case model for further analytic work. Current school schemes usually consist of a linear or U-shaped classroom building form with classroom blocks arranged around a central courtyard used as recreational or sport area. Typical classrooms dimensions are of 6 X 8m with pitched single roofs and fixed windows located adjacent to a shaded corridor. These schools are made of concrete blocks, supported by a steel structure and concrete floors. The roof consists of corrugated steel sheets. Windows are single glazed and doors simple metallic sheets. The model was set to follow the design criteria of the current Code of Construction for Educational Buildings (MINEDUC) in the hot tropical climate. According to this code the minimum area required is of 1.25 m² to 1.50 m² per student in primary schools, with a student capacity from 15, 20, 30 or a maximum of 40 students, which is not recommended [4]. In accordance to these guidelines the model assumed a 48 m² classroom with a 3.20m floor to ceiling height to accommodate 30 students and 1 teacher. Fig 2.1

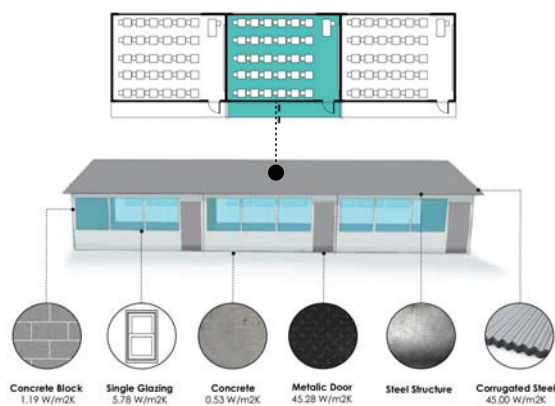


Fig. 2.1 Base Case Model

Analytic work was carried out to assess the environmental performance of a typical primary school model in the hot tropical climate of Izabal. The simulations encompassed different scenarios to represent various climatic seasons throughout the school year during the occupancy schedule with Meteororm climate data for Izabal. These included typical wet and dry weeks during the months of February and July. Design parameters were established with following the MINEDUC guidelines and the requirements for primary schools. Minimum air change per hour was set at 5.14 ACH, assuming an infiltration of 2 ACH. Other specifications included a window to floor ratio of 25% and 1.20m long overhangs. Construction materials were assumed the same as of current local practices, Fig. 2.1.

The comfort band was set between 24-29°C, according to the recommended range for adequate performance in schools in developing countries [5]. The thermal simulations show indoor overheating to occur in both the typical wet and dry seasons, exceeding well above the upper limit of the comfort band. Indoor temperatures peaks reached 34-37°C during the dry season, while outdoor peaks ranged between 25-29°C, and 36-39°C during the wet season, while outdoor peaks ranged between 28-34°C, Fig 2.2.

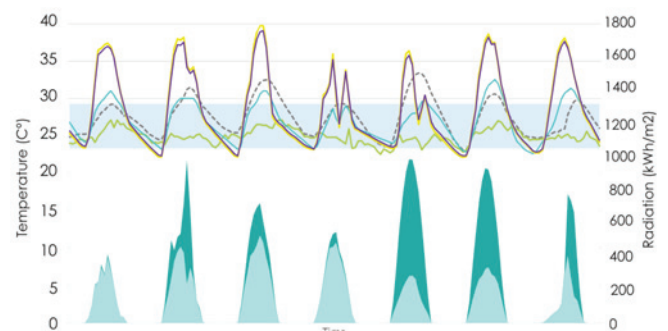


Fig 4.8 Wet Season Week Performance. Source: Open Studio

Legend

- Comfort Band
- DBT [C]
- Global Horizontal Radiation
- Diffuse Horizontal Radiation
- Mean Temperature
- Dew Point Temperature
- Operative Temperature
- Dry Bulb Temperature

Fig. 2.2 Current Practice Wet Season Thermal Study.

The study also demonstrated that the fixed windows used in the current practice do not allow the minimum air exchange per hour requirement (as set by MINEDUC) to be met and a minimum of a 25% window to floor ratio and a design reassuring cross ventilation is needed to meet these ventilation requirements. Daylighting analysis was carried out to determine the daylight availability during which 300 Lux required for primary schools are met during its occupancy. The UDI (Useful Daylight Illuminance) analysis shows that the 25% window to floor ratio allows a 77% of the occupancy hours to be achieved, 2.3.

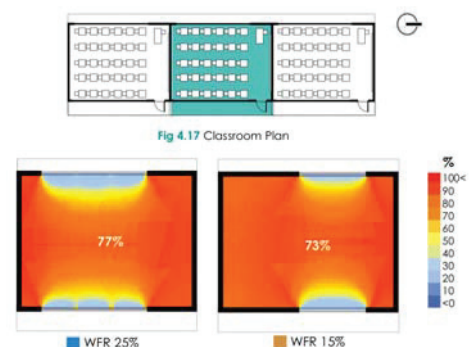
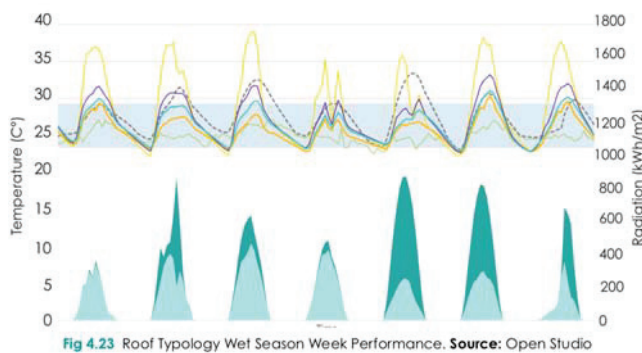


Fig. 2.3 UDI Analysis. Source: Ladybug

The analytical work highlights the main problematics of the current practice on the thermal performance of the typical school model in Guatemala.

Due to the high levels of global and diffuse horizontal radiation, humidity dry bulb temperatures as well as 5,500kwh internal casual gains, the most important factors which needs to be addressed to reach indoor comfort are introducing adequate ventilation strategies, a roofing strategy that can reduce heat transmissions and mitigate heat gains and careful selection of materials.

Due to the high sun angles, the roof design can play a major role in reducing heat gains. The effect on indoor temperature of different roof design solutions was compared. These included a pitched single roof, a double roof, an elevated roof and a ventilated double roof, Fig 2.4. The study shows that the latter option performs best providing indoor comfort with temperatures ranging between 21°C and 29°C throughout the year. Another benefit of this roof solution is that it also aids mitigating humidity discomfort. Although the overhangs do not have a significant impact on decreasing indoor temperatures this is an essential element to drain the heavy rainfall of Izabal's tropical climate and to provide protection to the classroom corridors and entrances.



Legend

- Comfort Band
- DBT [C]
- Global Horizontal Radiation
- Diffuse Horizontal Radiation
- Dew Point Temperature
- Base Case Mean Temp.
- Double Roof Mean Temp.
- Elevated Roof Mean Temp.
- Elevated Double Roof Mean Temp.

Fig.2.4 Roof Typologies Wet Season Thermal Study.

Further studies explored elevating the building structure from the ground to generate air flow below the ground floor level. This reduces relative humidity levels and also prevents damage to the structure due to flooding and heavy rainfalls.

Daylighting studies undertaken to assess a UDI analysis to assess if the elevated double roof could also improve daylight levels. The percentage of useful daylight illuminance increased from 77% to 84%, Fig 2.5.

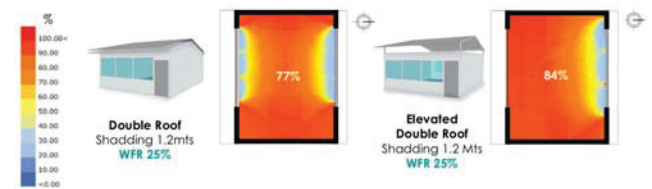


Fig. 2.5 UDI analysis for different roof design solutions

3. Self-Built Design Proposal

Based on the previous findings a design for a sustainable independent unit prototype in symbiosis with its local environmental context was developed. The main conceptual idea was to generate a self-built light weight unit that could be adapted to different site configurations and built with natural resources and materials available locally by the community and local workers, therefore reducing construction, planning and operational costs. The design development evolved from decision making studies to balance both thermal and daylighting indoor quality with Open studio and Ladybug/Honeybee.



Fig. 3.1 Hexagon Configuration Examples

The proposed design was based on a honeycomb grid. The hexagonal form is thought to be more stable structurally in comparison to a simple cube or rectangular module. This shape is also more stable and resistant to Guatemala's volcanic activity and earth movements. In addition, the honeycomb composition also opens the possibility to a more interesting configuration for primary school complexes. Hexagonal units allow flexibility and can be easily arranged in clusters to form various configurations with transitional spaces between units (Fig 3.1) allowing views, interaction between different age groups and creating an overall stimulating space for children to learn and grow. This shape reduces the total surface area by 36 m²

if compared to a 48 m² rectangular classroom, reducing planning, transportation and construction costs.

Thermal studies were carried out to compare the performance of a hexagon with a rectangular classroom shape with equivalent areas. The studies revealed that the hexagon shape performs similarly to a standard rectangular class, both achieving indoor temperatures ranging between 20°C to 31°C throughout the year. The proposed hexagonal unit was designed with a floor area of 48 m² to fit 30-35 pupils and one teacher. The materials used for the envelope are dry split and hollow bamboo, steel structure and a combination of canvas and bamboo walls. Set up on a concrete foundation, the floor steel structure is elevated 0.75m from the ground level to protect the bamboo structure and building from flooding from heavy rainfalls while also allowing air flow below the classroom floors to help dissipate internal heat gains. There is no glazing but openings are considered for natural ventilation and daylighting, and protection from insects, animals, rain and intruders is carefully thought out. The design incorporates 2 types of walls: one is a pivoting wall with a 360° rotation steel rod that offers students and teachers access to the adjacent outdoor green spaces of the complex.

This type of walls can be manipulated by the occupants for controlling ventilation, daylight penetration or to connect with adjacent classrooms to form a wider space for undertaking different activities.



The wall system proposed combines hollow bamboo and twill canvas, Fig 3.2. The hollow bamboo has 0.45m diameter and is positioned at a 45° angle across a 3mm steel rod along the wall to provide protection from rainfall while allowing air circulation. The second type of wall is made of solid split bamboo with a bamboo planter layer for growing vegetation on the external side. The vegetation provides protection from solar radiation and high outdoor temperatures thus help controlling external heat gains. In addition the planter system encourages children to plant their own “vertical garden” and embark on other activities involving vertical farming, plant growth etc. The classrooms floors are made of pressed bamboo planks fixed on the steel frame structure. The permeability of the pressed bamboo

allows underneath air flow and avoids direct contact with the ground. The pitched roof structure is a key environmental element of the design. It consists of an elevated double roof composed by 4 elements made of split dry bamboo and a galvanized steel sheet for rain, Fig 2.7. The indoor hot air can exist through the side opening through stack effect and diffused daylighting is allowed while protection from rain and solar radiation is still guaranteed. The pitched roof has a 1.20 m long overhang to protect the wall structures and interior spaces from heavy rainfalls and to provide shade throughout the classroom’s outdoor circulations. The interior face of the metallic roof is painted white to reflect and diffuse the daylight entering from the top opening to provide better indoor light quality. This layer acts as a “floating umbrella roof”. The second roof layer is made of canvas and a steel structure. The permeability of the canvas provides continuous ventilation thus helping relieve heat and dissipate moisture throughout the year. Materials properties are shown in Fig. 3.3.

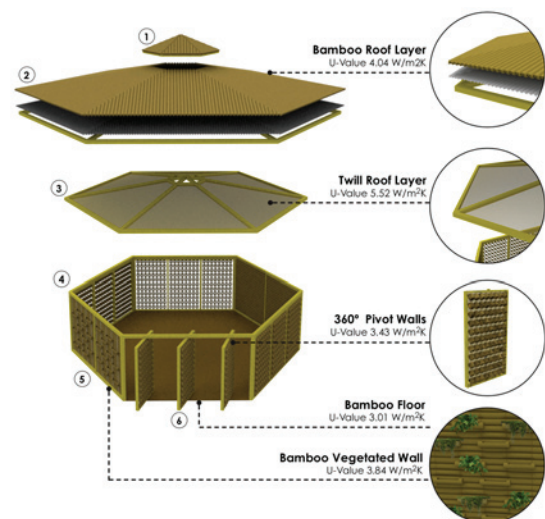


Fig.3.3 Classroom Materials & Properties

The classroom structures can be prefabricated off-site and transported to its location to be assembled on-site, promoting local jobs to its habitants. A tool kit manual explaining the construction methods and including step-by-step instructions on how to build and erect each classroom unit would be distributed. The module gives the flexibility to be mounted providing different configurations according to the community’s needs and preferences, and is adaptable to any site and local context.

4. Thermal & Daylight Performance

The final simulations to assess daylighting quality and the thermal performance of the proposed hexagonal

prototype unit are shown in Figures 4.1 and 4.2. The assumptions for the thermal model are shown in table 1.


		
Activity Sedentary (1 met)	Air Exchange 5.7 ach	Window to Floor Ratio 25%
Clo 1	Lighting 3.33 W/m ²	Occupancy 30 students + 1 teacher
Equipment 1 Watt /mts ²	Area: 48 mts ²	Occupancy Schedule 7:30 am to 3:30 pm

Table 4.1 Thermal & Daylight Model Parameters

Natural daylight in the classroom reaches 200-400 lux 89% during the total amount of school hours throughout the year. (Fig 4.2) Glare can be seen in the late afternoon, but this can be controlled by the pivoting doors.

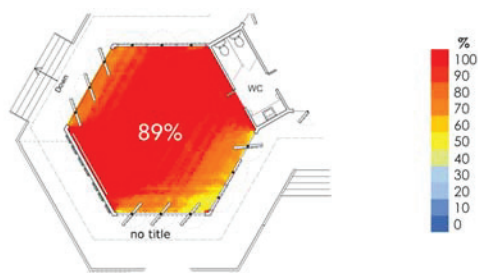


Fig. 4.1 Daylight Analysis

Indoor temperatures oscillate between 20°C and 28°C during the typical dry season week and between 24°C and 31°C during the wet season, Simulations also shows typical current practice performance as a reference for comparison Fig 4.2.

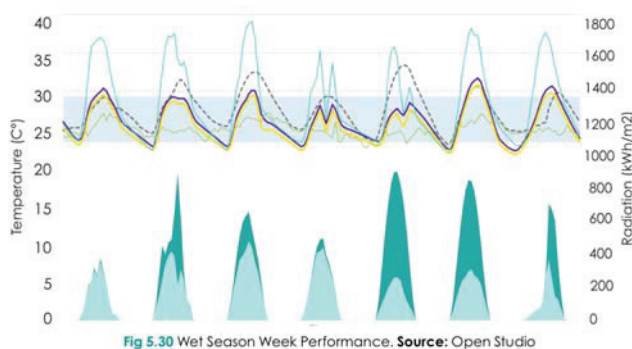


Fig 5.30 Wet Season Week Performance. Source: Open Studio

Legend

- Comfort Band
- DBT [C]
- Global Horizontal Radiation
- Diffuse Horizontal Radiation
- Class Mean Temperature
- Dew Point Temperature
- Class Operating Temperature
- Current Practice Mean Temperature

Fig. 4.2 Hex Classroom Thermal Performance Wet Season

5. CONCLUSIONS:

The hexagon shaped classroom design here proposed offers the possibility for an alternative design solution for educational buildings in Izabal. The design studies demonstrated that implementing passive design strategies and incorporating adaptive design solutions with a layout allowing cross ventilation (and 5.70 ach), a double roof structure, 1.20m overhangs, 3.20m building height, elevated floor structures, a 25% window to floor ratio and carefully selected envelope materials, can provide indoor comfort throughout the year. Simulations showed drops of indoor peak temperatures by up to 8K in a 48m² classroom with 30 children and 1 teacher in comparison to current practice in public schools in the area of Izabal, Guatemala. The honeycomb shape offers flexibility and various adaptable design configuration possibilities and an educational space which can also act as a tool to enhance the learning & teaching experiences, while providing a space which can be used by the community members. The proposed solution promotes sustainability by using natural local renewable materials such as bamboo and fabric. The use of twill canvas aids thermal performance and air flow while promoting local crafts and supporting local artisans. The proposed prototype can be self-built by the local community, thus reducing design and construction costs. The structure can be prefabricated off site and adapted according to specific community's needs.

REFERENCES

1. Monica, Cach. (2014). Historia de la educación en Guatemala. <https://www.monografias.com/trabajos94/historia-educacion-en-guatemala/historia-educacion-en-guatemala.shtml>
2. James Garfield. (2010). Without education, neither freedom nor justice can be <http://www.avivara.education/aboutguatemala/educationinguatemala.html>
3. Osoy Escobar, Maria Andree. (2019). Design of Educational Buildings in a Tropical Climate. MArch Dissertation. Pp 1-129
4. MINEDUC. (July, 2013). Manual del Aula de Calidad : Modalidad de Entrega Presencial. Ministerios de Educación vicedespacho Técnico Dirección general de Currículo - DIGECUR- .Guatemala. Pp. 6
5. ASHRAE (1999). Ventilation for Acceptable Indoor Air Quality. ASHRAE Standard 62-1999, Atlanta.

Embodied Energy and Carbon Assess in Passivhaus A UK Case Study

SERGIO GOMEZ-TORRES¹, FIONN STEVENSON¹,
JENNY BRIERLEY¹, FRAN BRADSHAW²

¹The University of Sheffield, Sheffield, UK

² Anne Thorne Architects, London, UK

ABSTRACT: As Passivhaus is widely accepted as high tier standard for reducing the energy consumption, it relies its strategy on a super insulated envelope and the inclusion of diverse assemblies and appliances. Although, the materials used to complete standards stipulated to comply the Passivhaus certification usually are made of highly intensive materials. This paper assesses the importance of the embodied energy and carbon contribution in the total Life Cycle of the building. By selecting a case study in the city of York UK, which has been operating for 3 years, the study contrasts the operational energy against the embodied energy. Besides, a substitution material approach was assessed in behalf to understand if the substitution of the present wall fabric for low-impact materials will decrease the levels of embodied carbon and energy.

KEYWORDS: Embodied Energy, Embodied Carbon, Passivhaus, Life Cycle Analysis, UK

1. INTRODUCTION

According to the latest IPCC report global temperature is expected to increase +1.5 degrees between 2030 and 2052 and is directly related to the Greenhouse Gas emissions (GHG) produced by human activities. The UK government has thus implemented different policies to reduce CO₂ emissions by 100 % from 1990 levels by the year 2050 [1]. The UK government plan "Reducing Emissions from Buildings" sets out the groundwork for increasing energy efficiency in homes [2].

The total energy use of buildings is composed of operating energy (OE) and embodied energy (EE). Various studies mainly focus on reducing OE and not the EE of the building elements [3,4]. However, studies differ on which stage of an EE LCA has the most impact [5]. According to [6] an average 80 m² house in the UK, EE accounts for 22% of total energy consumption and EC for 19 % of total carbon emissions, the study assessed 14 homes and found the average EE was 1483.33 kWh/m² and EC 110 CO₂Kg/m².

The Passivhaus (PH) standard has become a new reference for low-energy buildings and various local governments and organizations in the EU have now implemented Passivhaus as a requirement. Passivhaus certification requires an outstanding level of indoor environmental quality together with high-energy efficiency. Despite the low energy consumption of the operational energy, the impact of the embodied energy [EE] in PH assessment can be significant [7]. Due the high quantities of insulation required to reach PH

requirements for a Passivhaus the total EE can be as high as 56.9% of the total life cycle energy in a 80 years period using a input-output-based hybrid analysis[8].

The PH standard requires a maximum of 120 kWh/m² for the overall operational primary energy (OPE), of which a maximum of 15 kWh/m² should be used for the heating or cooling demand [9].

Key elements to achieve the Passivhaus standard are high insulation levels, draught free-construction, high performance windows and doors, and Mechanical Heat Recovery Ventilation (MVHR). MVHR systems account for between approximately 30 000 and 50 000 MJ in of initial and recurrent EE over a 50 year building lifespan, significantly reducing their benefit in a mild maritime climate like the UK [10].

The aim of this study is thus to understand the embodied energy relative to energy in use in a Passivhaus home and compare the concrete block structure with an alternative low EE timber/unfired brick structure. It will also take into consideration the embodied carbon.

2. LITERATURE REVIEW

2.1 Embodied energy

EE typically comprises all the energy involved in the extraction, production, and transportation processes of a product to the point of measurement, which is commonly the place of use. It may also include the secondary energy used for the production of all

materials embedded in the production of the elements of the given product. Three methods are generally used to calculate EE:

1. Input-output (IO) analysis, which uses national financial transactions to establish the energy intensity of economic sectors and attributes this to individual products.

2. Process-based analysis (PA), which collects all data, including direct and indirect energy inputs, related directly to the individual building product.

3. Hybrid analysis (HI-O) which combines both IO and PA processes, making it the most reliable and comprehensive embodied energy method [11].

The relationship between the LCA and EE is important, with energy being embodied in the intermediate products and materials that are passed on between producers, until these reach the final consumers.

Natural construction materials such as timber and organic fibres contain less EE compared to steel, concrete and polyurethane [12]. However, the energy involved in the maintenance procedures of these natural materials and their lifespan, needs to be taken into consideration. For example, an adobe house in New Delhi resulted in a cradle to gate EE of about 131,944 kWh for a 100 m² building and around 163,88.9 kWh for maintenance. When burnt brick, concrete and cement were substituted the building consumed a total of 200,000 GJ [13]. This shows that unfired clay materials could significantly reduce EE, despite their maintenance EE.

2.2 Embodied Carbon

While EE more typically accounts for 10-20% of overall energy use in homes, EC is often as high as 20-50 % of overall emissions in the same building [14]. EC can be measured from cradle-to-gate, cradle-to-site, cradle-to-end of construction, cradle-to-grave, or even cradle-to-cradle, and is usually assessed using an adapted form of Life Cycle Assessment (LCA) as defined by the International Standard ISO 14044:2006 . The Royal Institution of Chartered Surveyors (RICS) guidance used here calculates the EC per kilogram of product using the cradle to gate framework deriving from processing to the final product only, and not to site[15]. RICS suggests 60 years as a reference lifecycle period for buildings, broadly representative of typical replacement cycles for major building components, and finally, systems that stretch across a period into the future that is reasonably predictable. However, these components can also last for longer or shorter periods, depending on other activities.

2.3 Embodied carbon and energy data sources.

The Inventory of Carbon & Energy (ICE) is used in this study as one of the few open source databases available. It uses the process analysis method, which relies on the cradle to gate boundary [6].

The latest version of ICE (V.3.0 2019) does not consider embodied energy, as embodied carbon is now considered a more useful indicator. Additionally, the database only focuses on materials instead of components [16], and this affects reliability since the carbon factors used in the energy implemented in the combined materials manufacturing process for components can differ too.

Environmental Product Declarations (EPD) provide a more accurate assessment for a specific construction according to ISO 14025 standards [17]. However, the quality of these voluntary EPDs depends on manufacturer statements and this can result in a less valid assessment.

3. RESEARCH APPROACH AND METHODS

A single house exemplar case study approach was chosen [18], closely tied to local factors, such as climate, energy production process and local building material supply chains. This approach relies on multiple sources of evidence to validate the EE and EC findings and has advantages over predictive EE simulation, which focuses on limited variables and divorces the phenomenon from its context.

A classic post occupancy evaluation incorporated the following methods to more fully evaluate the EE and EC in context: a site visit, an interview with the owners of the house to understand the common use of the energy by the occupants, a photo survey, a construction survey, a document review, and a home demonstration tour to identify any possible changes between the design intentions and the construction in reality [19].

As the calculations for EE and EC include the amount of energy in an element (MJ) and kilograms of carbon emissions (kgCO₂/kg), this study used a causal-comparative research method to identify the various material intensities overall. The case study house was modelled in REVIT taking off quantitative measurements based on the documents and data gathered.

The embodied carbon calculation was made using the H/B:ERT [20] tool which uses the ICE 2.0 database. The volumes and specifications of materials were extracted from the bill of quantities. Meanwhile, EE and EC factors were obtained from EPDs and ICE databases. Energy consumption records from 2016 -2018 were converted to average annual carbon emissions using the latest UK carbon emissions factors for the national

grid, resulting in the Operational Carbon (OC) figure. Finally, the OE results were contrasted to the EE figures in the case study.

4. CASE STUDY

The case study is a 3 bedroom (127m² TIA), handmade brick Passivhaus detached house located in York, designed by Anne Thorne Architects, and completed in 2015 (Figs. 1-4). The designers specified a handmade brick produced just 15 Km away from the site. The clay for the brick was extracted on the factory site, significantly reducing carbon emissions for transportation.

This dwelling has 400 mm PIR high performance insulation in the ground flooring. The roof is equipped with high-density polyethylene between the battens and 300mm wool insulation. The external Walls comprise 300 mm mineral between 105mm handmade brick and 100mm aerated concrete block inner leaf resting on concrete foundations (Fig. 5).

The use of these materials enabled the case study to significantly surpass the PH requirements as discussed next.

The PH home was planned for four people but mainly only the owner now inhabits it: an older retired woman, studying for a PhD.

Figure 01: Views External views.



Figure 02: Section.

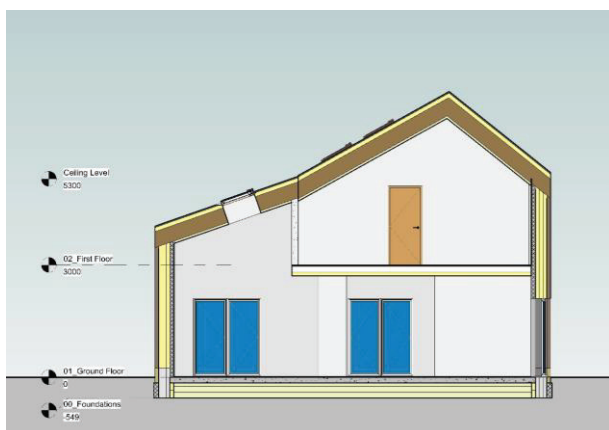


Figure 03: Ground Floor Plan (Anne Thorne architects).

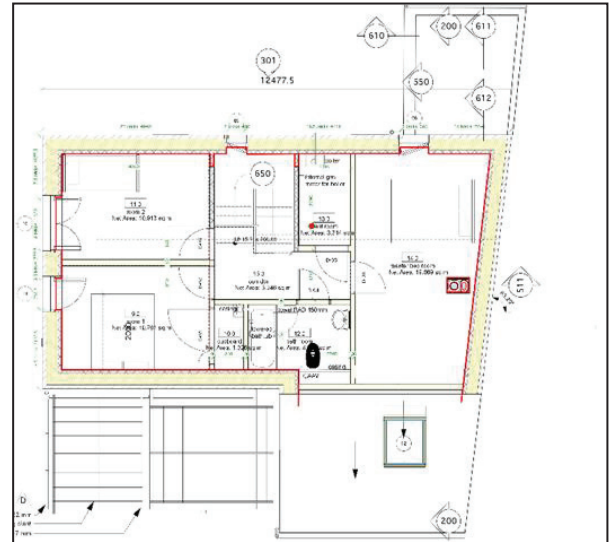


Figure 04: First Floor Plan (Anne Thorne architects).

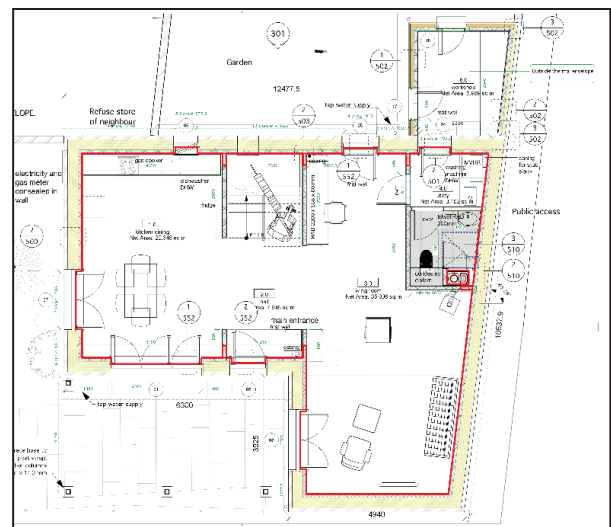
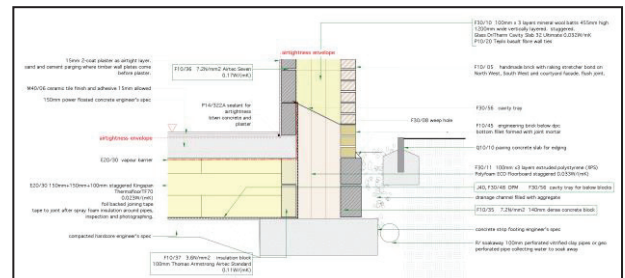


Figure 05: Detailed Section.



5. DISCUSSION AND RESULTS

5.1 Embodied Energy and Carbon

The initial total EE for the house, in the LCA cradle to gate framework stages A1-A3 according to the RICS parameters, is 159,291.61 kWh and 1,254.26 kWh/m².

The monitored operational energy for the home was 4,401.08kWh/pa or 34.65 kWh/m². The OE is far lower than the Passivhaus 120 kWh/m² primary energy target. The lifecycle of 100 years the OE is 440,107.50 kWh and the total EE is 159,291.61 kWh. Thus, EE represents 36.19 % of the total energy used over a predicted lifetime of this home, which is highly significant.

The EC was also calculated using the same ICE database V.3.0, EPDs and RICS parameters. The EC for the house works out as 59,295.95 kgCO₂e.

The total carbon emissions for the energy in use, (using 2018 UK conversion factors) were 973.34 kgCO₂e/ per year, and for a 100 years lifespan, this totals 97,333.50 kgCO₂e. This means that the EC represents 60.92 % of the total carbon emissions for this Passivhaus home, which is vastly significant (Table 1).

Even if the electricity energy used produced net zero carbon emissions, the EC is still considerable. This shows that when low carbon buildings are more realistically analysed from a life cycle approach they can have a much heavier environmental impact [21].

When comparing the percentage of EC established by H/B:ERT (41,550.00 KgCO₂) against the overall EC calculated through the bill of quantities (59,295.95 KgCO₂), the H/B:ERT tool accounts for 29.92% less EC. This is concerning as it shows inaccuracies in the tool. Moreover, the accounting for EC in the transport, construction and end of life is unclear in H/B:ERT.

What is apparent from the table in Figure 6 is that the substructure materials take up a disproportionate amount of EE, but less so in terms of EC, although this figures need to be updated as they rely on the ICE V.2, as the latest version does not include natural materials.

The figures for the sanitary equipment and lighting fixtures also seem highly out of proportion, yet these are taken from bona fide EPD certificates. This illustrates the difficulty of carrying out robust EE and EC calculations. However, the external wall comprised of clay brick and concrete block with extensive insulation is a major component of both EE and EC. On this basis, it was decided to carry out a substitution for these elements of the building that carried a significant amount of EE/EC.

Table 1. – Materials Take Off.

	Embodied carbon kgCO ₂ e	Embodied Energy kWh	Embodied carbon %	Embodied Energy %
Substructure Materials	10857.90	413.54	18.31%	0.26%
Ground floor Construction	4261.41	10461.18	7.19%	6.57%
Intermediate Floors	2555.63	16168.50	4.31%	10.15%
Roof	5090.22	7165.23	8.58%	4.50%
External Walls	19286.37	42788.47	32.53%	26.86%
Steel Structural Elements	574.17	4341.89	0.97%	2.73%
Internal Walls	2798.41	5695.88	4.72%	3.58%
Internal Doors	388.80	1777.22	0.66%	1.12%
External Doors	1876.62	9633.87	3.16%	6.05%
Windows	703.10	3609.45	1.19%	2.27%
Roof lights	1781.74	4710.56	3.00%	2.96%
Sanitary Equipment	4270.00	18709.74	7.20%	11.75%
MVHR Pipework	631.91	0.30	1.07%	0.00%
Plumbing	782.07	3482.42	1.32%	2.19%
Lighting Fixtures	3437.62	30333.36	5.80%	19.04%
Total	59,295.95	159,291.61	100%	100.00%

5.3 Substitution for clay material

The total embodied energy of concrete masonry located in the internal layer of the cavity wall, accounts for just 544.55 KgCO₂e and 1824.22 kWh in total, however the brick EPD used is generic which compromises these results to some degree.

A substitution approach was used to replace the internal walling aerated concrete blocks /earth wool insulation with unfired clay bricks /natural wool insulation in a timber-framed system (Fig. 6).

An unfired brick has EE of 0.35 kWh/Kg per unit, (105mm x 215mm x 65mm) and EC of 0.025 CO₂kge [22]. This compares with the aerated concrete block having an EE of 18.60 kWh/Kg per unit and EC of 8.33 KgCO₂e per unit. The unfired clay brick has fifty times less EE than its equivalent aerated concrete block, making a significant saving in EE. The Thermafleece TF35 natural wool insulation is composed of 60% wool, 30% recycled polyester, 10% polyester binder. It has an EE of 0.28 kWh/Kg and EC of 0.22 KgCO₂e/kg. This can be compared to the earth wool insulation EE value of 175.27kWh/kg and EC value of 36.40 KgCO₂e/Kg. The overall substitution accounts for EE of 35,083.20 kWh/Kg and EC of 12,781.45 KgCO₂e/Kg compared to the original EC of 19,286.37 KgCO₂e/Kg and EE of 42788.70 kWh/Kg. When this is compared to the overall saving for the substitution in relation to the house EE and EC values, there is a saving of 4.80 % EE and 18.07 % EC. Although this figure is less significant due to the external walling only accounting for around a third of the EE and EC of the house, it still demonstrates the importance of substituting high EE and EC materials with lower ones where possible.

Figure 6: Unfired clay brick and timber frame prior to insulating



Figure 7. – Wall fabric substitution material

	EC Retrofit KgCO ₂ e/kg	%	EE Retrofit kWh/kg	%
York Handmade Bricks	3513.29	27.49%	17356.45	49.47%
Mortar used in External Skin	594.59	4.65%	1321.32	3.77%
Natural insulation	1858.67	14.54%	2634.17	7.51%
Internal Face Timber Studs	1468.82	11.49%	2151.01	6.13%
Internal Layer Unfired bricks	619.11	4.84%	5259.92	14.99%
Concrete cavity filling	1705.00	13.34%	2553.29	7.28%
Performed Cavity Trays	633.92	4.96%	864.15	2.46%
Beds Cavity Trays	3.93	0.03%	540.64	1.54%
Movement Joints with Sealant	111.09	0.87%	145.32	0.41%
Precast Concrete Lintels	20.04	0.16%	59.25	0.17%
Precast Steel Lintels	523.62	4.10%	483.54	1.38%
Internal Coat plaster	1704.32	13.33%	1603.12	4.57%
Internal Paint	25.05	0.20%	111.02	0.32%
Total	12,781.45	100%	35,083.20	100%

6. CONCLUSIONS

6.1 Key findings

This low energy home has an OE of just or 32.32 kWh/m²/pa as primary energy and OC of 7.66 CO₂/m²/pa. A key finding, however, is that 60.92 % of the total carbon predicted to be emitted in a 100-year lifespan was produced upfront during the construction phase. This hidden factor is a major concern for the Passivhaus Standard, which does not include either EE or EC.

However, there is still not a standard methodology to accurately determine EE [23]. EC, by contrast, appears to have more standardised guidance.

Although the home meets the Passivhaus standard, the use of a gas boiler and MVHR system makes a significant impact on the EE and EC, including the need to replace MVHR filters regularly. As demonstrated, the high impact structural and insulation materials can play a major role in the EE in homes. The replacement of these materials with more natural materials can save up to 4.80% in their EE and 18.07% EC. This demonstrates the importance of considering these factors in the Passivhaus Standard and for future new build Passivhaus homes. They should also be considered for the EnerPHit retrofit standard.

6.2 Limitations of the study

The limitations in this study were numerous, showing that more research is required to standardise these areas:

1. Different tools had to be used for the calculation of embodied carbon (BIM, EPD, ICE, Bill of quantities) which can lead to multiple interpretation errors.

2. Different assumptions for OE consumption and energy CO₂ emissions conversion factors can lead to a wide variation in measurement figures.

3. Differences in the protocols and scope for EE and EC can lead to different outputs that can be out of context and produce unreliable data.

4. The H/B:ERT tool clearly aims to simplify the detailed accounting process. However, there are several limitations of this “plug-in”, such as the fixed number of materials and no figures for plumbing and electric fixtures, producing weak results.

7. REFERENCES

- Department for Business E and IS. *Amendment of the Target for 2050*. London, United Kingdom: Minister of State; 2019:Section 1 of the Climate Change Act 2008.
<https://www.legislation.gov.uk/uksi/2019/1056/signature/made>.
- Department of Energy and Climate Change. *The Carbon Plan: Delivering Our Low Carbon Future Presented*. London; 2011.
doi:10.1177/1468794113509262
- Dixit MK, Fernández-solís JL, Lavy S, Culp CH. Need for an embodied energy measurement protocol for buildings : A review paper. *Renew Sustain Energy Rev*. 2012;16(6):3730-3743.
doi:10.1016/j.rser.2012.03.021
- Stephan A, Crawford RH, Myttenaere K De. A comprehensive assessment of the life cycle energy demand of passive houses. *Appl Energy*. 2013;112:23-34. doi:10.1016/j.apenergy.2013.05.076
- Dixit MK. Life cycle embodied energy analysis of residential buildings : A review of literature to investigate embodied energy parameters. *Renew Sustain Energy Rev*. 2017;79(October 2016):390-413.
doi:10.1016/j.rser.2017.05.051
- Jones GPH and Cl. Embodied energy and carbon in construction materials. *Proc Inst Civ Eng - Energy*. 2008;161(2):87-98. doi:10.1680/ener.2008.161.2.87
- Thiers S, Peuportier B. Energy and environmental assessment of two high energy performance residential buildings. *Build Environ*. 2012;51:276-284.
doi:10.1016/j.buildenv.2011.11.018
- Crawford RH, Stephan A. The Significance of Embodied Energy in Certified Passive Houses. 2013;7(6):427-433.
- Kaklauskas A, Rute J, Kazimieras E, et al. Passive House model for quantitative and qualitative analyses and its intelligent system. *Energy Build*. 2012;50:7-18. doi:10.1016/j.enbuild.2012.03.008
- Baborska-Narozny M, Stevenson F. Continuous mechanical ventilation in housing - understanding the gap between intended and actual performance and use. *Energy Procedia*. 2015;83:167-176.
doi:10.1016/j.egypro.2015.12.207
- Treloar GJ. Extracting Embodied Energy Paths from Input – Output Tables : Towards an Input – Output-based Hybrid Energy Analysis Method based Hybrid Energy Analysis Method. 2006;5314.
doi:10.1080/09535319700000032
- Dequaire X. Passivhaus as a low-energy building standard : contribution to a typology. 2012:377-391.
doi:10.1007/s12053-011-9140-8
- Prakash R, Shukla KK. Life cycle energy analysis of buildings : An overview. 2017;(October):5-7.
doi:10.1016/j.enbuild.2010.05.007
- Thormark C. A low energy building in a life cycle — its embodied energy , energy need for operation and recycling potential. 2002;37:429-435.
- RICS. *Whole Life Carbon Assessment for the Built Environment*.; 2017.
http://www.rics.org/Global/Whole_life_carbon_assessment_for_the_BE_PG_guidance_2017.pdf.
- Schwartz Y, Eleftheriadis S, Raslan R, Mumovic D. Semantically Enriched BIM Life Cycle Assessment to Enhance Buildings ' Environmental Performance. In: *CIBSE Technical Symposium*, . Edinburgh; 2016:1-14.
- Schwartz Y. An Integrated Thermal Simulation & Generative Design Decision Support Framework for the Refurbishment or Replacement of Buildings : A Life Cycle Performance Optimisation Approach. 2018.
- Yin RK. *Case Study Research Design and Methods (5th Ed.)*. Vol 5. (Sage, ed.). Thousand Oaks, CA; 2014.
doi:10.3138/cjpe.30.1.108
- Stevenson F. *Housing Fit for Purpose: Learning through Design and Performance*. (RIBA Publishing, ed.). London; 2019.
- Hawkins\Brown;Yair Schwartz. Hawkins\Brown: Emission Reduction Tool \. Hawkins\Brown Emission Reduction Toolkit launch.
<https://www.hawkinsbrown.com/news-and-events/event/hawkins-brown-emission-reduction-toolkit-launch>. Published 2018. Accessed March 18, 2019.
- Hernandez P, Kenny P. From net energy to zero energy buildings: Defining life cycle zero energy buildings (LC-ZEB). *Energy Build*. 2010;42(6):815-821.
doi:https://doi.org/10.1016/j.enbuild.2009.12.001
- Morton T, Stevenson F, Taylor B, Smith NC. *Low Cost Earth Brick Construction - Partners in Innovation Research Project Final Report, Scotland*. Bracknell, Berkshire: Bracknell, Berkshire : IHS BRE Press, 2008; 2005.
- Stephan A, Crawford RH, Myttenaere K De. A comprehensive assessment of the life cycle energy demand of passive houses. *Appl Energy*. 2013;112:23-34. doi:10.1016/j.apenergy.2013.05.076

Evaluating Neutral, Preferred and Comfort Range Temperatures and Computing Adaptive Equation for Kano Region

SANI M ALI¹, BRETT D MARTINSON², SURA AL-MAIYAH³

¹Bayero University, Kano, Nigeria

²University of Portsmouth, Portsmouth, UK

³University of Salford, Manchester, UK

ABSTRACT: Provisions of international comfort standards may not be appropriate for all climates, it is therefore imperative to evaluate comfort requirements of indoor occupants in all regions, particularly where comprehensive standards are lacking. As part of an ongoing study on comfort in higher education facilities in Kano, involving lecture theatres and laboratories, an Indoor Environmental Quality field study was conducted by collecting a total of 1382 questionnaires in addition to physical measurements, covering a period of 10 months. In addition to measurements of air speed, air and radiant temperatures, relative humidity, a comfort survey was undertaken where activity levels and clothing insulations were obtained. Two neutral temperatures were arrived at based on operative and indoor running mean temperatures, 27.4 °C and 28.1 °C respectively. Similarly a comfort zone of 22 °C to 32 °C was realised. The results revealed that the adaptive equation using the weighted running mean outdoor air temperature had the highest coefficient of determination, with regression coefficient of 0.6, which is nearly twice those of ASHRAE 55 and EN 15251. The evaluated neutral and preferred temperatures show that subjects are comfortable even at 32 °C in naturally ventilated buildings in Kano region.

KEYWORDS: Neutral temperature, preferred temperature, comfort zone, adaptive equation, Sub-Saharan Africa

1. INTRODUCTION

The assessment of thermal comfort in buildings makes it possible to determine the acceptable range of environmental parameters and permitting architectural recommendations that best fit each type of climate. It is also known that daily climatic patterns in all regions require climate-conscious building design strategies to achieve a comfortable thermal environment, this is therefore apt for the tropics. As vividly captured by Nicol (2004), that “the climatic, cultural and the allowance for time means that comfort surveys are needed in every area of the world, particularly in the tropics where current standards are weakest”. He also stated that “.... the empirical findings of field surveys can be used as a guide for informing the design of buildings to provide comfortable conditions. Wherever possible this can be improved by the conduct of local field surveys to fully reflect local climate and culture”. Nonetheless, thermal comfort studies for naturally ventilated buildings in the tropical context, are relatively under represented, this is especially true for the Sub-Saharan African region.

Two main models are popularly used to define thermal comfort, the predicted mean vote (PMV) and the adaptive thermal comfort (ATC). PMV-PPD equation was used in arriving at the recommendations of some international comfort

standards, such as ISO 7730, EN 15251 and ASHRAE Standard 55. PMV is however confounded with the problem of limited applicability for predicting comfort temperatures in hot climates. Adaptive thermal comfort requirements for naturally ventilated (NV) spaces significantly differ from those defined by PMV/PPD model. An adaptive opportunity is the ability for the occupants to open doors or windows, put on/off ceiling fans, adjust clothing etc., as against the climate chamber-based assessment. The primary aim of this paper is to evaluate the neutral, comfort range and preferred temperatures, as well as developing an appropriate adaptive thermal comfort equation for naturally ventilated buildings in the hot (temperature ranges between 12 °C and 39 °C) and dry region (relative humidity ranges between 20% and 80%) of Nigeria.

1.1 Neutral temperatures from Nigeria

Thermal comfort studies identified from Nigeria that calculated the neutral and comfort range temperatures and adaptive equations are very few. Ogbonna & Harris (2008) conducted a fieldwork in university classrooms and residential houses in Jos, using linear regression of thermal sensation votes (TSV) on operative temperature (T_{op}) across their samples, the study yielded a neutral temperature of 26.27 °C and a comfort

range of between 24.88 °C and 27.66 °C. They also obtained a correlation $r^2 = 0.57$ from the regression line equation ($TSV = 0.3589T_{op} - 9.4285$). Efeoma et al. (2014) undertook a thermal comfort assessment of office buildings in Enugu, eastern Nigeria (in February, when average air temperature reaches 38 °C), and obtained a range of comfort temperature of 24.7 °C to 32.9 °C. Another study conducted in the rainforest of Nigeria by BRE (1978) in Port Harcourt yielded a neutral temperature of 23.13 °C, indicating a wide disparity of up to 3.14 °C between the Jos and the Port Harcourt figures. Some more thermal comfort studies were recently conducted in the country but mostly in residential houses, where clothing is casual and light (Abdulkareem et al., 2018; Adaji et al., 2015; Munonye & Ji, 2017).

2. METHODOLOGY

This study was carried out in Bayero University, a conventional university situated in Kano, Nigeria. Kano lies on latitude 12 °N and longitude 8.17 °E, in the Savannah region of West Africa. Being situated within lower latitudes combined with high solar radiation and low humidity, Kano region is classified as having a hot and dry climate according

to Koppen's classification. The fieldwork was undertaken from August 2016 to May 2017, and was conducted on three different occasions; during the rainy season of August, 2016 (warm and wet), then in January, 2017 (winter season) when it was cool and dry and finally in May, 2017 (summer season) when it was hot and dry. Both physical measurements of air speed, air and radiant temperatures, relative humidity (using spot and logging instruments) and surveys were conducted based on procedures consistent with ASHRAE standard 55-2013. The surveys were conducted via a paper-based questionnaire prepared and administered to 1382 respondents in six learning spaces in the university.

3. RESULTS

The PMV & PPD, operative temperature, AMV, and the adaptive comfort indices based on EN 15251 and ASHRAE Standard 55, the running mean temperature (T_{rm}) and the mean outdoor air temperatures ($T_{out,mean}$) of the entire survey months were derived and presented in Tables 1 to 3 and were used in arriving at the neutral and preferred temperatures.

Table 1: Derived Thermal Comfort Indices in Mid-season

Survey	LEARNING ENVIRONMENT	T_{op} °C	T_{rm} °C	PMV	PPD	T_{out} °C	AMV	T_n
Mid-season (first survey)	AKTH	27.4	27.4	+0.36	8%	27.9	-0.08	27.8
	Dandatti	29.8	28.8	+0.89	22%	29.1	0.12	28.3
	FEES	27.0	27.4	+0.24	6%	30.4	-0.20	27.8
	I H Umar	30.4	30.6	+1.28	39%	31.0	1.50	28.9
	MPL	30.0	29.2	+1.17	34%	32.8	0.77	27.8
	PHL	27.7	30.2	+1.00	26%	27.9	-0.38	28.2

Table 2: Derived thermal comfort indices in the Winter

	LEARNING ENVIRONMENT	T_{op} °C	T_{rm} °C	PMV	PPD	T_{out} °C	AMV	T_n
Winter season (Second survey)	AKTH	25.5	25.4	+0.38	8%	25.4	-1.03	27.2
	Dandatti	23.1	23.8	-0.21	6%	23.8	-0.74	26.7
	FEES	29.4	26.8	+1.35	43%	26.4	-0.75	26.7
	I H Umar	25.0	24.8	+0.25	6%	30.8	-1.03	27.0
	MPL	29.6	29.2	+1.42	47%	30.3	0.08	28.5
	PHL	23.7	25.4	+0.35	7%	23.6	0.33	26.8

Table 3: Derived thermal comfort indices in the Summer

Survey	LEARNING ENVIRONMENT	T_{op} °C	T_{rm} °C	PMV	PPD	T_{out} °C	AMV	T_n
Summer (third survey)	AKTH	34.9	36.5	+2.02	78%	35.6	0.93	30.8
	Dandatti	31.3	33.5	+1.03	27%	36.3	2.29	29.9
	FEES	33.2	34.4	+1.56	54%	34.8	1.44	30.2
	I H Umar	34.3	35.8	+1.46	49%	36.8	2.20	30.6
	MPL	33.6	36.3	+1.29	40%	35.6	1.23	30.8
	PHL	33.0	32.4	+1.11	31%	33.5	1.33	29.5

3.1 Neutral temperature

Two sets of regression analyses were conducted between the mean thermal sensation votes calculated as actual mean votes (AMV) and two different indoor temperatures (operative temperature = T_{op} , and running mean temperature = T_{indrm}) for comparison. This method was followed by Mishra & Ramgopal (2014) and Baruah et al. (2014). The neutral temperatures were calculated by equating the obtained equations of the comfort index (AMV) to zero, which is the point at which

most occupants felt neither warm nor cold, while the comfort temperature ranges are based on -1 to +1 on the 7-point scale. Figure 1 shows the fitted line plots of the relationships of the comfort index with the T_{op} and T_{indrm} . The equations formed by these relationships, the r^2 , p values, neutral and comfort range temperatures are tabulated and presented in Table 4. The T_n obtained by correlating the AMV and the indoor running mean temperature was the strongest with an $r^2 = 70\%$, as against that of T_{op} of 59%.

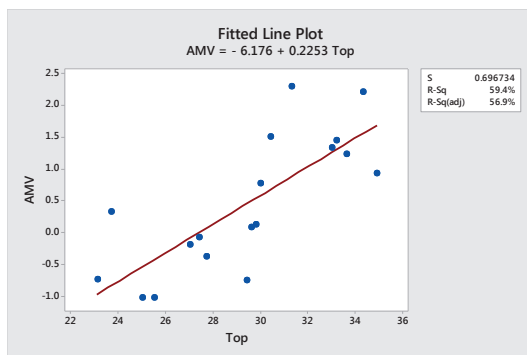


Figure 1a = AMV Vs T_{op}

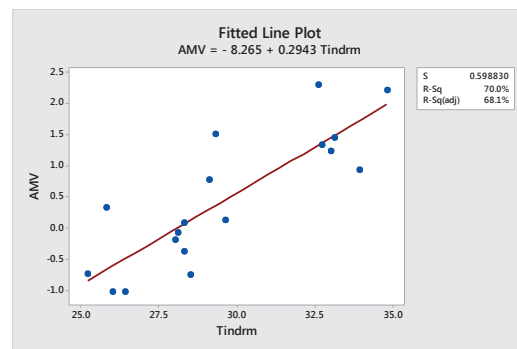


Figure 1b = AMV Vs T_{indrm}

Figure 1: Correlations of AMV versus T_{op} and T_{indrm}

Table 4: Neutral temperatures based on T_{op} and T_{indrm}

Equations	r^2 and P values	T_n (°C)	Comfort Range (°C)
AMV = $-6.176 + 0.2253 T_{op}$	$r^2 = 59.4\%$ ($P = 0.000$)	27.4	23.0 - 31.9
AMV = $-8.265 + 0.2943 T_{indrm}$	$r^2 = 70.0\%$ ($P = 0.000$)	28.1	24.7 - 31.5

3.2 Preferred temperature

To obtain the preferred temperature, further analysis was carried out based on the results of the preference votes on the seven-point McIntyre preference scale. According to the answers to the questions on the questionnaire: “this time what do you prefer in this space; much cooler, cooler, slightly cooler, no change, slightly warmer, warmer or much warmer”? In arriving at the want cooler and want warmer votes, the sum of all votes under “much cooler, cooler and slightly cooler” were merged to form the want cooler. Similarly, the sum of all the votes under “slightly warmer, warmer and much warmer” formed the want warmer category. This method was followed by a number of studies, such as de Dear et al. (2014); Tao & Li R. (2014); and Ye et al. (2010). During each season, operative temperatures of each space were

obtained, and in each space at each operative temperature there were people who preferred “wanting warmer”, “wanting no change” and “wanting cooler” conditions. Therefore, the cumulative frequencies of the “wanting warmer” and “wanting cooler” categories were classified into an operative temperature bin of 1 °C. These are shown in Figures 2 to 4, respectively for the winter season, the summer season and for the mid-season.

3.2.1 Winter preferred temperature

Figure 2 shows a chart with two quadratic equations obtained from the fitted line plots of wanting warmer and wanting cooler conditions for the winter season and the respective equations are shown as Equations 1 and 2:

$$\text{Equation 1: Want cooler} = -7.9957 + 0.5453T_{op} - 0.0082T_{op}^2 \dots (r^2 = 0.9851)$$

$$\text{Equation 2: Want warmer} = 0.2497 + 0.149T_{op} - 0.0052T_{op}^2 \dots (r^2 = 0.9775)$$

The preferred temperature for winter season was then calculated by equating the two quadratic equations obtained, this gave a value of 25.9 °C. This was further validated by the intersection of the two curves; “want cooler” and “want warmer” in Figure 2.

$$\text{Equation 3: Want cooler} = -53.433 + 3.5445T_{op} - 0.0577T_{op}^2 \dots (r^2 = 0.9774)$$

$$\text{Equation 4: Want warmer} = -16.926 + 0.8637T_{op} - 0.01T_{op}^2 \dots (r^2 = 0.9749)$$

The summer preferred temperature was also calculated by equating the two quadratic equations obtained, which gave 33.1 °C. This was also validated by the intersection of the two

3.2.2 Summer preferred temperature

Similarly Figure 3 shows two quadratic equations obtained from the fitted line plots of wanting warmer and wanting cooler conditions for the summer season and their respective equations are shown as Equations 3 and 4:

curves; “want cooler” and “want warmer” in Figure 3, this however has exceeded the comfort temperature of 32 °C.

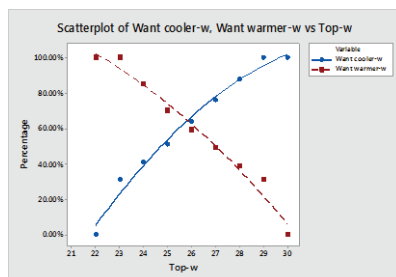


Figure 2: Winter preferred temperature

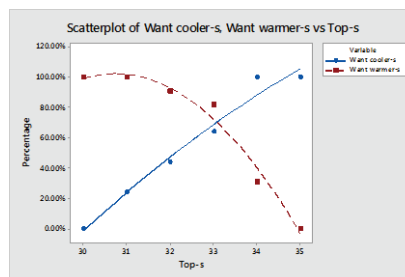


Figure 3: Summer preferred temperature

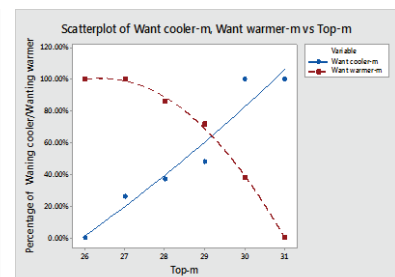


Figure 4: Midseason preferred temperature

3.2.3 Mid-season preferred temperature

Likewise Figure 4 shows two quadratic equations obtained from the fitted line plots of wanting warmer and wanting cooler conditions for the mid-season and their respective equations are shown as Equations 5 and 6. The mid-season preferred

temperature is then calculated by equating the two quadratic equations obtained, which is 29.3 °C. This is also approximately indicated by the intersection of the two curves; “want cooler” and “want warmer” in Figure 4.

$$\text{Equation 5: Want cooler} = -0.5366 - 0.1366T_{op} + 0.0061T_{op}^2 \dots (r^2 = 0.934)$$

$$\text{Equation 6: Want warmer} = -32.661 + 2.5482T_{op} - 0.0482T_{op}^2 \dots (r^2 = 0.997)$$

3.2.4 Adaptive comfort equation for Kano

This study used the Griffiths' equation and a 0.5 constant, the comfort temperatures were calculated on the day of each survey and were correlated with three different conditions to produce the adaptive equations appropriate for Kano. The conditions included the weighted running mean outdoor temperature (T_{rm}) and the outdoor mean temperature ($T_{out,mean}$), See

$$\text{Equation 7: } T_{comf} = T - AMV/\alpha$$

Figures 5 and 6 for the respective fitted line plots. This is done in line with the ASHRAE 55 and the EN 15251 standards with a view to finding which of them is most applicable in predicting the comfort temperature for the region. The obtained adaptive comfort equations, their r^2 and p values are further presented in Table 5.

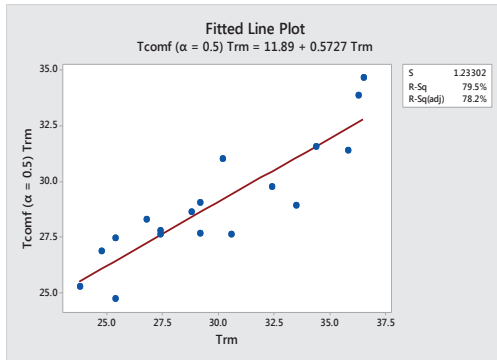


Figure 5: Regression line of $T_{comf}(\alpha = 0.5)$ Vs T_{rm}

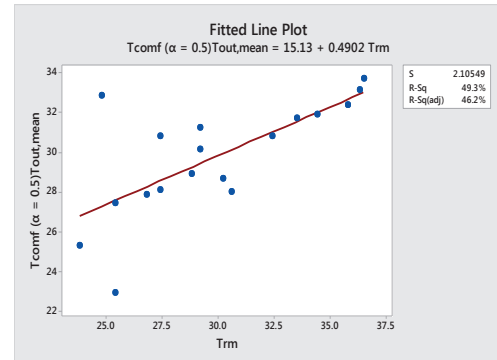


Figure 6: Regression line of $T_{comf}(\alpha = 0.5)$ Vs T_{rm}

Table 5: Adaptive Comfort Equations based on $\alpha = 0.5$	
$T_{comf}(T_{rm}) = 11.89 + 0.5727 T_{rm}$	$r^2 = 79.5\%$ ($p = 0.000$)
$T_{comf}(T_{out,mean}) = 15.13 + 0.4902 T_{rm}$	$r^2 = 49.3\%$ ($p = 0.001$)

Equation 8: $T_{comf} = 0.57T_{rm} + 11.89$ (Using T_{rm})

Equation 9: $T_{comf} = 0.49T_{rm} + 15.13$ (Using $T_{out,mean}$)

Equation 10: $Y = 0.49x + 15.13$ (Using $T_{out,mean}$)

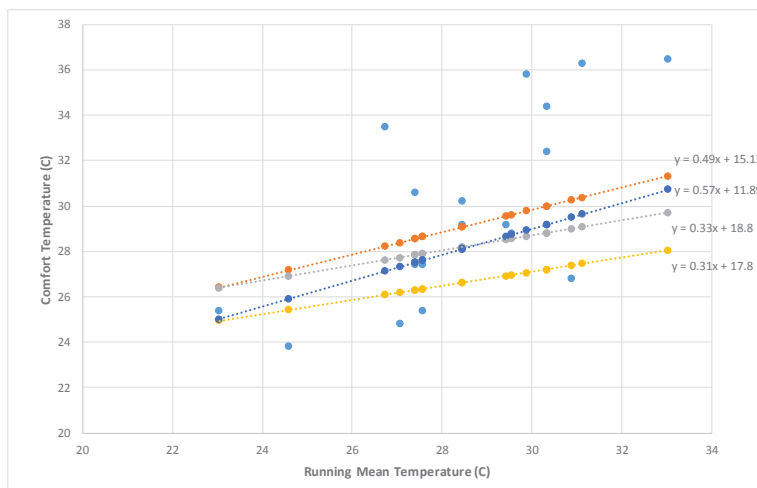


Figure 7: Comparison the obtained equation with adaptive thermal comfort standards' equations

4. DISCUSSION AND SUMMARY

From the foregoing analysis, two different neutral temperatures were obtained for Kano based on operative and indoor running mean temperatures, these are 27.4 °C, and 28.1 °C respectively. All the evaluated neutral temperatures are higher than two out of the three neutral temperatures earlier evaluated in Nigeria; Port Harcourt (23.13 °C) and Jos (26.27 °C), but that of Enugu (28.8 °C) is higher than both.

The obtained winter preferred temperature of 25.9 °C, as expected, is lower than the mid-season preferred temperature of 29.3 °C by 3.4 °C, and also lower than that of the summer (33.1 °C) by 7.2°C. Interestingly the preferred temperature during the winter falls below the neutral

temperature (27.4 °C), while the mid-season preferred temperature is slightly higher than its correspondent neutral temperature. Therefore using the said neutral temperature of 27.4°C, which is based on the operative temperature, a comfort zone of 23 °C to 32 °C with a range of 9 °C was realised and is found to be higher than the range of ASHRAE (7 °C) and that of EN 15251 (6 °C).

Using Griffiths' method, weighted outdoor running mean and outdoor monthly mean temperatures the adaptive comfort equation was obtained. Although the one based on the T_{rm} has the highest r^2 value, the one based on the $T_{out,mean}$ is closer to those of ASHRAE 55 and EN 15251. Nigeria with its tropical climate, electrical energy

issue and with a population size which demands more higher education facilities, could greatly benefit from the development and implementation of an adaptive comfort standard. This paper therefore recommends the adoption of

EN 15251 Equation for the country, and the use of Equation 10 (see Figure 7), obtained using the $T_{out,mean}$, however it could be further explored to ascertain its efficacy.

REFERENCES

- Abdulkareem, M., Al-Maiyah, S., & Cook, M. (2018). Remodelling Facade Design for Improving Daylighting and the Thermal Environment in Abuja's Low-Income Housing. *Renewable & Sustainable Energy Reviews*, 82(3), 2820-2833.
<http://dx.doi.org/10.1016/j.rser.2017.10.010>
- Adaji, M., Watkins, R., & Adler, G. (2015). *An Investigation into Thermal Comfort in Residential Buildings in the Hot Humid Climate of Sub-Saharan Africa: A Field Study in Abuja-Nigeria*. Paper presented at the Passive Low Energy Architecture, Boplogna.
- ASHRAE (2013). (2013). *ASHRAE 55: Thermal Environmental Conditions for Human Occupancy*. Atlanta, USA: American Society of Heating, Refrigeration, and Air-conditioning Engineers.
- Baruah, P., Singh, M. K., & Mahapatra, S. M. (2014). *Thermal Comfort in Naturally Ventilated Classrooms*. Paper presented at the Passive and Low Energy Architecture, Ahmedabad.
- Building Research Establishment, B. (1978). *4: Energy, Heating and Thermal Comfort*. London: Construction Press.
- CEN. (2007). *BS EN 15251:2007: Indoor Environmental Input Parameters for Design and Assessment of Energy Performance of Buildings Addressing Indoor Air Quality, Thermal Environment, Lighting and Acoustics*. Brussels.
- De Dear, R., Kim, J., Candido, C., & Deule, M. (2014). *Summer Thermal Comfort in Australian School Classrooms*. Paper presented at the Windsor conference: Counting the cost of comfort in a changing world, Cumberland Ldge, Windsor, UK.
- Efeoma, M. O., K. Ahadzie, D., A. Ankrah, N., & Uduku, O. (2014). Assessing Thermal Comfort and Energy Efficiency in Tropical African Offices Using the Adaptive Approach. *Structural Survey*, 32(5), 396-412.
<http://dx.doi.org/10.1108/ss-03-2014-0015>
- Griffiths, I. D. (1990). *Thermal Comfort in Buildings with Passive Solar Features: Field Studies*. University of Surrey Guildford Surrey, UK: Commission of the European Communities.
- Humphreys, M. A. (1976). Field Studies of Thermal Comfort Compared and Applied, Department of the Environment: Building Research Establishment, Watford, Uk *Journal of the Institute of Heating and Ventilation Engineering*, 44, 5-7.
- Mahdy, M. M., & Nikolopoulou, M. (2012). *From Construction to Operation: Achieving Indoor Thermal Comfort Via Altering External Walls Specifications in Egypt*. Paper presented at the International conference on green buildings technologies and materials, China.
- Munonye, C., & Ji, Y. (Eds.). (2017). *Rating the Components of Indoor Environmental Quality in Students' Classrooms in Warm Humid Climate of Uli, Nigeria*. Salford University, UK: IPGRC.
- Nicol, & Humphreys, M. (2010). Derivation of the Adaptive Equations for Thermal Comfort in Free-Running Buildings in European Standard En15251. *Building and Environment*, 45(1), 11-17.
<http://dx.doi.org/10.1016/j.buildenv.2008.12.013>
- Nicol, & Humphreys, M. A. (2002). Adaptive Thermal Comfort and Sustainable Thermal Standards for Buildings. *Energy and Building*, 34(563-572). [http://dx.doi.org/PII:S0378-7788\(02\)00006-3](http://dx.doi.org/PII:S0378-7788(02)00006-3)
- Ogbonna, A. C., & Harris, D. J. (2008). Thermal Comfort in Sub-Saharan Africa: Field Study Report in Jos-Nigeria. *Applied Energy*, 85(1), 1-11.
<http://dx.doi.org/10.1016/j.apenergy.2007.06.005>
- Ye, X., Lian, Z., Jiang, C., Zhou, Z., & Chen, H. (2010). Investigation of Indoor Environmental Quality in Shanghai Metro Stations, China. *Environmental Monitoring and Assessment*, 167(1-4), 643-651.

Performance of an air radiative cooling system in a residential building in Chile

MIGUEL A. GÁLVEZ¹, JORGE CONTERAS², RODRIGO BARRAZA³, DANIELA DÍAZ⁴

¹Department of Architecture, Federico Santa María Technical University, Valparaíso, Chile

² Fellow Researcher, Pontificia Universidad Católica, Valparaíso, Chile

³Department of Mechanical Engineering, Federico Santa María Technical University, Santiago, Chile

⁴Department of Architecture, Federico Santa María Technical University, Valparaíso, Chile

ABSTRACT: This paper analyses the performance of a low energy radiative cooling system in Chile. The cooling potential of these systems has not been addressed at all in the context of Chile's varied and complex climatic reality. For this purpose, an air radiative cooling system has been installed in an experimental housing prototype in the Valparaíso region. Ambient conditions, as well as the system variables evolution, have been measured along a complete summer week. Using this set of data and an analytical model, the paper describes the influence of the different parts (e.g., specialized radiator, thermal mass, heat transportation subsystem, and terminal unit) on the performance of the complete system, as well as its coupling with the indoor environment. The experimental results show that with this system, the ambient temperature can be lowered more than 5°C. Furthermore, it is experimentally proven that the system dissipates 50 W/m² when it reaches its maximum potential, and 4.3 MJ during the one-week functioning period. This job is the initial step towards a mature cooling system; thus, the next steps include several modifications and upgrades that need to be experimentally tested.

KEYWORDS: Radiative cooling, Social housing, Air conditioning systems, Energy efficiency

1. INTRODUCTION

The main challenge of the refurbishment of Chilean social houses built during the 1960 decade is to provide thermal comfort to vulnerable families living in situations of energy poverty within homes of deficient constructive quality. Under summer conditions, the implementation of passive or low-energy-consumption air conditioning systems is a great opportunity to reduce the overheating of spaces without increasing the electric demand due to air conditioning equipment. Two are the usual architectural strategies to achieve such a goal [1]: Reflective roofs (usually known as cool roofs) base their operation on a large solar reflectance and high thermal emission of the roof surface, which is achieved through low emissivity paintings. On the other hand, radiative roofs use the surface properties of a specialized radiator on the roof to cool a heat transfer fluid, mainly air or water. Of these systems, the present work only addresses the later. In such cases, the cooling effect is produced by heat losses from a surface exposed to the sky by the emission of longwave radiation that depends on its surface temperature. This process happens day and night, with the difference that during the day, the solar radiation absorbed by the surface, which depends on its short wave absorptivity coefficient, is greater than the energy losses due to air convection and longwave re-irradiation to the atmosphere, so it is heated. During

the night, the longwave radiation emitted by the surface is greater than the energy received from the atmospheric radiation. It produces a cooling effect by a net loss of longwave radiant heat, which reaches its maximum potential when the temperature difference between the surface and the sky is more considerable. As for the atmospheric radiation, it depends on the humidity of the air and especially the cloud conditions and the percentage of cloud cover. The significant influence of the ambient moisture on the atmospheric radiation value responds to the fact that the water vapor in the air absorbs the longwave radiation emitted by the surfaces, as it occurs with the higher temperature of the cloud cover, which reduces the heat losses [2]. A blackbody ($\epsilon_{\text{rad}} = 1$) at 27°C radiates approximately 460 W/m² when its temperature equals ambient temperature.

Given the need for maximum exposure and direct view to the sky to enhance the cooling effect, the roofs of the building are the appropriate location for the specialized radiator to be eventually placed. However, once the architectural integration is achieved, the following challenge is to transfer, and on many occasions to store, the cooling power into the building, so that comfort conditions are eventually obtained. Architecture has always seen this phenomenon as an opportunity and, accordingly, a great deal of passive radiative cooling systems has been proposed in

different parts of the world [2]. Accordingly, a great deal of passive radiative cooling systems has been proposed in different parts of the world [3]. From so extensive a catalogue, three different groups of night radiators can be identified: Massive roofs, Lightweight metallic nocturnal radiators, and water solar collectors, which differ in their way of producing, storing and transporting the cold [4].

Massive roofs with mobile or fixed insulation can be found the only system that has been commercialized and applied in various buildings such as the SKYTHERM in Arizona [5]. In such extremely dry ambient, indoor temperature results go from 20 to 27.8 °C, with outside temperatures ranging from 0 to 45 °C. Other similar applications are the Cool Pool system by Hammond applied in several houses designed by him in California [6] and the ESUSE - AC system by González [6]. Experimental data on the efficiency of this type of system in hot and humid climates can be found in [7], [8]. There are also some variations where the thermal mass is concentrated on the concrete of the roof slab with mobile insulation, which allows the buildings to be well insulated and easily keeping room temperature below ambient temperature [9], [10].

Lightweight metallic nocturnal radiators consist of a cavity that allows airflow under a metallic radiator plate cooled by longwave radiation and convection. There are several ways to store this cold within the building, for example, by directing the air at the outlet of the plate towards a structural mass inside the structure, which keeps cold during night-time and then absorbs heat during the day [11]. The application of these types of systems in hot and humid climates can be seen in [10], [12].

Water solar collectors cool the water during the night, which is then circulated using pipes through the roofs or walls [9]. A variation of this system is based on the circulation of water at night, by using a small electric pump, from an isolated pond located into the ceiling through fixed radiators placed on it. The water tank also serves as a mass for the thermal storage of the building [13].

The main disadvantage of all the systems is their daytime performance. These systems are unable to produce any cold due to being subjected to heating by solar radiation. It is alleviated by using mobile devices for shading or insulation. Other system designs dissipate the daytime gain to a second accumulator from which it can be used, or simply to release the energy. New selective materials, based on graphene, have recently come to answer this problem, which can cool below ambient temperature even receiving solar radiation. It allows optimizing the operation of the system during daytime hours, reopening the interest in these systems [14]. Nevertheless, the high cost means that the use of radiators with selective coatings

has not been considered in this project, which is primarily focused on the social housing sector.

In Chile, due to the lack of experimental research on the atmospheric radiation, with the sole exception of a 50-year old study [15], there is no recent data on the potential of night radiation in our country. This paper gives the first steps towards the development of a passive cooling system based on night sky radiation adapted to Chilean atmospheric conditions and setting the bases for mapping the cooling potential supported by measurements that could be used in future projects

2. MATERIAL AND METHOD

When designing the system to experiment, two main requirements have been considered: being easy to install, with conventional materials, and that it is possible to place it in a rehabilitation. The system has been implemented in prototype “Casa FÉNIX Fondef” [16], within the premises of the Renewable Energies Laboratory (LER) of the Federico Santa María Technical University (UTFSM), in the city of Quilpué, Valparaíso (Fig. 1).



Figure 1: FONDEF prototype. Northwest view

It has an area of 24 m² and was built with SIP panels on floors and walls, with 15% of windows on facades. The ceiling is constructed with sandwich panels 8 cm thick, formed by two metal sheets, and expanded polystyrene infill. Finally, the prototype has a ventilated pitched roof of the galvanized steel sheet, with a greater inclination facing north. So, it has been decided to place the radiator plates on the opposite side of the roof, facing south, avoiding direct exposure to the sun most times of the years.

The system uses a radiator plate, like the proposed by Gonzalez in the SECORA typology [12], connected to a network of ducts, through an air fan towards the thermal mass terminal unit.

The radiators' design is an empty structure that allows airflow from the inlet to the outlet of the collector. The objective is to reuse the structure from a broken flat plate solar collector. The structure is insulated at the bottom and on the sides. On the top, it has a black painted aluminium sheet that allows radiative heat exchange to the sky.

The radiator plate, with an area of 2 m², consists of a prismatic box constructed with a steel profile structure sheathed on three of its sides, the lateral faces, and the bottom, with 40 mm width mineral wool insulation. The side exposed to the sky is covered with an aluminium plate painted black ($\epsilon_{rad} = 0.9$). It is put in contact with the air that is driven through the interior of the collector. At both ends of the box, special metal plenums are adjusted for the inlet and outlet of air. The elements of the system are shown in Fig. 2.



Figure 2: Radiator insulation (left) and installation over the roof (right)

As it has been indicated in the introduction, air-based systems have difficulty in the accumulation phase, and more in this case where you want to cool down at night to cool down during the day. According to literature, this is solved by using an energy storage material that is capable of absorbing heat during the day and then releasing it at night through a ventilation system.

The cooled air is transported through PVC conduits DN 110 to the terminal unit, driven by a centrifugal fan in line with the duct, which operates at night, from 7 PM to 8 AM. Before being supplied to the room, the air passes through a thermal mass wall that stores nocturnal cold, which is intended to be released to ambient air during the following day. Inside the 1 m high, 1 m long, and 0.3 m wide stonewall, it has been placed a PVC collector with 110 mm horizontal pipes crossed by six 40 mm vertical pipes. So that the cooled air consequently cools the stones through eight slots of 3 mm for each tube has been made to release the air into the rocks effectively. The elements of the system are shown in Fig. 3.



Figure 3: PVC heat exchanger (left) and gravel wall for thermal mass (right).

Fig.4 shows the system's general operation. During the day, the gravel accumulator absorbs the heat of the surroundings, which allows reducing thermal gains of

the house during this period. Thus, at night, when the demand for refrigeration is minimal, the accumulator is cooled down using an air stream that comes from the radiator located at the roof so that the thermal mass accumulates the cooling loads during the daytime.

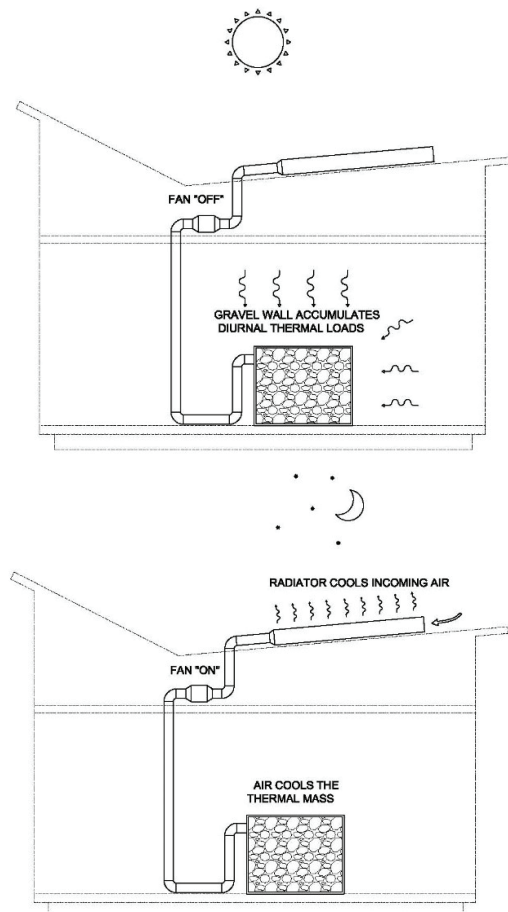


Figure 4: Diurnal (a) and nocturnal (b) system operation

2.1 Experimental

As for the measurements taken during the tests, sensors were placed at different points of the system, as Fig. 5 shows. The temperature sensors are of two types: PT-100 (Sv) and contact (Sc) sensors. Complementarily, a weather station was installed on the roof to have data on air temperature, relative humidity, solar radiation, and wind speed. The data from the indoor environment is taken using HOBO U12-012 dataloggers of temperature, and humidity placed in the centre of the prototype, as well as two thermocouples in the north elevation at heights of 0.3 meters and 2 meters.

The temperature sensors SV1, SV2, and SC1 installed in the radiator plate, and a hot wire anemometer installed in the airflow makes possible to know the actual cooling power of the collector using the previous data of temperature, flow and the specific heat of the air.

The airflow rate effect on the air outlet temperature was carried out with two different airflow rates: 34.8 m³/h and 43.1 m³/h. These values are in the range of ventilation rates recommended by the regulations of air quality for homes (nearly 0.5 ACH). Nevertheless, it should be remembered that the flows used in applications of passive conditioning mostly overcomes such values, so offering great potential for the improvement of the tested system.

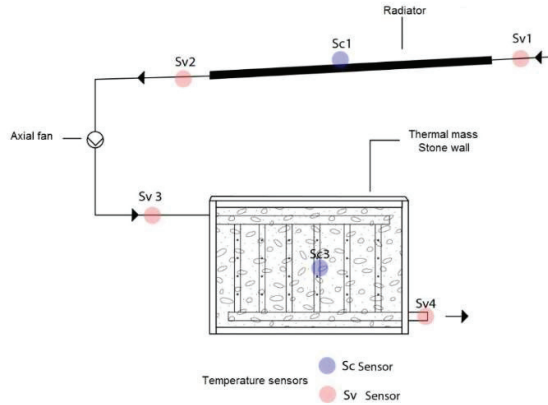


Figure 5: Temperature measurement points

2.2 Analytical

A numerical model of heat transfer was performed in Matlab to obtain an approximation of the operation of the radiator at night. It calculates the outlet temperature of the air, as shown in Eq. (1)

$$T_{air,out} = \frac{\dot{Q}_{cooling}}{h} + T_{air,in} \quad (1)$$

where (W/m^2) represents the energy rate to be removed from the air, and h ($W/m^2 \cdot ^\circ C$) is the overall convective heat transfer coefficient. It is obtained as presented in Eq. (2)

$$h = Nu \frac{k}{L_r} \quad (2)$$

where Nu is the Nusselt number (-), k is the thermal conductivity of air ($W/m \cdot ^\circ C$), and L_r is the length of the radiator (m). The Nusselt correlation in Eq. (3) is obtained from [17], assuming the flowing regime is turbulent

$$Nu = 0.0158 Re^{0.8} \quad (3)$$

where the Re is the Reynolds number (-), which is calculated using air density, ρ_{air} , the average air velocity v_{air} , the dynamic viscosity of air, μ , and the length of the radiator L_r as indicated in Eq. (4)

$$Re = \frac{\rho v_{air} L_r}{\mu} \quad (4)$$

The energy balance equation in the radiator is:

$$\dot{Q}_{conv-int} = \dot{Q}_{net rad} - \dot{Q}_{conv-ext} \quad (5)$$

where $\dot{Q}_{net rad}$ is the net radiation exchange flow between the plate and the sky, and $\dot{Q}_{conv-ext}$ is the heat flow exchanged by the plate and the surrounding air using natural convection. Considering inlet and outlet air temperatures in the air radiator are measured, then this heat flow, $\dot{Q}_{conv-int}$ (or \dot{Q}_{cool}) can be expressed as in Eq. (6)

$$\begin{aligned} \dot{Q}_{cooling} &= \dot{m} C_{p,air} (T_{outlet} - T_{inlet}) \\ \dot{Q}_{cooling} &= -\dot{Q}_{conv-int} \end{aligned} \quad (6)$$

Moreover, the net heat radiation exchange can be calculated as indicated in Eq. (7)

$$\dot{Q}_{net rad} = \dot{Q}_{panel rad} - \dot{Q}_{sky rad} \quad (7)$$

where panel to the atmosphere radiation, $\dot{Q}_{panel rad}$ and the radiation from the sky, $\dot{Q}_{sky rad}$, is given by Eq. (8) and Eq.(9).

$$\dot{Q}_{panel rad} = A_{rad} \epsilon_p \sigma T_p^4 \quad (8)$$

$$\dot{Q}_{sky rad} = A_{rad} \sigma T_{sky}^4 \quad (9)$$

Where

- ϵ_p - plate emissivity (-)
- T_{sky} - sky temperature (K)
- A_{rad} - plate area (m²)
- T_p - average plate temperature ($^\circ C$)
- σ - Stefan-Boltzmann constant ($W/m^2 K^4$)

The sky temperature is obtained from the ambient temperature and humidity through correlations, as shown in Eq. (10) [18]

$$T_{sky} = T_{air} + 0.69 T_{dp} - 18 \quad (10)$$

where the dewpoint temperature T_{dp} , in Eq. (11) depends on the ambient temperature and relative humidity, HR [19]

$$T_{dp} = \frac{243.5 \left[\ln \frac{RH}{100} + \frac{17.67 T_{amb}}{T_{amb} + 243.5} \right]}{17.67 - \ln \frac{RH}{100} - \frac{17.67 T_{amb}}{T_{amb} + 243.5}} \quad (11)$$

$$T_{dp}, T_{amb} [=] ^\circ C$$

The emissivity of the aluminium plate. ϵ_{rad} is 0.88.

3. RESULTS AND DISCUSSION

First tests have been carried out with two different airflow rates: 34.8 m³/h and 43.1 m³/h to evaluate its effect on the air outlet temperature in the radiator. These values are in the range of ventilation rates recommended by the regulations of air quality for homes (nearly 0.5 ACH). Nevertheless, flows used in regular applications of passive conditioning mostly overcomes such values. Thus, there is a high potential for the improvement of the tested system.

Fig. 6 shows ambient temperature, wind speed, and relative humidity for these two tests.

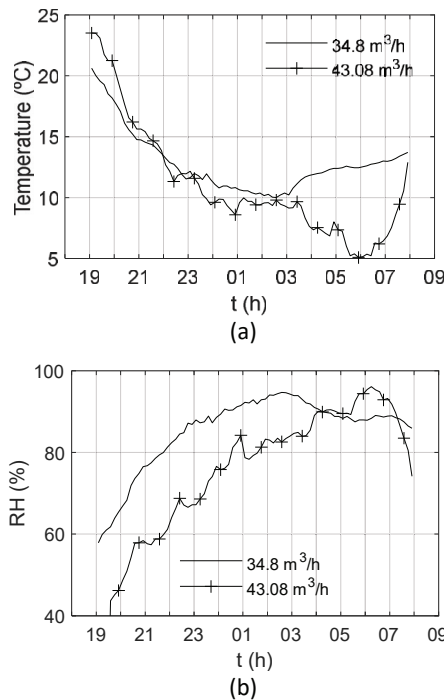


Figure 6: Environmental measured variables at each test: ambient temperature (a) and relative humidity (b).

Fig. 7 shows temperatures measures acquired on November 29 from 19:00 until November 30 at 08:00 for the 34.8 m³/h flowrate case, and on November 25 to 26 at the same hours for the 43.08 m³/h flowrate test.

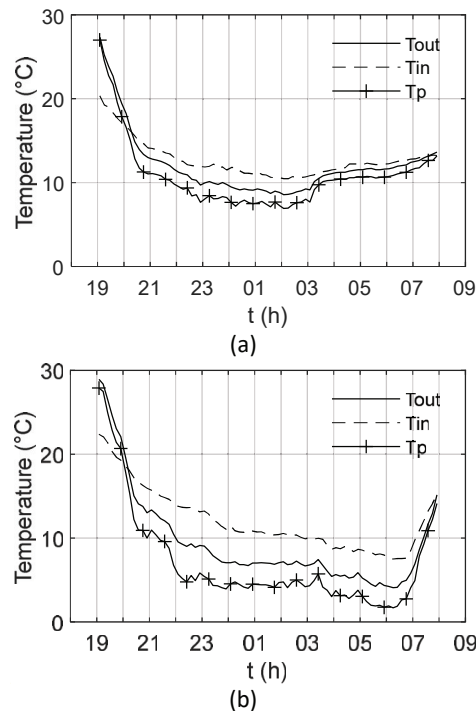


Figure 7: Inlet and outlet air temperature, and surface temperature for the air radiator at night using two different flowrates, 34.8 m³/h (a) and 43.08 m³/h (b)

Fig. 8 shows that the temperature difference is higher when the mass flow increases.

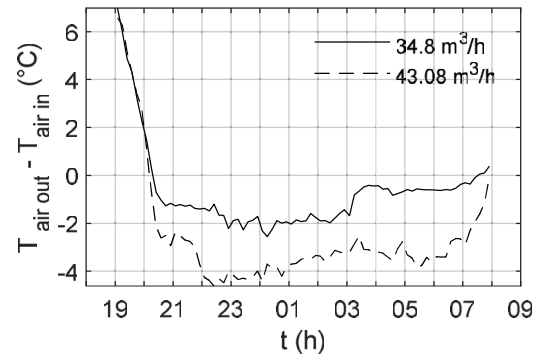


Figure 8: The temperature difference between the outlet and inlet for the air at each mass flow rate.

Nonetheless, it remains to be analysed if this phenomenon is a consequence of a higher heat transfer ratio, due to an increase of the turbulence inside the collector, or only a cooling potential effect due to the specific climatic conditions of the test day. Therefore, considering the radiation plate as the control volume, the energy rate extracted from inlet air $\dot{Q}_{conv-int}$ can be expressed as in Eq. (5). Thus, Fig. 9 shows each of these heat flows for this energy balance.

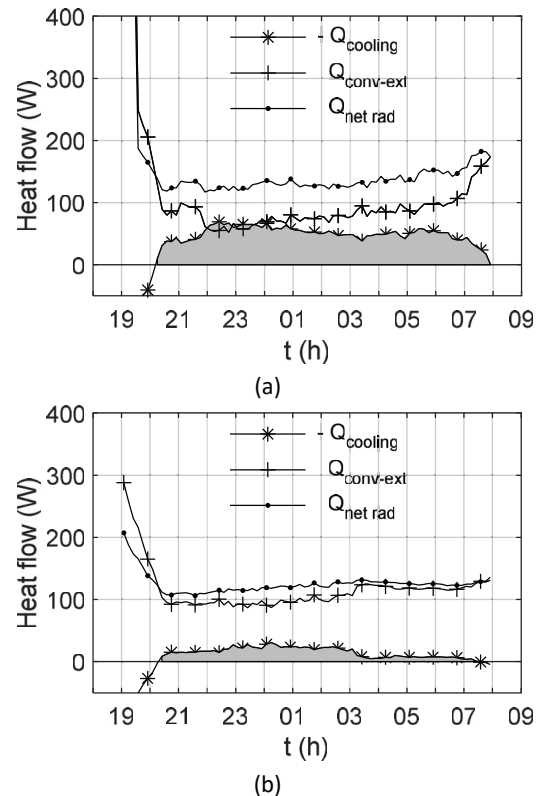


Figure 9: Heat flows components that belong to the energy balance in Eq. (5), 34.8 m³/h (above) and 43.08 m³/h (b), grey shaded areas show the energy removed from the air.

Results in Fig. 9 (a) indicates that the heat radiated by the plate is slightly higher than heat added by convection, which gives a lower cooling power to the air (comparing both grey shaded areas in Fig. 9. Fig. 6 shows that during the 34.8 m³/h test after 03:00, the ambient temperature rises significantly, which increases the magnitude of the convection component. This drawback reduces its cooling power during the test. Moreover, besides this ambient temperature increase, a higher relative humidity during that night (Fig. 6) also produces an increase in the sky radiation, $\dot{Q}_{sky,rad}$ in Eq. (7), which is due to an increase in the sky emissivity and sky temperature.

4. CONCLUSION

The feasibility of this technique in the Chilean context shows that the cooling power obtained with a standard radiant plate under the nonideal coastal Chilean climate makes the system feasible. The cooling capacity of the systems is expected to be higher for other Chilean environments, especially those hot and arid. Moreover, there is a wide margin of improvement for the components of the air radiator, mainly through the use of selective materials in the plate, the addition of windshields, the optimized design of the air inlets, and the improvement of forced convection heat exchange using fins and deflectors. Regarding the indoor system, special care must be taken when designing experimental tests and how to mitigate external variables that cannot be controlled.

ACKNOWLEDGMENTS

This research is part of the multidisciplinary internal project PI_M_18_16 entitled "Integración de la tecnología de enfriamiento pasivo por radiación infrarroja en viviendas sociales en Chile" which has been funded by the DGIIP of the Federico Santa María Technical University.

REFERENCES

- [1] K. M. Al-Obaidi, M. Ismail, and A. M. Abdul Rahman, "Passive cooling techniques through reflective and radiative roofs in tropical houses in Southeast Asia: A literature review," *Front. Archit. Res.*, vol. 3, no. 3, pp. 283–297, Sep. 2014, doi: 10.1016/j.foar.2014.06.002.
- [2] J. Cook, "Passive cooling," 1989.
- [3] X. Lu, P. Xu, H. Wang, T. Yang, and J. Hou, "Cooling potential and applications prospects of passive radiative cooling in buildings: The current state-of-the-art," *Renew. Sustain. Energy Rev.*, vol. 65, pp. 1079–1097, Nov. 2016, doi: 10.1016/j.rser.2016.07.058.
- [4] B. U. U. DJNGS, "The cooling potential of a metallic nocturnal radiator," *Energy Build.*, vol. 28, pp. 251–256, 1998.
- [5] H. R. Hay and P. Daniel, "SKYTHERM DESIGN EVALUATION II." SKYTHERM PRODUCTION RESEARCH," in *Proceedings of Annual Solar Heating and Cooling Research and Development Branch Contractors' Meeting*, 1979, p. 388.
- [6] J. Hammond, "Suncatcher and cool pool. Project report," 1981, doi: 10.2172/6825284.
- [7] E. González, "Técnicas de enfriamiento pasivo. Resultados experimentales en el clima cálido y húmedo de Maracaibo, Venezuela," *CIT, Inf. Tecnológica*, vol. 8, no. 5, pp. 99–103, 1997.
- [8] B. Givoni, "Experimental studies on radiant and evaporative cooling of roofs," in *Proceedings of the international passive and hybrid cooling conference, Miami Beach, FL*, 1981, pp. 279–283.
- [9] B. Givoni, *Passive low energy cooling of buildings*. John Wiley & Sons, 1994.
- [10] A. Dimoudi and A. Androustopoulos, "The cooling performance of a radiator based roof component," *Sol. Energy*, vol. 80, no. 8, pp. 1039–1047, Aug. 2006, doi: 10.1016/j.solener.2005.06.017.
- [11] M. I. Ahmad, H. Jarimi, and S. Riffat, *Nocturnal Cooling Technology for Building Applications*. Singapore: Springer Singapore, 2019.
- [12] E. González and B. Givoni, "Radiative and radiative/evaporative passive cooling systems for a hot humid climate--Maracaibo," *PLEA 2004*, 2004.
- [13] E. Erell and Y. Etzion, "Radiative cooling of buildings with flat-plate solar collectors," *Build. Environ.*, vol. 35, no. 4, pp. 297–305, 2000.
- [14] M. Zeyghami, D. Y. Goswami, and E. Stefanakos, "A review of clear sky radiative cooling developments and applications in renewable power systems and passive building cooling," *Sol. Energy Mater. Sol. Cells*, vol. 178, pp. 115–128, May 2018, doi: 10.1016/j.solmat.2018.01.015.
- [15] A. Castellanos, J. Fournier, and R. Valdivia, "Enfriamiento de un cuerpo negro radiante en dirección del espacio en el desierto de Atacama, Chile," 1972.
- [16] N. Hormazábal *et al.*, "Casa FÉNIX. From the SDE 2014 Competition to the reconstruction after the 2014 urban fire of Valparaíso," in *Passive and Low Energy Architecture Conference*, 2015.
- [17] W. M. Kays, *Convective heat and mass transfer*. Tata McGraw-Hill Education, 2012.
- [18] E. N. ISO, "10456: 2007," *Build. Mater. Prod. Hygrothermal Prop. Des. values Proced. Determ. Declar. Des. Therm. values*, 2007.
- [19] G. Harrison, *Meteorological Measurements and Instrumentation*. Wiley, 2014.
- [20] P. Berdahl and R. Fromberg, "The thermal radiance of clear skies," *Sol. Energy*, vol. 29, no. 4, pp. 299–314, 1982, doi: 10.1016/0038-092X(82)90245-6.

Single-Skin and Multi-Skin Building Envelopes in Extreme Sub-Arctic Climates

Biophilic, Healthy Lighting and Thermal Performance Evaluations

MOJTABA PARSAAE¹, CLAUDE MH. DEMERS¹, MARC HÉBERT², JEAN-FRANÇOIS LALONDE³,
ANDRÉ POTVIN¹

¹GRAP, School of Architecture, Laval University, Quebec, Canada

²CERVO Brain Research Centre, Faculty of Medicine, Laval University, Quebec, Canada

³Electrical and Computer Engineering Department, Laval University, Quebec, Canada

ABSTRACT: *This research aims at studying the potentials of single-skin and multi-skin envelopes with different window sizes to promote biophilic, healthy lighting and thermal performance of buildings in extreme sub-Arctic climatic conditions. Single-skin envelopes with low window-to-wall ratios (WWR) are most often recommended for sub-Arctic climates to reduce heating loads. Potentials of multi-skin envelopes to address biophilia and healthy lighting combined with energy-efficiency factors in such climates have not, yet, received sufficient attention. Five envelope models are evaluated including two single-skin envelopes with 20% and 40% WWR and three multi-skin envelopes with 80% WWR for the interior skin and a fully glazing external skin applied in different cavity depths. Biophilic and thermal performance of the envelopes are evaluated through developing numerical models of an open-plan office in Northern Canada, as a case study. Healthy lighting performance of the envelopes are evaluated through developing an experimental setup with 1:50 scale models under actual clear skies combined with numerical models of the office. The results reveal that multi-skin envelopes have promising potentials to promote biophilic, healthy lighting and thermal performance in sub-Arctic climates. However, such envelopes must be further developed by combining with adaptive insulated shading devices for higher lighting and thermal performance.*

KEYWORDS: *Climate responsive façade, High-performance building, human-centric lighting, Biophilic design*

1. INTRODUCTION

This research explores the performance of single-skin and multi-skin building envelopes under extreme sub-Arctic climatic conditions in terms of biophilic, healthy lighting and thermal indicators. Building envelopes in sub-Arctic climates, i.e. near and above 50° N towards the Arctic, must respond to biophilic, healthy lighting and thermal energy-efficiency factors in relation to the extreme cold weather and drastic seasonal day/night cycles. Envelopes' configuration and openings are main elements connecting indoors to outdoors which affect view and accessibility to the outdoor nature, daylighting, and day/night cycle, known as photoperiods [1]. Relationships with natural phenomena and the outdoor nature, identified as biophilia, are a contributing factor to building occupants' psychological wellbeing such as reducing stress and anxiety and improving cognitive performance [2-4]. Maximizing the use of daylighting and providing a proper lighting quality and sufficient darkness at the proper time of the day also contribute to occupants' photobiological wellbeing in terms of image-forming (IF) and non-image forming (NIF) responses [5, 6]. IF responses affect vision and visual performance. NIF responses regulate internal body clocks, wake-sleep cycles, alertness, and mood [5, 7]. Envelopes and openings also play key roles in

thermal performance and energy consumptions of buildings related to heating and cooling systems [8, 9]. Openings' characteristics and sizes have considerable impacts on building heat losses and solar heat gains. Northern Canada building codes and practices are mainly developed based on low window-to-wall ratios (WWR) to reduce heat losses from openings [1, 10]. Increasing the WWR of existing envelope practices could elevate energy consumption of Northern buildings. Potentials of multi-skin envelopes to improve biophilic, lighting and thermal performance of Northern buildings have not, yet, studied. Previous research has mostly evaluated multi-skin building envelopes under temperate and hot climatic conditions in terms of visual comfort and daylighting and thermal performance [8, 11-15]. Biophilic and healthy lighting performance of multi-skin envelopes combined with thermal and energy-efficiency indicators under extreme sub-Arctic climatic conditions has not, yet, adequately studied [1].

This research evaluates biophilic, healthy lighting and thermal performance of five fundamental models of single-skin and multi-skin building envelopes with different window sizes under sub-Arctic climatic conditions of Northern Canada. Experimental and numerical methods were employed to evaluate the

envelope models under actual and simulated Northern conditions. The results were discussed to provide a strategic overview for developing high-performance climate-responsive envelopes for Northern buildings which could promote biophilic qualities through efficient indoor-outdoor connections.

2. MATERIAL AND METHODS

Five fundamental envelope models applied to an open-plan office in Northern Canada were considered for performance evaluations. As depicted in Fig. 1, the proposed models include (1) a single-skin envelope with a low WWR of around 20%, as recommended by the national energy code of Canada for buildings [10, 16], (2) a single-skin envelope with an average WWR of around 40%, (3) a multi-skin envelope with a cavity depth of 40 cm and 80% WWR of internal skin, (4) a multi-skin envelope with an 80 cm intermediate space and 80% WWR of internal skin, similar to a covered corridor, and (5) a multi-skin envelope with a 200 cm intermediate space and 80% WWR of internal skin, as a habitable space similar to a covered balcony. A fully transparent single glazing skin is considered as the exterior skin of multi-skin envelopes.

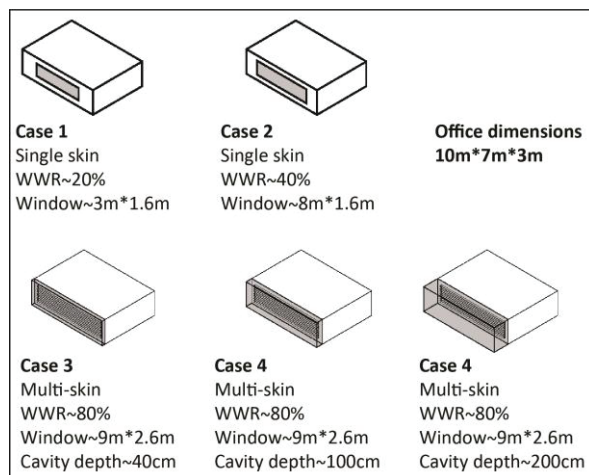


Figure 1: The proposed envelopes for the reference office

Biophilic performance indicators are mainly related to connectivity and contact with nature, especially outdoor natural phenomena [2-4]. Biophilic performance is, therefore, represented by occupants' field of view (FOV) towards outdoors. Biophilic features of indoors, such as using greenery, are considered as a constant independent variable remained unchanged for all models. Biophilic performance of the proposed envelope models was evaluated by using numerical methods in Autodesk AutoCAD (2020) to calculate occupants' view angle towards the window and outdoors. Horizontal and vertical view angles of occupants in different viewpoints in the reference office, from the middle to

sides and corners, were calculated. Vertical FOVs were calculated at the middle height of the space for all viewpoints (see Fig. 2). The overall FOVs were derived by multiplying horizontal and vertical view angles. FOVs were normalized in terms of human eyes' horizontal and vertical view angles corresponding to around 120°.

An experimental setup with 1:50 scale models of the open-plan office in different window sizes was developed to evaluate the healthy lighting performance under actual clear skies and direct sun lighting in Quebec, QC, Canada (Lat: 46° N, Long: 76° W). High dynamic range (HDR) imagery and post-processing techniques were employed to capture and compute healthy lighting parameters inside the models. Healthy lighting parameters are mainly related to photopic and melanopic units and colour temperature of lighting in the space. Photopic units represent potential IF responses. Melanopic units and colour temperature represent potential NIF responses [17, 18]. A proper lighting quality in terms of photopic and melanopic units and colour temperatures must be provided at different times of the day from the morning to evening [17]. Lighting with high melanopic units and colour temperature is, generally, recommended for the morning until noon. Lighting with low melanopic units and colour temperatures are, generally, recommended for the afternoon and evening. Complete darkness must be provided for nights and sleeping [1, 5]. The details of the experimental setup, HDR imagery, calibration and post processing were based on the previous studies of Parsaee, et al. [17], Jung and Inanici [18]. Photopic and melanopic units are normalized by the intensity of the photopic and melanopic luminance intensities of the exterior daylighting received at the vertical plan in the direction of the experimental set-up, i.e. towards the south. Furthermore, numerical models of the envelopes were developed by using an online tool offered by Marsh [19] to calculate spatial daylighting autonomy with a minimum threshold of 300 lux in the office, as an indicator of annual daylighting availability and penetration.

Numerical models were also developed in IES Virtual Environment Software [20] using the EnergyPlus engine to evaluate thermal and energy performance of the envelopes in terms of heating loads. Heating loads were calculated for the energy required to provide occupants with acceptable thermal comfort zones and indoor air qualities inside the case study of the open-plan office in Kuujuaq, Quebec, Canada (Lat: 58° N, Long: 68° W), as recommended by NRC [10], ASHRAE [21]. The details of the thermal model are offered in Table 1. Thermal performance of the envelopes was evaluated for applications on different façade directions by

calculating heating loads of the office directed towards the south, east, west, and north.

Table 1: Thermal model settings and characteristics

Item	Value
Wall total R-value	3.85 (m ² K/W)
Roof and floor total R-value	5.03 (m ² K/W)
Double glazing window net U-value	1.41
Double glazing window visual transmittance	0.71
Single glazing window (for the exterior skin) net U-value	5.81
Single glazing window (for the exterior skin) visual transmittance	0.76
Insulated panels R-value	2 (m ² K/W)
Heating set-point	21 °C
Heating set-back	18 °C
Opening setpoint for natural ventilation	21 °C (outdoor air temperature)
Occupancy density	14 (m ² /P)
Office occupancy hours	08:00 - 18:00
People (latent and sensible heat)	150 (W/P)
Lighting	12.00 (W/m ²)
Computer and equipment	12.00 (W/m ²)
Infiltration rate	0.35 (l/s/m ²)
Ventilation rate	8.5 (l/s/person)

3. RESULTS AND DISCUSSIONS

The results are discussed in terms of biophilic, healthy lighting and thermal performance of proposed cases as the following sections.

3.1 Biophilic performance of the envelopes

The envelope models proposed with higher WWRs, cases 2-5, are offered higher biophilic performance related to occupants FOVs to outdoors. As illustrated in Fig. 2, increasing the window size from 20% to 80% increases occupants' overall FOV from nearly 2% to 10% for viewpoints near the back wall. The window size of 20% WWR, case 1, offers significantly obstructed views towards the outdoor, especially in terms of horizontal FOVs of occupants near the side walls and corners. Increasing the window size from around 40%, case 2, to 80%, cases 3-5, increases the individual's overall FOV about 20% to 50% at different viewpoints in the middle and corner of the space. The results also show that the window size of near and above 80% offers relatively immersive views to the outdoor nature, especially for the spots near the window. As biophilic design calling for immersive views to nature, window sizes of above 40% are recommended for higher biophilic qualities.

3.2 Healthy lighting performance of the envelopes

The experimental results show the higher daylighting performance of envelopes with average and high window sizes, cases 2-5, in terms of the penetration, distribution and probabilities of photopic and melanopic units and colour temperatures inside the model. As illustrated in Fig. 3, increasing the window size from 20%, case 1, to 40% and 80%, cases 2-5, increases the frequency and probability of higher photopic and melanopic units in the space. The small size window of case 1 significantly obstructs daylighting penetration in the space. The normalized photopic and melanopic intensities are accumulated around 10% of the outdoor daylighting photopic and melanopic intensities. The probability of daylighting autonomy with above 300 lux in the space is less than 10% throughout the year (Fig. 3-d). Cases 2-5 with 40% and 80% WWRs enable daylighting to penetrate and distribute in the space. The frequencies of high photopic and melanopic units are significantly increased compared to case 1. The normalized photopic intensity in case 2 is distributed mostly between 20% to 40% within the side viewpoint and between 25% to 50% within the back viewpoint, which is significantly higher than the corresponding values for the case 1, i.e. 10%. In cases 3-5, the normalized photopic intensity is distributed between 30% to 60% within the side viewpoint and between 35% to 70% within the back viewpoint which is higher the case 2 and also the corresponding values for the case 1, i.e. 10%. The probability of daylighting

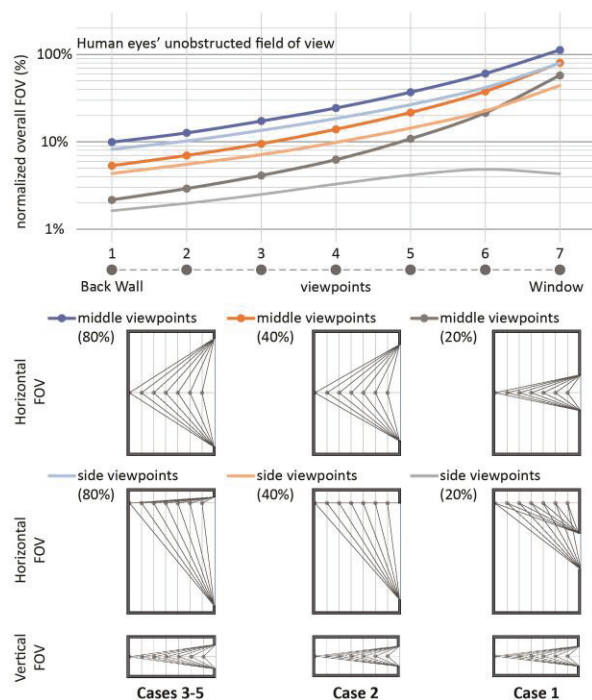


Figure 2: Impacts of different window sizes on occupants' field of view (FOV) to outdoors at different viewpoints in the space

autonomy with above 300 lux accounts for at least 20% of the space for cases 2-5 which is twice the corresponding value for case 1, i.e. less than 10%. Daylighting penetration in the space is highly increased for cases 2-5 reaching the back wall compared to case 1. Overall, the higher window size offers higher daylighting accessibility in the space. However, larger window sizes increase the risk of glare in the space demanding efficient shading devices such as blinds, curtains, or shutters.

3.3 Thermal performance of the envelopes

The results reveal the high thermal performance of the multi-skin building envelopes under the south, west and east directions in the extreme cold climatic conditions of Northern Canada. As illustrated in Fig. 4, heating loads of the reference office with a single skin façade and 20% to 40% WWRs, cases 1-2, are almost around 200 kWh/m²/yr under different directions. Applying a multi-skin envelope with 80% WWR and different cavity depths from 40 cm to 200 cm, cases 3-5, considerably reduces heating loads of the office by around 40 kWh/m²/yr under the south direction. This is mainly related to higher potentials of solar heat gains enabled by larger window sizes. Heating loads of the office with the multi-skin envelopes and the huge window size, cases 3-5, are almost similar to heating loads of the office with the single-skin

envelopes and small-average window sizes, cases 1-2. However, the multi-skin envelopes increase the heating loads of the office about 20 kWh/m²/yr under the north direction compared to the corresponding heating loads for the single-skin envelope offices. This is mainly related to higher heat losses from the high WWR of the proposed cases under the north direction where solar radiations are negligible. Note that cooling systems are not required in such extreme cold climates where opening the window for a few hours of natural ventilation could fulfil potential cooling demands in the summer. No overheating has also occurred inside the cavity.

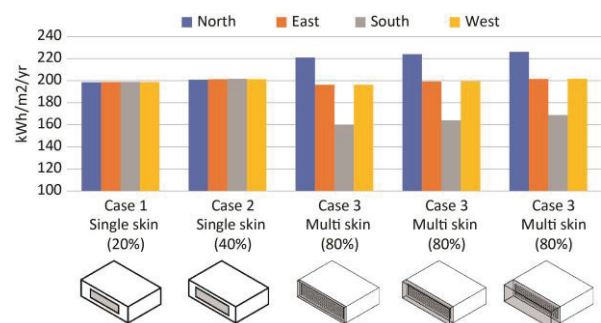


Figure 4: Annual heating loads of the reference office proposed with different envelope configurations and WWRs under various directions in Kuujuaq, Quebec, Canada.

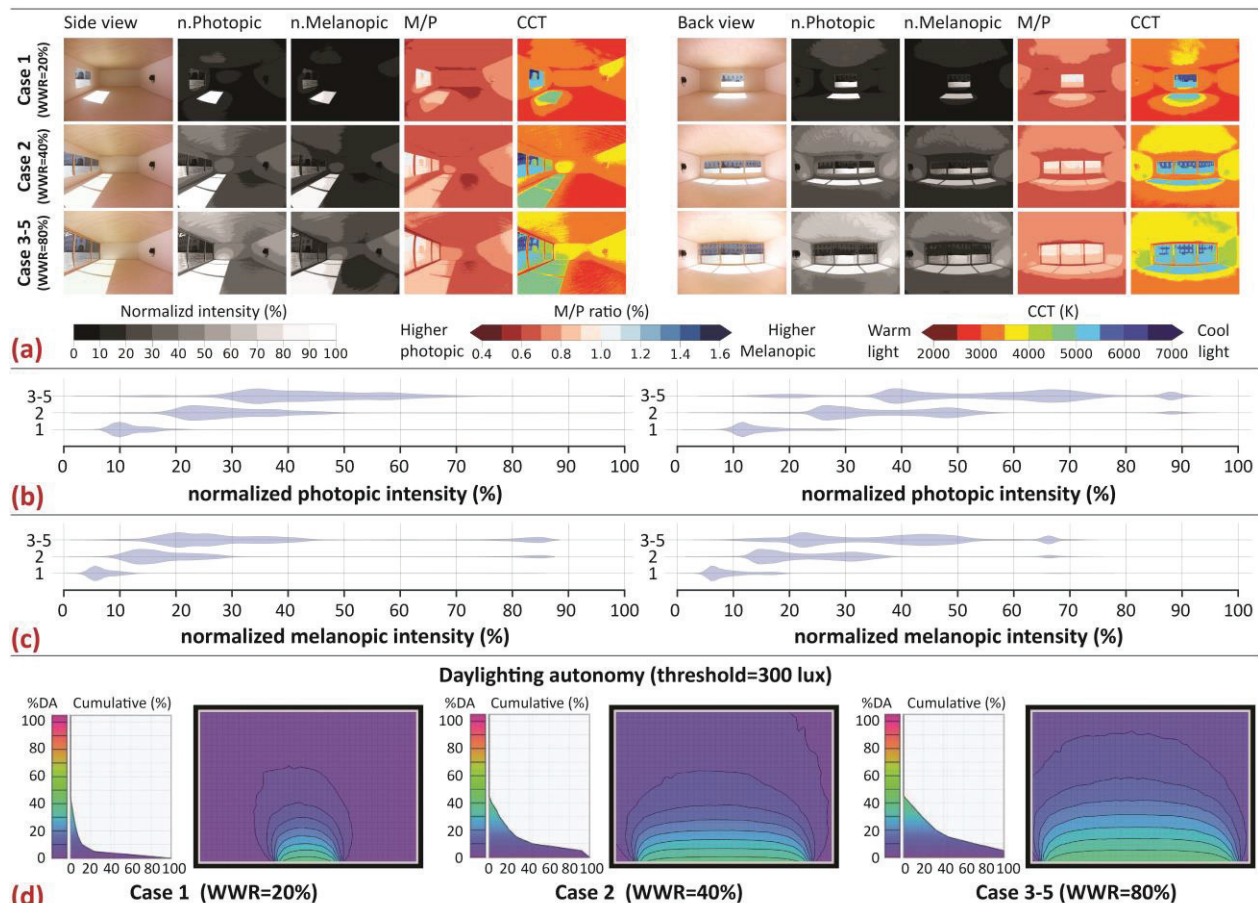


Figure 3: Impacts of window sizes on healthy daylighting parameters and daylighting autonomy inside the office

4. CONCLUSIONS

This research studied biophilic, healthy lighting and thermal performance of different single-skin and multi-skin envelopes under extreme sub-Arctic climatic conditions of Northern Canada. The results of research revealed the promising potentials of multi-skin envelopes with high WWRs to establish efficient indoor-outdoor connections offering higher biophilic, daylighting and thermal performance. Single-skin envelopes with the small opening size, as recommended by Canada building and energy codes, present very poor performance in responding to biophilic and healthy lighting requirements. Yet, higher window size increases the risk of glare and visual discomfort which demands efficient shading devices to control daylighting intensity. Shading devices are, generally, required for all envelopes with high or low window sizes to control the low-altitude sun lighting in Northern latitudes as well as to block daylighting during the long days of the summer. Future research must develop multi-skin envelopes with effective shading devices to improve the overall performance of the building in terms of biophilic, health lighting and thermal indicators. Multi-skin envelopes with habitable or transient intermediate spaces such as corridors and balconies must be further developed which could improve biophilic qualities of Northern buildings. Such spaces could, also, be developed as a cultivating area similar to greenhouses for Northern buildings. Adaptive shading panels with dynamic behaviours made of (super-) insulation materials could be developed to modify daylighting parameters related to occupants' photobiological needs as well as to cover openings and reduce heat losses when daylighting and views to outdoors are not required for the interior, for example during night times or weekends in the case of offices. The configurations and material of the external skin of multi-skin envelopes must also be further studied for extreme conditions of sub-Arctic climates.

ACKNOWLEDGEMENTS

This research was supported by the Sentinel North program of Université Laval, made possible, in part, thanks to funding from the Canada First Research Excellence Fund.

REFERENCES

1. Parsaee, M., Demers, C. M., Hébert, M., Lalonde, J.-F., & Potvin, A. (2020). Biophilic, photobiological and energy-efficient design framework of adaptive building façades for Northern Canada. *Indoor and Built Environment*. doi:10.1177/1420326X20903082
2. Browning, W., Ryan, C., & Clancy, J. (2014). *14 Patterns of biophilic design*. New York, US.
3. Kellert, S. R., & Calabrese, E. F. (2015). The practice of biophilic design. www.biophilicdesign.com
4. Yin, J., Yuan, J., Arfaei, N., Catalano, P. J., Allen, J. G., & Spengler, J. D. (2020). Effects of biophilic indoor environment on stress and anxiety recovery: A between-subjects experiment in virtual reality. *Environment International*, 136, 105427.
5. Parsaee, M., Demers, C. M. H., Hébert, M., Lalonde, J.-F., & Potvin, A. (2019). A photobiological approach to biophilic design in extreme climates. *Building and Environment*, 154, 211-226.
6. CIE. (2019). *Position statement on non-visual effects of light - recommending proper light at the proper time, 2nd edition (october 3, 2019)*. Retrieved from CIE Central Bureau, Vienna, Austria.
7. Khademagha, P., Aries, M., Rosemann, A., & van Loenen, E. (2016). Implementing non-image-forming effects of light in the built environment: A review on what we need. *Building and Environment*, 108, 263-272.
8. Barbosa, S., & Ip, K. (2014). Perspectives of double skin façades for naturally ventilated buildings: A review. *Renewable and Sustainable Energy Reviews*, 40, 1019-1029.
9. Konis, K., & Selkowitz, S. (2107). *Effective Daylighting with High-Performance Facades: Emerging Design Practices*: Springer.
10. NRC. (2015). National Energy Code of Canada for Buildings (NR24-24/2015E). In. Ottawa, Canada: National Research Council of Canada.
11. Joe, J., Choi, W., Kwak, Y., & Huh, J.-H. (2014). Optimal design of a multi-story double skin facade. *Energy and Buildings*, 76, 143-150.
12. Larsen, S. F., Rengifo, L., & Filippín, C. (2015). Double skin glazed façades in sunny Mediterranean climates. *Energy and Buildings*, 102, 18-31.
13. Pomponi, F., Piroozfar, P. A., Southall, R., Ashton, P., & Farr, E. R. (2016). Energy performance of Double-Skin Façades in temperate climates: A systematic review and meta-analysis. *Renewable and Sustainable Energy Reviews*, 54, 1525-1536.
14. Shameri, M., Alghoul, M., Elayeb, O., Zain, M. F. M., Alrubaih, M., Amir, H., & Sopian, K. (2013). Daylighting characteristics of existing double-skin façade office buildings. *Energy and Buildings*, 59, 279-286.
15. Wong, P. C. (2008). *Natural ventilation in double-skin façade design for office buildings in hot and humid climate*. (PhD), University of New South Wales, Australia, Australia.
16. NRC. (2015). National Building Code of Canada (NR24-28/2015). In. Ottawa, Canada: National Research Council of Canada.
17. Parsaee, M., Demers, C. M. H., Lalonde, J.-F., Potvin, A., Inanici, M., & Hébert, M. (2020). Human-centric lighting performance of shading panels in architecture: A benchmarking study with lab scale physical models under real skies. *Solar Energy*, 204, 354-368.
18. Jung, B. Y., & Inanici, M. (2019). Measuring circadian lighting through high dynamic range photography. *Lighting Research & Technology*, 51(5), 742-763.
19. Marsh, A. (2020). Software Development. <http://andrewmarsh.com/software/>
20. IESVE. (2019). IES Virtual Environment Software. <https://www.iesve.com/>
21. ASHRAE. (2017). ANSI/ASHRAE Standard 55-2017. In *Thermal environmental conditions for human occupancy*. Atlanta, US: American Society of Heating, Refrigerating and Air conditioning Engineers.

Conserving 20th Century Historic Places and Buildings of Jinja (Uganda) through Environmentally Sustainable Adaptive Reuse

ANTHONY K. WAKO

Faculty of the Built Environment, Uganda Martyrs University, Nkozi, Uganda

This paper examines Jinja's historic places and buildings as opportunities for conservation through environmentally sustainable adaptive reuse. Jinja is an important city located about 80km east of Kampala-Uganda, with an assemblage of historic places and buildings from the 20th century. The early to mid 20th century witnessed the founding and growth of Jinja as a Colonial Administrative Centre for the eastern region alongside colonial industrial developments. Buildings, which are an outcome of this period, are vital for their heritage significance value that is engrained in socio-cultural and socio-economic aspects. This paper thus argues for the inclusion of environmental sustainability as a component of heritage significance, an often-excluded concern at both micro and macro urban planning levels within the city. This gap stems from inadequate scholarship on planning, conservation and direct adaptation of historic environments in response to climate change, across sub-Saharan Africa. Through historical perspectives and environmental sustainability criteria, the paper maintains that reuse and continued improvement of dilapidated places and buildings is inherently a sustainable endeavour. It further proposes a working narrative for seemingly undervalued concepts of conservation and sustainability in Uganda, drawing on the experience of selected urban projects.

KEYWORDS: Historic Buildings, Jinja, Conservation, Adaptive Reuse, Sustainability

1. INTRODUCTION

This paper evaluates how Jinja's historic places and buildings can be assessed through the lens of the ongoing dialogue of environmental sustainability. Jinja, a major commercial city approximately 80km east of Kampala, is among the few cities in Uganda with a collection of early 20th century buildings within their central business district. Much as Jinja's colonial-era built heritage is in abundance, it is constantly under the pressure of being erased by developers and municipal authorities. Without historical conservation policy, this built heritage will likely be abandoned or replaced, "creating more of an eye-sore effect rather than one of pride and societal connection" [1].

This paper, hence, forms a basis for conservation policies from a historical perspective that could be a valuable addition to Jinja's long term urban development plans. In addition, conservation policies could include such considerations as environmental sustainability assessment criteria such as green heritage design, durability of materials and assemblies, life cycle assessment, embodied energy, sustainable communities and ecological concerns, among others. It can be argued that if one of the aims of sustainability is continuous improvement, then the reuse of old buildings instead of demolishing for new developments, is one of the means to achieve this [2].

In the last decade, there has been a growing body of research on a global scale that positions buildings in

ways other than by historic, cultural and architectural standards, and rather "... as repositories of energy worth preserving for their environmental value ..." [3]. This paper consequently contributes to the positive issues of urban heritage and historical buildings in a field where there have been significantly fewer platforms on a global scale. Much as historic buildings have long been classified as being significant when they meet the criteria associated with socio-cultural values, buildings that are on the borderline of significance or lack these values are therefore considered insignificant [3]. It is the exigency of this paper to argue for a re-evaluation of historical significance that takes into account environmental sustainability, while also considering that these buildings could be documentation of the architectural culture of communities that might need conservation criteria [4].

The section that follows gives a historical overview that situates the paper within socio-cultural and socio-economic contexts of Jinja's historic places and buildings. A gesture that draws parallels between heritage and environmental sustainability is developed in section 3. The methodological approach in section 4 addresses the extents and limits of both built heritage and sustainability of the study. Both possible and suggested strategies that have worked in some case study projects of buildings and places within Jinja are discussed in section 5.

2. JINJA'S BUILDINGS: HISTORICAL PERSPECTIVES

Jinja's surviving historic buildings are from different periods: the early 20th century, art deco period of the 1930s, modern period of the 1940s to 1960s and the late 20th century (Figure 1). The early 20th century period and art deco period of the 1930s was dominated by Indian industrial patronage and they played a pivotal role in developing Jinja's urban built heritage [5]. Through Indian-dominated trade and Indian-mercantile capital of this period, the economic lifeblood of Jinja and the larger Uganda Protectorate grew exponentially. These periods became dominated by construction techniques and materials such as corrugated iron sheets that were influenced by the arrival of colonial railways into East Africa. The modern period (the 1940s-1960s) coincided with the opening of the Owen Falls Dam in 1954 at Jinja and materials such as concrete and steel became more commonplace. Though this paper focusses on buildings from the early 20th century period which are the majority as indicated in a prominent street of Jinja (Main Street) in figure 1, it makes references to buildings and places from other time-periods. Historic buildings such as these are irreplaceable, providing character and identity to cities like Jinja.

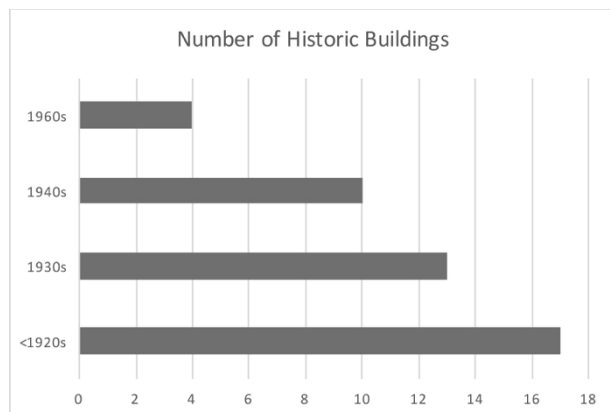


Figure 1: Historic buildings along Jinja's Main Street

3. MAKING A CASE FOR CONSERVATION AND SUSTAINABILITY

It is inherently more sustainable to adapt buildings and live in them than to start from scratch while in pursuit of environmental efficiency. An inclination that was expounded on by Bullen [2], who posited that extending the useful life of existing buildings supports key concepts of sustainability by lowering material utilisation, its transport, energy consumption and pollution [2]. Buildings that have been in existence since the beginning of the 20th century in Jinja, therefore, have promoted the retention and reuse of existing resources and continued the use of previous energy investments (embodied energy) and life cycle analysis. Figure 2 shows that 80% of a building's life cycle costs are integrated into planning. Jinja's colonial

buildings were built in an age when a 20-30-year service life was thought to be sufficient. Their original design may not necessarily be considered today as a sustainable approach, however conservation work that exposes the buildings' inherent energy components enhances and contributes to their thermal comfort level and energy conservation. The need for sustainability and conservation is further merited by Holland [6] who postulated that buildings built today use ancient techniques of responding to local microclimates.

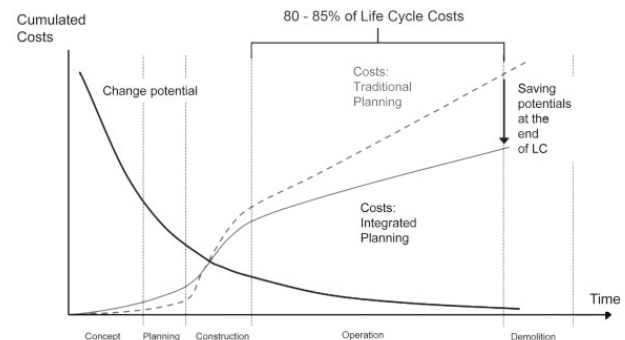


Figure 2: Building's life cycle cost amounts to 80%

This paper thus highlights the often-excluded concerns for sustainability and built heritage at both domestic and urban planning levels. An important gap that stems from few publications on conservation and direct adaptation of historic environments in response to climate change, more so in sub-Saharan Africa.

4. METHODOLOGICAL APPROACH

Examining how existing historic places and buildings can be adapted to complement 21st-century trends could identify the key factors needed to make necessary adjustments. Analysing these factors as stated by Bullen [2] increases the likelihood of a historic building being adapted and consequently becoming more sustainable [2]. To start with, before conservation works on historic places and buildings, a historical study must be conducted to situate the built heritage. Within the espoused criteria to restrict and justify the chosen places and buildings worthy of conservation (adapted to new uses); their historical significance, typological significance and exceptional craftsmanship take precedence and should be prioritised [7]. Although historical interpretive methodological approach sets a foundation that positions this paper in a socio-cultural context of heritage, it provides to a lesser extent the environmental sustainability aspects to be considered for adaptive reuse.

The second part of the methodological approach entails integrating key heritage, socio-cultural and community sustainability indicators into environmental-sustainability assessment tools (Figure 3). Though these tools, across the globe, cover a broad

range of different processes that are derived from environmental impact and strategic assessment, heritage and conservation consideration narrows the scope.

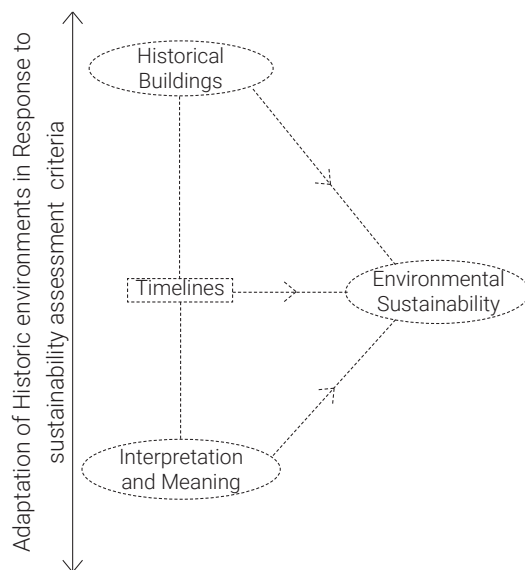


Figure 3: Methodological Strategies

By applying this methodological approach, the paper provides an appreciation of SDG 11: on Sustainable Cities and Communities. This endeavour matches former progress of Jinja's infrastructural development and maintains the significance of its existing green public spaces, to improve urban planning and management in introspective ways.

5. ADAPTIVE REUSE AND STRATEGIES: KEY HISTORIC BUILDINGS AND PLACES

Adaptive reuse for new functional programs, through the second lens of social-life in an economically viable and sustainable way [8], is evident in projects such as the Madhvani building (Figure 4), Source Café (Figure 5) and a series of buildings along Jinja's historic streetscapes. Accruing from the long-agreed impracticability of attempting to preserve all historic buildings [6], changes to these buildings may appear aesthetically minor but socio-culturally significant and adapted to 21st-century trends. This scheme is in line with the appreciation of heritage that pays homage to Jinja's industrial past, which is an approach that could be extended to iconic places like the Busoga Square (Figure 7). The Square could act as a convivial green space that adds character to the potential historic precinct. The Square houses the Town Hall (Figure 8), Jinja District Administrative building (Figure 9) and World War memorial (Figure 10) at the midpoint. These places and buildings are critical to Jinja's historical narrative, complement its tourist attractions such as the source of the River Nile and a series of cultural heritage sites.

5.1 Madhvani Building: Conservation Avenues

The first storeyed building in Jinja, completed in 1919, is the Madhvani building. The building is significant because it represents the cornerstone of the Madhvani family business empire in East Africa [5]. From the family business' inception in 1912, the building housed its main offices and headquarters for the different industries.



Figure 4: Arcade of the street-facing façade of the Madhvani building.

With some of the building components (timber posts, window frames, verge board and fascia boards) from the 20th century carefully replaced with replicas during 2010 restoration, it still stands as a true manifestation that pays reverence to the Madhvani's past and present industrial achievements within Jinja. Though the building's components like the timber doors and windows, with good workmanship, were partially replaced, the original cement-screed floor finish was entirely replaced by floor-clay tiles (Figure 4) to meet the quality of office spaces in the urban precinct. The choice of floor-clay tiles over re-cementing can be viewed as a response to environmental sustainability in two ways: first, manufacture and transport of the floor-clay tiles were within a delivery radius of 6km instead of cement from a factory that is located more than 80km from the building, and secondly, a manufacturing process that involved burning coffee husks as opposed to firewood.

The reasons for conserving this building, besides its historic and socio-cultural worth can, therefore, be extended to include the environmental value that stems from the choice of replacement-material and manufacturing processes.

5.2 The Source Café Building: Old Vs New

Completed in 1924, the Source Café building (Figure 5) in Jinja has been a testament to sustainable adaptive reuse throughout its life span of over 90 years. In a society where a 50-year period is

considered obsolete for a building, the source café durability is over the odds and stands as an example to emulate in a city whose built heritage is fast disappearing. The building derives its importance from its continued re-use during the early 20th century as a bakery, retail stores, a bar and now houses a restaurant, library, craft store and a multipurpose-space [5].



Figure 5: Timber Trellis at the entrance of The Source Café Building

Alterations to the buildings' exterior and interior showcase distinctions between the 'old' and 'new', thus highlighting great workmanship of the early 20th century alongside recent modifications. These include a timber trellis placed on an early 20th-century façade (Figure 5), exposed original roof trusses with a ceiling lining, a recent mosaic floor finish on the veranda and clay floor tiles that illuminate the interior space. The Source Café building retains workmanship, materiality, constructed features that bear witness to the early 20th century's way of life through the mid-century to the present day.

The Source Café and Madhvani buildings represent a non-renewable capital resource of materials, energy, financial investment and a socio-cultural role. Historic buildings such as these have a minimum intervention principle which is shared by "conservation and sustainability" [9]. This was a deliberate bottom-up approach that commenced with interventions on the existing buildings and sought to make it work in the 21st century.

5.3 Withering Heritage: Jinja's Streetscapes

The first 3 decades of the 20th century attest to Jinja's becoming an administrative centre for the Eastern Province of the Uganda Protectorate, albeit limited functions including the colonial administrative offices at the Busoga Square (Figure 7), a market (bazaar), an inland port on Lake Victoria and only one fully built-up street that traversed racially dominated urban zones [5], Main Street. Main Street stretches about 1.8km north from the Busoga Square and today

it is one of the few surviving streets whose heritage is in peril (Figure 6).



Figure 6: The Igar Building is an example of a recent 'Infill development' on Main Street that does not respect the existing historic urban fabric.

Recent Infill developments, for example, do not respond sympathetically to the predominant scale (Figure 6) of historic built-scape in terms of height, bulk, density and grain. The impact of suitably scaled buildings cannot be compensated for by building form, design or detailing thus, diminishing the 20th-century historic street character.

5.4 Revival Opportunities: The Square within the Town

Busoga Square (Figure 7), a significant open green space, gives Jinja a strong image. Like a myriad of green spaces in cities across sub-Saharan Africa, the square contributes to social activities, climate amelioration and ecological diversity without separating or isolating people from each other [10]. The presence of Jinja Town hall building, the District Administrative offices building and World War II Memorial, all within the Square, add to the civic composition of the city. All three projects, though derelict, substantiate the industrial achievements and administrative purposes of Jinja within the Eastern region.



Figure 7: Busoga Square in 1937

The Jinja Town Hall (Figure 8) is significant because it highlighted Jinja's transition from a township (1907) to a municipality (1956). It signified Jinja's urban division as administratively independent from the East Provincial administration. Completed in 1958, the

Town Hall was commissioned by the colonial-era Governor of Uganda, Sir Frederick Crawford (1957-1961). Designed in the tropical modernist architectural style that trended in the 1950s-60s in Uganda, the building design incorporated passive design strategies of cross ventilation and solar shading devices. The building has a rectilinear form and prominent clock tower at the entrance; a feature that is reminiscent of some of the first buildings to be erected in settlements by European colonialists across Africa [11]. The Town Hall's form and material-substance illustrate large scale building processes of the time including cement that was transported from Tororo Cement factory about 130km east of Jinja.

Commendation to the Jinja Municipal Council (JMC), the current occupants of the building, for attempting to paint most buildings' exterior such as this (Figure 8). However, these efforts could include and are complemented by life cycle assessment and durability of materials in determining the heritage significance of Jinja's historic buildings. Additionally, tropical modernist architecture characteristics like climate responsive design that are evident in the town hall building and are occasionally over-looked in recent designs across Uganda, present opportunities for conservation.



Figure 8: Jinja Town Hall Building. Completed in 1958

Representation of Jinja's historic buildings, in which colonialism pervaded various aspects of the built form, can be traced in the 1920s Jinja District Offices building (Figure 9). The building, with its simplicity, is aligned with subversion of neo-classical

columns on all facades. It is linked to the earliest governance of Uganda's regional administrative and political setting – the East Province Administration. Hence, the building derives its significance as one of the oldest continuously-functioning civic buildings district offices in Uganda, serving the community as the district and immigration offices.



Figure 9: Jinja District Offices completed in the 1920s

The Jinja District Offices building is of great individuality and the space around it provides an opportunity to appreciate it as a unique composition. The building, together with the World War Memorial monument (Figure 10) at the midpoint of the Busoga Square, within their landscape, is appreciated in the same way as sculpture, that is, by walking around them and viewing from all sides.



Figure 10: World War Memorial monument located at the centre of Busoga Square.

The physical and societal attributes of these buildings and the monument within the Square is inseparable. They represent a continuous timeline of the 20th century past, present and future by way of their heritage significant value which is expressed through memory, socio-cultural and socio-political

cohesion. They collectively represent an environmental capital that underscores their survival and that of society.

6. CONCLUSION

New buildings without links to the past may operate successfully, however they risk being thin and devoid of meaning that is engrained in the historical past. Understanding both historic and environmental values situates such buildings and places at the forefront of the sustainability movement. This paper has demonstrated that the success of Jinja can be curated historically while also concentrating on environmental concerns. It has presented an overview that not only unearths the meaning(s) and interpretation(s) which connect people to the fabric of place and time but act as crucibles of climate responsive approaches to planning, conservation and design considerations. In addition, the projects discussed in the previous sections are tangible examples of adaptive reuse, durability of material selection, manufacture, without detracting from the associated socio-cultural heritage significance. Such projects acknowledge Jinja as a city in the transition to having 'earmarks of a post-carbon city and in need of rigorous planning interventions'. Reflections and discussions that position heritage as a non-renewable landmark thus place heritage conservation alongside sustainable development. The paper has contributed to the holistic approach to conservation of historic places and buildings making certain that development is not sustainable without heritage conservation.

ACKNOWLEDGEMENTS

I would like to thank my mentors Mark Olweny and Achilles Ahimbisibwe for encouraging me to participate in this research exercise. To the Faculty of the Built Environment at Uganda Martyrs University for providing a favourable platform for a dialogue of sustainable built environments. To my reviewers and editors; Guy Mambo and Viola Kitabire, your invaluable input is much appreciated.

REFERENCES

1. Geva, A., (2008) Rediscovering Sustainable Design through Preservation: Bauhaus Apartments in Tel Aviv *The Journal of Preservation Technology*, 39(1): p. 43-49
2. Bullen, P.A., (2007). Adaptive reuse and sustainability of commercial buildings. *Facilities*, 25(2): p.20-31 [online], Available at <https://doi.org/10.1108/02632770710716911>
3. Merlino, R. K., (2014). (Re)Evaluating Significance: The Environmental and Cultural Value in Older and Historic Buildings, 36(3): p.70-85
4. Moschella P, Salemi A, Lo Faro A, Sanfilippo G, Detommaso M, & Privitera A., (2013). Historic Buildings in Mediterranean Area and Solar Thermal Technologies: Architectural Integration vs Preservation Criteria. In the Mediterranean Green Energy Forum. Catania, Italy.

5. Wako, A. K. and Olweny, M. R., (2019). Historical Study of Jinja, Uganda: A City influenced by Industrial Developments During the Early 20th Century. In *Structural Studies, Repairs and Maintenance of Heritage Architecture XVI*, 191, Seville, p.67-78
6. Holland, M., (2012). Conserving the Future: The Need for Sustainability in City Planning and Preservation. *The Journal of Preservation Technology*, 43(1): p3-6. Available: <https://www.jstor.org/stable/41548688>
7. Osasona, C., (2019). Architectural Renewal: A Rising Dawn in Ile-Ife. In *Structural Studies, Repairs and Maintenance of Heritage Architecture XVI*, 191, Seville, p.43-58
8. Jonge, W. D., (2017). Heritage for the Masses. About Modern Icons & Everyday Modernism, Historic Value & a Sustainable Future. In *The 6th Baltic Sea Region Cultural Heritage Forum: From Postwar to Postmodern*. Stockholm, Sweden, September
9. Rodwell, D., (2007) Conservation and Sustainability in Historic Cities. Oxford: Blackwell Publishing.
10. Yilmaz, M. and Keles R., (2004) Sustainable Housing Design and the Natural Environment. *Ekistics*, 71(429): p236-243. Available: <https://www.jstor.org/stable/43623436>
11. Folkers, A. S., (2019). Modern Architecture in Africa: Practical Encounters with Intricate African Modernity. Amsterdam: Springer.



SUSTAINABLE COMMUNITIES

Natural Capital Impact Assessment for New Urban Developments

PEPE PUCHOL-SALORT¹, MAARTEN VAN REEUWIJK², ANA MIJIC³

^{1,2,3} Civil and Environmental Engineering Department, Imperial College London, London, United Kingdom

ABSTRACT: Under pressures of climate change and population growth, it is crucial to address water security and sustainable urban development in our cities. This challenge is particularly important for London, where a shortage of housing has been experienced during last decades and the region is considered highly vulnerable to water shortages and floods. According to the Greater London Authority (GLA), an average of 66,000 new homes per year should be built until 2041. However, assessing impacts of such urban growth on environmental management and protection is complex and difficult to evaluate.

This creates a need to determine the extent to which Ecosystem Services (ES), or the benefits provided by the functioning natural environment in the form of Urban Natural Capital (UNC), are essential to the wellbeing of current and future urban dwellers and how costly it may be to provide them. This research aims to create an impact assessment framework for Urban Natural Capital (UNC) for new urban developments, which will provide crucial indicators to assess sustainability at an urban development scale. The results will be used to inform improved urban design in the context of water and environmental management, including Blue Green Infrastructure (BGI) solutions, and showcase the benefits that lead to better decisions and sustainable urban development.

KEYWORDS: Urban Natural Capital, Sustainability, Urban Developments, Ecosystem Services

1. INTRODUCTION

Under the increasing pressures of climate change and population growth at the global level, it is crucial to address water security and sustainable urban development. Urban Infrastructure Systems (UIS) involve multiple sectors, including water, land, transport and housing. These infrastructures interact with each other and put constant pressures on their surrounding environment and human wellbeing in the form of flood risk, water shortages, air and water pollution, and Urban Heat Island (UHI) effect [1].

Nowadays, more than 50% of the world's population live in urban areas, and this is predicted to reach 66% by 2050 [2]. This level of growth will be particularly critical in London, where population is projected to increase by 70,000 people every year, reaching 10.8 million citizens in 2041 [3].

The capital is one of the most at-risk UK's urban areas to future climate change, being particularly vulnerable to water scarcity, heat waves, flooding and air quality problems [3, 4, 5]. According to the Greater London Authority (GLA) and their new London Plan, an average of 66,000 new homes per year should be built in the city until 2041 [3].

However, the relationship between urbanisation and environmental management is very complex and has not been sufficiently addressed yet. Urbanisation is a difficult spatiotemporal process that influences areas beyond the urban cores, being a difficult process to control, quantify and plan [6]. Increased urbanisation can be detrimental to natural

environment's connectivity and condition, which are key components of resilience to climate change [7, 1].

Ecosystem Services (ES) and Natural Capital (NC) assessment is growing in popularity as an innovative and powerful method to evaluate the level of sustainability for new urban developments. The results from this type of assessment are generally presented as a series of numerical scores (positive or negative), but little evidence is available about their combination with spatial representation of the urban development. Hence, a valuable method that combines Urban Natural Capital (UNC) values with graphical Geographical Information Systems (GIS) maps is performed in this study, making the process for sustainable urban design more effective and reliable, which may ultimately lead to better planning decisions.

1.2 Sustainable urban infrastructure solutions

Nature Based Solutions (NBS) are broadly defined as solutions inspired and supported by nature that simultaneously provide environmental, social and economic benefits to citizens [8]. They also have a series of co-benefits, such as improving health and quality of life, and the attractiveness of the place [8]. The NBS concept includes Blue Green Infrastructure (BGI) and other sustainable concepts such as Sustainable Drainage Systems (SuDS), Ecological Engineering and Water Sensitive Urban Design (WSUD). Some examples of BGI include: street trees; parks and open spaces; permeable paving; engineered

stormwater controls (bioswales, rain gardens or retention ponds); green roofs; green facades; waterways and wetlands; or, urban gardens [9].

In parallel to this, Ecosystem Services (ES) are understood as all the benefits that citizens and human beings obtain from natural ecosystems [10]. In economic terms, natural ecosystems are also understood as a Natural Capital (NC), accounting for all the assets that the natural environment provides in the context of ES. These include soil, air, water and all living organisms [11].

BGI benefits can outweigh those of traditional hard infrastructure based on reinforced concrete, also known as grey infrastructure [12]. In order to achieve a good level of urban sustainability and a large number of ES, it would be necessary to evaluate the optimal combination of BG vs grey interventions to be implemented in our cities.

1.3 Complexity of urban interactions

Despite the fact that numerous investigations recently tried to integrate urban planning design with water and housing systems, many challenges still remain. These challenges are very clear if we analyse London's urban environment, which is currently in danger of critical deterioration due to climate change and a wide variety of constant pressures [3].

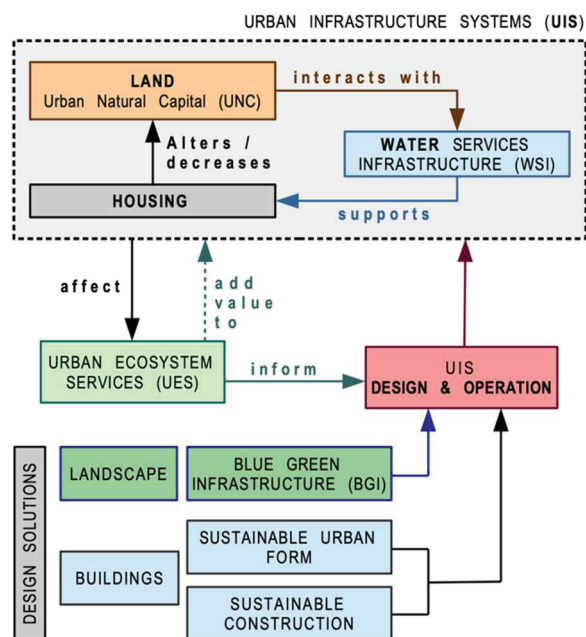


Figure 1: Systems thinking diagram that interlinks Urban Infrastructure Systems (UIS) with Urban Ecosystem Services (UES) and the relationship of sustainable design solutions to the design and operation of UIS.

More housing growth requires more water to be abstracted, which is finally converted into wastewater once it is treated, stored and consumed. This wastewater discharges from sewage treatment plants are released back to the natural environment and

affect the final amount of ES provided to citizens. In order to maintain a sustainable process and to manage urban water efficiently, it will be necessary to re-think the urban design concept from a systems perspective (see Fig. 1).

Although Urban Infrastructure Systems (UIS) might include transport or energy production, in this study they are comprised of the three main elements seen in Figure 1: 1) Housing, 2) Land, and 3) Water Services Infrastructure (WSI). These three urban elements are always interconnected and depend on, and affect each other. Land includes all the Blue and Green assets that are internal part of the system, that is the Urban Natural Capital (UNC); while housing includes all the building infrastructure and any impervious surface necessary to support it, such as parking, roads or paths. As conceptualised in Figure 1, UIS directly affect the Urban Ecosystem Services (UES), which at the same time also add value to the urban infrastructure (UIS). Therefore, the sustainable design solutions proposed for landscape and building areas will directly affect the performance and operation of the UIS.

1.4 CAMELLIA research project

This research is a key element of the Community Water Management for a Liveable London (CAMELLIA) research programme, which is focused on sustainable urban water management in London. CAMELLIA has four London-based case studies (Mogden, Enfield, Southwark and Thamesmead), each reflecting different key issues of urban water management (see Fig. 2). Among them, Thamesmead will be this work's main case study, where a major redevelopment plan is expected to emerge during the next 20 years [3].

CAMELLIA is supported by communities, policymakers and industry; it aims to transform collaborative water management to support the provision of lower cost and better performing water infrastructure in the context of significant housing development, whilst improving people's local environments and their quality of life.

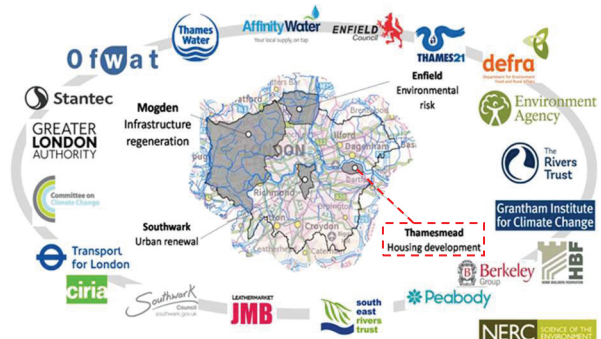


Figure 2: Case study areas inside CAMELLIA research project (London map with Thamesmead highlighted in red) and partners involved (logos around the map). (Source: CAMELLIA)

2. METHODOLOGY

2.1 Thamesmead as main case study area

Thamesmead is a 750-ha neighbourhood located in Shout-East London where around 150 ha are considered blue or green space. Following a report conducted by Vivid Economics, the total NC potential value provided by Thamesmead's blue and green-space is estimated to be at least £306 million or £257 per person per year [3]. Despite this abundant natural value, this blue and greenspace is not appropriately used by their citizens and large areas are even inaccessible.

As mentioned in Section 1.4, this district is undergoing a large urban regeneration programme and its major development will be Thamesmead Waterfront Development Plan (TMWDP). This scheme will include more than 11,500 new homes and a contemporary renovated masterplan carried out by the Peabody Housing Association. TMWDP, which comprises a total area of 100 ha and embraces almost 3 km of underdeveloped river waterfront, will be our main case study area to test our different urban design proposals.

2.2 Natural Capital impact assessment

Engineers and scientists need to determine the extent to which certain ES are essential to the welfare of current and future generations and how costly it may be to protect and conserve them. Accounting for the Urban Natural is a crucial indicator of our cities' level of sustainability and finding the most reliable type of assessment is a challenging task that needs to be analysed.

As already explained in previous sections, NC accounting will be this study's starting point in order to understand the environmental impact created by new housing developments. At this stage, the studies are focused only on the design aspect, leaving the operation of the system mentioned in Section 1.3 for future stages of the work (see Fig. 1).

There are different tools that evaluate Natural Capital (NC), two of the most commonly used being NCPT (Natural Capital Planning Tool; Hölzinger et al., 2019) and InVEST (Integrated Valuation of Ecosystem Services and Trade-offs; Sharp et al., 2018). Between them, NCPT is chosen because it is more appropriately designed for urban developments and fits within the general design process explained in Figure 1.

Despite its appropriate functionality, the NCPT only provides numerical scores for Ecosystem Services (ES) and lacks a graphical representation of land uses. Therefore, an important innovation presented in this work is the ability to link the pre- and post-development land-use areas of the site with a GIS software. For this, QGIS (Cavallini et al., 2019) is used

because it is a free-open source platform and can be easily shared with a range of professionals.

2.3 Urban design scenarios

Three different urban design scenarios of land uses are suggested in order to compare different levels of environmental impact. But, before presenting these three urban design scenarios, it is necessary to understand the pre-development land-use map, which will act as the initial baseline for all of them. This is represented based on research data previously collected and supplemented by OpenStreetMap and Google satellite maps.

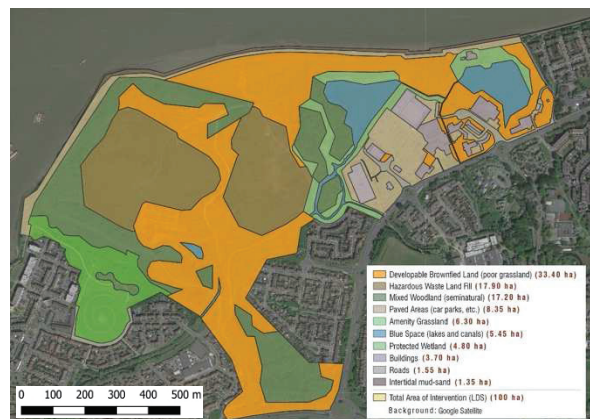


Figure 4: Pre-development land-use map for Thamesmead Waterfront Development Plan.

As seen in Fig. 4, most of the land at the pre-development state is currently developable brownfield land and hazardous waste land fill. The latter cannot be used for building, but it might be transformed into a natural reserve. On the other hand, the blue space (lakes and canals), the amenity grassland and the protected wetland must be preserved [7]. Apart from an existing and functioning water-pump station, all the existing buildings will be removed and redesigned in all three design options.



Figure 5: Post-development Land-Use map for Thamesmead Waterfront Development Plan. Scenario 1 – "Adverse".

Based on initial constraints previously explained such as the hazardous waste land fill areas or the protected wetlands, and in order to find a realistic but “adverse scenario”, the first urban layout is proposed (see Fig. 5). Scenario 1 represents a traditional way of building [14] and does not consider any sustainable urban form, such as appropriate orientation or green roofs. In this case, some land uses are transformed, such as developable brownfield or hazardous waste land; new ones emerge, such as built-up areas (high, medium and low density), gardens, mixed parkland or pond. These built-up areas with different types of densities are built with traditional ways of construction, being considered non-sustainable buildings.

As aforementioned, in Scenario 1 the blue space, protected wetland and intertidal mud-sand are preserved and have not been changed. Other land-uses, such as mixed woodland and amenity grassland, have been decreased in some parts but augmented elsewhere, especially where there is currently hazardous waste land fill.

The next scenario, called “intermediate”, has the same number of built-up hectares as Scenario 1, but instead of being high-, medium-, or low-density built-up areas, those are replaced by “buildings covered with green roofs” or “buildings with green walls” land uses. These two land uses are the only sustainable building options given by the NCPT. This is therefore seen as an important limitation of the tool, as BGI option cannot be implemented in the design properly. In the same way, the previous “roads” have been replaced by “local green roads”; while “paved areas (car parks, etc.)” are transformed into “gardens” (including the Thames path). NCPT does not give options for BGI land uses, such as “permeable paving” or “swales”, which constitutes another important limitation of the tool.

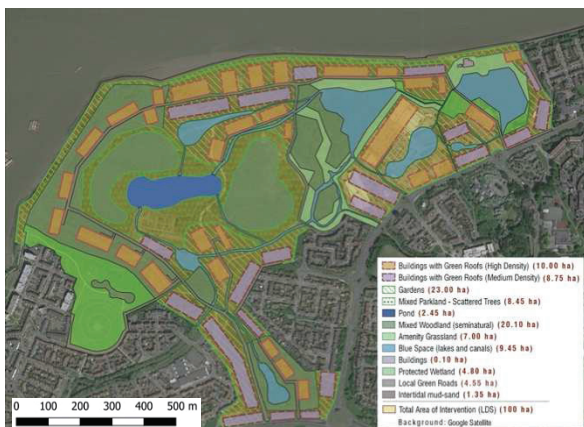


Figure 6: Post-development Land-Use map for Thamesmead Waterfront Development Plan. Scenario 3 – “Favourable”.

The third option, called “favourable”, is based on a completely new urban layout design (see Figure 6). In this case, instead of keeping the same areas and

changing only the “building typologies” (which would not be possible due to the already explained NCPT constraints); more green, blue and recreation spaces are arranged around the built-up areas to increase the ES received. This scenario is based on compact densities and BGI around them, which is proven to be a more sustainable option for future cities than low-density layouts [14].

Additionally, a series of further planning decisions is taken in Scenario 3: a) most existing woodland is preserved; b) more woodland and pond areas are added inside the parkland; c) gardens (which represent BGI) are placed around most of the building blocks; and, d) blue space is considerably increased with new lakes and a new canal network.

2.4 Densities for built-up areas

In terms of number of houses, the building developer, Peabody Housing Association, has a clear target of 11,500 new homes for this large urban development of TMWDP. It is demonstrated inside the literature that the concept of density is quite critical and is based on specific thresholds. Therefore, the values for high-, medium- or low-density can be defined differently depending on the author and always will depend on the particular context of the development and its surroundings [14].

ESTIMATED DENSITIES FOR EVERY URBAN DESIGN SCENARIO			
Scenario 1 - Adverse			
	N. of ha	Dwellings per ha	N. of dwellings
High-Density	31.65	280	8,862
Medium-Density	17.15	140	2,401
Low-Density	2.90	50	145
TOTAL N. DWELLINGS			11,408 / 11,500
Scenario 2 - Intermediate			
	N. of ha	Dwellings per ha	N. of dwellings
Buildings w. green roofs	31.65	280	8,862
Buildings w. green walls	20.05	130	2,607
TOTAL N. DWELLINGS			11,469 / 11,500
Scenario 3 - Favourable			
	N. of ha	Dwellings per ha	N. of dwellings
Buildings w. green roofs (HD)	10	800	8,000
Buildings w. green roofs (MD)	8.75	400	3,500
TOTAL N. DWELLINGS			11,500 / 11,500

Table 1. Estimated densities for the built-up areas for every urban design scenario studied and compared to Peabody's target of 11,500 new homes.

Hence, the number of dwellings per hectare inside these built-up areas has been estimated in order to achieve Peabody's target for each urban design scenario previously presented (Table 1). These estimated densities provide a general idea of the housing typologies that might be included in every urban design scenario.

3. RESULTS

The NCPT analyses ten Urban Ecosystem Services (UES), providing NC impact scores for each of them. These ten UES evaluated by the NCPT are: 1) harvested products, 2) biodiversity, 3) aesthetic values, 4) recreation, 5) water quality regulation, 6) flood risk

regulation, 7) air quality regulation, 8) local climate regulation, 9) global climate regulation and, 10) soil contamination.

Additionally, NCPT also gives the number of ES achieving Environmental Net Gain (ENG), which represents the environmental impacts of habitat change. It is important to highlight that, although these scores might be highly valuable indicators, they should always be deployed alongside with some expert knowledge in the field.

As explained in Section 2.3, the pre-development land-use map will be the initial baseline for all three scenarios. Once all the land-use data are processed using QGIS and the number of hectares for every land use are quantified in every scenario, these are introduced into the NCPT. This is combined with other types of data such as heat exposure, proportion of built-up area, flood risk zone, drinking water safeguard zone, air quality management area, accessibility, size of greenspace site, and soil drainage. At the end, the tool provides NC Impact Scores for every UES analysed and NC Net-gains for each designed urban scenario. At this point, it is remarkable to see how small changes in urban layout and land uses are able to provide significant variations in the NC impact assessment (see results in Table 2).

Natural Capital Impact of Thamesmead Waterfront Development						
Ecosystem Services (ES)	Scenario 1 "Adverse"		Scenario 2 "Intermediate"		Scenario 3 "Favourable"	
	NC Impact Score	NC Net-Gains	NC Impact Score	NC Net-Gains	NC Impact Score	NC Net-Gains
1. Harvested Products	-121	NO	-107	NO	-88	NO
2. Biodiversity	-54	NO	-11	NO	-12	NO
3. Aesthetic Values	299	NO	(+149)	YES	(+179)	YES
4. Recreation	(+1108)	YES	(+1154)	YES	(+1228)	YES
5. Water Quality Regulation	-156	NO	-25	NO	(+172)	YES
6. Flood Risk Regulation	-30	NO	-1	NO	(+119)	YES
7. Air Quality Regulation	-44	NO	(+128)	YES	(+146)	YES
8. Local Climate Regulation	-76	NO	(+1180)	YES	(+1176)	YES
9. Global Climate Regulation	(+31)	YES	(+361)	YES	(+365)	YES
10. Soil Contamination	0	NO	0	NO	0	NO
Natural Capital Net-Gains (number of services achieving net-gain)		2 / 10	5 / 10		7 / 10	

Table 2: NC Impact Scores and NC Net-gains for every ES analysed for the 3 different scenarios. (Source: NCPT)

As seen in Table 2, only two ES, Recreation and Global Climate Regulation, achieve NC net-gain for Scenario 1. The positive score achieved in Recreation in this scenario is easily explained because the Waterfront Development Plan site is currently inaccessible greenspace and the new urban design will directly provide new leisure and outdoor activity space to citizens. Regarding Scenario 2, Table 2 reveals that five ES achieve the NC net-gain. This indicates a significant improvement compared to Scenario 1, but there are still some ES in negative values.

Finally, in Scenario 3 most ES are positive and achieve NC net-gains. Harvested Products and Biodiversity are now the only ES with negative scores, although this is almost certainly due to the limitations discussed of the NCPT. Hence, it is seen that "gardens" (in this case understood as BGI) have a negative impact on biodiversity (compared to "poor grassland"). Recreation again has the highest positive score. This

can be explained firstly because the space was before inaccessible and, secondly, because there is an increase in green and blue space in this third urban design. As mentioned in Section 2.2, these scores are based only on the design aspect, although future studies on system operation will be conducted too.

3.1 Need for further methodological improvements

The analysis presented in previous sections, based on the TMWDP area and using the NCPT and QGIS tools, showed that the NCPT does not adequately account for important land uses to evaluate the benefits of BGI. For instance, the land use named "gardens" was introduced as the only form of BGI, but this generated negative scores of Biodiversity.

Therefore, it is suggested that new BGI typologies should be introduced in the NCPT land uses, for instance: "Permeable paving", "Detention basins", "Retention ponds", "Buildings with rainwater harvesting" or "Swales". It would also be useful to differentiate between "intensive green roofs" (deeper substrate and shrubby vegetation or even trees) and, "extensive green roofs" (thin layer of soil medium and plants like succulents, grasses or other low maintenance, low growing vegetation), as they might affect the final environmental performance of the buildings [14]. Additionally, "Buildings – area covered with green roof" and "Buildings - green walls" land areas should differentiate three different levels of density (high, medium and low). All of this will definitely deliver new and more accurate scores.

Finally, the tool is also lacking a systems thinking approach because it calculates each ES independently without considering interconnections between the three UIS elements (land, housing and water) presented in Figure 1. For all these reasons and the need for monetary valuation, a prototype for an Integrated Modelling Tool is introduced next.

3.2 New Integrated Modelling Tool

BEST (Benefits Estimation Tool; CIRIA, 2019) is a tool that provides an estimation of the profits that BGI can generate from an economic perspective; however, it also presents some limitations, such as not including sustainable building valuation side. A new Integrated Modelling Tool (IMT) which solves all the limitations presented in the NCPT and BEST, and also links their numerical results with a spatial representation of the development, is proposed. It will improve the vision and accuracy for suitable sustainable urban design solutions and enable more collaboration between urban design stakeholders. See the software architecture diagram of this Integrated Modelling Tool (IMT) and its functionality in Figure 7.

Both the NCPT and BEST are based on spreadsheet interface and the IMT will act as a software wrapper with Python code, enabling the user to design a new urban development layout and relate its spatial

representation with ES assessment and monetary prediction. The outputs of the tool will ultimately be compared against approved certification criteria, such as BREEAM Communities or LEED-ND.

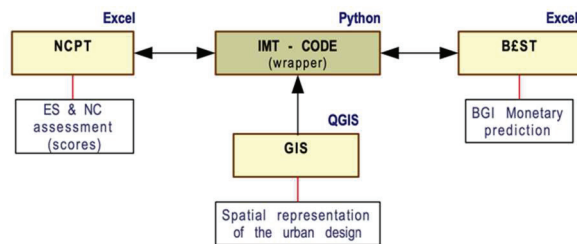


Figure 7: Integrated Modelling Tool (IMT) diagram to understand the software architecture of the prototype.

4. DISCUSSION

London needs to cope with its increasing housing demand to fulfil the expanding economic and social interests, but at the same time it must preserve its natural environment in order to be resilient and adapted to future climate change impacts. Its built environment should provide healthy and secure living-conditions to future generations and considerably reduce the risk of natural catastrophes, such as flooding and droughts. Sustainable urban development is considered crucial to tackle these stresses and its different types of sustainability assessment are still not sufficiently understood.

UIS (Urban Infrastructure Systems) are an interconnected entity and one of the best indicators of their functionality and impact into the environment is the evaluation of UES (Urban Ecosystem Services). This work starts from a systems approach concept in order to define a novel assessment framework for new urban developments, which has been initially outlined in Figure 1. The future steps should improve and redefine this framework and provide a quantitative evidence for optimal urban design solutions. This will require studying BGI and its multiple benefits, as well as the effects of urban form and vegetation within the context of Urban Ecosystem Services (UES) and Urban Natural Capital (UNC).

4. CONCLUSION

Urban Natural Capital (UNC) assessment is crucial to analyse the impacts of new urban developments on the environment. It will help housing developers, urban planners and policy-makers to make better decisions, especially at the early stages of the design. However, initial studies that combine NCPT numerical results with QGIS maps have shown that these tools are still lacking some important functionalities and there remains a need for a revised method. Hence, the next steps in this research work will focused on developing a new and integrated modelling tool for Urban Natural Capital (UNC) and Urban Ecosystem Services (UES) assessment in order to provide more

accurate and valuable results, all mapped from an overarching systems thinking perspective.

ACKNOWLEDGEMENTS

This work would not have been possible without funding from the Engineering and Physical Sciences Research Council (EPSRC) Centre for Doctoral Training (CDT) in Sustainable Civil Engineering. The research reported in this paper was taken as part of the CAMELLIA project (Community Water Management for a Liveable London), funded by the Natural Environment Research Council (NERC) under grant NE/S003495/1.

REFERENCES

1. Mijic, A. and Brown, K. (2019). Integrating Green and Blue Spaces Into Our Cities: Making It Happen. Grantham Institute Briefing Paper, No 30. Imperial College London.
2. United Nations (2014). World urbanization prospects: The 2014 revision, highlights. Population division, United Nations.
3. Greater London Authority (GLA), (2019). The Draft London Plan. Consolidated changes version – Clean July 2019. Report.
4. Clark, J., et al. (Policy Connect) (2018). Bricks & Water: A Plan of Action for Building Homes and Managing Water in England. Westminster Sustainable Business Forum.
5. Ford, A., et al. (2019). A multi-scale urban integrated assessment framework for climate change studies: A flooding application. *Computers, Environment and Urban Systems* 75.
6. Inostroza, L. and F. De la Barrera (2019). Ecosystem Services and Urbanisation. A Spatially Explicit Assessment in Upper Silesia, Central Europe. IOP Conference Series: Mater. Sci. Eng. 471 092028.
7. Lawton, J., et al. (2010). Making Space for Nature: A review of England's Wildlife Sites and Ecological Network. Report to Defra, UK.
8. Raymond, C. M., et al. (2017). A framework for assessing and implementing the co-benefits of nature-based solutions in urban areas. *Environmental Science & Policy* 77: 15–24.
9. Keeler, B. L., et al. (2019). Social-ecological and technological factors moderate the value of urban nature. Review Article. *Nature Sustainability* 2(1): 29–38.
10. Gómez-Baggethun, E. and D. N. Barton (2013). Classifying and valuing ecosystem services for urban planning. *Ecological Economics* 86: 235–245.
11. Mace, G. M., et al. (2015). Towards a risk register for natural capital. Review article. *Journal of Applied Ecology* 2015, 52, 641–653.
12. Maksimovic, C.; Bozovic, R.; Mijic, A.; Suter, I; Van Reeuwijk, M. (2017). Blue Green Solutions. A Systems Approach to Sustainable, Resilient and Cost-Efficient Urban Development. Imperial College London.
13. Ahmadian, E., et al. (2019). Sustainable cities: The relationships between urban built forms and density indicators. *Cities*: 95.
14. Oke, T., Mills, G., Christen, A., & Voogt, J. (2017). Urban Climates. Cambridge, Cambridge University Pres. ISBN: 9781107429536

Towards Developing Sustainable Maintenance Guidelines for Heritage Architecture of Northern Nigeria

OLUTOLA FUNMILAYO ADEKEYE,¹ AMINU ADAMU BENA, LUCELIA RODRIGUES, LORNA KIAMBA.

¹University of Nottingham, Nottingham, United Kingdom

² University of Nottingham, Nottingham, United Kingdom

ABSTRACT: Heritage buildings situated in various rural and urban settlements globally are continuously threatened by human and natural factors, which contribute to their gradual degradation and extinction. Globalization, population growth, climate, and the quest for land in traditional urban cities are some challenges experienced by these buildings in Nigeria. Emirs' Palaces in Northern Nigeria are important heritage building structures; they are houses for traditional monarchs with unique traditional designs, architectural characters, decorations/ornamentations, and planning that portray the cultural identity of northern Nigeria. In this paper, the authors outlined sustainable strategies for preserving these heritage buildings by timely intervention measures and maintenance initiatives. A survey was conducted on a case study of 'Gwandu' Emir's Palace located in North-Western Nigeria using a rating scale of variables to ascertain the rate of dilapidation of cultural identity features, the reflection of cultural character, the indigenous ornamentation situation, the use of traditional materials and the spatial planning. The study concludes that a strategic maintenance plan towards restoration initiative on the building fabric could guarantee the sustainable keeping of these palaces.

KEYWORDS: Heritage buildings, Palace Architecture, earthen architecture, traditional cities, vernacular buildings

1. INTRODUCTION

Traditional landscape of historic cities are strong and powerful cultural manifestations that show how society has existed in the past and developed into the present [12]. Heritage buildings are valuable assets that have legacy potentials of the past. They are deeply rooted in cultural artefacts, natural resources, and artistic motifs, architectural, historical, economic, and socio-cultural values [17]. The process of conservation and restoration of traditional heritage buildings of every community is of great importance and a serious task that often comes with challenges that need to be carefully studied and analysed [9].

A typical example of this is the Emir's palace building type found in the northern states of Nigeria (Fig. 2). The palace is a traditional house for a monarch, it is an official building designed and constructed with grandeur and traditional decorations. It is a prestigious monument with historical features symbolic to the culture and the history of Hausa people (Fig. 3). It is customarily located at the centre of traditional cities, in terms of orientation it is usually constructed in rich decorative motifs, abstract pieces of arts and symbols in various designs on the building facade (Fig. 2,3, 4 & 5).

The palace is also known as a traditional court where judgment is passed on locals from the authority (the Emir). Furthermore, it serves as an information dissemination center from the Emir to citizens.

In this study, the authors aimed to identify sustainable strategies towards heritage building technical maintenance for future implementation.

The Emir's palace of Gwandu covers an area of 45,000m², located in Birnin Kebbi the administrative headquarters and capital of Kebbi State, Nigeria. Birnin Kebbi town is approximately 150km southwest of Sokoto state (Fig. 1). The Emir of Gwandu is the chairman council of chiefs of Kebbi state. The palace houses 80-100 inhabitants, including the Emir's immediate family members, relatives, and staff (Fig. 2).

The research on the Emir's palace Gwandu in Birnin-kebbi, Kebbi State, was selected because it is an important heritage building associated with high cultural values, good historical background, and an eminent ranking as the second prominent in the hierarchy of traditional rulership of emirate councils in northern Nigeria, after the Sultanate palace in Sokoto.



Figure 1: Map of Nigeria Showing Birnin kebbi [11]

1.1 Historical evolution of Hausa land

Nigeria is a country in West Africa; it is at the northern hemisphere of the equator and east of the prime meridian. Nigeria is located in the tropics, the Hausa city-states comprise much of northern Nigeria, it is a territory north of Nigeria comprising Kano, Kastina provinces, and northwest of Sokoto. Hausa land was formed around the 11th-16th century under the Songhai Empire called the Hausa kingdom [5,12,15].



Figure 2: Emir's Palace Gwandu, Kebbi, Nig; façade without motifs after maintenance.



Figure 3: Emir's Palace Zazzau, Kaduna, Nig; façade decorated with motifs [5]

1.2 Evolution of Emirs palaces in Nigeria

According to Moughtin [12], historical background and evolution of palaces in northern Nigeria can be traced in two timelines: The Myth (*bayajidda*) around the 13th century and the expedition of religious reformer Uthman Bin Fodio in the 16th century. Many of these palaces emerged before the advent of colonial masters in Nigeria; they remained in their authentic and rich form in structure, planning, and composition. Furthermore, there are several other examples of traditional heritage buildings of Hausa society, including the Museum (*gidan tarihi*), Mosque, city gates, city walls, tombs/burial houses, and other eminent personality houses but palace architecture is more elaborate in providing futures that reveal historic resources such as age, rarity,

outstanding example associated with historic events, unique cultural building example and also connected to a personality. All these attributes of history and culture value are of great importance.

1.3 Emir's Palace structure and construction

In Hausa land, palaces are located at the centre of traditional cities and towns, they are surrounded by important building infrastructure of the traditional settlement and utility buildings that support the process of delivering community administration by the Emir as a traditional ruler. Many of the palace planning layout on-site are within 3 categories:

- Inner palace house (core),
- Immediate planning layout, and
- Town planning; within the fortified wall area.

The palace according to Dmochowski [5], is the most significant structure within the Hausa city layout that must be protected, followed by the forecourt (*Dandali*) which is an expanse of land between the palace (inner layout) and the immediate layout that is used for ceremonial sitting or sometimes a flat form for viewing *Durbar* (traditional horse riding processions) and other cultural displays.

Mud was used to construct elements of walls (*zanko*) pinnacles, roof dome (*soro*) parapet walls and spouts (*indararo*) (Figure 4); these are traceable in different Emir's palaces located in Zaria, Kano, Daura, and Katsina.

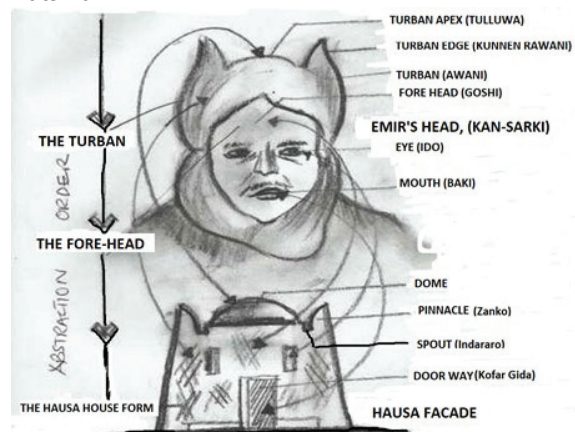


Figure 4: Symbolic abstract of the Emir's palace façade [2]

2. CONSERVATION AND RESTORATION GUIDELINES FOR PALACE BUILDINGS

According to Osasona [14], conservation is generally understood to mean "maintaining" while a more formal definition gives the meaning as "preservation", "safeguarding and protection". The salient issue inherent in this explanation is to maintain a building element without changing its appearance and outlook. And "restoration", is defined as "replacement; recovery; reconstruction; re-establishment", implying putting back of something to a former state or giving back a lost identity. The routine maintenance process is the

technical way to achieving the conservation of palace buildings. However, technical maintenance is challenging but it is also an important remedial treatment to be considered for traditional buildings.

Dennis [6] also defines the terms preservation, conservation, and restoration. He believes preservation means maintaining the fabric of a place in its existing state and retarding deterioration.

Where the scientific approach involves the instrumentation process to analyze, test, and produce a guideline result of the material and the component of the constituent structural parts, the technical approach starts with a process that covers the history and typology of buildings. The structural analysis of the building, the construction method, and application, material specification, the orthodox practice of the construction in terms of removal, restoring replacement, and periodic maintenance.

Deployment of these techniques on maintenance for the Emir's palace will involve the following processes:

- Documentation is regarded as an initial process in the conservation and restoration process according to [13] while suggesting that it must be guided in a manner not to alter the aesthetic, historical and physical integrity of the cultural property. However, all methods and materials for use during the process should be fully documented.
- Identification of the palace buildings (this may cover the condition of building before the intervention, which must be recorded),
- Description with sketches from observation stating climatic conditions, elements and other data relative to information,
- Examination of the materials, composition and construct falsified or removed, and suggestion of possible ways to conserve, treat or restore missing elements this intervention must be minimal, as this is necessary to avoid superficial furnishing of the building [13].

According to Fielden [8], the method of maintaining heritage buildings for conservation and restoration may also involve works for evaluation and treatment processes.

2.1 Maintenance Guidelines

Technical work guidelines for carrying out the conservation of historic buildings are provided by ICOMOS [16] policy document that involves the following:

- Analyzing the effects of climatic factors, on the building,
- Checking ground-level situation, foundation weakness, and drainages,

- Checking walls, types of openings, roofs, and other building elements,
- Suggesting method of restoration to be carried out E.g. removal of some elements and replacement with new durable materials,
- Treating building elements to eradicate chemical and biological attacks. The processes, procedures, methods, and techniques of restoration and conservation are ideal in carrying out the actual technical execution of restoration and conservation work on historic traditional buildings.
- Removing decayed building fragments and some elemental parts.
- Repairing and reconstructing the defective parts or completely making provision for restoring the lost elements.
- Periodic maintenance to be carried out as routine between 3-5 years.

According to ICOMOS, [16], these guidelines if applied in heritage buildings, will significantly promote sustainability, integration, and reflection of cultural identity.

2.2 Concept of Identity in Heritage Buildings

The expression of cultural identity in a building is significant in retaining its value in both cultural and traditional essence.

Mahgoub [10] describes symbolism as the reflection and transmission of cultural character to a building. Symbolizing built structure and arts/ornamentation are common features that classify Hausa architecture and Emir's palace unique in the purest form, (see Fig. 4 & 5). Therefore, these buildings need to be safeguarded because any effort aimed at retaining the motifs/ornamentation and decorations values on building elements (gates, walls, and façade), will be in an effort geared towards conservation and maintenance initiative.

2.3 Palace Ornamentation

Builders of Hausa traditional palaces in those days were saddled with the duties of carrying out routine maintenance on building fabrics largely on ornamentation. The builders are expert craftsmen skilled in their way. They are engaged in the construction of palaces across the region [4, 16].

Ornamentation, arts, and decoration on palaces (Fig 5) are significant elements that promote building identity, social status, cultural and religious essence to a traditionally heritage-built structure that are unique to individual Emir's palace [2,5]. One of the key questions asked in the questionnaire was the individual perception of the significance of ornamentations and motifs on Emir's palace buildings to promote and depict unique cultural identity, social status, and religious essence (Table 4).



Figure 5. Application of modern materials to produce motifs decorations on a mud wall [7]

3. METHODOLOGY

The authors have studied the Gwandu Emir's palace in Birnin Kebbi as a case study in Nigeria, which requires conservation and restoration maintenance.

A survey was developed and deployed to ascertain the rate of dilapidation and other characteristics. Interviews were conducted with the managers of the palace, its occupants, and building industry professionals. History of how palaces evolved overtime in a cultural setting, current challenges they face, and the theory of maintenance guidelines provided a source of primary data for in-depth analysis of the case study.

3.1 Case Study Building

This Emir's palace depicts the traditional planning pattern and orientation of Hausa city-states in both major and minor planning, it also maintains its traditional spatial location of cultural spaces and form character built substantially of local materials [3].

The case study was selected based on purpose and essential maintenance needs. The palace's physical character has been altered due to poor maintenance carried out, this brought about changes to its character and cultural identity features. The case study was analyzed in (Tables 1-4), based on two aspects:

- General history and documentation of Emir's palaces in the region.
- An assessment of the application of elements of cultural identity in the case study building.

3.2 Procedure

Out of 39 notable palaces with beautiful traditional outlooks in northern Nigeria, including the *Sultanate* palace in Sokoto, the palace of Gwandu in Birnin Kebbi town, Kebbi state was selected for evaluation. A questionnaire was prepared using cultural identity variables and participants were asked to vote for their level of acceptance and reflection of cultural character on palace buildings see (Table 2). A total

number of 180 questionnaires were distributed among palace administrators, workers, and staff of the state ministry of works (who are involved in routine maintenance of the facility) through government interventions. Form elements such as the palace gate, walls, and palace façade were compared with the variables. (Fig. 6) indicates a total loss of ornamentation from the graph.

Questions were asked in the form of interviews and questionnaires. Key questions asked where:

- Does the palace still maintain its traditional location from history to date?
- Does the palace still depict the Hausa architectural character?
- Does the palace have historic associations with local people?
- Can you affirm that traditional building materials are common materials used in palace construction?
- Are there indigenous ornamentation/ motifs on strategic walls on the present palace façade?
- Do you agree that the palace still maintains its cultural outlook?
- How significant are ornamentations/motifs on palace buildings to promote and depict unique Hausa cultural identity, social status, and religious values?

Table 1: General history and documentation of the case study building.

Case study	Description
Aspects	
General documentation	Documentation guidelines would reveal the history, culture, and challenges faced by the building that has led to the absence of ornamentation on it and also the identification of factors deterring cultural character and the process of attracting cultural identity to the building.
Assessment based on the application of cultural identity guided under the variables	<ul style="list-style-type: none"> • Spatial planning • Reflection of cultural character • Use of traditional materials • Presence of indigenous ornamentation. <p>The variables were rated in the questionnaire (Table 2).</p>

Table 2: Spatial planning (SP), Reflection of cultural character (RCC), Presence of indigenous ornamentation (IO), Use of traditional materials (TM), and Spatial Planning (SP)

VARIABLES	LEVEL OF APPLICATION	COMMENT
	Low Med High	
a) Spatial planning	✓	Illustration of an un-altered traditional city layout planning of Hausa Palace
b) Reflection	✓	Average

of cultural character	application of cultural character
c) Use of traditional materials ✓	Minimal use of local materials
d) Presence of indigenous ornamentation	Absence of art and decoration

Table 3: Scale ratio (SR), Reflection of cultural character (RCC), Presence of indigenous ornamentation (IO), Use of traditional materials (TM), and Spatial Planning (SP)

Scale (%)	100 = 5	75 = 4	50 = 3	25 = 2	0 = 1
Variables	Gate	Walls	Façade	SR (%)	
RCC	4	2	3	50	
IO	1	1	1	0	
TM	1	3	2	25	
SP	5	3	4	75	

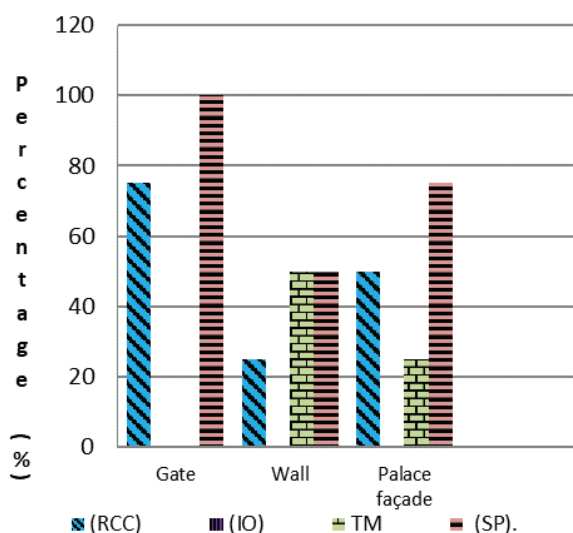


Figure 6: Graph showing the percentage score against the building elements

Table 4: Perception of the significance of ornamentations/motifs on palace buildings

Perception	No of respondents	Percentage score (%)
Significant	84	57
Less significant	36	24
Not significant	9	6
Indifferent	19	13
	148	100

About 82% of questionnaires were returned by the respondents of a population of 180 people. A guide was developed during the process of administering questionnaires to respondents by providing explanations for the questions asked in a language understood by the respondents.

4. RESULTS & DISCUSSIONS

Analysis of the Emir's palace building towards ascertaining the level of loss in cultural essence and traditional features over time is indicated on Table 3, which reveals that 50% reflection of cultural character was voted and recorded with the highest score on the gate and lowest on the walls, this is an indication that hausa building form has been symbolized on the palace main gate. The presence of indigenous ornamentation is non-existent on the palace, a score factor of 1, illustrated that the entire palace building has been defaced from its original state over time due to series of maintenance carried out without considering a technical and sustainable method of restoration.

Traditional building materials are sustainable materials. However, the use of traditional materials recorded a 25% score in the construction of the palace which indicates that a low amount of traditional materials were used in the construction. Palace buildings in traditional settlements of hausa land are located at the centre of the town and are surrounded by important adjoining structures with cultural values such as; Market square, mosque, prisons, and the foreground in between for cultural display during important ceremonies. This foreground always has its strongest hold on the gate in terms of planning because the gate is traditionally planned to serve as a podium for viewing events. "Dandali" as it is called in hausa language is significant in the palace planning because all other structures are located at the peripheral to it in the entire palace spatial composition; it is a combination of structures and the main gate surrounding a large stretch of land. Gwandu Emir's palace showcases efficient historic spatial planning and it was also voted during the survey as the highest variable of 75% for this study.

The format used in discussing the results (Table 4) was adopted from Idris [9] and modified by the authors shows that about 57% indicated that ornamentations and motifs are significant elements that portray their cultural identities and tradition as hausa people; 24% indicated that although it is a way of showcasing the hausa culture, it was also less significant as it requires maintenance and skilled men to sustain the motif. Furthermore, 6% of the respondents opined that the existing symbolic form of the palace building façade and the position/ spatial planning of the palace in the city makes the palace distinct already. However, 13% were indifferent.

From the analysis above, it shows that the presence of Motifs/ornamentations on Emir's palace buildings is an integral part of the architectural cultural character of the hausa tradition with an importance that cannot be over-emphasized. Thus, the absence and loss of these motifs/ornamentation on the Gwandu palace façade due to maintenance

over time depict that a strategic maintenance plan towards restoration initiative on the building fabric is needed. This can guarantee the sustainable development of other important building elements of the palace to salvage the continuous loss of unique cultural characters of the building to preserve the cultural identity of the area.

5. CONCLUSION

It is evident there are changes and challenges experienced by the palace of Gwandu, first, it is gradually losing motifs, ornamentation, and decorations indicated by the outcome of the survey carried out. From the survey results, 57% of respondents indicated that restoring the ornamentation on the palace is significant to depict the identity of the building. The façade should be where these traditional decorations are emphasized, however, it is an aspect that is worst hit by the complete absence of these ornamentations and decorations. This is caused by the gradual deterioration over time and the series of maintenance the palace has undergone which has substantially altered the quality of appearance and cultural identity features of the Gwandu Emir's palace. The building form still retains its original historic shape and location in a traditional setting (75% of the respondents agree that the spatial planning is great, which indicates that restoration of the building elements can easily be achieved). The guidelines provided are information acquired through a literature review of how symbolic a palace should be and ways to tackle the challenges towards accomplishing a technical conservation and restoration process not only to Gwandu palace but to the entire northern Nigeria palaces with similar problems. It is important to note that traditional buildings globally are good examples of sustainability and can be developed to meet high standards through building conservation and restoration to uplift the standards of heritage buildings, hence, there is a need for social, cultural, economic and environmental factors to balance sustainable maintenance objectives.

The following recommendations were made from this study on the restoration and maintenance of the Gwandu Emir's palace and other palaces with similar problems:

- Develop a thorough palace documentation process.
- Selection of motifs for the restoration process.
- Create a work plan and technical briefs for routine maintenance.
- Sourcing and making use of traditional artisan/builders in the active conservation and restoration process.

ACKNOWLEDGEMENTS

I wish to acknowledge the sponsors TETFUND Nigeria, Kwara State University (Nigeria) and the University of Nottingham (UK).

REFERENCES

1. Abubakar Y S., (2013) Online article available: <https://www.facebook.com/470393303000364/posts/40-influential-emirs-who-rule-northern-nigeria-alhaji-dr-ado-bayero-emir-of-kano/527956033910757>. [9 February 2013].
2. Adamu, A B. (2012). Integrating cultural identity in the upgrading of Argungu fishing and cultural festival centre, Kebbi state. Kebbi state. Nigeria. Unpublished MSc. Thesis. ABU Zaria, Nigeria.
3. Adamu, A B. (2009). Challenges of conservation and restoration of traditional building elements: A case study of, Emir's Palace, Gwandu, Kebbi State, Kebbi state. Nigeria. Unpublished Project. Abubakar Tafawa Balewa University Bauchi, Nigeria
4. Amira, E. and Ahmed, E., (2013). Sustainable Heritage Development Learning from Urban Conservation of Heritage projects of Non-Western Context. European journal of sustainable Development Vol2. No.2.
5. Dmochowski, Z.R., (1990). An Introduction to Nigerian Traditional Architecture: Northern Nigeria, Vol.1; London: Ethnographical Ltd. Pp. 1-20.
6. Dennis R, (2007). Conservation and Sustainability in Historic Cities, First edition. Blackwell Publishing Ltd, Oxford, UK. ISBN: 978-1-4051-2656-4
7. Ehrlich S. (2006). Multicultural Modernism; The Incubator of Change. (AIA) American Institute of Architect National Convention. Culver City, California, USA. Steven Ehrlich Architecture.
8. Fielden, B., (1994). Conservation of Historic buildings, Great Britain: Butter Worth, Heinemann.
9. Idris, I. I, (2015). Challenges of preservation of cultural landscapes in traditional cities: A case study of Kano city.
10. Mahgoub, Y. (2007). Architecture and Expression of Cultural Identity in Kuwait: Paper publication: Journal of Architectural Research. Volume 12- Issue2. New York: Routledge Taylor and Francis group.
11. Map of Nigeria. <https://www.weathersparks.com/location/bk>. Accessed; [17 April 2020].
12. Moughtin, J.C., (1985). Hausa Architecture. London, Ethnographica Ltd. Pp. 7-123.
13. Odiaua, I. (2005). *An Introduction to Architectural Conservation*. Seminar paper presentation, Architecture programme, ATBU, Bauchi.
14. Osasona, C. O. (2002). "Towards Conservation and Restoration of traditional building." A case study of Anglo African Building in Oyo Ibadan: AARCHES Journal, Vol.2, 1.
15. Salim, B.U. and Ismail, S, (2019). Conservation Challenges of Heritage Building Reuse in Nigeria: A review of decision-making models.
16. ICOMOS CHARTER (2003). Principle and Analysis, Conservation, and structural restoration of structural Heritage, 14th General Assembly, Victoria Falls, Zimbabwe.
17. I.N.T.B.A.U (2011). International Network for Traditional Building, Architecture, and Urbanism. [Online], Available: www.traditionalarchitecture.co.uk. [06 February 2012].

Urban Growth vs Density:

The case of a low – density and hot desert climate city

CARLOS LOPEZ-ORDOÑEZ,¹ ISABEL CRESPO CABILLO,¹ JAUME ROSET CALZADA,¹
HELENA COCH ROURA,¹

¹AIEM – E.T.S. de Arquitectura de Barcelona, Universitat Politècnica de Catalunya, Barcelona, Spain

ABSTRACT: One characteristic of sustainable urbanization is high density and compact city morphology. The actual global trend in urban growth is taking cities to lower densities. For hot desert climate cities, this form of dispersing growth is not beneficial. This work aims to evaluate urban sprawl and urban density behaviour of a dispersed city and provide solutions that could improve the quality of urban life. To this end, we analysed the case of Hermosillo, a low – density hot desert climate city with extreme temperatures and high solar radiation values (mean of 6,7 kWh/m² per day during the hot season). We evaluated the built density distribution and the distribution of vacant lots using GIS-based maps. The relation between its urban morphology and the incidence of solar radiation at street level was evaluated through simulations with Heliodon2. The results show that an urban policy that encourages the densification of the city centre by the infill of vacant lots, could be a strategy to contain the urban sprawl while improving the public space by providing shade through the own city form. The implementation of “mixed-use lots” and the vertical edificatory density could foster the creation of sub-centres where people enjoy a qualitative urban life.

KEYWORDS: Urban form, Urban density, Hot desert climate city, Disperse city, Urban infill.

1. INTRODUCTION

Urban density is commonly used to measure life quality in a city [1]. High density and a compact urban morphology are often seen as prerequisites for sustainable urbanization and economic growth [2]

Even though high density seems to be the best approach, nowadays actual trend at global scale follows the opposite way, an urban sprawl.

As shown in Figure 1, in almost all the selected cities for this study, the population density has decreased in a lapse of 15 years. This is due to that mean annual growth rate of the urban surface (4,3%) is higher than that of the population (2,8%) [3].

In numerous cases, the extension to metropolitan areas causes this reduction in density, for example, the case of Barcelona. When only the urban core is considered, the density is 159 inhab/ha. If analysing the metropolitan area, its density falls to 59 inhab/ha. The same happens with other cities, such as Paris (203 inhab/ha in Paris Centre – 40 inhab/ha in Grand

Paris) or New York (282 inhab/ha in Manhattan – 20 inhab/ha in New York) [3].

The current pace of urban growth is taking the centre of the cities to lower densities by increasing their suburbs with low – density residential and commercial development, this fractures them and creates great distances to cover increasing traffic [4].

In cities where the climate is one of the main parameters to take into account to achieve a quality urban life, a sprawl development that leads to low densities is not recommended. These cities are located in low medium latitudes (20°-33°) and concentrate a large part of the world population. [5]

Cities such as Phoenix, Tucson, Las Vegas, Hermosillo, Mexicali in America; Riyadh, Mecca, and Baghdad in the Middle East; Khartoum in Africa. In this framework, the study of the urban growth and density in hot desert climate cities (BWh, Köppen climate classification) takes big importance.

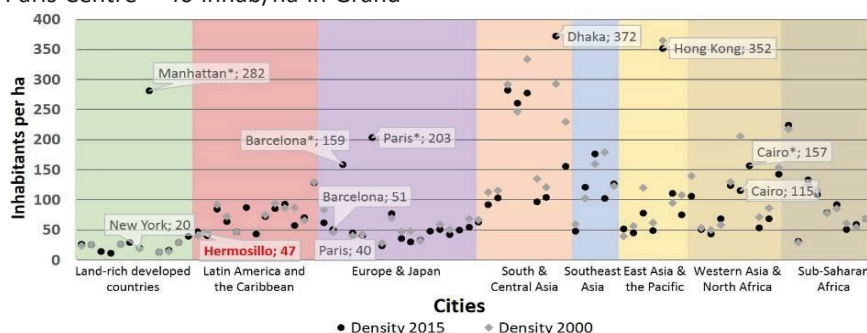


Figure 1: Urban density change 2000-2015. (*): urban core. Author's elaboration with data of Atlas of Urban Expansion [3].

2. OBJECTIVE

The goal of this work is to evaluate the urban growth and the change in urban density of the city of Hermosillo, Mexico, in the local and global context

This could help to provide urban planning that could improve the quality of life. To achieve this goal, it is also important to take into account the climatic conditions of the city. Given that in hot cities the direct component of solar radiation is one of the main parameters that affect the urban life quality, is analysed here.

3. METHODOLOGY

The methodology followed in this study focuses on different aspects to evaluate the urban growth:

- Urban density distribution
- Distribution of vacant lots within the city
- Urban form and climate

Divided into three phases where the two first phases consist of the data collection and it's processing and the third assesses the solar access at street level in a representative area of the city.

Data collection: the statistical data of 82 cities with more than 500,000 people used is from the Lincoln Institute of Land Policy [3]. The population data of Hermosillo is from the National Institute of Statistic and Geography (INEGI) [6] and the urban data is from the municipality of Hermosillo [7].

The climatological data is from the National Meteorological Service (SMN) [8] and from the Energy, Environment and Architecture Laboratory (LEMA) [9].

Data processing: The creation of GIS-based maps with the information processed is necessary to improve the comprehension of the data collected; this could be a useful tool in urban planning decision-making. The software used was ArcMap.

Solar access assessment: The solar radiation calculation program Heliodon2 [10] helps to assess the solar access at street level in the selected area (in this case, the streets of the city centre). For this assessment, 3D models must be built and simulated.

The solar access assessment takes place during the hot season (May 1st to October 31st). This period presents high temperatures and levels of direct solar radiation, which directly influences the comfort in the urban public space, conditioning its use by pedestrians during the day.

4. CASE STUDY

The city of Hermosillo (29° NL), shown in Figure 2, follows a scattered pattern of urban growth. It has a hot desert climate (BWh, Köppen climate classification) with an annual mean temperature of 25°C and a mean relative humidity of 43%. During the hot season, the city presents extreme temperatures of 40-45°C, sometimes reaching 50°C. It presents an

annual mean solar radiation of 5,85 kWh/m² per day, but during the hot season, the mean solar radiation is 6,7 kWh/m² per day (Table 1).

In the last century, in this region of North America, there has been recorded an increment in the mean temperature. In Hermosillo, this increment is more noticeable during the hot season. In the last 50 years, there has been an increment of around 2°C in the mean temperature of this season (Figure 3).



Figure 2: Satellite image of Hermosillo. Author's elaboration with Google Earth Pro.

Table 1: Monthly data (1980-2010) of average maximum temperature (AMT), mean temperature (MT), average minimum temperature (AmT), relative humidity (%) and global horizontal radiation (kWh/m²) [8, 9]

Month	AMT °C	MT °C	AmT °C	RH %	kWh/m ²
JAN	24,2	17,2	10,2	48	3,88
FEB	25,8	18,5	11,3	44	4,76
MAR	28,7	20,9	13,1	40	6,34
APR	32,3	24,1	15,9	34	7,45
MAY	36,3	27,9	19,4	31	7,73
JUN	39,8	31,8	23,8	34	7,59
JUL	39,3	32,5	25,8	48	7,07
AUG	38,3	31,9	25,6	53	6,88
SEP	37,5	31,0	24,6	48	5,74
OCT	33,9	26,9	19,8	42	5,23
NOV	28,6	21,6	14,0	43	4,11
DEC	24,0	17,1	10,2	49	3,25

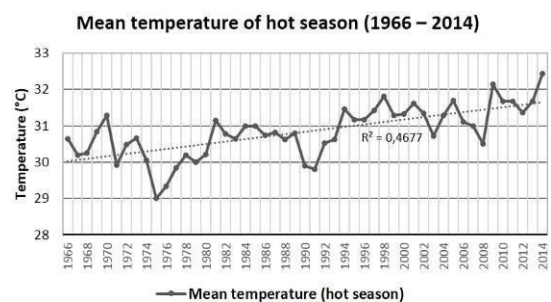


Figure 3: Mean temperature change (1966 to 2014). There is an increase of almost 2°C. Author's elaboration with data of the Municipality of Hermosillo [7].

Since the 20th century, the city has maintained an accelerated rate of urban and population growth. It has followed a housing policy that favours the construction of single-family dwellings in closed neighbourhoods.

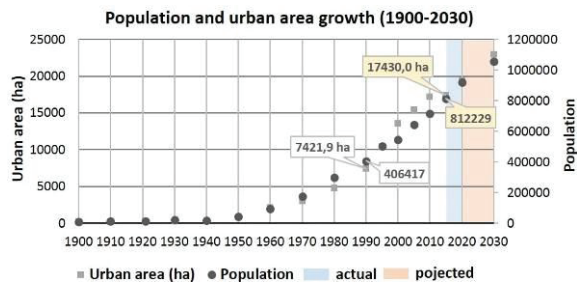


Figure 4: Evolution of the population and urban area of Hermosillo (1900 – 2030). Author's elaboration with data from INEGI [6].

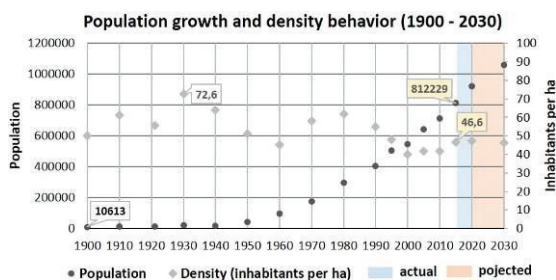


Figure 5: Evolution of the population and the behaviour of the urban density (1900 – 2030). Author's elaboration with data from INEGI [6].

As shown in figures 4 and 5, in 2015, the urban area was close to 17.500 ha with a population of over 800.000 inhabitants. The population and urban area will continue to grow at an accelerated rate maintaining a low urban density (less than 50 inhabitants per hectare).

But, how is Hermosillo located globally when comparing the relationship between its urban density and its climate?

It can be seen, in Figure 6, that the value of the urban density of Hermosillo (47 inhab/ha) is similar to

the one of Riyadh (43 inhab/ha). This value is far from that of historical cities such as Cairo (157 inhab/ha) and Alexandria (143 inhab/ha). In Mexico, this value is also behind recently founded cities, for example, the border city of Mexicali (87 inhab/ha).

5. RESULTS AND DISCUSSION

The behaviour of the last 30 years and the current social housing policy have led the city to present an irregular distribution of the population, displacing it from the city centre to suburban areas. At the same time, and due to its climate, it has transformed Hermosillo into a city that is not walkable and lacks quality public spaces.

5.1 Urban density distribution

The map in figure 7 shows the city's distribution of population density. While in most cities the density starts to decline while increasing the distance from the city centre [3], in Hermosillo, it is quite the opposite.

This low centrality effect is a characteristic of dispersed cities [11]. It means that inhabitants and certain economic activities tend to move from the city centre to the outskirts of the city. This causes the urban centre to lose economic and population weight compared to the suburban areas.

The city centre presents an urban density of 14 inhabitants per hectare, while the mean urban density of the rest of the city is 47 inhab/ha. These low densities remain around the city centre and create a donut effect in the urban area as higher densities surround it.

The growth of Hermosillo has been mainly in the north and south, while to a lesser extent in west directions. That is the reason why these areas present higher levels of urban density. The growth of the city follows this path since the city limits to the east with the Abelardo L. Rodríguez Dam, and to the northeast with the Bachoco hill, which is part of the Espinazo Prieto mountain range.

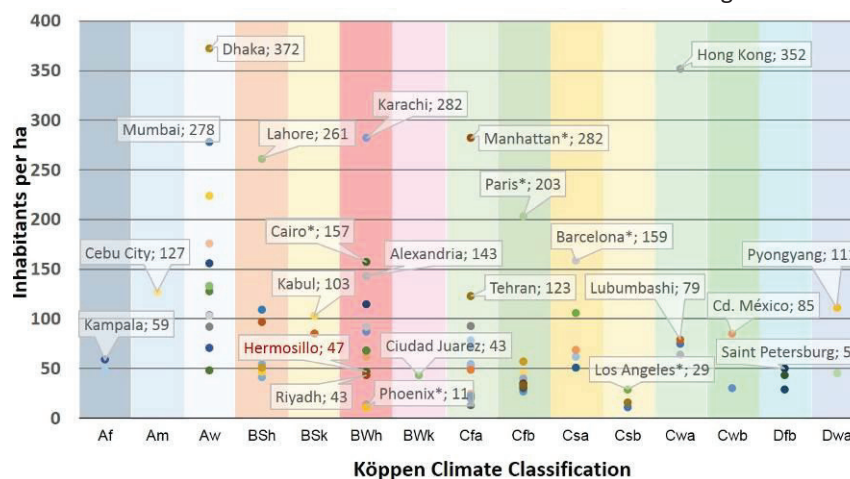


Figure 6: Population density by its climate. Hermosillo is located in the BWh strip. (*): Urban core. Author's elaboration with data from Atlas of Urban Expansion [3].

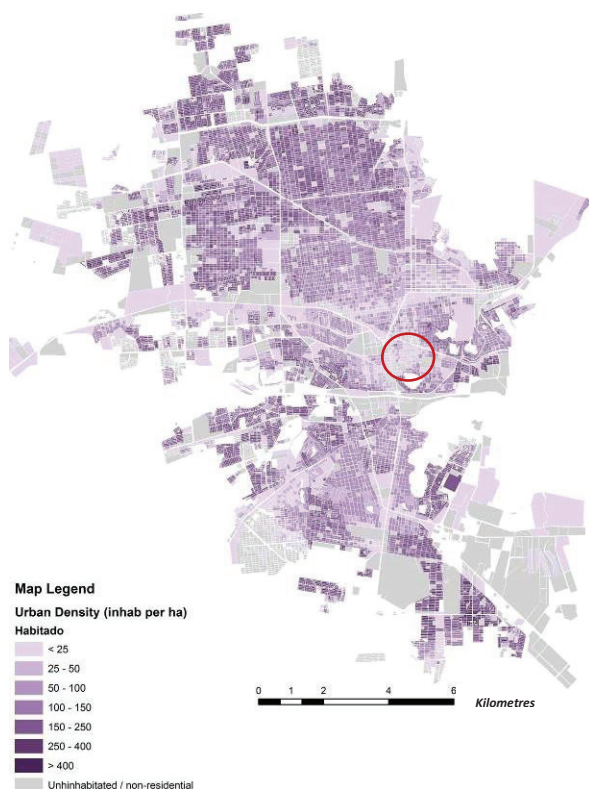


Figure 7: Urban density distribution by city blocks of Hermosillo. The red circle indicates the city centre location. Author's elaboration with data from INEGI [6].

Figure 7 shows that there are some city blocks listed as uninhabited or non-residential, but these city blocks are not necessarily empty. For instance, the industrial zone stands out in the southeast part, while the University is in the downtown area next to the city centre. There are other types of city blocks distributed throughout the city: industrial estates, housing reserves, urban equipment, etc.

5.2 Distribution of vacant lots within the city

Figure 8 shows the distribution of the existing vacant lots. We have considered a vacant lot the one that is within the urbanized area and does not have buildings, this, regardless of the type of land use. However, those listed as green areas by the municipality are not considered.

In Figure 8 we can see how most of the vacant lots are in the west, northwest and southeast areas. However, a strip (black rectangle) of vacant lots divides the city in two. The idea behind the development of this area was to create an urban megaproject that would detonate the area of the old riverbed of the Sonora River, making it the business centre of the city [12]. Currently, it has not been as successful as expected, and now more than being a business centre, it acts as a border between the north and south of the city.

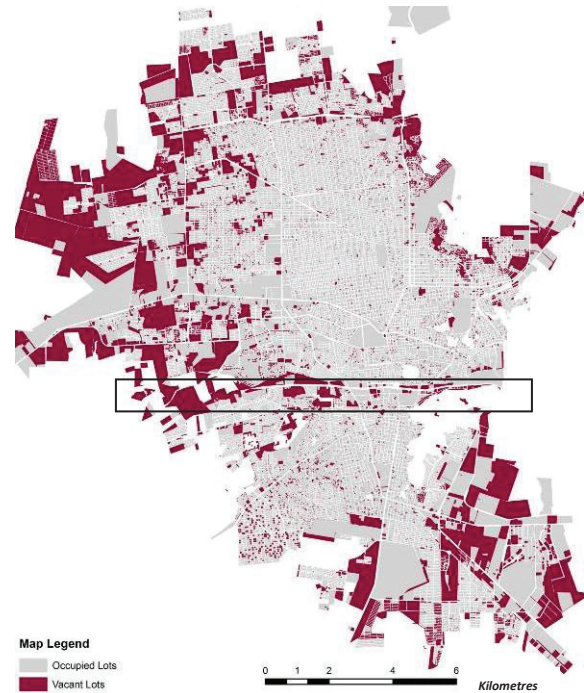


Figure 8: Vacant lots distribution of Hermosillo. The black rectangle indicates the Sonora River Project. Author's elaboration with data from INEGI [6].

There are 34,096 vacant lots in the city. This amount is equivalent to approximately 5,000 ha, that is, if we consider that the urban area is 17,500 ha, about 30% are vacant lots.

In this study, we did not find a single sample of the existence of mixed-use lots (i.e., commercial use on the ground floor and housing above).

5.3 Urban form and climate

Regarding the relationship between urban form and climate, Hermosillo follows the dispersed city model: single-story dwellings, wide streets, and low densities. All this driven by the use of the automobile, creating great distances to travel.

All this, together with a hot – desert climate, characterized by high temperatures and high levels of solar radiation, leads to a deficient public space and a continuous demand for land for housing developments [13, 14].

The area selected for the assessment of solar access at the street level is the city centre. This case study has been selected after considering that it is the area of the city with the highest construction density and the highest average building height. Therefore, this area should present the lowest levels of direct solar radiation on the streets.

The calculation was made considering 184 days (May 1st – October 31st), a grid precision of 15 minutes and a mesh size of 2 meters.

Figure 9 is a map that shows the results of simulating the behaviour of direct solar radiation in the selected area. The amount of energy displayed is that accumulated for square meter (kWh/m^2) throughout the hot season. As the figure shows, most of the streets receive a great amount of direct solar radiation.

As shown in Figure 9 and 10, the high level of penetration of solar radiation at the street level is due to two characteristics of the urban morphology of Hermosillo: the layout of its streets and the low height of its buildings (Figure 10).

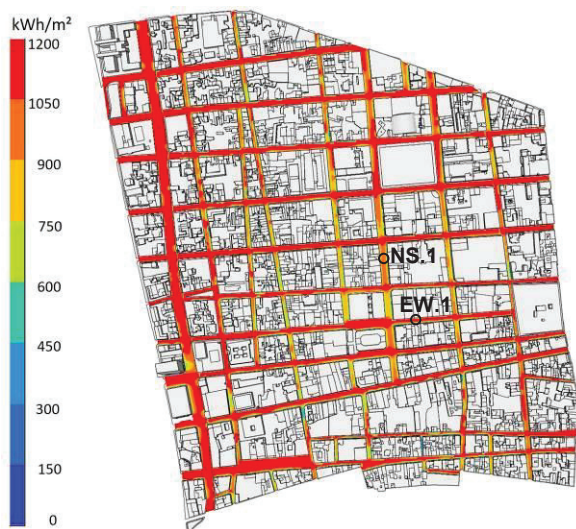


Figure 9: Results of the simulation of the direct solar radiation (kWh/m^2) at the street level during the hot season (1st May – October 31st). Author's elaboration with Heliodon2 [10].

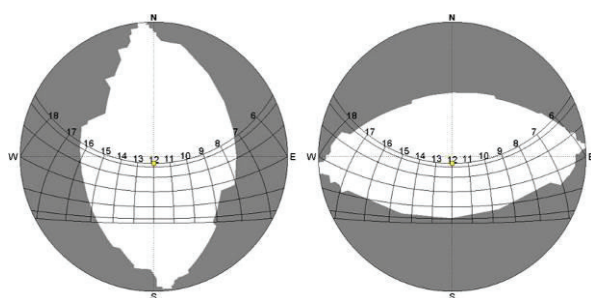


Figure 10: Solar path in stereographic diagrams of two streets with different orientations but similar aspect ratios ($h/w < 1$): the one on the left is the NS.1 point (North – South), on the right is the EW.1 point (East – West). Author's elaboration with Heliodon2 [10].

Figure 11 shows the maximum possible solar irradiance and the actual irradiance received for each day of the hot season. The maximum values range from $6,70 \text{ kWh}/\text{m}^2$ on May 1st, $7,29 \text{ kWh}/\text{m}^2$ on June 21st and $3,57$ on October 31st. These values are the maximums that a square meter can accumulate

throughout the indicated day. However, the actual values present a reduction occasioned by the obstruction produced by the own city form. On the same days, and order, the values are: $5,49 \text{ kWh}/\text{m}^2$ (18% less), $6,13 \text{ kWh}/\text{m}^2$ (16% less) and $2,42 \text{ kWh}/\text{m}^2$ (32% less).

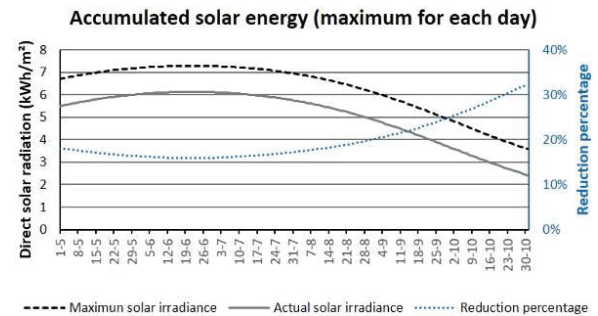


Figure 11: Maximum solar radiation accumulated daily during the hot season and the difference between the maximum possible solar irradiance and the actual solar irradiance. Author's elaboration with Heliodon2 [10]

5.4 Discussion

After observing the distribution of population density and vacant lots, as well as the relationship between urban form and climate, it seems necessary to define some strategies for an urban planning policy that includes these aspects. In this work, we propose two different strategies to help reduce urban distances, hence promoting the proximity in civic, administrative, social and daily life.

The first strategy is the infill of the vacant lots that are within the consolidated urban area. This approach could represent an improvement in terms of a slight increase in urban density. For this approach to work, it is necessary the implementation of mixed-use lots, that is, a lot that combines both commercial and residential use. This type of approach could help to reduce the typical zoning of land uses present in dispersed cities (large areas of a single type of land use).

The second strategy is the creation of urban sub-centres in different areas of the city. This approach attempts to change the current growth dynamics of the city, that is, to move from the dynamics of the typical dispersed city in continuous expansion to a new dynamic in which the creation of several sub-centres is encouraged to limit urban sprawl and thus increase urban density. These new sub-centres need to have a high density, both of construction and population. At the same time, they must have a morphology that allows the creation of shade in public space by the same urban form, protecting the pedestrian from the high incidence of solar radiation, and acting as an urban oases network (Figure 12).

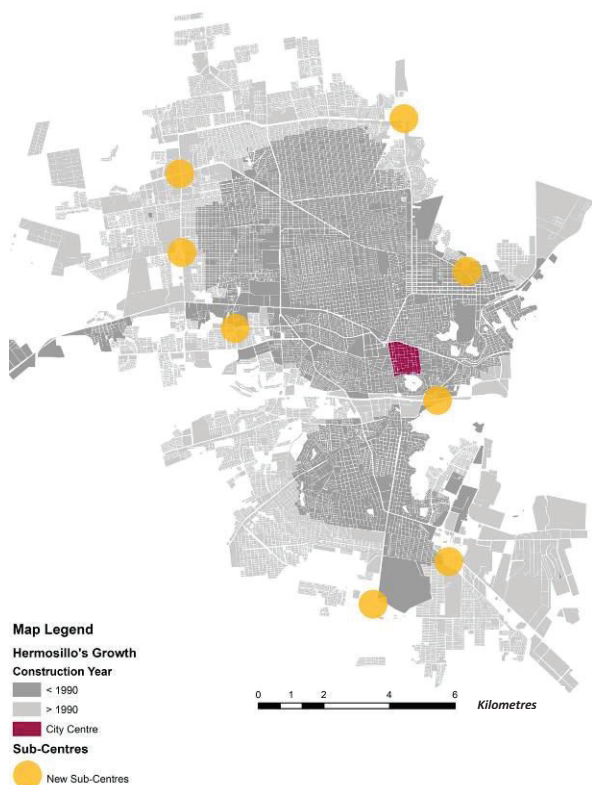


Figure 12: Possible hotspots for the creation of a network of sub-centres. Author's elaboration.

These two strategies, even though they can be used individually, should be considered complementary to each other, since they would be producing a synergy to achieve a common goal. Continuing with the example of the urban centre of Hermosillo, these two strategies could be applied in that area while taking advantage of the fact that it is an active commercial area and counts with all the public services. This can be done by the infill of vacant lots and the stacking of homes on top of current buildings whose construction permits it. This would allow the diversification of land uses and increasing building and population density. These interventions could lead to an improvement in the quality of public space, therefore, of urban life.

6. CONCLUSION

The behaviour of the last 30 years and the current social housing policy have led the city to present an irregular distribution of the population, displacing it from the city centre to suburban areas. At the same time, and due to its climate, it has transformed Hermosillo into a city that is not walkable and lacks quality public spaces.

Some strategies to densify could be applied to the city of Hermosillo to achieve a more regular distribution of the population density and contain urban sprawl while improving the public space by providing shade through the own city form.

These strategies act at two different scales:

- Filling the vacant lots within the city.
- The creation of sub-centres in different areas of the city.

For these strategies, the implementation of mixed-use lots (commerce at ground level and housing in upper levels) is necessary.

The urban mixed-use through the infill and the vertical densification through stacking in the city centre could help to raise the urban density (built and population density) of the area and act as a catalyser for other zones of the city.

A change in the housing policy could help to improve the situation, by favouring the construction of multifamily housing instead of just single-family.

ACKNOWLEDGEMENTS

This work is possible by the scholarship granted to C.F.L.O (CVU 469347) by the **CONACYT & SENER** of Mexico and by the **Spanish Ministry of Economy** under the MOET project, code *BIA2016-7765-R*.

REFERENCES

1. Dovey, K. and Pafka, E., (2014). The urban density assemblage: Modelling multiple measures. *Urban Design International*, 19: p. 66-76.
2. Berghauser, M. and Haupt, P., (2009). Space, Density and Urban Form. Technische Universiteit Delft: p. 15-18.
3. Angel, Shlomo et al., (2016). Atlas of Urban Expansion, The 2016 edition, Volume 1: Areas and Densities. New York: New York University, Nairobi: UN-Habitat, and Cambridge, MA: Lincoln Institute of Land Policy.
4. Conserve Energy Future, [Online]. Available: www.conserve-energy-future.com/causes-and-effects-of-urban-sprawl.php [30 April 2020].
5. López-Ordóñez, Carlos et al., (2020). The role of thermal insulation in the architecture of hot desert climates. *Sustainability in Energy and Buildings*: p. 433-444.
6. National Institute of Statistic and Geography, [Online]. Available: www.inegi.org.mx [29 July 2019]
7. IMPLAN Hermosillo, [Online]. Available: www.implanhermosillo.gob.mx/ [29 July 2019]
8. Servicio Meteorológico Nacional SMN, [Online]. Available: <https://smn.conagua.gob.mx/es/> [29 July 2019]
9. Laboratorio de Energía y Medio Ambiente LEMA, [Online]. Available: www.lemma-arq.unison.mx [29 July 2019]
10. Heliodon2, [Online]. Available: www.heliodon.net [10 March 2019]
11. Muñoz, Ivan et al., (2006). *SPRAWL. Definición, causas y efectos*. Universitat Autònoma de Barcelona and Universitat Politècnica de Catalunya.
12. Duarte, Alejandro., (2003). Historia Urbana de Hermosillo: cuatro fragmentos, una ciudad. In *Fiestas del Pitic*. Hermosillo May 29 – June 1.
13. López-Ordóñez, Carlos et al., (2019). Reshaping the city: Containing the urban sprawl and reducing solar access on the streets in a hot desert climate city. In *XIII CTV International Conference Virtual City and Territory*. Barcelona, October 2-4.
14. Jacobs, Jane., (1961). *The Death and Life of Great American Cities*. New York

The Contribution of Anthropogenic Heat on Urban Air Temperature Elevation: A Case Study of the Singapore Residential area

SHUO-JUN MEI¹, CHAO YUAN¹, RUIXUAN ZHU¹, WENHUI HE², XIAN-XIANG LI², TANYA TALWAR¹

¹National University of Singapore, Singapore

²Singapore-MIT Alliance for Research and Technology Centre

ABSTRACT: The contribution of anthropogenic heat emission on the street level air temperature elevation is evaluated in a residential area in Singapore. The Large-Eddy Simulation (LES) is used to calculate the wind and temperature field. A maximum air temperature elevation of 1.4 °C is found at the pedestrian level when the electricity consumption rate is about 8 W/m². The old type of residential buildings are found of higher temperature elevation even under much lower anthropogenic heat releasing rate. The pedestrian level temperature is even higher at a higher wind speed scenario. The main reason is the downward wind-driven flow at the low wind condition is change by buoyancy effect.

KEYWORDS: Anthropogenic heat; Buoyancy effect; Large eddy simulation; Realistic urban configuration; Urban ventilation;

1. INTRODUCTION

The urban air temperature was found higher than rural area by many field observation [1, 2]. Oke (1982) [3] summarize there are seven causes of the urban heat island, including:

- 1) Increased absorption of short-wave radiation;
- 2) Increased long-wave radiation from the sky;
- 3) Decreased long-wave radiation loss;
- 4) Anthropogenic heat source;
- 5) Increased sensible heat storage;
- 6) Decreased evapotranspiration;
- 7) Decreased total turbulent heat transport;

The measurement of the air temperature could not exclude the effect of anthropogenic heat from other factors, including solar radiation, shading and evaporation. The CFD modelling could separately investigate the contribution of each cause on local air temperature elevation. There are many researches on the contribution of solar radiation and shading on urban heat island [4]. However, the contribution of anthropogenic heat is not well understood. The analysis of climate data by Offerle et al., (2006) [5] shows that the anthropogenic heat is a significant input to the urban energy balance in the winter for European cities. The wintertime residential heating is the main source of anthropogenic heat in these cities. However, for the tropical cities, such as Singapore and Hong Kong, the residential cooling also results in intense heat releasing. Intense heat releases from the condensers of the air conditioners. The temperature elevation at such a hot climate is much more significant as the air temperature easily rises over the threshold for human health. A sustainable urban design needs to minimize the impact of anthropogenic

heat releasing on air temperature elevation at pedestrian level. The objective of the present study is to evaluate the contribution of anthropogenic heat on urban temperature elevation. A representative residential area in Singapore is selected to conduct the CFD (Computational Fluid Dynamics) simulations.

2. HEAT EMISSION RATE

The Housing & Development Board (HDB) is Singapore's public housing authority. HDB flats are home to over 80% of Singapore's resident population. The heat releasing rate was calculated from the residential energy consumption data. The energy consumption data of Singapore was obtained from the GIS data with a resolution of 200m × 200m grids. A residential area was selected for anthropogenic heat dispersion analysis,

As the main domestic energy consumption is on indoor cooling in Singapore, the air conditioner condenser could be regarded as the anthropogenic heat releasing position. A field survey was conducted to find out the condenser number of the target buildings. The number of floors and the number of condensers on each floor were presented in Figure 1. Table 1 summarizes the number of condensers and electricity consumption at each grid in Figure 1. The "Pinnacle@Duxton" buildings have a different electricity consumption rate of about 1200W. This is reasonable as multiple rooms share one condenser in "The Pinnacle@Duxton" buildings, while each room has its own condenser in other buildings. At grid 3 in figure 1, the electricity consumptions are composed by the target buildings and other non-residential buildings. As the electricity consumption of non-

residential buildings was unavailable, the electricity consumption rate of condensers were overestimated. As the residential building in Zone 3 is of the same type with the buildings in Zone 2, the electricity consumption rate of the condensers at Zone 2 could also be used for the target building in Zone 3. Therefore, a uniform electricity consumption rate of 600 W was used, except for the buildings in the “Pinnacle@Duxton”, which was specified as 1200 W in the CFD simulation.

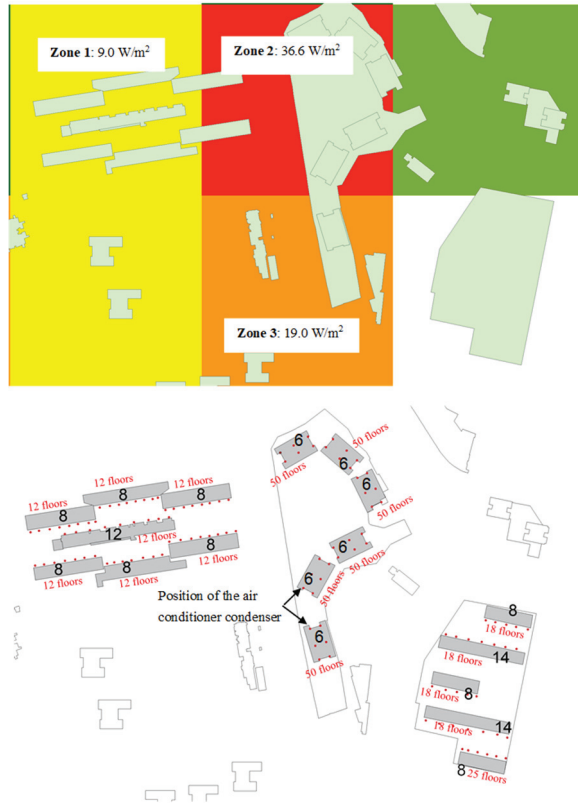


Figure 1. The number of floors and positions of air conditioner condensers of the medium-density area

Table 1. The computation of electricity consumption per releasing point based on GIS data and field survey.

Zone	Condenser number	Total electricity consumption rate	Electricity consumption per condenser
1	600	3.6×10^5 W	1220 W
2	1500	1.46×10^6 W	973 W
3	300	7.6×10^5 W	2533 W

The anthropogenic heat releasing from the condensers come from two part. The first part is the electricity consumption (E_c), which is mainly used to power the compressor. This part of energy will finally be transferred into heat and emit to our space. The second part (Q_c) is the heat transported from indoor to outdoor through heat engine cycle.

The anthropogenic heat emission rate from

condensers can be calculated as [6]:

$$Q = Q_c + E_c \quad (2)$$

where $Q_c = E_c \times COP$, and Coefficient of AC performance, $COP = 3.34$ [7]. Thus the anthropogenic heat emission rate per condenser is 2604W for the low rise HDB and 5208W for the Pinnacle@Duxton buildings.

3. CFD MODEL

3.1. Governing equations and turbulence model

The Large Eddy Simulation (LES) model was used to solve the turbulence atmospheric flow. Applying the filter operation to the incompressible Navier-Stokes equations leads to the following filtered equations:

$$\frac{\partial \hat{u}_i}{\partial x_i} = 0 \quad (1)$$

$$\frac{\partial \hat{u}_i}{\partial t} + \frac{\partial \hat{u}_i \hat{u}_j}{\partial x_j} = -\frac{1}{\rho} \frac{\partial \hat{p}}{\partial x_i} + \frac{\partial}{\partial x_i} \left(\tau_{ij}^{sgs} + \nu \frac{\partial \hat{u}_i}{\partial x_j} \right) + \beta g (\hat{\theta} - \theta_f) \delta_{i3} \quad (2)$$

The Boussinesq assumption was used to compute the buoyancy effect, \hat{u}_i the filtered velocity and \hat{p} the filtered pressure. The transport equation of filter temperature $\hat{\theta}$

$$\frac{\partial \hat{\theta}}{\partial t} + \frac{\partial \hat{\theta} \hat{u}_j}{\partial x_j} = -\frac{1}{\rho} \frac{\partial \hat{p}}{\partial x_j} + \frac{\partial}{\partial x_j} \left(\pi_j^{sgs} + \frac{\nu}{Pr} \frac{\partial \hat{\theta}}{\partial x_j} \right) + \Theta_s \quad (3)$$

Here, $\beta = 1/\theta_f$ is the thermal expansion coefficient of air, and θ_f is the reference temperature, Θ_s is the source term. Air density ρ is 1.2 kg m^{-3} , kinetic viscosity coefficient $\nu = 1.5 \times 10^{-5} \text{ m}^2 \text{ s}^{-1}$ and molecular Prandtl number Pr is 0.72.

The one equation subgrid model developed by [8] was used in this study. The turbulent viscosity ν_{sgs} is obtained by solving an additional transport equation for subgrid scale kinetic energy k_{sgs} :

$$\nu_{sgs} = C_k \Delta \sqrt{k_{sgs}} \quad (4)$$

where $C_k = 0.094$ is the model constant value.

The subgrid scale kinetic energy k_{sgs} is defined as:

$$k_{sgs} = \frac{1}{2} \tau_{kk} = \frac{1}{2} (\hat{u}_k \hat{u}_k - \hat{u}_k \hat{u}_k) \quad (5)$$

The transport equation is determined as:

$$\frac{\partial k_{sgs}}{\partial t} + \frac{\partial \hat{u}_j k_{sgs}}{\partial x_j} = \frac{\partial}{\partial x_j} \left((\nu + \nu_{sgs}) \frac{\partial k_{sgs}}{\partial x_j} \right) + 2C_v \Delta k_{sgs}^{1/2} \hat{S}_{ij} - C_\epsilon \frac{k_{sgs}^{3/2}}{\Delta} \quad (6)$$

Where $C_v = 0.05$ and $C_\epsilon = 1$ are model constants.

3.2. COMPUTATIONAL DOMAIN AND MESHING

For the anthropogenic heat dispersion modelling, it is important to resolve the flow around building and its near region. The 3D model of target buildings was built by geographic information system (GIS) data. The surrounding buildings were also explicitly modeled to consider the wake influence. An extended domain was built around the target buildings to allow the wake development. The criteria [9] was used to determine the domain size. Table 2 shows the computational domain size and spatial resolution.

Table 2. The domain size and mesh details

Domain size (m) (x, y, z)	1760×3000×1200
Upwind length (m)	600
Downwind length (m)	1800
Side length (m)	600
Mesh number	20,099,684
Maximum mesh size (m)	60
Minimum mesh size (m)	0.9

The meshes around complex urban geometries were generated by the snappyHexMesh tool. The meshes consisted of hexahedra (hex) and split-hexahedra (split-hex) cells. In cases with complex geometry the mesh was refined near the walls to produce cells with wall. Figure. 2 illustrates the computational mesh around target buildings.

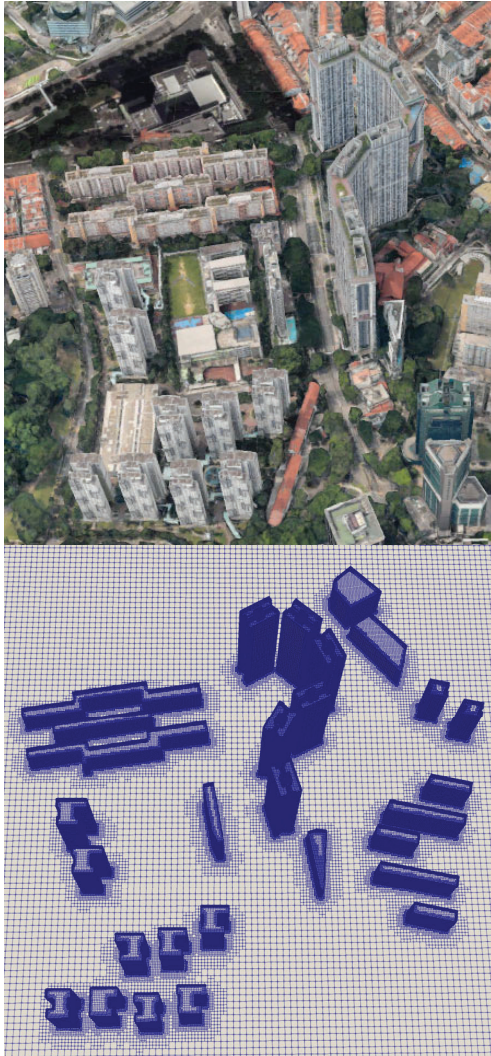


Figure 2. Satellite image, 3D model and computational geometry of the target area.

3.3. BOUNDARY CONDITIONS

The inlet boundary condition is of great importance in LES because the downstream flow development within the domain is largely determined by the prescribed in flow turbulence. The turbulence

structures at inlet boundary are coherent in space and time. The inflow velocity field should reproduce the turbulence structure as well as Atmospheric Boundary Layer (ABL) velocity profile.

The time-averaged horizontal velocity at the inlet of the computational domain was specified to represent an atmospheric boundary layer, where the turbulence originates only from friction and shear [10]

$$U(z) = \frac{u_{ABL}^*}{\kappa} \ln\left(\frac{z+z_0}{z_0}\right) \quad (7)$$

$$k(z) = \frac{u_{ABL}^{*2}}{\sqrt{C_\mu}} \quad (8)$$

$$\varepsilon(z) = \frac{u_{ABL}^{*3}}{\kappa(z+z_0)} \quad (9)$$

Here u_{ABL}^* is the atmospheric boundary layer friction velocity, z the height above the ground, z_0 the aerodynamic roughness length, k the turbulence kinetic energy, ε the turbulence dissipation rate $C_\mu = 0.09$ a constant of the turbulence model. Although the LES model does not include the turbulence variable k and ε , their profile are useful for specifying the Reynolds stress. Therefore, the vertical profiles of k and ε are also given.

The dominant wind directions of Singapore are North (N), North-northeast (NNE), and South (S), South-southwest, shown as Figure 5. These four dominant wind direction were used for the simulations. The annual wind speed 7.4 m/s and the lowest wind speed 1.1 m/s were measured with 300 m height at Changi station.

The turbulence structure of inflow conditions for the simulations were generated based on the method described in [11]. This method produces a velocity field with exponential correlation functions in space and time with length scale L and time scale T , given by

$$R(r, 0, 0) = \exp\left(-\frac{\pi r}{2L}\right) \quad (10)$$

$$R(t) = \exp\left(-\frac{\pi \Delta t}{2T}\right) \quad (11)$$

Three two-dimensional sets of random data with zero mean and unit variance are generated at each time step for calculating the fluctuating velocity components. These fluctuating velocity components are then filtered to obtain sets of data that have the exponential correlation functions with the prescribed length scale L_y and L_z in the two dimensions of the inflow plane. The correlations in time and the streamwise direction are reproduced by defining the data on the next time steps as a function of the data from the previous time step and a new set of random data.

For the outlet plane, the static pressure is fixed to a constant value and a zero normal gradient boundary condition is adopted for all other flow variables. The cyclic boundary condition was adopted to the lateral boundary planes. The surface shear stress on the ground is specified directly based on the logarithmic wall function with a roughness height of $z_0 = 0.5m$ which corresponds to the fairly level grass plains on

the real terrain site. The surface stress model predicts the total shear stress (including viscous and SGS stresses) based on the filtered velocity at the first cell center off the wall.

3.4. NUMERICAL SCHEME

OpenFOAM uses the finite volume method to solve the systems of partial differential. The temporal term of the governing equations is discretized using the Crank-Nicolson scheme, which is a second-order difference in time. Other terms of the governing equations were discretized using the second-order limited central difference. The governing equations were solved sequentially using the resulting Pressure-Implicit Splitting Operation (PISO) algorithm. The solution was performed implicitly by matrix inversion using the incomplete Cholesky conjugate gradient method. For the near-ground region, van Driest damping function was used in relation to the wall normal distance to the nearest ground surface.

An average Courant number $Co = 0.2$ is used. An initialization time of $10 L_x/U_{ref}$ is used to achieve a pseudo-steady state. Afterwards, the turbulence statistics are collected for a duration of $20 L_x/U_{ref}$.

3.5. VALIDATION OF THE PRESENT CFD MODEL

The aim of the present study is to simulate anthropogenic heat dispersion within three-dimensional building array considering the buoyancy effect. The wind tunnel experiment conducted by [12] measured the flow and temperature field within three-dimensional building array under bottom heating condition, which is used to verify our numerical model and numerical method. The array is composed by 10 rows and 6 columns of blocks, which are mounted on the floor. The cubical blocks are of uniform height $h = 0.1\text{ m}$. Distances between blocks are equal to h in streamwise direction and $0.5h$ in spanwise. The computational domain size of the validation case is of $33h \times 9h \times 7h$. The floor heating condition with $Ri = -0.19$ is simulated to study the effect of buoyancy force. The free stream velocity U_f is set as 1.5 m/s . The ground temperature $\theta_w = 332\text{ K}$ and free stream temperature $\theta_a = 292\text{ K}$ of the wind tunnel experiment are used in the validation case. The mean velocity profile at the inlet boundary was generated with $U_f = 1.5\text{ m/s}$ and $z_0 = 0.0033\text{ m}$ according to the wind tunnel experiment.

Simulations with two Reynolds-averaged Navier-Stokes (RANS) turbulence models, the realizable $k - \varepsilon$ model [13] and RNG $k - \varepsilon$ model [14], were also conducted on the same domain size and mesh. The vertical profiles of the streamwise velocity u_x and the time averaged temperature $\bar{\theta}$ along the centerline in the street canyon at the 8th row are compared with the wind tunnel results of [12] in Figure 3. The mean

velocity is normalized with free stream velocity U_f and the time averaged temperature is normalized by temperature elevation of the bottom surface by $(\bar{\theta} - \theta_w)/(\theta_a - \theta_w)$. The distribution of time-averaged temperature and velocity obtained by the experiment is well reproduced by LES. Both RANS model underestimated the air temperature and overestimated velocity in the canopy layer, especially at near ground level. Therefore, the LES model is used for the following parametric study.

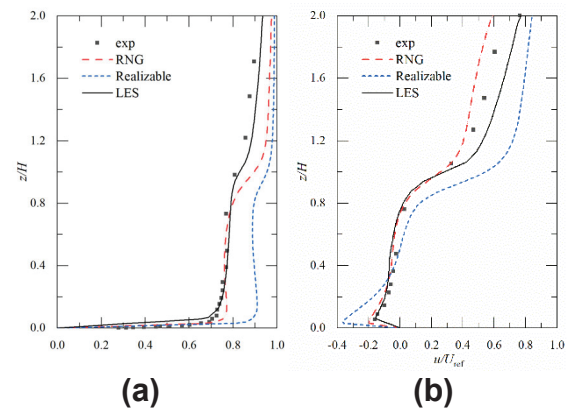


Figure 3. Comparisons of time-averaged horizontal velocity (a) and temperature (b) at the vertical centerline of 8th street canyon.

4. RESULTS AND DISCUSSION

4.1. Anthropogenic heat dispersion pattern

The warm air dispersion route was presented by plotting the iso-surfaces of temperature elevation in Figure 4. Only the air at the volume between closely spaced buildings was markedly warmed up. For the most cases, the effect of anthropogenic heat releasing only affect the air close to the buildings. The dispersion of anthropogenic heat is different from the pollutant dispersion due to the buoyancy effect. The upward motion of the warm air is obvious in the wind speeds. Especially, at the low wind speed, the warm air extended much higher than the rooftop. Therefore, the air-exchange of the street canyon at the position is very different from the previous wind-driven conditions, when the shear street at rooftop plays a major role. At the annual wind speed scenario, the warm air was transported to the ground level by the wake vortex behind the building [15]. At the extreme low wind speed scenario, upward motion is strong and breaks the original vortex behind the building. Therefore, the near-ground temperature could be higher for the higher wind speed.

4.2. Temperature elevation at pedestrian level

In this part, a qualitative evaluation was carried out for the temperature elevation caused by residential heat release. Figure 7 shows the temperature elevation field at 2 m height. This height is where most human activity happens.

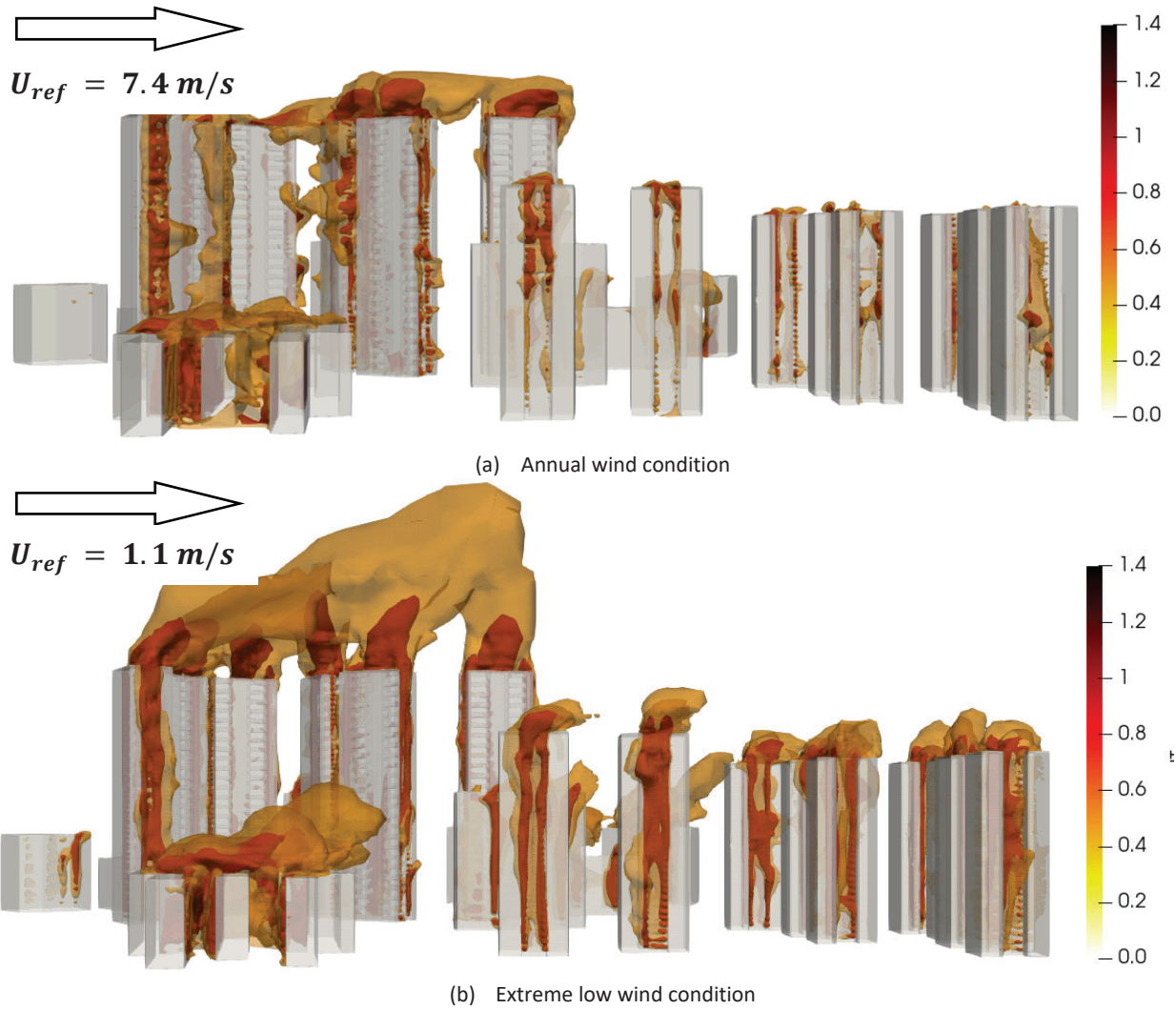


Figure 4. Instantaneous Iso-thermal surface of $\Delta T = 1^\circ \text{C}$, inside surfaces, $\Delta T = 0.5^\circ \text{C}$, outside surfaces under the annual wind speed $U_{ref} = 7.4 \text{ m/s}$ condition (a) and Extreme low wind $U_{ref} = 1.1 \text{ m/s}$ condition (b).

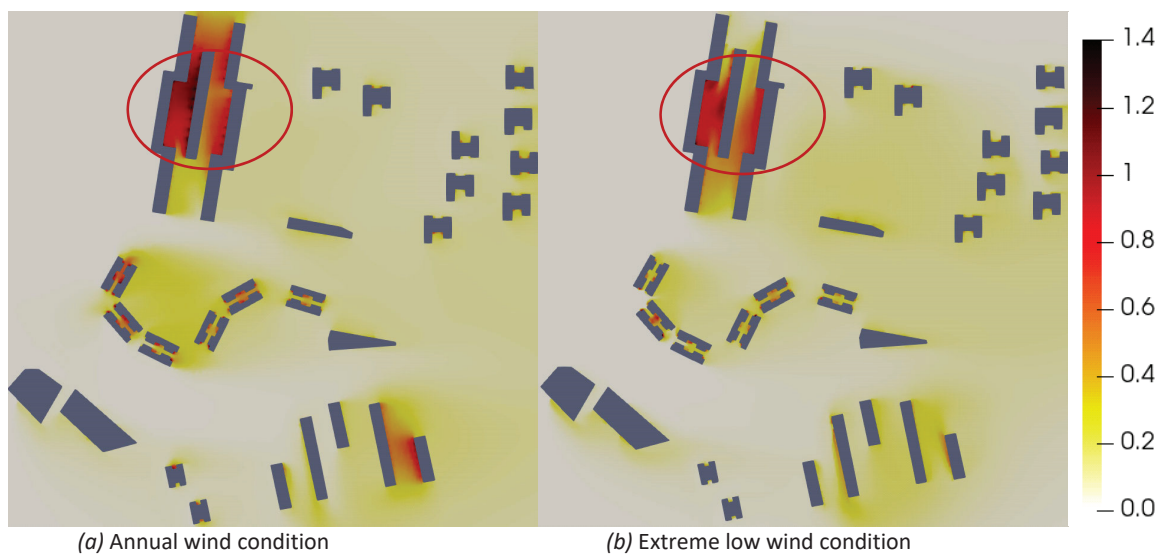


Figure 5. Time averaged temperature elevation distribution at pedestrian level ($z = 2 \text{ m}$) under the annual wind condition (a) and extreme low wind condition (b).

The highest temperature elevation was found at 1.2°C , which is located between two rows of buildings.

A typical “street canyon ” is formed by these buildings [16]. Vertically rotated vortices are generally formed within the street canyon, which significantly decreased the air exchange velocity [16]. The buildings of the warmest area were built in the 1970s, are the old type of HDB. The building heights are uniform of 24 m. Next to those buildings is the “Pinnacle@Duxton”, which is a new type of HDB built in 2001 with 150 m height. From the GIS data, the electricity consumption data is 5 times higher than the old HDB. However, the temperature elevation due to anthropogenic heat release is much lower. The comparison between these two residential areas demonstrates the urban street air warming could be mitigated by rational urban design.

5. CONCLUSION

The impact of anthropogenic heat emission induced by residential energy consumption on pedestrian level air temperature is investigated in this paper by CFD simulation. The heat releasing rate and urban configuration are obtained from electricity consumption. A Singapore residential area with both new and old type of HDB buildings is chosen for evaluation. The CFD model is validated by comparing with a non-isothermal wind tunnel experiment. The results show a maximum temperature elevation of 1.2 °C at the pedestrian level, which is located at the old type HDB. For the new type HDB with 5 times higher electricity consumption rate, the pedestrian level temperature is limited to 0.4 °C. Compared to the annual wind speed scenario, the extreme low wind speed generates lower temperature elevation at pedestrian level. The main reason is the vortex structure is destroyed to stronger buoyancy effect.

ACKNOWLEDGEMENTS

This research is supported by Singapore National Research Foundation under its two Campus for Research Excellence and Technological Enterprise (CREATE) programmes: 1) Intra-CREATE seed research grant (Grant no. NRF2018-ITS003-022) and Singapore ETH Centre, Future Resilience System II grant (Grant no. R-295-000-169-592). The computational work for this article was partially performed on resources of the National Supercomputing Centre, Singapore (<https://www.nscg.sg>).

REFERENCES

1. Oke, T.R., *City size and the urban heat island*. Atmospheric Environment (1967), 1973. 7(8): p. 769-779.
2. Wang, X., et al., *The street air warming phenomenon in a high-rise compact city*. Atmosphere, 2018. 9(10): p. 402.
3. Oke, T.R., *The energetic basis of the urban heat island*. Quarterly Journal of the Royal Meteorological Society, 1982. 108(455): p. 1-24.

4. Yang, X. and Y. Li, *The impact of building density and building height heterogeneity on average urban albedo and street surface temperature*. Building and Environment, 2015. 90: p. 146-156.
5. Offerle, B., et al., *Temporal variations in heat fluxes over a central European city centre*. Theoretical and Applied Climatology, 2006. 84(1): p. 103-115.
6. Kikegawa, Y., et al., *Development of a numerical simulation system toward comprehensive assessments of urban warming countermeasures including their impacts upon the urban buildings' energy-demands*. Applied Energy, 2003. 76(4): p. 449-466.
7. National Environment Agency (NEA). *Energy label and Tick Rating prior to 1 September 2014*. 2014;
8. Yoshizawa, A. and K.J.J.o.t.P.S.o.J. Horiuti, *A statistically-derived subgrid-scale kinetic energy model for the large-eddy simulation of turbulent flows*. 1985. 54(8): p. 2834-2839.
9. Tominaga, Y., et al., *AJ guidelines for practical applications of CFD to pedestrian wind environment around buildings*. Journal of Wind Engineering and Industrial Aerodynamics, 2008. 96(10): p. 1749-1761.
10. Richards, P.J. and R.P. Hoxey, *Appropriate boundary conditions for computational wind engineering models using the k-ε turbulence model*, in *Computational Wind Engineering 1*, S. Murakami, Editor. 1993, Elsevier: Oxford. p. 145-153.
11. Xie, Z.-T. and I.P. Castro, *Efficient Generation of Inflow Conditions for Large Eddy Simulation of Street-Scale Flows*. Flow, Turbulence and Combustion, 2008. 81(3): p. 449-470.
12. Uehara, K., et al., *Wind tunnel experiments on how thermal stratification affects flow in and above urban street canyons*. Atmospheric Environment, 2000. 34(10): p. 1553-1562.
13. Shih, T.-H., et al., *A new k-ε eddy viscosity model for high reynolds number turbulent flows*. Computers & Fluids, 1995. 24(3): p. 227-238.
14. Yakhot, V., et al., *Development of turbulence models for shear flows by a double expansion technique*. Physics of Fluids A: Fluid Dynamics, 1992. 4(7): p. 1510-1520.
15. Blocken, B. and J. Carmeliet, *Pedestrian wind environment around buildings: Literature review and practical examples*. Journal of Thermal Envelope and Building Science, 2004. 28(2): p. 107-159.
16. Mei, S.-J., et al., *Street canyon ventilation and airborne pollutant dispersion: 2-D versus 3-D CFD simulations*. Sustainable Cities and Society, 2019. 50: p. 101700.

Stall Prototype for Gandhi Street Market

Preserving the character of a humble Outdoor Market in the age of Supermarkets

ANJANA SURESH¹, PAULA CADIMA²

¹Urbanedge Architecture Ltd, Stamford, United Kingdom

² Architectural Association, London, United Kingdom

ABSTRACT: *The vendors and customers in the historic Gandhi market, Trichy, endure long hours of work in extreme environments, lack of urban amenities, lack of shelters and storage spaces, among other challenges. This paper looks at the current environmental and socio-economic conditions of the street vendors and discusses design solutions to increase their work efficiency and productivity while working outdoors in a hot and humid climate. The development of the design for a stall prototype is presented here. The main design concept aimed at utilising affordable strategies that could incorporate locally available materials for storage and cooling of the perishable produce to reduce expenses on transportation and refrigeration. Abundance of rainwater and solar energy has also been efficiently harvested for cooling purposes and energy consumption, respectively. The study involved analytic work to assess environmental and physiological parameters (without neglecting psychological issues) which could offer a stall capable of improving the working environment of the vendors and endure their livelihood in the long run to promote a better lifestyle.*

KEYWORDS: *Outdoor Comfort, Terracotta, Passive refrigeration, user-adaptability*

1. INTRODUCTION

Urbanization in a developing city like Trichy, India has been a boon and a bane to the society. It has created employment opportunities in the formal and informal sector. Informal sector that consists of street vendors represent a significant part of the economy. These vendors carry out their businesses in temporary or semi-permanent stalls and sell their goods in an unregulated and competitive market environment.

Since the advent of industrialisation and the rise of so called mega cities throughout the world, street vendors now strategically locate their workplaces in urban areas with steady pedestrian flows, often in central business districts or near crowded transport junctions. The presence of the street vendors is quite useful for a large section of the urban poor, as they provide goods, including food, at low prices. Subsequently, one can infer that one section of the urban poor, who typically operate as street vendors, subsidize the existence of the other sections of the urban poor by providing them cheap goods.

This paper addresses these issues and presents the development of design solutions aimed at increasing the market pedestrian experience in general, and the vendor's work efficiency and productivity while working outdoors in a hot and humid climate [2]. The paper focuses on the design development for a stall prototype made with locally available materials aimed at providing protection from rain and direct solar radiation while also integrating passive systems

using solar energy and collected rainwater for storage and cooling of the perishable produce. This is thought to reduce expenses on transportation and refrigeration.

2. THE CLIMATE OF TRICHY

Trichy is located at latitude 10.81 °N and longitude 78.69 °E and is categorised as 'Hot and Humid' climatic region with no major change in temperature between summer and winter. The high temperature and high humidity can be identified due to the presence of two rivers: Kaveri and Kollidam. As Trichy is situated on the Deccan plateau, the days are warm and dry with cooler evenings. The climate of Trichy can be divided into three periods in accordance to the monthly variations of the dry bulb temperature – Mild (November – February), Hot (June- October), Extremely Hot (March – May). The Mild period is the comfortable period wherein the dry bulb temperature lasts for a period of 4 months with temperatures ranging from 20°C to 30°C. The Hot period is characterised by outdoor temperatures ranging from 30°C to 37°C. which go above the calculated comfort range described in EN 15251 for hot and humid climates. Extremely Hot period is a highly uncomfortable period with high temperatures and high amounts of solar radiation where the temperature ranges from 35°C to 38°C. Trichy has high humidity levels that range from 55 to 80% throughout the year. High humidity combined with high temperatures can cause discomfort in vendors

and customers. Apart from high temperature and high humidity, Trichy also receives a significant amount of rainfall which lasts for six to eight months from May to December. The ensuing flooding and improper drainage cause an extraordinary amount of inconvenience for the vendors and pedestrians to carry out their daily work. Subsequently, the proposed design adopts various strategies to avoid flooding and harvest rainwater.

3. THE WAY OF LIFE AT GANDHI MARKET

The Gandhi Market in Trichy, Tamil Nadu, is a prime example of a community that has become subject to an uprooting and rehousing into a block like arrangement. It is a wholesale farmer's market selling vegetables, fruits and flowers where vendors sell to cities such as Chennai, Madurai and Tanjore. Its key clients and distributors include local store owners, restaurateurs, caterers. These vendors will have spent most of their lifetime selling their produces, much like their preceding generations did before them. Since they sell their produce in bulk, their day starts as early as 03:00am with the unloading of the produce and the arranging of their displays. They start selling throughout the morning and conclude by mid-day, as illustrated in Figure. 1. Apart from the vendors and customers, there are labourers/daily wage workers that help transport the produce from the trucks to their respective display spaces.

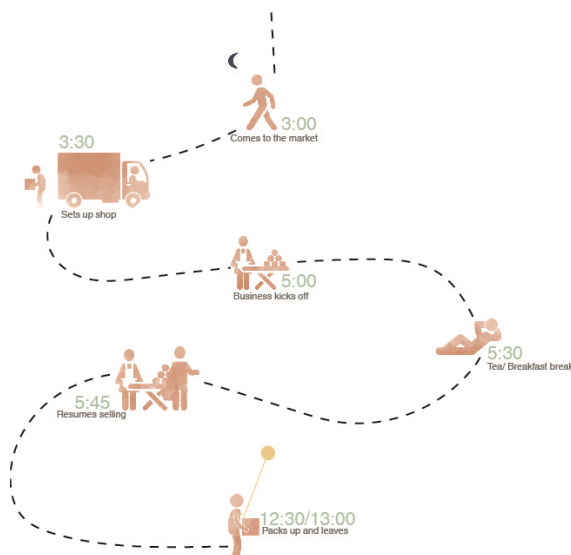


Figure 1: Daily routine of a vendor in Gandhi Street market.

The market is well known to be chaotic and unorganized due to the inflow and outflow of goods, customers, labourers and shopkeepers. There is a plethora of vendors who are found sitting on the ground, either a make-shift platform or a built platform. Vendors found seated on the ground are more exposed to conductive heat exchanges from the

ground when compared to the vendors sitting on a platform.

The vendors display their produce either on the ground or on a platform depending on convenience, whilst often sprinkling water on their produce to keep it fresh (Fig. 2). These fruits, vegetables and flowers are exposed to the harsh weather conditions most of the time and eventually lead to the reduction in their shelf life and an increase in organic waste; therefore, it was critical to devise a strategy to improve the freshness of their perishable produce.



Figure 2: Image of a vendor in Gandhi Street market.

The daily wage workers, shown in Fig. 3, help the vendors in transporting the produce from the unloading trucks to their display units. These workers are mostly men who carry bulky bags and travel for no more than five minutes by foot. As such, they are partly exposed to high solar radiation and increased metabolic rates, which can cause thermal discomfort during harsh weather conditions with no wind flow.

The current scenario does not offer sufficient strategies for storage, refrigeration, or protected shelter. The main objective of the redesign of this marketplace is therefore to provide methods for helping vendors store their produce fresh for a longer time without the hassle of transportation and create a better work environment.



Figure 3: A daily-wage worker in Gandhi Street market.

4. FINDINGS FROM FIELDWORK

Fieldwork was undertaken at the market space of Tamil Nadu, the site chosen for the redesign proposal [2]. The study included interviews, observations and spot measurements carried out to gather information on the present working environment that both the vendor and the customers must face in a daily basis. It also aimed at identifying the various environmental factors that affect the vendor's productivity and their perishable goods, their adaptive measures and strategies to improve thermal comfort, such as shading and enhancing ventilation, how vendors dealt with averting rain water, waste disposal and drainage patterns.

Spot measurements for air temperature, relative humidity, surface temperatures and wind velocity were recorded during the hot period of July, on a day with average temperature of 35 °C and average relative humidity of 60% during shopping times from 03:00 in the morning to 12:30pm.

Interviews were undertaken to gather information on challenges and issues market users faced when dealing with the effects of the varying climate swings day-to-day, the concerns they have with the storage of their produce considering climate variations and their preferences as to what they would like the marketplace to be able to accommodate in an ideal world situation.

The observations from the survey revealed that most of the vendors felt hot or warm at their current spot and only a handful of them felt comfortable. Extreme heat and rainfall were voted as the most uncomfortable parameters that affected their working conditions, both for the vendors and the customers.

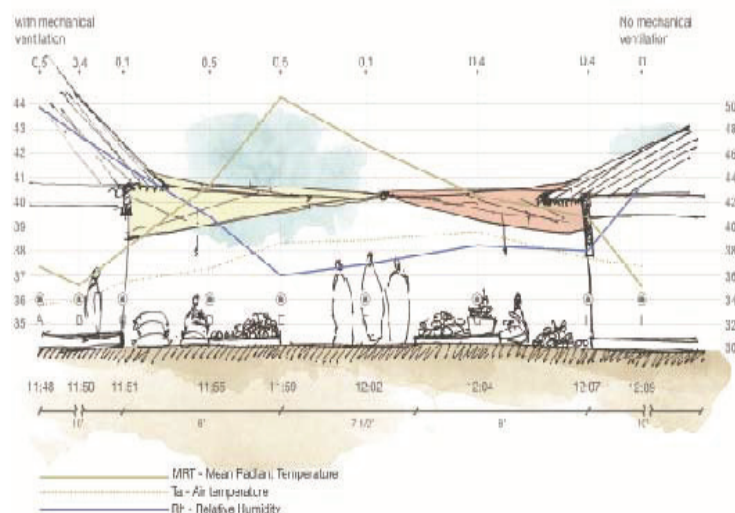


Figure 4: Conceptual sketch of a section in Gandhi market demonstrating the thermal conditions.

A combination of local roofing materials like thatch, gunny bag canopy and contemporary roofing materials like plastic canopy, asbestos cement roof sheets, etc. were commonly found in the market. The vendors prefer to use thatch or gunny bag canopy because it is easily available and cheap. However, during rainfall period, they end up placing a plastic canopy over it to provide protection from rain.

The recorded air temperature below the canopy was found to be 2-3K lower than the ambient air temperature. The air temperature measured at points A, B, C and I (Fig.4) was always lower than at other points due to the protected enclosure and a low sky view factor. However, the mean radiant temperature was found to be highest at the centre of this section throughout the marketplace. This was mainly due to the gaps in the plastic canopy above, exposing the pavement to direct solar radiation. Relative humidity at points E, F and G was observed to be lower than the relative humidity recorded under the solid asbestos canopy since the warm, humid air escapes through gaps in the plastic canopy combined with more wind movement at pedestrian level.

With regards to the waste disposal methods of the perishable items, it was found that most of the vendors sprinkled water on their fruits and vegetables to keep them temporarily fresh. After they had done this, the produce was either refrigerated at a rental storage space away from the market or thrown away. The latter method was found to be the most preferred method, due to the desire to economise on their business' expenditure.

5. OUTDOOR COMFORT STUDIES

Outdoor Thermal comfort is associated with environmental (air temperature, radiant temperature, wind speed and relative humidity) and personal (clothing and metabolism) factors and by a

variety of direct influences such as climate, geometry of the built-up spaces, materials, vegetation and indirect influences such as spatial, visual, acoustical, social and personal comfort.

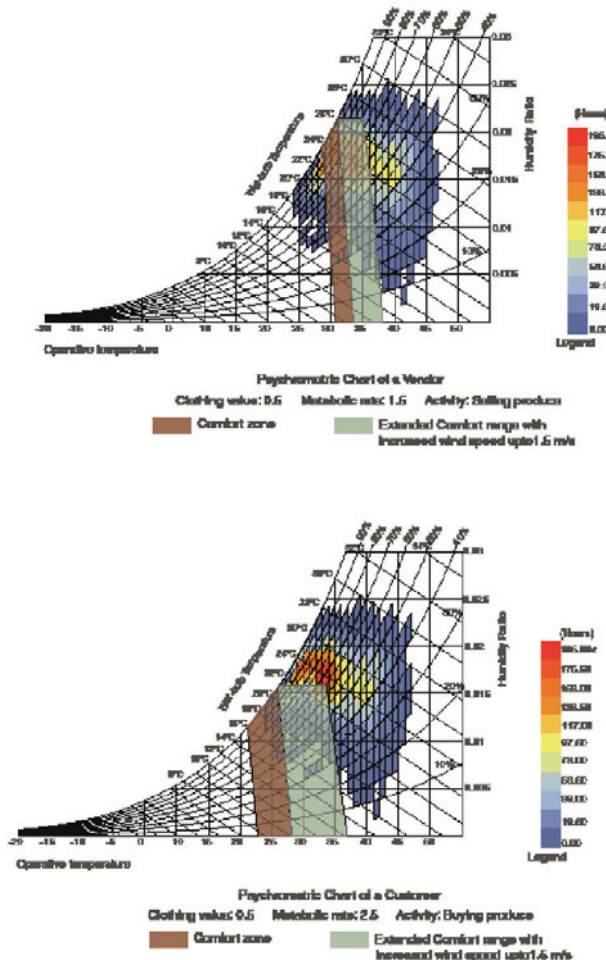


Figure 5: Psychrometric chart of a vendor and a customer with increased air movement.

Therefore, charts for different users, their respective clothing value, metabolic rate, body posture, and environmental factors were used to determine the comfort in Trichy's climate as shown in Figure 5.

To derive a comfort equation for hot and humid region, a literature review for this climate was done after which the EN 15251 comfort standard was chosen over the ASHRAE since it sets a comfort range for a free running mode derived from the equation below:

$$T_{\text{comf}} = 0.33 T_{\text{rm}} + 18.88 \quad (1)$$

Where the comfort equation is a function of the running mean of the outdoor temperature (T_{rm}). The comfort range is indicated as 2-3°C on either side of the optimum temperature. It also demonstrates how the comfort limits can be extended by increasing the wind speeds to provide psychological cooling. The limits can be extended up to 37°C with an air velocity of 1.5m/s.



Figure 6: Met rate and Clo value of the users of the market.

After analysing the various factors (Ref Fig. 6), both vendors and customers deal with while performing their daily activities, a more comfortable outdoor environment can be provided to improve their working conditions. Providing comfortable outdoor conditions can drastically help them improve their productivity and efficiency. Creating temporary relief methods for the customers from the harsh weather conditions can help in improving the economy of the market.

6. DESIGN DEVELOPMENT

The outdoor comfort preliminary studies and the fieldwork findings demonstrated that better shading and canopies are needed to provide a better environment for the vendors and customers. This will subsequently lead to an increase in their productivity. The fieldwork also revealed that keeping the vegetables and fruit fresh during the day is an important aspect for a successful business. Therefore, the design development for a stall-prototype here presented focused on two main strategies:

6.1. Providing appropriate shading methods and rainwater harvesting

The design proposal for shading was based on the nature and function of the market which started at 03:00 in the morning to 12:30pm. The sun altitude angles range from 10° early in the morning to 80° in the noon during mild and hot periods of Trichy. Due to the specific timings of their work, different geometries were tested to minimise direct solar radiation. The vertical plane is tilted as to reduce the surface area on the ground thereby, reducing the area exposed to solar radiation. Also, extending the roof outwards, helped in blocking the solar radiation up to 50%, thereby providing more hours of relief for the vendor.

The ventilated double roof option reduces heat fluxes transmitted by the exposed surface to solar radiation through the combined effect of shading and heat removed by the air flow in between surfaces. The butterfly roof helps in harnessing the potential of rainwater and solar energy. The lower sloped element is designed to shade during the working hours. The solar studies (Refer Fig. 7) show the sloped

roof to block almost 80% of the solar radiation from 10:00 to 13:00.

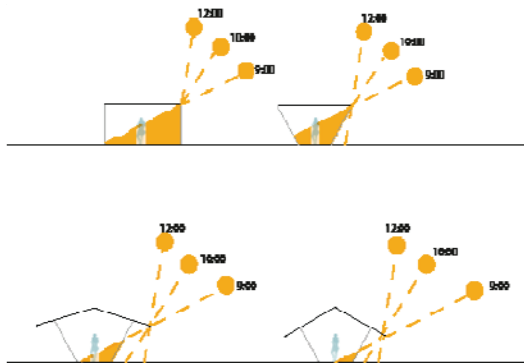


Figure 7: Conceptual graphic illustrating the sun altitude angles for various geometries.

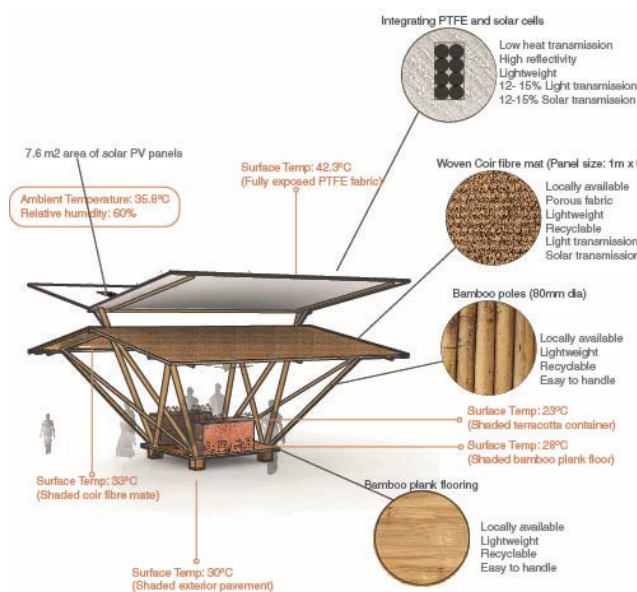


Figure 8: The proposed stall-prototype

The two roofs are united to form a concave roof with an air gap that acts like a buffer zone, allowing air movement which also helps in reducing the temperature of the overheated photovoltaic panel (Refer Fig. 8). The rainwater is collected by the butterfly roof and carried by hollow bamboo pipes to be stored in terracotta containers. In essence, these containers act as storage devices while also helping in extending the shelf life of the perishable items. The integrated photovoltaic panel on the outer canopy layer of the roof taps the abundant amount of solar energy available to Trichy. The panels receive solar radiation throughout the day and the energy is stored in batteries that can help in producing electricity to run the ceiling fans and light bulbs. The energy can also be harnessed to run motors to enable the pumping of flood water after torrential rains.

The canopy is projected to ensure reduced sky view factor, thereby reducing the effect of diffused radiation on the vendor. The projection also provides

temporary respite for the customers while stopping to buy the produce from the vendor during hot or rainy days. The stall is elevated by 0.3 metres from the ground to reinforce evaporative cooling of the terracotta containers. It also helps in decreasing heat gains received from the ground. The lateral sides are kept open to allow unobstructed wind flow.

6.2. Preservation of perishable goods using the concept of “passive-refrigeration”

Vendors found it extremely challenging to store and refrigerate their produce to sustain their freshness for longer periods. The process of repeatedly moving the produce to the storage and refrigeration facility was an extremely tedious and time-consuming process. Therefore, the stall-prototype design aimed at integrating an ecological cooling device that uses zero electricity to refrigerate fruits and vegetables.

Terracotta is a type of clay traditionally used in India to keep water cool using the principle of evaporative cooling. The porous surface of terracotta acts as a heat exchange where it absorbs water from the inside forming tiny droplets on the terracotta surface that evaporates in contact with air, thereby keeping the water cool. Under optimal conditions, cooling of up to 15°C can be obtained. Due to its proven historical effectiveness in India and its wide availability, the use of terracotta to develop cooling storage units is thought to be very suitable.

Two concepts were devised for the display and refrigeration of the produce using the principle of evaporative cooling, (Refer Fig. 9). The first concept is associated with the display of the produce since the vendors arrange their fresh harvest to maximise their customers. This harvest is open to the extreme weather conditions and tends to get rotten earlier than expected. By applying the similar principle explained above, the produce can be prevented from becoming rotten and unusable. A terracotta container filled with rain-water that uses convective and evaporative heat exchange to cool the surface of the container, on which the produce is displayed by 10 – 12K lesser than the ambient temperature, can extend the natural freshness of the produce for a longer time. The second concept was inspired by the “Terra-cooler” a cooling device invented by Stephan Augustin for food preservation. It incorporates the same principle that aids in storing the produce in a cool environment without the need for electricity or transportation. Studies by Vimala Beera et. Al (2011) demonstrated that storage of tropical fruits and vegetables require humid conditions that range from 80 to 95%. Therefore, this form of refrigeration is a viable solution because the humidity rises to 85% and reduces the air temperature by 10 to 15K inside the storage chamber due to evaporative cooling [1].

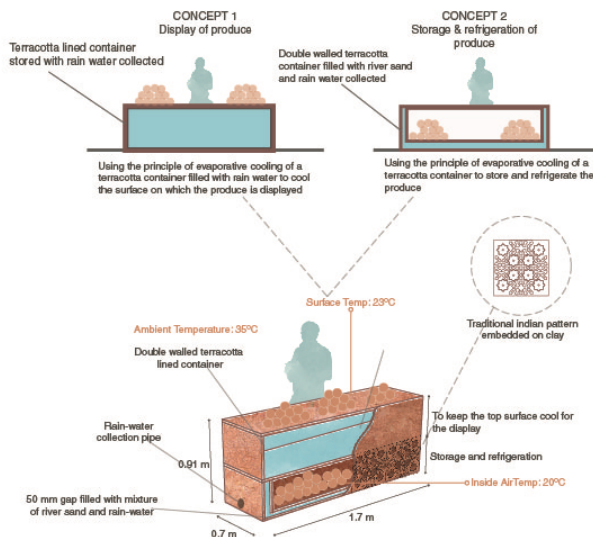


Figure 9: The proposed stall-prototype

The container is divided into two chambers filled with rainwater collected by the butterfly roofs through the bamboo elements that act as hollow pipes to carry the water from the gutters to the container. The top can be removed for the purposes of cleaning or repairing. The bottom chamber adopts the first concept of a functioning passive refrigerator with suitable temperature and humidity. This chamber can be opened from the inside by the vendor to store the produce. Fruits and vegetables can last twice as long, when compared to being stored at room temperature. The top chamber is filled with rainwater that adopts latent heat of evaporation to cool the surface of the displayed produce.

This zero-energy passive refrigerator utilizes low-cost, environment-friendly materials that are locally available to be constructed easily [2][3]. It must be kept under constant shade with regular air flow. In the absence of wind movement, mechanical ventilation installed in the ceiling of the stall can also help in accelerating the cooling effect. Every terracotta container can be personalised by the stall vendor by creating their own pattern on its exterior.

7. CONCLUSION

This study demonstrated a way in which sustainable environmental design can go beyond just providing comfort but also promote a better lifestyle. The paper reported on the design concept for a stall prototype (Refer Fig. 10) that can improve the working environment of the vendors and enhance their livelihood in the long run. It not only provides comfort for the vendors but also the customers who visit these markets often. It provides effective shading, ventilation for cooling, significant reduction in air temperatures and decreases the cost of living.

Affordable strategies that incorporate locally available materials for storage and cooling of the perishable produce leads to lesser expenses on transportation and storage for the vendors. Abundance of rainwater and solar energy has also been efficiently harvested for cooling purposes and energy consumption, respectively.



Figure 10: Proposed Gandhi market

The enduring presence of humble marketplaces such as Trichy are a testament to the men and women who dedicate themselves to serving the needs of the local community. The potential solutions presented provide a foundation for such an adaptation, whilst arguably retaining some of the key aspects of the markets layout that are so intrinsic to its ancient character. To put it another way, they are designed to be as unobtrusive and as beneficial to the physical wellbeing to those who gather within it as much as possible. The age of the marketplace does not need to be culled or suppressed, rather, it merely needs to undergo some adjustments that are both sustainable and capable to both accommodating a high-density population in the modern, fast paced 21st century.

With the adaptations, they will be able to sell the produce without it losing its freshness, something that its modern competitor, the supermarket, is currently able to boast, but at a cost of producing a carbon footprint. This solution will ensure the market is still a competitive, relevant, and crucially, environmentally friendly alternative in a fast-paced world that has little time to stand and stare and appreciate a sense of community and belonging.

REFERENCES

1. Beera, V., DV. Samuel and A. Lal Basediya, (2013). Evaporative cooling system for storage of fruits and vegetables – A review.
2. Suresh, A., (2018). Redesign of Gandhi Street market, Means to achieve outdoor thermal comfort.
3. Terra-cooler: Natural cooling with terracotta and water, [Online]

A Dynamic Analysis of Daylight Availability in Dense Urban Residential Areas: A Cross-region Study in China

LISHU HONG¹, XIN ZHANG¹, JIANGTAO DU²

¹School of Architecture, Tsinghua University, Beijing, China

²Liverpool School of Architecture, University of Liverpool, Liverpool, UK

ABSTRACT: Daylight utilization in cities is receiving increasing attention from urban planners and developers, architects, and engineers, especially in China. This article aims to study the daylight availability in highly dense residential areas across China with respect to current planning regulations. Using a method of climate-based analysis, frequencies of vertical daylight illuminance at building south façades in three urban layouts have been assessed according to five typical locations, one of which represents one daylight climate zone. Key findings are as follows: 1) Given the daylight availability, these layouts were proved as suitable for only two southern locations, but not appropriate for others. 2) Current regulations, focusing on ground floors in these layouts, would lead to excessive daylight illuminance and solar gain received at the higher façade. It is necessary to achieve a balanced level of daylight availability across various positions of building façade through an effective approach. 3) Under a situation of the highest building density allowed by current regulations, urban layouts (building forms) might not be able to take substantial effect on the overall daylight availability in buildings.

KEYWORDS: Daylight availability, Dense residential area, Daylight climate zone, Dynamic simulation, China

1. INTRODUCTION

Daylight utilization in urban areas is receiving increasing attention from urban planners and developers, architects, and engineers [1, 2]. China currently has two building regulations relating to daylighting planning: ‘Standard for daylighting design of buildings (2013)’ [3] and ‘Standard for urban residential area planning and design (2018)’ [4]. The first specifies daylight factors in terms of various functional spaces as the evaluation index for daylighting design, while the second quotes a minimum requirement of sunlight hours (calculated using sunpath diagram) in residential buildings. With the rapid urbanization in China, a great number of dense urban areas have recently emerged with high-rise buildings and narrow open spaces, resulting in very poor daylighting conditions [2]. However, with this new situation, it can be found that methods mentioned in two regulations [3, 4] are not able to help to achieve practical design and planning solutions, especially based on the response to local climates [2].

Several studies of planning regulations have been implemented in high dense cities in China. Ng [5] discussed daylight planning in terms of existing rules and policy in Hong Kong and found that these regulations had been applied ‘out of context’ with higher tower-like buildings. Other studies [6, 7] argued that the old version of the planning regulation [4] has very low potential to support practice due to the lack of detailed descriptions or adequate quantitative items, and on the other hand it could be

hard to apply it for locations dominant by non-clear sky conditions. In addition, in some areas of north China, this regulation resulted in excessive land waste [8]. These studies did not move beyond theoretical discussions and it seems that they might lack solid practical proofs to justify how to effectively improve the daylighting planning at an urban scale.

Some investigations provided in-depth analysis of application of the regulations [3, 4] relating to daylighting at specific Chinese locations. At a city of east China, a study [9] found that some high-rise residential buildings still got poor daylighting condition, even though they have been properly planned based on the regulation [4]. Using a dynamic analysis method, Lu and Du achieved more practical analyses according to daylight availability in a highly dense residential area in north-east China with a cold climate [2]. It seems that a cross-region study would be beneficial due to facts that planners could understand the limitations of current planning methods and thus more practical design activities could be effectively implemented.

This article presents a climate-based simulation analysis for daylight availability in five Chinese locations, each of which represents one of the five daylight climate zones in China [3]. Planned based on current regulations, three typical urban layouts (residential area) with high density were assessed. This study aims to find out the feasibility of daylighting planning at an urban scale and the possibility to produce new design guidelines and

strategies for achieving an effective daylighting planning at an urban scale in current China cities.

2. METHODS

2.1 Daylight climate zones and locations

As shown in Figure 1, five daylight climate zones in China [3] have been defined according to annual average total illuminance E_q (klx). They are zone I ($E_q \geq 45$), zone II ($40 \leq E_q < 45$), zone III ($35 \leq E_q < 40$), zone IV ($30 \leq E_q < 35$), and zone V ($E_q < 30$). This study selected five locations, each of which is the representative in one of these zones. The locations are: Lhasa (zone I), Yinchuan (zone II), Beijing (zone III), Guangzhou (zone IV), and Chengdu (zone V).

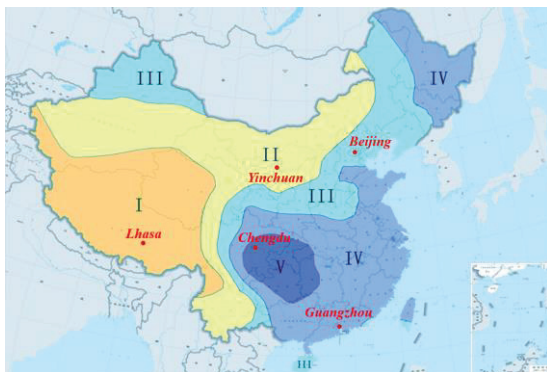


Figure 1: Daylight climate zones (I-V) and five Chinese locations.

2.2 Urban layouts studied

At each location, three typical urban layouts in residential areas were studied (Figure 2 & Table 1). Layout 1 and Layout 2 have square buildings ($27 \times 27 \times 72$ m) and rectangular buildings ($13 \times 60 \times 36$ m) respectively, while Layout 3 includes both two building types. The three layouts are used because they are currently typical urban layout forms applied in residential areas of most big Chinese cities [10]. Table 1 presents building distances in terms of locations and three layouts. The building dimensions and distances were defined to achieve the highest building density according to both national and local planning regulations [4, 11-17], with respect to the residential building design requirements of health and wellbeing, building structure, fire safety, etc.

Table 1: Building distances in three layouts.

Location	Building distance (m)							
	Layout 1		Layout 2		Layout 3			
	L1	L2	L1	L2	L1	L2	L3	L4
Lhasa	13	96	13	48	13	13	96	48
Yinchuan	13	119	13	58	13	13	119	60
Beijing	13	120	13	61	13	13	120	61
Guangzhou	22	45	13	38	13	22	45	27
Chengdu	22	36	16	30	16	22	36	30

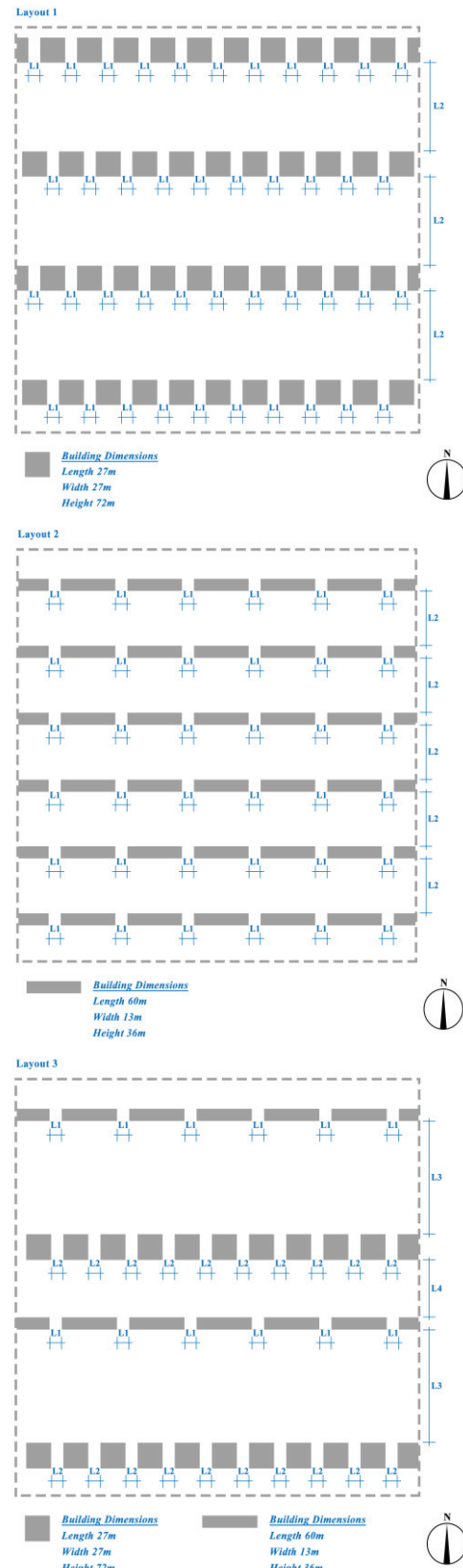


Figure 2: Three typical urban layouts studied.

2.3 Daylight availability and simulation

As mentioned in a previous study [2], there is a linear relationship between external vertical

illuminance at centre external window of building (E_v) and indoor average daylight illuminance at the working plane (I_{AI}). Thus, an equation can be used to describe this relationship as follows:

$$E_v = K \times I_{AI} \quad (1), \quad \text{where}$$

K is the coefficient factor, which is related to locations and climates. According to the method in the reference [2], the K value was achieved based on the regression analysis using local weather data. In this study, K values were used as 8.0 (Lhasa, Yinchuan, and Beijing), 9.0 (Guangzhou) and 9.5 (Chengdu). In addition, the daylight availability in these layouts was indicated by the external vertical illuminances at the centre south façade of square or rectangular buildings. As discussed in a study [18], when only receiving the daylight from windows, the range of 100 lx to 3000 lx for I_{AI} can be interpreted as a condition of 'useful daylight', while the ranges of > 3000 lx and ≤ 100 lx will be treated as 'excessive daylight' and 'inadequate daylight' respectively. Thus, with respect to the ranges of I_{AI} , E_v ranges were categorized using the Equation (1) at different locations as follows: 1) proper external vertical illuminance (PrVI) with ($K \times 100 \text{ lx} < E_v \leq K \times 3000 \text{ lx}$); 2) excessive external vertical illuminance (ExVI) with ($E_v > K \times 3000 \text{ lx}$); 3) poor external vertical illuminance (PoVI) with ($E_v \leq K \times 100 \text{ lx}$).

In the three layouts (Figure 2), the centre south façade of the buildings located in the middle was adopted as the studied position, due to a fact that the highest level of obstruction (worst daylight conditions) was found here. At this façade position, external vertical illuminance (E_v) was calculated using Daysim/Radiance and the method mentioned in a reference [2]. The annual occurrence (frequency) of the vertical illuminance (6:00 - 18:00) in each E_v range can be used to justify the potential of daylighting in buildings. A higher frequency of PrVI indicates a 'good' outdoor vertical illuminance that would result in a proper indoor illuminance across the working plane. If the frequency of ExVI has a higher value, the external façade surfaces will receive excessive solar gain and daylight illuminance, which means a higher risk to get visual discomfort and overheating problems in the indoor spaces. In addition, for PoVI, the higher is its frequency, the lower possibility is found to apply daylighting in the room.

3. RESULTS

This section presents frequencies of different ranges of vertical illuminance at south façades in terms of locations and three typical façade positions. Heights of these positions are: square building (s): 2.1 m (ground floor), 34.55 m (middle floor) and 69.95 m (top floor); rectangular building (r): 2.1 m (ground floor), 16.55 m (middle floor) and 33.95 m (top floor).

3.1 Daylighting availability: ground floor

Figure 3-5 show frequencies of PrVI and ExVI at ground floor in three layouts. It can be found that the three layouts could lead to relatively higher daylight availability at the ground floor for all locations (higher frequency of PrVI). Guangzhou has the highest PrVI frequency (over 71.65%), while Lhasa and Yinchuan have lower frequency of PrVI (still over 40.11%). However, ExVI frequencies of Lhasa and Yinchuan are both around 30%, which means at the two locations there are higher risk to get excessive solar gain and daylight illuminance, even at ground floor. On the contrary, Chengdu and Guangzhou have very low risk to get excessive solar gain (ExVI frequencies $\leq 7\%$). Beijing has PrVI frequency of over 55%, while its ExVI frequency is slightly lower than that of Lhasa and Yinchuan.

For Layout 1, the difference between PrVI frequency and ExVI frequency ranges from 14.12% (Yinchuan) to 68.90% (Guangzhou), whilst Yinchuan and Guangzhou see the differences of 11.08% and 64.61% for Layout 2 respectively. In Layout 3, these frequency differences have one range from 11.44% (Yinchuan) to 68.47% (Guangzhou) for square buildings, and another range from 8.58% (Lhasa) to 68.75% (Guangzhou) for rectangular buildings. Therefore, Guangzhou has higher possibility to achieve useful daylighting utilization under national and local regulations.

For one specific location, generally, PrVI frequencies of square and rectangular buildings are similar (absolute difference $\leq 3.67\%$). This finding could be reasonable since based on current regulations a similar level of obstruction could be found at the ground floor and thus the 'good' daylight condition will receive lower impact of urban layouts.

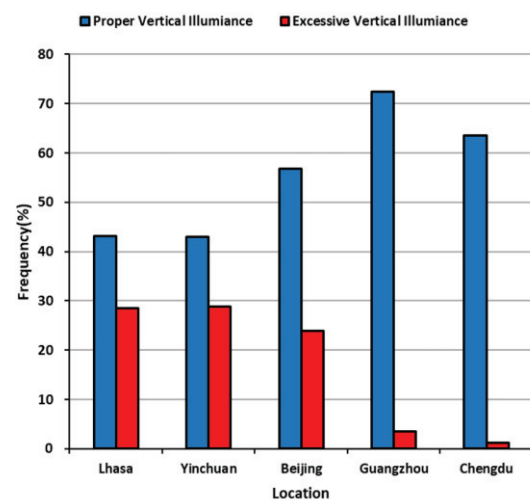


Figure 3: Frequencies of E_v ranges (Layout 1; ground floor).

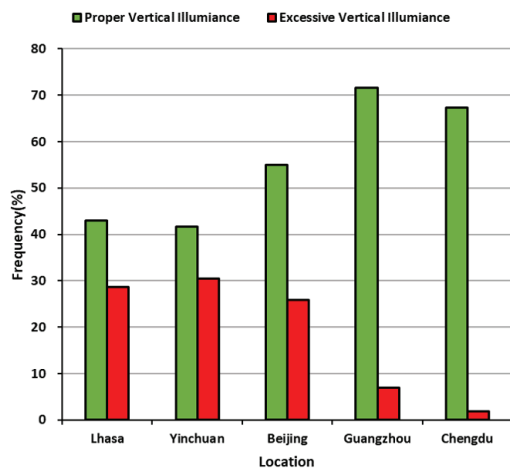


Figure 4: Frequencies of Ev ranges (Layout 2; ground floor).

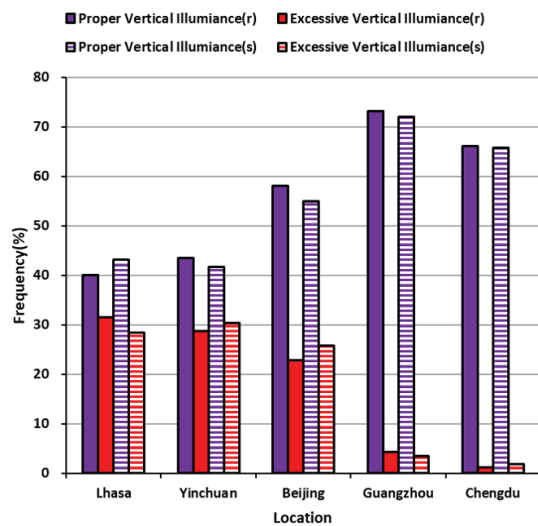


Figure 5: Frequencies of Ev ranges (Layout 3; ground floor).

3.2 Daylight availability: middle floor

Figure 6-7 present frequencies of two Ev ranges at middle floor in three layouts.

Apparently, the three layouts can still lead to relatively higher PrVI frequencies at the middle floor. Lhasa and Yinchuan have much lower PrVI frequencies than Guangzhou and Chengdu. In addition, ExVI frequencies have become higher at the middle floor. A higher level of solar gain and daylight illuminance will thus be found at middle floor for all locations, especially at Yinchuan and Lhasa. In Yinchuan, ExVI frequencies are generally higher, with the lowest value of 33% found at rectangular buildings in Layout 3. Lhasa sees that frequencies of PrVI and ExVI are very closed, and that 31% is the lowest ExVI frequency (rectangular buildings in Layout 3). These would clearly indicate that Lhasa and Yinchuan will have to deal with very high risk of overheating and visual discomfort at middle floor.

Compared with the ground floor, the middle floor sees increased ExVI frequencies for most buildings. For Layout 1 and Layout 2, the increase of ExVI frequency at Lhasa and Yinchuan have achieved over 6%, while Chengdu has a lower increase of around 2%. For Layout 3, the trend tends to be more complex. The increases of ExVI frequency at rectangular buildings are generally lower than square buildings. For rectangular buildings in Layout 3, Yinchuan has higher increase, but Lhasa does not have change. Square buildings see Lhasa and Yinchuan receive the highest increase, while the lowest increase is found at Chengdu. Thus, the daylight availability is significantly affected by the façade position in Lhasa and Yinchuan. The effect tends to be less in Chengdu.

At middle floor, there are no big differences of PrVI frequencies between Layout 1 and Layout 2 (< 0.4%) at all locations. This means that the layouts (with one type of building) will not significantly affect daylight availability at middle floor. For Layout 3 (mixed layout), rectangular buildings generally have higher PrVI frequencies than square buildings. Differences of PrVI frequency between rectangular and square buildings decreases with the decrease of E_q at five locations.

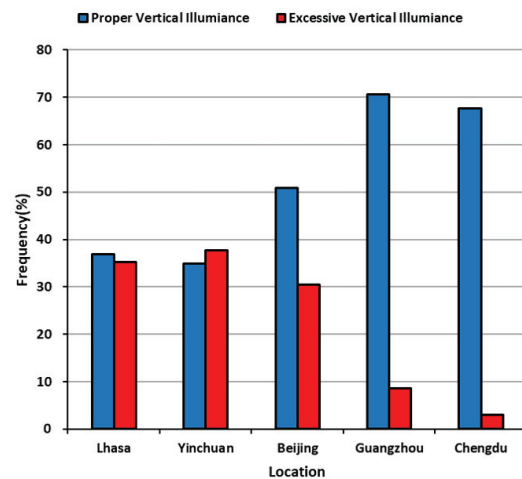


Figure 6: Frequencies of Ev ranges (Layout 1; middle floor).

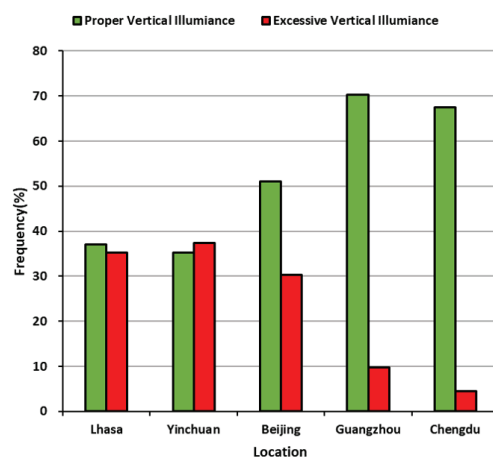


Figure 7: Frequencies of Ev ranges (Layout 2; middle floor).

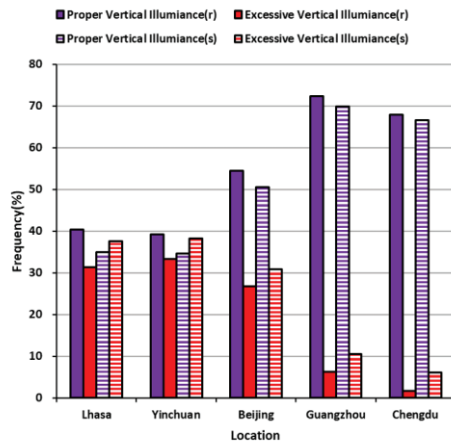


Figure 8: Frequencies of Ev ranges (Layout 3; middle floor).

3.3 Daylight availability: top floor

Frequencies of two Ev ranges at top floor in three layouts can be found in figure 9-11.

It can be found that only at three locations (Beijing, Guangzhou and Chengdu), the three layouts can lead to higher PrVI frequencies at top floor (above 45%). In addition, Lhasa and Yingchun can see higher ExVI frequencies ($\geq 35\%$), which are larger than their PrVI frequencies. For Beijing, Guangzhou and Chengdu, even though ExVI frequencies are still lower than PrVI frequencies, values of the former have significantly increased with positions moving to top floor. It is normal to agree that the top floor of buildings has highest risk of excessive solar gain and daylight illuminance.

Compared with middle floor, the decreases of PrVI frequency at top floor are larger in Lhasa and Yinchuan, but less clear in Guangzhou and Chengdu. The trend is similar to that of the middle floor, which can again enhance the fact that the daylight availability receives higher impact from the façade position in Lhasa and Yinchuan than Guangzhou and Chengdu.

At top floor, differences of PrVI frequency between Layout 1 and Layout 2 are insignificant (lower than 0.5%). Similar to the middle floor, the daylight availability at top façade will not be clearly influenced by the layout (with the same building in). In addition, for Layout 3, square buildings generally receive lower PrVI frequencies than rectangular buildings at all locations. The absolute differences of PrVI frequency between the two buildings are above 2.19%.

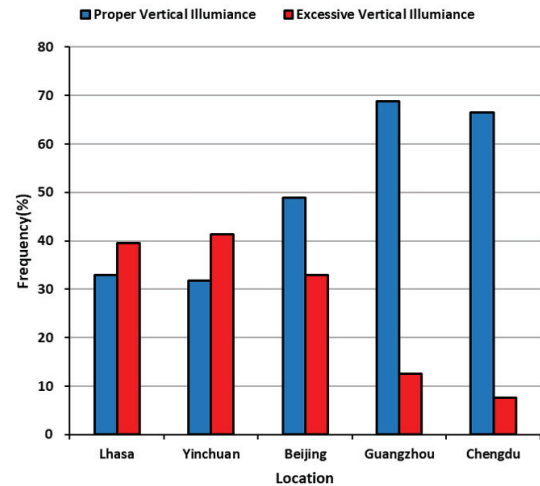


Figure 9: Frequencies of Ev ranges (Layout 1; top floor).

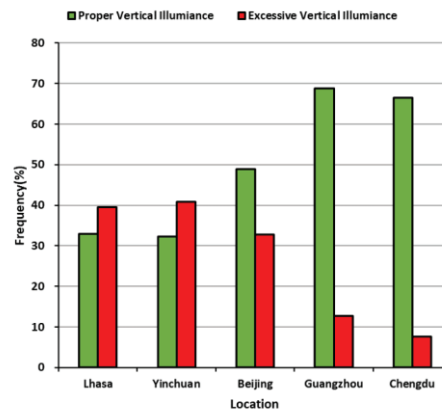


Figure 10: Frequencies of Ev ranges (Layout 2; top floor).

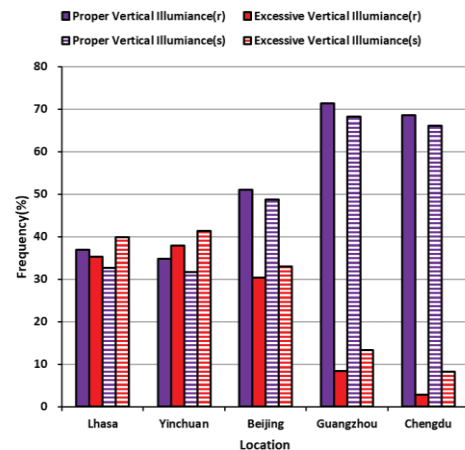


Figure 11: Frequencies of Ev ranges (Layout 3; top floor).

4. DISCUSSION AND CONCLUSION

Based on a climate-based analysis method, this study focuses on investigating the daylight availability of three urban residential layouts at five Chinese locations.

First, locations and climates play the most important role to achieve a proper daylighting utilization. In general, Guangzhou (Zone IV) and Chengdu (zone V) have the highest potential to

achieve ‘useful’ daylighting due to the achievement of the highest PrVI frequencies and relatively lower ExVI frequencies, while Lhasa and Yinchuan (Zone I and II) have the highest risk to get problems of overheating and visual discomfort due to the higher ExVI frequencies. Beijing’s has a medium potential for such ‘useful’ daylighting with the medium levels of PrVI and ExVI frequencies. These could indicate that the three layouts are very suitable for Guangzhou and Chengdu under current regulations but may not be appropriate for other locations. Without further modification of current regulations, it could be possible to give rise to environmental problems relating to land waste in some cities.

Second, during the early stage of urban design, it could be necessary to achieve a balanced level of daylight availability across the building façade, including lower, middle, and higher positions. The results have shown that the daylight availability in Lhasa and Yinchuan (Zone I and II) is much more sensitive to the façade positions than Guangzhou and Chengdu (Zone IV and V). Most planning regulations in China only focus on the ground floor, with the minimum requirement of sunshine hours at this position [4]. Without considering local climates and higher floor positions, there would be higher risk to get excessive solar gain and daylight illuminance for locations with high annual average illuminance (E_q).

Third, under the situation of the highest building density allowed by planning regulations [4, 11-17], urban layouts might not be able to take substantial effect on the overall daylight availability across the south façade in buildings. For the layouts using the same building type (Layout 1 and Layout 2), it has been found that daylight availabilities at three facade positions (ground, middle or top floor) are similar (Fig. 3-4, 6-7 and 9-10). However, for Layout 3 with two different buildings (Fig. 5, 8, 11), there are some differences found between square and rectangular buildings. Compared with square buildings, rectangular buildings would receive slightly higher levels of ‘useful’ daylighting at all locations. Thus, it seems that the type of buildings between adjacent rows may bring in some impacts to the daylight availability. According to most regulations [4, 12-15, 17], in general, the distance between two building rows is established based on the height of southern buildings without taking into consideration building forms. This could explain the insignificant differences of daylight availability between various urban layouts.

Limitation and future work: This study was implemented in three specific layouts. It would be interesting to check more parameters relating to the urban forms. Except for the south façade, other façades of buildings in the three layouts should be also studied. In addition, other typical orientations

(e.g. south-east or south-west) might deliver various impacts on the daylighting utilization in these layouts.

REFERENCES

1. Littlefair, P., (2001). Daylight, sunlight and solar gain in the urban environment. *Solar Energy*, 70(3): p. 177-185.
2. Lu, M. and Du, J., (2019). Dynamic evaluation of daylight availability in a highly-dense Chinese residential area with a cold climate. *Energy and Buildings*, 193: p. 139-159.
3. Ministry of Housing and Urban-Rural Development, (2013). GB 50033-2013, Standard for daylighting design of buildings. Beijing, China.
4. Ministry of Housing and Urban-Rural Development, (2018). GB 50180-2018, Standard for urban residential area planning and design. Beijing, China.
5. Ng, E., (2003). Studies on daylight design and regulation of high-density residential housing in Hong Kong. *Lighting Research and Technology*, 35(2): p. 127-139.
6. Yao, J., (2007). Suggestions and Regulations on Sunlight Analysis Methods for High-rise Buildings. *Building Science*, 23(5): p. 105-108.
7. Wang, X., and Duan Y., (2006). Sunlight Issues in Urban Planning Administration. *City Planning Review*, 9: p. 57-60.
8. Li, X., (2005). A Reflection of Some Problems in the Implementation of Code for Planning and Design on Urban Residential Areas. *Planners*, 8: p. 52-54.
9. He, Z., and Fan W., (2005). Sunshine Spacing and Building Setback. *Urban Planning Forum*, 2: p. 96-97.
10. Hu, W., (2007). Principle and Design of Residential District Planning. China Building Industry Press. Beijing, China, ISBN 978-7-112-08548-4.
11. Ministry of Housing and Urban-Rural Development, (1993). GB 50178, Standard of climatic regionalization for architecture. Beijing, China.
12. Ministry of Public Security, (2018). GB 50016–2014, Code for fire protection design of buildings. Beijing, China.
13. The People’s Government of Lhasa Municipality, (2007). Implementing Rules of Urban Planning Regulations in Lhasa (拉萨市城市规划条例实施细则). Lhasa, Tibet, China.
14. Bureau of Urban Planning of Yinchuan Municipality, (2016). Technical Regulations on Urban and Rural Planning Management in Yinchuan (银川市城乡规划管理技术规定). Yinchuan, Ningxia, China.
15. Beijing Municipal Commission of Planning, (2012). Revision of *General Rules for Planning and Design of Construction Projects in Beijing* and *Code of Urban Planning Management in Beijing* (《北京地区建设工程规划设计通则》《北京地区城市规划管理守则》修编). Beijing, China.
16. The People’s Government of Guangzhou Municipality, (2019). Technical Regulations on Urban and Rural Planning in Guangzhou (广州市城乡规划技术规定). Guangzhou, Guangdong, China.
17. Bureau of Urban Planning of Chengdu Municipality, (2015). Technical Regulations on Planning and Management of Towns and Villages in Chengdu (成都市城镇及村庄规划管理技术规定). Chengdu, Sichuan, China.
18. Mardaljevic, J., Andersen, M., Roy, N., and Christoffersen, J., (2013). Daylighting, Artificial Lighting and Non-Visual Effects Study for a Residential Building.

An Urban Usability Study for Exploring Socio-Cultural Sustainability in Contemporary Public Spaces: The Case of the New Abdali Development Project in Amman-Jordan

NEAMAT AL DISSI¹

Department of Architecture, University of Petra, Amman, Jordan

ABSTRACT: Public spaces are a key part of any city that defines its character. Historically, such areas located in downtowns are attractive destinations that contribute to connect people together, and allow to shape the cultural identity of the city. Recently, attention to public spaces around buildings in cities is less comparable to the unprecedented interest in creating iconic vertical structures and contemporary developments. However, these open areas need to offer the basic requirements of sustainability.

This research focuses on assessing the social and cultural dimensions of sustainability in contemporary public spaces. A usability study that is based on specific indicators; including social equity, satisfaction of human needs, quality of life, sense of place, culture identity, social interaction, and social mixing, is adopted to evaluate effectiveness, efficiency, and satisfaction of users. Moreover, the study entails other factors affecting the social life, such as hierarchy of spaces, privacy, place attachment, territoriality, personalization, control, and sensory of pleasure.

The New Abdali Project in Amman and the Boulevard specifically was taken as a case study, it is the newest and largest mixed-use development in the heart of the Jordanian capital, is one of its kind in Jordan, consisting of different services and functions.

KEYWORDS: Open Public Spaces, Cultural Identity, Social Sustainability, Urban Quality of Life, Social Behavior.

1. INTRODUCTION

Social sustainability is about designing for impact, and therefore, improving the quality of life [1,2]. Public spaces between buildings need to offer the basic requirements of social sustainability; such as improving community well-being, strengthening the social fabric of the community, creating a sense of belonging, reflecting the cultural identity of the city, and encouraging distinctive users' experience. However, assessing and measuring social and cultural dimensions at the urban scale of the city has considerably less attention than environmental and economic dimensions, and it was neither fully explored nor widely recognized. One of the challenges for achieving this aspect is the difficulty of identifying suitable measures that represent the social life. The study contributed to this field by identifying the different indicators that affect the quality of life in urban spaces, in addition to its impact on the spirit of the town. This study aims to find a mechanism to measure social and cultural sustainability in contemporary open public spaces. The Boulevard in Abdali development project, which is the newest public space in Amman, was chosen as a case study.

2. LITERATURE REVIEW

The term "sustainability" has been discussed in different sciences and disciplines. It became familiar and well-known after the Brundtland Commission of the United Nations on March 20, 1987, which defined sustainability as development that meets the needs of the present without compromising the ability of future generations to meet their own needs [3].

Sustainability concept embraces three equal pillars in importance; environmental, economic and social, which need to be all balanced. In early decades, the concept of sustainability was barely limited to the environmental and resource dimension. These very limited considerations were broadened by the UN-Conference on environment and development in the Rio de Janeiro in 1992. It was the first time that the social dimension and human development of sustainability were explicitly mentioned [4]. Yet, it attained importance after 2000 [5,6].

Social sustainability gained its origin from social community and the interaction with the environment they live in [7]. Chiu (2003) described the term as the conservation and development of the welfare of the present and forthcoming generations, and she agreed that social sustainability is both environment and people oriented [8]. Furthermore, it preserve a variety of important components, such as relationships people create with the environment, and their daily

lives, the social bonds, and senses of self-belonging [10].

2.1 Measuring Social Sustainability

Social and cultural dimensions of sustainability are more difficult to be assessed than other aspects. One of the best strategies to achieve that is to determine specific indicators that could be measured and quantified to represent the social dimension of the city and the urban space. Based on an intensive review of several studies [11-15]. Table 1 shows an explanation of the different social indicators and characteristics of each quality.

Table 1. Definitions and characteristics of social indicators (Author)

Social Indicators	Explanation, Definition and Characteristics		
1- Social equity	Includes equity of access to key services (including health, education, transport, housing, and recreation)		
2- Satisfaction of human needs	Basic needs and access to resources. It relates to both human and society. It follows Maslow's hierarchy of needs. It entails opportunities and available resources at the community level.	Human Needs	Spatial Qualities
		Physiological needs (Food, water, health and safety), and social needs (relationships, confidence, and mutual respect).	Comfort, public services, firmness, and balance.
		Safety needs	Privacy, legibility, and safety.
		Belongingness and love needs	Social amenities and facilities, sense of place and identity.
		Esteem needs	Inclusiveness, and preservation of local characteristics.
		Self-actualization needs (creativity and morality), opportunities and available resources in society).	Diversity, and public participation.
		Beauty and aesthetics needs.	Visual richness, visual proportions, and visual distinctiveness.
3- Well-being, happiness, and quality of life	It is the sum or factors that contribute to the social, environmental and economic wellbeing of citizens. It covers aspects such as healthy environment, wellbeing, happiness, and satisfaction.	Urban Quality of Life Principles	
		Environmental	Give the ability to enjoy natural landscape by providing a range of green areas distributed within the neighborhood.
		Physical	<ul style="list-style-type: none"> - Neighborhood should be compact, pedestrian friendly and mixed use. - Provide the access to adequate services and facilities that fulfill people's needs. - Provide well-defined streets and open spaces by a well-structured building layout, in addition to take density and crowd-ness into consideration in the design phase of open public spaces. - Provide the access to adequate eco-buildings and housings that fulfill people's needs and national building code. - Provide a hierarchy of complete street networks based on pedestrian and vehicle load. - Take into account projected management, maintenance and repair policies to ensure the sustainability of neighborhood.
		Mobility	<ul style="list-style-type: none"> - Provide alternatives to using car in order to reduce traffic load, minimize air pollution and conserve energy. - Provide activities of daily living and transit stops within walking distance to allow independence to elderly, young and who do not drive. - Provide fine network interconnecting streets to encourage walking. - Provide streets friendly with pedestrian, cycle and vehicle.

		Social	<ul style="list-style-type: none"> - Social justice and equity. - Remove all barriers that reduce the participation in daily - Life of certain social groups, such as those with disabilities, women, children and elderly. - Design of streets and buildings should reinforce safe environments. - Promote good relationships and daily interaction between people by providing civic buildings and public gathering places. - Promote the livability of streets by providing safe, comfortable, interesting streets and squares to the pedestrian.
		Psychological	<ul style="list-style-type: none"> - Promote community identity by preserving heritage and historic remains, making architecture and landscape responding to their context. - Provide the opportunity for people to have a place of their own by giving the ability to personalize the space.
		Economical	Provide job opportunities and promote local business by supporting locally owned stores and business, as well as by encouraging mixed use development, affordable housing, services and facilities.
		Political	<ul style="list-style-type: none"> - Promote integrated urban governance. - Provide codes and legislation to control evolution. - Promote the community involvement in council decision making.
4- Social interaction, social mixing (cohesion and inclusion)	Socially cohesive and physically integrated urban unit. It is about relational aspects of society, but also on individual and personal aspects.		
5- Pride, sense of place and cultural identity	It is about people's precipitations of a certain place. It mainly relates to a positive sense of attachment, dependent, and identity that people feel about the place they live.		
6- Sense of Community	It is about social interaction of people living in a given area, sense of community, and place attachment.		
7- Future Focus	Future Focus (or long term viability and promotion) It is indicated that social sustainability is primarily about valuing and protecting positive aspects of cultures and promoting current conditions-encompassing individuals, communities and societies, and also ensuring the qualities for generations to come.		

3. DEFINING THE CONTEXT OF THE STUDY

New Abdali Development project is the largest mixed-use project ever constructed in the heart of Amman, the capital of Jordan¹. Abdali Investment and Development PSC has managed to create a unique master plan that includes a studied mix of residential apartments, commercial offices, hotels and serviced apartments, retail outlets as well as medical and entertainment facilities.

Abdali seeks to flourish the image of Amman, to a modern city, and matching it with most of the world's renowned city centers, as this such project was missed in Amman, and it is one of a kind in Jordan in a valuable land at a central location, envisioned as a "New Downtown", high-end mixed use development and an important district with a major employment area, an active center, beside that it is a center for modern life and commerce[15].

The Boulevard, or the Pedestrian Spine Sector, strategically located at the heart of Abdali project. The spine includes restaurants and retail spaces at the

¹<http://www.abdali.jo>

ground level, and on the upper floor levels it includes residential and office spaces. It is a mixed-use complex that consists of a 370-meter-long and a 21-meter-wide outdoor pedestrian spine, bordered by 12 buildings.



Figure 1: Land-use plan for the Abdali Project

Source: <http://www.abdali.jo/index.php?r=site/page&id=20>

These buildings offer unique premium retail outlets, high street cafes and restaurants, contemporary office spaces, luxurious Arjaan by Rotana hotel serviced apartments and exclusive rooftop lounges. The Boulevard complement Abdali's vision in redefining modern living in the Jordanian capital, enhancing the capital's touristic and economic offering². The Boulevard is divided into three main squares. Furthermore, it contain two main plazas: the theater plaza; and the fountain plaza.



Figure 2: Spatial distribution of the Boulevard

Source: <http://www.pikasso.com/Jordan/en/Products/60-Malls/The-Boulevard/176-All-Accesses-Network>

4. ASSESSING SOCIO-CULTURAL INDICATORS IN THE BOULEVARD OF ABDALI PROJECT

Social and cultural aspects of sustainability need to be assessed to know what limits does the open space in the Boulevard can fulfill the indicators and achieve its common characteristics. A usability study was used to evaluate effectiveness, efficiency, and satisfaction of users. The study adopted a mixed method approach to map out the social behavior of users, and to understand the complexity of the cultural scene with its relation to the identity of the place. This methodological triangulation comprises two parts. The first is a qualitatively driven stage, which includes a photographic database, observations, and interviews with people who visit the study area. The second is a quantitative stage that has been performed through distributing questionnaires to visitors, and examining the cognitive maps of the participants. Parallel to this social-behavioral survey, 'space syntax' method was used to explore spatial and social relations between

the different zones in the study area, and discover any experiential significance implicit in the urban setting. Two computational tools were used for carrying out this analysis. Firstly, Syntax2D, to execute isovist analysis that addresses visual fields. Secondly, DepthmapX, which is a visibility graph analysis tool to understand the spatial configuration of the site, and the movement patterns of users.

5. RESULTS AND DISCUSSION

Based on the previously mentioned methods, the following are the main results of the study.

5-1. Social Equity, Social Mixing, Social Interaction, and Diversity

The Boulevard is a mixed use project with different services, uses and activities which enhance diversity and vitality. Based on multiple field visits, it was noticeable that some of the visitors prefer to set individually, others set with their families, beside that it was familiar to see elderly people set in one of the main plazas and chat together.

According to the questionnaire, 30% of the sample strongly agree that the Boulevard project allows visitors to interact and communicate with each other in a smoothly way, while 36% of the participants fairly agree about that. Also, Results of the survey showed that 52% of the asked sample see that the Boulevard is a place where people from different ages can enjoy the place and take advantage of its different services and facilities, and it is not restricted for a specific age group.

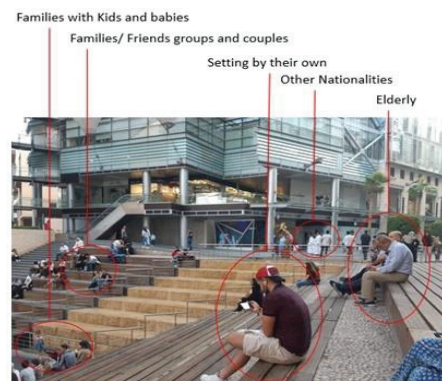


Figure 3: Diversity of users and activities in Boulevard
(Source: Author, August 2019)

5-2. Satisfaction of Human Needs

Human needs include different spatial qualities in urban design.

5-2-1. Safety, Security, and Legibility

Results showed that 62% of the sample strongly agree that they feel very safe while walking in the Boulevard due to the advanced security and protection systems. Also, the lighting quality in evenings and night hours plays an important role in providing safety and reducing crime rates in public

²<http://www.abdali-boulevard.jo/site/about>

spaces. Responses showed that 90% of the participants are comfortable with the lighting quality at Abdali Boulevard at evenings and night time, and it is convenient and gives an interesting atmosphere. Legibility in the Boulevard is developed by a well-defined pedestrian spine of movement, which has a clear direction and bounded by buildings and palm trees. Gateways are defined as well by the orientation of buildings and openness to the surroundings.

5-2-2. Comfort, Availability of Public Services, and Firmness

Most of the asked sample agreed that the Boulevard is a mixed-use development and an integrated project in terms of the variety of services, in addition to the different options for seating areas and the variety of retail shops. However, there is a lack in some facilities and services, and it could be added to the project, such as a public library, nursery, kids care area, indoor theatre, and other facilities. According to the number and the service quality of toilets in the Boulevard, 80% of the sample were satisfied about it and agreed that the services quality is adequate enough, and according to the number of trees and shading elements in the Boulevard public spaces, 20% of the asked sample find that the shading elements are not sufficient and not enough to protect visitors from the sun radiation, 20% were neutral, and 60% find them enough. Whereas From the field observation in a visit in the mid-day, it was noticeable that the tensile structure above the theatre plaza allows the sun radiation to penetrates and reach most the seating spaces in the theatre. Regarding the buildings heights overlooking the Abdali Boulevard, 74% of the sample do not cause any inconvenience or discomfort for them.

5-2-3. Social Facilities, Sense of Place, Identity, and Preservation of Local Characteristics

To make a sociable place, it is necessary to provide enough public seating areas with different types. Results showed most of the sample agreed that the seating areas are enough. Regarding how the Boulevard respects the identity of the place, and if it preserves the local characteristics of the context, the sample has been asked about how the facade design of the different buildings in the Boulevard makes them feel. Results showed that 60% of the participants find the facades reflect the technological advancement and civilization, while 16% answered that it is an imitation for the Western architectural style. From another point of view, specialists find that the new Abdali project made a massive change in the skyline of Amman, as it neglects the urban context and the architectural character through the different scale and image, especially that

it is adjacent to important buildings, such as King Abdullah Mosque, Palace of Justice building, and the Parliament building [15].



Figure 4. Abdali project and how it affects the skyline of Amman (Source: Ashour 2017)

Yet, in some interviews with visitors, they said that the design of the Boulevard reflects the modern life style, and there is nothing authentic about it. They added you can find the same spirit of the place in different modern cities around the world. That is why it may not be accepted by simple people, as they prefer the randomness and spontaneity of city centres. This point can also reflect the psychological aspect in the quality of life indicators as mentioned previously in (Table 1). However, when we focus on the design and heights of the buildings overlooking the Boulevard, the layout of the different buildings is united based on a grid and contributes to the overall character of the surrounding with a contemporary touch using a different materials. Besides that, it is worth to mention that the facades of the project are 6 floors above the ground level, which is not too much taller than other buildings that people used to see in Amman.

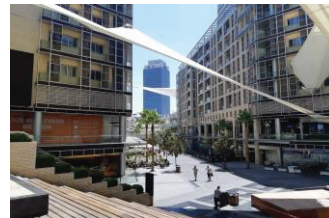


Figure 5. Design of building facades overlooking the Boulevard (Source: Author, August 2019)

5-2-4. Visual Richness, Visual Proportions, and Visual Distinctiveness

Despite of the unified image of the Boulevard buildings, there is a variety of façade treatments, and different alternatives for users' experience. Visual richness manifested in the variety of the used materials. Moreover, the variety of vegetation, beside the different scenes that some locations allow you to look for. According to the visual proportion, the use of advertising boards, trees and street furniture helps to make the Boulevard a 'human scale' place.

Regarding the sensory and pleasure, most of the participants were agreed that the variety of sound sources in the Boulevard give a lively and energetic atmosphere. Moreover, the changeable themes, and the flexibility of using the outdoor spaces for different

official events were what visitors like the most about the Boulevard according to 26% of the sample.

5-2-5. Quality of Life

Social, and environmental aspects have been discussed within the above tested factors and characteristics. Beside the physical aspects mentioned before, which relates to the mixed land use and pedestrian friendly neighbourhood, the density and crowding, in addition to compactness should be considered when measuring social sustainability in a public open space. Results showed that 52% of the sample find the area of the outdoor spaces in the Boulevard is appropriate with the number of users in regular days when there are no celebrations or festivals. On the other hand, 30% of the sample slightly disagree about if area of the outdoor spaces in the Boulevard is appropriate with the number of users when there are celebrations or festivals, and 14% were strongly disagree about that. In official celebrations, the Boulevard seems to be very crowded with people, as the space capacity is not enough for large number of visitors in a single time.

Mobility, Accessibility, and Connectivity

According to accessibility, most of the sample agreed that the Boulevard has an easy accessibility, as it is located near the city centre and there are no obstacles to get reached.

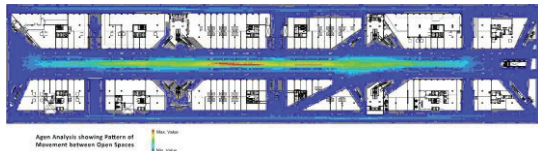


Figure 6. Patterns of movement between open spaces, which was produced using DepthmapX software.(Source: Author)

The project includes different options in the approach and accessibility for the Boulevard, there is an option to enter the Boulevard from Abdali mall directly through the tunnel under the street. Most of the asked sample found that the Boulevard and Abdali mall are interconnected as visiting one of them leads to visit the other.

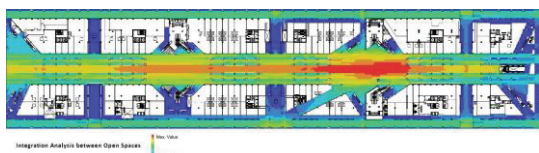


Figure 7. Integration between the Boulevard and Abdali Mall, which was produced using DepthmapX software (Source: Author)

It is important to check whether the Boulevard design allows for the independence to elderly people and individuals with special needs to walk and move

through it. Therefore, the sample was asked if the design of the Boulevard takes into account the circulation and movement needs for all groups, including them. Results showed that 40% strongly agreed and 42% agreed about that. However, despite of the sample opinion, and the high awareness in Boulevard project to attain a place with different alternatives for visitors to move and walk through, but the observation showed that, the main entrances from the Abdali Mall side and Rotana Tower side have only stairs without a ramps.

The signage system and the guiding panels are substantial located in the public space for way finding. Results showed that 44% of the sample find that the signage system was taken into consideration in the Boulevard, and they are enough to guide them for the location of different facilities.

5-3. Economic Aspect

One of the main goals of Abdali project is to create a sense of community ownership of the project and develop a district which is economically attractive for investors, and to increase businesses quality and quantity. Also to increase employment rates for the young and professional Jordanians³.

5-4. Future Focus

Abdali project including the Boulevard tries to create a modern and vibrant district with an attractive pedestrian spine which blend both, the traditional and the modern. Buildings overlooking external appearance combines contemporary architectural materials and models with traditional design elements, with a glimpse of traditional sense of place. Yet, the Boulevard promotes a higher standard of services and infrastructure within its mixed-use developments, and to improve employment, and also ensuring the qualities for generations to come[16].

6- CONCLUSION

Social sustainability is about designing for impact, and therefore, improving the quality of life.

Public spaces between buildings need to offer the basic requirements of social sustainability. One of the challenges for achieving this aspect is the difficulty of identifying suitable measures that represent the social life. The study contributed to this field by identifying the different indicators that affect the quality of life in urban spaces. Measuring such aspects is based on implementing a usability study, and also on realizing and analysing the social meanings of the spatial organization using advanced computational tools.

Based on the results of the study, Table (2) shows whether the Boulevard project in the current conditions fulfil those indicators or not, and suggests

³<http://www.laceco.me/work/the-boulevard>

strategies that could support social and cultural sustainability for the Boulevard and other future public spaces in Jordan.

Table 2. Degree of verification and suggestions for the different aspects of social and cultural sustainability in the Boulevard project in Amman. (Author).

Indicator	Degree of Verification	Indicators	Suggestions
1. Social Equity, Social Mixing, Social Interaction, and Diversity	Partially achieved (76.8 %)	The Boulevard project allows visitors to interact and communicate with each other in a smooth way regardless the differences between them. The Abdali project has enough public seating areas and seats.	75.6% It is important to integrate all people together not only from different ages and social statuses, but also to integrate people with low incomes in such projects. Most of the cafes and retail shops attract specific group of people who are capable to spend money on supplementary. Thus it is important to make a variety of services and provide affordable services and put those people into consideration. 78.0%
2. Satisfaction of Human Needs			
2.1. Safety, Security, and Legibility	Achieved (89.4 %)	I feel safe while walking in the Boulevard due to advanced security and protection systems. The lighting quality at the Boulevard at evenings and night time is convenient and gives an interesting atmosphere.	90.8% 88.0%
2.2. Comfort, Availability of Public Services, and Firmness	Partially achieved (78.6 %)	The number of trees and shading elements in the Boulevard public spaces is sufficient to protect visitors from the sun radiation. The Boulevard project is a mixed use development and an integrated project in terms of the variety of services, the different options for seating areas and the variety of retails. The number and the service quality of toilets in the Boulevard is adequate.	74.0% 81.2% 80.8% The cultural aspect was eliminated in the Boulevard. The available services are mainly limited for retail shops, restaurants and cafes, beside the open public spaces. Thus, other facilities could be added to the Boulevard, such as a library, nursery, kids care center, and indoor auditorium.
2.3. Social Facilities, Sense of Place, Identity, and Preservation of Local Characteristics	Partially achieved (77.6 %)	Buildings heights overlooking the Abdali Boulevard do not cause any inconvenience or discomfort for you.	77.6% It is a controversial topic. Although the facades reflect the technological advancement and civilization, the project is an imitation for the Western architectural style. The new Abdali project made a massive change in the skyline of Amman. People can find the same spirit of the place in different modern cities around the world.
2.4. Visual Richness, Proportions, and	Achieved (87.2 %)	The Abdali project reflects progress and technological advancement.	87.2%
2.5. Well-being, Happiness, and Sense of Pleasure	Achieved (85.2 %)	The variety of sound sources in the Boulevard (the sound of water features, trees, visitors' voices, etc.) give a lively and energetic atmosphere and do not disturb you.	85.2%
2.6. Density, Crowding, and Compactness	Partially achieved (64.5 %)	The site selection for the New Abdali Development project is not appropriate, and it was better to choose another location away from the city center, overcrowding and congestion of cars. The area of the outdoor spaces in the Boulevard is appropriate with the number of users on regular days when there are no celebrations or festivals.	56.0% 82.0% The Boulevard seems to be very crowded in official celebrations, as the space capacity is not enough and not prepared for large number of visitors in a single time.
2.7. Mobility, Accessibility, and Connectivity	Partially achieved (78.3 %)	The Boulevard has an easy accessibility, as it is located near the city center and there are no obstacles to be visited. The design of the Abdali Boulevard design takes into account the circulation and movement needs for all groups, including the elderly, mothers and individuals with special needs. The area of the outdoor spaces in the Boulevard is appropriate with the number of users when there are celebrations or festivals. The signage system and the guiding panels in the Boulevard are enough to guide you for the location of main plazas, landmarks and the public services such as w.c.s and praying rooms.	76.0% 82.8% 64.4% 72.8% Ramps should be provided in the main entries where there are different levels between the street and the entry zone for elderly peoples, people who use wheel chairs, and also parents who hold strollers.
3. Economic Aspect	Achieved	As discussed in Section 5.3 (Economic Aspect)	
4. Future Focus	Achieved	As discussed in Section 5.4 (Future Focus)	

REFERENCES

- Schwarz, M. and Krabbendam, D. (2013). *Sustainist Design Guide: How Sharing, Localism, Connectedness*

and Proportionality Are Creating a New Agenda for Social Design. Amsterdam: BIS Publishers.

- Woodcraft, S. (2012). Social Sustainability and New Communities: Moving from Concept to Practice in the UK. *Procedia - Social and Behavioral Sciences*. 68: 29–42.
- WCED (World Commission on Environment and Development). (1987). *Our Common Future*. Oxford: Oxford University Press.
- Harun, N. Z., Zakariya, K., Mansor, M., and Zakaria, K. (2014). Determining Attributes of Urban Plaza for Social Sustainability. *AMER International Conference on Quality of Life 153*. Kota Kinabalu: Elsevier, pp. 606–615.
- Ghahramanpouri, A., Lamit, H., Sedaghatnia, S. (2013). Urban Social Sustainability Trends in Research Literature. *Asian Soc. Sci.* 9: 185–193.
- Colantonio, A. (2007). Social Sustainability: An Exploratory Analysis of Its Definition, Assessment Methods Metrics and Tools. *EIBURS Working Paper Series*. Oxford: Oxford Brooks University, Oxford Institute for Sustainable Development (OISD), International Land Markets Group.
- Dempsey, N., Bramley, G., Power, S., Brown, C. (2009). The Social Dimension of Sustainable Development: Defining Urban Social Sustainability. *Sustainable Development*. 19: 289–300.
- Chiu, R.L.H. (2003). Social Sustainability, Sustainable Development and Housing Development: The Experience of Hong Kong. In *Housing and Social Change: East, West Perspectives*; Forrest, R. and Lee, J. (Editors). London: Routledge, pp. 221–239.
- Doğu, F. U. and Aras, L. (2019). *Measuring Social Sustainability with the Developed MCSA Model: Güzeyurt Case*. Lefke, Northern Cyprus: Department of Architecture, European University of Lefke.
- Mehan, A., and F. Soflei, (2016). Social Sustainability in Urban Context: Concepts, Definitions and Principles. *Proceedings of the EAAE ARCC 10th International Conference (EAAE ARCC 2016): Architectural Research Addressing Societal Challenges*. Lisbon, Portugal, 15-18 June 2016, pp. 293-299. CRC Press by Taylor and Francis Group.
- Serag El Din, H., Shalaby, A., Farouh, H., and Elarian, S. (2012). Principles of Urban Quality of Life for a Neighborhood. *HBRC Journal*, 9(1): 86-92
- Landorf, C. (2011). Evaluating Social Sustainability in Historic Urban Environments. *International Journal of Heritage Studies*, 17 (5), 463–477. Available online: <http://dx.doi.org/10.1080/13527258.2011.563788>.
- Colantonio, A. (2010). Urban Social Sustainability Themes and Assessment Methods. *Proceeding of the Institution of Civil Engineers: Urban Design and planning*, 163(2): 79–88. Available online: <http://dx.doi.org/10.1680/udap.2010.163.2.79>.
- Maslow, A. (1954). *Motivation and Personality*. Harper Row Publishers, Inc.
- Ashour, K. (2017). *Urban Regeneration Strategies in Amman's Core: Urban Development and Real Estate Market*. PhD Thesis. Dortmund: Faculty of Spatial Planning, Dortmund Technical University.
- Saba, N. (2019). *Abdali Investment & Development Project*. Available online: <http://www.abdali.jo/index.php?r=site/page&id=18>

“Are children independently mobile to school anymore?": A comparative study of two neighbourhoods in Kolkata, India Assessing the role of neighbourhood built-environment

MEGHA TYAGI¹, GAURAV RAHEJA¹

¹Department of Architecture and Planning, Indian Institute of Technology, Roorkee, India

ABSTRACT: This paper aims to provide empirical evidence on the existing levels of children's independent mobility (CIM) to school and its relationship with the neighbourhood-built environment in an Indian context. Taking a comparative analysis approach, the study situates itself within two typologies of inner-city and mid-rise neighbourhoods in Kolkata. Purposive sampling technique resulted in the recruitment of 271 school-children aged 7-12 years with prior parental permissions. CIM level differences across children's age and gender were analysed using chi-square tests, while relationships between CIM to school and objectively measured BE variables (land-use mix, street connectivity, traffic exposure, residential density) were analysed using logistic regression. The analysis reveals that older (10-12 years) children from both neighbourhoods experience higher CIM levels, irrespective of gender. In the inner-city neighbourhood, land-use mix and residential density were significantly associated with CIM to school. While in the mid-rise neighbourhood, only street connectivity was found to have an impact on CIM. Concludingly, this study re-looks at neighbourhood design and its characteristics from the viewpoint of children's mobility need, promoting independent and active transportation for sustainable cities. The findings have direct implications on India's neighbourhood policy guidelines and Child-Friendly Smart City initiative.

KEYWORDS: Children's independent mobility, urban neighbourhood, school, built environment, India

1. INTRODUCTION

Every day, 1.8 billion children travel to and from school around the world. Majority of these trips are characterised as motorized and highly dependent[1]. Globally, this phenomenon is leading to an increase in pressure on the existing environmental pollution levels, as well as traffic congestion near schools. Researchers argue that the factors responsible for this phenomenon range from lack of supportive physical infrastructure, distance to school, stranger danger, parental fear about neighbourhood safety to untamed vehicular traffic [2]. Consequently, these factors are leading to a decline in children's physical activity levels and cognitive skills [3], as well as a sharp rise in obesity and overweightness issues [4]. In India as well, children do not attain the recommended levels of 60 minutes of MVPA (moderate to vigorous physical activity) [5] and spend major part of their days in sedentary pursuits.

The concept of children's independent mobility (CIM), developed by Hillman et al. [6], offers opportunities of relooking at urban neighbourhood fabric from the perspective of children's mobility. It is defined as the right of a child to walk or cycle or use any public mode to transport to reach local destinations without any adult supervision. In the recent decade, CIM has gained a significant position globally as a concept, concern and tool for evaluating performances of urban cities concerning children's local mobility. Cities with higher CIM level tend to have a majority of children walking or cycling alone to

schools, adding 30 minutes of MVPA to their daily routine[7].

Recent research [8] has demonstrated that there exists a strong correlation between CIM and planning of urban neighbourhood. Studies support that efficiently designed streets and neighbourhood spaces can have a positive impact on CIM. Further, international initiatives such as UNICEF's Child-Friendly Cities Initiative, The New Urban Agenda (Habitat III) and Sustainable Development Goals (SDG goal no. 11) also highlights the significance of safe, accessible and sustainable infrastructure for catering to children's mobility needs within neighbourhoods[9]. Nationally, there have been attempts in India to investigate this correlation for adults, but an exclusive focus on children or adolescence remains under-researched.

To bridge this gap, the paper investigates and provides empirical evidence regarding the level of CIM to school and its relationship with the neighbourhood-built environment within the Indian context. Adopting a comparative analysis approach, the study situates itself within two typologies of inner-city and mid-rise urban neighbourhood in Kolkata. The key objectives of the paper are (i) to identify the level of CIM to school across the neighbourhoods, (ii) to examine the differences in CIM across children's age and gender and (iii) to determine and compare the association between built environment (BE) variables and CIM levels to school across different neighbourhood typologies.

2. RESEARCH DESIGN

2.1 Study context

This cross-sectional study is based in Kolkata, the erstwhile capital of British India with a 250-year-old history and presently the state capital of West Bengal. It is one of the fast urbanizing megacities of India, with a population density of 24,306 per square kilometre[10]. The city, with the world's 8th largest urban agglomeration, has a distinct land-use pattern dominated by residential land use[11]. Its spatial structure comprises of a compact design, and an extensive network of public/intermediate public transport (IPT) with limited road infrastructure. The city also exhibits a strong neighbourhood component with a predominant "para" culture within pre-independence inner-city neighbourhoods. A "Para" is a variant of the neighbourhood, not strictly adhering to the administrative boundaries[12]. The post-independence era saw the emergence of a mid-rise planned satellite township called 'Salt Lake' under Bidhannagar Municipal Corporation as a solution to accommodate unprecedented population growth in the main city of Kolkata [11]. This study situates itself in two such typical neighbourhood typologies of low-rise traditional inner-city (Khidirpur) and mid-rise planned satellite township (Salt Lake Sector-1).

Figure 1 and 2 show the figure-ground map of both selected neighbourhoods. Khidirpur is a port neighbourhood located in South Kolkata about 5kms from the city's Central Business district (CBD) and is adjacent to river Hooghly and Fort William. This neighbourhood, with narrow street widths, high population density and proximity to services like hospitals, school, shopping area and a city library is home to lower and upper-middle-class families. The housing typology can be categorised as low-rise and pre-independence structures. On the other hand, Salt Lake, located on the north-eastern fringes of the city, is a planned neighbourhood with a proper road network, that experienced organized urban growth due to well-defined land-use zoning. Divided into five sectors and 71 blocks, with each block having at least two parks and one playground, this neighbourhood has both individual houses and housing complexes. The housing typology can be characterised as mid-rise semi-detached structures. This study considers only Sector-1 as the focus area.

For this study, each child's neighbourhood is defined as the area within an 800m pedestrian network buffer around his/her home, following the protocols of several international studies related to children's mobility[1, 13].



Figure 1: Figure-ground map of Khidirpur (Inner-city neighbourhood).

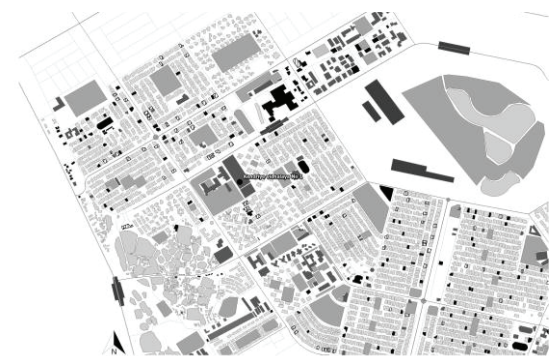


Figure 2: Figure-ground map of Salt Lake (mid-rise neighbourhood).

2.2 Participants

Purposive sampling technique was used to collect data from children of age 7-12 years (grade 3 to 7) and their parents, respectively. The multiple international and national studies [14] as well as psychological theories[15], establishing the fact that children in middle childhood are most physically active and can easily navigate through their local surroundings, guided the selection of this age group.

A total of eight schools were identified and approached in the two neighbourhoods for participation in the study. Out of these eight schools, three agreed, which included two private schools in Khidirpur and one government school in Salt Lake Sector-1. Before initiating the survey process, parents were asked to complete a questionnaire, obtaining their approval for their child's participation and reporting on socio-demographic information including residential address, gender, educational qualifications, child's age and gender, family type and vehicle ownership. Prior to the second part, the parents' addresses, thus received, were checked using Google Earth, confirming their residence within 800m from the school. In the second part, the selected children of consenting parents were asked to report on their mode of transport and accompaniment status for their daily journey to

school. Finally, the obtained data of 271 children and their parents was included in the analysis.

2.3 Mobility to school

Children were asked to select among seven options for the mode of transport while commuting to and from school every day. These options included 'walk', 'bicycle', 'school bus/van', 'local bus/tram', 'hand-pulled / auto-rickshaw', 'motorbike' or 'car'. They were next asked to report on their accompaniment status by selecting from the three options of 'alone', 'with other children like friends/sibling' or 'with adults like parents or grandparents'. Children who reported travelling to school 'alone' or 'with other children' using active/public mode of transport were coded as '1' (independent mobility), and rest were coded as '0' (dependent mobility).

2.4. Objectively measured built-environment (BE) variables

To obtain the BE variables, a GIS dataset containing street networks and land-use were developed for both neighbourhoods. The high-resolution aerial photographs were used for digitizing the neighbourhood maps in ArcGIS 10.7 (ESRI Inc., Redland, CA). The school locations and children's addresses were geocoded in the form of point shapefile. The following four BE variables were calculated, which were finalized through literature review and expert opinion: (i) Land-use mix: It was calculated using the entropy index, which is the most widely accepted and commonly used index for representing land use mix. Entropy is expressed, as shown by equation 1:

$$\text{Entropy index} = (-1) \times \sum_j \frac{P_j \times \log(P_j)}{\log(J)} \quad (1)$$

Where, P_j is the proportion of developed land in the j^{th} land-use type, and J is the total land uses considered in the study. Entropy index varies between 0 and 1, wherein 0 indicate single-use typology (homogeneous) and 1 indicate maximum mixed-use typology (heterogeneous). (ii) Street connectivity: It is calculated (using connected node ratio method) by dividing the number of the street intersections (real nodes) by the number of intersections plus cul-de-sacs (the total number of nodes). The maximum value for this variable is 1, with higher numbers indicating that there are few cul-de-sacs and dead ends and higher connectivity. (iii) Traffic exposure: In the absence of data on traffic volumes, 'road function' was used as proxy and traffic speed exposure is calculated as the ratio of high speed (>50 km/hour) road lengths to low speed (<50km/hour) road lengths within neighbourhood boundary. The data on the design speed of four urban

roads (arterial, sub-arterial, collector and local) was obtained from Indian Road Congress manual IRC:86-1983 (Geometric design standard for urban roads in plains, IRC, 1983). (iv) Residential density: It was calculated as the ratio of residential dwelling units to the total residential area of 800m network buffer around each child's residential addresses [16]. Values for these input measures were normalised using z-scores.

2.4 Analysis

Statistical analysis was performed using IBM SPSS Statistics version 25. Chi-square tests were conducted to test the differences between means of independent mobility to school by child's gender, child's age, parent's gender, parent's qualification, parent's profession, family type and vehicular ownership. Binary logistic regression was used to study the association between objectively measured BE variables of neighbourhood and CIM to school. A p-value threshold of 0.05 was used to determine statistical significance.

3. RESULTS

3.1 Sample

The descriptive characteristics of the participating children and their parents are shown in Table 1. Out of 271 children selected, almost half (55%) were girls equally distributed within the two age-group categories. Majority of respondents among parents were fathers (62.7%). Most parents had done graduation (70.8%) and were working (72.3%) while living in a nuclear family model (66.4%). Most households did not own any vehicle (37.6%) and among the rest, scooter or a motorbike ownership was the highest (34.7%).

Table 1: Socio-demographic characteristics of participating children and parents (n=144 for Khidirpur and n=127 for Salt Lake)

Characteristics	N	%
<i>Child's gender</i>		
Boy	122	45
Girl	149	55
<i>Child's age (years)</i>		
Younger (7-9)	137	50.6
Older (10-12)	134	49.4
<i>Parent's gender</i>		
Father	170	62.7
Mother	101	37.3
<i>Parent's qualification</i>		
Post-graduate	49	18.1
Graduate	192	70.8
Senior-secondary	30	11.1
<i>Parent's employment status</i>		
Working full-time	196	72.3
Homemaker	75	27.7
<i>Family Type</i>		
Joint	91	33.6

Nuclear	180	66.4
<i>Vehicular ownership</i>		
Car	65	24.0
Scooter/bike	94	34.7
Both	10	3.7
None	102	37.6

3.2 Objective 1: CIM levels to school

Travel modes and accompaniment levels on the journey to school in both neighbourhoods are presented in Table 2. Children in Khidirpur (36.1%) were found to have greater independent mobility to the school than in Salt Lake. However, on an average, the level of CIM to school in both cases remains 35%. Walking (56.9%) and public transport (11.8%) were the most popular modes of commuting in Khidirpur. Hand-pulled rickshaw, which is unique to the inner-city neighbourhoods of Kolkata, was found to be the preferred choice among public transport commuters to school. On the other hand, children in Salt Lake either walked (51.1%) or were driven in a school bus/van (23.6%) followed by motorbike or car (22.9%) to school.

Table 2: Level of CIM and usual mode of transport to and from school in the neighbourhoods

Characteristics	Mobility to school (%)	
	Khidirpur	Salt Lake
<i>Mobility to school</i>		
Independent	36.1	34.6
Dependent	63.9	65.4
<i>Mode of Transport</i>		
Walk	56.9	51.1
Bicycle	11.1	2.4
School bus/van	10.4	23.6
Public transport	11.8	0
Motorbike/car	9.8	22.9

3.3 Objective 2: CIM across child's age and gender

There was no significant difference found between CIM to school among boys and girls. However, on an average, older children (10-12 years) in both neighbourhoods were found to enjoy greater independent mobility to the school than the younger ones (Khidirpur, $\chi^2= 38.34$, $p=0.00$ and Salt Lake, $\chi^2= 26.52$, $p=0.00$). Other socio-demographic characteristics like parent's gender, qualification or employment, family type and vehicular ownership had no significant association with CIM to school. Since only children's age was significantly associated, level of CIM to school across the child's age is presented in Table 3. The table shows as the child's age increases, the percentage of children travelling to school alone also increases. An interesting positive shift can be seen between age-group of 9 and 10 years. It is noted that as the child moves from primary to the secondary school system, they are given more freedom to travel to school independently.

Table 3: Level of CIM across child's age in the neighbourhoods

Child's age (years)	CIM to school (%)	
	Khidirpur	Salt Lake
7	9.5	0
8	13.6	11.1
9	14.7	18.1
10	48.2	36
11	71.4	55
12	75	77.2

3.4 Objective 3: CIM and BE variables

The results of logistic regression analysis examining the association between neighbourhood BE variables and the odds of the child to travel independently to school are presented in Table 4. The analysis is controlled for the child's age since it had influence over CIM to school. The results reveal that in Khidirpur (inner-city neighbourhood), for each unit increase in land-use mix and residential density, odds for a child to travel independently to school increases by 2.65 and 1.91 times, respectively. On the other hand, in Salt Lake (mid-rise neighbourhood), land-use mix or residential density had no impact on CIM. It is the increase by each unit in Salt Lake's street connectivity that increases the odds of a child to travel independently to school by 2.94 times. Traffic exposure in both cases had no influence on the child's freedom to reach school.

Table 4: The association between CIM to school and built environment variables of the neighbourhoods

Neighbourhood Built Environment variables	CIM to school ^a	
	Khidirpur OR (95% CI)	Salt Lake OR (95% CI)
Land-use mix	2.65(1.46, 4.79)*	1.12 (0.65, 1.95)
Street connectivity	0.75 (0.40, 1.40)	2.94(1.70, 5.07)*
Traffic exposure	1.45 (0.89, 2.35)	1.09 (0.67, 1.78)
Residential density	1.91(1.19, 3.06)*	1.79 (0.95, 3.40)

^a Analyses controlled for child's age.

* the variables are significantly associated with CIM to school ($p<0.05$).

4. DISCUSSION

This paper examines children's mobility to school in Indian context with respect to its level of independence, extending the discussion beyond the existing travel modes.

The study reveals that only 35% of children travelled to school independently. This proportion of children with independent mobility is lower than reported in studies conducted in other countries. For example, in Western Australia, 71.8% of children travelled independently[17], while in New Zealand, 44.3% of children were allowed to travel outside without adult supervision [18], in Spain 57.2% of children reported independent commuting to school

both ways[19] and in Finland, 69% of children in inner-city travelled independently in their school journeys[20]. Moreover, walking was identified as the popular mode of transport in children's journey to school alone or with parents/caregivers. It aligns with the findings from another Indian study on children's everyday mobility to school in Hyderabad[21], where 57% of children were found to be walking to school daily. This finding underscores the importance of safe walkability, especially around schools along with improved transport-level neighbourhood environment through urban planning and policy.

While examining the influence of socio-demographic characteristics of both children and their parents, it was found that only the child's age was associated with CIM. Unlike previous studies[17, 22], both boys and girls were considered equal with respect to the parent's decision on their mobility to school. This phenomenon may be attributed to the parental fear for the child's safety from stranger danger and traffic, equally for both genders, fuelled by adverse media reports about child's abuse in India. As a result, though not covered in this study, consideration of parent's neighbourhood perception becomes essential within children's mobility studies.

It is also evident that objectively measured context-specific features of the neighbourhood's physical environment influence CIM to school and varies according to neighbourhood typology. For the inner-city neighbourhood, land-use mix and residential density were found to be significant predictors of CIM to school, supporting previous studies from developed countries[8, 23]. A higher land-use mix promotes 'eyes on the street' concept for children's mobility, creating a positive parental perception about their safety. It further reduces the distance of travel to various child-specific destinations. Similarly, residential density is essential for the walkability of the neighbourhood, as there will be higher service provisions (e.g. shops, hospitals, banks, schools) in areas where more people reside[24]. For the mid-rise neighbourhood, street connectivity was found to be significant in supporting CIM to school. As confirmed by other studies[17, 23], improved street network positively influences children's mobility behaviour by reducing distances to destinations and providing multiple route options. This difference between the two neighbourhood typologies can be attributed to their urban growth. The mid-rise neighbourhood had organised urban growth, hence instead of land-use mix or residential density; its street connectivity was an important criterion related to CIM. Concludingly, neighbourhoods in India, unlike developed countries, present multiple challenges to children's mobility experiences with respect to the social, cultural and physical dimension. Generalization of results by

taking only one typology of the neighbourhood in a diverse country like India, therefore, do not present an overall picture of CIM. Few studies have also highlighted the importance of safer traffic environments for CIM[22, 25], but this study found no association between traffic exposure and children's mobility to school in the cases of both neighbourhoods.

The study findings have important implications for Urban and Regional Development Plans Formulation and Implementation (URDPFI) guidelines which primarily governs India's neighbourhood laws and policies. To improve the land-use mix, it is essential to co-locate residences, businesses and associated services nearby, increasing safety parameters for children while going to school alone. Similarly, designing safe, 'walkable' neighbourhoods, with greater connected streets surrounding child-specific destinations like schools, are also an important precondition for children to be independently mobile. This may involve creating separate pedestrian and cycling pathways, thereby building confidence among parents to let their children move alone. Such promotion of active transport may translate into fewer motorized traffic and less pollution, thus laying the foundation for future sustainable cities.

5. CONCLUSION

Children's mobility data to school from Indian cities is presently limited to provide any valid evidence on their CIM position at the global level. However, this study, as a case, sheds light on the issue, revealing that only 35% of children aged 7-12 years are independently mobile to school today. Asserting the need to re-look at neighbourhood design and its characteristics from the point of children's mobility need, the study identifies neighbourhood typology as an important factor for consideration. 'Land-use mix', 'street connectivity' and 'residential density' are significant in enabling a supportive environment for CIM to school. Overall, the findings support not only India's urban policy guidelines but also Child-Friendly Smart Cities (CFSC) initiative that recognizes mobility as critical components for creating a child-friendly environment.

Future research is required to overcome the limitations of the study by considering the distance to school, street hierarchy, street width and other route characteristics as variables. As mentioned in the discussion, parent's perception is another significant component that plays a considerable role in children's independence and mode of transport to school. Hence, inclusion of parent's perception and attitude towards CIM is also essential. Additionally, the impact of climate on CIM to school through longitudinal studies involving diverse neighbourhood

typologies can further advance the in-depth understanding of CIM supporting post-carbon sustainable cities in the Indian context.

ACKNOWLEDGEMENTS

The authors would like to thank school principals, teachers, children and parents from St. Thomas' Boys' & Girls' School, Khidirpur and Kendriya Vidyalaya No. 1, Salt Lake for their participation in the study.

REFERENCES

- Carver, A., et al., *Independent mobility on the journey to school: A joint cross-sectional and prospective exploration of social and physical environmental influences*. Journal of Transport & Health, 2014. 1(1): p. 25-32.
- Malone, K., *The bubble-wrap generation: children growing up in walled gardens*. Environmental Education Research, 2007. 13(4): p. 513-527.
- Rissotto, A. and F. Tonucci, *Freedom of movement and environmental knowledge in elementary school children*. Journal of Environmental Psychology, 2002. 22(1-2): p. 65-77.
- WHO. *Facts and figures on childhood obesity*. 2016 [cited 2017 6 April]; Available from: <https://www.who.int/end-childhood-obesity/facts/en/>.
- WHO, *Global recommendations on physical activity for health*. 2010: Geneva, Switzerland. p. 60.
- Hillman, M., Adams, J, Whitelegg, J, *One false move: a study of children's independent mobility*. 1990, Policy Studies Institute: London.
- Cooper, A.R., et al., *Commuting to school: are children who walk more physically active?* 2003. 25(4): p. 273-276.
- Curtis, C., C. Babb, and D. Olaru, *Built environment and children's travel to school*. Transport Policy, 2015. 42: p. 21-33.
- Malone, K., *Child Friendly Cities: A model of planning for sustainable development*, in *Designing Cities with Children and Young People*. 2017, Routledge. p. 11-23.
- DCO, *District Census handbook Kolkata*. 2011, Directorate of census operations West Bengal: Kolkata.
- Mukherjee, M., *Urban growth and spatial transformation of Kolkata metropolis: a continuation of colonial legacy*. ARPN Journal of Science & Technology, 2012. 2: p. 365-380.
- Sengupta, K.M., *Community and Neighbourhood in a Colonial City*. South Asia Research, 2017. 38(1): p. 40-56.
- Oliver, M., et al., *Associations between the neighbourhood built environment and out of school physical activity and active travel: An examination from the Kids in the City study*. Health Place, 2015. 36: p. 57-64.
- Bhonsle, K. and V. Adane, *Assessing the Play Provisions for Children in Urban Neighborhoods of India: Case Study Nagpur, Maharashtra*. Buildings, 2016. 6(3).
- Piaget, J., *The construction of reality in the child*. 1955: Routledge.
- Ikeda, E., et al., *Assessment of direct and indirect associations between children active school travel and environmental, household and child factors using structural equation modelling*. Int J Behav Nutr Phys Act, 2019. 16(1): p. 32.
- Villanueva, K., et al., *Does the walkability of neighbourhoods affect children's independent mobility, independent of parental, socio-cultural and individual factors?* Children's Geographies, 2013. 12(4): p. 393-411.
- Mitchell, H., R.A. Kearns, and D.C.J.G. Collins, *Nuances of neighbourhood: children's perceptions of the space between home and school in Auckland, New Zealand*. 2007. 38(4): p. 614-627.
- Ayllón, E., et al., *Independent mobility to school and Spanish children: go, return, or both?* Children's Geographies, 2020: p. 1-15.
- Kyttä, M., et al., *The last free-range children? Children's independent mobility in Finland in the 1990s and 2010s*. Journal of Transport Geography, 2015. 47: p. 1-12.
- Tetali, S., P. Edwards, and G.V. Roberts, *How do children travel to school in urban India? A cross-sectional study of 5,842 children in Hyderabad*. BMC Public Health, 2016. 16(1): p. 1099.
- Smith, M., et al., *Children's Transport Built Environments: A Mixed Methods Study of Associations between Perceived and Objective Measures and Relationships with Parent Licence for Independent Mobility in Auckland, New Zealand*. Int J Environ Res Public Health, 2019. 16(8).
- Carver, A., et al., *How are the built environment and household travel characteristics associated with children's active transport in Melbourne, Australia?* Journal of Transport & Health, 2019. 12: p. 115-129.
- Giles-Corti, W., et al., *How walkable is Melbourne? The development of a transport walkability index for metropolitan Melbourne*. 2014.
- Giles-Corti, B., et al., *School site and the potential to walk to school: the impact of street connectivity and traffic exposure in school neighborhoods*. Health Place, 2011. 17(2): p. 545-50.

Greenway on Street Canyon of Residential Areas in Dhaka: Missing link of plausible impact in taming the thermal comfort

ZARRIN TASNIM¹, DR. MD ASHIKUR RAHMAN JOARDER¹

¹Department of Architecture, Bangladesh University of Engineering and Technology (BUET), Dhaka, Bangladesh

ABSTRACT: *Orchards and meadows featured ancient Dhaka city. Rapid urbanization replaces foliage with edifices harvesting microclimate of higher air temperature or dry bulb temperature (DBT) than rural surroundings. Dhaka's outdoor temperature is 1-1.5 K higher than adjacent regions. Integrating greenways on Dhaka's street canyons that are linear open spaces built along lush green, stream or similar features for non-motorized users ameliorating environment, is an implicit remedy alleviating the delinquents. Tropical studies confirmed that planted urban streets reduced DBT up to 1-3 K. This research concerns about the microclimatic impact of integrated greenways on street canyons at planned residential areas of Dhaka. Field study was steered at eight potential planted and bare street canyons. The microclimatic parameters were recorded from 10.00-18.00 hours during summer days using Thermo-Anemometer and Hygro-Thermometer. An existing bare street canyon and integrated greenway on same street canyon were simulated using Envi-met V4.3.2 Summer-18 software from 08.00-20.00 hours. The exploration reveals that integrated greenway reduced DBT and mean radiant temperature (T_{mrt}) up to 7.03-10.30 K, and 5.76-31.36 K respectively and increased relative humidity (RH) up to 7.90-18.47% of Dhaka's street canyon. This study unveils that greenways offer immense cooling effect on urban street canyon microclimate enhancing pedestrian thermal comfort.*

KEYWORDS: *Integrated greenway, Microclimate, Urban street canyon, Aspect ratio, Pedestrian thermal comfort*

1. PROLOGUE

Dhaka, the capital city of Bangladesh lacks pedestrian friendly environment. It's current morphology containing magnified edifices, ample hardscapes and meagre foliage, compels amplified outdoor temperature (1-1.5 K higher than adjacent areas) and uncomfortable urban spaces [1]. Residential usage hail in Dhaka besides farmlands. It can be silver-tongued that assessing the implicit integration of greenways (linear open spaces built along plush green, stream, or same traits for strollers) on planned residential (PR) Dhaka is invincible in lessening the elevated city temperature ensuing pedestrian thermal comfort. Tropical studies painted the avail of urban green infrastructure and permeable pavements integrated with irrigation systems during hot dry seasons (plus, for example, pervious concrete pavement, porous asphalt pavement, permeable interlocking concrete pavers and reinforced grass pavers) in altering outdoor human thermal comfort indices as dry bulb temperature (DBT), relative humidity (RH) and mean radiant temperature (T_{mrt}). Urban street trees reduced DBT up to 1-3 K, T_{mrt} up to 30 K and increased RH up to 10% [2-3]. Permeable pavement with evaporative cooling and tree shade mend human thermal comfort reducing surface temperature and T_{mrt} in hot periods [4]. In tropical Dhaka, outdoor human thermal comfort range regarding DBT is 28.5-32 °C, RH is 30%-70% preferably 50%-60%, and wind speed (WS) is 1.5 m/s for pedestrians walking under shade [5]. For outdoor

thermal comfort, 0.77 K drop in T_{mrt} can poise 0.56 K increase in DBT [6]. Manifold reviews conversed the greenway boons in storm water management, urban delight, biodiversity and amending environment [7-9]. Yet, research enunciating urban greenway pluses in enhancing thermal comfort, trading thermal comfort indices is rare. This study endeavours to connect the missing link amid greenways and their likely impact in taming the thermal comfort indices of urban street canyon (USC) microclimate. This study assesses the integrated greenway's plausibility in ameliorating thermal comfort indices of PR Dhaka's street canyon microclimate gracing pedestrian thermal comfort.

In Dhaka's context, various reviews explored green infrastructures, yet, no significant research quested urban greenway except the pilot and elaborate study of this research [10-11]. Several studies on outdoor climate, with or without foliage are available. This paper stands out from the rest, imparting a research beyond mere vegetation or outdoor climate. It addresses the bigger issue, the microclimatic impact of integrating greenways on USCs at PR areas. This research is distinct by delving the urban greenway graces on outdoor thermal comfort ensuring a pleasant urban walkway for the ambles. This study ushers the urbanites towards a plausible remedy that may strengthen the two pillars of a successful city, microclimatic thermal comfort and walkability, by enhancing urban microclimate and offering thermally comfortable sound urban walkway.

2. METHODOLOGY

Trailing mix method approach, this research embraced quantitative order blending experimental, simulation and analytical methods. The field survey explored the existing microclimatic parameters of Dhaka's selected street canyons ensuing the urban meteorological observation guidance [12]. Each site measured DBT, RH and WS at one hour interval from 10.00-18.00 hours from March 2017-2018 on several hot summer days, covering the critical periods (11.00-14.00 hours) of the day and the most thermally formidable periods (March, April and May) of tropical Dhaka [13]. This paper notes the compelling findings measured on 6th March 2018. The simulation study probed microclimatic impact of integrated greenways on PR Dhaka's street canyons. Envi-met software modelled and simulated the selected bare street canyon from 08.00-20.00 hours. Later, Albero 4.3 and Envi-met integrated greenway on the same model and simulated for same hours. This study concluded over analysing field and simulation data.

3. FIELD STUDY

The field study explored eight potential existing bare and greenway identical (GI) street canyons at PR Dhaka. The GI street canyons contained high leaf area density (LAD) and high leaf area index (LAI) trees densely planted on both sides. Thermo-Anemometer and Hygro-Thermometer logged the microclimatic parameters (DBT, RH and WS) from 10.00-18.00 hours during summer days.

3.1 Study area selection

Exploring Dhaka's various PR areas, street canyons of variant aspect ratios, Section-12, Pallabi (area: 17 km²; latitude: 23.495°N; longitude: 90.215°E) at Mirpur was selected for this study (Fig. 1). Once a plethora of green embodied this place. Housing and roads has invaded the greenery generating congested areas of deficient accessible green, gradually.

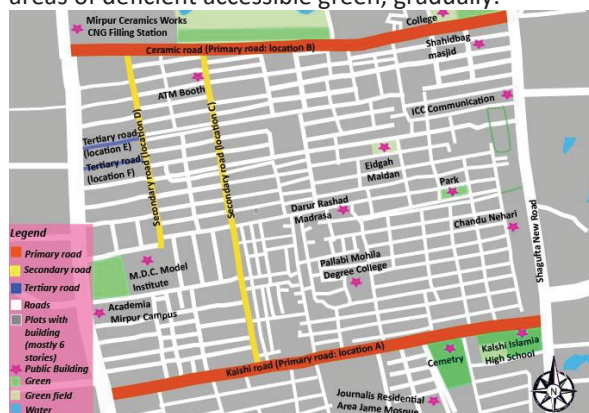


Figure 1: Selected sites of Section-12, Pallabi, Mirpur, Dhaka.

It is a lower middle-wage residential area, of high-density urbanization (1991: population 364000, density 21,412 per km²) and sparsely vegetation, exposed to high air temperature. The prevalent

hardscapes embodied by the site's huge open asphalt roads and concrete footpath, harvest harshly high thermal storage baring the residents to high surface temperature. The roads are widening chopping down the left-over tree shreds. Reviving the green is crucial in this nascent area of highly derelict green infrastructure. This lower wage area involving lower structures, less foliage, extra exposed concrete and asphalt surfaces and high sky view factors, is highly vulnerable to higher ambient, radiant, and surface temperatures, and inevitably translates into higher negative thermal comfort to the denizens [14]. Thus, these residential sites were modelled to muse the microclimatic impact of integrated greenway on USC.

3.2 Study area structure

The total (1.27 km² (1127 m X 1127 m approx.) study area was selected in view of three different pairs of representative street canyon aspect ratio (H/W). Ensuing the street hierarchy, primary, secondary, and tertiary roads were inspected namely location A, B, C, D, E and F in turn (Fig. 2). Buildings are mostly six stories made of brick wall, concrete slab, glaze window and metal. Roads are gridiron patterned, plot divisional representing the whole area. Both north south and east west oriented roads were assessed. As street orientation and street canyon aspect ratio play a major part in radiation exchange and heat storage [15]. Green and bare street canyons were evaluated.

The primary roads are mutually parallel serving heavy traffic alternatively. The secondary roads are similarly parallel serving light traffic. The tertiary roads are mostly pedestrian. The mainstream denizens, possessing no personal vehicle, use public transports and enter here by foot. Myriads of pedestrians use these streets. Therefore, these roads are suitable for integrating greenways and unearthing their impact on USC microclimate.

3.3 Study location A, B, C, D and F

Location A and B are east west oriented primary roads, namely Kalshi Road (36 m width) and Ceramic Road (24 m width) in turn. Location C and D are north south oriented secondary roads (24 m width) namely Road No. 12 and Road No. 5 in turn. Location E and F are east west oriented tertiary roads of 18 m width namely Road No. 4 and Road No. 6 in order. At all locations, buildings are mostly of 18 m height. Average street canyon aspect ratios (H/W) are nearly 1:2 (0.5), 3:4 (0.75), 3:4 (0.75), 3:4 (0.75), 1 and 1 at location A, B, C, D, E and F in order.

The microclimatic parameters were measured at eight points (Point-1, 2, 3, 4, 5, 6, 7 and 8) of selected street canyons at 1.5 m above ground level namely pedestrian level (Fig. 2). Point-2 was bare with no green nearby and Point-1 was near a green symmetry

covering many trees, at location A. Point-3 embraced buildings at one side and small tree stripe on other side; and Point-4 embodied buildings at one side and tree draped vast linear area on other side, at location B. Point-5 was on a bare road with no green near at location C. Point-6 was on a road lying many large trees linearly placed on both sides at location D. Point-7 was on a bare road with no green nearby at location E. Point-8 was on a road holding plentiful huge trees linearly set on both sides at location F.

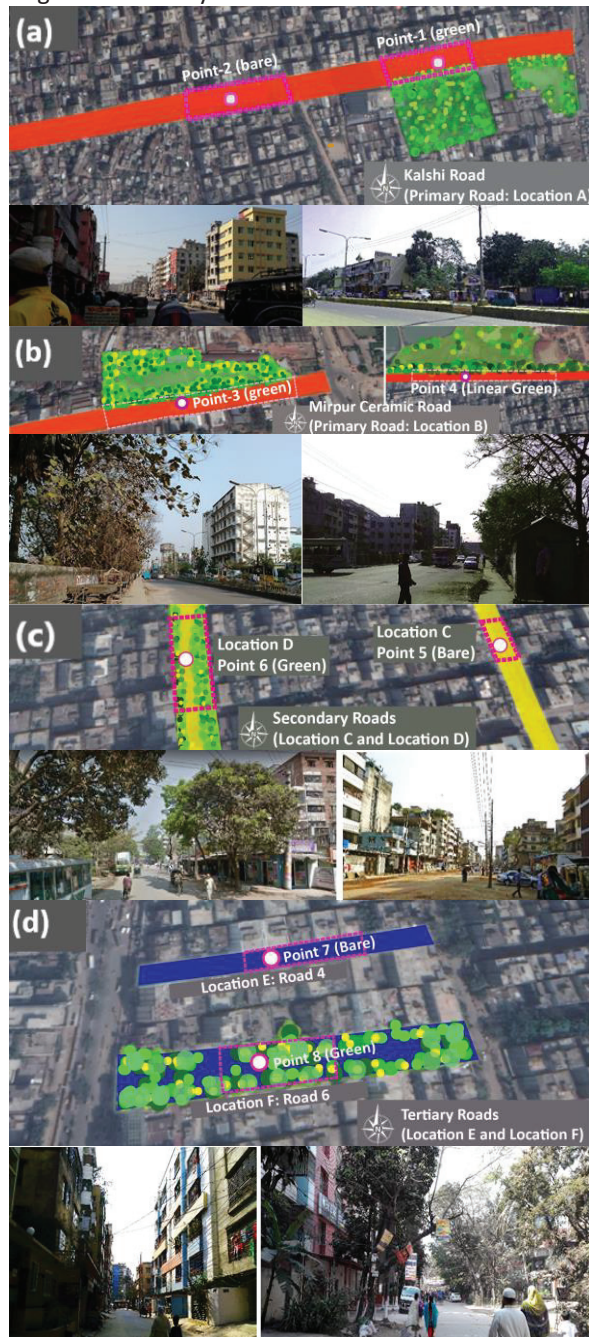


Figure 2: Six locations of selected sites at Section-12, Pallabi, Mirpur, Dhaka (a) Location A: green Point-1 (right) and bare Point-2 (left); (b) Location B: green Point-3 (left) and linear green Point-4 (right); (c) Location C: bare Point-5 (right) and Location D: green Point-6 (left); (d) Location E: bare Point-7 (top, left) and Location F: green point-8 (bottom, right).

3.4 Dry bulb temperature measurements

Average DBT was logged lower (0.73-1.34 K lower) at green or GI points than bare points from 10.00-18.00 hours. Point-7 and Point-8 showed the best result. The average DBT was 1.34 K lower at Point-8 than Point-7 from 10.00-18.00 hours. Point-8 was at a deep street canyon and more resembling to greenway with high LAD and high LAI trees arranged linearly on both sides of the road. Point-7 was at a bare and deep street canyon (Fig. 2).

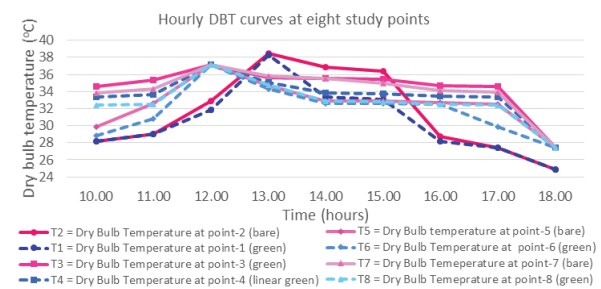


Figure 3: Field data analysis of hourly DBT at eight study points.

The linear green, more resembling greenway (MRG) Point-4 showed lower average DBT (average 1.02 K lower, maximum 1.7 K lower at 11.00, 14.00 and 15.00 hours, and minimum 0.5 K lower at 13.00 hours) than green, less resembling greenway (LRG) Point-3 from 10.00-18.00 hours (Fig. 2). The maximum DBT difference befell at 14.00 hours, when DBT was 3.5 K lower at green Point-1 than bare Point-2. The minimum DBT difference befell twice where DBT was 0.2 K lower, at 13.00 hours at green Point-1 than bare Point-2 and at 16.00 hours at green Point-6 than bare Point-5. Point-1 and Point-2 were at a shallow street canyon and Point-5 and Point-6 were at mid deep street canyons. Fig. 3 shows field data analysis of DBT at eight study points.

3.5 Relative humidity measurements

Average RH was logged nearly similar or higher (0.44%-1.58% higher) at green or GI points than bare points from 10.00-18.00 hours. Kalshi Road showed the finest result, noting the average RH 1.58% higher at green Point-1 than bare Point-2 from 10.00-18.00 hours. This was a shallow street canyon (Fig. 2). The maximum RH difference was spotted at 12.00 hours when RH was 7% higher at green Point-1 than bare Point-2. The minimum RH difference was spotted in two cases where RH was 1% higher at 13.00, 15.00 and 17.00 hours at linear green (MRG) Point-4 than green Point-3 and at 13.00, 16.00 and 17.00 hours at green Point-8 than bare Point-7. Point-1, Point-2, Point-3 and Point-4 were at shallow street canyons. Point-7 and Point-8 were at deep street canyons. RH was higher (average 1% from 10.00-18.00 hours, maximum 4% at 14.00 hours and minimum 1% at 13.00, 15.00 and 17.00 hours) at linear green (MRG) Point-4 than green Point-3. Fig. 4 shows field data analysis of hourly RH at eight study points.

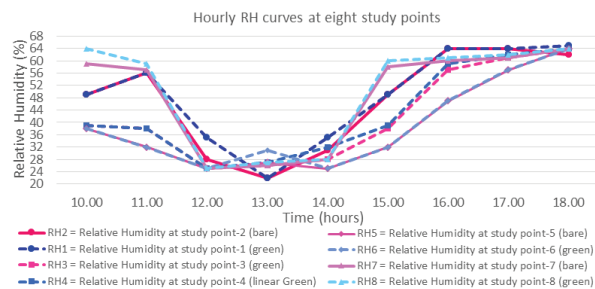


Figure 4: Field data analysis of hourly RH at eight study points.

3.6 Wind speed measurements

The GI street canyons showed lower average WS (0.44-0.81 m/s lower) from 10.00-18.00 hours. The maximum WS difference befell at 11.00 hours logging 2.2 m/s lower WS at green Point-1 than bare Point-2. The minimum WS difference befell at 12.00 hours noting 0.1 m/s lower WS at green Point-1 than bare Point-2. Unusually, at 15.00 hours, WS befell 0.2 m/s higher at green Point-1 than bare Point-2. Point-1 and Point-2 were at a shallow street canyon. Linear green (MRG) Point-4 showed higher average WS (average 0.74 m/s higher, maximum 0.9 m/s at 18.00 hours and minimum 0.6 m/s at 10.00 hours) than green (LRG) Point-3 from 10.00-18.00 hours (Fig. 2). Fig. 5 paints field data analysis of hourly WS at eight points.

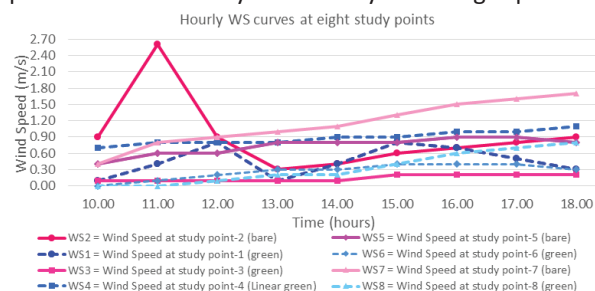


Figure 5: Field data analysis of hourly WS at eight study points.

4. SIMULATION STUDY

Given no existing greenway on Dhaka's street canyons, this study pondered the existing bare points for simulation. Envi-met Spaces 4.3.2 and Envi-met V4.3.2 Summer 18 software modelled and simulated one major existing bare street canyon, bare Point-2 at Kalshi Road from 08.00-20.00 hours (Fig. 6). The same software integrated greenway on same bare model, termed greenway Point-1 and simulated for same hours (Fig. 6 and Fig. 7). The simulation grasped field data as climatic parameters input. The greenway model was designed applying a pedestrian trail paved with permeable interlocking concrete pavement (PICP) hemmed in many densely planted Delonix regia using Albero 4.3.0 and Envi-met (64 bit). As the permeability and thermal properties of PICP allowing evaporative cooling leverage lessening DBT and T_{mrt} up to 12 K and enhance pedestrian thermal comfort [4]. Delonix regia (LAI 2.5), a popular street tree in

Dhaka and worldwide, aids reducing DBT and increasing RH in summer days honing pedestrian thermal comfort [16]. This model hatches all greenway features including storm water drainage. Leonardo 4.3.0 extracted the simulation maps.

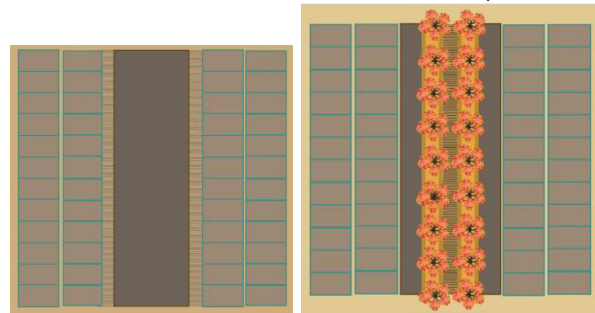


Figure 6: Simulation model of bare Point-2 (left) and greenway Point-1 (right) at Kalshi Road.

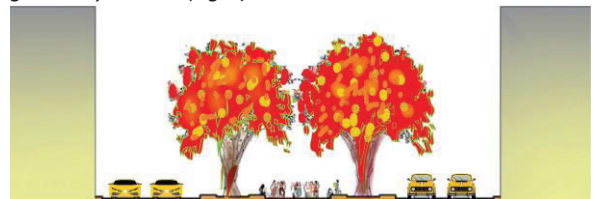


Figure 7: Sectional simulation model of greenway Point-1.

4.1 Dry bulb temperature simulation

The simulation study revealed that the average DBT was lower (9.07 K lower) at greenway Point-1 than bare Point-2 from 08.00-20.00 hours. The best result befell at 15.00 hours logging 10.30 K lower DBT at greenway Point-1 than bare Point-2. The least result ensued at 09.00 hours logging 7.03 K lower DBT at greenway Point-1 than bare Point-2. Fig. 8 shows comparative DBT simulation map specimen at Kalshi Road with bare Point-2 and greenway Point-1.

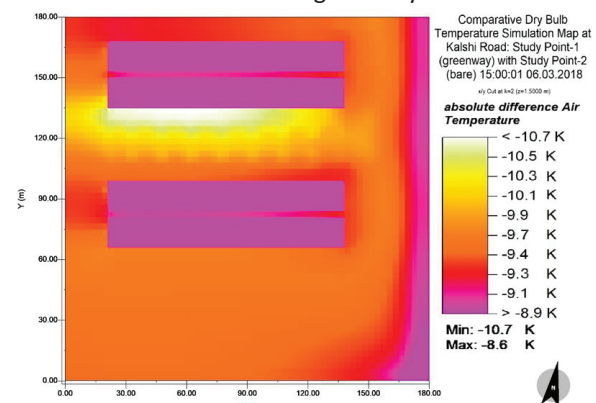


Figure 8: Comparative DBT simulation map at Kalshi Road, greenway Point-1 with bare Point-2 on 15.00.01, 06.03.2018.

4.2 Relative humidity simulation

The average RH was higher (13.06% higher) at greenway Point-1 than bare Point-2 from 08.00-20.00 hours. The best result ensued at 10.00 hours noting 18.47% higher RH at greenway Point-1 than bare Point-2. The least result befell at 11.00 hours noting 7.90% higher RH at greenway Point-1 than bare Point-

2. Fig. 9 shows comparative RH simulation map at Kalshi Road, greenway Point-1 with bare Point-2.

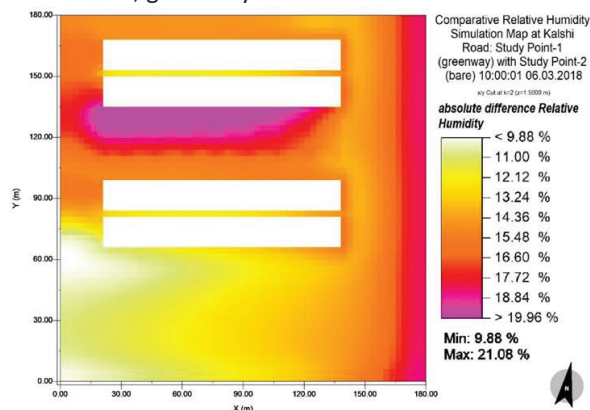


Figure 9: Comparative RH simulation map at Kalshi Road, greenway Point-1 with bare Point-2 on 10.00.01, 06.03.2018.

4.3 Mean radiant temperature simulation

Simulation study revealed that average T_{mrt} was lower (21.82 K lower) at greenway Point-1 than bare Point-2 from 08.00-20.00 hours. The best result befell at 18.00 hours logging 31.36 K lower T_{mrt} at greenway Point-1 than bare Point-2. The least result ensued at 18.00 hours recording 5.76 K lower T_{mrt} at greenway Point-1 than bare Point-2. Fig. 10 and Fig. 11 shows comparative hourly T_{mrt} simulation curves and T_{mrt} simulation map specimen respectively of bare Point-2 and greenway Point-1 at Kalshi Road.

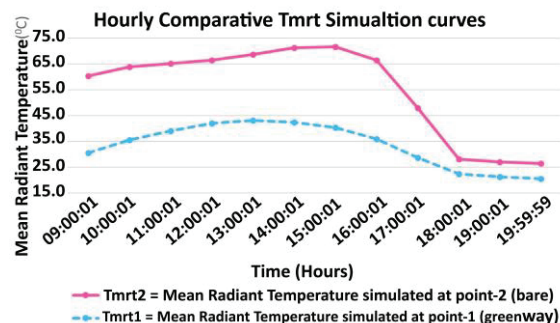


Figure 10: Comparative T_{mrt} simulation curves at Kalshi Road, bare Point-2 with greenway Point-1 from 08.00 to 20.00 hours.

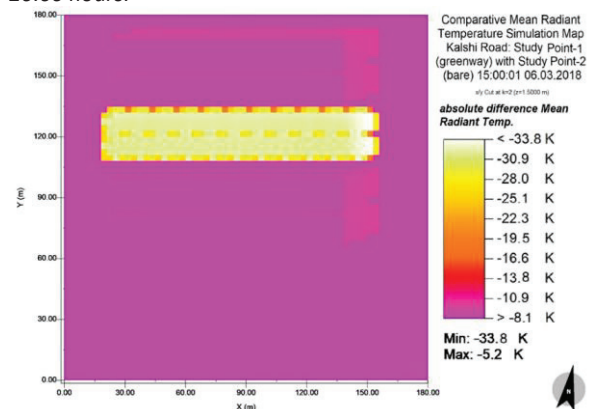


Figure 11: Comparative T_{mrt} simulation map at Kalshi road, greenway Point-1 with bare Point-2 on 15.00.01, 06.03.2018.

4.4 Wind speed simulation

The simulation study revealed that the average WS was lower (0.47 m/s slower) at greenway Point-1 than bare Point-2 from 08.00-20.00 hours. The maximum difference befell from 18.00-20.00 hours logging 0.5 m/s lower WS at greenway Point-1 than bare Point-2. The minimum difference ensued at 11.00 hours logging 0.40 m/s lower WS at greenway Point-1 than bare Point-2. Fig. 12 shows a comparative WS simulation map specimen at Kalshi Road with greenway Point-1 and bare Point-2.

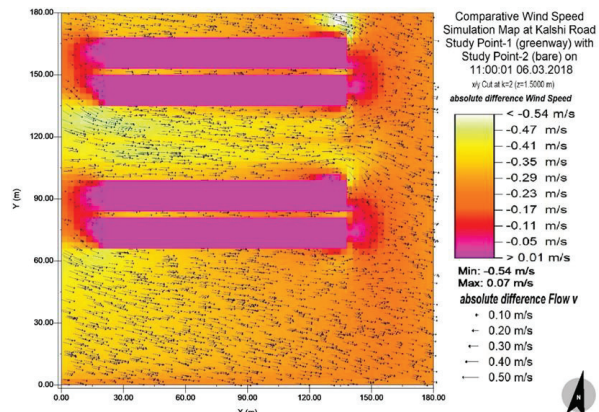


Figure 12: Comparative WS simulation map at Kalshi Road, greenway Point-1 with bare Point-2 on 11.00.01, 06.03.2018.

5. DISCUSSION

This research explores the microclimatic impact of integrated greenways on Dhaka's street canyons over field and simulation study. The field study reveals that at most street canyons of PR Dhaka, DBT exceeded thermal comfort level (above 32 °C) at daytime however, RH was within comfort range (30%-70%) for most of the daytime. Yet, from 12.00-14.00 hours, RH was below comfort range (below 30%-70%) at many points. At most points, blindly bare or green, WS was below comfort level (below 1.5 m/s) all day. Greenway identical features (GIF) as densely planted high LAD and high LAI trees on both sides contributed reducing DBT (up to 0.2-3.5 K) and increasing RH (up to 1%-7%) of the street canyons at daytime. At some points, GIF aided dropping DBT of the street canyons within or close to thermal comfort level (22.5-32 °C). Yet, GIF influenced reducing WS (up to 0.1-2.2 m/s) of the street canyons ensuing less thermal comfort. Harmonize greenway integration on USC can repeal this effect. GIF honed CE (up to 0.5-1.7 K lower DBT), RH (up to 1%-4% higher) and WS (up to 0.6-0.9 m/s higher) of the street canyon than scattered trees at same site condition. North south oriented street canyons were cooler (lower DBT) than east west ones.

The field study reveals a relationship between greenway and street canyon aspect ratio (H/W) at daytime [11]. The CE of greenway is inversely proportional to H/W (Eq. 1). Greenway holds a compelling CE (lower DBT) and IE (increment effect)

of RH when integrated on shallow street canyon. H/W is inversely proportionate with the IE of greenway on RH (Eq. 2). Deep street canyon mixed with greenway deliver consistent cool environment of lower DBT and higher RH. DE of greenway on WS is proportionate with H/W (Eq. 3). Greenway integrated on deeper street canyon has a higher DE on WS of USC. In shallow street canyon, greenway holds less or sometimes no DE on WS of USC.

$$(H/W)_{\text{greenway}} \propto 1/(CE)_{\text{DBT}} \quad (1)$$

$$(H/W)_{\text{greenway}} \propto 1/(IE)_{\text{RH}} \quad (2)$$

$$(H/W)_{\text{greenway}} \propto (DE)_{\text{WS}} \quad (3)$$

Where, H/W – street canyon aspect ratio (Height/Width); DBT – Dry Bulb Temperature; CE – Cooling Effect; RH – Relative Humidity; IE – Increment Effect; WS – Wind Speed; DE – Decrement Effect.

The field study investigated the available sites containing GIF. For deep insight of greenway impact in honing street canyon microclimate based on thermal comfort indices, a seamless greenway model was applied and compared with the existing bare street canyon model through simulation software Envi-met. The percentage deviation of field data and simulation data at Kalshi Road on bare Point-2 calculated regarding DBT, RH and WS are 1.83%, 8.62% and -4.44% in turn. This is anticipated, as Envi-met cannot imitate the entire microclimate settings.

The simulation study unveils that integrating greenway on USC holds immense CE (reducing DBT) and enormous RH increment than applying dispersed mere vegetation or cool pavements. Integrated greenway avails reducing DBT (up to 7.03-10.30 K) and increasing RH (up to 7.90%-18.47%) extensively of Dhaka's street canyons and forms comfortable microclimate. The integrated greenway containing densely planted high LAD and high LAI trees and cool pavement explicitly PICP made walking trail influenced lessening T_{mrt} (up to 5.76-31.36 K) immensely. This incident creates pedestrian thermal comfort during weak wind summer days [17]. However, the integrated greenway constrains reducing WS (up to 0.40-0.50 m/s lower) ensuing less thermal comfort. Again, integrated greenway can quash this effect honing thermal comfort through lower DBT, T_{mrt} and higher RH in USC microclimate. In corollary, synchronise integration of greenway on USC regarding DBT, RH, T_{mrt} and WS can ensure thermally comfortable USC microclimate.

4. CONCLUSION

This research clarifies that integrated greenways consist an inherent cooling effect on street canyons of PR Dhaka. Over field and simulation study, this research reveals that greenway leverages reducing DBT and T_{mrt} and increasing RH of USC microclimate. Integrated greenway on USC enhance pedestrian thermal comfort. However, greenway elicits reducing

WS of USC ensuing less thermal comfort. Coherent integration of greenways on USC regarding DBT, T_{mrt} , RH and WS rescind this effect. Concisely, integrated greenways on street canyons of PR Dhaka can deliver the urbanites thermally comfortable, benign, and pleasant urban walking environment.

ACKNOWLEDGEMENTS

This work is performed in the Department of Architecture, BUET. The authors thankfully acknowledge the support and facilities given by BUET.

REFERENCES

1. Tabassum, T. and Sharmin, S., (2011). The impact of green space declination in Dhaka 's local thermal environment. In *The Special Conference on Urbanization, Traffic Jam and Environment*, Dhaka, Bangladesh.
2. Shashua-Bar, L. and Hoffman, M.E., (2000). Vegetation as a climatic component in the design of an urban street: An empirical model for predicting the cooling effect of urban green areas with trees. *Energy and buildings*, 31(3): p. 221–235.
3. Werneck, D. and Romero, M., (2017). Microclimate on outdoor spaces in the context of tropical climate: a case study in Brasilia–Brazil. In *PLEA*, Edinburgh, 2: p. 1956–1963.
4. Li, H., (2012). Evaluation of Cool Pavement Strategies for Heat Island Mitigation. Ph.D. Dissertation, *University of California*, Davis.
5. Ahmed, K.S., (2003). Comfort in urban spaces: defining the boundaries of outdoor thermal comfort for the tropical urban environments. *Energy and Buildings*, 35(1): p. 103–110.
6. Emmanuel, R. and Fernando H.J.S., (2007). Urban heat islands in humid and arid climates: role of urban form and thermal properties in Colombo, Sri Lanka and Phoenix, USA. *Climate Research*, 34(3): p. 241–251.
7. Little, C.E., Greenways for America. (1995). *Johns Hopkins University Press*, Baltimore, MD, United States.
8. Marwa, S.M., (2012). Urban celebrations-greenway network for livable and sustainable cities. Master's thesis, *University of Nairobi*.
9. Searns, R.M., (1995). The evolution of greenways as an adaptive urban landscape form. *Landscape and Urban Planning*, 33(1), p. 65–80.
10. Tasnim, Z., (2017). Implicit integration of greenway on urban street canyon of Dhaka city. In *Arcasia Forum Journal*, Jaipur, India, May 23-25, p. 147.
11. Tasnim, Z., (2018). A study on potential integration of greenway on urban street canyon at planned residential area of Dhaka city. M.Arch. thesis, *Dept. of Architecture, BUET*, Dhaka, Bangladesh.
12. Oke, T.R., (2004). Initial guidance to obtain representative meteorological observations at urban sites. *World Meteorological Organization*, Canada, Report 81.
13. Ahmed, K.S., (1995). Approaches to bioclimatic urban design for the tropics with special reference to Dhaka, Bangladesh. Ph.D. thesis (unpublished), A. A., London, UK.
14. Harlan, S.L., Brazel, A.J., Prashad, L., Stefanov, W.L. and Larsen, L., (2006). Neighborhood microclimates and vulnerability to heat stress. *Social Science & Medicine*, 63(11): p. 2847–2863.
15. Nunez, M. and Oke, T.R., (1977). The Energy Balance of an Urban Canyon. *J. Appl. Meteor*, 16(1): p. 11–19.
16. Lin, Y. H. and Tsai, K.T., (2017). Screening of tree species for improving outdoor human thermal comfort in a Taiwanese city. *Sustainability*, 9(3): p. 340.
17. Gulyás, Á, Unger, J. and Matzarakis, A., (2006). Assessment of the microclimatic and human comfort conditions in a complex urban environment: Modelling and measurements. *Building & Environment*, 41(12): p. 1713–1722.

Urban and Building Integrated Vegetation and its impact on London's urban environment

JOAO SILVA, ROSA SCHIANO-PHAN, AMEDEO SCOFONE

The University of Westminster, London, UK

ABSTRACT: *Vegetation among cities has always been related to a higher quality of the environments since the beginning of urban planning discussions. This paper presents a work developed through literature review, fieldwork, and analytic work, using on-site measurements and computational simulation. The aim of the work is to quantify the impacts of vegetation in heavily built areas lacking green elements. The paper analyses various typologies of vegetation and their integration within the built environment, developing a definition for Urban and Building Integrated Vegetation (UBIVs). The research showed that different UBIVs have a distinct impact on the local urban scale and that the addition of vegetation was responsible in most of the outcomes to enhance the thermal comfort and worsen the air quality. The paper showed that the combination of vegetation and specific building geometries was the best strategy to improve both air quality and thermal comfort.*

KEYWORDS: *Vegetation, Thermal comfort, Air quality, Built environment.*

1. INTRODUCTION

Air pollution is a worldwide issue linkable to the economic growth speed. In developed countries, where economic growth is slower, air pollution levels recorded today are lower than in the past, while in developing countries the recorded levels are increasing according to the level of industrialization and urban growth [1]. Actions to mitigate this effect need to be taken globally: in London plans have already been presented through its government official documents to reduce the pollutants emission [2]. The measures adopted are largely addressed to public and private transportation, with the plan of using predominantly electric vehicles by 2050 [3].

An important factor inside urban areas today is biodiversity, 'which can be defined as a range of plants and animals living together in their habitats adding value to people's lives' [4]. Biodiversity can generate ethical, aesthetic, informational, economic and ecological value [4]. The focus of this research is its capacity of transforming cities' environment and enhancing thermal comfort inside urban centres, which will directly impact human health [4]. Biodiversity inside urban context has been discussed the past 100 years [5] and nowadays the green structures have been proven to mitigate discomfort caused by high temperature [5,6]. Regarding air pollution it can be more difficult to prove its impact due to the numerous variables that can influence the performance of greenery on its mitigation, as for example, wind velocities, wind directions, vegetation typologies and species [6].

The city of London is considered to have a rich biodiversity due to the existence of more than 300 bird species and over 1500 plants [4]. According to a research developed in 2018, London is considered to be the fourth greenest city in Europe [7] and the city's government has expressed, through official documents, the intention of transforming it into the greenest city in the world [8]. The project of making London even greener is expressed through projects as 'London National park city'. The project exists to raise the discussion of access to high quality natural spaces and make all types of green structures accessible throughout all areas of the city [9]. Considering the biodiversity characteristics explained above and the numerous heavily built areas of the city with very low amount of vegetation, London was chosen for the development of the studies. This research is dedicated to study the vegetation which needs to be implemented to the urban tissue and to the buildings facades due to the lack of space. This type of vegetation is called in this research 'Urban and Building Integrated Vegetation' (UBIVs) and was tested to quantify the impact on human comfort and health through the development of fieldwork and digital simulations.

2. FIELD WORK AND DIGITAL SIMULATIONS

The two studied UBIVs were the living walls and green pockets, due to the possibility of measuring the impacts with higher accuracy in the ground floor level. For the development of this work the green pockets were considered to be the

vegetated public squares surrounded by medium to tall buildings, usually having a large number of trees and plant species.

The developed work started with the study of the different densities within London considering the characteristics and patterns of the built environment, which helped to choose the areas for the experimentations. The same land size (approx. 44,800 sqm) was analysed from two different sites in London. The Red Lion square with of 12% vegetated area, against the City of London with a vegetation cover of 3%. Both studied areas presented similar plot coverage (42% in Red Lion square and 52% in the City of London), in the other hand the floor area ratio, which is related with the number of built floors showcased an expressive difference (10 in the City area against 3 in the Red Lion). This study demonstrated the impact of verticalization and how these factors can create two completely different urban environments, which this work had the aim to test. The fieldwork was conducted in The Red Lion Square and in the City of London and the measurements were taken on a rainy, overcast day and on a sunny day with clear sky.



Figure 1: Density Diagram of the City of London



Figure 2: Density Diagram of the Red Lion Square area.

For the digital simulations the Red Lion Square area was chosen due to being a vegetated area in the center of the city which could fulfill the exercise purpose of understanding how the different density of the scheme can affect the outcomes. This purpose was achieved through the addition of buildings, bringing the reality of the Red Lion area closer to other contexts of London which have higher density. The simulations was the 31st of august at 2pm was the period selected, representing a summer day with high temperatures and clear sky.

The following cases were studied to assess the effect of vegetation:

Case A: Existing condition of Red lion Square, considering the same amount of grass, number of trees and paved areas existent today.;

Case B: Removal of all the existing green structures and substitution of the grass with hard paving; and

Case C: Removal of trees, preserving the same amount of grass and paved areas inside the square in addition to the application of the living walls to the facades of adjacent buildings and restoring existing grass.

The last portion of the digital simulation exercise is related to the study of density and vegetation which resulted in the application of different building geometries occupying the area corresponding to the Red Lion Square. The buildings were defined by the plot ratio and site coverage, finally showcasing four distinct tested scenarios, all of them with a plot ratio of 2.0. The following scenarios were tested:

Four distinct buildings with site coverage of 50%;

Three buildings with site coverage of 37.5%;

Two buildings (one on each side of the site) representing 25% of site coverage;

A single tall building with site coverage of 12.5%;

As per the 50% site coverage scenario but developed as a 'courtyard building'; and

As above but organized as a 'U shape' instead.

All the studies with the addition of buildings there were two different scenarios: one with the grass in the open areas and living walls in all the facades, including the surrounding existent buildings; the other scenario, without the addition of green structures. To the further understanding of the impacts of diverse green structures on air quality and thermal comfort, in some of the cases, trees were also added to the schemes with living walls and grass.

3. RESULTS

The main fieldwork outcome was that the areas with a higher number of trees had a higher

concentration of pollutants. The adjacent areas which presented lower concentration of trees presented higher air quality. The outcomes indicated that trees in the urban tissue can decrease air quality, probably due to its capacity of trapping particles and reducing the wind velocities. With lower wind velocities fewer particles are removed from the studied areas.

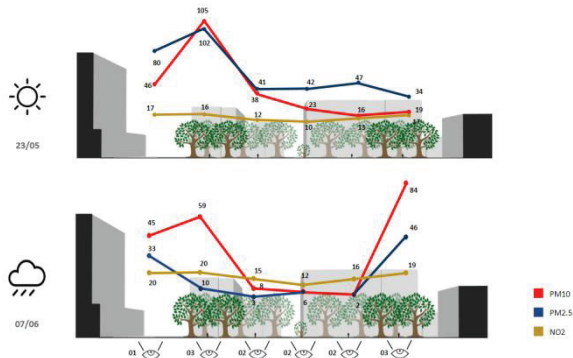


Figure 3: Diagram with the pollutants outcome of the fieldwork in different areas of the Red Lion Square.

The Digital Simulations shown that the living walls and grass caused a surface temperature reduction on all the walls where it was applied, leading to a drop in the mean radiant temperature of the studied square by 2°C (fig 4) in relation the case without any vegetation (fig. 5). The trees were the main factors to enhance thermal comfort reducing the mean radiant temperature of the square in 16.6C (fig. 6) in relation to the scenario with living walls (fig. 5). The UTCI (Universal thermal climate index) simulation showed that in the 'no vegetation' situation there is strong heat stress (32.2°C) inside the square area, against moderate heat stress (29.8°C) with the living walls and grass. When analysing the current situation (with trees) the temperature drops to a weighted average of 26.1°C which is considered to be comfortable.

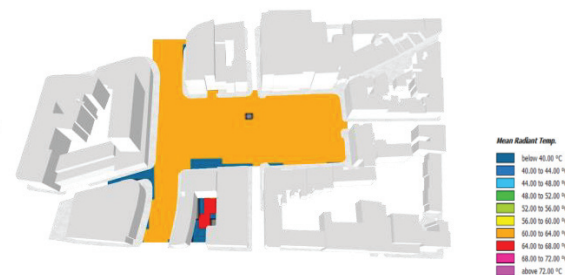


Figure 4: Diagram with the mean radiant temperature in the Red Lion Square without vegetation

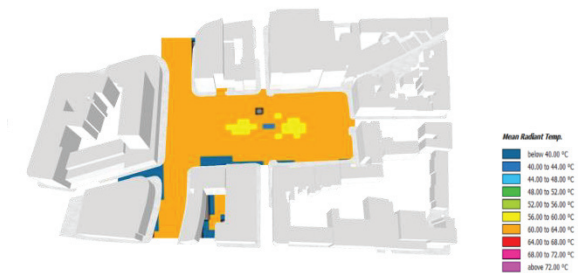


Figure 5: Diagram with the mean radiant temperature in the Red Lion Square with the addition of living walls

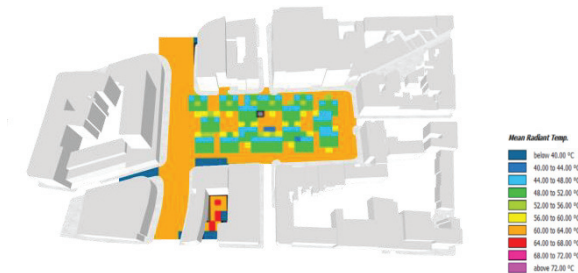


Figure 6: Diagram with the mean radiant temperature outcome of the digital simulation of the Red Lion Square as it is today (with grass and trees and no living walls).

Overall, the results indicate a substantial positive impact on thermal comfort thanks to the presence of trees, not displaying an expressive change with the addition of living walls on the Red Lion Square. However, studying the outcomes on the surrounding areas, considering all the surfaces covered with the living wall structure it was observed a drop on the average mean radiant temperature by 10% in one spot (indicated in fig 05). The result can suggest that in specific urban contexts (geometries) the building integrated vegetation (in this case the green walls) can indeed product impacts in the environment's thermal comfort.

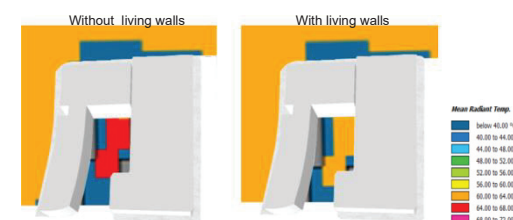
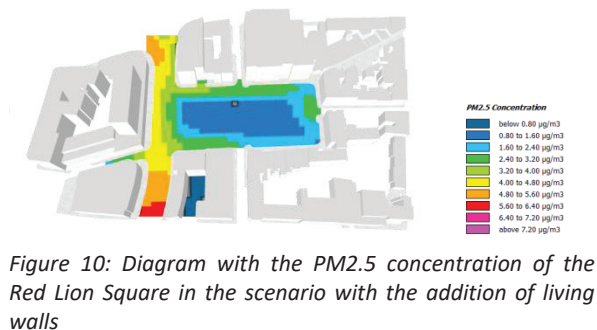
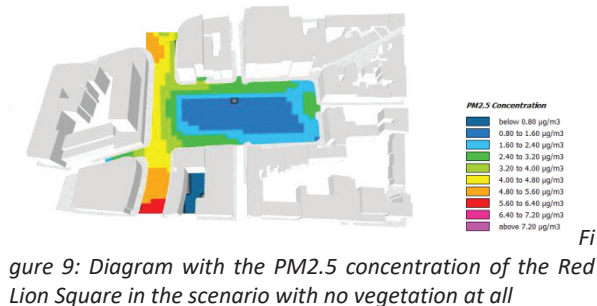
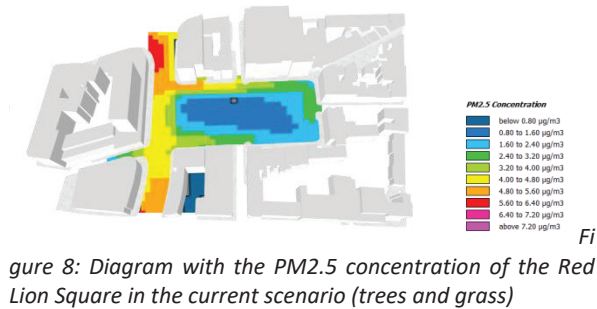


Figure 7: Diagram comparing the same building geometry with and without the application of living walls.

Analysing the pollutants concentrations in the outcomes, it was possible to see that even though the showcased levels for all pollutants (NO², PM2.5, and PM10) were not high, due to the World Health Organization (WHO) recommended standards, it was still possible to spot significant shifts between some of the scenarios. For the development of the comparison studies, the PM2.5 concentration levels

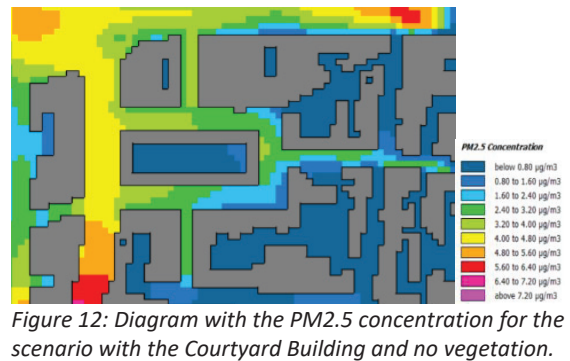
were the first pollutants to be analysed. The primary visible outcome was that the weighted average which was $1.5\mu\text{g}/\text{m}^3$ in the current scenario with trees (fig. 8) and in the situation with no vegetation at all the number drops to $0.87\mu\text{g}/\text{m}^3$ (fig. 9), finally, after adding living wall and grass the concentration level increases to $1.3\mu\text{g}/\text{m}^3$ (fig. 10).



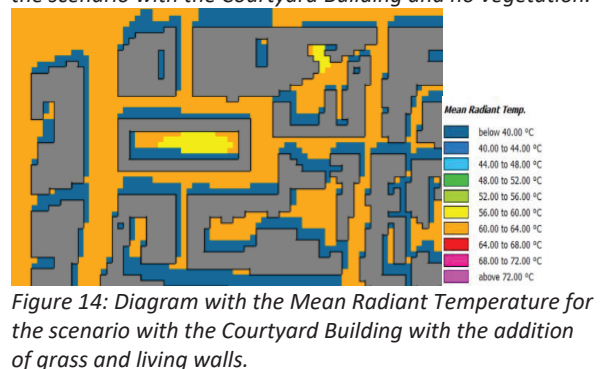
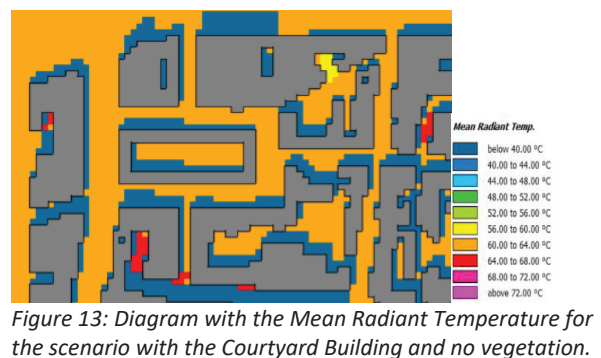
Comparing two of the different studied designs with vegetation (living wall, grass, and trees) the scenario with four buildings presented a weighted average mean radiant temperature of 55°C against 50.4°C on the second one. The same scenario also displays a slight increase in the PM2.5 concentration. Even though the building geometry acts as a barrier against the pollution sources the scenario with trees has lower air quality inside the areas between buildings.



With the implementation of the courtyard building (fig 06), it was possible to determine that the air quality inside the enclosed courtyard enhanced substantially. The result was a weighted average of $0.4\mu\text{g}/\text{m}^3$, representing a drop of 71% in comparison with the base case (Red Lion as it is today) and the lowest concentration from all outcomes in this research.



In the same case explained above, in relation to outdoor comfort, comparing the scenarios with and without vegetation the first result was a drop in the mean radiant temperature of 6°C (10.3%) when the living walls and grass were added.



The next important finding was that in this case the vegetation had a negligible effect on concentration levels of pm2.5 in the air.

This finding proves the impact of building geometry, as barriers, creating sheltered areas, even in city centers. The outcome indicates that Urban and building integrated vegetation can be added without possibly decreasing air quality. The 'U' shaped geometry showcased a weighted average PM2.5 concentration level of 0.7ug/m³ (fig. 15), only 0.3 higher than the completely enclosed building (scenarios with grass and living walls). The apertures to the courtyard reduced the mean radiant temperature to 2°C, probably due to the permitted wind circulation, considering that the prevailing winds come from the southwest. These findings displayed the possibility of having a space in the middle of the city, with significantly lower pollution levels than the surroundings.

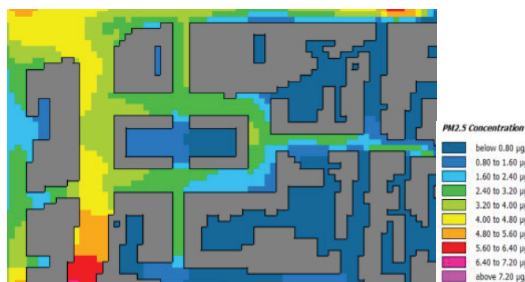


Figure 15: Diagram with the PM2.5 concentration for the scenario with the U building with living walls and grass.

The last issue in this scenario was still the high mean radiant temperatures, decreasing thermal comfort. For this reason, the last step of this research was to add trees in the protected courtyard area. With this addition the PM2.5 concentration only increased 0.05ug/m³ (6%), indicating no substantial change in the air quality. On the other hand, the mean radiant temperature drops from 51.3°C to 38.5°C, a decrease of 12.8°C; displaying an enhancement in thermal comfort by 25%. The last studied scenario presents a very successful strategy combining the building geometry design and the application of vegetation towards increasing thermal comfort and air quality simultaneously.

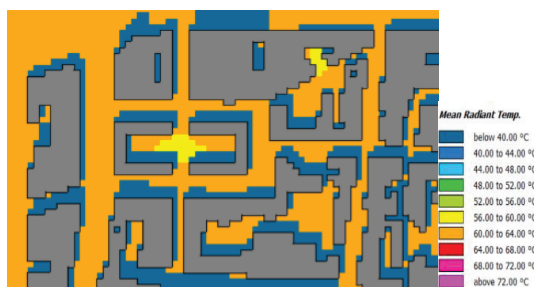


Figure 16: Diagram with the Mean Radiant Temperature for the scenario with the U building with living walls and grass.

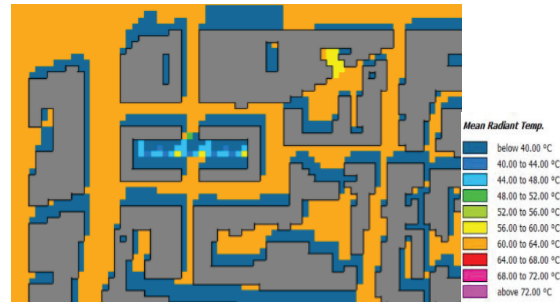


Figure 17: Diagram with the Mean Radiant Temperature for the scenario with the U building with trees

4. DISCUSSION

Considering a 26% reduction in the pollutant levels between scenarios with and without barriers it's possible to state that in a day with very poor air quality the courtyard environment could achieve high air quality levels. For example, if the surrounding area was presenting 10ug/m³ of PM2.5 concentration levels the outcome weighted average would be 2.5ug/m³, which is considered to be a low pollution level according to the London air quality network.

The outcomes presented in this paper regarding the impact of UBIVs on air quality showcased the negative impact of trees, the difficulty of quantifying the impact of living walls when studied in an open square and the effectiveness of the buildings as barriers against the main sources of pollution.

The combination between an enclosed geometry and the use of vegetation (grass and green walls) inside the courtyard area represent the best case scenario. When the trees were added in the open areas on the case study mentioned above, the pollutant weighted average concentration increased slightly. However, the mean radiant temperature dropped 12 C. In a hot day such as the one analysed in this paper the existence of trees are essential for the comfort of the users in the urban context. The research showed that even though trees are inside a "protected" environment the air quality can be reduced. One way to mitigate the negative impact of trees, according to the previous studies and findings presented in this paper, is the use of species with lower LADs, increasing wind velocity and consequently air quality. Even though the study showcased that reducing the LAD would not substantially change outdoor comfort, further research should be developed to accurately study the impact.

The study indicated the possibility of using buildings or other physical barriers against the main sources of pollution. Nowadays, the cars are still the main reason for low air quality, for this reason, the smaller streets can have the traffic reduced in addition to the use of UBIVs to create "safer zones" even in the polluted city centers.

5. CONCLUSION

By the end of the research, it was possible to conclude, confirming other researches' findings on the same topic that the vegetation inside an urban context can be useful to improve thermal comfort, reducing the heat island effect. It was demonstrated in this research that the improvement of thermal comfort conditions is directly connected with the materials used in the city and their capacity to transfer, absorb and emit heat to the environment. Vegetation can be ideal to decrease the perception of temperature in the environment. However, the capacity that trees have to shade the environment was shown to be the most precious asset, generating reductions of more than 10°C in the mean radiant temperature.

With regards to the air quality aspect of the research, green walls, trees and grass, were observed as a prejudicial addition in the first experiments, resulting in a 5% increase in concentration levels of pm2.5. By the end of the research, the combination of a building against the main source and the addition of green walls demonstrated no shifts in air quality.

The enclosed building with the addition of trees shows a reduction of 25% in the mean radiant temperature and an increase of only 6% in the concentration of the pollutants, indicating how the proper use of vegetation can be positive for both studied aspects inside the urban environment.

REFERENCES

1. Harrison, R.M., (2014). *Pollution: Causes, effects and control*.
2. Scorer, R., (1973). *Pollution in the air: problems, policies and priorities*.
3. Greater London Authority, (2017). *London Environment Strategy*, 17: p. 16-19, 38-40.
4. Greater London Authority, (2018). *Mayor's Transport Strategy*, 18: p. 107-111.
5. Hunt, J., (2005). *London's Environment, prospects for a sustainable world city*, 05: p. 123 – 126.
6. Pozo, S., (2018). *Vegetation as a Potential Tool for Improving Thermal Comfort and Exposure to Solar Radiation in the Streets of Quito*.
7. Santos, R., (2017). *Vegetation Cover and Surface Temperature in Urban Areas: An Analysis Using Remote Sensing in the City of Salvador, Bahia, Brazil*.
8. Abhijith, K.V., (2017). *Atmospheric Environment*, 162: p. 71-86.
9. *The Telegraph*. (2019). *London has become the world's first 'National Park City' – but what does that really mean?* [Online] Accessed 17/03/2020
<<https://www.telegraph.co.uk/travel/news/london-national-park-city/>>

The Logistics of Energy: Strategies for achieving Energy Optimisation within nZEB Mixed Use Urban Developments

MARTIN MURRAY¹, SHANE COLCLOUGH¹, PHILIP GRIFFITHS¹

¹ Belfast School of Architecture and the Built Environment,
Ulster University, Shore Road, Jordanstown, Belfast, Co Antrim, BT37 0QB

ABSTRACT: The recast European Directive for Energy Efficiency in Buildings requires that from December 31st 2020 all new buildings constructed within the European Union (EU) meet an nearly-Zero Energy Building (nZEB) standard. The defining characteristics of which place an emphasis on (a) Cost optimality, (b) Improved building controls, (c) Improved fabric performance, and (d) Substantive renewable energy provision, all based on a predictive energy performance. However the specific nZEB definition has been left 'open-ended', so as to allow variation across individual EU nation states. This paper suggests strategies to facilitate energy optimisation of the nZEB standard within mixed use urban developments located in a temperate oceanic climate. The paper derives from a concern that the nZEB standard, as practiced in Ireland, may inadvertently increase lock-in of current energy standards and use valuable resources now in an unplanned, profligate way. In so doing we reduce our future communal capacity to greater self-determination in regards to all forms of future energy, renewable and non-renewable, operational and embodied. These are pressing issues due to the necessary long service life of buildings and the thirty years to 2050 within which it is considered imperative that we bring greenhouse gas emissions to Zero.

KEYWORDS: nZEB, Energy-optimisation, Resource-optimisation, Urban, Mixed-Use.

1. INTRODUCTION

The European Union's overall Energy Policy and Legislation revolves around three major goals: (i) Energy security, (ii) Retention of competitiveness, and (iii) Support for sustainability. In this context it is noted that: *'Energy efficiency is the most cost effective way to reduce emissions, improve energy security and competitiveness, make energy consumption more affordable for consumers as well as create employment, including in export industries'* [1].

The specific energy aspirations for buildings as defined within current European Legislation, (principally Article 9 of the recast Energy Performance of Buildings Directive (EPBD), 2010, are framed by the eponymous definition of a nearly Zero Energy Building (nZEB), as one, whereby:- *'the point where the measures required to implement the standard are 'cost optimal' to achieve a balance between costs and energy performance in the current construction environment'*.

Additionally it is noted that in regard to such nZEB buildings:- *'the nearly zero or very low amount of energy required should be covered to a very significant extent by energy from renewable sources, including energy from renewable sources produced on-site or nearby'* [1]. To truly reflect this aim within our future post carbon cities, buildings will effectively need to achieve a zero use of non-renewable energy. This future reality appears significantly beyond the

aspirations of the current nZEB methodologies and this shortcoming is inadvertently acknowledged, within the most recent Renewable Energy Directive II (RED II), adapted by the EU in December 2018, which sets an increased binding target of 32% of the EU's energy demand, to be met by renewable technologies by 2030.

What is particularly notable is that the RED II Agreement also sets unequivocally, an *'energy efficiency first'* principle. It acknowledges that the *'cheapest and cleanest source of energy is the energy that does not need to be produced'*. This legislative evolution brings with it by default an evolved range of nZEB logistics also, namely (a) an improved standard of fabric performance, beyond the current concepts of cost optimality and (b) a heightened awareness of the carbon intensity of nZEB buildings, reflected in the passive embodied carbon, the active carbon utilised in its construction and the operational carbon ongoing. Calibrations of which are all quickly coming to the fore in the context of global climate disruption [2].

Unfortunately across almost 20 years, of European legislative policies, we have consistently failed to meet anticipated energy and carbon reduction targets. This is evident in regard to the 1.5% annual savings anticipated year on year by the main national energy providers and the simple energy performance of new and refurbished buildings. 'Low-energy' buildings built to legislative requirements have consistently failed to deliver the

savings anticipated in predictive softwares. In Ireland and the United Kingdom there has been a consistent deviation between the preliminary Energy Performance Certificates (EPC's) based on the modelled data and the Display Energy Certificates (DEC's), based on actual use data [3].

The question arises therefore as to the optimality of the current nZEB standard, which is uniquely energy centred and characterised by the most decidedly indefinite prologue 'nearly'. Is the current nZEB standard a justifiable foundation logistic, sufficiently robust, measurable and aspirational to facilitate a future where the embodied energy of our ultra-low energy buildings will approach significantly their operational energy? Is there a way forward which thematically allows for, (i) an ease of application in practice, (ii) a clear functionality in addressing energy usage and (iii) a reduction in GHG emissions, all in an immediate and practical way? How does one optimise policy decisions from the metric 'nearly'?

2. THE CURRENT nZEB STANDARD

In Ireland the current nZEB standard across non-domestic buildings, - policy effective in its totality from December 31st 2020 - reflects a 60% improvement on baseline 2005 regulations. For domestic buildings this improvement above the baseline 2005 figure, is 80%. Ostensibly all good; yet who in 2020 can even remember the reality of life in 2005? Who in 2005 was designing buildings to ensure some regulatory conformity for 2020, or even 2050, which effectively is the energy standard to which we must now adhere. Any building constructed or renovated now, must anticipate and meet the energy and resource capacities which will be operable in 2050.

The immediate challenge this represents for the Irish construction industry is reflected in the fact that while the domestic energy standard has been incrementally improved over the last 15 years, with a coherence of approach, incremental steps, adaptable technologies and a growing social awareness, the non-domestic standard has not. We enter therefore into a 2020 construction milieu, where design, material and technological advances have not been incrementally improved within the construction customs of our non-domestic building stock and the nZEB challenge will need to address a market which is predominantly investment led. These circumstances are further complicated by the wide variability of tenancy, use pattern, and physical form inherent to non-domestic building types; dependant on the 'love of strangers' for an optimality of use. All of which suggests that there is a real low energy challenge of significant proportions

for non-domestic buildings, new and old, new build and refurbishment.

The challenge represented by refurbishments - non-domestic and domestic alike - is particularly significant given the lack of construction skill-sets available, post-financial crash and the lack of new recruits coming into an industry which has a poor reputation for career regularity and generally reflects poor remuneration for that most valuable commodity and renewable of energies, man-labour. Furthermore (a) the low carbon challenge (environmental), (b) the financial structures to reflect the true cost of carbon, (economical), and (c) the need for closed loop supply chains, (social), reflects in microcosm the well-known venn-diagram triage, and perhaps also the illusion, of that elusive and long standing ideal:- 'Sustainable Development'.

2.1 The Practical Challenges of nZEB

nZEB (non-Domestic) buildings in Ireland are developed and energy analysed through the Non-domestic Energy Assessment Procedure (NEAP) using iSBEM v.5.5h software. This 1990's software is not a 'design tool' but rather facilitates a comparison between relative energy performances. It therefore lacks the rigour of analysis and performance metrics found in other standards such as *Passivhaus*. It also omits plug loads, (significant given our changing pattern of energy use), and has no elements of dynamic simulation, thus affecting an accuracy in follow through, from preliminary modelling to the reality of implementation and real use [4].

In a more direct way, treating our future building stock as a series of independent entities unrelated to their energy context and energy grid environment is unhelpful in understanding optimal energy solutions and fails to recognise the complexity of the challenges in front of us. The credentials therefore of credible nZEB buildings, sit on shifting sands.

Historically these 'nZEB credentials' encompass an Energy Performance Coefficient or Ratio, (EPC) and a Carbon Performance Coefficient, (CPC). If the EPC and CPC are 1.0 and 1.15 respectively the Renewable Energy Ratio (RER) to Primary Energy for the building must be 20% or greater. If the EPC and CPC coefficients improve by 10% to 0.9 and 1.04 respectively the RER can be reduced to 10%.

The implication of both RER percentages is that we are constructing buildings in 2020, which will be operable through to 2030/2050, and which have a grid dependency of anything from 80% to 90% respectively. In England where over 60 gigawatts of electricity is used every year, they would need to cover the whole of the English countryside with wind farms to ensure adequate 'renewable, decarbonised' electrical energy; whilst also being conscious that in times of wind

depletion the system would require an additional back-up capacity of 75% to meet needs. So while the principle of 'make it electric and make it green' is acceptable, the grid capacity will be challenged in supporting, not just the building needs, but also the emerging electrical vehicle (EV) market.

It is therefore deeply problematic that we have an energy resource standard in Ireland, nZEB, which measures itself against an historic 2005 standard, as opposed to practically addressing itself against future 2050 needs and relies on a currently carbon dependant electrical grid for success. Thus in setting its energy saving target too low the current nZEB approach will put significant future pressures on our electrical grid and ignores the reality that all new buildings, should effectively be achieving Zero Carbon Emissions now, so as to serve adequately the future 2050 needs [5].

A key bed rock consideration for nZEB, its radical justification, has been 'cost optimality'. Economically this expression and consideration can be used to justify a wide variety of policy directions depending on where one's perception of economic value lies [6]. It must however, *by obligation* be considered under the EPBD-recast 2010.

The resulting cost optimisation, as derived from the non-domestic reference building(s), ignores a whole range of multi-beneficial criteria, including benefits of improved indoor air quality, (IAQ), which in turn gives rise to increased productivity, reduced illness, reduced user absenteeism and increased well-being. In domestic buildings this list is longer, encompassing such inherent social benefits as fuel poverty alleviation and direct improved health benefits to occupants [7]. Inherent to this wider societal perspective, beyond cost-optimality, is a greater appreciation of 'energy optimality' which reflects energy used carefully, in contrast to an efficiency of production without deep consideration as to use, and more particularly, the implications for resource depletion and CO₂ emissions over time [8].

2.2 The End of Cost Optimality

'Change comes when the short term logic of events intersects with the long term evolution of ideas. Every ideology has its weaknesses but no human society can live without an ideology to make sense of its inequalities' [9]. As energy lies central to the equalities of life, it is critical that any energy solution enshrined in policy carries with it an ideology that ensures reasonable access for all. It is therefore also inevitable that the current market operation without fundamental change is not an option [10]. Notwithstanding this sobering reality, it is noted that all of the key variables, upon which cost optimality is structured, are themselves prone to significant change over relatively

short periods of time: the cost of renewables, the cost of money and the future cost of all energies are entirely unpredictable in the short term, and in the long term will be irrelevant as 'optimisation of energy use' and 'reduced carbon emissions' will be the key determinants in creating an energy performance 'step-change' within the construction industry.

In many ways, 'cost optimality' is a pseudonym for 'market optimality' and it is only with great reticence that we ought to follow the market. Such a lesson was learned by legislators drafting the 'Clean Air Act' in America in the 1960's and 1970's, where it was realised very early on, that if real intrinsic change was to be achieved, then standards must be set by the legislators, not the market place. The Market is not altruistic [11].

Undoubtably one possible alternative to 'cost optimality' would be 'societal optimality', where not just does operational efficiency come into play, but also the embodied energy of the construction materials evaluated in the context of long term resources and real carbon obligations. Future nZEB buildings must be energy-plus, smart-ready, and bio-material based, with plan dimensions to allow a relative ease of natural ventilation and multiple flexibilities of future use.

In this regard Passivhaus design is also based on cost optimality, as it too focuses on systems of operation that meet criteria of *value for money*; however the focus at all times starts with fabric first, interior thermal comfort, temperature symmetry, air tightness and optimal IAQ; in contrast the nZEB investigative software accepts more basic levels of internal comfort and airtightness but still uses significantly similar resources [12].

2.3 The Issue of Resources

It is this use of increasingly limited resources which is the real paradigm change necessary to nZEB policy. The new paradigm suggests a future where the social right to build customised, spatially independent, low energy buildings, dependent on technologies, and mono-utility, whose life span is short, relative to the building fabric investment, comes under question. Such adjusted criteria point irrevocably toward a fabric first principle as is central to the traditions of PHPP design; optimum orientation, airtightness, good heat recovery and a design format to allow optimal use, reuse and significant flexibility of operation.

The Sainsbury supermarket in Greenwich, UK, is a case in point. Built in the late 90's as a flagship low-energy building, when its owners out-grew the space, it was demolished and replaced by a furniture warehouse because the building's flexibility for other users was hindered by its bespoke low-energy architecture, focused on its initial design use. In contrast, Marks and

Spencer's environmental planning requires all new stores to be designed so that they have long-term future flexibility. An inclusive design approach such as this will change construction and design methodologies and allow different on-site and off-site craft and trade traditions to evolve thus forging different levels of speciality and allowing the emergence of authentic 'green collar' jobs. In a mechanised milieu we can lose sight of the fact that labour is the renewable energy resource par-excellence.

Mixed-use urban development incorporating both domestic and non-domestic uses, stitched unto brown field sites, facilitates an immediate ease of application and design context for such change. What then are the logistics of such an approach?

2.4 The Shifting Sands of Calibrating Energy Use

The singular metric of operational energy, which is central to nZEB policy, lacks relevance when faced with the greater proportionality of embodied carbon reflected in construction materials and methodologies. It can take approximately eighty tonnes of carbon emissions to build a typical 2 bed cottage style house in the UK [13]. Refurbishing a similar type cottage (from the 1930's/40's) would attract a carbon budget as low as eight tonnes. Even allowing for calculation variables, it is clear that the nonchalance by which we have demolished older buildings in the past can no longer be considered unimportant to the global carbon challenge. Investing in improvements to existing homes can be dramatically more cost-effective and operationally important for all of us than extensive new build [13].

The typical west European lifestyle is responsible for annual carbon emissions of c. ten tonnes of CO₂. In order to meet IPCC recommendations and achieve zero emissions by 2050 this figure must immediately reduce to five tonnes per annum. Allowing for an increased global population, (three billion additional by 2050), we would need to reduce our individual household energy consumption to one tonne of carbon per annum for a 100m² house. This represents 10Kg per m², if this particular house was 100% electric which would in turn reflect an energy usage of approximately 18kWh/m² per annum, a standard significantly lower than the nZEB standards currently applicable, and still dependant on grid electricity. Our new build constructions therefore are going to have to justify their use of resources by delivering significantly greater energy performance standards beyond those of nZEB and if possible, be themselves 'energy positive' [8].

Such 'energy plus' developments would be a key active element of future Smart Grids, if capable of large contributions of locally produced renewable energy, to the overall power grid. This then becomes another key

logistic for future low energy mixed-use buildings. Developments will therefore also need metrics to quantify building energy flexibility, combined with load shifting abilities, battery storage, power adjustment, energy efficiency and cost efficiency. Integral to these key performance indicators would be a constant dependable, indoor temperature modulation, where the fabric performance would be a most important determining parameter, allowing energy to be shared.

These emerging changes to the energy supply structure will also lead to a constantly changing primary energy factor, therefore a non-renewable primary energy demand will no longer be suitable for assessing buildings' energy efficiency. An emerging proposal by Prof Ronald Rovers, referencing resources in relation to the land units required to produce them, offers a potential route to an ethically based set of performance obligations [8].

3. ENERGY OPPORTUNITY OF URBAN MIXED USE DEVELOPMENTS

The current mismatch between energy use and on-site energy generation is one of the key challenges in bringing forward any optimisation of nZEB policy and the energy profile of a mixed-use development helps in a very direct way to address this anomaly. Intelligent energy storage and management become significant contributors in levelling out seasonal and use variations where the peak electrical generation can be either significantly higher or lower than the use requirements. This energy challenge is a particular opportunity for mixed use developments, where the different energy use profiles, (having been minimised through improved fabric design), can be combined to reduce the energy gap across the whole development and optimise its overall energy performance.

The practical nature of improved low energy design strategies such as PH design, can help to achieve these stated aims across a variety of scales. The greatest challenge and opportunity rests with small urban developments which could catalyse change at the level of the local grid, the village within the city where *'the whole is greater than the sum of the parts'*; a working definition of what constitutes good urban design for post-carbon cities.

3.1 The Changed Logistics of Mixed-Use Energy

To emphasise this point it is worth reflecting on the common definition of 'logistics' being *'the detailed organization and implementation of a complex operation'*. To progress an understanding of what the 'complex operation' of energy might be, we need to understand it as an integrated system; one where energy is no longer seen simply as a commoditised

product to be purchased as required and used to depletion.

To challenge this level of myopia, all new development must of itself reflect an underlying system of energy and resource use, promoting principles of reduce, reuse, recycle and regeneration, all inherent characteristics of an integrated system. This crucially will ensure that the return on resource investment is beneficial, if not optimal, in regards to carbon usage for society as a whole. There is unfortunately a perception in the market place, driven by current nZEB policy, that so long as the primary energy usage and carbon emissions are controlled through statutory regulations then the problem of climate change is being addressed and yet nothing could be further from the reality of the climate problem as it is now formulating [8].

The real problem, stated simply, is that we must now significantly flatten the curve of GHG emissions in order to buy time to use materials and resources in a coordinated and sustainable way to address the carbon emissions of our older building stock. We must effectively reduce waste, (by retaining fabric), reuse structures, (through refurbishment), recycle materials, (through careful demolition) and regenerate spaces (through energy-plus design). If policy consideration moves from an energy-centric policy to a resource-centric policy the key logistics of nZEB will move to save energy and optimise resource use. More significantly if we move from an entirely energy centric policy to a CO₂ elimination policy then renewable energy and material strategies take centre stage and we avoid the significant volumes of potential lock-in of poor standards which are in hand [14].

Current reviews of ninety-five residential buildings (assumed 50-year lifespans), identified a range of embodied carbon emissions between 179.3 kgCO₂e/m² to 1050 kg CO₂e/m², reflecting a share of between 9% to 80% to the total life cycle impact. Similar trends from the perspective of embodied energy followed, and ranged between 9% to 22% for conventional build, 32% to 38% for passivhaus and between 21% to 57% for low energy buildings. The 'normalised' results indicate a sensitivity to the electricity mix which could not be neutralised, and confirms the need for further understanding to facilitate LCA analysis.

The emerging decarbonised grid electricity in the UK currently produces around 0.096kg of CO₂ per kWh generated, while natural gas produces around 0.400kg per kWh. So while decarbonising of the grid is desirable and progressing, natural gas will still be necessary for peak use of the grid through to 2030. We will therefore have to pay, and balance, this use of fossil fuel by increased localised electrical generation. The immediate energy future lies therefore in fabric first

mixed use developments with significant generation of energy, used locally.

It is necessary in this emerging scenario to also recognise that "zero-energy" buildings, do require additional materials (e.g. insulation) or the installation of technologies (e.g. PV and mechanical ventilation) which further increase the embodied energy of these buildings and their related environmental emissions. However these materials are there for significant periods of time and can be analysed under various Life Cycle Assessment methodologies, using various environmental indicators: Global Warming Potential (GWP), Primary Energy Intensity (PEI), and Acidification Potential (AP). All of which indicate that subject to geographical location, carbon payback occurs quite quickly, within 5 to 6 years [14].

All societies by their nature, evaluate things through an underlying socially validated system, albeit stated clearly or metaphorically understood. Our current value system as expressed through nZEB is one derived from a perception of European economic growth, dating back as far as Renaissance times, and financed by vast amounts of accumulated wealth from overseas conquered nations. It brokers a belief system of progress and societal wealth based on such continued economic expansion, which we all know now to be myopic in nature. However the nZEB policy as currently framed, seeks not to endanger this viewpoint, and yet this is what is required.

Close to this viewpoint will be our future pricing of carbon to a level necessary to get the economic ship to change course. While the current value ranges from €25 to €29, the figure for action change needs to be closer to €70 a ton. Ronald Rovers suggests, (influenced by the works of Henry George), that carbon and all resources including wealth, can be measured and valued in a more fundamentally ethical way by reflecting its inherent land intensity. Furthermore the value benefit of anything lies in the ability of that thing to serve the needs of the greater community, for as long as possible, in regard to resources used. This is a society where generational wealth is created. However it is also a society which places real value on resources used with prudence. This would necessitate mixed use development with energy utilised with restraint, prioritising maintenance, repair and renewal [8].

The nZEB energy logistics currently operational appear to support the design of single-use buildings, inflexible, with moderate energy needs, necessitating significant associated social-wide energy use to justify their location and size. This approach prioritises rental value of property, over 'real' value, which is disguised by undervaluing all of the associated GHG emissions. Thus the system upon which nZEB is based, protects the

investment values of pension funds and banks. In the context of reducing GHG emissions within 30 years, maximum, these values are now redundant

4.0 nZEB FOR THE 'THIRTY YEAR' CHALLENGE

The opening up of national grids to renewable energy will allow urban energy-positive developments to thrive. In financial terms there are still obstacles however, the granular scale of activity which increasingly values and minimises energy use across the full spectrum of societal activities, living, commuting and commercial will find bedrock in such energy-positive developments.

Resilience is greatly valued at present. It reflects an ability to respond positively to system shocks. The systemisation necessary in supporting future low energy logistics must spread its net wide, utilising multiple energy generators, supporting a localised supply grid, and eventually leading the supply to an increasing localised, reduced energy, demand. Mixed use nZEB developments located on strategic inner-city brown sites, can in this way remain resilient and support resilience.

By focusing on energy operational use only, our current nZEB legislative controls are inadequate in scope to protect society from poorly constructed buildings and the growing carbon emissions challenge of all buildings. Mixed-use urban-developments built to fabric-first, energy-plus principles will create a future tradition of energy.

5. CONCLUSION

The theme of this paper has been to explore and understand the emerging logistics inherent in achieving energy optimisation within mixed use urban developments. Utilising proven design and implementation methodologies such as Passivhaus will be a key determinant in the planning of post carbon cities and therefore are central to addressing our vulnerabilities to climate change.

The nZEB policy strategy is in need of significant review if it is to meet this challenge. This is a challenge not just of energy use, but rather one of resource use to optimum benefit. The problem is social as well as scientific, it is psychological, physiological and cultural as well as political, financial or legislation. We therefore cannot progress a strategic change to logistics without changing our perception of the problem. Central to this is a change in the concept of value and labour. If we set value reflective of the current market place, the cost optimality of nZEB makes sense. If we see the final solution to fossil free energy as large scale nuclear or wind or PV, then labour as a renewable commodity does not even warrant calibration. And yet this last

reality is nonsense in the context that the biggest energy challenge is renovation of our existing building stock, without increasing levels of carbon lock-in [15].

It is not unusual that the existing technologies and methodologies of the market place act as a drag on any potential for radical transformation, however the current nZEB logistics fail in their creation of a real taxonomy of energy change and it is this which we must address, if we are to achieve a meaningful stepped approach to a transformational change.

We have an opportunity now in the midst of the enforced social change of Covid 19, to radically alter our perception of social and labour value. We have lived in an age of mass denial related to GHG emissions, we actively resist imagining the death of humanity much as we resist also dwelling on our own, however needs must, and resources and time have become both our enemy and friend. We must act and engage with both now.

ACKNOWLEDGEMENTS

This paper is intended as foundation research in support of Ph D Study at Ulster University, Jordanstown. I wish to thank the University for their sponsorship of these studies and their support in the development of this paper.

REFERENCES

1. Implementation of the Energy Efficiency Directive (2012/27/EU), *EPRS Review* 579.327, April 2016.
2. Amended Energy Performance of Buildings Directive (EPBD) (2018).
3. H. Richie, M. Roser (2020) - CO₂ and Greenhouse Gas Emissions. *OurWorldInData.org*. Retrieved from: 'https://ourworldindata.org/co2-and-other-greenhouse-gas-emissions' (Online Resource).
4. G. Wardell and K. Shanks, Energy Performance Survey of Irish Housing (2005), (*Unpublished*).
5. R. Rovers, People vs Resources. (*Eburon, Utrecht 2019*).
6. M Mazzucato, The Value of Everything. (*Allen Lane, 2018*).
7. Zero carbon Hub. Indoor air quality in highly energy efficient homes, (2008)
8. R. Rovers, People vs Resources. (*Eburon, Utrecht 2019*).
9. T. Piketty. Capital & Ideology. (*Belknap Press, 2019*)
10. J. Wainwright and G. Mann. Climate Leviathan, *Verso 2018*.
11. B. Gardiner. Choked, *University of Chicago Press, (2019)*
12. International Passive House Association. <https://passivehouse-international.org/>
13. M. Berners-Lee. How Bad are Bananas. *Profile Books 2010*
14. Renewable and Sustainable Energy Reviews, *ISSN: 1364-0321, Vol: 82, Page: 1774-1786 2018*
15. G. Unruh. Escaping Carbon Lock-in Energy Policy, 2002, (*vol. 30, issue 4, 317-325*)

Post Occupancy Evaluation Of Educational Buildings In Warm-Humid Climate: Using BUS Methodology To Understand The Implications Of Naturally Ventilated Building Design On Human Comfort

SUBHASHINI SELVARAJ

Thiagarajar college of Engineering, Madurai, Tamil Nadu, India

ABSTRACT: *Comfort in architecture can relate to many aspects of how a building gets designed. One of the main challenges in educational buildings in warm-humid climatic zones is to provide a thermally comfortable environment to satisfy the needs of the students and teachers involved in it. The present study has tried to analysis the occupants' perception on the thermal performance of the building using post occupancy evaluation (POE) survey results. This study has carried out POE survey using Building Use Studies (BUS) post occupancy evaluation methods in four separate building blocks located within an institutional campus in Madurai, out of which two are mixed mode (classified as Type I) and the other two are naturally ventilated (classified as Type II). A comparative analysis between the two types has been carried out by analysing the results from the POE survey. The results revealed that the occupants' satisfaction with respect to the thermal performance of both cases in summer was lower than the BUS benchmarks. The feedback from the occupants on other factors like image of the building, user needs, storage and other facilities, overall comfort (thermal, lighting and noise) and productivity served as a strong database which could be used for the effective design of educational buildings in future.*

KEYWORDS: *post occupancy evaluation; thermal comfort; warm-humid climate; natural ventilation; educational buildings.*

1. INTRODUCTION

In modern societies, people spend more time of the day in offices and schools than residences. Most offices are air-conditioned and provided with suitable infrastructure. In India most of the schools and universities have naturally ventilated classrooms with only fans for mechanical ventilation [1]. Our built environment has a profound impact on our health, wellbeing, and productivity. A built environment is a medium between the location where it is built and its users. Buildings must be designed in such a way as to provide healthy and comfortable environments for human activities. A building must fit the activities it is built for and provide spaces for function, comfort, and safety. Scientific research demonstrates how the physical classroom environment influences student achievement [2-4]. Inadequate lighting, noise, low air quality, and deficient heating in the classroom are significantly related to worse student's achievement. Similarly, the amount of light, air, heat entering a building affects the behaviour of its users. Be it a simple line or a complex form; buildings can change the state of mind of its user. Since olden days, natural lighting, ventilation, and thermal comfort play an inevitable role in the process of learning through the Gurukul system of learning in India. The students

were taught under the shades of huge banyan trees or neem trees, where they get fresh air, ambient lighting and thermal comfort. Nowadays, it is not possible to follow such a system due to various factors like air pollution, noise pollution, space constraints in the urban settings, climate change and so on [5,6]. A positive psychological impact on users can increase the productivity in the learning environment [7]. Hence the built environment should harmoniously blend with the positioning and the psychology of the users to satisfy the function for which the space is planned.

The present study has carried out POE survey in four separate building blocks located within a large institutional campus in Madurai out of which two are naturally ventilated (NV) and the other two are mixed mode(MM) using Building Use Studies (BUS) post occupancy evaluation (POE) methods. In the NV classrooms fans were used for promoting air circulation. In MM buildings there were spaces both NV and air-conditioned (AC). A review of various POE systems and their approaches with respect to their objectives and methodologies has been done in this paper. The efficiency of POEs in obtaining information on indoor environmental quality has also been addressed in the literature review. The results revealed that the occupants' satisfaction with respect

to the thermal performance of both cases (NV and MM) in summer was lower than the BUS benchmarks.

2. AN OVERVIEW OF POE SYSTEMS

The Post Occupancy Evaluation (POE) is a systematic process of evaluation of a building from the occupants' perspective [8]. In general, the system provides a procedure of collecting feedbacks from the occupants of an existing building to understand and evaluate the performance of the buildings in various aspects. There is also growing interest in post-occupancy evaluation (POE) in recent times. Post occupancy evaluations of buildings serve as a way to assess the building performance both in a qualitative and quantitative way. POE in educational buildings can help determine the facilities needed to be provided for proper management of the learning spaces in terms of planning aspects, thermal performance and indoor environmental quality (IEQ) [9]. It has been reported that the feedback on user satisfaction obtained through POE of low energy buildings are essential to understand the effectiveness of the built environment [10]. The performance of buildings can be analysed from three different aspects such as, occupants' perception, environmental performance and economic value. Generally, buildings are designed focussing on its environmental performance and economic value. The occupants' point of view is often neglected. Leaman et al (2010), states that it is essential to consider the building occupants' perspective for building performance evaluation [11]. Ng and Akasah (2013) have done a comprehensive post occupancy evaluation for a set of energy efficient and LEED rated buildings in Malaysia and reported that despite of the proper planning the occupants in these buildings were not satisfied with the performance of the building [12].

During the past decades POE methodology has been implemented as an important tool to evaluate the psychological, physical and environmental parameters that affect the Indoor Environmental Quality (IEQ) of a building. The advantages of POE over other conventional surveys are that, in this method the occupants of the building act as the main sources of information on the performance of buildings. Over the past few decades, the quality benchmarking of buildings as a feedback tool by POE systems has not only raised interest among architects, engineers and builders but also the building occupants as well [13]. There are different types of POE systems developed mainly in UK and USA to evaluate both domestic and non-domestic buildings. Alessandra et.al (2014) has done a critical analysis of various POE systems and highlighted their pros and cons [14]. The measurement indices used in POEs include questionnaire surveys, personal

interviews and time of assessment and physical measurements of the building, feedbacks from the occupants on user satisfaction and productivity, also on building performance measures such as thermal comfort, noise and lighting levels, adequate space, spatial relationships, etc. Hence, based on the study, POE can be suggested as the most preferable building performance assessment method with respect to overall comfort and environmental qualities.

3. THE POE METHODOLOGY OF THE PRESENT STUDY

Four separate building blocks located within a large institutional campus in Madurai out of which two are naturally ventilated (NV) and the other two are mixed mode (MM). A post occupancy evaluation in the case study buildings were carried out using the Building Use Studies Survey (BUS) Workplace Questionnaire developed by Leaman and Bordass 2005 [15]. The survey was administered to occupants in the NV and air conditioned classrooms in the selected case study buildings. The MM buildings were classified as Type I and NV buildings as Type II. The location of Type I numbered as 1 & 2 and Type II numbered as 3 & 4 are shown in Fig 1.



Figure 1: Location of case study building within the institutional campus

3.1 Description of case study buildings

The façade of the case studies 1-4 are represented in Fig.2. The structure of case study 1 (represented in Fig.1) alone is made of ashlar masonry for walls with inner surfaces plastered, RCC roofs, cement flooring and steel framed doors and windows. The AC seminar halls in MM buildings had wooden or glass doors fixed with aluminium frames. The other three case study buildings comprises of brick masonry walls plastered on both sides, RCC roofs with weathering proofing course on top, cement floorings, steel framed doors and windows. The occupant density of both NV and AC classrooms were between 1 and 1.3. In Case study I the classrooms and labs were enclosed by double banked corridors whereas, Case studies 2, 3 & 4 have cross ventilated single banked classrooms with standard corridor widths of 2.5m. The sizes of the windows are also same but the number of

windows; orientation of the windows and occupant density varies in all the cases. The aerial view of Case study 1 and 3 as seen in Fig.1 shows that the plan of both buildings are linear with no courtyards but shaded with vegetation on both sides, whereas Case study 2 & 4 have courtyards with aspect ratio 1:1 and 1:2. The implication of the building design on thermal comfort has been interpreted by doing a comparative analysis of the occupants' thermal perception collected through the POE survey and field study with respect to the location, orientation of windows, shading devices, building envelope materials of their classrooms in the case buildings.

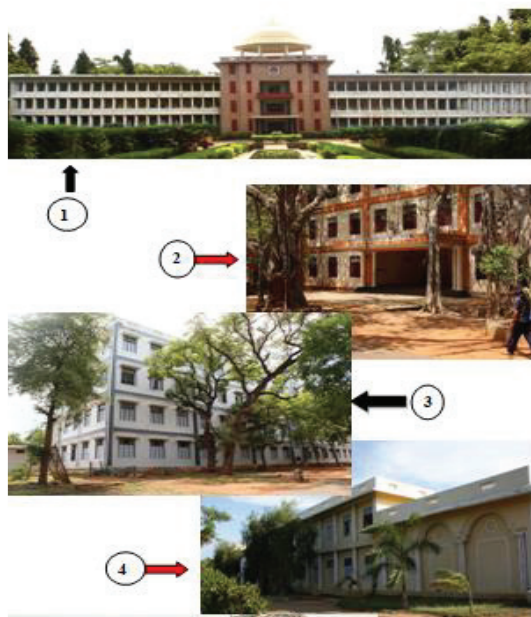


Figure 2: Facades of the case study buildings

3.2 The BUS Methodology

A total of 600 surveys (150 to each block) were distributed but only 210 occupants responded back, 110 from the Type I blocks, 100 from Type II blocks in the year 2016. The respondents were faculty members and under-graduate students of age group 18 to 55 years, 40% males and 60% females. The questionnaires were personally distributed to all occupants (students and teachers) during the morning hours of a day. The completed questionnaires were personally collected within half an hour time if the occupants were free or by the end of the day. The ratio of teacher to students amongst the respondents was in the ratio 1:4.

The BUS questionnaire provides a range of quantitative and qualitative data which includes the basic information of the users (age, sex, during of their stay in the building), the feedback on design of the buildings, user needs, storage and other facilities, overall comfort (thermal, lighting and noise) and productivity. The data gathered from manual questionnaire survey are transferred into pre-formatted Excel data files and processed by a series

of scripts to obtain the results. The results are derived from the mean scores and open ended comments given by the occupants on their satisfaction levels and perception of overall comfort (thermal, lighting and acoustical) during summer, winter and monsoon from the BUS survey data. The responses to the variables are sought on a 7-point scale (A type scale) [16].

Fig 3 represents the results of one of the variables derived from BUS questionnaire survey. The mean value from the survey is evaluated against upper and lower limits of the benchmarks and the scale midpoint as shown in Fig.3.

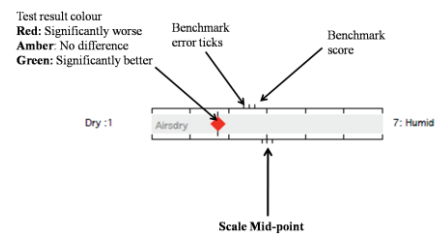


Figure 3: Key to BUS summary charts

The Benchmarks are denoted by three vertical lines on the top scale and the scale midpoint (MD) is denoted by three vertical lines at the bottom scale of each variable. The test results are denoted by three colours, the green, amber or red, where green squares show that the mean values are higher than the benchmark and scale midpoint and hence in good agreement. The amber circles represent no difference and red diamonds shows a poor score.

4. RESULTS AND DISCUSSIONS

Fig 4 & 5 represent the summary of the overall performance ratings of the 12 variables surveyed using BUS questionnaire. From the results, it is evident that the variables with mean scores higher than the benchmark levels, are denoted by green squares showing that the occupants feel 'significantly better'.

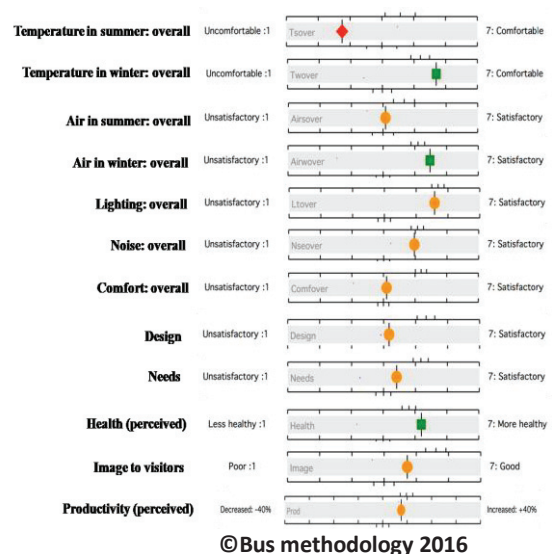
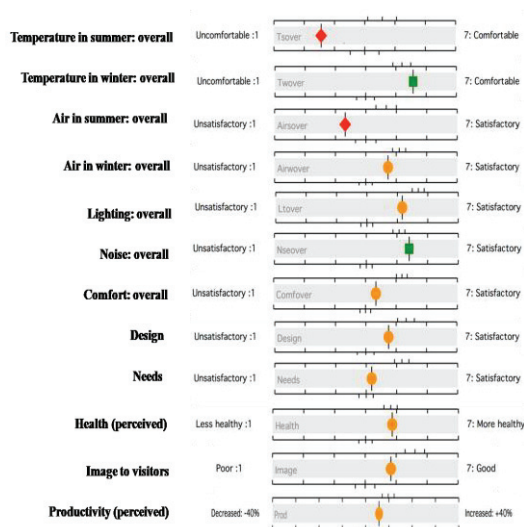


Figure 4: BUS summary chart for Type I buildings



©Bus methodology 2016

Figure 5: BUS summary chart for Type II buildings

The amber circles are closer to the benchmark and slightly higher than the scaled mid-point, representing 'no difference' in the occupant's sensation. The red diamonds denote 'significantly worse' sensations. In both Type I & II case study buildings, it was observed that the overall temperature in summer (Tsover) was 'significantly worse' and marked by red diamonds (see Fig 4 & 5). In Type II buildings it was observed that the overall air in summer (Airsover) was also lower than the benchmark and midpoint limits (see Fig 5). Fig 6a shows the BUS scores for temperature overall and air overall in summer for Type I building, and Fig 6b shows the BUS scores for the same variables as above for Type II buildings. The results were calculated based on the percentile of votes.

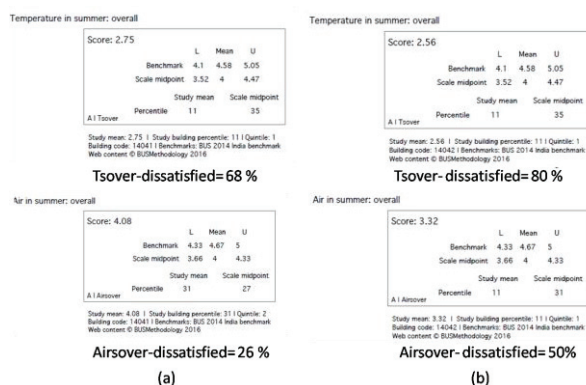


Figure 6: BUS scores for Type I and Type II buildings

It is noted that the 68% of occupants were dissatisfied with Tsover in Type I buildings in summer. In Type II building, 80% of the occupants were dissatisfied with temperature in summer.

The overall ratings for air in summer (Airsover) in NV classrooms of Type I building are lower than the bench mark (Score= 4.08; MD= 3.66, benchmark= 4.33; A type scale) and the results showed that 26% of the occupants are dissatisfied whereas, in Type II buildings, percentage of occupant dissatisfaction levels were higher compared to Type I buildings, up to 50% with the scores of Airsover lower than the midpoint and benchmark (Score= 3.32; benchmark= 4.33; MD= 3.66; A type scale).

The subjective measurements of thermal comfort levels revealed that the occupants in naturally ventilated classrooms had higher acceptability levels than the occupants in air conditioned classrooms. Although the students in naturally ventilated building expressed more adaptive behaviour, the interviews through POE revealed that thermal discomfort during the afternoon hours badly affected their performance. The students were not able to concentrate on the classes. There was more of sweating, and some students even complained on palpitations of the heart due to intolerable heat during afternoon hours.

4. BUILDING DESIGN IMPLICATIONS

Based on the observations on the building design of the case study buildings it could be inferred that the orientation of the buildings, presence of courtyards, thermo-physical properties of the building envelope, window to wall ratio (WWR) and shading devices might have an influence on the thermal performance of the building. It was identified from the responses that the occupants in NV classrooms that were enclosed around courtyards with aspect ratios 1:1 or 1:2 or had cross ventilation with windows oriented towards north and south, windows with proper shading; felt thermally comfortable whereas the occupants in NV classrooms that had windows on one side only or windows oriented towards east-west and/or higher WWR or windows with no shading devices; felt thermally uncomfortable.

5. CONCLUSIONS

The BUS survey techniques were very helpful in providing occupants' feedback on the total performance (thermal, air quality, lighting and noise) of the building in use. It was also helpful in identifying other issues related with furniture, storage, water quality, etc from the occupants of the building. The POE results revealed that the occupants in NV buildings were dissatisfied with the temperature and air in summer, whereas in Mixed-mode (Type I) the occupants were more dissatisfied with temperature alone. The students stated that they felt tired and restless due to increase in temperature in the afternoon hours in the NV lecture halls. In Type I (mixed-mode) blocks; the lecture halls were mostly

NV whereas computer labs, seminar halls and few faculty rooms were AC, so the combined results showed that temperature in summer was poor in mixed-mode. Moreover it was found that this drawback did not affect the productivity of the students since the students were adults and they exhibited adaptive behaviour to adjust their comfort needs. But there was one disadvantage; it was easy to collect back the questionnaire from faculties as they could be approached at their spaces during their free hours; on the contrary it was difficult to collect back the filled questionnaire from the students. Few students also hesitated to fill the three page questionnaire. Some of them just ticked all boxes without reading the questions; some left most of the boxes blank. Only few students responded properly, that is why the number of responses was lesser when compared to the occupant density. Another difficulty experienced by the authors was that it took a little time to transfer the data collected into the excel-sheet for getting the results. Thus the authors felt that if the questionnaires could be circulated through online mode, it would be less time consuming and easier for both the respondents and surveyors. Since the POE results showed occupant dissatisfaction in temperature and air in summer, it was decided to conduct a field study of the outdoor and indoor thermal environment of the learning spaces to identify the building design implication on thermal comfort. Thus the BUS POE results act as an effective database which can be used by architects for further investigation and development of research ideas for the efficient design of naturally ventilated educational buildings in warm-humid climatic regions.

ACKNOWLEDGEMENTS

I would like to acknowledge Prof. Adrian Leaman for having given permission to use BUS questionnaire under licence and his valuable support and feedback during the project.

REFERENCES

1. Subhashini S, Thirumaran K., (2018). A passive design solution to enhance thermal comfort in an educational building in the warm humid climatic zone of Madurai. *Journal of Building Engineering*, 18: p. 395-407.
2. Ramli, N.H., Ahmad, S., Masri, M.H., (2013) Improving the Classroom Physical Environment: Classroom users' perception, *Procedia - Social and Behavioral Sciences*, 101: p. 221 – 229.
3. Barrett, P., Fay Davies, F., Zhang, Y., Barrett, L., (2015). The impact of classroom design on pupils' learning: Final results of a holistic, multi-level analysis, *Building and Environment*, 89: p. 118-133.
4. Mustafa, F. A., (2017). Performance assessment of buildings via post-occupancy evaluation: A case study of the building of the architecture and software engineering departments in Salahaddin University- Erbil, Iraq, *Frontiers of Architectural Research*, 6(3): p. 412-429.
5. Shelly, K.J., (2015). Relevance of Gurukul Education System in Present Circumstance: A Philosophical Perception. *Journal of Philosophy, Culture and Religion*, 12: p.9-10.
6. Frederick, A.G., (2016). A Comparative Study between Gurukul System and Western System of Education. *International Journal of Education and Multidisciplinary Studies*, 03 (01): p. 51-58.
7. Mendell, M. and Heath, G., (2005). Do indoor pollutants and thermal conditions in schools influence student performance? A critical review of the literature. *Indoor Air*, 15: p. 27-52.
8. Preiser, W., (2001). The evolution of post-occupancy evaluation: Toward building performance and universal design evaluation. Learning from Our Buildings: A State-of-the-Practice Summary of Post-Occupancy Evaluation. Federal Facilities Council, National Academy Press, Washington D.C.
9. Tookaloo, A., Smith, R., (2015). Post Occupancy Evaluation in Higher Education. *Procedia Engineering*, 118: p. 515–521.
10. BRI 2001. Special Issue – Post-occupancy Evaluation. *Building Research and Information*, 29 (2): p. 79-174.
11. Leaman, A., Stevenson, F., & Bordass, B. (2010). Building evaluation: practice and principles. *Building Research & Information*, 38 (5): p.564–577.
12. Ng, B and Akasah, Z. A. (2013). Post occupancy evaluation of energy-efficient buildings in tropical climates – Malaysia. *International Journal of Architectural Research* 7 (2): p.08-21.
13. Gossauer, E and Wagner, A., (2007). Post-occupancy Evaluation and Thermal Comfort: State of the Art and New Approaches. *Advances in Building Energy Research*, 1: p. 151–175.
14. Alessandra, G., Giuliana, L, Daniele, M., Salvatore, P., and Vincenzo, F., (2014). Indoor environmental quality survey: a brief comparison between different Post Occupancy Evaluation methods. *Advanced Materials Research*. 864-867: p. 1148-1152.
15. Leaman, A. and Bordass, W., (2005). Productivity in Buildings: the Killer Variables, Revised 2005, for updated edition of Clemence-Croome D (ed), Creating the Productive Workplace, London.
16. Thomas, L and Baird, G., (2006). Post-occupancy evaluation of passive downdraft evaporative cooling and air-conditioned buildings at Torrent Research Centre, Ahmedabad, India. 40th Annual Conference of the Architectural Science Association ANZAScA, Adelaide, South Australia. November 22-25.

Participatory Processes Impelling Urban Socioecosystem Renewal

Social Sustainability from an Environmental Approach

MARIA LOPEZDEASIAIN¹, MARCOS CASTRO-BONAÑO², RUBEN MORA-ESTEBAN²,
MARIA LUMBRERAS-ARCOS³

¹Techonological Centre HABITEC, and University of Las Palmas de Gran Canaria, Las Palmas, Spain

²University of Malaga, Malaga, Spain

³University of Seville, Seville, Spain

ABSTRACT: *Understanding urban renewal as a participatory process enables to have a strong link between the technical proposal to improve habitability and the inhabitants' perception of the improvement of their quality of life related to their real needs. This research identifies obsolescence processes in neighbourhoods, including the definition of indicators and their intensity rates in relation to social metabolism; measures applicable in relation to such indicators; application to representative case studies which can be extrapolated to other situations; and assessment of the impact of measures applied to these case studies from a socioecosystemic approach. The main objective of this research is to define, develop and apply the aspects, criteria, processes and indicators derived from the adoption of the socioecosystemic approach. This approach is focused on the improvement of habitability and sustainability conditions— socially, economically and environmentally speaking- in obsolete urban areas. Although there is a broad technical knowledge, we should never forget the social point of view that is key when it comes to deciding the way an action can be designed and applied in order for it to be effective and perceived in a positive way by residents. This article explains the process and tools developed that can be extrapolated to any other Andalusian urban area.*

KEYWORDS: *urban regeneration; urban indicators; participative process; governance; resilience*

1. INTRODUCTION

Nowadays, technical architectural approaches are not sufficient for regeneration processes in our cities. There is a real and incontestable need of new tools for reaching more complex situations. Understanding urban renewal as a participatory process makes it possible to have a strong link between the technical proposal to improve habitability [1] and the inhabitants' perception of the improvement of their quality of life related to their real needs [2].

There are lots of research proposals of environmental indicators that define in a quantitative and qualitative way a neighbourhood's situation in sustainability terms [3]. They have been developed in a rigorous and objective process and we can understand and measure the sustainability situation of a neighbourhood by using them from a technical point of view [4].

On the other hand, when we take decisions from these studies to improve our neighbourhoods and cities, we quite often find citizens rejection on those improvements, since they do not feel the same necessities that could have been detected objectively.

This paper presents a process proposal to integrate environmental indicators with perceptive

information from citizens, in order to create a participative process [5] with more successful possibilities regarding a regenerative urban intervention.

The research has developed an initial state of the art on environmental indicators. Then several tools have also been developed for analysing the cities from an objective and technical environmental approach. In the same way, some participative tools have been introduced for the qualitative and perceptive approach. Finally the research has developed a proposal for a process that integrates all tools developed and other previous known and interesting ones to face the urban situations from a participative sustainable approach.

2. OBJECTIVE

The main objective of this research is to define, develop and apply the aspects, criteria, processes and indicators derived from the adoption of the socioecosystemic approach. This approach is focused on the improvement of habitability and sustainability conditions – environmentally, economically, and socially speaking- in those urban areas presenting signs of obsolescence in the Andalusian cities.

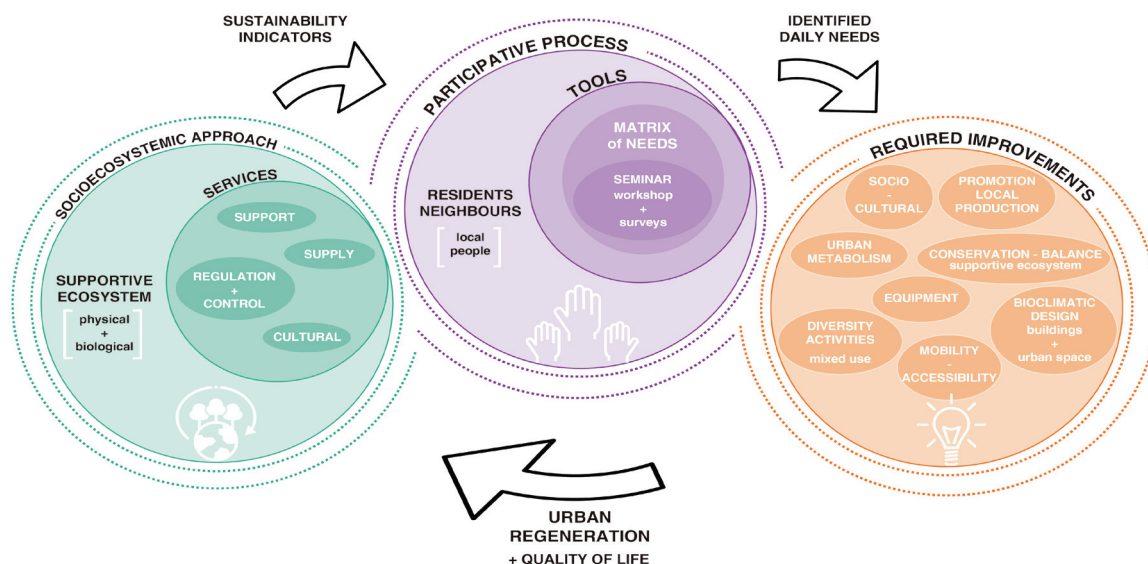


Figure 1: Process and tools developed

Adopting this approach, as it is directly connected to the physical and environmental supportive ecosystems of the territory, allows us to ensure the basic sustainability requirements linked to this ecosystem's balance and to benefit from its own resilient capacity.

Diverse working tools have been developed during the research. In this article, firstly, the validity of the approach is verified, and secondly, one of the considered tools is developed thanks to an experimental case study carried out in the Huelin neighbourhood in Malaga, Spain.

3. THE SOCIOECOSYSTEMIC APPROACH

To define ecosystem services, the concept of Service Provision Unit (SPU) is adopted, which can help to quantify them and therefore to develop variables and their subsequent indicators [6]. Therefore, an ecosystem service must be primarily quantifiable. The same would apply to an urban dimension of socioecosystemic services.

This research develops a method to link urban context conditions (including those related to the metabolism of natural resources) with the population's basic needs in a certain urban environment.

From an ecosystem approach, we define the socioecosystemic services of a neighbourhood as support services, supply services, regulation and cultural services, each of which is comprised by different aspects, allowing us to address all needs and requirements that must be provided in order to ensure a high quality life.

3.1 Support Services

These are the services required for the production of other SESs and the sustainability of the neighbourhood.

- Supportive urban ground. Balanced ecosystem rich in biodiversity. Geology, orography, hydrology, microclimate integrated with public spaces and buildings
- Balanced urban structure that allows an appropriate building - public space urban ratio in relation to the supportive ecosystem
- Functional Urban Diversity. Organisation and balance among different land uses
- Adequate, well-maintained streets and public spaces
- Adequate buildings, in good conditions and well-maintained
- Adequate infrastructure, in good conditions and well-maintained
- Appropriate and necessary institutions for social, environmental, and economic management

3.2 Supply services

Products and direct services obtained from the neighbourhood socioecosystem.

- Housing, schools, health and socio-cultural centres
- Retail, offices, small industries (exchange of goods and services)
- Supply of materials (food, equipment, materials for support maintenance), water, energy and information (telecommunications)
- Material, water and energy disposal
- Accessibility-Mobility
- Social exchange situations

3.3 Regulation / Control Services

Benefits obtained from the regulation of socioeconomic cycles.

- Urban land regulation. Management of the balance among land uses. Management of public green spaces
- Microclimate management and control
- Accessibility and mobility regulation
- Energy management and control
- Material flow management. Urban waste collection and treatment
- Water cycle management and control
- Information Management

3.4 Cultural Services

Intangible benefits obtained from the socioecosystems.

- Habitability, physical and psychological comfort
- Urban Landscape
- Neighbourhood identity
- Education
- Health and Safety
- Cultural Heritage
- Social interaction, leisure and entertainment
- Access to information

4. OBSOLESCENCE PROCESSES IN ANDALUSIA

The research method presented in this paper identifies obsolescence processes in selected Andalusian neighbourhoods; concluding with its application to a representative case study which can be extrapolated to other situations in Andalusia.

4.1 Sustainability Indicators and Obsolescence Index

A preliminary study of the state of the art was conducted in order to define the most suitable sustainability indicators that should be considered for this research. Different national and international resources have been studied, most of them already used in diverse urban situations and contexts. In addition, an obsolescence index has been defined which permits to catalogue each urban neighbourhood situation.

Several national and international indicator systems have been studied. The selection criteria for these systems are as follows:

- They are indicator systems developed by scientists who are specialists in the field and have a solid background in urban sustainability
- They are systems that allow an objective self-evaluation of progress in terms of sustainability for each urban situation
- These are indicator systems not developed for commercial purposes
- They define a broad organisation structure that covers all urban aspects and their complexity

- They define indicators in a specific way and develop them by using tables and sheets for calculation or data collection

All systems have been analysed in terms of: developer organisation, authors, objective, scale, approach, strengths and limitations, always with reference to the aims of this research.

The selected indicators were defined according to their quality; therefore they present the following properties:

- They have scientific validity
- They are easy to interpret
- They are sensitive to identified changes
- They are simple and easy to understand
- They are based on information that is available or accessible at a reasonable cost
- They are included within an organisation model or framework that explains the objectives and goals
- They are based, preferably, on intelligible units
- They can be revised over time

These properties are not all mandatory, but most of them can be observed.

Once the existing sustainability indicator systems have been analysed, as well as the real and daily needs of residents in a neighbourhood, an Obsolescence Index is defined. This index is useful for determining and defining the problems that affect Andalusian neighbourhoods, such as the inability to provide certain socioecosystemic services, in order to propose potential urban regeneration processes to improve residents' quality of life.

In defining this index, the most suitable indicators have been selected according to the areas of work predefined by the neighbourhood needs-based approach and which provide an opportunity to work on future improvements based on the corresponding strategies.

5. MEASURES AND TOOLS APPLICABLE

In order to find potential solutions to the problems detected by the obsolescence index previously defined following suitable sustainability indicators, a wide structure of potential strategies to develop has been constructed.

From this point, a technical analysis of situations and strategies to implement has been developed but it is also essential to include inhabitants' perception of the situation and potential possibilities for improvement. Some experiments have been conducted for this purpose, in order to define the most suitable approach to select the final tools.

Therefore, three different experiments, which try to get inhabitants involved into the renewal process of their neighbourhoods, have been considered:

- Online surveys to association leaders defining the problems on their neighbourhoods
- Surveys and interviews developed in local cases to neighbours
- Surveys and working tables or workshops developed in local cases and related to the assessment of potential improvements in the neighbourhood.

6. LOCATION AND CASE STUDIES

Diverse case studies have been selected presenting different scales. First of all, what a neighbourhood is, as a scale reference, has been defined. The main and most difficult issue has been to define the correct approach in order to represent all Andalusian neighbourhoods. For this purpose, statistical databases have been studied, although some nearby case studies has also been considered for experimental purposes. This second approach is the one addressed in this article.

Their application to representative case studies has proven how participative tools and strategies are necessary to properly apply technical architectural solutions for urban regeneration. In addition, those tools and strategies are definitely significant instruments to decide which architectural technical solutions are applicable for each particular situation and neighbourhood and which should be discarded.

On this basis, a specific tool is developed which relates the urban obsolescence indicators predefined in the obsolescence index to the daily needs of residents. The aim of this tool is to let residents decide the priority order for each neighbourhood problem or deficiency which has been previously detected by the obsolescence indicators applied.

7. TOOL DEVELOPMENT

The developed tool comprises a matrix of needs to be assessed and detected in a specific neighbourhood as well as the potentially necessary improvements defined from a technical point of view. This tool is supported by the development of a survey that allows the participatory verification of these needs and, more importantly, their prioritisation by the residents.

This matrix is structured through the initial elaboration of a table containing residents' basic needs, from which the link with the socioecosystemic services is established. These needs, defined by citizens in their daily lives, are then used as a starting point. When relating these needs to the indicators, we are capable of identifying a series of generic or tactical improvements which may be required in certain neighbourhoods and which can be defined in relation to different aspects:

- Socio-cultural improvements

- Urban Metabolism Improvements
- Equipment improvement
- Improvement in the diversity of activities
- Improvement in mobility - accessibility
- Improvement in conservation - balance of the supportive ecosystem
- Improvement in the promotion of local production
- Improvement in the bioclimatic design of buildings and urban space.

These improvements are related to certain defined levels of management that involve different agents to a greater or lesser extent and which are: Social management, metabolic balance management (energy, materials, water) and town planning management, determining whether or not the neighbourhood is providing the predefined socioecosystemic services.

Table 1: Required improvements according to identified needs. Source: Compiled by authors

NEEDS TO IDENTIFY AND EVALUATE	REQUIRED IMPROVEMENTS
Social diversity	Socio-cultural improvement
Local support for employment, information, housing	Socio-cultural improvement
Local asset management	Socio-cultural improvement
Urban metabolism	Urban metabolism improvement
Energy Management	Urban metabolism improvement
Appropriate health, education and social facilities	Equipment improvement
Ecological local business	Improvement in the diversity of activities
Mixed use facilities	Improvement in the diversity of activities
Proximity	Improvement in mobility and accessibility
Mobility based on public and pedestrian transport	Improvement in mobility and accessibility
Environmental quality	Conservation - balance of supportive ecosystem
Local organic production	Promotion of local production
Contact with nature	Conservation - balance of supportive ecosystem
Civic education	Socio-cultural improvement
Citizen participation	Socio-cultural improvement
Urban Landscape	Socio-cultural improvement
Bioclimatic urban design	Improvement in building design - urban space
Bioclimatic renovation of buildings	Improvement in building design - urban space
Bioclimatic renovation of urban space	Improvement in building design - urban space

Based on this matrix, a survey is simultaneously developed to translate the technical aspects to the

citizens so that they can assess in a simple, practical and understandable way, the deficiencies of their neighbourhood in socioecosystemic terms. The verification of this matrix tool, along with the complementary survey, is performed with fieldwork.

8. VERIFICATION. CASE STUDY: HUELING

This workshop focused on citizen participation called 'Workshop URBANA-te. Get involved in your neighbourhood!', took place in the neighbourhood of Huelin (Malaga, Spain), with the aim of raising awareness of the need to carry out participatory processes linked to urban regeneration, as well as serving as an experimental case for this research.

The Workshop was addressed to students and professionals, young people, elderly, unemployed, housewives/husbands, teachers, technicians, educators and all citizens of any field interested in discussing about improving the habitability and sustainability of their neighbourhoods through participatory processes.

The neighbourhood of Huelin in Malaga was selected as the object of study in this workshop. A seven-day workshop aimed to raise awareness among citizens of the need to carry out participatory processes linked to urban regeneration. In the first session, after analysing the current conditions of the neighbourhood through the perception of the people who live and/or move around it, using surveys, the purpose, was to establish a series of strategies. These strategies would subsequently help to identify the needs and opportunities that exist in the neighbourhood and to confirm their relevance by applying the matrix tool.

The Workshop, which involved a total of 35 hours, was divided into three phases that were structured and developed as follows:

During the first phase, several conferences were held involving the participation of diverse personalities who assisted us throughout this stage by sharing their real or academic experiences on participatory projects. From this first approach, and with the help of the participating agents, the first workshop was held. In it, guidelines were acquired to approach the first contact with the neighbourhood, needs and opportunities were analysed, and all of this as a result of the socioeconomic information previously obtained from diverse databases.

The second phase, dedicated to fieldwork, involved an approach to the neighbourhood, where a series of surveys were carried out on various residents and some representatives from social organisations who wanted to take part in this workshop. This sample attempted to incorporate neighbours aged between 16 and 60, men and women from all social backgrounds. Subsequently, a review of the initial survey is carried out among

residents of the neighbourhood by approaching them in the streets. It is performed during a three-day field trip, thanks to which the workshop participants are also able to walk around and discover the neighbourhood. This three-day stage included approximately two hundred surveys in addition to three personal interviews with representatives of neighbourhood associations: Asociación de Vecinos Torrijos and Asociación de Vecinos y de Iniciativas Ciudadanas Parque del Mar and the Federación Provincial Asociación de Mujeres Ágora. All the information collected during these days was analysed in subsequent workshops.

Finally, the third phase involved conferences both on real issues about citizen participation and the workshops on the analysis of the information gathered qualitatively through surveys. This is the point when an ideal atmosphere is generated for the development of ideas and proposals to improve the neighbourhood by all the agents present at the conferences. The matrix tool is tested and the final conclusions are edited and shared with the speakers, participants and researchers of the project as well as with the neighbours of Huelin.

9. STATISTICAL ANALYSIS

Working with qualitative data allows us to approach closer realities. Hence, we have used surveys to get closer to the social reality of a neighbourhood. Data is not always accurate and precise; it depends on how it is presented.

This data is used to search profiles, the profile of the neighbourhood. The defined survey provides a pattern. It also identifies the needs and deficiencies, i.e., orienting the statistics to the hierarchy of people's needs. For this reason, we used a series of qualitative questions oriented to this search for priorities.

An exploratory analysis of the data is carried out. we do not intend to describe the society, we group citizens to see how responses change according to each category, whether they are men or women, whether they work or are unemployed, etc. Firstly, a general descriptive analysis is carried out, secondly, an exploratory analysis by groups (sex, age interval, by home ownership...) and finally, a double entry analysis is carried out, meaning that two variables are considered (e.g. man and woman and a specific question) to establish whether there are significant correlations between the variables. The next step was to perform a multivariable analysis. There are filter questions to try to get answers to a question that is initially unanswered.

This survey tool, together with the matrix tool used during the workshop, allows to define in a unequivocal and prioritised way both the problems and needs detected by the social agents and technical

experts, as well as the opportunities and potential strategies to be developed to improve the neighbourhood.

10. RESULTS AND CONCLUSIONS

The obsolescence index obtained for Huelin showed the people's perception of obsolescence in the neighbourhood. Provision (economy, water, energy) and regulation services (accessibility, traffic, urban space) are the main areas where people identify deficiencies. On the other hand, cultural and recreational services are those with the highest scores.

From the experiment carried out in Huelin we can draw several conclusions regarding the validity of the implemented tools. The validity and usefulness of the selected obsolescence indicators to determine the deficiencies of the neighbourhoods from a technical point of view is confirmed. Nevertheless, the relative importance of these deficiencies does not always correspond with the appreciation of the neighbours. Moreover, it does not even have to coincide with the appreciation of the own neighbourhood associations, which theoretically represent the feeling of the neighbourhood.

Therefore, the experiment confirms that it becomes essential to consider the opinion from well-informed residents when it comes to define the deficiencies of their neighbourhood and propose improvements. This can only be done through participatory processes that directly involve the neighbours in gathering reliable information on their daily needs and above all in finding out what are the priorities that the neighbours perceive regarding the satisfaction of their daily needs.

For this purpose, the two developed tools are very useful. On one hand, the needs-indicators relation matrix highlights all the aspects to be considered from a technical point of view and defines potential solutions to be applied, which are then explained and discussed in a participative way. On the other hand, the survey tool provides a way to prioritise actions, discard specific solutions that are not widely accepted by the residents and strengthen the decisions reached by consensus during the participatory process.

It is important to highlight the need for a participatory process through which the tools are adapted to each specific case. This process should be managed in an informed manner to ensure and enable the effective participation of everyone, and the selected tools should be comprehensible, clear, dynamic and flexible to ensure citizens' involvement.

The process and methodology defined and the matrix and survey tools developed, allow a wide range of possibilities of extrapolation for different Andalusian cases. Most of them have been clearly

identified during this research and can be explained in further papers.

Although there is a broad technical knowledge that sets us up on the right track to reach the objective presented from a technical point of view, we should never forget the social point of view that is key when it comes to deciding the way an action can be designed and applied in order for it to be effective and perceived in a positive way by residents.

Understanding the urban renewal as a participative process makes possible the connection between technical proposals to improve habitability and inhabitants' perception of the improvement of their quality of life related to their real necessities.

ACKNOWLEDGEMENTS

The authors wish to acknowledge the work and contribution of all other members of staff and collaborators participating in EUObs: . Moreover the authors wish to acknowledge the Andalusian Regional Government (Consejería de Economía, Innovación, Ciencia y Empleo de la Junta de Andalucía) for funding the EUObs project research in 2014. EUObs is built on a consortium of four academic partners: GI-MAS-UMA, GI-LUOTUGR, GI-INGENTES-IUACC-US and HABITEC (private non-profit foundation); coordinated by the last one.

REFERENCES

1. Casals-Tres, M., J. Arcas-Abella, and A. Cuchí Burgos, (2013). Aproximación a una habitabilidad articulada desde la sostenibilidad. Raíces teóricas y caminos por andar. *INVI* 28, nº 77: p. 16.
2. Max-Neef, M., A. Elizalde, and M. Hopenhayn. Desarrollo a escala humana. Opciones para el futuro. Santiago de Chile: *Centro de Alternativas al Desarrollo CEPAUR*, 1986.
3. Cano Ruano, B. (2015). Methodology And Tools For Improving Neighbourhoods With Problems Of Obsolescence. Case Of Andalusia. *Plea 2015. Architecture in (R) Evolution*. Bologna, Italy. Association Building Green Futures.
4. Hernández Aja, A. (2009). Calidad de vida y medio ambiente urbano. Indicadores locales de sostenibilidad y calidad de vida urbana. *INVI* 24, nº 65: p. 79-111.
5. Latapié Sère, M. (2014). Propuestas para el empoderamiento de los ciudadanos; participación social ante el cambio climático desde un enfoque arquitectónico y urbano. In *Cambio climático y expansión territorial*. Memoria del XXXVI Encuentro RNIU, Colima. University of Colima: p. 266-281.
6. Haase, Dagmar, Neele Larondelle, Erik Andersson, Martina Artmann, Sara Borgström, Jürgen Breuste, Erik Gomez-Baggethun, et al. 2014. "A Quantitative Review of Urban Ecosystem Service Assessments: Concepts, Models, and Implementation." *Ambio* 43 (4): 413-33.

Urban Microclimatic Diversity and Thermal Comfort Do variations in sun and wind conditions correlate with PET grades?

ZHIKAI PENG and KOEN STEEMERS

The Martin Centre for Architectural and Urban Studies, University of Cambridge, Cambridge, United Kingdom

ABSTRACT: *Urban microclimatic diversity is of significance to understanding outdoor thermal satisfaction, as it offers a degree of freedom of choice for comfort seeking behaviour, thermal stimulation and potential alliesthesia. The existing assessment of thermal diversity has shown a strong relation to urban 3D geometry. A new workflow is proposed based on previous methods for strengthening the reliability in mapping urban microclimatic diversity. Two new indicators, the gross sun-wind diversity (D%) and the net diversity (d%) have been tested in three urban district models via Envi-MET simulation. The results are segmented by 9 grades of physiological equivalent temperature (PET), showing the value of including the range and variety of thermal sensations in the assessment of urban comfort. The preliminary findings point to a stronger link between microclimatic diversity and thermal neutrality in transitional seasons than in summer or winter.*

KEYWORDS: *Microclimatic Diversity Assessment, Urban Form, Dynamic Simulation*

1. INTRODUCTION

Outdoor thermal stimuli may be perceived negatively and thus to be avoided when they stress our bodies when exceeding the threshold of thermal comfort. Multiple studies have reported the degree of thermal dissatisfaction when experiencing strong heat or cold stress in the urban environment [1]. However, within a certain range, the diversity of thermal stimuli may positively influence our thermal sense through contrast, which has the potential to promote outdoor thermal adaptation and experiences [2].

Solar radiation and wind are two key observable thermal stimuli in the urban fabric [3]. The combinations of this pair of parameters vary in time and space, and characterise the microclimate on which our thermal experiences are based [4]–[6]. In hot weather, people seek solace in the shade as they perceive sunlight as a thermal penalty [7]. A breeze is considered desirable, especially in warm and humid conditions, and is a thermal reward by reducing heat stress [8]. Similarly, solar radiation can result in thermal satisfaction despite cold winter air [9]. Outdoor spaces have variable thermal characteristics, as buildings and vegetation can provide shade for pedestrians [10] and street canyons may serve as wind corridors [11]. Such changing patterns of microclimatic combinations offer adaptive opportunities [12]. People have different thermal needs, depending on their physical and metabolic conditions. Regardless of whether people prefer sun versus shade or wind versus stillness, an appropriate diversity of these combinations would provide users with more freedom of choice [13]. In contrast, isothermal spaces can give rise to thermal boredom and lower perceived control and alliesthesia [14]. Not only do isothermal spaces instil boredom, but such conditions may only ever

satisfy an average activity, and not the range of activities we find in urban spaces. Therefore, diverse patterns of outdoor thermal stimuli are presumed to enhance our thermal experience.

In this paper, the method for assessing microclimatic diversity at city district level is refined. Taking sun-wind diversity as an example, the paper defines and demonstrates the variation in urban microclimatic combinations in three urban districts in three European cities: London, Paris and Vienna.

2. RESEARCH QUESTIONS & METHODOLOGIES

The initial research on urban environmental diversity was conducted by Steemers et al [13]. More recently, Chatzipoulka et al. explored the relationship between thermal diversity, building density and urban coverage, comparing instantaneous and average diversity, overlapping solar insolation and wind shadow maps to capture the coverage values for the maximum thermal diversity in London and Paris [15]. Their findings have shown a strong, non-linear relationship between urban geometry and thermal diversity, but their model sensitivity is limited. One precondition to use their shadow casting algorithms is that their spatial diversity map represents an extended time period, accounted for by using averaged inputs for the model, e.g. the equinoctial and annual patterns of sun and wind exposure. Despite the simulation efficiency achieved by simplification and approximation in the researchers' shadow casting algorithms, the derived thermal diversity index (D%) is limited in addressing spatial diversity - the seasonal and diurnal variation of thermal sensations which plays an essential role in thermal diversity.

Here, scenarios beyond annually averaged spatial diversity [15] are explored to understand the dynamics

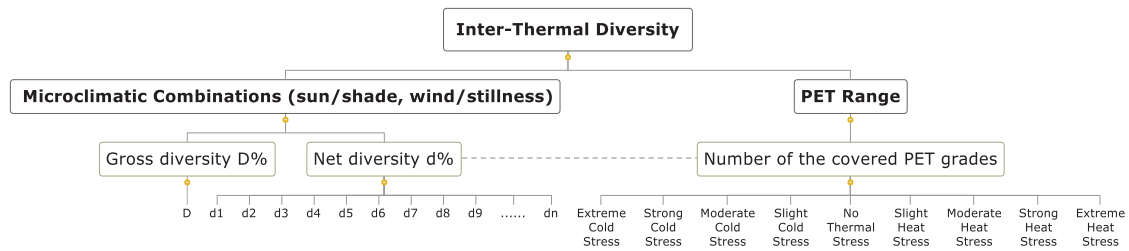


Figure 1: Inter-thermal diversity - two methodologies for mapping the diversity of sun and wind stimuli at district level.

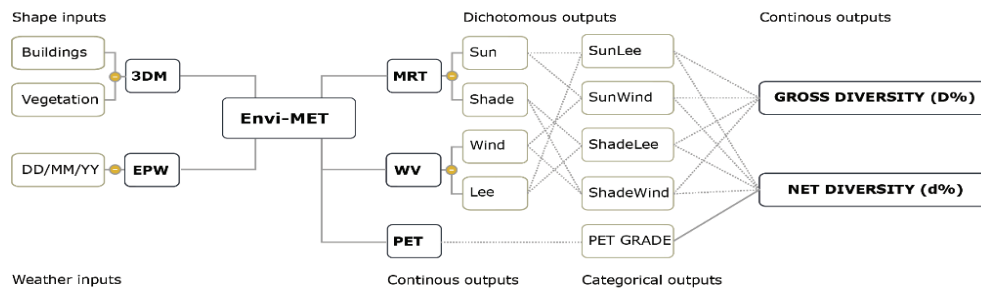


Figure 2: A workflow for measuring urban sun-wind diversity

of sun-wind diversity in various seasons. Furthermore, a new index is proposed, the net diversity $d\%$, scaled by the physiological equivalent temperature (PET) [16]. The PET has been widely utilised to evaluate heat and cold stress on a linear scale [17], [18]. To be specific, the proposed net index $d\%$ is designed to divide the gross diversity $D\%$ into smaller segments scaled by nine grades of PET. The segmentation reflects how hot, cold or neutral net indices ($d\%$) are allocated in terms of the thermal sensation. The new proposed index $d\%$ is not intended to replace the previous $D\%$, but to refine the model by considering the dynamics of thermal sensation which demonstrate the interconnection between microclimatic diversity and thermal neutrality in urban spaces. Additionally, whether the diversity of thermal stimuli is related to the diversity of thermal sensations is explored. Thus, these research questions are addressed:

- What inferences can be drawn from the diurnal and seasonal changes in the gross index $D\%$ and the net index $d\%$ of urban sun-wind diversity?
- Can a greater diversity in the quantity of sun and wind stimuli ($D\%$) lead to a wider range of thermal sensations in terms of the grades on the PET scale (Figure 1)?

2.1 Workflow

The Envi-MET program is used to simulate the microclimate in three urban districts. The mean radiant temperature (MRT) and wind velocity (WV) outputs have been assigned to the spatial units. The method for setting the threshold values taken from the existing literature has been refined [15]. Instead of adopting the averaged threshold in years, this paper specifies this value in seasons. The thresholds are calculated to be able to divide four microclimatic

combinations: 'Sun + Stillness' (SunLee), 'Sun + Wind' (SunWind), 'Shade + Stillness' (ShadeLee), and 'Shade + Wind' (ShadeWind). The spatial area of each combination is accumulated and segmented based on PET grades to be able to calculate the gross ($D\%$) and net ($d\%$) percentages of sun-wind diversity (Figure 2). The PET value is calculated for a 35-year-old male of 1.75 m and 75 kg. These default parameters were chosen for demonstration purposes only.

2.2 Study Areas

European theatre districts are characterised by their built forms and the mixed use of public spaces [19]. A theatre district is usually centred around a large landmark building, which is surrounded by a variety of smaller building blocks and public parks. The public spaces in between them create opportunities for social gatherings and outdoor activities. Apart from social and cultural experiences in these theatre districts, special attention is paid to the microclimate and its impact on visitors' thermal experience in outdoor spaces.

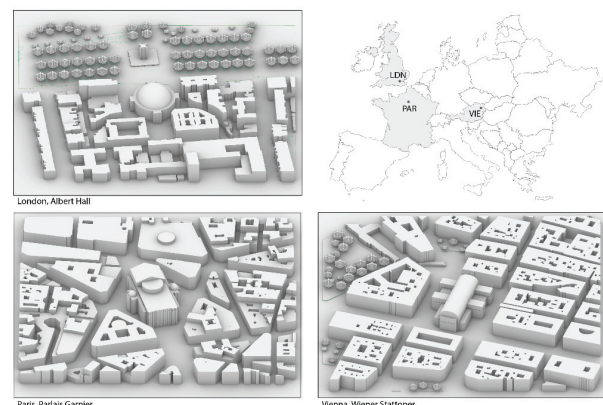


Figure 3: Three theatre districts for thermal diversity study

To explore microclimatic diversity, three European cities are selected on similar geographic latitudes - London, Paris and Vienna - as case studies for demonstrating the fine-tuned methods for assessing thermal diversity. Three theatre districts are chosen, of 500 by 500 meters (Figure 3): The Royal Albert Hall, the Palais Garnier and the Wiener Staatsoper. Their building density, coverage, pedestrian space density and parks percentages are shown in Table 1.

Table 1: Quantifying urban contexts.

Spatial metrics	Royal Albert Hall	Palais Garnier	Wiener Staatsoper
Density (M ³ /M ²)	6	15	13
Coverage (%)	28	54	44
Pavements by Area (M/M ²)	0.04	0.04	0.04
Parks (%)	38	0	16

Before carrying out the microclimatic simulation, three days close to the June solstice, September equinox and December solstice in 2019, are selected that meet our criteria, i.e.: no drastic diurnal fluctuation in wind directions, representative air temperature and humidity for the whole months, and a cloudless sky during daytime. The timeframe for diurnal simulation has been modulated according to each city's longitude and time zone. Since Paris shares a similar longitude but is situated in a different time zone than London, and, conversely, since Paris is on a different longitude but in the same time zone as Vienna, the time frame for Paris' simulation has been set to start and end one hour later than the simulations for London and Vienna.

Table 2: Weather profiles referenced from Energy-Plus.

Simulation Inputs	Royal Albert Hall	Palais Garnier	Wiener Staatsoper
Dates for simulation (DD/MM/YY)	29/06/19; 30/12/19; 21/09/19.	29/06/19; 30/12/19; 21/09/19.	29/06/19; 30/12/19; 21/09/19.
Hours of simulation (H)	15; 9; 12.	15; 9; 12.	15; 9; 12.
Mean wind velocity (M/S)	4.47; 2.68; 4.47.	2.23; 1.78; 4.47.	2.23; 1.78; 5.36.
Prevailing wind direction	W; SW; E.	W; SSE; E.	N; SSE; SE.
Range of air temperature (°C)	[16, 32]; [6, 12]; [11, 25].	[16, 35]; [0, 9]; [12, 27].	[12, 28]; [-3, 1]; [5, 19].
Range of humidity (%)	[33, 88]; [72, 100]; [39, 72].	[40, 88]; [58, 98]; [39, 58].	[26, 82]; [70, 80]; [40, 87].

2.3 Equations

To calculate the sun-wind diversity, the previously referenced method [15] is followed by simulations in Envi-MET. The equation (1) for the gross diversity D (%) has been reformatted by involving an integer k representing the amount of microclimatic combinations. The equation (2) has been duplicated to

calculate the net diversity d (%) by replacing the inputs x segmented by PET grades from the inputs X in equation (1). The difference between D and d lies in their sample sources N and n denoted in equation (3).

$$D = 1 - \sqrt{\frac{\sum(X-\bar{X})^2}{k(k-1) \cdot \bar{X}^2}} \quad (1)$$

$$d = 1 - \sqrt{\frac{\sum(x-\bar{x})^2}{k(k-1) \cdot \bar{x}^2}} \quad (2)$$

$$N_{ij} = \sum_{i=1}^j n_i \quad (3)$$

where

D is the gross index for evaluating sun-wind diversity; X is aggregated by the outdoor spatial units identified as one of four microclimatic combinations – 'Sun + Stillness', 'Sun + Wind', 'Shade + Stillness' and 'Shade + Wind';

k is an integer which represents the total amount of microclimatic combinations – here it equals 4;

x is the number of partial spatial units segmented from X by nine PET grades, sequenced by n and N respectively;

N_{ij} is the sample number added up from n_i to n_j , where the PET grade number $i < j \leq 9$ (Table 3).

Table 3: Nine ranges of physiological equivalent temperature (PET) for different grades of physiological stress [4], [5].

PET (°C)	Grade of physiological stress	Abbreviation
<4	Extreme cold stress	XtrmCS
[4, 8)	Strong cold stress	StrCS
[8, 13)	Moderate cold stress	ModCS
[13, 18)	Slight cold stress	SLCS
[18, 23)	No thermal stress	NTS
[23, 29)	Slight heat stress	SLHS
[29, 35)	Moderate heat stress	ModHS
[35, 41]	Strong heat stress	StrHS
41<	Extreme heat stress	XtrmHS

3. FINDINGS

A total of 108 hours of daytime simulations for the three districts were carried out, including 15 hours for the June solstice, 9 hours for the December solstice and 12 hours for the September equinox. The first and last hours of every day have been excluded, since nearly all spatial units are shaded. Representative urban sun-wind patterns were modelled in Envi-Met for the morning, noon and afternoon (Figure 4).

3.1 Summer scenarios

Figure 5 demonstrates the expected divergence in diurnal variation between the PET and the sun-wind diversity $D\%$ shared by the three cities. The highest PET (heat stress) occurred between 15:00 to 17:00 (40°C in London, 46°C in Paris and 37°C in Vienna) while the lowest was found at dawn (22°C in London, 29°C in Paris and 22°C in Vienna). The gross $D\%$ remained more stable throughout the day (60% for London, 65% for Paris and 80% for Vienna).

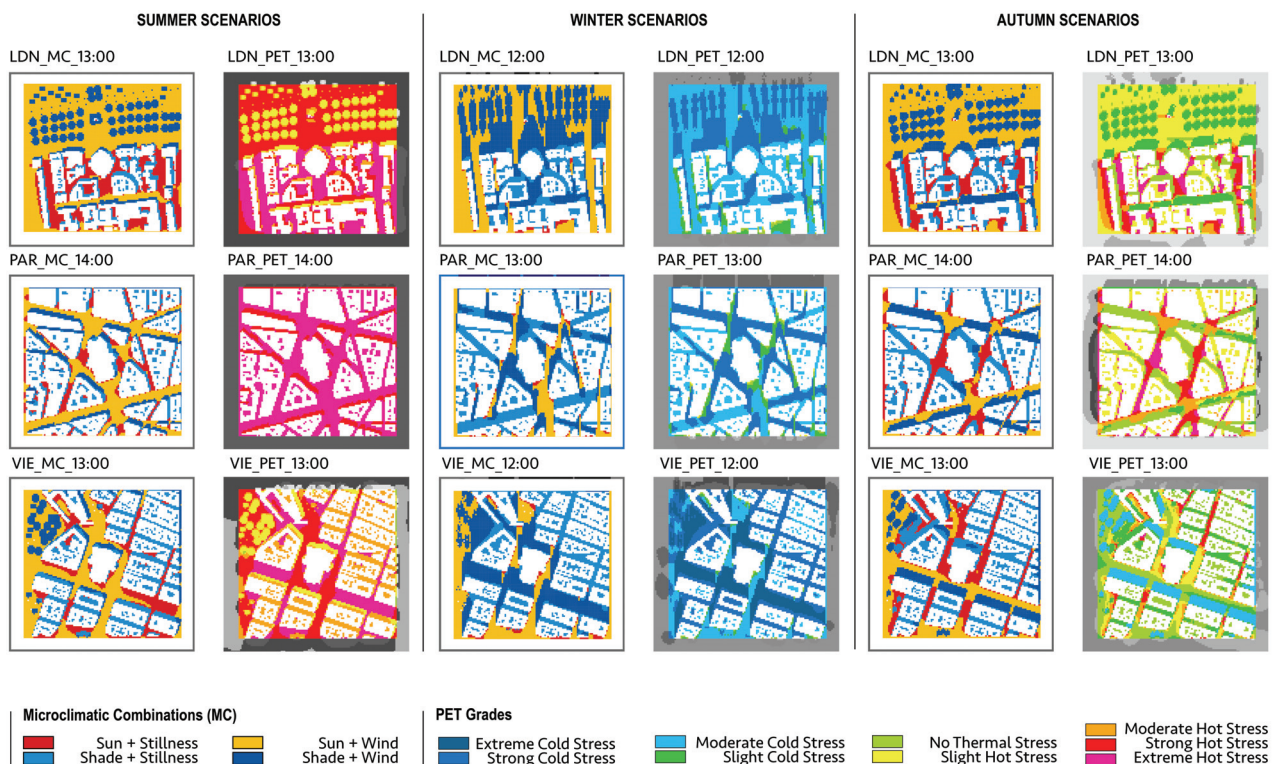


Figure 4: Microclimatic diversity maps vs PET maps at 12:00/13:00 (London, Vienna) and 13:00/14:00 (Paris) on a sunny day close to the Summer Solstice, Winter Solstice and September Equinox.

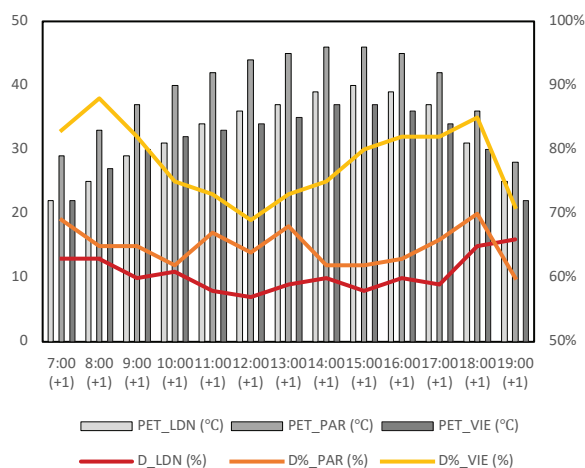


Figure 5: 13-hour daytime PET and the gross sun-wind diversity D (%) between three theatre districts in London, Paris and Vienna on a sunny day close to the June solstice.

3.2 Winter scenarios

In Figure 6, the diurnal fluctuation of PET in winter is much smaller than in summer (15 °C), with differences of less than 4 °C across the three cities. A shorter daytime is one of the main reasons for reduced PET variation in winter. The score of gross diversity D% in the three cities varied relatively little (55% for London, 67% for Paris and 70% for Vienna).

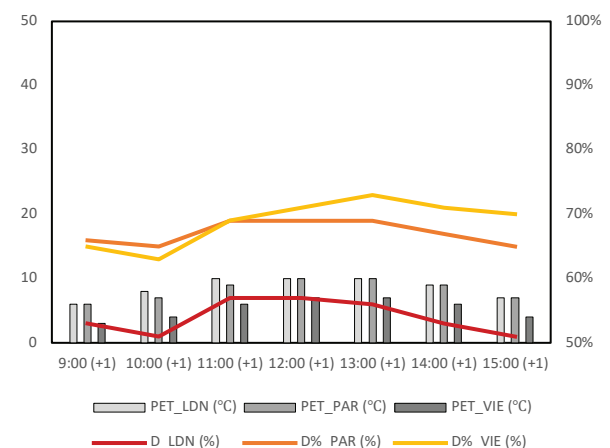


Figure 6: 7-hour daytime PET and the gross sun-wind diversity D (%) between three theatre districts in London, Paris and Vienna on a sunny day close to the December solstice

3.3 Autumn scenarios

Figure 7 summarises the findings of the autumn scenario. The gross sun-wind diversity fluctuated more drastically in Paris [70% - 96%] and Vienna [69% - 85%] than in London [63% - 67%], and the results are distinct from the more steady diversity in summer and winter.

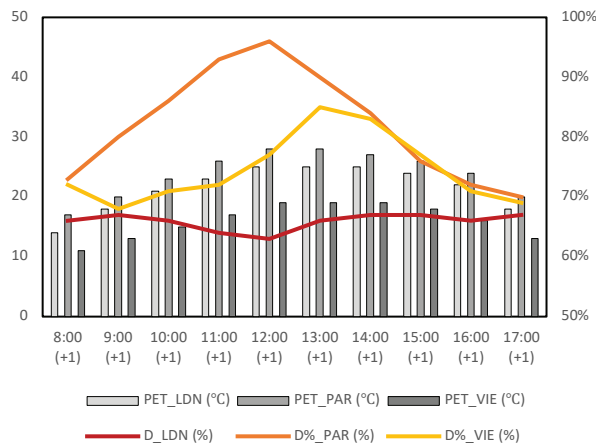


Figure 7: **10-hour** daytime PET and the gross sun-wind diversity D (%) between three theatre districts in London, Paris and Vienna on a sunny day close to the **September equinox**.

4. DISCUSSION

Previous research –based on shadow casting algorithms [15]– is limited in addressing the dynamics of microclimatic diversity. This work reveals more information on the variation of microclimates and thermal sensations on a diurnal and seasonal bases.

4.1 Microclimatic diversity vs thermal neutrality

Regardless of how thermal neutrality has been researched in past studies [20], it has rarely been analysed to explore its potential link to microclimatic diversity. This paper reveals both synergistic and deviated results on microclimatic diversity versus thermal neutrality based on the time series data. The cases—from autumn to winter (Figure 7 and 6)—demonstrate that the microclimatic combinations becomes less diverse in relation to a decrease in the averaged PET values. In addition, a deviation between diversity and neutrality can be observed in some cases. In summer there is a slight negative correlation between D and PET, though sufficient D is maintained to provide freedom of choice even under strong or extreme heat stress. In winter, the two marginally correlate, thus when cold the cities provide less microclimatic diversity and freedom of choice. At Equinox, there is the most chance to meet various stimuli preferences at positive correlation, i.e., as thermal stress decrease there is more diversity.

These synergistic and deviated results have been confirmed by aggregating all the datasets on bubble charts (Figure 8) to present the relationship between the net diversity $d\%$ and PET grades . A bifurcation of

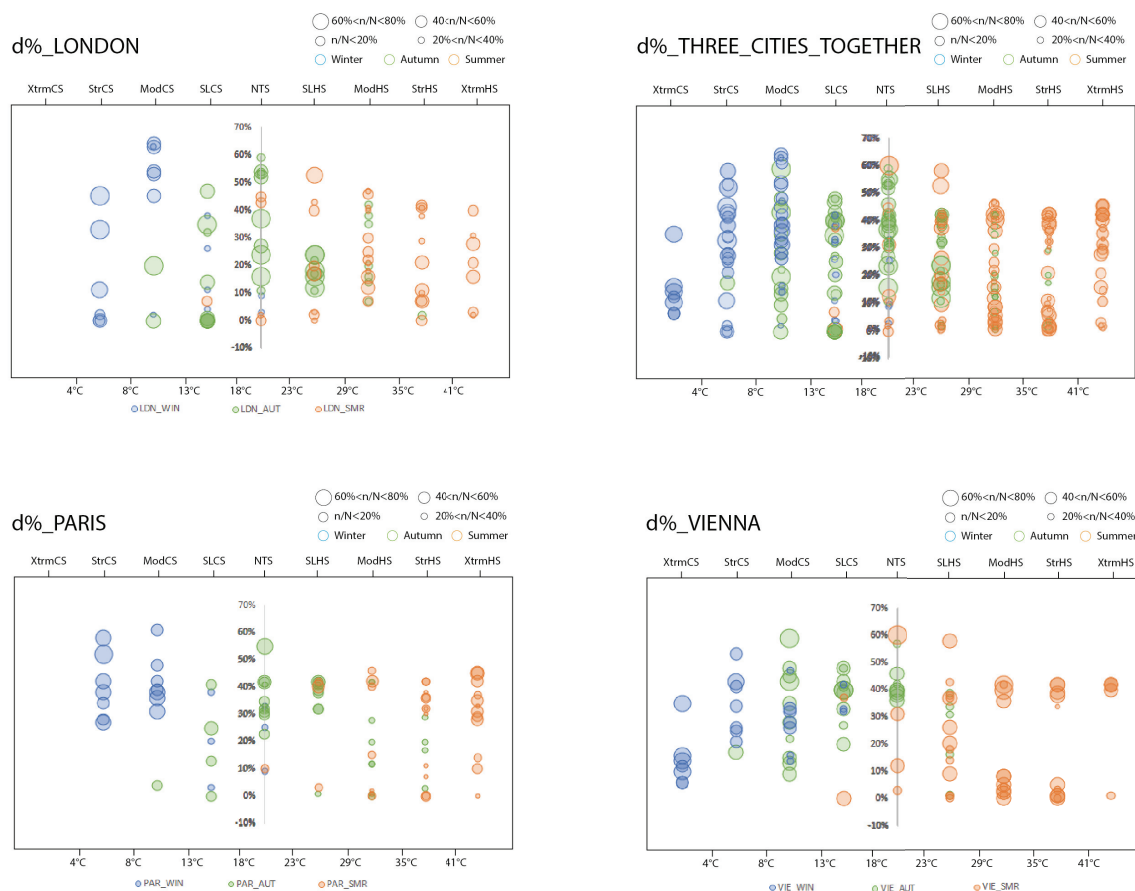


Figure 8: Bubble charts presenting the relationship between the net diversity $d\%$ (microclimatic diversity) and PET grades (thermal neutrality), aggregated by all datasets of **Summer Solstice (in orange)**, **Winter Solstice (in blue)** and **September Equinox (in green)**. London (top left), Paris (bottom left), Vienna (bottom right) and three cities together (top right). The bubble sizes emphasise the sample sizes.

data occurs during hot seasons, especially in Vienna, where there is a polarisation of high d% and low d% at higher temperature, alongside a strong heat stress. The bifurcation indicates the increase of the coexistence of the microclimatic monotony and diversity when PET value is higher.

4.2 Limitations

Due to the limited computational capacity for running CFD-based model, only three representative days has been selected for demonstration purpose for microclimatic diversity and PET analysis in three European cities. Comparability might be influenced as three theatre district samples own unique urban geometries, though share similar latitude but located in distinct climates. Besides, in-situ validation will be required to further improve the validity and reliability.

5. CONCLUSION

The purpose of this paper is to improve methods for assessing microclimatic diversity and outdoor thermal comfort. A CFD-based simulation tool has been adopted which has included previously missing environmental factors -e.g. air temperature and humidity- which influence thermal sensations. Diurnal and seasonal variations of microclimates have been demonstrated in time series and they have been compared with the dynamics in the resultant microclimatic diversity and PET ranges. Firstly, results show that urban microclimatic diversity (D%) is higher on equinox days than on solstice days by up to 30% for the three-city district showcases. A higher D% is also frequently found in early afternoon in autumn and around dawn and twilight in summer, but it remains steady during other times when thermal stress cannot be neglected. Secondly, using the net diversity index (d%) for correlation with PET grades, both synergistic and deviated results have been found across the urban samples. The preliminary finding in this study shows that the relationship between microclimatic diversity and thermal neutrality appears stronger in transitional seasons than summer and winter. Higher PET values are associated with polarised microclimatic diversity.

ACKNOWLEDGEMENTS

The CSC funding is gratefully acknowledged.

REFERENCES

1. Abdel-Ghany, A. M., Al-Helal, I. M., & Shady, M. R. (2013). Human thermal comfort and heat stress in an outdoor urban arid environment: a case study. *Advances in Meteorology*, 2013.
2. Nikolopoulou, M. (2011). Outdoor thermal comfort. *Frontiers in Bioscience*, 3, 1552-1568.
3. Mackey, C., Galanos, T., Norford, L., & Roudsari, M. S. (2017, August). Wind, sun, surface temperature, and heat island: critical variables for high-resolution outdoor thermal comfort. In *Proceedings of the 15th international conference of building performance simulation association. San Francisco, USA*.
4. Walton, D., Dravitzki, V., & Donn, M. (2007). The relative influence of wind, sunlight and temperature on user comfort in urban outdoor spaces. *Building and environment*, 42(9), 3166-3175.
5. Bosselmann, P., Flores, J., Gray, W., Priestley, T., Anderson, R., Arens, E., ... & Kim, J. J. (1984). Sun, Wind, and Comfort A Study of Open Spaces and Sidewalks in Four Downtown Areas.
6. Li, J., Niu, J., Mak, C. M., Huang, T., & Xie, Y. (2018). Assessment of outdoor thermal comfort in Hong Kong based on the individual desirability and acceptability of sun and wind conditions. *Building and Environment*, 145, 50-61.
7. Lin, T. P. (2009). Thermal perception, adaptation and attendance in a public square in hot and humid regions. *Building and environment*, 44(10), 2017-2026.
8. Matzarakis, A., & Mayer, H. (1997). Heat stress in Greece. *International Journal of Biometeorology*, 41(1), 34-39.
9. Klemm, W., Heusinkveld, B. G., Lenzholzer, S., Jacobs, M. H., & Van Hove, B. (2015). Psychological and physical impact of urban green spaces on outdoor thermal comfort during summertime in The Netherlands. *Building and environment*, 83, 120-128.
10. Andreou, E. (2014). The effect of urban layout, street geometry and orientation on shading conditions in urban canyons in the Mediterranean. *Renewable Energy*, 63, 587-596.
11. Ak, M. K., & Ozdede, S. (2016). Urban landscape design and planning related to wind effects. *Oxidation Communications*, 39(1), 699-710.
12. Shooshtarian, S., Rajagopalan, P., & Sagoo, A. (2018). A comprehensive review of thermal adaptive strategies in outdoor spaces. *Sustainable cities and society*, 41, 647-665.
13. Steemers, K., & Ramos, M. (2009). Urban Environment Diversity and Human Comfort. *Designing High-Density Cities: For Social and Environmental Sustainability*, 107.
14. De Dear, R. (2011). Revisiting an old hypothesis of human thermal perception: alliesthesia. *Building Research & Information*, 39(2), 108-117.
15. Chatzipoulka, C., Steemers, K., & Nikolopoulou, M. (2020). Density and coverage values as indicators of thermal diversity in open spaces: Comparative analysis of London and Paris based on sun and wind shadow maps. *Cities*, 100, 102645.
16. Walther, E., & Goestchel, Q. (2018). The PET comfort index: Questioning the model. *Building and Environment*, 137, 1-10.
17. Makaremi, N., Salleh, E., Jaafar, M. Z., & GhaffarianHoseini, A. (2012). Thermal comfort conditions of shaded outdoor spaces in hot and humid climate of Malaysia. *Building and environment*, 48, 7-14.
18. Hwang, R. L., Lin, T. P., & Matzarakis, A. (2011). Seasonal effects of urban street shading on long-term outdoor thermal comfort. *Building and environment*, 46(4), 863-870.
19. Whyte, W. H. (1980). The social life of small urban spaces.
20. Gagge, A. P., Stolwijk, J. A. J., & Hardy, J. D. (1967). Comfort and thermal sensations and associated physiological responses at various ambient temperatures. *Environmental research*, 1(1), 1-20.

Cooling Effect of Urban Parks in the Metropolitan Region of Barcelona:

The sample of Viladecans, Gavà and Castelldefels urban continuous

BLANCA ARELLANO¹, JOSEP ROCA¹, ALAN GARCÍA-HARO¹

¹Department of Architectural Technology, Polytechnic University of Catalonia, Barcelona, Spain

ABSTRACT: This study presents a multi-stage approach to quantify the cooling effect of urban parks in the metropolitan region of Barcelona from the Land Surface Temperature (LST) of Landsat-8 of a summer day. We quantified the cooling extent (L_{max}) and intensity (ΔT) of seven parks in the conurbation of Viladecans, Gavà and Castelldefels through three analytical methods based on a multi-stage spatial subdivision of the urban surroundings. First results show ΔT of 1.25°C and 1.50°C in relation to the 0-100m and 100-300m concentric urban annuli respectively. The L_{max} calculated by 10m-width concentric annuli registered 91.67m average with ΔT of 1.22°C. Last, 10m-width transversal sections to the park resulted in average ΔT of 2.21°C in industrial zones, 1.05°C in residential areas and 1.76°C adjacent to another park. Where the L_{max} resulted in 109.00m average to northeast and 129.67m to southwest, with maximum 170m in the industrial zone and 310m in the another park's area respectively. Conclusions discuss differences between methods applied and considerations to further replication in larger scale studies.

KEYWORDS: Global and Local Warming, Urban Heat Island, Cooling Effect of Green Spaces, Cool Island

1. INTRODUCTION

Urban parks play a fundamental role in climate change adaptation in cities. Commonly with the largest concentration of vegetation and unsealed surfaces in the cities, the parks increase humidity in the air and the shadow projected on the surfaces. Breaking the continuity of the Urban Heat Island effect (UHI), caused, in part, by the high absorption of direct sun-heat in the artificial surfaces [1]. Thus, parks register lower temperatures than the rest of urban spaces and generate a cooling effect that spreads to their surroundings creating a "cool island" effect [2].

The cooling effect of parks is quantified by the extent limit, which is the maximum distance reached by the cooling spread outside boundaries of the park; and the intensity, which is the difference in temperature between the park and a certain urban space in its near surroundings [2]. Divergences on the calculation of these cooling indicators are related to the scale of the study, the spatial distribution of the data and the method to register temperatures. There is a consensus on the calculation of the cooling intensity, but with slight differences on the spatial attribution of the temperature to the park and the one that represents the urban space. The cooling extent presents a lower consensus on its definition. Previous investigations pointed that the cooling extent of parks between 3 and 200ha size, is in the 50 to 300 meters (m) range, but larger parks go from 200 to 2000m. Whereas the cooling intensity registers values between 1 to 4°C during day and 2 to 5°C at night [3], with an average intensity between 0.94 and 1.15°C [4].

Previous studies are grouped in three general approaches. First, the survey of air temperature variations with weather stations and their relation to the distance to green spaces, limited to large-scale analysis and the need of interpolate information [5, 6]. Other studies performed field measurement campaigns with portable weather stations on routes that intersect parks and their surroundings, which is limited to specific cases [2, 7]. Second, studies that recur to numerical modelling and thermal simulation of parks and their surroundings, which allow higher number of cases and the assessment of hypothetical modifications to the current state of the spaces [8, 9]. Third, the remote sensing approaches, which has become one of the most frequent methods to obtain thermal and physical data of the territory. Particularly, the Land Surface Temperature (LST) has been applied to multiscale analysis of the UHI or in general urban climatology studies, due to the potential of the spatial continuity of the thermal data [10, 11].

2.2 Study area

In this study, we aboard the conurbation of Viladecans, Gavà and Castelldefels (VGC area) in the Metropolitan Region of Barcelona (41°20'16"N; 41°15'50"N; 1°55'29"E; 2°04'26"E). The area presents continuous and discontinuous urban fabric and industrial units (Figure 1). Castelldefels is mainly covered by discontinuous urban fabric; Gavà is predominantly agricultural and natural with industrial units as large as the urban fabric; and Viladecans is mainly covered by agricultural land.

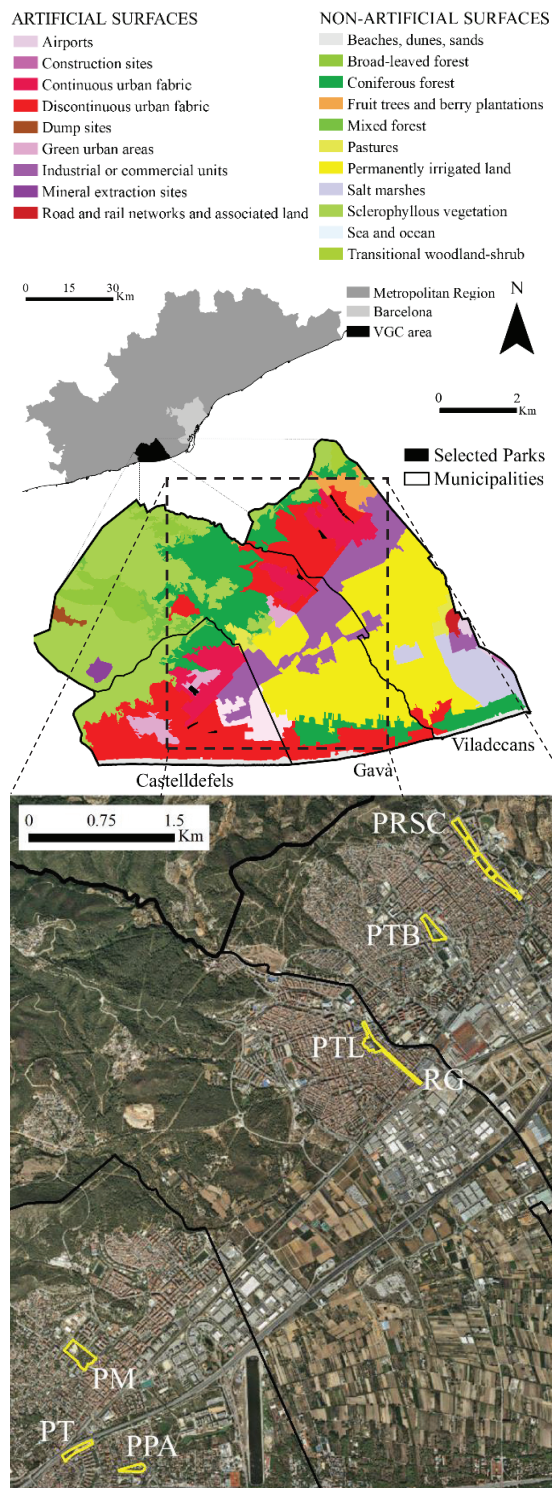


Figure 1: Selected parks and 2012 Corine Land Cover [12] [13]

The present work is part of a series of previous works that aim to quantify the microclimatic influence of the urban green spaces in the Metropolitan Region of Barcelona. First on the series, a study revealed differences of 4.28°C during day and 2.56°C at night in autumn between urban and rural areas LST [14]. Later, through measured air (T_A) and surface (T_S) temperature, a study registered that, during summer daytime, the Coll Favà Gardens with predominant paved surface and lower proportion of vegetation,

registered 5.03°C and 9.91°C higher T_A and T_S respectively than the Central Park mostly covered by dense vegetation, both in the Sant Cugat del Vallès municipality [15]. Likewise, the integration of field measurements, remote sensing and thermal simulation in two parks of Barcelona, registered that Turó Park, with abundant vegetation and dense built-up context, reaches a cooling extent of 80m with a 2.89°C intensity. While, the Parc del Centre del Poblenou Park, with sparse vegetation and mid-dense built-up and wooded surroundings, registered 90m of extent and 2.75°C of intensity [16].

2. METHODOLOGY

In this context, here we adapted three remote sensing analytical methods to quantify the cooling effect of seven parks at different scale approaches. With the purpose of define basic criteria for replication in the metropolitan region of Barcelona. The seven cases selected for this study correspond to green areas identified as points of interest because of their landscape value and differences of urban context (Figure 1). The cases of study are: *P. Riera de Sant Climent*, Viladecans (PRSC); *P. Torrent Ballester*, Viladecans (PTB); *P. Torre Lluch*, Gavà (PTL); *Rambla de Gavà*, Gavà (RG); *P. de la Muntanyeta*, Castelldefels (PM); *P. dels Tellinaires*, Castelldefels (PT); *P. de la Plaça d'Asturias*, Castelldefels (PPA).

2.1 LST retrieval

We retrieved LST from the Landsat-8 imagery of July 26 of 2018 acquired at 10:36 GTM+1 [17] and with the emissivity corrected algorithm [18]:

$$LST = T_B / [1 + (\lambda \times T_B / \alpha) \ln \epsilon] \quad (1)$$

where LST is in °C; T_B - at-sensor brightness temperature (°C) from thermal infrared one band (TIRS1); λ - wavelength value of TIRS1 band (10.895µm); α - surface radiation constant (1.4388×10⁻²mK); ϵ - surface emissivity estimated with the simplified NDVI threshold method [19] applying the emissivity values of [20].

2.2 Cooling effect indicators

The cooling effect is calculated by its extent and intensity. The cooling intensity (ΔT) is the difference between the temperature of the parks (T_P) and the urban areas (T_U), calculated as $T_U - T_P$ [2]. Cooling effect shows positive ΔT values. The cooling extent limit (L_{max}) is the maximum distance reached by the microclimatic influence of the park. Positive cooling effect implies lower temperatures near to the park and gradual increment according to more distance. In a fitted dataset of temperature of urban spaces ordered by distance to a park, the cooling effect generates a "cooling curve" [21, 22], which ends at the maximum ΔT (ΔT_{max}) and define the L_{max} point (Figure 2).

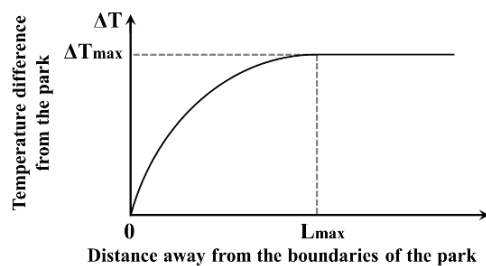


Figure 2: Conceptual model of the cooling effect [21].

2.3 Analytical methods

2.3.1 Delimitation of the surroundings by two concentric annuli

As first approach, we proposed a delimitation of the nearby surrounding areas by two concentric annuli for the cases of study. The aim of this division is to quantify the ΔT of each park, in relation to its particular context and make a first approach to identify potential ranges of distance of the L_{max} .

Here, we generated two concentric annuli from zero to 100 meters (A_1) and 100 to 300m (A_2) away from each park. Then, we calculated the mean LST of each annulus and park individually, excluding pixels of the other parks within annulus of another park.

2.3.2 Quantifying the cooling effect through 10m-width concentric annuli

In a more detailed approach, we proposed a 10m-width concentric annuli to homogenize LST of the surroundings and quantify L_{max} and ΔT of each park.

First, we created a 500m radius from the perimeter of the parks and divided it in 50 concentric 10m-width annuli. Then, we calculated mean LST for each park and annulus excluding LST pixels of parks and a six-degree polynomial curve fitting fixed fluctuations in the dataset of 51 LST values (park and 50 annuli). Here, we identified the L_{max} at the end of the cooling curve and estimated ΔT_{max} with the L_{max} point as T_U .

In this method, we excluded the Rambla de Gavà due to the narrowness of its section. Instead, we studied it with more detail in the following section.

2.3.3 Quantifying the cooling effect variations through transversal sections

Finally, we proposed transversal sections for a detailed analysis of ΔT and L_{max} of the Rambla de Gavà. As complement to the 50 concentric annuli, we placed 10m-width transversal sections to the Rambla throughout its extension. It resulted in a 10m-cells grid, distributed in 59 rows that correspond to the transversal sections and 101 columns that are the clipped annuli, 50 to northeast, 50 to southwest and one of the Rambla. Then, we resampled the LST cells to 5m-pixels and calculated average LST of the 10m-cells grid. In this case, we obtained two LST datasets for each section: the northeast and southwest. Both with the LST of the Rambla as first value. Where we also performed the curve fitting and cooling indicators calculations in both orientations.

3. RESULTS

The entire VGC area registered 35.64°C mean LST, just artificial surfaces 36.69°C and the non-artificial 35.06°C (Figure 3). Particularly, artificial surfaces in the municipalities registered 35.41°C in Castelldefels, 37.15°C in Gavà and 38.02°C in Viladecans.

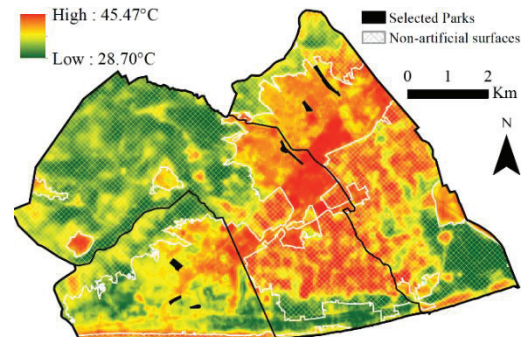


Figure 3: VGC area Landsat-8 LST of July 26 of 2018

The LST of the parks reflects the municipal variations, which decrease going from Viladecans to Castelldefels (Figure 4). In general, the parks resulted 1.08°C lower than the artificial surfaces of the conurbation. However, Viladecans registered the highest cooling effect and Castelldefels the lowest.

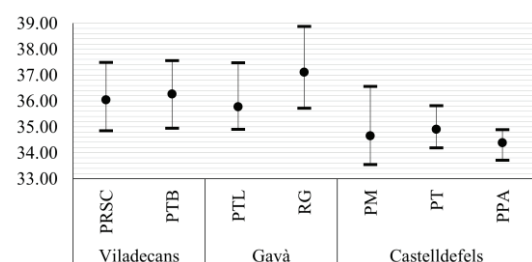


Figure 4: LST of the parks.

3.1 Cooling effect in the closest surroundings

The 0-100m (A_1) and 100-300m (A_2) annuli, indicate a 1.25°C and 1.50°C reduction of the parks in relation with these areas. In the particular results, annuli resulted in positive ΔT in all the cases (Figure 5).

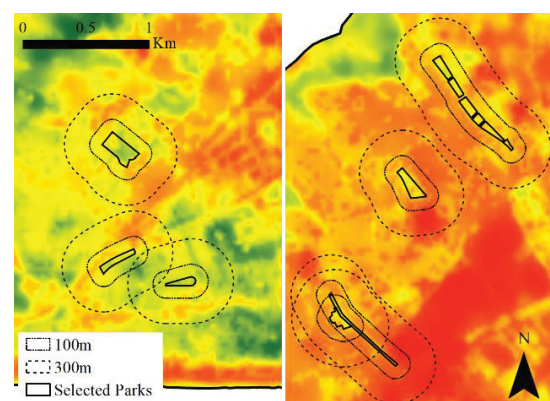


Figure 5: Concentric annuli of 100 and 300m.

The A_1 annulus registered the highest ΔT in the Parc Torre Lluch and the lowest in the Parc de la Plaça d'Astúries. While the A_2 registered its highest ΔT also in the Parc Torre Lluch and the lowest in the Parc dels Tellinaires (Table 1).

Table 1: LST of concentric annuli and ΔT .

Park	LST Park	LST A ₁	LST A ₂	ΔT A ₁ -P	ΔT A ₂ -P	ΔT A ₂ -A ₁
PRSC	36.03	37.12	37.55	1.09	1.52	0.43
PTB	36.27	37.97	38.24	1.70	1.97	0.28
PTL	35.77	37.92	37.99	2.15	2.22	0.07
RG	37.10	38.36	39.07	1.26	1.96	0.71
PM	34.65	35.82	36.18	1.17	1.53	0.36
PT	34.90	35.61	35.52	0.71	0.62	-0.08
PPA	34.39	35.05	35.04	0.66	0.65	-0.02

The higher ΔT values in the A₂ annulus, imply an extended increase of the temperature beyond the 100m, where the Lmax point is reached (Figure 6). However, the Parc dels Tellinares and the Parc de la Plaça d'Asturias, register their maximum ΔT in the A₁ area. Which imply that the cooling effect of the parks do not extents farther than 100m.

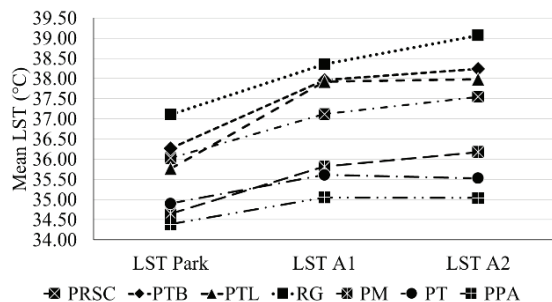


Figure 6: LST of parks and concentric annuli A1 and A2.

3.2 Cooling effect by the 10m-width annuli

The quantification by 10m-width concentric annuli registered positive cooling effect in the six parks assessed in this stage. Parks resulted in average 91.67m Lmax and 1.22°C ΔT . The maximum Lmax correspond to the Parc Torrent Ballester and the minimum to the Parc de la Plaça d'Asturias (Figure 7).

Comparison of the fitted LST datasets of the parks, show the decreasing trend of the cooling effect of the parks from Viladecans to Castelldefels (Figure 7). Nevertheless, important differences are appreciable in the LST of the urban surroundings (Figure 6). Which are those that define the cooling potential of the parks. Particularly, the Parc dels Tellinares and the Parc de la Plaça d'Asturias, with greener surroundings than the park, register the lower LST values which results in the lowest cooling Lmax and ΔT .

3.3 Cooling effect through transversal sections

The entire Rambla de Gavà registered an absolute mean LST of 37.10°C, the highest of the parks. Likewise, the divided Rambla by different urban contexts (Figures 8) registered a 2.21°C reduction in the industrial context, 1.05°C in the urban fabric and 1.76°C in the Parc Torre Lluch area.

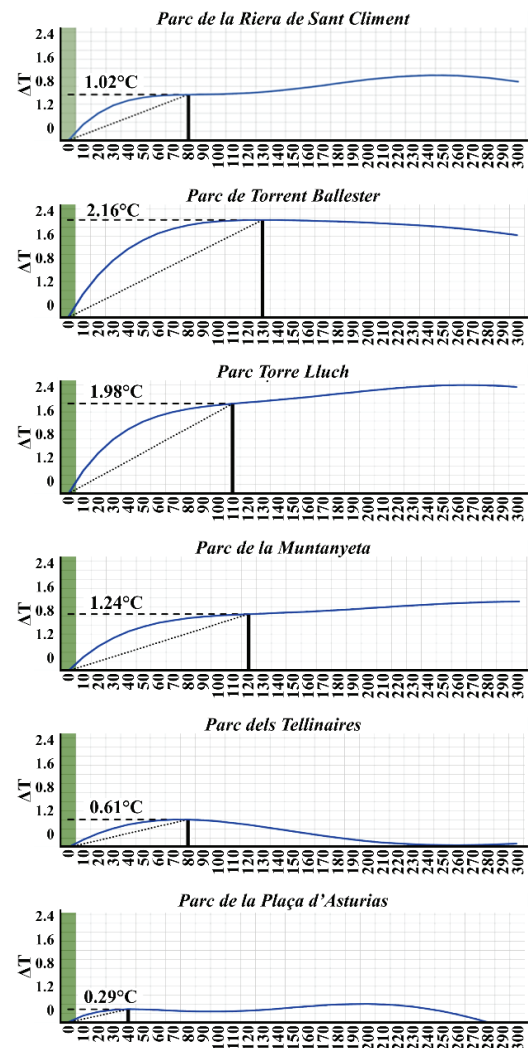


Figure 7: Fitted LST datasets (Park LST = 0) and cooling indicators calculation of the parks.

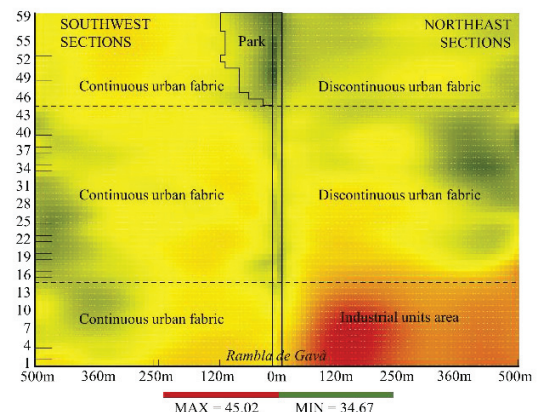


Figure 8: Fitted LST in the grid and context subdivisions.

The 3D visualization of the fitted LST in the transversal sections reveals the clear cooling effect of the Rambla de Gavà and the park (Figure 9). As well as the contrasting LST values in the industrial units.

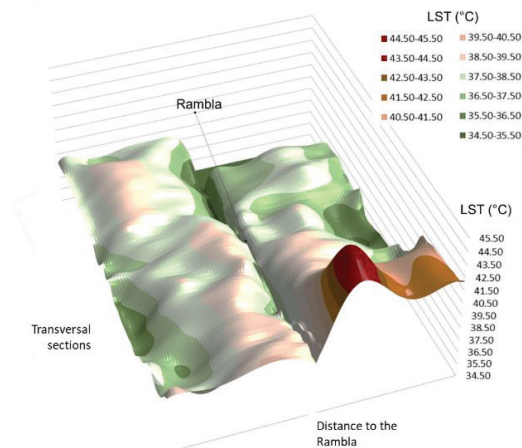


Figure 9: 3D chart of fitted LST of transversal sections

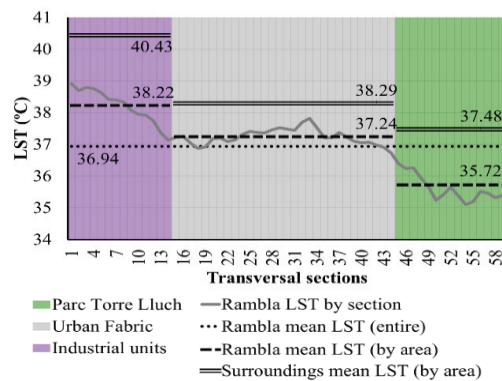


Figure 10: LST of the transversal section by urban context

The Rambla registered differences of ΔT in relation to the orientations of the surroundings (Figure 10). In the industrial area, it registered 3.91°C ΔT to north and 0.51°C to south. In the Parc Torre Lluch area, a 1.48°C of ΔT was registered to north and 2.03°C to south. Meanwhile, the urban fabric area registered a smaller variation with 1.16°C to north and 1.09°C to south.

The Lmax calculation for each transversal section, matched with the average LST reduction by type of urban context. The section 1 (Figure 11) registered a higher ΔT in the north sections with industrial units than in the south section with continuous urban fabric. Nevertheless, the extent resulted very close between both orientations. Meanwhile in the section 26 (Figure 12) corresponding to the urban fabric, values between northeast with discontinuous urban fabric and southwest with continuous urban fabric resulted very close. However, in this case, the Lmax registered a higher value in the discontinuous urban fabric. Likewise, the section 59 (Figure 13), regarding to the Parc Torre Lluch area, registered the effect of the Rambla and the park together. Here, in the southwest, the intensity and extent registered higher values than the northeast with discontinuous urban fabric.

Last, the quantification of cooling effect of all the sections in both orientations results in a detailed spatial delimitation of the Lmax throughout all the Rambla (Figure 14). Average Lmax reached 109.00m to the northeast and 129.67m average to the southwest.

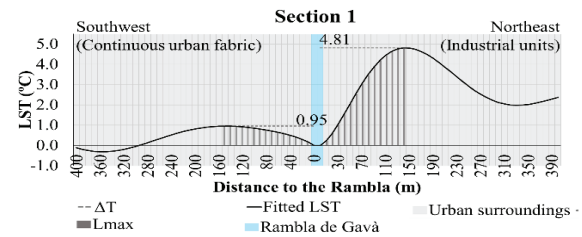


Figure 11: ΔT and Lmax in transversal section 1.

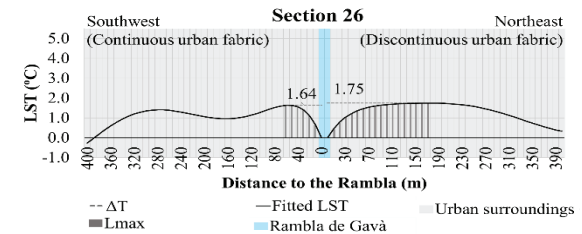


Figure 12: ΔT and Lmax in transversal section 26.

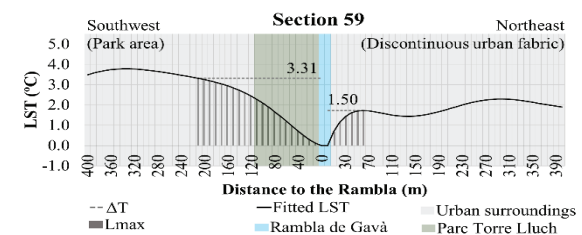


Figure 13: ΔT and Lmax in transversal section 59.

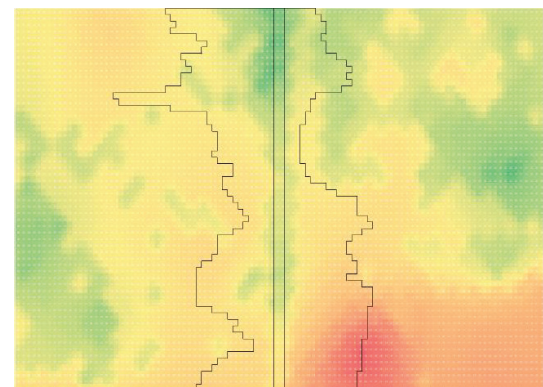


Figure 14: Lmax throughout all the transversal sections.

4 Conclusions

The three methods applied resulted in similar cooling potential of the parks. This multi-stage analysis, points that spatial analytical methods for measure the variations of temperature in the cities, are suitable to recognize the influence of the physical composition of the built environment.

The three methods are suitable for larger scales replication. However, the delimitation of the spaces through two concentric annuli allows a more generalized vision of the thermal environment, for which it results suitable for analyse a study area with a larger amount of data. Likewise, results on the first stage represent a general frame of the results of the other stages. In the other hand, the cooling extent calculation through transversal section is considered the more suitable to quantify influence of the built environment composition. As shown in the results, this method results in a detailed picture of the cooling

effect. However, processing the transversal sections demands several steps of spatial classification to analyse the data, and it is limited to particular cases.

The urban surroundings of the parks, registered more influence on the cooling effect than the LST of the parks. Particularly in this study area, the cooling effect resulted more related to the different variations of the temperature of the surrounding areas. Further research still necessary on this issue.

Higher temperatures in the urban context registered higher cooling effect. Nevertheless, higher LST in the closest urban spaces, cause a reduced cooling effect. This affirmation is related to the contention of the cooling, caused by the dense built spaces near to the park. In these cases, the parks cannot compensate the heat in their surroundings and their cooling effect is stopped.

Last, conclusions on the particular influence of the land cover classification are related to the observation that higher temperatures derive in higher cooling effect. Where the higher temperatures in the industrial units, resulted in the higher cooling intensity. As well as those in the discontinuous urban fabric with lower temperature. However, in the case of the Rambla, the continuous urban fabric caused a lower cooling effect than the discontinuous one, which is related to the detail of the analysis that reflects singularities of particular spaces.

Acknowledgements

The study is part of the project "Urban-CLIMPLAN. The urban heat island: effect on climate change and modelling for territorial and urban planning strategies. Application for the metropolitan region of Barcelona, Spain", supported by the Ministry of Economy and Competitiveness of Spain (MINECO) and the European Regional Development Fund (ERDF) with code of reference BIA2015-68623-R.

References

1. Oke, T., 1982. The energetic basis of the urban heat island. *Quarterly Journal of the Royal Meteorological Society*, Issue 108, pp. 1-24.
2. Spronken-Smith, R. & Oke, T., 1998. The thermal regime of urban parks in two cities with different summer climates. *International Journal of Remote Sensing*, XIX(11), pp. 2085-2104.
3. Kuttler, W., 2012. Climate Change on the Urban Scale – Effects and Counter-Measures in Central Europe. In: N. CHhetri, ed. *Human and Social Dimensions of Climate Change*. Rijeka: InTech, pp. 105-142.
4. Bowler, D., Buyung-Ali, L., Knight, T. & Pullin, A., 2010. Urban greening to cool towns and cities: A systematic review of the empirical evidence. *Landscape and Urban Planning*, pp. 147-155.
5. Jauregui, E., 1990. Influence of a Large Urban Park on Temperatures and Convective Precipitation in a Tropical City. *Energy and Buildings*, 15-16(3-4), pp. 457-463.

6. Anjos, M. & Lopes, A., 2017. Urban Heat Island and Park Cool Island Intensities in the Coastal City of Aracaju, North-Eastern Brazil. *Sustainability*, Issue 9, p. 1379.
7. Yan, H., Wu, F. & Dong, L., 2018. Influence of a large urban park on the local urban thermal environment. *Science of the Total Environment*, pp. 882-891.
8. Chow, W., Pope, R., Martin, C. & Brazel, A., 2011. Observing and modeling the nocturnal park cool island of an arid city: horizontal and vertical impacts. *Theoretical and Applied Climatology*, 103(1-2), pp. 197-211.
9. Declet-Barreto, J., Brazel, A. J., Martin, C. & Chow, W. T. L., 2013. Creating the park cool island in an inner-city neighborhood: heat mitigation strategy for Phoenix, AZ. *Urban Ecosystems*, 16(3), pp. 617-635.
10. Ren, Z. et al., 2013. Estimation of the Relationship between Urban Park Characteristics and Park Cool Island Intensity by Remote Sensing Data and Field Measurement. *Forests*, 4(4), pp. 868-886.
11. Cao, X., Onishi, A., Chen, J. & Imura, H., 2010. Quantifying the cool island intensity of urban parks using ASTER and IKONOS data. *Landscape and Urban Planning*, Volume 96, pp. 224-231.
12. Copernicus Land Monitoring Service, 2016. *Corine Land Cover 2012 Version 18*. [Online] Available at: <https://land.copernicus.eu/pan-european/corine-land-cover/clc-2012>
13. Arellano, B. & Roca, J., 2016. Identifying urban heat island: The Barcelona case. *Proc. XI CTV*. Cracovia, Centre de Política de Sòl i Valoracions, pp. 798-812.
14. Barcelona Regional, 2018. *Parcs Seleccionats*. Barcelona: s.n.
15. Roca, J., Arellano, B. & Batlle, E., 2018. Green areas and urban heat island: combining remote sensed data with ground observations. *Proc. SPIE 10767*, Remote Sensing and Modeling of Ecosystems for Sustainability XV, 1076705.
16. García-Haro, A. & Arellano, B., 2018. Isla de frío de los parques urbanos de Barcelona. Estudio de caso del Turó Parc y el Parc del Centre del Poblenou. *Proc. XII CTV*. Mendoza, Argentina, s.n., pp. 381-400.
17. U.S. Geological Survey (USGS), 2018. *Image of Metropolitan Area of Barcelona, Spain at July 26 of 2018*. s.l.:s.n.
18. Artis, D. A. & Carnahan, W. H., 1982. Survey of emissivity variability in thermography of urban areas. *Remote Sensing of Environment*, 12(4), pp. 313-329.
19. Sobrino, J., Jiménez-Muñoz, J. & Paolini, L., 2004. Land surface temperature retrieval from LANDSAT TM 5. *Remote Sensing of Environment*, 90(4), pp. 434-440.
20. Stathopoulou, M., Cartalis, C. & Petrakis, M., 2006. Integrating Corine Land Cover data and Landsat TM for surface emissivity definition: application to the urban area of Athens, Greece. *International Journal of Remote Sensing*, 28(15), pp. 3291-3304.
21. Lin, W. et al., 2015. Calculating cooling extents of green parks using remote sensing: Method and test. *Landscape and Urban Planning*, pp. 66-75.
22. Du, H. et al., 2017. Quantifying the cool island effects of urban green spaces using remote sensing Data. *Urban Forestry & Urban Greening*, Issue 27, pp. 24-31.

The environmental performance of temporary urban interventions:

Technical assessment of regeneration initiatives in the city centre of São Paulo, with focus on thermal and acoustic performance

RANNY L. X. N. MICHALSKI¹, LUCÉLIA RODRIGUES², JOANA C. S. GONÇALVES³, ROBERTA C. K. MULFARTH⁴, LEONARDO M. MONTEIRO⁵, RENATA TUBELO⁶, ALESSANDRA R. P. SHIMOMURA⁷, CAROLINA O. BLEY⁸, MARIANA S. VITTI⁹, DANIEL F. BILESKY¹⁰, MAYSA M. GUIMARAES¹¹
^{1,3,4,5,7,8,9,10,11} Faculty of Architecture and Urbanism, University of Sao Paulo, (FAUUSP, LABAUT), Sao Paulo, Brazil.
^{2,6} University of Nottingham, Faculty of Engineering, Department of Architecture, London, UK.

ABSTRACT: *Temporary urbanism is an approach to reactivate urban spaces through short-term interventions in a range of urban contexts. In central São Paulo, the Luz and Santa Ifigênia neighbourhoods, characterized by deprivation of their physical environments and social structures, were the focus of this investigation. The Mungunzá Container Theatre and the General Osório Square, located within these neighbourhoods, were selected as case-studies. Whilst the thermal performance of the container theatre itself was the main interest, in the case of the Square the fundamental issue was the environmental noise. The objective was to identify adequate strategies to improve environmental conditions in these locations in order to enhance positive social impact, and, then, contribute to the regeneration of these neighbourhoods. This research was based on fieldwork and analytical procedures of thermal and acoustic performances. In the container theatre building, the adoption of external shading and wider openings for ventilation reduced its indoor peak temperatures and delivered thermal comfort during the warmest period of the year. In the Square, sound absorber road surface material and an acoustic shell were proposed to reduce noise and promote better acoustic quality for outdoor performances.*

KEYWORDS: *Temporary urbanism, Thermal performance, Acoustic performance, Fieldwork, Analytical work.*

1. INTRODUCTION

Temporary urbanism is an approach to reactivate urban spaces through temporary and short-time interventions in a range of urban contexts [1]. Different from the conventional top-down master planning approach, temporary urbanism is flexible, innovative and more engaging with the local population. It often involves the erection of temporary buildings and/or changes to the landscape and urban furniture.

In the neighbourhoods of the city centre of São Paulo, Brazil, as in many megacities in the world, spaces between buildings and public squares are vastly used by informal business and street markets, or are abandoned and crime ridden [2]. Nevertheless, positive changes have recently been made on these spaces through the adoption of temporary interventions, promoted by a series of governmental and non-governmental institutions [3, 4, 5]. The provision of cultural and social spaces for the population to gather safely have proved to be helpful means to increase social cohesion and community capital in deprived urban areas [6, 7].

In this context, the work presented in this paper investigated the environmental performance of temporary design interventions for two nearby sites in

central São Paulo. Given the predominant warm conditions of São Paulo's humid subtropical climate, coupled with the magnitude of the problem of noise pollution, the environmental studies focused on thermal and acoustic performances. The technical work was based on fieldwork and analytical procedures, leading to environmental-focused design proposals.

2. CLIMATE

São Paulo (latitude 23.85° S; longitude 46.64° W; altitude 792 m) is located in a region of humid subtropical climate (*Cfa*) [8], being characterized by warm-humid summer days, with predominantly partially cloudy sky, and cool and drier winter days, with predominantly sunny sky. Air temperatures are moderate in most of the year with an annual average temperature of approximately 19 °C [9]. Due to the subtropical conditions, overcast sky occurs during 60% of the year, and diffuse radiation can reach 50% or more of the total global radiation on the horizontal plan in all seasons. January is the hottest month, followed by February, with an average of nearly 23 °C, absolute minimum of 14 °C and absolute maximum of 34 °C. Relative humidity varies between 31% and 100%. Maximum global solar radiation on the horizontal plan

is 1,068 W/m², being 578 W/m² diffuse. July is the coolest month, followed by August, with an average of 16 °C, absolute minimum of 8 °C and absolute maximum of 27 °C. Relative humidity varies between 26% and 100%. Maximum global radiation is 719 W/m², being the diffuse accountable for 435 W/m², more than half of the total [9].

Regarding acoustic conditions, noise pollution is one of the biggest environmental problems in urban centres considered a public health issue, affecting health and quality of life [10]. The main sources of noise in central areas of the cities are those related to transport. In order to tackle this issue, in São Paulo, a recent municipal law established the development of the first *city noise map*, to be finished in 2023 [11]. The noise map allows the diagnosis of the actual noise conditions and, therefore, it can inform potential interventions for improvement, as it already happens in Europe [10, 12]. Performance wise, the Brazilian standard ABNT NBR 10151 sets acoustic criteria for environments outside buildings [13]. The standard describes procedures for acoustic measurement and evaluation, and establishes limits for sound pressure levels for different outdoor environments, as a function of land use, occupation, and time of the day the exposure occurs.

3. CASE-STUDY INTERVENTIONS

In central São Paulo, the neighbourhoods of *Luz* and *Santa Ifigênia* are characterized by a high level of deprivation of their physical environments, with a significant number of degraded and vacant buildings alongside with underused public spaces mainly occupied by homeless and drug-addicts. On the other hand, they are also the location of important cultural facilities and listed buildings. In addition to that, the area encompassed by the two neighbourhoods is one of the main pool of jobs in the city and is well connected by public transportation modes to the edges of the city, where most of the poor population lives [14].

Given the nature of its physical and social problems, the area has been the focus of small-scale urban interventions as well as temporary urbanism initiatives [2, 3, 15]. In this context, the *Cultural Complex Mungunzá Container Theatre*, here called *Cultural Complex Mungunzá* (*Compania de Artes Teatro Mungunzá*) [3] and the *Open City Centre Square Largo General Osório*, here called *General Osório Square* (*Centro Aberto Largo General Osório*, CALGO) [2] were selected as case-studies. Figure 1 shows their locations and pictures. They were selected because a degree of temporary urbanism approach was undertaken on both cases. The first case, the *Mungunzá Container Theatre*, is a result of a bottom-up approach, dedicated to cultural and theatre related activities. It was built on an

abandoned site, supported by two light-weight structures, one made of industrial containers and another being a geodesic dome made of polycarbonate triangular structures and enclosed by a plastic layer.

The second case, *General Osório Square*, is a top-down approach initiative, implemented by the local city authorities, where a previously underused square was treated to accommodate different kinds of leisure activities, including the provision of movable outdoor furniture, such as beach chairs, tables and umbrellas, to be placed on a wooden deck used for short performances surrounded by wide pavements. Despite their different approaches, both projects aimed to increase the permanence of residents on their locations, by proposing cultural and social activities.



Figure 1: Locations and views: *General Osório Square* and *Cultural Complex Mungunzá*.

4. METHOD

This research was based on fieldwork and analytical work focusing on thermal and acoustic performances. In situ measurements recorded outdoor conditions in both case-study areas as well as inside the structures of the *Container Theatre* in August 2018. The measurements were cross-compared to time-lapse observations in order to understand how people interact with the built environment on specific climatic conditions, helping to inform about suitable temporary uses and potential improvements on the existing ones.

4.1. Thermal analysis

With regard to the thermal analysis, in the *Cultural Complex Mungunzá*, measurements of dry-bulb temperature (DBT), wet-bulb globe temperature (WGBT) and relative humidity (RH) were continuously taken in four locations: inside the container building (the theatre), the geodesic structure, outdoors under a tree and under the sun, from 11:45 am to 3:45 pm, with readings each 15 minutes. In the *General Osório Square*, spot measurements were taken in the middle of the day, between 12 am and 1 pm.

The equipment used for the external continuous monitoring consisted of data loggers Hobo Onset U23001 with weather shield. Internally, data loggers Hobo Onset U12 were adopted. In addition, grey globes

to measure mean radiant temperatures were adopted in both indoors and outdoors. The spot measurements were taken with thermo-hygrometer *Hanna*.

For the assessment of outdoors thermal comfort, the index of Predicted Thermal Sensation, developed by Monteiro to the climate of São Paulo [16] was adopted. In the sequence, thermal analytical studies addressed the performance of the container structure with focus on the intensity of its occupation and the risk of overheating during the warmest period of the year. For this purpose, indoor peak summer temperatures were calculated using the *Centre Scientifique et Technique du Bâtiment* (CSTB) method [17].

4.2. Acoustic analysis

The acoustic assessment consisted of sound pressure level evaluation, computational simulations and an intervention design proposal to improve the quality of the outdoor spaces. Sound pressure levels were measured in different points in order to characterise acoustic conditions in the selected locations. Results were also compared with the values established by the Brazilian Standard ABNT NBR 10151 [13]. For the measurements, a sound level meter Larson Davis model SLM 831 and a sound level meter calibrator Larson Davis model 200 CAL were used.

The A-weighted equivalent continuous sound pressure level (L_{Aeq}), maximum and minimum A-weighted sound pressure levels (L_{Amax} and L_{Amin}) and statistical levels (L_{AN}), where N is the percent exceedance level, were measured. L_{A90} is the A-weighted sound pressure level that is exceeded for 90% of the time interval considered and it is an indicator of the residual noise. On the other hand, L_{A10} is the A-weighted sound pressure level that is exceeded for 10% of the time interval and it is an indicator of events.

For the advanced analytical studies on urban noise, the software CadnaA was used. The software acoustically models the outdoor environment based on the following inputs: contour lines, buildings, roads and noise sources, ground and surfaces absorption, number of different types of vehicles per hour and speed limits of the roads. Then, based on these assumptions, it is possible to calculate and predict the environmental noise of the place. The purpose of the analytical simulations was to identify effective solutions to improve the acoustic outdoor environment of the case studies, in order to create appropriate and health conditions to the development of outdoor social/communal activities. Following the analysis of the base-case acoustic urban environment, alternative scenarios for the road surfaces, insertion of landscape and other strategies were compared.

In addition to the measurements and simulations analysis of potential uses, an acoustic shell for musical performance was proposed to be installed in *General Osório Square*, in order to adequately direct sound to the audience, located in the middle of the square.

5. FINDINGS: CULTURAL COMPLEX MUNGUNZÁ

5.1. Measurements

The measured data (Fig. 2) revealed comfortable conditions both indoors and outdoors during the time of the fieldwork, being consistent with a typical winter day for the city of São Paulo, with a clear sky and perceivable air movement, as per the adaptive comfort criteria [18]. The highest air and globe temperatures were found within the geodesic structure, followed by the container building (unoccupied during the measurements). The lowest temperatures were found outdoors, under the tree (Fig. 2). The geodesic dome had its poorer thermal performance associated to the high thermal transmittance of its plastic skin that combined to higher levels of global radiation significantly impacted on the amount of heat that passed through the structure. Whilst in the indoor measurements air temperatures were higher than (but very close to) the radiant ones (with the exception of one measurement in the geodesic) because of lack of internal thermal mass, outside it was the opposite: radiant temperatures were higher than the air ones due to the effect of the sky diffuse radiation.

The peak temperature inside the container reached 24.5 °C at 11h45 and 24 °C in the geodesic structure at 2 pm, 6 °C higher than under the tree, where the maximum temperature registered was 18 °C. Comparatively, the nearest weather station (located in a park area) had a measured air temperature value slightly lower by less than 0.5 °C (Fig. 2). Exposed to the sun, air temperature varied between 19 °C and 21 °C for most of the time, whereas the globe temperature reached 24 °C at 2 pm (Fig. 3). The results in the container and in the geodesic structure showed the potential risk of thermal discomfort in the warmest periods of the year, when external temperatures can reach as high as 34 °C and solar radiation can represent more than the double of a typical winter day (as the day of the fieldwork) [9]. Although only the results of temperatures are shown here, it is worth mentioning that relative humidity varied throughout the measurement points during the day, from 75% in the morning to 35% in the afternoon. Nevertheless, despite the typical dry conditions, the findings of relative humidity did not indicate any risk for comfort or health in any of the four measurement points.

The Physiological Equivalent Temperatures (PET) were calculated taking into account the hourly

predicted thermal sensation for the position under the sun and the respective comfort temperatures for the month of August. The results indicated the outdoor thermal conditions in the slightly cold band for most of the time (Fig. 4). Adding to the measurements, the time-lapse image series showed air movement of leaves of trees, whilst people were seating under the sun. It is important to consider that this was a typical winter day, with mild temperatures near 20 °C.

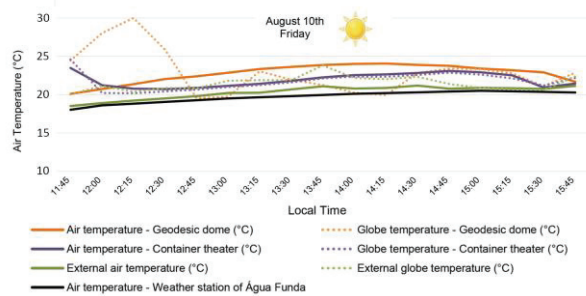


Figure 2: Measurements of DBT and WGBT in three locations at Cultural Complex Mungunzá: container theatre, geodesic dome, shaded outdoors (under the tree), compared to the closest weather station in São Paulo, on August 10th 2018, from 11:45 am to 3:45 pm.

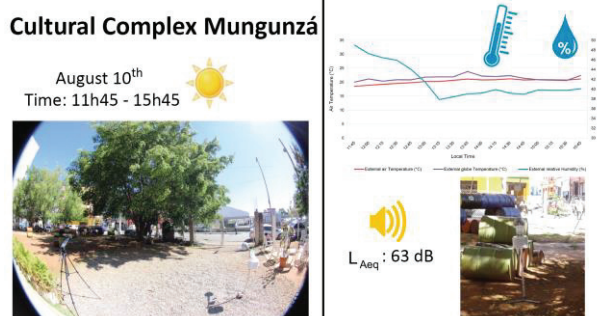


Figure 3: Cultural Complex Mungunzá, summary of measurements of temperatures, RH and L_{Aeq} recordings in the outdoor position, exposed to the sun on August 10th.

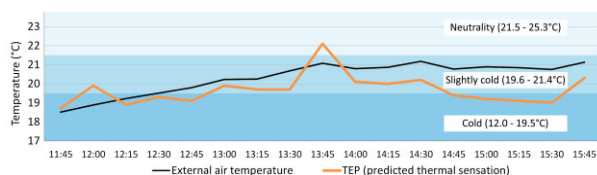


Figure 4: Calculated outdoor thermal comfort zone for the month of August with the predicted thermal sensation for the case-study area and air temperature under the sun [16].

Looking at noise conditions on site, the measured A-weighted equivalent continuous sound pressure level (L_{Aeq}) was 63 dB, lower than the 65 dB daytime limit established by ABNT NBR 10151 (2019) [13]. According to the standard, for outdoors, in mixed-use area with predominance of cultural activities, leisure and tourism, a 65 dB limit is allowed for L_{Aeq} for the daytime period, and a 55 dB limit is allowed for the night period. Maximum and minimum sound pressure levels were 87

and 52 dB. Considering the statistical levels, L_{A10} was 64 dB and L_{A90} was 56 dB. Recorded sounds were locksmiths in the surroundings, children playing outdoors on the site's external area and the adjacent road traffic. In this particular case, traffic was not identified as a problematic noise source in the surroundings of the cultural complex.

5.2. Design Optimisation

Alternative design scenarios were tested to reduce the solar gains and increase heat losses through the metal and glazed envelope of the container building. A set of opportunities to improve its thermal performance were also identified. The climate-responsive design strategies examined were: 1. the increase of ventilation, 2. addition of brise-soleil on east and west glazed facades, 3. addition of brise-soleil on east and west facades combined with the increase of ventilation, and, 4. increase of internal thermal mass in the ceiling (Fig. 5). Despite the unprotected glazed facades and the minimum aperture for ventilation, the current light reflective colour of the external cladding (specially in the roof) proved to be beneficial to the thermal performance of the base-case. Maximum indoor temperatures for each of the strategies and their potential thermal comfort conditions were calculated using the CSTB method [17].

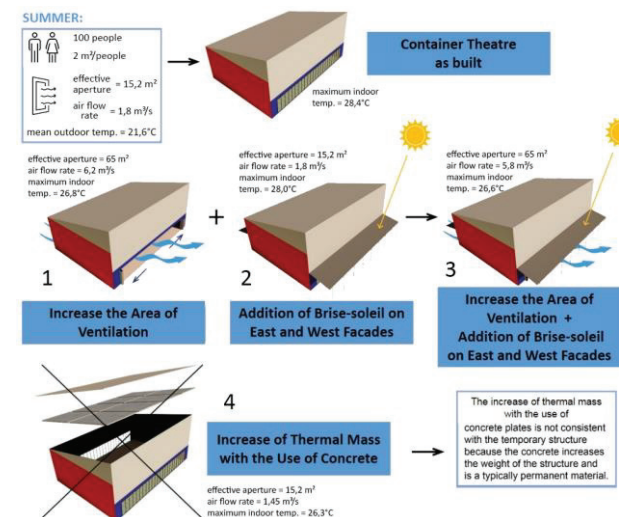


Figure 5: Analytical studies of the building of the container theatre, showing the range of design interventions tested to improve thermal performance.

The findings showed that the increase of the area of ventilation and adoption of shading (strategy number 3) would be able to reduce summer peak temperature from 28.4 °C (base case) to 26.6 °C, increasing the indoor thermal comfort conditions. The introduction of internal thermal mass reduces the peak temperature to 26.3 °C, a small improvement compared to the

combined effect of shading and ventilation. However, introducing the ventilation alone already results in comfortable conditions for 90% of the occupants. The thermal performance of the container in a typical autumn day is very similar to the summer one. As a result, more than 90% of the users would feel comfortable in both summer and winter periods. In the typical winter day, the external fixed horizontal shading over glazed areas coupled with the selective use of ventilation reduce peak temperatures from 24 °C to 21.9 °C, keeping the internal space comfortable.

6. FINDINGS: GENERAL OSÓRIO SQUARE

6.1. Measurements

In the *General Osório Square*, outdoor thermal conditions were within the neutrality zone, showing temperatures around 19 °C in the middle of the day, when the square is often used by local workers and residents (Fig. 6). Despite that, the time-lapse revealed people with different preferences, both under the shadow and exposed to the sun in a variety of activities such as talking, eating, resting, or just waiting. This is result from the environmental diversity provided by the landscape coupled with the availability of urban furniture and other public amenities, such as portable deck-chairs and umbrellas. Thermal conditions were not a problem to the square occupancy.

On the other hand, measurement results indicated the urban noise as an issue in the location, L_{Aeq} value was measured at 66 dB, and a L_{Amax} at 89 dB. L_{Amin} was 54 dB, L_{A10} was 69 dB, and L_{A90} was 59 dB.

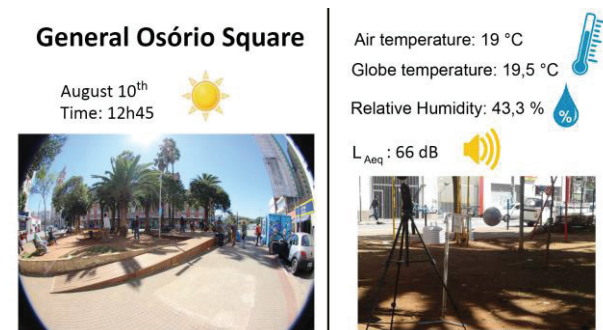


Figure 6: General Osório Square, summary of outdoor measurements on August 10th, including temperatures, RH and L_{Aeq} recordings.

For outdoors artistic performances in the *General Osório Square*, 66 dB is a high sound pressure level, compromising some activities such as listening to music and understanding speech. Therefore, the need of acoustic structures to qualify short-term music performances was identified. However, prior to the design of such structures, analytical studies on how to improve local urban noise were developed.

6.2. Design Optimisation

Acoustic computational simulations were undertaken to examine different scenarios with the aim of reducing urban noise levels and, thus, improving user's outdoor comfort. The alternative scenarios examined were: 1. vehicles prohibited at adjacent streets, 2. road's speed limit reduced to 10 km/h, 3. surface of the road changed to an asphalt with greater sound absorption, 4. circulation of heavy vehicles prohibited on the studied area, 5. road's speed limit reduced to 10 km/h and road's surface changed to an asphalt with higher sound absorption. Simulation results pointed out to the significant contribution of reducing speed limits and changing the sound absorption of the roads. Figure 7 shows the base case and the best alternative (number 5).

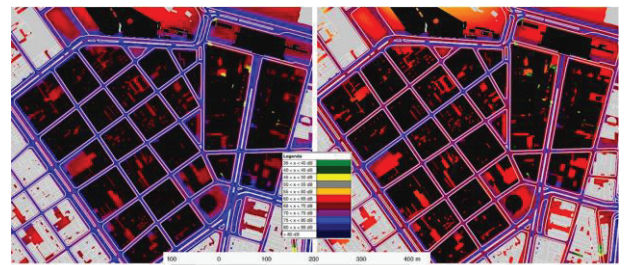


Figure 7: Simulations of urban noise in the area of the case-studies. On the left, base case. On the right, alternative 5. The darker the colour (closer to purple), higher the noise levels.

After testing the alternatives, the other potential temporary initiative proposed at *General Osório Square* was an acoustic shell to be placed on the existing stage of the square. The idea was to create a new urban equipment within the square that could have the same cultural *ethos* of the surroundings – a new equipment for artistic performances, where plays and music performances could be presented. The starting point considered an acoustic shell that could be easily assembled and disassembled and stored within the municipality container, located at the square and currently used to store the movable beach chairs used during the day. The form intention was to create a structure for musical performances which was able to take the sound up to the middle of the square and to reduce the interference of the streets' noise. Figure 8 shows the proposal: a planar acoustic system with its geometry allowing the reflected sound generated at the deck to reach up to the middle of the square.

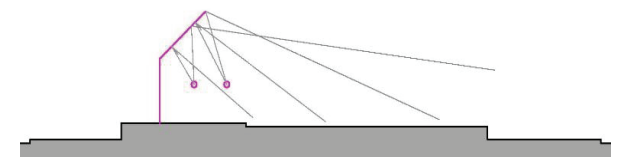


Figure 8: Final proposal - Section.

7. FINAL CONSIDERATIONS

The local remarkable social-economic complexity and a series of cultural initiatives found in the area of *Luz* and *Santa Ifigênia* neighbourhoods provide a potential for a programme of successful temporary structures, such as what can be observed in the *Cultural Complex Mungunzá* or in the *General Osório Square*. Different kinds of temporary structures already in place in the area of interest are showing signs of positive social changes in these deprived neighbourhoods. Nevertheless, the diversity and quality of these physical structures can be questioned and technically improved in order to enhance even further their positive social impact both inside buildings and in open spaces. This was the case of the container building, with the insertion of external shading and wider openings for ventilation, which improved its thermal performance. Strategic designed interventions were based on the temporary character of the building. For this reason, the increase of the internal thermal mass was disregarded due to its impact on the overall structure and its small contribution to the final thermal conditions of the internal space.

The external measurements revealed a thermal environment close to comfort on a typical sunny winter day in São Paulo, that favours outdoor activities. In addition, the diversified thermal conditions created in the *General Osório Square*, as well as in the area of the *Cultural Complex Mungunzá*, are important qualities that, coupled with the urban furniture and short-term events, invite pedestrians to stop and stay, effectively using these urban public spaces. However, the acoustic studies showed that there was room for improvement. Modifications of the surrounding urban surfaces proved to have a significant impact in reducing urban noise and promoting more comfortable and adequate acoustic environment for outdoor performances.

Proposing a temporary structure for the *General Osório Square* with a cultural focus, such as an acoustic shell, also allowed a social improvement to be carried out within the area. It would encourage new cultural activities and promote the continuance of the activities that have been developed there and that are widely accepted by the community, but with very little interference on the location, its social structure and use. Moreover, the facility of assembling and disassembling the proposed structure allows it to be transported and used in different places in the city, according to its necessity, making the intervention more feasible.

ACKNOWLEDGEMENTS

Thanks to FAPESP (no. 2017/08754-5), the University of São Paulo, the University of Nottingham,

and the University of Birmingham for supporting this research. Thanks to the Secretary of Urban Development of São Paulo City for the information provided. Thanks to *Cultural Complex Mungunzá* for the access to fieldwork. The authors would also like to thank the technician from FAUUSP, Ranieri Higa, for his support with the fieldwork.

REFERENCES

1. Andres, I. and Kraftl, P., (2018). New directions in the theorisation of temporary urbanism. American Association of Geographers, AAG.
2. PMSP - Prefeitura Municipal de São Paulo, (2017). Largo General Osório. *Programa Centro Aberto*. São Paulo: Prefeitura da Cidade de São Paulo.
3. COMPANHIA MUNGUNZA DE TEATRO, (2018). *Teatro de Container Mungunza*. [Online].
4. PMSP - Prefeitura de São Paulo, (2019). Centro Aberto - Experiências na escala humana, [Online], Available: <http://gestao urbana.prefeitura.sp.gov.br/centro-aberto> [16 December 2019].
5. PMSP - Prefeitura de São Paulo, (2016). Parklets: Políticas de Incentivo Parklets Municipais. Prefeitura de São Paulo. Available: <https://gestaourbana.prefeitura.sp.gov.br/> [20 May 2019].
6. Fontes, A. S., (2012). Intervenções temporárias e marcas permanentes na cidade contemporânea, *Arquitetura Revista*, 8, p 31-48.
7. Pacheco, P., (2018). *O poder de transformação do urbanismo tático*, [Online]. The City Fix Brasil.
8. Peel, M. C.; Finlayson, B. L.; McMahon, T. A., (2007). Updated world map of the Köppen–Geiger climate classification. In: *Hydrol. Earth Syst. Sci.* 11: 1633–1644.
9. LABEEE, UFSC, UFSC, (2005). Arquivos climáticos em formato TRY, SWERA, CSV e BIN. [Online].
10. EEA - European Environment Agency, (2020). EEA Report No 22/2019. Environmental noise in Europe. Luxembourg, [Online], Available: <https://www.eea.europa.eu/publications/environmental-noise-in-europe/> [10 April 2020].
11. PMSP - Prefeitura Municipal de São Paulo, (2016). Lei nº 16.499, de 20 de julho de 2016. Dispõe sobre a elaboração do Mapa do Ruído Urbano da Cidade de São Paulo e dá outras providências. Diário Oficial do Município de São Paulo, SP.
12. Gevú, N. V. et al, (2018). Mapa de ruído como ferramenta de diagnóstico e projeto. *Acústica e Vibrações*, v. 50, 93-106.
13. Associação Brasileira de Normas Técnicas, (2019). ABNT NBR 10151: Acústica - Medição e avaliação de níveis de pressão sonora em áreas habitadas - Aplicação de uso geral. Rio de Janeiro.
14. PMSP - Prefeitura Municipal de São Paulo, (2015). *Censo da População em Situação de Rua da Cidade de São Paulo, 2015: Resultados*, [Online]. São Paulo, Brazil: FIPE & PMSP.
15. Gonçalves, G. and Márcio Pinho, M., (2017). *Prefeitura instala contêineres da F1 para atendimento de usuários de drogas em estacionamento da GCM*, [Online]. São Paulo: G1.
16. Monteiro, L. M., (2008). *Modelos preditivos de conforto térmico: quantificação de relações entre as variáveis microclimáticas e a sensação térmica para a avaliação e projeto de espaços abertos*. [PhD Thesis], USP, Brazil.
17. Frota, A. B. and Schiffer, S. R., (2001). *Manual de conforto térmico (5ª edição)*. São Paulo: Editora Nobel.
18. Nicol, J., Humphreys, M., Roaf, S., (2012). *Adaptive thermal comfort: principles and practice*, Routledge.

Urban Growth with Greenhouse Gas Emissions Reductions Leveraging Passive House in the Commonwealth of Massachusetts

BLAKE JACKSON

Stantec Architecture & Engineering, LLC, Boston, Massachusetts, USA

ABSTRACT: *In an increasingly urbanizing world, cities play a key role in either mitigating climate catastrophe, or they will fall victim to it. Urban growth offers major opportunities to reduce greenhouse gas emissions through increased density, minimized per capita resource consumption and by providing the economic stimulus to transition from fossil fuel-dependency towards a post-carbon civilization. This paper demonstrates how large-scale North American developments are leveraging governmental initiatives, Passive House and utility incentives to prioritize ultra-high performing buildings, particularly mixed-use multifamily housing. It explains the drivers, using a case study in Boston, Massachusetts – indicative of other major North American cities, both in terms of the risks posed by climate change and due to its continued alignment with the 2015 Paris Agreement. The paper provides project-specific details in adherence to these principals, providing a calculation developed by the design team illustrating the return on investment for each residential project that factors in an early-phase economic analysis: first cost premium, energy savings, rebates and the return on investment for Passive House – useful in permitting and early design to influence decision-making, as well as leveraging the potential of urban growth to enhance the public realm and to curb, not exacerbate, climate change impacts.*

KEYWORDS: *Master Planning, Energy, Resiliency, Passive House, Greenhouse Gas Emissions*

1. INTRODUCTION

The Commonwealth of Massachusetts, located in the New England region of the northeast United States, is seeing unprecedented growth, with Boston – the regional centre – experiencing its third largest building boom in its 400-year history. This growth is spurred by a diverse economy, which includes over sixty area institutions of higher education (including Harvard and MIT), several major academic teaching healthcare institutions, robust financial and real estate investment trusts, excellent national rail and international air service and one of the densest biotech clusters anywhere in the world – Kendall Square. This growth expects to add 130,000 jobs to the Boston Metropolitan Area by 2030, growing twice as fast as the US average between 2010 and 2014 alone [1]; yet, such growth will invariably place major strains on a city plagued by rising income inequality, aged, decerped, underfunded public transportation infrastructure and the future impacts of climate change, which include increased heatwaves, increased precipitation and sea level rise. Boston is ranked by the World Bank as the fifth highest US city concerning at real estate value at risk from climate change impacts – 8th globally – equating to an estimated \$741million USD annually by 2050 [2].

This paper explores how local and regional governments are partnering, with private sector developers and institutions, to promote the use of Passive House (both Passive House Institute – PHI – and Passive House Institute US - PHIUS), adapted from use in Germany since the 1980's to the specificities of North American climate zones, to

leverage development growth to increase density while mitigating carbon emissions, providing better thermal comfort and indoor air quality, reducing noise and increasing passive survivability in buildings and which offers greater resiliency through increased social equity, more durable building stock and lowered utility bills. A case study 2.4million ft² (223,000m²) mixed-use development under permit (990 residential units) will illustrate how Passive House, as part of a transit-oriented development (TOD), can achieve these goals. The case study will explore the process of evaluating the cost benefit analysis of Passive House in this region to explain how the standard is “mainstreaming” there and across North America, looking specifically at the Boston market and drivers for ultra-high performing buildings there and throughout the US northeast.

2. CITY WITH A VISION

Boston learned from the 2012 impacts of Superstorm Sandy upon New York City. Since, local governments and the design community began mobilizing efforts to envision Boston's future, given new climate science and the opportunities created by the resurgence of the US economy after the global financial crisis of 2007-2009 [3]. This effort resulted in the creation of two key pieces of legislation: *Imagine Boston 2030* (2017) and *Carbon Free 2050* (2019). *Imagine Boston 2030* is the first comprehensive masterplan for the city in over fifty years, since the end of urban renewal, with the goal of providing better quality of life, equity and resilience for every unique Boston neighbourhood [4]. An extension of this plan, *Carbon*

Free 2050, specifically addresses strategies for eliminating greenhouse gas emissions by 2050 via electrification and upgrades to new and existing building stock, transitioning the power grid off fossil fuels towards being 80% renewables-based, zero waste and through comprehensive overhauls to the city's transportation infrastructure [5].

In addition, the Massachusetts Environmental Policy Act (MEPA) requires review of plans for permit when projects require involvement of state agencies, typically required for larger projects >5-acres (>0.02km²) where one of the following attributes are impacted [6]:

- development of agricultural land,
- alteration of endangered species habitat,
- alteration of wetlands,

- development of new utilities infrastructure,
- projects requiring federal controls,
- hazardous waste treatment, and/or
- significant historic/archaeological resources

Given that Boston, within the North America context, is a historically significant city with multiple projects >1million ft² (92,900m²) underway, MEPA is leveraging its power and oversight to enforce greater environmental commitments from these large projects to meet the more stringent environmental standards for approval, above the current minimum allowable: >10% better performance than energy code (ASHRAE 90.1) and demonstrating a >15% overall reduction in combined Scope 1, 2 and 3 greenhouse gas emissions.

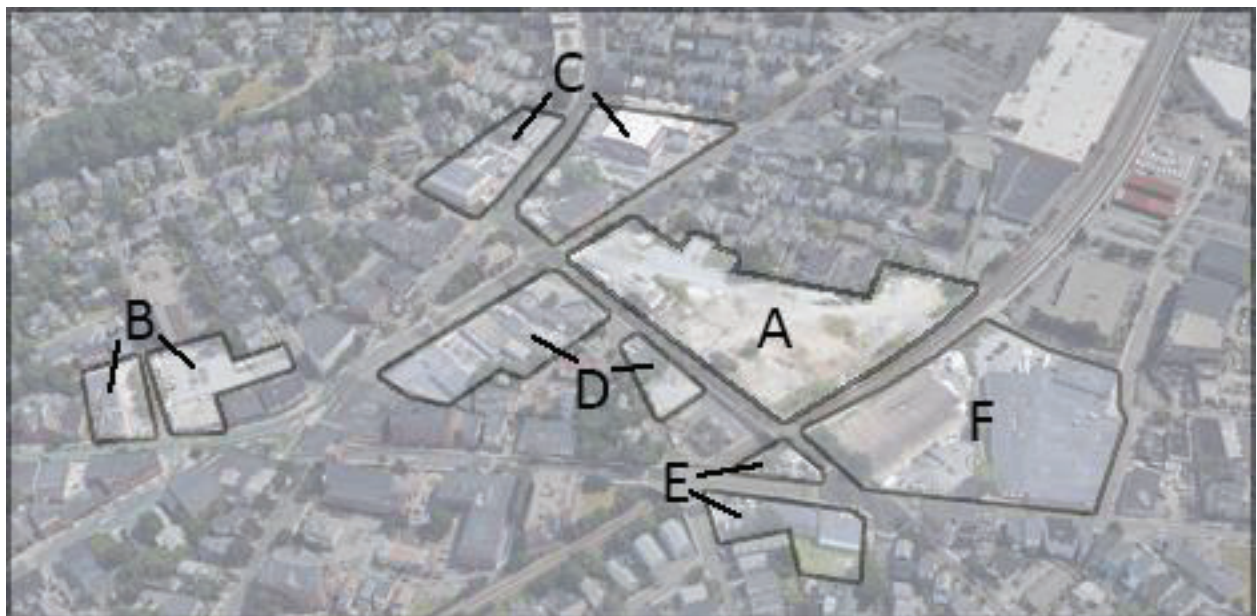


Figure 1: Aerial of the proposed site of the Union Square District: A) vacant lot/grade parking, B) single-level commercial/grade parking, C) single-level commercial structures, D) single-level commercial structures, E) grade parking/single-level commercial structures and F) warehouses.

3. DISCOVER UNION SQUARE

One such project under MEPA purview is Discover Union Square (Figures 1 and 2). Located in a city adjacent to Boston – Somerville, Massachusetts. The masterplan features seven residential buildings (990 units, 20% of which will be affordable stock), mixed-use commercial lab and office buildings and it is part of a transit-oriented development (TOD) catalysed by the new MBTA Green Line (subway) extension, which will connect the development directly into downtown Boston and the greater metropolitan region [7].

This project, given its size and scope, is under MEPA jurisdiction, and MEPA is leveraging its permitting power to request the development feature Passive House residential projects, Phase-2 and onward. This is a major leap beyond what is regularly required – 10% site energy use reduction

and 15% greenhouse gas reductions – towards >65% site energy reduction and >70% emissions reductions for the residential scope [8]. This project illustrates how governmental entities are leveraging plans, like *Carbon Free 2050*, to meet long-term emissions reductions targets aligned with the Paris Agreement, of which many US cities and states are still following – including Boston and the state of Massachusetts. However, this creates conflict between the desired outcomes of the government and the execution by developers because the government is essentially asking for design and performance commitments during permitting, when buildings are purely conceptual abstracts – masses only. The purpose of permitting so many parcels at once is to avoiding doing each building individually, with the ultimate

goal of enabling the developer to the right to either build their structures or sell parcels for development to other entities. Developers are typically reticent “over-commit” at this stage, which could tie the development to monetary and performance constraints (even technologies which may be outdated by the time of construction), as well as risking limiting the pool of potential interest later from both tenants and other developers. This is a common reason why master planning efforts seek to

only meet minimum code compliance levels during this early, visionary phase of development; however, the conundrum lies in that these commitments lock in outdated code minimums long-term, doing more to reduce the potential to leverage larger developments for their energy reduction potential. This is why government entities are now stepping in to leverage the permitting process – and eventual design of the individual buildings – to obtain greater climate action.

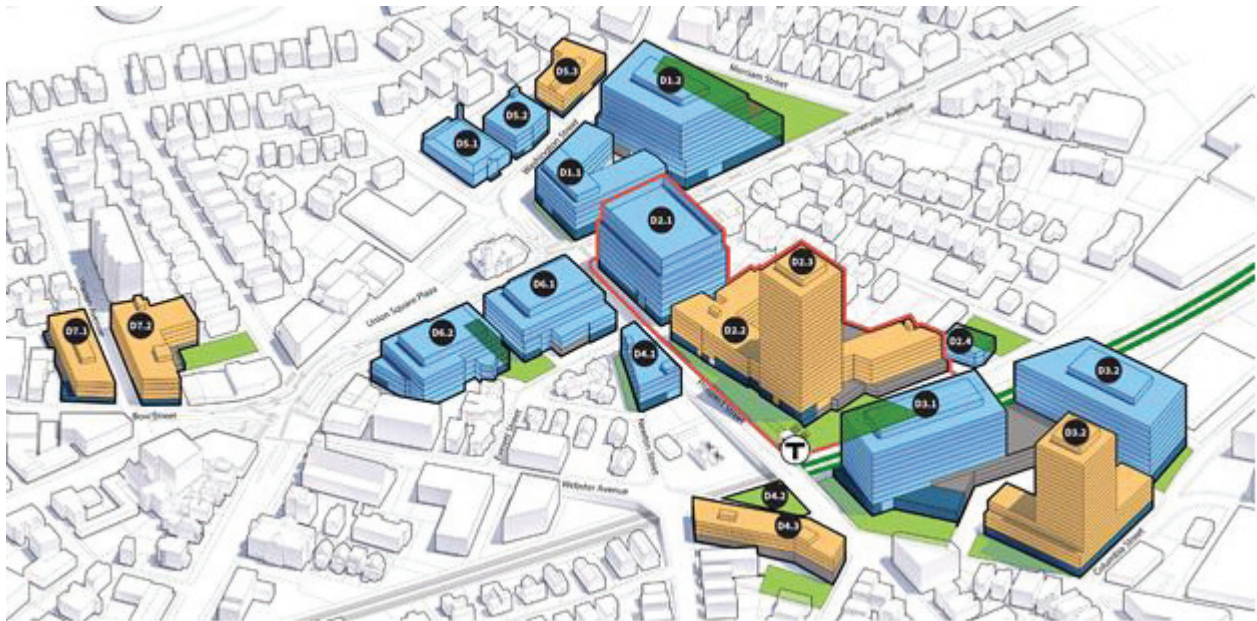


Figure 2: Proposed Discover Union Square: residential (orange), commercial (blue), subway extension (“T”) and Phase-1 (red).

4. PASSIVE HOUSE CALCULATOR FOR SCHEMATIC DESIGN

This project has been years in the making, begun prior to the publication of *Carbon Free 2050*; thus, the leap from 10% site energy/15% greenhouse gas emissions reductions to >65% site energy/>70% greenhouse gas emissions reductions meant the design/permitting team had to quickly assess the viability and impacts of the residential projects being designed to Passive House standards. Table 1, below, shows how the team leveraged Passive House energy

savings and two existing incentives programs (MassSaves and Alternative Energy Credits – AEC) to offset the first cost premiums for Passive House certification to make a business case for how this development could proceed without setbacks, aligned with the new regulatory goals. Note: MassAvaes at the time of the study offered \$0.50/kWh avoided; however, the new program – detailed later in this section – offers a higher amount.

Table 1: Phases-2 (and Onward) Passive House Results

Building Number See Figure-1	Residential Square Footage	Passive House Premium (USD)	Annual Energy Savings (kWh)	Mass Save Incentive (USD)	Alternative Energy Credit (USD)	Annual Electricity Savings (USD)	Premium Minus Rebates (USD)	Return With/without Incentives (Years)
3.2	333,000	\$2,957,040	3,220,558	\$1,610,278	\$86,300	\$547,494	\$1,260,461	5.4 – 2.3
4.3	54,000	\$479,520	522,253	\$261,126	\$86,300	\$88,782	\$132,093	5.4 – 1.5
5.3	30,000	\$266,400	290,140	\$145,070	\$86,300	\$49,323	\$75,473	5.4 – 1.5
7.1	40,000	\$355,200				765	\$75,474	5.5 – 1.2
7.2	77,000	\$683,760				418	\$266,816	6.1 – 2.4

Note: The Discover Union Square development is part of a state-wide shift towards the

use of natural gas for residential projects. This is a goal of the state by 2050.

Taking only the residential projects’ area (excluding retail and parking, as these are outside the

purview of Passive House, as well as the thermal envelope controlled by the design/permit team), the

team applied a \$8.88/sf (€8.13) first cost premium for Passive House to each building, based on *New York State Energy Research and Development Authority* (NYSERDA regional median costs for certified Passive Houses (2017 dollars). This methodology was approved by MEPA, as New York's and Massachusetts' construction cost indexes mirror each other – materials and union labour – and because New York has a larger critical mass of built Passive House certified projects to reference.

Of particular benefit to projects moving forward will be the Mass Save utility rebates for Passive House (increased from Table-1). Eligible to all projects >5-units registering and/or certifying with Passive House, generous rebates are being offered to usher in greater uptake at both the pre- and post-construction phases of projects. Up to \$25,000 (€22,875) can be obtained for use in feasibility studies and energy modelling. This is envisioned to overcome the knowledge gap present across the US industry regarding Passive House, as even though it has been employed in Europe since the 1980's, it is still relatively new to the North American market. Also, an additional \$500 (€458) per dwelling unit can be

earned during design, which for Discover Union Square (990 units) accounted for \$495,000 (€453,110). This helped compensate the team, as the effort incurred more time and fees than typical permitting, to perform more early-phase energy modelling, develop more envelope options with an overall weight >R-5, and options for mechanical systems, including VRF systems, heat pumps and onsite solar PV. Even greater offerings come post-construction phase. For certified Passive Houses, an additional \$2,500 (€2,289) per dwelling unit is awarded for, as well as performance bonuses of \$0.75 (€0.69) per kilowatt-hour (kWh) avoided and \$7.50 (€6.87) per therm avoided above a code-compliant baseline. This equated here to \$2,475,000 (€2,265,550) of post-construction rebates and a grand total of \$3,095,000 (€2,833,080) pre- and post-construction. While not entirely covering the development-wide Passive House premium, \$4,741,920 (€4,340,628), it offsets approximately 65%, reducing the hypothetical Passive House premium from \$8.88 (€8.13) per square foot to \$5.77 (€5.28) per square foot [9].



Figure 3: A view of the Phase 1 development, which shows a mid-rise office/lab building (left), a mid-rise residential building (centre) and a high-rise residential building adjacent to the proposed MBTA Green Line (subway) extension.

6. MOMENTUM

At the time of MEPA approval, awarded Fall 2019, only Building D4.3, which in Figure 1 is directly across

the street from the MBTA – “T” – transit hub and the Phase-1 tower, was officially committed to registering and certifying as a Passive House pilot within the development. This project was selected for several reasons:

- It is the smallest building within the development; thus, it represents the least financial risk.
- It has the simplest, most rectilinear geometry of any building within the development; thus, it makes the design, detailing and construction of a Passive House envelope more achievable.
- It is located at the confluence of three major streets, as well as the MBTA Green Line subway extension; thus, the noise reduction benefits, and improved indoor air quality potential, were seen to benefit this site the most of any other parcel.
- It's human scale at four floors made the expression of a Passive House façade with a 30%, maximum, window-to-wall ratio – expressed through punched openings – an aesthetically appropriate choice.
- It is being slated for 100% affordable units; thus, it leverages Passive House utility savings to have a maximum social impact for vulnerable populations.

The City of Somerville and the development team's negotiations are far from over. In fact, this effort was just the beginning. The good news is that the City will gain one new Passive House project that will demonstrate its viability for this growing area. While the developer has only committed this project – even though all were studied – the City of Somerville has since updated their code requirements (2019) to require net-zero energy new construction, as well as LEED Platinum lab buildings. This is a significant step in the right direction, as the next phases of development at Union Square of individual parcels will have to consider these measures moving forward.

Similar initiatives are gaining foothold within the Cities of Boston and Cambridge, Massachusetts, who together with Somerville represent the majority of the population (888,000 residents, or 13%) of the entire state of Massachusetts), and these communities are the economic engine of the state and are the areas most under development pressure. In May of 2019, this was codified when the mayors of each of these three municipalities signed letters urging developers to engage with their carbon neutrality goals, specifically now through 2030, to meet the overall 2050 goals, building on existing LEED-based ordinances, to utilize Passive House and/or, the Living Building Challenge, and/or LEED Zero and/or Architecture 2030 Zero Code options in conjunction with existing Massachusetts Stretch

Energy Code [10]. This legislation moves beyond LEED-based code equivalencies, which are still in place to help projects target a holistic framework for water, materials transportation and site parameters, towards performance-based verification of buildings (new and existing) to leverage development towards achievement of shared climate goals. This is a major shift seen in other major US markets – New York City, San Francisco, Washington DC, etc. – that is already being implemented in major Canadian markets. For instance, in Vancouver, British Columbia, Passive House compliance is now required by code, and certification (not just equivalency) means the City is allowing developers additional buildable area and/or height, further demonstrating that development and urban growth can help cities across North America, and beyond, achieve their 2050 targets.

7. CONCLUSION

This paper shows how to assess residential portions of masterplans for inclusion of Passive House within the US northeast using a simple methodology that can help project teams convince commercial real estate developers, and institutions, to utilize and promote Passive House as a means of achieving enhanced greenhouse gas emissions reductions, utilities savings and increased resiliency – with the help of municipal levers. Without current incentives, Massachusetts projects demonstrate a 5.4- to 6.1-years' return on investment for Passive House, which is outside of the typical 3-5 year acceptable payback period of most commercial real estate developers; yet, because of the strong incentives currently in place, in Massachusetts and elsewhere, coupled with long-term operational savings, this diminishes to 1.2- to 2.4-years' return on investment, which is considered palatable both for institutions and even for the most shrewd commercial real estate developers. Not surprisingly, the smaller the building, the quicker the return. Additional steps should be taken to validate this study, particularly in regard to solar control costs and performance impacts; however, as a quick reference for considerations shaping concept through schematic design, this paper should help in guiding early decision making. To keep up with this exciting project, you can follow its progress online at <https://discoverusq.com/>.

ACKNOWLEDGEMENTS

The author would like to thank the team who supported the creation of this research: Timothy Lowe (Stantec), Katie Raymond (Epsilon Associates), Tom Segundo (RWS Engineering), Greg Karczewski (Union Square Station Associates) and Justin Kunz (Union Square Station Associates).

REFERENCES

1. Housing a Changing City: Boston 2030, [Online], Available: <https://www.boston.gov/departments/neighborhood-development/housing-changing-city-boston-2030> [23 July 2019].
2. With Nowhere to Hide From Rising Seas, Boston Prepares for a Wetter Future: The Coastal City is Taking the Hint from Recent Storms and Floods, [Online], Available: <https://www.sciencenews.org/article/boston-adapting-rising-sea-level-coastal-flooding> [6 April 2020].
3. A New Age for an Old Town, [Online], Available: <https://www3.bostonglobe.com/business/2015/03/01/boston-historic-building-boom-redefining-skyline/Mxay21sRwTfYlN29GYLYjM/story.html?arc404=true> [23 July 2019].
4. Imagine Boston 2030: A Plan for the Future of Boston, [Online], Available: https://www.boston.gov/sites/default/files/imce-uploads/2018-06/imagine20-boston202030_pages2.pdf. [3 April 2020]
5. Ed. Hostetter, A. B. and M. Lubber, (2019). *Carbon Free Boston: Summary Report 2019*: p. 3.
6. Does My Project Require MEPA Review, [Online], Available: <https://www.mass.gov/service-details/does-my-project-require-mepa-review> [23 July 2019].
7. USQ: Redevelopment of 15 Acres in Union Square, Somerville, [Online], Available: <https://discoverusq.com/> [23 July 2019].
8. Ormond, Paul, (2019). *Union Square Redevelopment, Somerville, Massachusetts, EEA #15889*. p. 1-2.
9. Passive House Incentives: Take Energy Efficiency to a New Level, [Online], Available: <https://www.masssave.com/saving/residential-rebates/passive-house-incentives> [1 April 2020].
10. Anderson, Rob, (2019). *Joint Comments from the Cities of Boston, Cambridge, and Somerville on updating the Massachusetts Street Energy Code, pursuant to 780 CMR Chapter 115 AA*. p. 1-3.

Adaptive thermal comfort model suitable for outdoors considering the urban heat island effect

Urban and user approaches to enhance the outdoor thermal comfort

IVAN OROPEZA-PEREZ

Department of Architecture, Universidad de las Americas, Puebla, Mexico

ABSTRACT: In this work, an adaptive thermal comfort model is developed to consider the urban heat island effect upon outdoor occupants. Along with outdoor air temperature and outdoor relative humidity, other factors such as proper clothing and direct solar radiation are considered to assess the outdoor conditions in terms of thermal comfort. The study is carried out by developing a new model based on written surveys upon a study-group of 41 persons in an urban location with a Köppen classification of Cwb. Whereas the result values show a proper consistency (Conbrach's alpha of 0.91 and 0.93), this assessment shows that the UHI increases the thermal discomfort on the human body, while the use of urban and user-oriented approaches enhances in a great extent the thermal comfort. Then, a sensitivity analysis is carried out in order to find the most influencing factor upon this new adaptive thermal comfort model. With this, it is expected to consider urban-cooling and body-oriented approaches onto the cities in order to avoid thermal discomfort and its consequences, such as health issues, energy consumption, and the global warming, among other challenges.

KEYWORDS: Urban heat island, adaptive thermal comfort model, urban-layout approach, body-oriented approach

1. INTRODUCTION

The current situation in the world enforces new and better manners of dispatching energy for the every-day human activities. These manners should fulfil various characteristics that do not affect the environment like the increase of the so-called climate change, which is the most challenging issue faced by the human kind and whose origin is shared in a great extent by energy-related activities.

In addition, in a city context, the so-called urban heat island (UHI) is a phenomenon that grows every day in amount and intensity along over the world. This phenomenon comprises the increase of the local air temperature, the diffuse solar radiation and other physical characteristics that imply thermal discomfort upon the inhabitants. Other consequence of the UHI is the occurred onto the surrounding buildings, which are affected in their indoor environment, generally increasing the indoor temperature therefore enforcing the use of a cooling method such as fans and air-conditioning systems with the consequence of energy consumption.

In this sense, not only the indoor environments are affected by the UHI. The outdoor conditions, especially air temperature, relative humidity and global solar radiation are increased, which implies thermal discomfort among the outdoor occupants.

Therefore, in this document, an adaptive thermal comfort model suitable for outdoor conditions considering the UHI effect is developed in order to assess the thermal comfort performance of the users

as well as to propose solutions for this phenomenon and its consequences.

1.1 Characteristics of the UHI

The phenomenon of UHI consists in “an urban area or metropolitan area that is significantly warmer than its surrounding rural areas due to human activities” [1]. According to literature, the first cause of the temperature increase is the modification of land surfaces, followed by the waste heat from a certain energy activity. The main heat flows of the urban heat island can be seen in Figure 1.

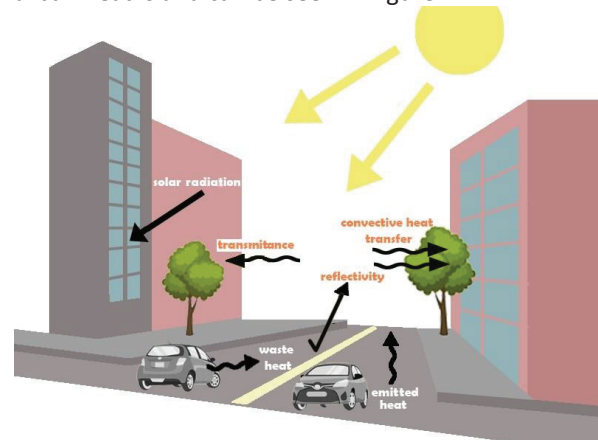


Figure 1: Main heat flows of an urban heat island.

From Figure 1, one can see the three main heat gains upon the urban area: the absorbed heat of the surface materials, which is almost immediately

emitted to their surroundings; the direct solar gains, mainly caused by high values of urban transmittance; and the heat waste due to human activities, especially motor traffic. Therefore, various manners to block and avoid these heat gains can be developed: high values of reflectivity in the urban surfaces; convective heat transfer throughout the urban morphology; and high values of urban thermal transmittance to decrease the direct heat gains are among the most used [2-3].

If these approaches are correctly applied, the UHI effect might be decreased therefore outdoor thermal comfort can be achieved [4].

On the other hand, various approaches can be applied upon the user her/his self. For instance, the variation of clothing could lead to an effective solution for thermal discomfort [5]. Different approaches regarding the metabolic rate also can drive to enhance thermal comfort [6].

Hence, in this document, an adaptive thermal comfort model that takes account the main features of both the urban layout and the users preferences is developed. This model is considered as novel since combines both the main features of the urban layout and the approaches that the user his/her self can apply onto his/her body in order to achieve the outdoor thermal comfort.

2. ADAPTIVE THERMAL COMFORT MODEL

2.1 Outdoor thermal comfort survey

In order to analyse the effect of the UHI onto a certain group of users, a written survey is hereby developed. This survey has the purpose of showing the most important aspects to consider when the UHI effect is present. The format of the survey can be seen in Table 1.

Table 1: Written survey sample for analysing the thermal comfort in an outdoor context.

Variable	No	Partial	Yes
1. Proper temperature			
2. Proper humidity			
3. Low direct radiation			
4. Low diffuse radiation			
5. Cool breeze			
6. Proper clothing			
7. Proper activity			
Thermal comfort			

This written survey was oriented to a study group of 41 persons (18 female and 23 male) with an age range of 19 - 22 years old.

The study group belongs to the Universidad de las Americas Puebla (UDLAP, initials in Spanish), located in the southern city of Puebla, Mexico, as students of bachelor in Architecture and Interior Architecture. Every member of the study group expressed her/his

willingness of participating on the survey and showed her/his proper health conditions through a health certificate issued by the Department of Medical Care of UDLAP.

Moreover, the city of Puebla has a latitude of 19°03'05"N and a longitude of 98°13'04"W, 106 km of distance from Mexico City. Its climate is classified as Cwb, i.e. dry-winter subtropical highland variety, according to the Köppen-Geiger classification, very similar to the Mexico City climate. This climate was chosen for geographical conveniences, but also for the high effect that the UHI has upon the urban areas of this kind of climate [7].

Thereby, the process of the analysis was the following: the study group was requested for answering the written questionnaire onto rural conditions (no UHI) and onto an urban context, considering the UHI, for the same hour at similar conditions of outdoor temperature (23 – 25 °C), relative humidity (50 – 60%) and global solar radiation (600 – 800 W/m²). Pictures of the two places of survey are shown in Figure 2.



Figure 2: Rural and urban conditions for the written questionnaires in Puebla City, Mexico.

The answers for the written survey are classified by the variables shown in Table 1. In this way, the number of answers of each variable as well as the general perception of thermal comfort for the group of study are displayed in Figure 3, upon the rural environment, and Figure 4, onto the urban environment considering the UHI effect.

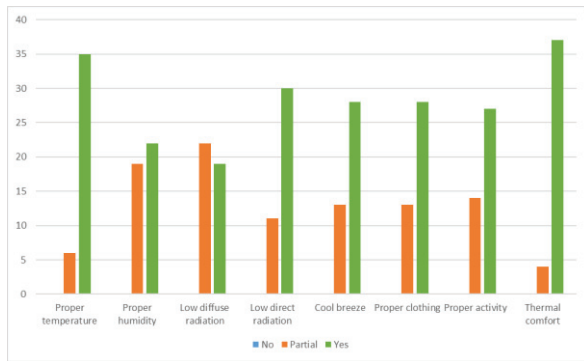


Figure 3: Number of answers for outdoor thermal comfort perception onto a rural environment.

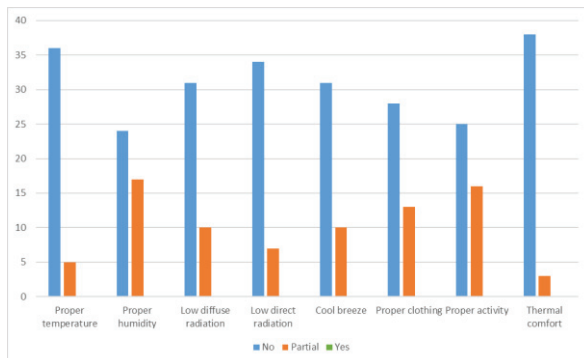


Figure 4: Number of answers for outdoor thermal comfort perception onto an urban environment considering the UHI.

In Figure 3 and 4 one can notice that none amongst the interviewed group answered for thermal discomfort in the rural area and thermal comfort in the urban area.

Thereby, the answers of the survey are analysed statistically to find the consistency of the results. Therefore, the Conbrach's alpha value is used. This value is highly used to find the correlation between a certain group of given results, generally subjective answers converted to numerical values [8]. In this way, to every answer in this study, a numerical value is given. For the answer "no" is 1, for "partial" is 2 and for "yes" is 3. With this, the Conbrach's alpha is estimated as follows:

$$\alpha = [n/n - 1] \cdot [1 - \sum \sigma_i^2 / \sigma_t^2] \quad (1)$$

Where α – Conbrach's alpha
 n – Number of items
 σ_i^2 – Variance of item i
 σ_t^2 – Variance of the total items

The variance of each item is calculated as the following:

$$\sigma_i^2 = 1/n \cdot \sum (x_i - \bar{x})^2 \quad (2)$$

Where x_i – Value of item
 \bar{x} – Mean value of the items

By using Eq. 1 and 2, a Conbrach's alpha value of 0.91 is estimated for the rural conditions, whereas for urban conditions a Conbrach's alpha value of 0.93 is estimated. This shows that the results can be seen as consistent, if it is considered that a Conbrach's value higher than 0.7 is necessary to find the reliability of the results [8]. Thus, with these results, an adaptive thermal comfort model is hereby developed, considering the influence of the different variables upon the interviewed students.

2.2 Adaptive thermal comfort model

A development of a new model of adaptive thermal comfort is hereby proposed. This model takes account of the adaptive equation developed by Oropeza-Perez et al. for a location with mild-temperate conditions as the presented by Köppen as a classification of Cwb [9]. In addition, the model is developed considering the answers of the written survey presented in Section 2.1.

The adaptive thermal comfort model for Cwb developed in [9] is shown as follows:

$$T_c = 0.53 \cdot T_{out} + 10.3 \quad (3)$$

where T_c - Temperature of comfort ($^{\circ}\text{C}$);

T_{out} - outdoor air temperature ($^{\circ}\text{C}$);

This equation is compared to the adaptive thermal comfort models of ASHRAE 55 and EN 15251, given by Eq. 4 and 5, respectively:

$$T_c = 0.31 \cdot T_{out} + 17.8 \quad (4)$$

$$T_c = 0.33 \cdot T_{out} + 18.8 \quad (5)$$

From Eq. 3 to 5, Figure 5 can be displayed, showing the comparison of the three adaptive thermal comfort models.

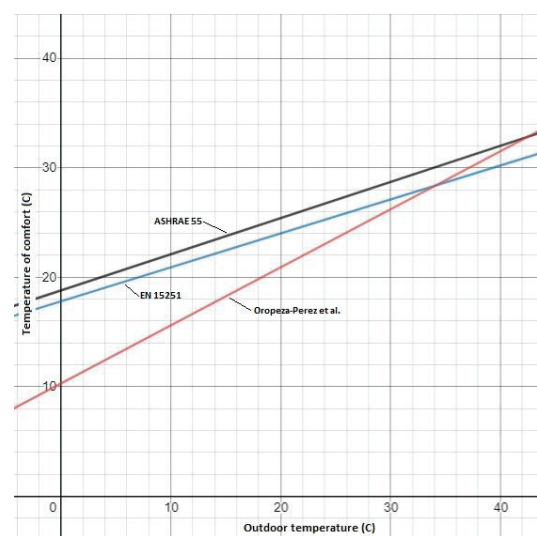


Figure 5: Comparison between three models of adaptive thermal comfort.

In Figure 5 it can be seen that the thermal comfort in climates such as Cwb presented by Oropeza-Perez

et al. is reached in a more difficult manner than those presented for ASHRAE 55 and EN 15251. This means that in this kind of climate people feel in thermal discomfort in an easier way when warm conditions are present.

Hence, when the UHI occurs in Puebla for instance, it is very likely that people would feel thermal discomfort. This statement is supported by Figures 3 and 4, where it can be seen that nobody feels thermal comfort in an urban context, whereas in rural conditions nobody feels thermal discomfort.

In this sense, the influence of the UHI is analysed in this manuscript considering not only the outdoor temperature, but also other features of the urban layout and the persons themselves.

2.3 Numerical outdoor thermal comfort model

In this manuscript, the variables of the written survey (proper temperature, proper humidity, low direct radiation, low diffuse radiation, cool breeze, proper clothing and proper activity) are quantified to find out the most influencing factor upon the people that stands on the UHI.

For doing this, a comparison between the answers given in the rural conditions and the urban context is carried out. This comparison is statistically analyzed with the difference of the average values for answers with UHI (urban) and the average values for answers without UHI (rural). As it was previously mentioned, to each answer (no, partial, yes) a numerical value was assigned (1, 2, 3, respectively). In addition, the standard deviation is calculated for every variable to determine the reliability of the differences.

In this sense, the values of the answers can be seen in Table 2:

Table 2: Comparison of the results for rural conditions (no UHI) and urban conditions (UHI)

Variable	Difference of values	Standard deviation No UHI	Standard deviation UHI
Proper temperature	1.73	0.36	0.33
Proper humidity	1.10	0.50	0.50
Low direct radiation	1.22	0.50	0.43
Low diffuse radiation	1.56	0.45	0.38
Cool breeze	1.41	0.47	0.45
Proper clothing	1.37	0.47	0.47
Proper activity	1.27	0.48	0.49

Table 2 shows that the answers given in the written surveys have similar results, since their standards deviations do not reach further than 0.5. This means that every variable has only two answers: either no/partial or yes/partial, which corroborates the opposite thermal sensations with UHI and without UHI.

Regarding the differences of values, a sort from the highest to the lowest value can be displayed in Table 3. With these differences of values, one can find out what is the variable that changes the most onto the occupants with and without UHI, therefore, one can suppose that is the variable with the highest influence upon the thermal comfort perception.

Table 3: Difference of the average values for answers with UHI and the average values for answers without UHI

Variable	Difference of values
Proper temperature	1.73
Low direct radiation	1.56
Cool breeze	1.41
Proper clothing	1.37
Proper activity	1.27
Low diffuse radiation	1.22
Proper humidity	1.10

From Table 3, one can see that the most influencing variable to measure outdoor thermal comfort is the outdoor temperature, followed by the direct solar radiation. Furthermore, another important variable that has an influence upon the thermal comfort of the outdoor occupants is the ventilation along with a proper clothing.

These variables, mainly, make that the outdoor occupants have a comfort feeling or not depending on the UHI presence.

Thereby, in order to develop an index that measures the thermal comfort considering the mentioned variables, Eq. 6 is developed, based on the written questionnaires:

$$\begin{aligned}
 EOSC = & 0.73 \cdot [|24^{\circ}\text{C} - T_{out}|/4^{\circ}\text{C}] + \\
 & 0.56 \cdot [|100 \text{ W/m}^2 - R_{Dir}|/100 \text{ W/m}^2] + \\
 & 0.22 \cdot [|100 \text{ W/m}^2 - R_{Dif}|/100 \text{ W/m}^2] + \\
 & 0.41 \cdot [|3 \text{ m/s} - v|/3 \text{ m/s}] + \\
 & 0.37 \cdot [|1.2 \text{ clo} - Clo|/0.5 \text{ clo}] + \\
 & 0.27 \cdot [|1 \text{ met} - Met|/0.5 \text{ met}] + \\
 & 0.10 \cdot [|60 \% - RH|/15 \%) \quad (6)
 \end{aligned}$$

where EOSC is the Equivalent Outdoor Sensation of Comfort (dimensionless); T_{out} is the outdoor temperature ($^{\circ}\text{C}$); R_{Dir} is the direct solar radiation (W/m^2); R_{Dif} is the diffuse solar radiation (W/m^2); v is the outdoor wind velocity (m/s); Clo is the clothing (Clo); Met is the metabolic rate (met); and RH is the relative humidity (%);

With Eq. 6 it is pretended to determine a thermal comfort index with values from 0 (total thermal comfort) until 12 (total thermal discomfort).

3. RESULTS

3.1 Values of EOSC

Using Eq. 6, Table 4 can be constructed. When the conditions of comfort stated in these documents are set, the value of EOSC is the minimum, whereas the conditions of the variables are considered as extreme, EOSC reaches the highest value. Furthermore, the comfort range of each variable is given by the denominator of every term in Eq. 6.

Table 4: Values of EOSC considering variables of comfort and variables at extreme conditions

Variable	Comfort values	Extreme values
Proper temperature	24 °C	45 °C
Proper humidity	60%	100%
Low direct radiation	100 W/m ²	700 W/m ²
Low diffuse radiation	100 W/m ²	600 W/m ²
Cool breeze	3 m/s	15 m/s
Proper clothing	1.2 clo	3 clo
Proper activity	1 met	3 met
EOSC	0	12.6

If the boundary values of the comfort ranges are considered, i.e. the values given by the denominators of Eq. 6, Table 5 can be constructed.

Table 5: Values of EOSC considering variables with values at boundary conditions of comfort

Variable	Upper boundary values
Proper temperature	28 °C
Proper humidity	75%
Low direct radiation	200 W/m ²
Low diffuse radiation	200 W/m ²
Cool breeze	6 m/s
Proper clothing	1.7 clo
Proper activity	1.5 met
EOSC	2.7

From Tables 4 & 5, one can see that the EOSC value gives a wider perception of thermal comfort considering the UHI effect. From 0 to 2.7, it is considered that the outdoor conditions are proper for thermal comfort. Beyond this value, it is very likely to perceive conditions of discomfort.

Moreover, as Eq. 6 depends on seven variables for both the outdoor and users conditions, a sensitivity analysis is carried out to find out the most influencing factor upon the EOSC.

3.1 Sensitivity analysis

Considering the values of the variables with conditions of comfort from Table 4, a sensitivity analysis is carried out. For each variable, the other six variables are set with their correspondent comfort values (Table 4, column 2), while the selected variable is modified from its value of comfort until its extreme value (Table 4, column 3). With this, Figure 6 is displayed.

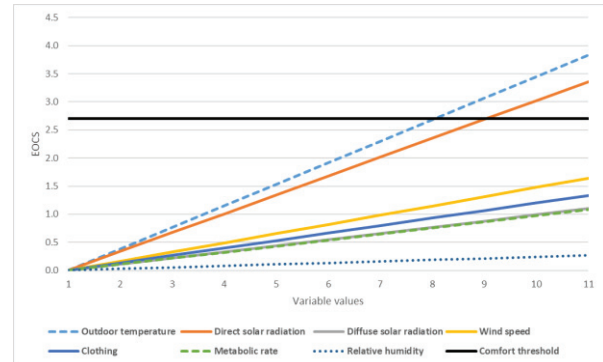


Figure 6: Sensitivity analysis of the variables of outdoor comfort.

In Figure 6 one can notice that only the outdoor temperature and the direct solar radiation are able to reach EOSC values higher than 2.7 (thermal discomfort). That means that although the other six variables were set within the comfort range, the increase of the outdoor temperature or the direct solar radiation could cause thermal discomfort upon the outdoor occupants.

Nevertheless, the clothing and the metabolic rate of the people have a certain influence on the EOSC. This means that even though the outdoor conditions are not the proper for achieving thermal comfort, the users are still able to do this if they apply certain approaches onto their bodies, including mechanical ventilation to increase the wind speed.

On the other hand, urban approaches such as green areas, vegetation and urban shading are essential to decrease the direct solar radiation, in specific, and with this to try to reach the proper outdoor conditions for thermal comfort.

In this sense, other urban approaches such as high reflectivity materials and urban canyons would help to lower the outdoor temperature by removing the waste and emitted heat (urban canyons) and reflecting both the direct and diffuse solar radiation, which increases the outdoor temperature on a UHI context.

In general, however, a combination of both urban and user approaches is necessary to decrease the thermal discomfort, reflected in this document as high values of the EOSC. The application of only one or two approaches would imply outdoor thermal discomfort.

3.1 Limitations of the model

The model presented here has a number of limitations: the written questionnaire was headed towards young healthy people. Other groups such as sensitive and elderly have to be considered to find a deeper analysis.

In addition, the model was applied upon a particular climate condition, Cwb (dry-winter subtropical highland). The variable of relative humidity would have more influence in conditions such as Af (tropical rainforest) or Cfa (humid subtropical) where relative humidity has a higher influence upon the users.

Because of this, it is expected to make a further analysis taking account of bigger groups of study and more climate conditions in order to develop a more complete model.

4. CONCLUSION

This paper shows the influence of various physical factors upon the thermal comfort of occupants of urban areas. The direct solar radiation and the increase of the outdoor air temperature are the most influencing factors to increase the thermal discomfort, while the use of urban shading and reflective materials as well as a proper clothing and metabolic rate (1 clo and 1 met, respectively) help to reduce these causes of discomfort.

After using a written questionnaire answered by healthy and young people, a mathematical model is developed to find the Equivalent Outdoor Sensation of Comfort, which gives a wider perspective of thermal comfort taking account of both outdoor and user variables.

Considering other thermal comfort models suitable for outdoor conditions such as the Physiological Equivalent Temperature (PET), the Predicted Mean Vote (PMV) or the Universal Thermal Climate Index (UTCI) [10-13], the model developed here has the advantage of being applicable with the outdoor conditions and the conditions of the outdoor occupants, and considering the UHI effect upon them.

REFERENCES

1. Mirzae, P.A., (2015). Recent challenges in modeling of urban heat island. *Sustainable Cities and Society*, 19: p. 200-206.
2. Morini, E., Touchaei, A.G., Rossi, F., Cotana, F., and Akbari, H., (2018). Evaluation of albedo enhancement to mitigate impacts of urban heat island in Rome (Italy) using WRF meteorological model, *Urban Climate*, 24: p. 551-566.
3. Yuan, J., Emura, K., Farnham, C., and Sakai, H., (2016). Application of glass beads as retro-reflective facades for urban heat island mitigation: Experimental investigation and simulation analysis. *Building and Environment*, 105: p. 140-152.
4. Fabiani, C., Pisello, A.L., Bou-Zeid, E., Yang, J., and Cotana, F., (2019). Adaptive measures for mitigating urban heat islands: The potential of thermochromic materials to

control roofing energy balance. *Applied Energy*, 247: p. 155-170.

5. Wang, Z., Cao, B., Ji, W., and Zhu, Y., (2020). Study on clothing insulation distribution between half-bodies and its effects on thermal comfort in cold environments. *Energy and Buildings*, 211: p. 109796.
6. Zhang, A., Huang, Q., Du, Y., Zhen, Q., and Zhang Q., (2019). Agent-Based Modelling of Occupants' Clothing and Activity Behaviour and Their Impact on Thermal Comfort in Buildings. *IOP Conf. Ser.: Earth Environ. Sci.*, 329: p. 012022
7. Jauregui, E., (1997). Heat island development in Mexico City. *Atmospheric Environment*, 31: p. 3821-3831.
8. Ummah, R., Sulisworo, D., Raharjo, W., Maruto, G., Nurul, and Huda Abd, R., (2020). The effect of informal cooperative activity through online learning on the understanding of physics concept. *Universal Journal of Educational Research*, 8(3 B): p. 69-77
9. Oropeza-Perez, I., Petzold-Rodriguez, A.H., and Bonilla-Lopez, C., (2017). Adaptive thermal comfort in the main Mexican climate conditions with and without passive cooling. *Energy and Buildings*, 145: p. 251-258.
10. Wu, J., Li, X., Lin, Y., Yan, Y., and Tu, J., (2020). A PMV-based HVAC control strategy for office rooms subjected to solar radiation. *Building and Environment*, 177: p. 106863.
11. Sharmin, T., Steemers, K., and Humphreys, M., (2019). Outdoor thermal comfort and summer PET range: A field study in tropical city Dhaka. *Energy and Buildings*, 198: p. 149-159.
12. Krüger, E.L., Silva, T.J.V., da Silveira Hirashima, S.Q., da Cunha, E.G., and Rosa, L.A., (2020). Calibrating UTCI'S comfort assessment scale for three Brazilian cities with different climatic conditions. *International Journal of Biometeorology*, Article in Press.
13. Li, J., Niu, J., Mak, C.M., Huang, T., and Xie, Y., (2020). Exploration of applicability of UTCI and thermally comfortable sun and wind conditions outdoors in a subtropical city of Hong Kong. *Sustainable Cities and Society*, 52: p. 101793.

Integrating landscape tactics into building energy performance evaluation based on urban morphometry

ULRIKE PASSE¹, HOSSEIN ENTEZARI², VICTORIA GOETZ², MIRA ENGLER²

¹Department of Architecture, Iowa State University, Ames, Iowa, USA

²Department of Landscape Architecture, Iowa State University, Ames, Iowa, USA

This paper presents a comparative analysis of urban landscape strategies to reduce building energy consumption to urban energy simulations for two climate zones in the US: Hot and dry Phoenix, Arizona and warm and humid, yet heating dominated Des Moines Iowa. Spatial strategies for high, medium and low density urban spatial typologies were tested to improve urban microclimate for buildings and surrounding environments. Other variables were window to wall ratio In the heating dominated climate of Iowa with about 6500 heating degree days, vegetative coverings are only effective for the warm summer months most effective with larger window to wall ratios. In the hot and arid climate of Arizona, the vegetative covering are effective across the whole year.

KEYWORDS: Microclimate, Vegetative Covering, Landscape strategies, Urban Energy Modeling

1. INTRODUCTION

This paper presents landscape strategies and spatial design guidelines for medium density urban and spatial typologies to improve urban microclimate for buildings and surrounding environments. The likelihood of extreme heat events is predicted to increase in the Midwest region of the US. This trend is exacerbated by the heat storage capacity of the dense built environment of urban area (urban heat island effect); and the fact, that many residences in low-income neighbourhoods do not have central air-conditioning systems (e.g., up to 50% of low-income homes in the study area). Vegetation can mitigate these effects by reducing reflected radiation, reducing surface heat fluxes, and increasing evapotranspiration. Efforts to integrate these effects in combined building-microclimate energy models have only recently been attempted, for example Kubilay et al., (2019) and Taleghani et al. (2016), [1, 2]. This project will add a design workflow to integrate climatic impact of landscape strategies into building energy modelling.

2. BACKGROUND AND RECENT LITERATURE

Current literature into natural ventilation and computational fluid dynamics (CFD) [3] and urban microclimate such as Erell and Pearlmutter (2011) [4] provided the basis for this investigation. The project proposed here is based on a multi-year effort to expand the microclimate and urban heat island modelling capacity of urban energy modelling tools as a collaboration between Architecture, Landscape Architecture, Urban Ecology, Data Science and Computational Fluid Dynamics to develop a workflow

for an urban energy model of a mid-size city in the Midwest of the USA integrating impact of trees and vegetation. Furthermore, landscape tactics as highlighted by Margolis and Robinson (2007) [5] provided the basis for this investigation into landscape-based regenerative strategies for urban climate mitigation. Remote-sensed satellite-derived urban surface temperatures for Urban Heat Island (UHI) prediction can be integrated as well as future typical meteorological year data sets (FTMY) to integrate climate change predictions into building energy simulations [6, 7]. The project uses the capacities of DIVA for Rhino [8] and the urban modelling interface (*umi*) developed at MIT [9] to improve heat flux prediction onto the building envelope for energy modelling [10]. This method will integrate qualitative landscape features, tactics and components in the urban landscape such as vertical garden membranes, green roofs, and other built surface considerations with thermal building and near-building environment data (surface temperature, vegetation, evapotranspiration) to construct a probabilistic model that predicts thermal fluxes on the building envelope.

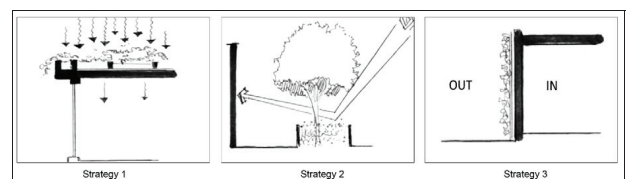


Figure 1: Landscape strategies. Strategy 1: Roof; Strategy 2: shade trees; Strategy 3: Green surface

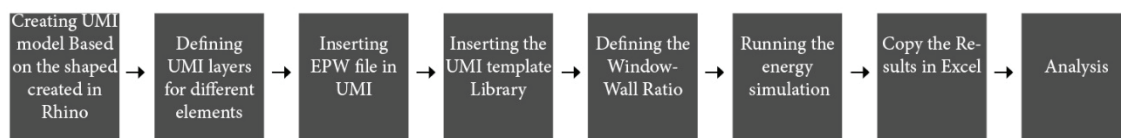


Figure 2: Workflow overview for simulation scenarios

2. METHODOLOGY

Spatial density as the proportion of the width and height of the street canyon is a known metric for urban climatology called urban morphometry [3, 4], yet the integration of trees and vegetation is not fully developed when considering this metric for building energy performance. This project thus used urban energy modelling techniques to integrate the combined effects of vegetation on building heat fluxes by shading the buildings from solar radiation as shade and by reducing temperature through evapotranspiration (transfer radiation into latent heat) to develop landscape characteristics (Figure 2).

Landscape design guidelines for spatial densities and three different climatic locations were developed based on solar radiation exposure in the urban canyon spaces which enables connection to urban energy modelling enhancing urban design capacities.

First, the vegetative features were investigated in each landscape strategy using drawings and models, including consideration of location and seasonal and temporal scale. Then specific qualitative landscape features and tactics on and around the building (facades, roofs) such as trees, ground cover, vertical gardens, and other surface considerations were noted for each urban typology. While outdoor comfort and microclimate can already be conducted using the tool Envi-MET, this project provides a novel investigation into qualitative and quantitative landscape design strategies for building energy consumption as well as outdoor climate in the age of climate change. This project will contribute to the improvement of design prediction capabilities for integration of vegetation into building and urban energy models. Metrics then predict reduced energy use intensity (EUI) for each proposed strategy per urban classification in three climates (Midwest, Arizona, Florida) (Figure 1 and Figure 3):

- 1.High height - High density: High rise: Multi story tower blocks in dense urban surroundings.
- 2.Low Height - High Density: Residential: one or two stories single houses, small shops, warehouse, light industrial, few trees.
- 3.Medium Height and Density: Residential: two or three story large and closely spaced, semidetached and

row houses, less than 5 story; blocks of flats with open surroundings, shops, schools.

- 4.High height and Low density: Residential: Less than 6 story row and block buildings and major facilities

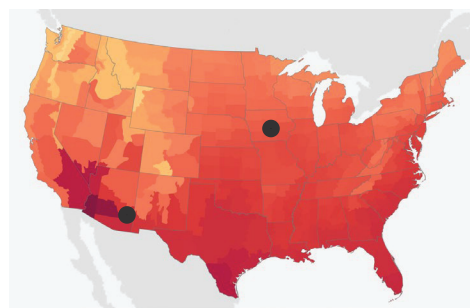


Figure 3: Map of the US with the two climate location (colors indicate altitudes (darker = lower))

Table 1: Overview of the simulation scenarios discussed here

Energy Simulation Scenarios		
Location: Des Moines, IA		
Scenario 1	Scenario 2	Scenario3
High Height, Low Density-Without Trees-40% Window to Wall Ratio	High Height, Low Density-With Trees-40% Window to Wall Ratio	High Height, Low Density-With Green Walls-40% Window to Wall Ratio
High Height, Low Density-Without Trees-50% Window to Wall Ratio	High Height, Low Density- With Trees-50% Window to Wall Ratio	High Height, Low Density- With Green Walls-50% Window to Wall Ratio
High Height, Low Density-Without Trees-60% Window to Wall Ratio	High Height, Low Density- With Trees-60% Window to Wall Ratio	High Height, Low Density With Green Walls-60% Window to Wall Ratio
High Height, Low Density-Without Trees-70% Window to Wall Ratio	High Height, Low Density- With Trees-70% Window to Wall Ratio	High Height, Low Density- With Green Walls-70% Window to Wall Ratio
High Height, Low Density-Without Trees-80% Window to Wall Ratio	High Height, Low Density- With Trees-80% Window to Wall Ratio	High Height, Low Density- With Green Walls-80% Window to Wall Ratio

Location: Phoenix, AZ		
Scenario 1	Scenario 2	Scenario3
High Height, Low Density-Without Trees-50% Window to Wall Ratio	High Height, Low Density- With Trees-50% Window to Wall Ratio	High Height, Low Density- With Green Walls-50% Window to Wall Ratio

3. SIMULATION SCENARIOS

For the comparative simulation scenarios for this paper, two climates were selected: Hot and dry Phoenix, Arizona and heating dominated Des Moines, Iowa with warm and humid summer as noted in Table 1. In the first set of simulations, a city block with an area around 78,000 m² was modelled for the climate of Des Moines, Iowa for high-height, high density (Figure 4). In the second set of simulations, high height – low density was computed for Des Moines using the same parameter as in Set 1. This scenario was selected as it is most receptive to all three selected scenarios (Figure 5).

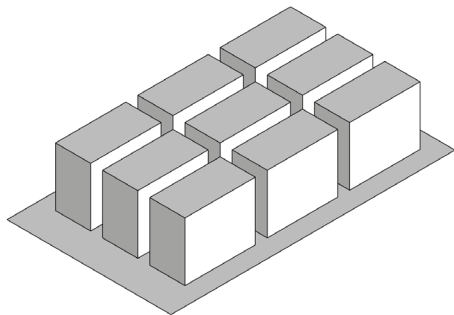


Figure 4: Modeling scenario for High-Height – High Density

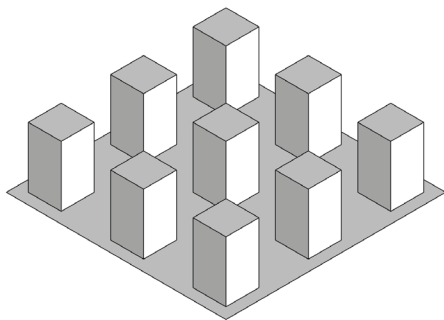


Figure 5: Modeling scenario for High-Height –Low Density

The model includes nine buildings and the related street canyons. EnergyPlus weather data for the location was uploaded in the software. The geometric shapes of buildings, trees, and living surfaces were created according to their real dimension such as building height and width, tree trunk and canopy) and then the appropriate software layers for various site elements were chosen. A typical individual tree was created to represent the structures of the species (*Amelanchier arborea* or *Acer palmatum*) in the site

including the total height, trunk height, canopy width, and canopy height. To evaluate the heat reduction and energy saving effect of both trees and living surfaces, a scenario of “bare ground” was created, which is devoid of any vegetation or natural elements. In addition, a scenario with trees around the buildings, and another one with green surfaces on/above buildings were modeled to determine the cooling effect of these natural features. The rectangular surfaces represented living walls and green roofs. The buildings’ façades and the green surfaces are the same size in the model (Green walls are 22×12 m² and green roofs are 12×12 m²). The green surfaces were attached to the building’s facades and roof with a short distance of 60 cm. In order to separate them from the buildings in the energy simulations modeling, SHADING was selected for them as the material. Additionally, in each scenario for Des Moines, Iowa, the window-wall ratio was adjusted from 40% to 80% to include the impact of building opening on its energy performance.

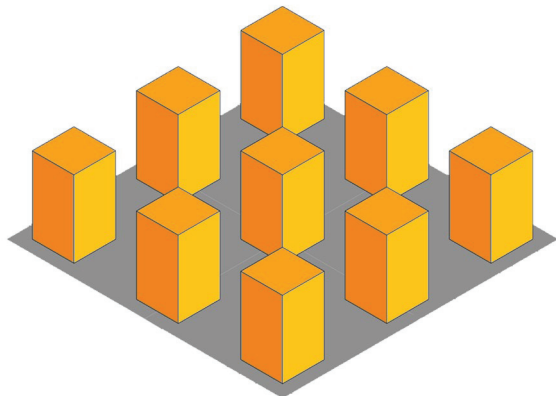


Figure 6: Scenario 1: High-Rise | Low-Density | No Trees

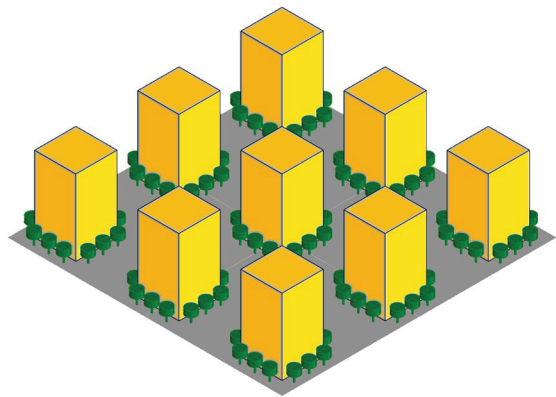


Figure 7: Scenario 2: High-Rise | Low-Density | With Trees

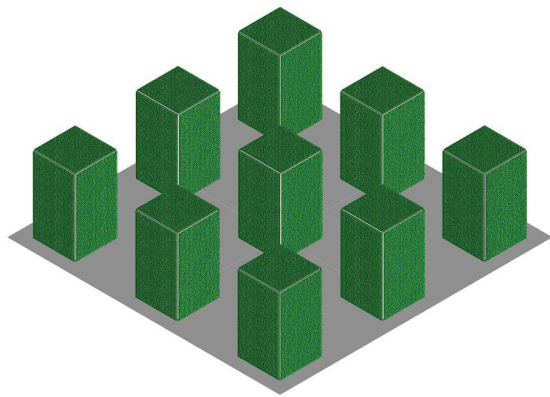


Figure 8: Scenario 3: High-Rise | Low-Density | Vegetative Surfaces

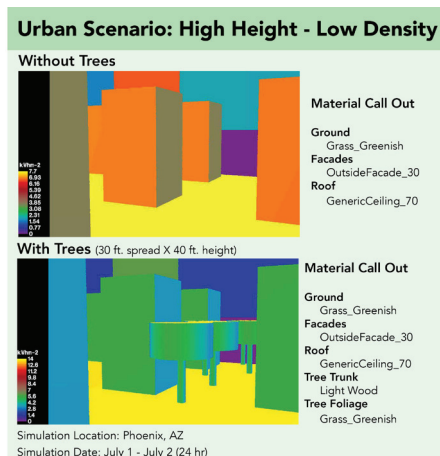


Figure 9: Exposure to solar radiation high height, low density, Phoenix AZ with and without landscape tactics

Urban Scenario: High Height - Low Density

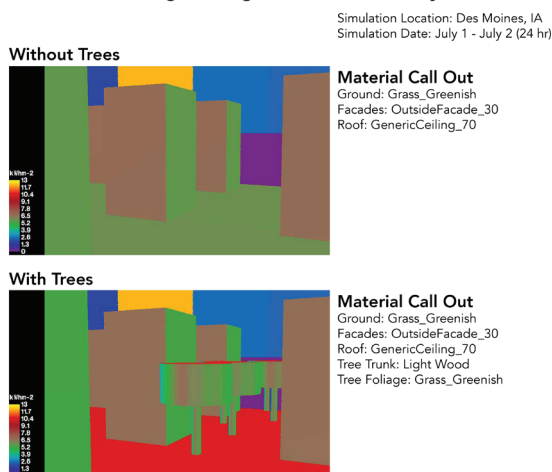


Figure 10: Exposure to solar radiation high height, low density Des Moines, IA, with and without landscape tactics

In the third set of simulations high height- low density urban morphometry was simulated for Phoenix, Arizona. For the Phoenix, Arizona scenarios, 50% window to wall ratio was selected. The results of the models illustrate the energy consumption for each building and the overall amount. The colours in the simulation scenarios in Figures 6 to 8 relate to the colours in Figures 11 to 12.

Based on the climatic data for the selected locations, the plant hardiness map was consulted and a design guide for of plant prepared. A selection is presented in Table 2 based on the three planting strategies noted in Figure 1.

Table 2: Exemplary selection of planting suggestion for the USDA planting zone 4 and the three planting scenarios (Fig. 1)

Green Roof	Miscanthus or Maiden Grass	Miscanthus sinensis cultivars
	Switchgrass	Panicum virgatum
Shade Trees	Hedge Maple	Acer campestre
	Lacebark Elm	Ulmus parvifolia
Vegetative Walls	Sweet Autumn Clematis	Clematis paniculata
	Baltic English Ivy	Hedera helix 'Baltica'

4.COMPARATIVE RESULTS

Once all simulations for Des Moines Iowa and Arizona were completed, comparative charts were created. Figure 12 on the next page shows the overall results for Des Moines, IA for the warm season June to August differentiated by window to wall ratio. Taken the barren built form as the baseline, the decrease in energy consumption with trees is between 2 to 3 %, but with complete vegetative covering on all five sides, a 41 to 45%, with the highest reduction of 41% related to the highest window to wall ratio (80%) during cooling season. In the heating dominated climate of Iowa with about 6500 heating degree days, vegetative coverings are only effective for the warm summer months, as noted in Figure 12. On the contrary in the hot and arid climate of Arizona, the vegetative covering of all five sides of the building has an effect across the whole year as can be noted in Figures 13 and 14. The simulations also indicate, that vegetative walls and roofs have the most impact with larger window to wall ratios.

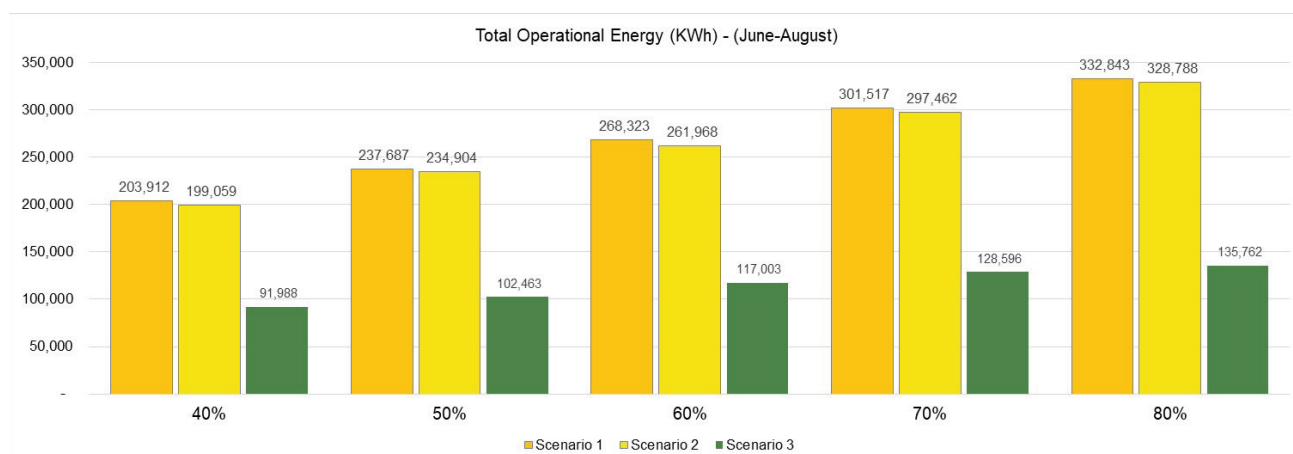


Figure 11: Simulation results in umi for the warm season (June to August) in Des Moines, Iowa

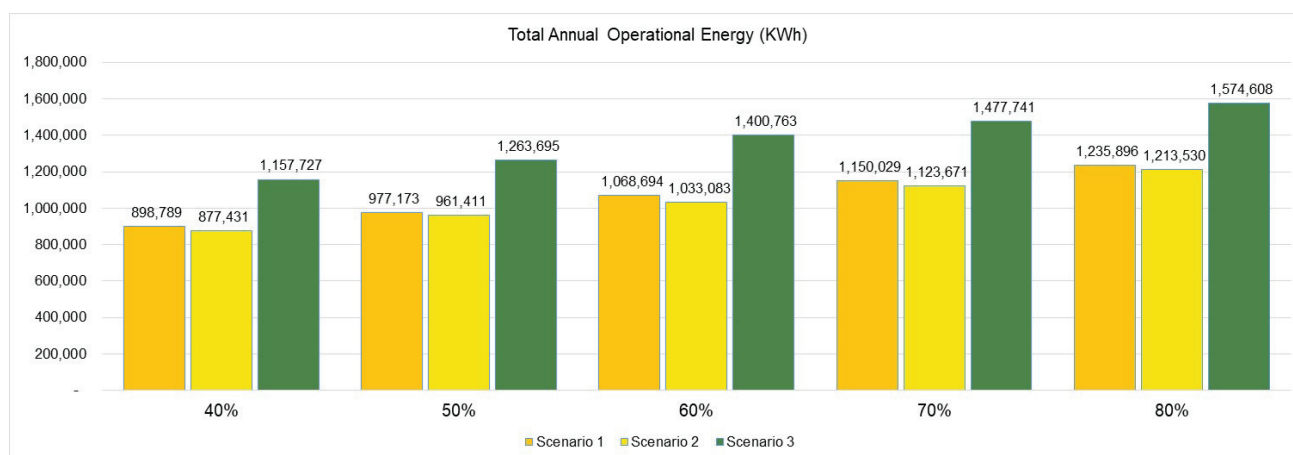


Figure 12: Simulation results in umi for the full year in Des Moines, Iowa

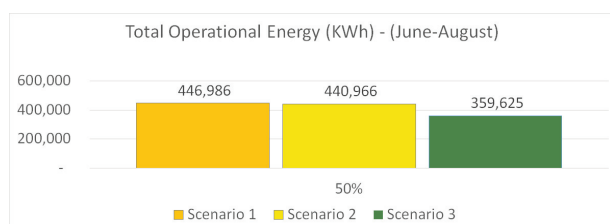


Figure 13: Simulation results in umi for the warm season June to August in Phoenix, Arizona

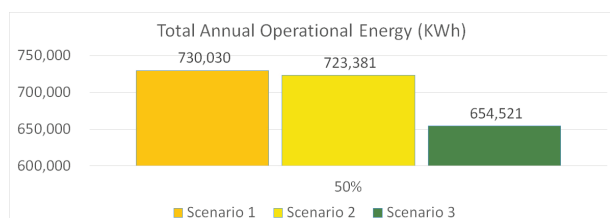


Figure 14: Simulation results in umi for the full year

5. RECOMMENDATION AND FUTURE WORK

The results derived from the presented simulations indicate an important relationship between urban morphometry, vegetative strategies and climate. It has also been noted, that measured data is not readily available. Therefore the research team will utilize a custom designed versatile Mobile Diagnostic Lab (MDL) designed for a variety of building energy research applications. It is composed of an 8'(W) × 10'(L) × 9'(H) experimental cabin and an attached mechanical room on a 19' long trailer with air suspension (Figures 15, 16). The MDL envelope is airtight, and part of the wall section is exchangeable. It houses a programmable HVAC system, and an expandable data acquisition system (DAS). The DAS can collect data at different frequencies with multiple sensors. Currently, about 250 data measurement points are able to collect data on interior air temperature and humidity, surface temperature and heat flux inside and outside the experiment cabin, power generation, and consumption.



Figure 15: Experimental set-up of the MDL testing climatic impact of vegetative covering



Figure 16: Experimental set-up of the MDL testing climatic impact of a green roof.

The research capacities of the MDL enable study of diverse heat transfer paths through building assemblies, heat transfer between building surfaces and surrounding microclimate, baseline energy consumption for different climates, and CFD models for natural ventilation and passive heating. A heat flux sensor will measure the impact of vegetative coverings on heat flux on the building enclosure first in Iowa, then next summer in Arizona.

6. CONCLUSION

The impacts or improvements expected from this research for regenerative and sustainable design are manifold. Considering three distinctly different urban typologies, densities, and climates this project made progress towards linking 'natural infrastructure' to building energy efficiency. This research has moved forward by developing a landscape design matrix that can be applied to four selected urban density scenarios in three climate related cities. By using climate data, assigning materiality and pinpointing nodes within DIVA and *umi* for Rhino, this study related landscape interventions to surface radiation and natural ventilation techniques. This project will contribute to the improvement of design prediction capabilities for integration of vegetation into building and urban energy models. Metrics will predict reduced energy use intensity (EUI) for each proposed strategy per urban morphometry classification.

REFERENCES

1. Kubilay, A., D. Derome, J. Carmeliet, (2019) Impact of evaporative cooling due to wetting of urban materials on local

thermal comfort in a street canyon, Sustainable Cities and Society, Volume 49, 2019, 101574, ISSN 2210-6707, <https://doi.org/10.1016/j.scs.2019.101574>

2. Taleghani, M., Sailor, D., & Ban-Weiss, G.A. (2016). Micrometeorological simulations to predict the impacts of heat mitigation strategies on pedestrian thermal comfort in a Los Angeles neighborhood, *Environ. Res. Lett.* Vol. 11, doi: 10.1088/1748-9326/11/2/024003
3. Passe, U., Battaglia, F. (2015). *Designing spaces for natural ventilation: An architect's guide*. London, New York: Routledge, Taylor and Francis.
4. Errell, E., Pearlmutter, D., & Williamson, T. (2015). *Urban microclimate: Designing the spaces between buildings*.
5. Margolis, L., & Robinson, A. (2007). *Living systems: Innovative materials and technologies for landscape architecture*. Basel: Birkhäuser.
6. Rabideau, S. L., Passe, U., & Takle, E. S. (2012). Exploring alternatives to the "typical meteorological year" for incorporating climate change into building design. *ASHRAE transactions*, 118(1), 384-391.
7. Kalvelage, K., Passe, U., Rabideau, S., & Takle, E. S. (2014). Changing climate: The effects on energy demand and human comfort. *Energy and Buildings*, 76(0), 373-380. doi: 10.1016/j.enbuild.2014.03.009
8. McNeel (2019) Rhinoceros v6, <https://www.rhino3d.com/>
9. Reinhart, C., Dogan, T., Jakubiec, J. A., Rakha, T., & Sang, A. (2013). Umi-an urban simulation environment for building energy use, daylighting and walkability. 13th Conference of International Building Performance Simulation Association, Chambéry, France.
10. Hashemi, F., Marmur, B. Thompson, J., Passe, U., (2018) Developing a Workflow to Integrate Tree Inventory Data into Urban Energy Models, *Proceedings of the 2018 Simulation in Architecture and Urban Design Conference, SimAUD 2018*, June 05-07 at TU Delft, the Netherlands. Society for Modeling & Simulation International.

Disruptive technologies on mobility raising new opportunities for urban design

MELISSA BELATO FORTES¹, MARCELO EDUARDO GIACAGLIA², DENISE HELENA SILVA DUARTE³

^{1, 2, 3} University of São Paulo, São Paulo, Brazil

ABSTRACT: *The subject of this research is the impact of disruptive technologies on mobility, mainly due to driverless vehicles and shared mobility. The objective is to investigate changes in urban design resulting from possible changes in road infrastructure. The method includes analysis of secondary data in the literature and in different databases, as well as propositions for the future scenario and its consequent impacts on urban design. The changes in road infrastructure (lanes and on-street parking) for the city of Sao Paulo, Brazil, were also quantified, between 15% and 25%, based on parameters and indicators selected from different urban contexts. With the urban design proposals applied in a central district in the city of Sao Paulo, it was found that the alteration of the road infrastructure validates the quantification carried out and demonstrates the potential to transform the existing urban design in favor of the qualification of public spaces and a more sustainable urban mobility.*

KEYWORDS: *Urban mobility, Driverless vehicle, Shared mobility, Road infrastructure, Urban mobility*

1. INTRODUCTION

There is significant speculation about how technologies, especially driverless cars and shared mobility, will be adopted and introduced in cities [1, 2]. There has been also disagreement regarding the impacts of such changes to the urban environment, thus the difficulty in making recommendations for the future [2, 3].

Approaches to technologies have focused mainly on technical aspects, such as algorithms for their operation, predictability and efficiency, so far there is a lack of studies on impacts on the urban environment.

However, some authors [2, 3] mention that this is a unique opportunity to rethink the city. This is because of the potential for reclaiming space from roads, including on-street parking.

This process is promising after a century of automobile-oriented transport policy, which has left a legacy in urban design focused on prioritizing road infrastructure, where pedestrians have often been neglected. As a result, public spaces, including sidewalks, have been reduced, road widths widened to accommodate vehicles, and pedestrian movement has become difficult and dangerous [4].

The arrival of driverless vehicles, alongside other initiatives or trends, such as travel sharing and a greater connection of people with modes of transport, will impact vehicle ownership, parking demand, and, consequently, urban space. This should culminate in less congestion, lower environmental impact, since new cars without motorization are powered by electric and silent engines [5, 6, 7].

Some authors mention that the effect of affordable travel sharing services, especially driverless vehicles will improve mobility and thus increase, instead of decrease road traffic. Other points identified as unfavorable are: 1) extinction of job types, such as drivers, or loss of jobs, e.g., in the automobile manufacturing and service industries; 2) favoring urban sprawl [8, 9, 10].

There are indications that innovative planning is capable of reversing problems into opportunities, in which the cost or lack of accessibility to transportation are considered the greatest barriers for people who do not drive, as well as for those people with physical, age or motor limitations. Driverless vehicles have the potential to provide access to employment, education, health and leisure, in an urban environment with fewer traffic accidents and less pollution.

Nowadays, the prospect of a widespread shift to driverless and shared mobility is heading in the same direction as unprecedented progress towards more sustainable urban mobility, as the way forward for the city's attractiveness and better quality of life in the urban realm.

2. QUANTIFICATION OF CHANGES IN ROAD INFRASTRUCTURE

In order to qualify and quantify the alterations of the road infrastructure to be used in the design scenarios, the following parameters were used: 1) the variation of the distance traveled; 2) the reduction in the number of vehicles in use; and 3) the alteration of the road infrastructure.

As for the “distance variation” parameter, most of the previous studies estimate its increase, which is expected since it can be caused by the convenience and cost-benefit associated with the use of driverless vehicles on shared and individual trips. However, even in the studies that estimate this increase, there is a considerable difference in the estimates, which vary between 6% and 35%, which may be related to the particularity of each urban context addressed by the literature [1, 5, 11, 12, 13, 14].

Regarding the parameter “reduction in the number of vehicles in use”, the majority of the researched studies show an oscillation in the percentage of reduction between 80% and 90% of private vehicles. This consensus among studies may be related to the expected performance of driverless vehicles, as well as the acceptance by people of the new model of shared mobility [5, 11, 15, 16, 17, 18, 19].

Regarding the parameter “alteration of the road infrastructure”, earlier studies found that between 12% to 20% of the space can be made available for other uses, mainly due to the reduction of street parking spaces, showing that. On-street parking should be eliminated or partially converted in pick up and drop off areas [5, 20, 21, 22].

3. MAIN EXISTING APPROACHES TO TECHNOLOGY IMPACTS ON THE URBAN ENVIRONMENT

Some authors [2, 23] provide guidelines, albeit incipient, about changes in the urban environment resulting from mobility technologies. Among the main ones are those related to: 1) road lane width reductions due to the tendency of intermodal use of travel and the use of a vehicle without a shared driver. These trends may lead to a reduction in the number of vehicles circulating, resulting in less road infrastructure; 2) on-street parking reduction or elimination, as the driverless vehicles will be constantly in circulation, especially during periods of high demand, reducing the need for parking closed to an owner.

Therefore, it is expected that new technologies in mobility can provide a new approach to urban design. One of the expected effects is the conversion of the released areas into other uses, such as for urban green and living spaces for pedestrians and cyclists.

4. METHOD

Recent work being produced by leading research centers such as the Massachusetts Institute of Technology (MIT), as well as the initiatives of, Bloomberg Philanthropies, and researchers addressing urban redesign guidelines combined with new technologies have been systematized [2, 23, 24].

The research continues with: 1) the selection of the urban context and the area of intervention; 2) the

analysis of parameters and indicators from different urban contexts; 3) the estimate of the alterations of the road infrastructure for the city of Sao Paulo; 4) the assessment of the intervention area; 5) the verification of results against initial estimates based on previous studies; and 6) the elaboration of the design scenarios for the road infrastructure resulting from disruptive technologies.

4.1 Criteria for the selection of the urban context and the intervention area

Mobility innovations become more favorable in large cities, where, in addition to conventional car traveling, it is possible to use a bicycle or other vehicle as a service and share trips.

In order to find a suitable real urban context in the city of Sao Paulo for testing the future scenario, data from densely occupied downtown areas, some of them under renovation, were initially raised. Busy and well-connected areas like this tends to benefit more from driverless vehicles and efficient mobility, in order to improve travel and commuting.

Central districts are crossed by main axes of the city, as road arteries, bus corridors, and subway lines, with the possibility of increasing and qualifying the different public transport systems, in order to articulate to non-motorized modes and to new mobility technologies.

4.2 Analysis of mobility parameters and indicators from different urban contexts

Indicators were chosen for each parameter:

1) for the “variation of the distance traveled”, the indicators are: number of trips per inhabitant, average travel distance, average travel time and population density. These indicators are intended to reveal how consolidated the city is in relation to urban mobility, point out the level of complexity for the adoption of shared driverless vehicles and express the feasibility of introducing shared mobility;

2) for the “reduction in the number of vehicles in use”, the indicators are: number of usage hours of the private vehicle per day, percentage of trips in a private vehicle, motorization rate, population and population density. These indicators exhibit impact on reducing the number of vehicles in use, reveal the potential for reducing travel by private vehicle, impact on vehicle ownership, underpin the distinction between medium, large and megacities and also express the feasibility of introducing shared mobility;

3) for the parameter “alteration of the road infrastructure”, the indicators are: percentage of reduction of private vehicles in use, percentage of the on-street parking area, percentage of the road infrastructure area and variation of the distance traveled. These indicators express the road space

needed and reveal the potential for its conversion to other uses.

4.3 Estimated change in road infrastructure for the city of Sao Paulo

To pose this estimate, the percentage study mentioned in item 2 was adopted, making it possible to adjust the parameters and indicators in relation to the different urban contexts. Among the reference studies, one can find Austin, Berlin, Lisbon, London, New York and Singapore [1, 5, 11, 12, 13, 14, 15, 16, 17, 18, 19, 20, 21, 22].

Considering the changes in road infrastructure (lanes and on-street parking) based on the results expected for other cities, it was estimated that the city of Sao Paulo may have an interval between 15% and 25%, due to the fact that the city has median percentages of road private vehicles in use and also in the area of road infrastructure, in addition to the high estimate of the variation in the distance traveled.

4.4 Assessment of the intervention area

All the roads in the intervention area were measured in order to obtain data regarding the weakness and qualities of the area to support the proposals for the future scenarios.

The potential for altering road infrastructure to be converted into other uses was verified, in order to propose an urban redesign.

4.5 Verification if the changes in the road infrastructure obtained in the surveys validate the initial estimate

It was estimated, based on previous studies [1, 5, 21], a 15% to 25% change in use of the road infrastructure.

With the urban redesign proposals for the intervention area, it was possible to obtain the following percentages of alteration of the road infrastructure: 17.5% of the on-street parking area and 5.3% of the vehicle circulation area, totaling 22.8%.

4.6 Elaboration of urban design scenarios

The analysis intervention area encompassed 294 roads of the selected central districts of the city of Sao Paulo, as show in Figure 1; all of them were mapped including road lanes, street parking, pedestrian paths, cycle routes, urban vegetation and the public transport system.

This information supported the propositions, making it possible to analyze the alterations in road infrastructure, revealing how much area is possible to convert into other uses, circa 22.8%, revealing the potential for transformation, with an increase of 45% in sidewalks' width and of 500% percent in bicycle lanes' extension.

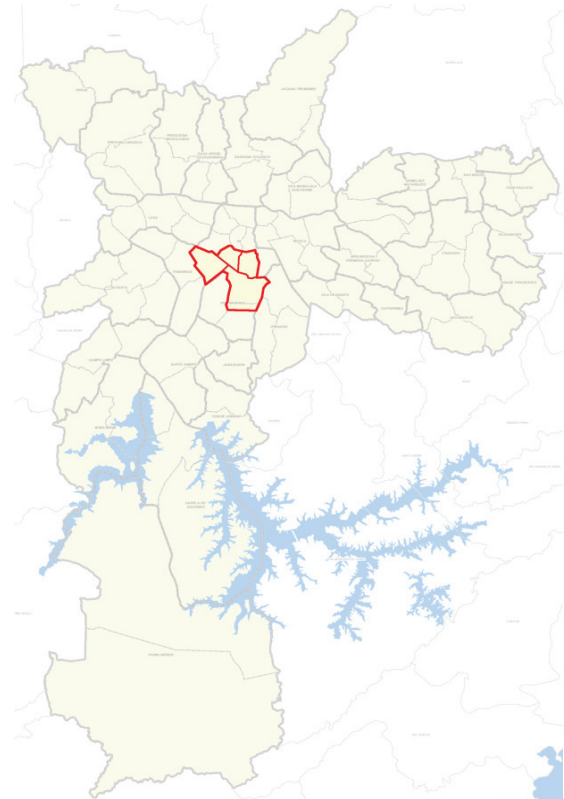


Figure 1: City map of Sao Paulo municipality with selected districts outlined in red.

It should be noted that the 294 streets were classified, as: 1) expressways, with no at-grade intersections or pedestrian crossings and no direct access to plots; 2) arterial roads, with controlled intersections and pedestrian crossings and the possibility of direct access to plots, connecting different city regions; 3) collector roads, collecting and distributing traffic entering or exiting from expressways or arterial roads, into city regions; 4) local roads, with uncontrolled intersections and crossings, for local or restricted access.

Of these, 17 roads were selected for detailed analysis, because of their representativeness in each class and of diversity of opportunities for redesign, such as increased vegetation, pedestrian circulation, on-street parking, number of lanes, including mass transit and bicycle and proximity to rail station. Figure 2 exhibit comparative cross sections for the existing conditions, intervention plan and final state.

This selection was important, not only for testing urban intervention proposals, but also to assure that the same can be done, or quickly estimated without the need for detailed analysis (São Paulo has tens of thousands of streets), for any road of the same class and features, within the study area, the city, or any other city, where the priority order is: pedestrian, bicycle, public transport, driverless vehicles, with planned transitional equipment along its border for the gradual abandonment of conventional vehicles.

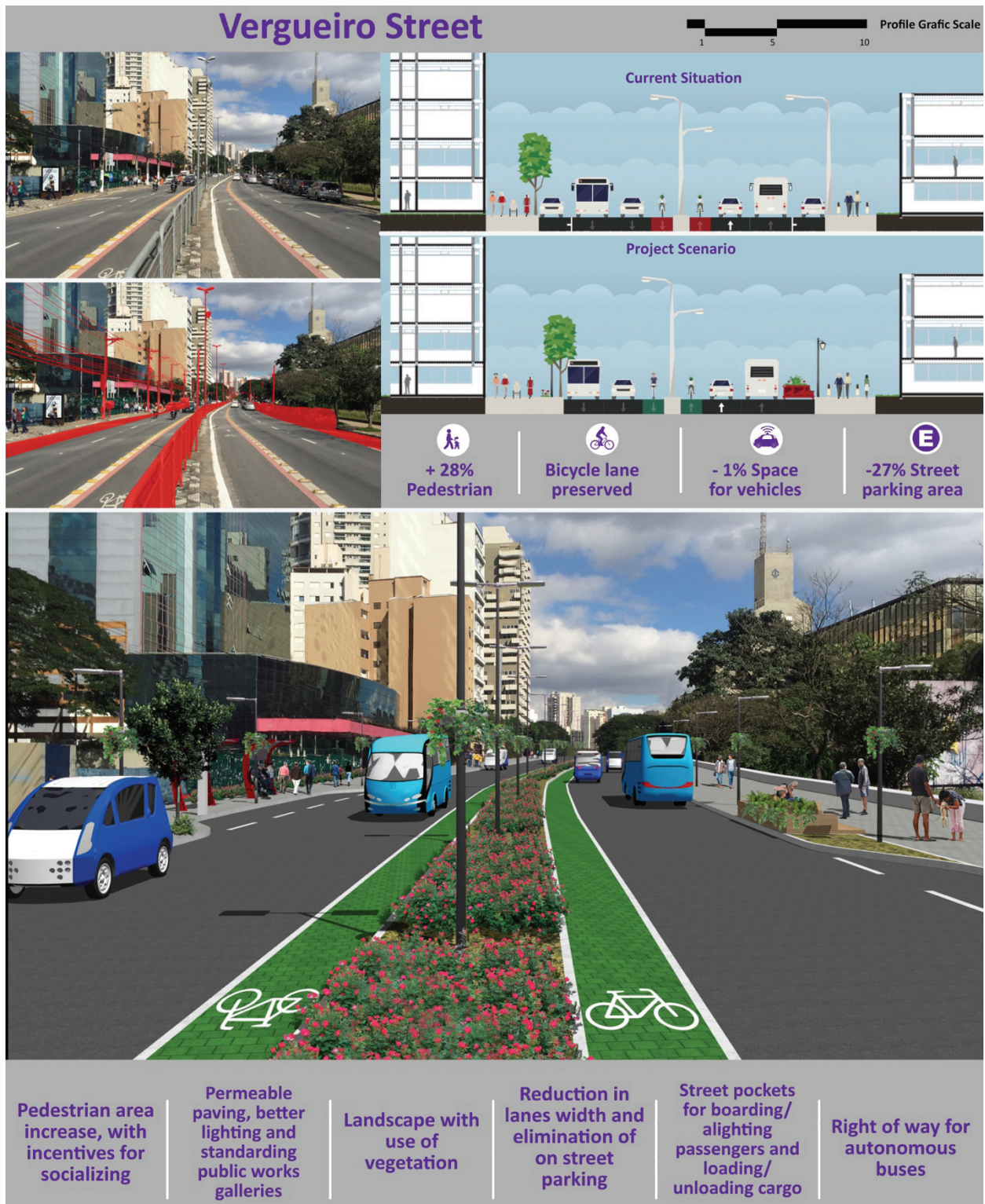


Figure 2: Current situation (top), project scenario (middle), and final design (bottom) example in the intervention area.

The study focused on a scenario where driverless and conventional vehicles do not run aside, although, in the expanding borders, they can use the same part of road, but not at the same time. This was assessed in longitudinal designs on selected roads, were signaling and other devices for such segregation can be installed and operated at reasonable costs [25].

Figure 3 exhibit a longitudinal section, where it is proposed that traffic on Vergueiro Street be allowed

for conventional vehicles and for vehicles driverless, in a segregated way, with separate lanes. Vergueiro Street already has underground parking with access to a Metro station, which was selected to be the hub, promoting a modal transfer. In addition, this hub will have spaces for vehicle charging, as well as a maintenance area and spaces for vehicles without driver.



Figure 3: Proposal for the road system of Rua Vergueiro, Rua Domingos de Moraes and surroundings.

5. OPPORTUNITIES FOR THE POST-COVID SCENARIO

In the past few months, much of the world has suddenly stopped, due to recommendations for people to stay home in response to the COVID-19 pandemic. Cities worldwide have experienced a significant reduction in circulation, oftentimes the retreat or end of congestion in transport systems.

From the second week of March until August first week, the city of Sao Paulo had a 77% reduction in circulation [26].

Whilst hoping to pass safely through the pandemic this crisis is undoubtedly an opportunity to rethink the habits of urban mobility.

To improve social distancing, some cities - Oakland and Boston to Minneapolis, in the United States and Milan, Italy - announced the expansion of their sidewalks, in order to temporarily block the road and street parking, as COVID-19 restrictions were lifted [27, 28, 29].

Because of the reduction in circulation, communities around the world are experiencing reduced air pollution. City planners have an opportunity to foresee the benefits of the changes, that could be permanent, provided the adequate shifts in infrastructure, services and urban design are made.

Public transport is facing its post-COVID challenges related to health and personal well-being, which can be addressed through best cleaning. Also, a concern, before Covid-19, the discussion regarding

the required hygiene and actions for ensuring it, in shared vehicles (driverless or not), requires added attention.

6. CONCLUSION

The propositions demonstrate the potential of the transformation of the current urban design in favor of more sustainable urban mobility, with the conversion of areas released by road infrastructure (lanes and on-street parking) to other uses, prioritizing pedestrians and cyclists and qualifying public spaces.

Besides road infrastructure, other hidden spaces for cars in parking lots and building garages can be explored and converted to urban amenities.

Through detailed street-by-street analysis, carried out in this assessment, the calculated 22.8% shift in road infrastructure use, validates the original estimate, from 15 to 25% for the city of Sao Paulo.

It can be inferred that the procedures applied for area calculations in the intervention area can be applied to other roads in each category. Such analysis could be extended to other areas of the city and, depending on the local context, to other cities.

Therefore, this work contributes to urban studies, especially but not restricted to large metropolitan areas, with the aim to consider the incorporation of disruptive technologies in mobility seeking opportunities for urban redesign.

ACKNOWLEDGEMENTS

This work was partially financed by FAPESP (Grant #2016/02825-5) and CNPq (Productivity Grant #309669/2015-4).

REFERENCES

1. Fagnant, D. J. and Kockelman, K. M., (2015). Preparing a nation for autonomous vehicles: opportunities, barriers and policy recommendations. *Transportation Research Part A: Policy and Practice*, v. 77, p. 167-181.
2. Schlossberg, M. et al., (2018). Rethinking the street in an era of driverless cars. <https://doi.org/10.13140/RG.2.2.29462.04162>.
3. Guerra, E., (2016). Planning for cars that drive themselves: metropolitan planning organizations, regional transportation plans, and autonomous vehicles. *Journal of Planning Education and Research*, v. 36, p. 210-224.
4. Gehl, J., (2013). Cidades para pessoas. São Paulo: Perspectiva.
5. The Organisation For Economic Co-Operation and Development – OECD; International Transport Forum – ITF, (2015). Urban mobility system upgrade: How shared self-driving cars could change city traffic, International Transport Forum Policy Papers, n. 6, OECD Publishing, Paris. <https://doi.org/10.1787/5jlwvzdk29g5-en>.
6. Staples, R., (2016). Driver(less) is more, [Online], Available: <http://www.iaacblog.com/programs/driverless-is-more/> [06 January 2016].
7. Ratti, C., (2017). Digital tools for the city of the future. ARQ (Santiago), n. 96, p. 48-51. <https://doi.org/10.4067/S0717-69962017000200048>.
8. Litman, T., (2018). Autonomous vehicle implementation predictions: implications for transport planning, [Online], Available: <https://www.vtpi.org/avip.pdf> [15 May 2018].
9. Arbib, J.; Seba, T., (2017). Rethinking transportation 2020-2030: the disruption of transportation and the collapse of the internal-combustion vehicle and oil industries, [Online], Available: <http://bit.ly/2pL0cZV> [05 March 2018].
10. Kockelman, K. et al., (2016). Implications of connected and automated vehicles on the safety and operations of roadway networks: a final report. Texas: The University of Texas at Austin, [Online], Available: <https://library.ctr.utexas.edu/ctr-publications/0-6849-1.pdf> [07 November 2017].
11. Massachusetts Institute Of Technology – MIT, (2014). HubCab, [Online], Available: <http://hubcab.org/#13.00/40.7219/-73.9484> [03 January 2019].
12. Fagnant, D. J.; Kockelman, K. M.; Bansal, P., (2015). Operations of Shared Autonomous Vehicle Fleet for Austin. *Transportation Research Record: Journal of the Transportation Research Board*, v. 2536, p. 98-106.
13. Chen, T. D., (2015). Management of a shared, autonomous, electric vehicle fleet: vehicle choice, charging infrastructure & pricing strategies. Dissertation - University of Texas at Austin, Austin.
14. Bierstedt, J. et al., (2014). Effects of next-generation vehicles on travel demand and highway capacity, [Online], Available: http://www.fehrandpeers.com/wp-content/uploads/2015/07/FP_Think_Next_Gen_Vehicle_WHITE_Paper_FINAL.pdf [06 August 2017].
15. Spieser, K. et al., (2014). Toward a systematic approach to the design and evaluation of automated mobility-on-demand systems: a case study in Singapore. In: MEYER, G.; BEIKER, S. (ed.). Road vehicle automation. Lecture notes in mobility. Springer International Publishing, p. 229-245.
16. Liu, J. et al., (2017). Tracking a system of shared autonomous vehicles across the Austin, Texas network using agent-based simulation. *Transportation*, v. 44, p. 1261-1278.
17. Boesch, P. M.; Ciari, F.; Axhausen, K. W., (2015). Autonomous vehicle fleet sizes required to serve different levels of demand. *Transportation Research Record*, v. 2542, p.111-119.
18. Bischoff, J.; Maciejewski, M., (2016). Simulation of city-wide replacement of private cars with autonomous taxis in Berlin. *Procedia Computer Science*, v. 83, p. 237-244.
19. Fagnant, D. J.; Kockelman, K. M., (2016). Dynamic ride-sharing and fleet sizing for a system of shared autonomous vehicles in Austin, Texas. *Transportation*, v. 45, p. 1-16.
20. Ambühl, L.; Ciari, F.; Menendez, M., (2016). What about space? A simulation-based assessment of AVs impact on road space in urban áreas. In: *16th Swiss Transport Research Conference*, 2016, Ascona.
21. WSP; Farrelis, (2016). Making better places: autonomous vehicles and future opportunities, [Online], Available: <http://www.wsp-pb.com/Global/UK/WSPPB-Farrelis-AV-whitepaper.pdf> [09 August 2017].
22. Zhang, W. et al., (2015). Exploring the impact of shared autonomous vehicles on urban parking demand: an agent-based simulation approach. *Sustainable Cities and Society*, v. 19, p. 34-45.
23. National Association of City Transportation Officials – NACTO, (2017). Blueprint for autonomous urbanismo, [Online], Available: https://nacto.org/wp-content/uploads/2017/11/BAU_Mod1_raster-sm.pdf [15 June 2018].
24. Massachusetts Institute of Technology – MIT, (2015). MCity Test Facility, [Online], Available: <https://mcity.umich.edu/our-work/mcity-test-facility/> [10 April 2016].
25. Fortes, M. B. (2019). Tecnologias disruptivas e mobilidade urbana: inovações para o desenho das cidades. Doctoral Thesis, Faculdade de Arquitetura e Urbanismo, University of São Paulo. <https://doi.org/10.11606/T.16.2020.tde-04022020-175103>.
26. Citymapper Mobility Index, (2020). [Online], Available: <https://citymapper.com/CMI> [01 May 2020].
27. Rudick, R., (2020). Oakland Paves Way for Open Streets Everywhere, [Online], Available: <https://sf.streetsblog.org/2020/04/20/oakland-paves-way-for-open-streets/> [02 May 2020].
28. Diaz, J., (2020). Cities Close Streets to Cars, Opening Space for Social Distancing. The New York Times, [Online], Available: <https://www.nytimes.com/2020/04/11/us/coronavirus-street-closures.html> [02 May 2020].
29. Laker, L. (2020). Milan announces ambitious scheme to reduce car use after lockdown. The Guardian, [Online], Available: <https://www.theguardian.com/world/2020/apr/21/milan-seeks-to-prevent-post-crisis-return-of-traffic-pollution> [02 May 2020].

Characterising living wall microclimate modifications in sheltered urban conditions

findings from two monitored case studies

KANCHANE GUNAWARDENA¹ KOEN STEEMERS¹

¹The Martin Centre for Architectural and Urban Studies, Department of Architecture, University of Cambridge.

ABSTRACT: Green infrastructure enhancements are widely advocated to address heat-related risks in cities. The challenge of implementing enhancements in dense cities has necessitated the development of surface greening, with living walls having gained increased prominence in recent years. This paper considered such in-situ applications to quantify the extents of their influence on the microclimates of two sheltered urban conditions. The results highlight the potency of hygrothermal modifications to be most apparent within the immediate zone, while the disparity in influence between the two studies suggest that with increased shelter the hygrothermal influence is likely to be relatively weaker. Surface temperature monitoring results from the Indoor case study presented significant variation. While these were not potent enough to cause radiation asymmetry associated discomfort, thermal sensation and diversity to occupants is probable. These findings therefore highlight the necessity for designers to take account of this proximity influence, and in future designs to increase building occupant access to installations.

KEYWORDS: Urban greening, vertical greening, living walls, living wall monitoring, microclimate modification

1. INTRODUCTION

To address the call for developing passive climate resilience strategies, the project investigates the influence and effectiveness of utilising vertical greening for reducing energy loads of urban buildings and surrounding microclimates. By examining this green infrastructure focus, the project aims to improve urban built environments that would in turn lead to health and wellbeing enhancements of their ever-growing populations.

Although vertical greening includes the two principal approaches of 'green facades' and 'living walls', recent interest is directed at the latter [1–2]. The plants in such systems root into a substrate (natural or synthetic porous/fibrous media) carrying support-work that includes irrigation and fertigation supply. The greater prominence of living walls is attributed to their flourishing aesthetic appeal, with recent installations introduced to various building typologies, scales, and outdoor, semi-outdoor, and indoor conditions [2–4].

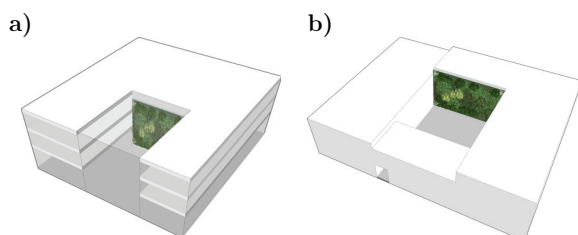


Figure 1. Diagrammatic representation of an installation in an indoor atrium (a); and a semi-outdoor courtyard (b).

The purpose of this conference paper is to present findings from monitoring campaigns carried out at two sheltered living wall (indoor and semi-outdoor) case studies that characterises their microclimate modifications (Figure 1). Key parameters monitored included soil, surface, and air temperature, as well as relative humidity.

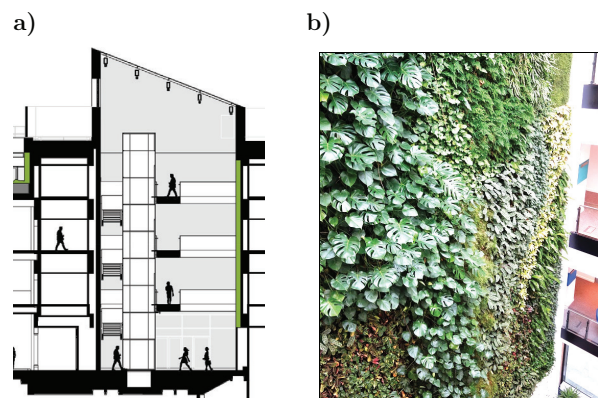


Figure 2. Extract from the building section showing the atrium (a); and the living wall in its current state (b).

1.1 Indoor atrium

Within urban buildings the general arrangement often includes a large atrium situated off the entrance. An example of such an atrium is located at a campus building in Cambridge, England (Cfb Köppen climate), where the northwest atrium surface is host to a flourishing three-storey living wall (Figure 2).

This installation is 13 m-high and 91 m² in coverage, with ~8,750 evergreen plants from 24 species planted onto a soil-based, modular interlocking crate system [5].

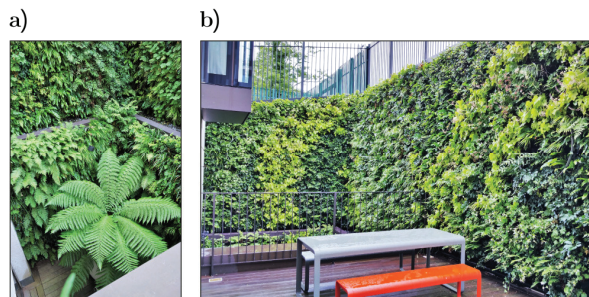


Figure 3. Residential courtyard in Primrose Hill, London, basement level court (a); east- and south-facing walls of the terrace court (b).

1.2 Semi-outdoor courtyard

The monitored courtyard is in Primrose Hill, London (Cfb) and has living walls installed on three bounding surfaces of the sheltered court, while the remaining north face is represented by the stone and glazed façade of the residential building. The arrangement includes a lower level which continues the living walls at the northwest corner down to form a basement court (Figure 3). The living walls have an average height of ~4 m and a total area of ~102 m²; with ~5,000 plants representing 14 species planted onto a soil-based, modular felt-pocket system [5].

2. METHODOLOGY

The monitoring of the indoor atrium case study in Cambridge included the measurement of soil (SoiIT), surface (ST), and air temperatures (AT), and relative humidity (RH); while absolute humidity (AH) was calculated. The hygrothermal observations were recorded between June 2018 to March 2019, with the period between June to September 2018 considered as summer, and between October 2018 to March 2019 considered as winter.

The monitoring of the semi-outdoor case study in Primrose Hill included the measurement of AT and RH, with absolute humidity (AH) calculated to characterise the courtyard's microclimate. The hygrothermal observations were recorded between August 2018 to December 2019, with the period between May-to-September considered as summer, and between October-to-April as winter.

The apparatus used for the exercises included manufacturer calibrated HOBO (Onset Computer Corporation, Bourne, MA, USA) and Tinytag (Gemini Data Loggers, Chichester, West Sussex, UK) AT, RH, and ST probes and loggers. All data was processed and analysed using Matlab R2019a (MathWorks, Natick, MA, USA) software. For large datasets (N>300), normality was determined with reference

to skewness and kurtosis thresholds, with failures assessed with nonparametric tests. Given that mean value datasets and their relation to probe locating parameters were limited (N<5), the relationships were plotted as profiles for discussion (see Figure 4 and Figure 5).

3. FINDINGS

3.1 Hygrothermal profiles

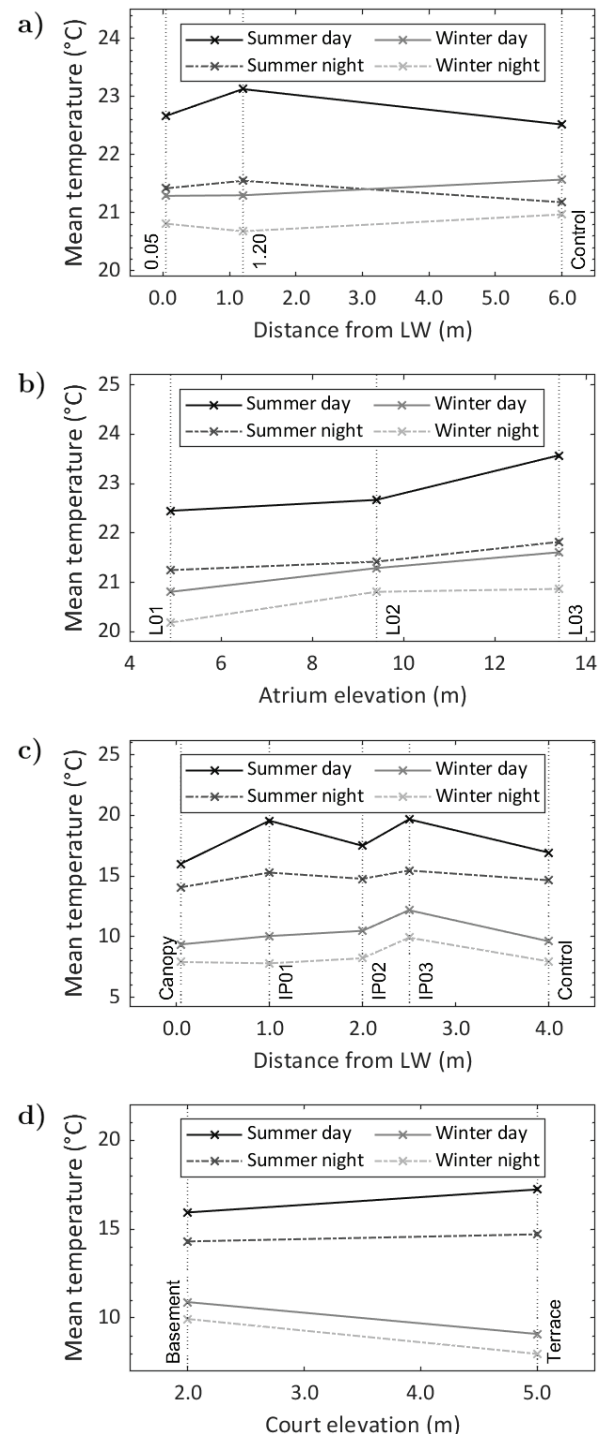


Figure 4. Mean AT profiles for indoor case study horizontal (a) and vertical (b) distribution; and semi-outdoor case study horizontal (c) and vertical (d) distribution.

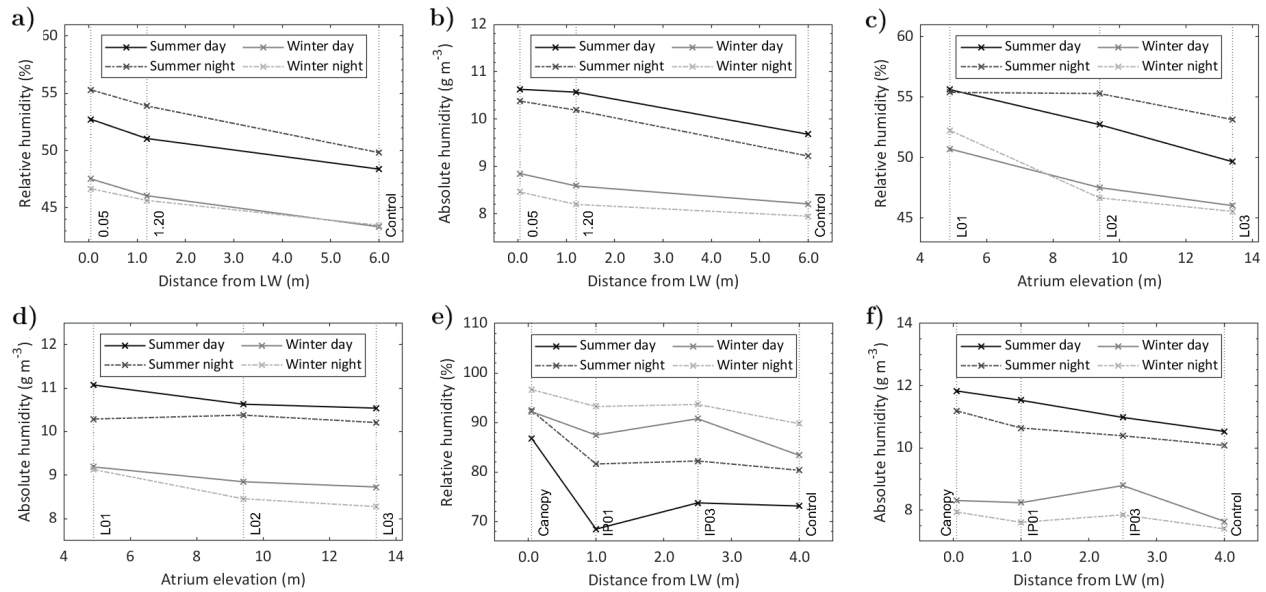


Figure 5. Mean RH and AH profiles for horizontal (a & b) and vertical (c & d) distribution at the indoor study; and for horizontal distribution at the semi-outdoor study (e & f).

3.2 Surface temperatures

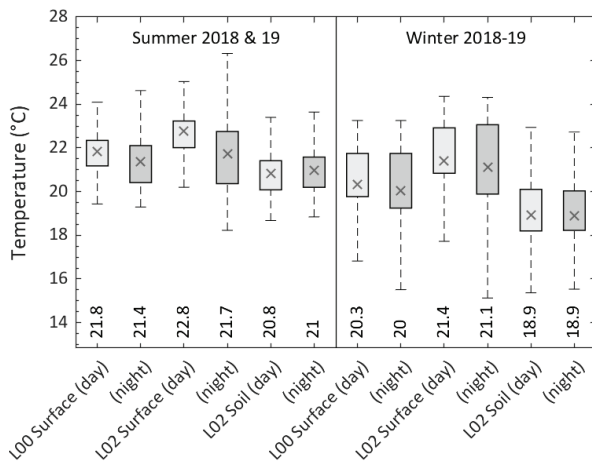


Figure 6. Atrium ST and SoilT datasets, with means ('x').

Table 1. Atrium ST and SoilT influence.

	SUMMER 2018 & 19		WINTER 2018-19	
Temp. (°C)	ST (L00 - L02)	L02 (ST - SoilT)	ST (L00 - L02)	L02 (ST - SoilT)
Daytime	-0.93 (±0.01), -4.2%	1.95 (±0.01), 8.6%	-1.09 (±0.02), -5.4%	2.48 (±0.02), 11.6%
{L00 ST}	{L02: 104.2%}		{L02: 105.4%}	
{L02 ST}		{L02 SoilT: 91.4%}		{L02 SoilT: 88.4%}
{L02 AT}		{L02 SoilT: 91.9%}		{L02 SoilT: 88.9%}
Night-time	-0.38 (±0.01), -1.8%	0.76 (±0.01), 3.5%	-1.08 (±0.02), -5.4%	2.23 (±0.02), 10.6%
{L00 ST}	{L02: 101.8%}		{L02: 105.4%}	
{L02 ST}		{L02 SoilT: 96.5%}		{L02 SoilT: 89.4%}
{L02 AT}		{L02 SoilT: 97.9%}		{L02 SoilT: 90.7%}

Note: '{ }' refer to values relative to L00 ST; L02 ST; L02 AT: 100%.

4. DISCUSSION

4.1 Air temperature influence

With the indoor case study, the Control demonstrated weak correlations and shared variance (r^2) with the outdoor climate. Mean ambient (Control) ATs still varied seasonally, with summer $M = 0.95, \pm 0.014$ K during the daytime and $M = 0.21, \pm 0.015$ K during the night-time warmer than winter. This modest variation is expected given that the atrium is mostly naturally ventilated. Control reading relationships with atrium probes on the other hand were very strong, and strongest with horizontal than vertical distribution probes. The weakest of these relationships were however during the summer daytime, which suggested interference from another source. Owing to this disruption, living wall horizontal AT distribution influence is best limited to the discussion between the 0.05 and 1.20 m probes, where the latter datasets showed >99% AT variability with the 0.05 m dataset. When mean AT profiles were examined (Figure 4a), the summer day and night-time, and winter daytime profiles agreed with Pérez-Urrestarazu *et al.* (2016) observations to present increased means at the 1.20 m probe (2.0, 0.1, and 0.05% respectively). Thus save for the winter night-time profile, all others presented cooler ATs immediate to the living wall ($M \sim 0.5$ K coolest AT difference during summer daytime), in agreement with previous vertical greening studies [1–7–8].

Vertical AT profiles showed the presence of a thermal gradient with means increasing with atrium floor levels L01-to-L03 (Figure 4b). L03 as a result presented the warmest canopy proximate ATs, with the summer presenting the highest means. The gradient confirms the presence of a buoyancy-driven

stack-effect, which had pronounced influence in the summer. This flow is also likely to be the principal contributor towards the summertime interference at the Control probe mentioned above. The dataset correlations showed that 63% of L02 and 38% of L03's AT variability to be explained by L01. The contributions from rising thermals from the lower level were therefore progressively supplemented by loading from intermediate floor level gains, as well as higher irradiance exposure from the installation upper region's proximity to the atrium rooflight.

With the semi-outdoor case study, the Control demonstrated strong correlations and r^2 (98.2%) with the outdoor climate. Control mean ATs as a result varied seasonally with summer $M = 7.31, \pm 0.02$ K during the daytime and $M = 6.69, \pm 0.02$ K during the night-time warmer than winter. The much greater mean difference relative to the indoor study is expected given the court's exposure to the elements, regardless of its sheltering boundaries. The Control readings however presented lower means for both day and night-time than intermediate horizontal distribution probes (Figure 4c). This suggested interference, which could be attributed to the influence of the building façade's thermal properties. The Control AT means however were still higher than the canopy probe, with the latter having presented the lowest means (coolest $M = 0.9$ K influence for summer daytime relative to Control). The lowest cooling influence was for the winter night-time ($M = 0.05$ K), which suggests significantly reduced cooling contribution from the evergreen cover. This is expected given that photosynthesis and transpiration is negligible during nocturnal hours, which is exacerbated by evergreen efficiencies being lower in winter [9–10]. Horizontal AT influence distribution was notably nonlinear in the summer, with the intermediate probes (IPs) presenting relatively higher means and a daytime drop at IP02 (Figure 4c). The reason for this daytime drop is unclear at present and could be due to mixing introduced from an unidentified source.

Given that only two vertical points were monitored at this study (~3 m elevational difference), a clear thermal disparity was evident with the Terrace presenting warmer day (1.29 K) and night-time (0.40 K) means relative to the Basement in summer, while in winter this was inverted (1.79 and 1.96 K respectively). This latter inverted profile (Figure 4d) contrasts with the indoor study, although is explained by the basement court's subterranean condition where it is subject to greater thermal conduction influences from its two retaining boundary walls (including living walls), and heat gains from adjoining basement living spaces. Daytime Terrace AT variance on the other hand highlighted the significance of irradiance loading variations.

4.2 Moisture influence

With the indoor case study, the recorded Control RH mean range between 43–55% is within the 40–60% range recommended for office environments [11], although is below the typical requirements (85–95%) to maintain evergreen foliage health [1–12]. The Control RH readings showed weak r^2 (~7%) with the outdoor climate, although seasonal variation was evident with summer $M = 5.03, \pm 0.06\%$ during the daytime and $M = 6.35, \pm 0.06\%$ during the night-time greater than winter; while AH presented summer $M = 15.2\%$ during the daytime and $M = 13.8\%$ during the night-time greater than winter. These variations are again expected given that the atrium is predominantly naturally ventilated. Notably, Control RH variation was explained mostly by AH ($r^2 = 61\%$) variance than AT (17%).

The horizontal RH distribution from the living wall to the Control decreased in winter and summer, and both day and night-time, with steeper gradients between the 0.05 and 1.20 m probes (Figure 5a). The highest RH was therefore always proximate to the living wall canopy ($M = 5.5\%$ L02 increase relative to the Control in summer night-time), in agreement with previous vertical greening studies [7–13]. AH profiles complemented this trend, with the maximum summer night-time mean increase for L02 relative to the Control at 13%. The summer daytime difference between 0.05 and 1.20 m probes however was notably marginal (2.5%), which suggests that during this period living wall proximate RH increase was mostly affected by AT cooling than by an increase in humidity. This is in agreement with the Susorova *et al.* (2014) study, where a significant fraction of the humidity from transpiration was found to be utilised to maintain foliage health in warmer conditions.

RH means at the indoor study also presented a vertical gradient with means decreasing from floor levels L01-to-L03 (Figure 5c). L01 therefore presented the highest RH ($M = 8.8\%$ summer night-time), as well as AH ($M = 14.5\%$ summer night-time relative to the Control). The AH mean difference between L02 and L03 however was notably minimal (<1%); thereby highlighting the RH reductions at the upper levels to be dominantly influenced by the AT increase of the thermal gradient.

With the semi-outdoor study, the Control RH showed strong correlation ($r^2 = 87\%$) with the outdoor climate (weaker than AT: 98.2%). Control mean RH as a result varied seasonally, with summer $M = 10.23, \pm 0.09\%$ during the daytime and $M = 9.40, \pm 0.07\%$ during the night-time lesser than winter; while AH presented summer $M = 27.4\%$ during the daytime and $M = 26.6\%$ during the night-time greater than winter. These larger variations in relation to the indoor study is again expected given the court's exposure. All RH means were as a result significantly

higher (68-97%) than at the indoor atrium (43-56%), with wintertime means exceeding the upper limit for comfort (70%). AH means however highlighted that humidity was only ~9% greater than at the indoor atrium over the summer, while in winter it was ~7% lesser. RH variation was therefore explained mostly by AT ($r^2 = 18\%$) variance than AH (1.4%).

In agreement with the indoor atrium, the highest RH means for all conditions was at the Canopy probe (summer daytime $M = 13.7\%$, highest relative to Control). The horizontal distribution showed RH reduction to be greatest ($M = 18.4\%$ for summer daytime) between the Canopy and IP01 probe, while at IP02, RH showed a relative increase (pronounced for summer profiles, Figure 5e), similar to the mean AT drop discussed earlier. For the summer profiles, examining AH means highlighted this RH increase to be influenced by the dip in AT. In winter however, IP02 demonstrated an increase in AH to disrupt the linear decay, as observed with summertime AH decay. This again highlighted interference from an unidentified source. Although AH decay in the summer was significant, it still showed substantial influence within the most frequented zone of the 4 m deep court. This is aided by the court's sheltered boundary conditions, where limited exposure to ambient airflow reduces opportunity for humidity advection. Summertime discomfort risk however is still to be reported by the residential occupants.

4.3 Surface temperature influence

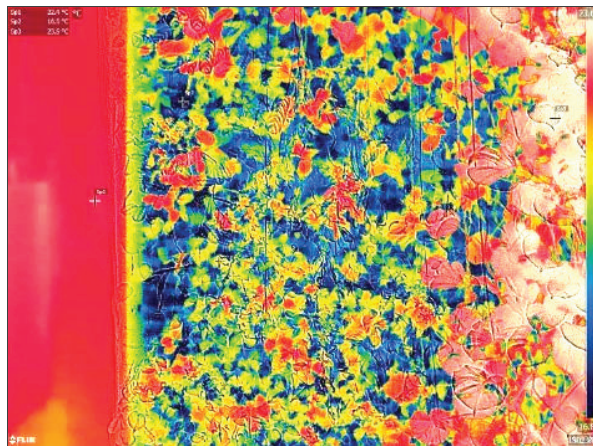


Figure 7. Thermogram of indoor study wall showing cooler (blue) substrate areas (5.9 K cooler than bare wall to left).

With indoor case study STs, an increase in means was recorded between L00 (base of the living wall) and L02 (vertical mid-point), both day and night-time, and in summer and winter (Figure 6 and Table 1). The relatively weaker correlations presented between the two floor levels in the summer suggests greater thermal contribution from another source to affect the ST increase. This could be partly attributed to the

midsection of the installation wall receiving greater summertime irradiance penetration from the rooflight above, relative to the L00 base condition. The relatively stronger correlations presented with wintertime data (which also presented higher mean STs) on the other hand suggests greater contribution from the AT thermal gradient within the atrium volume; which is further clarified by the marginally stronger correlations ($r_s > 0.97$) between L02 ATs and corresponding STs.

The recorded L02 SoilT means were notably lower than the corresponding ST and AT, both day and night-time and in summer and winter (Figure 6 and Table 1). This could be attributed to the moisture retention properties (increase in heat capacity) and continued evaporation from exposed soil surfaces. Passive qualitative thermography of the installation confirmed the soil substrate to be the coolest surface within the atrium volume, with some ST differences as large as ~6 K (e.g. Figure 7). Significant ST differences between areas could result in radiation asymmetry associated discomfort. The maximum differences recorded however were less than the threshold (>10 K) required to adversely affect comfort, although fell within the range where localised thermal sensation could be reported by proximate occupants [14]. The presence of a living wall could therefore result in occupants experiencing beneficial thermal sensations and diversity [15]; provided their presence is within the immediate zone of influence. The likelihood of the case study building occupants encountering this however is minimal, given that at higher floor levels proximity is restricted by the installation's default arrangement (presence of a void). The beneficial experience of living wall associated thermal diversity is therefore unavailable to this building's occupants.

5. CONCLUSION

Previous studies had presented experimental evidence to suggest significant thermal benefit from exterior vertical greening application. This study presents in-situ monitoring results in relation to an indoor atrium and semi-outdoor court to characterise living wall influence on the microclimates of sheltered conditions. The results highlighted a surface proximate cooling and humidifying influence at the indoor study (maximum AT: $M = 0.3$ K and RH: $M = 5.5\%$), and greater influence at the semi-outdoor study (maximum AT: $M = 0.9$ K and RH: $M = 13.7\%$). This disparity in influence suggests that greater the degree of shelter (enclosed system), the weaker the hygrothermal influence is likely to be. This is mostly attributed to the reduced influence of atmospheric advection, where in higher exposure conditions latent and sensible flux advection enhances transpiration associated microclimate influence.

The indoor study results established that most of the humidity generated from transpiration is repurposed to maintain good foliage health during the summer. This is particularly significant in indoor conditions where ambient RH is maintained at much lower values than would be required for evergreen plants. In general, the potency of hygrothermal modifications characterised by horizontal distribution was most apparent within the 1-2 m zone from installation surfaces. Beyond this range, other phenomena such as the stack flow at the indoor atrium, seem to cause interference and mixing to disrupt horizontal distribution. Hygrothermal gradation with installation height was also observed at both case studies, although the semi-outdoor court presented a wintertime inversion explained by its arrangement and resultant thermal exchanges. In general, vertical canopy temperature distribution is significantly influenced by exposure to irradiation loading, with remaining contribution from intermediate level thermal sources and sinks.

Although ST differences are not potent enough to cause radiation asymmetry associated discomfort, they are likely to be potent enough to present thermal sensation and diversity to occupants, which highlights an area that warrants further investigation. The design and arrangements of the installation at the indoor case study however precludes such benefits from being experienced by its building occupants at present. This in turn highlights the necessity for designers to take account of the proximity influence and increase building occupant access at future projects.

The monitoring study presented in this conference paper was subject to several limitations. A key limitation of carrying out in-situ monitoring was the inability to place sensors at ideal locations. At the indoor study for example, sensors were suspended across the atrium only where support structures were available. Furthermore, both studies were in occupied buildings, which meant that monitoring schedules had to be modified to not disrupt their day-to-day operation. This was critical at the indoor study, where the building has multiple occupancy and significant occupant and visitor traffic. Caution must also be raised here in relation to the interpretation of observations. Point-based ST readings for example are not truly representative of the distribution diversity of plant canopies, with quantitative thermography advocated as a comprehensive alternative where available.

ACKNOWLEDGEMENT

The work described in this paper is part of a doctoral studentship funded by the UK Engineering and Physical Sciences Research Council [1930753].

REFERENCES

1. K. Gunawardena & K. Steemers, Living walls in indoor environments. *Building and Environment*, 148 (2019) 478–487.
2. K. R. Gunawardena & T. Kershaw, Green and blue-space significance to urban heat island mitigation. In S. Emmitt, & K. Adeyeye, eds., *Integr. Des. Int. Conf.* (Bath: University of Bath, 2016), pp. 1–15.
3. R. Collins, M. Schaafsma, & M. D. Hudson, The value of green walls to urban biodiversity. *Land Use Policy*, 64 (2017) 114–123.
4. K. R. Gunawardena, M. J. Wells, & T. Kershaw, Utilising green and bluespace to mitigate urban heat island intensity. *Science of the Total Environment*, 584–585 (2017) 1040–1055.
5. K. Gunawardena & K. Steemers, Living wall influence on microclimates: an indoor case study. *CISBAT 2019, Spec. Issue J. Phys. Conf. Ser.* (IOP Science, 2019).
6. L. Pérez-Urrestarazu, R. Fernández-Cañero, A. Franco, & G. Egea, Influence of an active living wall on indoor temperature and humidity conditions. *Ecological Engineering*, 90 (2016) 120–124.
7. I. Susorova, P. Azimi, & B. Stephens, The effects of climbing vegetation on the local microclimate, thermal performance, and air infiltration of four building facade orientations. *Building and Environment*, 76 (2014) 113–124.
8. R. W. F. Cameron, J. E. Taylor, & M. R. Emmett, What's "cool" in the world of green façades? How plant choice influences the cooling properties of green walls. *Building and Environment*, 73 (2014) 198–207.
9. G. Öquist & N. P. A. Huner, Photosynthesis of Overwintering Evergreen Plants. *Annual Review of Plant Biology*, 54 (2003) 329–355.
10. H. Lamberts, F. Stuart Chapin, T. L. Pons, H. Lamberts, F. S. Chapin, T. L. Pons, H. Lamberts, F. Stuart Chapin, & T. L. Pons, *Plant Physiological Ecology*, Second (Springer New York, 2008).
11. CIBSE, *Guide A: Environmental design*, 8th ed (Norwich: Chartered Institution of Building Services Engineers, 2018).
12. K. Gunawardena & K. Steemers, Urban living walls: reporting on maintenance challenges from a review of European installations. *Architectural Science Review*, 0 (2020) 1–10.
13. R. Fernández-Cañero, L. P. Urrestarazu, & A. Franco Salas, Assessment of the cooling potential of an indoor living wall using different substrates in a warm climate. *Indoor and Built Environment*, 21 (2012) 642–650.
14. P. O. Fanger, B. M. Ipsen, G. Langkilde, B. W. Olesen, N. K. Christensen, & S. Tanabe, Comfort limits for asymmetric thermal radiation. *Energy and Buildings*, 8 (1985) 225–236.
15. K. Steemers & M. A. Steane, *Environmental diversity in architecture* (London: Spon Press, 2004).

Thermal Conditions In Urban Settlements In Hot Arid Regions: The Case Of Ksar Tafilalt, Ghardaia, Algeria

MOHAMED YACINE TELLI, GIRIDHARAN RENGANATHAN, RICHARD WATKINS

Kent School of Architecture and Planning, Canterbury, UK

This research investigates the influence of natural ventilation on the indoor thermal environment in the residential vernacular architecture of Ghardaia. The research was performed through a field study investigation during the hot summer period. The investigation included similar natural ventilation strategies, i.e. daytime, full-day and night-time ventilation. Two settlements, one historic and traditional and one contemporary but described as an “eco-city”, have been examined using field measurements and computer modelling. field air temperature and the relative humidity were measured using data loggers were the primary measurements taken in the field, comparing street's air temperature it was found the in Tafilalt was 4k higher than Beni Isguen, over one week and computer modelling of the settlements was conducted using VI-Suite software. The main part of the paper assesses the indoor comfort trends and implications of urban form, with a particular reference to the effect of varying density and presents strategic findings. It calls for continued research and development, particularly in the field of modelling the urban microclimate as a function of design. The results show that natural night ventilation in the traditional settlement is the most effective strategy for passive cooling in vernacular dwellings during the hot summer period.

KEYWORDS: Energy, Comfort, Urban form, Air temperature

1. INTRODUCTION

In an urban context, the main objective of environmental design is the creation of urban areas offering comfortable outdoor spaces. However, unlike the interior spaces of buildings, defined by relatively regular and controllable thermal conditions, exterior urban spaces are characterized by large daily and seasonal variations in microclimatic parameters, which are much more difficult to control (air temperature, wind and radiation for example). The specificities of the urban environment generate noticeable climatic changes at all levels. Therefore, understanding the relationships between urban morphology and the physical parameters of the local microclimate are essential.

This paper presents two case studies in Ghardaia city in the south of Algeria: **Tafilalt** and **Beni Isguen**. They were selected as they have two different patterns of neighborhoods, in a microclimate of about 1.5 km² (Figure 1). Comparisons are based on the urban thermal performance, to reveal how differences in urban patterns of land use and population densities affect the outdoor climate conditions and in turn pedestrian comfort and indeed indoor conditions. Subsequently, this will give real lessons and significant ideas on how the application of sustainable design maintains outdoor and indoor comfort. The choice of Ghardaia in this research is for the purpose of studying the improvement of outdoor thermal behavior based on thermal simulation and sensitivity analysis with peak outdoor temperatures as the criteria. The

findings in this study are pertinent to a building's ventilation strategy integrated into the building envelope design and optimization.



Figure 1: overview of the two settlements

2. METHODOLOGY

This study examines specific considerations of street orientation. The two case studies represent two types of architecture: the vernacular (Beni Isguen) and modern (Tafilalt) in Ghardaia City. The adopted steps are outlined in three simultaneous approaches being followed:

2.1 Site parameters

in order to simulate the urban canyons (Figure 1), site surveys were carried out in both locations. In particular measurements were made to determine the aspect ratio Height/Width, for both canyons which had similar orientations (NW-SE).

2.2 Model the radiation environment

The two settlements were modelled using ArchiCAD and applying it within VI-Suite Software, to study the simplified synthetic urban fabric of both settlements. This aims to provide an approach to quantifying the urban form design element and adapting the master plan for the present and future times. This is based on the thermal pedestrian comfort which shows the effect of the compactness of the settlements and the depth of the streets on solar gain received. The geometry of the two points A and B in the different settlements was input to ArchiCAD and uploaded to Vi-Suite to perform shadow mapping analysis. In this context shadow mapping is the prediction of how often points in space are in direct sunlight when the sun is above the horizon. Simulations in the VI-Suite were done for the summertime using mesh geometry within the scene as the calculation points, with four calculations per hour, using the urban building geometry as the calculation points.

2.3 Field monitoring

Conduct monitoring of the air temperature and relative humidity in the streets. HOBO data loggers were used to measure and record outdoor 15-minute climate data for one week during the summer: from 03/08/2018 to 09/08/2018. The monitoring targeted two points outdoors (two measurement stations) and two points in living rooms in both settlements. External measurements were made by placing each logger within a white (open beehive type) solar radiation shield, suspending this in the middle of each street at 2m height, and away from any heat source or another form of interference. Measurements were taken during representative days of summer conditions. This work presents the analysis only of the data corresponding to one week, in relatively low wind conditions. The data from these two stations characterize the local climatic effect of the streets, and this has been compared with the meteorological data from the airport, 2km away.

3. URBAN FORM OF THE CASE STUDIES

Ghardaia is located in the centre of the northern part of the Algerian desert. It is situated 600 km south of the capital Algiers at latitude 32° North and longitude 2°30' East. The climate of the Ghardaia city is a hot desert climate characterised by summers with torrid heats reaching 50°C and soft winters with the average minimum just above freezing point. The relative humidity is very low except for the winter months where 60% is common [1].

The valley of the "wadi" M'Zab " Ghardaia" includes five "Ksour" (small strengthened cities), founded over more than six and a half centuries (1011 until 1679) [2]. During all this period the knowledge of the local people adapted to the environment and

construction knowledge was undoubtedly refined to contribute to improving comfort in the local (thermally) very demanding conditions. The M'Zab Valley is situated in the south-east of Algeria, in the full desert and belongs to a hot dry climatic zone. Renowned for its secular architecture and remarkable integration of the urban forms to the whole conditions of the natural environment [3], it has today undergone extensive changes which have affected these exceptional characteristics.



Figure 2: View of Ksar Beni Isguen



Figure 3: View of Ksar Tafilelt

The organization of each city consists of three great layers: the ksar is generally established in the core of the settlement which is built overall out of traditional materials, the habitat of the palm grove at the edges with a variation of the building density, generally very far from the Ksar, and contemporary extensions with rather high densities and a horizontal spreading out. They are generally made out of traditional materials with little vegetation [4].

3.1 Beni Isguen

Located in the M'Zab Valley, Beni-Isguen city is one of its five strengthened cities. It is composed of juxtaposed morphological areas which have relatively clear limits and marked differences. Compact urban forms characterize the old city centres, especially in the Saharan cities. These centres are often very dense and appear as a large concentration of buildings in a dense urban radius. Depending on their morphology, there are: the traditional island, e.g. "Beni Isguen" with its irregular street network, and the Haussmannian island with a regular street network, e.g. Tafilelt. See Figures 2 and 3.

3.2 Tafilelt: Algeria's first eco-friendly desert city

Tafilelt is an "eco-city" in the Sahara and a 20-year project to make the desert bloom with all residents helping to plant trees and recycle waste. The ksar of Tafilelt, initiated in 1998 by the Amidoul foundation as part of a social project, is set on a rocky hill overlooking the ksar of Beni-Isguen. This urban complex, with 870 housing units, has plots, streets, alleys, walkways, playgrounds and accompanying structures, such as library, school, shops, community house [5], gym and leisure facilities (park). Considered to be the extension of the old Ksar of Beni-Isguen, this new ksar was built thanks to a financial arrangement involving: the beneficiary, the State (in the framework of the formula "Participative Social Housing") and the community through the **Amidoul** foundation. See Figure 4. To ensure thermal comfort, some traditional architectural and urban principles have been updated.



Figure 4: View of the edge of Ksar Tafilelt

4. RESULTS

4.1 The influence of compact shapes on outdoor conditions "A"

A compact urban fabric is generally narrow and deep in Beni Isguen. See Figure 2. It prevents the sun's rays from reaching public spaces (streets, squares or interior courtyards) and generates shadows which contribute to increasing the comfort of these spaces. conversely, in stable weather and in hot periods, these spaces favour the phenomenon of radiative trapping,

thereby increasing the surface and air temperatures and the risk of discomfort. This radiative trapping is due to the multiple reflections of the solar rays by urban surfaces.

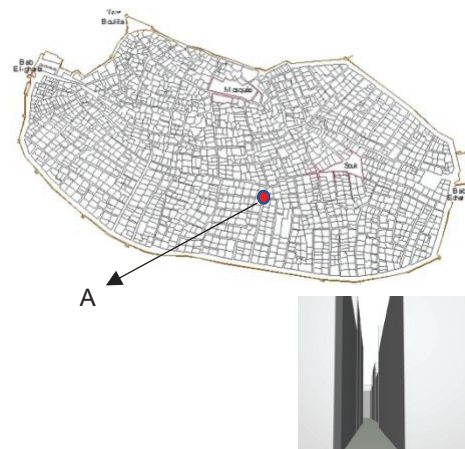


Figure 5: The location of house "A" in Beni Isguen

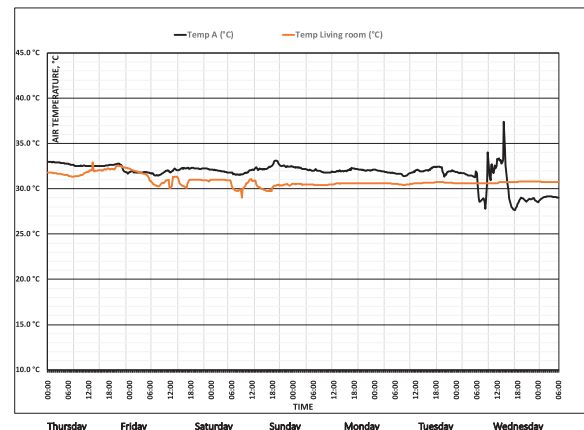


Figure 6: Comparison of the air temperature outdoors and a living room in location "A" for one week

4. 3 The influence of regular urban shapes on outdoor conditions "B"

In the case of Tafilelt (Figure 7), the streets are 80% wider compared to location A (Beni Isguen) by about 1,5 metres which in turn makes them more exposed to the sunlight (Figure 5).

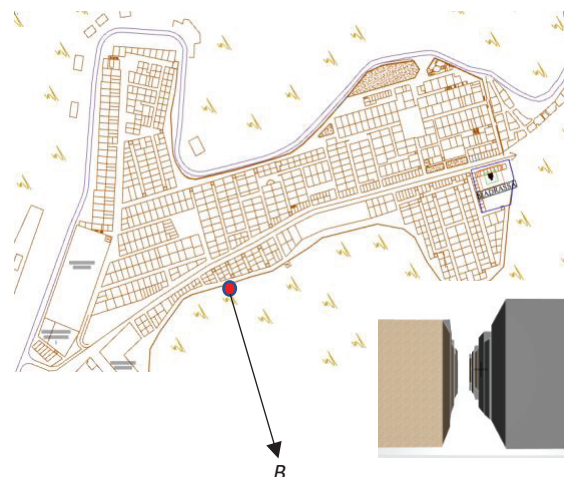


Figure 7: The location of house "B" in Tafilelt

In addition, an increase in temperature inside the buildings (Figure 8) was also observed which then has an impact on thermal comfort of their occupants.

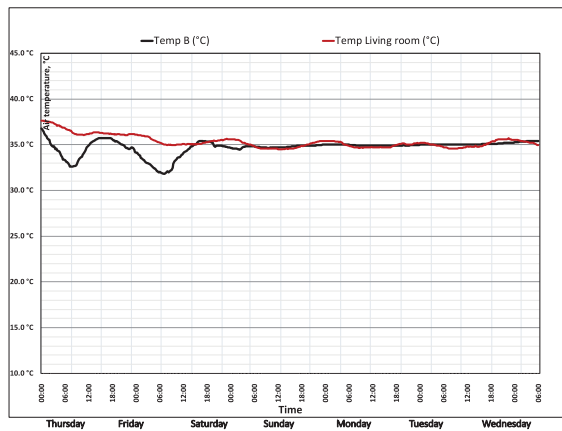


Figure 8: Comparison of the air temperature for outdoors and a living room in location B for one week

The orientation of urban fabric is a spatial parameter used to analyse the accessibility of solar energy and daylight within street gorges. It creates shaded and sunny surfaces leading to variations in ambient and surface temperatures



A: $H/W=3$

B: $H/W=1.7$

Figure 9: The width of the road at both sites

Morphologically, this indicator produces forms of sun protection or exposure in urban spaces. The protection is often effective, only at the start and end of the day, depending on the orientation of the building. Indeed, when the sun is at its zenith, the shaded areas are very reduced (Figure 10).

5. DISCUSSION

The results' analysis shows that location A has deep streets in dense urban tissue which act as heat traps. Solar protection, from the narrow street gorges ($H/W=3$) are very important in the thermal behaviour in the summer. Because of the reduced solar access, use of light brown colours, and the weak anthropogenic heat generation; air temperature decreases of 8°C were

recorded in summer compared to the meteorological airport data. Given the shading effects in "B", the temperatures outdoors are very different from those of "A". The average weekly temperature of "B" remains fairly similar to the meteorological airport data. The average temperatures of the two locations obtained during the week of the study were compared. This comparison shows that during the day the greatest difference between the two places amounts to 8°C on Sunday at 15:00. The H/W ratio of Tafilelt allows more solar radiation into the street gorge and moreover the upper part of the west façade receives the sun for longer (Figure 10).



Figure 10: The shading in both streets, each oriented southwest, at 3:00 pm

In a very similar way, the average temperature of the southwest façade remains slightly higher than that of the northeast façade (Figure 10). However, during the night the temperatures of the streets are lower than those of the other elements and that of the air probably because of the radiative deficit. On the one hand, the roofs have a wide view of the sky and in addition, they are highly exposed to the wind, thus returning more heat to the sky in infrared and by convection. During the cloudy days, the temperature of the surfaces is controlled more by the atmospheric infrared flux and the incident diffuse flux.

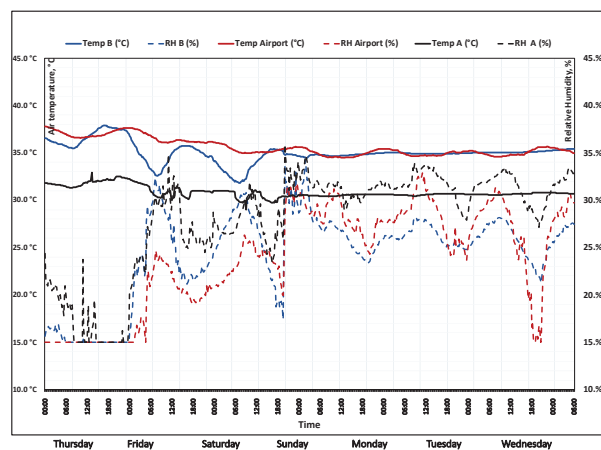


Figure 11: Comparing the outdoor temperature and humidity for both cases with meteorological airport data for one week



Figure 12: Shadow mapping for Beni Isguen

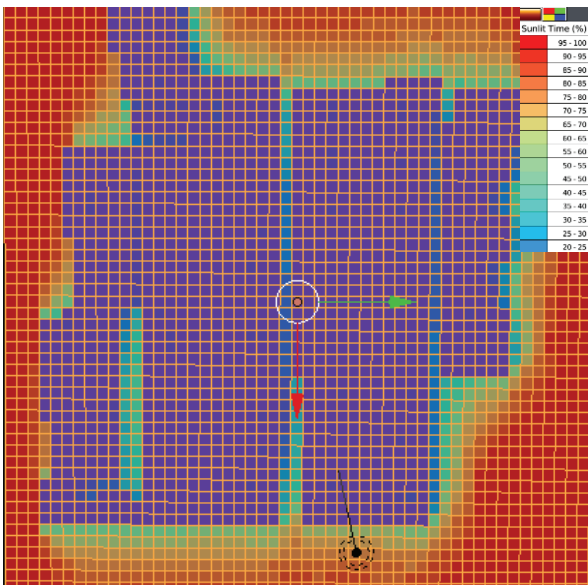


Figure 13: Shadow mapping with building removed for clarity, Beni Isguen

Streets in "A" are less exposed to the sun because of the height to width ratio of the narrow streets [9]. The roofs, characterized by a high sky view factor, still have the highest temperatures during the day. They thus play a major role in the absorption and return of solar energy especially in location "B".

In order to study microclimate for urban planning land use, the Compactness Degree for the built-up area was used as a parameter to measure the surface exposure to the sun. In both places, the same surface area and the same orientation were selected.

Based on shadow mapping in both places it was observed in case A (Figure 12, 13) that the ratio of the surface exposed to the sun to the surface in shadow was lower compared to case B (Figure 14, 15).

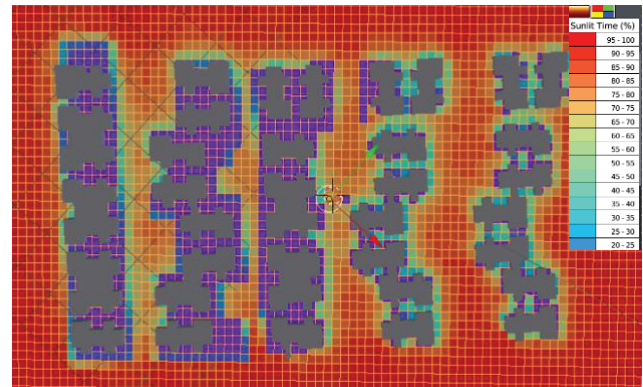


Figure 14: Shadow mapping for Tafilelt

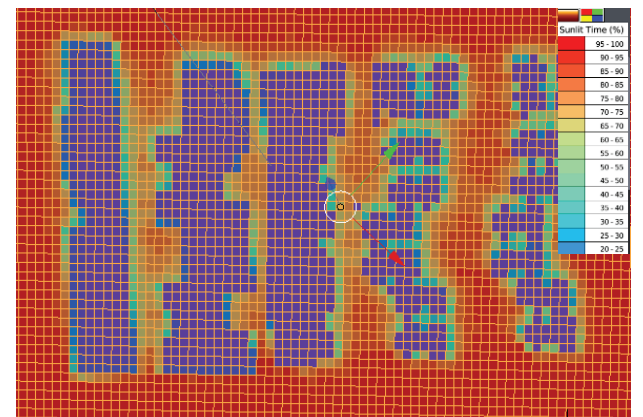


Figure 15: Shadow mapping with building removed for clarity, Tafilelt

The duration of sunshine indicates the sum of the time intervals during the day that buildings and streets are subjected to insolation during a given period. The duration of sunshine in a district can affect the average radiant temperature, a physical component of thermal comfort that integrates the flows of short and long wavelengths. The longer the duration of sunshine, the higher the amount of incident solar energy, which can increase the risk of discomfort. Figure 12 shows the results of the simulation of the duration of sunshine for one day, Wednesday. Location B in Tafilelt settlement is the one that receives the most solar radiation with 47.0% of the time, i.e. more than 6h35 min. In contrast, location "A" in Beni Isguen receives solar radiation for 32.2% of the time, i.e. 4h20 min. See Figures: 12,13,14,15. The shortest duration of sunshine is obtained for Beni Isguen, with only 4 hours of sunshine. This short duration is mainly due to the compactness of the urban tissue and the narrow width of the streets.

5. CONCLUSIONS

Two settlements, one historic and traditional and one contemporary but described as an "eco-city", have been examined using field measurements and computer modelling. In the context of a very dry and very hot climate the role of buildings and their

placement, i.e. the resulting urban morphology, must be to reduce the temperature and promote greater comfort in a passive way as far as is possible.

Tafilelt, although built using traditional materials, departs from the historic urban form found in Beni Isguen. The buildings were found to be more widely spaced, with streets almost 100% wider (3.5m rather than 2m). Building heights are similar, and this leads to a 50% reduction at Tafilelt of the H/W ratio. Street level solar exposure is thus much greater at Tafilelt – some 50% more than at Beni Isguen.

The impact of this on the air temperature experienced by pedestrians (and on the air entering buildings) was revealed by the air temperatures measured in the two streets. Over four days the air temperatures in the Tafilelt street were very similar to that of the airport's met station temperatures, and both locations were some 4-5K higher than in the Beni Isguen street. The traditional morphology of the latter clearly provides a major benefit in terms of comfort and reducing the need mechanical cooling.

Given that Tafilelt was designed as an eco-city, it is surprising to find, albeit based on the evidence of short-term monitoring, that it results in higher urban temperatures. Whilst the choice of materials for the town (very traditional) and its emphasis on planting of vegetation must be commended, allowing much greater solar radiation to enter the urban structure is unhelpful. The width streets give access for the vehicle to access houses, clearly width streets allow better access for vehicles but that's comes as its cost highest urban temperature. It would be worth investigating options to counter this effect, e.g. street shading, more reflective materials, etc. This is the subject of ongoing research.

REFERENCES

1. Ali-Toudert F, Mayer H (2005) Numerical study on the effects of aspect ratio H/W and orientation of an urban street canyon on outdoor thermal comfort. *Building Environ* (in press)
2. Djenane M (1998) Participation of the urban form in the control of solar irradiation. Particular reference to the role of the street in hot and dry regions. Magister's memory. university of Mohamed Khider, Biskra
3. Oke T. Street design and urban canopy layer climate. *Energ Buildings* 1988; 11:103–13.
4. Donnadieu, al (1977), *Living in the desert, the mozabite Houses*, édit. Pierre Mardaga, Bruxelles. p91
5. Benyoucef Brahim (2009), *New cities, Autopsy of a local experience*, *Lives of Cities*, n° 18, p 61.
6. Bakarman M, Chang J. The influence of height/width ratio on urban heat island in hot-arid climates. *Procedia Eng* 2015;118:101–8.

Energy transition challenges in under-occupied homes Assessment of two peri-urban neighbourhoods of single-family houses

JUDITH DROUILLES, EMMANUEL REY

Laboratory of architecture and sustainable technologies (LAST),
Ecole Polytechnique fédérale de Lausanne (EPFL), Switzerland

ABSTRACT: Current planning policies aim at putting a stop to urban sprawl by favouring densification processes. In this context, future developments are more likely to happen in strategic urban areas than in existing peri-urban neighbourhoods of single-family houses. There, a possible path of development is the inertia and the submission to demographic evolutions of population ageing and reduction of household sizes. Under those unfavourable conditions, the evolution of two case-studies located in the Swiss context is measured by 2050. The paper investigates the energy transition potential of two off-centred residential areas by assessing the environmental impacts owing to construction/retrofit and operation of dwellings, and to the induced daily mobility of the inhabitants. The innovative methodology implemented for this research project supports a spatiotemporal data management that allows establishing an annual assessment throughout the 35-year period of study (2015-2050). The results highlight the submission of the transition potential to the alternation of household's life-cycles. This study underlines the importance of considering over-time assessments for a more reliable prospective evaluation, and it questions the transition slowness of owner-occupied dwellings.

KEYWORDS: Energy transition, single-family homes, under-occupation, retrofit, life-cycle analysis

1. INTRODUCTION

1.1 Context and challenges

Facing climate change issues, cities appear as one of the major energy consumers. Transport and households are particularly responsible for this high urban energy footprint, especially in off-centred low-density residential areas [1].

Energy-retrofitting of single-family houses, which are mostly heated with fossil fuels, represent a major topic for coming years. The issue is even more urgent in peri-urban areas highly dependent on individual car mobility. Under those conditions, inhabitants are vulnerable to potential future crisis. Therefore, investigating straight away the energy transition potential of areas of single-family houses is important, since they too have a role to play in meeting global emission targets. Locally, exploring the possibility of more resilient peri-urban communities would help mitigate future socioeconomic downsides.

However, among multiple challenges faced by peri-urban residential areas, the paper addresses: 1) the low energy-efficiency of their building stock, mainly built between the 1960s and 1980s, 2) the issues of the mismatch between single-family houses typologies and current demographic and societal evolutions towards population ageing and reduction of household size [2].

1.2 Research framework

The findings presented in this paper are part of a broader research [3] which investigated the future of

peri-urban neighbourhoods of single-family houses in light of five prospective scenarios. The research questioned the sustainability transition potential of car dependent residential areas created mainly in the second half of the 20th century.

The first step of the research identified *peri-urban residential municipalities* according to several criteria recurrent in European and Swiss definitions. They gather towns that are physically separated from the compact central urban fabric, but connected to them through functional relationships (commuting). They also present significative population density and proportion of single-family houses in their building stock. Finally, they met a strong demographic growth between 1950 and 2000 [4]. The main body of research was the conception, application and assessment of the following prospective scenarios, presented in depth in [5]. Two scenarios – *Caducity* and *Exclusivity* – investigate a future inertia of neighbourhoods and the preservation of current lifestyles. The scenario *Opportunity* focuses on effects of emerging soft-densification practices. *Urbanity* and *Mutuality* propose deeper transitions based on weak signals of mentality and society changes. The scenarios are systematically applied in real case-studies and assessed according to all aspects of sustainability and to their implementation feasibility. Altogether, the research outcomes help anticipating how future planning decisions might maintain or improve the situation of existing peri-urban neighbourhoods.

1.3 Aim and structure

The present paper however focuses only on the *Caducity* scenario and investigates more deeply the effect of a *status quo*, which may concern some of the neighbourhoods less integrated within metropolitan dynamics, which are not considered as future land resources. Hence, the paper aims at assessing the energy transition potential of such areas submitted to unfavourable conditions of development. The novelty of the approach lies in part in considering the effects of inertia or negative trends [6], also in conducting a prospective analysis at neighbourhood scale based on a research by design methodology combined with an extensive data management. It results in the spatiotemporal assessment of the scenarios implementation process and outcomes.

The following section of the paper presents the material and methods used for the implementation of the *Caducity* scenario into two existing case-studies, located in the urban region of Lausanne. Starting from a theoretical basis, it sets the conditions for attractiveness and value losses, then it gives the hypotheses selected for the scenario implementation at neighbourhood scale and for the assessment of its environmental impacts.

The next section provides the results in terms of demographic trend, building transformations and environmental assessment. The results highlight the impacts of a wide spread under-occupation of single-family houses on the energy transition extent and speed.

2. METHOD

A panel of eighteen academy and industry experts was consulted to gather arguments supporting diverse future perspectives for neighbourhoods of single-family houses. The five scenarios resulted from the identification of coherent future visions for an application in the Swiss context. They are representative of the issues discussed in the interviews and collected across the literature. The *Caducity* scenario, is therefore, representative of the current and foreseen evolution of some peri-urban areas [7]. It considers the following context and hypotheses.

2.1 Loss of attractiveness

According to current trends, neighbourhoods of single-family houses are likely to face stagnation or decay in the coming years [8,9]. Arguments supporting this hypothesis are owing to external circumstances such as the global demographic transition known in European countries. The growing proportion of small households and elderlies questions the maintenance of the attractiveness of single-family houses typologies

[2,10,11]. As shown in a Dutch study, population ageing and the reduction of household size is highly correlated to an over-consumption of housing, i.e. to dwelling under-occupation [12]. The authors indicate how older households tend to stay in their homes after children departure and that the phenomenon is more common in owner-occupied homes.

Regarding peri-urban neighbourhoods of single-family houses a higher risk of inertia exists due to the high dependence to individual motorized transport [8], and to the common political opposition to change meant to preserve the electorate's living environment [13]. Moreover, current trends in urban and territorial planning tend to reorient future developments in strategic urban areas well connected to public infrastructures. This inward densification is a guiding principle of current Swiss planning policies [14]. Those evidences witnessed at large scale suggest that some dynamics relating to the shrinking city phenomenon (such as population decrease) could apply to some peripheral or off-centred built areas [15].

2.2 Loss of value

At a closer scale, the *Caducity* scenario embraces those hypotheses, which induce a loss of economic value of existing buildings due to the conditions of low attractiveness and of delayed retrofits.

1. As a direct consequence of longer occupation periods, many small elderly households, with limited resources live in single-family houses. Retrofit actions are delayed until new occupants get involved.

2. Living in central areas close to a richer offer of local amenities becomes more appealing than the landscape qualities of peri-urban areas. Hence, a slight disarticulation of the real-estate market in those areas induces longer vacancies between owners: prices drop and insertion time of houses in the market increases.

3. For a similar reason, the scenario assumes that the demand is not sufficient for the empty plots to be built. It only allows the refurbishment of existing houses.

2.3 Implementation in two case studies

Further than identifying those theoretical hypotheses, the added value of the research lies in implementing the scenario into existing case-studies in order to observe actual effects on the building stock. To do so, the study is focused on the urban region of Lausanne, Switzerland.

Selected among a typology of peri-urban neighbourhoods of single-family houses [16], the case-studies presented here belong to two contrasted types, showing opposite features. The neighbourhood located in Chavornay (CHA) (Fig. 1a) is close to a regional train

station, its urbanisation started long before 1975. Quite large, with an area of nine hectares, it gathered in 2015, 213 inhabitants in 93 dwellings. The neighbourhood located in Jorat-Mézières (MEZ) (Fig. 1b) is only accessible by bus. Its urbanisation started around 1975. It is a small neighbourhood, with an area of three and a half hectares. It was composed in 2015, of 29 dwellings occupied by 72 persons.

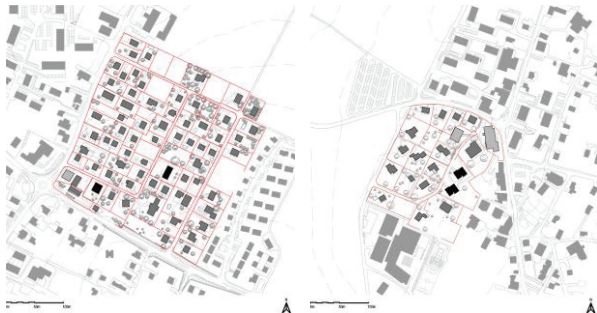


Figure 1: L: Neighbourhood in Chavornay (CHA) VD-CH (2015)
R: Neighbourhood in Jorat-Mézières (MEZ) VD-CH (2015)

The evolution of owner-occupied houses is very dependent on the inhabitant's evolving needs along the different life-stages. It is especially conditioned by the entry into the family phase, since the purchase of a house usually precedes or follows the birth of the first child [2]. By considering neighbourhoods of owner-occupied houses built in the second half of the 20th century, many houses are still occupied by their initial owners. Simulating the house occupation, and the alternance of cycles (Fig. 2) is possible thanks to the definition of turning points and pivotal ages when changes are more likely to happen. Two elements have significant effects on the assessment of environmental impacts:

- The departure of the children. Afterwards, the house is occupied by a small household of retired people.
- Life expectancy [17]. Even though local data have shown that some households wish to relocate, the scenario assumes that 100% of them stay as long as possible in their houses. Indeed, in this scenario, the real-estate market lengthens the insertion time of houses and prevents a fast and easy rotation of households.

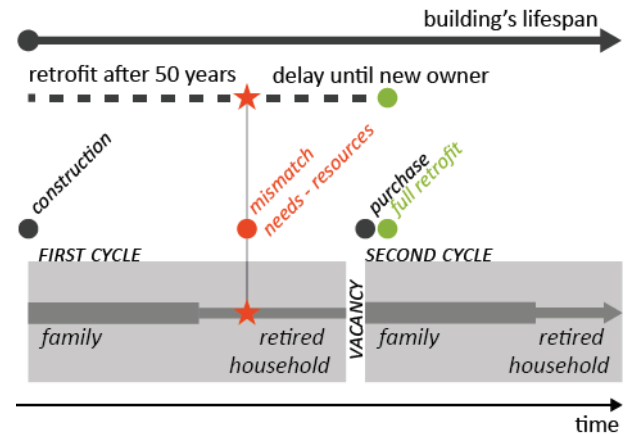


Figure 2: Occupation cycles in owner-occupied single-family houses, and effect on building's state. Hypotheses considered for the entire building stock in Caducity scenario.

2.4 Environmental impact assessment

The environmental impact assessment is built at neighbourhood scale according to the framework set by the Swiss 2000-watt society concept applied to the built environment [18]. Non-renewable primary energy (NRPE) demand and subsequent greenhouse gas (GHG) emissions for construction/retrofit and operation of the buildings, as well as for induced daily mobility of the dwelling's occupants are considered within the assessment. Global targets for those three items are set for 2050 at 7,200 kWh.pers.yr and 960 kgCO₂e.pers.yr.

Considering the complexity of conducting environmental assessments at larger scales than the building's, the evaluation relies on reference values provided by [1]. The latter gives a reference database to establish indicative large-scale energy assessments. This work provides reference values in square-meter per year for operation and construction/retrofit of representative Swiss residential buildings of the late 20th century (Tab. 1).

Table 1: Indicative and non-exhaustive reference data used to estimate the environmental impacts at neighbourhood scale. Values expressed in kWh(NRPE).sqm.yr and in kgCO₂e.sqm.yr. OI: Operational impacts, EI: embodied impacts assessed for a 60 years lifespan, SFH: single-family houses, MFH: multi-family house. Whole tables in [1]'s complementary files.

OI	As built (E0)		Retrofit S0		Retrofit S1	
	NRPE	CO ₂ e	NRPE	CO ₂ e	NRPE	CO ₂ e
SFH	435.98	92.65	175.58	29.67	102.65	4.15
MFH	266.78	53.72	138.83	22.61	99.93	4.04

EI	As built (E0)		Retrofit S0		Retrofit S1	
	NRPE	CO ₂ e	NRPE	CO ₂ e	NRPE	CO ₂ e
SFH	5.58	1.42	7.93	1.99	11.17	2.92
MFH	3.09	0.74	4.00	0.97	6.56	1.72

According to the hypotheses mentioned in figure 2, the state of both case-studies' building stock is assessed throughout the 2015-2050 period. The external circumstances considered for this particular prospective scenario provide other clues such as the household's limited resources and their lower capability to retrofit their house to highly efficient energy standard. Consequently, this scenario considers that 90% of retrofitted buildings will simply comply with legal requirements in terms of energy efficiency that are progressively more restrictive i.e. S0 before 2015 and S1 until 2050 (Tab. 1). The remaining buildings (10%) are retrofitted to higher standards towards passive or positive energy buildings.

The proposed assessment considers all residential buildings in the neighbourhood according to their heating fuel, gross floor area (GFA) and mean occupation. Unlike what Table 2 presents, the assessment is conducted annually for each individual building. Consequently, every variation in occupation or energy performance induced by principles shown in Figure 2 are precisely accounted for.

Table 2: Aggregated data representative of each case-study's building stock. Mean gross floor area (GFA), majority heating fuels in 2015; in 2050, heat-pumps are mostly used. The last two columns show the mean building occupation in 2015 and 2050, considering under-occupation by small households and transitional vacancy.

Case-study	Nb. buildings	Mean GFA	Heating fuels	2015 occup.	2050 occup.
CHA	75	251sqm	oil/gas	2.8	2.5
MEZ	20	319sqm	oil	3.6	3.8

The assessment of mobility related environmental impacts rely on the method detailed in [19]. Based on mean annual impacts established for 2015 and 2050 car fleets, the method considers nine adjustment factors related to location and other project features. Half of them are stable among case-studies and/or scenarios. Table 3 presents impacts and factors used for *Caducity* scenario.

Table 3: NRPE demand and subsequent GHG emissions for 2015 and 2050 car fleets. Indicative adjustment factors used to assess 2050 GHG emissions owing to induced daily mobility in both case-studies PT: public transport.

Car fleet	NRPE kWh.pers.yr	GHG kg.CO2e.pers.yr
2015	4060	860
2050	2190	390

Adjustment (e.i. 2050 GHG)	CHA	MEZ
Location	1.04	1.04
Quality of access by PT	0.99	0.99
Intensity of PT use	1	1
Intensity of car use	1.28	1.28

Access to leisure	0.99	1.06
Access to supermarket	1.08	1.1
Access to car-sharing	1.12	1.16
Parking spot per dwelling	1.02	1.01
Income	0.72	0.72

3. RESULTS

3.1 Neutral or decreasing demographic trend

The conditions of implementation of *Caducity* scenario induce an overall demographic stability between 2015 and 2050 (Fig. 3). In CHA (grey line), the population steadily decreases, while newer houses are under-occupied. Contrary to MEZ, the building stock has grown regularly since the 1960s. It allows a continuous renewal of the population, and a limitation of the under-occupation to 17% to 50% of the building stock. In MEZ (black line), a demographic trough between 2015 and 2042 is related to the progressive under-occupation of 70% of houses. They were built in a short 10-year period and they follow similar occupation cycles. The vacancy reaches its highest level in 2036 with seven unoccupied homes. The increase in population noticed from 2040 on, corresponds to the beginning of new occupation cycles, and the reduction to 5% of under-occupation.

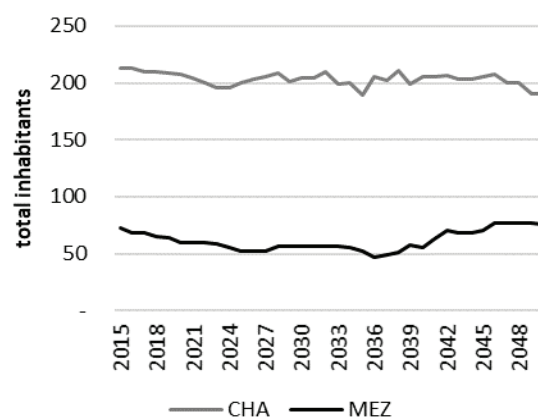


Figure 3: Demographic evolution in number of persons, in both case-studies (CHA: grey, MEZ: black line) between 2015 and 2050, according to the above-mentioned hypotheses.

3.2 Slow transition

The evolution of the building stock is submitted to these demographic conditions. Both case-studies present different features in terms of transition slowness. In CHA, only 47% of the building stock is retrofitted by 2050. It relates to the fact that the neighbourhood is composed of many houses built after the year 2000. In MEZ however, the slowness is due to the homogeneity of the neighbourhood since 95% of the houses are retrofitted in fifteen years, but the process starts in the second half of the considered period.

Table 4: Building retrofit process in both case-studies.

	CHA	MEZ
Retrofits before 2015	13%	0%
Retrofits 2015-2050	33%	95%
As built houses in 2051	53%	5%
Theoretical retrofit time limit	50 yr	
Actual mean retrofit timeout	60.68 yr	62.53 yr
First retrofit 2015-2050	2023	2033
Last retrofit 2015-2050	2050	2048

3.3 Environmental impacts in 2050

The assessment by 2050 aims at showing the transition potential and at what extent *Caducity* scenario achieves complying to 2050 requirements in energy efficiency. Figure 4 shows the average NRPE demand and GHG emissions per person in 2015 and 2050. In 2015, the assessment shows a very low average performance across the building stock of both case-studies. NRPE demand is at least 3.5 times higher than targets. In MEZ, GHG emissions exceed by 6.4 tons the annual target. The high reliance on fossil fuels for heating is clear throughout those results. By 2050, demand and emissions are significantly reduced in both case studies. In the case of CHA, environmental impacts in 2050 are still more than 10,000 kWh and one ton of CO₂e per person per year higher than targets. The improvement is more obvious in MEZ, with a reduction of about 25,000 kWh and 5.5 tons per person between 2015 and 2050.

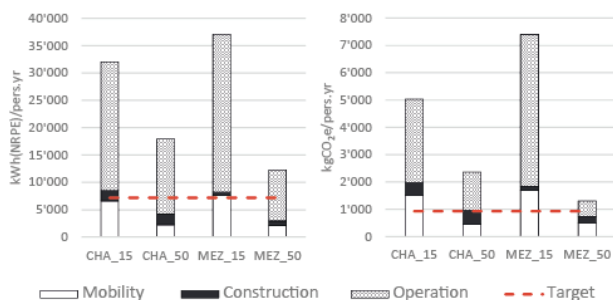


Figure 4: Evolution of NRPE demand and GHG emissions per person between 2015 (15) and 2050 (50), in both CHA and MEZ, owing to induced daily mobility of inhabitants, construction/retrofit of dwellings and their operation. Comparison with 2000-watt society targets for 2050.

3.4 Annual assessment and evolution trends

Figure 5 highlights the reduction trend of GHG emissions on an annual basis between 2015 and 2050, according to the assumptions of *Caducity* scenario. Whereas emissions are steadily decreasing in CHA, in MEZ average individual emissions increase until 2025 when a first dwelling is left vacant. The bell-shape distribution is linked to the drop of about one-third of the neighbourhood's population in the first years of the

considered period. The decrease of GHG emission is very fast once the building renovation process starts in the neighbourhood.

An illustration of those distinct trends also appears in the comparison of cumulated GHG emissions during the whole 2015-2050 period. On average, a resident of CHA emits 3.8 tons of CO₂e per year, whilst in MEZ the annual individual average emissions for the 35-year period are of 6.1 tons of CO₂e.

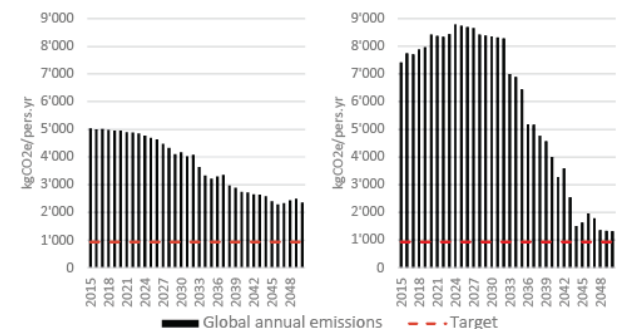


Figure 5: Annual evolution of GHG emissions for both neighbourhoods between 2015 and 2050. L: CHA, R: MEZ.

4. DISCUSSION

In line with international objectives to mitigate carbon emission by 80% to 90% by 2050, it is crucial that single-family houses located in remote areas also engage into building retrofit processes. Average environmental impacts in 2015 in both case-studies are far from meeting the targets set in the framework of the 2,000-watt society concept. Although, results show a clear improvement by 2050, they remain above targets. Optimizations should concern mobility practices and building occupation in priority.

The results of the implementation of the *Caducity* scenario highlight the importance of considering over-time assessments for a more reliable prospective sustainability evaluation. Focusing on the starting and finishing points of the assessment suggests that MEZ performs much better than CHA, and that it is more efficient in its renovation process. Nonetheless, the annual results over the 35-year period underline the steady improvement of the situation in CHA and its lower cumulated GHG emissions. The slowness of the energy transition appears clearly in this assessment and it raises the questions of ways to speed-up the process in owner-occupied buildings.

This study finally points out the need of further studies on turnkey real-estate developments in order to mitigate and better anticipate the alternation of occupation cycles in such homogeneous neighbourhoods. Energy efficiency is only one of the affected topics. On a sociodemographic level, small residential municipalities must also face an evolving

demand for equipment such as child care facilities, schools or nursing homes.

5. CONCLUSION

This paper outlines conditions and effects of future stagnation or decay of peri-urban neighbourhoods of single-family houses. It underlines how those existing built areas might be submitted to losses in attractiveness and real-estate value due to a mismatch between single-family houses typologies and the growing proportions of small households and elderlies. The dynamic assessment of the scenario implementation highlights that inhabitants' life cycles determine the amplitude of the transformations engaged. Based on specific restrictive assumptions for *Caducity* scenario, the considered 35-year period (2015-2050) is nevertheless sufficient to witness a population renewal and the retrofit of most dwellings.

Because single-family houses are usually owner-occupied dwellings, similar energy transition trends are witnessed for more proactive scenarios. Even in cases of higher municipal implication (*Urbanity* scenario), transformations are submitted to the life cycles of households and to the temporality of their needs. To play their part in achieving the energy transition challenge globally, neighbourhoods of single-family houses must engage in retrofitting processes despite the complexity related to land fragmentation and to individual property.

ACKNOWLEDGEMENTS

The Swiss National Science Foundation supported this research in the framework of the "Living Peripheries" project (Project n°100013_152586/1).

The authors acknowledge the contributions of Dr Frederic Frank and Dr Sophie Lufkin in the successful completion of the above-mentioned research project.

REFERENCES

1. J. Drouilles, S. Aguacil, E. Hoxha, T. Jusselme, S. Lufkin, E. Rey, Environmental impact assessment of Swiss residential archetypes: a comparison of construction and mobility scenarios, *Energy Effic.* 12 (2019) 1661–1689. <https://doi.org/10.1007/s12053-019-09811-0>.
2. M. Beyeler, *Métamorphose : transformer sa maison au fil de la vie*, Presses Polytechniques et Universitaires Romandes, Lausanne, 2014.
3. J. Drouilles, Quartiers résidentiels périurbains en transition : Comparaison multicritère de scénarios prospectifs à l'horizon 2050, EPFL (Ecole Polytechnique Fédérale de Lausanne), 2019. <http://infoscience.epfl.ch/record/269159> (accessed September 2, 2019).
4. J. Drouilles, S. Lufkin, E. Rey, Energy transition potential in peri-urban dwellings: Assessment of theoretical scenarios in the Swiss context, *Energy Build.* (2017) 379–390. <https://doi.org/10.1016/j.enbuild.2017.05.033>.

5. J. Drouilles, S. Lufkin, E. Rey, Peri-urban residential neighbourhoods at the margins of current trends in urban growth: towards sustainable transition paths?, *Int. J. Sustain. Dev. Plan.* 13 (2018) 954–966. <https://doi.org/10.2495/SDP-V13-N7-954-966>.
6. M. Antal, G. Mattioli, I. Rattle, Let's focus more on negative trends: A comment on the transitions research agenda, *Environ. Innov. Soc. Transit.* (in press) 4. <https://doi.org/10.1016/j.eist.2020.02.001>.
7. M. Dumont, *Le périurbain : un milieu en perpétuelle évolution*, (2018). <https://www.millenaire3.com/interview/Le-periurbain-un-milieu-en-perpetuelle-evolution> (accessed September 26, 2018).
8. P. Filion, Suburban Inertia: The Entrenchment of Dispersed Suburbanism, *Int. J. Urban Reg. Res.* 39 (2015) 633–640. <https://doi.org/10.1111/1468-2427.12198>.
9. E. Rey, Quartiers de villas, friches du futur ?, *Tracés. Zones villas* (2009) 7–8.
10. ARE, R. Gilgen Thétaz, M. Kellenberger, *Tendances et défis: faits et chiffres relatifs au Projet de territoire Suisse*, ARE (Federal Office for Spatial Development), Bern, 2018.
11. P. Rérat, *Habiter la ville: evolution démographique et attractivité résidentielle d'une ville-centre*, Alphil, Neuchâtel, 2010.
12. W.A.V. Clark, M.C. Deurloo, Aging in place and housing over-consumption, *J. Hous. Built Environ.* 21 (2006) 257–270. <https://doi.org/10.1007/s10901-006-9048-3>.
13. M. Ströbele, M. Hunziker, Are suburbs perceived as rural villages? Landscape-related residential preferences in Switzerland, *Landscape Urban Plan.* 163 (2017) 67–79. <https://doi.org/10.1016/j.landurbplan.2017.02.015>.
14. CH, Federal law on territorial planning (LAT), 22 June 1979, RO 1979 1573, Berne: Swiss Federal Council, 2013.
15. S. Schetke, D. Haase, Multi-criteria assessment of socio-environmental aspects in shrinking cities. Experiences from eastern Germany, *Environ. Impact Assess. Rev.* 28 (2008) 483–503. <https://doi.org/10.1016/j.eiar.2007.09.004>.
16. J. Drouilles, S. Lufkin, E. Rey, Towards a sustainable renewal of peri-urban neighbourhoods of single-family houses in Switzerland, in: *Proc. Int. Conf. Sustain. Des. Built Environ.* 2017, London, UK, 2017: pp. 776–786.
17. J. Menthonnex, *Estimation des durées de vie par génération : Evolution 1900-2150 et tables de mortalité par génération 1900-2030 pour la Suisse*, OFS (Federal Statistical Office), Pully, 2015.
18. SIA, *SIA 2040:2017, La voie SIA vers l'efficacité énergétique*, SIA Swiss society of engineers and architects, Zurich, 2017.
19. SIA, *SIA 2039:2016, Mobilité - Consommation énergétique des bâtiments en fonction de leur localisation*, SIA Swiss society of engineers and architects, Zurich, 2016.

Sustainable communities through an innovative renovation process:

Subsidy retention to improve living conditions of captive residents

LEONTIEN BIELEN, ALEXIS VERSELE

KU Leuven, Ghent, Belgium

ABSTRACT: In many European cities, one of the main urban challenges is the lack of affordable, qualitative and energy-efficient housing for people with a low income. Prices on the private rental market are increasing and waiting lists for social housing are growing. Population ageing and a rising proportion of single- and two-person households result in a rising demand for more compact housing types. For vulnerable residents, the affordable private market segment is narrow and shrinking fast. Captive residents are living in poor quality houses and do not have the means and skills to renovate. This research focuses on how to tackle this main urban challenge by renovating the houses of captive residents through the innovative system of subsidy retention. The analysis of case studies in the city of Ghent shows the preliminary results of the positive impact on housing quality and energy efficiency. The methodology for upscaling these projects is discussed, based on a case study of 100 housing renovations of captive residents in Ghent. This research is formulating an optimization of the renovation works through the financial policy instrument of subsidy retention for improving housing conditions of captive households.

KEYWORDS: Renovation, Subsidy retention, Housing quality, Innovation

1. HOUSING MARKET

The Flemish region of Belgium (Flanders) counts a huge number of homeowners: in 2013, 70,5% of the Flemish households was living in his own property. However, a descending trend is visible since 2005, when 74,4% of the households had a property of their own [1]. The numbers for 2018 show no significant changes compared to 2013 with 72% owner-occupants [2]. The private rental market in Flanders is for 95% owned by private landlords. The majority of them (64%) is renting out only one house. In 2018, 10.990 houses were on the social rental market, rented via Social Rental Agencies (SRAs) [3]. From 2005 to 2013, prices of private rent increased by 8%, which is 1% on top of the inflation. Winters S. et al. [1] observed that the most vulnerable groups are suffering the most from this evolution. Even though private rental prices have increased the most, residents also encounter growing problems on the social rental market and as owner-occupant. Differences between property and rental market can be found in a combination of the evolution of income and housing expenses. While income did not change significantly, rental prices were increasing more than repayment of loans [1]. Regarding the social rental market, waiting lists for renting from social rental agencies are growing: in 2014, 120.504 people were waiting for social housing; in 2018, this number increased to 153.910 [4].

A growing proportion of elderly people and single- and two-person households results in a rising demand for more compact housing types such as apartments [5]. Population ageing and socialization of healthcare create a growing need for an adjusted living environment for elderly people.

For vulnerable residents, the affordable private market segment is narrow and is shrinking fast. Captive residents are living in poor quality houses and do not have the means and skills to renovate. Traditional support tools (premiums, tax benefits,...) do not reach the most vulnerable inhabitants since they require seed money to pre-finance renovation costs or need to pay taxes to be able to enjoy a tax reduction. Without external intervention, the situation is getting worse for these citizens, their future and the neighbourhood. Research about housing shortage in Flanders has estimated the proportion of captive owners in the cities of Antwerp and Ghent around 4,3% on average [6]. In Ghent, about 6.000 owners would be captive residents. On the rental market, there are about 93.000 captive renters (households) in Flanders [7].

2. ENERGY PERFORMANCE AND HOUSING QUALITY

The largest single energy consumer in Europe is the building sector with 36% of EU CO₂ emissions. By 2030, the European Commission aims to cut CO₂ emissions by at least 40% [8]. To reach this goal, the

EU has established a legislative framework including the Energy Performance of Buildings Directive 2018/844 (EPBD). The EPBD requires all new buildings from 2021 (public buildings from 2019) to be nearly zero-energy buildings (NZEB). The nearly zero or very low amount of energy required in these buildings, should be coming to a very significant extent from renewable sources, including sources produced on-site or nearby.

According to the Government of Flanders, around 80% of the newly built houses could be classified as an NZEB [9-10]. However, the energy performance of the existing building stock is extremely poor. In 2019, only 5% of the existing residential buildings in Flanders reached the target for maximum energy consumption in 2050 of 100 kWh/m²year [5].

In Flanders, 33% of the houses of owner-residents do not meet the minimum requirements of the Flemish Housing Standard [11]. In the private rental sector, 47% of the houses are of inadequate quality [1]. The cost of renovating the Flemish housing stock conform the Flemish Housing Standard is estimated at 137 – 145 billion euros [12].

These results clearly show that improving the energy performance of the existing housing stock is crucial. Especially for people with a low income in low quality housing, the Flemish Housing Standard and the stipulated energy objectives are hard to achieve [6]. The probability of performing deep energy renovations appears to be much lower in houses with renters or vulnerable residents such as low-income groups, elderly people, singles or unemployed inhabitants. Financial obstacles seem to hinder renovation works. Moreover, a lack of knowledge and information about existing policy support can obstruct renovation works. Finally, the practical organisation of a renovation process could be an obstacle, especially in multi-family housing [13]. Considering these hindrances, Ryckewaert et al. [14] stressed the need for diverse policy measures, including specific financial support, information, guidance and unburdening.

Housing and income inequalities can also be seen in other European countries. In a majority of EU Member States, house prices are growing faster than income and housing has become the highest expenditure. In 2015, about 39.3% of EU households at risk of poverty were overburdened by housing costs [15]. Two-thirds of the European Union's population is living in urban areas. The EU's urban renewal activities aim at rehabilitating urban areas to improve the living environment, covering social inclusion and sustainable development. In many of these cities, the process of gentrification is changing the character of neighbourhoods: the influx of more affluent residents and businesses is forcing locals to move due to unaffordable housing prices.

A growing demand for affordable housing for low income residents in combination with a shortage of qualitative and energy efficient housing opportunities is one of the main urban challenges today. Therefore, this paper focuses on how to tackle this challenge with the innovative financial concept of subsidy retention. The paper will give an overview of the findings and results of the cases of the Dampoort KnapT OP! - projects (DKO). Furthermore, the methodology for upscaling these projects will be discussed (GKO-project). The analysis of the data results in clear trends that are used to shape the GKO-project progress and direct it towards a successful outcome. More data will be analysed in the next stages of the research.

3. SUBSIDY RETENTION FOR CAPTIVE HOMEOWNERS

Since a few years the concept of subsidy retention has been used in a partnership between civil society organisation, researchers from different universities and with policy makers from different local authorities as well as from the Flemish region to improve the living conditions of captive residents [16-17].

For each captive homeowner, selected based on a number of social requirements, the public authorities are providing a subsidy to execute renovation works that are agreed in advance between local authority and homeowner. The principle of subsidy retention is based on an allowance that is recurring over time to the public authorities. In described projects, the 'recurring' happens when the official ownership of the property changes (sale/disposal/donation/inheritance). Through this concept, public finance is not only used for a limited group, but it will allow the authorities to reuse the fund for new renovation projects in the future. After an initial intervention, the value of the recurring allowance at the time of repayment must be able to guarantee the same improvement in housing quality as before. To realise this, the homeowner has to pay back the initial allowance increased with a part of the realized added value of the property. This added value is based on the value of the property at the moment of reimbursement decreased with the nominal value of the allowance and an exempted amount (the inflation-adjusted value of the property before renovation works).

3.1 Cases

This concept was first implemented in the city of Ghent where it was tested in the projects of DKO 1 (2015) and 2 (2018). After this testing phase, the approach was adopted by several Flemish cities and realised in another neighbourhood of Ghent and in different municipalities in the province of Vlaams-Brabant. The European funded 'Urban Innovation

Actions'-project 'Gent knapt op' (GKO) (2019 – 2021) [18] aims to explore the impact of upscaling of this concept on macro-economic and social level. The GKO-project aims to renovate 100 houses of captive residents in different neighbourhoods of Ghent through the principle of subsidy retention. Before, during and after the renovation process, the residents are unburdened and supported technically, financially, administrative and socially.

3.2 Neighbourhood analysis to reach different target groups

In order to have a well-organized communication strategy and an efficient recruitment process in the GKO-project, priority neighbourhoods were identified based on quantitative analysis of neighbourhood economic, social and housing indicators as well as on qualitative input. Therefore, many key stakeholders were contacted and cases were examined in collaboration with field workers. In addition, similar projects such as a pilot project (Dampoort KnapT OP!) were investigated. From this survey, a set of indicators was derived to identify the profile of potential beneficiaries. Detailed mapping was conducted based on demographic data, neighbourhood evaluation and property statistics [19-20]. Data from the public centre for social welfare, such as the number of inhabitants with debt mediation, a living wage or a winter premium for energy costs, were mapped with the prosperity index and unemployment rates. As an additional criterion, the presence of 'boots on the ground' – non-profit organisations offering social assistance to inhabitants – was considered in the final choice of the target neighbourhoods. Since a renovation process demands a lot of administration, negotiation skills, commitment and know-how, professional social workers can offer private support to guide participants through the renovation process. The collaboration between a local government and private partners offers a lot of advantages. The government is an independent and neutral key stakeholder. Civil society organisations have know-how and expertise in specific disciplines and can be more flexible and responding to individual needs. As a result of the analysis of these data, 4 densely populated urban areas were selected for the implementation of the project: Brugse Poort - Rooigem, Rabot - Blaisantvest, Dampoort – Sint Amandsberg and Muide – Meulestede - Afrikaalaan.

3.3 Target groups

The main target group in this research is captive residents, for whom a differentiation can be made into 4 categories. The first category exists of owner-occupant who are stuck in their house due to the lack of affordable housing in the city where rents are high

but loan charges are relatively low. Or they own a house of poor quality because of their personal situation (divorce, sickness, unemployment,...). They don't have the financial means to improve their housing situation. The second group is the co-owners in apartments, who don't have the possibility of financially contributing to renovation works decided by the community of co-owners. Thirdly, there are captive renters whose landlord doesn't have the possibility to improve his property. With their low income, these renters are not able to improve their housing situation without external support. A fourth category is elderly people whose houses are not adapted to their physical needs.

Before the recruitment phase could start, the terms and conditions for participation had to be defined. For each target group, a set of conditions was listed. These conditions are grouped in 2 categories: mandatory application requirements and criteria that are weighted and scored to create a ranking in order to identify the most vulnerable candidates.

3.4 Financial sensitivity analysis

The sensitivity and risks of the recurring fund, i.e. the creation of sufficient added value, depend on several aspects: whether or not there is a mortgage loan on the property, the extent to which the intervention increases the value of the property, the real interest rates and inflation, the amount of the allowance in relation to the value of the property before the renovation works and the evolution of real estate prices compared to the inflation.

After analysing the sensitivity of the recurring fund, the following suggestions were made. Firstly, in the case of reimbursement of the fund after a period of ten years, a renovation would result in sufficient added value at the moment of reimbursement. A shorter period of reimbursement would imply a high risk and will reduce the value of the fund. Moreover, renovation projects where the allowance is used for adjustments that would not result in an added value of the property will pose a risk to the fund. Secondly, market dynamics play an important role in maintaining the value of the fund and generally show a decrease in the relative value of the reimbursements [21-22]. This is partly due to decreasing real interest rates. Thirdly, to limit risks, an allowance of 30.000 EUR per household is chosen. On the one hand, this was determined based on the experience from previous projects (i.e. 'Dampoort KnapT OP!' 1 & 2 and 'Rabot KnapT OP') [17]. This experience demonstrated that a minimum amount of 30.000 EUR was needed to renovate the houses with the poorest quality conform the standards of the Flemish Housing Code. Ryckewaert et al. [12] estimated that Flemish houses with a need for

restoration or renovation, would require an average renovation cost of 22.000 EUR per house to meet the Flemish Housing Standard. On the other hand, the sensitivity analysis shows that increasing this amount over 30.000 EUR reduces the renovation capacities of the recurring fund in the future.

4. IMPROVING THE HOUSING QUALITY IN THE SELECTED NEIGHBOURHOODS

To achieve successful results, the project does not use a predetermined set of renovation works, but starts from the individual needs of the occupants and the necessary renovation works. Each house completes a screening process to see if it complies with the Flemish Housing Standard in which the basic housing needs are defined [11]. Additionally to this screening, also the energy performance is mapped. Based on these results, a set of prioritized renovation works related to the safety and health of the occupants is proposed. To diminish the risks of the recurring fund, some works such as decoration or renovation of rooms without residential function, are not considered.

Once the candidates have successfully completed the selection process and agreed on the proposed renovation plan, tenders are requested from contractors and, if necessary, the application of permits is arranged. Candidates are guided throughout the entire renovation process. Technical assistants are in charge of communication between homeowners, architects and contractors. When complex renovation works are required, such as a new roof construction or a structural reinforcement of the house, families are offered a temporary housing facility. Afterwards, they will be assisted in the preparatory work for subsidy applications.

Because the renovation works often include little fragmented activities, engaging interested and adequate contractors is difficult as they prefer larger renovation works. Combining activities is not always successful because different tasks that have to be carried out at different moments are involved. Therefore, the tender process was shifted from submission of two different offers to a tender request sent to at least two contractors. In that way, a contractor can be appointed earlier in time and the renovation process will not be delayed.

5. EVALUATION

Based on the ambitious climate plans of the city of Ghent, the GKO-project sets the goal for primary energy consumption after renovation to a maximum of 70 kWh/(m².a) for heating [23]. Monitoring before and after renovation aims to understand the comfort and energy performance of the building and the applied renovation measures.

For the GKO-project, the authors are monitoring the indoor climate (temperature, relative humidity) and energy performance (infra-red scans) in different dwellings. This data will be collected for at least 4 weeks during heating season, with a 10 minutes interval. The consumption of fossil fuels and electricity will be monitored through collection of data from meters in the houses and data from the energy supply services. An energy survey will be conducted in each house to map the user behaviour.

Breesch et al. [24] applied this monitoring strategy when analysing the impact of the renovation measures on the indoor climate and energy use in similar houses from the DKO 2 - project. This research shows that it is difficult to draw general conclusions from comparable renovation actions in the three studied houses. The measurements of air tightness, indoor temperature and the energy use for heating presented different results after renovation. Therefore, the monitoring process for the GKO - project will be extended to a study of ten dwellings with varying characteristics, most of them terraced single-family houses. Furthermore, cash flow simulations will weigh costs and expected energy savings to define the most cost-optimal renovation scenarios.

5.1 First preliminary results of housing quality and energy performance (DKO-project)

During the DKO 1-project, 9 dwellings of captive residents were renovated. Housing quality improvements and energy efficiency were analysed [17].

In most of the houses, residents were exposed to serious safety and health risks such as danger of electrocution (60% of the houses), risk for carbon monoxide (CO) intoxication (70%) and humidity problems (100%). All these risks were eliminated after renovation works, except for one house where risk of collapse was prioritized over electricity works.

In order to be in line with the Flemish Housing Standard, houses should remain under 15 penalty points. When a defect of 15 penalty points or two defects of 9 points are not renovated timely, this will lead to a declaration of inadequate or even uninhabitable housing. Before renovation works, the houses reached an average of 51 penalty points. After renovation, this could be reduced to an average of 11 points.

Thanks to the renovation works, the energy efficiency of the houses has improved. The average energy performance of 519 kWh/m² before renovation could be reduced to 244 kWh/m². This is below the Flemish average of 296 kWh/m². As expected, the most impact was realized in the houses that scored worst on the Flemish Housing Standard.

Different energy saving measures were implemented during the renovation of the 9 dwellings. The percentage of houses with implementation of these measures before and after renovation can be found in Table 1.

Table 1: Implementation of energy saving measures

	% of houses before renovation	% of houses after renovation
Insulation pitched roof or attic floor	30%	90%
Insulation flat roof	20%	100%
Double (or triple) glazing	50%	100%
Efficient heating system	30%	100%
Insulation of (part of) exterior walls	0%	50%
Insulation of (part of) floor	0%	40%

The improvement of the energy efficiency is linked as much as possible to the housing quality. The share of investments in energy savings relative to housing quality for each house is visualized in Figure 2. Investment costs are based on the invoices of performed renovation works. By means of a smart renovation plan, both the housing quality and the energy performance of the houses strongly increased. E.g. the renovation of a leaking roof in 8 houses was combined with roof insulation measures.

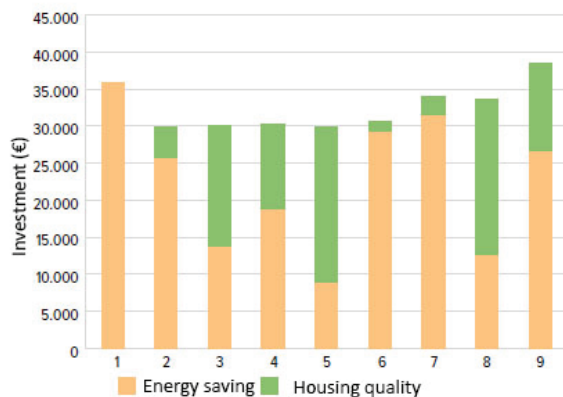


Figure 2: Investments in energy savings (under) vs housing quality (top) [17]

5.2 Impact of upscaling project

The impact of housing renovations using a recurring fund will be analysed socially, technically, financially and operationally. For measuring the qualitative impact of the recurring fund, a holistic impact assessment process is set up.

Besides impact measurements for the participants, also the situation of drop-outs and not selected candidates will be evaluated. This monitoring process starts with the assessment of the reasons for not completing the selection process. It will clarify causes of success or failure and will show if the project is reaching the right target group. This

might have impact on the selection procedure (different calls, steps and timings) but also on the terms and conditions for participation.

Furthermore, the operation and management of the recurring fund will be evaluated. All investments, both financial and human resources, are registered through the entire process. Cost-effectiveness of public spending in the project will be calculated and compared with other policy instruments.

Results of the GKO – project will be compared with the outcomes of the pilot projects in 2015 (DKO 1) and 2018 (DKO 2). The impact measurements will be key for upscaling of the project in the future. Not only for improvement of the financial instrument, but also to encourage public authorities to replicate and implement this system.

6. CONCLUSION

This paper focuses on how to tackle the urban housing challenge through renovation works following the innovative financial concept of subsidy retention. Based on previously implemented renovation projects for captive residents in Ghent, this research shows the preliminary results of improved housing quality and energy efficiency and describes the methodology for upscaling the concept.

Terms and conditions for participation ensure that the most vulnerable target groups are reached. A neighbourhood analysis was conducted based on information and data from key stakeholders, demographic data, property statistics and the presence of social workers in the neighbourhoods. A flexible timetable would facilitate the building of trust relationships and mitigate drop-outs. To reach the requirements of the Flemish Housing Standard, technical support is of utmost importance. Energy monitoring of the houses reveals the technical impact of the renovation works. Through the renovation works, safety and health risks could be eliminated in nearly all houses. The average of penalty points according to the Flemish Housing Standard could be reduced from 51 to 11. The average energy performance of the houses could be reduced from 519 kWh/m² to 244 kWh/m² through different energy saving measures. By means of a smart renovation plan, both housing quality and energy performance of the houses strongly increased. A holistic impact measurement process is set up for measuring the impact of upscaling the concept. To clarify causes of success or failure in the recruitment process, not only the situation of participants but also drop-outs and not selected candidates will be evaluated. Regarding the financial aspects of the fund, the sensitivity analysis shows that the reimbursement period should be at least 10 years to mitigate the risk of loss of value of the fund. Renovation works that would result in an added value of the property should be given preference. Market dynamics have their impact on

the fund. At least 30.000 EUR is needed to renovate the houses with the poorest quality conform the standards of the Flemish Housing Code. Cost-effectiveness of the fund will be calculated in order to improve the financial instrument to ensure that the system of subsidy retention will meet the demand for a stable structure of financial support for comprehensive renovation works for vulnerable groups.

Compared to a traditional fund which is only made available once for one household, this recurring fund endeavours that public money benefits many vulnerable families. This fund can be spread over several generations and several households. In this way, it supports a sustainable, inclusive urban regeneration that could be continued on a permanent basis. The use of subsidy retention leads to a win-win situation for households, neighbourhoods and policy makers.

ACKNOWLEDGEMENTS

This research is possible thanks to a collaboration between the city of Ghent, the Public Center for Social Welfare of Ghent, KU Leuven, the University of Ghent, AP Hogeschool Antwerp, de Energiecentrale and non-profit organizations SIVI, Samenlevingsopbouw and Domus Mundi. It is part of the ICCARus project and is co-financed by the European Fund for Regional Development through the Urban Innovative Actions (UIA) initiative.

REFERENCES

1. S. Winters, W. Ceulemans, K. Heylen, I. Pannecoucke, L. Vanderstraeten, K. Van den Broeck, P. De Decker, M. Ryckewaert and G. Verbeeck, "Wonen in Vlaanderen anno 2013. De bevindingen uit het Grote Woononderzoek 2013 gebundeld," Steunpunt Wonen, Leuven, 2015.
2. K. Heylen and L. Vanderstraeten, "Wonen in Vlaanderen anno 2018.," Steunpunt Wonen, Leuven, 2019.
3. Vlaanderen, "Cijfers over sociale huisvesting in Vlaanderen," 2020. [Online]. Available: <https://www.wonenvlaanderen.be/woononderzoek-en-statistieken/cijfers-over-sociale-huisvesting-vlaanderen>. [Accessed 2020].
4. Vlaamse Maatschappij voor Sociaal Wonen, "Over sociale huisvesting - statistieken," 31 December 2018. [Online]. Available: <https://www.vmsw.be/statistieken>. [Accessed 2020].
5. Vlaams Energieagentschap, "Vlaamse renovatiestrategie 2050: de weg naar energiezuinige en koolstofarme gebouwen," VEA, Brussels, 2019.
6. P. De Decker, B. Meeus, I. Pannecoucke, E. Schillebeeckx, J. Verstraete and E. Volckaert, Woonnood in Vlaanderen : Feiten/Mythen/Voorstellen., Antwerp, Belgium: Garant Uitgevers nv, 2015.
7. L. Vanderstraeten and M. Ryckewaert, "Noodkopers, noodeigenaars en captive renters in Vlaanderen. Nadere analyses op basis van het GWO2013," Steunpunt Wonen, Leuven, 2019.
8. "European Commission," 9 March 2020. [Online]. Available: https://ec.europa.eu/info/news/new-energy-performance-buildings-directive-kicks-2020-mar-09_en. [Accessed 2020].
9. Vlaams Energieagentschap, "EPB-eisentabellen per aanvraagjaar," [Online]. Available: www.energiesparen.be/EPB-pedia/eisen-per-aanvraagjaar. [Accessed 2020].
10. VEA, "EPB-CIJFERRAPPORT (Cijfers over EPB-aangiften van woongebouwen ingediend vanaf 01-01-2006 tot en met 31-12-2019)," Vlaams Energieagentschap, 2020.
11. Vlaamse Regering, "Vlaamse Wooncode: Geconsolideerde versie oktober 2009," Department Ruimtelijke Ordening, Woonbeleid en Onroerend Erfgoed, Brussels, 1997.
12. M. Ryckewaert, K. Van den Houde, L. Vanderstraeten and J. L. m.m.v. Leysen, "Inschatting van de renovatiekosten om het Vlaamse woningpatrimonium aan te passen aan de woningkwaliteits- en energetische vereisten," Steunpunt Wonen, Leuven, 2019.
13. K. Van den Broeck, "Drempels voor renovatie aan de vraagzijde," Steunpunt Wonen, Leuven, 2019.
14. M. Ryckewaert, K. Van de Broeck and F. Vastmans, "Renovatie van de Vlaamse woningvoorraad: vaststellingen en beleidsaanbevelingen," Steunpunt wonen, Leuven, 2019.
15. The Housing Europe Observatory, "The State of Housing in the EU," Housing Europe, the European Federation of Public, Cooperative and Social Housing, Brussels, 2017.
16. Provincie Vlaams-Brabant, "Renovatielening met uitgestelde betaling," Provincie Vlaams-Brabant, [Online]. Available: <https://www.vlaamsbrabant.be/wonen-milieu/wonen-en-ruimtelijke-ordening/leningen-premies-subsidies/renovatielening/index.jsp>. [Accessed April 2020].
17. A. Morbee and K. Maes, "Dampoort KnapT OP! Wijkrenovatie met noodkopers.," OCMW Gent, Ghent, 2016.
18. European Union (UIA), "ICCARus (Gent knapt op) - Improving housing conditions of captive residents in Ghent," Urban Innovative Actions, [Online]. Available: <https://www.uia-initiative.eu/en/uia-cities/ghent-call3>. [Accessed April 2020].
19. Statbel, "Belgium in figures," [Online]. Available: <https://statbel.fgov.be/en>. [Accessed 2020].
20. The city of Ghent, "Buurtmonitor Gent," [Online]. Available: <https://gent.buurtmonitor.be/>.
21. F. Vastmans, E. Buyst, R. Helgers and S. Damen, "Woningprijzen: woningprijs-mechanisme & marktevenwichten. De logica, nood en valkuilen van betaalbaarheid als woningprijs determinant," Steunpunt Wonen, Leuven, 2014.
22. R. Helgers, E. Buyst and F. Verboven, "The Relation between Housing Characteristics and Housing Prices: A New Light into the Recent Evolution of Housing Prices in Flanders," Larcier, 2019.
23. D. Termond and T. Heyse, "Gents Klimaatplan 2014 - 2019," Stad Gent, Gent.
24. H. Breesch, A. Beyaert, A. Callens and A. Versele, "Impact of Renovation Measures on the Indoor Climate and Energy Use in Single Family Dwellings in Belgium," in PLEA 2020: Planning Post Carbon Cities, 2020.

Designing the Future to Predict the Future: An 'urban-first' approach to co-creating zero-carbon neighbourhoods

ANDREW JENKINS*¹, GREG KEEFFE*¹, CRAIG LEE MARTIN², ANDY VAN DEN DOBBELSTEEN³,
SIEBE BROERSMA³, RICCARDO MARIA PULSELLI⁴

¹Queen's University Belfast, Belfast, United Kingdom

²The Grenfell-Baines Institute of Architecture, UCLan, Preston, United Kingdom

³TU Delft, Delft, The Netherlands

⁴The University of Siena, Siena, Italy

ABSTRACT: *The natural ecotone between people, community and carbon reduction is the zero-carbon community. Over recent decades, the design of zero-carbon communities has focussed too greatly on carbon emissions and not enough on building communities. Anthropogenic climate change is a human problem, yet people are seldom placed at the centre of design solutions. The City-zen Roadshow is an intensive co-creational approach to creating zero-carbon communities, which places stakeholders at the very centre of the design process. The methodology uses an 'urban-first' approach and champions urban design as the main driver to deliver change. Carbon accounting and energy analysis sit in adjacency with the urban design proposals to deliver interventions that are net zero-carbon, low energy, low waste, socially rich, ecologically diverse, economically robust, resilient, fit for purpose and engaging. The paper describes this novel approach using one roadshow as a case study to illustrate the urban interventions proposed. Living in zero-carbon communities is not just about photovoltaic panels and wind turbines. It is, instead, about thinking differently about the way in which people live and the decisions they make, to provide people with alternative ways of living that are more desirable than those currently available.*

KEYWORDS: *Urban, Neighbourhood, Co-creation, Zero-carbon, Stakeholders*

1. INTRODUCTION

The European Union and the United Kingdom have both pledged to reduce carbon emissions to zero by 2050 [1,2]. This reduction in carbon emissions is critical in reducing the effects of climate change and maintaining a global temperature increase of less than 2°C [3]. The European Union has seen a fall in carbon emissions of 22 percent between the years of 1990 and 2017 [4] and the United Kingdom has seen a reduction of 44 percent between the years of 1990 and 2018 [5]. To date, big investments in renewable technologies, such as on-shore and off-shore wind farms alongside bioenergy, have led to significant carbon savings [6].

Although these figures represent a significant contribution to reducing carbon emissions, the rate of reduction is not sufficient to achieve net-zero carbon emissions by 2050. To meet this goal, the performance and efficiency of renewable technologies will need to improve, and the cost of those technologies will need to reduce. The burden of reducing carbon emissions, however, does not rest solely on the advancement of technological solutions. The human element of what is a human problem needs to be considered and addressed, and individual people need to understand their role in mitigating carbon emissions.

2. THE ROLE OF THE INDIVIDUAL

Anthropogenic climate change is the cumulative effect of all human decisions made over the past two hundred years. Consequently, the potential impact of

small changes in behaviour and lifestyle choices in the future can accumulate to a large overall reduction in carbon emissions. For example, it is estimated that becoming car-free could save at least 1 ton of CO₂e per capita per annum and that eating a plant-based diet could reduce carbon equivalent emissions by up to 1.6 tons per capita per annum. Avoiding a single transatlantic return flight could save at least 0.7 tons of CO₂e per annum whilst purchasing electricity from a renewable provider could save between 0.1 and 2.5 tons per capita per annum [7]. Behavioural change will be instrumental in achieving net-zero carbon emissions, and this has to be driven by education and engagement to empower individuals to take control of future change within their local community.

3. ZERO-CARBON COMMUNITIES

The natural ecotone between people, community, and carbon reduction is the 'zero-carbon community'; otherwise known as a one-planet community, an ecopolis, an ecodistrict, or an ecocity [8]. The idea of an eco-city was first explored in 1898 by Ebenezer Howard in his book 'Garden Cities of To-morrow' [9]. This idea re-emerged during the 1960s and 1970s and was later formalised in 1987 by Richard Register when he published the book 'Ecocity Berkeley: Building cities for a healthy future' [10]. These early ideas focussed on compact developments and mixed land use, a reprioritisation of pedestrians, along with the increased use of public transport and a focus on mitigating ecological damage. Early eco-city principles

also included the formations of ecologically and socially just economic development, conservation, and increased resource efficiency [11].

Since then, the idea of an eco-city has developed into a vehicle to directly reduce carbon emissions and energy use through the design and implementation of 'place' [12]. Unfortunately, very few examples encompass the holistic approach of eco-cities due to an over-emphasis on reducing energy use as the primary driver of mitigating climate change [13, 14, 15]. Whilst it is important to understand energy use at a neighbourhood and city scale, renewable energy and its efficient conversion into heat, light, and work does not provide any meaningful depth to a community.



Figure 1: The first UK eco-town, 'North-West Bicester'.

This can be seen in examples such as North-West Bicester in England, which can be used as an example to illustrate the shortcomings of current zero-carbon developments (fig. 1). This project was the first eco-town to be completed in the UK and it boasts rooftop photovoltaic panels, an on-site combined heat and power plant, efficient insulation, rainwater harvesting and green garage roofs. It is a zero-carbon development but there is no green space for families to enjoy, neither is there a central square to facilitate community activities. The site is awash with hard surfaces and there are no on-site conveniences to reduce car journeys. Bicester town centre is a 30-minute walk away, or a 9-minute bike ride, with no cycle routes running through, to, or from, the development. The development is disconnected from its surroundings and offers no incentives for residents to change their behaviours. North-west Bicester, therefore, is a traditional English development with the gilt of zero-carbon credentials. Residents who live there are unlikely to take a walk because there is nowhere to walk to, and they would be unlikely to go for a bike ride due to the lack of safe bicycle routes. Although the development will save many tons of carbon over its useful life, it could have saved many more if it had considered the impacts of providing a healthier, happier and more connected lifestyle to the residents that would ultimately bring the site to life.

4. THE CITY-ZEN ROADSHOW

The built environment plays a significant role in how people choose to live their lives and the decisions they make [16, 17, 18]. Therefore, to create zero-carbon neighbourhoods that holistically address economic, social, ecological and environmental issues, new methodologies are required that are holistic in nature. In addition to this, these new methodologies need to consider the human element of the challenges ahead to help deliver zero-carbon developments that are net zero-carbon, low energy, low waste, socially rich, ecologically diverse, economically robust, resilient, fit for purpose and engaging places to live.

This was the premise of the City-zen Roadshow, which formed part of the wider EU initiative 'City-zen'. The City-zen Roadshow combined local stakeholder knowledge with global expertise to co-create future zero-carbon communities. The City-zen Roadshow aimed to work closely with people from the hosting city, such as city leaders, neighbourhood associations, urban planners, and residents to co-create future zero-carbon propositions that were fit for purpose, both in terms of carbon savings and improvements to the communities. The philosophy behind this approach is to leverage zero-carbon development to improve the quality of life and to include stakeholders from the very beginning to maximise the impact and the advocacy of the interventions proposed. Over four years, the roadshow has visited ten cities: Belfast, Izmir, Dubrovnik, Menorca, Roeselare, Preston, Nicosia, Sevilla and Amersfoort. These were chosen due to already engaging in zero-carbon initiatives and the prior enthusiasm of the municipalities and stakeholders regarding the roadshow methodology.

5. AN 'URBAN-FIRST' APPROACH TO ZERO-CARBON

In addition to the co-creational nature of the City-zen Roadshow, the methodology utilises an 'urban-first' approach, which champions the role of urban design to deliver widespread change. Although urban design is at the forefront of this methodology, carbon accounting and urban energy systems work in adjacency to the urban design proposals to deliver holistic and meaningful interventions (fig 2.)

The methodology begins with separate analyses of existing carbon emissions, energy use and the urban form, alongside societal and contextual considerations. These investigations are driven by guided tours around the city, insights provided by local residents and conversations with local stakeholders and city leaders. These elements, when combined, derive an overall brief for the project, including urban challenges, the carbon footprint and overall energy use. After this, a series of urban explorations are developed alongside local stakeholders to address the key social, economic and environmental challenges within the neighbourhood. These explorations are

then developed further with the assistance of carbon accounting and urban energy systems to improve the carbon mitigation of each intervention. After this, the methodology returns to the urban explorations to include additional elements such as energy centres and community farms, in addition to assigning areas for photovoltaic panels, vehicle charging points, and wind turbines. The carbon mitigation of each intervention is calculated and combined to give an overall carbon mitigation value for the urban design strategy. Finally, a transition roadmap is developed, which identifies a series of annual goals to achieve net-zero carbon emissions by 2050.

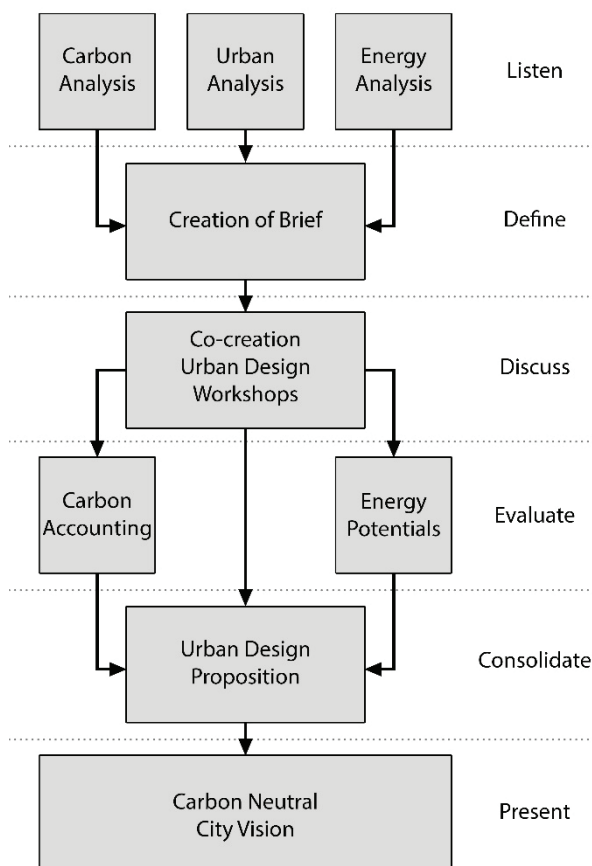


Figure 2: The 'urban-first' zero-carbon design methodology

6. ROESELARE, BELGIUM: CASE STUDY

To contextualise the urban-first approach of the City-zen Roadshow, a case study will be used to illustrate some of the urban interventions developed alongside local stakeholders. The city of Roeselare in Belgium will be used for this purpose due to the extensive participation of stakeholders and the breadth of urban interventions proposed. The city of Roeselare invited the roadshow to visit them to engage creatively with stakeholders and reduce their carbon footprint to zero.

6.1 Listen and Define

Upon arriving in Roeselare, the 'roadies' were taken on a tour around the urban centre to see the

carbon reduction measures that are currently in place or under construction. Later, the roadies were shown around the neighbourhood that would be the focus of the investigations and met with several local stakeholders who spoke about their neighbourhood. The neighbourhood was located south-west of the city centre in between the two ring roads that define the structure and form of the city. When walking around the neighbourhood it became clear that several key characteristics defined it. These included disconnections both from the city and the adjacent natural landscapes, low building density, periodic flooding, the lack of a defined centre, poor legibility, and low quality public green space. These key challenges would help form the brief for the project and define the scope and scale of the interventions.

Through detailed conversation with the municipality, the energy use and resulting carbon footprint of the city was calculated. The energy use of the city was estimated to be 2.28×10^6 kWh per annum. The life cycle analysis emission factor of the energy produced to power the city was calculated to be $0.181 \text{ kgCO}_2\text{e/kWh}$ based upon a 33 percent contribution from gas, a 17 percent contribution from renewables, and a 50 percent contribution from nuclear energy. The carbon emissions of Roeselare were estimated to be 412,396 tons of CO_2e per annum and the carbon footprint was equivalent to 30,548 hectares of forest, which is five 5.1 times larger than the city's geographic area of 5979 hectares (fig. 3). The area of forest was calculated based upon the ability of forest land to sequester 1.35 kg of CO_2e per square metre per annum [19].

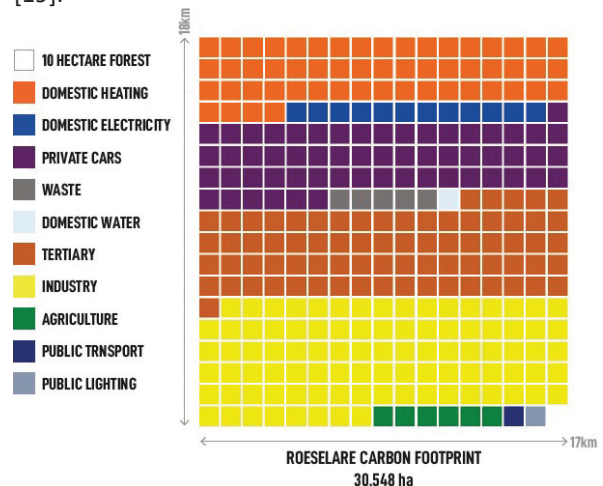


Figure 3: The carbon footprint of Roeselare. Each square represents ten hectares of forest land.

6.2. Discuss, Evaluate and Consolidate

To tackle the key challenges of the neighbourhood, a series of urban design workshops took place in several locations at different times of day to maximise stakeholder engagement. In collaboration with local stakeholders, a number of urban interventions were

developed with a focus on providing relevant infrastructures to facilitate walking and cycling to and from the city in order to minimise car use, to increase the density of the neighbourhood, to create a defined neighbourhood centre in order to provide both public open space and to provide opportunities for local businesses, and to address the periodic flooding of the adjacent culvert.

The culvert that was in place was very narrow and offered very little capacity to deal with peak rainfall. Due to the lack of green space in the neighbourhood, water runoff was also very high. Therefore, it was proposed to widen the culvert and create an elevated walkway along one side to create a nature walk to and from the city (fig. 4). The culvert would also be fed by a new sustainable drainage system that would incorporate swales and ponds to maximise water attenuation and minimise discharge into the culvert, which would also create new habitats for local wildlife.

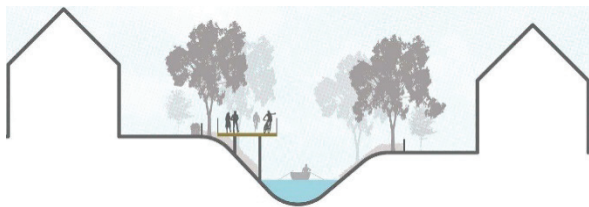


Figure 4: Widening of the culvert to create a nature walk and improve connectivity.

The neighbourhood was in desperate need of a direct route towards the city to greatly reduce the number of needless car journeys taken. The neighbourhood suffers from poor urban planning that favoured the creation of multiple cul-de-sacs, which generally pushes people towards making needless car journeys to travel relatively small distances. To address this, several cul-de-sacs were connected together with minimal loss of private land, to create an uninterrupted route to the city centre.

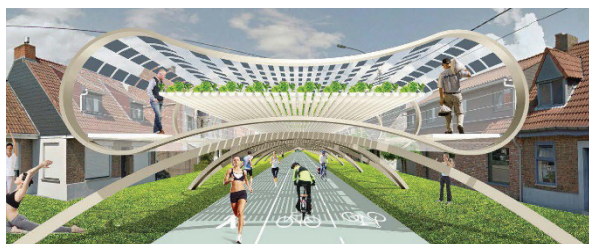


Figure 5: The neighbourhood cycle route with a food and energy producing canopy.

This route could be used by those walking, running or cycling and was covered by a canopy to make it useable regardless of the weather. The canopy also produced food and electricity for the local neighbourhood. When paired with an electric bicycle sharing scheme, this intervention would be capable of greatly reducing vehicle carbon emissions (fig. 5).

The intensity of the neighbourhood was very poor, offering almost no space for local amenities or recreational activities. To address this, a neighbourhood centre was proposed that could facilitate these requirements (fig. 6). This centre would offer a supermarket, retail space, a large open park and a boating lake to further increase water attenuation. Large greenhouses in addition to a large rooftop urban farm on the retail unit would help to grow food for the local population; not only creating jobs but also reducing food miles. The creation of a centre helps to reorient and reinvigorate the neighbourhood, whilst providing the residents with access to nature and much needed open space.



Figure 6: The new neighbourhood centre including retail space, a rooftop farm, open green space, and a boating lake.

Low building density is considered to be a problem because it forces people to spread out over a large area and, as a result, some residents can be much further away from the goods and services they require, which increases travel distances and the number of car journeys made. Low-density settlements also promote urban sprawl, which eats into natural landscapes over time. In the north-east of the neighbourhood there are some pockets of land and several old buildings that were unoccupied that could facilitate the development of apartment blocks placed between the neighbourhood centre and the city centre. This would help provide the space needed for additional amenities such as doctors, schools, and places to meet. These new blocks would create large areas of flat roofs that would be perfect locations for rooftop farming.



Figure 7: A row of 'technoterps' including aquaponic flood defences and rooftop greenhouses.

Many of the properties in the neighbourhood benefit from flat roofs, which offer potential opportunities for other rooftop farms. The idea of the

‘technoterp’ was created, which incorporated flood defences made of raised beds and fish tanks to run aquaponic systems that grew food on the roof (fig. 7). Where flat roofs were not present, community block farms were created to increase the overall resilience of the neighbourhood.

In addition to the urban interventions proposed, the supporting energy infrastructures were also a key component of decarbonising the neighbourhood. The output of these interventions was not simply to quantify the scale of renewable technologies required, but also to break down those vast numbers into annual deliverables. This manifested as the installation of seven hectares of roof- and ground-based photovoltaic panels every year, one hectare of thermal photovoltaic panels every year, and one 4MW wind turbine every year before 2050 to meet the electricity needs of the city. To meet the high-temperature heating demands of the city, it would need to increase the existing district heating network by 10 GWh and connect 850 homes per year, increase industrial waste heat capture by 10GWh per year, install 4GWh per year of solar collectors, and install an additional 4GWh of high-temperature storage per year up to 100GWh. To meet the medium- and low-temperature demands of the city it would be necessary to thermally renovate 1100 properties per year, capture 2.5GWh of medium-temperature waste heat per year up to 35GWh, and increase aquifer and borehole heat storage by 3GWh per year up to 80GWh for both medium- and low-temperature heat by 2050. These deliverables were also proposed at the urban scale to determine where these technologies could be positioned (fig. 8).

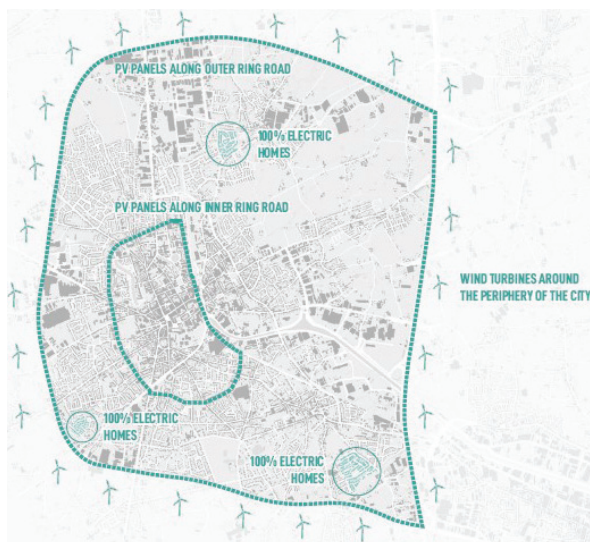


Figure 8: The energy production plan for the city including two rings of photovoltaic panels alongside highways, a ring of wind turbines, three 100% electric communities in addition to rooftop and ground-based photovoltaic panels.

6.4. Carbon Savings

Both the urban and energy interventions proposed have varying impacts when considering the reduction in carbon emissions. Each intervention reduces carbon emissions outright, but factors such as increased energy consumption in the future must also be taken into consideration. In addition to this, it can be difficult for municipalities to determine which interventions would have the largest impact and which should be prioritised. For example, the carbon emission savings brought about by improving the thermal performance of building skins would be fifteen times greater than those provided by the combined savings of increased recycling, LED streetlights and electric buses (tab. 1)

Table 1: Impact of urban interventions on the carbon footprint of Roeselare, Belgium (initially 30,548 hectares)

Energy Intervention	Carbon Reduction
Building envelope improvements	15 %
Wind Turbines	12 %
Solar collectors and MT storage	10 %
Electric cars	10 %
Thermal photovoltaic panels	6 %
Rooftop photovoltaic panels	6 %
LT heat grids with aquifer heat storage	5 %
Cycle routes and electric car share	5 %
Waste incineration for district heating	4 %
Solar collectors and HT storage	4 %
HT industrial waste heat for district heating	4 %
Biomass for industry	3 %
Urban trees and green spaces	3 %
Ground level photovoltaic panels	2 %
Recycling, LED Lights and Electric Buses	1 %
Energy use increase	-3 %
TOTAL	87%

The remaining 13 percent of carbon emissions would need to be taken up by forest land planted specifically to sequester these emissions. An area beyond the outer ring road of the city was allocated for this, which would provide residents with a place to recoup and spend quality time with loved ones; a strange by-product of developing zero-carbon communities by typical standards.

7. CONCLUSIONS

The City-zen Roadshow is a holistic approach to designing future zero-carbon communities that focusses on the multifaceted drivers of society, environment, ecology, and economy that helped drive the first explorations into eco-city design. The roadshow created a platform to experiment with intensive co-creational design methodologies as a way to meaningfully engage with local stakeholder, who would ultimately play out the strategies of future zero-carbon communities. The urban-first approach developed as part of the roadshow took the power of urban design and used it to reshape ‘sustainability’,

enabling stakeholders to view it through the lens of health, wellbeing and quality of life, rather than simply using the car less, spending money on LED bulbs or investing in building insulation.

What was found through the roadshow is that, not surprisingly, local stakeholders are deeply passionate about the places in which they live, and that to be given an opportunity to shape that place – whilst simultaneously reducing its carbon footprint as well as improving the quality of life – is something stakeholders are very thankful for. Not only that, but the process has been well received in each city and enjoyable for all involved. The symbiotic relationship that was created between stakeholders and global experts through the vehicle of the roadshow not only allowed for the quick prototyping of ideas, due to efficient and effective feedback loops, but it also enabled local stakeholders to feel connected to their city, which is a key component of civic wellbeing and achieving ‘eudaimonia’ [20]. This approach helped build a lexicon amongst stakeholders, enabled advocacy of zero-carbon strategies, and created a foundation from which meaningful debate can occur before such interventions are formalised by municipalities. Enabling meaningful collaborations at such an early stage in the zero-carbon transition process also makes it possible to strengthen communities that were open to change and ensures that momentum continues to occur after the roadshow leaves.

The redesign of the neighbourhood in Roeselare provides local residents with an improved quality of life whilst reducing net carbon emissions to zero. It is hoped that the interventions proposed are put into practice within a short space of time across the city, and that the ideas developed help other cities address their own climate challenges in the future. Living in a zero-carbon community is not just about photovoltaic panels and wind turbines. It is, instead, about thinking differently about the way in which people live and the decisions they make out of convenience and habit, which not only detract from their health and happiness, but also cause undue strain on the environment. Ultimately, someone has to design the places in which people live, and the City-zen Roadshow has proven that guiding stakeholders along an engaging design process can bring about impactful designs that are fit for purpose, net zero-carbon, socially accepted, and rather interesting to engage with and live amongst.

ACKNOWLEDGEMENTS

The City-zen Roadshow is a collaborative research project run by Queen’s University Belfast, TU Delft, The University of Siena, Vito Energyville and ThInk E.

REFERENCES

1. European Commission (2019) *The European Green Deal*, Brussels, European Commission.
2. *The Climate Change Act 2008 (2050 Target Amendment) Order* 2019, Available at: https://www.legislation.gov.uk/ukdsi/2019/9780111187654/pdfs/ukdsi_9780111187654_en.pdf [accessed 11th March 2020].
3. United Nations / Framework Convention on Climate Change (2015) *Adoption of the Paris Agreement*, 21st Conference of the Parties, Paris: United Nations.
4. European Environment Agency (2019) *Annual European Union greenhouse gas inventory 1990–2017 and inventory report 2019*, Brussels, European Commission.
5. Department for Business, Energy and Industrial Strategy (2019) *2018 UK Greenhouse Gas Emissions, Provisional Figures*, Newport, Office for National Statistics.
6. Department for Business, Energy and Industrial Strategy (2019) *UK Energy Statistics, Q1 2019*, Office for National Statistics.
7. Wynes, S., Nicholas, K. A. (2017) The climate mitigation gap: Education and government recommendations miss the most effective individual actions, *Environmental Research Letters*, 12 (7), DOI: 10.1088/1748-9326/aa7541.
8. Holden, M., Li, C., Molina, A. (2015) The emergence and spread of ecourban neighbourhoods around the world, *Sustainability*, 7, pp. 11418–11437 doi:10.3390/su70911418.
9. Howard, E. (1902) *Garden cities of to-morrow*, London, Swan, Sonnenschein & Co.
10. Roseland, M. (1997) Dimensions of the eco-city, *Cities* 14(4), pp. 197–202.
11. Roseland, M. (1997) Dimensions of the eco-city. *Cities*, 14, pp.197–202.
12. Joss, S (2011) Eco-cities: The mainstreaming of urban sustainability – key characteristics and driving factors, *International Journal of Sustainable Development and Planning*, 6(3), pp.268–285
13. Hachem, C., Athienitis, A., Fazio, P. (2012) Evaluation of energy supply and demand in solar neighbourhoods, *Energy and Buildings*, 49, pp.335–347.
14. Marique, A.-F., Penders, M., Reiter, S. (2013) From zero energy building to zero energy neighbourhood. Urban form and mobility matter, *13th Passive and Low Energy Architecture Conference*, Munich, Germany, 10th – 12th September 2013.
15. Marique, A.-F., Reiter, S. (2014), A simplified framework to assess the feasibility of zero-energy at the neighbourhood/community scale, *Energy and Buildings*, 82(2014), pp.114–122.
16. Guan, C., Srinivasan, S., Nielsen, C. P. (2019) Does neighbourhood form influence low-carbon transportation in China, *Transportation Research Part D*, 67, pp.406–420
17. Newman, P., Kenworthy, J. (1999) *Sustainability and cities: Overcoming Automotive Dependence*, Washington DC, Island Press
18. Williams, K., Burton, E., Jenks, M, eds. (2000) *Achieving sustainable urban form*, London, Spon Press.
19. Pulselli, R. M., Marchi, M., Neri, E., Marchettini, N., Bastianoni, S. (2019) Carbon accounting framework for decarbonisation of European city neighbourhoods, *Journal of Cleaner Production*, 208, pp.850–868
20. Montgomery, C. (2013) *Happy city: Transforming our lives through urban design*, 2nd ed., London, Penguin.

Influence of High-Density Mixed-Use Residential Neighborhood Building Layout on Building Energy Consumption: Taking ChuangZhiFang in Shanghai, China as an Example

TIAN NANNAN^{1,2}, YANG FENG^{* 1,2}

¹ College of Architecture and Urban Planning (CAUP), Tongji University, Shanghai, China;

² Key Laboratory of Urban Renewal and Spatial Optimization Technology, Shanghai, China

ABSTRACT: In 2016, Shanghai released the "Shanghai Planning Guidance of 15-Minute Living Community Circle". This concept means that there are basic public service facilities such as education, commerce, transportation, culture and sports within a 15-minute walk around the home to improve the quality of life of residents. High-density mixed-use residential areas may be a better choice owing to their dense road network and multiple functions. This paper analyses the impact of building layout (height/width ratio of urban canyon, courtyard aspect ratio, courtyard layout and community functional distribution) on the energy consumption of the high-density mixed-use residential area research case in the context of Shanghai through preliminary field investigations and numerical simulations, in an attempt to supporting energy-sensitive and low-carbon urban design in the future.

KEYWORDS: High-density mixed-use neighborhood, Building layout, Building operational energy consumption, UMI

1. INTRODUCTION

Building energy consumption is affected by many interrelated factors such as climate, urban setting, building massing and envelope, system and users' behaviour. Buildings are in an urban context rather than isolated. Different building layouts will form different shadows and different ventilation conditions between buildings, which will affect the microclimate around buildings and then affect the building energy consumption.

Previous research has been carried out to explore the relationship between building layout and building energy consumption. Some through numerical simulation of the ideal architectural layout prototypes, some through observation, and some have used a combination of the two methods. Leslie Martin et al. proposed six archetypal forms in the late 1960s, and they raised the question of "which block form is the best way to use land". This method has brought great inspiration to later researchers. Ratti reassessed the results using newly developed computer techniques, and his analysis addressed the following parameters: shape factor, shadow density, direct daylight factor and sky view factor [1]. Muhaisen evaluated the shading performance of different proportions of the courtyard form in different climatic regions [2]. Strømman-Andersen studied the impact of urban canyon geometry on building energy use in

Copenhagen and found that the effect on office buildings is as high as +30%, while the housing impact is +19% [3]. In addition, smaller surface-to-volume ratio is found beneficial to reduce building energy consumption in Beijing [4]; the parameter that has the greatest impact on cooling and total energy consumption is the height of the western building in Wuhan [5].

Shanghai is situated in an area with hot summer and cold winter. It must prevent overheating in summer and properly consider heat preservation in winter. The composition of energy consumption varies in different climates, so the priority factors will also be different. Although the focus is on Shanghai, China, the methods and research results are relevant to global urban development and architectural design.

In addition, the reason for the research based on the Chuangzhifang community is the positive development trend of high-density mixed-use blocks. In 2016, Shanghai released the "Shanghai Planning Guidance of 15-Minute Living Community Circle" [6] to improve the quality of life. However, prevalent large-scale enclosed residential areas in Chinese cities can hardly meet this requirement. High-density mixed-use residential areas like Chuangzhifang (Fig.1) may be a better choice owing to their dense road network and multiple functions. In this article, the effect of building layout on

building operational energy demand of the studied case in the context of Shanghai is analyzed and potential to optimize energy performance explored, in an attempt to supporting energy-sensitive and low-carbon urban design in the future.



Figure 1: ChuangZhiFang Community, Shanghai. It integrates residential, retail and small office and shows a wealth of walking space and community vitality.

2. METHODS & ANALYSIS

This study has been divided into two parts. The first part begins by a field survey of Shanghai Chuangzhifang, investigating the users' energy use habits through questionnaires and building typical envelope parameters through site survey. It will then go on to set the parameters of the simulation software UMI based on the data obtained from the survey. Take the ideal block model simplified from the real block Chuangzhifang as simulation object and select four neighbourhood-scale factors affecting building energy consumption, namely height/width ratio of urban canyon (H/W), courtyard aspect ratio, courtyard layout and community functional distribution. The experimental procedure includes determining constants and variables, establishing models, numerical simulation and data statistics, and finally using the annual energy consumption per unit area (EUI, kWh/ m²·yr) as an evaluation index to analyse the impact of different building layouts on building energy consumption.

The second part optimizes the original plan of Chuangzhifang community according to the conclusions drawn in the first part to verify the results through numerical simulation.

2.1 Ideal block model simulation

2.1.1 Software introduction

UMI (Urban Modeling Interface, developed by MIT's Sustainable Design Lab) is a new Rhinoceros-based urban modeling design tool, which allows users to carry out operational energy, daylighting and walkability evaluations of complete neighborhoods. The underlying simulation engines are EnergyPlus, Radiance/Daysim as well as a series of Grasshopper and Python scripts[7]. Its biggest feature is the algorithm for generation and simulation of abstracted rapid multi-zone urban

building energy model called "shoebboxer"[8]. Its workflow is:

(1) Firstly, geometric input and non-geometric input. The geometric input includes the street grid and mass model of the building group, and buildings are subdivided into units according to the functions in the building (for example, a building with retail below and residences above contains at least two units). Each unit should have a non-geometric input, including "Unit Properties" (floor-to-floor height, window-to-wall ratio, perimeter offset, etc.) and "Zone Template" (the material and structure of the building envelope, the number of occupants, schedules and the equipment system and control strategies, etc.).

(2) After that, determine the position and shape of the shoebox. The reference of Shoebox is to simplify the complexity of model to speed up the simulation. Usually the building is abstracted into a set of shoebox models located in representative positions. Shoebox placement and clustering standard is radiation. The closest point of median radiation value is the center of mass position, which is the ideal position of a typical indoor thermal model. In addition, the shape of the shoebox is determined by facade-area to floor-area ratio of the unit, etc. Then use ray casting technology to pull the visible part around the shoeboxes into the EnergyPlus simulation as contextual shading.

(3) Finally, simulation, summary and visualization of results. The shoebox model is simulated as an editable EnergyPlus model. The simulation results of each shoebox model are summarized by weighing the results of each shoebox and the floor area of its associated cluster. The final energy simulation results can be mapped back to the visualization scene of Rhinoceros.

The above method considers diverse urban forms without losing geometric details, can obtain more accurate and reliable simulation results in a shorter time, and is more suitable for block and urban building energy simulation.

2.1.2 Parameter settings

Based on the data obtained from 118 valid resident questionnaires and 130 valid questionnaires for business and office users and related building energy efficiency codes, the setting parameters are as follows.

Table 1: Window-to-wall ratio.

Orientation	Window-to-wall ratio
North/South	0.4
East/West	0.3

Table 2: Building envelope performance.

Building Envelope	Heat transfer coefficient (W/m ² ·K)
Ground Floor	0.61
Interior Floor	2.00
Roof	0.49
Facade	0.77
Window	2.60

Table 3: Indoor temperature setting.

Season	Temperature(°C)
Summer	24
Winter	20

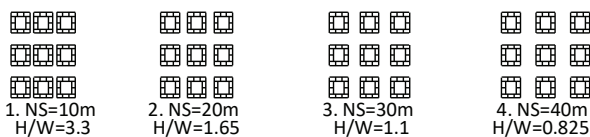
Table 4: The schedules of air-conditioning system.

Building Type	Summer		winter	
	Start	End	Start	End
Residential	Jun. 1st	Sept.30th	Nov. 20th	Mar.1st
Business	Jun. 1st	Sept.30th	Dec. 1st	Feb.15th
Office	Jun. 1st	Sept.30th	Nov. 20th	Mar.1st

2.1.3 Numerical simulation and data analysis

(1) Height/width ratio of urban canyon (H/W). Establish 3D models which are all composed of 9 identical courtyards and each courtyard consisting of 10 single buildings (16m*10m*33m). The constants are building height (H: 11*3m=33m) and total building volume (475200m³), and the variables are north-south street width and east-west street width. The change of H/W is illustrated in Fig.2. In the simulation, these buildings were set to three types: residential, office and retail. The setting of multiple functions was to study the influence level of H/W on energy consumption of different types of buildings. Take the annual energy consumption per unit area(EUI) of the inner courtyard for comparison and analysis.

EW Street Width=30m H=33m



NS Street Width=20m H=33m

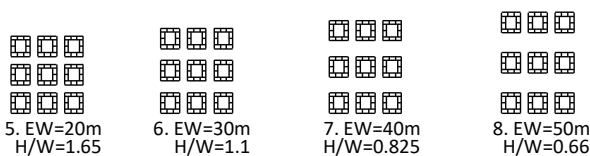


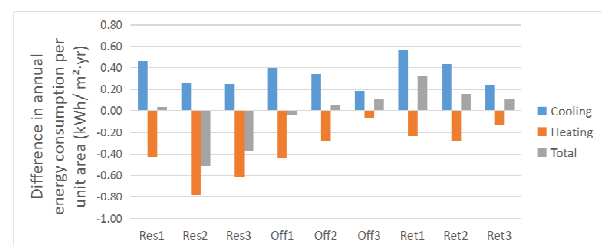
Figure2 : height/width ratio of urban canyon (H/W).

As the H/W changes, the difference in annual cooling, heating and total energy consumption per unit area (the simulated value of the latter model minus the former model) is shown in Fig.3. It can be seen that regardless of north-south or east-west streets, whether

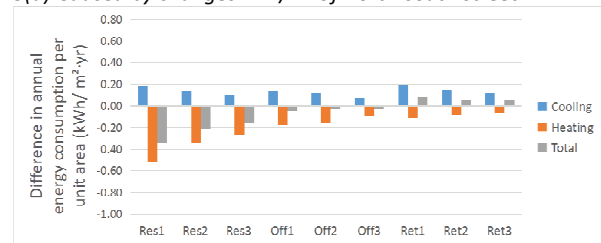
residential, office or commercial buildings, as the H/W decreases, cooling energy consumption increases while heating energy consumption decreases. The reason for this trend may be that as the street becomes wider, the solar radiation received by the building increases and the shadows between the buildings decrease. On the whole, the influence of H/W of north-south street on building energy consumption is more obvious than that of east-west direction.

However, The trend of EUI of different types of buildings varies slightly with the change of H/W. For commercial buildings, the EUI increases as H/W decreases. The reason for this phenomenon is that the cooling energy consumption of commercial buildings is approximately 7 times (according to simulation data) the heating energy consumption, leading to the H/W has a greater impact on the cooling energy consumption, and the cooling energy consumption increases as H/W decreases, which causes an increase in the total energy consumption per unit area. For residential buildings, the EUI generally decreases as the H/W decreases. For office buildings, the EUI decreases with the decrease of the H/W of east-west street, and generally increases with the decrease of the H/W of north-south street.

Although the change values of the EUI are less than 1 kWh/ m²·yr and the highest value is only 0.51 kWh/ m²·yr, for a block with a total area of about 178,500m² like Chuangzhifang, it can also save 91035 kWh of energy every year, and the energy-saving benefit is considerable.



3(a) Caused by changes in H/W of north-south street.

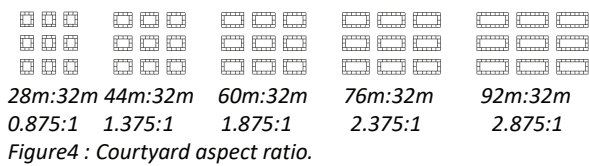


3(b) Caused by changes in H/W of east-west street.

Figure3: Difference in annual energy consumption per unit area caused by changes in H/W.

(2) Courtyard aspect ratio. The constants are building height (H: 11*3m=33m) and H/W(1.1), and the

variable is the courtyard aspect ratio(Fig.4). The EUI of the inner courtyard was taken for analysis.



Whether it is residential, office or commercial building, the EUI decreases with the increase of courtyard aspect ratio. The change in courtyard aspect ratio has a relatively greater impact on the EUI of the residence (Fig.5), and the maximum change is 1.17 kWh/ m²-yr, which appears when the residential courtyard aspect ratio changes from 1.375:1 to 1.875:1.

In addition, compared to cooling energy consumption, changes in courtyard aspect ratio have a greater impact on heating energy consumption. The larger change value of EUI appears in courtyard aspect ratio from 1.375:1 to 2.375:1, however, for buildings of different scales, there may be differences in this range. In practical applications, the specific impact trend and degree will depend on the specific situation (local climate, building scale, etc.).

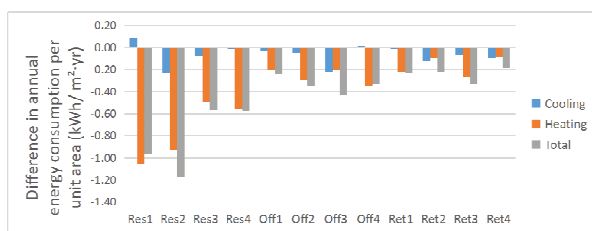
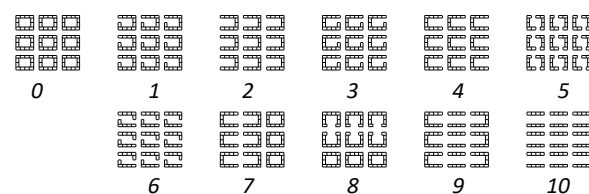


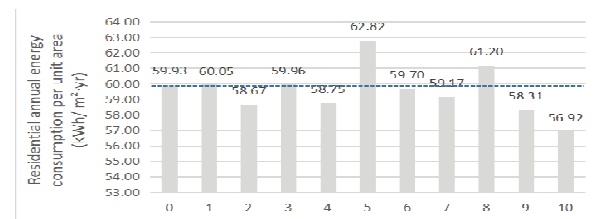
Figure5: Difference in annual energy consumption per unit area caused by changes in courtyard aspect ratio (the simulated value of the latter model minus the former model).

(3) Courtyard layout. The constants are building height(H: 33m) and H/W(1.1), and the variable is courtyard layout(Fig.6). 0 is the basic model and 1-10 are the variant models. Take the EUI of the building clusters for comparison and analysis, trying to find a more energy-efficient courtyard layout.

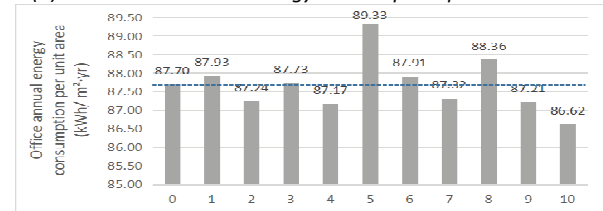


Compared to model 0, the models with better EUI of residence are 10,9,2,4,7,6 (Sort by EUI from low to high)

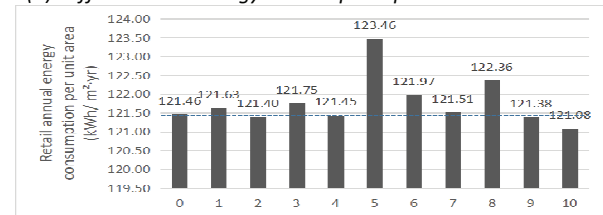
(Fig.7(a)), of office buildings are 10,4,9,2,7 (Fig.7(b)), of commercial buildings are 10,9,2,4 (Fig.7(c)), and the models that perform poorly are 5,8. The trend is roughly as follows: building clusters with fewer east-west buildings have smaller EUI. Therefore, in order to be more energy-efficient, should we minimize east-west buildings and eventually turn all buildings into slabs (like model10)?



7 (a): Residential annual energy consumption per unit area.



7(b): Office annual energy consumption per unit area.



7 (c): Retail annual energy consumption per unit area.

Figure7: Annual energy consumption per unit area with different courtyard layouts.

The answer I think is negative, and the reasons are as follows: the model 6 with a smaller ratio of east-west building area to total area(0.25) has higher EUI than the model 7 with a larger proportion of east-west building area(0.31). In addition, models 2,4 and 6 with the same proportion of east-west building area(0.25) also have different EUI. Therefore, in addition to the proportion of east-west building area, the position of east-west building in the building group also has an impact on the EUI. Moreover, the introduction of a small amount of east-west buildings increases the energy consumption slightly, but it can also enrich the street space and pedestrian environment at the same time. For example, Chuangzhifang block is a typical courtyard layout with dense road network. Inside the courtyard is a relatively private and well-greened space that belongs only to the residents, and outside the courtyard are commercial walking streets of suitable scale and lively atmosphere. Compared with the large-scale enclosed community

with single form arranged in slabs, the courtyard layout with dense road network undoubtedly has a more convenient and dynamic living space.

(4) Community functional distribution. Except for the variable functional distribution, all parameters remain unchanged: building height (H:11*3m=33m), H/W(1.1), total building area (158400m²) and percentage of building function (residential45%, office22%, commercial33%). The building function distribution is shown in Fig.8. In models 1,2,3, an entire building is occupied by a function, and in models 4,5,6, commercial function is placed from ground floor to third floor (a part to the fourth floor), and the other functions are distributed above the business.

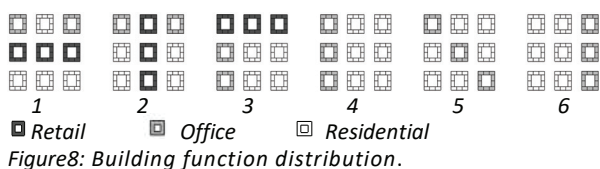


Figure8: Building function distribution.

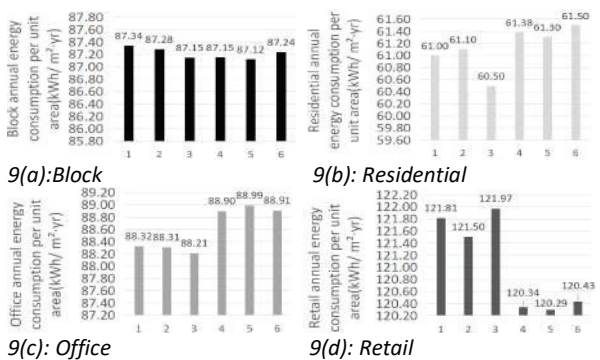


Figure9: Annual energy consumption per unit area with different building function distribution.

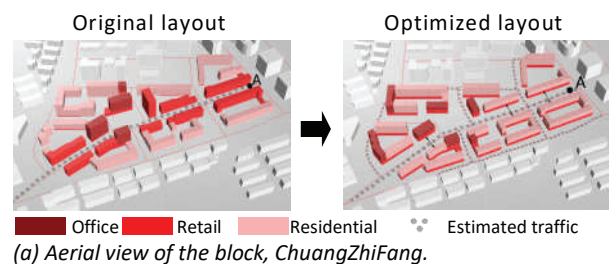
Different building functional distribution can bring different EUI to the building cluster (Fig.9(a)). The energy consumption of model 5 is relatively good (87.12kWh/ m²-yr), which is 0.22kWh/ m²-yr less than the relatively poor model 1 (87.34kWh/ m²-yr), so a reasonable functional distribution can also appropriately reduce building energy consumption, which is one of the means of energy saving.

An obvious trend in Fig.9(b), Fig.9(c), and Fig.9(d) is: the EUI of residential and office buildings of model 4,5,6 is higher than model1,2,3, and for commercial buildings, model4,5,6 is lower than model1,2,3, and the reduction is greater, which is the main reason for the reduction in energy consumption of the entire building cluster. So what is the reason for the lower energy consumption when the business is distributed on the lower floor? The lower floors receive less solar radiation and more shadows, which leads to a decrease in cooling energy

consumption, so its annual energy consumption per unit area will be dropped due to the energy consumption structure characterized by cooling in summer and almost no heating in winter.

2.2 Energy consumption optimization of real block Chuangzhifang

Based on the above analysis, the original planning layout and functional distribution of the real block Chuangzhifang were adjusted. The original plan of Chuangzhifang is composed of seven small groups (Fig.10). When adjusting the original plan, the cluster division was generally followed. Without changing the original planning path and design concept, only the east-west street width was increased from 26m to 40m, and the aspect ratio of each courtyard was appropriately increased. In terms of community functional distribution, businesses are placed on the ground floor to the third floor, on which residential and offices are placed. The two layouts have the same proportion of building function which is 45% for residential, 37% for retail and 18% for office. The total building area of the two models is 178,633m² and 178,649 m².



(a) Aerial view of the block, ChuangZhiFang.



(b) Perspective view of the street at point A.

Figure10 : Energy consumption optimization of real block.

The simulation result shows that the annual total energy consumption of the original scheme is 15153039kWh, and the annual total energy consumption of the optimized scheme is 15027542kWh, which can save 125497kWh in one year. The simulation results can show that optimizing the layout of buildings and the distribution of building types can be used as one of the potential energy saving methods. Of course, in the planning and design of a block, there is not only a reference indicator of energy saving. In the process of generating a plan, low-carbon energy saving is certainly a good vision and can be used as an auxiliary

optimization method, but various factors must still be considered comprehensively. For example, in the optimization plan, in addition to energy-saving considerations, widening the main road has also expanded the crowded pedestrian space caused by tables and chairs outside the catering shops, so that the pedestrian street has a suitable scale, and flower beds can also be placed along the street to plant green plants to beautify the street, and resting seats can also be placed for pedestrians to rest, increasing people's stay time and stimulating the vitality of the street. In addition, extending the distribution of shops to the branch roads beside the main road helps to attract residents of surrounding communities, makes the branch roads also walkable, and expands the vitality space of the community.

3. RESULTS

(1) As the H/W of street decreases, cooling energy consumption increases while heating energy consumption decreases, the annual total energy consumption per unit area of commercial buildings increases while residential buildings generally decreases. Moreover, the influence of the H/W of north-south street on building energy consumption is more obvious than east-west direction.

(2) Whether it is residential, office or commercial buildings, with the increase of the aspect ratio of the courtyard, the annual energy consumption per unit area shows a downward trend. Furthermore, the change in the courtyard aspect ratio has a relatively greater impact on the annual energy consumption per unit area of the residence.

(3) In general, building clusters with fewer east-west buildings have smaller annual energy consumption per unit area. Moreover, the position of east-west buildings in the cluster also has an impact on annual energy consumption per unit area..

(4) Under the condition that the proportion of each building type of the building cluster is unchanged, different building functional distribution will affect the annual energy consumption per unit area of the building cluster. In general, business on the lower floor consumes less energy than when it is distributed throughout the building.

There are many factors that affect building energy consumption and their interactions are complex. This article mainly discusses the impact of height/width ratio of urban canyon (H/W), courtyard aspect ratio, courtyard layout and community functional distribution on the energy consumption of different types of buildings (residential, office and commercial), with a view to lay the foundation for the follow-up research work on low-carbon energy-saving design of

high-density mixed-use residential neighborhood. In fact, there are "almost infinite combinations of different climatic contexts, urban geometries, climate variables and design objectives. Obviously there is no single solution, i.e. no universally optimum geometry". as Oke said.

In addition, different building layouts have an impact on the urban microclimate and thus on building energy consumption. Therefore, the climatic conditions entered in the simulation should be the local microclimate affected by the building layout. In this regard, the research has its limitations. Except for solar radiation, other climate data such as wind environment and temperature have not changed with the adjustment of the building layout, so the results may be affected to some extent. Nevertheless, with its simulation speed and accuracy, it can still be regarded as a better choice for block and urban building energy modeling. Finally, the impact of a single factor on building energy consumption is still clear, but when the factors are considered in combination, more detailed simulation and sensitivity analysis must be performed.

ACKNOWLEDGEMENTS

The research is supported by the National Natural Science Foundation of China (NSFC) Project (No.: 51678413).

REFERENCES

1. Carlo Ratti, Dana Raydan, Koen Steemers, (2003). Building form and environmental performance: archetypes, analysis and an arid climate. *Energy and Buildings*, 35:p.49–59.
2. Ahmed S. Muhaisen, (2006). Shading simulation of the courtyard form in different climatic regions. *Building and Environment*, 41:p.1731–1741.
3. J. Strømmand-Andersen, (2011). The urban canyon and building energy use: Urban density versus daylight and passive solar gains. *Energy and Buildings*, 43:p.2011–2020.
4. HU Shan, YAN Da, CUI Ying, (2015). Influence of building space form on the energy consumption of residential buildings. *Building Science*, 31(10):p.117–123+145.
5. HE Cheng, ZHU Li, TIAN Wei, (2018). Sensitivity analysis of urban building layout on energy consumption. *Journal of Harbin Institute of Technology*, 50(4):p.174–180.
6. Shanghai Urban Planning and Land Resources Administration Bureau, (2016). *Shanghai Planning Guidance of 15-Minute Living Community Circle*.
7. Reinhart, (2013). UMI - An urban simulation environment for building energy use, daylighting and walkability. *13th Conference of International Building Performance Simulation Association, Chambéry, France*: p.476–483.
8. Timur Dogan, Christoph Reinhart, (2017). Shoeboxer: An algorithm for abstracted rapid multi-zone urban building energy model generation and simulation. *Energy and Buildings*, 140:p.140–15.

Optimizing Social Benefit of Vertical Greening System in Open Residential Neighborhood Using a Multiple Raster Data Based Viewshed Analysis: A Case Study in Southern China

YIPENG FENG^{1,2} and FENG YANG^{1,2}

¹College of Architecture and Urban Planning (CAUP), Tongji University, Shanghai, China;

²Key Laboratory of Urban Renewal and Spatial Optimization Technology, Shanghai, China

ABSTRACT: Vertical greening system (VGS) can effectively alleviate the conflict between urban greening and urban construction land in the process of urban development. Excellent VGS design can bring environmental, economic and social benefits to the city. Among them, the environmental and economic benefits of VGS are easier to quantify and study, but social benefits are often overlooked because of its particularity. The aim of this study is to develop a method that can quantify the social benefits of VGS and visualize the results. This method is based on a fast viewshed analysis technology using multiple GIS raster data, which can be used to calculate the distribution of pedestrian sight lines in urban space and the visibility of VGS in various areas of the city, providing a powerful Data support for the optimal design of VGS social benefits.

KEYWORDS: Vertical Greening System, Viewshed Analysis, Social-benefit Analysis, Urban Environment.

1. INTRODUCTION

Landscape plants have an important position in Chinese culture since ancient times. But the conflict between greening and construction land continuously increase with the urbanization progress in China. Vertical Greening System (VGS) is a modern building façade which uses vegetation to green and beautify the facade of buildings and structures [1]. For its advantages of saving land, many countries, especially those in Asia, have begun to research into the policy, laws and technology of vertical greening [2,3]. Through decades of development, VGS is now being applied more and more in practice.

VGS has economic benefits (e.g. building energy saving), environmental benefits (e.g. heat island mitigation and thermal comfort improvement) and social benefits (e.g. aesthetic, visual comfort and landscape effect). However, the social benefits of VGS are often overlooked in previous research, compared with others.

The main way to optimize the environmental and economic benefits of VGS is to enable the VGS to fully respond to local natural climate and urban environment, and improve the urban microclimate and reduce building energy consumption. While, the social benefits of VGS are realized through sight contact with pedestrians. Because visual contact with green vegetation can bring benefits to people who are anxious and under stress, and even directly affect people's health [4]. Therefore, when designing a VGS, we need to fully think about where the VGS can be

more easily to have eye contact with people. We also need to know where in the block, people have insufficient visual contact with green plants, so that we can make subsequent improvements to it.

This paper aims to develop a viewshed analysis method for the optimization design and social benefits assessing of VGS. Social benefits of VGS involve many complicated subjective factors, making it difficult to be quantified. To simplify the problem and facilitate theoretical analysis, this paper assumes that in high-density urban environment, there is a positive correlation between VGS social benefits and its visibility from major public spaces and pedestrian areas, as better view to greenery is beneficial to one's mental and physical health [4].

The social benefits of VGS are closely related to the distribution of people's sightlines in the city. By analyzing people's sightlines, we can determine which part of facades in the block are easier to draw people's attention, in other words, is more worthwhile to reform. Conversely, we can also analyze how different VGS designs will generate visual feedback in the neighborhood. Today, viewshed analysis technology is relatively mature and has been widely used in urban design and planning field.

Gabriele Garnero uses a raster-based approach to analysis the visibility in the city of Turin, Italy[5]. Kwang Youn Lee, Jung Il Seo, Kyoung-Nam apply viewshed and spatial aesthetic analyses to forest

practices for mountain scenery improvement in the Republic of Korea [6].

Most GIS software has DEM (Digital Elevation Model)-based calculation modules for visibility and sight analysis. But, subject to computational efficiency, its function is often limited to the analysis of the relationship between point elements. Therefore, this paper will make improvements on the basis of traditional view analysis algorithms, and propose a new general-purpose fast view analysis algorithm, and apply it to the research of VGS optimization design.

This article will take the Opening Residential Neighborhood (ORN), which is representative in the development of contemporary urban development and features smaller block sizes, denser and narrower street grids, mixture of residential with commercial, and pedestrian-friendly streets and pocket parks right in block[7], as research object, introduce the basic principle of the fast view analysis algorithm above-mentioned and the corresponding design method of VGS social benefit optimization.

2. METHODS

2.1 Parameters

The optimization method can be divided into two parts, establishing a VGS design reference system, and establishing a VGS design social benefit evaluation system.

To achieve these goals, firstly, this paper presents Greening View Factor (GVF) and Facade Sight Density (FSD) as calculation and appraisal parameters for VGS design and assessment.

GVF is defined as the fraction of the overlying sphere in a panoramic view image that are occupied by the facades with vertical greening (Fig.1). The change in its value can reflect the proportion of the vertical greening facade in the view of pedestrians at different positions, which is very similar to the concept of the sky view factor(SVF).

while FSD is the number of times per unit of area the facade seen by people in a random moment of daytime. Its value can reflect which part of the facades in the street can appear in the pedestrian's sight more frequently, which also implies which positions are more worthy of our efforts in design. Its numerical value is mainly affected by factors such as the shape of the block, the architectural modeling and the distribution of people flow. Therefore, to calculate FSD, in addition to the DEM of the block, we also need to obtain the Pedestrian Flow Density (PFD) data, which is the density of pedestrians per unit area. This data can be obtained through field measurements, drone images, or crowd counting. As shown in Fig.2, PFD mainly describes the distribution of people in the site, and provides a necessary pre-parameter for subsequent calculation.



Figure 1: The value of GVF of a certain point can be understood as the ratio of the white area (which represents greening) to the area of the panoramic sphere.

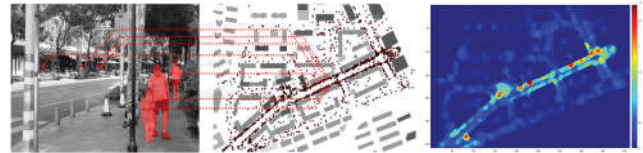


Figure 2: PFD raster data generation flowchart, points elements in the figure represent the locations of pedestrians in the site.

The storage, calculation and visualization of relevant parameters will be carried out in the form of raster data. To calculate and store GVF and FSD, GIS tools is needed to create multiple raster data to record the building elevation, the facade greening density and PFD distribution respectively. Then, MATLAB and Python programs will be used to accomplish the data processing work.

2.2 Mathematical preparation

In order to calculate the GVF and FSD, a famous visibility analysis algorithm in Earth Science and Radar Science was introduced into this research. Combine with traditional Shadowing-Volume algorithm widely used in urban analysis [8], this paper developed a View Factor algorithm on DEM. The way it works:

First, visibility judgement, make a half-line from view point V to target point T, and identify the relation between the height of points on the half-line and corresponding elevation on the map. If there is any point on the half-line, its height is smaller than the correspond elevation, these two points are invisible to each other. Conversely, visible to each other [9-11] (Fig. 3a).

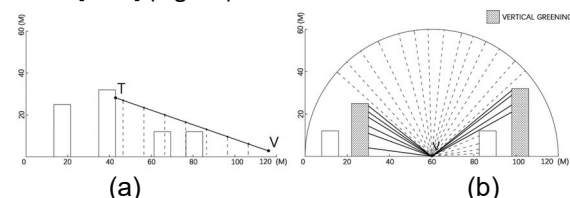


Figure 3: (a) Principle of visibility analysis; (b) Principle of view factors calculation.

Based on this, we select one point as view point, and draw a large number of half-lines by random angles from this point. Then record how many half-lines were blocked by facades with vertical greening. Then, divide this number by the total number of half-lines and we have the quotient approximated as the GVF value (Fig. 3b), the more the half-lines the higher the accuracy.

Considering two different VGS may have different greening rate, which will also bring about differences in visual quality, we should have a scoring system. For example, if a half-line hits a facade with a higher Greening to Wall Ratio (GWR), it will score a higher point (Less than or equal to 1. e.g. 0.9), meanwhile, if it hits a facade with lower GWR, will score a lower point. Then the GVF approximately equals to the total score divided by the total number of half-lines.

Similar to the calculation process of GVF, By recording the times each facade was hit by half-lines and dividing the number by facade area, we get the approximate FSD of each façade. If the half-line came from a view point with higher PFD value, the half-line will have a higher weight during the counting process. When calculating FSD, we have to consider the range of people's perspective. In this scenario, the height angle of the half-line emission is limited to between +50 degrees and minus -70 degrees to simulate the line of sight.

It should be noted that the main purpose of this algorithm is to reduce the space-time complexity required for calculation as much as possible and reduce the dependency on computer hardware. As a result, when calculating the FSD, we can only get the relative relationship between the points on the facade, rather than the value with actual physical significance.

FSD can provide a reference for our design, while GVF can be used as a good social benefit assessment index. Data processing programs are written by MATLAB (2D Analysis) and Python (3D Analysis) , and they are available upon request.

2.3 Research on Ideal Models :

Through the above procedures, a set of VGS social benefit optimization design process can be formed. The basic framework is shown in Fig.4, which is mainly divided into two parts:

1. Generate design based on FSD.
2. Assessment and iterate the design based on the GVF calculation results.

In order to demonstrate the practical steps of this method, we establish a set of idealized models that can represent typical parts of ORN.

As shown in Fig.5, type-A is the prototype of the reference group, which represents a typical intersection in the ORN. It consists of four 6-storey 18-meter-high buildings and 18-meter-wide urban roads. The pedestrian flow density in the site is evenly distributed, 0.2 people / m². Type-B is based on Type-A, which widens the road. A 4-meter wide sidewalk is added along the side of the building. The pedestrian flow density on the sidewalk is higher than that on the main street, 0.6 people / m². Type-C adds a pocket park on the basis of Type-A. The density of people in the centre of the park is 0.6 people / square

meter. Type-D adjusts the height of one of the buildings to 12 storeys, simulating the high-rise business format in a mixed-used block.

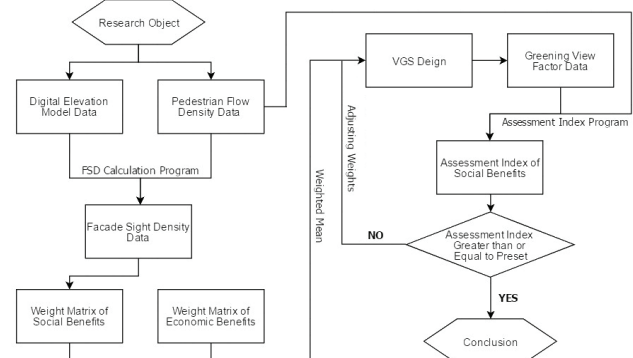


Figure 4: Experimental Block Diagram.

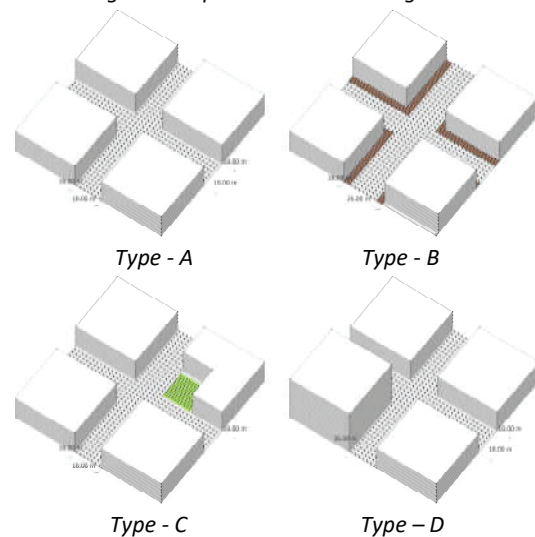


Figure 5: ORN Ideal Models.

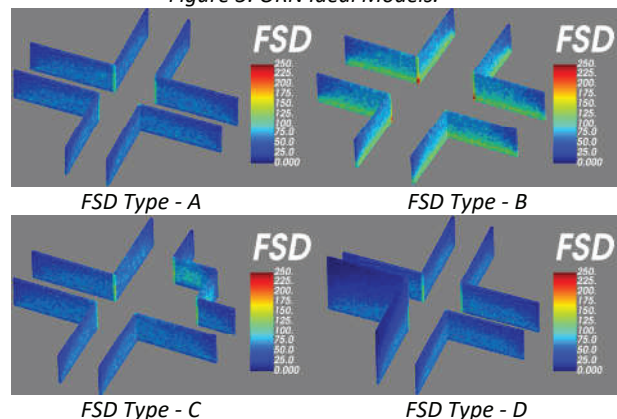


Figure 6: FSD Analytical Diagram of Ideal Models.

First of all, we need to establish the corresponding DEM and PFD raster data according to the model scenario and input it into the FSD calculation program to obtain the FSD data in each model. The visualization results are shown in Fig.6.

According to the FSD calculation results, we can design a reasonable VGS system for different facades (Fig.7). Nowadays, VGS systems are gradually standardized and modularized. Therefore, we may

achieve changes in GWR (Greening to Wall Ratio) by adjusting the density of VGS modules. In addition, FSD data can also be imported into the parametric design software, such as Grasshopper, as design parameters to obtain more interesting design effects.

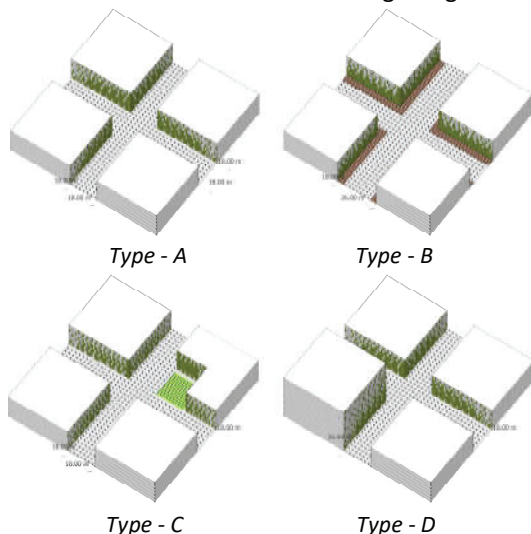


Figure 7: VGS Designs of Ideal Models.

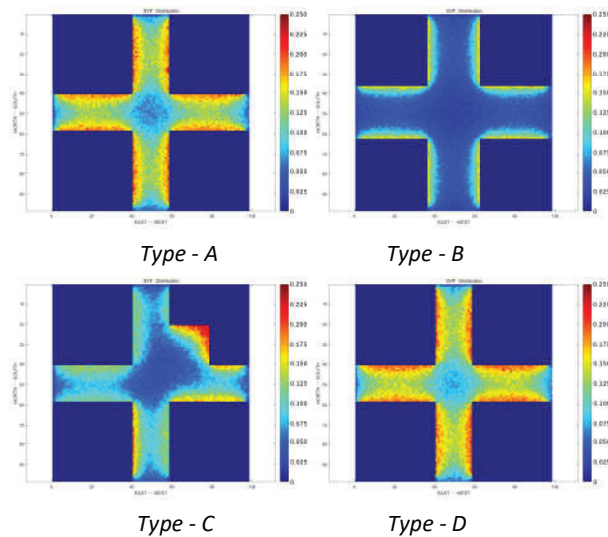


Figure 8: GVF Analytical Diagram of Ideal Models.

When the design plan is initially completed, we need to store the spatial shape and GWR data of the VGS into a three-dimensional raster grid (Volume Pixel Model), import it into the GVF calculation program, and run the program to obtain the GVF distribution map (Fig.8). According to the GVF calculation result, we can constantly fine-tune and update the VGS design to obtain the final optimized design.

Through the above research, we can obtain the VGS social benefit optimization design rule of typical parts in the ORN, as a reference for future practical application. In the actual design and application process, this method can be more flexible. Moreover, the real ORN environment will be more complicated

than the idealized model. In order to further explore the design method of social benefit optimization based on the above-mentioned viewshed analysis algorithm, it is necessary to test and analyze the method through actual case.

3. EXPERIMENTAL PROCEDURE

This paper selected a block named Chuangzhifang in Yangpu District, Shanghai, China as a case study, for its typical ORN pattern, which lead to the natural formation of space nodes. This paper wants to use this case to find a design method for optimizing Social Benefit of Vertical Greening System in ORN.

Chuangzhifang Block (Fig.9), located on the Daxuelu Road of Wujiaochang Commercial Circle in the north of Shanghai, adopts a typical enclosed layout. Buildings there mainly are multi-storey, along with a few high-rise buildings.

Through fieldwork, author's team collected the necessary basic information of Chuangzhifang, including building layout, business format, and pedestrian flow density. All of those are stored as raster data by GIS software. According to the preliminary calculation of the DEM model, the total building facade area of the Chuangzhifang block is about 100,710 m². This paper hopes to complete the VGS design of this block through technological methods.

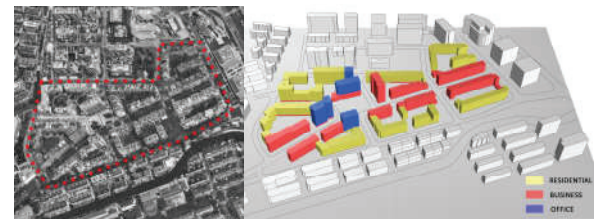


Figure 9: ChuangZhiFang Community, Shanghai.

As can be seen from Fig.10a and Fig.10b, the distribution of pedestrians in Chuangzhifang Block is closely related to the architectural layouts and business formats. The flow of pedestrians mainly gathers in the Daxuelu commercial street, the central square and the small square at the exit of the subway.

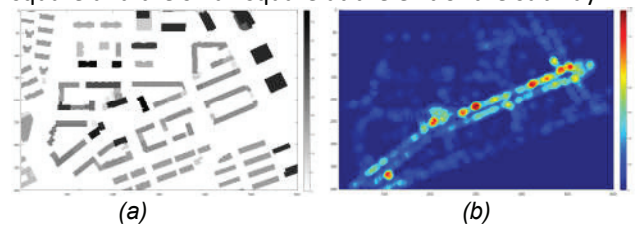


Figure 10:(a) Digital Elevation Model and
(b) Pedestrian Flow Density in Chuangzhifang Block

Among these places, the flow of pedestrians on the Daxuelu Road showed a distinct point aggregation (The red part in Fig. 10b). The main reasons can be divided into two points. First, there are many semi-open-air restaurants on Daxuelu Road. Restaurants with good reputations often attract people and cause

a crowd gathering on the street. On the other hand, the coexistence of people and vehicles on the Daxuelu Road led to the dense distribution of traffic lights on the road. So, lots of people will gather at the intersections because of the traffic. Thus, reasonable design of VGS can effectively alleviate the anxiety of customers waiting for meals and pedestrians waiting for traffic lights, and improve the quality of pedestrian experience in a targeted manner.

As mentioned, urban digital elevation and Pedestrian Flow Density (PFD) data have been well prepared in two raster grids with the same size. We start the previously written Python program to achieve the 3-D FSD data (Fig.11).

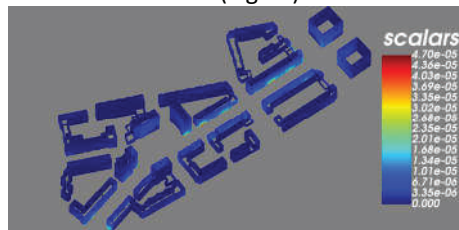


Figure 11: FSD distribution in Chuangzhifang Block.

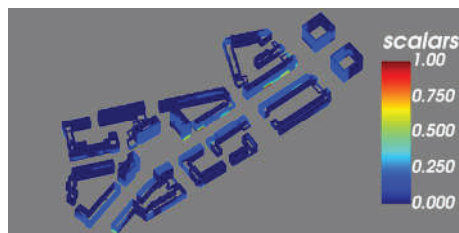


Figure 12: VGS Visual Design Reference Matrix of Chuangzhifang Block. This matrix represents the weights of VGS design of different façade, considering social benefits.

Fig. 11 shows the FSD of Chuangzhifang block. The matrix intuitively reflects the distribution of sightlines on the building facades of Chuangzhifang block. In order to facilitate the analysis and calculation, we take each floor of each building unit as the basic unit, average the FSD on each basic unit and carry out normalization processing on it to obtain the visual design reference matrix (Fig.12).

Fig.12, the visual design reference matrix, reflects the relative proportion of the density of sightlines on different facades in the block. The higher the value, the higher the sightline flux per unit area on the facade unit, which means that the facade there has higher visual renovation value. Based on the previous assumptions, in order to maximize the social benefits of VGS, these facades should be preferentially allocated to higher greening densities. In program, it can be expressed as increasing the façade's GWR.

Considering the environmental and economic benefits of VGS, we set up another weight matrix to describe which facades should be given priority to VGS renovation when considering environmental and economic benefits. Refer to the previous research results on the energy saving effect of VGS [12]. This

article assigns the corresponding design reference weights to the facades with different orientations (Table.1).

Orientation	North	South	West	East
Weight	0.20	0.25	0.30	0.25

Table 1: Design weights on facades with different orientations.

Finally, we added these two raster matrices with weight and normalized the result matrix to obtain a final VGS Comprehensive Design Reference Matrix.

In the addition process, the weight coefficients of different design reference matrices can be flexibly determined according to the architect's design intention. In this case, the author assigned a weight coefficient of 0.7 to the Visual Design Reference Matrix, and 0.3 to the Environment and Economic Benefits Design Reference Matrix, because in this case, the visual benefit of VGS has priority over the consideration of environmental and economic benefits. So far, we get the final VGS Comprehensive Design Reference Matrix (Fig.13).

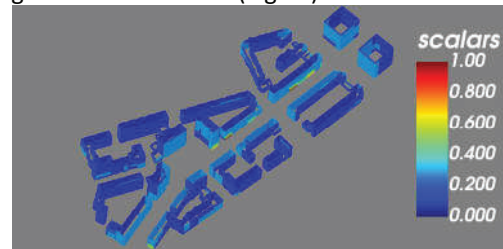


Figure 13: VGS Comprehensive Design Reference Matrix of Chuangzhifang Block, higher value means that the facade here is worth investing more design resources.

Pattern	GWR	Cost of Retrofit	Aesthetic value
A	0.00	No cost	No change
B	0.20	little	Slightly improved
C	0.40	Low	Relatively improved
D	0.60	Medium	Obviously improved
E	0.80	High	Greatly improved

Table 2: Modularized Vertical Greening System patterns.

This information can be a good design indicator by helping we assign each facade a social benefit optimum VGS pattern. Different average GWR of different walls can be achieved by adjusting the density of VGS module units, while, by adjusting the arrangement of VGS units, a rich artistic modeling can also be generated.

The author has designed 5 different VGS patterns with ascending levels of GWR and cost for the three business formats of buildings in the Chuangzhifang Block (Table.2, Fig. 14). Each façade in this block will be assigned a suitable VGS pattern according to its format and corresponding VGS Comprehensive Design Reference Weight Matrix value (Fig. 14, Fig.15), while, the Greening-to-Wall Ratio should be restored by another raster grid. After this, GVF can also be calculated and visualized, providing a way to assess the VGS social benefits (Fig. 16).

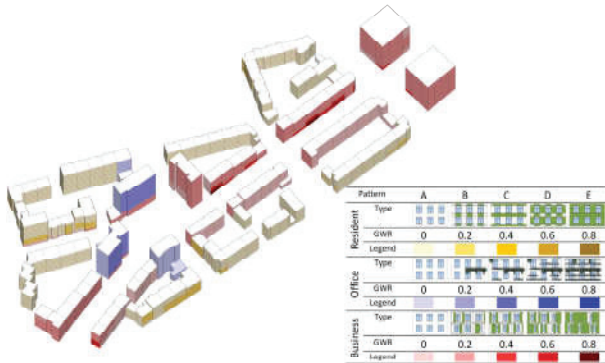


Figure 14: VGS pattern assignment in Chuangzhifang Block;



Figure 15: VGS Design Rendering of Chuangzhifang Block

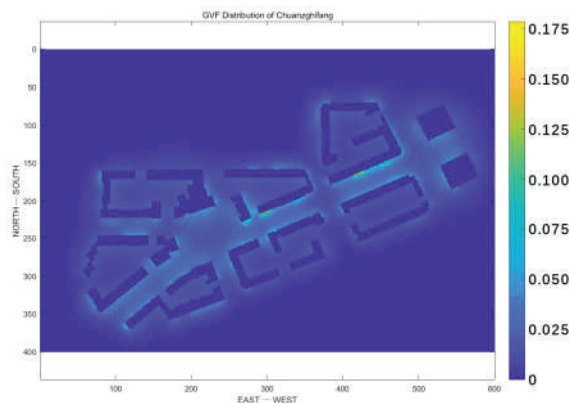


Figure 16: Greening view factors in Chuangzhifang Block

In this scenario, it can be seen that most open space with high pedestrian density (Red and yellow area in Fig.10b) were given a reasonable GVF value (Fig.16) to match their PFD. This means this vertical greening strategy can match the viewshed distribution of flow of people. This also means the social benefits of a given VGS investment (in terms of VGS size and category) can be optimized.

4. RESULTS AND DISCUSSION

In summary, this paper presents two parameters, FSD and GVF, and a fast-mathematical method for calculating these parameters. So, we may analyze the distribution of pedestrian sight lines in urban blocks before proceeding with VGS design to ensure that pedestrians can have sufficient view of vegetations and optimize the social benefits of VGS. On this basis, this paper takes Shanghai Chuangzhifang Block as a

case study to develop a method to study the optimal design of VGS social benefits.

This article provides a scientific calculation method with low space-time complexity, means it can be operated on a personal computer even a laptop. Take this research as an example, it only takes about 1 hour to complete the FSD and GVF calculation of Chuangzhifang Block (600m * 400m * 50 m)

At the same time, the View Factor Algorithm also has considerable potential in other research studies. In addition to the calculation of GVF, it can also calculate the view factor of any other objects (E.g. Billboards, Landscape sculptures, Placards and so on.) on city scale. All we need to do is replace the VGS raster with raster data that stores information about other objects.

In addition, with rapid development of computer technology nowadays, it has great practical significance to digitize design parameters and use parameters to guide design, for it provides parameter preconditions for the participation of AI technology.

ACKNOWLEDGEMENTS

The research is supported by the National Natural Science Foundation of China (NSFC) Project (No.: 51678413)

REFERENCES

1. Ministry of housing and construction. Vertical Greening Engineering Technical Schedule. CJJ/T236-2015. 2016.
2. Special Greening Joint Seminar[C]. Neo-green space design: Seibundo-shinkosha; 1995.
3. Yang F, Lau SSY, Baharuddin. Background study: Vertical greening consultancy report prepared for Urban Renewal Authority, Hong Kong. Department of Architecture, The University of Hong Kong, 2006.
4. Ulrich R.S. Human responses to vegetation and landscape. Landscape and Urban Planning . 1986, Vol.13, p.29-44
5. Gabriele Garnero. Visibility analysis in urban spaces: a raster-based approach and case studies. 2015, 42(4):688-707.
6. Kwang Youn Lee, Jung Il Seo, Kyoung-Nam Kim, et al. Application of Viewshed and Spatial Aesthetic Analyses to Forest Practices for Mountain Scenery Improvement in the Republic of Korea. 2019, 11(9)
7. Yang, B., Discussion on Opening up gated communities. City Planning Review, 2016. 2016(12): p. 113-117.
8. Ratti C F. Urban analysis for environmental prediction. PhD thesis, Darwin College, University of Cambridge, 2001: 331.
9. Fawad S. Adapting Bresenham Algorithm [J]. Journal of Theoretical and Applied Information Technology. 2006(2) p.27.
10. Zhang Gang. Research on DEM based distributed parallel algorithm for visual analysis, Geography and Geo-Information Science, 2013(4): p. 81-85.
11. A Viewshed Analysis Algorithm for 3D Urban Buildings, Bulletin of Surveying and Mapping, 2018(1):p.103-106
12. Zhan Yi, Chen Jiaqi, Zeng Liurui. Comparative Study on Different Forms of Vertical Greening of Building External Walls (Taking Guangzhou as an Example) [J]. Guangdong Architecture Civil Engineering, 2019,26(07):6-11.

A Critical Discussion of Sustainable Assessment Methods as Applied to Communities with Dual Urban-rural Characteristics: Case studies of two villages in Southwest China

YUN GAO¹ ADRIAN PITTS¹ ZHOU ZOU² XIN CHEN² LING ZHOU¹

¹University of Huddersfield, Huddersfield, United Kingdom

²Yunnan Arts University, Kunming, China

ABSTRACT: Rural revitalisation in China has led to new village developments that incorporated more and more dual urban-rural characteristics. Increasingly young villagers move to cities to work and villages have been developed as attractions that draw people from cities as visitors or new residents. A range of frameworks and assessment methods have been developed to guide the new rural or urban developments and evaluate the performance. However rigid regulations and building codes may not be flexible enough to assess complex situations brought about by the mobility of people, materials, sources and transportation between urban and rural areas. By using the concepts of the interface between the urban and the rural, this paper analyses two case studies in Yunnan Province, Southwest China. This project is to consider how the study of development of two villages can bridge the gap that frequently exists between research on urban and rural studies. In this it also compares the sustainability codes for urban and rural areas in Yunnan province to help identify missing and conflicting aspects if the sustainability codes were to be used for a mixed rural and urban area.

KEYWORDS: dual urban-rural area, sustainable criteria, China, urban village, peri-urban

1. INTRODUCTION

Mixed urban and rural communities in China become common because rural to urban migration has become a constant social phenomenon in China since the 1990s. Traditional urban and rural distinctions and relations in Chinese history were less defined than those set up today. China's household registration system, the 'hukou' system was set up in 1949. It categorizes citizens into urban (non-agricultural) and rural (agricultural) residents of a particular location. Historically, the urban residents were favoured in resource allocation compared to the rural residents and migrants. Major and persistent gaps between rural and urban populations therefore existed in terms of employment, social insurance and social welfare benefits [1]. In 2014, China's government issued a new policy to reform the hukou system to support a faster urbanization process [2]. New government regulations removed the limits on the rural migrants to urban labour markets. At the same time, the rural *hukou*-based village land rights have been open up for renting by urban residences and for outside developers and agribusiness companies [Andreas and Zhan 2016]. As a result, many mixed urban and rural communities formed inside cities or along the peri-urban areas.

The existing sustainability criteria systems, however, have been limited in their ability to analyze a series of characteristics of the areas that combined

with urban and rural areas. For example, the BREEAM (Building Research Establishment Environmental Assessment Method) Communities Technical Manual defines "Urban" as "a settlement with a population of 10,000 or more located within a tract of predominantly built up land"; and "Rural" as "any settlement or land that does not meet the definition of urban" [3]. There are few common criteria in assessment indications between rural and urban characteristics. In addition, the existing assessment criteria focused more on environmental and economic aspects; with few considering the social aspects. As a result, the assessment for new rural development projects might reveal aspects that are excluded by the definition of either 'rural' or 'urban'.

Therefore, rather than using a generic tool to assess projects that would yield generic results, this paper carried out specific research in two case studies of urban villages in Kunming, capital city of Yunnan Province in Southwest China. Yunnan is located in a region where 25 minority ethnic groups live in relative proximity. Many villages in the region engaged in low-input agriculture in rocky mountainous areas which led to rural poverty [4]. The lack of natural endowments, poor geographic conditions and fragile ecological environment are often the main driving forces behind persistent poverty in many villages in the region [4]. Many young villagers migrated to cities to find jobs with

better payments, at the same time, villages close to the city centers also attracted outsiders to rent the accommodation because of the low housing rent price and better natural environment.

Two villages were chosen in Kunming as case studies: Damoyu village where mainly Yi ethnic people live, and Haiyang village occupied by the Han ethnic group. Both villages are well known for the beauty of their landscape with surroundings of lake and mountain. The traditional settlements were formed to be in an harmonious relationship with the surrounding environment and also had a unique cultural and social heritage. Those characteristics and their close link with the urban areas attracted members of the urban population to rent houses in the village and investors, who were interested to develop various tourist projects in the villages.

The case studies therefore analyse the process of a rural village being developed and transformed into a combined rural and urban residential community. In the processes of transformation, these two villages retained their distinctiveness and some rural activities, but at the same time, they were integrated into the urbanization process that affected a much larger area. This new process calls for a redefinition of traditional urban and rural distinction and sustainable guidance that is suitable to use in the dual rural and urban areas. The study also made comparisons between the *Code for improving rural settlement* and the *Assessment Standard for Green Building in Yunnan province* where the two case studies are located.

The research of urban villages highlighted that rather than disappearing the rural-urban boundary now overlaps in different aspects. As part of the research the authors carried out interviews with village management groups, villagers, and planners who helped set up future development plans for the two villages. Our inter-disciplinary research into the historical changes of two places highlighted the fast-changing nature of the significant imbalances between urban and rural areas regarding their sustainability, and therefore require new focus on the sustainable criteria to assess those newly formed places.

2. SUSTAINABLE ASSESSMENT METHODS

Existing studies argue that different from those in the West, Chinese sustainability concepts and the official discourse of sustainability focused more on economic prosperity and the interests of the state, and placed less emphasis on individuals' rights, and is encompassed in the Chinese concept of the "ecological civilization." [5] Sustainable design codes

for urban and rural areas in Yunnan province in China also have very different focuses [6].

The Chinese sustainable assessment criteria include rural assessment and guidance for improving conditions in existing rural settlements, and a code for design of sustainable buildings in urban areas. Comparing the codes designed for urban and rural areas, the rural assessment categories generally focus on protecting the natural environment and providing for essential daily needs such as the supply of water, drainage, electricity and waste collection. In terms of built environment, it focuses on the safety of the structure, and construction making use of local materials and skills. The social and culture aspects include religious, social and cultural life associated with agricultural communities, and memory and history of the place. Sustainable tourism is also another focus for communities in Yunnan, an area that is famous for its diversity of ethnic culture and beautiful natural environment. A study of sustainable tourism development at one UNESCO site in Yunnan suggested that rural tourism and ecotourism, and its overall philosophy, reaches far beyond the limits of tourism development. It should generate a framework for ecological, economic, and social issues which balance development and conservation in the longer term [7].

Table 1 compares the Technical Guide for Improving Human Settlement in Rural Areas in Yunnan (IHSRAY) published in March 2018, and Yunnan Provincial Assessment Standard for Green Building (ASGB), published in May 2015 for the location of the two case studies [6]. It should be noted that rural areas of Southwest China are less well-developed compared to those of the East coast/Pacific Rim areas, and sustainable development is therefore different from the eastern areas [4].

In Table 1, assessment categories that are considered for rural settlements are not specifically included for those in the urban areas. In order to compare the changes in the two case studies, it should be noted that one was identified as a rural village which had historically close links with urban life; and the other is a village attracted a large number of urban residents: one fifth of residents in the village are urban population and work in the city centre. Many of those are artists and small family hotel owners. The study focuses on the comparison of social and economic wellbeing of these two communities.

2. CASE STUDIES

2.1 Haiyang village

One case study is in the Chenggong area of Kunming, in Yunnan Province. Haiyang village is

located at 1840m above sea level [9]. It has a history of about 700 years stretching back to the Ming dynasty (1368-1644). The name Haiyang means “Banquet by the Sea” which evolved from its history as an official location for providing banquets by the Dian Lake for local government events. Apart from agriculture, villagers made a living from fishing and the village used to be a busy port for salt trade to the adjacent old city Kunming. After the introduction of modern transportation systems in the 1950s, trade and transportation through river and lake came to an end. The village stagnated because it used to depend on that trade route and its fishing business, and only limited development had taken place since then. Because of the close distance with Kunming city, many social and cultural traditions inherited in the village echoed those in traditional Chinese urban life. During the anti-Japanese war in the 1940s, the first girls’ school in Kunming city was relocated to the

village to avoid the bombing as the village was only 10 km away from the urban centre. After the war, the school carried on running until 2000 which made the village well known to the local area.

Despite agriculture remaining as the important source of income for villagers in the Province more generally, it only counted for about 50% income in Haiyan village [8]. Villagers now plant vegetable and flowers to supply the needs of the urban centre.

By 2016, there were 883 families with 2550 ethnic Han population. More than half of the houses in the village were traditional timber or adobe brick houses, about 350 houses were made from bricks and concrete structure and about 70 houses were combined timber and bricks (Fig. 1). Like other villages in China, many young villagers now work in cities. Other villagers work in agriculture. The average per capita yearly income lies at approximately US\$608 in 2016.

Table 1 Comparison of the technical guides in Yunnan for rural areas and urban areas

Criteria assessed	Criteria assessed in more details	IHSRAY Rural	ASGB Urban
Land use and outdoor environment	Land saving and outdoor environment		✓
Material	Building materials and construction methods	✓	✓
Water supply and drainage	Water supply and drainage, water saving	✓	✓
Electricity	Electricity supply and energy saving	✓	✓
Building design	Climate in regions considered for building thermal design		✓
Architectural Design	Rational space utilization	✓	
Indoor environment quality	Lighting, ventilation, building envelop, acoustical environment, air quality and industrialized construction products, building life extension		✓
Construction	Construction management	✓	✓
	Structural safety: building envelope	✓	
	Demolish and improve unsafe buildings	✓	
Operation management	Management procedure Technical management Environment management		✓
Styles and features	Control colour, style and height for public space, courtyard space and green areas	✓	
Hygiene	Waste and sewage collection	✓	
	Public space and facilities hygiene	✓	
	Disaster resistance	✓	
Transportation and safety	Transportation and safety	✓	✓
Ecology	Protect natural landscape and water bodies	✓	
	Development of local industries considering natural environment	✓	
	Protect natural landscape and water bodies	✓	
Protect local cultural heritage	Protect local listed buildings, such as temples and old pagoda, wells, trees etc	✓	
	Protect buildings and space used for local rituals	✓	
Promotion and innovation			✓

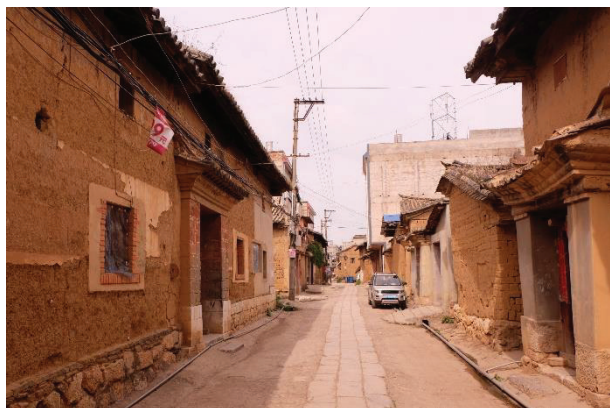


Figure 1: Haiyang village

The established Fengshui location and landscape attracted outside investment for various development projects, including urban fishing park, a public cemetery, and various design projects attributed to high end academic and renown designers from as far away as Beijing. Their design solutions involved renovation of the traditional houses in strategic locations within the village, thus improving the 'edge' of the settlement, nodes that link various roads and traffic routes. Those renovated houses include a study centre, a local agriculture product centre, and an eco-tourism centre that works as both a small hotel and a training studio for discussing eco-friendly lifestyles. However, those projects will need further funding to implement and exploit their initiatives.

2.2 Damoyu village

The second case study, Damoyu village historically is a Yi ethnic people village, set up in the 18th Century. Damoyu means "Black bamboo forest" in the Yi language. It is located next to Qipanshan National Forest Park, and a large water reservoir. The village is to the west of the city of Kunming about 15 Km away at an elevation of 2200m [10].

The village has 250 families and about 800 residents. The original villagers were all Yi ethnic people with only a small number of clans with the same surnames. In 2008, about 95 houses were made from bricks and concrete structure, 21 houses were made from brick and timber structure and about 126 houses were combined timber and adobe brick. There is a Tuzu temple in the village, where is still busy during various festivals during the year. Despite agriculture remaining as an important source of income for villagers, it only counted for about 18% of income in Damoyu village; the primary produce is vegetables for the city. Average personal income for local residents was about 570 USD [10].

Since 2010, the village has gone through fundamental change from a village based on agriculture to a village with one fifth of residents coming from nearby cities. It has increasingly become a popular place for city dwellers to rent and renovate properties as their second homes (Figure 2). Due to the low housing rent price, it has attracted some scholars, artists, and handicraftsmen, and encouraged family hotel owners to rent houses. The increased population from outside and their associated life styles have been converted into opportunities for development in the village. For example, people started to rebuild public space in the village, renovate façades along the streets, and organise various social activities such as festivals and symposium in the village. Villagers and immigrants shared the facilities and public space under the management of the village management group. Many renovated houses changed function to become, for instance, family hotels or in some cases eco-life style training centres. The main positive aspect of the place is the common recognition that the protection of cultural and natural heritage could become a valuable development mechanism.

The high-altitude location means it can only produce crops once a year, but the area does have some special plants and landscape which have a good potential for tourists from the city. The village management group have tried to develop initiatives for the conservation of tangible built and natural heritage to encourage the long-term tourism development of the village. This is also linked to the official plan to develop the adjacent Qipanshan National Forest Park.



Figure 2: Damoyu village

The research carried out in the village case studies revealed that despite intentions to develop rural and urban villages in more sustainable ways, there was a lack of formal procedures to be applied to provide guidelines or to evaluate outcomes.

Table 2: Suggestions for sustainable criteria for urban village or peri-urban areas

Sustainable considerations for mixed "urban-rural" communities	Suggested sustainable criteria for mixed urban and rural communities
Definitions of 'urban' and 'rural': Treat 'peri-urban' or urban village as an independent category in the assessment, something apart from existing 'urban' and 'rural'	Consider settlements in 'urban', 'rural' and also 'urban village' or 'peri-urban' categories. Urban village areas are variable in size and nature, with alternating elements of both urbanised and rural agriculture environments, which maintained close links with the ecological footprints of both urban and rural areas.
Governance: Community involvement in decisions and the importance role of the community management on managing shared facilities and benefits in the communities	In China, the combined top-down process and bottom-up processes affected the perceptions of sustainable construction. Compared to the emphasis on personal responsibilities in the West, sustainable development was linked to economic development and good governance with management of shared facilities and benefits
Hukou-based and market-based land right: Consider rural property rights as collective rights of the communities that are benefit to the rural population as a whole community rather than individual benefit for a short term or urban benefits.	Rural hukou-based village land rights have been open up for renting by urban residences and for outside developers and agribusiness companies to facilitate land concentration. The shift from hukou-based to market-based land rights has resulted in a hybrid system that combines the two. Villagers have gained limited but significant rights to lease, mortgage and sell the rights to use their land, which attracted urban residents and outside developers
The formal and informal multi-functions and to accommodate heterogeneous social composition: Consider villagers and immigrants or people who use the facilities in communities as various groups, who have different life styles with associated space and time in village.	Understanding and abilities of the stakeholder and representative group of communities to pursue the benefits individually and collectively for locals. Local villagers and immigrants' life styles and needs in the villages are varied, but their relationships are closely associated because of the shared village management system, facilities and spaces. A residential community may include local residents and other habitants. A socially cohesive community for both local villagers and other stakeholders, where social composition may change rapidly. Various groups with diversity of incomes.
Flows of population and materials: Include policies for mixed urban and rural characteristics and consider economic footprint in areas beyond the site location. The urban villages can both benefited or disadvantaged from both urban and rural systems but may have very flexible and less fixed methods to make use of those systems or to avoid responsibilities.	To consider flow of migrants, commuters, construction materials, food and energy sources over the short-term that have substantial impact on locals' life. Consider flow of migrants, commuters, and shifts in human spatial and material relationship with the urban areas and the rural landscape. The distance between people's housing and their workplaces.
Long-term and short-term economic success and importance of the community management group, may need to assess on a case by case basis	Separate the assessment of short and long term benefits for the communities. For example, rent acquisition has a short-term return rather than long term production; the knowledge and design styles from urban area may either support or destroy the local landscape and life styles.
Training and skills: Consider impacts on both local and temporary inhabitants in the local site and beyond	To consider training and skills that can create diversity of income including those from both farming or urban jobs. Knowledge and skills relate to job opportunities, e.g. training programmes for both farming and urban jobs
Housing provision: Include the formal and informal functions of properties	Consider the changed function of the properties, and those of domestic and public spaces. Consider the hygiene and safety of existing proprieties
Delivery of services, facilities and amenities: Ensure essential facilities are provided and that they are located within a reasonable and safe	Take into account of local variation for different social groups in welfare, participation rights, and relative value

walking distance. This is particular important during the periods that have been affected by the Covid-19	
Local vernacular: Ensure that the development relates to the local character whilst reinforcing its own identity, which is essential to attract visitors, investors and other groups. It was perceived as a pre-condition for the level of <i>beautiful environment</i> .	Historical memories and new identity for various social groups Protect local listed buildings or important landmarks such as pagoda, wells, and trees etc. and protect buildings and spaces used for local rituals.

3. CONCLUSION

Through analyzing the development of two urban villages, the study has established that sustainable assessment criteria should include more considerations with regard to communities with dual urban and rural characters. This can be observed in Table 2 which summaries the key aspects.

As a result, the authors suggest to set up 'rural-urban' transition areas as an independent category in the application of sustainability assessment methods. For the transition between rural and urban areas, the authors suggest to include more details in terms of: incorporation of the close links to rural and city areas beyond the local site; understanding of the diversity of population living in the mixed urban and rural communities; and the need to separate long-term and short-term time benefits for the communities.

These four aspects cannot be assessed in existing building codes in Yunnan or other existing assessment criteria. This study therefore concludes that it is important to consider communities with dual 'rural-urban' characters as an independent concept in the assessment, and to define a set of indicators for sustainable design for those dual urban and rural areas.

ACKNOWLEDGEMENTS

This research was part funded by the University of Huddersfield, UK; the British Academy, UK Award Reference CRFG\101033; and the Arts and Humanities Research Council, UK grant number AH/R004129/1.

REFERENCES

1. Afridi, F., Li, S X., Yufei Ren, (2015). Social identity and inequality: The impact of China's hukou system. *Journal of Public Economics*, 123: p. 17–29

2. State Council on further advancement Views on the Reform of the Household Registration System, [Online], Available: http://www.gov.cn/zhengce/content/2014-07/30/content_8944.htm. [8th December 2019].
3. BREEAM (Building Research Establishment Environmental Assessment Method) Communities Technical Manual SD202-1.22012. [online], Available: https://www.breeam.com/communitiesmanual/content/resources/otherformats/output/10_pdf/20_a4_pdf_screen/sd202_breeam_communities_1.2_screen.pdf
4. Liu, Y., Jilai Liu, J., Zhou, Y. (2017) Spatio-temporal patterns of rural poverty in China and targeted poverty alleviation strategies, *Journal of Rural Studies* 52: 66-75
5. Liu, C., Chen, L., Vanderbeck, R., Valentine, G., Zhang, M., Diprose, K., and McQuaid, K. (2018) A Chinese route to sustainability: Postsocialist transitions and the construction of ecological civilization, *Sustainable Development*. 26: 741-748.
6. Editor group of Yunnan Provincial Residential and Urban and Rural Construction Bureau and Yunnan Provincial Planning and Design Research Institution, *Code for improving rural settlement and the Assessment Standard for Green Building in Yunnan province*. Yunnan Provincial Residential and Urban and Rural Construction Bureau, Kunming, China. 2018.
7. Jacques P. Feiner , Shiwen Mi & Willy A. Schmid (2002) Sustainable Rural Development Based on Cultural Heritage, *disP - The Planning Review*, 38:151, 79-86,
8. Yunnan Provincial Architectural Science Research Institution, *Yunnan Provincial Assessment Standard for Green Building (DBL 53/T-49-2015)*. Yunnan Publish Press and Yunnan Science and Technology Press, Kunming, China. 2015.
9. Haiyang village, [online], Available: <https://baike.baidu.com/item/%E6%B5%B7%E6%99%8F%E6%9D%91/62949> [18 July 2019].
10. Damoyu village's, [online], Available: <https://baike.baidu.com/item/%E5%A4%A7%E5%A2%A8%E9%9B%A8%E6%9D%91> [18 July 2019]

Modelling and Testing Extendable Shading Devices to Mitigate Thermal Discomfort in a Hot Arid Climate

A case study for the Hajj in Makkah, Saudi Arabia

MOHAMMED ALHARTHI^{1,2}, STEVE SHARPLES²

¹Umm Al Qura University, Makkah, Saudi Arabia

² University of Liverpool, Liverpool, UK

ABSTRACT: Due to the annual pilgrimage of Hajj, the city of Makkah attracts around 2.5 million people from diverse backgrounds around the world. Many of these pilgrims may not have experienced conditions like the hot arid summer climate of Makkah. The pilgrims spend long hours exposed to high air temperatures and intense solar radiation levels while travelling between the Holy Sites of Makkah. The thermal discomfort they face can become extreme, leading to heat exhaustion or heatstroke that is severe enough to cause death. This research investigated a digitally-modelled expandable shading system that sort to mitigate this thermal stress at a microclimate level. The simulations used local data weather and quantified comfort conditions in terms of the Universal Thermal Comfort Index (UTCI) and operative temperature. The results showed a significant improvement in the thermal comfort when the expandable shades were applied, with the average yearly operative temperatures reducing by around 16%. For the most arduous and populated pilgrimage day of Hajj, the results indicated a 35% temperature difference between shaded non-shaded areas at the peak times and, for the same day, the solar radiation analysis yielded a reduction of around 90% between the shaded and the non-shaded areas.

KEYWORDS: Makkah, Hajj, Thermal Comfort, Expandable Shades, Outdoor

1. INTRODUCTION

The Saudi Arabian city of Makkah hosts the annual Islamic pilgrimage event of the Hajj. Around 2.5 million pilgrims assemble in Makkah over a 1-week period. Pilgrims visit four holy sites, walking significant distances (as much as 50 km) and spending, in total, 20 to 30 hours outside. Hajj can take place during the Saudi summer when Makkah's air temperatures may exceed 43°C [1].

Illness at Hajj associated with heat stress is a major concern [2] that will only increase with predicted future climate change in the region [3]. Adapting the pilgrim routes to provide adequate thermal comfort conditions is crucial as a wide range of people - young and old, healthy, and poorly, from countries all around the world – go to Makkah [4].

This study investigated how the microclimate experienced by pilgrims walking between the holy sites might be improved. A parametric analysis of different urban solar shading options was undertaken digitally using a range of simulation software to identify the best combinations of shade shape, size and height. Significant improvements in local air temperatures under the shading systems were achieved, which could then be related to improved thermal comfort conditions.

2. LITERATURE REVIEW

One of the main goals of designing and planning urban spaces is to make them comfortable and attractive to the people who use them [5]. The main factor that determines whether an urban space is comfortable is the microclimate. A major case study related to this research is the shading of the Prophet's Mosque in Madinah, Saudi Arabia [6].

The work of Otto and Rasch helped in mitigating the discomfort of the prayers within the semi-urban context of two courtyards within the Mosque by the use of kinetic shading devices (Fig. 1) [6].



Figure 1: The Inner courtyard of the Mosque of Madinah showing its shading system [6].

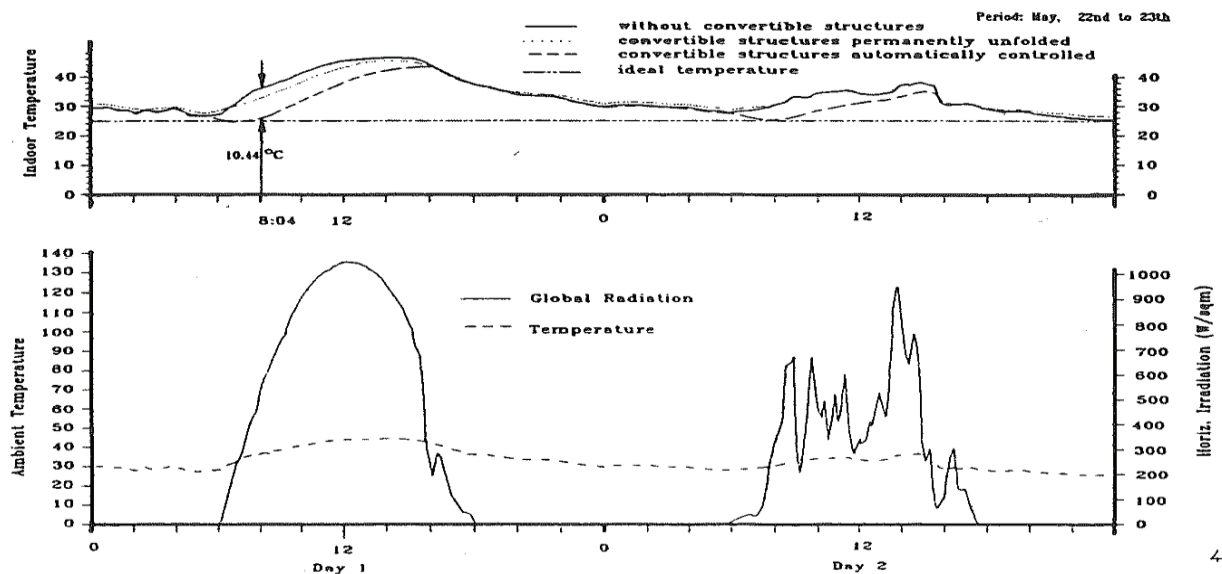


Figure 2: A microclimate regulation study for the courtyard in the Prophet's Mosque in Madinah [7].

The shading of the Prophet's Mosque took the form of retractable white canopies that could be either kept closed, remain unfolded and opened throughout the day or opened intermittently in response to environmental conditions via the use of automatic controls. The results from the study by Rasch [7], as seen in Fig. 2, shows how the canopies could reduce shade air temperatures by 10.4°C in the morning by around 08:00 compared to the ambient value.

Sijiny [8] examined pedestrian flows between the Hajj's holy sites and considered various lightweight shading alternatives to protect the pilgrims. It was noted that the shaded route will increase the number of pedestrians and decrease vehicle usage. As well as the severe climatic conditions, the density of the people gathering for Hajj can increase microclimatic temperatures within the crowd. A modelling study by Chen et al [9] simulated the conditions of the Hajj disaster on 24th September 2015, where crowds collided at the intersection of two roads. The study estimated that the temperature in the middle of the crowd might have almost reached 50°C. The potential risk to life for pilgrims to Hajj highlights the importance of trying to improve their microclimate as they move between the holy sites to reduce thermal stress. In this study, the effectiveness of large expandable shading systems along the pilgrim routes that open and retract in a manner similar to a parasol is considered. A recent review of other mitigating strategies to improve the thermal environment and thermal comfort of urban outdoor spaces has been given by Lai et al [10], who found that shading from trees was one of the most effective mitigating strategies.

3. THE ROUTE OF HAJJ

When people arrive at Makkah, they start performing a series of religious tasks, while wearing the garment of Hajj (two white pieces of clothes that are wrapped around the upper body and the lower body for men with no other layers). Most people keep this garment on until the end of Hajj, which starts after the declaration of Hajj [6].

On the morning of the eighth day of the Islamic lunar month of Thul-Hijjah, on which the actual Hajj (pilgrimage) starts, the pilgrims begin to go to Mina. On the next morning, often before sunrise to avoid the later heat of the sun, people in Mina usually start travelling the 14 kilometres to Arafat toward Namirah Mosque. The percentage of the pilgrims who choose to walk this route exceeds 30% of the total travellers [7]. After the sunset of the ninth day, people go back to Muzdalifah where around 85% of pilgrims stay the night. On the tenth day, people who spent the night in Muzdalifah, go to the three individual places of Al-jamarat, where they perform a religious rite of stoning the devil's pillars. After that, the pilgrims go back to Mina to rest. During the eleventh and twelfth-days people start going back to Makkah from Mina.

The distances walked by pilgrims during the five days of Hajj can be significant – perhaps 30 to 50 km in total. In particular, people endure a great deal of walking and tiring activities during the 14 km journey between Mina and Arafat (Fig. 3) [11]. For that reason, this route was the proposed location for the shading system investigated in this study. The advantage of allocating objects in this location is that it will protect the vast majority of pilgrims from heat stress. This is particularly important as many of the pilgrims come from places around the world where

they are physiologically adapted to their own cooler climates and so are likely to find Makkah's hot and arid climate very discomfoting [12].

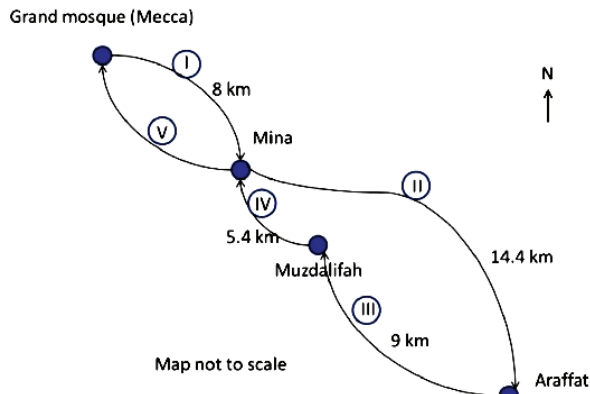


Figure 3: Routes and distances of Hajj pilgrimage [11].

4. METHODOLOGY

4.1 Climate analysis

The climatic analysis of this study focused on the holy sites in Makkah, especially during the Hajj 2019 period of 9th – 14th August. Two software were used for the study: Climate Consultant 6.0 and LadyBug Grasshopper [13]. The weather file for Arafat was chosen for the analysis as it was the closest site for this research. These data analyses were acquired using historical weather data and were logged in Grasshopper and LadyBug's components to illustrate different data for the 2019 Hajj, such as dry bulb temperature, relative humidity, global horizontal solar radiation and wind speed (Fig. 4). The weather analysis for August shows that for most times between 6:00AM and 6:00PM the conditions are thermally uncomfortable.

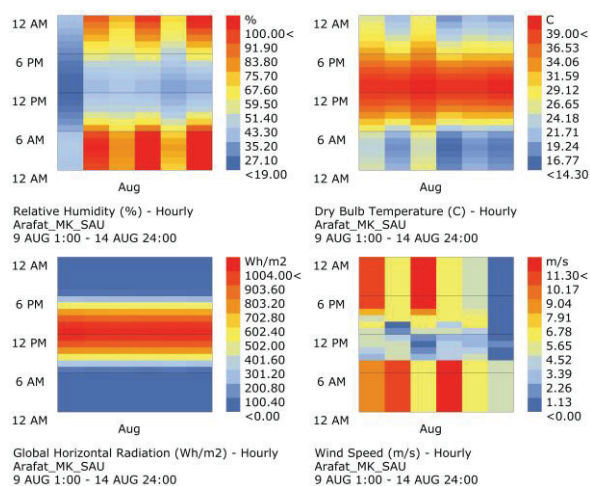


Figure 4: Arafat, Makkah - August hourly output of the dry bulb temperature (top right), relative humidity (top left), global horizontal radiation (bottom left) and global wind speed (bottom right).

The Arafat weather file that was obtained from the LadyBug website (ladybug.tools/epwmap2019)

was in a standard EnergyPlus EPW weather file format. The data readings gave a clear picture of the climatic behaviour for the years provided, and it was clear that the Arafat climate was hot and arid climate. After analysing the Arafat climate data, four hourly worst-case scenarios (in terms of thermal comfort) were identified, when the dry bulb temperatures and the relative humidity were at their highest and lowest values (Fig.5).

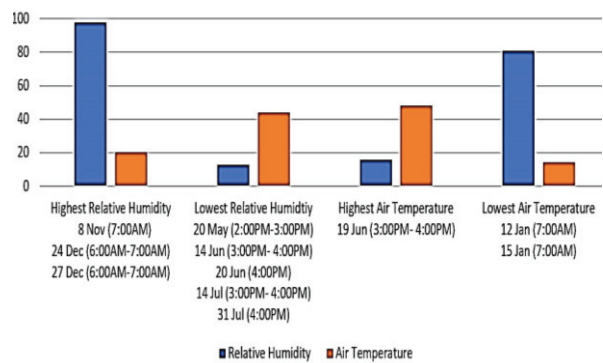


Figure 5: Worst-case scenarios of air temperature and relative humidity from the Arafat weather file.

4.2 The Universal Thermal Comfort Index (UTCI)

In order to study the impact of the proposed shading system on microclimate comfort, it was necessary to identify an outdoor thermal comfort index. Although many such indices have been developed over the last twenty years, most of them only consider the role of a single climatic parameter, such as solar radiation or wind speed, on comfort.

The Universal Thermal Climate Index (UTCI) has the benefit of combining four climatic variables (air temperature, radiant temperature, humidity, and wind speed) and calculating a temperature that 'feels like' being exposed to those combined weather conditions [14]. Another advantage of the Universal Thermal Climate Index for this study, when compared to other indices, such as the Physiologically Equivalent Temperature (PET), is its capability to adjust the assumed outdoor clothing level of people, whereas the PET uses a standard clothing level [15]. The advantage here is knowing that the Makkah context embraces different cultures with different clothing expectations besides the clothing of Hajj, where men are expected to wear two white garments during the days of the pilgrimage. This suggests that the UTCI is more appropriate to illustrate the thermal physiological stress than the PET. It is also a more recently developed thermal model [15].

Table 1 shows the range of UTCI 'feels like' temperature values and the equivalent thermal stress categories.

Table 1: The UTCI 'feels like' temperatures in °C and the equivalent thermal stress.

UTCI range in °C	Stress category
above +46	extreme heat stress
+38 to +46	very high heat stress
+32 to +38	high heat stress
+26 to +32	moderate heat stress
+9 to +26	no thermal stress
0 to +9	slight cold stress
-13 to 0	moderate cold stress
-27 to -13	high cold stress
-40 to -27	very high cold stress
Below -40	extreme cold stress

4.3 Modelling procedure for the shading devices

The modelling and simulation of the proposed shading systems were undertaken using Rhinoceros 3D software with Grasshopper to calculate values of UTCI, operative temperatures and incident solar radiation levels. The simulations were based on an example performed by Mackey using LadyBug Tools [16]. The climatic data were obtained from the LadyBug Tools LLC website for EPW maps [17] where the climatic data of Arafat - the nearest location of the tested area - was connected to the algorithmic process of the simulation. For modelling purposes, a square-shaped shading canopy model was found to be the most practical. The canopy was 15m high and 30 x 30m in plan, giving an extendable area of up to 900m² (Fig. 6). These dimensions were suggested based on the size of the pedestrian paths between Mina and Arafat, Makkah. The canopies were formed as a 9-unit (3x3) cluster to shade the chosen location around Arafat. The materials were assumed to be solid with zero transmittance properties as it was found that, in terms of shade benefits, the shades' materials had minimal impact when made of a low thermal mass fabric [18].

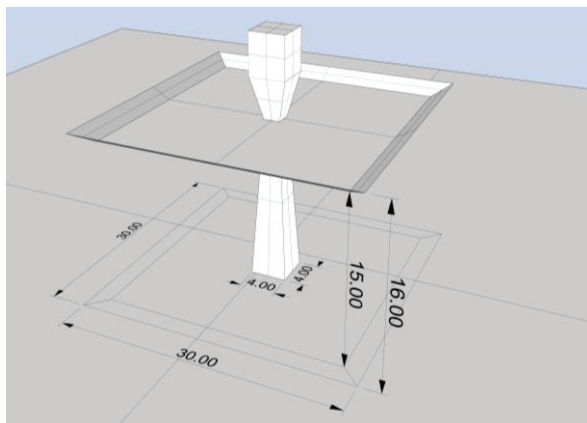


Figure 6: Details of the modelled canopy shading device.

5. RESULTS

5.1 The UTCI temperatures

The performance of the proposed device was quantified in terms of the UTCI values created under the canopy measured over a grid of 5m at a height of 1m above the ground for the 10th August 2019 (max/min DBT of 37°/31°C, RH 48-62%, wind speed 1.9 to 5.5 m/s). Fig. 7 shows the average UTCI values with the canopy retracted and extended. Average UTCI dropped from 36.5°C (strong heat stress) to 31.5°C (moderate heat stress).

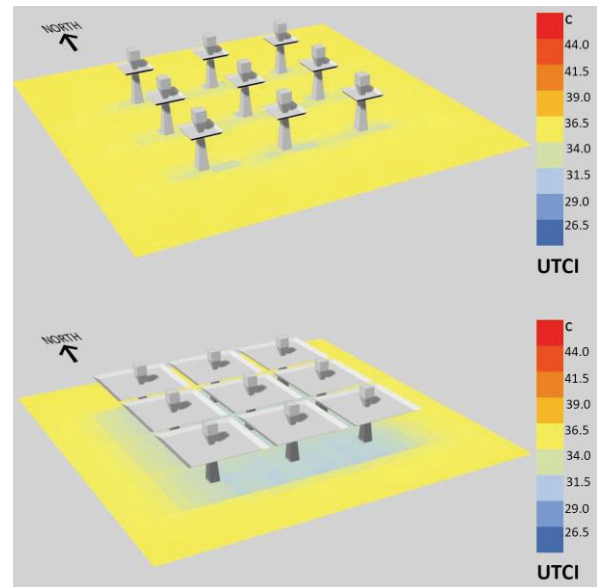


Figure 7: Average UTCI for 9-cluster shading of the site on 10th August (retracted [above] and extended [below]).

Hourly operative temperatures for the 10th August for extended and retracted canopy scenarios were also examined (Fig. 8). Temperature differences between shaded and sunlit areas start to appear at 07:00, where the sunlit area was around 38.6°C while the shaded area was around 34.5°C. The biggest difference in operative temperatures between the shaded and non-shaded areas was around 16°C at 09:00 and 17:00. The last time to record a difference was 18:00, when the non-shaded area was around 46.8°C while the shaded area was around 38.6°C (Fig. 9). After that time, the sun had set, and no further differences were found.

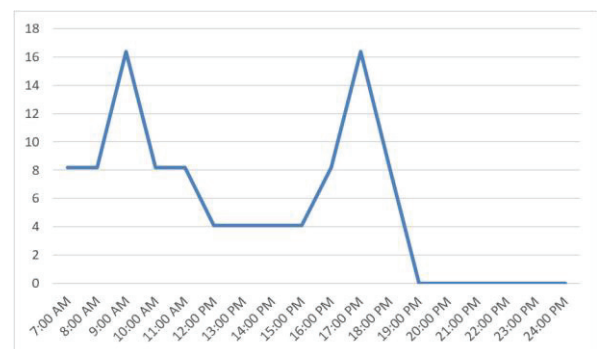


Figure 8: Hourly operative temperatures differences (°C) between the shaded and non-shaded areas, 10th August.

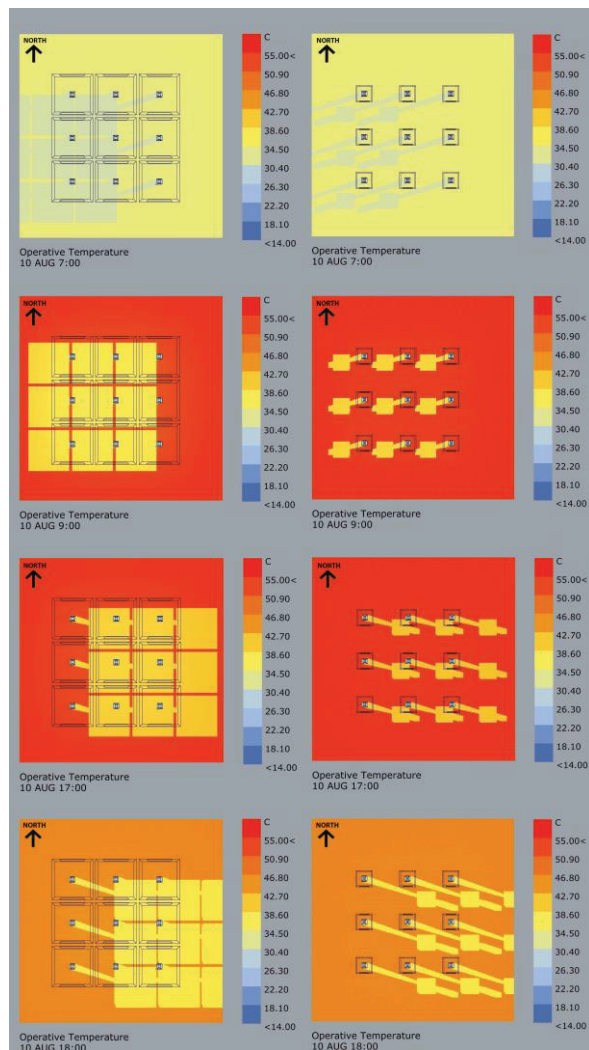


Figure 9: Operative temperatures at the site on 10th August at (top to bottom) 07:00; 09:00; 17:00 and 18:00 (shading extended [left] and shading retracted [right]).

5.2 The solar radiation analysis

The solar radiation analysis results showed large difference between shaded areas and the exposed sunlit areas. The analysed period was between the 9th – 13th August for the hours 09:00 – 15:00. The shades affected the radiation levels significantly. Solar radiation values outside the shaded area exceeded 24 kWh/m², while inside the shaded area they were between 9.41kWh/m² and 2.35kWh/m² toward the central area of the shades, rising to 16.47kWh/m² at the boundary of the shaded/unshaded areas (Fig. 10).

5.3 The shading benefits analysis

For a whole year, a visual scale of comfort (-3 to +3, where -3 indicates extremely cold and +3 extremely hot), was produced for shade and no shade areas, which showed the year-round benefits of shading the chosen urban area in Makkah (Fig. 11). It showed that there was an extreme discomfort for most of the year between the hours of 09:00 and 18:00. The simulation showed that for around 41% of

the time during the year people felt heat stress outdoors, around 19% of the time people felt cold stress and around 27% of the time people felt comfortable outdoors. During the Hajj period, people felt heat stress for almost all the time outdoors. The shading system helped mitigating the thermal discomfort for the pedestrians walking beneath them during the year (Fig. 11 below).

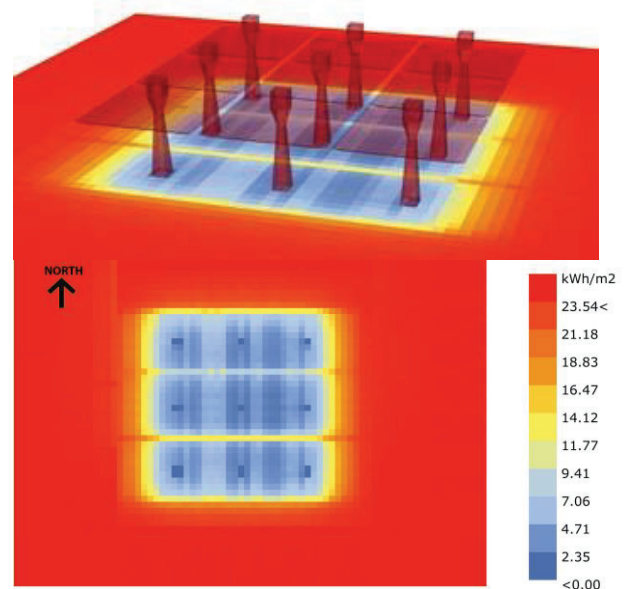


Figure 10: Solar radiation levels for the modelled canopy shading device, 9-13 August, between 09:00 and 15:00.

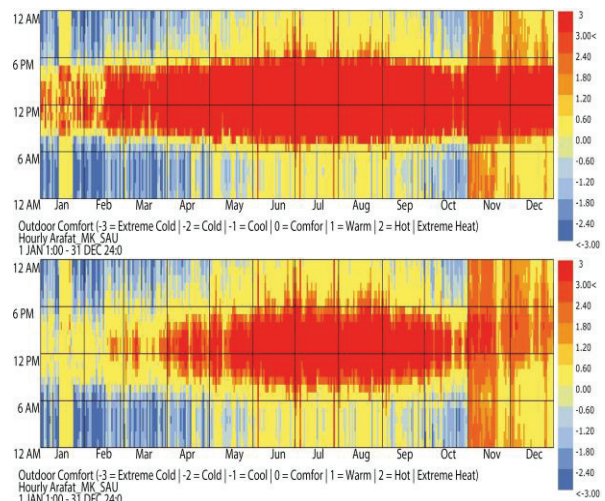


Figure 11: Annual outdoor comfort levels without (above) and with (below) the shading canopies.

A visual illustration with a scale of degree days/m² was made to show the best location to walk beneath the shade and was calculated for the whole year (Fig. 12). The degrees per day are representing the balance temperature difference between the external air temperature and the temperature at a point under the shade on an hourly basis for the analysed period per square metre. The smaller the temperature difference then the less good that spot.

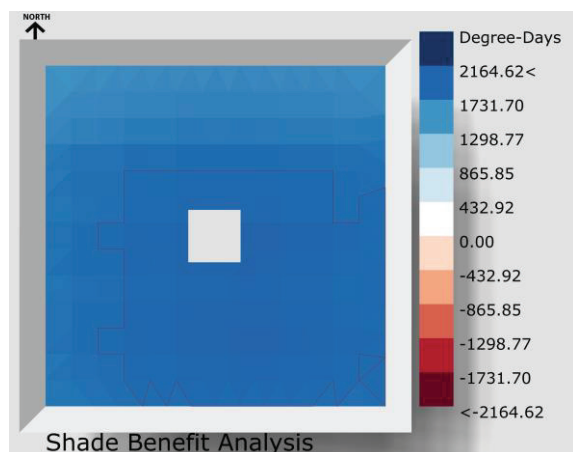


Figure 12: The shade benefit analysis, where the darker blue areas are the best locations to walk beneath the shading device.

Finally, an analysis calculated the number of hours of direct sunlight received at the site on 10th August from 9:00AM to 15:00PM when the shading devices were expanded and retracted. Fig. 13 shows how the very minimal shade provide by the support stands and the folded shading led to sunshine hours on the ground of between 9 and 10+ hours of direct sunlight. Conversely, with the shading fully extended, the direct sunlight hours were typically 1 to 2 hours.

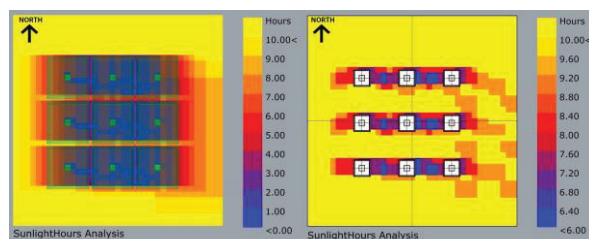


Figure 13: Sunshine hours for 10 August from 9:00AM to 3:00PM for the extended (left) and retracted (right) shading.

6. CONCLUSION

This study has examined the effect on outdoor pedestrian comfort of a cluster of prototype shading canopies. There was a significant improvement in the thermal comfort when the canopies were opened, for both daily and yearly periods. A significant increase in the thermal comfort was found when the canopies were applied. The benefits outreached the Hajj period to be suitable for the most year. Further work will investigate integrating other passive cooling measures into the canopies, such as evaporative cooling.

REFERENCES

1. Abdou, A. E. A., (2014). Temperature trend on Makkah, Saudi Arabia. *Atmos. Clim. Sci.*, 4: p. 457–481.
2. Abdelmoety D. A., N.K. El-Bakri, W. O. Almowallid, Z. A. Turkistani, B. H. Bugis, E. A. Baseif, M. H. Melbari, K. AlHarbi

- and A. Abu-Shaheen, (2018) Characteristics of heat illness during Hajj: A cross-sectional study. *Biomed Res. Int.*, 2018: p. 1-6.
3. Kang, S. J. S. Pal and E. A. B. Eltahir, (2019). Future heat stress during Muslim Pilgrimage (Hajj) projected to exceed 'Extreme Danger' levels," *Geophys. Res. Lett.*, 46: p. 10094–10100.
4. General Authority for Statistics in Saudi Arabia, (2019). Hajj Statistics Report 1440H-2019G, *Hajj Stat. 2019 - 1440*, 2019, p. 51.
5. Maruani, T. and I. Amit-Cohen, (2007). Open space planning models: A review of approaches and methods. *Landsc. Urban Plan.*, 81: p. 1–13.
6. Werkbund Bayern and Museum Villa Stuck(1995)., *Frei Otto, Bodo Rasch : finding form : towards an architecture of the minimal : the Werkbund shows Frei Otto, Frei Otto shows Bodo Rasch : exhibition in the Villa Stuck, Munich, on the occasion of the award of the 1992 Deutscher Werkbund Bayern prize to F.*, 3. ed. Axel Menges.
7. Rasch, B., (1980). Die Zeltstädte des Hadsch/The Tent Cities of the Hajj, Stuttgart 1980 (= Universität Stuttgart, Mitteilungen des Instituts für leichte Flächentragwerke, no. 29)
8. R. S. Sijiny, (2016). Lightweight interventions as solutions to the annual pilgrimage to Makkah (The Hajj): The role of shading structures for pedestrians walkways. Unpublished Masters dissertation, University of Vienna.
9. Chen, L., C. R. Jung, S. R. Musse, M. Moneimne, C. Wang, R. Fruchter, V. Bazjanac, G. Chen and N. I. Badler, (2017). Crowd simulation incorporating thermal environments and responsive behaviors. *Presence*, 26, No. 4: p. 436–452.
10. Lai, D., W. Liu, T. Gan, K. Liu and Q. Chen, (2019). A review of mitigating strategies to improve the thermal environment and thermal comfort in urban outdoor spaces. *Science of the Total Environment*, 661: p. 337–353.
11. El Hanandeh, A. (2013). Quantifying the carbon footprint of religious tourism: the case of Hajj. *Journal of Cleaner Production*, 52: p. 53-60.
12. General Authority for Statistics in Saudi Arabia, (2018). Hajj Statistics, *Hajj Stat. 2018-1439*.
13. LadyBug Tools LCC, (2019). LadyBug for Grasshopper, <https://mostapharoudsari.gitbooks.io/ladybug-primer/content/>.
14. Mackey, C., T. Galanos, L. Norford and M. S. Roudsari, (2017). Wind, sun, surface temperature, and heat island: critical variables for high-resolution outdoor thermal comfort. Proc. 15th IBPSA Conference, San Francisco, CA, USA, Aug. 7-9: p. 985-993.
15. Matzarakis, A., S. Muthers and F. Rutz, (2014). Application and comparison of UTCI and PET in temperate climate conditions. *Finisterra*, 49: p. 21–31.
16. LadyBug Tools LLC, (2019). Urban Microclimate - Simple Spatial UTCI. Available at: http://hydrashare.github.io/hydra/viewer?owner=chriswackey&fork=hydra_2&id=Urban_Microclimate_-_Simple_Spatial_UTCI&slide=0&scale=1&offset=0,0.
17. LadyBug Tools LLC, (2019). EPWMAP - Arafat :: 410320 :: ISD-TMYx. <https://www.ladybug.tools/epwmap/>.
18. Mackey, C., M.S. Roudsari, P. Samaras, (2015). ComfortCover: A Novel Method for the Design of Outdoor Shades. https://www.ladybug.tools/assets/pdf/ComfortCover_SIMA_UD_2015.pdf/.

Using textile canopy shadings to decrease street solar loads

ELENA GARCIA-NEVADO¹ ANTOINE BUGEAT¹ EDUARDO FERNANDEZ² BENOIT BECKERS¹

¹ Urban Physics Joint Laboratory, Université de Pau et des Pays de l'Adour, E2S UPPA, Anglet, France

² Universidad de la República. Montevideo, Uruguay

ABSTRACT: One of the main design goals of bioclimatic urbanism in locations suffering from excessive heat is providing shade. In the Mediterranean region, a common strategy to achieve this goal is the use of textile shading devices over the street. This work aims to evaluate the potential of these 'sun sails' in decreasing street solar loads. To this end, we analyse an actual street in Cordoba, a city with extreme summer conditions, using climate-based simulations. We compare the distribution of solar loads over the urban canyon surfaces with and without sun sails under several scenarios of street and tissue reflectance. Results show that the use of sun sails, especially if high-mounted, is an effective strategy to limit street solar loads with simultaneous benefits for pedestrians and building comfort. In absolute terms, the outcomes of sun sails are similar in streets with dark or light-coloured façades, and better than whitening interventions. The effectiveness of these devices not only depends on the openness of the tissue but also on its colour.

KEYWORDS: Sun sails, Shading, Urban cooling, Heat mitigation, Mediterranean region.

1. INTRODUCTION

Cities with temperate and hot climates are already home for the majority of humans on Earth and will concentrate the population growth of the next few decades. In these areas, the excessive heat poses a seasonal or all year long comfort problem, which will worsen as the climate change progresses, due to global warming and the increase in extreme heat events. Therefore, one of the main challenges of sustainable urban planning worldwide consists of implementing strategies to cool the city.

Under excessive warm conditions, limiting the solar loads received by urban surfaces constitutes a major design goal. Shading has demonstrated to be an effective strategy in this sense, regardless of the way to generate it [1]. At the urban scale, literature has mainly focused on the positive effect of self-shading urban morphologies [5] and shade trees [6], while the attention paid to urban shading devices has been far more limited [2].

Textile canopy shadings may constitute an interesting choice when dealing with some design constraints, such as water shortage or the need for removable protections. In Mediterranean cities, typically affected by these limitations, the use of street sun sails is common (Fig. 1). Up to date, studies have mainly assessed the benefits of this kind of device on pedestrian comfort relying on point analyses [2-3]. More spatialized analyses covering the global street scale are essential, though, for a comprehensive evaluation of sun sails effects. In this vein, shadows cast by sun sails may also affect buildings, helping to limit their overheating, and hence, their cooling energy consumption [11].



Figure 1: Urban sun sails in Sierpes St (Sevilla, 1918) and Gondomar St (Cordoba, 2018).

2. OBJETIVE

The present work aims to assess the effectiveness of textile canopy shadings in limiting the solar loads absorbed by the street surfaces. Specifically, the goal of this paper is to answer three questions:

- What is the most effective urban intervention: adding urban shading devices or whitening the street?
- Are sun sails equally effective in dark and light-coloured urban environments?
- How does the sun sail colour affect its cooling potential?

To provide realistic insights on the subject, we analyse an existing street in Cordoba, a city with extreme summer conditions. We simulate the solar loads absorbed by façades and the pavement, comparing results with and without sun sails for the complete warm season under different scenarios.

3. METHOD

The present study relies on computer simulations over a 3D mock-up of an actual street. To complete these simulations, we followed three steps.

First, we created a 3D model of the investigated urban environment. Using CAD tools, we generated two versions of this urban model: with and without sun sails. To create buildings, we extruded the 2D footprints from cadastral sources, using the individual building heights retrieved from Google Earth Pro. Sun sail pieces were modelled as two offset surfaces, extremely close to one another, meshed in the same way, with variable tilt and elevation.

Second, we assigned the optical properties to the surfaces comprised in the model. In the most general case, materials can transmit (directly and diffusely), reflect (directly and diffusely) and absorb the impinging solar energy. Coefficients τ_r , τ_d , ρ_r , ρ_d and α express, respectively, the ratio between these options ($\tau_r + \tau_d + \rho_r + \rho_d + \alpha = 1$). For this work, we assume that ground and façade surfaces are opaque perfect diffusers ($\tau_r = \tau_d = \rho_r = 0$), verifying then Equation (1):

$$\rho_d + \alpha = 1 \quad (1)$$

Regarding sun sails, we consider them as open wave tissues that partially block the incident radiation. According to Kotey's experimental measurements [7], this kind of tissues transmits radiation both directly (τ_r) and diffusely (τ_d), while the radiation blocked is whether absorbed and/or reflected backwards purely diffusely ρ_d ($\rho_r = 0$). This work models the optical behavior of sun sails tissues accordingly, as expressed in Equation (2):

$$\tau_r + \tau_d + \rho_d + \alpha = 1 \quad (2)$$

For this study, we assume that the value of the diffuse transmission (τ_d) and reflection (ρ_d) is constant regardless of the incident angle θ , being dependent on the tissue color. Conversely, the tissue direct transmission (τ_r) is angular-dependent feature of the tissue. Its maximum value happens at a normal incidence ($\theta = 0^\circ$) and corresponds to the openness factor of the tissue ($A_0 = \tau_{r0}$). As the incidence angle increases, τ_r gradually diminishes to zero at $\theta > 65^\circ$ [7].

Third, we proceed to the calculation of the solar loads absorbed by surfaces in the model. To this end, we use the algorithm detailed in [10], based on radiosity method [8]. This technique requires the meshing of the complete urban scene: sky and built surfaces. In this study, we use a fine mesh ($< 0.5\text{m}^2$) for the surfaces of interest (façades, sun sails and the ground) and a coarser one for the rest of the scene ($> 4\text{m}^2$). We subdivided the sky into a 5000-element mesh following the equal-area partition proposed by [4]. To calculate the radiance of each sky patch, we used the Perez All-Weather model [9], using as inputs the climatic data of the selected location (*epw file), and the position of the Sun at each time step.

Another prerequisite of the radiosity method is the computation of the *view factors* (F_{ij}) between all the pairs of elements i - j in the scene. In this paper, we chose instead to use '*extended view factors*' (F_{ij}^*). This technique allows for accounting not only diffuse radiation exchanges (ρ_d , τ_d) but also the specular ones (ρ_r , τ_r). Thanks to this approach, we can perform accurate computations of the radiative exchanges in the complete urban scene (not view dependent), taking into account in detail all the optical properties of the sun sails (τ_r , τ_d , ρ_d , α).

Once fulfilled the basic prerequisites of the Radiosity method, we calculate the irradiance (E_i) received by any patch i of the scene. To this end, we need to solve the system of linear equations under the form of Equation (3). The first term of this expression accounts for the radiation from the sky vault, the second and third terms, the reflected and transmitted parts from the built environment, respectively.

$$E_i = \sum_j (F_{ij}^* M_j + F_{ij}^* \rho_{d,j} E_j + F_{ij}^* \tau_{d,j'} E_{j'}) \quad \forall \text{ patch } i \quad (3)$$

where E_i , E_j - irradiances on patch i / j (Wm^{-2});
 F_{ij}^* - extended view factor from patch i to j ;
 M_j - exitance of the patch j (Wm^{-2});
 $\rho_{d,j}$ - diffuse reflectance of the patch j ;
 $\tau_{d,j'}$ - diffuse transmittance of the patch j' .

*Patches j and j' represent a pair of identical patches in the two offset surfaces of sun sails.

Finally, we compute solar loads (A_i), that is, the fraction of the incident solar radiation that ends up being absorbed by each street surface. To do this, we multiply the irradiance of each surface by their total solar absorptance, following Equation (4).

$$A_i = \alpha_i E_i \quad (4)$$

where A_i - solar load of patch i (Wm^{-2});
 E_i - irradiance on patch i (Wm^{-2});
 α_i - absorptance of the patch i .

4. CASE STUDY

4.1 Site description

Cordoba is a historical city located in the South of Spain ($37^\circ 53' \text{N}$). It presents a Mediterranean climate with mild winters and a warm and dry season running from May to September (Fig. 2). During this period, the average high exceeds 30°C , and heatwaves and air temperature peaks over 40°C are recurrent.

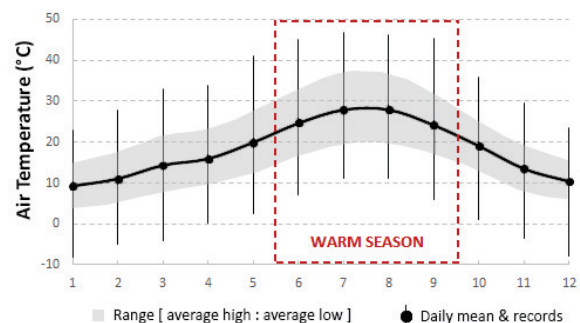


Figure 2: Climate data from Cordoba Airport.

To mitigate these extreme conditions, every year, the city council and a local commerce association promote the installation of textile canopy shadings over several commercial streets of the city centre. This work focuses on one of them: *Gondomar St*. This street is a deep urban canyon ($W/H=0.6$), bounded by North and South facing façades (Fig. 3a).

Gondomar St is mainly composed of high reflective façades (white, beige, yellow), as shown in Fig. 1. Occasionally, some dark façades appear, typically made of bare brick, a common cladding in the city. The street ground is a low reflectance surface made of a dark grey granite paving.



Figure 3: Plans (up) and aerial views (down) of *Gondomar St* (source: Google Earth Pro) and its 3D model.

The sun sails installed in this street consist of white triangle-shaped pieces of micro-perforated PVC tissue. Individual pieces are fixed to the upper part of façades through metallic tensors, leaving gaps between them to reduce wind-drag effects and air stagnation. Due to the difference in height among opposing buildings, the tilt of sun sails varies along the street, creating additional gaps (Fig. 3d).

Until now, the shading devices installed in *Gondomar St* only shelter the street partially (Fig. 3b). The city council is currently studying the possibility of an extension project to cover the street along its entire length for the next years.

4.2 Simulation model and scenarios

Following Section 3, we created two geometrical models of *Gondomar St*: one without sun sails, another with them. The latter model included not only the existing sun sails but also the projected ones, as shown in Fig. 3c.

To address the design-related questions posed in the present work, we analysed the street solar loads under six different scenarios (Fig. 4).

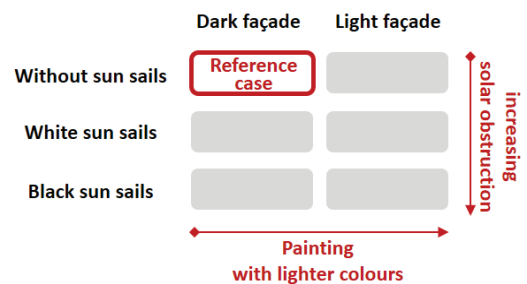


Figure 4: Case scenarios studied through simulations.

Based on the features of this urban area, we defined two idealistic scenarios regarding the façade reflectance: dark and light-coloured. For both cases, we run simulations between 15 May and 15 September without sun sails, and with two types of them: black and white. Table 1 summarises the optical properties considered for each scenario. Notice that ground and roof properties, as well as the tissue openness, were the same in all the simulations.

Table 1: Optical properties of urban surfaces and sun sail tissues at normal incidence ($\theta = 0^\circ$).

Model surface	τ_r	τ_d	ρ_d	α
Dark façade	0	0	0.30	0.70
Light façade	0	0	0.70	0.30
Ground	0	0	0.10	0.90
Roof	0	0	0.40	0.60
White sun sail ¹	0.18	0.12	0.62	0.08
Black sun sail ²	0.18	0	0.08	0.74

Tissue with an openness factor of $A_0 = 18\%$, made of white fibers ($\rho=0.90$)¹ or black fibers ($\rho=0.10$)²

5. RESULTS

This section presents the simulation results of the solar loads absorbed by street surfaces for all the investigated scenarios. The order of graphs in Figs. 5 and 6 follows the scheme in Fig. 3. This makes it possible to compare the impact of whitening façades and increasing solar protection at a glance (by reading from left-to-right or top-to-bottom, respectively).

5.1 Distribution of solar loads over façades

Fig. 5 presents the distribution of solar loads over the façades of the investigated street. Results show that the south façade of a dark street with no sun sails has the highest solar gains. In contrast, the north façade of a light-coloured street with black sun sails presents the lowest solar gains.

In the absence of sun sails, north and south-facing façades present differentiated behaviours. The south façade absorbs higher solar loads than the north one, and with a more uniform distribution. Differences between orientations decrease when façades are lighter due to the multiple reflections.

When sheltered by sun sails, both façades present a similar distribution of solar loads, characterized by two differentiated zones: below and above the shading devices. Façade areas below the sun sails absorb significantly less solar radiation than those above it, regardless of the façade and sun sail

colour. These two parameters affect, though, their effectiveness as a heat mitigation strategy.

For the same openness factor, black tissues have lower global transmittance and reflectance than white ones. Therefore, the tissue colour affects the absorption of solar radiation of surfaces both below and above sun sails. In both cases and for both façades, solar loads are lower when using black tissues instead of the white ones. In fact, façade solar loads above white sun sails exceed those without sun sails at all due to an increase in reflected radiation.

The results also indicate that the effectiveness of sun sails varies depending on the reflectance of the street. The reduction in solar loads due to sun sails on the façades is more evident the darker they are, especially on the south-facing one.

5.2 Distribution of solar loads over the pavement

Fig. 6 depicts the solar loads absorbed by the pavement of the investigated street for the different scenarios assessed. Solar loads over the pavement are maximum in the street with no solar protection and white façades, due to the multiple inter-reflections between these surfaces. Conversely, the dark street sheltered by black sun sails presents the lowest solar loads over the pavement.

The installation of sun sails reduces significantly the solar radiation absorbed by the ground, regardless of the façade and sun sail colour. This

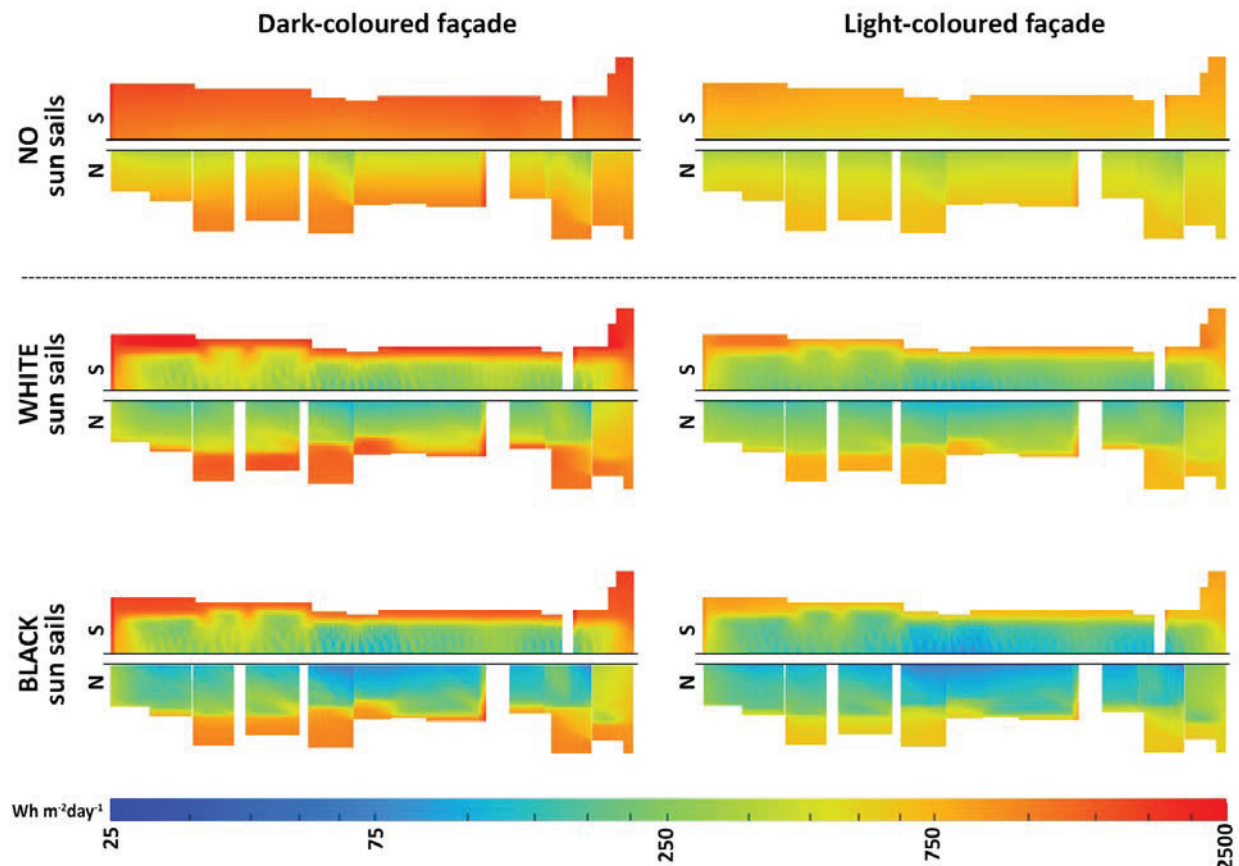


Figure 5: Solar loads absorbed by street surfaces with and without sun sails (Wh m²day⁻¹, from 15/05 to 15/09).

decrease is especially noticeable on the area close to the base of the building facing south, that is, the pavement area receiving direct solar radiation.

5.3 The global effect of sun sails on solar street loads

Since the use of sun sails affects the solar gains of façades and pavement simultaneously, it has a global impact on the street scale. To discuss this aspect, we introduce the concept of *street solar loads*, as the sum of the solar loads (MWh/season) accumulated by the ground and façade surfaces bounding the studied street during the investigated period. In this sense, Fig. 7 compares the effect of whitening the façades or installing sun sails on the *street solar loads* of the street with dark façades (base scenario). Results show that, regardless of their colour, the use of sun sails is the best alternative to reduce street solar loads. Though painting and installing sun sails have a similar impact over the façade solar loads, the former intervention increases ground solar gains (+20%) while the latter reduces them (up to -65%).

Fig. 8 compares the impact of sun sails on the solar loads of streets with a different reflectance. Results show that, in absolute terms, the reduction in solar loads due to the installation of sun sails is similar for streets with light and dark façades, being only slightly higher in the latter environment. The reason is that sun sails avoid radiation from

penetrating into the canyon and being absorbed by surfaces whether directly (dark façades) or after multiple reflections (light façades).

These results also demonstrate that the colour of sun sail plays a secondary - but not negligible - role in the global effectiveness of these devices. The use of black sun sails instead of the white ones helps to reduce street solar loads between 8-12%. This means that roughly 20% of the total decrease in streets solar loads due to the presence of sun sails depends on their colour.

6. DISCUSSION

Results in this work indicate that the darker the sun sails, the more effective they are in reducing solar gains over the street surfaces. However, black tissues absorb more solar radiation than the white ones, therefore overheating to a greater extent and emitting more longwave radiation towards buildings and pedestrians. This counter effect diminishes the effectiveness of black sun sails somehow.

The assessment of the impact of sun sails on the longwave exchanges between the street surfaces and users is beyond the scope of this paper since it would require thermal simulations. However, a complete evaluation of the cooling potential of this kind of urban shading devices should take into account this aspect.

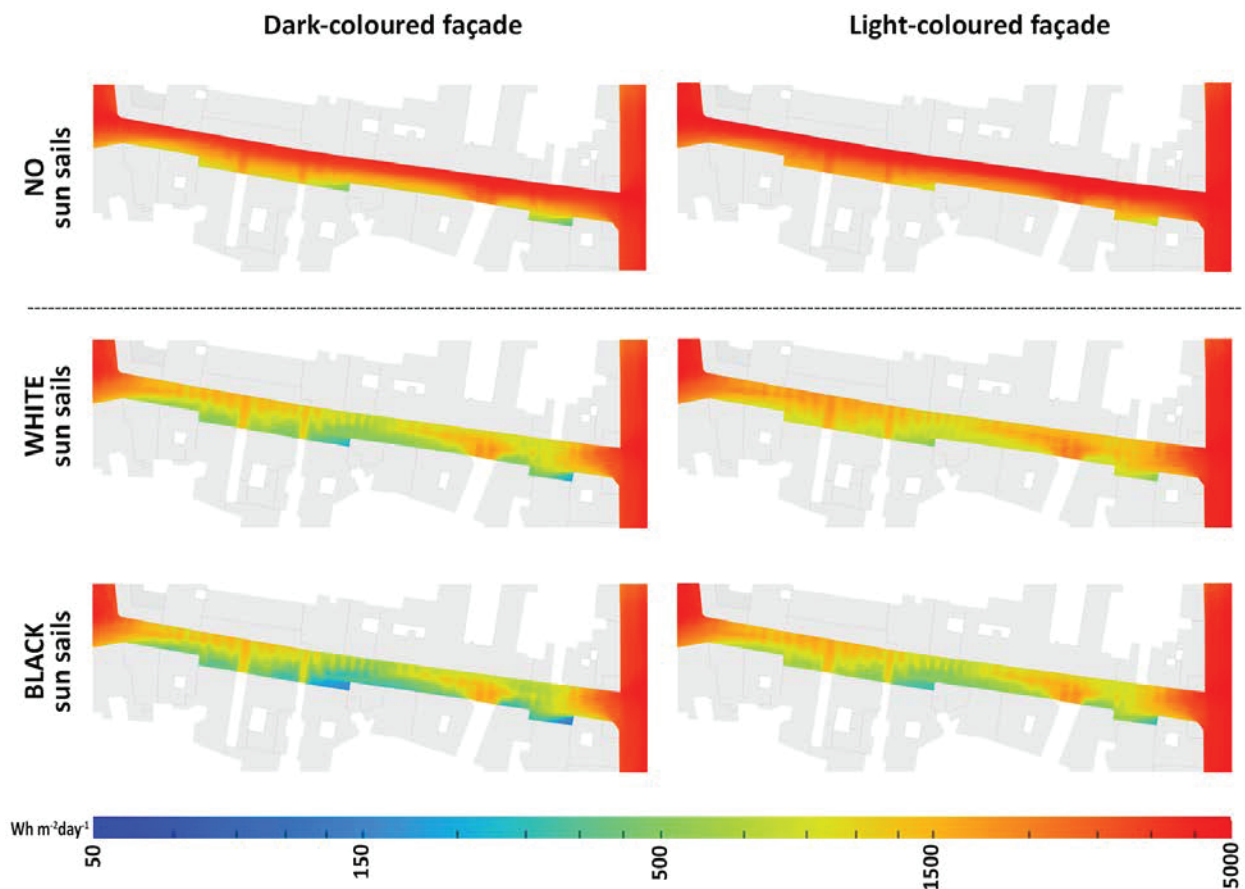


Figure 6: Solar loads absorbed by street surfaces with and without sun sails ($\text{Wh m}^{-2}\text{day}^{-1}$, from 15/05 to 15/09).

The use of sun sails will decrease wind speeds within the street, a key aspect for indoor and indoor comfort. Further investigations in this matter are needed.

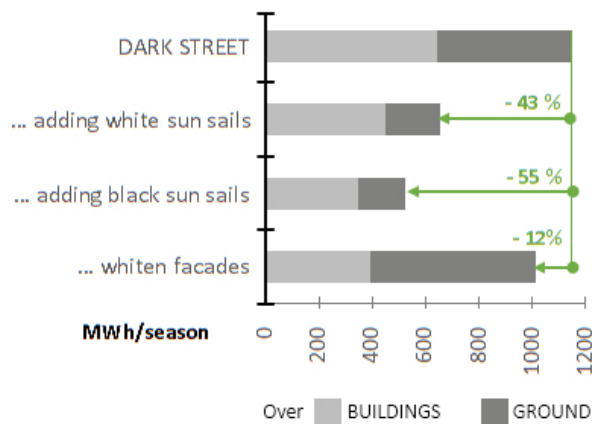


Figure 7: Impact of painting or installing sun sails on solar loads of the 'dark street'.

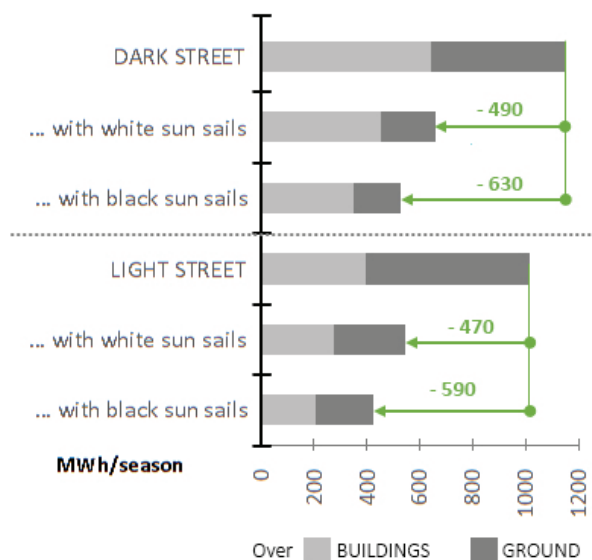


Figure 8: Impact of adding sun sails on the solar loads depending on façade reflectance.

7. CONCLUSIONS

This paper assessed the impact of urban sun sails over the solar loads of façades and ground, as critical parameters for cooling energy consumption and pedestrian comfort. Based on the results of our simulations, we conclude that:

- Installing sun sails is a highly effective way to reduce street solar loads, with decreases between 43-64%. Sun sails are more effective than whitening façades because they limit not only the solar gains over façades but also over the ground.
- At the local scale, shading is more effective, the darker a surface is. However, at a street level, sun sails are almost equally effective in environments with dark or light-coloured façades, making them an exportable heat mitigation strategy.

- The sun sail colour affects its cooling potential in a not negligible way ($\pm 20\%$). Darker tissues have a better performance than the lighter ones, due to their reduced transmittance and reflectance. Regardless of the tissue colour, high-mounted sun sails are always desirable, but this is especially important with light-coloured tissues.

Urban interventions may have opposing effects on building and street users. Therefore, it is crucial to take into account both aspects when assessing their suitability. The main potential of sun sails is their simultaneous benefits for outdoor and indoor summer comfort, without affecting the street appearance or winter solar gains. Additionally, sun sails balance solar loads between buildings, helping to "democratise" urban cooling needs.

ACKNOWLEDGEMENTS

This work was funded by the *Communauté d'agglomération du Pays Basque* and the *Nouvelle-Aquitaine* region.

REFERENCES

1. Middel, A. et al., (2016). Impact of shade on outdoor thermal comfort—a seasonal field study in Tempe, Arizona. *Int J of Biometeorol*, 60(12): pp.1849–1861.
2. Paolini, R. et al., (2014). Assessment of Thermal Stress in a Street Canyon in Pedestrian Area with or without Canopy Shading. *Energy Procedia*, 48: pp.1570–1575.
3. Kántor, N., et al., (2018). Human-biometeorological significance of shading in urban public spaces—Summertime measurements in Pécs, Hungary. *Landscape and Urban Planning*, 170(2018): pp.241–255.
4. Beckers, B. and P. Beckers, (2014). Sky vault partition for computing daylight availability and shortwave energy budget on an urban scale. *Lighting Res. and Technol.*, 46(6): p.716-28.
5. Bourbia F, Boucheriba F (2010). Impact of street design on urban microclimate for semi arid climate (Constantine). *Renew Energy* 35:343–347.
6. Akbari H, Pomerantz M, Taha H (2001). Cool surfaces and shade trees to reduce energy use and improve air quality in urban areas. *Solar Energy* 70:295–310
7. Kotey N., Wright. J.L., Collins M. (2009). Determining off-normal solar optical properties of roller blinds. *ASHRAE Trans* 115 PART 2:3–17.
8. Goral C.M., Torrance K.E., Greenberg D.P. and Battaile B. (1984). Modeling the interaction of light between diffuse surfaces. In: *ACM SIGGRAPH* 18:3 213-222.
9. Perez, R., Seals, R. and Michalsky, J., 1993. All-weather model for sky luminance distribution—preliminary configuration and validation. *Solar energy*, 50(3):235-245.
10. Bugeat, A., Fernández, E., Beckers, B. and Aguerre, J., (2019). A Multi-Scale Consideration of Daylight in a Real Urban Context. In: *Proceedings of BS2019: 16th IBPSA Building Simulation Conference*, Rome, Italy.
11. Garcia-Navado, E. (2013). *Toldo urbano: Posibilidades de reducción de la demanda de refrigeración* (Master Thesis). Universidad Politecnica de Catalunya (UPC).

Thermally-activated water-based lattices: Thermal control of exterior urban areas through evaporative cooling, shading and ventilation

A MARCOS ¹, J A TENORIO ¹, M C GUERRERO ², M C PAVÓN ²,
J SÁNCHEZ-RAMOS ³ AND S ÁLVAREZ ²

¹ Eduardo Torroja Institute-CSIC, Madrid, Spain

² Thermal Engineering Group, School of Engineering, University of Seville, Seville, Spain

³ Cádiz University, Cadiz, Spain

ABSTRACT: The CartujaQanat project represents the necessity to rethink the way our cities are conceived as time passes by and the world evolves. Current and future needs demand up-to-date solutions that combine the knowledge obtained from experience and tradition with innovative research. Cities have the responsibility to contribute to a better environment for their inhabitants while minimizing resource consumption. Passive techniques and bioclimatic solutions have significant benefits for the health and well-being of humans, making them ideal when properly adapted to their suitable climates. Keeping this in mind, CartujaQanat pursues the creation of open-air spaces that provide a comfortable environment in hot and dry weather conditions with minimal negative impacts. Strategies developed for the project utilize water as a heat transfer fluid in open and closed systems to enable the acclimatization of exterior spaces. The project includes the use of physical barriers in the form of bioclimatic lattices that act as a solar screen, enabling natural ventilation and providing a certain level of confinement to the air. These effects are enhanced with the hygrothermal capabilities of water, which is incorporated for direct and indirect evaporative cooling as well as thermally activated elements.

KEYWORDS: Urban Comfort, Evaporative Cooling, Bioclimatic Lattice

1. INTRODUCTION

As global temperature rises, cities in general are becoming warmer, with the urban heat island increasing this effect due to the abundance of artificial surfaces. These surfaces accumulate heat from solar radiation but are not able to fully dissipate it during the night, therefore resulting in higher average temperatures over time. It becomes necessary to incorporate strategies that improve the liveability of cities.

The CartujaQanat project intends to recover street life through a new model of urban governance in the hot climate of Seville. The street is used as a social revitalizer that tries to involve in its transformation citizens along with public and private agents.

The main objective of the project is the renovation of a small urban area in Isla de la Cartuja, next to the Guadalquivir River. This territory was not urbanized until 1992, when the Universal Exposition took place. Since then, different uses have been established in the island, among which educational has a significant role. Examples of this are the Cartuja Scientific and Technological Park (PCT Cartuja) and the University of Seville, this last one being one of the main institutions involved in the CartujaQanat project.

However, some areas have not been redeveloped yet and remain partly unattended, becoming interesting starting points for urban actions such as the one presented in this paper. Once finished, the instructive nature of CartujaQanat is expected to promote the revitalization of the area while encouraging citizens to demand spaces with analogous characteristics in terms of comfort and social benefits.

Within the intervention there are three characteristic elements to develop: an amphitheater, a multipurpose marketplace and a water qanat. The first two are unenclosed buildings at the service of people that are designed to accommodate diverse activities and serve as pioneer examples of mitigation of inclement weather in exterior spaces. The latter, conceived as an open-air channel, is part of a passive acclimatization system designed to mitigate energy demands from these buildings and their users.

CartujaQanat provides a holistic approach towards a conception of urban areas where the focus is set on citizens and their current and future needs, especially with Climate Change affecting many cities due to the Urban Heat Island. To pursue these objectives, bioclimatic techniques are reinterpreted for their implementation in urban spaces. Traditional elements like the Asian qanats are combined with

passive cooling techniques to improve comfort conditions in outside areas.

The present investigation studies the potential of bioclimatic lattices that incorporate water for thermal activation in order to reduce temperature in a specific and partially controlled environment. Lattices have a passive design that enables natural ventilation while protecting from direct sunlight. This is combined with the evaporative cooling effect of water and its latent heat characteristics during phase-change for a better overall performance.

2. METHODS

The island of Cartuja has previously had experience with bioclimatization of exterior spaces. In the original design in 1992, the aim was to make the most out of the available natural resources, including vegetation, evaporative cooling, shadowing and thermal inertia, in order to create a comfortable microclimate. Several of the structures originally built for the Expo '92 remain as they were, while others have been modified or removed. CartujaQanat sets its focus on one of the parks from the original project, along with its elements, to perform a renovation that revitalizes the surrounding areas.

For the development of the project, it was crucial to understand the weather conditions of Seville, which is located in the South of Spain. The city has a Mediterranean climate modified by the proximity and influence of the Atlantic Ocean. This combination results in mild and rainy winters as well as hot and dry summers, with average maximum temperatures of 35 degrees Celsius during the months of July and August [1]. Prevailing winds, originated in the Atlantic Ocean, blow from the South West following the direction of the Guadalquivir river valley.

If comfort was to be pursued in these conditions, two concepts had to be considered: shading and confinement. They ought to serve as the base for the constructive development of the project.

Using elements to generate a shaded area is one of the most basic and adequate strategies in hot climates, given that most energy gains originate from solar irradiance. On the other hand, when working with outer spaces, confining the air is key to avoid constant renovation of air when its temperature is above or below comfortable parameters. Aside from generating roofed areas to avoid direct sunlight, a characteristic element is incorporated to the project to contribute to the mitigation of weather: the bioclimatic lattice.

CartujaQanat introduces the lattice as an active element of climate control by combining it with water, thus creating an evaporative cooling lattice.

Lattices can be found in several cultures around the world acting as barriers against the sun while enabling ventilation, mostly in areas with hot and dry weather. They have been used mainly in traditional architecture in areas such as the Mediterranean. These lattices can have different designs in order to adapt to site-specific conditions meaning that the solution achieved can be modified to satisfy demands in different countries, conferring it a certain level of scalability worldwide.

One of the reasons for the usefulness of latticed geometries is that they enable the Venturi effect, which promotes airflow and decreases air temperature [2].

To take this Venturi effect a step forward, the lattice in this project has been developed in contact with water, which has interesting thermal potential due to its heat storage capacity [3]. It acts as a great heat transfer fluid for sensible and latent heat. When in touch with hot air from the environment, water absorbs heat, resulting in cooler air that can be used for acclimatisation of the desired space.

Water utilized in the cooling system would therefore absorb heat during the day. For a full-day cycle to work, water needs to be cooled down at night so that it dissipates the heat that has been absorbed during the day. This is achieved at night through its pulverisation along with radiative cooling [4]. Both processes have a positive effect in the decrease of water temperature and heat dissipation due to the night sky temperature depression.

The performance of the evaporative cooling effects and their effectiveness have been studied theoretically and experimentally for the project. The entire evaporative cooling lattice system was set to work on daily cycles so that it could provide enough cooling capacity every day to satisfy energy demands.

Firstly, a computerized analysis was performed in relation to factors involved in pulverization such as optimal water droplet size for proper cooling with minimal evaporation, as well as water temperature variation and ranges. The intention was to allow deciding the optimal starting point, which lead to the verification of these results in an experiment that completed the knowledge and understanding of the system.

The experiment that followed was developed to target the cooling effectiveness of the evaporative

effect of the qanat. This qanat contains the water that will be used as a heat transfer fluid in contact with the lattice.

3. RESULTS

Water is used as an energy-transferring fluid. During the day, it is utilized to cool down the environment by moistening elements such as the lattice and others. While flowing through the moist lattice, air temperature is lowered by transferring heat to the water, part of which therefore evaporates.

Given that water temperature is increased throughout the day, it becomes necessary to lower it. This is done by exposing it to the night sky at the previously mentioned qanat, when the ambience temperature drops. Water is cooled down due to the radiative cooling effect. For the system to function, it is necessary for it to work in cycles on a daily basis.

One of the main concerns in the project was to achieve proper temperature drop in water within the available hours of night sky, which are limited. The surface of exposition needed to be increased for high effectiveness. After considering several options, the optimal solution consisted of spraying it into the qanat. Not only was the qanat surface exposed to the sky, but also the outer surface of every droplet into which water was sprayed.

Smaller drops of water mean that more water will evaporate, resulting in water loss, which needs to be replaced. This results in a higher consumption of water. If drops were too big, on the contrary, the system might not have enough cooling power. The smaller the droplets, the better efficiency, but also higher evaporation. A balance had to be achieved.

The balance between evaporation rate and cooling performance was analysed through a computerized software, narrowing down the search for optimal pulverization systems for the experiment.

To study the performance of the cooling system, two water basins of equal volumes were created and compared on daily cycles (Figure 1). One of them served as a reference, letting its content stand still, while the other was the active basin through pulverization.

During the day, and keeping in mind the weather conditions at the time of the experiment, water was heated in both basins above 25 degrees Celsius, allowing for proper temperature drop at night.

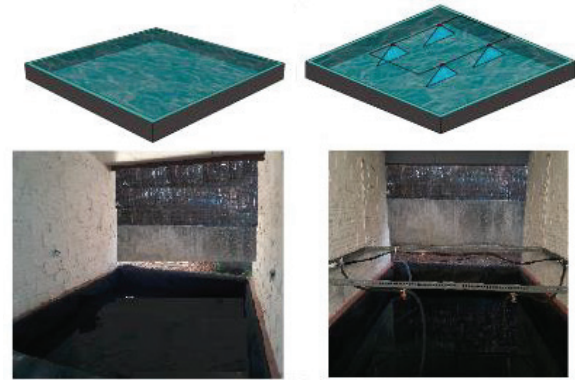


Figure 1: Comparison of passive basin (left) and active basin (right)

For the experiment, water was sprayed into one of the basins using nozzles with varying levels of pulverization. Along with a water pump that enabled modifying the water supply pressure, the system provided information to analyse the cooling capabilities of the different misting effects.

For a complete comparison, the study was monitored and measurements were taken for a series of parameters, including temperature, humidity, volume of water flow, spraying height and pressure. In addition, the total volume of evaporated water after each cycle was also analysed in search of the optimal ratio of cooling effectiveness and evaporated water. Figure (2) shows the results obtained during a standard cycle of spraying that took place between the evening and the following morning.

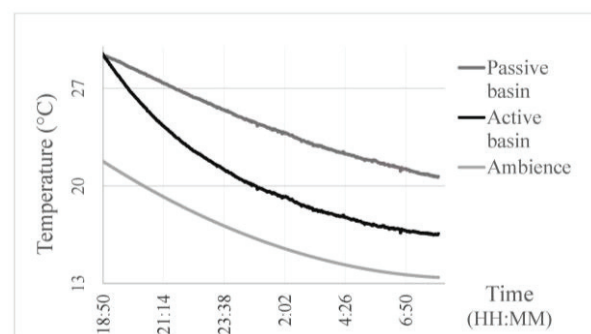


Figure 2: Daily water pumping cycle comparing the active basin and the reference basin

Once the benefit of the evaporative cooling system for the bioclimatic lattice was confirmed, the project moved on to analyse the lattice design.

As part of a CFD analysis, the lattice was studied within a wind tunnel with a geometrical section of 1m x 1m. Different options varying in shape and size of mass and hollows were designed to evaluate the

pressure drop before and after the lattice in relation to the speed of air, following Equation (1).

$$\Delta P = a * v^2 + b * v \quad (1)$$

where ΔP - pressure drop (Pa);
 v - air velocity (m/s);

Figures (3) and (4) show a sample of the type of graphs and results obtained with this analysis for pressure and velocity respectively.

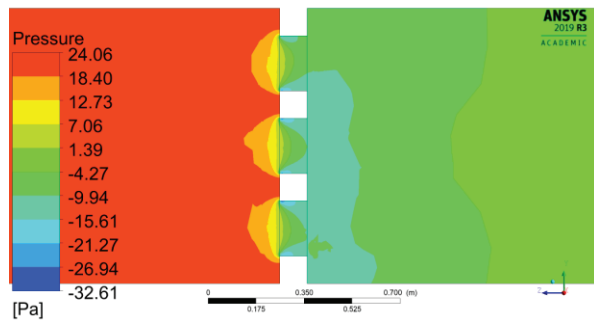


Figure 3: Lattice CFD analysis for pressure

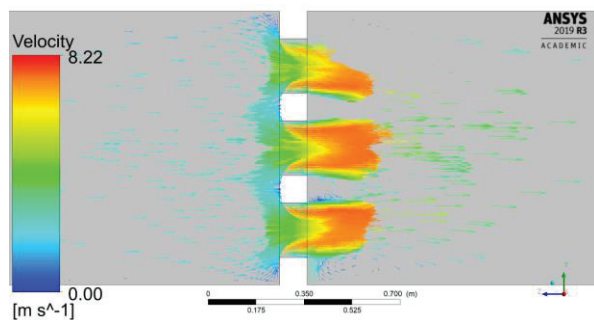


Figure 4: Lattice CFD analysis for velocity

The values obtained with this calculation were utilized to create graphs to characterize the efficiency of the system that represent Equation (1), such as Figure 5:

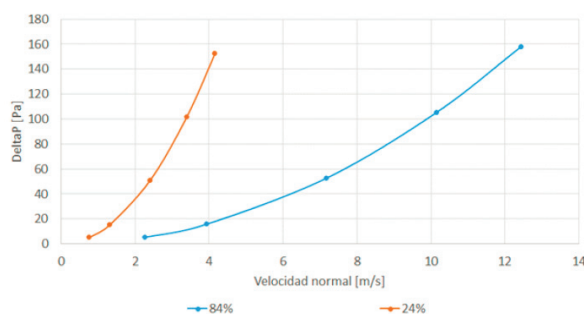


Figure 5: Velocity-Pressure Drop graph

The success of the study encourages the implementation of the bioclimatic evaporative cooling lattice in the CartujaQanat project. Water is one of the key elements for the correct performance of the bioclimatic system, which is why this study was decisive. The results obtained throughout the

different stages of the project have confirmed the initial approach regarding the possibility to utilize passive techniques such as evaporative cooling for the acclimatization of exterior spaces with minimal energy consumption.

Having proved that it is possible to use water in cycles to improve the thermal performance of the system, the next step is to work on the geometry and design of the lattices in parallel with CFD analysis for best results. Moist lattices developed under this project in the following months are expected to be highly effective in reducing the temperature of the air that passes through them: water, cooled at night, lowers the surface temperature of the lattice, absorbing heat from the air.

The incorporation of water creates a complex system that takes advantage of the sensible and latent heat involved in phase change of water from liquid to vapour and vice versa. The materials used for the fabrication of the lattice need to have a certain level of porosity, which was solved by the utilization of ceramic and concrete.

4. CONCLUSION

CartujaQanat is an ambitious project that encompasses all stages of research, from theoretical approach and experimental study to building a real case study that will be monitored over time. This will enable to obtain further information and results from the prototype, as well as its applications.

The project has studied the performance of the presented water-based systems and serves as a pilot experience to analyse their suitability and potential implementation in cities with hot and dry weather where water availability might not be troublesome. Once the project is finally built and put to the test, if it becomes a success, it may encourage analogous cities to adapt it to their own conditions.

Research developed under this project has proven the effectiveness of combining lattices with water to reduce heat and promote thermal comfort in a partly enclosed urban area. It is increasingly important to develop strategies that minimize energy demand and consumption, while at the same time favouring comfort conditions for citizens and users in general.

CartujaQanat is a complex project with different points of interest. While attempting to create a highly efficient bioclimatic system, it also tries to involve people, creating a connection between the importance of these kind of urban actions and the positive effect that areas with comfortable conditions can have in society. Furthermore, the interventions will be educational and self-explanatory for visitors to

comprehend. Urban open spaces have always been places for social and cultural interchange, and they need to be vindicated and designed as an essential part of a liveable city.

ACKNOWLEDGEMENTS

Project funded by the European Commission under the Urban Innovative Actions program, which is financed through the European Regional Development Fund. Urban Innovative Actions is an Initiative of the European Union promoting pilot projects in the field of sustainable urban development.

REFERENCES

1. Igawa, N. and H. Nakamura, (2001). All Sky Model as a standard sky for the simulation of daylight environment. *Building and Environment*, 36: p. 763-770.
2. Kittler, R., (1985). Luminance distribution characteristics of homogeneous skies: a measurement and prediction strategy. *Lighting Research and Technology*, 17(4): p. 183-8.
3. Perraudau, M., (1988). Luminance models. In *National Lighting Conference*. Cambridge, UK, March 27-30.
4. International Daylight Monitoring Programme, [Online], Available: <http://idmp.entpe.fr/> [16 June 2008].

The effect of street grid form and orientation on urban wind flows and pedestrian thermal comfort

YARA AYYAD^{1,2}, STEVE SHARPLES¹

¹University of Liverpool, Liverpool, UK

²Al-Ahliyya Amman University, Amman, Jordan

ABSTRACT: Rapid urbanisation puts pressure on urban planning to create layouts that are sustainable, healthy and thermally comfortable for urban occupants. This study explores the influence of street grid form, as a single aspect of the urban layout, on wind flow, solar access and thermal stress in a hot climate. Four street scenarios based in Amman, Jordan were simulated under the same climatic conditions using the CFD modelling software Envi-MET. The analysis included different orientations for the designed grids to assess the effect of sun angle and wind direction. The results were compared in terms of average wind speed and physiological equivalent temperature (PET). Although wind speeds were found to change greatly for different orientations, PET was more sensitive to the different grid geometries rather than their orientation.

KEYWORDS: outdoor thermal comfort, Envi-MET, wind flow, urban layout, physiological equivalent temperature.

1. INTRODUCTION

Industrial, technological and economic growth in recent decades has led to a large increase in the world's population, with a projected global population by 2050 of 9.7 billion [1]. Most people will live in cities, creating problems of overcrowding, pollution and poor outdoor urban environments. Better informed and more sustainable planning might help improve comfort conditions for urban pedestrians as they move around city centres. This study explores how different street grid systems, as a single aspect of urban layout, can affect wind flow and thermal stress. Four scenarios were simulated under the same climatic conditions in the CFD modelling software Envi-MET. The analysis included two different street orientations to assess the effect on solar access, wind speed and wind direction. The results were compared in terms of average wind speed and the thermal comfort index physiological equivalent temperature (PET).

2. BACKGROUND

Designing an urban space that considers the wellbeing of its occupants goes through several stages, starting with the design phase and followed by the testing phase. Testing can be performed using the CFD modelling software Envi-MET— an urban modelling software that assesses the interaction between the selected site's microclimate and its built environment [2-5]. The impact of the generated microclimate on the thermal comfort of pedestrians can be assessed using the physiological equivalent temperature (PET) [6]. Unlike some other comfort metrics, PET values are influenced by local wind speeds and solar radiation conditions [7]. PET groups include 8-13°C (cold); 18-23°C (comfortable); 23-29°C

(slightly warm); 29-35°C (warm); 35-41°C (hot) and >41°C (very hot).

3. METHODOLOGY.

The study site was Amman in Jordan, which has a climate of long hot summers and short cool winters. Four common urban layouts (three grid and one radial) on a 150 x 150m plot were modelled to quantify the effect of street grid form and street orientation on wind flow and PET (Fig. 1). The grids were simulated twice, once with streets running north to south and, by rotating the grid by 45° counter-clockwise, with the streets running NE-SW, creating two different wind directions. The data were extracted based on a human height of 1.75m.

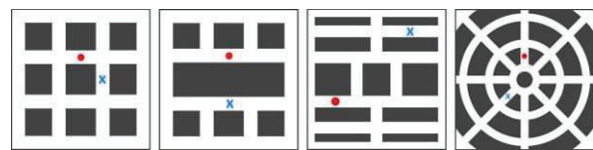


Figure 1: Grid layouts A (left) to D (right), receptor 1 is shown as a red dot and receptor 2 as a blue cross X.

All the Envi-MET inputs, apart from the grid layout, were kept the same: a building height to street width ratio of 1; the buildings' cladding material was white limestone (the most common choice in Jordan); street albedo was 10% (asphalt); and the dominant wind direction was westerly for all the layouts. The simulation results were compared in terms of wind speed distribution for each layout at 11:00 am, and PET thermal comfort over a 24-hour period for the two street receptors. The simulation date was 23rd September, with a minimum air temperature of 18°C, a maximum of 30°C, a 4 m/s starting wind speed, a minimum relative humidity of 50% and a maximum of 70%.

4. RESULTS AND DISCUSSION

The layouts were labelled from A-D and each orientation was given the number 1 for 45° orientation from the North and 2 for 0° orientation from the North. For each of the layouts, wind behaviour analysis was performed in terms of the speed and flow.

4.1 Street grid layout A

For the 45° direction from North layout, the wind enters the plot at an incidence angle of 45°, creating a flow separation when it reaches the sharp edge of the buildings. Vortices are formed in the cavity zone at the rear side façades of the buildings due to the lower surface pressures, causing wind speeds to reduce significantly compared to the mean flow in streets. As the wind flow progresses across the plot, a helical wind pattern is created throughout the streets - this phenomenon is the vector sum of the vortices and the channelling flows created by the external wind flow. Fig. 2 indicates the flow patterns, although the figure is too small to flows and speeds clearly.

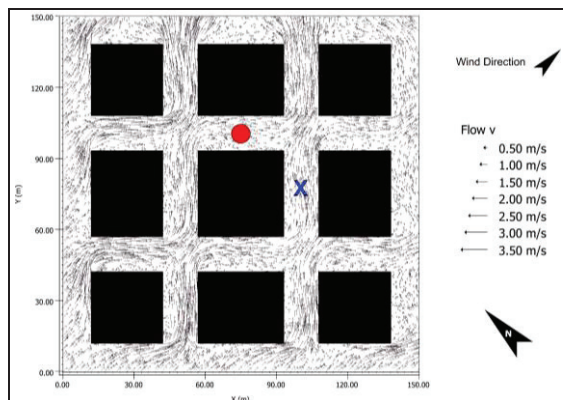


Figure 2: Wind flows and speeds for scenario A.1.

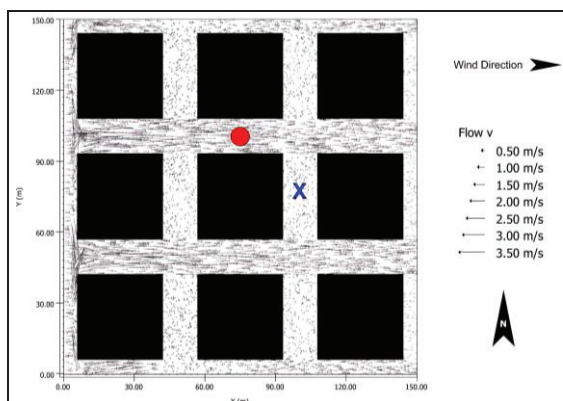


Figure 3: Wind flows and speeds for scenario A.2.

For scenario A.2, the wind enters the plot at 0° incidence angle, creating a channelling flow (Fig. 3). This flow produces a high pressure in the streets that are oriented in the flow path, which in turn, restricts the wind flow into the streets perpendicular to the flow. The high wind speed flow coming from the West in the West-East oriented streets create low velocity

corner vortices in North-South streets. In the North-South streets, two vortices are created with opposite rotation directions, but because they have low velocity, they do not affect each other's flows. Scenario A.2 shows a higher percentage of higher wind speed than scenario A.1 (Fig. 4), but also a high percentage of low wind speed. Scenario A.1, with its more even distribution of wind speeds, has a better chance of providing comfort for pedestrians. Fig. 5 shows the range of PET values for the two receptors and the two wind direction scenarios A.1 and A.2. The dashed lines are the upper (23°C) and lower (18°C) PET values for comfort.

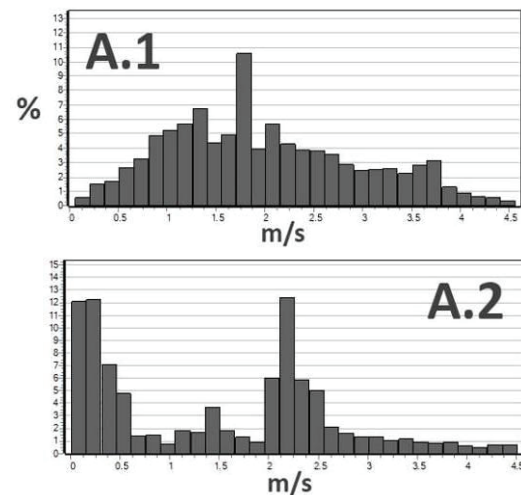


Figure 4: Wind speed distribution (%) for A.1 and A.2.

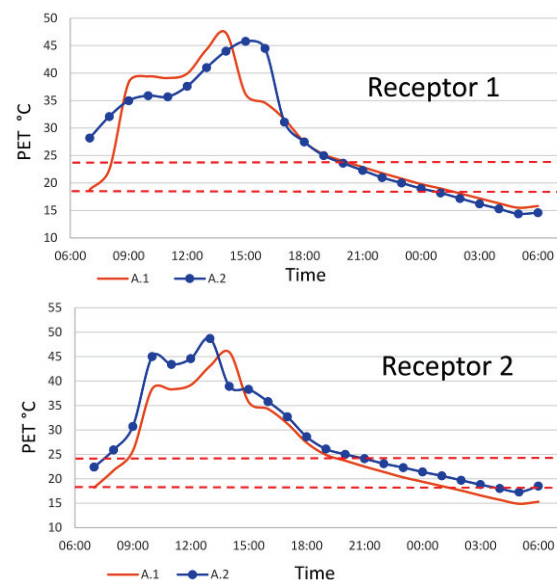


Figure 5: PET for receptors 1 and 2 for scenarios A.1 and A.2

Scenario A.2 has higher PET values than scenario A.1 during the early hours of the day and later on between the hours of 15:00 and sunset, the raise in PET values in this situation is due to the location of receptor 1, where it is situated on the west-east axis with no shading from the morning and evening sun, the opposite can be seen in A.1, where higher PET

levels were recorded during midday, due to the location of the receptor on the northern western-southern eastern axis which means it would not be shaded during the high sun from the south. The change of orientation of the plot changed the areas that sun would reach in different times of the day, and when inspecting the shadows casted by the buildings for both of the scenarios, it was concluded that scenario A.1 have the least time duration of direct sun radiation.

4.2. Street grid layout B

For scenario B.1 a flow separation occurs when the wind strikes the SW corner of the buildings, causing vortices to form in the cavity zone located at the rear of the buildings, where wind speeds are lower than the rest of the plot (Fig. 6). As wind flow enters the plot, it gets disturbed by the central attached building row and forms a flow that gets fed by the wind coming from the detached buildings and maintains high speeds. The wind flow is strong when it enters the street on the leeward side of the row buildings, however, it gets weaker as it loses its intensity moving forward due to its flow direction that allows flow separation when it hits the edges of the detached buildings.

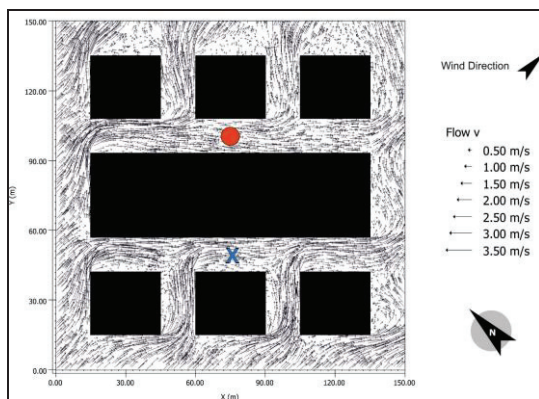


Figure 6: Wind flows and speeds for scenario B.1.

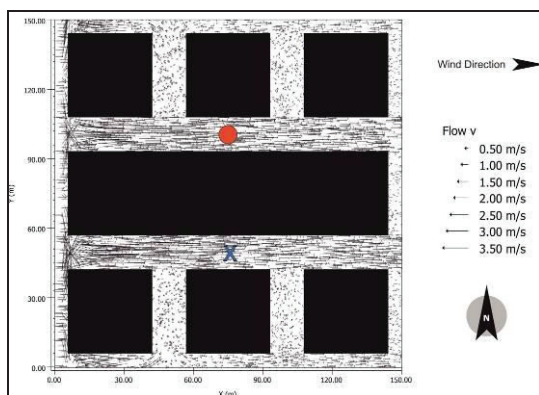


Figure 7: Wind flows and speeds for scenario B.2.

With scenario B.2 (Fig. 7) the wind is channelled along the W-E streets and the constriction increases the wind speeds to values slightly higher than scenario A.2. The high intensity of the channelled

flows prevents strong flows entering the N-S streets, creating very low wind speeds. This is reflected in the high percentage frequency of low winds shown for scenario B.2 in Fig. 8, while B.1 shows a much better distribution (13% of wind speeds >2 m/s).

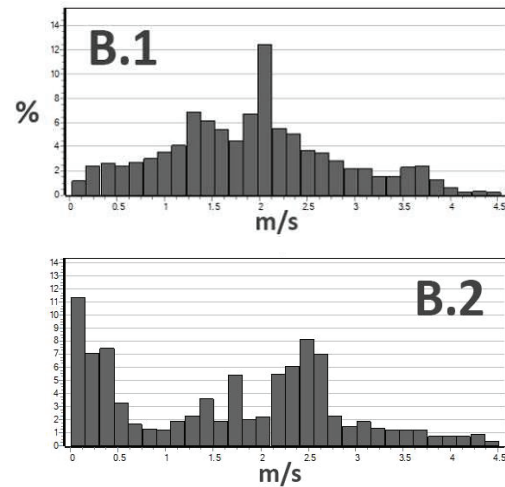


Figure 8: Wind speed distribution (%) for B.1 and B.2.

PET values in B1.1 and B.2 range from slightly cool to very hot and are heavily affected by solar access. The peak in PET for both receptors in Fig. 9, between 18:00 and 06:00, reflects the direct solar irradiation in the day. Wind speeds at both receptors were very similar, giving close night-time PET values. Daytime PET values are much higher in the more open layout of B.1 and B.2. The dashed lines are the upper (23°C) and lower (18°C) PET values for comfort.

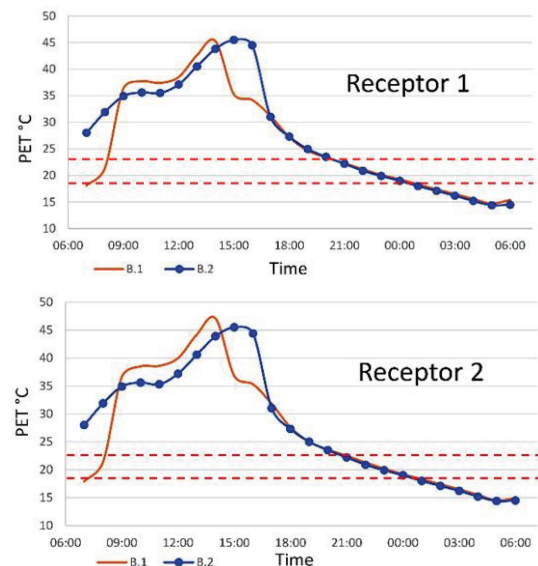


Figure 9: PET for receptors 1 and 2 for scenarios B.1 and B.2

4.3 Street grid layout C

The geometry in scenario C.1 introduces the effect of linear buildings against a cluster of square buildings. Fig. 10 shows wind flow enters SW corner of the plot and splits into two streams - the left stream, free of obstacles, accelerates while the right stream decelerates. Wind speeds increases in the

between the linear buildings compared to the big cluster of buildings in the middle of the plot. This is explained by the size of the cavity area cast by the bigger cluster of buildings where vortices are formed, and wind speed is reduced. Low wind speed can be seen in the NE corner due to the strong wind flow coming from street opening, which gets reinforced by the helical vortices from the adjacent canyons, all of this create strong pressures that prevent strong wind flows into the receptor 2 location.

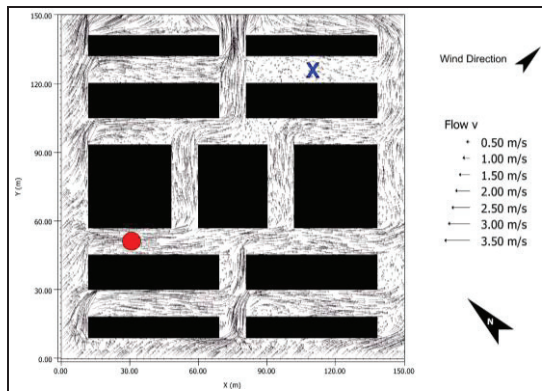


Figure 10: Wind flows and speeds for scenario C.1.

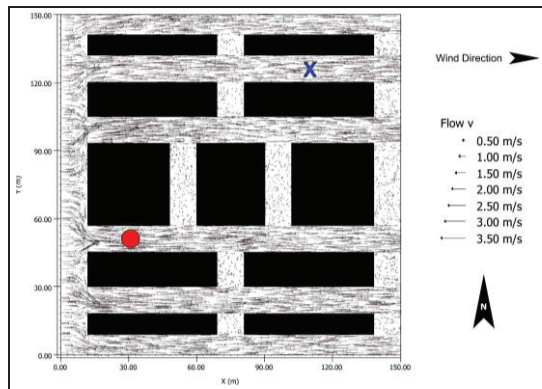


Figure 11: Wind flows and speeds for scenario C.2.

For scenario C.2, the west wind is channelled and accelerated through the West-East streets, which limits wind penetration into the N-S streets (Fig. 11). Low speed vortices are formed in the shorter N-S streets, while longer N-S streets have two vortices forming from each end with opposite rotations. The C.2 orientation may raise the overall wind speed, but it produces areas with very low air movement. The percentage frequency distribution of wind speeds across the site for C.1 is almost normal, with a spike around 2.2 m/s (Fig. 12). In scenario C.2 the distribution clusters tightly around higher speeds (2 to 2.5 m/s). However, the distribution also shows a higher count of low speeds than scenario C.1.

Fig. 13 shows the hourly PET values levels for C.1 and C.2. Daytime PETs range from comfortable to very hot, and are heavily influenced by incident solar radiation, and orientation is crucial in determining the site's sunlit and shaded areas. With receptors 1

and 2, the PET values for scenario C.2 spike at 09:00 and again before sundown at 17:00. The sun directly these receptors when in the east and west (i.e. morning and late afternoon). However, these receptors are shaded when the sun is between SE and SW (09:00-14:00). PET values drop drastically at night due to the lack of solar radiation.

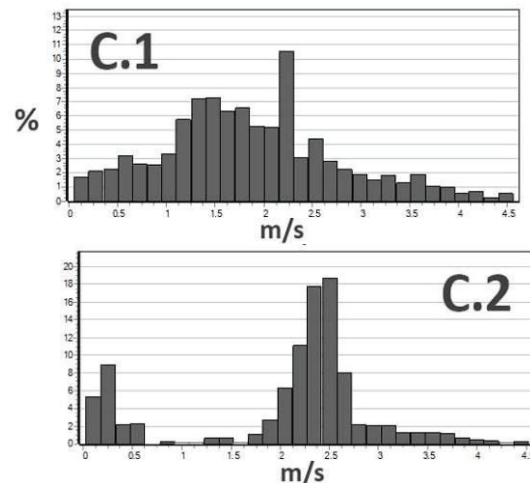


Figure 12: Wind speed distribution (%) for C.1 and C.2.

The night-time PET levels vary from comfortable to slightly cool and show the effect of wind speed. Receptor 2 has a higher PET value for scenario C.1 than C.2 due to C.1's lower wind speeds, while receptor 1 has similar C.1 and C.2 PET levels due to similar wind speed values. The dashed lines are the upper (23°C) and lower (18°C) PET values for comfort.

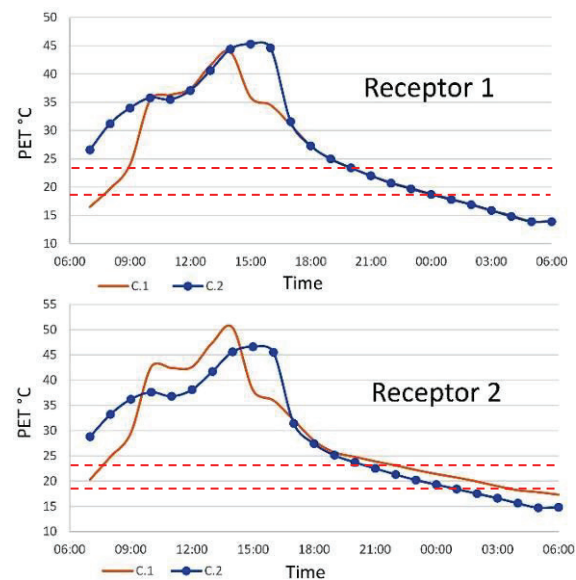


Figure 12: PET for receptors 1 and 2, scenarios C.1 and C.2

4.4 Street grid layout D

A radial street geometry was tested to see if it offered any advantages over the grid layouts. Fig. 14 for the rotated plan (D.1) shows wind entering the plot from the SW corner and slowing as it progresses along the street due to a lack of reinforcing flows from other streets. The main wind flow passes

receptor 2 with a low velocity to reach the centre of the plot before splitting into two flows. These two flows have higher wind speed values because they are joined by two streams passing through the W-E and N-S streets. Wind speeds across the plot average 0.15 to 1.4 m/s compared to the 4 m/s initial speed.

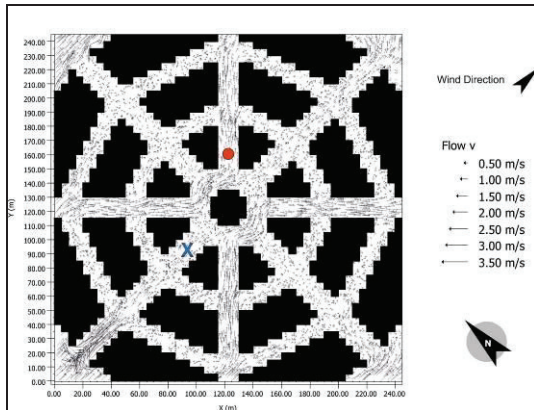


Figure 13: Wind flow for scenario D.1.

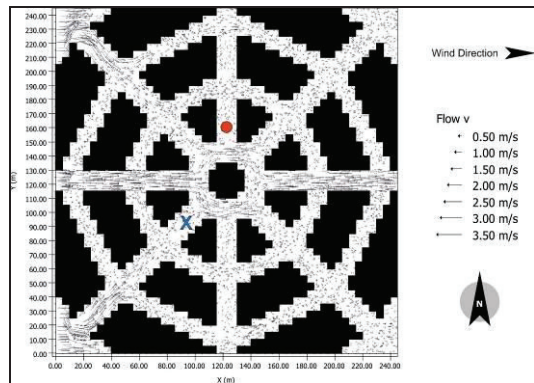


Figure 14: Wind flow for scenario D.2.

For scenario D.2 (Fig. 15) wind enters the plot from the west and maintains its speed along the street until it reaches the centre of the plot, then the flow divides into two streams moving around the centre of the plot and exiting through the end of the west oriented street. For scenario D.1 the flow leaves the plot through two streets passing through the north oriented and west oriented streets; but in Scenario D.2 the flow separates and then recombines in the same line of motion. This might have happened as a shortcoming in Envi-MET, which read the edges of the building as small ridges rather than a continuous line. The average wind speeds inside the plot are low, from 0.1-1.25 m/s.

The wind speed percentage distributions (Fig. 16) show that for the radial plan most speeds are lower than for the grid layouts. Scenario D.1 did have some areas with wind speeds of 0.5-1.5 m/s, but the majority of speeds for scenario D.2 were in the range 0 to 0.75 m/s. Both scenarios show low air flow, which raises the risk of poor pollutant dispersion.

Fig. 17 shows the PET values over the 24 hours of simulation, ranging from slightly warm to slightly cool

during the night, and from slightly warm to very hot during the day. The radial layout allows the sun to shine on the location of the receptors at various times during the day, and this produces spikes in the PET curves as the receptors are irradiated. This is more apparent for receptor 2 due to its location.

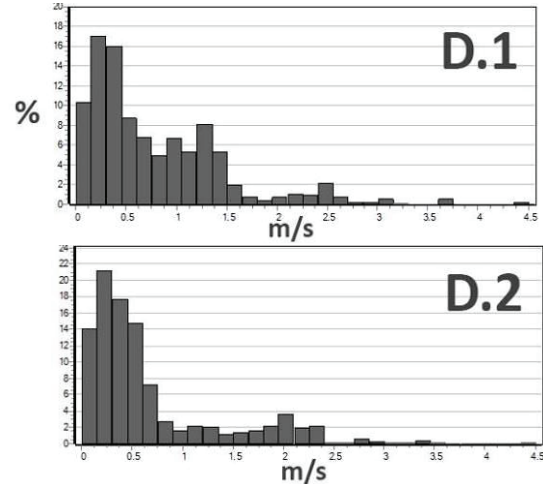


Figure 15: Wind speed distribution (%) for D.1 and D.2.

PET values for scenario D.1 are noticeably higher than for scenario D.2 between 06:00-09:00 and 15:00-18:00. This is due to its location being on the West-East axis, where direct sun reaches the receptors in the morning and evening. Receptor 1 shows the same tendencies as receptor 2 where there is a spike when the sun reaches the location. However, the location of the receptor limited the morning and evening solar access, and this resulted in high PET levels from 10:00 to 14:00 in D.1 and from 10:00 to 13:00 in D.2. The dashed lines are the upper (23°C) and lower (18°C) PET values for comfort.

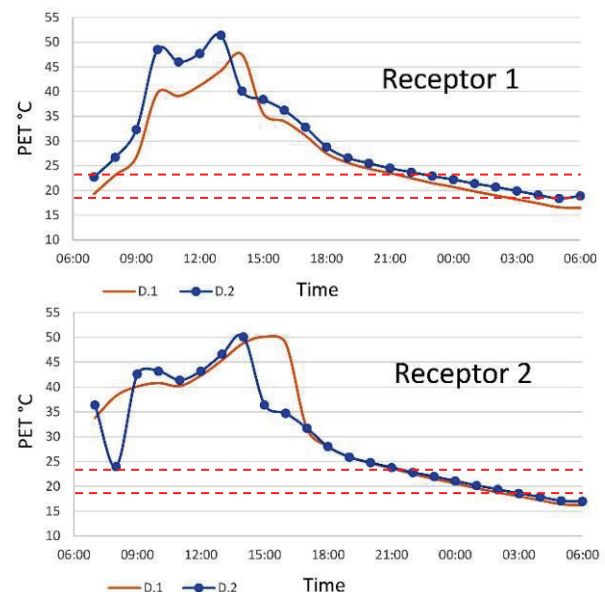


Figure 16: PET for receptors 1 and 2, scenarios D.1 and D.2

PET levels for both scenarios are reduced at night and have very close values, as was seen for all of the previous layouts. This can be explained by the close

night-time values of the meteorological factors - air temperature, wind speed, mean radiant temperature and relative humidity. It has been noticed that some of the meteorological factors, like the air temperature and relative humidity, are difficult to influence in an urban layout through geometrical modification. However, other meteorological factors, like wind speed and mean radiant temperature, vary significantly from one urban form to the other, which creates the big difference in PET values at day and the small difference at night.

4. CONCLUSION

Street grid layouts are comprised of a multitude of variables that impact upon their environmental performance. These included orientation, wind direction, albedo and height to width ratio. For the sake of containing the quantity of results in this study, some variables were assumed as having fixed values for each grid. The street grid analysis covered the geometrical composition of four designs - three orthogonal grids and one radial grid. The building properties and starting meteorological conditions for every grid were the same to ensure all results reflected changes only due to the grid layout and the wind direction.

The street grid analysis showed interesting results for the different layouts. Wind speed was affected greatly by the change of orientation, where the 45° counter-clockwise rotation from North showed a major improvement in wind flow distributions. However, the change in orientation did not play a key role in changing PET levels, even though the change in orientation changed the shadow patterns. The main reason behind the rise and fall of PET levels was the geometry of the plot, whether it was rotated from the original orientation or not. Understanding the geometry of the site is a key component in determining the thermal stress on the human body, Jiang, et al, 2020, concluded similar findings with their study on parallel and staggered urban layouts, where the staggered layout performed better based on the shape and spacing they proposed. Table 1 shows the percentage of the 150 x 150m plot area that experienced low wind speeds (0 to 0.5 m/s) for the various geometrical layouts.

Table 1: Percentage area of plot with wind speeds 0-0.5 m/s

LAYOUTS	A		B		C		D		E	
SCENARIOS	A.1	A.2	B.1	B.2	C.1	C.2	D.1	D.2	E.1	E.2
AREA PERCENTAGE	6%	36%	8%	29%	9%	18%	52%	68%	42%	60%

All of the scenarios 1, with a 45° counter-clockwise rotation from the north, showed improved wind flow results when compared to scenarios 2 with no turn from the north. Layout A scenario 1 showed better results across all layouts and scenarios with only 6% of the plot area having low wind speeds, while layout D showed the worst results across all

layouts due to its curved streets that obstructed wind flow, with 68% of plot area having low wind speeds.

Table 2 shows the average PET values for all the layouts over the 24 period of simulations.

Table 2: Average PET values for all layouts.

LAYOUTS	A		B		C		D		E	
SCENARIOS	A.1	A.2	B.1	B.2	C.1	C.2	D.1	D.2	E.1	E.2
PET	26.1	27.2	26.6	27.6	26.7	28.3	28.2	29.3	28.4	29.6

The average PET values shown in Table 2 do not convey how well the layouts present their comfort level, but rather they show how in the same layout the different orientation (scenarios 1 and 2) shifts the comfort levels. An increase in PET values is noticed in all of the layouts in scenario 2, which is caused by the North-South orientation streets that receive the highest levels of solar radiation throughout the day. In terms of the most favourable range of PET values for comfort over the 24 hours of the studied day, the simple layout A (a 3 x 3 array of square buildings) had slightly better PET values than the other grid layouts.

REFERENCES

1. United Nations, (2019). World population prospects: The 2019 revision, New York, UN Population Division. https://population.un.org/wpp/Publications/Files/WPP2019_Highlights.pdf
2. Bruse, M., (2019), ENVI-met. <https://www.envi-met.com/>
3. Ayyad Y.N. and S. Sharples, (2019). Envi-MET validation and sensitivity analysis using field measurements in a hot arid climate. In *Proc. SBE19 Conference*, Cardiff, 24-25 September 2019. IOP Conference Series: Earth Environ. Sci., **329** 012040
4. Wasim Yahia, M.W. and E. Johansson, (2013). Influence of urban planning regulations on the microclimate in a hot dry climate: The example of Damascus, Syria. *J Hous and the Built Environ*, **28**: p.51-65
5. Hamdan D.M.A. and F.L. Oliveira, (2019). The impact of urban design elements on microclimate in hot arid climatic conditions: Al Ain City, UAE. *Energy and Buildings*, **200**: p.86-103.
6. Hoppe, P., (1999). The physiological equivalent temperature – a universal index for the biometeorological assessment of the thermal environment. *Int J Biometeorol*, **43**(2): p. 71-75.
7. Lee, H., H. Mayer, and W. Kuttler, (2019). To what extent does the air flow initialisation of the ENVI-met model affect human heat stress simulated in a common street canyon? *Int J Biometeorol*, **63**: p. 73-81.
8. Jiang, Y., C. Wu and M. Teng, (2020). Impact of residential building layouts on microclimate in a high temperature and high humidity region. *Sustainability*, **12**(3), article no. 1046.

Impact of urban albedo on microclimate Computational investigation in London

AGNESE SALVATI¹ MARIA KOLOKOTRONI¹ ALKIS KOTOPOULEAS² RICHARD WATKINS²
RENGANATHAN GIRIDHARAN² MARIALENA NIKOLOPOULOU²

¹ Brunel University London, London, United Kingdom

² University of Kent, Canterbury, United Kingdom

ABSTRACT: The urban albedo (UA), defined as the ratio of the reflected to the incoming shortwave radiation at the upper edge of urban canyons, quantifies their ability to reflect solar radiation towards the sky. This research investigates the impact of real-world urban geometries and optical properties of facades and roads materials on the UA and street level microclimate in London. The Indexed Sphere (IVS) algorithm of ENVI-met 4.4.4 is used to compute the UA of several canyon configurations. The accuracy of the IVS algorithm is evaluated against measurements on a 1:10 physical model reproducing the geometry and materials of the case study area. The simulation results show that reflective materials applied to the canyon surfaces are more effective in increasing the UA of canyons with low aspect ratios. The use of reflective materials in urban canyons always increases the amount of reflections at the street level, increasing the mean radiant temperature in most cases. Air temperature is not affected by the canyon's façades reflectivity while it shows a significant daytime reduction for increased roads' reflectivity. The results provide preliminary guidelines for the control of UA and the improvement of microclimate in London.

KEYWORDS: Urban Albedo, reflective materials, Heat island, microclimate, ENVI-met

1. INTRODUCTION

The increase of absorption of solar radiation and heat storage by urban structures are significant contributing factors to the urban heat island (UHI) intensity in cities [1] [2]. The UHI, although more pronounced in high radiation and high ambient temperature cities, has negative impacts on thermal comfort, health and building energy use also in cities of high latitudes such as London (Lat 51.5 N) [3], [4]. For this reason, tackling urban warming and overheating risk is one of the priorities of the city's climate change adaptation strategy [5].

There exist two major strategies for UHI mitigation, based on two physical principles: (1) decreasing solar absorption in the urban environment and (2) increasing evapotranspiration using greenery and water. The first strategy is based on the use of reflective urban surfaces, which reduce solar absorption and surface temperature and, consequently, air temperature [1], [6].

In the urban context, the cooling potential of reflective materials can be decreased due to the interaction of solar radiation with urban geometry [7]–[9]. The concept of “Urban Albedo” (UA) was thus developed to bring together the effect of urban geometry and materials' optical properties on the overall ability of urban areas to reflect short-wave radiation toward the sky. The UA is defined as the ratio of the outgoing to the incoming shortwave radiation at the upper edge of the urban canopy layer

[10]. The variability of UA in urban areas has been investigated using experimental models [11], [12] and numerical models [10], [13], [14]. These studies agree that, for a given site coverage ratio, the UA decreases for an increase of façade density, average building height and building height variability. This is explained by the increase of multiple reflections and radiation trapping within vertical surfaces. In fact, simulation studies have also shown that the urban textures with higher density of vertical surfaces have higher UHI intensity [15]. The limitation of these studies on UA is that urban areas are always simplified to symmetric canyon geometries or equal size squared footprint buildings on orthogonal grids with uniform material cover for roads, walls and roofs.

Some studies also highlighted that using reflective materials in the urban context may worsen the outdoor thermal conditions due to the increase of reflections and mean radiant temperature at the street level [16], [17].

For these reasons, the correlation between the reflection coefficients of roads' and facades' materials and the canyon UA is not straightforward, as well as the impact of UA on the street level microclimate.

This study investigates the impact of real-world urban geometries and optical properties of facades and roads materials on UA and microclimate in a residential area of London. This is intended to provide

guidelines for the control of UA to improve outdoor thermal comfort in London.

2. MATERIALS AND METHODS

This research is based on microclimate simulations with ENVI-met V4.4.4 and measurements on a physical model of the studied urban area. The experimental and computational data are used to achieve the following objectives:

- 1) Evaluate the performance of the new ENVI-met IVS algorithm for radiation transfer
- 2) Assess the net impact of different spatial distributions of reflective materials on the UA of canyons with different geometries
- 3) Understand the net impact of UA change on the street level thermal environment

2.1 Physical model

A 1:10 physical model of the real urban area was built at the University of Kent (Canterbury, UK). The physical model accurately reproduces the geometry and material distribution of the real urban area (Figure 1). The model is located outdoors and equipped with pairs of pyranometers – one looking upward and the other looking downward - to measure the incoming and reflected radiation in three points: in the middle of the model at the equivalent height of 10m above the tallest building (Point 1) and at the eaves level in two urban canyons (Point 2 and 3).

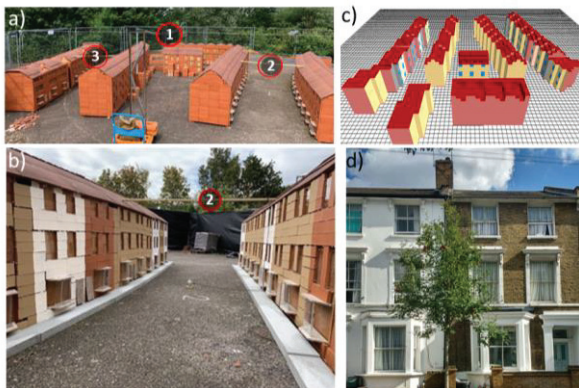


Figure 1: a) physical model and location of the pyranometers 1, 2 and 3; b) detail of the physical model materials; c) ENVI-met model for the IVS algorithm evaluation; d) Detail of the facades of the case study area

Table 1: Model's materials specification

Materials	Reflection coefficient
Asphalt	0.11
Roof tiles	0.21
Concrete paving	0.27
Red Bricks	0.31
Buff lime painted Bricks	0.42
Magnolia painted Bricks	0.52
White painted Bricks	0.78

2.2 Evaluation of the ENVI-met IVS algorithm

An ENVI-met model reproducing the geometry and materials of the physical model (Figure 1) was used to assess the model's accuracy in the calculation of solar radiation reflections within urban canyons.

To this aim, the forcing global solar radiation was adjusted based on the incoming solar radiation measured on top of the physical model and the simulation output "Reflected short-wave radiation from the lower hemisphere" was compared to the reflected solar radiation measured on the physical model. The comparison was performed for the three construction phased reported in table 2, using the reflection coefficients of table 1, so as to compare ENVI-met' sensitivity to material change.

Table 2: Physical model construction phases

Model phases	Materials
1- As Built	tiles, red bricks and glass
2- With Paving	Concrete paving was added
3- Façade Colours	Façade colour were added and paving removed

All ENVI-met simulations were run using the Indexed Sphere (IVS) algorithm of ENVI-met 4.4.4. The IVS algorithm calculates the reflected shortwave radiation and emitted longwave radiation from any element (walls, roofs, ground surface and vegetation) proportional to the view factor of those elements and considering the actual state of the element (i.e. surface temperature and solar irradiation). This method is thus much more accurate than the simplified method which calculates uniform reflections within urban canyons based on the average albedo of the materials.

2.2 ENVI-met model for UA and microclimate investigations

The physical model has some limitations such as the absence of vegetation and a limited number of buildings compared to the real urban area. Therefore, a more complete ENVI-met model of the case study area was built to provide realistic boundary conditions to assess the impact of material change on UA and microclimate (Figure 2). The ENVI-met model has vegetation, covers a larger portion of the urban area and is forced with local air temperatures measured on site [18].

A number of scenarios with reflective materials applied to the roads and the facades of the case study area were simulated to assess the impact on the canyons UA and on the street level microclimate. The microclimate impact was assessed in terms of air temperature and mean radiant temperature change at the pedestrian level. The tested scenarios for material distribution are reported in table 3. These were tested on two canyon geometries: low-rise

canyons with aspect ratio of about 0.75 and high-rise canyons with aspect ratio of about 1.5. The low-rise canyons correspond to the aspect ratio of the canyons in the case study area. The high-rise configuration was obtained keeping the same building footprint of the case study area and doubling the height of the buildings. The results of these 8 combinations of geometry and reflective material distribution have been analysed for the canyons 1, 2 and 3 highlighted in figure 2, which have also different orientation.

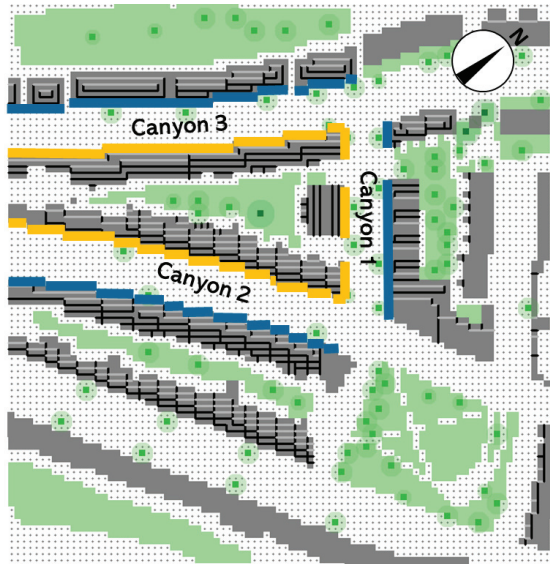


Figure 2: Plan of the ENVI-met model used to test the impact of reflective materials on the canyons' UA and the microclimate at street level.

Table 3: Simulated scenarios to assess the impact of reflective materials applied to different canyons' surfaces

Model ID	Reflection Coeff.	Distribution of reflective material
A1 out	r=0.6	Reflective material applied to the outer marked facades (Fig 2)
A1 centre	r=0.6	Reflective material applied to the inner marked facades (Fig 2)
A1 top	r=0.6	Reflective material applied to the top half of the canyons' facades
A2	r=0.5	Reflective material applied to the roads

3. RESULTS AND DISCUSSION

3.1. Performance of the ENVI-met IVS algorithm

The comparison between the reflected radiation measured at the physical model and computed by ENVI-met is shown in Figure 3. The comparison shows that ENVI-met slightly underestimates the reflections of solar radiation at the eaves level of urban canyons while it overestimates the reflections on top of the model from noon and until sunset. Therefore, ENVI-met tends to overestimate the UA of urban canyons in the afternoon compared to the measurements. In spite of these discrepancies, the overall performance of the IVS algorithm is in good

agreement with the measurements in terms of daily UA. The daily UA is calculated as the ratio of the total reflected radiation to the total incoming radiation over the reference day. On top of the model, the daily UA measured and calculated was 0.12 and 0.15 respectively. At the eaves level, the measured and calculated UA was 0.09 - 0.1 and 0.07 respectively.

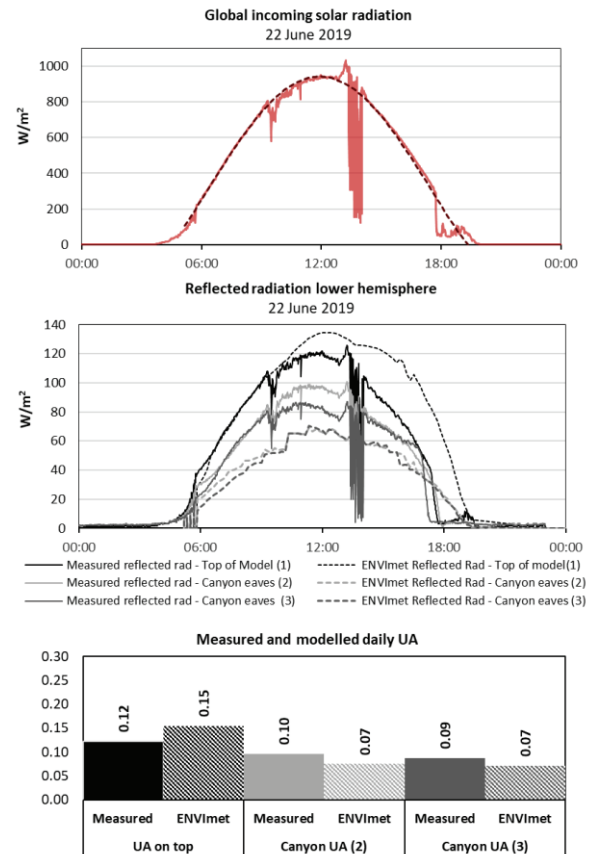


Figure 3: Comparison of measured and simulated incoming global solar radiation (graph on top), reflected solar radiation (graph in the middle) and daily urban albedo

Table 1: Sensitivity of the ENVI-met IVS algorithm to material change on roads and facades in the computation of canyon reflections compared to measurements

	Measured		ENVI-met	
Model ID and Ref Day	Canyon UA (2)	Δ UA	Canyon UA (2)	Δ UA
As built				
23/07/2019	0.100	-	0.077	-
Paving				
20/09/19	0.123	23%	0.105	37%
Facade colours				
06/10/19	0.156	56%	0.114	48%

The comparison shown in figure 3 correspond to the construction phase named "As built" (table 2). The impact of road and façade materials on the canyon UA as measured and computed by ENVI-met is reported in table 4. The results show that ENVI-met captures the increase of UA due to materials change, even if the percentage of UA change is slightly

different compared to those measured on the physical model. This can be also due to the unavoidable geometry differences between the physical model and the ENVI-met model due to the orthogonal mesh constraints.

3.2 Impact of reflective materials on UA for different canyon aspect ratios

The results of the simulations testing the impact of reflective materials on the canyons' UA for different aspect ratios, are reported in figure 4. The canyon daily albedo has been calculated as the ratio of the total reflected to the total incoming short-wave radiation in the three canyon sections presented in figure 4. For each canyon, the hourly incoming and reflected radiation was computed as the mean value of all the cells of the section (cell size 2x2 m) and the daily sum of the mean reflected and incoming radiation was used to calculate the daily UA of the three canyons.

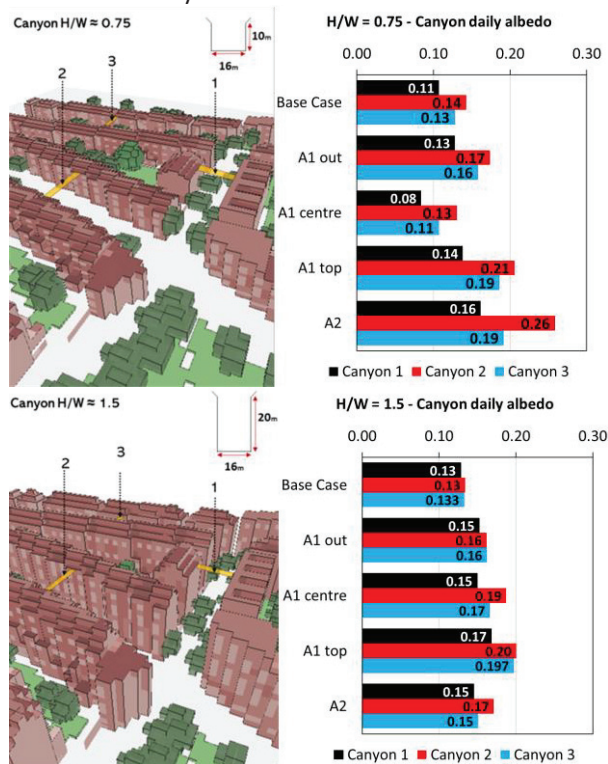


Figure 4: Impact of the reflective material scenarios on the three canyons' daily urban albedo

The simulation results show some interesting differences on the impact of reflective materials in different canyon geometries. The reflective materials have a larger impact on low-rise aspect ratio canyons compared to high-rise ones. This is particularly evident for the scenario A2 – reflective roads – which determines a much higher relative increase of UA in the canyons with aspect ratio of 0.75 compared to the ones with aspect ratio 1.5. However, when the reflective materials are applied to the top half of the canyon's facades (A1 TOP), the two canyon

geometries show a similar relative and absolute variation of the UA. This might be explained by the fact that the top half of the canyon facades receive a similar amount of solar radiation despite the different geometry. The results presented in figure 4 indicate that the two canyon geometries have less variation of the UA for the base case materials compared to variations for other cases examined. However, this similarity does not result to the same microclimate at the street level, because the increase of building height determines a significant reduction of the solar radiation reaching the street level in the high-rise urban area.

The results also indicate that the highest relative increase of UA is achieved with scenario A2 in the low-rise canyons and with the scenario A1 TOP in the high-rise canyons. Some differences exist in the UA of the three different canyons due to their orientation. Canyon 2 shows the highest variations of UA with the use of reflective materials since it is the canyon receiving the highest amount of solar radiation among the three analysed.

3.3 Impact of UA on microclimate

The microclimate impact of the tested scenarios has been analysed in terms of air temperature and mean radiant temperature change at the street level (1.5 m high) compared to the base case material distribution. The thermal environment of the base case configurations is reported in figure 5 for the two canyon aspect ratios.

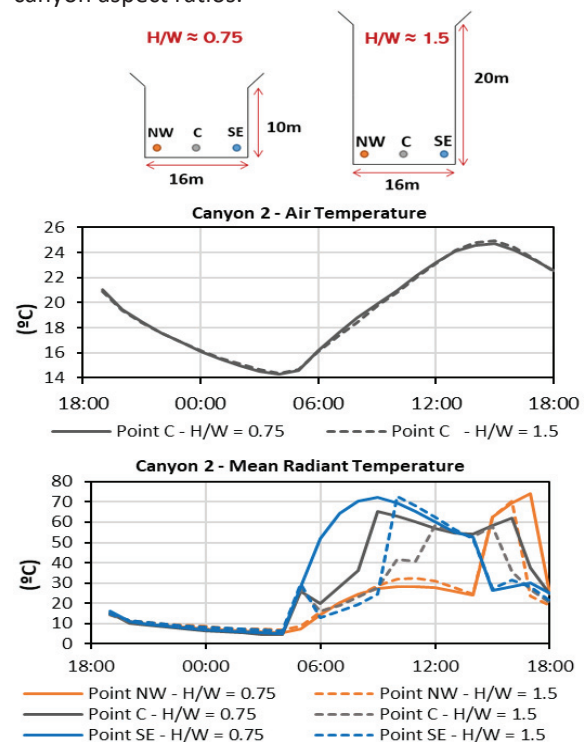


Figure 5: Air temperature and mean radiant temperature in different points of the two canyons configurations with the base case material distribution. NW and SE indicate the orientation of the adjacent façade.

The comparison presented in figure 5 highlights that the increase of building height determines a significant decrease of mean radiant temperature in the morning and the afternoon, due to the reduction of solar radiation reaching the street level. Conversely, the two canyon geometries with the base case material distribution have the same air temperature; this is due to the fact that the simulations were forced with the same air temperatures, measured in the case study area. In reality, a change in the canyon aspect ratio would probably determine variations in the daytime and night-time air temperatures; however this is not the aim of this study and the base case air temperature should be interpreted just as a term of comparison for the tested scenarios.

The most representative results of the microclimate impact of the tested scenarios are reported in Figure 6. The graphs refer to the street level thermal environment of the canyon 2 (Figure 2), which showed the maximum change in UA for the tested reflective materials scenarios.

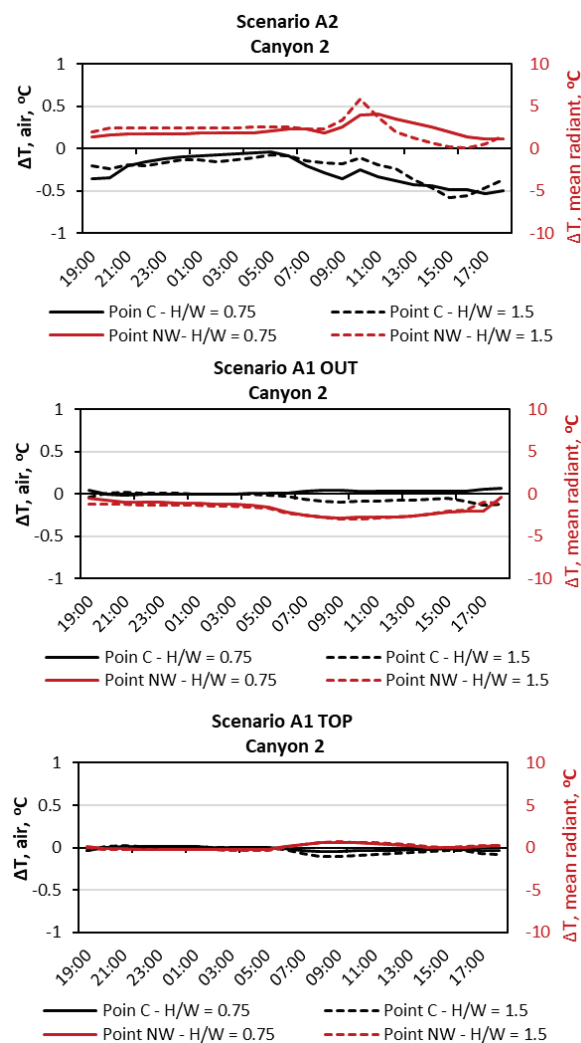


Figure 6: ENVI-met results of the impact of reflective materials on roads (A2) and facades (A1 OUT and A1 TOP) on the air temperature and mean radiant temperature change at the street level compared to the base case.

The graphs show that increasing the reflectivity of roads or facades has a different impact on air temperature and mean radiant temperature. This is due to the geometry of urban canyon surfaces that, in most cases, reflects solar radiation towards other urban surfaces instead to the sky. In fact, all the tested scenarios show an increase of reflections at the street level which determines an increase of the mean radiant temperature in most cases.

The first graph in figure 6 shows that increasing the road reflectivity results to an increase of mean radiant temperature but also a decrease of air temperature during daytime. Despite the different aspect ratios, the relative difference is similar in high-rise and low-rise urban canyons. This result can be explained by the fact that a higher reflection coefficient of the road material allows a reduction of the surface temperature during daytime, with a positive impact on air temperature. However, it also results to an increase of the reflected solar radiation received by the building facades, resulting to an increase of the mean radiant temperature. Similar results have been reported by previous studies carried out at lower latitudes locations [16], [17].

The impact of increased façade reflectivity on air temperature is negligible in all the scenarios analysed. Similarly, the impact of increased façade reflectivity on the mean radiant temperature is smaller compared to the one determined by the increase of roads' reflectivity. In some cases, increasing the reflectivity of facades also allows to reduce the mean radiant temperature, as shown in figure 6 for the scenario A1 OUT. However, this does not happen in all the canyons analysed and seems to depend on the facades' orientation. The use of reflective materials on the top half of the canyon façade has almost no impact on air temperature nor mean radiant temperature at the street level. This scenario also allowed a significant increase of the canyons' UA.

The microclimate results presented in this study do not allow to draw any conclusion on the net impact of the use of reflective materials on outdoor thermal comfort in London, because of the contrasting impacts on mean radiant temperature, reflections and air temperature at the street level. A further elaboration of the microclimate outputs into comprehensive indices such as the Physiological Equivalent Temperature (PET) is needed to compare the performance of the different scenarios on the outdoor thermal comfort. For a comprehensive analysis, the impact of the reflective material scenarios on UA and outdoor thermal comfort needs to be investigated also in the winter seasons. These will be the next steps of this research.

4. CONCLUSION

This paper presented results from experimental and computational investigations on the impact of real-world urban geometries and optical properties of facades and roads materials on the urban albedo and the street level microclimate in a case-study area of London. The results provided insights on the real cooling potential of reflective materials in the urban context at London's latitude. Different scenarios involving the use of reflective materials on roads and facades were tested on low-rise and high-rise urban canyon configurations.

The results indicate that increasing the reflectivity of roads has the highest impact on the increase of urban albedo in low-rise urban canyon configurations. Instead, in canyon with higher aspect ratio, increasing the reflectivity of the top half of the canyon's facades allows the highest increase of urban albedo.

In terms of microclimate, the daytime air temperature shows a reduction for an increase of the road reflectivity while it is not affected by the facades' reflectivity. All the scenarios determine an increase of reflections at the street level which reduces or erases the positive impact of surface temperature reduction on the mean radiant temperature. Instead, the use of reflective materials only on the top half of the canyon façades does not affect the street level microclimate. Therefore, it can be concluded that this could be an effective strategy to increase UA and potentially mitigate the UHI intensity at the urban scale without compromising the street level microclimate.

The study also provided a novel evaluation of ENVI-met IVS algorithm for detailed radiation transfer calculation. The comparison with measurements showed a good agreement and confirmed its suitability for investigations on the impact of reflective materials on urban albedo and microclimate in urban canyons.

These results provide novel insights into the interrelationships between urban form, material properties and urban microclimate in high latitude locations. Further developments will be aimed at developing design guidelines for the control of UA and the improvement of the outdoor thermal environment in London and cities of similar latitudes.

ACKNOWLEDGEMENTS

This work was funded by EPSRC UK under the project 'Urban albedo computation in high latitude locations: An experimental approach' (EP/P02517X/1).

REFERENCES

1. Akbari, H. and Kolokotsa, D. (2016). Three decades of urban heat islands and mitigation technologies research, *Energy and Buildings*, 133: p. 834–852

2. Oke, T. R., Mills, G., Christen, A. and Voogt, J. A., (2007). *Urban Climates*. Cambridge University Press

3. Kolokotroni, M., Ren, X., Davies, M., and Mavrogianni, A., (2012). London's urban heat island: Impact on current and future energy consumption in office buildings, *Energy and Buildings*, 47: p. 302–311.

4. Mavrogianni, A., Davies, M., Batty, M., Belcher, S. E., Bohnenstengel, S. I., Carruthers, D., ... Ye, Z. (2011). The comfort, energy and health implications of London's urban heat island. *Building Services Engineering Research and Technology*, 32(1):p. 35–52.

5. Nickson, A., Woolston, H., Daniels, J., Dedring, I., Reid, K., Ranger, K., ... Roger Street, T. R. (2011). *Managing risks and increasing resilience. The Mayor's climate change adaptation strategy*. Greater London Authority, London.

6. Santamouris, M., (2014). Cooling the cities - A review of reflective and green roof mitigation technologies to fight heat island and improve comfort in urban environments, *Solar Energy*, 103: p. 682–703.

7. Rosado, P. J., Ban-Weiss, G., Moheggh, A., and Levinson, R. M. (2017). Influence of street setbacks on solar reflection and air cooling by reflective streets in urban canyons. *Solar Energy*, 144:p. 144–157.

8. Yang, J., Wang, Z.-H., and Kaloush, K. E. (2015). Environmental impacts of reflective materials: Is high albedo a 'silver bullet' for mitigating urban heat island? *Renewable and Sustainable Energy Reviews*, 47:p. 830–843.

9. Yaghoobian, N., & Kleissl, J. (2012). Effect of reflective pavements on building energy use. *Urban Climate*, 2:p. 25–42.

10. Yang, X., and Li, Y. (2015). The impact of building density and building height heterogeneity on average urban albedo and street surface temperature. *Building and Environment*, 90: p.146–156.

11. Aida, M., and Gotoh, K. (1982). Urban albedo as a function of the urban structure — A two-dimensional numerical simulation. *Boundary-Layer Meteorology*, 23(4):p. 415–424.

12. Steemers, K., Baker, N., Crowther, D., Dubiel, J., & Nikolopoulou, M. (1998). Radiation absorption and urban texture. *Building Research and Information*, 26(2): p. 103–112.

13. Groleau, D., and Mestayer, P. G. (2013). Urban Morphology Influence on Urban Albedo: A Revisit with the Solene Model. *Boundary-Layer Meteorology*, 147(2): p. 301–327.

14. Qin, Y., Tan, K., Meng, D., and Li, F. (2016). Theory and procedure for measuring the solar reflectance of urban prototypes. *Energy and Buildings*, 126, 44–50. <https://doi.org/10.1016/j.enbuild.2016.05.026>

15. Salvati, A., Monti, P., Coch Roura, H., and Cecere, C. (2019). Climatic performance of urban textures: Analysis tools for a Mediterranean urban context. *Energy and Buildings*, 185: p. 162–179.

16. Alchapar, N. L., and Correa, E. N. (2016). The use of reflective materials as a strategy for urban cooling in an arid "OASIS" city. *Sustainable Cities and Society*, 27: p. 1–14.

17. Erell, E., Pearlmutter, D., Boneh, D., and Kutiel, P. B. (2014). Effect of high-albedo materials on pedestrian heat stress in urban street canyons. *Urban Climate*, 10: 367–386.

18. Salvati, A., and Kolokotroni, M., (2019). Microclimate Data For Building Energy Modelling : Study On ENVI-Met Forcing Data, in *Proceedings of the 16th IBPSA Conference*, pp. 3361–3368.

Architectural and social potential of urban lighting

A field study of how brightness can affect the experience of waiting for public transportation

METTE HVASS¹, ELLEN KATHRINE HANSEN¹

¹Aalborg University, Copenhagen, Denmark

ABSTRACT: *This paper reveals how perceived brightness of urban lighting influences the experience of waiting for public transportation at night. Through a field study of two tram stations in Aarhus, Denmark, the waiting area and the immediate surroundings have been analyzed through descriptive observations and interviews with users. Three brightness parameters have been located. First, the study illustrates the importance of the brightness hierarchy when observing the changes in the visual appearance of the surroundings when the light transitions from natural to artificial light. Second, the study illustrates how the brightness ratios between the waiting area and the immediate surroundings influence users' perceptions of the two areas. Third, the study illustrates how the brightness level influences visual appearance of travelers waiting together. The architectural potential of light is connected to the perception of immediate surroundings and the waiting area, whereas the social potential is connected to a user's perceptions of other waiting travelers. The three brightness parameters define a future lab experiment. Synchronizing and reducing the brightness level can be used to explore how light promotes a pleasant atmosphere in waiting areas and thereby helps more people choose public transportation.*

KEYWORDS: *Lighting design, urban design, public waiting areas, brightness, urban lighting.*

1. INTRODUCTION

At night, lighting contributes to the visual appearance of urban spaces. However, lighting is often designed primarily to meet lighting regulations, while its influence on atmosphere, behavior and mood is secondary. There is a need for research into the psychological effects of light within real-world contexts (i.e., a public transport context) [1], and knowledge about how people perceive light [2] and the atmosphere that lighting creates in the urban context.

Public transportation is one of the focus areas in the United Nations Development Program's sustainable development goals. Goal 11, "sustainable cities and communities" [3], refers to making cities inclusive, safe, resilient and sustainable, which includes helping more people choose public transportation.

As cities become denser, new sustainable urban infrastructures can improve mobility [4], and dynamic lighting scenarios can support infrastructure to create livable and socially sustainable spaces designed for everyday activities [5].

Investigating lighting in waiting areas helps obtain an understanding of how people experience lighting with the aim to improve the waiting situation and help more people choose public instead of private transportation.

A new urban infrastructure, the tram in Aarhus, Denmark, is used as a case study to gain knowledge of the stations, the people using them, and the users' actions. In this setting, we investigate the role of lighting when perceiving the waiting area and the

immediate surroundings, the architectural potential [6] and the role of lighting when perceiving other people waiting, the social potential of light [7].

Hervé Descottes states that "lighting should be designed for the specific space, for people in the space and their actions, building on an awareness of how we can use various lighting principles in the urban context" [8]. According to Descottes, lighting principles can be divided into six categories: illuminance, luminance, color and temperature, height, density, and direction and distribution. By varying these principals, numerous lighting designs can be created according the needs. This paper focuses on the importance of one of the lighting principles connected to brightness levels: how brightness hierarchy, ratio and level influences how we perceive space and people. Descottes explains that "luminance is the objective measure of light intensity per unit area, brightness is the subjective sensation that we, the viewer, experience when looking at an object or a surface" [8].

Some may argue that advanced light-source and lighting control technology can provide dynamic lighting scenarios for almost any need. However, we lack definitions and possible ways of developing and validating the potentials concerning the architectural and social needs for lighting for complex urban spaces. Understanding how brightness of lighting can meet specific needs in the urban space and can become a design tool to address the complexity of a case study and further research on brightness.

2. AIM

The aim of this field study is to investigate how lighting can influence travelers' perceptions of the surrounding space and fellow travelers while waiting at a station. With a focus on brightness, the aim is to define parameters for brightness that can be used to inform further research.

3. BACKGROUND

The first tram traffic line opened in December 2017 in Aarhus, and traffic lines for trams in Odense and Copenhagen will be completed in 2021 and 2025. The new traffic structures aim to increase public transportation in the cities and their connections to the suburbs and thereby increase the use of public transportation [9]. This paper reveals findings from field studies of two tram stations in Aarhus, Skolebakken and Nørreport. The stations are placed in the urban context with a visual connection to the surroundings, aiming to break down visual boundaries between people waiting and urban space. The field study is part of a PhD project on urban architectural lighting around public transportation. In the project, scenography is used as a metaphor to describe the contexts in which lighting is used in connection with everyday activities in the city. At the theatre, the architect and scenographer Adolpe Appia described light as the element that gives "life" to the stage, the actor and the drama [10]. Similarly, the lighting at night can give "life" to the urban space (the stage) and pedestrians (the actors) by targeting and illuminating their actions (the drama) [11]. At the theatre, lighting principals such as illuminance, luminance, color and temperature, height, density, and direction and distribution [8] are used to give "life" to a play. Another important aspect to take into consideration is that the eye is sensitive to contrasts of light at low light levels and perceives the environment differently when it is daylight (photopic vision), dusk (mesopic vision) or night (scotopic vision) [12]. In the northern countries (e.g., Denmark), there is large variation of daylight during the year. The long dusk periods and the lack of daylight during the winter leads to the fact that during these periods everyday activities (e.g., commuting to and from work) are performed in electrical light or darkness.

Urban architecture designed for daytime often changes visually into completely different setups when electrical lighting is turned on at night [6]. The urban space must be designed for people and their everyday activities and made livable [13]. The lighting must support the architecture, add visibility where necessary to be able to read the space and introduce a new architectural layer in the selection of what to illuminate, and thereby take advantage of the architectural potential of light.

The waiting area at a tram station can be characterized as a "node", referring to Kevin Lynch [14] and his urban mental maps. Nodes are strategic focal points for orientation, and the stations analyzed can be characterized as such because of the visual contact between the waiting area and the surrounding urban context. Waiting travelers are therefore both in visual contact with the waiting area and the immediate surroundings, and the waiting time will be influenced by the appearance of this physical context and the lighting at night.

The lighting in the urban space must be planned in a way that supports making surroundings visible, but lighting designers agree that urban lighting can do much more than fulfil our need to navigate and feel safe at night. Lighting can beautify urban spaces, support activities in the spaces, and create a safe and comfortable atmosphere that encourages social engagement [6, 15].

The interactions between people in everyday urban activities have been studied in various research fields. In sociology, Erving Goffman studied meetings between people in the public space and described how face-to-face interactions happen constantly in the urban space, as people interact and "perform" their public role [16, 17]. These social interactions happen all the time, and in the dark hours the lighting influences facial expressions; therefore, lighting has an influence on how other people's intentions are perceived. Jane Jacobs describes these interactions between people as a choreography (e.g., on the pavement where many people pass by each other) [18]. Our actions on the pavement are pre-studied roles we perform as we move through the city. In the lighting design research area, Daria Casciani looked into the social aspects of lighting, studying how lighting can have an effect on social intimacy/inclusion or social exclusion. Lighting has a potential to support meetings between people and the actions that result, as well as to introduce an atmosphere that can encourage social interactions. [7]. This leads to the study of how brightness levels influence how we perceive the urban space around a station (the architectural potential of light) and how we perceive fellow travelers in a waiting area (the social potential of light).

4. METHOD

4.1 Selection of stations and timing of tests

Two tram stations were selected for the study to examine the role of lighting in different urban contexts. Skolebakken station is located between the city and the harbor. On one side of the station is the city, a two-lane road and five-story facades, and on the other side is a park adjacent to a port area. One side is illuminated by the city lights (traffic lights, road lights and cars lights), and on the other side of the

station the light is dimmed on the park area and the water in the harbor area, forming a dark space.

Nørreport station is located with two-lane roads on each side, pavement and then facades of two to five stories on each side of the station. Next to the station, there is a well-lit intersection. Road lighting is available for cars, but the pavement is quite dark and the lights from the facades and cars dominate when one looks towards the facades from the station.

Observations were conducted over two days in January 2019 and interviews over two days in February 2019, during rush hour from 06:00–08:00 and from 16:00–18:00. The choice of intervals allowed the researcher to collect data in daylight, during transition hours and at night.

4.2 Observations

The data were collected using descriptive observations based on James P. Spradley's ethnographic methods [19]. When recording observations, Spradley's nine-dimension descriptive question matrix was used to structure observed impressions. The matrix provides a map for making action-based data collection and consists of the space, actor, activity, object, act, event, time, goal and feeling dimensions. The dimensions of space, actor and activity were primarily used for recordings of observations in this analysis and recordings of light in the nightscape [19].

At each station, the observations took place at six points, or scenes: three scenes on the way to the station and three scenes in the station. Ten minutes were spent at each urban scene where the space, the people and their activities were observed, as well as the experience of light. Because the observations were registered in daylight, transition hours and in the dark, the contrast between the day-lit space and the space lit by electrical light is revealed in the photos. The recordings consisted of photos describing each observed scene as well as field notes describing the observers' impressions in words. By photographing the movement in the vicinity of the station and several points at the station, the intention was to capture a pedestrian's experience of moving through the built environment and, as Gordon Cullen describes in his term "serial vision", to describe how a pedestrian's various views affect the experience of the city [20].

4.3 Interviews

The data were collected using descriptive interviews based on Spradley's ethnographic methods [21]. The semi-structured interviews were conducted at the stations during the morning and evening rush hours. Twenty test subjects were interviewed (nine men and 11 women between 20–60 years old). Interviews were conducted while travelers waited for trams to arrive, between 5–10 minutes. The questions were designed to prompt

answers about the informants' typical experience of the station and, more specifically, how they experienced details in the present moment [21].

An interview guide included the following guiding questions about space, actor, activity and light:

1. Where do you stand at the station, how is the station's space and surroundings (space) experienced? 2. How do you perceive passengers at the station, can you see them clearly (actor)? 3. What do you do during while waiting (activity)? 4. Does the lighting at the station have any influence on your answers? Each interview began by collecting general information about gender and age. Then a question about the travelers' preferred locations at the station was asked and, from there on, the participants' answers determined in which direction the interview moved. The answers were gathered in written field notes during the interviews, which were in Danish.

4.4 Data analysis

The data were analyzed through a traditional coding method, where observation and interview data were analyzed in four steps: organizing, recognizing, coding and interpretation. Collecting field notes and photos was Step 1, finding themes and categories was Step 2, coding the text for focus areas was Step 3, and Step 4 was explaining the findings of the analysis [22]. In the analysis, the observations and interviews are supplemented with references to research to support and frame the findings.

5. ANALYSIS / EVALUATION OF FIELD STUDY

Through observations and interviews with a focus on the space, the people, their actions and light, it was possible to define three brightness parameters based on the architectural and social potential of light.

5.1 Observations

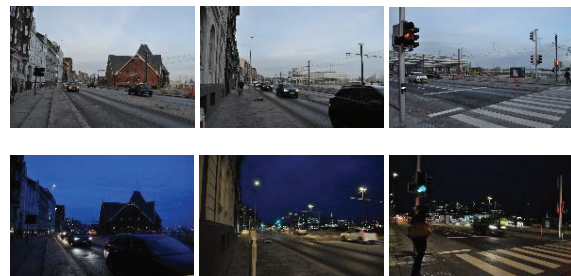


Figure 1. Brightness hierarchy. Approaching the station during the day and at night, Skolebakken station.

The serial vision [20], when walking towards the station in daylight and in darkness, is illustrated in Figure 1. In daylight, vertical facades, a freestanding building and visual contact with the harbor area define the space. At night, the visual identity of the space changes. The facades turn dark and light from windows is seen as light spots. Important architectural details disappear and the demarcation of the space towards the harbor is invisible in the

darkness. Chris Cuttle describes how a planned gradation of illumination can express a lighting designer's intentions and that an ordered distribution of lighting is necessary to achieve an illumination or brightness hierarchy in the design [23].

The brightness hierarchy should be taken into consideration when designing with light. In daytime, the visual appearance of urban surfaces is shaped by the dynamism of natural light [24]. There are potentials in creating a visually perceived space with a brightness hierarchy that refers to what is perceived in natural light. This hierarchy can become unbalanced if the brightness levels are not adjusted.



Figure 2. Brightness ratios. The brightness contrast between the waiting area and the immediate surroundings, Nørreport station.

The brightness contrast between the waiting area and the immediate surroundings is perceived as high. As day turns into night, the waiting area becomes very bright compared to the surrounding city, which can give a feeling of being in the spotlight and not being able to see details in the surrounding city. Descottes describes the brightness contrast: "The careful control of illumination levels across spatial trajectories is crucial in ensuring visual and spatial continuity, comfort and one's ability to see." [8]. Research reveals that the appearance of light in a space may be affected by adjacent areas [25] and that subjective assessments of brightness in adjoining spaces, a sequential experience, may be influenced by previous adaptation [26].



Figure 3. Brightness, a visual barrier, Skolebakken station
Light can act as a visual barrier. Figure 3 illustrates how light on the station railing, to the left, prevents one from seeing the surrounding area. To the right, the light on the railing is broken and a visual contact with the surrounding space occurs.

Navaz Davoudian discussed the connection between luminance ratios and the visual perception of a space in relation to the coherence between a lit object in the urban space and the density of background light patterns. Results show that when the density of the background light pattern is increased, the visual saliency of an illuminated object is reduced [27]. In this case, the background disappears because of the lit detail in the railing, which is a part of the design

identity of the station but in this case it forms a visual barrier.

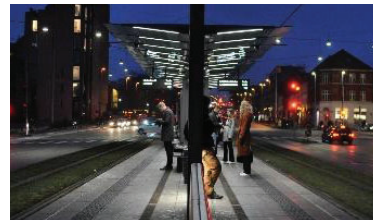


Figure 4. Brightness level. Illumination of people, Nørreport.

The bright, diffuse light installed in the shelter roof over the waiting area lightens up the people waiting for the tram. The faces appear without shadows and therefore without form, and the space is in great contrast with the immediate surroundings. Figure 4 illustrates how a face is perceived in the shadow when a person is looking down and how only the legs are lit by light on the railing if one is placed outside the shelter and only lit up by the railing light. Within indoor lighting research, tests have shown that lower lighting levels and warm white light induce calmer and more relaxed feelings, which also influence a positive social attitude [28]. Through her research on social lighting, Daria Casciani concluded that "light acts to enforce interpersonal relationship, supports social negotiations, contributes in communicating proxemics information and defining more socially including or excluding environments". [7]

5.2 Interviews

Of the surveyed respondents, 14 out of 20 people placed themselves under the roof of the platform and either sat or stood. The remaining people moved around or positioned themselves in relation to where they exited the tram when they arrived at their destination. However, most of the subjects choose to position themselves under the roof where there is shelter, light and the opportunity to sit.

Subjects described how the station, at a distance, is perceived as bright, easy to see and as something that lights up in the dark. On the other hand, the surroundings were described as dark, unsafe and in contrast, when the city is observed from the station.

The answers concerning the light at the station are harder to process because they relate to the personal experience of the light. Some respondents found the topic very interesting and others were very surprised to be asked about it. The analysis of the responses showed that eight people found the lighting too bright (e.i., a negative attitude to the bright light). Eleven people associated the light with safety and one person had no opinion about the lighting. The term "public light" was associated with something positive (e.i., how lighting must be a public place) or something negative (e.i., impersonal). There is a difference in how safety is perceived in relation to light. Some travelers find it safe to be in the "spotlight" and others find it safe to be able to perceive the surroundings. In lighting research, three

lighting modes are considered the most important to human perception and are often used for tests: the illumination level (bright vs. dim), the distribution (uniform vs. non-uniform) and the position (overhead vs. peripheral) [29]. The current paper is focused on the brightness level (bright vs. dim). Brightness levels are often discussed in relation to safety and much research in urban lighting shows that a high light level is related to the feeling of safety [30]. Yet others state that designers can produce a cold, impersonal public space with light or they can use light to help reinforce an impression of a warm, intimate place where users feel a greater sense of privacy [29]. We lack knowledge to understand the connection between lighting and feelings of safety to be able to determine lighting design possibilities that are socially acceptable [31].

6. FINDINGS

Three brightness parameters were found important for the experience of waiting for public transportation. The importance of the brightness parameters is supported by quotes from the interviews.

6.1 Observations

The observations resulted in the definition of three brightness parameters when observing the waiting area and the immediate surroundings. It was found that lighting principles related to the brightness ratios in connecting scenes in the urban space are of great importance for the perception of the immediate surroundings, the near physical surroundings, the waiting area and the people nearby.



Figure 5. Brightness parameters

A. Brightness hierarchy in the immediate surroundings. The urban scenes change character from day to night. When the brightness hierarchy is out of balance, important urban details can disappear because of a too high or a too low brightness level in a certain area (Figure 1).

B. Brightness ratios between the immediate surroundings and the waiting area. High brightness contrast between the waiting area and the immediate surroundings makes the urban context invisible (Figure 2).

C. Brightness level in the waiting area. High brightness level and sole use of diffuse light on people waiting makes faces appear too brightly illuminated, so details disappear or recede into complete shadow, when people are looking down (e.g., at their phones; Figure 4).

6.2 Interviews

The interviews were conducted in the waiting area under the lights from the shelter. The following quotes from the interviews relate to the three brightness parameters presented in the section above. One participant stated, “At a distance the station is easy to spot, bright and welcoming, as you walk towards it”. One could argue that when approaching the station the brightness hierarchy is perfect. However, when looking from the waiting area towards the immediate surroundings, a subject stated, “The facades are in darkness, seen from the station, you can’t see people on the sidewalk”. The brightness ratios are not adjusted, and as another person said, “During the day, it is good that the station is open to the harbor (visually), but in the evening, it is unsafe because it is dark (in the surroundings)”. Nevertheless, safety is perceived in different ways when it comes to lighting. One subject stated the station had “much better light than bus stops, safer and not gloomy. Comfortable light, like daylight. Late in the evening, I take the tram because of the light and traffic around. It’s safer. I feel like other people can see if something happens. I’d rather be at the tram station than at a dark bus stop”. Some people feel safe when they are in the spotlight and some people would prefer to be able to see the surroundings. Concerning the brightness level, again people have different focuses and different backgrounds for answering. One person stated, “People look a bit like corpses; a different light could make people look more normal and friendly,” whereas another said the light seemed like “sterile light, but it is probably energy efficient as it should be today.”

7. DISCUSSION

Results from observations and interviews reveal a connection between brightness hierarchy, brightness ratios and brightness level in relation to how users perceive the space they are situated in, fellow travelers and the immediate surroundings. The study illustrates that at high light levels, the visual contact with the surroundings and the impression of people in the waiting area is impaired. This approach can lead to further investigation of how low the light level should be to be able to see the immediate surroundings and fellow travelers in a pleasant light. According to Kaplan and Kaplan, “The drivers for people to interact with the environment are the possibility of understanding the space and the possibility of exploring it” [32]. To explore a space, it has to be visible. Therefore, light ratios take on importance. Hierarchy of luminance can be objectively controlled using luminance ratios, a comparative system of numbers that describes a surface’s brightness in relation to another, as described by Descottes. In a list of predetermined

design objectives, Cuttle mentions (a) overall perceived brightness or dimness of illumination, (b) perceived difference of brightness of illumination between the design space and adjacent spaces, and (c) an illumination hierarchy. The illumination hierarchy involves creating a light distribution to give graded levels of perceived difference of illumination between selected room surfaces or objects and their surroundings [25], stressing the importance of the brightness hierarchy, brightness ratios and the brightness level of light.

The observations and interviews were conducted over four days and therefore must be regarded as a pilot study. To obtain data that are more valid, a larger sample of observations and interviews is needed. The results are found valid for directing future research on brightness and how brightness can influence travelers' perceptions of the surrounding space and fellow travelers in a waiting situation.

8. CONCLUSION

The aim of this field experiment and literature review was to examine the architectural and social potential of using lighting in public transportation waiting areas. The brightness hierarchy and brightness ratios are connected to how people perceive the waiting area and the immediate surroundings (i.e., the architectural potential of light) at two tram stations in Aarhus, Denmark. Furthermore, the brightness level was connected to how users perceived fellow travelers in a waiting area (i.e., the social potential of light). The findings from the field study have led to a framework for testing brightness in a laboratory experiment that will be performed in the lighting laboratory facilities at Aalborg University, Copenhagen.

ACKNOWLEDGEMENT

This research is part of a Ph.D. project in urban architectural lighting funded by the industrial partners Schröder (BE) and Holscher Design (DK).

REFERENCES

- Hughes, N., (2020) Identifying new concepts for innovative lighting-based interventions to influence movement and behaviours in train stations. *Lighting Res. Technol.* 2020; 0: 1–15
- Johansson, M., (2013). Perceived outdoor lighting quality (POLQ): A lighting assessment tool. *Journal of Environmental Psychology*.
- United Nations, Sustainable Development Goals, <https://sustainabledevelopment.un.org/>
- Jensen, O.B., (2016). *Mobilities Design: Urban Designs for Mobile Situations*. Routledge
- Dempsey, N., (2009). *The social dimension of Sustainable Development: Defining Urban Social Sustainability*. Wiley InterScience
- Brandi, U., (2006). *Light for Cities*. Birkhäuser Arch.
- Casciani, D., (2017). What Light Does: Reflecting on the active social effects of lighting design and technology. Conference paper 6th STS Italia Conference.
- Descottes, H., (2011). *Architectural lighting: Designing with light and space*. Architecture Briefs
- Jensen, B., (2017). Aarhus Letbane, fra vision til virkelighed. Aarhus Letbane I/S
- Palmer, S., (2013). *Light. Readings in theatre practice*. Palgrave Macmillan
- Hvass, M., & Hansen, E.K., (2020). Potentials of light in urban spaces defined through scenographic principles. NAF/ NAAR Symposium: *Approaches and Methods in Architectural Research*. Chalmers University Technology. Gothenburg, 13-14 June 2019. (Forthcoming)
- Boyce, P.R., (2014). *Human Factors in Lighting*, Third Edition. CRC Press
- Gehl J.,(2010). *Cities for people*. Washington DC: Island Press
- Lynch, K. A., (1960). *The Image of the City*. MIT Press
- Narboni, R., (2004). *Lighting the landscape*. Birkhäuser
- Goffman, E., (1959). *The Presentation of self in everyday life*. Anchor Books
- Goffman, E., (1967). *Interaction ritual : essays on face-to-face behaviour*. Harmondsworth : Penguin
- Jacobs J., (1961). *The death and life of great American cities*. New York : Modern Library
- Spradley, J.P., (1980). *Participant observation*. New York. Holt, Rinehart and Winston
- Cullen, G.,(1961). *Concise Townscape*. Taylor&Francis Ltd
- Spradley, J.P., (1979). *The ethnographic interview*. New York. Holt, Rinehart and Winston
- Bjørner, T., (2015). *Qualitative methods for consumer Research*. Hans Reitzels
- Cuttle, C., (2015). *Lighting Design, A perception-based approach*. Routledge, Taylor & Francis Group
- Shrum, G., (2017). *Natural light and architecture. Lighting, Illumination in Architecture*, Vol 49
- Cuttle, C., (2013). A new direction for general lighting practice. *Lighting Research & Technology*, 45(1)
- McKenna, G.T., (1981). A study of the sequential experience of different lighting. *Lighting Research & Technology*
- Davoudian, N., (2019). *Urban lighting for people, evidence-based lighting design for the built environment*. RIBA publishing Theories, Research, & Applications. Cambridge: Cambridge University Press.
- Baron, R., (1992). Effects of Indoor Lighting (Illuminance and Spectral Distribution) on the Performance of Cognitive Tasks and Interpersonal Behaviors: The Potential Mediating Role of Positive Affect. *Motivation and Emotion*, 16 (1), 1–33.
- Flynn, J., (1988). Lighting Design Decisions as Interventions in Human Visual Space. In Nasar, J.(ed.), *Environmental Aesthetics*.
- Nasar, J.L., (2017). Impressions of lighting in public squares after dark. *Environment and Behavior*, 2017.Vol 49
- Stone, T., (2018). The Value of Darkness: A Moral Framework for Urban Nighttime Lighting. *Sci Eng Ethics* (2018) 24:607–628
- Kaplan, R & Kaplan, S., (1989). *The Experience of Nature: A Psychological Perspective*. University Press, Cambridge.

Decarbonising our transport system: Vehicle use behaviour analysis to assess the potential of transitioning to electric mobility

JULIE WALDRON¹, LUCELIA RODRIGUES¹, MARK GILLOTT¹, SOPHIE NAYLOR¹, ROB SHIPMAN¹

¹Department of Architecture and Built Environment, Buildings, Energy and Environment Research Group,
University of Nottingham, Nottingham, UK

ABSTRACT: *The transport sector is responsible for over 20% of the global carbon emissions. One of the strategies to reduce its impact includes transitioning to electric vehicles (EV). However, this represents several challenges to existing cities, such as the lack of a charging network compatible with different vehicles archetypes, the increase in energy demand, and the aged infrastructure that can result in power shortages. In this paper is presented a behaviour analysis covering a 49-vehicle fleet of a university in the UK. One year data was analysed, including 150,656 journeys undertaken by various taskforces. The results indicate that 96.3% to 99.8% of the time, the pattern of use fit within the current range of capacity of EVs. Stationary time analysis showed that most of the vehicles remained parked overnight (+10 hours) and during daytime the vehicles were not used simultaneously. This is a convenient scenario to implement vehicle-to-grid, which would allow the users to monetise their vehicles by using their batteries as assets. A vehicle-parking location analysis identified potential locations for charging infrastructure. Finally, reductions of 79.6% in carbon emissions were estimated if the fossil-fuelled vehicles were to be replaced by EVs. This reduction may increase as grid energy is decarbonised.*

KEYWORDS: *Electric Vehicles, Vehicle to Grid, Renewable Energy, Energy Storage, Decarbonising the Grid*

1. INTRODUCTION

The World Health Organisation estimates that 92% of the world's population lives in places where the pollution exceeds the recommended air quality levels [1]. Recently, as a result of the pandemic-related restrictions on movement, average air pollution levels have fallen to unprecedented levels all over the world [2], [3] and by up to 60% in the UK [4], [5], where experts predict a consequent dramatic reduction in incidences of asthma and hospital admissions related to non Covid-19 respiratory conditions [6]. The pandemic effect on air pollution provides us with a glimpse of how a low-carbon future could look like.

The transport sector alone is currently responsible for 20.5% of the global carbon emissions [7]. The Intergovernmental Panel on Climate Change has warned that rapid changes are required in all aspects of society in order to limit global warming to 1.5°C [8]. Even though the pandemic demonstrated that the reduction in economic activity and traffic restrictions effectively reduced carbon emissions, it is estimated that emissions levels could exceed the pre-pandemic levels as soon as the economy and transport are reactivated, if no measures are taken to avoid this [9].

In order to reduce carbon emissions generated by the transport system, many governments have set targets to phase out fossil fuel vehicles and replace them with electric vehicles (EV). Some of the most

ambitious plans have been established by Norway to suspend the sale of internal combustion engine (ICE) vehicles by 2025, followed by Germany, Netherlands, India and Israel by 2030, UK by 2035, and France, Taiwan and China by 2040.

In order for this transition to electric mobility to be successful, much has to be changed in our cities. In particular, we will need to install charging networks compatible with different vehicles archetypes, increase the generation of renewable energy to compensate for the added demand, and prevent energy shortages by appropriately using the vehicles' batteries to balance the grid [10].

According to Noel et al [11], it has been reported that 'range anxiety' is a prominent concern of users considering adopting electric vehicles, as well as, price, charging infrastructure and consumer perception. Over the last decade, new technologies, such as vehicle-to-grid (V2G), have been trialled to integrate the transport system with the energy system in order to overcome some of the barriers for the uptake of electric vehicles [10].

V2G refers to using the bi-directional capacity of EVs to store energy and sell it to the grid on demand [12]. It aims to use "EV battery packs as aggregated distributed grid-based energy storage" [13 p.1]. Some of the benefits include: a) the support it can provide to the energy grid by help regulating the peak demand; b) economic incentives to the end user from selling the energy back to the grid; c) the optimisation

of the energy cost; and, more importantly, d) renewable energy storage (particularly wind and solar sources), which is essential to decarbonise the energy grid [10].

In this paper, the authors present a user behaviour analysis of a university fleet of 49 vehicles looking at the patterns of stationary time, parking location and simultaneous use. The fleet was chosen because it provides various services for the university's large estate, reflecting, albeit in a smaller scale, the situation found in a city. The authors then assess the compatibility of the fleet with available EV and V2G technology, undertake a feasibility assessment of the charging infrastructure, and produce an estimate of the potential carbon emissions reduction if EV was to be adopted where possible.

2. METHODOLOGY

The sample evaluated was a fleet of 49 vehicles from the University of Nottingham (40 diesel and 9 electric vans). These vehicles were tracked using Trakm8 telematics system [14]. The vehicles were split into six clusters according to the service provided, named Fleet 1 to 6, in order to anonymise the data (Table 1). One year of historical data was extracted for five of the fleets and six months data for the remaining fleet (as this was the only data available for Fleet 6 at the time of this research). In total, 150,656 journeys were analysed. The telematics retrieved consisted of start and end date of the journey, duration, initial and final location and distance travelled, among others. A journey was defined as the event when the vehicle travelled from one location to other; journeys with distance equal to zero were excluded.

Table 1 – Dataset Summary

Cluster	# vehicles	Dataset	# Journeys
Fleet 1	5	12 months	22,111
Fleet 2	22	12 months	54,976
Fleet 3	8	12 months	17,576
Fleet 4	4	12 months	18,494
Fleet 5	3	12 months	12,379
Fleet 6	7	6 months	25,120
Total	49	-	150,656

The data analysis included descriptive statistics, stationary time analysis, vehicle parking location likelihood and simultaneous use analysis. Sensitive information, such as individual characteristics of the vehicles or tasks details were anonymised. This study was approved by the Ethics committee from the Faculty of Engineering of the University of Nottingham and the University Estates team.

3. RESULTS

The dataset was filtered to identify the patterns of behaviour of the fleets. The frequency use of the vehicles according to the day of the week was extracted by looking at the percentage distribution from Monday to Sunday. It was found that five of the fleets have more than 93% of their active time from Monday to Friday, and Fleet 6 registered a relatively uniform distribution of the journeys across the seven days of the week (variation of 2.5% between days). Therefore, the analyses for Fleets 1 - 5 were conducted only for weekdays.

Table 2 presents a summary of the descriptive statistics of the distances travelled per journey and per day. The *Journey Distance* refers to the miles registered per trip. Fleet 5 registered the highest mean distance (2.5 miles, SD = 3.6), which means that these vehicles are used for longer journeys in comparison to the other fleets. The maximum distance travelled in a single journey was 162.8 miles, registered by a vehicle from Fleet 3.

Table 2 – Descriptive Statistics: Journey Distance and Day Distance registered per fleet.

	Fleet	Mean	Std. Deviation	Maximum
Journey Distance (miles)	1	0.8	1.5	58.4
	2	1.4	2.1	40.1
	3	1.7	3.5	162.8
	4	1.5	2.9	47.5
	5	2.4	3.6	23.8
	6	1.9	2.5	59.1
Day Distance (miles)	1	13.9	9.5	121.1
	2	15.4	10.3	92.6
	3	16.4	14.1	326.3
	4	27.9	17.7	100.9
	5	42.3	23.9	99.5
	6	43.3	23.7	126.3

The *Day Distance* is the cumulative distance travelled in a day per vehicle. This was analysed per fleet. Fleet 6 recorded the highest mean (43.3 miles, SD = 23.7), followed by Fleet 5 (42.3 miles, SD = 23.9). The maximum distance travelled in a day was 326.3 miles, registered by a vehicle from Fleet 3. However, it was noted that the very long journeys that populate the maximum column were rare, which is why the mean day distances are low.

3.1. Stationary Time Analysis

The average percentage of *Stationary Time* provides a view on the probability of a vehicle to be stationary at a specific moment. In Figure 1, each line represents the calculated average per fleet during weekdays. In this graph, 100% means that all the vehicles of the fleet remained stationary during the time evaluated, while a case of 0% of stationary time would mean that all the vehicles were in use.

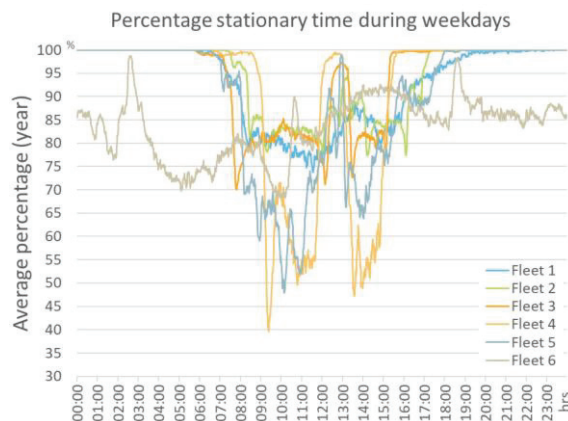


Figure 1 - Stationary Time during weekdays, 100% means that all the vehicles are stationary. As the percentage is lower, the probability of the vehicles to be used is higher.

Fleet 6 was the only group of vehicles that remained active 24 hours across the year; the rest of the fleets remained stationary overnight. Peak usage occurred between 8:00 to 12:00hrs, and 13:00 to 16:00 hrs.

3.2. Vehicle Parking Location

During the operation of the vehicles, they use different parking locations in order to deliver their services. The dwell time at these sites can significantly vary according to the services provided. If the fleet was to be electric, the location of the parking and charging stations would become a crucial factor to be considered, because of the feasibility of the installation and the amount of infrastructure investment required. Therefore, this work included a *Vehicle Parking Location* analysis that aimed to identify the main parking site of the vehicles in a 24 hours period. To achieve this, the postcode registered at the end of each journey and the dwell time of the vehicles in these locations were overlapped. For example, Figure 2 presents the *Average Likelihood* of Fleet 2 of being at specific locations in a 24 hours period during a year.

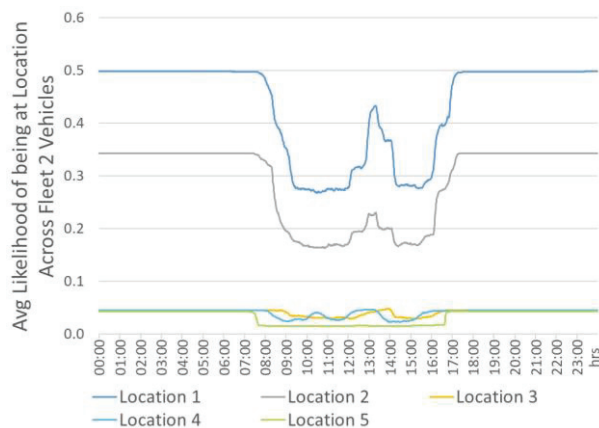


Figure 2 - Average likelihood of being at Locations (1-5) across all the vehicles of Fleet 2

Location 1 and 2 were the sites where Fleet 2 vehicles presented a highest likelihood to be parked overnight (Figure 2), indicating also that the vehicles returned to this location between 12:30 - 14:00 hrs.

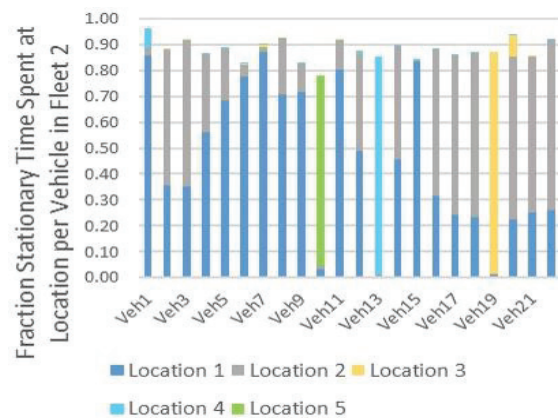


Figure 3 - Fraction of Stationary Time at Locations (1-5) for each vehicle of Fleet 2

Figure 2 would suggest that Locations 1 and 2 would be good candidates for charging points to serve the whole of Fleet 2. However, a breakdown of time spent per location for each vehicle in the fleet, shown in Figure 3, indicated that three vehicles in this fleet stay overnight at locations other than 1 and 2, suggesting the need for additional chargers. This highlights some of the challenges in transitioning a diverse fleet of vehicles to EV.

This analysis was repeated with the other fleets using other locations in order to identify the main parking sites and best possible location of charging stations for each of them.

3.3. Simultaneous Use

The *Simultaneous Use* analysis aimed at identifying the behaviour patterns of the vehicles and the most active hours of the fleets. In Figure 4, the colour scale represents the number of vehicles used simultaneously per minute, white means zero vehicles and red all vehicles (the total number of vehicles varies according to the fleet size). The vertical axis corresponds to the months evaluated (January to December 2018 for Fleets 1 to 5, and December 2018 to May 2019 for Fleet 6), and the horizontal axis refers to a 24 hours period.

In Figure 4 is observed that each fleet presents a different pattern of behaviour. For instance, Fleet 1 does not have a specific start and end of the operation, while Fleet 2 has a sharp starting time around 7:30 am and is finishing activities at 5:00 pm. As previously reported in the *Stationery Time* analysis, Fleet 6 operates 24/7. It is also noticed that during the active periods, there are different gaps occurring across the year for all fleets, usually a round midday for Fleets 1-5. These gaps are different for Fleet 6 happening at 3:00 am, 11:00 am and 7:00pm.

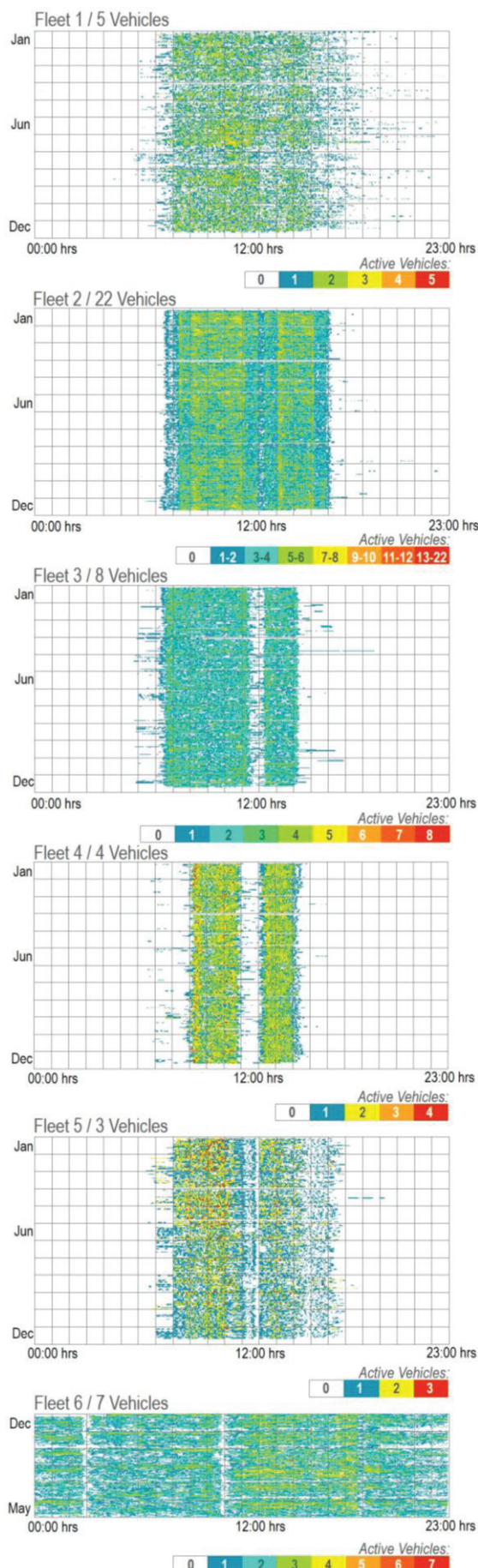


Figure 4 - Simultaneous Use Analysis Fleet 1 to 6

4. DISCUSSION

As seen in Table 2, the mean *Journey Distance* of the fleets varied between 0.8 and 2.4 miles, and the mean *Day Distance* were between 13.9 to 43.3 miles. If only these values were considered to decide whether the fleets function is compatible with an electric version of the vehicles, then it could be determined that the transition to EVs would be possible as a 40 kWh battery van has a range of 115 miles [15]. This range could cover almost three times the average range required for the busiest fleet in a day (e.g. Fleet 6: 43.3 miles). However, 'range anxiety' has been reported as a combination of feeling stressed by the possibility of the battery running low, and the situation when the "...driver needs to drive a longer distance than the EV is usually capable of going in a single charge" [11 p.97].

In order to analyse the situations that may cause 'range anxiety', the maximum distance values from Table 2 were reviewed. According to Pearre et al [16] and Gonder et al [17], an EV could fit 95% of the required daily mileage, assuming a *Day Distance* of 100 miles. Therefore, this assumption was considered for each fleet. For most of the fleets, exceeding 100 miles in a day was rare; for instance: Fleet 1 exceeded 100 miles two times in a year, Fleet 3 six times and Fleet 4 once. This means that 99.8% of the time the operation of these vehicles would fit with the range capacity of an EV. On the other hand, Fleet 6 exceeded 100 miles 46 times in a year; however, this represented 3.7% of the time, meaning that 96.3% of the time this fleet would fit current EV range capacity. In addition, the *Stationary Time* analysis provided evidence of several opportunities to charge the vehicles during the daytime, which could also support to alleviate the 'range anxiety'. It must also be noted that EV technology is progressing quickly, and range capacity is increasing significantly with every new vehicle model.

4.1. Charging Infrastructure

The *Stationary Time* analysis showed that, with the exception of Fleet 6, the vehicles remained stationary for at least 10 hours during the nights over the year. This time would allow for a full charge of the vehicles to take place assuming a wall box charger (6.6 kWh). In addition, according to the results presented in Figure 1 and 2, during the day, many of the vehicles were stationary between 12:30 and 14:00 hrs. This period could be used to connect the vehicles to the grid. Figure 3 indicates that the vehicles returned to the same main location during midday. Therefore, the charging infrastructure could be centralised in the main building where the fleets operate.

The *Simultaneous Use* analysis provides a view of the peak time during the operation of the fleets, as

well as an insight on the number of vehicles available to connect to the chargers. As an example of this, Fleet 2 rarely operates 22 vehicles at the same time, and during peak time around 7-8 vehicles are in use. This means a potential to have the remaining 14 vehicles connected to the grid during the daytime if they are located at the main parking site.

Considering the bi-directional power flow between the vehicles and the energy grid provided by V2G technology, the *Simultaneous Use* analysis, allowed the identification of compatible fleets. For instance, Fleet 1 to 5 are good candidates for bi-directional charging, as they presented a very predictable stationary time throughout the year. V2G can help facilitate the integration of renewable energy sources; therefore, fleets that remained stationary during midday, such as Fleets 1 to 5 could be used as storage of energy produced by, for example, photovoltaic panels.

Conversely, Fleet 6 would not be compatible with a V2G system, as it presents high usage 24/7. Moreover, as this fleet has a frequent use, the drivers would require to connect and disconnect the vehicles often. This action could interfere with the operation and efficiency of the fleet. Therefore, a wireless charging system would be a better fit for this fleet.

The main parking location is a key factor for V2G aggregation services [18], as the efficiency of the system relies on the availability of vehicles for the connection to the grid, as "it must be parked close enough to an available charging station to be plugged in" [19 p.2]. This work's exploration of the vehicle main locations determined preliminary optimal location charging points to be installed at the university campus (Figures 2 and 3). The outcomes of the *Vehicle Parking Location* analysis were discussed with the electrical services manager from the university to assess the feasibility to install charging stations at different locations. Three types of scenarios were identified:

1. High feasibility sites: locations that would require minor investments (e.g. parking site located close to a power station, enough power capacity, minor ground works).
2. Medium feasibility: sites that would require some investment to adequate installations (e.g. soft ground works required to reach power station).
3. Low feasibility: installations that would require high investments (e.g. power station located far requiring high investments in groundworks, limitation on power supply).

The infrastructure costs are a key factor of V2G systems, as this will define the success of the business models. Therefore, it is estimated that only locations with high or medium feasibility are apt for installation.

4.2. Reduction of Carbon Emissions

It has been reported that uncontrolled charging of EVs can overload the demand on the grid and increase carbon emissions [10]. According to Jochem et al [20] at an early stage, the uncontrolled unidirectional charging of EVs will be adequate to penetrate the market. However, it is expected that system will evolve to a controlled stage where the unidirectional charging allows reducing pollutants by postponing the charging process to an optimal time (e.g., when the grid has a low energy demand and/or high renewable energy production). Nevertheless, bi-directional controlled charging (V2G) will be required to achieve a scenario where the vehicle batteries can support the national energy grid by storing intermittent sources of energy (e.g. wind and solar) [20]. This will allow reducing carbon emissions not only by stopping burning fossil fuels to power vehicles, but also to decarbonise the grid system by better integrating renewable sources.

In order to assess the carbon savings from replacing a fossil-fuelled vehicle to EVs, the carbon emissions of one of the vehicles from Fleet 1 were extracted from Trakm8. The vehicle evaluated was a Peugeot Boxer HDI 335. This vehicle travelled 7,200 km in a year generating 1,505 kg of carbon (CO₂) emissions. The results were compared with an equivalent EV in the market, a Nissan e-NV200 [15]. With a battery capacity of 40 kWh, this vehicle has a range of 115 miles and a consumption of 330 Wh/miles. This vehicle would require 1,476 kWh of energy to travel 7,200 km in a year. Assuming an overall grid factor of 0.208 kg of CO₂/kWh [21] multiplied by 1,476 kWh, results in 307 kg of CO₂ emissions in a year. This means a reduction of 79.6% of the carbon emissions, if the diesel vehicle is replaced by an EV. These calculations are estimated values as carbon emissions from the energy grid fluctuate depending on the annual average mix, time-dependent sources and balancing strategies from political measures [20].

In order to reduce carbon emissions, cities will need to optimise the generation, storage, sharing and distribution of energy. The integration of the transport and energy systems was firstly envisaged by Letendre and Kempton [22] twenty years ago; however, the combination of EV technology development, feasible energy storage and renewable energy infrastructure was required to realise this future [10].

5. CONCLUSIONS

In this work, the authors developed a methodology using behaviour analysis to identify key aspects of vehicle use in order to assess the potential for a transition to electric mobility. Stationary Time, Vehicle Parking Location and Simultaneous Use were

explored to identify the compatibility of EV technology with the studied fleet, the feasibility of a charging infrastructure and the environmental benefits that could be obtained.

This study demonstrated that between 96.3% and 99.8% of the time the current diesel vehicles use were compatible with the range of capacity of EVs. This means that 'range anxiety', a common challenge for the uptake of EV technology, was usually caused by a very small amount of events in a year. Dwelling times of 10 hours during the night, low simultaneous use and frequency of parking locations demonstrated the suitability of V2G technology. In addition, it was estimated that a change from diesel to EVs would result in a reduction in carbon emissions of around 79.6%. This could be reduced further by a decarbonised energy grid, which could be helped by a better integration of renewable energy through the use of the storage available within the vehicle batteries.

Although this study was undertaken using a relatively small fleet, the lessons learnt are application to city-scale challenges.

ACKNOWLEDGEMENTS

This paper is an outcome of the research activities of EV-elocity funded by the Office for Low Emissions Vehicles (OLEV), the Department for Business, Energy and Industrial Strategy (BEIS) and facilitated by Innovate UK.

REFERENCES

- [1] World Health Organization, "WHO releases country estimates on air pollution exposure and health impact," 2016. [Online]. Available: <https://www.who.int/en/news-room/detail/27-09-2016-who-releases-country-estimates-on-air-pollution-exposure-and-health-impact>. [Accessed: 27-Sep-2019].
- [2] H. Regan, "Air pollution falls by unprecedented levels in major global cities during coronavirus lockdowns," *CNN World*, 23-Apr-2020.
- [3] S. Kugel and R. Feeser, "How the pandemic is changing air pollution levels," *CBS News*, 29-Apr-2020.
- [4] BBC News, "Lockdown 'halves pollution' in central London," *Pollution*, 06-May-2020.
- [5] P. Monks, "Coronavirus: lockdown's effect on air pollution provides rare glimpse of low-carbon future," *The Conversation*, 15-Apr-2020. [Online]. Available: <https://theconversation.com/coronavirus-lockdowns-effect-on-air-pollution-provides-rare-glimpse-of-low-carbon-future-134685>. [Accessed: 13-May-2020].
- [6] G. Davies, "Coronavirus has shown us just how bad air pollution is for our health," *The Independent*, 2020.
- [7] The World Bank, "CO2 emissions from transport (% of total fuel combustion) | Data," 2019. [Online]. Available: <https://data.worldbank.org/indicator/en.co2.tran.zs?end=2014&start=1960&view=chart>. [Accessed: 04-Jul-2019].
- [8] M. Allen *et al.*, "IPCC, 2018: Summary for Policymakers. In: Global Warming of 1.5°C. An IPCC Special Report on the impacts of global warming of 1.5°C above pre-industrial levels and related global greenhouse gas emission pathways, in the context of strengthening the global," Geneva, 2018.
- [9] Q. Wang and M. Su, "A preliminary assessment of the impact of COVID-19 on environment – A case study of China," *Sci. Total Environ.*, vol. 728, p. 138915, 2020, doi: <https://doi.org/10.1016/j.scitotenv.2020.138915>.
- [10] J. Waldron, L. Rodrigues, M. Gillott, S. Naylor, and R. Shipman, "Towards an electric revolution: a review on vehicle-to-grid, smart charging and user behaviour," in *Sustainable Energy Towards the New Revolution: Proceedings of the 18th International Conference on Sustainable Energy Technologies*, 2019, pp. 1–9.
- [11] L. Noel, G. Zarazua de Rubens, B. K. Sovacool, and J. Kester, "Fear and loathing of electric vehicles: The reactionary rhetoric of range anxiety," *Energy Res. Soc. Sci.*, vol. 48, no. April 2018, pp. 96–107, 2019, doi: [10.1016/j.erss.2018.10.001](https://doi.org/10.1016/j.erss.2018.10.001).
- [12] Y. Zheng, S. Niu, Y. Shang, Z. Shao, and L. Jian, "Integrating plug-in electric vehicles into power grids: A comprehensive review on power interaction mode, scheduling methodology and mathematical foundation," *Renewable and Sustainable Energy Reviews*, 2019, doi: [10.1016/j.rser.2019.05.059](https://doi.org/10.1016/j.rser.2019.05.059).
- [13] H. Krueger and A. Cruden, "Multi-layer event-based Vehicle-to-Grid (V2G) scheduling with short term predictive capability within a modular aggregator control structure," *IEEE Trans. Veh. Technol.*, vol. 69, no. 5, pp. 4727–4739, 2020, doi: [10.1109/tvt.2020.2976035](https://doi.org/10.1109/tvt.2020.2976035).
- [14] Trakm8, "Fleet Management, Telematics Insurance, Optimisation, Automotive & Cameras." [Online]. Available: <https://www.trakm8.com/>. [Accessed: 29-Apr-2020].
- [15] Nissan, "Nissan e-NV200." [Online]. Available: https://www-europe.nissan-cdn.net/content/dam/Nissan/gb/brochures/Vehicles/Nissan_e-NV200_van_UK.pdf. [Accessed: 30-Apr-2020].
- [16] N. S. Pearre, W. Kempton, R. L. Guensler, and V. V. Elango, "Electric vehicles: How much range is required for a day's driving?," *Transp. Res. Part C Emerg. Technol.*, vol. 19, no. 6, pp. 1171–1184, 2011, doi: [10.1016/j.trc.2010.12.010](https://doi.org/10.1016/j.trc.2010.12.010).
- [17] J. Gonder, T. Markel, M. Thornton, and A. Simpson, "Using global positioning system travel data to assess real-world energy use of plug-in hybrid electric vehicles," *Transp. Res. Rec.*, no. 2017, pp. 26–32, 2007, doi: [10.3141/2017-04](https://doi.org/10.3141/2017-04).
- [18] R. Shipman, S. Naylor, J. Pinchin, R. Gough, and M. Gillott, "Learning capacity: predicting user decisions for vehicle-to-grid services," *Energy Informatics*, vol. 2, no. 1, pp. 1–22, 2019, doi: [10.1186/s42162-019-0102-2](https://doi.org/10.1186/s42162-019-0102-2).
- [19] R. Shipman, J. Waldron, S. Naylor, J. Pinchin, L. Rodrigues, and M. Gillott, "Where Will You Park? Predicting Vehicle Locations for Vehicle-to-Grid," *Energies*, vol. 13, p. 1933, 2020.
- [20] P. Jochem, S. Babrowski, and W. Fichtner, "Assessing CO2 emissions of electric vehicles in Germany in 2030," *Transp. Res. Part A Policy Pract.*, vol. 78, no. 2015, pp. 68–83, 2015, doi: [10.1016/j.tra.2015.05.007](https://doi.org/10.1016/j.tra.2015.05.007).
- [21] Department for Business Energy and Industrial Strategy, "Fuel mix disclosure data tables," 2019.
- [22] S. E. Letendre and W. Kempton, "The V2G concept: a new for model power? Connecting utility infrastructure and automobiles," *Public Util. Fortn.*, 2002.

Analysis of Shrubby-Arboreal Species as a Barrier to Wind for Comfort in Open Spaces

HELENA CRISTINA PADOVANI ZANLORENZI¹ LEONARDO MARQUES MONTEIRO

¹Faculdade de Arquitetura e Urbanismo da Universidade de São Paulo – FAUUSP, São Paulo, Brazil

²Faculdade de Arquitetura e Urbanismo da Universidade de São Paulo – FAUUSP, São Paulo, Brazil

ABSTRACT: Urban microclimatic studies are important bases for optimizing thermal comfort conditions in open spaces. This study is part of the author's doctoral research, by collecting empirical data on wind velocity attenuation by shrub-arboreal species, located on the campus of the Institute for Technological Research (IPT) at the São Paulo University (USP) in São Paulo city, SP, Brazil. The 16 studied samples were chosen by the variety of available species, as well as the different densities of the crown composition. This research refers to isolated elements (in the case of trees) or small alignments (in shrub elements). The attenuation index obtained was divided into 4 classification ranges for future comparison to the Leaf Area Index (LAI) looking for the correlation: 33 to 39%, 40 to 45%, 46 to 49% and 50 to 54%, with 4 sampling species in each range. Results indicate that the chosen species are representative for the continuity of wind barrier studies and the possibility of obtaining the desired correlation. New measurements will be carried out concomitantly to the measurement of the LAI's species, as well as tests on wind tunnel to improve and validate the obtained results.

KEYWORDS: Outdoor comfort, thermal comfort, wind barriers, vegetable barriers, green infrastructure

1. INTRODUCTION

Outdoor spaces that provide a pleasant thermal comfort experience for pedestrians effectively improve the quality of urban life. [4] reviewed the research of the last decade on outdoor thermal comfort and the use of outdoor spaces in the context of urban planning. [6-16-23-24] studied air flow through urban environments as one of the most important factors affecting human health and thermal comfort.

Knowing and quantifying urban microclimatic variables is an object of interest to obtain optimized thermal comfort conditions in open spaces. Locating objects with appropriate characteristics to act as barriers to winds is an efficient practice; it is known that the landscape can be modified to be adapted to human comfort, specially in urban spaces where it is required. Vegetation has a significant effect on wind flows, affecting speed and direction. [25] made an important global compilation of the studies already carried out about plant barriers, seeking relationships between the barrier's shelter capacity and its porosity, with the similar approach given by [9-17]. [15-19] performed several experiments with wind tunnel barriers, relating different heights and shapes. [1-14-18] also varied densities and the distance of tree barriers to analyze the resultant effects. Windbreaks can reduce wind speeds up to 30 times their height (H), according to [8]. These experiments serve as an important basis for current studies and is detailed in the bibliographic review of the author's master's thesis [27].

The performance of barriers is also related to other factors such as porosity and its position in relation to the incident winds. The larger and denser the vegetation, the greater the barrier effect [2], and density is an important feature in the effectiveness of the hole shelterbelt [13]. An average porosity is more efficient [1-18]: around 35% according to [5-21-26] or 27% in experiments with the *Grevillea robusta* made by [22].

The present study is part of the author's doctoral research, by collecting empirical data on wind velocity attenuation by shrub-arboreal species to provide subsidies for studies of plants as wind barriers. The results will be related to the Leaf Area Index (LAI) of the species for applicability in other species. LAI is the ratio of half of the total needle surface area per unit ground area, a primary parameter used in ecophysiological and biogeochemical models to describe plant canopies [3-7].

2. MATERIALS AND METHODS

2.1 Study area

The shrubby-arboreal species studied are located on the campus of the Institute for Technological Research (IPT), at the São Paulo University (USP) in São Paulo city, SP, Brazil (Fig. 1). This site was chosen for containing representative plant species, within the viable options for local measurements.

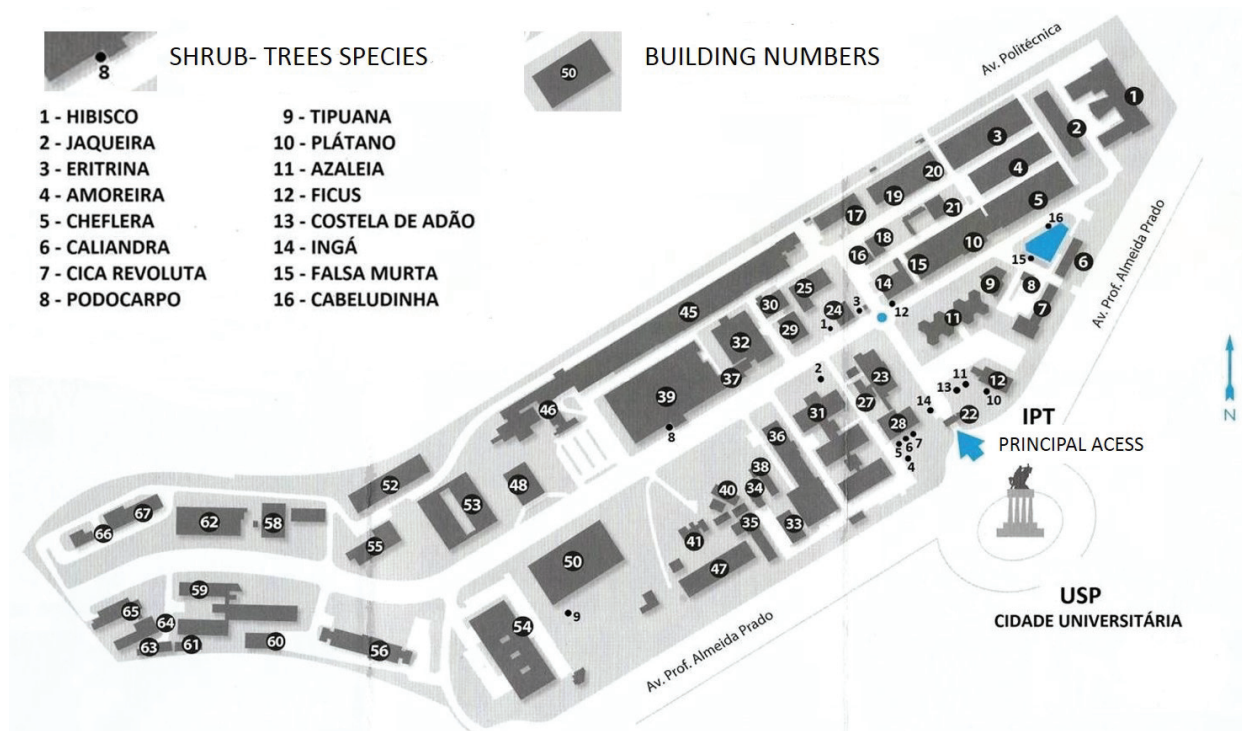


Figure 1: Location of the 16 studied species

2.2 Species selection criteria

Among the 42 pre-selected plant samples with the possibility of functioning as plant barriers, 16 species were chosen for effective measurements, by the variety of available species, as well as the different densities of the crown composition. It was also part of the criterion to be shrub-tree elements with a crown at the height of pedestrians, in order to be characterized as a barrier to winds for thermal comfort.

Among the options of the same species, the one with the best location and best composition at pedestrian height was chosen, making measurements feasible.

This research refers to isolated elements (in the case of trees) or small alignments (in shrub elements).

Although trees as a barrier to winds for thermal comfort are more important in the winter period, studies were carried out on the species available on campus in the summer period, when they are most vigorous; the reason is that the main objective of this research stage was to divide the species into ranges of different LAI values, seeking a correlation with the wind barrier effect. Subsequent measurements on species in the winter period will be adequate.

2.3 Field data collection

In this empirical study, measurements were made on shrub-trees species by assessing the wind speed attenuation index; as basic variables, air temperature (°C) and relative humidity (%) were also measured.

All measurements were made specially from 8:30 am to 4:30 pm, 1 day per species, between January 15

and February 12, 2019. All the microclimatic variables were recorded every 5 minutes.

The data collectors were located before and after each plant barrier for simultaneous measurements, using a Campbell Scientific Station (Fig. 2a) composed by datalogger (CR800) and solar collector for battery power. The station was connected to 2 sets of equal data collectors, one for each side of the plant barrier; each set (Fig. 2b) contained 1 thermohygrometer (HMP45C) properly protected from direct solar radiation (ventilated protection) and 1 sonic anemometer (Windsonic) to survey the intensity and direction of winds, marking the true north and collecting the wind direction every 45°.

All the scientific station is weather resistant, ensuring the data collection schedule.

The data obtained from air temperature and relative humidity will be analyzed as complementary data for possible correlations.

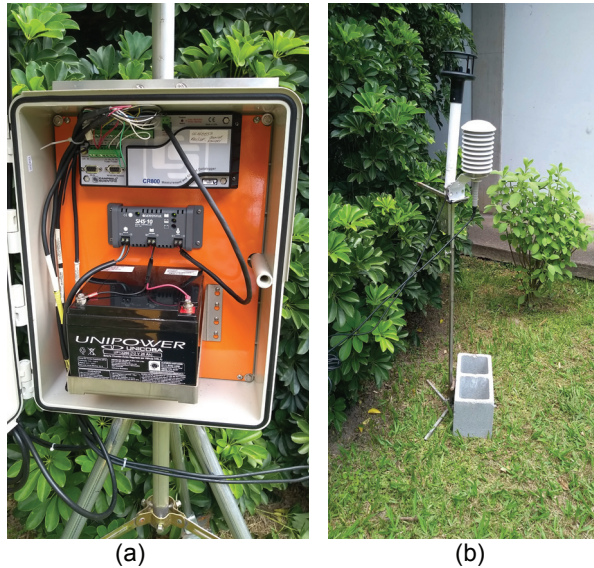


Figure 2: (a) Campbell Scientific Station datalogger; (b) 1 set data collector (thermohygrometer + sonic anemometer)

The data collectors were placed in tripods at a height of 1.50 m, near the plant barrier, at two opposite points (Fig. 3).



Figure 3: Location of station datalogger and data collectors

3. RESULTS AND DISCUSSION

The 16 measured shrubby-arboreal elements are listed in Table 1 with the respective wind attenuation results, with popular and scientific names.

Results presented in column (A) are those obtained throughout the measurement period in all wind incidence directions; in column (B), the results are restricted to the range of 8:30 am to 16:30 pm period, also in all wind incidence directions.

The column (C) shows the results restricted to the range of 8:30 am to 16:30 pm period, but only considering the normal wind incidence direction.

Table 1: Plant species and wind attenuation results. In (A) considering the total measurements in all wind incidence directions; in (B) the results in the 8:30am~4:30pm period, in all wind incidence directions, and in (C) the results in the 8:30am~4:30pm period, only considering the normal wind incidence direction.

POPULAR NAME & MEASUREMENT POINT	SCIENTIFIC NAME	FAMILY	% ATTENUATION			CLA SSIF.
			A	B	C	
1 HIBISCO	<i>Malvaviscus arboreus</i> Cav. [12]	MALVACEAE	44	45	58	8
2 JAQUEIRA	<i>Artocarpus heterophyllus</i> Lam. [28]	MORACEAE	40	40	51	5
3 ERITRINA	<i>Erythrina speciosa</i> var. <i>rosea</i> N.F.Mattos [28]	FABACEAE	48	48	55	11
4 AMOREIRA	<i>Morus nigra</i> L. [28]	MORACEAE	44	44	54	7
5 CHEFLERA	<i>Schefflera arboricola</i> [29]	ARALIACEAE	39	39	47	4
6 CALIANDRA	<i>Calliandra brevipes</i> Benth. [12]	FABACEAE - MIMOSOIDEAE	50	50	56	12
7 CICA	<i>Cycas revoluta</i> Thunb. [12]	CYCADACEAE	53	55	58	15
8 PODOCARPO	<i>Podocarpus macrophyllus</i> (Thunb.) Sweet [12]	PODOCARPACEAE	49	50	63	13
9 TIPUANA	<i>Tipuana tipu</i> (Benth.) Kuntze [28]	FABACEAE	46	46	57	9
10 PLÁTANO	<i>Platanus hispanica</i> Ten. [28]	PLATANACEAE	35	33	46	1
11 AZALEIA	<i>Rhododendron simsii</i> Planch. [12]	ERICACEAE	35	35	46	2
12 FIGUEIRA	<i>Ficus benjamina</i> L. [20-28]	MORACEAE	46	46	60	10
13 COSTELA DE ADÃO	<i>Monstera deliciosa</i> Liebm. [12]	ARACEAE	40	40	53	6
14 INGÁ	<i>Inga marginata</i> Willd. [10]	FABACEAE	39	38	46	3
15 FALSA MURTA	<i>Murraya paniculata</i> (L.) Jack [30]	RUTACEAE	54	54	61	16
16 CABELUDINHA	<i>Myrciaria glazioviana</i> (Kiaersk.) G.M. Barroso ex Sobral [11]	MYRTACEAE	50	51	60	14

The results obtained in column (B) were adopted as a pattern by considering similar conditions to those obtained in the relevant bibliography, measuring free incidence of winds and not just the normal incidence.

Results listed in column (C) will be used for specific purposes in the research in progress, and has been quoted to indicate how it affects the resulting global data.

All the results obtained were divided into 4 classification ranges for future comparison with the LAI to be measured looking for the correlation. Considering all of the obtained data (A), the classification ranges are: 35 to 39%, 40 to 44%, 45 to 49% and 50 to 54%, with 4 sampling species in each range. If we only consider measurements restricted to the 8:30 am to 4:30 pm schedule (B, adopted), the ranges are adjusted to: 33 to 39%, 40 to 45%, 46 to 49% and 50 to 54%.

Measurement of winds before and after the plant elements portrayed the attenuation of the winds by the barriers. In this case, the most relevant is not the intensity of the wind itself, but how much were attenuated by the barrier. Therefore, in case of wind direction inversion, the values were also inverted in

such a way that it is always considered the relation from the highest to the lowest intensity of incident winds. The same criteria was practiced in the measurements of the author's master [27].

The graphic below (Fig. 4) shows the attenuation percentages listed in (A), (B) and (C) conditions, in the 16 measures vegetable species.

All the species are located as 1 to 16 in the graphic according to the attenuation results, indicated in the last column of Table 1.

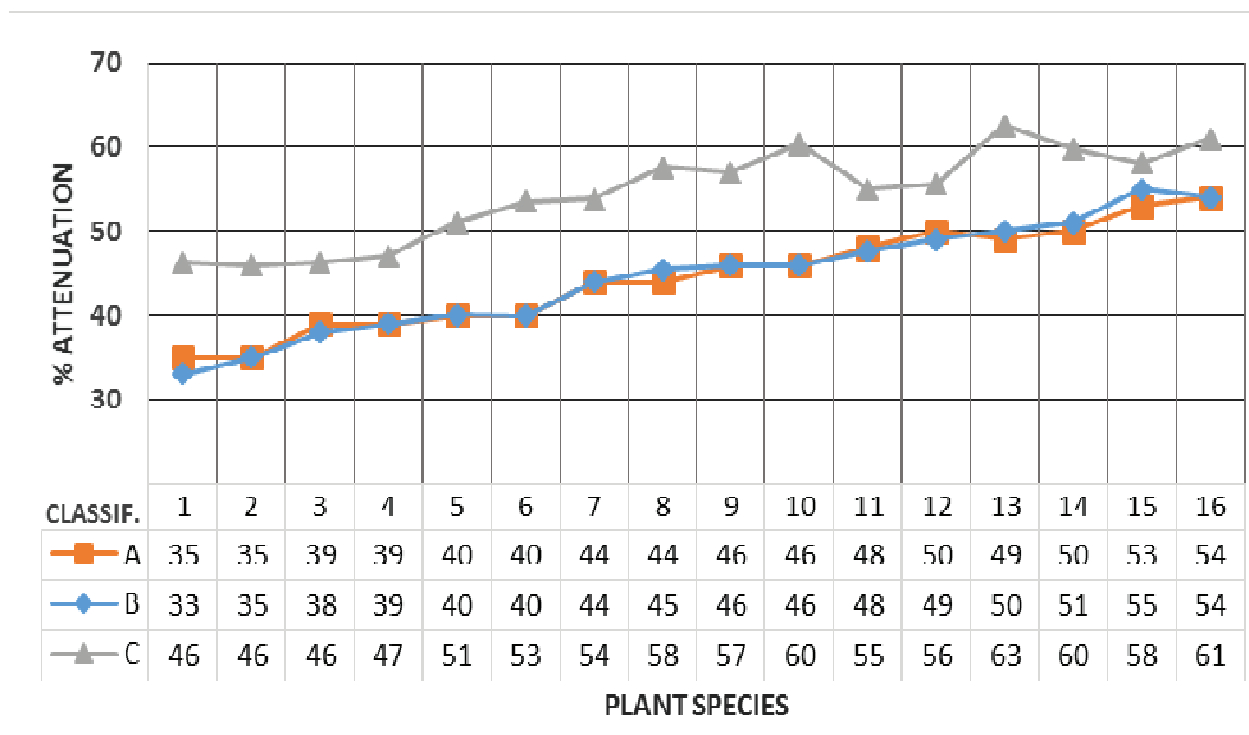


Figure 4: The attenuation percentages obtained in (A), (B) and (C) conditions, in the 16 measures vegetable species.

In the (C) situation, the wind attenuation results even 14% higher than in the (B) considerations; this result is expected, since only the incidence of winds that effectively cross the vegetation is considered.

4. CONCLUSION

The results indicate that the chosen species are representative for the continuity of wind barrier studies and the possibility of obtaining the desired correlation.

Additional measurements are planned to increase and validate the data obtained so far, and will be carried out concomitantly to the measurement of the LAI's species, as well as tests on wind tunnel to improve and validate the obtained results.

ACKNOWLEDGEMENTS

The authors thank the Faculty of Architecture and Urbanism of the University of São Paulo (FAUUSP) for the support and loan of measuring equipment. The authors are also grateful for the important support of the Institute for Technological Research (IPT) in allowing measurements on its campus, making this research feasible.

REFERENCES

- 1 Bonan, G., (2002). *Ecological climatology: concepts and applications*. Cambridge: Cambridge University Press, 690 p.
2. Brown, R.D. and Gillespie, T.J., (1995). *Microclimatic landscape design: creating thermal comfort and energy efficiency*. New York: John Wile. 193 p.

3. Chen, J. M., Rich, P. M., Gower, T. S., Norman, J. M. and Plummer, S., (1997). Leaf area index of boreal forests: Theory, techniques and measurements. *Journal of Geophysical Research* 102, 429–443.
4. Chen, L.; Ng, E., (2012). Outdoor thermal comfort and outdoor activities: a review of research in the past decade. *Cities*, Hong Kong, v. 29, p. 118-125.
5. Errell, E., Pearlmutter, D. and Williamson, T., (2011). *Urban microclimate: designing the spaces between buildings*. London: MPG Books. 266 p.
6. Gao, Y.; Yao, R.; Li, B.; Turkbeyler, E.; Luo, Q.; Short, A., (2012). Field studies on the effect of built forms on urban wind environments. *Renewable Energy*, Cambridge, v. 46, p. 148-154.
7. Jensen, R.R., Hardin, P.J., Bekker, M., Farnes, D.S., Lulla, V. and Hardin, A., (2009). Modeling urban leaf area index with AISA+ hyperspectral data. *Applied Geography* 29, 320–332.
8. Kuhns, M., (2008). Planting trees for energy conservation: the right tree in the right place. *Utah State of University* [Online], Available: <https://forestry.usu.edu/trees-cities-towns/tree-selection/plant-trees-energy-conservation/> [28 Mai 2020].
9. Lee, J.-P., Lee, E.-J., Lee, S.-J., (2014). Shelter effect of a fir tree with different porosities. *Journal of Mechanical Science and Technology* 28 (2), 565-572.
10. Lorenzi, H. (a), (2009). *Árvores brasileiras: manual de identificação e cultivo de plantas arbóreas nativas do Brasil*, vol.2, 3 ed. Nova Odessa, SP: Instituto Plantarum.
11. Lorenzi, H. (b), (2009). *Árvores brasileiras: manual de identificação e cultivo de plantas arbóreas nativas do Brasil*, vol.3, 1 ed. Nova Odessa, SP: Instituto Plantarum.
12. Lorenzi, H., (2013). *Plantas para jardim no Brasil: herbáceas, arbustivas e trepadeiras*. Nova Odessa, SP: Instituto Plantarum.
13. Ma, R., Wang, J., Qu, J. and Liu, H., (2010). Effectiveness of shelterbelt with a non-uniform density distribution. *Journal of Wind Engineering and Industrial Aerodynamics* 98, 767-771.
14. Martins, G.B., Costa, A.B. da, Jabardo, P.J.S. and Nader, G., (2018). Medição em túneis de vento da velocidade do ar próxima à parede para estudos de conforto de pedestres. *Revista IPT | Tecnologia e Inovação* v.2, n.1.
15. McClure, S., Kim, J.J., Lee, S.J. and Zhang, W., (2017). Shelter effects of porous multi-scale fractal fences. *Journal of Wind Engineering and Industrial Aerodynamics* 163, 6-14.
16. Nikolopoulou, M., (2004). Designing open spaces in the urban environment: a bioclimatic approach; RUROS: Rediscovering the Urban Realm and Open Spaces. Greece: *Centre for Energy Resources*, Department of Buildings. 53 p.
17. Nord, M., (1991). Shelter effects of vegetation belts – Results of field measurements. *Boundary-Layer Meteorology* 54, 363-385.
18. Oke, T. R., (1987). *Boundary layer climates*. 2ed. Routledge and John Wiley & Son; London, New York. 435 p.
19. Olgyay, V., (1963). *Design with climate – bioclimatic approach to architectural regionalism*. New Jersey: Princeton University Press. 190 p.
20. Pradella, D.Z.A., Silva, J.W.F., Nisi [et al.], (2015). *Arborização urbana*. São Paulo: SMA/CEA. 200 p.
21. Santiago, J.L., Martín, F., Cuerva, A., Bezdeneznykh, N., Sanz-Andrés, A., (2007). Experimental and numerical study of wind flow behind windbreaks. *Atmospheric Environment*, Madrid 41, 6406-6420.
22. Simões, J.W. and Durigan, G., (1987). Quebra-ventos de *Grevillea robusta* A. CUNN: efeitos sobre a velocidade do vento, umidade do solo e produção do café. *IPEF*, Piracicaba 36, 27-34.
23. Szűcs, A., (2013). Wind comfort in a public urban space: case study within Dublin Docklands. *Frontiers of Architectural Research*, Dublin, v. 2, p. 50-66.
24. Wu, H.; Kriksic, F., (2012). Designing for pedestrian comfort in response to local climate. *Journal of Wind Engineering and Industrial Aerodynamics*, Guelph, v. 104/106, p. 397-407.
25. Wu, T., Zhang, P., Zhang, L., Wang, J., Yu, M., Zhou, X. and Wang, G.G., (2018). Relationships between shelter effects and optical porosity: A meta-analysis for tree windbreaks. *Agricultural and Forest Meteorology* 259, 75–81.
26. Wu, X., Zou, X., Zhang, C., Wang, R., Zhao, J. and Zhang, J., (2013). The effect of wind barriers on airflow in a wind tunnel. *Journal of Arid Environments*, Beijing 97, 73-83.
27. Zanlorenzi, H.C.P., (2015). *Áreas verdes e conforto térmico: o papel da vegetação no controle dos ventos*. 129 p. Dissertação (Mestrado em Ciências) – Escola Superior de Agricultura Luiz de Queiroz, Universidade de São Paulo ESALQ / USP, Piracicaba.
28. [Online], Available: <http://www.ipni.org/ipni/> [2 Mar 2019].
29. [Online], Available: <http://meueternoceu.blogspot.com/2016/06/483-cheflera.html/> [2 Mar 2019].
30. [Online], Available: http://servicos.jbrj.gov.br/flora/search/Muraya_paniculata/ [2 Mar 2019].

Energy sharing between sustainable residential and conventional commercial buildings cluster

Case study for energy hub design

KULJEET SINGH¹, CAROLINE HACHEM-VERMETTE¹

¹Solar Energy and Community Design Lab, School of Architecture, Planning and Landscape (SAPL), University of Calgary, 2500 University Drive NW, Calgary, Alberta, CANADA T2N 1N4

ABSTRACT: In this work, the energy sharing potentials between various conventional commercial (no building integrated photovoltaic, BIPV) and two high performance (BIPV installed + non-electrical space heating and hot water equipment) multi-storey residential (MSR) buildings are determined in a mixed-use cluster. The space heating and domestic hot water requirements of MSR buildings is assumed to be met using natural gas (or other clean energy resource), whereas, for conventional commercial buildings (i.e., office, retail and supermarket) all the energy needs are satisfied using electricity. The MSR buildings is equipped with BIPV panels, for which roof area is used. After meeting the electricity needs of MSR, the excessive generation could be used to serve some commercial floor area. The commercial to MSR floor area fraction served using excess electricity can vary due to loads, seasons, months and other weather conditions. Accounting for all these conditions, this study analyses the variable average fraction of floor area of given commercial building to MSR buildings, that can be electrified from the excessive electricity by MSR-BIPV. The results indicate that maximum energy sharing is possible in July for all the commercial and residential mixtures, whereas least sharing is possible in December. In all the commercial and residential combinations, the maximum energy sharing is possible in MSR-retail combination followed by MSR-office and MSR-supermarket mixtures. The maximum dependent supermarket to MSR floor area fraction representing the area of commercial building that can be served using excess BIPV generation, is only 22% of maximum dependent retail to MSR area fraction during summer season.

KEYWORDS: Energy sharing, mixed-use cluster, energy hub, solar energy,

1. INTRODUCTION

As part of the worldwide efforts of transitioning towards sustainable low environmental impact environment, net-zero energy building concept (NZEB) is evolving rapidly. A NZEB building can be categorized either as newly developed building or an upgrade to a conventional building [1]. Upgrade may include high performance envelope and PV generation systems on roof and facades. NZEBs equipped with building-integrated photovoltaic (BIPV) might have excessive electricity generation during the daytime, at different hours depending on the PV system orientation. As such, the potential for energy sharing with neighbouring buildings arises [2].

Energy sharing can play a key role in sustainable neighbourhood developments. Energy hub is a concept that enables the energy sharing within the cluster of buildings depending upon demands and generations [3]. Energy hubs can be applied to variety of applications from commercial and residential buildings to agricultural applications. Rasregar and Firuzabad [4] studied a home managing the energy flows from various sources such as combined heat and power (CHP), PV panels and electrical storage. Hanafizadeh *et al.* [5] proposed the design of energy

hub for commercial buildings leading to the sizing of combined cooling, heating and power systems. Bozchalui *et al.* [6] proposed a hierarchical control approach for greenhouse within energy hub using energy optimization methodology. Similar studies on energy hubs covering various perspectives such as decision making for residential energy hubs within smart grid network [7], multi-objective optimization [8], and expansion strategies [9] were also reported in literature. Collectively it is recognized that due to the difference in energy demand profiles, energy sharing potential can be significant between residential and commercial buildings.

Under the purview of sustainable building design and energy sharing among buildings, it is beneficial to study the energy sharing potential between upgraded (BIPV installed with non-electrical space heating and hot water equipment) and conventional buildings (no BIPV and all electrical equipment). Consequently, this work presents a case study where two high performance multi-storey residential (MSR) buildings equipped with BIPV is considered. These buildings are assumed to be in existing bunch of commercial buildings such as offices, retails and supermarkets. Based upon the demand and generation profiles of

MSR buildings, during the hours of excessive electricity generation from BIPV, the equivalent commercial area (i.e., offices, retails and supermarkets) that can be electrified is estimated after evaluating commercial load profile. This analysis is conducted on the hourly basis for various months of the year.

2. METHODOLOGY

As illustrated earlier, this work estimates the energy sharing potential among high performance MSR buildings and various types of conventional commercial buildings using energy hub. This section explains the case study location, building cluster, simulation and estimation of energy sharing potential method.

2.1 Case study location

The case study is conducted for Calgary, Canada (51°N and 114°W). The climate for this location is cold for most of the year. The lowest temperature of the considered location is around -31°C, whereas, the highest temperature reaches around 36°C [10]. The potential of solar energy generation in Calgary is significant (peak solar intensity about 1200 W/m² [11]) as compared to other sites in Canada.

2.2 Definition of cluster

In mixed-use cluster, two high performance MSR buildings and variety of commercial buildings are included. The commercial buildings are defined by three types of uses such as office, retail and supermarket catering diverse energy requirements. The details of both types of buildings are discussed below.

2.2.1 Multistorey residential building

Two MSR buildings consist of total 64 apartments (32 apartments per building). Each apartment has floor area of 110 m², consequently the total floor area for two MSR buildings is estimated as 7040 m². Each building has four floors, and each floor has 8 apartment units. The equatorial facing façade width to perpendicular width ratio is kept around 1.3 for each apartment unit [12]. Further, the MSR buildings assumes high performance envelope. High performance energy efficient building design seeking net-zero energy level is adopted in this study [12]. The space heating and domestic hot water (DHW) demands for both residential buildings are served using natural gas or other clean energy resource. [13]. The MSR buildings are also equipped with BIPV to generate electricity. For this purpose, total roof area is used for the installation of PV panels. The tilt angle of the PV panels is taken as 45° (optimum as per location) and their efficiency is assumed to be around 18% [14]. Further, it is assumed that no self-shading is

caused by the PV panels. The cooling demands of both MSR buildings are fulfilled using electricity.

2.2.2 Commercial buildings

Three types of commercial buildings such as offices, retails and supermarket are analysed in this work. Each type of commercial building is assumed to be dependent upon grid electricity for all energy needs (such as cooling, space heating, DHW, equipment/appliances, etc.). However, high performance building envelopes are also considered for all types of commercial buildings to improve energy efficiency. The occupancy and other loads for the commercial buildings are considered as per ASHRAE standards [15].

2.3 Simulation

In order to study the energy performance of MSR and commercial buildings EnergyPlus [16] is used, whereas, SketchUp with Legacy OpenStudio plugins [17] are implemented as modelling tool. The hourly energy demand and PV electricity generation profiles for the whole year are obtained for MSR buildings. Thereafter, the hourly yearlong energy intensity profiles (energy consumption per unit area) are determined for each type of commercial building using the EnergyPlus simulations. After estimating hourly MSR energy consumption and energy generation profiles along with energy intensity profiles for office, retail and supermarket, the estimation of energy sharing potential is made for various MSR and commercial building mixtures.

2.4 Energy sharing potential estimation

After obtaining the energy consumption and generation profiles for residential and commercial buildings, the energy sharing potential (dependent area that can be relied on MSR-BIPV) is estimated using in-house Matlab program. The program uses the average monthly energy profiles for both types of buildings (coded as subroutines). Series of objective function for each hour (as given in Eq. 1) estimating the commercial area that can be served using supplementary electrical production by BIPV of MSR buildings are minimized using fminunc Matlab toolbox [18].

$$\min: f = [P_{BIPV} - P_{MSR} - P_c(A_c)] \leq 10^{-6} \quad (1)$$

where, P_{BIPV} and P_{MSR} are BIPV power generation and consumption by MSR buildings, respectively. While, P_c is electricity consumption by a particular type of commercial building (offices, retails, or supermarket), which is function of commercial area A_c (in m²). The Eq. 1 is minimized using variable A_c , intending to yield near zero value of f (10^{-6}). For instance, if no excess electricity is available from MSR

buildings, no commercial area can be served by MSR-BIPV. As a result, the function f in Eq. 1 is minimized by commercial area, $A_c = 0$, which eventually means that no commercial area electricity demand can be served using MSR-BIPV electricity production. In other words, A_c represents the amount of commercial area that can be dependent upon on MSR-BIPV for its electricity needs. Whenever there is excess generation of electricity than what MSR buildings consume, the dependent commercial area of given type can be served by excess generation.

3. RESULT AND DISCUSSION

As discussed earlier, the energy sharing potential is measured in this work in terms of dependent

(after fulfilling their own energy needs) in different seasons are presented. In winter months (Fig. 1a), the maximum average dependent office to MSR floor area fraction varies from 0.64 to 1.15 (or 64-115% of MSR floor area). It is least in December followed by January due to high energy required for heating load. In January and February, the peak dependency is at 1:00 pm, whereas in December maximum dependent floor area fraction can be yielded at 2:00 pm. Referring Fig. 1b, the maximum dependent office floor for electricity is above 1.28 times of MSR floor area, with maximum sharing potential in April (floor area fraction = 1.43). For March, the energy sharing enables at 9:00 am till 5:00 pm, whereas, for April and May the energy sharing is possible from 8:00 am

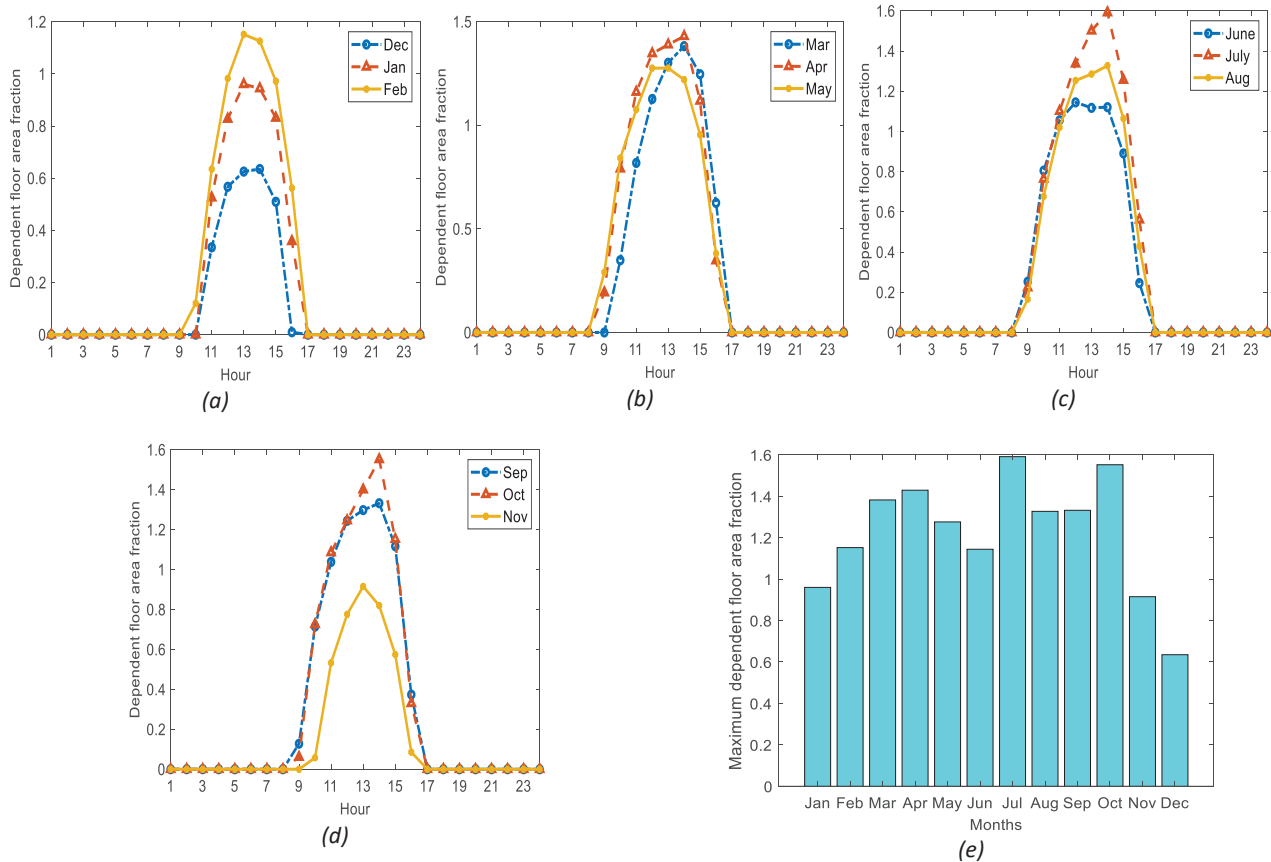


Fig. 1 Dependent office floor area on high performance multistorey residential building in various seasons (a) winter, (b) spring, (c) summer, and (d) fall

commercial area that can be served using excessive generation by MSR-BIPV. Accordingly, its fraction with respect to MSR buildings' total floor area is estimated. The average hourly variation in dependent commercial to residential area fractions are studied for various months in different seasons.

In Fig. 1, the dependent average conventional office to MSR floor area fractions served by MSR-BIPV

to 5:00 pm. After 5:00 pm, the load of MSR increases beyond on-site generation by BIPV. As shown in Fig. 1c, for summer months, the energy sharing potential peaks in July by dependent office floor area as 1.6 times of MSR floor area, due to significant electricity generation by BIPV. During June and August, the maximum peak of office dependent areas found as 1.14 and 1.33, respectively. In June, the peak

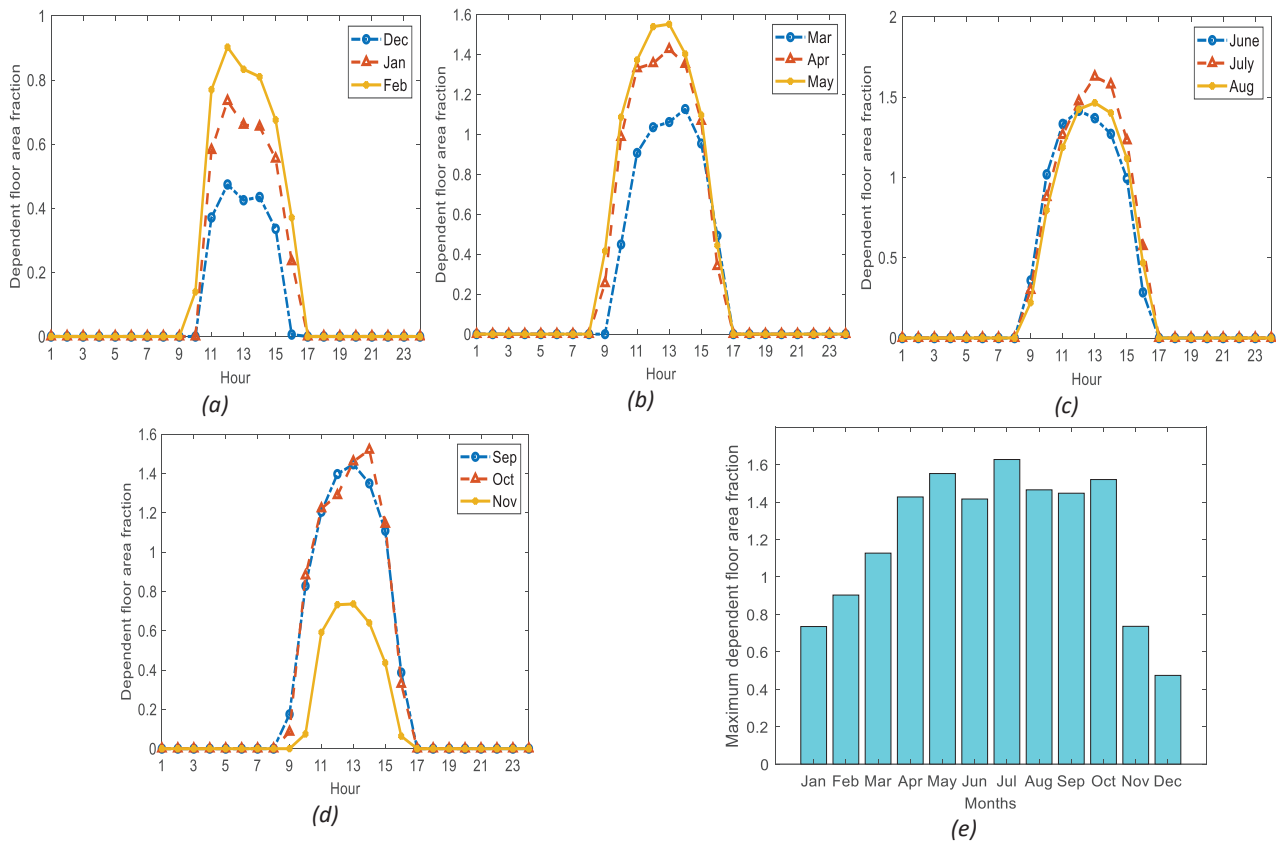


Fig. 2 Dependent retail floor area on high performance multistorey residential building is various seasons (a) winter, (b) spring, (c) summer, and (d) fall

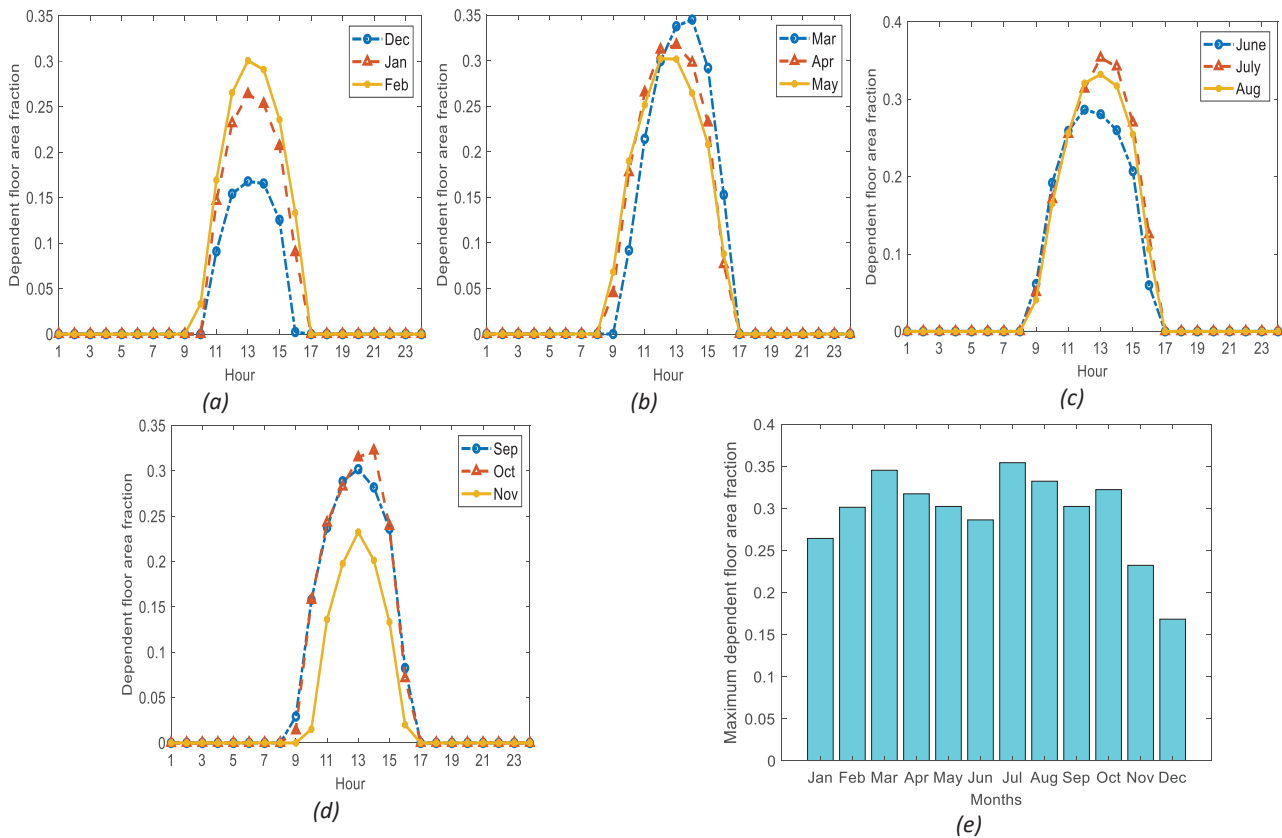


Fig. 3 Dependent supermarket floor area on high performance multistorey residential building is various seasons (a) winter, (b) spring, (c) summer, and (d) fall

dependent area ratio is less due to less comparative generation by BIPV, while, in August tendency of rain

excess electricity during 9am-5pm. Fig. 2e presents the variation of maximum dependent retail to MSR

Table 1 Summary of peak dependent commercial to MSR floor fractions for various seasons

Combination Season	MSR-Office fraction				MSR-Retail fraction				MSR-Supermarket fraction			
	Least	Month	Max	Month	Least	Month	Max	Month	Least	Month	Max	Month
Winter	0.64	Dec	1.15	Feb	0.47	Dec	0.90	Feb	0.17	Dec	0.30	Feb
Spring	1.28	May	1.43	Apr	1.13	Mar	1.55	May	0.30	May	0.35	Mar
Summer	1.14	Jun	1.59	Jul	1.42	Jun	1.63	Jul	0.29	Jun	0.35	Jul
Fall	0.92	Nov	1.55	Oct	0.74	Nov	1.52	Oct	0.23	Nov	0.32	Oct

reduces the production of electricity. Referring Fig. 1d, the dependent office floor area ratio trend for September is similar to August. However, due to reduction in electricity used for cooling, the dependent office floor area fraction reaches 1.55 times of MSR floor area. In Fig. 1e, the maximum (or peak) possible dependent office to MSR floor area fractions for various months are presented. Maximum potential is in July, while minimum is in December.

In Fig. 2, the dependent retail floor area fraction that can be served by excessive electricity generation of MSR-BIPV is presented for various seasons. In Fig. 2a, it can be seen that in winter the peak dependent retail area fraction reaches 0.47, 0.73, and 0.90 in December, January and February, respectively, around 12:00 pm. For December, January, and February, the availabilities of excessive power from MSR-BIPV are respectively for 10am-4pm, 10am-5pm, and 9am-5pm. As compared to February, in March the maximum dependent retail area fraction increases from 0.90 to 1.13 of MSR floor area (refer Fig. 2b). Nevertheless, in the consecutive months such as April and May, the maximum dependent retail area fraction increases to 1.43 and 1.55, respectively, with the availability of electricity from 8am to 5 pm. During summer months (shown in Fig. 2c), due to less comparative generation in June (compared to July and August), the maximum retail dependent area fraction is 1.42 of MSR floor area, with peak at 12 pm. For July and August, the peak dependent retail area fractions of 1.63 and 1.46, respectively, served by excessive generation of MSR-BIPV are observed around 1 pm. In September also the value of peak retail served area by excess power of BIPV is around 1.45 of MSR floor area with the peak at 1 as revealed in Fig. 2d. In October, due to significant reduction in cooling load of MSR buildings, the dependent floor area of retail increases to 1.52 during 2 pm. The duration of availability of excessive electricity from BIPV is from 8 am to 5 pm during September and October. However, in November, due to less generation by MSR-BIPV along with increased heat load of retail, the dependent maximum retail area fraction reduces to 0.74, with the availability of

floor area fraction along various months. The peak dependent retail floor area can be served by excess BIPV generation is achievable in July, whereas least dependency is present in December.

In Fig. 3, the hourly average dependent supermarket to MSR floor area fractions served by MSR-BIPV are presented. Due to high energy intensity of supermarket, less floor area can be served using excessive electrical generation by MSR-BIPV, as compared to office and retail buildings. As shown in Fig. 3a, in winter, the maximum dependent floor area fraction varies between 0.17 and 0.3, with least in December and maximum in February. Interestingly, during spring months (in Fig. 3b), irrespective to previous cases of office and retail, the maximum dependent supermarket area fraction served by MSR-BIPV is observed in March (0.35 times of MSR floor area). Further, it decreases to 0.32 and 0.30 in April and May, respectively. This is due to excessive cooling demand of supermarket building as compared to office and retail. Similarly, as shown in Fig. 3c, the maximum dependent supermarket to MSR floor area fractions varies from 0.29 to 0.35, with the availability of excessive electricity from MSR-BIPV from 8 am to 5 pm. However, as revealed in Fig. 3d, the peak varies between 0.23 to 0.32, with the least in November and maximum in October. Fig. 3e indicates maximum dependent supermarket floor area fraction for various months.

Table 1 summarizes the results for various seasons, indicating least possible and maximum possible dependent commercial to MSR floor area fractions. In conclusion, the maximum energy sharing between office and MSR buildings is possible in summer during the month of July, whereas, least during December in winter season. Similarly, results are indicated for other seasons in Table 1.

4. CONCLUSION

This paper presents the potential for energy sharing in two high performance multi-storey residential (MSR) buildings (installed with BIPV and non-electrical space heating + DHW) with various conventional commercial buildings. The MSR buildings are assumed to be installed with BIPV on

roof along with space heating and DHW served by natural gas. After fulfilling its own electricity requirement, MSR building could supply excess electricity to neighbouring commercial buildings (i.e., office, retail and supermarket). Accordingly, dependent commercial to MSR floor area fractions are estimated that can be served using excessive electricity generation. Below are the key conclusions of the work:

- For the combination of MSR and office buildings, the least and maximum possible dependent office area fractions are 0.64 and 1.59 during December and July, respectively. Maximum least dependent office area fraction is 1.28 during spring season.
- In case of MSR-retail combination, the maximum sharing is possible in July and least in December, when the retail area fractions are 1.63 and 0.47, respectively. The maximum sharing is enabled in the summer season where the peak dependent retail to MSR floor area fractions vary between 1.42 to 1.63.
- Significant reduction in energy sharing potentials is observed for MSR-Supermarket combination as compared to the other two combinations, where the dependent supermarket to MSR area proportion varies from 0.17 to 0.35. In March as well as in July, a maximum energy sharing is possible with the same value of area fraction (0.35).
- Overall maximum energy sharing is possible between MSR and retail buildings during the month of July, when the maximum retail floor area of 1.63 times the MSR can be served using excess electrical generation by MSR-BIPV. However, least energy sharing opportunities are observed in MSR-Supermarket combination.

This work is useful to determine the possible synergy between modern BIPV-equipped residential and conventional commercial (no BIPV installed), enabling energy sharing in retrofiting projects. Ultimately, the basis of energy hub design for mixed-use cluster can be driven using the proposed methodology. Future scope of this work includes the study of energy sharing potential from other carrier such as heat along with synergy between multiple types of commercial and residential buildings.

ACKNOWLEDGEMENTS

This work acknowledges the funding received from Natural Sciences and Engineering Research Council (NSERC), Canada, under Discovery Grant Program.

REFERENCES

1. Asaee SR, Nikoofard S, Ugursal VI, Beausoleil-Morrison I (2017) Techno-economic assessment of photovoltaic (PV) and building integrated

photovoltaic/thermal (BIPV/T) system retrofits in the Canadian housing stock. *Energy Build* 152:667–679.

2. Mohammadi M, Noorollahi Y, Mohammadi-ivatloo B, et al (2018) Optimal management of energy hubs and smart energy hubs – A review. *Renew Sustain Energy Rev* 89:33–50.

3. Mohammadi M, Noorollahi Y, Mohammadi-ivatloo B, Yousefi H (2017) Energy hub: From a model to a concept – A review. *Renew Sustain Energy Rev* 80:1512–1527.

4. Rastegar M, Fotuhi-Firuzabad M (2015) Load management in a residential energy hub with renewable distributed energy resources. *Energy Build* 107:234–242.

5. Hanafizadeh P, Eshraghi J, Ahmadi P, Sattari A (2016) Evaluation and sizing of a CCHP system for a commercial and office buildings. *J Build Eng* 5:67–78.

6. Bozchalui MC, Cañizares CA, Bhattacharya K (2015) Optimal energy management of greenhouses in smart grids. *IEEE Trans Smart Grid* 6:827–835.

7. Hadjsaid N, Sabonnadière JC (2013) Optimal operation of residential energy hubs in smart grids. *Smart Grids* 3:1755–1766.

8. La Scala M, Vaccaro A, Zobaa AF (2014) A goal programming methodology for multiobjective optimization of distributed energy hubs operation. *Appl Therm Eng* 71:658–666.

9. Zhang X, Shahidehpour M, Alabdulwahab A, Abusorrah A (2015) Optimal expansion planning of energy hub with multiple energy infrastructures. *IEEE Trans Smart Grid* 6:1–10.

10. calgary.weatherstats.ca (2019) Temperature - Monthly data for Calgary. <https://calgary.weatherstats.ca/charts/temperature-monthly.html>. Accessed 1 Aug 2019

11. Hachem-vermette C, Singh K (2019) Mixed-use neighborhoods layout patterns: Impact on solar access and resilience. *Sustain Cities Soc* 51:101771.

12. Hachem C (2016) Impact of neighborhood design on energy performance and GHG emissions. *Appl Energy* 177:422–434.

13. Hachem-Vermette C (2018) Multistory building envelope: Creative design and enhanced performance. *Sol Energy* 159:710–721.

14. Hachem C, Fazio P, Athienitis A (2013) Solar optimized residential neighborhoods: Evaluation and design methodology. *Sol Energy* 95:42–64.

15. Hachem C, Cubi E, Bergerson J (2016) Energy performance of a solar mixed-use community. *Sustain Cities Soc* 27:145–151.

16. National Renewable Energy Laboratory (NREL) (2016) EnergyPlus. <https://energyplus.net/>. Accessed 28 Nov 2018

17. Chopra A, Town L, Pichereau C (2012) Introduction to Google SketchUp. Wiley, Hoboken

18. MathWorks (2016) Unconstrained minimization (fminunc). <http://in.mathworks.com/help/optim/ug/fminunc-unconstrained-minimization.html>. Accessed 18 Apr 2016

Characterization and mitigation through Urban Climatic Map:

Investigations on the urban climate of Curitiba - Brazil.

LISANA KATIA SCHMITZ¹, FRANCINE AIDIE ROSSI², LUTZ KATZSCHNER³,
ALESSANDRA MEL⁴ AND GABRIELA ALMEIDA⁵

¹Federal University of Paraná, Curitiba, Brazil

²Federal University of Paraná, Curitiba, Brazil

³Institut for Climate and Energy Concepts, Kassel, Germany

⁴Federal University of Paraná, Curitiba, Brazil

⁵Architect and Urbanist, Curitiba, Brazil

ABSTRACT: The increase of temperature in the urban areas due the urbanization process has been object of several researches. The enlargement of the built area, the verticalization and the suppression of the green areas negatively influence the local climate and reduce the thermal comfort. Curitiba is a city of Southern America and it is known by its urban planning and plans, although, the city still does not possess a strategic plan for adaptation and mitigation of the effects of the climatic changes. This study aims to investigate mitigation strategies to maximize the thermal comfort in the urban space. The methodology used was the Urban Climatic Map (UCMap). The data were processed in Geographic Information System (GIS) generating raster data sets with resolution of 30 x 30 m. For the analysis was considering three situations: the 2019 occupation and two mitigation scenarios considering the intensification of the urban forestation. The results show that the vegetation leads to an improvement of comfort in the areas with larger thermal load. In addition, the comparison between the 2019 map and the two scenarios shows a decrease of 5.65% of the areas with larger discomfort for heat in the scenario 1 and 6.53% in the scenario 2.

KEYWORDS: UCMap, Mitigation Strategies, Urban Climate, Urban Planning, Envi-Met

1. INTRODUCTION

The city of Curitiba is in South of Brazil and it is the coldest capital of the country. The city is in the south of the Tropic of Capricorn, in an altitude of 934 m above the sea level and its climate is classified as Cfb (Köppen-Geiger). The city is famous for its urban planning and plans. The city growth is guided by the tripod use of the soil, road system and public transportation. This leads to structural axes, from the centre to the periphery, with high occupancy density [1]. The occupation of Curitiba city is regulated by a zoning law, through the creation of axes, zones and special sectors of use and occupation of the soil and differentiated densities.

Data of Brazilian institute of Geography and Statistics (IBGE) demonstrate that Curitiba's population grew in 10%, between the years of 2010 and 2019, passing of the 1.751.907 inhabitants for 1.933.105 [2], promoting the expansion of the urbanization with the consequent extinction of the rural areas and enlargement of the urban area to 100% of the surface's city. Such urban growth alters the urban climate and elevate the medium temperatures. The comparison of the temperatures of Temperature Reference Year 1969 [4] with the 1999 [5],

demonstrating the increase of 0.9°C in the medium temperatures of summer and 1.3°C in the winter.

It is perceptible the increment in the maximum medium temperature in all seasons, the reinforcement of the variability and frequency of the extreme events. To illustrated that, in last 12 September (wintertime) the maximum temperature achieved 32.8°C (typical of summer). The maximum average temperature observed in September in the period 1981-2010 was 21.4°C [5].

Considering the high degree of occupation of the city area and the estimated population growth in 2.151.040 inhabitants to the year of 2050 [6], the public administration foresees an elevation in the population density and verticalization. Which will enlarge the built volume in the central areas and will suppress green areas, influencing the local climate and the thermal comfort. In the face of this scenario, using the methodology of the Urban Climatic Map, the present study intends to characterize the urban climate of Curitiba and to investigate mitigation strategies to maximize the thermal comfort in the urban space.

2. CLIMATIC CHANGES AND MITIGATION

The larger cities contribute to the global warming and its population face the impacts of the changes of the climate. The metropolises consume 75% of all energy produced in the world and emit 70% of CO₂ [7]. Thus, in October of 2005 was formed the C40, Group of Leadership of the Big Cities for the Climate, that gathers the 40 larger metropolises of the planet and Curitiba is part of this group [8].

Although the engagement of Curitiba, the engagement of Curitiba, the city still does not possess a strategic plan for adaptation and mitigation of the effects of the climatic changes.

2.1 Changes in the temperature and precipitation

According to AR4, the projection for changes in average temperatures for the South area of South America, indicated an increase for the winter (June to August) from 0.6°C to 1.1°C for 2020, from 1°C to 2.9°C for 2050 and from 1.8°C to 4.5°C for 2080. For the summer (December to February) the projected increase is from 0.8°C to 1.2°C for 2020, from 1.0°C to 3.0°C for 2050 and, from 1.8°C to 4.5°C for 2080. [8]

Concerning the regime of rains, the regional climatic projections show much higher degree of uncertainty, showing variations that are going from the reduction to the increment of the pluviosity index. For 2020 winter (June to August), the index diverges between -5% and 3%, for 2050, between -12% and 10% and, for 2080, between -12% and 12%. For 2020 summer (December to February), the variation is going from -3% to 5%, in the same period of 2050, it oscillates between -5% and 10% and for 2080, from -10% to 10%. [8].

2.2 Mitigation strategies to improve the thermal environment

Thinking the urban expansion through an adaptative urban design is important, so that urban expansion does not affect the thermal environment in a wide scale. Although there is no one solution, it is necessary geographically appropriate strategies to approach the problem [9] and the seasonal effects of vegetation must be considered [10].

The four major strategies [11] to mitigate the thermal environment are changing the urban geometry, using cool surface, incorporating bodies of water, and planting vegetation. These strategies improve the thermal environment by modifying the radiative and convective heat exchange within urban spaces, by reducing the absorption of short-wave radiation, by decreasing the air temperature due the evaporative effect and by blocking the solar radiation, reducing the wind speed, and lowering the air temperature, respectively.

Mills et al. [12] stated that where the urban geometry is consolidated the scope for changes is constrained and therefore, efforts have focused on

changing the properties of the urban surface to modify its radiative and evaporative properties. Vegetation is an alternative because can provide shade, evaporative cooling, manage noise and air pollution, etc.

Lobaccaro and Acero [13] presented several studies demonstrate how green actions have a crucial role in the process of sustainable passive cooling of urban planning as well as in saving energy and progressing human thermal comfort. The vegetation collaborates to preventing flooding [14].

Recent studies shown that the composition and configuration of the trees can affect the land surface temperature, both in daytime and night-time [15]; the correct choice of vegetation type can potentialized the cooling effect [16], also improving the thermal comfort [17].

Researches using numeric simulation software show the importance of the urban green areas to mitigate the UHI, regarding thermal performance in outdoor spaces and reduce energy consumption [18]; relation between vegetation ratio and street ratio (H/W) [19]; surface vegetation and green roof [20] [21]; and coverage ratio by trees, grass, green roofs and thermal sensation in a high-rise environment [22].

3. METHODOLOGY

The Urban Climatic Map - UCMaP system consists of a series of basic input layers (analytical maps of climatic and meteorological elements, geographic terrain data, greenery information, and planning parameters) and two main UCMaP components: the UC-AnMap, which visualizes and spatializes various climatic evaluation and assessment by different Climatopes and the UC-ReMap, which includes planning instructions from the urban climatic point of view [23].

From the mid-1980s, countries in Europe, such as Switzerland, Austria, Sweden, Hungary, Czechoslovakia, Poland, Portugal, and the United Kingdom have carried out UCMaP studies. After 1990s has also been adopted and developed in South America. More than 15 countries have conducted their own UCMaP studies and recently, UCMaP has attracted increasing interest in the world. [23].

3.1 The study area

In this study two scales of research were included. In the local scale, the entire city (434,892 km²) was analysed through the UCMaP. And, in the microclimatic scale, three blocks of the Neighbourhood Batel (fig.1) was investigated to evaluate the thermal comfort. The blocks are conformed by wide avenues (object of intensification of the forestation) and urban canyons and the software Envi-met was used for the microclimatic simulation.

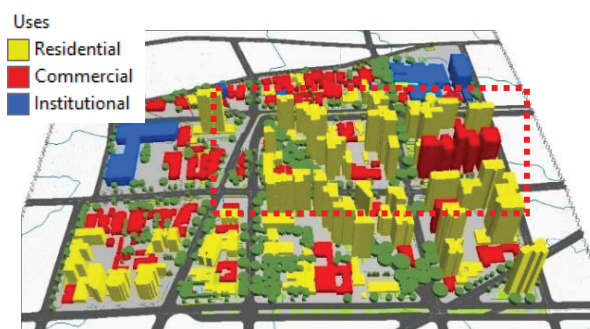


Figure 1: Area of neighborhood Batel. Curitiba.

3.2 The data and process

To producing an Urban Climatic Map representing the current city, cartographic data from 2019 were used, available by the Institute of Research and Urban Planning of Curitiba (IPPUC), relative to the occupation and use of the soil, road system, blocks, altimetry, green areas and hydrography.

The climatic data (air temperature, air humidity, wind, and precipitation) were obtained from the Meteorological System of Paraná (SIMEPAR) and National Institute of Meteorology (INMET). The characterization of occupation of the blocks, built areas, uses and heights of buildings were obtained from orthophotos supplied by IPPUC, updated and complemented with support of Google Earth or Street View, and, the green areas were obtained by the extraction of the Foliar Area Index of Image Landsat 8.

The processing was made in Geographic Information System (GIS), software ArcGIS, version 10.8, generating raster data sets with resolution of 30 x 30 m. The layers with negative effects have positive values, and positive effects have negative values. The UC-AnMap was generated through direct raster sum.

The layers used in the formulation of the Thermal Load Map were the building bulk, anthropogenic gains, altitude and elevation, and bioclimatic effects related to urban green space, as well their classes, and the corresponding weights were presented in figure 2.

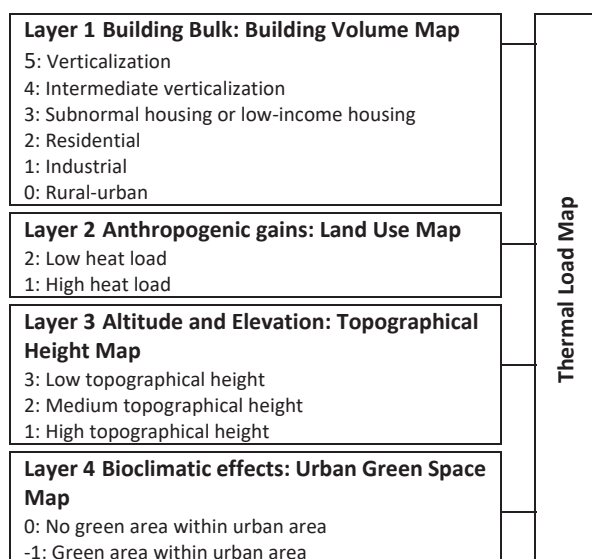


Figure 2: Layers of Thermal Load Map

The Layer1 - Building Volume Map – was one of larger acquisition difficulty, because in Curitiba there are 241 occupation zones with variations of uses, constructive potential, population density etc. Then, it was made the aggregation in six different classes: Rural-urban, Industrial, Residential, Subnormal housing or low-income housing, Intermediate verticalization and Verticalization. Also considered the uses of the buildings, population density, permeability of the soil and constructive potential.

The layers used in the formulation of the Dynamical Potentials map, such as urban permeability, bioclimatic effects related to cool air movement, downhill air movement, and reduced ventilation, as well their classes and the corresponding weights were presented in figure 3.

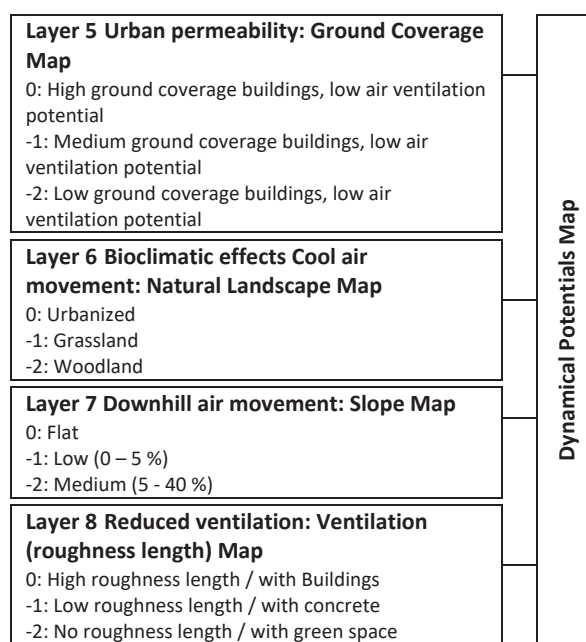


Figure 3: Layers of Dynamical Potentials Map

To generate the mitigation scenarios through the intensification of the urban streets forestation two new scenarios were generated for the Layer 6 - map of natural landscapes, being added forestation of great load in the main roads, of larger width and wider sidewalks, and forestation of medium load for the other streets. The two scenarios were converted for the same used format, raster, and was added to the IAF. Then, two mitigation scenarios for the Layer 6 were created, and the UCMap, using these scenarios, was processed again:

- Scenario 1: the increase of the street's forestation, with 18 m of cup diameter, 15 m of height and attenuation coefficient above 80% (summer), considering trees typologies used in the Curitiba's forestation, such as *Tipuana tipu* and *Caesalpinia peltophoroides*.
- Scenario 2: mitigation scenario 1 plus the increase forestation of all other streets with medium trees,

with 8 m of cup diameter, 10 m of height, besides attenuation coefficient above 80% (summer), including typologies used in the Curitiba's forestation, such as *Granular Tibouchina*, *Tebebuia crysotricha*, *Tebebuia impetiginosa*.

Intending to generate three different UCMaP scenarios, the model it was run three times, remaining the Thermal Load Map 2019 and changing the Layer 6 of the Dynamic Potentials Map, being generated three different dynamical potential maps (fig.4): to the year 2019, scenario 1, scenario 2.

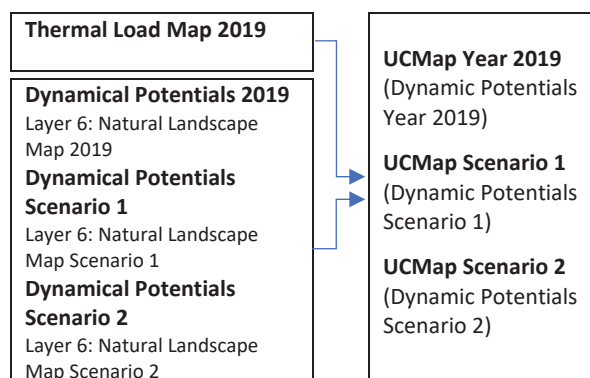


Figure 4: Procedures to generate the scenarios of UCMaP

The Envi-met software, version 4.4.5, was used to simulate the effects of the mitigation strategies in the microclimate, because in the raster, the simulated effect is restricted to the streets cells that contains the forestation, although the vegetation has influence on the neighbourhood scale.

4. RESULTS AND DISCUSSION

The areas of smaller thermal load, better ventilation potential and comfort, are concentrated on the peripheries, close to the borders of the city (west and south), where are the sources of water supply and where the use of the soil inhibits the occupation (fig.5). The data demonstrate that the vegetation lead to an improvement of comfort, enlarging the percentage of area in the classes of smaller thermal load and larger thermal comfort, classes 2, 3, 4, and especially in the class 2.

A simple visual comparison of images in figure 5, shows a reproduction of the same patterns of use. The change occurs locally or in the microscale, in the public open spaces, wide roads and avenues. The scenarios of mitigation 1 (fig.5B) and 2 (fig.5C) promote the enlargement of area of the classes with smaller thermal load and larger thermal comfort (classes 1 to 4), and the reduction in the percentage of area of the classes 5 to 8 (highest thermal load) is observed.

When comparing the 2019 map with the scenarios 1 and 2 (tab. 1) we can verify the increase of classes 2 and 3 and a decrease in the classes 4, 5, and, mostly, in class 6.

Table 1: Percentage of area from each class x scenarios.

CLASSES	2019	SCENARIO 1	SCENARIO 2
CLASS 1	0.08%	0.60%	0.77%
CLASS 2	4.37%	5.64%	6.65%
CLASS 3	18.75%	19.65%	19.58%
CLASS 4	30.51%	30.43%	29.72%
CLASS 5	30.59%	29.92%	29.74%
CLASS 6	14.02%	12.45%	12.24%
CLASS 7	1.44%	1.11%	1.10%
CLASS 8	0.24%	0.20%	0.20%

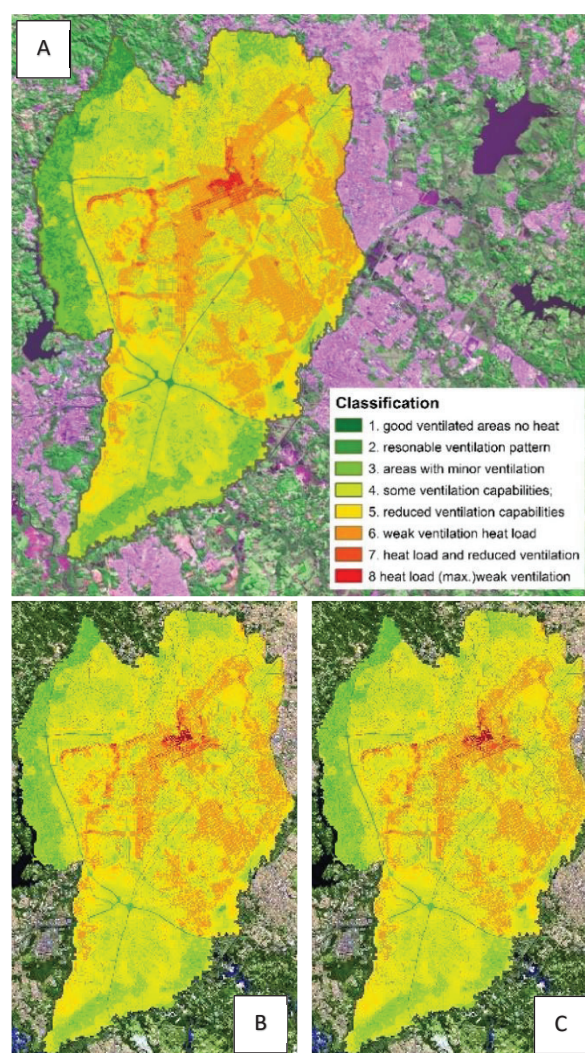


Figure 5: UC-AnMap resulting scenarios to 2019 (A) Mitigation Scenario 1 (B) and Mitigation Scenario 2 (C).

The figure 6 presents the distribution of the classes 1 to 4 (classes of larger comfort) and 5 to 8 (classes of larger discomfort for heat) in the downtown area, the place more built and waterproofed of the city. In the public open spaces of the downtown area it is evident the reduction of the discomfort spaces (highlighted in red) in the scenario 2 (fig. 6B) when compared to the year 2019 (fig. 6A).

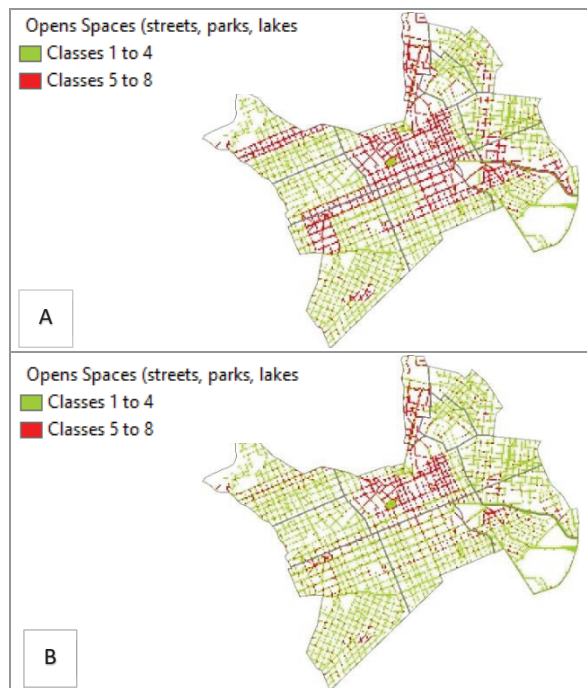


Figure 6: Effects on the open public spaces year 2019 (A) e Scenario 2 (B).

In the table 2 are presented the percentage of the classes of larger comfort (1 to 4) and discomfort (5 to 8) for the whole city and for the public open spaces (streets, pedestrians areas, squares, etc).

Table 2: Percentage of area classes 1 to 4 and 5 to 8.

Scenario	ENTIRE CITY		OPEN SPACES	
	Classes 1-4 [%]	Classes 5-8 [%]	Classes 1-4 [%]	Classes 5-8 [%]
Year 2019	53.70	46.30	88.56	11.44
Scenario 1	56.32	43.68	91.89	8.11
Scenario 2	56.72	43.28	92.54	7.46

The percentage of discomfort areas (classes 5 to 8) in the entire city it is superior to the verified in the public open spaces, over 43% against less than 12%, and it is also verified that the largest reduction in the percentage of discomfort it happens in the scenario 1, with 3.33%, however, when compared the scenarios 1 and 2 the reduction it is smaller than 0.65%.

The model developed with Envi-met was updated from version 3.1 to 4.4.5 and were considered the variation (min x max) of air temperature, relative humidity from air, and wind speed from February 2011 [27] and 2019, besides of Roughness Length (tab.3):

Table 3: Input data simulation Envi-met.

Model	Ta [°C]	RH [%]	WS [m/s]	Roughness Length [Z ₀]
Year 2011	18.7 - 28.6	54 - 90	0.4-4.2	0.96
Year 2019	18.3 - 26.8	63 - 96	1.0-2.6	1.2

Both studies, Schmitz [26] from 2011 (fig.8A) and the present (fig.8B), consider the same species for the forestation and same attenuation factor, increasing

three times the land cover area of urban street forestation (tab.4).

Table 4: Land cover areas from simulations 2011 and 2019.

Land cover	2011		2019	
	Area (m ²)	[%]	Area	[%]
Buildings	11,223.4	23.08	11,223.4	23.08
Urban forestry	7,128.58	14.66	20,952.6	43.09
Ground vegetation	4,327.98	8.90	4,327.98	8.90
Impermeable areas	15,598.9	32.08	5,888.91	12.11
Streets	10,345.2	21.28	6,231.25	12.82
Simulated area	48,624.2	100.0	48,624.2	100.0

The spatial resolution of both models (fig.8) was: 126 x 62 x 26 (x,y,z) units of 2.5m x 2.5m x 3.0m (dx,dy,dz).

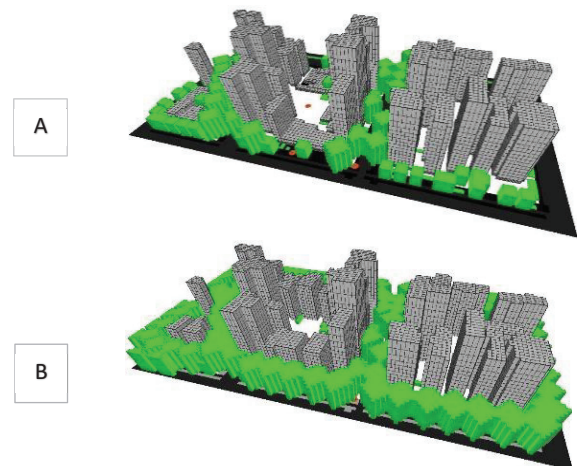


Figure 8: Model of Envi-met (A) scenario 2011 (B) Scenario 2019 - intensification of the urban street's forestation.

The results demonstrate significant decrease in the medium and maximum values of Air Temperature (Ta): 1.9°C and 2.2°C, respectively. The Wind Speed (Ws), as expected, is reduced between 12 and 28%; while the relative humidity (RH) increases about 5%, also expected face the forestation (tab.5).

Table 5: Comparison of air temperature (Ta), Wind Speed (Ws) and relative humidity (RH) – 2011 x 2019.

	Ta [°C]	Ta [°C]	Ws [m/s]	Ws [m/s]	RH [%]	RH [%]
	2011	2019	2011]	2019	2011	2019
Min.	20.8	20.8	0.7	0.5	74.2	74.1
Med.	25.0	23.1	0.7	0.6	77.6	81.1
Max.	27.0	24.8	0.8	0.7	86.2	90.8

The Universal Thermal Comfort Index (UTCI). presented significant improvement in all the values. The minimum value decrease in 2 °C from equivalent temperature, while the maximum value is reduced of 8.6 °C. moving of the strong to moderate stress caused by the heat, being only 2.5 °C above the state of thermal comfort. The main reason for such significant reduction is the shadowing promoted by the forestation that makes to fall down the mean radiant temperature (tab.6).

Table 6: Comparison of Mean Radiant Temperature (MRT) and Universal Thermal Comfort Index (UTCI) – 2011 x 2019.

	MRT [°C] 2011	MRT [°C] 2019	UTCI [°C] 2011	UTCI [°C] 2019
Min.	17.4	13.3	22.9	20.9
Med.	43.1	24.3	31.5	25.2
Max.	61.0	34.5	37.5	28.9

The improvement in the index of thermal comfort, by the intensification of the urban forestation, means the improvement in each class of UC-AnMap. In this new panorama, the resulting UCMAP would have only five classes (class 1 to 5) and therefore the discomfort for heat would be limited to the moderate stress.

5. CONCLUSION

The present investigation provides two positive results. The first is that the UC-AnMap for Curitiba spatially presents the different degrees of comfort and discomfort in the urban space. The second is that the method allowed to simulate in a simplified way the potential mitigation by the intensification of the urban forestation. The percentage of area that presented increment in the dynamic potential and in the thermal comfort it seems reduced, because it varies from 5.6 to 6.5% of the total area of the city. Despite the affected areas located along the roads have little representativeness front the total area, there was real gain of thermal comfort, especially for the pedestrians.

Finally, through the microclimatic simulation it was possible to understand the effects of the mitigation strategies, demonstrating that the introduction of full forestation in the open public spaces (avenues and streets) can mean an improvement about two to eight degrees of thermal comfort (UTCI index) as much for the public spaces as for their neighbours.

ACKNOWLEDGEMENTS

To CNPq and Fundação Araucária for the research support to the students of the Program of Scientific Initiation.

REFERENCES

1. DANNI-OLIVEIRA. I.M. (2000). Considerações sobre a poluição do ar em Curitiba-PR face a seus aspectos de urbanização. RA'E GA: o espaço geográfico em análise. 4: p. 101-110. UFPR: Curitiba.
2. IBGE (2019). Cidades@. Available: <https://cidades.ibge.gov.br> [18 September 2019]
3. Goulart. S.V.G.; Lamberts. R.; Firmino. S. (1998) Dados climáticos para projeto e avaliação energética de edificações para 14 cidades brasileiras. 2ª ed. Florianópolis: UFSC.
4. Rossi. F. A.; Krüger. E. I.; Dumke. E. (2009) Atualização do ano climático de referência para Curitiba. In: ENCAC. 11. p-199-207.
5. INMET (2019). Normal climatológica do Brasil 1981-2010. <http://www.inmet.gov.br> [18 September 2019].
6. IPPUC (2019). Infocuritiba. Available: Disponível em: <http://infocuritiba.ippuc.org.br>. [18 September 2019].
7. C40 CITIES (2011). Climate Action in Megacities: C40 Cities Baseline and Opportunities. ARUP. version1. June/2011.

8. PBMC (2014). Impactos. vulnerabilidades e adaptação às mudanças climáticas. COPPE. UFRJ. Brasil. Available: <http://www.pbmc.coppe.ufrj.br/> [02 August 2020]
9. Georgescu. M.; Morefield. P.E.; Bierwagen. B.G.; Weaver. C.P. (2014). Urban adaptation can roll back warming of emerging megapolitan regions. Proc. Nat. Acad. Sci.. 111(8): p-2909–2914.
10. Chun. B.; Guldman. J.M. (2018). Impact of greening on the urban heat island: Seasonal variations and mitigation strategies. Comput. Environ. Urban Syst.. 71: p-165–176.
11. Lai. D.; Liu. W.; Gan. T.; Liu. K.; Chen. Q. (2019). A review of mitigating strategies to improve the thermal environment and thermal comfort in urban outdoor spaces. Sci. Total Environ.. 661: p-337–353.
12. Mills. G.; Cleugh. H.; Emmanuel. R.; Endlicher. W.; Erell. E.; McGranahan. G.; Ng. E.; Nickson. A.; Rosenthal. J.; Steemer. K. (2010). Climate information for improved planning and management of mega cities (Needs Perspectives). Procedia Environ. Sci.. 1: p-228-246.
13. Lobaccaro. G. and Acero. J.A. (2015). Comparative analysis of green actions to improve outdoor thermal comfort inside typical urban street canyons. Urban Climate. 14: p-251–267.
14. KATZSCHNER. L. (2007) New developments in applied urban climatology. In: ENCAC. (9). p. 01-10.
15. Chen. J.; Jin. S.; Du. P. (2020). Roles of horizontal and vertical tree canopy structure in mitigating daytime and nighttime urban heat island effects. Int J Appl Earth Obs Geoinformation. 89: 102060.
16. Richards. D.R.; Fung. T.K.; Belcher. R.N.. Edwards. P.J. (2020). Differential air temperature cooling performance of urban vegetation types in the tropics. Urban Forestry & Urban Greening. 50: 126651.
17. Zhang. L.; Zhang. Q.; Lan. Y. (2018). Effects of the tree distribution and species on outdoor environment conditions in a hot summer and cold winter zone: A case study in Wuhan residential quarters. Build. Environ.. 130: p- 27–39.
18. Aboelata. A.; Sodoudi. S. (2019). Evaluating urban vegetation scenarios to mitigate urban heat island and reduce buildings' energy in dense built-up areas in Cairo. Build. Environ.. 166: 106407.
19. Aboelata. A. (2020). Vegetation in different street orientations of aspect ratio (H/W 1:1) to mitigate UHI and reduce buildings' energy in arid climate. Build. Environ.. 172: 106712.
20. Arghavani. S.; Hossein M.; Abbas-Ali A. A. B. (2020). Numerical assessment of the urban green space scenarios on urban heat island and thermal comfort level in Tehran Metropolis. Journal of Cleaner Production. In press
21. Sk Ziaul. Swades Pal (2020). Modeling the effects of green alternative on heat island mitigation of a meso level town. West Bengal. India. Adv. Space Res.. 65: p-1789–1802
22. Kim. H.; Gu. D.; Kim. H. Y. (2018). Effects of Urban Heat Island mitigation in various climate zones in the United States. Sustainable Cities and Society. 41: p-841–852.
23. Ren C.. Ng E.. Yan Y.. Katzschner. L. (2011). Urban climatic map studies: a review. Int. J. Climat.. 31:p-2213–2233.
24. SCHMITZ. L.K. (2014) Reestruturação Urbana e Conforto Térmico em Curitiba/PR: diagnóstico. modelagem e cenários. 307 f. Tese (Doutorado em Geografia). UFPR.
25. INMET (2020). Temperatura média mensal período jan./2019-feb/2010. BDMEP <http://www.inmet.gov.br> [28 February 2020].

Multidisciplinary Local Teams and Technologies for Participatory Processes in Sustainable Territorial Strategies

The Integral Regeneration of an Agrarian Valley in the Galician Diffuse City

DAVID PEREIRA-MARTÍNEZ^{1 2}

¹ University of Porto (UPorto), Center for Studies in Architecture and Urbanism (CEAU), Portugal

² University of A Coruña (UDC), Group of Territorial Studies (GET), Spain

ABSTRACT: Galician territory is an old agrarian complex in which urbanisation is developing as a diffuse city. These peri-urban spaces show great resilience but present difficult governance, i.e. opportunities and challenges for sustainability. In this explicit context, an integral regeneration strategy for a valley was carried out using participatory processes. According to literature, the strategy uses multidisciplinary, transdisciplinarity, and medium levels of participation. The empirical approach has taken into account three main aspects: a multidisciplinary team, local professionals, and new technologies. As territorial studies need to combine several disciplines, the multidisciplinary team is made up of two architects, a biologist, and an archaeologist, all of whom have transdisciplinary profiles. In this specific case, there is a strong sense of ownership and a highly involved civil society, so the team included local professionals in order to reinforce mutual trust. This proximity had risks, but it enabled a closer participatory process through meetings, events, discussions and presentations. Technologies were used to share information and to manage a GIS customised database. These approaches illustrate the positive effects of participation in sustainable territorial strategies, but also the difficulties in their implementation.

KEYWORDS: Multidisciplinary, Small communities, Participation, Sustainable territorial strategies, Galicia

1. INTRODUCTION

This study presents a discussion about the implementation of participatory processes in sustainable territorial strategies, using a case study in Galicia. The introduction characterises this region and justifies the participatory approach. The first part explains the implications of multidisciplinary in participation. The second section studies the advantages and disadvantages of local teams. The third part analyses the potential of technologies to manage participation inputs and outputs. Finally, the conclusions highlight the opportunities and difficulties of participation in territorial strategies.

The approach to a territory and the management of its activities should take into account its specific characteristics and processes. Galicia is a peripheral European region in the North-West of the Iberian Peninsula, which is characterised as an old agrarian complex (Bouhier 1979). This is an atomised and rich habitat with a long history of communities who have developed an interesting and subtle balance their activities and environment. In recent decades, the rural territorial structure was used as basis for an urban development in the form of a *diffuse city*, the primary example being the Rías Baixas (Dalda, Docampo, and

Harguindey 2005). This peri-urban space was studied at a local scale in its territorial forms and processes (Barreiro 2012), and shows great resilience but presents difficult governance, i.e. opportunities and challenges in becoming a sustainable community.

In this context, an environmental intervention was proposed for an agrarian valley in the municipality of Moaña (Fig. 1), which serves as a case study to discuss alternative approaches to the territory.

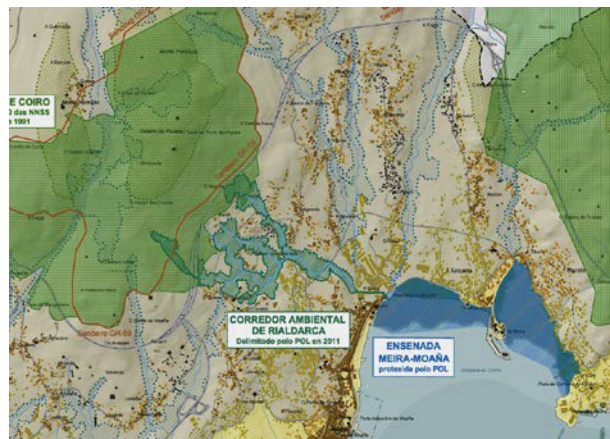


Figure 1: The valley as a green corridor joining the hill forests and the intertidal ecosystem (areas to be protected in POL).

Too often, these territorial interventions are either conventional unilateral projects, inapplicable by governments, or excessively complex master plans, difficult to be understood and supported by residents and land owners (Innes and Booher 2004). Both approaches follow a top-down scheme (Plante, Boisjoly, and Guillemot 2009) based on experts' opinions, and need decades to be implemented. Other interventions, such as urban parks or conservation areas, are normally imposed as a result of general interest, and do not adapt to local conditions and needs, thus having negative consequences on the balance between community and nature. The peripheral touristic areas, such as Moaña and this valley in particular, usually encounter infrastructure and urban development projects. In order to avoid these risks and form a realistic framework for sustainability, an regeneration strategy was developed using participation.

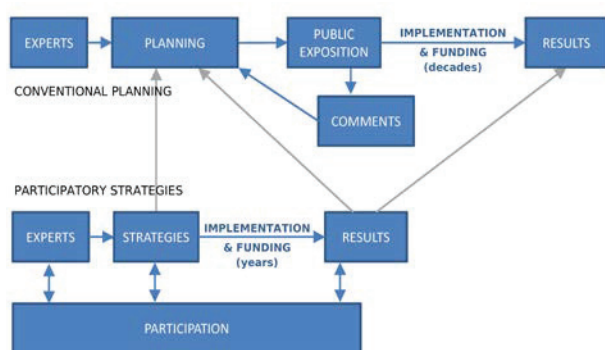


Figure 2: Conventional planning vs. participatory strategies.

Participation has been proposed as an alternative (Fig. 2) to the classic rational planning model (Friedmann 1973). Participatory processes are relevant in sustainable territorial strategies because they allow professionals and agents to share ideas and common objectives (Innes and Booher 2010). Bottom-up propositions can be an efficient and effective complement to top-down policies

(Esparcia, Escribano, and Serrano 2015). Thus, the strategy for the integral regeneration of this valley was conceived as an alternative (compatible) approach, based on local knowledge, participation, and short-term change. This constitutes important differences in planning:

- no imposed expert solution
- no change in land ownership
- no exchange of public and private areas
- actions are concentrated to the next few years

These more rapid actions and tangible change can create a connection with the community and between stakeholders (Plante, Boisjoly, and Guillemot 2009), and produce a better situation to discuss long-term sustainable planning (Fig. 2). Participation needs substantial time and money, and then it is necessary to start with limited actions before implementing major measures (Maier 2001). Thus, in this framework, the stakeholders can discuss actions before planning implementation. Avoiding a radical interventionist expert master plan, the strategy can propose participative win-win soft deals with short-term benefits for both the community and the environment: plantation of local species, new pathways, school activities, wildlife studies, etc.

The strategic document was designed as a basis to develop and promote internal and external funding. It compiles participation inputs and analyses natural and social systems (including constraints and possibilities) in order to make a diagnosis. From this, several measures and indicators are proposed for the sustainable development of the area, which also have to be re-discussed before implementation. These complex peri-urban contexts (Fig. 3) need sensible approaches for real sustainability. As a consequence, the empirical participatory strategy has especially taken into consideration three main aspects: a multidisciplinary team, local professionals, and technologies.

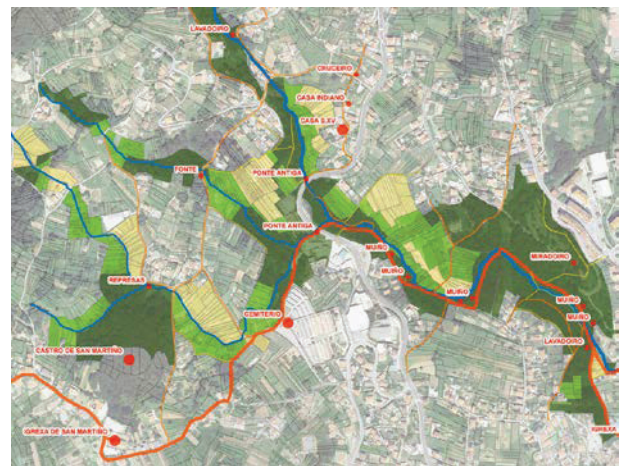


Figure 3: Environmental and social systems in the valley.

2. MULTIDISCIPLINARY TEAMS AND PARTICIPATION

After the conventional top-down understanding based on expert opinion, other collaborative approaches emerged. In this case, the integral strategy for the regeneration of this valley in Moaña uses the notions of multidisciplinary and transdisciplinarity (Lucca 2017), since the four members of the team are professionals of different disciplines and each of them have expertise in various fields needed in this holistic strategy: urbanism, forestry management, strategic planning, heritage, history, natural ecosystems, and invasive species.

Territorial studies need to combine several disciplines (Lucca 2009) to study environmental and social systems (Fig. 3), e.g. biology, cultural and heritage studies, urbanism, architecture, territorial planning, and agriculture management. Thus, the multidisciplinary team is made up of two architects, a biologist, and an archaeologist. The several specialties of each member of the team – forest management, technologies for sustainability, educational divulgation in natural sciences, and visitor management – assures transdisciplinarity. These different sensitivities represent and naturalise the tension between ecology and land use within the team itself, and encourage consensus during the participatory process.

This participatory strategy can take advantage of multidisciplinary and transdisciplinarity, but it also needs to adjust the degree of participation according to local conditions. Some initiatives have been undertaken before in this municipality, but they were an exception and there was a lack of participative culture amongst both the decision makers and the civil society. This situation is also common in other contexts within rural frameworks (Esparcia, Escribano and Serrano 2015).



Figure 4: Neighbourhood leaders in a participatory meeting.

Thus, this strategy could only implement certain processes to include the community (Fig. 4), which are classified as medium levels of participation according to literature (Maier 2001, Díaz 2008): advisory positions

and partnerships, information, consultation, discussion, co-decision, and strategic alliances. These processes are insufficient when developing a shared sustainable model in the community, but, at least they promote a culture of participation, which is necessary to achieve more advanced levels in the future. Thus, participation fosters a bottom-up approach and the empowerment of local society (Esparcia 2015).

Nevertheless, participation faced many difficulties and dilemmas. Participatory processes are especially difficult to implement in contexts without this tradition:

Currently citizens have a say but their involvement seldom exceeds mere opposition towards active involvement. Their attempts to be heard in the decision-making process are perceived as a nuisance by developers and some local governments as well. (Maier 2001)

Ordinary citizens usually care more about their immediate future and day-to-day gains rather than any long-term effort or investment with higher risk (Maier 2001). There is ambivalence in the literature about the different ways of implementing participation. In fact, collaborative participation “is an ideal which will never be fully attained” (Innes and Booher 2004).

3. LOCAL PROFESSIONALS IN PARTICIPATION

Participatory processes in smaller communities are different than the “dialogue in big cities and regions” (Maier 2001) due to the intense relationships between stakeholders (Plante, Boisjoly and Guillemot 2009). In participation, trust between professionals and agents is important, and this requires a direct and close contact (Lucca 2017); people feel more comfortable with professionals with whom they already share a link.

In order to build bonds with the community, the team consisted of professionals with experience in social movements, some of whom were even related to this space. This closeness has advantages, such as the understanding of agents’ roles that “makes it possible to apprehend the governance mode” and facilitates “both formal and informal institutional arrangements” (Plante, Boisjoly, and Guillemot 2009).

Moreover, in this case, there is a strong sense of ownership, and a large amount of work was carried out over many years by a highly involved civil society. The traditional mobilisation of the community was “due to necessity” (Poupeau 2012) and against negative intervention in the territory. Several urban developments and infrastructures were presented in this peripheral valley of the metropolitan area, which ironically was formally viewed as a green corridor by the administrations (Fig. 5). As a result, agents expressed a widespread mistrust between one another.

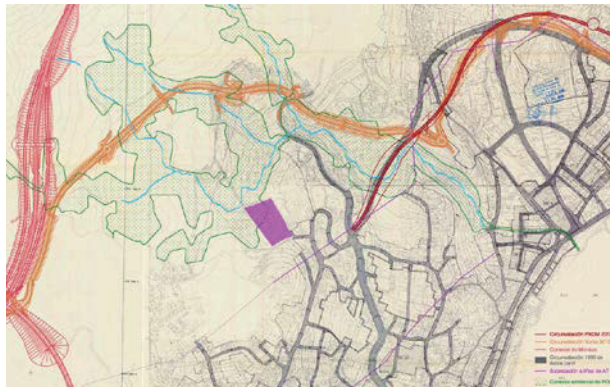


Figure 5: Successive urban plans and infrastructure projects.

During the process, several groups of stakeholders were identified to take into account the largest range of concerns (Plante, Boisjoly, and Guillemot 2009):

- residents (including associations' members)
- local experts and social leaders
- environmental activists and associations
- the owners of the fields and forestry lots
- the local government of the municipality
- other administrations and parties

Scientific literature highlights the importance of farmers (Defrancesco et al. 2008, Corsi et al. 2014), but the image of a farm does not correspond to this territory. Decades ago there were peasants who exploited various separate fields and bred a few animals in stables – the ground floor of their small houses. In Moaña, agriculture was a part-time job complemented with monetary activities; an organisation that has survived here and in other peri-urban contexts to this day (Pérez-Rúa 2018; Corsi et al. 2014). The owners – land tenants and users of the fields – are the protagonists of the landscape's management in this territory, to whom the participatory strategy pays special attention.

Smaller communities with intense relationships between the tenants have positive effects on the adoption of agri-environmental measures (Defrancesco et al. 2008). The involvement of the community is a continuous process and the inclusion of the groups is achieved through a “snow-ball effect” (Maier 2001). In these smaller communities, the difficulty is “to join together the differences around various stakes, without forcing the consensus, or negating problems and conflicts” (Plante, Boisjoly, and Guillemot 2009).

This closeness to the local agents enabled a living participatory process through several meetings where the strategy was discussed. This is relevant in territorial strategies because it enables people to re-discover and to re-evaluate their environment, and, as a consequence, abandoned pathways were recovered. Several tours were organised in the area to explain the proposals, critique them, and ask for the support of

citizens. One of these events brought together almost 1% of the municipality's residents, who could directly talk in situ with the team and local politicians. The whole process was widely covered by local media (Fig. 6), increasing social awareness about the environment.



Figure 6: Coverage of a participatory activity by local media.

As a result, mutual trust was reinforced and many interviews were carried out. Life stories were included in an intangible heritage appendix, and were complemented by an analysis of the toponyms using cadastral information. The density of the names related to water, relief forms, and vegetation, proves an intense relationship between community and territory.



Figure 7: Modern cadastre and density of toponymic data.

Due to participation, it was possible for the study to take into account traditional, local, and scientific knowledge (Plante, Boisjoly, and Guillemot 2009). The great work done by conservationists during the previous decades was increased and complemented in the study. Other important historical information was collected from the community and experts, such as a historical cadastre description (Fig. 8). Material heritage was also analysed, characterising pre-roman, medieval, and vernacular elements. Thus, the strategy could take into account the historical evolution of the valley.



Figure 8: Cadastre description (1754), found by a resident.

The feeling of belonging, and family and friendship relationships promote “actors’ mobilization”; however, “such closeness does not always favour dialogue” (Plante, Boisjoly, and Guillemot 2009). Close relationships between professionals and communities appear both as advantages – sometimes a necessity – and epistemological difficulties (Poupeau 2012). In these cases, involved professionals have to ask themselves about the “conditions of possibility and impossibility” when working in the community (Poupeau 2012). In this strategy, the team’s coordinator was chosen from another municipality, without any relation to the involved agents. In successive phases, coordination is previewed by other university researchers to reinforce neutrality.

4. TECHNOLOGIES IN PARTICIPATORY PLANNING

In participation processes, professionals should act above all as mediators. Their professional skills and training with technologies can be used to balance the traditional lack of information and cartography in peri-urban spaces. In this strategy, GIS was used to develop a customised database with information from national services and input received from civil agents.

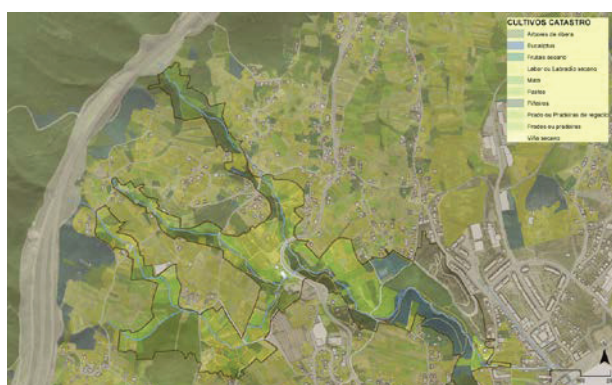


Figure 9: Detailed land uses (crops and forests) in the area.

In this participatory strategy, local knowledge and traditional understanding of the exploitation of the territory was confirmed by advanced systems in GIS (Fig. 9-11). These contacts with the real builders of the territory enriched all of the involved disciplines.

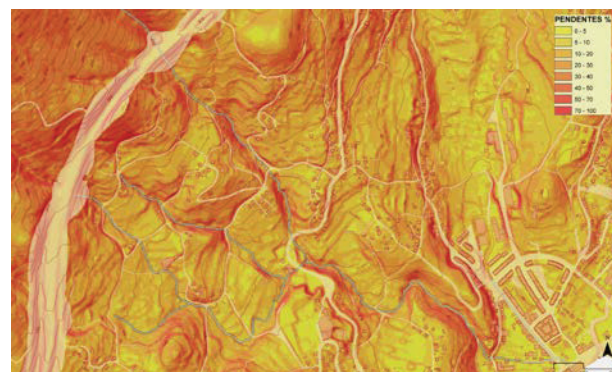


Figure 10: Slope analysis of vegetation and crops studies.



Figure 11: Orientation analysis for the same studies.

The specific psychology of owners’ attitudes and beliefs has to be taken into account when designing and communicating agri-environmental measures (Defrancesco et al. 2008). Thus, the strategy acknowledges current planning and (the very atomised) land ownership, and within this framework, secondary policies and local agreements have been proposed. Within this space, various degrees of protection have been proposed for the areas different uses: river margins, sustainable forests, organic crops. This has enabled the promotion of deals between owners and public administration in order to create a free-access productive park integrated in a green infrastructure (Corsi et al. 2014). The agreements with owners are non-monetary: a long-term release in forest areas, and flexible short-term release for abandoned fields. These ongoing agreements will enable the council to create a sustainable landscape park on private terrains, avoid the fields’ neglect, and promote organic agriculture.

The GIS database made it possible to manage plots, owners, fire buffer zones, and possible legal crops by

informative maps (Fig. 12), which increased transparency during the participatory process.



Figure 12: Lots, owners, and crops are managed by GIS.

This initiative can lend a hand when promoting actions to revive agriculture, and better manage territory in peri-urban areas (Corsi et al. 2014). However, as other studies highlight, “some gaps still remain between rhetoric and practical implementation” (Esparcia, Escribano, and Serrano 2015). There is a lack of technological training in both private and public sectors, thus GIS systems can only be used inside the team and to export maps. The coexistence between new bottom-up approaches and traditional top-down concepts in both civil society and amongst decision makers generates tension and conflicts (Esparcia, Escribano, and Serrano 2015). Participatory processes require more transparency and better communication (Esparcia, Escribano, and Serrano 2015), including this strategy. Finally, this participatory process was carried out with a reduced budget and an enormous effort from the community, the strategic team, and the Council of Moaña. This case is not an exception (Plante, Boisjoly, and Guillemot 2009)

In addition, this participatory process has suffered from restrictions due to the COVID-19 pandemic, which provoked the delay of events and physical activities planned for the strategy in 2020. Public health alerts present an uncertain future for on-site participation.

5. CONCLUSIONS

Participation is a key factor in sustainable territorial strategies for real environmental, social, and heritage restitution. Three aspects were taken into account:

- a multidisciplinary experienced team
- local professionals related to the community
- the use of technologies

These approaches have shown a certain efficacy throughout the first phase and the outlook is promising. However, participation processes, environmental issues, and smaller communities face many difficulties, which the effort of the agents compensated for.

It is still necessary to work on a wider culture of participation in both society and public administration, and this approach has to be promoted and applied in smaller communities.

ACKNOWLEDGEMENTS

This paper is the result of the aforementioned strategy, in which the other authors, Alexandre Farto Fernández, Antonio López Nogueira, and Alexandre Paz Caamaño, did magnificent work. This project was by order of the government of the Municipality of Moaña, who showed a great interest and sensitivity around these issues. The support of the University of A Coruña and its School of Architecture (ETSAC), especially the contribution of its Dean, Plácido Lizancos, in the participation area, are fully acknowledged. The great labour of English editors, Emma Jean Sankey and Amy Lavender, is recognised as essential. The authors of the paper and the strategy thank all the experts, residents, activists, owners, and attendees of meetings and participatory events.

REFERENCES

1. Barreiro, M. (2013). Configurazione della città diffusa in Galicia: Il caso di O Morrazo [...]. Milano, POLIMI.
2. Bouhier, A. (1979). La Galice, essai géographique d'analyse et d'interprétation [...]. La Roche-sur-Yon, Impr. Yonnaise.
3. Corsi, S. et al. (2014). Farmers' Participation in Territorial Planning. In *Advanced Engineering Forum*, 11: p.351-355
4. Dalda, J.L., Docampo, M.G., and Harguindey, J.G. (2005). Cidade difusa en Galicia. Santiago de Compostela, Xunta.
5. Defrancesco, E. et al. (2008). Factors Affecting Farmers' Participation in Agri-environmental Measures. In *Journal of Agricultural Economics*, 59: p.114-131.
6. Díaz, V.J. (2008). Participación ciudadana y vivienda: El programa de autoconstrucción [...]. Las Palmas, ULPGC.
7. Esparcia, J., Escribano, J., Serrano, J. (2015). From development to power relations and territorial governance. In *Journal of Rural Studies*, 42: p.29-42.
8. Friedmann, J. (1973). *Retracking America: a Theory of Transactive Planning*. New York, Anchor Press.
9. Innes, J.E. and Booher, D.E. (2004). Reframing Public Participation. In *Planning Theory&Practice*, v.5 (4): p.419-436.
10. Innes, J.E. and Booher, D.E. (2010). *Planning with Complexity*. London, Routledge.
11. Maier, K. (2001). Citizen Participation in Planning: Climbing a Ladder? In *European Planning Studies*, v.9 (6): p.707-719.
12. Lucca, E. (2017). Estrategias y metodologías de formación de equipos interdisciplinarios. *Hábitat y Sociedad*, 10: p.15-34.
13. Plante, S., Boisjoly, J., Guillemot, J. (2009). Participative governance and integrated coastal management. In *Journal of Coastal Conservation*, 13: 175-183
14. Poupeau, F. (2012). Una mirada retrospectiva sobre una investigación en las periferias urbanas, El Alto (Bolivia). In *Bulletin de l'Institut Français d'Études Andines*. 41 (3).
15. Pérez-Rúa, M. (2018). Creación e transformación da cidade litoral: Moaña 1950-1987. [...]. Santiago de Compostela, USC.

Energy Democracy in Practice

A Participatory Approach to the Community Governance of Renewables

SUZANNA TÖRNROTH¹, ADOLFO SOTOCÁ²

¹ Suzanna Törnroth, Luleå University of Technology, Luleå, Sweden

² Adolfo Sotoca, Universitat Politècnica de Catalunya, Barcelona, Spain

ABSTRACT: *Energy democracy as an energy planning paradigm proposes that citizens play a major role within the governing of their local energy resources. Previous research indicates that local governments are in a key position to drive these collaborative and bottom-up approaches in community energy governance. The key challenge lies in mobilising abstract democratic ideals in a practical manner. Creating socio-material platforms for democratic participation within contemporary energy planning is a prominent research gap to be filled in light of the global energy transition towards post-carbon societies. This paper draws on the field of design-driven research and the framework of “democratic design experiments” to propose a possible line of departure on how energy democracy can be practiced at a local governmental scale. Using this framework, a pilot study was conducted in a neighbourhood in the north of Sweden to explore future potential solar photovoltaic panel landscapes in the area. The workshop revealed opportunities for creative and playful methods in producing situated imaginings of solar panel futures that is built upon meaningful local collaboration. On a systemic level, the paper discusses potential challenges in motivation and participation in the framework’s wider scope of implementation.*

KEYWORDS: *Energy democracy, co-design, local governance, renewable energy, collaborative planning*

1. INTRODUCTION

Energy democracy is a concept that proposes that energy technologies are not simply value-free physical structures, but embedded within a larger socio-ecological framework [1]. In here, these structures can play a key role in building just and democratic futures for local communities, where communities can participate in the control of their energy resources and shape energy systems that are sensitive to the local context [1]. This key idea has been reflected within a plethora of political frameworks at both the levels of regional and local governance, for example, the EU Roadmap 2050 [2].

However, apart from being distinctly articulated within the political sphere, literature has shown that the operationalisability of energy democracy at a community and grassroots level is lacking in an equivalent sense of clarity and advancement [3]. Advancing the vision of the energy democracy movement would therefore require prioritising local and community governance [3-4] through systemic bottom-up social mobilisation, disputes as well as collaboration and civiness [5]. This begins with the creation of arenas for a meeting of perspectives, debates and discussions between different social groups in society on how renewables can be integrated into their urban environment [5].

This paper tackles the challenge of creating a socio-material platform in which energy democracy can occur in a practical manner. The authors propose a method that embodies democratic and

participatory ideals on which energy democracy is built upon. The method put forth, called ‘*democratic design experiments*’, is intended for the early stages of collaborative municipal energy planning. The key thrust of the method is the inclusion of a bottom-up understanding of local energy resources.

In the ‘Background’ section, the paper elaborates on energy democracy and exposes research gaps in how contemporary energy planning is carried out. In ‘Theoretical Framework’, the paper expounds on democratic design experiments vis-à-vis energy democracy. It presents fundamental understandings on which the pilot study is based upon. In ‘The Method’, the paper details the execution of a pilot study using a democratic design experiment in the neighbourhood of Mjölkudden, in the northern city of Luleå, Sweden. The ‘Analysis’ section delineates how the empirical data collected through the workshop was analysed. Finally, the ‘Findings and Discussion’ section pits some key findings, challenges and arenas for future research.

2. BACKGROUND

Energy democracy as part of a socio-technical energy transition most fundamentally refers to civic engagement and collaboration in the energy planning process that is more democratic, sustainable, bottom-up, equitable, and responsible [4,6]. Discussing energy issues alongside climate change concerns often presents a series of challenges. Some of these challenges include the need for a clear

communication portal with the community, establishing public acceptance of policy and technological mediations, encouraging positive change in consumption habits and behaviour, as well as marshalling local public and grassroots organisation efforts [6]. These challenges can be tackled through enforcing democratic interventions and public culpability [1,3,6]. With energy research moving from a purely technological focus to the more socio-cultural implications of the transition, “what publics think, know, say and do have become core concerns of energy research, policy and practice,” [6].

Many cities currently plan for their low-carbon, renewable energy futures through a combination of top-down and bottom-up approaches. National and regional political frameworks bound local governments to reach certain pre-defined targets. Local governments, although limited in power, are in an optimal position to concentrate efforts in energy planning in a direction most suited to the local context and resources [7]. Here, in the following paragraphs, the authors draw research gaps and lessons from two contemporary energy planning case studies, in Italy and in Denmark.

According to a study conducted on 12 municipal energy plans in Italy [8], it appears that local governments undergo three key stages during the planning of their municipal low-carbon energy plans, which are; 1. Territorial energy diagnosis of the local area, 2. Compilation and analysis of low-carbon measures, and finally, 3. CO₂ reduction target assessment. Within these stages, bottom-up data collection derives through questionnaires from the public, energy auditing, fuel and electricity retailers, and the municipal database. With increasing liberalisation of the energy market, the study shows that information from private companies are increasingly difficult to collect. The key findings from the study therefore push that a coordinated energy planning at national, regional and local level is required, and that a combination of a decentralised and centralised approach to renewable energy technologies and alternative sources is ideal [8]. Local governments are in a position to develop and implement pilot renewable energy installations that would aid in educating the public in renewable energy potentialities in the urban environment, as well as aid in tackling potential unacceptance and NIMBYism that could surface in the widespread installation of renewable energy technologies [8]. This view is also further supported by previous research that propose that local governments have the capacity to cultivate a social identity that promotes positive perceptions of the energy transition [7,9] and local energy initiatives, attributed to “symbolic, affective and socially-constructed aspects,” [10].

In Denmark, a study conducted on 11 municipal plans [11] views the current role of the municipality within national energy planning process to be problematic and underdeveloped. There is little or unclear direction towards the exact tasks, responsibilities and roles the municipalities should take in order to become potential strategic energy planning authorities [11]. This is attributed to municipal energy plans not being formal planning documents, and thus, are not binding [11]. The main thrust of this study is to argue for heightened collaboration and synergy between central and local energy planning, in order to position local governments as strategic players within national energy planning efforts. The authors of the case study argue that the implementation of national renewable energy strategies is entirely dependent on tangible work done at the local level, and without which, long-term goals on fossil fuel independence will not be reached [11]. Ideally, the role of the municipality would be to receive support from the central level whilst having the sovereignty and flexibility to incorporate local municipal suggestions and experiences [11]. This would mean that a feedback loop would be created, where learnings from on-the-ground experiences would feed into overarching institutional frameworks and the drafting of national energy policy [11].

From the two case studies presented above, some key called-for action measures within the current energy governance rhetoric have been summarised:

1. Need for concrete work done at the local level to provide contextual, empirical data for higher levels of governance to work with (i.e. a strategic feedback loop system).
2. Developing an effective democratic communication platform with the public to improve information accessibility.
3. Increased sovereignty for local governments that allow flexibility to implement local adjustments and policies in line with context and resources.

In the next few sections, this paper puts forth a method, some findings and a discussion that contribute to the points above.

3. THEORETICAL FRAMEWORK: DEMOCRATIC DESIGN EXPERIMENTS FOR ENERGY DEMOCRACY

Borrowing from constructive design research, ‘*democratic design experiments*’ have been identified as potential avenues for persons to meet, converse and collaborate on envisioning energy futures [12]. These experiments stem from a participatory design heritage, where the role of the designer is to work collaboratively with stakeholders and locals who have situated experiential knowledge of a desired topic, in

order to bring about meaningful, co-produced solutions to societal problems.

The aim of these design experiments is to create an environment that is non-threatening, inclusive and creative, which addresses inherent power dynamics and local particularities in a sensitive manner. This way, genuine and critical discussions can take place. Democratic design experiments aim to make issues experientially available, such that possible solutions become tangible, formable, and within reach of engaged yet diverse public [12]. The communication tools and methods that are selected, combined, and performed are crucial in shaping an environment viable for agonistic pluralism [12]. Due to the methodological nature of democratic design experiments, researchers that conduct democratic design experiments are deeply entangled within the process and the issues that they set out to explore [12].

When optimally integrated into the urban planning process, the hypothesis lies in the idea that these democratic design experiments would aid in the development of a bottom-up, community energy planning approach that focuses on social justice. These prototypical democratic design experiments exist in many different forms and in different examples across the world today, all of which emphasise and begin with the inclusion of multiple perspectives from the different stakeholders. It begins with the experiences and knowledge the locals have of their resources and spaces that bolster further discussions on how to shape future clean energy systems according to the local context. For the scope of the pilot study, the democratic design experiment took the form of a workshop, where a combination of methods were utilised: participatory mapping, a generative design exercise, back-casting, and an unstructured round-table discussion.

4. THE METHOD: A PILOT STUDY

The pilot study was held in the fall of 2019, in the neighbourhood of Mjölkudden, located in the northern city of Luleå, in Sweden. The neighbourhood has approximately 3,683 total inhabitants [13], and public outreach for the workshop occurred through flyer distribution to approximately 400 apartment households and community organisations (the church, main shopping area, an elementary school, an elderly home), email communications, and announcements on social media. The neighbourhood of Mjölkudden was selected due to an expression of interest from the local housing council to install collective solar photovoltaic panels on the roofs of the apartment complexes within the area. Explicitly, the aim of the pilot study was to understand the possible design and aesthetics of solar photovoltaic panel installations within the neighbourhood,

influenced and shaped by local perceptions of - and needs for - the pre-existing urban, public spaces in the area. Implicitly, the authors sought to uncover possibilities for creative collaboration to operationalise principles of energy democracy at a community level. The intimate workshop saw an attendance of four individuals, three males and one female, all between the ages of 48 to 63. Their careers range from a union leader, a local vegetable farmer, and two engineers. The workshop was arranged in the evening, after conventional work hours, in a bid to draw a larger crowd.

The workshop does not offer – and does not attempt to offer – a representative pilot study. Ethnographically, a qualitative, place-based approach was taken over a quantitative approach within the scope of this research in order to facilitate an in-depth learning of the urban narratives of the participants involved. This included the learning of their lived experiences of their local urban public spaces, their values and priorities concerning renewable energy and its infrastructure, and finally, their creative capacities in imagining different energy landscapes. Each context poses local particularities that differ from another context, calling for design-specific solutions to be responsive and shaped according to local needs.

GDPR guidelines were followed by attaining verbal permissions for data use from participants. Empirical data was collected through annotated cartographic maps, researcher's field notes of participants' actions and reactions throughout the workshop, filled-in sheets of paper from the back-casting exercise, as well as an extended voice recording of the entire workshop. One researcher led the workshop, accompanied by another facilitator who aided in language and communication.

The workshop followed the framework of a democratic design experiment, where the socio-material setting was organised for inspiration, material reflexivity and social inclusivity. Attendees were seated around a table with workshop materials in the middle: maps, paper, pens, markers, Post-Its and photographs of innovative solar photovoltaic designs. The workshop followed three stages over the duration of two hours:

- Stage 1: Participatory mapping.
- Stage 2: Envisioning local solar panel landscapes.
- Stage 3: Discussion and reflections.

For Stage 1 and Stage 2, several A3 maps were provided of the area, printed out in different scales to visualise and emphasise different aspects of the neighbourhood. The different maps included a large-scale aerial view over the entire neighbourhood, magnified aspects of the different housing cooperatives within the area (or more formally

known as *bostadsrättföreningen* in Swedish), as well as magnified aspects of the central public amenities and commercial activities to the area. For Stage 3, the participants were provided with an A4 sheet of paper each, to conduct a back-casting exercise together.

4.1 Stage 1: Participatory mapping

Participatory mapping was selected as a key method used in the workshop due to its capacity to serve as a visual communication platform for ideas and experiences that are rooted in the built, urban environment. In this exercise, the participants were asked to map where they live, their most frequently used routes in the area and areas that they found attractive/unattractive (Fig. 1). The purpose of this exercise was to understand the area better from the perspective of a local, and the spaces and experiences that affect them most on a daily basis. Understanding the major mobility routes and areas of high activity would facilitate urban planners in directing efforts towards key points for improvement.

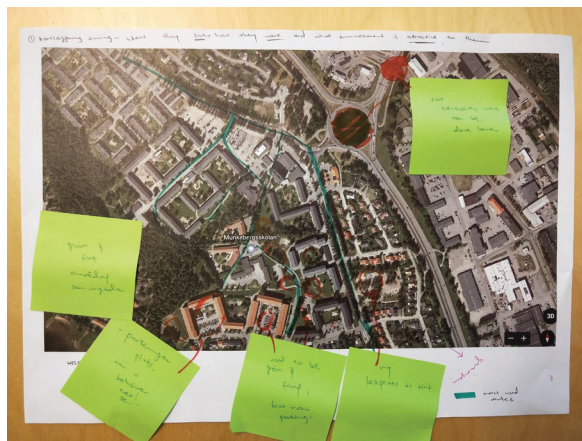


Figure 1: Collaborative mapping of daily routes and spaces frequently used.

4.2 Stage 2: Envisioning local solar panel landscapes

In this exercise, a new map was provided (Fig. 2), in which the most suitable areas for solar photovoltaic panels have been shaded (i.e. roofs and facades facing south, and open land areas with low susceptibility to shade). Logistical feasibility issues aside, the participants were then asked to select and discuss the areas in which they could possibly foresee solar photovoltaic panels being installed. The participants were shown visionary and innovative design ideas concerning small-scale solar panel systems in order to inspire the future design of the area. They were then asked to give their inputs before and after being shown these ideas. The purpose of this exercise was to brainstorm a collaborative plan for future hypothetical solar photovoltaic panel projects; combining experiential knowledge from the inhabitants, innovative design

solutions, and technical knowledge of solar accessibility of the present area.

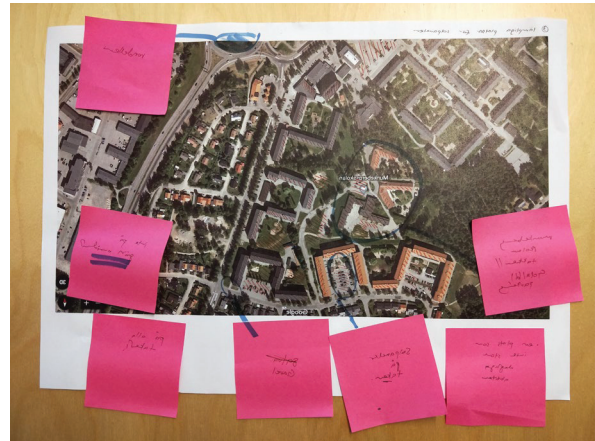


Figure 2: Collaborative mapping of potential sites for solar photovoltaic panel installation.

4.3 Stage 3: Discussion and reflections

During Stage 3, the participants were asked to conduct a back-casting exercise [14], where the participants were given an A4 paper to list and explain possible steps that can be taken from the current state, in order to achieve their envisioned solar panel landscape within the neighbourhood. The purpose of this activity was to convert seemingly unfeasible energy futures into small, concrete steps that can be taken, in a bid to motivate and mobilise the public into action. The activity entailed an open and unstructured qualitative round-table discussion that was documented through the continuous voice recording, researchers' field notes as well as through the A4 back-casting exercise paper. The findings provided insight into the values, priorities and context-specific needs within the community on the local energy transition.

5. ANALYSIS

The workshop voice recording was transcribed and then analysed via a thematic content analysis. The transcript was sequentially marked with the words, phrases and short passages where the researcher had "observed something of special interest" [15]. All "special interest" markings were coded to different themes, which then set the structure for the creation of a workshop summary document. The same process was conducted for the map annotations, the researcher's field notes, and the filled-in sheets of paper resulting from Stage 3's back-casting exercise. The document was then sent out to all workshop participants, to seek a collective analysis based on individual interpretations of the workshop event. Requests were made for edits and feedback. The document was finalised and then used as a foundation for this paper. The document was also distributed to a major local energy authority

(Luleå Energi) and the municipal planning authority (Luleå Municipality) for input into future local governance and planning processes.

6. FINDINGS AND DISCUSSION

6.1 Motivation and participation

The participatory mapping process had set the stage for an open and meaningful dialogue among the participants, providing a material space for their perspectives to meet. However, the participants to the workshop were few in number, totalling to four persons, despite extensive public outreach efforts to over 400 households. The small sample size of the workshop could be attributed to a variety of factors. One possible discussion point could be the motivation or pro-activeness to participate. Here, the authors would like to draw upon a significant question worth reflecting upon, “What are the incentives [for locals to] participate in a planning procedure, as individuals and groups?” [16].

In the workshop, the participants posed questions as to what the next steps will be after the workshop: “How will my input affect the municipality decision-making process?”, “What outcomes will result from this?”, “Are they planning future projects for the area...and when?”, “Will there be further communication and collaboration on potential projects in this area?”. This was particularly evident during Stage 3. The participants appeared concerned about their ultimate influence on future community energy plans, possibly attributed to past negative experiences associated with the local urban planning process. The key challenge here appears to be providing the confidence that pro-activeness and participation in such community-planning decisions would lead to a visible impact, i.e. a joint ownership of the final decision made.

Although the workshop reflects situated knowledge for the local context of Luleå, Sweden, these are key issues that relate a wider scope of public participation rhetoric in collaborative urban planning. There appears to be a need to challenge the existing model of local participation if it is not embodying a shared belief in the process. This could be addressed through the re-framing and re-formulation of the local public participation process. If not that, the “conception of the preferable” [16], which in this case, is collaborative local governance on energy issues, perhaps needs to be revisited altogether. As posed by planning theorist, Nikhil Kaza, “if it is not preferable to large segments of the society, how can it be socially preferable?” [16].

6.2 Leveraging design interventions for energy democracy

The small sample size allowed for intimate and honest discussions on their views and perspectives on

current and future governmental efforts. To uphold anonymity, no photographs were taken of the participants. It was found that the participants were hesitant to express themselves by creative means via drawing on the maps, but were more comfortable with expressing their ideas through speech. The researcher took on an initial facilitating role by converting their speech to ideas on the map, which then motivated the participants to follow in cue by adding and editing the ideas after. As speech appeared to be the common comfortable mode of communication between the participants, the voice recording proved useful in capturing all ideas and nuances in speech.

The participatory mapping process entailed a creative and playful approach to how the inhabitants perceive and characterise the spaces. The visual method, known to elicit design ideas, associations, metaphors, narratives, and memories [15] proved successful in its use. The participants drew on personal stories and memories through the use of descriptive phrases such as, “attractive green areas”, “nice playground area for the children”, “boring roundabouts”, “idyllic forested walking paths”, among others (phrases were translated from the workshop voice recording, and some can be seen on Post-Its in Fig. 1). Here, creativity and playfulness proves to expedite an informal and honest approach to how the inhabitants evaluate their social milieu during this workshop, through dissolving any trace of a formal and strict atmosphere.

It was discovered that the material component of the workshop; material interactivity with maps, Post-Its, pens and markers, facilitated discussions in non-threatening medium. Using these materials, participants were able to negotiate tensions between some contradicting views. For example, this was done by using the materials to explain their thoughts in an approachable and pedagogical manner. In some instances, the materials served as objects that the participants fidgeted with, which could indicate the materials’ role in providing minor distraction and sense of comfort for individuals within a workshop environment. Furthermore, taking the creative approach had also aided in bridging any communication or language gaps, because the map provided as a visual tool that supplemented verbal explanations.

6.3 Co-creating situated urban energy landscapes

The results from Stage 2 of the experimental workshop revolved around three key themes in envisioning solar panels within the urban neighbourhood: visibility, aesthetics, and solar accessibility. The participants generally agreed that the visibility of solar panels was not considered a problem, unless the panels obstructed pedestrian

views and walking paths. For example, the participants were strongly against solar panels being placed on the wide green lawns, as it would disrupt pedestrian views and access to recreational areas for the children. On the map, the participants highlighted roofs (e.g. of buildings and parking garages) to be generally optimal areas for solar panel installations since they were considered “dead space” whilst being accessible to high solar irradiance. Aesthetically, facades were considered as potential areas for solar panels to be placed in a visually pleasing way. Roundabouts, because currently empty and considered unattractive, were also pointed out as potential areas for new solar panel projects as they were largely unshaded and therefore could provide for high solar accessibility.

Overall, the participants expressed specific ideas to how they could envision solar panels within their neighbourhood, which indicates the benefit of working with energy governance on-the-ground. Detailed, meaningful and realisable designs can be co-produced from such democratic design experiments. The workshop had also shed light on the values and meanings that the local participants attached to the urban landscape of the neighbourhood, which can be utilised as guidance for future renewable energy projects. The participants generally agreed that introducing small-scale solar photovoltaic panels within the neighbourhood was a feasible way forward in providing clean energy to the neighbourhood, and in supporting municipal goals (i.e. Luleå Vision 2050) of achieving sustainable neighbourhoods.

7. CONCLUSION

The learnings from this workshop provide a preliminary step forward in the conversation on how urban planners can begin to operationalise energy democracy and capitalise on local knowledge for the future energy planning of renewables. For the scope of this study, small-scale solar photovoltaic panel systems was utilised as an example. However, this study shows preliminary feasibility in applying democratic design experiments to the planning of other renewable energy models in the urban environment, for example, small-scale windmills.

This pilot study exercised energy democracy through design interventions at a small and intimate scale. Taking the research a step further, a possible line of departure would be to test democratic design experiments as a form of participation that is situated within the larger ecology of public participation processes. This study was a step forward in lending to the idea that community-level governance of energy resources can be more than an opportunity to meet technical and political demands in producing clean energy – it can also serve to fundamentally reshape

social, economic and political relations in order to deliver community benefits.

ACKNOWLEDGEMENTS

This paper was supported by Energimyndigheten through Project Grant 46355-1.

REFERENCES

1. Thombs, R. P. (2019). When democracy meets energy transitions: A typology of social power and energy system scale. *Energy Research and Social Science*, 52(March): p. 159–168.
2. European Climate Foundation. (2010). *Roadmap 2050 - A practical guide to a prosperous, low-carbon Europe*. Technical analysis. Europe, I, 100.
3. Stephens, J. C. (2019). Energy democracy: Redistributing power to the people through renewable transformation. *Environment*, 61(2): p. 4–13.
4. Van Veelen, B. (2018). Negotiating energy democracy in practice: governance processes in community energy projects. *Environmental Politics*, 27(4): p. 644–665.
5. Mouffe, C. (2000). *The Democratic Paradox* (First). London, UK: Verso Books.
6. Chilvers, J., Pallett, H., & Hargreaves, T. (2018). Ecologies of participation in socio-technical change: The case of energy system transitions. *Energy Research and Social Science*, 42(February): p. 199–210.
7. Balest, J., Pisani, E., Vettorato, D., & Secco, L. (2018). Local reflections on low-carbon energy systems: A systematic review of actors, processes, and networks of local societies. *Energy Research and Social Science*, 42(March): p. 170–181.
8. Brandoni, C., & Polonara, F. (2012). The role of municipal planning in the regional energy-planning process. *Energy*, 48(1): p. 323–338.
9. Wolsink, M. (2007). Planning of renewables schemes: Deliberative and fair decision-making on landscape issues instead of reproachful accusations of non-cooperation. *Energy Policy*, 35(5): p. 2692–2704.
10. Devine-Wright, P. (2005). Beyond NIMBYism: Towards an integrated framework for understanding public perceptions of wind energy. *Wind Energy*, 8(2): p. 125–139.
11. Sperling, K., Hvelplund, F., & Mathiesen, B. V. (2011). Centralisation and decentralisation in strategic municipal energy planning in Denmark. *Energy Policy*, 39(3): p. 1338–1351.
12. Binder, T., Brandt, E., Ehn, P., & Halse, J. (2015). Democratic design experiments: between parliament and laboratory. *CoDesign*, 11(3–4): p. 152–165.
13. Luleå Municipality. (2019). *Befolkningen Statistik i Luleå*. Luleå, Sweden.
14. Robinson, J. B. (1982). Energy backcasting: A proposed method of policy analysis. *Energy Policy*, 10(4), 337–344.
15. Simonsen, J., & Friberg, K. (2014). Collective Analysis of Qualitative Data. In J. Simonsen, C. Svabo, S. M. Strandvad, K. Samson, M. Hertzum, & O. E. Hansen (Eds.), *Situated Design Methods* (First, p. 400). London, UK: MIT Press.
16. Kaza, N. (2006). Tyranny of the median and costly consent: A reflection on the justification for participatory urban planning processes. *Planning Theory*, 5(3): p. 255–270.

Can Planning Mitigate UHI?

A “Remote Sensing” and “Local Climate Zones” Analysis for Barcelona

ROLANDO BIERE¹, BLANCA ARELLANO², JOSEP ROCA³

^{1,2,3} Centre for Land Policy and Valuations(CPSV), Universitat Politècnica de Catalunya (UPC), Barcelona, Spain

ABSTRACT: Warming of the climate system is unequivocal [1]. There is a consensus on the fact that cities have a special role in Climate Change (CC). In this context maybe one of the most relevant climatic factors is the Urban Heat Island effect. For this reason, the introduction of climate assessment in urban and territorial planning can serve to mitigate the effects of the UHI. The main objective of this paper is to study, using remote sensing techniques, how urban planning affects the generation of the Urban Heat Island in the Metropolitan Area of Barcelona (MAB), as well as the determination of LCZ specifically adapted to this area with more than 30 municipalities, bringing together about 3.5 million inhabitants. The paper shows the methodology used to define “local climate zones”, or “climatopes”, and their insertion in metropolitan urban planning. Its inclusion in urban planning can be a decisive step to reduce the city's climate impacts, increasing its resilience to heat waves. The results allow to know the climatic behaviour of the different land uses, as well as to elaborate criteria that increase the efficiency of urban planning from the perspective of Climate Change.

KEYWORDS: Climate Change, Urban Heat Island, Regional and Urban Planning

1. INTRODUCTION

Warming of the climate system is unequivocal, and since the 1950s, many of the observed changes are unprecedented over decades to millennia. The atmosphere and ocean have warmed, the amounts of snow and ice have diminished, and sea level has risen [1]. The global emissions of GHG due to the effects of human activities have increased, since the pre-industrial era, by 70% between 1970 and 2004. The result of the different models of the evolution of the temperatures of the earth's surface, show the prominence of anthropogenic forcing origin, with respect to those of a natural nature.

There is a consensus on the fact that cities have a special role in the Climate Change (CC). According to the Center for Human Settlements, cities are responsible for 75% of global energy consumption, as of 80% of GHG emissions [2]. The contribution of the urbanization to the climatic change is of double nature: on the one hand, by the urban generation of GHG, a factor that contributes in a decisive way to the global warming of the planet; on the other, by the radiation generated by the surface of the urbanized land, which determines a marked flow of sensible and latent heat according to the type of urban covers, as well as their degree of humidity. Although the climate of cities depends mainly on factors of regional character, the local and micro-scale factors, such as the different characteristics of the urban structure, the topography and surface of the ground cover, vegetation, as well as the anthropogenic heat generated by urban metabolism, among other factors, can modify the regional climate and generate urban microclimates. There are significant differences in the climate of urban areas compared to rural areas: The

Urban Heat Island (UHI) describes the influence of urban surfaces on the temperature patterns in contrast to the surrounding areas.

One of the main causes is the sealed land and artificial materials (e. asphalt and concrete) used in urban areas. Two types of UHI can be distinguished (Fig. 1): a) “canopy layer heat island”, which depends on the roughness of the soil generated by the buildings and the canopy of the trees, with an upper limit located just above the level of the roofs of the buildings, and b) “boundary level heat island”, situated above the first, with a lower limit subject to the influence of the urban surface.

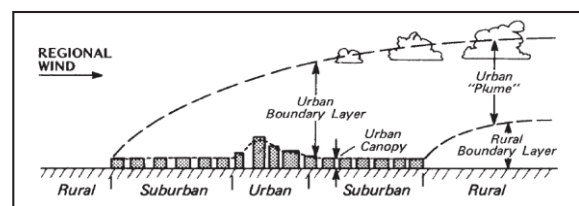


Figure 1: Urban Canopy & Urban Boundary Layers [3]

Urban planning has a fundamental transcendence to inform, coordinate and implement measures to improve the climate quality of cities in the face of global climate change [4]. There have been some initiatives to introduce methodologies, in the spatial planning, aimed at mitigating climate change. Especially on the “small scale”, there is an extensive experience of urban bioclimatic design. In turn, at the building level there has been a significant effort in recent years to increase energy efficiency, with the aim of reducing the generation of GHG. On the “large scale”, however, that of urban and territorial planning, there does not seem to be a parallel awareness, with

few initiatives to adapt it in order to increase urban resilience to climate change.

The development of the so-called climatopes has become one of the most effective mechanisms for the introduction of climate in territorial and urban planning to the "large scale" (meso-scale, in climatic terms). The beginnings of this technique are found in the pioneering works developed by German researchers at the end of the 70's, which developed the new technique of the Climatopes [5, 6].

This technique, called in the English-language literature, Local Climate Zones (LCZ) has highlighted the importance of integrating climate assessment into territorial and urban planning [7]. The traditional approach that differentiated exclusively the "urban" from the "rural" has been definitively overcome. In this sense, the incorporation of "climatopes" (typical of Central European culture) in the official (Anglo-Saxon) discourse of urban climatology has been especially relevant [8].

These are defined as all classes to emerge from the division of the landscape universe [8]. The classes are local in scale (Fig. 2), climatic in nature, and zonal in representation.

Built types	Definition	Land cover types	Definition
1. Compact high-rise	Dense mix of tall buildings to tens of stories. Few or no trees. Land cover mostly paved. Concrete, steel, stone, and glass construction materials.	A. Dense trees	Heavily wooded landscape of deciduous and/or evergreen trees. Land cover mostly pervious (low plants). Zone function is natural forest, tree cultivation, or urban park.
2. Compact midrise	Dense mix of midrise buildings (3–9 stories). Few or no trees. Land cover mostly paved. Stone, brick, tile, and concrete construction materials.	B. Scattered trees	Lightly wooded landscape of deciduous and/or evergreen trees. Land cover mostly pervious (low plants). Zone function is natural forest, tree cultivation, or urban park.
3. Compact low-rise	Dense mix of low-rise buildings (1–3 stories). Few or no trees. Land cover mostly paved. Stone, brick, tile, and concrete construction materials.	C. Bush, scrub	Open arrangement of bushes, shrubs, and short, woody trees. Land cover mostly pervious (bare soil or sand). Zone function is natural scrubland or agriculture.
4. Open high-rise	Open arrangement of tall buildings to tens of stories. Abundance of pervious land cover (low plants, scattered trees). Concrete, steel, stone, and glass construction materials.	D. Low plants	Featureless landscape of grass or herbaceous plants/crops. Few or no trees. Zone function is natural grassland, agriculture, or urban park.
5. Open midrise	Open arrangement of midrise buildings (3–9 stories). Abundance of pervious land cover (low plants, scattered trees). Concrete, steel, stone, and glass construction materials.	E. Bare rock or paved	Featureless landscape of rock or paved cover. Few or no trees or plants. Zone function is natural desert (rock) or urban transportation.
6. Open low-rise	Open arrangement of low-rise buildings (1–3 stories). Abundance of pervious land cover (low plants, scattered trees). Wood, brick, stone, tile, and concrete construction materials.	F. Bare soil or sand	Featureless landscape of soil or sand cover. Few or no trees or plants. Zone function is natural desert or agriculture.
7. Lightweight low-rise	Dense mix of single-story buildings. Few or no trees. Land cover mostly hard-packed. Lightweight construction materials (e.g., wood, thatch, corrugated metal).	G. Water	Large, open water bodies such as seas and lakes, or small bodies such as rivers, reservoirs, and lagoons.
8. Large low-rise	Open arrangement of large low-rise buildings (1–3 stories). Few or no trees. Land cover mostly paved. Steel, concrete, metal, and stone construction materials.	VARIABLE LAND COVER PROPERTIES	
9. Sparsely built	Sparse arrangement of small or medium-sized buildings in a natural setting. Abundance of pervious land cover (low plants, scattered trees).	b. bare trees	Leafless deciduous trees (e.g., winter). Increased sky view factor. Reduced albedo.
10. Heavy industry	Low-rise and midrise industrial structures (towers, tanks, stacks). Few or no trees. Land cover mostly paved or hard-packed. Metal, steel, and concrete construction materials.	s. snow cover	Snow cover >10 cm in depth. Low admittance. High albedo.
		d. dry ground	Parched soil. Low admittance. Large Bowen ratio. Increased albedo.
		w. wet ground	Waterlogged soil. High admittance. Small Bowen ratio. Reduced albedo.

Figure 2: Local Climate Zones defined by Oke [10]

These LCZ can be understood as regions of uniform surface cover, structure, material, and human activity that span hundreds of meters to several kilometres in the horizontal scale. Each LCZ has a characteristic screen-height temperature regime that is most apparent over dry surfaces, on calm, clear nights, and in areas of simple relief. Each LCZ is individually named and ordered by one (or more) distinguishing surface

property, which in most cases is the height/packing of roughness objects or the dominant land cover [9]. The physical properties of all zones are measurable and nonspecific as to place or time. The analysis using Local Climate Zones (LCZ) to understand the UHI effect in the city is relevant, considering the difference in temperatures of the classes between them. LCZ have served as a link between both approaches, previously separated.

The introduction of climate assessment in urban and territorial planning can serve to mitigate the effects of the UHI. The practice of planning must include measures such as the limitation of urban expansion, the increase of green areas (including the roofs and facades of buildings) as well as the percentage of pervious land. It is also important to include the modification of the albedo of the built areas (increasing the degree of reflection of incoming solar radiation), the integration of artificial water bodies, the promotion of urban ventilation, the architectural composition of the building and, in general, the composition of urban morphology in a way that facilitates air circulation, generates urban canyons and softens temperatures. All these are measures that must be included in the daily practices of urban and territorial planning.

2. OBJECTIVE AND METHODOLOGY

The general objective of the research is to study, using remote sensing techniques, how urban planning affects the generation of the Urban Heat Island in the Metropolitan Area of Barcelona (MAB), as well as the determination of LCZ specifically adapted to the case of study. MAB (Fig. 3) includes more than 30 municipalities bringing together about 3.2 million inhabitants and an extension of 636 km².

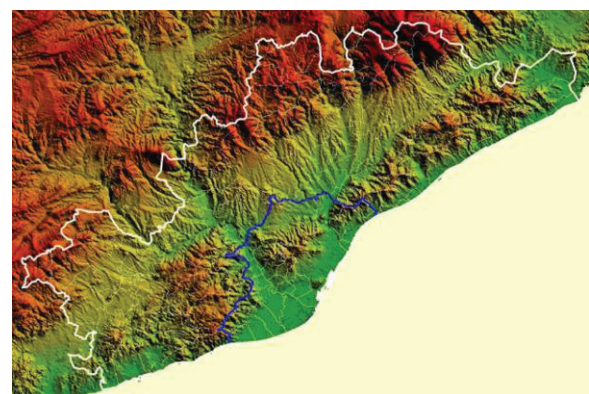


Figure 3: MRB (in white) and MAB (in blue)

The Metropolitan Area is the economic and political heart of the Metropolitan Region of Barcelona (MRB), which includes 164 municipalities with a population of 4.8 million people and an extension of 3,200 square kilometres (Fig. 3). At this metropolitan scale, the spatial configuration of the UHI will be studied.

The objective of this work is to integrate the evaluation of the urban climate in the metropolitan planning of Barcelona. It is necessary to overcome the traditional vision of urban zoning, from a strictly morphological vision, from the regulation of land uses to a more integral perspective, which incorporates the environmental assessment (including generation of GHG) and climate of the urban territory.

The methodology of this work combines the use of remote sensing technologies with the analysis of the attributes that characterize the different areas of urban planning. The combination of both approaches, remote and local data allow the construction of the different LCZ or “climatopes”, as well as incorporate climate analysis in urban planning.

Specifically, the research methodology is developed in the following steps:

- Remote sensing analysis: 1) LST is obtained from LANDSAT 8; 2) the information obtained through the satellites allows knowing some indices that affect the UHI, such as the NDVI, NDBI, Urban Index and others indicators, and; 3) LST and the other obtained indexes by remote sensing allow a detailed approximation of the UHI of the MRB and MAB.
- Local Analysis. The objective of this second stage of the research is to integrate the different indicators obtained through remote sensing in the analysis of the built environment. The aim is to develop a methodology of urban-climatic zoning, which integrates the main components of urban climate in the traditional urban zoning. Among others, the following indicators has been used at the local level: Albedo, Sky View Factor, Pervious/impervious surface, LST, Air Temperature, three canopy and quality of vegetation, NDBI and other indices of building intensity and Floor Area Ratio.

The integration of the previous indicators with the data obtained through remote sensing allows obtaining the regional climate or LCZ of Barcelona.

3. OBTAINING THE LST FOR THE MRB AND MAB

The method to obtain the LST has been based on obtained information from LANDSAT.

3.1 Day-time LST Obtaining Process

The numerical coding (Digital Number-DN) of the thermal band (infrared heat) has been converted into physical units i.e. in Celsius degrees, as follow (Fig. 4):

- Transformation of DN into spectral radiance.
- Calculation of brightness temperature at-sensor. This temperature does not consider the type of material or land that emits the energy captured. Therefore, it would be equivalent to the temperature emitted by a black body.

- Correction of the numerical value obtained in the previous steps, by introducing the emissivity of the soil materials. The emissivity is obtained from the normalized difference vegetation index, NDVI. The use of this index respect to other alternatives, such as land use classification has two main advantages: 1. both, temperature and vegetation index come from the same moment in time, and 2. the immediacy of the calculation of this index.

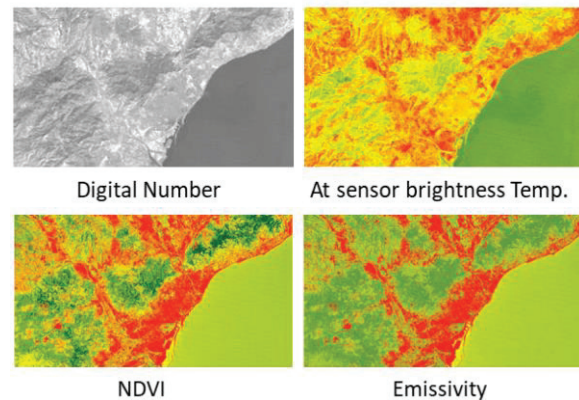


Figure 4: Stages of the LST Process

Once finished this process, the UHI for the Metropolitan Region of Barcelona is obtained (Fig. 5).

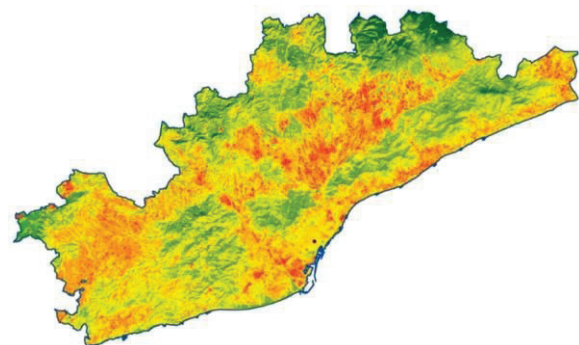


Figure 5: LST of the Metropolitan Region of Barcelona.

3.2 Improving the Spatial Resolution of the LST

The resolution of Landsat (30 m/pixel in the visible and infrared bands, 100 m/pixel in the thermal band) does not allow a detailed knowledge of the LST (Fig. 6). Sentinel 2 (10 m/pixel) offers the possibility of resizing the thermal image to a higher level of spatial resolution. To change the resolution from 30 to 10 m/pixel, two different OLS models are developed:

- On the one hand, a strictly geographical model is tested. Such model incorporates, as independent variables, the altitude (DTM), orientation, slope and distance to the sea. The model explains 38.5% of the variation of the LST.
- In a similar way, an “urban model” can be constructed to explain the day-time LST (Landsat). The best model of the tested ones

explains 55% of the variation of the LST, with the NDVI (-), NDBI and UI (+), and the average LST of the urban planning areas (which appears as the most significant variable).

- The integration of the two previous models, allows to improve the R^2 up to 0.572. The change of scale from 30 (Landsat 8) to 10 meters (Sentinel2) allows to substantially improve the visibility of the UHI.
- Finally, a "hybrid" model at 10 meters / pixel is tested (Fig. 5). This model explains 64% of the spatial variation of the LST, improving in a sensible way the visualization of the UHI of Barcelona. The model is constructed with the NDVI (-), NDBI (+), orientation (-), slope (+), UI (+), altitude (-), distance to the coast (-), emissivity (-), distance to the centre of the city (+), albedo (-) and the average LST of the different zones of metropolitan planning (+).

All the variables are significant (except for the Urban Index, due to its high collinearity with the NDBI) and appear with the expected sign. It is noteworthy that, at the scale of the municipality of Barcelona, the distance to the centre appears with a positive sign, due to the existence of (hot) industrial zones in the periphery of the city.

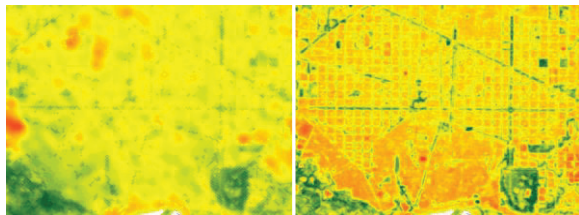


Figure 6: LST (Landsat 8) vs "Hybrid" Model

3.3 Night-time LST Obtaining Process

Once the LST was obtained at day-time by means of Landsat (30 m/pixel) and Sentinel (10 m/pixel), the LST at night-time was obtained through MODIS (1 km/pixel). In this step is possible make a comparison between day-time LST (Landsat) with night-time LST (MODIS). This comparison (Fig. 7) shows the sharp differences between the morphology of the UHI in day-time and night-time.

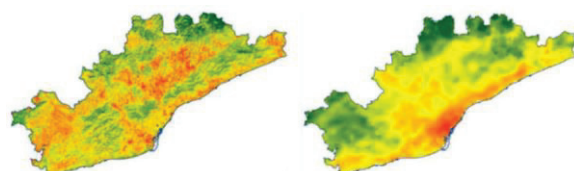


Figure 7: Comparison Day-time LST vs Night-time LST.

During the day, the metropolitan centre (the city of Barcelona) does not show the highest metropolitan LST. They are the industrial areas of the first metropolitan ring (that surrounds the city except for the North side, where *Collserola Park* closes the ring) that reveal the highest surface temperatures. The

extreme LST are also located in the industrial areas and in the compact centers located in the Pre-Coastal Depression, which runs parallel to the sea, beyond the Coastal Mountains (*Garraf, Collserola* and so on). The agricultural areas of the Pre-Coastal Depression, especially the vineyards, also observe elevated LST. On the opposite side, the forested areas show the lowest temperatures at metropolitan scale: the spaces characterized by a high quantity and quality of the vegetation observe the most moderate LST in the MRB, as evidenced by the high negative correlation between the NDVI and the day-time LST.

During the night (Fig. 8), the spatial distribution of the LST varies in a meaningful way. The compact urban centers, and especially the city of Barcelona, denote the highest LST.

On the other hand, in rural areas, the reduction of night temperatures is pronounced. The agrarian zones, and especially the vineyards, observe a much more pronounced cooling than the urban spaces. And the highest LSTs move from the Pre-Coastal Depression to the Coastline. The industrial areas, on the other hand, also show a marked reduction of the LST: they cool much more sharply than the compact residential fabrics. And the wooded areas, except for those located at very high altitudes (>1,000 meters), also observe, like the urban centers, a greater thermal inertia. Forests preserve surface temperature much more than open spaces.

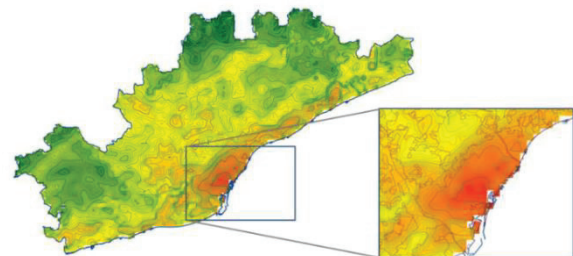


Figure 8: MAB Night-time UHI

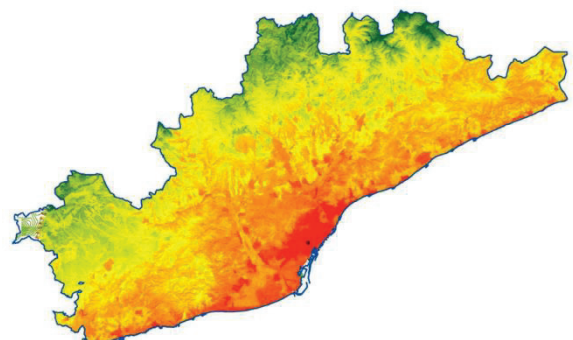


Figure 9: Night-time LST (30 meters/pixel)

The nocturnal LST, with a spatial resolution of 30 m/pixel (Fig. 9), confirms the different geographical distribution of the metropolitan UHI in relation to the day-time LST. There is a clear relative warming (less cooling) of the coastal areas and the main urban centres of the pre-coastal depression. The city of

Barcelona, the metropolitan centre, obtains the highest LST. On the other hand, the industrial areas of the urban periphery as well as the agricultural ones are cooled down sharply, forming a marked UHI.

3.4 Analysis and results

Once obtained the LST is possible to know the UHI of the MRB, differenced by uses. The hottest uses are: Logistics Activity, 34.40%; Industry, 33.29%; Dev. Land (economic activities), 31.89%; Tertiary, 31.39%; Roads and Streets, 31.34%; Compact City, 31.05%; Mixed Area, 31.04%; Mixed Use Development, 30.82%; and Old City, 30.32%. In the other extreme the coolest areas are: Rural (protection), 28.16%; Green Areas, 28.23%; Hydrographic system, 28.61%; Detached Houses, 28.62%; Agricultural Land, 29.08%; Residential Blocks, 29.6%; Dev. Land (residential), 29.71%; and Semi-Detached Houses, 30.3%. From this distribution, the most highlighted is that:

- The “economic activities & logistics” (34.40°C), “industrial” (33.29°C), “tertiary” and “services” (31.37°C) represent the hottest land uses.
- At the same time the “roads network” (31.34°C) as well as the “compact residential” (31.05°C), LST is clearly higher than the average of the MRB (28.58 °C).
- The “non-developable land of special protection”, the “undeveloped land with protection”, the “open spaces and green areas” as well as the “Hydrographic system”, are the best rated land uses from a climate perspective.

In summary: the artificialized areas observe an average LST that is 7.2% higher than the non-artificialized zones.

The combination of the LST with the remaining indexes used (NDVI, NDBI, albedo, SVF, Floor Area Ratio, ...) allows the establishment of the LCZ in the MAB.

The average LAST (day and night time) of the different Corine Land Covers of the MRB is also compared (Table 1).

Table 1: LST (day and night) by CLC.

Corine Land Cover	LST		Difference
	Day-time	Night-time	
High and medium density	30.35	17.63	12.72
Urban Sprawl	28.80	16.17	12.63
Industrial and commercial	31.21	16.52	14.69
Other Urban Land Uses	29.72	17.06	12.66
Agricultural Areas	30.07	15.06	15.01
Forest Areas	26.93	15.23	11.70
Other Rural Land Uses	28.35	15.32	13.03

The preceding analysis allows the elaboration of LCZ that simultaneously attend urban planning and climate behaviour.

4. LOCAL CLIMATE ZONES OF THE MAB

The results of the previous epigraph confirm the existence of a pronounced UHI in the metropolitan area of Barcelona. It is convenient, therefore, to propose (in urban planning) measures aimed at refreshing highly artificialized covers. For this, it is convenient the introduction of “climatopes” or “local climate zones” in urban planning.

The methodology used to delimit the LCZs of the MRB differentiates the following categories:

1. *Urban fabrics*. a) Residential (Fig.10): i. Old cities, ii. “Ensanches” (high and medium density compact urban fabrics), iii. Isolated Blocks, and iv. Urban Sprawl, and b) Industrial (Fig.11): i. In urban continuum, and ii. Industrial parks.
2. *Open spaces*. a) Agricultural lands, b) Urban Parks, and c) Forest Areas.

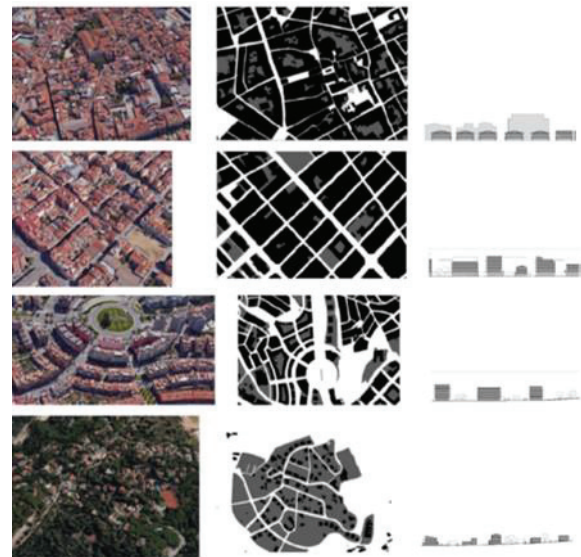


Figure 10: Urban Fabrics. Residential

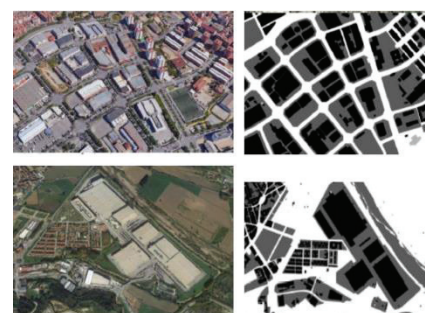


Figure 10: Urban Fabrics. Industrial

This analyse, has been carried out in the MAB, and also in detailed specific areas. Has been overlapped different information sources: Metropolitan General Plan (current urban planning from de the Urban Map of Catalonia, MUC), Corine Land Cover (land uses), blocks, lots, LST, NDBI, and NDVI.

Different specific areas have been analysed. One of them in Viladecans, Gavà, and Castelldefels Urban Continuum. Here has been compared the obtained

“Climatopes” (Fig. 11) with the LST of the same area (Fig. 12).

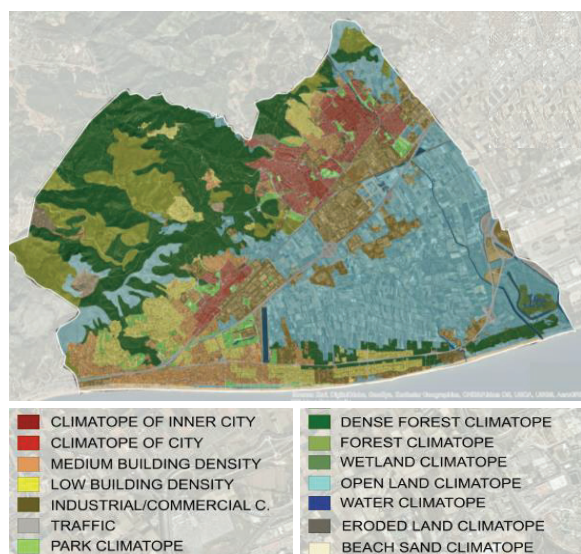


Figure 11: Specific Definition of Local Climate Zones

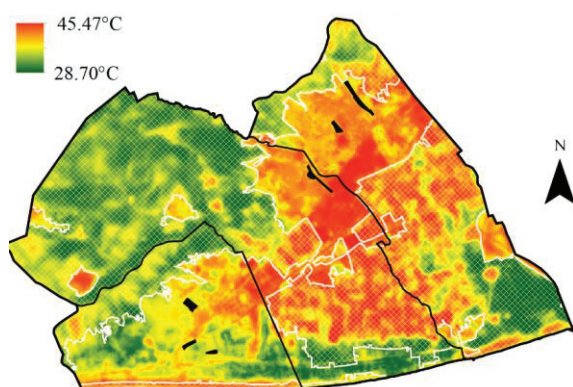


Figure 12: LST of Viladecans, Gavà, and Castelldefels

Has been clearly detected that the Climatopes related with open green areas “dense forest” and “forest” are in coincidence with the coolest temperatures obtained in the LST analysis. In the other extreme a clear correspondence exists too between the hottest temperatures with “inner city” and “city”, but is not so clear in the “medium building density, as also occurs in “open land”. Growing areas are warmer than extensive green areas. In a very detailed scale has been detected than the disposition of urban green areas in central zones helps to reduce the temperature of the immediate built areas around of these.

5. CONCLUSION

The study carried out allows to know the climatic behaviour of the different land uses, as well as to elaborate criteria that increase the efficiency of urban planning from the perspective of Climate Change. The paper shows the methodology used to define “local climate zones”, or “climatopes”, and its insertion in metropolitan urban planning. Its inclusion in urban

planning can be a decisive step to reduce the city's climate impacts, increasing its resilience to climate change. In synthesis we can conclude that: a) the use of both analysis, remote sensing technologies and “local climate zones” or “climatopes”, can help to identify in detail, general and specific areas of the UHI; b) at local scale urban morphology and land uses play a key role to generate and control UHI, c) urban planning and landscape design, the selection of materials and vegetation, at urban scale has a particular relevance to promote resilience to heat waves and reduce the UHI, considering the specific characteristics of the central areas of the city.

ACKNOWLEDGEMENTS

The authors wish to thank to the Ministry of Economy and Competitiveness of Spain (MINECO) and the European Regional Development Fund (ERDF) that finance the project “Urban-CLIMPLAN. The urban heat island: effects on climate change and modelling towards strategies of territorial and urban planning. Application to the Metropolitan Region of Barcelona” (Ref. BIA2015-68623-R).

REFERENCES

1. Intergovernmental Panel on Climate Change (2014). *Climate Change 2014. Synthesis Report*, Fifth Assessment Report. Geneva, Switzerland, 151 pp.
2. United Nations, General Assembly, Second Committee [Online] Available at <http://www.un.org/press/en/2007/gaef3190.doc.htm>
3. Oke, T.R. (1987). *Boundary Layer Climates*. Second, Taylor & Francis, 416 pp.
4. Alcoforado, M. J. & Matzarakis, A. (2010). Planning with Urban Climate in Different Climatic Zones, *Geographica*, 57: p. 5-39.
5. Baumüller, J.; Flassak, T.; Schädler, G.; Keim, M. & Lohmeyer, A. (1998). ‘Urban climate 21’ - Climatological basics and design features for ‘Stuttgart 21’. *Report of Research Center for Urban Safety and Security*, Kobe University, 1: p. 42-52.
6. Scherer, D., Fehrenbach, U., Beha, H-D. & Parlow, E. (1999). Improved concepts and methods in analysis and evaluation of the urban climate for optimizing urban planning process, *Atmospheric Environment*, 33: p. 4185-4193.
7. Chao, R. et al (2010). Urban Climatic Map Studies: A review. *International Journal of Climatology*, 31: P. 2213-2233. DOI <https://www.doi.org/10.1002/joc.2237>
8. Stewart, I.D. & Oke, T.R. (2012). ‘Local climate zones’ for urban temperature studies. *Bulletin of the American Meteorological Society* 93: p. 1879-1900.
9. Stewart, I.D. (2011). Redefining the urban heat island. Ph.D. dissertation, Department of Geography, University of British Columbia, 352 pp. [Online] Available at <https://circle.ubc.ca/handle/2429/38069>.
10. Oke, T.R. (2004). Initial guidance to obtain representative meteorological observations at urban sites. IOM Rep. 81, WMO/TD-No. 1250, 47 pp.

Outdoor thermal comfort approach in summer season for the city of Madrid

Influence of urban typologies in microclimate and the outdoor thermal sensation

HELENA LÓPEZ MORENO^{1,2}, MARÍA NURIA SÁNCHEZ EGIDO¹, EMANUELA GIANCOLA¹, JOSÉ ANTONIO FERRER TEVAR¹, FRANCISCO JAVIER NEILA GONZÁLEZ², SILVIA SOUTULLO CASTRO¹

¹ Center of Energy, Environmental and Technological Research, CIEMAT

² Department of Construction and Architectural Technology, Universidad Politécnica de Madrid, UPM

The influence of different urban typologies in the microclimate and the outdoor thermal comfort in the city of Madrid has been evaluated for a summer typical day. Thus, meteorological variables from the Climatic Network of Madrid have been interpolated and assigned to each urban typology. The urban microclimate analysis reveals variations of air temperature, relative humidity and wind velocity for each typology; being significative during the night, when it is reached differences of 2°C for air temperature and 16% for relative humidity between compacted-high rise and dispersed typologies. Through the urban microclimate data, the thermal comfort is calculated according to the UTCI index. Two representative neighbourhoods of each urban typology are hourly simulated through the SkyHelios-Pro software. Results are assessed through the weighted averages for the selected neighbourhoods' area. They show that during the night there is "no thermal stress", but variations between the urban categories are found. From 12:00 am to 19:00 pm the thermal sensation is "strong heat stress", however there are areas for all typologies where a "very strong heat stress" is achieved. Considering the daily UTCI behaviour, Historical Buildings present the worst values. On the other hand, Modern Closed Blocks respond better to the thermal stress.

KEYWORDS: Urban typologies, urban indicators, outdoor thermal comfort, urban microclimate, SkyHelios simulation.

1. INTRODUCTION

Climate change is related to extreme weather events, which have become more frequent, intense and longer [1]. Heat waves are even worse in urban environments, where the global mean temperature is higher [2]. The Urban Heat Island (UHI) effect based on urban temperatures is widely studied, and it is associated with the urban surface characteristics [3][4]. However, other meteorological variables as humidity, wind and radiation are also modified by the urban morphology and the materials 'properties. This phenomenon, known as urban microclimate, impacts on the energy consumption, productivity and the human health [2][5][6][7].

Although some urban patterns had been related to the influence in the environmental performance at the micro level [8][9], the urban microclimate behaviour is not considered globally through real urban structures. This novel perspective could help cities, where live the 55% of the global population[10], to ensure a thermal quality for both to implant new strategies to reduce the greenhouse emissions and to adapt the environment to the new climatic scenarios.

2. OBJECTIVES

This study assesses the influence of the real urban typologies' characteristics in the urban microclimate behaviour and its impact on the outdoor thermal comfort in cities. The city of Madrid has been taken

as case of study because of their urban complexity and its high summer temperatures, associated to a heat stress. The main objectives of this study are: a) Definition of the current urban typologies in Madrid and their characteristics, b) Knowledge the characteristics of the microclimate behavior for the studied urban typologies and c) Evaluation of outdoor thermal comfort for different urban typologies.

3. MATERIALS AND METHODS

The present methodology is conducted as follows:

3.1 Urban typologies

Different urban classifications are widely available in the scientific literature. Corine Land Cover (CLC) [11] is an inventory based on the visual interpretation of high-resolution image satellite that classifies the land cover in 44 classes, including artificial areas as urban fabric. Other classifications as Local Climate Zones (LCZ) classify a city and its surrounding areas into 17 types, ten of which are urban [12].

Although these urban areas organizations present great advantages in terms of microclimate assessment process, they don't describe the urban typologies according to the peculiarities of the country or the city that facilitate the adaptation strategy process to increase environmental comfort to stakeholders. Thus, more detailed urban classifications for the city Madrid have been assessed.

The Spanish General Directorate of Cadastre (SGDC) divided the built environment depending on its constructive typology in a) collective buildings – open or closed block – and b) individual buildings – terraced and semi-detached house. The General Urban Planning Plan of the city of Madrid (PGOUM) has diverse norms for each type of constructions, with a total of 9 Zonal Norms and other specific classifications for built areas. Finally, the Statistical Institute of the Community of Madrid (SICM) [13] delimits geographically residential areas in 8 typological sectors.

The SICM classification had been selected for being the most updated and tailored for this study. Table 1, Figure 1 and Figure 2 shows the typologies description, visual characteristics and location.

Table 1. SICM classification: Urban typologies description

Name	Description. Urban characteristics	
	Plot, urban grid	Buildings
HB Historical buildings	Irregular plot Medium urban grid Adjoining blocks	High rise Apartment blocks Ancient age
PS Primary settlements	Irregular plot Small-medium urban grid Mix of blocks	Medium rise Single houses or new apartment blocks Ancient age
DS Developed settlements	Semi-irregular plot Big urban grid Adjoining blocks	High rise Apartment blocks Middle age
RC Regular Closed blocks	Regular plot Big urban grid Adjoining blocks	High rise Apartment blocks Ancient age
MC Modern Closed blocks	Regular plot Big urban grid Separate blocks	Medium-high rise Apartment blocks Modern age
OB Open blocks	Variable plot Big urban grid Separate blocks	High rise Apartment blocks Medium-modern age
SH: Single/semi-detached houses	Regular plot Small urban grid Separate blocks	Low rise Single houses Medium-modern age
TH Terraced houses	Regular plot Small urban grid Adjoining blocks	Low rise Single houses Medium-modern age



Figure 1. Residential areas of SICM classification. Distribution and visual characteristics.

3.2 The micro-climate characterization of Madrid

Thermal comfort in urban areas must be assessed from a micro-scale point of view. Urban distributions, morphology, materials or surfaces shape local climatic variables [12]. However, most of the climatic database doesn't consider these variations from a micro level perspective. On the contrary, they offer a general information based on the most frequent values, gathered by macroscale climatic values. Hence, real climatic data for Madrid have been analyzed through Climatic Network of the Madrid's City Hall (CNM) [14] characterized by distributed points along the urban area. It has been selected the maximum of viable CNM's points, without considering their relationship with the urban typology. The Figure 2 presents for each selected CNM's point: the number point, the location, the height of sensors above the ground level (H) and meteorological variables available as the air temperature (Ta), relative humidity (RH), wind velocity (Wv) and global solar radiation (G).

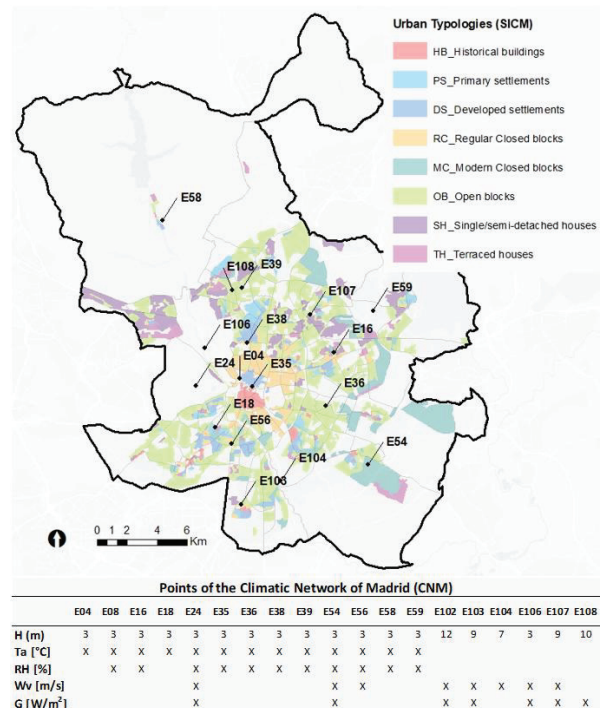


Figure 2. Location and details of the CNM's point and SICM urban typology classification

According to the Köppen climate classification, Madrid is categorized as Csa, Mediterranean climate with mild cool winters and hot summers. Thus, critical episodes in terms of external thermal comfort are related to summer season worsened by extreme weather events and the urban microclimatic effect.

Therefore, it is selected a summer representative day (SRD) for the study through the Typical Meteorological Year methodology (TMY). It is used the registered data in the weather station of CIEMAT facilities, in Madrid [5][15]. The TMY have been developed by the method PASCOOL, gathering data

for 10 years (2008-2017). June 12, July 03 and August 25 had been representative days of the summer months. July 03 is selected as the SRD for the whole season because it shows high mean temperatures along all day, graphed in the Figure 3.

In order to ensure a correct comparison between meteorological data only the values at the same height above the ground are considered for Ta and RH assessment. For the Wv parameters, a height correction is calculated through the Hellman's exponential with a friction coefficient of 0,4 used in urban areas [16].

In addition, to get a distribution map of Ta, RH, Wv and G, their values have been georeferenced and interpolated by Geographic Information System tools (GIS). To this end, it is used the kriging method, where the distributed variables are modelled by a Gaussian process governed by prior covariances [17]. As an example of this process, the Figure 3 and the Figure 4 show CNM's values for July 03. Figure represents hourly Ta values and Figure 4 shows the interpolated results for Ta and RH at 8:00 am.

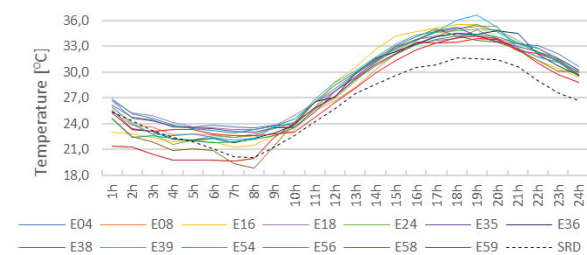


Figure 3. Hourly air temperature (Ta) values for the CNM's points and SRD for the 03 July

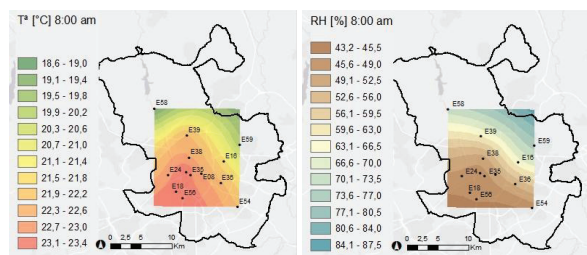


Figure 4. Air temperature (Ta) and Relative Humidity (RH) interpolated values for the CNM's points. 03 July at 8:00 am

3.3 Outdoor Thermal Comfort

Thermal perception of humans must be considered from both the thermoregulatory system and the characteristics of the surroundings. Thus, some thermal indexes have been developed based on the energy balance between our body and the environmental conditions. The most used are Predicted Mean Vote (PMV), the Standard Effective Temperature (SET), the new Modified Equivalent Temperature (mPET) or the Universal Thermal Comfort Index (UTCI). They are all based on the characteristics of the human body and its basal metabolism (height, weight, sex, activity or quantity of cloths), and the microclimatic variables (air and

surface temperature, humidity, wind speed and direction or short and long wave radiation) [18]. Furthermore, properties materials (albedo, emissivity or transparency) and morphological conditions (sky view factor or the sun visible), are determinant in the definition of the urban microclimate.

UTCI has been selected for this study because it is independent of a person's characteristics and it is valid in all climates, seasons and scales. These considerations ease further comparisons in other regions. UTCI is based on the concept of equivalent temperature (ET) comparing current and hypothetical conditions. It depends on the actual values of Ta, Wv, humidity expressed as water vapour pressure (vp) or relative humidity (RH) and mean radiant temperature (MRT) [19]. UTCI values belong to a thermal perception scale divided in 10 categories that goes from extreme cold stress (inferior -50 °C ET) to extreme heat stress (superior +50 °C ET), being no thermal stress values between 9°C ET to 26°C ET.

4. RESULTS

The result's methodology is structured as follows:

4.1 Definition of the urban typologies

The described urban typologies offered by the SICM are analysed from diverse urban indicators. Data from SGDC and the distribution uses from PGUOM are used to this end. Figure 5 represents the mean height of buildings and the representativeness of residential constructions for the SICM classification. Figure 6 indicates the percentage of the surface that is distributed for public spaces and private zones destined to residential areas.

The analysis of Figure 5 and Figure 6 reveals compacted urban typologies for HB, PS, DS and RC, where most of the public surface is occupied by roads (mean of 43%) and private areas are mostly destined to the built zone (mean of 40%). A compacted-high rise typology is presented for the HB, DS and RC buildings (mean of 13m), its representativeness sums up a total of 34% of buildings. PS is characterized to be a compacted-medium rise typology (9 m), with a representativeness of 10% from the total of blocks. Otherwise, MC, OB, SH and TH are disperse urban typologies, where there are more green areas in public spaces (mean of 24%) and private areas have more spaces of pavement (mean of 11%) and garden specially for single-family houses (mean of 26%). Diverse height types are found; disperse-high rise typology belongs to MC and OB (mean of 14m), with a low representativeness for MC (3%) and a high one for OB (30%). The disperse-low rise typology corresponds to SH and TH (6 m), with a 23% number of buildings from the total. However, through a visual analysis some morphological and height variation

within the neighbourhoods is appreciated, especially in DS, OB and TH classifications (Figure 9).

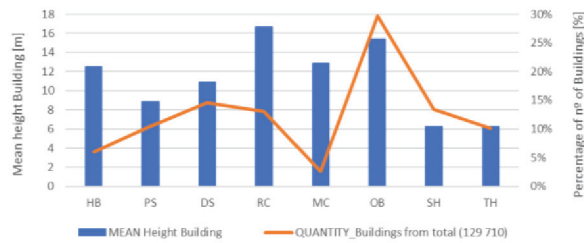


Figure 5. Mean height buildings and percentage of buildings from the total for SICM's urban typologies

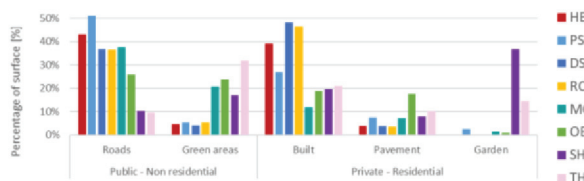


Figure 6. Surface distributions for each urban typology of the SICM classification

4.2 Microclimate behaviour for urban typologies

In order to describe the urban microclimate behaviour, the following graphs show T_a , RH, W_v and G values according to the diverse urban typologies (Figure 7). The weighted mean values for each climatic variable are calculated for the diverse urban zones using the previous interpolation maps.

Notably, all urban typologies present inverse behaviours of T_a and RH. During the day the highest value of T_a is 35°C and the lowest for RH (15%). In the night it is observed slight differences between urban typologies. Temperature values for HB, DS and RC are up 2°C higher than OB, MC, SH and TH. In contra, humidity values for HB, DS and RC are up 16% higher than OB, MC SH and TH. There are modest differences in wind velocity values in the early hours of the night (1:00 -4:00 am) and during the day (14:00 - 19:00 pm), being MC and PS superior to TH with max differences of 0,4 m/s at 2:00 am. No significant changes are found in the solar radiation behaviour. The maximum incidence is at 15:00 pm with a mean of 970 W/m².

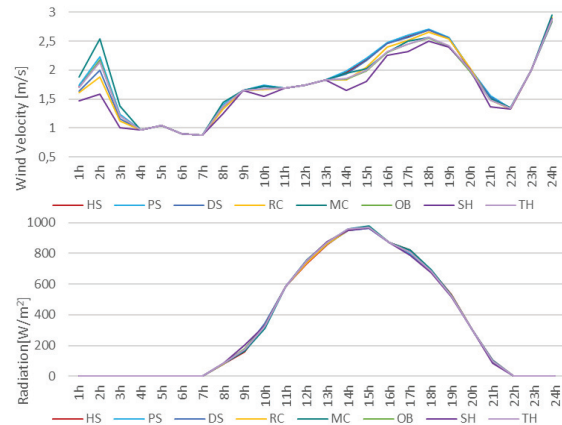
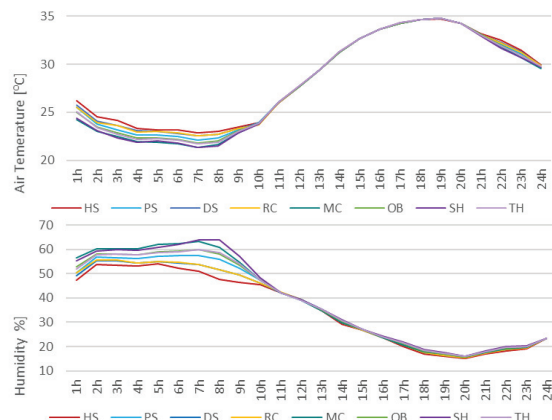


Figure 7. Weighted Mean values of Air temperature (T_a), Relative Humidity (RH), Wind velocity (W_v) and Global Solar Radiation (G) values for urban typologies of Madrid for a typical summer day

4.3 UTCI index for representative typologies

UTCI aim is knowing the physiological reaction of the body to current thermal conditions. Thus, it is developed by a complex multi-node model of human thermoregulation augmented by an adaptation clothing model [18]. In contrast to other indexes, the physiological parameters of the UTCI cannot be set. It is assumed in all cases a fix activity (walking speed of 4km/h) and internal heat production (135 W/m²).

The SkyHelios Pro software is used to define the UTCI index [20]. The model allows the calculation and visualization of continuous results for each point of a complex area. For this purpose, two representative neighbourhoods of each urban typology defined by SICM are selected to be simulated on July 03. TH typology has not been considered because of its similarity to SH. The program has been fed in each simulated area by a) Hourly urban meteorological variables T_a , RH, W_v and G . The weighted means of these values for each neighbourhood are used for the interpolated CNM's points. b) Urban morphology through 3D representation and its material properties (Table 2).

Table 2. Material properties for the UTCI simulation

Material	Asphalt	Concrete	Plaster	Grass	Soil	Tree
Albedo	0.13	0.23	0.30	0.23	0.30	0.20
Emissivity	0.95	0.80	0.92	0.93	0.87	0.98
Transparency	1.00	1.00	1.00	1.00	1.00	0.90

Conducted results are displayed for the whole representative neighborhood through 5 x 5 m grid at 1.1 m of height. The grid size is selected to be the most effective solution between the available resources and the accuracy of results. The obtained outcomes include atmospheric, sunshine and biometric approaches as albedo (α), emissivity (ϵ), sky view factor (SVF), surface temperature (TS), short and

long wave (SW, LW), mean radiant temperature (MRT), wind direction (Wd), visible sun (Sv) and UTCI .

The hourly mean UTCI behavior is represented in Figure 8.a, considering the weighted mean values of the two representative neighborhoods per typology, named with the “r” suffix. Furthermore, in the graph it is included the thermal sensation equivalent scale. From 22:00 pm to 10:00 am all urban classifications are in the category of “No thermal stress”, with a minimum of 20°C ET, finding slightly differences during the night of approximately of 2°C ET between the lowest urban typology (MCr) and the highest (HBr). The rest of the day the thermal sensation according to UTCI scale belongs to “moderate stress” and “strong heat stress” from 12:00 am to 19:00 pm, with not remarkable variations between urban typologies. However, as it is graphed in the Figure 8.b and Figure 8.c, which represents the minimum and the maximum UTCI values in the representative areas of the neighborhoods, some areas modify the hourly UTCI behavior previously described. Minimum values attenuate the UTCI curve until the 18°C ET at 02:00 am. On the other hand, the maximum results show that in all typologies a “very strong heat stress” is reached from 12:00 am to 18:00 pm with the highest value of 42°C ET at 15:00 pm.

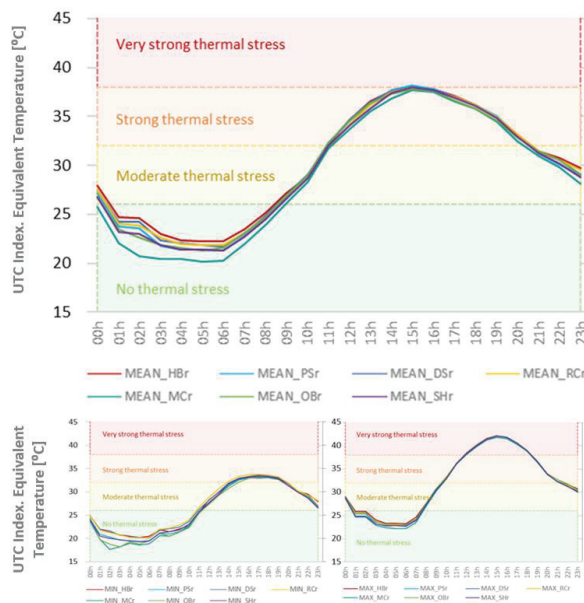


Figure 8. Hourly UTCI index values for urban typologies through the simulation of representative neighbourhoods. a) Mean (top), b) Minimum (left) and c) Maximum (right)

The Figure 9 represents the UTCI index distribution in an example area of the selected 14 neighbourhoods where building scales, distributions and morphologies at 2D are displayed. As an example, 05:00 am and 15:00 am are chosen times because they correspond to the lowest and highest UTCI values from the Figure 8.a. At 05:00 am more variations in the UTCI values are found, being lower

for MCr, OBr and SHr (about an ET of 20°C) and higher for HBr, DSr and RCr (about an ET of 22°C). On the other hand, at 15:00 pm no appreciable differences between values are shown being about 38°C ET. Only these values are reduced to an ET of 32-34°C in areas shaded by high buildings or trees.



Figure 9. UTCI values through a 5 x 5 m grid distribution at the height of 1.1 m for representative neighbourhoods

Finally, Figure 10 portrays the accrued UTCI values per day that are shown in Figure 8.a. It illustrates bigger values of UTCI for HBr, DSr and RCr and smaller for MCr, SHr and OBr, confirming the previous analysis (Figure 8 and Figure 10). So, the highest UTCI values are usually linked to compact-high rise typologies. In contrast, the lowest values are linked to disperse high rise or low zones.

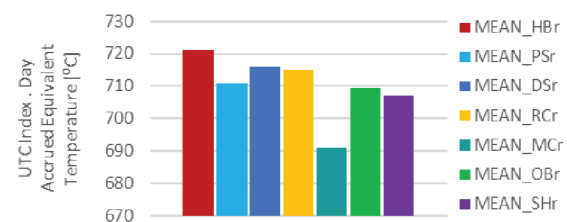


Figure 10. Accrued hourly per day UTCI values for the representative neighbourhoods.

4. CONCLUSION

The microclimate and the outdoor thermal comfort in the city of Madrid are evaluated for a summer typical day in different urban areas. Based on the Statistical Institute of the Community of Madrid (SICM) classification, the urban typologies of Madrid have been divided into compact-high rise, compact-medium rise, disperse-high rise and disperse-low rise zones. Nonetheless, morphological and height differences between the representative neighbourhoods are found, suggesting a review of the SCIM classification.

The urban microclimate is studied for these urban typologies though hourly Ta, RH, Wv and G values for the representative summer day. These interpolated data, from the CNM's points, show slight differences of approximately 2°C Ta between urban classifications during the night, being the highest results to compacted-high rise typologies and the lowest results to disperse typologies as it may be expected due to the urban heat island. This behaviour is the opposite for the RH values with until 16 % of difference.

Outdoor thermal comfort is evaluated according to the UTCI index. To this end, two representative neighbourhoods of each urban typology are simulated by the software Sky Helios Pro. The conducted data are approached hourly by 5 x 5 m grid at the height of 1.1 m through urban microclimate data. Values are analysed considering UTCI distribution within the neighbourhood and globally for the urban typology. Both approaches show differences during the night, being higher for compact- high rise typologies (about ET of 22°C) than disperse typologies (about ET of 20°C) but are classified as "no thermal stress". Hardly UTCI variations are found during the day (about ET of 38°C at 15:00 pm), only reduced by the trees or building's shadows. Although the mean thermal sensation in the central day hours (12.00 am-19:00 pm) is "strong heat stress", for all typologies a "very strong heat stress" is reached in some areas.

Some considerations should attend for further studies, as the fixed physical values and adaptation clothing model of the UTCI index, which should hide some current comfort variations. Besides the found limitations, this study presents a first approach to study the outdoor thermal comfort for the urban typologies of Madrid. It justifies the need to plan strategies to reduce thermal stress, especially in compacted-high rise urban typologies that represent the 34% of buildings. These frameworks will be even more crucial for the forecasted extreme events as the heat waves.

REFERENCES

1. "IPCC: Global Warming of 1.5°C," 2018.
2. "IPCC: Climate Change 2014. Synthesis Report " 2018.

3. C. S. B. Grimmond *et al.*, (2010). "Climate and more sustainable cities: Climate information for improved planning and management of cities" *Procedia Environ. Sci.*, vol. 1, no. 1, pp. 247–274.
4. Y. Wang, Q. Zhan, and W. Ouyang, (2017) "Impact of Urban climate landscape patterns on land surface temperature in Wuhan, China," *Sustain.*, vol. 9, no. 10
5. M. N. Sánchez, S. Soutullo, R. Olmedo, D. Bravo, S. Castaño, and M. J. Jiménez, (2020) "An experimental methodology to assess the climate impact on the energy performance of buildings: A ten-year evaluation in temperate and cold desert areas," *Appl. Energy*, vol. 264, no. February, p. 114730.
6. D. Fröhlich and A. Matzarakis, (2012) "Modeling of changes in thermal bioclimate: Examples based on urban spaces in Freiburg, Germany," *Theor. Appl. Climatol.*, vol. 111, no. 3–4, pp. 547–558, 2013.
7. C. Linares and J. Díaz, (2008) "Impact of high temperatures on hospital admissions: Comparative analysis with previous studies about mortality (Madrid)," *Eur. J. Public Health*, vol. 18, no. 3, pp. 317–322.
8. Z. J. Heng CK, Malone-Lee LC, (2017) "Relationship between density, urban form and environmental performance," *Grow. Compact urban form, density Sustain. Routledge*. In J. H. Bay S. Lehmann
9. S. Ghosh and R. Vale, (2009) "Typologies and Basic Descriptors of New Zealand Residential Urban Forms," *J. Urban Des.*, vol. 14, no. 4, pp. 507–536
10. U. Nations, *World Urbanization Prospects*, vol. 12. 2018.
11. "CLC 2018 — Copernicus Land Monitoring Service," 2018. [Online], Available: <https://land.copernicus.eu/pan-european/corine-land-cover/clc2018> [Apr. 17, 2020].
12. I. D. Stewart and T. R. Oke, (2012) "Local climate zones for urban temperature studies," *Bull. Am. Meteorol. Soc.*, vol. 93, no. 12, pp. 1879–1900.
13. "SICM - Statistical Institute of the Community of Madrid" [Online], Available: <http://www.madrid.org/> [Apr. 17, 2020].
14. "Climatic Network of the Madrid's City Hall." [Online], Available: <http://www.mambiente.madrid.es> [Apr. 17, 2020].
15. Soutullo, S.; Sánchez, M.N.; Enríquez, R.; Jiménez, M.J.; Heras, M.R. (2017). Empirical estimation of the climatic representativeness in two different areas: Desert and Mediterranean climates. *Energy Proc.*, vol. 122, pp. 829–834.
16. S. Zare, N. Hasheminejad, H. E. Shirvan, R. Hemmatjo, K. Sarebanzadeh, and S. Ahmadi, (2018) "Comparing Universal Thermal Climate Index (UTCI) with selected thermal indices/environmental parameters during 12 months of the year," *Weather Clim. Extrem.*
17. K. Johnston, J. M. Ver Hoef, K. Krivoruchko, and N. Lucas, (2004) "Using ArcGIS geostatistical analyst," *Analysis*, vol. 300, no. January 2004, p. 300, 2001
18. D. Fröhlich and A. Matzarakis, (2018) "SkyHelios - A model for the rapid calculation of spatially resolved micro scale climate factors," p. 66.
19. "UTCI - Universal Thermal Climate Index." [Online], Available: <http://www.utci.org/> [Apr. 17, 2020].
20. D. Fröhlich and A. Matzarakis, (2018) "Spatial estimation of thermal indices in urban areas-basics of the skyhelios model," *Atmosphere (Basel)*, vol. 9, no. 6, pp. 1–14.

Effective Food: Design and Urban Agriculture in the Post Carbon City

SEÁN CULLEN¹, GREG KEEFFE¹

¹ School of Natural and Built Environment, Queen's University Belfast, Belfast, United Kingdom

ABSTRACT: *Urban agriculture has the potential to unlock new content and form in the new programmatic and spatial dynamics of the post carbon city. It will be one defined by new use of post-industrial and post-retail buildings and sites. We propose the growth and engagement with urban agriculture as a way of creating new ecological and sustainable futures. Through the design of a technical food system in the urban context of Belfast, the paper demonstrates how local food production can reduce food miles, limit packaging and waste, thereby optimising food, energy and water (FEW) resources use while offering new possibilities for how residents live, work and access food. Firstly, the paper analyses the impact of residents' food consumption by quantifying land use for production and the area of forest to sequester full lifecycle carbon emissions, called the 'foodprint'. Secondly, the paper examines how efficient the integration of a technical food system in the city is in reducing the ecological footprint of food consumption. The paper finds that urban agriculture is effective rather than efficient. The importance of food production rests in the opportunities it creates in fostering new economic, social and cultural opportunities while enhancing ideas related to the circular economy, reduce waste and make visible the provenance of food.*

KEYWORDS: *Urban agriculture, design practice, productive neighbourhood*

1. INTRODUCTION

Historically, food has shaped and transformed the urban environment because of its social, cultural and economic importance. Food previously anchored the development of our cities, constrained by the movement of live animals or grain via ports to markets. Contemporary food production, supply and distribution, however, have detached the city from its hinterland, fed instead by global systems characterised by intensive farming practices and complex logistical operations. Consumers are distant from landscapes of production; the U.K.'s five biggest supermarkets account for 75.3% of total market share on food – bottlenecks in the supply chain and indifferent experiences [1]. At the same time, diets are changing. Convenient and highly processed food becoming more common and causing long-term health issues. A consequence of this cultural shift, however, is the impact of food on the ecological footprint of the city. When London completed its first ecological footprint in the early 21st Century, 40% was attributed to food, for which it had no policy to address [2]. Here we argue that urban agriculture can effectively transform our cities and reduce environmental impact attributed to food by examining how the design of a technical food system in Belfast can reduce our ecological footprint but also change our connection to and perception of food.

Our research uses design practice to alter how the food-energy-water (FEW) nexus is operationalised in the city [3]. This paper proposes how urban design interventions can produce effective synergies, create

closed loop waste streams, enhance circular economies and engage residents with food provenance. Furthermore, the quantifies the impact of food consumption by analysing land use and carbon emissions of our diets – split across various stages of the supply chain – to qualify the efficiencies provided by a design intervention. We find that while the productive neighbourhood can improve the efficiency of our FEW resources, its value lies in effectiveness, producing new social, economic and environmental opportunities for residents.

2. FOODPRINT: SPATIALISING THE IMPACT OF FOOD CONSUMPTION IN CITIES

The consumption of food in cities is often measured in metrics that are problematic for urban designers to deal with – millions of tonnes, thousands of calories per minute or billions of Pound Sterling per day. Therefore, we propose translating the impact of food on our cities into spatialised information that can measure the current consequences of food consumption in addition to measuring how a design intervention can affect it. Spatialising data is important because it is the language of urban design and architecture. It also offers a way to capture the complex nature of food that comes from distant and distributed landscapes.

The 'foodprint' spatialises average annual per capita consumption (PCC) of food for residents in Northern Ireland in two ways [4]. Firstly, the area of land required to produce food for annual PCC. Secondly, the area of forest to sequester full lifecycle

PLEA 2020 A CORUÑA

Planning Post Carbon Cities

carbon emissions of food for annual PCC (Table 1). The assumed sequestration rate of 3.6 tC/ha/year is based on planting Sitka Spruce YC 16 [5].

Table 1: Annual PCC food consumption for N.I. [6] translated to land use for production [7, 8] and area to sequester the full lifecycle emissions [9]

Food item	Annual PCC consumption (kg/l/#)	Land use (m ²)	Area to sequester full lifecycle emissions (m ²)
Beef (kg)	21.18	487	423.10
Lamb (kg)	1.03	19	29.96
Pork(kg)	15.06	111	134.89
Chicken (kg)	18.59	136	94.94
Turkey (kg)	1.34	10	10.79
Fish (kg)	6.49	2	25.94
Whole Milk (l)	93.64	111	131.66
Cheese (kg)	4.84	49	48.33
Yoghurt (ml)	10.01	5	16.30
Eggs (#)	105.87	41	15.04
Fresh Fruit (kg)	51.57	26	41.97
Fresh vegetables (kg)	47.17	14	76.80
Potatoes (kg)	105.01	21	225.34
Tomatoes (kg)	1.43	0	1.17
Cereals (kg)	57.43	80	72.25
Rice (kg)	5.06	3	10.12
Butter (kg)	2.62	36	-
Margarine (kg)	0.66	14	-
Vegetable Oil (l)	2.71	56	-
Sugar (kg)	3.24	4	-
Tea (kg)	1.60	56	-
Coffee (kg)	1.05	17	-
Beer (l)	5.80	3	-
Wine (l)	10.13	15	-
Total		1317	1359

The data is spatialised to the scale of the individual (PCC), the household (2.5 PCC) and the street (65 PCC) compared to their physical footprint in the city (Fig. 1). It demonstrates the influence food consumption has on distant, distributed landscapes that often utilise intensive farming practices and carbon hungry supply, processing and distribution processes that consumers are often unfamiliar with – feed lots in the American mid-west, glasshouses in the Hook of Holland, plastic greenhouses in Alermía, Spain or poultry broiler houses in Northern Ireland.

In total, 61% of emissions in food lifecycle assessment comes from the farm alone [10].

However, growing food locally can significantly reduce transportation and packaging emissions; these vary with different food types. For example, emissions for tomatoes (1.4 kg CO₂e per kg) are from: farm (50%); land-use change (29%); transport (14%); packaging (7%) [10, 11]. The importance of spatialised data also lies in its ability to act as a metric in order to assess the impact of a design intervention. Of interest to us, is how a design intervention in the city can bring measurable improvements to emissions reductions and land use while also assessing the wider social, cultural and economic benefits in the city.



Figure 1: Spatialised 'foodprint' measured at the scale of the individual (PCC = 0.27ha), the household (2.5 PCC = 0.67ha) and the average terrace street in Belfast (65 PCC = 17.34ha), depicting land-use (red) and area of forest for sequestering full lifecycle carbon emissions from annual food consumption of average resident.

3. DESIGN PRAXIS AND THE FWE NEXUS

Our research looks at urban design practice as a way of unlocking potential futures for regions, cities and neighbourhoods. It seeks to proposition how we transform neighbourhoods to mitigate and adapt to climate change while capitalising on productive synergies in the urban environment. Much of this is done through proposing radical, speculative futures that open dialogue with stakeholders. By asking 'what if...' we try to set out principles that go beyond

PLEA 2020 A CORUÑA

Planning Post Carbon Cities

constraints of traditional forms of engagement with place. We use Belfast, the site on which we are basing much of our ongoing research, as an example of how to utilise the 'foodprint' for assessing the impact of a design intervention. It is a post-industrial city – the birthplace of the Titanic – and is currently undergoing radical spatial transformations due to the changing nature of economic activity and peacebuilding activities.

The design proposition reimagines an existing typology seen across the city and a prominent piece of infrastructure in neighbourhoods: the peacewall (Fig. 2). Built in the second half of the 20th Century, during a period known as The Troubles, peacewalls were constructed by the state in Northern Ireland to separate Unionist and Nationalist communities where violence typically flared up. Increasingly difficult to deal with in local communities, their future remains contentious and divisive. Here we propose the operationalisation of a peacewall on Bryson Steet in East Belfast, turning them into productive spaces with the aim of creating a politically neutral zone where food can bring people together.

The design utilises an aquaponic growing system for tomato production. On a footprint of 45m² and over three floors, the structure is 30m in length (Fig. 3). The proposal can produce crops year-round at an

average yield of 30 crops/m², equating to a total annual output of 32,400 kg.



Figure 2: The Bryson Street peacewall in East Belfast, the site of the design intervention. Typically, used to divide communities, they are contentious and problematic to deal with.

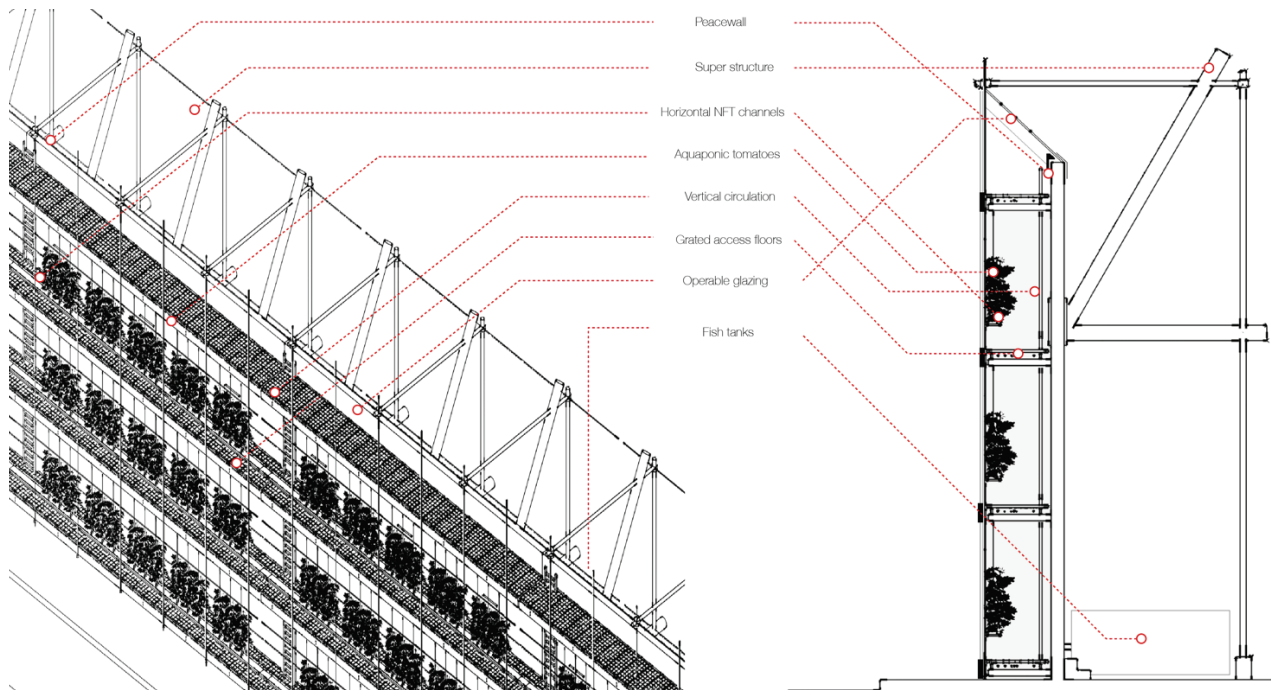


Figure 3: Productive peacewall on Bryson Street for shared food growing spaces in the neighbourhood.

4. MEASURING EFFICIENCIES OF URBAN AGRICULTURE

The following demonstrates how the design intervention alters an individual's 'foodprint'. It visualises how a *productive peacewall* can change CO₂e emissions and land use associated with the consumption of a single vegetable – in this case tomatoes. Currently, using traditional farming practices, an individual consumes 1.43 kg of tomatoes per annum and requires an area of 0.04m² to grow. Should the resident now eat the tomatoes from the *productive peacewall*, this reduces to 0.004m² – 10% of the area compared to traditional growing process.

The *productive peacewall* also changes the full lifecycle emissions for tomato consumption of the resident. Firstly, food miles are reduced, eliminating 14% of the emissions associated with tomato production. Secondly, packaging is eliminated, as all the tomatoes from the *productive peacewall* are sold loose to residents. This reduces full lifecycle emissions by a further 7% [10, 11]. Two key assumptions are made in this calculation: firstly, that the emissions from the farm (50%) remain the same – the new vertical system will use as much energy as a

traditional farm per kilogram of output; secondly, that the land-use change (29%) remains the same – which accounts for the embodied emissions in the construction of the new vertical system in the neighbourhood and balanced out over the lifespan of the building. Consequently, the CO₂e from a resident's tomato 'foodprint' goes from 2kg CO₂e per annum to 1.56kg CO₂e – or 1.48m² and 1.15 m² of forest respectively, to sequester the carbon [5]. This is a reduction of 22% for an individual's tomato consumption.

While these numbers are significant for tomato consumption, within the whole picture of food consumption they affect the 'foodprint' in a very small way (Fig. 4). In an individual's total 'foodprint', land use reduced by 0.036m² (0.0027%) and area to sequester CO₂e emissions by 0.33m² (0.024%) – extremely small improvements in efficiency. Therefore, urban agriculture requires design to be effective rather than efficient [12]. It must envisage new possibilities that enable systems to thrive, particularly through the synergies it creates and new ways in which residents live.



Figure 4: Assessing the effectiveness of the design intervention through the foodprint of the individual (PCC) – the original (left) versus the new foodprint based on the *productive peacewall* (right). The new food print of the individual provides efficiencies of 90% for land use and 22% in area for sequestering carbon emissions when considering tomato consumption – the reduction is shown in shaded red area. However, only provides small efficiencies of overall food print; therefore, design must be effective for the city and its residents in other ways.

5. DELIVERING EFFECTIVE FOOD

Firstly, urban agriculture must be viewed as collective, complementary forms of production that provide synergies in outputs and waste streams. The system operates in close proximity to waste streams which are otherwise unused. The reuse and recycling potential in the city are immense and offers vast opportunities for urban agriculture to reduce emissions from the farm and from land use change. For example, packaging and refrigeration used in the supply chain can be negated – saving energy and material waste. Furthermore, and not considered in the above re-calculation of the ‘foodprint’, is the potential to harvest fish in the aquaponic system. Although they require feed, which might come from waste food in the neighbourhood, it provides further reduction in food miles and packaging for fish consumption. Energy cascading systems may also support the reduction in operational costs and energy losses in the neighbourhood. For example, waste heat from intensive industrial processes could be captured for heating of the aquaponic system during the winter. It could aid in raising the temperature of the growing space as well as the water temperature of the fish tanks. Secondly, the opportunities offered by creating a circular economy are immense; money spent in the neighbourhood stays in the neighbourhood. Currently, multinational shops and supermarkets extract money from the city – retail ‘sinks’. Value is created through local production and enables multiplier effects. The system produces a crop worth £90,000 a year at current retail rates for tomatoes. This money could be used to support employment and operation in the neighbourhood.

Similarly, new possibilities for engagement with the provenance of food are created. The shortening of the supply chains enables residents to see where their food is coming from and see how it is produced; it also allows for resilience. Devastating weather events on harvests and disruptions to just-in time supply chains results in a fragile food system which requires cities to become somewhat autonomous to reduce risk. Likewise, central to future urban environments is the experience economy; it will redefine how we engage with buildings, spaces and the operation of urban settings across the globe over the next century [13]. No longer requiring goods or services, people desire and crave experiences. These experiences are staged, offering memorable and personal forms of engagement to the guest and reveal complexity, unexpectedness and joy over time. The four ‘Es’ of the experience economy are: educational, esthetic, escapist and entertainment. Food production, purchasing and consumption have historically been celebrated and enjoyed in our cities.

They offer forms of social and civic interaction unique to a people, place and culture that must return to our neighbourhoods. The post carbon city requires food to: enhance what we know about its production and value (education); embrace its smell, sounds and tastes unique to a place (esthetic); allow us to immerse ourselves in unexpected ways of production and consumption (escapist); and, to sing, laugh and cry with friends and family over a meal (entertainment).

Critically, design must transform how residents live in a place. The *productive peace wall* seeks to make an interface a new, productive and working zone where residents from both communities can engage in a dynamic and neutral way – buying, selling or making food. It offers new content and form to the typology evident right across the city. The city has long-term ambitions to transform these areas to enhance community cohesion and interaction through a neutral function. The ‘foodprint’ demonstrates that growing locally can only slightly reduce the ecological impact of food, so relies on more effective narratives and dynamics in the city and between residents.

6. FUTURE WORK: QUESTIONS OF PRODUCT, SERVICE AND TYPOLOGY

The design intervention and the evaluation of how it affects the ‘foodprint’ demonstrates that a reduction in carbon emissions are primarily through reduced transportation and packaging. However, it is predicated on a critique solely of the service – in this case the production of food. What is not considered, is the embodied energy in the fabrication and production of the architecture or infrastructure. It is important to note that our research on the FEW-nexus looks not at the cost implicit in the product – in this case the construction – but in the service it offers through its operational lifespan. Future work will critique this approach, particularly through the lens of cradle to cradle concepts in order to imagine possibilities of reuse or biodegradable materials.

Other future work will look at different urban typologies coupled with technical food systems that will utilise the ‘foodprint’ as a form of assessment. It will go on to explore new ways of adapting the neighbourhood to unlock radical food futures that are effective. These will explore the *food producing forecourt* – a key food-energy interface – and the *adapted terrace* – a core FWE consumptive typology. The interfaces of infrastructural systems with consumers have emergent trajectories with which urban design must deal with. Firstly, the forecourt as a loss leading resource (fuel) to get shoppers to large superstores. Secondly, the house of the 20th century

has outdated technologies in relation to energy consumption and comfort but also in terms of how food is delivered – takeaway meals (JustEat, Deliveroo) or fresh food boxes (Gusto). Lastly, it will explore how we value underlying principles or design ethos when considering the future challenges of the city? As shown here, depending on whether we value a reduction in CO₂ or whether we value profit, it alters the form of a design proposition in the neighbourhood. Critically however, no matter the ethos, the proposition must respond to climate change at all levels of engagement, constantly questioning the role new climate futures will have on influencing the emergent city.

7. CONCLUSION

Food is a vital metric to consider in the post carbon city because it relies on a global, rural hinterland for production and supply. The city of the 21st century is dealing with new paradigms of operation, production, processing, supply and consumption that, arguably, must transform how we live for the benefit of the environment. The urban context presents opportunities for productive, effective urban agriculture; it offers new typologies of urban spaces that are experimental and connects citizens with systems of food production that is ordinarily global, intensive and unbeknownst to the consumer.

Design, planning and architecture do not only attempt to improve the efficiency of resources but also to promote visions for new ways of living. Notably, as made evident through the quantification and spatialization of the ‘foodprint’, design typically operates as an effective, heuristic practice. Effectiveness of urban design in the post carbon city rests on the creation of circular economies, closed waste streams and evidencing food provenance – all enabled through urban agriculture. The experience of food in the post carbon city is focused primarily on the later stages of the supply chain – purchase and consumption. However, food production can be a future experience of urban life that subsumes our neighbourhoods and daily activities; forming new types of economies, tourist activities and employment opportunities.

Around the world, cities will have to deal with food as an urban metric as it affects health, well-being and lifestyle in significant, long-term ways. Urban design must begin to operate systematically to effect change. For this reason, the practice of measuring and visualising the extremities of design potential in the neighbourhood allow for a more radical neighbourhoods of the future. Stakeholders are traditionally static; design practice should unlock, quantify and qualify design practice that utilises food,

energy and water in an effective way beyond the paradigms already present in the minds of citizens.

ACKNOWLEDGEMENTS

M-NEX is a granted project of Collaborative Research Area Belmont Forum (no. 11314551). We are grateful to JPI Europe Urban for initiating the “Sustainable Urbanization Global Initiative—Food-Water-Energy Nexus” and making the M-NEX project possible.

REFERENCES

1. Kantar World Panel. Great Britain: Grocery Market Share (12 weeks ending). Available: <https://www.kantarworldpanel.com/grocery-market-share/great-britain>. [06 April 2020]
2. Best Foot Forward, 2002. *City Limits: A resource flow and ecological footprint analysis of Greater London*. Chartered Institution of Wastes Management Environmental Body.
3. Yan, W. and R. Roggema. (2019). Developing a Design-Led Approach for the Food-Energy-Water Nexus in Cities. *Urban Planning*, 4(1): p.123-135.
4. Cullen, S. and G. Keeffe, (2020) 'Spatialised method for analysing the impact of food', in Roggema, R. and Yan, W. (ed.) *TransFEWmation*. Switzerland: Spring International Publishing. (accepted)
5. Dewar, R.C. and M.G.R. Cannell, (1992). Carbon sequestration in the trees, products and soils of forest plantations: an analysis using UK examples. *Tree Physiology*, 8, pp. 239–258.
6. Office for National Statistics, (2017). *Family and Food Survey: purchased quantities of household food and drink per person per week (three-year averages) 2016-17*. London, U.K.
7. Gerbens-Leenes, P.W. and S. Nonhebel, 2002. Consumption patterns and their effects on land required for food. *Ecological Economics*, 42(1), pp. 185-199.
8. Williams, A.G., Audsley, E., and D.L. Sandars, 2006. *Determining the environmental burdens and resource use in the production of agricultural and horticultural commodities*. Main Report. Defra Research Project ISO205. Bedford: Cranfield University and Defra.
9. Hamerschlag, K., 2011. Meat eaters guide to climate change and health. *Environmental Working Group*, pp. 19.
10. Poore, J. and T. Nemecek, (2018). Reducing Food's Environmental Impacts through Producers and Consumers. *Science*, 360(6392): p. 987-992
11. Ritchie, H., (2020). You want to reduce the carbon footprint of your food? Focus on what you eat, not whether your food is local. *Our World in Data*, [Online]. Available: <https://ourworldindata.org/food-choice-vs-eating-local> [6 April 2020]
12. Keeffe, G. and S. Cullen. (2020) 'A flexible scaffold: design praxis in the FEW-nexus', in Roggema, R. (ed.) *TransFEWmation*. Switzerland: Spring International Publishing. (accepted)
13. Pine, B. J., 2nd and J.H. Gilmore, (1998). 'Welcome to the experience economy'. *Harvard Business Review*, vol. 76(4): p. 97-105.

Simulation Based Support for the Urban Energy Transition

Predicting Heating Energy Needs for Residential Building Clusters Using a Non-Linear Data-Driven Approach

ANDREAS KOCH¹, MARIE SEVENET¹

¹EIFER Europäisches Institut für Energieforschung EDF-KIT EWIV,
Emmy-Noether-Strasse 11, 76131 Karlsruhe, Germany

1. INTRODUCTION

In the context of an increasing importance of cities in the global debate on climate change [1], opportunities for urban mitigation actions emerge at the scale of building clusters and neighbourhoods as a distinct target scale for urban energy planning.

[2] provide a detailed assessment of a number of applied models to support urban energy planning. In their analysis of quantitative energy assessment methods for existing buildings [3] point out the difficulties of acquiring reliable input data for forward models. At the scale of urban neighbourhoods, detailed building descriptions often lack reliable data and are in many cases over-parameterised for the planning tasks [4]. In the same line of thought [5] states that “the different physical and administrative scales and actors induce scarce, dispersed and low quality physical data, which reduces the quality of models”.

The conducted research investigates the applicability of a data-driven approach, based on a limited amount of input data at the scale of building clusters. The paper argues to apply such simplified yet accurate models in urban energy planning to allow for continuous benchmarks for monitoring the urban energy transition.

2. URBAN ENERGY PLANNING

Following a global energy transition needed, different stakeholder are involved at different scale from local to global, building to city to intervene on the production of renewable energy and the control of energy use. While the macro level provides objectives, regulation and subsidies for the transition, communities must implement these objectives, and developers and owners must comply with the new standards in force.

For the implementation of energy strategies, IEA EBC Annexes 51 and 63 [6] pointed out the need for new approaches that allow planners to adopt a consensus position among all stakeholders and actors. During Annex63¹, a number of challenges related to barriers for planners have been identified [7].

1. Setting environmental targets and objectives for urban development.
2. Developing a feasible strategy around the use of renewable energy.
3. Create and use a legislative framework to encourage the transition process.
4. Create the framework for competitive design that maximises environmental benefits.
5. Develop and use planning and decision support tools based on available information.
6. Establish a feasible program for the establishment of an observatory.
7. Obtain the commitment of stakeholders.
8. Monetizing the non-financial benefits of the transition process
9. How to structure the organization to ensure fluidity of action.

These measures refer to all scales of involvement: city, district and project scale. However, they are not implemented in the same way at each scale. At city scale, municipalities set the overall objectives and trends. While at project scale, targets have to be operational and measurable in order to be monitored over time. Table 1 shows differences in planning process for each scale.

¹ <http://annex63.iea-ebc.org/www.annex63.org/index.html>

Table 1: Measures at District Scale Compared to City and Project Scales [8]

City Scale	District Scale	Project Scale
Targets in form of broad strategic statements	Targets in form of setting up planning framework	Targets in form of specific configurations at site
Development-oriented	Planning-oriented	Action-oriented
Strategic representatives	Local representatives	Professional stakeholders
Outlining	Framing	Configuring
Decision and Information	Analysis and Regulation	Execution and Monitoring

In a consistent urban energy planning approach, climate and energy targets have to be defined at city scale, to then be applied on energy concepts at district level which eventually become the framework for building and infrastructure concepts for implementation projects. Especially with regard to local production and the use of renewable energy the district emerged as a planning object in its own right [9]. In the following planning support at both district and city scale will be regarded considering a quantitative planning support method.

Urban energy planning at district level involves multiple actors such as planners, architects, developers, local representatives and businesses sometimes local citizens. Such situation often result in “wicked problems” [10] with multiple objectives, values, problems tactics, complexity and uncertainty. To avoid conflicts and misunderstanding, a data-driven approach, based on a limited amount of input data helps to build a comprehensive and common vision on modelling.

3. METHODOLOGY AND DATA

Planning processes aims to anticipate and build an adequate trajectory for the energy transition. In the previous section, the tasks at different levels have been discussed. From these identified needs [7], it is deducted that quantifiable energy needs at city and district scale are necessary prerequisites to set realistic environmental targets (1.) and develop realistic strategies for the use of renewable energies (2.). Eventually, planning support tools (5.) should be usable by planners to integrate them in a multi-stakeholder process and deliver robust results based on available data. A main difficulty identified by [3] is that detailed data on the energy performance of buildings is most of the time dispersed and incomplete. In the current practice, this is especially an issue for bottom up or physical models, describing the building stock. More importantly existing tools are often complicated and difficult or costly to maintain.

For the strategic energy planning at the scale of districts or cities in this study preference was thus given

to a data-driven approach described by [11, 12] as it is based on the annual heating needs of buildings as well as mean daily outdoor temperature data that is readily available in most urban areas.

The selected energy signature calculates mean daily energy needs as a function of the mean outdoor temperature (Figure 1). Equation 1 describes the distribution function for the heating energy needs over the simulated period resulting in the normalised daily energy needs for each day (h_a). Mostly annual heating periods represent the periods for which data is available and useful for planning strategies.

$$h_a = \frac{A}{1 + \left(\frac{B}{\vartheta_a - \vartheta_0}\right)^C} + D \quad (\text{eq. 1})$$

The mean daily outdoor temperature (ϑ_a) is the single regressor variable and is calculated as a geometric series over the past four days. The three parameters “A”, “B” and “C” are defined in relation to the type of building. Parameter “D” shifts the curve along the y-axis and thus describes the non-temperature dependant part of the energy needs (e.g. domestic hot water). The temperature ϑ_0 describes the point of discontinuity with T equals 40°C.

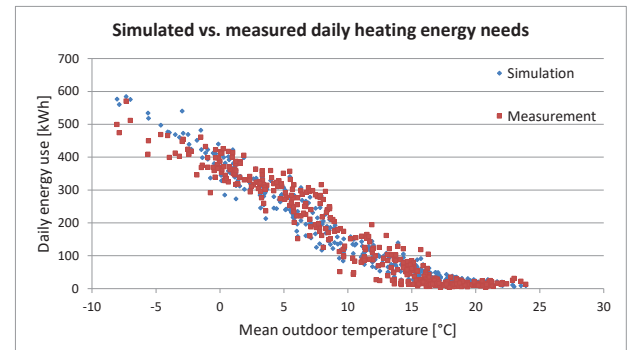


Figure 1: Simulated and measured daily heating energy needs vs. outdoor temperature for five single dwelling units [12]

For the parametrisation a number of parameter sets can be found [12, 13] that differ by typical performance of the building, here the ones proposed by [11] were used which are provided in Table 2. The parameters are in all cases derived from the analysis of larger samples representative for specific usages.

Table 2: Factors for the model parametrisation

Factor	A	B	C	D
Value	2.79	-37.17	5.40	0.17

The described method was initially developed for regional prediction of gas loads and is used for example in Germany [13], a similar statistical method is used in the UK or Austria. It represents a tested model for the application at a regional scale.

For the described use case, it is therefore most relevant to test the lower limit of its applicability. Due to the nature of statistic models such a lower limit is reached when the model fails to predict aggregated values of energy needs with an acceptable error. In order to test the suitability, daily heating energy needs were calculated for a number of residential buildings in Southern Germany using the non-linear, single variant energy signature model. Simulation results were then evaluated against measured data at different aggregation scales from single buildings to a cluster of five buildings.

4. RESULTS

The statistical analysis shows an improvement of all considered indicators with increasing sample size (Table 3). As can be expected, the simulation for individual buildings showed high values for the coefficient of variation of the root mean square error (CV RSME) of up to 44%. By adding further buildings, the error was reduced to a value of 19% for the whole sample. The decreasing error with larger sample size indicate that already the very small sample shows aggregating effects in which high and low consuming units even out towards a mean daily energy use.

The coefficient of determination (R^2) shows a strong correlation and improved from 0.83 to a value of 0.95 for the full sample size. The Bravais-Pearson correlation coefficient (p) showed a slight increase to 0.97 from an already high value of 0.91.

The ratio of the standard deviations of simulated and measured data series (σ_s/σ_m) improved to a value 0.98 indicating a similar spread of measured and simulated data. This indicates that the model depicts the maximum and minimum energy needs well. While this paper focuses on the energy needs, this leads to conclude that a similar approach could be suitable for determining the maximum power requirements in e.g. district heating schemes. Figure 2 shows the time series of the aggregated daily energy needs against the mean daily outdoor temperature.

Table 3: Statistic analysis of the simulation results at different aggregation scales

Daily Series	CV RMSE	R^2	P	σ_s/σ_m
Single Bldg A	35 %	0.87	0.93	1.10
Single Bldg B	25 %	0.92	0.96	1.02
Single Bldg C	24 %	0.96	0.98	0.85
Single Bldg D	30 %	0.88	0.94	1.00
Single Bldg G	44 %	0.83	0.91	0.78
All Bldgs.	19 %	0.95	0.97	0.98

With regard to the application for the aggregated building cluster the approach proved to deliver good results within the range of acceptability suggested for building simulation by ASHRAE Guideline 14-2002 [14].

5. DISCUSSION

In all considered cases, individual buildings were less well represented than the full sample. The work supports the research hypothesis of a sensitivity to scale of data-driven models. Yet the results presented in this paper provide evidence that for heating needs

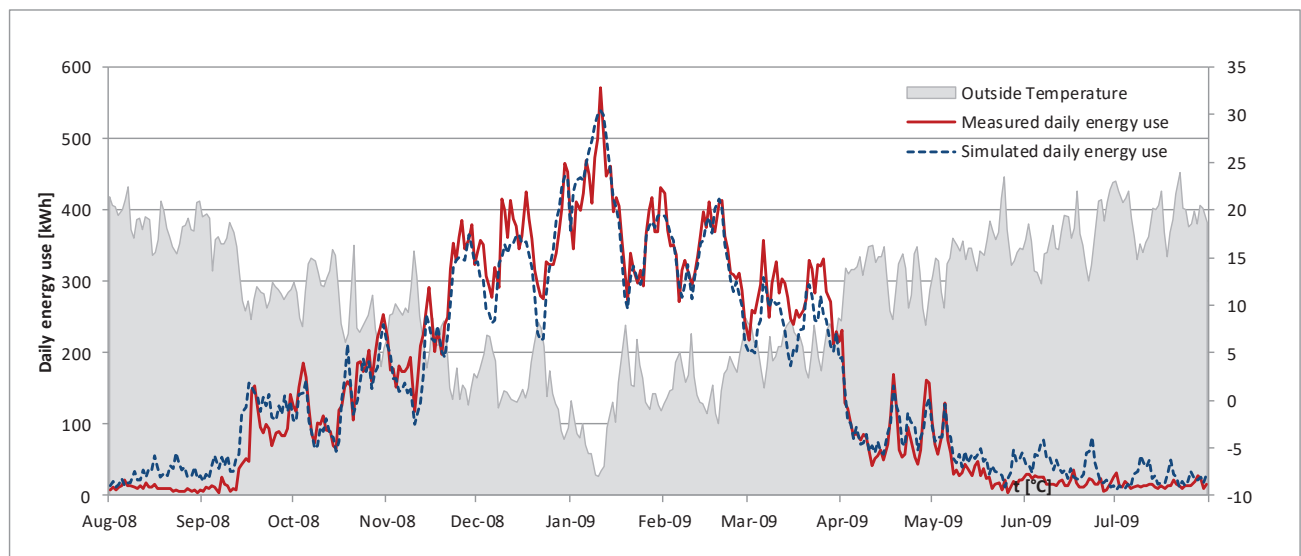


Figure 2: Time series of measured and simulated daily energy needs for five dwellings against mean daily outdoor temperature [12]

small sample size might be sufficient to employ data-driven approaches. This is especially true as results can be expected to be even more robust at larger scales of districts or urban areas. The results indicate an applicability of the model at the even larger scale of neighbourhoods or cities.

In comparison to simpler linear energy signatures the non-linear model describes the behaviour at cold temperatures well (*Figure 1*). The non-linear behaviour of heating energy needs can be described by a number of factors, [15] describe changes in ventilation behaviour in residential buildings as one possible cause.

While the shown application case was based on default, model parameters the calibration of the energy signature model for specific sites could further improved the results. This can be of interest for example for monitoring schemes for specific development projects. In addition to providing a fast yet robust model for heating energy needs, the results indicate a possible applicability in the context of continuous commissioning as this kind of model can be easily updated and does not require an expert user for maintenance. The model requires few variables and dataset used are common and frequently available at city scale. This allows planners to follow up performance of implemented measures and consequently to monitor target fulfilment at larger scales. In this way the level of achievement of the goals at project, district or city scale can be tracked over time in a continuous monitoring. In the context of urban planning, data driven models like the discussed energy signature can support planners at community level to evaluate results for a large number of projects or neighbourhoods. This enables the community to verify the achievement of the targets and where necessary adjust the projects' performance to manage the overall energy transition strategy at city level.

ACKNOWLEDGEMENTS

The authors would like to express their thanks to Niklas Griebßbaum for his kind support in the treatment of the monitoring data.

REFERENCES

1. United Nations, Sustainable Development Goals, 2017. Available from: <http://www.un.org/sustainabledevelopment/cities/> (viewed 01.02.2020).
2. Mendes, G., C. Ioakimidis and P. Ferrão (2011). On the planning and analysis of Integrated Community Energy Systems: A review and survey of available tools. *Renewable and Sustainable Energy Reviews* 15(9), 4836-4854.
3. Wang, S., C. Yan and F. Xiao (2012). Quantitative energy performance assessment methods for existing buildings. *Energy and Buildings* 55, 8.
4. Coakley, D., P. Raftery and M. Keane (2014). A review of methods to match building energy simulation models to measured data. *Renewable and Sustainable Energy Reviews* 37, 123-141.
5. Cajot, S., Peter, M., Bahu, J. M., Guignet, F., Koch, A., & Maréchal, F. (2017). Obstacles in energy planning at the urban scale. *Sustainable Cities and Society*, 30, 223-236. doi:<https://doi.org/10.1016/j.scs.2017.02.003>
6. Strasser, H., Kimman, J., Koch, A., Mair am Tinkhof, O., Müller, D., Schiefelbein, J., & Slotterback, C. (2018). IEA EBC annex 63—implementation of energy strategies in communities. *Energy and Buildings*, 158 (Supplement C), 123-134. doi:<https://doi.org/10.1016/j.enbuild.2017.08.051>
7. Quitzau, M.-B., Hoffmann, B., Petersen, J.-P., Heller, A., Olesen, B. W., C., R., . . . J. Kimman, J. (2018). Implementation of Energy Strategies in Communities (Annex 63) Volume 2: Development of strategic measures. International Energy Agency.
8. Quitzau, M.-B., Hoffmann, B., Petersen, J.-P., Heller, A., Olesen, B. W., C., R., . . . J. Kimman, J. (2018). Implementation of Energy Strategies in Communities (Annex 63) Volume 2: Development of strategic measures. International Energy Agency.
9. Koch, A., Girard, S., & McKoen, K. (2012). Towards a neighbourhood scale for low-or zero-carbon building projects. *Building Research & Information*, 40(4), 527-537.
10. Cajot, S., Koch, A., Marechal, F., & Peter, M. (2015). Energy planning in the urban context: challenges and perspectives. Paper presented at the 6th International Building Physics Conference, IBPC 2, Torino.
11. Hellwig, M. (2003). Entwicklung und Anwendung parametrisierter Standard-Lastprofile. (PhD), Technische Universität München, München.
12. Koch, E. A. (2016). Continuous Simulation for Urban Energy Planning Based on a Non-Linear Data-Driven Modelling Approach. (PhD), Karlsruher Institut für Technologie (KIT), Karlsruhe.
13. BDEW, VKU, & GEODE. (2014). BDEW/VKU/GEODE Leitfaden - Abwicklung von Standardlastprofilen Gas. Bundesverband der Energie- und Wasserwirtschaft e.V.; Verband kommunaler Unternehmen e.V, Groupement Européen des entreprises et Organismes de Distribution d'Énergie, Berlin.
14. ASHRAE (2002). Guideline 14-2002, Measurement of Energy and Demand Savings. Atlanta, Georgia, American Society of Heating, Ventilating, and Air Conditioning Engineers.
15. Schnieders, J., W. Feist, R. Pflug and O. Kah (2001). CEPHEUS - Wissenschaftliche Begleitung und Auswertung, Endbericht. Darmstadt, Passivhaus Institut.

Promoting a dispersed urban mobility approach for rehabilitation of historic Cairo

DOAA SALAHELDIN ISMAIL ELSAYED¹, WALAA S.E. ISMAEEL²

¹ Faculty of Engineering, Department of Architecture, Kafrelsheikh University, Kafr el-Sheikh, Egypt

² Faculty of Engineering, Department of Architecture, The British University in Egypt, Sherouq city, Egypt

ABSTRACT: A linear mobility approach has been adopted for Al-Muiz Street according to the proposed rehabilitation plan for historic Cairo by the United Nations development program (UNDP) initiative. Nevertheless, this study shows that promoting dispersed mobility flows leads to more sustainable options. Hence, three routes are proposed to connect two points of attraction along Al-Muiz Street to another point of attraction in a dispersed urban fabric, these are; 'Khisro sabil' and 'Khatkhoda Sabil' to 'Beet Elqadi' square, respectively. The three proposed routes are investigated in terms of urban and environmental analysis to achieve better environmental quality, less carbon emissions and maximum visual exposure to cultural heritage buildings using validated software programs. The result shows the optimum route where further sustainable rehabilitation initiatives are advised to promote a dispersed urban mobility approach. This microscale analytical study can be replicated to develop the sustainable capacity of historic Cairo.

KEYWORDS: Carbon emissions, Environmental quality, Historic Cairo, Urban mobility, Visual exposure

1. INTRODUCTION

Historic quarters in contemporary cities are perceived through mobility and flows as much as sedentary places. Since the 1980s, more cities assigned pedestrian itineraries as the dominant mobility in historic quarters [1]. After the United Nations Educational, Scientific and Cultural Organization (UNESCO) selected historic Cairo area as a World Heritage Site in 1979, conservation and rehabilitation plans were assigned to regenerate the historic centre and ameliorate the living conditions of its local community [2]. The latest was the United Nations development program (UNDP) initiative, which proposed a rehabilitation plan for historic Cairo in 1997 [3]. The plan focused on Al-Muiz Street; being the major spine extending north-south the Fatimid capital, of rich architectural, cultural and social potentials. The UNDP dedicated this touristic route for pedestrian-use only; aiming to achieve a car-free historic centre [4]. Nevertheless, there is a rich network of cultural heritage buildings and urban spaces located beyond the touristic route but are paid less attention. Hence, this study draws the attention that promoting a dispersed urban mobility approach for rehabilitation of old Cairo may prove a better sustainable solution that would eventually lead to fewer carbon emissions, better environmental quality and maximum visual exposure to cultural heritage buildings. The study introduces a micro-scale analysis for three proposed routes for dispersed mobility that lead from 'Khisro sabil' and 'Khatkhoda Sabil' located in Al-Muiz Street to 'Beet Elqadi' square located in a dispersed urban fabric; noting that this sector has been defined with the highest potentials

for sustainable rehabilitation initiative according to a previous study by Elsayed et. al (2019) [5].

2. LITERATURE REVIEW

Previous studies have promoted the application of sustainable forms of mobilization for historic areas [4,6,7]. This has many benefits to support local businesses [8] and maximize the urban experience [9]. Furthermore, other scholars have pointed out the importance of considering the environmental aspects as well [1,10]. In this regard, the rehabilitation of Al-Muiz Street has been investigated in terms of some parameters in which sabil buildings have been looked upon as nuclei of urban units. This helped characterize urban sectors in an attempt to determine those with the highest sustainable rehabilitation potentials [5].

Several approaches and lessons have been discussed for the benefits of promoting sustainable forms of urban mobility [11,12]. Thus, some indicators and models have been applied to assess the impact of pedestrianization and walkability in historic cities [13–15]. Also, several tools and methods have been used. On one hand, graphical means have been applied to map walkability potentials based on a Transient oriented approach as a sort of assessment for the quality of the urban environment [16]. On the other hand, models have been used to assess the visual performance of a neighbourhood in historic Cairo [17]. Also, the Geographic Information System Mapping (GIS) has been used to map carbon emissions [18] and along with spatial regression, a walking model has been developed [19]. Furthermore, numerical modelling

has been applied to evaluate outdoor microclimatic conditions [10].

Furthermore, the literature review includes the following types of spatial analysis that can be categorized for the purpose of the study into;

- Environmental analysis: this aims at investigating the environmental quality and carbon emissions of the space defined. The former includes criteria related to achieving outdoor thermal comfort conditions and others
- Urban analysis: this aims at investigating visual exposure to cultural heritage buildings. It is noted that the most significant characteristic in the urban fabric of historic Cairo is its organic and

irregular pattern that was generated according to levels of privacy and social needs [20]. Accordingly, the number of deviation points reflects the authenticity of the urban fabric revealing how far it recalls the Arabic culture within the urban morphology [21,22]. Hence, an isovist or viewshed analysis investigates the area in a spatial environment directly visible from a location within the space [21].

3. STUDY AREA

The surroundings of Al-Muiz Street in Al-Gamaliya district (720,000m²) has great potentials for diffused pedestrian mobility- refer to Fig. (1).

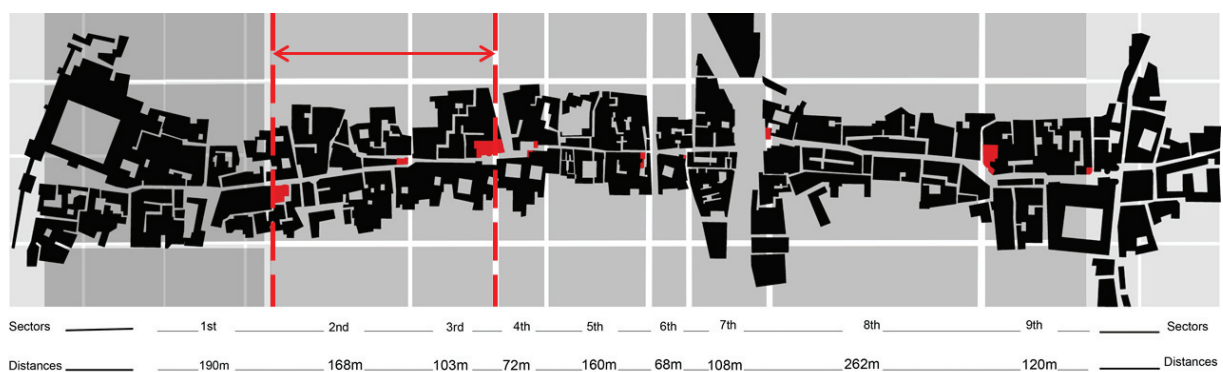


Figure 1. shows the urban spine of Al-Muiz street and the sector under study [5]

In this regard, an urban sector of area 62,000 m² (linking 'Khisro Sabil' and 'Khatkhoda Sabil' located in Al-Muiz Street to 'Beet Elqadi' square) has been defined by a previous study to be the most sustainably rehabilitated urban sector along Al-Muiz Street. Hence, the following three routes-shown in Table (1)-have been pinpointed to link the three defined points.

- Khisro Sabil: point 1
- Khatkhoda Sabil: point 2
- Beet Elqadi: point 3

Furthermore, a detailed micro scale-analysis level has investigated the linear mobility of the urban sector understudy in Al-Muiz Street which is 2,517m² of area and 761 m length as shown in Fig. (2). This aims to assess the potential of the three proposed routes for diffused mobility approaches in terms of urban and environmental performance using validated software programs to be able to recommend the route with the greatest potentials for rehabilitation activities as part of establishing a futuristic dispersed urban flow to serve Al-Muiz Street.

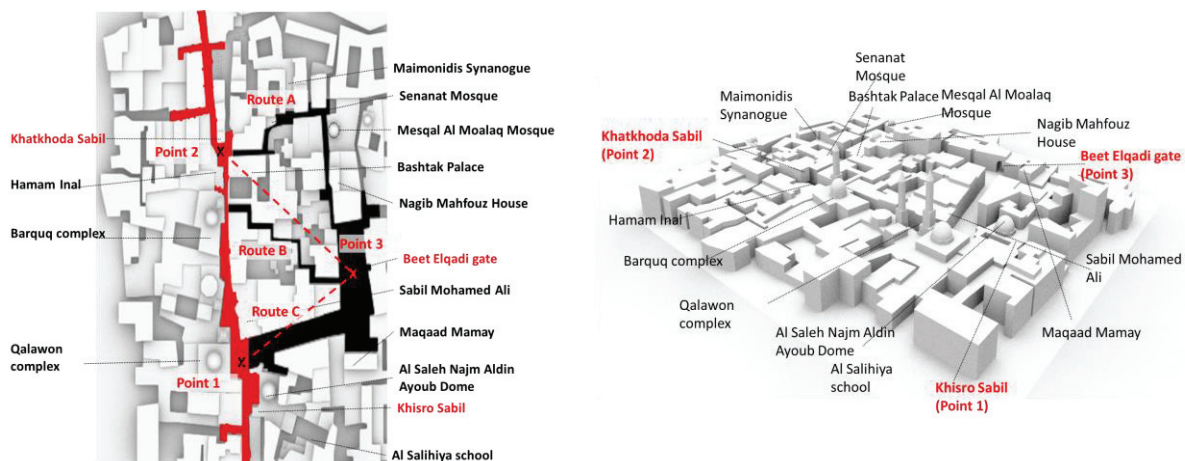


Figure 2. The urban context showing the three proposed routes

Table 1. Spatial variations for the three defined routes

Routes	Area (m ²)	Distance (m)
A	859.89	207.36
B	477.16	220.93
C	1549.50	177.46

4. METHOD

Based on previous literature [1,4,17], three parameters have been defined for sustainable rehabilitation of historic districts; less carbon emissions, better environmental quality and maximum visual exposure to cultural heritage buildings.

Hence, the assessment criteria of the sustainability potentials of the three proposed routes are determined based on the following types of analysis:

- The urban analysis is used to determine the visual exposure to the cultural heritage buildings. This is done using parametric analytical tools (ladybug-grasshopper) to study urban visibility and exposure through the isovist field analysis and view analysis.
- The environmental analysis: for the purpose of this study, this analysis includes investigating the environmental quality of the defined route using parametric analytical tools (ladybug-grasshopper). These are used to validate the outdoor thermal comfort conditions-particularly using the outdoor solar radiation analysis. It is noted that other measures such as air temperature, relative humidity, wind speed and direction contribute to outdoor thermal comfort [23,24], however, for

this micro-scale analysis, this had an equal effect in all three routes but focusing on calculating solar radiation provided significant variations. Another study is carried to measure the amount of estimated carbon emissions for each route. This is determined based on multiplying the route length by the sum of emissions produced by different means of transportations crossing the route on an annual basis.

4.1. Solar radiation analysis

The solar radiation analysis is a component provided by the ladybug software program to enable calculating the radiation falling on an input geometry using a selected sky matrix in a specific analysis period. This analysis is carried for the purpose of the study for the summer period, from June till September. The selected test geometries represent street surfaces where the surrounding buildings are designed as the sunlight blocking geometries. A grid size of 3x3 m is set to perform solar radiation analysis on the tested surface. The offset distance of the test point from the input test geometry is set at 0.01 m. The analysis of the three routes is shown in Fig. (3).

According to the literature review [25,26], thermal comfort is achieved within a range of 21-27.5°C temperature and maximum 30-65% relative humidity and wind speed up to 5 m/s. Also, the range of acceptable solar radiation is increased by a scale of 1 unit for an increase of each 200 W/m² [27].

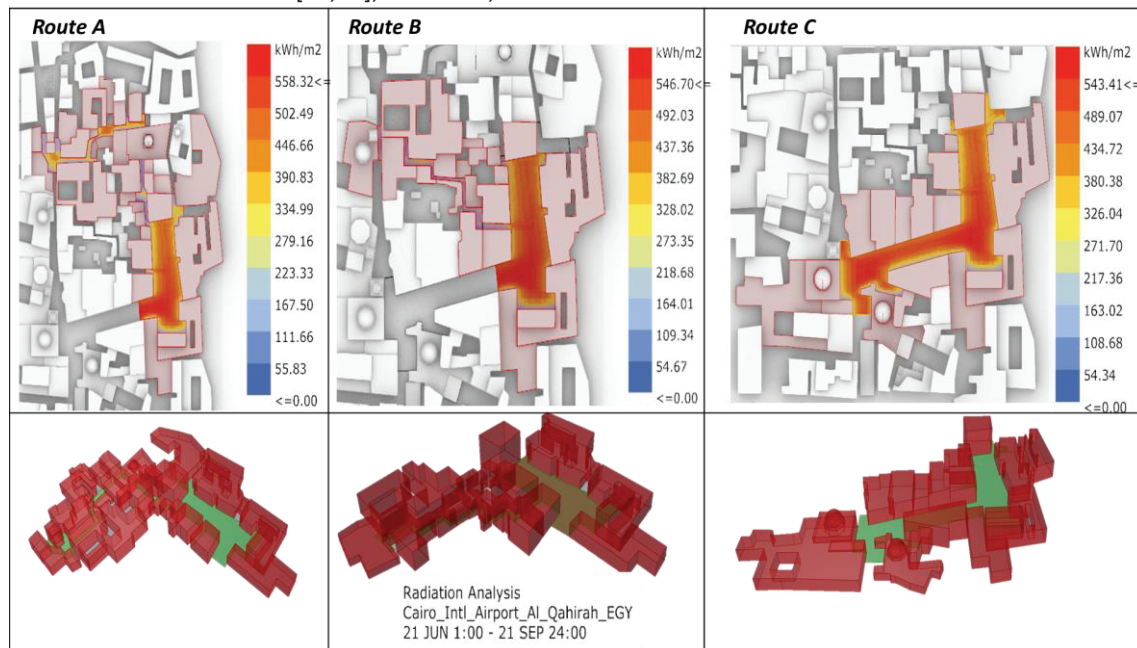


Figure 3. The solar radiation analysis of the three proposed routes

4.2. Isovist field analysis

The isovist field analysis is a component supported in grasshopper software aiming to compute an isovist sampling at a certain location. It is used in this study

to enable studying the visible urban fabric within a sequence of test points along each path. This illustrates the value of the urban heritage besides that of the architectural buildings. The extent of the visibility radius was set at 500 meters. The study

achieved the isovist field analysis over a grid of 320mx260m, which reflects the study area of Al-Muiz Street and its surroundings. The test points were inserted according to the deviation points along the path as follows;

- Route A: 5 test points
- Route B: 7 test points
- Route C: 2 test points

An example of an isovist field analysis is shown in Fig. (4).

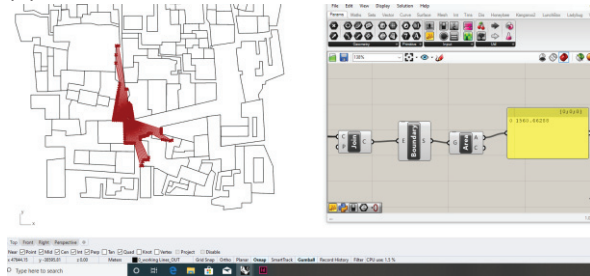


Figure 4. Isovist field analysis

4.3. View analysis

The Ladybug view analysis is a component evaluating the visibility of an input geometry from a set of key viewing points. In the current study, the analysis is set for evaluating and calculating the average percentage of the test geometry seen by the test viewpoints. The study selected a test geometry composed of the hidden cultural heritage buildings existing beyond or adjacent to Al-Muiz Street but not visible (these are 15 buildings). The key viewing points are inserted on the 3D Rhino model to reflect visual points along each path as shown in Fig. (5) and (6). The study sets a grid size of 5 meters which represents the average size of the grid cell for visibility analysis on the test geometry. A distance from the base is set to 0.01 m, representing the offset distance of the test point grid from the input test geometry. An average of 5 to 7 view test points was set along each path. Accordingly, the study investigates the average percentage of visibility to the hidden cultural heritage buildings in relation to each path to select the path of the highest average views.

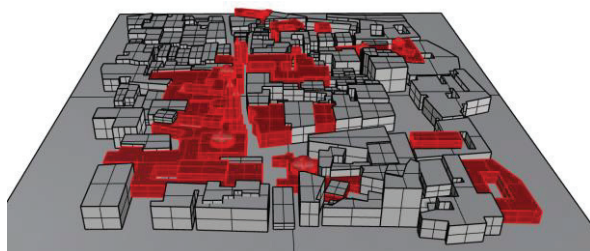


Figure 5. View analysis-contextual model

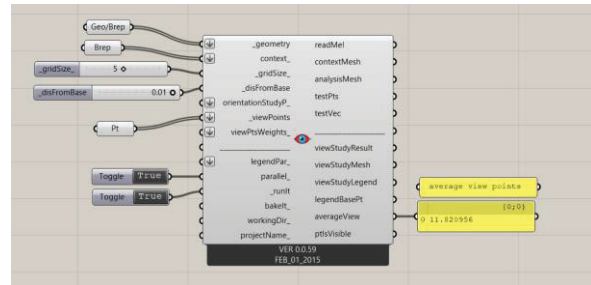


Figure 6. View analysis-parametric model

4.4. Carbon emission analysis

By observation, an average number of means of transportation has been estimated for each route daily as follows; noting that private cars are not allowed.

Route A = 50 motorcycles

Route B = 50 motorcycles

Route C = 100 motorcycles and 56 shuttle buses and 112 vans.

Then a model is used to compute the carbon emissions generated in each route based on its length and the existing means of transportation crossing it on an annual basis according to Mahmoud and El-Sayed (2011)[28].

5. RESULTS

The results of the spatial studies are presented in Fig. (7) as follows;

5.1. Solar radiation analysis

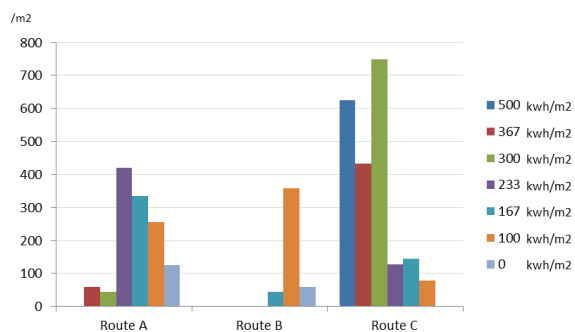


Figure 7. comparing the solar radiation for the three proposed routes

The result of comparing the solar radiation analysis for the three routes shows that route A achieves a balance of favourable intensity of solar radiation that achieves outdoor thermal comfort.

5.2. Isovist field analysis

The result of the isovist analysis indicates that route C has the greatest field area which allows the greatest exposure to cultural heritage buildings in the surrounding area as follows;

- Route A: 5 test points and isovist area of 4426m²
- Route B: 7 test points and isovist area 3961m²
- Route C: 2 test points and isovist area 5071 m²

5.3. View analysis

The average percentage of visibility was calculated as follows:

Route A = 2.20%

Route B = 0.77%

Route C = 1.64%

Hence, it can be concluded that route A achieves the highest average view percentage to the hidden cultural heritage buildings- existing beyond Al-Muiz Street.

5.4. Carbon emission analysis

The result of comparing the three routes in terms of carbon emissions is shown in Table (2). This shows that route A has the least contribution of carbon emissions compared to the other two routes.

Table 2. Comparing the carbon emissions for the three routes

	CO ₂ equivalent
Route A	0.39 ton/year (for motorcycles)
Route B	0.42 ton/year (for motorcycles)
Route C	0.338 (for motorcycles)+ 1.748 (vans)+ 3.68 (shuttle buses)=5.76 ton/year total

5.4. Comparing the three routes

Hence, by comparing the three routes according to the predefined assessment criteria shown in Table (3), it shows that route A is the optimum route in terms of solar radiation analysis, least carbon emissions and providing views and exposure to the urban context but its performance is lower in terms of Isovist field analysis. Assuming equal weights for the four aforementioned criteria, then Route A has obtained 75%, followed by route C then route B. This helps draw prioritisation plan for sustainable rehabilitation of the entire pedestrian spine of Al-Muiz while promoting diffused pedestrian mobility is sub-routes to enrich the urban and visual experience.

Table 3. shows a comprehensive comparison for the assessment of the three routes in terms of the defined parameters

		Route A	Route B	Route C
Urban studies	Solar radiation analysis	Optimum performance	Poor performance	Average performance
	Carbon emissions analysis	Optimum performance	Average performance	Poor performance
	View analysis	Optimum performance	Poor performance	Average performance
	Isovist field analysis	Average performance	Optimum performance	Poor performance

By comparing the results to previous literature, it shows that both the urban and environmental parameters may result in pedestrian deviation from the shortest planned route as stated by [1]. The study completes the micro-scale numerical model for an outdoor urban which discussed the prevailing climate, the urban form and roughness of Al-Muiz Street [10]. Further visual analysis was carried using the isovist analysis to pinpoint the importance of urban analysis as well [21]. This can be used to promote sustainable tourism [7,9]. It also confirms the Sabil building as an urban unit as suggested by [5].

6. CONCLUSION

The study investigates alternative urban mobility approaches that are capable of exploring the cultural, historic, urban and environmental potentials hidden beyond the linear corridor of Al-Muiz Street. It suggests alternative circulation scenarios therein. This methodology can be applied in similar contexts aiming to promote the urban and environmental performances of historic urban centres and eventually expand beyond the nine clusters proposed by the UNDP. On the district level, the study selects the surroundings of Al-Muiz Street in Al-Gamaliya district (720,000m²) to act as the reference case study for exploring the diffused pedestrian mobility. On the neighbourhood level, an urban sector of around 62,000m² has been studied to assess the potentials of the proposed routes through three defined parameters; less carbon emissions, better environmental quality and maximum visual exposure to the cultural heritage buildings. A series of investigations are carried based on quantitative and qualitative analysis. This promotes a sustainable urban circulation which pinpoints the potentials of the diffused pedestrian network in offering richer users' experiences. This is considered as a pilot study to investigate the capacity of historic Cairo to act as a sustainable historic quarter of less carbon emissions and better environmental quality.

ACKNOWLEDGEMENTS

The authors would like to thank associate professor Marwa Adel from the British University in Egypt for her help and support with the research.

REFERENCES

- [1] Foltête JC, Piombini A. Deviations in pedestrian itineraries in urban areas: A method to assess the role of environmental factors. Environ Plan B Plan Des 2010. doi:10.1068/b35015.
- [2] Salama AM. Cultural Sustainability of Historic Cities: Notes on Conservation Projects in Old Cairo. 16th Int Assoc People-Environment Stud Conf, 2000.

- [3] UNDP. The rehabilitation of Historic Cairo, Final Report. 1997.
- [4] Lamei S. Regeneration of historic Cairo & the sustainable development process. *City Time* 2011;5:49–53.
- [5] Elsayed DS, Ismaeel WSE, Elsayed MA. Revisiting sabil buildings as nuclei of urban units. *ARCHCAIRO 8 Build Futur Now Rights to Better Living, Archit Context*, 2019, p. 565–88.
- [6] Although I, Boundaries UG. Cultural Heritage of Urban Definitions : Centres and Borders. *Int Conf Urban Chang Iran* 2012.
- [7] Fahmi W. Sustainable Tourism and the Rehabilitation of Cairo's Historical Districts: the Case of the Bazaar Area and the Cities of Dead, 2019. doi:10.3390/wsf2-00906.
- [8] Elfouly HA, Ghaly AA. The perceived impact of pedestrianization on local businesses in Al-Muizz Egypt : A case study. *Int Journal Dev Sustain* 2015;6:399–411.
- [9] Samadi Z, Yunus RM, Omar D, Bakri AF. Experiencing Urban through On-street Activity. *Procedia - Soc Behav Sci* 2015;170:653–8. doi:10.1016/j.sbspro.2015.01.067.
- [10] Elnabawi MH, Hamza N, Dudek S. Numerical modelling evaluation for the microclimate of an outdoor urban form in Cairo, Egypt. *HBRC J* 2015. doi:10.1016/j.hbrj.2014.03.004.
- [11] Refaat MH, Kafafy NA. Approaches and Lessons for enhancing walkability in cities : a Landscape Conceptual Solution for Talaat Harb Street , Cairo. *Educ Res* 2014.
- [12] Dias JA, Silva LMC da, Morais TC de. Urban Mobility to Improve the Center of a Brazilian Historic Town. *Procedia - Soc Behav Sci* 2014. doi:10.1016/j.sbspro.2014.12.128.
- [13] Cambra P. Pedestrian Accessibility and Attractiveness Indicators for Walkability Assessment. 2012.
- [14] Haghi MR, Izadi mohammad saeid, Molavi E. Assessment and comparison of two policies: pedestrianization and walkability in CBDs (Case Study: Hamedan CBD). *Sci J Manag Syst* 2015.
- [15] Khalighi N. Assessing the Impacts of Pedestrianisation on Historic Urban Landscape of Tehran TT -. *IUST* 2018. doi:10.22068/ijaup.28.1.91.
- [16] Serra-Coch G, Chastel C, Campos S, Coch H. Graphical approach to assess urban quality: Mapping walkability based on the TOD-standard. *Cities* 2018;76:58–71. doi:10.1016/j.cities.2018.01.007.
- [17] Almaiyah S, Elkadi H. Study on the Visual Performance of a Traditional Residential Neighborhood in Old Cairo. *J Urban Technol* 2012;19:59–86. doi:10.1080/10630732.2011.649913.
- [18] Lee JK, Christen A, Ketler R, Nesic Z. A mobile sensor network to map carbon dioxide emissions in urban environments. *Atmos Meas Tech* 2017. doi:10.5194/amt-10-645-2017.
- [19] Sanni T, Abrantes PAL. Estimating walking modal share: A novel approach based on spatial regression models and GIS. *J Maps* 2010;6:192–8. doi:10.4113/jom.2010.1080.
- [20] Attia A, El-Shalat MF. The Influence of the Islamic Culture on the Urban Fabric of Alexandria. *First Int Conf Archit Dep Fac Eng Ain Shams Univ*, 2006.
- [21] Turner A, Doxa M, O'Sullivan D, Penn A. From isovists to visibility graphs: A methodology for the analysis of architectural space. *Environ Plan B Plan Des* 2001;28:103–21. doi:10.1068/b2684.
- [22] Malhis S. Narratives in Mamluk architecture: Spatial and perceptual analyses of the madrassas and their mausoleums. *Front Archit Res* 2016;5:74–90. doi:10.1016/j.foar.2015.11.002.
- [23] Ghaffarianhoseini A, Berardi U, Ghaffarianhoseini A, Al-Obaidi K. Analyzing the thermal comfort conditions of outdoor spaces in a university campus in Kuala Lumpur, Malaysia. *Sci Total Environ* 2019. doi:10.1016/j.scitotenv.2019.01.284.
- [24] Canan F, Golasi I, Ciano V, Coppi M, Salata F. Outdoor thermal comfort conditions during summer in a cold semi-arid climate. A transversal field survey in Central Anatolia (Turkey). *Build Environ* 2019. doi:10.1016/j.buildenv.2018.11.008.
- [25] Katafygiotou MC, Serghides DK. Bioclimatic chart analysis in three climate zones in Cyprus. *Indoor Built Environ* 2015. doi:10.1177/1420326X14526909.
- [26] Al-Azri NA, Zurigat YH, Al-Rawahi NZ. Development of bioclimatic chart for passive building design. *Int J Sustain Energy* 2013. doi:10.1080/14786451.2013.813026.
- [27] Hodder SG, Parsons K. The effects of solar radiation on thermal comfort. *Int J Biometeorol* 2007. doi:10.1007/s00484-006-0050-y.
- [28] Mahmoud AHA, El-Sayed MA. Development of sustainable urban green areas in Egyptian new cities: The case of El-Sadat City. *Landsc Urban Plan* 2011. doi:10.1016/j.landurbplan.2011.02.008.

Analysis of courtyards heat mitigation potential in warm and dry urban locations.

Diurnal Thermal Range variants on the porosity of the city.

Diz-Mellado, Eduardo¹; Galán Marín, Carmen¹; Rivera Gomez, Carlos¹; Rojas-Fernández, Juan Manuel¹; Nikolopoulou, Marialena².

¹Departamento de Construcciones Arquitectónicas 1, Escuela Técnica Superior de Arquitectura, Universidad de Sevilla, Avda. Reina Mercedes, 2, 41012 Seville, Spain.

²Centre for Architecture and Sustainable Environment, Kent School of Architecture, University of Kent, Canterbury, UK.

ABSTRACT: Studies on climate change establish the average daily temperature as a universal measure. However, the complexity of climatic variations is not adequately defined by the average air temperature alone. In addition, changes in daily maximum and minimum temperatures are related to the average surface temperature, while the urban heat island (UHI) effect is related to urban versus rural diurnal thermal range (DTR) variations for similar geographical locations. While the greatest differences in the temperature of the radiant surface are observed during noon, the differences in urban and rural air temperature are observed predominantly at night. Quantifying the importance of thermal tempering generated in the microclimate of the courtyard is the fundamental objective of this work. In this way, it is significant to consider not only the hours of maximum outdoor temperature (MOT), but also the entire DTR in relation to the thermal performance of the courtyard. To this end, monitoring campaigns have been carried out in courtyards with different geometry but in an urban environment of the same geographical area. The main novelty is the assessment of these thermal parameters: MOT and DTR with courtyard Aspect Ratio (AR) in order to determine thermal behaviour patterns able to quantify thermodynamic performance and courtyards potential as passive cooling tools.

KEYWORDS: Courtyard; Aspect ratio; Diurnal Temperature Range; Thermal Comfort.

1. INTRODUCTION

The generation and recovery of transitional spaces such as the courtyards is a fundamental bioclimatic strategy. The courtyard is an architectural resource linked to a geographical and cultural environment. In the warm areas of the earth, it provides shade; in the cold areas, it breaks the continuity of the wind generating microclimates; and in humid climates, it contributes to generating cross ventilation by increasing the constructed porosity, understood as the courtyards (pores) in the buildings. The courtyard is, therefore, an essential space for cities, and an ultimate synergy between architecture, culture and sustainability. Paradoxically, although climate adaptation is a functional characteristic of the courtyard linked to its origin, there are no quantifying tools that can reliably estimate its microclimatic behaviour [1].

A reduction of the energy demand of the buildings is possible thanks to the existence of different passive strategies in the design of the cities to improve the users' thermal comfort [2]. The courtyard or other transitional spaces between the interior and the exterior of the building, acquire great importance as passive cooling systems in architecture.

Their design and construction characteristics help as thermal regulators for buildings and cities by mitigating the heat island effect. In hot climates, the courtyard helps to improve the conditions of light and ventilation in the buildings.

The daily mean temperature is generally used as a universal measurement for climate change study. However, mean temperature alone is insufficient to reflect the complicated variations of climate. In fact, trends in mean surface temperature are often due to changes in daily maximum and minimum temperatures [3]. Therefore, the Diurnal Thermal Range (DTR) becomes an important indicator of climate change [4], as well as an important meteorological index relating to global climate change and weather variation [5]. DTR is defined as the intra-day difference between the maximum and minimum temperatures according to the following Equation (1):

$$T_{\max} - T_{\min} = \text{DTR } (^{\circ}\text{C}) \quad (1)$$

Changes in DTR have multiple possible causes (cloud cover, urban heat island, aerosols, water vapour and greenhouse gases) with different regions affected by different factors.

Urban Heat Island (UHI) is one of the anthropogenic phenomena most directly related to changes in cities' temperatures. Research has highlighted that different types of heat island effect occur at different levels of the city: in the surface layer, in the canopy layer below roof level and in the boundary level [6]. Thermal behaviour of urban surfaces is directly related to the UHI effect and environmental aspects, such as heat stress and air pollution. Urban and rural air temperature differences are observed mainly at night, while the greatest differences in surface radiant temperature are observed during midday. Moreover, the surface temperature differences strongly vary in microscale up to dozens of degrees, because of the varying radiant load. In contrast, the UHI intensity in the canopy and boundary layers is much less [7].

Even though the inner courtyard is one of the most suitable passive-cooling systems used in warm climates, this thermal tempering effect is positive during both winter and summer [8], despite being more significant in the latter. In fact, there is a relationship between urban geometry, specifically in the layout and proportion of full and empty volumes, and the distribution of urban heat island in cities. In this sense, some particularities can be identified in different urban scenarios, considering the effects of climate zoning on the real urban densification [9].

The aim of the present paper is to quantify the extent in which the courtyard microclimate indicates a thermal variation capable of not only of qualifying the higher outdoor thermal stress hours, but also the entire outdoor DTR. To address this, field monitoring campaigns have been carried out in different courtyard geometries in a warm and dry climate urban environment. The main novelty is the assessment of Maximum Outdoor Temperature (MOT) and DTR with courtyard aspect ratio (AR) in order to determine thermal behaviour patterns within the courtyards.

2. MATERIALS AND METHODS

2.1 Site location and climate description

This study is carried out in the Spanish city of Seville, (37° 22' 58" N 5° 58' 23" W, elevation 16 m above sea level); located in climatic zone B4 according to Spanish standards [10]. This climatic zone is characterized by mild winters and warm summers. According to the Köppen classification, Seville is located in an area of category Csa, characterized by dry summers and especially hot and warm temperatures.

The absolute maximum and minimum temperatures have been obtained from the historical climatic database of Spanish Meteorological Agency (AEMET) [11] to analyse the thermal behaviour of the city, where the case studies are located (Table 1). It is a city in

which summers are quite hot, and where the thermal regulation of the courtyards is considered to be fundamental to the thermal tempering of the city. The meteorological data obtained are from measurement areas in the outskirts of the city, so it would be reasonable to assume the urban heat island effect can further accentuate the effect of the thermal increase inside the city.

On the other hand, the worrying prospects reported by the IPCC for the city, with a significant increase in the average temperature, will cause thermal peaks in the summer heat waves that will be detrimental for thermal comfort.

Table 1: Maximum and minimum absolute historic temperatures in Seville.

	Jan	Feb	Mar	Apr	May	Jun
T _{MAX}	24,2	28	32,9	35,4	40,8	45,2
T _{MIN}	-4,4	-5,5	-2	1	3,8	8,4

	Jul	Aug	Sep	Oct	Nov	Dec
T _{MAX}	46,6	45,9	44,8	36,6	31,2	24,5
T _{MIN}	11,4	12	8,6	2	-1,4	-4,8

2.2 Field measurement methodology

The monitoring campaigns have been carried out in two different seasons; spring, with generalized maximum temperatures lower than 37°C, and during the summer, with generalized maximum temperatures higher than 37°C.

The measurements have been made with a portable weather station, PCE-FWS, whose data have been confirmed with those provided by AEMET [11]. The thermal data inside the courtyards have been measured with portable sensors. Sensors have been placed at different heights to check the thermal stratification of the courtyard. TESTO 174 T temperature sensors have been used for the upper heights, 3 m and 4,5 m, respectively from the courtyard pavement and TESTO 174 H humidity and temperature sensors at the lower levels, placed at 1,5m. To avoid the effect of direct radiation they have been protected with breathable shields.

Five case studies with different geometries were monitored in two separated seasonal field monitoring campaigns. The measurements were conducted according to a previously developed protocol; thermal differences between summer and autumn campaigns help to understand the thermal behaviour of the courtyard in terms of MOT and DTR parameters [12].

3. RESULTS AND DISCUSSION

3.1 Case Studies

A set of five case studies (CS1-CS5) had been selected, each with a different AR interval, but with the same characteristics of orientation and albedo [13], and were monitored for a two-week period. The selected courtyards CS1 and CS2 were located in public buildings while the rest of case studies (CS3, CS4 and CS5) were located in residential buildings. These are different building typologies and use, highlighting disparate uses, i.e. residential or educational (Fig. 1).

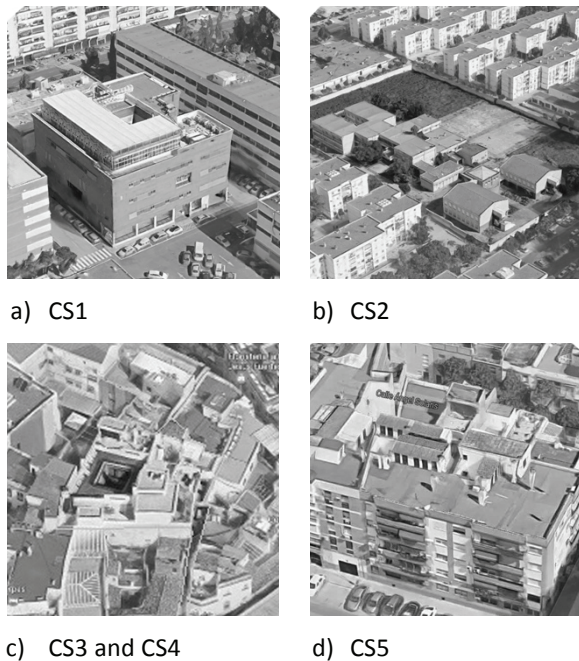


Figure 1: Case Studies

The case studies geometrical differences were expressed in terms of Aspect Ratio (AR), which is defined as the ratio of height to width of the courtyards according to the following Equation (2):

$$AR = H/W \quad (2)$$

AR was used to detect the influence of this parameter on the thermal behaviour of the courtyards (Table 2).

Table 2: Geometric characteristics and AR of the courtyards.

Case	dimensions (m)	height (m)	AR (H/W)
CS 1	7,3 x 6,6	14,0	2,02
CS 2	6,9 x 5,2	5,0	0,84
CS 3	2,0 x 3,8	14,3	5,77
CS 4	1,9 x 5,6	14,1	4,84
CS 5	3,5 x 3,5	16,0	4,54

Case studies results show an improved behaviour during the warmer campaign in terms of Thermal Gap (TG). The TG, expressed by the Equation (3):

$$TG(^{\circ}C) = \text{Outdoor } T^a - \text{Mean Courtyard } T^a \quad (3)$$

When the thermal gap during MOT is analysed, the higher the outdoor temperature, the higher is the gap (Fig. 2). The measured DTR results are even more relevant, since outside the courtyard, for most of the case studies, there are DTRs greater than 20°C, while inside the courtyards the DTR barely exceeds 3°C in some cases (Fig. 3). Moreover, TG results show greater difference between the outdoor and courtyard temperature in case studies with higher aspect ratio. It is noticeable that the case studies with the higher AR, i.e. higher than 3, demonstrate a greater thermal gap (Fig. 4).

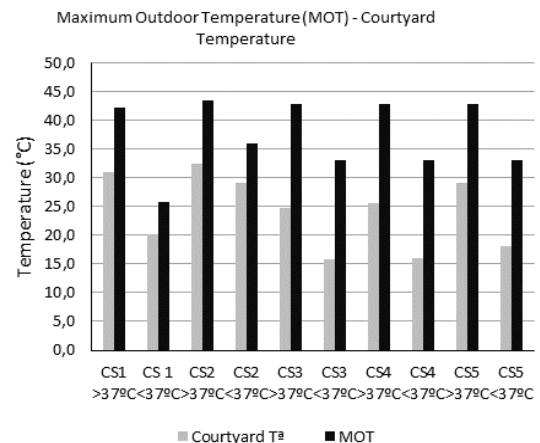


Figure 2: Maximum Outdoor Temperature (MOT) and Courtyard Temperature for each case study for the different temperature categories (i.e. >37°C and <37°C).

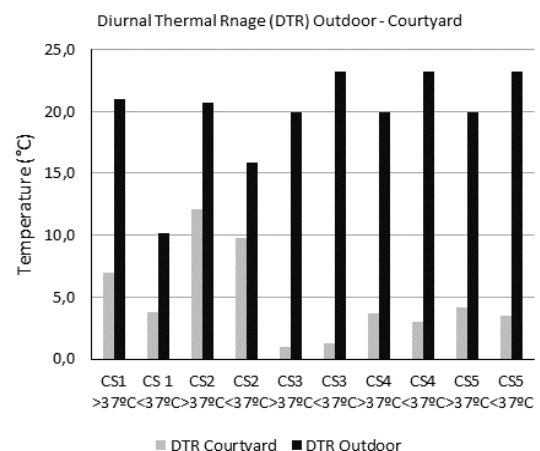


Figure 3: Outdoor versus Courtyard Diurnal Thermal Range (DTR) for each case study for the different temperature categories (i.e. >37°C and <37°C).

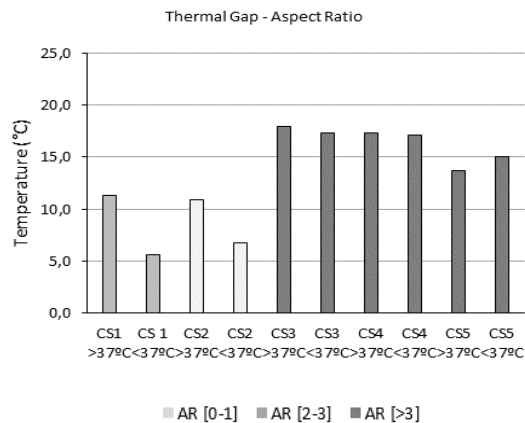
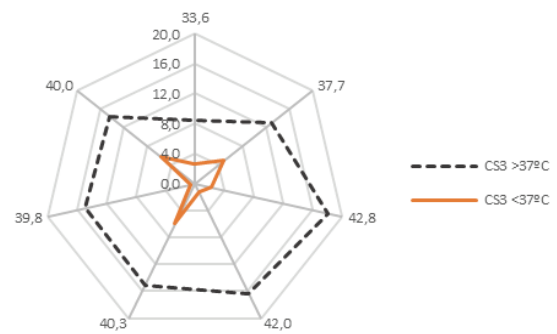


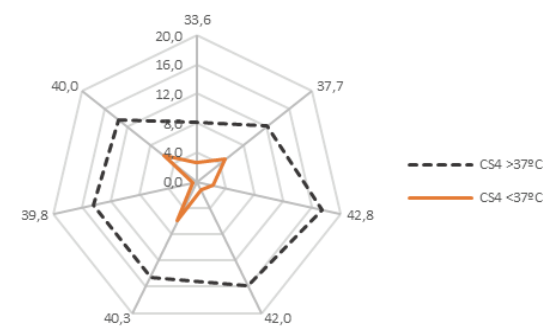
Figure 4: Correlation Thermal Gap (TG) and Aspect Ratio (AR) for each case study for the different temperature categories (i.e. $>37^{\circ}\text{C}$ and $<37^{\circ}\text{C}$).

3.2 Results and Discussion

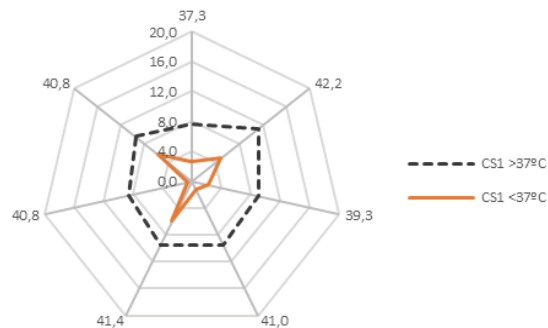
Results show that courtyards present better behaviour at warmer temperatures. These results have been studied in detail as shown (Fig. 5) with the same two thermal ranges. In light colour, the TG is reflected with a temperature below 37°C and in dark colour with outdoor temperature values greater than 37°C .



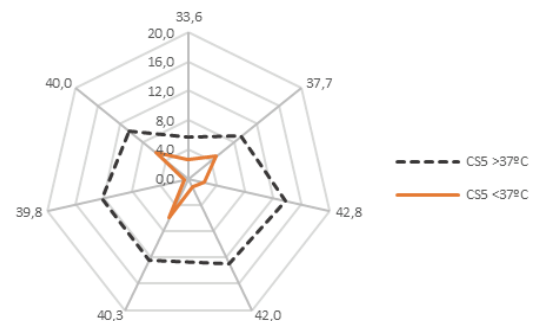
c) Case 3. Aspect Ratio: 5,77.



d) Case 4. Aspect Ratio: 4,84.

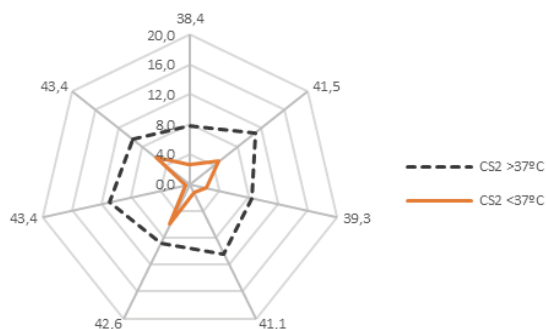


a) Case 1. Aspect Ratio: 2,02.



e) Case 5. Aspect Ratio: 4,54.

Figure 5: Courtyard behaviour according outdoor temperature



b) Case 2. Aspect Ratio: 0,84.

The data reflected in Fig.5, according to the central dispersion, show the tempering potential capacity of each courtyard. With maximum outdoor temperatures up to 37°C , courtyards show a rather homogeneous behaviour. Moreover, with maximum outdoor temperatures above 37°C , the courtyards manage to reduce extreme heat temperatures. This means that there is a thermal value from which the thermal regulating component of the courtyard is really effective. In addition, a large difference in the capacity of thermal regulation is detected in each case study, the biggest difference being in cases with a higher aspect ratio.

Analysing the results obtained, courtyard behaviour appears to improve with increasing MOT and AR (Fig. 6). Represented MOT on the horizontal axis and Thermal Gap (TG) on the vertical axis, the greater the MOT, the higher is the Thermal Gap (TG).

Outdoor temperature (in terms of DTR) and courtyard geometry (as AR), both parameters combined, have a significant influence in courtyard microclimate performance. This effect is shown in the following graph, where DTR gap between outdoor and courtyard is represented against MOT (Fig. 7). This behaviour varies for different AR of the courtyard.

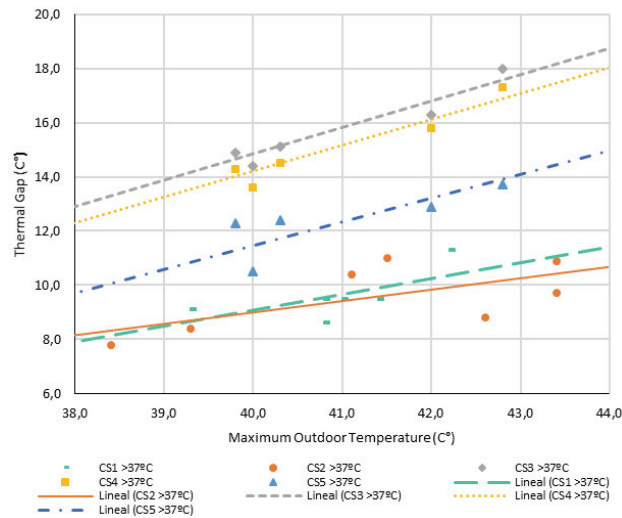


Figure 6: Correlation between TG and MOT for 5 case study

In this case, the slopes represented for the five case studies show that the TG is accentuated as MOT increases. In addition, case studies CS1 and CS2, with the smallest AR, show a TG of 10 °C approximately, while the case study with higher AR has a TG greater than 18 °C.

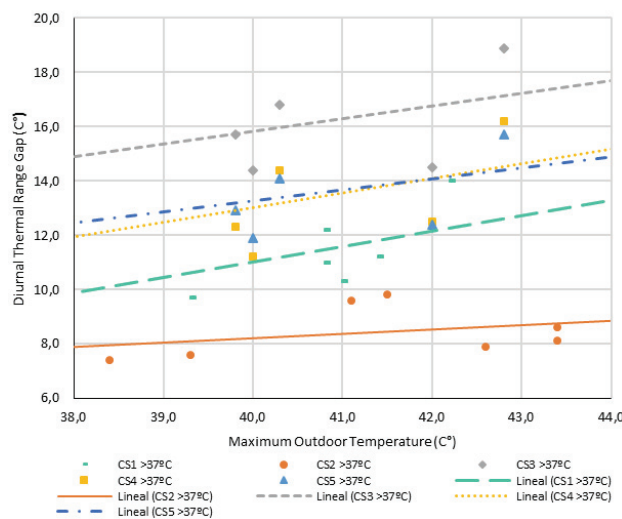


Figure 7: DTR Gap and MOT correlation for each case study

The same as before, the tempering potential of courtyard is better in CS5. DTR gap is less affected by MOT than TG, but the aspect ratio is again determinant in the courtyard behaviour.

4. FINAL REMARKS AND CONCLUSION

The tempering potential of courtyards highlighted in this work suggests a potential energy deficit, which in the context of global average temperature increases, must be promoted to address the complexity of the warming climate. The tempering effect of courtyards is not reflected in the buildings of the last decades around the world, as these had been conceived exclusively as lighting and ventilation resources, and not due to their thermoregulatory potential. The courtyards act as thermal regulators of buildings and cities, so that a control over their design strategies, always in accordance with the geographical location, can improve such capacities. Future lines of research can help to establish design patterns for each location, controlling the thermal savings achieved from simple strategies implemented during the development of such architectural design.

The case studies selected, all located in Seville, have been selected based on their different geometries. In this paper the AR influence on the thermal behaviour of these spaces has been demonstrated. Hence, the higher the temperature of the city along with a higher aspect ratio of courtyards, the more influential is the courtyard as a tool for minimizing the effects of climate change.

It could be concluded that the maximum deviation between outdoor and courtyard temperature coincides with MOT. This factor is important to establish the tempering potential in a given courtyard. On the other hand, the daily overview through DTR analysis allows evaluating complete cycles assessing the courtyard behaviour from a perspective of comfort throughout the day. Furthermore, the courtyard thermal tempering mechanism becomes more evident when outdoor DTR increases and it can be stated that, for certain geometries, the courtyard thermal buffer effect is important to consider in order to improve temperatures in the cities.

ACKNOWLEDGEMENTS

The authors wish to acknowledge the IUACC “Instituto Universitario de Arquitectura y Ciencias de la Construcción” for the necessary support to develop this research. They thank the two anonymous reviewers whose comments/suggestions helped to improve and clarify this manuscript. This work was supported by the National Government of Spain Research Projects MTM2015-64577-C2-2-R and RTI2018-093521-BC33.

The authors also gratefully acknowledge AEMET (State Meteorological Agency) for the data supplied and the financial support of the Spanish Ministry of Education, Culture and Sport via one pre-doctoral contract granted to Eduardo Diz Mellado (FPU 18/04783).

Author Contributions: C.G.-M., C.R.-G. JM.R-F and M. N. conceived and designed the experiments; E.D.-M. performed the experiments and analysed the data; E.D.-M., C.G.-M. and C.R.-G. wrote the paper. C.G.-M., M. N. and C.R.-G. edited the paper. All authors have read and agreed to the published version of the manuscript.

Conflicts of Interest: The authors declare no conflict of interest. The funders had no role in the design of the study; in the collection, analyses, or interpretation of data; in the writing of the manuscript, or in the decision to publish the results.

REFERENCES

1. V.P. López-Cabeza, C. Galán-Marín, C. Rivera-Gómez, J. Roa-Fernandez. Courtyard microclimate ENVI-met outputs deviation from the experimental data. *Building and Environment* 2018. 144, 129-141; <https://doi.org/10.1016/j.buildenv.2018.08.013>
2. H. A. Abdulkareem, 'Thermal Comfort through the Microclimates of the Courtyard. A Critical Review of the Middle-eastern Courtyard House as a Climatic Response', *Procedia - Soc. Behav. Sci.*, vol. 216, no. October 2015, pp. 662–674, Jan. 2016.
3. Sun, D., Pinker, R., Kafatos, M., 2006. Diurnal temperature range over the United States: a satellite view. *Geophys. Res. Lett.* 33, L05705.
4. Easterling DR, Horton B, Jones PD, et al. Maximum and minimum temperature trends for the globe. *Science* (80-). 1997;277(5324):364-367. doi:10.1126/science.277.5324.364.
5. Braganza, K., et al., 2004. Diurnal temperature range as an index of global climate change during the twentieth century. *Geophys. Res. Lett.* 31, 405–407.
6. T.R. Oke, The heat island of the urban boundary layer: characteristics, causes and effects, in: J.E. Cermak, A.G. Davenport, E.G. Plate, D.X. Viegas (Eds.), *Wind Climate and Cities*, (1995) NATO ASI Series, pp. 81–107.
7. J.A. Voogt, T.R. Oke, Complete urban surface temperatures, *Journal of Applied Meteorology* 36 (9) (1997) 1117–1132.
8. Martinelli, L.; Matzarakis, A. Influence of height/width proportions on the thermal comfort of courtyard typology for Italian climate zones. *Sustain. Cities Soc.* 2017, 29, 97–106
9. J. Rojas-Fernández, C. Galán-Marín, J. Roa-Fernández and C. Rivera-Gómez. Correlations between GIS-Based Urban Building Densification Analysis and Climate Guidelines for Mediterranean Courtyards. *Sustainability* 2017, 9(12), 2255; <https://doi.org/10.3390/su9122255>
10. Documento Básico HE. CTE. Código técnico de la Edificación. Documento Básico HE Ahorro de Energía. <https://www.codigotecnico.org/images/stories/pdf/ahorro-Energia/DBHE.pdf> [18 July 2019]
11. Resúmenes climatológicos - España - Anuales - Agencia Estatal de Meteorología - AEMET. Gobierno de España. http://www.aemet.es/es/serviciosclimaticos/vigilancia_clima/resumenes?w=0&datos=2. Accessed 15.01.2019.
12. E. Diz-Mellado, C. Galán-Marín and C. Rivera-Gómez. Adaptive Comfort Criteria in Transitional Spaces. A Proposal for Outdoor Comfort. *Proceedings*, 2020, 38, 1, (12); <https://doi.org/10.3390/proceedings2019038013>
13. C. Rivera-Gómez, E. Diz-Mellado, C. Galán-Marín and V.P. López-Cabeza. Tempering potential-based evaluation of the courtyard microclimate as a combined function of aspect ratio and outdoor temperature. *Sustainable Cities and Society* 2019, 51, 101740; <https://doi.org/10.1016/j.scs.2019.101740>.

Stakeholder engagement in nature-based public space design

Sustainable regeneration of urban environments

GLORIA OSEI¹, FEDERICA PASCALE¹, ALISON POOLEY¹,
NEZHAPI DELLE-ODELEYE¹

¹Anglia Ruskin University, Chelmsford, UK

ABSTRACT: The purpose of this paper is to present an argument for the theory of community and nature as key stakeholders in sustainable regeneration of urban environments, needed for a profitable Post Carbon City. This aim is achieved by exploring the real-world practices of creating community-driven nature-based public spaces from pre-construction to post-implementation. The paper adopts a narrative literature review method to build and analyse discourse within stakeholder engagement in Nature Based Solutions (NBS). A stakeholder model is presented for use of engagement, based on the phases of the project lifecycle against the effected internal and external stakeholders for NBS. A generalised understanding of the involvement of community and nature, as nature-based public space stakeholders, is offered. The research finds that for the optimal design of nature-based public spaces in urban environments, socio-environmental perception is essential. Therefore, the societal and natural sets of the Sustainability Venn Diagram are interdependent.

The assessment incorporates a focused search of books and articles from academia and practice, providing a novel perspective for the role of nature-based public space as an NBS in Post Carbon Cities.

KEYWORDS: Sustainability, NBS, Stakeholder engagement, Socio-Environment, Nature-based public space

1. INTRODUCTION

Urban regeneration can come at a great cost to the global environment [1, 2]. The UN World Commission on Environment and Development reported in 1987 that to achieve a sustainable future, development must not only be mindful of the current needs, but also the needs of future generations [3]. This account inspired the creation of models such as the Sustainability Venn Diagram [4]. These models give equal and overlapping value to natural, societal, and economical factors. Others have however contested for a sustainability model based on the necessary requirements and the level of dependency to accomplish sustainability. The Nested Sustainability Model [5] holds that economy is dependent on society, and society (and so therefore economy) is dependent on the environment. Decades later, it is currently evident that the economic factor of regeneration projects is valued above the others, superseding the others when there is a clash of interests [6]. The discourse on Post Carbon Cities explores urban life where the use of carbon is responsible and at a durable rate. This includes the need for urban environments to partake in mitigation methods such as Nature Based Solutions (NBS).

NBS are approaches stimulated by nature, with the use of green and/or blue spaces and interventions. Nature-based designs are therefore 'inspired, supported or copied from nature' [7]. The implementation of NBS in urban environments has been considered for: climate change adaptation by

aiding heat, energy and flood regulations [8]; natural disaster regeneration by allowing ecosystems to restore and increase [9]; agricultural sustainability by improved integrity of water management and food security [10].

Nature-based public spaces, a form of NBS, has provided a list of benefits in urban environments, including economic development [11], improvement of environmental conditions and comfort [12], aesthetics [13,14], social cohesion [15], and human health and wellbeing [16]. Research in the immersion of humans with nature, however, shows that basic physical walks through a natural environment have little effect on human's connectedness with nature [17]. This research notes that amplified contact with nature by emotional and sensory activities provides a greater bond with nature, potentially resulting in increased human benefits. Availability has an impact on the community-nature experience. The size of the natural environment and the distance the individual must travel to access the amenities are vital [18, 19], therefore post carbon cities will need to consider increasing the availability of nature-based public spaces for enhanced community sustainability.

Chatterton [20] notes that to achieve Post Carbon Cities, it is necessary to incorporate holistic initiatives, democratic actions, political cohesion, proactive process-based approaches, replicable planning, and networking of local and global links. Chatterton states that it is necessary for the dynamics of Post Carbon

Cities to incorporate community empowerment and control. To achieve community empowerment and control, urban planning often requires stakeholder engagement.

Two types of stakeholders are identified as necessary for the management and process of development [21, 22, 23]. Internal stakeholders form the intimate structure of decision-making management within the system [24,25]. External stakeholders, on the other hand, create the outer performance network with the potential to drive value and progress [26, 27]. Stakeholder engagement enables a project to become more relevant and impactful to stakeholders. These benefits are most successful in projects reliant on uptake in activities [28], such as nature-based public spaces. Recently, advancements have been made to produce methods of community involvement in the planning process of public space regeneration [29, 30, 31]. There has been a shift from the conventional use of external stakeholders as actors of benefit to achieve internal goals. Outreach to external bodies from diverse positions are being employed to create links of broad engagement [32].

Nevertheless, there are counterclaims of a lack of stakeholder engagement in regeneration. Project management literature has often reported on external stakeholders and their actions in negative and opposing terms [33, 34, 35]. These actions are mainly driven by stakeholder concerns about a project's long-term value achievement, and the impact on social, environmental, and economic sustainability [33]. These concerns regularly lead management teams to adopt disengagement strategies with external stakeholders, such as dismissal or concealment [36]. This is because management is primarily driven by short-term goals, such as budget, schedule and performance [37], and the need to reach key milestones [38].

The aim of this paper is to analyse the theory of community and nature as key stakeholders, for a sustainable regeneration of urban environments. In support of this aim, two research objectives are presented:

1. To explore **theoretical planning practices** of creating community-driven nature-based public spaces.
2. To assess how the **realities of stakeholdership** is adapted within these planning practices.

The paper argues for the need to represent the functions nature and society play in encouraging sustainable communities from pre-construction to post-implementation. A generalised understanding on the involvement of community and nature, as nature-

based public space stakeholders, is offered. The paper therefore considers the linked set, between nature and society, in the original Sustainability Venn Diagram. A stakeholder model is presented for engagement, based on the phase of the project (within its lifecycle) against the effected internal and external stakeholders for NBS.

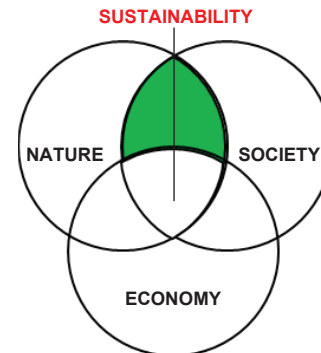


Figure 1: Sustainability Venn diagram highlighting the nature/social link.

2. METHODOLOGY

To investigate the process of nature and community involvement in urban regeneration, this paper adopts a narrative literature review method to build and analyse discourse within stakeholder engagement in NBS. This assessment incorporates a focused search of books and articles from academia and practice.

For the scope of this paper it is considered that society is the collection of impacted human beings, internal and external to the space considered. Nature is measured as land naturally or artificially inhabited by vegetation, also incorporating the numerous habitants that occupy it [39].

3. THEORETICAL PLANNING PRACTICES

3.1 Nature Design Elements

Land uses are considered in site development design planning as they impact on and are impacted by developments such as new nature-based public spaces. Land ownership occupies practical and political requirements in nature-based public space design. The owner of the land is relevant for information on incorporating impacting and impacted land use, as well as for the necessary maintenance collaborations. The share of land ownership is predominantly occupied by limited companies and corporate bodies [40]. Ownership is therefore relevant in nature-based public space design in considering the depths that could be taken for community-driven motives. It is questioned the extent in which community 'place attachment' can be achieved in view of existing land ownership [13, 41].

External environmental settings such as nature-based public spaces give rise to a degree of quality of

life. Lynch [42] pioneered 5 visual elements for human understanding of space: edges – the outer end limits of space; Paths – the ground structure; Nodes – key places; Landmarks – notable fixtures such as statues; and Districts. For the sustainable regeneration of urban environments, mindful planning of the resultant environment is therefore paramount. This planning requires engagement as nature-based public spaces can have some notable disadvantages to communities, such as a lack of control of events/space, fear of loss, and physical dislikes of the space (e.g. lack of colour) [43].

Maintenance is important as poorly maintained sites can also lead to misuse or degeneration of land. Effective maintenance plans are necessary to institutionalise reputable maintenance and renovation regimes [44]. It is argued that to ensure maintenance of nature-based public space, integrating the evolution and growth of their natural elements [45] is required. However, updating public space through maintenance can lead to place identity issues [46]. These issues can be aided with consultation through stakeholder engagement.

Elements of design that should be replaced or removed can be realised through engagement. Beer and Higgins [47] provide a guide of 5 possible views for a potential nature-based public space site for planning practices. These, if considered within a nature-based public space design, allows collaboration between the extent to which the community can view parts of the site, with the availability of each section of the site:

- **Very good views** - must be kept open
- **Good views** - ought to be kept open
- **Moderate views** - used with advantage
- **Poor views** - ought to be screened
- **Very poor views** - must be screened

3.2 Community Design Elements

As a subset of society, communities are a relevant part of site planning within the built environment [47]. The community that may be considered within planning range between residents, local workers, visitors, interested citizens, passers-by, etc. Data collected from communities provides information on design considerations that are necessary and to what extent they are so. The data can be used to analyse the factors of community-nature experience.

Human perception, through community engagement, can be incorporated within the design process, assisting in the inclusion and exclusion of design elements. The perception of the community helps to identify questions such as: **What will encourage me to use/ not use/ or misuse this space?**

In gaining perceptions, Sharp [48] investigates the use of public artists as a medium between the community and authorities within urban regeneration projects. In the UK these means are being increasingly explored. Glasgow, the UK City of Architecture and Design 1999, shows the success of community-driven regeneration from the offset. The use of the new genre public art approach allows creators to produce identity and ownership through engagement with community. Sharp reflects that for urban regeneration to succeed, there should be “processes through which communities are activated and stimulated into action” (2007, p.288).

(Malone, 2002) notes that age variation can form a diversity in social perception between generations; a concern in development planning for community approval. These differing needs have also progressed an increase in the sense of insecurity between the elderly and the younger generation. Though there are differences in the preferences and needs of people dependent on their age, status etc., Levy-Storms, Chen and Loukaitou-Sideris (2018) found that there were similarities in basic desires between the older and younger generations. The availability of public spaces to every type of user means that design should aim to be sensitive to all abilities and vulnerabilities. Many vulnerable individuals identify little differentiation between their physical and psychological wellbeing; and speak of both aspects as critical factors when using open spaces [50].

4. REALITIES OF STAKEHOLDERSHIP

4.1 Community stakeholder engagement

For the full benefits of public spaces to be realised, direct communication with the community is necessary [51]. It has been argued that the built environment pays little attention to the community as relevant agents when it comes to planning and design [52]. In *Remaking Cities*, Ravetz [52] gives an analysis of the urban environment and the use of the built environment as a control mechanism for groups within society over others in the community. Some have highlighted the role communities play as stakeholders to present this argument [33]. The hierarchy of external stakeholder importance implies that local communities are often disregarded. (Di Maddaloni and Davis, 2017) state that local communities’ inability to influence resources needed for a development project means that project managers concentrate heavily on the organisation of time and cost, rather than community values. In the evaluation of their systematic review, it is stated that local communities can play a beneficial role in the planning stages by limiting time and cost disruptions. Open-ended, personal communication prior to development is the ideal strategy to involve the public in development

projects [53]. Community inputs are necessary for post-psychological responses from both long-term and recent residents [54, 55]. There is a need for careful design aesthetics to incorporate culture, place identity, and place attachment aimed at recognising the individuality of the community [13, 41]. Otsuka and Reeve (2007), identify that Town Centre Managers are influential to local authorities in regeneration by providing information on local community needs and interests. However, their knowledge is limited as their work does not see them directly communicating with the users for development purposes but reporting through observation.

Ball [57] explores the negative views associated with community-driven regeneration and expressed the concern of non-representative data; where the middle class, elderly and Caucasian people, are greatly represented. Individuals with dominant personalities and/or unrealistic aims also contribute to the un-representative data. Other negative experiences researched are that community-driven processes are time consuming, over democratic, and hindered by a lack of trust between community and authority. Timely disengagement is therefore also required [32]. Design teams must be aware of the need to place effort in shared long-term value interests with external stakeholders and enhance the process of engagement and disengagement through prior protocols to establish flexibility [28, 32].

4.2 Nature stakeholder engagement

Stakeholders are commonly described using exclusively human representation. In the wider context they represent the social and economic set of a project [58]. The social set of the sustainability diagram have representation through the community, end user, and in part, the local council and media. The economic set of the sustainability diagram is represented through the investors that fund the project and also the contractors, suppliers, and other key workers that are employed to deliver the project. Nature as a stakeholder is lacking in representation [58]. Commonly represented merely by the presence on interested organisations [59], such as environmental agencies, they are kept informed of the progress of the project. These agencies often have opposing interests but are capable of influencing action from management [37], such as the enforcement to complete Environmental Impact Assessments [60]. There is however no representation of nature as an 'impacted stakeholder', yet the environmental set are usually impacted significantly and permanently when urban spaces are developed. Within the confines of nature-based public spaces, however, nature plays a responsible stakeholder role

as a type of supplier, for the project, as well as an impacted stakeholder.

Non-human creatures whose habitats are imposed on by development also form an impacted nature stakeholder. There is argument to consider these species as stakeholders due to the disruption and/or displacement they face due to urban development. Within the study of development, however, the habitat and habitants' role as stakeholders have been largely neglected in studies [60]. Sage et al. [60] express that this lack of research in the field has led to limited relevant data on the process of encountering habitants in development projects. Their case studies show that considering habitants as stakeholders and therefore 'proactively accommodating wildlife', produces positive results on both a project and organisational level. As nature is given a voice through human agencies amidst conflicting issues, nature is a vulnerable stakeholder in developments.

4.3 Stakeholder model for engagement

It is evident that local communities as external stakeholders may benefit from a more effective engagement. The role they play as stakeholders is crucial to the survival of the project after implementation. Yet when designing community-driven, nature-based, public spaces for the interactive use of humans and nature, it is essential to incorporate careful planning and maintenance. These design plans can mitigate potential drawbacks through examples like using low allergen vegetation and high safety playgrounds [61]. Modified from Di Maddaloni and Davis's recognised stakeholders [27], the stakeholder model below represents the required extent of engagement with various stakeholders, within NBS development projects.

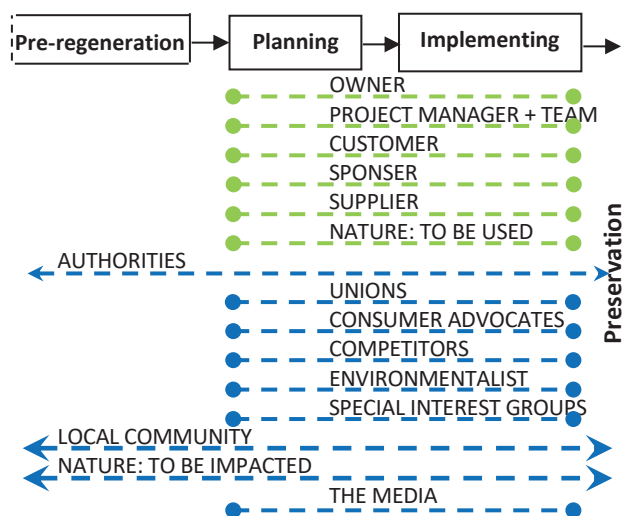


Figure 2: Stakeholder model: based on project phase against the effected stakeholders for NBS

5. FINDINGS

The research reveals that to achieve sustainable communities in post carbon cities, emphasis on effective design process of nature-based public spaces is necessary. The theme of 'community-nature stakeholdership' gives rise to the theory of place creation through socio-environmental perception. This concept holds that for the optimal design of nature-based public spaces in urban environments, social engagement must be a key focus. However, the natural environment is also essential in encouraging the basic elements of community participation by enhancing social cohesion. Therefore, the sets of society and nature in the Sustainability Venn diagram are interdependent.

Local communities' inability to influence resources needed for a project means that project managers often disregard the community's position as stakeholders [27]. It is evident that to achieve systematic outcomes, projects should use a balanced approach of engagement and disengagement [37, 62, 63]. As community and nature are crucial stakeholders for the continuity of NBS projects, efficiently organised disengagement through protocol is vital.

Carefully planned natural infrastructure, with local community stakeholder engagement, could bring extensive benefits to urban regeneration projects. This paper argues that achieving nature/social factors of development can provide positive impacts on other sustainability factors. These benefits include emotional, intellectual, social, and physical benefits [43].

The review identifies that a lack of maintenance in nature-based public spaces can lead to misuse or degeneration of land. Also commented on, is the necessity for design to incorporate facilities that allow for easy use by the more vulnerable in society. Further, there are few assessments into the psychological effects of the exposure to nature, compared to physical affects [16].

5.1 Implication and originality

This paper highlights that community-driven nature based public spaces are fundamental to breaking the boundaries needed for profitable Post Carbon Cities. It brings academia and the practice of urban regeneration together, to argue that public spaces can and will hold a key position in creating Post Carbon Cities. The utilisation of a community-driven approach will aid the complex process of constructing nature-based public spaces. It highlights the importance of social factors in the future of urban regions and represents the role of nature in propelling sustainable communities.

The value of this paper to academia and practice alike is that it provides a novel perspective examining the combination of nature and social factors to

provide practical answers on how current practice can be altered and enhanced, aiding a revised thinking for urban regeneration models.

The research is limited as it reviews research and practice papers and books but no other documents.

6. CONCLUSION

This paper concludes in proposing that sustainable communities can be achieved in Post Carbon Cities by placing an increased priority on the benefits nature has on social issues. The research argues that the most critical portion of the Sustainability Venn Diagram is the link of nature and society, for NBS in Post Carbon Cities. When incorporating NBS in urban regeneration, projects can subsequently benefit from a strengthened proposal at the planning stages, a limited chance of community-instigated delays at the implementation stage, and a potentially valued design at completion.

REFERENCES

1. Winkless, L., (2016). *Science and the city: The mechanics behind the metropolis*. Bloomsbury Publishing.
2. Moore, R., (2016). *Slow burn city: London in the twenty-first century*. Pan Macmillan.
3. WCED, S.W.S., (1987). *World commission on environment and development*. Our common future, 17, pp.1-91.
4. Elkington, J., (1998). *Cannibals with Forks: The Triple Bottom Line of 21st Century Business*. Paperback edition ed. Gabriola Island: John Wiley & Sons, Ltd.
5. Giddings, B., Hopwood, B. and O'Brien, G., (2002). *Environment, economy and society: fitting them together into sustainable development*. Sustainable Development, 10 (4), pp.187-196.
6. Adams, J., Bosselmann, K., Cartwright, W., Davis, P., Hertnon, S., Howell, R., Lawton, M., Peet, J., Reid, W. and Salinger, J., (2009). *Strong Sustainability for New Zealand: principles and scenarios*.
7. ECDG, (2015). *Towards an EU research and innovate policy agenda for nature-based solutions and re-naturing cities*. Luxembourg: European Commission.
8. Kabisch, N., Korn, H., Stadler, J. and Bonn, A., (2017). *Nature-Based Solutions to Climate Change Adaptation in Urban Areas: Linkages between Science, Policy and Practice*. Cham: Springer.
9. Asian Development Bank, (2016). *Nature-Based Solutions for Building Resilience in Towns and Cities: Case Studies from the Greater Mekong Region*. Manila: Asian Development Bank Institute.
10. Sonneveld, Ben G J S, Merbis, M.D., Alfarrá, A., Unver, O. and Arnal, M.F., (2018). *Nature-Based Solutions for agricultural water management and food security 12 Nature-Based Solutions for agricultural water management and food security*. FOOD AND AGRICULTURE ORGANIZATION OF THE UNITED NATIONS, Rome, 2018. Unpublished.
11. Buckley, R.C. and Brough, P., (2017). *Economic Value of Parks via Human Mental Health: An Analytical Framework*. Frontiers in Ecology and Evolution, 5 (16), pp.1-9.
12. Boeri, A., Gaspari, J., Gianfrate, V. and Longo, D., (2017). *Accelerating urban transition: An approach to greening the built environment*. WIT Transactions on Ecology and the Environment, 223, pp.3-14.
13. Julier, G., (2005). *Urban designscapes and the production of aesthetic consent*. Urban Studies, 42 (5-6), pp.869-887.
14. Kim, S. and Kwon, H., (2018). *Urban Sustainability through Public Architecture*. Sustainability, 10 (4), pp.1249.
15. Ivanova, E., (2016). *Public Gardening and the Challenges of Neighbourhood Regeneration in Moscow*. Critical Housing Analysis, 3 (2), pp.26-32.
16. Van den Bosch, M. and Ode Sang, Å., (2017). *Urban natural environments as nature-based solutions for improved public health – A systematic review of reviews*. Environmental Research, 158, pp.373-384.
17. Lumber, R., Richardson, M. and Sheffield, D., (2017). *Beyond knowing nature: Contact, emotion, compassion, meaning, and beauty are pathways to nature connection*. PloS one, 12 (5), pp.1-24.

18. Ekkel, E.D. and de Vries, S., (2017). *Nearby green space and human health: Evaluating accessibility metrics*. Landscape and Urban Planning, 157, pp.214-220.
19. Russo, A. and Cirella, G., (2018). *Modern compact cities: how much greenery do we need?* International journal of environmental research and public health, 15 (10), pp.2180.
20. Chatterton, P., (2013). *Towards an agenda for post-carbon cities: lessons from Lilac, the UK's first ecological, affordable cohousing community*. International Journal of Urban and Regional Research, 37 (5), pp.1654-1674.
21. Ayuso, S., Ángel Rodríguez, M., García-Castro, R. and Ángel Ariño, M., (2011). *Does stakeholder engagement promote sustainable innovation orientation?* Industrial Management & Data Systems, 111 (9), pp.1399-1417.
22. Bal, M., Bryde, D., Fearon, D. and Ochieng, E., (2013). *Stakeholder Engagement: Achieving Sustainability in the Construction Sector*. Sustainability, 5 (2), pp.695-710.
23. Collinge, W.H. and Harty, C.F., (2014). *Stakeholder interpretations of design: semiotic insights into the briefing process*. Construction Management and Economics: ARCOM Conference Issue, 32 (7-8), pp.760-772.
24. Chinyio, E.A. and Akintoye, A., (2008). *Practical approaches for engaging stakeholders: findings from the UK*. Construction Management and Economics: STAKEHOLDER MANAGEMENT IN CONSTRUCTION, 26 (6), pp.591-599.
25. Eskerod, P., Huemann, M. and Ringhofer, C., (2015). *Stakeholder Inclusiveness: Enriching Project Management with General Stakeholder Theory*. Project Management Journal, 46 (6), pp.42-53.
26. Fassin, Y., (2009). *The Stakeholder Model Refined*. Journal of Business Ethics, 84 (1), pp.113-135.
27. Di Maddaloni, F. and Davis, K., (2017). *The influence of local community stakeholders in megaprojects: Rethinking their inclusiveness to improve project performance*. International Journal of Project Management, 35 (8), pp.1537-1556.
28. Haddaway, N.R., Kohl, C., Rebelo da Silva, N., Schiemann, J., Spök, A., Stewart, R., Sweet, J.B. and Wilhelm, R., (2017). *A framework for stakeholder engagement during systematic reviews and maps in environmental management*. Environmental Evidence, 6 (1), pp.1-14.
29. Cilliers, E.J. and Timmermans, W., (2014). *The importance of creative participatory planning in the public place-making process*. Environment and Planning B: Planning and Design, 41 (3), pp.413-429.
30. Cilliers, E.J. and Nicolene, D.E., (2016). *Planning for lively spaces: Adding value to old spaces*. 2016. 49th ISOCARP Congress Brisbane, October 2014, The Netherlands: ISOCARP.
31. Stratigea, A., Kikidou, M., Patelida, M. and Somarakis, G., (2017). *Engaging Citizens in Planning Open Public Space Regeneration: Pedio Agora Framework*. Journal of Urban Planning and Development, 144 (1), p.05017016.
32. Lehtinen, J., Aaltonen, K. and Rajala, R., (2019). *Stakeholder management in complex product systems: Practices and rationales for engagement and disengagement*. Industrial Marketing Management, 79, pp.58-70.
33. Chan, A.P.C. and Oppong, G.D., (2017). *Managing the expectations of external stakeholders in construction projects*. Engineering, Construction and Architectural Management, 24 (5), pp.736-756.
34. Teo, M.M. and Loosmore, M., (2017). *Understanding community protest from a project management perspective: A relationship-based approach*. International Journal of Project Management, 35 (8), pp.1444-1458.
35. Di Maddaloni, F. and Davis, K., (2018). *Project manager's perception of the local communities' stakeholder in megaprojects. An empirical investigation in the UK*. International Journal of Project Management, 36 (3), pp.542-565.
36. Aaltonen, K., Kujala, J., Havela, L. and Savage, G., (2015). *Stakeholder Dynamics During the Project Front-End: The Case of Nuclear Waste Repository Projects*. Project Management Journal, 46 (6), pp.15-41.
37. Aaltonen, K. and Kujala, J., (2010). *A project lifecycle perspective on stakeholder influence strategies in global projects*. Scandinavian Journal of Management, 26 (4), pp.381-397.
38. Flyvbjerg, B., (2014). *What You Should Know About Megaprojects and Why: An Overview*. Project Management Journal, 45 (2), pp.6-19.
39. Nicol, C. and Blake, R., (2000). *Classification and Use of Open Space in the Context of Increasing Urban Capacity*. Planning Practice & Research, 15 (3), pp.193-210.
40. HM Land Registry, (2018). Open data revolution: harnessing the power of land ownership insights. [on-line] Available at: <<https://hmlandregistry.blog.gov.uk/2018/10/18/open-data-revolution-harnessing-the-power-of-land-ownership-insights/>> [Accessed: 26 February 2020].
41. Mihaylov, N. and Perkins, D.D., (2014). *Community place attachment and its role in social capital development*. In: L.C. Manzo and P. Devine-Wright, eds. 2014. Place attachment: Advances in theory, methods and applications. London and New York: Routledge New York, NY. Chapter: 5. pp.61-74.
42. Lynch, K., (1960). *The image of the city*. Cambridge, Mass: MIT Press.
43. Mostyn, B., (1980). *Personal Benefits and Satisfaction Derived from Participation in Urban Wildlife Projects: A Qualitative Evaluation Undertaken on Behalf of the Nature Conservancy Council*. London: British Association of Social Workers.
44. Douglas, O., Lennon, M. and Scott, M., (2017). *Green space benefits for health and well-being: A life-course approach for urban planning, design and management*. Cities, 66, pp.53-62.
45. Charras, K., Bébin, C., Laulier, V., Mabire, J. and Aquino, J., (2018). *Designing dementia-friendly gardens: A workshop for landscape architects*. Innovative Practice: Dementia. London, pp.1-9.
46. Carmona, M., (2015). *Re-theorising contemporary public space: a new narrative and a new normative*. Journal of Urbanism: International Research on Placemaking and Urban Sustainability, 8 (4), pp.373-405.
47. Beer, A.R. and Higgins, C., (2000). *Environmental Planning for Site Development*. 2nd ed. ed. GB: Spon (E&F).
48. Sharp, J., (2007). *The life and death of five spaces: public art and community regeneration in Glasgow*. Cultural Geographies, 14 (2), pp.274-292.
49. Malone, K., 2002. Street life: youth, culture and competing uses of public space. Environment and Urbanization, 14 (2), pp.157-168.
50. Levy-Storms, L., Chen, L. and Loukaitou-Sideris, A., (2018). *Older adults' needs and preferences for open space and physical activity in and near parks: a systematic review*. Journal of Aging and Physical Activity, 26 (4), pp.682-696.
51. Chalmers, H. and Colvin, J., (2005). *Addressing environmental inequalities in UK policy: an action research perspective*. Local Environment, 10 (4), pp.333-360.
52. Ravetz, A., (1980). *Remaking Cities*. 1st ed. London: Routledge Ltd.
53. Golden, S.M., (2014). *Occupied by Design: Evaluating Performative Tactics for More Sustainable Shared City Space in Private-led Regeneration Projects*. WIT Transactions on Ecology and the Environment, 191, pp.441-452.
54. Bélanger, H., Cameron, S. and de la Mora, C., (2012). *Revitalization of Public Spaces in a Working Class Neighbourhood: Appropriation identity and urban imaginary*. In: H. Casakin and F. Bernardo, eds. 2012. The Role of Place Identity in the Perception, Understanding, and Design of Built Environments. United Arab Emirates: Bentham Science. Chapter: 4. pp.47-62.
55. Salone, C., Baraldi, S.B. and Pazzola, G., (2017). *Cultural production in peripheral urban spaces: lessons from Barriera, Turin (Italy)*. European Planning Studies, 25 (12), pp.2117-2137.
56. Otsuka, N. and Reeve, A., (2007). *The contribution and potential of town centre management for regeneration: Shifting its focus from management to regeneration*. Town Planning Review, 78 (2), pp.225-250.
57. Ball, M., (2004). *Co-operation with the community in property-led urban regeneration*. Journal of Property Research, 21 (2), pp.119-142.
58. Starik, M., (1995). *Should Trees Have Managerial Standing? Toward Stakeholder Status for Non-Human Nature*. Journal of Business Ethics, 14 (3), pp.207-217.
59. Phillips, R.A. and Reichart, J., (2000). *The Environment as a Stakeholder? A Fairness-Based Approach*. Journal of Business Ethics, 23 (2), pp.185-197.
60. Sage, D., Dainty, A., Tryggvason, K., Justesen, L. and Mouritsen, J., (2013). *"All That Fuss, Just for Some Bloody Badgers?" The politics of wildlife in infrastructure construction*. 2013. Procs 29th Annual ARCOM Conference. Reading, UK: Association of Researchers in Construction Management. pp.839-848.
61. Braubach, M., Egorov, A., Mudu, P., Wolf, T., Ward Thompson, C. and Martuzzi, M., (2017). *Effects of Urban Green Space on Environmental Health, Equity and Resilience*. In: N. Kabisch, H. Korn, J. Stadler and A. Bonn, eds. 2017. Nature-Based Solutions to Climate Change Adaptation in Urban Areas. London: Springer. pp.187-205.
62. Miles, S., (2012). *Stakeholder: Essentially Contested or Just Confused?* Journal of Business Ethics, 108 (3), pp.285-298.
63. Zeng, R.C., Zeng, S.X., Ma, H.Y., Lin, H. and Tam, V.W.Y., (2015). *Social responsibility of major infrastructure projects in China*. International Journal of Project Management, 33 (3), pp.537-548.

The Mixed-use matrix

Developing design guidelines for the mixed-use typology for Mumbai

SHRUTI SHIVA

Terra Viridis, Hyderabad, India

Morphologically, the mixed-use typology is a stepping stone to sustainable urban design. Designed keeping accessibility, program, mobility and foremost, pedestrians in mind, a mixed-use typology generates compact clusters, where a live-work-play relation is established, giving great scope for performance optimization, owing to typological advantage. This paper is an on-going research to produce the 'mixed-use matrix' for the city of Mumbai, aimed at providing planners guidelines at early design stages. An explorative research, this paper proposes a method, introduces the base case and puts forth the direction for the research to follow. An iterative study assessing urban heat island effect through Dragonfly, followed by energy simulation for cooling load was conducted. In conclusion the paper puts forth a set of design guidelines as a form of a matrix, where massing strategies such as –high rise, mid-rise and low-rise are assessed based on their outdoor and indoor performance. Simple architectural interventions that can be adopted at early stages are alluded to, thus providing designers a quick manual to start assessing their massing and master-planning strategies for mixed-use development in Mumbai.

KEYWORDS: Mixed-use developments, urban heat island, early stage design performance, Mumbai

1. INTRODUCTION

Morphologically, the mixed-use typology is a stepping stone to sustainable urban design. Designed keeping accessibility, program, mobility and foremost, pedestrians in mind, a mixed-use typology generates compact clusters, where a live-work-play relation is established, giving great scope for performance optimization, owing to typological advantage. Grant [1] exalts the mixed use typology as a smart and sustainable approach to urban planning. Hachem [2] seconds this while elucidating the lack of adequate research and guidelines about designing mixed-use types. This paper is an on-going research to produce the 'mixed-use matrix' for the city of Mumbai, aimed at providing planners guidelines at early design stages. An explorative research, this paper proposes a method, introduces the base case and puts forth the direction for the research to follow.

2. RESEARCH QUESTION

The research aims to create guidelines for mixed use typology design. As mixed use types are sizable clusters, the research is divided into two scopes of study- Microclimate and building level. The first part outlines the key agenda of the outdoor/microclimate study, which are the following:

- 1) Assessing the impact of built form on microclimate through the lens of urban heat island effect
- 2) Deriving and defining parameters that impact the heat island for generative massing strategies

The second part aims to link the effect of microclimate massing studies to its impacts on building level decisions through cooling loads and daylight metrics.

2.1 The base case

In order to create a base case, a precedent was required to be established. As this study is conducted for Mumbai, the only existing in-construction proposal for a high performance mixed-use development was chosen as the base case.

The development is called Kohinoor Square (Fig.1) and is located in the central area of Dadar in the city. It consists of a high-rise module and its mixed-use parameters are as follows:

Site Coverage Ratio: 0.6, Tree Coverage Ratio: 0.01, Grass Coverage Ratio: 0.09

4% retail, 29% parking, 4% F&B, 57% commercial and 7% residential.



Figure 1: View of the proposal (source: SSA architects)

2.2 Method-Part 1

The base case was evaluated using Dragonfly and the urban weather generator tool to see the adjusted

weather conditions created for that specific microclimate. The tool uses factors like typology distribution, ground and green cover, building facets to arrive at an adjusted weather file, which is site specific. This was then compared to the weather data for the city for two representative weeks- one in monsoon and one in summer (Fig.2).

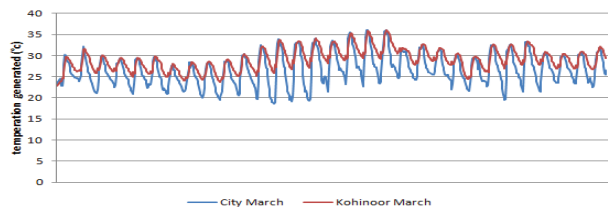


Figure 2: Comparison between dry bulb for weather file against base case, summer week.

An average of dry bulb temperature for both, base case and city weather data was calculated (ΔT) and this metric was further used for sensitivity studies. As summers are more oppressive in Mumbai, further studies were conducted for the summer week.

$\Delta T = DBT_{site} - DBT_{city}$; where DBT is dry bulb temp.

While keeping the mixed-use proportions constant, the impact of various factors, such as- site coverage ratio, green cover ratio and facade cover ratio, was studied by generating the ΔT . Parametric studies were conducted which would help in identifying the parameter most critical in creating an ambient microclimate. Tendency lines were plotted for ΔT for each parameter and a point of diminishing returns was arrived upon in each case (Fig.3)

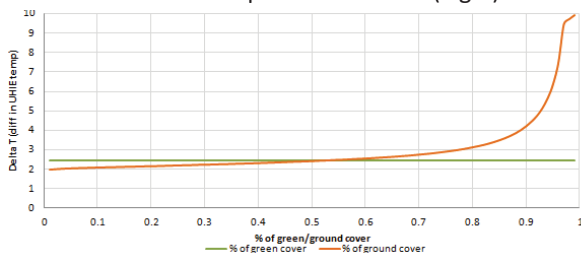


Figure 3: Tendency plots for site cover, green cover against ΔT

It was observed that while the impact of changing ground cover was significant, the change in green cover percentage was not yielding any palpable results. Upon further testing, it was deduced that this was a limitation of the tool, wherein it was simulating the ground underneath grass closer to a pavement than soil, despite applying soil properties as per Energyplus materials. Therefore, it was concluded that the factor to be studied would be the ground cover and thereby, the impact of density on heat island would be measured.

2.3 Iterative massing studies

Using grasshopper's native Galapagos solver, a set of iterative studies to generate massing options for

the given site was conducted. The idea was to obtain massing strategies that were informed by the previous studies to obtain ambient outdoor conditions. Table 1 illustrates the parameters that were tested, the resultant metric chosen for evaluations and other fixed constants.

Table 1: Parameters -fixed and constant

Geometric parameters changed	Parameters fixed	Studied metric for comparison
Height of blocks	Ground cover=0.5	Incident irradiation on ground (kwh/sq.m annual)
No. of blocks	Green cover= 0.5	
Aspect ratio	FAR= 2.5	

2.4 Results and findings

The iterative studies largely explored the correlation between density and its subsequent effect on heat island. Select results were uploaded onto design explorer to clearly see the correlation between the various factors and the resultant irradiation produced. (Fig.4)

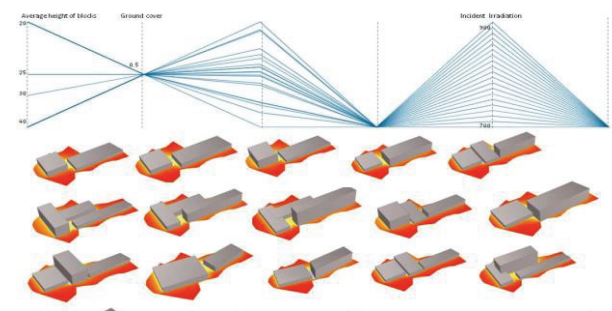


Figure 4: Massing iterations correlated to height and ground cover ratio (after: design explorer interface)

It was then noted that a more favourable density in Mumbai as opposed to the extremely high-rise-low-rise scheme deployed in the base case, is multiple blocks of mid to high rise. Of the many iterations generated, the worst and best massing were considered and then compared to the existing base case. The parameter for comparison was both, the incident irradiation and ΔT obtained through the weather generator. Table 2 illustrates the comparative results.

Table 2: Comparative results of iterative studies

	Irradiation (kwh/sq.m)	ΔT (K) for summer week
Base case	978.3	2.39
Worst case	884.9	1.53
Best case	796.1	0.61

3. INFERENCES FROM MICROCLIMATE STUDIES

The following inferences can be culled out from the massing studies:

- Density has a negative correlation; a midrise to moderate high rise is preferred over extremely high rise massing schemes.
- Massing resulting in enclosed courts is preferred over strip massing.

While the ambient conditions favour a mid-rise to moderate high rise combination approach, a corpus of literature favours compactness from a cooling load perspective [3-4]. Therefore, in the next set of studies, the impact of density on cooling load was observed. Of the massing iterations, twenty cases were taken forward to be further studied on a building level.

4. BUILDING LEVEL METHOD

Twenty iterations from the massing studies representing typical cases of high-low rise combination, sprawl and medium density, were further studied to assess the impact of density on cooling loads. This was done by analysing the relationship between surface to volume ratio and cooling loads. The analysis was conducted using the parametric study chain used in part one and then connected to honeybee's energy simulation studio that leverages energy plus. The adjusted weather file generated for each massing case through Dragonfly was used in energy analysis, to account for urban heat island and its impacts on cooling loads. Figure 5 illustrates the method.

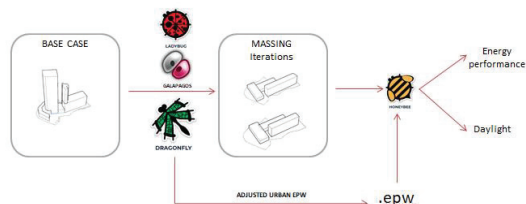


Figure 5: Flow of processes applied for energy study.

As it is a mixed use building, the proportions of mixed use were maintained in the various iterations and the internal conditions of those masses were applied accordingly. The following table lists the assumptions of construction, schedule and internal conditions applied for the energy modelling.

Table 3: assumptions for energy modelling

Default energyplus set – Office applied to 57% of massing. Schedule, setpoint, construction : Office default
Default energyplus set- Midrise apartment applied to 7% of massing
Default energyplus set – FullServiceRestaurant

applied to 7% massing

Remaining was modelled as a dummy zone (parking)

4.1 Results- Energy simulations

The cooling load for each massing condition obtained was extracted. The weighted average of the loads for each typology in the mixed use was calculated in proportion to their area. This weighted average cooling load produced for all iterations was then plotted against surface to volume ratio of the built form. A regression plot was generated (Fig.6) which showed a strong acceptance rate, as was hypothesized through literature.

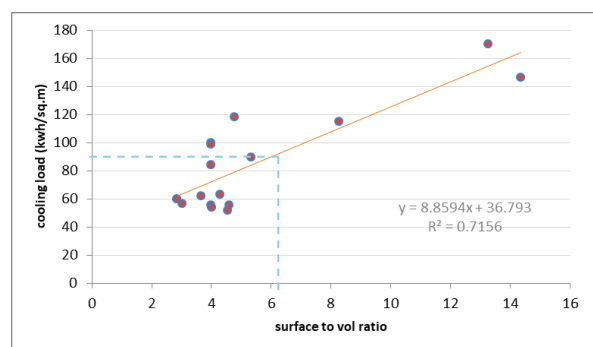


Figure 6: Plot of cooling load against surface to volume ratio.

The linear relationship of lower surface to volume ratio – lower cooling load is clearly established.

4.2 Results- Daylight simulations

A further set of studies extracting the daylight levels of the massing were conducted to observe if more compact forms resulted in impacted or enhanced daylight levels. The following assumptions were made for daylight studies. Note, these are commonly used characteristics in Indian commercial spaces.

Table 4: assumptions for daylight modelling

Element	Characteristic
Wall	Reflectivity : 0.5
Floor plate	Reflectivity : 0.3
Windows	VLT : 0.6, WWR: 40%
Ceiling	Reflectivity : 0.7
Other assumptions :	
- Entire floor plate was run in all blocks	
- Floor plate at half of total Height was selected	

The analysis was conducted using Honeybee and the same massing iterations run in the previous studies for cooling load were run for daylight performance. The results for a Daylight Autonomy of 300 lux were used as a metric. The average DA_300

achieved across the massing blocks was plotted against Surface to volume ratio. (Fig. 7)

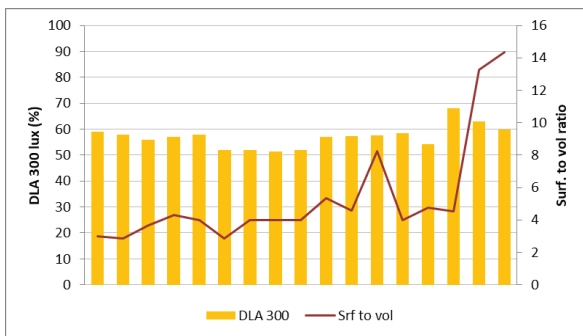


Figure 7: Daylight performance against Surf to vol ratio

It can be observed that while the surface to volume ratio changes, the daylight levels remain more or less constant. A further regression plot (Fig. 8) showed an R² value of 0.16, revealing that daylight performance was not strongly correlated to the massing parameter of surface to volume, thereby making energy performance the critical variable to assess the overall performance of a mixed use massing.

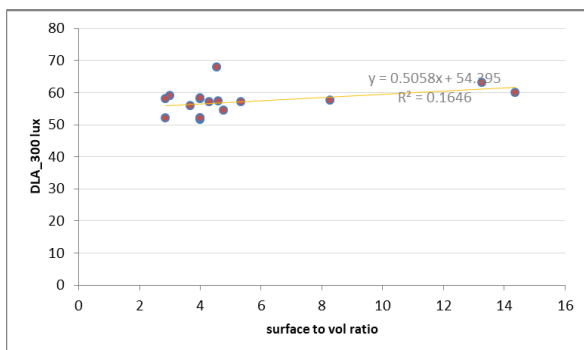


Figure 8: Daylight performance against Surface to vol ratio

4.3 Inferences and finding

The key findings from the two stage studies were as follows:

- It was observed that massing that creates more overlaps and over-shading reduces the incident radiation thereby reducing the urban heat island effect.
- The over-lapping forms of medium density showed better results in outdoor studies.
- Low density, sprawl buildings also performed better than high-rise massing in terms of urban heat island; however these massing schemes had a high cooling load due to increased surface to volume exposure.
- Medium dense building, with longer facades flanking interior courts had lower cooling

loads compared to more exposed mid-rise schemes, despite their surface to volume ratio more median value than in the lower half

- High rise with more surface to volume ratio do not benefit in urban heat island reduction and produce high cooling loads as well.
- Intersecting geometry with medium to high surface to volume ratio also produced median cooling loads. This can be attributed to self-shading of forms that impact cooling loads.

These inferences were used to generate a set of preliminary design guidelines for mixed-use buildings in the context of Mumbai, India. An example of the guidelines is illustrated below. The aim of the guideline is to not only encourage cluster-based mixed use development in the city, but also to provide design directives that have positive performance implications.

5. THE MATRIX

The set of studies conducted were conducted with an aim to produce a set of guidelines for designers to refer to in the early stages of designing mixed –use developments in Mumbai. The following grid (Table.5) is a summary of studies. This grid aims to be read as a manual to guide massing and planning strategies during master-planning and concept stages of design. By using only two major metrics – Urban heat island effect and cooling load, the grid provides the designer the ability to quickly discern the performance capability of their early design from an outdoor and indoor perspective.

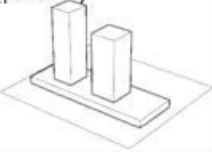




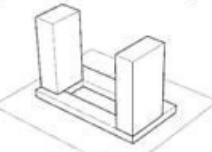


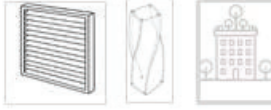











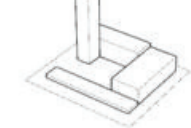




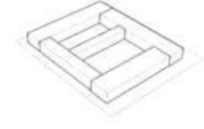




The way to interpret the grid is as follows:









- The massing is primarily divided into density based typologies: high rise, mid-rise and low rise.
- Each of those types are further divided into podium type or courtyard enclosing
- Each massing strategy is evaluated for its performance against urban heat island effect and cooling load (as suggested by the studies conducted)
- They are graded by least to most impact by growing sizes of circles, indicative of the measure of impact
- The circles are colour coded for outdoor, indoor and overall

For each strategy a set of design features that can adopted for improving the performance of that strategy is provided. These features are restricted to – shading, form alteration from orientation or twisting perspective, and increase

in green cover through landscape or green roof.
The features are limited to those which have
direct impact on early stage design decisions.

Table 5: The mixed-use matrix

Massing strategy	Reduces urban heat island	Reduces cooling load	Architectural interventions required for implementation	Overall preference
High rise- low rise (podium) 				
High rise- low rise (court yard enclosed) 				
Medium rise (podium) 				
Medium rise (court enclosed) 				
High rise-mid rise 				
Low rise (sprawl/grid) 				


Most to least impact

Not recommended

Outdoor

Cooling

Overall

Shading

Form twisting

Green cover

Canada.” *Buildings*, vol. 4, no. 3, 9 July 2014, pp. 336–354, 10.3390/buildings4030336.

6. CONCLUSION

Mumbai being a dense city and the country’s most rapidly growing city in terms of population and built environmental growth, has scope to embrace the mixed-use model to tackle challenges of housing deficit whilst providing occupants a sustainable environment. This paper aims to provide early insight into massing strategies for these mixed-use developments from a performance perspective in order to aid designers in their decision making.

While high density is considered the solution for housing problems in many developing nations, it is important to understand its implications on performance from both an urban and building level. In highlighting the pros and cons of commonly used massing strategies, a more performance conscious approach can be adopted from the conceptual stages itself, preventing additional costs and effort at later stages.

REFERENCES

1. Grant, J. (2007). Chapter 3. Encouraging mixed-use in practice. In *Incentives, Regulations and Plans: the role of states and nation-states in smart growth planning*, Edwin Elgar Publishers UK, pp 57-76.
2. Hachem, C. (2015). *Design of a base case mixed-use community and its energy performance*, IBPC, Elsevier, pp 663-668
3. Duarte, G., Fonseca, L., Goliatt, P. and Lemonge, A., (2017) *Comparison of machine learning techniques for predicting energy loads in buildings*, *Ambiente Construído*, 17(3), pp.103-115.
4. Suraya, W, et al, (2015) “*Analysing Optimum Building Form in Relation to Lower Cooling Load.*” Annual Serial Landmark International Conferences on Quality of Life ASEAN-Turkey ASLI QoL2015, 2015.
5. Nault, E., Rey, E. and Andersen, M., (2016). *A Multi-Criteria Decision-Support Workflow for Early-Stage Neighborhood Design based on Predicted Solar Performance*. In: *PLEA*, Los Angeles
6. Takkanon, Pattaranan (2016). *A Study of Height to Width Ratios and Urban Heat Island Intensity of Bangkok* Vol. 1, 2016, pp. 30–31. Accessed 02 April 2020.
7. McKeen, Philip, and Alan Fung (2014). “*The Effect of Building Aspect Ratio on Energy Efficiency: A Case Study for Multi-Unit Residential Buildings in*

8. Bande, Lindita, et al (2019) “*Validation of UWG and ENVI-Met Models in an Abu Dhabi District, Based on Site Measurements.*” *Sustainability*, vol. 11, no. 16, 13 Aug. 2019, p. 4378, 10.3390/su11164378.

Building Performance Simulation Supporting Typical Design Activities The Case of 'Volume Massing'

PIL BRIX PURUP¹, STEFFEN PETERSEN², ANDREW FERGUSON DUNN¹, MYRTA GKAINTAZI-MASOUTI², ONDREJ VISA²

¹ NIRAS A/S, Aarhus, Denmark

² Department of Engineering, Aarhus University, Aarhus, Denmark

ABSTRACT: Recent research have revealed that common tools for building performance simulation (BPS) are not fit to support typical design activities that architects conduct during early design. This paper presents the development of a prototype for a BPS tool aimed to support the design activities during 'volume massing', in which architects define outer boundaries of new building(s) relative to the landscape. The prototype was developed using a mix of methods: Semi-structured interviews, paper prototypes, user workshops and a test case. The results indicates that the prototype has potential to support design activities during design activities related to 'volume massing'.

KEYWORDS: Building performance simulation, Design support, Design activities, Volume massing, Thermal comfort

1. INTRODUCTION

Building performance simulations (BPS) is a powerful tool to support design decisions in the early stages of low-energy building design [1]. Despite of this ability, the use of BPS tools in the early design stage seems to be rare in design practice. Recent research suggests that one way to ensure better integration of BPS into the early design stage is a development that focus more on the building designer as the potential user, rather than the simulation expert [2-3]. Interviews conducted among architects in Scandinavia concludes that architects are willing to use BPS to inform their early decisions if the tools are conformed to fit their design process [4-5]. Therefore, Purup and Petersen [6] conducted nine semi-structured interviews of Danish architects to identify ways of bridging the gap between design practice and BPS tools. The interviews identified a (finite) number of design activities (e.g. 'Research', 'Modelling', 'Analysis' and 'Evaluation'). Furthermore, a set of requirements for development of BPS tool fit for building design practice (early stage) – in the view of practicing building designers – was defined based on the interviews [6]:

- **Independent of the design process:** The BPS tool must support a typical architectural design activity, i.e. support what architects actually do when they design – not dictate a certain process or workflow.
- **Fast and imbedded BPS modelling:** Use geometrical data from architectural CAD models at a different level of detail, and make the BPS tool a plug-in to the CAD tool (no manual export of data).
- **All geometrical shapes are possible:** No need for simplifying the architectural expression of the CAD model to enable BPS.
- **Independent of chosen CAD tool:** The BPS tool should (at least) work in Rhino, SketchUp and Revit.

- **Differentiated input interface:** Make the tool usable to non-experts who want to apply BPS by making simple interfaces for setting up simulation parameters (e.g. by using templates or wizards) but make all input variables accessible in another interface for the advanced user.

- **Fast versus precise simulations:** The BPS tool for the early design stage should build on feasible trade-offs between precision and simulation speed.

- **Intuitive visualisation of simulation results:** Visualisations of simulation results should 1) be presented in a way that non-expert immediately can decode it 2) allow experts to assess the output in detail, and 3) support stakeholder collaboration.

- **Auto-generate documentation:** An export function that generates reports containing input/output data for documentation purposes.

Design activities related to 'Volume massing' where architects arrange the new overall building volume in relation to the existing context and landscape was often mentioned in the interviews. The interviewed architects switches between two types of design activities during 'Volume massing': '3D volume shaping' (push/pull surfaces, scaling blocks, moving corner points or edges, etc.) and 'Lego/Duplo' (arrangement of predefined blocks or shapes, either room size blocks (Lego) or larger sections of buildings (Duplo)) [6].

The purpose of this paper is to present the development of a prototype BPS tool for generation of decision support when conducting design activities related to 'Volume massing'.

2. METHODOLOGY

The research reported in this paper follows the research framework presented by Purup and Petersen [2], in which a 'reflective researcher(s)' investigates a relevant research question related to a chosen research theme and

topic by iteratively looping through the action research activities ‘planning, acting, observing and reflecting’. This way researchers incrementally refine the knowledge base for answering the research question. The theme of the research reported in this paper is ‘implementation of the BPS in early design practice’ with the special attention to the topic ‘BPS support for the early design activities during volume massing’. The specific research question to be answered was:

How shall a BPS tool be conformed in order to provide timely and useful information regarding thermal indoor climate during the design activities related to the design task ‘Volume massing’?

To answer this question, we chose a co-creation approach in which we invited architects and other potential users to participate actively in the development. A mix of different research activities for the development of the initial prototype was therefore planned: A semi-structured interview among architects and paper prototyping in a co-creation workshop. Thereafter, a BPS-based method fit for simulating the thermal indoor climate during the ‘Volume massing’ design task was prototyped and tested in a case study. The following sections provide more detail on the abovementioned research activities.

2.1 Semi-structured interviews among architects

Information about ‘Volume massing’ and its associated design activities was gathered through semi-structured interviews of six practising architects working in a larger Danish architect firm. We conducted the interviews following the interview guide in table 1 which follow the principles of [7-8], by initiating with a narrative approach asking about their last massing project, before continuing with questions on tool capabilities. All interviews were audio recorded, transcribed and analysed with respect to the listed research questions. The interviews were conducted by two researchers with engineering background under supervision from another researcher with experience in qualitative research.

2.2 Co-creation workshop with potential users

Based on data from the interviews, a series of paper prototypes of a BPS tool to support the ‘Volume massing’ activities was generated during a two hour co-creation workshop with a group of three simulation experts (the researchers) and five architects. Three workshop activities were planned using techniques from research in user experience [9]: 1) A group discussion on priority of input and output using post-its, 2) brainstorming on various ideas, and 3) sketching paper prototypes for graphical user interfaces (GUI) and desired functionalities of the (real) BPS tool. Figure 1 is a photo from this workshop.



Figure 1: Photo of paper-prototyping process at workshop

Table 1: Interview guide.

Theme: Demographic data
<u>Interview question:</u>
<ul style="list-style-type: none"> • What is your role in the office?
Theme: Volume massing activity
<i>Research question: What is the activities during volume massing?</i>
<u>Interview question:</u>
<ul style="list-style-type: none"> • Could you walk me through your last massing activities? What did you do first? Next? • What information do you have at the beginning? (Materials, purpose, shape)
Theme: Building performance simulation tool
<i>Research question: What should be the characteristics of the thermal simulation tool that we should design?</i>
<u>Interview question:</u>
<ul style="list-style-type: none"> • Which simulation tools are you using, if any and what do you simulate? • Have you used Grasshopper? If yes, did you use it for simulations? • What do you like and do not like about current simulation tools? (interface, results, input, calculation speed) • How would you improve them? • How would you like the results to be visualized? • What kind of input would you like to have (eg function, glazing type, glazing area, U values, airflow, number of people)? Do you prefer templates of to choose everything? • What kind of output would you like to see (eg temperatures, PMV, compliance with standards)? • How much time would you spend on setting and running a simulation during the volume massing?
Conclusion
<ul style="list-style-type: none"> • Do you have something to add? • Do you have some suggestions for our project?

2.3 Proposed BPS method for ‘Volume massing’

The main challenge in establishing a BPS-based method fit for simulating the thermal indoor climate during ‘Volume massing’ is that thermal indoor climate must be simulated on room level, while the ‘Volume massing’ design activities – by definition – is about manipulating whole-building geometry. Therefore, we needed to formulate a method that relates room performance to whole-building geometric manipulation. Inspiration was found in a study by Dogan and Reinhart [10] who represent building energy need distributed into room level by a clustering technique of external sun load into thermal ‘shoebox’ models. But instead of simulating energy performance, we simulated the quality of the thermal indoor climate in terms of overheated hours throughout the year. The approach outlined in Figure 2 was to 1) simulate external annual sun load in a room-size grid extruded on the building façade using Ladybug [11] or Honeybee [11] (i.e. DaySim), 2) use a clustering technique (Owl, [12]) to generate groups grid cells with similar external annual sun load, 3) make BPS of rooms representing each cluster in a loop consisting of Anemone [13], DIVA [14], and ICEbear [15-17], and 4) make an interpolation of the BPS results and external sun load, and project it back on the facade grid to illustrate how the whole-building geometry and its context affects room-level thermal indoor climate.

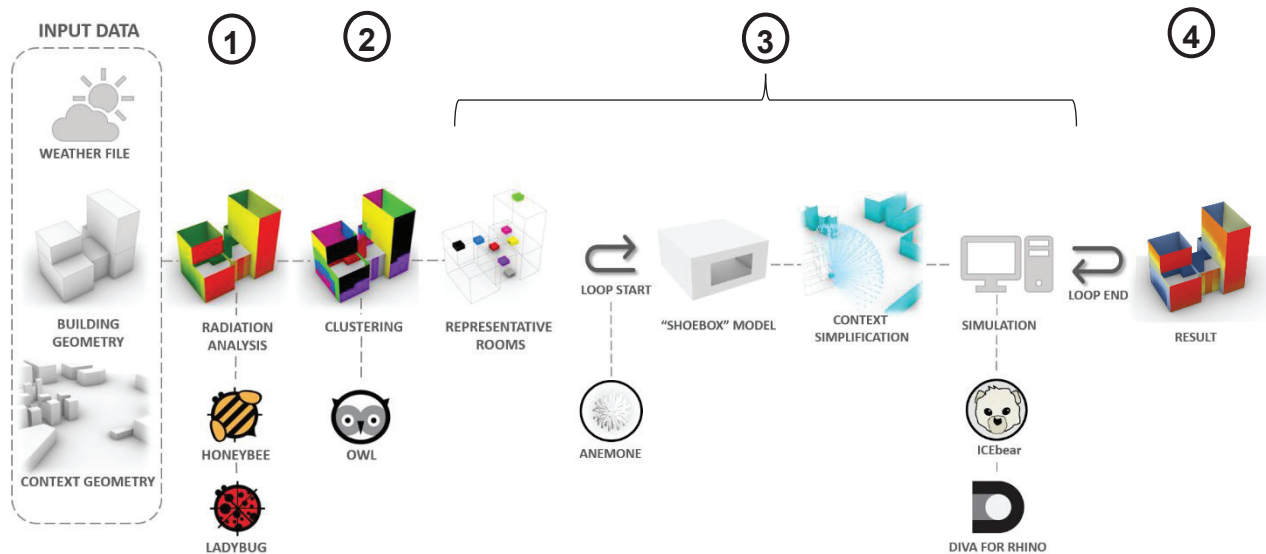


Figure 2: The proposed BPS method for automated simulation procedure during volume massing design activities.

2.4 Test case

The performance of the proposed simulation method was benchmarked against BPS of all rooms in the case illustrated in figure 3. The case building had 561 rooms distributed on its facades and multiple surrounding buildings that cast shadows and reflect solar energy onto the case building. It was assumed that all rooms were alike. The geometry of the room is illustrated in figure 3. Window wall ratio was 30 % and formed into one window with dimensions $H/W = 1.64/3.28$ m located in the centre of the façade. The performance data for the glazing was $U=1.1$ W/(m²K), $g=0.35$ and $LT=0.65$. The window frame was 60 mm thick with $U=1.0$ W/(m²K), and a linear loss from the spacer profile of 0.03 W/(m·K). The envelope insulation was $U=0.16$ W/(m²K), and the linear loss from window joints was 0.06 W/(m·K). Thermal capacity was estimated according to EN13790:2008 as 'Very light'. The room was assumed to have six occupants doing office work with an activity level of 1.2 Met during the hour 8-16 all workdays, however with an hour lunch break at noon with 50 % occupation. The occupants were dressed after season: 1 clo during winter and 0.5 clo during summer. Each of their workstation had an equipment heat load of 100 W/station and a work lamp of 15 W/station turning on if daylight level was below 500 lx. The energy need for the ambient light was adjusted linearly between 0.5 W/m² and 5 W/m² according to daylight level in order to fulfil a light demand of 300 lx. Light sensor was located at work desk 0.85 m above floor in the centre of the room. The HVAC system was assumed to have an in-zone heating system (a convector supplied by district heating) of 25 W/m² heating to 20°C. Furthermore, the HVAC system included a variable air volume (VAV) ventilation system including:

- Heating coil for heating the air to a minimum of 18°C in order to prevent draught from ventilation inlet.
- Cooling coil for cooling inlet air down to 18°C, if operative room temperature exceed cooling setpoints at 26°C during summer or 24.5°C during winter. The cooling system had a COP=3.0.
- Heat recovery unit with an efficiency of 80%

- VAV pump with an annual average specific fan power (SFP) of 1500 J/m³ provided an air flow in occupation hours of 60-200 L/s adjusted according to air quality fulfilling EN15251 class II and according to cooling set points for room temperature.

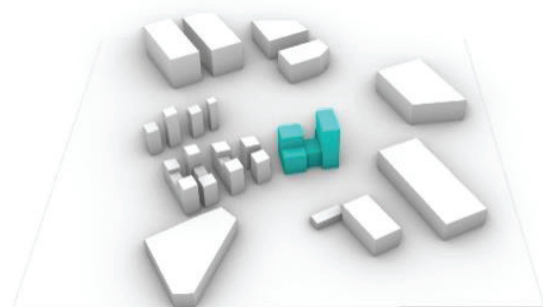


Figure 3: Illustration of test case; 'Volume massing' model (blue) and existing context (white).

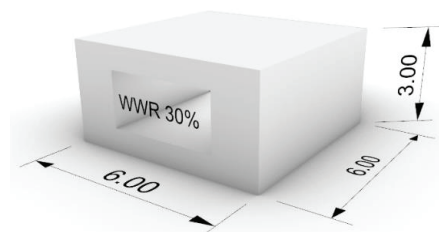


Figure 4: Room geometry used in case study.

Ventilation was turned off outside occupation hours. The infiltration level was set to 2.5 L/s during occupied hours and 1.1 L/s outside occupied hours. External reflectance was 0.1 for ground (Albedo) and 0.2 for external shadings (surrounding building). The internal reflectance was 0.70 on ceiling, 0.50 on wall and 0.20 on floor.

It is noted that program default input was used for the Ladybug solar estimation, and the radiance settings of Honeybee was set to $ab=2$, $ad=4096$, $as=1024$, $aa=0.15$, $ar=144$.

3. RESULTS

3.1 Supporting 'Volume massing' design activities

The semi-structured interviews and the co-creation workshop revealed that it was evident that architects want somehow to inform their volume massing activities if they are integrated in their process, easy to use, works fast and provide nice graphical results, as illustrated in the following quote:

'Sometimes you just need something very simple that looks nice, that works fast, and is not something like a separate stage of the project. It's just integrated.'

The desired traits for a BPS tool for supporting 'Volume massing' was similar to those found by Purup and Petersen [6]. They expressed a need for a dynamic GUI in terms of level of detail as described in following quote:

'There are many factors that we do not take into consideration in the early stages. If it should really work, we need some basic general settings and the minute we know a little bit more about the project we could start changing the things. (...) Maybe you could turn on and off the complexity of the program, depending on where you are in the process'. The need for 'basic general setting' could be met by introducing templates for room settings.

Furthermore, the output should be presented graphically to be understood by the designers:

'Well, as an architect I am very visual, and all my colleagues are that too.'

'I always want to see what's happening visually. That's just how my mind works.'

'We are architects, we are thinking in a graphical way.'

Though they desire the execution time of the simulation to be unnoticeable, they seem to accept a tolerance of approximately 10 minute, and put this in relation to how slow the communication runs when getting the results through a collaborating engineer which is how these analysis are obtained today:

'I mean, we tried it with the engineers and we were waiting days to get the results, and after these days, when we got the results our concept was looking completely different, that is always the problem.'

In relation to accuracy, they are less concerned. They need a clarification of the direction their project are moving – not the exact performance:

'The indication of where the project is going, both regarding thermal comfort, daylight, wind, whatever, is much more important for us to know. Whether we are going totally wrong direction or actually a good direction.'

Compared to Purup and Petersen [6], we went into further detail on the known and unknown parameters during a 'Volume massing' (Table 2), as well as the level of detail in their actual CAD models. Their CAD models are simplified shapes without windows, wall thickness or internal walls often created as stacked boxes to define floor levels. The CAD models are manipulated by copying, pasting, deleting and moving these boxes around (like the 'Lego/Duplo' modelling activity [6]) and by scaling or shaping these boxes (like the 'Transforming 3D shapes' modelling activity [6]).

3.2 Test case results

Figure 5 illustrates the simulated overheating hours of the benchmark model at 651 different location on the facade surface. These simulations took a total of approximately three hours to execute mainly due to time-

consuming simulation of indoor daylight levels in the reference points and detailed solar heat gains. The suggested BPS method relying on clustering using Ladybug or Honeybee to identify a total of eight representative rooms for BPS simulation decreased simulation time to a total of approx. 3 minutes and 5 minutes, respectively, whereof Ladybug and Honeybee used approx. 17 seconds and 2.5 minutes, respectively.

Though interpolation based on Ladybug solar irradiation were the fastest method of those suggested, there is a noticeable difference when comparing the interpolated results of Ladybug (Figure 6b) with the simulated results in Figure 5. Interpolation based on external solar irradiation simulated in ICEbear and Honeybee were more similar to the benchmark result in Figure 5.

Table 2: Known and unknown parameters during volume massing activity.

Known	An idea of	Unknown
Square meters of building	Floor height	Room design
functionality (e.g. office area, housing area etc.)	Room depth	Materials (U-values, structure etc.)
	Window wall ratio (WWR)	
Landscape	Glazing type	Window design (Facade system, shading device etc.)
Building boundaries/shell	Thermal capacity	
		Wall thickness

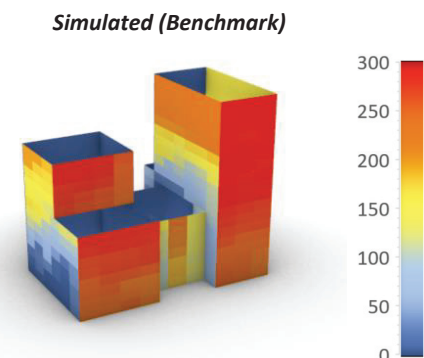


Figure 5: Simulated results [hours above 26 °C] in rooms at different facade locations (view from south-west)

The difference between the simulated and interpolated results is illustrated in Figure 7. The interpolation based on Ladybug caused a difference of up to 112 hours overheating (excluding outliers), while interpolation based on ICEbear or Honeybee only caused a difference of up to 20 and 67 hours (excluding outliers), respectively. The difference in the interpolation results was caused by dis-correlation between overheating and external solar irradiation (Figure 6d). Applying ICEbear solar irradiation for interpolation illustrates the potential minimum error of the suggested clustering and interpolation method, since the solar algorithms are the same as in the benchmark estimation.

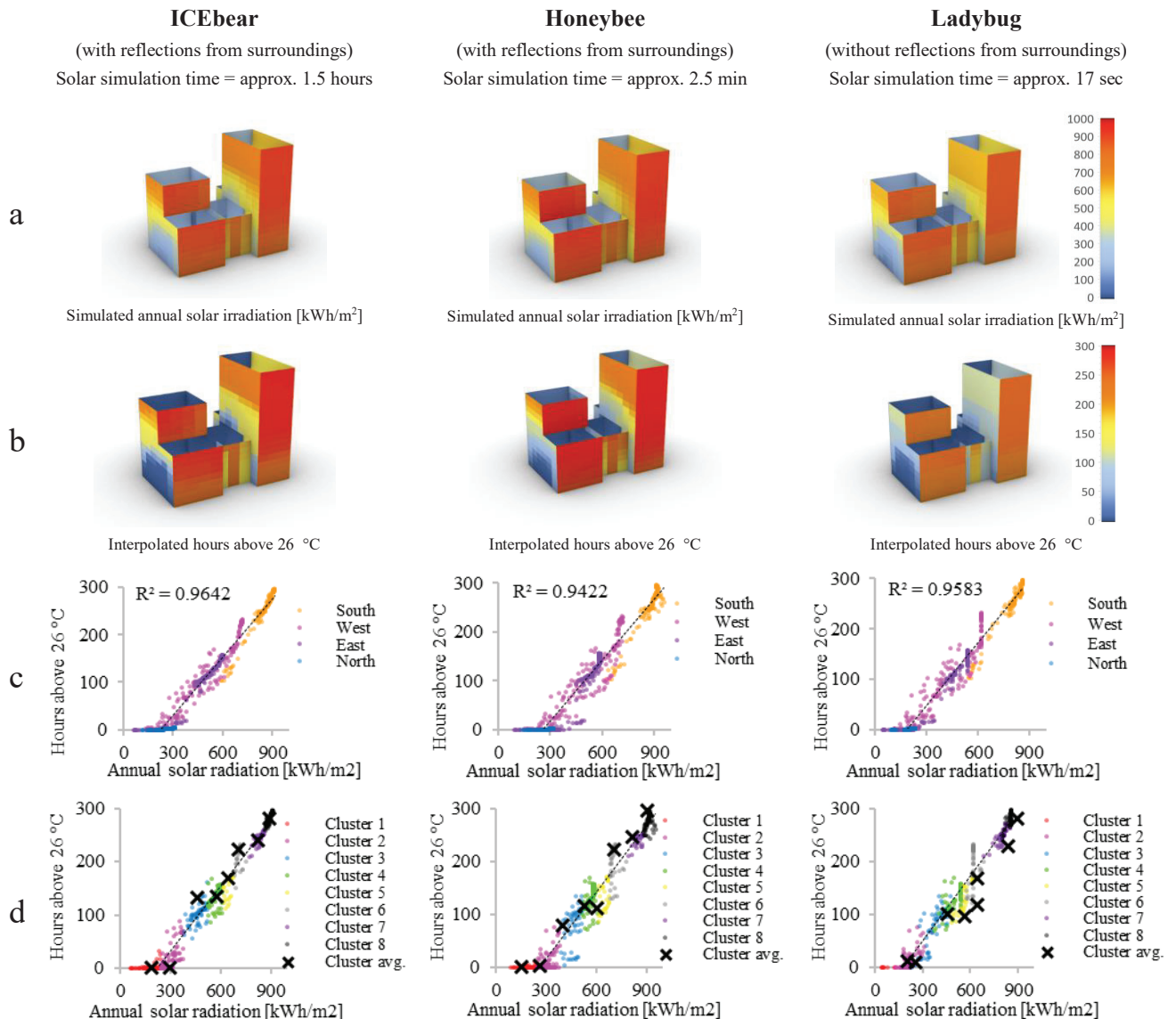


Figure 6: (a) Simulated solar irradiation with ICEbear, Honeybee and Ladybug (view from south-west). (b) Interpolated results based on solar irradiation (view from south-west). (c) Correlation between simulated results and solar irradiation, divided into clusters divided into orientation. (d) Correlation between simulated results and solar irradiation, divided into clusters.

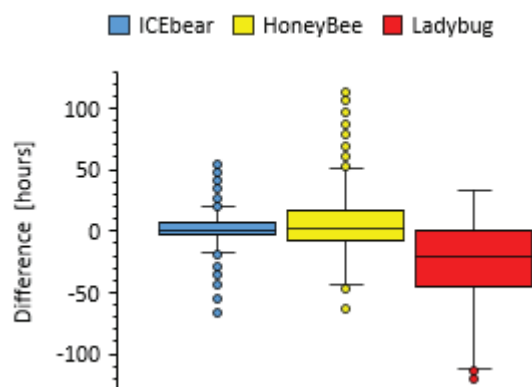


Figure 7: Distribution of difference between interpolated and simulated results for each program.

The difference between ICEbear and Ladybug solar irradiation was highest at locations in which reflections from external obstructions have a significant impact (Figure 6a). This illustrates how important reflections from external obstacles become in an urban setting. It is therefore critical for the proposed prototype that Ladybug do not include external reflection.

Figure 6c illustrates the correlations divided into facade orientations. There seems to be a small gap between orientations that could improve the interpolation even further by considering sun load in relation to time of the day and not just as a sum of the annual solar load, or by clustering in each orientation.

4. DISCUSSION

Findings from the interviews and workshop confirmed what other researchers have also found [4-6]: the architects are willing to use BPS tools if they are conformed to fit their design practice. This desire was manifested quite clearly in

the workshop where the architects participated dedicated and actively, and provided an ideal offset for the development of a more user-oriented BPS interface.

The test case results showed a difference of up to 112 hours when using Ladybug for clustering and interpolation. This is unacceptable for practical application. The reason for the large deviation is that Ladybug lacks the inclusion of external reflections which is crucial for the performance of a building in an urban context. Including reflections in the solar irradiation calculation – using sun loads from Honeybee for clustering and interpolation instead – decreased the error to 67 hours of overheating, which could be considered a reasonable precise result in the initial stages of the building design process. Clustering and interpolating based on ICEbear solar irradiation reduced the error to only 20 hours but the simulation time was significantly longer due to the way ICEbear calculates solar reflections from surrounding [17]. The solar algorithm of ICEbear could be modified/simplified for clustering purpose and thereby ending up having a similar trade-off between simulation time and accuracy as Honeybee. However, different Radiance settings for Honeybee could also be investigated for improvement of the trade-off between simulation precision and speed.

Future studies should also investigate whether annual external sun load is an appropriate metric for the correlation method. An alternative could for example be the time of the day when sun load peaks. Studies into the number of necessary clusters needed to represent the whole-building performance is also needed. Finally, the influence of other design parameters such as window form and properties, shading systems, heat capacity and different HVAC systems on the proposed method also needs to be investigated.

5. CONCLUSION

This paper describes the development of a BPS-prototype intended to support the design activities related to 'Volume Massing' with information regarding the consequence on indoor climate performance. Based on needs defined in semi-structured interviews and a co-creation workshop including practicing architects, the proposed prototype was developed to:

- handle the simplicity of early massing models without windows, wall thickness or internal walls, by predefining a shoebox room-model which then are placed at different locations at the facade,
- run with few and default settings by categorizing simulation inputs into room type templates, and suggesting window wall ratio and glazing type,
- visualize results graphically and directly on the building geometry facade surface inside the CAD-tool.

The results of a test case indicate that the prototype has a potential to support the design activities related to 'Volume massing'.

ACKNOWLEDGEMENT

The authors gratefully appreciate the funding for this study provided by the NIRAS ALECTIA Foundation and the Industrial Ph.D. program at Innovation Fund Denmark. We also thank C.F. Møller Architects for their conductive participation in the workshop and interviews, as well as their offer of massing model.

REFERENCES

1. Petersen, S. and S. Svendsen, (2010). Method and simulation program informed decisions in the early stages of building design. *Energy and Building*, 42: p. 1113–1119.
2. Purup, P.B., and S. Petersen, (2019). Research framework for development of building performance simulation tools for early design stages. *Automation in Construction*, 109: p. 1-15.
3. de Souza, C. B., (2011). Contrasting paradigms of design thinking: The building thermal simulation tool user vs. the building designer. *Automation in Construction*, 22: p. 112–122.
4. Petersen, S., J. Bryder, K. Levinsen, and J. Strunge, (2014). Method for Integrating Simulation-Based Support in the Building Design Process. In *Design in Civil and Environmental Engineering*. Copenhagen, DK, August 22-23.
5. Kanters, J., M. Horvat, and M.C. Dubois, (2014). Tools and methods used by architects for solar design. *Energy and Buildings*, 68: p. 721-731.
6. Purup, P.B., and S. Petersen, (2020). Requirement analysis for building performance simulation tools conformed to fit design practice. *Automation in construction*, 116: p. 1-12.
7. Blommaert, J., and J. Dong, (2010). Ethnographic fieldwork: A beginner's guide. *Multilingual Matters*.
8. Brinkmann, S. and L. Tanggaard, (2010). Kvalitative metoder: en grundbog. (in Danish). 1. edition, *Hans Reitzels forlag*, Copenhagen
9. Hartson, R. and P.S. Pyla, (2012). The UX book: Process and guidelines for ensuring a quality user experience. *Elsevier*, Boston.
10. Dogan, T., and C. Reinhart, (2013). Automated conversation of architectural massing models into thermal 'shoebox' models. In *Building Simulation*. Chambéry, FR, August 26-28.
11. Ladybug-tools, [Online], Available: Food4rhino.com/app/Ladybug-tools [11 May 2020].
12. Owl, [Online], Available: Food4Rhino.com/app/Owl [11 May 2020].
13. Anemone, [Online], Available: Food4Rhino.com/app/anemone [11 May 2020].
14. DIVA-for-Rhino, [Online], Available: <http://diva4rhino.com/> [11 May 2020].
15. Lauridsen, P.K.B. and S. Petersen, (2014). Integrating Indoor Climate, daylight and Energy Simulations in Parametric Models and Performance-Based Design. In *Design in Civil and Environmental Engineering*. Copenhagen, DK, August 22-23.
16. Purup, P.B., and S. Petersen, (2017). Rapid simulation of various types of HVAC systems in the early design stage. *Energy Procedia*, 122: p. 469–474.
17. Petersen, S, T.H. Broholt, L. Christensen, P.B. Purup, (2018). Thermal Performance Simulation of Complex Fenestration Systems in the Early Design Stage. in *Building Simulation and optimization*. Cambridge, UK, September 11-12

When water does not cool: A Different Use of Water in Urban Design

JOÃO CORTESÃO¹, SANDA LENZHOLZER¹

¹Wageningen University and Research, Wageningen, The Netherlands

ABSTRACT: This paper explores the implications that recent evidence on the negligible cooling effects of water can have for urban design practice. It tackles the misconception of using small urban water bodies to cool down urban areas and addresses a different approach to employing water in climate-responsive urban design. The “Nieuwe Mark” project, Breda, The Netherlands, is presented as to illustrate and develop these ideas. The results of an online questionnaire sent out to the design team of Nieuwe Mark show an unanimous acceptance about the misconception of using water as a coolant and indicate a change of mindset for future water-related projects. The article discusses the results obtained and concludes about the long-term implications that such change of mindset can have to the employment of water in urban design. The main outcome is that when water is not necessarily a coolant, urban design practice has the opportunity to rethink its approach to small urban water bodies by embracing holistic design approaches combining water body, shade, wind and water vaporisation.

KEYWORDS: urban water bodies, climate-responsive, design tools, Research Through Design, transdisciplinary

1. INTRODUCTION

Water bodies and water features are particularly popular and appealing design elements [1]. Aesthetical and recreational considerations are frequently considered during its employment in urban design. Water is also often employed as a coolant, based on the assertion that it necessarily leads to cooling effects. However, new knowledge on the cooling effects of water has been challenging the way landscape professionals commonly use it in their designs.

Excluding the cooling effects of the sea [2,3], water seems not to have a significant cooling effect. Previous research indicates that large urban water bodies, such as rivers or lakes, have quite limited daytime cooling effects and might originate night-time warming [4-6]. Research on the cooling effects of small urban water bodies, like ponds or canals, indicates that the cooling effects of water are negligible [7,8]. These studies basically point out that the cooling effects of water should not be taken for granted.

But when water is not necessarily a coolant, what does that imply for urban design practice? To answer this question, this paper presents the “Nieuwe Mark” project as an illustration of what to do when water is not a coolant, and to explore what long-term implications this can have to the employment of water in urban design.

The *Nieuwe Mark* project (Fig. 1) redesigned and daylighted the river Mark, in Breda, The Netherlands. The goal was to create added value to the area on

different parameters, amongst which cooling microclimates along the water body. To assist the municipal design team with achieving this goal, the municipality of Breda assigned Wageningen University (WU) to develop evidence-based design tools tailored to the area.



Figure 1: The Provisional Design of the Nieuwe Mark (the blue circles indicate the seven areas focused in the research). Source: Breda municipality.

The tools were to be applied into the project's provisional design (PD). For the sake of efficiency, these

tools were developed for seven areas within the PD (Fig. 1) that represented typical spatial layouts of the project. These areas were defined upfront by the design and research teams together, based on two criteria: need for climate-responsive measures and replicability within the PD.

The tools developed by WU were meant to communicate generic climate-responsive design measures. These measures dealt with adding or revising design elements in designated areas of the PD (see Methodology) and were indicated over 3D perspectives of those areas (Fig. 2). A colour code ranked the effectiveness of each measure in order to help prioritising design decisions, if necessary. Dark blue conveyed the highest potential for microclimatic improvement. The expected summer effects were indicated for all measures. Winter effects were not indicated when no significant effect was likely to result from a design measure.

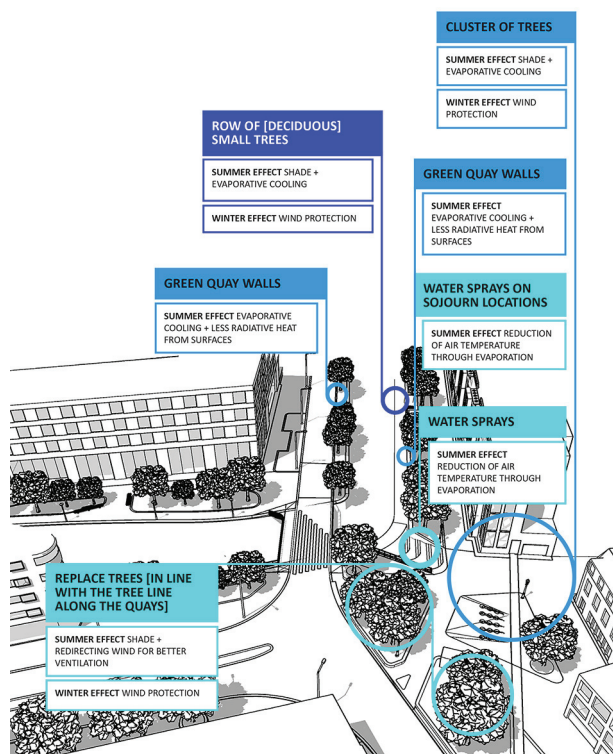


Figure 2: Example of a climate-responsive design tool for the Provisional Design of the Nieuwe Mark project.

Eventually, the *Nieuwe Mark* project was an interplay between design research and practice around up-to-date knowledge on the cooling effects of small urban water bodies. It provided a real-life 'lab' to new knowledge on the cooling effects of water, shedding light upon the misconception of using water as a coolant and, on that basis, upon a different approach to designing urban water bodies. This paper addresses the

likely long-term implications this had for the design activities of the *Nieuwe Mark*'s design team. The article concludes by expanding this subject beyond the *Nieuwe Mark* project.

2. METHODOLOGY

2.1 Overview on the *Nieuwe Mark*

The project was developed within a consortium bridging research and practice. On the research side, the WU team gathered experts on climate-responsive urban design and meteorology. Design practice was represented by the landscape design team of Breda municipality. The project's consortium also gathered experts on urban ecosystems, project management, heritage, and representatives of local associations of residents and businesses.

The design tools were developed with Research Through Design (RTD) [9] along three iterations comprising the production of potential design solutions and their testing (Fig. 3). The first iteration looked into achieving ideal microclimate effects. Operability aspects were excluded in order to apply evidence-based design knowledge on the topic as integrally as possible. The second iteration focused on finding a realistic match between the microclimate effects developed in iteration 1 and operability parameters such as maintenance requirements, traffic circulation or underground infrastructures. The third iteration refined this compromise as to achieve applicable design tools.

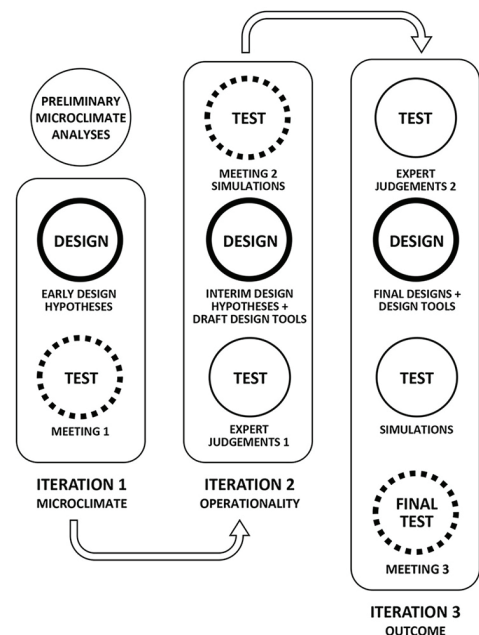


Figure 3: The Research Through Design process of the *Nieuwe Mark* project.

The research started with preliminary microclimate analyses. These preceded the RTD as to adequately inform the designing activities about the measures to be implemented. The analyses dealt with sun and wind, the variables mostly influencing the microclimate of small urban water bodies, and were made with consideration to a typical heatwave day in the Netherlands. The chosen date was July 01, thus, near the annual maximum of solar elevation. The sun/shadow analyses were made with the Sketchup model. As the model indicated 1 p.m. to present the highest exposure to sun, this was the period that the design measures referred to regarding excessive solar radiation. The meteorology and climate-responsive urban design experts from WU discussed the analyses. The results of these discussions were synthesised graphically in 3D perspectives produced with the Sketchup model (Fig. 4).

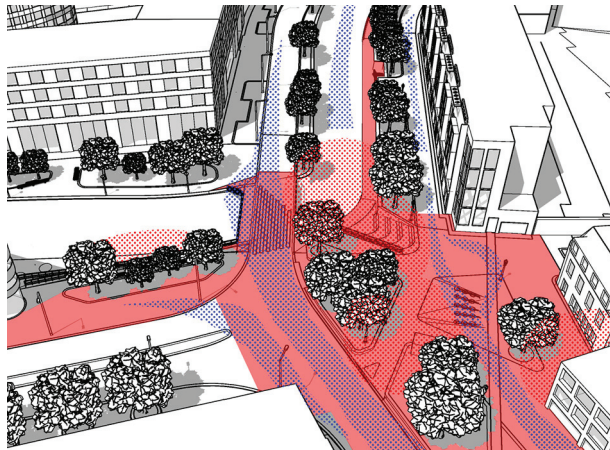


Figure 4: Preliminary microclimate analysis for area D, within the Provisional Design of the Nieuwe Mark project.

Within the RTD, the different potential design solutions dealt with increasing shade with trees along the quays and on their walls; allowing air to flow as unobstructed as possible; introducing water mist in sojourn locations; and depaving areas without heavy motorised traffic. These design measures were retrieved from the design prototypes for cool urban water environments developed in the “Really cooling water bodies in cities” (REALCOOL) research project [7], [10]. In REALCOOL, the combination of these design measures reduced the Physiological Equivalent Temperature (PET) around water by as much as 9°C [10].

The potential design solutions were subsequently evaluated through two expert judgements sessions, micrometeorological simulations with the Envi-met model, and during three meetings with the project’s consortium. In more detail:

- The expert judgements dealt with educated-guesses, within the research team, on the main micrometeorological issues behind the potential design solutions. This allowed evaluating the cooling potential of each potential design solution before plotting it into Envi-met.
- The simulations with Envi-met described and quantified the micrometeorological processes of the PD and of the design solutions with highest potential for cooling effects. This potential was assessed by comparing the design solutions with the PD (reference situation). Figure 5 shows an example of these simulations, made for one of the areas within the PD of the *Nieuwe Mark* project. In line with the results of REALCOOL, all simulations showed negligible reductions in air temperature from water itself, but that the design measures applied in *Nieuwe Mark* – the combination of shading with trees, natural ventilation and water vaporisation – led to PET reductions by as much as 14°C. No field measurement was conducted due to the time available for the study. The follow-up project GreenQuays, co-funded by the European Regional Development Fund through the Urban Innovative Actions Initiative, is conducting field measurements for validating new design solutions.
- The consortium meetings were used for discussing the potential design solutions and the results of the Envi-met simulations with the project’s stakeholders. These meetings provided insights on the operability issues raised by the potential design solutions, and on how well did these meet the stakeholders’ expectations and the goals of the project. Each meeting resulted in bringing down the three to four potential design solutions developed per area to one design solution per area.

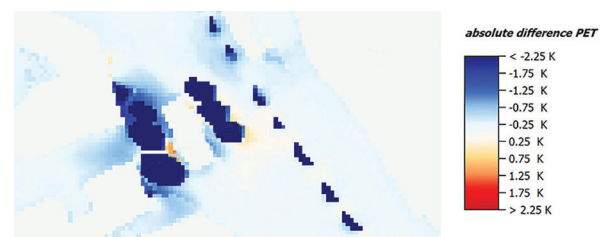


Figure 5: PET map obtained with the micrometeorological simulations with Envi-met for area B, within the Provisional Design of the Nieuwe Mark project.

The consortium meetings were of particular importance in addressing the question: when water is not necessarily a coolant, what does that imply for urban design practice?

The cooling effects of water was a recurrent topic of discussion during these meetings, fuelled by the results of the simulations with Envi-met. From the first meeting, light was shed upon the misconception of using water as a coolant based on evidence on its negligible cooling effects. Because the design measures applied in *Nieuwe Mark* led to significant PET reductions, these measures were presented and discussed as what to do when water is not a coolant.

The consortium meetings adopted an open and clear communication, where professional jargon was replaced by laymen terms. The aim was to actively engage the stakeholders, to keep their expectations real, and to building a base of trust and mutual understanding with the research team. The outcome were design tools based on (scientific) evidence around their expected cooling effects, endowed with the necessary (practical) conditions for real-life implementation.

2.2 Ex-post online questionnaire

Albeit their relevance, the consortium meetings did not look into the broader impacts that a new view on designing with water would have on long-term design activities beyond the *Nieuwe Mark* project. To address this issue and, thus, answer the research question explored in this paper, a short online questionnaire was sent via email to the design team after completion of the project.

The questionnaire, originally in Dutch, included two close-ended statements and one close-ended question:

1. *"The design tools fulfil your needs and expectations"*, in order to understand if the research had successfully answered its assignment and fitted properly the current and future goals of the project;
2. *"This project changed your perception about the cooling effects of water (namely that water does not necessarily cools its surroundings)"*, to confirm whether the misconception on the cooling effects of water had been accepted;
3. *"If your perception about the cooling effects of water is now different, which changes will it bring to your design activity beyond the Nieuwe Mark project?"*, in order to understand if the new knowledge provided with the research would have only short-term effects (i.e. *Nieuwe Mark*) or long-term effects (i.e. future projects) on design decisions.

Statements 1 and 2 were answered on a seven-point Likert scale, ranging from "strongly agree" to "strongly disagree". Question 3 was answered with multiple choice, namely: *"you will use urban water bodies the same way you have been using so far (e.g. for aesthetics or recreation)"*; *"you will start designing urban water bodies based on a combination of water, shade, wind and water features (e.g. sprays)"*; and *"you will no longer use urban water bodies"*. Question 3 also included an optional open-ended possibility for indicating missing aspects in the questionnaire. The questionnaire was built with the online tool Typeform.

3. RESULTS

Regarding the first statement, all respondents to the questionnaire indicated that the research fulfilled their needs and expectations, i.e. climate-responsive design measures applicable to the PD.

Relatively to the second statement, all respondents referred that the project changed their perception about the cooling effects of water.

For question 3, all respondents indicated that they will start designing urban water bodies in future projects based on a combination of water, shade, wind and water features.

4. DISCUSSION

Regarding the first statement, earlier positive feedback given by Dutch designers on the applicability of the REALCOOL prototypes can help interpreting the results obtained. Two aspects revealed by that feedback on REALCOOL can be called forth in interpreting the results obtained for the first statement: RTD process and communication options for the design tools.

First, the design tools are the outcome of a cumulative RTD process systematically steering the research towards evidence and applicability. The effects of each design measure on both cooling effects and applicability to practice were secured throughout the RTD. This is a procedural matter complying with the principle that, in design, phenomena are investigated through modelling, pattern-formation and synthesis, under the values of practicality and appropriateness [11]. Second, the design tools embody knowledge on how to perform tasks around the design of cooling urban water environments, expressed visually. This was to respond to visual thinking, an essential design activity [12]. Furthermore, as the challenges currently posed to urban areas prevent designers to collect, assimilate and process alone all information needed to solve design problems [13], visual tools and appraisal methods hold the potential to more effectively

communicate to practitioners than, for example, textual resources [14].

Together, the development of potential design solutions with a good understanding of each design measure, and the option to communicate them visually, allowed creating the aimed applicable evidence-based design tools. This can explain why all respondents indicated that the design tools fulfilled their needs and expectations.

The feedback given on the second statement suggests that the misconception on the cooling effects of water was realised and accepted. This result can be explained with three activities carried out during the consortium meetings: informing the design team about the misconception of using water as a coolant; informing the design team about the creation of cooling urban water environments; developing the design measures for the PD through a close cooperation between WU and the design team.

The consortium meetings constituted moments of transdisciplinary cooperation where experts, designers and the project commissioner were engaged in steering the project towards its goal. Questioning the conception of water as a coolant and informing about a different approach to designing urban water bodies took place smoothly. Progressively, this new knowledge sunk into the design team. Building trust and mutual understanding was the key, which can be understood in light of the benefits of participatory process reflecting the knowledge of experts and the wishes of a project commissioner [15].

The results obtained for question 3 further substantiate the feedback obtained on the second statement. These indicate long-term effects resulting from the new knowledge provided, i.e. a new mindset for the design of urban water bodies. Beyond the fact that all respondents stated that they will “*start designing urban water bodies based on a combination of water, shade, wind and water features*”, no respondent chose the option “*you will use urban water bodies the same way you have been using so far*”. Furthermore, the absence of votes on the option “*you will no longer use urban water bodies*”, suggests that water kept its attractiveness to designers.

The unanimity of responses to the questionnaire suggests that the *Nieuwe Mark* project was able of making the design team aware that water is not necessarily a coolant. More importantly, it informed about a different approach to designing urban water bodies. This approach was synthesised in evidence-based design tools expressing visually the application of shading, ventilation and water vaporisation measures around the river Mark.

5. CONCLUSION

The *Nieuwe Mark* project confirmed in real-life evidence from previous research on the cooling effects of water: water does not seem to significantly reduce air temperature in the air layer adjacent to the water surface. However, it is possible to create cooler urban water environments by zooming out from the water body itself. Significant PET reductions, therefore improved conditions for outdoor thermal comfort, may be achieved by combining water body, shading with trees, natural ventilation and water vaporisation. The results obtained are valid for typical heatwave days in the Netherlands. We would expect variations to the results obtained for other climatic regions, and between different properties of water (e.g. turbidity) and characteristics of the water body (e.g. flow rate or depth).

Based on this study, the likely long-term implications that such change of mindset can have to the employment of water in urban design are:

- Water bodies and features will keep being employed but the decision to do so will no longer be made under the assumption that water necessarily leads to cooling effects;
- The mindset of landscape professionals engaged in water-related urban design projects will be widened from the water body itself to the whole environment surrounding it, e.g. an urban canyon;
- The designing of these urban water environments will be holistic – it will synergistically combine water body, shade, natural ventilation, and water vaporisation in ways to be specified by each project;
- This holistic designing will count on more and better transdisciplinary practices, bringing urban design closer together to fields as varied as architecture, built heritage or hydraulic engineering;
- Aesthetical, recreational and symbolic considerations often made around the use of water are not excluded in this new mindset.

The underlying message of this article is: when water is not necessarily a coolant, urban design practice has the opportunity to rethink its approach to urban water bodies by embracing holistic design approaches combining water body, shade, wind and water vaporisation. When water does not cool down, urban water environments designed under this frame are likely to. The climate adaptation of urban areas can largely benefit from implementing these cooling urban water environments.

The different approach to designing urban water bodies has the potential to gain momentum in practice. The change can take place smooth and swiftly provided that: firstly, evidence on the negligible cooling effects of water is shown to practitioners; secondly, that practitioners are appropriately informed on what to do then, through evidence-based design principles for cooling urban water environments. Design research can play a vital role here by providing landscape professionals with the appropriate conceptual tools [16]. But perhaps more importantly, as illustrated with the *Nieuwe Mark* project, a close cooperation between researchers and practitioners in developing these tools can *per se* trigger such role as much as the tools themselves.

Research indicates that there is room for expanding the benefits of urban water bodies from common purposes to climate-resilience. The principles to be utilised by landscape professionals in their designs should be distilled from further systemic thinking with porous boundaries between academia and practice.

ACKNOWLEDGEMENTS

The authors would like to express their gratitude to all parties of the project's consortium for the valuable feedback given throughout the RTD and for the open communication process, and to the WU research team member Sytse Koopmans for the Envi-met simulations.

REFERENCES

1. Backhaus, A., T. Dam and M.B. Jensen (2012). Stormwater management challenges as revealed through a design experiment with professional landscape architects. *Urban Water Journal*, 9(1): p. 29-43.
2. Cuadrat, J.M. and M.F. Pita (2009). Climatología. Madrid: Ediciones Cátedra.
3. Lenzholzer, S. and R. Brown (2016). Post-positivist microclimatic urban design research: A review. *Landscape and Urban Planning*, 153: p. 111-121.
4. van Hove, L.W.A., C.M.J. Jacobs, B.G. Heusinkveld, J.A. Elbers, B.L. van Driel and A.A.M. Holtslag (2015). Temporal and spatial variability of urban heat island and thermal comfort within the Rotterdam agglomeration. *Building and Environment*, 83: p. 91-103.
5. Steeneveld, G.J., S. Koopmans, B.G. Heusinkveld and N.E. Theeuwes (2014). Refreshing the role of open water surfaces on mitigating the maximum urban heat island effect. *Landscape and Urban Planning*, 121: p. 92-96.
6. Solcerová, A. (2018). Water as a coolant of cities. PhD thesis: Technische Universiteit Delft.
7. Cortesão, J., S. Lenzholzer, L. Klok, C. Jacobs and J. Kluck (2019). Cooling Urban Water Environments: Design Prototypes for Design Professionals. Proceedings of the 34th International Conference on Passive and Low Energy Architecture. p. 520-525.
8. Solcerova, A., F. van de Ven and N. van de Giesen (2019). Nighttime cooling of an urban pond. *Frontiers in Earth Science*, 7: p. 1-10.
9. Lenzholzer, S., I. Duchhart and J. Koh (2013). Research through designing' in landscape architecture. *Landscape and Urban Planning*, 113: p. 120-127.
10. Cortesão, J., S. Lenzholzer, L. Klok, C. Jacobs and J. Kluck (2019). Generating applicable urban design knowledge. *Journal of Urban Design*, [Online], DOI: <https://doi.org/10.1080/13574809.2019.1650638>
11. Cross, N. (1982). Designerly ways of knowing. *Design Studies*, 3(4): p. 221-227.
12. Nijhuis, S., E. Stolk and M. Jan Hoekstra (2016). Teaching urbanism: the Delft approach. Proceedings of the *Institution of Civil Engineers*: p. 1-11.
13. Jonas, W. (2007). Design Research and its Meaning to the Methodological Development of the Discipline, in *Design research now. Essays and Selected projects*, R. Michel, Ed. Berlin: Birkhäuser. p. 187-206.
14. Cortesão, J., F.B. Alves and K. Raaphorst (2018). Photographic comparison: a method for qualitative outdoor thermal perception surveys. *International Journal of Biometeorology*, [Online], DOI: <https://doi.org/10.1007/s00484-018-1575-6>
15. Raaphorst, K. (2018). Knowing your audience: the contingency of landscape design interpretations. *Journal of Urban Design*, 23(5): p. 654-673.
16. Inam, A. (2011). From dichotomy to dialectic: Practising theory in urban design. *Journal of Urban Design*, 16(2): p. 257-277.

Energy efficiency and comfort on a deprived neighbourhood in Madrid (Spain)

The gap between a predictive model and measured data on energy consumption, addressing indoor environmental quality assessment

FERNANDO DE FRUTOS¹, FERNANDO MARTIN CONSUEGRA¹, IGNACIO OTEIZA¹, CARMEN ALONSO¹, BORJA FRUTOS¹, JAVIER GALEANO²

¹ Instituto Ciencias de la Construcción Eduardo Torroja. CSIC, Madrid, Spain

² Grupo Sistemas Complejos, Universidad Politécnica de Madrid, Spain

ABSTRACT: The work presented here analyses the energy consumption and indoor environmental quality (IEQ) of four dwellings in a vulnerable neighbourhood on the outskirts of Madrid. It is focused on exploring the gap between predicted and measured energy consumption in three steps: generation of theoretical models, monitoring campaign and gap estimation. The theoretical approach consists of a simplified energy model on an urban scale using the ISO 13790 standard, with the results aggregated by dwelling, block and neighbourhood. Monitoring collects actual information on the energy consumption, indoor environmental quality (IEQ) and climate conditions of a representative building over a year. The gap is defined as the difference between the two values, and the analysis of results, in relation to the observed IEQ, points to different strategies for addressing energy inefficiency and improving the quality of life in these dwellings.

KEYWORDS: Indoor environmental quality, Energy consumption, Energy modelling, Monitoring, Performance gap.

1. INTRODUCTION

Housing stock context. In Spain the number of housing units built according to the 2011 census is more than 2 million units; 61% of them were built before 1979, when the NBE CT-79 standard introduced the first energy efficiency requirements [1]. It is estimated that 9 million people can be affected by an insufficient indoor environmental quality (IEQ) situations related to their type of housing. and with probable negative consequences for health. (Fig. 1)

In the city of Madrid, the total number of residential buildings used for housing were built prior to the appearance of the NBE-CT-79 standard. More than 85% of homes have a heating installation, either individual or centralized, and about 15% do not have an adequate heating systems. In terms of space cooling, 23% of households have cooling systems, and 75% do not [2]. This building stock requires comprehensive rehabilitation to achieve the objectives of the European directives on energy efficiency and climate change. Energy poverty studies in Madrid point at 23% of the population with an energy expenditure higher than 10% of incomes; 10% of households cannot maintain their home in adequate temperature conditions during the winter [3-4]; in summer, due to climate change, heat waves are increasing every year.

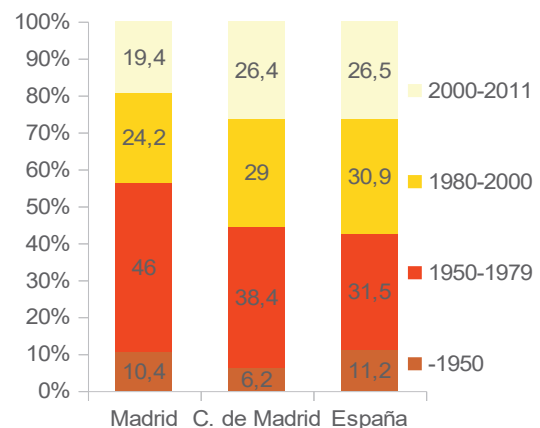


Figure 1: Number of buildings by year of construction.

Source: INE 2011

On previous projects (REFAVIV and REVEN [5-6]), the thermal envelope characteristics from residential buildings in social housing developments was collected from a wide sample built between 1939 and 1979. Monitoring energy consumption, IEQ, and user behaviour reveal significant differences from the energy performance standards. Also shortcoming in IEQ, inaccuracies in assumptions about users' behavior and flaws in construction were identified [7].

The current project (HABITARES [8]) aims to improve the habitability and health conditions of the population by reducing energy dependency in vulnerable neighbourhoods in Madrid. It is based on the hypothesis that rehabilitation at an urban scale can improve the environmental quality of housing and reduce energy vulnerability with a greater impact than rehabilitation done building by building.

An urban Energy Loss Evaluating Method (Spanish initials, MEPEC) has been developed in a previous stage. It establishes a theoretical model of the space heating consumption of existing urban fabrics, using precise energy indicators developed with pooled data collected building by building from the cadastre [9].

2. OBJETIVE

This work aims to develop an assessment method to compare the gap between a theoretical energy consumption model (TEC) and measured energy consumption data (MEC). The theoretical model is based on calculations of the energy needs to meet comfort conditions on an entire vulnerable neighbourhood located in the south of Madrid. Measured data were obtained by monitoring during one year a representative residential building in the same neighbourhood. The campaign includes climate data (CD) and IEQ monitoring to analyse the causes of this gap.

3. METHODOLOGY

This section introduces the case study and presents the methodological approach.

3.1 Case study

The case study is a social housing conjoint of 190 units, erected in 1950 and situated in a vulnerable quarter on the southern outskirts of Madrid, in Villaverde district (Fig. 2). One of the buildings was selected for the monitoring campaign: the monitored building (MB).



Figure 2: Case study

The buildings form a large central courtyard, have two floors with four houses per door, two on the ground floor and two on the first floor. The construction characteristics of the thermal envelope can be summarized as follows: 1) gabled roofs; 2)

semi-vaulted and interlocking ceramic vault and floor slab on the ground floor; 3) facades made of one foot thick ceramic brick walls with external plastered coating (in a poor state of conservation) without any type of insulation; 4) windows, mostly with aluminum frames and simple glass. The houses have a kitchen, bathroom, living room and three bedrooms [10].

2.2 Methodological approach

The methodology is divided into four main parts: Surveys, Energy needs approach, Monitoring approach, and Gap calculation. The process is summarized in the following flow chart (Fig. 3)

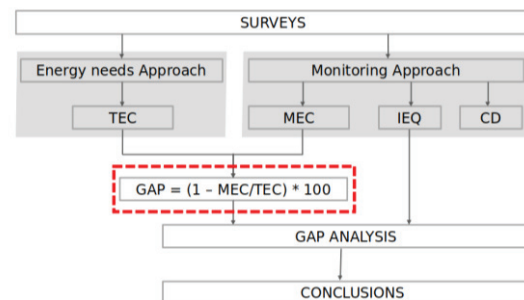


Figure 3: Methodological chart

Surveys. A survey was conducted in each dwelling of MB. It included building and household characteristics, energy habits, HVAC systems and the Universal Supply Point Code (CUPS). CUPS is a unique code, used by Smart Metering Technology (SMT), which identifies an energy supply point (whether electricity or piped gas) to access historical energy consumptions. In this paper, SMT were used to compare with monitored data [11].

Energy needs approach. The average energy consumption of a Spanish household is 10521 kWh per year, while the continental area (Madrid) is 13141 kWh per year [12]. Space heating demand indicator (kWh/m²) is calculated for each building from the sample using MEPEC [9]. Using these estimated values, the surface of each dwelling and the data on thermal installations collected in the surveys, it is possible to calculate the approximate theoretical consumption (TEC) necessary to satisfy basic energy needs for each dwelling. TEC is the energy for space heating plus consumption for other uses. Primary energy and associated CO₂ emissions are also calculated [13].

Monitoring approach. The aim of the monitoring approach is to obtain information on energy consumption, IEQ and climate data. Data was received every 10 minutes during one year (from January to December 2019) using internet of things technology (IOT). IOT has allowed to reduce costs and intrusion. User's willingness and availability has been

essential for developing the study. Finally, of the four homes studied, only three could be finally monitored.

MEC. Energy consumption of electricity (kWh) and natural gas (m³) is measured. In order to compare the consumption of natural gas and electricity, the conversion factor used was 11.70 kWh for each m³ of natural gas, corresponding to a Higher Calorific Power (HCP). The value of the HCP is not always the same, and there may be slight variations in each bill [14].

Accuracy/range consumption sensors:

- Electricity (kWh): Transmitter <3×300A/1W, clamp sensor <80A, 20W-20kW/-
- Natural gas (m³): Transmitter 232 counter imp/W1, clamp sensor >10ms pulse interval/-

IEQ. Living room and main bedroom were monitored. IEQ data from the living room were analyzed as representative of each dwelling.

Accuracy/range IEQ sensors:

- Temperature (T°C): ±0.4°C
- Relative Humidity (HR%): ±4%
- Air quality (CO₂ ppm): ±0ppm

CD. A weather station was located on the roof of the MB to gather data from the local microclimate.

Accuracy/range CD sensors:

- Temperature (T°C): ±1°C
- Relative Humidity (HR%): ±5%

Gap. The gap is set as the difference between TEC and MEC, expressed as a percentage [15].

$$GAP = \left[1 - \frac{MEC}{TEC} \right] \times 100$$

4. RESULTS

Results are shown by Surveys, Energy needs approach, Monitoring approach and Gap. Dwellings are identified as v1 in green color, v2 in blue, v3 could not be monitored, v4 in red and CD in light-grey color.

4.1 Surveys

Surveys gather useful information for the TEC calculation and planning MEC (Table 1, 2 and Fig. 4)

Table 1: Household size, space heating energy source and system of each dwelling.

	size	source	system
v1	2	Diesel	Individual combined
v2	4	Electricity	Individual
v3	1	Natural gas	Individual combined
v4	3	Electricity	Inadequate heating equipment

Table 2: Average annual electricity (SMT) and gasoil consumptions (kWh year) of each dwelling.

	Electricity	Gasoil
v1	530.26	10180*
v2	9852.25	
v3	-	-
v4	4519.46	
Total	14901.97	10180

* Estimation based on the information declared in the survey

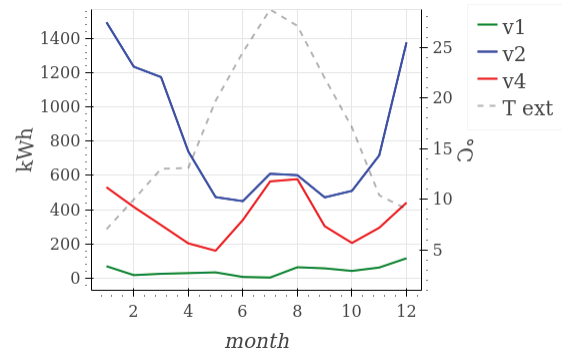


Figure 4: Average consumption profile (kWh SMT) and outdoor T(°C). Monthly data

4.2 Energy needs approach

TEC results represent the calculated energy consumption for satisfying basic energy needs. MEPEC estimates 125,6 kWh/m² heating demand for the MB. Heating consumption represents 55% of total energy consumption on an average dwelling located in Madrid [12]. The amount of energy for “other uses” is set as an average value per square meter, similar for every dwelling. Table 2 summarizes the net area of heated space (m²), the calculated heating demand (HD), efficiency of the heating systems (EF), heating consumption (H) and the amount of energy for other uses (OU) on each dwelling. All the consumptions are expressed in kWh.



Figure 5: Heating demand per building kWh/m²

Table 2: m^2 , Heating demand (HD), Efficiency (EF), heating (H) and other uses (OU) consumptions (kWh) of each dwelling

	m^2	HD	EF	H	OU
v1	48	6028.8	0.70	8612.57	2618.18
v2	48	6028.8	1.00	6028.80	2618.18
v3	68	8540.8	0.75	11387.73	3709.09
v4	51	6405.6	1.00	6405.60	2781.82

The methodology allows to calculate the theoretical consumptions for satisfying basic energy needs and associated environmental impact (Table 3-4)

Table 3: Conversion factors, from final energy to primary energy and CO₂ heating emissions [13]

source	kWh EP.tot/ kWh E.final	kg CO ₂ / kWh E. final
Diesel	1.18	0.31
Electricity	2.37	0.33
Natural gas	1.20	0.25

Table 4: Final energy (TEC), Primary Energy (PEC) consumptions and Kg CO₂ Emmision associated (CO₂-EM) of heating and other uses in each dwelling

	TEC	PEC	CO ₂ -EM
v1	11230.75	16379.91	3492.76
v2	8646.98	20476.05	2862.15
v3	15096.82	22391.47	3804.4
v4	9187.42	21755.81	3041.04
Total	44161.97	81003.24	13200.35

4.3 Monitoring approach

Results obtained from energy consumption (MEC) and IEQ are shown here, including, hygrothermal comfort and air quality records.

MEC. The gathered consumption results are resumed in Table 5.

Table 5: Electricity (kWh year), Gasoil (kWh year) and MEC (kWh) of each dwelling.

	Electricity	Gasoil	MEC
v1	1760.92	10180*	11940.92
v2	5515.15		5515.15
v3	-	-	-
v4	4436.32		4436.32
Total	11712.39	10180	21892.39

* Estimation based on the information declared in the survey

IEQ. Hygrothermal confort. T (°C) and RH (%). Código Técnico de la Edificación (CTE) [16] estipulates winter (20-17°C) and summer (27-25°C) target temperatures and relative humidity (30-70%) in housing. See Fig. 6-7 and Table 6 shows the percentage of hours. MB does not meet comfort

during summer months of Jun, Jul, Aug, Sept. v2 does not meet comfort in Feb y v4 in Jan and Feb.

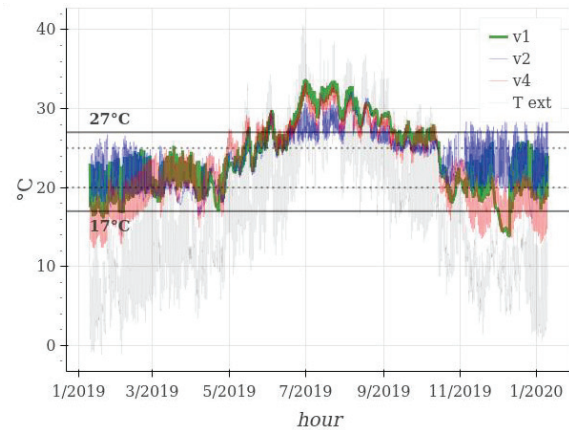


Figure 6: T(°C). Hourly data

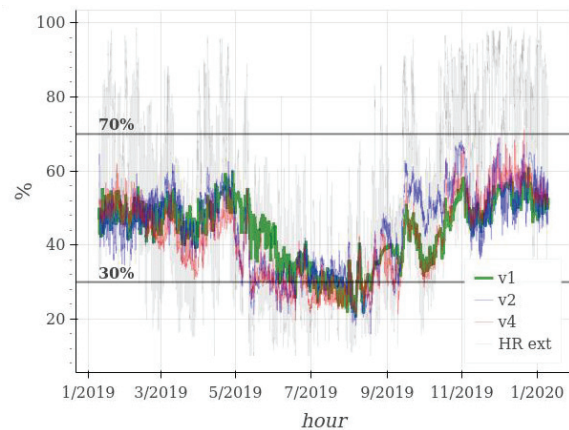


Figure 7: RH(%). Hourly data

Table 6: % hours in each dwelling.

	T≤17°C	T>27°C	RH≤30%	RH>70%
v1	3.49%	22.92%	6.87%	0.00%
v2	1.15%	17.94%	11.48%	0.19%
v3	-	-	-	-
v4	13.17%	23.09%	19.16%	0.02%

IEQ. Air quality. CO₂ ppm. A sufficient flow of outdoor air must be provided in residential premises to ensure that the average annual concentration of CO₂ does not exceeded 900ppm. Also the annual accumulation over 1600ppm does not exceed 500.000ppm.h [16]. (Fig. 8, table 7). MB results of the air quality show evidences of poor air quality in each dwelling.

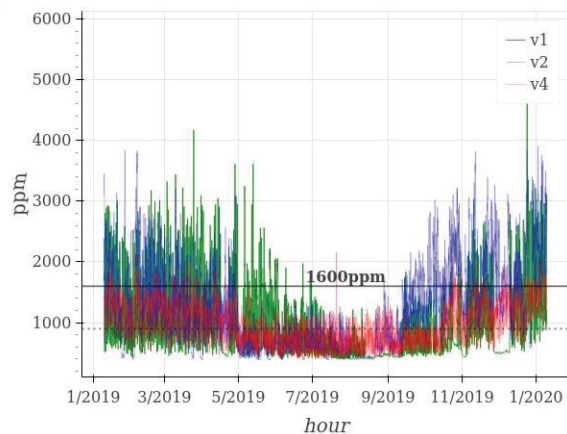


Figure 8: CO₂ ppm of each dwelling

Table 7: Average and accumulated annual CO₂ ppm of each dwelling

	Average	Accumulated
v1	1039.92	31716.20
v2	1316.00	6979078.29
v3	-	-
v4	1047.38	83774.73

4.3 Gap

Figure 9 and Table 8 represent the results of the gap according to the proposed methodology.

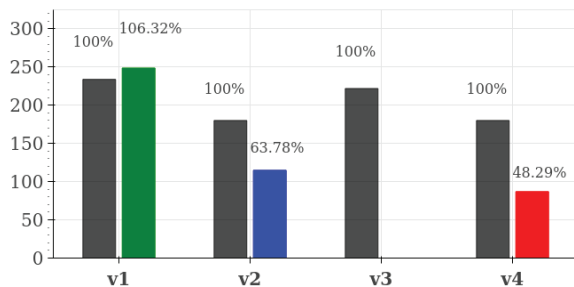


Figure 9: Gap plot

Table 8: Final energy (TEC kWh), MEC (kWh) and Gap for each dwelling.

	TEC	MEC	Gap
v1	11230.75	11940.92	-6.32%
v2	8646.98	5515.15	36.22%
v3	15096.82	-	-
v4	9187.42	4436.32	51.71%
Total	44161.97	21892.39	

DISCUSSION

The analyses relates gap and IEQ. There are six possible scenarios (Fig. 10); values of Gap may be less than, equal to or greater than zero. IEQ may or may not meet with the CTE [16-17].

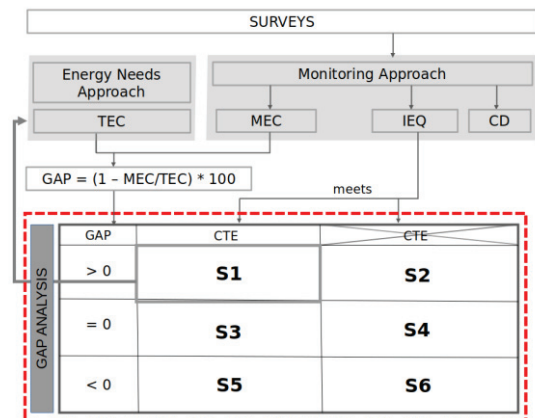


Figure 10: Gap analysis

S1. Scenario 1: Gap is greater than zero and IEQ meets CTE. This scenario points the need of a model calibration, MEC allows to adjust TEC.

S2. Scenario 2: Gap is greater than zero and IEQ does not meet the CTE. Energy vulnerability scenario. The greater the gap, the greater the risk of energy vulnerability.

S3. Scenario 3: Gap equals zero and IEQ meets the CTE. It complies with the requirements of the regulations.

S4. Scenario 4: Gap equals zero and IEQ does not meet the CTE. Energy efficiency improvement measures are needed.

S5. Scenario 5: Gap is less than zero and IEQ meets the CTE. Excessive energy consumption to reach comfort, it is necessary to improve the energy efficiency of the building to reach comfort.

S6. Scenario 6: Gap is less than zero and the IEQ does not meet the CTE. High environmental impact. Urgent refurbishment of the building is needed.

Table 9: Diagnostico for each dwelling

	Gap	CTE	Scenario
v1	-6.32%	No	S6
v2	36.22%	No	S2
v3	-	-	-
v4	51.71%	No	S2

Table 10: Recommended improvement methods

	CTE
v1	Cooling and humidifying in summer months. Ventilation needed during winter months (afternoon - evening)
v2	Cooling supply and humidifying in summer months. Ventilation urged needed (summer and winter)
v3	-
v4	Heating needed. Cooling and humidifying in summer months

The poor energy efficiency of MB confirms that neither increasing the energy consumption in v3 and v4 would achieve the comfort as seen in v1.

4. CONCLUSION

MEPEC, CUPS and IEQ are the minimum data needed to make the detailed energy profile per dwelling. In Spain, only energy trading companies have access to the consumption records of the smart meters, this makes it necessary to monitor consumption, so the price of monitoring is increased.

Relating Gap and IEQ, allow to extend the scale of the analysis of both the theoretical models and the monitoring. From this analysis, it is concluded that urgent measures are needed to improve energy rehabilitation. At this moment, the different strategies are being defined together with the social agents involved.

By applying this research methodology to 8 more blocks of houses, a total of 23 monitored houses, we will be able to go deeper into the calibration of urban models and the efficiency of the measures used in rehabilitation.

ACKNOWLEDGEMENTS

This document was funded by Spanish Ministry of Economy and Competitiveness project: HABITA-RES BIA 2017-83231-C2-1-R. And Acknowledgment of the Project i-LINK A 20220- CSIC. "Nanotechnology based Thermochromic Materials for Adaptive Building envelopes". The authors wish to thank EMVS, the occupants of MB and the Energy Service Company-Stechome.

REFERENCES

1. Oteiza, I., Alonso, C., Martín-Consuegra, F., Monjo, J., González Moya, M., y Buldón, A., La envolvente Energética de la vivienda social. El caso de Madrid en el periodo 1937-1979, vol. 428, 1 vols. Madrid: Editorial CSIC, 2018.
2. Martín-Consuegra, F. Hernández-Aja, A., Oteiza, i., and Alonso, C. «Distribución de la pobreza energética en la ciudad de Madrid (España)», Rev. EURE - Rev. Estud. Urbano Reg., vol. 4, n.o 13, may 2019.
3. Sánchez-Guevara, C., Fernández, A.S., and Hernández-Aja, A. «Income, energy expenditure and housing in Madrid: retrofitting policy implications», Build. Res. Inf., vol. 43, n.o 6, pp. 737-749, nov. 2015, doi: 10.1080/09613218.2014.98473.
4. Luxán García De Diego, M, Sánchez-Guevara C., Román López, E, Gómez Muñoz, G, y Barbero Barrera, M., Rehabilitación exprés para hogares vulnerables. Soluciones de bajo coste, Fundación Gas Natural Fenosa. Madrid, 2017.
5. REFAVIV project - "Energy rehabilitation of deteriorated social housing facades in large Spanish cities, applying innovative national and European products (2012-2016). Available from: <https://proyectorrefaviv.ietcc.csic.es/>
6. RE-VEN project - "Energy rehabilitation of social housing, applying innovative window products with CE marking" (2013-2017). Available: <https://proyectorhabitares.ietcc.csic.es/>

7. Alonso, C., Oteiza, I., Martín-Consuegra, F., and Frutos, B. «Methodological proposal for monitoring energy refurbishment. Indoor environmental quality in two case studies of social housing in Madrid, Spain», Energy Build., vol. 1, pp. 492-02, nov. 2017, doi: 10.1016/j.enbuild.2017.09.042.
8. HABITA-RES project - "New integrated assessment tool for vulnerable urban areas. Towards energy self-sufficiency and in favour of a bio-healthy habitability model" (2018-2020). Available: <https://proyectoraven.ietcc.csic.es>
9. Martín-Consuegra, F., de Frutos, F., Oteiza, I. and Hernández Aja, A. «Use of cadastral data to assess urban sca jul. 2018 le building energy loss. Application to a deprived quarter in Madrid», Energy Build., vol. 171, pp. 0-63, jul. 2018, doi: 10.1016/j.enbuild.2018.04.007.
10. Empresa Municipal de la Vivienda y Suelo (EMVS)
11. Martín-Consuegra, F., Gouveia, J.P., de Frutos, F., Alonso, C. and Oteiza, I. «Energy consumption and comfort gap in social housing in Madrid, through smart meters and surveys information», en Transition, Vitoria-Gasteiz (Spain), 2019.
12. Consumos del Sector residencial en España. Resumen de información básica. Proyecto SECH-SPAHOUSEC. IDAE. 2011.
13. Report on the calculation of the cost-optimal levels of the minimum energy performance requirements for buildings in the new Spanish regulations and their comparison with the current requirements. Available: https://ec.europa.eu/energy/sites/ener/files/documents/e_s_2018_cost-optimal_en_version.pdf
14. www.unionfenosagas.com. Mar-2020.
15. Cuerda, E., Guerra-Santín, O., Sendra, J., , and Neila, F. «Understanding the performance gap in energy retrofitting: Measured input data for adjusting building simulation models», Energy Build., vol. 209, 109688, feb. 2020, doi: 10.1016/j.enbuild.2019.109688.
16. CTE-DB-HE. «Código técnico de la Edificación. Documento Básico HE Ahorro de energía». Dic-2019.
17. CTE-DB-HS 3. «Código técnico de la Edificación. Documento Básico HS Salubridad Calidad del aire interior». Dic-2019.

Reference Weather Data Selection in Urban Weather Generator Model

NOELIA ALCHAPAR¹, CLAUDIA PEZZUTO², SANTIAGO BALLARINI³, ERICA CORREA¹

¹Institute of Environment, Habitat and Energy (INAHE-CONICET), Mendoza, Argentina

²Potifical Catholic University of Campinas, Brazil

³National University of Cuyo, Mendoza, Argentina

ABSTRACT: The precision and degree of detail of input urban area parameters and meteorological files directly affect the final result of a simulation. The objective of the research is to evaluate the performance of the Urban Weather Generator v4.1 model (UWG) for urban climate analysis in two cities. Experimental measurements during the summer period in two cities (Mendoza -desert climate- and Campinas -warm temperate-) were used to verify the accuracy of the model. A comparison with two types of weather files (.epw) was used to verify the performance of the input data. The Typical Meteorological Year (TMY) weather data, which is the weather file commonly used with this software, and a weather data based on the year of collection of the experiment (Single_Year) were used. This research showed how the use of the one-year measurement weather file (Single_Year) greatly reduces errors between observed and simulated data. The air temperature registers an $R^2=0.96$ (Mendoza) and 0.98 (Campinas). Whereas if the simulation is performed with typical long-term weather data (TMY), the coefficient of determination is null ($R^2 = 0.43$ in Mendoza and $R^2 = 0.11$ in Campinas). The same was verified with the relative humidity in both cities. The underestimation or overestimation of temperature and humidity leads to errors in calculating the use of equipment for interior conditioning of buildings. Therefore, to obtain accurate results at a given location, it is necessary to know the local climate at short intervals, usually at an hourly rate, during a given year.

KEYWORDS: Urban Microclimate, UWG Software, Weather Data.

1. INTRODUCTION

The urban heat island (UHI) phenomenon has energy, environmental and social consequences, deteriorating the quality of life of citizens [1]. Knowledge of its magnitude and characteristics is an essential requirement for urban planning aimed at mitigating and adapting to climate change [2–4].

Urban simulation models play an important role in the design, analysis, and optimization of the shape and technology of cities in order to improve energy use and reduce the impact on the environment. However, due to the extreme complexity of built environments and many parameters that interact in a city, it is difficult to obtain an accurate representation of them. Therefore, the calibration of climate models and the analysis of their predictive capacity are of particular interest since it is necessary to assess the extent to which simulation models are capable of representing real situations before implementing derived results and conclusions on the urban planning process.[5]

Thus, the main focus of this investigation was to study the Urban Weather Generator v4.1 (UWG) model [6] that is based on the Town Energy Balance Model (TEB) [7] and which includes a

building energy model derived from EnergyPlus algorithms [6]. The UWG performance is comparable to computationally expensive models at the mesoscale and its relatively fast algorithm makes it suitable for the applications of iterative design tools. The UWG model simplifies the specific microclimatic effects of the site, however, it is sufficiently robust as to produce plausible values through urban morphology and vegetation parameters. This model is flexible and compatible with other energy simulators. This information allows a veracity and adjustment of studies on the building thermal behavior inserted in an urban environment, as well as on the effect of the heat island in the construction of building energy consumption profiles.

This paper examines the complexity of estimating the actual air temperatures inside urban canyons from measurements at a Rural Weather Station. Here, we investigated the accuracy of the UWG v4.1 model (UWG) that predicts canopy-level urban air temperature by four submodules: the rural station model, the vertical diffusion model, the urban boundary-layer (UBL) model and the urban canopy and building energy model [8]. Therefore, the precision and degree of detail of input urban

area parameters and meteorological files directly affect the final result of the simulation

Experimental measurements during the summer period in two cities (Mendoza -desert climate- and Campinas -warm temperate-) were used to verify the accuracy of the model. A comparison with two types of weather files (epw) was used to verify the performance of the input data. The Typical Meteorological Year (TMY) weather data, which is the weather file commonly used with this software together with weather data based on the year of collection of the experiment (Single_Year) were used

2. METHODS

To achieve the stated objective, the average air temperature values of the observed rural weather station and the simulated ones were initially checked; secondly, the recorded air temperature inside the observed and simulated canyon was compared over a typical summer period in both cities.

2.1. Description of the study area

This research was carried out under two climatic contexts, that of the city of Mendoza, Argentina (32°54'48 "S, 68 °50 '46 "W) and that of the city of Campinas, Brazil (22°53'20 "S, 47°04 '40 "W). According to the Köppen climate classification, Mendoza, Argentina corresponds to a desert climate with cold steppe (BWk), while Campinas, Brazil, has a warm temperate climate with dry winters and hot summers (Cwa).

One suburban neighborhood was selected in Mendoza and others in Campinas. These areas are located in a region with low horizontal building density and residential zoning.

The selected neighbourhood in Mendoza is found in the northwest of the metropolitan area. The average building height is 3.2 m, with a street width ranging from 12 to 16 m and 3 m of sidewalk. The H/W aspect is 0.17. The species *Morus alba* blanco is the predominant urban afforestation.

The area studied in Campinas is found in the northwest of the metropolitan region. The buildings have an average height of 4 m, with street width between 9 and 12 m, sidewalk – 3 m and frontal setback 2-3 m. The H/W aspect ratio is approximately 0.20. (Figure 1).

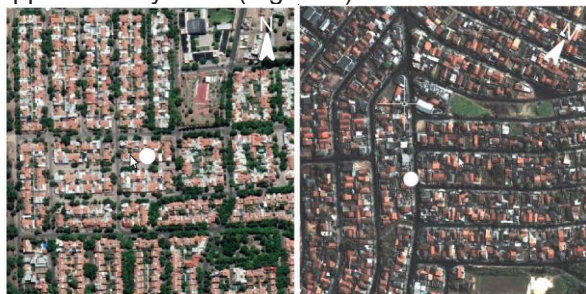


Figure 1: Mendoza -left- and Campinas -right- Study areas

(acquisition point)

2.2. Microclimatic monitoring

With the purpose of obtaining the environmental performance of the sector, a fixed sensor was placed within each studied area. Each sensor recorded air temperature (Ta) and relative humidity (RH) values during the month of January 2014 (Mendoza) and 2013 (Campinas) every 15 minutes in (Mendoza) and 20 minutes (Campinas) respectively. The measuring devices were installed in places with the minimum interference of physical barriers and building materials. All the instruments were installed within protectors to avoid direct incidence of solar radiation and to protect them against bad weather conditions (Onset HOBO RS1 Solar Radiation Shield).

2.3. Input parameters

Two input files are selected to perform the calculation with the UWG software: (i) an XLSM file that describes the characteristics of the urban reference site -meteorological, urban, vegetation and building typology parameters-; (ii) and a rural weather file in EnergyPlus format EPW.

2.3.1. Urban site characteristics

The meteorological parameters describe the characteristics of the urban boundary layer of the reference city. Urban parameters include morpho-material factors such as urban geometry, albedo level of materials, and parameters of an anthropogenic nature such as the heat produced by traffic. Vegetation parameters define the percentage of plant and tree cover and the albedo of the vegetation. Finally, building typology parameters define the percentage of different building types in the reference area.

To obtain the urban and vegetation parameters needed to run a UWG model, a GIS procedure was used to model the studied area (Table 1).

Table 1: Urban Weather Generator parameters

Urban Characteristics	Campinas	Mendoza
Average Building Height	3.44 m	3.62 m
Building Density	0.45	0.27
Vertical to Horizontal Ratio	0.34	0.37
Urban Area Characteristic Length	507.5 m	507.5 m
Road Albedo	0.2	0.2
Vegetation Parameters		
Urban Area Vegetation Coverage	0.06	0.05
Urban Area Tree Coverage	0.02	0.24

2.3.2. Rural weather file

For the analyses, two types of weather data were used: a one year measurement weather archive - Single Year- (base year of measurement) and typical long-term weather data, - Long-term weather-, both EPW-type meteorological data.

The EPW_Single_Year files were manually constructed with climatic variables of a specific year, these variables coincide with the monitoring period of the fixed sensor within the study area: Mendoza (2014) according to the El Plumerillo observatory and Campinas (2013) according to the Viracopos Observatory.

EPW_Long_term_weather files were downloaded from Climate One Building .Org, a repository of free climate data for building performance simulation (<http://climate.onebuilding.org/>) The files, which correspond to Typical Meteorological Years, (TMY) are calculated according to ISO 15927-4:2005 methodologies [9]

A typical meteorological year (TMY) is a set of 12 typical meteorological months. The typicality of a month is based on Finkelstein-Schafer statistics which present daily rates of maximum, minimum and average dry bulb, maximum speed and average wind and global solar radiation [10]. The archive of the city of Mendoza corresponds to the period 2003 to 2017, and that of Campinas to the period 2004 to 2018.

Figure 2 shows the wide differences obtained by contrasting the Ta and HR obtained from an EPW_Single_Year and EPW_Long_term_weather file.



Figure 2: Comparison of air temperature (°C) and relative humidity (%) data obtained from a Single_Year

climate file and a Long-term weather file, according to the analyzed city.

In the city of Mendoza, the average differences of Ta reach 1.3°C and in Campinas -1.1°C. In contrast, the differences in the average HR records are -20% in Mendoza and 6% in Campinas.

In other words, in Mendoza -desert climate city- the EPW_Long_term_weather file underestimates the Ta and greatly overestimates the HR compared to the EPW_Single_Year. On the other hand, in the city of Campinas -war temperate city- the opposite occurs since the Ta is overestimated and the HR is underestimated.

2.4. Output parameters

The UWG model -through Matlab code- generates two output files. The first is an XLSX file which contains the daily average of hourly values of microclimatic parameters related to the urban canyon layer (UCL). The second is a modified EPW file with the urban parameters of the reference sitewhich is compatible with various building thermal simulators (i.e. EnergyPlus).

3. RESULTS

This section compares the air temperature of urban sensors installed in the cities of Mendoza and Campinas with the values estimated by the UWG model.

Tables 2 and 3 show the comparison between the values of air temperature and relative humidity at the observed point (fixed point) and the estimated point above the Urban Canopy Layer. (UCL_point). The values correspond to a simulation day and those of the same day collected at the fixed point in the study area. These show that the city of Mendoza is hotter and drier than the city of Campinas. When comparing air temperatures at the fixed point, values in the range of 24.8 °C and 37.9 °C were found for the city of Mendoza with the relative humidity between 15.0% and 33.8%. The city of Campinas showed air temperature values in the range of 18.9 °C and 32.7 °C and relative humidity between 35.3% and 91.1%. When comparing the simulated data in the UWG model and the monitored point, a better adjustment is observed for both air temperature and relative humidity when using the weather file of the year of measurement (Single_Year). However, it is observed that the UWG model tends to overestimate the temperature for the city of Mendoza (ΔT_{min} 1.30 °C, ΔT_{max} 0.70 °C), and to underestimate Campinas' temperature. (ΔT_{min} -0.70 °C, ΔT_{max} -0.70 °C). In contrast, it overestimates the relative humidity for Campinas (ΔRH_{min} 5.6%, ΔRH_{max} 6.10%), it underestimates the minimum relative humidity (ΔRH_{min} 2.7%) and it overestimates the maximum relative humidity (ΔRH_{min} 5.0%) for the city of Mendoza. Figures 3

and 4 show this daily behavior of the air temperature and the relative humidity data

Table 2: Minimum, maximum and mean temperatures and thermal amplitude of Urban Canopy Layer estimated (UCL_point) by the UWG and observed (Fixed_point)

	Temperature (°C)			
	Min	Max	Mean	Amplitude
Mendoza				
Fixed_point	24.8	37.9	31.6	13.1
UCL_point (Single_Year)	26.1	38.6	32.8	12.5
UCL_point (Long-Term Weather)	22.5	36.0	29.8	13.6
Campinas				
Fixed_point	18.9	32.7	25.1	13.8
UCL_point (Single_Year)	18.3	32.0	24.4	13.7
UCL_point (Long-Term Weather)	19.3	27.0	21.1	7.7

Table 3: Minimum, maximum and mean relative humidity of Urban Canopy Layer estimated (UCL_point) by the UWG and observed (Fixed_point)

	Relative Humidity (%)		
	Min	Max	Mean
Mendoza			
Fixed_point	15	33.8	20.2
UCL_point (Single_Year)	12.3	38.8	22.9
UCL_point (Long-Term Weather)	34.6	75.7	53.1
Campinas			
Fixed_point	35.3	91.1	65.2
UCL_point (Single_Year)	40.9	97.2	69.8
UCL_point (Long-Term Weather)	69.6	97.4	85.7

In order to evaluate the accuracy of the model (tables 4 and 5 and figures 3 y 4) for the collected values (Fixed_point) in comparison with the estimated data (UCL_point (Single_Year) and UCL_point (Long-Term Weather)) the following statistical methods were performed: the coefficient of determination (R²), the mean bias error (MBE); and root mean square error (RMSE). The results show that the model presents a good performance in air temperature for both cities when using the weather file of the year of measurement (Single Year), with coefficient of determination (R²) values

estimated for the two types of weather files compared to the observed data

of 0.96 (Mendoza) and 0.98 (Campinas). On the other hand, for relative humidity, Campinas presented a better performance (R² 0.98) when compared with Mendoza. (R² 0.87). The model presented a low performance in both cities when using the Long-Term Weather file (UCL_point (Long-Term Weather),

El MBE informa el desempeño a largo plazo del modelo. Su valor positivo para la temperatura del aire en Mendoza (1,16) demuestra el promedio sobrevalorado, aunque muestra una subestimación de 0,67 para Campinas. In assessing the relative humidity, the performance of the two cities shows overestimated values, 2.64 and 4.64 in Mendoza and Campinas respectively. The low magnitudes of the RMSE for both cities when assessing the air temperature and relative humidity with the weather file of the year of measurement (Single_Year) reinforce the good performance of this model.

Table 4: R², MBE and RMSE calculation between the Air Temperature above the Urban Canopy Layer estimated by the UWG and observed point during the summer

	R ²	MBE	RMSE
UCL_point (Single_Year) versus Fixed_point			
Mendoza	0.96	1.16	1.47
Campinas	0.98	-0.67	1.00
UCL_point (Long-Term Weather) versus Fixed_point			
Mendoza	0.43	-1.84	3.93
Campinas	0.11	-3.95	6.03

Table 5: R², MBE and RMSE calculation between the Relative Humidity above the Urban Canopy Layer estimated by the UWG and observed point during the summer

	R ²	MBE	RMSE
UCL_point (Single_Year) versus Fixed_point			
Mendoza	0.73	2.64	4.60
Campinas	0.98	4.64	5.80
UCL_point (Long-Term Weather) versus Fixed_point			
Mendoza	0.17	9.56	12.99
Campinas	0.08	24.59	35.35

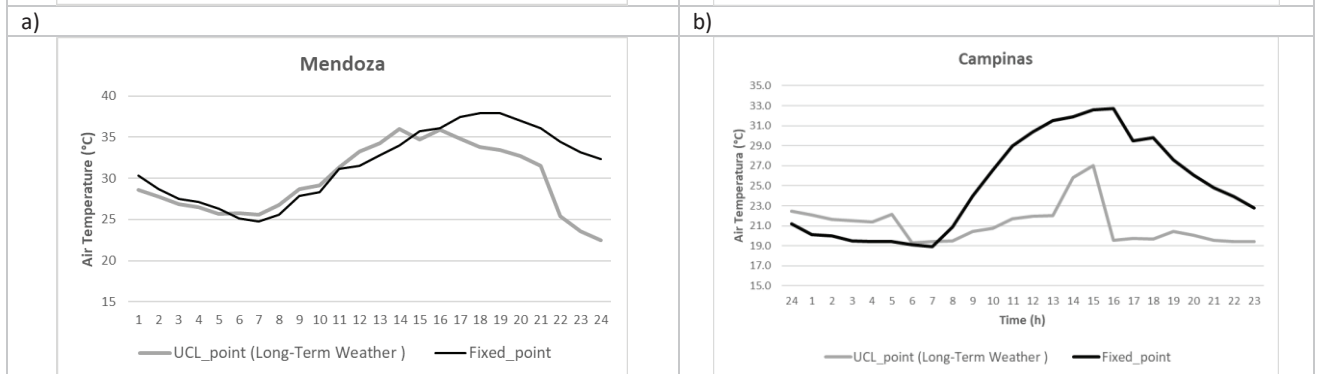
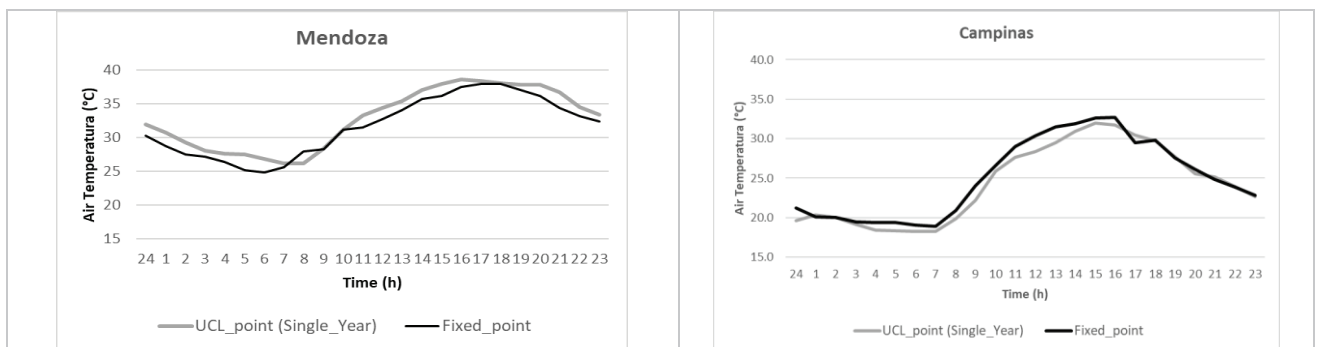


Figure 3: Diurnal cycle of air temperature above the Urban Canopy Layer estimated (UCL_point) by the UWG and observed (Fixed_point) for the summer. a) Data between UCL_point (Single_Year) and Fixed_point in Mendoza, b) Data between UCL_point (Single_Year) and Fixed_point in Campinas, c) Data between UCL_point (Long-Term Weather) and Fixed_point in Mendoza, d) Data between UCL_point (Long-Term Weather) and Fixed_point in Campinas

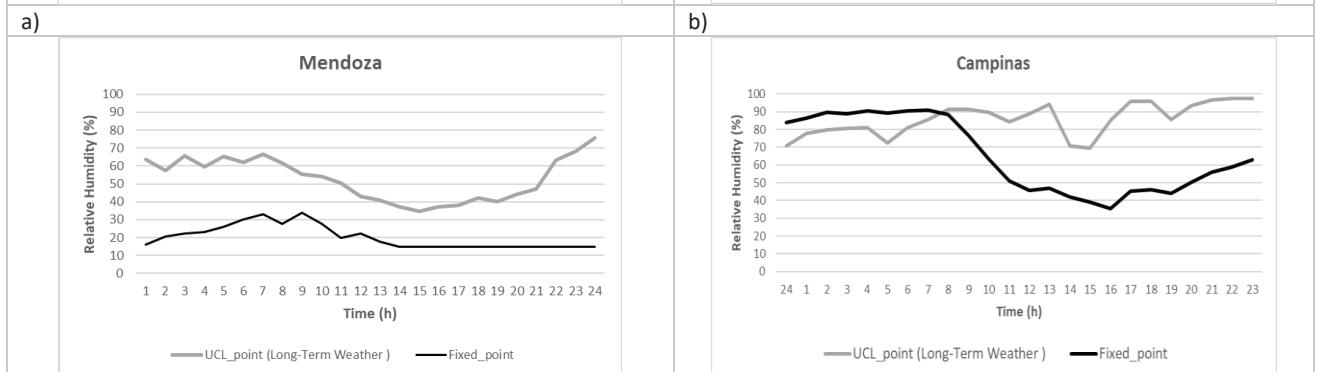
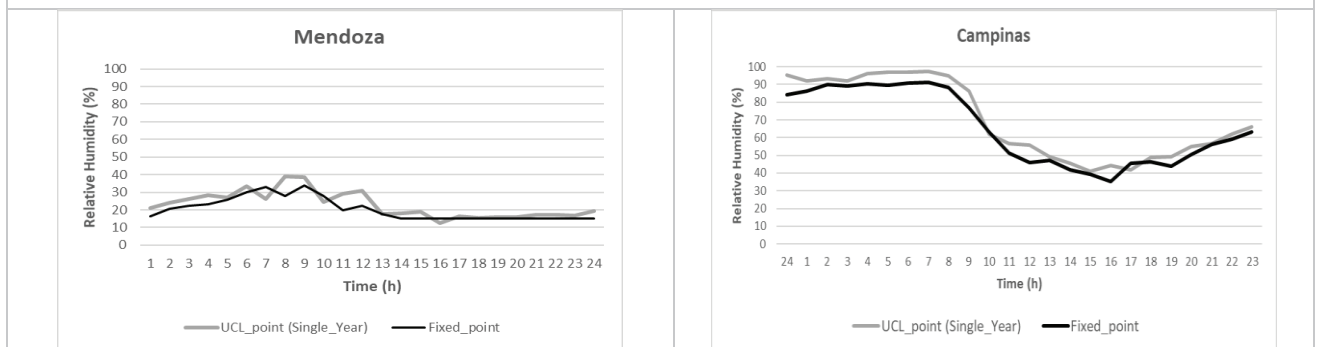


Figure 4: Diurnal cycle of Relative Humidity above the Urban Canopy Layer estimated (UCL_point) by the UWG and observed (Fixed_point) for the summer. a) Data between UCL_point (Single_Year) and Fixed_point in Mendoza, b) Data between UCL_point (Single_Year) and Fixed_point in Campinas, c) Data between UCL_point (Long-Term Weather) and Fixed_point in Mendoza, d) Data between UCL_point (Long-Term Weather) and Fixed_point in Campinas.

4. CONCLUSION

This research showed how the use of the one-year measurement weather file (EPW_Single_Year) greatly reduces errors between observed and simulated data. The air temperature registers an $R_2=0.96$ (Mendoza) and 0.98 (Campinas). Whereas if the simulation is performed with typical long-term weather data (EPW_Long_term_weather), the coefficient of determination is very low ($R_2 = 0.43$ in Mendoza and $R_2 = 0.11$ in Campinas). The same was verified with the relative humidity in both cities.

Academia and the professional sector concerned with evaluating building energy efficiency generally use long-term sources of climate consultation (Long_term_weather) without knowing the problems that these data can have on the energy consumption of a building. The underestimation or overestimation of temperature and humidity leads to a misleading calculation in the conditioning equipment of interior spaces. Therefore, for accurate results at a given location, it is necessary to know the local climate at short intervals - usually with an hourly frequency - throughout a given year as typical.

It should be noted that in cities with high heliophany and a large percentage of urban Area Tree Coverage, as is the case of Mendoza, the adjustment possibilities, in the summer period, are conditioned if only humidity and temperature variables in the climate files are modified. Future works envisage building a climate file with specific data on global solar radiation, direct normal and diffuse for the measurement year.

The research will be continued by estimating building energy consumption associated with the selection of Single_Year and Long_term_weather climate files, for different climatic contexts.

ACKNOWLEDGEMENTS

This work was supported by the National Agency for Scientific and Technological Promotion-ANPCyT- of Argentina, through the Fund for Scientific and Technological Research -FONCyT and the State of São Paulo Research Foundation – FAPESP (2019/10308-9).

REFERENCES

- [1] M. Santamouris, (2015) Analyzing the heat island magnitude and characteristics in one hundred Asian and Australian cities and regions, *Sci. Total Environ.* 512–513 582–598. doi:10.1016/j.scitotenv.2015.01.060.
- [2] D.E. Bowler, L. Buyung-Ali, T.M. Knight, A.S. Pullin, (2010) Urban greening to cool towns and cities: A systematic review of the empirical evidence, *Landsc. Urban Plan.* 97 147–155.

- doi:10.1016/j.landurbplan.2010.05.006.
- [3] C.R. Chang, M.H. Li, (2014) Effects of urban parks on the local urban thermal environment, *Urban For. Urban Green.* 13 672–681. doi:10.1016/j.ufug.2014.08.001.
- [4] K. Perini, A. Magliocco, (2014) Effects of vegetation, urban density, building height, and atmospheric conditions on local temperatures and thermal comfort, *Urban For. Urban Green.* 13 495–506. doi:10.1016/j.ufug.2014.03.003.
- [5] J. Mao, Y. Fu, A. Afshari, P.R. Armstrong, L.K. Norford, (2018) Optimization-aided calibration of an urban microclimate model under uncertainty, *Build. Environ.* 143 390–403. doi:10.1016/j.buildenv.2018.07.034.
- [6] B. Bueno, L. Norford, J. Hidalgo, G. Pigeon, (2013) The urban weather generator, *J. Build. Perform. Simul.* 6 269–281. doi:10.1080/19401493.2012.718797.
- [7] V. Masson, (2000) A physically-based scheme for the urban energy budget in atmospheric models, *Boundary-Layer Meteorol.* 94 357–397. doi:10.1023/A:1002463829265.
- [8] A. Nakano, B. Bueno, L. Norford, C.F. Reinhart, (2015) Urban weather generator - A novel workflow for integrating urban heat island effect within urban design process, 14th Int. Conf. IBPSA - Build. Simul. 2015, BS 2015, Conf. Proc. 1901–1908.
- [9] European Committee for Standardization (CEN), (2005) ISO 15927-4: Hygrothermal performance of buildings -- Calculation and presentation of climatic data -- Part 4: Hourly data for assessing the annual energy use for heating and cooling, ISO.
- [10] F. Bre, M.G.G.S. Cruz, V.D. Fachinotti, (2017) Generación del año meteorológico típico para la ciudad de la plata, argentina, in: ENCAC/ELACAC (Ed.), XVI Encontro Nac. Tecnol. Do Ambient. Construído X ELACAC Encontro Latino-Americano Conforto No Ambient. Construído, Balneário Camboriú, SC.,

Building performance, climatic variables, and indices: identification of correlations for social housing across the Mexican territory

DANIEL ZEPEDA-RIVAS¹, ROEL LOONEN³, JORGE RODRÍGUEZ-ÁLVAREZ^{1,2}

¹ Universidade A Coruña, A Coruña, Spain

² Architectural Association School of Architecture, London, UK

³ Eindhoven University of Technology, Eindhoven, The Netherlands

ABSTRACT: Building energy codes rely on climate zoning to establish regional requirements and benchmarks for building performance. Nevertheless, there is neither an accepted methodology for this purpose nor a scientific agreement when considering variables that provide quantitative results. This paper explores the relationships between the environmental performance of a free-running housing prototype, simulated in 240 locations across the Mexican territory, and climatic variables: latitude, altitude, and diurnal range, as well as the climatic indices of continentality, oceanity, and aridity. Correlations were found and analysed through statistical methods to define the significance of the selected variables to be used to predict the effectiveness of a free-running dwelling. The simulation outputs were processed as the percentage of time in comfort and overheating/overcooling hours. The results proved that latitude and altitude had a stronger correlation than the diurnal range and the climatic indices which showed similar but inferior effect sizes for all cases. None of the obtained correlation effect sizes reached a strong significative value. The results demonstrate that the highest correlation values were from the variables of Latitude and Altitude, with both effect sizes within the moderate correlation range, therefore, these variables can be used as guidelines in the prediction of a general trend when predicting thermal comfort in free-running buildings.

KEYWORDS: Climate zoning, free-running buildings, Social housing, tropical climate

1. INTRODUCTION

As part of the global efforts to reduce CO₂ emissions, building energy efficiency programmes have been implemented across the world. Among the purposes of this programmes, is to regulate and distribute energy policies throughout territories using climate zoning as a mechanism. However, there is not an established method to do this. Previous studies have identified as many as 19 parameters as determining factors for developing criteria for climatic zoning methodologies for building energy efficiency applications. As a consequence, there is no consensus in which factors and how many of them should be included. Moreover, there is neither a correlation between the number of zones nor their sizes among countries [1], [2].

The most utilized zoning approaches have been developed in climates located at higher latitudes where active methods for heating and cooling are necessary means to create and maintain thermal comfort in building interiors. Consequently, the criteria in them are focused on energy-saving rather than proposing completely passive methods. The application of such methods becomes counterproductive when they are applied in warmer climates, such as the one in Mexico, where thermal

comfort can be achieved by exploiting the bioclimatic potential.

Mexico occupies the 13th place in global territorial extension and it encompasses 14 of the 31 possible climates according to Köppen's climate classification. Historically speaking, vernacular architecture in the Mexican territory has been free-running, relying only on passive means to create thermal comfort. Nevertheless, nowadays due to the low quality of the novel social housing, there is a constant increase in the need and use of energy consumption for cooling purposes regardless of the mildness of the climate [3], and the fact that over 70% of the population suffers some kind of poverty [4]. This can be considered a consequence of impractical regulations, that excludes a pragmatic passive approach, as well as punitive measures or legislation to ensure its implementation.

The problem with the increasing use of Air Conditioning (A/C) is in part because of the socio-economical situation of the population, but mainly because of the wasted climate potential across the country. Recent research that evaluated the Mexican construction sector concluded that, on the longer-term, it is more profitable to make an energy-efficient modification to the building envelope of a dwelling, than the installation of an operational cost of an A/C

unit [5], Other studies elaborated by [6]–[9] explore the energy-saving and bioclimatic potential of the territory through passive strategies, while further research made by [10], [11] conclude that even at the locations with the warmer climates and the most extreme conditions, there are effective and functional passive strategies to achieve thermal comfort. Moreover, it is also important to consider, that the United Nations Environment Programme (UNEP) has encouraged and suggested in different occasions the implementation and promotion of better building energy standards as means to reduce energy consumption [12], [13]

The most utilized climate zoning methodologies use different parameters such as climate variables, climate indices, and bioclimatic variables as indicators to characterize the climate. A climate variable is an average or an accumulative count of a specific variable such as temperature or rainfall. A bioclimatic variable is a value derived from a specific calculation of a climate variable through a certain period to characterize a specific aspect, such as maximum monthly temperature or a yearly diurnal index. A climate index is a value derived from a calculation involving different climate variables and/or bioclimatic variables within a formula to characterize and state the possible changes in a climate system through a location, such as continentality, oceanity, and aridity.

The objective of this paper is to explore the correlation between the environmental performance of a free-running dwelling and different selected parameters. These parameters are the variables of latitude and elevation, the bioclimatic parameter of diurnal range, and the indices of continentality, oceanity, and aridity. For a deeper analysis, two different versions for each climatic index will be analysed.

2. METHODOLOGY

The followed methodology was elaborated based on the work by [14] in which a set of climatic variables and indices were related to passive measures and further translated into design recommendations. For the present work, a reference building is considered, in a similar way it was done in the work by [15], [16] where a reference building was simulated in different locations and the results are used to create a zoning distribution.

As a first step, weather data from 240 locations was collected in the format of EPW weather files. The calculation periods for all the files covered a 20-year period for radiation (1991-2010) and 10 years for temperature (2000-2009). Despite the fact that all the locations were selected according to the official localization of weather stations published by the Mexican government [17], the information in them

is comprised differently, 68 of them are fully equipped weather station, and the information from them is completely composed by on-site collected observations, 105 of them did not include solar radiation, therefore, these values were interpolated, and for the case of 67 of them it was not possible to obtain any data, thus the weather files were completely interpolated. All the interpolation work was done using the software Meteonorm 7.2. [18] In Figure 1, it is possible to appreciate a map of the Mexican territory with the location of the 240 weather station.

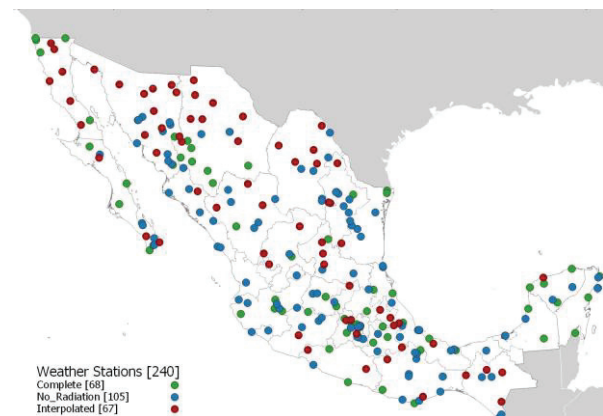


Figure 1: The location and types of the 240 weather stations where data was gathered.

As the following step, a reference building was established. The initial floor plan distribution, as well as the building envelope specifics, were taken from the Incremental Housing project elaborated by Studio Elemental [19]. The initial design of the project was originally conceived in 2003 considering Chilean socio-economic statistics for its dimensioning and constructive specifications, however, leaning on the fact that situation is similar across the Latin-American territory, in 2008 Studio Elemental created an adapted version for the Mexican context. A floor plan of the housing prototype is presented in Figure 2 and Table 1 provides a summary of the physical dimensions of the building.



Figure 2: Floorplan of the house prototype

Table 1: Physical dimensions of the housing prototype building

Area	54 m ²
Perimeter	30.3 m
Volume	145.4 m ³
Interior height	2.7 m
Window to Wall Ratio	0.25

Because of the predominant warmth and the tropicity of the country, the floor plan was modelled as a single and free-standing ground floor with no immediate context, assuming the worst-case scenario for overheating. The building materials were assigned considering the traditional building methods, as well as the population's poverty indicators published in the last national housing census [20]. Table 2 provides a summary of the building element's resistance values.

Table 2: Building element's resistance values of the housing prototype

	Resistance values
External Walls	3.09 W/m ² K
Windows	5.20 W/m ² K
Roof	3.23 W/m ² K
Floor	5.53 W/m ² K

The internal conditions of the dwellings were also modelled according to the last census data. It was assumed that the dwelling is occupied by a family of four people with regular daytime activities with the typical heat gains values during the occupancy and non-occupancy time. The house was modelled as naturally ventilated free-running buildings completely relying on passive strategies, considering an infiltration rate of 0.75 air changes per hour, a 50% fraction of operable window glazing area and a stack discharge coefficient of 0.25, the window opening and closing algorithm, was automated with schedules emulating the occupant's behaviour and the minimum and maximum interior temperatures for natural ventilation were programmed according to the comfort band.

The comfort assessment was elaborated according to the European Standard EN-16798 (previously EN-15251) for naturally ventilated buildings. It was decided to employ the European comfort standard, rather than the North American, following the concept that the original comfort algorithm of the EN-15251 has a higher operative temperature tolerance of 33.5°C, as a consequence of considering the exponentially weighted running mean of the past days mean outdoor air temperature ($T_{r,m}$)

rather than the monthly mean temperature ($T_{o,m}$) considered by ASHRAE, which only allows a maximum operative temperature of 31.4°C [21]. Additionally, an acceptability limit of 80% was also assumed and it was applied as a comfort band-width of 8°K. Finally, to assess the indoor thermal comfort in a quantitative way, and due to the lack of a comfort standard for free-running naturally ventilated dwellings, the general comfort assessment was elaborated following the EN-16798 standard for naturally ventilated office buildings.

In the final phase, a set of parameters were selected and the climatic indices were calculated according to each location. The parameters were:

- Latitude: The geographical latitude of the location according to the distance to the equator. This feature was selected since it is the main one used by the current Mexican normative [22] with the intention of determining its adequacy.
- Altitude: The geographical height of the locations in relation to the sea level. Previous work by [23] aimed at an Indian context, found that there is a correlation between the altitude and the environmental performance of an active dwelling. The objective is to investigate if this same relation applies to the Mexican context and for free-running homes.
- Diurnal Range: The temperature variation between the highest value and the lowest value occurring within one day. The objective is to explore to what extent this feature can predict the possible effectiveness of passive strategies, in climates characteristically arid, the diurnal range can provide the necessary means to tackle the daytime overheating with the night's coldness and vice versa [24].
- Continentality: The quantification of the degree to which a location is influenced by the surrounding landmass. The selected indices are the Johansson Continentality Index and the Conrad Continentality Index [25], [26], even when the second was intended to be an improvement of the first one, over the time, it has been found that they are equally useful for different purposes [27]. Both equations include latitude, Thermal Amplitude (T_{amp}) and arithmetic fixed values, T_{amp} is defined as the difference between the maximum monthly temperature and the minimum monthly temperature during the year. The difference between the two formulas lies in the fixed arithmetic values.
- Oceanity: The quantification of the degree to which a location is influenced by the proximity of the sea. The selected indices are the Kerner Oceanity Index and the Mars Oceanity Index

[28], [29], both in a similar condition as the previously mentioned, in which they are still used nowadays for different purposes. Their formulas follow the same general structure, and they both consider the T_{amp} in the same way. Their differences are in the fixed arithmetic values, and in the fact that Kerner's Index considers the resultant value of the subtraction of October's mean monthly temperature minus April's, while Mars consider the latitude degrees minus a fixed value [27].

- **Aridity:** The quantification of the degree to which a location is influenced by the lack of effective or life-promoting moisture. The selected indices are the De Martonne Aridity Index and Pinna Combinative Index [30], [31], both of them used for different purposes, De Martonne's index provides a simple general overview since it's the resultant of the division of the mean yearly values of precipitation and air temperature plus ten, while the Pinna Combinative Index provides a more accurate number with respect to the extent of the aridity since it considers the mean monthly values of precipitation and temperature of the driest months additionally to the yearly values of precipitation and air temperature.

3. RESULTS

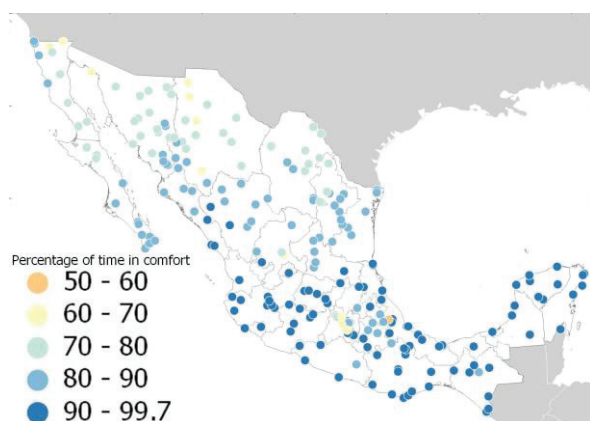


Figure 3: Percentage of time in comfort of each location

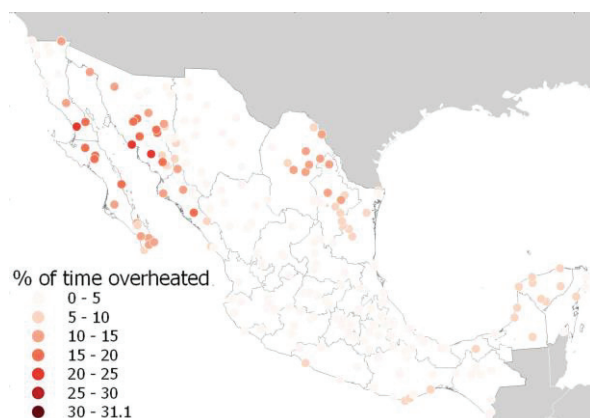


Figure 4: Percentage of time in overheated of each location

The simulation results were processed according to the resultant Operative Temperature (T_o). The total percentage of time in comfort (figure 03) was calculated as well as the percentage of time overheated, or above the upper comfort limit (figure 04), and the percentage of time overcooled or below the lower comfort limit (figure 05). A dataset was created including the station's general information, the selected parameters and simulation results.

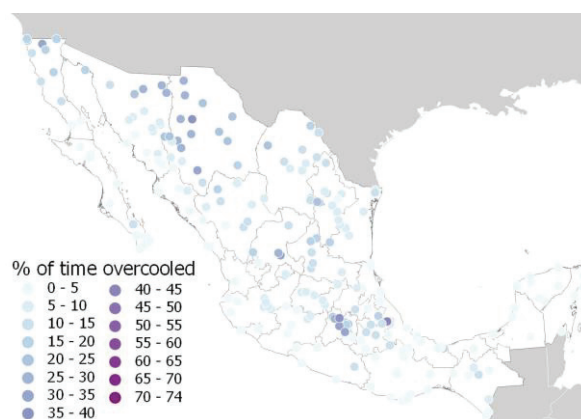


Figure 5: Percentage of time in overcooled of each location

Table 3: r values of Spearman's rank correlation coefficient test results

	% in comfort	Overheating hours	Overcooling hours	Average effect size
Latitude	-0.71	0.38	0.50	0.53
Altitude	-0.32	-0.73	0.67	0.58
Diurnal range	-0.53	-0.36	0.68	0.52
Johansson's Continentality	-0.65	0.42	0.45	0.50
Conrad's Continentality	-0.67	0.41	0.47	0.52
Kerner's Oceanity	-0.06	0.65	-0.29	0.34
Marsz's Oceanity	0.65	-0.42	-0.45	0.51
De Martonne's 's Aridity	0.51	-0.50	-0.22	0.41
Pinna's Aridity	0.49	-0.48	-0.21	0.39

For the statistical analysis, the simulation results were considered as dependent variables and the selected parameters were considered as independent variables. As a first step, a Shapiro-Wilk test together with a non-parametric Kolmogorov-Smirnov test were performed to all elements of the dataset. As a result, it was established that all of the elements of the dataset were non-normally distributed. Sequentially, with the interest of establishing the relation between the dependent and independent variables, Q-Q plots were elaborated followed by the Spearman's rank correlation coefficient test. The resultant correlation coefficients were tabulated (Table 3) and the effect sizes were

interpreted following the recommendations of [32], [33], where an effect size value of 0.1 to 0.2 is considered as very small, 0.2 to 0.5 as small, 0.5 to 0.8 as medium and 0.8 to 1 large. All the resultant effect sizes determined that none of the tested correlations presented values above -0.73, positioning all the effect sizes in the medium, small, and very small categories. None of the independent variables demonstrated a constant medium effect or higher size across the independent parameters.

The highest correlation values obtained with respect to the simulation results were all within the medium effect size classification. The parameter of Latitude presented the highest value of the chart with a -0.71 and also with respect the percentage of time in comfort, the parameter of altitude presented a value of -0.73 with respect of overheating and for the case of overcooling the highest effect sizes were the ones of altitude of 0.67 and diurnal range of 0.68. The parameters with the highest effect sizes were Latitude and Altitude, from which it is possible to establish that there is a monotonic relationship between the latitude and percentage of time in comfort, although, it is not possible to determine accurately if this lack of comfort correspond to overheating and overcooling. On the contrary, with the resultant effect sizes of altitude, it is possible to establish that there is also a relationship between the increase of meters above sea level of a location and the overheating and overcooling hours, but not necessarily neither in an equative manner nor a proportional way according to the total percentage of time in comfort. For the case of the Diurnal range, it presented two mediums or moderate effect sizes and one small correlation value, from which we can establish that the diurnal range might predict in a non-accurate way the total percentage of time in comfort and overcooling hours, and even in a more imprecise way the overheating hours. None of the Climatic Indices, presented a strong or large correlation value, the highest averages correspond to Johansson's Continentiality index, Conrad's Continentiality Index and Marsz's Oceanity Index. The three of them presented a medium or moderate effect size for the percentage of time in comfort and a small correlation in overheating and overcooling with similar values between -0.42 and -0.47. Kerner's Oceanity index presented the highest correlation value among indices with a 0.65 for overheating hours and the lowest value in the chart of -0.06 for the percentage of time in comfort, being the closest value to a no-correlation result, the three values of Pinna's Aridity index remained in the small correlation category, and together with Kerner's Oceanity index presented the two lowest averages values of the table.

4. CONCLUSION

The study presented in this paper investigates the relationship between nine different variables and the time in comfort of a naturally ventilated free-running house. For the investigation, weather data of 240 different location across the Mexican territory, was collected and it was first used to calculate climate indices, sequentially; a reference free-running naturally ventilated building was simulated in these locations, and the simulation results were used to test the correlation of the environmental performance of a free-running dwelling and different climatic parameters: latitude, altitude, diurnal range and the indices of continentality, oceanity and aridity.

The study considered the Mexican territory as a single geographical area, which is in contrast to the observations of Köppen's climate classification that divides the country into three main different areas based on their climate generalities. This subdivision will be investigated in further studies since the sources of discomfort may concur according to general climate zoning. Similarly, further research needs to be followed, since the simulation results or total percentage of time in comfort together with the total overheating and overcooling time, may vary when considering a different building configuration closer to what can be found in an urban or suburban area.

The present research considered the correlation of nine different variables and thermal comfort simulation results. The highest correlation values were obtained for Latitude and Altitude. Meanwhile, the average correlation values for the bioclimatic feature of diurnal range and the climate indices are within the medium and small effect size categories. Hence their results can be considered more ambiguous and uncertain compared with Latitude and Altitude.

One of the secondary objectives of this work was to test the parameter of Latitude as it is used in the Mexican normative. In the normative Latitude is employed as the main variable to define the building envelope resistance value of a dwelling. After looking at the results obtained, it is possible to conclude that while the parameter of latitude encompasses a level of uncertainty, it showed a closer relation to predict the total percentage of time in comfort. Nevertheless, the pertinence of the building regulations' suggested resistance values remains in question since they seem to be unrelated to the socioeconomic situation and they fail to consider the typical construction systems in the country.

REFERENCES

- [1] A. Walsh, L. Labaki, and D. Cóstola, "Panorama do Zoneamento Bioclimático nas Américas," *XV Encontro Nac. Tecnol. do Ambient. Construído*, no. 1, pp. 994–1003, 2014.
- [2] A. Walsh, D. Cóstola, and L. C. Labaki, "Review of methods for climatic zoning for building energy efficiency programs," *Build. Environ.*, vol. 112, pp. 337–350, 2017.
- [3] CONUEE, "Estudio de Caracterización del Uso de Aire Acondicionado en Viviendas de Interés Social en México," 2016.
- [4] CONEVAL, "Informe de Evaluación de la Política de Desarrollo Social 2018," *Coneval*, p. 60, 2018.
- [5] O. A. Preciado-Pérez and S. Fotios, "Comprehensive cost-benefit analysis of energy efficiency in social housing. Case study: Northwest Mexico," *Energy Build.*, 2017.
- [6] D. Morillón-Gálvez, R. Saldana-Flores, and A. Tejeda-Martínez, "Human bioclimatic atlas for Mexico," *Sol. Energy*, vol. 76, no. 6, pp. 781–792, 2004.
- [7] I. Oropeza-Perez and P. A. Østergaard, "The influence of an estimated energy saving due to natural ventilation on the Mexican energy system," *Energy*, vol. 64, pp. 1080–1091, 2014.
- [8] I. Oropeza-Perez and P. A. Østergaard, "Active and passive cooling methods for dwellings: A review," *Renew. Sustain. Energy Rev.*, vol. 82, no. September 2017, pp. 531–544, 2018.
- [9] R. M. Rivera and G. L. H., "Improvement of Thermal Comfort by Passive Strategies . Case Study : Social Housing in Mexico," no. October, 2019.
- [10] I. Marincic, J. M. Ochoa, M. G. Alupuche, and G. Gómez-Azpeitia, "Adaptive Thermal Comfort in Warm Dry Climate : Economical dwellings in Mexico," *26th Conf. Passiv. Low Energy Archit. Quebec City, Canada*, no. June, pp. 22–24, 2009.
- [11] G. Gómez-Azpeitia, G. Bojórquez-Morales, P. Ruiz, I. Marincic, E. González, and A. Tejeda, "Extreme adaptation to extreme environments: case study of hot dry, hot sub-humid, and hot humid climates in Mexico," *Proc. 7th Wind. Conf. Chang. Context Conf. an Unpredictable World.*, vol. 8, no. 8, pp. 12–15, 2012.
- [12] U. SBCI, "Greenhouse Gas Emissions Baselines and Reduction Potentials from Buildings in México," p. 65, 2009.
- [13] UNEP, "Annex C - UNEP Emissions Gap Report 2019 Recent policy changes in selected G20 members," pp. 1–58, 2019.
- [14] J. Rodríguez Álvarez and S. Pintos Pena, "A Climatic Cartography for Sustainable Housing : Development of a meteorological classification in Galicia , Spain," vol. 1, 2016.
- [15] F. J. S. de la Flor, S. Á. Domínguez, J. L. M. Félix, and R. G. Falcón, "Climatic zoning and its application to Spanish building energy performance regulations," *Energy Build.*, vol. 40, no. 10, pp. 1984–1990, 2008.
- [16] M. Carpio, J. Jódar, M. L. Rodríguez, and M. Zamorano, "A proposed method based on approximation and interpolation for determining climatic zones and its effect on energy demand and CO₂ emissions from buildings," *Energy Build.*, vol. 87, pp. 253–264, 2015.
- [17] SMN-CONAGUA, "Estaciones Meteorológicas Automáticas (EMAS)," *Servicio Meteorológico de la CONAGUA*, 2010. [Online]. Available: <https://smn.conagua.gob.mx/es/observando-el-tiempo/estaciones-meteorologicas-automaticas-emas>. [Accessed: 02-May-2020].
- [18] METEOTEST, *Handbook part II: Theory Global Meteorological Database Version 7 Software and Data for Engineers , Planers and Education*, no. January. 2019.
- [19] S. Elemental, "Elemental," 2019. [Online]. Available: <http://www.elementalchile.cl/en/>. [Accessed: 02-May-2020].
- [20] INEGI, "Instituto Nacional de Estadística y Geografía," *México en cifras*, 2018. [Online]. Available: <http://www.inegi.org.mx/>. [Accessed: 09-Sep-2018].
- [21] F. Nicol, M. Humphreys, and S. Roaf, *Adaptive Thermal Comfort, Principles and Practice*. London: Routledge, 2012.
- [22] CONUEE, "Norma Oficial Mexicana NOM-020-ENER-2011, Eficiencia energética en edificaciones.- Envoltente de edificios para uso habitacional," *D. Of. la Fed.*, no. NOM-020-ENER-2011, pp. 1–4, 2011.
- [23] R. Jayapalan Nair, E. Brembilla, C. Hopfe, and J. Mardaljevic, "Weather Data for Building Simulation : Grid Resolution for Climate Zone Delineation Loughborough University , Loughborough , United Kingdom Abstract," *16th IBPSA Build. Simul. Conf.*, pp. 1–8, 2019.
- [24] S. V. Szokolay, *Introduction to architectural science: the basis of sustainable design*, vol. 8. Elsevier, 2008.
- [25] O. V. Johansson, "Über die Asymmetrie der meteorologischen Schwankungen," *Soc. Sci. Fenn. Comment. Physico-Mathematicae*, vol. 3, 1926.
- [26] V. Conrad, *Methods in Climatology*, 2nd ed., vol. 1, no. 3. Cambridge, Massachusetts, 1946.
- [27] C. Andrade and J. A. Corte-Real, "Spatial distribution of climate indices in the Iberian Peninsula," *AIP Conf. Proc.*, vol. 1648, no. September, pp. 11–16, 2015.
- [28] F. Kerner, "Thermoisodromen, Versuch einer kartographischen Darstellung des jährlichen Ganges der Lufttemperatur (Wien)," *K. K. Geogr. Gesellschaft*, vol. 6, no. 3, p. 30, 1905.
- [29] A. Marsz and S. Rakusa-Suszczewski, "Charakterystyka ekologiczna rejonu Zatoki Admiralicji (King George Island, South Shetland Island)," *Kosmos*, vol. 36, no. 1, p. 103–127, 1987.
- [30] E. de Martonne, *Traité de géographie physique - tome 3 : Biogéographie*, vol. 42, no. 9. Paris: Armand Colin, 1925.
- [31] J. Zambakas, *General Climatology*, vol. 11, no. 2. Athens, Greece.: Department of Geology, National & Kapodistrian University of Athens, 1992.
- [32] C. J. Ferguson, "An Effect Size Primer: A Guide for Clinicians and Researchers," *Prof. Psychol. Res. Pract.*, vol. 40, no. 5, pp. 532–538, 2009.
- [33] S. S. Sawilowsky, "New Effect Size Rules of Thumb," *J. Mod. Appl. Stat. Methods*, vol. 8, no. 2, pp. 597–599, 2009.

CFD Analysis for Appropriate Positions of Wind Turbines on Tall Building in an Urban Environment

PATTARANAN TAKKANON, PHARPOOM PIMOLVICHAYAKIT

Department of Building Innovation, Faculty of Architecture, Kasetsart University, Bangkok, Thailand

ABSTRACT: Wind is a source of renewable energy and also a source of clean, non-polluting, electricity. This study aims to find appropriate position to install wind turbine on high-rise building for highest electricity generation. The study was based on an experimental method using Computational Fluid Dynamics (CFD) software package to simulate airflow around the wind turbine areas. There were 4 options of wind turbine installation: 1) Roof installation (Type A) Height 130 m., 2) Wall installation (Type B) Height 80-130 m., 3) In the middle of openings (Type C) Height 80, 100, 120 m., and 4) Between 2 towers (Type D) Height 70-130 m. Each type had subtypes and each of them was considered for energy performance by its average wind velocity. Under an urban wind condition and possible location for skyscrapers and tall buildings, results from the study show that installation type A1 and A2 gave the highest amount of electricity at 2,920.85 kWh/Year. Type B4 generated 6,283.44 kWh/Year as the highest. Type C3 gave the highest amount of electricity at 3,869.62 kWh/Year and type D3 gave the highest at 11,968.34 kWh/Year. Therefore, D3 showed the highest amount of electricity generated of all options.

KEYWORDS: Wind Power, Wind Turbine, Building-Integrated Wind Turbine, Computation Fluid Dynamics (CFD)

1. INTRODUCTION

Wind energy is one of the renewable sources with the greatest potential for clean and efficient power. Wind turbine technology is increasingly important and has gained attention in recent years. While offshore wind farms continue to expand, urban and sub-urban areas are becoming interesting locations for wind energy harvesting [1-8]. However, urban environment has some limitations on application of wind turbines. The potentials, challenges and concerns regarding urban wind energy have been extensively reviewed by many researchers [9-14]. Thailand Alternative Energy Development Plan (AEDP) 2015-2036 also increases targets for installed alternative energy to 19.635 MW in 2036. The wind energy sector alone will be accounted for 15.25% of total alternative energy by 2036 compared to 4.99% in 2014 [15]. Nonetheless, not every area in Thailand can rely on wind energy. Urban areas are characterised by low-speed wind resulting in an inefficient power generation of wind turbines and Bangkok is no exception. By considering that wind speed increases with height, it is possible to install wind turbines on tall buildings in the city to gain benefit of their heights. Based on literature review, there are mainly 3 options to install wind turbines [16]: 1) on top of buildings, 2) integrated in the construction of buildings, and 3) between two buildings. While there are a few cases of wind turbine installation in Bangkok, they are in form of stand-alone wind turbines placed in open areas such as public park and car parking lot. The wind turbines for such conditions produce only small amount of energy. Research on the usage of wind turbines on tall buildings especially in

high-density and low-speed wind environment of Bangkok is still lacking. Therefore, the current study is an initiative to find appropriate position to install wind turbines on tall buildings in Bangkok for best energy performance.

2. CASE STUDY AND EXPERIMENTAL METHOD

The study was based on an experimental method using Computational Fluid Dynamics (CFD) to simulate airflow around the wind turbine areas. Models of various built forms and heights possible under the bulk control of building regulation for a selected area in Bangkok were created.

2.1 Site selection and case study

The site in Bangna district was selected for wind studies as it was the business district and close to the main meteorological station. Models of up to 130-meter-high buildings were created to comply with the height limit in Bangna district. All case study buildings had 6 to 12-meter span as a standard structure of tall buildings. Each floor is of 24m x 24m. According to Thai building regulations, building height from any point shall not be more than twice the horizontal distance from such point which is perpendicular to the boundary of the opposite side of the nearest public road. Therefore, the total building height for the study must not exceed 130 m as calculated from 30 m wide road and height restriction for Bangna zone. Weather data of 2018 of the study area were obtained from Bangna Meteorological Station. There were 4 options of wind turbine installation: 1) Roof installation (Type A) Height 130 m., 2) Wall installation (Type B) Height

80-130 m., 3) In the middle of openings (Type C) Height 80, 100, 120 m., and 4) Between 2 towers (Type D) Height 70-130 m [17]. Each type had subtypes and each of them was considered for power generation by its average wind velocity. Subtype A1-A4 were differentiated by rooftop shapes: flat roof (A1), tilted roof (A2), gable roof (A3), and hip roof (A4), as they could be aerodynamic buildings or bluff buildings [18]. Subtype B1-B5 were varied with shapes of floor plan or the building footprint i.e. circle (B1), triangle (B2), hexagon (B3), octagon (B4), and square (B5). Subtype C1-C3 were varied by different sizes of the openings or the building's holes. They consisted of the square-shaped building with 6m x 6m openings at 80m high (C1), the building with 9m x 9m openings at 100m high (C2), and the building with 12m x 9m openings at 120m high (C3). Subtype D1-D4 were two towers with different distances: 6m (D1), 12m (D2), and 24m (D3). There were 15 subtypes in total (Fig. 1). The wind turbine location and measurement points were at 3m and 6m away from the building edge [19].

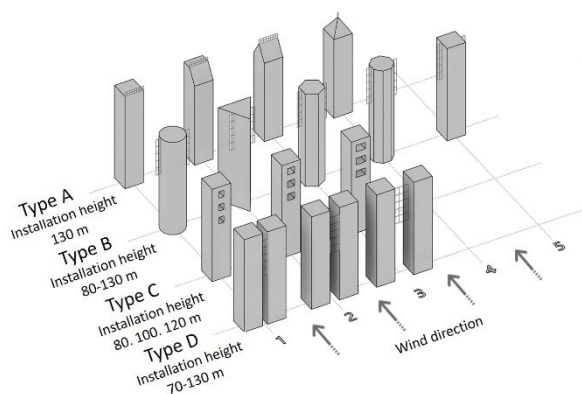


Figure 1: Building types for wind studies

2.2 CFD simulation

The setting condition for wind simulation studies was urban area formed by high-rise buildings (10-storey buildings) which provided inverse power of exponent (n) for roughness category index at 2.8571 [20]. The commercial CFD simulation program, scStream, was employed for calculation. The program has been widely used for numerical simulation especially for forecasting wind field in and around buildings [21-24]. It is based on structured grid and finite difference method, with high precision and high calculation speed [25]. The computational domain was $k-\epsilon$ which was for turbulence modeling. It was suggested to provide 10-20 times of building size as the area around building with wind turbines to avoid boundary layer effect [26]. The computational domain was then set for 270m x 270m x 500m to locate the studied model in the middle. Average wind velocity obtained at the reference height (11 m above ground) was 1.44 m/s. Wind direction for the simulation was always set to come from the front and be

perpendicular to the wind turbines in all cases. Performances of 1 kW and 10 kW wind turbines for the study were based on manufacturer's data [27].

The studies compared both vertical axis wind turbine (VAWT) and horizontal axis wind turbine (HAWT). In order to generate power, the average wind velocity around the wind turbine must be at least 3 m/s which was a criterion for considering appropriate positions of the wind turbines on tall buildings. The distance between wind turbines must be at least 3 times of the wind turbine swept area. Therefore, within the same size of space allowed for installation, the number of wind turbines to be placed may be different depending on their types and sizes. Whether the wind turbines were mounted on the roof or alongside the building, they must be within 6-meter distance from the building edge (Fig 2).

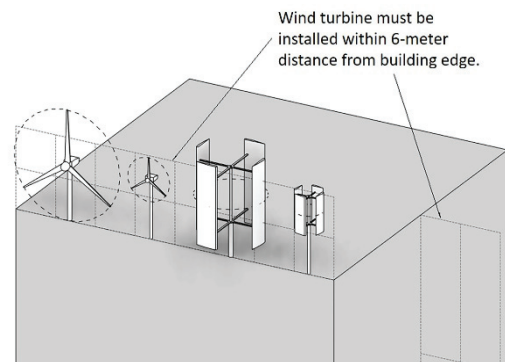


Figure 2: Types of wind turbines and their installation area within 6 m distance from the building edge

The parameters set for the experiment can be summarised in Table 1.

Table 1: Case study details and experimental parameters

Topic		Detail
Building	Type	Office
	Height	130 m
	No. of floors	47
	span	6-12 m
	Floor plan	24m x 24m
Site location	Bangna District	Bangkok
	Land Use	Commercial, medium density
	FAR	7:1
	OSR	4.5%
Wind	Average velocity	1.44 m/s
	directions	(at 11m above ground) SSW, S, NE
CFD	Roughness Category Index	V
	Surrounding	high-rise buildings (10 or more storeys)
	Inverse power of exponent (n)	2.8571
	Upper wind altitude (Z_G)	650 m
	Computational domain	270m x 270m x 500m

3. WIND AVAILABILITY AND WIND TURBINE

The weather data from Bangna district in 2018 showed that there were 3 prevailing wind directions: south-southwest (SSW), southwest (S), and northeast (NE). There were 196 days or 54% of the entire year that wind velocities were in range of 3 to 6 m/s which had potential to drive wind turbines and generate electricity. It is suggested that average wind speed for the low-speed wind turbines should range from 3.00 to 4.00 m/s. By considering the moderate wind situation in the city, the wind turbine models with cut-in wind speed ranging from 1.00 to 3.00 m/s were selected. Too high wind speed can become cut-out speed, thus stopping power generation. Details of the 10kW and 1kW of HAWT and VAWT were shown in Table 2.

Table 2: Details of selected wind turbines [28]

Type	HAWT		VAWT	
	10kW	1kW	10kW	1kW
Diameter (D)	8	3.2	5	2
Radius/Height (r)/(h)	4	1.6	6	2.8
Area Blade (A)	25.12	10.048	30	5.6
Hub Height (m)	12,15,18,24,30	3,6,9,12,15	5,9,12,18	2,3,6,9,12
Starting Wind Speed (m/s)	2.5	2.5	2.5	2
Cut-in Speed (m/s)	2.5	3	2.5	2
Cut-out Speed (m/s)	none	25	none	none
Rated Wind speed (m/s)	10	12	11	10
Survival Wind Speed (m/s)	50	45	55	50
Wind Power (w)	10-13kW	1kW	10kW	1500
Weight (kg)	520	60	680	78
Noise (dB)	< 45	< 46	<38	0

Wind turbine selection was based on its rotor diameter, rotor width, rotor height, and load on building structure. Only 1kW wind turbines were allowed to be installed on Type A and Type B buildings.

When compared with HAWTs, VAWTs produce less electricity due to their size. Nonetheless, more of them can be installed on site with less spacing. With maximum wind speed at 9.00-10.00 m/s, they can generate electricity up to 1000 Watts, the same as those from HAWTs.

4. RESULTS

The study aimed to find appropriate positions to mount wind turbines on tall buildings by comparing the energy output of each position while considering

the investment of the system. The energy performance results of wind turbine installation options were studied as well as their payback period.

Since the product manufacturer only provided performance data in forms of annual energy output (kWh/year) based on different wind velocities in range of 3-10 m/s and 3-12 m/s for HAWT and VAWT, respectively, it is essential to find energy output from cut-in wind speed which is below 3 m/s up to 4 m/s. Therefore, based on information provided from the product manufacturer [28], a relationship between wind speed and energy output of each wind turbine model was established as shown in Equations (1)-(4). All equations were then be used to calculate energy output from the wind velocity obtained by CFD simulation.

For 10kW HAWT

$$y = 818.85x^2 - 1363x \quad (1)$$

For 1kW HAWT

$$y = 94.935x^2 - 165.85x \quad (2)$$

For 10kW VAWT

$$y = 117.68x^3 - 282.02x^2 + 123.76x \quad (3)$$

For 1kW VAWT

$$y = 11.746x^3 + 13.457x^2 - 53.029x \quad (4)$$

Where x - wind speed (m/s)

y - energy output (kWh/year)

Results show that the areas with wind velocities above 3 m/s were higher than 70 m and around 6 m away from the building edges. Roof-installation type A1 (flat roof) and A2 (tilted roof) with vertical axis wind turbines gave their highest amount of electricity at 2,920.85 kWh/Year (Fig. 3). Wall-installation type B4 (octagon as the aerodynamic plan shape) with horizontal wind turbines generated 6,283.44 kWh/Year as the highest (Fig. 4). Inside-opening-installation type C3 with horizontal wind turbines gave the highest amount of electricity at 3,869.62 kWh/Year (Fig. 5) and between-towers-installation type D3 with horizontal wind turbines gave the highest at 11,968.34 kWh/Year which was the highest amount of electricity generated of all options (Fig. 6).

Energy results of all types of wind turbines and positions were summarised in graphical format as shown in Fig 7. It was evident that C1 did not give sufficient wind velocity for electricity generation. Building Type C and Type D were flexible for both horizontal axis and vertical axis wind turbines selected for the study.

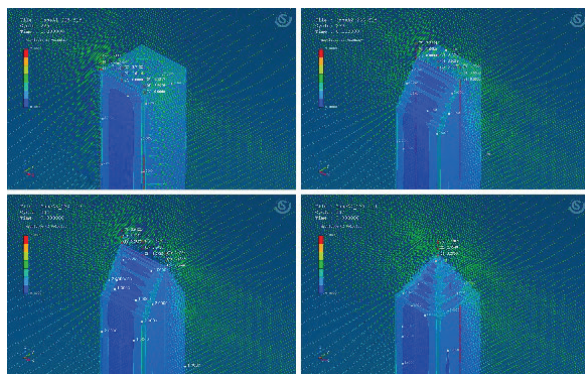


Figure 3: Roof installation (Type A1-A4)

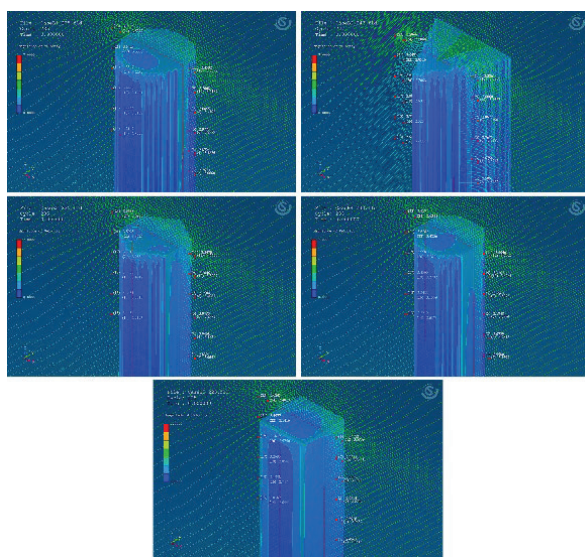


Figure 4: Wall installation (Type B1-B5)

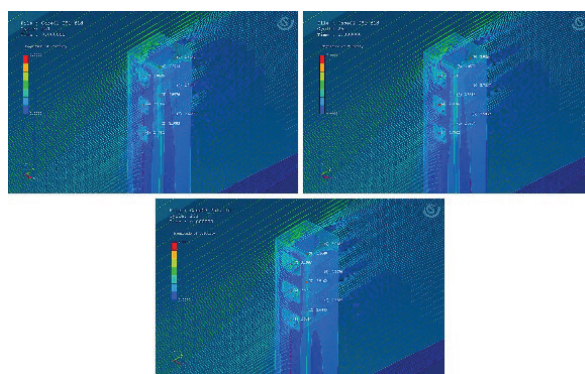


Figure 5: Inside-openings installation (Type C1-C3)

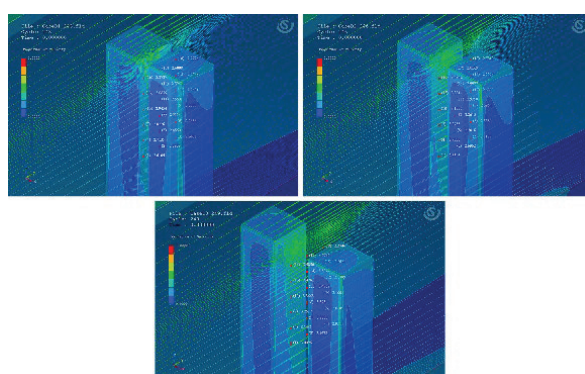


Figure 6: Between-towers installation (Type D1-D3)

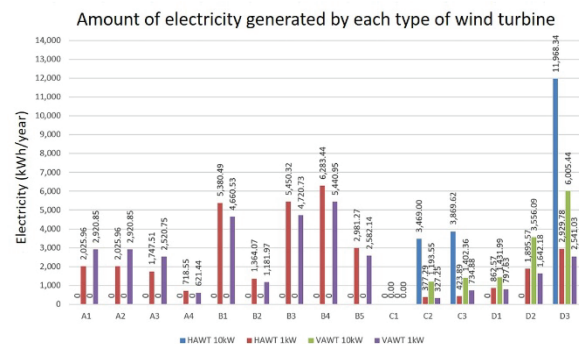


Figure 7: Wind turbine performance

The amount of energy output from each option can be explained by many factors namely area size, building form, and opening.

Area size for wind turbine installation controls number and type of wind turbines possibly installed on the building. Within a limited space and at the same amount of generated electricity, VAWT should be installed rather than HAWT because VAWT is smaller and there could be more of them mounted in the specified area. The more installed wind turbines, the more electricity generated.

Aerodynamic building forms that correspond to the prevailing wind can induce wind velocities higher than the bluff forms that are against the wind direction. Providing openings such as in cases of Type C and Type D will create wind channel and steady wind which is important for electricity generation.

Taking the best option of each type, the alternative energy generated by wind turbine could be utilised in different building systems as specified in Table 3. However, since the wind energy in the urban area of Bangna district could rely on natural wind for only 54% of one year's time, the amount of wind energy contributed to the whole energy demand in percent (in brackets) was still very small.

Table 3: Amount of electricity for building systems

Type	AC	Lighting	Lift	Whole building
	kWh/yr /sqm	kWh/yr/ sqm	kWh/yr/ person-height	kWh/yr /sqm
A1 and A2	21.45	97.85	1,281.07	13.37
	(0.08%)	(0.36%)	(4.73%)	(0.05%)
B4	46.15	210.50	2,755.89	28.76
	(0.17%)	(0.78%)	(10.18%)	(0.11%)
C3	28.42	129.64	1,697.20	17.71
	(0.10%)	(0.48%)	(6.27%)	(0.07%)
D3	87.91	400.95	5,249.27	54.78
	(0.32%)	(1.48%)	(19.39%)	(0.20%)

The area of building type A, B, and C was 27,072 sqm while building type D had two towers, thus occupying 54,144 sqm which doubled the size of the

others. In order to make a fair comparison, all cases were compared in terms of electricity per year per area (kWh/yr/sqm).

Based on the price in 2019, the investment cost to install each type of wind turbine was demonstrated in Fig 8. The economic analysis was conducted by taking initial cost, capacity factor of the wind turbine, 50-year maintenance cost as well as interest rate into account in order to calculate net present value and benefit cost ratio. Payback period of each installation option could then be calculated and shown in Table 4. It should also be noted that the investment and payback periods were varied depending on numbers of wind turbines possibly installed for each option. Even though D4 gave the highest amount of electricity, it had the biggest area to consume energy and the cost for installing 3 of 10-Kw HAWTs was high. Therefore, its payback period was the longest.

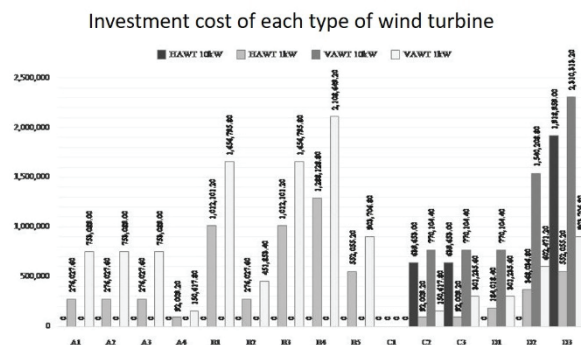


Figure 8: Investment cost

Table 4: Payback periods of various wind turbine positions

Type	Wind turbine type	No. of Wind turbines	Payback period (year)
A1 and A2	1kW-VAWT	5	4.72
B4	1kW-HAWT	12	4.95
C3	10kW-HAWT	1	5.33
D3	10kW-HAWT	3	5.41

In conclusion, appropriate positions to install wind turbines on tall building were recommended in Fig 9.

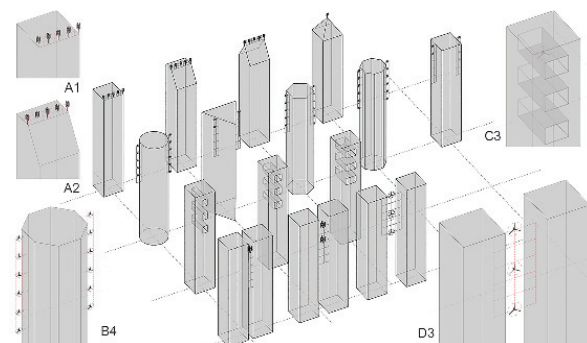


Figure 9: Summary of recommended types of wind turbine installation on building

With wind speed of over 3 m/s, wind turbines at the height above 70 m and within 6 m distance from the building edge could function well for power generation. Amount of wind energy ranking from the highest to the lowest were D3, B4, C3, and A1 and A2, respectively. The payback period ranking from the shortest to the longest were A1 and A2, B4, C3, and D3, respectively. Rooftop shape was insignificant as there were only slight differences among results from A1-A4. Size of the rooftop area was more important. Wall-mounted wind turbines could be a good option as type B provided more space for installing small wind turbines, thus more electricity, while the overall cost was not too high. Providing wind channel through building as type C required at least a 9m x 9m opening at 100 m above ground. The wind condition was steady which was good for power generation. The between-towers-installation, type D, gave the maximum energy output as it provided an opportunity to install more than one big wind turbines between two buildings. The suggested distance between the two towers was 24 m in order to create steady airflow in the middle of the space.

4. CONCLUSION

It is possible to use wind energy in a moderate-wind urban environment by installing wind turbines on tall buildings. Positions and types of wind turbines to be installed on tall buildings should be considered as an integral part during building design process. The mounting position is relevant to wind turbine type and size, resulting in energy output. Amount of power generated depends on area size for wind turbine installation, building form, and opening or wind channel that keeps the wind speed steady. Vertical axis wind turbines produce less energy but require less area for installation and are suitable for roof installation. Aerodynamic building forms provide unlimited space for small wall-mounted wind turbines while installing big wind turbines inside openings or between two towers potentially produce much higher amount of electricity.

REFERENCES

- Balduzzi, F., Bianchini, A., Carnevale, E.A., Ferrari, L. and S. Magnani, (2012). Feasibility analysis of a darrieus vertical-axis wind turbine installation in the rooftop of a building. *Applied Energy*, 97: p. 921–929.
- Zanforlin, S. and S. Letizia, (2015). Improving the performance of wind turbines in urban environment by integrating the action of a diffuser with the aerodynamics of the rooftops. *Energy Procedia*, 82: p. 774–781.
- Tabrizi, A.B., Whale, J., Lyons, T. and T. Urme, (2014). Performance and safety of rooftop wind turbines: Use of CFD to gain insight into inflow conditions. *Renewable Energy*, 67: P. 242–251.
- Mithraratne N., (2009). Roof-top wind turbines for microgeneration in urban houses in New Zealand. *Energy Build*, 41(10): p. 1013–1018.

5. Mertens, S., Kuik, G.V. and G.V. Bussel, (2003). Performance of an H-Darrieus in the skewed flow on a roof. *Journal of Solar Energy Engineering*, 125: p. 433–440.
6. Lee, K.Y., Tsao, S.H., Tzeng, C.W. and H.J. Lin, (2018). Influence of the vertical wind and wind direction on the power output of a small vertical-axis wind turbine installed on the rooftop of a building. *Applied Energy*, 209: p. 383–391.
7. Ledo, L., Kosasih, P.B. and P. Cooper, (2011). Roof mounting site analysis for micro-wind turbines. *Renewable Energy*, 36(5): p. 1379–1391.
8. Sunderland, K., Mills, G. and M. Conlon, (2013). Estimating the wind resource in an urban area: a case study of micro-wind generation potential in Dublin, Ireland. *Journal of Wind Engineering and Industrial Aerodynamics*, 118: p. 44–53.
9. Micallef, D. and G. van Bussel, (2018). A review of urban wind energy research: aerodynamics and other challenges. *Energies*, 11(9): p. 2204.
10. Anup, K.C., Whale, J. and T. Urmee, (2019). Urban wind conditions and small wind turbines in the built environment: a review. *Renewable Energy*, 131: p. 268–283.
11. Toja-Silva, F., Kono, T., Peralta, C., Lopez-Garcia, O. and J. Chen, (2018). A review of computational fluid dynamics (CFD) simulations of the wind flow around buildings for urban wind energy exploitation. *Journal of Wind Engineering and Industrial Aerodynamics*, 180: p. 66–87.
12. Walker, S.L., (2011). Building mounted wind turbines and their suitability for the urban scale—A review of methods of estimating urban wind resource. *Energy and Buildings*, 43(8): p. 1852–1862.
13. Stathopoulos, T., Alrawashdeh, H., Al-Quraan, A., Blocken, B., Dilimulati, A., Paraschivoiu, M. and P. Pilay, Urban wind energy: some views on potential and challenges. *Journal of Wind Engineering and Industrial Aerodynamics*, 179: p. 146–157.
14. Fields, J., Oteri F, Preus, R. and Baring-Gould, I. (2016), Deployment of wind turbines in the built environment: Risks, lessons, and recommended practices, National Renewable Energy Laboratory (NREL).
15. Department of Alternative Energy Development and Efficiency, (2015). Alternative Energy Development Plan: AEDP2015. Ministry of Energy, Thailand.
16. Bošnjaković, M., (2013). Wind Power Building Integration. *Journal of Mechanics Engineering and Automation*, 3: p. 221–226.
17. Mertens, S., (2006). Wind Energy in the Built Environment: Concentrator Effects of Buildings. Multi-Science, UK.
18. Abdolhossein-Pour, F., Alaghmandan, M. and R.J. Krawczyk, (2013). Enabling Form to be Adjusted Based on Performance. In *The 47th International Conference of the Architectural Science Association (ANZAScA)*, Australia, November 13–16.
19. EnConLab King Monkut's University of Technology Thonburi, (2004). Consideration Criteria for Issuing Licenses for Wind Power Generation in Bangkok.
20. Tominaga, Y., Mochida, A., Yoshie, R., Kataoka, H., Nozu, T., Yoshikawa, M. and T. Shirasawa, (2008). AIJ Guidelines for Practical Applications of CFD to Pedestrian Wind Environment around Buildings. *Journal of Wind Engineering and Industrial Aerodynamics*, 96: p. 1749–1761.
21. Ding, C. and K. P. Lam, (2019). Data-driven model for cross ventilation potential in high-density cities based on coupled CFD simulation and machine learning. *Building and Environment*, 165: 106394.
22. He, Y., Tablada, A. and N. H. Wong, (2018). Effects of non-uniform and orthogonal breezeway networks on pedestrian ventilation in Singapore's high-density urban environments. *Urban Climate*, 24: p. 460–484.
23. He, Y., Tablada, A., and N. H. Wong, (2019). A parametric study of angular road patterns on pedestrian ventilation in high-density urban areas. *Building and Environment*, 151: p. 251–267.
24. Yang, J., Shi, B., Shi, Y., Marvin, S., Zheng, Y., and G. Xia, (2020). Air pollution dispersal in high density urban areas: Research on the triadic relation of wind, air pollution, and urban form. *Sustainable Cities and Society*, 54: 101941.
25. Yao, W.L., Fan, Q.Y., Zhang, Y.W. and Y.B. Xue, (2012). The Research of CFD applications for thermal fluid simulation of Building Environment. In *ASim2012 Conference*. Shanghai, China, November 25–27.
26. Waewsak, J., (2015). Wind Energy Technology. Chulalongkorn University Printing House, Bangkok.
27. Aeolos Wind Energy Ltd. (Producer). (2009). Wind Turbine Brochure.
28. Lotus Energy Technology Co., Ltd., [Online], Available: <http://www.windturbinestar.com/> [10 May 2020].

Investigating the Impact of Urban Fabric on Urban Albedo: Case Study of London

MUHAMMED YENINARCILAR, MARIALENA NIKOLOPOULOU, ALKIS KOTOPOULEAS,
RICHARD WATKINS, GIRIDHARAN RENGANATHAN

Centre for Architecture and Sustainable Environment (CASE), Kent School of Architecture and Planning,
University of Kent, Canterbury CT2 7NZ, United Kingdom

ABSTRACT: The paper presents the preliminary work in developing an Urban Albedo Calculator, an empirical model to predict changes in urban albedo in relation to changes in the urban fabric, materials, solar geometry, etc. It investigates experimentally, through a 1:10 scale model a case study in central London, and computationally, through RADIANCE, the impact of urban geometry and materials' reflectance. Following the successful calibration of the model, the results highlighted the substantial impact of urban materials and their placement on urban albedo, demonstrating the dominant weighting of horizontal ground surfaces in the case of low rise environments. The effect of geometry was investigated through different scenarios, at ground and roof levels, as well as through changes in the H/W ratio. The results demonstrated that increasing the H/W ratio has the most significant impact on urban albedo, with the albedo changes varying under different sky conditions due to the orientation of the blocks.

KEYWORDS: Urban albedo, microclimate, materials, geometry, RADIANCE

1. INTRODUCTION

Urban albedo - defined as the ratio of incoming to outgoing short wave radiation - has major implications for the urban microclimate [1]. It is one of the most important contributors to changes in outdoor temperature, intensifying the urban heat island phenomenon [2, 3]. This is the reason that the Greater London Authority has identified urban albedo as one of the most significant parameters for mitigating the Urban Heat Island in London [4].

In an urban environment, the incoming solar radiation undergoes multiple reflections, with part of it being absorbed by the incident surface, and another portion reflected back into the environment (Fig. 1). It is assumed that the radiation is completely absorbed in an urban canyon after 50 reflections [5]. Multiple factors affect this photometric process [6-14];

- Building block geometry,
- The reflectance of the roof,
- Canyon geometry,
- The reflectance of the ground,
- The reflectance of the walls,
- Solar altitude,
- Solar azimuth,
- Urban vegetation,
- Soil moisture.

Considering the wide range of parameters, it is not advisable to predict the urban albedo from literature, especially in cities where surface changes are substantial. However, professionals in the urban environment need to know the urban albedo of the

final urban setting in advance, in order to develop appropriate alternative development scenarios, as well as to incorporate it in energy and thermal simulations of buildings.



Figure 1: The photometric process of incoming radiation in an urban environment.

The project addresses this gap by developing an empirical model to predict changes in urban albedo in relation to changes in the urban fabric, materials, solar geometry, etc. The Urban Albedo Calculator (UAC) will be developed for application in high latitude locations, using London as a representative urban environment in the UK. This is done through employing different methodologies: laboratory, field measurements and computational methods.

The objective of this paper is to investigate and present the preliminary experimental and computational results on the impact of urban geometry, and reflectance of different materials in a case study located in central London. Initially, it

presents the calibration process, the comparison of radiation measurements from the 1:10 scale model built at the University of Kent campus and simulation results from the advanced lighting simulation tool, RADIANCE. Following the successful calibration with the experimental model, the paper proceeds to analyse and present the impact of changes in the reflectance of materials and geometry on the urban albedo as examined with lighting simulations in RADIANCE.

2. METHODOLOGY

2.1 Experimental model

Preliminary surveys were conducted to identify critical locations within the Greater London area. Stanley Terrace, a residential area in the London Borough of Islington, comprising terraced houses, was selected as a representative residential area. The case study was extensively surveyed and scanned using a 3D scanning camera to obtain detailed data on block geometry, canyon geometry and urban materials, which fed into the development of the 1:10 scaled physical model (Fig. 2).

The experimental model was built at the University of Kent campus for logistical reasons as the latitudinal difference between London (51.5074°) and Canterbury (51.2802°) is insignificant. The model was built within a 5m radius representing a 50m radius of an urban area which is considered a suitable area for the investigation of urban climate change in a London setting. Brick, the most common building material in London, was used as a module for the construction of building blocks structured with cut-to-size plywood and roofed with clay roof tiles. Windows and doors were framed with plywood while the development of windows was completed using 4mm clear float glass (Fig.2).



Figure 2: The 1:10 scaled physical model at the University of Kent campus in Canterbury.

2.2 Data collection from the experimental model

To capture the incoming solar irradiance and reflected irradiance, 8 pyranometers were located at critical points within the experimental model (Fig. 3). Five pyranometers facing up measured the incoming radiation and three pyranometers facing down measured the reflected irradiance.

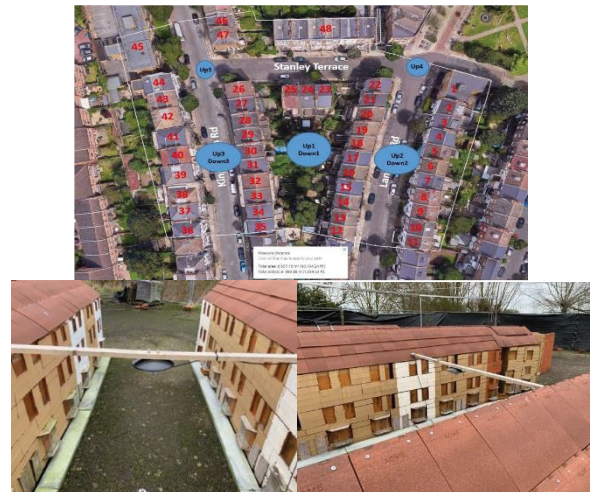


Figure 3: The location of the pyranometers (above) and the pyranometers on the experimental model (below).

Two back-to-back pyranometers (*Up1* and *Down1*) suspended at the centre of the model, at a height of 1m above the tallest building, measured total incoming and total reflected irradiance. A pair of pyranometers (*Up2* - *Down2* and *Up3* - *Down3*) was installed in the middle of two canyons (i.e. Landseer Road and Kingsdown Road), measuring incoming radiation at street level and outgoing radiation at eaves level. In addition, two more pyranometers (*Up4* and *Up5*) were located on the two junctions measuring incoming solar radiation at street level (Table 1, Fig. 3). To prevent noise radiation from reaching the downward-looking pyranometers several black shades of different shape and size were tested during the fine-tuning of the measurement protocol, while the experimental site was surrounded by black tarpaulins to block extraneous radiation from the surrounding areas.

Table 1: The height of the different pyranometers from the ground.

Pyranometers	Height (m)
Up1	2.05
Up2	0.09
Up3	0.09
Up4	0.09
Up5	0.09
Down1	1.84
Down2	0.96
Down3	1.00

2.3 3D modelling

To model the radiation exchanges in RADIANCE, it was essential to prepare a 3D model of the geometry in 3D drawing software. This was accomplished through a point cloud data based 3D scan carried out to determine the height of the blocks, block geometry,

street canyon and surface materials. The scanning system used Autodesk Recap software [15]. Moreover, a 3D scanning survey was also conducted at the 1:10 scale model and the point cloud data were used to prepare a 3D geometry of the physical model in Sketch-Up (Fig. 4) [16]. The 3D geometry was further developed in RADIANCE for advanced lighting simulations to enable calibration of the model. The calibrated model will be used to generate data for the Urban Albedo Calculator. The experimental site (1:10) 3D model was used to assess the impact of scaling on radiation.



Figure 4: The 3D model of the 1:10 scale model built at the University of Kent campus.

2.4 Lighting simulations in RADIANCE

RADIANCE is a collection of programmes for advanced lighting analysis and visualization. The software was first developed as a research tool to investigate advanced rendering techniques for lighting design at the Lawrence Berkeley National Laboratories (LBNL) [17]. The capability of the software has been enhanced over the years, and nowadays is capable of running highly sophisticated lighting simulations. Unlike other programs that use the radiosity algorithm, RADIANCE uses ray-tracing techniques to simulate parameters related to lighting visualization from object modelling to rendering, point calculation, image processing and display.

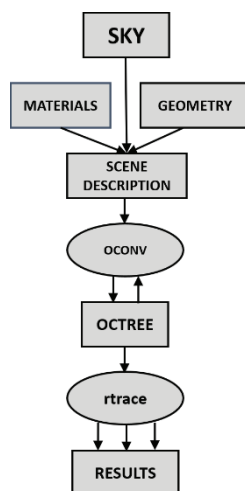


Figure 5: The workflow for lighting simulation in RADIANCE.

The workflow of the computational lighting simulation in RADIANCE consisted of several steps (Fig. 5). Firstly, the geometry of the model to be simulated was created in Sketch-Up and thereafter imported into RADIANCE.

The second step was to create the desired sky conditions. RADIANCE enables different sky types such as a sunny sky with or without sun, cloudy sky, intermediate sky with or without sun, and a uniform cloudy sky. The input parameters required in the RADIANCE command are the global horizontal irradiance value (measured by the Up1 pyranometer in the physical model), site latitude and longitude, simulation month, day and time.

The third step was to specify the material properties for all surfaces of the scene geometry (e.g. reflectance of materials). RADIANCE’s material library provides more than 30 material types. Materials’ reflectance can be obtained from the library. However, since the RADIANCE model was to be calibrated against the results obtained from the scale model, the reflectance values from the physical model were used instead. These were obtained through onsite spot measurements by means of an albedometer (Table 2).

Table 2: The reflectance of the materials used in the experimental model and imported into RADIANCE.

Materials	Reflectance
Asphalt	0.21
Red Brick	0.31
Roof Tiles	0.21
Glass (on tarmac)	0.21
Pavement	0.27

The next step included the definition of viewpoints and view directions in RADIANCE. Viewpoints were defined to coincide with the location of the pyranometers in the experimental model. A rendering file (octree file) was then produced through the “oconv” command. Finally, numerical results were obtained after running the “rtrace” command.

3. RESULTS AND DISCUSSION

3.1 Calibration

The successful calibration of the model was essential to ensure that lighting simulations of the 3D model in RADIANCE produce results similar to the measurements from the physical model.

The calibration process involved simulations of the 3D model under three different sky conditions: (i) sunny sky, (ii) partly cloudy sky with sun and (iii) cloudy sky without sun. Tables 3-5 present the onsite measurements for these three sky types. The study included a different number of inter-reflections, using

a single, three and five inter-reflections. The results discussed in this paper focus on data collected from pyranometers Up1, Up2, Up4, Up5 and Down2.

Table 3: The calibration results from RADIANCE under sunny sky conditions in June, for different inter-reflections.

Clear sunny sky - 01/06/2019, 13:00							
	On-site (W/m ²)	RADIANCE-Number of Inter-reflections (W/m ²)					
		1	% diff	3	% diff	5	% diff
Up1	904.2	901.7	-0.3	901.8	-0.3	901.6	-0.3
Up2	904.6	875.2	-3.3	882.9	-2.4	883.0	-2.4
Up4	898.8	876.0	-2.5	880.8	-2.0	880.7	-2.0
Up5	895	879.8	-1.7	885.8	-1.0	885.5	-1.1
Down2	95.4	64.8	-	82.1	-	82.4	-
			32.1		14.0		13.6

Table 4: The calibration results from RADIANCE under partly cloudy sky conditions in June, for different inter-reflections.

Partly cloudy sky - 27/06/2019, 13:00							
	On-site (W/m ²)	RADIANCE-Number of Interreflection (W/m ²)					
		1	% diff	3	% diff	5	% diff
Up1	494.7	489.7	-1.0	489.8	-	489.5	-
Up2	401.6	412.1	2.6	420.5	4.7	420.6	4.7
Up4	439.8	429.2	-2.4	435.5	-	436.3	-
Up5	418.4	428.8	2.5	438.3	4.8	437.7	4.6
Down2	46.3	8.3	-	43.2	-	43.5	-
			82.1		6.7		5.9

Table 5: The calibration results from RADIANCE under cloudy sky conditions in June, for different inter-reflections.

Cloudy sky - 25/06/2019, 13:00							
	On-site (W/m ²)	RADIANCE-Number of Inter-reflection (W/m ²)					
		1	% diff	3	% diff	5	% diff
Up1	227.7	224.9	-1.2	224.9	-	224.8	-
Up2	168.3	172.4	2.5	178.2	5.9	178.6	6.1
Up4	189.2	190.7	0.8	194.6	2.8	194.3	2.7
Up5	178.4	183.9	3.1	189.3	6.1	189.4	6.2
Down2	19.2	0.3	-	19.8	3.0	19.7	2.8
			98.2				

The results (Tables 3-5) show that the difference between measured and simulation values was predominantly within the $\pm 10\%$ margin, which is considered adequate for calibration purposes. More specifically, the difference was around 2% for sunny sky conditions and slightly higher for partly cloudy and cloudy sky conditions. The latter can be attributed to the significantly smaller radiation intensities under partly cloudy and cloudy conditions, where small differences reflect noticeable percentage differences (e.g. a 4 W/m² difference, from 178.4 to 189.3 W/m², indicates a 6% difference). The analysis also highlighted the importance of inter-reflections in modelling; the differences between measured and simulated figures were seen to reduce with increasing

the numbers of inter-reflections, and this was particularly so in the case of Down2 pyranometer.

The results suggested that the RADIANCE model with the material properties, geometry, and sky definition had been calibrated successfully against the physical model. Accordingly, this model was employed for further analysis to evaluate changes in materials and geometry along with their respective impact on albedo.

3.2 The impact of material reflectance on albedo

Two different simulations were conducted in RADIANCE to investigate the impact of material reflectance on urban albedo. Firstly, the reflectance of the brick wall was changed from 0.31 to 0.6, to indicate a highly reflective material. Then, the reflectance values of the vertical and horizontal surfaces were swapped, i.e. the reflectance of the horizontal surface (asphalt) was increased to 0.31, while the reflectance of the vertical surfaces (walls) was decreased to 0.11.

Table 6: The impact of material reflectance on albedo, α .

Sky Types	α , base case	Highly reflective walls		Replacing asphalt with brick	
		α	% diff	α	% diff
sunny	0.093	0.113	20.78	0.193	106.81
partly cloudy	0.104	0.131	26.98	0.205	97.57
cloudy	0.111	0.142	28.44	0.210	89.95

Focusing on Landseer Road, Table 6 compares base case albedo (i.e. the ratio of incoming radiation measured by Up2 pyranometer to outgoing radiation measured by Down2 pyranometer) against the albedo values for the different scenarios. The results demonstrate that using highly reflective material for the walls results in an approximately 20% increase of albedo in sunny sky conditions. The impact was found to be highest for partly and cloudy sky conditions, where albedo increased by almost 30%.

When the reflectance of asphalt and walls are interchanged (i.e. $r_{\text{walls}} = 0.11$ and $r_{\text{asphalt}} = 0.31$), the results showed that the amount of radiation trapped within the street gorge decreased significantly. Under sunny sky conditions, for instance, Landseer Road's albedo doubled with the increase being over 100% while the respective increase of albedo under partly and cloudy sky was also high, at 98% and 90% respectively.

The findings highlight the importance of material reflectance and material distribution in an urban setting in changing urban albedo. The capacity of an urban environment to reflect solar radiation can be

increased with a rise of material reflectance. More importantly, its placement, i.e. horizontally or vertically has a bigger impact, with the reflectance of horizontal surfaces appearing to have the largest influence on urban albedo.

3.3 The impact of geometrical changes on albedo

The simulations aimed at assessing the impact of geometrical changes on albedo were divided into two strands. Firstly, the impact of having pavement and flat roof was investigated (Fig. 6), followed by the impact of adding three more storeys on the buildings in Landseer Road (Fig. 7).

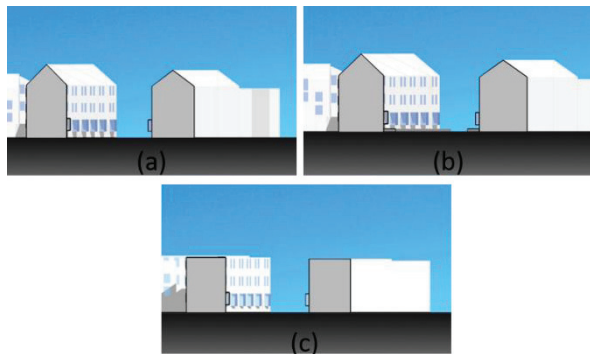


Figure 6: The geometrical changes; a) the base case, b) pavement added, c) pitched roof replaced with a flat roof.

Table 7: The impact of geometrical changes on albedo, α .

Geometrical changes on Landseer Road					
Sky Types	α , base case	with pavement		with flat roof	
		α	% diff	α	% diff
sunny	0.093	0.100	6.70	0.092	-1.44
partly cloudy	0.104	0.112	8.62	0.106	2.67
cloudy	0.111	0.119	7.99	0.113	2.48

The introduction of concrete paving (with a reflectance of 0.27) on the simulated street saw the albedo increasing by about 7-8% under all-sky conditions. Conversely, the replacement of the pitched roof in the original 3D geometry with a flat roof, had a much smaller impact on albedo, which varied under the different sky conditions. The albedo decreased by 1.44% under a sunny sky, whereas it increased by about 2-3% under a partly cloudy and cloudy sky, suggesting that geometrical changes at ground level have a much bigger effect than changes at roof level.

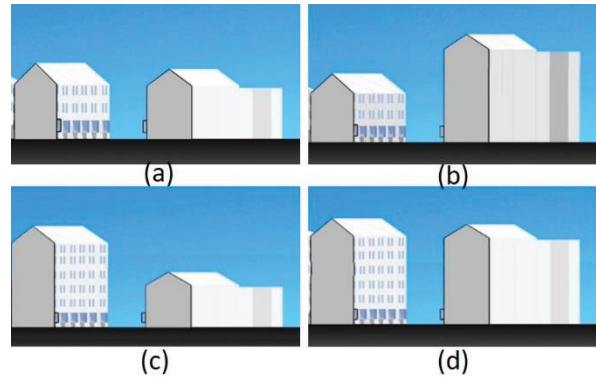


Figure 7: The geometrical changes of the buildings on Landseer Road; a) base case, b) extra 3-storeys to the buildings on the right side, c) extra 3-storeys to those on the left side, and d) extra 3-storeys on all buildings.

Table 8: The impact of geometrical changes through increased height on albedo, α .

Sky Types	α , base case	Increased height on Landseer Road					
		right side		left side		all	
		α	% diff	α	% diff	α	% diff
sunny	0.093	0.073	-21.71	0.093	0.54	0.074	-20.27
partly cloudy	0.104	0.100	-3.64	0.105	1.16	0.078	-24.53
cloudy	0.111	0.111	0.37	0.113	1.90	0.080	-28.31

With respect to the impact of increased building height through the addition of three more storeys, separate simulations were run with the height increased (a) on either side of the street gorge, and (b) on both sides, thus changing the H/W ratio from 1:2 to 1:1.

The addition of three storeys on the buildings on the right side of the street gorge was seen to decrease its albedo by about 22% under the sunny sky conditions and by only 4% under a partly cloudy sky (Table 8). No significant albedo change was found for cloudy sky conditions. On the other hand, the addition of three extra storeys on the buildings on the left side did not have a significant impact on albedo under all sky conditions, with the observed changes being 1-2%. Moreover, the addition of the extra storeys on both sides of the street gorge resulted in a decreased albedo (-21%) under sunny sky conditions and showed a higher decrease in albedo under partly cloudy and cloudy sky conditions, by 24% and 28% respectively (Table 8).

The analysis suggests that changing the urban geometry changes the urban albedo and this is very much sensitive to orientation. Further, reduction in urban albedo is high in deep street canyons. These findings are in line with existing premises and this gives a very high level of confidence to generate the necessary data base for the urban albedo calculator taking into account urban geometrical variations in London.

4. CONCLUSION

The main objective of this paper was to investigate experimentally and computationally the impact of urban geometry and materials' reflectances using a case study located in central London. A 3D experimental 1:10 scale model was built and clad using actual building materials. The study used radiation measurements from the physical model to calibrate the digital model and examine computationally some of the parameters affecting urban albedo by means of the highly sophisticated lighting simulation tool, RADIANCE.

Following the successful calibration of the model, the results highlighted the substantial impact of urban materials and their placement on urban albedo and demonstrated the dominant effect of horizontal ground surfaces. The effect of geometry was investigated through different scenarios, at ground and roof levels, as well as through changes in the H/W ratio. The results demonstrated that increasing the H/W ratio has the most significant impact on urban albedo, with the albedo changes varying under different sky conditions due to the orientation of the blocks.

The study is a part of a large-scale ongoing project. The impact of different materials is currently being investigated along with different types of urban geometries on the urban albedo, all of which will inform the debate. Ultimately, this knowledge can feed into the development of the urban albedo calculator, an empirical model to predict changes in urban albedo in the urban fabric, which can be used by a range of stakeholders in the early stage of design processes.

ACKNOWLEDGEMENTS

This project has been funded by the UK Engineering and Physical Sciences Research Council (EPSRC) contract no. EP/P025145/1. Moreover, the PhD researcher is funded by the Republic of Turkey, Ministry of National Education.

The bricks used in the experimental model have been donated by IBSTOCK Bricks Plc, and the roof tiles by Marley Ltd Roof specialists.

REFERENCES

- [1] Oke T.R. (1987). *Boundary Layer Climates*, Methuen, USA.
- [2] Santamouris, M., Synnefa, A. and Karlessi, T. (2011). Using advanced cool materials in the urban built environment to mitigate heat island and improve thermal comfort conditions. *Solar Energy* 85, 3085-3102.
- [3] H. Akbari, H.D. Matthews. Global cooling updates: Reflective roofs and pavements. *Energy and Buildings* 55 (2012) 2-6.
- [4] GLA, Greater London Authority (2006). *London Urban Heat Island (LUHI): A Summary for Decision Makers*. UK.
- [5] Aida M. and Gotoh K. (1982). Urban albedo as a function of the urban structure- a two-dimensional numerical simulation. *Boundary-Layer Meteorology*, Vol. 23.
- [6] Steemers, K., Baker, N., Crowther, D., Dubiel, J. and Nikolopoulou, M. (1998). Radiation absorption and urban texture. *Building Research and Information*, Vol. 26(2), pp. 103-112.
- [7] Aida M. (1982). Urban albedo as a function of the urban structure-a model experiment *Boundary-Layer Meteorology*, Vol. 23.
- [8] Swaid H. and Hoffman M.E. (1990). Climatic impacts of urban design features for high and mid latitude cities, *Energy and Buildings*, Vol. 14.
- [9] Taha H. (1997). Urban climate and heat islands: albedo, evapotranspiration, and anthropogenic heat, *Energy and Buildings*, Vol. 25.
- [10] Kondo A., Ueno M., Kaga A. and Yamaguchi K. (2001). The influence of urban canopy configuration on urban albedo, *Boundary-Layer Meteorology*, Vol. 100.
- [11] Sailor D.J. and Fan H. (2002). Modelling the diurnal variability of effective albedo for cities, *Atmospheric Environment*, Vol. 36.
- [12] Yang X. and Li Y. (2015). The impact of building density and building height heterogeneity on average urban albedo and street temperature, *Building and Environment*, Vol. 90.
- [13] Chimklai P., Hagishima A. and Tanimoto J. (2004). A computer system to support albedo calculation in urban areas, *Building and Environment*, Vol. 23.
- [14] Taha H. (1997). Urban climate and heat islands: albedo, evapotranspiration, and anthropogenic heat, *Energy and Buildings*, Vol. 25.
- [15] Autodesk ReCap software. Autodesk Inc.
- [16] SketchUp software, (2000). Trimble Inc.
- [17] Larson, G., and Shakespeare, R., (2011). *Rendering with RADIANCE The art and Science of Lighting Visualization*, pp. 3-7.

Improving Hyperlocal Air Quality in Cities Impact of vegetation on pollutants concentration at pedestrian level

MEHRDAD BORNA¹, ROSA SCHIANO-PHAN¹

¹School of Architecture and Cities, University of Westminster, London, United Kingdom

ABSTRACT: Recent estimates published by WHO report that in 2016 outdoor air pollution caused 4.2 million premature deaths worldwide and urged urban planners, policymakers, and environmentalist to make health and wellbeing their number one priority when designing cities. In view of this, the current paper explores the effectiveness of trees and vegetation in dispersing air pollutants at pedestrian level by administering detailed fieldwork and spot measurement of both pollutants and microclimatic parameters close to one of the most polluted roads in London (Euston Road); followed by modelling a variety of real-life scenarios by using computational simulation application for validation and prediction. Whilst many studies agree in general on the mitigation of urban air pollutants by vegetation, the result of the current study contradicts this common understanding and demonstrates drastic increases in the concentration of particulate matters in the vicinity of trees. The results highlight that trees reduce wind velocity and air movement, causing pollutants to trap inside urban canyons. Therefore, planting more trees does not necessarily mean less pollution, at least locally. Instead, to alleviate air quality problems, more attention should be given to vegetation configuration, type, scale and most importantly, their locations and distributions within active urban pockets.

KEYWORDS: Air pollution, Vegetation, Urban form, ENVI-met, Particulate matters

1. INTRODUCTION

The recent Lancet report (2018) highlighted air pollution as the major cause of cardiovascular and respiratory illnesses and premature death in the world today. For instance, in 2015 pollutants such as Nitrogen Dioxide (NO₂) and Particulate Matter (PM₁₀, PM_{2.5}) have caused 64,000 premature deaths in the UK, out of which, 9000 belongs to a developed city like London. The health impacts of outdoor and indoor air pollution are well researched and established by a substantial body of research worldwide. In contrast, relatively little research has investigated the role that the built environment can potentially have on the concentration and dispersion of air pollutants [1].

Whilst the best way to tackle air pollution is to reduce and stop the pollutants at their sources, which must always be the primary focus of air quality policies, a secondary method, and one which has been increasingly perceived as effectively removing pollutants and improving urban life, is urban greenery [2]. There is a large body of studies referring to trees and their air purifying power and the fact that planting more trees is a cost-effective way to tackle urban air pollution [3]. In view of this assumption, the current paper explores the effectiveness of trees and vegetation in dispersing air pollutants at pedestrian level by administering detailed fieldwork and spot measurement of both pollutants and

microclimatic parameters; followed by modelling a variety of real-life scenarios by using computational simulation software for validation and prediction.

2. METHODOLOGY

As an empirical basis for this investigation, this paper intentionally conducted its research far from the roadside and within an open courtyard (plaza) which was identified as a high-quality active pocket [4] which encourages the users to stay for longer periods of time, therefore increasing the risk of being exposed to pollutants. Accordingly, the Regent's Place pedestrian plaza which is located adjacent to one of the most polluted roads in London (Euston Road), was chosen as the fieldwork site for this paper. The fieldwork was conducted during a time when the Square was expected to be much busier than other times. In that respect, the on-site spot measurements were only carried out on the locations with the highest activities and a greater number of people density.

The Regent's Place characterised by street canyon configuration with an aspect ratio (height over width) of 1.81 and Sky View Factor of 0.35 and the built-up areas are 15 times greater than the green spaces (including trees, hedges, green roofs). Based on previous studies done by other researchers, the high aspect ratio and low SVF have a direct impact on the microclimate of a

particular urban location (at a hyperlocal scale) [5]; specifically, on wind speed and its direction and accordingly influence the rate of dilution and dispersion of pollutants. Based on a scheme (Local Climate Zone) developed by Stewart and Oke in 2012, the study site classified as ‘compact high-rise’ where tall buildings are tightly packed beside each other with little green spaces and a few trees between them.

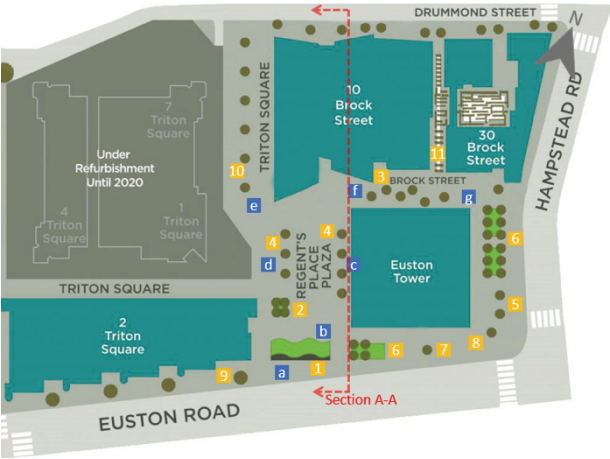


Figure 1: The Regent’s Place Plaza.
 ■ Locations where the measurements were taken
 ■ Location of trees; description provided in table 02
 Section A-A illustrated in figure 05

In terms of population density and activities, close to 12,000 visitors, workers, and residents passing through the plaza each day. Despite its mixed-use, the square is mainly being used by office workers throughout the weekdays and getting populated during lunchtime (11:30 am – 3:00 pm). With its high quality and stylish sitting areas which have mainly sited under the trees, more people are attracted to stay, sit, eat, meet, enjoy, and interact with each other. The square also enjoys access to a number of restaurants, and during the summer/warmer season the restaurants offer more tables and chairs for people to have their meals in the outside open air. There is also an annual events programme, involving summer events during lunchtimes, charity events, farmers markets and other social events. For that reason, this study conducted during the lunchtime (11:00 am – 3:00 pm) and over the summer period (August 2018) where the square was expected to be much busier than other times. In that respect, the site divided into two characteristics and the on-site spot measurements were carried out on, first, locations with the highest activities and a greater number of people density, i.e. location b, c, and d, fig. 1. Second, locations which were seen to offer a better understanding of how air pollutants enter the site or disperse from the site, i.e. location a, e, f and g.

The concentration of particulate matter has increasingly become more significant inside the urban canyons where the urban form and urban features (i.e. solid and porous barriers) are intensifying the concentration of pollutants and increasing health problems [6]. For that reason, apart from Nitrogen Dioxide (NO₂) which is a major concern for Euston road; this study has considered to measure and evaluate two further key urban pollutants; these are particulate matter with a diameter of 10 microns (PM₁₀) and particulate matter with a diameter of 2.5 microns (PM_{2.5}).

2.1 Micro-meteorological observation and monitoring of street-level air pollutant concentration

In this study, two portable real-time monitoring devices have been used: Aeroqual Series 200, which is a Portable Air Quality Monitor and Vane Anemometer and Thermo hygrometer, Testo 410-2. Air pollutants and micro-meteorological parameters measured for the period of 30 minutes at each point with readings taken every 5 minutes and average values have been logged-in for further use in the computational analysis at modelling stage (Table 01).

Sunny Day		Meteorological conditions on 3 rd August 2018 - Fri								Street-level air pollutant concentration					
Location	Time (hrs:mins)	Air Temperature (°C)		Relative Humidity (%)		Wind Velocity (m/s)		Wind Direction (m/s)		NO ₂ (µg/m ³)		PM ₁₀ (µg/m ³)		PM _{2.5} (µg/m ³)	
		P*	S**	P	S	P	S	P	S	P	S	P	S	P	S
a	11:00 – 11:30	29	27	56	54	2.2	2	SSW	SSW	119	94.6	34	23	14	14
	11:35 – 12:05	28	27	60	54	1.4	2	SSW	SSW	76	94.6	22	23	6	14
b	12:10 – 12:40	25	28	63	51	0.4	2	-	SSW	51	137.3	47	21.3	29	18.1
	12:45 – 13:15	24	28	60	51	1.2	2	W	SSW	43	137.3	19	21.3	18	18.1
c	13:20 – 13:50	24	29	67	43	1.0	2	S	SSW	52	94.9	31	24.6	20	19.3
	13:55 – 14:25	26	29	58	43	2.8	3	WSW	SW	57	94.9	26	24.6	9	19.3
d	14:30 – 15:00	27	30	57	38	1.5	3	-	SW	101	72.5	30	30.4	16	16.3

Table 01. Meteorological and air pollution data for 3rd August 2018. *P = Primary data, **S = Secondary data related to mereological conditions extracted from www.metoffice.gov.uk and air pollution data obtained from londonair.org.uk ‘Westminster - Marylebone Road – kerbside’ monitoring station operated by King’s College London.

Both air quality and microclimatic parameters have been compared and ratified against live official data from www.metoffice.gov.uk and the nearest fixed meteorological and air quality monitoring station to the study site. In this case, ‘Westminster - Marylebone Road – kerbside’ monitoring station operated by King’s College London has been chosen, which sits within a kilometre distance from the study site. The equipment sets are placed with a reference height of 1.5 meter above ground level. The study also captured data in several days and weather conditions, i.e. sunny, rainy, and relatively windy day. However, in this paper, only data and results pertaining to the 3rd August are used for

illustration. On this particular day, the wind direction was the same as London prevailing wind direction, making this day a good representation of typical London wind behaviour for most of the year.

2.2 Computer simulations for validation and prediction

Parallel to the spot measurements and data collection, the complex microclimate phenomena and a range of issues, including air pollution dispersal/concentration, air movement in and around buildings, pedestrian level wind environment and the impacts of non-morphological features on air movement, i.e. vegetation, bus stops and cantilevered shading structures, which project at least one meter beyond the side of a building have been modelled and simulated on ENVI-met version 4.4.3. In order to correlate the relationship between vegetation and pollutants concentration, in addition to modelling the current scenario, a no-green scenario has also modelled and simulated for the plaza.

ENVI-met, which is a 3D CFD (Computational Fluid Dynamics) application, has been selected as air pollution dispersion simulation tool due to its proven reliable outcomes that were examined by previous researchers [7,8,9]. This Eulerian, time- dependant dispersion model uses RANS equation as its turbulence modelling and is capable of computing a large number of air plume particles as they emit from their original source [10]. Moreover, it uses the Finite Difference Method (FDM) to solve the multitude of partial differential equations in the model, which allows ENVI-met to use relatively large time steps but still remaining numerically stable. Moreover, with its fine resolution between half a meter to 10 meters and a typical time frame of 24-48 hours and a time step of 1-5 seconds, the model is able to simulate complicated scenarios and display the interactions between solid and porous barriers at various levels and resolutions in a very graphical format. The graphical representation of various scenarios created and produced by the LEONARDO tool included in ENVI-met package. As it was mentioned, the field spot measurement only conducted for 4 hours (11:00 am – 3:00 pm), therefore, in order to cover the total simulation time the data inserted in ENVI-met collected from ‘Westminster - Marylebone Road – kerbside’ monitoring station. The result of the ENVI-met simulation were thereafter compared with the field spot measurement values and further analysis and validation is provided in Result & Discussion section of this paper.

Data related to roads, buildings, vegetation, and surfaces material recorded and gathered through conventional field measurement, satellite-based

measurement and official GIS documents/maps (Ordnance Survey which is the UK governmental mapping agency). Collected data from official GIS checked and verified against conventional field measurement data, and in some cases, aerial perspective published by Bing Maps and Google Maps used to minimise possible errors. Information related to vegetation characteristics such as species name, height, crown shape/size, clear stem height, and Leaf Area Density (LAD), leaf persistence and surface cover have been described in Table 02.

Vegetation Location	Vegetation Scientific name	Vegetation Common name	Vegetation Height (meter)	LAD (High/Low – Dense/Sparse)	Hairiness 0 (Smooth) – 10 (Silky)	Stickiness 0 (Leathery) – 10 (Highly viscid)	Evergreen /Deciduous	Trunk Size	Crown shape/Size	Clear Stem height (meter)
1	Buxus	Box Hedging	1	High	0	1	Evergreen	N/A	Hedge	0
2	Hedera helix	English Ivy	0.3	High	0	1	Evergreen	N/A	N/A	0
3	Platanus x acerifolia	London Plane	10	Low	5	3	Deciduous	Medium	Broadly Oval (Heart-Shaped)	2.5
4	Platanus x acerifolia	London Plane	10	Low	5	3	Deciduous	Medium	Broadly Oval (Heart-Shaped)	2.5
5	Prunus	Cherry Tree	4	Low	3	2	Deciduous	Small	Irregular (Heart-Shaped)	2
6	Tilia	Lime Tree	8	High	4	6	Deciduous	Medium	Broadly Round (Spherical)	2.5
7	Tilia	Lime Tree	8	High	4	6	Deciduous	Medium	Broadly Round (Spherical)	2.5
8	Platanus x acerifolia	London Plane	4	Low	5	3	Deciduous	Small	Irregular (Heart-Shaped)	2
9	Platanus x acerifolia	London Plane	10	Low	5	3	Deciduous	Medium	Broadly Oval (Heart-Shaped)	2
10	Quercus cerris	Turkey Oak	15	Low	2	2	Deciduous	Medium	Broadly Oval (Heart-Shaped)	4
11	Buxus	Box Hedging	2	High	2	1	Evergreen	N/A	Hedge	0

Table 02. Description of the study site's vegetation characteristic. Locations shown on fig. 01 in yellow numbered label

It is worth mentioning that the ENVI-met models are not working reliably at their model borders and the grids very close to them. For that reason, the nesting area of all simulation scenarios chosen sufficiently large to increase the accuracy and numerical stability of the simulation result [11]. Based on the guideline prescribed by previous researchers [12] five nesting grid cells were empirically set on each side of the model and accordingly the z-grid set to 3 times higher than the tallest building in the model site [13]. In order to accelerate the computational (rendering) time of the simulation, it was decided to lower the resolution to 4 for all axis (dx, dy and dz). Other setting and configuration considerations have been summarised in Table 03.

Modelling area file (.inx) settings		Simulation file (.sim) settings	
Model Location		Start and duration of model run	
Location	Central London	Start Date (DD.MM.YYYY)	03.07.2018
Latitude (deg.-N,-S)	51.49	Start time (HH:MM)	06:00
Longitude (deg.-W,+E)	-0.31	Total simulation time (h)	16
Model Geometry		Initial meteorological conditions	
Grid dimension (x, y, z)	75 x 75 x 60	Wind speed at 10m height (m/s)	2.5
Grid cells size (dx, dy, dz)	4m; 4m; 4m	Wind direction (deg)	225
Model rotation out of grid north	-19.00	Air Temperature (°C)	17 (min.) – 32 (max.)
Nesting Grids		Relative Humidity in 2m (%)	36 (min.) – 94 (max.)
Number of nesting grids	5	Pollution Dispersion	
		Operation mode	Multi Pollutant
		Chemistry (NO-O3-NO2)	Dispersion & Action Chemistry

Table 03. Study site input file in ENVI-met 4.4.3.

3. RESULTS & DISCUSSION

The first item revealed from the fieldwork spot measurement was that, 3rd August which was a sunny day recorded as the most polluted day in comparison to 9th (rainy day) and 24th August (windy day). This is more distinct when we look at the PM₁₀ and PM_{2.5} levels and less noticeable in the case of NO₂ levels. Interestingly, the result of 9th August which was the rainy day scenario recorded PM₁₀ and PM_{2.5} at even lower level than a windy day, but still, NO₂ was relatively high, and this has been identified as a reoccurring pattern for all other study days. In order to investigate this results further, the results of fieldwork spot measurements for the three study days of 3rd, 9th and 24th August 2018 were compared against the ENVI-met simulation of the same dates and times to firstly validate ENVI-met simulations and secondly to evaluate the effects of trees on the concentration of mentioned pollutants at the monitoring site (Regent's Place) (in this paper only data and results pertaining to the 3rd August are used for illustration). As Table 04 shows, there is a slight difference between the simulation values and measured data. The level and value of the various meteorological parameters and air pollutants simulated by ENVI-met are consistently lower than what has been measured on-site.

Sunny Day		Meteorological conditions on 3 rd August 2018 - Fri										Street-level air pollutant concentration					
Location	Time (hrs:mins)	Air Temperature (°C)		Relative Humidity (%)		Wind Velocity (m/s)		Wind Direction (m/s)		NO ₂ (µg/m ³)		PM ₁₀ (µg/m ³)		PM _{2.5} (µg/m ³)			
		FM*	EM**	FM	EM	FM	EM	FM	EM	FM	EM	FM	EM	FM	EM		
1	11:00 – 11:30	29	27	56	54	2.2	1	SSW	SSW	119	90	34	15	14	9		
2	11:35 – 12:05	28	27	60	54	1.4	0.5	SSW	SSW	76	90	22	10	6	6		
3	12:10 – 12:40	25	25	63	57	0.4	0.5	-	NNW	51	30	47	10	29	6		
4	12:45 – 13:15	24	25	60	58	1.2	1	W	WSW	43	30	19	5	18	3		
5	13:20 – 13:50	24	25	67	59	1.0	1	S	SSW	52	30	31	5	20	3		
6	13:55 – 14:25	26	25	58	55	2.8	2.5	WSW	SW	57	30	26	5	9	3		
7	14:30 – 15:00	27	25	57	59	1.5	2	-	SSE	101	60	30	10	16	6		

Table 04. Comparison between data gathered during fieldwork measurement and data extracted from ENVI-met simulation result. *FM = Field measurements **EM= ENVI-met simulation.

This ratio changes depending on the given meteorological conditions on the given days; however, in general, the pollution values in ENVI-met are always lower in value than the fieldwork spot measurement data. For example, the NO₂ and PMs concentration are respectively 1.4 and 3.2 times higher in recorded fieldwork spot measurements. In the case of meteorological parameters in most cases, the values are closely similar. These differences were expected as the background concentration data (for pollutants) and meteorological data which have been added in ENVI-met were extracted from the meteorological station which was located about a kilometre away from the study site ('Westminster - Marylebone Road – kerbside'), moreover, there were various simplification and

assumption had to be made while modelling the site in ENVI-met. However, the most interesting aspect of this comparison which is also the main interest of this research is that the measured data and simulation data conclusively and broadly correspond to each other and more precisely confirmed and aligned over the pollution concentration zones.

In order to analyse the simulation results in more detail and understand the impact of trees on air pollution concentration, it was decided to compare the microclimate parameters both in the current urban configuration and in a scenario where there are no trees or vegetation. In this paper, the simulations with a greater significance have been presented in the next pages. For that reason, the data selected for illustration is also related to the busiest (activity and population wise) time of the plaza, which was 1 pm (lunchtime).

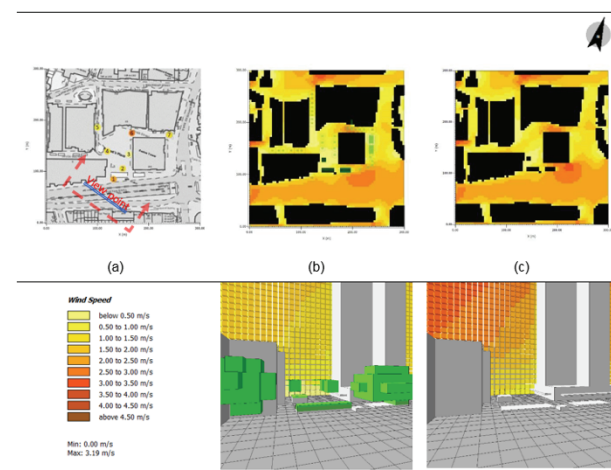


Figure 02. Snapshot of wind velocity and direction map at pedestrian level (1.5 m height from ground) for August 3rd, 2018, 13:00 h. (a) fieldwork spot measurements (b) ENVI-met simulation of current scenario (c) ENVI-met simulation of no-green scenario.

The simulation outcomes are quite revealing in several ways. First, the relative humidity is much lower in the no-green scenario, and this supports previous findings which have shown a decrease in relative humidity in no-green scenarios. Meanwhile, in the case of air temperature, the changes are not noticeable, and we do not see a great temperature difference between the two scenarios. This can be related to the low leaf area index of the trees and their clean stem height. This has been highlighted in Table 02. The wind aspect is the most interesting finding. Based on the result of the fieldwork and ENVI-met simulation, it is clear that trees in high and low density urban areas affect the wind velocity and its behaviour. As illustrated in Fig. 03 wind

velocity and vegetation have inverse correlation meaning that the wind velocity decreases with an increase in vegetation volume especially in the case of trees with high leaf area density (LAD). This drop of velocity has a direct impact on a higher concentration of pollutants, and in the case of Regent's Place, the high level of pollutants concentration can be found around the sets of trees which are located on the east and west side of the plaza (fig. 01 - location c and d). This scenario is exacerbated during the London prevailing wind direction of SSW and those trees planted in north and northeast of the square (fig. 01 – location e and f) slow down air velocity further and avoid pollutants to disperse from the plaza, therefore, led to a higher concentration of pollutants under the group of trees located in the east and west side of the plaza. Specifically, $PM_{2.5}$ is 120% greater around the group of trees in location (c) and PM_{10} values are even higher and stand at 175%. It has been noted that there is not much difference in NO_2 concentration values and the two scenarios (current and no-green) are almost the same but still around trees we can observe that the values are slightly higher than no-green scenario. It is worth mentioning that, the impact of trees on wind flow greatly depend on the vegetation shape and species, as well as the density of the urban context, i.e. planting high LAD heart-shape or spherical crown shape trees with low clear stem height and little space from each other, could slow down air velocity at pedestrian level (the urban canopy layer) and increase the concentration of pollutants. Previous research done by Edward NG [14] and several other studies [5,15,16] on designing for urban ventilation and urban thermal comfort, has established that a high-density urban area induces a weak wind flow and the current study shows that planting more trees will only exacerbate this already-slow wind speed reducing it even further.

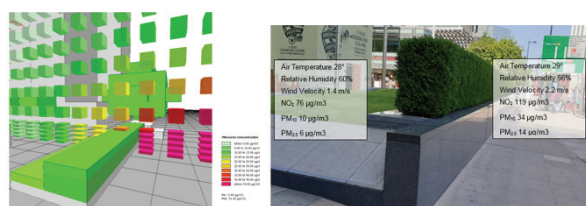


Figure 03. Snapshot of PM_{10} concentration map around hedgerow at the south side of the Regent's Place (left). Fieldwork spot measurements (right). August 3, 2018, 11:00 h.

Further analysis of the result showed that the large hedgerow located at the south side of the site (fig. 01 – location a) is the most effective element in dispersing or blocking (depositing) pollutants. In accord with the result of fieldworks, the ENVI-met simulation with the exception of NO_2 , have indicated the same and showed

a substantial improvement in air quality in location (b) (immediately after the hedgerow) (Fig 04). Previous studies conducted by a number of researchers [16,17] are in support of the above findings. In addition to that, in 2018 similar experiment conducted by King's College London has found levels of NO_2 reduced by 23% when an ivy screen wall was installed and placed between school playground and a busy road [18]. For that reason, it has been decided to take this strategy a step further and pilot scenarios where hedgerows which have proven to be even more effective than ivy screen [19] can be employed as a barrier and stop the PMs from congregation under the group of trees at Location (c).

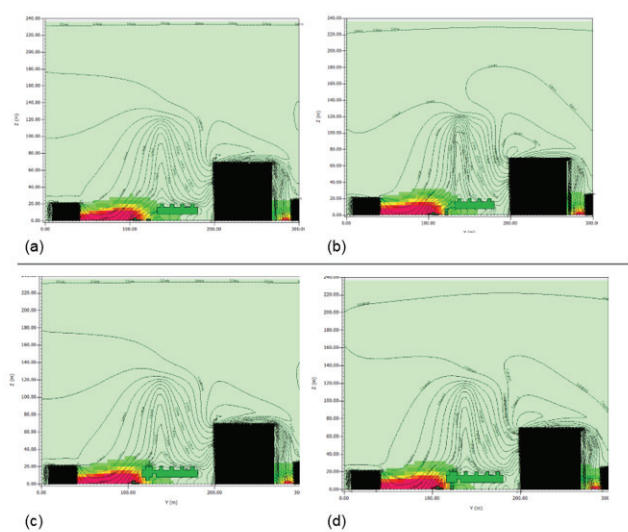


Figure 04. Section a-a illustrating PM_{10} concentration map at pedestrian level with (a) adding a 2-meter height hedgerow; (b) adding a 4-meter height hedgerow; (c) adding an 8 meter Tilia tree (lime tree); (d) adding a 2-meter height hedgerow and an eight-meter lime tree, immediately after the existing hedgerow on the south side of the site.

The first scenario (a) was to add a parallel hedgerow immediately after the 'near wake' of the existing hedgerow (fig 04 - a). the result shows a pronounced reduction in pollution level (PM_{10}) and has limited the distance which air pollution can travel (downwind). Furthermore, it has been noticed that the inlet airflow partly blocked by the two rows of hedges and partly separated upward and generated skimming flow. In the second attempt and in order to avoid the formation of skimming flow, the 2-meter hedgerow increased to 4-meter height. However, the simulation outcome showed that 4 meter height porous barrier is not enough to influence the flow turbulence as minimal reduction in terms of pollution level has been observed. In the third attempt, a 4 meter hedgerow has been replaced with an eight meter Tilia tree (lime tree, similar species as to the group of trees at East side of the site) to offer protection

over a larger distance downwind. The result showed a further reduction in the distance which air pollution can travel but not much difference in terms of air pollution concentration at pedestrian level. For that reason and as a final mitigation strategy, both hedgerow and tall trees put back in their suggested places to provide the maximum protection in terms of distance, downwind and pollution concentration at the pedestrian level (Fig 04 d).

4. CONCLUSION

Whilst many studies agree in general on the mitigation of urban air pollutants by vegetation through their deposition and dispersion properties, the result of the current research contradicts this common understanding and demonstrates drastic increases in the concentration of particulate matters in the vicinity of trees. The results highlight that trees reduce wind velocity and air movement, causing pollutants to settle around and under trees' canopy. This is more distinct when we look at the PM₁₀ and PM_{2.5} levels and less noticeable in the case of NO₂ levels. Therefore, planting more trees does not necessarily mean less pollution, at least locally. Instead, to alleviate air quality problems, more attention should be given to vegetation configuration, type, scale and most importantly, their locations and distributions within the given active urban pocket. The findings from this research provide a fruitful area for further work to determine the exact effectiveness of vegetation in urban spaces throughout the year (summer and winter scenarios). Further investigation and modelling in different urban form with diverse vegetation type and spatial quality are required to be conducted to establish a better understanding of this matter. Needless to say that, we need more effective tree planting policy which takes the above challenges into account, and urban planners need to consider the impact of urban trees and green spaces on air quality at hyperlocal scale.

ACKNOWLEDGEMENTS

The authors would like to thank the University of Westminster, Graduate School and The 125 Fund Award for providing instruments and high-performance computing facility to conduct this research. We thank Dr Krystallia Kamvasinou for her helpful comments on a draft of this paper.

REFERENCES

1. Hankey, S. and Marshall, J.D. (2017). Urban Form, Air Pollution, and Health. *Environmental health reports*, 4 (4): p. 491–503.
2. Berardi, U., G. Hoseini. 2013. State-of-the-art analysis of the environmental benefits of green roofs. *Journal of Applied Energy* 115: p. 411–428.

3. Nowak, D. and Heisler, G. (2010). Air Quality Effects of Urban Trees and Parks. *National Recreation and Park Association*, 1 (1), p. 48.
4. Gehl, J. (2011). *Life between buildings: using public space*. Washington, DC: Island Press, 200.
5. Edussuriya, P., Chan, A. and Malvin, A. (2014). Urban morphology and air quality in dense residential environments: Correlations between morphological parameters and air pollution at street-level. *Journal of Engineering Science and Technology*, 9 (1), p. 64–80.
6. WHO (2018), Ambient (outdoor) Air Pollution, available from <https://www.who.int/news-room> [June 2019]
7. Jin, H. et al. (2017). The effects of residential area building layout on outdoor wind environment at the pedestrian level in severe cold regions of China. *Sustainability (Switzerland)*, 9 (12), p. 1–18.
8. Vos, P.E.J. et al. (2013). Improving local air quality in cities: To tree or not to tree? *Environmental Pollution*, 183. Elsevier Ltd 113–122.
9. Tsoka, S., Tsikaloudaki, K. and Theodosiou, T. (2017). Urban space's morphology and microclimatic analysis: A study for a typical urban district in the Mediterranean city of Thessaloniki, Greece. *Energy and Buildings*, 156. Elsevier B.V. 96–108.
10. Bruse, M. (2004). ENVI-met 3.0: Updated Model Overview (March), p. 1–12.
11. ENVI-met (2019). Nesting Grids. [envi-met.info](http://www.envi-met.info). available from <http://www.envi-met.info/doku.php?id=kb:nesting> [June 2019]
12. Conry, P. et al. (2015). Chicago's heat island and climate change: Bridging the scales via dynamical downscaling. *Journal of Applied Meteorology and Climatology*, 54 (7), 1430–1448.
13. Evyatar, E., David, P. and Terry, W. (2011). *Meteorology and Urban Design* Erelletal 1950_2010., p. 23–24.
14. Ng, E. et al. (2011). Improving the wind environment in high-density cities by understanding urban morphology and surface roughness: A study in Hong Kong. *Landscape and Urban Planning*, 101 (1), Elsevier B.V. 59–74.
15. Chatzidimitriou, A. and Yannas, S. (2017). Street canyon design and improvement potential for urban open spaces; the influence of canyon aspect ratio and orientation on microclimate and outdoor comfort. *Sustainable Cities and Society*, 33 (June), Elsevier 85–101.
16. Abhijith, K. V. et al. (2017). Air pollution abatement performances of green infrastructure in open road and built-up street canyon environments – A review. *Atmospheric Environment*, 162, Elsevier Ltd 71–86.
17. Hewitt, C.N., Ashworth, K. and MacKenzie, A.R. (2019). Using green infrastructure to improve urban air quality (GI4AQ). *Ambio*, Springer Netherlands.
18. Temper, A.H. and Green, D.C. (2018). The impact of a green screen on concentrations of nitrogen dioxide at Bowes Primary School, Enfield Prepared for the London Borough of Enfield (January), 1–19.
19. Chen, L. et al. (2017). Variation in Tree Species Ability to Capture and Retain Airborne Fine Particulate Matter (PM_{2.5}). *Scientific Reports*, 7 (1), Springer US 1–11.

Impact of built density and surface materials on urban microclimate for Sao Paulo, Brazil:

Simulation of different scenarios using ENVI-met Full Forcing tool

CAROLINA S. GUSSON¹, HELGE SIMON², DENISE H. S. DUARTE¹

¹School of Architecture and Urbanism, University of Sao Paulo, Brazil;

²Geographisches Institut, Johannes Gutenberg-Universität Mainz, Germany

ABSTRACT: The objective of this work is to quantify the verticalization impact onto microclimate and thermal comfort at pedestrian level. Geometry and thermal behaviour of building components and surface finishes alter the local microclimate and thus have the potential to mitigate urban heating at microscale level and to improve pedestrian thermal comfort conditions. To examine the effects of different geometries, building components and surface finishes onto microclimate and pedestrian thermal comfort, field measurements in one of the most densely built areas of Sao Paulo as well as modelling, calibration, and simulation of parametric scenarios in the ENVI-met 4.4.3 model have been carried out. The results showed that geometry strongly interferes with microclimate on pedestrian level. During daytime; streets orientation, courtyards, height differences and plot ratio have impacts that, if put together, can increase or decrease the mean radiant temperature (MRT) by up to 14 K and the temperature of equivalent perception (TEP) up to 7.7 K. Combined differences in construction components and surface finishes different can reach differences of up to 8.1 K in MRT and 4.3 K in TEP at daytime and at least 3,9 K in MRT and 2 K in TEP at night time.

KEYWORDS: Verticalization, Urban Geometry, Building Envelope, Urban Microclimate, Thermal Comfort

1. INTRODUCTION

Currently 54% of the world's population lives in urban areas and the projection is, that by 2050 66% of the world's population will be living in cities. In recent years, urbanization has been particularly great in tropical climates and it is likely to even increase [1]. The combination of tropical climates and urbanization leads to new challenges in mitigating the intensity of urban heat island effects. Since similar climates can be found in Brazil where 85% already live in urban area, the climatic problems in Brazilian cities today are showcases to other developing urban areas in tropical climates. One of those showcases is São Paulo being the fourth urbanized region in the world with the largest population of around 21 million inhabitants [1]. It is situated at 23° 32' 56" South and 46° 38' 20" West and is, according to the Köppen classification, characterized by a humid subtropical climate (Cfa).

The urban area of Sao Paulo is very heterogenous – from slums and high-rise buildings to large urban parks and sparsely build-up areas with large green spaces. This results in a variety of different urban microclimates, so is particularly important to do measurements and model calibration in the study interest area before going to parametric simulations using the ENVI-met model [2]. This research has two approaches: measurements and simulation and how to combine them to achieve more accurate results.

2. METHOD

2.1 Field Campaign

In order to calibrate the ENVI-met model and to establish values to be used as input for the full forcing, a field campaign was undertaken in the most densely built area of the city (Fig. 1). The variables collected in the field surveys were air temperature (°C), relative air humidity (%), wind speed (m/s), wind direction (in degrees from North) and gray globe temperature (°C).



Figure 1 - Aerial photo of the two measurement sites.
Google Earth (2016).

The measurements were taken during 20 consecutive days from April 5th to April 25th, 2016. This month represents average climatic conditions as it is close to the autumnal equinox. According to the IAG Bulletin [3], April 2016 covered significantly more days with maximum temperature above 30°C (there were 21 days under these conditions) than the long-term

average and was the driest April since measurements begun in the city, in 1933.

2.2 Calibration

The variables required for the ENVI-met V4.4.3 model calibration with full forcing tool are direct and diffuse short-wave radiation, long wave radiation, air temperature and humidity, wind speed and direction [4]. The analysis of the direct and indirect short-wave radiation data from April 5 to 25, 2016 showed that, on April 17, there was no occurrence of clouds. Thus, the days selected for the simulation input data in full forcing was from 4 am on April 16 to 4 am on April 18, 2016 resulting in a simulation time of 48 hours.

The input data for hourly air temperature and relative humidity were obtained from the average values measured at the two points (Paulista and Bela Vista). The input data for the direct and diffuse short wave radiation and long wave radiation were recorded by the station of the Laboratory of Micrometeorology (LabMicro), located on a platform on the top of the building of the Institute of Astronomy, Geophysics and Atmospheric Sciences (IAG), at Cidade Universitária, University of São Paulo (USP) in a different neighbourhood from the two measurements site (Fig. 1). Input data for wind speed and direction were kept constant over the course of the simulation, since tests performed by [5], the model did not run with different data in each hour for wind speed and direction. As the wind speed in the measurement area is very low, it was decided to maintain the dominant direction of 135° and an entry wind speed at 2m high of 1,15 m/s that will represent in the middle of the court the lowest value measured.

The materials used on the surfaces of roads and blocks were surveyed on site and average values were adopted for them. All building walls were digitized using concrete hollow blocks with an albedo of 0.3. All buildings slabs were digitized using concrete with an albedo of 0.4. The model area covered an area of 702 meters x 621 meters horizontally and 256 meters meters vertically (see Table 1). The simulation took 12 days to run on an Intel core i7 - 6700 16GB RAM computer, 3.41 GHz, with 8 logic processors and 4 cores.

Table 1: Calibration model geometry

Model dimensions (grids)	234 x 207 x 40
Grid size (meters)	3 x 3 x 4
Telescoping Factor (%)	3
Start telescoping after (m)	20
Lowest grid box split into 5 sub cells	

2.3. Scenarios


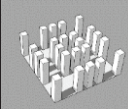
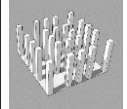
After model calibration, fifteen different parametric scenarios were generated combining three different height of tower's blocks (Table 3), with five different surface building components most used in

Sao Paulo, Brazil featuring different values for radiative properties (Table 4).

The design of the three building scenarios started from the adopted ENVI-met modulation grids (2.5m x 2.5m) to fit the 100m x 100m blocks. The next step was the definition of heights and spacing between buildings based on the São Paulo's building code which defines conditions of aeration and insolation. The site coverage was based on what is allowed by the municipality's zoning, but it was necessary to extrapolate the maximum plot ratio values allowed by the current zoning law (now 4) so that the scenarios could have greater variations in height and could reflect an already built city due to previous legislation. The scenarios buildings increase in height and maintain similar plot ratio by decreasing the site coverage. All the three building scenarios should have a plot ratio like the field campaign areas (Paulista and Bela Vista) (Table 3).

Because in city zoning the areas that can be densified have to be close to transportation axes, with bus corridors, subways stations, bike lanes which is characteristics of great avenues, the scenarios main blocks are surrounded by a road with the dimensions of a large avenue, like Paulista Avenue (30 m).

Table 3: Scenarios high, site coverage, plot ratio and 3D.

Buildings high	44m	81m	119m
Site Coverage	0,5	0,32	0,18
Plot Ratio	7,3	8,6	7,1
3D			

The buildings components chosen to be simulated in the scenarios are part of the most used in the built surfaces in São Paulo, the concrete hollow block, the ceramic hollow brick, and the laminated glass. The surface finishes to be simulated, however, are composed of two extreme values for albedo: A more reflective finish and a less reflective one. In the case of masonry, the albedo of 0.02 was selected to represent a surface all painted in black and an albedo of 0.9 as a surface all painted in white. In case of laminated glass, a glass with more heat reflective properties and another with more heat transmissive properties were selected. The two extremes will thus give the dimension of effects on external climate with the variation of these elements in buildings. In preliminary tests, the white ceramic hollow brick presented similar behaviour as the white concrete hollow block, so for the simulations, we opted for only one component with a white finish (Table 4).

Table 4: Most used building facade components in Sao Paulo, Brazil, and different values for radiative properties.

Materials	Concrete hollow block	Ceramic hollow brick	Laminated Glass		
Reflection	0,02	0,9	0,02	0,4	0,07
Transmission	-	-	-	0,15	0,76

The scenarios aim to quantify the impact of changes in the built geometry and surface materials properties by analyzing the values of mean radiant temperature (MRT), air temperature and Temperature of Equivalent Perception (TEP) in the pedestrian level. TEP is a thermal index developed for local conditions, which allows the prediction of thermal adequacy in urban outdoor spaces for subtropical climates [6]. The scenarios model geometry is described below (Table 5).

Table 5: Scenarios model geometry

Height	44m	81m	119m
Model dimensions (grids)	132 x 132 x 30	132 x 132 x 40	132 x 132 x 45
Grid size (meters)	2.5 x 2.5 x 3	2.5 x 2.5 x 4	2.5 x 2.5 x 4
Telescoping Factor (%)	-	1	4
Start telescoping after (m)	-	10	30

Lowest grid box split into 5 sub cells

3. RESULTS ANALYSIS AND DISCUSSION

3.1 ENVI-met Calibration

Figure 2 shows a comparison between measured and simulated data for the two points, Paulista and Bela Vista. Air temperature behaved practically the same in the night until 11 am when, due to the influence of the incoming solar radiation, the measured temperature was slightly higher than the simulated one, reaching +1.2 K at 1 pm at Bela Vista point and +0.6 K at 1 pm at Paulista point. In the case of the MRT, the model followed the curve of the measured data, but always slightly below the value calculated by the measured globe temperature. As the MRT is mostly sensitive to radiation, and the model represents only the average of the materials that are in place and not exactly each material value, this may have influenced the results as well.

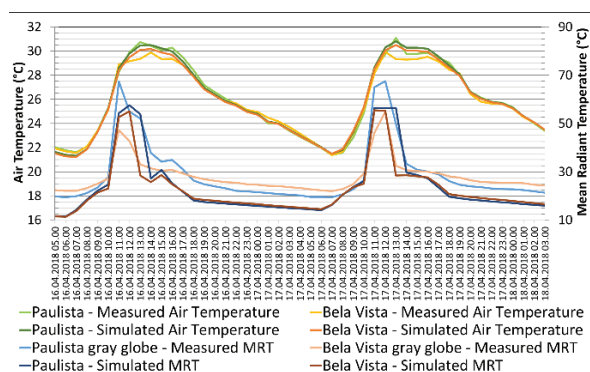


Figure 2 – Measured and simulated air temperature and mean radiant temperature

Table 2 shows results of the statistical analysis R^2 (coefficient of determination) and RMSE (root mean square error) for the two points. The R^2 for air temperature of 0.99 for the two points constitutes a very high correlation. The RMSE value was very small, which means that the model represents air temperature very well. Looking at R^2 values of MRT, the model performed well representing both locations with values of 0.93. RMSE values of MRT are higher which is mainly caused by greater differences at nighttime.

Table 2: Statistical analysis between measured and simulated data

	R^2	RMSE [K]
Air temperature Paulista	0.99	0.26
Air temperature Bela Vista	0.99	0.35
MRT Paulista (gray globe)	0.93	6.22
MRT Bela Vista (gray globe)	0.93	7.04

3.2 Parametric scenarios

For the results analysis, average air temperatures were obtained at pedestrian level (1,5m height) for the coldest time (5am) and the hottest time (12pm). The data was extracted for five outdoor spaces of each scenario: north-south axis (right and left), east-west axis (above and below) and the middle of the court (Fig. 3). The statistical method variance analysis (ANOVA) was applied to analyse the results. The ANOVA model was adjusted only with main effects and the average influence of each isolated factor on the response variable was obtained.

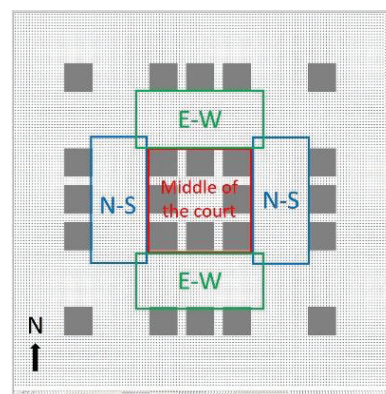


Figure 3 – Results analysis areas

3.2.1 Built geometry

For 12h the 81m height scenario and the East-West axis presented the best results. Due to the shading of the N-S axis for this time of year and hour, the MRT and TEP obtained at noon is greater on the N-S axis than on the E-W axis - average difference are around 11.6 K for MRT and 6.1 K for TEP. The middle of the court is more shaded than the N-S axis, but less shaded than the E-W axis, presenting an intermediate result between the two axes (2.5 K for MRT and 1.8 K for TEP higher than the E-W axis and 9.1 K for MRT and 4.3 K for TEP less than the N-S axis) (Table 6).

Table 6: Axes results in relation to the MRT and TEP average for 12h

Axes	Ranking	MRT and TEP differences [K]
North-South	3	11.6 / 6.1
Middle of the court	2	2.5 / 1.8
East-West	1	0 / 0

Regarding height, the 81m height scenarios resulted in lower TEP and MRT at 12pm, followed by scenarios of 119m height and, lastly, of 44m height. The increase in TEP and MRT in the 119m scenario happens because the buildings are taller, but also slimmer, thus the spaces between buildings are greater than the one in 81m, causing more direct short-wave radiation reaching pedestrian level. The 44m scenario, even with the smallest setbacks, is the one with the highest TEP and MRT, since the buildings provide less shade due to their relative height (Table 7).

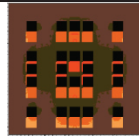

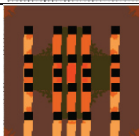
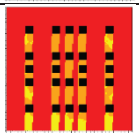
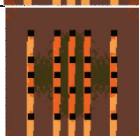
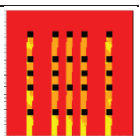

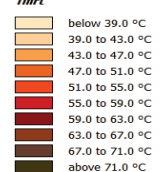
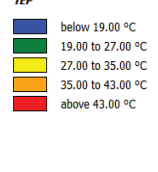
Table 7: Height and site coverage results in relation to the MRT and TEP average for 12h

Heights (m)	Ranking	MRT and TEP differences [K]
44	3	2.4 / 1.5
119	2	2.0 / 0.9
81	1	0 / 0

In the coldest period, at night, the building geometry had a small influence on MRT and TEP. The height showed a difference of 0.2 K in MRT and 0.15 K in TEP, while the axes did not show differences in MRT and TEP: Only the middle of the court showed a difference of 0.6 K in TEP and 0.15 K in MRT compared with both axes. The building geometry influences on air temperature for the scenarios showed an average increase of 0.8 K in the 44m scenario compared to other heights and 0.4 K higher values in the N-S axis compared to the other axes at 12h. At night, the building geometry had no influence on the air temperature between the simulated scenarios, mainly because their close ranges of built volume and plot ratio.

Table 8 shows the distribution of MRT and TEP at the pedestrian level, at 12 noon, for the white concrete hollow brick scenarios. Great influence of geometry is observed due to the shading of buildings. The red areas in the TEP images indicate areas with a very hot sensation. Orange indicates hot, yellow warm sensation. During this hour there are no spaces with neutrality or cool sensation. It is observed that for the North-South axis there is no difference in the thermal sensation with the change in height and site coverage. This can be explained by the absence of shade for the entire axis at this time. Only the shaded areas in the E-W axis and in the middle of the court show hot sensations.

Table 8: MRT and PET distribution at 12 pm at pedestrian level (1.50 m)

Building component and finish		White Concrete hollow block	
Variable (°C)		MRT	TEP
Height (m)	44		
	81		
	119		
Subtitles		Tmrt 	TEP 

The effect of building geometry over a 24h cycle was analyzed in Fig. 4 from the average hourly TEP values in each scenario at the pedestrian level. It is observed that the E-W axis presented less hours (1%) in the very hot sensation than the N-S axis (6%), representing the hottest hours of the day. Evaluating the N-S axis over the course of the day, the amount of sensation of discomfort due to heat (30%) is lower than for the E-W axis (32%). This indicates, that at certain times the N-S axis has a better behavior than the E-W due to the influence of solar position.

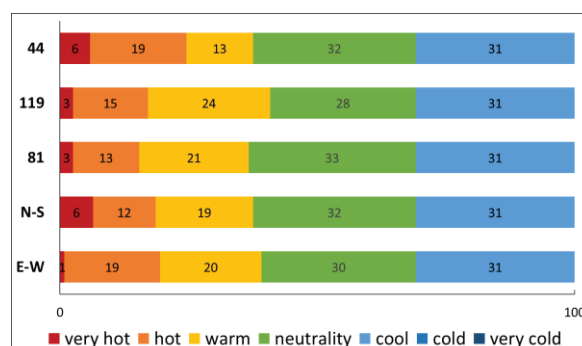


Figure 4 – thermal sensation in average percentage of hours for a period of 24h due to build geometry

The analysis of the height effect in a 24-hour cycle, shows that the 119m height scenarios present less time in a neutrality sensation than the other scenarios. The 44m scenario, despite showing almost the same time in neutrality as the 81m, presents more hours of very hot sensation (6%) than the other scenarios (3%). Thus, it can be concluded that at noon, the hottest period of the day, the 44m scenario is the worst

scenario among the 3. However, over 24 hours the 119m scenario presented longer times of discomfort due to heat (42%) than the 44 m scenario (38%). This mainly stems from the wider space between buildings that impact the solar heat gain at other times of the day in the 119m scenario.

3.2.2 Building surface components and finishes

The building surface components and finishes behavior for the hottest time showed that the transmissive laminated glass had a lower MRT and TEP values, whereas the component that resulted in the highest MRT and TEP was the concrete hollow block with a white finish with average increases of MRT 8.1 K and TEP 4.3 K over the laminated transmissive glass (Table 9).

The white concrete hollow block and the reflective laminated glass reflect much of the incoming short-wave radiation. The black ceramic hollow brick and concrete hollow block, despite having a higher surface temperature than the previous components, emit more longwave radiation with less impact on the MRT and TEP to the external environment. Considering the interior/exterior relationship, it is worth mentioning that with transmissive laminated glass, most of the radiation is transmitted to the interior of the building, and it is important to seek compatibility between the best thermal performance between the two scales.

Table 9: Building surfaces components and finishes results in relation to the MRT and TEP average for 12h

Building surfaces components and finishes	Ranking	MRT and TEP differences [K]
White concrete hollow block	5	8.1 / 4.3
Reflective laminated glass	4	3.5 / 1.9
Black ceramic hollow brick	3	1.9 / 1
Black concrete hollow block	2	0.3 / 0.1
Transmissive laminated glass	1	0 / 0

The effect of different building surface components and finishes for the coldest time of the day showed that the transmissive laminated glass produced generally lower MRT and TEP values. The highest MRT and TEP were found for the concrete hollow block with a black finish, which, on average, showed an increase of 3.9 K in the MRT and 2 K in TEP for 5am compared to transmissive laminated glass. The results also show that, during the night, MRT and TEP are mostly influenced by the building surface component. At the coldest time (5 am) both glass types present the best results, because the material has compared to the concrete hollow block, and ceramic hollow brick lower capability of heat storage (Table 11).

Table 11: Building surfaces components and finishes results in relation to the MRT and TEP average for 5h

Building surfaces components and finishes	Ranking	MRT and TEP differences [K]
Black concrete hollow block	5	3.9 / 2
Black ceramic hollow brick	4	2.9 / 1.5
White concrete hollow block	3	2.6 / 1.4
Reflective laminated glass	2	0.2 / 0
Transmissive laminated glass	1	0 / 0

Table 10 shows the influence of surface finishes on both MRT and TEP values for the hottest period (12 pm). Scenarios with more reflective surfaces make spaces in the shade more uncomfortable than those same spaces in scenarios with less reflective surfaces.

Table 10: MRT and PET distribution at 12 pm at pedestrian level (1.50 m)

Height		44	
Variable (°C)		MRT	TEP
Construction component and finish	White concrete hollow block		
	Black ceramic hollow brick		
	Transmissive laminated glass		
Subtitles		Tmrt below 39.0 °C 39.0 to 43.0 °C 43.0 to 47.0 °C 47.0 to 51.0 °C 51.0 to 55.0 °C 55.0 to 59.0 °C 59.0 to 63.0 °C 63.0 to 67.0 °C 67.0 to 71.0 °C above 71.0 °C	TEP below 19.00 °C 19.00 to 27.00 °C 27.00 to 35.00 °C 35.00 to 43.00 °C above 43.00 °C

Table 12 shows data for the coldest period (5am), the building surface components have a great influence on MRT and TEP. MRT and TEP area higher in scenarios with components that store more heat as concrete hollow block compared to the glass scenarios. As already mentioned in item 2.2 calibration, the ENVI-met model underestimated the values of MRT and TEP at night, so it is possible that the thermal sensation obtained with the scenarios is underestimated for the night period.

Table 12: MRT and PET distribution at 5 am at pedestrian level (1.50 m)

Height		44	
Variable (°C)		MRT	TEP
Construction component and finish	Black concrete hollow block		
	White concrete hollow block		
	Transmissive laminated glass		
Subtitles		Tmrt below 10.75 °C 10.75 to 11.50 °C 11.50 to 12.25 °C 12.25 to 13.00 °C 13.00 to 13.75 °C 13.75 to 14.50 °C 14.50 to 15.25 °C 15.25 to 16.00 °C 16.00 to 16.75 °C above 16.75 °C	TEP below 12.00 °C 12.00 to 19.00 °C 19.00 to 26.00 °C above 26.00 °C

The effect caused by building surface components and finishes in a 24-hour cycle (Fig.5) shows that during the day, the white concrete hollow block had a longer period in the very hot sensation (7%) than the other 4 scenarios (3%). When analyzing the total hours in discomfort due to heat throughout the day, the behavior ranking follows the same ranking for 12h, with longer time in discomfort for reflective finishes than for more absorptive ones. The sensation of neutrality occurred in less hours in scenarios with more reflective finishes (28% and 29%) and reaching 33% in those with finishes that result in greater absorption of radiation. During the coldest period of the day, the building components that store less heat (glass) were the ones that provided the longest times of cool sensation outside.

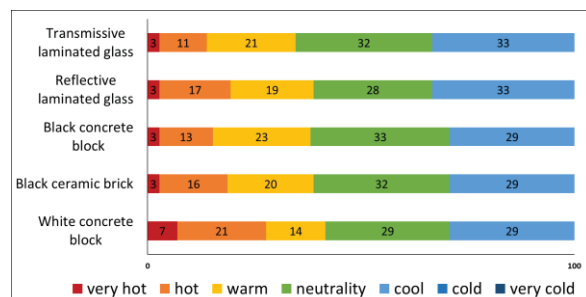


Figure 5 – thermal sensation in average percentage of hours for a period of 24h due to building surface components and finishes

4. CONCLUSIONS

The research showed that the ENVI-met model, despite underestimating the MRT at night, presented

good statistical results in the calibration. Regarding the combined effect of geometry, building components and surface finishes, the daytime differences between the scenarios was up to 22.1 K in MRT and 11.9 K in TEP. During nighttime differences were of at least 4.1 K in MRT and 2.7 K in TEP. Site coverage and height were the dominant factors that most influenced the microclimate during daytime. It showed that the resulting differences in shading and ventilation, could considerably improving the thermal sensation at the pedestrian level.

Surface finishes had a considerable effect on both daytime and nighttime. In the daytime they effect both the inside and the outside of building. The reflective finish causes discomfort for pedestrians in open spaces, but it can improve conditions in indoor spaces, whereas darker finishes improve conditions in open spaces, but can contribute substantially to the air temperature increase inside the building. The building components, on the other hand, have a greater impact on the microclimate and nighttime thermal comfort in the urban environment due to their heat storage properties. The next steps will discuss the relationship between the results achieved and the built density of subtropical cities regarding geometry and building facades.

ACKNOWLEDGEMENTS

To Micrometeorology Group of IAG USP for the radiation data. This study was financed in part by the Coordenação de Aperfeiçoamento de Pessoal de Nível Superior - Brasil (CAPES) - Finance Code 001, FAPESP (Grant #2016/02825-5) and CNPq (Produtivity Grant 309669/2015/4).

REFERENCES

- United Nations, Department of Economic and Social Affairs, Population Division (2014). *World Urbanization Prospects: The 2014 Revision*, CD-ROM Edition.
- ENVI-met model, [Online], Available: <https://www.envi-met.com/> [02 October 2019].
- Instituto de Astronomia, Geofísica e Ciências Atmosféricas da Universidade de São Paulo, (2016). *Estação Meteorológica do IAG-USP - Resumo Mensal – Abril/2016*. 46° Edição. São Paulo: IAG-USP. Available: <http://www.estacao.iag.usp.br/Mensais/Abril2016.pdf>. [29 July 2019].
- SIMON, H. (2016). *Modeling urban microclimate: development, implementation and evaluation of new and improved calculation methods for the urban microclimate model ENVI-met*. 218 p. Thesis (Doktor der Naturwissenschaften) – Johannes Gutenberg-Universität Mainz, Mainz.
- SHINZATO, P. et al, (2019). Calibration process and parametrization of tropical plants using ENVI-met V4–Sao Paulo case study. *Architectural Science Review*, v. 62, n. 2, p. 112–125, 2019.
- Monteiro, L., Alucci, M., (2011). *Proposal of an outdoor index: empirical verification in the subtropical climate*. In: 27th Conference on Passive and Low Energy Architecture PLEA, July 2011. Louvain-la-neuve, Belgium

Shading and temperature of urban canyons An analysis in the downtown area of Passo Fundo-Brazil

SINARA FURLANI, DANIELA MARONI, VANUSA TEBALDI, GRACE TIBÉRIO CARDOSO

Postgraduation Program of Architecture and Urbanism, School of Engineering and Applied Sciences, IMED, Passo Fundo, Brazil.

ABSTRACT: *This article aimed to analyze the influence of shading on the variable temperature in different urban canyons in the downtown area of Passo Fundo, Brazil. This research includes part of the pilot study of the project “Microclimatic Zoning of the city of Passo Fundo”. This article presents the results collected at two points on the public sidewalk, on two different blocks of the road. The methodology consisted of collecting the morphological characteristics, and measuring climatic variables such as solar radiation, air temperature and humidity, in addition to the surface temperature of buildings and asphalt pavement, using a thermographic camera. In addition, the work consisted of verifying the possible influence of vegetation on temperatures, since one collection point has vegetation along the public sidewalk, and the other collection point does not. The results showed that most of the shading is provided due to the narrowing of the canyons and tall buildings. However, the existing vegetation is insufficient to provide thermal comfort at the pedestrian level, and in addition, there is a possible influence of the materials of the facade of the buildings both in their surface temperature and in the reflection of the incident radiation.*

KEYWORDS: *Urban Canyons. Thermal Comfort. Urban Climate. Vegetation.*

1. INTRODUCTION

Measuring the impacts of urbanisation on the climatic conditions of cities is of great importance for proposing adaptation or mitigation solutions that aim to reduce negative consequences to urban quality of life, such as urban heat island phenomena (UHI). Despite having typical characteristics, heat island phenomena vary in intensity and moment of occurrence, according to location, urban morphology, energy flows and weather conditions [1,2]. The results obtained by Gäal *et al.* [3] showed that surface shading, provided by urban densification and afforestation could modify and even control the solar incidence in urban canyons, interfering mainly in microclimatic conditions, such as air temperature.

Urban morphology is an important multidimensional variable to consider in climate modeling and observations, because it significantly drives the local and micro-scale climatic variability in cities. Urban form can be described through urban canopy parameters (UCPs) that resolve the spatial heterogeneity of cities by specifying the 3-dimensional geometry, arrangement, and materials of urban features [4].

The study of the morphological characteristics of urban canyons is essential for microclimatic analyses,

since verticalization and constructive densification influence the temperature range, air humidity, solar radiation, among others, acting directly on the environmental and human quality of urban spaces, and conditioning their uses and appropriations. In addition, according to Romero *et al.* [2], the different materials used in the constructions, causes the city to present different patterns of heat emission, or albedo. The higher the albedo, the more heat will be emitted from the surfaces, mainly in city centers, favoring higher temperatures and the so-called urban heat islands.

When we talk about urban climate, the phenomenon of urban heat island (UHI) is the most documented in relation to climate change. The term “heat island” describes the hottest areas within urban perimeters in relation to the nearest non-urbanized areas, due to the fact that urban areas have typically darker surfaces and with less vegetation than in semi-urban and non-urban environments [5]. This daily temperature difference between urban and non-urban areas affects the microclimate and consequently the use of energy and the habitability of cities [5].

Urban Heat Islands (UHIs) have been recognised as influencing minimum air temperatures in cities, and are noted in IPCC's Fifth Assessment Report for their

possible impact on global warming. As cities increase in size and built density, especially in developing countries, these impacts would be expected to increase [6].

Whilst the UHI phenomenon is understood, in general ways, to be associated with the physical properties of urban surfaces, buildings, anthropogenic heat release, and sky view factors within urban canyons, detailed studies in particular locations can add to our understanding and, potentially, point to ways of mitigating the effect [7].

In this context, the presence of vegetation areas can affect the urban energy balance shading the surfaces and blocking the long-wave radiation from the sky, reducing air speed and providing moisture by evapotranspirational cooling. However, the extent of these influences on urban microclimate vary widely depending on the vegetation type and water availability [1,8].

According to Yu *et al.* [9], the vegetation inserted in the urban morphological composition, directly influences the climatic conformation of the place, since it acts as a transforming element of the heat energy, through the process of photosynthesis, in water vapor resulting in the humidification of the air. The cooling effect of green spaces is an important ecosystem service, essential to mitigate the effect of the urban heat island (UHI) and, thus, increase urban resilience to climate change.

Also in this context, Ribeiro *et al.* [10] observed tree shading and thermal comfort indexes in hot-dry and hot-humid periods in the city of Cuiabá, Brazil, and concluded that there was a better thermal performance in areas with tree shading, reinforcing the importance of afforestation in cities to provide better thermal comfort to users.

In a study by Shinzato and Duarte [11], it proves the influence and the positive impact exerted by vegetation on the microclimate and consequently on the comfort of open spaces, a result obtained through the shading caused by the treetops that directly influences the surface temperatures below of the canopy, affecting, in turn, the average radiant temperature.

According to this scenario, the present article aims to analyse the influence of shading on the temperature variable in two different urban canyons in the downtown area of Passo Fundo/RS. The research includes part of the pilot study of the project "Microclimatic Zoning of the city of Passo Fundo". The two points analyzed in this study are positioned in two consecutive canyons on the road, located in the central area of the city, and have similar morphological configurations with respect to the average height of the buildings and the width of the roads. The main difference is in the presence of vegetation at one of the points, in addition to the

materials of the building surfaces being different, and therefore contributing to a different energy balance between the two canyons.

2. METHODOLOGY

According to Köppen's classical classification, the climate of Passo Fundo's region is Cfa, in other words, with humid subtropical characteristics, with rainfall distributed throughout the year. Passo Fundo is located at 28°22' South latitude and 52°40' West longitude, and its altitude is about 683 meters above sea level (INMET, 2019). The maximum annual temperature is 29 °C and the minimum temperature is 0°C. However, only in June, the month in which this survey was done, the minimum temperature was 5°C and the maximum 24°C. The annual relative humidity is approximately 73% [12].

The first stage of the research was performed in loco, in order to collect information regarding the morphological characterisation of the site, to define the point of collection of pedestrian level shading data and environmental variables (solar radiation, temperature and humidity, relative air temperature and surrounding surface temperature). To collect the climatic variables inside the canyons, as well as the common photographic records and with the thermographic camera, each point was located on the right side of the road, inside the canyon. The environmental variables were collected by the IMED Faculty Mobile Automatic Weather Station. Data collection took place over three days, between 8 am and 8 pm. The measurements consisted of staying 15 minutes at each point, on the right side of the road, moving to the next one afterwards. Testo 865 thermographic camera was used to collect the surface temperatures of the asphalt paved road, and the building close to the point, due to the shading caused by the other constructions around the collection point. The images of the buildings registered by the thermographic camera are those located on the left side of the road, in front of the point of collection of climatic variables. Due to the solar orientation of the canyons, the facades on the left side receive more incidence of solar radiation than those on the right. The surfaces of the buildings were characterized as masonry with plaster, from light to dark colors, and glass. In canyon 2, there was a larger glass area due to the presence of stores and commercial establishments.

The meteorological conditions during the analysis period demonstrated the dominance of an Atlantic polar front, which increased the cloudiness of the sky, decreased the thermal amplitudes and raised the relative humidity.

The analysed canyons have a width/height (W/H) ratio of 0.80 (Fig. 1), considered "claustrophobic", according to Romero's classification [13]. The

predominant material of the buildings is masonry with white paint, with emissivity (ϵ) of approximately 0.90, and on the road, the pavement is asphalt, with emissivity (ϵ) around 0.90 to 0.98. Only at point 2 there is the presence of vegetation in its immediate surroundings. The trees that are part of the road, located on the public sidewalk, are of the *Bauhinia Fortificata* species and they are about 4 meters high.

According to the satellite images and survey of the area, the built density of the four blocks that form the canyons below was calculated (Fig. 1), which refers to the ratio between the built area, considering the projection of the buildings and the number pavements, and the court area. In the canyon of point 1, the block density to the northwest is 4.5, denser than the block to the southeast, with a density of 2. It is noticed that the area of the block to the northwest is smaller in relation to the others, and has some taller buildings. In canyon 2, the block to the northwest has a density of 2.54 and the block to the southeast 2.29.

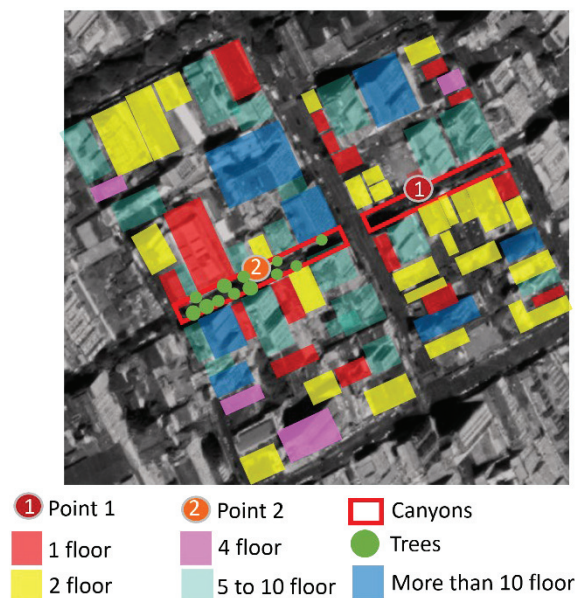


Figure 1: Height map of buildings and location of analysis points in the channels.

3. RESULTS AND DISCUSSION

In the morning (9 am), the measured radiation was around 30 W/m^2 , air temperature and relative humidity 13.5°C and 80%, respectively.

In point 1, part of the asphalt pavement was shaded by the buildings, and registered a surface temperature of 8°C , while in the part with solar incidence, the registered temperature was 9°C . The buildings, exposed to solar radiation, had a surface temperature of 12°C (Fig. 2).



Figure 2: View at 9 am no ponto 1. Testo camera focus on asphalt road and building.

In point 2, most of the road was shaded by buildings and trees, with surface temperatures around 9°C (Fig. 3). Buildings were more exposed to radiation with surface temperatures around 13°C (Fig. 3).

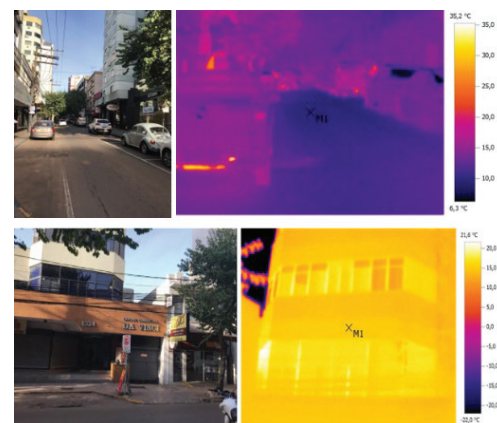


Figure 3: View at 9 am no ponto 2. Testo camera focus on asphalt road and building.

The Figure 4 illustrates the simulation of shading at 9 am, of the buildings in front of points 1 and 2, respectively.

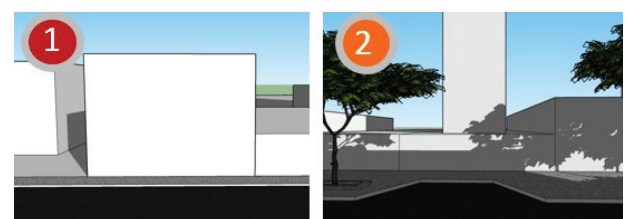


Figure 4: View at 9 am in points 1 and 2. Shading study carried out in the Google Sketchup program.

Thus, it was observed that the surface temperatures of both the asphalt pavement and the buildings of the analyzed canyons were similar during the morning. As the measurements were made in the winter period, the early morning occurred around 7 am and the angle of the

solar height for 9 am was approximately 15 degrees. These conditions possibly contributed to the similarity of the air temperatures collected in the two canyons, since the angles of incidence of the radiation conditioned more to the reflection of the solar rays than the absorption by the surfaces.

In the afternoon (2 p.m), the measured radiation was around 50 W/m², air temperature 20 °C and relative humidity 60%.

At point 1, the asphalt surface, despite being totally shaded by the canyon buildings, had a temperature of 11.6 °C (Fig. 5), compared to its surface temperature at 9 am. The buildings, however, having been exposed to solar radiation for a longer time, had a temperature of 27.5 °C (Fig. 5). Asphalt has great heat absorption and, consequently, greater emissivity. The temperature of this surface possibly increased due to the absorption of the heat emitted by the surrounding surfaces.

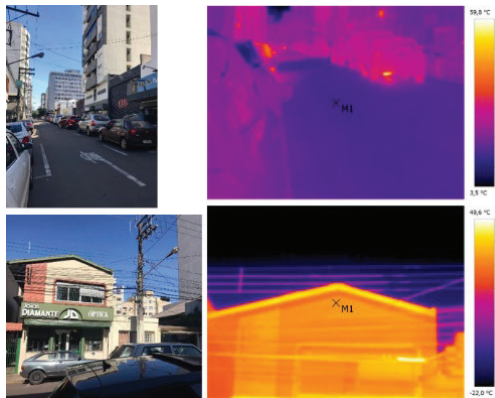


Figure 5: View at 2 pm no ponto 1. Testo camera focus on asphalt road and building.

At this time, in point 2, most of the road was also shaded by buildings and trees, with a surface temperature of 19 °C (Fig. 6). The buildings had higher surface temperatures than in the morning, around 33 °C (Fig. 6). The same thermal behavior of the surfaces was observed in point 2, with a high temperature of the asphalt even shaded by the surroundings and trees. Possibly, due to the higher height of the buildings in this canyon, the heat is reflected and reabsorbed more times by the surfaces.



Figure 6: View at 2 pm no ponto 2. Testo camera focus on asphalt road and building.

The Figure 7 simulates the shading of buildings in front of the collection point, from points 1 and 2, during the afternoon. In this case, despite the taller trees and buildings being higher than in point 1, the shading generated is not enough to decrease the surface temperature of the asphalt, due to the greater reflection of the heat inside the canyon.

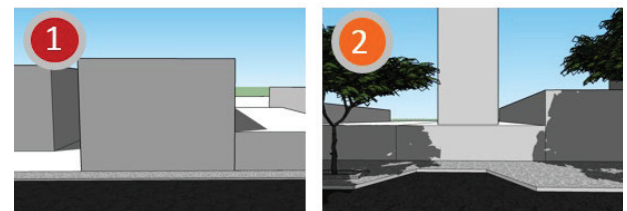


Figure 7: View at 2 am in points 1 and 2. Shading study carried out in the Google Sketchup program.

In the afternoon (5 pm), the value recorded for the environmental variables were: radiation 8 W/m², air temperature 19 °C and relative humidity 66%.

In the late afternoon, the surface temperature of the asphalt at point 1, which was completely shaded, was 11.8 °C, and that of the building was 29.2 °C (Fig. 8).

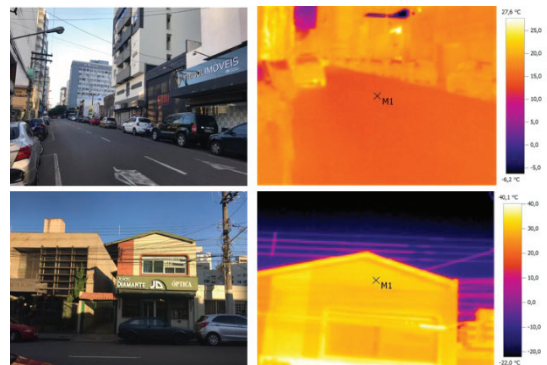


Figure 8: View at 5 pm no ponto 1. Testo camera focus on asphalt road and building.

In this situation, the shading and the lower height of the buildings in the canyon at point 1 kept the asphalt surface temperature more uniform, as it allowed the absorbed radiation to be emitted into the atmosphere. The building, as it was more exposed to the sun, as expected registered a higher surface temperature. There is an undeveloped plot in front of the measured building at point 1, which allowed solar incidence for a longer time, since the solar height at this time was approximately 5 degrees.

At point 2, the temperature of the asphalt surface also decreased to 17 ° C (Fig. 9), but it remained higher compared to the temperature of the asphalt surface at point 1. However, the building's surface temperatures were around 21 ° C (Fig. 9). Possibly, due to the larger glass area of canyon 2 and the angle of incidence of the sun's rays to be smaller than normal, there was more reflection of solar radiation than absorption by the building's surface, and more absorption and emissivity by asphalt surface. In addition, due to the lower solar height at this time, the buildings in the surroundings have made greater shading in the measured building.

The Figure 10 shows the shading study of buildings in front of the collection points, in the late afternoon.



Figure 9: View at 5 pm no ponto 2. Testo camera focus on asphalt road and building.

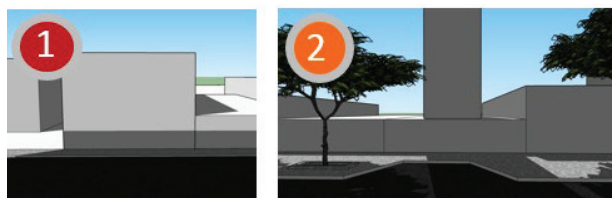


Figure 10: View at 5 pm in points 1 and 2. Shading study carried out in the Google Sketchup program.

When analyzing these two canyons, it was noticed that the higher average height of the buildings in point 2, and the presence of vegetation, were not enough to decrease the surface temperature of the road and the building in front of the collection point. This fact,

however, can contribute to greater reflection of the heat in the public space, instead of allowing the loss of night radiation.

Although not all canyon surfaces have been analyzed, with this exercise it was possible to see that the materiality of the buildings and the pathway contributes to the thermal behavior observed in the two points.

4. CONCLUSION

This study aimed to investigate the impact of urban morphology on the predominant surface temperatures of the urban canyons analyzed, as part of the pilot study of the microclimate characterization of the central area of Passo Fundo-RS, Brazil.

It was concluded that, in colder periods with dominance of polar air mass, added to the canyon's claustrophobic profile and constructive density of the area, a part of the solar radiation reached the surfaces of the buildings and the road ahead collection points, raising surface temperatures throughout the day. However, due to the materiality of these same surfaces, and the higher average height of the buildings in point 2, there was possibly a greater reflection of the heat emitted by the surfaces to the asphalt of the road, than in point 1.

It was also observed that the existing vegetation is insufficient to avoid overheating the road, and possibly will not provide thermal comfort to the pedestrian during the summer. With adequate urban afforestation, there could be a significant improvement in the microclimate, through humidification and evaporative cooling.

Due to the scenario we witnessed in the cities of an intentional urbanization process, the study becomes relevant because it presents data and analyzes of the correlation of the morphological configurations of urban canyons and their interference in the local microclimate composition, exposing the need to plan environments that have configurations that assist in climatic balance according to the physical and meteorological needs of the place, providing qualitative environments for its population.

ACKNOWLEDGEMENTS

Thanks to the Rio Grande Do Sul State Research Support Foundation - FAPERGS for the acquisition of the equipment that supported this research.

REFERENCES

1. Erell, E., Pearlmuter, D., Williamson, T., (2015). Urban Microclimate: Designing the Spaces between Buildings. Routledge, 1: 288 p.

2. Romero, M. A. B., Baptista, G. M. M., Lima, E. A., Werneck, D. R., Vianna, E. O., and Sales, G. L., (2019). Mudanças climáticas e ilhas de calor urbanas. Brasília: *ETB*, 1: p. 75.
3. Gäal, L. P. M., Leonhardt, C. R., Pezzuto, C. C., (2016). Influência da geometria urbana no microclima de cânions urbanos. *2016 Brazilian Technology Symposium*. Campinas, BR, December 1-2.
4. Middel, A., Lukasczyk, J., Maciejewski, R., Demuzere, M., Roth, M., (2018). Sky View Factor footprints for urban climate modeling. *Urban Climate*, 25: p. 120-134.
5. Kaloustian, N., Diab, Y., (2015). Effects of urbanization on the urban heat island in Beirut. *Urban Climate*, 14: p. 154-165.
6. Nichol, J., Choi, S. Y., Wong, M. S., Sawaid, A., (2020). Temperature change and urbanisation in a multi-nucleated megacity: china's pearl river delta.: China's Pearl River Delta. *Urban Climate*, 31: p. 100592-100592.
7. Clay, R., Guan, H., (2020). The urban-parkland nocturnal temperature interface. *Urban Climate*, 31: p. 100585-100585.
8. Krayenhoff, E. S., Jiang, T., Christen, A., Martilli, A., Oke, T. R., Bailey, B. N., Nazarian, N., Voogt, J. A., Giometto, M. G., Stastny, A., Crawford, B. R., (2020). A multi-layer urban canopy meteorological model with trees (BEP-Tree): street tree impacts on pedestrian-level climate.: Street tree impacts on pedestrian-level climate. *Urban Climate*, 32: p. 100590-100590.
9. Yu, Z., Guo, X., Jørgensen, G., Vejre, H., (2017). How can urban green spaces be planned for climate adaptation in subtropical cities? *Ecological Indicators*, 82: p. 152-162
10. Ribeiro, K. F. A., Valin, M. O. J., Santos, F. M. M., Nogueira, M. C. D. J. A., Nogueira, J. D. S., (2018). Estudo da influência do sombreamento arbóreo nos índices de conforto térmico na cidade de Cuiabá – MT. *Ambiência*, 14(2): p. 300-314.
11. Shinzato, P., Duarte, D. H. S., (2018). Impacto da vegetação nos microclimas urbanos e no conforto térmico em espaços abertos em função das interações solo-vegetação-atmosfera. *Ambiente Construído*, 18(2): p. 197-215
12. Instituto Nacional de Meteorologia do Brasil [INMET], Estações Automáticas. Brasília: EMBRAPA, [Online], Available: http://www.inmet.gov.br/portal/index.php?r=home/page&page=rede_estacoes_auto_graf [02 September 2019].
13. Romero, M. A. B., (2016) Arquitetura bioclimática do espaço público. Brasília: *UNB*, 4: 226 p.

No Retreat from Change: Landscape Information Modelling as a Design Tool for a Resilient Community: The Case of Poço da Draga in Fortaleza, Brazil.

NEWTON CÉLIO BECKER DE MOURA, TAINAH FROTA CARVALHO

Architecture and Urbanism Department, Universidade Federal do Ceará, Fortaleza, Brazil

ABSTRACT: *Considering adaptation to the challenges of climate change, this paper presents a case study that explores the concept of Landscape Information Modeling (LIM) as a decision-making and design tool to assess strategies of resilience for a local informal settlement in Brazil. LIM theory provides a novel approach for urban design and employs computer intelligence systems to analyze environmental data as inputs and propose scenarios from which the optimal arrangement may be selected. Poço da Draga is a historical community located in the coast of the City of Fortaleza, Brazil. As a result of inequality, this community has long settled into an unfavorable housing area that suffers with usual floods throughout the year and is also threatened by sea level rise. Although significant researches and projects have assessed the balance of environmental and society in Brazil, this work prospects a new point of view to access the dialectic between these issues.*

KEYWORDS: *Intelligent Landscapes, Flood Risk, Parametric Modeling, Landscape Information Modelling.*

1. INTRODUCTION

1.1. CLIMATE CHANGE

The challenge imposed to researchers and professionals of many areas in the XXI century regarding the creation of alternative solutions for city design is now, more than ever, in evidence. The search for a safe and good environment for human living implies a change in the way we think and plan our urban infrastructure. It is necessary to ally artificial and natural strategies in order to reduce human impact in the natural environment and those strategies must also be accessible and feasible to every social sector.

Like in other large urban centers, the city of Fortaleza, Brazil (Fig.1). environmental problems are already facts of their own and deserve further study. According to the PBMC (2016), throughout the 21st century, temperatures at Fortaleza grew as the concentration of greenhouse gases also increased. Climate change related to greenhouse gases puts in evidence the necessity for more green infrastructures in urban spaces as, according to ONU (2018), it is predicted that by 2050 68% of the world's population will be living in cities.



Figure 1: Poço da Draga top view. Source: Google Maps, edited by author, 2019.

1.2. THE SITE

Brazilian cities have a part of its population neglected by the government regarding housing and basic infrastructure rights. Low-income settlements condition of informality result from the lack of infrastructure, consequently affecting quality of life. Such negligence comes from an urban legislation that acts as an exclusion agent which does not guarantee basic life needs, such as access to the sewage collection and treatment. These settlements are often built in unstable and environmentally sensitive areas since those areas are usually unoccupied and not thoroughly inspected by local governments (Freitas, 2015).

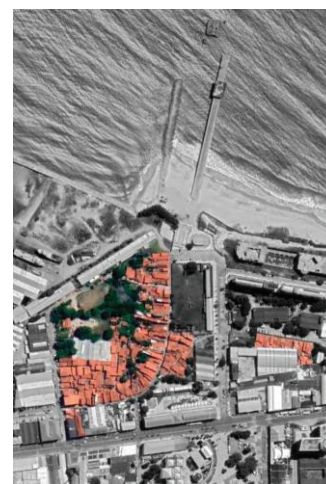


Figure 2: Poço da Draga top view. Source: Google Maps, edited by author, 2019.

Poço da Draga (Fig.2) is a historical community, dating from more than 100 years, located at the coast of Fortaleza, Brazil. As a result from social and economic inequality, this community has long settled into an unfavorable housing area that suffers with usual floods throughout the year. Such occurrences were never dealt by the local government as the houses are considered being illegal today, although, by the time the first houses were built, there was no official legislation to the site. Besides the flooding issue, the community does not have access to public sewage system which, along with the presence of a hydrological body of water nearby, increases their exposure to different diseases (Barreira *et al.*, 2019). This puts this community situation at constant and rising risk, considering how climate change consequences can possibly aggravate flooding occurrences (Fig. 3).



Figure 3: 2011's first flood, images recorded in April. Source: Images available on the "Ilhadadrage" Youtube channel.

Despite Poço da Draga proximity to Fortaleza historical and economical center, it is considered one of the first segregation spaces within the city. The community's background takes part in the history of a fishing village that used to exist at the central coast and from which most of the current elder residents descend (Almeida, 2014). Besides being considered an informal settlement today, at the time the first houses were built, there was no official legislation to the site.

1.3. LIM STRATEGY

Considering the continual change in urban landscape of 21st century cities, the quality of traditional urban planning is questioned, as the difference between legal and real city increases (Freitas C. *et al.* 2016). This challenge is imposed at an even greatest importance in cities like Fortaleza where there is great housing inequality, as mentioned before. Faced with this issue, it is necessary for researchers and workers to produce data and generate models to base decisions within urban projects and highlight for a more inclusive city (Freitas C. *et al.* 2016).

The identification of urban problems must be continuous, due to the current scenario of constant change, designers must be able to work with increasingly changeable data. Finally, design decisions should no longer be a linear process; on

the contrary, they should be a looping visualization and readjustment of hypotheses, based on feedback. To this purpose, the development of intelligent systems based on informational design are key to achieving urban systems that can represent this city space that is in constant change and adaptation. This type of mechanisms can be used as mediators, supporting design decisions in urban and landscape plans (Moreira *et al.*, 2018).

The present work explores one type of informational design mechanism, the Landscape Information Modelling (LIM), which as an intelligent design tool that looks forward to bringing automatization to landscape modelling and urban planning (Ahmad M. *et al.* 2012). The goal is to create a system of bioretention cell implementation by using computer algorithm systems associated with 3D visualization for it to be used by designers and planners. The bioretention cell solution allied with the cities traditional drainage system opens a path to better optimization of public resources and effort. Such green alternatives should increase resilience of spaces and communities like Poço da Draga.

2. METHODOLOGY

The chosen platform to develop the algorithm consists of the interoperability between the programs Rhinoceros® plus Grasshopper® from McNeel and Associates. Rhinoceros 3D® program (CAD platform solution), besides being a complete modeler, giving exporting and importing options in a big amount of renderers (which is important in image production) possesses Grasshopper® free plugin, a visual programming interface (Souza, 2018) (Fig. 4).

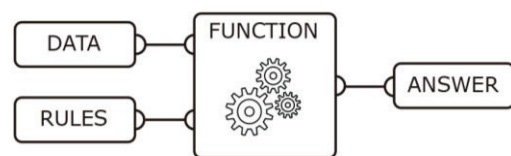


Figure 4: Diagram representing the working scheme of a visual programming language syntax. Created by the authors.

In this specific study it was created a complex algorithm which is divided into 3 main steps. First the user can analyze the site in question and how rain behaves, as a result is possible to understand how the flood tend to occur and where this rainwater comes from. As a second step, the effective precipitation is calculated from an empirical equation, as a result it is possible to predict or define (depending on the user's intention) the amount of rainwater that the green infrastructures should absorb. Finally, the bioretention cells amount and composition are defined, finally the algorithm gives as an answer the volume absorbed by the green infrastructures.

With the data collected in steps one, two and three the designer can make effective decisions for any site in which the algorithm is implemented (fig. 3).

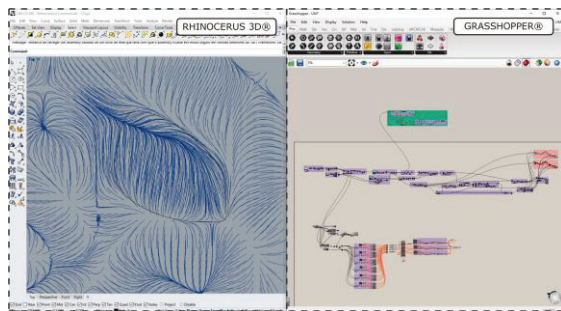


Figure 5: desktop screenshot in which programs Rhinoceros (left) and Grasshopper® plugin (right) are working simultaneously. Created by authors.

3. CASE STUDY

3.1. THE SITE

Poço da Draga (Fig. 6) is a community which suffers with constant flooding problems. A pond forms within this territory every year in rainy season. This water body partially runs to the sea nearby, but it still gets accumulated for some time at the community region, being a catalyst for diseases, in other words, a constant risk for people's lives (Fig. 3). Walking through the streets and alleys it can be seen houses with raised floors, already prepared for the next flooding period (Barreira *et al.*, 2019).

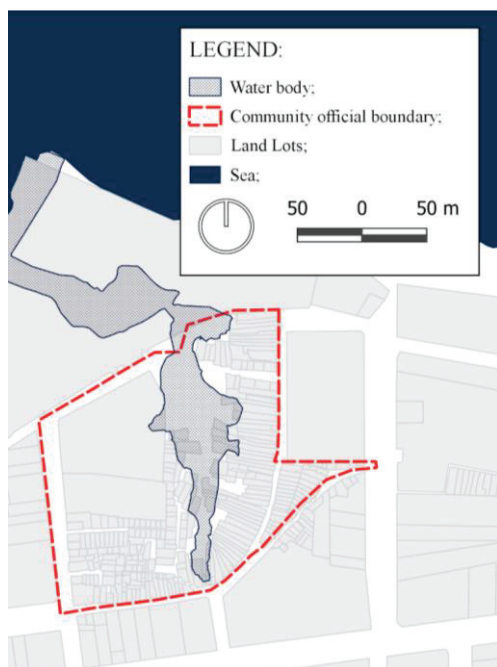


Figure 6: Map representing Poço da Draga. Created by authors.

3.2. RAIN SIMULATION

At the algorithm's first stage it is necessary to use the region's topography as the input to analyze the rainwater behavior, as shown in figure

7. As a result to this simulation it has been observed that a great area (here named "flow impact area") was responsible for the floodings and the water retention area present in Poço da Draga's region. This "boundary area" is established by the researcher based on his or her interpretation of the simulation.

The flow impact area is composed majorly by a city dense downtown area of Fortaleza, consequently it is a mostly impervious region. This situation has proven itself to be good for the implementation of green infrastructure, in this case, bioretention cells, and the algorithm was key to understanding where and how-to better act in this specific situation.



Figure 7: Map representing Flow Impact Area calculated by algorithm. Created by authors.

3.3. FLOW RATE CALCULATION

Next, an empirical equation is used to calculate the surface runoff at the flow impact water area on a time range of one hour (Silva *et al.*, 2013). In this equation it was used as parameters the impact area, the flow rate of the 100 years

return period for this specific region and the runoff coefficient as shown in figure 8.

$$R = (A \times \alpha \times f)$$

Figure 8: Surface runoff equation. R = surface runoff; A = surface area; α = runoff coefficient; f = flow rate; Δt = duration (Silva *et al.*, 2013).

Type of ground surface	Coefficient of surface runoff, F_{re}
Road:	
Pavement	0.70–0.90
Permeable pavement	0.30–0.40
Gravel road	0.30–0.70
Shoulder or top of slope:	
Fine soil	0.40–0.65
Coarse soil	0.10–0.30
Hard rock	0.70–0.85
Soft rock	0.50–0.75
Grass plot of sand:	
Slope 0–2%	0.05–0.10
Slope 2–7%	0.10–0.15
Slope 7%	0.15–0.20
Grass plot of clay:	
Slope 0–2%	0.13–0.17
Slope 2–7%	0.18–0.22
Slope 7%	0.25–0.35
Roof	1.00
Unused bare land	0.20–0.40
Athletic field	0.40–0.80
Park with vegetation	0.10–0.25
Mountain with a gentle slope	0.30
Mountain with a steep slope	0.50
A paddy field or water	0.70–0.80
Farmland	0.10–0.30

Figure 9: Table used as reference to define the runoff coefficient (Jinno *et al.*, 2009).

The previous topic established the impact area, in this case the area has 445877.24m². The flow rate for 100 years return period for Fortaleza is 95.6mm/h (Silva *et al.*, 2013). Finally, the runoff coefficient used was 0.7, based on figure 9 and considering the case study site (Jinno *et al.*, 2009). As a result, the surface runoff was defined by the algorithm as 2.98 * 10⁷L/h, illustrated in figure 10.

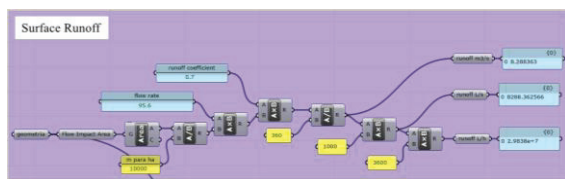


Figure 10: Image captured from Grasshopper® workspace where the equation takes place. Created by authors.

3.4. GREEN INFRASTRUCTURE

The final step of the algorithm defines the amount of water that will be retained by the green infrastructures, in this case it was used as reference the value of 2.98 * 10⁷L/h, found previously. It is important to remember that this value is decided by the researcher in use of the algorithm, for example, the return period in the surface runoff calculation can be set for 50 years instead of 100 and the researcher is also free to choose between working with the full value or not.

At this specific case study, the choice of working with a 100 year return period comes from the need for resilience when it comes to vulnerable

communities like Poço da Draga, which do not receive constant financing and support from the government as explained previously.

Besides the water reservation input it is also necessary a street network shapefile of the site. With this file the program is able to use the different roads characteristics as inputs, in this case the input necessary is the width of the road, so that the extension of bioretention cell use can be calculated. There is not a predefined width for those infrastructures, these must be defined by the user, in this study case a proportionate width was chosen for each type of street. With that explained, there is still a last input, and this one must be a choice of the researcher, it is the depth of the bioretention cells.

Bioretention cells are formed by a series of layers in the following order (from top to bottom): (i) vegetation, (ii) vegetation subtract; (iii) coarse sand; (iv) thermal blanket; (v) gravel (Fig. 12). Gravel layer is the one where water is absorbed and its depth defined to set an end value (Moura *et al.*, 2015). So, as a resume, that are 3 types of data that are not predefined, the amount of water that must be handled and the width and depth of the infrastructures. Those are meant to be tested back and forward to better attend the project's goals (Fig. 11).

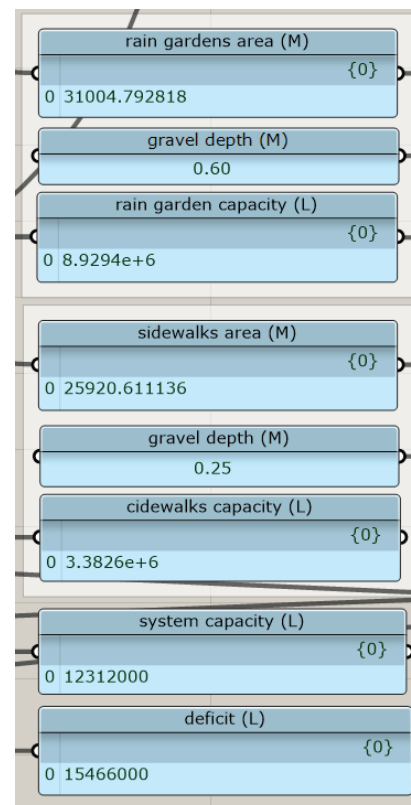


Figure 11: Image from Grasshopper® workspace where data can be manipulated and visualized. Created by authors.

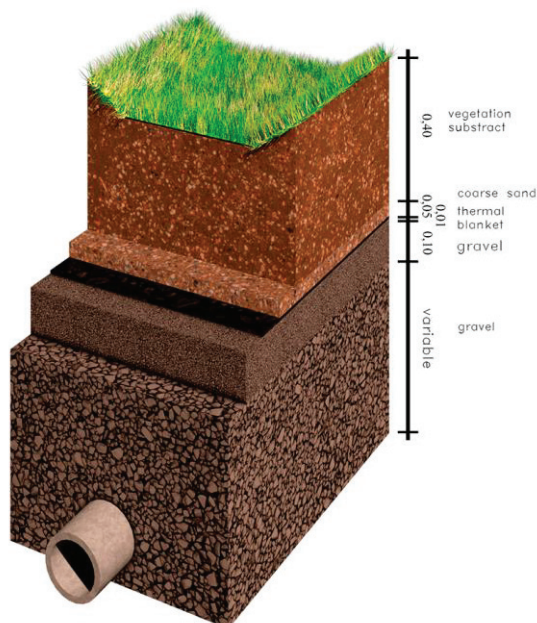


Figure 12: Bioretention cell. Created by authors.

3.5. CLOSURE

The three steps explained previously support one another and, once the user processes each one the first time, parameters can be redefined and readjusted in any one of them at any given order. In this case study the design plan was to adapt all streets inside the flow impact area to receive the green infrastructures in order that they could work in their full potential.

4. CONCLUSION

Achieving the creation of a LIM platform is a challenge due to the complexity of landscape design. This paper is an example of how this concept can be applied to a specific issue, such as green infrastructure for flood risk areas. It is important to highlight that in Brazilian cities, as in other countries that have a great social inequality, there are other factors such as the presence of informal settlements which enhances negative impacts due to climate change. These factors make the need for more intelligent and precise urban interventions, that is why the Landscape Informational Modelling proves itself to be a good tool that helps making decisions to increase city resilience in front of future change.

This initial study works only with drainage aspects of the urban space, with further research development we look forward to enhancing the research reach to other aspects of landscape and urban design such as mobility and vegetation specific interventions through parametric modelling.

REFERENCES

1. PBMC (2016). Impacto, vulnerabilidade e adaptação das cidades costeiras brasileiras às mudanças climáticas: Relatório Especial do Painel Brasileiro de Mudanças Climáticas [Marengo, J.A., Scarano, F.R. (Eds.)]. PBMC, COPPE - UFRJ. Rio de Janeiro, Brasil. 184 p. ISBN: 978-85-285-0345-6.
2. United Nations, Department of Economic and Social Affairs, Population Division (2019). World Urbanization Prospects: The 2018 Revision (ST/ESA/SER.A/420). New York: United Nations.
3. Freitas, C. F. S. (2015a). Fighting for planning for the first time, in Fortaleza, Brazil. *Progressive Planning*, 204, 11–14. Available: http://www.plannersnetwork.org/wp-content/uploads/2015/09/PPM_Sum2015_Freitas.pdf [Google Scholar]
4. Universidade Federal do Ceará, Fundação Cetrede (2019). Plano Integrado de Regularização Fundiária da Zeis do Poço da Draga: Caderno de Diagnóstico Socioeconômico, Físico-Ambiental, Urbanístico e Fundiário. Brazil, Fortaleza.
5. Almeida, A. A. (2015). Segregação urbana na contemporaneidade: o caso da Comunidade Poço da Draga na cidade de Fortaleza. (dissertation). Available: <http://tede.mackenzie.br/jspui/handle/tede/389>.
6. Lima, M. Q. C., Freitas, F. S. (2016). Modelagem paramétrica e os limites dos mecanismos tradicionais de regulação da forma urbana. *Revista Políticas Públicas & Cidades*, v. 4, n. 1, pp.117 – 138.
7. Moreira, E., Cardoso, D. R., & Simões, P. J. A. (2018). Information technologies applied to the assessment of the visibility of historical heritage in urban contexts/Tecnologias da informação aplicadas à avaliação da visibilidade de bens tombados em contextos urbanos. *Brazilian Journal of Information Design*, 15(1), 1+.
8. Ahmad, Ahmad & Aliyu, Abdullahi (2012). The Need for Landscape Information Modelling (LIM) in Landscape Architecture. *Digital Landscape Architecture Conference*. Dessau, Germany, May 31 - June 2.
9. Silva, F. O. E., Palácio, F. F. R., Campos, J N. B. (2013). Equação de chuvas para Fortaleza-CE com dados do pluviógrafo da UFC. *Revista DAE*, v. 192. DOI: 10.4322/dae.2014.106
10. Jinno, K., Tsutsumi, A., Alkaeed O., Saita S. & Berndtsson R., (2009). Effects of land-use change on groundwater recharge model parameters. *Hydrological Sciences Journal*, 54:2, 300-315. DOI: 10.1623/hysj.54.2.300
11. Moura, N., Pellegrino, P., & Martins, J. (2015). Best management practices as an alternative for flood and urban storm water control in a changing climate. *Journal of Flood Risk Management*, 9(3), 243-254. doi:10.1111/jfr3.12194

‘Urban Lab City’: Investigating the Role of Built Form on Air Quality and Urban Microclimates— City of London Case Study

JULIE ANN FUTCHER¹, GERALD MILLS²

¹ Urban Generation, London, United Kingdom

² University College Dublin, Dublin, Ireland

ABSTRACT: Here we report on the preliminary findings from a pilot project titled ‘Urban Lab City’. The project investigates the influence of built form on air quality (Nitrogen Dioxide) and daytime air temperatures in the City of London. The study employs a network of 80 diffusion tubes that are installed along a network of streets that form a transect through a complex urban setting. This street network is also part of an ‘urban climate walk’, which is used to teach urban climatology and has previously been used to measure aspects of the microclimates. Results show that the dimensions and layout of buildings (built form) have a significant influence on the outdoor environment. The research presented here forms part of a series of connected projects on aspects of urban sustainability that focus on building groups rather than individual buildings. Together these projects demonstrate buildings are not energy-islands but have a dynamic relationship with their wider environment.

KEYWORDS: Built Form, Urban Microclimate, Urban Air Quality, Passive Resources, Field Measurements

1. INTRODUCTION

London, like many cities, is experiencing a remarkable transformation to its urban landscape as tall and very tall buildings (< 20 storeys) are inserted into its relatively low-lying setting (>25 meters) (Figure 1). Whilst it can be argued that these transformations address the need for additional floor area (both residential and commercial), they coincide with concerns over air quality and overheating risks, aggravated further by the climate emergency. In addressing these issues, the influence of the spatial characteristics of built form (the dimensions of buildings and their placement in relation to each other), on both air temperature and pollution dispersal, is often overlooked in favour of solutions that focus on the individual building. These solutions are often described as generic as they are ‘non-specific to actual geographic locations or climatic conditions’ (Blakely 2007). The effects of this building-scale focus are compounded where policies do not consider the aggregate impact of built form on the surrounding neighbourhood. The absence of policy is a result of a number of factors, including our limited understanding of the environmental outcomes that arise from building interactions and the primacy of building needs over those of other buildings and the intervening outdoor spaces. As a consequence, policy does not avail of opportunities to use built form to the benefit of the neighbourhood. This paper examines the aggregate impacts of buildings on outdoor spaces in the City of London, which has a diverse and complex built form.

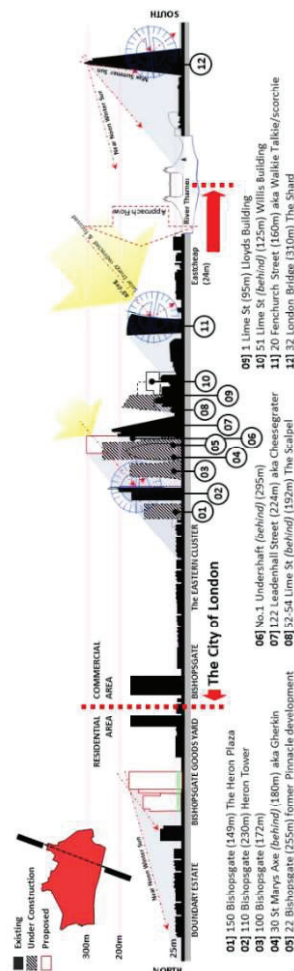


Figure 1: Conceptual section of the City of London through the Eastern Cluster

The City of London is both the historic core of Greater London and a world-leading financial district. As a result, its built form accommodates high-end office space that is housed in both older mid-rise buildings and modern tall and very tall buildings (Figure 1). The emerging built form is highly heterogeneous over short distances and results in diverse urban microclimates. This heterogeneity alongside its central urban location and its daytime 'office hours' function¹, which makes it an ideal location for a monitoring study to improve our understanding of the effects of built form on the wider environment.



Figure 2: Map showing average building heights (meters) and tube locations (stars) along the route of the London Urban Climate Walk (thick dashed line)

2. THE CITY OF LONDON MICROCLIMATE STUDY

The diversity of the City's urban microclimates provides the context for the development of an Urban Climate Walk (CIBSE 2015) that demonstrates the role of urban form on outdoor climates (Figure 2). The Walk was designed to promote conversations around the spatial and temporal influence of built form on access to passive resources (day and sun

¹ The City has a residential population of 7,5000 However a working population of over 510,000 Monday to Friday 9 to 5 giving the area an interesting dynamic on day to day energy flows

light, wind and temperature) and in turn, its influence on the dispersal of heat and pollution. The route of the Walk was designed to maximize exposure to different microclimates and has been used as a framework for measuring urban climate effects.

A series of indicative daytime observations of wind (average and maximum) and air temperatures using simple equipment (name). These variables were recorded at various locations along the Walk route between December 2016 and January 2017 (Winter) and over a 10 day period in August 2017 (Summer). The instrument was exposed until the air temperature readings had settled. All readings were taken in the shade 1.5 meters above ground, facing due north. These measurements capture a sample of the daytime microclimates within the urban canopy, which are highly dynamic over space and time.

These microclimate surveys identified areas where tall buildings create strong winds at ground level. In addition, these findings indicated that the location and timing of these effects depends on the direction and strength of the ambient wind. The surveys also identified areas of gustiness, of channelling and of calm. By comparison, there is little variation in air temperature along the Walk, despite the highly variable shadowing pattern indicating the effectiveness of mixing within the canopy.

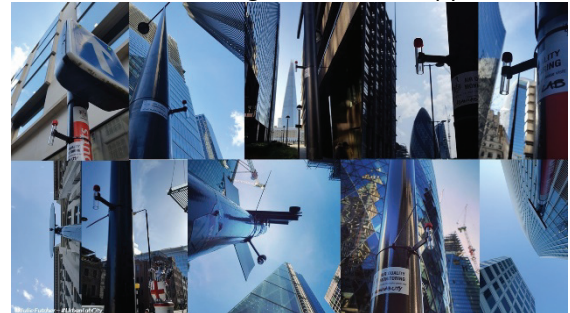


Figure 3: An example of a tube locations

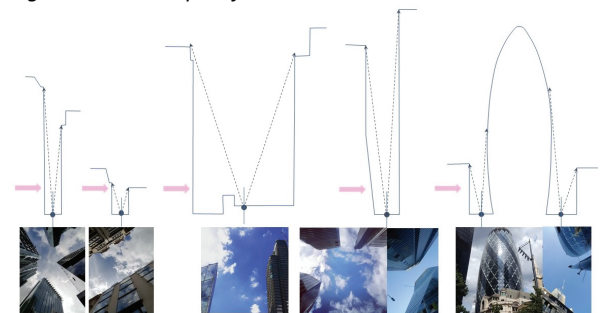


Figure 4: An example of a mean building H/W ratio along the walk (arrow represents 25meter average building height)

The microclimate measurements from each location along the route were compared against conditions at a base location (Moorgate) marked on Figure 2 (①). This site was chosen as it represents a simple urban setting with a long north south street (20 meters) lined by terraced buildings of the same

height (25 meters); the mean building height to street width (H/W) ratio is close to 1.

All other measurements were made in streets with varying orientations, symmetry and H/W ratios (Figure 4). In addition, each is associated with varying daytime functions (i.e., office use) and associated pedestrian and motor traffic.

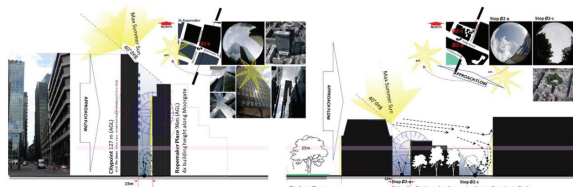


Figure 5: Section through Ropemaker place and Eldon Place

3. MICROCLIMATE RESULTS

Ropemaker Place (96m), the Heron Plaza (112m) and Citypoint (127m) is a small cluster (S02b) of relatively tall buildings (Figure 5). In winter the site is gustier than the base site although both record winds of 4 ms^{-1} ; the air temperatures varies by about a degree either side of 9°C , recorded at the base. In summer, the winds at this location are lower. During the summer walks, lower range of wind speeds were recorded ($0.4 \pm 0.9 \text{ ms}^{-1}$) compared to the average 1.4 ms^{-1} and a higher range of daytime T_{air} (within $\pm 2^\circ\text{C}$ range) against (ØS01) average summer daytime T_a 23°C for the same period.

However, at the other end of the street (Eldon Street (S02-a), little variation in wind movement was recorded for both winter and summer, and daytime T_{air} showed no significant difference against ØS01 for both periods (Figure 5). These findings are in line with much urban climate research which suggests that daytime urban air temperatures are likely to be similar due to local scale mixing.

Table 1. Number and location of the diffusion tubes and microclimate measurements

Site (S)	Site Location	Number of tubes
S02	South Place /Eldon St	6 of 20
	Ropemaker Place	12 of 20
	Moorgate, North end.	2 of 20
S04	Worship Street	4 of 9
	North Broadgate	5 of 9
S06	Camomile St	5
S07	Heron Tower and 100 Bishopsgate	5
	30 St Mary's Axe (Gherkin)	4 of 16
	Eastern Cluster	4 of 16
S08	South Bishopsgate	8 of 16
S09	20 Fenchurch	5 of 7
S10	Old Watermans Walk	3 of 6
	Lower Thames St	3 of 6
	Mid to South Moorgate includes London wall Junction and Gresham St north Bank Junction	6 of 17
	Bank	11 of 17

In our sample studies, slightly more dynamic effects on summer T_{air} were found at the sites of the taller buildings, i.e., Principle Place (ØS04) ($-2 \pm 2^\circ\text{C}$); the Heron Tower (S06) ($-1 \pm 1^\circ\text{C}$); the Eastern Cluster (S07) ($-2 \pm 1^\circ\text{C}$) and 20 Fenchurch Street (S08) ($-2 \pm 1^\circ\text{C}$). These results indicate the potential to tall buildings to deflect cooler higher winds down to street level.



Figure 6: An example of a tube deployment. The sensor is the red capped device attached to a lamppost at 2m height.

4. THE CITY OF LONDON AIR QUALITY STUDY

Diffusion tubes were installed along the street network in the City (Figure 2 and 3). The sites were chosen to represent common pedestrian routes alongside streets with different levels of traffic; they also capture a range of microclimates identified through the Urban Walk. Table 1 shows the number of tubes placed at seven different sites, which record airborne Nitrogen Dioxide (NO_2) passively (see Figure 6 & 10). Each device is attached to a lamppost close to the road (Figure 6 & 10) and is left in place for a month, after which they are replaced.

Inevitably not all tubes were mounted in the ideal location, nor at the desired 2 meters off the ground. There was also ongoing loss of data due to the theft of the tubes. Finally, it is worth noting that results suffer from missing data, which can distort the

findings. This has been addressed using the recommended 'Annualised' adjustment method, and the 'Bias Adjustment Factor' (DEFRA 2018) has also been applied to the annual results.

Table 2. Average NO₂ values for both May and the annual values for the tube sites.

Station	May	Annual	Station	May	Annual
S02-01	52	50	S07a-7b	66	68
S02-02	54	54	S07a-7c	66	66
S02-03	42	49	S07a-7d	66	67
S02-04	41	45	S07-01	35	38
S02-05	43	44	S07-02	49	49
S02-06	41	43	S07-03	46	44
S02-07	42	41	S07-04	40	41
S02-08	40	43	S07-05	39	43
S02-09	84	77	S07-06	44	43
S02-10	51	46	S07-a	45	49
S02-11	50	55	S07-b	31	40
S02-12	51	52	S08-01	38	39
S02-13	44	44	S08-02	51	51
S02-14	50	50	S08-03	49	49
S02-16	48	48	S08-04	49	43
S02-17	58	60	S08-06	57	45
S02-19	69	80	S08-07	35	46
S02-20	52	53	S08-08	44	49
S02-21	46	57	S09-01	37	39
S02-22	48	57	S09-02	45	41
S02-30	41	47	S09-03	68	53
S04-01	43	43	S09-04	86	67
S04-02	46	47	S09-05	74	73
S04-03	46	46	S09-06	54	54
S04-04	42	50	S10-01	77	77
S04-07	73	82	S10-02	72	77
S04-08	65	73	S10-03	79	79
S04-09	57	68	S10-03a	77	79
S04-09a	63	67	S10-04	78	77
S04-10	55	65	S10-05	49	58
S06-01	85	79	S10-06	39	47
S06-02	62	68	S10-07	69	69
S06-03	65	67	S10-08	65	65
S06-03	63	68	S10-09	55	66
S06-05	75	80	S10-10	81	83
S07a-01	76	86	S10-11	63	61
S07a-02	86	87	S10-12	43	43
S07a-03	80	80	S10-13	63	63
S07a-04	78	85	S10-14	114	115
S07a-05	78	80	S10-15	67	68
S07a-7a	76	76	S10-16	59	59

4.1 Air Quality Results

Here we report on our key observations of the study. Generally, the study found results to correlate well with those identified in the urban microclimate

studies, with better air quality recorded near the windy sites around the base of the tall buildings. Although air quality overall is poor, several sites had good air quality during all months, and others moderately good some of the time. As expected, air quality at road junctions was worse than those recorded nearby.

Of the 80 sites 17 recorded 40 µg/m³ or less (Table 2), which is the annual limit identified in air quality management plans (DEFRA 2018). Two of these sites are located Old Watermans Walk a very narrow (H/W ratio >2) pedestrian route (S09-01 and S09-02) next to the Thames Path, but the rest were located directly at the base of tall buildings, in areas with low levels of traffic i.e., Ropemaker (S02); Worship Street (S04); and at the Eastern Cluster (S07).

In addition, low levels were recorded at the two standalone towers, to the south of 20 Fenchurch Street (S08) and to the west of the 'Old Stock Exchange' (S10-12). The best average air quality reading of 31 µg/m³ (Table 2 and Figure 7) was recorded along Lime Street (S07-B) in the centre of the Eastern Cluster. We hypothesise that this is due to both relatively low levels of traffic and ventilation caused by the surrounding tall buildings. It is worth noting in part 2 of this study that for the City of London low levels of traffic alone where not enough to ensure low levels of NO₂.

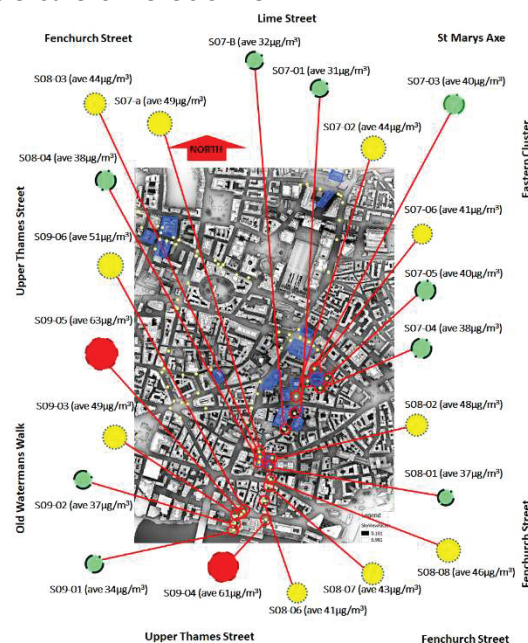


Figure 7 annual average NO₂ values for the Eastern Cluster (S07), Fenchurch Street (S08) and S10 and Old Watermans Walk (S09). The size of symbol is proportional to value and colours indicate levels (µg m⁻³): green (<40), yellow (<60), red (<100) and black (>100).

The worst air quality, 110 µg/m³ (Table 2 and Figure 8) was recorded at the junction of Moorgate and London Wall (S10-14), where a temporary

overhang acts as a barrier to pollution dispersal, generated at or near the junction. This result is 30 % higher than the second highest level $82 \mu\text{g}/\text{m}^3$ (S07a-3) further west along London Wall, followed closely by (S07a-01), directly at the north of the Bishopsgate/London Wall junction.

The highest average levels were recorded along the two major N/S thoroughfares along Moorgate (S02 & S10) and Bishopsgate and Gracechurch Street (S07) (Figure 8); these include the junction at the north of Moorgate (S02-09 and 19); the junction at the south of Moorgate (S10-04 and 03); at the Bank of England along Princes Street (S10-02 and 03a); at Bank Junction (S10-10); at the junction of London Wall and Bishopsgate (S07a-01 to 05); along Bishopsgate and Gracechurch Street (S07a) and at the junction of Liverpool Street and Bishopsgate (S04-07); and along Camomile Street (S06-05 and 03).

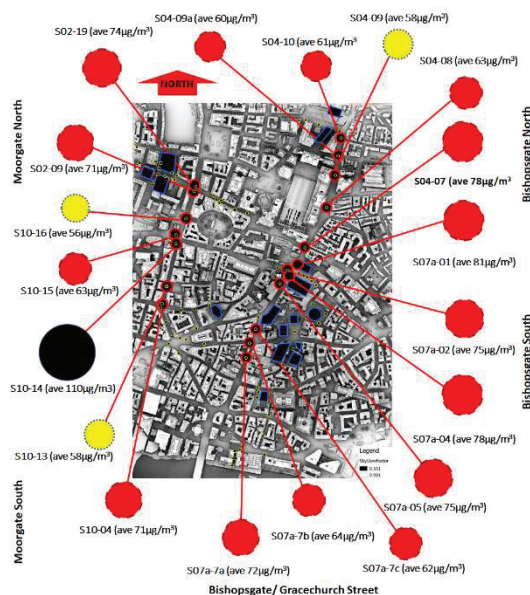


Figure 8 [5] annual average for Moorgate (S02 and S10) and Bishopsgate (S04 and S07a) two major N/S thoroughfares through the City of London.

The two major north-south thoroughfares along Moorgate (S02 & S10), and along Bishopsgate and Gracechurch Street (S07), included in the study, make interesting comparisons (Figure 8). Both are major routes through the City but the built form of each is very different, as are the traffic flows; with Bishopsgate having much higher levels of congestion, including a large number of buses, compared to Moorgate. However, these differences in congestion are not reflected in the measured levels of NO₂ (Figure 8); the average reading for Moorgate and Bishopsgate are 72 and 70 $\mu\text{g}/\text{m}^3$, respectively. Moorgate is a symmetrical street with a mean building height (H) of 25 m, and a mean street width (W) of 20 m; mean H/W ratio is close to 1 along its entire length. The surrounding area has a similar form

(compact mid-rise). Bishopsgate is found in a compact high rise area with an average H/W ratio >2. Along Bishopsgate there is considerable variation in building height and street width along its length. The street is flanked by various tall buildings (greater than 7 stories) with a series of very tall buildings at its centre, including 110 Bishopsgate (230 m) and One Bishopsgate Plaza, 100 and 22 Bishopsgate (135, 172 and 278 m, respectively). These different forms affect airflow and pollutant dispersal and suggest that the Bishopsgate form lowers near-surface air quality close to that found in Moorgate.

The peak levels of recorded NO₂ for July are found at all sites located along Bishopsgate, north of the emerging tower at 22 Bishopsgate (Figure 8). These peak levels suggest an increase in traffic flow, rather than a weather driven event, as this effect is not picked up by the City's the continuous monitoring sites.

To verify results from the field study, measurements taken from around the Bank of England (S10) were correlated against a computational fluid dynamic (CFD) simulation study performed using a steady state, Reynolds Averaged Navier Stokes' K-Omega SST model. Figure 9 shows the wind speeds at 2 m, with the prevailing wind coming from the South-West based on the CFD study. The results from the simulation indicate that areas of low winds are associated with high NO₂ values and vice versa. This is evident at the Old Stock Exchange (S10-12), and areas of recirculation and stagnant flow are easily identified. Further results of this study can be found on the consultancies webpage (Salientedge 2018).

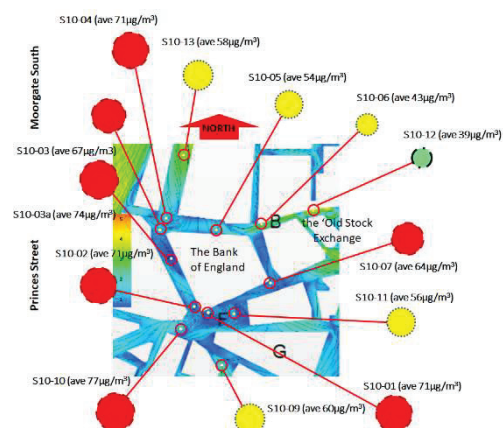


Figure 9: CFD of Bank Area (S10) courtesy of Salient Edge. The figure shows wind velocity (m/s) at 2 meters above ground, the location of the tubes (S10 - 01 to 13), for R1-R12. Prevailing Wind direction from the South West.

5. CONCLUSIONS

Here we report on the initial findings identified in the pilot 'Urban Lab City' project. The focus of this component has been the detailed examination of ambient air quality (NO₂) at over 80 sites placed

along a street network located in the City of London. This area is distinguished by extreme variation in aspects of built form (dimensions of streets and of buildings) over short distances.

The observations show that tall buildings and street geometry have an impact on air quality. General observations from this study indicate;

- Built form has a localised effect on air quality.
- The best urban air quality is found where there is both low levels of traffic and a cluster of tall buildings.
- The air quality at junctions was worse than those recorded nearby.
- Localised built form influences air quality at pedestrian level
- Minor obstructions (such as construction canopies) to ventilation can significantly affect air quality

Overall, the findings demonstrate not only how the surface structure of built form influences local climate through airflow, but that in turn these effects impact spatially on air quality.



Figure 10: The site (S10-02) BANK

This pilot project has identified the important role of urban built form on levels of air pollution in the City of London. In contrast to other studies, it takes the perspective of the pedestrian and purposefully samples the street network based on microclimate knowledge. Moreover, it uses an inexpensive system to gather spatially precise averaged information on ambient air quality. The results show considerable variation over short distances that cannot be

explained only by traffic emissions. The dynamic relationship of the buildings on near-surface airflow created patterns of ventilation and calm that affect the mixing of emissions. However, the prevailing airflow patterns produce areas of sustained poor air quality. The results indicate that tall buildings can improve near surface air quality however at a cost of increased gustiness for pedestrians.

ACKNOWLEDGEMENTS

The author would like to acknowledge the City of London Corporation for commissioning the study and the contribution to this study from Salient Edge an engineering and aerodynamics consultancy company that provided the CFD of Bank (S10).

REFERENCES

1. Fitcher J., and Mills, G. (2015) Walking-Among-Giants CIBSE journal
2. <https://www.metoffice.gov.uk/climate/uk/regional-climates/so>
3. DEFRA (2018) Local Air Quality Management Technical Guidance (TG16) February 2018
4. <https://salientedge.com/blog/2018cleaning-up-the-big-smoke>
5. Aristodemou, E., Boganegra, Luz L., Mottet, L., Pavlidis, D., Constantinou, A., Pain, C., Robins, A. and ApSimon, H. (2018) How tall buildings affect turbulent air flows and dispersion of pollution within a neighbourhood Environmental Pollution 233 782e796
6. Daniel R. Drew, D., Barlow, J. and Lane, S., (2013) Observations of wind speed profiles over Greater London, UK, using a Doppler lidar J. WindEng.Ind.Aerodyn.121 98–105

A simplified approach for designing sustainable Near Zero Energy Settlements

Environmental impact analysis applied in the framework of the European ZERO-PLUS project

GLORIA PIGNATTA¹

¹Faculty of the Built Environment at the University of New South Wales (UNSW), Sydney, Australia

ABSTRACT: In Europe, more than one-third of greenhouse gas emissions are produced by buildings, that are also responsible for approximately 40% of the total energy consumption. In the framework of the European project ZERO-PLUS, that contributes to meet the policy goals of the European directives on new buildings, an innovative method to design, built, operate, and monitor high energy performing residential buildings has been developed and applied at the community level in four European countries; UK, France, Italy, and Cyprus. ZERO-PLUS, tackling climate change, aims to demonstrate that it is possible to achieve cost-effective near-zero energy settlements without forgetting the environmental aspects. One of the activities implemented in ZERO-PLUS concerns the environmental impact assessment of near-zero energy settlements designs in Europe. This activity has been carried out by developing and applying a simplified Life Cycle Assessment (LCA) technique and a pre-assessment of the LEED rating system to the four ZERO-PLUS case studies at the end of their preliminary design stage. This to encourage the integration of green building practices in the ZERO-PLUS design. In this paper, the Italian case study has been chosen to present the novel simplified LCA approach applied at the settlement level. **KEYWORDS:** Environmental impact analysis, Near Zero Energy buildings, LCA analysis, IPCC method, Cumulative Energy Demand (CED) method

1. INTRODUCTION

Nowadays, environmental considerations and analyses are becoming extremely important in the building sector due to the increasing awareness of the negative impact that buildings produce on the environment.

Net-zero energy or net zero carbon concepts have been developed in recent years at the international level with the aim to reduce to zero both the energy consumption and the greenhouse gas emissions that are associated with the building sector [1]. Cost barriers are associated with the implementation of these high energy and environmental performing buildings, thus limiting their development and diffusion. One possibility to overcome these cost barriers consists in applying the same net-zero energy or net zero carbon concept from the scale of the building to the scale of the settlement, where the economy of scale may be easily implemented. Numerous advantages may be registered when moving from the scale of the building to the scale of the settlement, such as the improvement of the social organisation, the optimization of the maintenance cost, the more reliable supply of energy, and the

optimization of the quality of the outdoor environment by mitigating the local microclimate thanks to the application of passive mitigation strategies at the settlement level [2].

In Europe, a large number of projects have been carried out to achieve net-zero energy or net zero carbon residential buildings [3-5], especially to meet the requirements set by the European directives on new buildings [6].

One European project of the energy efficiency H2020 program is ZERO-PLUS "Achieving near Zero and Positive Energy Settlements in Europe using Advanced Energy Technology" [7]. This project contributes to the practical implementation of 4 new residential net-zero energy settlements in Italy, France, Cyprus, and the UK aiming at reducing the energy consumption, the CO₂ emissions, and the cost of achieving net-zero energy requirements in the demonstration buildings. In this project, innovative and advanced technologies for energy conservation and energy production, that can facilitate the achievement of the energy and environmental ZERO-PLUS targets, are proposed and integrated into the design of the 4 settlements. The ZERO-PLUS project

aims also to i) contribute to the mitigation of the climate change and the urban heat island (UHI) phenomenon, thanks to a dedicated climate-responsive and affordable design and ii) demonstrate that it is possible to achieve cost-effective and high energy performing buildings without forgetting the quality of life and the health of the residents, the energy security, and the environmental impact [8-10].

Due to the significant environmental impact produced by buildings, it is of fundamental importance to introduce the life cycle perspective in the building and settlement design [11].

The present paper presents the novel and simplified approach that has been developed in the ZERO-PLUS framework to design sustainable Near Zero Energy Settlements by means of a dedicated environmental impact analysis.

2. METHODOLOGY AND METHOD

As anticipated in the introduction, the ZERO-PLUS project is a framework composed of a series of approaches, novel materials and technologies, tools, guidelines, among others, that aims to achieve the future energy and environmental requirements for new sustainable residential buildings and settlements.

One of the activities implemented in ZERO-PLUS deals with the environmental impact assessment of the preliminary designs of the near-zero energy settlements in Europe by means of the Life Cycle Assessment (LCA) technique and the LEED (Leadership in Energy and Environmental Design certification) assessment protocol developed by the U.S. Green Building Council (USGBC) [12]. This activity has been carried out by developing and applying a simplified Life Cycle Assessment (LCA) technique, together with the LEED pre-assessment evaluation, to the 4 ZERO-PLUS case study settlements at the end of their optimized preliminary design stage. This to encourage the integration of green building practices in the ZERO-PLUS design. The aim of the simplified LCA approach is to compare the environmental performance of the proposed ZERO-PLUS designs for the near-zero energy settlements with the same near-zero energy settlements designs where the ZERO-PLUS concept (e.g., ZERO-PLUS guidelines, technologies, and solutions for settlement optimization) [13] is not applied.

In the project, the standardized LCA methodology [14,15] is applied to all the innovative ZERO-PLUS materials and renewable energy systems (RESs) by following the cradle-to-gate approach that includes only the pre-use phase (e.g., raw material extraction and manufacturing process). Due to a lack of reliable data, not yet available for the novel ZERO-PLUS

materials and technologies, the use phase, demolition, and recycling disposal were not considered in the environmental analysis.

The simplified LCA analysis has been performed by using the SimaPro software [16], where the Intergovernmental Panel on Climate Change (IPCC) [17] and Cumulative Energy Demand (CED) [18] methods have been selected as environmental impact assessment methods for the purpose of the project. In this study, the first method (i.e. IPCC) represents the climate change impact category and it is related to emissions of greenhouse gases (GHGs) to air and their global warming potential with a timeframe of 100 years (GWP 100a). The second method (i.e. CED) aims to evaluate the total primary energy input for the production of each technology by considering the energy resources divided into the following five impact categories:

- Non-renewable - fossil;
- Non-renewable - nuclear;
- Renewable - biomass;
- Renewable - wind, solar, geothermal;
- Renewable - water.

In order to get the value of the Cumulative Energy Demand, each impact category has been given the weighting factor 1 without normalization.

The first step of the simplified environmental analysis is the estimation of the standardized cradle-to-gate environmental impact of each ZERO-PLUS renewable energy production technology that has been integrated into each ZERO-PLUS settlement as RES installation at the community level.

The second step of the simplified approach consists in the comparison between the environmental impact produced by the following two scenarios, both elaborated for each settlement:

- ZERO-PLUS SCENARIO: where the environmental impact is associated with the primary energy produced by the ZERO-PLUS renewable energy technologies installed within the settlement to serve the community;
- REFERENCE SCENARIO: where the environmental impact is associated with the primary energy (same amount of primary energy produced by the ZERO-PLUS renewable energy technologies) produced by the national energy carrier mix.

To perform the comparison, the REFERENCE SCENARIO has been elaborated by means of the SimaPro software as follows:

- Selection, from the SimaPro database, of the appropriate data sets related to the national

power generation energy mix for each case study settlement;

- Adaptation of each data set in order to consider the pre-use phase and not the recycling disposal phase. This modification is necessary for comparison purposes since the recycling disposal has not been considered in the ZERO-PLUS technologies' environmental analysis either;
- Input the cumulative primary energy production values, generated in each settlement by the ZERO-PLUS renewable energy technologies, as the multiplier of each variable of the selected data sets;
- Selection of the LCA methods in SimaPro software, i.e. both the IPCC_{GWP 100a} and the CED methods;
- Run the simulations for each REFERENCE SCENARIO associated with the investigated net-zero energy settlements;
- Set the outputs with the appropriate units of measure.

In the final step, the environmental performance of the new residential demonstration case study dwellings has been evaluated by means of the pre-assessment of the rating system LEED v4 for Building Design and Construction (BD+C): Homes and Multifamily Low-rise [19]. This rating system consists in attributing a maximum of 100 points to each demonstration building across 8 LEED credit categories: i) Location and Transportation, ii) Sustainable Sites, iii) Water Efficiency, iv) Energy and Atmosphere, v) Materials and Resources, vi) Indoor Environmental Quality, vii) Innovation in Design, and viii) Regional Priority. Other 4 and 6 additional points may be added at the maximum for Regional Priority and Innovation in Design credits, respectively.

Figure 1 shows the 4 levels of LEED certification that can be assigned to a building with respect to the associated number of achieved points.



Figure 1: LEED certification levels.

2.1 Italian case study settlement

This paper presents the results of the simplified LCA approach and the LEED pre-assessment evaluation applied to the preliminary design of the Italian ZERO-PLUS settlement. The Italian case study settlement is

located in Granarolo dell'Emilia (Bologna), in the northern part of Italy and it is characterized by a Temperate and Mediterranean climate (Köppen-Geiger climate classification Cfa) [20] with an annual global solar radiation on a horizontal surface equal to 1429 kWh/sqm. According to the Italian zoning defined in the D.P.R. 412/1993 [21], the settlement falls into the climatic zone E characterized by 2162 Heating Degree Days (HDDs) and about 110 Cooling Degree Days. The Italian ZERO-PLUS settlement belongs to a flat residential area of 9,600 sqm and consists of 8 single-family villas. Among those villas, 2 have been selected as the demonstration case study villas of the ZERO-PLUS project. The 2 demonstration villas are characterized by a similar architectural and technical design specifically adapted to meet the ZERO-PLUS requirements. Each villa presents a total floor area of approximately 240 sqm and a net floor area of approximately 125 sqm.

Figure 2 shows the elevations of the 2 demonstration single-family villas of the Italian ZERO-PLUS settlement at the preliminary stage of the design.

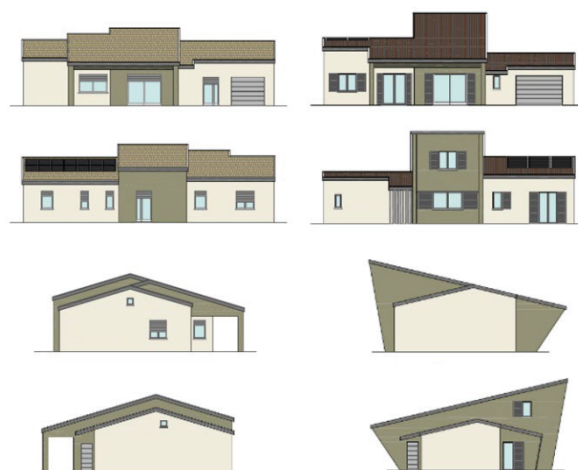


Figure 2: Elevations of the 2 Italian demonstration ZERO-PLUS villas (from the top to the bottom: West, East, North, and South elevation).

In the preliminary design stage, the ZERO-PLUS renewable energy production technology that has been selected for the Italian settlement is the WindRail® B60 system, a solar and wind-driven energy system produced by Anergdy. This innovative technology is able to produce electricity in all seasons under a range of different weather conditions and even with a low value of wind speed [22].

Figure 3 shows the initial design of one module of the WindRail® B60 system installed on the pitched rooftop of a building where the two main renewable energy components are clearly visible: i) the micro

wind turbine (composed by two rotors) able to automatically align with the prevalent wind direction, and ii) 4 photovoltaic panels.

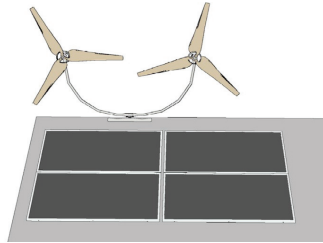


Figure 3: Visual representation of 1 module of the initial design of the WindRail® B60 produced by Anergdy [23].

To achieve the energy production target set by the ZERO-PLUS project at settlement level (i.e. 50 kWh/sqm per year), the Italian settlement has been provided with 2 modules of WindRail® B60 system and 28 sqm of traditional photovoltaic panels. Each WindRail® B60 module has been considered for installation on the pitched rooftop of each villa, close to the photovoltaic panels.

2.2 LCA results for the WindRail® B60 system

The GHG (i.e. IPCC_{GWP 100a}) and the primary energy (i.e. CED) embodied in 1 module of the WindRail® B60 system are presented in Table 1 together with its thermal and electric energy production. All the values reported in Table 1 have been provided by the technology provider Anergdy for the initial version of the WindRail® B60 system and for the specific installation in the Italian settlement.

Table 1: Summary of the LCA results for the WindRail® B60 system.

ZERO-PLUS renewable energy production technology	WindRail® B60
Functional Unit (f.u.)	1 module
Lifetime [y]	30
Electric energy prod. [kWh/y]	1908
Net thermal energy prod. [kWh/y]	-
IPCC _{GWP 100a} [kgCO _{2eq}]	2540
CED [MJ]	36,109

2.3 Results of the environmental impact analysis at the settlement level

The total electric energy production generated at the settlement level by the 2 modules of the WindRail® B60 system when installed on the rooftop of the 2 demonstration villas has been estimated to be equal to 3816 kWh/y, the double of the electric energy production generated by a single module of the WindRail® B60 system (i.e. 1908 kWh/y as in Table 1).

The total thermal energy production generated at the settlement level by the 2 modules of the WindRail® B60 system is equal to zero, as per 1 single module.

The two total electric and thermal energy production values have been used to estimate the settlement' total primary energy production generated by the 2 modules of the WindRail® B60 system. More in the detail, the total primary energy production, produced at the settlement scale, has been calculated based on the electric and thermal energy production associated with the 2 modules of the WindRail® B60 system opportunely converted into primary energy through the use of the national grid coefficient (i.e. in Italy, 2.5 for the conversion of the electric energy and 1.11 for the conversion of the thermal energy).

The environmental impact analysed in terms of the same two single indexes, i.e. IPCC and CED, has been estimated for the 2 modules of the WindRail® B60 system by applying the principle of superposition of the embodied energy and GHG emission outputs at the settlement level (see the ZERO-PLUS SCENARIO in Table 2). The results of the environmental impact analysis summarized for the ZERO-PLUS SCENARIO in Table 2 are presented in terms of embodied energy, as in Table 1.

The amount of primary energy produced at the settlement level by the 2 modules of the hybrid electrical renewable energy system WindRail® B60 (i.e. Settlement primary energy production, in Table 2) has also been used as an input for the SimaPro software to calculate the environmental impact of the REFERENCE SCENARIO considering the two selected independent indexes, i.e. IPCC and CED.

Table 2 allows the comparison between the results of the simplified environmental analysis for the ZERO-PLUS SCENARIO and the simulated results, obtained as SimaPro outputs, for the REFERENCE SCENARIO. All the values reported in Table 2 refer to the entire ZERO-PLUS settlement.

Table 2: Summary of the simplified LCA results for the Italian ZERO-PLUS and REFERENCE scenarios.

SCENARIO	ZERO-PLUS	REFERENCE
Settlement primary energy production [kWh/y]	9540	9540
Settlement IPCC _{GWP 100a} [kgCO _{2eq}]	5080	6820
Settlement CED [MJ]	72,218	106,000

2.4 Result of the LEED pre-assessment

Prerequisites and credits have been assigned to the preliminary designs of the 2 Italian demonstration villas according to the LEED v4 certification with the aim to obtain the potential LEED certification level. The result of the LEED pre-assessment for the Italian case study is presented in Table 3. The categories where the ZERO-PLUS design solutions have contributed to the collection of LEED points are ii) (e.g., use of cool and permeable materials to reduce the heat island and for rainwater management), iv) (e.g., use of energy conservation measures and PV panels), v) (e.g., use of local materials), vi) (e.g., use of the radiative system and ventilation system), and viii) where 4 regional priority credits are achieved for the Annual energy use, Active solar-ready design, Site selection, and Rainwater management. ZERO-PLUS does not address any other category, including water efficiency where 3 points are achieved because the design of the Italian dwellings meets the national building regulation requirements for what concerns the water use.

Table 3: LEED pre-assessment for both Italian demonstration villas.

Category (*ZERO-PLUS contribution)	Possible credits	Earned credits
Integrative process	2	1
i) Location and transportation	15	6.5
ii) Sustainable sites*	7	4
iii) Water efficiency	12	3
iv) Energy and atmosphere*	38	35
v) Materials and resources*	10	6.5
vi) Indoor Environm. Quality*	16	12
vii) Innovation	6	1
viii) Regional priority*	4	4
Total	110	73
LEED for Homes certification: GOLD		

3. DISCUSSION OF THE RESULTS

The environmental efficacy of the novel WindRail® B60 system has been demonstrated in this study by observing the results of the environmental impact comparison between the ZERO-PLUS and the REFERENCE scenarios, that refers to the common national solutions (i.e. Italian power generation energy mix) for the energy production. In Table 2, it is possible to note that, even if the 2 modules of the WindRail® B60 system produce an environmental impact that can be considered as equivalent (meaning low differences between the two scenarios) to the one associated to the Italian power generation energy mix (considering the same amount of primary energy produced at settlement level), both IPCC and CED indexes are lower for the ZERO-PLUS SCENARIO.

The Gold LEED certification potentially achievable by the 2 Italian demonstration villas highlights instead that the ZERO-PLUS framework when applied is able to produce environmentally friendly buildings.

4. CONCLUSION

The people's awareness about climate change is growing as well as the number of demanding energy and environmental regulations that are coming in force in Europe and all around the world. Through the H2020 energy efficiency program, the European Commission is supporting projects, like ZERO-PLUS, which aims to achieve sustainable buildings and reduce energy consumption and greenhouse gas emissions in Europe by means of new research approaches and technology innovation applied on a large scale in the building sector.

In this paper, a novel and simplified LCA approach and a pre-assessment evaluation of the green building program LEED have been presented applied to the ZERO-PLUS settlement of Granarolo dell'Emilia (Bologna), Italy. The same has been applied also to the other 3 ZERO-PLUS case study settlements to facilitate the assessment of the sustainability level of novel renewable energy systems (RESSs) when implemented for community use.

As a result of the simplified environmental impact analysis presented in this paper, the ZERO-PLUS SCENARIO, defined as the scenario where the primary energy demand of the settlement is covered by the energy produced by the novel renewable energy system (e.g., the WindRail® B60 system for the Italian case study), presents lower values of both IPCC and CED indexes with respect to the same values estimated for the REFERENCE SCENARIO, defined as the scenario where the primary energy demand of the settlement is covered by the energy supplied by the national electricity grid.

According to the rating system LEED v4, both Italian demonstration villas are capable to earn the Gold LEED certification thanks to the ZERO-PLUS preliminary design. As further development, the new rating system LEED v4.1 Residential: Single Family Homes should be applied to the completed demonstration buildings with the aim to pursue the LEED certification for the demonstration buildings of the ZERO-PLUS project.

Even if the simplified environmental analysis proposed in this study presents not negligible limitations in terms of accuracy and completeness of the results with respect to the traditional Life Cycle Assessment, it presents also the advantages of being simple and quick to be performed during the preliminary stage of the settlement design, when the renewable energy production technologies need to be

integrated at the community level to achieve the target of a net-zero or positive energy settlement.

As a general conclusion, the ZERO-PLUS project offers a prominent solution for sustainable buildings and settlements. It demonstrates, through the real implementation of the 4 near-zero energy settlements, that it is already possible to obtain more energy efficient, reliable, sustainable, and cost-effective residential buildings. Thus, the key message of the project is that, by moving the design from the building to the settlement scale, it is feasible to create future residential communities that are affordable and able to minimize the environmental impact.

ACKNOWLEDGEMENTS

This work has received funding from the European Union Horizon 2020 Programme in the framework of the “ZERO-PLUS project: Achieving near Zero and Positive Energy Settlements in Europe using Advanced Energy Technology”, under grant agreement n° 678407. The author thanks CONTEDIL and Sven Koehler from Anergdy for providing the data, the ZERO-PLUS partnership and the University of Athens group for the cooperation and coordination effort.

REFERENCES

- Voss, K., E. Musall, (2013). Net Zero Energy Buildings: International Projects of Carbon Neutrality in Buildings. *DETAIL Green Books*, ISBN-978-3-0346-0780-3. Munich, 2011.
- Artopoulos, G., G. Pignatta, M. Santamouris, (2018). From the Sum of Near-Zero Energy Buildings to the Whole of a Near-Zero Energy Housing Settlement: The Role of Communal Spaces in Performance-Driven Design, *Architecture_MPS*, 14(1).
- Ascione, F., N. Bianco, F. De Rossi, R.F. De Masi, G.P. Vanoli, (2016). Concept, Design and Energy Performance of a Net Zero-Energy Building in Mediterranean Climate. *Procedia Engineering*, 169: p. 26-37.
- Ascione, F., N. Bianco, R.F. De Masi, M. Dousi, S. Hionidis, S. Kaliakos, E. Mastrapostoli, M. Nomikos, M. Santamouris, A. Synnefa, G.P. Vanoli, K.Vassilakopoulou, (2017). Design and performance analysis of a zero-energy settlement in Greece. *International Journal of Low-Carbon Technologies*, 12(2): p. 141–161.
- Ascione, F., N. Bianco, O. Böttcher, R. Kaltenbrunner, G.P. Vanoli, (2016). Net zero-energy buildings in Germany: Design, model calibration and lessons learned from a case-study in Berlin. *Energy and Buildings*, 133: p. 688-710.
- Directive (EU) 2018/844 of the European Parliament and the Council on the energy performance of buildings and Directive 2012/27/EU on energy efficiency, [Online], Available: <http://data.europa.eu/eli/dir/2018/844/oj> [5 May 2020].
- ZERO-PLUS project website, [Online], Available: www.zeroplus.org/ [5 May 2020].
- Pisello, A.L., C. Piselli, G. Pignatta, C. Fabiani, F. Ubertini, F. Cotana, M. Santamouris, (2016). Net Zero Energy settlements in Europe: first findings of the Zero-Plus Horizon 2020 project. In *16th CIRIAF National Congress*. Assisi, Italy, April 7-9.
- Castaldo, V.L., A.L. Pisello, C. Piselli, C. Fabiani, F. Cotana, M. Santamouris, (2018). How outdoor microclimate mitigation affects building thermal-energy performance: A new design-stage method for energy saving in residential near-zero energy settlements in Italy. *Renewable Energy*, 127: p. 920–935.
- Isaac, S., S. Shubin, G. Rabinowitz, (2020). Cost-Optimal Net Zero Energy Communities. *Sustainability*, 12(6): p. 2432.
- Hernandez, P., P. Kenny, (2010). From net energy to zero energy buildings: Defining life cycle zero energy buildings (LC-ZEB), *Energy and Buildings*, 42: p. 815–821.
- U.S. Green Building Council (USGBC) website, [Online], Available: www.usgbc.org/ [5 May 2020].
- Synnefa, A., M. Laskari, R. Gupta, A.L. Pisello, M. Santamouris, (2017). Development of Net Zero Energy Settlements Using Advanced Energy Technologies. *Procedia Engineering*, 180: p. 1388-1401.
- ISO 14040:2006, Environmental management – Life cycle assessment – Principles and framework. *International Organization for Standardization*, [Online], Available: www.iso.org [5 May 2020].
- ISO 14044:2006/AMD 1:2017, Environmental management – Life cycle assessment – Requirements and guidelines – Amendment 1. *International Organization for Standardization*, [Online], Available: www.iso.org [5 May 2020].
- SimaPro software, [Online], Available: www.pre-sustainability.com/simapro
- M. Jefferson, (2015). IPCC fifth assessment synthesis report ‘Climate change 2014: Longer report’: Critical analysis, *Technological Forecasting and Social Change*, 92: p. 362-363.
- Brecheisen T., T. Theis, (2015). Chapter 10 - Life cycle assessment as a comparative analysis tool for sustainable brownfield redevelopment projects: Cumulative energy demand and greenhouse gas emissions. *Assessing and Measuring Environmental Impact and Sustainability*: p. 323-365.
- LEED v4 rating system selection guidance - LEED BD +C: Homes and Multifamily Lowrise, [Online], Available: www.usgbc.org/leed-tools/rating-system-selection-guidance [5 May 2020].
- Peel, M.C., B.L. Finlayson, T.A. McMahon, (2007). Updated world map of the Köppen–Geiger climate classification. *Hydrology and Earth System Sciences*, 11: p. 1633–1644.
- The D.P.R. no. 412/93 “Norme per la progettazione, l'installazione e la manutenzione degli impianti termici degli edifici ai fini del contenimento dei consumi di energia” – Italian climatic zones, [Online], Available: www.certifico.com/component/attachments/download/6600 [5 May 2020].
- Anergdy WindRail® system website, [Online], Available: www.anerdy.com/en/solutions/building [5 May 2020].
- ZERO-PLUS Public Deliverables (2016). A full report of the outdoor energy technologies and renewable systems at NZE settlement, [Online], Available: www.zeroplus.org/pdf/ZERO%20PLUS_D4.1.pdf [5 May 2020].